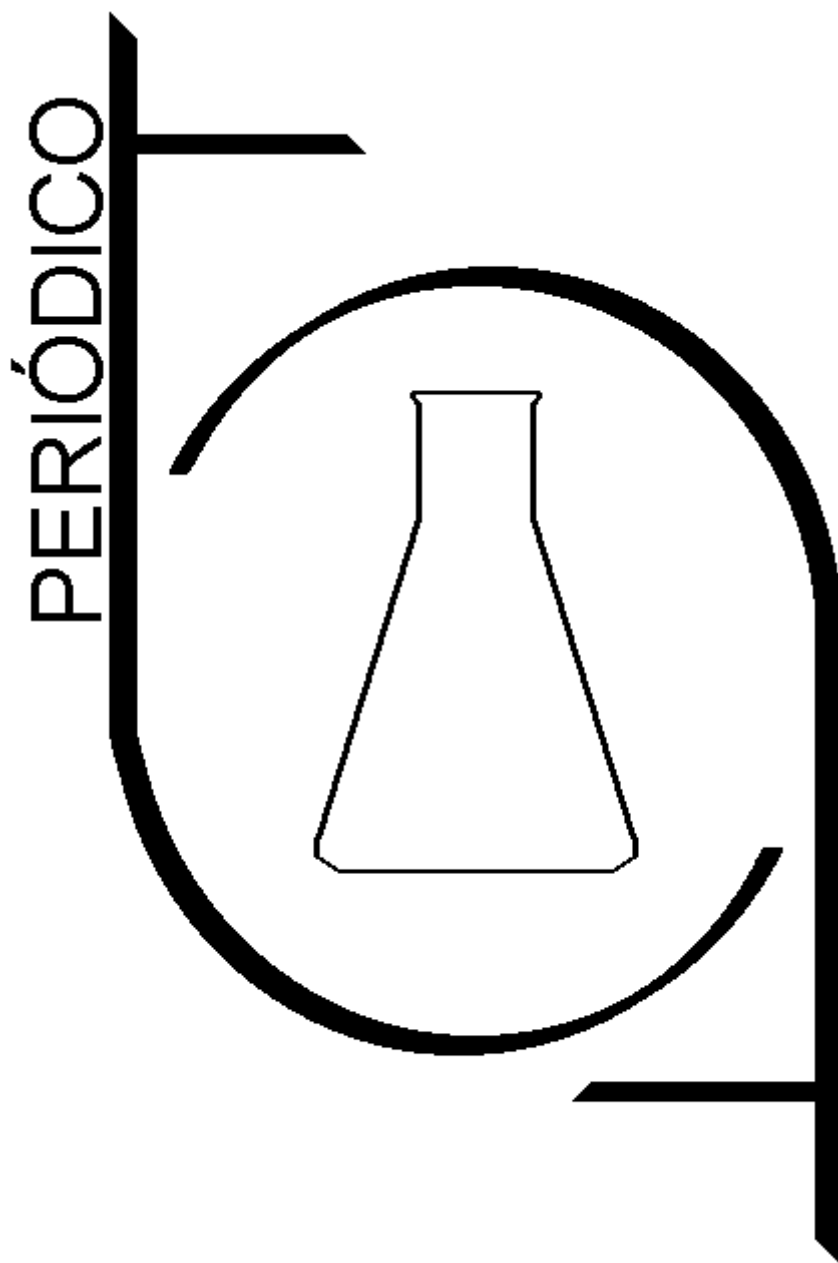


PERIÓDICO TCHÊ QUÍMICA



Volume 17

-

Número 34

-

2020 ISSN 2179-0302

Órgão de divulgação científica e informativa

www.periodico.tchequimica.com

PERIÓDICO TCHÊ QUÍMICA

ISSN - 1806-0374 (Impresso) - ISSN - 2179-0302 (Online)

Volume 17

Número 34 – 2020

ISSN 2179 - 0302

Órgão de divulgação científica e informativa.

Dados Internacionais de Catalogação na Publicação (CIP)

Periódico Tchê Química: órgão de divulgação científica e informativa [recurso eletrônico] / Grupo Tchê Química – Vol. 1, n. 1 (Jan. 2004)- . – Porto Alegre: Grupo Tchê Química, 2005 - Semestral.

Sistema requerido: Adobe Acrobat Reader.

Modo de acesso: World Wide Web:

<<http://www.tchequimica.com>>

Descrição baseada em: Vol. 14, n. 28 (ago. 2017).

ISSN 1806-0374

ISSN 2179-0302

1. Química. I. Grupo Tchê Química.

CDD 540

Bibliotecário Responsável

Ednei de Freitas Silveira

CRB 10/1262



Welcome to the TCHÊ QUÍMICA JOURNAL

International multidisciplinary scientific journal

*The Tchê Química Journal publishes original research papers, review articles, short communications (scientific publications), book reviews, forum articles, technical reports, articles on chemical education, interviews, announcements or letters. Articles suitable for publication in the Tchê Química Journal are those that cover the traditional fields of **Chemistry, Physics, Mathematics, Biology, Pharmacy, Medicine, Engineering and Agriculture**. We are especially interested in those submissions that are highly relevant to theoretical and applied contributions in the area of chemistry and related disciplines.*

PERIÓDICO TCHÊ QUÍMICA

Volume 17

Número 34 – 2020

ISSN 2179 - 0302

Órgão de divulgação científica e informativa.

Comissão Editorial

Editores-chefe

- Dr. Luis Alcides Brandini De Boni,
deboni@tchequimica.com
- Dr. Eduardo Goldani,
goldani@tchequimica.com

Editores técnicos

- Ednei de Freitas Silveira
– *Bibliotecário Responsável*
- Dr. Francisco José Santos Lima,
lima@tchequimica.com, Brasil, UFRN.
- Dr. Carlos Eduardo Cardoso,
cardoso@tchequimica.com, Brasil, USS.
- Dr. Sérgio Machado Corrêa,
correa@tchequimica.com, Brasil, UERJ.

Corpo Editorial

Membros

- Teresa M. Roseiro Maria Estronca, Dr.,
roseiro@tchequimica.com, Portugal, UC.
- Monica Regina da Costa Marques, Dr.,
aguiar@tchequimica.com, Brasil, UERJ.
- Ketevan Kapatadze, Dr.,
kapatadze@tchequimica.com, Geórgia, ISU.
- Márcio von Mühlen, Dr.,
vonmuhlen@tchequimica.com, EUA, MIT.
- Élcio Jeronimo de Oliveira, Dr.,
elcio@tchequimica.com, Brasil, CTA.

- José Carlos Oliveira Santos, Dr.,
zecarlosufcg@tchequimica.com, Brasil, UFCG.
- Alcides Wagner Serpa Guarino, Dr.,
guarino@tchequimica.com, Brasil, UNIRIO.
- Roseli Fernandes Gennari, Dr.,
gennari@tchequimica.com, Brasil, USP.
- Rafael Rodrigues de Oliveira, Dr.,
oliveira@tchequimica.com, Brasil, Brava Biosciences.
- Lívio César Cunha Nunes, Dr.,
nunes@tchequimica.com, Brasil, UFPI.
- João Guilherme Casagrande Jr, Dr.,
casagrande@tchequimica.com, Brasil, EMBRAPA.
- Denise Alves Fungaro, Dr.,
fungaro@tchequimica.com, Brasil, IPEN.
- Murilo Sérgio da Silva Julião, Dr.,
juliao@tchequimica.com, Brasil, UVA.
- Amit Chaudhry, Dr.,
chaudhry@tchequimica.com, Índia, Panjab University.
- Hugo David Chirinos Collantes, Dr.,
chirinos@tchequimica.com, Peru, UNI.
- Carlos E. de Medeiros J., Dr.,
jeronimo@tchequimica.com, Brasil, PETROBRAS.
- Walter José Peláez, Dr.,
pelaez@tchequimica.com, Argentina, UNC.
- Rodrigo Brambilla, Dr.,
brambilla@tchequimica.com, Brasil, UFRGS.
- Joan Josep Solaz-Portolés, Dr.,
solaz@tchequimica.com, Espanha, UV.
- José Euzébio Simões Neto, Dr.,
simoes@tchequimica.com, Brasil, UFRP.
- Aline Maria dos Santos Teixeira, Dr.,
santos@tchequimica.com, Brasil, UFRJ.

- César Luiz da Silva Guimarães, Me., guimaraes@tchequimica.com, Brasil, IBAMA.
- Daniel Ricardo Arsand, Dr., arsand@tchequimica.com, Brasil, IFSul.
- Paulo Sergio Souza, Dr., souza@tchequimica.com, Brasil, Fundação Osorio.
- Moisés Rômolos Cesário, Dr., romolos@tchequimica.com, França, ULCO.
- Andrian Saputra, Dr., saputra@tchequimica.com, Universidade de Lampung, Indonésia.
- Vanessa Barbieri Xavier, Dr., xavier@tchequimica.com, Brasil, PUCRS.
- Danyelle Medeiros de Araújo Moura, Dr., moura@tchequimica.com, Brasil, UFRN.
- Gabriel Rubensam, Me., grubensam@tchequimica.com, Brasil, UFRGS.
- Masurquede de Azevedo Coimbra, Me., coimbra@tchequimica.com, Brasil, Sec. de Saúde do Estado - RS.
- Oana-Maria Popa, Me., popa@tchequimica.com, IPN, Romênia.

Esta revista é indexada e resumida pelo CAS, EBSCO, Latindex, Sumários, Index Copernicus, Scopus, OAIJ, CAB Abstracts, EuroPub e Reaxys.

Missão

O Periódico Tchê Química (PTQ) publica artigos de pesquisa originais, artigos de revisão, notas curtas (publicações científicas), revisões de livros, artigos de fórum, editoriais e entrevistas. Pesquisadores de todos os países são convidados a publicar nas páginas do PTQ.

A responsabilidade sobre os artigos é de exclusividade dos autores.

Correspondências

Rua Anita Garibaldi, 359/603.
Bairro Mon't Serrat. CEP: 90450-001
Porto Alegre – RS. Brasil.
Skype: tchequimica
www.periodico.tchequimica.com
tchequimica@tchequimica.com

Periódico Tchê Química

ISSN - 1806-0374 (Print)
ISSN - 2179-0302 (Online)

LCCN: 2010240735

Divulgação *on-line* em
<http://www.periodico.tchequimica.com>
<http://www.journal.tchequimica.com>
<http://www.tchequimica.com>

Índice

1 - Artigo / Article

SANTOS, ANDRÉIA GREGÓRIO DA SILVA; NAVARRO, DANIELA DO AMARAL FERRAZ; MAGALHÃES, NEREIDE STELA SANTOS; MELO-SANTOS, MARIA ALICE VARJAL; BRANDÃO, SOFIA SUELY FERREIRA

BRASIL

ATIVIDADE LARVICIDA DE ÓLEO ESSENCIAL DE CROTON RHAMNIFOLIOIDES (PAX & ENCAPSULADO EM NANOSSISTEMA POLIMÉRICO FRENTE AO MOSQUITO AEDES AEGYPTI

LARVICIDAL ACTIVITY OF CROTON RHAMNIFOLIOIDES (PAX & HOFFM) ESSENTIAL OIL ENCAPSULATED IN A POLYMERIC NANOSYSTEM AGAINST THE MOSQUITO AEDES AEGYPTI

Página – 1

3 - Artigo / Article

ARJMANDI, ZAHRA; MAHMOODI, ZOHREH; BEHBOODI MOGHADAM, ZAHRA; MAHMOODZADEH, HABIBOLLAH; QORBANI, MOSTAFA;

IRÃ

O EFEITO DO PROGRAMA EDUCACIONAL BASEADO NO CONCEITO DE INTIMIDADE SEXUAL ATRAVÉS DE SMARTPHONE EM MULHERES PÓS-MASTECTOMIA: UM ESTUDO CLÍNICO RANDOMIZADO CONTROLADO

THE EFFECT OF EDUCATIONAL PROGRAM-BASED ON SEXUAL INTIMACY CONCEPT VIA SMARTPHONE IN WOMEN FOLLOWING MASTECTOMY: A RANDOMIZED CONTROLLED TRIAL

Página – 23

5 - Artigo / Article

SUKMAWATI, FATMA; SETYOSARI, PUNAJI; SULTON, SULTON; PURNOMO; PURNOMO

INDONÉSIA

O EFEITO DA APRENDIZAGEM COLABORATIVA BASEADA EM PROJETOS NO DOMÍNIO DO CONCEITO DE COGUMELO: O CASO DE ESTUDANTES DE ENSINO MÉDIO NA INDONÉSIA

THE EFFECT OF PROJECT-BASED COLLABORATIVE LEARNING ON CONCEPT MASTERY OF MUSHROOM: THE CASE OF SENIOR HIGH SCHOOL STUDENTS IN INDONESIA

Página – 45

2 - Artigo / Article

PRASETYA, AGUNG TRI; CAHYONO, EDY; SUDARMIN; HARYANI, SRI

INDONÉSIA

COMO OS PROCEDIMENTOS DE QUALIDADE DE LABORATÓRIO AFETAM A COMPETÊNCIA DOS ESTUDANTES COM GRADUAÇÃO EM QUÍMICA?

HOW LABORATORY QUALITY PROCEDURES AFFECT THE COMPETENCE OF CHEMISTRY UNDERGRADUATE STUDENTS?

Página – 10

4 - Artigo / Article

BOGDANOVA, EKATERINA V.; MELNIKOVA, ELENA I.; KOSHEVAROVA, IRINA B.;

RUSSIA

ESTUDO DAS FORMAS DE CONEXÃO À UMIDADE DE COMPONENTES EM CONCENTRADOS DE PROTEÍNA-CARBOIDRATO DE SORO DE QUEIJO

THE RESEARCH OF THE TYPES OF MOISTURE BONDS IN PROTEIN-CARBOHYDRATE CONCENTRATES OF CHEESE WHEY

Página – 33

6 - Artigo / Article

PORTELA, LINO WAGNER CASTELO BRANCO; ALMEIDA, ANA FABIOLA LEITE; BARBOSA, ERILSON DE SOUSA; CEZAR, KLEBER LIMA; OLIVEIRA, PATRICK ABREU

BRASIL

ANÁLISE ENERGÉTICA E DESEMPENHO DE UM COLETOR SOLAR CILÍNDRICO PARABÓLICO AUXILIADO POR SISTEMA DE RASTREAMENTO SOLAR

ENERGY ANALYSIS AND PERFORMANCE OF A PARABOLIC CYLINDRICAL SOLAR COLLECTOR AIDED BY SOLAR TRACKING SYSTEM

Página – 53

7 - Artigo / Article

BATALINI, CLAUDEMIR; DE GIOVANI, WAGNER FERRARESI

BRASIL**OXIDAÇÕES ELETROQUÍMICAS DE SUBSTÂNCIAS ORGÂNICAS USANDO COMO CATALISADOR UM NOVO AQUACOMPLEXO DIARSÍNICO DE RUTÊNIO (II)**

ELECTROCHEMICAL OXIDATIONS OF ORGANIC SUBSTANCES USING A NEW RUTHENIUM (II) DIARSENIC AQUACOMPLEX AS CATALYST

Página – 62

9 - Artigo / Article

BUDEIZ, VICTOR; AGUIAR, ANDRÉ

BRASIL**MONITORAMENTO E RELACIONAMENTO DOS PARÂMETROS DQO E DBO₅ EM AFLUENTE E ESGOTO TRATADO DAS CIDADES DE ITAJUBÁ E PEDRALVA, MG**

MONITORING AND RELATIONSHIP OF COD AND BOD₅ PARAMETERS IN AFLUENT AND TREATED SEWAGE FROM ITAJUBÁ AND PEDRALVA CITIES, MG

Página – 80

11 - Artigo / Article

HIND MAHDI SALEH

IRAQUE**INVESTIGAÇÃO DAS CARACTERÍSTICAS DO POLIFURFURAL PREPARADO ATRAVÉS DO PROCESSO DE POLIMERIZAÇÃO**

CHARACTERISTICS INVESTIGATION OF PREPARED POLYFURFURAL THROUGH THE POLYMERIZATION PROCESS

Página – 112

13 - Artigo / Article

SEVBITOV, ANDREI; TIMOSHIN, ANTON; DOROFEEV, ALEKSEI; DAVIDYANTS, ALLA; ERSHOV, KIRILL; KUZNETSOVA, MARIA

RÚSSIA**CARACTERÍSTICAS COMPARATIVAS DO ESTADO DE TECIDOS DENTÁRIOS DUROS EM PACIENTES DEPENDENTES DE DROGAS QUE USAM HEROÍNA, E METADADONA COMO TERAPIA DE SUBSTITUIÇÃO**

COMPARATIVE CHARACTERISTICS OF THE STATE OF HARD DENTAL TISSUES IN DRUG-DEPENDENT PATIENTS WHO USE HEROIN, AND METHADONE AS REPLACEMENT THERAPY

Página – 135

8 - Artigo / Article

KENZHEBEK AKMALAIULY; ZHANAR ZHUMADILOVA

CAZAQUISTÃO**INFLUÊNCIA DA QUALIDADE DO FILLER NA CONDUTIVIDADE TÉRMICA DO CONCRETO**

INFLUENCE OF FILLER QUALITY ON CONCRETE THERMAL CONDUCTIVITY

Página – 67

10 - Artigo / Article

MUSSABEKOVA, SAULE AMANGELDIEVNA

CAZAQUISTÃO**POSSIBILIDADES DE IDENTIFICAÇÃO DE MANCHA DO SÊMEN APÓS A LAVAGEM DE ROUPAS E ROUPAS DE CAMA EM CASOS DE INVESTIGAÇÃO DE ABUSO SEXUAL**

POSSIBILITIES OF SEMEN STAIN IDENTIFICATION AFTER CLOTHING AND BEDDING WASHING IN INVESTIGATING CASES OF SEXUAL ASSAULT

Página – 93

12 - Artigo / Article

MOUSAVIE, SEYED HAMZEH; BEIGI RIZI, KAMRAN; HOSSEINPOUR PARISA; NEGAHI ALI REZA.

IRÃ**COMPARAÇÃO DE ABORDAGENS CIRÚRGICAS E NÃO CIRÚRGICAS AO TRAUMA ESPLÊNICO**

COMPARISON OF SURGICAL AND NON-SURGICAL APPROACHES TO SPLENIC TRAUMA

Página – 125

14 - Artigo / Article

FONSECA, JEMIMA GONÇALVES PINTO; EITERER, LUCAS PRUDÊNCIO; OTENIO, MARCELO HENRIQUE; PASSOS, LEÔNIDAS PAIXÃO; SILVA, JÚLIO CÉSAR JOSÉ

BRASIL**INFLUÊNCIA DE PARÂMETROS METEOROLÓGICOS NA CONCENTRAÇÃO DE METAIS PESADOS E AGENTES ETIOLÓGICOS EM AMOSTRAS DE LODO DE ESGOTO COMO FERRAMENTA PARA SEU USO NA AGRICULTURA**

INFLUENCE OF METEOROLOGICAL PARAMETERS ON THE CONCENTRATION OF HEAVY METALS AND ETIOLOGICAL AGENTS IN SEWAGE SLUDGE SAMPLES AS A TOOL FOR THEIR USE IN AGRICULTURE

Página – 147

15 - Artigo / Article

ALAM, ASHRAF

ÍNDIA

**PEDAGOGIA DO CÁLCULO NA ÍNDIA: UMA INVESTIGAÇÃO
EMPÍRICA**

*PEDAGOGY OF CALCULUS IN INDIA: AN EMPIRICAL
INVESTIGATION*

Página – 164

17 - Artigo / Article

DORSKAIA, ELENA VLADIMIROVNA; PESTOV, SERGEI
MIHAYLOVICH

RÚSSIA

**ESTUDO DA PLASMASORÇÃO IN VITRO DE LIPOPROTEÍNA E
PROPRIEDADES FÍSICO-QUÍMICAS DE SORBENTES
POLIMÉRICOS COM GRUPOS AMINO SUBSTITUÍDOS**

*STUDY OF THE IN VITRO LIPOPROTEIN PLASMASORPTION
AND PHYSICO-CHEMICAL PROPERTIES OF POLYMERIC
SORBENTS WITH SUBSTITUTED AMINO GROUPS*

Página – 188

19 - Artigo / Article

FERNANDEZ-MAESTRE, ROBERTO

COLÔMBIA

**A IMPORTÂNCIA DO ENSINO DAS CURVAS DE TITULAÇÃO NA
QUÍMICA ANALÍTICA**

*THE IMPORTANCE OF TEACHING TITRATION CURVES IN
ANALYTICAL CHEMISTRY*

Página – 213

21 - Artigo / Article

MAZANKO, MARIA S.; CHISTYAKOV, VLADIMIR A.;
ALESHUKINA, IRAIDA S.; EID, MOEZ ALI; ABDULKADHIM,
KAREEM ABBOOD ZEJAWI;

RÚSSIA

**AValiação de PROPRIEDADES ANTIOXIDANTES E PRÓ-
OXIDANTES DE ESTIRPES DE LACTOBACILLUS E
ENTEROCOCCES USANDO O MÉTODO DE ORAC E
LUXBIOSENSOR**

*ASSESSING ANTIOXIDANT AND PROOXIDANT PROPERTIES
OF LACTOBACILLI AND ENTEROCOCCI STRAINS BY USING
ORAC AND LUX-BIOSENSOR METHODS*

Página – 240

16 - Artigo / Article

MARZANOV, Nurbiy S.; MARZANOVA, Saida N.; BAITLESSOV,
Yerbulat U.; BOZYMOVA, Aigul K.; DAVLETOVA, Ainur M.;

RÚSSIA

**CARACTERÍSTICAS DAS RAÇAS AUTÓCTONES DA RÚSSIA E
DO CAZAQUISTÃO DE ATRAVÉS DO TESTE DE
MICRONÚCLEOS**

*CHARACTERISTICS OF AUTOCHTHONOUS BREEDS OF
RUSSIA AND KAZAKHSTAN BY MICRONUCLEAR TEST*

Página – 181

18 - Artigo / Article

BAEHAKI, FARHAN; RUDIBYANI, RATU BETTA; AENI, SUCI
RIZKI NURUL PERDANA, RYZAL; AQMARINA, SHINDY NUR;

INDONÉSIA

**UTILIZAÇÃO DE SEMENTES DE *Salacca zalacca* COMO
ADSORVENTES DE CHROMIUM(VI)**

*UTILIZATION OF *Salacca zalacca* SEEDS AS CHROMIUM(VI)
ADSORBENTS*

Página – 200

20 - Artigo / Article

RUOSO, ANA CRISTINA; LHAMBY, ANDRESSA; MISSAGGIA,
ANDRÉ BRUM; KLUNK, MARCOS ANTÔNIO; CAETANO, NATAN
ROBERTO

BRASIL

**ANÁLISE ENERGÉTICA E ECONÔMICA DA UTILIZAÇÃO DO
ETANOL HIDRATADO**

*ENERGETIC AND ECONOMIC ANALYSIS OF USE OF
HYDRATED ETHANOL*

Página – 220

22 - Artigo / Article

AKHMEDOVA SAIDA R., OMAROV NABI S-M.;

RÚSSIA

**DETERMINAÇÃO DE INDICADORES DE ESTADO DE CITOCINA
E FATORES DE ANGIOGÊNESE EM PACIENTES COM
ENDOMETRIOSE GENITAL EXTERNA E DEFICIÊNCIA DE
VITAMINA D**

*DETERMINATION OF CYTOKINE STATUS INDICATORS AND
ANGIOGENESIS FACTORS IN PATIENTS WITH EXTERNAL
GENITAL ENDOMETRIOSIS AND VITAMIN D DEFICIENCY*

Página – 251

23 - Artigo / Article

OREKHOVA, YELENA YURIEVNA; GREBENKINA, LIDIA KONSTANTINOVNA; ZHOKINA, NADEZHDA ALEKSEEVNA; KUSHNYR, LIUBOV ALEKSANDROVNA; SAMOTAEV, PAVEL IGOREVICH

RÚSSIA

FORMAÇÃO DA ATITUDE BASEADA NOS VALORES DOS ALUNOS EM RELAÇÃO À FUTURA PROFISSÃO DOCENTE COMO BASE MORAL DA ÉTICA PEDAGÓGICA

FORMATION OF STUDENTS' VALUES-BASED ATTITUDE TO THE FUTURE TEACHING PROFESSION AS MORAL BASIS OF PEDAGOGICAL ETHICS

Página – 260

25 - Artigo / Article

YATSENKO, ALEXANDR SERGEEVICH;

RÚSSIA

O ESTUDO DA AGRESSIVIDADE BIOLÓGICA DO PÓ DE COMPOSIÇÕES FORMADAS E SEM AMIANTO, AMBOS EM SUA PRODUÇÃO E OPERAÇÃO

THE STUDY OF THE BIOLOGICAL AGGRESSIVENESS OF DUST OF ASBESTOSFORMED AND ASBESTOS-FREE COMPOSITIONS, BOTH IN THEIR PRODUCTION AND OPERATION

Página – 282

27 - Artigo / Article

GANEEV TIMUR IREKOVICH.; KABIROVA MILYAUSHA FAUZIEVNA; YUNUSOV RENAT RAMIZOVICH; GALIULLINA MARINA VLADIMIROVNA;

RÚSSIA

ALTERAÇÕES NO METABOLISMO DE FOSFORO-CÁLCIO NO HIPOTIROIDISMO EXPERIMENTAL

CHANGES IN PHOSPHORUS-CALCIUM METABOLISM IN EXPERIMENTAL HYPOTHYROIDISM

Página – 303

29 - Artigo / Article

TYULEPBERDINOVA, GULNUR A.; ORALBEKOVA, ZHANAR O.; GAZIZ, GULNUR G.; MAXUTOVA, BOTA A.; BAITENOVA, SALTANAT A.;

CAZAQUISTÃO

ANÁLISE COMPARATIVA DE MÉTODOS NUMÉRICOS DA SOLUÇÃO DE UM PROBLEMA INVERSO UNIDIMENSIONAL DE ACÚSTICA

COMPARATIVE ANALYSIS OF NUMERICAL METHODS OF THE SOLUTION OF A ONE-DIMENSIONAL INVERSE PROBLEM OF ACOUSTICS

Página – 321

24 - Artigo / Article

VENIAMINOVNA, KUROPTEVA ZOIA; MICHAILOVNA, BAYDER LARISA; LEONIDOVNA, BELAYA OLGA; TOKTOMAMATOVNA, ZHUMABAEVA TAASILKAN

RÚSSIA

AUMENTO DA SÍNTESE DE ÓXIDO NÍTRICO EM MACROFAGAS PERITONEAIS SOB A AÇÃO DO ÁCIDO ASCÓRBICO

INCREASED NITRIC OXIDE SYNTHESIS IN PERITONEAL MACROPHAGES UNDER THE ACTION OF ASCORBIC ACID

Página – 273

26 - Artigo / Article

OREKHOVA, YELENA YURIEVNA; GREBENKINA, LIDIA KONSTANTINOVNA; SUVOROVA, NATALYA ALEXANDROVNA ; STAVRUK, MARINA ALEXANDROVNA

RÚSSIA

CONDIÇÕES PEDAGÓGICAS PARA A FORMAÇÃO DE COMPETÊNCIA PROFISSIONAL DE ESTUDANTES DE UMA UNIVERSIDADE TÉCNICA

PEDAGOGICAL CONDITIONS OF FORMATION OF PROFESSIONAL COMPETENCE OF STUDENTS OF A TECHNICAL UNIVERSITY

Página – 291

28 - Artigo / Article

AITKALDUJAILI, NAWFAL HUSSEIN AND BANOON, SHAIMA RABEEH

IRAQUE

CARACTERIZAÇÃO ANTIBACTERIANA DE NANOPARTÍCULAS DE TITÂNIO NANOSSINTETIZADAS POR STREPTOCOCCUS THERMOPHILUS

ANTIBACTERIAL CHARACTERIZATION OF TITANIUM NANOPARTICLES NANOSYNTHESIZED BY STREPTOCOCCUS THERMOPHILUS

Página – 311

30 - Artigo / Article

SKVORTSOV, ARKADIY A.; KORYACHKO, MARINA V.; ZUEV, SERGEI M.; RYBAKOVA, MARGARITA R.;

RÚSSIA

PROCESSOS DE DEGRADAÇÃO NO SISTEMA AI-TI-SI SOB CHOQUE TÉRMICO

DEGRADATION PROCESSES IN THE AI-TI-SI SYSTEM UNDER THERMAL SHOCK

Página – 335

31 - Artigo / Article

UTYUZH, ANATOLY S.; YUMASHEV, ALEXEY V.; ISAKOV, ESENALI I.; MAKAROV, ALEXEY L.; MATVEEVA, ELENA A.

RÚSSIA**DIAGNÓSTICO E TRATAMENTO DE DOENÇAS PERIODONTAIS INFLAMATÓRIAS**

DIAGNOSIS AND TREATMENT OF INFLAMMATORY PERIODONTAL DISEASES

Página – 343

33 - Artigo / Article

ARISTIAWAN, YOSI; PUTRI RAMADHANINGTYAS, DILLANI; KOMALASARI, ISNA; STYARINI, DYAH; HAMIM, NURYATINI

INDONÉSIA**MÉTODO DE VALIDAÇÃO PARA DETERMINAÇÃO DE INSETICIDAS ORGANOCLORADOS EM GINSENG USANDO A CROMATOGRAFIA GASOSA ACOPLADA À ESPECTROMETRIA DE MASSA DE DILUIÇÃO ISOTÓPICA (ID-GC-MS)**

METHOD VALIDATION FOR ORGANOCHLORINE INSECTICIDES DETERMINATION IN GINSENG BY USING ISOTOPE-DILUTION GAS CHROMATOGRAPHY-MASS SPECTROMETRY (ID-GC-MS)

Página – 362

35 - Artigo / Article

SOBOLEV VLADIMIR D.; YUSHKIN ALEXEY A.; SABBATOVSKIY KONSTANTIN G.; SERGEEVA INESSA P.;

RÚSSIA**PROPRIEDADES DE TRANSPORTE DA PERCOLAÇÃO DE FASE LÍQUIDA EM RAMOS DE POLÍMEROS VÍTREOS ALTAMENTE PERMEÁVEIS**

TRANSPORT PROPERTIES OF LIQUID PHASE PERCOLATION CLUSTER IN HIGHLY PERMEABLE GLASSY POLYMERS

Página – 379

37 - Artigo / Article

BAKHSHALIYEVA, KONUL FARRUKH; NAMAZOV, NIZAMI RZA; HASANOVA, ARZU RASUL; MAMMADOVA, FIDAN RASIM; MURADOV, PANAH ZULFIGAR

AZERBAIJÃO**AVALIAÇÃO DAS PERSPECTIVAS DE ESTUDAR E USAR COGUMELOS DO AZERBAIJÃO COMO PRODUTORES EFICAZES DE SUBSTÂNCIAS BIOLÓGICAMENTE ATIVAS**

ASSESSMENT OF THE PROSPECTS OF STUDYING AND USING MUSHROOMS OF AZERBAIJAN AS EFFECTIVE PRODUCERS OF BIOLOGICALLY ACTIVE SUBSTANCES

Página – 403

32 - Artigo / Article

ZHAKATAYEVA, ALTYNAY; IZTAYEV, AUYELBEK; MULDABEKOVA, BAYAN; YAKIYAYEVA, MADINA; HRIVNA LUDEK

CAZAQUISTÃO**AVALIAÇÃO CIENTÍFICA DA SEGURANÇA DO RISCO DE SEGURANÇA DOS PRODUTOS DE AÇÚCAR BRUTO**

SCIENTIFIC SECURITY ASSESSMENT OF SAFETY RISK OF RAW SUGAR PRODUCTS

Página – 352

34 - Artigo / Article

OLIVEIRA JÚNIOR, CHARLES IVO DE; OIVEIRA, GUSTAVO FÉLIX; REZENDE, GLÁUCIA APARECIDA ANDRADE; ALVES, BLYENY HATALITA PEREIRA

BRASIL**COMPOSTOS FENÓLICOS TOTAIS E CAPACIDADE ANTIOXIDANTE *IN VITRO* DA CASCA E POLPA DE ABACAXI PÉROLA E ABACAXI HAVAIANO**

*TOTAL PHENOLIC COMPOUNDS AND *IN VITRO* ANTIOXIDATING CAPABILITY OF PEARL PINEAPPLE AND HAWAIIAN PINEAPPLE*

Página – 373

36 - Artigo / Article

SYROMYATNIKOV, MIKHAIL YURIEVICH; GUREEV, ARTYOM PETROVICH; MIKHAILOV, EVGENY VLADIMIROVICH; PARSHIN, PAVEL ANDREEVICH; POPOV, VASILY NIKOLAEVICH

RÚSSIA**EFEITO DE PESTICIDAS NO NÍVEL DE DANOS AO MTDNA EM CABEÇAS DE ABELHAS (*BOMBUS TERRESTRIS* L.)**

*PESTICIDES EFFECT ON THE LEVEL OF MTDNA DAMAGE IN BUMBLEBEES HEADS (*BOMBUS TERRESTRIS* L.)*

Página – 395

38 - Artigo / Article

KALIZHANOVA, ANNA; MARYSHKINA, TAISSIYA; ISHMURATOVA, MARGARITA; IBRAYEVA, BAYAN; SEMBIYEV, KURMANGAZY;

CAZAQUISTÃO**INTEGRANDO O COMPONENTE LINGUO-CULTURAL E O MÉTODO DO MAPA DA MENTE PARA DESENVOLVER UM E-DICIONÁRIO TRILÍNGUE DE TERMOS BIOLÓGICOS**

INTEGRATING THE LINGUOCULTURAL COMPONENT AND MIND-MAP METHOD TO DEVELOP A TRILINGUAL E-DICTIONARY OF BIOLOGICAL TERMS

Página – 412

39 - Artigo / Article

KHUSAINOV, ABILZHAN; SARSENOVA, ANARA; SINDIREVA, ANNA; YESSSENZHOLOV, BAURZHAN; ZHARKINBEKOV, TEMIRKHAN;

CAZAQUISTÃO

RACIONAMENTO ECOLÓGICO DE DOSES DE UMA PREPARAÇÃO CONTENDO CARBONO DE MÚLTIPLOS COMPONENTES ATRAVÉS DE CONTEÚDO DE METAIS PESADOS E ATIVIDADE MICROBIOLÓGICA DO SOLO

ECOLOGICAL RATIONING OF DOSES OF A MULTICOMPONENT CARBON-CONTAINING PREPARATION THROUGH HEAVY METAL CONTENT AND SOIL MICROBIOLOGICAL ACTIVITY

Página – 425

41 - Artigo / Article

AMORIM NETO, JUAREZ POMPEU DE; LIMA, RICARDO JOSÉ PONTES; ROCHA, PAULO ALEXANDRE COSTA; MARINHO, FELIPE PINTO; SILVA, MARIA EUGÊNIA VIEIRA DA

BRASIL

ANÁLISE EXPERIMENTAL DE UM SISTEMA SOLAR TÉRMICO UTILIZANDO NANOFLUIDO HÍBRIDO DE PRATA E DIÓXIDO DE TITÂNIO.

EXPERIMENTAL ANALYSIS OF A SOLAR HEAT SYSTEM USING HYBRID SILVER NANOFLUID AND TITANIUM DIOXIDE

Página – 448

43 - Artigo / Article

GEVORGYAN, SILVA A.; HAYRAPETYAN, SERGEY S.; HAYRAPETYAN, MARTIN S.; KHACHATRYAN, HAMBARDZUM G.

ARMÊNIA

AValiação EXPRESSA DO MECANISMO DE SORÇÃO EM MATERIAIS QUE CONTÊM TURFA

EXPRESS EVALUATION OF SORPTION MECHANISM ON PEAT CONTAINING MATERIALS

Página – 469

40 - Artigo / Article

OLIVEIRA, ADRIENE KELLY GOIS, SANTOS, ADRIANA PAULA BATISTA, CALDEIRA, VINÍCIUS PATRÍCIO DA SILVA

BRASIL

APLICAÇÃO DE NANOMATERIAIS À BASE DE TITANATO DE SÓDIO PARA ADSORÇÃO DE CORANTES

APPLICATION OF SODIUM TITANATE BASED NANOMATERIALS FOR DYE ADSORPTION

Página – 436

42 - Artigo / Article

BYTSSENKO, OKSANA A.; STESHENKO, IGOR G.; PANOV, VLADIMIR A.; TISHKOV, VICTOR V.; MARKOV, ALEXEY B.;

RÚSSIA

ALTERAÇÕES ESTRUTURAIS E DE FASE NAS CAMADAS DE SUPERFÍCIE DA COBERTURA MULTICOMPONENTE RESISTENTE AO CALOR DO REVESTIMENTO DE ÍONS DE PLASMA NI-CR-AL-Y APÓS MODIFICAÇÃO POR FEIXES DE ELÉTRONS DE CORRENTE FORTE COM DURAÇÃO DE MICROSSEGUNDOS

STRUCTURAL AND PHASE CHANGES OF THE SURFACE LAYERS OF HEAT-RESISTANT MULTICOMPONENT COATING OF ION-PLASMA COATING Ni-Cr-Al-Y AFTER MODIFICATION BY HIGH-CURRENT ELECTRON BEAMS MICROSECOND DURATION

Página – 459

44 - Artigo / Article

GIONGO, CAMILA NASCIMENTO; LOPES, VANESSA FALCHETTI; GRIGOLETTO, DIANA FORTKAMP; MIRANDA, EDUARDO HÖSEL.

BRASIL

APOCININA, UM INIBIDOR DO COMPLEXO DE NADPH OXIDASE

APOCYNIN, AN INHIBITOR OF THE NADPH OXIDASE COMPLEX

Página – 478

45 - Artigo / Article

BRKICH, GALINA EDUARDOVNA; PYATIGORSKAYA, NATALIA VALERYEVNA; DEMINA, NATALYA BORISOVNA; BAKHRUSHINA, ELENA OLEGOVNA; LAVROV, MSTISLAV IGOREVICH;

RÚSSIA**DESENVOLVIMENTO DA COMPOSIÇÃO E TECNOLOGIA PARA A PRODUÇÃO DE DROGAS ENCAPSULADAS COM BASE EM 3,7-DIAZABICICLO[3.3.1]NONANO**

DEVELOPMENT OF THE COMPOSITION AND TECHNOLOGY FOR THE PRODUCTION OF ENCAPSULATED DRUGS BASED ON 3,7-DIAZABICYCLO[3.3.1]NONANE

Página – 502

47 - Artigo / Article

AUBAKIROVA, GULZHAN; ADILBEKOV, ZHANAT; NARBAYEV, SERIK;

CAZAQUISTÃO**INFLUÊNCIA DA MINERALIZAÇÃO DA ÁGUA NA PRODUTIVIDADE DE ZOOPLÂNCTON NOS RESERVATÓRIOS DA REGIÃO DE AKMOLA**

INFLUENCE OF WATER MINERALIZATION ON ZOOPLANKTON PRODUCTIVITY IN RESERVOIRS OF AKMOLA REGION

Página – 520

49 - Artigo / Article

KHAIBULLINA, KARINA SHAMILEVNA; SAGIROVA, LYAISAN RUSTAMOVNA; SANDYGA, MIKHAIL SERGEEVICH;

RÚSSIA**SUBSTANCIAÇÃO E SELEÇÃO DE UM INIBIDOR PARA EVITAR A FORMAÇÃO DE DEPÓSITOS DE ASFALTO-RESINA-PARAFINA**

SUBSTANTIATION AND SELECTION OF AN INHIBITOR FOR PREVENTING THE FORMATION OF ASPHALT-RESIN-PARAFFIN DEPOSITS

Página – 541

51 - Artigo / Article

APRYATINA KRISTINA V.; TKACHUK EKATERINA K.; SMIRNOVA LARISA A.

RÚSSIA**CONDIÇÕES CONFORMACIONAIS DE MACROMOLECULAS QUITOSANAS E SUA INFLUÊNCIA NA EFICIÊNCIA DO PROCESSO DE POLIMERIZAÇÃO DA QUITOSANA COM 2-HIDROXIETIL METACRILATO E N-VINILPIRROLIDONA**

CONFORMATIONAL CONDITIONS OF CHITOSAN MACROMOLECULES AND THEIR INFLUENCE ON THE EFFICIENCY OF CHITOSAN POLYMERIZATION PROCESS WITH 2-HYDROXYETHYL METHACRYLATE AND N-VINYLPYRROLIDONE

Página – 562

46 - Artigo / Article

AL-SHAHEEN, AHMAD HASHIM

IRAQUE**GANHO E MELHORIA DA LARGURA DE BANDA DE FRAGMENTO RETANGULAR DA ANTENA MICROSTRIP**

GAIN AND BANDWIDTH ENHANCEMENT OF RECTANGULAR PATCH MICROSTRIP ANTENNA

Página – 512

48 - Artigo / Article

JASIM, EKHLAS Q.; DHAIF, HAWRAA K.; MUHAMMAD-ALI, MUNTHAR A.

IRAQUE**SÍNTESE, CARACTERIZAÇÃO, ATIVIDADE ANTIFÚNGICA E RELACIONAMENTO ESTRUTURA-ATIVIDADE: ESTUDO DE ALGUMAS BASES MONO E DI-SCHIFF**

SYNTHESIS, CHARACTERIZATION, ANTIFUNGAL ACTIVITY AND STRUCTURE ACTIVITY RELATIONSHIPS: STUDY OF SOME MONO- AND DI-SCHIFF BASES

Página – 528

50 - Artigo / Article

BOLSHAKOVA, LARISA SERGEEVNA; LISITSYN, ANDREY BORISOVICH; CHERNUHA, IRINA MIHAILOVNA; SHELEPINA, NATALIA VLADIMIROVNA; PARSHUTINA, INNA GRIGOREVNA

RÚSSIA**EFEITO DE COMPOSTOS ORGÂNICOS E INORGÂNICOS DE IODO NA PRODUTIVIDADE DE PORCOS E NA QUALIDADE DA CARNE**

EFFECT OF ORGANIC AND INORGANIC IODINE COMPOUNDS ON PIG PRODUCTIVITY AND MEAT QUALITY

Página – 552

52 - Artigo / Article

DUTOVA, SVETLANA VYACHESLAVOVNA; SARANCHINA, JULIA VLADIMIROVNA; KILINA, OKSANA YURYEVNA; KHANARIN, NIKOLAI VLADIMIROVICH; KULAKOVA, TATIANA SERGEEVNA;

RÚSSIA**OPORTUNIDADES MODERNAS DE FARMACOTERAPIA ATEROSCLEROSE: NOVAS DIREÇÕES**

MODERN OPPORTUNITIES OF ATHEROSCLEROSIS PHARMACOTHERAPY: NEW DIRECTIONS

Página – 578

53 - Artigo / Article

SHUKURLU, YUSIF H.;

AZERBAIJÃO**EFEITO DO SELÊNIO NA ESTRUTURA SUPRAMOLECULAR E CARACTERÍSTICAS TÉRMICAS DA FIBROÍNA BOMBYX MORI L**

THE EFFECT OF SELENIUM ON THE SUPRAMOLECULAR STRUCTURE AND THERMAL CHARACTERISTICS OF FIBROIN BOMBYX MORI L

Página – 591

55 - Artigo / Article

THAQEEF MURTADA JAWAD AND LUMA MAJEED AHMED

IRAQUE**SÍNTESE ULTRASSÔNICA DIRETA DE NANOCOMPOSITOS WO₃/TiO₂ E APLICANDOOS NA FOTODECOLORIZAÇÃO DO CORANTE AMARELO DE EOSINA**

DIRECT ULTRASONIC SYNTHESIS OF WO₃/TiO₂ NANOCOMPOSITES AND APPLYING THEM IN THE PHOTODECOLORIZATION OF EOSIN YELLOW DYE

Página – 621

57 - Artigo / Article

ZHUMALINA, AKMARAL K.; TUSUPKALIEV, BALASH T.; ZAME, YULIYA A.; VOLOSHINA, LYUDMILA V.; DARZHANOVA, KLARA B.

RÚSSIA**ASPECTOS CLÍNICOS E IMUNOLÓGICOS DA ADAPTAÇÃO DO RECÉM-NASCIDO DE MÃE COM INFECÇÃO INTRAUTERINA**

CLINICAL AND IMMUNOLOGICAL ASPECTS OF NEWBORN ADAPTATION BORN FROM MOTHERS WITH INTRAUTERINE INFECTION

Página – 656

59 - Artigo / Article

ZHUGINISOV, MARATBEK T.; ZHUMADILOVA, ZHANAR O.

CAZAQUISTÃO**AGREGADO LEVE E CONCRETO A BASE DE ESCÓRIAS, COM ALTO CONTEÚDO RESIDUAL DE COMBUSTÍVEL**

LIGHTWEIGHT AGGREGATE AND ASHES SLAG BASED CONCRETE WITH HIGH RESIDUAL FUEL CONTENT

Página – 678

54 - Artigo / Article

BIDAIBEKOV, YESSEN; GRINSHKUN, VADIM; BOSTANOV, BEKTAS; UMBETBAYEV, KAIRAT; MYRSYDYKOV, YERLES;

CAZAQUISTÃO**PATRIMÔNIO MATEMÁTICO DE AL-FARABI E UMA ABORDAGEM ALGORÍTMICA À SOLUÇÃO DE PROBLEMAS EM CONSTRUÇÕES GEOMÉTRICAS NO AMBIENTE GEOGEBRA**

AL-FARABI'S MATHEMATICAL LEGACY AND ALGORITHMIC APPROACH TO RESOLVING PROBLEMS REGARDING GEOMETRICAL CONSTRUCTIONS IN GEOGEBRA ENVIRONMENT

Página – 599

56 - Artigo / Article

SABUKEVICH, VIOLETTA SERGEEVNA; PODOPRIGORA, DMITRY GEORGIEVICH; SHAGIAKHMETOV, ARTEM MARATOVICH

RÚSSIA**JUSTIFICATIVA PARA A SELEÇÃO DE UM SISTEMA ÓTIMO DE DESENVOLVIMENTO DE CAMPO DE ÓLEO NA PARTE ORIENTAL DO MAR DE PECHORA E SEU CÁLCULO**

RATIONALE FOR SELECTION OF AN OIL FIELD OPTIMAL DEVELOPMENT SYSTEM IN THE EASTERN PART OF THE PECHORA SEA AND ITS CALCULATION

Página – 634

58 - Artigo / Article

HIBA KHALEEL SAEED AL-SHAKARCHI AND YOUSEF JABBAR AL-SHAHERY

IRAQUE**AVALIAÇÃO DA HABILIDADE DE CRESCIMENTO DE ARTHROSPIRA SP. EM SAIS DE METÁIS PESADOS E SEU EFEITO EM ALGUNS COMPONENTES CELULARES**

EVALUATION OF ARTHROSPIRA SP. GROWTH ABILITY ON HEAVY METAL SALTS AND THEIR EFFECT ON SOME CELLULAR COMPONENTS

Página – 667

60 - Artigo / Article

HAYAWI, MOHAMMED KAREEM; KAREEM, MOHANAD MOUSA, AND AHMED, LUMA MAJEED

IRAQUE**SÍNTESE DOS NANOCOMPOSITOS ESPINÉLIO Mn₃O₄ E ESPINÉLIO Mn₃O₄/ZrO₂ E USANDO-OS NA DECOLORIZAÇÃO FOTO-CATÁLICA DO COMPLEXO Fe(II)-(4,5-DIAZAFLUOREN-9-ONA 11)**

SYNTHESIS OF SPINEL Mn₃O₄ AND SPINEL Mn₃O₄/ZrO₂ NANOCOMPOSITES AND USING THEM IN PHOTO-CATALYTIC DECOLORIZATION OF Fe(II)-(4,5-DIAZAFLUOREN-9-ONE 11) COMPLEX

Página – 689

61 - Artigo / Article

CHOKIN, KANAT SH.; YEDILBAYEV, ABDAMAN I.; YEDILBAYEV, BAIMURAT A.; YUGAY, VLADIMIR D.

CAZAQUISTÃO**SEPARAÇÃO MAGNÉTICA SECA DE MINÉRIO DE MAGNETITA**

DRY MAGNETIC SEPARATION OF MAGNETITE ORES

Página – 700

63 - Artigo / Article

ABETOV, Auez E.; UZBEKOV, Abylay N.; GRIB, Nicolay N.; MELNIKOV, Andrey E.; MALININ, Yury A.;

CAZAQUISTÃO**VARIABILIDADE ESPACIAL DE PROPRIEDADES FÍSICAS E MECÂNICAS DE MASSA ROCHOSA NO CAZAQUISTÃO CENTRAL**

SPATIAL VARIABILITY OF PHYSICAL AND MECHANICAL PROPERTIES OF ROCK MASS IN CENTRAL KAZAKHSTAN

Página – 718

65 - Artigo / Article

SALTABAYEVA, ULBOSSYN; YUMASHEV, ALEXEI

CAZAQUISTÃO**CARACTERÍSTICAS COMPARATIVAS DA SEGURANÇA DOS MÉTODOS DE IMUNOTERAPIA SUBLINGUAL E PARENTERAL**

COMPARATIVE CHARACTERISTICS OF SAFETY OF SUBLINGUAL AND PARENTERAL IMMUNOTHERAPY METHODS

Página – 736

67 - Artigo / Article

JASSIM ABAS AL-HILFI, ZAIDON JAWAD KAHDIM, TAHSEEN SADDAM FANDI, AND LUMA M.AHMED

IRAQUE**ESTUDO ESTRUTURAL DE COMPLEXOS DE HEXAFLUOROACETILACETONA, PIRAZOL E DERIVADOS DE PIRAZOL COM ALGUNS METAIS POR FT-IR E ¹H-RMN**

STRUCTURAL STUDY OF COMPLEXES FROM HEXAFLUOROACETYLACETONE, PYRAZOLE, AND ITS PYRAZOLE DERIVATIVE WITH SOME METALS BY FT-IR, AND ¹H-NMR

Página – 756

62 - Artigo / Article

YULIANTI, DWI; WIYANTO; RUSILOWATI, ANI; NUGROHO, SUNYOTO EKO;

INDONÉSIA**DESENVOLVIMENTO DE MATERIAIS DE ENSINO-APRENDIZAGEM DE FÍSICA BASEADOS EM TECNOLOGIA CIENTÍFICA DE ENGENHARIA E MATEMÁTICA PARA DESENVOLVER HABILIDADES DE APRENDIZAGEM DO SÉCULO XXI**

DEVELOPMENT OF PHYSICS LEARNING TEACHING MATERIALS BASED ON SCIENCE TECHNOLOGY ENGINEERING AND MATHEMATICS TO DEVELOP 21ST CENTURY LEARNING SKILLS

Página – 711

64 - Artigo / Article

PERDANA, RYZAL; BUDIYONO; SAJIDAN; SUKARMIN, RUDIBYANI, RATU BETTA

INDONÉSIA**FINVESTIGAÇÃO DE COMPLEXIDADE SOCIAL (ISC): PROJETO INSTRUCIONAL PARA REFORÇAR AS COMPETÊNCIAS CRÍTICAS E CRIATIVAS (CCT) NA QUÍMICA**

INQUIRY SOCIAL COMPLEXITY (ISC): DESIGN INSTRUCTIONAL TO EMPOWERMENT CRITICAL AND CREATIVE THINKING (CCT) SKILLS IN CHEMISTRY

Página – 727

66 - Artigo / Article

LOBANOV, GRIGORY V.; AVRAMENKO, MARINA V.; PROTASOVA, ALINA P.; DROZDOV, NIKOLAI N.

RÚSSIA**ALTERAÇÕES SAZONAIS E A LONGO PRAZO DO ÍNDICE DE VEGETAÇÃO DE TERRAS ARÁVEIS DA REGIÃO DE BRYANSK (RÚSSIA CENTRAL): REGULARIDADES E FATORES DINÂMICOS**

SEASONAL AND LONG-TERM CHANGES OF VEGETATION INDEX OF ARABLE LANDS OF BRYANSK REGION (CENTRAL RUSSIA): REGULARITIES AND DYNAMICS FACTORS

Página – 745

68 - Artigo / Article

KHAIBULLINA, KARINA SHAMILEVNA; KOROBV, GRIGORY YURIEVICH ; LEKOMTSEV ALEKSANDR VIKTOROVICH;

RÚSSIA**DESENVOLVIMENTO DE UM INIBIDOR DE DEPÓSITO DE ASFALTO-RESINA-PARAFINA E SUBSCANTIAÇÃO DOS PARÂMETROS TECNOLÓGICOS DE SUA INJEÇÃO NA ZONA DE FORMAÇÃO DE FURO INFERIOR**

DEVELOPMENT OF AN ASPHALT-RESIN-PARAFFIN DEPOSITS INHIBITOR AND SUBSTANTIATION OF THE TECHNOLOGICAL PARAMETERS OF ITS INJECTION INTO THE BOTTOM-HOLE FORMATION ZONE

Página – 769

69 - Artigo / Article

MARDASHOV, DMITRY; ISLAMOV, SHAMIL, NEFEDOV, YURY

RÚSSIA

**DETALHES DA TECNOLOGIA DE CONTROLE DE POÇO
DURANTE A OPERAÇÃO EM CONDIÇÕES COMPLICADAS**

*SPECIFICS OF WELL KILLING TECHNOLOGY DURING WELL
SERVICE OPERATION IN COMPLICATED CONDITIONS*

Página – 782

71 - Artigo / Article

GAPSALAMOV, ALMAZ RAFISOVICH; BOCHKAREVA, TATYANA
NIKOLAEVNA; AKHMETSHIN, ELVIR MUNIROVICH; VASILEV,
VLADIMIR LVOVICH; ANISIMOVA, TATYANA IVANOVNA;

RÚSSIA

SOCIEDADE DIGITAL: NOVOS DESAFIOS PARA A EDUCAÇÃO

DIGITAL SOCIETY: NEW CHALLENGES FOR EDUCATION

Página – 803

73 - Artigo / Article

BELAIA, OLGA FEDOROVNA; GUTKIN, DENIS SERGEEVICH;
KAREVA, ELENA NIKOLAEVNA; VOLCHKOVA, ELENA
VASILYEVNA; VAKHRAMEEVA, MARIA SERGEEVNA

RÚSSIA

**NÍVEIS SÉRICOS DE IL-8 EM PACIENTES COM GASTRITE
CRÔNICA ATIVA E DOENÇA ÚLCERA PÉPTICA**

*SERUM LEVELS OF IL-8 IN PATIENTS WITH CHRONIC ACTIVE
GASTRITIS AND PEPTIC ULCER DISEASE*

PÁGINA – 826

75 - Artigo / Article

KHAZIEV, DANIS; GADIEV RINAT; GALINA, CHULPAN;
VALITOV, FARIT; KAZANINA, MARINA; KOPYLOVA, SVETLANA;
IVANOV, EFIM

RÚSSIA

**EFICÁCIA DA APLICAÇÃO DE SAPROPEL EM DIETAS DE
GANSOS**

*EFFECTIVENESS OF SAPROPEL APPLICATION IN DIETS OF
GEESE*

Página – 845

70 - Artigo / Article

POGODIN, VENIAMIN A.; ASTAPOV, ALEXEY N.; RABINSKIY,
LEV N.

RÚSSIA

**ESTIMATIVA DE SUPERFÍCIE ESPECÍFICA DE MCCC NO
PROCESSO DE OXIDAÇÃO A BAIXA TEMPERATURA**

*TCCCM SPECIFIC SURFACE ESTIMATION IN PROCESS OF
LOW-TEMPERATURE OXIDATION*

Página – 793

72 - Artigo / Article

MAKHMETOVA, ARDAK S.; AGZAMOV, FARIT A.; KOMLEVA,
SVETLANA F.; ISMAILOV, ABDULAKHAT A.; ISMAILOVA,
JAMILYAM A.

RÚSSIA E CAZAQUISTÃO

**ANÁLISE DAS RAZÕES DA PRESSÃO ENTRE COLUNAS COM
O EXEMPLO DE CAMPO DE ZHANAZHOL**

*INTERCASING PRESSURE CAUSES ANALYSIS ON THE
EXAMPLE OF ZHANAZHOL FIELD*

Página – 817

74 - Artigo / Article

ASTUTI, ELSA ARI; WORO, SUMARNI; WIYANTO

INDONÉSIA

**INTELIGÊNCIA INTERPESSOAL DE ESTUDANTES DA ESCOLA
PROFISSIONAL EM APRENDIZAGEM QUÍMICA: UM ESTUDO
DE CASO**

*INTERPERSONAL INTELLIGENCE OF VOCATIONAL HIGH
SCHOOL STUDENTS ON CHEMISTRY LEARNING: A CASE
STUDY*

Página – 835

76 - Artigo / Article

SHYIAN, NADIYA I.; KRYVORUCHKO, ALINA V.; STRYZHAK,
SVITLANA V.; KRYKUNOVA, VALENTYNA YE.; ANTONETS,
OLEKSANDR A.

UCRÂNIA

**MODELO ESTRUTURAL E FUNCIONAL DA METODOLOGIA DE
PREPARAÇÃO DE PROFESSORES DE QUÍMICA PARA A
APLICAÇÃO DE TECNOLOGIAS DE NUVEM NA ATIVIDADE
PROFISSIONAL**

*STRUCTURAL AND FUNCTIONAL MODEL OF THE
METHODOLOGY FOR PREPARING FUTURE CHEMISTRY
TEACHERS FOR THE USE OF CLOUD TECHNOLOGIES IN
PROFESSIONAL ACTIVITIES*

Página – 856

77 - Artigo / Article

ALSHAYBAN, DHFER; JOSEPH, ROYES

ARÁBIA SAUDITA

O IMPACTO DA ADESÃO À MEDICAÇÃO NA QUALIDADE DE VIDA RELACIONADA À SAÚDE DE PACIENTES DIABÉTICOS NO REINO DA ARÁBIA SAUDITA: CONCLUSÕES DE UM ESTUDO TRANSVERSAL

THE IMPACT OF MEDICATION ADHERENCE ON HEALTH-RELATED QUALITY OF LIFE OF DIABETIC PATIENTS IN THE KINGDOM OF SAUDI ARABIA: FINDINGS FROM A CROSS-SECTIONAL STUDY

Página – 867

79 - Artigo / Article

KURBATOV, ALEXEY S.; OREKHOV, ALEXANDER A.; RABINSKIY, LEV N.; TUSHAVINA, OLGA V.; KUZNETSOVA, EKATERINA L.

RÚSSIA

ESTUDO DO PROBLEMA DE PERDA DE ESTABILIDADE DE ESTRUTURAS CILÍNDRICAS DE PAREDES FINAS SOB EXPOSIÇÃO TÉRMICA LOCAL INTENSA

RESEARCH OF THE PROBLEM OF LOSS OF STABILITY OF CYLINDRICAL THIN-WALLED STRUCTURES UNDER INTENSE LOCAL TEMPERATURE EXPOSURE

Página – 884

81- Artigo / Article

KUZMIN, PETR A.; BUKHARINA, IRINA L.; KUZMINA, AJGUL M.

RÚSSIA

INVESTIGAÇÃO DA COMPOSIÇÃO BIOQUÍMICA DO BORDO DA NORUEGA (ACER PLATANOIDES L.) NAS CONDIÇÕES DE ESTRESSE TECNOLÓGICO

AN INVESTIGATION OF THE BIOCHEMICAL COMPOSITION OF NORWAY MAPLE (ACER PLATANOIDES L.) IN THE CONDITIONS OF TECHNOGENIC STRESS

Página – 905

83 - Artigo / Article

SKVORTSOV, ARKADIY A.; LUK'YANOV, MIKHAIL N.; SKVORTSOVA, ANNA A.

RÚSSIA

CARACTERÍSTICAS DA DEFORMAÇÃO E DESTRUIÇÃO DE CERÂMICAS POROSAS À BASE DE DIATOMITO

THE FEATURES OF DEFORMATION AND DESTRUCTION OF POROUS DIATOMITE-BASED CERAMICS

Página – 925

78 - Artigo / Article

GAPSALAMOV, ALMAZ RAFISOVICH; MERZON, ELENA EFIMOVNA; KUZNETSOV, MAKSIM SERGEYEVICH; VASILEV, VLADIMIR LVOVICH; BOCHKAREVA, TATYANA NIKOLAEVNA

RÚSSIA

O SISTEMA EDUCACIONAL NO CONTEXTO DAS TRANSFORMAÇÕES SOCIOECONÔMICAS

THE EDUCATION SYSTEM IN THE CONTEXT OF SOCIO-ECONOMIC TRANSFORMATIONS

Página – 874

80 - Artigo / Article

KUANGALIEV, ZINON A.; DOSKASIYEVA, GULSIN S.; MARDANOV, ALTYNBEK S.

RÚSSIA

PESQUISA DO MECANISMO DE PRODUÇÃO DE PETRÓLEO A PARTIR DE DEPÓSITOS DE HIDROCARBONETOS COM COLETORES DE BAIXA PERMEABILIDADE

RESEARCH OF THE MECHANISM OF OIL RECOVERY FROM HYDROCARBON DEPOSITS WITH LOW PERMEABILITY RESERVOIRS

Página – 892

82 - Artigo / Article

PRISCHEPA, OLEG M.; NEFEDOV, YURY V.; KOCHNEVA, OLGA E.;

RÚSSIA

MATÉRIA-PRIMA BASE DE RESERVAS DE ÓLEO DE DIFÍCIL EXTRAÇÃO DA RÚSSIA

RAW MATERIAL BASE OF HARD-TO-EXTRACT OIL RESERVES OF RUSSIA

Página – 915

84 - Artigo / Article

SHAGIAKHMETOV, ARTEM MARATOVICH; PODOPRIGORA, DMITRY GEORGIEVICH; TERLEEV, ANDREY VICTOROVICH

RÚSSIA

O ESTUDO DA DEPENDÊNCIA DAS PROPRIEDADES REOLÓGICAS DAS COMPOSIÇÕES DE FORMAÇÃO EM GEL NA ABERTURA DE FENDAS AO MODELAR SEU FLUXO EM UM VISCÔMETRO ROTACIONAL

THE STUDY OF THE DEPENDENCE OF THE RHEOLOGICAL PROPERTIES OF GEL-FORMING COMPOSITIONS ON THE CRACK OPENING WHEN MODELING THEIR FLOW ON A ROTATIONAL VISCOMETER

Página – 933

85 - Artigo / Article

TASHPULATOV, SALIKH S.; SABIROVA, ZIYODA A.;
CHERUNOVA, IRINA V.; NEMIROVA, LYUBOV F.; MUMINOVA,
UMIDA T.

RÚSSIA E REPÚBLICA DO UZBEQUISTÃO**DISPOSITIVO PARA ESTUDO DAS PROPRIEDADES
TERMOFÍSICAS DE MATERIAIS TÊXTEIS DE VOLUME E SUAS
EMBALAGENS PELO MÉTODO DE MODO REGULAR NO AR**

*A DEVICE FOR STUDYING THE THERMOPHYSICAL
PROPERTIES OF BULK TEXTILE MATERIALS AND THEIR
PACKAGES BY THE REGULAR MODE METHOD IN AIR*

Página – 940

87- Artigo / Article

86 - Artigo / Article

AGZAMOV, FARIT A.; KABDUSHEV, ARMAN; TOKUNOVA,
ELVIRA; MANAPBAYEV, BAUYRZHAN ZH.; KOZHAGELDI,
BOLAT ZH.

RÚSSIA E CAZAQUISTÃO**CORROSÃO DE MAGNÉSIA DE MATERIAIS DE ENCHIMENTO**

MAGNESIA CORROSION OF GROUTING MATERIALS

Página – 951

88 - Artigo / Article

AVDEEV, YURI MIKHAILOVICH; GOROVOY, SERGEY
ALEKSEEVICH; KARPENKO, ELENA; KUDRYAVTSEV, VALERY;
KOZLOVSKY, LYDIA;

RÚSSIA**AVALIAÇÃO DO ESTADO DAS PLANTAS VERDES SOB AS
CONDIÇÕES DE URBANIZAÇÃO**

*EVALUATION OF THE STATE OF GREEN PLANTS UNDER THE
CONDITIONS OF URBANIZATION*

Página – 966

89 - Artigo / Article

SHUYUSHBAYEVA, NURGUL N.; SAGIMBAEVA, SHYNAR ZH.;
MUSSENOVA, ELMIRA K.; BIZHANOVA, KARLYGASH B.;
ZHANTURINA, NURGUL N.

CAZAQUISTÃO**REDUÇÃO DAS CONDIÇÕES DEFEITUOSAS DE OPERAÇÃO
DA PLANTA DE ENERGIA EÓLICA AO RESERVAR OS MODOS
DE OPERAÇÃO DE ENERGIA ALTERNATIVA**

*REDUCTION OF DEFECTIVE CONDITIONS OF THE WIND
POWER PLANT OPERATION AT RESERVING THE OPERATION
MODES OF ALTERNATIVE ENERGY*

Página – 976

91- Artigo / Article

90 - Artigo / Article

RYNDIN, VLADIMIR V.

CAZAQUISTÃO**APLICAÇÃO DO POSTULADO DE NÃO-EQUILÍBRIO PARA
CALCULAR O NÃO-EQUILÍBRIO DE SISTEMAS DE VÁRIOS
GASES E LÍQUIDOS**

*APPLICATION OF THE POSTULATE OF NONEQUILIBRIUM TO
CALCULATE THE NONEQUILIBRIUM OF SYSTEMS OF
DISSIMILAR GASES AND LIQUIDS*

Página – 998

92 - Artigo / Article

NAZARABADI, ROSHANAK BAHRAMI; MEHRABANPOUR,
MOHAMMAD JAVAD; EDALATMANESH, MOHAMMAD AMIN;
SHARIATI, MEHRDAD

IRÃ**UMA INVESTIGAÇÃO SOBRE O EFEITO DO VÍRUS INFLUENZA
H9N2 NA APOPTOSE DE CÉLULAS TESTICULARES EM
EMBRIÃO DE GALINHA USANDO SYBR VERDE PCR EM
TEMPO-REAL**

*AN INVESTIGATION INTO THE EFFECT OF H9N2 INFLUENZA
VIRUS ON APOPTOSIS OF TESTICULAR CELLS IN CHICKEN
EMBRYO USING SYBR-GREEN REAL-TIME PCR*

Página – 1003

93 - Artigo / Article

OSPANOV, ABDYMANAP; MUSLIMOV, NURZHAN;
TIMURBEKOVA, AIGUL; MAMAYEVA, LAURA; JUMABEKOVA,
GULNARA

CAZAQUISTÃO**COMPOSIÇÃO DE AMINOÁCIDOS DE FARINHA POLI-CEREAL
NÃO CONVENCIONAL PARA MASSA**

*THE AMINO ACID COMPOSITION OF UNCONVENTIONAL
POLY-CEREAL FLOUR FOR PASTA*

Página – 1012

95 - Artigo / Article

BITARAF, NEGIN; SAADATMAND, SARA; MEHREGAN, IRAJ;
AHMADVAND, RAHIM; EBADI, MOSTAFA

IRÃ**AVALIAÇÃO DOS EFEITOS DE MITIGAÇÃO DE GLOMUS
MOSSEAE EM TRITICUM AESTIVUM L., CV. CHAMRAN SOB
ESTRESSE SECA**

*EVALUATION OF MITIGATION EFFECTS OF GLOMUS
MOSSEAE ON TRITICUM AESTIVUM L., CV. CHAMRAN UNDER
DROUGHT STRESS*

Página – 1033

97- Artigo / Article

BABAYTSEV, ARSENIY V.; KUZNETSOVA, EKATERINA L.;
RABINSKIY, LEV N.; TUSHAVINA, OLGA V.;

IRÃ**INVESTIGAÇÃO DE DEFORMAÇÕES PERMANENTES EM
COMPOSITOS NANOMODIFICADOS APÓS A MOLDAGEM EM
TEMPERATURAS ELEVADAS**

*INVESTIGATION OF PERMANENT STRAINS IN NANOMODIFIED
COMPOSITES AFTER MOLDING AT ELEVATED
TEMPERATURES*

Página – 1055

94 - Artigo / Article

ROYTBERG, GRIGORY EFIMOVICH; SHARKHUN, OLGA
OLEGOVNA; PLATONOVA, OKSANA EVGENYEVNA;
STEPANOVA, ANNA ALEXANDROVNA;

RÚSSIA**A TOMOGRAFIA DE EMISSÃO DE POSITRONS NO
DIAGNÓSTICO PRECOCE DOS TRANSTORNOS
METABÓLICOS DO MIOCÁRDIO EM PACIENTES RESISTENTES
À INSULINA COM DOENÇA HEPÁTICA GORDUROSA NÃO
ALCOÓLICA**

*THE POSITRON EMISSION TOMOGRAPHY IN EARLY
DIAGNOSTICS OF THE METABOLIC MYOCARDIAL DISORDERS
IN INSULIN-RESISTANT PATIENTS WITH NON-ALCOHOLIC
FATTY LIVER DISEASE*

Página – 1026

96 - Artigo / Article

SHAHEED, IHSAN MAHDI AND DHAHIR, SAADIYAH AHMED

IRAQUE**EXTRAÇÃO E DETERMINAÇÃO DE TEBUCONAZOL EM
AMOSTRAS AMBIENTAIS DA CIDADE DE KARBALA NO
IRAQUE E EM SUA FORMULAÇÃO USANDO
CROMATOGRAFIA LÍQUIDA DE ALTO DESEMPENHO (HPLC)**

*EXTRACTION AND DETERMINATION OF TEBUCONAZOLE IN
ENVIRONMENTAL SAMPLES FROM THE CITY OF KARBALA,
IRAQ AND IN ITS FORMULATION USING HIGH- PERFORMANCE
LIQUID CHROMATOGRAPHY (HPLC)*

Página – 1046

Author instructions

**INSTRUCTIONS FOR AUTHORS - PREPARATION
OF MANUSCRIPTS**

Página – 1068

**PAGE CHARGES (1), DISCOUNTS (2), AND FREE
PUBLICATION OPPORTUNITIES (3)**

Página – 1072

Publication Ethics

Dear readers and authors

We are sorry for the inconvenience, but some manuscripts were removed from this issue in the last minute. We have fail in some reviewing processes. We did not request some specific pieces of information in some papers. Therefore, to avoid causing any damage to the authors or the journal, and to be equally fair with everyone, we decided to move those specific manuscripts to the next issue.

As a result of this unexpected and unprecedented problem, we have taken this as a precious and important lesson. Because of that, we are now changing and improving our review process. We do apologize for any inconvenience that this may have caused to the authors and readers.

Thank you, everyone, for trusting and supporting Tche Quimica Journal

Editors:

Luis A. B De Boni

Eduardo Goldani

ATIVIDADE LARVICIDA DE ÓLEO ESSENCIAL DE *CROTON RHAMNIFOLIOIDES* (PAX & HOFFM) ENCAPSULADO EM NANOSSISTEMA POLIMÉRICO FRENTE AO MOSQUITO *AEDES AEGYPTI*

LARVICIDAL ACTIVITY OF *CROTON RHAMNIFOLIOIDES* (PAX & HOFFM) ESSENTIAL OIL ENCAPSULATED IN A POLYMERIC NANOSYSTEM AGAINST THE MOSQUITO *AEDES AEGYPTI*

SANTOS, Andréia Gregório da Silva^{1*}; NAVARRO, Daniela do Amaral Ferraz²; MAGALHÃES, Nereide Stela Santos³; MELO-SANTOS, Maria Alice Varjal⁴; BRANDÃO, Sofia Suely Ferreira⁵

^{1,5}Instituto Federal de Educação, Ciência e Tecnologia de Pernambuco, Mestrado Profissional em Gestão Ambiental.

² Universidade Federal de Pernambuco, Departamento de Química Fundamental

³ Universidade Federal de Pernambuco, Laboratório de Imunopatologia Keizo-Asami (LIKA).

⁴Fundação Oswaldo Cruz-PE/Instituto Aggeu Magalhães – IAM – PE, Laboratório do Serviço de Referência em Controle de Culicídeos Vetores

* Autor correspondente
e-mail: andreia2007@gmail.com

Received 26 July 2019; received in revised form 25 November 2019; accepted 12 February 2020

RESUMO

Aedes aegypti é uma espécie de mosquito com ampla distribuição mundial, envolvida nos ciclos de transmissão da dengue, Zika e chikungunya. A inexistência de vacinas para a maioria destas arboviroses realça a importância do controle vetorial como medida para reduzir a incidência dessas doenças. Diversas pesquisas têm sido realizadas no intuito de encontrar substâncias de origem vegetal candidatas ao controle de *A. aegypti*. Neste sentido, as plantas medicinais que também apresentam ação inseticida têm se mostrado promissoras para o desenvolvimento de novos produtos, ambientalmente mais seguros do que os inseticidas químicos tradicionais. O objetivo deste trabalho foi avaliar a atividade larvicida do óleo essencial das folhas de *Croton rhamnifolioides* e de sua formulação em nanocápsulas para *A. aegypti*. O óleo essencial foi extraído por hidrodestilação e analisado por cromatografia gasosa acoplada a um espectrômetro de massas (CG/MS). Foram produzidas formulações contendo concentrações do óleo puro, que variaram de 40 a 80 µg/mL e nanocápsulas de policaprolactona com concentrações de 30 a 120 µg/mL. Os ensaios larvicidas foram realizados utilizando concentrações variadas de uma suspensão aquosa, em triplicatas, contendo 20 larvas/concentração, além de um controle não tratado. Como resultados, o óleo essencial apresentou teor médio que variou entre 1,4% e 0,58%, em função da época da coleta e, como principais constituintes, eucaliptol (16,57%) e (E)-cariofileno (11,32%). Os valores de CL₅₀ variaram de 26,3 µg/mL a 52,2 µg/mL e de CL₉₀ de 37,8 µg/mL a 68,7 µg/mL para o óleo puro. No óleo encapsulado, a CL₅₀ = 63,4 µg/mL e a CL₉₀ = 104,8 µg/mL. O óleo puro de *Croton rhamnifolioides* foi considerado mais ativo contra as larvas de *A. aegypti* do que o encapsulado, embora ambos tenham demonstrando grande potencial para aplicação como larvicida.

Palavras-chave: atividade larvicida; plantas medicinais; nanopartículas.

ABSTRACT

Aedes aegypti is a species of mosquito with wide distribution worldwide, involved in the cycles of transmission of dengue, Zika and chikungunya. The lack of vaccines for most of these arboviruses highlights the importance of vector control as a measure to reduce the incidence of these diseases. Several researches have been carried out in order to find substances of plant origin that are candidates for the control of *A. aegypti*. In this sense, medicinal plants that also have an insecticidal action have shown promise for the development of new products, environmentally safer than traditional chemical insecticides. The objective of this work was to evaluate the larvicidal activity of the essential oil of the leaves of *Croton rhamnifolioides* and its formulation in nanocapsules for *A. aegypti*. The essential oil was extracted by hydrodistillation and analyzed by gas chromatography coupled

to a mass spectrometer (CG/MS). Formulations were produced containing concentrations of pure oil, which ranged from 40 to 80 µg/mL and polycaprolactone nanocapsules with concentrations from 30 to 120 µg/mL. Larvicide tests were performed using varying concentrations of an aqueous suspension, in triplicates, containing 20 larvae / concentration, in addition to an untreated control. As a result, the essential oil had an average content that varied between 1.4% and 0.58%, depending on the time of collection and, as main constituents, eucalyptol (16.57%) and (E)-cariophyllene (11, 32%). LC50 values ranged from 26.3 µg/mL to 52.2 µg/mL and CL90 from 37.8 µg/mL to 68.7 µg/mL for pure oil. In encapsulated oil, the LC50 = 63.4 µg/mL and the LC90 = 104.8 µg/mL. The pure oil of *Croton rhamnifolioides* was considered more active against the larvae of *A. aegypti* than the encapsulated one, although both have great potential for application as a larvicide.

Keywords: larvicidal test; medicinal plants, nanoparticles.

1. INTRODUÇÃO:

Modificações antrópicas, quase que irreversíveis, no ambiente têm afetado a qualidade de vida das pessoas (Pontes, 1994) e propiciado o aumento da densidade populacional de alguns insetos sinantrópicos. Entre estes, destacam-se os mosquitos, a exemplo de *Aedes aegypti*, adaptados aos centros urbanos, onde em função do seu hábito alimentar antropofílico, têm atuado como vetor de arbovírus (Souza, Silva e Silva, 2010; Prezoto, 2016).

Para prevenir doenças como dengue, Zika e febre chikungunya se faz necessário o controle vetorial da principal espécie envolvida em seus ciclos de transmissão, *A. aegypti*. Para tanto, foram instituídas no Brasil, nas décadas de 1980/1990, políticas Públicas de Saúde para o controle desta espécie de mosquito, uma vez que não existem vacinas disponíveis para proteger as populações humanas expostas (Braga e Valle, 2007; Chiarella, 2016).

Nesse sentido, o controle do mosquito vem sendo realizado por meio do uso de inseticidas químicos das classes dos organofosforados e piretroides desde 1996, quando foi lançada a primeira versão de erradicação/controle de *A. aegypti* no país (Brasil, 2002; Rose, 2001; Penna, 2003; Braga e Valle, 2007). O uso contínuo de tais produtos tem levado à seleção de populações do mosquito resistentes (Araújo *et al.*, 2013; Chediak *et al.*, 2016) e ocasionado diversos danos ao ambiente, seja no ar ou na água, interferindo diretamente na saúde do ser humano, além de ocasionar vários transtornos ambientais, sociais e econômicos (Jintana *et al.*, 2015).

Tendo em vista a necessidade de alternativas a estes compostos químicos, que reduzam significativamente os impactos ambientais e econômicos, e que ao mesmo tempo sejam efetivos contra o mosquito, surgem as plantas medicinais (Corrêa e Salgado, 2011; Lima *et al.*, 2013; Castillo *et al.*, 2017). Segundo Santos (2014), algumas destas plantas apresentam

atividade larvicida contra o mosquito *A. aegypti* devido à presença de várias substâncias orgânicas que agem de forma isolada ou sinérgica. Ainda segundo Soloway (1976), os vegetais são importantes fontes de substâncias bioativas que possuem estruturas químicas diferentes e com distintas atividades contra insetos.

Em revisão realizada por Dias e Moraes (2014), foi observado que de 361 óleos essenciais já estudados quanto a sua bioatividade larvicida, 60% destes foram considerados ativos e obtidos de espécies de vegetais das famílias *Myrtaceae*, *Lamiaceae* e *Rutaceae*.

Da família *Euphorbiaceae*, *Croton rhamnifolioides* é uma espécie vegetal conhecida popularmente como “quebra-faca” ou “catinga-branca” (Randau *et al.*, 2004), apresentando atividade antimicrobiana (Da Costa *et al.*, 2013), acaricida (Da Câmara *et al.*, 2017) e inseticida, inclusive para culicídeos vetores, como o mosquito *A. aegypti* (Santos, 2014).

Aliada a este fato, a biotecnologia tem investido no desenvolvimento de nanopartículas biodegradáveis, tendo como objetivo obter a liberação controlada de ativos, com uma concentração ideal (Soppimath *et al.*, 2001; Peng *et al.*, 2014). Sendo assim, a nanoencapsulação de óleos essenciais pode representar uma alternativa viável na proteção deste princípio ativo, quando disponibilizado como larvicida em criadouros de mosquitos (Pavela, 2016).

Diante do exposto, o presente trabalho avaliou a atividade larvicida do óleo essencial de folhas de *C. rhamnifolioides*, formulado ou não em nanocápsulas, em sistema de liberação controlada, para o controle do mosquito *A. aegypti*, visando a obtenção de novos biolarvicidas, ambientalmente mais seguros.

2. PARTE EXPERIMENTAL:

2.1 Coleta e armazenamento de material botânico

Croton rhamnifolioides foi coletada no município de Serra Talhada, localizado no sertão de Pernambuco, entre os meses de janeiro a março de 2017. Foi realizada a identificação botânica da planta pela professora Dra. Elba Ferraz, sendo uma exsicata depositada no Herbário Professor Vasconcelos Sobrinho na Universidade Federal Rural de Pernambuco, sob número de tombamento 49855. As folhas da planta foram separadas manualmente e, posteriormente, realizada a secagem natural por três dias consecutivos, à sombra e sem incidência de luz solar. Uma vez secas, as folhas foram distribuídas em sacos plásticos e conservadas em refrigeração até o momento da sua utilização.

2.1.1 Extração do óleo essencial de *Croton rhamnifolioides*

Para a extração do óleo essencial, foi utilizada a técnica da hidrodestilação, adaptada do sistema de Clevenger (Santos *et al.*, 2015). As folhas secas foram cortadas e, introduzidas em um balão de fundo redondo com capacidade de 5L, sendo adicionada posteriormente água destilada. O processo de extração ocorreu em duas horas, sob aquecimento em manta aquecedora Lucadema 5000. No condensador de bolas foi utilizada água refrigerada proveniente de uma unidade de refrigeração Biothec BT SOUR. O óleo foi separado em tubo de Dean Stark, seco em sulfato de sódio anidro e armazenado sob refrigeração até o momento do uso.

2.1.2 Identificação dos constituintes químicos do óleo essencial

Os componentes do óleo essencial de *C. rhamnifolioides* foram quantificados e identificados através dos métodos de CG e CG-MS no Departamento de Química Fundamental da UFPE, utilizando um cromatógrafo a gás GC HP5890 Series II com detector de ionização de chamas e uma coluna capilar Ultra 1 (25mx0,32mmx0,52µm). Utilizando o hidrogênio como gás de arraste, as condições de programação foram de inicialmente 60 °C, variando 10 °C/minuto até 280 °C, mantida por 35 minutos. A temperatura do injetor foi de 200 °C e do detector de 290 °C. Utilizou-se um cromatógrafo a gás acoplado a um espectrômetro de massas Finnigan GCQ Mat tipo quadrupolo-ion trap, 70 eV de energia de ionização e Coluna capilar DB5 (25mx32mmx0,52µm), para a identificação dos componentes do óleo essencial. O hélio foi utilizado como gás de arraste e as condições de programação foi inicialmente 60° C, variando 10° C/minuto até 275° C, mantida por 30

minutos. A temperatura do injetor foi de 250° C. Os componentes foram identificados por meio de comparação com aqueles encontrados na biblioteca NIST (Adams, 2001; Lago *et al.*, 2006).

2.1.3 Preparação das nanocápsulas

As nanocápsulas de policaprolactona contendo o óleo essencial (NP-PCL/OE) foram preparadas segundo o método de deposição interfacial do polímero pré-formado conforme descrito por Flores *et al* (2011), com algumas modificações. Solubilizados, 50 mg de polímero (PCL), 77 mg de Span 80 e 100 mg de óleo essencial foram dissolvidos em 5 mL de acetona. Esta fase orgânica foi introduzida lentamente numa solução aquosa (10 mL) contendo o 77 mg de Tween 80, sob agitação magnética durante 10 min. Em seguida, a acetona foi removida por evaporação sob pressão reduzida para retirada do solvente. O volume final das formulações foi fixado em 10 mL para obter uma concentração final de óleo de 10 mg/mL (1%). As formulações sem o OE (NC-PCL) também foram preparadas.

2.1.4 Caracterização das formulações contendo óleo essencial

O diâmetro médio de partícula e o índice de polidispersão das nanocápsulas foram determinados no equipamento Zetasizer Nano-ZS90 (Malvern, Worcestershire, UK), utilizando a técnica de espectroscopia de autocorrelação de fótons (PCS), após diluição adequada da amostra em água ultrapura. O potencial zeta foi medido pela técnica de mobilidade eletroforética usando o mesmo aparelho a 25°C, após diluição da amostra em NaCl 10 Mm adequada da amostra.

2.1.5 Determinação do conteúdo de óleo nas nanocápsulas

O conteúdo de OE nas nanocápsulas foi determinado por duas técnicas: cromatografia líquida de alta performance (CLAE) e espectrofotometria de absorção no UV-Visível (Natrajan *et al.*, 2015). Para quantificação, uma curva padrão do OE foi preparada em acetonitrila em concentrações variando de 50 a 250 µg.mL⁻¹. Para efetuar a quantificação do OE, uma curva analítica foi inicialmente preparada com concentrações variando de 50 a 300 µg/mL. Posteriormente, estabeleceu-se correlação linear entre concentração, considerada variável independente (x), e relação entre as áreas dos picos cromatográficos do fármaco e do padrão interno, considerada variável dependente (y). A linearidade foi avaliada através de análise de

regressão linear, utilizando ajuste dos dados pelo método dos mínimos quadrados. Os limites de detecção (LD) e quantificação (LOQ) foram estimados de acordo com as diretrizes do ICH. O limite de detecção foi calculado através da fórmula: $LD = 3,3 (\sigma / I)$, e o limite de quantificação foi calculado através da fórmula: $LQ = 10 (\sigma / I)$, onde σ é o desvio padrão do intercepto com relação ao eixo dos Y e I é o valor da inclinação da curva analítica. Quanto ao doseamento do óleo essencial nas nanocápsulas foi utilizado 0,1 mL da suspensão das nanocápsulas as quais foram solubilizadas em 5 mL de acetonitrila. A solução foi, posteriormente, submetida à sonicação por 5 min, filtrada em filtros Millex® (0,22 µm) e quantificada. Os experimentos foram realizados em triplicata. Para a eficiência da encapsulação do OE nas nanocápsulas foi empregado 0,4 mL da suspensão das nanocápsulas onde foram ultrafiltradas em filtros de filtrantes Microcon® (Millipore, Billerica, EUA) e submetidas a ultrafiltração associada com centrifugação a 10.000 rpm durante 1h. A concentração de OE no ultrafiltrado foi determinada por CLAE e a eficiência de encapsulação (%) calculada pela diferença entre a concentração total do fármaco usada na preparação da formulação e a quantidade não encapsulada (livre no ultrafiltrado). Quanto as condições cromatográficas sua análise foi realizada em equipamento Alliance 2695 (Waters, EUA) acoplado a um detector de arranjos de diodos (PDA) 2998 (Waters, EUA), operado a 263 nm. Uma coluna de fase reversa C₁₈ (250 mm × 4,6 mm, 5 mm, XBridge™ Waters) protegida por uma pré-coluna da mesma composição (20 mm × 4,6mm). A fase móvel foi composta por água: acetonitrila (20:80) (v/v). O fluxo utilizado foi de 1,5 mL/min a 30°C e um volume de injeção de 50 µL. Para as condições espectrofotométricas sua análise foi realizada em equipamento Ultrospec® 3000 pro (Amersham Biosciences, Alemanha) em um comprimento de onda de 236 nm a temperatura ambiente.

2.1.6 Determinação da atividade larvicida

Os testes larvicidas foram realizados de acordo com as recomendações do protocolo da Organização Mundial de Saúde (OMS, 2006). As larvas de *Aedes aegypti*, linhagem RecL, foram obtidas no insetário do Departamento de Entomologia do Instituto Aggeu Magalhães/FIOCRUZ/PE. O ensaio biológico foi realizado em condições controladas, sendo as larvas do terceiro estágio mantidas a $26 \pm 1^\circ \text{C}$. Todos os bioensaios foram realizados utilizando uma solução de 2g do óleo essencial para cada

14 mL de etanol do óleo puro e PCL para as nanocápsulas, e o controle negativo foi realizado apenas com etanol. Para a realização dos bioensaios preliminares, preparou-se uma solução inicial de 200 µg/mL de emulsão do óleo essencial, dissolvendo-se 50 mg da amostra de óleo essencial de *C. rhamnifolioides* puro em 3,5 mL de etanol, completando-se para 250 mL com água destilada. A partir da solução inicial foram preparadas diferentes concentrações do óleo essencial puro (40 a 80 µg/mL) e do óleo essencial encapsulado (30 a 80 µg/mL), testadas em três réplicas com 20 larvas/concentração. Os níveis de mortalidade foram registrados após 24h e 48h de exposição. As larvas eram consideradas mortas quando não respondiam ao estímulo de toque ou não emergiam à superfície da solução. Os valores de mortalidade por concentração foram utilizados para estimar, por regressão linear Log-Probít, as concentrações letais para 50% e 90% das larvas expostas (CL₅₀ e CL₉₀), pelo programa estatístico SPSS for Windows versão 21.0, a um nível de confiança de 95%.

3. RESULTADOS E DISCUSSÃO:

3.1 Extração do óleo essencial de *Croton rhamnifolioides*

A partir das extrações realizadas com as folhas de *C. rhamnifolioides* foi determinado o teor do óleo essencial, que apresentou valor médio variando entre 1,4% e 0,58%, em função da época da coleta. Santos *et al.* (2014) obtiveram, para a mesma espécie do gênero *Croton*, um teor de 0,80%. Souza *et al.* (2017), avaliando três espécies de *Croton* verificaram a influência da pluviosidade, temperatura e incidência solar sobre o rendimento e a composição dos seus óleos essenciais. Diversos fatores como horário de coleta da amostra, idade da planta, condições climáticas, influenciam tanto o teor de óleo essencial como a sua composição química (Kerrola, 1994; Carvalho, 2006).

3.1.1 Identificação dos constituintes químicos do óleo essencial

Os constituintes químicos do óleo essencial foram identificados por cromatografia gasosa acoplada à espectrometria de massas (CG-MS). Após análise dos cromatogramas, observou-se que os principais componentes do óleo essencial identificados foram o eucaliptol ou 1,8-cineol (16,57%), o (E)-cariofileno (11,32 %), o α -felandreno (5,52%) e o espatulenol (5,35%). Tais resultados estão de acordo com dados obtidos anteriormente na literatura para *C.*

rhamnifolioides, reportados por Santos *et al.* (2014) e Vidal *et al.* (2017), que verificaram, para o eucaliptol, porcentagem de 7,24 e 18,32%, respectivamente.

3.1.2 Preparação das nanocápsulas e caracterização das formulações contendo óleo essencial

Os resultados obtidos na caracterização das nanopartículas estão apresentados na Tabela 1.

As NC-PCL e NC-PCL/OE apresentaram um tamanho de $200,7 \pm 6,04$ nm e $222,2 \pm 0,53$ nm, respectivamente. Um aumento de cerca de 10% foi observado após a adição do óleo, provavelmente, devido a formação do núcleo oleoso na nanopartícula. Os valores de índice de polidispersão foram menores que 0,2 indicando a presença de populações monodispersas de partículas ou apresentando uma faixa estreita de distribuição do tamanho das partículas.

Os valores de potencial zeta das nanopartículas foram de $-10,1 \pm 2,09$ mV (NC-PCL) e $-15,5 \pm 3,45$ mV (NC-PCL/OE), respectivamente. Estes resultados indicam uma boa estabilidade das formulações. A eficiência de encapsulação das nanocápsulas foi avaliada por CLAE e por espectrofotometria, nos quais foram observadas diferenças nos resultados quando comparados os dois métodos. A curva analítica utilizada para efetuar a quantificação do óleo essencial foi ajustada por análise de regressão linear, as quais estão apresentadas na Tabela 2.

O método mostrou-se linear entre as concentrações de 50 a 300 $\mu\text{g/mL}$. A equação da regressão linear obtida foi $y = -0,0024 + 0,0027 x$ por espectrofotometria e $y = -0,088 + 0,052 x$, em que y é a absorbância ou área e x a concentração ($\mu\text{g/mL}$) em equivalentes de OE, respectivamente (Figuras 1 e 2).

O coeficiente de correlação obtido foi de 0,9993, significando que 99,93% da variação total em torno da média é explicada pela regressão linear, comprovando a adequação do método ao intervalo avaliado. Os dados da análise de regressão são resumidos na Tabela 3.

A eficiência de encapsulação do OE nas nanocápsulas foi de $51,66 \pm 1,76$ % (espectrofotometria) e $32,78 \pm 1,56$ % (CLAE), o que equivale a uma concentração de fármaco na formulação de 5,17 mg/mL e 3,28 mg/mL, respectivamente. De acordo com estes resultados, sugere-se que o sistema ficou saturado pela grande quantidade de óleo

(10mg/mL), com uma proporção polímero/OE de 1:2 (p/p). Além disso, ha uma volatilização natural do óleo essencial, que é intensificada com o processo de rotaevaporação. Sundararajan *et al.* (2018), observou uma diminuição do tamanho na nanoemulsão após 30 dias de armazenamento, ficando a partícula abaixo de 200nm.

3.1.3 Determinação da atividade larvicida

Após uma série de extrações, foram obtidos quatro lotes de óleo essencial, que, para uso nos testes larvicidas, foram identificados em função dos diferentes tempos de armazenamento a 4°C (refrigeração), sendo A (1 ano), B (2 meses), C (uso imediato) e D (uso imediato). Os dois últimos lotes, embora utilizados logo após a extração do óleo, foram obtidos em dias diferentes.

Os valores de concentração letal estimados para os óleos experimentais variaram entre os diferentes lotes de produção (Tabela 4), sendo as amostras C e D consideradas as de maior toxicidade, por exibirem valores médios de CL_{90} menores do que 39 $\mu\text{g/mL}$, após 24h de exposição. Estas mesmas amostras também corresponderam as extrações mais recentes (C e D). Para as amostras dos Lotes A e B a expressão máxima da mortalidade larval em cada concentração foi alcançada de forma tardia, ou seja, após 48h de exposição.

A atividade larvicida apresentada pelo óleo essencial utilizado no presente estudo pode estar relacionada à ação sinérgica de seus constituintes químicos (Andrés *et al.*, 2017). No caso do óleo de *C. rhamnifolioides*, os estudos prévios realizados por Santos (2014) demonstram que a presença do α -felandreno, na composição química do óleo, pode ter relação com sua atividade larvicida. Ainda neste estudo, verificou-se que o efeito inibitório da atividade da tripsina pode estar associado à atividade larvicida.

Para os bioensaios com as nanopartículas (NC-PCL/OE), foi utilizado apenas o Lote D, pois este apresentou o menor valor de CL_{90} nos testes com o óleo essencial. Os valores de concentração letal revelaram uma diminuição importante da toxicidade, bem como um aumento no tempo requerido para alcançar a mortalidade final nas concentrações testadas de até 48h, comparados ao óleo essencial puro não encapsulado. Nossos resultados são em parte semelhantes aos observados por Sundararajan *et al.* (2018), embora os mesmos tenham referido o início da mortalidade a partir das 48h. O mesmo comportamento foi constatado por Kanés (2011),

ao utilizar o polímero sintético PCL na nanoencapsulação do óleo de copaíba, observou um retardo da liberação do princípio ativo no período de 48h. De acordo com este autor, estudos sobre a atividade larvica residual do produto seriam necessários para saber se o óleo está sendo liberado de forma constante ou se a formação da membrana polimérica impossibilitou a liberação do princípio ativo. Neste mesmo estudo Kanés *et al.* (2011) demonstram que a utilização de gelatina possibilitou uma liberação mais rápida do óleo quando comparada a outros polímeros, fato que pode estar associado a espessura e integridade da partícula formada ao redor do princípio ativo. Outra variável a ser considerada neste contexto, segundo os autores, é o fato da gelatina ser uma proteína, e que as proteínas fazem parte da alimentação das larvas e isso pode ter potencializado a atividade larvica.

Christofoli *et al.* (2015) avaliando nanoesferas de PCL com óleo essencial de *Zanthoxylum rhoifolium* e de *Z. riedelianum*, obteve aproximadamente 80% de difusão em 72h de ensaio.

Em nossos bioensaios não foram observadas diferenças em ambos os controles, ou seja, nanopartículas vazias e etanol, demonstrando assim que o produto utilizado nas nanopartículas não promoveu qualquer mortalidade larval. Apesar disso, as nanopartículas contendo o óleo essencial de *C. rhamnifolioides* retardaram a mortalidade das larvas (L3) de *A. aegypti* e exigiram uma quantidade maior do composto quando comparado ao óleo puro. Embora isso tenha acontecido, a atividade larvica descrita para o óleo nanoencapsulado foi maior do que o referido para outros compostos de origem vegetal (Manimaran *et al.*, 2012; Soonwera, 2015).

Uma grande vantagem do uso das nanopartículas foi promover a solubilidade do produto em água sem a necessidade da adição de solventes. Estudos complementares podem revelar ainda vantagens adicionais desta nanoencapsulação do óleo de *C. rhamnifolioides*, relacionadas a atividade residual, ligada por exemplo, à proteção do princípio ativo e sua liberação gradual no ambiente aquático. Outro aspecto importante seria a redução do contato do larvica com o homem (Vishwakarma *et al.*, 2016).

4. CONCLUSÕES:

A prospecção de compostos naturais com atividade larvica para mosquitos representa uma importante área do conhecimento, necessária ao desenvolvimento de produtos mais seletivos e ambientalmente seguros, como alternativa ao uso de inseticidas químicos sintéticos. A redução da carga de uso destes compostos no combate ao mosquito *A. aegypti* surge como uma tendência mundial, nos últimos cinco anos, sobretudo em função da resistência da espécie a tais inseticidas, largamente documentadas na última década.

Os resultados encontrados para o óleo essencial das folhas de *C. rhamnifolioides* mostraram-se promissores tanto em sua apresentação pura quanto em nanocápsulas de policaprolactona, cujos valores de CL₅₀ foram <30 µg/mL e <75 µg/mL, respectivamente. Assim, o óleo de *C. rhamnifolioides* pode ser uma alternativa viável, embora estudos complementares sejam necessários para compreender o efeito de variáveis como: idade do vegetal, período de coleta, fatores climáticos, volatilização do óleo, técnica de obtenção do óleo, tempo de armazenamento e forma de conservação do óleo, sobre sua performance larvica.

É possível ainda sugerir quanto à nanopartícula testada que, outros polímeros sintéticos possam promover um perfil de liberação mais adequado do princípio ativo e, consequentemente, possam potencializar a ação larvica do óleo de *C. rhamnifolioides*.

Diante do exposto, investir no desenvolvimento de um produto à base de óleos essenciais de *C. rhamnifolioides*, empregando nanotecnologia para o controle da liberação e prolongamento da ação do ativo, como já ocorre com diversos fármacos, poderá aumentar sua estabilidade e atividade tóxica para larvas de *A. aegypti*. Contudo, a destruição e eliminação de criadouros larvais desta espécie de mosquito devem continuar a ser a principal ação de controle, trabalhada junto à população, a fim de reforçar a importância do papel de cada um no combate ao mosquito.

5. AGRADECIMENTOS:

Ao IFPE pela oportunidade de realizar o Curso de Graduação e Pós Graduação; às parcerias envolvidas com os laboratórios da UFPE e o IAM/Fiocruz-PE. À tecnóloga Ana Paula Araújo do Laboratório do Serviço de Referência em Controle de Culicídeos Vetores

(SRCCV)/IAM/Fiocruz-PE, pelo apoio nos testes biológicos.

6. REFERÊNCIAS:

- Adams, R. P. Identification of Essential Oil Components by Gas Chromatography/Quadrupole Mass Spectroscopy. Carol Stream: Allured Publ. Corp. **2001**.
- Araujo, A.P., Araujo Diniz, D.F., Helvecio, E., De Barros, R.A., De Oliveira, C.M., Ayres, C.F., De Melo-Santos, M.A., Regis, L.N. and Silva-Filha, M.H., *Parasit Vectors*, **2013**, 6,297.
- Andrés, M.F., Rossa, G.E. Cassel, E., Vargas, R.M.F., Santana, O., Díaz, C.E., González-Coloma, A. *Food Chem. Toxicol.*, **2017**, 109,1086.
- Braga, I. A., Valle, D., *Epidemiol. Serv. Saúde* **2007**, 16, 279.
- Brasil. Ministério da Saúde. Fundação Nacional de Saúde (FUNASA). Programa Nacional de Controle da Dengue. Brasília. **2002**, 154 p.
- Castillo, R., Stashenko, E., Duque, J. *J. Am. Mosquito Contr.*, **2017**, 33, 25.
- Carvalho Filho, J. L. S., Blank, A. F., Alves, P. B., Ehlert, P. A. D., Melo, A. S., Cavalcanti, S. C. H., Arrigoni-Blank, M. F.; Silva- Mann, R. *Rev. bras. farmacogn.*, **2006**, 16, 24.
- Chediak, M., G. Pimenta F, J., Coelho, G.E., Braga, I.A., Lima, J.B., Cavalcante, K.R., Sousa, L.C., Melo-Santos, M.A., Macoris Mde, L., Araujo, A.P., Ayres, C.F., Andrighetti, M.T., Gomes, R.G., Campos, K.B. and Guedes, R.N., *Mem Inst Oswaldo Cruz*, **2016**, 111, 321.
- Christofoli, M., Costa, E. C. C., Bicalho, K. U., de Cássia Domingues, V., Peixoto, M. F., Alves, C. C. F., Araújo, W. L., De Melo Cazal, C. *Ind. Crops Prod.*, **2015**, 70, 301.
- Chiarella, J. M. *Rev. Ciênc. Méd. Sorocaba*, **2016**, 18, 123.
- Corrêa, J. C. R.; Salgado, H. R. N. *Rev. Bras. Pl. Med.*, **2011**, 13, 500.
- Da Câmara, C. A. G., De Moraes, M. M., De Melo, J.P.R., Da Silva, M.C. *J. Essent. Oil-Bear. Plants*, **2017**, 20, 1434.
- Da Costa, A. C. V., Melo, G. F. D., Madruga, M. S., Da Costa, J. G. M., Garino, F., Neto, V. Q. *Semina: Ciênc. Agrár.* **2013**, 34, 2853.
- Dias, C. N., Moraes, D. F. C. *Parasitol. Res.* **2014**, 113, 565.
- Flores, F. C., Ribeiro, R. F., Ourique, A. F., Rolim, C. M. B., Silva, C. B., Pohlmann, A. R., Beck, R. C. R., Guterres, S. S. *Quim. Nova*, **2011**, 34, 968.
- Jintana, Y., Saowanne, C., Nongkran, L., Pradya, S. *Acta Trop.* **2015**, 149, 232.
- Kanes, LA; Prophiro, JS; Guerreiro, K; Clemes, I; Silva, OS; Vieira, ES; Nascimento, MP; Zepon, KM; *Parasitol. Res.* **2011**, 108, 1.
- Kerrola, K; Galambosi, B; Kallio, H; J. *Agr. Food Chem.* **1994**, 42, 775.
- Lago, J. H. G., Soares, M. G., Batista, P. L. G., Silva, M. F. G. F., Corrêa, A. G., Fernandes, J. B., Vieira, P. C., Roque, N. F. *Rev. Phytochem.* **2006**, 67, 589.
- Lima, G., Souza, T. Paula Freire, G., Farias, D., Cunha, A., Nágila, R., Moraes, S., Carvalho, A. *Parasitol. Res.*, **2013**, 112, 1953.
- Manimaran, A., Cruz, M. J. J., Muthu, C., Vicent, s., Ignacimuthu, S. *Adv. Biosci. Biotechnol.*, **2012**, 3, 855.
- Natrajan, D., Srivasan, S., Sundar, K., Ravindran, A. *J. food drug anal.*, **2015**, 23, 560.
- Organização mundial de saúde. Pesticide and Their Application. For the Control of Vectors and Pests of Public Health Importance. Geneva, Switzerland. WHO/CDS/NTD/WHOPES/GCDPP, **2006**.
- Pavela, R., *Curr. Org. Chem.*, **2016**, 20, 2674.
- Penna, M. L. F. *Cad. Saúde Pública*, **2003**, 19, 305.
- Peng, C., Zhao, S-Q., Zhang, J., Huang, G.Y., Chen, L.Y., Zhao, F-Y. *Food Chem.*, **2014**, 165, 560.
- Pontes, R. J.S., Ruffino, N. A., *Rev. Saúde Públ.*, **1994**, 28.
- Prezoto, F. *Ces Revista*, **2016**, 30, 267.
- Randau, K. P., Florêncio, D. C., Ferreira, C. P., Xavier, H. S. *Rev. Bras. Farmacogn.*, **2004**, 14, 89.
- Rose, R. I. *Emerg. Infect. Dis.* **2001**, 7, 17.
- Sundararajan, B., Thamaraselvi, R., Anil, K. M., Ranjitha, K. B. D. *Rev. Microb. Pathog.* **2018**, 125.
- Santos, G. K. N., Dutra, K. A., Lira, C. S., Lima, B. N., Napoleão, T. H., Paiva, P. M. G; Maranhão, C. A., Brandão, S. S. F., Navarro, D. M. A. F. *Molecules*, **2014**, 19, 16573.

33. Santos, A. G. S., Dutra, K. A., Dutra, m. T. D., Silva, F. S. V. C. B., Maranhão, C. A., Navarro, D. M. A. F., Frutuoso, M. N. M. A., Brandão, S. S. F. *Holos*, **2015**, 31, 36.
34. Soloway, S. B. *Environ. Health Perspect*, **1976**, 14, 109.
35. Soonwera, M. *Parasitology Research*, **2015**, 114, 4531.
36. Soppimath, K. S., Aminabhavi, T. M.; Kulkarni, A. R., Rudzinski, W. E., *J. Control. Release*, **2001**, 70, 1.
37. Souza, G.S., Bonilla, O.H., Lucena, E.M.P., Barbosa, Y.P. *Cienc. Rural*, **2017**, 47, 1.
38. Souza, S. S., Silva, I. G., Silva, H. H. G. *Rev. Soc. Bras. Med. Trop.*, **2010**, 43, 152.
39. Vidal, C. S., Martins, A. O. B. P. B., Silva, A. A., Oliveira, M. R. C., Ribeiro-Filho, J., Albuquerque, T. R., Coutinho, H. D. M., Almeida, J. R. G. S., Junior, L. J. Q., Menezes, I. R. A. *Biomed. Pharmacother.* **2017**, 89, 47.
40. Vishwakarma G. S., Gautama, N., Babub, J. N., Mittala, S., Jaitakc, V., *Polym.Rev.*, **2016**, 56, 668.

Tabela 1 - Tamanho de partícula, índice de polidispersão (PDI), potencial Zeta, doseamento eficiência de encapsulação (EE %) determinado por cromatografia líquida de alta performance (CLAE) e espectrofotometria de absorção no UV-Visível (UV-Vis) nas nanocápsulas sem (NC-PCL) e com óleo essencial (NC-PCL/OE).

Formulação	Tamanho de Partícula (nm)	PDI	Potencial Zeta (mV)	Doseamento (%)	EE% (CLAE)
NC-PCL	200,7 ± 6,04	0,160	-10,1 ± 2,09	-	-
NC-PCL/OE	222,2 ± 0,53	0,116	-15,5 ± 3,45	52,5 ± 1,44	70,7 ± 1,86

Autoria: Milena Ferraz, 2018

Tabela 2- Curva analítica do óleo essencial de *Croton rhamnifolioides* a 236 nm.

Concentração teórica de OE (µg/mL)	Valor da absorbância	Valor da Área OE (mAU/min)
50	0,135	2,69
100	0,262	5,05
150	0,392	7,65
200	0,532	10,27
250	0,654	12,97
300	0,802	15,69

Autoria: Milena Ferraz, 2018

Tabela 3- Parâmetros do método espectrofotométrico e CLAE para a quantificação do óleo essencial (OE).

Parâmetros	Espectrofotometria	CLAE
Comprimento de onda de medição (nm)	236	236
Faixa linear (µg/mL ⁻¹)	50-300	50-300
Intercepto ± (desvio padrão)	-0,0024 (± 0,006)	-0,088 (± 0,118)
Inclinação ± (desvio padrão)	0,0027 (± 0,00003)	0,052 (± 0,0006)
Coefficiente de correlação (r ²)	0,9993	0,9993
Limite de detecção, LD, (µg/mL ⁻¹)	7,33	7,49
Limite de quantificação, LQ, (µg/mL ⁻¹)	22,22	22,69

Autoria: Milena Ferraz, 2018

Tabela 4 - Toxicidade de diferentes lotes de produção do óleo essencial de folhas de *Croton rhamnifolioides* para larvas de *Aedes aegypti*, provenientes da colônia Recife-Laboratório (RecL).

Lote	Tempo de exposição (h)	CL ₅₀ ² (Intervalo de confiança 95%)	CL ₉₀ ² (Intervalo de confiança 95%)
A	48	48,2 (38,8 – 60,5)	60,7 (47,6 – 76,4)
B	48	52,2 (45,0 – 62,0)	68,7 (53,7 – 93,7)
C	24	26,3 (20,2 – 30,8)	39,0 (27,8 – 51,0)
D	24	26,4 (23,5 – 29,9)	37,8 (31,7 – 46,1)
D ¹	48	63,4 (51,6 – 74,0)	108,8 (84,5 – 146,4)

1 = Amostra de óleo essencial do lote D nanoencapsulada.

2 = Concentração letal média (µg/ml) para 50% (LC₅₀) ou para 90% (LC₉₀) das larvas expostas.

Autoria: Melo-Santos, 2019

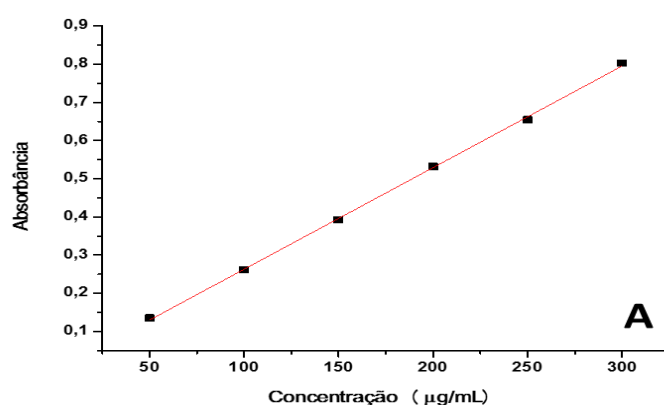


Figura 1 - Análise de regressão linear do óleo essencial por espectroscopia (A). A linha vermelha representa o ajuste à regressão linear.

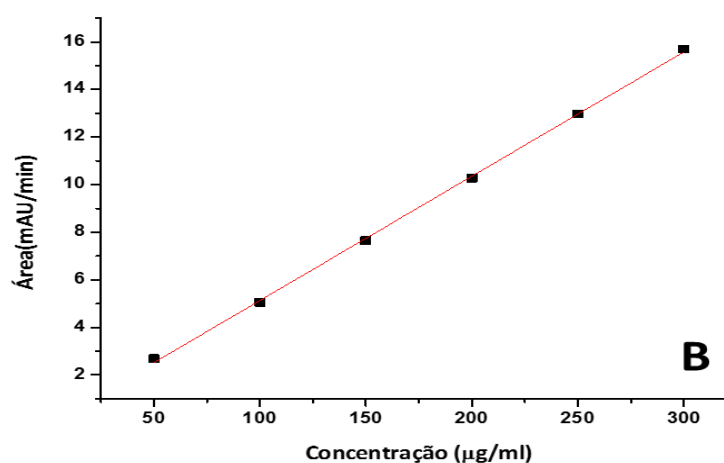


Figura 2- Análise de regressão linear do óleo essencial por CLAE (B). A linha vermelha representa o ajuste à regressão linear.

COMO OS PROCEDIMENTOS DE QUALIDADE DE LABORATÓRIO AFETAM A
COMPETÊNCIA DOS ESTUDANTES COM GRADUAÇÃO EM QUÍMICA?HOW LABORATORY QUALITY PROCEDURES AFFECT THE COMPETENCE OF
CHEMISTRY UNDERGRADUATE STUDENTS?PRASETYA, Agung Tri^{1*}; CAHYONO, Edy²; SUDARMIN³; HARYANI, Sri⁴¹Graduate study of Science Education Program, Universitas Negeri Semarang, Indonesia^{2,3,4} Chemistry Department, Faculty of Mathematics and Natural Science, Universitas Negeri Semarang, Indonesia

* Correspondence author

e-mail: agungchem@mail.unnes.ac.id

Received 05 December 2019; received in revised form 15 December 2019; accepted 08 January 2020

RESUMO

De acordo com as competências do século XXI, a reforma do sistema educacional nas universidades é necessária para melhorar a qualidade dos graduados. O objetivo deste estudo foi aprimorar a competência dos graduados em química empregando um modelo de aprendizado baseado em projetos através da aplicação de procedimentos de qualidade laboratorial (PBL-ALQP). O modelo PBL-ALQP foi utilizado no experimento de instrumentação para análise química e foi realizado em duas etapas. Na fase preliminar, foram observadas atividades dos alunos na preparação de soluções de trabalho e na análise de instrumentação para medir o nível de realização das habilidades laboratoriais necessárias e habilidades de análise de instrumentação, respectivamente. No trabalho do projeto, os alunos dos grupos receberam um projeto para resolver problemas relacionados à análise de instrumentação. Ao se referir aos artigos científicos que eles deviam procurar, os alunos tinham que ser capazes de compilar projetos de projetos, implementar projetos, relatar resultados do projeto, implementando procedimentos de qualidade de laboratório, para que os resultados das análises realizadas possam ser confiáveis e válidos. Através de uma avaliação autêntica, observou-se a atividade do aluno para medir o nível de realização de habilidades de pensamento crítico, habilidades de comunicação e habilidades de trabalho científico. O nível de realização de habilidades básicas de laboratório, habilidades de análise de instrumentação, habilidades de pensamento crítico, habilidades de comunicação e trabalho científico de estudantes de química estão em categorias altas. Os resultados indicaram que o modelo PBL-ALQP pode ser usado para melhorar a competência dos graduados em química.

Palavras-chave: *Aprendizagem Baseada em Projetos; Procedimentos de Qualidade Laboratorial; Competências de Graduação; Condutometria de Titulação Ácido-Base; Espectrofotometria UV-Vis*

ABSTRACT

Reform of the education system in universities is needed to improve the quality of graduates according to 21st-century competencies. The purpose of this study was to enhance the competence of chemistry graduates by applying a project-based learning model through the application of laboratory quality procedures (PBL-ALQP). The PBL-ALQP model has been used for the chemical analysis instrumentation experiment and was carried out in two stages. In the preliminary stage, student activities in working solutions preparation and conducting instrumentation analysis were observed to measure the achievement level of necessary laboratory skills and instrumentation analysis skills, respectively. In project work, students in groups were given a project to solve problems related to instrumentation analysis. By referring to the scientific articles that they must look for, students must collaboratively be able to compile project designs, implement projects, report project results by implementing laboratory quality procedures so that the results of the analysis carried out can be trusted and valid. Through authentic assessment, student activity was observed to measure the achievement level of critical thinking skills, communication skills, and scientific work abilities. The achievement level of basic laboratory skills, instrumentation analysis skills, critical thinking skills, communication skills, and scientific work abilities of chemistry students are in high categories. The results showed that PBL-ALQP model could be used to improve the competence of chemistry graduates.

Keyword: *Project-Based Learning; Laboratory Quality Procedures; Undergraduate Competencies; Acid-Base Titration Conductometry; UV-Vis Spectrophotometry*

1. INTRODUCTION

Globalization has caused significant changes in the field of education. Higher education institutions are required to reform the education system to improve the quality of graduates following 21st-century competencies (Cavinato, 2017). Competencies of graduates in analytical chemistry are high order thinking skills and strong instrumentation analysis skills to accommodate the needs of the workforce according to 21st-century competencies (Prasetya, Haryani, Cahyono, & Sudarmin, 2019).

The preliminary study results of students work from the Chemistry Study program - at the Faculty of Mathematics and Natural Sciences Universitas Negeri Semarang (FMIPA UNNES) located in Central Java Indonesia - in the period 2017-2019, found that there were students who did not understand the concepts and principles of instrumentation analysis (Haryani, Liliarsari, Permanasari, & Buchari, 2010). Students' instrumentation analysis skills are still low, this is indicated by the measurement results that have not yet been tested for accuracy and precision, and the validation of the test methods for the quality of measurement results has not been validated. Critical thinking skills of students are also still low, as shown by their weak ability to design proposals, implement and report research results. Efforts should be made to improve the competence of undergraduates from Chemistry study programs at the FMIPA UNNES to be equal and be able to compete with undergraduates from other tertiary institutions in the global era (Haryani, 2011; Haryani, Prasetya, & Bahron, 2017).

Project-based learning models are widely applied in chemical analysis practices to develop undergraduate competencies (Bagheri, Ali, Chong, & Daud, 2013; Bowden et al., 2012; Cavinato, 2017; Chun, Kang, Kim, & Kim, 2015; Frederick, 2013; Lee, Blackwell, Drake, & Moran, 2014). The application of project-based learning models can provide authentic experiences for students in developing critical thinking skills to solve problems through collaboration (Cesarino, Mulholland, & Francisco, 2018; Jollands, Jolly, & Molyneaux, 2012; Wurdinger & Qureshi, 2015). Utilization of project-based learning models through accredited laboratory simulations to obtain valid measurement results (Taylor et al., 2015). The forensic science model is used to increase student involvement in Experiment activities

(Frederick, 2013). The results provide more enormous benefits and experience compared to traditional experiments; students are more critical and competitive. Chemical analysis instrumentation experiment utilizing environmental issues has been used to see misconceptions in modern chemical instrumentation. It was used to train instrumentation analysis skills accurately, foster motivational, collaborative, and communication attitudes (Carbó, Adelantado, & Reig, 2010; Robinson, 2013).

Classical and instrumental analysis results categorized as valid if the analysis carried out by following the principles of scientific work through the applying of laboratory quality procedures. Validation of testing methods as the applying of laboratory quality procedures needs to be trained for students so that graduate competencies can be improved. It is necessary to develop a chemical analysis instrumentation experiment model that can increase the competence of undergraduates through a project-based learning model by applying laboratory quality procedures (ALQP) (Bowden et al., 2012; Jiang, 2005; Taylor et al., 2015).

The development of the PBL-ALQP model aims to improve the mastery of instrumentation analysis concepts, basic laboratory skills, instrumentation analysis skills, critical thinking skills for problem-solving, communication skills, and scientific work abilities. The PBL-ALQP model was divided into two stages, namely the preliminary stage and project work. The preliminary stage was intended to introduce various instrumentation to students as well as to measure the level of basic laboratory skills and instrumentation analysis skills. Project work was aimed at providing authentic experiences for students in solving problem-related to daily life, developing a correct understanding of scientific processes, critical thinking skills, communication skills, and scientific work abilities (Wurdinger & Qureshi, 2015). The PBL-ALQP model that is implemented in blended learning, which combines experiment learning in the laboratory with online learning. Learning begins with giving open-ended, complex, and related problems with daily life, and is designed so that students work collaboratively, disciplined, and responsibly. New knowledge needs to be possessed by students to search for literary literature in solving problems, as well as critical thinking skills for making hypotheses, compiling

and carrying out experiment procedures, conducting data analysis and making conclusions based on information collected to solve problems (Cavinato, 2017; Frederick, 2013).

2. MATERIALS AND METHODS

2.1 Data Collecting Instruments

This research is a development of the PBL-ALQP model, which is proven to improve the competence of chemistry undergraduates (Creswell, 2010). The implementation of the PBL-ALQP model was carried out using a one-group pretest-posttest design in 2 classes consisting of 65 students during 12 class meetings, as presented in Table 1. All the students are bind as a participant of the instrumentation analysis course (required course as undergraduate students in chemistry). At the initial meeting, learning agreement covers their willingness as a subject in current research without affecting their final mark. Individual assignments given online include drafting and experiment reports, discussions, and self-assessments through *elena.unnes.ac.id*. In the preliminary stage, an authentic assessment, which is a method of assessing all student activities during the experiment, is carried out by ten observers. The authentic assessment consists of evaluating the design and experiment report and observing student activities during the experiment activity. An authentic assessment in weeks 1-3 was used to measure the level of basic laboratory skills through observing the activities of students in taking, weighing, dissolving, and diluting chemicals and how to do titrations. An authentic assessment in the 4th-6th week is used to measure the level of instrumentation analysis skills through observation of student activities in stringing, calibrating, and operating pH-meter, conductometer, and UV-Vis spectrophotometer in verification practice activities.

In project work, authentic assessment is used to measure the level of critical thinking skills, communication skills, scientific work abilities, and the attitude of discipline and responsibility of students. All authentic assessment instruments used in the study have been validated by learning and evaluation experts with valid results, and have been tested to determine their reliability through interrater reliability testing.

Study material as a source of problems that are open-ended, complex, and related to daily life that must be revealed and sought for resolution by students include analysis of well water quality, analysis of tap water quality, analysis of iodine levels in table salt, analysis of essential minerals in fruit/vegetables, and analysis of heavy metals in waste. Collaborative students must be able to find literature related to one of the study materials from various sources of reference as a basis for developing project designs. Implementation of project work must be carried out by applying laboratory quality procedures, namely by using the principles of scientific work to obtain valid data. One way to apply laboratory quality procedures is to validate testing methods, which include a limit of detection (LoD) tests, a limit of quantization (LoQ), linearity ranges, and precision and accuracy tests.

2.2 Data Analysis

All the results were classified into the group of design assessment and experiment, as well as student activities and experiment observation. Furthermore, authentic assessment rubrics were used in the form of *Likert* scales that have been prepared, the achievement level of basic laboratory skills, instrumentation analysis skills, communication skills, scientific work abilities, and the attitude of discipline and responsibility of students can be measured (Hake, 2008). Students' abilities in designing, implementing, and reporting on project work are used as a basis for measuring the level of critical thinking skills.

3. RESULTS AND DISCUSSION

Basic laboratory skills and instrumentation analysis skills can be built through the active role of students in the preliminary Experiment (Lee et al., 2014). The integration of preliminary experiments and project work carried out with the application of laboratory quality procedures can also improve critical thinking skills, communication skills, and scientific work abilities (Cavinato, 2017). The PBL-ALQP model can develop critical thinking skills through the ability to search the scientific literature, translate scientific articles, compile experimental steps, operate instrumentation to collect data, perform data calculations and analyzes, validate testing methods, and draw conclusions (Frederick, 2013; Taylor et al., 2015). Students' skills in presenting and writing

scientific articles as a product of project work can improve communication skills. In the end, the improvement of critical thinking skills and communication skills in completing project work affects the growth of scientific work skills.

3.1 Implementation of the PBL-ALQP Model in the Preliminary Stage

The results of the assessment and observation of student activities during the preliminary experiment obtained information that there were 64 (99%) and 58 (89%) students who had basic laboratory skills and instrumentation analysis skills with high and very high criteria. From those three achievement groups (determined based on cumulative performance index), the achievement level of basic laboratory skills and instrumentation analysis skills did not differ significantly. Detailed information is presented in Table 2.

Student activities in designing experiments include analyzing the needs of working solutions and preparing descriptions of how to make working solutions. Students can recap the needs of working solutions and describe how to make working solutions properly. The percentage of errors observed in the description of the making of working solutions due to calculation factors of 9%, the material purity (18%), solution volume (6%), and molecular formula errors (32%). The difficulty level experienced by students in describing the preparation of working solutions increases sequentially from liquid raw materials (for example, HCl), solid raw materials (for example, NaOH), and solid raw materials from polyfunctional compounds (for example oxalic acid and sodium tetraborate). Student activities in making working solutions and standardization run smoothly. Some student activities recorded during observation and not following work instructions include the process of weighing, dissolving, thinning, and titrating. Considering chemicals with an analytical balance in an open condition, the container used is not suitable, stirring carelessly, and doing titration with only one hand (Robinson, 2013). Students from each achievement group have an excellent ability to make experiment reports.

The next activity in the preliminary stage is a verification experiment to determine the ionization constant (K_a) of acetic acid with pH-meter, acid-base titration with a conductometer, and to determine the concentration of copper(II)

sulfate with UV-Vis spectrophotometer. An understanding of instrumentation components, analytical techniques, data analysis, concluding the focus of observation (Robinson, 2013). The information obtained from Table 2 shows that the instruments that were mastered by students in succession were the pH-meter, conductometer, and UV-Vis spectrophotometer. The highest achievement level of instrumentation analysis skills obtained by students when operating instruments in the sequence are the pH-meter, conductometer, and UV-Vis spectrophotometer. The same sequence of two former instruments makes students ease to be mastery. However, the operation procedure of the UV-Vis spectrophotometer is still complicated. The results can be seen from the level of instrumentation analysis skill achievement with very high criteria in operating the highest pH-meter compared to the conductometer and UV-Vis spectrophotometer. There are 4, 10, and 11 students who are not yet skilled in operating the pH-meter, conductometer, and UV-Vis spectrophotometer, respectively.

There are no significant mistakes observed while observing and evaluating the experiment design. However, some little mistakes, such as the carefulness of student planning for borrowing glasswares for the experiment. In advance, the number of members in the student groups impact on collaboration skills of students, particularly in shared-tasks contribution by each person. In the experiment, the ideal number in a group consists of a maximum of 3 people (Santos, Montes, Sánchez-Coronilla, & Navas, 2014). The ability of students to operate the pH-meter and conductometer is no different, because the two instruments have similar shapes, sizes, and ways of working, even though they have different functions. The similarity between the pH-meter and the conductometer helps and facilitates students in operating. Different conditions occur at the lab reporting stage with a pH-meter compared to conductometric titration. It'd, was revealed that students had difficulty in making conductometry titration charts.

The biggest mistake occurred in the lab reporting phase using a UV-Vis spectrophotometer, which is when making the calibration curve. There are several steps students must work to be able to calculate the concentration of copper(II) sulfate. This leads the errors in making reports. Difficulties

experienced by students in processing data and calculations have an impact on the decline in the achievement level of instrument analysis skills with very high criteria. This condition is very similar to the results of research conducted by Robinson (2013) and Cavinato (2017) (Cavinato, 2017; Robinson, 2013).

Authentic experience gained by students in operating the pH-meter, conductometer, and UV-Vis spectrophotometer can increase understanding of the principles and practical operational ways of the instrument (Fakayode, 2014). A thorough evaluation of the preliminary experimental findings is used as feedback at the end of the experiment. Through feedback, knowledge, and understanding of analytical chemistry concepts, especially in the context of making working solutions and standardization can be improved, and mistakes in using basic laboratory equipment can be avoided (Dalgarno, Bishop, Adlong, & Bedgood Jr, 2009; Karataş, 2016). By giving feedback, instrumentation analysis skills can be improved again, mistakes made by students during an experiment can be corrected and not repeated in project work and can increase retention (Carvalho, Fiuza, Gama, & Salema, 2015; Sharples, 2019).

3.2 Implementation of the PBL-ALQP Model in the Project Work Phase

Following the syntax of project-based learning, learning begins with giving open-ended and complex problems. Students collaboratively make project designs, determine schedules, implement, and make project reports. The project design begins with compiling issues, hypotheses, and proceed with searching scientific literature relating to the themes in the discourse. From the scientific research obtained, each student proposes an instrumentation analysis method as an alternative method of analysis that can be applied to answer the problem. Through discussion in groups, they were required to decide on one way of instrumentation analysis to be used in project design. The choice of instrumentation analysis method must pay attention to the availability and condition of the instrument, as well as the availability of supporting chemicals in the laboratory (Cavinato, 2017; Fakayode, King, Yakubu, Mohammed, & Pollard, 2011; Frederick, 2013; Henderson, 2010; Robinson, 2013; Taylor et al., 2015). Following the PBL-ALQP model developed, the project work design must apply laboratory quality procedures in the activities of

taking samples, making working solutions, preparing samples, making calibration curves, measuring samples, calculating and analyzing data, and validating testing methods. The validation activities of the testing methods carried out include linearity tests, LoD and LoQ calculations, precision, and accuracy tests (Carbó et al., 2010; Fakayode, 2014; Jiang, 2005; Taylor et al., 2015).

The results of observations and assessments during project work obtained information that there were 63, 82, 74, 98, and 82% of students who possessed critical thinking skills, communication skills, and scientific work abilities, as well as discipline and responsibility with high and very high criteria. Between the upper and middle achievement groups have significantly different levels of critical thinking skills and scientific work abilities. Differences also occur in the achievement level of communication skills between the upper and lower achievement groups. Of the three achievement groups, the attainment level of discipline and responsibility did not differ significantly. Detailed information is presented in Table 3.

3.2.1 Critical thinking skills

Critical thinking skills are measured using criteria consisting of five dimensions, namely 1) elementary, 2) in-depth clarification, 3) judgment, 4) inference, and 5) strategies (Perkins & Murphy, 2006; Saripudin, Haryani, & Wardani, 2015; Sarwi & Liliyasi, 2010; Sarwi, Rusilowati, & Khanafiyah, 2012; Tawil & Liliyasi, 2013). Analysis of the achievement level of critical thinking skills in completing projects of each dimension is presented in Figure 1.

The elementary dimension is measured by looking at the systematic suitability of the project design and experimental objectives. There are 2 out of 19 groups that have not made hypotheses and data analysis techniques in the project design. As most references are still in the form of scientific articles, there are only two groups whose references are in the form of standard methods. The ability of students to develop hypotheses has the lowest achievement level. The assumption made by students is still not connecting between variables and has not been measured. The dimensions of in-depth clarification have the lowest performance compared to other dimensions. The systematic foundation of

literature, relationships between concepts, and accuracy of the formulas use was used to measure this dimension. The ability of students to make problem formulations is still low. The formulation of a good problem must be made clearly, related to the topic in the discourse, and made in question sentences. The dimension of judgment is measured by looking at the suitability of experimental tools and materials used, the steps of the experiment, and the way data is collected. Language constraints are the main cause of students' difficulties in compiling work steps, primarily work steps for precision and accuracy tests. However, students have no difficulty in using simple laboratory equipment (taking solids, taking liquid, weighing, dissolving, and diluting), and operating instrumentation equipment. This can be understood because students have been trained in the preliminary experiment.

The dimension of inference is assessed based on depth in conducting data analysis, discussion, and conclusions. This dimension is measured through the assessment of project reports related to making working solutions, making calibration curves, as well as the results of the validation of testing methods that include linearity, LoD, LoQ, accuracy, and precision. Students were able to prepare working solutions, calibration curves, and LoD and LoQ calculations correctly. However, they still need intensive guidance from the lecturer to determine precision and accuracy. The validation results of the test method on the calibration curve (with $r^2 > 0.9$) and LoD-LoQ calculation are 68% and 37%, respectively. In advanced, there are only 21% and 26% of students meet the requirement for precision and accuracy determination, respectively. The results indicate that students still need more practice to validate the testing method. The dimensions of strategies re-assessed through the systematic and quality of report appearance prepared by students are following existing guidelines. The lowest indicator is in the appearance of the report that is less interesting, consistency, and shallow discussion.

In the PBL-ALQP model, students are required to search literature through various sources to find instrumentation analysis techniques, so that it will require a person to think critically to be able to obtain, choose, and process the information effectively (Henderson, 2010). Through scientific articles obtained can be used to make work steps in project design (Cavinato, 2017), increase understanding of the

instruments used (Fakayode, 2014), as well as to develop analytical methods (Frederick, 2013). The excellent project design will produce objective truth when it is supported by a reliable analytical method. Further, the analysis results will be then guaranteed quality, and valid data will be obtained.

The performance of the analysis method was evaluated by testing linearity, LoD, LoQ, precision, and accuracy (Jiang, 2005). Through assigning project design tasks to validate the testing method, students develop critical thinking skills. Giving open-ended, complex, and daily-related problems that must be resolved helps students hone critical thinking skills because students are required to interact directly with the real world collaboratively. Through discussion is an effective way to train and develop critical thinking skills, because in the discussion there is an exchange of opinions and in the process of exchange of opinions that students can consider, reject, or accept the opinions themselves or others to match the opinions of the group. This is what ultimately fosters students' critical thinking skills (Arfianawati, Sudarmin, & Sumarni, 2016). The achievement level of students' critical thinking skills is influenced by the ability to formulate hypotheses, formulate problems, seek reference to standard methods, translate the contents of scientific articles into work steps, perform calculations, and data analysis. The achievement level of students' critical thinking skills can still be improved through training.

3.2.2 Communication skills

The communication skills achievement level is high, with the distribution of high categories with 53 students (82%). Measurement of the achievement level of student communication skills is done through 2 methods, namely observation at the time of presentation and assessment of the quality of scientific articles that have been prepared. The average achievement level of verbal communication skills for each indicator is higher than non-verbal communication skills. The verbal communication skills result found that students: 1) already have skills in delivering presentation material in front of the class and collaboration well; 2) having confidence, being open to ideas from other groups; 3) questioning skills' need to be developed because there are still many students who are not yet involved in the discussion; 4) managing time is needed for groups who are presenting the results of the

project need.

On the other hand, the assessment of non-verbal communication skills results find that 1) students are citing the references mostly from textbooks and only a small portion of recent scientific articles; 2) sub-chapter method is still the same as working procedure as it stated in the project report; 3) discussion part is still shallow, only in the form of results of the test method validation, and have not to correlate between all variables and objectives to be achieved. The results indicate that students' communication skills were still needed to be developed. Some activities, including writing scientific papers and scientific articles training, as well as preparation and timing in presentations/discussions. Project-based learning can also be used to improve communication skills, both delivering presentations and writing scientific reports (Fakayode, 2014; Gusarova, Kopytova, & Reshetnikova, 2019; Henderson, 2010; Sojka & Che, 2008).

3.2.3 Scientific work abilities

Scientific work abilities are measured through project design evaluation, observation of project implementation, and assessment of project results. Scientific work abilities are measured using criteria consisting of 5 dimensions, namely 1) observation and asking questions, 2) planning an experiment, 3) conducting an experiment, 4) communicating, and 5) applying (Cahyani, Rustaman, Arifin, & Hendriani, 2014; Luzyawati, 2014). The measurement level results of the scientific work abilities of students after participating in the experiment using a PBL-ALQP model are 48 students (74%) in the high category. Analysis of achievement level of scientific work abilities in completing projects of each dimension is presented in Figure 2.

The achievement of observation and question dimensions was measured through the quality of references used, the appropriateness of reference content, instrument condition and the availability of supporting chemicals, the background in preparing the hypothesis, the choice of analytical methods to solve the problem, as well as the formulation of the problems raised in the project design. The contents of the references obtained by students are under the problem, although the amount is very minimal. The instrument chosen was under the characteristics of the sample. The choice of

instrumentation analysis method should have considered the appropriateness of the instrument's function, operational range, type of sample, ease, accuracy, selectivity, and detection limits of the instrument. The analysis techniques selection should consider the complexity of the sample, potential for interference, and the level of analytes in the sample. The results of the background assessment in preparing the hypothesis still have not paid attention to these factors carefully.

The dimensions of planning an experiment are measured through project objectives, hypotheses, completeness of tools and materials, classification of types of variables, work steps in project design, and project implementation schedules. The results obtained indicate that the chemical specifications for making working solutions are not detailed. The ability to form hypotheses is still low because it has not been able to link the relationships between variables and cannot be measured. Students also find it challenging to develop precision and accuracy test methods and how to analyze data.

The dimensions of experimenting are measured by looking at the work result data, which consists of making working solutions, sample preparation, making a calibration curve, measuring samples, testing accuracy, precision, as well as observation sheets and data analysis methods. Data from the manufacture of working solutions have used chemicals with pro analyst grade and traceable standard solutions. Students have been skilled in grouping data in tables. In making calibration curves, it is found that the standard concentration used is under the working range of the instrument. Students have been able to interpret the calibration curve obtained by looking at the correlation coefficient. There are 6 out of 19 groups whose calibration curves have a correlation coefficient (r^2) of less than 0.9. Students are not yet skilled in interpreting the results of validation of test methods, although students have been able to calculate the amount of LoD and LoQ, they cannot explain the further use of the amount. Students still cannot utilize the information obtained when validating the testing methods that have been done. The validation parameters of the test methods, which include linearity, LoD, LoQ, accuracy, and precision, can be used to assess whether the analytical method is chosen and used for analytical analysis in the sample is appropriate and appropriate. From 19

groups, there were only five groups that obtained good precision and accuracy test results ($RSD < 2\%$, recovery 80-120%). This result shows that most students still need to practice in making calibration curves, testing precision, and accuracy.

Students' ability to discussing, presenting data, making graphics/drawings, and compiling reports are parameters for measuring the communicating dimension. The results obtained illustrate that between members in the group, there has been a division of tasks and good cooperation. Students are still not actively asking questions in discussions and tend to be passive. The presentation material that is displayed is good because it has combined information in the form of graphs, tables, and images, as well as the appropriate font size. The presentation atmosphere is less than optimal because the presenter has not been able to utilize time well and lacks confidence. Scientific articles compiled by students are good. The observed shortcomings were the method of writing, the results and discussion, and the references used.

The dimension of applying is measured by the ability of students to explain events using concepts and to apply to new situations. The results obtained indicate that the ability of students to discuss the correlation between absorbance and concentration in *Lambert-Beer* law and analysis techniques still needs to be improved. There are only a few students discussed UV-Vis spectrophotometer or atomic absorption spectrophotometer sample requirements in their report nor discussion.

The scientific work abilities of students still need to be improved, especially the dimensions of observation and asking questions. This fact shows that students have difficulty in finding and understanding the contents of scientific articles. Students need to be given the task of searching scientific articles through the internet network because supporting facilities are complete such as the availability of internet networks and computing laboratories that can be accessed by each student. The dimensions of planning an experiment need to be improved, especially the ability of students to form hypotheses, formulate problems, and arrange work steps for validation of testing methods. Students need to be stimulated in the form of assignments to translate the contents of scientific articles and present them in front of the class. Through discussion and collaboration in groups, they are

asked to arrange work steps in project work based on selected scientific articles. The same step has been proven by Bramer (2001) to improve the ability of scientific work (Bramer, 2001). Project-based learning with problems related to daily life can also be used to improve life skills, develop analytical skills, and scientific work skills (Akinoglu & Tandogan, 2007; Baumgartner & Zabin, 2008; Smith & Dragojlovic, 2013; Wurdinger & Qureshi, 2015).

3.2.4 Discipline and responsibility

The level of discipline and responsibility of students in the PBL-ALQP model is very high. The disciplinary attitude of students is observed through assessment of attendance, the accuracy of completing assignments, and uploading them to *elena.unnes.ac.id*. It was observed that the time most used by students to upload assignments was in the evening before the experiment and in the morning before the experiment began. This fact shows that students are still not optimal in managing learning time, although the PBL-ALQP model, combined with blended learning, can improve discipline (Assis, Silva, & Ribeiro, 2017; Eskrootchi & Oskrochi, 2010; Medeiros, Júnior, Bender, Menegussi, & Curcher, 2017). The attitude of responsibility from students is measured by the participation of students in preparing practical tools and materials, and care in maintaining cleaning the laboratory. The PBL-ALQP model that is applied can increase the sense of responsibility of students and give freedom in exploring practically responsibly, although there are still students who have low levels of participation in preparing practical tools (Bagheri *et al.*, 2013; Cavinato, 2017; Doppelt, 2003; Frederick, 2013; Wurdinger & Qureshi, 2015).

4. CONCLUSIONS

The PBL-ALQP model developed can improve graduate competencies which can be seen from the achievement level of basic laboratory skills, instrumentation analysis skills, critical thinking skills, communication skills, scientific work abilities by 99, 89, 63, 82, and 74% respectively, and attitudes discipline and responsibility of 98 and 92% in the high and very high categories. The assignment of searching scientific articles related to the problem really helped students in developing project designs and developing critical thinking skills and scientific work abilities. Presentation

and writing of scientific articles from the work of the project also help communication skills of students. However, students still have difficulties in finding scientific literature, translating scientific articles, converting the contents of literature into work steps, compiling hypotheses, conducting data analysis, and drawing conclusions. Further study will then conduct to overcome the issues.

5. REFERENCES

1. Akinoglu, O., & Tandogan, R.O., *Eurasia J. Math. Sci. & Tech. Ed.*, **2007**, 3(1), 71–81.
2. Arfianawati, S., Sudarmin, & Sumarni, W., *Jurnal Pengajaran MIPA*, **2016**, 21(1), 46–51.
3. Assis, A.F., Silva, M.D., & Ribeiro, N.S., *Periódico Tchê Química*, **2017**, 14(27), 162–170.
4. Bagheri, M., Ali, W.Z.W., Chong, M.B.A., & Daud, S.M., *Contemporary Ed. Technol.*, **2013**, 4(1), 15–29.
5. Baumgartner, E., & Zabin, C.J., *Environ. Ed. Res.*, **2008**, 14(2), 97–114.
6. Bowden, J.A., Nocito, B.A., Lowers, R.H., Guillet, L.J., Williams, K.R., & Young, V.Y., *J. Chem. Ed.*, **2012**, 89, 1057–1060.
7. Bramer, S. Van., *J. Chem. Ed.*, **2001**, 78(9), 1167–1174.
8. Cahyani, R., Rustaman, N.Y., Arifin, M., & Hendriani, Y., *JPII*, **2014**, 3(1), 8–11.
9. Carbó, A.D., Adelantado, V.J.G., & Reig, F.B., *US-China Ed. Rev.*, **2010**, 7(7), 15–29.
10. Carvalho, C., Fiuza, E., Gama, P., & Salema, M., *TUSED*, **2015**, 12(2), 21–31.
11. Cavinato, A.G., *Anal. Bioanal. Chem.*, **2017**, 409(6), 1465–1470.
12. Cesarino, E.C., Mulholland, D.S., & Francisco, W., *Periódico Tchê Química*, **2018**, 15(30), 221–240.
13. Chun, M.S., Kang, K. Il, Kim, Y.H.M., & Kim, Y.H.M., *Universal J. Ed. Res.*, **2015**, 3(11), 937–942.
14. Creswell, J.W., *Research Design Pendekatan Kualitatif, Kuantitatif, dan Mixed*. Yogyakarta: Pustaka Pelajar, **2010**.
15. Dalgarno, B., Bishop, A.G., Adlong, W., & Bedgood Jr, D.R., *Comput. Ed.*, **2009**, 53, 853–865.
16. Doppelt, Y., *Int. J. Technol. Des. Ed.*, **2003**, 13(3), 255–272.
17. Fakayode, S.O., *Anal. Bioanal. Chem.*, **2014**, 406(5), 1267–1271.
18. Fakayode, S.O., King, A.G., Yakubu, M., Mohammed, A.K., & Pollard, D.A., *J. Chem. Ed.*, **2011**, 89, 109–113.
19. Frederick, K. A., *Anal. Bioanal. Chem.*, **2013**, 405(17), 5623–5626.
20. Gusarova, M. S., Kopytova, A. V., & Reshetnikova, I. G., *Periódico Tchê Química*, **2019**, 16(31), 903–912.
21. Hake, R.R., *Handbook of Design Research Methods in Education*. (A. E. Kelly, R.A. Lesh, & J.Y. Baek, Eds.). New York: Madison Ave, **2008**.
22. Haryani, S., Liliarsari, Permanasari, A., & Buchari. *Jurnal Pendidikan Matematika dan Sains*, **2010**, XV(1), 35–42.
23. Haryani, S., Prasetya, A.T., & Bahron, H. *JPII*, **2017**, 6(2), 229–236.
24. Henderson, D.E., *J. Chem. Ed.*, **2010**, 87(4), 412–415.
25. Jiang, W., *J. Am. Sci.*, **2005**, 1(2), 93–94.
26. Jollands, M., Jolly, L., & Molyneaux, T., *Project-Based Learning as a Contributing Factor to Graduates' Work Readiness*, **2012**.
27. Karataş, F., *Chem. Ed. Res. Practice*, **2016**, 17(1), 100–110.
28. Lee, J.S., Blackwell, S., Drake, J., & Moran, K.A., *Interdisciplinary J. PBL*, **2014**, 8(2), 18–34.
29. Luzyawati, L., *Wacana Didaktika*, **2014**, III(17), 21–32.
30. Medeiros, F., Júnior, P., Bender, M., Menegussi, L., & Curcher, M., *A Blended Learning Experience Applying Project-Based Learning in an Interdisciplinary Classroom*, ICERI2017 Proceedings, 8665–8672, **2017**.
31. Perkins, C., & Murphy, E., *Educational Technology and Society*, **2006**, 9(1),

- 298–307.
32. Prasetya, A.T., Haryani, S., Cahyono, E., & Sudarmin, J. *Physics: Conference Series*, **2019**, 132 (032055):1-7.
 33. Robinson, J.K., *Anal. Bioanal. Chem.*, **2013**, 405(1), 7–13.
 34. Santos, D.M.D.L., Montes, A., Sánchez-Coronilla, A., & Navas, J., *J. Chem. Ed.*, **2014**, 91(9), 1481–1485.
 35. Saripudin, A., Haryani, S., & Wardani, S., Characterized Project Based Learning to Improve Critical Thinking Skills, ICMSE 2015, **2015**.
 36. Sarwi, & Liliarsari., *Forum Kependidikan*, **2010**, 30(1), 37–44.
 37. Sarwi, Rusilowati, A., & Khanafiyah, S., *JPFI*, **2012**, 8(1), 41–50.
 38. Sharples, M., *OEB Insights*, **2019**, 1–3.
 39. Smith, O.L., & Dragojlovic, V., *J. Lab. Chem. Ed.*, **2013**, 1(2), 25–33.
 40. Sojka, Z., & Che, M., *J. Chem. Ed.*, **2008**, 85(7), 934–940.
 41. Tawil, M., & Liliarsari., Berpikir Kompleks dan Implementasinya dalam Pembelajaran IPA, Badan Penerbit Universitas Negeri Makassar: Makasar, **2013**.
 42. Taylor, P.D.P., Barańkiewicz, D., Bettencourt Da Silva, R., Brodnjak Vončina, D., Bulska, E., Camoes, M. F., ... Perämäki, P., *Anal. Bioanal. Chem.*, **2015**, 407(23), 6899–6907.
 43. Wurdinger, S., & Qureshi, M., *Innovative Higher Ed.*, **2015**, 40(3), 279–286.

Table 1. The PBL-ALQP model implementation schedule

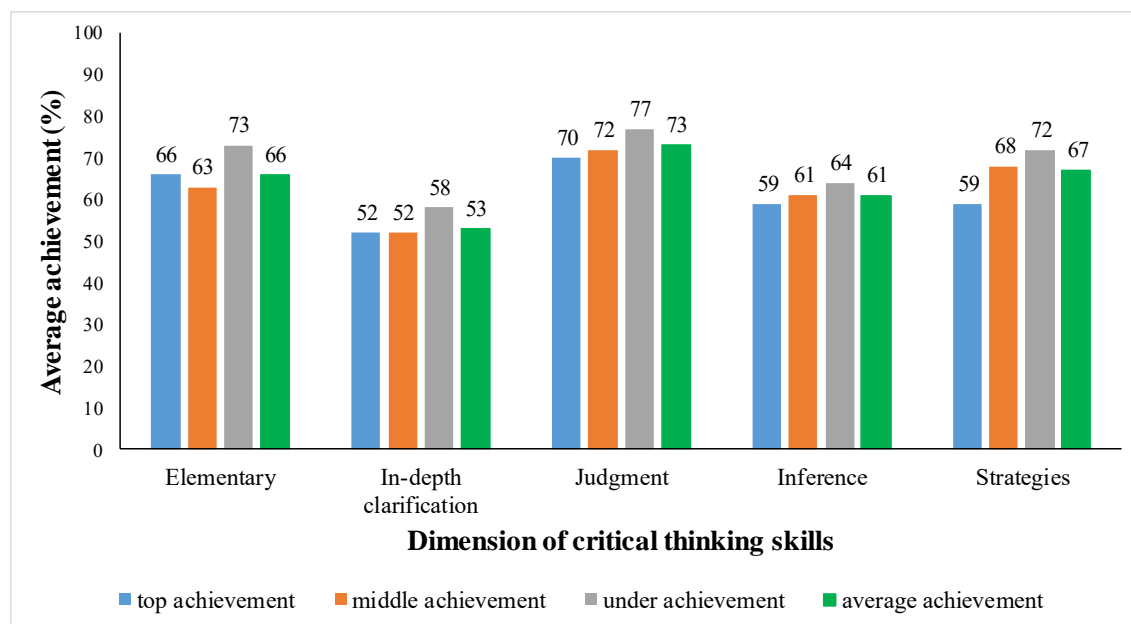
Meeting	Experiment event	Student activities	Observer activity
<u>Preliminary experiment</u>			
1 st Week	Preparation	a. Reviewing chemical requirements (including the type, concentration, and volume of working solutions needed) b. Compiling a description of making working solutions	Authentic assessment to measure the level of basic laboratory skills
2nd week	Making a working solution	Making working solutions (weighing, taking, dissolving, diluting chemicals)	
3rd week	Standardize of working solutions	a. Standardization of working solutions (taking, pipetting, diluting chemicals, titration) b. Making a report	
4th week	Determination of Ka acetic acid with a pH-meter	a. Compiling a list of experimental equipment b. Practical activities (stringing, calibrating, and operating the pH-meter) c. Making a report	Authentic assessment to measure the level of instrumentation analysis skills
5th week	Acid-base titration with a conductometer	a. Compiling a list of experimental equipment b. Practical activities (stringing, calibrating, and operating the conductometer) c. Making a report	
6th week	Determination of [Cu ²⁺] by UV-Vis spectrophotometer	a. Compiling a list of experimental equipment b. Practical activities (stringing, calibrating, and operating the UV-Vis spectrophotometer) c. Making a report	
<u>Project work</u>			
7th week	Lab project	Designing the project, taking data with the appropriate instrumentation analysis method, validating the testing method, analyzing the data, and concluding as an answer to the problem given.	Authentic assessment to measure the level of critical thinking skills, communication skills, and scientific work abilities
8th week	Lab project		
9th week	Lab project		
10th week	Lab project		
11th week	Project reporting and presentation		
12th week	Compilation of scientific articles		

Table 2. The achievement level of basic laboratory skills and instrumentation analysis skills

No	Skills which was observed	Achievement score (%)			
		Less	Mid	High	Very high
1.	Basic laboratory skills	-	1	65	34
2.	Instrumentation analysis skills				
a.	pH-meter	-	6	51	43
b.	Conductometer	3	12	59	26
c.	Spectrophotometer UV-Vis	2	15	72	11

Table 3. The achievement level of critical thinking skills, communication skills, scientific work abilities, discipline, and responsibility

No	Skills which was observed	Achievement score (%)			
		Less	Mid	High	Very high
1.	Critical thinking skills	2	35	63	-
2.	Communication skills	-	18	82	-
3.	Scientific work abilities	-	26	74	-
4.	Discipline	-	2	6	92
5.	Responsibility	-	8	12	80

**Figure 1.** Distribution of achievement level in critical thinking skills dimensions each achievement group

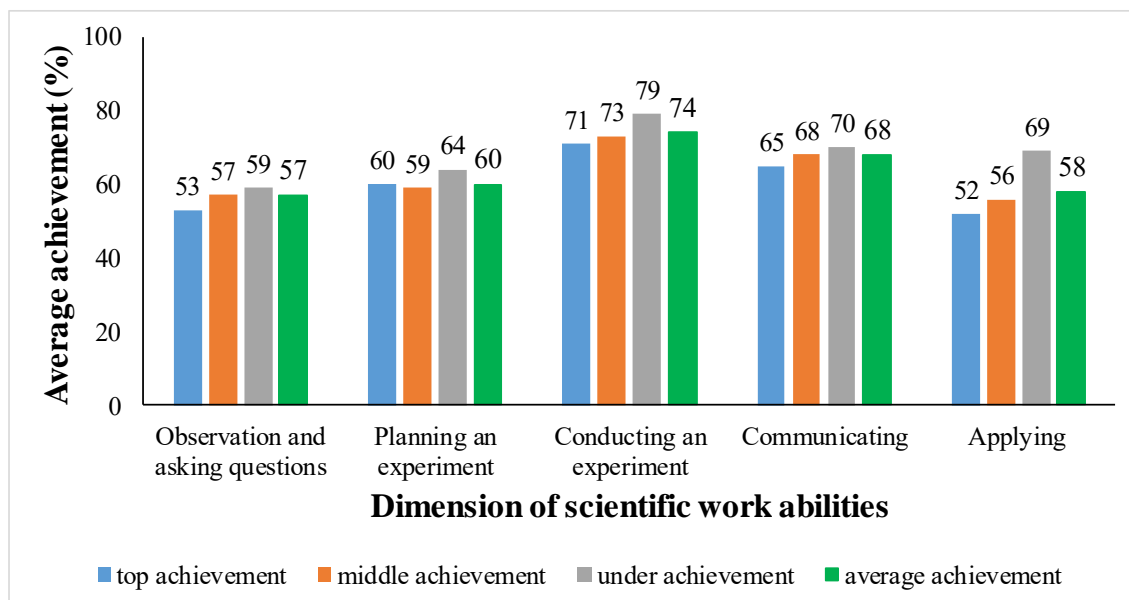


Figure 2. The achievement level distribution of the scientific work abilities dimensions of each achievement group

O EFEITO DO PROGRAMA EDUCACIONAL BASEADO NO CONCEITO DE INTIMIDADE SEXUAL ATRAVÉS DE SMARTPHONE EM MULHERES PÓS-MASTECTOMIA: UM ESTUDO CLÍNICO RANDOMIZADO CONTROLADO**THE EFFECT OF EDUCATIONAL PROGRAM-BASED ON SEXUAL INTIMACY CONCEPT VIA SMARTPHONE IN WOMEN FOLLOWING MASTECTOMY: A RANDOMIZED CONTROLLED TRIAL**

ARJMANDI, Zahra¹; MAHMOODI, Zohreh^{2*}; BEHBOODI MOGHADAM, Zahra³; MAHMOODZADEH, Habibollah⁴; QORBANI, Mostafa^{5, 6};

¹ MSc, School of Nursing and Midwifery, Tehran University of Medical Sciences, Tehran, Iran

² Social Determinants of Health Research Center, Alborz University of Medical Sciences, Karaj, Iran

³ School of Nursing and Midwifery, Tehran University of Medical Sciences, Tehran, Iran

⁴ Tehran University of Medical Sciences, Tehran, Iran

⁵ Non-Communicable Diseases Research Center, Alborz University of Medical Sciences, Karaj, Iran

⁶ Endocrinology and Metabolism Research Center, Endocrinology and Metabolism Clinical Sciences Institute, Tehran University of Medical Sciences, Tehran, Iran

* Correspondence author

e-mail: Zohrehmahmoodi2011@gmail.com

Received 22 October 2019; received in revised form 11 December 2019; accepted 23 December 2019

RESUMO

A malignidade mais comum entre mulheres em todo o mundo é o câncer de mama. A mastectomia é um dos tratamentos de câncer de mama mais comumente usados, com impacto direto no desempenho sexual desses pacientes. O objetivo deste estudo foi examinar o impacto do programa Educacional por meio do *smartphone* na intimidade sexual de mulheres com câncer de mama. Em um estudo controlado randomizado, 60 mulheres com mastectomia foram encaminhadas ao Hospital Imam Khomeini entre abril e julho de 2018 e foram divididas aleatoriamente em duas intervenções (intimidade sexual com educação de rotina em mastectomia e quimioterapia) e grupos de controle (mastectomia de rotina e educação em quimioterapia) usando quatro blocos aleatórios. Foram realizadas seis sessões via *smartphone* para ambos os grupos; o questionário de intimidade sexual foi preenchido pelos participantes antes e após a intervenção. Os dados foram analisados pelo SPSS 21 em nível de significância de $p < 0.05$. De acordo com os achados, o escore médio da intimidade sexual geral antes da intervenção não foi significativamente diferente ($p = 0.143$) entre os dois grupos. No entanto, após a intervenção, o escore médio da intimidade sexual geral foi significativamente diferente nos grupos controle e intervenção, sendo maior no grupo intervenção ($p < 0.001$). O presente estudo mostrou que a educação via *smartphone* foi eficaz para melhorar a intimidade sexual de mulheres com câncer de mama e, consequentemente, melhorar as relações sexuais dos casais.

Palavras-chave: Educação sexual; Intimidade sexual; Smartphone; Mastectomia;

ABSTRACT

The most common malignancy among women around the world is breast cancer. Mastectomy is one of the most commonly used breast cancer treatments, which has a direct impact on the sexual performance of these patients. The purpose of this study was to examine the impact of Educational program through Smartphone on the sexual intimacy of women with breast cancer. In a randomized controlled trial, 60 women with mastectomy referred to Imam Khomeini Hospital from April to July 2018 and were randomly divided into two intervention (sexual intimacy with routine mastectomy and chemotherapy care education) and control groups (routine mastectomy and chemotherapy care education) using four randomized blocks. Six sessions via smartphone were held for both groups the sexual intimacy questionnaire was completed by participants before and after the intervention. The data were analyzed by SPSS 21 at a significance level of $p < 0.05$. According to the findings, the mean score of overall sexual intimacy before intervention was not significantly different ($p = 0.143$) between the

two groups. However, after the intervention, the mean score of total sexual intimacy was significantly different in the control and intervention groups being higher in the intervention group ($p < 0.001$). The present study showed that education via smartphone was effective in improving the sexual intimacy of women with breast cancer and consequently enhancing the couples' sexual relations.

Keywords: Sex education; Sexual intimacy; Smartphone; Mastectomy;

1. INTRODUCTION:

Breast cancer is one of the most common malignancies among women and has the highest mortality rate in this group throughout the world. More than 7 million people in the world are currently affected by breast cancer, and the number of new cases is expected to reach 10-15 million by 2020 (Hummel *et al.*, 2018, Ghoncheh *et al.*, 2016, Li *et al.*, 2016).

This malignancy accounts for 33% of all cancers in women, and its prevalence in the general population is estimated to be between 8% and 10% in different countries (Boyd *et al.*, 2007, Society, 2017, Khalkhali *et al.*, 2019). Evidence suggests that about 60% of breast cancer cases in Iran occur in women under the age of 50 (Esfandiari *et al.*, 2015).

Mastectomy is one of the most commonly used treatments for this malignancy that directly affects the sexual performance of these patients (Rojas *et al.*, 2017; Pérez *et al.*, 2010). In this method, the body image of patients is affected, and this has a profound effect on their mental status (Traun-Vogt and Herdina, 2010; Safarpour *et al.*, 2018; Fouladi *et al.*, 2018). This disease is associated with many problems that can affect mental health and quality of life of these patients (Berek, 2002, Norouzirad *et al.*, 2018; Moghaddam Tabrizi *et al.*, 2018,). These individuals also have difficulties in their sexual and marital relationships, and this significantly affects the relationship between women and men and their families (Galbraith *et al.*, 2005, Kaviani *et al.*, 2014, Boquiren *et al.*, 2019, Brandão *et al.*, 2017, Male *et al.*, 2016).

One of the most critical factors affecting sexual function is sexual intimacy (Cairo Notari *et al.*, 2018; Nordvig *et al.*, 2019; Bois *et al.*, 2016). Sexual intimacy is the need to share and express sexual thoughts, feelings, and imagination with the spouse. (Kalra *et al.*, 2011) This kind of intimacy is mainly in the direction of sexual stimulation and requires communication, and exchange and expression of thoughts, feelings tendencies, and imaginations that have sexual nature (Ali *et al.*, 2004). Sexual intimacy is a complex subject that needs special attention because satisfaction from

sexual intimacy affects other relationships in couples (Bagarozzi, 2014; Tat *et al.*, 2018).

Lack of proper information and inadequate training on sexual activity, and consequently the inappropriate communication, wrong sexual beliefs, and anxiety about sexual performance play an essential role in the emergence and continuation of these disorders (Hummel *et al.*, 2017, Perz *et al.*, 2013, Crowley *et al.*, 2016). Findings show that sexual intimacy helps to reduce the burden of cancer diagnosis and treatment and the recovery process (Weijmar Schultz and Van de Wiel, 2003; Ussher *et al.*, 2013).

There are different ways to increase sexual intimacy, including education and sexual counseling on marital relationships, which help healthy sexual growth, marital health, interpersonal relationships, affection, sex, body image and gender roles (Jun *et al.*, 2011, Zareipour *et al.*, 2018, Boswell and Dizon, 2015). Different methods that are used for patient counseling include written, oral, photo, film, telephone, internet, and other means. The upward trend in mobile phone use in human societies had caused this device to be considered as a new tool in care, education, and counseling, which can be used from a distance for communication between patients and health care providers (Barak, 2003, Yazdani *et al.*, 2019).

This process is similar to in-person counseling and psychotherapy, but there are some differences. In this method, there are no barriers that are usually caused by social status, geographical location, and physical and emotional characteristics. Therefore, it can be instrumental in improving sexual problems (Barak and Cohen, 2002). This study aimed to investigate the impact of sexual counseling by Smartphone on the sexual intimacy of women attending the selected center of Tehran.

2. MATERIALS AND METHODS:

2.1. Design

A Parallel randomized clinical trial was conducted on women with breast cancer attending

the Imam Khomeini Hospital in Tehran from April to July 2018. This center is a referral for patients with cancer. Human rights were respected following the Helsinki Declaration 1975, as revised in 1983. The informed consent was taken from the participants. The Medical Ethics Committee has approved current studies of Alborz University of Medical Sciences and Health Services on 23 December 2017 (code: 1396.147)

2.2 Participants and recruitment

Sample size was determined based on the previous study of Shahkarami *et al.* By considering type I and II errors (0.05, 0.2), the mean change (standard deviation) score of sexual intimacy before and after intervention were 6.6(5.2) and 0.5(10.80) in intervention and control groups respectively, and a 10% attrition rate determined a sample size of 35 subjects in each as described in equation 1.

$$n = \frac{\left(Z_{1-\frac{\alpha}{2}} + Z_{1-\beta} \right)^2 (\delta_1^2 + \delta_2^2)}{(\mu_1 - \mu_2)^2} \quad \text{eq.1}$$

2.3 Inclusion criteria

There were included in this study 20 to 60 years old married woman, having a mastectomy due to breast cancer, not having prosthesis, having reading and writing skills, not having chronic diseases (heart, diabetes, kidney, liver), obtaining medium to low score based on gender intimacy questionnaire, having access to Smartphone and internet, knowing how to use Smartphone, and having the consent of spouse. In this study, information was collected by using a standard sexual intimacy questionnaire (Botlani *et al.*, 2010), and a personal-social information checklist.

Sexual intimacy questionnaire is a one-dimensional questionnaire, which consists of 30 questions and is analyzed based on the score obtained from the survey. So that, the score between 30 and 50 indicate the low level of sexual intimacy, between 50 and 100 shows the moderate level of sexual intimacy, and rating of above 100 reflects the high level of sexual intimacy (Botlani *et al.*, 2010). In Iran, the reliability of the components of this questionnaire was obtained by Cronbach's alpha (0.84) for the entire poll (Botlani *et al.*, 2010).

The sociodemographic checklist included questions about age, level of education, occupation, income level, number of partners,

marital status

2.4 Processors

After obtaining the necessary permissions, the researcher attended the cancer center of Imam Khomeini Hospital and selected 60 eligible participants, between 80 patients, by convenience sampling, then, the study objectives were expressed to them, and if they wished to participate in the study, written consent was obtained from them and their spouses. The patients were then asked to complete the Sexual Intimacy Questionnaire.

This information was used as a baseline score for comparison and also for identifying qualified individuals. If the score of the subjects was moderate and low (scores of 100 and less), they were included in the study and randomly divided into the intervention and control groups by using Permuted block randomization. Before allocating people in each group, a telegram channel was designed by the researcher, and she was the only one who had access to the telephone numbers of the participants.

The participants did not have access to each other's phone number. In the next step, to allocate people in the groups, the researcher obtained the telephone number from each participant for education. The intervention group received sexual intimacy education under the supervision of a sexologist along with routine mastectomy and chemotherapy care education according to the protocol of the cancer center. They received this intervention twice a week through the telegram channel, which allowed them to enter into discussions and express their comments. The control group underwent routine mastectomy and chemotherapy care education according to the protocol of the center through the telegram channel.

To observe ethic, an educational package related to sexual intimacy (all contents presented in the intervention group) was given to the control group at the end of an informative session. An admin managed the telegram channel for one month for six educating sessions (two sessions per week) and related contents were uploaded. The materials included audio files, text file and associated images. In order to ensure that the participants have used the topics uploaded to the telegram channel in each session, several questions were asked from each participant privately by the researcher, which were related to the subject, of course. If any participant needed more advice or had question, their need was met

individually on their page, but general questions were answered in the group (Table 1).

At the end of the sessions, (After the six-session) the participants were contacted again and both groups were asked to complete the sexual intimacy questionnaire once again. After completion, the post-intervention scores were kept for analysis. The information of 60 people was analyzed in both groups (Figure. 1). To make the participants communicate more with each other and use each other's experiences, another telegram channel was designed for their peers.

2.5 Statistical Analysis

Intention to treat analysis (ITT) considered dealing with noncompliance and missing. Outcomes in this randomized controlled trial (RCT) were sexual intimacy, and the collected data were analyzed by SPSS software using independent and paired t-tests.

3. RESULTS AND DISCUSSION:

In the present study, 60 women with mastectomy due to breast cancer who remained until the end of the research in the intervention and control groups were examined. After examining the normality by K-S, variables tested by Fisher exact test and chi-square test, no significant difference was found between the two groups in terms of mean age, education level, and duration of breast cancer diagnosis. In other words, the two groups were homogeneous. (Table 2)

There was no significant difference between the mean overall score of sexual intimacy in the control and intervention groups before the study. In other words, both groups were similar in terms of sexual intimacy. However, after the intervention, the comparison of the mean overall score of sexual intimacy was significantly different between the two groups ($p = 0.000$), so that the mean score of sexual intimacy in the intervention group was significantly higher than the pre-intervention time. This difference indicated the positive impact of counseling (Table 3).

To examine the hypothesis of the study, "sexual counseling affects the sexual intimacy of women with breast cancer," the covariance analysis was used. After reviewing the premises, the result of the test indicated the significance of F for the scores of sexual intimacies. Accordingly, the zero hypotheses were ruled out and we could conclude that the mean scores of the two groups (control and intervention groups) after the intervention (after moderating the pre-intervention

scores) were significantly different from each other (Table 4).

Breast cancer is associated with many individual, social, and familial complications for patients and their families. (Wassermann *et al.*, 2019, Ataollahi *et al.*, 2015) For example, it can be a significant contributor to sexual problems due to the weakening of physical strength, decreasing ability to perform daily activities, hospitalization, and cancer-induced depression (Kwait *et al.*, 2016, Alappattu *et al.*, 2015).

In the present study, after considering the individual-social and familial variables of the participants in the two groups, we found that the majority of variables such as; age, education, occupational status, first gestation age, number of children, history of breastfeeding, duration of marriage, type of contraception, type of medications used during treatment, time of filling the questionnaire, level of income, age of the first menstruation, place of residence, history of breast cancer in the family, and duration of the disease, were not significantly different from each other. In other words, the two groups were homogeneous in terms of the variables mentioned earlier, and this was one of the strengths of the study.

According to the findings of the study, there was no significant difference in the score of sexual intimacy before consultation in the two groups of control and intervention. In other words, the two groups, at the time of entering the study, were homogeneous in terms of sexual intimacy. However, after the intervention, the mean of overall sexual intimacy score in the intervention group showed a significant increase compared to the control group.

Study of Moradi *et al.* (2014) entitled: "Investigating the Impact of Consultation on the Sexual Function of Women with Type 2 Diabetes in 2014" showed that counseling improves the sexual function of women with type 2 diabetes. They found a significant difference between the mean sexual performance scores before and after the intervention in the intervention group compared to the control group (Moradi *et al.*, 2016).

Also, Mohammad Shakarami *et al.* (2013) researched the effect of sexual education on the sexual intimacy of married women attending the Hamyaran center of Bojnourd. They found a significant difference between the mean scores of sexual intimacy in the intervention and control group in the post-test and follow up stages. They also found that sexual education increased the sexual intimacy of women in the intervention group

(Shakarami *et al.*, 2014).

The results of the present study are also consistent with the findings of an investigation by Jennifer Barski *et al.* (2015). They conducted a study as a randomized pilot trial on sexual intimacy and concerns of patients with colorectal cancer. They found a positive effect of internet intervention on sexual performance and self-efficacy of the participants(Reese *et al.*, 2014).

Women's sexual satisfaction is closely related to psychological intimacy than physical acts of sexual intercourse(Gilbert *et al.*, 2013), and The result of this study is similar to Masoumi and *et al.* (2017). They expressed sexual education can be used as a method of intervention in the sexual relationship of spouses particularly in marital dissatisfaction(Masoumi *et al.*, 2017).

One of the leading causes of sexual problems after cancer is the problem in establishing communication and expressing needs and wishes (Zee *et al.*, 2008). According to studies, modern communication technologies provide a new opportunity for individuals to create a private space in cyberspace, where people communicate with one another and form a wide range of online relationships in social networking channels(Ebert *et al.*, 2015). On the other hand, concerning the culture of patients, speaking about sexual problems with someone else in a face-to-face manner can be difficult for some patients, and that is why the use of these social networks such as telegrams can have a more significant effect during information gathering, evaluation and treatment (Taylor and Luce, 2003). According to Marlene Elias, online counseling is the most controversial change that has taken place in the consultation and treatment(Barak and Cohen, 2002).

4. CONCLUSIONS:

Consultation as an effective procedure of solving problems can improve the quality of sexual life, and the social networks, especially mobile phones, are everywhere and have been well accepted as a communication tool. The results of the present study indicated the effectiveness of sexual intimacy education on marital problems of women after mastectomy. Education by health cares like nurses and midwives can help to increase the sexual intimacy of women and their spouses, as the primary care providers of women, Also, considering the expansion of cyberspace and convenient of access to Smartphone, the use of such device is useful for reducing costs, and

resolving time and space constraints for educating. In the present study, we tried to homogenize the participants, but the existence of other social networks could be considered as a limitation of this study.

5. ACKNOWLEDGMENTS:

The authors like to thank Research Deputy of Alborz University of medical sciences for funding support

6. REFERENCES:

1. Alappattu, M. J., Coronado, R. A., Lee, D., Bour, B. & George, S. Z. *Physical therapy*, **2015**, 95, 526-538.
2. Ali, S. R., Liu, W. M. & Humedian, M.. *Islam Professional Psychology: Research and Practice*, **2004**, 35, 635.
3. Ataollahi, M., Sharifi, J., Paknahad, M. & Paknahad, A. *Journal of medicine and life*, **2015**, 8, 6.
4. Bagarozzi, D. A. *Enhancing intimacy in marriage: a clinician's guide*, routledge. **2014**
5. Barak, A. *Journal of Career Assessment*, **2003**, 11, 3-21.
6. Barak, A. & Cohen, L. *Journal of Career Assessment*, **2002**, 10, 387-400.
7. Berek, J. Early pregnancy loss and ectopic pregnancy. Novak's Gynecology. Philadelphia. Lippincott: Williams and Wilkins. **2002**.
8. Bois, K., Bergeron, S., Rosen, N., Mayrand, M.-H., Brassard, A. & Sadikaj, G. *Health Psychology*, **2016**, 35, 531.
9. Boquiren, V.M., Esplen, M.J., Wong, J., Toner, B., Warner, E., Malik, N, *Psycho-Oncology*, **2016**, 25, 66-76.
10. Boswell, E.N. and Dizon, D.S., Breast cancer and sexual function. *Translational andrology and urology*, **2015**, 4, 160.
11. Botlani, S., Ahmadi, A., Bahrami, F., Shahsiah, M. & Mohebbi, S. *Journal of Fundamentals of Mental Health*, **2010**, 12, 496-505.
12. Boyd, N. F., Guo, H., Martin, L. J., Sun, L., Stone, J., Fishell, E., Jong, R. A., Hislop, G., Chiarelli, A. & Minkin, S. *New England Journal of Medicine*, **2007**, 356, 227-236.

13. Brandão, T., Pedro, J., Nunes, N., Martins, M.V., Costa, M.E., Matos, P.M., *Psycho-oncology*, **2017**, 26, 2019-2029.
14. Cairo Notari, S., Favez, N., Notari, L., Panes-ruedin, B., Antonini, T. & Delaloye, J. F. *European journal of cancer care*, **2018**, 27, e12607.
15. Crowley, S.A., Foley, S.M., Wittmann, D., Jagielski, C.H., Dunn, R.L., Clark, P.M., *et al.*, *Journal of Cancer Education*, **2016**, 31, 588-594.
16. Ebert, D. D., Zarski, A.-C., Christensen, H., Stikkelbroek, Y., Cuijpers, P., Berking, M. & Riper, H. *PloS one*, **2015**, 10, e0119895.
17. Esfandiari, Z., Joulaee, A. & Asli Azad, M. A. *Journal of health research in community*, **2015**, 1, 63-71.
18. Fouladi, N., Pourfarzi, F., Dolattorkpour, N., Alimohammadi, S., Mehrara, E., *Psycho-oncology*, **2018**, 27, 434-441.
19. Galbraith, M. E., Archiga, A., Ramirez, J. & Pedro, L. W. Prostate cancer survivors' and partners' self-reports of health-related quality of life, treatment symptoms, and marital satisfaction 2.5-5.5 years after treatment. *Oncology Nursing Forum*, **2005**.
20. Ghoncheh, M., Pournamdar, Z. & Salehiniya, H. *Asian Pac J Cancer Prev*, **2016**, 17, 43-46.
21. Gilbert, E., Ussher, J. M. & Perz, J. *Psychology & health*, **2013**, 28, 603-619.
22. Hummel, S. B., Hahn, D. E., Van Lankveld, J. J., Oldenburg, H. S., Broomans, E. & Aaronson, N. K. *The journal of sexual medicine*, **2017**, 14, 1248-1259.
23. Hummel, S. B., Van Lankveld, J. J., Oldenburg, H. S., Hahn, D. E., Kieffer, J. M., Gerritsma, M. A., Kuenen, M. A., Bijker, N., Borgstein, P. J. & Heuff, G. *Journal of sex & marital therapy*, **2018**, 1-000.
24. Jun, E.-Y., Kim, S., Chang, S.-B., OH, K., Kang, H. S. & Kang, S. S. *Cancer nursing*, **2011**, 34, 142-149.
25. Kalra, G., Subramanyam, A. & Pinto, C. *Indian journal of psychiatry*, **2011**, 53, 300.
26. Kaviani, M., Rahnavard, T., Azima, S., Emamghoreishi, M., Asadi, N. & Sayadi, M. *International journal of community based nursing and midwifery*, **2014**, 2, 94.
27. Khalkhali, H.R., Gharaaghaji, R., Valizadeh, R., Kousehlou, Z., Ayatollahi, H., *Asian Pacific Journal of Cancer Prevention*, **2019**, 20, 1345-1351.
28. Kwait, R. M., Pesek, S., Onstad, M., Edmonson, D., Clark, M. A., Raker, C., Stuckey, A. & Gass, J. *Annals of surgical oncology*, **2016**, 23, 3403-3411.
29. Li, T., Mello-thoms, C. & Brennan, P. C. *Breast cancer research and treatment*, **2016**, 159, 395-406.
30. Male, D.A., Fergus, K.D. and Cullen, K., *Current opinion in supportive and palliative care*, **2016**, 10, 66-74.
31. Masoumi, S. Z., Kazemi, F., Nejati, B., Parsa, P. & Karami, M. *Electronic physician*, **2017**, 9, 3598.
32. MoghAddam Tabrizi, F., Alizadeh, S. and Barjasteh, S., *Avicenna Journal of Nursing and Midwifery Care*, **2018**, 26, 1-10.
33. Moradi, M., Geranmayeh, M., Mirmohammadali, M. & Mehran, A. *Journal of hayat*, **2016**, 22, 148-158.
34. Nordvig, A., Goldberg, D. & Huey, E. The Cognitive Aspects of Sexual Intimacy in Dementia Patients: A Neurophysiological Review and Insights for Diagnosis and Treatment. *neurology*, **2019**.
35. Norouzirad, R., Khazaei, Z., Mousavi, M., Adineh, H.A., Hoghooghi, M., Khabazkhoob, M., *et al.*, *Immunopathologia Persa*, **2018**, 4, 7.
36. Perez, M., Liu, Y., Schootman, M., Aft, R. L., Schechtman, K. B., Gillanders, W. E. & Jeffe, D. B. *Menopause (New York, NY)*, **2010**, 17, 924.
37. Perz, J., Ussher, J. M. & Gilbert, E. *BMC cancer*, **2013**, 13, 270.
38. Reese, J. B., Porter, L. S., Regan, K. R., Keefe, F. J., Azad, N. S., Diaz, L. A., Herman, J. M. & Haythornthwaite, J. A. *Psycho-Oncology*, **2014**, 23, 1005-1013.
39. Rojas, K., Onstad, M., Raker, C., Clark, M. A., Stuckey, A. & Gass, J. *Breast cancer research and treatment*, **2017**, 163, 273-279.
40. Safarpour, M., Tiyyuri, A., Mohamadzade, M., *Iranian Journal of Health Sciences*, **2018**, 6, 1-9.

41. Shakarami, M., Davarnia, R., Zaharakar, K. & Gohari, S. The effect of sex education on sexual intimacy of married women. **2014**.
42. Society, A. C. 2017. Breast cancer facts & figures 2017–2018. American Cancer Society Atlanta, GA.
43. Tat, S., Doan, T., Yoo, G.J., Levine, E.G., *Journal of Cancer Education*, **2018**, 33, 477-484.
44. Taylor, C. B. & Luce, K. H. *Current directions in psychological science*, **2003**, 12, 18-22.
45. Traun-vogt, G. & Herdina, P. F.. *Wien Med Wochenschr*, **2010**, 160, 182-5.
46. Ussher, J. M., Perz, J., Gilbert, E., Wong, W. T. & Hobbs, K. *Cancer Nursing*, **2013**, 36, 454-462.
47. Wassermann, J., Gelber, S. I., Rosenberg, S. M., Ruddy, K. J., Tamimi, R. M., Schapira, L., Borges, V. F., Come, S. E., Meyer, M. E. & Partridge, A. H. Nonadherent behaviors among young women on adjuvant endocrine therapy for breast cancer. *Cancer*. **2019**.
48. Weijmar Schultz, W. & Van De Wiel, H. *Journal of sex & marital therapy*, **2003**, 29, 121-128.
49. Yazdani, M., Mahmoodi, Z., Azin, S. A. & Qorbani, M. *International Journal of Community Based Nursing & Midwifery*, **2019**, 7, 231-240.
50. Zareipour, M.A., Mahmoodi, H., Valizadeh, R., Ghorooji, M.G., Moradali, M.R., Zare, F. *Asian Pacific journal of cancer prevention: APJCP*, **2018**, 19, 2717.
51. Zee, B., Huang, C., Mak, S., Wong, J., Chan, E. & Yeo, W. *Asia-Pacific Journal of Clinical Oncology*, **2008**, 4, 218-226.

Table1. The content provided in each educating session

Number of sessions	Content of each Session
Session 1	Welcome to the group, the goals and rules of the channel are expressed, self-introduction, determination of communication, importance of marital relations, education of sexuality and marital affairs
Session 2	Teaching the correct sexual relations technique, sexual aspects of life and behaviors which can lead to marital satisfaction .
Session 3	Familiarity with the common sexual disorders of women
Session 4	Familiarity with Physiology of Sexual Exercise, Physical Education
Session 5	Focusing skills training, Attention and awareness of sensory symptoms, Expression of expression, Sexual self-expression
Session 6	Confronting Negative Thought and Reviewing Past Sessions. open Chanel for one heure in order to ask their question

Table 2. Distribution of demographic characteristics of women with breast cancer

Variables		Intervention group (n=30)	Control group (n=30)	Total (n=60)	P
		n (%)	n (%)	n	
Age	Less than 40 years old	11(36.7)	9(30)	20	0.768
	40 to 44	6(20)	8(26.7)	14	
	45 to 49	6(20)	4(13.3)	10	
	50 and above	7(23.3)	9(30)	16	
Education	Reading and writing	6(20)	6(20)	12	0.670
	Secondary school	8(26.7)	10(33.3)	18	
	High school diploma	11(36.7)	12(40)	23	
	Bachelor and master degree	5(16.7)	2(6.7)	7	
Employment	Housekeeper	24(80)	26(86.7)	50	0.748
	Clerk	5(16.7)	3(10)	8	
	Others	1(3.3)	1(3.3)	2	
Age at the first menstruation	8-13years	24(80)	20(66.7)	44	0.382
	>14 years	6(20)	10(33.3)	16	
Age at the first pregnancy	Below 18 years old	4(13.3)	3(10)	7	0.640
	18 to 20 years old	11(36.7)	10(33.3)	21	
	21 to 35 years old	12(40)	15(50)	27	
	35 and above	0(0)	1(3.3)	1	
	No answer	3(10)	1(3.3)	4	
History of	Yes	23(76.7)	25(83.3)	48	
	No	7(23.3)	4(13.3)	11	

lactation	No answer	0(0)	1(3.3)	1	0.386
History of breast cancer in the family	Yes	4(13.3)	6(20)	10	0.731
	No	26(86.7)	24(80)	50	
Type of medication	Tamoxifen	3(10)	6(20)	9	0.352
	Letrozole	5(16.7)	2(6.7)	7	
	Other	5(16.7)	8(26.7)	13	
Duration of cancer diagnosis	Less than one year	17(56.7)	14(46.7)	31	0.795
	More than one year	16(53.3)	18(60)	34	

Table 3. Comparison of the mean overall score of sexual intimacy in the two groups of control and intervention before and after the intervention in women with breast cancer

Variable		Before intervention	After intervention	p*
Sexual intimacy	Control group	69.10±9.7	68.57±9.70	0.118
	Intervention group	72.37±6.86	80.33±5.55	0.000
p **		0.14	0.000	

*= pair T-test ** = In depended test

Table 4. Testing the hypothesis of the effect of sexual counseling on the sexual intimacy of women with breast cancer based on covariance analysis

Reference	Sum of squares	Degree of freedom	Mean of squares	F value	P-value
Modified model	4898.421	2	2449.211	220.048	0.000
The width from the origin	199.625	1	199.625	17.935	0.000
Before intervention	2821.605	1	2821.605	253.506	0.000
group	1183.516	1	1183.516	106.333	0.000
Error	634.429	57	11.130	-----	-----
Total	338101	60	-----	-----	-----

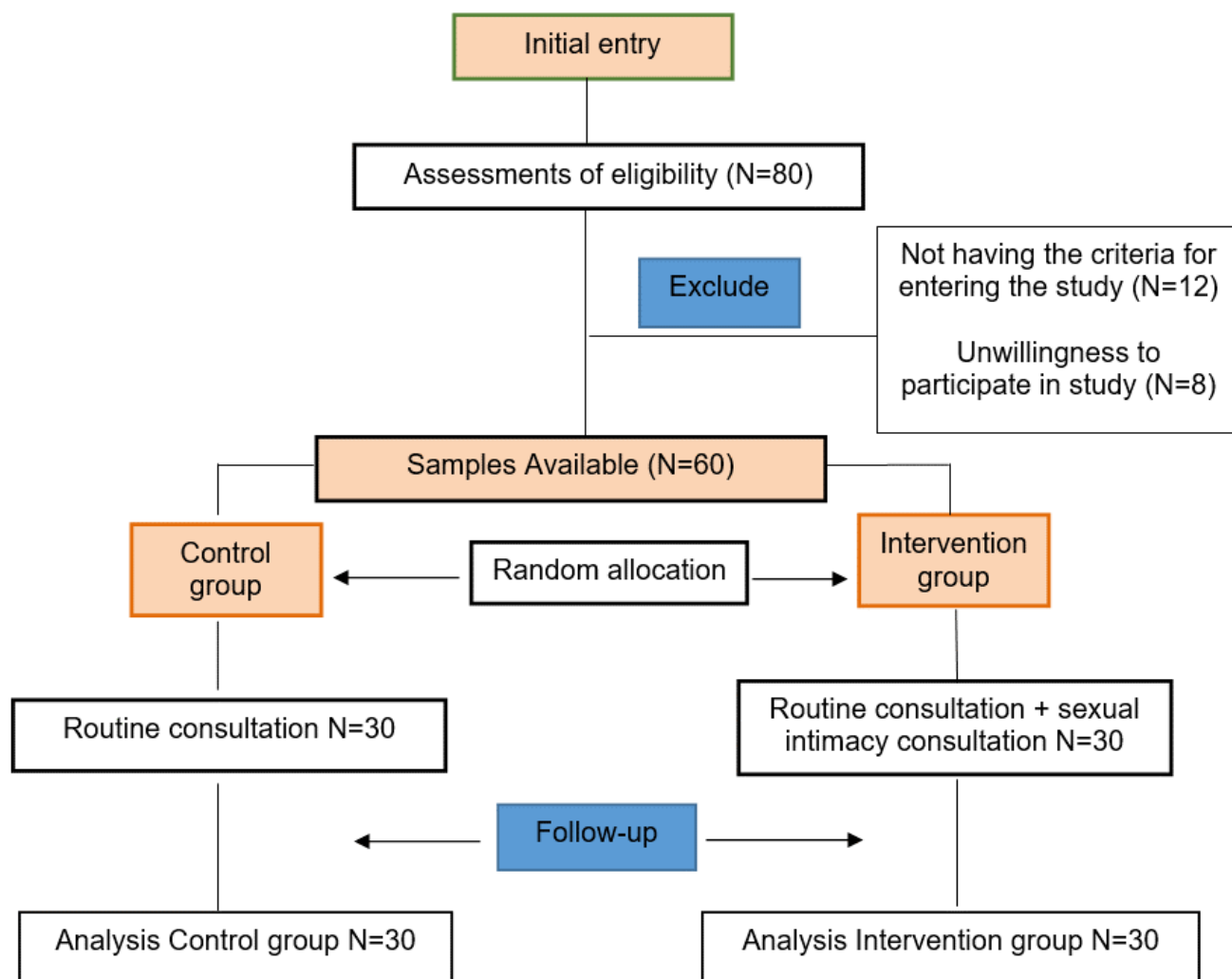


Figure 1. CONSORT flow diagram of the participants

ESTUDO DAS FORMAS DE CONEXÃO À UMIDADE DE COMPONENTES EM CONCENTRADOS DE PROTEÍNA-CARBOIDRATO DE SORO DE QUEIJO

THE RESEARCH OF THE TYPES OF MOISTURE BONDS IN PROTEIN-CARBOHYDRATE CONCENTRATES OF CHEESE WHEY

ИЗУЧЕНИЕ ФОРМ СВЯЗИ ВЛАГИ КОМПОНЕНТОВ В БЕЛКОВО-УГЛЕВОДНЫХ КОНЦЕНТРАТАХ ПОДСЫРНОЙ СЫВОРОТКИ

BOGDANOVA, Ekaterina V.^{1*}; MELNIKOVA, Elena I.²; KOSHEVAROVA, Irina B.³;

^{1,2} Voronezh State University of Engineering Technologies, Chair of Animal-Derived Food Technology, Voronezh, Russia

³ Voronezh State University of Engineering Technologies, Chair of Foreign Languages, Voronezh, Russia

* Correspondence author

e-mail: bogdanova.77.77@bk.ru

Received 31 October 2019; received in revised form 04 December 2019; accepted 14 December 2019

RESUMO

O objetivo da pesquisa é melhorar a tecnologia de produção de concentrados de proteína-carboidrato de soro de queijo, em termos de ligação da umidade com os principais componentes. Os objetos da pesquisa foram soro de queijo natural obtido na produção de queijos Rossiyskii e soro de ultrafiltração com percentual de 35 e 55% de matéria seca de proteínas, produzido com o uso da unidade industrial de ultrafiltração MMS Swissflow UF com membranas cerâmicas. A composição química e as propriedades físico-químicas das matérias-primas e do produto acabado foram estudadas usando métodos padrão. Foram identificados três estágios de desidratação da amostra. Eles estão em conformidade com a liberação de umidade com diferentes ligações e energia. O estágio I é a área de produção em que a umidade não ligada é aquecida e removida, e as moléculas de água são mantidas por forças capilares fracas. O estágio II é a área de produção para remoção de umidade imobilizada. O estágio III é a área de produção para remoção de água quimicamente ligada, que se adapta à umidade residual após a secagem da amostra. Um aumento na água menos móvel e uma mudança na proporção entre os diferentes tipos de ligação à umidade foram observados com um aumento na fração de massa protéica na matéria seca das amostras. Verificou-se que a reação de Maillard ocorreu em concentrados de soro de queijo com percentagem de matéria seca de proteína de 35 e 55% nas temperaturas acima de 78 e 70 °C, respectivamente. A faixa de temperatura da liberação de umidade não ligada estava aumentando durante o processo de secagem devido ao aumento do teor de proteínas nos concentrados, bem como à taxa de interação entre proteínas e lactose, levando ao escurecimento não enzimático dos produtos secos. Foi estabelecido que a secagem de proteína-carboidrato de soro de queijo concentrada com percentagem de 35% de matéria seca de proteína é inconveniente a temperaturas superiores a 130 e 173 °C, respectivamente.

Palavras-chave: *matérias-primas lácteas secundárias, características de secagem, concentrado de proteína-carboidrato.*

ABSTRACT

The purpose of the research is to improve the technology of producing cheese whey protein-carbohydrate concentrates, in terms of binding moisture with the main components. Objects of the research were natural cheese whey obtained in the production of *Rossiyskii* cheese and ultrafiltration cheese whey concentrates with protein dry matter percentage of 35 and 55%, produced with the use of MMS Swissflow UF industrial ultrafiltration unit with ceramic membranes. The chemical composition and Physico-chemical properties of raw materials and the finished product have been studied using standard methods. Three stages of sample dehydration have been identified. They conform to moisture release with different bonds and energy. Stage I is the production area where unbound moisture is heated and removed, and water molecules are held by weak capillary forces. Stage II is the production area for immobilized moisture removal. Stage III is the production area for chemically bound water removal, which conforms to the residual moisture after drying the

sample. An increase in the least mobile water and a change in the ratio between different types of moisture-binding have been observed with an increase in the protein mass fraction in the dry matter of the samples. It has been found that the Maillard reaction occurred in cheese whey concentrates with protein dry matter percentage of 35 and 55% at the temperatures above 78 and 70 °C, respectively. The temperature range of the unbound moisture release was increasing during the drying process due to an increase of the protein content in concentrates as well as the rate of interaction between proteins and lactose leading to non-enzymatic browning of dry products. It has been established that drying cheese whey protein-carbohydrate concentrates with protein dry matter percentage of 35, and 55% is inexpedient at temperatures exceeding 130 and 173 °C, respectively.

Keywords: *secondary dairy raw materials, drying features, protein-carbohydrate concentrate*

АННОТАЦИЯ

Цель исследований – совершенствование технологии получения белково-углеводных концентратов подсырной сыворотки с учетом форм связи в них влаги с основными компонентами. Объекты исследований: натуральная подсырная сыворотка, полученная при производстве сыра «Российский», ультрафильтрационные концентраты подсырной сыворотки с массовой долей белка в сухом веществе 35 и 55%, выработанные на промышленной ультрафильтрационной установке MMS Swissflow UF с керамическими мембранами. Химический состав и физико-химические показатели сырья и готового продукта изучены по стандартным методикам. По результатам исследований установлены три ступени дегидратации образцов, которые соответствовали высвобождению влаги с различной формой и энергией: I ступень – участок, на котором происходил нагрев и удаление свободно связанной влаги, а также молекул воды, удерживаемых слабыми капиллярными силами; II ступень – участок, где удалялась иммобилизованная влага; III ступень – участок, на котором удалялась химически связанная вода, что соответствовало остаточной влаге после высушивания навески. Наблюдалось повышение количества наименее подвижной воды и изменение соотношения между различными формами связи влаги с увеличением массовой доли белка в сухом веществе образцов. Установлено, что реакция Майяра протекала в концентратах подсырной сыворотки с массовой долей белка в сухом веществе 35 и 55% при температурах более 78 и 70 °C соответственно. С увеличением массовой доли белка в концентратах повышался температурный диапазон высвобождения удаляемой влаги в процессе сушки и увеличивалась скорость взаимодействия между белками и лактозой, приводившая к неферментативному покоричневению сухих продуктов. Установлено, что сушка белково-углеводных концентратов подсырной сыворотки с массовой долей белка в сухом веществе 35 и 55% при температуре более 130 и 173 °C соответственно нецелесообразна.

Ключевые слова: *вторичное молочное сырьё, особенности сушки, белково-углеводные концентраты*

1. INTRODUCTION

Current market trends show an increase in the intensive production of milk protein products, the technology of which is accompanied by the production of large volumes of whey (Tihomirova, 2017). The problem of complete and rational processing of secondary raw materials in the dairy industry, including whey, is taking a special value in the conditions of the whole milk shortage. It contains about 50% of milk solids, more than 80% of whey proteins, which determine its high biological value (Ponomarev *et al.*, 2018).

The most common technologies of whey processing include the usage of all its components. These are the technologies of dry whey production, including demineralized ones, which are implemented in Russia. Thus, 129,000 tons of these products were produced in the

Russian Federation in 2017 (Kharitonov, 2019). Nevertheless, the domestic production of whey powder does not satisfy the needs due to the weak development of secondary raw milk processing. Most of the whey produced in the country (59%) is used to feed farm animals, 20% is drained into fields or wastewater, and only 21% is used to further processing (Khramtsov, 2018).

The fractionation of whey protein-carbohydrate-mineral complex is a prospective technique. This technological method enables to obtain of food ingredients with high added value, for example, concentrates and isolates of whey proteins, microparticulate, lactose, dry permeate, mineral salts, including lactates and calcium phosphates, which are in high demand. World production of the ingredients manufactured by such technologies is characterized by high average annual growth rates, at the level of 5 – 10% (Božanic *et al.*, 2014; Topalov *et al.*, 2016;

Barukcic, 2018). They are in high demand in the Russian market but are hardly ever produced in our country. The demand for these products is satisfied mainly by imports.

The implementation of this direction requires the use of membrane technologies, which allow fractionation of whey components according to the size of their molecules. The obtained semi-finished products can be processed using traditional lines, including film-type vacuum evaporators, characterized by a minimal thermal effect on the raw materials, and modern drying units, carrying out multi-stage drying using efficient systems of preparation and purification of the drying agent.

Import volumes of whey protein concentrates and isolates are increasing steadily every year. This is determined by their essential physical and chemical properties, such as fat- and moisture retention, emulsifying capacity, and a number of technological functions in food systems, which depend on the degree of their hydration, surface activity and type of protein-protein interactions in partially unfolded structures (degree of denaturation) (Kassem, 2015). The functional properties of whey proteins are induced by peculiarities of the tertiary structure formation and its flexibility, in particular, the presence of a hydrophobic pocket inside the β -cylinder of the β -lactoglobulin tertiary structure, as well as the activity of surface areas and the presence of disulfide bonds and partially buried sulfhydryl group. Moreover, the ability of whey proteins to exhibit amphiphilic properties makes a significant contribution to the stabilization of their structure (Damodaran *et al.*, 2012).

Whey protein concentrates and isolates do not have the status of food additives and, as a consequence, lack the "E" indexed letter, providing a "clean" label of the finished food product. Whey proteins are the source of essential amino acids and branched-chain amino acids (valine, leucine, and isoleucine) in terms of physiological effects on the human body. Their amino acid profile is very similar to the composition of human muscle tissue; therefore, these nutrients are characterized by a high rate of cleavage in comparison with other proteins. The usage of these components in the production of various food products makes it possible to increase their nutritional and biological value (Damodaran *et al.*, 2012).

The use of whey protein concentrates is determined by the protein mass fraction content. Russian standard GOST R 53456-2009 "Whey

protein concentrate powders. Specifications" provides the production of concentrates with dry protein matter (PDM) percentage not less than 35.0 and 55.0%. Such products are widely used in baby food, gerodietetic food, sports nutrition, and confectionery production for the enrichment and as stabilizers in the production of meat and dairy products.

Since irreversible denaturation of whey proteins reduces their solubility and affects adversely the technological properties, which require high surface activity, a number of research on observation of the stability factors of whey proteins, as well as the features of the individual components interaction of cheese whey during heat treatment have been conducted by Russian and foreign scholars (Bannikova and Evdokimov, 2016; Budanina *et al.*, 2017; Bull *et al.*, 2017; Cabral *et al.*, 2019; Henriques *et al.*, 2017; Kumar *et al.*, 2013; Meena *et al.*, 2017; Savadkoobi *et al.*, 2014; da Silva *et al.*, 2015; Schön *et al.*, 2017; Torres *et al.*, 2017; Wijayant *et al.*, 2014). However, the problem of obtaining ultrafiltration concentrates (UF-concentrates) from cheese whey and justification of technological modes of their processing are still urgent issues. Thus, the purpose of this research was to improve the technology of UF-concentrates obtained from cheese whey and to study the forms of binding moisture with main components. Based on this data, it is possible to prevent irreversible structural changes in the whey protein molecules during subsequent evaporation and drying process to ensure their maximum structural stability and preservation of fat- and moisture retention and emulsification.

In the furtherance of this goal, the following tasks have been defined:

- to justify the modes of technological processing of cheese whey for production of UF-concentrates with various protein mass fractions;
- to study the forms of moisture-binding in UF-concentrates of cheese whey with various protein mass fractions;
- to determine the chemical composition, properties, and quality characteristics of the obtained UF-concentrates of cheese whey.

2. MATERIALS AND METHODS

Natural cheese whey obtained in the production of *Rossiyskii* cheese at the PSC Dairy Plant "Voronezhskii" (Kalacheevskii Cheese Factory, Kalach, Voronezh Region) and UF-

concentrates of cheese whey with various protein mass fractions, produced using MMS Swissflow UF industrial ultrafiltration unit with ceramic membranes were the objects of the study. The research was carried out in the laboratories of the Core Facility Center of the Voronezh State University of Engineering Technologies and Mollab Ltd.

The chemical composition, physical and chemical properties of raw materials and the finished product were studied in compliance with the standard and generally used methods, as well as modified and improved techniques.

The nephelometric method, based on the removal of denatured whey proteins from the system by precipitation with a saturated solution of sodium chloride, was used to determine the whey protein nitrogen index (WPNI) (Sikand *et al.*, 2008). The precipitate was separated; a saturated solution of sodium chloride (10 cm³) and 2 drops of hydrochloric acid solution (10% wt) were added into a test tube containing 1 cm³ of the filtrate. The optical density of the test sample was measured at 420 nm using the PE-5400 UF spectrophotometer (Russia) and compared to a standard curve obtained by analyzing the samples with a known WPNI value. The whey protein nitrogen index characterizes the content of non-denatured whey proteins in the sample.

The types of moisture-binding in UF-concentrates of cheese whey were investigated using the STA 449 F3 Jupiter simultaneous thermal analyzer (Germany) in the laboratory of the Core Facility Center "Control and Management of Energy-efficient Projects" at the Voronezh State University of Engineering Technologies under the state order No 10.8678.2017/7.8. This device combines the advantages of a highly sensitive thermobalance and a differential scanning calorimeter. The analysis consisted of the curves plotting for temperature changes in the sample with a weight of 10 ± 0.5 g during drying. The method of differential scanning calorimetry (DSC) is based on the registration of thermal effects of physicochemical and structural transformations occurring in the sample during a programmed change in temperature regime. The software, such as NETZSCH Proteus and MS Excel, was used for processing the obtained data of DSC and thermogravimetric (TG) curves. Subsequently, dDSC and dTG differential curves were plotted. The experiments were carried out by heating from 25 to 300 °C at a speed of 5 K/min in an oxidized aluminum pan in a gaseous

nitrogen medium of class 5 with a purge gas flow rate of 60 cm³/min. The accuracy of temperature measurement by DSC and TG methods was 0.1 °C.

The content of 5-hydroxymethylfurfural was determined using a photometric method with a PE 5400 UF spectrophotometer (Russia) in accordance with GOST 29032-91. The optical density of the samples was measured at a wavelength of 540 nm, using vessels having a working length of 30 mm (Zhang *et al.*, 2017).

Statistical analysis of the results was carried out using methods of mathematical statistics according to the data obtained from 5 to 10 experiments in three replications. The MathCad 16.0 application package was used for information processing and graphical interpretations of the results.

3. RESULTS AND DISCUSSION:

Whey protein concentrates (WPC) were produced by ultrafiltration according to the process flow chart in Figure 1. Cheese whey samples with the active acidity of 6.4 – 6.8 and the protein content of 0.8% were subjected to preliminary purification in a clarifying centrifuge at a temperature of 43 - 45 °C to remove the protein dust and fat. The fat content in skimmed whey should not exceed 0.05%. Then pasteurization was carried out at a temperature of 76 ± 2 °C for 15 sec. Pasteurized cheese whey was collected in a storage tank. Microfiltration was included in the manufacturing cycle due to the necessity of having a low-fat content in UF WPC.

The cheese whey ultrafiltration was carried out at $t = (10 - 12)$ °C under pressure of 0.3 – 0.6 MPa in order to obtain WPC with various protein content. The concentration factor for protein was 4.4 - 4.5 and 8.8 - 8.9 to obtain concentrates with a PDM percentage of 35 and 55%, respectively. The choice of the ultrafiltration mode was justified by the necessity to minimize the effect on the native protein structure to prevent bacterial growth in the retentate and calcium phosphate precipitation in the pores of the membrane modules.

Since high content of mineral substances in UF-concentrates can contribute to solubilization of lactose causing poor dehydration, diafiltration is a compulsory technological operation, which allows reduction of the mass fractions of lactose and mineral salts (Nesterenko *et al.*, 2014).

Including lactose pre-crystallization into the process flow chart in the form of condensed mixture enables to prevent dry product clumping during storage. The concentrate should be cooled to 30 – 32 °C quickly at the end of evaporation. Crystallization of lactose is advisable to carry out by subsequent slow cooling to 20 °C with fine-crystalline lactose seed in an amount of 0.02 – 0.1%. Then the condensed mixture should be mixed at the agitator speed rate of 10 rpm for 30 sec. clockwise and 30s. counter-clockwise with intermediate switching off periods for 30 sec. between them (Nesterenko *et al.*, 2014).

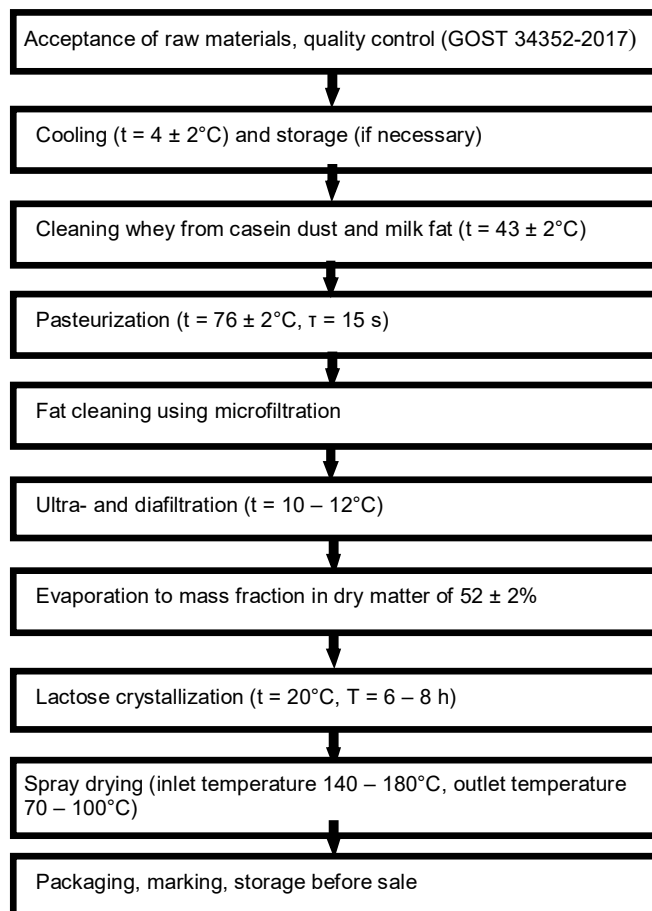


Figure 1. Process flow chart for production of whey protein UF-concentrates

The chemical composition and properties of cheese whey and the obtained UF-concentrates are given in Table 1.

The amphiphilicity of whey proteins, being an integral part of UF-concentrates, explains their ability to bind water molecules in solutions. The water is known to have a more structured form in concentrated systems due to the changes in protein conformation. These changes depend on whether the moisture content is critical or can be caused by the influence of lactose crystallization on the specific heat capacity (Kramer, 2012).

Hydrophobic group assemblage and hydrophobic interaction have an adverse effect on thermodynamics in such solutions. It is the mainspring of protein folding, forcing many hydrophobic residues to occupy positions that are deep inside the protein. However, non-polar groups of globular proteins usually cover about 40-50% of their surface area, and with the decrease in temperature, hydrophobic interactions weaken, whereas hydrogen bonds strengthen (Damodaran *et al.*, 2012).

Differential thermal analysis (DTA) and thermogravimetry (TG) were used to study the free and bound moisture ratio in cheese whey and its UF-concentrates. Thermograms (heating curves) are the result of thermal analysis; these curves depend mainly on the chemical composition and the structure of the investigated material. The thermogram has a number of critical points (Figure 2). The peaks on the DTG curve characterize temperature limits for the removal of free moisture and bound moisture of various types. Capillary moisture is removed at a constant temperature at the initial stage of drying. The inflection of curve characterizes moisture removal in cable and abutting phases. At the initial stage, the linear section is determined by the removal of multi-molecular adsorption moisture, and then monomolecular adsorption moisture (Karam *et al.*, 2017). There is one endothermic effect observed on the DSC curves, which is accompanied by heat absorption and mass changes of the samples on the TG-curves. The dDSC peak area is proportional to the change of the reaction enthalpy and to the mass of the samples and inversely proportional to their thermal conductivity (Niftaliev *et al.*, 2018; Pozhidaeva *et al.*, 2018; Rodionova *et al.*, 2018), see Table 2.

The analysis of the DTG curves made it possible to assume that at the temperature above 129 °C, the peaks determine lactose melting and proteins thermolysis in the samples. Moreover, endo-effect peaks grow up with an increase in PDM percentage in the studied systems. Dehydration of UF WPC was carried out at higher temperatures than for the initial cheese whey, which proved a larger degree of moisture-binding in them. Whereas the hydrophobic effect is caused only by entropy at room temperature, with rising temperature, the energy of hydrogen split bonds with non-polar groups on the surface of globular proteins is of increasing importance (Finkel'stein and Ptitsyn, 2012). In addition, the dependence of reducing energy costs for moisture removal from the samples on the

increase in PDM percentage in UF WPC has been identified.

The primary hydration for most proteins is 0.2-0.5 mol of water/100 g of polymer, and it is an integral part of its structure. There are several hypothesis concerning the nature of these primary binding sites, such as monomolecular adsorption on the polar sites (arg, his, lys, asp, gly, cys, met, ser, thr, tyr, trp) and multimolecular adsorption on the specific sites, where water molecules can bind with two, three or four hydrophilic molecular groups simultaneously. The existence of such binding sites depends on the specific geometric arrangements in the macromolecules. A hydrogen bond donator or an acceptor can act as a hydrophilic group.

Probably, sites that provide only singular hydrogen bonds with water molecules do not serve as primary sites for the formation of any bond with a certain free energy. Thus, depending on the geometry of the hydrophilic groups in the vicinity, a particular group may or may not form the primary binding site. Weak bonds, such as cysteine or methionine, are hardly considered as hydrogen bonds in this respect; they can only serve as weak additional stabilizing interactions (Damodaran et al., 2012).

Using TG curves, the transformation degree of α (ratio of mass at the time t to the total mass change at the end of the process) has been calculated depending on the temperature (Figure 3). The dependencies obtained were S-shaped, which indicated the complex nature of the interaction between water molecules and whey proteins and between low molecular weight components of cheese whey and its UF-concentrates and suggested a different water release rate at the dehydration stages.

Figure 4 shows the dependencies of the logarithm of the degree of substance conversion (α) on the temperature $\lg \alpha = f(1/T)$, which were used for quantitative evaluation of the types of moisture bonds in the samples.

Three stages of sample dehydration have been established, corresponding to various forms of moisture release and energy (Figure 3). Stage I is the production area, where free-bound moisture was heated and removed, and water molecules were held by weak capillary forces. Stage II is the production area where immobilized moisture (water molecules forming more distant adsorption layers) was removed. Stage III is the production area, where chemically bound water was removed, which characterized the monomolecular water layer associated with polar

groups, and the water-dipole interaction took place, which corresponded to the residual moisture after drying the sample (Niftaliev et al., 2018; Andiç-Çakir et al., 2014).

Thus, with an increase in PDM percentage in UF WPC, the amount of least mobile water increased, and the ratio between different types of moisture changed. The shape of the curve for a sample with a PDM percentage of 55% (Figure 4) indicates the maximum monolayer in it, which is formed only over the easily accessible components of the dry matter with a pronounced polarity.

Lactose contributed to an increase in protein hydration through non-covalent interaction with water and protein molecules by hydrogen bonds (Aalaei et al., 2018). This additionally makes it possible to increase the stability of whey proteins against denaturation and to inhibit lactose crystallization during subsequent concentration and drying (Yazdanpanah and Langrish, 2011; Amdadul Haque et al., 2018; Lisitsyn et al., 2016; Liu et al., 2016; Norwood et al., 2017; Abd El-Salam and El-Shibiny, 2018; Lin et al., 2018; Swarnalatha and Mor, 2019). However, increased protein content in UF-concentrates can lead to the faster flow of the Maillard reaction.

A complex peak on the DSC curves (Figure 2) takes into account the conversions that occurred with lactose during the drying process of the studied samples: glass transition, crystallization, and the course of the Maillard reaction. To isolate non-enzymatic browning on dDSK curves upon reaching effect temperatures, the presence of 5-hydroxymethylfurfural was determined in the samples as an indicator of the Maillard reaction onset. It was established that the reaction of non-enzymatic browning proceeded in UF WPCs with PDM percentage of 35 and 55% at temperatures above 78 and 70°C, respectively. Numerous peaks on the dDSK curve for a sample of UF WPCs with PDM percentage of 55% are likely to characterize different stages of the Maillard reaction. However, their speed is low, which is associated with a low mass fraction of lactose in this sample.

4. CONCLUSIONS:

Thus, the moisture content of various bonds in protein-carbohydrate concentrates of cheese whey is influenced by the protein dry matter percentage, including minerals, in the protein-lactose ratio. With a change in this ratio

when concentrating cheese whey proteins, the temperature range of moisture release in the process of drying grows, and the rate of interaction between proteins and lactose increases, leading to non-enzymatic browning of the products. According to the results of the conducted research, it has been established that drying of cheese whey protein-carbohydrate concentrates with PDM percentage of 35 and 55% at the temperatures over 130 and 173 °C, respectively, is inexpedient, since it may result in the occurrence of the defects in color, taste, and odor in the finished product.

5. ACKNOWLEDGMENTS:

The study was conducted as part of the scientific research work of the staff of the Chair of Animal-Derived Food Technology of the Voronezh State University of Engineering Technologies, Voronezh, Russian Federation.

6. REFERENCES:

1. Aalaei, K.; Rayner, M.; Sjöholm Aalaei, K.I. *Critical Reviews in Food Science and Nutrition*, 2018. <https://www.tandfonline.com/doi/full/10.1080/10408398.2018.1431202?scroll=top&needAccess=true/>, accessed 17 April 2019, DOI: 10.1080/10408398.2018.1431202.
2. Abd El-Salam, M.H.; El-Shibiny, S. *Int. J. Biol. Macromol.* 2018, 112, 83–92. DOI: <https://doi.org/10.1016/j.ijbiomac.2018.01.114>.
3. Amdadul Haque, M.; Chen, J.; Aldred, P.; Adhikari, B. *Drying Technol.* 2015, 33, 10, 1243. DOI: 10.1080/07373937.2015.1023311.
4. Andiç-Çakir, Ö.; Sarikanat, M.; Tüfekçi, H.B.; Demirci, C. *Composites Part B: Engineering* 2014, 61, 49, doi: 10.1016/j.compositesb.2014.01.029.
5. Bannikova, A.V.; Evdokimov, I.A. Innovation Technologies of Functional *Molochnokhozyaistvenny Vestnik [Dairy Bulletin]* 2016, 2 (22), 67. (In Russian), <https://elibrary.ru/item.asp?id=26336756>, accessed June 2019.
6. Barukcic, I. *Journal of Food Biotechnology Research* 2018, 2, 1-2, <http://www.imedpub.com/articles/whey-as-a-potential-functional-foodproperties-processing-and-future-perspective.pdf>, accessed June 2019.
7. Božanic, R.; Barukcic, I.; Jakopovic, K.L.; Tratnik, L. *Austin J. Nutri. Food Sci.* 2014, 2, 7, 1036, <https://pdfs.semanticscholar.org/477b/d2d3c3f627292e550fcc115371618647f4b2.pdf>, accessed September 2019.
8. Budanina, L.N.; Vereshchagin, A.L.; Bychin, N.V. *Food Processing: Techniques and Technology* 2017, 44, 1, 93. DOI: 10.21179/2074-9414-2017-1-93-99. (In Russian).
9. Bull, S.P.; Hong, Y.; Khutoryanskiy, V.V., Parker, J.K. *Food Quality and Preference* 2017, 56, part B, 233. DOI: 10.1016/j.foodqual.2016.03.008.
10. Cabral, S.R.; de Brito de Azevedo, B.M.; Pereira da Silva, M.; et al. *J. Membr. Sci. Res.* 2019, 5(2), 172, doi: 10.22079/JMSR.2018.92367.1208.
11. da Silva, A.N.; Perez, R.; Minim, V. P. R.; Martins, D. *Food Research International* 2015, 3(10), 177, doi: 10.1016/j.foodres.2015.03.009.
12. Damodaran, S.; Parkin, K.L.; Fennema, O.R., eds.; *Fennema's Food Chemistry*. 4th ed. Taylor & Francis Group: London – New York, 2008.
13. Finkel'stein, A.V.; Ptitsyn, O.B. *Protein physics*, Knizhnyy dom Universitet Publ.: Moscow, 2012, (In Russian).
14. Henriques, M.; Gomes, D.; Pereira, C. *Food Technol. Biotechnol.* 2017, 55 (4), 454; DOI: 10.17113/ftb.55.04.17.5248.
15. Karam, M.C.; Hosri, C.; Hussain, R., et al. *J. Food Process. Preserv.* 2017, 41(5), <https://onlinelibrary.wiley.com/doi/abs/10.1111/jfpp.13200>, accessed March 2019. doi: 10.1111/jfpp.13200.
16. Kassem, J. *International Journal of Dairy Science* 2015, 10(4), 139, doi: 10.3923/ijds.2015.139.159.
17. Kharitonov, D.V. Problems and Prospects of the Domestic Dairy Sector Development. *Dairy Industry* 2019, 4, 50, (In Russian), <http://moloprom.ru/2019/04/problemny-i-perspektivy-razvitiya-otchestvennoy-molochnoy-promyshlennosti/> accessed September 2019.
18. Khramtsov, A.G. *Food Technology*, 2018, 2-3 (362-363), 9–12. (In Russian). <https://elibrary.ru/item.asp?id=35186331>, accessed September 2019.
19. Kramer, R.M.; Shende, V.R.; Motl, N.; Pace, C.N.; Scholtz, J.M. *Biophys. J.* 2012, 18, 102 (8), 1907, doi: 10.1016/j.bpj.2012.01.060.

20. Kumar, P.; Sharma, N.; Ranjan, R.; Kumar, S. *Asian-Australas. J. Anim. Sci.*, 2013, 26(9), 1347, doi: 10.5713/ajas.2013.13082.
21. Lin, Y.W.; Liu, Y.H.; Wang, L.; Xie, Y.K.; Gao, Z.; et al. *Int. J. Agr. Biol. Eng.* 2018, 11(2), 214–218, doi: 10.1016/j.ijabe.2018.11.027.
22. Lisitsyn, A.; Kuznetsova, O.; Minaev, M.; Prosekov, A. *Orient. J. Chem.* 2016, 32(2), 867, doi: 10.13005/ojc/320212.
23. Liu, F.; Teodorowicz, M.; van Boekel, M.A.; Wichers, H.J.; Hettinga, K.A. *Food Funct.* 2016, 7, 239, doi: 10.1039/C5FO00718F.
24. Meena, G.S.; Singh, A.K.; Panjagari, N.R.; Arora, S. *J. Food Sci. Technol.* 2017, 54(10), 3010, doi: 10.1007/s13197-017-2796-0.
25. Nesterenko, P.G.; Khramtsov, A.G.; Evdokimov, I.A.; Ryabtseva, S.A.; Lodygin, A.D. *Dairy Industry*, 2014, 1, 66 (In Russian), <http://moloprom.ru/2017/03/kompleksnoe-ispol-zovanie-komponentov-molochnoj-syvorotki/> accessed September 2019
26. Niftaliev, S.I.; Peregodov, Yu.S.; Mejri, R.; Saranov, I.A. *Sorption and chromatographic processes* 2018, 18(4), 598, DOI: 10.17308/sorpchrom.2018.18/568. (In Russian).
27. Norwood, E.A.; Pezennec, S.; Burgain, J.; Briard-Bion, V.; Schuck, P.; et al. *J. Food Eng.* 2017, 195, 206, DOI: 10.1016/j.jfoodeng.2016.10.010.
28. Ponomarev, A.N.; Melnikova, E.I.; Bogdanova, E.V. *Dairy Industry*, 2018, 7, 38, (In Russian) <http://moloprom.ru/2018/07/molochnaya-syvorotka-kak-sy-r-evoj-resurs-dlya-proizvodstva-pishhevy-h-ingredientov/>, accessed September 2019
29. Pozhidaeva, E.A.; Popov, E.S.; Ilyushina, A.V.; Bolotova, N.V.; Ivanova, E.V. *Food Industry*, 2018, 11, 73 (In Russian), <https://elibrary.ru/item.asp?id=41241516> accessed September 2019
30. Rodionova, N.S.; Popov, E.S.; Pozhidaeva, E.A.; Pynzar, S.S.; Ryaskina, L.O. *IOP Conf. Series: Journal of Physics: Conf. Series* 2018, 1015, 032107. DOI: 10.1088/1742-6596/1015/3/032107.
31. Savadkoobi, S.; Bannikova, A.; Kasapis, S.; Adhikari, B. *Food Chem.* 2014, 150, 469, doi: 10.1016/j.foodchem.2013.11.029.
32. Schön, A.; Clarkson, B. R.; Jaime, M.; Freire, E. *Proteins* 2017, 85(11), 2009, doi: 10.1002/prot.25354.
33. Sikand, V.; Tong, P.; Walker, J. *Dairy Sci. Technol.* 2008, 88, 1, 105, doi: 10.1051/dst:2007011.
34. Swarnalatha, G.; Mor, S. *Int. J. Curr. Microbiol. Appl. Sci.*, 2019, 8(4), 1679, doi: 10.20546/ijcmas.2019.804.196.
35. Tihomirova, N.A. *Dairy Industry* 2017, 5, 24, (In Russian), <http://moloprom.ru/2017/05/formirovanie-assortimenta-i-planirovanie-ob-emov-proizvodstva-otchestvennoj-molochnoj-produktsii/>, accessed September 2019.
36. Topalov, V.K.; Chablin, B.V.; Evdokimov, I.A.; Zolotareva, M.S.; Volodin, D.N. *Milk Processing*, 2016, 7 (201), 17, (In Russian), <https://elibrary.ru/item.asp?id=26508504>, accessed September 2019.
37. Torres, J.K.F.; Stephani, R.; Tavares, G.M.; et al. Technological Aspects of Lactose-hydrolyzed Milk Powder. *Food Res. Int.*, 2017, 101, 45, DOI: 10.1016/j.foodres.2017.08.043.
38. Wijayant, H.B.; Heni, B.; Hilton, C. Deeth Stability of Whey Proteins during Thermal Processing: A Review. *Compr. Rev. Food Sci. Food Saf.* 2014, 13, 1235, doi: 10.1111/1541-4337.12105.
39. Yazdanpanah, N.; Langrish, T. *Dairy Sci. Technol.* 2011, 91, 323, doi: 10.1007/s13594-011-0015-8.
40. Zhang, H.; Ping, Q.; Zhang, J.; Lia, N. *J. Bioresour. Bioprod.* 2017, 2 (4), 170, doi: 10.21967/jbb.v2i4.84.

Table 1. Chemical composition and properties of the samples

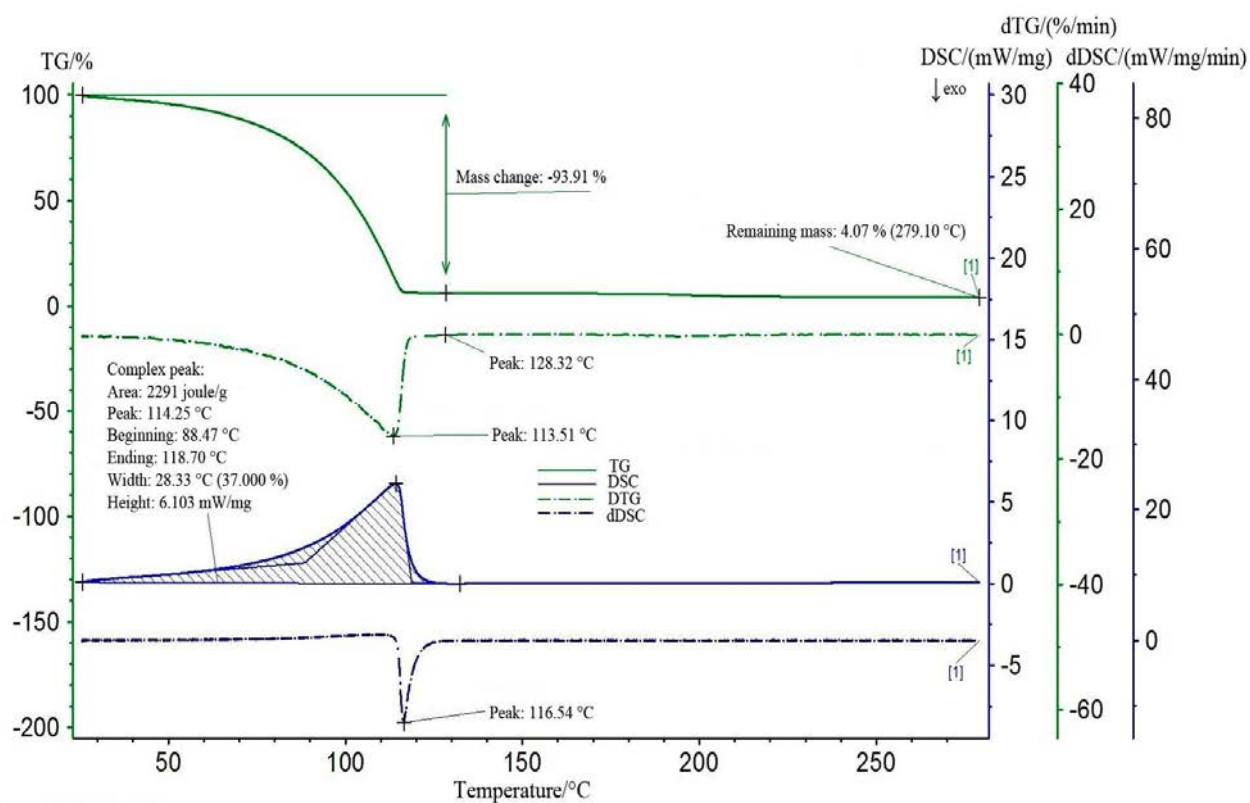
Indicator	Cheese whey	UF-WPC with PDM percentage of 35%	UF-WPC with PDM percentage of 55%
Milk in dry matter, %	6.09	10.11	12.37
Fat in dry matter, %	0.05	0.40	0.65
Total protein in dry matter, %	0.74	3.55	6.83
Lactose in dry matter, %	4.54	5.17	3.14
Protein-lactose ratio	1 : 6.1	1 : 1.4	2.2 : 1
Acidity, °T	16	21	28
WPNI, mg of nitrogen/g	5.5	5.3	5.2

Table 2. Enthalpies and mass changes during the process of heating cheese whey and its UF-concentrates

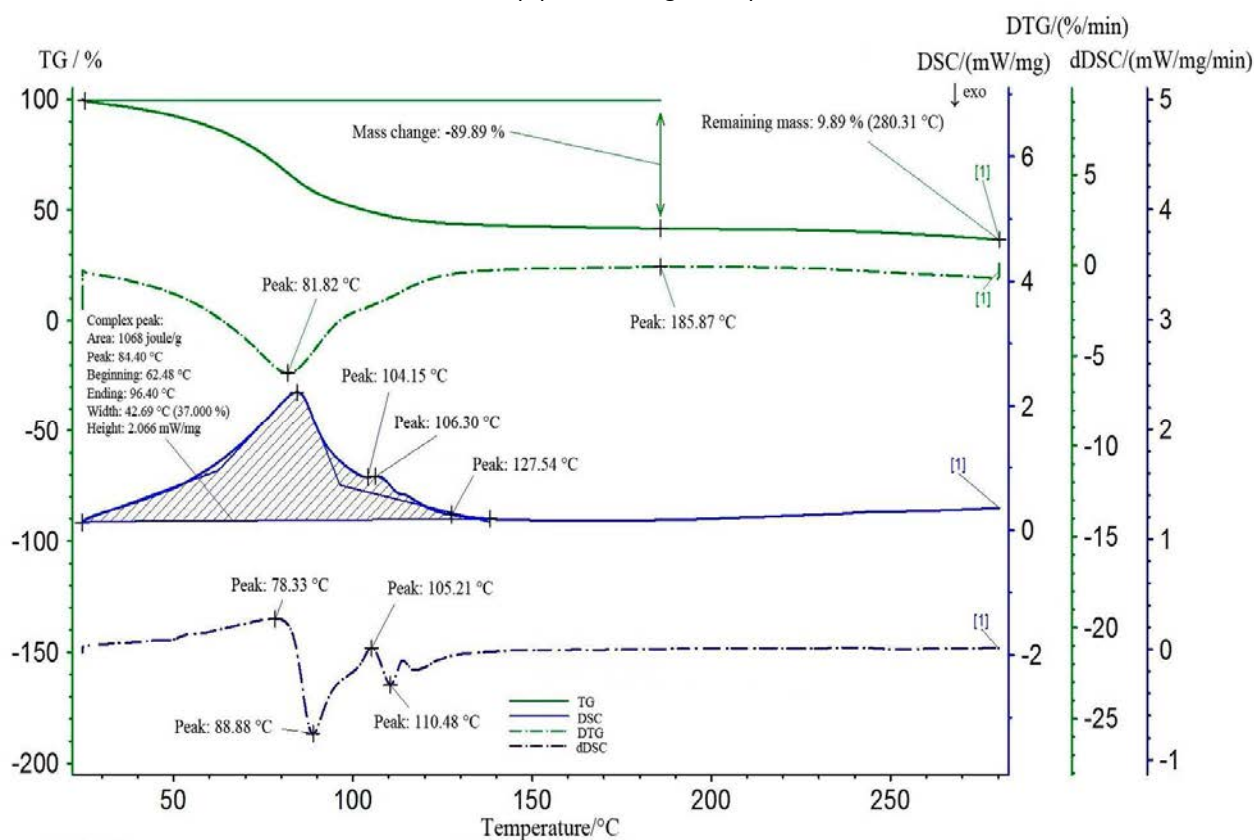
Sample	Temperature range ΔT , °C	Enthalpy ΔH , joule/kg (DSC curve)	Sample mass change, % (TG curve)
Cheese whey	30 – 132	2.291	93.91
UF-WPC with PDM percentage of 35%	25 – 140	1.068	89.89
UF-WPC with PDM percentage of 55%	25 – 205	0.635	87.63

Table 3. Quantitative characteristics of kinetically unequal water in the studied samples

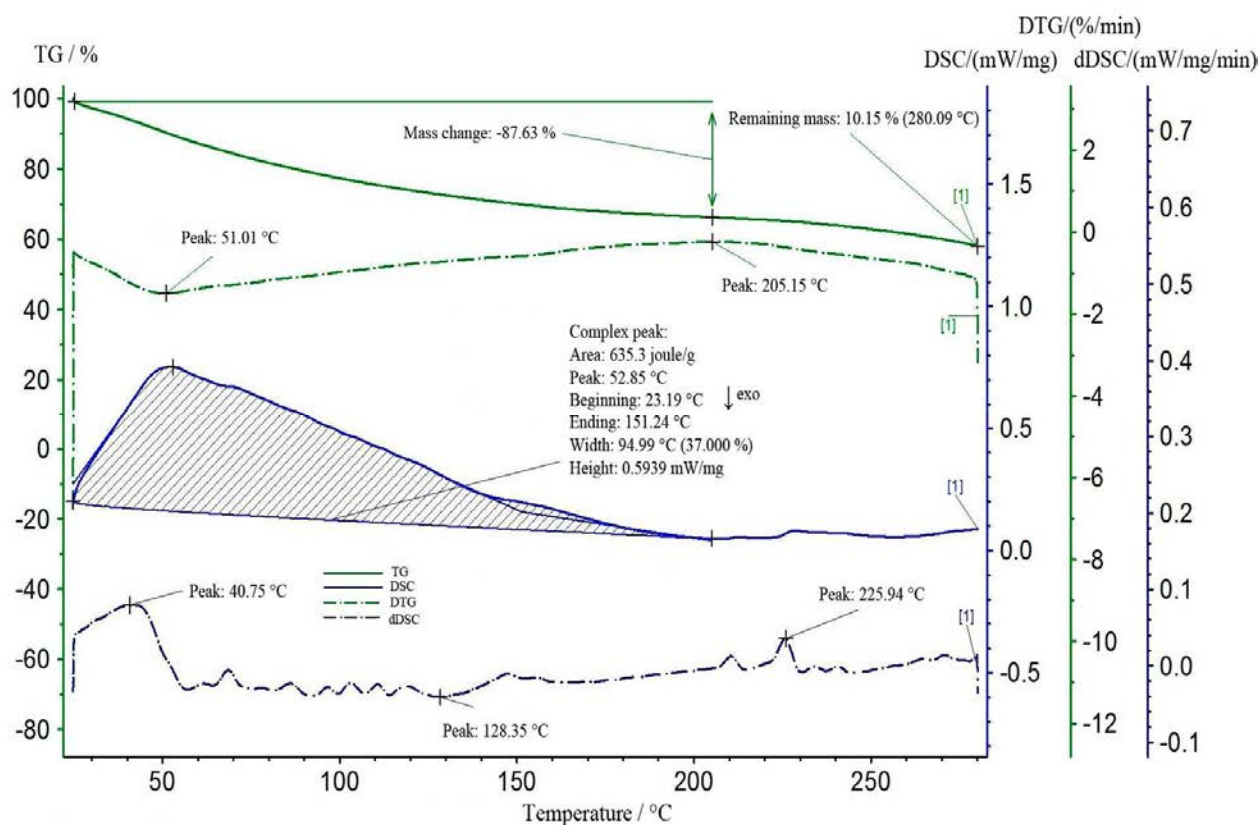
Dehydration degree	ΔT , K	Δt , °C	$\Delta \alpha$	Mass fraction of free moisture, %
Cheese whey				
I	298 – 346	25 – 73	0 – 0.135	13.491
II	346 – 397	73 – 124	0.135 – 0.999	86.406
III	397 – 402	124 – 129	0.999 – 1.000	0.104
UF-WPC with PDM percentage of 35%				
I	298 – 323	25 – 50	0 – 0.130	13.047
II	323 – 402	50 – 129	0.130 – 0.970	83.537
III	402 – 458	129 – 185	0.970 – 1.000	3.416
UF-WPC with PDM percentage of 55%				
I	298 – 313	25 – 40	0 – 0.170	12.778
II	313 – 445	40 – 172	0.170 – 0.950	81.878
III	445 – 478	172 – 205	0.950 – 1.000	5.344



a) (Part of Figure 2)



b) (Part of Figure 2)



c)

Figure 2. Thermograms of the examined samples:

a) cheese whey; b) UF-WPC with PDM percentage of 35%; c) UF-WPC with PDM percentage of 55%

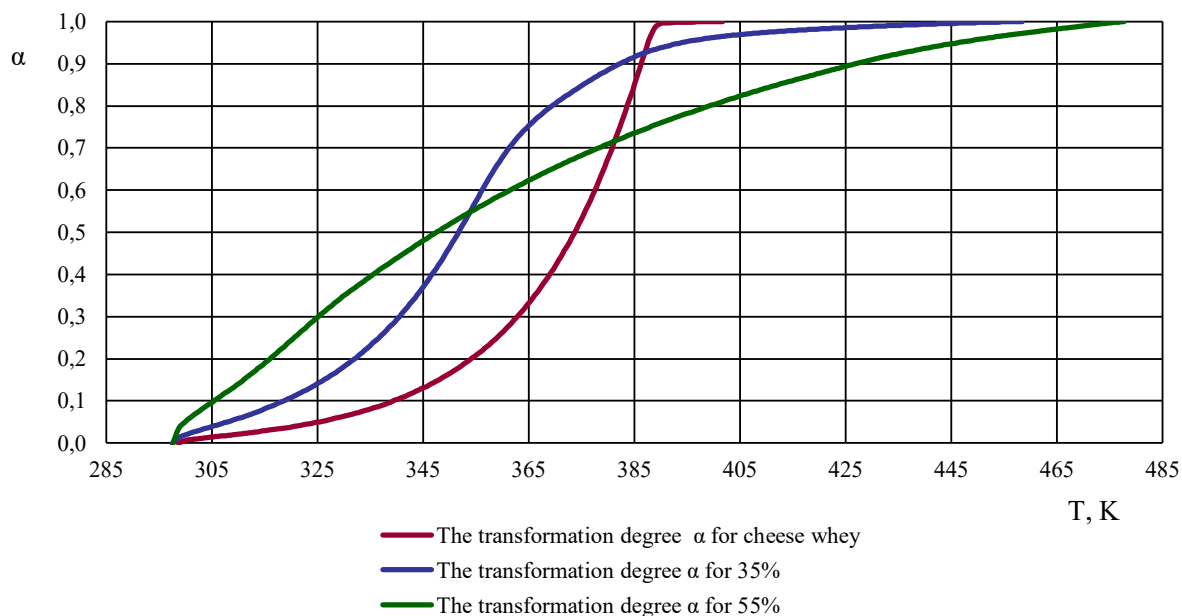


Figure 3. The dependence of the transformation of substance α on temperature

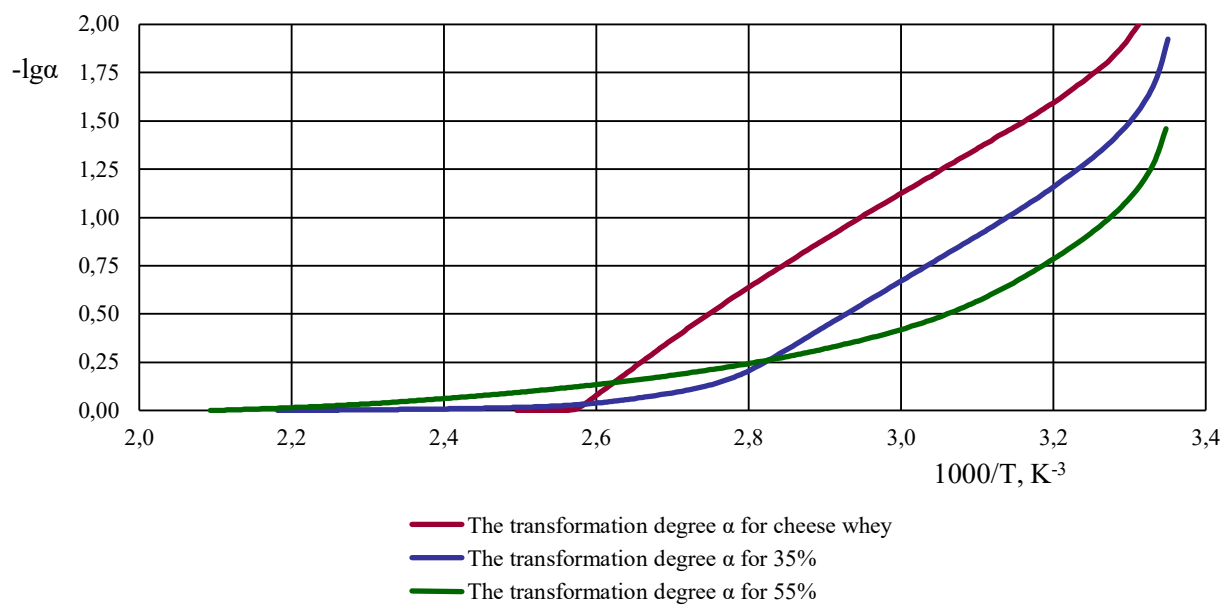


Figure 4. The dependence of the transformation of a substance ($-\lg \alpha$) on the value of $1000/T$ when heated

O EFEITO DA APRENDIZAGEM COLABORATIVA BASEADA EM PROJETOS NO DOMÍNIO DO CONCEITO DE COGUMELO: O CASO DE ESTUDANTES DE ENSINO MÉDIO NA INDONÉSIA**THE EFFECT OF PROJECT-BASED COLLABORATIVE LEARNING ON CONCEPT MASTERY OF MUSHROOM: THE CASE OF SENIOR HIGH SCHOOL STUDENTS IN INDONESIA**

SUKMAWATI, Fatma^{1*}; SETYOSARI, Punaji²; SULTON, Sulton³; PURNOMO, Purnomo⁴

1, 2, 3, * Department of Instructional Technology, Faculty of Education, Universitas Negeri Malang, Indonesia

⁴ Department of Mechanical Engineering, Faculty of Engineering, Universitas Negeri Malang, Indonesia

* Correspondence author
e-mail: fatmasukma76@gmail.com

Received 30 November 2019; received in revised form 21 December 2019; accepted 12 January 2020

RESUMO

É altamente recomendável que o aprendizado de biologia seja apresentado contextualmente após experimentação e observação dos fenômenos diários. Este estudo, uma pesquisa quase-experimental utilizando um projeto de grupo de controle não equivalente pré-teste e pós-teste, objetivou entender o efeito do aprendizado colaborativo baseado em projetos no domínio do conceito de cogumelos. Os sujeitos do estudo foram 75 alunos da décima série do ensino médio na cidade de Surakarta, Indonésia, divididos em duas turmas: 38 alunos da turma experimental 37 da turma de controle. Na aula experimental, os alunos foram tratados com estratégias de aprendizagem colaborativa baseadas em projetos. Na estratégia de aprendizagem colaborativa baseada em projetos, os alunos foram desafiados a criar um projeto de cultivo de cogumelos ostra (*Pleurotus ostreatus*) com os resíduos de hortas como serragem, por exemplo. Na aula controle, os alunos foram tratados com instrução direta. O instrumento utilizado foi um teste e ensaio de múltipla escolha desenvolvido por pesquisadores para medir o domínio conceitual dos estudantes em relação aos cogumelos. Os dados da pesquisa foram analisados pelo teste t de amostra independente. Os resultados mostraram que o escore médio *n-gain* para as classes experimental e controle foi de 63,09% e 45,73%, respectivamente. Além disso, todos os indicadores de domínio do conceito de cogumelo mostraram os escores *n-gain* para a classe experimental maiores que a classe controle. A análise do teste t de amostra independente provou que existiram diferenças significativas entre a instrução direta e a aprendizagem colaborativa baseada em projetos para melhorar o conceito de domínio do cogumelo. Finalmente, esta pesquisa concluiu que a aprendizagem colaborativa baseada em projetos é mais eficaz para enriquecer o domínio do conceito do que a instrução direta.

Palavras-chave: *Aprendizagem Colaborativa Baseada em Projetos; Domínio de Conceito; Cogumelo; Biologia*

ABSTRACT

Biology learning is highly recommended to be presented contextually following daily experience and phenomena. This study, a quasi-experimental research using a pretest-posttest non-equivalent control group design, aimed to understand the effect of project-based collaborative learning towards the concept mastery of mushrooms. The subjects of the study were 75 tenth grade of high school students in Surakarta City, Indonesia, divided into two classes: 38 students in the experimental class 37 in the control class. In the experimental class, the students were treated with project-based collaborative learning strategies. In project-based collaborative learning strategy, students were challenged to create a project on oyster mushroom cultivation (*Pleurotus ostreatus*) With the media garden waste such as sawdust. In the control class, the students were treated with direct instruction. The instrument used was a multiple-choice test and essay developed by researchers to measure students' concept mastery towards mushrooms. Research data were analyzed by independent sample t-test. The results found that the average *n-gain* score for the

experimental and the control classes were 63.09% and 45.73%, respectively. Moreover, all indicators of mushroom concept mastery showed the n-gain scores for the experimental class higher than the control class. Analysis of independent sample t-test proved that the significant differences existed between direct instruction and project-based collaborative learning in improving the concept mastery of mushroom. Finally, This research concluded that project-based collaborative learning is more effective in enriching the concept mastery than direct instruction.

Keywords: *Collaborative Project-Based Learning; Concept Mastery; Mushroom; Biology*

1. INTRODUCTION:

Teaching and learning science focuses on joyful, meaningful, and contextual learning (Muammer, 2012; King & Henderson, 2018; Chin & Osborne, 2008). It means that science concepts, including biology, need to be associated with everyday problems or real-life phenomena (Ertikanto *et al.*, 2017). Contextual learning facilitates an opportunity for students to interpret events, conducting experiments and investigations in understanding the concepts (Suryawati & Osman, 2018; Yildiz & Baltaci, 2016; O'Sullivan, 2006; Klassen, 2006; Glynn & Winter, 2004). To introduce meaningful and contextual learning, project-based learning and collaborative learning are recommended to improve students' understanding of the concepts of science correctly including biology (Lee *et al.*, 2014; Donnelly & Fitzmaurice, 2012; Rogers *et al.*, 2011).

Project-based collaborative learning (PBCL) is learning to integrate project-based learning with cooperative learning strategies (Sankaranarayanan, 2019; Avouris *et al.*, 2010; Chan & Chen, 2010; Ellis & Hafner, 2017; Jeremić *et al.*, 2009). PBCL strategy was conducted with project-based learning phase with a form of teamwork through a collaborative approach. According to Jeremić *et al.* (2009) said that when teachers use project-based learning by way of individual work, students do not have the ability to Collaboration. It makes collaborative learning is also necessary for carrying out duties on project-based learning. Integrate project-based learning to collaborative learning produces positive results for students is one learning outcome students' understanding of concepts (Baser, Ozden, & Karaarslan, 2017). Many studies have shown how project-based collaborative learning activities can improve students' understanding of the idea (David, 2018; Baser, Ozden, & Karaarslan, 2017; Donnelly & Fitzmaurice, 2012). PBCL is the potential to create a learning environment that develops the knowledge and skills needed for the twenty-first century, and features of the learning environment plays a vital role in achieving this potential (Garba, Byabazaire, & Busthami, 2015).

Problem-based collaborative learning (PBCL) has advantages such as: involving learners to be active in education, improve cooperative skills, improve academic skills, develop higher-level thinking skills and build positive relationships between students and teachers (Jalinus & Nabawi, 2019). This learning strategies suitable to be applied in learning biology because the material requires skills in problem-solving and creative thinking skills that can be understood by the learner.

In studying the biology subject matter, especially mushroom, students often find it challenging to master the material. According to Çimer (2012), biological materials such as Mushroom have a lot to learn and too complicated. Also, several types of mushroom cannot be observed directly, and the content is a widely used term that is difficult to understand the students. Many students who have misconceptions on biological materials such as morphology and physiology of low-level plants such as mushroom (Karagoz & Cakir, 2011; Shinysheroova, 2018; Bulunuz, Jarrett, & Bulunuz, 2008), Another difficulty experienced by students in learning biology is to apply the knowledge gained in school to real life. When students learn a new knowledge in the classroom, they do not understand what is learned (Bahar, 2003; Çimer, 2012), They memorize the material that makes them bored (Chavan & Patankar, 2018). In mushroom material, students are required to master the competencies such as identifying characteristics of mushroom, explaining how mushroom obtain nutrients, disclose how the reproduction of fungus and explains the role of mushroom in life. Therefore, to achieve these competencies, the project needs to be done to cultivate mushrooms by implementing strategies collaborative project-based learning in biology.

2. MATERIALS AND METHODS:

2.1 Research design and sample

This research was a quasi-experimental study with a pre-test post-test non-equivalent

control group design. Research subjects were high school students in class X Surakarta, Indonesia. The number of students involved was 75, with 37 students in the control group and 38 students in the experimental group. All the participants have filled the agreement to participate in this research as research sample. The experimental group was treated with a Project-based collaborative learning strategy while the control group was treated with direct instruction.

At the research implementation stage, data collection activities were carried out by providing a pretest in the experimental class and the control class to measure students' initial abilities. In the experimental group (PBCL strategy group), students create a project in the form of oyster mushroom cultivation (*Pleurotus Ostreatus*) within four weeks. While in the control class (direct instruction), students do not make projects, but students work on assignments given by the teacher.

The procedure used a strategic research PBCL through five stages adapted by Baser *et al.* (2017) namely: (a) dividing the working groups and identify problems; (b) designing the project and create the project schedule; (c) carry out the project; (d) presenting the project in front of the class; (e) evaluate the project. Students were given a worksheet to guide students' projects.

During the first week, students created a small group of four people. Teachers provided stimulus-related projects. Teachers gave explanations about the plans to be undertaken. Afterward, at the stage of identifying, students were asked to solve the problem of a nutrient-rich food source. They were given the challenge to the issue: "What should be done by high school students to utilize the biological sciences in the field of food and industry?". The next stage, students designed a project and made project schedule activities.

In the second and third weeks, the students carried out the project. Students chose a type of mushroom, the planting medium, and material tools used in the project. All the activities carried out by a group discussion. At this stage, students created a planting medium with the material of sawdust, and oyster mushroom was selected. Furthermore, the students planted seedlings mushroom into sterilized media. All the project activities were recorded and monitored every day.

At the present stage of the project was done in the fourth week. Each group was required to present the results of the project to the class.

The other group provided feedback in the form of suggestions and criticism. Furthermore, teachers gave advice and evaluate the results of the student project. At the end of the meeting, teachers provided post-test evaluation form understanding of the concept to measure student success in learning.

The control group (direct instruction) had four stages according step (Baghcheghi, Koohestani, & Rezaei, 2011) namely (a) the teacher to the learning objectives, (b) teachers ask information to students about the material being studied, (c) the teacher check student understanding and provides feedback and (d) the teacher gives an evaluation. In this research, this learning activity was conducted for four weeks, and in the last week, teachers offered post-test students' understanding of the concept.

2.2 Data Collection Tools

The measurement scale of the data tool consisted of 35 items adjusted to achieve the research objectives. The items consisted of 30 multiple choice questions and five essay item questions originating from literature reviews related to biology subjects, especially mushroom material. Assessment This measurement instrument is used to measure the effectiveness of learning in the classroom. This instrument consisted of 35 items that measure six concepts explained in the literature, namely: identifying the characteristics of mushroom (6 items), describing body structure (5 items), describing how mushrooms obtain nutrients (7 items), explaining how to reproduce mushroom (7 items), interpreting mushroom classification (5 items), and describe the role of fungi in economics (5 items). Validity and reliability were investigated by biologists and learning technology experts.

2.3 Data Analysis

This research is a quantitative research with a descriptive approach. Biologists and educational technologist have analyzed validity and reliability. Analysis of the data used is the Independent Sample T-Test to see differences in the average value of concept understanding between the experimental class and the control class. Research data were analyzed using a statistical tool that is SPSS 24.0, with a statistical significance value of 0.05. Before the t-test was carried out, the homogeneity test stage was carried out with the Kolmogorov-Smirnov test and the data normality test stage used the Levene test.

3. RESULTS AND DISCUSSION:

The results of this study describes the oyster mushroom cultivation project undertaken PBCL students through learning and student learning outcomes after completing the learning.

3.1 The oyster mushroom cultivation project

According to Chitamba *et al.* (2012), there are several steps in the cultivation of oyster mushrooms; (a) renders the seeds; (b) renders a spot fungus; (c) the manufacture of mushroom growing media; (d) sterilization of the media park; (e) seed inoculation; (f) incubation; (g) harvesting. The prepared mushroom seed is F3. Mushroom growing media using necessary materials of sawdust mixed with limestone (CaCO_3), rice bran, TSP, mixed with water evenly. Once evenly mixed, media is inserted into the plastic (poly) measuring 25x30cm.

The next process was done with steamed Sterilization 95-100°C temperature for 12 hours. Sterilization was performed to avoid any contamination of other organisms that can affect the growth of mushroom. After that, seed inoculation process. Inoculation is a step to fill mushroom seed into the planting medium already cold. The next process is incubation. In this process, polybag arranged in the room with the sleeping position. The room temperature was set 0-26 C. During the incubation process, performed maintenance. Within one month of mycelium, already meet the polybag. If the mycelium already reaches polybag, a cotton cap can be opened. The last stage is harvesting. Harvesting should be done early morning by removing the entire body of the fungus, and then cleaned.

Oyster mushroom cultivation process takes approximately four weeks. Fungal seedling growth in the first week, day 5 (Figure 1a) looks hyphae began to emerge. Hyphae are tubular fungal structures formed from spore growth. Hyphae that appears can be seen clearly when viewed using a microscope. On week 2, on the 15th day (Figure 1b), mycelium was seen. Mycelium is a collection of hyphae. Mycelium can be seen with the eye without the aid of a microscope. At week 3, day 25 (Figure 1c) a fruit body was formed. The fruit body is a collection of hypha that arises from the planting media. Fruit bodies on white oyster mushrooms with a length of 3 cm. Day 29 (Figure 1d) fruitbody length of 5 cm and mushroom hood began to appear with a diameter of 1 cm. At week 4, day 32 (Figure 1e), it was seen that the fruit body began to elongate by

8 cm and the hood began to widen with a diameter of 4 cm. As for the characteristics of oyster mushrooms that can be observed are shaped like a hood/umbrella, growing in groups, and white, the fruitbody has a stem that grows sideways.

3.2 Assessment of Concept Mastery

Learning outcomes are abilities that have been achieved by students after the learning process has been completed. In this study, learning outcomes are the understanding of the concept of mushroom material in biology subjects obtained by students, both those taught using PBCL strategies and those shown with direct instruction. The concept mastery of students in experimental and control classes can be seen in Figure2.

From Figure 2, it can be observed that the n-gain of the experimental class is higher than the n-gain of the control class for all indicators of concept mastery of mushroom. In more detail, the n-gain scores of the innovative class and the control class for the identifying characteristics of function indicators are 81.14 and 75.18, describing the structure of the body are 78.67 and 72.41, the index explaining how to function nutrients is 78.44 and 70.28, signs explain how reproduction of mushroom are 79.57 and 67.63, indicators defining the classification of fungus are 80.57 and 69.67, and indicators describe the role of mushroom in economics 83.28 and 73.06, respectively.

Moreover, the data from the pretest and posttest were analyzed using the Kolmogorov-Smirnov for normality test and a Levene test for homogeneity analysis. The statistical result showed that the significance value for the normality test (p-value) of the control and experimental classes was 0.200 ($p > 0.05$). It means that the data resulting from concept mastery test were normally distributed. As for the homogeneity test of the Levene test, each in control and experimental classes was 0.268 and 0.207 ($p > 0.05$). It means that the research data in the control and experimental classes are homogeneous. Based on this prerequisite test, hypothesis testing can be done.

Hypothesis testing is done by using an independent sample t-test to determine the difference between before and after treatment in each control class and experimental class. Table 1 showed the posttest value of the experimental and control classes using the value in the first row is 0.000. Furthermore, the t-value of 4.614 is compared with the T_f table of 1.993 with $\alpha = 0.05$.

It can be concluded that there is a significant difference in understanding the concept of mushroom material between the experimental group taught with PBCL and the control group trained with direct instruction.

Therefore, we can conclude there are differences in the results understanding the concept of learners who learn to use project-based collaborative learning with direct instruction. Students are learning to use strategies. Collaborative Project-Based Learning has an understanding of the idea of higher than students learning with direct instruction. The results are consistent with previous research that the implementation of project-based learning strategies integrated with collaborative learning, improve student learning outcomes (Ellis & Hafner, 2017; Holmes & Hwang, 2016; Shadiev, Hwang, & Huang, 2015; Jamal, Essawi, & Tilchin, 2014; Donnelly & Fitzmaurice, 2012; Avery *et al.* 2010).

Project-based learning and collaborative learning have characteristics such as solving and exploring the projects faced, learning outcomes in the context of student life, and using teams (Abdulwahed *et al.*, 2015). In this learning scheme, students have many opportunities to generate and discuss ideas, make plans, exchange ideas, find solutions, create projects, satisfy curiosity, and develop creativity. This is different from direct instruction where students tend to learn individually and more passive in receiving information from a teacher or just student worksheets (Nayereh *et al.*, 2011).

PBCL is learning the design stage of the project. This stage involves an attempt by the students to apply the knowledge that students master concepts with or without the guidance of teachers (Baser *et al.*, 2017; Kai *et al.*, 2017), Activity oyster mushroom cultivation project work starts from identifying the problem, reviewing the literature, formulate a problem-solving or design products, collect materials, conduct experiments, and evaluation can encourage students' creativity and motivation that affect their competence in solving problems. Additionally, PBCL applied correctly can make students active in class, providing an opportunity for students to integrate theory that has been obtained, learn to solve a contextual, work collaboratively, to help students learn in a fun way, helping them gain the depth of the concept of a material and help them to use higher-order thinking (Lee, Huh, & Reigeluth, 2015),

PBCL strategy is suitable to be applied in

high school. This is because learning biology regarding how the discovery and apply the knowledge gained. Thus, biology is not just about the mastery of experience in the form of a collection of facts, concepts, or principles but also about the application process. Biology education is expected to be a tool for students to learn about themselves and their environment to implement them in their daily life (Peterson & Myer, 2011).

Project-based collaborative learning can bring the students active and feel a more intellectual challenge. This strategy encourages students to work together in groups, exchanging ideas to solve problems, increase self-confidence, as well as train students to appreciate the differences and the lack of other students, so the role of peers in the group will encourage the spirit of learning, as well as reducing the dominance of the individual. Based on these results, the researchers recommend the adoption of PBCL, especially for biology, to improve students' understanding of the concept.

4. CONCLUSIONS:

The oyster mushroom cultivation project with sawdust waste media has been successfully designed by students in the scheme of PBCL strategy. PBCL strategy showed a better improvement of the concept mastery of the biology students in the topics of mushroom compared with the direct instructions. The highest concept mastery score has been found on the indicator of the role of mushrooms in economics and identification of mushroom characteristics. Although the implementation of PBCL strategy required more time than direct instruction, it gave a better and positive impact on students learning. PBCL strategy made learning more fun, creative, effective, fostering mutual cooperation, and adaptive to the real-life situation.

The recommendation for further research is that PBCL can be applied to primary and junior high school students. Also, in implementing PBCL, it is also necessary to consider external (family, economic capability, and environment) and internal (motivation, talent, and independence) factors. Furthermore, future research needs to explore the implementation of PBCL to improve students' thinking as higher-order thinking and creativity.

5. ACKNOWLEDGMENTS:

This research was supported by the Ministry of Finance of the Republic of Indonesia

through BUDI-DN Scholarship.

6. REFERENCES:

1. Abdulwahed, M., Hasna, MO, & Froyd, JE. *Advances in Engineering Education in the Middle East and North Africa: Current Status and Future Insights*. **2015**, 441-446
2. Avery, Z., Castillo, M., Guo, H., Guo, J., Warter-Perez, N., Won, DS, & Dong, J.. *Proceedings of Frontiers in Education Conference*, **2010**, 1-7.
3. Avouris, N., Kaxiras, S., Koufopavlou, O., Sgarbas, K., & Stathopoulou, P. *14th Panhellenic Conference on Informatics*, **2010**, 237-241.
4. Baghcheghi, N., Koohestani, H. R., & Rezaei, K. A. *Nurse Educ. Today*, **2011**, 31(8), 877-882.
5. Bahar, M. *Educ. Sci.-Theor. Pract.*, **2003**, 3(1), 55-64.
6. Baser, D., Ozden, MY, & Karaarslan, H. *Res. Sci. Technol. Educ.*, **2017**, 35(2), 131-148.
7. Bulunuz, N., Jarrett, O. S., & Bulunuz, M. J. *Turk. Sci. Educ.*, **2008**, 5(3), 32-46.
8. Chavan, R., & Patankar, P. *Aarhat Multidis. Int. Educ. Res. J.*, **2018**, 7(23), 144-153.
9. Chan, L. H., & Chen, C. H. *Performance Improvement*, **2010**, 49(2), 23-28.
10. Chin, C., & Osborne, J. *Stud. Sci. Educ.*, **2008**, 44(1), 1-39.
11. Çimer, A. *Educ. Res. Rev.*, **2012**, 7(3), 61-71.
12. David, A. A. *Am. Biol. Teach.*, **2018**, 80 (4), 278-284.
13. Donnelly, R. & Fitzmaurice, M. *Emerging Issues in the Practice of University Learning and Teaching*, **2005**, 87-98.
14. Ellis, T., & Hafner, W. *Interdisc. J. e-Skills Lifelong Learn.*, **2017**, 4(1), 167-190.
15. Ertikanto, C., Herpratiwi, Yunarti, T. & Saputra, A. *Int. J. Instr.*, **2017**, 10(3), 93-108.
16. Garba, S. A., Byabazaire, Y., & Busthami, A. H. *Int. J. Emerg. Technol. in Learn.*, **2015**, 10(4), 72-79.
17. Glynn, S. M., & Winter, L. K. *J. Elem. Sci. Educ.*, **2004**, 16(2), 51-63.
18. Holmes, V., & Hwang, Y. *J. Educ. Res.*, **2016**, 109(5), 449-463.
19. Jalinus, N., Syahril, S., & Nabawi, R. A. A. *J. Technic. Educ. Train.*, **2019**, 11(1), 36-43.
20. Jamal, A. H., Essawi, M., & Tilchin, O. *Int. J. High. Educ.*, **2014**, 3(1), 127-135.
21. Jeremić, Z., Jovanović, J., Gašević, D., & Hatala, M. *European Conference on Technology Enhanced Learning*. **2009**, 441-446.
22. Kai, S., Chu, W., Zhang, Y., Chen, K., Keung, C., Wing, C., ... Lau, W. *Internet High. Educ.*, **2017**, 33, 49-60.
23. Karagoz, M., & Cakir, M. *Kuram Egitim ve Uygulamada Bilimleri*, **2011**, 11(3), 1668-1674.
24. King, D., & Henderson, S. *Int. J. Sci. Educ.*, **2018**, 40(10), 1221-1238.
25. Klassen, S. *Interchange*, **2006**, 37(1-2), 31-62.
26. Lee, J. S., Blackwell, S., Drake, J., & Moran, K. A. *Interdisc. J. Problem-Based Learn.*, **2014**, 8(2), 2.
27. Lee, D., Huh, Y., & Reigeluth, C. M. *Instruc. Sci.*, **2015**, 43(5), 561-590.
28. Muammer, C. A. *J. Sci. Educ. Technol.*, **2012**, 21(6), 686-701.
29. O'Sullivan, M. *Int. J. Educ. Develop.*, **2006**, 26(3), 246-260.
30. Peterson, S. E., & Myer, R. A. *Couns. Educ. Supervis.*, **1995**, 35(2), 150-158.
31. Rogers, M. A. P., Cross, D. I., Gresalfi, M. S., Trauth-Nare, A. E., & Buck, G. A. *Int. J. Sci. Math. Educ.*, **2011**, 9(4), 893-917.
32. Sankaranarayanan, S. *Proceedings of the 50th ACM Technical Symposium on Computer Science Education*, **2019**, 1296-1296.
33. Shadiey, R., Hwang, W. Y., & Huang, Y. M. *Austral. J. Educ. Technol.*, **2015**, 31(2), 123-139.
34. Shinysheroova, G. B., Yessimov, B. K., Tuleubayev, Z., Seitbayev, K. Z., Sagyndukova, S. Z., & Dyussekenova, A. B. *Period. Tche Quim.*, **2018**, 15(30), 322-329.
35. Suryawati, E., & Osman, K. *Eur. J. Math. Sci. Technol. Educ.*, **2018**, 14(1), 61-76.
36. Yildiz, A., & Baltaci, S. *Online J. New Horiz. Educ.*, **2016**, 6(4), 155-166.

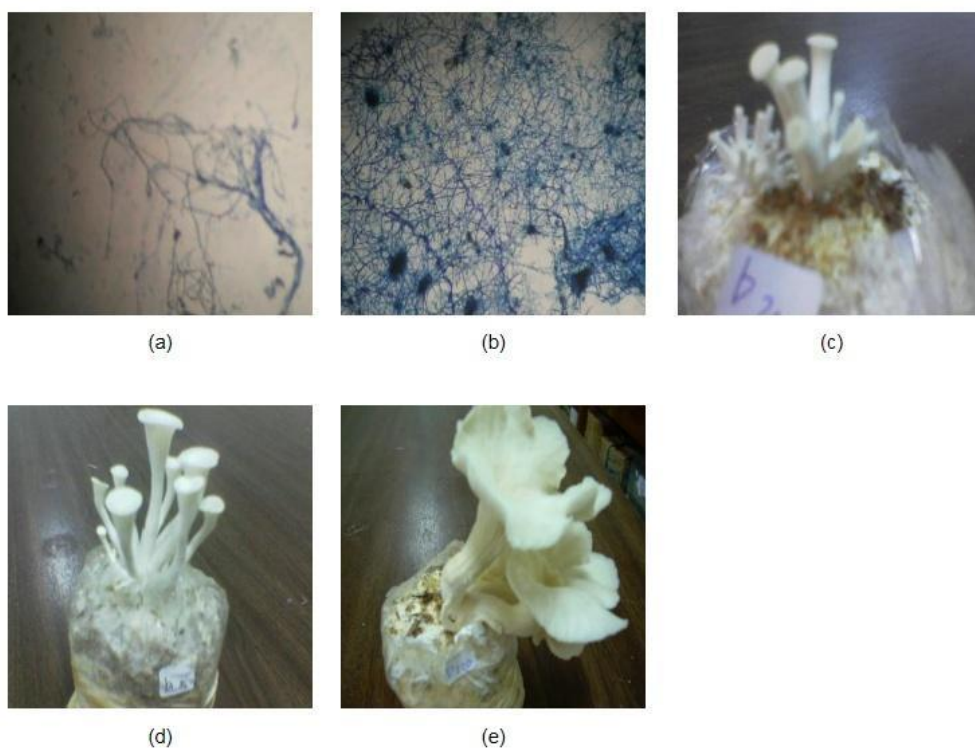


Figure 1. Oyster mushroom cultivation process. (a) Observation day 5, (b) day 15, (c) day 25, (d) day 29, (e) day 32

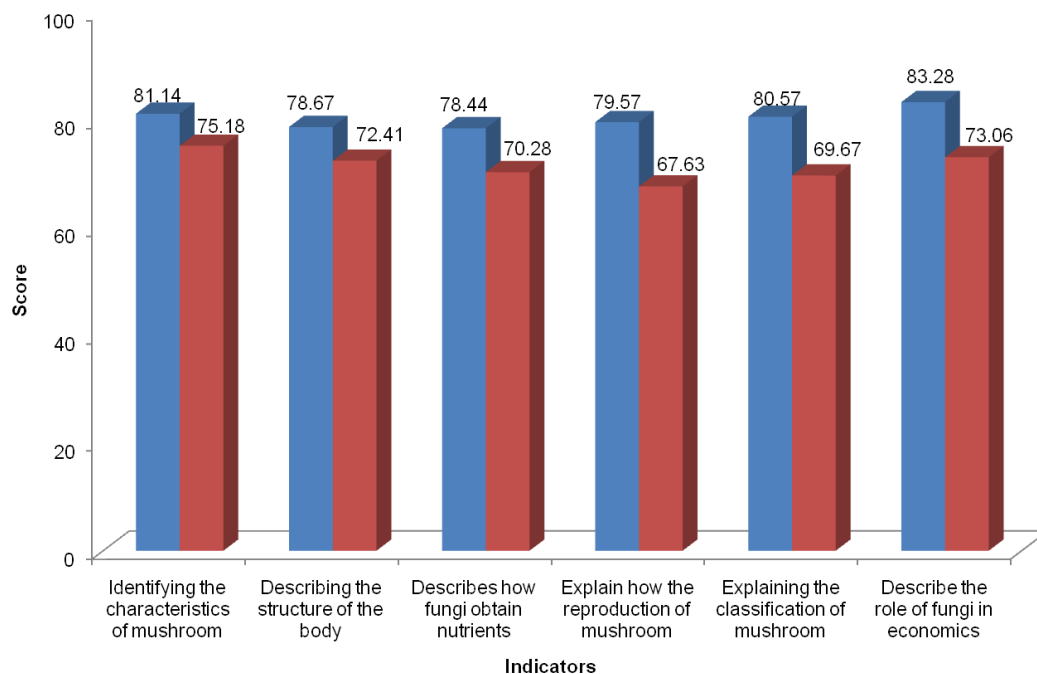


Figure 2. n-gain score of experimental (blue) and control (red) classes for each indicators

Table1. The result of independent samples T-test

	Levene's Test for Equality of Variances		T-test for Equality of Means		Sig. (2- tailed)	Mean Difference	SE Difference
	F	sig	T	df			
Equal variances assumed	1.622	.207	4.614	73	.000	8.05477	1.74554
Equal variances not assumed			4.629	69.909	.000	8.05477	1.73997

Note: F = Fisher test or Fisher distributions; Sig = significance; T = Tukey test or Tukey distributions; df = degree of freedom; SE = standard error

ANÁLISE ENERGÉTICA E DESEMPENHO DE UM COLETOR SOLAR CILÍNDRICO PARABÓLICO AUXILIADO POR SISTEMA DE RASTREAMENTO SOLAR**ENERGY ANALYSIS AND PERFORMANCE OF A PARABOLIC CYLINDRICAL SOLAR COLLECTOR AIDED BY SOLAR TRACKING SYSTEM**

PORTELA, Lino Wagner Castelo Branco^{1*}; ALMEIDA, Ana Fabíola Leite²; BARBOSA, Erilson de Sousa³; CEZAR, Kleber Lima⁴; OLIVEIRA, Patrick Abreu⁵

^{1,2} Universidade Federal do Ceará, Departamento de Engenharia Mecânica, Campus do Pici, Fortaleza - CE, Brasil

³ Instituto Federal de Educação, Ciência e Tecnologia do Ceará, Itapipoca - CE, Brasil

^{4,5} Universidade Federal do Piauí, Departamento de Engenharia Mecânica, Grupo Interdisciplinar de Pesquisa em Energia Solar (GIPES), Campus Petrônio Portella, Teresina - PI, Brasil

* Autor correspondente
e-mail: linowcbp@gmail.com

Received 13 November 2019; received in revised form 20 December 2019; accepted 10 January 2020

RESUMO

Ao longo dos últimos anos, países como Brasil, Estados Unidos, Alemanha e China vêm recebendo grandes investimentos para o avanço da utilização de fontes energéticas renováveis como, por exemplo, a energia solar, biomassa e eólica. Isso tem ocorrido devido ao crescimento das demandas por energia em função do aumento populacional e evolução das atividades industriais. A energia solar pode ser aproveitada com a utilização de concentradores solares que são comumente utilizados em sistemas solares térmicos nos quais o fluido de trabalho atinja temperaturas mais elevadas do que as que podem ser obtidas em outros coletores. Esses concentradores são os responsáveis por proporcionarem o fornecimento de energia térmica. Esta pesquisa analisou a influência energética da tecnologia Concentrador Solar Parabólico auxiliado por um sistema de rastreamento solar, levando em consideração seu balanço de energia e o cálculo de eficiência térmica. O concentrador apresentou uma eficiência óptica de 81 % e conseguiu atingir valores de eficiência térmica média entre 21,8 % e 24,7 % sob condições de radiação solar máxima entre 900 W/m² e 990 W/m². A temperatura do tubo absorvedor utilizado para receber a concentração dos raios solares alcançou temperaturas entre 80 °C e 98,6 °C, proporcionando a temperatura do fluido de trabalho do sistema atingir valores acima de 100 °C. Esses resultados apresentam a capacidade desse tipo de coletor solar de fornecer energia para aplicações térmicas como, por exemplo, aquecimento de água para processos industriais ou domésticos, desidratação e secagem de alimentos, refrigeração, dessalinização térmica e microgeração de energia elétrica. Além disso, a eficiência térmica (entre 21,8 % e 24,7 %) mostrou-se satisfatória quando levado em consideração o tipo de concentrador, o que também valida o sistema eletrônico de rastreamento já que ele conseguiu acompanhar o movimento relativo do sol e favorecer o aumento da eficiência térmica do sistema.

Palavras-chave: Fontes energéticas renováveis, Energia solar, Concentradores solares, Balanço de energia, Eficiência térmica.

ABSTRACT

Over the last few years, countries such as Brazil, the United States, Germany, and China have been receiving significant investments to advance the use of renewable energy sources, such as solar energy, biomass and wind. This has been due to the growing demand for electricity due to population increase and the evolution of industrial activities. Solar energy can be enjoyed by using solar concentrators that are commonly used in solar thermal systems where the working fluid reaches higher temperatures than can be obtained from other collectors. These concentrators are responsible for providing the thermal energy supply. This research analyzed the energy influence of Parabolic Solar Concentrator technology aided by a solar tracking system, taking into account its energy balance and thermal efficiency calculation. The concentrator had an optical efficiency of 81 % and was able to achieve average thermal efficiency values between 21.8 % and 24.7 % under maximum solar radiation conditions between 900 W/m² and 990 W/m². The temperature of the absorber tube used to receive the concentration of sunlight reached temperatures between 80 °C and 98.6 °C, allowing the system working fluid a

temperature to reach values above 100 °C. These results show the ability of this type of solar collector to provide power for thermal applications such as heating water for industrial or domestic processes, food dehydration, and drying, refrigeration, thermal desalination and microgeneration of electricity. Besides, the thermal efficiency (between 21.8 % and 24.7 %) was satisfactory when considering the type of concentrator, which also validates the electronic tracking system as it was able to track the relative movement of the sun and favor the increase of thermal efficiency of the system.

Keywords: *Renewable energy sources, Solar energy, Solar concentrators, Energy balance, Thermal efficiency.*

1. INTRODUÇÃO:

Ao longo dos últimos anos, países como Brasil, EUA, Alemanha e China, vêm recebendo grandes investimentos para o desenvolvimento de fontes energéticas renováveis como, por exemplo, a energia solar, biomassa e energia eólica (IEA, 2017). As fontes renováveis, quando comparadas aos combustíveis convencionais (gás natural, petróleo, carvão mineral), se mostram benéficas em relação ao equilíbrio do ciclo de produção energética e à diminuição da poluição ambiental (Ge *et al.*, 2018). No entanto, conforme a Agência Nacional de Energia Elétrica (ANEEL) no ano de 2019, a principal fonte de energia do Brasil ainda é proveniente de hidrelétricas (60,8 %), como também de combustíveis fósseis, sendo os mais utilizados o gás natural (7,7 %), petróleo (5,1 %) e carvão mineral (1,9 %).

O valor comercial de fontes renováveis, como a energia solar, tem se mostrado em recessão, principalmente pela ampliação da sua utilização e do avanço tecnológico nessa área, o que tem favorecido o seu desenvolvimento. No decorrer das próximas décadas, as fontes limpas tendem a representar grande parcela da matriz energética brasileira (Schaeffer *et al.*, 2016). Segundo Tiepolo *et al.* (2016), a capacidade de geração de energia elétrica por hidrelétricas vem caindo a cada ano – cerca de 20 pontos percentuais em relação ao total gerado, nos últimos 10 anos.

A energia solar é notavelmente a fonte energética de maior abundância, e considerando o grande potencial energético solar do Brasil, a aplicação dessa energia pode representar estimada contribuição na evolução sustentável da sociedade (Santos *et al.*, 2018). O número de aplicações da energia solar é diversificado, levando em consideração os diversos níveis de temperatura e demandas por energia (Schlecht; Meyer, 2012). No entanto, o recurso solar pode ser altamente variável em algumas regiões, seja pela posição das nuvens, pelos gases presentes na atmosfera, como também outros fatores naturais. Com essa variação, problemas relacionados à produção e confiabilidade de

sistemas solares podem existir (Inman *et al.*, 2013). Isso justifica a necessidade de muitos sistemas solares serem auxiliados por sistemas de rastreamento solar. A aplicação de sistemas de rastreamento solar afetam significativamente o aumento da eficiência, como também a utilização de matérias com boa refletividade e condutividade (Bazak; Sazak, 2014; Sekhar, 2015).

Uma das formas de se aproveitar a energia solar é através da tecnologia Concentrador Solar Parabólico (CSP), eles são amplamente explorados para produzirem calor a grandes níveis de temperatura (Kalogirou, 2014; Azzouzi *et al.*, 2018). As aplicações desse tipo de energia podem ser desde processos agropecuários, dessalinização de água, processos industriais e até mesmo refrigeração e climatização (Pereira *et al.*, 2017). Em trabalhos como Fernández-García (2010), Palenzuela *et al.* (2015), Arunkumar *et al.* (2016), Giglio e Lamberts (2016), Montenon *et al.* (2017), Fan *et al.* (2018), Elakhdar *et al.* (2019) e Abdessemed *et al.* (2019) são apresentados exemplos de aplicações com esse tipo de energia. O pesquisador Werner (2006) constatou que em 32 países da Europa, 57 % dos processos de aquecimento industrial demandavam fluidos em temperatura próxima de 400 °C, portanto, a utilização de concentradores solares parabólicos também representa uma economia de energia elétrica para o setor industrial.

Este trabalho apresenta o potencial energético de uma aplicação solar e contribui para o desenvolvimento da pesquisa na área de energias renováveis. Algumas pesquisas buscaram investigar o aumento da eficiência térmica de concentradores solares parabólicos, conforme os trabalhos de Duff *et al.* (1975), Schwarzer *et al.* (2000), Price *et al.* (2002), Kalogirou (2002), Lupfert (2007), Sintali *et al.* (2014), Al-Nimr e Dahdolan (2015), Behar *et al.* (2015) e Hassan *et al.* (2019). O objetivo desta pesquisa foi analisar a capacidade energética e o desempenho de um coletor solar cilíndrico parabólico auxiliado por um sistema de rastreamento a partir da utilização de energia solar.

2. MATERIAIS E MÉTODOS:

2.1. O Concentrador Solar Parabólico

O concentrador solar parabólico utilizado na pesquisa foi fabricado com uma estrutura a partir de perfis quadrados e retangulares de aço carbono e foi utilizada uma chapa de aço inox espelhada AISI 430 de 0,8 mm de espessura como superfície refletora. No foco da calha parabólica foi montado um tubo de cobre com diâmetro de 5/8", com distância focal de 200 mm. A abertura do concentrador é de 900 mm de largura e 1800 mm de comprimento. A eficiência óptica do concentrador é de 81 %. A Figura 1 apresenta o concentrador solar parabólico.

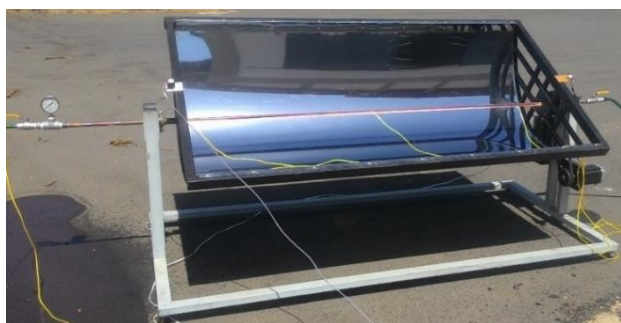


Figura 1. O concentrador solar parabólico.

2.2. O Sistema de Rastreamento Solar

Para rastrear o sol ao longo do dia, foi desenvolvido um sistema de rastreamento o qual foi fixado à estrutura do concentrador parabólico. O sistema de rastreamento é controlado por um microcontrolador Arduino Mega 2560 R3, associado a um módulo de dois sensores de luminosidade NORPS-12 do tipo LDR (*Light Dependent Resistor*). Conforme o *datasheet* desse módulo, o LDR é uma célula fotocondutiva de sulfeto de cádmio (CdS), a qual tem uma resposta espectral similar à do olho humano. Segundo Dally *et al.* (1993), o LDR é fabricado a partir de materiais semicondutores, normalmente CdS ou seleneto de cádmio (CdSe), pois eles apresentam uma excelente resposta fotocondutora. A precisão de rastreamento solar é aumentada com o auxílio de eletrônica sensível à luz (Jagoo, 2013). Na Figura 2 é ilustrada a superfície de um LDR.

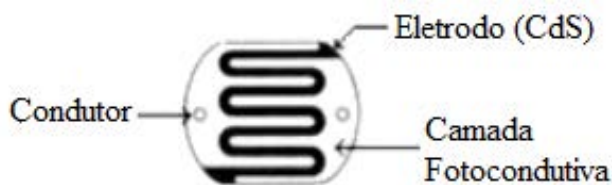


Figura 2. A superfície de um LDR.

O módulo com os sensores LDR's tem a função de enviar à placa de controle as informações necessárias ao rastreamento do nível de radiação solar. Esses sensores apresentam uma resistência variável conforme a intensidade luminosa que incide sobre sua superfície (Barbosa, 2009). A principal vantagem dos sensores LDR's está na geração do sinal na magnitude da tensão de referência do microcontrolador, além do seu baixo custo. Por outro lado, a desvantagem da sua utilização é a sua alta sensibilidade às pequenas variações de luminosidade (Prinsloo; Dobson, 2014). A Figura 3 apresenta o módulo de sensores com os LDR's utilizados no sistema de rastreamento do concentrador solar parabólico.

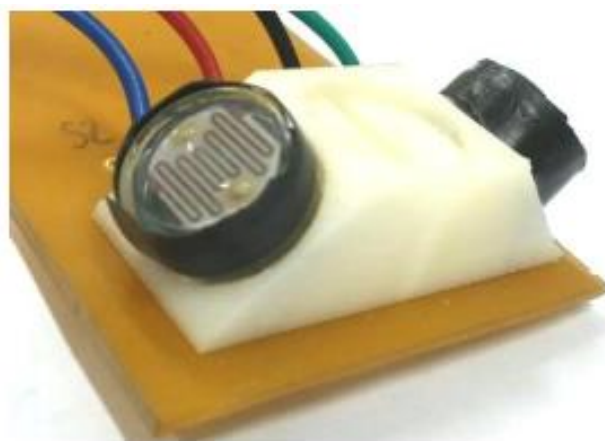


Figura 3. Módulo de sensores de luminosidade.

Os LDR's localizados nos planos inclinados (45° em relação à base) são responsáveis por fornecer a resistência elétrica que determinará em qual sentido o concentrador deverá girar.

2.3. Os Sensores e a Instrumentação para Coleta de Dados

Foram coletados dados de temperatura na parede externa do tubo de cobre localizado no foco da calha parabólica, e a temperatura de entrada e saída do fluido de trabalho como também dados de radiação solar. Na coleta de dados de temperatura, foram utilizados termopares do tipo K. Eles possuem faixa de leitura de -270 °C a 1372 °C (erro máximo entre 0,5 – 1 °C) e são formados por dois fios metálicos, Níquel e Crômio, que foram unidos em sua extremidade e fixados no concentrador solar parabólico. No sistema, foram utilizados cinco sensores termopares, o primeiro medindo a temperatura de entrada da água que alimentava o sistema, outros três foram fixados ao longo do tubo e o último na saída do sistema medindo a

temperatura final. Já a aquisição dos dados de radiação solar (W/m^2), ocorreu a partir de um sensor piranômetro Kimo™ – modelo CR 110, esse piranômetro apresenta uma faixa de leitura de 0 a 1500 W/m^2 (precisão de 5%). A Figura 4 ilustra a localização desses sensores.

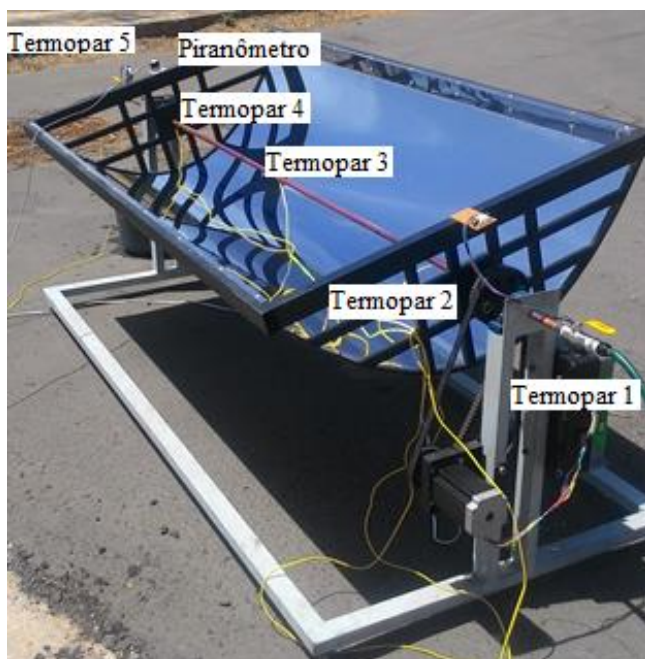


Figura 4. Localização dos sensores termopares e do piranômetro.

2.4. Transmissão de movimento para o coletor solar

Na transmissão de movimento, capaz de movimentar o concentrador parabólico em sentido que aumentasse a concentração dos raios solares, foi utilizado um motor de passo bipolar (modelo 86BHH1500-424E-37BS). Ele possui como características 4 bobinas (8 fios) para uma tensão de 12 V e um torque de 100 kgf.cm. Os motores de passo também possuem como característica a alta precisão em seus movimentos, sendo aplicado em sistemas onde o controle do ângulo de rotação é muito importante, tal qual o sistema de rastreamento deste trabalho. A Figura 5 apresenta o motor de passo.



Figura 5. Motor de passo bipolar.

2.5. Balanço de Energia no Coletor Solar

A análise térmica do desempenho do tubo absorvedor utiliza um balanço de energia que inclui todas as equações e correlações necessárias para relacionar os termos do balanço; que depende do tipo de coletor, parâmetros do tubo, propriedades ópticas e também condições atmosféricas. A energia, proveniente das propriedades ópticas, está diretamente relacionada com as possíveis imperfeições na superfície refletora da calha parabólica, erros de rastreamento, incidência de nuvens e também de limpeza nas superfícies do sistema. No balanço, a energia solar efetiva (energia solar menos as perdas ópticas) é absorvida pela superfície do tubo absorvedor. Essa energia é conduzida pelo tubo e transferida ao fluido pelo fenômeno de convecção; a energia remanescente é transmitida de volta ao ambiente por radiação e convecção e também parte dela é perdida através da condução entre o suporte de fixação do coletor cilíndrico parabólico (Forristall, 2003). Na Figura 6 é mostrado o balanço de energia em uma seção transversal do tubo e também o modelo de resistência térmica.

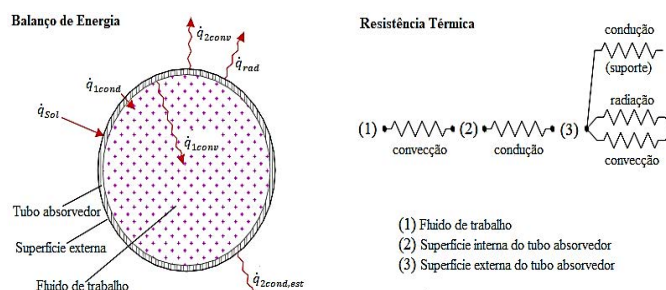


Figura 6. Balanço de Energia e Resistência Térmica.

Com base na Figura 6, é possível equacionar a conservação de energia do sistema, as equações são:

$$\dot{q}_{1\text{conv}} = \dot{q}_{1\text{cond}} \quad (\text{Eq. 1})$$

$$\dot{q}_{\text{Sol}} = \dot{q}_{2\text{conv}} + \dot{q}_{\text{rad}} + \dot{q}_{1\text{cond}} + \dot{q}_{2\text{cond,est}} \quad (\text{Eq. 2})$$

$$\dot{q}_{\text{perda}} = \dot{q}_{2\text{conv}} + \dot{q}_{\text{rad}} + \dot{q}_{2\text{cond,est}} \quad (\text{Eq. 3})$$

Os termos do equacionamento são definidos na Tabela 1.

2.6. Eficiência Térmica

A eficiência térmica é o termo utilizado na termodinâmica que procura quantificar uma estimativa do nível de aproveitamento em um

sistema que envolve transferência de calor (Moran *et al.*, 2005; Çengel; Ghajar, 2015). Em um coletor solar térmico, a eficiência térmica no absorvedor que ocorre a conversão de energia solar em calor, é possível ser calculada pela relação:

$$\eta_t = \frac{\dot{Q}_{\text{útil}}}{I} \quad (\text{Eq. 4})$$

em que $\dot{Q}_{\text{útil}}$ representa a taxa de transferência de energia na forma de calor útil e I é a taxa de radiação solar que incide sobre a superfície de abertura do concentrador solar parabólico. Esses termos podem ser calculados conforme as equações a seguir (Kreith; Bohn, 2003; Incropera *et al.*, 2008).

$$\dot{Q}_{\text{útil}} = \dot{m} \cdot C_{\text{med}} \cdot (T_{\text{ent}} - T_{\text{sai}}) \quad (\text{Eq. 5})$$

$$I = G \cdot A_a \quad (\text{Eq. 6})$$

onde \dot{m} representa a vazão volumétrica do fluido de trabalho, C_{med} o calor específico médio do fluido de trabalho, T_{ent} a temperatura de entrada do fluido de trabalho no sistema, T_{sai} a temperatura de saída do fluido de trabalho no sistema, G o valor de irradiação total no sistema e A_a a área de abertura do coletor solar (calculada pelo produto da sua largura do coletor com o seu comprimento).

3. RESULTADOS E DISCUSSÃO:

Para verificar o desempenho do concentrador parabólico foram coletados dados de radiação solar, temperatura na superfície externa do tubo absorvedor e temperatura do fluido de trabalho (água). O funcionamento do concentrador foi analisado sob duas condições. A primeira com a presença de muitas nuvens e a segunda com nuvens em intervalos pouco menores de tempo em relação à primeira. A Figura 7 apresenta a distribuição de radiação solar, a temperatura média na superfície do tubo absorvedor e a temperatura de entrada e saída do fluido em um dia com muitas nuvens.

É possível perceber que apesar da incidências de muitas nuvens os índices de radiação solar teve períodos em que permaneceu próximo de 800 W/m² em média, conseguindo chegar em 900 W/m². Em relação à temperatura do tubo, conseguiu atingir temperatura de 80 °C, nesse ponto a temperatura da água ficou acima de 100 °C – deixando sua fase líquida e passando a ser vapor. Pode-se observar também que nos períodos em que a incidência de nuvens

foi maior, a temperatura da água e do tubo diminuíram consideravelmente – como no período entre 12h08min e 12h43min, e também no período entre 15h02min e 15h28min.

A Figura 8 apresenta a distribuição de radiação solar, a temperatura média na superfície do tubo absorvedor e a temperatura de entrada e saída do fluido em condição com menos nuvens. Nesse período os índices de radiação solar teve momentos em que permaneceu próximo a uma incidência de 800 W/m² na média, conseguindo chegar em 900 W/m². Em relação à temperatura do tubo, conseguiu atingir temperatura média de 80 °C. Pode-se observar também que nos períodos em que a incidência de nuvens foi por um período maior, a temperatura da água e do tubo diminuíram consideravelmente – como no período entre 12h29min e 12h38min, e também no período entre 13h50min e 13h54min.

Foi possível analisar a eficiência do concentrador solar parabólico nessas duas situações, as Figuras 9 e 10 apresentam o resultado das eficiências ao longo do período.

No primeiro período (Figura 9), a eficiência térmica do concentrador solar variou entre diversos picos, como o representado no intervalo de 41,9 % no horário de 15h29min e 0,6 % no horário de 15h30min, essa variação se deve principalmente à constante presença de nuvens nesse período. Apesar disso o concentrador conseguiu manter sua eficiência térmica média em 21,8 %.

No segundo período (Figura 10), a eficiência térmica do concentrador variou entre picos de 40 % e 6 %, como no período de 12h35min e 12h38min. O concentrador conseguiu manter sua eficiência média em 24,7 %.

4. CONCLUSÕES:

A partir da pesquisa realizada, foi possível constatar que o concentrador solar parabólico apresentou desempenho satisfatório nos períodos em que a radiação solar se manteve acima de 700 W/m² e também na presença de poucas nuvens sobre o sistema. Em condições como essa, a temperatura do tubo absorvedor apresentou variações máximas entre 80 °C e 98,6 °C, tornando possível a temperatura do fluido de trabalho atingir valores acima de 100 °C, o que torna capaz o coletor solar de fornecer energia para aplicações de térmicas como, por exemplo, aquecimento de água para processos industriais ou residenciais, desidratação e secagem de alimentos, refrigeração, dessalinização térmica e

microgeração de eletricidade.

Com a aplicação do concentrador solar de pequeno porte, dos sensores de instrumentação e do balanço de energia desenvolvido, foi possível determinar a eficiência térmica do sistema. A eficiência média alcançada entre 21,8 % e 24,7 % é considerada satisfatória, quando levado em consideração o tipo de concentrador ser o parabólico.

O sistema eletrônico de rastreamento utilizando LDR's e a placa arduino, apresentou bom desempenho, pois conseguiu acompanhar o movimento relativo do sol e favorecer o aumento de eficiência térmica do sistema.

5. AGRADECIMENTOS:

Os autores agradecem à Coordenação de Aperfeiçoamento de Pessoal de Nível Superior (CAPES) pelo apoio financeiro na forma de bolsa de estudos e ao Conselho Nacional de Desenvolvimento Científico e Tecnológico (CNPq) pela promoção da pesquisa por meio do edital nº 18/2013 MCTI / CNPq / SPM-PR / Petrobras - Meninas e jovens fazendo ciências exatas, engenharia e computação.

6. REFERÊNCIAS:

1. Agência Nacional de Energia Elétrica. *Matriz de Energia Elétrica*. **2019**.
2. Abdessemed, A., Bougriou, C., Guerraiche, D., Abachi, R. *Renewable Energy*, **2019**, 132, 1134-1140.
3. Al-Nimr, M.A., Dahdolan, M.E. *Solar Energy*, **2015**, 114, 8-16.
4. Arunkumar, T., Velraj, R., Denkenberger, D.C., Sathyamurthy, R., Kumar, K.V., Ahsan, A. *Renewable Energy*, **2016**, 88, 391-400.
5. Azzouzi, D., Bourorga, H.E., Belainine, K.A., Boumeddane, B. *Renewable Energy*, **2018**, 125, 495-500.
6. Barbosa, E.S. Desenvolvimento de um Sistema de Controle para Concentradores Parabólicos de Baixo Custo Aplicados à Refrigeração. Dissertação de mestrado (UFC), **2009**.
7. Bazak, O.D., Sazak, B.S. *International Journal of Research in Engineering and Technology*, **2014**.
8. Behar, O., Khellaf, A., Mohammedi, K. *Energy Conversion and Management*, **2015**, 106, 268-281.
9. Çengel, Y.A., Ghajar, A.J. *Heat and Mass Transfer: fundamentals & applications*. New York: McGraw-Hill Education, **2015**.
10. Dally, J.W., Riley, W.F., McConnel, K.G. *Instrumentation for Engineering Measurements*. John Wiley & Sons, Inc., **1993**.
11. Duff, W.S., Lameiro, G.F., Löf, G.O.G. *Solar Energy*, **1975**, 17, 47-58.
12. Elakhdar, M., Landoulsi, H., Tashtoush, B., Nehdi, E., Kairouani, L. *A combined thermal system of ejector refrigeration and Organic Rankine cycles for power generation using a solar parabolic trough*. *Energy Conversion and Management*, **2019**.
13. Fan, M., Liang, H., You, S., Zhang, H., Yin, B., Wu, X. *Applied Energy*, **2018**, 100-111.
14. Fernández-García, A., Zarza, E., Valenzuela, L., Pérez, M. *Renewable and Sustainable Energy Reviews*, **2010**, 14, 1695-1721.
15. Forristall, R. *Heat Transfer Analysis and Modeling of a Parabolic Trough Solar Receiver Implemented in Engineering Equation Solver*. Golden, CO: National Renewable Energy Laboratory, **2003**.
16. Ge, T.S., Wang, R.Z., Xu, Z.Y., Pan, Q.W., Du, S., Chen, X.M., Ma, T., Wu, X.N., Sun, X.L., Chen, J.F. *Renewable Energy*, **2018**, 126, 1126-1140.
17. Giglio, T., Lamberts, R. *Energy and Buildings*, Lausanne, **2016**, 130, 434-442.
18. Hassan, H., Ahmed, M.S., Fathy, M. *Renewable Energy*, **2019**, 135, 136-147.
19. Incropera, F.P., DeWitt, D.P., Bergman, T.L., Lavine, A.S. *Fundamentos de Transferência de Calor e de Massa*. Rio de Janeiro: LTC, **2008**.
20. Inman, R.H., Pedro, H.T.C., Coimbra, C.F.M. *Prog. Energy Combust. Sci*, **2013**, 39, 535-576.
21. International Energy Agency. *Key World Energy Statistics 2017*. Paris, **2017**.
22. Jagoo, Z. *Tracking Solar Concentrators – A Low Budget Solution*. Springer, **2013**.
23. Kalogirou, S.A. *Energy*, **2002**, 27, 813-830.
24. Kalogirou, S.A. *Solar Energy Engineering: Processes and Systems*. Academic Press,

2014.

25. Kreith, F., Bohn, M.S. *Princípios de Transferência de Calor*. Pioneira Thomson Learning, **2003**.
26. Lupfert, E.E., Pottler, K., Ulmer, S., Riffelmenn, K.J., Neumann, A., Schiricke, B. J. *Sol. Energy Eng*, **2007**, 129, 147-152.
27. Moran, M.J., Shapiro, H.N., Munson, B.R., DeWitt, D.P. *Introdução à engenharia de sistemas térmicos: termodinâmica, mecânica dos fluidos e transferência de calor*. Rio de Janeiro: LTC, **2005**.
28. Montenon, A.C., Fylaktos, N., Montagnino, F., Paredes, F., Papanicolas, C.N. *Concentrated Solar Power in the Built Environment*. AIP Conference Proceedings, **2017**.
29. Palenzuela, P., Zaragoza, G., Alarcón-Padilla, D.C. *Energy*, **2015**, 82, 986-995.
30. Pereira, E.B., Martins, F.R., Gonçalves, A.R., Costa, R.S., Lima, F.J.L., Rüther, R., Abreu, S.L., Tiepolo, G.M., Pereira, S.V., Souza, J.G. *Atlas brasileiro de energia solar*. São José dos Campos: INPE, **2017**.
31. Price, H., Lupfert, E., Kearney, D., et al. *J. Sol. Energy Eng*, **2002**, 124 (5), 109-125.
32. Prinsloo, G., Dobson, R. *Solar tracking*. Stellenbosch University, **2014**.
33. Santos, A.P.S., Albuquerque Jr, D.M., Braga, R.A.P., Lima, R.A., Medeiros, S.S. *O encolhimento das águas: o que se vê e o que se diz sobre crise hídrica e convivência com o semiárido*. Campina Grande: INSA, **2018**.
34. Schaeffer, R., et al. [R]evolução Energética: Rumo a um Brasil com 100 % de energias limpas e renováveis. São Paulo, **2016**.
35. Schlecht, M., Meyer, R. Site selection and feasibility analysis for concentrating solar power (CSP) systems. Lovegrove, K., Stein, W. *Concentrating solar power technology*. Cambridge, UK: Woodhead, **2012**, Cap. 4.
36. Schwarzer, K., Vieira, M.E., Farber, C. *Solar termal desalination system with heat recovery*. Euromed 2000, Jerbas, Tunisia, **2000**.
37. Sekhar, T. *International Journal of Novel Research in Electrical and Mechanical Engineering*, **2015**, 2, 38-45.
38. Sintali, I.S., Egbo, G., Dandakouta, H. *American Journal of Engineering Research (AJER)*, **2014**, 3, 25-33.
39. Tiepolo, G.M., Urbanetz, J., Pereira, E.B., Pereira, S.V., Alves, A.R. *Energia solar no Estado do Paraná – Potencial, barreiras e políticas públicas*. X CBPE, Gramado, **2016**.
40. Werner, S. *The European heat market, work package 1*. Euroheat & Power, **2006**.

Tabela 1. Termos do equacionamento do balanço de energia

Fluxo de calor (W/m)	Fenômeno de transferência de calor	Região de transferência de calor	
		Desde	Para
\dot{q}_{1conv}	Convecção	superfície interna do tubo absorvedor	fluido de trabalho
\dot{q}_{1cond}	Condução	superfície externa do tubo absorvedor	superfície interna do tubo absorvedor
\dot{q}_{2conv}	Convecção	superfície externa do tubo absorvedor	ambiente
\dot{q}_{rad}	Radiação	superfície externa do tubo absorvedor	ambiente
$\dot{q}_{2cond,est}$	Condução	superfície externa do tubo absorvedor	suporte de fixação do coletor
\dot{q}_{Sol}	Irradiação solar absorvida	incidência de irradiação solar	superfície externa do tubo absorvedor
\dot{q}_{perda}	Radiação e convecção	coletor cilíndrico parabólico	ambiente

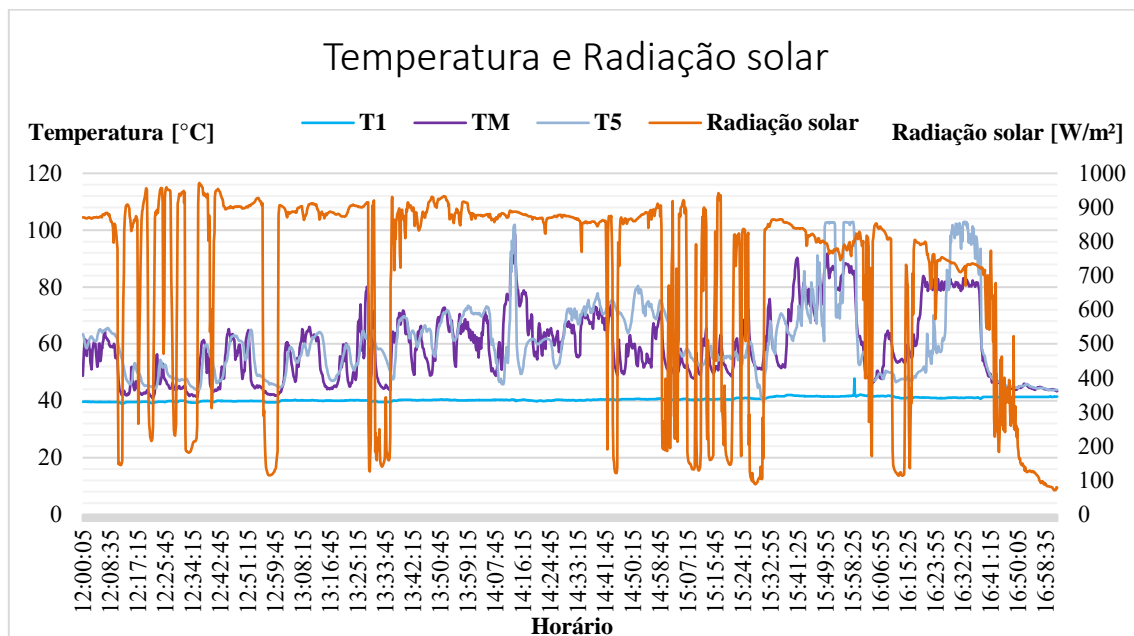


Figura 7. Radiação solar e temperatura sob muitas nuvens.

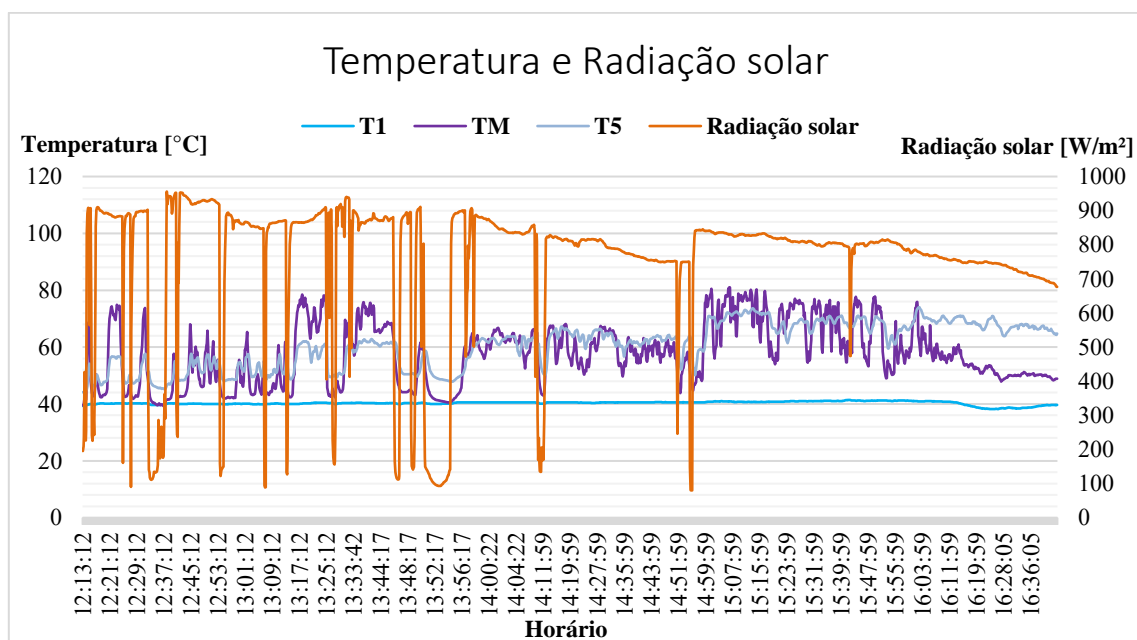


Figura 8. Radiação solar e temperatura com a presença de nuvens em intervalos menores

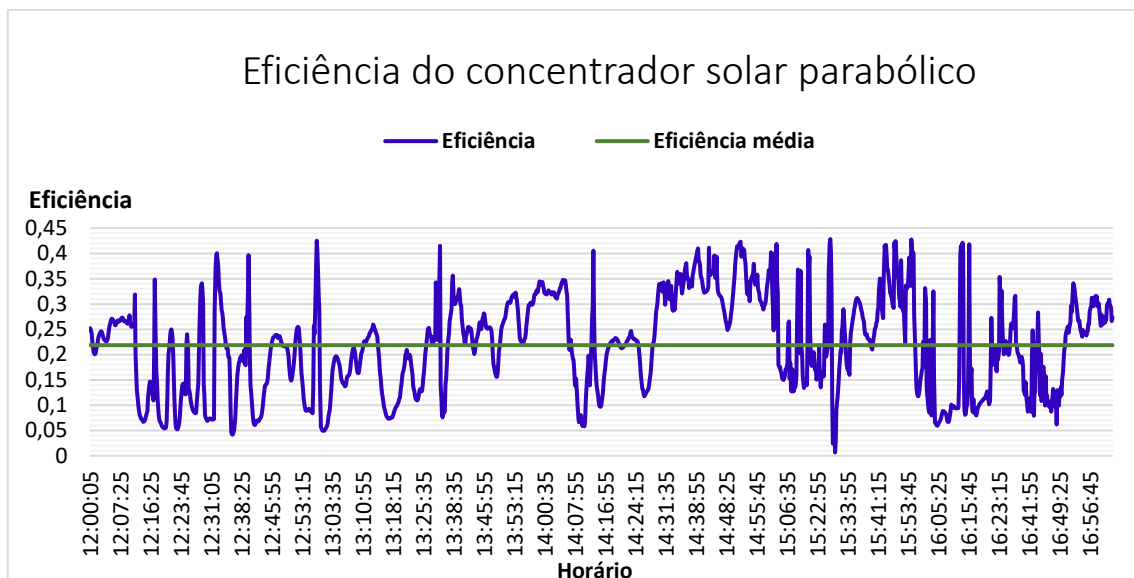


Figura 9. Eficiência térmica do concentrador solar sob muitas nuvens.

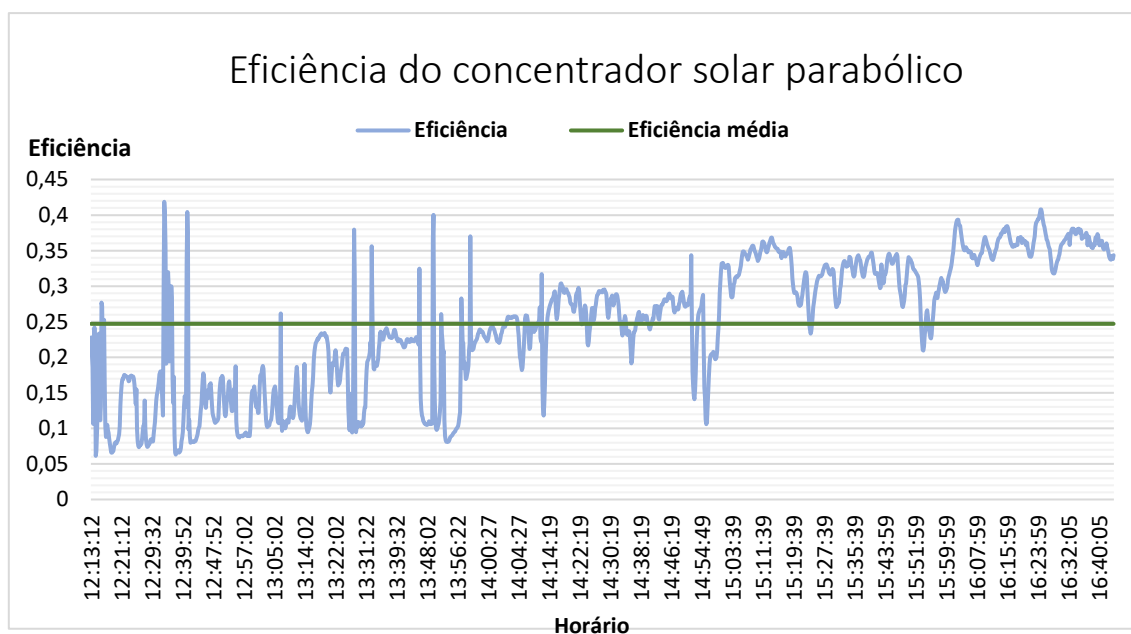


Figura 10. Eficiência térmica do concentrador solar com a presença de nuvens em intervalos menores.

OXIDAÇÕES ELETROQUÍMICAS DE SUBSTÂNCIAS ORGÂNICAS USANDO COMO CATALISADOR UM NOVO AQUACOMPLEXO DIARSÍNICO DE RUTÊNIO (II)

ELECTROCHEMICAL OXIDATIONS OF ORGANIC SUBSTANCES USING A NEW RUTHENIUM (II) DIARSENIC AQUACOMPLEX AS CATALYST

BATALINI, Claudemir^{1*}; DE GIOVANI, Wagner Ferraresi²;

¹ Universidade Federal de Mato Grosso - ICET/CUA, LAPQUÍM - Unidade II - Pontal do Araguaia - MT - Brasil

² Universidade de São Paulo, FFCLRP - Ribeirão Preto - SP - Brasil

* Autor correspondente
e-mail: pirapotimao@msn.com

Received 20 November 2019; received in revised form 19 December 2019; accepted 06 January 2020

RESUMO

Várias funções orgânicas podem sofrer reações de oxidação e a indústria química procura desenvolver cada vez mais processos que se ajustam na conduta da chamada Química Verde na busca de processos mais sustentáveis. Os processos eletroquímicos de transferência de elétrons usando complexos metálicos surgem assim como uma alternativa importante nesses processos oxidativos uma vez que exploram muitas reações em meio aquoso e utilizam-se de quantidades catalíticas do complexo. O objetivo deste trabalho foi testar a habilidade como eletrocatalisador de um novo aquacomplexo diarsênico de rutênio (II), $[\text{Ru}(\text{L})(\text{totpy})(\text{OH}_2)](\text{ClO}_4)_2$ ($\text{L}=\text{Ph}_2\text{AsCH}_2\text{CH}_2\text{AsPh}_2$; $(\text{totpy})=4'-(4\text{-toluyl})-2,2':6',2''\text{-tripiridina}$), em experimentos de eletroxidação de substâncias orgânicas de diferentes funções. As eletroxidações foram conduzidas sob potencial constante de +1,00 V (vs ECS), em solução 7:3 tampão fosfato:t-butanol, pH 8,1, com a proporção de 1,00 mmol.L⁻¹ do aquacomplexo $[\text{Ru}(\text{L})(\text{totpy})(\text{OH}_2)](\text{ClO}_4)_2$ para 50,00 mmol.L⁻¹ de cada substrato orgânico. As substâncias orgânicas de partida oxidadas e os respectivos produtos obtidos foram o álcool benzílico (benzaldeído), benzaldeído (ácido benzóico), éter benzilbutílico (benzaldeído e ácido benzóico) e 1-feniletanol (acetofenona). Observou-se reações seletivas e com bons rendimentos para os produtos. O processo eletroquímico utilizado revelou algumas vantagens frente a outros métodos oxidativos clássicos, como os biológicos e os oxidantes inorgânicos, ressaltando-se a rapidez, a possibilidade de utilizar meio aquoso nas reações, a seletividade na formação dos produtos e a possibilidade de se usar pequena escala de catalisador.

Palavras-chave: complexo metálico, eletrocatalise, eletroxidação, funções orgânicas, rutênio.

ABSTRACT

Various organic functions can undergo oxidation reactions, and the chemical industry increasingly seeks to develop processes based on the Green Chemistry approach in the search for more sustainable practices. Electrochemical electron transfer processes using metal complexes thus appear as an important alternative in these oxidative processes since they exploit numerous reactions in aqueous media and use catalytic amounts of the complex. The purpose of this work was to test the electrocatalytic ability of a new ruthenium (II) diarsenic aqua complex, $[\text{Ru}(\text{L})(\text{totpy})(\text{OH}_2)](\text{ClO}_4)_2$ ($\text{L}=\text{Ph}_2\text{AsCH}_2\text{CH}_2\text{AsPh}_2$; $(\text{totpy})=4'-(4\text{-tolyl})-2,2':6',2''\text{-terpyridine}$), in electrooxidation experiments of organic substances with different functions. The experiments were conducted at a constant potential of +1.00 V (vs ECS) in a solution of 7:3 phosphate buffer: t-butanol, pH 8.1, with a ratio of 1.00 mmol.L⁻¹ of the aqua complex $[\text{Ru}(\text{L})(\text{totpy})(\text{OH}_2)](\text{ClO}_4)_2$ to 50.00 mmol.L⁻¹ of each organic substrate. The oxidized organic starting materials and the respective products obtained therefrom were benzyl alcohol (benzaldehyde), benzaldehyde (benzoic acid), benzyl butyl ether (benzaldehyde and benzoic acid) and 1-phenylethanol (acetophenone). Selective reactions with good yields for the products were observed. The electrochemical process used here revealed some benefits over other classic oxidative methods, such as biological advantages and inorganic oxidants, emphasizing the speed, the possibility of using aqueous media in the reactions, selectivity in the formation of products, and the possibility of using small amounts of catalyst.

Keywords: metal complex, electrocatalysis, electrooxidation, organic functions, ruthenium.

1. INTRODUCTION:

Over the past two decades, investigations and applications of metal complexes in catalytic reactions have increased significantly in academic research and in the chemical industry, largely due to the selectivity exhibited by most of these reactions (Wang *et al.*, 2019), and more recently in the search for more sustainable processes that align with some of the principles of Green Chemistry (Song *et al.*, 2017).

Research on the subject has shed increasing light on the process that takes place between the substrate and the metallic complex (Thompson *et al.*, 1984; Nunes *et al.*, 2008; Roudesly *et al.*, 2017). In many cases, this has enabled the sequential steps of the stages of reactions to be determined and intermediate compounds to be identified, following changes in the oxidation state of the complex during the catalytic process and providing quantitative descriptions of the metal-substrate coupling (Efimov & Streelets, 1990; Manikandan *et al.*, 2015; Dhawa *et al.*, 2018).

Among the metal complexes used in the indirect electrooxidation of organic compounds, the ones that stand out are the high oxidation state polypyridine oxo/aqua complex systems that are widely used as electrochemical mediators in the transformation of organic substrates (Carrijo & Romero, 1994; Seok & Meyer, 2005; Tong & Thummel, 2016). The application of a suitable potential enables the transformation of an aqua into an oxo complex. This, in turn, oxidizes the organic substrate in aqueous medium, and is reduced to aqua complex, maintaining the catalytic cycle. Ruthenium complexes usually preserve their integrity in solution because the nature of ruthenium allows for a reversible electron transfer without ligand exchange (Seddon & Seddon, 1984).

Terpyridine ligands such as 2,2':6',2''-terpyridine and its substituted derivatives are often employed in the preparation of ruthenium complexes, rendering the complex highly stable against the loss of these ligands (Meyer, 1984; Tse *et al.*, 2005; Ezhilarasu *et al.*, 2017). Diarsenic and diphosphinic bidentate ligands also reportedly offer some advantages over their monodentate analogues by allowing for better control of the coordination number and stereochemistry of the resulting complex and by decreasing intra- and intermolecular exchange processes (Chaudret *et al.*, 1988; Gao *et al.*, 1996). It has been proposed that the hydrophobic

nature of arsines and phosphines makes it difficult to solvate the active oxo center of the complex to which it is bonded. Thus, in electrocatalytic reactions, upon leaving the aqueous phase, the substrate enters the non-solvated region of the active site ($\text{Ru}^{\text{IV}}=\text{O}$); this proximity facilitates the catalytic effect of the complex (Marmion & Takeuchi, 1988; Tong & Thummel, 2016).

Some systematic electrocatalytic studies conducted by our research group on organic substrates have shown that ruthenium polypyridine oxo/aqua complexes mixed with phosphines or arsines were more selective than those containing only polypyridines as ligands (Lima *et al.*, 1998; Sussuchi *et al.*, 2006). Therefore, it was proposed to test the electrocatalytic ability of a ruthenium terpyridine aqua complex containing an innovative combination with a diarsenic bidentate ligand (Figure 1): $[\text{Ru}(\text{L})(\text{totpy})(\text{OH}_2)](\text{ClO}_4)_2$ ($\text{L}=\text{Ph}_2\text{AsCH}_2\text{CH}_2\text{AsPh}_2$; ($\text{totpy}=4'-(4\text{-tolyl})-2,2':6',2''\text{-terpyridine}$), in electrooxidation experiments of organic substances with different functions in homogeneous aqueous phase.

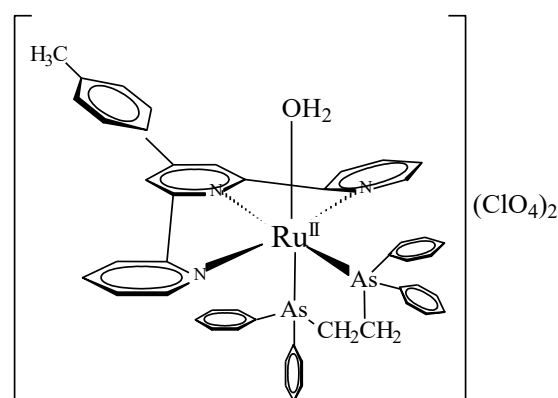


Figure 1. Chemical structure of ruthenium (II) diarsenic aqua complex $[\text{Ru}(\text{L})(\text{totpy})(\text{OH}_2)](\text{ClO}_4)_2$.

2. MATERIALS AND METHODS:

2.1. Reagents and Solvents

Double distilled water was prepared by treating distilled water with an alkaline solution of potassium permanganate (KMnO_4), which was then distilled (Morita & Assumpção, 2007). Ethyl ether was previously distilled in sulfuric acid medium in order to remove impurities (Morita & Assumpção, 2007). Dichloromethane was dried on an aluminum trioxide column (Al_2O_3) for the cyclic voltammetry experiments. All the other reagents and solvents, from Merck, Aldrich, Mallinckrodt and Sigma, were used in their

commercial form (P.A.), without further purification. A mixture of salts, $\text{NaH}_2\text{PO}_4/\text{Na}_2\text{HPO}_4 \cdot \text{H}_2\text{O}$, with ionic strength of 0.25 mol.L^{-1} (phosphate buffer) in a solution of 70:30 mL of double distilled water:t-butanol was used for the preparation of a solution with pH 8.1. This pH level for the phosphate buffer solution was measured directly by a pH meter and is therefore an apparent pH value.

2.2. Equipment

The electrochemical studies were carried out at atmospheric temperature and pressure in a FAC-200 A potentiostat/galvanostat coupled to an Intralab current data logger. The electrooxidation experiments were carried out in a two-compartment electrochemical cell containing saturated calomel as reference electrode, and a platinum plate (1.00 cm^2 area, 0.20 cm thickness) as auxiliary electrode inside a sintered glass tube. The working electrode was a platinum mesh electrode with 164.00 cm^2 of area and a wire diameter of 0.16 mm . ^1H NMR spectra were recorded in Bruker AC-80 nuclear magnetic resonance spectrometer (80MHz) using deuterated chloroform (CDCl_3) as solvent and tetramethylsilane (TMS) as internal standard (0 ppm on the δ scale). The CG analysis was performed in a Varian 3400 gas chromatograph equipped with a flame ionization detector (FID), using OV-17 Chrom W-HP (3% in Chromosorb W, 80-100 mesh) and Carbowax 20M (10% in Chromosorb W, 80-100 mesh) metal columns, both 2.00 m long and 3.00 mm in diameter, and the values obtained were compared with commercially available standards.

2.3. General Method of Electrochemical Oxidations

All the experiments were performed at ambient temperature and pressure in a 7:3 phosphate:t-butanol buffer solution at pH 8.1. The ratio of the concentrations was 1.00 mmol.L^{-1} of the diarsenic aqua complex $[\text{Ru}(\text{L})(\text{totpy})(\text{OH}_2)](\text{ClO}_4)_2$ to $50.00 \text{ mmol.L}^{-1}$ of the organic substrates. After sufficient charge had passed through to oxidize the aqua complex ($\text{Ru}^{\text{II}}\text{-OH}_2 \rightarrow \text{Ru}^{\text{IV}}\text{=O}$) dissolved in the aqueous medium with the solution under stirring, the organic substrate was added and a sufficient amount of charge (Coulombs) was passed to trigger the desired reaction or until the current dropped to values close to the residual currents. At the end of each electrooxidation process, the pH of the solution was raised to approximately 10 by adding an aqueous solution of 1.00 mol.L^{-1} of sodium

hydroxide (NaOH) and the organic phase was extracted five times with portions of 5 mL of ethyl ether. For the experiments leading to benzoic acid (as either a product or a byproduct of the oxidation reaction), the remaining aqueous phase was acidified with hydrochloric acid concentrated to a pH level of about 2.0, and another extraction was carried out with ethyl ether. After evaporation of the solvent, the products were identified and the yield of the reactions was calculated by means of gas chromatography, using a known amount of cyclohexanol as an internal standard, or weighed material, melting point and/or ^1H NMR.

2.4. Synthesis of the ruthenium (II) diarsenic aqua complex $[\text{Ru}(\text{L})(\text{totpy})(\text{OH}_2)](\text{ClO}_4)_2$ ($\text{L}=\text{Ph}_2\text{AsCH}_2\text{CH}_2\text{AsPh}_2$) (totpy=4'-(4-tolyl)-2,2':6',2''-terpyridine)

The complete synthesis of diarsenic aqua complex $[\text{Ru}(\text{L})(\text{totpy})(\text{OH}_2)](\text{ClO}_4)_2$, with an innovative combination of a substituted terpyridine ligand (totpy) and a bidentate arsine ligand (L), involved three steps, based on the $[\text{Ru}(\text{OH}_2)_3\text{Cl}_3]$ complex, which is described in the literature (Batalini & De Giovani, 2019).

3. RESULTS AND DISCUSSION:

Table 1 describes the electrochemical oxidation experiments of organic substances with different functions. The oxidations were performed at pH 8.1 because of the better reversible behavior of the $\text{Ru}^{\text{IV/III}}\text{-Ru}^{\text{III/II}}$ redox pairs of the complex, which was revealed in the cyclic voltammetry experiments in aqueous medium when the complex was characterized (Batalini & De Giovani, 2019). The applied potential chosen for all the electrooxidation experiments was $+1.00 \text{ V}$ (vs ECS). This potential, which is higher than the half-wave potential of the $\text{Ru}^{\text{IV/III}}$ redox pair of the aqua complex at pH 8.1, suffices to generate the oxo complex from the aqua complex. The results described in Table 1 indicate reactions that behaved selectively in the formation of a single product. This selectivity was particularly visible in the oxidation experiments of benzyl alcohol and 1-phenylethanol, where the formation of benzoic acid was not observed in the process. In these two experiments, there appeared to be a control that explains this non-formation of benzoic acid, given that benzaldehyde was oxidized to benzoic acid under the same reaction conditions. Thus, the selectivity observed here appears to be a combination of the control of the number of Coulombs applied in the reaction and the excess of substrate during oxidation, when the oxo complex was preferentially oxidized, instead of the

product undergoing subsequent oxidation.

Table 2 describes the data obtained in some electrooxidation processes of organic substrates, in the same conditions as those of the results presented in Table 1, albeit in the absence of the aqua complex $[\text{Ru}(\text{L})(\text{totpy})(\text{OH}_2)](\text{ClO}_4)_2$. Note that there was practically no oxidation of the organic substrates without the presence of the ruthenium aqua complex synthesized as catalyst. These experiments appeared to function as a direct electrooxidation process of the substrate by the electrode; the applied potential of +1.0 V was insufficient to trigger oxidation. A comparison of the results obtained in the "blank" experiments (Table 2) with the substrates listed in Table 1 clearly shows the importance of the role of the ruthenium oxo/aqua complex system in the electron transfer process, which leads to the formation of products with much higher yields and greater selectivity in the formation of a single product, at lower potentials than that required for the direct oxidation of the substrate by the electrode.

4. CONCLUSIONS:

This study demonstrates the importance of using metallic complexes as electrocatalytic systems in organic reactions. The four organic substances underwent selective oxidation against the new diarsenic aqua complex employed here in a homogeneous aqueous phase. The yields of the catalytic electrooxidation processes varied from good to excellent in the electrolytic processes that did not require bond breaking (benzylbutyl ether), which follows the hydride abstraction step. In addition to the advantages of this process, the use of electrooxidation in an aqueous system such as the one used in this research contributes to render the chemical process less aggressive to the environment.

5. ACKNOWLEDGMENTS:

The authors gratefully acknowledge the Federal University of Mato Grosso, UFMT, for its scientific support, and Brazil's Federal Agency for the Support and Improvement of Higher Education, CAPES, for awarding a doctoral grant.

6. REFERENCES:

1. Batalini, C.; De Giovani, W. F. *Periódico Tchê Química*, **2019**, 16, 130.
2. Carrijo, R. M.; Romero, J. R. *Synth. Commun.*, **1994**, 24, 433.
3. Chaudret, B.; Delavaux, B.; Poilblanc, R. *Coord. Chem. Rev.*, **1988**, 86, 191.
4. Dhawa, U.; Zell, D.; Yin, R.; Okumura, S.; Murakami, M.; Ackermann, L. *Journal of Catalysis*, **2018**, 364, 14.
5. Efimov, O. N.; Streelets, V. V. *Coord. Chem. Rev.*, **1990**, 99, 15.
6. Ezhilarasu, T.; Sathiyaseelan, A.; Kalaichelvan, P. T.; Balasubramanian, S. *Journal of Molecular Structure*, **2017**, 1134, 265.
7. Gao, J. X.; Wan, H. L.; Wong, W. K.; Tse, M. C.; Wong, W. T. *Polyhedron*, **1996**, 15, 1241.
8. Lima, E. C.; Fenga, P. G.; Romero, J. R.; De Giovani, W. F. *Polyhedron*, **1998**, 17, 313.
9. Manikandan, R.; Anitha, P.; Prakash, G.; Vijayan, P.; Viswanathamurthi, P.; Butcher, R. J.; Malecki, J. G. *J. Molec. Catalysis A: Chemical*, **2015**, 398, 312.
10. Marmion, M. E.; Takeuchi, K. J. *J. Chem. Soc., Dalton Trans.*, **1988**, 2385.
11. Meyer, T. J. *J. Electrochem. Soc.*, **1984**, 131, 221-C.
12. Morita, T.; Assumpção, R. M. V. *Manual de soluções, reagentes e solventes*, 2 ed., São Paulo: Ed. Blucher, 2007.
13. Nunes, G. S.; Alexiou, A. D. P.; Toma, H. E. *Journal of Catalysis*, **2008**, 260, 188.
14. Roudesly, F.; Oble, J.; Poli, G. *J. Molec. Catalysis A: Chemical* **2017**, 426 - Part B, 275.
15. Seddon, E. A.; Seddon, K. R. *The Chemistry of Ruthenium*, New York: Elsevier, 1984.
16. Seok, W. K.; Meyer, T. J. *Inorganic Chemistry*, **2005**, 44, 3931.
17. Song, Q. W.; Zhou, Z. H.; He, L. N., *Green Chem.*, **2017**, 19, 3707.
18. Sussuchi, E. M.; Lima, A. A.; Giovani, W. F. *Journal of Chemical Catalysis A, Chemical*, **2006**, 259, 302.
19. Thompson, M. S.; De Giovani, W. F.; Moyer, B. A.; Meyer, T. J. *J. Org. Chem.*, **1984**, 49, 4972.
20. Tong, L.; Thummel, R. P. *Chemical*

Science, **2016**, 7, 6591.

21. Tse, M. K.; Klawonn, M.; Bhor, S.; Doebl, C.; Anilkumar, G.; Hugl, H.; Maegerlein, W.; Beller, M. *Organic Letters*, **2005**, 7, 987.

22. Wang, B.; Duke, K.; Scaiano, J. C.; Lanterna, A. E. *Journal of Catalysis*, **2019**, 379, 33.

Table 1. Electrooxidation of organic substances in 7:3 phosphate buffer:t-butanol solution, pH 8.1, using as catalyst the diarsenic aqua complex $[Ru(L)(totpy)(OH_2)](ClO_4)_2$ ($L=Ph_2AsCH_2CH_2AsPh_2$), (totpy=4'-(4-tolyl)-2,2':6':2''-terpyridine).

Substrate	I_i / I_f (mA)	Time (h)	% Applied charge	Product (s)	Yield (%) ^a
benzyl alcohol	17/11	6	100 ^b	benzaldehyde	90
benzaldehyde	14/2	14	100 ^b	benzoic acid ^d	46
benzylbutyl ether	12/4.8	14.5	100 ^c	benzaldehyde	18
				benzoic acid ^d	20
1-phenylethanol	11/5	8.5	100 ^b	acetophenone	83

^a Yield calculated based on the charge applied (in Coulombs) (electric yield).

^b Percentage of Coulombs for a process involving two electrons.

^c Percentage of Coulombs for a process involving four electrons.

^d Melting point obtained: 119-121 °C (literature: 121-122 °C); ¹H RMN (δ , CDCl₃): 12.0 (s, 1H); 8.20-8.10 (m, 2H) and 7.60-7.50 (m, 3H).

Table 2. Electrooxidation of organic substances in 7:3 phosphate buffer:t-butanol solution, pH 8.1, in the absence of diarsenic aqua complex $[Ru(L)(totpy)(OH_2)](ClO_4)_2$ ($L=Ph_2AsCH_2CH_2AsPh_2$), (totpy=4'-(4-tolyl)-2,2':6':2''-terpyridine) (blank experiments).

Substrate	I_i / I_f (mA)	Time (h)	% Applied charge ^a	Product	Yield (%) ^b
benzyl alcohol	12/0.3	4	3.4	benzaldehyde	01
benzaldehyde	5/0.1	15	3.6	benzoic acid ^c	02
1-phenylethanol	10/0.2	17	4.5	acetophenone	04

^a Percentage of Coulombs for a process involving two electrons.

^b Yield calculated based on the charge applied (in Coulombs) (electric yield).

^c Melting point obtained: 119-121 °C (literature: 121-122 °C); ¹H RMN (δ , CDCl₃): 12.0 (s, 1H); 8.20-8.10 (m, 2H) and 7.60-7.50 (m, 3H).

INFLUÊNCIA DA QUALIDADE DO FILLER NA CONDUTIVIDADE TÉRMICA DO CONCRETO

INFLUENCE OF FILLER QUALITY ON CONCRETE THERMAL CONDUCTIVITY

ВЛИЯНИЕ КАЧЕСТВА ЗАПОЛНИТЕЛЯ НА ТЕПЛОПРОВОДНОСТЬ БЕТОНА

KENZHEBEK AKMALAIULY¹; ZHANAR ZHUMADILOVA²

^{1,2} Satbayev University, Institute of Architecture and Civil Engineering, Department of Civil Engineering and Construction Materials, Kazakhstan

** Corresponding author*
e-mail: zhanar_85@mail.ru

Received 12 June 2019; received in revised form 30 November 2019, 27 December 2019 ; accepted 09 January 2019

RESUMO

Estudos sobre o efeito da composição de grãos na condutividade térmica de concreto leve, demonstraram que a composição mineral do material de enchimento (agregados) reflete substancialmente a condutividade térmica e a densidade do concreto. Os grãos do componente têm um efeito ligeiramente mais alto na condutividade térmica do que o próprio material. A prova dessa posição é que a condutividade térmica de materiais a granel é sempre um pouco menor que dos materiais celulares da mesma densidade média. Em um corpo poroso absolutamente seco, a transferência de calor pode ocorrer não apenas através da condutividade térmica através do esqueleto sólido do corpo e localizado nos poros do ar, mas também por convecção e radiação entre as paredes dos poros. Com um diâmetro de poro inferior a 1 mm, a transferência de calor por convecção é praticamente zero, e o coeficiente de condutividade por calor radiante pode ser desprezado apenas quando o diâmetro de poro é inferior a 0,5 mm. Portanto, com a mesma porosidade, o coeficiente de condutividade térmica será maior, maiores serão os poros do material. Portanto, a criação de uma estrutura finamente porosa de concreto leve e o uso de agregados finamente porosos contribuem para a produção de concreto com condutividade térmica reduzida. A prova pode ser o resultado de experimentos e as curvas apresentadas. Um aumento no tamanho dos poros na superfície dos grãos dos agregados leva a um aumento nos vazios intergranulares das misturas. Como resultado dos estudos mineralógico-petrográficos de agregados porosos artificiais, foi estabelecido que as fases de aluminossilicato com uma estrutura desordenada - argila amorfizada com queima e vidros ácidos - predominam na argila expandida, agloporita e perlita expandida. A escória é caracterizada por uma predominância de fases cristalinas - silicatos com baixo teor de cálcio básico do que aluminossilicatos de cálcio e magnésio. A fase vítrea está presente apenas na forma de impureza de 15 - 20%. Ao analisar os dados experimentais, concluiu-se que a condutividade térmica da argila expandida aumenta com o aumento da densidade. No entanto, na mesma densidade, argila expandida de diferentes lotes da mesma planta e especialmente de plantas diferentes diferem nos valores do coeficiente de condutividade térmica.

Palavras-chave: *density, porosity, slag concrete, thermal conductivity coefficient, crystalline phase.*

ABSTRACT

Studies on the effect of grain composition on the thermal conductivity of lightweight concrete, it was shown that the mineral composition of filler (aggregates) substantially reflects the thermal conductivity and density of concrete. The grains of the component have a slightly higher effect on the thermal conductivity than the material itself. The proof of this position is that the thermal conductivity of bulk materials is always slightly lower than cellular materials of the same average density. In an absolutely dry porous body, heat transfer can occur not only through thermal conductivity but also through the solid skeleton of the body, located in the air pores, but also by convection and radiation between the pore walls. With a pore diameter of less than 1 mm, convective heat transfer is practically zero, and the coefficient of radiant heat conductivity can be neglected only when the pore diameter is less than 0.5 mm. Therefore, with the same porosity, the thermal conductivity coefficient will be the greater, the larger the pores of the material. Therefore, the creation of a finely porous structure of lightweight concrete and the use of finely porous aggregates contributes to the production of concrete with reduced thermal conductivity. The proof can be the results of experiments and the curves

presented. An increase in the pore size on the surface of the grains of the aggregates leads to an increase in intergranular voids of the mixtures. As a result of mineralogical-petrographic studies of artificial porous aggregates, it was established that aluminosilicate phases with a disordered structure — clay amorphized with firing and acidic glasses — predominate in expanded clay, agloporite, and expanded perlite. Slag is characterized by a predominance of crystalline phases - low-basic calcium silicates than calcium and magnesium aluminosilicates. The glassy phase is present only in the form of an impurity of 15 - 20%. When analyzing the experimental data, we came to the conclusion that the thermal conductivity of expanded clay increases with increasing density. However, at the same density, expanded clay of different batches of the same plant and especially of different plants, differ in the values of the coefficient of thermal conductivity.

Keywords: *density, porosity, slag concrete, thermal conductivity coefficient, crystalline phase.*

АБСТРАКТ

Исследования влияние зернового состава на теплопроводность легкого бетона показали, что минеральный состав заполнителей, существенно отражает теплопроводностью и плотности бетона. Зерна составляющего оказывает несколько большее влияние на теплопроводность, чем самого материала. Доказательством этого положения служит то, что коэффициенты теплопроводности сыпучих материалов всегда несколько ниже, чем ячеистых материалов той же средней плотности. В абсолютно сухом пористом теле, передача тепла может происходить не только теплопроводностью через твердый скелет тела и находящийся в порах воздуха, но и путем конвекции и излучения между стенками пора. При диаметре поры меньше 1 мм конвективный теплообмен практически равен нулю, а коэффициентом лучистой теплопроводности можно пренебречь лишь в случае, когда диаметр поры менее 0,5 мм. Следовательно, при одинаковой пористости величина коэффициента теплопроводности будет тем больше, чем крупнее поры материала. Поэтому создание мелкопористой структуры легкого бетона и применение мелкопористых заполнителей способствует получению бетона пониженной теплопроводности. Доказательством могут служить результаты экспериментов и представленные кривые. Увеличение размера пор на поверхности зерен заполнителей приводит к увеличению межзерновых пустотностей смесей. В результате минералого-петрографических исследований искусственных пористых заполнителей установлено, что в составе керамзита, аглопорита и вспученного перлита преобладают алюмосиликатные фазы с неупорядоченным строением - аморфизированное обжигом глинистое вещество и кислые стекла. Для шлака характерно преобладание кристаллических фаз - низкоосновных силикатов кальция, чем алюмосиликатов кальция и магния. Стекловидная фаза присутствует лишь в виде примеси 15 - 20%. При анализе экспериментальных данных пришли к выводу, что коэффициент теплопроводности керамзита повышается с увеличением его плотности. Однако при одной и той же плотности керамзиты разных партий одного завода и особенно разных заводов отличаются значениями коэффициента теплопроводности.

Ключевые слова: *плотность, пористость, шлакобетон, коэффициент теплопроводности, кристаллическая фаза.*

1. INTRODUCTION

The lighter the concrete, the usually less thermal conductivity, since a decrease in concrete density is associated with an increase in porosity. Noting the presence of a certain general relationship between the density and thermal conductivity of concrete, it is necessary to keep in mind the possible significant deviations from this dependence. In blast-furnace slag containing a large number of different impurities, it is possible that there is such a frequent violation of the crystal lattices formed in the mineral slag when their thermal conductivity becomes close to the thermal conductivity of the glasses, in addition, the fact that the slag especially acidic, there is

always a certain amount of glass enveloping the crystals. In addition, the introduction of granular slag into concrete instead of porous slag led to an increase in the thermal conductivity of concrete, while increasing its average density (Petrov, 2009; GOST 9758 – 2012, 2012; CN&R 23-02-2003 and 2004).

The thermal conductivity of concrete is determined by the type of aggregate used. The production of porous aggregates for lightweight concrete was made by the use of lightweight concrete wall panels of exterior walls in the construction of heat-insulating lightweight concrete for various purposes.

Factors can be divided into groups according to the degree of their influence on the thermal

conductivity of slag concrete, with decreasing significance: the first group is the porosity of concrete and aggregate, particle size distribution and phase composition of the aggregate; the second group - the type and consumption of cement; the third group is mixing water consumption; the fourth group - conditions for hardening concrete. According to leading experts, the factors of the fourth group have a slight effect on the thermal conductivity of lightweight concrete (CN&R 23-02-2003, 2004; Dvorkin, 2013; Bazhenov, 2013).

With an increase in the glass phase content, the thermal conductivity of the slag decreases. So, as an increase in the glass phase by 10-20% reduces the coefficient of thermal conductivity of the backfill from slag pumice by 8-12%. According to (GOST 32496-2013, 2013; Zotkin, 2014; Nesvetaev, 2012), at the same density and grain composition, the thermal conductivity coefficient of the backfill from completely crystallized slag is 16–20% higher than that of vitrified slag. The predominant influence on the coefficient of thermal conductivity of slag is provided by the isotropic glass. A small amount of denitrified glass enhances the effect of isotropic glass, and its content of more than 25% causes a weakening of the effect of the glass phase on the thermal conductivity of slag (STO 08.23.02-2009, 2009).

According to (Maksimov, 2004; Gorin, 2010), the thermal conductivity coefficients of concrete with a density of 1250 kg/m³ on blast furnace slag and a density of 800 kg/m³ on expanded clay gravel are the same.

According to (GOST 10832-2009, 2009; Gorin, 2011), the improved thermophysical properties of expanded clay of one plant are due to the fact that it contains only 10 - 15% of crystalline quartz compared to 30 - 40% in comparison with expanded clay of another plant, in addition, depending on the type of expanded clay, the thermal conductivity of concrete is its identical density can vary by 0.06 - 0.12 W/(m·°C).

2. MATERIALS AND METHODS

2.1 Effect of porous filler on the properties of lightweight concrete

A highly active component of the crystalline phase is residual quartz. The quartz content in the solid phase of the high-strength aggregate

(filler) varies from 20 to 26%. The grain size of quartz varies on average from 2-3 to 120-200 mcm. Usually, the surface of quartz grains is fused and corroded by feldspar melt. In the presence of active feldspar melt and sufficient firing temperature, the thickness of the margin of fusion of the grains of residual quartz is 2–5 mcm. Grains smaller than 2 mcm, as a rule, pass into the melt. It has been established that quartz grains and the vitreous component experience uniform tension in all directions: radial tensions in the entire region are tensile; the tangential tensions in the glass phase at the boundary with quartz grain are compressive. Special individual studies and processing of the results using equations characterizing the stress state and radial deformations determined the magnitude and distribution of tensions in the quartz component and the surrounding glass phase (Petrov, 2009; Rogovoi, 2016). As they move away from quartz, they decrease, pass through zero, and become tensile at the boundary of the region. The resulting micro tensions are directly proportional to the content of residual quartz. These tensions are proportional to the total surface of all quartz grains per unit volume of the rock and are manifested to the greatest extent when the radius of the quartz grains is three times the thickness of the dissolved layer. Therefore, the most dangerous place is the interphase boundary of contact of quartz grains with the glass phase.

As a result of studies of porous aggregates of various plants, it was found that the average pore diameter of slag is higher, in addition, the average porosity is lower, and the content of the glassy component is much lower than that of expanded clay. Meanwhile, as follows from Figure 1, the thermal conductivity of slag and expanded clay with a density of 900 and 600 kg/m³, respectively, is the same.

The solid phase may be in a crystalline or glassy state. The thermal conductivity of glasses is a function of their chemical compound; the limits of its change are small. The minimum and maximum values of the thermal conductivity coefficient of the studied glasses are between 0.7 and 1.3 W/(m·°C).

The highest thermal conductivity has transparent quartz glass - 1.3 W/(m·°C). Various oxides introduced into the glass change the thermal conductivity of the glasses. Other conditions being the same, refractory materials have higher thermal conductivity. The bigger the content of MgO, SiO₂, Al₂O₃ constituents with high thermal conductivity, and the higher the

firing temperature, which contributes to an increase in the content of crystalline substance.

2.2 Thermal conductivity of lightweight concrete

Studies of establishing the dependence of the density of lightweight concrete on the thermal conductivity for concrete with a density of 1300 kg/m³ and a lower coefficient of thermal conductivity have slag concrete (Figure 1).

Thermal conductivity is the most important essential property of lightweight concrete, the lighter the concrete, the lower its thermal conductivity, since a decrease in concrete density is associated with an increase in porosity, i.e., involving air in the concrete volume, which is a good heat insulator in small pores (Figure-2).

From this, we see that the thermal conductivity of concrete is significantly affected by the mineralogical composition of the aggregate. Thus, quartz has the highest thermal conductivity, limestone, and dolomite - medium, trachyte, and basalt - the lowest, which also depends on the directions of the heat flux with respect to the orientation of the crystals. Since the thermal conductivity of water is greater higher than the thermal conductivity of air, the degree of saturation of concrete with water is of great importance. For example, an increase in the level of humidity in lightweight concrete leads to an almost twofold increase in thermal conductivity.

The thermal conductivity coefficients of crystals and glasses with the same chemical composition differ very significantly. As compiled from the data, the thermal conductivity coefficients of the crystals of the main compounds, which are usually part of building materials, are several times higher than the same value for glasses of the same chemical compound (Table 1).

There is a relationship between density and thermal conductivity, but there may be deviations from this dependence. For example, those amorphous materials are less thermally conductive than crystalline. Therefore, from the point of view of thermal insulation requirements, aggregates are preferable, in which there is more glass, for example, slag pumice.

Table 2 shows data on the dependence of the coefficient of thermal conductivity of air in closed pores on the pore diameter at 0 °C.

The thermal conductivity of the material in pores up to 1 mm in size varies little, and in

pores, with a diameter of more than 1 mm, it increases sharply. Therefore, with the same porosity, the thermal conductivity coefficient will be the greater higher, the larger the pores of the material. Therefore, the creation of a finely porous structure of lightweight concrete and the use of finely porous aggregates contribute to the production of concrete with reduced thermal conductivity (Mikulsky, 2007).

In addition, the thermal conductivity of lightweight concrete is affected by the particle size distribution of the aggregate, because the nature of the porosity and pore size depends on it.

It was found that the thermal conductivity coefficients of concrete with a density of 1450 kg/m³ with aggregate made of slag and the same concrete in which fine sand (fractions below 1.2 mm) is replaced by quartz sand are within respectively 0.42-0.56 and 0.57-0.72 W/(m·°C) (Figure 3).

Sodium - calcium glass (69% - SiO₂, 15% - Na₂O, 16% - CaO) in the form of a tile 2 cm thick, heated to 900 °C, partially crystallized and cooled to 50 °C, has a thermal conductivity 40% higher than the original (Bazhenov, 2002). The thermal conductivity of dump blast furnace slag with a crystalline phase content of 85-90% and 3-5% at an equal density in a piece is respectively 1.23 and 0.87 W/(m·°C) (Bobrov, 2003).

The effect of the amount of glass phase on the thermal conductivity of the slag filling of fractions of 0-10 mm was determined (Figure 4). Significant changes in thermal conductivity are observed when the glass phase content is less than 35 - 40%.

It was found that the optimal combination of heat-shielding and physical-mechanical indicators of slag concrete is determined by the content of 50-60% glass phase and 40-50% of the crystalline phase in the slag since this depends on the type of slag used (Bazhenov, 2004).

The dependence of the thermal conductivity of the slag on the glass phase content in it is extreme, i.e., the slag has a low thermal conductivity with a low content of crystals and with a sufficiently high, which implies that in order to reduce the thermal conductivity of the slag, it is not necessary to strive to increase the glass phase content in it or to maintain its amount in a narrow range. Unwanted combinations of pore diameter and degree of crystallized slag should only be avoided (Eremkin, 2000).

When studying the effect of slag quality on

concrete properties, a tendency was found to decrease the thermal conductivity coefficient with an increase in the content of the vitreous phase in the slag (Figure 5).

The separation of the slag into vitreous (less than 20% of crystals) and crystalline (more than 35% of crystals) is conventionally accepted (20 - 35% of crystals is glass crystalline) 0.190 W/(m·°C). The content of the crystalline phase in the slag is 50 -70%.

The use in the concrete of two types of crushed stone from slowly and quickly cooled slag (hence, with different glass phase contents) does not significantly affect the value of the thermal conductivity coefficient. And when granular slag is replaced with slag sand in concrete, the value of thermal conductivity even decreases slightly. The introduction of granular slag into concrete instead of porous slag led to an increase in the thermal conductivity of concrete by 14%, while its density increased by 13.2%.

Structural and heat-insulating concrete was studied at various plants. The thermal conductivity coefficient of concrete in one plant is 14% higher than concrete in another plant, with concrete density increased by 7%. At the same time, slag at one plant is characterized by a glass phase content of 60 - 85% than at another plant 45 - 70%.

Therefore, under other unchanged conditions, the thermal conductivity of the material is determined not only by the amount of glass phase, which was ascertained by the researchers but also by other parameters of the phase structure of the material.

The researchers found that to reduce thermal conductivity, not only the total amount of glass contained in the aggregate but also its distribution is significant.

The most advantageous from this point of view is the case when the vitreous membranes cover the walls of pores and capillaries with at least a thin layer since, in this case, the heat transfer by radiation will decrease. It is also important essential that the pore walls have not only a porous but also a porous structure, i.e., so that crystalline inclusions would be separated from each other by at least thin glassy layers. Then there will be no "cold bridges" - the most intense direct heat transfer paths through adjacent crystals.

According to (GOST 25820-2014, 2014), the size of the material's crystals is assigned an important role in influencing the thermal

conductivity. With a decrease in the crystal size, the thermal conductivity of the slag decreases. In addition, the thermal conductivity of the material is significantly affected by its mineralogical composition.

This is explained by the low, close to glass thermal conductivity of crystallized slag. In blast-furnace slag's containing a large number of various impurities, it is possible that there is such a frequent violation of the crystal lattices of minerals formed in the slag when their thermal conductivity becomes close to the thermal conductivity of the glasses. In addition, the decrease in the thermal conductivity of the slag is also influenced by the fact that in the slag, especially acidic, there is always a certain amount of glass enveloping the crystals. The enveloping component has a slightly greater higher effect on thermal conductivity than the enveloped. The proof of this position is that the thermal conductivity of bulk materials is always somewhat lower than cellular materials of the same density.

With increasing porosity of a material, the effect of its phase composition on thermal conductivity decreases, and the influence of porosity increases. If within the limits of the density of slag concrete 1300 - 1600 kg/m³, which corresponds to the range of the total concrete porosity of 0.4 - 0.5, the value of the glassy structure of the aggregate is most affected, and then the influence of concrete porosity prevails in the region of lower density values.

In an absolutely dry porous, heat transfer can occur not only through thermal conductivity through the solid skeleton of the body and the air in the pores, but also by convection and radiation between the walls of the pore. With a pore diameter of less than 5 mm in a temperature difference of 10 °C, convective heat transfer is practically zero, and the coefficient of radiant heat conductivity can be neglected only when the pore diameter is less than 0.5 mm.

Figure 6 shows the curves, from which it follows that for a material with the same density, the dependence of the coefficient of thermal conductivity on porosity is higher for fired bricks, characterized by rough porosity due to the introduction of large significant burnable additives than for finely divided masses in which pores smaller and formed due to the introduction of a large amount of water.

So, with an increase in the density of concrete, for example, from 314 to 415 kg/m³, the value of

the coefficient of thermal conductivity does not change, provided that the average diameter of the cell decreases from 1.86 to 0.81 mm.

According to the author (GOST 27005 – 2014, 2014), an increase in the pore size on the surface of the aggregate grains leads to an increase in the intergranular voidness of the mixtures, which causes an additional consumption of the binder. A decrease in the density of aggregates with increasing pore size leads to an increase in the density of concrete, and, consequently, its coefficient of thermal conductivity.

The nature of porosity also affects thermal conductivity. Closed porosity not only reduces the thermal conductivity of the air trapped in it but also prevents water absorption.

The thermal conductivity of lightweight concrete is significantly affected by the particle size distribution of aggregates since it determines the structure of concrete and the nature of porosity.

On the question of the rational grain composition of slag concrete from the point of view of obtaining concrete with minimal thermal conductivity, there are various views (Davidyuk, 2010; Orentlicher, 2010). Special individual studies to determine the influence of the particle size distribution of slag concrete aggregates showed that with the addition of slag sand with a bulk density of more than 1000 kg/m³, the thermal conductivity of concrete increases in proportion to the amount of sand introduced into concrete (Figure 7), which is caused by an increase in concrete density.

Therefore, obtaining concrete of a cohesive structure is advisable only in the presence of fine aggregate with a density not exceeding that of slag.

The thermal conductivity of concrete on slag increases by 10%, with an increase to 0.45 of the fraction of fine aggregate in the total volume of aggregates of slag concrete. With a further increase in the sand content in concrete, its thermal conductivity does not change.

Studies of concretes based on expanded clay gravel have shown that the coefficient of thermal conductivity of expanded clay concrete can fluctuate over a fairly reasonably wide range (up to 30%) depending on the selected structure at the same density. The decisive factor in the structure formation of lightweight concrete, according to the authors, is the content of fine aggregate in concrete.

The experts came to the same conclusion in the study of slag concrete (Alekseev, 2010; Surkov, 2009). For slag concrete, the linear relationship between density and thermal conductivity is not fair. With a decrease in the size of the slag fraction, the average pore size decreases and, consequently, the proportion of large pores in concrete. Since the thermal conductivity of air in pores with a diameter of more than 1 mm (up to 3 mm) is 15-20% higher than in pores with a diameter of up to 1 mm, the presence of large pores will be less effective obstacle to heat transfer in concrete than small pores of the same volume.

The thermal conductivity coefficient is also affected by the size of the contact areas between the individual particles of the material: the larger these sites are, the higher the thermal conductivity of the material will be. For example, an increase in grain size from 5 to 30 mm increases the thermal conductivity of slag filling by 36% at the same density.

An increase in the fraction of the fine fraction in the concrete of the composite structure contributes to an increase in the interface between the cement stone and the aggregate; thermal resistances arise on the interface, which will increase in proportion to the increase in the interface. Therefore, slag concrete on aggregate with a lower average fineness has a thermal conductivity coefficient lower than concrete on a larger aggregate (Figure 8).

The optimal value of the fraction of fine aggregate for obtaining concrete of the lowest density is 0.25, the lowest coefficient of thermal conductivity is 0.50. With an increase in the fraction of fine aggregate from 0.25 to 0.50, the coefficient of thermal conductivity of slag concrete decreases by 10-12%, with an increase in the density of concrete by 5-6%.

The conducted studies suggest that the use of slag sand as fine aggregate for structural and heat-insulating concrete with optimal composition selection should not lead to an increase in the thermal conductivity, despite a significant increase in density. This is due to the increased, against slag crushed stone, the glass content in the slag sand, the phenomenon is explained by the fact that, firstly, with an increase in the cooling rate of the slag melt, the glass content in the composition of the slag material increases. Thus, the part of the sand resulting from granulation upon direct contact of the slag melt with a large amount of water is more glass-containing than the slag crushed stone formed at

a relatively low cooling rate of the melt with a lack of water.

Secondly, when crushing a slag block, glass-containing inclusions are subject to greater more considerable grinding, which, when sifted, are also released into slag sand.

According to (Fedoseev, 2010) the lowest thermal conductivity is characterized by lightweight concrete with aggregate containing 20% of grains of 1.2–5 mm fraction and 80% of grains of 5–20 mm while maintaining the strength of concrete.

In mortars and concrete, cement particles surround the aggregate, so the thermal conductivity of cement stone has a significant effect on the thermal conductivity of concrete.

Concrete of the same composition, in different Portland cements, has different thermal conductivity coefficients. Thus, the thermal conductivity on slag cement was 30% lower than when using conventional Portland cement (Figure 9).

This is due to the fact that cement has a different amount of fiberglass slag. In addition, the increase in the number of crystals can lead to an increase by an average of 10% in the thermal conductivity of cement stone, the same density with an increase in the type of cement.

Studies of the effect of cement on the thermal conductivity of heavy concrete revealed that with an increase in the amount of cement, an increase in thermal conductivity is initially observed, which is a consequence of filling air voids. Then, having reached a certain limit (about 500 kg/m³), a decrease in thermal conductivity occurred, since concrete aggregates have higher thermal conductivity than cement stone.

3. RESULTS AND DISCUSSION

The aggregate has a noticeable effect on the structure formation of lightweight concrete after hardening of the concrete mix. He creates a rigid frame, strengthening the structure at the first stage of its formation; its presence significantly affects the hardening conditions of cement stone. In concrete, the interaction of cement and water and its hardening occur in thin layers between the grains of the aggregate with full interaction with it.

The thermal conductivity coefficients of the grains of porous aggregates depend on their type, density, and pore structure. The conducted studies suggest that the use of slag sand as fine

aggregate for structural and heat-insulating concrete with optimal composition selection should not lead to an increase in the thermal conductivity, despite a significant increase in density.

Increasing the thermal resistance of the walls of the solid base by reducing their cross-section, the deterioration of the contacts between the walls of the skeleton also significantly improve its thermal conductivity. The most important goal of thermal insulation of building structures is to reduce energy consumption for heating a building. In construction, thermal insulation reduces the thickness of building envelopes.

4. CONCLUSIONS

The thermal conductivity of porous aggregates, like other porous bodies, is affected by the quantity and quality (size) of air pores and humidity. The phase composition of the material has a noticeable effect. An anomaly in the coefficient of thermal conductivity is associated with the presence of a vitreous phase. The larger the glass, the lower the thermal conductivity coefficient for the aggregate of the same density. In order to stimulate the production of aggregates with the best thermal insulation properties for concrete claddings, it is proposed to standardize the content of slag glass (for example, for high-quality slag pumice stone 60-80%).

Therefore, with other conditions unchanged, the thermal conductivity of the material is determined not only by the amount of glass phase but also by other parameters of the phase structure of the material. For example, it was found that to reduce thermal conductivity, not only the total amount of glass contained in the aggregate is significant, but also its distribution. The most advantageous from this point of view is the case when the vitreous membranes cover the walls of pores and capillaries with at least a thin layer since, in this case, the heat transfer by radiation will decrease. It is also important that the pore walls not only have a porous and porphyritic structure so that crystalline inclusions are separated from each other by at least thin glassy layers. The thermal conductivity coefficients of crystals and glasses with the same chemical composition differ very significantly.

5. ACKNOWLEDGMENTS:

The authors are grateful to the leadership of the Kazakh National Research Technical

University named after K. I. Satpayev (Satbayev University) for creating the conditions for carrying out this work at an accredited research laboratory of architecture and construction (NILAS).

6. REFERENCES:

1. Petrov V. P., Makridin N. I., Yarmakovskiy V. N. Porous aggregates, and concrete. Materials science. Production technology. Tutorial. Samara State University of Architecture and Civil Engineering, EBS DIA. 2009.
2. GOST 9758 – 2012. Inorganic porous aggregates for construction work. Test methods. 2012.
3. CN&R 23-02-2003. Thermal protection of buildings. M.: Gosstroy of Russia, 2004. 40 p.
4. Dvorkin L. I., Dvorkin O. L. Special concretes. Infra Engineering. 2013.
5. Bazhenov Yu. M., Alimov L. A., Voronin V.V. The structure and properties of concrete with nanomodifiers based on industrial waste. Monograph. Moscow State University of Civil Engineering, EBS DIA. 2013.
6. GOST 32496 – 2013. Porous aggregates for lightweight concrete. Technical conditions. 2013.
7. Zotkin A. G. Concrete with effective additives. Infra Engineering. 2014.
8. Nesvetaev G.V., Davidiyuk A.N. Effective glassy porous aggregates, and concrete based on them. Monograph. RSSU. 2012.
9. STO 08.23.02-2009. Wall stones from light sandless expanded clay concrete. Samara: SSASU, 2009. 282 p.
10. Maksimov B.A., Korenkova S.F., Petrov V.P. The effect of crystallization on the properties of slag-sites. University News. Construction and architecture. 2004. No. 4. p.p. 61–65.
11. Gorin V. M., Tokareva S. A., Vytchikov Yu.S., Shiyonov L.L., Belyakov I. G. The use of wall stones from sandless expanded clay concrete in housing construction // Builds. materials. 2010. No. 2. p.p. 12–13.
12. GOST 10832 – 2009. Sand and expanded perlite crushed stone. Technical specifications.
13. Gorin V. M., Tokareva S. A., Vytchikov Yu. S. Modern building envelopes made of expanded clay for energy-efficient buildings // Building materials. 2011. No. 3. P. 34–36.
14. Petrov V. P., Makridin N. I., Yarmakovskiy V. N. Porous aggregates, and lightweight concrete. Materials Science. Production technology. Tutorial. Samara: SSASU, 2009. 436 p.
15. Rogovoi M. I. Technology of artificial porous aggregates and ceramics. Transport company. 2016. 320 p. ISBN: 9785436500201.
16. Mikulsky V. G. and other Building materials and products - M.: Publishing house ASV, 2007. -520 p.
17. Bazhenov Yu.M. Concrete technology. – M.: Higher. school, 2002. - 500 p.
18. Bobrov Yu. L., Ovcharenko E. G., Shoikhet B. M., Petukhova E. Yu. Thermal insulation materials and structures. – M.: INFRA - M, 2003. -- 268 p.
19. Bazhenov Yu. M., Alimov L.A., Voronin V. V., Magdeev U. Kh. Technology of concrete, building products, and structures. - M.: DIA, 2004. - 256 p.
20. Eremkin A. I., Koroleva T. I. Thermal conditions of buildings: a manual. - M.: Publishing House ACB, 2000 - 368 p.
21. GOST 25820-2014. Light concrete. Technical conditions.
22. GOST 27005 – 2014. Concrete light and cellular. Rules for controlling average density.
23. Davidiyuk A. N. Structurally-heat-insulating lightweight concrete based on glassy porous aggregates. Abstract of dissertation for the degree. Rostov-on-Don, 2010.
24. Orentlicher L. P. XXI century - the century of light concrete: Concrete technology, 2010. No. 01-02, p.p.29-31.
25. Alekseev V. A. Lightweight concrete technology with aggregate based on granular foam glass: abstract book. MGSU (NRU). 2010. p.p. 54-58.
26. Surkov V. N. Prospects for the development of cellular concrete: Concrete and reinforced concrete, 2009. No. 4, p.p.12-15.
27. Fedoseev A. S. Development of new building materials: collection of abstracts. MGSU (NRU), 2010. 157-160 p.p.

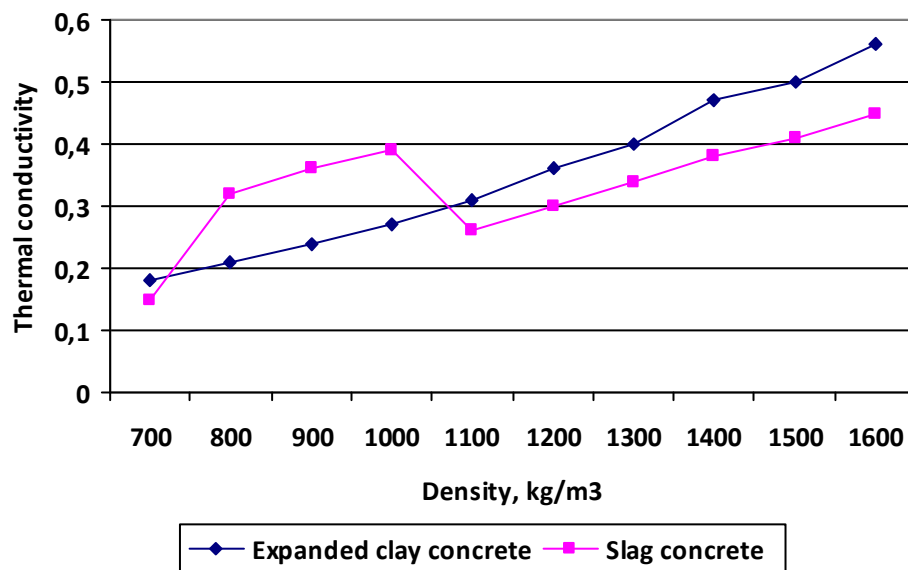


Figure 1. The dependence between thermal conductivity and density

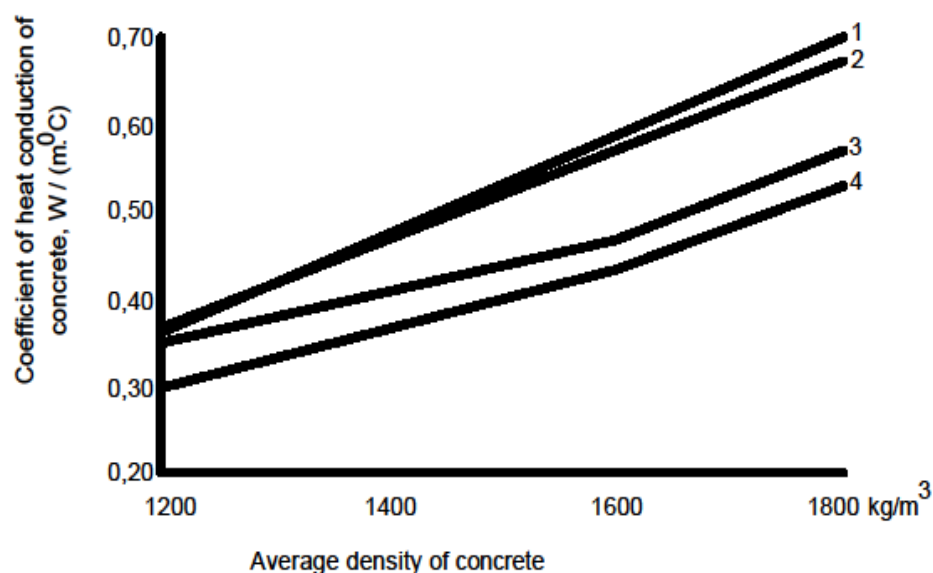


Figure 2. The dependence of the thermal conductivity (heat conduction) of concrete on their density (according to CN&R P-3-79).

1 - agloporiton concrete and concrete on fuel (boiler) slag; 2 - expanded clay concrete on expanded clay sand; 3 - concrete on blast furnace granulated slag; 4 - slag concrete.

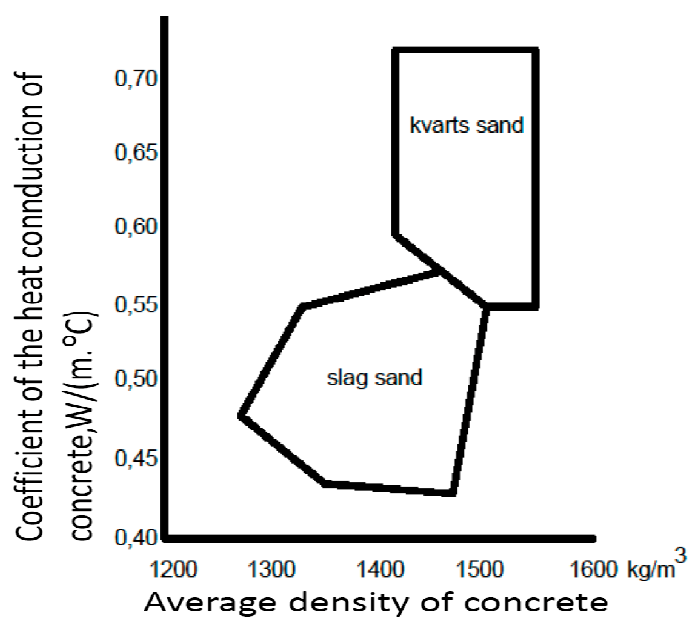


Figure 3. The thermal conductivity (heat conduction) of concrete with different fine aggregate

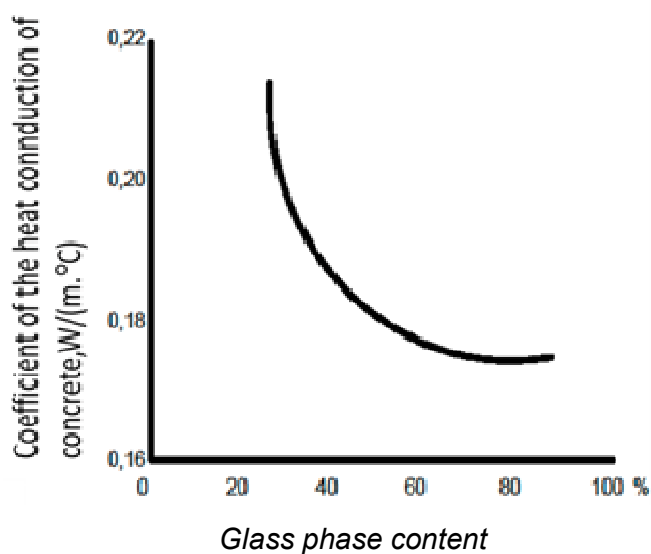


Figure 4. The effect of the glass phase content on the thermal conductivity (heat conduction) of the slag fraction 0-10 mm

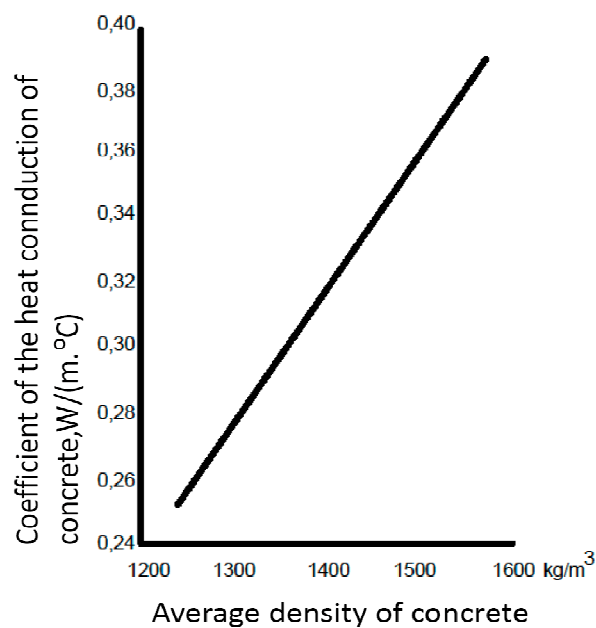


Figure 5. The dependence of the thermal conductivity (heat conduction) of concrete on its density and quality of slag pumice

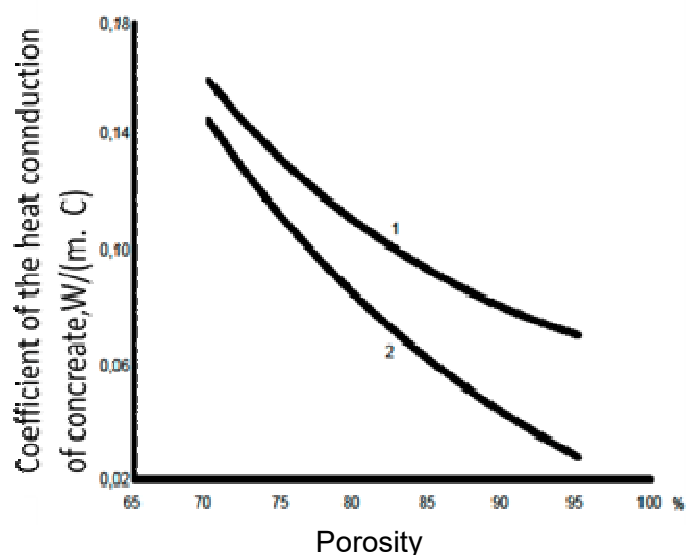


Figure 6. The dependence of the coefficient of thermal conductivity (heat conduction) on porosity for materials of cellular structure.
1 - burnt brick; 2 - heat-insulating masses

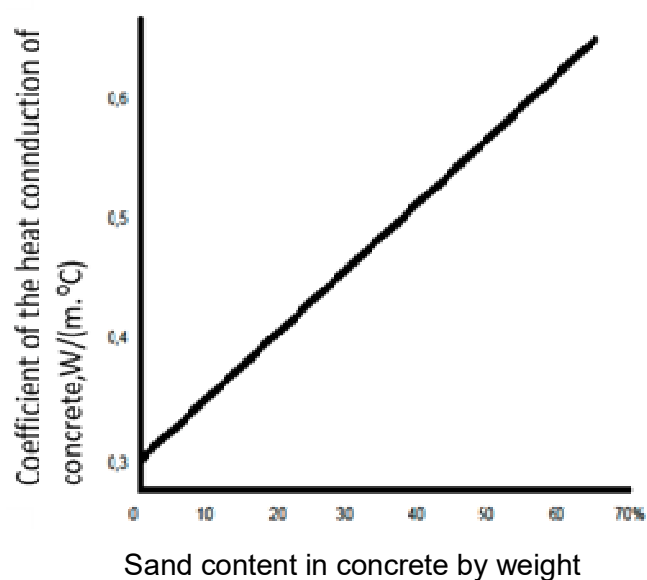


Figure 7. Dependence of the thermal conductivity (heat conduction) of slag concrete on the particle size distribution of aggregates

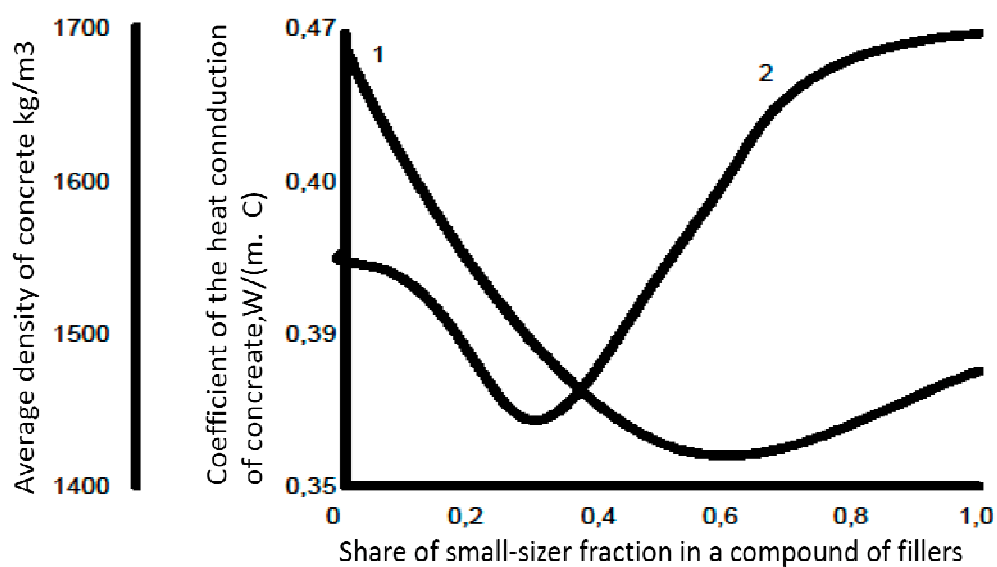


Figure 8. The dependence of the density and thermal conductivity (heat conduction) coefficient of structural and heat-insulating slag concrete on the fraction of the fine fraction

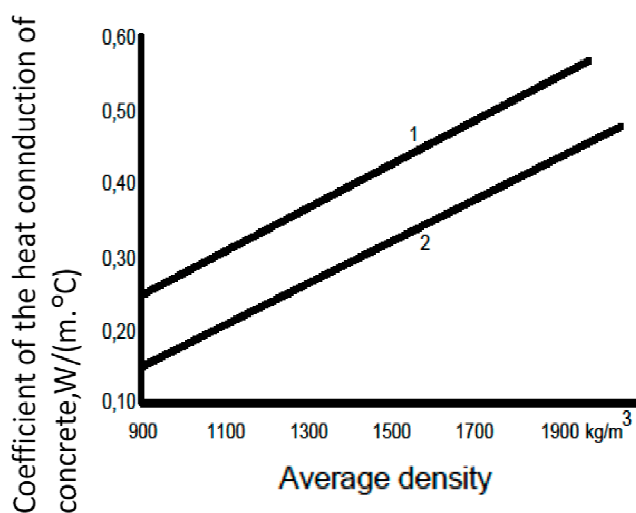


Figure 9. The dependence of thermal conductivity (heat conduction) of concrete
1 - on portland cement; 2- on slag cement

Table 1. The thermal conductivity of compounds at 0 °C

Condition	Compound	Coefficient of thermal conductivity, W/(m·°C)
Crystalline	SiO ₂	9.3
	MgO	38.8
	Al ₂ O ₃	9.1
	CaO	7.98
Vitreous (glassy)	SiO ₂	1.49
	MgO	1.2
	Al ₂ O ₃	0.55
	CaO	0.72

Table 2. The dependence of the coefficient of thermal conductivity of air in closed pores on the pore diameter at 0 °C

Thermal conductivity, W/(m·°C)	Pore diameter, mm					
	Without pore	0.1	0.5	1	2	5
Absolute	0.02	0.022	0.023	0.03	0.03	0.04
Relative	0.92	1.02	1.12	1.14	1.34	1.90

MONITORAMENTO E RELACIONAMENTO DOS PARÂMETROS DQO E DBO₅ EM AFLUENTE E ESGOTO TRATADO DAS CIDADES DE ITAJUBÁ E PEDRALVA, MG

MONITORING AND RELATIONSHIP OF COD AND BOD₅ PARAMETERS IN AFLUENT AND TREATED SEWAGE FROM ITAJUBÁ AND PEDRALVA CITIES, MG

BUDEIZ, Victor; AGUIAR, André*

Universidade Federal de Itajubá, Instituto de Recursos Naturais

* Autor correspondente

e-mail: andrepiranga@yahoo.com.br

Received 30 July 2019; received in revised form 09 January 2020; accepted 29 January 2020

RESUMO

Uma das principais características avaliadas no tratamento de esgotos municipais consiste no teor de matéria orgânica, geralmente baseado nas análises de Demandas Química e Bioquímica de Oxigênio, DQO e DBO respectivamente. O objetivo deste trabalho foi analisar e comparar a relação entre os parâmetros DQO e DBO₅ para esgotos domésticos brutos (afluentes) e tratados de duas estações de tratamento de esgoto (ETEs) pertencentes às cidades de Itajubá e Pedralva, ambas localizadas no sul de Minas Gerais, Brasil. Em função dos dados obtidos ao longo de dois anos junto à companhia de saneamento do Estado, analisaram-se as razões e a correlação linear entre DQO e DBO₅, assim como suas remoções percentuais como forma de verificar a eficiência das ETEs. Foram verificadas razões médias DQO/DBO₅ de 2,13 e 2,20 para os afluentes das ETEs de Itajubá e Pedralva, respectivamente. Esses valores estão na faixa típica de esgoto bruto doméstico, não sendo encontrados indícios de contribuição industrial. Os valores de coeficiente de correlação linear (R^2) entre os parâmetros DQO e DBO₅ para o esgoto bruto de Itajubá e Pedralva foram 0,8585 e 0,4863, respectivamente, sugerindo que pode-se estimar a DBO₅ a partir da DQO para a ETE da primeira cidade ($R^2 > 0.8$). Para as amostras de esgoto tratado de ambas as ETEs não se recomenda tal abordagem, pois os valores de R^2 foram menores que 0.3. De acordo com a legislação estadual vigente (COPAM/CERH nº 1), as duas ETEs removeram eficientemente a DBO₅, enquanto a ETE de Itajubá apresentou remoção de DQO levemente abaixo do estipulado. Em relação à legislação federal (CONAMA nº 430), ambas as ETEs reduziram eficientemente a DBO₅.

Palavras-chave: *Demanda química de oxigênio; Demanda bioquímica de oxigênio; Índice de biodegradabilidade; Esgoto doméstico; Efluente industrial.*

ABSTRACT

One of the main characteristics evaluated in municipal sewage treatment is the organic matter content, usually based on the analysis of Chemical and Biochemical Oxygen Demands, COD, and BOD respectively. The objective of this work was to analyze and compare the relation between the COD and BOD parameters for raw sewage (effluent) and treated sewage of two wastewater treatment plants (WWTPs) of the cities of Itajubá and Pedralva, both localized in the south of Minas Gerais, Brazil. Due to the data obtained over two years from the state sanitation company, the analysis of ratios and linear correlation between COD and BOD₅ were performed, as well as their removal (%) to verify the WWTP efficiencies. The COD/BOD₅ value of 2.13 was obtained for the affluent of Itajubá city, while for Pedralva was 2.20. These values are common at the typical range of raw domestic wastewater, and no evidence of industrial contribution was found. The values of the linear correlation coefficient (R^2) between the COD and BOD₅ parameters for affluent of Itajubá and Pedralva were 0.8585 and 0.4863, respectively, suggesting that BOD₅ value can be estimated from COD only in the first case ($R^2 > 0.8$). For treated sewage samples from both WWTPs, this approach is not appropriate because the R^2 values were lower than 0.3. According to current state legislation (COPAM/CERH nº 01), the two WWTPs efficiently removed the BOD₅, while Itajubá WWTP showed COD removal slightly below the stipulated. Following federal legislation (CONAMA nº 430), both WWTPs have efficiently removed BOD₅.

Keywords: *Chemical oxygen demand; Biochemical oxygen demand; Biodegradability index; Domestic wastewater; Industrial effluent.*

1. INTRODUÇÃO:

Atualmente, em torno de 4,5 bilhões de pessoas não usufruem de um sistema de coleta e tratamento de esgoto gerido de forma segura no mundo (ONU, 2019). No Brasil, a falta de saneamento básico em determinadas localidades, principalmente em regiões mais carentes como a Norte, favorece a manifestação de diversas doenças de veiculação hídrica (Sousa *et al.*, 2018). Problemas correlatos à falta de saneamento também são comuns na região Sul (Rudy e Goulart, 2018). Nesse contexto, a ausência ou até mesmo a ineficiência de tratamento de esgoto e saneamento básico podem contribuir para a propagação de inúmeras doenças parasitárias e infecciosas, além da degradação do corpo hídrico (Pinho *et al.*, 2017; Rudy e Goulart, 2018). Projeto, instalação e operação confiáveis de um sistema de coleta e tratamento de esgoto devem propiciar a melhoria do saneamento básico e da saúde global, que por sua vez levam à diminuição da proliferação dessas doenças de veiculação hídrica e com isso aliviar o sistema de saúde (Soares *et al.*, 2002; Pereira *et al.*, 2018).

O lançamento sem tratamento prévio do esgoto num corpo hídrico pode ser muito danoso também ao meio ambiente. Alta concentração de matéria orgânica favorece a multiplicação de bactérias heterotróficas, reduzindo o oxigênio dissolvido necessário para a sobrevivência de organismos aquáticos superiores. O excesso de nutrientes a base de nitrogênio e fósforo pode proporcionar a eutrofização, que corresponde ao crescimento acelerado de organismos aquáticos autotróficos, particularmente algas planctônicas e ervas aquáticas. Esses organismos conferem odor, turbidez, reduzem a penetração de luz, a fotossíntese e consequentemente o oxigênio do meio, aspectos esses que impactam de forma negativa o ecossistema (Jordão e Pessoa, 2011). Apesar de os mananciais possuírem capacidade de autodepuração, ou seja, degradação de matéria orgânica carbonácea e remoção de nutrientes, os mesmos não toleram concentrações elevadas desses poluentes (Pinho *et al.*, 2017). A partir disso, o tratamento do esgoto sanitário é uma medida fundamental para se prevenir as inúmeras patologias e desequilíbrios possíveis de um descarte incorreto de esgoto sanitário e de efluentes.

Existem diversos métodos que permitem o tratamento de águas residuárias. As instalações com esse propósito são conhecidas por Estações de Tratamento de Esgoto (ETEs). Os tratamentos

podem ser preliminares, visando principalmente a remoção de materiais mais grosseiros; como exemplo tem-se o uso de grades e os desarenadores. Em seguida, têm-se os tratamentos primários para remoção de material sedimentável ou flutuante; podem ser usados os decantadores ou flotadores, respectivamente. Tratamentos secundários consistem na remoção de matéria orgânica biodegradável, dissolvida ou em suspensão, por ação predominante de bactérias. Polimentos ou tratamentos terciários podem ser empregados, a depender da eficiência das etapas anteriores, assim como das características do corpo receptor (Archela *et al.*, 2003; Jordão e Pessoa, 2011; Pinho *et al.*, 2017). Em resumo, a decisão de quais operações unitárias requeridas deve se basear nas características do curso d'água, capacidade de autodepuração do mesmo e dos limites definidos pela legislação para o descarte (Pinho *et al.*, 2017; Moraes e Santos, 2019).

A nível federal, a resolução nº 357 do Conselho Nacional do Meio Ambiente (CONAMA, 2005) dispõe sobre a classificação dos corpos hídricos e diretrizes ambientais para o seu enquadramento, além de estabelecer as condições e padrões de lançamento de efluentes. No ano de 2011, a resolução nº 430 complementou e alterou a resolução de 2005, dispondo sobre as condições e padrões de lançamento de efluentes (CONAMA, 2011). Além disso, cada estado ou município pode apresentar sua legislação própria ou complementar à federal (Moraes e Santos, 2019). Por exemplo, o Conselho Estadual de Política Ambiental (COPAM) e o Conselho Estadual de Recursos Hídricos (CERH) de Minas Gerais fazem uso da Deliberação Normativa Conjunta COPAM/CERH-MG nº 01 (2008) que dispõe sobre a classificação dos corpos hídricos e diretrizes ambientais para o seu enquadramento, bem como estabelece condições e padrões de lançamento de efluentes nesse estado.

O conhecimento sobre as características dos esgotos que chegam às ETEs é fundamental para o projeto e a operação de forma eficiente das mesmas. Usualmente para se determinar a quantidade de matéria orgânica presente em águas residuárias faz-se uso dos parâmetros de Demandas Bioquímica e Química de Oxigênio, DBO e DQO respectivamente. A DBO é a quantidade de oxigênio necessária para oxidar a matéria orgânica por meio da decomposição microbiana aeróbia em um determinado tempo e temperatura estabelecidos. Para efeitos de comparação e praticidade, padronizou-se o

ensaio incubando-se a amostra à 20 °C por 5 dias (DBO₅). A DBO₅ em mg L⁻¹ pode ser calculada pela equação 1:

$$DBO_5 = (OD_1 - OD_2)/P \quad (1)$$

onde OD₁ corresponde a concentração de oxigênio dissolvido da amostra diluída; OD₂ à concentração residual de oxigênio dissolvido na amostra após transcorridos 5 dias e; P é a fração de amostra em relação ao volume total do frasco (Jordão e Pessoa, 2011).

A DQO refere-se à quantidade de oxigênio necessária para a oxidação da matéria orgânica por um agente químico, geralmente dicromato de potássio (Jordão e Pessoa, 2011). A oxidação de uma determinada substância orgânica (C_xH_yO_z) contida em águas no ensaio de DQO pode ser representada pela equação 2, onde $n = 4x + y - 2z$. Por convenção, o número de equivalentes de dicromato reduzido (n) corresponde ao número de equivalentes de oxigênio que seria consumido. Após a reação, a DQO é determinada a partir do dicromato residual (titulometria) ou do Cr³⁺ formado (colorimetria) (Zuccari *et al.*, 2005).

A DBO corresponde ao teor de matéria orgânica biodegradável, enquanto a DQO ao teor de matéria orgânica biodegradável mais a fração não-biodegradável (Jordão e Pessoa, 2011; Zuccari *et al.*, 2005; Quintana *et al.*, 2018; von Sperling, 2014). O custo envolvido na análise de DBO é cerca de 4,5 vezes o custo de uma análise de DQO. Além disso, o tempo necessário para a obtenção de resultados de DBO é de 5 dias no mínimo, enquanto o de DQO é no mínimo 2 h (Silva e Mendonça, 2003).

Uma relação importante entre esses parâmetros, a razão DQO/DBO₅, varia de acordo com o uso ao qual a água foi submetida. Para águas residuárias de origem doméstica, essa razão varia de 1,7 a 2,4. Com base nesse intervalo, uma fração significativa da matéria orgânica poderia ser removida por tratamentos biológicos, os quais são eficientes e de baixo custo (von Sperling, 2014). Por outro lado, valores acima desta faixa indicam recalcitrância dos componentes ou também pode indicar contribuição de efluente industrial (Jordão e Pessoa, 2011), o que prejudicaria a execução de tratamentos biológicos nas ETES devido à toxicidade de certas substâncias sobre os microrganismos. Ao inverter essa razão, ela é conhecida por índice de biodegradabilidade (DBO₅/DQO), a qual também serve para mensurar a biodegradabilidade de águas residuárias (Silva e Mendonça, 2003).

Em vista do exposto, o presente trabalho teve como objetivo realizar um estudo envolvendo os parâmetros DQO e DBO₅ nos afluentes e esgotos tratados das cidades de Itajubá e Pedralva, localizadas no sul do estado de Minas Gerais. A primeira possui aproximadamente 96 mil habitantes, além de contar com um parque industrial, enquanto a segunda possui em torno de 11 mil habitantes (IBGE, 2019), mas isenta de indústrias. A eficiência das ETES de cada município será verificada com base na redução desses parâmetros, enquanto a razão entre eles poderá fornecer indícios de presença ou não de efluente industrial, além da biodegradabilidade dos esgotos a serem tratados. Também foi verificada a presença ou não de correlação linear entre os valores de DQO e DBO₅ como forma de facilitar a caracterização de águas residuárias com base no primeiro parâmetro.

2. MATERIAIS E MÉTODOS:

Os dados utilizados referentes ao monitoramento dos parâmetros DQO e DBO₅ dos afluentes e esgotos tratados das ETES Capim Fino, pertencente ao município de Pedralva, e Sapucaí, de Itajubá, foram fornecidos pela COPASA (Companhia de Saneamento de Minas Gerais), a qual é responsável pela operação e administração de ambas as estações.

A Figura 1 consiste num fluxograma contendo as etapas envolvidas na ETE de Pedralva, a qual possui tratamentos preliminares (gradeamento seguido de desarenador), secundários (reator anaeróbio de fluxo ascendente – RAFA seguido de lagoa de estabilização facultativa) até etapas finais de polimento (duas lagoas de polimento em série). Além disso, a mesma possui tratamentos do lodo (leito de secagem) e queimador do biogás, ambos gerados no reator. Para a ETE de Itajubá as etapas são as mesmas, exceto pela ausência das lagoas facultativa e de polimentos, sendo que o esgoto tratado que sai do reator é descartado diretamente no corpo receptor.

As Figuras 2 e 3 mostram imagens por satélite de ambas as ETES constando suas principais etapas em destaque.



Figura 2. Vista aérea da ETE Capim Fino (Pedralva-MG): A – Grade + Desarenador; B – Reator Anaeróbio; C – Lagoa de Estabilização Facultativa; D e E – Lagoas de Polimento em Série; F – Leito de Secagem do Lodo; G – Queimador do Biogás. Fonte: Google Earth.



Figura 3. Vista aérea da ETE Sapucaí (Itajubá-MG): A – Gradeamento + Desarenador; B – Reatores Anaeróbios em Paralelo (4); C – Leitos de Secagem do Lodo; D – Queimador do Biogás. Fonte: Google Earth.

Para a ETE Sapucaí, a COPASA coletou 25 amostras mensais, no período de maio de 2016 a maio de 2018, realizando análises dos parâmetros supracitados. Para a ETE Capim Fino, a COPASA coletou 11 amostras, uma vez que o monitoramento dos parâmetros é realizado a cada dois meses para a mesma. Os dados para esta ETE compreenderam de junho de 2016 a abril de 2018. Ainda segundo a COPASA, utilizaram-se os métodos 5210 B e 5220 D para se determinar respectivamente DBO_5 e DQO. Esses métodos estão descritos no *Standard Methods for the Examination of Water and Wastewater* (Clesceri et al., 1998).

A interpretação destas informações foi realizada por meio do *software Microsoft Excel 2016*, o qual permitiu o desenvolvimento matemático dos dados de DBO_5 e DQO para verificar a presença ou não de correlação linear. Além disso, foram calculadas as porcentagens de remoção desses parâmetros e as razões entre os mesmos.

A partir dos valores de DBO_5 e DQO, verificou-se o atendimento do tratamento de esgoto frente às legislações vigentes estadual (COPAM/CERH-MG nº 01, 2008) e federal (CONAMA nº 430, 2011).

3. RESULTADOS E DISCUSSÃO:

Além dos dados de DBO_5 e DQO referentes aos afluentes e efluentes das ETES Sapucaí e Capim Fino, a COPASA informou a data de coleta das amostras e o tempo meteorológico para eventuais discussões. Em seguida, realizaram-se os cálculos das razões DQO/DBO_5 , DBO_5/DQO e das remoções percentuais de DBO_5 e DQO com base no mesmo dia de coleta. As Tabelas 1 e 2 apresentam os dados descritivos da ETE de Itajubá e Pedralva referentes aos afluentes, respectivamente.

O parâmetro DBO_5 para esgotos predominantemente sanitários situa-se na faixa de 250 a 400 $mg\ L^{-1}$ (von Sperling, 2014), e no presente trabalho o valor médio observado para a ETE de Itajubá foi de 300 $mg\ L^{-1}$. Com relação à DQO, o valor médio foi de 609 $mg\ L^{-1}$, dentro da faixa da literatura, a qual compreende de 450 a 800 $mg\ L^{-1}$ (von Sperling, 2014). Dessa forma, os valores médios para essa ETE estão dentro da faixa usual. No entanto, os resultados apresentados pela ETE de Pedralva possuem valores médios acima da faixa típica, uma vez que a DBO_5 e a DQO nos afluentes foram respectivamente 420 e 911 $mg\ L^{-1}$. Por outro lado, em algumas amostragens observaram-se

também valores de DBO₅ e DQO abaixo da faixa típica. Não foi possível encontrar padrões de interferência de sazonalidade que justificassem os valores apresentados para a ETE de Pedralva. No entanto, foi possível observar que em dias chuvosos ou nublados os valores de DQO e DBO₅ para esgoto bruto de Itajubá foram geralmente menores.

A razão DQO/DBO₅ para o afluente da ETE de Itajubá está compreendida entre 1,37 a 3,39, com média de 2,13. Para o afluente da ETE de Pedralva a razão possui média de 2,20, com valores entre 1,65 e 3,21. Segundo von Sperling (2014), esses valores médios estão de acordo com o valor típico de esgotos domésticos brutos e também está justificada a utilização do tratamento biológico pelas estações, uma vez que o índice médio é menor que 2,5. Tais valores médios são um indicativo de alta biodegradabilidade das amostras de esgoto e, portanto, a realização de tratamento biológico para os mesmos é apropriada (von Sperling, 2014). Penido *et al.* (2018) encontrou um valor médio de 1,7 para DQO/DBO₅ a partir de esgoto da ETE Onça de Santa Luzia (MG), representando uma maior biodegradabilidade frente às amostras de esgoto de Itajubá e Pedralva. Os valores médios de DQO e DBO₅ reportados por esses autores estão praticamente na faixa típica, assim como foi observado para a ETE de Itajubá.

Ambas as ETEs apresentaram valores de razão DQO/DBO₅ acima de 2,5 em alguns dos meses. Segundo a literatura (Jordão e Pessoa, 2011; Zucacari *et al.*, 2005; Quintana *et al.*, 2018; Von Sperling, 2014), esses valores podem indicar a presença de efluentes industriais no esgoto ou, mais comumente, a uma menor fração de matéria orgânica biodegradável inerente à amostra. No entanto, sabe-se que a cidade de Pedralva não conta com a instalação de indústrias. Sendo assim, essa razão pode não ser apropriada para afirmar se há contribuição de efluente industrial em ETEs, inclusive para cidades industrializadas, como é o caso de Itajubá, no presente trabalho, e também Jundiaí (SP), para a qual também foram verificados valores DQO/DBO₅ acima de 2,5 (Giansante, 2002).

Apesar da razão mencionada anteriormente indicar a biodegradabilidade de esgotos domésticos e efluentes industriais, o seu inverso (DBO₅/DQO) é também usual. Observou-se que os índices médios de biodegradabilidade dos afluentes das ETEs de Itajubá e de Pedralva foram respectivamente 0,50 e 0,47. Silva e Mendonça (2003) monitoraram seis ETEs na região da grande Vitória-ES, obtendo para esgoto

bruto um índice de biodegradabilidade médio igual a 0,47, mesmo valor encontrado para duas ETEs de Araraquara-SP (Scalize *et al.*, 2004). Índices nessa faixa indicam que os esgotos brutos das quatro cidades, incluindo Itajubá e Pedralva, podem ser tratados biologicamente (von Sperling, 2014). Ao estudar oito ETEs do Egito, Abdalla e Hammam (2014) encontraram índices numa faixa de 0,30 a 0,96, com valor médio igual a 0,67. Desta forma, os índices de biodegradabilidade apresentados pelas ETEs de Itajubá e Pedralva estão entre os valores observados por outros autores.

Os dados referentes às amostras de esgoto tratado são apresentados nas Tabelas 3 e 4. Ao compará-los com aqueles encontrados para afluentes, foram observadas reduções de DBO₅ e DQO em função dos tratamentos empregados nas duas ETEs para todos os meses avaliados. De acordo com a Deliberação Normativa Conjunta COPAM/CERH-MG nº 1, de 05 de Maio de 2008, o descarte de matéria orgânica deve atender os limites máximos de 60 mg L⁻¹ para DBO₅ e 180 mg L⁻¹ para DQO. Conforme os dados para esgoto tratado, a maior parte deles atende a deliberação do COPAM/CERH-MG. No entanto, quando não se atende a remoção estipulada, a mesma deliberação determina para sistemas de esgotos sanitários uma remoção mínima de 60% para DBO₅, com média anual de 70%, e de 55% para DQO, com média anual de 65%. Baseado neste critério, casos pontuais de não atendimento à legislação ocorreram por parte da ETE de Itajubá, enquanto a ETE de Pedralva atendeu totalmente no período avaliado.

Quanto às remoções médias, obtiveram-se os valores para a ETE de Itajubá de 76% e 63% para DBO₅ e DQO, respectivamente, enquanto para a ETE de Pedralva foram 93% e 77%. A maior eficiência da segunda ETE é provavelmente devida aos tratamentos biológicos adicionais: uma lagoa de estabilização facultativa e duas lagoas de polimento. Geralmente, processos anaeróbios como o RAFA costumam remover até 70% de matéria orgânica, necessitando muitas vezes de tratamentos posteriores (Jordão e Pessoa, 2011; von Sperling 2014). No caso da ETE de Pedralva, a mesma conta com etapas adicionais que promoveram mais de 90% e quase 80% nas remoções de DBO₅ e DQO, respectivamente. As remoções de DBO₅ apresentadas pelas ETEs atenderam a deliberação nº 01 COPAM/CERH-MG, uma vez que são maiores do que os 70% de média anual exigido. Contudo, a remoção de DQO pela ETE de Itajubá está levemente abaixo de 65%. É importante frisar que as amostras

coletadas e analisadas de esgoto bruto e tratado foram realizadas em intervalos mensais, podendo não representar precisamente a remoção de matéria orgânica ocorrida. Estudos realizados anteriormente, com o propósito de avaliar outras ETEs brasileiras, também observaram eficiência (Oliveira *et al.*, 2016; Marçal e Silva, 2017; Ribeiro e Silva, 2018), mas também ineficiência na remoção de matéria orgânica (Orssatto *et al.*, 2009; Tardivo, 2009; Lopes, 2015; Michalake *et al.*, 2016). Essa é uma constatação de que muitas delas necessitam de melhorias.

A cidade de Pedralva é cortada pelo Ribeirão Anhumas, que nasce nas matas próximas à mesma. Esse ribeirão possui pequeno porte, tendo uma vazão média de aproximadamente 500 L s^{-1} . Por possuir tais características, o tratamento de efluentes realizado na ETE Capim Fino deve possuir de fato uma maior remoção de matéria orgânica quando comparado à ETE Sapucaí, a qual despeja o esgoto tratado no Rio Sapucaí, de maior porte e vazão de $21,33 \text{ m}^3 \text{ s}^{-1}$ próxima à Itajubá (Resumo Executivo, 2010).

Quanto à resolução CONAMA nº 430, as duas ETEs analisadas atenderam o limite máximo de 120 mg L^{-1} de DBO_5 para esgoto tratado ou remoção mínima de 60% do mesmo parâmetro. Entretanto, limite de lançamento ou remoção mínima de DQO não constam na resolução federal. Assim como Minas Gerais, para outros estados e municípios os padrões de lançamento de efluentes são mais rígidos que a legislação federal, adotando padrões adicionais, como é o caso da DQO. Esse aspecto é uma forma de adequação a cada contexto econômico e ambiental (Morais e Santos, 2019).

As amostras de esgoto tratado das ETEs de Itajubá e Pedralva apresentaram índices de biodegradabilidade médios de 0,34 e 0,15 respectivamente. Para a cidade de Vitória (ES), os valores encontrados variaram entre 0,18 e 0,27 (Silva e Mendonça, 2003). Observou-se aqui uma já esperada diminuição nos índices de biodegradabilidade, justificado pelo emprego de tratamentos secundários nas ETEs, os quais visam principalmente a remoção de matéria orgânica biodegradável do esgoto por atuação microbiana e desta forma reduzir mais acentuadamente a carga de DBO_5 em relação à fração de matéria orgânica não biodegradável. Baseado nessa mesma interpretação, a razão DQO/DBO_5 se elevou para os esgotos tratados das duas ETEs.

Procurou-se avaliar também nesse

trabalho uma correlação linear entre os dados de DQO e DBO_5 , pois a obtenção do primeiro parâmetro é mais rápida e prática (Silva e Mendonça, 2003; von Sperling, 2014). Realizou-se então a plotagem dos valores DQO *versus* DBO_5 para os afluentes e também para as amostras de esgoto tratado de cada cidade separadamente. A Figura 4 mostra a plotagem dos dados do afluente da ETE de Itajubá. As equações de ajuste linear dos parâmetros supracitados de ambas as ETEs são mostradas na Tabela 5.

Os parâmetros coletados de DBO_5 e DQO para o esgoto bruto de Itajubá permitiram a obtenção de uma equação de reta que permite estimar a DBO_5 por meio da determinação de DQO, uma vez que o coeficiente de correlação linear é alto. Esse aspecto é bastante relevante, pois a análise de DQO é mais rápida que a DBO_5 e mais barata, podendo conduzir a redução de custos operacionais e maior agilidade em tomadas de decisão sobre medidas de correção operacional. Entretanto, para o afluente da ETE de Pedralva, assim como para o esgoto tratado das duas ETEs, os coeficientes de correlação linear observados foram baixos, contraindicando as respectivas equações obtidas para estimar um parâmetro em função do outro. É importante frisar que a correlação para uma mesma ETE pode variar, pois os parâmetros de DQO e DBO_5 sofrem mudanças condicionadas ao clima, costumes sociais, disponibilidade de água, tamanho da população, presença de indústrias, etc (Abdalla e Hammam, 2014).

A literatura também reporta valores altos de correlação linear entre esses dois parâmetros, principalmente para afluentes. Abdalla e Hammam (2014) observaram para ETEs do Egito valores de R^2 entre 0,64 e 0,983, sendo a maioria deles acima de 0,8. Silva e Mendonça (2003) verificaram que os valores de R^2 para afluentes da maioria das ETEs da grande Vitória (ES) foram entre 0,80 e 0,89, enquanto para a maioria das amostras de esgoto tratado os valores foram inferiores a 0,6. Ao estudar uma ETE de Cascavel (PR), Orssatto *et al.* (2009) obtiveram valores de R^2 iguais a 0,987 e 0,76 para afluente e esgoto tratado, respectivamente. Por outro lado, para uma das ETEs do município de Araraquara (SP) foi possível obter um R^2 igual a 0,81 para o esgoto tratado, enquanto para o esgoto bruto observou-se um valor abaixo de 0,6 (Scalize *et al.*, 2004).

Para efluentes industriais também é possível existir correlação linear entre parâmetros de análise de águas. Para efluentes brutos de diferentes laticínios mineiros, Batista e Aguiar

(2018) observaram um R^2 de 0,9231 a partir dos dados de DBO₅ e DQO. Para efluentes brutos provenientes de quatro indústrias têxteis da China, Liang *et al.* (2018) observaram correlação linear entre DQO e o parâmetro de toxicidade ao obter valores de R^2 superiores a 0,82 para todas elas separadamente.

4. CONCLUSÕES:

Com base nos valores médios dos parâmetros de DBO₅ e DQO, apenas a ETE de Itajubá apresentou valores dentro das faixas típicas de esgoto predominantemente domésticos brasileiros. Esporadicamente, ambas as ETEs apresentaram valores fora da faixa típica. Em termos de eficiência de tratamento, as remoções médias de DBO₅ e DQO foram respectivamente 76% e 63% para a ETE de Itajubá e 93% e 77% para a ETE de Pedralva. A maior remoção na segunda ETE é justificada pelo emprego adicional de uma lagoa facultativa e duas de polimento em série, etapas inexistentes na primeira. Em termos legais, com exceção da remoção um pouco abaixo de 65% de DQO pela ETE de Itajubá (63%), todos os valores estão de acordo com a Deliberação Normativa Conjunta COPAM/CERH nº 01. Em relação à resolução CONAMA nº 430, praticamente todos os valores de DBO₅ para esgoto tratado estão de acordo com a mesma. Os valores médios de DQO/DBO₅ encontrados justificam a viabilidade de tratamentos biológicos empregados nas duas ETEs. Ainda, ressalta-se que foram observados valores de DQO/DBO₅ acima de 2,5, sobretudo para a ETE de Pedralva. Tal razão pode não ser apropriada para assegurar a presença de efluentes industriais na rede de esgoto de nenhuma delas, uma vez que a cidade de Pedralva não possui indústrias. Ao confrontar os dados de DBO₅ e DQO, apenas houve correlação linear para afluentes da ETE de Itajubá ($R^2 = 0,8585$). Desta forma, pode-se usar a equação de reta obtida para estimar a DBO₅ a partir da DQO, de forma a auxiliar na tomada de decisões de operação da própria ETE.

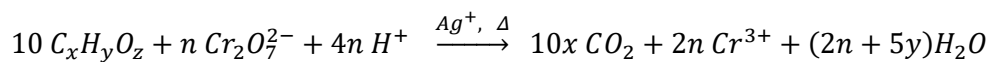
5. AGRADECIMENTOS:

Os autores agradecem à COPASA pelo fornecimento dos dados referentes às ETEs Sapucaí e Capim Fino.

6. REFERÊNCIAS:

1. Abdalla, K. Z., Hammam G. *Int. J. Sci.: Basic Appl. Res.*, **2014**, 13, 42.
2. Archela, E., Carraro, A., Fernandes, F., Barros, O. N. F., Archela, R. S. *Geografia*, **2003**, 12, 517.
3. Batista, N. B. S., Aguiar, A. Trabalhos do 22º Encontro Latino Americano de Iniciação Científica, São José dos Campos, Brasil, **2018**.
4. Clesceri, L. S., Greenberg, A. E., Eaton, A. D. *Standard Methods for the Examination of Water and Wastewater*, 20th ed., American Public Health Association: Washington, **1998**.
5. COPAM/CERH - Conselho Estadual de Política Ambiental/Conselho Estadual de Recursos Hídricos, Deliberação Conjunta nº 01, 2008. Disponível em: <http://www.mma.gov.br/port/conama/processos/EFABF603/DeliberaNormativaConjuntaCOPAM-CERHno01-2008.pdf>, acessada em junho **2019**.
6. Giansante, A. E. Trabalhos do 6º Simpósio Ítalo Brasileiro de Engenharia Sanitária e Ambiental (SIBESA), Espírito Santo, Brasil, **2002**.
7. IBGE - Instituto Brasileiro de Geografia e Estatística. Disponível em: <https://cidades.ibge.gov.br/brasil/mg/pedralva/panorama>, acessada em abril de **2019**.
8. Jordão, E. P., Pessoa, C. A. Tratamento de esgotos domésticos, 6ª ed., ABES: Rio de Janeiro, **2011**.
9. Liang, J., Ning, X., Sun, J., Song, J., Lu, J., Cai, H., Hong, Y. *Ecotoxicol. Environ. Saf.*, **2018**, 166, 56.
10. Lopes, T. R. Dissertação de Mestrado em Tecnologias Ambientais, Universidade Tecnológica Federal do Paraná, Brasil, 2015.
11. Marçal, D. A., Silva, C. E. *Eng. Sanit. Ambient.*, **2017**, 22, 761.
12. Michalake, A. E., Silva, C. R., Silva, F. F. *Ciênc. Nat.*, **2016**, 38, 1560.
13. Morais, N. W. S., Santos, A. B. *Revista DAE*, **2019**, 67, 40.
14. Oliveira, E. M. S., Andrade, E. L. B., Fernandes, A. I. A., Varela Neto, R. F., Villar, S. B. B. L. Trabalhos do 7º Congresso Brasileiro de Gestão Ambiental, Campina Grande, Brasil, **2016**.

15. ONU (2019). Disponível em: <https://nacoesunidas.org/mais-de-2-bilhoes-de-pessoas-no-mundo-sao-privadas-do-direito-a-agua/amp/>, acessada em novembro de **2019**.
16. Orssatto, F., Hermes, E., Vilas Boas, M. A. *Engenharia Ambiental: Pesquisa e Tecnologia*, **2009**, 6, 155.
17. Penido, D. L. A., Marques, M. V. A., Matos, A. T., Costa, M. T. M., Silvério, T. H. R. *Periódico Tchê Quím*, **2018**, 15, 95.
18. Pereira, R. C., Lima, F. C., Rezende, D. *Revista da Faculdade de Educação e Meio Ambiente*, **2018**, 9, 852.
19. Pinho, E. A. S., Ferreira, L. F. R., Américo-Pinheiro, J. H. P., Torres, N. H. *Bioenergia em Revista: Diálogos*, **2017**, 7, 46.
20. Quintana, G. O., Fagnani, E., Candello, F. P., Guimarães, J. R. *J. Braz. Chem. Soc.*, **2018**, 29, 490.
21. Resolução CONAMA nº 430 de 13 de maio de 2011. Disponível em: <http://www2.mma.gov.br/port/conama/legiabre.cfm?codlegi=646>, acessada em novembro de **2019**.
22. Resolução CONAMA nº 357 de 17 de março de 2005. Disponível em: <http://www2.mma.gov.br/port/conama/legiabre.cfm?codlegi=459>, acessada em novembro de **2019**.
23. Resumo Executivo. Disponível em: http://www.igam.mg.gov.br/images/stories/planos_diretores_BH/sapucai.pdf, acessada em janeiro de **2020**.
24. Ribeiro, J. C., Silva, G. H. R. *Eng. Sanit. Ambient.*, **2018**, 23, 27.
25. Rudy, L. M., Goulart, A. A. *Revista UniANDRADE*, **2018**, 20, 18.
26. Scalize, P. S., Leite, W. C. A., Rodrigues, J. M., Correa, M. S., Venuzo, S. B., Lombardi, R., Oliveira, S. C., Santos, M. F. *Trabalhos da 34ª Assembleia Nacional da ASSEMAE*, Rio Grande do Sul, Brasil, **2004**.
27. Silva, S. R., Mendonça, A. S. F. *Eng. Sanit. Ambient.*, **2003**, 8, 213.
28. Soares, S. R. A., Bernardes, R. S., Netto, O. M. C. *Cad. Saúde Pública*, **2002**, 18, 1713.
29. Sousa, E., Ramos, G. O., Santos Júnior, J. S., Beltrão, N. E. S. *R. Gest. Sust. Ambient.*, **2018**, 7, 487.
30. Tardivo, M. Tese de Doutorado em Ciências, Universidade de São Paulo, Brasil, 2009.
31. von Sperling, M. *Introdução à qualidade das águas e ao tratamento de esgotos*. 4ª ed. UFMG: Belo Horizonte, **2014**.
32. Zuccari, M. L., Graner, C. A. F., Leopoldo, P. F. *Eng. Agr.*, **2005**, 20, 69.



Equação 2. Reação envolvida na determinação da DQO a partir do dicromato residual. Fonte: Zuccari et. al (2005).

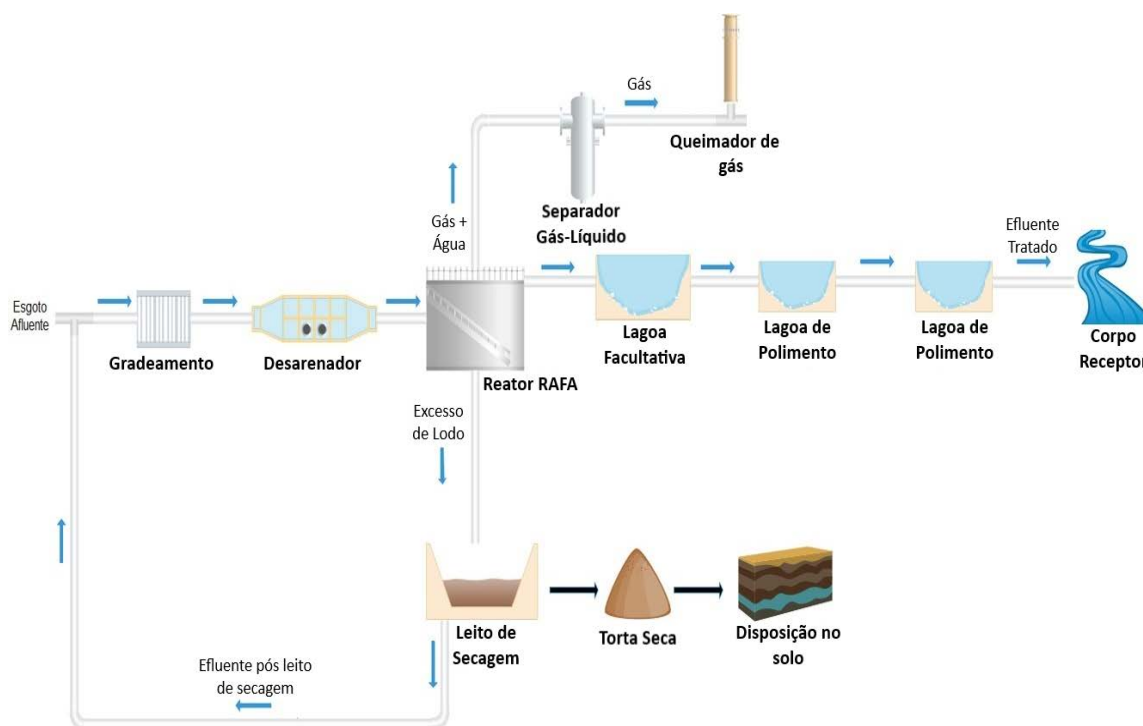


Figura 1. Etapas envolvidas na ETE Capim Fino – Pedralva (MG). RAFA – reator anaeróbico de fluxo ascendente.

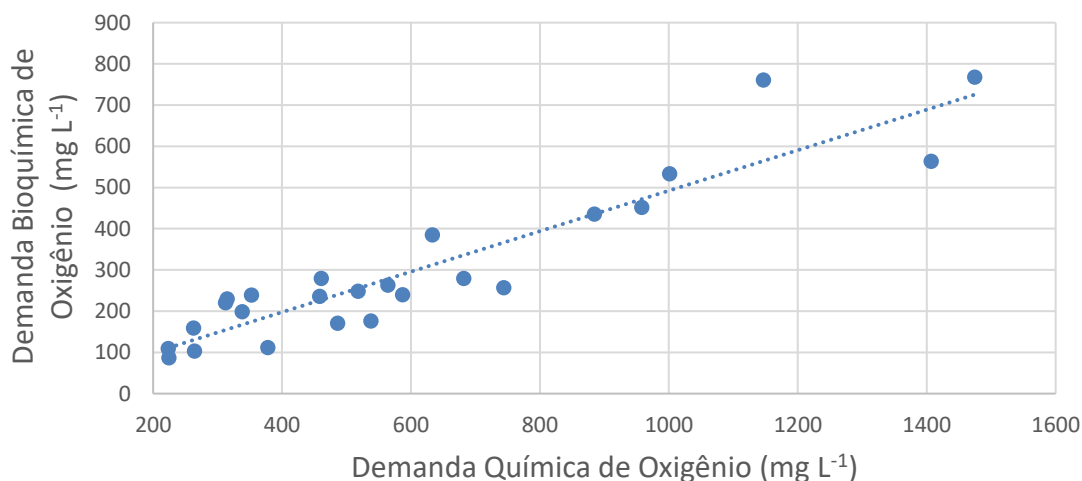


Figura 4. Dados de DQO × DBO₅ para amostras de afluente da ETE Sapucaí – Itajubá (MG).

Tabela 1. Dados descritivos referentes ao afluente da ETE Sapucaí – Itajubá.

Data da coleta	Tempo	DBO ₅ (mg L ⁻¹)	DQO (mg L ⁻¹)	DQO/DBO ₅	DBO ₅ /DQO
11/05/2016	Nublado	257,0	744,0	2,89	0,35
14/06/2016	Bom	248,0	518,0	2,09	0,48
12/07/2016	Bom	278,8	460,8	1,65	0,61
03/08/2016	Bom	451,7	958,3	2,12	0,47
14/09/2016	Bom	384,6	633,0	1,65	0,61
04/10/2016	Nublado	158,6	262,6	1,66	0,60
23/11/2016	Nublado	235,4	458,4	1,95	0,51
06/12/2016	Bom	170,6	486,1	2,85	0,35
18/01/2017	Chuvoso	108,8	223,3	2,05	0,49
15/02/2017	Bom	111,4	377,8	3,39	0,29
07/03/2017	Nublado	86,8	224,7	2,59	0,39
05/04/2017	Bom	175,8	537,7	3,06	0,33
02/05/2017	Bom	229,6	315,1	1,37	0,73
07/06/2017	Bom	239,1	352,8	1,48	0,68
04/07/2017	Bom	278,9	681,9	2,44	0,41
09/08/2017	Bom	563,4	1407,1	2,50	0,40
13/09/2017	Bom	435,3	884,5	2,03	0,49
16/10/2017	Bom	767,9	1474,7	1,92	0,52
07/11/2017	Nublado	220,2	312,2	1,42	0,71
05/12/2017	Bom	532,9	1001,5	1,88	0,53
02/01/2018	Nublado	103,1	264,1	2,56	0,39
20/02/2018	Nublado	198,8	338,0	1,70	0,59
06/03/2018	Bom	760,4	1146,7	1,51	0,66
03/04/2018	Bom	263,1	564,3	2,14	0,47
08/05/2018	Bom	239,6	587,2	2,45	0,41
Média	-	300,0 ± 188,4	608,6 ± 355,3	2,1 ± 0,6	0,5 ± 0,1

Fonte: Dados da pesquisa.

Tabela 2. Dados descritivos referentes ao afluente da ETE Capim Fino – Pedralva.

Data da coleta	Tempo	DBO ₅ (mg L ⁻¹)	DQO (mg L ⁻¹)	DQO/DBO ₅	DBO ₅ /DQO
14/06/2016	Bom	331,0	685,0	2,07	0,48
02/08/2016	Bom	535,7	1081,8	2,02	0,50
08/11/2016	Bom	279,4	658,1	2,36	0,42
20/12/2016	Bom	216,3	553,6	2,56	0,39
07/02/2017	Bom	543,7	1101,5	2,03	0,49
05/04/2017	Bom	411,5	764,6	1,86	0,54
07/06/2017	Bom	454,2	1229,0	2,71	0,37
01/08/2017	Bom	442,4	1419,6	3,21	0,31
05/12/2017	Nublado	440,3	728,2	1,65	0,60
19/02/2018	Nublado	394,8	778,8	1,97	0,51
03/04/2018	Bom	562,6	1019,2	1,81	0,55
Média	-	419,3 ± 110,0	910,9 ± 274,2	2,2 ± 0,5	0,47 ± 0,09

Fonte: Dados da pesquisa.

Tabela 3. Dados descritivos referentes ao esgoto tratado da ETE Sapucaí – Itajubá.

Data da coleta	DBO ₅ (mg L ⁻¹)	DQO (mg L ⁻¹)	DQO/DBO ₅	DBO ₅ /DQO	Remoção de DBO ₅ (%)	Remoção de DQO (%)
11/05/2016	54,0	120,0	2,22	0,45	79,0	83,9
14/06/2016	116,0	255,0	2,20	0,45	53,2	50,8
12/07/2016	74,5	172,3	2,31	0,43	73,3	62,6
03/08/2016	117,6	447,4	3,80	0,26	74,0	53,3
14/09/2016	85,4	239,0	2,80	0,36	77,8	62,2
04/10/2016	45,8	94,0	2,05	0,49	71,1	64,2
23/11/2016	80,2	164,0	2,04	0,49	65,9	64,2
06/12/2016	21,4	123,6	5,78	0,17	87,5	74,6
18/01/2017	33,3	114,6	3,44	0,29	69,4	48,7
15/02/2017	31,3	156,0	4,98	0,20	71,9	58,7
07/03/2017	24,0	101,1	4,21	0,24	72,4	55,0
05/04/2017	41,3	139,3	3,37	0,30	76,5	74,1
02/05/2017	67,3	229,0	3,40	0,29	70,7	27,3
07/06/2017	35,9	243,6	6,79	0,15	85,0	31,0
04/07/2017	85,1	285,4	3,35	0,30	69,5	58,1
09/08/2017	77,4	588,5	7,60	0,13	86,3	58,2
13/09/2017	111,6	170,0	1,52	0,66	74,4	80,8
16/10/2017	55,4	201,0	3,63	0,28	92,8	86,4
07/11/2017	56,5	83,0	1,47	0,68	74,3	73,4
05/12/2017	57,9	237,9	4,11	0,24	89,1	76,2
02/01/2018	29,6	132,1	4,46	0,22	71,3	50,0
20/02/2018	36,20	133,90	3,70	0,27	81,8	60,4
06/03/2018	29,40	64,50	2,19	0,46	96,1	94,4
03/04/2018	97,20	201,20	2,07	0,48	63,1	64,3
08/05/2018	48,00	236,40	4,93	0,20	80,0	59,7
Média	60,5 ± 29,5	197,3± 115,4	3,5 ± 1,6	0,3 ± 0,2	76,3 ± 9,6	62,9 ± 15,7

Fonte: Dados da pesquisa.

Tabela 4. Dados descritivos referentes ao esgoto tratado da ETE Capim Fino – Pedralva.

Data da coleta	DBO ₅ (mg L ⁻¹)	DQO (mg L ⁻¹)	DQO/DBO ₅	DBO ₅ /DQO	Remoção de DBO ₅ (%)	Remoção de DQO (%)
14/06/2016	21,0	160,0	7,62	0,13	93,7	76,6
02/08/2016	41,1	205,3	5,00	0,20	92,3	81,0
08/11/2016	24,8	178,0	7,18	0,14	91,1	73,0
20/12/2016	43,0	244,8	5,69	0,18	80,1	55,8
07/02/2017	20,9	100,2	4,79	0,21	96,2	90,9
05/04/2017	36,2	177,6	4,91	0,20	91,2	76,8
07/06/2017	16,2	238,1	14,70	0,07	96,4	80,6
01/08/2017	19,6	308,4	15,73	0,06	95,6	78,3
05/12/2017	33,2	227,7	6,86	0,15	92,5	68,7
19/02/2018	17,8	142,3	7,99	0,13	95,5	81,7
03/04/2018	21,3	140,3	6,59	0,15	96,2	86,2
Média	26,8 ± 9,7	193,0 ± 59,1	7,9 ± 3,8	0,15 ± 0,05	92,8 ± 4,7	77,2 ± 9,3

Fonte: Dados da pesquisa.

Tabela 5. Ajuste linear a partir dos dados de DBO₅ e DQO para as duas ETEs em estudo.

ETE	Esgoto	Equação de reta	Coefficiente de correlação linear (R ²)
Sapucaí (Itajubá)	Bruto	DBO ₅ = 0,491*DQO + 1,057	0,8585
	Tratado	DBO ₅ = 0,140*DQO + 32,926	0,2992
Capim Fino (Pedralva)	Bruto	DBO ₅ = 0,280*DQO + 164,490	0,4863
	Tratado	DBO ₅ = 0,727*DQO – 113,488	0,0512

Fonte: Dados da pesquisa.

POSSIBILIDADES DE IDENTIFICAÇÃO DE MANCHA DO SÊMEN APÓS A LAVAGEM DE ROUPAS E ROUPAS DE CAMA EM CASOS DE INVESTIGAÇÃO DE ABUSO SEXUAL**POSSIBILITIES OF SEMEN STAIN IDENTIFICATION AFTER CLOTHING AND BEDDING WASHING IN INVESTIGATING CASES OF SEXUAL ASSAULT**

MUSSABEKOVA, Saule Amangeldievna

Ph.D. in Medical Sciences, Assistant Professor, Pathology Department, NCJSC "Karaganda Medical University,"
Kazakhstan, Karaganda city,

** Corresponding author*
e-mail: mussabekova.kmu@bk.ru

Received 04 December 2019; received in revised form 10 January 2020; accepted 10 February 2020

RESUMO

Identificar manchas de sêmen em roupas e roupas de cama é um componente crucial na investigação de casos de agressão sexual. Em alguns casos, roupas e roupas de cama já foram lavadas antes de serem removidas e enviadas para exame forense. Não há dados suficientes sobre as melhores práticas para lidar com vestígios de sêmen nas roupas após a lavagem. O objetivo desse trabalho foi estudar a possibilidade de identificar vestígios de sêmen nas roupas após a lavagem usando técnicas amplamente utilizadas. Para simular evidências físicas típicas, amostras de sêmen de doadores foram aplicadas a peças de roupas feitas de vários tecidos. As roupas foram lavadas sob várias condições (com a ajuda de agentes não biológicos e biológicos (contendo enzimas) e em várias máquinas de lavar). Após a lavagem, as manchas de lavagem foram caracterizadas pela presença de sinal de fluorescência, espermatozoides (método Koren - Stokis), determinação de fosfatase ácida, antígeno prostático específico e semenogelina, além de resultados de pesquisas sorológicas de acordo com o sistema AB0 e Análise de DNA. A análise de roupas usando esses métodos mostrou-se eficaz em condições experimentais. No entanto, a presença de enzimas como componentes detergentes projetados para destruir manchas biogênicas afeta significativamente os resultados da identificação de manchas de sêmen. Foi estabelecido que o perfil genético completo pode ser obtido a partir de manchas de sêmen, mesmo após lavar três vezes. São necessárias estratégias diferentes para detectar, selecionar e identificar manchas de sêmen, dependendo das circunstâncias de um caso. Recomenda-se examinar roupas e roupas de cama, mesmo que as amostras tenham sido previamente lavadas.

Palavras-chave: *medicina forense, abuso sexual, identificação de manchas de sêmen, lavagem, perfil genético.*

ABSTRACT

Identifying semen stains on clothing and bedding is a crucial component in investigating cases of sexual assault. In some cases, clothing and bedding have already been washed before they were removed and sent for forensic examination. There is insufficient data on best practices for handling traces of semen on clothes after washing. This work aimed to study the possibility of identifying traces of semen on clothes after washing using widely used techniques. To simulate typical physical evidence, donor semen samples were applied to pieces of clothing made from various fabrics. The clothes were washed under multiple conditions (with the help of non-biological and biological (enzyme-containing) agents, and across numerous washing machines). After washing, the washing stains were characterized by the presence of fluorescence signal, spermatozoa (Koren – Stokis method), the determination of acid phosphatase, prostate-specific antigen and semenogelin, as well as the results of serological research according to the AB0 system and DNA analysis. Clothing analysis using these methods was shown to be effective in experimental conditions. However, the presence of enzymes as detergent components designed to destroy biogenic stains significantly affect the results of the identification of semen stains. It has been established that the full genetic profile can be obtained from semen stains even after washing three times. Different strategies are needed to detect, select and identify semen stains depending on the circumstances of a case. It is recommended to examine clothing and bedding, even if the specimens were previously washed.

1. INTRODUCTION:

Identification of traces of a crime with the use of physical evidence, in particular, biological fluids such as blood and semen, is an essential point in forensic examination and is often the key in criminal investigations. Subsequently, the findings are used as evidence in court (Rainn.org., 2014). Sometimes traces of sexual violence are present in small quantities or mixtures or have been previously destroyed, so their identification is often tricky (Martínez et al., 2015). Currently, amid a general increase in the number of sexual assaults, especially against children, the number of targeted removal of crime evidence by criminals has increased. The use of such simple measures as washing in an automatic washing machine with the addition of laundry detergent leads to difficulties in the subsequent identification of traces of the crime. The use of enzyme-containing synthetic detergents further complicates this task and forces experts to improve forensic techniques and expand the range of research methods used (Galitsky, Mussabekova, 2007; Hofmann et al. 2018). Enzymes are designed to destroy stains of biological origin, including group-specific antigens and DNA structure. Detergents containing enzymes remove stains faster than other detergents and are very useful in washing at low temperatures (Gurtovaya, 2007).

Serological, immunological, and molecular genetic methods are traditionally used to identify traces of semen, including micro traces of biological origin (Harbison, Fleming, 2016). Development of molecular biology methods provides an improvement in genetic analysis methods and expands expert capabilities (Harbison, Fleming, 2016; SWGDAM Recommendations for the Efficient DNA Processing Of Sexual Assault Evidence Kits Scientific Working Group on DNA Analysis Methods, 2016) since genetic material (DNA) is a stable biological structure and retains its ability to be tested for three years (Karni et al., 2013). In some cases, biogenic traces on bedding or clothes which can prove the fact of

sexual violence are preliminarily and purposefully destroyed by washing, which leads to a decrease in the amount of DNA available for forensic examination (Brayley-Morris et al., 2015). Clothing after wash is often not investigated since it is assumed that prolonged storage of physical evidence also leads to the impossibility of detecting traces of semen and their subsequent identification (Forensic evidence collection in sexual assault & rape, 2014). However, in recent years, the possibilities of genetic analysis have improved significantly, and studies have shown that a small amount of DNA is required to obtain a full genetic profile from semen stains efficiently. This analysis is feasible despite several preliminary washes of clothing (Rainn.org., 2014; Harbison, Fleming, 2016; SWGDAM Recommendations for the Efficient DNA Processing Of Sexual Assault Evidence Kits Scientific Working Group on DNA Analysis Methods, 2016; Brayley-Morris et al. 2015, Farnen 2008). The empirical studies published have shown that biogenic stains can persist on pieces of clothing after washing in a washing machine using various washing programs, detergents and temperatures (Galitsky, F. Mussabekova, 2007; Hofmann et al. 2018; Gurtovaya, 2007; Brayley-Morris, 2015; Schlagetter, Glynn, 2012), and that DNA profiles can be obtained by examining traces on washed pieces of clothing, and bedding (Farnen, 2008; Schlagetter, Glynn 2012; Jobin, De Gouffe, 2003; Nussbaumer et al., 2003; Edler et al., 2017; Kulstein, Wiegand, 2018) However, not enough information has been published about the possibilities of using traditional methods to study semen stains after washing.

The purpose of this work was to study the influence of modern synthetic detergents on semen stains, as well as to evaluate the effectiveness of using various traditional forensic medical research methods and the possibility of carrying out a molecular genetic examination in the study of physical evidence (clothing, bedding) after washing. The results of such experimental studies can be used as the basis for the development of forensic protocols

in the investigation of specific types of crimes (Rainn.org., 2014; SWGDAM Recommendations for the Efficient DNA Processing Of Sexual Assault Evidence Kits Scientific Working Group on DNA Analysis Methods, 2016).

2. MATERIALS AND METHODS:

2.1. Sample preparation

To simulate a typical physical evidence, semen samples were used (for a period not exceeding 1 hour) from 12 donors who did not take further part in the experiment. All donors were anonymous, and samples were labeled with letters A–M. The material was taken following the rules adopted by the Ethical Commission of KSMU. In all cases, written informed consent was obtained from semen donors. The research bioethics committee approved the study of the National Research Ethics Service (Protocol No. 56, dated December 21, 2017) for the use of human tissues. Donor ejaculate was preliminarily checked for semen. To create the experimental samples listed in Table 1, several ejaculates of each donor were used.

Therefore, to ensure consistency, the ejaculates of each donor were initially pooled to obtain a stock solution before applying it on the pieces of clothing. Semen was placed on various items of new children's school clothes from different fabrics: cotton (T-shirts, 100% cotton), semi-synthetic (blouses, gabardine), synthetic (tights, 100% nylon), wool (pants, wool 90%, viscose 10%), wool blend (socks, 70% wool, 20% cotton, 10% Coolmax) and blended (shirts, cotton 65%, polyester 30%, elastane 5%). Before the experiment, all clothes were previously washed twice in a washing machine and dried to remove the surface treatment of the fabric and allow the semen to be absorbed deeper into the fabric. All applied semen stains were dried for at least 24 hours before washing. In some cases, 1 ml of semen from different donors was applied to clothing, and 2 ml of semen were combined as a 1:1 mixture of semen from two donors. The first applied stain of one donor was dried, and then the second semen was additionally applied to it to imitate traces of semen from two different sources. After applying the stains, clothes have been dried for

48 hours at room temperature. Prepared experimental samples of clothing with semen stains were stored individually in paper bags at room temperature in a dark room. Tables 1a, 1b and 1c summarize the main parameters and results of the study.

Before the first wash, all clothes were examined using an alternative light source (Forensic Light Source – Mini-Crimescope Advance) at a wavelength of CSS (532 nm) using an orange filter. To indicate the position of semen stains and provision of the subsequent accuracy of sampling for the study, the location of semen stains on clothes was marked by a water-insoluble pen.

2.2. Washing conditions

For the research, three brands of household automatic washing machines with different types of loading were used (top-loading 1: Whirlpool TDLR 70220; frontal loading 1: Bosch WLG 2416 M; frontal loading 2: Siemens WS12T540OE). The standard wash mode lasting 90 min (~ 30 ° C) and the spin cycle 1200 rpm were used; the quantity of detergent was assigned according to the manufacturer's recommendations. Three brands of regionally popular synthetic detergents were used for washing: biological (enzyme-containing) liquid detergent Persil® Power-Liquid®, enzyme-containing detergent Tide Original and non-biological washing powder ECOVER ZERO NON-BIO. Fabric conditioners were not used in experimental washes. After washing, clothes were dried for 12 hours at room temperature and stored individually in paper bags until the next wash. Clothes # 19-23 without applied stains (clean) were also washed with clothes having semen stains to study the possibility of transferring DNA from clothes with semen stains to other clothes inside the washing machine. To identify the source of any reconstituted DNA, buccal smears were taken from all semen donors and from a laboratory technician directly working with experimental samples. For further research, the clothing was conditionally divided into five sections, from which the materials for the study were taken.

2.3. Sample processing and analysis

After each test washing, experimental clothing samples were examined using alternative light sources (Forensic Light Source - Mini-Crimescope Advance), were tested for the presence of acid phosphatase (Phosphatesmo K) (Macherey-Nagel, Germany) and semen using immunological tests SERATEC[®] PSA Semiquant (Seratech, Germany) and RSID[™] - Semen for serological determination of blood group in the AB0 system with the use of polyclonal reagents (anti-A, anti-B, anti-H) (Hematolog LLC, Moscow, Russia) and DNA analysis. Since soluble components of seminal fluid tend to migrate outwards (Kobus et al., 2002), a systematic approach was used for identification accuracy. Plots with semen stains and with an area of 0.8 cm² have been cut out on each piece of clothing. Microscopic sections were taken in the middle between the center and the edge of stains to test for the presence of the acid phosphatase (AP), PSA, Sg and establishing the group of AB0 system, and for DNA analysis that has been done at stain centers and the edge according to the present scheme blots (Figure1).

2.4. Research methods

After each wash, clothes No. 1-18 in the areas designated by the marker were examined using an alternative light source (Forensic Light Source - Mini-Crimescope Advance). The fluorescence intensity of each stain was evaluated using a relative scale as negative, weak, moderate, and strong. Then, ten semen stains (1 cm²) were tested on each sample of clothing according to the instructions for use. The following tests were conducted: on the presence of acid phosphatase using Phosphatesmo K indicator paper, Koren – Stokis spermatozoa staining (0.5% solution of erythrosine in 25% ammonia), followed by microscopy using a light microscope (detection of whole semen cells was used as evidence which clearly distinguished the red-painted head, neck, tail, or its fragment), and also SERATEC[®] PSA Semiquant, RSID[™] -Semen tests. For the serological study of semen stains according to the AB0 system, an absorption/elution reaction was used with anti-A, anti-B polyclonal reagents with a titer of 1: 200, anti-H with a titer of 1: 128.

Results were evaluated using the criteria shown in Table 2.

To estimate the amount of DNA extracted, samples were taken after each washing. Two methods of material removal were used: flushing (sample was wiped back and forth with a moistened swab once over the entire surface of the stain) and cutting (chopped pieces removed according to the scheme, Figure 1). The amount and profile of the extracted DNA were determined. All samples were subjected to the genetic analysis: DNA was extracted using the EZ1 DNA Test Kit (Qiagen) with the BioRobot EZ1 (Qiagen) according to the manufacturer's instructions. Before applying BioRobot EZ1 during the cell lysis stage, 1M DTT was added to all samples to improve DNA release. Extracted DNA was eluted in 50 µl of sterile deionized water.

Additionally, DNA was extracted from buccal samples using the EZ1 and BioRobot DNA Test Kit under the manufacturer's instructions. DNA was eluted in 100 µl of sterile deionized water. Negative control was used to monitor possible contamination during DNA extraction. Evaluation of the quality and quantity of human DNA isolated from biological material was performed using the Quantifiler[™] Human DNA Quantification Kit reagent kit on the ABI Prism[™] 7500 Sequence Detection System manufactured by Applied Biosystems (USA).

2.5. Statistical analysis

Comparisons of the parameters under study depending on the fabrics, the type of washing machine used, the type of load, the kind of washing powder, and the differences in the amounts of DNA obtained from semen stains under different washing conditions were evaluated using the Kraskel - Wallis H-test.

3. RESULTS AND DISCUSSION:

3.1. Analysis of semen stains after several washes using traditional methods

3.1.1 Semen stain detection with an alternative light source

To establish the effectiveness of using an alternative light source when detecting semen stains after washing, 180 semen stains were

examined with an estimate of their fluorescence. After the first (single) washing, most of the dyes (75%) showed strong fluorescence, 25% - 5%, and moderate - weak (Figure 2).

However, with each subsequent wash, the fluorescence intensity decreased. After the second wash, the fluorescence intensity was 35%, 40%, and 20%, respectively, while 5% of the stains showed a negative result. After triple washing, a negative result was obtained for 22% of the stains. A large part of the semen stains (50%) demonstrated weak fluorescence signal, while the percentage of stains with moderate fluorescence decreased to 25%. The fluorescence intensity varied significantly depending on the size of the semen stain (the stains formed by the mixture of two donors were more extensive in diameter), while the stains of smaller diameter (from one donor) had less intense fluorescence. Different washing conditions, such as washing machine brand or type of loading as well as the model and brand of washing powder, did not have a statistically significant effect on the fluorescence intensity. No acid phosphatase was detected in traces of semen with weak fluorescence. This suggests that fluorescent components are easily removed. Besides, it should be noted that the white color of clothes was optimal for observing fluorescence. It is known that after several washes, low-intensity fluorescence on colored fabrics can be missed out (Kobus et al., 2002). Consequently, the use of an alternative light source to identify semen stains on washing clothes can only be considered as a preliminary examination result, which will provide an expert with additional opportunities to find traces of the crime.

3.1.2 Detection of the acid phosphatase presence in semen stains

A study of semen stains for the acid phosphatase (AP) presence has shown that after a single wash, 84% of the semen stains were AP-negative (Table 3).

Most of the semen stains after a single wash in a top-loading machine or a non-biological washing powder were AP-positive with a moderate or strong degree of color, with statistically significant differences between groups ($p \leq 0.05$). In this connection, it can be

assumed that these type of wash are less effective in removing biogenic traces. However, precise conclusions are impossible due to limited resources and an insufficient number of comparative studies (other brands of washing machines and non-biological washing powder). After the second wash, AP-negative results were found in 95% of cases, and only 5% of stains showed a slightly positive effect. After the third wash, the results were negative in 100% of cases. In previous studies, it has been reported that AP testing results may be negative or positive (Harbison, Fleming, 2016; Schlagetter, Glynn, 2012; Kobus et al., 2002; Crowe et al., 2003; Stefandou et al., 2010). However, experimental studies showed that only 16% of semen stains were AP-positive as a result of a single wash, 3% of which had strong fluorescence signal, that fully confirms previous studies (Noël et al., 2019) on the ineffectiveness of using tests for detecting acid phosphatase in identifying semen stains after washing.

3.1.3 Detection of spermatozoa in semen stains after washing using microscopy

In the morphological study, spermatozoa were identified microscopically only in 2% of semen stains after washing (Table 4)

The staining intensity of spermatozoa in semen stains after laundry was identical to the color of spermatozoa found in normal conditions. It should be noted that positive results were obtained in semen stains on cotton fabrics, which is most likely due to the heterogeneous structure of the fabric fibers. Studies have shown that the use of synthetic detergent, regardless of its brand or form (powder, liquid) according to the instructions for a single wash in an automatic washing machine, increases the likelihood of destruction of whole spermatozoa up to 98%. This indicates that this method has low efficiency in the study of semen stains after washing. Also, in some cases, spermatozoa may initially be absent in some diseases or be destroyed as a result of putrefactive changes due to improper storage of physical evidence or exposure to environmental factors (Martínez et al. 2015; Harbison, Fleming, 2016; Forensic evidence collection in sexual assault & rape, 2014; Chambers et al., 2010; Dale et al., 2008)

3.1.4 Detection of prostate-specific antigen in semen stains

Tests for the detection of prostate-specific antigen (PSA) and semenogelin (Sg) can be used in the absence of spermatozoa. Identification of semen stains after a single wash using the SERATEC® PSA Semiquant test showed positive results in 92% with varying degrees of the color of the test line (Table 5).

60% of PSA-positive results were characterized by a moderate degree of the test line color, 30% - intensive and only 2% - weak. As a result of double washing, the number of PSA-negative results increased to 57%, while PSA-positive results of different intensities were 10%, 30%, and 3%, respectively. After triple washing, only 12% of PSA-positive semen stains were observed, of which 9% had mild color intensity.

It should be noted that PSA-positive results were observed while analyzing semen stains on mixed and cotton fabrics. Analysis of the results did not reveal significant differences depending on the type of detergent or brand, or type of washing machine loading. The presence of PSA-positive semen stains after three washes confirms previous studies (Schlagetter, Glynn, 2012; Edler et al., 2017). Although the detection of PSA remains a highly effective method for detecting the semen presence, the interpretation of the results should take into account the presence of false-positive results with other human biological secretions (Dale et al., 2008; Hochmeister et al., 1999).

3.1.5 Identification of semen stains using the RSID® Semen test

Identification of semen stains after a single wash using RSID® Semen test showed positive results with varying degrees of the color of the test line in 94% of stains (Table 6) and only 5% of them showed negative results.

As a result of the second washing, the number of negative results is significantly increased and reached 52%, while the test line has a weak coloring in 8% of cases, moderate - 35% and intensive in 5 % of cases. As a result of a triple washing when samples have been tested using RSID® Semen, the number of negative results increased to 85%, which is

most likely due to the excess of the endpoint of the semen dilution. Despite this, the obtained results confirmed the results of previous studies (Cooper et al., 2014; Suttiposit, Wongwittayapanich, 2018; Honggang et al., 2012) and showed that the RSID® Semen test is highly useful for identifying semen on clothes or bedding after washing. Besides, the lack of cross-reactivity concerning other substrates and biological fluids is also a key factor, which is of great importance in cases of sexual violence when mixing of various human secretions is possible (Forensic evidence collection in sexual assault & rape, 2014; Suttiposit, Wongwittayapanich, 2018).

Experimental data have shown that PSA and Sg detection tests are quick and sensitive methods for identifying semen stains after washing. However, the sensitivity of the RSID® Semen test in this study was slightly higher than that of the SERATEC® PSA Semiquant test, regardless of whether the stain test result was negative or positive. These results show that SERATEC® PSA Semiquant and RSID® Semen immunochromatographic tests are very effective in identifying traces of semen after washing due to high sensitivity, while cross-reaction with other biological fluids is not typical for RSID® Semen (Hochmeister et al., 1999; Cooper et al., 2014; Suttiposit, Wongwittayapanich, 2018).

3.1.6 Detection of group antigens A, B, H in the semen stains

Further, we performed a serological analysis to determine the blood group in the ABO system in tested samples. The corresponding group, antigens A, B, and H, were detected in all semen stains with a positive PSA and Sg test results. Notably, each subsequent wash led to a decrease in the group antigens titer value and a subsequent reduction in t agglutination intensity from intensive (++++) after a single wash to a weakly expressed (+) after a triple wash. Additionally, good fixation of group antigens (medium and robust agglutination intensity) was shown by semen stains on cotton and mixed fabrics (T-shirts, shirts, pants) in contrast to synthetic ones. That is also most likely related to the structure and surface characteristics of the fibers. The natural heterogeneous structure of natural fibers contributes to a stronger fixation

of antigens. It was established that the serological detection of the blood group is quite effective in the study of semen stains after washing, but since this method is routine, its use can be justified only in certain circumstances, including for the preliminary selection of traces before subsequent DNA analysis.

3.2. DNA analysis of semen stains after washing

3.2.1 Efficiency of DNA extraction from the samples

For DNA analysis, differential DNA extraction was performed. DNA yield was quantified only for the spermatozoa fraction. The results of sample analysis obtained by flushing show that this method is not suitable for the study of clothes after washing since the results obtained were significantly inferior to the results obtained in the study of the cut stains (Tables 7 and 8).

Negative results were obtained regardless of the washing conditions, apparently due to an insufficient amount of DNA. After a single wash of cotton and blended fabrics, the DNA concentration obtained from the spermatozoa fraction ranged on average from 0.018 to 0.021 ng / μ l. Despite this, genetic profiles were obtained in the traces with the maximum DNA concentration after a single wash. The DNA concentration obtained from the semen fraction after the second wash decreased significantly (0.002-0.005 ng / μ l). As a result, in 92% of the samples tested, the amount of DNA was insufficient for subsequent analysis.

On the contrary, the cut-off stains taken after a single wash contained enough DNA to establish the genetic profile (Table 8).

Even though with each subsequent washing, the amount of extracted DNA was continually decreasing, the minimum concentration of DNA required for amplification and obtaining a full profile has been maintained. Analyzing the sums of ranks presented in the resulting report, we can talk about the impact of the method for material removal on the research results. The necessary study performance was ensured when cutting the material with the stain for research, and the worst one was in the case of the removal of the material by flushing the stain (Tables 7 and 8).

Although detergents for washing, in general, have a similar composition, however, the number and ratio of components in them can be very different depending on the brand. The results of the study showed that different detergents could have a different effect on DNA detection and recovery in semen stains. Thus, after the use of non-biological washing powder, it was possible to recover higher amounts of DNA than in the study of semen stains after washing with enzyme-containing agents (Tables 9a and 9b).

As a result, 2.8 - 3.9 ng/ μ l of DNA corresponding to the DNA profiles of semen donors was isolated from the stains removed by cutting after one wash, regardless of the washing conditions. Depending on the number of washes, the overall decrease in the average amount of DNA extracted from semen stains has steadily decreased. Thus, the whole amounts of DNA in dyes on cotton fabrics recorded at each subsequent washing was lowering on the average from 3.9 ng / μ l after the first washing to 2.57 after the second washing and to 2.07 ng / μ l after the third washing. After triple wash, the amount of extracted DNA in some samples remained high and amounted to 1.5-2 ng / μ l, regardless of the brand and type of loading characteristic to a washing machine. It should be noted that similar trends were observed in the study of semen stains on mixed fabric types. However, the amount of isolated DNA in them was significantly lower. In stains on synthetic fabrics, a sufficient amount of material for DNA identification was not obtained, which is most likely associated not only with the DNA degradation under the influence of enzymes contained in the detergent but also with the smooth structure of the fibers in this type of fabric. Previous studies have already proved the ability of biological body fluids, such as blood, saliva, and semen to be preserved on the fabrics after a single wash, and showed that in most cases enough DNA could be recovered to establish the genetic profile (Brayley-Morris et al., 2015; Nussbaumer et al., 2003; Edler et al., 2017; Kulstein, Wiegand, 2018; Andrews, Coquoz, 1994). In the present study, cut-off semen stains having washed once yielded sufficient amounts of DNA, which in some cases reached 3.9 ng / μ l. As have been previously reported (Brayley-Morris et al., 2015; Nussbaumer et al., 2003), this amount of DNA

is sufficient to obtain a genetic profile. The results of the study show that under standard washing conditions, the DNA amount required for identification and establishing the full genetic profile can be obtained from semen stains after triple washing. It can be assumed that with such high amounts of DNA collected, complete genetic patterns can be established after a higher number of washes, especially if the area of the surface under investigation is large (Brayley-Morris et al., 2015).

3.2.2 Efficiency of DNA profile recovery from several donors

To study the possibilities of distinguishing DNA profiles in cases of sexual violence committed by several persons at the same time (Chambers et al., 2010), semen stains from two donors were applied to cotton and various types of mixed tissues (T-shirts, pants and shirts). Clothing samples tested are described in Table 1.

Since the amount of DNA obtained from semen stains on mixed tissues (trousers, shirts) was less (2.1–2.5 ng / μ l) than on T-shirts (3.5–3.9 ng / μ l), it was in the study of semen stains obtained from two donors that sufficient quantities of DNA were obtained from T-shirts, allowing to establish complete DNA profiles of both donors, regardless of the number of washes. Although the amount of DNA extracted from pants and shirts was lower than the amount removed from semen stains on cotton fabrics (T-shirts), for some of the samples, full DNA profiles were obtained, which have been corresponded, however, to the profile of only one of the donors. At the same time, the most significant differences in the entire range of the DNA amount for the studied stains were obtained on cotton fabrics ($p \leq 0.05$). Although the study of traces on shirts and trousers showed a wide range of the amount of isolated DNA, it was not possible to establish full profiles of both donors (Table 10b).

This most likely depends on the individual qualities of the donor semen and the type of fabric. At the same time, there are practically no significant differences between the mixed, semi-synthetic, and half-wool material in the entire range of the studied amounts of DNA, throughout all washes. However, in some cases,

DNA mixtures of two people were isolated, which could not be reliably divided into major and minor components, and therefore, no precise results were obtained.

3.2.3 Determination of secondary DNA transfer when washing in a washing machine

Previous studies suggest that spermatozoa from semen stains on women's underwear can be found on other underwear when washed in the same washing machine (Kafarowski et al., 1996; Kamphausen et al., 2015; Voskoboinik et al., 2017). To study the possibility of transferring DNA from one clothes to another when washing in a washing machine, clean clothes were washed together with experimental clothes with semen stains (Table 10a). The analysis results for the studied clothes (№№ 19–23) after washing at 30 ° C are presented in table 10b. When conducting the research, tests for fluorescence, semen microscopy, and acid phosphatase were negative. However, tests for the presence of PSA and Sg showed positive results on cotton fabrics, weakly positive in some traces on mixed fabrics, and negative on synthetic fabrics.

At the same time, the difference in the amount of recovered DNA was established depending on the type of material. The amount of DNA on a T-shirt varied over a wide range, but in general, it was higher than on shirts and trousers; trace amounts of DNA found on the toes and pantyhose were unsuitable for analysis. Upon that, full DNA identification was obtained only in the study of cotton T-shirts. The results of the study depend, most likely, not only on the type of fabric but also on the qualities of donor semen. Since the calculated value is higher than the critical one, there are statistically significant ($p < 0.05$) differences in the amount of DNA depending on the number of washes and the type of fabric. Nonetheless, these data are not sufficient to describe any categorical findings, and they confirm the preliminary results available in the literature on the secondary DNA transfer (Nussbaumer et al., 2003; Kamphausen et al., 2015; Voskoboinik et al., 2017; L.T. Brown Migration Patterns of Seminal Fluid Components and Spermatozoa in Semen Stains Exposed to Water and Blood, 2016) and support previously proposed concept on "owner's DNA" transfer between items of

clothing in the washing machine (Kulstein, Wiegand, 2018). However, this concept has not yet been confirmed and requires additional research.

Collectively, DNA profiling is the method mostly affected by the washing of the clothing samples. Differences in the amounts of DNA obtained in our and other similar studies (Brayley-Morris et al., 2015; Jobin, De Gouffe, 2003; Nussbaumer et al., 2003; Stefandou et al., 2010; Andrews, Coquoz, 1994) may be due to differences in the washing programs used (temperature, brand, and type of detergent, a washing machine brand, etc.), as well as the storage time of material evidence with traces of semen, clothing composition, and various donors. DNA transfer between pieces of clothing in a washing machine could also affect the amount of DNA extracted. Some studies show (Brayley-Morris et al., 2015; L.T. Brown Migration Patterns of Seminal Fluid Components and Spermatozoa in Semen Stains Exposed to Water and Blood, 2016) that multiple washes of cotton fabric with semen stains only lead to minimal loss of recovered DNA, which suggests that numerous washing may not have a significant effect on DNA recover. In this study, three brands of automatic washing machines with identical cycles and a washing temperature regime (30 °C) were used, and the results show that some devices can remove DNA better than others. However, the type of washing powder and washing machine, as well as the temperature of the water during washing in different regions may vary depending on the area, national characteristics, various economic factors. For example, previous studies have shown that similar amounts of DNA can be extracted from semen stains, blood or saliva, when washing at 30°C, 40°C and 60°C (Brayley-Morris et al., 2015; Edler et al., 2017; Andrews, Coquoz, 1994), however, it is possible to use 90°C during washing. It is possible that the use of such a high temperature along with longer wash cycles may more significantly affect semen stains and reduce the amount of remaining DNA more strongly.

The research results showed that there are significant differences in the ability to preserve the traces of semen subjected to washing, depending on the type of fabric of the carrier object. Thus, semen stains located on

natural fabrics are preserved better, as confirmed by previous studies (Harbison, Fleming, 2016; Brayley-Morris et al., 2015; Nussbaumer et al., 2003; Crowe et al., 2003). It has been shown that washed cotton fabrics hold semen better than washed Capron or nylon (Schlagetter, Glynn, 2012; Edler et al., 2017). When semen stains are placed on synthetic fabrics, the possibility of their subsequent group and individual identification is almost wholly absent. In our study, we found that the type of fabric affects the efficiency of semen stain detection when examining them using the serological determination of blood groups and DNA analysis, which corresponds to published data.

Additionally, we analyzed the effect of enzyme-containing and non-biological detergents on the effectiveness of the examination. It is found that enzyme-containing detergents significantly reduce the possibility of identifying semen stains, thus reducing its effectiveness (Table 11).

4. CONCLUSIONS:

The results demonstrate that the efficiency of semen stains analysis by traditional methods vary depending on the conditions of washing. For all means, a decrease in detection efficiency depending on the number of washes performed, was observed. Among traditional morphological and immunological methods, laundry has the most significant effect on the possibility of carrying out a microscopic analysis of semen stains and conducting a reaction to the detection of acid phosphatase. Some methods retain their effectiveness regardless of the use of different types of laundry detergent (determination of fluorescence, PSA, and Sg detection), which confirms the results of previous studies. Enzyme-containing detergents affect biogenic traces and the consequences of forensic examination significantly reducing the effectiveness of some screening methods and the amount of DNA detected.

Nevertheless, this study shows that it is possible not only to identify semen stains but also to recover DNA in the quantities sufficient for further DNA profiling even after three washes. This can be achieved by the suitable sample

preparation, and the success is dependent on to differences in the washing programs used (temperature, brand and type of detergent, a washing machine brand, etc.), as well as the storage time of material evidence with traces of semen, fabric composition, and variation between donors.

Collectively it is recommend a mandatory examination of clothing after washing. At the same time, all suspicious traces with negative microscopy results (taking into account possible vasectomy or aspermia) require further testing to exclude false-negative results. Besides, when pre-wash information is available, screening methods should be chosen with care to ensure that they are appropriate.

Reliability, specificity, and objectivity in the study of traces that have been destroyed are today one of the most urgent problems. Therefore, a systematic approach and the correct choice of research strategy in combination with operational information obtained during the investigation will help to prove the facts of sexual violence. Based on the above, it can be assumed that the use of traditional research methods in combination with an appropriate screening strategy and a suitable material removal method is effective and allows a positive, informative result to get in cases of examining clothes after their washing when proving the facts of sexual violence.

5. REFERENCES:

1. Andrews, C. Coquoz, R. *Advances in Forensic Haemogenetics*, **1994**, 343–345, https://doi.org/10.1007/978-3-642-78782-9_90.
2. Brayley-Morris, H.A., Sorrell, A.P., Revoir, G.E., Meakin, D.S., Court, R.M. *Forensic Sci. Int. Genet.*, **2015**, 19, 165–171, 10.1016/j.fsigen.2015.07.016.
3. Chambers, J.C., Horvath, M.A.H., Kelly, L. *A Crim. Justice Behav.*, **2010**, 37, 1114–1139.
4. Cooper, P., Spruce, C., Webb, L. and Borowitzka, A. *Identification of Human Semen. A comparison of the ABA card, P30 and Rapid Stain Identification (RSID)-Semen Test Kits*. 1st ed. **2014**. Available at:
http://www.seiddon.com/Semen_archivo_1.pdf (Accessed 05 Dec. 2014).
5. Crowe, G., Moss, D., Elliot, D. *Can. Soc. Forensic Sci. J.*, **2003**, 33, 1–5, <https://doi.org/10.1080/00085030.2000.10757498>.
6. Dale, L., Laux, M.S., Sarah E. *Forensic Detection of Semen III. Detection of PSA Using Membrane Based Tests: Sensitivity Issues with Regards to the Presence of PSA in Other Body Fluids. Midwestern Association of Forensic Scientists*. **2008**. Retrieved from <http://mafs.net/pdf/forensicedetectionsemen3.pdf>. (Accessed 11 May 2018).
7. Edler, C., Gehl, A., Kohwagner, J., Walther, M., Krebs, O., Augustin, C., Klein, A. *Int. J. Legal Med*, **2017**, 131, 1179–1189, <https://doi.org/10.1007/s00414-017-1549-y>.
8. Farmen, R.K., Cortez, P., Frøyland, E.S. *Forensic. Sci. Int. Genet. Suppl.*, **2008**, 1, 418–420, <https://doi.org/10.1016/j.fsigss.2007.10.218>.
9. *Forensic evidence collection in sexual assault & rape*. **2014**. Available at: http://www.lifecentre.uk.com/police_info/gathering_forensic_evidence.html (Accessed 12 Dec. 2018).
10. Galitsky, F., Mussabekova, S.A. *Journal of Forensic Medicine*, **2007**, 50(1), 22–23.
11. Gurtovaya, C.B. *To a question about the possible effects of various detergents on the definition of specific and blood group*. Moscow, Collected Works of doctors of forensic biologists, **2007**, 16–19.
12. Harbison, S., Fleming, R. *Res. Rep. Forensic Med. Sci*, **2016**, 6, 11–23.
13. Hochmeister, M.N., Budowle, B., Rudin, O., Gehrig, C., Borer, U., Thali, M., Dirnhofer, R. *J Forensic Sci.*, **1999**, 44(5), 1057–60.
14. Hofmann, M., Adamec, J., Anslinger, K., Bayer, B., Graw, M., Peschel, O., Schulz,

- M.M. *Int. J. Legal Med.*, **2018**, 133(1), 3-16. <https://doi.org/10.1007/s00414-018-1897-2>.
15. Honggang, L., Chunlin, W., Xiuli, G., Chengliang, X. *Human Reproduction*, **2012**, 27(4), 991–997, <https://doi.org/10.1093/humrep/der481>.
 16. Jobin, R.M., De Gouffe, M.D. *Can. Soc. Forensic Sci. J.*, **2003**, 36 (1), 1-10, 10.1080/00085030.2003.10757551.
 17. Kafarowski, E., Lyon, A.M., Sloan, M.M. *Can. Soc. Forensic Sci. J.*, **1996**, 29, 7–11, <https://doi.org/10.1080/00085030.1996.10757042>.
 18. Kamphausen, T., Fandel, S.B., Gutmann, J.S., Bajanowski, T., and Poetsch, M. *Int. J. Legal Med.*, **2015**, 129, 709–714, <https://doi.org/10.1007/s00414-015-1203-5>.
 19. Karni, M., Zidon, D., Polak, P., Zalevsky, Z., Shefi, O. *DNA Cell Biol*, **2013**, 32 (6), 298-301, 10.1089/dna.2013.2056.
 20. Kobus, H. J., Phil, D., Silenieks, E., Scharnberg, J.B. *J. Forensic Sci.*, **2002**, 47, 819–823, <https://doi.org/10.1520/JFS15467J>.
 21. Kulstein, G. Wiegand, P. *Int. J. Legal Med.*, **2018**, 132, 67–81, <https://doi.org/10.1007/s00414-017-1691-6>.
 22. L.T. Brown. *Migration Patterns of Seminal Fluid Components and Spermatozoa in Semen Stains Exposed to Water and Blood (M.Sc.)*. **2016**. Retrieved from Boston University <https://hdl.handle.net/2144/16806> (Accessed 05 Dec. 2018).
 23. Martínez, P., Santiago, B., Alcalá, B., Atienza, I. *Science & Justice*, **2015**, 55 (2), 118-123.
 24. Noël, S., Lagacé, K., Raymond, S., Granger, D., Loyer, M., Bourgoin, S., Jolicoeur, C., Séguin, D. *Forensic Sci Int Genet.*, **2019**, 38, 9-14, doi: 10.1016/j.fsigen.2018.10.002. Epub 2018 Oct 4. PMID: 30312967.
 25. Noël, S., Lagacé, K., Rogic, A., Granger, D., Bourgoin, S., Jolicoeur, C., and Séguin, D. *Forensic Sci. Int. Genet.*, **2016**, 23, 240–247, <https://doi.org/10.1016/j.fsigen.2016.05.004>.
 26. Nussbaumer, C., Halama, T., Ostermann, W. *Forensic Sci. Int.*, **2003**, 136, 47.
 27. Rainn.org. *Preserving and Collecting Forensic Evidence*. RAINN. Rape, Abuse and Incest National Network. **2014**. Available at: <https://www.rainn.org/get-information/aftermath-of-sexual-assault/preserving-and-collecting-forensic-evidence> (Accessed 21 Dec. 2018).
 28. Schlagetter, T.G. Glynn, C.L. *Int. J. Forensic Sci*, **2012**, 2.
 29. Stefandou, M., Alevisopoulos, G., Spiliopoulou, C. *West Indian Med J.*, **2010**, 280, 3.
 30. Suttipasit, P., Wongwittayapanich, S. *Journal of Forensic and Legal Medicine*, **2018**, 54, 102-108, <https://doi.org/10.1016/j.jflm.2017.12.017>.
 31. SWGDAM *Recommendations for the Efficient DNA Processing Of Sexual Assault Evidence Kits Scientific Working Group on DNA Analysis Methods*. **2016**. Available at: <https://www.swgdam.org/publications> (Accessed 24 July. 2019).
 32. Voskoboinik, L., Amiel, M., Reshef, A., Gafny, R., Barash, M. *Int. J. Legal Med.*, **2017**. <https://doi.org/10.1007/s00414-017-1617-3>.

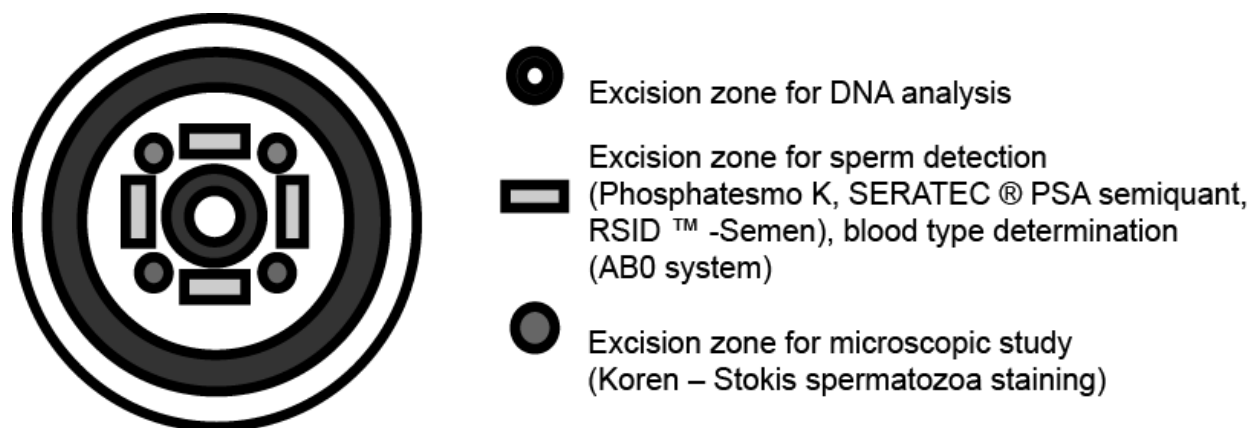


Figure 1. The scheme of material removal from an experimental stain depending on the type of study

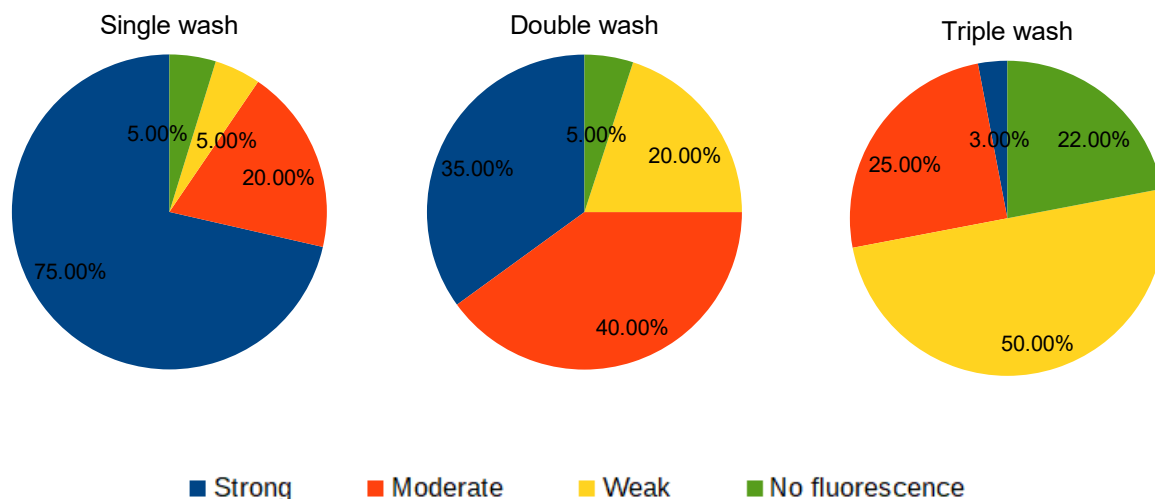


Figure 2. Evaluation of the fluorescence degree for semen stains using an alternative light source (Forensic Light Source - Mini-Crimescope Advance) depending on the number of washes

Table 1a. Summary table of the main parameters used in the study (a type of clothing, semen donors (A–M), a brand of a washing machine, type of washing powder, washing conditions, number of washes) ($n = 430$)

Type of clothes	Donors	Number of stains	Washing machine, brand, type of loading	Detergent	Parameters (T°C)	Number of washes
T-shirt 1	A, D, H, L	8	Whirlpool TDLR 70220, top	Persil® Power-Liquid®	30° C	3
	A: D	1				
	H: L	1				
	B, C, G, I	8				
T-shirt 2	B: I	1	BoschWLG 2416 M, frontal	Laundry detergent Tide Original	30° C	3
	C: G	1				
	E, F, K, M					

T-shirt 3	K: M	1	SiemensWS12T540OE, frontal	Washing powder ECOVER ZERO NON BIO	30° C	3
	E: F	1				
Blouse 4	A, D, H, L	10	WhirlpoolTDLR 70220, top	Persil ® Power-Liquid ®	30° C	3
Blouse 5	B, C, G, I	10	BoschWLG 2416 M, frontal	washing powder TIDE ORIGINAL	30° C	3
Blouse 6	E, F, K, M	10	SiemensWS12T540OE, Frontal	washing powder ECOVER ZERO NON BIO	30° C	3
Tights 7	A, D, H, L	10	WhirlpoolTDLR 70220, top	Persil ® Power-Liquid ®	30° C	3
Tights 8	B, C, G, I	10	BoschWLG 2416 M, frontal	washing powder Tide original	30° C	3
Tights 9	E, F, K, M	10	SiemensWS12T540OE, frontal	washing powder ECOVER ZERO NON BIO	30° C	3
Trousers 10	A, D, H, L	8	WhirlpoolTDLR 70220, top	Persil ® Power-Liquid ®	30° C	3
	A: L	1				
	D: H	1				
Trousers 11	B, C, G, I	8	BoschWLG 2416 M, frontal	washing powder TIDE ORIGINAL	30° C	3
	G: C	1				
	B: I	1				
Trousers 12	E, F, K, M	10	SiemensWS12T540OE, frontal	washing powder ECOVER ZERO NON BIO	30° C	3
	E: F	1				
	K: M	1				
A pair of socks 13	A, D, H, L	1	WhirlpoolTDLR 70220, top	Persil ® Power-Liquid ®	30° C	3
A pair of socks 14	B, C, G, I	10	BoschWLG 2416 M, frontal	washing powder TIDE ORIGINAL	30° C	3
A pair of socks 15	E, F, K, M	10	SiemensWS12T540OE, frontal	washing powder ECOVER ZERO NON BIO	30° C	3
Shirt 16	A, D, H, L	8	WhirlpoolTDLR 70220, top	Persil ® Power-Liquid ®	30° C	3
	D: H	1				
	A: L	1				
Shirt 17	B, C, G, I	8	BoschWLG 2416 M, frontal	washing powder TIDE ORIGINAL	30° C	3
	B: G	1				
	C: I	1				
Shirt 18	E, F, K, M	8	SiemensWS12T540OE, frontal	washing powder ECOVER ZERO NON BIO	30° C	3
	E: K	1				
	F: M	1				

Table 1b. Summary table of the main results of semen stain detection (including stain detection methods) (spots, n = 430)

Type of clothes	Semen detection					Blood type determination using the ABO system
	Fluorescence (Forensic light source)	Microscopy (Koren - Stockis)	AP (Phosphatesmo K)	SERATEC ® Psa semi quant	RSID ™ - Semen	
T-shirt 1	30	20	30	30	30	27
T-shirt 2	30	20	30	30	30	21
T-shirt 3	30	20	30	30	30	24

Blouse 4	25	20	25	25	25	14
Blouse 5	25	20	25	25	25	15
Blouse 6	25	20	25	25	25	15
Tights 7	19	16	19	19	19	9
Tights 8	19	16	19	19	19	9
Tights 9	21	17	21	21	21	11
Trousers 10	28	20	28	28	28	18
Trousers 11	26	20	26	26	26	16
Trousers 12	24	20	24	24	24	14
A pair of socks 13	21	20	21	21	21	11
A pair of socks 14	20	20	20	20	20	10
A pair of socks 15	20	20	20	20	20	10
Shirt 16	23	20	23	23	23	13
Shirt 17	21	20	21	21	21	11
Shirt 18	23	20	23	23	23	14
Total	430	349	430	430	430	262

Table 1c. Summary table of the main results of DNA detection in semen stains

Type of clothes	Donors	DNA analysis			
		Flush, number of stains	DNA profiles	Cutting, number of stains	DNA profiles
T-shirt 1	A, D, H, L	4	100% one source with a matching donor profile	4	100% one source with a matching donor profile
		1	A mixture of 1: 1A1 (15): D2 (15)	-	-
		-	-	1	1: 1 mixture H1 (15): L2 (15)
T-shirt 2	B, C, G, I	4	100% one source with a matching donor profile	4	100% one source with a matching donor profile
		1	A mixture of 1: 1B1 (15): I2 (15)	-	-
		-	-	one	A mixture of 1: 1 C1 (15): G2 (15)
T-shirt 3	E, F, K, M	4	100% one source with a matching donor profile	4	100% one source with a matching donor profile
		1	1: 1 mixture	-	-

		K1 (15): M2 (15)			
		-	-	1	1: 1 mixture E1 (15): F2 (15)
Blouse 4	A, D, H, L	5	-	5	100% one source with a matching donor profile
Blouse 5	B, C, G, I	5	-	5	100% one source with a matching donor profile
Blouse 6	E, F, K, M	5	-	5	100% one source with a matching donor profile
Tights 7	A, D, H, L	5	-	5	-
Tights 8	B, C, G, I	5	-	5	-
Tights 9	E, F, K, M	5	-	5	-
		4	-	4	100% one source only with donors A, H, D
Trousers 10	A, D, H, L	1	-	1	Major D1 (15) and minor (1)
		4	-	4	100% one source only with donors B, I
Trousers 11	B, C, G, I	1	-	1	Major I2 (15) and minor (1)
		4	-	4	100% one source only with donors K, F, M
Trousers 12	E, F, K, M	1	-	1	Major K1 (15) and minor (1)
A pair of socks 13	A, D, H, L	5	-	5	-
A pair of socks 14	B, C, G, I	5	-	5	-
A pair of socks 15	E, F, K, M	5	-	5	-
		4	-	4	100% one source only with donors A, D, L
Shirt 16	A, D, H, L	1	-	1	Major A1 (15) and minor (1)
		4	-	4	100% one source only with donors B, I, C
Shirt 17	B, C, G, I	1	-	1	Major C1 (15) and minor (1)
		4	-	4	100% one source only with donors F, K, M
Shirt 18	E, F, K, M	1	-	1	Major F1 (15) and minor (1)
Total		90		90	

Table 2. Standard criteria for evaluating results concerning AP, PSA and Sg

Category	Phosphatesmo K (AP)	SERATEC [®] PSA Semiquant	RSID [™] -Semen
	Colouring appearance, time	Test line appearance	Test line appearance
Strong	1 - 30 seconds	1-3 minutes	1-3 minutes
Moderate	31 - 60 seconds	4-7 minutes	4-7 minutes
Weak	61 - 120 seconds	8-10 minutes	8-10 minutes
Negative	Colouring is absent for 2 minutes	The line is absent for 10 minutes.	The line is absent for 10 minutes.

Table 3. The results of studies on the detection of acid phosphatase in semen stains depending on the number of washings (n = 430).

Number of washes	Acid Phosphatase (AP)			
	Negative result	Positive result		
		Appearance coloring		
		weak	moderate	intense
Single wash (n = 180)	84%	5%	8%	3%
Double wash (n = 169)	95%	5%	0%	0%
Triple wash (n = 81)	100%	0%	0%	0%

Table 4. The results of studies on the detection of spermatozoa in semen stains depending on the number of washings (n = 430).

Number of washes	Microscopy	
	Negative result	Positive result
Single wash (n = 180)	98%	2%
Double wash (n = 169)	100%	0%
Triple wash (n = 81)	-	-

Table 5. The results of studies on the detection of PSA in semen stains depending on the number of washings (n = 430).

Number of washes	SERATEC [®] PSA			
	Negative result	Positive result		
		Test line colouring		
		weak	moderate	intense
Single wash (n = 180)	8%	2%	60%	30%
Double wash (n = 169)	57%	10%	30%	3%
Triple wash (n = 81)	89%	9%	2%	0%

Table 6. The results of studies on the detection of Sg in semen stains depending on the number of washings (n = 430).

Number of washes	RSID TM -Semen			
	Negative result	Positive result		
		Test line colouring		
		weak	moderate	intense
Single wash (n = 180)	6%	5%	55%	34%
Double wash (n = 169)	52%	8%	35%	5%
Triple wash (n = 81)	85%	10%	5%	0%

Table 7. DNA extraction efficiency in samples obtained by flushing

# of washes	Washout (DNA concentration), ng / μ l (+ CO)					
	Cotton n = 30	Semi-synthetic n = 30	Synthetic n = 30	Wool n = 30	Wool blend n = 30	Mixed n = 30
1	0.021 \pm 0.003	0.01 \pm 0.005	-	0.018 \pm 0.001	0.016 \pm 0.001	0.018 \pm 0.003
2	0.005 \pm 0.001	0.010 \pm 0.001	-	0.015 \pm 0.001	0.015 \pm 0.001	0.015 \pm 0.001
3	0.0002 \pm 0.001	-	-	-	-	-

Table 8. DNA extraction efficiency in samples obtained by cutting

# of washes	Cutting (DNA concentration), ng / μ l (+ CO)					
	Cotton n = 30	Semi-synthetic n = 30	Synthetic n = 30	Wool n = 30	Wool blend n = 30	Mixed n = 30
1	3.9 \pm 0.1	2.5 \pm 0.1	0.021 \pm 0.003	2.1 \pm 0.01	1.9 \pm 0.01	2.5 \pm 0.1
2	2.5 \pm 0.1	1.6 \pm 0.1	-	1.7 \pm 0.01	1.5 \pm 0.01	1.8 \pm 0.01
3	2.07 \pm 0.1	0.016 \pm 0.001	-	0.016 \pm 0.001	0.015 \pm 0.001	0.021 \pm 0.001

Table 9a. DNA extraction efficiency after enzyme-containing washing means

# of washes	Enzyme-containing washing means (DNA concentration), ng / μ l					
	Cotton n = 30	Semi-synthetic n = 30	Synthetic n = 30	Wool n = 30	Wool blend n = 30	Mixed n = 30
1	3.5 \pm 0.1	2.5 \pm 0.1	0.021 \pm 0.003	1.8 \pm 0.1	1.9 \pm 0.01	2.5 \pm 0.1
2	2.0 \pm 0.1	1.6 \pm 0.1	-	1.1 \pm 0.1	1.5 \pm 0.01	1.1 \pm 0.1
3	1.5 \pm 0.1	0.016 \pm 0.001		0.8 \pm 0.1	0.015 \pm 0.001	0.8 \pm 0.1

Table 9b. DNA extraction efficiency after non-biological washing means

# of washes	Non-biological washing means (DNA concentration), ng / μ l					
	Cotton n = 30	Semi-synthetic n = 30	Synthetic n = 30	Wool n = 30	Wool blend n = 30	Mixed n = 30
1	3.9 \pm 0.1	2.8 \pm 0.1	0.05 \pm 0.01	2.1 \pm 0.1	2.0 \pm 0.01	2.5 \pm 0.1
2	2.5 \pm 0.1	1.8 \pm 0.1	0.021 \pm 0.003	1.5 \pm 0.1	1.7 \pm 0.01	1.7 \pm 0.1
3	2.07 \pm 0.1	0.021 \pm 0.001	0.015 \pm 0.001	1.0 \pm 0.1	0.018 \pm 0.001	1.2 \pm 0.1

Table 10a. The parameters of the study on semen transfer inside a washing machine (a type of clothing, semen donors, a brand of a washing machine, type of washing powder, washing conditions, number of washes)

Type of clothes	Donors	Number of stains	Washing machine, brand, type of loading	Detergent	Parameters (T°C)	Number of washes
T-shirt 19	A,D,H,L	0	WhirlpoolTDLR 70220, top	Persil [®] Power-Liquid [®]	30°C	2
Tights 20	A, D,H,L	0	BoschWLG 2416 M, frontal	washing powder TIDE ORIGINAL	30°C	1
Trousers 21	A,D,H,L	0	SiemensWS12T540OE, frontal	washing powder ECOVER ZERO NON BIO	30°C	1
Socks 22	A,D,H,L	0	BoschWLG 2416 M, frontal	washing powder tide original	30°C	1
Shirt 23	A,D,H,L	0	SiemensWS12T540OE, frontal	washing powder ECOVER ZERO NON BIO	30°C	1

Table 10b. Summary table of the main results of semen stain and DNA detection.

Type of clothes	Semen detection					Blood type (AB0)	DNA analysis	
	Fluorescence (Forensic light source)	Microscopy (Koren - Stockis)	AP (Phosphates-mo K)	SERATEC [®] PSA semiquant	RSID [™] -Semen		Type of material withdrawal - cutting	DNA profiles obtained
T-shirt 19	-	-	-	+	+	+	5 places	Mixture A 1 (15), D2 (15), H 3 (15), L4 (15)
Tights 20	-	-	-	-	-	-	-	-
Trousers 21	-	-	-	+	+	+	5 places	- Major D2 (15), H3 (15) and minor L (2), A (2)
Socks 22	-	-	-	-	+	±	-	-

Shirt 23	-	-	-	+	+	+	5 places	Major D1 (15) A3 (15) and minor L (2), H (2)
----------	---	---	---	---	---	---	----------	--

Table 11. The results of semen trace identification after washing, depending on the type and consistency of synthetic detergents.

Type of fabric	Type and consistency of synthetic detergents		
	Non-biological	Biological	
	(without enzymes)	(with enzymes)	
	Powder	Powder	Liquid
	ECOVER ZERO NON	Tide Original	Persil® Power-
	BIO.		Liquid®
	One wash		
Cotton (100% cotton)	+++	++	++
Semisynthetic (gabardine)	+++	++	++
Synthetic (100% nylon)	++	+	+
Wool (wool 90%, viscose 10%)	+++	++	++
Wool blend (70% wool, 20% cotton, 10% coolmax)	+++	++	++
Mixed (65% cotton, 30% polyester, 5% elastane).	+++	++	++
	Two washes		
Cotton (100% cotton)	++	+	+
Semisynthetic (gabardine)	++	+	+
Synthetic (100% nylon)	+	±	±
Wool (wool 90%, viscose 10%)	++	+	+
Wool blend (70% wool, 20% cotton, 10% coolmax)	++	+	+
Mixed (65% cotton, 30% polyester, 5% elastane).	++	+	+
	Three washes		
Cotton (100% cotton)	+	±	±
Semisynthetic (gabardine)	+	±	±
Synthetic (100% nylon)	±	-	-
Wool (wool 90%, viscose 10%)	+	±	±
Wool blend (70% wool, 20% cotton, 10% coolmax)	±	-	-
Mixed (65% cotton, 30% polyester, 5% elastane).	+	±	±

+ - weak possibility of identifying results

++ - moderate (medium) possibility of identifying results

+++ good (strong) possibility of identifying results

INVESTIGAÇÃO DAS CARACTERÍSTICAS DO POLIFURFURAL PREPARADO ATRAVÉS DO PROCESSO DE POLIMERIZAÇÃO

CHARACTERISTICS INVESTIGATION OF PREPARED POLYFURFURAL THROUGH THE POLYMERIZATION PROCESS

فحص خواص متعدد الفوفورال لج ضرر الل عجي قلوبل مة

¹Hind Mahdi Saleh

¹Department of Chemistry, College of Science, University of Misan, Misan, Iraq.

* Correspondence author

e-mail: hind1980@uomisan.edu.iq

Received 12 November 2019; received in revised form 14 January 2020; accepted 20 January 2020

RESUMO

Recentemente, o furfural é o produto químico industrial mais comumente produzido, devido à sua produção ser muito flexível. Neste estudo, o furfural foi convertido em poli-furfural através do processo de polimerização em meio ácido. Algumas características mecânicas e térmicas foram investigadas para o polímero viscoso. O polímero foi caracterizado pelo espectro de FTIR da resina furana preparada neste estudo, mostrando várias bandas devido ao anel furano, que aparece em (3116,1508,1149 e 735) cm^{-1} . Além disso, o espectro mostrou uma banda a 3450 cm^{-1} devido ao grupo hidroxil e uma banda a 1714 cm^{-1} devido ao grupo carbonil que foram gerados por clivagem do anel furano sob polimerização no meio ácido. A análise de CHN, condição de cura do polímero, foi seguida pela técnica DSC, e a temperatura de transição vítrea da resina curada foi estimada (246 °C). A análise termogravimétrica (TGA) fornece uma boa abordagem para acelerar o teste de vida útil do polímero que monitora as alterações de peso nos materiais. O TGA e o DSC da resina furana são compostos após aquecimento a 250 °C, 300 °C, 350 °C e 400 °C; teve uma etapa de decomposição. Por outro lado, o tratamento térmico do polímero foi realizado em diferentes temperaturas e tempos, e vários parâmetros térmicos foram determinados

Palavras-chave: *condição de reação, Perda por ignição, síntese, viscosidade, teste de tração, cargas*

ABSTRACT

Recently, furfural is the most commonly produced industrial chemical because of its production is very flexible. In this study, furfural was converted into poly furfural through polymerization process under acidic medium. Some mechanical and thermal characteristics were investigated for the viscous polymer. The polymer was characterized by the FTIR spectrum of the furan resin prepared in this study showed several bands due to the furan ring, which appears at (3116,1508,1149 and 735) cm^{-1} . In addition, the spectrum showed a band at 3450 cm^{-1} due to the hydroxyl group and band at 1714 cm^{-1} due to carbonyl group which was generated by cleavage the furan ring under polymerization at the acid medium. The CHN analysis, curing condition of the polymer, was followed by the DSC technique, and the glass transition temperature of cured resin was an estimate (246 °C). Thermo Gravimetric Analysis (TGA) provides a good approach to accelerate the polymer lifetime testing that monitors weight changes in materials. The TGA and DSC of the furan resin compounds after heating at 250 °C, 300 °C, 350 °C, and 400 °C; had one decomposition step. On the other hand, thermal treatment of polymer was done at different temperatures and times, and several thermal parameters were determined.

Keywords: *reaction condition, Loss on Ignition, synthesizing, viscosity, tensile testing*

ال لخص

في الآونة الأخيرة، فوفورال هو المادة الكيميائية الأكثر شيوعاً لصناعة الأكرشيو وعلب سبب مرون قن إنتاج ه. في هذه الدراسة تم تحويل الفوفورال إلى بولي فوفورال من خلال عملية التلمر في الوس طال حمضي، وتفحص خصائص الخصر لخصائص الفوفورال والحرارة في بولي مة اللزج. شُخص بولي مة الفوفورال في هذه الدراسة بوس طة طيف FTIR لخصائص بولي مة الفوفورال الذي أظهر عدة خصائص بوليمرية الفوفورال، والتي يتظم

عدد 6113، 1051، 1111، و 560 (سم⁻¹). الصفلة إلى، أظهر الطيف حزمة عند 6105 سم⁻¹ بسبب مجموعة الهيدروكسيل وحزمة عند 1511 سم⁻¹ بسبب مجموعة الكاربونيل التي ترتبط بسلسلة الشارح لدرجة حرارة التحلل الحراري الوسيط لحمض بيتا لاهل CHN، ظروف معالجه بلوليمر أشعة تحت الحمراء DSC وكثرت درجة حرارة التحلل الحراري للزجاج لبلوليمر (613 درجة مئوية). (يفتح لاهل لاجلانية لحرارة (TGA) طريقة جديدة لتسريع اختبار عمل بلوليمر لمرحلة تلك غيرات الوزني في المواد. إن TGA و DSC لمرافقات ريثق في ورايب عدد التسخين عند 605 درجة مئوية، 655 درجة مئوية، 605 درجة مئوية، و 155 درجة مئوية؛ خطوط لاهل واحدة. من ناحية أخرى تمت المعالجة لحرارة لاهل وليمروفي درجات حرارة ووقت استمخفة بمتحدي لاهل من لاهل مانت لحرارة.

للتلخيصات في الملحق: ظروف اللصق لاهل وفق داب الاشتعال لاف في الاشتعال ليكرلي ب، للزوج أختبار لاهل.

1. INTRODUCTION

Furfural has captured extreme attention as one of the most important organic compounds, and it is exclusively produced from lignocelluloses biomass by dehydrating pentose (Dashtban *et al.*, 2012; Ahmad *et al.*, 1995; Feather *et al.*, 1972; Win, 2005), Lignocelluloses biomass has drawn a lot of attention because of its high carbohydrate content. It contains approximately 42-45 % cellulose, 23-36 % hemicelluloses and 22-28 % lignin (Orlov *et al.*, 2017; Cai, *et al.*, 2017). Furfural can be produced by a one-step or a two-step process. In a one-step process, pentosan is hydrolyzed into xylose and then dehydrated into furfural simultaneously. However, in the two-step process, hydrolysis of pentosan occurs under mild conditions followed by dehydration of xylose into furfural (Poddar *et al.*, 2014; Agirrezabal-Telleria *et al.*, 2014a). The commercial production of furfural is by the acid hydrolysis of pentose polysaccharides from non-food residues of food crops and wood wastes from fibrous residues of food crops, in terms of industrial production batch or continuous reactors has been used for that. The reaction condition for furfural production is 3% acid solution to lignocelluloses mass ratio of between 2:1 and 3:1 at 170 -185 °C, the maximum furfural yields are within (45 - 50) % (Barbosa *et al.*, 2014; Agirrezabal-Telleria, 2014b) . The schematic for this process is presented in Figure 1.

Furfural (furan-2 – carboxaldehyde) is a viscous, colorless liquid with a boiling point of about 160 °C. It has a pleasant aromatic odor and turns dark, brown, or black when exposed to air (Morone *et al.*, 2005; Lakra *et al.*, 2014), furfural is natural precursor to arrange furan – based chemicals and solvents (Lakra *et al.*, 2014) as it is illustrated schematically in Figure 2. Additionally, furfural is the sleeping beauty of all the bio-renewable chemicals, bioplastics, and polymers, it as well as its derivatives, has been utilized in a wide range of applications, for instance, plastic, pharmaceuticals, and

agrochemicals (Tsanaktsis *et al.*, 2015; Aït-Aïssa and Aïder, 2014). Furthermore, it can be used for the synthesis of particular polymers depending on the chemistry of the furan ring. Moreover, furfural alcohol is most of these derivatives that have been used in reinforced carbon-carbon composites (Aït-Aïssa and Aïder, 2014; Mascal, 2015; Fleute-Schlachter *et al.*, 2015; Chen *et al.*, 2014). The aim of the proposed research was to synthesizing poly furfural using acid polymerization process, also studying some physical and thermal features of the prepared polymer. Furthermore, the new composite material was synthesized by using industrial waste silica and the polymer as a binder material.

2. MATERIALS AND METHODS

2.1. Materials

Furfural 98%, absolute ethanol, and sulphuric acid 98% were purchased from Fluka company, whereas other chemicals such as acetone, methanol were obtained from Merck company. Silica reinforced filler was obtained from fluorescence tube waste as powder form with a density of 2.33 kg/m³ and a mesh size of 200 micrometers.

2.2. Viscosity Measurements

The viscosity of the furan resin prepared in this study was measured using brook-field rotary viscometer type Alpha series code V 100002 with a spindle at 252 °C. An average value of three replicated measurements was reported (Alshawhi and Hanoosh, 2019).

2.3. Fourier Transform Infra-Red (FTIR) spectroscopy

The FTIR spectra of cured resin were performed using Shimadzu FTIR – 84005, and each spectrum was recorded in a frequency range of 500 – 4000 cm using potassium bromide (KBr) disc. The KBr was previously oven-dried at

300 °C to lessen the interference of water (Bobrowski *et al.*, 2018).

2.4. Differential Scanning Calorimetry (DSC)

DSC measurements were conducted by Shimadzu DSC-60. Dynamic scans were performed within the temperature range (25 – 350) °C at a constant heating rate of 10°C /min. Under the N₂ atmosphere at a flow rate of 20 ml/min, about 10 – 15 mg of uncured resin was used in an aluminum crucible (Abdul Razak *et al.*, 2016).

2.5. Thermo Gravimetric Analysis (TGA)

TGA measurements were computed using TGA Q SOV 20-13. The dynamic scan was measure within temperature range (25 – 700) °C, at a constant heating rate of 10 °C/min. All measurements have been performed under the nitrogen atmosphere at a flow rate of 30 ml/min (Garay *et al.*, 2011).

2.6. Resin Solid Content

The percentage of solid resin content (s) was calculated by the Equation 1:

$$\%S = S1/S0 \times 100\% \quad (\text{Eq. 1})$$

Where S0, and S1 are the weight of the resin before and after dried 3 hours at 105 °C, respectively (Lin *et al.*, 2014).

2.7. Samples Preparation for Primitive Mechanical Test

Amounts of silica filler and resin were weighted by using a digital scale and poured into mixer Shimadzu were blended for 1 minute, then an amount of generated mixture was put into molds for tensile, compression, and harden test. The samples were subjected to the curing process before they were extracted from the molds. A total of three samples were prepared for numbering, tensile testing of the sample in a shape of dumbbly was carried out after 24 hours of the molding and curing processes. Tensile force and elongation were applied until the samples were broken into two parts for compressive strength test samples, for the test were cylindrical shape with 50 mm diameter and 50 mm height. Each sample was pressed at a load of 1200 N until the breakdown occurred (Arbaoui *et al.*, 2016).

Synthesizing of Poly Furfural Resin

Furan resin was prepared by using 50g of freshly distilled furfural in 250 ml round flask fitted with a reflux condenser, mechanical stirrer, and a digital thermometer. To furfural monomer 5ml of Sulfuric Acid (2M) was added and heated at 100 °C with a suitable stirrer until a brown viscose material was obtained (after 2.5 hours) then this resin was soluble in hexane and washed several times with water in order to remove untreated monomer and acid residue. Finally, a hexane layer was separated and dried under magnesium sulfate then it filtrated and evaporated to provide a brown viscose material. Sample from the produced furan resin will be subjected to DSC study (Choura *et al.*, 1996).

2.8. Final Mechanical Test

The silica and furan resin amounts were weighted by using a digital scale (different weight ratio of waste industries silica 10,20,30 and 40% with furan resin as a binder. They were mixed for 3 minutes, then the amount of the generated mixture was put into molds for tensile and compression. Finally, the sample was cured at 130 °C for about 4 hours and post-cure at 150 °C for about 3 hours (Arbaoui *et al.*, 2016).

2.9. Curing Process of Poly Furfural

The curing process of the prepared furan resin was achieved by heating, and firstly the resin was heated at 100 °C for 5 hours then at 120 °C for 3 hours. Finally, post-cure at 150 °C for 3 hours, a sample from the processed resin will be taken to the TGA study (Tasan and Kaynak, 2004).

2.10. Weight Loss Investigation Test

For study purposes, the cured poly furfural resin was subjected to the heating test under temperatures of 200 °C, 250 °C, 300 °C, 350 °C, and 400 °C respectively. The test was conducted to investigate the influence of heating on the loss of weight of the processed resin. The quantitative weight of the cured resin was put in the oven at a constant time (1 hour), then weight residue was measured (Dhinakaran *et al.*, 2010).

2.11. Loss on Ignition (LOI)

Loss on ignition was performed in order to determine the presence of organic or other gas-

forming materials in the silica furane resin. A 10 g of sample was weighted and put into a crucible, and then it was heated at 1000 °C for 30 minutes. After that, it was taken out of the oven and placed immediately in desiccators. The sample was weighted for a second time, LOI was measured according to the initial weight minus final weight and divided by the initial weight in unit gram.

3. RESULTS AND DISCUSSION:

3.1. Reaction scheme

Schematically as demonstrated below, furan resin was obtained by the polymerization process of freshly distilled furfural under acid medium, leading to the formation of brown viscose material with some physical properties presented in Table 1.

Then this polymer after heating over than 100 °C cross-linked polymer may be obtained as shown schematically is infusible and non-soluble in most organic solvents.

3.2. Mechanical Study.

Tensile testing of the processed samples in a shape of dumbbell was performed after 24 hours of the curing process, and the samples were subjected to clamp between attachments, as shown in Figure 3. The tensile force was applied until the samples were broken into two parts. Table 2 shows the results for tensile strength, elongation, compressive strength and hardness, and these values were averaged from 3 samples for each set of percentage ratio except for hardness test

It was observed that the value of tensile strength for cured poly furfural alone was 7.8 kg/cm², while this value increased consistently with an additional percentage of waste silica. It was 21 kg/cm² for a 40% weight percentage of silica filler. In the case of elongation, the value will be reduced with increasing fillers due to the most brittle behavior of polymers. While a compressive strength test was performed using a universal testing machine (UTM), samples were cylindrical shapes with 50 mm diameter and 50 mm height, as shown in Figure 4. Each sample was placed between compression holders until it was broken. The result was displayed from the aided software. The obtained results have shown that the compressive strength of the composite increased consistently with a rising percentage of

silica filler due to the more bonded between silica and furan resin after curing.

3.3. FTIR-Study

The FTIR spectroscopy is an important and common technique to identify the most functional group. So, the FTIR spectrum of the furan resin prepared in this study showed several bands due to the furan ring, which appeared at (3116, 1508, 1149 and 735) cm⁻¹. Also, band at 3450 cm⁻¹ due to the presence of hydroxyl group and band at 1714 cm⁻¹ due to carbonyl group presence through cleavage of some furan ring under polymerization at acid medium. Figure 5 shows the spectrum of uncured furan resin.

3.4. Heat treatment of cured poly furfural resin

Table 3 shows the weightless of the cured polymer at different temperatures (250, 300, 350, 400 °C) within a range of times. According to Table 3, the maximum weight loss was 46% at 400 °C when the cured polymer was held for 1 hour at this temperature, then this percentage decreased to 10% at the same temperature but at 6 hours holding. That means these types of polymers have a good char yield due to the presence of fused aromatic structure after heating.

3.5. TGA and DSC study

Polymers can be employed to predict the lifetime of 16 products; Thermo Gravimetric Analysis (TGA) provides a good approach to accelerate the polymer lifetime testing that monitors weight changes in materials. Figures (8 -11) and Table 4 show the TGA and DSC of the furan resin compounds after heating at 250 °C, 300 °C, 350 °C and 400 °C, furan resin compounds had one decomposition step. The percentages of the char content of cured resin at 600 °C were more than 35%, which indicates that those materials can be used as thermal insulators. Furthermore, the glass transition temperature (T_g) of the cured furan resin was 246 °C as explained in figure.7 that also may indicate more cross-linking occur after curing. Figure 6 shows the DSC thermogram of uncured furan resin, and the uncured sample presented an exothermic peak may due to the reaction among hydroxyl groups in polymer chains. The optimum curing temperature was around 125 °C. Also, the values of T_g are directly proportional to

temperatures of the resin, which attribute to more crosslink formation (Li *et al.*, 2017; Saha *et al.*, 2014; Kandola *et al.*, 2015; Celikbag *et al.*, 2017). Table 5 illustrates that.

3.6. Loss on Ignition (LOI)

Table 6 shows the LOI results for furan resin and furan resin-bonded silica, LOI obtained was less than 2 %, and that confirms the distinct values of LOI according to (Anthonia and Philip, 2015; Nastac *et al.*, 2016; Sun *et al.*, 2019). LOI must be kept below 3%, and the results demonstrate that LOI is inversely proportional to the added percentage of silica.

4. CONCLUSIONS:

The proposed research has utilized the polymerization process to convert furfural to ploy furfural under acidic medium, and particular mechanical and thermal characteristics were investigated. The tensile strength for processed poly furfural alone was 7.8 kg/cm², and it was directly proportional to added percentages of waste silica, which was used as a filler. In terms of thermal features, the thermal decomposition of prepared polymers showed that the char content of cured resin was more than 35% at 600 °C, the thermal study was implemented within a considerable range of temperatures.

5. REFERENCES:

1. Dashtban, M., Gilbert, A., Fateh, P. *J. Sci. Technol. Forest Prod. Process.*, **2012**, *2*, 44–53.
2. Ahmad, T., Kenne, L., Olsson, K., Theander, O. *Carbohydr. Res.*, **1995**, *276*, 309–320.
3. Feather, M. S., Harris, D. W., Nichols, S. B. *J. Org. Chem.*, **1972**, *37*, 1606–1608.
4. Win, D. *Aust. J. Technol.*, **2005**, *8*, 185–190.
5. Orlov, D. V., Lomovskiy, I. O., Lomovskiy, O. I. *Periód. Tchê Quím.*, **2017**, *14*(27), 83–90.
6. Cai, J., He, Y., Yu, X., Banks, S. W., Yang, Y., Zhang, X., Yu, Y., Liu, R., Bridgwater, A. V. *Renew. Sustain. Energy Rev.*, **2017**, *76*, 309–322.
7. Poddar, S., Kamruzzaman, M., Sujan, S. M. A., Hossain, M., Jamal, M. S., Gafur, M. A., Khanam, M. *Fuel*, **2014**, *131*, 43–48.
8. Agirrezabal-Telleria, I., Requies, J., Güemez, M. B., Arias, P. L. *Appl Catal B-Environ*, **2014a**, *145*, 34–42.
9. Barbosa, B. M., Colodette, J. L., Longue Júnior, D., Gomes, F. J. B., Martino, D. C. *J Wood Chem Technol*, **2014**, *34*(3), 178–190.
10. Agirrezabal-Telleria, I., Gandarias, I., Arias, P. L. *Catal Today*, **2014b**, *234*, 42–58.
11. Morone, A., Apte, M., Pandey, R. A. *Renew. Sustain. Energy Rev*, **2005**, *51*, 548–565.
12. Lakra, R., Kiran, M. S., Usha, R., Mohan, R., Sundaresan, R., Korrapati, P. S. *Int J Biol Macromol*, **2014**, *65*, 252–257.
13. Tsanaktsis, V., Vouvoudi, E., Papageorgiou, G. Z., Papageorgiou, D. G., Chrissafis, K., Bikiaris, D. N. *J Anal Appl Pyrol*, **2015**, *112*, 369–378.
14. Aït-Aissa, A., Aïder, M. *International journal of food science & technology*, **2014**, *49*(5), 1245–1253.
15. Mascal, M. *ChemSusChem*, **2015**, *8*(20), 3391–3395.
16. Fleute-Schlachter, I., Merlet, S., Baldauf, K. J., Mainx, H. G., Abribat, B. Washington, DC: U.S. **2015**. *Patent No. 9,107,403*.
17. Chen, B., Li, F., Huang, Z., Lu, T., Yuan, Y., Yuan, G. *ChemSusChem*, **2014**, *7*(1), 202–209.
18. Anthonia, E. E., Philip, H. S. *Int. J. Adv. Chem*, **2015**, *3*(2), 42–47.
19. Nastac, L., Jia, S., Nastac, M. N., Wood, R. *Int. J. Cast Met. Res*, **2016**, *29*(4), 194–201.
20. Sun, J., Li, L., Li, J. *Chem. Eng. J.*, **2019**, *369*, 150–160.
21. Li, Y. L., Wu, G. H., Liu, W. C., Chen, A. T., Zhang, L., Wang, Y. X. *China Foundry*, **2017**, *14*(2), 128–137.
22. Saha, D., Li, Y., Bi, Z., Chen, J., Keum, J. K., Hensley, D. K., Grappe, H. A., Meyer III, H. M., Dai, S., Paranthaman, M. P., Naskar, A. K. *Langmuir*, **2014**, *30*(3), 900–910.
23. Kandola, B., Ebdon, J., Chowdhury, K. *Polymers*, **2015**, *7*(2), 298–315.
24. Celikbag, Y., Meadows, S., Barde, M., Adhikari, S., Buschle-Diller, G., Auad, M. L., Via, B. K. *Ind Eng Chem Res*, **2017**, *56*(33), 9389–9400.
25. Bobrowski, A., Drozynski, D., Grabowska, B., Kaczmarska, K., Kurlito-Kozioł, Z., Brzezinski, M. *China Foundry*, **2018**, *15*(2).
26. Abdul Razak, A. A., Saleh, N. J., Emad, M. *Eng. & Tech. Journal*, **2016**, *34* Part(A) (9), 1731–1743.

27. Garay, A. C., Heck, V., Zattera, A. J., Souza, J. A., Amico, S. C. *J. Reinf. Plast. Compos*, **2011**, 30(14), 1213-1221.
28. Lin, R., Sun, J., Yue, C., Wang, X., Tu, D., Gao, Z. *Maderas. Ciencia y tecnología*, **2014**, 16(2), 159-174.
29. Tasan, C. C., Kaynak, C. In *Proceedings of the International Symposium of Research Students on Materials Science and Engineering ISRS 2004*.
30. Arbaoui, J., Moustabchir, H., Vigué, J. R., Royer, F. X. *Mater. Res. Innov.*, **2016**, 20(2), 145-150.
31. Alshawi, F. M., Hanoosh, W. S. *Revista Innovaciencia*, **2019**, 7(1), 1-15.
32. Choura, M., Belgacem, N. M., Gandini, A. *Macromolecules*, **1996**, 29(11), 3839-3850.
33. Dhinakaran, M., Dasaradan, B. S., Subramaniam, V. *JTATM*, **2010**, 6(3).

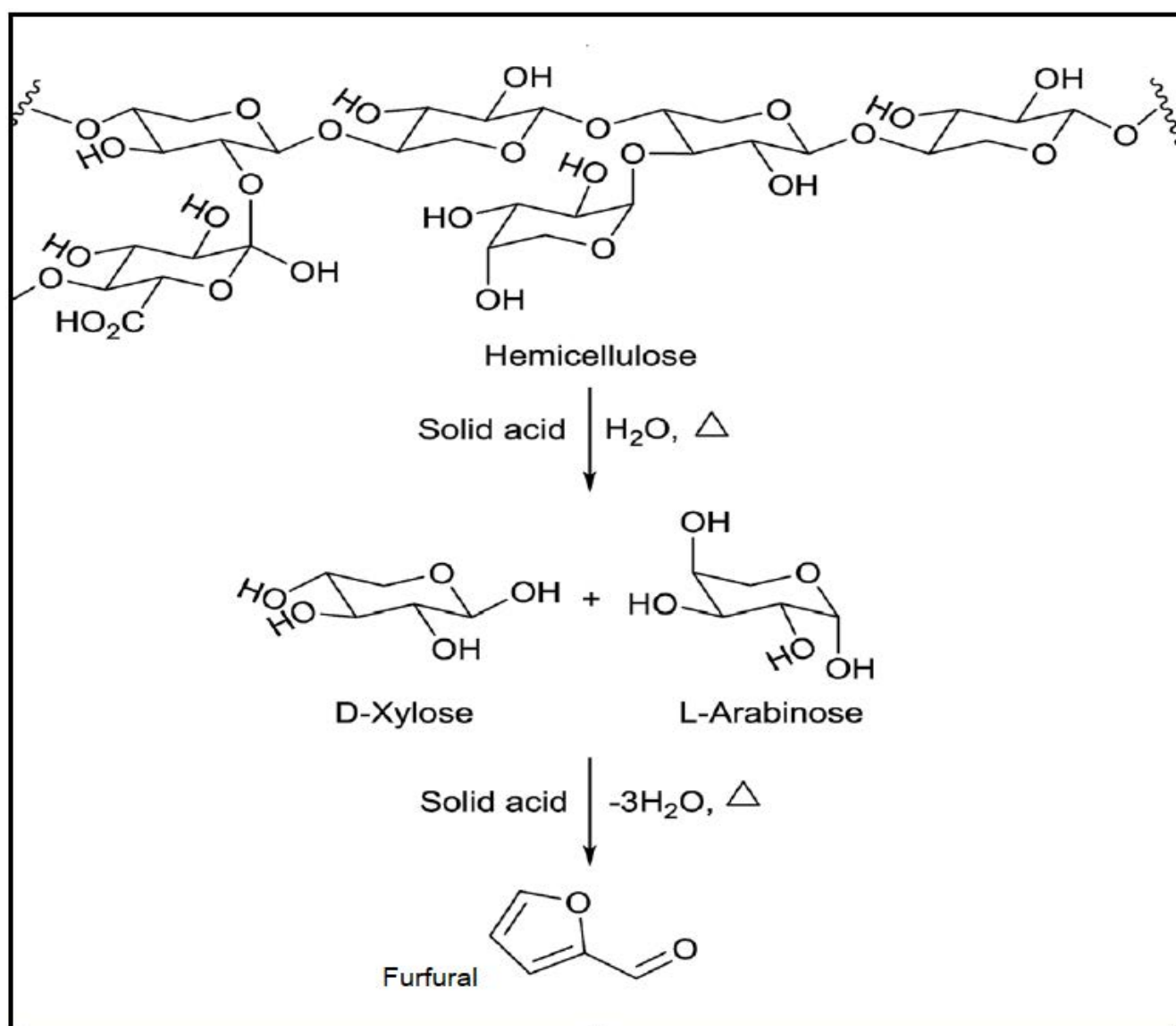


Figure 1. The reaction for the acid-catalyzed the conversion of hemicellulose into furfural

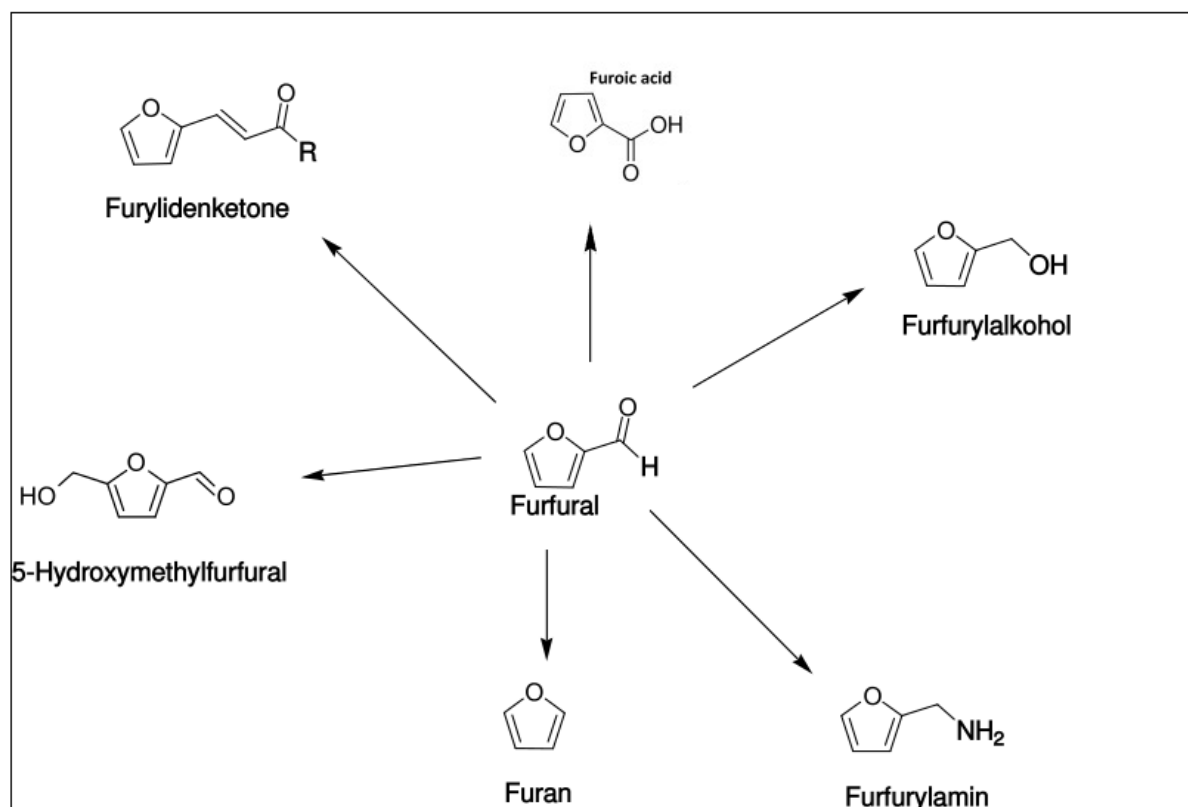


Figure 2. Conversion of furfural into some important chemical compounds



Figure 3. The sample was clamped between the attachments of the universal silica strength machine

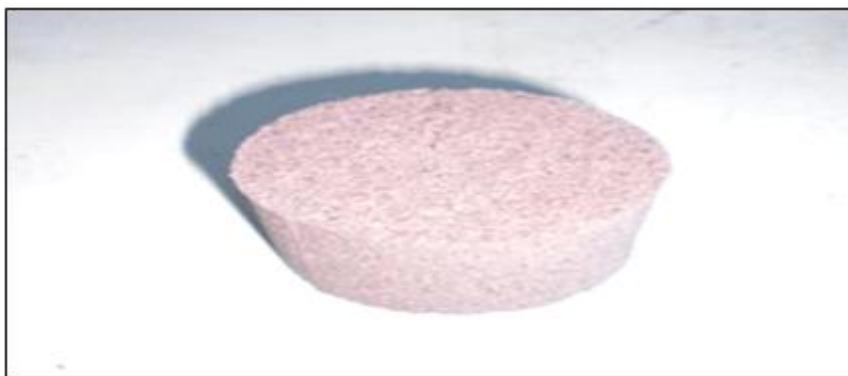


Figure 4. Sample for compressive strength.

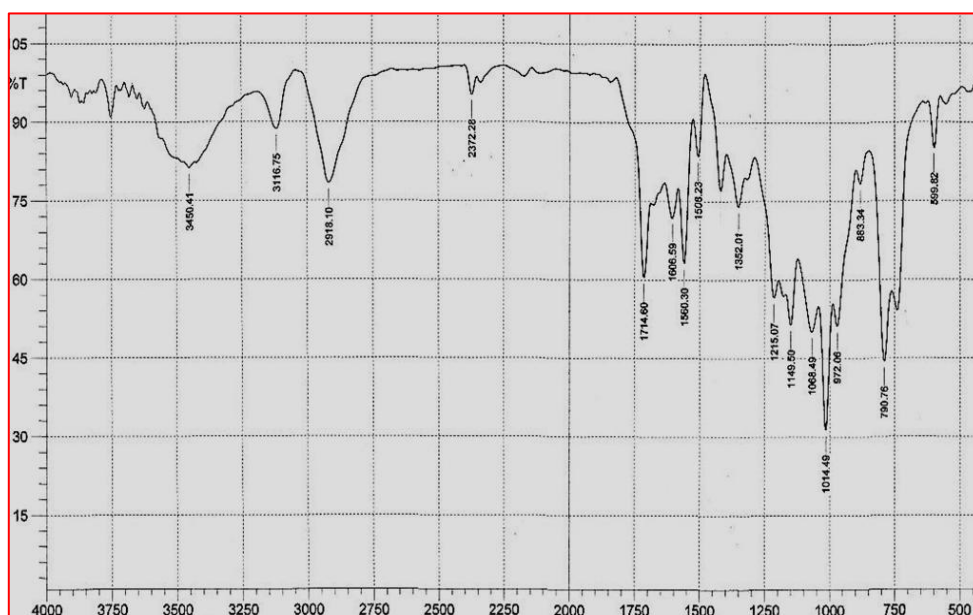


Figure 5. FTIR spectrum of polyfurfural

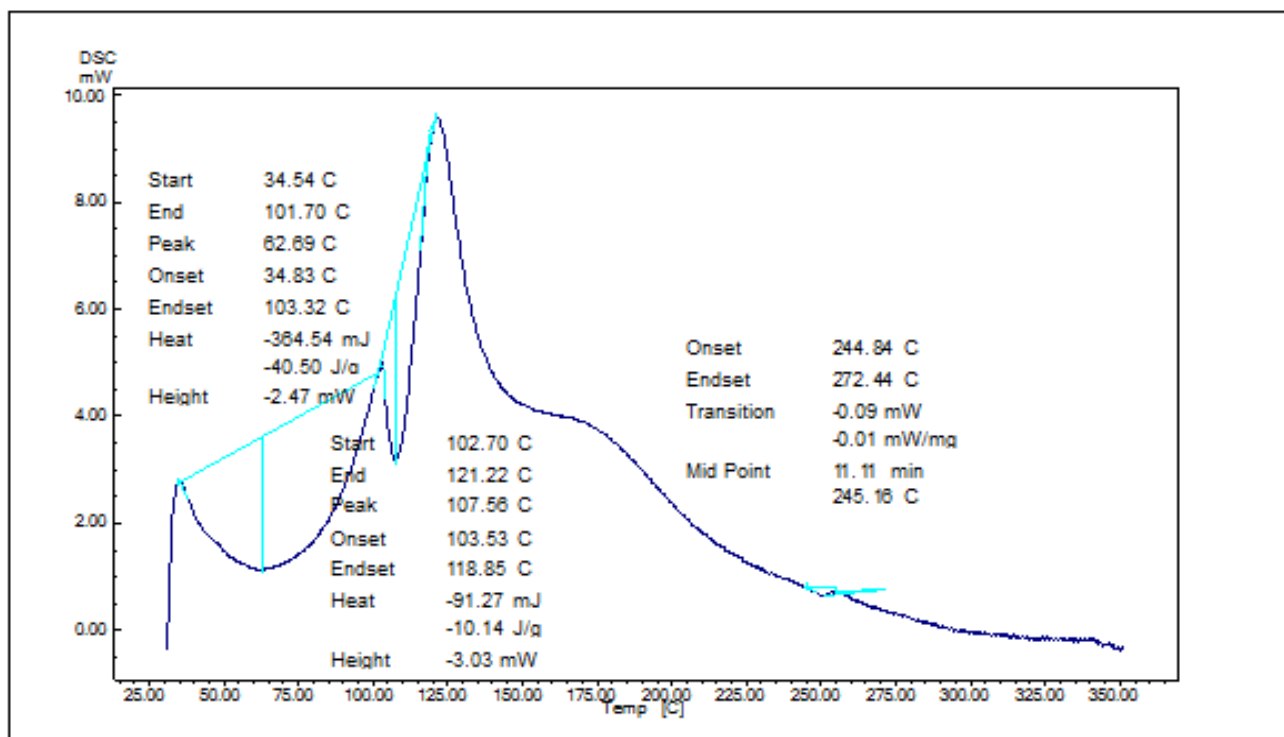


Figure 6. DSC thermogram of furan resin

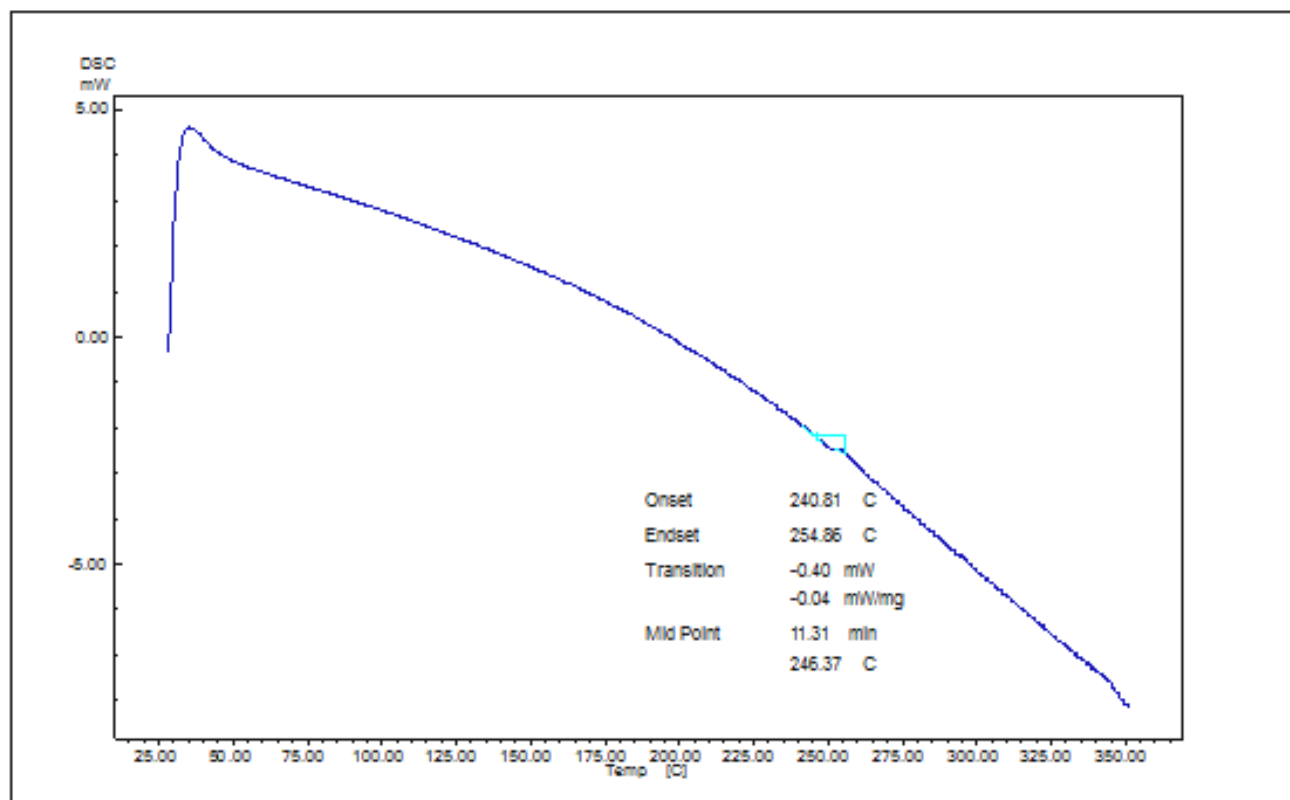


Figure 7. DSC thermogram of Cured poly furfural.

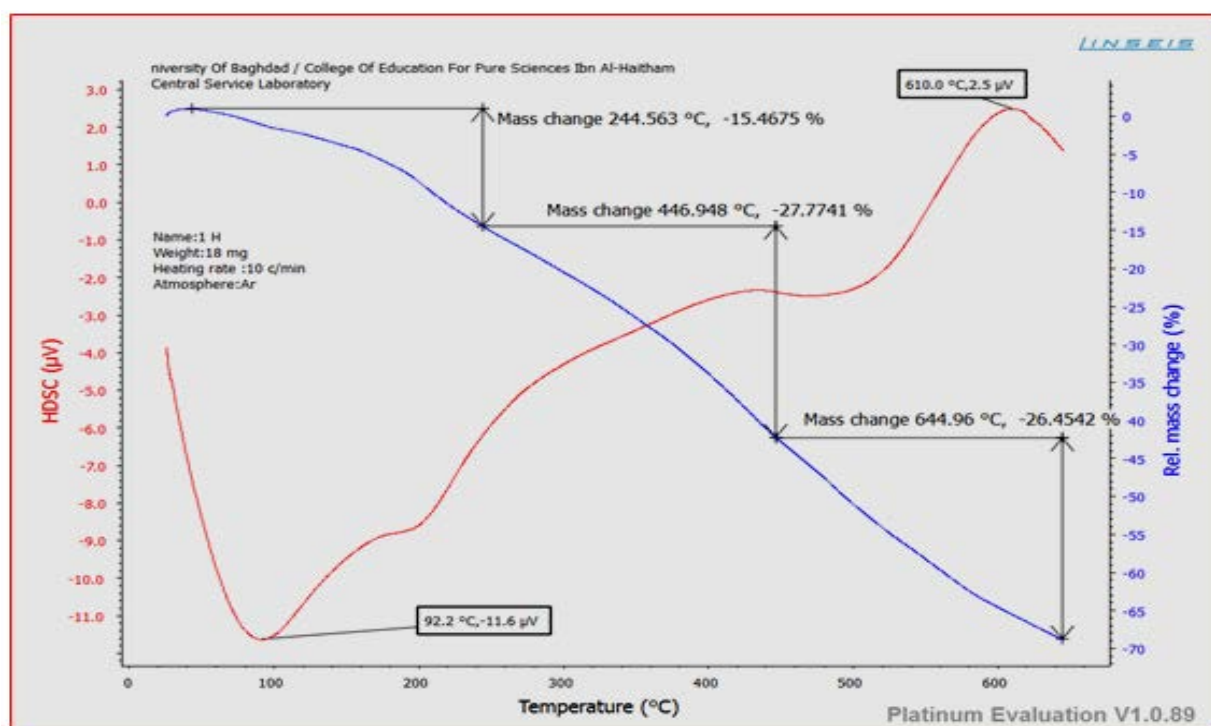


Figure 8. TGA and DSC thermogram of furan resin after heat treatment at 250°C

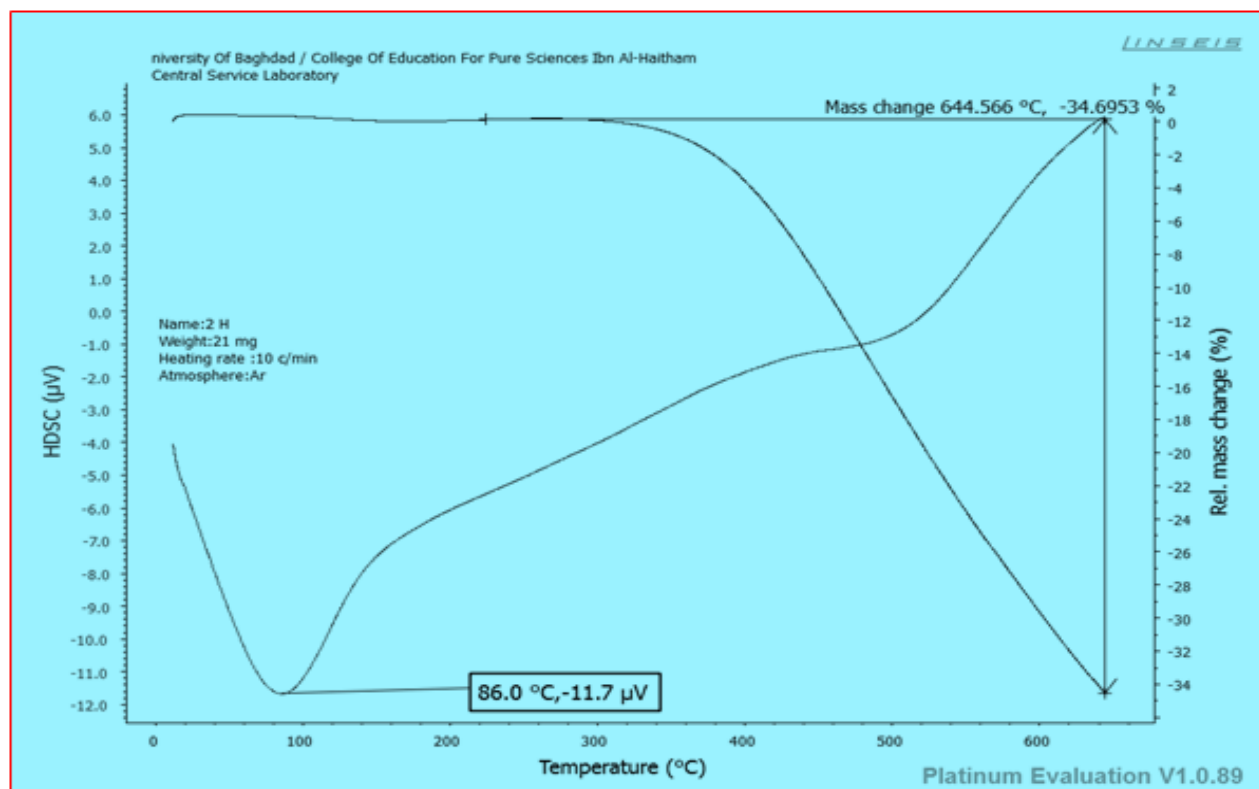


Figure 9. TGA and DSC thermogram of furan resin after heat treatment at 300 °C

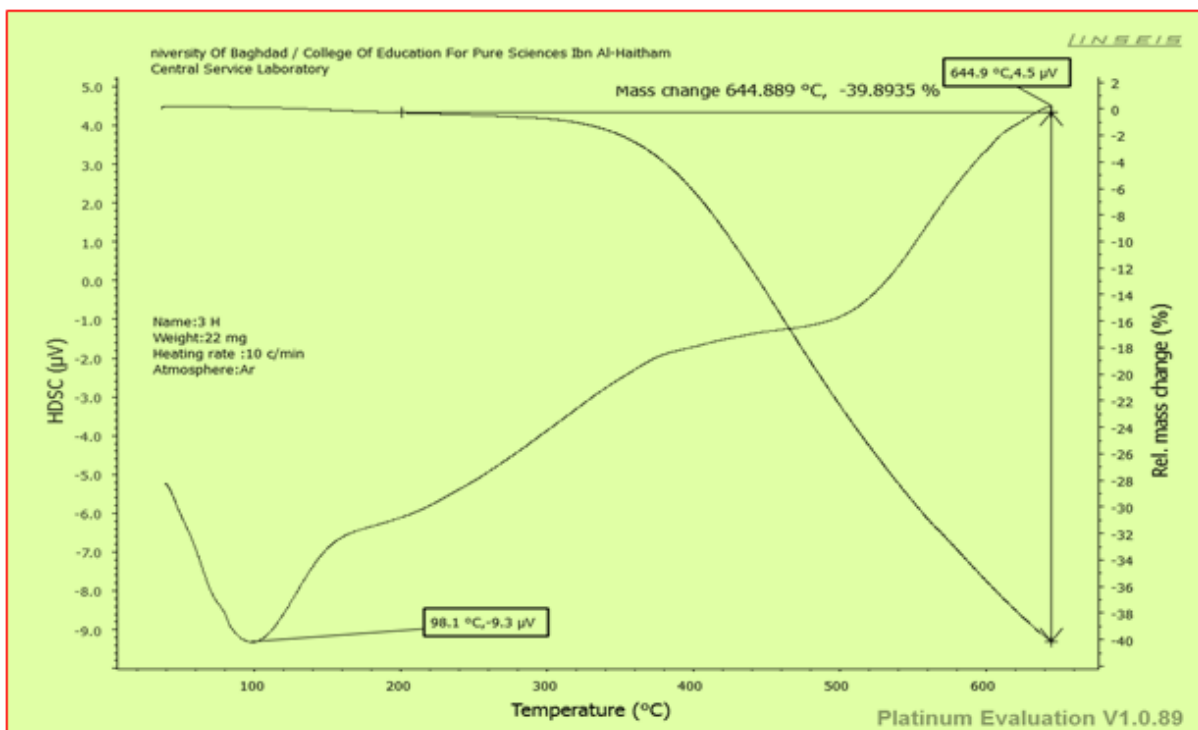


Figure 10. TGA and DSC thermogram of furan resin after heat treatment at 350 °C

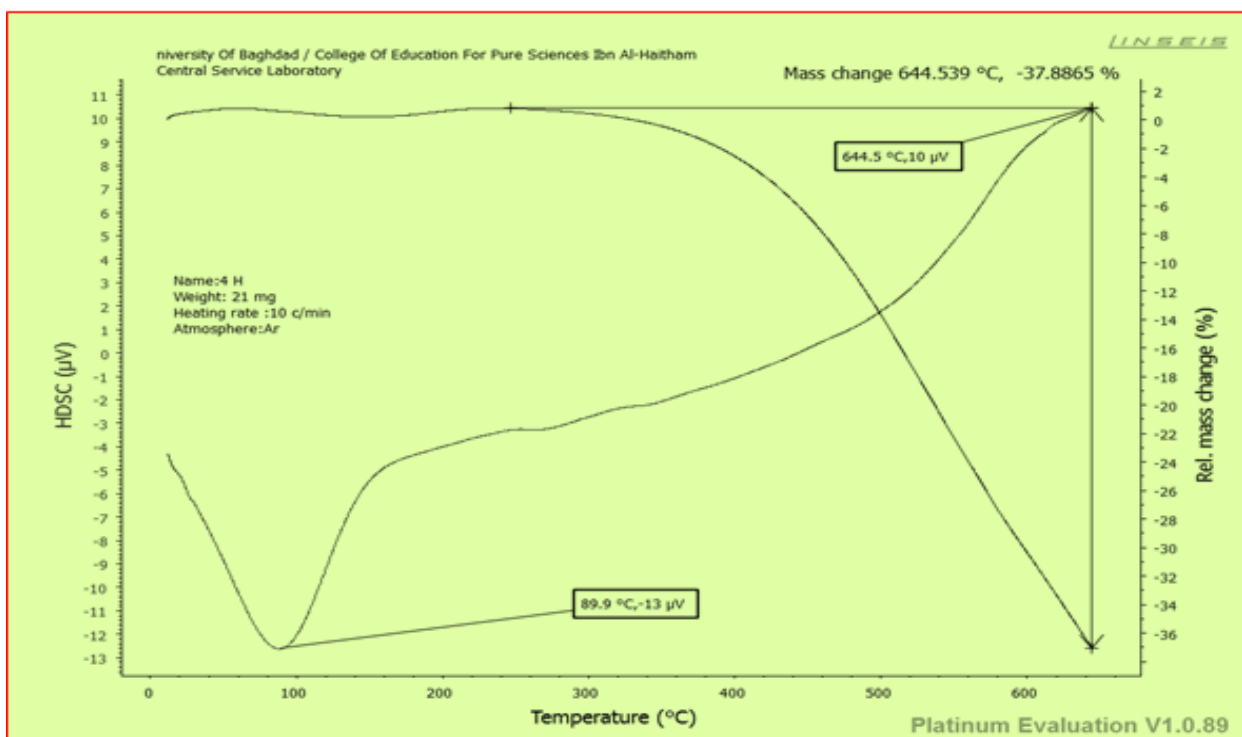


Figure 11. TGA and DSC thermogram of furan resin after heat treatment at 400 °C

Table 1: Some physical properties of uncured furan resin

Gel time min. (loss of fluidity) at 100 °C	Viscosity (mpa.s) at 25 °C	Dry solid content % at 105 °C. 3hrs
21 min	327	51.32

Table 2. Tensile strength, elongation, compressive strength and hardness of silica casting mold

Sample No	Tensile strength Kg/cm ²	Elongation %	Compressive strength Kg/cm ²	Hardness Shor D
Cured furan resin alone	7.80	2.1	14.72	63
10% silica	10.32	1.9	17.32	69
20%	12.73	1.8	20.11	71
30%	17.52	1.5	24.32	75
40%	21.00	1.4	28.56	77

Table 3: Weight loss of furan resin at different temperatures and times

Temperature °C	Weight loss %					
	1h	2h	3h	4h	5h	6h
250	6.38	0.49	0.42	0.24	0.19	0.08
300	10.56	5.57	1.91	0.41	0.37	0.23
350	14.16	10.08	4.79	2.32	2.06	1.22
400	46.45	28.15	27.94	23.46	12.17	10.74

Table 4: Thermal parameter obtained from TGA /DSC thermogram of cured poly furfural after heat treatment at different temperatures

Resin No.	Decomposition temperature °C	Char content at 600 °C %	Temp. of 50% weight loss °C
1H	244	35	495
2H	380	70	>600
3H	380	64	>600
4H	450	70	>600

Table 5. Tg value of cured poly furfural obtained from DSC thermogram

Resin No.	Tg °C
Cured polymer alone.	246
1H	200
2H	270
3H	256
4H	254

Table 6. LOI values for furan resin and its composites

Resin. NO.	LOI %
Cured polymer alone.	1.94
10 % silica	1.83
20 %	1.54
30 %	1.42
40 %	1.27

COMPARAÇÃO DE ABORDAGENS CIRÚRGICAS E NÃO CIRÚRGICAS AO TRAUMA ESPLÊNICO**COMPARISON OF SURGICAL AND NON-SURGICAL APPROACHES TO SPLENIC TRAUMA**

MOUSAVIE, Seyed Hamzeh¹; BEIGI RIZI, Kamran²; HOSSEINPOUR Parisa³; NEGAHI Ali Reza^{*1}.

¹ Hazrat Rasoul Medical Complex, Iran University of Medical Sciences, Tehran, Iran

² Department of surgery, Rasool-Akram Hospital, Iran University of Medical Sciences, Tehran, Iran

³ Student Research Committee, School of Medicine, Iran University of Medical Sciences, Tehran, Iran

** Corresponding author
e-mail: arneghahi@gmail.com*

Received 24 August 2019; received in revised form 13 January 2020; accepted 02 February 2020

RESUMO

A perda do baço acarreta em aumento do risco de sepse, pielonefrite, pneumonia e embolia pulmonar ao longo da vida de pacientes com trauma esplênico. Com relação à sensibilidade do baço e à importância de terapias apropriadas para trauma espástico, este estudo teve como objetivo determinar as consequências do trauma raquimedular com base em diferentes métodos terapêuticos. Este estudo de coorte retrospectivo foi realizado em pacientes com trauma esplênico que foram encaminhados ao Hospital Rasool Akram em Teerã, Irã, durante 2011-2017. Todos os registros médicos de 133 pacientes com trauma esplênico foram coletados entre 2011 e 2017. Os dados foram coletados relacionados à ultrassonografia e tomografia computadorizada ou a outros métodos de diagnóstico dos pacientes admitidos na enfermaria cirúrgica. Finalmente, pacientes com trauma esplênico com abordagem cirúrgica foram comparados com indivíduos com abordagem não cirúrgica. As abordagens cirúrgicas e não cirúrgicas foram realizadas em 80% (n = 104) e 20% (n = 26) dos indivíduos, respectivamente. Houve diferença significativa entre os dois grupos em relação ao tempo de permanência na unidade de terapia intensiva e duração total da internação. A comparação entre os dois grupos mostrou que não houve diferença significativa em termos dos efeitos colaterais relacionados ($P > 0,05$). No geral, 80,8% (n = 84) e 96,4% (n = 27) dos pacientes receberam alta nos grupos cirúrgico e não cirúrgico, respectivamente. Além disso, 19,2% (n = 20) e 3,6% (n = 1) dos casos morreram em grupos cirúrgicos e não cirúrgicos. A comparação dos pacientes sobreviventes mostrou que houve uma diferença significativa entre os grupos ($P = 0,045$). Este estudo mostrou que não houve diferença em relação às consequências de abordagens cirúrgicas e não cirúrgicas nos pacientes com trauma esplênico. O tempo de internação hospitalar foi menor no grupo não cirúrgico, comparado ao grupo cirúrgico. A causa mais comum de trauma nos dois grupos foi acidente de carro. O hematoma retroperitoneal foi o trauma intra-abdominal mais comum. A taxa de mortalidade foi maior no grupo cirúrgico em comparação com o grupo não cirúrgico.

Palavras-chave: *Trauma abdominal contuso, Tratamento não cirúrgico, Esplenectomia esplênica, Trauma esplênico.*

ABSTRACT

The spleen loss leads to increase the risk of sepsis, pyelonephritis, pneumonia, and pulmonary embolism throughout the lifetime of patients with splenic trauma. Regarding the sensitivity of the spleen and the importance of appropriate therapies for spastic trauma, this study aimed to determine the consequences of spinal trauma based on different therapeutic methods. This retrospective cohort study was conducted on the splenic trauma patients who were referred to Rasool Akram Hospital in Tehran, Iran, during 2011-2017. All medical records of 133 splenic trauma patients were gathered from 2011-2017. The data were gathered related to ultrasound, and computed tomography scan or other diagnostic methods of the patients admitted in the surgical ward. Finally, splenic trauma patients with a surgical approach were compared to the subjects with a non-surgical approach. Surgical and non-surgical approaches were performed on 80% (n=104) and 20% (n=26) of the subjects, respectively. There was a significant difference between the two groups regarding the length of intensive care unit stay and total hospitalization duration. The comparison between the two groups showed that there was no significant difference in term of the related side effects ($P > 0.05$). Overall, 80.8% (n=84) and 96.4% (n=27) of the

patients were discharged in surgical and non-surgical groups, respectively. In addition, 19.2% (n=20) and 3.6% (n=1) of the cases died in surgical and non-surgical groups. The comparison of survived patients showed that there was a significant difference between the groups ($P=0.045$). This study showed that there was no difference regarding the consequences of surgical and non-surgical approaches in patients with splenic trauma. The length of hospital stay was shorter in the non-surgical group, compared to that of the surgical group. The most common cause of trauma in both groups was car accidents. Retroperitoneal hematoma was the most common intra-abdominal trauma. The mortality rate was higher in the surgical group in comparison to that of the non-surgical group.

Keywords: *Blunt abdominal trauma, Non-surgical management, Splenectomy, Splenic, Splenic Trauma*

1. INTRODUCTION:

Trauma has some type resulting in superficial and deep injuries that can threaten the lives of people of all ages (Khazaei *et al.*, 2016). The most common blunt abdominal trauma is splenic trauma. The spleen loss leads to increase the risk of sepsis, pyelonephritis, pneumonia, and pulmonary embolism throughout the lifetime of these patients. Spinal injury is observed in more than 3% of all the cases referring to trauma centers and 40% of laparotomies are performed due to blunt abdominal trauma, which occurs with unknown causes. Previously, splenorrhaphy was the dominant technique of spleen preservation (Hoefnagel, 1956). Despite the uncommon infection after splenectomy (0.5-3.2%), the mortality rate of the patients with postoperative infection is reported between 50% and 75% indicating an increase in the complications of this approach utilization (Bisharat *et al.*, 2001). The risk of sepsis, pneumonia pyelonephritis, pulmonary pneumonia, and pulmonary embolism throughout the patient's lifetime increased in the patients without the spleen, compared to that in the general population (Renzulli *et al.*, 2009).

Regarding the advancements in imaging and increasing use of computed tomography (CT) scan in trauma cases, surgical treatment has been introduced as an applicable technique in patients with spleen trauma. First, this approach was used in the treatment of children and then for adults since the early 1990s (El Khoury *et al.*, 2011). In cases with unstable hemodynamic condition and the use of diagnostic techniques, such as ultrasound, splenectomy is considered as an option. However, in patients with stable vital symptoms, if there is a doubt about the abdominal visceral injury, CT scan is the best diagnostic method. With the detection of spleen injuries in a patient's CT scan, the surgeon deals with the issue of surgical intervention or the use of non-surgical treatment (Oyo-Ita *et al.*, 2015).

The sensitivity of the spleen organs, choosing appropriate therapies for trauma patients

to prevent complications, such as bleeding, infections, and deaths and the existence of some controversial information considering the choice of surgical and non-surgical procedures are essential issues in this regard. With this background in mind and the inadequate number of studies about this issue in Iran, the present study aimed to determine the consequences of splenic trauma based on different therapeutic methods in Iranian population.

2. MATERIALS AND METHODS:

This retrospective cohort study was conducted on the splenic trauma patients, who were referred to the Rasool Akram Hospital in Tehran, Iran, 2011-2017. All medical records of 143 splenic trauma patients were gathered from 2011-2017. The inclusion criteria were trauma diagnosis, surgical or non-surgical treatment, and the availability of patients' records. First, the data of 143 splenic trauma patients admitted in the surgical ward were gathered related to ultrasound and CT scan or other diagnostic methods. Then, some cases were excluded from the study due to incomplete information, and 133 patients remained. The Data, including age, gender, trauma grade, the type of treatment intervention, duration of hospitalization, re-referral to the hospital, number of times and volume of blood transfusion, and rate of postoperative mortality were gathered and then entered into a researcher-made questionnaire. Finally, splenic trauma patients with a surgical approach were compared to the cases with a non-surgical procedure.

2.1. Statistical analysis

All the data were analyzed in SPSS software (version 24) using Chi-square test, t-test, and Mann-Whitney U test. P-value less than 0.05 was considered statistically significant.

2.2 Ethical considerations

The Ethics Committee approved this study of the Iran University of Medical Sciences

(IR.IUMS.FMD.REC.1398.101). All procedures performed in studies involving human participants following the ethical standards of the institutional and national research committee and with the 1964 Helsinki declaration and its later amendments. All participants provided written and informed consent.

3. RESULTS AND DISCUSSION:

The mean age of the subjects was reported as 25.6 ± 11.26 years within the range of 2-63 years. In total, 113 (85%) and 20 (15%) subjects were male and female, respectively. Table 1 tabulates other demographic and diagnostic data. The mean scores of systolic blood pressure, diastolic blood pressure, respiratory rate, body temperature, and heart rate were 108.62 ± 18.261 mmHg, 69.54 ± 11.9 mmHg, 18.27 ± 5.57 breaths/min, $39.63 \pm 29.31^\circ$, and 98.51 ± 20.57 beat/min, respectively. Moreover, the mean scores of length of intensive care unit (ICU) stay and ward hospitalization were 5.78 ± 9.11 and 10.64 ± 11.7 days, respectively. Also, the mean score of the Glasgow Coma Scale was calculated as 13.45 ± 3.105 . Surgical and non-surgical approaches were used in 80% ($n=104$) and 20% ($n=26$) of the patients, respectively. Table 2 demonstrates the distribution of concurrent Intra- and extra-abdominal traumas based on surgical and non-surgical approaches.

There was no significant difference between intra- and extra-abdominal injuries ($P=0.006$). Moreover, Table 3 tabulates the mean scores of basic information according to surgical and non-surgical approaches. Based on the obtained results, there was a significant difference between the two groups in terms of length of ICU stay and total hospitalization duration. The comparison of disease grade between the two groups showed that there was no significant difference between surgical and non-surgical approaches ($P=0.21$). The related side effects were observed in 26% and 11.5% of the patients in the surgical and non-surgical groups, respectively. No significant difference was observed between the two groups in terms of the side effect ($P>0.05$).

Table 4 presents different side effects based on surgical and non-surgical approaches. Overall, 30.8%, 61.5%, and 7.7% of the subjects were in Grade 1, Grade 2, and Grade 3, respectively. The frequency of disease grade based on surgical and non-surgical approaches is presented in Table 5. The CT scan was performed in 53.5% ($n=53$) and 82.1% ($n=23$) of the cases in

surgical and non-surgical groups, respectively. According to the conduction of CT scan, no significant difference was observed between surgical and non-surgical approaches ($P=0.006$).

Penetrating trauma, blunt trauma, car accident, fight, and fall were the causes of trauma in 5.8%, 1%, 48.1%, 3.8%, and 41.3% of the cases in the surgical group, respectively. In the non-surgical group, 5.3%, 1.5%, 50%, 3%, and 40.2% of the patients were injured due to penetrating trauma, blunt trauma, car accident, fight, and fall, respectively. Finally, 80.8% ($n=84$) and 96.4% ($n=27$) of the subjects were discharged in surgical and non-surgical groups, respectively. In addition, 19.2% ($n=20$) and 3.6% ($n=1$) of the cases died in surgical and non-surgical groups. The comparison of survived patients demonstrated a significant difference between the two groups ($P=0.045$).

Based on the obtained results of this study, there was no significant difference between intra- and extra-abdominal traumas in surgical and non-surgical approaches. The length of ICU stay and total hospitalization duration were shorter in the non-surgical group, compared to those of the surgical group. Car accidents were the most common cause of trauma in both groups. Retroperitoneal hematoma was the most common intra-abdominal trauma and the most common extra-abdominal trauma was related to organs in both groups. The rate of mortality was higher in the surgical group.

The non-surgical approach in patients with splenic trauma is a controversial issue. This approach has some benefits; however, the careful selection of cases is difficult due to level I scientific evidence. The leading cause of this approach failure is the errors in the clinical assessment. In some instances, with acute spastic trauma, the patient is transferred to the operating room without a CT scan. The advancements in imaging approaches leads to the use of non-surgical technique in recent years.

Similar to the findings of the present study, in a study carried out by Lyas *et al.*, it was shown that non-surgical approach was successful and there was no difference between the prognosis of patients in surgical and non-surgical groups (Lyass *et al.*, 2001). Future studies should be conducted regarding the role of CT scan in the patients with the non-surgical approach. More effective outcomes and higher success rates have been reported in the comparison of surgical and non-surgical techniques for patients with Grade III and IV injuries (Tugnoli *et al.*, 2015).

However, the risk of non-surgical

management failure even after artery embolization increased in large lesions, which probably leads to worse parenchymal injury. On the other hand, according to the development of splenic abscess due to splenic ischemia and necrosis, the splenic trauma patients may need splenectomy. Artery embolization is associated with the increasing risk of non-surgical management failure rate; therefore, its use should be extensive (DuBose *et al.*, 2014). Based on a study conducted by Cinquantini *et al.*, the clinical success rate was reported as 95% for non-surgical management. Similar to the present study, in the study mentioned above, non-surgical management and splenic surgical management in dealing with hemodynamically stable patients with splenic injuries were compared and the results revealed no significant difference between them (Cinquantini *et al.*, 2018).

In the present study, the patients in the surgical group were similar to those in the non-surgical group in term of the lesion severity, while in a study performed by Cinquantini *et al.*, the patients in the surgical group had remarkable higher severity, compared to those in the non-surgical group. The surgical approach treated all cases with Grade IV with a clinical success rate of 100%. In a study carried out by Cinquantini *et al.*, it was suggested that a high chance of success is achieved by embolization that is confirmed by other reports (Rajani *et al.*, 2006; Davis *et al.*, 1998; Dent *et al.*, 2004).

According to the literature, the success rate of non-surgical management is estimated between 85–94% (Requarth *et al.*, 2018). However, a higher percentage of non-surgical approach is likely to be related to the treatment of patients with lower grades using these approaches. In fact, the majority of cases treated with embolization were in Grade III (Cinquantini *et al.*, 2018). Based on the results of the present study, no difference was observed between non-surgical and surgical approaches in terms of disease grade. Nonetheless, Banerjee *et al.* suggested the surgical procedure for the patients with Grade III (Banerjee *et al.*, 2013).

In a study conducted by Brillianto *et al.*, it was indicated that the success rates of patients with surgical and non-surgical approaches were reported as 91.6% and 95.4%, respectively, that was not different between the patients with various Grades. This finding confirmed by Bhullar *et al.* study (Bhullar *et al.*, 2012) showed that non-invasive measures for patients with high or low trauma grades under the standard protocol could be very safe and successful (Brillantino *et al.*,

2016). The management of Grade III lesions is very controversial. Although some studies supported the surgical approach (Banerjee *et al.*, 2015; Bhullar *et al.*, 2012; Brilliantino *et al.*, 2016; Miller *et al.*, 2014), some of them reported no remarkable advantages in this regard (Stassen *et al.*, 2012; Crichton *et al.*, 2017).

Some studies suggested the surgical approach associated with non-surgical management to increase the clinical success rate (Rajani *et al.*, 2006; Dent *et al.*, 2004). However, no improvement in splenic salvage rate was reported in other studies (Harbrecht *et al.*, 2007; Duchesne *et al.*, 2008; Smith *et al.*, 2006). In some studies, proximal and distal splenic embolization is compared (Bessoud *et al.*, 2006; Frandon *et al.*, 2014; Schnüriger *et al.*, 2011); however, due to different conditions of using these approaches, the comparison is misleading. Technically, distal embolization leads to safer hemostasis; therefore, with the observation of one or two target lesions in angiography, it should be preferred. Since there is a limited number of studies regarding the combined embolization (Rong *et al.*, 2017), it is recommended to carry out future studies in this regard.

In a retrospective registry review, 926 patients with splenic injury were assessed. Similar to the results of the present study, the study as mentioned earlier, indicated the same distribution of splenic injury grade between two groups. An improvement was observed in non-operative management by the increasing use of angiography and embolization. An aggressive utilization of splenic embolization in patients with appropriate indications will result in low rates of failure and mortality (Rosati *et al.*, 2015). Some advantages have been observed regarding the non-surgical approach. In the present study, total hospitalization duration was shorter in the non-surgical group, compared to that of the surgical group. Shorter hospitalization time was confirmed by another similar study (Tugnoli *et al.*, 2015), leading to a decrease in the risk of hospital infections, costs, and missed working days for each patient.

Moreover, there was no need for blood transfusion, platelet count, fresh frozen plasma, and Ringer's serum in the non-surgical approach that results in decreasing the risk of hospital infections and faster treatment. The survival of patients is the main goal of therapy focused on the traumatic patients; however, the mortality rate in cases with non-surgical management is not specified in the literature (Peitzman *et al.*, 2016). A primary concern in the case of patients with

splenic injuries is the possibility of a delayed rupture after discharge. Based on the evidence, it was concluded that there is no difference between the survival rate in splenic trauma patients with surgical and non-surgical approaches (Rialon *et al.*, 2016).

The present study demonstrated that 80.8% and 96.4% of the subjects in surgical and non-surgical approaches survived, respectively indicating no difference between the two in terms of survival. The survival rate was higher in the non-surgical group than that of the surgical group and the difference was not statistically significant. Therefore, both techniques are useful in the treatment of the patients. In this regard, the proper selection of cases for each type of treatment (surgical or non-surgical) is essential. In another retrospective study carried out by Kaufman *et al.* on 2587 patients, it was indicated that there is no relationship between the survival rate and use of ICU equipment (Kaufman *et al.*, 2016). According to the results of a retrospective study conducted by Alamri *et al.* on 238 patients, the mortality rate was higher among the patients older than 46 years, compared to that of the younger ones. The findings of the study as mentioned above showed that the splenectomy rate decreased; therefore, radiation therapy has been a successful method for the treatment of patients with high grades (Kaufman *et al.*, 2017), consistent with the results of some other studies (Robinette *et al.*, 1977; Ein *et al.*, 1977; HALLER, 2018; Aksnes *et al.*, 1995; Neuwirth *et al.*, 2016; Lolle *et al.*, 2016).

Based on the findings of a study carried out by Girard *et al.*, the non-surgical approach is the first-line treatment for splenic trauma patients with stable hemodynamic condition (Girard *et al.*, 2016). This result was confirmed by another review study conducted by Maboutly *et al.* that showed the increase of non-surgical approach in traumatic patients with stable hemodynamic condition. However, the use of non-surgical techniques in patients with high Grades may lead to an increase in the risk of failure, prolonged hospitalization, risk of delayed bleeding, and transfusion-related infections. Therefore, an appropriate therapeutic approach should be performed based on the patient's clinical condition, radiological findings, and surgeon's experience (El-Matbouly *et al.*, 2016).

Qu *et al.* assessed the postoperative consequences in patients who underwent splenectomy. According to the findings of the study above, it was revealed that 1.1% of the subjects who experienced splenectomy had intra-abdominal hemorrhage 21.43% of whom died.

Besides, a significant relationship was observed between the post-operative bleeding and mortality rate. According to the result as mentioned earlier, abdominal bleeding as the leading risk factor should be a matter of concern in patients with splenic trauma (Qu *et al.*, 2013), consistent with the results of some other studies (Krausz *et al.*, 2003; Solomonov *et al.*, 2000; Pusateri *et al.*, 2003).

In a study conducted by Ochsner, the stable hemodynamic conditions, absence of peritoneal damage signs in CT scan, and absence of significant peritoneal symptoms in abdominal examinations were introduced as the main criteria regarding the use of non-surgical approach in patients with splenic trauma (Ochsner *et al.*, 2001), consistent with the results of some other studies (Federle *et al.*, 1998; Notash *et al.*, 2008; Upadhyaya *et al.*, 2003; Sharma *et al.*, 2005; Krause *et al.*, 2000; Sclafani *et al.*, 1991). The present study provided more information considering non-surgical management in patients with splenic trauma and more details on the consequences of splenic trauma. Because the present study was a retrospective observational study; therefore, the obtained results cannot be generalized to other populations. The small sample size was considered another limitation of this study. It is suggested to carry out further studies to assess the value of ultrasound and CT scan in non-operative management of blunt splenic injuries.

4. CONCLUSIONS:

The obtained results of this study showed that there was no significant difference in the consequences of patients with splenic trauma between the surgical and non-surgical approaches. The length of hospitalization stay was shorter in the non-surgical group, compared to that of the surgical group. The most common cause of trauma in both groups was car accidents. Retroperitoneal hematoma was the most common intra-abdominal trauma. Furthermore, the mortality rate was higher in the surgical group, compared to that of the non-surgical group.

5. REFERENCES:

1. Aksnes, J., Abdelnoor, M. and Mathisen, O. *The European journal of surgery= Acta chirurgica*. **1995**, 161(4), 253-258.
2. Alamri, Y., Moon, D., Yen, D.A., Wakeman, C., Eglinton, T. and Frizelle, F. *The New*

- Zealand Medical Journal (Online)*, **2017**, 130(1463), 11-18.
3. Banerjee, A., Duane, T.M., Wilson, S.P., Haney, S., O'Neill, P.J., Evans, H.L., Como, J.J. and Claridge, J.A. *Journal of Trauma and Acute Care Surgery*. **2013**, 75(1), pp.69-75.
 4. Bessoud, B., Denys, A., Calmes, J.M., Madoff, D., Qanadli, S., Schnyder, P. and Doenz, F. *American journal of roentgenology*. **2006**, 186(3), 779-785.
 5. Bhullar, I.S., Frykberg, E.R., Siragusa, D., Chesire, D., Paul, J., Tepas III, J.J. and Kerwin, A.J. *Journal of the American College of Surgeons*. **2012**, 214(6), 958-964.
 6. Bisharat, N.O.H.L.I.R.R., Omari, H., Lavi, I. and Raz, R. *Journal of Infection*. **2001**, 43(3), 182-186.
 7. Brillantino, A., Iacobellis, F., Robustelli, U., Villamaina, E., Maglione, F., Colletti, O., De Palma, M., Paladino, F. and Noschese, G. *European Journal of Trauma and Emergency Surgery*. **2016**, 42(5), 593-598.
 8. Cinquantini, F., Simonini, E., Di Saverio, S., Cecchelli, C., Kwan, S.H., Ponti, F., Coniglio, C., Tugnoli, G. and Torricelli, P., *Cardiovascular and interventional radiology*. **2018**, 41(9), 1324-1332.
 9. Crichton, J.C.I., Naidoo, K., Yet, B., Brundage, S.I. and Perkins, Z., *Journal of Trauma and Acute Care Surgery*. **2017**, 83(5), 934-943.
 10. Davis, K.A., Fabian, T.C., Croce, M.A., Gavant, M.L., Flick, P.A., Minard, G., Kudsk, K.A. and Pritchard, F.E., *Journal of Trauma and Acute Care Surgery*. **1998**, 44(6), 1008-1015.
 11. Dent, D., Alsabrook, G., Erickson, B.A., Myers, J., Wholey, M., Stewart, R., Root, H., Ferral, H., Postoak, D., Napier, D. and Pruitt Jr, B.A. *Journal of Trauma and Acute Care Surgery*. **2004**, 56(5), 1063-1067.
 12. DuBose, J.J., Brenner, M. and Scalea, T.M., **2014**. Minimally Invasive Approach and Endovascular Techniques for Vascular Trauma. In *Trauma Surgery* (pp. 109-119). Springer, Milano.
 13. Duchesne, J.C., Simmons, J.D., Schmieg Jr, R.E., McSwain Jr, N.E. and Bellows, C.F. *Journal of Trauma and Acute Care Surgery*. **2008**, 65(6), 1346-1353.
 14. Ein, S.H., Shandling, B.A.R.R.Y., Simpson, J.S., Stephens, C.A., Bandi, S.K., Biggar, W.D. and Freedman, M.H. *Annals of surgery*. **1977**, 185(3), 307.
 15. El Khoury, M.Y., Gandhi, R., Dandache, P., Lombardo, G. and Wormser, G.P. *Ticks and tick-borne diseases*. **2011**, 2(4), pp.235-238.
 16. El-Matbouly, M., Jabbour, G., El-Menyar, A., Peralta, R., Abdelrahman, H., Zarour, A., Al-Hassani, A. and Al-Thani, H. *The Surgeon*. **2016**, 14(1), 52-58.
 17. Federle, M.P., Courcoulas, A.P., Powell, M., Ferris, J.V. and Peitzman, A.B. *Radiology*. **1998**, 206(1), 137-142.
 18. Frandon, J., Rodière, M., Arvieux, C., Michoud, M., Vendrell, A., Broux, C., Sengel, C., Bricault, I., Ferretti, G. and Thony, F. *Diagnostic and interventional imaging*. **2014**, 95(9), 825-831.
 19. Girard, E., Abba, J., Cristiano, N., Siebert, M., Barbois, S., Létoublon, C. and Arvieux, C. *Journal of visceral surgery*. **2016**, 153(4), 45-60.
 20. HALLER JR, J.A. *Transplantation*. **1964**, 2(2), 287-291.
 21. Harbrecht, B.G., Ko, S.H., Watson, G.A., Forsythe, R.M., Rosengart, M.R. and Peitzman, A.B. *Journal of Trauma and Acute Care Surgery*. **2007**, 63(1), 44-49.
 22. Hoefnagel, R., **1956**, March. Susceptibility to infection after splenectomy performed in childhood. In *Clinical proceedings-Children's Hospital of the District of Columbia* (Vol. 12, No. 3, p. 48).
 23. Kaufman, E.J., Wiebe, D.J., Martin, N.D., Pascual, J.L., Reilly, P.M. and Holena, D.N. *Journal of Surgical Research*, **2016**, 203(2), 338-347.
 24. Khazaei, Z., Khazaei, S., Valizadeh, R., Mazharmanesh, S., Mirmoeini, R., Mamdohi, S., Pordanjani, S.R., Nili, S., Ayubi, E., Mansori, K. and Goodarzi, E. *International Journal of Pediatrics*. **2016**, 4(7), 2213-2220.
 25. Krause, K.R., Howells, G.A. and Bair, H.A. *The american surgeon*, **2000**, 66(7), 636
 26. Krausz, M.M. and Hirsh, M. *Journal of Trauma and Acute Care Surgery*, **2003**, 55(1), 62-68.

27. Lolle, I., Pommergaard, H.C., Scheffe, D.F., Bulut, O., Krarup, P.M. and Rosenstock, S.J. *Diseases of the Colon & Rectum*, **2016**, 59(12), 1150-1159
28. Lyass, S., Sela, T., Lebensart, P.D. and Muggia-Sullam, M. *IMAJ-RAMAT GAN*, **2001**, 3(10), 731-733.
29. M Gage Ochsner, M.D. *World journal of surgery*, **2001**, 25(11), 1393-1396.
30. Miller, P.R., Chang, M.C., Hoth, J.J., Mowery, N.T., Hildreth, A.N., Martin, R.S., Holmes, J.H., Meredith, J.W. and Requarth, J.A. *Journal of the American College of Surgeons*, **2014**, 218(4), 644-648.
31. Neuwirth, M.G., Bartlett, E.K., Newton, A.D., Fraker, D.L., Kelz, R.R., Roses, R.E. and Karakousis, G.C. *Journal of Surgical Research*, **2016**, 205(1), 155-162.
32. Notash, A.Y., Amoli, H.A., Nikandish, A., Kenari, A.Y., Jahangiri, F. and Khashayar, P. *Emergency Medicine Journal*, **2008**, 25(4), 210-212.
33. Oyo-Ita, A., Chinnock, P. and Ikpeme, I.A., **2015**. Surgical versus non-surgical management of abdominal injury. Cochrane Database of Systematic Reviews, (11).
34. Peitzman, A.B., Ferrada, P. and Puyana, J.C. *Surgical infections*, **2009**, 10(5), 427-433.
35. Pusateri, A.E., McCarthy, S.J., Gregory, K.W., Harris, R.A., Cardenas, L., McManus, A.T. and Goodwin Jr, C.W. *Journal of Trauma and Acute Care Surgery*, **2003**, 54(1), 177-182.
36. Qu, Y., Ren, S., Li, C., Qian, S. and Liu, P. *International surgery*, **2013**, 98(1), 55-60.
37. Rajani, R.R., Claridge, J.A., Yowler, C.J., Patrick, P., Wiant, A., Summers, J.I., McDonald, A.A., Como, J.J. and Malangoni, M.A. *Surgery*, **2006**, 140(4), 625-632.
38. Renzulli, P., Hostettler, A., Schoepfer, A.M., Gloor, B. and Candinas, D. *British Journal of Surgery: Incorporating European Journal of Surgery and Swiss Surgery*, **2009**, 96(10), 1114-1121.
39. Requarth, J.A., D'Agostino Jr, R.B. and Miller, P.R. *Journal of Trauma and Acute Care Surgery*, **2011**, 71(4), 898-903.
40. Rialon, K.L., Englum, B.R., Gulack, B.C., Guevara, C.J., Bhattacharya, S.D., Shapiro, M.L., Rice, H.E., Scarborough, J.E. and Adibe, O.O. *The American Journal of Surgery*, **2016**, 212(4), 786-793.
41. Robinette, C.D. and Fraumeni JR, J. *The Lancet*, **1977**, 310(8029), 127-129.
42. Rong, J.J., Liu, D., Liang, M., Wang, Q.H., Sun, J.Y., Zhang, Q.Y., Peng, C.F., Xuan, F.Q., Zhao, L.J., Tian, X.X. and Han, Y.L. *Military Medical Research*, **2017**, 4(1), 17.
43. Rosati, C., Ata, A., Siskin, G.P., Megna, D., Bonville, D.J. and Stain, S.C. *The American Journal of Surgery*, **2015**, 209(2), 308-314.
44. Schnüriger, B., Inaba, K., Konstantinidis, A., Lustenberger, T., Chan, L.S. and Demetriades, D. *Journal of Trauma and Acute Care Surgery*, **2011**, 70(1), 252-260.
45. Sclafani, S., Weisberg, A., Scalea, T.M., Phillips, T.F. and Duncan, A.O. *Radiology*, **1991**, 181(1), 189-196.
46. Sharma, O.P., Oswanski, M.F., Daniel, S., Raj, S.S. and Daoud, Y.A. *The American surgeon*, **2005**, 71(5), 379-386.
47. Smith, H.E., Biffl, W.L., Majercik, S.D., Jednacz, J., Lambiase, R. and Cioffi, W.G. *Journal of Trauma and Acute Care Surgery*, **2006**, 61(3), 541-546.
48. Solomonov, E., Hirsh, M., Yahiya, A. and Krausz, M.M. *Critical care medicine*, **2000**, 28(3), 749-754.
49. Stassen, N.A., Bhullar, I., Cheng, J.D., Crandall, M.L., Friese, R.S., Guillaumondegui, O.D., Jawa, R.S., Maung, A.A., Rohs Jr, T.J., Sangosanya, A. and Schuster, K.M. *Journal of Trauma and Acute Care Surgery*, **2012**, 73(5), S294-S300.
50. Tugnoli, G., Bianchi, E., Biscardi, A., Coniglio, C., Isceri, S., Simonetti, L., Gordini, G. and Di Saverio, S. *Surgery today*, **2015**, 45(10), 1210-1217.
51. Upadhyaya, P. *Pediatric surgery international*, **2003**, 19(9-10), 617-627.

Table 1. Demographic and diagnostic data of splenic trauma patients

Variable		n	%	Variable		n	%
Education	Below high school	40	43.0	Occupation	Self-employed	35	40.7
	High school	32	34.4		Employed	7	8.1
	Associate Degree	9	9.7		Housewife	3	3.5
	Bachelor	9	9.7		Student	41	47.7
	Master or higher	3	3.2	Cause of trauma	Penetrating trauma	7	5.3
Diagnosis	Computed tomography scan	43	34.1		Blunt trauma	2	1.5
	Ultrasound	63	50.0		Accident	66	50.0
	Other	7	5.6		Fight	4	3.0
	Both	13	10.3		Fall	53	40.2

Table 2. Distribution and comparison of concurrent intra- and extra-abdominal traumas based on surgical and non-surgical approaches

Intra-abdominal trauma		n	%	n	%	Extra-abdominal trauma		n	%	n	%
Intestine	Surgical	3	2.9	4	3.1	Chest	Surgical	10	9.6	12	9.2
	Non-surgical	1	3.8				Non-surgical	2	7.7		
Liver	Surgical	7	6.7	11	8.5	Head	Surgical	5	4.8	7	5.4
	Non-surgical	4	15.4				Non-surgical	2	7.7		
Diaphragm	Surgical	3	2.9	3	2.3	Limb	Surgical	17	16.3	24	18.5
	Non-surgical	0	0				Non-surgical	7	26.9		
None	Surgical	60	57.7	79	60.8	Pelvis	Surgical	4	3.8	4	3.1
	Non-surgical	19	73.1				Non-surgical	0	0		
Kidney	Surgical	4	3.8	4	3.1	None	Surgical	31	29.8	40	30.8
	Non-surgical	0	0				Non-surgical	9	34.6		
Retroperitoneal hematoma	Surgical	11	10.6	11	8.5	Spine	Surgical	7	6.7	9	6.9
	Non-surgical	0	0				Non-surgical	2	7.7		
Stomach	Surgical	2	1.9	2	1.5	Limb, head, and neck	Surgical	17	16.3	20	15.4
	Non-surgical	0	0				Non-surgical	3	11.5		
Pancreas	Surgical	1	1.0	1	0.8	Limb and chest	Surgical	9	8.7	10	7.7
	Non-surgical	0	0				Non-surgical	1	3.8		
Intestine and liver	Surgical	1	1.0	1	0.8	Chest, limb, and head	Surgical	1	1.0	1	0.8
	Non-surgical	0	0				Non-surgical	0	0		
Intestine and retroperitoneal hematoma	Surgical	2	1.9	2	1.5	Head and pelvic	Surgical	1	1.0	1	0.8
	Non-surgical	0	0				Non-surgical	0	0		
Liver and kidney	Surgical	4	3.8	6	4.6	Pelvic and spine	Surgical	2	1.9	2	1.5
	Non-surgical	2	7.7				Non-surgical	0	0		
Liver and retroperitoneal	Surgical	4	3.8	4	3.1	Kidney, intestine,	Surgical	2	1.9	2	1.5
	Non-surgical	0	0				Non-surgical	0	0		

neal hematoma						and retroperiton eal hematoma					
------------------	--	--	--	--	--	--	--	--	--	--	--

Table 3. Mean score of basic information according to surgical and non-surgical approaches

Variables	Treatment approach	n	Mean	Standard deviation	P-value
Systolic blood pressure	Surgical	104	108.16	19.18	0.57
	Non-surgical	26	110.42	14.15	
Diastolic blood pressure	Surgical	104	69.62	12.20	0.88
	Non-surgical	26	69.23	10.83	
Respiratory rate	Surgical	102	18.49	6.05	0.36
	Non-surgical	25	17.36	2.76	
Body temperature	Surgical	103	40.301	32.80	0.61
	Non-surgical	26	37.01	0.25	
Heart rate	Surgical	103	100.02	21.1	0.09
	Non-surgical	26	92.54	17.41	
Length of intensive care unit stay (day)	Surgical	101	6.40	10.08	0.01
	Non-surgical	28	3.57	3.27	
Total hospitalization duration (day)	Surgical	104	11.40	12.9	0.02
	Non-surgical	28	7.82	4.42	
Blood loss in operating room (cc)	Surgical	102	1430.39	1416.78	0.000
	Non-surgical	26	0	0	
Whole blood transfusion (cc)	Surgical	103	86.41	458.26	0.35
	Non-surgical	28	5.36	28.34	
Packed red blood cells transfusion in operating room (cc)	Surgical	103	434.99	549.96	0.000
	Non-surgical	26	0	0	
Packed red blood cells transfusion except in operating room (cc)	Surgical	102	133.33	273.34	0.03
	Non-surgical	26	40.38	162.49	
Fresh frozen plasma transfusion in operating room (cc)	Surgical	102	288.24	443.72	0.000
	Non-surgical	26	0	0	
Fresh frozen plasma transfusion except in operating room (cc)	Surgical	103	159.22	436.88	0.01
	Non-surgical	26	30.77	156.89	
Platelet transfusion in operating room (cc)	Surgical	103	14.08	82.37	0.000
	Non-surgical	26	.00	.000	
Platelet transfusion except in operating room (cc)	Surgical	103	8.74	56.63	0.43
	Non-surgical	26	0	0	
Normal saline injection in operating room (cc)	Surgical	103	2107.28	1584.25	0.000
	Non-surgical	26	0	0	
Normal saline injection except in operating room (cc)	Surgical	103	441.75	1015.32	0.002
	Non-surgical	26	76.92	306.34	
Urine output in operating room (cc)	Surgical	103	703.40	607.561	0.000
	Non-surgical	26	0	0	
Ringer's lactate solution injection in	Surgical	103	924.76	972.108	0.000

operating room (cc)	Non-surgical	26	0	0	
Ringer's lactate solution injection except in operating room (cc)	Surgical	103	53.40	312.42	0.387
	Non-surgical	26	0	0	
Ringer's serum injection in operating room (cc)	Surgical	103	1316.5	998.73	0.000
	Non-surgical	26	0	0	
Ringer's serum injection except in operating room (cc)	Surgical	103	33.98	175.205	0.91
	Non-surgical	26	38.46	196.11	
Number of computed tomography scans	Surgical	98	0.67	0.75	0.03
	Non-surgical	28	0.96	0.57	
Number of ultrasounds	Surgical	99	1.23	0.71	0.31
	Non-surgical	26	1.08	0.62	

Table 4. Different side effects based on surgical and non-surgical approaches

Variables	Treatment approach	n	%	Total	
				n	%
Infection and fever	Surgical	15	14.4	17	13.1
	Non-surgical	2	7.7		
Bleeding	Surgical	3	2.9	3	2.3
	Non-surgical	0	0		
No splenic embolization	Surgical	77	74.0	100	76.9
	Non-surgical	23	88.5		
Seizure	Surgical	3	2.9	4	3.1
	Non-surgical	1	3.8		
Perforation	Surgical	2	1.9	2	1.5
	Non-surgical	0	0		
Tachycardia and tachypnea	Surgical	1	1.0	1	0.8
	Non-surgical	0	0		
Bronchiectasis	Surgical	1	1.0	1	0.8
	Non-surgical	0	0		
Infection and bleeding	Surgical	2	1.9	2	1.5
	Non-surgical	0	0		

Table 5. Grades of lesions based on surgical and non-surgical approaches

Treatment approach		Grade			Total
		2	3	4	
Surgical	n	1	6	1	8
	%	12.5	75.0	12.5	100
Non-surgical	n	3	2	0	5
	%	60.0	40.0	0.0	100
Total	n	4	8	1	13
	%	30.8	61.5	7.7	100

CARACTERÍSTICAS COMPARATIVAS DO ESTADO DE TECIDOS DENTÁRIOS DUROS EM PACIENTES DEPENDENTES DE DROGAS QUE USAM HEROÍNA, E METADADONA COMO TERAPIA DE SUBSTITUIÇÃO**COMPARATIVE CHARACTERISTICS OF THE STATE OF HARD DENTAL TISSUES IN DRUG-DEPENDENT PATIENTS WHO USE HEROIN, AND METHADONE AS REPLACEMENT THERAPY****СРАВНИТЕЛЬНАЯ ХАРАКТЕРИСТИКА СОСТОЯНИЯ ТВЕРДЫХ ТКАНЕЙ ЗУБОВ У НАРКОЗАВИСИМЫХ ПАЦИЕНТОВ, УПОТРЕБЛЯЮЩИХ ГЕРОИН И МЕТАДОН В КАЧЕСТВЕ ЗАМЕСТИТЕЛЬНОЙ ТЕРАПИИ**

SEVBITOV, Andrei*;TIMOSHIN, Anton; DOROFEEV, Aleksei; DAVIDYANTS, Alla; ERSHOV, Kirill; KUZNETSOVA, Maria

Department of Propaedeutic of Dental Diseases
of I.M. Sechenov First Moscow State Medical University (Sechenov University)

* Correspondence author
e-mail: avsevbitov@mail.ru

Received 12 November 2019; received in revised form 19 January 2020; accepted 22 January 2020

RESUMO

De acordo com o serviço Federal de controle de drogas da Rússia, atualmente, 8,5 milhões de pessoas consomem drogas, incluindo maconha - 6,2 milhões, drogas sintéticas - 1,5 milhão e heroína - 800.000 pessoas. De acordo com a literatura estrangeira e nacional, o consumo de narcóticos na população cresce continuamente, principalmente na juventude e na adolescência: na estrutura dos drogados, 20% são pacientes com idades entre 9 e 16 anos, 60% - 17 a 30 anos, 20% - 30 anos ou mais. Além disso, muitos autores observam o fato de que mesmo em jovens com uso a por um curto período de metadona, aumenta acentuadamente a intensidade de cárie dental com subsequente perda rápida de dentes. Desde 2005, a OMS incluiu a droga metadona na lista de medicamentos essenciais para o tratamento da dependência de opióides. No entanto, de acordo com a literatura mais recente, o efeito negativo da metadona no corpo como um todo e a saúde bucal são muito mais pronunciados do que quando se toma heroína. As alterações na cavidade oral ao consumir heroína e metadona na literatura não são suficientemente abordadas, portanto, é considerado relevante estudar a patologia dentária nesse grupo de pacientes. Este artigo apresenta os resultados de uma análise comparativa dos efeitos adversos da heroína e da metadona nos tecidos duros dos dentes de pacientes dependentes de drogas. Nos pacientes que tomavam heroína e metadona, houve uma deterioração nos indicadores de status dentário. As principais manifestações do uso de narcóticos são o desenvolvimento do processo carioso, doenças inflamatórias da cavidade oral, violação da salivação, formação e disseminação de infecção odontogênica crônica. O efeito negativo da metadona é mais pronunciado em comparação com a heroína devido ao contato da droga em forma de comprimido com a mucosa oral.

Keywords: *cárie dentária, toxicodependência, heroína, metadona.*

ABSTRACT

According to the Federal service for drug control in Russia, currently, 8.5 million people take drugs, including marijuana-6.2 million, synthetic drugs-1.5 million, and heroin-800,000 people. According to foreign and domestic literature, the population's consumption of narcotic drugs is continuously growing, especially in the youth and adolescence: in the structure of drug addicts, 20% are patients aged 9-16 years, 60% - 17-30 years, 20% - 30 years and older. Besides, many authors note the fact that even in young people with short-term use of methadone sharply increases the intensity of dental caries with subsequent rapid loss of teeth. Since 2005, the WHO has included the drug methadone in the list of essential medicines for the treatment of opioid dependence. However, according to the latest literature, the negative effect of methadone on the body as a

whole, and dental health is much more pronounced than when taking heroin. Changes in the oral cavity when taking heroin and methadone in the literature are not covered enough, so it is considered relevant to study dental pathology in this group of patients. This article presents the results of a comparative analysis of the adverse effects of heroin and methadone on the hard tissues of the teeth of drug-dependent patients. In patients taking heroin and methadone, there was a deterioration in dental status indicators. The main manifestations of taking narcotic drugs are the development of the carious process, inflammatory diseases of the oral cavity, violation of salivation, the formation and spread of chronic odontogenic infection. The negative effect of methadone is more pronounced in comparison with heroin due to the contact of the tablet form of the drug with the oral mucosa.

Keywords: *dental caries, drug addiction, heroin, methadone.*

АННОТАЦИЯ

По данным Федеральной службы по контролю за оборотом наркотиков в России в настоящее время наркотики принимают 8,5 млн. человек, из них марихуану — 6.2 млн., синтетические наркотики — 1,5 миллиона, а героин — 800 000 человек. По данным зарубежной и отечественной литературы потребление населением наркотических препаратов постоянно растет, особенно в молодежной среде и подростковом возрасте: в структуре наркозависимых 20% составляют пациенты в возрасте 9–16 лет, 60% — 17–30 лет, 20% — от 30 лет и старше. Кроме того, многие авторы отмечают тот факт, что даже у лиц молодого возраста при непродолжительном приеме метадона резко увеличивается показатель интенсивности кариеса зубов с последующей быстрой потерей зубов. С 2005 года ВОЗ был включен препарат метадон в перечень основных лекарственных средств для лечения опиоидной зависимости. Однако по последним данным литературы, отрицательное влияние метадона на организм в целом и на стоматологическое здоровье значительно более выражено, чем при приеме героина. Изменения в полости рта при приеме героина и метадона в литературных источниках освещены недостаточно, поэтому актуальным считается изучение стоматологической патологии у данного контингента пациентов. В данной статье приведены результаты сравнительного анализа отрицательного воздействия героина и метадона на твердые ткани зубов у наркозависимых пациентов. У пациентов, принимающих героин и метадон, отмечено ухудшение показателей стоматологического статуса. Основными проявлениями приема наркотических препаратов являются развитие кариозного процесса, воспалительных заболеваний ротовой полости, нарушение саливации, формирование и распространение хронической одонтогенной инфекции. Отрицательное влияние метадона более выражено по сравнению с героином вследствие контакта таблетированной формы препарата со слизистой оболочкой полости рта.

Ключевые слова: *кариес зубов, наркомания, героин, метадон.*

1. INTRODUCTION

According to foreign and domestic literature, the population's consumption of narcotic drugs is constantly growing, especially in the youth and adolescence: in the structure of drug addicts, 20% are patients aged 9-16 years, 60% - 17-30 years, 20% - 30 years and older. [Silva *et al*, 2019; Gupta *et al*, 2012; Mateos-Moreno *et al*, 2013]. According to sociological research in recent years, every seventh student has tried drugs at least once. Over the past ten years, the number of adolescents with drug addiction has increased 13 times [Evstratenko *et al*, 2018; Sevbitov *et al*, 2019].

According to the Federal service for drug control in Russia, currently, 8.5 million people take drugs, including marijuana - 6.2 million, synthetic drugs - 1.5 million, and heroin-800,000 people.

Since 2005, WHO has included the drug methadone in the list of essential medicines for the treatment of opioid dependence. However, according to the latest literature, the negative effect of methadone on the body as a whole and dental health is much more pronounced than when taking heroin. Changes in the oral cavity when taking heroin and methadone in the literature are not covered enough, so it is considered relevant to study dental pathology in this group of patients [Martusevich *et al*, 2014; Mazzeo *et al*; 2013].

Methadone (6dimethylamino-4,4-diphenyl-3heptanon) is a synthetic opioid, an analgesic with narcotic properties, first obtained in 1946. Initially, the drug was supposed to be used as a substitute for morphine due to the similarity of the physiological effects caused, except for analgesia, less pronounced in cases of methadone use. Nevertheless, in 1949, the effectiveness of reducing doses of methadone for

the treatment of heroin withdrawal was shown. In 1964 V. P. Dole and M. A. Nyswander offered methadone for the treatment of patients with heroin addiction, and since then, the drug has been used in medicine mainly for the relief of heroin withdrawal attacks and as a means of replacement therapy [Simonova *et al*, 2014; Timoshin *et al*; 2018].

In the mid-60s of the last century, methadone programs were proposed, which are still being implemented in the United States, Great Britain, Denmark, Sweden, the Netherlands and other countries. The goal of these programs is not drug withdrawal, but social rehabilitation, reducing the level of criminogenic behavior, as well as inhibiting HIV infection and the development of AIDS. Also, in several countries in Europe, Latvia, Lithuania, Ukraine, and the United States, there are similar programs that aim to gradually transfer patients who use heroin to another synthetic drug, such as methadone. In Russia, such programs are banned or are limited in their use. In Ukraine, the methadone program lasted about nine years. In Crimea, during this time, the number of patients receiving an opium antagonist has increased from 9 to 800 people. After the return of Crimea to the Russian Federation, this program was discontinued. When adapting patients after methadone addiction, many drug addicts were further rehabilitated in other cities of Russia (Moscow, St. Petersburg, Rostov-on-don). Moreover, this process continues today because it turned out that the dependence on methadone is long-lasting and much more severe than on other opiates [Vaijayanthimala *et al*, 2015; Voloshina *et al*, 2018; Dos Silva *et al*; 2019].

According to the results of foreign studies of the effectiveness of methadone replacement therapy programs, it was noted that about 60% of the patients who participated in them, together with the use of methadone, continued to use "street" drugs. Besides, after replacement therapy, only 5-10% of patients with heroin addiction have remission of more than one year. Despite the above, it is stated that currently, methadone is used by drug users mainly for substitution purposes against the background of already formed heroin addiction [Silva *et al*, 2019; Gigena *et al*, 2015; Walter *et al*, 2015].

It should be borne in mind that systematic uncontrolled use of methadone for only one month due to the parallel development of tolerance to the drug and addiction to it, can lead to an increase in a single dose of methadone five times (1 g). It is also shown that the rate of

development of tolerance and dependence in the use of methadone is proportional to the length of use and the daily dose of heroin. Besides, if heroin withdrawal lasts for several days, then methadone-a few weeks. Unlike heroin, when you cancel methadone, the addict is not able to give up the drug on their own. Also, methadone overdose is much more common than heroin due to the slowness of its action and the unpredictable rate of development of tolerance to the drug. This does not allow you to assess the necessary dose, which does not threaten fatal consequences [Yang *et al*, 2015; Gupta *et al*, 2012].

Rapid acquisition of tolerance to the drug is also a problem of substitution therapy since many patients are subsequently forced to take methadone for years. It should be noted that while methadone maintenance therapy significantly increased mortality from overdoses. With increasing rates, acute methadone poisoning also prevails in the structure of acute opiate drug poisoning (the ratio of heroin/methadone was 3/1 in 2011, 1/3 in 2012 and 1/5 in the first six months of 2013).

To date, the spread and non-medical use of narcotic substances naturally leads to an increase in social tension and personal and public danger: an increase in crime, accidents, and suicides, severe problems with their health and the health of future offspring, a decrease in life expectancy, prostitution, the spread of HIV infection, hepatitis C [Mateos-Moreno *et al*, 2013; Protrka *et al*; 2013].

It is stated that drug addiction of any nature is a severe threat not only to the mental, somatic but also to the dental status of patients. It was found that the frequency and severity of oral diseases significantly increased in patients with drug dependence who use heroin [Du M. *et al*, 2001; Dukić *et al*, 2013].

Significant changes in the dental status of heroin-dependent patients are associated with the reluctance to lead a healthy lifestyle, comply with basic hygiene standards of oral care, and regularly visit the dentist. An important role is played by the reduction of the body's immunity, its protective and adaptive abilities against the background of taking drugs [Vehkalahti *et al*; 1996].

According to most authors, the main problems of dental heroin-dependent patients are the following [Girardin *et al*, 2019]:

- destruction of hard tissues of teeth;

- development of periodontal diseases of inflammatory origin;
- changes in the oral mucosa;
- violation of salivation;
- spread of foci of chronic odontogenic infection.

Based on the above, the purpose of the work is to conduct a comparative analysis of the negative impact on the hard tissues of the teeth of patients taking heroin and methadone as replacement therapy based on a set of objective studies [Di Fazio *et al*, 2018; Fiorentin *et al*, 2018].

2. MATERIALS AND METHODS

All research methods under this article have been conducted in accordance with the relevant guidelines and regulations. All experimental protocols were approved by the Local Ethics Committee of I. M. Sechenov First Moscow State Medical University (Sechenov University) protocol number № 05-16 from 18.05.2016. Prior to the study, informed consent was obtained from all patients for the upcoming study.

A set of clinical material was carried out from 2015 to 2017 in the clinic for the treatment and rehabilitation of drug-dependent patients of the medical center "Profmed". These were patients with various types of drug addiction, but the bulk - using opioid drugs (97%)

A total of 110 patients aged 20 to 50 years and more were examined, men-68, women-42, who are in the rehabilitation period.

According to the goals and objectives of the study, patients were selected who in addition to heroin mainly did not take other drugs (group 1-53 patients), and patients who received methadone as replacement therapy at different times (group 2-57 patients) Their distribution by sex, age, and duration of use of the drug are presented in Table 1 and 2.

Depending on the duration of the drug, group 1 patients are divided into two subgroups: 1A-patients with a duration of administration from 1 to 3 years and 1B-with a duration of administration of 3-5 or more years.

Similarly, patients were divided into two groups. Patients in subgroups 2A and 2B were taken mainly oral methadone, according to the scheme prescribed by the doctor-narcologist in the form of syrup or tablets.

Examination of the oral cavity included the determination of the hygienic state, detection of pathological changes in the oral mucosa, periodontal, hard tissues of the tooth.

At the same time, it was revealed that all 100% of the examined patients need various types of dental care. It was also revealed that all their previous visits to the dentist were motivated by the development of pain syndrome, that is, for emergency indications and, mainly, to the dentist to remove an inappropriate tooth treatment or to open an abscess.

Based on a survey of patients, it was found that planned oral sanitation was rejected, as a rule, due to problems of adaptation to dental treatment, fear of pain, and there were various life restrictions due to drug use and the duration of stages of dental treatment.

To assess the hygienic state of the oral cavity, the Green-Vermillion index was calculated, which includes the plaque index and the Tartar index.

An instrumental survey was also conducted. The teeth were examined using a dental mirror and a probe. When analyzing the intensity of the carious process, we used the values of the CFR indices of teeth, where C – the number of carious (untreated) teeth, F (filling) - the number of treated (sealed) teeth, R - the number of removed or to be removed teeth. The sum (C+F+R) of all affected and lost teeth characterizes the intensity of the carious process in a particular person.

The prevalence of caries was also assessed. The prevalence of dental caries is the ratio of the number of persons who have at least one of the signs of dental caries (carious, filled or removed teeth) to the total number of examined, expressed as a percentage.

3. RESULTS AND DISCUSSION:

Among the 100 people examined in the rehabilitation center for drug addicts, there was not a single person who did not complain about the general state of health and did not have pathological changes in the oral cavity. All 100% of those examined needed dental care. When conducting a survey of patients, it was found that women were motivated to take drugs for economic reasons in 32.7% of cases, moral and psychological in 43.2%, the influence of a drug-dependent husband, or another sexual partner.

In men, the main reasons were: interest to

try something "new" - 71.4%, dissatisfaction with work, career, family life-17.3%, the influence of friends, and the environment-11.3%.

Age-related terms of initiation of drug use in men and women were not revealed – the average age was 17.3 years, which has a substantial negative impact on the development of the body as a whole and, in particular, in the formation of the dental system.

It was revealed that the expressed drug dependence and the appearance of signs of withdrawal syndrome for the first time in women were formed approximately 6-8 months, in men-in 1-1.2 years, that is, two times later, which can be explained by the different frequency of taking drugs.

The negative manifestation of drug use men noted as the development of various somatic diseases (weakness, fatigue, heart pain, violation of the chair), women-the development of female dysfunction, memory loss, anorexia.

In the structure of complaints about hard tissues of the teeth, complaints about the destruction of teeth prevailed. All the examined patients had an unsatisfactory state of oral hygiene. Against the background of the general pathology of the body of drug-dependent patients, this is one of the main factors in the development of inflammatory processes in the oral cavity (Fig. One).

It was found that supragingival and subgingival deposits were reliably encountered in patients of both groups (100%), while solid supragingival and subgingival deposits prevailed.

Hygienic state of the oral cavity when using heroin and methadone.

The hygienic state of the oral cavity is not only a reflection of the general state of the body but also, in a certain way, plays a role in the prediction and development of major dental diseases. This indicator was evaluated by calculating the Green-Vermilion index (1964). The data obtained are presented in Tables 3 and 4 and Figure 1.

As can be seen from table 3, the hygienic state of the oral cavity in patients taking heroin can be assessed as "bad" and "very bad" - in 49% of patients in subgroup 1A and 45.2% of patients in subgroup 1B. Satisfactory hygiene was observed only in 5.7% of patients in subgroup 1A.

In a comparative analysis of hygiene indicators in different age groups of subgroup 1A,

it was found that 20-40 year-old patients had a level of hygiene with a rating of "bad" and "very bad" 2 times more often than in the age group of 41-50 years (33.9% and 15.1% of patients, respectively). A similar pattern is observed in subgroup 1B (33.9% and 11.3%).

The dependence of the hygiene index on the duration of drug use was not revealed by us: "bad" and "very bad" hygiene was detected in 49% of the examined patients with drug use lasting up to 3 years and in 45.2 patients taking drugs for more than three years.

Similarly calculated indicators of hygiene in the 2nd group (Tab. 4).

From the data obtained in table 4, it can be seen that satisfactory oral hygiene in patients of subgroup 2A is 3.4%, in subgroup 2B - 5.2%

"Bad" and "very bad" hygiene was found in 49.2% of patients in subgroup 2A and 41.9% of patients in subgroup 2A and 41.9% of patients in subgroup 2B, satisfactory-in 3.4% of patients in group 2A and 5.2% of patients in group 2B.

In group 2, there is also a dependence on the state of oral hygiene on age, as in group 1 ("bad" and "very bad" hygiene in 36.9% of patients 20-40 years and 12.3% aged 41-50 years). In subgroup 2B, these figures were 29.7% and 12.2%, respectively.

Thus, a poor and very poor state of oral hygiene has been established in all patients. At the same time, the indicators in both groups do not have much difference. It should be noted that patients often did not pay attention to such factors as the need to rinse the mouth after eating, a certain choice of toothpaste and brushes, because no preventive work was done with them [Cone *et al*, 2012; Kunkel *et al*, 2015; Grabenauer *et al*, 2018].

Features of the clinic of the carious process in the use of drugs.

Parenteral use of heroin contributes to an increase in the prevalence (96-100%) and intensity of dental caries due to toxic effects on the oral cavity. There was a correlation between the experience of heroin use and the intensity of dental caries: the longer the experience, the more likely the development of multiple caries, which later turns into pulpitis and periodontitis of a sluggish course [Pesce *et al*, 2012; Rook *et al*, 2005; Wasels *et al*, 1994; Presley *et al*, 2003; Sordi *et al*, 2017].

A characteristic feature of this group of patients is the absence of dental complaints and

the development of "pain-free caries".

The prevalence of caries in the examined patients was 100%, CFR-16.7%

The index of prevalence and intensity of caries was calculated separately for each subject, and then the average values were derived. The results are presented in Table 5.

As follows from table 5 in subgroup 1A (29 patients), the prevalence of caries was 87.8 in the age group of 20-40 years%.

In the age group from 41 to 50 years of this subgroup, the same figure was 98.1%.

The prevalence of caries in subgroup 1B was: at the age of 20-40 years, the prevalence was 87.9%, over 41 years - respectively 98.8%.

Thus, from the presented data, it can be stated that according to the WHO assessment, these values indicate a high prevalence of caries in people who take drugs. In this case, the indicators tend to increase depending on the age of patients and the timing of drug use.

The rate of caries intensity was 4.3 in subgroup 1A in the age group 20-40 years, and 5.8 in the age group 41-50 years.

In subgroup 1B, this indicator was 6.3 in the age group of 20-40 years and 6.8 in the age group of 41-50 years, i.e., the same relationship is observed as in the prevalence of caries: the intensity index tends to increase depending on the age of the patient and the duration of heroin use.

Similarly, we studied the prevalence and intensity of caries in patients transferred to methadone replacement therapy (group 2).

As can be seen from Table 6, the following data were obtained in group 2: in subgroup 2A, the prevalence in patients aged 20-40 years was 89.3%, in group 41-50 years – 94.2%.

The intensity index was in subgroup 2A in the age group 20-40 years - 5.8; and in the age group 41-50 years - 7.1.

In subgroup 2B, the prevalence of caries in people aged 20 to 40 years was 96.6%, and in the older age group, 99.6%. Accordingly, the intensity – 6.7, and in the older age group-8.7.

Thus, in the 2nd group, as in the 1st, there is a dependence (deterioration) of the prevalence and intensity of caries on the age of patients and the duration of drug use.

4. CONCLUSIONS:

Heroin use has a toxic effect on the oral organs: clinically, there are high rates of prevalence and intensity of caries, especially in the age group of 41-50 years. When using methadone as replacement therapy, the prevalence of caries in 41-50 year olds is slightly higher than in the age group of 20-40 years (by 4%), the intensity of caries is similar (by 1.3 points or higher). The use of methadone as a replacement therapy has a more negative effect on the hygiene of the oral cavity and the condition of the hard tissues of the teeth than with the use of heroin.

A special feature of the treatment of patients suffering from drug addiction is the need for rapid preventive measures, rehabilitation of the oral cavity, including the removal of destroyed teeth and teeth with 3 degrees of mobility, treatment of dental caries and its complications. Given the high prevalence of dental diseases in drug-dependent patients, it is recommended to use high-quality care with annual planned rehabilitation to improve the quality of life. The use of modern therapeutic and orthopedic materials will improve the quality of dental care.

Given the peculiarities of caries in drug-dependent patients, the occurrence of which is connected, including, with hypocalvaria recommended as a filling material to use polyalkenoate blocks of cement having series-production properties due to the content of fluoride ions.

5. ACKNOWLEDGMENTS:

This work was done at Sechenov University with supported by the "Russian Academic Excellence Project 5-100".

6. REFERENCES:

1. Evstratenko, V. V., Sevbitov, A. V., Platonova, V. V., Selifanova, E. I., Dorofeev, A. E. The characteristics of crystallization of mixed saliva in patients using heroin and methadone. *Klinicheskaya Laboratornaya Diagnostika*, **2018**, 63(4), 223-227.
2. Sevbitov A.V., Dorofeev A.E., Kuznetsova M.Yu., Timoshin A.V., Ershov K.A. Comparative characteristics of the crystallogram of the oral fluid in patients who use heroin and methadone. *Periodico Tchê Química*, **2019**, 16(33), 94-101

3. Martusevich, A. K., Yanchenko, V. A., Zhdanova, O. B., Artese, F., Napisanova, L. A., Virbalene, R. Crystallization characteristics of biological fluids of patients with postoperative alveococcosis. *Sovremennye Tehnologii v Medicine*, **2014**, 6(2), 38-42.
4. Mazzeo, M. A., Linares, J. A., López, M. M., Bachmeier, E., Wietz, F. M., Galván, V., Valentinuzzi, M. C., Riveros, J. A., Finkelberg, A. Analysis of saliva samples from oncological patients treated with 5-fluorouracil and leucovorin calcium by scanning electron microscopy with energy dispersive system. *Journal of Oral Pathology and Medicine*, **2013**, 42(10), 788-792.
5. Simonova, Z. G., Martusevich, A. K., Shubina, O. I., Emanuel, V.L. Structuring characteristics of biological fluids of patients with combined cardiovascular and gastrointestinal pathology. *Sovremennye Tehnologii v Medicine*, **2014**, 6(3), 64-70.
6. Timoshin, A. V., Dorofeev, A. E., Davidyants, A. A., Ershov, K. A., Pustokhina, I. G., Danshina, S. D. Features of the dental status of patients taking narcotic smoking mixtures. *Indo American Journal of Pharmaceutical Sciences*. **2018**, 5(9), 9114-9117.
7. Vijayanthimala, V., Lee, D. K., Kim, S. V., Yen, A., Tsai, N., Ho, D., Chang, H.-C., Shenderova, O. Nanodiamond-mediated drug delivery, and imaging: Challenges and opportunities. *Expert Opinion on Drug Delivery*. **2015**, 12(5), 735-749.
8. Voloshina, I. M., Borisov, V. V., Sevbitov, A.V., Davidyants, A.A., Mironov, S. N., Kuznetsova, M. Yu., Ergesheva, E. V. Distinctive features of microcrystallization of mixed saliva in children with different levels of activity of carious process. *Asian Journal of Pharmaceutics*, **2018**, 12(S3), 1017-1020.
9. Dos Silva, D. S., De Yamaguchi, K. K. L. Drug chemistry, and self-medication awareness as a tool in teaching organic functions. *Periodico Tchê Química*, **2019**, 16(31), 223-234
10. Silva, P. D. C., Santos, B. L. C. D., Soares, G.L., Oliveira, W.A.D. Anti-Candida albicans activity of the association of citronelal with anfotericin B or with cetoconazole. *Periodico Tchê Química*, **2019**, 16(31), 250-257
11. Gigena, P. C., Cornejo, L. S., Lescano-de-Ferrer, A. Oral health in drug addict adolescents and non-psychoactive substance users. *Acta Odontol Latinoam*, **2015**, 28(1), 48-57.
12. Walter M., Bentz D., Schick Tanz N., Milnik A., Aerni A., Gerhards C., Schwegler K., Vogel M., Blum J., Schmid O., Roozendaal B., Lang UE, Borgwardt S., de Quervain D. Effects of cortisol administration on craving in heroin addicts. *Transl Psychiatry*. **2015**, 28(5), 610.
13. Yang T., Guo X., Wang H., Fu S., Wen Y., Yang H. Magnetically optimized SERS assay for rapid detection of trace drug-related biomarkers in saliva and fingerprints. *Biosens Bioelectron*. **2015**, 15(68), 350-357.
14. Gupta T., Shah N., Mathur V. P., Dhawan A. Oral health status of a group of illicit drug users in Delhi, India. *Community Dent Health*, **2012**, 29(1), 49-54.
15. Mateos-Moreno M. V., Del-Río-Highsmith J., Riobóo-García R., Solá-Ruiz M. F., Celemin-Viñuela A. Dental profile of a community of recovering drug addicts: Biomedical aspects. Retrospective cohort study. *Med Oral Patol Oral Cir Bucal*. 2013 Jul 1;18(4):e671-9
16. Protrka N., Katunarić M., Filipović I., Verzak Z. Caries prevalence in heroin addicts. *Acta Clin Croat*. **2013**, 52(4), 436-43.
17. Du M., Bedi R., Guo L., Champion J., Fan M., Holt R. Oral health status of heroin users in a rehabilitation centre in Hubei province, China. *Community Dent Health*, **2001**, 18(2), 94-8.
18. Dukić W., Dobrijević T. T., Katunarić M., Lesić S. Caries prevalence in chronic alcoholics and the relationship to salivary flow rate and pH. *Cent Eur J Public Health*, **2013**, 21(1):43-7.
19. Vehkalahti M., Nikula-Sarakorpi E., Paunio I. Evaluation of salivary tests and dental status in the prediction of caries increment in caries-susceptible teenagers. *Caries Res*, **1996**, 30(1), 22-8.
20. Girardin F., Hearmon N., Negro F., Eddowes L., Bruggmann P., Castro E. Increasing hepatitis C virus screening in people who inject drugs in Switzerland using rapid antibody saliva and dried blood spot testing: A cost-effectiveness analysis. *J Viral Hepat*. **2019**, 26(2), 236-245.

21. Di Fazio V., Wille S. M. R., Toennes S. W., van Wel J. H. P., Ramaekers J. G., Samyn N. Driving under the influence of cocaine: Quantitative determination of basic drugs in oral fluid obtained during roadside controls and a controlled study with cocaine users. *Drug Test Anal*, **2018**, 10.
22. Fiorentin T. R., Scherer J. N., Marcelo M. C. A., Sousa T. R. V., Pechansky F., Ferrão M. F., Limberger R. P. Comparison of Cocaine/Crack Biomarkers Concentrations in Oral Fluid, Urine, and Plasma Simultaneously Collected From Drug Users. *J Anal Toxicol*, **2018**, 42(2), 69-76.
23. Cone E. J. Oral fluid results compared to self reports of recent cocaine and heroin use by methadone maintenance patients. *Forensic Sci Int*. **2012**, 10(215), 88-91.
24. Kunkel F., Fey E., Borg D., Stripp R., Getto C. Assessment of the use of oral fluid as a matrix for drug monitoring in patients undergoing treatment for opioid addiction. *J Opioid Manag*. **2015**, 11(5), 435-42.
25. Grabenauer M., Moore K. N., Bynum N. D., White R. M., Mitchell J. M., Hayes E. D., Flegel R. Development of a Quantitative LC-MS-MS Assay for Codeine, Morphine, 6-Acetylmorphine, Hydrocodone, Hydromorphone, Oxycodone and Oxymorphone in Neat Oral Fluid. *J Anal Toxicol*. **2018**, 42(6), 392-399
26. Pesce A., West C., Gonzales E., Rosenthal M., West R., Mikel C., Almazan P., Latyshev S., Horn P. Illicit drug use correlates with negative urine drug test results for prescribed hydrocodone, oxycodone, and morphine. *Pain Physician*, **2012**, 15(5), E687-92.
27. Rook E. J., Hillebrand M. J., Rosing H., van Ree J. M., Beijnen J. H. The quantitative analysis of heroin, methadone, and their metabolites and the simultaneous detection of cocaine, acetylcodeine, and their metabolites in human plasma by high-performance liquid chromatography coupled with tandem mass spectrometry. *J Chromatogr B Analyt Technol Biomed Life Sci*. **2005**, 824(1-2), 213-21.
28. Wasels R., Belleville F. Gas chromatographic-mass spectrometric procedures used for the identification and determination of morphine, codeine, and 6-monoacetylmorphine. *J Chromatogr A*. **1994**, 674(1-2), 225-34.
29. Presley L., Lehrer M., Seiter W., Hahn D., Rowland B., Smith M., Kardos KW, Fritch D., Salamone S., Niedbala R. S., Cone E.J. High prevalence of 6-acetylmorphine in morphine-positive oral fluid specimens. *Forensic Sci Int*, **2003**, 133(1-2), 22-5.
30. Sordi M. B., Massochin R. C., Camargo A. R., Lemos T., Munhoz E. A. Oral health assessment for users of marijuana and cocaine/crack substances. *Braz Oral Res*, **2017**, 31, 102.

Table 1. Distribution of heroin users by gender, age, and duration of use (group 1)

Drug	Total patients	Gender	Age	Duration of use		Total
				1-3 years (group 1A)	3-5 or more years (group 1B)	
Methadone	53	M	20-30 years	6	6	12
		W		3	3	6
		M	31-40 years	7	7	14
		W		4	2	6
		M	41-50 and more	5	3	8
		W		4	3	7
Total:				29	24	53

Table 2. Distribution of methadone users by gender, age, and duration of use (group 2)

Drug	Total patients	Gender	Age	Duration of use		Total
				1-3 years (group 1A)	3-5 or more years (group 1B)	
Methadone	57	M	20-30 years	5	5	10
		W		5	4	9
		M	31-40 years	8	6	14
		W		4	4	8
		M	41-50 and more	5	5	10
		W		3	3	6
Total:				30	27	57

Table 3. Indicators of the hygienic state of the oral cavity in patients of the 1st group (previously used heroin)

The index level of hygiene, the rate of indicators	Group 1 (n=53)			
	Subgroup 1A		Subgroup 1B	
	20-40 year n-20	41-50 year n-9	20-40 year n-18	41-50 year n-6
Good 0-0,6	-	-	-	-
Satisfactory 0,7-1,6	2 (3,8%)	1 (1,9%)	-	-
Bad 1,7-2,5	7 (13,2%)	2 (3,8%)	4 (7,5%)	3 (5,6%)
Very bad >2,6	11 (20,7%)	6 (11,3%)	14 (26,4%)	3 (5,7%)

Table 4. Indicators of the hygienic state of the oral cavity in patients of the 2nd group (substitution therapy with methadone)

The index level of hygiene, the rate of indicators	Group 1 (n=53)			
	Subgroup 1A		Subgroup 1B	
	20-40 year n-22	41-50 year n-8	20-40 year n-19	41-50 year n-8
Good 0-0,6	-	-	-	-
Satisfactory 0,7-1,6	1 (1,7%)	1 (1,7%)	2 (3,5%)	1 (1,7%)
Bad 1,7-2,5	3 (5,3%)	2 (3,5%)	9 (15,7%)	1 (1,7%)
Very bad >2,6	18 (31,6%)	5 (8,8%)	8 (14%)	6 (10,5%)

Table 5. Prevalence of caries in patients taking heroin and methadone, depending on age and duration of use

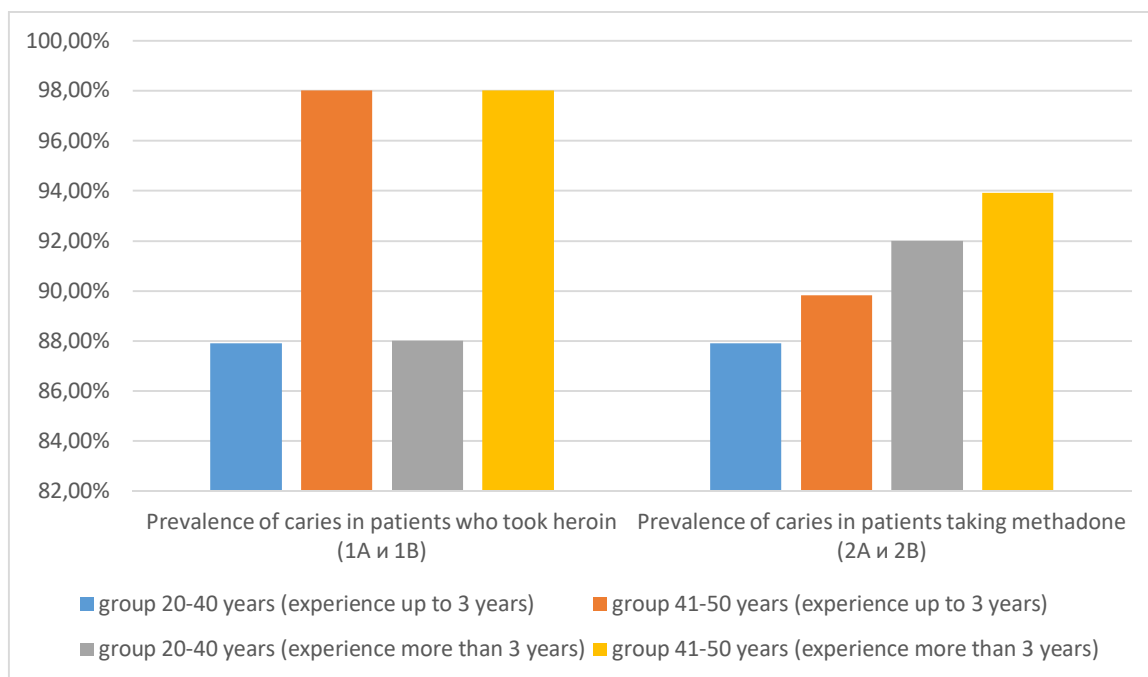


Table 6. The intensity of caries in patients who took heroin and methadone, depending on the age and duration of use

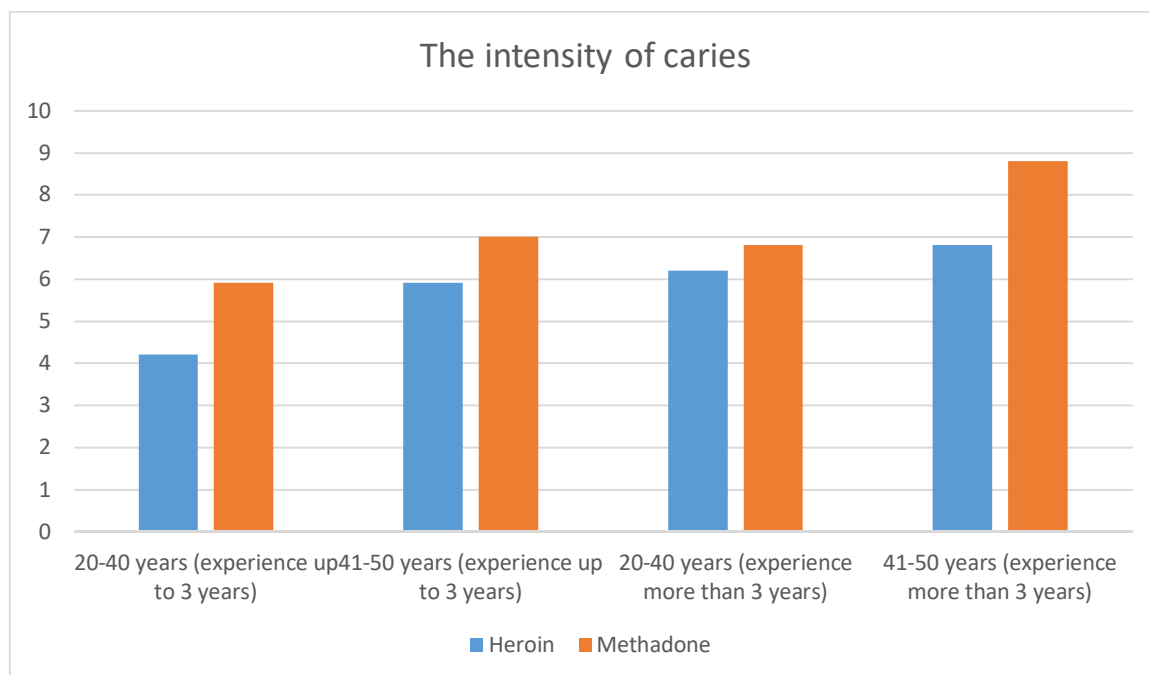




Figure 1. Patient P. Methadone replacement therapy for 6 years. Chronic periodontitis of the upper dentition, chronic generalized periodontitis

INFLUÊNCIA DE PARÂMETROS METEOROLÓGICOS NA CONCENTRAÇÃO DE METAIS PESADOS E AGENTES ETIOLÓGICOS EM AMOSTRAS DE LODO DE ESGOTO COMO FERRAMENTA PARA SEU USO NA AGRICULTURA**INFLUENCE OF METEOROLOGICAL PARAMETERS ON THE CONCENTRATION OF HEAVY METALS AND ETIOLOGICAL AGENTS IN SEWAGE SLUDGE SAMPLES AS A TOOL FOR THEIR USE IN AGRICULTURE**

FONSECA, Jemima Gonçalves Pinto¹; EITERER, Lucas Prudêncio²; OTENIO, Marcelo Henrique³; PASSOS, Leônidas Paixão⁴; SILVA, Júlio César José^{5*}

^{1,5} Universidade Federal de Juiz de Fora, Departamento de Química

² Centro de Ensino Superior, Departamento de Biologia

^{3,4} Embrapa Gado de Leite de Juiz de Fora, Laboratório de Biotecnologia e Fisiologia Vegetal

* Autor correspondente
e-mail: julio.silva@ufjf.edu.br

Received 27 November 2019; received in revised form 22 January 2020; accepted 23 January 2020

RESUMO

O trabalho verificou ao longo de 24 meses, a influência da temperatura e da precipitação pluviométrica sobre os níveis de nutrientes e metais pesados em amostras de lodo de esgoto coletadas na Estação de Tratamento de Esgoto de Juiz de Fora, Minas Gerais, Brasil. Os resultados revelaram altos teores de nitrogênio (4,7-5,2 %), fósforo (1,4-2,2 %), potássio (0,076 - 0,106 %), magnésio (0,113-0,386 %), ferro (1,84-5,03 %) e zinco (38,2 - 6902,1 mg kg⁻¹). Para a maioria das amostras investigadas a concentração de zinco ficou acima do valor máximo permitido (2.800 mg Kg⁻¹). As concentrações de Arsênio cádmio, cromo, cobre e chumbo ficaram abaixo dos valores máximos permitidos pela legislação. As análises parasitológicas identificaram coliformes termotolerantes (0,49-160 NMP g⁻¹) e ovos de helmintos, porém, em quantidades abaixo do permitido pela legislação. Esses resultados são um indicativo da eficiência do processo de tratamento do esgoto empregado. Adicionalmente, os resultados demonstraram influência significativa dos parâmetros meteorológicos sobre as concentrações de nitrogênio, cobre, chumbo, zinco e agentes patogênicos no lodo. Os resultados demonstraram também forte correlação entre as concentrações de cobre, chumbo e zinco, indicando que a presença desses elementos no lodo de esgoto tem origem comum. Os resultados demonstraram a viabilidade do uso da matriz investigada como fertilizante quando coletada em períodos chuvosos, quando favorece a diluição dos elementos presentes em suas formas solúveis.

Palavras-chave: *Elemento Tóxicos, Nutrientes, Contaminação, Variação Sazonal*

ABSTRACT

The influence of temperature and rainfall on nutrient levels, heavy metals, and etiologic agents in sludge samples collected at the Sewage Treatment Station of Juiz de Fora, Minas Gerais, Brazil, was verified over 24 months. The results showed high levels of nitrogen (4.7-5.2%), phosphorus (1.4-2.2%), potassium (0.076-0.106%), magnesium (0.113-0.386%), iron 5.03%) and zinc (38.2-6902.1 mg Kg⁻¹). For most of the investigated samples, the concentration of zinc was above the maximum allowed value (2,800 mg Kg⁻¹). The concentrations of arsenic, cadmium, chrome, copper, and lead were below the maximum values allowed by the legislation. Parasitological analyzes identified thermotolerant coliforms (0.49-160 NMP g⁻¹) and helminth eggs (1 egg), however, in amounts less than allowed by legislation. These results are indicative of the efficiency of the sewage treatment process. The results showed a significant influence of the meteorological parameters on the concentrations of nitrogen, copper, lead, zinc and pathogens in the sludge. The results also showed a strong correlation between the concentrations of copper, lead and zinc indicating that the presence of these elements in the sewage sludge has a common origin. The results demonstrated the feasibility of using the investigated matrix as fertilizer when collected in rainy periods when

it favors the dilution of the elements present in their soluble forms.

Keywords: *Toxics Elements, Nutrients, Contamination, Seasonal Variation*

1. INTRODUÇÃO

No que diz respeito a gestão de águas residuais em todo mundo, hoje, a destinação do lodo de esgoto (LE) é considerada um dos principais desafios ambientais (CHEN e KUO, 2016). Sua composição predominantemente orgânica pode contribuir para a manutenção da fertilidade do solo, em função da elevada concentração de nutrientes (Sharma, *et al.*, 2017). Uma alternativa que vem sendo considerada viável em muitos países é a utilização desta matriz como fertilizante em processos agrícolas, em função da elevada concentração de nitrogênio, fósforo e potássio, descritos na literatura como macronutrientes essenciais para as espécies vegetais (Kelessidis e Stasinakis, 2012). Esta premissa se torna relevante, desde que os teores de metais pesados e agentes patogênicos presentes estejam de acordo com as condições propostas na legislação ambiental vigente (Resolução do Conselho Nacional do Meio Ambiente [CONAMA] 375 de 29 de agosto de 2006).

Um aspecto importante na avaliação desses materiais é a realização de estudos específicos para cada ETE, em virtude das diferenças que ocorrem na composição mineral do LE conforme - dentre outros fatores - a localização geográfica e os procedimentos de coleta e manejo. As avaliações sazonais e as correlações entre os teores de substâncias inorgânicas no lodo de esgoto com os parâmetros meteorológicos são importantes para estabelecer os períodos em que a coleta dessa matriz seria apropriada para a utilização agrícola, e os períodos de alerta, em que seria necessário um controle mais rigoroso dessas concentrações, quer no produto obtido (LE), quer nas fontes geradoras (Pinheiro e Sígolo, 2007; Kasina *et al.*, 2017).

Poucos trabalhos têm discutindo o impacto dos parâmetros meteorológicos sobre os teores de nutrientes e metais pesados no LE. Chen *et al.* (2017) avaliou, por exemplo, a relação temporal entre 5 parâmetros presentes no LE dos EUA e confirmou uma correlação negativa entre 3 estudados com a temperatura. Kasina *et al.* (2017) estudaram as mudanças sazonais na composição química e mineralógica de resíduos

de processo de incineração do LE e constataram diferenças para alguns analitos especialmente durante o verão.

No Brasil, Pinheiro e Sígolo (2007) realizaram um estudo da influência da precipitação pluviométrica em São Paulo no teor de metais pesados em LE, e encontraram correlação estatística apenas com Ni e Zn. Nenhum dos trabalhos citados, no entanto, avaliou a influência de parâmetros sazonais nas concentrações de agentes patogênicos, que são listados como um dos 4 critérios de padrão essenciais para avaliação de um LE destinado a processos agrícolas (CONAMA, 2006).

Considerando a necessidade de métodos alternativos para a disposição final do LE e a escassez de matérias-primas para a fabricação de fertilizantes, o presente trabalho teve como objetivo investigar a influência sazonal sobre a concentração de nutrientes, metais pesados e agentes patogênicos no lodo, visando obter uma importante ferramenta de avaliação da viabilidade da utilização deste resíduo como fonte potencial de nutrientes para cultivos agrícolas. A introdução deve apresentar o problema, as razões para a realização do trabalho, as hipóteses ou previsões que estão sendo consideradas e um histórico de maneira clara e compreensível. Não deverá conter equações ou notações matemáticas. Deverá constar uma breve pesquisa da literatura que seja relevante ao trabalho de modo que um leitor não-especialista possa compreender o significado dos resultados apresentados.

2. MATERIAL E MÉTODOS

2.1. Área de Estudo

Juiz de Fora é a terceira cidade mais populosa do Estado de Minas Gerais, com uma área total de 1.429,875 km², distribuídos em 446,551 km² de área urbana e 983,324 km² de área rural, na Mata Atlântica. O clima da região é o tropical de altitude, com dois períodos distintos, o quente e chuvoso (outubro a abril) e o frio e seco (maio a setembro). A população segundo censo do Instituto Brasileiro de Geografia e Estatística (IBGE) de 2016 gira em torno de

559.636 habitantes. Além do fluxo de veículos, a região apresenta diversos setores industriais, que incluem atividades de fabricação de produtos têxteis, alimentos e bebidas e setores de metalurgia e montagem de veículos, tornando-se assim um importante pólo comercial e industrial no Estado de Minas Gerais (Portal PJF, 2018). A cidade gera o equivalente a 124 L de esgoto/habitante-dia, ou seja, aproximadamente 3700L de esgoto por cada pessoa em um mês, o que transforma a destinação do resíduo em uma problemática ambiental urgente.

2.2. Coleta e acondicionamento das amostras

As amostras foram coletadas mensalmente na ETE da Companhia de Saneamento de Juiz de Fora (CESAMA –JF), unidade Mercedes – Benz/Barreira do Triunfo, a partir de janeiro de 2015 até dezembro de 2016. Para o acondicionamento do resíduo, utilizaram-se frascos de polietileno previamente descontaminados em solução de HNO_3 10% v/v durante 24 horas. No laboratório a amostra foi estocada em geladeira, a 4 °C e em seguida foram preparadas para análise. Para todas as análises, foram quarteadas, secas em estufa a 40 °C por 3 dias, peneiradas em peneiras de aço inox com malha de 2 mm e maceradas em gral de ágata com pistilo para completa homogeneização.

2.3. Instrumentação e técnicas analíticas

Com o objetivo de identificar quais elementos poderiam ser empregados como indicadores da influência de parâmetros meteorológicos sobre a concentração de espécies tóxicas nas amostras de LE foi realizada uma varredura inicial usando um espectrômetro de emissão óptica em plasma indutivamente acoplado (ICP AES) modelo Optima™ 7000DV (Perkin Elmer – Waltham, MA, USA). As técnicas utilizadas neste trabalho para a determinação sazonal dos analitos escolhidos estão sintetizadas no mapa conceitual descrito na Figura 1.

2.4. Reagentes e curvas analíticas

Todos os reagentes utilizados foram grau analítico e as soluções preparadas com água deionizada (ELGA Optimus Milipore), com resistividade igual a 18,2 MΩ.cm e menos que 2

μg.L⁻¹ de carbono orgânico total (TOC). Para o preparo das soluções padrões intermediárias de Cu, Cr, Fe, K, Mg, P, Pb e Zn foram usadas soluções padrões monoelementares de 1000 mg L⁻¹ em meio HNO_3 2% v/v (MERCK). As faixas de concentrações para as curvas analíticas foram: P (2-40 mg.L⁻¹), K (2-30 mg.L⁻¹), Cu, Cr e Pb (0,1 – 4 mg.L⁻¹), Fe e Zn (0,5 – 8 mg.L⁻¹) e Mg (0,06 – 6 mg.L⁻¹). Todas as vidrarias foram descontaminadas em solução de HNO_3 (Isotar, Duque de Caxias, RJ) 10% v/v por no mínimo 24 horas

2.5. Preparo das amostras

Para a digestão das amostras de LE empregou-se o método oficial do *Deutsches Institut für Normung* (DIN EN) 13346. Para a análise de P empregou-se o método utilizado por Salinas e Garcia (1985). Utilizou-se o método de Kjeldhal para a concentração de N (Yanu e Jakmune, 2017).

2.6. Figuras de Mérito

Os limites de detecção (LD) e de quantificação (LQ) instrumentais nas análises por espectrometria de absorção atômica por chama (FAAS) foram calculados multiplicando o desvio padrão de 10 leituras do branco analítico por 3 e 10, respectivamente, e dividindo-se o resultado pelo coeficiente angular da curva analítica. Para calcular os valores de LD e LQ do método proposto, utilizou-se um fator de correção considerando a massa de LE utilizada no método e o volume final da amostra digerida, considerando também os fatores de diluição envolvidos. Para as técnicas de espectrometria por emissão atômica por chama (FAES) e espectrofotometria no UV/Vis os LD e LQ instrumentais foram calculados utilizando a estimativa do desvio padrão do coeficiente linear no lugar do desvio padrão do branco. A detectabilidade ou sensibilidade para a técnica FAAS nas condições avaliadas foi verificada através do cálculo da concentração característica (c_0). Os valores foram calculados pela divisão do valor 0,0044 pelo coeficiente angular da curva analítica. A linearidade das curvas analíticas foi avaliada pelo coeficiente de determinação (r^2). A precisão foi avaliada através da estimativa do coeficiente de variação (CV), realizado em ensaios independentes, repetidos de amostras em replicatas. Testes de adição e recuperação

de analitos foram realizados, em dois níveis de concentração, para avaliar a exatidão do método (Lourdes *et al.*, 2016).

2.7. Análises Estatísticas

As curvas de calibração foram validadas e a significância estatística foi determinada pela Análise de Variância (ANOVA) e o pressuposto de normalidade verificado pelo teste de Shapiro – Wilk. A fim de comparar as variações das concentrações ao longo do período de estudo, utilizaram-se gráficos de barras. Para verificar o grau de correlação entre as variáveis (precipitação pluviométrica e temperatura com a concentração das substâncias inorgânicas), calculou-se o coeficiente de correlação de Pearson (Action Stat, Versão: 3.5.152.34 build 4), uma vez que os dados obtidos obedecem ao pressuposto da Normalidade. A significância do coeficiente de correlação foi calculada para cada analito utilizando o teste de hipóteses, com $n-2$ graus de liberdade na tabela *t* de *Student* em um nível de confiança de 95 %.

2.8. Análises microbiológicas

Para a análise de ovos de helmintos utilizou-se a técnica de centrifugo-flutuação conforme sugerido por Sloss e Kemp (1978). Para as análises de coliformes termotolerantes, empregou-se a técnica do número mais provável (NMP) também conhecido como método de tubos múltiplos, ambas preconizadas pela resolução CONAMA (375/2006). A fim de avaliar a eficiência de redução de coliformes termotolerantes pelo tratamento aeróbico realizado no lodo de esgoto de Juiz de Fora/MG, empregou-se a técnica de semeadura por espalhamento em superfície *spread plate* (Vanderzant e Splitoesser, 1992) em meios EMB (*Eosin Methylen Blue Agar*) e *MacConkey*, preparado previamente e esterilizado.

2.9. Dados meteorológicos

Os dados meteorológicos da cidade de Juiz de Fora/MG (precipitação pluviométrica e temperatura) foram obtidos junto ao Instituto Nacional de Meteorologia (INMET).

3. RESULTADOS E DISCUSSÃO:

3.1. Caracterização inicial do LE

Os resultados da varredura realizada no LE estão apresentados na tabela 1, juntamente com as concentrações máximas de substâncias inorgânicas permitidas pelas legislações dos EUA, Comunidade Europeia e Brasileira. A escolha dos elementos para o estudo sazonal baseou-se na concentração nas amostras, na exigência da legislação e na importância do elemento para o estado nutricional da planta (CONAMA, 2006; Alexandre *et al.*, 2012). Com base nesses parâmetros foram escolhidos para o estudo N, P, K e Mg (classificados como macronutrientes essenciais), Cu, Fe e Zn (classificados como micronutrientes), e Cr e Pb (considerados metais tóxicos). Os elementos As, Ba, Cd não foram incluídos porque apresentaram concentrações abaixo dos respectivos LD's do método e do máximo permitido pela legislação brasileira.

3.2. Validação dos métodos utilizados

Os testes de Shapiro - Wilk nas curvas apresentaram uma distribuição normal com p -valores maiores que 0,05. Nas variâncias, os valores de F calculado foram menores que F tabelado para a falta de ajuste e para a significância do método foram obtidos valores de F calculado significativamente maiores do que os de F tabelados, indicando assim bom ajuste e linearidade do método, observado também pelo coeficiente de determinação (r^2) (Tabela 2).

Os LD's e LQ's para Cd, Cr, Cu, Fe, K, Mg, P, Pb e Zn variaram entre $(1,18 \cdot 10^{-3} - 1,40 \text{ mg} \cdot \text{L}^{-1})$ instrumental e $0,127 - 1,81 \text{ mg} \cdot \text{kg}^{-1}$ método) e $(0,212 - 1,81 \text{ instrumental e } 0,707 - 6,04 \text{ mg} \cdot \text{kg}^{-1})$ método) respectivamente. Esses valores ficaram abaixo dos valores permitidos pelas legislações indicando que o método é apropriado para determinação dos analitos. Para a sensibilidade, os valores encontrados ficaram na mesma ordem de grandeza dos valores do manual do equipamento e obtidos por outros autores indicando que os métodos utilizados apresentaram sensibilidade adequadas. Os valores de CV para todas as amostras analisadas por FAAS foram menores que 6%. Já para as demais técnicas os valores ficaram abaixo de 1,5 %. As recuperações variaram de 83 – 116 % demonstrando que os métodos utilizados apresentaram precisão e exatidões

adequadas (Lourdes *et al.*, 2016).

3.3. Avaliação dos parâmetros meteorológicos

Na Figura 2 e na Tabela 3 são apresentados os dados meteorológicos (precipitação e temperatura do ar) no período de janeiro de 2015 a dezembro de 2016. A cidade de Juiz de Fora está localizada em uma região de transição climática, no qual recebe a influência do oceano Atlântico, da continentalidade e da latitude. Levando, ainda em consideração a dinâmica dos sistemas atmosféricos, esta é influenciada por quatro massas de ar (massa tropical atlântica (mTa), massa polar atlântica (mPa), massa tropical continental (mTc) e Massa Equatorial Continental (mEc)) e pelo sistema frontal (Borsato e Mendonça, 2015). Desta forma, a ação das massas de ar enfatiza a sazonalidade das precipitações anuais, criando um período mais seco e com menor aquecimento continental no qual prevalecem sob influência das massas de ar de alta pressão atmosférica, que se caracterizam por promover estabilidade atmosférica, céu limpo e baixa umidade (Musk, 1988) o que prevalece ao longo do outono e inverno como pode ser observado na Figura 2.

Por outro lado, de setembro a março, ocorre maior aquecimento continental o que propicia a atuação de sistemas atmosféricos de baixa pressão, acarretando em maiores volumes de precipitação e instabilidade atmosférica. Destaca-se também nesse período a atuação da Zona de Convergência do Atlântico Sul (ZCAS), que se caracteriza por uma faixa de nebulosidade convectiva que pode se estender desde o sul da Amazônia até o sudeste, sendo considerado um fenômeno típico de verão na América do Sul e favorece a ocorrência de significativos volumes de precipitação (Borsato e Mendonça, 2015). O comportamento das precipitações nos dois anos analisados seguiu um padrão habitual, com duas sazonalidades bem distintas, uma mais seca e outra mais chuvosa (Figura 1). Com relação ao total de precipitação anual, o ano de 2015 teve um comportamento de tendente a seco e o ano de 2016 foi habitual, quando comparados à média de precipitações registradas na cidade que são de 1646,6 mm. Quanto à temperatura do ar em ambos os anos foi habitual, isto é próximo à média do período de 1981-2010, que é de 19,3° C (Normais Climatológicas, 2010).

3.4. Concentração sazonal dos nutrientes e metais pesados no LE

A Tabela 4 mostra as concentrações obtidas (em base seca) dos elementos investigados (N, P, K, Mg, Cu, Fe, Zn, Cr e Pb) no LE durante 24 meses de coleta. Para melhor visualização das variações das concentrações de cada analito no período investigado utilizaram-se gráficos de barras (Figura 3) contendo as concentrações tabeladas através do sistema de normalização de dados (Caldas, Brum, Paula e Cassella, 2013). Na análise dos macronutrientes, os resultados obtidos para o N indicaram variações entre 4,71 e 5,18 %, valores de 1,40 a 2,44 % para P e de 0,076 a 0,11 % para K. Para o Mg, os resultados obtidos apresentaram uma faixa de variação de 0,11 – 0,38%. Analisando o gráfico de barras, é possível perceber que as concentrações dos elementos N, P e K variam apenas em pequena extensão (CV < 9,0 %). O fato das concentrações variarem muito pouco ao longo de 2 anos de coleta atestam, em um primeiro momento, que o resíduo investigado pode ser considerado uma fonte promissora destes nutrientes independente da época do ano. A legislação brasileira (CONAMA 375/2006) não especifica uma concentração limite para os elementos N, P, K, Mg e Fe em amostras de LE utilizado para fins agrícolas (Kelessidis e Stasinakis, 2012). Porém, segundo a literatura (Malavolta, 2006) admite-se que de 1 a 4 % do total de N orgânico possa ser mineralizado e fornecido à cultura durante seu ciclo anual. Logo, quanto maior o teor de N no solo/substrato utilizado, maior será disponibilizado para as espécies vegetais.

Os valores encontrados de P no LE investigado foram bem superiores aos disponíveis nos solos de um modo geral (0,005 a 0,2%). No entanto, deve ser considerado que o uso de uma matriz com altos teores de P pode ocasionar processos eutróficos, decorrentes da lixiviação dos solos pela ação das chuvas e pelo intemperismo (Oliveira e Matiazzo, 2001). As amostras contendo K, por outro lado, foram as que apresentaram as menores concentrações desse elemento em comparação com N, P e Mg. Tsutiya (1999) relatou que a baixa concentração de K no LE é decorrente do mineral ser solúvel em água, permanecendo na fase líquida durante o processo de secagem na ETE. As espécies vegetais absorvem grandes quantidades de K trocável, podendo acumular no tecido foliar concentrações na faixa de 0,5 – 5%, demonstrando a necessidade deste nutriente

para a manutenção das culturas, o que nem sempre pode ser suprida pelo LE, havendo necessidade de complementação por parte de outras fontes (Malavolta, 2006).

Em relação aos micronutrientes, o Fe foi o elemento que apresentou maior concentração, com teor na faixa de 1,8 – 5,0 % e um CV na ordem de 24%, já para o Cu foi observado uma variação de 104 a 602 mg kg⁻¹ com CV de 31%. Nas determinações de Zn, foram observados, assim como no Fe e Cu, altos teores desse analito. Embora tenha sido observada uma variabilidade na concentração de Fe (Figura 3), essas variações não afetaram a importância do caráter nutricional do resíduo uma vez que os teores de Fe foram elevados independentemente da época do ano. Há relatos na literatura sobre a toxidez do Fe em comparação com outros elementos, no entanto, sabe-se que em solos muito ácidos pode ocorrer a fitotoxidez desse elemento (Nogueirol, Melo, Bertoncini e Allconi, 2014). Outra característica do Fe são os efeitos de toxidez indireta ocasionados pelo seu excesso que pode alterar a absorção de outros nutrientes como Ca, Mg, K e P (Zhang, Zhang e Mao, 1999). A concentração de Cu, embora seja requerida na ordem de µg kg⁻¹, dependendo da origem das águas residuais e do local aonde são produzidas, podem originar lodos com altas concentrações desse elemento (na ordem de mg kg⁻¹ ou até mesmo % m/m), como é o caso do lodo de Juiz de Fora/MG. Segundo Nogueirol *et al.* (2014) elementos metálicos podem ser considerados um problema em particular, porque não são biodegradáveis como algumas substâncias orgânicas, podendo se acumular no ecossistema em que está inserido (solo e plantas), principalmente quando se faz o uso continuado, em doses crescentes, em áreas cultiváveis. Segundo a literatura, a aplicação de LE promove o aumento da concentração de metais no solo, dentre eles Fe, Cu e Zn (Rangel, Silva, Bettiol e Dynia, 2003). Por outro lado, há estudos que apontam que, embora este aumento seja evidente, a mobilidade dos metais em solos tratados com lodo de esgoto é baixa. No entanto, a capacidade do solo de reter tais elementos, em função do tempo, dos fatores climáticos, da capacidade de troca catiônica, dentre outros, é um importante fator que deve ser questionado e avaliado para a utilização deste resíduo *in natura* em sistemas agrícolas (Oliveira e Mattiazzo, 2001).

O comportamento do Zn nas amostras de LE investigadas foi distinto em relação aos demais micronutrientes. A concentração de Zn

variou de 38,2 mg kg⁻¹ até um valor máximo em torno de 7000 mg kg⁻¹, um valor 2,5 vezes maior que o valor máximo permitido (VMP) de 2800 mg kg⁻¹, com exceção para os meses de janeiro, fevereiro e novembro de 2015 e fevereiro e dezembro de 2016. O Zn também foi o elemento que apresentou um perfil mais heterogêneo no período investigado (Figura 3) e o que apresentou o maior número de valores anômalos (Tabela 4, sublinhado em negrito). Essa variação significativa de concentração (CV de 52%) só não foi maior que a variação do volume de precipitação pluviométrica, com um CV de 81,3% em 2015 e de 105,3% em 2016 (Tabela 3 e Figura 3), porém, considerando que a cidade de Juiz de Fora possui duas estações bem definidas de precipitação pluviométrica (estação seca e estação úmida), essa variação pode ser considerada dentro do padrão esperado (Mimura *et al.*, 2016). A alta concentração de Zn no lodo não pode ser considerada incomum. Segundo Alexandre *et al.* (2012) o Zn é o 23º elemento mais abundante na crosta terrestre, sendo encontrado em praticamente todos os compartimentos do meio ambiente. Outro fator que pode acarretar o aumento significativo de Zn no substrato é a origem do lodo. Em águas residuais industriais, a quantidade deste mineral pode aumentar em decorrência das atividades produtivas. Ignatowicz (2017) relata a presença de Zn em amostras de lodos municipais com concentração variando entre 220,3 e 227 mg kg⁻¹, já Sharma *et al.* (2017), comparando as propriedades físico-químicas entre lodos de diversos países, observou variações de Zn de 161 a 2050 mg kg⁻¹ na Índia, de 0,21 a 1350 mg kg⁻¹ na China, de 210 – 3060 mg kg⁻¹ na Austrália e de 560 a 1100 mg kg⁻¹ na Espanha. Nissim *et al.* (2018) observou concentrações de Zn em torno de 961 mg kg⁻¹ em amostras de LE coletadas na Itália. Segundo o Departamento nacional de Produção Mineral (DNPM), no Brasil o Zn tem grande utilidade em virtude de seu potencial anticorrosivo, sendo assim, é um elemento intensamente empregado em indústrias automobilísticas, construção civil e de eletrodomésticos. Tais fatores podem favorecer a produção de lodos industriais com altos teores do metal. De acordo com os dados obtidos pode se afirmar, para as amostras investigadas, que o Zn é um elemento determinante na escolha da melhor época do ano para a coleta do lodo destinado ao uso agrícola.

As análises demonstraram que as concentrações de Cr e Pb variaram na faixa de 71- 158 mg kg⁻¹ e de 17 - 106 mg.kg⁻¹ com CV's de 17 e 32% para Cr e Pb, respectivamente. A

legislação brasileira possui valores de referência apenas para o Cr ($1000 \text{ mg}\cdot\text{kg}^{-1}$), sendo os valores encontrados considerados aceitáveis, tanto para Cr quanto para Pb. De acordo com a Tabela 5 foi possível observar que os resultados encontrados para os macronutrientes (N, P, K, e Mg e Fe), micronutrientes (Zn e Cu) e metais pesados (Cr e Pb) para as amostras de LE coletadas na ETE de Juiz de Fora/MG foram comparáveis com os resultados obtidos para amostras de LE de outros países e de outras regiões do Brasil, exceto para K e Zn. Nota-se que são poucos os registros do teor de Mg e Fe nos estudos de destinação do LE para uso agrícola, apesar da relevância destes elementos para a nutrição vegetal (Malavolta, 2006).

3.5. Concentração sazonal dos agentes patogênicos no LE

Os resultados relativos a concentração dos coliformes termotolerantes estão descritos na Tabela 6. Os dados foram obtidos a partir de testes com tubos múltiplos, referentes aos meses de julho, agosto, outubro, novembro e dezembro de 2016, compreendendo meses com diferentes características climáticas (verão, outono e inverno) para controle de qualidade de agentes patogênicos. Os valores foram comparados com a tabela de índice de NMP de amostra e indicaram, com um nível de confiança de 95%, a presença dos coliformes termotolerantes a 100 mL ou 100 gramas de LE base seca. Segundo a resolução CONAMA 375/06, o LE do tipo "A", adequado para a agricultura deve apresentar valores menores que 10^3 NMP g^{-1} de ST (sólidos totais). Na análise de ovos de helmintos, avaliando a presença dos micro-organismos indicadores de contaminação fecal, encontrou-se apenas um único ovo em todas as amostras coletadas para este estudo. De acordo com a literatura, a concentração dos elementos presentes no LE depende do tipo de efluente que chega à ETE. Os de origem industrial podem gerar lodos com alta concentração de metais pesados, principalmente metais, em contrapartida, com menor teor de agentes patogênicos, como é o caso do LE deste estudo (Zielinska, Oleszczuk, Charnas, Skubiszewska-Zieba e Pasieczna-Patkowska, 2015).

Na contagem de colônias de coliformes totais em meio MacConkey e EMB os resultados demonstraram que o processo de tratamento aeróbico empregado na ETE Barreira do Triunfo de Juiz de Fora/MG causou uma diminuição considerável no número de coliformes totais (Tabela 7), diminuindo, consequentemente, os

riscos de contaminação e propagação de doenças, além de possibilitar a utilização deste lodo como fertilizante para o solo. A legislação brasileira não especifica um valor máximo para contagem de colônias a partir dos métodos MacConkey e EMB, sendo o procedimento utilizado apenas para avaliar a eficácia do processo de tratamento do esgoto empregado para minimizar a presença de contaminantes microbiológicos. Todos os resultados apresentaram valores abaixo do especificado pelas legislações, embora tenha sido observado que nos meses mais chuvosos a quantidade de coliformes termotolerantes reduz drasticamente o que implicaria em uma influência expressiva do ciclo pluviométrico.

3.6. Correlação entre os parâmetros meteorológicos e as variáveis investigadas no LE

A matriz de correlação de Pearson (Tabela 8) indicou a 95% de confiança que os elementos analisados, em geral, se mostraram pouco sensíveis às variações sazonais. No entanto, os dados indicaram uma correlação positiva entre o N e a precipitação pluviométrica (0,54). Na atmosfera podem ocorrer formas combinadas de N, como amônia e formas orgânicas em resíduos finamente subdivididos, principalmente em áreas industriais. A ocorrência de chuvas mais fortes pode carrear para os tanques de produção e equalização do LE essas formas combinadas, aumentando assim o teor de nitrogênio neste resíduo. Horttanainen e Havukainen (2017) afirmam que o N presente nos sistemas de esgotos é originado principalmente da ureia que rapidamente se hidrolisa em nitrogênio amoniacal. O nitrogênio amoniacal em águas residuais está presente concomitantemente em ambas às formas: NH_3 e NH_4^+ e o equilíbrio entre as duas formas em uma solução líquida é dependente do pH e da temperatura, o que explicaria as mudanças de concentração com a variação de precipitação pluviométrica. A avaliação estatística dos dados também demonstrou uma correlação negativa entre Cu (-0,55), Zn (-0,55) e Pb (-0,51) e a temperatura. Esse comportamento antagônico indica que em meses chuvosos (mais quentes) a concentração é menor provavelmente devido ao efeito da diluição das frações solúveis (Pinheiro e Sígolo, 2007). Porém, considerando as altas concentrações de Zn durante todo o ano, o período de coleta do lodo deve privilegiar os meses mais quentes compreendidos entre novembro e fevereiro em decorrência dos

maiores índices de precipitação (Tabela 3), como demonstrado pela correlação (0,58) entre a temperatura e o índice de precipitação. Os resultados demonstraram a viabilidade da utilização do LE como fertilizante quando coletado em períodos chuvosos, quando favorece a diluição dos elementos presentes em suas formas solúveis. A adoção dessa estratégia poderia ser um meio de potencializar o uso do LE na agricultura evitando, concomitantemente, etapas exaustivas e custosas de pré-tratamento para redução da concentração desse contaminante (Nascimento *et al.*, 2014; Pires *et al.*, 2014).

A falta de correlação entre as concentrações de K, Mg, Fe e Cr no LE com os fatores climáticos estudados, em comparação com os outros elementos, é um indicativo que a presença dos metais no biossólido não é proveniente do intemperismo das rochas ocasionado pela ação das chuvas e da temperatura, mas outros fatores como os descartes de efluentes industriais ou a presença de frações não solúveis (Pinheiro e Sígolo, 2007). No caso do P, a falta de correlação pode ser explicada pelo fato das principais contribuições das frações de fósforo (orgânico e inorgânico) encontrados no LE não serem provenientes dos ciclos naturais, mas do acesso da população a produtos industrializados (detergentes à base de polifosfatos) e dieta alimentar (Jordão e Pessoa, 2011). Como o LE da ETE Barreira do Triunfo é 90% proveniente de atividades industriais, tais fatores possivelmente não influenciariam no aumento ou diminuição da concentração de P no resíduo. Os testes estatísticos indicaram também correlações positivas entre os elementos analisados, como por exemplo, moderadas entre Zn e Pb (0,60), P e Mg (0,50), K e Pb (0,48) e entre P e Cr (-0,61), bem como forte entre Cu e Zn (0,74) e Cu e Pb (0,93). Como correlações positivas indicam fontes comuns entre os elementos investigados, é possível afirmar que tanto o Zn, quanto Cu e Pb, são provenientes de contribuições industriais. Esses resultados chamam a atenção, tanto para a eficiência dos processos de tratamento de efluentes industriais, bem como dos processos de tratamento desses efluentes quando chegam a ETE.

4. CONCLUSÕES:

O estudo demonstrou que o LE produzido na cidade de Juiz de Fora/MG é uma fonte

altamente promissora de macronutrientes e micronutrientes essenciais e que pode ser utilizado como fertilizante através da coleta nos meses mais chuvosos uma vez que os fatores sazonais auxiliam na diluição, não somente do Zn, mas de vários outros elementos, além de restringir drasticamente o teor de agentes patogênicos prejudiciais à saúde que poderiam ocasionar contaminação em espécies vegetais. Essa estratégia, adicionalmente, evitaria etapas exaustivas e custosas de pré-tratamento para redução da concentração de contaminantes. Esta utilização do lodo seria extremamente benéfica para a região uma vez que reduziria a geração de resíduo sólido e diminuiria a dependência de adubos comerciais, favorecendo a agricultura familiar e pequenas empresas. É de suma importância que estudos específicos em diferentes ETE's do país sejam realizados a fim de se avaliar futuras possibilidades de obtenção de um LE que esteja dentro dos padrões legais, ambientais e sanitários a fim de garantir uma utilização segura em atividades agrícolas e promover práticas ambientais sustentáveis. Por fim, é possível concluir que contribuições industriais é a possível fonte elementos importantes, tais como, Cu, Pb e Zn, no LE investigado.

5. AGRADECIMENTOS

Os autores agradecem a Sebastião de Castro Evaristo pelo auxílio na condução dos experimentos. Fonseca, J. G. P., agradece a CAPES (Coordenação de Aperfeiçoamento de Pessoal de Nível Superior) pela bolsa de doutorado concedida. Os autores também agradecem as agências de fomento CNPq (Conselho Nacional de Desenvolvimento Científico e Tecnológico), FAPEMIG (Fundação de Amparo à Pesquisa do Estado de Minas Gerais), Rede Mineira de Química, INCT Aqua (Instituto Nacional de Ciência e Tecnologia: Recursos Minerais, Água e Biodiversidade e Mineração), Embrapa (Empresa Brasileira de Pesquisa Agropecuária) e CAPES pelo suporte financeiro.

6. REFERÊNCIAS BIBLIOGRÁFICAS

1. Alexandre, J.R., Oliveira, M.L.F., Santos, T.C., Canton, G.C., Conceição, J.M., Eutrópio, F., Cruz, Z.M.A.; Dobbs, L.B., e

- Ramos, A.C. *Natureza on line*, **2012**, 10, 23.
2. Borsato, V.A., e Mendonça, F.A. *Geosp*, **2016**, 19, 585.
 3. Brito, J.M.C., Lopes, R., Machado, A.M.V., Guerrero, C.A.C., Faleiro, L., e Beltrao, J. *Bio. Life Sci*, **2007**, 86, 205.
 4. Caldas, F.S., Brum, D.M., Paula, E.R., e Cassella, R.J. *Talanta*, **2013**, 110, 21.
 5. Ciélisk, M.B.; Namie'snik, J.; e Konieczka, P. *J. Clean. Prod*, **2015**, 90, 1.
 6. CHEN, Y.C.; KUO, J. *J. Clea. Prod*, **2016**, 196.
 7. Chen, Y., Wang, M., Wang, G., Chen, M., Luo, D., Li, R. *Soil Tillage Res*, **2012**, 123, 35.
 8. Horttanainen, M., e Havukainen, J. *J. Clea. Prod*, **2017**, 142, Part 4.
 9. <https://www.mma.gov.br/>, acessada em Agosto de 2018.
 10. <http://www.inmet.gov.br/portal/index.php?r=clima/normaisClimatologicas.>, acessada em Novembro de 2018.
 11. Ignatowicz, K. *Environ. Res*, **2017**, 156, 19.
 12. Jordão, E.P., Pessoa, C.A., Tratamento de esgotos domésticos, 6 ed., ABES: Rio de Janeiro, 2011.
 13. Kasina, M., Kovalski, R.P., Michalik, M. *Energy Procedia*, **2017**, 125, 34.
 14. Kelessidis, A., Stasinakis, S.A. *Waste Management*, **2012**, 32, 1186.
 15. Lakdhar, A.; Scelza, R., Scotti, R., Rao, M.A., Jedidi, N., Gianfreda, L., Abdely, C. *Rev. Cie. Suelo Nutri. Veg*, **2010**, 10, 40.
 16. Lima, T.M., Neves, C.A.R. *Sumário Mineral – Departamento Nacional de Produção Mineral*, **2015**, 35, 1.
 17. Lourdes, A., Mimura, A., Sousa, R., Silva, J. *Atomic Spec*, **2016**, 37, 120.
 18. Malavolta, E. *Manual de Nutrição Mineral das Plantas*, 3 ed., Agronomica Ceres: São Paulo, 2006.
 19. Mimura, A. S., Fazaa, L. P., Marqueza, R., Hyarica, M.L., Oliveira, M. A. L., Silva, J.C. *Quim. Nova*, **2016**, 15, 1.
 20. Musk, L., *Weather systems*. Cambridge: Cambridge University Press, 1988.
 21. Nascimento, A. L., Sampaio, R. A., Cruz, S. F. Junio, G. R. Z., Barbosa, C. F., Fernandes, L. A. *Rev. Bras. Enga. Agríc. Amb*, **2014**, 18, 694.
 22. Nash, D., Butler, C., Cody, J., Warne, M.St.J., McLaughlin, M.J., Heemsbergen, D., Broos, K., Bell, M., Barry, G., Pritchard, D., Penny, N. *Appl. Environ. Soil Sci*, **2011**, 11, 1.
 23. Nissim, W.G., Cincinelli, A., Martellini, T., Alvisi, L., Palm, E., Mancuso, E., Azzarello, E. *Environ. Res*, **2018**, 164, 356.
 24. Nogueirol, R. C., Melo, W.J., Bertoncini, E.I., Allconi, L.R.F. *Environ. Monit. Asses*, **2015**, 185, 2015.
 25. Oliveira, F.C., Matiazzo, M.E. *Sci. Agríc*, **2001**, 58, 807.
 26. Pinheiro, C.H.R., Sígolo, J.B. *Geochim. Bras*, **2007**, 21, 151.
 27. Pires, A. M. M., Mattiazzo, M. E., Berton, R. S., Guilherme, L. R. G., Marchi, G. *Embrapa Com. Tec*, **2014**, 28, 1.
 28. <https://www.pjf.mg.gov.br/>, acessada em Novembro de 2018.
 29. Rangel, O.J.P., Silva, C.A., Bettiol, W., Dynia, J.F. *Rev. Bras. Cie. Solo*, **2006**, 30, 2006.
 30. Salinas, J. G., Garcia, R. Métodos químicos para el análisis de suelos ácidos y plantas forrajeras. Centro Internacional de Agricultura Tropical. Programa de Pastos Tropicales, 1 ed., Cali: Colombia, 1985.
 31. Sharma, B., Sarkar, A., Singh, P., Sing, R.P. *Waste Management*, **2017**, 64, 117.
 32. Sloss, M. W., Kemp, R. L. *Veterinary clinical parasitology*, 5. ed., Ames: Iowa State University, 1978.
 33. Sommers, L.S. *J. Environ. Quality*, **1985**, 6, 1977.
 34. Tsutyia, M.T. *Resumo do 20^o Congresso Brasileiro de Engenharia Sanitária e Ambiental*, São Paulo, Brasil, 1999.
 35. Vanderzant, C., Splittstoesser, D.F. (1992). *Compendium of methods for the microbiological examination of foods*, 3. ed., American Public Health Association: Washington, 1992.

36. Xue, D., Huang, X. *Chemosphere*, **2013**, 93, 583.
37. Yanu, P., Jakmunne, J. *Food Chem*, **2017**, 230, 572.
38. Zhang, X., Zhang, F., Mao, D. *Plant, and Soil*, **1999**, 209, 187.
39. Zielinska, A., Oleszczuk, P., Charnas, B., Skubiszewska-Zieba, J., Pasieczna-Patkowska, S. J. *Anal. Appl. Pyrolysis*, (2015), doi:10.1016/j.jaap.2015.01.025.

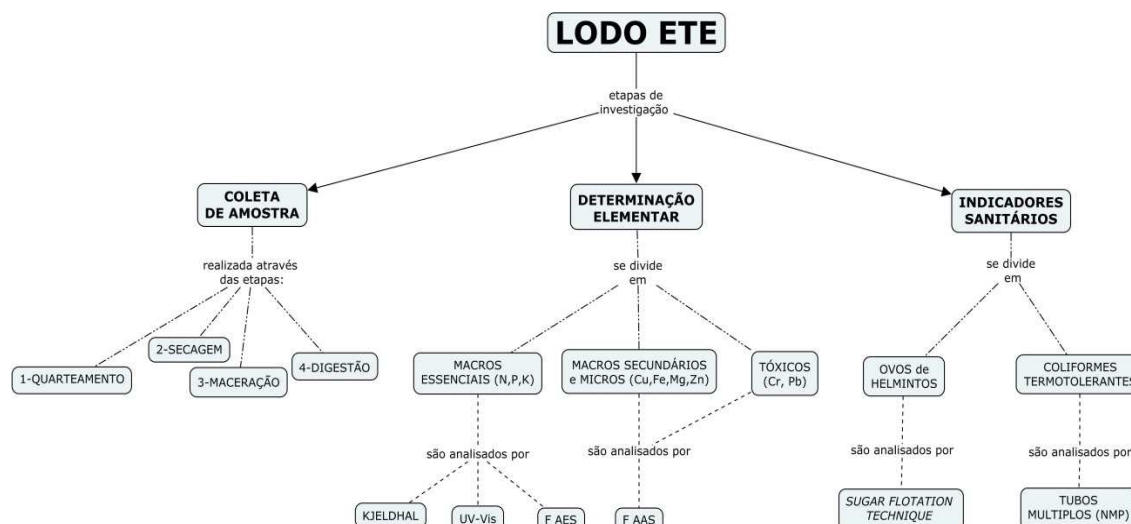


Figura 1. Mapa conceitual das técnicas e procedimentos utilizados no estudo

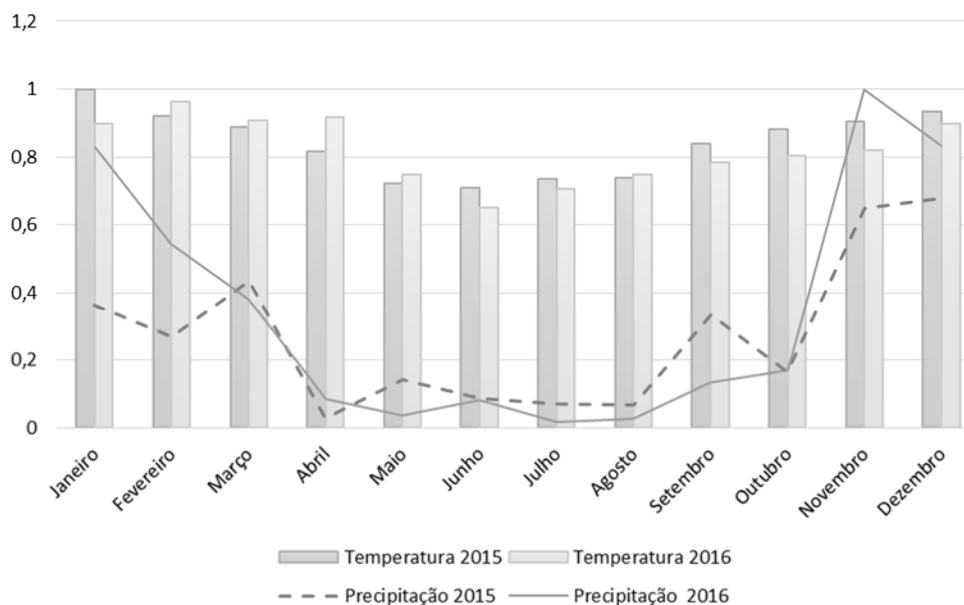


Figura 2. Variação da precipitação pluviométrica e da temperatura na cidade de Juiz de Fora/MG durante o período de estudo (2015 e 2016).

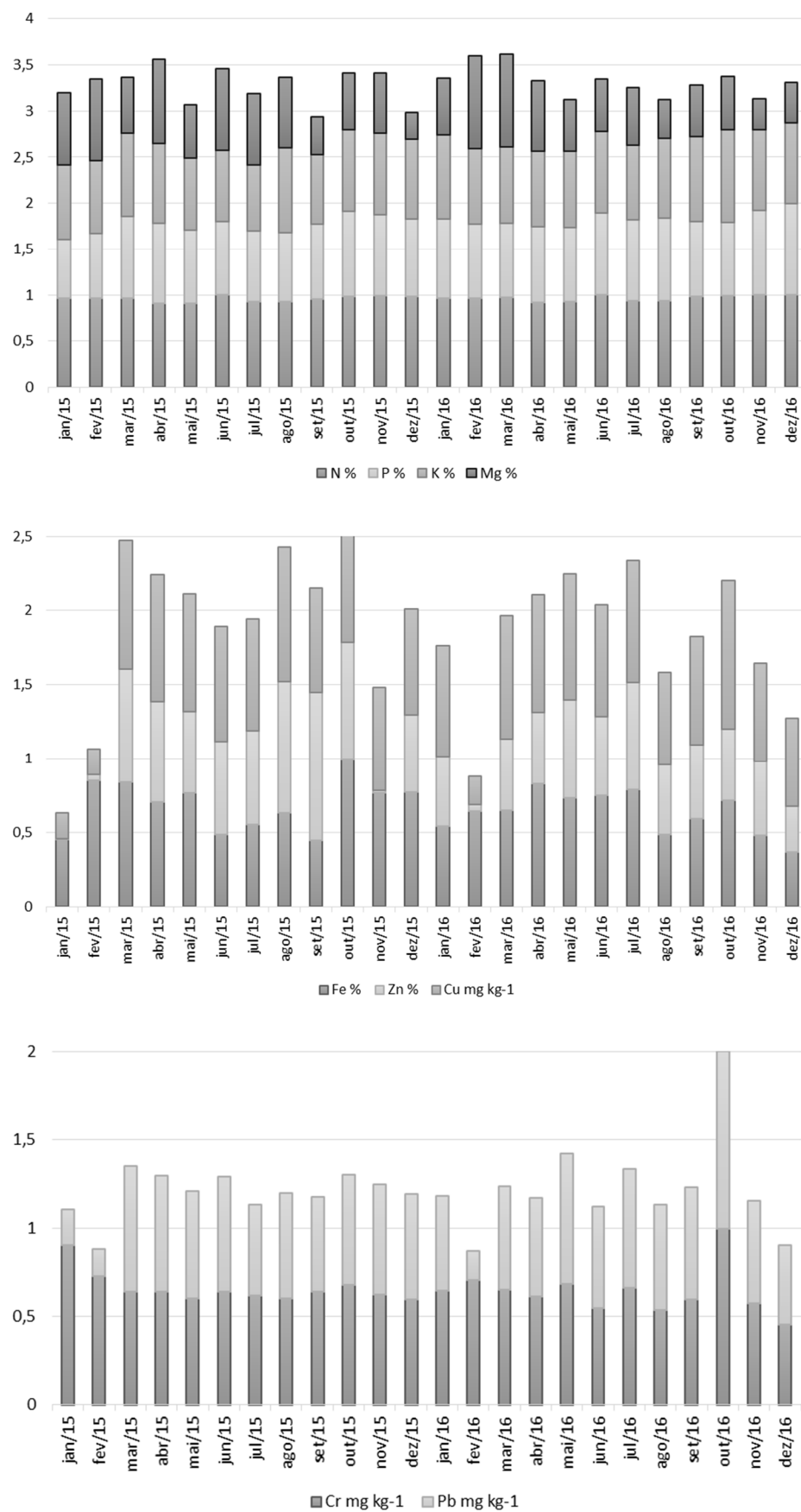


Figura 3. Variações das concentrações de N, P, K, Mg, Cu, Fe, Zn, Cr e Pb do LE de Juiz de Fora/MG durante o período de estudo (2015 e 2016).

Tabela 1. Determinação de macro e micro-elementos em LE por ICP AES. Apenas os valores disponíveis nas legislações são apresentados. Valores em mg kg⁻¹ base seca.

Parâmetros	Valores máximo permitidos (VMP)			
	^a EUA	^b Europa	^c Brasil	Este estudo
Arsênio	41	-	41	< LD
Bário	-	-	1300	< LD
Cádmio	39	20-40	39	< LD
Cálcio	-	-	-	1,06. 10 ⁴
Chumbo	300	750 -1200	300	71,5
Cobre	1500	1000 -1750	1500	307,7
Cromo	-	-	1000	87,5
Estrôncio	-	-	-	128,2
Ferro	-	-	-	2,3.10 ⁴
Fósforo	-	-	-	1,3.10 ⁴
Magnésio	-	-	-	1,1.10 ³
Mangânes	-	-	-	438,2
Molibdênio	-	-	50	5,4
Níquel	420	300-400	420	77,6
Potássio	-	-	-	780
Sódio	-	-	-	580
Zinco	2800	2500-4000	2800	2,3.10 ³

^aEUA – USEPA 40 CFR/50; ^bComunidade Européia - Diretiva 86/278 EEC; ^cBrasil - CONAMA 375.

Tabela 2. Resultados dos testes estatísticos para os nutrientes e metais pesados presentes no LE

Analitos	p-valores	Ajuste da curva		Significância da curva		r ²
		F tabelado	F calculado	F tabelado	F calculado	
P	0,2292	3,97	3,05	4,38	1,42.10 ³	0,9917
K	0,9711	3,33	3,03	4,45	4,92.10 ³	0,9991
Mg	0,0671	3,97	3,73	4,84	1,86.10 ⁵	0,9995
Cu	0,3396	3,71	2,67	4,67	4,09.10 ⁴	0,9992
Fe	0,3909	3,71	3,25	4,67	1,34.10 ⁴	0,9989
Zn	0,8245	3,97	3,85	4,96	6,2.10 ³	0,999
Cr	0,3944	3,33	2,94	4,96	2,5.10 ³	0,9997
Pb	0,2107	3,33	3,24	4,96	2,4.10 ⁵	0,9994

Tabela 3. Parâmetros meteorológicos em Juiz de Fora durante o período de 2015 e 2016 (INMET, 2017)

Mês	Precipitação pluviométrica (mm)		Temperatura Média (°C)	
	2015	2016	2015	2016
Jan	146,8	334,8	23,8	21,4
Fev	108,8	219,0	21,9	22,9
Mar	175,2	153,4	21,1	21,6
Abr	11,2	35,0	19,4	21,8
Mai	58,0	15,6	17,2	17,8
Jun	35,8	33,0	16,9	15,5
Jul	29,0	6,8	17,5	16,8
Ago	27,4	11,4	17,6	17,8
Set	135,2	54,6	20,0	18,7
Out	66,4	68,8	21,0	19,1
Nov	261,4	402,8	21,5	19,5
Dez	273,4	335,6	22,2	21,4
Média	110,717	139,233	20,0083	19,525
¹ Min.	27,4	6,8	16,9	16,8
² Máx.	273,4	402,8	23,8	22,9
³ S	90,0	146,6	2,3	2,3
⁴ CV(%)	81,2945	105,262	11,3939	11,7952
Total anual	1328,6	1670,8	240,1	234,3

¹Mínimo, ²Máximo, ³Desvio padrão, ⁴Coefficiente de variação

Fonte: Instituto Nacional de Meteorologia.

Tabela 4. Concentração dos elementos no LE (n=3), precipitação pluviométrica e variação da temperatura no período de janeiro de 2015 a dezembro de 2016. Valores anômalos em sublinhado em negrito

Mês	Macroelementos (%)					Microelementos (mg kg ⁻¹)			
	N	P	K	Mg	Fe	Cu	Zn	Cr	Pb
jan/15	4,97	1,41	0,086	0,302	2,26	107,6	<u>38,2</u>	143,0	22,0
fev/15	5,00	1,55	0,083	0,341	4,28	104,7	<u>268,2</u>	114,3	17,1
mar/15	4,99	1,95	0,096	0,236	4,24	522,4	5251,3	101,0	76,4
abr/15	4,72	1,91	0,092	0,351	3,56	515,3	4680,5	101,1	70,1
mai/15	4,71	1,75	0,083	0,221	3,85	476,9	3830,6	95,2	64,8
jun/15	5,17	1,77	0,081	0,341	2,43	467,8	4354,2	101,1	69,8
jul/15	4,79	1,69	0,076	0,297	2,79	454,4	4374,7	97,4	55,4
ago/15	4,78	1,65	0,099	0,294	3,18	547,5	6131,9	95,1	64,2
set/15	4,93	1,80	0,079	0,161	2,25	424,7	6902,1	100,7	57,8
out/15	5,11	2,02	0,094	0,236	5,03	448,6	5425,2	106,7	67,1
nov/15	5,15	1,92	0,094	0,250	3,85	420,5	<u>116,8</u>	98,4	67,0
dez/15	5,07	1,85	0,092	0,113	3,88	429,8	3631,1	93,7	64,3
jan/16	4,99	1,89	0,096	0,240	2,73	451,5	3246,7	101,4	58,1
fev/16	5,01	1,77	0,087	0,385	3,23	116,9	<u>305,7</u>	111,3	18,1
mar/16	5,02	1,78	0,088	0,386	3,26	500,1	3345,6	102,4	63,1
abr/16	4,76	1,81	0,087	0,293	4,16	479,2	3345,8	96,6	60,1
mai/16	4,79	1,77	0,088	0,217	3,68	513,2	4581,5	107,9	79,4
jun/16	5,17	1,95	0,094	0,219	3,78	452,2	3694,0	86,4	61,8
jul/16	4,83	1,93	0,086	0,241	3,97	494,0	5033,6	104,0	72,2
ago/16	4,84	1,97	0,092	0,158	2,45	376,4	3255,5	84,6	63,8
set/16	5,09	1,79	0,097	0,215	2,99	441,8	3430,6	93,7	68,4
out/16	5,14	1,75	0,106	0,224	3,60	602,2	3355,0	158,2	106,9
nov/16	5,18	2,01	0,093	0,129	2,41	402,6	3449,5	90,2	62,9
dez/16	5,16	2,18	0,093	0,171	1,84	356,8	<u>2168,5</u>	71,2	48,3
Média	4,97	1,83	0,086	0,251	3,32	421,1	3509,0	102,3	60,8
³ Min.	4,71	1,41	0,076	0,113	1,84	104,7	38,2	71,2	17,1
⁴ Máx.	5,18	2,18	0,106	0,386	5,03	602,2	6902,1	158,2	106,9
⁵ S	0,160	0,163	0,007	0,076	0,80	131,6	1840,4	17,5	19,4
⁶ CV(%)	3,2	8,9	8,0	30,3	24,2	31,3	52,4	17,1	31,9
⁷ VMP	⁸ ND	ND	ND	ND	ND	1500	2800	1000	300

¹Precipitação pluviométrica; ²Temperatura; ³Mínimo, ⁴Máximo, ⁵Desvio padrão; ⁶Coeficiente de variação;

⁷Valores máximos permitidos pela legislação brasileira (CONAMA 375); ⁸Não determinado.

Tabela 5. Concentração das substâncias inorgânicas no LE em diferentes países

País	Elementos									Fonte ³
	N ¹	P ¹	K ¹	Mg ¹	Fe ¹	Zn ¹	Cu ²	Cr ²	Pb ²	
Brasil (JF)	4,7-5,2	1,4-2,2	0,08-0,11	0,11-0,40	1,8-5,0	0,004-0,7	105-602	71-158	17-107	-
Brasil (SP)	2,2-5,5	0,6-3,7	0,10	0,38	24-54	0,1-0,3	1058	823	364	2
Austrália	2,50	0,83	---	---	1,3-1,8	0,02-0,3	92-1996	308	323	1
Bélgica	---	---	---	---	---	0,1	100	150	600	2
Canadá	5,90	3,80	0,63	---	---	0,05	100	210	150	3
Chile	0,49	0,14	0,36	0,09	$4,4 \cdot 10^{-4}$	0,068	239,6	11,74	0,89	4
China	2-6,50	2,18	0,62	---	$2,4 \cdot 10^{-4}$	0,13	975	288	49-186	5
Espanha	3,5-4,5	0,58	0,60	1,30	31	0,06-0,1	450	1-400	43-300	6
EUA	3,30	2,30	0,30	0,40	38	0,04	300	100	150	7
Portugal	4,00	1,70	0,40	---	---	---	---	---	---	8
Tunísia	3,87	0,01	0,09	---	28	---	0,059	---	101,7	9

¹%, ² mg kg⁻¹, ³. Fonte: (1) Nash *et al.* (2011); Sharma *et al.* (2017); (2)(3) Sharma *et al.* (2017); (4) Celis *et al.* (2008); (5) Xue e Huang (2013); Sharma *et al.* (2017); (6) Sharma *et al.* (2017); (7) Sommers (1977); Sharma *et al.* (2017); (8) Brito *et al.* (1999); (9) Lakhdar *et al.* (2010).

Tabela 6. Resultados dos testes para coliformes termotolerantes pela técnica do número mais provável (NMP)

Amostras	Nº de tubos com resultado positivo			NMP/100 mL
	Etapa 3 - Ensaio Confirmativo			
	Meio E.C - Diluições			
	10 ⁻¹	10 ⁻²	10 ⁻³	
Julho	5	4	5	430
Agosto	5	5	5	>1600
Outubro	5	2	0	49
Novembro	5	3	0	79
Dezembro	5	3	0	79

Tabela 7. Contagem de colônias de coliformes totais em meio MacConkey e BEM

Diluição do meio de cultura	1ª duplicata	2ª duplicata	Meio de cultura	Tipo de amostra
10 ⁻²	Incontáveis	Incontáveis	MacConkey	Entrada
10 ⁻⁴	5 F / 2 NF	2 F / 4 NF	MacConkey	Entrada
10 ⁻⁶	0 F / 0 NF	0 F / 0 NF	MacConkey	Entrada
10 ⁻²	4 F / 2 NF	2 F / 3 NF	MacConkey	Saída
10 ⁻⁴	0 F / 0 NF	0 F / 0 NF	MacConkey	Saída
10 ⁻⁶	0 F / 0 NF	0 F / 0 NF	MacConkey	Saída
10 ⁻²	Incontáveis	Incontáveis	EMB	Entrada
10 ⁻⁴	45 F / 10 NF	39 F / 5 NF	EMB	Entrada
10 ⁻⁶	0 F / 0 NF	0 F / 2 NF	EMB	Entrada
10 ⁻²	43 F / 21 NF	36 F / 12 NF	EMB	Saída
10 ⁻⁴	2 F / 0 NF	0 F / 3 NF	EMB	Saída
10 ⁻⁶	0 F / 0 NF	0 F / 0 NF	EMB	Saída

F: fermentadores; NF: Não fermentadores.

Tabela 8. Matriz de correlação de Pearson entre parâmetros físico-químicos, elementos-traço e maiores no lodo de esgoto. Apenas as correlações com significância $p < 0,05$ são apresentadas

	N	P	K	Mg	Cu	Fe	Zn	Cr	Pb	PP (mm)	T(°C)
N	1										
P	-	1									
K	-	-	1								
Mg	-	-0,50	-	1							
Cu	-	-	-	-	1						
Fe	-	-	-	-	-	1					
Zn	-	-	-	-	0,74	-	1				
Cr	-	-0,61	-	-	-	-	-	1			
Pb	-	-	0,48	-	0,93	-	0,60	-	1		
PP (mm)	0,54	-	-	-	-	-	-	-	-	1	
T(°C)	-	-	-	-	-0,55	-	-0,55	-	-0,51	0,58	1

- abaixo do nível de significância; PP: Precipitação pluviométrica; T: Temperatura.

PEDAGOGIA DO CÁLCULO NA ÍNDIA: UMA INVESTIGAÇÃO EMPÍRICA

PEDAGOGY OF CALCULUS IN INDIA: AN EMPIRICAL INVESTIGATION

ALAM, Ashraf*

University of Delhi, Department of Education. India.

* Correspondence author
e-mail: ashraf_alam@live.com

Received 29 December 2019; received in revised form 01 January 2020; accepted 01 February 2020

RESUMO

Quando os alunos aprendem uma construção de cálculo, tanto uma imagem conceitual quanto uma definição de conceito são impressas em sua mente e, por causa disso, exemplos concretos e da vida real se tornam um pré-requisito para um ambiente de aprendizado contextualmente rico para as abstrações inerentemente presentes no cálculo. À luz das proposições mencionadas, o presente estudo se concentra em investigar várias questões, algumas das mais importantes incluem a natureza epistemológica do currículo de cálculo nas escolas de ensino médio da Índia, papel dos professores de cálculo indianos na cognição dos alunos, possibilidade de enumeração de características de um professor de cálculo bem-sucedido em relação ao meio sociocultural da Índia, desafios relacionados à imersão completa do cálculo na manipulação de símbolos que eventualmente dão origem a obstáculos cognitivos, inter-relação entre o conhecimento do conteúdo de cálculo dos professores e suas práticas pedagógicas, efeito do cálculo da escola secundária sobre o desempenho do cálculo da faculdade de estudantes indianos e a natureza do efeito em alunos indianos que fazem cálculo na escola sobre seu desempenho processual e conceitual. Para este extenso estudo, foram coletados dados de PGTs e Professores Auxiliares / Associados com mais de 8 anos de experiência em ensino de cálculo em 76 escolas, faculdades e universidades diferentes, pertencentes a 23 estados e territórios sindicais da Índia. Participaram deste estudo 323 professores. Múltiplos métodos de coleta de dados foram utilizados, incluindo observação naturalista, entrevistas estruturadas, observações em sala de aula, entrevistas em grupo focadas e discussões informais, e estas foram realizadas antes e depois do ensino em sala de aula. O pesquisador transcreveu as entrevistas, identificou temas emergentes e repetidos e utilizou o software NVivo e Concordance para conduzir a análise de conteúdo e discurso em sala de aula, com métodos simples de contagem e abordagem aplicada à teoria fundamentada, na qual os dados empíricos foram categorizados tematicamente e, no processo, empregados a abordagem de indução. O pesquisador analisou as transcrições usando N5 (NUD * IST 5.0; QSR International, Melbourne) com a abordagem da teoria fundamentada. Este estudo de pesquisa é de natureza puramente qualitativa e sua estrutura está dentro do paradigma interpretativo. O estudo atual foi realizado entre junho de 2016 e março de 2019. Os resultados indicam que existem muitos obstáculos cognitivos na compreensão dos conceitos incorporados no cálculo: dois dos mais destacados que saíram do estudo incluem o relacionado às intuições e o outro relacionados a aspectos lingüísticos / representacionais.

Palavras-chave: *Currículo; Diferenciação; Avaliação; Integração; Educação Matemática.*

ABSTRACT

When students learn a calculus construct, both a concept image as well as a concept definition is imprinted in their mind, and because of it, concrete and real-life examples become a prerequisite for a contextually rich learning environment for the abstractions inherently present in calculus. In the light of aforementioned propositions, the current study focusses on delving into several issues, few of the prominent ones include the epistemological nature of calculus curriculum in India's senior-secondary schools, role of Indian calculus teachers in students' cognition, possibility of enumeration of characteristics of a successful calculus teacher with regards to India's socio-cultural milieu, challenges regarding complete immersion of calculus in manipulation of symbols that eventually give rise to cognitive obstacles, interrelationship between teachers' calculus content knowledge and their pedagogical practices, effect of secondary school calculus on performance of Indian students' college calculus, and the nature of effect on Indian learners having calculus in school on their procedural and conceptual performance. For this extensive study, data were collected from

PGTs and Assistant/Associate Professors having more than 8 years of calculus teaching experience drawn from 76 different schools, colleges and universities belonging to 23 different states and union territories of India. A total of 323 teachers took part in this study. Multiple methods of data collection were used including naturalistic observation, structured interviews, classroom observations, focussed group interviews, and informal discussions, and these were done both before and after the classroom teaching. The researcher transcribed the interviews, identified emerging and repeated themes, and used NVivo and Concordance software to conduct content and classroom discourse analysis, with simple counting methods and applied grounded theory approach using which empirical data were thematically categorized and in the process of it, employed the induction approach. The researcher analyzed the transcripts using N5 (NUD*IST 5.0; QSR International, Melbourne) with the grounded theory approach. This research study is purely qualitative in nature and its framework lies within the interpretative paradigm. The current study was carried out between June 2016 and March 2019. Findings indicate that there are lots of cognitive obstacles in understanding the concepts inbuilt in calculus: two of the prominent ones that came out from the study include the one related to intuitions and the other related to linguistic/representational aspects.

Keywords: *Curriculum; Differentiation; Evaluation; Integration; Mathematics Education*

1. INTRODUCTION

It's been several years that researchers have been discussing and debating about the very nature and purpose of making school and college students learn mathematics (Dossey, 1992; Orton & Wain, 1994). In most of the countries be it developed or developing, it is seen that mathematics in school has a position that is privileged over other subjects and that the status which it enjoys is because of its usefulness and application which is in stark contrast to others' beliefs who view mathematics as the highest form of culture and that which emphasizes abstractness having formal proof and that it focusses inside of itself (Gardiner, 1995; Neumark, 1995).

The recurrent problem of introducing integration and differentiation to newbies is the frequent reinforcement of certain typical questions that involves asking them to solve, graph, calculate, plot, compute, differentiate, sketch, determine, etc. (Ferrini-Mundy & Graham, 1991). Students' learning a concept or a construct without knowledge and comprehension of its meaning has been the issue of research for several decades (Hiebert & Carpenter, 1992). In the 1980s, because of the visible crisis pertaining to learning and teaching of calculus, the US witnessed a movement that inspired changes in the manner in which calculus was taught to students (A. Tucker & Leitzel, 1995).

There has been an attempt by several authors to expand the "Rule of Three" to incorporate enactive and formal representation (David Tall, 1996); representations using animations (Bowers, 1999; Leinbach, 1997); representation of real data (Kaput, 1998) wherein learners experiencing states of affairs that are

close to reality and natural phenomenon and implanting the usage of functions in data that are real and representations that are verbal (Kennedy, 2000). (Asiala, Cottrill, Dubinsky, & Schwingendorf, 1997) have talked about what existing literature says with regards to learner's understanding of functions and reports that students have a conception or mental representation of functions that are pretty infirm and that they show a tendency of relying on algebraic formulas while evolving and formulating their conception of functions. (Koirala, 1997) sets the students' conceptual understanding while teaching calculus in the theoretical account that (Skemp, 1976) gave about the relational and instrumental cognition involving giving rules and formulas to students in solving problems on calculus and the application of those formulas by students in solving calculus problems that are of routine-nature which does not require students to put any brain to delve into its basics.

(Schwalbach & Dosemagen, 2000) emphasizes the use of concrete examples giving students a contextually rich environment to inquire into the abstractions inherently present in calculus. When a student learns a certain construct, a concept image, as well as a concept definition, is built in her mind (David Tall & Vinner, 1981). It is mostly by accident that process of concept construction occurs among learners because they learn using identical textbook problems which lead to naïve or intuitive structures that are immune to transformation and the belief of abstractions that are reflective (Piaget, 1985), which (Dubinsky, 2002) had conceptualized for summarization of traits that is present in constructively reflective abstractions emanating from the viewpoint of mathematical thinking of higher-order, constitutes co-ordination, encapsulation, internalizing, reversibility and

generalization.

Using Dubinsky's model, (Repo, 1994) has come up with an explanation of reflective abstraction in the construction of cognitive structures on constructs pertaining to derivatives. It is very much possible that if learners could internalize concepts that are specific to derivatives, and work towards development of capabilities in conceiving a function of derivatives as the nodal unit for processing, they can in subsequence easily fabricate a novel inverse process for delving in operations of differentials, thus making it pretty alike to determination of integration of the originally chosen function. (David Tall, 1996) delineates the proposition given by (Sfard, 1992) that viewing of mathematics operationally is preceded by structurally viewing it, considering objects and the formal definitions and this could have prominent implications with regards to theories of teaching. The difference which is there among "*concept definition*" and the holistic impression of "*concept image*" is reprised by (David Tall, 1996) and this distinguishing difference made some mathematicians (David Tall & Vinner, 1981; Vinner & Dreyfus, 1989) explicate certain lack of successes in students' understanding of it. (Gray & Tall, 1994) propounded and used the notional belief of "*procept*", describing it as an amalgamation of process and concept, thereby laying claim that it is, in particular, conformed to the contemplation of calculus learning and its initial analysis. They opined that functions, integrals, derivatives and the notions of fundamental limits are all examples of *procepts*. When concepts are viewed in more than one setting and from diverse viewpoints, it becomes an essential noetic state of cognition that is visualized as the facet of "general idea of flexibility" talked about by (Dreyfus & Eisenberg, 2012). In their study, (De Guzmán, Hodgson, Robert, & Villani, 1998) show that at different stages of an individual's learning and education, students show varying levels of maturity while proving a theorem. It is specifically expected from tertiary level learners to showcase correct formalism while engaging with non-trivial proofs. An attempt was made, applicable to diverse mathematical areas to teach analysis. And was showcased in the study carried out by Legrand and the approach under consideration, often referred to as "scientific debate" (Artigue, 2001; Legrand, 1993), has its roots in a particular type of discourse among learners with regards to theorems' validity. If students encounter arguments that are structured with regards to mathematical content, deeper development of

cognition of fundamental concepts is seen.

(Praslon, 1999) in his study has examined the excogitation of derivatives as a case study of non-continuities in transitioning from the school to university and the findings attest to the attempts that students make in adjusting their mathematically sound learning aids to situations that are baffling and complicated leading these attempts towards oversimplifications that are consequences of their limited field of experience. Most of the researches carried out till date are towards reforming calculus, emphasizing majorly on opinions made or descriptions given either on software programs that ease calculus learning, or of the contemporary curricula which eventually lead to mere informing the readers of *what* and *how* of calculus learning and teaching, relevant examples to which can be found in (A. H. Schoenfeld, 1995), (Douglas, 1995), and (Solow, 1994). In many instances of research in calculus education, the evaluations have made use of experimental and quasi-experimental designs that are straightaway borrowed from physical or natural sciences. They have used two groups, one where exposure is given and other where no exposure is given and comparison is drawn between the pre-test and post-test scores where randomization techniques were used for selection of samples in a relatively controlled environment making use of the reform approach. Tests sometimes were specifically designed for assessment of certain specific kinds of students' performance, like their proficiency in handling traditional algorithms or in the determination of their ability to solve problems that are conceptually driven. Relevant examples to it can be found in (Armstrong, Garner, & Wynn, 1994) and (Bookman & Friedman, 1994). Comparative studies of this kind have certain long-familiar limitations, [see e.g., (A. Schoenfeld, 1994)] prominent one is its poor suitability in studying a phenomenon that is as complicated as students' learning and teaching. Prima facie it is found that, in many cases of researches done towards improvement of pedagogy of calculus, what is identified turns out to be an interesting phenomenon but the findings, results and conclusions has less of bearing when it comes to its contribution on cognition of effective techniques to be implanted in teaching and learning of calculus. Identification of interesting occurrences, say for instance, determination of differential performance of students from different courses on exam questions wherein the study is using diverse designs of experimental research or observations of learners' problem-solving behavior while they are in calculus class, have

the potential for generation of results possessing explanatory power for uncovering differences in performances of learners. In few of the researches, such methods are used in examining research questions that are non-comparative in nature, to read more on non-comparative studies and examples of it see (Selden, Selden, & Mason, 1994); (Palmiter, 1991); (Park & Travers, 1996); and (Bonsangue & Drew, 1995). It is unfortunate though that studies yielding results possessing impregnable explanatory power are scarcely available and studies that are comparative in nature undertaken on the teaching of calculus and reform in its curriculum have not been able to effectively advance our cognition about students' calculus learning and on how diverse pedagogical circumstances can positively impact their understanding.

It has been documented in several types of research that what appears to be pupils' impuissance in the cognition of concepts of calculus might not actually be the case; in fact, it may just be the manifestations of their pre-existent comprehension of associated concepts. Learners may, for example, comprehend the conceptions of functions in a certain way that serves them considerably in few particular situations but are not in consonance with, or are not supportive of the developments of a sturdy inference of derivatives, illustrations related to it are witnessed in (David Tall, 1992), (S. Monk & Nemirovsky, 1994), (Ferrini-Mundy & Graham, 1994), (Williams, 1991), and (White & Mitchelmore, 1996). A study conducted by (Kuh, Kinzie, Schuh, & Whitt, 2011) found that to accelerate pupil learning and collegiate excellence; thought-provoking and intellectually stimulating creative work is fundamental.

There are certain beliefs that are commonly held by secondary school students of mathematics that were outlined by (Garofalo, 1989) based on observations and conversations he engaged with his students during his long career as a mathematics teacher. These beliefs include: teachers and textbooks are the sole authority of knowledge and that most of the mathematical problems could be solved by directly applying the facts, theorems, rules, formulas and procedures emanating directly from teachers and textbooks, (p. 502); formulas rather than their derivations are important (p. 503); and that the teachers/textbooks are the sole dispensers of knowledge (p.503), concomitantly the way students engage with mathematics, the approach with which they solve math problems and their expectations with the nature of a

mathematics classroom are directly affected by the belief systems students hold (Bookman, 1993; A. H. Schoenfeld, 1995). It has been recommended by (Smith & Moore, 1990, 1991) that school/college teachers shall involve less in delivering lectures and more on encouraging them engaging in group tasks/activities [see also (Bookman & Blake, 1996)].

Most of the prominent contemporary researches in mathematics education that focusses on reformation leading to enhancement of teaching efficiency are works that are either on mathematics pedagogy at elementary or secondary level or on calculus learning at school and university level (Douglas, 1986; N. C. o. T. o. M. C. o. S. f. S. Mathematics, 1989; N. C. o. T. o. M. C. o. T. S. f. S. Mathematics, 1991; M. Tucker, 1990), mathematical fraternity thus are now recognizing the immense importance of calculus and are thus getting all the more connected in the process (Young, 1987). A constructivist mathematician would state that learning math is a process in which students engage in reorganization of their activities for resolving problem areas that are found excessively difficult to them (Cobb et al., 1991) and in alignment with this take, constructivists agree on construction of mathematical knowledge in the classrooms via reflective abstraction, and that there is continuous development of cognitive structures (Noddings, Maher, & Davis, 1990).

In the field of mathematics education, it has been found that several researchers have showcased their interest in facets of learners' cognition of functions at the senior-secondary schools and colleges (Buck, 1970; Dreyfus & Eisenberg, 1983, 1984; D. H. Monk, 1987). Findings of these researches have shown that most of the learners at this level are stuck to a single definition of functions that is being staged by the correspondence rule whose domain is unvarying in its entirety (Ferrini-Mundy & Graham, 1991; Markovits, Eylon, & Bruckheimer, 1986; Vinner & Dreyfus, 1989). When there is movement in thought process from graphical mode to algebraic mode, piecewise definition of functions bring about massive difficulty for the learners (Ferrini-Mundy & Graham, 1991; Markovits et al., 1986; Vinner & Dreyfus, 1989), and additionally, learners for most of the time, ascertain whether or not graphs represent functions by its measure of acquaintance (Ferrini-Mundy & Graham, 1991). In the settings where students have both graphical and algebraic data, they often view them independently and oftentimes find comfortability using methods

whose reasoning is contradictory (Ferrini-Mundy & Graham, 1991). Tendency of students have been noted by researchers, and while examining their behavior about a graph both locally and at any one point and also algebraically, students have shown the tendency of evaluating formulas for one domain value, while on the contrary, a holistic rendition is usually of utmost importance in cognizing concepts in calculus (Bell & Janvier, 1981; D. H. Monk, 1987).

It has been observed that researches on pupils' cognition of limits are not very extensive and learners often encounter conflicts among precise/formal and informal definitions that use interpretations in simple language and in natural discourses (Confrey, 1981; Graham & Ferrini-Mundy, 1989; D Tall & Schwarzenberger, 1978; Williams, 1991) and pupils often have this feeling that a limit can never be reached and are mostly anxious for the fear of encountering a mismatch between their instinctual knowledge and the solutions they come up with via mathematical processing (Ferrini-Mundy & Graham, 1991) and in connection to it (Davis & Vinner, 1986) figured out that learners keep holding a very similar visceral perception regarding limits of sequences. Easy accessibility and inexpensiveness of graphics calculators make students of pre-calculus and calculus, studying in formal educational institutions; use this technology extensively, thereby showcasing a substantial impact on classroom instruction.

It is widely claimed that usage of graphics calculators makes room for enhanced conceptual approaches to a problem-solving, refined understanding of the bond between graphic representation and symbolic algebra, and sharpened ability among students in solving mathematical problems. Students now take all the benefits emanating from it because earlier they were asked to solve problems the way traditional and formal mathematics required (Demana, Waits, & Clemens, 1993; N. C. o. T. o. M. C. o. S. f. S. Mathematics, 1989; David Tall & Blackett, 1986).

Considering the aforementioned issues egressing from the literature, the researcher aims to investigate the epistemological nature of calculus curriculum in India's senior-secondary schools, role of Indian calculus teachers in students' cognition, possibility of enumeration of characteristics of a successful calculus teacher with regards to India's socio-cultural milieu, challenges regarding complete immersion of calculus in manipulation of symbols that eventually give rise to cognitive obstacles,

interrelationship between teachers' calculus content knowledge and their pedagogical practices, effect of secondary school calculus on performance of Indian students' college calculus, and the nature of effect on Indian learners having calculus in school on their procedural and conceptual performance.

Research assumptions

Frid, in his research, focuses on teaching the principles of calculus with different approaches: a study of comparisons of conceptual and infinitesimal approaches vs. technique-oriented approach of understanding calculus (Frid, 1994). This *frame of reference* reflects the diverse impact it has on using different approaches to students' sources of conviction and language use. There are a lot of cognitive obstacles in understanding the concepts of calculus, two of the prominent being: one related to intuitions and the other related to linguistic/representational aspects. Now that calculus is completely immersed in the manipulation of symbols, that too at the expense of students' mathematical understanding, consequently giving rise to cognitive obstacles through linguistic and/or representational aspects. Students are often pretty curious to know what they are being asked to learn (here it is calculus), and the possession of their intuition has an emphatic role to play in their construction of calculus concepts. (Norman & Prichard, 1994) in their research propose that a framework that is useful to fix securely the considerations of cognitively demanding obstacles that confines in the realm of the framework proposed by Krutetskian cognitive processes of flexibility, generalization and reversibility and to develop the understanding of calculus among learners, the importance underlying the connections between different representations be it visual-spatial, graphical, concrete, algebraic or numeric is bobbing up into existence.

Harvard Consortium Calculus text gave a guiding principle by the name "Rule of Three", which states that topics of the syllabus, as far as possible, shall be transacted using all three techniques, namely graphically, numerically and analytically whose rationale is to come up with a course where all the three viewpoints are balanced, and students get to view all the major concepts from all possible angles (Hallett, 2006). The most significant takeaway from the analyses of the researches done so far in learning and

teaching of calculus is that the students before they immerse into symbolic manipulations, more emphasis they should place on learning conceptually and making use of multiple representations and connections.

2. MATERIALS AND METHODS

The author has traced the development of calculus-teaching at schools and colleges and identified commonalities and differences. For this extensive study, data were collected from post-graduate teachers (PGTs) and Assistant/Associate Professors having more than 8 years of calculus teaching experience, drawn from 76 different schools, colleges, and universities, belonging to 23 different states and union territories of India. Data were mostly collected using a schedule consisting of 24 items. A total of 323 teachers took part in this study. Data were also amassed making use of structured interviews, classroom observations, focussed group interviews, and informal discussions that were done both before and after classroom teaching. Semi-structured interviews were audio-taped and were carried out with each of 323 teachers (its duration was close to one hour per teacher).

Along with that, the researcher took field notes of their observations from teaching sessions that were conducted by 62 calculus teachers. Towards the end, the researcher was in possession of a large amount of data. This research study is purely qualitative in nature and lies within an interpretative paradigm/framework. This study was carried out between March 2016 and May 2019.

It was specifically taken care of that the 76 educational institutions chosen for the study were geographically separated from one another - this was done to ensure that the sample was a true representation of India. Interviews were transcribed, and those themes that kept egressing and echoing were keyed out. NVivo and Concordance software programs were used for the analysis of contents and classroom discourses, making use of plain enumeration methods.

The grounded theory approach was employed, using which, thematic categorizations of empirically derived data were done using the inductive approach. Validity checks allowed apparent cogency of the authors' experiential accounts, assaying *éclaircissement* and

illustration of central ideas throughout the interview process, and devotion of concentration to aberrant illustrations, cases, and examples was done in extreme minute detail.

The teachers were selected after being granted due permission from the principals, directors, HoDs of schools, colleges, and universities. The time period of the study was 2 years and 9 months, i.e., from June 2016 till March 2019. Focused group interviews were conducted through schedules that were pre-designed as per the objectives of the research. Semi-structured designs were used in focussed group interviews. The length of each interview was between 90 and 120 minutes. Teachers were asked to consecrate to concealment by not quoting what other participants in their focus group discussed. Teachers were promised by the investigator of the prudence of what they revealed and were inspired with confidence to be as frank, forthright, blunt, and honest as existing in possibility. Tape-recording of interviews were done, they were then amply rewritten in a different script, and were examined for initial analysis by the researcher.

The final analytical investigation disclosed that the themes from the first two analyses, even though they were contrastingly clubbed, excerpted exactly identical situations and events from the empirically derived data. This the researcher took as ratification of the basing of the investigation of the data. To include it as a theme, affirming data were contained in focus groups from all 76 educational institutions and in all of the focus groups. Indexing of the extracts of the interviews was done, e.g., EdInt1, EdInt2, etc. Participants represented a mix of both the genders, and their ages varied from 29 to 57 years. In order to prevent the identification of the participating institutions, teachers were advised to make anonymous the details of the educational institutes and hide any such materials that could lead to the recognition of their schools/universities.

Researcher was an integral part of all the focus group interviews and ahead of each meeting, the researcher explicated the agenda of the research. It was clearly and categorically stated beforehand that each of the participants will be anonymized. After the interview got over, no contact was established with the participants. Copies of the transcripts were returned to the groups, and each participant understood that if the content in it is not what they intended to convey, the transcripts, in that case, will be discarded and won't be used in the study.

Separate analyses were done of transcribed tapes of each of the interviews and meetings. The grounded theory approach was used by the researcher in the development of theoretical and explanatory principles.

The coding of themes was done consistently and robustly following grounded theory rules, and all the emerging themes directly supported the verbatim data coming from the interviews. The overarching aim of generating theory from the findings was never an objective of this study. Probing questions were asked in the middle of the focus group interviews so that they easily open up and that no elements remain untouched. To establish rapport and to make them feel at ease, informal chit chat was done to attract their interest and it was ensured to them that whatever they say will be out in the open anonymously. These strategies were used to stimulate healthy discussion during focussed group interviews. A total of seven participants refused to participate after reading through the transcribed data, and 16 respondents did not differ in key characteristics.

After all the teachers were communicated about the goals and design of the research, a consent letter was taken into possession from the participants for interviewing them, which states that they were free to leave the focus group or interview sessions, if they wished to, at any stage of the research. Approvals were obtained from 11 local ethics committees, and in order to shield the identity of the teachers as well as that of the educational institutions, pseudonyms were rendered to them. Constant comparative method (Bogdan & Biklen, 2003) was used to analyze the transcribed verbatim interviews. Data were analyzed inductively, and the identification of common themes and concepts were made across experiences (Lincoln & Guba, 1985).

Once the researcher was done with the coding, and drawing up of the themes were accomplished, the comparison of all the themes was made. It eventually resulted in the final six themes for the expatiated study. Although identification of several codes was made, only the ones with the strongest bearing were expended (assorted with more than 50% of the interview sample). The array of codes that were with me in the beginning, the excerpts were aggrouped and gestated utilizing them and were then made part of the adoption factors. Complemental codes and constructs were, however, admitted if they were to egress in the analysis.

After the initial coding was discharged, the database of excerpts underneath every factor was reread again and again to ascertain coherent applications of excerpts, and the factors were systematically framed. In the course of these scrutinies, certain transfigurations to the coding were brought in. As an example, certain excerpts were situated underneath a dissimilar code. Multiple techniques of data collection were utilized by blending focussed group interviews, in-depth interviews, and naturalistic observation. Investigator analyzed transcripts making use of N5 (NUD*IST 5.0; QSR International, Melbourne) accompanying the approaches employed in grounded theory methodologies. For the purpose of revision, transcribed transcripts were returned to each of the respondents.

The researcher formulated themes from the transcripts. Marking and linking of the segments of texts were executed from different interviews that addressed similar concerns or mattes or experiences making use of NUD*IST. Considering the contexts of all the interviews, themes were conceived. It was impossible to develop inter-rater reliability scores because the interviews had very little similarity with respect to complex composition—scores of this nature are inappropriate for the data that have minuscule or no predefined coding. Triangulation method employing diaries, questionnaires, and interviews were consecrated to get over powerful criticisms of common method bias in the methods that were used predominantly. Diaries were effectively used in recording the data. This tool has been opted in spite of the complemental exertion demanded in the collection of data. In this case, diaries also playacted as a think-aloud mechanism, which eventually helped the researcher in effectively capturing teachers' cognitive processes.

3. RESULTS AND DISCUSSION

Integration and differentiation has two distinct conceptual settings, one geometric and the other dynamic. Calculus teachers are sufficiently comfortable moving between them that they often forget how difficult it can be for students to grasp their equivalence. It has been found that intervention programs like calculus workshops promoting excellence in academia and fruitful classroom interaction have a direct bearing on pupil's academic achievement on both basic calculus courses as well as advanced-level calculus courses and thus supports the suggestions detailed in (N. C. o. T. o. M. C. o. S.

f. S. Mathematics, 1989; N. C. o. T. o. M. C. o. T. S. f. S. Mathematics, 1991) and (Weissglass, 1992). Looking at the persistence, performance, and cost findings, the current study emphasizes on needs in schools and colleges to possess the facility to accurately pursue the scholastic achievement of the pupils across time. The achievement among students in calculus learning appears to be linked less to pre-college aptitude than to their in-college scholastic occurrences, activities, performances, and anticipations; and it has prominently surfaced that when students are taught calculus by "discovery" approach, they do as well on problems and manipulative skills as those with traditional instructions, but in addition, they have increased understanding thereby making discovery approach to hold possession of a superior knowledge of the fundamental theory and logical relations among parts of the calculus, consequently, leading to students, experiencing the thrill of discovery and the satisfaction of producing results through creative effort - all of which lead to greater enjoyment of mathematics and a deeper understanding of its nature and use thereby making students express ideas of calculus in their own language and undergo the stimulating and disciplinary experience of having their expressions and ideas sharpened through examination by other students as well as by the teacher.

The integration of digital tools in calculus learning and teaching has been initiated by a few schools in India. However, in most of the Indian schools, classroom teaching of calculus is traditional, and thus emphasize those aspects of knowledge that are truly procedural. In those instances where the emphasis is more on the application of concepts in calculus teaching, often contradictions exist with other contextual matters like for example, our evaluation system presses calculus learners to perform relatively fair in regular problems, thus indicating that it is being operated at the action level. It came along from the interviews from calculus teachers that, even though, pupils have the right answers, yet they lack understanding of the concepts.

Learners based on their previous mental assimilations frequently constructed their knowledge, relying by and large on thinking procedurally and not on thinking conceptually while solving tasks on calculus. (Hobden, 2006) in his research stressed on plausible reasons of learners successfully engaging with mathematical constructs, it is emphasized that learners require to be efficient and competent in both conceptually understanding the constructs as well as in

developing procedural fluency. The current study found out that some groups successfully construct their knowledge of derivative with the notations' (e.g., dy/dx) instrumental understanding and for them it is the representation in every context with regards to derivatives and it appeared that construction of their mathematical knowledge took place as facts that were isolated and they found difficulty in seeing interrelationships between different constructs. Learners' responses to teachers' queries made the researcher believe that they struggled to build a connection between maxima/minima and different functions.

In few other cases, it appeared that calculus students were struggling to accommodate those concepts that they newly learned with the ones they had previously learned; e.g., the concept of minima/maxima is taught to students of 11th grade, but they find it difficult in applying that know-how to 12th-grade calculus, and if learners have quadratic equations at hand and to them as they have learned it, it helps generate parabolas and it is known how can one ascertain the turning point in similar cases but now when they engage in learning calculus, minima/maxima has altogether different meaning, and are in search of other mechanisms to deal with it which led the researcher to come up with few issues pertaining to calculus cognition that emerged in the research findings. Few of these include: 1) there was a lack in understanding about notations (e.g., $\frac{dy}{dx}$ by the learners, 2) construction of schema for derivative and maxima/minima is missing among the learners 3) modeling the problems is a weak spot for the calculus learners 4) preference learners give more to rules and formulas, and 5) incorrect application of algebraic notations are seen in calculus students. In this research, responses of teachers brought out that the functioning of the majority of the students is at the phase of action and wherever there is a requirement of rules and formulas, they effectively solve all the questions. Repeated substitution of area and volume formulas into the problems and application of differentiation rules are seen to be done by students to find the derivatives. Whereas on the other hand, some learners often interiorize the formulas on volumes in a process where volume is visualized as a cubic function and encapsulating derivatives as an object in finding the minima. It is evident that this schema has partial assimilation in learners' memory structure, yet mostly they fail in coordinating with schemas that are there already present, for instance, that

of functions and gradients that are essential in solving questions on optimization and in viewing its schema.

Calculus teachers in their interviews revealed that learners have instrumental knowledge of optimization that occurs with both the action stage and with APOS theory's process stage. Most of the time, the learners' knowledge creation is confined only by action conception. This is mainly for the fact that they could solve only such problems that are in the requirement of extraneous stimulation. Causes of it may be attributed to the creation of stimulus within the organized nature of the problems: coordination of others with complete totality in respective objects making other actions and processes act on them. The findings revealed that the entire basis of learners' knowledge creation is rooted in those conceptions and procedural functions that are totally detached from one another.

This possibly is the consequence of the mannerisms in which learning and teaching occur, which bestow greater vehemence on aspects that are procedural in nature. Disregarding conceptual inferences of the constructs of calculus and the questions that pupils are solving in their calculus classrooms encourage their instrumental understanding. Learners eventually broaden their inferences into different aspects of their areas of knowledge. This occurs: 1) when learners are demanded to find out a curve's gradient which is delineated by $y = ax^2 + bx + c$; here learners cite 'a' as the first term's coefficient and contradicting by iterating that the coefficient in the first term of $y = mx + c$ is employed for straight line's gradient, and 2) to find the minima/maxima at the turning point for $y = ax^3 + bx^2 + cx + d$, learners use the formula $x = -b/2a$ to find the x value at the local maxima/minima. Evidently, the learners made use of the knowledge they acquired when they learned quadratic functions. Now, talking about teacher knowledge and its role in teachers' practices, the findings indicate that both have an effect on actual teaching because teachers have to deploy both mathematical as well as pedagogical knowledge in her teaching in order to take "effective" decisions.

3.1 Significance of Learning Calculus in Schools, Colleges, and Universities

To study the phenomenal changes in the physical world, calculus plays a pivotal role in effective engagement with advanced physics and

students who major in mathematics start off with introductory calculus as a groundwork in engagement with advanced calculus which helps in examining the underlying theory which runs in the background of it and in comprehending more complex problems including partial and directional derivatives and the geometry of three-dimensional spaces. Certain advanced courses in statistics and computer programming require expertise in calculus, and in spite of mathematical subspecialty, all specialized disciplines have a profound background in problem-solving techniques and thought processes of calculus. Since the problems that are solved with the help of calculus are continuously evolving, studying calculus becomes all the more crucial for students majoring in computer science, and as a consequence, computer programmers specifically will be able to define and involve in problem-solving in a stepwise fashion using methods of calculus.

The subtleties of numerical analysis require the usage of calculus, and the basic logical and analytical processes that are fundamental to calculus are thus having incalculable worth for the many careers that are available for computer science engineers and programmers. Talking about America of early 1980s, there came a movement to replace first-year graduate calculus with discrete mathematics but this move faced massive resistance by defenders of calculus who powerfully and effectively defended the importance and requirement of including calculus to the core of university curriculum for mathematics and eventually this matter was resolved and calculus in the first year of college again found its place in the curriculum. (Bressoud, 1992) found it apt but was a little dissatisfied. He believed that if systemic changes are to be carried out to improve undergraduate mathematics education, then mathematics teachers must be clear about the "Why?" of teaching calculus. It was found that the recommendation of CUPM was completely wrong in not changing the syllabus of the first semester of calculus and the current syllabus was inadequate as it stands. A feeling of alarm or dread and expectation was there among the students in their approach to calculus.

Students believe that the road ahead in learning calculus is going to be tough, but at the same time, they expect that the course will draw together from the mathematics that they have learned in high school and that their learning of college calculus will transform their earlier gathered knowledge of mathematics in better

comprehension of the world around them by acting as a potent instrument. This tool actually exists in calculus but is often missed by the students. Owing to this, the students are left disillusioned and disappointed. Two answers came up to the question - *Why Do We Teach Calculus?* The first is that, for now many disciplines are using calculus and that too in many different contexts, so if the mathematicians don't teach it to the pupils, then Biologists, Engineers and Physicists will have to take up the job of teaching calculus to them. So the mathematics teachers, shall not shy away from teaching calculus. The usefulness of calculus in varied disciplinary areas is an insufficient answer to the question - *Why Do We Teach Calculus?* If this is the sole criterion, then by this logic, linear programming, and more so statistical analysis will turn out to be even more useful to a majority of college mathematics students, so mathematics teachers should teach only the topics on discrete mathematics instead of teaching calculus! Thereby, there came the second answer to the question. This answer had consequences that were revolutionary to the way mathematics teachers make students learn calculus.

Calculus is situated at the core of mathematical paradigm and concepts of calculus have helped develop modern scientific thought and to see mathematics outside the context of calculus is somewhat meaningless, and thus calculus positions itself at the very foundation of scientific world view and by that means, development of calculus brought mathematics into being. The second answer emphasizes the reason for the teaching of calculus on the vehemence of calculus in learning of locating ourselves in the society that constitutes us. It will be tremendously gross conduct against the first-year pupils of calculus if the teachers of mathematics aren't able to convey the excitement of making them uncover the secrets of nature using calculus.

3.2 Main Issues in Learning and Teaching of Calculus

The following questions attempt to throw light on the importance of learning calculus while transitioning from senior-secondary school to college mathematics: What are the effective policies and practices to remove obstacles and to overcome difficulties that students face in such transitioning? What can be done to place students in the appropriate course when they join

college? What can be done to ensure that the chosen course enables students to move up the ladder in the courses that are built upon them? The transition from senior-secondary school to college mathematics is often damaging to pupils' sense of self-efficacy and also of their mathematical identity, especially in the case of women. What could be the core issues here, and what could be done to address them? Is there a relationship between currently taught calculus at the senior secondary school and its true needs in effective learning of mathematically intensive university courses? How shall colleges and university departments respond to the increasing number of students taking up calculus in senior-secondary schools in designing/shaping what to teach and how they are to be taught? What measures shall be opted to ensure that both senior-secondary school and college/university teachers make use of the most effective/efficient methods for teaching calculus? How to make certain that there is ample opportunity for the students to develop their abilities pertaining to mathematical practices that are critical in nature when they transition from senior-secondary school to college mathematics?

It came out from the interview of calculus teachers that students shall learn calculus not because there is some significant residual associated with it; instead, they must have the drive to learn it. Where the very purpose of learning calculus is not to develop a deeper and abiding understanding or to playfully learn while engaging with the tools of calculus, and to mere pass the exams with good marks, reasons of it could either be that students undervalue calculus as an integral part that will help direct their career path or could be because they know that they will be studying calculus again when they join college, the learning in both the cases will be quite superficial. Consequently, many of the mathematics students who get themselves enrolled in calculus in senior-secondary schools are inadequately prepared for calculus when they join college. In the best case, the learning trajectory shall unfold among students in such a way that the formal mathematics emerges in every mathematical activity a student undertakes and this ideal case is associated with (Freudenthal, 1991), wherein this contention states that mathematics should start and shall stay within common sense and he wished that this adage be understood dynamically, further arguing that common sense is dynamic and not static and remarked that what is common sense for a mathematician may not be what it is for a layperson and that common sense is something

that evolves in the course of learning.

3.3 Alternative Methodologies for Teaching Calculus

It is stressed by many calculus teachers that sophisticated knowledge of elementary functions, including trigonometric, algebraic, logarithmic, and exponential functions, should be taught thoroughly before taking up teaching and learning of calculus. Our school mathematics curriculum has never come up with a satisfactory program in geometry. To effectively teach calculus in schools, full treatment of analytic geometry should be made an essential prerequisite. Understanding of analytic geometry is extremely important, so much so that teaching of finite mathematics and matrix algebra shall be done only after rigorously presenting analytic geometry to the students. (Allendoerfer, 1963) therefore contends that 1) complete abandonment of analytic geometry by colleges is their greatest loss and if at all analytic geometry is to be taught, it must appear in the curriculum of high school mathematics. 2) being a straightforward subject, analytic geometry, vis-à-vis calculus and probability, makes all the mathematics teachers of all the schools to easily handle the teaching content without the need for any specialized training. The question then comes regarding the time of the academic life of a student when she/he shall be taught calculus and who should be bestowed with the responsibility of teaching calculus to the school students? With regard to the former question, it is maintained that until the school students are well versed with the concepts of analytic geometry and elementary functions, they shouldn't be introduced to calculus. If by marathon teaching, these concepts are taught before Grade-12, the teaching of calculus shall be considered. It has been long advocated for a 6-week short course in calculus towards the end of Grade-12, as a fresh transition to 1st year in college. It is feared of this course getting any longer than 6 weeks and shorter than 10-12 months, for then it will simply replace the college course and will waste student's time and consequently the appetite for college calculus will be lost. Now from the teacher's viewpoint, the teaching of calculus effectively is a tough task and thus, calculus should be handled by the best trained, most efficient and shall be chosen from "the lot" of most thoroughly experienced mathematics teachers. Findings to the research bewails the appointment of average mathematics school

teachers for a course in calculus and laments teaching of inexperienced students who takes up calculus in their 1st year of college.

Learning calculus can be a wonderful and exciting experience when it is taught well by experienced teachers and contrarily a horrible one otherwise. It is therefore urged to school authorities to not offer calculus as a course if they don't have efficient and experienced teachers, and it is advised to teachers to ask their students to diligently choose colleges where the college employs their most able teaching staffs for the course in calculus. It is commonly believed that differentiation and integration is what is there in the study of calculus, but in the true sense, this viewpoint is superficial and rather completely flawed. The prominent idea of calculus emerges from the concept of *limits* and without the systematic understanding of *limits*, a course in calculus is a complete failure. A course in calculus often begins with little or no preparation or forethought to *limits* as something which is difficult to comprehend by the students and consequently, calculus teachers get marveled considering the reasons for student's inability to handle even the routine aspects of calculus.

Using the epsilon-delta technique for problems on limits is usually done at the beginning of the course in calculus. An intuitive preparation is required, for it being a difficult new idea, if the epsilon-delta technique is to be dealt in full detail. The very idea and notion among students about the concept of absolute value and inequality is naively understood and is utterly oppressive. There is a dire need for alternatives because both the aforementioned approaches lead to failure. Mathematics teachers shall start off calculus by solving a substantial number of problems on limits which students are familiar with, but care shall be taken that those problems shall not be trivial. The triviality of problems can be understood with an illustration like this:

$$\lim_{x \rightarrow 3} \frac{5x^2 - 8x - 13}{x^2 - 5}$$

Presenting such problems is a futile exercise in learning *limits*. Understanding of real number system in general and completeness property, in particular, is crucial that could be least said in the cognition of the concepts of *limits*. The least upper bound is how students at this stage will grasp about completeness property. With regards to the collection of

examples on plane geometry dealt in the first set, often referred to in popular discourse as “*incommensurable cases*”, shall be made an integral part of the calculus course, in their very first few weeks.

The theorem worth examining in greater depth and understanding is “*a line that is parallel to any one side of a triangle will divide the other two sides of the triangle into proportional segments*”, and another problem to be extensively understood is of “*defining the area of a rectangle, one of whose side is irrational*”. From here, calculus teachers can move on to define the length of an arc of a circle. Another interesting problem to be followed could be on irregular inscribed and circumscribed polygons: “*to show that the length of any inscribed polygon is less than that of any circumscribed polygon and that there is a pair consisting of an inscribed and a circumscribed polygon whose lengths are arbitrarily close together*”. Here nothing is being done, but integral calculus. Till here, calculus teachers have not introduced the concepts of integrals and the formal machinery of integral calculus, i.e., comprehension and articulation of *ideas* without being hung up to the complex formulas. After these geometry examples, it is expected from calculus teachers to shed light on the infinite series. To come up with an answer or solution on summing the elements of infinite series is always pretty fascinating for students of senior secondary schools, consequently leading to a meaningful payoff in their cognition of *limits*.

There was a time when infinite series had a place in every algebra book. Before a student starts to learn basic calculus, it was earlier understood both by publishers of mathematics textbooks as well as by the mathematicians that *limits* had to be introduced in the above mentioned way. It is contended that their experiences have just been bluntly ignored. At this stage, only the series on constants shall be treated, but then calculus teachers also shall immediately jump on to power series as it couldn't be postponed for long. Now the time is ripe for introducing students to examples and illustrations on limits of functions, such as the ones shown below:

$$\lim_{x \rightarrow 0} \frac{\tan x - \sin x}{x^3}$$

$$\lim_{x \rightarrow 5} \frac{\sqrt{x^2 + 11} - 6}{x - 5}$$

After learning the aforementioned, students must have gained the understanding so well that it will enable them to use freely the epsilon-delta

notation. Also, they will be in a position to understand and comprehend the concept of continuous functions and their properties. This is the stage in mathematics student's life when the traditional concepts of differentiation, integration, differential equations shall be brought to them.

Another important point to make here is with regards to the popular college textbooks. The introduction of integration after differentiation is seen in them, which is pretty disturbing. It is the least effective way to teach calculus as it is suggested to start with integration and finding areas and volumes of infinite series by summing the series the same way as discussed above. This is said to be the best takeaway: “*an integral is the limit of the sequence of sums*”. After the establishment of this idea, calculus teachers shall then move on to solve the differentiation of polynomials and establish its connection with integration and consequently prove the Fundamental Theorem. Transcendental functions shall be introduced only after discussing Taylor's theorem, power series, and the interval of convergence. Now the calculus teachers shall expand by their series, the exponential and trigonometric functions, and derive their calculus without investing any further time. There is no other better or more refined approach to teach calculus with understanding vis-à-vis the aforementioned proposed approach.

4. SUGGESTIONS AND RECOMMENDATIONS

Envisioning of learning in a socio-cultural context by breaking down complex calculus concepts into parts similar to the idea vigorously pressed by Vygotsky, and such similar innovative techniques shall be emphasized for student's cognition that is all together process-related that uses scaffolding and classroom dialogue. Calculus reform needs to concentrate not only on increasing the success rate of all students but also on improving their ability, to apply calculus creatively, and to accomplish this, might well require calculus teaching to be structured differently. The author recommend the incorporation of videos in calculus teaching wherever required, for it is common knowledge that teachers too enjoy when more students with better preparation turn up for their class.

For students looking out for quality resources online when not fetched forthwith by educators makes it essential for the educators to acquire familiarity with such online content and to

learn to develop online tools of their own for easy navigation of course materials for their students. Calculus modules that call for a little bit of background understanding make the flipped classroom model effective and all the more important. For students to recall before class what was taught in previous calculus classes, effective use of videos and web resources can be made, eventually saving a lot of time to be dedicated to the topic actually thought of by the teacher to be taught in the class thereby providing learners, who are having fewer time and greater social pressure limitations, an invaluable learning opportunity.

Calculus teachers need to keep in mind the Guershon Harel's Necessity Principle, which states that students are most likely to learn when they see a *need* for what teachers intend to teach them, where, by '*need*', it is meant *intellectual need*. Students require experience with a variety of problems for which the easiest and most natural approach is in terms of accumulation that can be modeled with a sum of products, multiplying the rate of accumulation by the small increment in the independent variable, problems for which the evaluation of the definite integral is the last step. The heart of the intellectual activity should be on converting a problem into an accumulation that can be calculated via a limit of appropriate sums. The focus of calculus teachers shall be first on the dynamic understanding, and then to use this to build the geometric realization of the theorems in calculus.

The analysis of this study on course-repeating patterns among workshop and non-workshop students suggest that time-effective, cost-effective, and a highly academic intervention program, if carried out near the learners' college career, could improve this unfortunate picture. Findings to this study suggest that a good calculus teacher is one who provides explanations that are understandable, who listens carefully to pupils' questions and comments, who help students become a better calculus problem solver, who allows time to students for understanding of difficult calculus ideas, who makes the students feel comfortable in asking calculus questions during class, who presents more than one method for solving the same calculus problem, who makes the calculus class interesting, who asks questions to students to determine whether they understood what was being discussed, and discusses and emphasizes more on the applications of calculus.

To be an effective calculus teacher, ambitious teaching strategies require strong

student-teacher rapport. The practices that a calculus teacher shall opt include frequently allowing students to work on calculus problems with one-another, assignments that are to be completed outside class time shall frequently be submitted as a group project, exam questions shall require students to mostly solve word problems on calculus, calculus teachers shall frequently ask students to pen-down the explanations of their solution in the notebook, both home assignments and exam questions shall require students to solve calculus problems that are unique and different unlike those done in class or are present in the book, calculus teachers shall hold whole-class discussions giving students the opportunity to explain and justify their solution to the entire class and also clear the doubts of their fellow mates who wishes for further clarification.

Calculus problems which have problem situations that are experientially real to the learners are referred to as context problems, and in concurrence with it is the overall goal of realistic mathematics education (RME) instructional design which is used to support the gradual emergence of a taken-as-shared mathematical reality and opting for RME will consequently make the calculus experience for its learners enriching, for now, they can reinvent their expanding common sense, thereby making these experiences non-dichotomous between their everyday life experiences and the calculus problems they solve while learning in school from textbooks written by foreign authors; making both part of the same reality and thereby arriving at a reflexive relationship between usage of context problems and development of experiential reality among calculus students making the context problems on calculus rooted in reality and consequently if more the context problems students solve on calculus, the larger they expand their reality. This connection that calculus offers to its students is incisively the cause that makes calculus students act in a meaningful manner from the very beginning. The researcher suggests that concern for understanding rather than manipulative skill alone is a matter of utmost importance in encouraging the attainment of the quality which calculus education should provide.

To continue the teaching of calculus by methods which are antithetical to those of the experience-discovery approach may deprive our students of the richness of mathematical education which they deserve and which is so imperative that they shall have it. To develop conceptual understanding and cognition of

principles of advanced calculus and possibilities in teaching those to school students and to effectively teach “Visual Calculus” course which comprises mathematical topics few of which are multivariable calculus concepts on differentiation and integrated 3-D geometry, integration and optimization, etc., a reform in calculus teacher preparation is required so that efficient teachers could be tailor-made for teaching school calculus.

The perception of calculus teachers needs to be examined with regards to the early development of calculus concepts among learners. The correlation between teachers’ pedagogic knowledge and their content knowledge and examining their preparedness, and consequently, their confidence in teaching school students the concepts of calculus, requires profound attention. The onus lies on the teachers to be mindful of students’ internal conflicts in dealing with mathematical problems to help them strengthen the novel constructs students come across; and to help them counter it effectively, the teachers shall devise Itemised Genetic Decompositions (IGDs) for the tasks at hand, because it is these IGDs that make teachers learn about the mental configurations of their students and this critical assessment of their learners eventually help educators in gauging the effectiveness of their teaching.

5. CONCLUSIONS

It has been found that calculus under normal conditions in India is taught by inefficient teaches, at a fallacious time and in an inaccurate manner. In mathematics education, time is ripe to examine calculus teaching. Reasons for the same that came out from this research include: (1) calculus in today’s time is pretty common to be taught to senior secondary school students, and (2) the very nature and character of calculus being taught in senior secondary schools and colleges has a bearing on the nature and character of pre-calculus courses taught in middle and high schools. A marathon discussion needs to be initiated for the greater good. For now, the researcher sees how our schools and colleges are troubled by nature and approach to teaching calculus to the learners. Some of the pressing questions that the current study has found include: What is the nature of senior-secondary school calculus? Is there a rationale behind opting for one senior-secondary school calculus curriculum over another that helps better prepare students in the successful learning of

university mathematics? What is the role of calculus teacher, and is it really the teacher who plays the most important role in making students learn calculus? If it is so, can the characteristics of a successful calculus teacher be enumerated? Under the present conditions of early introduction of calculus in the senior-secondary school mathematics curriculum, are the students *actually* encouraged to study mathematics and engineering sciences? Is it so that the students studying in schools wherein calculus is taught are significantly better mathematically, compared to those students, in whose school, calculus is not offered or to those students who do not take up calculus course in senior-secondary class e.g., those who choose to study humanities and social sciences after their 10th board exams? Concerning pedagogical approaches, what is the mathematical nature of teachers’ knowledge with regards to derivatives? What are teachers’ commonly used pedagogical practices? What are teachers’ views as for teaching and learning of calculus? Can different kinds of interrelationships be keyed between teachers’ mathematical knowledge and their pedagogical practices? Why teachers find it extremely difficult to come up with novel solutions to sort out the difficulties that a student face, and is it in anyway correlated to their mathematical and/or pedagogical knowledge? Does secondary school calculus affect performance in college calculus? What is the effect of the level of secondary school calculus background on the measures of their learning outcome? What is the nature of this effect on procedural competency and on conceptual performance? Is there a relationship between secondary school calculus background and continuation to first-semester college calculus?

These are some of the pressing issues vis-à-vis calculus learning and teaching, that require immediate attention and deliberation.

6. REFERENCES:

1. Allendoerfer, C. B. (1963). The case against calculus. *The Mathematics Teacher*, 56(7), 482-485.
2. Armstrong, G., Garner, L., & Wynn, J. (1994). Our experience with two reformed calculus programs. *Problems, Resources, and Issues in Mathematics Undergraduate Studies*, 4(4), 301-311.
3. Artigue, M. (2001). What can we learn from educational research at the university level? *The teaching and*

- learning of mathematics at university level* (pp. 207-220): Springer.
4. Asiala, M., Cottrill, J., Dubinsky, E., & Schwingendorf, K. E. (1997). The development of students' graphical understanding of the derivative. *The Journal of Mathematical Behavior*, 16(4), 399-431.
 5. Bell, A., & Janvier, C. (1981). The interpretation of graphs representing situations. *For the learning of mathematics*, 2(1), 34-42.
 6. Bonsangue, M. V., & Drew, D. E. (1995). Increasing minority students' success in calculus. *New Directions for Teaching and Learning*, 1995(61), 23-33.
 7. Bookman, J. (1993). An expert-novice study of metacognitive behavior in four types of mathematics problems. *Problems, Resources, and Issues in Mathematics Undergraduate Studies*, 3(3), 284-314.
 8. Bookman, J., & Blake, L. (1996). Seven years of Project CALC at Duke University approaching steady state? *Problems, Resources, and Issues in Mathematics Undergraduate Studies*, 6(3), 221-234.
 9. Bookman, J., & Friedman, C. P. (1994). A comparison of the problem-solving performance of students in lab-based and traditional calculus. *Research in collegiate mathematics education I*, 4, 101-116.
 10. Bowers, D. (1999). Animating web pages with the TI-92. Retrieved July.
 11. Bressoud, D. M. (1992). Why do we teach calculus? *The American Mathematical Monthly*, 99(7), 615-617.
 12. Buck, R. (1970). A generalized Hausdorff dimension for functions and sets. *Pacific Journal of Mathematics*, 33(1), 69-78.
 13. Cobb, P., Wood, T., Yackel, E., Nicholls, J., Wheatley, G., Trigatti, B., & Perlwitz, M. (1991). Assessment of a problem-centered second-grade mathematics project. *Journal for research in mathematics education*, 3-29.
 14. Confrey, J. (1981). CONCEPTUAL CHANGE, NUMBER CONCEPTS, AND THE INTRODUCTION TO CALCULUS.
 15. Davis, R. B., & Vinner, S. (1986). The notion of limit: Some seemingly unavoidable misconception stages. *The Journal of Mathematical Behavior*.
 16. De Guzmán, M., Hodgson, B. R., Robert, A., & Villani, V. (1998). *Difficulties in the passage from secondary to tertiary education*. Paper presented at the Proceedings of the International Congress of Mathematicians.
 17. Demana, F. D., Waits, B. K., & Clemens, S. R. (1993). *Precalculus: Functions and graphs*: Addison Wesley.
 18. Dossey, J. A. (1992). The nature of mathematics: Its role and its influence. *Handbook of research on mathematics teaching and learning*, 39, 48.
 19. Douglas, R. G. (1986). *Toward a lean and lively calculus: conference/workshop to develop alternative curriculum and teaching methods for calculus at the college level, Tulane University, January 2-6, 1986* (Vol. 6): Mathematical Assn of Amer.
 20. Douglas, R. G. (1995). The first decade of calculus reform. *UME Trends*, 6(6), 1-2.
 21. Dreyfus, T., & Eisenberg, T. (1983). The function concept in college students: Linearity, smoothness, and periodicity. *Focus on learning problems in mathematics*, 5(3), 119-132.
 22. Dreyfus, T., & Eisenberg, T. (1984). Intuitions on functions. *The Journal of experimental education*, 52(2), 77-85.
 23. Dreyfus, T., & Eisenberg, T. (2012). On different facets of mathematical thinking *The nature of mathematical thinking* (pp. 269-300): Routledge.
 24. Dubinsky, E. (2002). Reflective abstraction in advanced mathematical thinking, *Advanced mathematical thinking* (pp. 95-126): Springer.
 25. Ferrini-Mundy, J., & Graham, K. (1994). Research in calculus learning: Understanding of limits, derivatives, and integrals. *MAA notes*, 31-46.
 26. Ferrini-Mundy, J., & Graham, K. G. (1991). An overview of the calculus curriculum reform effort: Issues for learning, teaching, and curriculum development. *The American Mathematical Monthly*, 98(7), 627-635.
 27. Freudenthal, H. (1991). *Revisiting Mathematics Education* (Dordrecht: D. Reidel Publishing, Co).
 28. Frid, S. (1994). Three approaches to undergraduate calculus instruction: Their nature and potential impact on students' language use and sources of conviction. *Research in Collegiate Mathematics Education I, Providence, RI: AMS*.
 29. Gardiner, T. (1995). Mathematics hamstrung by long divisions. *The Sunday Times*, 22.
 30. Garofalo, J. (1989). Beliefs and their

- influence on mathematical performance. *The Mathematics Teacher*, 82(7), 502-505.
31. Graham, K. G., & Ferrini-Mundy, J. (1989). *An exploration of student understanding of central concepts in calculus*. Paper presented at the Annual Meeting of the American Educational Research Association, San Francisco, CA.
 32. Gray, E. M., & Tall, D. O. (1994). Duality, ambiguity, and flexibility: A "proceptual" view of simple arithmetic. *Journal for research in mathematics education*, 116-140.
 33. Hallett, D. H. (2006). What have we learned from calculus reform? The road to conceptual understanding. *MAA notes*, 69, 43.
 34. Hiebert, J., & Carpenter, T. P. (1992). Learning and teaching with understanding. *Handbook of research on mathematics teaching and learning: A project of the National Council of Teachers of Mathematics*, 65-97.
 35. Hobden, S. (2006). *Forewarned is forearmed-previewing the 2006 Grade 10 mathematical literacy cohort*. Paper presented at the 14th Annual meeting of the Southern African Association for Research in Mathematics, Science and Technology Education (SAARMSTE), Pretoria.
 36. Kaput, J. J. (1998). Representations, inscriptions, descriptions, and learning: A kaleidoscope of windows. *The Journal of Mathematical Behavior*, 17(2), 265-281.
 37. Kennedy, D. (2000). AP calculus for a new century: Consultado el.
 38. Koirala, H. P. (1997). Teaching of calculus for students' conceptual understanding. *The Mathematics Educator*, 2(1), 52-62.
 39. Kuh, G. D., Kinzie, J., Schuh, J. H., & Whitt, E. J. (2011). *Student success in college: Creating conditions that matter*. John Wiley & Sons.
 40. Legrand, M. (1993). Débat scientifique en cours de mathématiques. *Repères irem*, 10, 123-159.
 41. Leinbach, C. (1997). The curriculum in the age of CAS. *The state of computer algebra in mathematics education*. Bromley, England: Chartwell-Bratt.
 42. Markovits, Z., Eylon, B.-S., & Bruckheimer, M. (1986). Functions today and yesterday. *For the learning of mathematics*, 6(2), 18-28.
 43. Mathematics, N. C. o. T. o. M. C. o. S. f. S. (1989). *Curriculum and evaluation standards for school mathematics*: Natl Council of Teachers of.
 44. Mathematics, N. C. o. T. o. M. C. o. T. S. f. S. (1991). *Professional standards for teaching mathematics*: Natl Council of Teachers of.
 45. Monk, D. H. (1987). Secondary school size and curriculum comprehensiveness. *Economics of Education Review*, 6(2), 137-150.
 46. Monk, S., & Nemirovsky, R. (1994). The case of Dan: Student construction of a functional situation through visual attributes. *CBMS Issues in Mathematics Education*, 4, 139-168.
 47. Neumark, V. (1995). For the love of maths. *Times Educational Supplement*, 8.
 48. Noddings, N., Maher, C. A., & Davis, R. B. (1990). *Constructivist views on the teaching and learning of mathematics*: National Council of Teachers of Mathematics.
 49. Norman, F. A., & Prichard, M. K. (1994). Cognitive obstacles to the learning of calculus: a Kruketskiian perspective. *MAA notes*, 65-78.
 50. Orton, A., & Wain, G. (1994). The aims of teaching mathematics. *Issues in teaching mathematics*, 1-20.
 51. Palmiter, J. R. (1991). Effects of computer algebra systems on concept and skill acquisition in calculus. *Journal for research in mathematics education*, 151-156.
 52. Park, K., & Travers, K. J. (1996). A comparative study of a computer-based and a standard college first-year calculus course. *CBMS Issues in Mathematics Education*, 6, 155-176.
 53. Piaget, J. (1985). The equilibration of cognitive structures (T. Brown & KJ Thampy, Trans.). *Cambridge: Harvard University Press*.
 54. Praslon, F. (1999). *Discontinuities regarding the secondary/university transition: The notion of derivative as a specific case*. Paper presented at the PME CONFERENCE.
 55. Repo, S. (1994). Understanding and reflective abstraction: Learning the concept of derivative in a computer environment. *International DERIVE Journal*, 1(1), 97-113.
 56. Schoenfeld, A. (1994). *Some notes on the enterprise (research in collegiate*

- mathematics education, that is*). Paper presented at the Conference Board of the Mathematical Sciences Issues in Mathematics Education.
57. Schoenfeld, A. H. (1995). A brief biography of calculus reform. *UME Trends*, 6(6), 3-5.
 58. Schwalbach, E. M., & Dosemagen, D. M. (2000). Developing student understanding: Contextualizing calculus concepts. *School Science and Mathematics*, 100(2), 90-98.
 59. Selden, J., Selden, A., & Mason, A. (1994). Even good calculus students can't solve nonroutine problems. *MAA notes*, 19-28.
 60. Sfard, A. (1992). Operational origins of mathematical objects and the quandary of reification-the case of function. *The concept of function: Aspects of epistemology and pedagogy*, 25, 59-84.
 61. Skemp, R. R. (1976). Relational understanding and instrumental understanding. *Mathematics teaching*, 77(1), 20-26.
 62. Smith, D. A., & Moore, L. C. (1990). Duke University: Project calc. *Priming the calculus pump: Innovations and resources*, 51-74.
 63. Smith, D. A., & Moore, L. C. (1991). Project CALC: An integrated laboratory course. *The laboratory approach to teaching calculus. The Mathematical Association of America, Washington, DC*, 81-92.
 64. Solow, A. E. (1994). *Preparing for a new calculus: Conference proceedings*: Mathematical Assn of Amer.
 65. Tall, D. (1992). The transition to advanced mathematical thinking: Functions, limits, infinity, and proof. *Handbook of research on mathematics teaching and learning*, 495-511.
 66. Tall, D. (1996). *Functions and Calculus (Vol. 1)*: Dordrecht, Netherlands: Kluwer Academic.
 67. Tall, D., & Blackett, N. (1986). Investigating graphs and the calculus in the sixth form. *Exploring mathematics with microcomputers*, 156-175.
 68. Tall, D., & Schwarzenberger, R. (1978). Conflicts in the learning of real numbers and limits. *Mathematics teaching*, 82.
 69. Tall, D., & Vinner, S. (1981). Concept image and concept definition in mathematics with particular reference to limits and continuity. *Educational studies in mathematics*, 12(2), 151-169.
 70. Tucker, A., & Leitzel, J. R. (1995). *Assessing calculus reform efforts: A report to the community*: Mathematical Assn of Amer.
 71. Tucker, M. (1990). *Out there: Marginalization and contemporary cultures (Vol. 4)*: MIT Press.
 72. Vinner, S., & Dreyfus, T. (1989). Images and definitions for the concept of function. *Journal for research in mathematics education*, 356-366.
 73. Weissglass, J. (1992). Changing the Culture of Mathematics Instruction. *Journal of mathematical behavior*, 11(2), 195-203.
 74. White, P., & Mitchelmore, M. (1996). Conceptual knowledge in introductory calculus. *Journal for research in mathematics education*, 27, 79-95.
 75. Williams, S. R. (1991). Models of limit held by college calculus students. *Journal for research in mathematics education*, 22(3), 219-236.
 76. Young, G. S. (1987). Present problems and future prospects. *Calculus for a new century*, 172-175.

CARACTERÍSTICAS DAS RAÇAS AUTÓCTONES DA RÚSSIA E DO CAZAQUISTÃO DE ATRAVÉS DO TESTE DE MICRONÚCLEOS**CHARACTERISTICS OF AUTOCHTHONOUS BREEDS OF RUSSIA AND KAZAKHSTAN BY MICRONUCLEAR TEST****ХАРАКТЕРИСТИКА АВТОХТОННЫХ ПОРОД РОССИИ И КАЗАХСТАНА ПО МИКРОЯДЕРНОМУ ТЕСТУ**

MARZANOV, Nurbiy S.¹; MARZANOVA, Saida N.²; BAITLESSOV, Yerbulat U.³; BOZYMOVA, Aigul K.³; DAVLETOVA, Ainur M.⁴;

¹Laboratory for Molecular Bases of Selection, Ernst Federal Science Center for Animal Husbandry, Podolsk, Russian Federation

²Department of Immunology and Biotechnology, Skryabin Moscow State Academy of Veterinary Medicine and Biotechnology, Moscow, Russian Federation

³Department of Ecology and Biotechnology, West-Kazakhstan Innovative-Technological University, Uralsk, Republic of Kazakhstan

⁴Department of Higher School of Livestock Production Technology, Zhangir Khan West Kazakhstan Agrarian-Technical University, Uralsk, Republic of Kazakhstan

* Correspondence author
e-mail: nmarzanov@yandex.ru

Received 26 November 2019; received in revised form 22 January 2020; accepted 30 January 2020

RESUMO

O artigo é dedicado aos resultados do teste de micronúcleos em duas raças autóctones bem conhecidas da Federação Russa e da República do Cazaquistão: Romanov e Edilbay. Nas ovelhas Romanov, as maiores taxas de ocorrência de micronúcleos foram encontradas em cordeiros ($8,7 \pm 0,9$), depois em ovelhas produtivas ($5,6 \pm 0,03$ ‰) e ovinos ($4,8 \pm 0,3$ ‰). A raça Edilbay apresenta diferenças nos resultados da análise de micronúcleos nos eritrócitos, os quais são mais pronunciados nos dois tipos da mesma raça: "Birlik" e "Suyunduk". A coudelaria "Birlik" está localizada nos Urais, na região oeste do Cazaquistão. Ovelhas Edilbay da raça Suyunduk são criadas na coudelaria "Makash", na região (óblast) de Atyrauz, na República do Cazaquistão, localizada próximo ao local de teste nuclear de Azgir. A diferença no teste de micronúcleos deve-se ao fato de que as ovelhas Suyunduk serem expostas a fatores de estresse ambiental devido à proximidade de locais com alto nível de contaminação por radionuclídeos. O efeito constante da seleção natural promove a reprodução de animais com maior resistência a fatores de estresse ambiental. Isso explica a baixa ocorrência de células com anormalidades citogenéticas em ovelhas do tipo "Suyunduk" Edilbay. Esse tipo tem maior potencial de adaptação a condições desfavoráveis de reprodução do que as ovelhas da raça Edilbay Birlik. Um alto nível de indicadores de teste de micronúcleos nas ovelhas Romanov está associado às características do sexo e faixas etárias, bem como à carga ambiental das condições climáticas na Rússia Central. A classificação dos micronúcleos é proposta. Acredita-se que os micronúcleos grandes e médios sejam formados sob a influência de vários mutagênicos no corpo, causando uma grande divisão de cromossomos individuais na metáfase e na anáfase. Pequenos micronúcleos indicam uma diminuição na viabilidade celular potencial.

Palavras-chave: ovelhas, eritrócitos, estresse ambiental, distúrbios citogenéticos.

ABSTRACT

The article is devoted to the results of the micronucleus test in two well-known autochthonous sheep breeds of the Russian Federation and the Republic of Kazakhstan: Romanov and Edilbay. In Romanov sheep, the highest rates of micronucleus occurrence were found in lambs (8.7 ± 0.9 ‰), than in producing rams (5.6 ± 0.03 ‰) and ewes (4.8 ± 0.3 ‰). The Edilbay breed has the differences in micronucleus test results in erythrocytes are most pronounced between two intrabreed types: "Birlik" and "Suyunduk". The breeding plant "Birlik" is located in the Ural,

the West Kazakhstan region. "Suyunduk" type of Edilbay breed sheep are raised in the breeding plant "Makash" in the Atyrauz region of the Republic of Kazakhstan, located near the Azgir nuclear test site. The difference in the micronucleus test is due to the fact that sheep of the "Suyunduk" type are exposed to environmental stress factors due to the proximity of places with high levels of radionuclide contamination. The constant action of natural selection contributes to the reproduction of animals with increased resistance to environmental stress factors. This explains the low occurrence of cells with cytogenetic abnormalities in sheep of the "Suyunduk" Edilbay breed sheep type. This type has a higher potential for adaptation to adverse breeding conditions than the Birlik type of Edilbay breed sheep. The high level of micronucleus test indicators in sheep of the Romanov breed is associated with the peculiarities of gender and age groups, and also the environmental stress of climatic conditions in Central Russia. A classification of micronucleus is proposed. It is believed that large and medium-sized micronucleus are formed by the action of various mutagens on the body, causing a large in the division of individual chromosomes in metaphase and anaphase. Small micronucleuses indicate a decrease in potential cell viability.

Keywords: *sheep, red blood cells, environmental stress, cytogenetic abnormalities.*

АННОТАЦИЯ

Статья посвящена результатам микроядерного теста у двух известных автохтонных пород овец Российской Федерации и Республики Казахстан: романовской и эдильбаевской. У овец романовской породы самые высокие показатели встречаемости микроядра были обнаружены у ягнят ($8,7 \pm 0,9$), затем у баранов-производителей ($5,6 \pm 0,03$ %) и овцематок ($4,8 \pm 0,3$ %). Эдильбаевская порода имеет различия в результатах анализа микроядра в эритроцитах, которые наиболее выражены у двух внутривидовых типов: «Бирлик» и «Суюндук». Племенной завод «Бирлик» расположен на Урале, в Западно-Казахстанской области. Овец эдильбаевской породы типа «Суюндук» разводят на племенном заводе «Макаш» в Атырауской области Республики Казахстан, расположенном недалеко от Азгирского ядерного полигона. Разница в микроядерном тесте связана с тем, что овцы типа «Суюндук» подвержены факторам стресса окружающей среды из-за близости к местам с высоким уровнем радионуклидного загрязнения. Это способствует размножению животных с повышенной устойчивостью к факторам стресса окружающей среды, что объясняет низкую встречаемость клеток с цитогенетическими аномалиями у овец типа «Суюндук» эдильбаевской породы. Этот тип обладает более высоким потенциалом для адаптации к неблагоприятным условиям размножения, чем овцы типа «Бирлик». Высокий уровень показателей микроядерного теста у овец романовской породы связан с особенностями половой и возрастной групп, а также с экологической нагрузкой климатических условий в Центральной России. Предложена классификация микроядра. Считается, что крупные и средние микроядра образуются под действием различных мутагенов на организм, вызывая большое деление отдельных хромосом в метафазе и анафазе. Мелкие микроядра указывают на снижение потенциальной жизнеспособности клеток.

Ключевые слова: *овцы, эритроциты, экологический стресс, цитогенетические нарушения.*

1. INTRODUCTION

Bioindication, as an integral part of biomonitoring, has developed as a methodology for scientific research, and this is especially important since today, consequence of scientific and technological progress have become an objective reality (Gorovtsov *et al.*, 2017; Jiyeubekov *et al.*, 2018; Minakova *et al.*, 2018; Hodov *et al.*, 2019). The use of methods based on morphogenetic indicators of developmental stability and cytogenetic homeostasis are a promising direction since they meet practically all the requirements of biomonitoring (Udroiu, 2007; Udroiu and Sgura, 2017; Bakhtiar *et al.*, 2017; Cox *et al.*, 2019; Belhadj Slimen *et al.*, 2019).

Morphogenetic indicators characterize the level of cytogenetic stability of an individual organism and can form its phenotype under the conditions of a specific environment (Zakharov,

and Trofimov, 2017; Kolosov *et al.*, 2017; Mukhametzharova *et al.*, 2018). Cytogenetic homeostasis can be studied using a micronucleus test, the essence of which is to calculate the number and volume of cells with micronuclei (Shapiro *et al.*, 2003; Astafieva, 2017; Glden Yilmaz and Gl, 2017; Monte *et al.*, 2019; Sabbioni *et al.*, 2018; Maass *et al.*, 2018; Wu *et al.*, 2019).

The micronucleus test is one of the methods for determining substances that exhibit genotoxic effects on the body (Hristova *et al.*, 2017; McAllister *et al.*, 2017; Luijten *et al.*, 2018; Lu *et al.*, 2018). Literary data indicate that the micronucleus test is not inferior, and sometimes even exceeds the chromosomal aberration tests in terms of informativeness and efficiency (Ilinskikh *et al.*, 2011; Sabbioni *et al.*, 2019). The micronucleus test developed by W. Schmid (Schmid, 1975). It is based on using in vivo bone marrow cells of higher vertebrates, fish, and

amphibians as biomarkers (Albarella *et al.*, 2019; Žaja *et al.*, 2019). However, in recent years, it has been replenished with a number of new techniques (analysis of micronuclei obtained by a block of cytokinesis, analysis of rodent erythrocytes micronuclei, and other similar techniques) that cover animal and plant cells, as well as various types of smear staining (Schmid, 1975; Fenech, 2000; Ilinskikh *et al.*, 2011; Astafieva *et al.*, 2015; Hayashi, 2016; Wilde *et al.*, 2017; Afusat *et al.*, 2017; Arieli, 2017; Dossybayev *et al.*, 2019).

2. MATERIALS AND METHODS

Peripheral blood samples for research were taken from 69 sheep of two breeds: Romanov and Edilbay. Sheep (n=35) belonged to the Romanov breed were taken from breeding plants Yaroslavl region. The Edilbay breed was represented by two interbreed types: "Birlik" (n = 16) and "Suyunduk" (n = 18) from the breeding plant "Volgograd–Edilbay" Volgograd region. This farm purchased sheep of the "Birlik" type from the "Birlik" breeding enterprise of the West Kazakhstan region, and "Suyunduk" from the "Makash" of the Atyrauz region the Republic of Kazakhstan. Blood from the jugular vein was taken in tubes with a 0.5% EDTA solution. Smears were made on glass slides, thoroughly washed and degreased using a mixture of Nikiforov (a mixture of equal volumes of ethyl alcohol and anhydrous sulfuric ether; It is used for fixing blood products, bacterial preparations and organ prints).

To count erythrocytes with micronucleus, a drop of peripheral blood was diluted with the physiological solution (1:1), and smears were prepared on the glasses, which were fixed with methyl alcohol and dried at room temperature. Smears were stained using the Pappenheim method using Mai-Grunwald and Giems solutions (Romejs, 1953; Sarkisov and Perov, 1996; Tabecka-Lonczynska *et al.*, 2019; Younas *et al.*, 2013).

Red blood cells with micronuclei were counted for each test animal in 37 workers. In each field, approximately 80 erythrocytes were found, which is 3000 cells. For the convenience of analysis, the total figure was divided by three. The results are presented per 1000 cells. The obtained data were expressed in ppm (‰) – the ratio of the number of erythrocytes with micronucleuses to the total number of cells counted. Cell analysis was carried out using a Motic binocular microscope with a built-in digital camera (DMBA300), an increase of 1000 (Astafieva *et al.*, 2015; Astafieva,

2017).

The statistical significance of differences in the frequencies of cytogenetic anomalies between breeds and groups of animals was evaluated by Student's t-test. A difference of $P < 0.05$ and more were considered statistically significant (Glanc, 1999).

3. RESULTS AND DISCUSSION:

The results of the micronucleus test on the Romanov breed of sheep are presented in Table 1. It was found that the highest rates of occurrence of micronucleuses were detected in lambs (8.7 ± 0.9), then in rams (5.6 ± 0.03 ‰), and in third place were ewes (4.8 ± 0.3) (Table 1).

There is a significant difference in micronucleus dough between rams and ewes ($P < 0.01$) and between adult groups of animals and young animals ($P < 0.01$), which may be due to the rigid selection of producers for the tribe and age since blood was taken from old sheep. We believe this is due to the relative immaturity of the cellular component of the immune system in lambs, which is responsible for the elimination of red blood cells with micronucleus. Our results for young animals confirm the data on the increased level of micronucleus in comparison with adults. Two interbreed types of Edilbay breed "Birlik" and "Suyunduk" were studied in comparison with the obtained materials on Romanov breed (Table 2).

The differences in the results of the micronucleus test in erythrocytes are most pronounced between different interbreeding types. In the Edilbay sheep breed "Birlik" type, the frequency of occurrence of erythrocytes with micronucleus (4.6 ± 0.3) was higher compared to "Suyunduk" sheep type (3.5 ± 0.2). According to the presented data, it is clear that the frequency of occurrence of erythrocytes with micronucleus in individuals of the Romanov breed (5.8 ± 1.18 ‰) is even higher than that of interbreeding types of the Edilbay breed. The reason for the differentiation of the "Suyunduk" and "Birlik" sheep breed types may be that the breeding plants were located in different environmental conditions. The breeding plant "Birlik" is located in the Ural region, in the West Kazakhstan region.

The "Suyunduk" type of Edilbay sheep breed were descended from the breeding plant „Makash" in the Atyrauz region of the Republic Kazakhstan. The breeding plant "Makash" is located next to the well-known Azgir nuclear test site of the Volgograd region Russian Federation. The observed micronucleus differentiation is due

to the fact that sheep of the “Suyunduk” Edilbay sheep breed type were subjected to constant environmental stress factors due to the proximity of their breeding sites to the region with high levels of radionuclide contamination (Astafieva *et al.*, 2015; Astafieva, 2017).

The chronic action of natural selection contributes to the reproduction of animals with increased resistance to environmental stress factors. This probably explains the relatively low frequency of occurrence of cells with cytogenetic abnormalities in animals of “Suyunduk” Edilbay sheep breed type. The “Suyunduk” type of Edilbay sheep breed has a higher potential for adaptation to unfavorable breeding conditions than the “Birlik” type, which is the result of the action of natural selection in generations. As for the high level of performance in Romanov sheep along with the characteristics of gender and age groups, the environmental stress of the climatic conditions of Central Russia is possible. Thus, the micronucleus test is one of the methods for determining the influence of substances that exhibit genotoxic effects on the body. Microkernels are fragments of the nucleus in eukaryotic cells that do not contain the complete genome necessary for its survival (Figures 1 and 2).

The size of micronucleus depends on the reasons underlying their formation. It is believed that large and medium micronucleus are formed by the action of various mutagens on the body, which causes a large in the division of individual chromosomes in metaphase and anaphase. At the same time, small micronucleuses indicates a decrease in the potential viability of cells (Figure 3).

4. CONCLUSIONS:

As a result of the study, in accordance with the sizes of micronucleus and the forms of their occurrence, a classification consisting of 5 points was proposed. When determining the size of a micronucleus, they proceeded from the average size of the normoblast core, averaging 1.5 microns. The classification includes the presence of five types of occurrence of micronucleus in the cell:

1. The first type is one or several large micronuclei in erythrocytes, up to 1/4 the size of an average normoblast nucleus.
2. The second type is one micronucleus in the erythrocyte, ranging in size from 1/15 to 1/10 of the average size of the normoblast core.
3. The third type is one small micronucleus

in the erythrocyte, 1/40 of the average size of the normoblast nucleus.

4. The fourth type – micronucleus, which are several small formations, in an amount from 2 to 10 pieces, the size of a microkernel of the 2nd and 3rd types, i.e., from 1/40 to 1 / 15– 1/10 of the average size of the nucleus of a normoblast.

5. The fifth type is when both large and small micronucleuses are detected simultaneously in the studied red blood cells.

In the studied blood smears of sheep of two breeds, the Romanov and Edilbay, mainly large micronucleus were found. Most often, large micronucleus were one in a red blood cell, less often two. Small micronucleus were found in the amount of two, rarely three in one erythrocyte. In 5% of the total number of cells with micronucleus, there was a large micronucleus and one or two small sizes next to it. Only 10% of the total number of cells with micronucleus revealed the formation of small and medium sizes. Thus, a micronucleus test was carried out on the instability of the genetic apparatus in the erythrocytes of the blood of two autochthonous sheep breeds from the Russian Federation and the Republic of Kazakhstan. In Romanov sheep, the relationship between the level of micronucleus in erythrocytes and the age of animals was determined. A comparative characteristic is given for the occurrence of micronuclei in known sheep breeds of two countries: the Russian Federation and the Republic of Kazakhstan.

5. REFERENCES:

1. Afusat, J.J., Theodora, O.O., Adewole, A.A. *Journal of Advanced Veterinary and Animal Research*, **2017**, 4(3), 281-287. DOI: 10.5455/javar.2017.d225.
2. Albarella, S., D'anza, E., Galdiero, G., Esposito, L., De Biase, D., Paciello, O., Ciotola, F., Peretti, V. *Animals*, **2019**, 9(10), Article number 776.
3. Arieli, R. *Frontiers in Physiology*, **2017**, 8(AUG), Article number 591.
4. Astafieva, E.E. *Genetic evaluation of species and breeds of animals bred in different environmental conditions*. Moscow: Moscow State Academy of Veterinary Medicine and Biotechnology, **2017**.
5. Astafieva, E.E., Komkova, E.A., Petrov, S.N., Adamyan, K.K., Marzanov, N.S. *Russian Agricultural Sciences*, **2015**, 1, 33-35.

6. Bakhtiar, R., Abdolmohammadi, A., Hajarian, H., Nikousefat, Z., Kalantar-Neyestanaki, D. *Meta Gene*, **2017**, *104*, 186-191.
7. Belhadj Slimen, I., Chniter, M., Najar, T., Ghram, A. *Livestock Science*, **2019**, *229*, 179-187.
8. Cox, J.F., Navarrete, F., Carrasco, A., Dorado, J., Saravia, F. *Theriogenology*, **2019**, *123*, 159-166.
9. Dossybayev, K., Orazymbetova, Z., Mussayeva, A., Saitou, N., Zhapbasov, R., Makhmatov, B., Bekmanov, B. *Archives Animal Breeding*, **2019**, *62*(1), 305-312.
10. Fenech, M. *Fundamental, and Molecular Mechanisms of Mutagenesis*, **2000**, *455*(1-2), 81-95. DOI: 10.1016/S0027-5107(00)00065-8.
11. Glanc, S. *Biomedical statistics*. Moscow: Praktika, **1999**.
12. Gorovtsov, A., Rajput, V.D., Gorbov, S., Vasilchenko, N. Bioindication-based approaches for sustainable management of urban ecosystems. In: R. Singh, S. Kumar (Eds.), *Green technologies and environmental sustainability (pp. 203-228)*, Luxembourg: Springer International Publishing, **2017**.
13. Gülden Yilmaz, S., Gül, M. *Journal of Applied Biological Sciences*, **2017**, *11*(1), 45-53.
14. Hayashi, M. *Genes, and Environment*, **2016**, *38*(1), 18. DOI: 10.1186/s41021-016-0044-x.
15. Hodov, V.I., Abylkasymov, D., Sudarev, N.P., Abrampalskaya, O.V., Migulev, P.I. *International Journal of Innovative Technology and Exploring Engineering*, **2019**, *9*(1), 3897-3901.
16. Hristova, D., Metodiev, S., Nikolov, V., Vassilev, D., Todorovska, E. *Genetika*, **2017**, *49*(1), 247-258.
17. Ilinskikh, N.N., Vasiliev, S.A., Kravtsov, V.Ju. *Micronuclear test in screening and monitoring of mutagens. Methodological features of micronuclear analysis in assessing the state of cytogenetic instability*. Saarbrücken: Lap Lambert Academic, **2011**.
18. Jiyenbekov, A., Barinova, S., Bigaliev, A., Nurashov, S., Sametova, E., Fahima, T. *Applied Ecology and Environmental Research*, **2018**, *16*(6), 7799-7831.
19. Kolosov, Y.A., Klimenko, A.I., Vasilenko, V.N., Shirokova, V., Getmantseva, L.V., Kolosov, A.Y., Aboneev, V.V., Chizhova, L.N., Marchenko, V.V., Mikhailenko, A.K., Aboneev, D.V. *OnLine Journal of Biological Sciences*, **2017**, *17*(4), 343-347.
20. Lu, T., Pei, W., Zhang, S., Wu, Y., Chen, F., Han, X., Guan, W. *Pakistan Journal of Zoology*, **2018**, *50*(5), 157-168.
21. Luijten, M.N.H., Lee, J.X.T., Chen, S., Crasta, K.C. *Methods in Molecular Biology*, **2018**, *1769*, 183-195.
22. Maass, K., Rosing, F., Ronchi, P., Willmund, K.V., Devens, F., Hergt, M., Herrmann, H., Lichter, P., Ernst, A. *Experimental Cell Research*, **2018**, *371*(2), 353-363.
23. McAllister, E.J., Apgar, J.R., Leung, C.R., Rickert, R.C., Jellusova, J. *Journal of Immunology*, **2017**, *199*(8), 2998-3003.
24. Minakova, E.A., Shlychkov, A.P., Arinina, A.V. *IOP Conference Series: Earth and Environmental Science*, **2018**, *107*(1), Article number 012065.
25. Monte, A.P.O., Barros, V.R.P., Santos, J.M., Menezes, V.G., Cavalcante, A.Y.P., Gouveia, B.B., Bezerra, M.E.S., Matos, M.H.T. *Genetics and Molecular Research*, **2019**, *129*, 61-69.
26. Mukhametzharova, I., Islamov, Y., Shauyenov, S., Ibrayev, D., Atavliyeva, S., Tarlykov, P. *OnLine Journal of Biological Sciences*, **2018**, *18*(3), 341-348.
27. Romejs, B. *Microscopic technique*. Moscow: Foreign Literature Publishing House, **1953**.
28. Sabbioni, A., Beretti, V., Ablondi, M., Righi, F., Superchi, P. *Small Ruminant Research*, **2018**, *159*, 69-74.
29. Sabbioni, A., Beretti, V., Zambini, E.M., Superchi, P., Ablondi, M. *Small Ruminant Research*, **2019**, *174*, 141-147.
30. Sarkisov, D.S., Perov, Ju.L. *Microscopic technique*. Moscow: Medicina, **1996**.
31. Schmid, W. *Mutation Research*, **1975**, *31*, 9-15.
32. Shapiro, N.A., Bogatyrev V.N., Petrov, A.S. *News of Clinical Cytology of Russia*, **2003**, *7*(1-2), 32-39.
33. Tabecka-Lonczynska, A., Mytych, J., Solek, P., Kowalewski, M.P., Koziorowski, M. *Theriogenology*, **2019**, *126*, 199-205.
34. Udroi, I.A. *Povolzhskiy Journal of Ecology*, **2007**, *1*, 75-77.

35. Udrioiu, I.A., Sgura, A. *Animal Genetics*, **2017**, 48(5), 505-515. DOI: 10.1111 / age.12581.
36. Wilde, S., Dambowsky, M., Hempt, C., Sutter, A., Queisser, N. *Environmental and Molecular Mutagenesis*, **2017**, 58(9), 662-677.
37. Wu, X., Gao, F., Wu, Y., Sun, R., Guan, W., Tian, X. *Cytotechnology*, **2019**, 71(2), 539-551.
38. Younas, U., Abdullah, M., Bhatti, J.A., Pasha, T.N., Ahmad, N., Nasir, M., Hussain, A. *Journal of Animal and Plant Sciences*, **2013**, 23 (1), 40-44.
39. Žaja, I.Ž., Vince, S., Milas, N.P., Lobpreis, I.R.A., Špoljarić, B., Vugrovečki, A.S., Milinković-Tur, S., Šimpraga, M., Pajurin, L., Mikuš, T., Vlahović, K., Popović, M., Špoljarić, D. *Animals*, **2019**, 9(12), Article number 1130.
40. Zakharov, V.M., Trofimov, I.E. *Russian Journal of Developmental Biology*, **2017**, 48(6), 369-378.

Table 1. The frequency of occurrence of erythrocytes with micronucleus in the studied sheep of the Romanov breed (in ‰)

No.	Group of discovered animals	n	The average number of micronucleus per 1000 cells
1	Rams	8	5.6 ± 0.3
2	Ewes	20	4.8 ± 0.3
3	Lambs 2 months age	7	8.7 ± 0.9
4	Group average	35	5.8 ± 1.8

Table 2. The frequency of occurrence of erythrocytes with micronucleus in studied sheep breeds (‰)

Sheep breeds and interbreeding types	n	Number of micronucleuses per 1000 cells
Edilbay interbreeds types:		
Birlik	16	4.6 ± 0.3
Suyunduk	18	3.5 ± 0.2
Romanov	35	5.8 ± 1.8

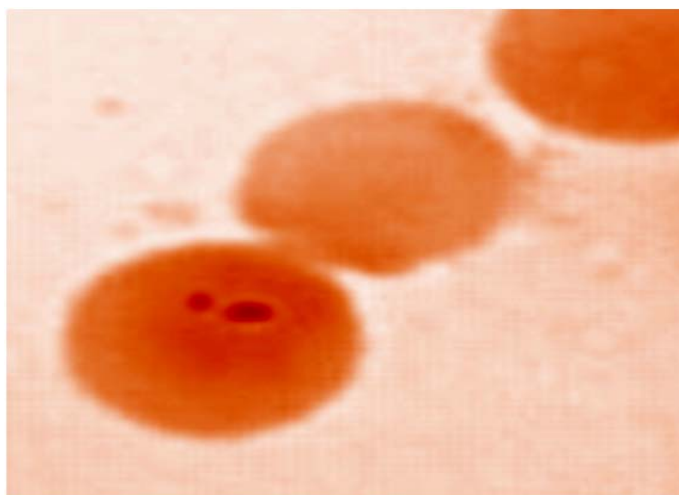


Figure 1. The sheep in the erythrocyte are represented large and medium micronucleuses

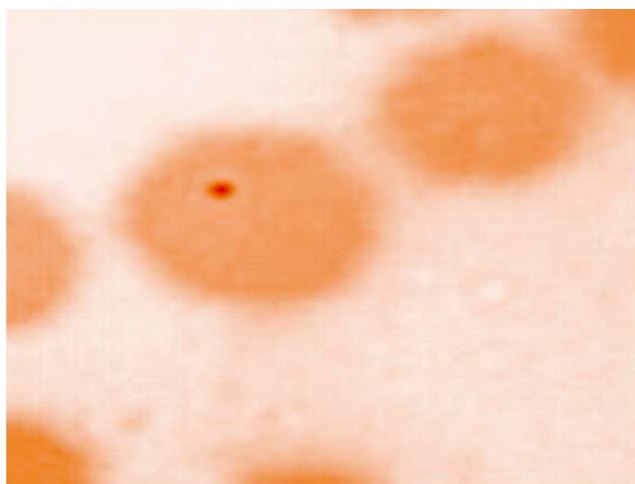


Figure 2. Middle micronucleus in a sheep erythrocyte

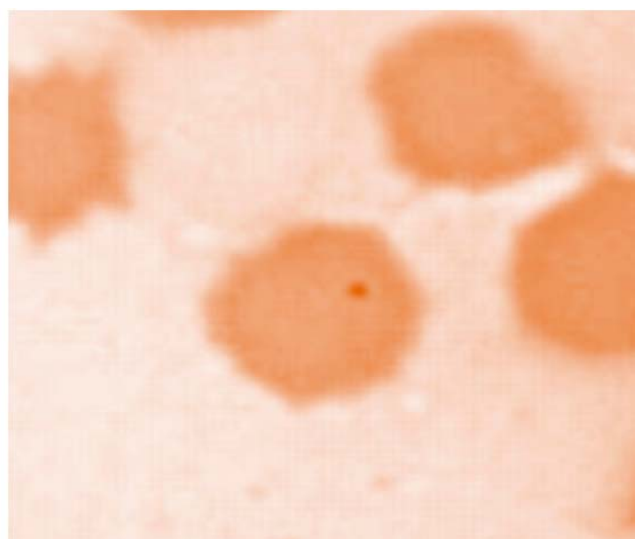


Figure 3. Erythrocyte in a sheep with a small micronucleus

ESTUDO DA PLASMASORÇÃO *IN VITRO* DE LIPOPROTEÍNA E PROPRIEDADES FÍSICO-QUÍMICAS DE SORBENTES POLIMÉRICOS COM GRUPOS AMINO SUBSTITUÍDOS**STUDY OF THE *IN VITRO* LIPOPROTEIN PLASMASORPTION AND PHYSICO-CHEMICAL PROPERTIES OF POLYMERIC SORBENTS WITH SUBSTITUTED AMINO GROUPS****ИЗУЧЕНИЕ СОРБЦИИ ЛИПОПРОТЕИНОВ ИЗ ПЛАЗМЫ *IN VITRO* И ФИЗИКО-ХИМИЧЕСКИХ СВОЙСТВ ПОЛИМЕРНЫХ СОРБЕНТОВ С ЗАМЕЩЕННЫМИ АМИНОГРУППАМИ**

DORSKAIA, Elena Vladimirovna^{1*}; PESTOV, Sergei Mihaylovich²

¹ Mendeleev University of Chemical Technology of Russia, Faculty of Technology of Organic Substances and Chemical Pharmaceutical Compounds, Department of Expert Examination in Drug Testing and Narcoanalysis. Russia.

² Russian Technological University, Institute of Fine Chemical Technology, Department of Physical Chemistry. Russia.

* Correspondence author
e-mail: edrhtu@mail.ru

Received 12 December 2019; received in revised form 28 January 2020; accepted 02 February 2020

RESUMO

Atualmente, o método de plasmassorção é amplamente utilizado na prática clínica para remover quantidades excessivas de metabólitos que causam várias patologias. No entanto, os plasmasorbentes aplicados muitas vezes podem fornecer vários efeitos colaterais para o paciente, como a coagulação do sangue, a liberação de partículas de poeira e a absorção de componentes úteis do plasma. Além disso, eles podem ser bastante caros. O objetivo do trabalho foi criar plasmasorbentes disponíveis com boa hemocompatibilidade para a adsorção de lipoproteínas do plasma. Foram sintetizados vários trocadores de ânions com grupos de trimetilamina, monoetanolamina e trietanolamina. Para os sorventes obtidos, foram investigadas as propriedades de adsorção e físico-química. Densidade aparente, volume específico no intumescimento, coeficiente de intumescimento em vários solventes (água, etanol, isopropanol, propilenoglicol, acetona) foram determinados e os cálculos teóricos da capacidade total de troca e massa de reticulação e frações molares foram realizados. Verificou-se que o melhor inchaço é alcançado no propilenoglicol. Para os sorventes LP27 e LP29, foram determinadas as capacidades nas frações de triglicerídeos e lipoproteínas e o coeficiente de distribuição dos componentes do perfil lipídico entre as fases sólida e líquida. É mostrado que ambos os sorventes têm boas propriedades de sorção, sendo a amostra LP29 bastante promissora para a extração dos componentes do perfil lipídico. Presume-se que os sorventes desenvolvidos sejam mais baratos que os atualmente utilizados, pois são sintetizados com base na matriz disponível comercialmente. Espera-se que os resultados obtidos sejam úteis para investigações adicionais visando à melhoria da qualidade da moderna tecnologia de plasmassorção.

Palavras-chave: *Extração de LDL e VLDL, sorção de colesterol, aterosclerose, hipercolesterolemia, doenças cardiovasculares.*

ABSTRACT

Currently, the plasmasorption method is widely used in clinical practice to remove excessive amounts of metabolites that cause various pathologies. However, the plasmasorbents applied often can give a number of side effects for the patient, such as the blood clotting, the release of dust particles, and the sorption of useful components from the plasma. Besides that, they can be quite expensive. The aim of the work was to create available plasmasorbents with a good hemocompatibility for the lipoprotein adsorption from the plasma. A number of anion exchangers with groups of trimethylamine, monoethanolamine, and triethanolamine were synthesized. For the sorbents obtained, adsorption and physico-chemical properties were investigated. Bulk

density, specific volume at swelling, the swelling coefficient in various solvents (water, ethanol, isopropanol, propylene glycol, acetone) were determined and the theoretical calculations of total exchange capacity and crosslinking mass and molar fractions were made. It was found that the best swelling is achieved in propylene glycol. For the sorbents LP27 and LP29, the capacities on triglyceride and lipoprotein fractions and the coefficient of distribution of lipid profile components between the solid and liquid phases were determined. It is shown that both sorbents have good sorption properties, the sample LP29 being quite promising for the lipid profile components extraction. The developed sorbents are assumed to be cheaper than currently used ones as they are synthesized on the basis of commercially available matrix. The results obtained are expected to be useful for further investigations aimed at the modern plasmasorption technology quality improvement.

Keywords: *LDL and VLDL extraction, cholesterol sorption, atherosclerosis, hypercholesterolemia, cardiovascular diseases.*

АННОТАЦИЯ

В настоящее время метод плазмасорбции широко используется в клинической практике для удаления избыточного количества метаболитов, вызывающих различные патологии. Однако используемые плазмасорбенты зачастую могут вызывать ряд побочных эффектов, таких как повышение свертываемости крови, выделение частиц пыли и извлечение полезных компонентов из плазмы. Кроме того, они могут быть достаточно дороги. Целью данной работы было создание доступных плазмасорбентов, обладающих хорошей гемосовместимостью, для извлечения липопротеинов. Был синтезирован ряд анионитов с группами триметиламина, моноэтаноламина и триэтаноламина и исследованы их адсорбционные и физико-химические свойства. Определены насыпная плотность, удельный объем при набухании, коэффициенты набухания в различных растворителях (вода, этанол, изopropanol, пропиленгликоль, ацетон), а также рассчитаны теоретические значения полной обменной емкости и массовой и мольной долей сшивающего агента. Показано, что наилучшее набухание достигается при использовании в качестве растворителя пропиленгликоля. Для образцов ЛБ27 и ЛБ29 определены адсорбционные емкости по триглицеридам и фракциям липопротеинов и рассчитаны коэффициенты распределения компонентов между твердой и жидкой фазами. Показано, что оба сорбента имеют хорошие сорбционные свойства. Наиболее перспективным для извлечения компонентов липидного спектра является образец ЛБ29, имеющий достаточно высокие емкости по всем компонентам. Предполагается, что разрабатываемые сорбенты будут дешевле, чем используемые в настоящее время, благодаря использованию для их синтеза доступного промышленного анионита. Полученные результаты могут быть полезны для дальнейших исследований, направленных на улучшение качества и доступности современных плазмасорбционных технологий.

Ключевые слова: *извлечение ЛПНП и ЛПОНП, сорбция холестерина, атеросклероз, гиперхолестеринемия, сердечно-сосудистые заболевания.*

1. INTRODUCTION

The plasmasorption method is widely used in clinical practice for the treatment of pathologies caused by the increased content of certain substances in the blood. In particular, it is prescribed for the treatment of atherosclerosis caused by an increased content of low- and very low-density lipoprotein cholesterol (LDL and VLDL) in blood plasma.

The surface of lipoprotein particles is negatively charged; accordingly, copolymers with substituted amino groups having a positively charged quaternary nitrogen atom were chosen as plasmasorbents. Various nitrogen atom substituents affecting the electron density shift were used. In that way, it was possible to adjust the magnitude of the positive charge of the sorption center and its hydrophilic-

hydrophobic properties.

There are a number of studies into this subject that have been carried out in recent times; (Bereli *et al.*, 2011; Cao *et al.*, 2011; Dorskaia *et al.*, 2019a; Dorskaia *et al.*, 2019b; Gan *et al.*, 2016; Hou *et al.*, 2013; 2015; Huang *et al.*, 2010; Huang *et al.*, 2011; Huang *et al.*, 2009; Khattari, 2016; Lan *et al.*, 2012; Li *et al.*, 2014; Li *et al.*, 2011; Li *et al.*, 2013; Liu *et al.*, 2016; Liu *et al.*, 2012; Liu *et al.*, 2015; Lu *et al.*, 2013; Lu *et al.*, 2011a; Lu *et al.*, 2011b; Ma *et al.*, 2011; Ma *et al.*, 2008; Teruel *et al.*, 1995; Wang *et al.*, 2016; Wang *et al.*, 2014; Wang & Lan, 2014; Yu, 2013; Yu *et al.*, 2014; Zheng *et al.*, 2011) can be noted. In (Lu *et al.*, 2011a; Lu *et al.*, 2011b) the extraction of lipid profile components by sorbents based on carbon nanotubes modified with various agents was studied. Papers (Hou *et al.*, 2013; 2015; Huang

et al., 2010; Huang *et al.*, 2011; Huang *et al.*, 2009; Lan *et al.*, 2012; Li *et al.*, 2014; Li *et al.*, 2011; Liu *et al.*, 2015; Ma *et al.*, 2011; Ma *et al.*, 2008; Wang *et al.*, 2016; Zheng *et al.*, 2011) are devoted to the binding of LDL with heparin. In (Yu *et al.*, 2014), the authors synthesized the amphiphilic adsorbent based on polyvinyl alcohol (PVA) containing cholesterol ligand and sulfonic dextran ligands. In (Li *et al.*, 2013; Wang *et al.*, 2014; Wang & Lan, 2014) sorbents with ligands of other saccharides are described. In (Lu *et al.*, 2013) authors offered the modified by L-tryptophan carbon sorbent for the extraction of LDL.

Contacting with biological fluids, medical sorbents must be hemocompatible, stable, chemically resistant, standardized, have sorption activity, and not emit toxic substances. However, currently used plasmasorbents often to some degree do not meet these requirements, besides that they can be quite expensive. The developed sorbents are assumed to be cheaper than currently used ones as they are synthesized on the basis of commercially available matrixes. The results obtained are expected to be useful for further investigations aimed at improving the quality and the availability of modern plasmasorption methods.

2. MATERIALS AND METHODS

2.1. Synthesis of the sorbents LP23-30

At the first stage, eight sorbents with groups of trimethylamine, monoethanolamine, and triethanolamine were synthesized. The anion exchanger Lewatit® Monoplus M 500 (see Table 1) was being affected by solutions of amines at heating for 1 h. Water or mixtures of water with isopropanol, propylene glycol, or acetone in a volume ratio of 1:1 were used as solvents. Table 2 presents the synthesis conditions. The choice of the synthesis temperature of 65 °C for the sorbents LP23-25 and LP27-29 was limited by the maximum operating temperature of the Lewatit® Monoplus M 500 (70 °C), and the temperature of 50 °C for LP26 and LP30 – by the acetone boiling point (56 °C). Figure 1 shows the synthesis reactions. Table 1 presents the monomer composition of the copolymers synthesized.

2.2. Determination of the lipoprotein adsorption of the sorbents LP23-30

An in vitro experiment on the sorption of the lipid profile components from plasma was

carried out for the sorbents LP27 and LP29. The samples of sorbents were converted in OH-form and washed by 0.14 N sodium chloride solution. Then the samples were interacting with donor plasma for 3 h. Further, the content of triglycerides (TG), total cholesterol (TC), and high-density lipoprotein cholesterol (HDL) in initial plasma and in plasma after sorption was determined. The analyses were carried out in the Laboratory and Diagnostic Center LDC on the analyzer Architect c8000 (Abbot, USA, manufactured in Japan by Toshiba Medical Systems Corporation) by enzymatic colorimetric methods. The content of LDL and VLDL cholesterol was determined according to Fridvald's (Equations 1 and 2):

$$C_{LDL} = C_{TC} - C_{HDL} - C_{TG} / 2.2 \quad (\text{Eq. 1})$$

$$C_{VLDL} = C_{TG} / 2.2 \quad (\text{Eq. 2})$$

where, C_{LDL} , C_{TC} , C_{HDL} , C_{TG} , C_{VLDL} – concentrations of LDL cholesterol, total cholesterol, HDL cholesterol, triglycerides and VLDL cholesterol correspondingly, mmol·l⁻¹.

3. RESULTS AND DISCUSSION:

3.1. Study of the physico-chemical properties of the LP23-30 sorbents

The following theoretical characteristics were calculated for the initial and synthesized sorbents in chloride and hydroxyl forms:

- total exchange capacity, mmol·g⁻¹ (Equation 3, Figure 2):

$$TEC_f = TEC_0 / (1 + \Delta) \quad (\text{Eq. 3})$$

where, TEC_0 – total exchange capacity of the initial copolymer Lewatit® Monoplus M 500, mmol·g⁻¹; Δ – weight gain per 1 g of the initial copolymer during synthesis, g·g⁻¹.

- crosslinking mass fraction (Equation 4, Figure 3):

$$q_m = 1 - TEC \cdot M \quad (\text{Eq. 4})$$

where, TEC – total exchange capacity, mol·g⁻¹; M – the molar mass of a copolymer unit, g·mol⁻¹.

- crosslinking molar fraction (Equation 5, Figure 4):

$$q_v = q_m / (1 + TEC (M_s - M)) \quad (\text{Eq. 5})$$

where, M_s – the molar mass of the crosslinking agent, $\text{g}\cdot\text{mol}^{-1}$.

Crosslinking molar fraction of the initial and all the synthesized sorbents have the same values since only functional groups replaced during the synthesis, but the ratio of the main-chain units and the crosslinking agent did not change.

For these characteristics, the minimum, the average, and the maximum values were determined, because the ranges of values used for the calculation were given in the Lewatit® Monoplus M 500 product detail sheet. Consequently, also ranges of the calculated values were obtained. For the synthesized sorbents, these parameters were calculated with the assumption that the degree of conversion is 100%. In fact, the degree of conversion is less, and the real values of these indicators are in the range between the values calculated for the initial sorbent Lewatit® Monoplus M 500 (the degree of conversion 0%) and for the full degree of conversion.

The following characteristics, for the studied samples¹:

- bulk density, $\text{g}\cdot\text{ml}^{-1}$ (Equation 6, Figure 5a):

$$\rho = V / m \quad (\text{Eq. 6})$$

where, V – sorbent volume, ml; m – sorbent mass, g.

- specific volume, $\text{ml}\cdot\text{g}^{-1}$ (Equation 7, Figure 5b):

$$V_{sp} = V_{sw} / m \quad (\text{Eq. 7})$$

where, V_{sw} – volume of a sorbent in the swollen state, ml.

As can be seen, the bulk density of the sorbents LP24-26 with groups of triethanolamine is greater than the bulk density

of the sorbents LP28-30 with groups of monoethanolamine. This can probably be explained by the influence of the molar mass of functional groups: in the case of the sorbents LP24-26 functional groups with a greater molar mass than in the case of LP28-30 fall on the same site of the polymer matrix.

The specific volume is the parameter reciprocal of the density of the sorbent in the swollen state. Accordingly, for this parameter, the inverse relationship is observed: for the sorbents LP24-26 with a greater molar mass of functional groups, it is slightly less than for LP28-30.

- coefficient of swelling in water and in various solvents (Equation 8, Figure 6):

$$K_{sw} = V_{sw} / V \quad (\text{Eq. 8})$$

As can be seen, the swelling coefficient of the synthesized sorbents LP23-30 decreases in a row of solvents: water>ethanol>isopropanol. Apparently, this is due to the fact that these sorbents contain both groups of trimethylamine (unreacted groups of the initial copolymer Lewatit® Monoplus M 500) and of triethanolamine (in the case of the sorbents LP23-26) or monoethanolamine (in the case of the sorbents LP23-26). Hydroxyl groups of ethanolamines increase the hydrophilicity of the sorbents, therefore, being more hydrophilic compared to the initial copolymer, the sorbents LP23-30 better swell in a more polar solvent (water) than in a less polar one (isopropanol).

A similar situation is observed for the swelling of sorbents in propylene glycol and acetone. The swelling coefficient decreases in the row: propylene glycol>water>acetone, respectively, reducing the number of hydroxyl groups in this row of solvents (in propylene glycol – 2, in water – 1, in acetone – 0).

As can be seen from figure 6, the difference between the swelling coefficients in ethanol and isopropanol is small, because these solvents are close in structure homologs, differing by only one CH_2 -group. In the case of propylene glycol and acetone, the swelling coefficient differs significantly – by 1.4-1.7 times, which can be explained by a significant difference in the structure of these solvents belonging to different classes of organic compounds.

Further, the sorption exchange capacities

¹ The sorbents were dried to a nominal air-dry state, when the mass decrease was less than 2.1% per week.

on chloride ion of the samples obtained were estimated, and their average values were 2-2.5 mmol·g⁻¹.

3.2. Study of the lipoprotein adsorption by the sorbents LP27 and LP29

The two sorbents – LP27 (with groups of monoethanolamine, solvent – water) and LP29 (with groups of monoethanolamine, solvent – water+propylene glycol) were selected for the experiment on plasmasorption in static conditions. The choice of monoethanolamine groups is due to the fact that earlier studies of a wide range of sorbents of different classes showed good sorption capacity of these groups. The choice of water as a solvent (in the case of LP27) is caused by the fact that it is the most common and available substance, and the mixture of water and propylene glycol (in the case of LP29) – because previous studies showed good results when using the latter.

For these sorbents, the static sorption capacity on the lipid profile components (μmol·g⁻¹) were calculated (Equation 9, Figure 7):

$$S = (C_0 - C_f) V_p / m \quad (\text{Eq. 9})$$

where, C_0 , C_f – initial and final concentrations of a component in plasma, mmol·l⁻¹; V_p – plasma volume, ml; m – sorbent mass per dry weight, g.

As can be seen, the sorbent LP29 has larger capacities on all lipid profile components than the sorbent LP27.

Figure 8 shows the distribution of the sorption capacities of the sorbents LP27 and LP29 by lipoprotein fractions. More than 1/3 of the capacities of both sorbents are spent on the extraction of atherogenic LDL cholesterol, this being a positive factor in terms of the treatment of atherosclerosis. 1/3 of the capacities is spent on HDL cholesterol extraction. Of the two studied sorbents, LP27 has a larger part of the capacity occupied by LDL cholesterol than LP29, and the latter has a larger part of the capacity spent on VLDL cholesterol.

The coefficient of distribution of lipid profile components between the solid and liquid phases (I of plasma : I of sorbent) was determined for the investigated sorbents by Equation 10 (Figure 9).

$$K_d = S / C_f \quad (\text{Eq. 10})$$

As can be seen, the distribution coefficient of all lipid profile components is greater for the sorbent LP29, indicating its good ability to concentrate these substances in its volume.

4. CONCLUSIONS:

The eight sorbents LP23-30 with trimethylamine, monoethanolamine, and triethanolamine groups were synthesized. Their following theoretical characteristics were calculated: exchange capacity (2.63-4.75 mmol·g⁻¹), crosslinking mass, and molar fractions (0.048-0.286 and 0.104-0.375 correspondingly). Physico-chemical properties of the sorbents LP23-30 (bulk density, specific volume at swelling, the swelling coefficient in various solvents) are determined. The experiment on plasmasorption of the lipid profile components for the sorbents LP27 and LP29 in static conditions is carried out. High sorption capacity of these anionites, especially of LP29, was revealed.

The offered sorbents are assumed to be cheaper than currently used ones. The results obtained can be helpful for further investigations aimed at creating modern affine plasmasorbents for cardiovascular diseases treatment.

5. ACKNOWLEDGMENTS

The authors are grateful for the assistance in research providing and conducting to A. A. Anisimova, A. N. Zhuravleva (Mendeleev University of Chemical Technology of Russia), P. A. Sem'ashkina, A. A. Kupr'ashov (A.N. Bakulev National Medical Research Center of Cardiovascular Surgery, Moscow), A. E. Zezerov (Laboratory and Diagnostic Center LDC, Moscow).

The work was supported by Mendeleev University of Chemical Technology of Russia. Project Number 017-2018.

6. REFERENCES:

1. Bereli, N., Şener, G., Yavuz, H. & Denizli, A. (2011) Oriented immobilized anti-LDL antibody carrying poly(hydroxyethyl methacrylate) cryogel for cholesterol removal from human plasma. *Materials Science and Engineering C*, 31, 1078–1083.

2. Cao, Y., Wang, H., Yang, C., Zhong, R., Lei, Y., Sun, K. & Liu, J. X. (2011) In vitro studies of PBT Nonwoven Fabrics adsorbent for the removal of low-density lipoprotein from hyperlipemia plasma. *Applied Surface Science*, 257(17), 7521-7528.
3. Dorskaia, E. V., Leykin, Y. A., Pestov, S. M. & Kovalenko, A. E. (2019a) Extraction of lipid profile components from plasma by various forms of polymeric sorbents with the ammonium and phosphonium base groups. *Periódico Tchê Química*, 16(31), 595-606.
4. Dorskaia, E. V., Pestov, S. M. & Leykin, Y. A. (2019b) Study of the in vitro lipoprotein plasmasorption by polymeric sorbent with monoethanolamine groups. *Periódico Tchê Química*, 16(32), 1-7.
5. Gan, N., Multia, E., Siren, H., Ruuth, M., Oorni, K., Maier, N. M., Jauhiainen, M., Kemell, M. & Riekkola, M. L. (2016) Tailor-made approach for selective isolation and elution of low-density lipoproteins by immunoaffinity sorbent on silica. *Analytical Biochemistry*, 514, 12-23.
6. Hou, X., Zhang, T. & Cao, A. (2013) A heparin modified polypropylene non-woven fabric membrane adsorbent for selective removal of low-density lipoprotein from plasma. *Polymers for Advanced Technologies*, 24(7), 660-667.
7. Hou, X., Zhang, T. & Cao, A. (2015) Preparation of new amphiphilic macroporous nonwoven polymeric adsorbents aimed for selective removal of low-density lipoprotein from plasma. *Journal of Biomedical Materials Research Part B-Applied Biomaterials*, 103(1), 52-61.
8. Huang, X.-J., Guduru, D., Xu, Z.-K., Vienken, J. & Groth, T. (2010) Immobilization of heparin on polysulfone surface for selective adsorption of low-density lipoprotein (LDL). *Acta Biomaterialia*, 6(3), 1099-1106.
9. Huang, X.-J., Guduru, D., Xu, Z.-K., Vienken, J. & Groth, T. (2011) Blood compatibility and permeability of heparin-modified polysulfone as potential membrane for simultaneous hemodialysis and LDL removal. *Macromolecular Bioscience*, 11, 131-140.
10. Huang, X. J., Guduru, D., Groth, T. & Vienken, J. (2009) Immobilization of heparin on polysulfone membranes for preferential adsorption of low-density lipoprotein (LDL). *International Journal of Artificial Organs*, 32(7), 419-419.
11. Khattari, Z. (2016) Adsorption kinetics of low-density lipoproteins with Langmuir monolayer. *Journal of Biological Physics*, 42(4), 539-550.
12. Lan, P., Ji, J., Huang, X. J., Guduru, D., Groth, T., Vienken, J. & Ding, H. (2012) Adsorption/desorption of low-density lipoprotein on a heparinized surface of gold sensors. *Chemical Research in Chinese Universities*, 28(2), 323-328.
13. Li, J., Hou, Y., Chen, X., Ding, X., Liu, Y., Shen, X. & Cai, K. (2014) Recyclable heparin and chitosan conjugated magnetic nanocomposites for selective removal of low-density lipoprotein from plasma. *Journal of materials science: materials in medicine*. Available online: [Accessed].
14. Li, J., Huang, X.-J., Lan, P., Vienken, J., Groth, T. & Xu, Z.-K. (2011) Covalent heparin modification of a polysulfone flat sheet membrane for selective removal of low-density lipoproteins: a simple and versatile method. *Macromolecular Bioscience*, 11, 1218-1226.
15. Li, J., Huang, X.-J., Vienken, J. r., Xu, Z.-K. & Groth, T. (2013) Bioinspired multiple-interaction model revealed in adsorption of low-density lipoprotein to surface containing saccharide and alkanesulfonate. *Langmuir*, 29(26), 8363-8369.
16. Liu, Q., Sun, S., Yang, T. T., Han, M., Lin, L. P., Zhao, C. S. & Su, B. H. (2016) A novel adsorbents for selective removal of low-density lipoprotein. *Nephrology Dialysis Transplantation*, 31, 229-229.
17. Liu, X. F., Zeng, A. R., Li, L., Yang, F., Wang, Q. & Wu, B. (2012) Synthesis of O-Oleoyl-Chitosan and Its Sorption Properties for Lipoproteins. *Journal of Biomaterials Science-Polymer Edition*, 23(1-4), 267-280.
18. Liu, Y., Qiu, W.-Z., Yang, H.-C., Qian, Y.-C., Huang, X.-J. & Xu, Z.-K. (2015) Polydopamine-assisted deposition of heparin for selective adsorption of low-density lipoprotein. *Rsc Advances*, 5(17), 12922-12930.
19. Lu, Y. M., Gong, Q. M., Liang, J. & Nie, Q. D. (2013) Modification carbon nanotubes composite beads by L-

- tryptophan and their adsorption capacity for low-density lipoprotein. *Chinese Journal of Inorganic Chemistry*, 29(10), 2034-2042.
20. Lu, Y. M., Gong, Q. M., Lu, F. P., Liang, J., Ji, L. J., Nie, Q. D. & Zhang, X. M. (2011a) Preparation of sulfonated porous carbon nanotubes/activated carbon composite beads and their adsorption of low-density lipoprotein. *Journal of Materials Science-Materials in Medicine*, 22(8), 1855-1862.
 21. Lu, Y. M., Gong, Q. M., Lu, F. P., Liang, J., Nie, Q. D. & Zhang, X. M. (2011b) Preparation of sulfonated carbon nanotubes/activated carbon composite beads and their adsorption capacity for low-density lipoprotein. *Acta Physico-Chimica Sinica*, 27(3), 683-688.
 22. Ma, K.-w., Dai, X.-z., Feng, S.-y., Jing, A.-h. & Yang, J.-y. (2011) Heparinized polyvinyl alcohol to specifically adsorb low-density lipoprotein from plasma. *Transfusion and Apheresis Science*, 44, 3-9.
 23. Ma, K. W., Ma, L., Cai, S. X., Wang, X., Liu, B., Xu, Z. L., Dai, X. Z., Yang, J. Y., Jing, A. H. & Lei, W. J. (2008) Preparation of heparin-immobilized PVA and its adsorption for low-density lipoprotein from hyperlipemia plasma. *Journal of Materials Science-Materials in Medicine*, 19(10), 3255-3261.
 24. Teruel, J. L., Lasuncion, M. A., Navarro, J. F., Carrero, P. & Ortuno, J. (1995) Pregnancy in a patient with homozygous familial hypercholesterolemia undergoing low-density-lipoprotein apheresis by dextran sulfate adsorption. *Metabolism-Clinical and Experimental*, 44(7), 929-933.
 25. Wang, L., Fang, F., Liu, Y., Li, J. & Huang, X. (2016) Facile preparation of heparinized polysulfone membrane assisted by polydopamine/polyethyleneimine co-deposition for simultaneous LDL selectivity and biocompatibility. *Applied Surface Science*, 385, 308-317.
 26. Wang, W., Huang, X. J., Cao, J. D., Lan, P. & Wu, W. (2014) Immobilization of sodium alginate sulfates on polysulfone ultrafiltration membranes for selective adsorption of low-density lipoprotein. *Acta Biomaterialia*, 10(1), 234-243.
 27. Wang, W. & Lan, P. (2014) Surface glycosylation of poly(3-hydroxybutyrate-co-4-hydroxybutyrate) membrane for selective adsorption of low-density lipoprotein. *Journal of Biomaterials Science, Polymer Edition*, 25(18), 2094-2112.
 28. Yu, Y. (2013) Adsorbents in blood purification: from lab search to clinical therapy. *Chinese Science Bulletin*, 58(35), 4357-4361.
 29. Yu, Y. T., Zhu, H. J. & Wang, S. Q. (2014) Amphiphilic polyvinyl alcohol adsorbent for the removal of low-density lipoprotein. *Artificial Cells Nanomedicine and Biotechnology*, 43(2), 117-123.
 30. Zheng, X. M., Huang, X. J. & Xu, Z. K. (2011) Surface heparinization of polypropylene microporous membranes for selective adsorption of low-density lipoprotein. *Acta Polymerica Sinica*(7), 791-798.

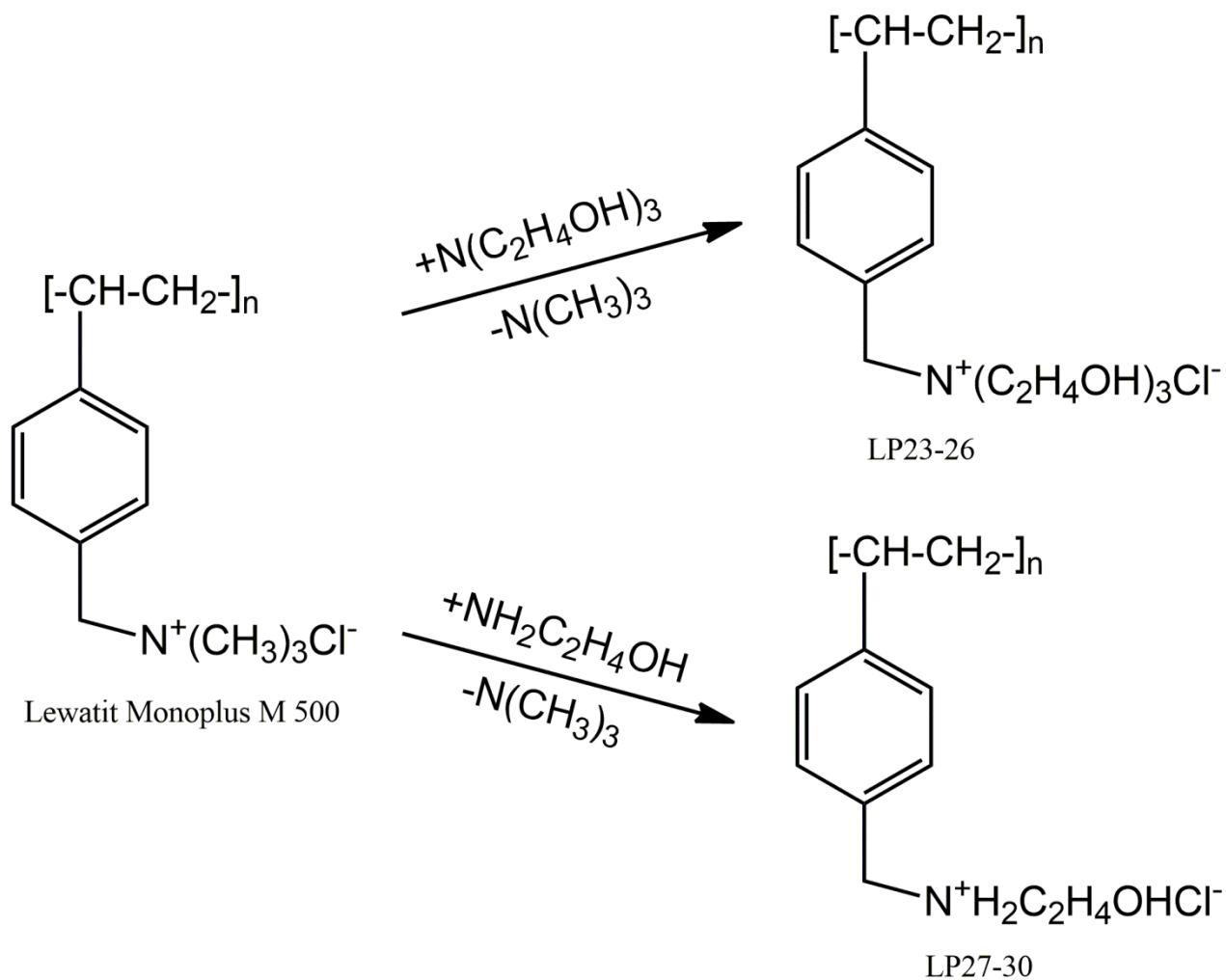


Figure 1. Reactions of syntheses of the sorbents LP23-30

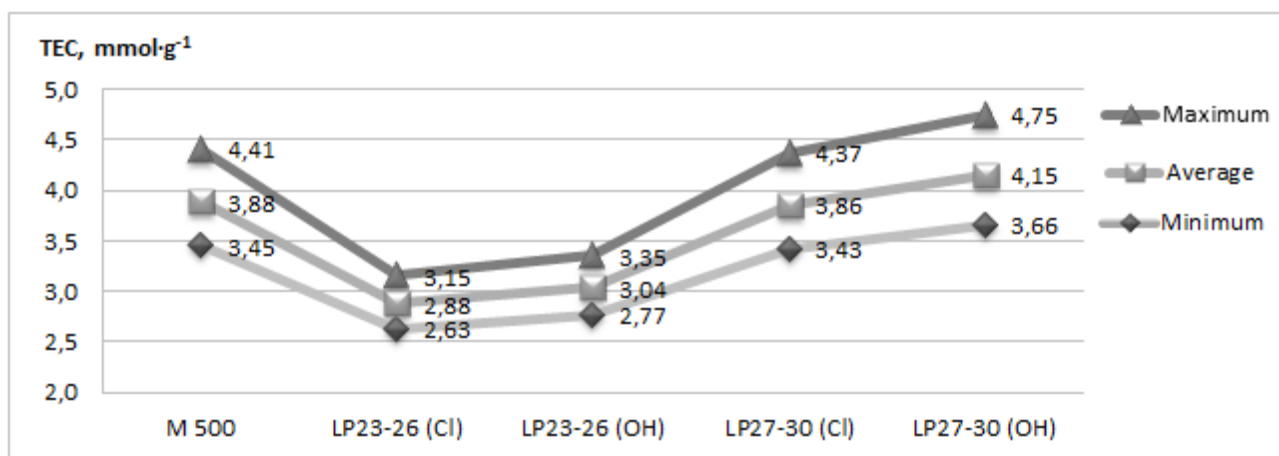


Figure 2. Theoretical total exchange capacity of the initial and synthesized sorbents in chloride and hydroxyl forms

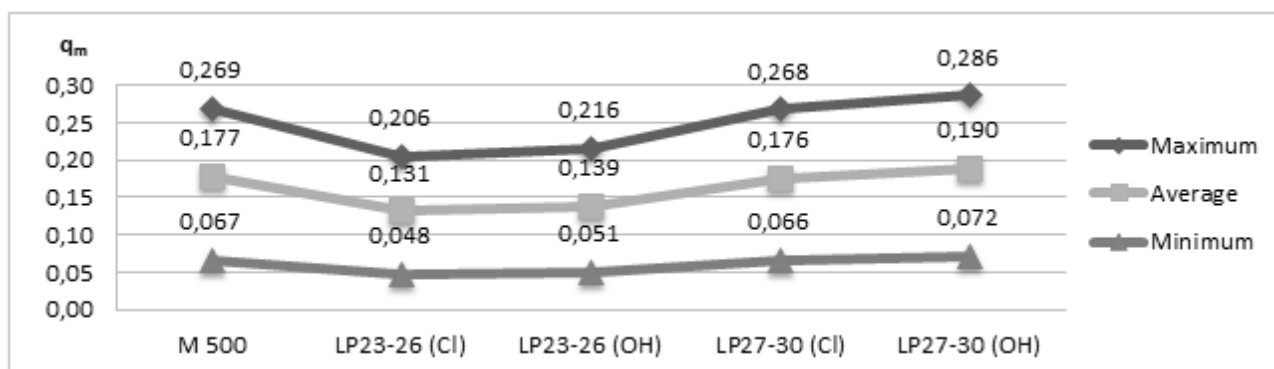


Figure 3. Theoretical crosslinking mass fraction of the initial and synthesized sorbents in chloride and hydroxyl forms

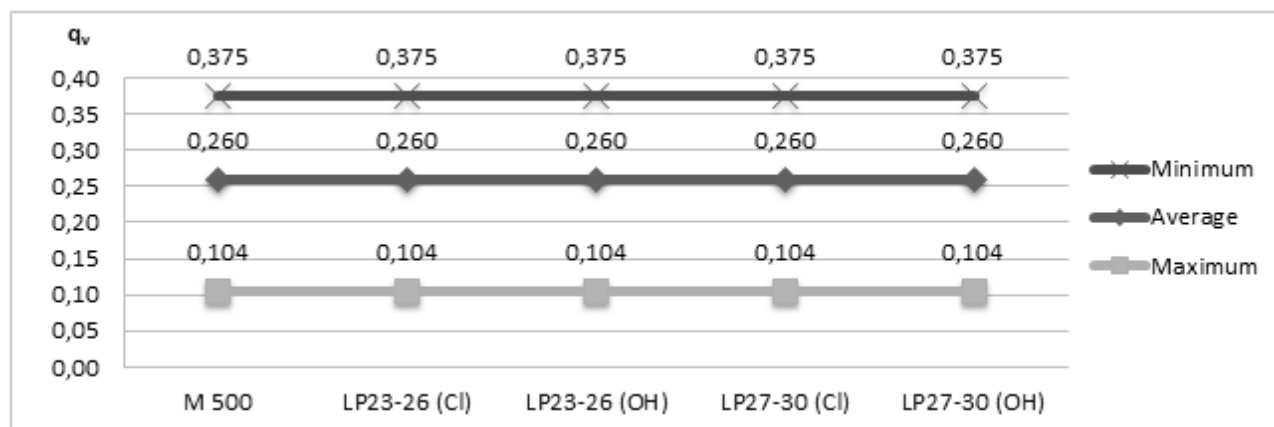


Figure 4. Theoretical crosslinking molar fraction of the initial and synthesized sorbents in chloride and hydroxyl forms

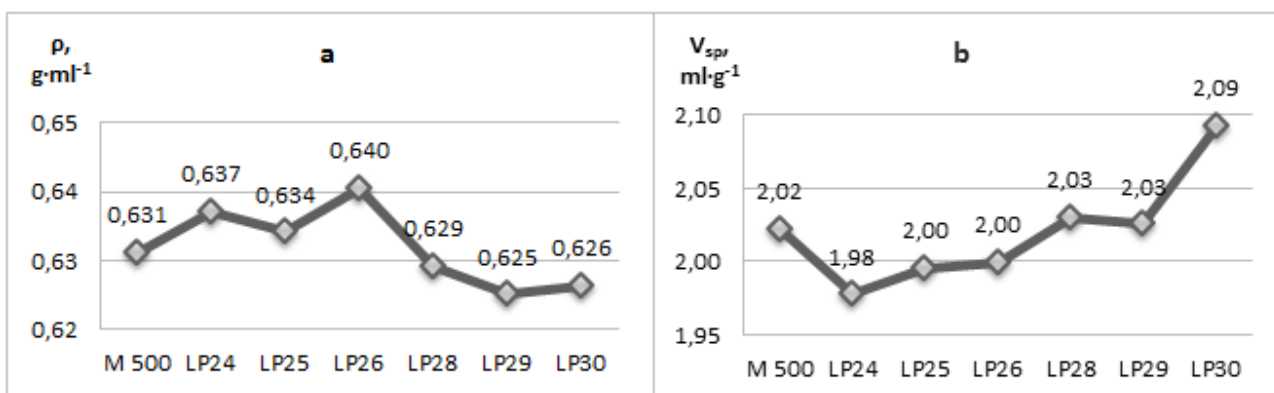


Figure 5. Bulk density (a) and specific volume (b) of the initial and synthesized sorbents in a nominal air-dry state

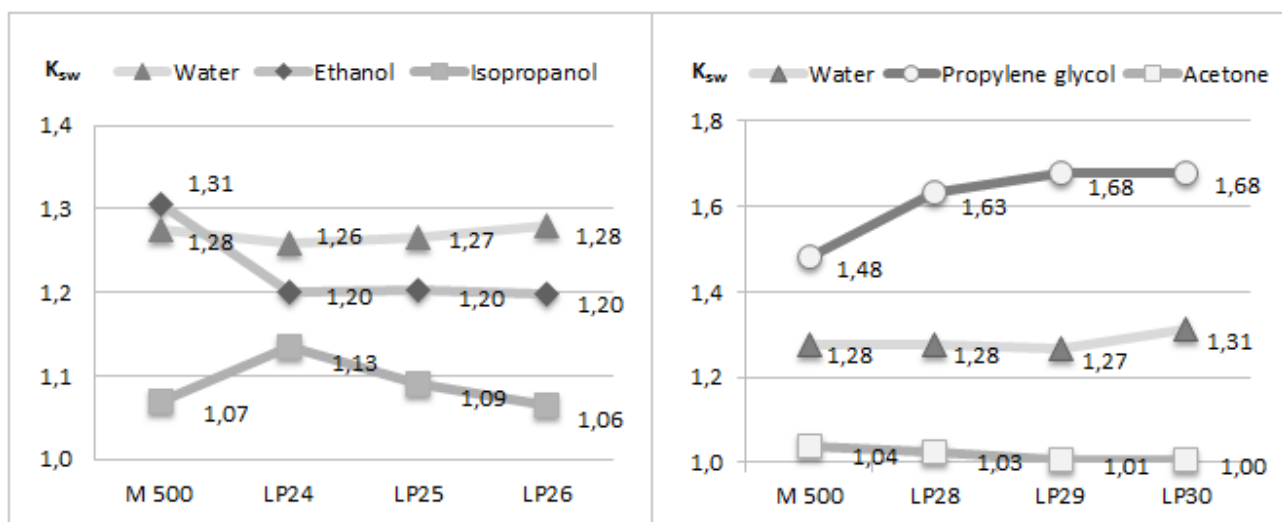


Figure 6. Coefficient of swelling in water and in various solvents of the initial and synthesized sorbents

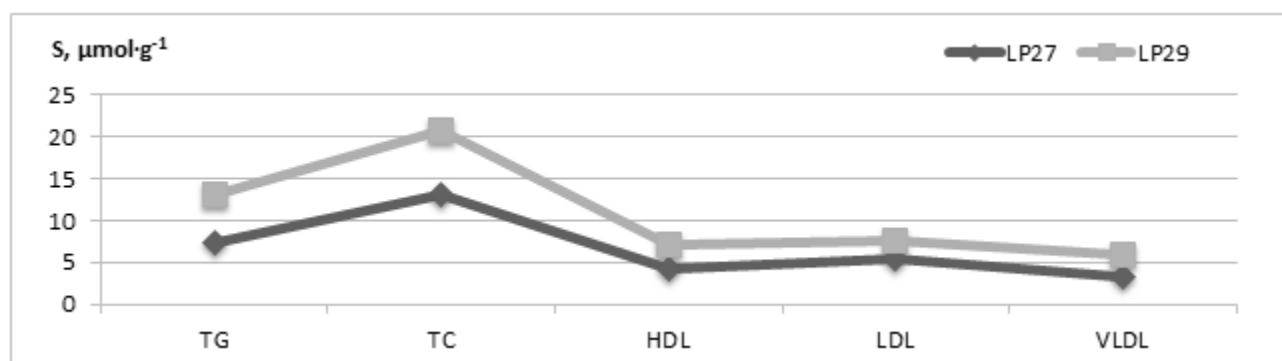


Figure 7. Static sorption capacity of the sorbents LP27 and LP29 on the lipid profile components



Figure 8. Distribution of the sorption capacities of the sorbents LP27 and LP29 by lipoprotein fractions

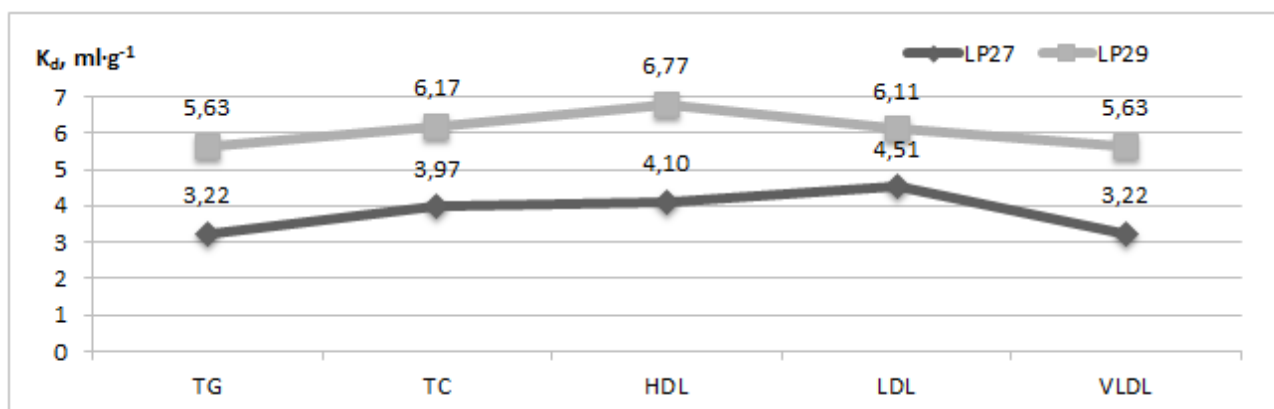


Figure 9. The distribution coefficient of the lipid profile components

Table 1. The composition of the copolymers

Copolymer	Monomer units		
	Matrix (initial links)	Matrix (modified links)	Crosslinking agent
Lewatit® Monoplus M 500		-	
LP23-26			
LP27-30			

Table 2. *The conditions of syntheses of the sorbents LP23-30*

Sorbent	Reactant	Solvent	Temperature, °C
LP23	Triethanolamine	Water	65±0,1
LP24		Water+isopropanol	65±0,1
LP25		Water+propylene glycol	65±0,1
LP26		Water+acetone	50±0,1
LP27	Monoethanolamine	Water	65±0,1
LP28		Water+isopropanol	65±0,1
LP29		Water+propylene glycol	65±0,1
LP30		Water+acetone	50±0,1

UTILIZAÇÃO DE SEMENTES DE *Salacca zalacca* COMO ADSORBENTES DE CROMO(VI)

UTILIZATION OF *Salacca zalacca* SEEDS AS CHROMIUM(VI) ADSORBENTS

BAEHAKI, Farhan^{1*}; RUDIBYANI, Ratu Betta^{2*}; AENI, Suci Rizki Nurul³; PERDANA, Ryzal⁴; AQMARINA, Shindy Nur⁵,

^{1,3,5} Medical Laboratory Technology, Rajawali School of Allied Science, Rajawali Barat St. 38, Bandung, West Java, Indonesia

² Chemistry Education, University of Lampung, Road Prof. Dr. Sumantri Brojonegoro No. 1, Bandar Lampung, Indonesia

⁴ Doctoral Program of Educational Science, Sebelas Maret University, Road Ir. Sutami 56 A, Jebres, Surakarta, Indonesia

* Correspondence author
e-mail: farhanbaehaki71@gmail.com

Received 12 December 2019; received in revised form 23 January 2020; accepted 3 February 2020

RESUMO

O sistema de tratamento de resíduos de cromo(VI) nas atividades da indústria têxtil na Indonésia é um problema ambiental que realmente precisa de atenção. Isso ocorre porque o cromo(VI) é um metal pesado que se enquadra na categoria de materiais perigosos e tóxicos. Para que possa ter um impacto negativo no meio ambiente e na saúde do corpo. Um simples esforço de processamento para reduzir a quantidade de cromo (VI) nos resíduos é o método de bioabsorção usando adsorventes orgânicos. Um desses adsorventes orgânicos são as sementes de *Salacca zalacca*. As sementes de *Salacca zalacca* podem ser usadas como um adsorvente alternativo porque possuem fibras de celulose que podem adsorver íons de cromo(VI) nos resíduos. Esta pesquisa foi realizada com uma amostra de resíduos de corantes de roupas obtidos em uma das escolas de engenharia têxtil de Bandung, na Indonésia. Além disso, também foram realizadas pesquisas sobre a determinação da dosagem correta, para que os resultados de adsorção fossem máximos. Os resultados mostraram que o pó de sementes de *Salacca zalacca* foi capaz de absorver até 76,21% da quantidade de cromo(VI) em 100 mL de amostras de resíduos com uma dose de 4 gramas. Estes resultados indicam o nível de eficácia e boa absorção de sementes de *Salacca zalacca* em pó. Para que este método possa ser usado como um método alternativo para tratar os resíduos de cromo(VI) de uma maneira mais simples e barata.

Palavras-chave: Bioabsorção, Crômio (VI), Tratamento de resíduos, Águas residuais.

ABSTRACT

The Chromium(VI) waste treatment system in the textile industry activities in Indonesia is an environmental problem that really needs attention. This is because Chromium(VI) is a heavy metal that falls into the category of hazardous and toxic materials. So that it can have a negative impact on the environment and health of the body. One simple processing effort to reduce the amount of Chromium(VI) in waste is the biosorption method using organic adsorbents. One of these organic adsorbents is *Salacca zalacca* seeds. *Salacca zalacca* seeds can be used as an alternative adsorbent because they have cellulose fibers that can adsorb Chromium(VI) ions in waste. This research was conducted using a sample of clothing coloring waste obtained from one of the textile engineering schools in Bandung, Indonesia. In addition, research was also conducted on determining the right dosage so that the adsorption results were maximal. The results showed that *Salacca zalacca* seed powder was able to adsorb as much as 76.21% of the amount of Chromium(VI) in 100 mL of waste samples with a dose of 4 grams. These results indicate the level of effectiveness and proper absorption of powdered *Salacca zalacca* seeds. So that this method can be used as an alternative method to treat Chromium(VI) waste in a simpler and cheaper way.

Keywords: Biosorption, Chromium(VI), Waste treatment, Wastewater.

1. INTRODUCTION

In Indonesia, the growth of the textile industries has grown very rapidly. The development of these textile industries can cause an increased risk of environmental pollution by the waste produced. Waste is a leftover from the activity of organisms, one of which originates from industrial activities. There are three types of waste that are usually produced by human activities, namely solid waste, liquid waste, and gas waste. The type of waste produced will depend on the type of activity carried out. To reduce the impact caused by the resulting waste, it is necessary to do the right treatment. However, the high cost of waste management is an obstacle to industrial activity. So that middle and lower level industries prefer to dispose of waste directly into the environment without being treated. This phenomenon causes a very alarming environmental pollution, such as rivers, seas, lakes, and so on. Data compiled by CNBC Indonesia states that nearly 349,000 tons of liquid waste enter the river flow every day from 1900 factories around the Citarum River, Indonesia. In addition, household waste and other wastes also enter the river body. However, despite these conditions, the Citarum river remains a source of water for the surrounding community. This condition is hazardous because the community can be infected with various diseases.

In industrial activities, waste generally will contain substances or contaminants that are produced from the rest of the raw materials, solvents or additives, failed products, washing equipment, and so on. In addition, the waste can also contain heavy metal ions (Pb, Hg, Cr, and so on) which are very dangerous because they are toxic (Abdi and Kazemi, 2015; Loukidou, Zouboulis, Karapantsios, and Matis, 2004; Lichtfouse and Schwarzbauer, 2012; Kizilo, 2019; Ordouee and Hazheminezhad, 2019). Heavy metals are a group of metals weighing more than 5 g/cm^3 (Olukanni, Agunwamba, and Ugwu, 2014). This group of metals has no biological function in plants and cannot decompose in the soil (Rodríguez, Cárdenas-González, Juárez, Pérez, Zarate, and Castillo, 2018). Some examples of industrial activities that have the potential to produce heavy metal waste are clothing, refineries, fertilizers and pesticides, metallurgy, iron and steel, leather-working, photography, electric appliance manufacturing, metal surface treating, and wastewater treatment plants (Olukanni, Agunwamba, Ugwu, 2014; Rodríguez, Cárdenas-González, Juárez, Pérez,

Zarate, Castillo, 2018; Acar and Malkoc, 2004; Ordouee and Hazheminezhad, 2019).

The textile industry is one sector that has a large share in producing Chromium (Cr) waste. The Indonesian Ministry of Health states that industrial waste produced is usually in the form of liquid waste containing Cr(III) and Cr(VI) ions. Cr(III) ion is the most stable form and important component for humans and animals as a glucose tolerance factor (GTF) in insulin, lipid, and protein metabolism. But Cr(VI) ion has very high toxicity because it has an affinity for red blood cells (Nagaraj, Aradhana, Svivakumar, Shrestha, and Gowda, 2009; Hua, Chan, Wu, and Wu, 2009). Cr(VI) ion is one of the ions that are nephrotoxic and carcinogenic (Abdi and Kazemi, 2015; Gautam, Mudhoo, Lofrano, and Chattopadhyaya, 2014). Even by its nature which has a high solubility in the water, it is possible to be adsorbed into the well water of residents living near the river so that it can be consumed by humans and cause interference with the health of the body. The toxic effects that can be caused by these ions are gastrointestinal bleeding, liver necrosis, renal tubular necrosis, allergic reactions, loss of breath, shortness of breath, headache, coughing, pulmonary congestion, sneezing, kidney damage, conjunctivitis, eyes burning, corneal damage until blindness, ulcers, in-infection of the respiratory tract, tooth discoloration, and cancer (Palar, 2012). Chromium that enters the body will undergo physiological and metabolic processes. Chromium metal or chromium compounds will interact with various biological elements contained in the body so that it can cause disruption of certain functions that work in the body's metabolism (Sharov, Plotnikova, Evseev, Rykova, 2019). In the process of metabolism, Cr(VI) ions will block or inhibit the work of the benzopyrene hydroxylase enzyme (Palar, 2012). Barriers to the performance of these enzymes can result in changes in cell growth, so cells grow wild and uncontrolled. These cells are called cancer. Based on its highly toxic nature, an appropriate treatment system is needed, so that it can minimize the level of environmental pollution and consumption risks.

Various methods of processing heavy metal waste have been carried out, such as chemical precipitation, solvent extraction, ion exchange, cementation and reverse osmosis, but usually require expensive costs and not environmentally friendly (Olukanni, Agunwamba, Ugwu, 2014; Acar and Malkoc, 2004; Kocasoy and Guvener, 2009; Ordouee and Hazheminezhad, 2019). One method of

processing waste that can be done economically and simply is the biosorption method (Ordouee and Hazheminezhad, 2019). Adsorption or biosorption is considered more economical, high efficiency, simplicity of design, and selectivity (Ordouee and Hazheminezhad, 2019). Biosorption is a process for removing heavy metals through a passive binding process in a solution so that it does not involve metabolic processes (Kocasoy and Guvener, 2009). Organic adsorbents can be used in this method. The use of microorganisms as adsorbents has been widely used, for example, such as *Aeromonas caviae* (Loukidou, Zouboulis, Karapantsios, and Matis, 2004), *Pseudomonas aeruginosa* (Olukanni, Agunwamba, Ugwu, 2014), *Fagus orientalis* L. (Acar and Malkoc, 2004), and so on. In addition, the use of other adsorbents such as peanut husk (Abdelfattah, Ismail, Al Sayed, Almedolab, and Aboelghait, 2016) can also be done. The other potential adsorbents are *Salacca zalacca* seeds. The availability of *Salacca zalacca* seeds is very abundant because it is usually not used by *Salacca zalacca* fruit processors. In *Salacca zalacca* seeds it contains cellulose which can adsorb metal ions quite well.

Cellulose compounds consist of active groups that are charged so that they can adsorb metal ions, such as Cr(VI) ions. This is because Cr(VI) has an empty orbital that can be filled by electrons from the active compound on cellulose (Ordouee and Hazheminezhad, 2019). Thus a bond can be formed between Cr(VI) with the active compound. Several factors can affect the adsorption process, namely interaction time, the surface area of adsorbent, the molecular size of adsorbate, pH of the solution, and concentration of heavy metals. Adequacy of interaction time can maximize the adsorption process. To streamline the interaction time, the stirring process is usually carried out first. With the stirring process, the adsorbent will increasingly spread and can enlarge the contact zone with the Cr(VI) ion. The pH value of the solution will affect the type of chemical interactions that occur in the adsorption process between metal ions and the surface of the biomass. Each metal has its own pH value that allows it to be adsorbed strongly. Concentration is related to the degree of saturation of the solution. If the saturation of the solution has been reached, the ability of the adsorbent to absorb will decrease due to the limited surface capacity of the adsorbent. These five factors must be considered to be able to maximize the adsorption process.

2. MATERIALS AND METHODS

2.1. Making *Salacca zalacca* Seed Adsorbents

Making *Salacca zalacca* seeds adsorbent is done through the process of destruction and washing (Widhianingrum, Inawati, Usakinah, Andriyati, and Nugraheni, 2016). At the stage of destruction, *Salacca zalacca* seeds are washed and dried, then smoothed using a blender. The *Salacca zalacca* powder produced is filtered using a sieve so that its size is relatively the same. Furthermore, the seed powder was washed using ethanol 99% and distilled water several times. The *Salacca zalacca* powder that has been washed is then dried using an oven.

2.2. Waste Water Sample Preparation

Wastewater samples were obtained from the College of Textile Technology in Bandung, Indonesia. The sample is waste from the process of coloring clothes and contains Chromium. In order for the sample to remain stable and last long, a solution of nitric acid (HNO₃) was added as a preservative.

2.3. Making Stock Solution

The sample is filtered using filter paper to separate the residue. As much as 100 mL of filtrate is taken and put in a 1000 mL volumetric flask to be diluted. This solution labeled **Solution I**. Then 80 mL of H₂SO₄ 2 M and 20 mL of Diphenylcarbazide were added. The addition of diphenyl carbazide aims to maximize the absorption of waves where Cr ions will bind to form complex compounds with these molecules. Add distilled water to the limit mark on the measuring flask and let it sit for 30 minutes. At this stage, the condition of the solution must be maintained at pH 3.

2.4. Making Standard Curve

Standard curves are created to obtain straight-line equations based on plot data between absorbance and concentration of standard solutions. The equation of the line can be used to determine Cr (VI) levels that are not known after adsorbed (Andrea, 2015). Making a standard curve is done by making a standard solution of K₂Cr₂O₇ 0.3 ppm; 0.6 ppm; 0.9 ppm; 1.2 ppm and 1.5 ppm in a 10 mL volumetric flask. Then 2 mL of H₂SO₄ 2M solution and 0.5 mL diphenyl carbazide were added. All of these standard solutions measured the absorbance value using a UV-Vis spectrophotometer with a wavelength of 540 nm.

2.5. Measurement of Cr(VI) Ion Concentration

2.5.1. Measurement of Cr(VI) Ion Concentration Before Adsorption

Measuring the concentration of Cr(VI) ions before adsorption was carried out by taking *Solution I*. The *Solution I* was centrifuged for 15 minutes, and then the obtained supernatant was inserted into the cuvette. The adsorbance measurements were carried out using a UV-Vis spectrophotometer at a wavelength of 540 nm (Minarsih, 2009; Andini, 2017). Measurements were taken twice so that the results were accurate. The calculation of solution concentration is done by using mathematical equations on a standard curve.

2.5.2. Measurement of Cr(VI) Ion Concentration After Adsorption

The *Solution I* was divided into five beakers with a volume of 100 mL each. In the five beakers, each of them was added with *Salacca zalacca* seed powder with 1 gram, 2 gram, 3 gram, 4 gram, and 5 gram. Then, the sample was stirred at a speed of 300 rpm with stirring time for 20 minutes. After that, the sample is left to stand for 15 minutes, then filtered using filter paper. The resulting filtrate was

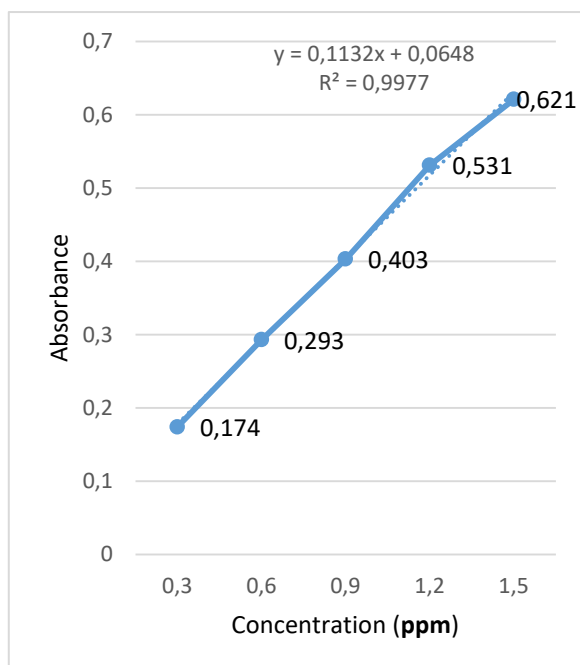


Figure 1. Chromium(VI) Standard Curve At Wavelengths of 540 nm.

centrifuged for 15 minutes. Measuring the concentration of Cr(VI) is done by taking the supernatant and entering it into the cuvette. This procedure is done twice to obtain more accurate data.

3. RESULTS AND DISCUSSION

3.1 Standard Curve $K_2Cr_2O_7$ Solution

The standard curve is obtained by measuring the standard solution of $K_2Cr_2O_7$. The value of R in **Figure 1** shows a strong correlation coefficient because the value of R is 0,997 (approaches the value of 1). This shows that the calibration curve produces lines that are linear and the errors that occur are smaller. The line equation $y = 0.1132x + 0.0648$ is a straight-line equation that can be used to measure the concentration of Cr(VI) in the sample. The standard curve method is used in this study because the spectrophotometer is standardized before it is used for the sample measurement process. This certainly will affect the measurement results because each tool has different conditions. If the resulting curve does not show a linear straight-line equation, then it is necessary to check the condition of the device or possibly check the reagents used.

In the line equation in **Figure 1**, variable y is the adsorbance value, and variable x is the value of the Cr(VI) concentration. So in this case, we must calculate the value of variable x to obtain the value of the concentration of Cr(VI) ions (the calculation results are presented in **Table 3**).

3.2. *Salacca zalacca* Seed Adsorption Ability Against Cr(VI) Ions

3.2.1. The Concentration of Cr(VI) Ions Before Adsorption

The adsorbance value obtained through three measurements is 0.630; 0.618; and 0.616. Measurements made three times repetition aimed to obtain more accurate data on the spectrophotometer. The three data values are calculated so that the average adsorbance value of 0.620 is obtained. This value is entered into the line equation in **Figure 1**, the value of the concentration of Cr(VI) is 4.92 ppm.

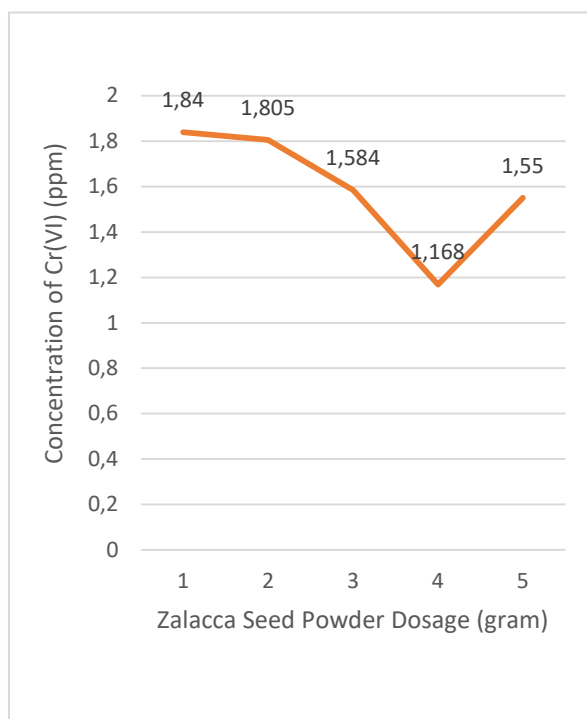


Figure 2. Graph of Decreasing Cr(VI) Ion Concentration After Adsorption Process with *Salacca zalacca* Seed Powder Dose Variation.

3.2.2. The Concentration of Cr(VI) After Adsorption

The biosorption process of the sample was carried out using five different dosages of *Salacca zalacca* seed powder. It aims to obtain dosage data where the salacca seed powder can adsorb Cr(VI) metal ions maximally. The amount of adsorbent is one of the factors that greatly influence the process of adsorption of heavy metals in solution. This is because of the number of adsorbent particles that can absorb heavy metals are increasing. Increasing the amount of adsorbent will cause an increase in the percentage of heavy metal that is absorbed because of the active center of the biosorbent that reacts so much too. **Figure 2** shows a decrease in the concentration of Cr(VI) ions are directly proportional to the increasing dose of *Salacca zalacca* seed powder used. This shows that the metal ion Cr(VI) can be well absorbed by the adsorbent. Significantly decreased levels of Cr(VI) were seen at doses of 3 grams and 4 grams (**Figure 2**). The amount of Cr(VI) ions adsorbed at this dose showed a very good adsorption ability from *Salacca zalacca* seeds with an absorption percentage of 68.61% and 76.21% (**Table 3**). However, at a dose of 5 grams, the concentration of Cr(VI) metal ions read by the spectrophotometer has increased again. This becomes something very interesting

because it should increase as the amount of adsorbent increases, the amount of Cr (VI) ions will continue to decrease. However, the facts show different results. This phenomenon occurs because the amount of adsorbent is not balanced with the number of samples, or in other words the solution has passed the saturation. Other results might be different if the number of samples used becomes more. Of course, this greatly affects the results of the waveform absorption readings on

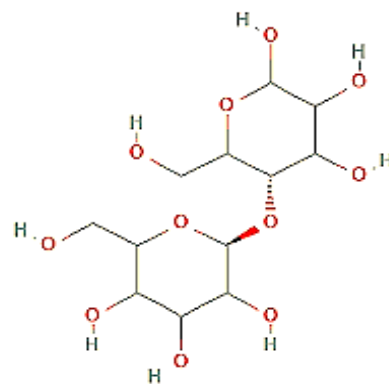


Figure 3. Structure of Cellulose Compounds

Reference: <https://pubchem.ncbi.nlm.nih.gov/compound/CELLULOSE>

the spectrophotometer. The remaining *Salacca zalacca* seed powder that is not bound to Cr(VI) remains in the solution and causes the solution to become more turbid, thereby affecting the measurement of absorbance of the sample.

Looking at the data in **Table 3**, in this case, a dose of 4 grams of *Salacca zalacca* powder is the maximum dose that can be given to adsorb Cr (VI) ions in 100 ml samples at pH 3. At this dose, the final Cr(VI) concentration after the adsorption process read by the spectrophotometer is 1.168 ppm. This means that as many as 3.752 ppm or 76.21% Cr(VI) ions have been successfully adsorbed by the adsorbent of *Salacca zalacca* seed powder.

This good adsorption ability is because the powder of *Salacca zalacca* seeds is composed of cellulose. Cellulose is a polysaccharide compound containing the hydroxide group (OH) (**Figure 3**). The oxygen atom in the hydroxide group in cellulose has a strong affinity. Meanwhile, heavy metal ions are positively charged. With the properties of the oxygen atom, heavy metal ions that are positively charged will be adsorbed on the cellulose surface. This absorption occurs because of the formation of bonds between the surface of cellulose and heavy metal ions. This process plays a role in the biosorption process of heavy metals. However, there has been a decline in the quality of absorption. At a dose of 5 grams (5th

data in **Figure 2**), the concentration of Cr(VI) ions read by the spectrophotometer increases again. In this case, This is not caused by the increasing Cr(VI) ion in the samples, but the dosage of the powder of *Salacca zalacca* seed is too excessive so that the remaining adsorbent affects the measurement of adsorbance of the sample.

4. CONCLUSIONS

Based on the data obtained in this study, *Salacca zalacca* seed powder can be used as an adsorbent for Cr(VI) ions. The adsorption ability of *Salacca zalacca* powder can be used in simple waste treatment to reduce the content of Cr(VI) ions. By setting the right conditions and dosages, the number of Cr(VI) ions can be maximally adsorbed. Thus, this method can be used as a cheaper and simpler method of processing Cr(VI) metal waste, so that it can be used by middle and lower level industries to reduce environmental damage.

5. ACKNOWLEDGMENTS

The authors are grateful to The Rajawali School of Allied Science, University of Lampung and Sebelas Maret University, who were willing to cooperate in completing this research. The authors also want to thank all those who have helped both material and moral so that this research can be carried out well.

6. REFERENCES

1. Abdi, O., Kazemi, M. J. *Mater. Environ. Sci.* **2015**, 6(5), 1386-1399.
2. Loukidou, M. X., Zouboulis, A.I., Karapantsios, T.D., Matis, K.A. *Eng. Aspects*, **2004**, 242, 93-104
3. Lichtfouse, E. and Schwarzbauer, J. "Environmental Chemistry For A Sustainable World Volume 1: Nanotechnology And Health Risk", New York: Springer, **2012**.
4. Olukanni, D. O., Agunwamba, J. C., Ugwu, E. C. *American Journal Of Scientific And Industrial Research*, **2014**, 5(2), 81-87.
5. Rodríguez, I. A., Cárdenas-González, J. F., Juárez, V. M. M., Pérez, A. R., Zarate, M. G. M., Castillo, N. C. P. *Advances in Bioremediation and Phytoremediation* , **2018**, 43-62.
6. Acar, F. N. And Malkoc, E. *Bioresource Technology*, **2004**, 94 13-15
7. Nagaraj, P., Aradhana, N., Svivakumar, A., Shrestha, A. K., Gowda, A.K. *Environmental Monitoring and Assessment*, **2009**, 157, 575-582.
8. Hua, L., Chan, Y. C., Wu, Y. P., and Wu, B. Y. *Journal of Hazardous Materials*, **2009**, 163, 1360-1368.
9. Gautam, R. K., Mudhoo, A., Lofrano, G., and Chattopadhyaya, M. C. *Journal of Environmental Chemical Engineering*, **2014**, 2, 239-259.
10. Palar, H. "Pencemaran Dan Toksikologi Logam Berat 4th Ed., Jakarta: Rineka Cipta, **2012**.
11. Kocasoy, G. and Guvener, Z. *Environmental Geology*, **2009**, 57(2), 291-296.
12. Davis, T. A., Volesky, B., and Mucci, A. *Water Research*, **2003**, 37, 4311-4330.
13. Abdelfattah, I., Ismail, A. A., Al Sayed, F., Almedolab, A., Aboelghait, K.M. *Environmental Nanotechnology, Monitoring & Management*, **2016**, 6, 176-183.
14. Kiziloz, B. *Periodico Tche Quimica*, **2019**, 16(31), 381-389.
15. Ordouee, B., Hazheminezhad, H. *Periodico Tche Quimica*, **2019**, 16(32), 228-238.
16. Sharov, A. V., Plotnikova, O. M., Evseev, V. V., Rykova, A. I., *Periodico Tche Quimica*, **2019**, 16(32), 516-528.
17. Widhianingrum, W.A., Inawati, Usakinah, K. N., Andriyati, V., Nugraheni, B., *Inovasi Teknik Kimia*, **2016**, 1(2), 84-87.
18. Andrea, C. *World Journal of Chemical Education*, **2015**, 3(3), 70-73.
19. Minarsih, T. *Jurnal Farmasi Indonesia*, **2009**, 6(3), 1-5.
20. Andini, A. *Jurnal Sain Health*, 2017, 1(2), 1-4.

Table 1. STANDARD CR(VI) MEASUREMENT RESULTS

Concentration (mg/L)	Absorbance
0,3	0,174
0,6	0,293
0,9	0,403
1,2	0,531
1,5	0,621

The data in **Table 1** is plotted into a standard curve (**Figure 1**) so that it produces a straight-line equation.

Table 2. MEASUREMENT RESULTS OF CR(VI) HEAVY METAL LEVELS ON WASTE WATER SAMPLE BEFORE ADSORPTION

Absorbance before dilution	Average	Cr(VI) metal concentration before dilution (mg/L)	Absorbance after dilution	Average	Cr(VI) metal concentration after dilution (mg/L)
1,193	1,191	9,97	0,630	0,620	4,92
1,190			0,618		
1,190			0,616		

Table 3. RESULTS OF EXAMINATION OF CR(VI) METAL ADSORPTION IN TEXTILE WASTE WATER USING *Salacca zalacca* SEED POWDER

Mass of adsorbent (gram)	Stirring Speed	Initial Absorbance of Waste Samples	Initial Cr(VI) Metal Concentration (mg/L)	Final Absorbance of Wastewater Samples		Final concentration of Cr(VI) metal (mg/L)		Percentage of Adsorption (%)
				I	II	I	II	
1	Low	0, 620	4,920	0,596	0,516	4,707	4	11,52
	Medium			0,382	0,378	2,814	2,778	33
	High			0,377	0,272	2,769	1,840	53,17
2	Low	0, 620	4,920	0,420	0,458	3,150	3,486	32,56
	Medium			0,396	0,353	2,938	2,557	44,16
	High			0,389	0,268	2,876	1,805	52,43
3	Low	0, 620	4,920	0,422	0,403	3,168	3	37,31
	Medium			0,312	0,300	2,194	2,088	56,48
	High			0,234	0,243	1,504	1,584	68,61
4	Low	0, 620	4,920	0,402	0,403	2,991	3	39,12
	Medium			0,228	0,224	1,451	1,415	70,87
	High			0,198	0,196	1,185	1,168	76,21
5	Low	0, 620	4,920	0,363	0,360	2,641	2,619	46,54
	Medium			0,273	0,271	1,849	1,831	62,60
	High			0,243	0,240	1,584	1,550	68,15

Research Data Processing

a. Calculation of Standard Cr(VI) Solution Series

Dilution :

$$M_1 V_1 = M_2 V_2$$

Note :

M_1 = Early molarity

V_1 = The volume of the initial solution used

M_2 = Final molarity

V_2 = The volume of solution to be made

- $100 \text{ mg/L} \times V_1 = 0,3 \text{ mg/L} \times 10 \text{ mL}$

$$V_1 = \frac{0,3 \times 10}{100} = 0,03 \text{ mL}$$

- $100 \text{ mg/L} \times V_1 = 0,6 \text{ mg/L} \times 10 \text{ mL}$

$$V_1 = \frac{0,6 \times 10}{100} = 0,06 \text{ mL}$$

- $100 \text{ mg/L} \times V_1 = 0,9 \text{ mg/L} \times 10 \text{ mL}$

$$V_1 = \frac{0,9 \times 10}{100} = 0,09 \text{ mL}$$

- $100 \text{ mg/L} \times V_1 = 1,2 \text{ mg/L} \times 10 \text{ mL}$

$$V_1 = \frac{1,2 \times 10}{100} = 0,12 \text{ mL}$$

- $100 \text{ mg/L} \times V_1 = 1,5 \text{ mg/L} \times 10 \text{ mL}$

$$V_1 = \frac{1,5 \times 10}{100} = 0,15 \text{ mL}$$

Table 4. Calculation of Cr(VI) Heavy Metal Content in Textile Waste Water Samples Before Adsorption

Absorbance before dilution	Average	Cr(VI) metal concentration before dilution (mg/L)	Absorbance after dilution	Average	Cr(VI) metal concentration after dilution (mg/L)
1,193			0,630		
1,190	1,191	9,97	0,618	0,620	4,92
1,190			0,616		

Linear Equation (from standard curve, **Figure 1**):

$$y = 0,113x + 0,064$$

Cr(VI) concentration before dilution:

$$1,191 = 0,113x + 0,064$$

$$0,113x = 1,191 - 0,064$$

$$x = \frac{1,191 - 0,064}{0,113} = 9,97 \text{ mg/L}$$

Cr(VI) concentration after dilution:

$$0,620 = 0,113x + 0,064$$

$$0,113x = 0,620 - 0,064$$

$$x = \frac{0,620 - 0,064}{0,113} = 4,92 \text{ mg/L}$$

Calculation of Cr(VI) Heavy Metal Content in Textile Waste Water Samples Using Salak Seed Powder

- **Calculation of Cr (VI) concentration with 1 gram of *Salacca zalacca* seed mass**

Low stirring speed

I. $0,596 = 0,113x + 0,064$

$$0,113x = 0,596 - 0,064$$

$$x = \frac{0,596-0,064}{0,113} = 4,707 \text{ mg/L}$$

II. $0,516 = 0,113x + 0,064$

$$0,113x = 0,516 - 0,064$$

$$x = \frac{0,516-0,064}{0,113} = 4,00 \text{ mg/L}$$

Medium stirring speed

I. $0,382 = 0,113x + 0,064$

$$0,113x = 0,382 - 0,064$$

$$x = \frac{0,382-0,064}{0,113} = 2,814 \text{ mg/L}$$

II. $0,378 = 0,113x + 0,064$

$$0,113x = 0,378 - 0,064$$

$$x = \frac{0,378-0,064}{0,113} = 2,778 \text{ mg/L}$$

High stirring speed

I. $0,377 = 0,113x + 0,064$

$$0,113x = 0,377 - 0,064$$

$$x = \frac{0,377-0,064}{0,113} = 2,769 \text{ mg/L}$$

II. $0,272 = 0,113x + 0,064$

$$0,113x = 0,272 - 0,064$$

$$x = \frac{0,272-0,064}{0,113} = 1,840 \text{ mg/L}$$

- **Calculation of Cr (VI) concentration with 2 gram of *Salacca zalacca* seed mass**

Low stirring speed

I. $0,420 = 0,113x + 0,064$

$$0,113x = 0,420 - 0,064$$

$$x = \frac{0,420-0,064}{0,113} = 3,150 \text{ mg/L}$$

II. $0,458 = 0,113x + 0,064$

$$0,113x = 0,458 - 0,064$$

$$x = \frac{0,458-0,064}{0,113} = 3,486 \text{ mg/L}$$

Medium stirring speed

I. $0,396 = 0,113x + 0,064$

$$0,113x = 0,396 - 0,064$$

$$x = \frac{0,396-0,064}{0,113} = 2,938 \text{ mg/L}$$

II. $0,353 = 0,113x + 0,064$

$$0,113x = 0,353 - 0,064$$

$$x = \frac{0,353-0,064}{0,113} = 2,557 \text{ mg/L}$$

High stirring speed

$$\text{I. } 0,389 = 0,113x + 0,064$$

$$0,113x = 0,389 - 0,064$$

$$x = \frac{0,389-0,064}{0,113} = 2,876 \text{ mg/L}$$

$$\text{II. } 0,268 = 0,113x + 0,064$$

$$0,113x = 0,268 - 0,064$$

$$x = \frac{0,268-0,064}{0,113} = 1,805 \text{ mg/L}$$

- **Calculation of Cr (VI) concentration with 3 gram of *Salacca zalacca* seed mass**

Low stirring speed

$$\text{I. } 0,422 = 0,113x + 0,064$$

$$0,113x = 0,422 - 0,064$$

$$x = \frac{0,422-0,064}{0,113} = 3,168 \text{ mg/L}$$

$$\text{II. } 0,403 = 0,113x + 0,064$$

$$0,113x = 0,403 - 0,064$$

$$x = \frac{0,403-0,064}{0,113} = 3,00 \text{ mg/L}$$

Medium stirring speed

$$\text{I. } 0,312 = 0,113x + 0,064$$

$$0,113x = 0,312 - 0,064$$

$$x = \frac{0,312-0,064}{0,113} = 2,194 \text{ mg/L}$$

$$\text{II. } 0,300 = 0,113x + 0,064$$

$$0,113x = 0,300 - 0,064$$

$$x = \frac{0,300-0,064}{0,113} = 2,088 \text{ mg/L}$$

High stirring speed

$$\text{I. } 0,234 = 0,113x + 0,064$$

$$0,113x = 0,234 - 0,064$$

$$x = \frac{0,234-0,064}{0,113} = 1,504 \text{ mg/L}$$

$$\text{II. } 0,243 = 0,113x + 0,064$$

$$0,113x = 0,243 - 0,064$$

$$x = \frac{0,243-0,064}{0,113} = 1,584 \text{ mg/L}$$

- **Calculation of Cr(VI) concentration with 4 gram of *Salacca zalacca* seed mass**

Low stirring speed

$$\text{I. } 0,402 = 0,113x + 0,064$$

$$0,113x = 0,402 - 0,064$$

$$x = \frac{0,402-0,064}{0,113} = 2,991 \text{ mg/L}$$

$$\text{II. } 0,403 = 0,113x + 0,064$$

$$0,113x = 0,403 - 0,064$$

$$x = \frac{0,403-0,064}{0,113} = 3,00 \text{ mg/L}$$

Medium stirring speed

$$\text{I. } 0,228 = 0,113x + 0,064$$

$$0,113x = 0,228 - 0,064$$

$$x = \frac{0,228-0,064}{0,113} = 1,451 \text{ mg/L}$$

$$\text{II. } 0,224 = 0,113x + 0,064$$

$$0,113x = 0,224 - 0,064$$

$$x = \frac{0,224-0,064}{0,113} = 1,415 \text{ mg/L}$$

High stirring speed

$$\text{I. } 0,198 = 0,113x + 0,064$$

$$0,113x = 0,198 - 0,064$$

$$x = \frac{0,198-0,064}{0,113} = 1,185 \text{ mg/L}$$

$$\text{II. } 0,196 = 0,113x + 0,064$$

$$0,113x = 0,196 - 0,064$$

$$x = \frac{0,196-0,064}{0,113} = 1,168 \text{ mg/L}$$

- **Calculation of Cr (VI) concentration with 5 gram of *Salacca zalacca* seed mass**

Low stirring speed

$$\text{I. } 0,363 = 0,113x + 0,064$$

$$0,113x = 0,363 - 0,064$$

$$x = \frac{0,363-0,064}{0,113} = 2,641 \text{ mg/L}$$

$$\text{II. } 0,360 = 0,113x + 0,064$$

$$0,113x = 0,360 - 0,064$$

$$x = \frac{0,360-0,064}{0,113} = 2,619 \text{ mg/L}$$

Kecepatan Pengadukan *medium*

$$\text{I. } 0,273 = 0,113x + 0,064$$

$$0,113x = 0,273 - 0,064$$

$$x = \frac{0,273-0,064}{0,113} = 1,849 \text{ mg/L}$$

$$\text{II. } 0,271 = 0,113x + 0,064$$

$$0,113x = 0,271 - 0,064$$

$$x = \frac{0,271-0,064}{0,113} = 1,831 \text{ mg/L}$$

High stirring speed

$$\text{I. } 0,243 = 0,113x + 0,064$$

$$0,113x = 0,243 - 0,064$$

$$x = \frac{0,243-0,064}{0,113} = 1,584 \text{ mg/L}$$

$$\text{II. } 0,240 = 0,113x + 0,064$$

$$0,113x = 0,240 - 0,064$$

$$x = \frac{0,240-0,064}{0,113} = 1,550 \text{ mg/L}$$

b. Calculation of Cr (VI) Heavy Metal Absorption Percentage

$$\% = \frac{\text{Initial Concentration} - \text{Final Concentration}}{\text{Initial Concentration}} \times 100 \%$$

- **Percentage decrease in Cr(VI) concentration with 1 gram *Salacca zalacca* seed mass**

Low Stirring Speed

$$X = \frac{4,707 + 4}{2} = 4,353$$

$$\% = \frac{4,920 - 4,353}{4,920} = 11,52 \%$$

Medium Stirring Speed

$$X = \frac{3,814 + 2,778}{2} = 3,296$$

$$\% = \frac{4,920 - 3,296}{4,920} = 33 \%$$

High Stirring Speed

$$X = \frac{2,769 + 1,840}{2} = 2,304$$

$$\% = \frac{4,920 - 2,304}{4,920} = 53,17 \%$$

- **Percentage decrease in Cr(VI) concentration with 2 gram *Salacca zalacca* seed mass**

Low Stirring Speed

$$X = \frac{3,150 + 3,486}{2} = 3,318$$

$$\% = \frac{4,920 - 3,318}{4,920} = 32,56 \%$$

Medium Stirring Speed

$$X = \frac{22,938 + 2,557}{2} = 2,747$$

$$\% = \frac{4,920 - 2,747}{4,920} = 44,16 \%$$

High Stirring Speed

$$X = \frac{2,876 + 1,805}{2} = 2,340$$

$$\% = \frac{4,920 - 2,340}{4,920} = 52,43 \%$$

- **Percentage decrease in Cr(VI) concentration with 3 gram *Salacca zalacca* seed mass**

Low Stirring Speed

$$X = \frac{3,168 + 3}{2} = 3,084$$

$$\% = \frac{4,920 - 3,084}{4,920} = 37,31 \%$$

Medium Stirring Speed

$$X = \frac{2,194 + 2,088}{2} = 2,141$$

$$\% = \frac{4,920 - 2,141}{4,920} = 56,48 \%$$

High Stirring Speed

$$X = \frac{21,504 + 1,584}{2} = 1,544$$

$$\% = \frac{4,920 - 1,544}{4,920} = 68,61 \%$$

- **Percentage decrease in Cr(VI) concentration with 4 gram *Salacca zalacca* seed mass**

Low Stirring Speed

$$X = \frac{2,991+3}{2} = 2,995$$

$$\% = \frac{4,920-2,995}{4,920} = 39,12 \%$$

Medium Stirring Speed

$$X = \frac{1,451+1,415}{2} = 1,433$$

$$\% = \frac{4,920-1,433}{4,920} = 70,87 \%$$

High Stirring Speed

$$X = \frac{1,185+1,168}{2} = 1,176$$

$$\% = \frac{4,920-1,176}{4,920} = 76,21 \%$$

- **Percentage decrease in Cr(VI) concentration with 5 gram *Salacca zalacca* seed mass**

Low Stirring Speed

$$X = \frac{2,641+2,619}{2} = 2,63$$

$$\% = \frac{4,920-2,63}{4,920} = 46,54 \%$$

Pada Kecepatan *medium*

$$X = \frac{1,849+1,831}{2} = 1,84$$

$$\% = \frac{4,920-1,84}{4,920} = 62,60 \%$$

High Stirring Speed

$$X = \frac{1,584+1,550}{2} = 1,567$$

$$\% = \frac{4,920-1,567}{4,920} = 68,15 \%$$

A IMPORTÂNCIA DO ENSINO DAS CURVAS DE TITULAÇÃO NA QUÍMICA ANALÍTICA**THE IMPORTANCE OF TEACHING TITRATION CURVES IN ANALYTICAL CHEMISTRY****FERNANDEZ-MAESTRE, Roberto**

Universidad de Cartagena, Programa de Química, Campus de San Pablo, Cartagena, Colombia.

e-mail: rfernandezm@unicartagena.edu.co

Received 09 December 2019; received in revised form 17 January 2020; accepted 05 March 2020

RESUMO

As curvas de titulação são um assunto importante de um curso de Química Analítica. O principal objetivo do cálculo das curvas de titulação é a seleção de um indicador para essas titulações. O cálculo dos erros de titulação é imperativo porque eles estabelecem se um determinado indicador pode ser usado para uma determinada titulação. Este estudo revisa a literatura disponível sobre curvas de titulação e calcula seus erros. Seu objetivo é chamar a atenção para a importância de que os estudantes de graduação em química terem competências para determinar os erros de titulação, em vez de competências para criar curvas de titulação, pois o objetivo final dessas curvas é determinar o erro cometido ao usar um determinado indicador para determinar seus pontos finais. Este estudo mostra que o cálculo do pH e do potencial no ponto de equivalência nas titulações ácido-base e redox, respectivamente, não é necessário para escolher o indicador de titulação, que gera um erro aceitável de acordo com o tipo de aplicação. São apresentados métodos para calcular esses erros nos quatro principais tipos de titulações; aqueles para titulações complexométricas e de precipitação são mais simples que os da literatura. Aqui, também é demonstrado que cálculo dos pontos imediatamente após e antes da inflexão da curva são mais importantes para esta seleção nesses dois tipos de titulações. Além disso, é mostrado que as curvas complexométricas e de precipitação não são necessárias para selecionar indicadores para essas titulações. Essas demonstrações são importantes porque os professores de química analítica podem desconsiderar o ensino de tópicos significativos gastando tempo calculando curvas de titulação desnecessárias (titulações complexométricas e de precipitação) ou pontos desnecessários de curvas de titulação (titulações redox e ácido-base) quando o cálculo dos erros de titulação dessas reações é mais importante. Este tópico é negligenciado pela maioria dos livros de química analítica. Os programas de graduação em química devem se concentrar mais no cálculo dos erros de titulação do que na construção de curvas de titulação.

Palavras-chave: erro de titulação; erro indicador; seleção de indicadores; erro de ponto final**ABSTRACT**

Titration curves are an essential subject of an Analytical Chemistry course. The main objective of calculating titration curves is the selection of an indicator for such titrations. The calculation of titration errors is imperative because they establish if a given indicator can be used for a given titration. This study reviews the available literature on titration curves and calculating their errors. Its purpose is to draw attention to the importance of undergraduate chemistry students having competencies to determine the titration errors rather than skills to build titration curves as the ultimate purpose of these curves is to determine the failure committed when using a given indicator to assess their endpoints. It is shown that the pH and potential calculation at the equivalence point in acid-base and redox titrations, respectively, are not required to choose the titration indicator, one that yields an acceptable error according to the type of application needed. Methods to calculate these errors in the four main types of titrations are presented; those for complexometric and precipitation titrations are simpler than in the literature. Here, it is also demonstrated that calculating points immediately after and before the curve inflection are more critical for this selection in these two types of titrations. Also, it is deducted that complexometric and precipitation curves are not required to select indicators for these titrations. These demonstrations are essential because analytical chemistry teachers may disregard teaching important topics by spending time calculating unnecessary titration curves (complexometric and precipitation titrations) or additional points of titration curves (redox and acid-base titrations) when the calculation of titration errors of these reactions is more critical. Most analytical chemistry textbooks neglect this topic. Undergraduate chemistry programs should focus more on calculating titration errors than on the construction of titration curves.

Keywords: titration error; indicator error; indicator selection; end-point error

1. INTRODUCTION:

The calculation of titration curves is a topic that demands a large portion of the time available for teaching an Analytical Chemistry course. This calculation allows a perspective of the changes in analyte or titrant along the titration, the estimation of the unknown analyte concentration, or, more importantly, the selection of an indicator for such titration. These titration curves are not entirely required or not at all to select an indicator and, in these cases, their calculation is just an academic exercise. By spending time in the calculation of these titration curves, significant subjects in Analytical Chemistry courses are ignored.

In his response to Daniel Harris about the importance of titration curves (Harris, 2008), Stephen Hawkes states that "choosing an indicator for an acid-base titration requires only calculation of the pH of the salt solution that is formed at the endpoint. Calculating the whole titration curve merely complicates the issue. ...Similar considerations apply to other kinds of titration" (Hawkes, 2008).

This study demonstrates that more information than this pH is required to choose an indicator. Also, Harris states that he has eliminated the titration curve calculations for EDTA and redox reactions in writing a lower-level analytical chemistry textbook (Harris, 2008). This elimination might complicate the selection of indicators in the case of redox reactions; however, because his is a lower-level analytical chemistry textbook, these types of titrations were not going to be considered, but only acid-base titrations. Harris also states that calculating titration curves allows the teacher to select the right indicator and to estimate the titration error in using that indicator (Harris, 2008), but this does not apply to precipitation and EDTA titrations, as demonstrated in the present study.

Better than calculating equivalence point concentrations in redox and acid-base titrations and complexometric and precipitation titration curves is the calculation of the indicator errors, subjects that many analytical chemistry textbooks skip. In this paper, it is shown that to select the right indicator of acid-base and redox titrations, the pH and the potential at the equivalence points are not needed but only calculating these parameters immediately after and before the curve inflection. In analytical chemistry, teachers might disregard teaching other vital subjects by committing time to the calculation of needless portions of the titration curves.

Consequently, this study aimed to highlight

the significance of determining the titration errors rather than building titration curves as the main objective of them is to determine the titration error when using a given indicator.

2. MATERIALS AND METHODS:

This study reviews the available literature on titration curves and calculating their errors. Its purpose is to draw attention to the importance of undergraduate chemistry students having competencies to determine the titration errors rather than competencies to build titration curves as the ultimate purpose of these curves is to determine the error committed when using a given indicator to assess their endpoints.

3. RESULTS AND DISCUSSION:

3.1. Acid-base and redox titrations

Figure 1 shows the acid-base titration of 20.00 ml of HCl with NaOH at several concentrations using phenolphthalein as an indicator. It can be seen that phenolphthalein works well for the titration of 0.100 mol L⁻¹ HCl but may introduce an indicator error as large as 0.4 ml in the titration of 0.0100 mol L⁻¹ HCl, the volume between the endpoint, 20 ml, and the dotted line (insert in Figure 1), which indicates the highest pH at which a regular person could visualize the endpoint at those concentrations.

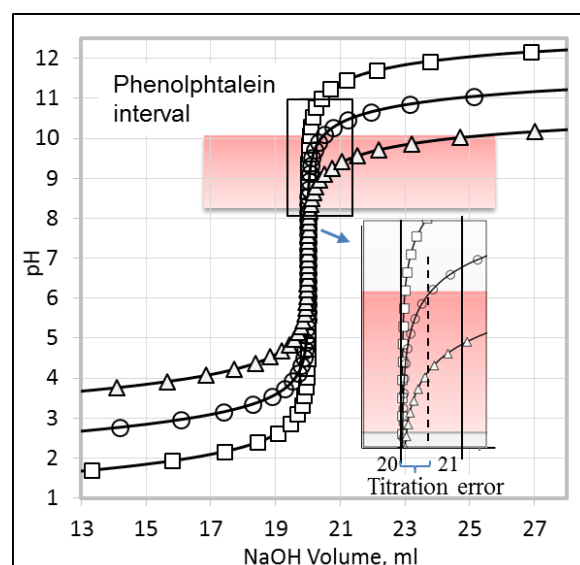


Figure 1. Acid-base titration of 20.00 ml of 0.100 (□), 0.0100 (○) and 0.00100 (Δ) mol L⁻¹ HCl with 0.100, 0.0100 and 0.00100 mol L⁻¹ NaOH, respectively. The shaded area indicates the pH interval at which an average person could visualize the titration end point. In the insert, the

volume between the dotted line and the end-point volume, 20 ml, shows the error occurring when using phenolphthalein as indicator, up to 0.4 ml for HCl 0.0100 mol L⁻¹ and larger for smaller concentrations (Gutz, 2010).

The titration at the lowest concentration in Figure 1, 0.00100 mol L⁻¹ HCl, might yield a more significant indicator error, or might not even be visualized. Similar problems can be found using other indicators or with indicators at the beginning of the end-point inflection of acid or base titrations. Table 1 shows the pK_a at which some acid-base indicators change colors. Following the same reasoning, other indicators from this table could not be used for titrations at concentrations lower than those in Figure 1. For example, cresol violet, which changes between pH 7.6-9.2, may introduce an indicator error of up to ~1.5 ml in the titration endpoint of 0.00100 mol L⁻¹ HCl. Methyl red, which changes color between pH 4.2- 6.3, at the beginning of the end-point inflection, may introduce a 0.5 ml-error in the titration of 0.0100 mol L⁻¹ HCl and a ~3 ml-error in that of 0.00100 mol L⁻¹ HCl in Figure 1. The origin of the indicator error of acid-base titration lies in the finite sensitivity of end-point indicators (Roller, 1932).

Table 1. Some acid-base indicators 5. (Skoog *et al.*, 2015; Harris, 2007; pH meter info, 2019; Streuli, 1963)

Common name	Transition Interval	pK _a
Cresol red	0.2–1.8	1.0
Thymol blue	1.2–2.8	1.65
Thymol blue	8.0–9.6	8.96
Methyl orange	3.1–4.4	3.46
Bromocresol green	3.8–5.4	4.66
Ethyl orange	3.4–4.8	
Methyl red	4.2–6.3	5.00
Bromothymol violet	5.2–6.8	6.12
Bromothymol blue	6.2–7.6	7.10
Phenol red	6.8–8.4	7.81
Cresol violet	7.6–9.2	
Phenolphthalein	8.3–10.0	9.4
Thymolphthalein	9.3–10.5	
Alizarin yellow	10–12	11.2

Equations for the calculation of titration errors in acid-base reactions have been derived (Butcher and Quintus, 1966; Gonzalez *et al.*, 1990).

Redox titrations require similar calculations immediately after and before the curve inflection to

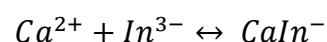
find the right indicator. In this case, the potential calculation at the equivalence point is the hardest of all titrations for students to understand and unnecessary to select an indicator for which, again, it might be better to use the time teaching this subject in more essential topics.

For complexometric and precipitation titrations, it is not required to calculate the titration curve to select the right indicator.

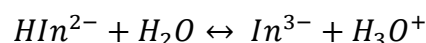
3.2. Complexometric titrations

For a titration with EDTA, the only data required are the initial metal concentration, the pH, the formation constant of the metal-indicator complex, and the indicator K_a for the dissociation reaction between the two main species involved in the color change at the titration pH. The calculation of the end-point metal concentration in a titration of 0.0100 mol L⁻¹ Mg²⁺ with EDTA and Eriochrome Black T (EBT) as the indicator at pH 10 has been reported (Skoog *et al.*, 2013) but the indicator error occurring in this titration at these conditions was not calculated. Following, there is a similar example solved for Ca²⁺, but the error occurring in using EBT to detect the endpoint is calculated demonstrating that EBT is not the right indicator for Ca²⁺ at these conditions.

Example 1. Determine the transition intervals for EBT in the titration of 25.00 mL of 0.0100 mol L⁻¹ Ca²⁺ with 0.0100 mol L⁻¹ EDTA at pH 10. The CaIn⁻ formation constant, K_f, and the second acid dissociation constant of the indicator, K₂, are:



$$K_f = \frac{[CaIn^{-}]}{[In^{3-}][Ca^{2+}]} = 2.5 \times 10^{-5}$$



$$K_2 = \frac{[In^{3-}][H_3O^{+}]}{[HIn^{2-}]} = 2.8 \times 10^{-12}$$

Solution. Multiplying K_f by K_a:

$$K_2 \times K_f = 2.5 \times 10^{-5} \times 2.8 \times 10^{-12} = \frac{[CaIn^{-}]}{[HIn^{2-}]} \frac{[H_3O^{+}]}{[Ca^{2+}]} = 7.0 \times 10^{-7}$$

Solving for Ca²⁺ and replacing the H₃O⁺ concentration at pH 10.0:

$$[Ca^{2+}] = \frac{[CaIn^-]}{[HIn^{2-}]} \frac{1.0 \times 10^{-10}}{7.0 \times 10^{-7}} \quad (eq. 1)$$

It can be considered that a given color in a mixture of two species with different colors can be detected by the average human eye when the concentration of the species with that color is 10 times the concentration of the species with the other color. Because $CaIn^-$ is red and HIn^{2-} is blue, the solution will be red if $[CaIn^-]/[HIn^{2-}] = 10$ and blue if $[CaIn^-]/[HIn^{2-}] = 0.1$. Replacing these two values of $[CaIn^-]/[HIn^{2-}]$ in Equation 1, it is found that the endpoint can be detected at a Ca^{2+} concentration as high as $0.0014 \text{ mol L}^{-1}$ (between 0.0014 and $1.4 \times 10^{-5} \text{ mol L}^{-1}$ or pCa values of 2.85 and 4.84). The indicator error for $0.0100 \text{ mol L}^{-1} Ca^{2+}$ could be as high as 14% (between 0.14 and 14%):

$$E = 100 - \frac{(0.0100 - 0.0014)}{0.0100} \times 100 = 14\%$$

A Ca^{2+} concentration of $0.0014 \text{ mol L}^{-1}$ is obtained when adding only 21.5 mL of the 25.0 mL of EDTA required to reach the endpoint in this example. Figure 2 shows the transition intervals for EBT of the titration of Example 2 and the range of change of the indicator. An Excel spreadsheet In Supporting Information shows the plotting of this curve.

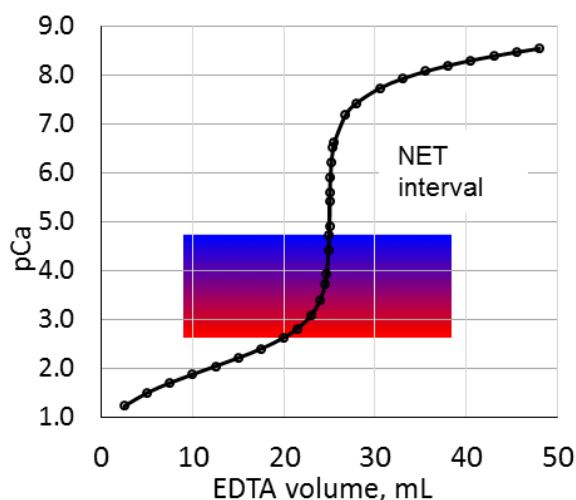


Figure 2. Color transition for EBT from red, the color of $CaIn^-$, to blue, the color of HIn^{2-} , for the titration of Example 2: 25.00 mL of $0.0100 \text{ mol L}^{-1} Ca^{2+}$ with $0.0100 \text{ mol L}^{-1} EDTA$ at $pH 10$. The limits of the colored area correspond to Ca^{2+} concentrations of $0.0014 \text{ mol L}^{-1}$ (below) and $1.4 \times 10^{-5} \text{ mol L}^{-1}$ (above), or pCa values of 2.85 and 4.84 , the range where the average person can detect the EBT color change. The color change

can be perceived 3.5 mL before the endpoint introducing an indicator error of up to 14%

Therefore, EBT is not the right indicator for $0.0100 \text{ mol L}^{-1} Ca^{2+}$, and it is not necessary to calculate the titration curve to find the right indicator in complexometric titrations of this type because the only data used in the preceding example were only those annotated above: initial Ca^{2+} concentration, titration pH , K_f and K_a . For Mg^{2+} , in contrast, the same procedure in the same conditions yields a maximum indicator error of 0.36% . Skoog, *et al.*, 2013 (Figure 17.10) also shows the transition intervals for EBT in the titration of 50.00 mL of Ca^{2+} and Mg^{2+} with EDTA and the 14% indicator error calculated in Example 1 can be visualized. Again, it can be seen from this figure that EBT is not suitable for the titration of Ca^{2+} but it is right for that of Mg^{2+} .

3.3. Precipitation titrations

In the case of precipitation titrations, the endpoint can be determined by the Mohr, Volhard, and Fajans methods. These methods use sodium dichromate, iron and adsorption indicators such as dichlorofluorescein as the end-point indicators, respectively (Christian, 2004). None of them require the calculation of the titration curve. More important than this calculation is calculating the indicator error at the endpoint for a particular precipitation titration. This calculation is not given in conventional textbooks of analytical chemistry in precipitation or complexometric titrations (Skoog *et al.*, 2015; Harris, 2007; Christian, 2004; Skoog *et al.*, 2013; Harvey, 2000; Fifield and Kealey, 2000).

3.3.1 Mohr Method

In this method, to determine halides titrating with Ag^+ , K_2CrO_4 , or other soluble chromate salt is added to the analyte solution; the formation of a reddish-brown Ag_2CrO_4 precipitate determines the endpoint.

Example 2. Determine the indicator error in the titration of 10.0 mL of $0.100 \text{ mol L}^{-1} Cl^-$ solution with 0.100 mol L^{-1} silver nitrate by the Mohr method.

Solution. The silver nitrate concentration at the endpoint is:

$$[Ag^+] = \sqrt{Ksp} = \sqrt{1.82 \times 10^{-10}} \\ = 1.35 \times 10^{-5} \frac{\text{mol}}{\text{L}} \quad (\text{eq. 2})$$

The K_2CrO_4 concentration required to precipitate Ag_2CrO_4 at the endpoint is:

$$[CrO_4^{2-}] = \frac{Ksp}{[Ag^+]^2} = \frac{1.2 \times 10^{-12}}{1.35 \times 10^{-5}} \\ = 6.6 \times 10^{-3} \frac{\text{mol}}{\text{L}} \quad (\text{eq. 3})$$

But K_2CrO_4 must be more diluted ($\sim 10^{-6}$ mol L^{-1}) than 6.6×10^{-3} mol L^{-1} because this concentration turns yellow the analyte solution, concealing the endpoint. This systematic error is corrected, analyzing a blank to determine the volume of titrant required to show the indicator's color. The blank consists of a small amount of chloride-free calcium carbonate, to replicate the white $AgCl$ precipitate, and the indicator (Harvey, 2000). This K_2CrO_4 concentration, ($\sim 10^{-6}$ mol L^{-1}), requires silver and chloride concentrations at the endpoint of:

$$[Ag^+] = \sqrt{\frac{Ksp}{[CrO_4^{2-}]}} = \sqrt{\frac{1.2 \times 10^{-12}}{1 \times 10^{-6}}} \\ = 1.1 \times 10^{-3} \frac{\text{mol}}{\text{L}} \quad (\text{eq. 4})$$

$$[Cl^-] = \frac{Ksp}{[Ag^+]} = \frac{1.82 \times 10^{-10}}{1.1 \times 10^{-3}} \\ = 1.6 \times 10^{-7} \frac{\text{mol}}{\text{L}} \quad (\text{eq. 5})$$

This chloride concentration would decrease the indicator error when compared to the initial chloride concentration, 0.100 mol L^{-1} because most of the original chloride has precipitated. However, to reach a silver concentration of 1.1×10^{-3} mol L^{-1} , the endpoint must be passed, adding an excess of silver, producing an indicator error. Two ways can be used to determine if the Mohr method is adequate to detect the endpoint in Example 2.

MOHR-ERROR, METHOD 1. To reach a silver concentration of 1.1×10^{-3} mol L^{-1} , the concentration required at the endpoint to precipitate Ag_2CrO_4 , with a $\sim 10^{-6}$ mol L^{-1} K_2CrO_4 concentration in 21.0 ml (total volume at the endpoint, including 1 ml of indicator solution), an excess of $\sim (1.1 \times 10^{-3} \text{ mol } L^{-1} \times 1.35 \times 10^{-5} \text{ mol } L^{-1}) \times 0.0200 \text{ L} = 2.3 \times 10^{-5}$ mol of silver must be added.

This amount of silver corresponds to a volume of $V = n M^{-1} = 2.3 \times 10^{-5} \text{ mol } Ag^+ / 0.100 \text{ mol } L^{-1} Ag^+ \cong 0.23 \text{ mL}$ of titrant. This volume corresponds to a 2.3% error for the 10.0 ml calculated to reach the endpoint and does not depend on the volume at the endpoint. This error increases with decreasing reagent concentrations, e.g., to 23% when 0.0100 mol L^{-1} Cl^- is titrated with 0.0100 mol L^{-1} silver nitrate. Therefore, the final formula to calculate the indicator error in the Mohr method is:

$$\text{Error} = \frac{(1.1 \times 10^{-3} - \sqrt{Ksp_a})V_T}{(V_{Ag^+})[Ag^+]}$$

Where 1.1×10^{-3} is the concentration of Ag^+ at the endpoint using 1×10^{-6} mol L^{-1} of K_2CrO_4 as the indicator; Ksp_a the solubility product of the analyte salt that precipitates (for 1:1 salts); $\sqrt{Ksp_a}$ the concentration of Ag^+ at the endpoint without using indicator (for 1:1 salts); V_T the total volume at the endpoint, the added volumes of analyte and silver nitrate; V_{Ag^+} the volume of Ag^+ to reach the endpoint; and $[Ag^+]$ the concentration of Ag^+ titrant.

MOHR-ERROR, METHOD 2. Here, the most significant indicator error that can be accepted is specified; let say 1%. Then, the approximate limits of the end-point inflection are calculated in terms of silver concentration, to obtain the 1% indicator error. In the titration of 10.0 mL of 0.100 mol L^{-1} Cl^- solution with 0.100 mol L^{-1} silver nitrate, these limits are 0.1 ml after and before the equivalence point where the indicator error is $(0.1 \text{ ml} / 10 \text{ ml}) \times 100 \leq 1\%$. The silver concentrations 0.1 ml after and before the equivalence point of this titration are 5.0×10^{-4} mol L^{-1} and 3.62×10^{-7} mol L^{-1} , respectively. If the silver concentration at the endpoint found using the chromate indicator, 1.1×10^{-3} mol L^{-1} (Equation 4), is within this concentration range, then the indicator can be used with an error $\leq 1\%$. In this case, the indicator should not be used because 1.1×10^{-3} mol L^{-1} , calculated above, is not within the said concentration range.

Equations for the calculation of titration errors in precipitation reactions using the Mohr method have been derived (Belcher *et al.*, 1957).

3.3.2 Volhard Method

In the Volhard method, the analyte is added with an excess of standard Ag^+ , which is titrated with standard SCN^- in a strongly acidic solution in the presence of Fe^{3+} . At the endpoint, a reddish complex, $Fe(SCN)^{2+}$, is formed. The

does not require the calculation of the titration curve (Harvey, 2000). Again, this error neither depends on the volume at the endpoint nor the K_{sp} of the analyte-titrant salt nor the analyte-titrant precipitation reaction.

Example 3. Calculate the concentration of Fe^{3+} required to produce a ~zero indicator error in the following titration: 15.00 ml of 0.100 mol L^{-1} Cl^{-} are added with 30.00 ml of 0.100 mol L^{-1} Ag^{+} ; the 15.0 ml excess of 0.100 mol L^{-1} Ag^{+} is back-titrated with 15.00 ml of 0.100 mol L^{-1} KSCN.

Solution. At the back-titration end point:

$$[Ag^{+}] = [SCN^{-}]$$

If Fe^{3+} is used as the indicator, part of the SCN^{-} will be present as $Fe(SCN)^{2+}$ at the endpoint and, therefore:

$$[Ag^{+}] = [SCN^{-}] + [Fe(SCN)^{2+}]$$

Replacing in the solubility product expression $K_{sp} = [Ag^{+}][SCN^{-}]$:

$$[Ag^{+}] = \frac{K_{sp}}{[SCN^{-}]} = \frac{1.1 \times 10^{-12}}{[SCN^{-}]} \\ = [SCN^{-}] + [Fe(SCN)^{2+}]$$

Replacing the $Fe(SCN)^{2+}$ concentration required to detect the endpoint, 6.4×10^{-6} mol L^{-1} , and solving for SCN^{-} in the last two terms:

$$[SCN^{-}]^2 + 6.4 \times 10^{-6}[SCN^{-}] - 1.1 \times 10^{-12} = 0 \\ [SCN^{-}] = 1.7 \times 10^{-7} \text{ mol } L^{-1}$$

This concentration yields a small indicator error: the SCN^{-} concentration at the endpoint without using indicator is $(K_{sp})^{1/2} = (1.1 \times 10^{-12})^{1/2} = 1.04 \times 10^{-6}$ mol L^{-1} . The difference in mmoles between this concentration and the one calculated above, using the indicator, 1.7×10^{-7} , is $(1.04 \times 10^{-6} - 1.7 \times 10^{-7})$ mmol $mL^{-1} \times 60 \text{ mL} = 5.2 \times 10^{-5}$ mmol of SCN^{-} , which requires only 5.2×10^{-5} mmol $SCN^{-} / (0.100 \text{ mmol } SCN^{-} \text{ mL}^{-1}) = 5.2 \times 10^{-4}$ ml of SCN^{-} titrant. This volume corresponds to an indicator error of $[5.2 \times 10^{-4} \text{ ml of KSCN} / 15.00 \text{ ml of KSCN}] \times 100 = 0.0035\%$. Then, $[SCN^{-}]$ is replaced by 1.7×10^{-7} mol L^{-1} and $[Fe(SCN)^{2+}]$ by 6.4×10^{-6} mol L^{-1} in the formation constant expression of $Fe(SCN)^{2+}$ to obtain the Fe^{3+} concentration required to visualize the endpoint:

$$K_f = \frac{[Fe(SCN)^{2+}]}{[Fe^{3+}][SCN^{-}]} = \frac{6.4 \times 10^{-6}}{[Fe^{3+}] \times 1.7 \times 10^{-7}} \\ = 1.05 \times 10^3$$

Solving for Fe^{3+} , a value of 0.036 mol L^{-1} is obtained. If the Fe^{3+} concentration is kept between 0.02 and 1.6 mol L^{-1} an indicator error $\leq 0.1\%$ is obtained.¹³ Therefore, the final formula to calculate the indicator error in the Volhard method, similar to the one derived above for the Mohr method, is:

$$Error = \frac{\left(1.04 \times 10^{-6} - \frac{6.4 \times 10^{-6}}{1.05 \times 10^3 [Fe^{3+}]}\right) V_T}{(V_{SCN^{-}})[SCN^{-}]} \\ = \frac{\left(1.04 \times 10^{-6} - \frac{6.1 \times 10^{-9}}{[Fe^{3+}]}\right) V_T}{(V_{SCN^{-}})[SCN^{-}]}$$

Where 1.04×10^{-6} is the SCN^{-} concentration at the equivalence point of the back-titration without the addition of Fe^{3+} ; 6.4×10^{-6} the $Fe(SCN)^{2+}$ concentration required to detect the endpoint; 1.05×10^3 the $Fe(SCN)^{2+}$ formation constant; V_T the total volume at the back-titration endpoint, the added volumes of analyte, silver nitrate and SCN^{-} ; $V_{SCN^{-}}$ the volume of SCN^{-} to reach the back-titration endpoint; and $[SCN^{-}]$ the concentration of the KSCN back-titrant. This formula is similar to that derived for the Mohr method because the terms of the subtraction, in parenthesis, are the SCN^{-} concentration at the equivalence point of the back-titration without the addition of indicator and adding it, respectively. In Supporting Information, a spreadsheet shows the calculation of this concentration and the indicator error associated.

3.3.3 Fajans Method

In the Fajans method, an adsorption indicator changes color when adsorbed onto the precipitate. For example, when titrating Cl^{-} with Ag^{+} , the anionic dye dichlorofluorescein is used as the indicator. Before the endpoint, the $AgCl$ precipitate has a negative surface charge due to the adsorption of excess Cl^{-} . The anionic indicator is repelled by the precipitate and remains in solution where it has a green-yellowish color. After the endpoint, the precipitate has a positive surface charge due to the adsorption of excess Ag^{+} . The anionic indicator now adsorbs onto the precipitate's surface where its color is pink, signaling the endpoint (Harvey, 2000). The indicator error in this method is small and is related to the amount of Ag^{+} in excess required to turn the

precipitate surface charge to positive to allow the adsorption of enough dichlorofluorescein to become the solution greenish-pinkish.

4. CONCLUSIONS:

In a regular analytical course, the teacher must consider teaching the calculation of the titration curve in complexometric and precipitation experiments because it is not required to choose the chemical indicator. For redox and acid-base titrations, at least, the points 0.1 ml before and after the equivalence point must be calculated to select the chemical indicator. In argentometric experiments using the Mohr method, the lowest concentrations to be used for the titrant and analyte are 0.1 M to avoid indicator errors more significant than 2.2%. Ways to calculate indicator errors in complexometric and precipitation titrations are presented that are simpler than those in the literature (Butcher and Quintus, 1966; Gonzalez, G. G.; Jimenez, *et al.*, 1990; Belcher *et al.*, 1957; Butler, 1963).

5. REFERENCES:

1. Harris, D. C. *J. Chem. Ed.* **2008**, 82, 498
2. Hawkes, S. J. *J. Chem. Ed.* **2008**, 82, 499.
3. Roller, P. S. *J. Am. Chem. Soc.* **1932**, 54, 3485.
4. Butcher, J., Quintus, F. *J. Chem. Ed.* **1966**, 43, 546.
5. Gonzalez, G. G.; Jimenez, A. M.; Asuero, A. G. *Microchem. J.* **1990**, 41, 113.
6. Skoog, D. A., West D. M., Holler F. J., Crouch, S. R. *Fundamentals of Analytical Chemistry*, 9th ed., Cengage Learning: Mexico, 2015.
7. Harris, D. *Quantitative Chemical Analysis*, 7th ed., Freeman: New York, 2007.
8. <http://www.ph-meter.info/pH-measurements-indicators>, accessed August 2019.
9. Streuli, C. A. In *Handbook of Analytical Chemistry*; Meites L., ed., McGraw-Hill: New York, 1963, pp. 3-35 and 3-36
10. Gutz, I. G. R. *Curtipot pH Calculator + Acid-Base Titration*. <http://www.iq.usp.br/gutz/Curtipot.html>; Universidade de São Paulo, Brazil, 2010
11. Christian, G. *Analytical Chemistry*, 6th ed., Wiley: New York, 2004.
12. Skoog, D. A., West D. M., Holler F. J., Crouch, S. R. *Fundamentals of Analytical Chemistry*, 8th ed., Thomson: Mexico, 2013.
13. Harvey, D. *Modern Analytical Chemistry, International Edition*, McGraw-Hill: Boston, 2000.
14. Fifield, F. W., Kealey, D. *Principles and Practice of Analytical Chemistry*, 5th ed., Blackwell Science: Cambridge, 2000.
15. Belcher, R., Macdonald, A. M. G., Parry, E. *Anal. Chim. Acta.* **1957**, 16, 524.
16. Butler, J. N. *J. Chem. Ed.* **1963**, 40, 66.

ANÁLISE ENERGÉTICA E ECONÔMICA DA UTILIZAÇÃO DO ETANOL HIDRATADO

ENERGETIC AND ECONOMIC ANALYSIS OF USE OF HYDRATED ETHANOL

RUOSO, Ana Cristina¹; LHAMBY, Andressa¹; MISSAGGIA, André Brum¹; KLUNK, Marcos Antônio^{2*}; CAETANO, Nattan Roberto¹

¹ Federal University of Santa Maria, Roraima Av. 1000, 97105-900 Santa Maria, RS, Brazil

² University of Vale do Rio dos Sinos, Unisinos Av. 950, 93020-190 São Leopoldo, RS, Brazil

* Correspondence

e-mail: marcosak@edu.unisinos.br

Received 17 December 2019; received in revised form 03 February 2020; accepted 04 February 2019

RESUMO

O interesse em biocombustíveis está crescendo e o etanol tem sido o biocombustível mais utilizado como aditivo e substituto da gasolina, sendo considerado uma alternativa potencial aos combustíveis tradicionais. O etanol representa 17% do consumo de energia em transporte no Brasil, a participação do setor de transporte na matriz energética é de 32,4%, que é o segundo setor que consome mais energia. A produção de etanol de primeira e segunda geração na mesma planta industrial apresenta melhores resultados econômicos em comparação aos processos isolados. Além disso, o etanol obtido da cana-de-açúcar apresenta biodegradabilidade e propicia a mitigação das emissões de CO₂. O objetivo do trabalho é realizar uma análise do etanol com vários níveis de hidratação, em termos energéticos, econômicos, ambientais e de segurança. Os resultados mostraram que a cada 10% de água em diluição em etanol, a temperatura na chama ao redor diminui 4%. Além disso, o etanol com 20% de diluição em água emite 20% menos radiação em comparação com 10% da diluição em água. De fato, a energia consumida na destilação para produzir etanol com 10% de água é o dobro. Por outro lado, essa diferença de energia na produção de etanol diluído com 30% de água não é suficiente para compensar as perdas no processo de uso de energia. Além disso, grandes quantidades de água na diluição do etanol podem inviabilizar o uso devido ao custo total do transporte. Portanto, o etanol com 20% de água representa o combustível mais eficiente, limpo e seguro em aplicações de chama livre.

Palavras-chave: *Bio-combustível, Biomassa, Uso da Energia, Combustão Segura, Cana-de-açúcar.*

ABSTRACT

Interest in biofuels is growing, and ethanol has been the most used biofuel as an additive and as a gasoline substitute and, it is considered a potential alternative to traditional fuels. Ethanol represents 17% of energy consumption in transportation in Brazil, the transport sector's share in the energy matrix is 32.4%, which is the second most energy-consuming sector. The production of first and second-generation ethanol in the same industrial plant presents better financial results compared to the isolated processes. Also, ethanol obtained from the sugarcane has renewability, biodegradability and provides CO₂ emissions mitigation. The objective of the work is to perform an analysis of the ethanol with several levels of hydration in terms of energetic, economic, environmental and safety. The results showed that each 10% of water in ethanol dilution the temperature in the flame surround decreases by 4%. Besides, the ethanol with 20% of water dilution emits 20% less radiation compared to 10% of water dilution. Indeed, the energy consumed in the distillation to produce ethanol with 10% of water is double. On the other hand, this energy difference in the production of ethanol diluted with 30% of water is not enough to compensate for the losses in the energy use process. Also, large amounts of water in ethanol dilution might be unfeasible the use due to the total cost of transportation. Therefore, ethanol with 20% of water represents the more efficient, cleaner and safe fuel in free flame applications.

Keywords: *Biofuel, Biomass, Energy Use, Combustion Safety, sugarcane.*

1. INTRODUCTION

Concerns about climate, environmental, technological, economic, political, demographic and social changes directly affect the world energy matrix (Shah *et al.*, 2019; Cataluña *et al.*, 2018; Moraes *et al.*, 2014). Interest in biofuels is growing, and ethanol has been the most used biofuel as an additive and as a gasoline substitute and, it is considered a potential alternative to traditional fuels (Chuepeng *et al.*, 2016; Goldemberg *et al.*, 2014; Breaux and Acharya, 2013; Nigam and Singh, 2011; Haq *et al.*, 2016). Ethanol represents 17% of energy consumption in transportation in Brazil, the transport sector's share in the energy matrix is 32.4%, which is the second most energy-consuming sector (EPE, 2017; Belincanta *et al.*, 2016). Hydrated ethanol had a share of 19.3 billion liters, at an alcoholic content range between 92.5 and 93.8° INPM (CONAB, 2016; Caetano *et al.*, 2015a).

The practical use of hydrated ethanol represents an essential factor for the reducing costs related to the energy consumed in the process (Venturini *et al.*, 2018; Tura *et al.*, 2018; Matugi *et al.*, 2018; Robertson and Pavlath, 1985; Fagundez *et al.*, 2017; Cataluña *et al.*, 2017). The production of first and second-generation ethanol in the same industrial plant presents better financial results compared to the isolated processes (Silva *et al.*, 2017; Caetano *et al.*, 2015b; Dias *et al.*, 2012; Ojeda *et al.*, 2011; Seabra *et al.*, 2010). Also, ethanol obtained from the sugarcane has renewability, biodegradability and provides CO₂ emissions mitigation (Klunk *et al.*, 2018a; Ponomarev *et al.*, 2017; Caetano and Silva, 2017; Tura *et al.*, 2018; Idrees *et al.*, 2014; Banerji *et al.*, 2014; Quintero *et al.*, 2008).

In social aspects, the advantage is due the processes involved in ethanol production create up to four times more jobs if compared with fossil fuels (Ruoso *et al.*, 2019; Pollin *et al.*, 2008). The ethanol from sugarcane generated six times more jobs than oil fuel (Farina *et al.*, 2013). Regarding the safety of use and storage, fires with ethanol represent dangerous situations for surrounding structures and people (Fossa and Devia, 2008). The flashpoint limit is an essential factor for the fire's prevention and unexpected explosions because this point is inversely proportional to the water concentration at the ethanol produced (Velásquez *et al.*, 2017).

The ethanol production stages are investigated continuously in order to obtain optimizations related to energy consumed in the

biofuel life cycle (Khawiwada *et al.*, 2016; Bansal *et al.*, 2016). The distillation stage has great industrial importance since its energy consumption is high (La-Salvia *et al.*, 2015; Jana, 2014). In this way, the optimization of the operating conditions in the distillation stage contributes to economic success (Klunk *et al.*, 2019a; Saffy *et al.*, 2015; Werle *et al.*, 2009).

The energy required to distill a mixture of up to 80% ethanol in water shown linear behavior. However, an abrupt increase in energy consumption is observed at concentrations up to 80% of ethanol (Fagundez *et al.*, 2017; Rahman *et al.*, 2016). As it is up to 95.6% by volume of ethanol, the energy for dehydration increases exponentially, raising the final value of the product (Aceves and Flowers, 2007; Mayer *et al.*, 2015; Pal *et al.*, 2018). The energy consumed in ethanol distillation with a concentration of 95% corresponds to 50% of the energy contained within the ethanol (Pimentel and Patzek, 2008).

Figure 1 shows the energy consumed in the distillation industrial phase in the function of the ethanol concentration in water. The costs of distillation for the ethanol production, with up to 80% ethanol in water, accounts for 20% of the total costs related to the energy used in the processes (Robertson and Pavlath, 1985). From this point, the distillation and dehydration processes account for approximately 37% of the energy production costs (Breaux and Acharya, 2011). In environmental terms, the use of biomass contributes to the low emissions of carbon dioxide (CO₂) (Klunk *et al.*, 2019b; Klunk *et al.*, 2018b; Klunk *et al.*, 2017a; Demirbaş, 2004). These low carbon dioxide emissions can be predicted by geochemical modeling (Klunk *et al.*, 2019c; 2019d; 2019e; Klunk *et al.*, 2018c; Klunk *et al.*, 2017b; Klunk *et al.*, 2015).

The use of ethanol as fuel or additive also reduces the CO₂ emissions when compared to fossil fuels (Melo *et al.*, 2012; Wang *et al.*, 2015). The CO₂ emitted burning biomass products are recycled through photosynthesis, which acts on biomass growth (Mandegari *et al.*, 2018; Zhang *et al.*, 2010). Thus, biofuel use has reduced carbon emissions by 10% throughout the energy sector (Flórez-Orrego *et al.*, 2015; Szklo *et al.*, 2005).

Ethanol, with 20% of water, shown a significantly increase in thermal efficiency (Chuepeng *et al.*, 2016). Meanwhile, 30% of water in ethanol represents an optimum dilution, being the most energy-efficient fuel to be produced, with the best actual use of the available chemical energy. Also, it presents

advantages in terms of energy balance and cost reduction (Fagundez *et al.*, 2017). Perhaps, this concentration should provide a large amount of water to transport in dynamic applications. Also, the heat release for ethanol from 96% to 100% is approximately the double of the values measured for 50% ethanol, so the radiation is directly proportional to the ethanol concentration (Hakkarainen *et al.*, 2017).

Therefore, this work aims to perform energy, economic, environmental, and safety analysis on the use of hydrated ethanol, considering the whole ethanol cycle, from planting to energy production. Thus, there is an interest in determining the relationship between the energy consumed in the production process and the calorific fuel value, the most representative production total costs, environmental factors, safety assurance, and, finally, concentration hydrous ethanol for industrial applications.

2. MATERIALS AND METHODS

2.1. Background

Information on sugarcane planting, transport and ethanol production in the plant, as well as energy balance, CO₂ equivalent (eq) emissions, and total costs were obtained from a bibliographic review. The Bibliographic Portfolio selection for this bibliographic study survey consists of three stages: (i) articles bank gross selection; (ii) articles database filtering (Cardoso *et al.*, 2015).

The selection was composed of three main stages: i) keywords definition; ii) database selection; iii) according to the defined keywords search for articles (Ensslin *et al.*, 2012). The results obtained in the literature review were converted according to CONAB, where 76 ton/ha corresponds to 5.928 L/ha, and 68 L/ton corresponds to 0,078m³/ton. Thus presenting uniformity in the measures, and thus it was possible to discuss the results (CONAB, 2016).

In this way, it was possible to identify the stages in which the energy used, the emissions, and the costs were more relevant. Therefore, with the information analyzed, the most efficient ethanol dilution for the pool fire condition was identified.

2.2. Safety analysis

The temperature, combustion rate, and

flash point were plotted for the different dilutions of ethanol. The flashpoint was determined to apply ASTM D92-16B (American Society for Testing and Materials, 2016).

In the experimental phase, temperature measurements were performed, and information about the flame was obtained at the different dilutions of ethanol. For this, the hydrated ethanol samples were made with 92% ethanol in water, using a 25 mL burette (resolution 0.1 mL) and KERN weighing-machine (resolution 0.001 g).

The tests used the samples had the following concentrations of ethanol in water: E90W10, E80W20, E70W30, E60W40, E50W50, E40W60, E30W70. A cylindrical aluminum vessel, 14 mm high (h) and 64.98 mm diameter (D), was used to perform the pool fire since the pool fire experiment is defined as a flame that has its spread established on top of a fuel surface (Nakakuki *et al.*, 2002; Sikanen and Hostikka, 2016).

Note that, the flame was under environmental conditions and over an open surface. Three-point thermocouples were used at distances of D/8, D/4, and D/2 from the edge of the fuel container and also at two points in height h and h + D/2, at the same distances in order to measure the ambient temperature in the vicinity of the flame. The thermocouples used were of the K model due to the suitability to the environment (from -270 °C to +1200 °C), the high sensitivity (41 mV/°C) and the associated low measurement uncertainty (0.75%) (Kus *et al.*, 2015; Fialho, 2013).

A camera and a thermal imager were employed to identify flame visual characteristics, such as color, brightness, radiation intensity, and shape. The FLIR model TG165's thermal imager is also 50 x 60 pixels resolution, and it measures temperatures ranging from - 25 to 380 °C, with an accuracy of 1.5%, with a minimum distance of 26 cm.

2.2.1. Radiation

The Radiation is often expressed as a fraction of the total rate of heat release and is vital for the burning rate determination, which is the mode of dominant heat transfer in large scale fires (Fialho, 2013; Hu, 2017; Yang *et al.*, 2017; Chatterjee *et al.*, 2011). Thus, the thermal radiation of the pool fire depends on the combustion products, CO₂, and water, which after the reaction, are at high temperatures, and soot particles (Drysdales *et al.*, 2011).

Therefore, to determine the dosage of radiation during a time interval of exposure and minimum safe distance for people and equipment, Equations 1 and 2 are used. The radiation dosage was obtained with Equation 1. The radiation dose is represented by J (W/m^2), and the energy portion radiates given by Q_R (W).

$$J = \int Q_R^{4/3} dt \quad (\text{Eq. 1})$$

From this equation, in addition to the radiation dosage, it is possible to determine the maximum exposure time and distance to safeguard people and materials. The radiation dose of $5 \text{ kW}/\text{m}^2$ can be tolerated during one minute Lowesmith *et al.* (2007). Also is recommended that objects and operators remain at a minimum distance “d” from the source in order to control the exposure, represented by Equation 2, according to the American Petroleum Institute (API, 1969; Caetano *et al.*, 2018; Caetano *et al.*, 2015c).

$$d = \sqrt{\frac{Q_T \tau F_R}{4\pi q_T}} \quad (\text{Eq. 2})$$

In Equation 2, τ corresponds to the transmissivity of the medium, dimensionless, q_r is the radiation that the object is exposed (W/m^2), and Q_T is the total energy emitted (W) (API, 1969). The energy fraction of the flame that is emitted into the environment is expressed by F_r .

3. RESULTS AND DISCUSSION

3.1. Data collected from the literature

For all the databases selected, a search was carried out with the keywords, with the search fields title (summary) and keywords (keywords). It had a temporary delimitation of 10 years (from the year 2010 to 2017), only publications of scientific articles, thesis, monographs, and dissertations. The files were selected without a database were submitted to a test of adherence and representativeness of the files, and filtering of the database was performed, and thus, the bibliographic file was presented, a later step consisted in the process of debugging the articles selected.

3.1.1. Energy balance

The bibliographic review was compiled in the agricultural phase, industrial phase, and the

ethanol distribution phase, corresponding to approximately 54, 28, and 18%, respectively. The energy of the agricultural phase includes the share of energy consumed by planting, cultivating, harvesting, and transporting. Also, it was evaluated the spending on machines, diesel oil, fertilization, seeds, herbicides, insecticides, transport of inputs and cane. The cultivation of sugar cane requires an area preparation for six consecutive harvests. This yields low energy utilization at this stage when compared to the energy available from ethanol (Salla *et al.*, 2010). Figure 2 shows the energy balance of ethanol, according to some authors.

The values presented a discrepancy, i.e., until nine units of renewable energy per unit fossil energy, are due to the particularities considered by each researcher. These are related to the year, the use of bagasse, energy cogeneration, planting regions, the size of the plants, distribution of biofuel, facilities, maintenance, labor, among other components.

However, considering 30% of the sugarcane bagasse was used for the replacement of wood in the boiler plants so that the rest of the bagasse was used in silage production Turdera *et al.* (2013). Also, it was evaluated the energy used for the production of ethanol in five different plants, obtaining an average energy balance of 6.8. The author considered the energy consumed in the distribution phase of ethanol as $2.82 \text{ GJ}/\text{ha}$. This distribution is made from the plant to the ethanol distribution stations. In addition, the author considered only the production of energy resulting from the use of ethanol, not considering the production of surplus electricity and the use of excess bagasse.

Donke *et al.* (2017) obtained values around 40% higher than García *et al.* (2011) and Donke *et al.* (2017). However, it was considered for the calculation the cogeneration, and the production process multipurpose plant of this study may have had better performance because it ignores the infrastructural aspects and occurs considering a technology. Besides, this case study was conducted in a region where sugarcane production is only expanding, which can result in above-average performance. Also, García *et al.* (2011) is a study carried out in Mexico using direct juice ethanol using bagasse and generating surplus electricity from cycle five years with $70 \text{ t}/\text{ha}$.

Fuel consumption by agricultural machinery is $22.3 \text{ L}/\text{ha}/\text{year}$ of diesel

corresponding to 1,062.7 MJ/ha (Soares *et al.*, 2009). The majority of this fuel is used in the implantation of the crop. In addition, transportation of sugar cane from the field to the plant has a high fossil fuel expense, corresponding to 2,058 MJ/ha/year (Boddey *et al.*, 2008).

The industrial phase considers the processes of extraction and treatment of the liquid from the sugarcane pressing, fermentation, distillation, dehydration, and maintenance. A large amount of energy is used in the phases of cleaning, crushing of the raw material, mats, and heating of the raw material in the plant. The global efficiency of the sugar cane ethanol production process is about 70%. The main losses are in the vapor generation and distillation, with 30% each (Saffy *et al.*, 2015). Besides, sugarcane straw and bagasse from the plantation can be used directly to produce energy. This biomass waste is burned in boilers to generate energy, in biodigesters, or for the production of second-generation ethanol (Leal *et al.*, 2013; Sordi *et al.*, 2013). Another essential factor of the use of biomass is to include the residues in the process of synthesis of zeolites to be used in industrial processes (Klunk *et al.*, 2020; Klunk *et al.*, 2019f).

The energy used in ethanol distribution increases representatively with the distance traveled by the finished product from the plant to the destination. Thus, in order to simplify the studies, most authors do not consider the distribution phase of ethanol for the evaluation of the energy used in the ethanol cycle, as this can vary widely due to the conditions in different regions.

Besides, these values also vary according to ethanol dilution. According to work (Kun-balog *et al.*, 2017), the production of the E92W8 instead of the E96W4 results in an energy saving of 154%. Also, the production of less concentrated ethanol such as the E52W48, increases this energy savings by 169%. An economy of 31% on the energy consumption was verified in comparison regarding ethanol E0W20 and anhydrous applied in an engine (Lanzanova *et al.*, 2016). López-Plaza *et al.* (2014) shown that 30% of energy economy can be reached using E80W20, while Saffy *et al.* (2015) indicates that the best rate is E86W14 due the thermal energy consumption, which is reduced in 10% (from 7.7 to 6.9 MJ/L), then, the financial energy spends decrease 8% in comparison to the anhydrous. The difference between the authors' results is a consequence of the production process which

Saffy *et al.* (2015) use corn in a sub-tropical country. Therefore, the production of hydrated ethanol can significantly increase the energy balance.

3.1.2. Dioxide equivalent emissions

Greenhouse gas (GHG) emissions from the entire ethanol production chain were evaluated in terms of CO₂ eq. The eight articles found containing emission results were compiled in Figure 3. These surveys considered emissions from direct consumption of fuels and electricity, emissions from the production of inputs such as fertilizers, herbicides, lubricants, and seeds. In addition to emissions related to the plant during the industrial process and the mechanization level of the harvest.

The majority of the cultivated areas use the burning of the straw for the harvest, and this conventional technique is still used. Soares *et al.* (2009) emissions by the manual harvesting system for burnt sugarcane and raw cane harvesting were compared. The replacement of the burning by the mechanized harvest represented less pollution. In this paper, the average considered the harvest burning and mechanized was 1.1 kgCO₂ eq/L and 0.4 kgCO₂ eq/L respectively, which represents 60% of reduction in the pollution.

Total CO₂ emissions considering the burning, have obtained 0.6 kgCO₂ eq/L, 1.4 kgCO₂ eq/L and 1.0 kgCO₂ eq/L and 1.3 kgCO₂ eq/L respectively by (Crago *et al.* (2010), Guerra *et al.* (2014), Munoz *et al.* (2014) and Donke *et al.* (2017)). However, Crago *et al.* (2010) included in the industrial phase values approximately 84% lower than those of Donke *et al.* (2017), and finally, the total emissions of kgCO₂ eq and found values around 53% lower than the other authors.

The aspects that most influenced its outcome were the emissions from the expansion of the agricultural area, the use of diesel oil in transport, and operations Donke *et al.* (2017). Also, the emissions from the burning of the straw in the pre-harvest stage of sugarcane were considered. These works were performed at distinct regions considering the climate and level of mechanization.

Total CO₂ emissions considering mechanized harvesting, obtained 0.2 kgCO₂ eq/L, 0.5 kgCO₂ eq/L and 0.5 kgCO₂ eq/L and 0.3 kgCO₂ eq/L, respectively (Paula *et al.*, 2010; Cavallet *et al.*, 2012; Turdera, 2013; Manochio *et al.*, 2017). Indeed, no GHG emission due to the

use of fossil fuels in the plants that generate the energy itself from the burning of the sugar cane bagasse Manochio *et al.* (2017). Direct CO₂ eq emissions related to bagasse burning and broth fermentation are not considered in the total emission, so the carbon released in the burning and fermentation will be sequestered by photosynthesis and will compose the vegetation during the next crop Manochio *et al.* (2017).

The average equivalent CO₂ emissions were 0.7 kgCO₂ eq/L during the production of ethanol, which corresponds to 3.6 t/ha. Thus, from the perspective of greenhouse gases during the entire production cycle of ethanol, it has been verified that there is a gain since the CO₂ equivalent, which is sequestered is higher than the amount of CO₂ emitted when the emissions generated, by the production of electric energy are not considered. The production of hydrated ethanol E86W14 decreases 8%, and, also, when there is cogeneration, the reduction of emissions reaches 25% in comparison to E100, when compared to gasoline this value reaches 72% (Saffy *et al.*, 2015; Hinton *et al.*, 2018). On the other hand, Kaliyan *et al.* (2011) conclude that the reduction of emissions in the production of hydrated ethanol E80W20 can reach 40%, considering the distribution from planting, which was also verified in the work of Roy *et al.* (2015) and López-Plaza *et al.* (2014). In addition to CO₂ eq emissions during ethanol production, the use of hydrated ethanol shows changes in the concentrations of other pollutants emitted during the burning of the biofuel. NO_x emissions decrease by more than 50% when ethanol dilution increases. Meanwhile, CO and hydrocarbon emissions increase significantly from the E60W40, 58% and 267%, respectively, when compared to E80W20 (Munsin *et al.*, 2013). This is because the use of more diluted ethanol has inefficient combustion. However, the E70W30 up to E96W4 ethanol has extremely low and insignificant CO and hydrocarbon emissions when burned. Therefore, the increase of hydration of ethanol up to 30% of water favors the reduction of pollutant emissions (Kun-balog *et al.*, 2017).

3.1.3. Costs

Since the 2007/2008 harvest, the projection of the agro-industrial production costs of the sugar-energy sector has been performed (Bigaton *et al.*, 2015; Bigaton *et al.*, 2016; Bigaton *et al.*, 2017). The forecast of the total costs for the production of ethanol anhydride and

hydrate of the 2015/2016, 2016/2017, and 2017/2018 crops of the Central-South region of Brazil was presented.

In predicting the harvest of 2015/2016, the authors indicated that the production mix of the sugar-energy sector was directed to hydrated ethanol. The forecast for 2016/2017 showed that the increase in costs was related to the decline of agricultural productivity and the low level of renewal and aging in the sugarcane plantations.

For the reduction of costs, the main activities required is the cogeneration of electricity Bigaton *et al.* (2016). Thus, the bagasse is burned, generating electricity. Also, the fall in harvested area and productivity in the forecast for the 2017/2018 harvest, as well as the fall in ethanol production costs.

Figure 4 represents the total costs of producing ethanol for some authors and the average costs. The average found among the authors was 3.2 USD/L.

This work realized research with the costs of ethanol production in the agricultural, industrial, and distribution phases were found three articles of the authors Crago *et al.* (2010), Mayer *et al.* (2016), and Manochio *et al.* (2017). The costs related to the agricultural phase were lower compared to the costs of the industrial phase, which depends on the renewal of the sugar cane plantation. The literature has shown that this renewal occurs every six harvests.

The price is a premium press approximately 0.23 USD/L Crago *et al.* (2010). Moreover, the refinery cost is USD 0.17 per liter, and the transportation of the finished product is US\$ 0.80 per liter. The cost of USD 0.4 per liter of ethanol is produced by low expenses for raw material cultivation, energy cogeneration, and second-generation ethanol production Manochio *et al.* (2017).

The production of ethanol and the sale of bagasse accounting for investment costs, maintenance, and operating costs, as well as the minimum, average and maximum cost of the raw material Mayer *et al.* (2016). Raw material costs are 0.27, 0.53 and 0.80 USD/L, with a 12% variation. However, the investment cost for a microdistillery with a capacity of 720.0 L/day was estimated at 0.11 USD/L. Thus, the cost of maintenance and operation was 0.33 USD/L, of which this amount is discounting the sale price of bagasse, in which the minimum is 0.03, average 0.05, and maximum 0.08 USD/L. The authors declare that a variation of 50% in raw material

cost results in a 26% change in the cost of ethanol. It is estimated that the final cost to the consumer is 1.80 USD/L, including ethanol production costs, taxes and profit margin on the producer, distributor and gas station. This makes the product unfeasible compared to the price of gasoline (Mayer *et al.*, 2016).

This sales value proposed by Mayer *et al.* (2016) is around 55% higher than that found by Crago *et al.* (2010), and 77% higher than that found by Manochio *et al.* (2017), due it was considered a micro-distillery and its final value of 1.80 USD/L corresponds to the final price of ethanol Mayer *et al.* (2016). On the other hand, Manochio *et al.* (2017) considered the costs of biomass, processing and conversion rate, excluding transport costs, which contributed to the cost difference between the other authors.

The cost of distribution affects the final price of biofuel. This relationship is influenced by the fact that ethanol production is located mainly in the Center-South region of Brazil. Thus, ethanol can have up to 40% variation in cost due to transport (ANP, 2016).

A relationship between costs, energy consumed, and energy supplied in the combustion by the biofuel were observed. E90W10 provides a reduction of 31% and 19% when compared to anhydrous ethanol and E95W5, respectively. The E80W20 is the dilution with the lowest production cost. However, mixtures between 85% and 90% of ethanol in water have the best operating cost, because volumetric fuel consumption increases with the water content and less efficiency of the engine (Lanzanova *et al.*, 2016; López-Plaza *et al.*, 2014). Thus, it is possible to perform an estimation of the optimum dilution of ethanol in terms of transport, considering general scenery. The energy released can be calculated by active power during the operation time (Fraga *et al.*, 2014; Klunk *et al.*, 2012).

3.1.4. Safety analysis

Safety analysis related to the ethanol combustion temperature, flame temperature with ethanol dilution, burning time and distance to the source, and fire point, according to section Safety analysis and Radiation.

Figure 5 shows the ethanol combustion temperature, which is related to energy. The temperature is related to the radiation and the transmission of heat by the radiation mechanism to the surroundings.

The ethanol dilution increases the temperature in the surroundings decreases by approximately 4% for each step measured, i.e., 10% (Figure 5). This relationship between dilutions and the reduced temperature is also observed in the work of Li *et al.* (2019). At the distances D/2 and D/4, the temperature behavior is similar, having a difference of approximately 10 °C. At the distance D/8, which is closer to the flame, the temperature increases by approximately 20 °C of D/4 and 30 °C of D/2, as well as a more pronounced increase concerning the dilutions.

The use of fuel ethanol with high hydration (above 5% v/v of water) leads to a reduction in the calorific value of the fuel, consequently increasing the energy fraction corresponding to the latent heat of water vaporization and increasing the fuel consumption (Breaux and Acharya, 2011). That way, the temperature of the hydrated ethanol is lower than that of pure ethanol, which is 1920 °C (Balki and Sayin, 2014). Thus, it is verified the measured temperatures shown in Figure 5, since, in addition to the hydration, the value was obtained around the flame.

The flashpoint limit depends on several factors, such as temperature. In order to evaluate the influence of temperature on the flashpoint limit, only the temperature was modified. The temperature at this point is not responsible for the instantaneous combustion of the whole volume of liquid, because, for the ignition, some external energy supply is necessary.

Mixtures at lower dilutions reach the flashpoint at temperatures lower than ambient, while more diluted mixtures should be heated to reach that point. This information is essential for maintaining the storage safety of ethanol and for defining which dilution of ethanol is most appropriate for storing, in order to prevent fire incidents around the storage areas.

Figure 6 shows the flashpoint in the function of dilutions from the 90% to 30% of ethanol in water, at where noteworthy that the E30W70 sample was heated up to the environment temperature for the definition of the flashpoint.

Figure 7 represents the behavior of the burning time as a function of the ethanol fraction in water. The firing time corresponds to the duration of the combustion until all the ethanol present in the mixture is consumed, or until the mixture becomes so weak that even the high-temperature values of the mixture are not

sufficient to achieve the flashpoint limit. The samples with higher water presence burned faster and represented dilutions that would give more safety in storage environments. Also observed by Oliveira *et al.* (2019), in which the simulated burning time was almost three times greater than the experimental time for hydrated ethanol. For Rahman *et al.* (2016) the addition of 30% or more of water has a significant influence on the initial combustion reaction and on the burning rate, the presence of small amounts of water (20% or less) resulted in faster combustion. The results presented by the authors are consistent with those presented in Figure 7.

Figure 8 represents the percentage difference of radiant energy by the flames at different dilutions, regarding the sample E90W10 as a reference to the comparison. The tests were performed with a free flame at ambient temperature and pressure. The calculation of the radiant energy depends on the shape, the emissivity, and the temperature. The shape factor is very susceptible to changes in the structure of the flame, as well as emissivity. Therefore, the approximate values of these parameters were estimated and considered constant for all the cases approached in this study, since they exert less influence on the results when compared with the temperature.

The difference in radiation between ethanol E90W10 and E80W20 is approximately 20% and approximately 50% for E70W30. The exposure time and distance react non-linearly for the dilutions presented. In mixtures with higher concentrations of ethanol, the water passed from the liquid to the vapor state and irradiated with the ethanol. In the case of the more dilute ethanol, the water remained liquid and did not radiate, cooling the flame and lowering the radiation.

Besides, the radiation is proportional to the flame volume. The container in which the ethanol was burned was a small container with a small sample. With the percentages between the dilutions of ethanol, it is possible to estimate the adequate exposure time and distance, aiming at safeguarding operators and equipment, according to the ratios and dose limits mentioned in Radiation, Equations 1 and 2. Figure 9 represents the maximum exposure time in minutes.

The maximum exposure time in fire situations to safeguard people and equipment increases with increasing ethanol hydration, as shown in Figure 9. This is because increasing the

hydration of ethanol decreases the dosage of radiation and consequently increases the exposure time to this dosage. Just as the more distant a person or equipment is from the flame, the smaller the radiation dosage emitted by the flame, so the longer the exposure time can be compared to distances closer to the flame.

For example, in the case where the radiant energy of the higher flame temperature was around 700 W/m^2 , the operator could remain exposed to the flame for about 7 minutes to E90W10. While for the radiant energy of the E40W60 in the D/2 position was approximately 520 W/m^2 , with a maximum exposure time of approximately 10 minutes.

Considering the laboratory conditions, the distance calculated for the flame of the experiment, according to API (1969), it was millimeters. For the situation that presented higher radiation dosage, E90W10, the safe distance was 12 mm, already for the E40W60 distance value was 8 mm approximately. The distance decreases with ethanol hydration, the difference between the E90W10 for the E80W20 and the E70W30 is 5% and 10%, respectively. Meanwhile, for high hydrates, this difference reaches 30%.

In this work, the values 0.52 to 0.7 kW/m^2 were obtained for the flame radiation, 7 to 9 min of exposure time, 12 to 8 mm of safe distance. Values of 10 to 12 kW/m^2 and from 0.3 to 0.5 min and, also, 12.5 to 37.5 kW/m^2 and 0.13 to 0.40 min of radiation dosage and maximum exposure time were found by Hakkarainen *et al.* (2017) and Fontenelle (2012), respectively. This indicates that the radiation from the flame is inversely proportional to the exposure time and around the same proportion. However, different levels of irradiance and the depth of the pool considered. While, Fontenelle (2012) performed a simulation of a fire in a storage tank, with real dimensions, which considered some standards such as API 650:2007 (2007) and NFPA 30:1996 (1996). Then, due to the dimensions of the pool of the present work, radiation was obtained around 95% lower and with an exposure time around 96% higher than the other works.

4. CONCLUSIONS

The study was conducted to evaluate the optimal dilution of ethanol and water in terms of storage, transport, and energy use. The analysis of CO_2 emissions was based on studies that evaluated the life cycle for ethanol, in terms of the phases, namely: agricultural, industrial, and

distribution. Also, the behavior of the limits of inflammability, the burning time and the radiation emission of the flames in relation to the dilution were analyzed.

The distillation of ethanol up to 80% consumes approximately 10% of the energy equivalent to the calorific value to be produced. Ethanol E90W10 consumes about 20% of this same energy, which increases energy consumption in the industrial phase, reducing energy balance and thus increasing the production costs. The distillation sector had the highest direct energy consumption concerning the industrial sector. Therefore, the production of hydrated ethanol reduces energy consumption and, consequently, reduces the costs of these sectors. Thus, this production strategy contributes to the increase of energy efficiency in the distillation stage.

The E80W20 ethanol flames emitted 20% less radiation compared to the E90W10, so considering the safety of operators and equipment, there is a gain in exposure time and the limit distance in case of fire incidents. However, this study suggests that ethanol E80W20 represents a significantly more efficient, cleaner, and safer fuel than the E90W10, regarding free flame applications.

It was also verified that there is no simple model that determines the levels of dilution that generate greater efficiency. The analyzes available in the literature do not follow a standard, and even if the life cycle phases for ethanol are similar, there are particularities in each work that drastically alter the results, such as the harvest, the region of planting, the scale of production, agricultural techniques, use of by-products and distribution of the finished product. Thus, for future work, it is suggested that ethanol tests vary the hydration of the samples every 2%. Also, to use pool fires with larger diameters, and to simulate situations with the influence of the wind, increase of the ambient temperature and change of pressure.

5. ACKNOWLEDGMENTS

The authors acknowledge the Brazilian agencies CNPq (National Council of Technological and Scientific Development – Brasília, DF, Brazil), CAPES (Coordination for the Improvement of Higher Education Personnel) for the research funding, and the generous assistance of all the people from the company who granted us access to their database and perception information.

6. REFERENCES

1. Shah, Z., Cataluña, R., Vaggetti, J. C. P., Amorim, V. D. A., Da Silva, R. Preparation of jet engine range fuel from biomass pyrolysis oil through hydrogenation and its comparison with aviation kerosene. *International Journal of Green Energy*. **2019**, 1-11.
2. Cataluña, R., Shah, Z., Venturi, V., Caetano, N. R., Da Silva, B. P., Azevedo, C. M. N., Da Silva, R., Suarez, P. A. Z., Oliveira, L. P. Production process of di-amyl ether and its use as an additive in the formulation of aviation fuels. *Fuel*. **2018**, 228, 226-233.
3. Moraes, M. A. F. D., Nassar, A. M., Moura, P., Leal, R. L. V., Cortez, L. A. B. Jet biofuels in Brazil: Sustainability challenges. *Renewable and Sustainable Energy Reviews*. **2014**, 40, 716-726.
4. Chuepeng, S., Srisuwan, S., Tongroon, M. Lean hydrous and anhydrous bioethanol combustion in the spark-ignition engine at idle. *Energy Conversion and Management*. **2016**, 128, 1-11.
5. Goldemberg, J., Mello, F. F. C., Cerri, C. E. P., Davies, C. A., Cerri, C. C. Meeting the global demand for biofuels in 2021 through sustainable land-use change policy. *Energy Policy*. **2014**, 69, 14-18.
6. Breaux, B. B., Acharya, S. The effect of elevated water content on swirl-stabilized ethanol/air flames. *Fuel*. **2013**, 105, 90-102.
7. Nigam, P. S., Singh, A. Production of liquid biofuels from renewable resources. *Progress in Energy and Combustion Science*. **2011**, 37(1), 52-68.
8. Haq, F., Ali, H., Shuaib, M., Badshah, M., Hassan, S. W., Munis, M. F. H., Chaudhary, H. J. Recent progress in bioethanol production from lignocellulosic materials: A review. *International Journal of Green Energy*. **2016**, 13(14), 1413-1441.
9. EPE – Empresa de Pesquisa Energética. Balanço Energético Nacional 2016: Ano Base 2016. Rio de Janeiro: EPE, **2017**.
10. Belincanta, J., Alchorne, J. A., Teixeira da Silva, M. The Brazilian experience with ethanol fuel: aspects of production, use, quality, and distribution logistics. *Brazilian Journal of Chemical Engineering*. **2016**, 33(4), 1091-1102.
11. CONAB – Companhia Nacional de Abastecimento. Acompanhamento da

- safra brasileira: cana-de-açúcar, safra 2016/15. Brasília, **2016**, 2(4), 1-76.
12. Caetano, N. R., Cataluña, R., Vielmo, H. A. Analysis of the Effect on the Mechanical Injection Engine Using Doped Diesel Fuel by Ethanol and Bio-Oil. *International Review of Mechanical Engineering*. **2015a**, 9(2), 124-128.
 13. Venturini, M. S., Bageston, J. V., Caetano, N. R., Peres, L. V., Bencherif, H., Schuch, N. J. Mesopause region temperature variability and its trend in southern Brazil. *Annales Geophysicae*. **2018**, 36(2), 301–310.
 14. Tura, A., Montipó, S., Fontana, R. C., Dillon, A. J. P., Camassola, M. Ethanol production from sugar liberated from Pinus SP. and Eucalyptus SP. biomass pretreated by ionic liquids. *Brazilian Journal of Chemical Engineering*. **2018**, 35(2), 467-476.
 15. Matugi, K., Chiavone-Filho, O., Ribeiro, M. P. A., Soares, R. P., Giordano, R. C. Vapor-liquid equilibrium calculation for simulation of bioethanol concentration from sugarcane. *Brazilian Journal of Chemical Engineering*. **2018**, 35(2), 341-352.
 16. Robertson, G. H., Pavlath, A. E. Dehydration of Ethanol. **1985**, U.S. Patent, (4), 556-460.
 17. Fagundez, J. L. S., Sari, R. L., Mayer, F. D., Martins, M. E. S., Salau, N. P. G. Determination of optimal wet ethanol composition as a fuel in spark-ignition engine. *Applied Thermal Engineering*. **2017**, 112, 317-325.
 18. Cataluña, R., Shah, Z., Pelisson, L., Caetano, N. R., Da Silva, R., Azevedo, C. Biodiesel Glycerides from the Soybean Ethylic Route Incomplete Conversion on the Diesel Engines Combustion Process. *Journal of the Brazilian Chemical Society*. **2017**, 00, 1-8.
 19. Silva, J. F. L., Selicani, M. A., Junqueira, T. L., Klein, B. C., Vaz Júnior, S., Bonomi, A. Integrated furfural and first-generation bioethanol production: process simulation and techno-economic analysis. *Brazilian Journal of Chemical Engineering*. **2017**, 34(3), 623-634.
 20. Caetano, N. R., Soares, D., Nunes, R. P., Pereira, F. M., Schneider, P. S., Vielmo, H. A., Van der Laan, F. T. A comparison of experimental results of soot production in laminar premixed flames. *Open Engineering*. **2015b**, 5, 213-219.
 21. Dias, M. O. S., Junqueira, T. L., Cavalett, O., Cunha, M. P., Jesus, C. D. F., Rossell, C. E. V., Bonomi, A. Integrated versus stand-alone second-generation ethanol production from sugarcane bagasse and trash. *Bioresource Technology*. **2012**, 103(1), 152-161.
 22. Ojeda, K., Ávila, O., Suárez, J., Kafarov, V. Evaluation of technological alternatives for process integration of sugarcane bagasse for sustainable biofuels production—Part 1. *Chemical Engineering Research and Design*. **2011**, 89(3), 270-279.
 23. Seabra, J. E. A., Tao, L., Chum, H. L., Macedo, I. C. A techno-economic evaluation of the effects of centralized cellulosic ethanol and co-products refinery options with sugarcane mill clustering. *Biomass and Bioenergy*. **2010**, 34(8), 1065-1078.
 24. Klunk, M. A., Dasgupta, S., Das, M., Shah, Z. System of Adsorption of CO₂ in Coalbed. *Southern Brazilian Journal of Chemistry*. **2018a**, 26, 2-9.
 25. Ponomarev, A.A., Bubnova, A.V., Klunk, M.A. The Use of X-Ray Microtomography to Assess Changes in the Voids Structure of Rocks. *Southern Brazilian Journal of Chemistry*. **2017**, 25, 12-16.
 26. Caetano, N. R., Silva, B. P. Technical and Economic Viability for the Briquettes Manufacture. *Defect and Diffusion Forum*. **2017**, 380, 218-226.
 27. Idrees, M., Adnan, A., Bokhari, S. A., and Qureshi, F. A. Production of fermentable sugars by combined chemo-enzymatic hydrolysis of cellulosic material for bioethanol production. *Brazilian Journal of Chemical Engineering*. **2014**, 31(2), 355-363.
 28. Banerji, A., Kishore, V. V. N., Balakrishnan, M. A comparison of pretreatments on release of sugars from sweet sorghum bagasse for bioethanol production. *International Journal of Green Energy*. **2014**, 14(6), 522-527.
 29. Quintero, J. A., Montoya, M. I., Sánchez, O. J., Giraldo, O. H., Cardona, C. A. Fuel ethanol production from sugarcane and corn: Comparative analysis for a Colombian case. *Energy*. **2008**, 33(3), 385-399.
 30. Ruoso, F. S., Bittencourt, L. C., Sudati, L. U., Klunk, M. A., Caetano, N. R. New Parameters for the Forest Biomass Waste Ecofirewood Manufacturing Process

- Optimization. *Periódico Tchê Química*. **2019**, 16(32), 560-571.
31. Pollin, R., Garrett-Peltier, H., Heintz, J., Scharber, H. Green Recovery – A Program to Create Good Jobs and Start Building a Low-Carbon Economy. Centre for American Progress and Political Economy Research Institute (PERI), University of Massachusetts, Washington, DC and Amherst, MA, USA, **2008**.
 32. Farina, E., Rodrigues, L., and Sousa, E. L. A política de petróleo e a indústria de etanol no Brasil. *Interesse Nacional*. **2013**, 22, 64-75.
 33. Fossa, M., Devia, F. A model for radiation evaluation and cooling system design in case of fire in tank farms. *Fire Safety Journal*. **2008**, 43(1), 42-49.
 34. Velásquez, E. I. G., Coronado, C. J. R., Quintero Cartagena, J. C., Carvalho, J. A., Mendiburu, A. Z., Andrade, J. C., Santos, J. C. Prediction of flammability limits for ethanol-air blends by the Kriging regression model and response surfaces. *Fuel*. **2017**, 210, 410-424.
 35. Khatiwada, D., Venkata, B. K., Silveira, S., Johnson, F. X. Energy and GHG balances of ethanol production from cane molasses in Indonesia. *Applied Energy*. **2016**, 164, 756-768.
 36. Bansal, A., Illukpitiya, P., Tegegne, F., Singh, S. P. Energy efficiency of ethanol production from cellulosic feedstock. *Renewable and Sustainable Energy Reviews*. **2016**, 58, 141-146.
 37. La-Salvia, N., Lovón-Quintana, J. J., Valença, G. P. vapor-phase catalytic conversion of ethanol into 1,3-butadiene on cr-ba/mcm-41 catalysts. *Brazilian Journal of Chemical Engineering*. **2015**, 32(2), 489-500.
 38. Jana, A. K. Advances in heat pump assisted distillation column: A review. *Energy conversion and management*. **2014**, 77, 287-297.
 39. Klunk, M.A., Dasgupta, S., Nunes, B.V.G., Wander, P.R. Synthesis of Sodalite Zeolite to Treatment of Textile Effluents. *Periódico Tchê Química*. **2019a**, 16(31), 778-783.
 40. Saffy, H. A., Northrop, W. F., Kittelson, D. B., Boies, A. M. Energy, carbon dioxide, and water use implications of hydrous ethanol production. *Energy Conversion and Management*. **2015**, 105, 900-907.
 41. Werle, L. O., Marangoni, C., Teleken, J. G., Sayer, C., Machado, R. F. Control Strategy with Distributed Action for Minimization of Transients in Distillation Column. *10th International Symposium on Process Systems Engineering: Part A*. **2009**, 1527-1532.
 42. Rahman, K. M., Kawahara, N., Tsuboi, K., Tomita, E. Combustion characteristics of wet ethanol ignited using a focused Q-switched Nd:YAG nanosecond laser. *Fuel*. **2016**, 165, 331-340.
 43. Aceves, S. M., Flowers, D. Improving ethanol life cycle energy efficiency by direct utilization of wet ethanol in HCCI engines. *Journal of Energy Resources Technology*. **2007**, 129, 332-337.
 44. Mayer, F. D., Feris, L. A., Marcilio, N. R., Hoffmann, R. Why small-scale fuel ethanol production in Brazil does not take off? *Renewable and Sustainable Energy Reviews*. **2015**, 43, 687-701.
 45. Pal, P., Kumar, R., Ghosh, A. K. Analysis of process intensification and performance assessment for fermentative continuous production of bioethanol in a multi-staged membrane-integrated bioreactor system. *Energy conversion and management*. **2018**, 171, 371-383.
 46. Pimentel, D., Patzek, T. Ethanol production: energy and economic issues related to U.S. and Brazilian sugarcane. *Biofuels, Solar, and Wind as Renewable Energy Systems*. **2008**, 5(14), 357-371.
 47. Breaux, B. B., Acharya, S. The effect of elevated water content on ethanol combustion: a feasibility study. ASME 2011 Power Conference collocated with JSME ICOPE 2011. *American Society of Mechanical Engineers*, **2011**.
 48. Klunk, M. A., Shah, Z., Wander, P. R. Use of Montmorillonite Clay for Adsorption Malachite Green Dye. *Periódico Tchê Química*. **2019b**, 16(32), 279-286.
 49. Klunk, M. A., Dasgupta, S., Das, M. Slow Pyrolysis of Rice Straw: Analysis of Biochar, Bio-Oil and Gas. *Southern Brazilian Journal of Chemistry*. **2018b**, 26, 17-25.
 50. Klunk, M. A., Dasgupta, S., Das, M. Influence of Fast Pyrolysis with Temperature on Gas, Char and Bio-oil Production. *Southern Brazilian Journal of Chemistry*. **2017a**, 25, 1-11.
 51. Demirbaş, A. Ethanol from Cellulosic Biomass Resources. *International Journal of Green Energy*. **2004**, 1(1), 79-87.
 52. Klunk, M. A., Dasgupta, S., Das, M., Wander, P. R. Computer Codes of

- Geochemical Modeling used to Water-Rock Interaction Simple and Complex Systems. *Periódico Tchê Química*. **2019c**, 16(32), 108-118.
53. Klunk, M. A., Dasgupta, S., Schropfer, S. B., Nunes, B. V. G., Wander, P. R. Comparative Study of Geochemical Speciation Modeling Using GEODELING Software. *Periódico Tchê Química*. **2019d**, 16(31), 816-822.
 54. Klunk, M. A., Shah, Z., Caetano, N. R., Conceição, R. V., Wander, P. R., Dasgupta, S., Das, M. CO₂ sequestration by magnesite mineralization through interaction between Mg-brine and CO₂ : integrated laboratory experiments and computerized geochemical modeling. *International Journal of Environmental Studies*. **2019e**, 1-18.
 55. Klunk, M. A., Dasgupta, S., Conceição, R. V. Computerized geochemical modeling of burial diagenesis of the Eocene turbidite reservoir elements: Urucutuca Formation, Espírito Santo Basin, southeastern Brazil passive margin. *Journal of Palaeogeography*. **2018c**, 7, 12-26.
 56. Klunk, M. A., Ponomarev, A. A. Dasgupta, S., Das, M. Arsenic Speciation in Groundwater using the Softwares PHREEQC, GWB and GEODELING. *Southern Brazilian Journal of Chemistry*. **2017b**, 25, 30-35.
 57. Klunk, M. A., Damiani, L. H., Feller, G., Rey, M. F., Conceição, R. V., Abel, M., De Ros, L. F. Geochemical modeling of diagenetic reactions in Snorre Field reservoir sandstones: a comparative study of computer codes. *Brazilian Journal of Geology*. **2015**, 45, 29-40.
 58. Melo, T. C. C., Machado, G. B., Belchior, C. R. P., Colaço, M. J., Barros, J. E. M., De Oliveira, E. J., De Oliveira, D. G. Hydrous ethanol-gasoline blends – Combustion and emission investigations on a Flex-Fuel engine. *Fuel*. **2012**, 97, 796-804.
 59. Wang, X., Chen, Z., Ni, J., Liu, S., Zhou, H. The effects of hydrous ethanol-gasoline on combustion and emission characteristics of a port injection gasoline engine. *Case Studies in Thermal Engineering*. **2015**, 6, 147-154.
 60. Mandegari, M., Farzad, S., Görgens, J. F. A new insight into sugarcane biorefineries with fossil fuel co-combustion: Techno-economic analysis and life cycle assessment. *Energy conversion and management*. **2018**, 165, 76-91.
 61. Zhang, Q., Wang, T., Wu, C., Ma, L., Xu, Y. Fractioned Preparation of Bio-Oil by Biomass Vacuum Pyrolysis. *International Journal of Green Energy*. **2010**, 7(3), 263-272.
 62. Flórez-Orrego, D., Silva, J. A. M., Oliveira Jr. S. Exergy and environmental comparison of the end-use of vehicle fuels: The Brazilian case. *Energy conversion and management*. **2015**, 100, 220-231.
 63. Szklo, A. S., Schaeffer, R., Edgar Schuller, M., Chandler, W. Brazilian energy policies side-effects on CO₂ emissions reduction. *Energy Policy*. **2005**, 33(3), 349-364.
 64. Hakkarainen, T., Korhonen, T., Vaari, J. Heat release characteristics of ethanol-water mixtures: Small-scale experiments. *Fire Safety Journal*. **2017**, 91, 174-181.
 65. Cardoso, T. L., Ensslin, S. R., Ensslin, L., Feliu, V. M. R., Dutra, A. Reflexões para avanço na área de Avaliação e Gestão do Desempenho das Universidades: uma análise da literatura científica. Seminários em Administração (XVIII SEMEAD) São Paulo-SP, **2015**.
 66. Ensslin, L., Ensslin, S. R., Pacheco, G. C. Um estudo sobre segurança em estádios de futebol baseado na análise bibliométrica da literatura internacional. *Perspectivas em Ciência da Informação*. **2012**, 17, 71-91.
 67. ASTM – D92-16B American Society for Testing and Materials: standard test method for flash and fire points by Cleveland open cup tester. West Conshohocken, **2016**.
 68. Nakakuki, A. Heat transfer in pool fires at a certain small lip height. *Combustion and Flame*. **2002**, 113(3), 259-272.
 69. Sikanen, T., Hostikka, S. Modeling and simulation of liquid pool fires with in-depth radiation absorption and heat transfer. *Fire Safety Journal*. **2016**, 80, 95-109.
 70. Kus, A., Isik, Y., Cakir, M., Coşkun, S., Özdemir, K. Thermocouple and Infrared Sensor-Based Measurement of Temperature Distribution in Metal Cutting. *Sensors*. **2015**, 15(1), 1274-1291.
 71. Fialho, B. A. Instrumentação industrial: conceitos, aplicações e análises, edition 7, São Paulo, **2013**.
 72. Hu, L., A review of physics and correlations of pool fire behaviour in wind

- and future challenges. *Fire Safety Journal*. **2017**, 91, 41-55.
73. Yang, Z., Adeosun, A., Kumfer, B. M., Axelbaum, R. L. An approach to estimating flame radiation in combustion chambers containing suspended-particles. *Fuel*. **2017**, 199, 420-429.
 74. Chatterjee, P., Ris, J. L., Wang, Y., Dorofeev, S. B. A model for soot radiation in buoyant diffusion flames. *Proceedings of the Combustion Institute*. **2011**, 33(2), 2665-2671.
 75. Drysdale, D. An Introduction to Fire Dynamics, United Kingdom: John Wiley & Sons, edition 3, **2011**.
 76. Lowesmith, B. J., Hankinson, G., Acton, M.R., Chamberlain, G. An Overview of the Nature of Hydrocarbon Jet Fire Hazards in the Oil and Gas Industry and a Simplified Approach to Assessing the Hazards. *Process Safety and Environmental Protection*. **2007**, 85(3), 207-220.
 77. API - American Petroleum Institute, Guide for Pressure-Relieving and Depressuring Systems – American Petroleum Institute Recommended Practice 521, Washington, D.C., edition 1, **1969**.
 78. Caetano, N. R., Centeno, F. R., Kyprianidis, K. Assessment of Thermal Radiation Heat Loss from Jet Diffusion Flames. *Thermal Science and Engineering Progress*. **2018**, 7, 241-247.
 79. Caetano, N. R., Stapasolla, T. Z., Peng, F. B., Schneider, P. S., Pereira, F. M., Vielmo, H. A. Diffusion Flame Stability of Low Calorific Fuels. Defect and Diffusion Forum. **2015c**, 362, 29-37.
 80. Salla, D. A., Cabello, C. Análise energética de sistemas de produção de etanol de mandioca, cana-de-açúcar e milho. *Energia na Agricultura*. **2010**, 25(2), 32-53.
 81. Turdera, V. M. Energy balance, forecasting of bioelectricity generation and greenhouse gas emission balance in the ethanol production at sugarcane mills in the state of Mato Grosso do Sul. *Renewable and Sustainable Energy Reviews*. **2013**, 19, 582-588.
 82. Mayer, F.D., Brondani, M., Hoffmann, R., Feris, L.A., Marcilio, N.R., and Baldo, V., Small-scale production of hydrous ethanol fuel: Economic and environmental assessment. *Biomass and Bioenergy*. **2016**, 93, 168-179.
 83. Manochio, C., Andrade, B. R., Rodriguez, R. P., Moraes, B. S. Ethanol from biomass: A comparative overview. *Renewable and Sustainable Energy Reviews*. **2017**, 80, 743-755.
 84. Oliveira, E. C. Balanço energético na produção de álcool da cana-de-açúcar: comparativo com a produção norte americana de etanol por meio da utilização de milho. PhD thesis, State University of Mato Grosso do Sul, Dourados, MS, **2010**.
 85. Grego, L. B. M., Eficiência energética do etanol e sua produção: análise comparativa entre Brasil e EUA, **2017**.
 86. García, C. A., Fuentes, A., Hennecke, A., Riegelhaupt, E., Manzini, F., Maser, O. Life-cycle greenhouse gas emissions and energy balances of sugarcane ethanol production in Mexico. *Applied Energy*. **2011**, 88(6), 2088-2097.
 87. Donke, A., Nogueira, A., Matai, P., Kulay, L. Environmental and Energy Performance of Ethanol Production from the Integration of Sugarcane, Corn, and Grain Sorghum in a Multipurpose Plant. *Resources*. **2017**, 6(1), 1-19.
 88. Soares, L. H. B., Alves, B. J. R., Urquiaga, S., Boddey, R. M. Mitigação das emissões de gases efeito estufa pelo uso do etanol da cana-de-açúcar produzido no Brasil. *Circular Técnica*. **2009**, 27, 1-14.
 89. Boddey, R. M., Soares, L. H. B., Alves, B. J. R., Urquiaga, S. Bio-Ethanol Production in Brazil. *Biofuels, Solar and Wind as Renewable Energy Systems*. **2008**, 321-356.
 90. Leal, M. R. L. V., Galdos, M. V., Scarpere, F. V., Seabra, J. E. A., Walter, A., Oliveira, C. O. F. Sugarcane straw availability, quality, recovery and energy use: A literature review. *Biomass and Bioenergy*. **2013**, 53, 11-19.
 91. Sordi, R. A., Manechini, C. Utilization of trash: a view from the agronomic and industrial perspective. *Scientia Agricola*. **2013**, 70(5), 1-2.
 92. Klunk, M. A., Das, M., Dasgupta, S., Impiombato, A. N., Caetano, N. C., Wander, P. R., Moraes, C. A. M. Comparative study using different external sources of aluminum on the zeolites synthesis from rice husk ash. *Materials Research Express*. **2020**, 7(015023), 1-18.
 93. Klunk, M. A., Dasgupta, S., Das, M., Cunha, M. G., Wander, P. R. Synthesis of

- Sodalite Zeolite and Adsorption Study of Crystal Violet Dye. *ECS Journal of Solid State Science and Technology*. **2019f**, 8(10), N144-N150.
94. Kun-balog, A., Sztankó, K., Józsa, V. Pollutant emission of gaseous and liquid aqueous bioethanol combustion in swirl burners. *Energy Conversion and Management*. **2017**, 149, 896-903.
 95. LanzaNova, T. D. M., Dalla Nora, M., Zhao, H. Performance and economic analysis of a direct injection spark ignition engine fueled with wet ethanol. *Applied Energy*. **2016**, 169, 230-239.
 96. Crago, C. L., Khanna, M., Barton, J., Giuliani, E., Amaral, W. Competitiveness of Brazilian sugarcane ethanol compared to US corn ethanol. *Energy Policy*. **2010**, 38(11), 7404-7415.
 97. Guerra, J. P. M., Coleta, J. R., Arruda, L. C. M., Silva, G. A., Kulay, L. Comparative analysis of electricity cogeneration scenarios in sugarcane production by LCA. *The International Journal of Life Cycle Assessment*. **2014**, 19(4), 814-825.
 98. Muñoz, I., Flury, K., Jungbluth, N., Rigalsford, G., Canals, L. M., King, H. Life cycle assessment of bio-based ethanol produced from different agricultural feedstocks. *The International Journal of Life Cycle Assessment*. **2014**, 19(1), 109-119.
 99. Paula, M., Pereira, F. A. R., Arias, E. R. A., Scheeren, B. R., Souza, C. C., Mata, D. S. Fixação de carbono e a emissão dos gases de efeito estufa na exploração da cana-de-açúcar. *Ciência e Agrotecnologia*. **2010**, 34(3), 633-640.
 100. Cavalett, O., Chagas, M. F., Seabra, J. E. A., Bonomi, A. Comparative LCA of ethanol versus gasoline in Brazil using different LCIA methods. *The International Journal of Life Cycle Assessment*. **2012**, 18(3), 647-658.
 101. Hinton, N., *et al.* Aqueous ethanol laminar burning velocity measurements using constant volume bomb methods. *Fuel*. **2018**, 214, 127-134.
 102. Kaliyan, N., Morey, R. V., Tiffany, D. G. Reducing life cycle greenhouse gas emissions of corn ethanol by integrating biomass to produce heat and power at ethanol plants. *Biomass and bioenergy*, **2011**, 35(3), 1103-1113.
 103. Roy, P., Dutta, A., Deen, B. Greenhouse gas emissions and production cost of ethanol produced from biosyngas fermentation process. *Bioresource technology*, **2015**, 192, 185-191.
 104. López-Plaza, E. L., Hernández, S., Barroso-Muñoz, F. O., Segovia-Hernández, J. G., Aceves, S. M., Martínez-Frías, J., Dibble, R. Experimental and Theoretical Study of the Energy Savings from Wet Ethanol Production and Utilization. *Energy Technology*, **2014**, 2(5), 440-445.
 105. Munsin, R., Laoonual, Y., Jugjai, S., Imai, Y. An experimental study on performance and emissions of a small SI engine generator set fuelled by hydrous ethanol with high water contents up to 40%. *Fuel*, **2013**, 106, 586-592.
 106. Bigaton, A., Danelon, A. F., Xavier, L. F. S., Fanton, M., Da Silva, H. T. P. Previsão de custos do setor sucroenergético na região Centro-Sul do Brasil: safra 2015/16. *Revista iPecege*. **2015**, 1, 146-156.
 107. Bigaton, A., Danelon, A. F., Bressan, G., Silva, H. J. T., Rosa, J. H. M. Previsão de custos do setor sucroenergético na região Centro-Sul do Brasil: safra 2017/18. *Revista iPecege*. **2016**, 2(3), 106-113 (2016).
 108. Bigaton, A., Oliveira, A. M. P. F. L., Xavier, F. S., Da Silva, H. J. T. P., Marques, V. Previsão de custos do setor sucroenergético na região Centro-Sul do Brasil: safra 2016/17. *Revista iPecege*. **2017**, 3(3), 65-70.
 109. ANP- Agência Nacional do Petróleo, Gás Natural e Biocombustíveis. Sistema de Levantamento de Preços. **2016**.
 110. Fraga, A., Klunk, M. A., Oliveira, A., Furtado, G., Knornschild, G. H., Dick, L. F. P. Soil corrosion of the AISI1020 steel buried near electrical power transmission line towers. *Materials Research*. **2014**, 17, 1637-1643.
 111. Klunk, M. A., Oliveira, A., Furtado, G., Knornschild, G. H., Dick, L. F. P. Study of the Corrosion of Buried Steel Grids of Electrical Power Transmission Towers. *ECS Transactions*. **2012**, 43, 23-27.
 112. Li, M., Shu, Z., Yi, L., Chen, B., Zhao, Y., & Geng, S. Combustion behavior and oscillatory regime of flame spread over ethanol aqueous solution with different proportions. *Fuel*, **2019**, 253, 220-228.

113. Balki, M. K., Sayin, C. The effect of compression ratio on the performance, emissions, and combustion of an SI (spark ignition) engine fueled with pure ethanol, methanol and unleaded gasoline. *Energy*. **2014**, 71, 194-201.
114. Oliveira, R. L. F., Doubek, G., Vianna, S. S. V. On the behaviour of the temperature field around pool fires in controlled experiment and numerical modeling. *Process Safety and Environmental Protection*, **2019**, 123, 358-369.
115. Fontenelle, A. M. F. Análise térmica em estruturas de tanques de armazenamento de etanol em situação de incêndio, Master Thesis, Federal University of Rio de Janeiro, Rio de Janeiro, **2012**.
116. ISO 5660-1:2015. Reaction-to-fire tests – Heat release, smoke production and mass loss rate – Part 1: Heat release rate (cone calorimeter method) and smoke production rate (dynamic measurement). *International Organization for Standardization*. **2015**, 1-55.
117. API STD 650:2007 - American Petroleum Institute, Welded tanks for oil storage, edition 11, **2007**.
118. NFPA 30 - Flammable and Combustible Liquids Code. *National fire protection association*. **1996**.

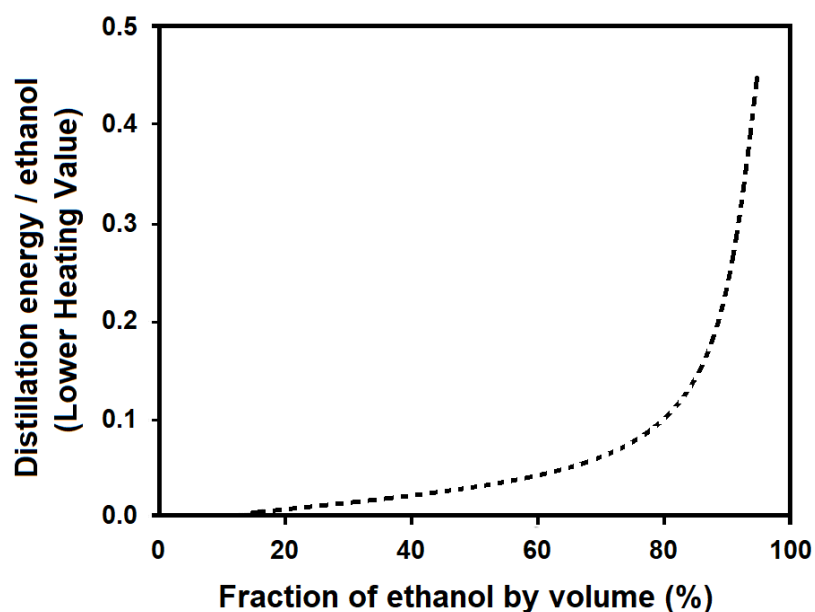


Figure 1. Energy consumption in the ethanol distillation process (Aceves and Flowers, 2007).

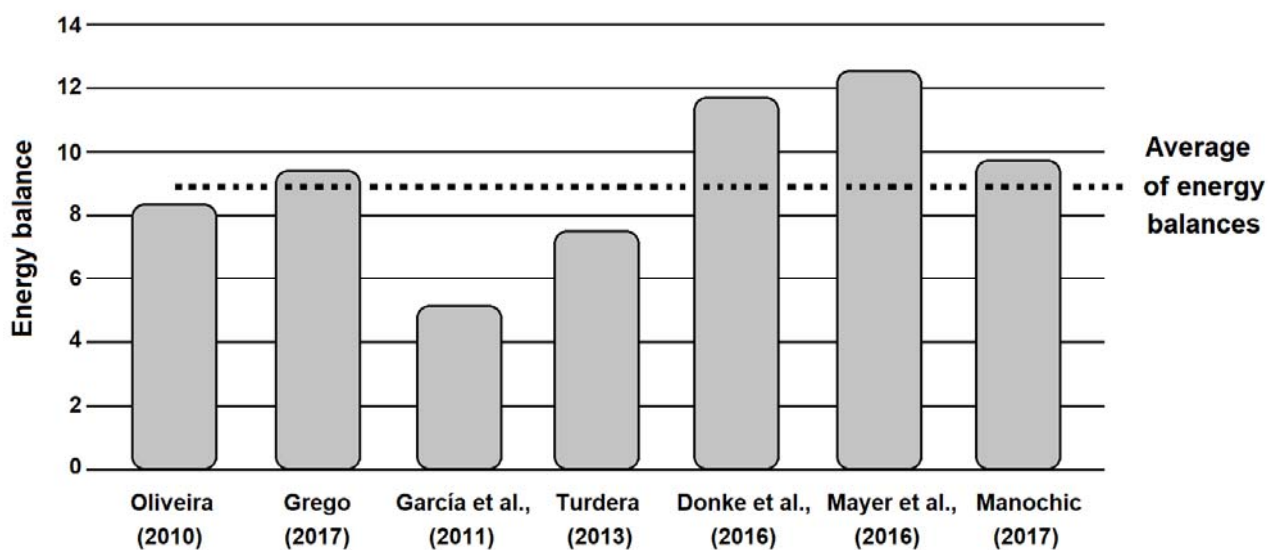


Figure 2. Energy balance over the last decade, for several authors (Oliveira, 2010; Grego, 2017; García et al., 2011; Turdera et al., 2013; Donke et al., 2017; Mayer et al., 2016; Manochio et al., 2017).

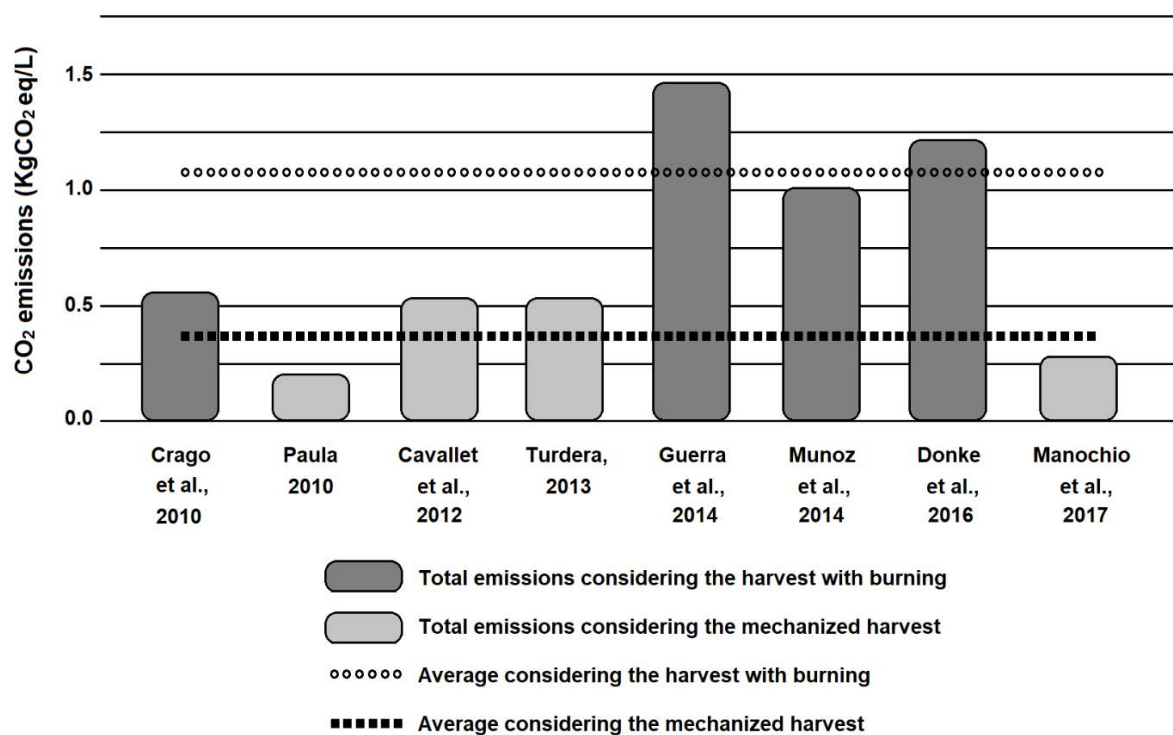


Figure 3. Total CO₂ emissions (kgCO₂ eq/L) for ethanol production (Crago et al., 2010; Paula et al., 2010; Cavallet et al., 2012; Turdera, 2013; Guerra et al., 2014; Munoz et al., 2014; Donke et al., 2017; Manochio et al., 2017).

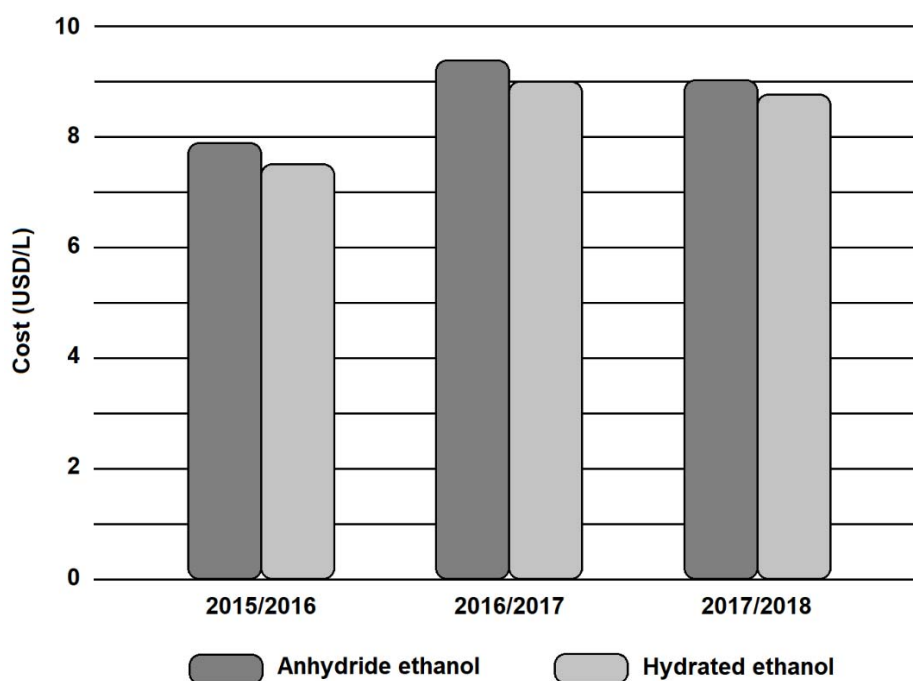


Figure 4. Total cost forecast for ethanol production (Bigaton et al., 2015; Bigaton et al., 2016; Bigaton et al., 2017).

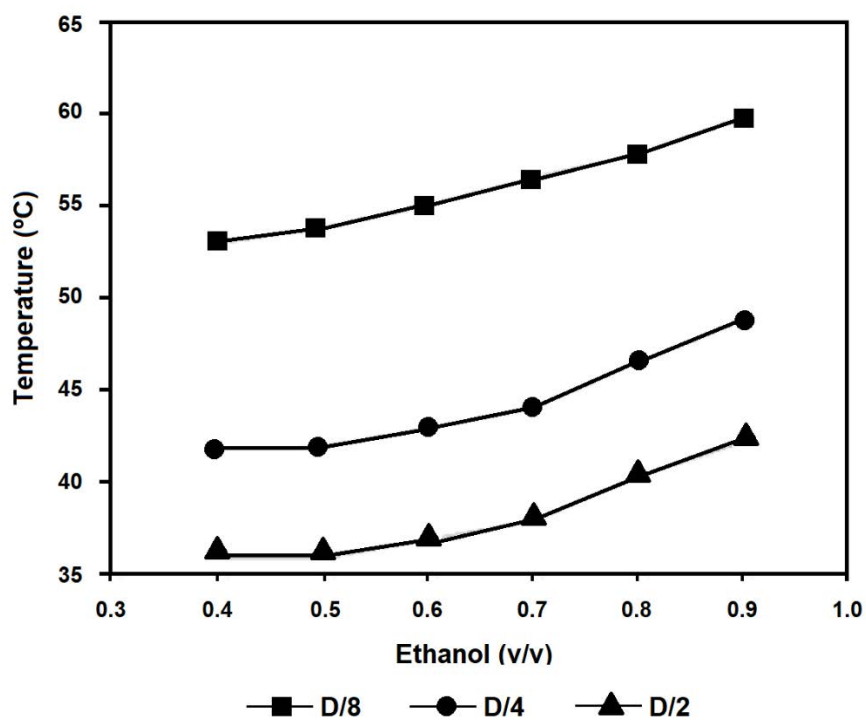


Figure 5. Surrounds temperature at different distances from the flame.

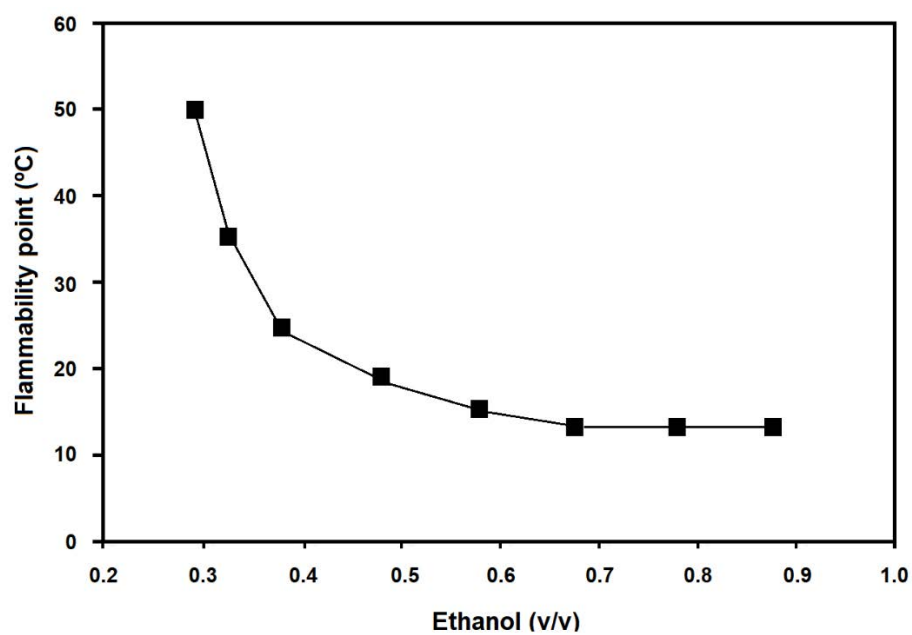


Figure 6. Flashpoint for dilutions from 90% to 30% of ethanol in water.

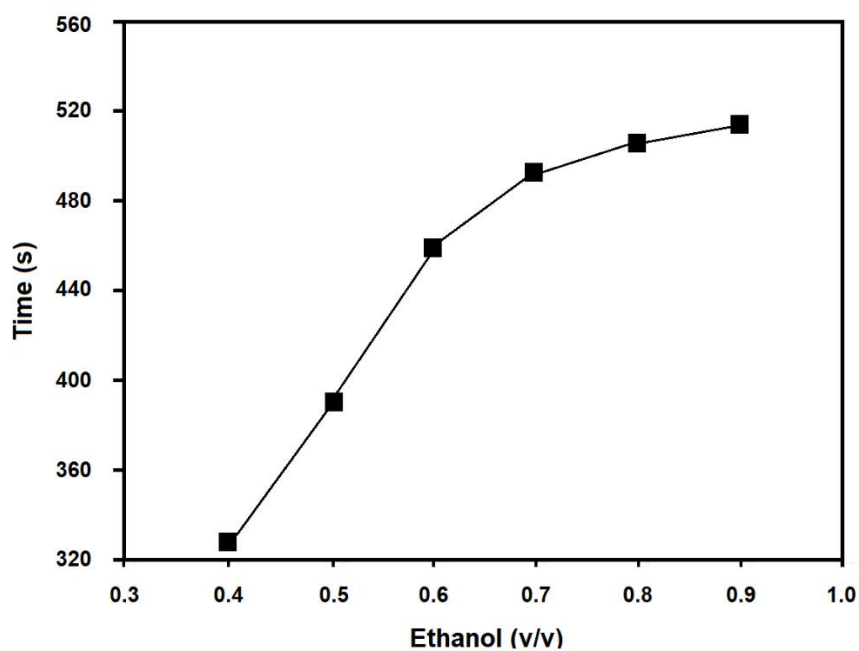


Figure 7. The behavior of the burning time as a function of the ethanol fraction in water.

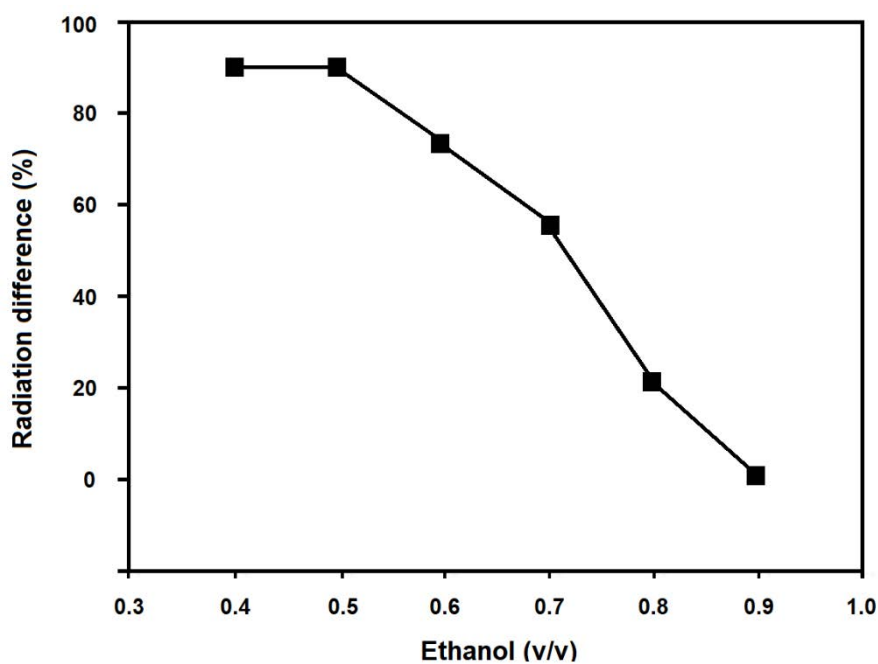


Figure 8. The difference of radiant energy (RE) between the flames in relation to E90W10 with the other dilutions of ethanol.

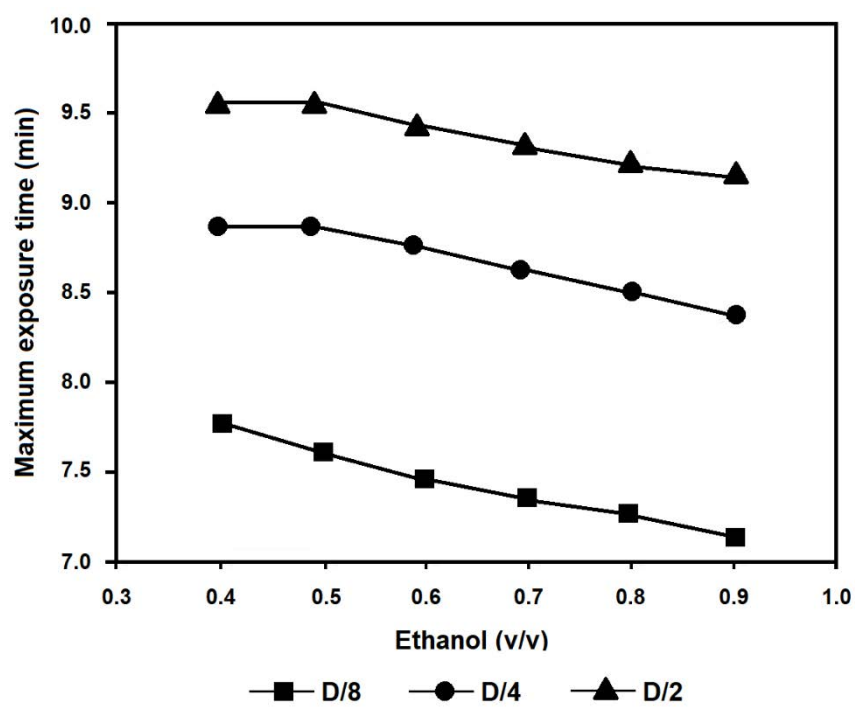


Figure 9. Exposition limits in the function of dilution.

AVALIAÇÃO DE PROPRIEDADES ANTIOXIDANTES E PRÓ-OXIDANTES DE ESTIRPES DE LACTOBACILLUS E ENTEROCOCCUS USANDO O MÉTODO DE ORAC E LUX-BIOSENSOR**ASSESSING ANTIOXIDANT AND PROOXIDANT PROPERTIES OF LACTOBACILLI AND ENTEROCOCCI STRAINS BY USING ORAC AND LUX-BIOSENSOR METHODS****ОЦЕНКА АНТИОКСИДАНТНЫХ И ПРООКСИДАНТНЫХ СВОЙСТВ ШТАММОВ ЛАКТОБАЦИЛЛ И ЭНТЕРОКОККОВ С ПОМОЩЬЮ МЕТОДОВ ORAC И LUX-БИОСЕНСОР**

MAZANKO, Maria S.^{1*}; CHISTYAKOV, Vladimir A.²; ALESHUKINA, Iraida S.³; EID, Moez Ali⁴; ABDULKADHIM, Kareem Abbood Zejawi⁵;

^{1,2}Southern Federal University, Academy of Biology and Biotechnology, Laboratory of Experimental Mutagenesis, 194/1 Stachka Ave., zip code 344090, Rostov-on-Don – Russian Federation

³Rostov Research Institute of Microbiology and Parasitology, Laboratory of Virology, Microbiology and Molecular-Biological Methods of Research, 119 Gazetny Lane, zip code 344000, Rostov-on-Don – Russian Federation

^{4,5}Southern Federal University, Academy of Biology and Biotechnology, Department of Genetics, 194/1 Stachka Ave., zip code 344090, Rostov-on-Don – Russian Federation

* Correspondence author
e-mail: mmazanko@sfedu.ru

Received 06 December 2019; received in revised form 22 January 2020; accepted 06 February 2020

RESUMO

Os lactobacilos são amplamente utilizados na medicina como bactérias probióticas. Os lactobacilos são considerados um dos tipos mais importantes de micróbios intestinais. Essas bactérias têm um efeito antioxidante e protetor de genes no sistema imunitário e nervoso de seus portadores. Mas algumas estirpes de enterococos podem ser patógenos e causar doenças como infecções do trato urinário, bacteremia, infecções no local da cirurgia, infecções na corrente sanguínea, diarreia. A necessidade de estudar as propriedades benéficas e prejudiciais das bactérias para os seres humanos determina a relevância do estudo. As propriedades antioxidantes e pró-oxidantes de 11 estirpes de *Enterococcus* e 7 metabólitos das estirpes de *Lactobacillus* foram analisadas utilizando uma análise de capacidade de absorção de radicais de oxigênio (ORAC) e um teste de biossensor lux. As bactérias foram incubadas no leite de vaca. Leite não fermentado foi usado como controle. O estudo mostrou que o leite fermentado com enterococos não apresentou diferenças significativas na capacidade antioxidante em comparação ao controle. Por outro lado, quase todos os lactobacilos aumentaram a capacidade antioxidante do leite coalhado em comparação com o leite não fermentado. Ou seja, os metabólitos das estirpes de *Lactobacillus* mostraram fortes propriedades antioxidantes, mesmo em baixas concentrações. Os metabólitos das estirpes de *Enterococcus* possuíam propriedades pró-oxidantes. Eles aumentaram a ação de outros pró-oxidantes, como paraquat, peróxido de hidrogênio, dioxidina, e mostraram um efeito sinérgico. O teste do biossensor lux, usado para avaliar o efeito de substâncias em células vivas com um metabolismo complexo, foi mais informativo do que a análise ORAC, que nos permitiu avaliar as propriedades antioxidantes e pró-oxidantes dos metabólitos de bactérias probióticas. O estudo revelou não apenas a influência do efeito direto da substância de teste na molécula alvo, mas também o efeito da ação indireta, interferindo em outros processos bioquímicos de uma célula viva, o que confirmou a necessidade de usar o teste de biossensor lux para trabalhos adicionais ao escolher estirpes de bactérias probióticas.

Palavras-chave: *Lactobacillus*, *Enterococcus*, produto de leite fermentado, antioxidante, pró-oxidante.

ABSTRACT

Lactobacilli are widely used in medicine as probiotic bacteria. Lactobacilli are considered one of the

most important types of intestinal microbes. These bacteria have an antioxidant, gene protective effect on the immune and nervous systems of the host. But some strains of enterococci can be pathogenic microorganisms and cause diseases such as urinary tract infections, bacteremia, infections at the surgical sites, bloodstream infections, diarrhea. The need to study the beneficial and harmful properties of bacteria for humans determines the relevance of the study. The antioxidant and prooxidant properties of 11 *Enterococcus* strains and 7 metabolites of *Lactobacillus* strains were analyzed using an oxygen radical absorption capacity (ORAC) analysis and a lux biosensor test. Bacteria were incubated in cow's milk. Unfermented milk was used as a control. A study showed that milk fermented with enterococci did not have significant differences in antioxidant ability compared to control. In contrast, almost all lactobacilli increased the antioxidant ability of sour milk compared to unfermented milk. That is, the metabolites of *Lactobacillus* strains have demonstrated strong antioxidant properties even at low concentrations. The metabolites of *Enterococcus* strains possessed prooxidant properties. They enhanced the action of other prooxidants, such as paraquat, hydrogen peroxide, dioxidine, and showed a synergistic effect. The Lux biosensor test, used to evaluate the effect of substances on living cells with a complex metabolism, was more informative than the ORAC analysis, which allowed to evaluate the antioxidant and prooxidant properties of probiotic bacteria metabolites. The study revealed not only the influence of the direct effect of the test substance on the target molecule, but also the effect of indirect action by interfering with other biochemical processes of a living cell, which confirmed the need to use the biosensor lux test for further work when choosing strains of probiotic bacteria.

Keywords: *Lactobacillus*, *Enterococcus*, fermented milk, antioxidant, prooxidant.

АННОТАЦИЯ

Бактерии р. *Lactobacillus* широко применяются в медицине в качестве пробиотических бактерий. Они, а также бактерии р. *Enterococcus*, составляют важную часть кишечной микробиоты, обладают антиоксидантной, генопротекторной активностью и влияют на иммунную и нервную систему хозяина. С другой стороны, некоторые представители р. *Enterococcus* могут оказаться патогенными и вызывать такие заболевания, как диарея, инфекции мочевыводящих путей, инфекции, развивающиеся при хирургических вмешательствах, в т.ч. инфекции кровотока. Именно поэтому важно изучить как положительные, так и негативные свойства данных бактерий. 11 штаммов энтерококков и 7 штаммов лактобацилл были исследованы на антиоксидантную и прооксидантную активность с помощью метода ORAC и Lux-биосенсорного теста. Бактерии инкубировали в коровьем молоке. В качестве контроля использовали неферментированное молоко. Молоко, ферментированное энтерококками, не имело существенных различий в антиоксидантной способности по сравнению с контролем. Напротив, почти все лактобациллы даже при низких концентрациях значительно увеличивали антиоксидантную активность ферментированного молока по сравнению с неферментированным. Метаболиты штаммов бактерий р. *Enterococcus*, напротив, обладали прооксидантными свойствами. Они показали синергетический эффект с действием других прооксидантов, таких как паракват, перекись водорода, диоксидин. Lux-биосенсорный тест, использованный для оценки действия метаболитов на живые клетки, оказался более информативным, чем метод ORAC. Он позволил оценить не только антиоксидантные, но и прооксидантные свойства метаболитов пробиотических бактерий. Lux-биосенсорный тест выявил не только прямое действие метаболитов на молекулу-мишень, но и опосредованное, происходящее путем вмешательства метаболитов в другие биохимические процессы живой клетки. Это подтверждает необходимость использования lux-биосенсорного теста при дальнейшей работе с пробиотическими штаммами.

Keywords: *Lactobacillus*, *Enterococcus*, кисломолочный продукт, антиоксидант, прооксидант.

1. INTRODUCTION

Lactobacilli are widely used in medicine and veterinary as probiotic bacteria (Acurcio *et al.*, 2014; Ruzicka *et al.*, 2016; Alfaia *et al.*, 2018; Beatrice *et al.*, 2018; Maldonado *et al.*, 2018; Tarabees *et al.*, 2019; Zhu *et al.*, 2019; Mekadim *et al.*, 2019; Petrut *et al.*, 2019; Barbieri *et al.*, 2019). The World Health Organization defines probiotics as “live microorganisms which when

administered in adequate amounts confer a health benefit on the host” (Report of a joint..., 2006).

Lactobacilli are considered one of the most important types of intestinal microbes. Previous studies have proven that these bacteria have an antioxidant, genoprotective effect on the immune and nervous system of the host (Rybalchenko *et al.*, 2014; Liévin-Le Moal and Servin, 2014; Saez-Lara *et al.*, 2015; Wang *et al.*,

2016; Wang *et al.*, 2017; Chistyakov *et al.*, 2018; Mekadim *et al.*, 2018). In addition to lactobacilli, bifidobacteria are actively used as probiotics, and they have similar properties (Saez-Lara *et al.*, 2015; Wang *et al.*, 2016).

Probiotics affect the balance of intestinal microflora, suppressing enhanced inflammatory responses, immune system stimulation, prevent diarrhea instead of using antibacterial drugs (Bin, 1995; Burns and Rowland, 2000; de Roos and Katan, 2000; Marteau, 2001; Liévin-Le Moal and Servin, 2014; Saez-Lara *et al.*, 2015; Wang *et al.*, 2016). In addition to medications, often in everyday life people get probiotic bacteria and their metabolic products in their daily food. This is why cow milk was chosen as a culture medium for probiotic bacteria in this study. Milk itself has a rather high antioxidant activity (Khan *et al.*, 2017).

Currently, researchers are interested in studying enterococci, which are also main types of the intestinal microbiome (Dominguez-Bello *et al.*, 2010; Franz *et al.*, 2011). It is known that enterococci can also affect immune system regulation, normal intestinal microflora maintenance, antitumor activity, antimicrobial activity, antioxidant activity, and lowering cholesterol levels (Pieniz *et al.*, 2014; Molina *et al.*, 2015; Guo *et al.*, 2016; Li *et al.*, 2017). According to the literature, strains of all the presented lactobacilli species are able to exhibit a different spectrum of antioxidant activity (Corsetti *et al.*, 2008; Amaretti *et al.*, 2013; Mishra *et al.*, 2015).

On the other hand, some strains of enterococci can be pathogens and cause diseases such as urinary tract infections, bacteraemia, surgical site infections, bloodstream infections, diarrhea (Schaberg *et al.*, 1991; Foulquié Moreno *et al.*, 2006), and can be toxic in food production (Franz *et al.*, 2001). Disputes about the applicability of various strains of enterococci as probiotics are still ongoing (Ghosh and Zurek, 2015; Anadón *et al.*, 2016; Joshi and Biswas, 2017; Carasi *et al.*, 2017; Li *et al.*, 2018; Igonina *et al.*, 2018; Sparo *et al.*, 2018; Popovic *et al.*, 2018; Braňek *et al.*, 2019).

In this work, the antioxidant activity of lactobacilli and enterococci strains metabolites were investigated using two different methods. Oxygen Radical Absorbance Capacity (ORAC) assay, which is a common method for assessing the antioxidant activity of different substances and compounds, including bacterial metabolites (Mishra *et al.*, 2015); and the lux-biosensor test, a promising method to identify the interaction of

substances occurring in vivo in a living cell (Manukhov *et al.*, 1999; Prazdnova *et al.*, 2015; Chistyakov *et al.*, 2018).

2. MATERIALS AND METHODS

2.1. Probiotic strains

The metabolites of 11 *Enterococcus* strains and 8 *Lactobacillus* strains were analyzed. 6 *Enterococcus* strains: *E. durans* 6380, *E. durans* 6363, *E. durans* 6379, *E. durans* 6413, *E. durans* 6451, *E. faecium* 9683, and 2 *Lactobacillus* strains: *L. rhamnosus* RH and *L. paracasei* 2647 were obtained from the collection of experimental mutagenesis laboratory. 5 *Enterococcus* strains: *E. durans* 61, *E. faecium* 67, *E. faecium* 75, *E. faecium* 81, *E. faecium* 115 and 6 *Lactobacillus* strains: *L. plantarum* 83, *L. acidophilus* 94, *L. casei* 100, *L. rhamnosus* 108, *L. casei* 116, *L. brevis* 122, were clinical isolates, kindly provided by Pokudina Inna Olegovna, laboratory "Biomedicine", SFedU. All strains were identified by MALDI-TOF mass spectrometry on a Microflex LT instrument (Bruker Daltonics GmbH, Leipzig, Germany) with Biotyper software (version 3.0) (Bruker Daltonics).

All bacteria were cultured at 37°C in 10 ml cow milk for 3 days. Ultra-pasteurized cow milk brand "Prostokvashino", Danone-Unimilk, fat content of 2.5% was used. Supernatants were collected by centrifugation (Minispinplus; Eppendorf, Leipzig, Germany) of fermented milk at 6000 rpm for 7 min.

2.2. Lux-biosensor test

Escherichia coli strains MG1655 (pSoxS-lux) (obtained from Manukhov, State Scientific Center Genetika, Moscow, Russia) were used as Lux biosensors, identifying induction of Sox operon, which is involved in SOS-reparation and serve as a part of the cellular antioxidant defense system (Zavilgelsky *et al.*, 2007). Antioxidant activity was evaluated by the ability of bacterial metabolites to reduce Sox-response, stimulated by addition of dioxidine (2,3-Quinoxalinedimethanol,1,4-dioxide, Biosintez, Penza, Russia) up to 2.25×10^{-5} M, paraquat (N,N'-dimethyl-4,4'-bipyridinium dichloride, Sigma Aldrich, Saint-Louis, MO) up to 10^{-3} M and hydrogen peroxide (Ferrain) up to 10^{-3} M concentrations respectively (Prazdnova *et al.*, 2015). The obtained supernatants were consecutively diluted 10, 100, 1000 times with the above reagents. Milk and its dilutions was used as a control.

The methodology for Lux biosensors bioluminescence detection was thoroughly described by Manukhov *et al.* (1999). A brief description is provided below. Pre-incubation of supernatant with culture was performed for 30 min. For luminescence measurements, an LM-01A automatic microplate luminometer (Immunotech, Praha, Czech Republic) was used. Measurements were carried out every 10 min for 120 min. To evaluate the influence of studied factors on Sox operon expression, the induction factor (Is) was calculated according to Equation 1:

$$Is = (Le/Lk) - 1 \quad (\text{Eq. 1})$$

where Lk and Le are luminescence intensities of control (without any substances, only lux-biosensors and water) and experimental samples (lux-biosensors with inducer or probiotic metabolites or both) respectively.

To characterize the protective activity of the studied concentration, the mean value of P during the whole duration of measurements was used. Each experiment was conducted at least three times in triplicate and the statistical analysis was performed using Student's t-test. Confidence intervals were calculated using MICROSOFT EXCEL (Microsoft Corporation, Redmond, WA) for P = 0.05.

2.3. ORAC assay

The total antioxidant capacity (TAC) was assessed using ORAC assay. It was carried out using an ORAC Assay Kit (ab233473) (Abcam plc., UK). The fluorescence intensity measurement was performed using a FLUOstar Omega, (BMG Labtech, Germany). The supernatants were diluted with fluorescein consecutively by 10, 100, 1000 times. Milk and its dilutions were used as a control (Amorati and Valgimigli, 2015; Mellado-Ortega *et al.*, 2017).

3. RESULTS AND DISCUSSION:

3.1. Determining antioxidant activity of microorganisms by the ORAC assay

The antioxidant capacity of studied microorganisms is shown in Table 1. Milk was used as a control, all bacteria were grown on milk. Milk fermented with enterococci had no significant differences in antioxidant capacity compared to control. In contrast, almost all lactobacilli increased the antioxidant capacity of

fermented milk compared to not-fermented. There were no significant differences in ORAC value in the case of strains *L. casei* 100 and *L. brevis* 122, they did not significantly differ from non-fermented milk, while strains *L. plantarum* 83 and *L. rhamnosus* RH showed the most significant increase in antioxidant capacity compared to control by about two times. It should be noted that the activity of lactobacilli did not depend on the species.

3.2. Determining antioxidant activity of lactobacilli using lux-biosensors

Lactobacillus metabolites did not show prooxidant activity - the change in the luminescence induction factor of the biosensor did not significantly differ from the control (Table 2). The addition of an inducer (paraquat) caused a high increase in the luminescence of biosensors, (Is) paraquat ranged within 23.9-27.4. For estimations, an average value of 24.2 was used. Unfermented milk showed a high protective activity, reducing the luminescence level of the lux-biosensor by 26% at a volume in solution of 10% (Table 2). In less concentrated solutions, the protective activity of milk decreased to 9%. Almost all lactobacilli demonstrated varying antioxidant properties and protected the biosensor cells from the action of superoxide. The greatest protective effect showed by *L. plantarum* 83 (91%), *L. rhamnosus* RH (84%) and *L. acidophilus* 94 (70%). *L. casei* 100 and *L. brevis* 122 did not show significant results compared to the control.

The direct reaction of *E. coli* MG1655 PSoxS-lux with the lactobacilli and enterococci metabolites, and the ability of these metabolites to protect cells from the action of paraquat causes superoxide generation in the cell (Dinis-Oliveira *et al.*, 2008). Paraquat in reaction with enzymes of the respiratory chain of the cell leads to the superoxide generation (Dinis-Oliveira *et al.*, 2008). Hydrogen peroxide and dioxidine are also able to activate the SoxRS in vivo (Manchado *et al.*, 2000; Sycheva *et al.*, 2004). As the volume of supernatant in solution decreased, its effect also decreased. However, with a decrease in volume from 10% to 1%, the protective activity of the supernatant practically did not decrease. Even with a supernatant volume of 0.01%, the protective activity of fermented milk was still recorded, significantly exceeding the activity of unfermented milk (10-42%, depending on the strain).

3.3. Determining antioxidant activity of enterococci

using lux-biosensors

The supernatant of *Enterococcus* fermented milk in a volume of 10% caused a significant increase in induction factor of the *E. coli* MG1655 PSoxS-lux (Table 3). *E. durans* 6380, *E. durans* 6413, *E. faecium* 9683 had the maximum prooxidant effect (3.7, 3.4, 3.2, respectively). A decrease in the supernatant content to 1% led to the disappearance of this effect. The simultaneous action of fermented milk and paraquat led to a significant increase in the induction factor. If (Is) of paraquat was 25.2, then adding 10% of supernatant and paraquat at the same time increased (Is) to 45.5 in the case of *E. faecium* 9683. The biggest increase was caused by *E. faecium* 9683, *E. durans* 6380, *E. durans* 6413, *E. faecium* 67 (an increase of 81%, 75%, 69% and 63%, respectively).

A decrease in the concentration of supernatant to 1% neutralized this effect in half of the studied strains, and a decrease to 0.1% neutralized this effect in all of these strains. When superoxide appears in the cell, the production of soxS gene products increases and the cell begins to glow brighter. Luminosity correlates with the amount of superoxide in the cell (Chistyakov *et al.*, 2018).

3.4. Studying the effect of enterococcal metabolites on the Sox response induced by various inducers

Hydrogen peroxide and dioxidine were used as inducers. The *Enterococcus* metabolites had a prooxidant effect. For comparison, (Is) of *E. durans* 6380 was - 3.5-3.7, (Is) of hydrogen peroxide at a concentration of 10-3 M – 5.4. The effect was observed only in high concentrations of the supernatant - 10%, sometimes 1% and quickly disappeared upon dilution. When superoxide inducer was introduced into the solution, *Enterococcus* metabolites led to a significant increase in the Sox response. Table 4 clearly showed that this is not a simple addition of the activity of metabolites and paraquat, but a synergistic effect. That is, the metabolites of *Enterococcus* do not have a strong prooxidant effect directly, but significantly increase the effect of paraquat. To find out if this effect is specific to paraquat, or it works similarly on other types of prooxidants, other inducers, such as hydrogen peroxide and dioxidine were used.

(Is) of the hydrogen peroxide was 5.4, of the dioxidine – 5.1. It is significantly lower than (Is) of paraquat. The fact is that *E. coli* MG1655 PSoxS-lux responds primarily to superoxide.

Paraquat in reaction with enzymes of the respiratory chain of the cell leads to the superoxide generation. Hydrogen peroxide and dioxidine are also able to activate the SoxRS *in vivo*, therefore, they generated a similar response, but their induction factor was lower. However, enterococcal metabolites also showed a synergistic effect with these inducers, significantly increasing (Is) when combined.

Paraquat was used as a positive control, the obtained induction factors of paraquat slightly differ from those presented above, since this is a different experiment. In general, differences between different replicates are not significant. The metabolites of these strains significantly increased (Is) of dioxidine (up to 96% in the case of *E. faecium* 9683), and also increased (Is) of hydrogen peroxide (up to 52% in the case of *E. durans* 6451).

4. CONCLUSIONS:

Considering that milk itself has a rather high antioxidant activity, in all experiments the effect of metabolites of probiotic bacteria was studied by using unfermented milk as a control. The ORAC assay was used to evaluate antioxidant and prooxidant properties of probiotic bacteria metabolites. The metabolites of *Enterococcus* bacteria did not show any antioxidant activity compared to non-fermented milk. *Lactobacillus* bacteria varied greatly in their ability to synthesize substances with antioxidant properties.

The ability to form antioxidant metabolites in high concentrations is a feature of the strain rather than a species. Therefore, it seems promising to isolate the genetic characteristics of highly active strains in order to create a super-producer strain in the future. The same characteristics were evaluated by using another method, which allows to evaluate the effect of bacterial metabolites on the metabolism of living cells. Lux-biosensor *E. coli* MG1655 PSoxS-lux cells carrying plasmids with luxCDABE operon from the photobacterium *Photobacterium luminescens* under the control of *E. coli* promoters. The production of soxS gene products increases and the cell begins to glow.

The direct reaction of *E. coli* MG1655 PSoxS-lux with the lactobacilli and enterococci metabolites, and the ability of these metabolites to protect cells were evaluated from the action of paraquat. *Lactobacillus* metabolites are powerful antioxidants significantly protect cells from the action of superoxide radical formed by paraquat.

Moreover, they themselves do not negatively affect the Sox-response of the cell. Even in small concentrations (0.01% supernatant), a significant protective effect was observed. The strains that showed the highest antioxidant capacity when using the ORAC assay showed the most significant protective effect in the bioluminescent test. This suggests the possibility of comparing the results of studies obtained in these different methods.

Enterococcal metabolites also showed a synergistic effect with these inducers, significantly increasing (Is) when combined which means that these metabolites do not affect the stage of interaction of paraquat with the enzymes of the respiratory chain, but the stage of cell response to the appearance of free radicals. This effect should be considered when choosing enterococcal strains to create probiotic preparations. After all, the body is constantly exposed to prooxidants obtained from food and air, as well as produced in the cells of the body, and an increase in the number of intestinal enterococcus can increase the oxidative load on the body.

The lux-biosensor test was more informative than ORAC. It evaluates the effects of substances on living cells with a complex metabolism. Therefore, the study can reveal not only the effects of the direct action of test substance on the target molecule, but also the effects of the indirect action through intervention in other biochemical processes of the living cell. Therefore, it's recommended to use the lux-biosensor test while selecting probiotic bacteria strains for further work.

5. ACKNOWLEDGMENTS:

This publication was financially supported by the Southern Federal University.

6. REFERENCES:

1. Acurcio, L.B., Souza, M.R., Nunes, A.C., Oliveira, D.L.S., Sandes, S.H.C., Alvim, L.B. *Arquivo Brasileiro de Medicina Veterinária e Zootecnia*, **2014**, 66(3), 940–948.
2. Alfaia, C.M., Gouveia, I.M., Fernandes, M.H., Fernandes, M.J., Semedo-Lemsaddek, T., Barreto, A.S., Fraqueza, M.J. *Journal of Food Science*, **2018**, 83(10), 2544–2549.
3. Amaretti, A., di Nunzio, M., Pompei, A., Raimondi, S., Rossi, M., Bordoni, A. *Applied Microbiology and Biotechnology*, **2013**, 97, 809–817.
4. Amorati, R., Valgimigli, L. *Free Radical Research*, **2015**, 49(5), 633–649.
5. Anadón, A., Martínez-Larrañaga, M.R., Ares, I., Martínez, M.A. Probiotics: safety and toxicity consideration. In: R.C. Gupta (Ed.), *Nutraceuticals: efficacy, safety and toxicity* (pp. 777–798). Hopkinsville: Elsevier Inc., **2016**.
6. Barbieri, F., Montanari, C., Gardini, F., Tabanelli, G. *Foods*, **2019**, 8(1), 17.
7. Beatrice, T., Francesca, P., Barbara, T., Filippo, F., Roberta, N. *European Food Research and Technology*, **2018**, 244(4), 721–728.
8. Bin, L.X. *Annales de Pédiatrie*, **1995**, 42, 96–401.
9. Braňek, O.B., Smaoui, S., Papadopoulou, C. *BioMed Research International*, **2019**, 2019, article number5938210.
10. Burns, A., Rowland, I., *Current Issues in Intestinal Microbiology*, **2000**, 1, 13–24.
11. Carasi, P., Racedo, S.M., Jacquot, C., Elie, A.M., Serradell, M.L., Urdaci, M.C. *Frontiers in Immunology*, **2017**, 8, 88. doi: 10.3389/fimmu.2017.00088.
12. Chistyakov, V.A., Prazdnova, E.V., Mazanko, M.S., Bren, A.B. *Biosensors*, **2018**, 8(1), 25. doi: 10.3390/bios8010025.
13. Corsetti, A., Caldini, G., Mastrangelo, M., Trotta, F., Valmorri, S., Cenci, G. *International Journal of Food Microbiology*, **2008**, 125(3), 330–335. doi: 10.1016/j.ijfoodmicro.2008.04.009.
14. de Roos, N.M., Katan, M.B. *The American Journal of Clinical Nutrition*, **2000**, 71, 405–411.
15. Dinis-Oliveira, R.J., Duarte, J.A., Sánchez-Navarro, A., Remião, F., Bastos, M.L., Carvalho, F. *Critical Reviews in Toxicology*, **2008**, 38(1), 13–71.
16. Dominguez-Bello, M.G., Costello, E.K., Contreras, M., Magris, M., Hidalgo, G., Fierer, N., Knight, R. *Proceedings of the National Academy of Sciences of the United States of America*, **2010**, 107(26), 11971–11975.
17. Foulquié Moreno, M.R., Sarantinopoulos, P., Tsakalidou, E., De Vuyst, L. *International Journal of Food Microbiology*, **2006**, 106(1), 1–24.

18. Franz, C.M., Huch, M., Abriouel, H., Holzapfel, W., Gálvez, A. *International Journal of Food Microbiology*, **2011**, 151(2), 125–140.
19. Franz, C.M., Muscholl-Silberhorn, A.B., Yousif, N.M., Vancanneyt, M., Swings, J., Holzapfel, W.H. *Applied and Environmental Microbiology*, **2001**, 67(9), 4385–4389.
20. Ghosh, A., Zurek, L. Antibiotic resistance in Enterococci: a food safety perspective. In: C.-Y. Chen, X. Yan, C.R. Jackson (Eds.), *Antimicrobial resistance and food safety: methods and techniques* (pp. 155–180). Wyndmoor: Elsevier Inc., **2015**.
21. Guo, L., Li, T., Tang, Y., Yang, L., Huo, G. *Microbial Biotechnology*, **2016**, 9(6), 737–745.
22. Igonina, E.V., Marsova, M.V., Abilev, S.K. *Russian Journal of Genetics: Applied Research*, **2018**, 8(1), 87–95.
23. Joshi, S.R., Biswas, K. Enterococci prevalent in processed food products: From probiotics to food safety. In: V.C. Kalia, Y.S. Shouche, H.J. Purohit, P. Rahi (Eds.), *Mining of microbial wealth and metagenomics* (pp. 287–299). Singapore: Springer Singapore, **2017**.
24. Khan, I.T., Nadeem, M., Imran, M., Ayaz, M., Ajmal, M., Ellahi, M.Y., Khalique, A. *Lipids in Health and Disease*, **2017**, 16(1), 163.
25. Li, B., Zhan, M., Evvie, S.E., Jin, D., Zhao, L., Chowdhury, S., Sarker, S.K., Huo, G., Liu, F. *Frontiers in Microbiology*, **2018**, 9, 1943. doi: 10.3389/fmicb.2018.01943.
26. Li, P., Niu, Q., Wei, Q., Zhang, Y., Ma, X., Kim, S.W., Lin, M., Huang, R. *Scientific Reports*, **2017**, 7, 41395.
27. Liévin-Le Moal, V., Servin, A.L. *Clinical Microbiology Reviews*, **2014**, 27(2), 167–99. doi: 10.1128/CMR.00080-13.
28. Maldonado, N.C., Ficooseco, C.A., Mansilla, F.I., Melián, C., Hébert, E.M., Vignolo, G.M., Nader-Macías, M.E.F. *Livestock Science*, **2018**, 212, 99–110.
29. Manchado, M., Michán, C., Pueyo, C.J. *Journal of Bacteriology*, **2000**, 182(23), 6842–6844.
30. Manukhov, I.V.; Eroshnikov, G.E.; Vissokikh, M.Y.; Zavilgelsky, G.B. *FEBS Letters*, **1999**, 448, 265–268.
31. Marteau, P., *Clinical Nutrition*, **2001**, 20, 41–45.
32. Mekadim, C., Killer, J., Mrázek, J., Bunešová, V., Pechar, R., Hroncová, Z., Vlková, E. *Archives of Microbiology*, **2018**, 200(10), 1427–1437.
33. Mekadim, C., Killer, J., Pechar, R., Mrázek, J. *Folia Microbiologica*, **2019**, 64(1), 113–120.
34. Mellado-Ortega, E., Zabalgoceazcoa, I., Vázquez de Aldana, B.R., Arellano, J.B. *Analytical Biochemistry*, **2017**, 519, 27–29.
35. Mishra, V., Shah, C., Mokashe, N., Chavan, R., Yadav, H., Prajapati, J. *Journal of Agricultural and Food Chemistry*, **2015**, 63(14), 3615–3626. doi: 10.1021/jf506326t.
36. Molina, M.A., Díaz, A.M., Hesse, C., Ginter, W., Gentilini, M.V., Nuñez, G.G., Canellada, A.M., Sparwasser, T., Berod, L., Castro, M.S., Manghi, M.A. *PLoS One*, **2015**, 10(5), e0127262.
37. Petrut, S., Rusu, E., Tudorache, I.S., Pelinescu, D., Sarbu, I., Stoica, I., Vassu, T. *Revista de Chimie*, **2019**, 70(7), 2434–2438.
38. Pieniz, S., Andreazza, R., Anghinoni, T., Camargo, F., Brandelli, A. *Food Control*, **2014**, 37, 251–256. doi: 10.1016/j.foodcont.2013.09.055.
39. Popovic, N., Dinic, M., Tolinacki, M., Mihajlovic, S., Terzic-Vidojevic, A., Bojic, S., Djokic, J., Golic, N., Veljovic, K. *Frontiers in Microbiology*, **2018**, 9, 78.
40. Prazdnova, E.V., Chistyakov, V.A., Churilov, M.N., Mazanko, M.S., Bren, A.B., Volski, A., Chikindas, M.L. *Letters in Applied Microbiology*, **2015**, 61, 549–554.
41. Report of a joint FAO/WHO expert consultation on evaluation of health and nutritional properties of Probiotics in food including powder milk with live lactic acid bacteria (2001). *FAO Food and Nutrition paper*, **2006**, 85. <http://www.fao.org/3/a-a0512e.pdf>.
42. Ruzicka, F., Horka, M., Hola, V., Mlynarikova, K., Drab, V. *Food Analytical Methods*, **2016**, 9(12), 3251–3257.
43. Rybalchenko, O.V., Bondarenko, V.M., Orlova, O.G. *Zhurnal Mikrobiologii, Epidemiologii, i Immunobiologii*, **2014**, 4, 87–92.
44. Saez-Lara, M.J., Gomez-Llorente, C., Plaza-Diaz, J., Gil, A. *BioMed Research*

International, **2015**, 2015, 505878. doi: 10.1155/2015/505878.

45. Schaberg, D.R., Culver, D.H., Gaynes, R.P. *The American Journal of Medicine*, **1991**, 91(3B), 72S–75S.
46. Sparo, M., Delpech, G., Allende, N.G. *Frontiers in Microbiology*, **2018**, 9, 3073.
47. Sycheva, L.P., Kovalenko, M.A., Sheremet'eva, S.M., Durnev, A.D., Zhurkov, V.S. *Bulletin of Experimental Biology and Medicine*, **2004**, 138(8), 165–167.
48. Tarabees, R., Gafar, K.M., EL-Sayed, M.S., Shehata, A.A., Ahmed, M. *Probiotics and Antimicrobial Proteins*, **2019**, 11(3), 981–989.
49. Wang, H., Lee, I.S., Braun, C., Enck, P. *Journal of Neurogastroenterology and Motility*, **2016**, 22(4), 589–605. doi: 10.5056/jnm16018.
50. Wang, Y., Wu, Y., Wang, Yu., Xu, H., Mei, X., Yu, D., Wang, Y., Li, W. *Nutrients*, **2017**, 9(5), 521.
51. Zavgelsky, G.B., Kotova, V.Yu, Manukhov, I.V. *Mutation Research – Genetic Toxicology and Environmental Mutagenesis*, **2007**, 634(1–2), 172–176.
52. Zhu, H.-M., Li, L., Li, S.-Y., Yan, Q., Li, F. *Journal of Ethnopharmacology*, **2019**, 237, 182–191.

Table 1. Oxygen radical antioxidant capacity (ORAC) values of supernatants of fermented milk

Strain	ORAC value (μmol TE/100 g)
Milk (control)	1012±210
<i>E. durans</i> 61	912±56
<i>E. faecium</i> 67	1265±112
<i>E. faecium</i> 75	1252±43
<i>E. faecium</i> 81	948±108
<i>E. faecium</i> 115	1143±97
<i>E. durans</i> 6363	1024±144
<i>E. durans</i> 6379	1255±86
<i>E. durans</i> 6380	940±84
<i>E. durans</i> 6413	869±132
<i>E. durans</i> 6451	1020±208
<i>E. faecium</i> 9683	1186±44
<i>L. plantarum</i> 83	2086±163*
<i>L. acidophilus</i> 94	1668±212*
<i>L. casei</i> 100	1066±104
<i>L. rhamnosus</i> 108	1841±91*
<i>L. casei</i> 116	1465±124*
<i>L. brevis</i> 122	1112±64
<i>L. paracasei</i> 2647	1342±110*
<i>L. rhamnosus</i> RH	2145±84*

Data represent average values ± standard deviation (SD).

* $p < 0.05$ vs. control.

Table 2. Induction factor (Is) of the *E. coli* MG1655 PSoxS-lux strain with the addition of lactobacilli-fermentated milk supernatants with and without inducer (paraquat). The values of increased (↑) and decreased (↓) (Is) compared to (Is) of control are given in parentheses, %

Strain		Volume of supernatant in solution, %			
		10	1	0.1	0.01
Control	no paraquat	0			
	with paraquat	25.2			
Milk	no paraquat	1.2	-1.4	1.1	1.0
	with paraquat	18.6 (26%↓)	20.9 (17%↓)	21.4 (15%↓)	22.9 (9%↓)
L. plantarum 83	no paraquat	0.9	1.1	-0.8	1.0
	with paraquat	2.3* (91%↓)	2.8* (89%↓)	7.6* (70%↓)	14.6* (42%↓)
L. acidophilus 94	no paraquat	0.3	0.7	0.2	0.9
	with paraquat	7.6* (70%↓)	9.1* (64%↓)	13.1* (48%↓)	19.9* (31%↓)
L. casei 100	no paraquat	-0.4	0	-0.3	0.4
	with paraquat	16.9 (33%↓)	18.9 (25%↓)	20.9 (17%↓)	23.2 (8%↓)
L. rhamnosus 108	no paraquat	1.3	0.4	0.9	-0.7
	with paraquat	8.3* (67%↓)	11.6* (54%↓)	12.9* (49%↓)	18.4* (27%↓)
L. casei 116	no paraquat	0.8	0.7	-0.4	0.8
	with paraquat	11.3* (55%↓)	13.9* (45%↓)	19.2* (24%↓)	22.7* (10%↓)
L. brevis 122	no paraquat	-0.5	0.5	1.1	-0.3
	with paraquat	17.1 (32%↓)	18.2 (24%↓)	20.7 (18%↓)	23.2 (8%↓)
L. paracasei 2647	no paraquat	1.4	-0.2	0.3	1.1
	with paraquat	16.1* (36%↓)	16.9* (33%↓)	20.4 (19%↓)	23.2 (9%↓)
L. rhamnosus RH	no paraquat	0.8	0.2	0.5	1.2
	with paraquat	4.0* (84%↓)	5.8* (77%↓)	7.3* (71%↓)	22.9* (38%↓)

* $p < 0.05$ vs. paraquat + milk.

Table 3. Induction factor (Is) of the *E. coli* MG1655 PSoxS-lux strain with the addition of enterococci fermented milk supernatants, with and without inducer (paraquat). The values of increase (↑) and decrease (↓) (Is) compared to (Is) of control are given in parentheses, %

Strain	Inducer	Volume of supernatant in solution, %			
		10	1	0.1	0.01
Control	no paraquat	0			
	with paraquat	25.2			
Milk	no paraquat	1.2	-1.4	1.1	1.0
	with paraquat	18.6 (26%↓)	20.9 (17%↓)	21.4 (15%↓)	22.9 (9%↓)
<i>E. durans</i> 61	no paraquat	2.6	0.4	1.1	-0.3
	with paraquat	39.1** (55%↑)	27.3** (8%↑)	24.7 (2%↓)	23.2 (8%↓)
<i>E. faecium</i> 67	no paraquat	3.8*	1.2	0.6	0.8
	with paraquat	41.1** (63%↑)	27.7** (10%↑)	25.0 (1%↓)	22.8 (10%↓)
<i>E. faecium</i> 75	no paraquat	2.7*	0.9	-0.6	0.1
	with paraquat	31.2** (24%↑)	21.7 (14%↓)	21.4 (15%↓)	23.5 (7%↓)
<i>E. faecium</i> 81	no paraquat	3.1*	0.7	0.4	1.2
	with paraquat	35.1** (39%↑)	24.2 (4%↓)	20.7 (18%↓)	23.6 (6%↓)
<i>E. faecium</i> 115	no paraquat	3.0*	0.4	0.6	1.0
	with paraquat	38.1** (51%↑)	27.2** (8%↑)	24.0 (5%↓)	22.8 (9%↓)
<i>E. durans</i> 6363	no paraquat	2.9*	-0.7	1.1	0.3
	with paraquat	38.8** (54%↑)	28.3** (12%↑)	23.5 (7%↓)	23.1 (9%↓)
<i>E. durans</i> 6379	no paraquat	2.3	0.9	0.6	-0.3
	with paraquat	33.6** (33%↑)	21.4 (15%↓)	22.2 (12%↓)	22.5 (11%↓)
<i>E. durans</i> 6380	no paraquat	3.7*	0.2	0.8	1.2
	with paraquat	44.0** (75%↑)	29.2** (16%↑)	27.8** (10%↑)	21.6 (14%↓)
<i>E. durans</i> 6413	no paraquat	3.4*	0.7	0.8	0.9
	with paraquat	42.5** (69%↑)	29.6** (17%↑)	27.6** (10%↑)	22.1 (12%↓)
<i>E. durans</i> 6451	no paraquat	2.7*	0.6	0.6	0.9
	with paraquat	35.3 (40%↑)	22.6 (10%↓)	22.7 (10%↓)	23.4 (7%↓)
<i>E. faecium</i> 9683	no paraquat	3.2*	0.8	0.8	1.1
	with paraquat	45.5** (81%↑)	27.9** (11%↑)	22.8 (10%↓)	22.4 (11%↓)

* $p < 0.05$ vs. (Is) of milk

** $p < 0.05$ vs. (Is) of paraquat + milk

Table 4. Induction factor (Is) of the *E. coli* MG1655 pSoxS-lux strain with the addition of enterococci fermented milk supernatants with and without different inducers. The values of increase (↑) and decrease (↓) (Is) compared to (Is) of control are given in parentheses, %

Inducer	No fermented milk	Milk	<i>E. durans</i> 6380	<i>E. durans</i> 6451	<i>E. faecium</i> 9683
No inducer	0	1.0	3.5*	2.8*	3.2*
Paraquat	25.4	19.1 (24%↓)	43.2** (70%↑)	43.4** (71%↑)	44.9** (77%↑)
Hydrogen peroxide	5.4	4.8 (11%↓)	7.5** (39%↑)	8.2** (52%↑)	7.7** (43%↑)
Dioxidine	5.1	4.3 (15%↓)	9.4** (84%↑)	9.5** (86%↑)	10.0** (96%↑)

* $p < 0.05$ vs. (Is) of milk

** $p < 0.05$ vs. (Is) of inducer + milk

DETERMINAÇÃO DE INDICADORES DE ESTADO DE CITOCINA E FATORES DE ANGIOGÊNESE EM PACIENTES COM ENDOMETRIOSE GENITAL EXTERNA E DEFICIÊNCIA DE VITAMINA D**DETERMINATION OF CYTOKINE STATUS INDICATORS AND ANGIOGENESIS FACTORS IN PATIENTS WITH EXTERNAL GENITAL ENDOMETRIOSIS AND VITAMIN D DEFICIENCY****ОПРЕДЕЛЕНИЕ ПОКАЗАТЕЛЕЙ ЦИТОКИНОВОГО СТАТУСА И ФАКТОРОВ АНГИОГЕНЕЗА У ПАЦИЕНТОК С НАРУЖНЫМ ГЕНИТАЛЬНЫМ ЭНДОМЕТРИОЗОМ И ДЕФИЦИТОМ ВИТАМИНА D**AKHMEDOVA Saida R.^{1*}, OMAROV Nabi S-M.²;^{1,2} Dagestan State Medical University, Department of Obstetrics and Gynecology;

* Correspondence author

e-mail: saida.ahmedova2017@yandex.ru

Received 12 June 2019; received in revised form 30 December 2019; accepted 29 January 2020

RESUMO

O estudo foi realizado para encontrar uma associação entre alguns indicadores de status de citocinas, nível de fatores de crescimento endotelial vascular e vitamina D, em mulheres com infertilidade e endometriose genital externa (EGE), a fim de aumentar a efetividade do tratamento dessa patologia. O baixo nível de vitamina D na dinâmica foi determinado em 240 pacientes com idades entre 25 e 35 anos com EGE planejando a gravidez, determinando o nível de 25 (OH) D no soro sanguíneo pelo método quimioluminescente. O status de interleucina (IL-1 β , IL-6, IL-4), TNF- α , VEGF-R1 no soro sanguíneo foi determinado usando imunoensaio enzimático múltiplo. Os resultados dos estudos revelaram um nível aumentado de IL-6, IL-1 β e TNF- α em grupos com baixo teor de vitamina D. Na vitamina D normal, foram registrados níveis significativamente mais baixos de fator de crescimento endotelial vascular (VEGF-R1) no soro sanguíneo. As taxas de gravidez foram maiores nos grupos com níveis normais de 25 (OH) D no soro sanguíneo. O nível sérico médio de VEGF-R1 em mulheres grávidas que engravidaram sozinhas foi 1,3-1,5 vezes menor.

Palavras-chave: *endometriose genital externa, citocinas, VEGF, vitamina D.***ABSTRACT**

The study was performed to find an association between some cytokine status indicators, level of vascular endothelial growth factors, and vitamin D in women with infertility and external genital endometriosis (EGE) in order to increase the effectiveness of treatment of this pathology. The low vitamin D status in the dynamics was determined in 240 patients aged 25 to 35 years with EGE planning pregnancy by determining the level of 25 (OH) D in the blood serum using the chemiluminescent method. Interleukin status (IL-1 β , IL-6, IL-4), TNF- α , VEGF-R1 in blood serum were determined using enzyme-multiple immunoassay. The results of the studies revealed an increased level of IL-6, IL-1 β , and TNF- α in groups with low vitamin D content. In normal vitamin D significantly lower levels of vascular endothelial growth factor (VEGF-R1) in the blood serum were registered. Pregnancy rates were higher in groups with normal 25 (OH) D levels in the blood serum. The mean serum VEGF-R1 level in pregnant women who became pregnant on their own was 1.3-1.5 times lower.

Keywords: *external genital endometriosis, cytokines, VEGF, vitamin D.***АННОТАЦИЯ**

Исследованы цитокиновые показатели (IL-1 β , IL-4, IL-6, ФНО- α) и VEGF-R1 у 240 пациенток с наружным генитальным эндометриозом (НГЭ), проживающих в Республике Дагестан и планирующих беременность, с выявленным дефицитом витамина D. В результате проведенных исследований установлено повышение уровня IL-6, IL-1 β и ФНО- α в группах с низким содержанием витамина D. Низкие показатели фактора роста эндотелия сосудов (VEGF) в сыворотке крови достоверно коррелировали с

Ключевые слова: наружный генитальный эндометриоз, цитокины, фактор роста эндотелия сосудов, витамин D.

1. INTRODUCTION

Endometriosis is a multifactorial pathology that occurs in 7-17% of women, leading in 30-50% of cases to impaired reproductive function (Adamyany and Aznaurova, 2015; Yarmolinskaya and Ailamazyan, 2017; Giudice, 2010). Its pathogenesis results in the disturbance of steroid hormones, the immune imbalance caused by inflammation and / or infection, increased the peritoneal activity of vascular growth factors (Adamyany and Aznaurova, 2015; Demir *et al.*, 2010; Huang *et al.*, 2014; Laschke *et al.*, 2011; Orazov, 2015; Radzinskiy *et al.*, 2016). The anti-inflammatory, antiproliferative and immunomodulatory vitamin D effects are known, thus allowing to consider it as an effective targeted endometriosis therapy (RAoE, 2015; Almassinokiani *et al.*, 2016; Ciavattini *et al.*, 2017; Lerchbaum and Rabe, 2014; Pike and Meyer, 2012). There is evidence that the expression of a large number of genes encoding proteins involved in proliferation, differentiation, and apoptosis are regulated by vitamin D (Denisova and Yarmolinskaya, 2017; Gysemans *et al.*, 2014; Irani *et al.*, 2015; Merhi *et al.*, 2014). Studies proving vitamin D effect on the immune system (Delvin *et al.*, 2014; Gysemans *et al.*, 2014; Irani *et al.*, 2015; Orazov, 2015) suggest that correction of its deficiency positively affects the fertility of patients with external genital endometriosis (EGE) (Paffoni *et al.*, 2014).

Objective: to assess the association of cytokine status, the level of angiogenesis factors, and vitamin D status in women with infertility and EGE. An analysis of the association between immunological parameters in infertility on the background of endometriosis and vitamin D status will clarify further the understanding of the pathogenesis of the disease, predict and realize its rational prevention and treatment.

2. MATERIALS AND METHODS

A prospective comparative analysis of the results of 240 patients of reproductive age management, who had a histologically confirmed diagnosis of external genital endometriosis and infertility depending on the treatment methods

from 2016 to 2019, was made. The study was approved by the ethics committee protocol number has no conflict of interest and was performed without financial support from pharmaceutical companies.

All patients were examined and treated in the departments of operative gynecology No. 1 and No. 2 of the Republic Clinical Hospital in Makhachkala, and in the Family Planning and Reproduction Room. All patients, depending on management tactics, were divided into groups of 60 persons: group 1 - after surgical treatment (ST), but without correction of vitamin D deficiency, group 2 - ST + vitamin D, 3- group - ST + dienogest (without correction of vitamin D deficiency), 4 - ST + dienogest + vitamin D. The mean age of patients from the 1st group was 30.7 ± 0.5 years and did not statistically differ from the mean age of patients from the 2nd group (31.4 ± 1.1 years), 3rd group (28.4 ± 1.2 years) and 4th group (30.1 ± 0.7 years). Inclusion criteria were age 25-35 years, 25 (OH) D blood serum level below 30 ng/ml, surgical removal of foci of endometriosis, the patient's desire to become pregnant, written consent of women to participate in the study. Exclusion criteria were pregnancy, varicose veins, systemic autoimmune diseases, mental disorders, malignant diseases, concomitant genital and endocrine pathologies, male infertility factors.

Low vitamin D status in dynamics was revealed by determining 25 (OH) D level in blood serum 3 days after taking vitamin D preparations by chemiluminescent method using kits and calibrators from Roche Diagnostics (Germany) for Architect 2000 analyzer (USA) according to the international standardization program for the determination of vitamin D - DEQAS. Vitamin D deficiency was determined as 25 (OH) D blood serum level less than 20 ng / ml, vitamin D deficiency was revealed at 25 (OH) D $> 21 < 29$ ng / ml blood serum concentration, normal vitamin D level at 25 (OH) D blood serum concentration more than 30 ng / ml. Severe vitamin D deficiency is classified as a condition in which the concentration of 25-hydroxycalciferol in the blood is less than 10 ng / ml (RAoE, 2015). It should be noted that none of the patients included in the study had a normal vitamin D concentration D in the body during the initial examination. The interleukin status (IL-1 β , IL-6, IL-4), TNF- α ,

VEGF-R1 in the blood serum of the examined women was determined using enzyme-multiplied immunoassay using the appropriate standard reagents (Cloud-Clone Corp., China; R&D Systems Inc., USA).

Cholecalciferol dosage of was determined according to the degree of vitamin D deficiency detected during the initial examination (1300 U per 10 ng / ml), and the course dose according to the recommendations (RAoE, 2015) was 200 thousand MU for therapy of insufficiency and 400 thousand MU - vitamin D deficiency. Therapy with dienogest in a dose of 2 mg once a day was carried out continuously for 3-6 months (Adamyan and Aznaurova, 2015).

Statistical data processing was performed by Statistica v.6.0 program using Student's criterion for groups with parametric values, and Spearman's method for rank, nonparametric values for assessing the correlation. The results of the study are presented as mean \pm standard deviation ($M \pm SD$). Considering that the number of compared groups is four, a critical significance level was $p < 0.0085$.

3. RESULTS AND DISCUSSION

Vitamin D concentration level in the body during the initial examination in the 1st group was 18.2 ± 0.4 [6.7; 27.3] ng / ml, in the 2nd group - 17.6 ± 0.6 [5.2; 27.9] ng / ml, in the 3rd group - 16.1 ± 0.8 [4.6; 25.8] ng / ml and in the 4th group 17.01 ± 0.8 [5.1; 27.3] ng / ml.

Moreover, the low vitamin D status was found with equal frequency and severity in seasonality and region of permanent residence of the examined patients. Besides, there was no dependence on the vitamin D level on age and social conditions.

In this study, obese women were not included. However, overweight patients (BMI 25-29.9 kg / m²) with almost the same frequency as normal growth and weight indicators were observed. It should be noted that there were no patients with insufficient body weight (BMI <18.5 kg / m²).

The duration of infertility averaged 6.4 ± 2.8 years in the 1st group, 5.8 ± 3.1 years in the 2nd group, 6.1 ± 2.4 in the 3rd group and 6.5 ± 3.7 years in the 4th group with fluctuations from 2 to 16 years in groups. Moreover, in the examined groups, primary infertility significantly prevailed: in the 1st group - in 81.7% of cases, in the 2nd

group - in 86.7%, in the 3rd group - in 80.0% and in the 4th - in 83.3% ($p < 0.0085$). The duration of primary infertility averaged 6.9 ± 1.2 years in the 1st group, 6.3 ± 0.5 years in the 2nd group, 6.7 ± 0.7 years in the 3rd group and 6.9 ± 0.8 years in the 4th group ($p < 0.0085$), and the secondary - 3.7 ± 0.8 years in the 1st group, 4.0 ± 0.3 years in the 2nd group, 3.2 ± 0.4 in the 3rd group and 3.8 ± 0.7 years in the 4th group ($p < 0.0085$).

During surgery, unilateral salpingo-ovariolysis was performed in 33.3% of cases in the 1st group, in 48.3% in the 2nd group, in 51.7% in the 3rd group and in 38.3% in the 4th group, ($p > 0.05$); in 20.0% of patients in the 1st group, in 18.3% in the 2nd group, in 16.7% in the 3rd group and in 33.3% in 4 group 2 - bilateral salpingo-ovariolysis was made ($p < 0.05$). When ovarian cysts were detected, cystectomy within healthy tissues was performed in 100% of cases using bipolar energy. Left-sided cystectomy was performed in 13.3-26.7% of patients in the groups, right-sided - in 21.7-31.7%, respectively. Bilateral cystectomy was performed in 8.3-18.3% of patients, respectively.

Analysis of the ratio of different color heterotopies revealed that violet and red dominated in the frequency of occurrence and size in all groups. Most often, they were located in the Douglas space, much less often (in 6.7-11.7% of cases in groups ($p < 0.05$)) in the area of the vesicoureteral fold, and (in 5.0-8.3% of cases in groups ($p < 0.05$)) were dispersed along the peritoneum of the pelvis.

Therapy of low vitamin D status was effective, and it was possible to reach the level of 30 ng / ml, which is characterized as normal, within 4-8 weeks. Subsequently, maintenance therapy was carried out.

A 3 months after colecalciferol appointment in order to restore vitamin D status, indicators were compared. Blood serum content of 25 (OH) D was 17.3 ± 0.7 [6.9; 24.8] ng / ml in the 1st group, 38.6 ± 0.7 [32.7; 57.7] ng / ml in the 2nd, 17.2 ± 0.7 [5.4; 24.8] ng / ml in the 3rd group and 35.6 ± 0.5 [31.9; 61.9] ng / ml in the 4th ($p < 0.0085$). Moreover, in the 2nd group, 25-hydroxyvitamin D level over 50.0 ng / ml was observed in 41.7% of the examined, and in the 4th group - in 38.3% ($p < 0.0085$). The patients did not follow any strict or special diets.

One month after the surgical treatment, no complaints of pain were in the 2nd and 4th groups of patients. In the first and third groups, where no correction of vitamin D deficiency was performed, several patients complaints of pain in

the absence and during menstruation remained, but their intensity decreased significantly. Three months after laparoscopy, the pain syndrome recurred in 5 patients in the 1st group, in 3 patients in the 2nd and third groups, and in 2 women in the 4th group. After 6 months, the recurrence of pain syndrome was in frequency quite different in the groups. Thus, in groups that did not receive dienogest, the recurrence rate of pain was 1.6 times higher in the group without vitamin D deficiency correction. In groups (in the 3rd and 4th), where the hormonal treatment was used in complex therapy, the frequency of pain was 2.2 times more rear comparing the 3rd group with the 1st one, 1.7 times when comparing the 4th group with the 2nd group, and 2.7 times when comparing the 4th groups with the 1st group ($p < 0.0085$). After a year of observation, the maximum number of patients with pain in the 1st group increased (by $15.0 \pm 7.8\%$ compared with 6 months), in the 2nd group - by $10.0 \pm 1.7\%$, in the 3rd group - by $6.7 \pm 1.8\%$ and in the 4th group - by $5.0 \pm 0.7\%$ ($p < 0.0085$). As a result, the best indicators in pain relief were noted in the 4th group, which received combined therapy with dienogest on the background of a normal vitamin D level in the body.

In this group of patients, complaints of pain a year after surgical treatment were 2.8 times less than in the 1st group, 1.8 times less than in the 2nd group, and 1.3 times less than in the 3rd group. The intensity of pelvic pain, estimated by VAS in women with pain syndrome, corresponded to an average of 3.9 ± 0.7 points in the 1st group, 3.1 ± 0.3 points in the 2nd, 3.5 ± 0.6 points in the 3rd group and 2.8 ± 0.4 points in the 4th group and was 1.3 times weaker in groups with normal vitamin D levels. Thus, the correction of vitamin D status positively affects pain syndrome treatment, as well as dienogest appointment in the postoperative period, however, the effectiveness of complex interaction is evident.

Complaints of spotting before and after menstruation disappeared in all patients after surgical treatment, but 12 months later these symptoms recurred in 25.0% of women of the 1st group, 13.3% of women of the 2nd group, 11.7% of patients of the 3 group and 6.7% of the 4th group ($p < 0.0085$).

One month after the treatment and diagnostic laparoscopy, menstrual irregularities were observed in 3 patients in the 1st group and 2 in the 2nd group. After 3 months, the frequency of complaints of menstrual dysfunction in these groups increased to 8.3% in the 1st group and

remained at the same level of 3.3% in the 2nd group ($p = 0.04$). After complex therapy, during 6 months this complication occurred in all patients - in 10.0% of cases in the 1st group, in 6.7% in the second group, in 3.3% in the 3rd group and in 1, 7% in the 4th group ($p < 0.0085$).

The year of observation yielded the following results - vitamin D administration allowed to reduce the frequency of menstrual dysfunction by 1.6 times in cases where no hormone therapy was carried out, and by 1.7 times when the restoration and monitoring of vitamin D status was accompanied by dienogest intake of. A low vitamin D level and lack of hormonal correction resulted in this indicator decrease by 4 times when comparing the 1st and 4th groups.

After therapeutic measures aimed at restoring an adequate vitamin D level, some indicators of cytokine status were performed, which showed that IL-6, IL-1 β and TNF- α concentration in the groups with a normal vitamin D level was lower compared with group 1 and 3, where vitamin D status was not corrected, their higher level was registered in the group with only surgical treatment. The level of pro-inflammatory IL-4 was higher in the groups in which the normal vitamin D status was restored, however, the difference between the groups was not as pronounced as when comparing other interleukins in groups. IL-4 blocks the stimulated and spontaneous production of other pro-inflammatory cytokines (IL-1 β , IL-6, TNF- α), but its activity in these studies was not very pronounced. Probably, the high IL-6 level in the 1st group is compensatory and could indicate antitumor processes activation on the background of increased inflammatory processes and restoration of neoangiogenesis (Radzinskiy *et al.*, 2016), confirmed by high VEGF-R1 level of. The lowest VEGF-R1 level was observed in the group of women receiving the correction of vitamin D deficiency together with hormone therapy. However, the assessment of the plasma level of the vascular endothelial factor was ambiguous. In general, it was found that cytokine status indicators significantly differed in groups depending on the saturation of the body with vitamin D.

Pregnancy rates varied markedly in groups. In the first group, the fact of spontaneous pregnancy was recorded in 21.7% (13) of the observations, in the second - in 35.0% (21) of the patient, in the third - in 48.3% (29) and in 4th - 51.7% (31). At the same time, the frequency of undeveloped pregnancy in the groups, in general,

was higher in 13.3% (8) in the 1st group and in the 2nd group - 10.0% (6), and much less frequently in the 3rd group 6.7 % (4) and in the 4th group - 5.0% (2) ($p = 0.94$). Repeated determination of VEGF-R1 level in these patients showed a sharp increase by 1.3-2.1 times at the time of pregnancy termination. Thus, in the 1st group it was 257.4 ± 21.4 ng / ml, in the 2nd group - 203.2 ± 14.2 ng / ml, in the 3rd group - 246.4 ± 17.7 ng / ml and in the 4th group - 221.4 ± 19.2 ng / ml ($p < 0.0085$). According to Cöl-Madendag *et al.* (2014), early abortion at the early sate of pregnancy termination is a result of a disturbance in the interaction of VEGF with its receptors in the mother-fetus system (VEGFR1 and VEGFR2): a significant decrease in receptor expression occurs (Volkova and Alyautdina, 2011).

Mean VEGF-R1 level in the blood serum of spontaneously pregnant women was 1.3-1.5 times lower than in the groups in general and amounted to 134.9 ± 35.5 ng / ml in the 1st group and 94.7 ± 11.9 ng / ml in the 2nd group, 114.4 ± 25.9 ng / ml in the 3 group and 95.1 ± 15.5 ng / ml in the 4 group, which significantly correlated with the pregnancy rate in groups ($r_1 = - 0.45$; $r_2 = - 0.55$; $r_3 = - 0.48$; $r_4 = - 0.41$; $p 0.40.0085$). The IVF procedure was completed in 28.3% of the patients in the 1st group, 25.0% in the 2nd group, 21.7% in the 3rd group, and 21.7% in the 4th group. As a result of IVF, pregnancy occurred in 8.3% in the 1st group, 8.3% in the 2nd group, 10.0% in the 3rd group, and 11.7% in the 4th group. It was found that in women who became pregnant as a result of IVF, the level of the vascular endothelial factor was 1.2 - 1.7 times higher and amounted to 227.1 ± 13.4 ng / ml, 215.3 ± 32.3 ng / ml, 228.5 ± 27 , 175.4 ± 38.1 ng / ml in groups, respectively.

The observed total vitamin D deficiency in women with EGE is consistent with the results of studies by other authors. For example, a prospective cohort study in the USA that included 70,566 patients showed that there is an inverse correlation between 25 (OH) D level and the incidence of endometriosis. In women with normal vitamin D levels (located in the upper quartile), the incidence of endometriosis was 25% lower than in those in whom the vitamin D plasma level was within the lower quartile (RR = 0.76; 95% CI: 0.60- 0.96; $p = 0.004$) (Merhi *et al.*, 2014). The absence of difference in vitamin D saturation of the body of the examined women by seasons is most likely due to the fact that the study was performed in a region without marked fluctuation in the length of day and night in

seasons, which can be observed in more northern regions, the number of sunny days does not depend on the time of the year, and there are also cultural characteristics of nutrition, with prevalence of flour foods, and wearing clothes covering most of the body, including the head.

Modern ideas on endometriosis pathogenesis of show that this disease meets all the criteria for autoimmune diseases, because inflammation is observed on the background of impaired immune regulation. Studies by C.A. Gysemans *et al.* (2014) prove the anti-inflammatory, antiproliferative, and immunomodulatory features of vitamin D the effect on the body by affecting the synthesis of certain pro-inflammatory cytokines, preventing transcription of a number of their genes (Gysemans *et al.*, 2014). IL-6, IL-1 β , and TNF- α activation, registered in our study in women with vitamin D lack or deficiency, shows systemic inflammation leading to changes in the peritoneal fluid, which, in turn, affects the quality and activity of sperm , slows down the acrosomal interaction and association of sperm with oocyte, decreased fertility (Delvin *et al.*, 2014; Gysemans *et al.*, 2014; Irani *et al.*, 2015; Orazov, 2015; Paffoni *et al.*, 2014). Normalization of vitamin D status leads to changes in the cytokine ratio, which is confirmed by epy increases number of pregnancies in the examined groups by 1.6 times only with the correction of vitamin D deficiency and 2.4 times with correction of insufficiency on the background of hormonal treatment with dienogest.

Modern literature indicates the special role of neovascularization in endometriosis pathogenesis (Radzinskiy *et al.*, 2016). The processes of significant neovascularization and neurogenesis activation in ectopic foci in external genital endometriosis were revealed. Already in the early stage of endometrioid heterotopia, an increased density of blood vessels, widening of their lumen, and increase in the number of "immature vessels" are observed (Burlev, 2016; Huang *et al.*, 2014). The main trigger factor for angiogenesis and vasculogenesis in physiological conditions and pathology is the vascular endothelial growth factor. Besides, VEGF as a strong factor in vascular permeability and leukocyte mobilization is involved in the development of the inflammatory process (Cöl-Madendag *et al.*, 2014; Demir *et al.*, 2010; Laschke *et al.*, 2011; Radzinskiy *et al.*, 2016). The decreased parameters of vascular endothelial growth factor in the groups with normal vitamin D levels and the inverse

relationship between the moderate rate of pregnancy and VEGF level in the blood can confirm the effectiveness of the indirect vitamin D effect on neovascularization processes. However, the literature data is ambiguous. Thus, in non-pregnant patients with tubal-peritoneal infertility factor, a 1.5-fold increase in serum VEGF in comparison with women who have positive ECF treatment results (Gerilovich *et al.*, 2013). In our study, in women who became pregnant as a result of ECF, the level of the vascular endothelial factor was 1.2 - 1.7 times higher. Such multidirectional parameters may indicate that in infertility on the background of endometriosis, pregnancy can only occur on the background of pronounced stimulation of angiogenesis.

4. CONCLUSIONS

The data obtained show that correction of vitamin D insufficiency on the background of dienogest therapy allows increasing efficiency of EGE symptom treatment and favors impregnation.

In vitamin D status correction in women with EGE and infertility, the best indicators of immune (cytokine) status were noted. IL-6, IL-1 β and TNF- α high level in groups with a low vitamin D content indicates a high immune tension in the body, which negatively affects impregnation.

The deficiency of vitamin D correction is accompanied by the increased the number of pregnancies in the examined groups by 1.6 times only with the correction of vitamin D deficiency and 2.4 times with the correction of insufficiency on the background of hormonal treatment with dienogest.

A significantly moderate inverse correlative relationship was found between VEGF-R1 serum level and the probability of pregnancy in women with EGE after surgical treatment (from -0.41 to -0.55).

Thus, the obtained data indicate the need for further study, the generalization of data on vitamin D role in the pathogenesis of external genital endometriosis, infertility associated with it, and its therapeutic effects.

5. REFERENCES

1. Adamyan, L. V., Aznaurova, Ya. B. Molecular aspects of endometriosis

- pathogenesis. *Problems of reproduction*, **2015**, 2, 66–77.
2. Almassinokiani, F., Khodaverdi, S., Solaymani-Dodaran, M., Akbari, P., Pazouki, A. Effects of vitamin D on endometriosis-related pain: a double-blind clinical trial. *Med Sci Monit*, **2016**, 22, 4960–4966.
3. Burlev, V. A. Proliferative and angiogenic activity of endometrioid ovarian cysts. *Problems of reproduction*, **2016**, 3, 91–100.
4. Ciavattini, A., Serri, M., DelliCarpini, G., Morini, S., Clemente, N. Ovarian endometriosis, and vitamin D serum levels. *Gynecol Endocrinol.*, **2017**, 33(2), 164–167.
5. RAoE (Russian Association of Endocrinologists). Clinical recommendations "Vitamin D deficiency in adults: diagnosis, treatment, and prevention". Moscow: Russian Association of Endocrinologists Publ, **2015**.
6. Cöl-Madendag, I., Madendag, Y., Altinkaya, S. Ö., Bayramoglu, H., Danisman, N. The role of VEGF and its receptors in the etiology of early pregnancy loss. *Gynecol. Endocrinol.*, **2014**, 30(2), 153–156.
7. Delvin, E., Souberbielle, J. C., Viard, J. P., Salle, B. Role of vitamin D in acquired immune and autoimmune diseases. *Crit Rev Clin Lab Sci.*, **2014**, 51, 232–247.
8. Demir, R., Yaba, A., Huppertz, B. Vasculogenesis and angiogenesis in the endometrium during menstrual cycle and implantation. *Acta Histochem.*, **2010**, 112, 203–214. DOI: 10.1016/j.acthis.2009.04.04.004.
9. Denisova, A. S., Yarmolinskaya, M. I. Vitamin D role in genital endometriosis pathogenesis. *Journal of Obstetrics and Women's Diseases*, **2017**, 66(6), 81–88.
10. Gerilovich, L. A., Salmina A. B., Egorova A. T., Bazina M. I., Morgun A. V., Syromiatnikova S. A. The role of angiogenesis markers in patients with various forms of infertility in reproductive technology programs. *Problems of Reproduction*, **2013**, 5, 60–63.
11. Giudice, L. C. Clinical practice. Endometriosis. *N. Engl. J. Med.*, **2010**, 362(25), 2389–2398. doi: 10.1056/NEJMcp1000274.
12. Gysemans, C. A., Cardozo, A. K., Callewaert, H., Giulietti, A., Hulshagen, L., Bouillon, R., Eizirik, D. L., Mathieu, C. 1,25-Dihydroxyvitamin D3 modulates the expression of chemokines and cytokines in pancreatic islets: implications for prevention

- of diabetes in nonobese diabetic mice. *Endocrinology*, **2014**, *146*(4), 1956–1964. DOI: 10.1210/en.2004-1322
13. Huang, T. S., Chen, Y. J., Chou, T. Y., Chen, C. Y., Li, H. Y., Huang, B. S., Tsai, H. W., Lan, H. Y., Chang, C. H., Twu, N. F., Yen, M. S., Wang, P. H., Chao, K. C., Lee, C. C., Yang, M. H. Oestrogen-induced angiogenesis promotes adenomyosis by activating the Slug-VEGF axis in endometrial epithelial cells. *J. Cell. Mol. Med.*, **2014**, *18*(7), 1358–1371. DOI: 10.1111/jcmm.12300
 14. Irani, M., Seifer, D. B., Grazi, R. V., Julka, N., Bhatt, D., Kalgi, B., Irani, S., Tal, O., Lambert-Messerlian, G., Tal, R. Vitamin D supplementation decreases TGF- β 1 bioavailability in PCOS: a randomized placebo-controlled trial. *J Clin Endocrinol Metab.*, **2015**, *100*(11), 4307–4314. DOI: 10.1210/jc.2015-2580.
 15. Laschke, M. W., Giebels, C., Menger, M. D. Vasculogenesis: a new piece of the endometriosis puzzle. *Hum. Reprod.*, **2011**, *17*(5), 628–636. DOI: 10.1093/humupd/dmr023.
 16. Lerchbaum, E., Rabe, T. Vitamin D, and female fertility. *Curr Opin Obstet Gynecol.*, **2014**, *26*, 145–150
 17. Merhi, Z., Doswell, A., Krebs, K., Cipolla, M. Vitamin D alters genes involved in follicular development and steroidogenesis in human cumulus granulosa cells. *J Clin Endocrinol Metab.*, **2014**, *99*(6), 1137–1145.
 18. Orazov, M. R. To the question of some serologic markers in pelvic pain caused by adenomyosis. *Moskovskij khirurgicheskij journal*, **2015**, *2*, 31–33.
 19. Paffoni, A., Ferrari, S., Viganò, P., Pagliardini, L., Papaleo, E., Candiani, M., Tirelli, A., Fedele, L., Somigliana, E. Vitamin D deficiency, and infertility: insights from in vitro fertilization cycles. *J Clin Endocrinol Metab.*, **2014**, *99*, 2372–2376. DOI: 10.1210/jc.2014-1802
 20. Pike, J. W., Meyer, M. B. The vitamin D receptor: new paradigms for the regulation of gene expression by 1,25-dihydroxyvitamin D3. *Rheum Dis Clin North Am.*, **2012**, *38*, 13–27. <https://doi.org/10.1016/j.ecl.2010.02.007>
 21. Radzinskiy, V. E., Orazov, M. R., Nosenko, E. N. Expression of vascular endothelial growth factor (VEGF) in uterine tissues as one of the mechanisms of algogenesis in adenomyosis, associated with chronic pelvic pain. *Patologicheskaya fiziologiya i eksperimentalnaya terapiya*, **2016**, *1*, 32–35.
 22. Volkova, L. V., Alyautdina, O. S. Clinical and diagnostic value of vascular endothelial growth factor in unsuccessful ECF attempts. *Obstetrics and Gynecology*, **2011**, *4*, 126–129.
 23. Yarmolinskaya, M. I., Ailamazyan, E. K. Genital endometriosis. Different aspects of the problem. St. Petersburg: Eco-Vector, **2017**.

Table 1. The cytokine composition in the blood serum of patients with EGE in groups with and without vitamin D deficiency

Parameter	Group 1	Group 2	Group 3	Group 4
IL-1 β , pg/ml	15.94 \pm 2.41	8.27 \pm 2.75	11,82 \pm 1.24	6.36 \pm 1.87
Significance of differences	p1-2=0.0041	p2-4=0.0076	p3-4=0.0061	p1-4=0.0015
IL-6, pg/ml	7.51 \pm 2.18	4.17 \pm 2.74	5.93 \pm 2.27	4,35 \pm 1,71
Significance of differences	p1-2=0.0001	p2-4=0.0087	p3-4=0.0035	p1-4=0.0019
TNF- α , pg/ml	15.49 \pm 2.73	9.23 \pm 3.51	11.01 \pm 3.68	7.75 \pm 2.79
Significance of differences	p1-2=0.0052	p2-4=0.0071	p3-4=0.0078	p1-4=0.0024
IL-4, pg/ml	14.35 \pm 4.17	18.73 \pm 5.77	13.48 \pm 4.83	17.87 \pm 4.92
Significance of differences	p1-2=0.0075	p2-4=0.0094	p3-4=0.0043	p1-4=0.0076
VEGF-R1, ng/ml	198.1 \pm 72.1	127.2 \pm 69.1	176.3 \pm 74.7	103.4 \pm 61.2
Significance of differences	p1-2=0.0055	p2-4=0.0074	p3-4=0.0028	p1-4=0.0021

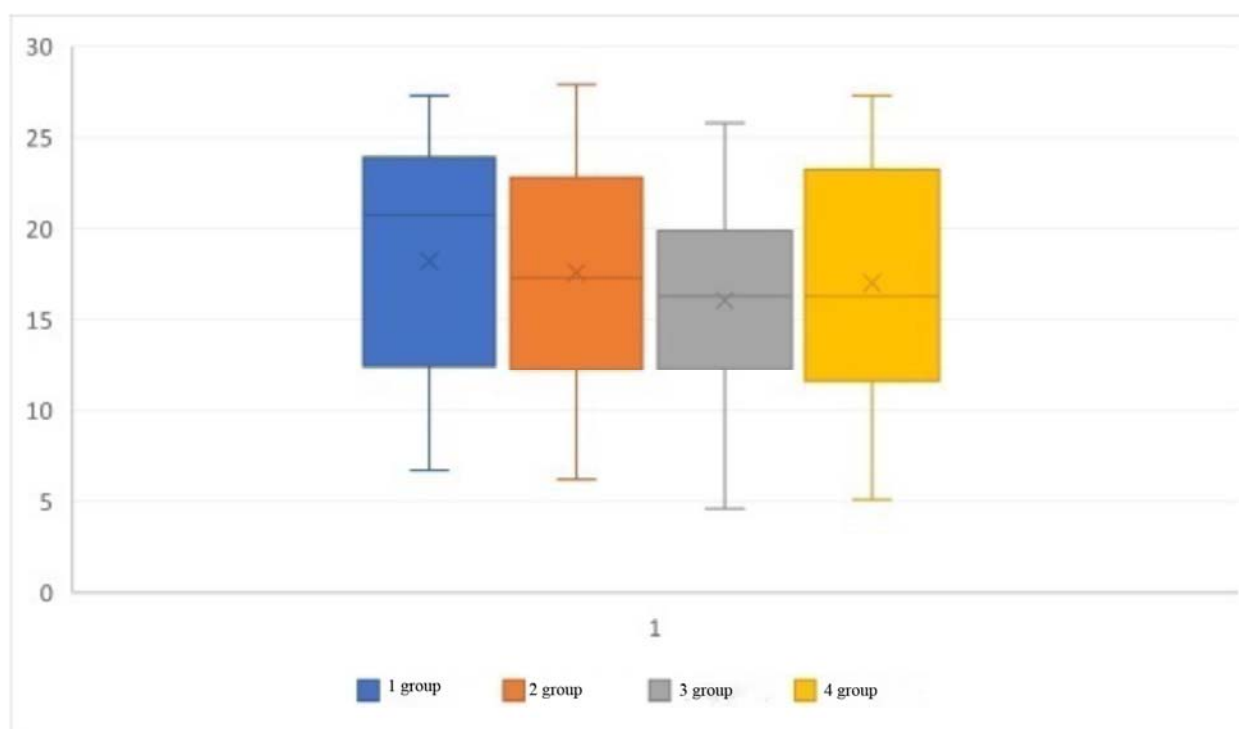


Figure 1. The level of concentration of vitamin D in the examined groups during the initial examination (ng / ml)

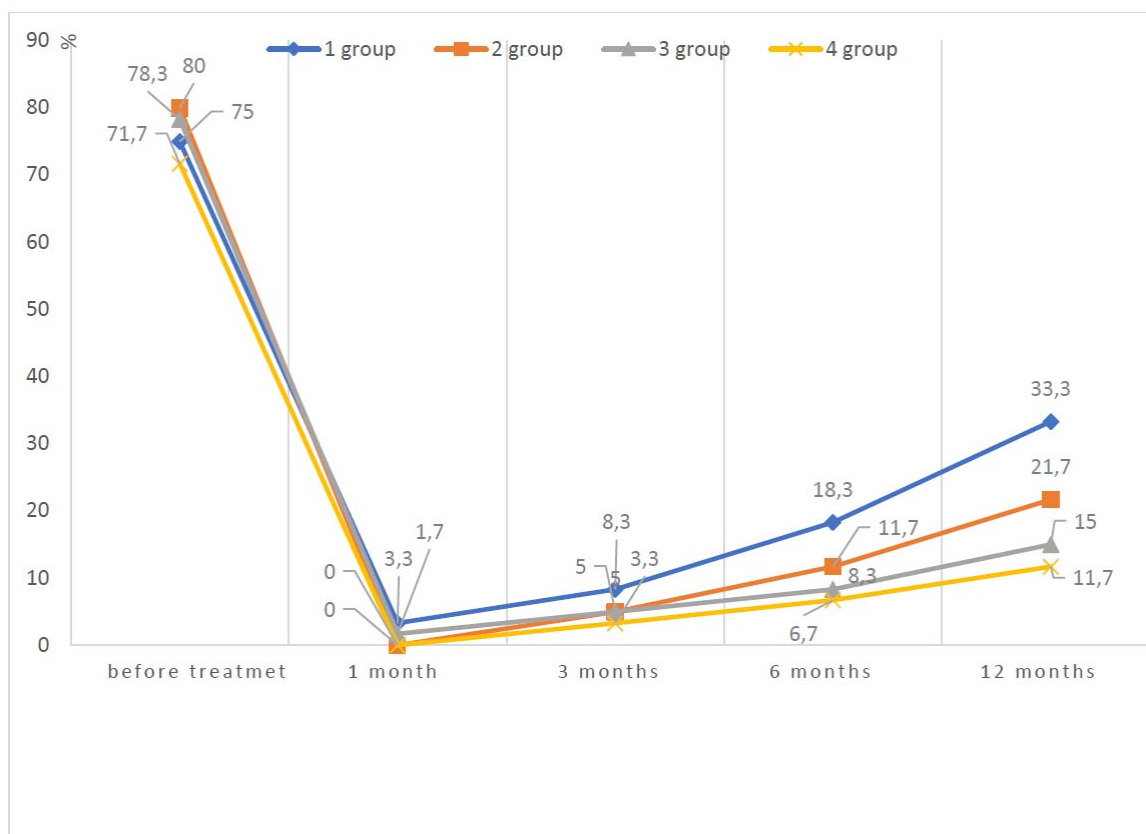


Figure 2. Pain syndrome dynamics in the examined patients depending on the treatment methods during one year after surgery.

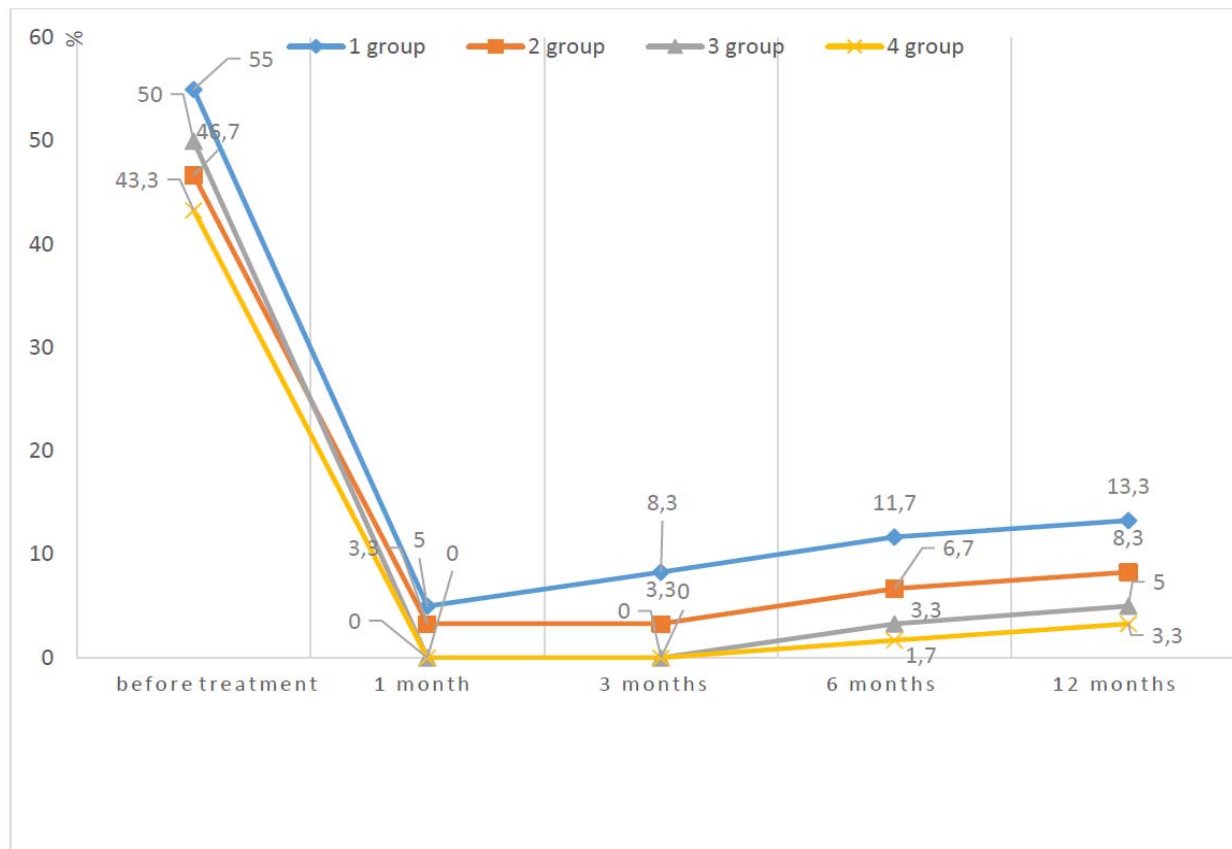


Figure 3. Dynamics of menstrual cycle disturbance in the examined patients depending on treatment methods during one year after surgery

FORMAÇÃO DA ATITUDE BASEADA NOS VALORES DOS ALUNOS EM RELAÇÃO À FUTURA PROFISSÃO DOCENTE COMO BASE MORAL DA ÉTICA PEDAGÓGICA**FORMATION OF STUDENTS' VALUES-BASED ATTITUDE TO THE FUTURE TEACHING PROFESSION AS MORAL BASIS OF PEDAGOGICAL ETHICS****ФОРМИРОВАНИЕ ЦЕННОСТНОГО ОТНОШЕНИЯ СТУДЕНТОВ К БУДУЩЕЙ ПРОФЕССИИ УЧИТЕЛЯ КАК МОРАЛЬНОЙ ОСНОВЕ ПЕДАГОГИЧЕСКОЙ ЭТИКИ**

OREKHOVA, Yelena Yurievna¹; GREBENKINA, Lidia Konstantinovna²; ZHOKINA, Nadezhda Alekseevna³; KUSHNYR, Liubov Aleksandrovna⁴; SAMOTAEV, Pavel Igorevich⁵

¹Department of Foreign Languages, Surgut State University, Surgut, Russia

²Department of Pedagogics and Management in Education, Ryazan State University named for S.A. Yesenin, Ryazan, Russia

³Department of Pedagogics and Management in Education, Ryazan State University named for S.A. Yesenin, Ryazan, Russia

⁴Department of Foreign Languages, Surgut State University, Surgut, Russia

⁵ Department of Physical Education and Health, Ryazan State Medical University named after I.P. Pavlov, Ryazan, Russia

* Corresponding author
e-mail: elena8778@mail.ru

Received 13 November 2019; received in revised form 04 February 2020; accepted 14 March 2020

RESUMO

O artigo é dedicado ao estudo do problema da formação da atitude baseada em valores dos estudantes modernos em relação à futura profissão. A ética pedagógica é a base teórica, metodológica e moral da formação dos valores humanísticos dos futuros professores que são considerados diretrizes "eternas" na formação profissional e na atividade pedagógica. A urgência do problema é justificada pelos requisitos modernos de educação profissional que visam melhorar as qualidades individuais de uma pessoa para formar seu pensamento inovador e autoconsciência moral. O objetivo do estudo foi considerar a praticabilidade de incluir a disciplina "Ética Pedagógica" no currículo do programa de treinamento "Educação Pedagógica" como um dos componentes importantes que criam uma base moral para dominar o sistema de valores profissionais humanísticos e entrar na comunidade profissional. As características do desenvolvimento da orientação humanística da personalidade dos alunos e a estrutura de sua esfera de valores são descritas e as conexões entre vários tipos de valores, orientação geral, componente criativo e auto-estima são reveladas. Os métodos de humanização da formação da personalidade dos jovens estudantes são propostos no quadro do sistema educacional moderno e das realidades sociais. Os resultados diagnósticos dos estudantes modernos apresentados no artigo permitem propor uma série de tarefas inovadoras de treinamento e educação profissional na universidade. Em particular, a formação de competências profissionais entre os alunos está associada à necessidade de dominar os valores humanísticos tradicionais, que muitas vezes não coincidem com as características pessoais modernas dos futuros professores. O desenvolvimento de valores, o conhecimento do mundo e a formação da própria imagem com base na cultura da sociedade estão se tornando componentes importantes da educação moderna e da auto-educação profissional.

Palavras-chave: *filosofia da educação, ética pedagógica, valores da educação profissional, orientações baseadas em valores.*

ABSTRACT

The article is devoted to the study of the problem of the formation of the values-based attitude of modern students to the future profession. Pedagogical ethics is the theoretical, methodological, and moral basis for the creation of prospective teachers' humanistic values, which are considered "eternal" guidelines in vocational

training and pedagogical activity. The urgency of the problem is justified by the modern requirements for professional education, which is aimed to improve a person's individual qualities to form his innovative thinking and moral self-awareness. The purpose of the study was to consider the practicability of including the discipline "Pedagogical Ethics" in the curriculum of the training program "Pedagogical Education" as one of the essential components that create a moral basis for mastering the system of humanistic professional values and entering the professional community. The features of the development of the humanistic orientation of students' personality and the structure of their value sphere are described and the connections between various types of values, general orientation, creative component and self-esteem are revealed. The methods of humanization of the formation of young students' personalities are proposed in the framework of the modern education system and social realities. The diagnostic results of advanced students presented in the paper make it possible to put forward a number of innovative tasks of vocational training and education at the university. In particular, the formation of professional competencies among students is associated with the need to master traditional humanistic values, which often do not coincide with the modern personal characteristics of future teachers. The development of values, the knowledge of the world and the formation of one's image based on the culture of the society are becoming essential components of modern education and professional self-education.

Keywords: *philosophy of education, pedagogical ethics, values of professional education, values-based orientations.*

АННОТАЦИЯ

Статья посвящена исследованию проблемы формирования ценностного отношения к будущей профессии у современных студентов. Педагогическая этика является теоретической, методологической и моральной основой формирования гуманистических ценностей будущих учителей, которые считаются «вечными» ориентирами в профессиональной подготовке и педагогической деятельности. Актуальность проблемы обоснована современными требованиями к профессиональному образованию, которое направлено на повышение индивидуальных качеств человека, формирование его инновационного мышления и нравственного самосознания. Цель исследования - рассмотреть возможность включения дисциплины «Педагогическая этика» в учебный план направления подготовки "Педагогическое образование" как одного из важных компонентов, создающих нравственную основу освоения системы гуманистических профессиональных ценностей, вхождения в профессиональное сообщество. Авторы раскрывают особенности развития гуманистической направленности личности студентов и структуру их ценностной сферы. Выявлены связи между различными видами ценностей, общей направленностью, творческой составляющей и самооценкой. Предлагаются способы гуманизации формирования личности студенческой молодежи в рамках современной системы образования и социальных реалий. Представленные в статье результаты диагностики современных студентов позволяют выдвинуть ряд инновационных задач профессионального обучения и воспитания в вузе. В частности, формирование у студентов профессиональных компетенций связано с необходимостью освоения традиционных гуманистических ценностей, что зачастую не совпадает с современными личностными свойствами будущих педагогов. Освоение ценностей, познание окружающего мира и формирование собственного образа на основе культуры общества становятся важными компонентами современного образования и профессионального самообразования.

Ключевые слова: *философия образования, педагогическая этика, ценности профессионального образования, ценностные ориентации*

1. INTRODUCTION:

New conditions for the formation of future teachers are characterized by a high intensity of sociocultural processes, which, of course, leads to a change in the values of society, affects both the development of pedagogical science as a whole and the content of teacher education. Meanwhile, the basis for the development of any profession is the adoption of precisely those moral standards that determine the attitude to professional activity, a person's place in it, understanding and fulfillment of professional duty based on spiritual and moral self-improvement. That is why, as never before,

the most important goal of modern university education is self-education, moral self-education, and self-development of the personality of the future teacher. Consequently, the preparation of a future teacher for professional activities at a university should be aimed not only at improving the quality of education, when knowledge, skills become absolute value, and, first of all, at enhancing an individual's personal qualities, the formation of his innovative thinking, and moral self-awareness of future teachers (Pasternak, 2008).

Modern researchers conclude that the urgent problem of university education is the creation of conditions for solving the issues of

ethical training of future professionals (Greibenkina *et al.*, 2016). This study aimed to formulate concerning the modern requirements for preparing a future teacher, consider the conditions and features of including "Pedagogical Ethics" in the curriculum as one of the essential disciplines that create the basis for mastering the system of professionalism values and entering the professional community.

The concept "value" was introduced into scientific terminology by the German philosopher I. Kant in the eighteenth century. In his work "Critique of Practical Reason" (1788), he considers value as a goal, as a meaning, as an ideal to strive for: "The knowledge of value, their mental perception and experience are based on fundamental feelings, primarily such as feelings of Love, and striving for Good, Truth and Beauty." He formulated the universal moral principle of humanistic education (the principle of freedom) and defined the humanity of relations as a sense of good and communication between a teacher and a student in the educational process (Kant, 1965).

The Austrian philosopher, psychologist W. Frankl (XX century) argued that values act as conceptual universals, playing the role of the meanings of human life. These include values of creativity, values of experience, values of attitude (New values of education, 1995: 109, 110). American psychologist A. Maslow (XX century), the founder of humanistic psychology, created a system of values and needs. Human uniqueness he considered to be the principal value of an individual's personality (New values of education, 1995).

Representatives of sociological science were also actively involved in the development of value problems, having made the most critical conclusion about social values. They believed that social values being interpreted through the prism of individual life activity, become personal values and a source of motivation for behavior. So, M. Weber thought that values are not only the motive of a human act but also are the fundamental norms of all types of actions. Values form beliefs expressed in specific commandments or requirements, according to which a person creates his life, follows his duty (Kravchenko, 2001). Of course, this conclusion is important for the study of the features of vocational education.

In the '80s of the twentieth century, pedagogical axiology began to develop as an independent branch in the national philosophy of education, as a philosophical doctrine of values.

Russian philosophers, teachers, and psychologists (L.A. Belyaeva, V.I. Zagvyazinsky, A.I. Kochetov, N.B. Krylova, V.A. Slastenin, G.I. Chizhikova, and others) comprehensively considered the idea of value and its development, value priorities for the modernization of Russian education, justified the need and the path to the transition to a value educational paradigm. V.A. In the textbook for students of higher educational institutions, "Introduction to Pedagogical Axiology," Slastenin and G. I. Chizhikova examined the substantive and functional components of pedagogical axiology as an interdisciplinary field of psychological and pedagogical knowledge. They show the values-based priorities of the modernization of Russian education, give proof of the need and consider the ways of moving from the authoritarian to the humanistic educational paradigm (Slastenin *et al.*, 2003).

In the '90s of the XXth century and at the beginning of the XXIst, the Institute of Pedagogical Innovations of the Russian Academy of Education published the scientific series "New values of education" ("Thesaurus-95"; "Thesaurus-2005"), devoted to the problems of philosophy of education. It included many issues briefly characterizing the philosophical doctrine of values, the content of which contains the general idea of an axiological approach to modern culture.

The first issue of "The Thesaurus for Teachers and School Psychologists" provides a brief description of the key concepts of the axiology of modern education, personality-oriented pedagogy, and psychology, didactics, and design theory of innovative educational systems. It reveals new meanings of educational activities in different countries. The second issue describes the new approaches (subjective, communicative, cultural, problematic) to the analysis of the content of humanistic education based on the goals of personality-oriented pedagogy. The third and fourth issues are characterized by various concepts of modernization of modern education; new ideas of pedagogy, psychology, and philosophy of education, problems of the interaction of the environment, education and development of children and adolescents, interconnections of communities and education are noted, foreign practical experience of different countries of Europe and the USA is widely represented.

In Thesaurus 2005, tasks are formulated, and the characteristic of the new situation in the development of education is described, in particular, new ideas of values-based education,

purposes of humanization and individualization of educational processes, cultural values and cultural-like methods of education and training are described, interest in the development of the socio-cultural space of the school is noted.

Currently, many scientists in their pedagogical studies show constant interest in the problem of the formation of values-based orientations of a person, values-based attitude to the teaching profession. The need to solve this problem of higher education is indicated by many teachers and psychologists, researchers and practitioners, founders of scientific schools (V.I. Andreev, E.I. Artamonova, M.A. Galaguzova, A.I. Kochetov, N.B. Krylova and many others). In particular, their conceptual ideas of updating the higher education system, training future specialists based on universal values, are presented in modern educational concepts, education programs, and vocational training.

Integrated psychological and pedagogical knowledge on the reorientation of the interaction of subjects of training and education towards innovative professional activities, subject-subject relationships in modern society, and the development of innovative educational technologies are of particular importance. A well-known teacher, A.I. Kochetov wrote that three "pillars" will be the foundation of pedagogy of the future: self-knowledge, creativity, and self-improvement, he also emphasized that "education as creativity, self-knowledge as self-study in the process of exploring life itself" will be created" (Kochetov, 1996).

A detailed analysis of the conceptual ideas of scientists and teachers on the problem under study is presented in the theoretical part of our research.

Thus, the formation of students' values-based attitude to the future teaching profession is the basis of professional education. This study aimed to consider the features of the introduction of the discipline "Pedagogical Ethics" in the curriculum as one of the essential subjects that create a moral basis for mastering the system of professional values and entering the professional community.

2. MATERIALS AND METHODS:

In determining the methodological base of the study, the authors relied on the philosophy of education, which focuses on the study of the most significant objects such as the problems of the essence and content of education, training and

upbringing in their interconnection, as well as the issue of man as a subject of pedagogical activity. An equally crucial methodological problem under current conditions is the refinement and concretization of the conceptual apparatus for further developing of pedagogical theory, updating the content and improving the quality of professional education.

The subject of this research is the formation of professional values of the future teacher in the system of pedagogical ethics (moral standards of human behavior, individual's attitude to his profession). When organizing a holistic pedagogical process at a university (training and education of bachelors) to form values-based orientations and treat the pedagogical job as values, the authors relied on a combination of the following methodological approaches: axiological, humanistic, cultural, competent, communicative, personality-oriented, systemic active, professionally-oriented, creative, technological, integrative. All of them are interconnected and, altogether, provide a professionally oriented, cultural-like, moral, and communicative-integrative orientation of the process of forming value-based adjustments. Consider the substantive aspects of these approaches.

The importance of the axiological (value) approach is very significant as it provides support for the philosophical doctrine of the nature of benefits, their place in reality and the structure of the value world, i.e., about the relationship of various values among themselves, their dependence on social and cultural factors and an individual's structure. The axiological approach in the study includes orienting the teacher to universal, national and professional values, a values-based orientation in pedagogical activity. Considering education as a multi-aspect value, scientists distinguish its universal, state, social and personal values. When solving a scientific problem, the following principles were used as a whole: humanization, creativity, unity of theory and practice, integration, continuity (Ravkin, 1995). The conceptual apparatus presented in the Federal Law "On Education in the Russian Federation" (Federal Law "On Education in the Russian Federation" 2012) and the updated requirements of the Federal State Standard for Higher Education of a New Generation for the Training of Future Teachers were also taken into consideration.

For example, the principle of humanization requires orientation on humanism as the worldview and moral basis for the formation and development of the personality of the teacher and

his students. Humanism, as a quality and ideological principle of personality, is the theoretical basis of the category of "humanitarian," meaning human individuality, its spirituality, upbringing, and education. Humanistic pedagogy aims to educate a free, creative person who can live and create in a democratic society. A personality-oriented approach in vocational education provides the creation of humanistic conditions aimed at developing a competent person, the organization of educational interaction between a teacher and a student when a student is considered as a universal human value and everyone is capable of self-education, self-development, self-determination, the formation of creative abilities.

No less important and relevant is the principle of cultural conformity, proclaimed by Disterweg in the XIX century, which became the basis of the culturological approach. The essence of the policy of cultural compliance lies in the fact that education meets the needs of the times, human development and the degree of culture the people are at. The culturological approach involves introducing the personality of the teacher into universal learning, the teacher's self-realization in culture and the development of his own social and professional position on this basis. In turn, the teacher's culture is a means and condition of the pedagogical activity, the foundation of educational mastery. The theory of the culturological approach, developed by V.A. Slastenin and his scientific school (XXI century), is used in the given study to determine the influence of the general and pedagogical culture on the development of teacher's professional competence when using interactive technologies in the learning process to achieve high performance. The system-activity approach in the implementation of the Federal State Educational Standard is oriented to the final result. It is a system-forming factor of activity and a component of forming the standards that consider professional education primarily as mastering professional experience.

The main methods of our research were a retrospective analysis and review of the literature on the problem, observation, questioning, interviews, interviewing, designing, modeling, monitoring, experiment, generalization of the experience of pedagogical activity.

3. RESULTS AND DISCUSSION:

In the theoretical part of the research, the essence of the problem of studying the values of modern professional education and pedagogical

ethics as the moral basis for the formation of future teachers' values-based attitude to their pedagogical activity and profession was studied in detail.

As it was written above, the category "value" has a semantic closeness with the category "values-based orientations." It is a multi-valued concept, reflecting everything that is realized and experienced by a person as actual significance, as meaning, as an ideal, as the essential characteristics of an individual's consciousness and behavior, and as target constructs of social activity. Values-based orientations appear to be a system of personality aspirations and as a character of this aspiration. They can also be considered as the highest level of ideas about ideals, about the meanings of life and activity that determine the activity of each person. In the category "values-based orientations," there is a direct indication of the existence of a life guide that defines the vector of personal development.

Value can also serve the purpose of human existence. In this regard, the authors agree with the opinion of V.A. Slastenin and E.I. Artamonova, who write about the significance of the characteristics of spiritual values. According to their viewpoint, building a hierarchy of values is associated with a personal worldview, the formation of self-awareness, and is based on the analysis of axiological structures vital for a person: ideals, beliefs, principles (Slastenin, Artamonova, 2002).

Considering pedagogical activity as a value for the development of the personality of the teacher and university students, it was necessary to review the content and methods of training and education. As a result, the future specialist will be "equipped" with knowledge and skills, moral standards, which prepare them for life and practical work. Therefore, it is vital to consider the essence of the term "ethics" (theoretical and practical philosophical science of morality) that has a rather long history: in the 4th century BC, the ancient Greek philosopher Aristotle introduced it to designate a field of knowledge that studies various virtues. It is noteworthy that even then Aristotle had in mind that ethics is aimed at human activity, and it is important to examine it not to know what virtue (moral) is, but to become virtuous, that is, to adopt a specific system of values, to cultivate noble qualities. The measure of real value, according to Aristotle, is "virtue and virtuous man as he is."

Today, research on professional ethics and the formation of the attitude of future specialists to

education as a value is very relevant. Professional ethics is the specific requirement of morality associated with the characteristics of various professions. The concept of "Pedagogical Ethics" was first formulated in Russia in the 70s of the XX century by E.A. Grishin. He argued that Pedagogical Ethics is the science of the laws of development of moral requirements generated by the characteristics of pedagogical work. These requirements are manifested in the relationships between a teacher and students, teachers and students' parents, between teachers and the administration, as well as in the existing relations of the teaching staff itself. Moral requirements are determined by the personal and professional qualities of the teacher (Grishin, 1973).

According to V.I. Andreev's opinion, under modern conditions, "Pedagogical Ethics is the science of the laws of development (self-development) and self-realization of a teacher's moral culture, which manifests itself in various situations of moral choice and moral activity in the process of solving pedagogical problems. Pedagogical ethics aims to identify, justify and formulate basic ethical laws and on their basis such professional and pedagogical principles and rules that would contribute to highly moral behavior and activities of the teacher and the work of the teacher to create a comfortable environment for all participants in the educational process". V.I. Andreev considers the preparation of a teacher for profoundly human pedagogical activity in all possible situations, at all stages of education and upbringing of the younger generation to be the final goal of "Pedagogical Ethics" (Andreev, 2012).

Scientist-teacher L.L. Shevchenko, the author of the book "Practical Pedagogical Ethics" (experimental didactic study guide, a book for teachers and parents, 1997) defines pedagogical ethics as part of ethics, the subject of which is the pattern of morality in the consciousness, behavior, relationships, and activities of the teacher. It is emphasized that the main objectives of the study guide are: "study of the theoretical problems of pedagogical morality; development of moral aspects of pedagogical work; identification of the requirements for the moral character of the teacher; the study of the moral consciousness of the teacher; study of the nature of the teacher's moral relations; development of issues of moral education and self-education of a teacher. The teacher reveals the basic concepts of pedagogical ethics: pedagogical justice, professional-pedagogical duty, professional honor and conscience, dignity, pedagogical authority, and self-discipline (Shevchenko, 1997).

In the pedagogical research of scientists, there is constant interest in the problem of the formation of a value attitude to the pedagogical profession. At the turn of the 21st century and the beginning of the 21st century, international scientific and practical conferences were held, such as: "Pedagogical education for the 21st century" (Moscow, 1994), "Problems of the formation and development of teacher's values-based orientations at the turn of the 21st century" (Tula, 1997), "Teacher Education: Challenges of the 21st Century", "Teacher Education: Challenges of the 21st Century" (dedicated to the memory of Academician of the Russian Academy of Education V. Slavenin, Ryazan, 2017), where Russian scientists and practical trainers of educational institutions (B.S. Gershunsky, L.K. Grebenkina, N.A. Zhokina, I.F. Isaev, N .V. Martishina, N.D. Nikandrov, A.A. Orlov, V.A. Slavenin, I.L. Fedotenko, E.N. Shiyanov and others) discussed the problems of the importance of the formation of values-based orientations in the process of psychological and pedagogical preparation of the future professionals and their professional activities. An analysis of conference materials allows us to note the constant attention of scientists to ethical issues, as well as highlight, in our opinion, the most significant values of professional training of future teachers.

It is essential to draw attention to a collective monograph "The conceptual apparatus of pedagogy and education" annually published by the scientists of the Ural State Pedagogical University (edited by M. A. Galaguzov, E. V. Tkachenko). It is devoted to conceptual and terminological problems and summarizing research on the challenge of future formation specialists of the values of education, the values of the teaching profession and teaching activities, due to the large-scale processes of modernization of domestic education (The conceptual apparatus of pedagogy and education, 2010).

The need for such studies was due to the adoption of the Concept for the modernization of Russian education for the period until 2010 in 2002. However, after this period, it became evident that the problems of modernization have not lost their relevance; on the contrary, they are acquiring new aspects that require further research and comprehensive understanding. To participate in the discussion of these problems, scientists are invited to explore new pedagogical phenomena and concepts that reflect the various aspects of modernization of education, its substantial and technological renewal following continually changing social realities and the latest

trends in its development. As a rule, four sections are proposed in the monograph: "Pedagogy methodology," "General pedagogy," "Professional pedagogy," and "Social and special pedagogy." So, the sixth issue of this publication (2010) is wholly devoted to the study of the problem of values and values-based orientations in education. In particular, it is considered:

1) axiological approach as a new research method in pedagogy;

2) understanding of education as a value, as a person's property, as a means of one's self-realization in life; as a means of making a person's career;

3) personal orientation of education, the idea of a person as the highest objective (value) of education;

4) direction of education on the spiritual and moral values of student's development and education.

The section "Professional Pedagogy" reveals the features of the axiological approach in vocational education: orientation on humanistic values, the formation of creativity among students in the process of university education, axiological orientation; values-based attitude to the pedagogical process and all its participants. The following values are highlighted: desire for truth; social well-being of society; social justice; moral humanistic norms; knowledge acquisition; respect for talents; decency (honesty); own dignity; personality value; social activity; your health and those around you; nature conservation; moral health of the team and society; the value of other peoples and their culture; goodwill in relationships, mutual assistance, etc. (The conceptual apparatus of pedagogy and education, 2010).

Discussing the essence of values, their place, and role in people's lives, V.A. Slastenin and the representatives of his scientific school argue that the category of value applies to the human world and society. Outside of a man and without a man, the concept of value cannot exist, since it represents a particular human type of significance of objects and phenomena. Values are not primary; they are derived from the correlation of the world and a man, confirming the relevance of what a man created in the process of history (Slastenin, Shiyanov, 1996).

Universal, state, social, and personal values are considered to be a universal priority, determining the essence of modern education, including higher education (Gershunsky, 1997: 6). Pedagogical activity is a particularly important

value of contemporary Russian society, aimed primarily at educating a humanist, patriot of Russia, focused on the priority of Russian national values with due respect for the importance of other cultures (Nikandrov, 1997).

The values of pedagogical activity serve as a guide for the teacher's social and professional event aimed at achieving socially meaningful humanistic goals in teaching and educating students. Scientists distinguish groups of universal and national values of pedagogical activity that influence the development of pedagogical skills of a teacher (Table 1):

Similar classifications are found in the works of other researchers. So, Z.I. Ravkin, classifying the pedagogical values of education, singles out the following groups: socio-political, intellectual, moral, and the group of values of professional-pedagogical activity. The scientist writes that their structure includes:

- a vocation to work as a teacher-educator,
- a consciousness of personal and social responsibility for the chosen profession;
- the talent of the teacher, his search and research, innovative activity;
- high moral personal qualities of a teacher;
- communicative abilities, a style of communication with students, based on democratic and humanistic principles (the teacher is called to love those he teaches and love what he teaches);
- the professionalism of the teacher, a high level of special and general cultural training, broad professional and broad erudition, pedagogical skills that ensure its competitive qualities in the labor market;
- consistent orientation towards the development and strengthening in the integral pedagogical process of social, intellectual, moral, and aesthetic values of education (Ravkin, 1995).

These ideas are largely reflected in recent documents. Thus, the Federal Law "On Education in the Russian Federation" (2012) affirms the humanistic nature of education among the main principles of state policy and legal regulation of relations in the field of education. However, sociological studies conducted in different years in different regions of the country show that, quite often, teachers only confine themselves to talking about humanism and recognizing the rights of schoolchildren. On the other hand, about half of the teachers surveyed do not conceal the fact that they use authoritarian methods (Timonina, 2014).

In other words, this indicates a contradiction that has existed in the education system for a long time. It also manifests itself in the professional problem: the affirmation of the humanistic principle puts the school teacher in a situation of constant sharp contradictions. Experience shows that the teacher's respect for the student does not guarantee the opposite: the teacher's respect for the student forms a consumer's attitude to teachers instead.

According to the Article 48 of the Law "On Education in the Russian Federation" "teaching staff must: comply with legal, moral and ethical standards, follow the requirements of professional ethics; respect the honor and dignity of students and other participants in educational relations (Federal Law "On Education in the Russian Federation" 2012). This requirement also can be found in the professional standard "Teacher" (Professional Standard "Teacher," 2013). Of course, these statements are specific grounds for the formation of the tasks of professional education.

The relevance of adopting the rules of professional behavior also relates to the fact that young people who choose a pedagogical profession for themselves come with their value system, which rejects the traditional ideas about social norms, as well as about the job. Each society forms its system of values, which helps a person to choose socially approved behavior in vital situations. It is worth mentioning a critical observation noted by a researcher of the youth, I.M. Ilyinsky, who argued against the traditional perception of the youth as a product of society, believing that the young generation is a social accumulator and produces community, concentrating future ideas and values in their views (Ilyinsky, 2001). That is, there is a need to bring the value system of the young generation with the value system established in professional activity.

It is worth noting that getting higher education for a young man today is one of his life goals, and is also considered by him as a condition of professional and personal self-determination, the possibility of self-development. This is also proved by the results of our study of a young student (Martishina *et al.*, 2016). For example, one can note particular dynamics in the judgments of young people about their life goals, perceptions of the future profession. So, the initial ideas about the future profession expressed by freshmen are superficial, based on their school perception of teachers. Studies show that in the judgments of young people, on the one hand, there are idealized

characteristics, and on the other, a negative perception of the future teaching profession, fear of interacting with children, rejection of the teacher's traditional norms of behavior. In many respects, such positions reflect the existing public opinion about the teaching profession. Note that the motives for choosing a pedagogical university among applicants are very diverse: only half of the applicants have a desire to be a teacher.

Often young people postpone the decision to choose the workplace they will decide after graduating from a university, while the status of a person with higher education attracts the majority of applicants. Also, boys and girls who enter the university have a high level of dependence on parents, who influence the choice of young people and materially support their studies. In this regard, first-year students demonstrate a lack of professional orientation during the period of schooling, as well as a certain infantilism, a lack of desire to be independent, to consider a future profession seriously, and to build a career. Meanwhile, career growth should be presented precisely as a process of achieving goals. In other words, at this stage of personality formation, a particular discrepancy is noted: young people talk about their dreams or goals, build an image of the future, but they do not always adequately choose the ways to achieve the desired result, they can develop their current actions as a movement towards the goal.

In this regard, in the study, the authors used the method of revealing the life values by Milton Rokich, who proposed to consider two types of benefits: "values-goals," or terminal, and "values-means," or instrumental (Lapin, 2002). According to the scientist, the former express in general terms the most important goals, ideals, and self-valuable meanings of people's lives, for example, the value of human life, family, interpersonal relationships, freedom, labor, etc. Instrumental values reflect the means approved by society for achieving goals; these are moral standards of behavior, as well as specific qualities of a person (such as independence, initiative, authority, etc.).

This approach helps to determine the mechanisms of professional and personal formation of the future expert. The conducted study made it possible to record in modern students who are mastering the program of teacher education, the characteristic dominance of personal life values over the values of professional self-realization (Ilyinsky, 2001). Young people put happy family life in the first place, and among professional values, they highlight the possibility of self-realization. The dynamics taking place in the

selection of benefits among students of 1-2 courses of bachelor's degree, students of the four-course of bachelor's degree and among graduate students is shown in Table 2.

As it is presented in Table 2, conformist, humane values, as well as communication values, are in the first place. Ethical values are in the last place for young students; in the future, their rating increases, but slightly. Modern trends in the youth environment include students' concentration on their problems, the need for self-development, personal success, and recognition. Ethical values take the last place among junior students; they have the least interest in following the norms. Self-affirmation, self-expression among the youth are much more critical.

The rating of ethical values is rising, but not significantly. Respondents note that sometimes or only "periodically," they think about compliance with moral standards, but they understand that this is important for the future profession. Thus, there is an absolute contradiction that arises among students in the process of mastering the next trade. The difficulty of adopting moral standards, reassessing values takes time. When asked what prevents people from living, observing ethical standards, students answered that this was due to a lack of education, as well as selfishness and "herd instincts."

On the one hand, it can be noted that older students, having an individual experience of interaction in professional activities, begin to realize the importance of adopting ethical standards. But on the other hand, such results confirm the need to pay special attention to the development of the values of the future profession, to create conditions for entering the professional community, which is characterized by a system of norms, rules of behavior, communication, relationships (Martishina *et al.*, 2016).

Thus, the introduction of the "Pedagogical Ethics" in the curriculum of the teacher education program is not only justified from the point of view of vocational training tasks but also becomes a very important condition for mastering pedagogical activity, providing an adequate understanding of the interaction of participants in educational relations.

This course is based on studies of modern deontology, which is based on general ethical standards and determines the normative moral position of the teacher. Note that the focus is precisely on "oughtness" (from Greek *deon* - duty), in other words, the profession dictates the observance of specific rules, sets codes of

conduct, prescribes a particular type of moral relationship between people, requires internal self-regulation of the person based on ethical ideals. Modern textbooks on pedagogical ethics affirm the traditional categories of pedagogical justice, professional duty, honor, and conscience, pedagogical authority, dignity, and self-discipline (Vekkesser *et al.*, 2017; Timonina, 2014).

Under current conditions of professional education, "Pedagogical Ethics" as a subject reflects the specificity of moral requirements for pedagogical activity. Note that this discipline includes not only the theoretical basis for the formation of pedagogical values but also involves a large number of practical tasks and independent work of students. For example, students get acquainted with the model code of the teacher (Letter of the Ministry of Education and Science of the Russian Federation of 2014) and also develop options for the professional system for teachers working in various educational institutions. Such work involves a certain "dipping" in the professional community, acquaintance with pedagogical situations, analysis of the characteristics of the interaction of participants in educational relations, the development of requirements that can become the basis for choosing value orientations, professional self-education of future teachers.

The training course "Educational Ethics" formerly was worked out to learn for students at the final course. However, young people need to orient themselves in professional requirements much earlier: in the first pedagogical practice, students find themselves in situations of difficult choice of behavior in the professional community, the choice of solving problems of interaction with children and their parents. In this regard, the study of the course "Pedagogical Ethics" is placed to an earlier stage in the curricula of various training profiles in the direction of "Pedagogical Education."

It is also worth noting that the quality of the educational process as a whole is of great importance in the training of future teachers. Ethical standards should be mastered not only within the framework of academic discipline but also presented in the real relationships of the teaching staff.

The task of modern professional education is to form not only certain competencies but also a system of professional values, without which it is impossible to imagine the fulfillment of the mission of pedagogical activity. In this regard, it is necessary to talk about the saturation of the

educational process with professional values, which should ensure the formation of the personality of the future teacher under certain conditions. It should be remembered that the values of education are goals, meanings, ideal forms of pedagogical activity aimed at professionally-personal formation and development of a specialist based on universal values (Zhokina, 2015).

4. CONCLUSIONS:

The study allows us to draw some conclusions that are important for improving the training of future teachers. In the process of scientific research, the presence of a constant interest of scientists in the problem of the formation of the values-based attitude to the teaching profession was confirmed.

A retrospective analysis of the positions of scientists in the interpretation of the axiological approach as a methodological condition for studying the values of professional education shows its unique significance. The axiological approach provides support on the philosophical doctrine of the nature of values, their structure and place in reality. This allows to orient the teacher to universal, national and professional values to form a value-related attitude to professional activities.

Pedagogical ethics constitutes a theoretical and methodological moral basis for the formation of the humanistic values of future teachers. These values are the "eternal" guidelines of their professional activity. The creator and bearer of values is a professional teacher whose primary function is to discover and improve human qualities in a person through the development of values, the knowledge of the world around him and the formation of his image based on the culture of society (Bykova, 2018).

The consistent and systematic learning of ethical principles of the profession is possible due to studying the subject "Pedagogical Ethics," plays an essential role in future teachers' training.

The analysis of theoretical sources and pedagogical experience shows that at present, goal-oriented pedagogical requirements are aimed to form a competently developed creative personality of future specialists. These goal-oriented pedagogical requirements are becoming integrative in the practical activities of university teachers. The formation of students' values-based attitude to the future teaching profession faces many obstacles associated with changing sociocultural conditions. In this regard, for the

preparation of students, a full-fledged "immersion" in the professional community is necessary. The discipline "Pedagogical Ethics" becomes the basis in the development of a system of values, rules and norms. The saturation of the educational process with events, interactions peculiar to professional activities should also be a valuable addition.

The preparation of students for the future teaching profession in modern conditions is characterized by an increase in the culture-forming function of education as a universal value. The role of a teacher with a high general and professional culture, capable of mastering and improving the culture of society as a value, passing it on to young generations is changing qualitatively.

5. REFERENCES:

1. Andreev, V.I.; Pedagogical Ethics: an innovative course for moral self-development, Kazan: Center for Innovative Technologies, **2012**, 20, 21, 24.
2. Belyaeva, L.A.; The philosophy of education and pedagogy in their relationship: The conceptual apparatus of pedagogy and education; Proceedings, Issue 5; Tkachenko, E.V., Galaguzova, M.A., eds; Moscow: Humanitarian Publishing Centre VLADOS. **2007**.
3. Bykova, S.S.; Deontological principles for the process of preparing a future teacher, taking into account the requirements of the ethical code of a pedagogical worker: Law and Education, No. 12. **2018**, 71-80.
4. Doroshenko, V.Yu.; Zotova, L.I.; Psychology and ethics of business communication: Textbook for universities; 2nd ed; Moscow: Culture and sport, UNITI, **1997**.
5. Federal Law "On Education in the Russian Federation". No. 273. December 29, **2012** http://www.consultant.ru/document/cons_doc_LAW_140174/ (Date of access - October 23, 2018).
6. Gershunsky, B.S.; The philosophy of education in the system of professional training of a future teacher: Problems of the formation and development of teacher's value orientations at the turn of the 21st century: Abstracts of the International Scientific and Practical Conference; Tula: TSPU named after L.N. Tolstoy. **1997**.

7. Grebenkina, L.K.; The formation of teacher professionalism in the system of continuous pedagogical education: monograph, 2nd edition. Ryazan: Ryazan State University, **2006**.
8. Grebenkina, L.K.; Zhokina, N.A.; Eremkina, O.V.; Introduction to pedagogical activity. Ryazan: Ryazan State University, **2009**.
9. Grebenkina, L.K.; Martishina, N.V.; Conceptual approaches to the study of value orientations of a modern teacher: Conceptual apparatus of pedagogy and education: Proceedings. Tkachenko, E.V.; ed. Yekaterinburg: "SV-96". **2010**.
10. Grebenkina, L.K.; Lesin, A.M.; Some features of the orientation and value sphere of the personality of first-year students of higher education: Russian Scientific Journal. **2015**. 1 (44). 88 - 94.
11. Grebenkina, L.K.; Zhokina, N.A.; Actual issues of professional and personal development of a student of a pedagogical university // University education of a modern teacher: Collection of scientific articles October 13, 2016; Gladkaya, I.V., Pisareva, S.A., eds. SPb: Publishing House of the Russian State Pedagogical University named after A.I. Herzen. **2016**, 118-124.
12. Grebenkina, L.K.; Zhokina, N.A.; Humanistic Values of Vocational Education at the University: Pedagogical Education: Challenges of the 21st Century: Proceedings of the International Scientific-practical Conference, dedicated to the memory of Academician of the Russian Academy of Education V.A. Slastenin; Samara. October 4-5, **2018**.
13. Grebenkina, L.K.; Zhokina, N.A.; Professional education in the pedagogical process of the university: The conceptual apparatus of pedagogy and education: collective monograph; Tkachenko, E.V.; Galaguzov, M.A.; eds; Ural State Pedagogical University. **2018**. 10.
14. Grebenkina, L.K.; Zhokina N.A.; To the question of the formation of pedagogical ethics in the professional and personal development of a student // Problems of spiritual and moral education in the modern world: collection of articles (April 24, 2018). Kolomna: SSGU. **2019**.
15. Grishin, E.A.; Professional and ethical teacher training in higher education. Vladimir, 1973.
16. Ilyinsky, I.M.; Youth and youth policy. Philosophy. History. Theory. Moscow: Voice, **2001**.
17. Isaev, I.F.; Scientific school of professional and pedagogical culture in the context of the development of ideas V.A. Slastenin, **2013**.
18. Kant, I.; The Works in 6 volumes. Moscow: "Mysl", **1965**. V. 4. Part I, 311-501.
19. Kochetov, A.I.; The culture of pedagogical research. Minsk: "Adukatsiya i subjects", **1996**.
20. Kravchenko, E.I.; Theory of social action: from Max Weber to phenomenologists: Sociological Journal. **2001**. 3, 121 - 141.
21. Kushnyr, L.A.; Motivation as instrument of students-biologists' bilingualism formation during foreign language teaching. EpSBS. Ardashkin, I.B.; Martyushev, N.V.; Klyagin, S.V.; Barkova, E.V.; Massalimova, A.R.; Syrov, V.N. **2018**. 690-697.
22. Lapin, N.I.; On the many and the same in the Russian transformation: Social Sciences and Modernity. **2002**. 2. 107.
23. Letter of the Ministry of Education and Science of the Russian Federation of February 6, **2014** No. 09-148 "On the direction of materials" - <https://www.garant.ru> (accessed 03.03.2019).
24. Martishina, N.V.; Eremkina, O.V.; Grebenkina, L.K.; Adzhieva, E. M.; Ganina, T.V.; Zhokina, N.A.; Professional and personal development of students in higher education: textbook; Eremkina, O.V. ed.; Ryazan: Publishing House "Concept", **2016**.
25. New values of education: a thesaurus for teachers and school psychologists. Issue 1. Moscow: Publishing center "Cicero", **1995**, 109, 110.
26. Nikandrov, N.D.; Russian teacher and his values: Problems of the formation and development of teacher's value orientations at the turn of the 21st century; Abstracts of the ISPC; Tolstoy, L.N.; ed; Tula. **1997**, 8.
27. Orekhova, Y.; Grebenkina, L.; Eremkina, O.; Badelina, M.; Sysoev, S.; Training the future teacher-researcher for professional

- activity at Master's degree level. *Revista Espacios*. 40 (29). **2019**. 10.
28. Orekhova, Y.; Grebenkina, L.; Zhokina, N.; Badelina, M.; Forming competences of students in educational process of a higher education institution. *Revista Espacios*. 39 (46). **2018**. 28.
 29. Orekhova, Y.; Grebenkina, L.; Martishina, N.; Badelina, M.; Implementation of competency-based approach in interactive teaching of future Masters of Education. *Revista Espacios*. 40 (29). **2018**. 15.
 30. Orekhova, Y.; Using Blended Learning in Higher Education: from Theory to Practice. Global Scientific potential. Saint-Petersburg. 6 (75). **2017**.
 31. Pasternak, N.A.; Psychology of education: Textbook for students at high school; Asmolov, A.G. ed.; Moscow. Publishing Center "Academy", **2008**, 125-160.
 32. Professional standard "Teacher" (pedagogical activity in the field of preschool, primary, basic, basic, secondary general education) (educator, teacher" (approved by the order of the Ministry of Labor and Social Protection of the Russian Federation of October 18, **2013** N 544n) - <http://professionalstandardteacher.rf> (Date of treatment 09.07.2019).
 33. Timonina, I.V.; Professional ethics of the teacher: Study guide. Kemerovo, **2014**.
 34. Ravkin, Z.I.; The constructive-genetic approach to the study of educational values is one of the directions of development of the modern Russian theory of pedagogy. Education: ideals and values (historical and theoretical aspect). Ravkin, Z.I.; ed; Moscow: ITPiO RAO, **1995**, 9.
 35. Scientific schools of the Institute of Pedagogy: Collection of articles of the third All-Russian pedagogical (Herzen) readings on April 18, 2019; Gladkaya, I.V.; Pisareva, S.A.; Tryapitsina A.P.; eds; St. Petersburg: Publishing House of Herzen RSPU. **2019**.
 36. Selevko, G. K.; Encyclopedia of educational technologies; 2 volumes. Moscow: Scientific and Research Institute of School Technologies, **2006**. V.1.
 37. Shevchenko, L.L.; Practical pedagogical ethics. Experimental didactic complex. Moscow: Sobor, **1997**, 11-13, 15.
 38. Slastenin; V.A.; Shiyarov, E.N.; The humanistic paradigm of education as the basis for the formation of a national strategy for teacher training // National values of education: history and modernity; Materials of the XVII Session of Scientific Council on the problems of the history of education and pedagogical science. Ravkin, Z.I.; ed. M.: ITOP RAO. **1996**.
 39. Slastenin, V.A.; Artamonova, E.I.; Axiological aspect of the content of modern pedagogical education: Pedagogical education and science. **2002**. No. 3. 4-9.
 40. Slastenin, V.A.; Chizhikova, G.I.; Introduction to pedagogical axiology: Textbook. manual for students of higher ped. institutions. Moscow.: Publishing Center "Academy", **2003**.
 41. Slastenin, V.A.; Professionalism of the teacher as a phenomenon of pedagogical culture. Pedagogical education and science. **2004**. № 5. 13.
 42. The conceptual apparatus of pedagogy and education; Proceedings; Tkachenko, E.V.; Galaguzova, M.A.; eds; Vol. 6. Yekaterinburg: Publishing house "SV-96", **2010**, 86.
 43. Veknesser, M.V.; Slavkina, I.A.; Firer, N.D.; Kharitonova, N.G.; Shmul'skaya, L.S.; Professional ethics in pedagogical activity: textbook. Guidebook; Krasnoyarsk: Sib. Feder. un-t, **2017**.
 44. Zhokina, N.A.; Fundamentals of professional education in high school // *Izvestiya RAO*. 2015. 2 (34). 73-78.
 45. Zhokina N.A. Fundamentals of professional education in high school // *Izvestiya RAO*, 2015, No. 2 (34). S. 73-78. Zhokina, N.A.; Petukhov, N.A.; Modern problems of the preparation of scientific and pedagogical personnel; *Drucker Bulletin: Scientific, Educational and Applied Journal*. **2019**, No. 3. 155-163.
 46. Zagvyazinsky, V. I.; Zakirova, A.F.; Pedagogical dictionary: studies. manual for students of higher educational institutions; Zagvyazinsky, V. I.; Zakirova, A.F.; eds; Moscow: Publishing Center "Academy", **2008**.
 47. <http://www.values-edu.ru/wp->

Table 1. *Groups of universal and national values of pedagogical activity influencing the development of pedagogical skills of a teacher*

N	Value description	Examples
11.	values associated with the adoption in society, the immediate social environment	the social significance of the teacher's work, the prestige of the teacher's professional activity, recognition of relatives, friends, etc.
22.	values related to meeting the need for communication	constant work with children, children's love and affection, opportunities to communicate with interesting people, parents, colleagues, exchange of spiritual values, etc.
33.	values related to self-improvement	the possibility of developing creative abilities, culturation with spiritual culture, doing one's favorite thing, the ability to enrich one's knowledge, etc.
44.	values associated with self-expression	(the possibility of developing creative abilities, culturation with spiritual culture, doing one's favorite thing, the ability to enrich one's knowledge, etc.
55.	values associated with utilitarian-pragmatic requests	opportunities for self-affirmation, interpersonal communication, professional growth, promotion, (Slasterin, Shiyanov, 1996: 233).

Table 2. *Comparison of the importance of values for modern students*

Types of values	Students		
	1-2 courses of bachelor's degree (134 students)	4 course of bachelor's degree (101 students)	graduate students (41 students)
	Importance of values for students (rating)		
Ethical values	8	5	6
Communication values	3	2	2
Values of work	4	3	5
Individualistic values	6	8	7
Conformist values	1	1	4
Altruistic values	2	6	1
Values of Self-Affirmation	7	7	8
Other people's acceptance values	5	4	3

AUMENTO DA SÍNTESE DE ÓXIDO NÍTRICO EM MACROFAGAS PERITONEAIS SOB A AÇÃO DO ÁCIDO ASCÓRBICO**INCREASED NITRIC OXIDE SYNTHESIS IN PERITONEAL MACROPHAGES UNDER THE ACTION OF ASCORBIC ACID****ПОВЫШЕНИЕ ПРОДУКЦИИ ОКСИДА АЗОТА В ПЕРИТОНЕАЛЬНЫХ МАКРОФАГАХ ПОД ДЕЙСТВИЕМ АСКОРБИНОВОЙ КИСЛОТЫ**

KUROPTOVA, Zoia Veniaminovna^{1*}; BAYDER, Larisa Michailovna²; BELAYA, Olga Leonidovna³; ZUMABAEVA, Taasilkan Toktomamatovna⁴

^{1,2} Emanuel Institute of Biochemical Physics, Russian Academy of Sciences. Russia.

³ Moscow State medico-stomatological University, Department of Hospital Therapy No. 2. Russia.

⁴ Osh State University. Russia.

* Correspondence author
e-mail: zvk@sky.chph.ras.ru

Received 24 December 2019; received in revised form 30 January 2020; accepted 12 February 2020

RESUMO

Foi estudado o efeito do ácido ascórbico (AA) na formação de óxido nítrico (NO) em macrófagos peritoneais de camundongos da linha SHK. A espectroscopia de RSE e UV revelou um aumento significativo na formação de óxido em uma suspensão de macrófagos com AA incubado à temperatura ambiente. Nos estudos de VHS, a hemoglobina adicionada a uma suspensão de macrófagos foi usada como uma armadilha de NO, e o óxido nítrico resultante foi detectado pela formação dos complexos de hemoglobina Heme-NO. A avaliação quantitativa mostrou que nessas condições, sob a ação de AA, $1,5 \times 10^9$ moléculas de NO por célula são produzidas em macrófagos. O aumento da síntese de óxido nítrico sob a ação do AA também foi estabelecido por espectroscopia UV no sobrenadante após a incubação do macrófago com AA. Considerando os dados conhecidos sobre o efeito citotóxico do NO em vírus e bactérias, pressupõe-se que o efeito do aumento da síntese de óxido nítrico nos tecidos peritoneal, MP tecidual e leucócitos sob a ação do AA seja o principal no efeito preventivo e terapêutico do AA no uma série de doenças, como um doente de frio.

Palavras-chave: *óxido nítrico, ácido ascórbico, macrófagos peritoneais, método ESR, complexos nitrosil Hb Hem-NO.*

ABSTRACT

The effect of ascorbic acid (AA) on the formation of nitric oxide (NO) in peritoneal macrophages of SHK line mice was studied. ESR and UV spectroscopy revealed a significant increase in oxide formation in a suspension of macrophages with AA incubated at room temperature. In ESR studies, hemoglobin added to a suspension of macrophages was used as a NO trap, and the resulting nitric oxide was detected by the formation of hemoglobin complexes Heme-NO. The quantitative assessment showed that under these conditions, under the action of AA, 1.5×10^9 molecules of NO per cell are produced in macrophages. The increase in nitric oxide synthesis under the action of AA was also established by UV spectroscopy in the supernatant after incubation of MP with AA. Considering the known data on the cytotoxic effect of NO on viruses and bacteria, it is assumed that the effect of increasing nitric oxide synthesis in peritoneal, tissue MP and leukocytes under the action of AA is the main in the preventive and therapeutic effect of AA in a number of diseases, such as a sick of cold.

Keywords: *nitric oxide, ascorbic acid, peritoneal macrophages, ESR method, nitrosyl complexes Hb Hem-NO.*

АННОТАЦИЯ

Исследовано влияние аскорбиновой кислоты (АК) на процесс образования оксида азота в перитонеальных макрофагах мышей линии SHK. Методами ЭПР- и УФ-спектроскопии было

зарегистрировано значительное повышение образования оксида в инкубированной при комнатной температуре суспензии макрофагов с АК. В исследованиях методом ЭПР качестве ловушки NO использовали гемоглобин, добавленный в суспензию макрофагов, и образующийся оксид азота регистрировали по образованию нитрозильных комплексов гемоглобина Гем-NO. Количественная оценка показала, что в этих условиях, под действием АК в макрофагах вырабатывается $1,5 \times 10^9$ молекул NO на клетку. Увеличение синтеза оксида азота под действием АК было установлено также методом УФ-спектроскопии в надосадочной жидкости после инкубации МФ с АК. Учитывая известные данные о цитотоксическом действии NO на вирусы и бактерии предполагается, что эффект увеличения синтеза оксида азота в перитонеальных, тканевых МФ и лейкоцитах под действием АК является основным в профилактическом и лечебном действии АК при ряде заболеваний, в частности, при простудных заболеваниях.

Ключевые слова: оксид азота, аскорбиновая кислота, перитонеальные макрофаги, метод ЭПР, нитрозильные комплексы Hb Гем-NO.

1. INTRODUCTION

In the 80s, it was found that activated MP, cultured together with target tumor cells, kill target cells (Krahenbuhl and Remington, 1974). And the agent responsible for the death of tumor cells is nitric oxide (NO) synthesized by macrophages. The participation of NO in the cytotoxic activity of macrophages to tumor cells was one of the first functional properties described for this molecule (Hibbs *et al.*, 1987a, 1987b; Stuehr and Marletta, 1987b; Stuehr and Nathan, 1989). It was shown that inhibition of NO synthesis in macrophages leads to a decrease in the antitumor resistance of the body, and the discovery of this basic fact made a great contribution to the increased number of studies devoted to the formation and function of NO in normal and pathological conditions. Although there are various, sometimes contradictory data on the role of NO in the development of tumors, it has definitely been established that NO synthesized by leukocytes and macrophages plays a main role in their ability to destroy tumor cells (Stuehr and Nathan, 1989; Hibbs *et al.*, 1987a; Stuehr and Marletta, 1987a; Keller, 1993; Farias-Eisner, *et al.*, 1994).

It was shown that sustained continuous production of NO in macrophages ensures their cytotoxic/cytostatic activity not only to tumor cells, but also to viruses, bacteria, fungi, protozoa, and helminths (Croen, 1993; Bi and Reiss, 1995; Vazquez-Torres *et al.*, 2000; Sibille and Reynolds, 1990; Nathan, 1995).

On cell lines and mouse, lines were found that resistance to microbes is often associated with the expression of the induced NO synthase (iNOS). More direct evidence of the iNOS role was obtained first by Hibbs J. and his colleagues (Hibbs *et al.*, 1987a, 1987b), and then by many

other researchers. They used iNOS inhibitors and showed that inhibitors worsen the course of diseases caused by many viruses and bacteria. The mechanisms of nitric oxide action were established. They included inhibition of mitochondrial respiration (MR) and DNA synthesis, iron loss by cells, and inhibition of enzymes involved in the Krebs cycle (Billiar *et al.*, 1989a, 1989b; Kwon *et al.*, 1991; MacMicking *et al.*, 1997; Beltran *et al.*, 2000; Fang, 1997).

NO is obviously not the only anti-pathogenic immune defense effector, but in most cases, it is either an inducer or an executor of a bactericidal program.

Therefore, the increased (NO) synthesis in the cells of the immune system is important in raising the body's resistance to infectious diseases, and, possibly, due to the available literary data, the prevention of tumor diseases.

There have been reports that in a number of cells, NO synthesis can be enhanced by the AA. Studies of the AA effect on the activity of NO synthesis in cells are few, and the data are quite contradictory. Thus, in (Nakai *et al.*, 2003), AA the role in iNOS induction and NO synthesis in macrophages of RAW 264.7 line mice was studied, and it was found that AA did not increase or decrease iNOS protein expression in these cells, in contrast to (Mizutani and Tsukagoishi, 1999) where AA increased protein induction in a macrophage-like cell line J 774.1. It has also been shown that AA inhibits iNOS induction in rat endothelial cells of the skeletal muscle (Wu *et al.*, 2002). Increased NO production in endothelial cells, animal and human leukocytes, and *E. Coli* cells were described in (Kuropteva *et al.*, 2000, Heller *et al.*, 1999; Huang *et al.*, 2000). Such inconsistency of data may depend on the type of cells. Therefore, the study of the AA effect on NO

synthesis in the cells that can express iNOS is still important.

2. MATERIALS AND METHODS

Peritoneal macrophages were isolated by the standard method of washing the contents of the abdominal cavity of SHK mice (The SHK male mice Swiss-H mice from nursery Kriukovo, Russia) with a 0.9% NaCl solution. The collected cells were washed twice with the same solution and centrifuged at 250 g for 10 min (Wasley *et al.*, 1972). The precipitate was suspended in saline. The cell concentration was 2×10^9 in 1 ml. To feed the cells, 2% serum solution of cattle was added (Biowest, France). The macrophage suspension was divided into 2 parts. AA solution (AA from Sigma) in Tris-HCl buffer with pH 7 was added to one part. AA concentration in the MP suspension was 9–10 mM. The second part to which Tris-HCl buffer was added served as a control.

MP suspensions with and without AA were incubated at room temperature. After 20 and 48 hours of incubation, samples of the supernatant were taken, and absorption was measured on the Shimadzu spectrophotometer (Japan).

To study ESR Hb solution in a concentration of 10^{-5} M was added as a NO trap. After certain periods of times of incubation, samples were taken, and specimens were prepared in the form of columns in Teflon tubes with a diameter of 3 mm and a height of 30 mm. They were frozen at liquid nitrogen temperature. Then, the specimens were freed from Teflon tubes, and macrophage suspension samples frozen at liquid nitrogen temperature were obtained in the form of columns with a diameter of 3 mm and a height of 30 mm. The ESR spectra of the prepared samples were recorded on ESR-300 spectrometer (Bruker-Analitishe-Messtechnik, Germany) at a temperature of liquid nitrogen.

3. RESULTS AND DISCUSSION

Rodent macrophages (MP) were one the first cell types for which nitric oxide (NO) formation from L-arginine was shown with the involvement of the inducible NO synthase enzyme (iNOS). In response to the administration of lipopolysaccharides (LPS) with or without gamma interferon, these cells synthesized iNOS mRNA and the enzyme itself. At the same time,

the accumulation of a significant number of nitrites and nitrates was registered (Krahenbuhl and Remington, 1974).

But it turned out that peritoneal MP isolated in a standard way, incubated at room temperature, can also synthesize a small amount of NO without additional stimulation, which could be detected by the presence of nitrites and nitrates, which are stable products of NO oxidation and are registered by UV spectroscopy upon absorption of 330–340 nm. This MP ability was used in this work to study the effect of AA on NO synthesis in these cells. UV and ESR spectroscopy methods were used for recording NO formed in MP suspension incubated at room temperature with and without AA. When studying the formation of NO by ESR, Hb was used as an NO trap, which has a high affinity to NO, and interacting with it, forms stable nitrosyl Heme-NO complexes (Heme-NO NCs), which determine the well-known ESR signal — a wide singlet with g-factor 2.02 and characteristic triplet splitting of 17 G with a g-factor of 2.01.

ESR spectra of suspension of peritoneal macrophages (MP) specimens of mice incubated with AA (10 mM) (Figure 1 (1)) and without it (Figure 1 (2)) within 48 hours are shown in Figure 1. Comparison of the spectra in Figure 1 (1) and Figure 1 (2) show that in the MP specimens incubated with AA for 48 hours, the intensive ESR signal is observed, in samples without AA, the signal is of low intensity.

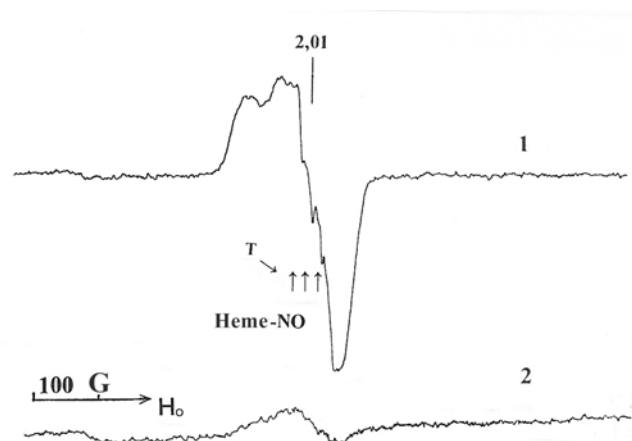


Figure 1. ESR spectra of samples of a suspension of peritoneal macrophages incubated for 48 hours at room temperature: (1) with AA (10 mM in 0.01 M Tris-buffer); (2) without AA (0.01 M Tris buffer). Spectrum registration conditions: microwave power 20 mW, the amplitude of magnetic field modulation 5 G, measurement temperature 77 K

The ESR signal in MP samples incubated with AA is due to nitrosyl complexes of Heme-NO NC, and its appearance indicates the formation of nitric oxide in the studied cell systems. Figure 2 shows the change in the intensity of the ESR signal in the MP suspension incubated for 20 and 48 hours, both with and without AA.

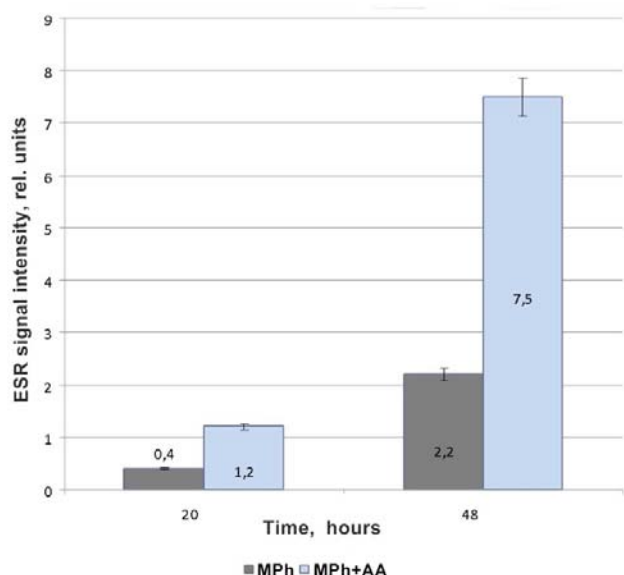


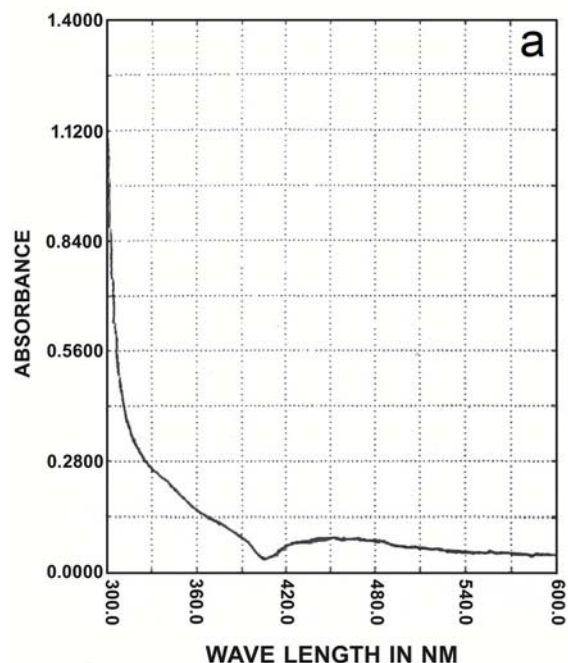
Figure 2. Change in ESR intensity signals of peritoneal macrophages suspension incubated for 20 and 48 hours at room temperature: in with and without AA.

By 48 h, the intensity of the ESR signal of Heme-NO NC and, consequently, the amount of NO formed in the samples incubated with AA was more than three times higher than the intensity of this signal in samples without AA.

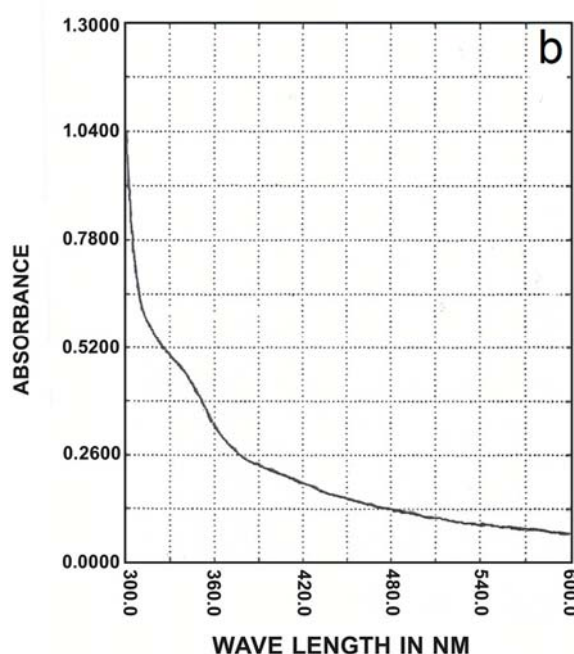
A quantitative assessment showed that in these conditions, 1.5×10^9 NO molecules are produced in macrophages per cell by 48 hours under the action of AA.

The optical absorption spectra of the supernatant of MP suspensions incubated at room temperature for 48 hours with and without AA were also analyzed. Figure 3 shows the optical absorption spectra of the MP supernatant in the region of 330-340 nm.

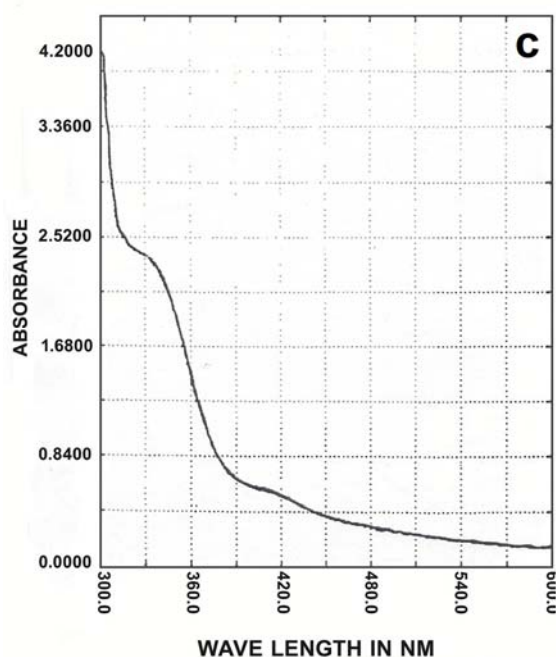
In samples incubated with AA (Figure 3 (b)), absorption was significantly higher (more than twice) than in supernatant samples of macrophages incubated without AA (Figure 3 (a)).



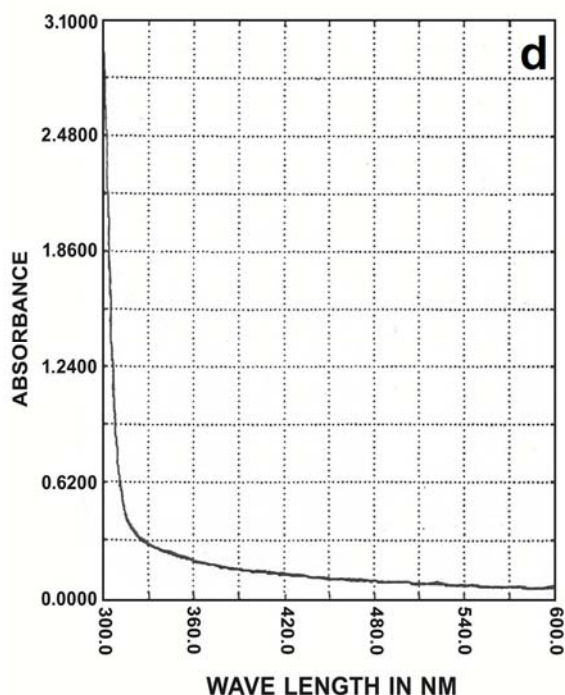
(a)



(b)



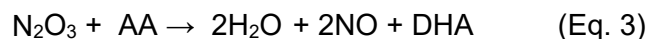
(c)



(d)

Figure 3. Spectra of optical absorption of the supernatant suspension of macrophages incubated: (a) - without AA (control); (b) - with AA; (c) - with AA + L-arginine; (d) - to samples of the supernatant (AA + arginine), the spectrum of which is shown in 3(c), immediately before the measurement, AA was added.

The incubation medium consisted of Tris buffer with the addition of 2% cattle serum solution in control samples. AA or AA + L-arginine were added in test samples, all in Tris buffer. It should be noted that the amount of nitrite formed in the samples in which the absorption spectrum is shown in Figure 3 (b) actually should really be more than registered since AA has not yet been used completely, part of the formed nitrite decomposes again under the action of AA with the formation of NO following the reactions in Equations 1 - 3 (Archer *et al.*, 1975):



And although nitrite can again be formed from the resulting NO, part of the NO is yet lost (leaves as a gas). Therefore, in experiments using the ESR method, when the formed NO molecules are accepted by hemoglobin, by 48 hours, there was a more than 3-fold increase in NO amount compared to control samples, in contrast to the data shown in Figure 3(b), when the increase was slightly more than 2 times. Figure 3(c) shows the absorption spectrum of the supernatant of macrophages incubated in the presence of AA with the addition of L-arginine (10^{-3} mM), NO- synthase substrate and an additional source of NO, and in this case the absorption value (and, therefore, the amount of nitrite formed) was higher than in samples of macrophages incubated only with AA. After addition to the supernatant of MP incubated with AA and L-arginine, the absorption spectra of which are shown in Figure 3(c), ascorbic acid at the concentration of $\geq 5 \times 10^{-3}$ mM, this absorption completely disappeared (Figure 3(d)) within 2-3 minutes confirming that the absorption in the region of 330-340 nm was due to nitrite ions, which rapidly decompose under the action of AA by the decomposition reaction of nitrites under the action of AA according to the above equations (Eq. 1 – Eq. 3).

Figure 4 shows the absorption spectra of macrophage supernatant samples after incubation with AA (10 mM) recorded regarding a control cuvette containing MP supernatant incubated without AA. Absorption in the region of

330-340 nm, due to nitrite and nitrate ions, the products of NO oxidation can be observed. This is one more evidence of the increased production of NO in MF under the influence of AA.

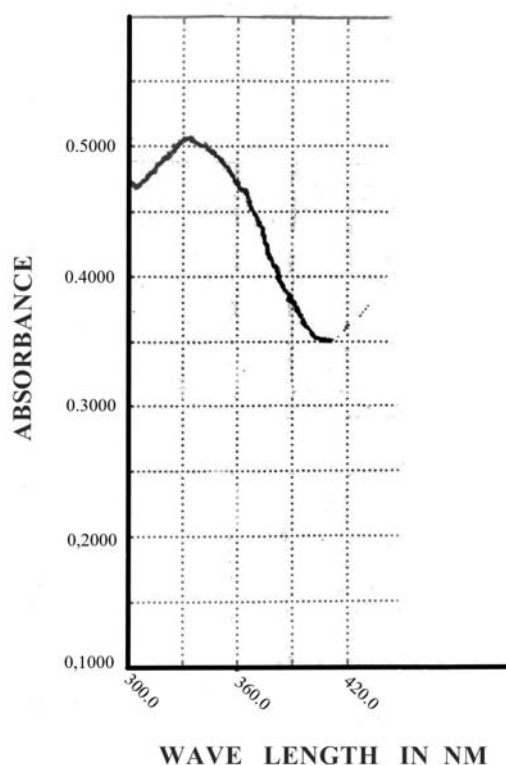


Figure 4. The optical absorption spectrum of the supernatant suspension of macrophages incubated with AA for 48 hours, measured relative to a control cuvette containing a supernatant suspension of macrophages incubated without AA under the same conditions.

The studies performed have shown that in peritoneal MP of SHK mice, NO synthesis in small amounts proceeds continuously without additional stimulating factors. And this is not a unique case. In the 1980s of the last century before the discovery of NO synthases, the formation of nitrosyl Heme-NO complexes was always observed during ESR study of the biotransformation of various biologically active compounds in isolated mouse liver tissues, and their number increased with the time of tissue incubation (Kuropteva and Pastushenko, 1985; Zhumabaeva and Kuropteva, 1986). Different hypotheses were made on NO appearance in the studied systems, but this effect became clear only after the discovery of NO-synthases. Now it is already well known that almost all cells in the liver tissue are able to express iNOS -

hepatocytes, Kupffer cells, endothelial cells, Ito cells. The appearance of intense signals of Heme-NO NC during incubation of liver tissues indicated that NO synthesis in liver cells proceeds continuously without additional stimulating factors. It was also reported in (MacMicking *et al.*, 1997) that some rat kidney cells or rat ovarian follicles during certain phases of the cycle, just like airway epithelium, are able to express iNOS normally. But previously, there were no reports that iNOS is expressed in MP normally, without induction.

The data obtained showed that AA is able to increase the synthesis of nitric oxide in peritoneal macrophages significantly and, therefore, activate NO-synthase. Using ESR, it was shown that after 48 hours incubation of MP with AA, the amount of NO formed was more than 3 times higher than in the samples incubated without AA. A quantitative assessment showed that each MP cell could synthesize up to 1.5×10^9 NO molecules under the experimental conditions (in 48 hours). Due to the absorption spectra of nitrites / nitrates, less increase in NO synthesis was recorded than by ESR. This is due to the fact that in the ESR experiments, all formed NO molecules are accepted by Hb, leading to the appearance of stable Heme-NO NCs, whereas when recording absorption spectra, the formed nitrites can partially be decomposed under the action of AA until all AA in the supernatant is consumed according to scheme 1.

To answer the question of the mechanisms of AA action, further studies are necessary. However, according to the data obtained and those available in the literature, it is possible to suggest that the main role of AA is to restore iNOS cofactors. NO-synthase is a carefully regulated enzyme, and for its normal functioning, 6 cofactors are necessary: FMN, FAD, NADH, BH₄, NADPH, and calmodulin connected with the active center. Moreover, tetrahydrobiopterin (BH₄), which is considered a necessary participant in the synthesis of NO as an active redox cofactor, is a key cofactor of iNOS (Heller *et al.*, 1999; Huang *et al.*, 2000; Hebel and Marletta, 1992).

This suggestion is based on the literature data on the increase in the NADPH content under the action of AA and on its participation in the maintenance of BH₄ in the reduced state. AA is necessary to prevent the irreversible oxidation of the key cofactor of the NO-synthase of tetrahydrobiopterin BH₄ to dihydrobiopterin BH₂ and thereby maintain the iNOS activity.

Really, there are experimental data showing that the increased iNOS activity is associated with maintaining the iNOS key cofactor - BH₄ in the reduced state (Nakai *et al.*, 2003; Huang *et al.*, 2000; Hebel and Marletta, 1992; Heller *et al.*, 2001; Toth *et al.*, 2002; D'Uscio *et al.*, 2003). The data obtained in (Wu *et al.*, 2002) that AA does not affect iNOS expression also confirm the suggestion of its participation as a reducing agent of the iNOS cofactors.

This assumption is indirectly supported by data on the functioning of the cycle of the NO and arginine synthesis in MP, as in the active work of the cycle, the need in BH₄ and NADPH increases significantly (Kuropteva *et al.*, 2019).

Previously there were reports on stimulation of NO formation by ascorbic acid in immunocompetent cells - animal and human leukocytes and some types of macrophages (Nakai *et al.*, 2003; Mizutani and Tsukagoishi, 1999; Kuropteva *et al.*, 2000). We believe that this effect plays a main role in the stimulation of the human immune system by ascorbate. In bacterial and viral infections, both iNOS induction and induction of humoral factors, cytokines, occur (Nathan, 1995; Bogdan, 2001). Cytokines activate NO formation in white blood cells and macrophages. NO, inhibiting the respiratory system and DNA synthesis in target cells (pathogenic bacteria, tumor cells) slows their reproduction and contributes to the death of these cells. AA, the content of which is high in leukocytes and MP, supports the process of NO production. But at the same time, AA is consumed. Therefore, in order for leukocytes and MP to be able to synthesize NO in sufficient amounts, it is necessary to maintain a sufficient level of AA in the organism.

The connection of the animal immune system with AA is confirmed by the fact that under adverse conditions in animals able to synthesize AA themselves AA immediately increases, the need in this vitamin increases several times.

The fact that AA can support the human immune system has been known for many years. AA turned to be especially effective in the prevention and control of colds. But the mechanism of AA action and its involvement in antibacterial action was earlier unclear. We believe that established in the recent

two decades effect of nitric oxide synthesis increase under AA action is the main one in the prevention and therapeutic effect of

this compound, at least for colds. The fact observed in practice.

5. CONCLUSION

Thus, it was shown that AA increases NO synthesis in the peritoneal macrophages of SHK mice. The amount of synthesized NO depends on the duration of AA activity. Maintenance of NO production in the cells of the immune system is very important since it was established that NO produced by leukocytes and macrophages is their main means for the destruction of bacteria, viruses, tumor cells, and other pathogenic organisms (Farias-Eisner *et al.*, 1994; Croen, 1993; Bi and Reiss, 1995; Vazquez-Torres *et al.*, 2000; Sibille and Reynolds, 1990; Nathan, 1995).

In mice macrophages and other immunocompetent cells, iNOS can synthesize NO for a long time after cell stimulation - for several hours or even days if there is a sufficient amount of arginine substrate and enzyme cofactors (Nathan, 1995; MacMicking *et al.*, 1997). In (Kuropteva *et al.*, 2019), data were obtained that suggested that in cells capable of expressing iNOS, there is a special cyclic process for the synthesis of arginine and nitric oxide, in which citrulline formed with iNOS can again be used for the synthesis of L-arginine and NO formation. The existence of such a cycle in MP allows us to explain how immunocompetent cells provide high necessities for L-arginine, necessary for NO synthesis. Thus, macrophages provide themselves with arginine. But in addition to arginine, oxygen and 6 cofactors, including tetrahydrobiopterin and NADPH, are also required for the normal functioning of iNOS. With the depletion of reserves of compounds that ensure the operation of this molecular machine - iNOS, NO production decreases. This results in the decreased functional activity of leukocytes and macrophages and a decrease in their cytotoxic / cytostatic effect on pathogenic organisms. As suggested above, AA action is probably associated with maintaining iNOS cofactors (in particular, BH₄ and NADPH) in the reduced working condition.

Therefore, the possibility of increasing NO production in the cells of the immune system using AA is important for increasing the effectiveness of prevention and control of bacteria, viruses, tumor cells, and other pathogenic organisms.

6. REFERENCES

1. Archer, M. C., Tannenbaum, S. R., Fan, T. Yi., Weisman, M. Reaction of nitrite with ascorbate and its relation to nitrosamine formation. *J Natl Cancer Inst.*, **1975**, 54(5), 1203-1205.
2. Beltran, B., Mathur, A., Duchon, M. R., Erusalimsky, J. D., Moncada, S. The effect of nitric oxide on cell respiration: A key to understanding its role in cell survival or death. *Proc. Natl. Acad. Sci. The USA*, **2000**, 97, 14602-14607.
3. Bi, Z., Reiss, C. S. Inhibition of vesicular stomatitis virus infection by nitric oxide. *J. Virol.*, **1995**, 69, 2208-2213.
4. Billiar, T. R., Curran, R. D., Stuehr, D. J., West, M. A., Bentz, B. G., Simmons, R. L. An L-arginine dependent mechanism mediates Kupffer cell inhibition of hepatocyte protein synthesis in vitro. *J. Exp. Med.*, **1989a**, 169(4), 1467-1472. doi: 10.1084/jem.169.4.1467
5. Billiar, T. R., Curran, R. D., West, M. A., Hofmann, K., Simmons, R. L. Kupffer cell cytotoxicity to hepatocytes in coculture requires L-arginine. *Arch. Surg.*, **1989b**, 124(12), 1416-1420. DOI: 10.1001/archsurg.1989.01410120062013
6. Bogdan, C. Nitric oxide and the immune response. *Nat. Immunol.*, **2001**, 2, 907-916.
7. Croen, K. D. Evidence for an antiviral effect of nitric oxide. *J. Clin. Invest.*, **1993**, 91, 2446-2452.
8. D'Uscio, L. V., Milstein, S., Richardson, D., Smith, L., Katusic, Z. S. Long-term vitamin C treatment increases vascular tetrahydrobiopterin levels and nitric oxide synthase activity. *Circ. Res.*, **2003**, 92, 88-95.
9. Fang, F. C. Perspectives series: host/pathogen interactions. Mechanisms of nitric oxide-related antimicrobial activity. *J. Clin. Invest.*, **1997**, 99, 2818-2825.
10. Farias-Eisner, R., Sherman, M. P., Aerberhard, E., Chaudhuri, G. Nitric oxide is an important mediator of tumoricidal activity in vivo. *Proc. Natl. Acad. Sci. The USA*, **1994**, 91, 9407-9411.
11. Hebel, J. M., Marletta, M. A. Macrophage nitric oxide synthase: the relationship between enzyme-bound tetrahydrobiopterin and synthase activity. *Biochemistry*, **1992**, 31, 7160-7165.
12. Heller, R., Munsher-Paulig, F., Grabner, R., Till, U. L-ascorbic acid potentiates nitric oxide synthesis in endothelial cells. *J. Biol. Chem.*, **1999**, 274, 8254-8260.
13. Heller, R., Unbehauen, A., Schellenberg, B., Mayer, B., Werner-Felmayer, G., Werner, E. R. L-ascorbic acid potentiates endothelial nitric oxide synthesis via a chemical stabilization of tetrahydrobiopterin. *J. Biol. Chem.*, **2001**, 276, 40-47.
14. Hibbs, J. B. Jr., Taintor, R. R., Vavrin, Z. Macrophage cytotoxicity: Role for L-arginine, deiminase, and imino nitrogen oxidation to nitrite. *Science*, **1987a**, 235(4787), 473-476.
15. Hibbs, J. B. Jr., Vavrin, Z. Taintor, R. R. L-arginine is required for expression of the activated macrophage effector mechanism causing selective metabolic inhibition in target cells. *J. Immunol.*, **1987b**, 138(2), 550-565.
16. Huang, A., Vita, J. A., Venema, R. C., Keaney, J. F. Jr. Ascorbic acid enhances endothelial nitric oxide synthase activity by increasing intracellular tetrahydrobiopterin. *J. Biol. Chem.*, **2000**, 275, 17399-17406.
17. Keller, R. The macrophage response to infectious agents: mechanisms of macrophage activation and tumor cell killing. *Res. Immunol.*, **1993**, 144, 271-273.
18. Krahenbuhl, J. L., Remington, J. S. The role of activated macrophages in specific and nonspecific cytostasis of tumor cells. *J. Immunology*, **1974**, 113, 507-516.
19. Kuropteva, Z. V., Bayder, L. M., Nagler, L. G., Bogatyrenko, T. N., Belaya, O. L. Synthesis of arginine and nitric oxide in cells with inducible NO synthase. *Izv. RAS. Ser. Chem.*, **2019**, 1, 174-180.
20. Kuropteva, Z. V., Bayder, L. M., Zhumabaeva, T.T. The effect of ascorbic acid on the production of leukocytes of nitric oxide. *Biophysics*, **2000**, 45(4), 671-674.
21. Kuropteva, Z. V., Pastushenko, O.N. Changes in paramagnetic complexes of blood and liver of animals under the influence of nitroglycerin. *Rep. USSR Academy of Sciences*, **1985**, 281(1), 189-192.
22. Kwon, N. S., Stuehr, D. J., Nathan, C. F. Inhibition of tumor cell ribonucleotide reductase by macrophage-derived nitric oxide. *J. Exp. Med.*, **1991**, 174, 761-767.
23. MacMicking, J., Xie, Q.-w., Nathan, C. Nitric oxide, and macrophage function. *Annu. Rev. Immunol.*, **1997**, 15, 323-350.

24. Mizutani, A., Tsukagoishi, N. Molecular role of ascorbate in the enhancement of NO production in the activated macrophage-like cell line, *J774.1. J. Nutr. Sci. Vitaminol. (Tokio)*, **1999**, *45*, 423-435.
25. Nakai, K., Urushihara, M., Kubota, Y., Kosaka, H. Ascorbate enhances iNOS activity by increasing tetrahydrobiopterin in RAW 264.7 cells. *Free radical Biology and Medicine*, **2003**, *35*, 929-937.
26. Nathan, C. Natural resistance and nitric oxide. *Cell*, **1995**, *82*, 873-876.
27. Sibille, Y., Reynolds, H. Y. Macrophages and polymorphonuclear neutrophils in lung defense and injury. *Am. Rev. Respir. Dis.*, **1990**, *141*, 471-501.
28. Stuehr, D. J., Marletta, M. A. Induction of nitrite/nitrate synthesis in murine macrophages by BCG infection, lymphokines, interferon-gamma. *J. Immunol.*, **1987a**, *139*, 518-525.
29. Stuehr, D. J., Marletta, M. A. Synthesis of nitrite and nitrate in Murine macrophage cell lines. *Cancer Res.*, **1987b**, *47(21)*, 5590-5594.
30. Stuehr, D. J., Nathan, C. F. Nitric oxide. A macrophage product is responsible for cytostasis and respiratory inhibition in tumor target cells, *J. Exp. Med.*, **1989**, *169*, 1543-1555.
31. Toth, M., Kukor, Z., Valent, S. Chemical stabilization of tetrahydrobiopterin by L-ascorbic acid: contribution to placental endothelial nitric oxide synthase activity. *Mol. Hum. RESRod.*, **2002**, *8*, 271-280.
32. Vazquez-Torres, A., Jones-Carson, J., Mastroeni, P., Ischiropoulos, H., Fang, F. C. Antimicrobial actions of the NADPH phagocyte oxidase and inducible nitric oxide synthase in experimental salmonellosis. I. Effects on microbial killing by activated peritoneal macrophages in vitro. *J. Exp. Med.*, **2000**, *192*, 227-236.
33. Wasley, G. D. Animal Tissue Culture. Williams & Wilkens Co., Baltimore, **1972**.
34. Wu, F., Timl, K., Wilson, J. X. Ascorbate inhibits iNOS expression in endotoxin- and IFN-gamma-stimulated rat skeletal muscle endothelial cells. *FEBS Lett.*, **2002**, *520*, 122-126.
35. Zhumabaeva, T. T., Kuropteva, Z. V. On the molecular mechanisms of the radiosensitizing effect of nitro compounds. *Radiobiology*, **1986**, *26(5)*, 671-674.

O ESTUDO DA AGRESSIVIDADE BIOLÓGICA DO PÓ DE COMPOSIÇÕES FORMADAS E SEM AMIANTO, AMBOS EM SUA PRODUÇÃO E OPERAÇÃO

THE STUDY OF THE BIOLOGICAL AGGRESSIVENESS OF DUST OF ASBESTOS-FORMED AND ASBESTOS-FREE COMPOSITIONS, BOTH IN THEIR PRODUCTION AND OPERATION

ИССЛЕДОВАНИЕ БИОЛОГИЧЕСКОЙ АГРЕССИВНОСТИ ПЫЛЕЙ АСБЕСТОФОРМОВАННЫХ И БЕЗАСБЕСТОВЫХ КОМПОЗИЦИЙ, КАК ПРИ ИХ ПРОИЗВОДСТВЕ, ТАК И ПРИ ИХ ЭКСПЛУАТАЦИИ.

YATSENKO, Alexandr Sergeevich^{1*};

¹ Federal State Budgetary Educational Institution of the Higher Education Ural State University of Railway Transport, Department of Technosphere Safety Yekaterinburg, Russian Federation

* Correspondence author

e-mail: al3ksandr.yatsenko@yandex.ru

Received 22 December 2019; received in revised form 04 February 2020; accepted 10 February 2020

RESUMO

Este manuscrito fornece informações básicas sobre o uso do amianto. Algumas propriedades físico-químicas do principal componente do amianto serpentino (AS, 95% de todo o amianto usado) e a agressividade biológica dos seguintes itens são consideradas: tipos de poeira na tecnologia de criação de produtos que contêm amianto e durante sua operação. Também foi dada atenção ao uso de substitutos do amianto existentes em produtos similares. Os autores apresentam dados que verificam que a incidência de doenças relacionadas ao amianto, incluindo asbestose de natureza profissional e não profissional, aumenta, principalmente em idosos, nos locais de produção de uma variedade de SA - amianto crisotila {CA, silicato de magnésio aquoso - $Mg_6[Si_4O_{10}](OH)_8$ }. Os autores prestam atenção especial ao uso de CA na produção de peças / produtos formados por amianto (AFP), por exemplo, lonas de freio contendo CA e seus substitutos. Sabe-se que esses produtos sofrem tensões zonais significativas durante a operação. As fibras CA perdem água higroscópica e constitucional. ($H_2O = 13,04 - 14,80\%$) no processo de frenagem do carro devido à alta pressão e aumento da temperatura local. Como resultado, eles se transformam quase totalmente em um material não agressivo (no sentido biológico) chamado forsterita. Estudos de pó de freio emitidos durante a frenagem de veículos leves VAZ não revelaram transformações semelhantes da degradação de CA. Podem ocorrer ao travar veículos pesados com massa superior a 2,5 toneladas e ao travar trens de alta velocidade com massa superior a 60 toneladas.

Palavras-chave: Amianto crisotila (AC), itens de fricção por atrito, forsterita, asbestose, basalto.

ABSTRACT

This manuscript provides basic information on the use of asbestos. Some physicochemical properties of the main component of serpentine asbestos (SA, 95% of all used asbestos) and the biological aggressiveness of the following are considered: dust types in the technology of creating asbestos-containing products and during their operation. Attention is also paid to the use of existing asbestos substitutes in similar products. The authors present data verifying that the incidence of asbestos-related diseases, including asbestosis of a professional and unprofessional nature, is increased, especially in the elderly, in the places of production of an SA variety – chrysotile asbestos {CA, aqueous magnesium silicate - $Mg_6[Si_4O_{10}](OH)_8$ }. The authors pay particular attention to the use of CA in the production of asbestos-formed parts/products (AFP), for example, brake linings containing CA and its substitutes. It is known that such products undergo significant zonal stresses during operation. CA fibers lose hygroscopic and constitutional water ($H_2O = 13.04 - 14.80\%$) in the process of car braking due to high pressure and increased local temperature. As a result, they almost entirely turn into a non-aggressive (in the biological sense) material called forsterite. Studies of brake dust emitted during the braking of lightweight VAZ vehicles did not reveal similar transformations of CA degradation. They may occur when braking heavy vehicles with a mass of more than 2.5 tons and when braking high-speed trains with a mass of more than 60 tons.

Keywords: *Chrysotile asbestos (CA), frictional braking items, forsterite, asbestosis, basalt.*

ABSTRACT

В статье представлены основные сведения об использовании асбеста. Рассмотрены некоторые физико-химические свойства основного компонента серпентинового асбеста (СА, 95% всего используемого), биологическая агрессивность: выделяющихся видов пыли в технологии создания асбестосодержащих изделий и при их эксплуатации, обращено также внимание на использование существующих заменителей асбеста в аналогичных изделиях. Представлены данные, что в местах добычи разновидности СА - хризотил-асбеста {ХА, водный силикат магния - $Mg_6[Si_4O_{10}](OH)_8$ } повышена заболеваемость асбест-обусловленными болезнями, а также асбестозом- профессионального и непрофессионального характера, особенно у лиц пожилого возраста. Особое внимание уделено использованию ХА в производстве асбестоформованных деталей/изделий (АФД), например, изготовление и использование тормозных накладок с содержанием ХА и его заменителей. Известно, что такие изделия в процессе эксплуатации подвергаются значительным зональным напряжениям. В процессе торможения автомашин в следствии возникающего высокого давления и повышенной локальной температуры в волокнах ХА происходит потеря гигроскопической и конституционной воды ($H_2O = 13,04 - 14,80\%$) в результате чего они практически полностью превращаются в неагрессивный в биологическом смысле материал под названием форстерит. Проведенные исследования тормозной пыли, выделяющейся при торможении легковых автомашин марки ВАЗ, подобные превращения деградации ХА не выявили, возможно они имеют место при торможении тяжеловесных автомашин с массой более 2,5 т и при торможении высокоскоростных, железнодорожных составов массой более 60 т.

Keywords: *Хризотил-асбест (ХА), Фрикционные тормозные изделия, Форстерит, Асбестоз, Базальт.*

1. INTRODUCTION

Chrysotile asbestos (CA) is a fine fiber mineral of the silicates class. Serpentine asbestos is of the greatest importance since it accounts for 95% of the asbestos that is used, commonly called "mountain flax". This is a mineral of the serpentine group – aqueous magnesium silicate $Mg_6[Si_4O_{10}](OH)_8$, which contains silicates of calcium, iron, sodium, and possibly other metals as impurities, and there is usually no free silicic acid (SiO_2), but it can appear in an amorphous form upon ignition. CA filamentary crystals are capable of splitting into very thin fibers, chemically resistant and resistant to high temperatures, which are widely used in engineering and in households: fireproof asbestos textile materials, types of workwear, asbestos cement products; friction products (brake linings, rings containing CA not less than 40-50%); paronite, electron for heat and electrical insulating gaskets, asbestos paper, and asbestos board; heat-insulating materials, asbestos-bitumen materials (roofing material, waterproofing materials).

The rapid development and improvement of all types of transport have led to an increase in the production of asbestos-formed parts (AFP), which are used in braking systems of various modes of transport, and in asbestos content, which can reach up to 75%. The latter depends on the mass and speed of a given means of transport:

the greater the speed and the weight of a given transport unit, the greater the amount of asbestos used in its CA brake linings.

During the operation of a transport unit, as well as in the manufacture of AFP (machining), a disintegration aerosol with CA content, which is officially recognized as professional harmful throughout the world, is released into the working area and the external environment. CA fibers can invade the epidermis, leading to the development of hyperkeratosis and cell proliferation. In asbestos textile production, asbestos formations are often localized on the flexion surfaces of the limbs. Car mechanics involved in the repair of braking systems and exposed to brake dust have shown an increased risk of cancer (pleural mesothelioma or lung cancer). CA long and short fibers, as well as coated with Bakelite or cement, have increased fibrogenicity and cytotoxicity compared to amphibole asbestos.

However, information on the incidence of asbestosis among these workers is controversial: from the recognition of a moderate asbestos hazard to a pronounced risk of its development after a relatively short exposure period. At the same time, in several epidemiological studies, even with prolonged dust exposure, and the increased oncological risk was not detected; however, some data in the literature indicate pronounced toxic, fibrogenic, and carcinogenic effects of CA, effects which are greatest on the cell

structure of macrophages and erythrocyte suspension (Yatsenko, 1995). Consequently, the biological aggressiveness of dust containing CA requires further in-depth study.

The term asbestos is currently understood to mean a group of minerals having a fibrous structure. Most of the mined asbestos belongs to the serpentine group – the serpentine and is called chrysotile asbestos CA – white asbestos (Fig. 1, 2) (Nikitina, 1991).



Figure 1. Chrysotile asbestos

Source: Nikitina, 1991

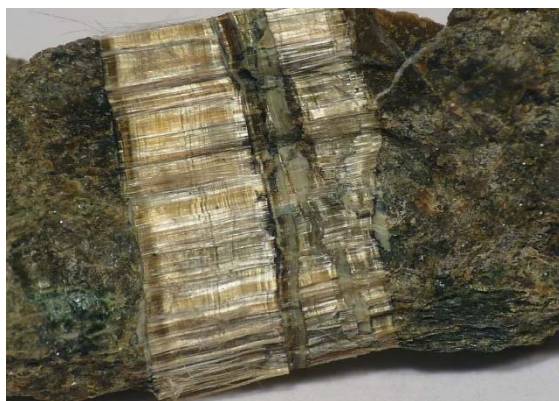


Figure 2. Asbestos vein in a mountain mineral

Source: Nikitina, 1991

The amphibole (hornblende) asbestos group differs significantly from the latter in several physicochemical properties. This group includes the following: anthophyllite, amosite, tremolite, actinolite, crocidolite, cape blue asbestos, rhodusite, and magnesio-arfvedsonite. The amphibole group of asbestos, which is practically not excreted from the lungs, poses the greatest danger to human health. CA, unlike amphiboles,

decomposes under the influence of tissue fluids and therefore is more rapidly excreted from the body and can pose a lower risk to human health. The greatest industrial value, both in Russia and abroad, is accounted for by CA. Currently, deposits in Bazhenovskoye (Sverdlovsk region, Russia), Quebec (Canada), Zimbabwe, South Africa, northern Kazakhstan, China, the United States, Brazil, Italy, and Japan are of the greatest global importance. However, at present, due to the increased consumption of asbestos in large cities, in addition to asbestosis, the number of malignant tumors – pleural mesothelioma and peritoneum – is also increasing. Therefore, asbestos is considered by many countries as characteristic of the hazards of contemporary urban life (Modern urban hazard) (Khazbiev, 2012). Such a statement is undoubtedly exaggerated.

International Labor Organization (ILO) Convention No. 162 (Geneva, 72nd Session of the ILO General Conference, 1986) on Occupational Health and Safety when Using Asbestos, covering all activities related to the effects of asbestos on workers, defined measures to prevent harmful effects on human health. In addition, in the Recommendations of the above conference, it was determined that the prohibition or authorization of the use of asbestos and asbestos-containing products should be based on a scientific assessment of their health hazards. Based on studies of carcinogens, The International Agency for Research on Cancer classifies asbestos in the first, most dangerous category of the list of carcinogens.

The most dangerous asbestos amphibole minerals are Amosite and Crocidolite (blue asbestos). Chrysotile fiber is easy to fluff in the air and in water, has a high adsorption capacity, and exhibits active adhesion to several carcinogens. This fiber is endlessly divided into very small sizes and is carried over very long distances in the air. The presence of CA fibers was established even at the north and south poles, where there is no human activity. Such negligibly small CA fibers easily penetrate the human body and carry various carcinogens.

The biological carcinogenic effect of CA substantially depends on its fiber length and diameter, which affects retention, clearance, and phagocytosis (Le Bouffant, 1980). For many years, the prevailing opinion abroad was that only hard, relatively long particles of asbestos penetrated the lung tissue, violating its integrity and causing proliferative inflammation with the gradual development of fibrosis in the area of fiber accumulation in bronchioles and in places where

the ciliated epithelium becomes cuboid. Short fibers ($<3\ \mu\text{m}$) cause a very weak reaction. Long particles cannot be removed by phagocytosis. Lingering in bronchioles, these long particles cause permanent tissue injury with respiratory movements. However, the introduction of short asbestos fibers also develops fibrosis, both nodular and diffuse-interstitial types.

Electron microscopy of sections of the lungs of experimental animals revealed a huge number of submicroscopic particles, which are hardly capable of injuring tissues. The development of fibrosis in areas where very long asbestos fibers very rarely settle does not have an explanation: around blood vessels, interalveolar septa, etc. A correlation between 1 gram of mineral residue in a dry lung and the severity of asbestosis has not been established (Nikitina, 1991). In addition, the decisive biological aggression is determined not by the needle structure and hardness of the asbestos, but by its solubility in tissue fluids.

In the case of prolonged contact of CA with tissue fluid, some dissolution of silicic acid occurs, causing damage and death of lung tissue cells. The above-mentioned effects of asbestos on the body led to a decrease and even a complete stoppage of its use in advanced countries of Europe (Platpnova, 2018). For example, in 1997, asbestos was completely banned in France, and since 2005, the countries of the European Union refuse to use asbestos (Dodson and Hammer, 2011; Castleman and Berger, 2005). However, for many products containing CA, there is no substitute for its properties today, and they are extremely necessary for several industries.

Previously accumulated asbestos-containing products in these countries should be regulated to neutralize the biological effects of asbestos or bury it in special places. Numerous methods have been proposed for special processing of asbestos-containing materials and their waste and use, such as CA calcination at 600-800°C, microwave radiation (Colangelo *et al.*, 2011; Gramat *et al.*, 2011), sulfuric acid treatment (Nam Nam *et al.*, 2014) and carbonization (Gadikota *et al.*, 2014), which alter the chemical and biological properties that reduce fibrogenicity and cytotoxicity.

After special treatment, asbestos-containing cement materials can be used as additives in building structures. For the disposal of asbestos-containing materials and their waste, the use of inactive mines has been proposed, which is being used in Greece, England, Italy, Germany,

and other EU countries (Gidakos *et al.*, 2008). However, despite the West recognizing asbestos as dangerous, the Rotterdam Convention does not include CA in the list of hazardous substances, and it continues to be used in the national economy in Russia and in developing countries, where up to 80% of the world's population lives. It should also be noted that based on ILO Convention No. 162, in many countries, another way has been proposed, consisting of replacing asbestos with other artificial mineral fibers. In Russia, Nikitina O.V. (1991) carried out such works by replacing CA with basalt fibers (AFC, Fig. 3, 4). In an animal experiment, it was possible to reduce the number of peritoneal mesotheliomas, but, unfortunately, the number of other malignant neoplasms increased about the same amount, especially in comparison with super-thin basalt fibers (STBF). In a comparative assessment of fibrogenicity, the results obtained also indicated relatively high rates compared with the control.



Figure 3. Characteristic columnar separateness of basalt
Source: Nikitina, 1991



Figure 4. Basalt
Source: Nikitina, 1991

Considering all the above, it can be inferred

that when replacing CA with AFC, where it is expedient from a technical and economic point of view, the requirements for safety measures should be similar to those in production with CA. Therefore, it is not yet possible to completely replace CA in technology. For example, when replacing CA with basalt fibers in brake products, the stopping distance of cars will be significantly increased, the latter, given the number of vehicles, speed limits, and tension on roads, of course, cannot be allowed. Basalt fibers can be used as a substitute for CA only where appropriate (Muzafarov, 1979).

The possible effect of dust on the nearby human and animal populations should also be considered in the hygienic assessment of asbestos processing plants. The former also confirms the increase in pleural forms of unprofessional asbestosis, mainly in older people (Ginzburg, 1970). The authors attribute this pathology to the weathering of the soil, and in particular, asbestos, which is likely present in these areas (Republic of Khakassia). A substantial amount of manufactured road and rail transportation can be a source of CA, both in residential zones and in the whole environment.

The purpose of the research is to study the biological aggressiveness of asbestos-containing and asbestos-free friction products in both their production and actual use.

Technological progress, including the rapid development of all types of transportation, steadily leads to an increase in the production of asbestos-molded parts intended for use in brake and vehicle coupling systems.

For the first time, it has been experimentally shown that the dust of asbestos-containing and basalt-containing (non-asbestos) compositions of friction products has equally pronounced moderate fibrogenic, weak carcinogenic, and noticeable toxic effects (Sudo, 2011). Additionally, in first-time animal experiments, the biological aggressiveness of dust was compared with the content of asbestos and non-asbestos dust based on basalt fibers (including those that were artificially created) (Nikitina, 1991; Yatsenko, 1994).

Asbestos, undoubtedly, is one of the leaders among materials that symbolize the progress of science and technology. Due to its unique properties (strength, the elasticity of fibers, heat and electrical conductivity, and chemical and thermal resistance), it is widely used in various industries. In industrialized countries, around 10% of asbestos is used for the preparation of

asbestos-shaped parts containing 15–72% of chrysotile asbestos. Technological progress, including the rapid development of all types of transportation, is steadily leading to an increase in the production of asbestos-molded parts intended for the brake and vehicle clutch system sectors (Yatsenko, 1994).

It was also experimentally shown for the first time that the dust from asbestos-containing and basalt-containing (asbestos-free) compositions of friction products, as well as the dust released during the repair of brake systems, have equally pronounced moderate fibrogenic, weak carcinogenic, and noticeable toxic effects. In this case, the degree of toxicity is determined by the content of chrysotile asbestos and phenol in the dust. The fibrogenicity does not depend on the presence of chemical additives used in the production of asbestos-formed parts. In addition, the biological aggressiveness of dust with asbestos and asbestos-free dust based on basalt fibers and artificially created ones was first experimentally compared in animals.

2. MATERIALS AND METHODS

The study of the degradation of chemical agents during the mechanical processing of brake products in production and their abrasion during braking of vehicles was carried out on ordinary asbestos-formed products of the Vehicle Textile Goods Plant in the town of Asbest, Russia. The study of structural changes in the CA crystal structure was carried out by X-ray phase analysis using a powder method (Gorelik, 1994; Mikheev, 1957; Mirkin, 1976) in the angle range V from 5 to 50° on a DRON-2.0 diffractometer by Burevestnik Research and Production Enterprise, St. Petersburg) in filtered copper $K\alpha$ -radiation and infrared spectroscopic analysis on a spectrometer "Specord JK-75" (manufactured by Analytik Jena, Germany) in the range of 400 - 4,000 cm^{-1} using pastes in paraffin oil in air at room temperature.

The authors used "Statistics in hygienic research Express method for estimating average values" by E. L. Notkin to assess the statistical significance. In acute and long-term experiments on toxicity, fibrogenicity, and carcinogenicity, the dust of brake products, containing CA and its substitutes, mice and white outbred rats were used.

The severity of the toxic effect was studied in an acute experiment on LD 50 (lethal dose = death of 50% of animals) with intraperitoneal administration in mice. The fibrogenic effect of

brake dust samples was studied in rats with an initial weight of 160-180 g, which were injected with 50 mg of various types of dust, in the form of a suspension in 1 ml of physiological solution. The control group of rats, respectively, was administered 1 ml of saline, without dust. Oncogenic evaluation of dust was studied in chronic experiments on similar rats, with an intraperitoneal injection. This experiment used two types of control: A). Rats that were injected with Bazhenov's CA powder, the carcinogenicity of which has been proven in several scientific studies and B). Rats that were injected with physiological saline only. Asbestos and asbestos-free dust samples were injected twice, in a single dose of 25 mg, with an interval of one month (Yatsenko and Sherstyuchenko, 2019).

Observation of animals lasted until the end of their lives (Yatsenko, 2017). The severity of the toxic effect was studied in an acute experiment on LD50 with intraperitoneal injection.

3. RESULTS AND DISCUSSION:

Brake dust released both during braking and machining does not lose its biological aggressiveness. CA does not turn into biologically safe forsterite. According to the data of IR spectroscopy, CA fibers do not completely lose constitutional water during mechanical processing. This is especially evident when considering the interval of deformation vibrations of water at $1,600\text{--}1,650\text{ cm}^{-1}$. Intense absorption in the region of $3,200\text{--}3,500\text{ cm}^{-1}$ and a weak band with a maximum at $1,600\text{ cm}^{-1}$ in the spectrum of asbestos and bakelite dust are due to the presence of labile interlayer water coordinated to metal (Figs. 5 and 6) (Mikheev, 1957).

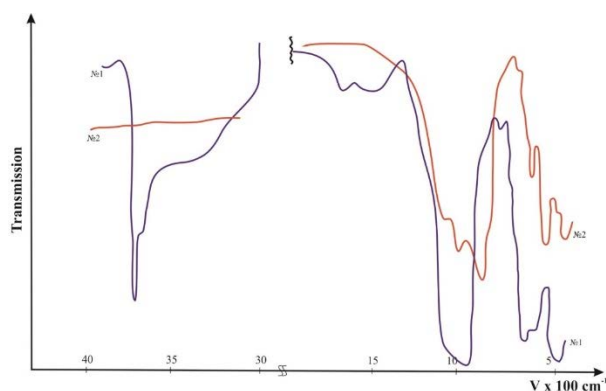


Figure 5. IR transmission spectra of samples of Bazhenovsky CA (No. 1) and CA calcined in a muffle furnace at $T = 900^{\circ}\text{C}$ (Fig. 2)

Source: Mikheev, 1957

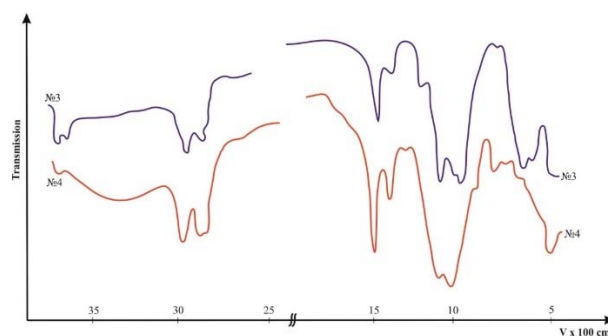


Figure 6. IR transmission spectra of dust samples collected from brake drums of cars (No. 4) and brake pad (Fig. 3)

Source: Mikheev, 1957

Based on the X-ray mineral determinant (Mikheev, 1957), the three lines related to forsterite and all the studied samples have very close interplanar spacings. In this regard, unambiguous radiographic identification of forsterite is difficult. The authors can only assume that if the latter is present, then its content is less than 10%.

The results of the toxic effect are presented in Table 1.

Table 1. Toxic effect of dust from friction products

Dust sample	The toxic effect of dust brake composites, depending on the dose, %					LD50, g/kg
	0.5	2.0	6.0	10.0	14.0	
Chrysotile-asbestos (CA)	20	80	100	100	-	1.5 ± 0.3
Asbestos Bakelite (AB)	-	16.6	50	100	-	5.4 ± 0.5
Basalt-containing compositions	-	-	50	70	100	6.2 ± 0.8
407-10	-	0	40	90	-	6.5 ± 0.4
E-251	-	-	-	-	-	-
Asbestos rubber	-	-	-	-	-	-

(AR)	-	0	33.	80	-	7.2 ±
T-167	-	-	3	60	93.	0.5
42-975			0		3	10.2 ± 0.5
Basalt fibers (STBF)	-	0	0	0	-	Over 10.0

Notes: 0 – no fallen animals

(-) – the specified dose was not injected

The fibrogenicity of dust released both during the production of AFP and during their usage was measured by the total hydroxyproline content in rat lungs, three and six months after injecting the test samples. The oxyproline content in rat lungs is shown in Tables 2 and 3.

Table 2. The content of oxyproline in the rat lungs with an intratracheal dusting (per 100 g of body weight) 3 months after injection

Samples of injected dust	Oxyproline, mcg
CA	2,290.0 ± 130.0
AR	1,890.0 ± 60.0
AB	3,199.5 ± 212.6
Dust collected from brake drums	3,208.2 ± 177.2
Control	1,220.0 ± 900
Asbestos-free compositions (AFC)	2,180.0 ± 210.0

Table 3. The content of oxyproline in the rat lungs with an intratracheal dusting (per 100 g of body weight) 6 months after injection

Samples of injected dust	Oxyproline, mcg
Control	1,520.0 ± 100.0
AR	2,150.0 ± 190.0
AB	3,924.2 ± 203.8
Dust collected from brake drums	3,527.4 ± 97.4
CA	2,980.0 ± 100.0
Quartz	4,600.0 ± 240.0
Asbestos-free compositions (based on basalt)	1,960.6 ± 160.6

Indicators of total hydroxyproline in the lungs make it possible to judge the degree of development of the fibrous process and, therefore, dust fibrogenicity. Tables 2 and 3 show that the dust collected from the brake drums has significant fibrogenic potential, even compared with CA, particularly with asbestos-free compositions. However, the fibrogenic potential of quartz is the highest. The data of experiments to determine the oncogenicity of the studied dust samples are presented in Table 4.

Table 4. The results of experiments on the comparative assessment of oncogenic properties of the studied dust

No. of the experiment	Injected substances	Number of rats	% of rats with malignant tumors
1	Control	110	-
	CA	60	45.0 ± 6.4
2	AR dust collected from the brake drums (T-167)	65	3.0 ± 2.1
	Basalt-containing composition s:		
	407-10	64	3.1 ± 2.1
	E-251	65	4.6 ± 2.5
	Superthin basalt fiber	50	14.0 ± 1.6

Table 4 shows that asbestos-containing dust released during the braking of vehicles has a significantly lower potential for oncogenicity compared to CA and even compared to basalt-containing compositions.

The toxic effect of asbestos-containing dust is determined by the percentage of CA in

them. There is no significant difference in the LD50 values between compositions based on asbestos and basalt. The mortality rate depends on the duration of contact with CA, the dustiness of the working area and the dust content, and also, apparently, on the impurities present in asbestos (tenths and hundredths of a percent) (e.g., zinc, chromium, vanadium, and other metals). It can be assumed that the inflammatory reaction with the activation of macrophages and leukocytes, and the increased release of oxygen compounds (i.e., radicals that can damage DNA and proteins and cause lipid peroxidation), can play a major role in the development of the toxic effect of CA (Platonova, 2018).

No significant difference was found in the fibrogenic activity of dust samples on both an asbestos and asbestos-free basis. The additives used in the manufacture of brake products do not have a noticeable effect on the fibrogenic activity of dust. Indicators and oxyproline content, as well as histological observations (Yatsenko, 2017), clearly demonstrate the significantly lower fibrogenic activity of dust released during the production of AFP and their operation, in comparison with Bazhenov's CA.

A significant decrease in the fibrogenicity of dust on an asbestos-free basis has not been established. The dust released during braking, as can be seen from the experiments, does not lose its biological aggressiveness and shows a sufficiently high fibrogenic activity. The quartz dust also shows its fibrogenic potential. The oncogenic properties of the studied dust samples show a significantly lower potential compared to chrysotile asbestos. This is due to the coating of CA fibers with binders: either Bakelite or rubber. Repeated experiments on oncogenic potential prove this (Yatsenko, 1994). When replacing chrysotile asbestos with basalt fibers, it was not possible to reduce the oncogenic potential of friction products, and when using super thin basalt fibers, oncogenicity even increased.

An epidemic analysis of mortality from malignant diseases, of both sexes, found that neither the workers of the Ural Vehicle Textile Goods Plant nor the workers of the Yaroslavl Vehicle Textile Goods Plant faced an increased oncological risk, according to the indicators of standardized relative risk (SRR). However, when analyzing mortality from oncological diseases in various subcohorts, differing in the predominance of different types of asbestos-containing dust, an increased risk was established among people of both sexes, where CA dust predominates (preparatory workshops). In the other subcohorts,

where there is mainly asbestos-Bakelite or asbestos-rubber dust, there is no increased cancer risk - these are workers engaged in molding, pressing, and machining (Yatsenko, 1994). Also, in general, it should be noted that cancer mortality rates are at the control level at both plants.

4. CONCLUSIONS:

Given the technical characteristics of CA and natural deposits, both in Russia and abroad, and the absence of substitutes that completely satisfy the main areas of production associated with CA in technical properties and biological aggressiveness, the authors can assume that it will be used for a long time in the national economy. Currently, there have been significant changes in the technology of friction products, which can significantly affect the physico-chemical properties of the dust emitted during machining. The speed of vehicles has also changed, and the mass of vehicles has increased significantly.

The studies were carried out on dust samples released during the operation of VAZ passenger cars weighing no more than 700 kg. Currently, jeeps weighing ~ 3 tons are being used more and more, and the number of freight rail and motor vehicles is also increasing. The weight of which can exceed 60 tons, which increases pressure and increases local temperature during braking. These factors in the released dust will ensure the conversion of CA to forsterite, and the dust will lose its biological and potential aggressiveness.

In addition, it is well known that some workers with a comparatively low dust exposure developed malignant tumors relatively quickly, while others with extensive work experience did not. This means that it can be assumed that the potential of antimutational mechanisms in the oncologically exposed workers varies significantly, which is the basis for explaining the occurrence of malignant tumors. Therefore, in this direction, it is also necessary to research the following: identifying criteria for the risk of tumors, which can subsequently be used in professional medical screenings for cancer hazardous professions.

6. REFERENCES:

1. Castleman, B.I., Berger, S.L.; *Asbestos: Medical and Legal Aspects*. Boston, Aspen Publishers, 2005.
2. Dodson, R.F., Hammar, S.P.;

- Asbestos: Risk Assessment, Epidemiology, and Health Effects*. CRC Press, New York, 2011.
3. Khazbiev, A. *Expert*, **2012**, 49, 102-117.
 4. Colangelo, F., Cioffi, R., Lavorgna, M., Verdolotti, L., De Stefano, L. *J. Haz. Mat*, **2011**, 195, 391-397.
 5. Granat, K., Nowak, D., Pigiel, M., Florczak, W., Opyd, B. *Archives of Civil and Mech. Eng*, **2015**, 15, 188-194.
 6. Nam, S.N., Jeong, S., Lim, H. *J. Haz. Mat*, **2014**, 265, 151-157.
 7. Gadikota, G., Natali, C., Boschi, C., Park, A.H.A. *J. Haz. Mat*, **2014**, 264, 42-52.
 8. Gidarakos, E., Anastasiadou, K., Koumantakis, E., Nikolaos, S. *J. Haz. Mat*, **2008**, 153, 955-965.
 9. Ginzburg, E.A. *Clinical Medicine*, **1970**, 12, 55-60.
 10. Le Bouffant, L. *IARS Sci.Publ*, **1980**, 2, 15-33.
 11. Gorelik, S.S.; *X-ray and electron-optical analysis*. MISIS: Moscow, 1994.
 12. Mikheev, V.I.; *The radiographic determinant of minerals: scientific and technical publishing house of literature on geology and mineral protection*. Moscow, 1957.
 13. Mirkin, L.I.; *X-ray analysis (Reference Guide)*. Science: Moscow, 1976.
 14. Nikitina, O.V.; *The main issues of occupational health in the production of basalt fibers and some products from them. Abstract of the Candidate of Medical Sciences Thesis 14.00.07*. St. Petersburg, 1991.
 15. Yatsenko, A.S.; *Biological aggressiveness of asbestos-containing dust in the production of AFP. Physiological, pedagogical and environmental health and healthy lifestyles. Collection of scientific works. X All-Russian Practical Conference*. Yekaterinburg, Russian Federation, 2017.
 16. Yatsenko, A.S.; *Hygienic assessment of the dust factor in the production of asbestos-formed parts. Abstract of the Candidate of Medical Sciences Thesis 14.00.07 - "Hygiene"*. St. Petersburg, 1994.
 17. Yatsenko, A., Sherstychnenko, O. *Life Safety*, **2019**, 1, 9-14.
 18. Platonova, A. *Meduza*, **2018**, June, 11-14.
 19. Muzafarov, V.G. *The list of minerals, rocks, and fossils*. Moscow: Ripol Classic, 1979.
 20. Sudo, M.M.; *General Geology*. Moscow, IIEPU Publishing, 2001.

CONDIÇÕES PEDAGÓGICAS PARA A FORMAÇÃO DE COMPETÊNCIA PROFISSIONAL DE ESTUDANTES DE UMA UNIVERSIDADE TÉCNICA**PEDAGOGICAL CONDITIONS OF FORMATION OF PROFESSIONAL COMPETENCE OF STUDENTS OF A TECHNICAL UNIVERSITY****ПЕДАГОГИЧЕСКИЕ УСЛОВИЯ ФОРМИРОВАНИЯ ПРОФЕССИОНАЛЬНОЙ КОМПЕТЕНТНОСТИ СТУДЕНТОВ ТЕХНИЧЕСКОГО ВУЗА**

OREKHOVA, Yelena Yurievna^{1*}; GREBENKINA, Lidia Konstantinovna²; SUVOROVA, Natalya Alexandrovna³; STAVRUK, Marina Alexandrovna⁴

¹ Department of Foreign Languages, Surgut State University, Surgut, Russia

² Department of Pedagogics and Management in Education, Ryazan State University named for S.A. Yesenin, Ryazan, Russia

³ Department of Construction of Engineering structures and mechanics, Ryazan State Agrotechnological University, Ryazan, Russia

⁴ Department of Foreign Languages, Surgut State University, Surgut, Russia

** Corresponding author
e-mail: elena8778@mail.ru*

Received 12 November 2019; received in revised form 05 February 2020; accepted 15 March 2020

RESUMO

Documentos fundamentais do governo estabelecem a prioridade do sistema educacional em políticas públicas, declarando a necessidade de treinamento científico e profissional bem-sucedido e atividades educacionais inovadoras de futuros especialistas. O artigo tem como objetivo propor uma solução para a formação de competência profissional de futuros especialistas de universidades técnicas na fase de modernização da educação na sociedade russa moderna. O trabalho revela a essência das principais abordagens metodológicas para resolver o problema em estudo como abordagens por competência, criativa, orientada para a personalidade, atividade do sistema, tecnológica e baseada em tarefas. Uma análise retrospectiva possibilitou revelar as condições pedagógicas, simulando a real atividade profissional de estudantes de uma faculdade técnica. São descritas as formas de desenvolvimento bem-sucedido da competência profissional de futuros especialistas (estabelecimento de ambiente criativo inovador, desenvolvimento da posição de sujeito de uma personalidade, fortalecimento de atividades orientadas para a prática, organização de reflexão e autorreflexão, uso de tecnologias e sistemas de computação, informação e telecomunicações, gestão eficaz das atividades acadêmicas, científicas e profissionais dos alunos). Com base nos princípios importantes, nas abordagens metodológicas, nos requisitos do Padrão Educacional Federal do Ensino Superior para a preparação de futuros especialistas na Federação Russa, o artigo apresenta a experiência inovadora da organização do processo educacional que visa formar uma competência profissional entre estudantes de graduação do Instituto Ryazan da Universidade Politécnica de Moscou, bem como da Universidade Agrotecológica do Estado de Ryazan, em homenagem a PA Kostychev. Este estudo possibilitou o desenvolvimento e a implementação de uma estrutura modular em bloco e do conteúdo de treinamento em engenharia e construção de estudantes, que inclui competências criativas de design, organizacionais e gerenciais, aplicadas à informação e criativas, correspondentes aos tipos de atividade profissional.

Palavras-chave: *metodologia de pesquisa, competência, abordagem baseada em competências, ambiente inovador-criativo, atividade profissional.*

ABSTRACT

Fundamental government documents set the priority of the educational system in public policy, declaring the need for successful scientific and professional training and innovative educational activities of future specialists. The article is aimed to propose a solution to the formation of professional competence of future specialists of technical universities at the stage of modernization of education in modern Russian society. The

work reveals the essence of the leading methodological approaches to solving the problem under study: competency, creative, personality-oriented, system-activity, technological, task-based approaches. A retrospective analysis made it possible to reveal the pedagogical conditions, simulating the real professional activity of students of a technical college. The ways of successful development of professional competence of future specialists are described (establishing innovative-creative environment; developing the subject position of a personality; strengthening practice-oriented activities; organizing reflection and self-reflection; using computing, information and telecommunication technologies, and systems; effective management of students' academic, scientific, and professional activities). Based on the leading principles, the methodological approaches, the requirements of the Federal State Educational Standard of Higher Education for the preparation of future specialists in the Russian Federation, the article presents the innovative experience of the organization of educational process, which is aimed to form a professional competence among graduate students of Ryazan Institute of Moscow Polytechnic University, as well as Ryazan State Agrotechnological University named after P.A. Kostychev. This study made it possible to develop and implement a block-modular structure and content of engineering and construction training of students, which includes design, organizational and managerial, information-applied, creative competencies corresponding to the types of professional activity.

Keywords: *research methodology, competence, competence-based approach, innovative-creative environment, professional activity.*

АННОТАЦИЯ

Основополагающие государственные документы устанавливают приоритет системы образования в государственной политике, заявляют о необходимости успешной научно-профессиональной подготовки и инновационной образовательной деятельности будущих специалистов. Статья посвящена решению актуальной проблемы, а именно формированию профессиональной компетентности будущих специалистов технических вузов на этапе модернизации образования современного российского общества. В ней раскрывается сущность ведущих методологических подходов к решению исследуемой проблемы: компетентностный, креативный, личностно ориентированный, системно-деятельностный, технологический, задачный. Методом ретроспективного анализа литературы выявлены педагогические условия, которые моделируют реальную профессиональную деятельность будущих специалистов технических вузов. Раскрыты пути успешного формирования профессиональной компетентности будущих инженеров-строителей (создание инновационно-креативной среды; становление субъектной позиции личности; усиление практико-ориентированной направленности деятельности; организация рефлексии и саморефлексии; использование вычислительных, информационных и телекоммуникационных технологий и систем; эффективное целенаправленное руководство учебной, научной и профессиональной деятельностью студентов). На основе ведущих принципов, методологических подходов и требований Федерального государственного образовательного стандарта высшего образования (ФГОС ВО) по подготовке будущих специалистов-инженеров представлен инновационный опыт организации учебного процесса в технических вузах г. Рязани, направленный на формирование профессиональной компетентности у студентов-выпускников Рязанского института Московского политехнического университета, а также Рязанского государственного агротехнологического университета имени П.А. Костычева. На основе проведенного исследования была разработана и реализована блочно-модульная структура и содержание инженерно-строительной подготовки студентов, которая включает проектно-конструкторскую, организационно-управленческую, информационно-прикладную, творческую компетентности, соответствующие видам профессиональной деятельности.

Keywords: *методология исследования, компетентность, компетентностный подход, инновационно-креативная среда, профессиональная деятельность.*

1. INTRODUCTION:

Fundamental government documents set the priority of the educational system in public policy, declaring the need for successful scientific and professional training and innovative educational activities of future specialists. In the Law of the Russian Federation "About Education in the Russian Federation" (2012), it is emphasized that the Russian educational system is given a decisive role in the formation of

professional personnel. The Concept of the Federal target program of the development of education for 2006–2010 states that to ensure the quality of teaching and its equal availability for all citizens, the institutional restructuring of the educational system is needed based on effective interaction with the labor market. In the Federal Targeted Program "Scientific and Scientific-Pedagogical Personnel of Innovative Russia (2014–2020)" and the "National Doctrine of Education in the Russian Federation" for the

period up to 2025, the focus is on the need for high-quality scientific, innovative educational activities and personnel training.

Engineering education in the 21st century is associated with dynamic changes in science and industry, based on the integrative role of training a competent specialist, including understanding of engineering activity as an integrative process, analytical thinking; set of abilities; critical assessment of facilities and production problems; contextual knowledge of the educational sphere and situation; the ability to supplement their expertise throughout their work and to adapt to changes in the technical and technological environment, the requirements of the world market; the ability to synthesize innovations at the stages of their design and production (Novikov, Zuev, 2000).

Professional competence of graduates of a technical university is a level-integrative personal education, including a set of system knowledge, practical skills that are used in the process of solving professional problems using computational, information and telecommunication technologies and systems. It is determined by the Federal State Standard of Higher Professional Education, which sets forth specific requirements for the training of technical specialists, including the formation of a set of universal, general and specific professional competencies (The federal state educational standard of higher professional education in the specialty 270800 "Construction" dated January 18, 2010, No. 54).

Formation of professional competence of the future specialist as an integrated system of in-depth expert knowledge, abilities, and skills consists in mastering specialized knowledge and skills, universal actions, social relations, intellectual skills, readiness to show personal qualities and is solved by implementing a set of tasks of a scientific, methodological and practical nature.

At present, the organization of the pedagogical process at a higher educational institution is a complex, multifactorial, constantly changing holistic phenomenon that combines the methods of preparing a future specialist and the means of educating, training, upbringing, and personal development. These processes are all based on the complex of necessary pedagogical conditions for the formation of professional competence of students of a technical university that meet the requirements of the Federal educational standards (Abulkhanova-Slavskaya,

1980).

Consequently, the relevance and significance of the research are due to the new requirements for the professional training of competitive specialists (bachelors and masters) of a technical university in higher education, formulated in the language of the competence-based approach, the formation of competencies and competence (Greibenkina, Suvorova, 2012).

In pedagogical science in current conditions, the problems of the competence-based approach, the formation of professional technical competence of a technical university, and its components are studied in Russia by such scientists as K.A. Abulkhanova-Slavskaya, E.I. Artamonova, V.I. Baidenko, A.A. Verbitsky, M.A. Galaguzova, L.K. Grebenkina, E.F. Zeer, I.A. Zimnyaya, N.V. Kuzmina, V.A. Slastenin, A.V. Khutorskoy, and others. They studied a wide range of problems, in particular, improving the quality and effectiveness of training future specialists, including a technical university.

The set of the components of professional competence reflects not only various aspects of professional activity, but also valuable personal qualities: the ability to self-change and self-development based on self-reflective organization; communication skills (initiative, collaboration, teamwork); ability to criticism and self-criticism; the ability to receive, consume, update informational knowledge, etc.

The continuous complication of activities based on reflexive self-organization creates new problems of a cognitive nature, as objective activity is always aimed at creation (Abulkhanova-Slavskaya, 2008; Baidenko, 2004; Verbitsky, 1991; Galaguzova., 2011; Grebenkina, Suvorova, 2012; Zeer, 1988, Zimnyaya, 2006; Kuzmina, 1990; Khutorskoy, 2003).

The creation and spread of innovations is a purposeful process of exploring the new, suggesting its creative understanding and improving practical results. In the works of scientists (G.S. Altshuller, I.M. Vertkin, V.P. Delia), it is emphasized that in the process of training and educating in a university, when preparing professionals, it is essential to create an innovative and creative environment as a high need for innovations and students' creativity. The researchers consider pedagogical conditions to be external and internal circumstances contributing to the action of personality development factors, for example, readiness for activity, stimulating environment, logistical and resource support, etc. In a broad sense, conditions

are interpreted as causes, development factors, technologies, methods, means training and education, management support, pedagogical support, interaction of the subjects, their joint activities (Altshuller, Vertkin, 1994; Delia, 2007).

The diversity of approaches and the complexity of the new stage of the formation of professional competence oblige a higher technical school to make adjustments to the training of competent specialists to acquire innovative business experience and the ability to make rational decisions. In our study, it was essential to determine the nature, structural components and features of the pedagogical conditions of a technical college. They simulate the real professional creative activity of bachelors and masters, going beyond the limits of learning situations and allowing future engineers to be included in it, developing their personal qualities, and ultimately forming their professional competence based on state educational standards in the training direction - "Construction."

So, the aim of the study was the introduce a competency-based approach and to implement the requirements of the Federal State Educational Standard of higher professional education of the third generation in the professional training of specialists in higher education. In the language of competencies, it is updated content, generalized methods of action when integrating different types of professional activity and solving technical problems of the all-Russian intersectoral association of employers "Russian Union of Builders," the requirements of the Employment Centers, the State Educational Establishment of Higher Education for the level of professional knowledge and skills of a modern specialist and prescriptive requirements of a competency-based approach.

2. MATERIALS AND METHODS:

The process of integrating Russian higher education into the world education system actualizes the problem of the formation of professional competence of future specialists of technical universities. Its solution involves the development and successful implementation of the new pedagogical conditions of training and educating in the integrated pedagogical process of a technical university. The application of these pedagogical conditions in practice ensures the active formation of the main components (competencies) of the professional competence of bachelors and masters, synchronization of methodological approaches and principles.

In modern conditions, scientists-methodologists and teachers (V.I. Zagvyazinsky, V.V. Kraevsky, A.I. Kochetov, G.K. Selevko, V.A. Slastenin) suggest using various methodological approaches and an integrated methodology set, aimed to achieve and solve theoretical and practical problems of modern education, in particular, to solve the problem of forming the professional competence of future specialists of technical universities (Zagvyazinsky, 2008; Kraevsky, 2006; Kochetov, 1996; Selevko, 2006; Slastenin, 2000).

The analysis of the use of the possibilities of various methodological approaches in the process of the formation of professional competence among students of a technical university showed that activities aimed at solving professional problems could not be built based on only one of them.

The following methodological approaches were leading in our study: a competency-based approach (based on the requirements of modern educational standards, as well as on innovative experience in solving professional problems); a creative approach (necessary for the organization of a creative approach in the educational process of the university); an axiological approach (value approach including orientation of the teacher to universal, national and professional values, value orientation in pedagogical activity); a personality-oriented approach (associated with the development of creative abilities, personal qualities and professional mobility of each of the subjects of the educational process); a system-activity approach (characterizing the theoretical and practical experience, scientific and useful results, the criteria development process, the formation of competencies); a technological approach (providing for the possibility of generalization of pedagogical modern technologies in the educational process); a task-oriented approach (to analyze and successfully solve technical problems of production activities). It can be concluded that these approaches are closely interrelated, interdependent and are necessary for the formation of students' professional competence in a technical university.

To solve the aims of the study and obtain reliable results, the sophisticated methodology of scientific research was used (theoretical and empirical methods): a retrospective analysis and review of the literature, observation, questioning, testing, interviews, designing, modeling, monitoring, experiment.

The requirements of the all-Russian

intersectoral association of employers "Russian Union of Builders," employment centers, Federal State Educational Standards of Higher Education for the level of professional knowledge of a modern specialist and directive requirements for the implementation of a competency-based approach were taken into consideration.

The educational environment of technical universities, new scientific, theoretical, and practical areas of the educational process (leading professional activities) of the Ryazan Institute (branch) of the Moscow Polytechnic University, as well as the Ryazan State Agrotechnological University, were chosen the research base of the study.

The teachers of the Department of Industrial and Civil Engineering of Ryazan Institute (branch) of the Moscow State Open University and Surgut State University took part in the experiment. In total, 256 people took part in the study, including 85 students in control groups and 87 students in experimental groups.

The Scientific Department and the Head of the Department of the University have approved this research, and all participants have agreed to participate and consented about the research.

3. RESULTS AND DISCUSSION:

The research was conducted within the educational system of technical universities, recent scientific, theoretical, and practical activities of the educational process (leading professional activities) of the Ryazan Institute (branch) of the Moscow Polytechnic University, as well as the Ryazan State Agrotechnical University.

The research program included the analysis and identification of the requirements and pedagogical conditions developed by scientists for the formation of professional competence of bachelors and undergraduates of Higher technical school, taking into consideration the Federal State Educational Standard of Higher Education 3+, 3++.

In the standards of bachelor's degree in the training program «Construction» it is stated that "when developing a bachelor's plan, the university formulates the requirements for the results of its development in the form of universal competences (systemic and critical thinking; project development and implementation; teamwork and leadership; communication; intercultural interaction; self-organization and self-development; life safety); general

professional and professional competencies of graduates. "As part of mastering the program, graduates can prepare to solve professional activity problems of the following types: survey; project; technological; organization and management; service and operation; expert-analytical.»

In the Federal State Educational Standards of Higher Education in master's training program "Construction," it is noted: a magister should be prepared to solve professional tasks of a higher level also following the types of professional activity: innovation and research, design and settlement; industrial and technological research and teaching; project management; professional expertise and regulatory-methodological."

These standards set forth requirements for the conditions of the implementation of undergraduate and graduate programs, which include the system-wide needs, the requirements for material and technical and educational and methodological support, the requirements for personnel and financial conditions for the implementation of programs, as well as the requirements for the mechanisms used to assess the quality of educational activities and the preparation of students by programs.

"The uniqueness of the master's program lies in the use of the CDIO ("planning - design - implementation - operation") approach in the learning process. The preparation process is formed as follows: the planning stage is for thinking over the technology, the project design strategy, regulatory requirements, developing concepts, technical and business plans; the second stage of the design is devoted to the development of the project, including ideas, drawings, and algorithms, structural materials; at the scene of implementation and operation, the project is being transformed into a housing and utilities facility (residential building, environmental protection enterprise, infrastructure facility, etc.)" (Annotation of the leading educational program for master's training 08.04.01 "Construction." Program name 08.04.01_16 "Design and construction of facilities."

During the analysis, we realized the need to create some interrelated conditions that simulate real professional activities that go beyond learning situations and allow students to be included in it, to develop their personal qualities, to form skills and abilities, to improve the professional experience. As a result, a set of pedagogical conditions was determined that contribute to the successful formation of professional competence

of future specialists (civil engineers: the example of the training of civil engineers:

- creation of an innovative and creative environment, which forms the high need of students for cognition and creative activity;

- formation of the subjective position of the student's personality capable of self-improvement and self-realization by involving him/her in the decision-making process, taking into account the characteristics of the contingent and the specifics of the educational process of a technical university;

- strengthening the practice-oriented direction of the activities carried out in the course of solving professional problems in construction, for example in designing and calculating bases and foundations using data of Ryazan region;

- use of computing, information and telecommunication technologies and systems, which allows combining traditional and innovative ways of mastering specialized knowledge, the development of professional skills as the basis of professional competence;

- organization of students' reflection and self-reflection, manifested in the ability to analyze, regulate their behavior and independent professional activities consciously;

- effective targeted management of educational, research, and professional activities of students.

Let us dwell upon the characteristics of the most significant pedagogical conditions. In our opinion, the creation of an innovative and creative environment at the university has an integrative nature, since this environment is, above all, socio-educational. It solves the tasks of professional training (and self-study), education (and self-education), and development (and self-development) of the future specialist. The innovative and creative environment in the context of the modernization of education is based on a particular social and mental readiness of the teacher's personality for such a change in the situation when both the teacher and the learner can effectively interact in joint activities, reach mutual understanding, eliminate conflicts. Pedagogical creativity assumes that the teacher has a high level of competence, as a result of which creative pedagogical activity becomes more efficient and successful. "The most important indicators of teacher's pedagogical creativity are creative well-being and pedagogical creativity" (Altshuller, 1987; Altshuller, Vertkin, 1994; Morozov, 2004; Delia,

2007).

Attention should be paid to the fact that future specialists need to be taught and developed comprehensively, taking into account their level of talent so that they display latent abilities. Teaching creative activity in a technical university is regarded as an activity that contributes to the improvement of personal qualities: mental activity; ingenuity; the desire to obtain new knowledge necessary for specific practical work; independence in the choice and solution of technical problems; diligence and responsibility; competitiveness, etc. It follows that it is essential to consider the development of the creativity of the individual as a continuous creative process and rely on the previously formed creative abilities.

Considering that the creation of an innovative and creative environment in mentioned technical universities is facilitated by the potential of training, general professional and unique disciplines, as well as the whole range of professional problem solving, we have implemented the necessary conditions for the successful formation of universal and professional competencies responsible for the success of mastering new knowledge and skills. In the educational process being organized, the experience of innovation activity was formed among the students who became its subjects. At the same time, the development of subject-subject relations, the subjective position of the personality of the future engineer, capable of self-realization and self-improvement, took place.

The formation of the subjective position of the individual was realized in the course of dialogic communication through the student's ability to perform all types and forms of learning activities (listen and outline lectures, speak to an audience, solve technical problems, lead discussions, defend their position), plan and organize their work, thoroughly learn and to communicate.

No less critical condition for the formation of professional competence of future civil engineers is the incentive to reflect, which is manifested in the ability to regulate their professional behavior and activities consciously. Teaching and educational activities of the teacher and student's cognitive and creative activities changed with the creation and improvement of an innovative, creative environment, encouraging the student to self-reflection and improve creative abilities. In the course of research, we considered reflection as an essential mechanism of productive thinking; as an exclusive organization of the processes of

understanding what is happening in a broad system context, including an assessment of the situation and actions, finding methods and operations for solving problems; as a process of introspection and active reflection on the state and activities of the individual and other people involved in solving problems (Greibenkina et al., 2004). Reflection characterizes the constant comprehension, transformation, and change of consciousness of the student based on the analysis of their actions. The reflexive activity makes it possible to most effectively and adequately carry out reflexive processes ensuring the development and self-development of an individual, contributes to the realization of a creative approach to professional activity, the achievement of its maximum efficiency and effectiveness (Stepanov, 2006).

Another essential condition for the successful formation of professional competence of future specialists of a technical university is the effective management of students' educational, scientific and practical activities. As a rule, when organizing professional events of students, the teacher provides and implements several levels: teaching and informative (experimental and theoretical), creative, practical, technological, and functional (Suvorova, 2011).

It is known that one of the critical provisions of the system-activity approach to teaching at a technical university is the clearly defined focus of the educational process on shaping students' logical thinking when making decisions related to the nature of their work. The basis of students' professional competence should be considered the ability to acquire knowledge and apply skills in various life situations, establish links between dynamically updated culture in theoretical and practical activities, and find an algorithm for solving professional problems. Consequently, the formation of professional competence of the future modern construction engineer is impossible without new information technologies and computer-aided design (CAD) systems based on the use of computer technology, information, particular, methodological support, which is one of the features of the pedagogical conditions of a technical university. The difference in the modern process of forming professional competencies in the field of telecommunications is that this young progressive field of pedagogical knowledge does not contain "ready-made knowledge" (Glubokova et al., 2008). For example, in our experience, organizing education through the active introduction of computer equipment and network communications into the educational process has become an indispensable element of pedagogical

activity, which determines the construction of interactive forms and teaching methods that meet the needs of the information society, the labor market, the pace of modernization of higher education. The use of computing, information, telecommunication technologies, and systems effectively influences the solution of professional tasks and the graphic design of project solutions, expands communication capabilities, actualizes the needs of the functional interaction of educational subjects.

When forming the professional competence of students, the role of modeling and solving technical problems is enormous, which strengthens the practical orientation as one of the conditions for the success of training in specialized disciplines and serves as a criterion of the level of knowledge and competence measurement. At the same time, the used teaching aids contribute to the development of not only knowledge but also personal qualities and abilities. In the process of practical work, solving technical problems, the student gains the experience of the work that he chose, and tries to determine whether the nature of this work corresponds to his abilities and skills.

The federal standard of higher education records the results of education, the requirements for solving the professional tasks of the future engineer at the level of his/her theoretical and practical experience. The undergraduate training program determines the content of higher education in the "Construction" area of study. In developing the undergraduate training program, the requirements for the results of its development in the form of universal, general and specific professional competencies of graduates were taken into consideration. The graduates should be ready to meet the challenges of professional activity: survey work; project; technological; organization and management; service and operation; expert-analytical.

For the successful formation of professional competence, the traditional list of the curriculum "Industrial and civil construction" was revised and modified, a particular course on "Computer-aided design of computer systems" was introduced.

In the curriculum "Urban construction and economy," "Roads," the discipline "Information technology for the calculation of building structures" was introduced.

As an integral element of the new information technologies, these courses offer to explore the extensive scientific system of civil

settlements, «Base,» which allows getting an innovative professional experience.

The purpose of these courses is to combine traditional and informational techniques of knowledge acquiring; identify the information needs for solving specific professional tasks; train the educational material interpretation and the analysis of situations, the application of further calculation results; develop the skills of applying the previously studied material, the ability to combine, apply theoretical knowledge to obtain a result that has a novelty, "the subject potential of the individual" in the new interdisciplinary conditions.

The specificity of the disciplines is in providing practical solutions to solving professional problems using the "Base" software package. In this regard, the effectiveness of the pedagogical influence becomes higher, since the computer acts as a component of the system of pedagogical management; as a means of increasing the efficiency of scientific and pedagogical research. The ability to find the necessary information and apply it in professional activities is a mandatory requirement of the employer for a modern specialist since the transition from knowledge to action is much faster. Therefore, information technologies and computer-aided design systems are a necessary tool and a specific condition that provides practical orientation using new information technologies and systems (Suvorova, 2011).

It is considered the ability and desire to communicate, interact in a networked electronic environment as competence and means of realizing professional reflection. It opens up vast opportunities for professional self-development and requires systematically organized, intellectual, communicative, reflexive, moral qualities from a future specialist, allowing to successfully set up activity in broad social, economic and cultural contexts.

As a result, the subject-subject interaction is changing, the role of the teacher is increasing not only as a carrier of social experience but also as an active subject which studies the newest adventure, conducts scientific research, interprets current trends, carries out professional approbation of the latest achievements, etc.

The comparison of the pedagogical and construction professional activities of an engineer and a bachelor engineer makes it possible to show the similarities and differences in the types of

events that are determined by the content of educational programs (Table 1).

As already noted, depending on the types of professional activity, a university graduate should be prepared to solve specific occupational tasks. Therefore, modern requirements for professional activity are the conceptual basis for structuring professional competence.

For example, implementing major methodological approaches and modern scientific-theoretical and practical activities in the educational process at the Ryazan Institute of the Moscow Polytechnic University, we realized the need to create conditions simulating real professional activity, extending beyond learning situations outside and allowing to include students in it, to develop their personal qualities, to form skills and to improve professional experience.

The professional activities of technical universities, according to their specificity, are associated with the state policy in education, regional characteristics, fundamental and industry science. Among the practical results of the implementation of the federal target program, the interaction with the real sector of the economy (in our study, the construction sector) can be admitted. For example, the All-Russian Intersectoral Association of Employers "Russian Union of Builders" includes several organizations in the Ryazan Region, aimed at the innovative way of professional and personal development of each employee, his/her skills to direct and organize his activities; use software to improve competitiveness. As a result, the requirements of Russian employers and All-Russian inter-sectoral association "Russian Union of Builders" to the level of professional competence of graduates of a technical university have been formulated:

to know:

- the theoretical foundations of general and specific professional disciplines;
- the trends and the main tendencies of science and technology development;

to be able to:

- transform acquired knowledge into innovative technologies,
- independently find, perceive and analyze new information, taking into account existing legislative and socio-legal norms;
- work with global information sources based on computer and information-communication tools;

- make decisions in uncertain, suddenly complicated professional conditions;

- determine the information needs, use and give them a professional assessment for solving specific problems.

to master:

- the CAD systems;

- the methods of system analysis;

- the means of conducting scientific research;

- the software packages for technical solutions;

- the adequate ways of professional communication and behavior, the ability to cooperate and work in a group for a typical result.

The analysis of the requirements has shown that employers consider the ability of a university graduate to solve non-standard professional tasks, use computer tools, information and communication technologies and have such personal qualities as initiative, communication, reflexivity, creativity as the main requirements in raising the level of employees' competence. The disadvantage of higher professional education in Russia was indicated as the closeness of the education system, obsession with the internal university criteria for training specialists without regard to the requirements of employers and the labor market, which cannot be ignored when forming the professional competence of future specialists.

The study has shown that improving the system of the stated pedagogical conditions contributes to a targeted, systemic formation of a competitive personality. The absence of any of the components reduces the level of motivational readiness to solve the problem of forming students' professional competence. All this was subsequently taken as the basis for the concept and model of the successful formation of the professional ability of bachelor students and undergraduates of a technical university.

4. CONCLUSIONS:

Modernization of higher technical education actualizes the problem of developing and implementing new pedagogical educational conditions into the university's educational process, which ensure the synchronization of principles, methodological approaches, the formation of personal qualities and professional competencies of future specialists (in our research, future civil engineers).

In current conditions, the professional competence of graduates of higher educational institutions of a professional profile is determined by the Federal State Standards of the new generation, which formulate specific requirements for graduates, in particular, the formation of universal, general, and professional competencies. At the same time, the methodology of the implemented transformations represents a competence-based approach that provides for innovative changes, both in the content of education and in the technology of management of the educational process.

When organizing and conducting a holistic pedagogical process, research and professional-practical activity, the following conditions for the successful formation of professional competence among students on an innovative basis proved their effectiveness: the current trends in the structure of professional expertise; the educational character of pedagogical process; the subject-subject interaction of teachers and trainees; the creation of innovative and creative environment, creative relationships; practice-oriented activities; the ability to reflection and self-reflection.

It is proved that the creation of an innovative and creative environment is an essential integrated condition for the organization of the educational process, in which the statement of the problem is a stage of activity, and the solution of a problem is the result of the stage. The use of non-standard creative technical tasks of an open type (absence of a single correct answer), problem analysis, modeling of professional situations and stimulation of self-confidence among students supposes that they have a specific knowledge, skills, abilities, and experience, that is, not only the application of subject-practical content of such tasks but also examples of the search for creative solutions and creative behavior, in other words, professional competence. Learning becomes the creativity of students when the teacher's influence is aimed at attracting them in acquiring the necessary integrated professional experience and is of a targeted nature. A student can gain professional competence when solving problems independently, which requires him to be ready to apply the necessary knowledge and skills in practical activities. Psychologists note that only by entering into useful contact with the outside world, purposefully and creatively transforming it, a student in the process of this complex interaction can change not only the surrounding world but also himself" (Sonin *et al.*, 2002).

Thus, the formation of universal and

professional competencies in technical university students is the degree of students' involvement into complex types of educational, cognitive and practical professional activities, where the development of goals, tasks, content, and technology of independent study of particular disciplines with the support and assistance of a teacher is fundamental; mastering the types of independent work, self-control and self-esteem as a result of the pedagogical interaction of the teacher and the student, implying continuity. The teacher is of great importance to the content and methods of organizing such activities; it is his qualification competency that contributes to the modernization processes in the education system.

The study showed that the establishment and improvement of the system of the stated pedagogical conditions contribute to the targeted, systemic formation of a competitive personality, the absence of any of the components reduces the level of motivational readiness to solve the problem of forming students' professional competence. All this was subsequently taken as the basis for the concept and model of the successful formation of professional ability of bachelor students and undergraduates of a technical university.

5. REFERENCES:

1. Abulkhanova-Slavskaya, K.A.; Activity, and personality psychology. Moscow: Nauka, **1980**, 336.
2. Altshuller, G.S; Daring formulas of creativity. Petrozavodsk: Karelia, **1987**, 269.
3. Altshuller, G.S.; Vertkin, I.M.; How to become a genius: The life strategy of a creative person. Minsk: Belarus, **1994**, 479.
4. Artamonova, E.I.; Competence-based approach in the formation of the personality of the teacher professional. Pedagogical education and science, **2008**, 10, 4 - 9.
5. Baidenko, V.I.; Competences in professional education: Higher education in Russia, **2004**, 11, 3 - 17.
6. Delia, V.P.; Innovative education of a humanitarian university: theoretical and methodological foundations. Moscow: OOO «PKTS Alteks», **2007**, 508.
7. Federal Law "On Education in the Russian Federation". No. 273. December 29, **2012** http://www.consultant.ru/document/cons_doc_LAW_140174/ (Date of access - October 23, 2018).
8. Galaguzova, M.A.; Doctoral research on pedagogy: about asks and answers: scientific and practical guide. Ekaterinburg: "SV-96", **2011**, 256.
9. Glubokova, E.N.; Kondrakova, I.E.; Mosolova, L.M.; Noskova, T.N.; Pavlova, T.B.; Pisareva, S.A.; Tryapitsina, A.P.; Tumalev, A.V.; Tumaleva, E.A.; Humanitarian technologies in higher professional education: scientific and methodological materials for the preparation of higher education teachers. SPb.: Akademiya Issledovaniya Kultury, **2008**, 118.
10. Grebenkina, L.K.; The path to mastery: psychological and pedagogical practicum. Ryazan: RSPU named after S.A. Yesenin, **2004**.
11. Grebenkina, L.K.; Suvorova, N.A.; Formation of professional competence of technical high school students in modern conditions. Ryazan: RSU named after S.A. Yesenin, **2012**.
12. Grebenkina, L.K.; Zhokina, N.A.; Humanistic Values of Vocational Education at the University: Pedagogical Education: Challenges of the 21st Century: Proceedings of the International Scientific-practical Conference, dedicated to the memory of Academician of the Russian Academy of Education V.A. Slastenin; Samara. October 4-5, **2018**.
13. Grebenkina, L.K.; Kopylova, N.A.; Conceptual ideas and innovative technologies for the interaction of stakeholders in the educational process of the university: Teacher professionalism: essence, content, development prospects, Moscow: MANPO, **2019**, 262-272.
14. Khutorskoy, A.V.; Didactic heuristics. Theory and technology of creative learning. Moscow: Izdatelstvo MGU, **2003**, 416.
15. Kochetov, A.I.; Culture of pedagogical research. Minsk: Journal reduction "Adukatsyya i vykhovanne", **1996**, 326.
16. Kraevsky, V.V.; Methodology of pedagogy: a new stage: study guide for students of higher school. M.: Academia, 2006.
17. Kuzmina, N.V. The professionalism of the personality of the teacher and master of industrial training. Moscow: Vysshaya

- shkola, **1990**, 119.
18. Lapin, N.I.; On the many and the same in the Russian transformation: Social Sciences and Modernity. **2002**. 2. 107.
 19. Letter of the Ministry of Education and Science of the Russian Federation of February 6, **2014** No. 09-148 "On the direction of materials" - <https://www.garant.ru> (accessed 03.03.2019).
 20. Morozov, A.V.; Creativity of a higher education teacher. Higher education today, **2004**, 3, 64 – 68.
 21. Novikov, P.M.; Zuev, V.M.; Advance professional education: scientific-practical guide. Moscow: RGATiZ, **2000**, 266.
 22. Orekhova, Y.; Grebenkina, L.; Zhokina, N.; Badelina, M.; Forming competences of students in educational process of a higher education institution. **Revista Espacios**. **39 (46)**. **2018**. **28**.
 23. Orekhova, Y.; Grebenkina, L.; Martishina, N.; Badelina, M.; Implementation of competency-based approach in interactive teaching of future Masters of Education. **Revista Espacios**. **40 (29)**. **2018**. **15**.
 24. Orekhova, E.Yu.; Grebenkina, L.K.; Badelina, M.V.; Kopylova, N.A.; Sysoev, S.M.; Innovative technologies of teachers and students' interaction in the educational process of the university, Amazonia Investiga, **2019**, 8, 19, 325-332.
 25. Pedagogical dictionary edited by V.I. Zagvyazinsky. Moscow: Izdatelskiy tsenter "Academiya", **2008**, 352.
 26. Selevko, G.K.; Encyclopedia of educational technologies: In 2 Volumes. Moscow: NII shkolnykh technology, **2006**.
 27. Slastenin, V.A.; Pedagogy. Moscow: Shkola PRESS, **2000**, 488.
 28. Slastenin, V.A.; Artamonova, E.I.; Axiological aspect of the content of modern pedagogical education: Pedagogical education and science. **2002**. No. 3. 4-9.
 29. Sonin, V.A.; Ivanov, S.P.; Nikitin, O.S.; Korolkova, V.A.; Psychology of professional activity. Smolensk, **2002**, 320.
 30. Stepanov, S.A.; Choose the right paths: Educational Policy, **2006**, 7, 54-57.
 31. Suvorova, N.A.; Preparation of students of a technical university based on the use of information educational resources. Russian scientific journal, **2011**, 4/23, 141-145.
 32. Suvorova, N.A.; Didactic features of the formation of professional competence of students of a technical university: Russian Scientific Journal, **2011**, 216-221.
 33. Suvorova, N. A.; Technical task is the basis of vocational training in a technical university: Trends in engineering and technological development of the agro-industrial complex: materials of the National Scientific and Practical Conference. Ryazan: FSBEI HI RSATU, **2019**, 362-365.
 34. The conceptual apparatus of pedagogy and education; Proceedings; Tkachenko, E.V.; Galaguzova, M.A.; eds; Vol. 6. Yekaterinburg: Publishing house "SV-96", **2010**, 86.
 35. Verbitsky, A.A.; Active education in higher school: a contextual approach. Methodological guide. Moscow: Vysshaya shkola, **1991**, 204.
 36. Zagvyazinsky, V. I.; Zakirova, A.F.; Pedagogical dictionary: studies. manual for students of higher educational institutions; Zagvyazinsky, V. I.; Zakirova, A.F.; eds; Moscow: Publishing Center "Academy", **2008**.
 37. Zeer, E.F.; Professional formation of the personality of the engineer-teacher. Sverdlovsk: Izdatelstvo Uralskogo Universiteta, **1988**, 120.
 38. Zimnyaya, I.A.; Competence approach. What is its place in the system of modern approaches to the problem of education? (theoretical and methodological aspect). Higher education today, **2006**, 8, 20-26.

Table 1. *Types of professional activity*

Types of professional activity	
Pedagogical activity	<ul style="list-style-type: none">• educational and methodical• managerial• research• project
Engineer activity	<ul style="list-style-type: none">• engineering design• organizational and managerial• production and technological• research
Bachelor - engineer activity	<ul style="list-style-type: none">• survey and design• production technology and production management• experimental research• installation-commissioning and service-operational

ALTERAÇÕES NO METABOLISMO DE FOSFORO-CÁLCIO NO HIPOTIREOIDISMO EXPERIMENTAL

CHANGES IN PHOSPHORUS-CALCIUM METABOLISM IN EXPERIMENTAL HYPOTHYROIDISM

ИЗМЕНЕНИЕ СОСТОЯНИЯ ФОСФОРНО-КАЛЬЦИЕВОГО ОБМЕНА В КОСТНОЙ ТКАНИ ПРИ ЭКСПЕРИМЕНТАЛЬНОМ ГИПОТИРЕОЗЕ

GANEEV Timur Irekovich.¹; KABIROVA Milyausha Fauzievna^{2*}; YUNUSOV Renat Ramizovich³; GALIULLINA Marina Vladimirovna⁴;

^{1,3,4} Bashkir State Medical University, Department of Orthopedic Dentistry and Oral - Maxillofacial Surgery

² Bashkir State Medical University, Department of Therapeutic Dentistry

* Correspondence author
e-mail: kabirova_milya@list.ru

Received 09 December 2019; received in revised form 30 January 2020; accepted 11 February 2020

RESUMO

O objetivo deste trabalho foi estudar mudanças no estado do metabolismo fósforo-cálcio, indicadores de certos hormônios, perfil de citocinas e estrutura histológica do tecido ósseo no hipotireoidismo experimental em ratos. O hipotireoidismo experimental foi causado pela administração intragástrica diária de tiamazol na dose de 2,5 mg / 100 g de peso corporal por 21 dias. O método colorimétrico foi utilizado para determinar o teor sérico de cálcio, fósforo e magnésio no sangue. Marcadores do metabolismo ósseo, nível de tireotropina, T3 e T4 total, testosterona, hormônios folículo-estimulantes (FSH) e luteinizante (LH), hormônio paratireóide (PTH), interleucina-1 β (IL-1 β) e -6 (IL-6), os tumores alfa de fator de necrose (TNF- α) foram estudados usando um imunoensaio enzimático. Para determinar a estrutura histológica do tecido ósseo, seções preparadas da diáfise femoral foram estudadas sob um microscópio da série MZ-300 (Áustria). Verificou-se que o desenvolvimento do hipotireoidismo é confirmado pela diminuição do teor de tiroxina e triiodotironina no contexto do aumento da secreção do hormônio estimulador da tireóide. O hipotireoidismo experimental é acompanhado por uma diminuição na concentração de fosfatase alcalina óssea no soro sanguíneo, mantendo os telopeptídeos C-terminais tipo 1 de colágeno, refletindo processos de remodelação prejudicados, há também uma diminuição na secreção de testosterona, um aumento nas gonadotrofinas, hormônio da paratireóide, citocinas pró-inflamatórias (IL-1 β , IL-6 e TNF- α). Sinais característicos do desenvolvimento da osteoporose displásica são revelados histologicamente na diáfise dos ossos tubulares.

Palavras-chave: *hipotireoidismo experimental, fosfatase alcalina óssea, telopeptídeos C-terminais tipo 1 de colágeno, interleucinas, ossos tubulares.*

ABSTRACT

The aim of this work was to study changes in the state of phosphorus-calcium metabolism, indicators of certain hormones, cytokine profile, and histological structure of bone tissue in experimental hypothyroidism in rats. Experimental hypothyroidism was caused by daily intragastric administration of Thiamazole in a dose of 2.5 mg / 100 g body weight for 21 days. The colorimetric method was used to determine blood serum calcium, phosphorus, and magnesium content. Bone metabolism markers, thyrotropin level, total T3 and T4, testosterone, follicle-stimulating (FSH) and luteinizing (LH) hormones, parathyroid hormone (PTH), interleukin-1 β (IL-1 β) and -6 (IL-6), necrosis factor tumors-alpha (TNF- α) were studied using an enzyme immunoassay. To determine the histological structure of bone tissue, prepared sections of the femoral diaphysis were studied under a microscope of the MZ-300 series (Austria). It was found that hypothyroidism development is confirmed by decreased content of thyroxine and triiodothyronine on the background of the increased secretion of thyroid-stimulating hormone. Experimental hypothyroidism is accompanied by a decrease in the concentration of bone alkaline phosphatase in the blood serum while maintaining the collagen C-terminal telopeptides type 1, reflecting impaired remodeling processes, there is also a decrease in testosterone secretion, an increase in gonadotropins, parathyroid hormone, pro-inflammatory cytokines (IL-1 β , IL-6, and TNF- α). Signs characteristic for the developing dysplastic osteoporosis are histologically revealed in the diaphysis of the tubular bones.

Keywords: *experimental hypothyroidism, bone alkaline phosphatase, collagen C-terminal telopeptides type 1, interleukins, tubular bones.*

АННОТАЦИЯ

Целью исследования явилось изучение изменений состояния фосфорно-кальциевого обмена, показателей некоторых гормонов, цитокиновый профиль и гистоструктуры костной ткани при экспериментальном гипотиреозе у крыс. Экспериментальный гипотиреоз, вызвали путём ежедневного внутрижелудочного введения мерказолила в дозе 2,5 мг/100 г массы тела в течении 21 дня. В сыворотке крови крыс в сыворотке крови колориметрическим методом исследовали содержание общего кальция, фосфора, магния. Содержание маркеров костного обмена, уровень тиреотропина, общий Т3 и Т4, тестостерона, фолликулостимулирующего (ФСГ) и лютеинизирующего (ЛГ) гормонов, паратгормона (ПТГ), интерлейкинов-1 β (IL-1 β) и - 6 (IL-6), фактора некроза опухолей- альфа (TNF- α) изучали методом иммуноферментного анализа. Для определения гистологической структуры костной ткани изучали подготовленные срезы диафиза бедренной кости под микроскопом серии МЗ-300 (Австрия). Было выявлено, что развитие гипотиреоза подтверждается снижением содержания тироксина и трийодтиронина на фоне увеличения секреции тиреотропного гормона. Экспериментальный гипотиреоз сопровождается уменьшением концентрации в сыворотке крови костной щелочной фосфатазы при сохранении С-концевых телопептидов коллагена типа 1, отражая нарушение процессов ремоделирования, также происходит снижение секреции тестостерона, увеличение - гонадотропинов, паратиреоидного гормона, провоспалительных цитокинов (IL-1 β , IL-6 и TNF- α). В диафизах трубчатых кости гистологически выявляются признаки, характерные для развивающегося диспластического остеопороза.

Ключевые слова: *экспериментальный гипотиреоз, костная щелочная фосфатаза, С-концевые телопептиды коллагена типа 1, интерлейкины, трубчатые кости.*

1. INTRODUCTION

Iodine deficiency diseases are among the most common noncommunicable diseases and is a serious problem in protecting public health. In more than 50% of the Russian Federation territory, there is an iodine deficit, and about 100 million people live in these regions in a state of chronic insufficiency. The territory of the Bashkortostan Republic is a region with iodine deficiency and associated goiter endemic. Iodine deficiency endemic conditions include a wide range of pathologies characterized by a decrease in the functional activity of the thyroid gland. Iodine deficiency manifests in a variety of pathologies from defects in physical and intellectual development, reproductive disorders to specific thyroid diseases (Kazimirko *et al.*, 2006; Farkhutdinova, 2005; Eriksen, 1986).

Hypothyroidism and hyperthyroidism are associated with a risk of osteoporosis (Marova, 2003; Nochevnaya *et al.*, 2011; Cardoso *et al.*, 2014; Wong and Steffes, 1984). Expression of the receptors of iodinated thyroid hormones was found both in osteoblasts and osteoclasts (Platonova and Troshina, 2015; Meunier *et al.*, 2005). Hypothyroidism is accompanied by a decrease in the number of basic multicellular

units in the bones in which local resorption and bone formation are associated with time. The duration of the phases of the remodeling cycle is increased, and the duration of the mineralization time of the newly formed osteons is significantly prolonged (Eriksen, 1986; Belyakov, 2014). The process of bone remodeling is a wonderful mechanism that simultaneously contributes to maintaining calcium homeostasis and bone integrity, and it's adaptive restructuring according to mechanical stimuli, and the needs of the body. Imbalance of remodeling cycles in hypothyroidism ultimately leads to a decreased bone mass, microarchitecture violation with an increase in bone tissue fragility and risk of fractures (Pavlova *et al.*, 2012; Bassett *et al.*, 2010; Nicholls *et al.*, 2012). There are literary data that in hypothyroidism, the spongy bone mainly affected, and excessive mineralization occurs in the cortical bone (Gouveia *et al.*, 1997; Schwarz *et al.*, 2006; Zimmermann and Anderson, 2011), which, however, does not reduce the risk of fractures. Mechanisms of these phenomena are not fully understood (Cardoso *et al.*, 2014; Wong and Steffes, 1984). Probably thyroid hormones affect the bioavailability and action of estrogens and / or androgens (Freitas *et al.*, 2003; Krassas *et al.*, 2010; Zhang and Lazar, 2000). Other authors (Nicholls *et al.*, 2012; Zhdo

et al., 2012) associated disturbances in the course of remodeling under the action of thyroid hormones with a change of D2 deiodinases (activator of T3 formation) in bone tissue activity and D3 (T3 inactivator) in osteoblasts.

Aim of the study: to characterize changes in phosphorus-calcium metabolism and bone tissue, its structure in experimental hypothyroidism in rats.

2. MATERIALS AND METHODS

The 26 white mongrel sexually mature male rats weighing 200-210 g were involved in experiments. Requirements and ethical standards on humane attitude to laboratory animals (order of the Ministry of Health of the Russian Federation dated 06/19/2003 No. 267 "On approval of laboratory practice." The animals were kept in standard vivarium conditions with a natural light mode, on a standard laboratory animal diet (GOST 50258-92). In the experimental group of animals, hypothyroidism was modeled by daily intragastric administration of Thiamazole at the rate of 2.5 mg / 100 g of body weight for three weeks by a metallic probe (Kozlov, 2006). On day 22, animals were decapitated under ether anesthesia. The content of total calcium, phosphorus, magnesium was studied in blood serum, using colorimetric method HUMAN company (determination of Ca - using D-cresolphatein-complexone, ammonium P-molybdenum acid, Mg - 1- (2-hydroxyazo) -2-naphthol-3- (2,4-dimethyl) -carboxiamide). Enzyme multiplied immunoassay was used to analyze the content of bone metabolism markers - bone alkaline phosphatase (reagents "Metra BAFKit Quidel Corporation), C - terminal collagen telopeptides type 1 (Serum Cross Laps Elisa reagents, Nordie Biosince Diagnostic A / S), and levels of thyrotropin (TSH), total T3 and T4, testosterone, follicle-stimulating (FSH) and luteinizing (LH) hormones, parathyroid hormone (PTH, reagents of Vector-Best CJSC, Russia), interleukins-1 β (IL-1 β) and - 6 (IL-6), tumor necrosis factor-alpha (TNF- α , reagents LLP "Cytokine circuit ", Russia) using Stat Fox 2100 analyzer (USA) and the Uniplan semi-automatic analyzer (Russia) according the producer's protocols. To characterize the histological structure of bone tissue, the femoral pieces were fixed in 10% neutral formalin, decalcified for 3 weeks in a 7% solution of nitric acid (with a change of solution every week), washed, poured paraffin into blocks, made slices 7-8 microns

thick. Sections were stained with hematoxylin and eosin. Microscopic sections were studied under a microscope of the MZ-300 series (Austria), micrographs were made using a Nikon Coolpix 4500 camera.

Statistical processing was carried out using the Statistica 6.0 software package (Stat Soft), with the calculation of arithmetic mean (M), standard error of arithmetic mean (m) with the estimation of the significance of intergroup differences by Student t-criterion.

3. RESULTS AND DISCUSSION

Table 1 shows the content of thyrotropin and thyroid hormones in the blood serum of white male rats in intoxication with Thiamazole. The results were obtained by enzyme multiplied assay.

Table 2 presents the indicators of mineral metabolism and markers of bone metabolism in experimental Thiamazole hypothyroidism in male rats, determined by the colorimetric method.

PTH, testosterone, FSH, LH, and cytokines blood serum content in male rats is shown in Table 3.

Figures 1 - 4 show microphoto-histostructures of femoral bones diaphysis in control and experimental groups of animals

Determination of thyroid-stimulating hormone (TSH), total thyroxine (tT4) and total triiodothyronine (tT3) in the blood serum of the experimental group of animals confirmed the development of thyroid hypofunction with a decrease in hormone secretion on the background of increased TSH at the end of 3-week Thiamazole administration (Table 1)

The results of determination of mineral metabolism indicators in blood serum and bone remodeling (Table 2) showed that with the development of Thiamazole hypothyroidism, statistically significant changes in serum calcium, phosphorus and magnesium are not observed, but there is a tendency to a decrease in the level of Ca and P (Marova, 2003; Bassett and Williams, 2009; Pantazi and Papapetrou, 2000).

In hypothyroidism, an increase in the secretion of parathyroid hormone has been established as an adaptive reaction to a slowdown in bone remodeling with the development of hypocalcemia, a decrease in calcitonin levels and an increase in calcitriol

(Kazimirko *et al.*, 2006; Vanderpump *et al.*, 2011).

The content of bone resorption marker - C - terminal collagen telopeptides type 1 (β -Cross Laps) in rats of the experimental group decreases slightly, and the bone formation marker - bone alkaline phosphatase decreases statistically significantly. The obtained results show the disturbance of bone remodeling with significant inhibition of bone tissue formation phase. This results in the disturbance of bone tissue structure, which was found in its histological study. Figures 1-4 show the microphoto-histostructure of the femoral bone diaphysis of animals in the control and experimental groups.

Thyroid hormones are likely to influence the metabolism of bone tissue and mineral metabolism indirectly, affecting other systemic hormones and tissue regulatory factors. In addition to the established counter-regulatory phenomenon between thyroid hormones and parathyroid hormone, it was shown that T_3 and calcitriol synergistically affects osteoclastogenesis (Samsonova, 2007; Gruber *et al.*, 1999; Wang and Sum, 1980). There are indications of changes in the levels of growth hormone, insulin-like growth factor, interleukin-6, prostaglandin- E_2 , sex hormones under the influence of T_3 (Bassett and Williams, 2009; Gruber *et al.*, 1999). Analysis of the level of certain hormones and cytokines in the serum of rats with Thiamazole hypothyroidism also indicates the effect of thyroid hormones on the hormonal status of the body (Table 3). In the experimental group, all the studied parameters (PTH, FSH, LH, IL-1 β , IL-6, and TNF- α) were significantly increased except for the main sex hormone in the male body, testosterone. An increased level of gonadotropic hormones of the pituitary gland, on the background of a slight decrease in testosterone, indicates that in rats of the experimental group with hypothyroidism, the central regulation of the synthesis and secretion of androgens and reciprocal physiological relationships between the components of the hormonal axis hypothalamus-pituitary gonad is preserved.

It should be stressed that in the case of Thiamazole intoxication, the content of pro-inflammatory cytokines in the blood serum increases in animals with hypothyroidism: IL-1 β , IL-6, and TNF- α . Pro-inflammatory cytokines in bone tissue induce the production of matrix metalloproteinases, inhibit the synthesis of their inhibitors, increase the production of RANKL, inhibit the migration of osteoblasts, induce

apoptosis of osteocytes and activate osteoclastogenesis and osteoclast functions (Cardoso *et al.*, 2014; Wei *et al.*, 2005). Whether the increased secretion of pro-inflammatory cytokines is associated with the development of hypothyroidism under the action of Thiamazole or the direct effect of the toxicant on the cells – producers of the studied cytokines requires further research. Nevertheless, the results of the studies show that with the development of hypothyroidism, disturbance of bone remodeling and mineral metabolism is a consequence of not only the direct influence of thyroid hormones on osteoblasts and osteoclasts, but they can also be associated with other mechanisms of their action.

In rats of the control group (Figure 1), the cortical bone is represented by a developed network of multidirectional havers channels with different calibers. Under the periosteum and endostomy, the outer and inner layers of the compact substance formed by the system of bone plates are located parallel to the bone surface. Osteocytes located between the outer and inner common plates have a process shape. Osteons are interconnected by insertion plates. Blood vessels are located in the center of the osteon, perforating canals are found.

In experimental hypothyroidism, a significant change in the histostructure of the diaphysis of the tubular bones is determined. The thickness of the wall of the femur is uneven. There is an alternation of a fairly thick section with a section of bone thinning. The cementing (joint) lines located between common plates and osteons and between packages of bone plates undergo a particularly significant change (Figure 2). Loss of bone mass is seen. Bone plates, combined in bone packs, have, in some places, a bright zone, sometimes exfoliate from each other, indicating the presence of dystrophic changes with demineralization of bone tissue. There are deformed sections of common (general) plates (Figure 3.). The disorder of bone tissue formation (bone formation) is revealed, which is manifested by focal changes in the mass of bone structures. At the same time, the narrowing of osteons gaps is observed (Figure 4).

Thus, in the group of animals with experimental Thiamazole hypothyroidism, changes characteristic of dysplastic osteopenia were observed in the bone tissue.

4. CONCLUSIONS

1. Three-weekly daily intragastric administration of Thiamazole in a dose of 2.5 mg / 100 g of the animal mass causes the development of changes characteristic to hypothyroidism in white mongrel rats: decreased blood serum level of thyroid hormones and increase in the level of thyrotropin.

2. In animals, experimental hypothyroidism is accompanied by insignificant changes (decrease) in blood serum levels of phosphorus and total calcium, a significant reduction in bone alkaline phosphatase levels while maintaining C-terminal telopeptides of collagen type 1 concentration, reflecting disturbances in remodeling processes.

3. Experimental Thiamazole hypothyroidism in male rats is accompanied by a decrease in testosterone secretion, an increase of gonadotropins, parathyroid hormone, pro-inflammatory cytokines (: IL-1 β , IL-6, and TNF- α), thus showing a complex mechanism for the development of bone and mineral metabolism disorders.

4. The study of the histostructure of the tubular bone diaphysis in experimental hypothyroidism, reveals signs characteristic for the developing dysplastic osteoporosis.

The work has been approved by the Local Ethics Committee of the Bashkir State Medical University Ministry of Health of the Russian Federation

6. REFERENCES

1. Bassett, J. H., Boyde, A., Howell, P. G. *Proc. Natl. Acad. Sci USA*, **2010**, 107(6), 7604–7609.
2. Bassett, J. H., Williams, G.R., **2009**, 42, 269–282.
3. Belyakov, Yu. A., Maxillofacial system in endocrine diseases, 2nd ed., Moscow: BINOM, **2014**.
4. Cardoso, L. F., Maciel, L. M., de Paula, F. J. A., *Arg. Bras. Endocrinol. Metab*, **2014**, 58(5), 452–463.
5. Eriksen, E. F., *Endocr. Rev*, **1986**, 7, 251–263.
6. Farkhutdinova, L. M., Goiter as a biomedical problem (on the example of the Republic of Bashkortostan), Ufa: Gilem, **2005**.
7. Freitas F. R. S., Moriscot A. S., Jorgetti V., Soares A. G., Passarelli M., Scanlan T. S., Brent G. A., Bianco A. C., Gouveia C. H. A., *Am.J.Physiol.Endocrinol*, **2003**, 285(5), E1135–1145. <https://doi.org/10.1152/ajpendo.00506.2002>
8. Gouveia, C. H., Jorgetti, V., Bianco, A. C., *J.Bone Miner.Res*, **1997**, 12, 2098–2107.
9. Gruber R, K Czerwenka, F Wolf, G.-M Ho, M Willheim, M Peterlik, Expression of the vitamin D receptor, of estrogen and thyroid hormone receptor α - and β -isoforms, and of the androgen receptor in cultures of native mouse bone marrow and of stromal/osteoblastic cells, *Bone*, **1999**, 24, 465–473. [https://doi.org/10.1016/S8756-3282\(99\)00017-4](https://doi.org/10.1016/S8756-3282(99)00017-4)
10. Kazimirko, V. K., Kovalenko, V. N., Maltsev, V. N., Osteoporosis: pathogenesis, clinical picture, prevention, and treatment, 2nd ed., Kiev: Morion, **2006**.
11. Kozlov, V. N., *Siberian Medical Journal*, **2006**, 5, 27–30.
12. Krassas, G. E., Poppe, K., Glioner, D. *Endocrine Reviews*, **2010**, 31(6), 702–736
13. Marova, E. I. Manual for osteoporosis, In L. I. Benevolenskaya (ed). Moscow: BINOM Laboratory of knowledge, **2003**.
14. Meunier N., Beattie J. H., Ciarapica D., O'Connor J. M., Andriollo-Sanchez M., Taras A., Coudray C., Polito A. Basal metabolic rate and thyroid hormones of late-middle-aged and older human subjects: the zenith study. *Eur journal clin nutr.*, **2005**, 59(2), 53–57.
15. Nicholls, J. J., Brassili, N. J., Williams, G. R., *J.Endocrinol*, **2012**, 214, 209–221.
16. Nochevnaya, L. B., Pavlenko, O. A., Kalinina, O. Yu., Stolyarov V. A., *Siberian Medical Journal* **2011**, 4(26), 189–193.
17. Pantazi, H., Papapetrou, P. D., *J.Clin. Endocrinol. Metab*, **2000**, 85(3), 1099–1106.
18. Pavlova, T. V., Peshkova E. K., Kolesnikov D. A. *Basic research*, **2012**, 4, 97–100.
19. Platonova, N. M., Troshina E. A., *Consilium medicum*, **2015**, 17(4), 44–50.
20. Samsonova L. N., *Problems of endocrinology*, **2007**, 53(6), 40–43.
21. Schneider, O. T., *Dentistry*, **2002**, 4, 55–57.

22. Schwarz, A. N., Sellmeyer, D. E., Strotmeyer, E. S. *J. Bone Miner Res*, **2006**, 20(4), 596–603.
23. Vanderpump, M. P., Lazarus J. H., Smyth P. P. Iodine status of UK schoolgirls: a cross-sectional survey. *Lancet*, **2011**, 377, 2007
24. Varga, F., Rumpler, M., Kiaushofer, K., *FEBS Lett*, **1994**, 345, 67–70.
25. Wang, K. W., Sum, C. F., *Singapore Med. J.*, **1980**, 30(5), 476–478.
26. Wei S., Kitaura H., Zhou P., Ross F. P., Teitelbaum S. L., IL-1 mediates TNF-induced osteoclastogenesis. *J. Clin. Invest*, **2005**, 115, 282–290. DOI: 10.1172/JCI23394
27. Wong, E. T., Steffes, M. W., *Clin. Lab. Med*, **1984**, 4, 655–670.
28. Zhang, J., Lazar, M. A., *Annu. Rev. Physiol*, **2000**, 62, 439–466.
29. Zhao B., Grimes S. N., Li S., Hu X., Ivashkiv L. B. TNF-induced osteoclastogenesis and inflammatory bone resorption are inhibited by transcription factor RBP-J. *J. Exp. Med*, **2012**, 209(2), 319–334. <https://doi.org/10.1084/jem.20111566>
30. Zimmermann, M. B., Anderson M. Prevalence of iodine deficiency in Europe in 2010. *Ann Endocrinol (Paris)*, **2011**, 72, 164–166.

Table 1. Blood serum thyrotropin and thyroid hormones content in white male rats in Thiamazole intoxication

Hormones	Control group n=10	Experimental group n=8	P
TTH, ml ME/l	1.11 ± 0.105	1.98 ± 0.166	<0.01
tT4, nmol/l	76.6 ± 3.33	61.9 ± 3.30	< 0.05
tT3, nmol/l	3.11 ± 0.19	1.8 ± 0.156	< 0.01

Table 2. The level of indicators of mineral metabolism and markers of bone metabolism in experimental Thiamazole hypothyroidism in male rats

Indicators	Control group	Experimental group n=8	P
Total Ca, mmol/l	2.24 ± 0.087	2.01 ± 0.166	> 0.2
P, mmol/l	1.81 ± 0.054	1.74 ± 0.065	> 0.5
Mg, mmol/l	0.86 ± 0.063	0.88 ± 0.053	> 0.5
ABP, E/l	6.1 ± 0.46	4.8 ± 0.36	< 0.05
β- Cross Laps, mgr/ml	0.87 ± 0.06	0.78 ± 0.04	> 0.1

Table 3. Content of some hormones and cytokines in rat blood serum in experimental hypothyroidism

Indicators	Control group, n=10	Experimental group, n=16	P
PTH	16.4 ± 0.22	22.1 ± 0.19	0.003
Testosterone nmol/l	23.6 ± 0.88	20.5 ± 0.72	0.048
FSH, ME/l	2.86 ± 0.116	3.70 ± 0.245	0.024
LH, ME/l	2.26 ± 0.195	2.98 ± 0.161	0.051
IL-1β, pg/ml	12.1 ± 1.07	18.7 ± 0.81	0.036
IL-6, pg/ml	15.2 ± 0.48	18.2 ± 0.39	0.050
TNF-α, pg/ml	15.9 ± 0.79	23.1 ± 0.91	0.026

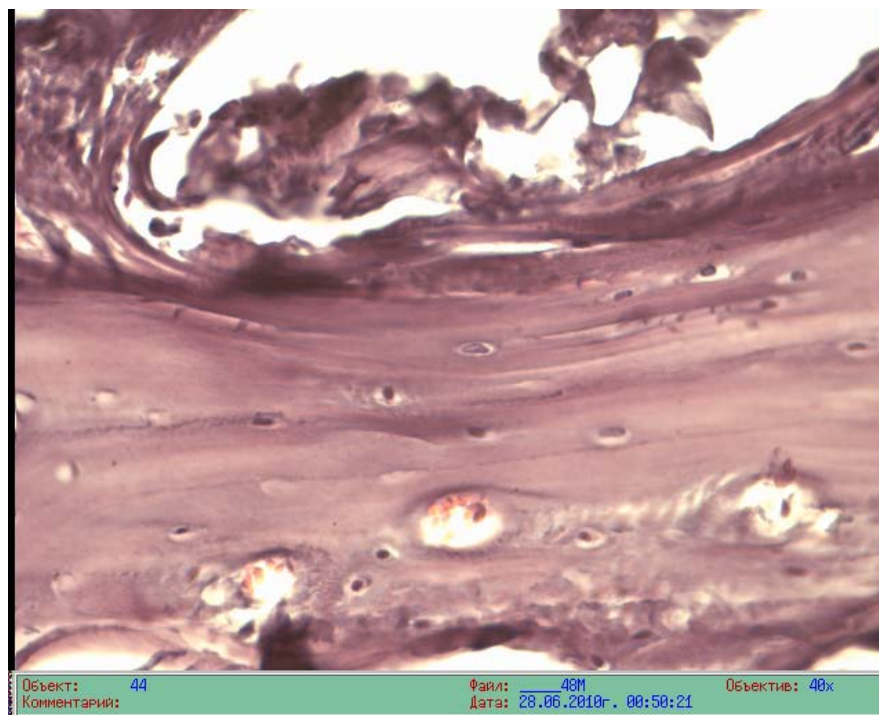


Figure 1. *Periosteum, compact bone, and endostasis of tubular bone diaphysis in the control group of animals. Hematoxylin and eosin stain. Microphoto, OK10, 40x*

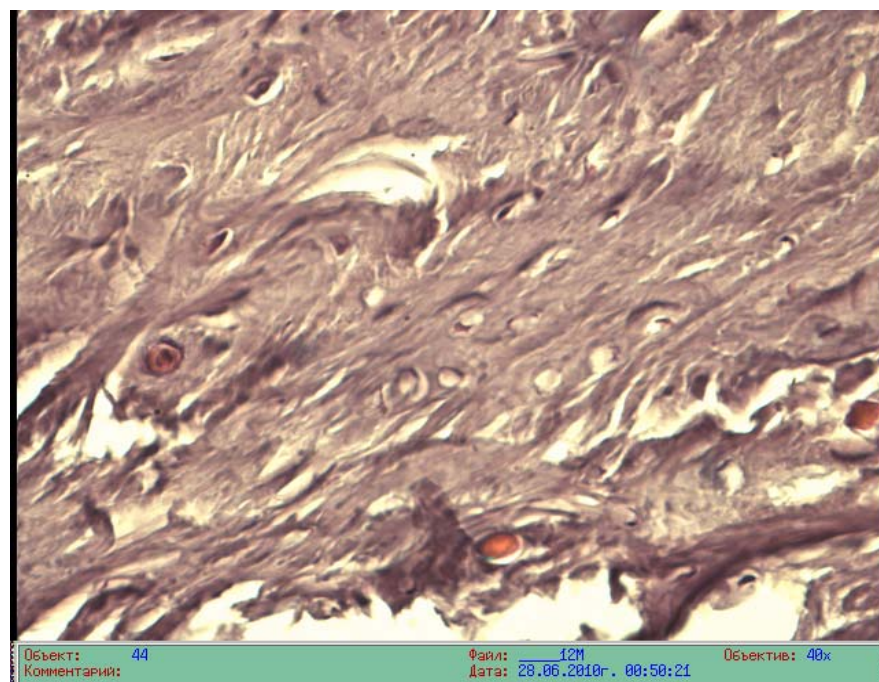


Figure 2. *Dilatation of tubular bones cementing lines of during hypothyroidism in experimental animals. Hematoxylin and eosin stain. Microphoto, OK10, 40x*

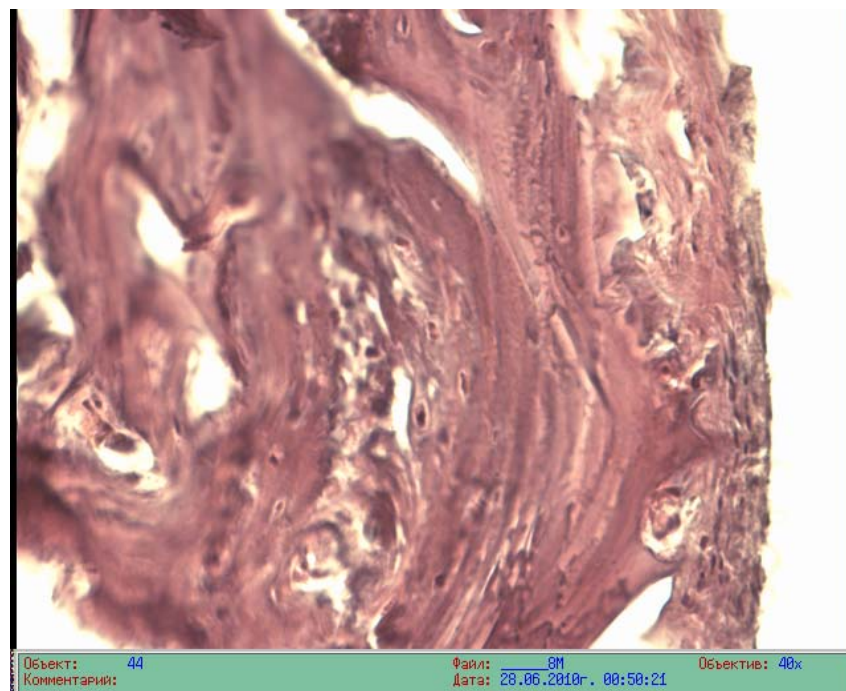


Figure3. Deformation zone of tubular bones structures in hypothyroidism in experimental animals. Hematoxylin and eosin stain. Microphoto, OK10, 40x

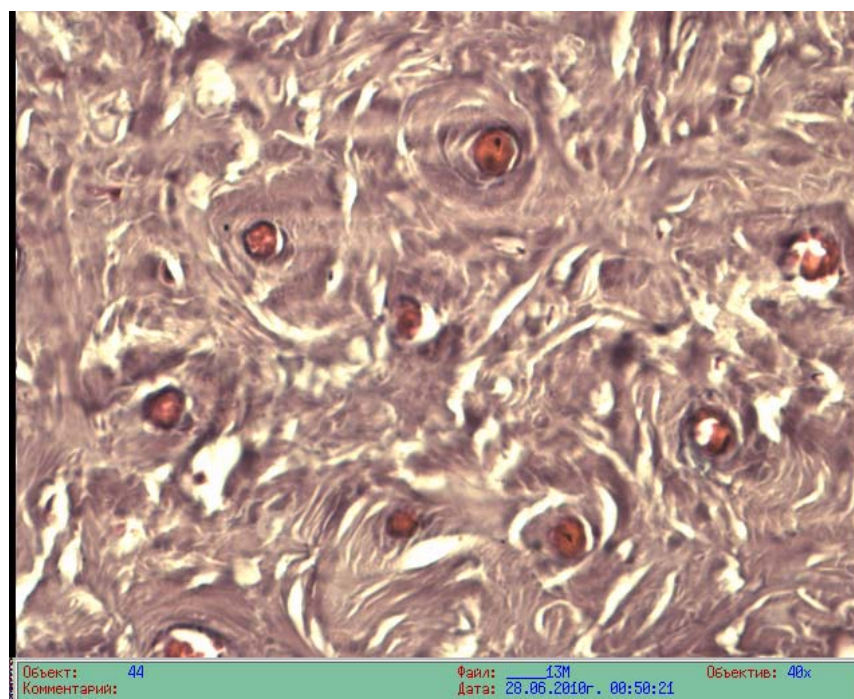


Figure 4. Narrowing of osteons gaps of with disturbance of the soldering line of the tubular bone in hypothyroidism in experimental animals. Hematoxylin and eosin stain. Microphoto, OK10, 40x

CARACTERIZAÇÃO ANTIBACTERIANA DE NANOPARTÍCULAS DE TITÂNIO
NANOSINTETIZADAS POR *STREPTOCOCCUS THERMOPHILUS*

ANTIBACTERIAL CHARACTERIZATION OF TITANIUM NANOPARTICLES
NANOSYNTHESIZED BY *STREPTOCOCCUS THERMOPHILUS*

التوصيف ضد البكتيري لجزيئات التيتانيوم النانوية الحبيوية المصنعة من بكتيريا
THERMOPHILUS

ALDUJAILI, Nawfal Hussein¹ and BANOON, Shaima Rabeeh^{2*}

¹ Department of Biology, Faculty of Science, University of Kufa, Najaf, Iraq

² Department of Biology, College of Science, University of Misan, Maysan, Iraq

* Correspondence author

e-mail: shimarb@uomisan.edu.iq

Received 22 December 2019; received in revised form 30 January 2020; accepted 11 February 2020

RESUMO

Os metais que contêm nanomateriais têm potencial para serem empregados no controle de diferentes tipos de infecções; no entanto, informações limitadas são conhecidas sobre suas propriedades antibacterianas. Este estudo foi realizado para investigar a nanossíntese de nanopartículas de titânio (NPTi) (utilizando *Streptococcus thermophilus* e analisando suas ações biológicas como antibacterianas). As colônias bacterianas isoladas foram identificadas usando os primers universais 16S rRNA; posteriormente as sequências nucleotídicas do gene 16S rRNA foram alinhadas com as sequências nucleotídicas das cepas obtidas no GeneBank através do software CLUSTAL X (versão 1.82). Nanopartículas de titânio foram nanossintetizadas por adição de dióxido de titânio 0,025M (TiO₂) ao sobrenadante livre de células de *Streptococcus thermophilus*. O TiO₂ foi utilizado como precursor para a nanobiossíntese de NPTi. A formação de NPTi foi indicada pela alteração da cor da solução do marrom claro para marrom escuro, indicando a produção de NPTi. A caracterização da nanobiossíntese foi realizada com UV-Visível (absorbância em 377 nm), Microscopia Eletrônica de Varredura, Difração de raios-X, Microscopia de Força Atômica, Espectroscopia de raios-X dispersiva de energia para distinguir a dimensão, forma (esférica) por MEV, análise de dispersão (homogênea) e elementar de nanopartículas. As NPTi biogênicas apresentaram atividade antibacteriana e antibiofilme contra a pneumonia por *Klebsiella* resistente a múltiplas drogas e ao *Staphylococcus aureus*. Como atividade antibacteriana, as NPTi inibiram significativamente *K.pneumoniae* (20 mm) na concentração de 500 µg/ml e *S. aureus* (16 mm) na mesma concentração e aumentando a concentração de NPTi, a zona de inibição aumentou. Enquanto a atividade antibiofilme das NPTi utilizando o método de tubos, nos tubos contendo suspensões bacterianas de *K.pneumoniae* e *S.aureus* com NPTi, os resultados demonstraram que a formação de biofilme foi impedida e removida pelo efeito das NPTi.

Palavras-chave: TiNPs biogênicos, nanopartículas, *Streptococcus thermophilus*, Atividade antibacteriana, Antibiofilme.

ABSTRACT

Metals that contain nanomaterials have the potential to be employed in controlling different kinds of infection, however, very limited information is known about their antibacterial properties. This study has been done to investigate the nanosynthesis titanium nanoparticles (TiNPs) using *Streptococcus thermophilus* and analyzing their biological actions as antibacterial. The bacterial isolates identified using universal primers 16S rRNA; then the 16S rRNA gene nucleotide sequences were aligned with the nucleotide sequences of strains obtained from the GeneBank through the software CLUSTAL X (version 1.82). Titanium nanoparticles were nanosynthesized by adding 0.025M titanium dioxide (TiO₂) into cell-free supernatant for *Streptococcus thermophilus*. TiO₂ was used as a precursor for nanobiosynthesis TiNPs. The formation of TiNPs was indicated by the color alteration of the solution from the light brown into dark brown indicates for the production of TiNPs. The Characterization of nanobiosynthesis was accomplished with UV-Visible (absorbance at 377nm), Scanning Electron Microscope, X-ray diffraction, Atomic Force Microscope, Energy-dispersive X-ray spectroscopy was used to distinguish the dimension, form (spherical) by SEM, dispersal (homogenous) and elemental analysis of

nanoparticles. Biogenic TiNPs have displayed antibacterial and antibiofilm activity against both multidrug-resistant *Klebsiella pneumonia* and *Staphylococcus aureus*. As an antibacterial activity, the TiNPs inhibited significantly *K.pneumoniae* (20 mm) with concentration (500 µg/ml), and *S. aureus* (16 mm) with the same concentration and increasing the concentration of TiNPs the inhibition zone increased. While as antibiofilm activity of TiNPs using the tube method, the tubes containing bacterial suspension *K.pneumoniae* and *S.aureus* with TiNPs, the results demonstrated that the biofilm formation was prevented and removed by the effect of TiNPs.

Keywords: Biogenic TiNPs, nanoparticles, *Streptococcus thermophilus*, Antibacterial Activity, Antibiofilm.

الملخص

المعادن التي تحتوي على مواد متناهية الصغر لديها القدرة على أن تستخدم في السيطرة على أنواع مختلفة من العدوى ، ومع ذلك ، هناك معلومات محدودة للغاية معروفة عن خصائصها المضادة للبكتيريا. تم إجراء هذه الدراسة لاستقصاء جسيمات التيتانيوم النانوية (TiNPs) باستخدام بكتيريا *Streptococcus thermophilus* (العقيدة المحبة للحرارة) وتحديد فعاليتها البيولوجية كمضادات للبكتيريا. تم تحديد العزلات البكتيرية باستخدام باديء عام 16S rRNA؛ ثم تمت محاذاة متواليات النيوكليوتيدات الجينية 16S rRNA مع متواليات النيوكليوتيدات الخاصة بالسلالات التي تم الحصول عليها من بنك الجينات من خلال برنامج CLUSTAL X (الإصدار 1.82). تم تصنيع جزيئات التيتانيوم النانوية عن طريق إضافة 0.025 M ثاني أكسيد التيتانيوم إلى راسح حار فقط على خلايا بكتيريا *Streptococcus thermophilus*. تم استخدام ثاني أكسيد التيتانيوم كبداء لجزيئات التيتانيوم النانوية الحيوية. إن الدليل على تكوين جزيئات التيتانيوم النانوية تم بواسطة تغيير لون المحلول من البني الفاتح إلى البني الداكن الذي يشير إلى إنتاج جزيئات التيتانيوم النانوية. تم تشخيص التركيب النانوي الحيوي باستخدام الأشعة فوق البنفسجية المرئية (الامتصاص عند 377 نانومتر) ، المجهر الإلكتروني الماسح ، حيود الأشعة السينية ، مجهر القوة الذرية ، ومطياف الأشعة السينية المشتتة للطاقة لتمييز البعد والشكل (كروي) بواسطة المجهر الإلكتروني الماسح ، التشتت (متجانسة) والتحليل الأولي للجسيمات النانوية. لقد أظهرت جزيئات التيتانيوم الحيوية المنشأ فعالية ضد بكتيرية وضد الغشاء الحيوي لكل من بكتيريا *K.pneumoniae* و *S.aureus* المتعددة المقاومة للأدوية. كفعالية ضد بكتيرية؛ لوحظ أن جزيئات التيتانيوم النانوية تثبط *K.pneumoniae* معنوياً بقطر (20 ملم) عند تركيز (500 µg/ml) وبكتيريا *S. aureus* بقطر (16 ملم) عند نفس التركيز ومنطقة التثبيط تزداد بازدياد تركيز جزيئات التيتانيوم النانوية. بينما فعالية ضد الغشاء الحيوي لجزيئات التيتانيوم النانوية باستخدام طريقة الأنبوب، أظهرت النتائج أن الأنابيب التي تحتوي على معلق بكتيري *K.pneumoniae* و *S.aureus* مع جزيئات التيتانيوم النانوية، بأنه تم منع تكوين الأغشية الحيوية وإزالتها بواسطة تأثير جزيئات التيتانيوم النانوية.

الكلمات المفتاحية: جزيئات التيتانيوم النانوية الحيوية ، جزيئات نانوية، *Streptococcus thermophilus* ، فعالية ضد بكتيرية، ضد غشاء حيوي.

1. INTRODUCTION

Due to the high photocatalytic activity of titanium dioxide TiO₂, it has been used in most daily life applications (Allen, 2008). It is well-known that titanium nanoparticles have incredible gas-sensitive properties (Chen and Mao, 2007). TiO₂ shows perfect stability and non-toxicity behavior (Sugimoto, 2003). Titanium dioxide is suitable to split H₂O due to its optical properties (Rao et al., 1980). It exhibits broadband UV absorption and sunscreen applications (Sung et al., 2002). The cure for infectious diseases is still concerned. Consequently, resistance has expanded because of the insensible take of antimicrobial agents (Jain et al., 2009).

Antimicrobial Resistance (AMR) is triggered by antimicrobial-resistant microorganisms. Many antimicrobials that are treated numerous microbial infections are quickly mislaying their efficiency, as bacterial species and further microbes improve resistance (O'Neill, 2016; Ali, 2018).

More than 700,000 persons in the world

die from AMR. Death could increase to 10,000,000 persons by 2050. Essentially, people should decrease the danger of bacteria emerging resistance by reducing the overuse and misuse of antibiotics and avoiding the infection (O'Neill, 2016).

The antimicrobial characteristics of metals such as zinc, silver, titanium, and copper have been known for the last decades, which facilitate the way to be exploited in many modern medical applications in order to control some microbial infection diseases (Weber & Rutala 2001). Several chemical forms have arisen from these metal-containing nanomaterials, including either solid nanoparticles (NPs) of metal or metal oxides such as Ag NPs and TiO₂ NPs (Han et al. 2010).

To- date, the specific mechanism of bacterial toxicity of nanometals is still not fully understood, but there is a theory saying that the free metal ion toxicity arising from the surface of the nanoparticles may play a vital role in infection control (Kim et al. 2007). In the case of using the titanium nanoparticles, by photocatalysis, the TiO₂ surface reacts with water to enable the release of the hydroxyl radical, which leads

subsequently to form the superoxide (Linsebigler *et al.* 1995). This superoxide could then be a potential element that able to attack the polyunsaturated phospholipids in bacteria (Wong *et al.* 2006) and lead to site-specific DNA damage (Hirakawa *et al.* 2004).

It has been proved that TiNPs have inhibition actions and avoidance the biofilm development, in addition to distinctive physicochemical and biological chattels (Wijnhoven *et al.*, 2009). Development of nanobiosynthesis that can be potential in many biomedical applications and development novel materials that inhibit the Multidrug resistance (MDR) microbe (Chaudhari *et al.*, 2012 and Franci *et al.*, 2015). That why use bacterial species in nanobiosynthesis (Gade *et al.*, 2008).

S. thermophilus have antibacterial and antioxidative possessions, regulating the balance of intestinal flora (Songisepp *et al.*, 2004).

The primary goal of this study was to nanobiosynthesis of TiNPs with *S. thermophiles*, and these TiNPs were chosen for their variety physico-chemical properties and, therefore, likely modes of action, TiO₂ NPs is a stable metal oxide. A secondary goal of this study was to come up with the ongoing test methods by evaluating both the antibacterial and antibiofilm activity.

2. MATERIALS AND METHODS

The Materials and Methods for this study as shown below in paragraphs:

2.1. 16S rRNA gene sequencing of Bacterial Isolates

The identification of species sequence was revealed via PCR with universal primers. The 16S rRNA was imperiled to DNA sequencing. Favour Prep total DNA Kit (Presto™ Mini gDNA Bacteria Kit, Geneaid ,Taiwan) was used to extract DNA following the company's instructions. PCR reaction mixture with final volume 20 µl consisted of 2µl for each 27F and 1492R primers (10 picomole), 9µl De-ionized water, and 7µl the DNA of the isolate were added into the AccuPower® Taq PCR PreMix tubes (Bioneer, South Korea); that contain (Taq DNA polymerase, dNTPs, KCl, MgCl₂, and buffer). PCR was done under the following conditions: 96°C, 6 min with 38 cycles: 35 sec at 96°C, 65 sec at 57°C, and 125 sec at 72°C, 5min 72°C. The products were separated at 1.5 % agarose

gel, then 16S rRNA was sent for sequencing (Sambrook and Rusell, 2001).

The 16S rRNA gene nucleotide sequences were aligned with the nucleotide sequences of reference strains obtained from the GeneBank database through the software CLUSTAL X (version 1.82) (Phalakornkule and Tanasupawat, 2006). The SnapGene tool was used for overall applications of editing and analysis. The similarity between the 16S rRNA gene nucleotide sequence and the most related species was exposed from the NCBI public database. BLASTn tool was used for accomplishing nucleotide sequences similarity against nucleotide sequence references that available in the Genbank database (Hall, 1999; Altschul *et al.*, 1997).

2.2. Preparation of cell-free supernatant of *Streptococcus thermophilus*

S. thermophilus was inoculated in prepared and autoclaved broth. Then, the culture was incubated in aerobic conditions at 37°C for 18 hrs. After the incubation period, centrifugation at 6000 rpm, 10 min. The cells were precipitated at the bottom of the tube and were discarded later, calmed was filtrated to TiNPs nanobiosynthesis (Chaudhari *et al.*, 2012).

2.3. Nanobiosynthesis of TiNPs with supernatant

Titanium dioxide (TiO₂) was used as originator to TiNPs nanobiosynthesis by *S. thermophilus*. 5 ml of titanium dioxide (0.025M) solution were added to 5 ml of cell-free supernatant of *S. thermophilus* that distributed in sterilized test tubes and mixed well. The resultant solutions were incubated at 37 °C for 18 h in a shaking incubator at 160 rpm. After incubation, the color has changed, then the reaction mixture was centrifuged at 10000 rpm for 20 minutes, the cell-free filtrate was rejected and substituted with water and re-centrifuged for several times, the precipitated pellets which represent the assemblage of TiNPs and then dryness, 40°C for 18-24 hours. The residues were assemblage plus kept aimed at use (Prasad *et al.*, 2007).

2.4. Nanocharacterization of TiNPs

The color of the reaction mix was observed by determining the absorbance of the reaction mix. TiNPs were examined with UV-Vis Spectra. (Shimadzu,1600). X-ray diffraction (XRD) was used to analyze the purity of the TiNPs (Huang *et al.*, 2018). Atomic Force Microscope (AFM) was accomplished for the examination of the TiNPs. Scanning Electron Microscope (SEM) was employed to determine

the morphology properties of TiNPs (Caroling *et al.*, 2013).

2.5. Antibacterial activity of TiNPs

Nanobiosynthesized TiNPs were tested to evaluate their antimicrobial activity against Multidrug resistance (MDR) *K. pneumoniae* and *S. aureus* using agar well diffusion method. Four different concentrations of TiNPs (100, 300, 400, and 500 µg/ml) were used, and the experiment has been done using a well plate of 6 mm. 100µl of each concentration was added into each well. One Petri-dish subcultured for each pathogenic bacteria and used as a control (without testing for antibacterial activity), and incubation conditions were at 37 °C for 24 h. (Rajeshkumar and Malarkodi, 2014).

2.6. Antibiofilm activity of TiNPs

Tube method (TM) was achieved to evaluate the biofilm development and antibiofilm action by TiNPs as follows: BHI was prepared and sterilized by autoclave, then inoculated each pathogenic bacteria and keep warm for 24 hrs at 37°C. The next day, BHI was prepared again, 2% of sucrose was added to BHI after sterilization by filtration, 60 µl from BHI was distributed in sterilized tubes, then 30 µl of each overnight bacterial suspension and 30 µl of TiNPs with concentration of 500 µg/ml were added separately to each tube, the control tube normally contained only the bacterial suspension without TiNPs and incubated under the same incubation conditions (Kumar *et al.*, 2012). After incubation, discharge the bacterial suspension and phosphate buffer saline (PBS) pH 7.4 from the tube and dryness at room temperature. The tubes were dealt with 1% crystal violet for 10 min and incubated at room temperature, and the excess stain was removed and washed with distilled water, the tubes were placed upside down to drain. Biofilm formation was observed as a positive when a visible film lined the wall and bottom of the tubes. The effect of TiNPs on biofilm formation of clinical bacteria was observed through inhibition of the formation of biofilm (Mathur *et al.*, 2006).

3. RESULTS AND DISCUSSION:

3.1 Results

The results of this study as shown below in paragraphs:

3.1.1. 16S rRNA gene sequencing of Bacterial Isolates

The 16S rRNA sequence was considered as a

more discerning. Thus, 1260 bp of 16S rRNA was amplified with PCR. From alignment with the database in GenBank by the BLAST program, bacteria were recognized with 99 % certainty to be *S. thermophilus* (Chagnaud *et al.*, 2001).

3.1.2. Nanobiosynthesis of TiNPs

The supernatant of *S. thermophilus* demonstrated ability in synthesis for TiNPs using Titanium dioxide (5mM) as an initiator for nanosynthesis TiNPs, and after shaking incubation for 18 hrs, 150 rpm 38°C, *S. thermophilus* changed the color from light brown into dark brown as an indicator for nanosynthesis of the TiNPs.

3.1.3. UV-visible spectrophotometer analysis

UV-Visible spectrophotometric is a proven technique that is usually used for the analysis of the nanoparticles. After 24 hours of incubation of the reaction mixture, color-changing was observed, which indicated the formation of the nanoparticles in the reaction mixture. The absorption spectrum has a peak at 377nm for TiNPs. This is an indication of the TiNPs formation.

3.1.4. SEM exploration of TiNPs

SEM enables the high-resolution imaging of single nanoparticles (NPs) with sizes well below 10 nm, In the current study, SEM analysis exhibited well-spread of TiNPs, regular with 18-30nm in diameter to each nanoparticle, with inconstant shape mostly spherical form (Figure 1).

3.1.5. EDS analysis of TiNPs

Titanium was quantified by Energy-dispersive X-ray spectroscopy (EDS) analysis through observing the optical absorption peaks of titanium elements. The presence of elemental titanium indicated the reduction of titanium ions in the reaction mixture. The EDS appeared solid indications from Ti atoms. The weight proportion of TiNPs was 70.50 % Titanium and 29.50% for O2 (Figure 2). The peak appeared at 4.5keV for TiNPs.

3.1.6. XRD analysis of TiNPs

The average size of TiNPs was detected by X-ray crystallography diffraction (XRD) analysis, and the *S. thermophilus* produce TiNPs with average size was 21 nm (Figure 3).

3.1.7. AFM analysis of TiNPs

The average diameter and the three-dimensional structure of TiNPs were detected by the Atomic Force Microscope (AFM) analysis, and the *S. thermophilus* produce TiNPs with an average diameter of 54.32 nm (Figure 4).

Depending on description and nano-characterization of nanoparticles by the color-changing, XRD and AFM. The morphology, size, distribution, and presence of metals nanoparticles were nanocharacterized and therefore, TiNPs were used for further study.

3.1.8. Antibacterial activity of TiNPs

Antibacterial activity of nano-biosynthesized TiNPs was used to evaluate their ability for inhibition growth of clinical bacteria. Agar well diffusion method was used for detecting the antibacterial activity of different concentrations of TiNPs. The study presented that TiNPs inhibited bacterial growth (Table 1; Figure 5). TiNPs inhibited significantly *K.pneumoniae* (20mm) with concentration (500µg/ml), and *S. aureus* (16mm) with the same concentration. It was observed when increased the concentration of TiNPs the inhibition zone increased, (500 µg/ml) showed a large inhibition zone than 100 µg/ml, 300 µg/ml and 400 µg/ml respectively.

3.1.9. Antibiofilm activity of TiNPs

The tube method (TM) was used for impost of biofilm creation by MDR *K.pneumoniae* and *S.aureus* and antibiofilm by TiNPs.

Results revealed that biofilm formation was observed in control tubes containing only bacterial suspension (without nanoparticles), which was considered positive by showing a visible film lined the wall and bottom of the tube in tested bacteria, as showed in Table 2.

While the tubes containing bacterial suspension *K.pneumoniae* and *S. aureus* with TiNPs, the results showed biofilm formation was prevented and removed by the effect of TiNPs, that have the ability on formation biofilm in moderate and weak degree respectively.

3.2. Discussions

Nano-biosynthesis of titanium nanoparticles by *S. thermophilus* supernatant

was indicated by changing the color of reaction mixture from light brown color into dark brown, the changing in color may be attributed to reduction of (TiO₂) into Titanium nanoparticles due to the action of extracellular proteins, and other biomolecules present in the culture of *S. thermophilus* mediated the hydrolysis of the anionic complexes and resulted in the nanobiosynthesis of titanium nanoparticles (Jha and Prasad, 2010; Ahmad *et al.*, 2013).

Not all the organisms are found to be competent for the nanobiosynthesis of nanoparticles. The exact process in nanobiosynthesis by all organisms is yet to be elucidated (Gurunathan *et al.*, 2009).

The nano-characterization of the biogenic nanoparticles was performed by UV-visible spectroscopy, SEM, and EDS analysis. The preliminary confirmation of the extracellular nanobiosynthesis of nanoparticles was obtained by the contrast color change due to the surface Plasmon resonance (SPR) phenomenon. This was observed with the UV spectroscopic study of the colloidal solution, the maximum absorption peak of the Titanium nanoparticles centered at 377nm (Vidyasagar *et al.*, 2018).

The plasmon resonance band showing the sharp absorbance and indicates little aggregation of the particles in solution. The absorption of brown color due to excitation of surface plasmon vibration in particles, surface plasmon absorption strongly depends on the particle size, shape dielectric medium, and chemical surrounding the UV-Vis absorption spectra of nanoparticles dispersed in water (Mariselvam *et al.*, 2013).

The current study displayed well-dispersed TiNPs with 50-150nm with spherical shape (Ibrahim and Salman, 2014; Aldujaili *et al.*, 2015). The weight percentage of Ti was 70.50%. indicated to elemental titanium that directed the reduction to Ti metals in the mix (Bhakya *et al.*, 2016; Chaudhari *et al.*, 2012).

Due to the appearance and rise of AMR, nanomaterials are a substitute for antibiotics. Nano-particles (NPs) were reflected good-looking for the making of a novel Antibacterials (Rai *et al.*, 2012). The TiNPs seemed to have particular effects on *K. pneumoniae* (20 mm) with concentration (500 µg/ml), and *S. aureus* (16 mm) (Silhavy *et al.*, 2010; Taglietti *et al.*, 2012).

Results from the present study and other studies showed differences in inhibition zones of bacterial species to TiNPs, and this may be

returned to the variances liability of bacterial species depends on commotion of elements (Gad *et al.*, 2007; Blake and Neill, 2013; Hadi and Melconian, 2013). As well as when increase concentration of TiNPs showed an increase in the inhibition activity (Shrivastava *et al.*, 2007).

The steady release of ions from the degradation of nanoparticles is a critical function of nanoparticles. Ions bind to the protein and genomic negative charge, causing changes in the cell wall, membrane, DNA, and RNA of bacteria. Ion interacts with functional groups such as imidazoles and indoles. The TiNPs also injury membranes and encourage the discharge of ROS (Wu *et al.*, 2014). It has been proposed that NPs inhibit DNA replication, Ribosomes Denaturation, and modulation the signal transduction in bacteria (Shrivastava *et al.*, 2007; Jung *et al.*, 2008; Davod *et al.*, 2011).

Nanosized particles showed more inhibition activity than large particles. Bactericidal activity of AgNPs of Nanosized particles (<30 nm) was optimum alongside *S. aureus* and *K. pneumonia* (Wu *et al.*, 2014).

The morphology of nanomaterials has important characterization in the inhibition commotion of TiNPs. Hexagonal NPs showed a high effect in comparison with further shapes, and this was endorsed to the particular surface areas (Hong *et al.*, 2016).

Several different mechanisms that may work together to confer resistance which include prevention of the antimicrobial from reaching its target by reducing its ability to penetrate the cell or expulsion of antimicrobial from the cell via general or specific efflux pumps or by modification or degradation of antimicrobial (Alekshun and Levy, 2007).

Organisms generally possess mechanisms for detoxifying metals. this including exclusion from the cell, isolating the metal in the cytoplasm by concentrating it in granules, precipitating it in the cell wall, or transforming it (e.g., by oxidation or reduction) into a harmless form in the organism (Brown, 1991).

Other studies have demonstrated that TiNPs failed to exhibit antibacterial activity, but upon combination with antibiotics, they were able to inhibit the growth of microorganisms (Roy *et al.*, 2010), contrary with some studies that revealed TiNPs have the ability to inhibit the microbial growth without any kind of combination (Vincent *et al.*, 2014).

Microbial biofilms are communities that

have resistance to antibiotics and immunity. Nanoparticles may be used TiNPs to inhibition activity (Vincent *et al.*, 2014).

Clinical bacteria appeared their capability to create biofilm without treated by the nanoparticles, with TiNPs biofilm was disallowed in *K.pneumoniae* and *S. aureus*, TiNPs maybe alter genes regulation of biofilm, the effect on initial formation and maturation, leading to inhibition of biofilm-related infections (Martinez-Gutierrez *et al.*, 2013; Fayaz *et al.*, 2010; Sadekuzzaman *et al.*, 2015). More or less strains of species may be sensitive or resistant to nanoparticles (Vanaja and Annadurai, 2013; Aldujaili, 2017).

4. CONCLUSIONS:

16S rRNA is a sensitive and reliable method for the identification of *Streptococcus thermophilus*. The Bacteria *S. thermophilus* competent for Nanobiosynthesis of nanoparticles because Not all the organisms are found to be competent for the nanobiosynthesis of nanoparticles. The TiNPs have particular effects on Multidrug-resistant *Klebsiella pneumonia* and *Staphylococcus aureus*, thus are a substitute for antibiotics.

5. REFERENCES:

1. Ahmad, R., Khatoon, N., Sardar, M. *Journal of Proteins & Proteomics.*, **2013**, 4(2).
2. Aldujaili, N. H., Abdullah, N.Y., Khaqani, R. L., Al-tfaly, S. A., Al-Shammary, A.H. *Int J Recent Sci Res.* **2015**,6(12):7741-7751.
3. Aldujaili, N. H., Alrufa, M.M., Sahib, F.H. *Journal of Pharmaceutical Sciences and Research.* **2017**, 9(7):1220-1228.
4. Alekshun, M.N., Levy, S.B. *Cell.* **2007**, 128(6):1037-1050.
5. Ali A. *Journal of Pure and Applied Microbiology.* **2018**,12(2):577-586.
6. Allen, N.S., Edge, M., Verran, J., Stratton, J., Maltby, J., Bygott, C. *Polymer degradation, and stability.* **2008**, 93(9):1632-1646.
7. Altschul, S.F., Madden, T.L., Schäffer, A.A., Zhang, J., Zhang, Z., Miller, W., Lipman, D.J. *Nucleic acids research.* **1997**, 25(17):3389-3402.
8. Bhakya, S., Muthukrishnan, S., Sukumaran, M., Muthukumar, M. *Appl Nanosci.* **2016**, 6(5):755-766.
9. Blake, K.L., O'Neill, A.J. *J. Antimicrob.*

- Chemother.* **2013**, 68(1):12-16.
10. Brown, M.J. *Harvard Academic Publishers*. **1991**:567-579.
 11. Caroling, G., Tiwari, S.K., Ranjitham, A.M., Suja, R. *Asian J Pharm Clin Res.* **2013**, 6(4):165-172.
 12. Chagnaud, P., Machinis, K., Coutte, L.A., Marecat, A., Mercenier, A., *Journal of Microbiological Methods.* **2001**, 44(2):139-148.
 13. Chaudhari, P.R., Masurkar, S.A., Shidore, V.B., Kamble, S.P. *Journal of Applied Pharmaceutical Science.* **2012**, 2(3):25-29.
 14. Chen, X., Mao, S.S. *Chemical reviews.* **2007**, 107(7):2891-2959.
 15. Davod, T., Reza, Z., Ali, V.A., Mehrdad, C. *International Journal of Agriculture and Biology.* **2011**, 13(6):986-990.
 16. Fayaz, A.M., Balaji, K., Girilal, M., Yadav, R., Kalaichelvan, P.T., Venketesan, R. *Nanomedicine: Nanotechnology, Biology and Medicine.* **2010**, 6(1):103-109.
 17. Franci, G., Falanga, A., Galdiero, S., Palomba, L., Rai, M., Morelli, G., Galdiero, M. *Molecules.* **2015**, 20(5):8856-8874.
 18. Gad, G., El-Domany, R.A., Zaki, S., Ashour, H.M. *Journal of antimicrobial chemotherapy.* **2007**, 60(5):1010-1017.
 19. Gade, A.K., Bonde, P., Ingle, A.P., Marcato, P.D., Duran, N., Rai, M.K. *Journal of Biobased Materials and Bioenergy.* **2008**, 2(3):243-247.
 20. Gurunathan, S., Lee, K.J., Kalishwaralal, K., Sheikpranbabu, S., Vaidyanathan, R., Eom, S.H. *Biomaterials.* **2009**, 30(31):6341-6350.
 21. Hadi, A.M., Melconian, A.K. *Iraqi Journal of Science.* **2013**, 54(5):1090-1095
 22. Hall, T. A. *Nucleic acids symposium series*, **1999**, 41(41): 95-98.
 23. Han, D.M., Song, C.F., Guo, G.S., Li, X.Y. *Sci China Chem.* **2010**, 53:1055-1059.
 24. Hirakawa, K., Mori, M., Yoshida, M., Oikawa, S., Kawanishi, S. *Free Radic Res.* **2004**, 38:439-447.
 25. Hong, X., Wen, J., Xiong, X., Hu, Y. *Environmental science and pollution research.* **2016**, 23(5):4489-4497.
 26. Huang Y, Hu Y, Chen L, Yang T, Huang H, Shi R, Lu P, Zhong C. *PloS one.* **2018**, 13(3): e0193659.
 27. Ibrahim, K.H., Salman, J.A., Ali, F.A. *European Scientific Journal.* **2014**, 10(9):1857-1881.
 28. Jain, D., Daima, H.K., Kachhwaha, S., Kothari, S.L. *Digest journal of nanomaterials and biostructures.* **2009**, 4(3):557-563.
 29. Jha, A.K., Prasad, K. *Biotechnology journal.* **2010**, (3):285-291
 30. Jung, W.K., Koo, H.C., Kim, K.W., Shin, S., Kim, S.H., Park, Y.H. *Appl. Environ. Microbiol.* **2008**, 74(7):2171-2178.
 31. Kim, J.S., Kuk, E., Yu, K.N., Kim, J.H., Park, S.J., Lee, H.J., Kim, S.H., Park, Y.K., Park, Y.H., Hwang, C.Y., Kim, Y.K. *Nanomedicine: Nanotechnology, Biology and Medicine.* **2007**, 3(1):95-101.
 32. Linsebigler, A.L., Lu, G., Yates, J.T. *Chem Rev.* **1995**, 95:735-758.
 33. Mariselvam, R., Ranjitsingh, A.J., Nanthini, A.U. *Int J Adv Res.* **2013**, 1(8):56-61.
 34. Martinez-Gutierrez, F., Boegli, L., Agostinho, A., Sánchez, E.M., Bach, H., Ruiz, F., James, G. *Biofouling.* **2013**, 29(6):651-660.
 35. Mathur, T., Singhal, S., Khan, S., Upadhyay, D.J., Fatma, T., Rattan, A. *Indian journal of medical microbiology.* **2006**, 24(1):25-29.
 36. O'Neill J. *Wellcome Trust and the Department of Health of UK Government.* **2016**.
 37. Phalakornkule, C., Tanasupawat, S. *Journal of Culture Collections.* **2006**, 5:46-57
 38. Prasad, K., Jha, A.K., Kulkarni, A.R. *Nanoscale Research Letters.* **2007**, 2(5):248-250.
 39. Rai, M.K., Deshmukh, S.D., Ingle, A.P., Gade, A.K. *Journal of applied microbiology.* **2012**, 112(5):841-852.
 40. Rajeshkumar, S., Malarkodi, C. *Bioinorganic chemistry and applications.* 2014, 10pp.
 41. Rao, M.V., Rajeshwar, K., Verneker, V.P., DuBow, J. *The Journal of Physical Chemistry.* **1980**, 84(15):1987-1991.
 42. Roy, S.C., Varghese, O.K., Paulose, M., Grimes, C.A. *Acs Nano.* **2010**, 4(3):1259-1278.
 43. Sadekuzzaman, M., Yang, S., Mizan, M.F., Ha, S.D. *Comprehensive Reviews in Food Science and Food Safety.* 2015, 14(4):491-509.
 44. Sambrook. J., Russell, D.W., Sambrook, J. *Cold Spring Harbor, NY: Cold Spring Harbor Laboratory Press.* **2006**.
 45. Shrivastava, S., Bera, T., Roy, A., Singh, G., Ramachandrarao, P., Dash, D.

- Nanotechnology*. **2007**, 18(22):225103-225112.
46. Silhavy, T.J., Kahne, D., Walker, S. *Cold Spring Harbor perspectives in biology*. **2010**, 2(5):a000414.
 47. Songisepp, E., Kullisaar, T., Hütt, P., Elias, P., Brilene, T., Zilmer, M., Mikelsaar, M. *Journal of dairy science*. **2004**, 87(7):2017-2023.
 48. Sugimoto, T., Zhou, X., Muramatsu, A. *Journal of colloid and interface science*. **2003**, 259(1):43-52.
 49. Sung, L.P., Scierka, S., Baghai-Anaraki, M., Ho, D.L. *MRS Online Proceedings Library Archive*. **2002**;740.
 50. Taglietti, A., Diaz Fernandez, Y.A., Amato, E., Cucca, L., Dacarro, G., Grisoli, P., Necchi, V., Pallavicini, P., Pasotti, L., Patrini, M. *Langmuir*. **2012**, 28(21):8140-8148.
 51. Vanaja, M., Annadurai, G. *Applied Nanoscience*. **2013**, 3(3):217-223.
 52. Vidyasagar D, Ghugal SG, Kulkarni A, Mishra P, Shende AG, Umare SS, Sasikala R. *Applied catalysis B: environmental*. **2018**, 221:339-48.
 53. Vincent, M.G., John, N.P, Narayanan, P.M., Vani, C., Murugan, S. *Journal of Applied Pharmaceutical Science*. **2014**, 4(7):41-46.
 54. Weber, D.J., Rutala, W.A. *Lippincott Williams and Wilkins*. **2001**. pp. 415–427.
 55. Wijnhoven, S.W., Peijnenburg, W.J., Herberts, C.A., Hagens, W.I., Oomen, A.G., Heugens, E.H., Roszek, B., Bisschops, J., Gosens, I., Van De Meent, D., Dekkers, S. *Nanotoxicology*. **2009**, 3(2):109-138.
 56. Wong, M.S., Chu, W.C., Sun, D.S., Huang, H.S., Chen, J.H., Tsai, P.J., Lin, N.T., Yu, M.S., Hsu, S.F., Wang, S.L., Chang, H.H.. *Appl Environ Microbiol*. **2006**, 72:6111–6116.
 57. Wu, D., Fan, W., Kishen, A., Gutmann, J.L., Fan, B. *Journal of endodontics*. **2014**, 40(2):285-290.

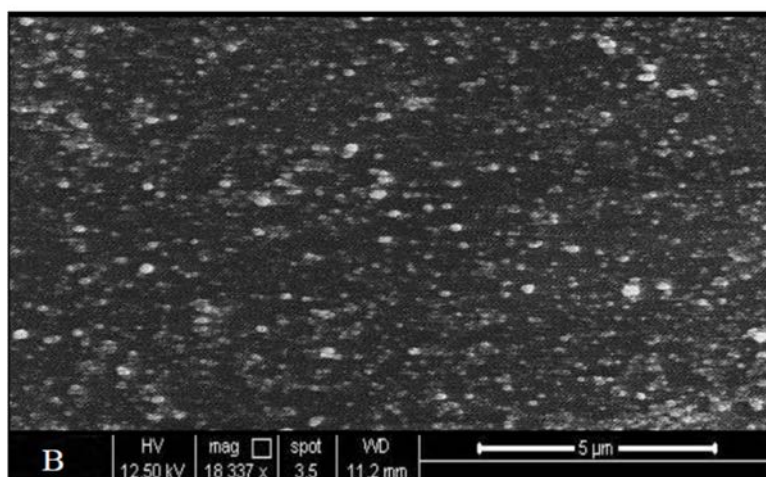


Figure 1. SEM micrograph of nanobiosynthesized TiNPs from *S. thermophilus*

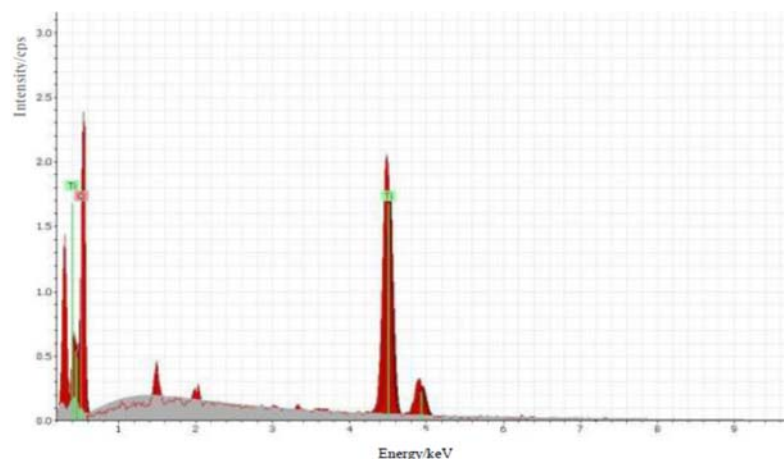


Figure 2. EDS analysis of nanosynthesized TiNPs using *S. thermophilus*

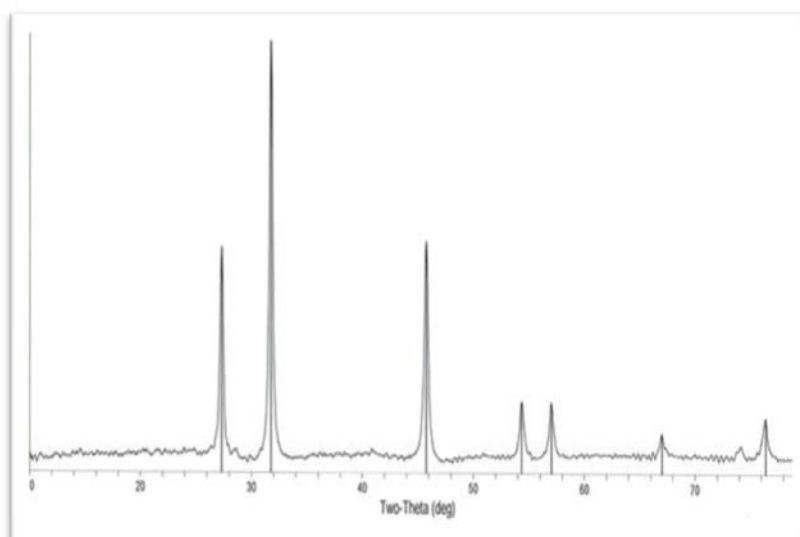


Figure 3. XRD analysis of biosynthesized TiNPs from *S. thermophilus*

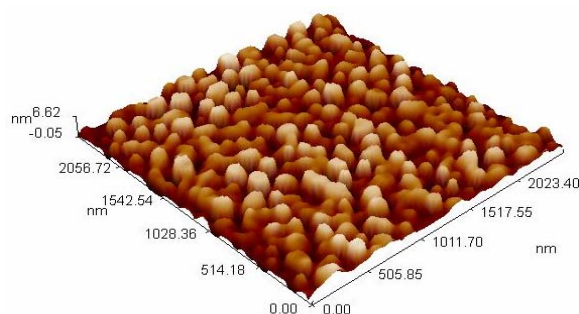


Figure 4. AFM analysis of nanobiosynthesized TiNPs from *S. thermophilus*

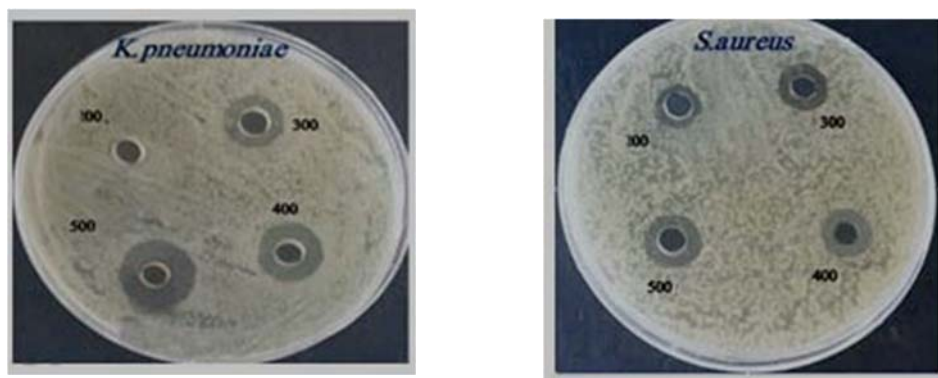


Figure 5. Inhibition zones of different concentrations of TiNPs against MDR *K.pneumoniae* and *S.aureus*.

Table 1. Inhibition zones of different concentrations of TiNPs against MDR *K.pneumoniae* and *S.aureus*

TiNPs con.(µg/ml)	100	300	400	500
<i>K.pneumoniae</i>	12	15	16	20
<i>S.aureus</i>	12	13	14	16

Table 2: Antibiofilm activity of TiNPs

Pathogenic bacteria	Qualitative of biofilm formation	Antibiofilm by TiNPs
<i>K.pneumoniae</i>	2	0
<i>S.aureus</i>	1	0

ANÁLISE COMPARATIVA DE MÉTODOS NUMÉRICOS DA SOLUÇÃO DE UM PROBLEMA INVERSO UNIDIMENSIONAL DE ACÚSTICA

COMPARATIVE ANALYSIS OF NUMERICAL METHODS OF THE SOLUTION OF A ONE-DIMENSIONAL INVERSE PROBLEM OF ACOUSTICS

СРАВНИТЕЛЬНЫЙ АНАЛИЗ ЧИСЛЕННЫХ МЕТОДОВ РЕШЕНИЯ ОДНОМЕРНОЙ ОБРАТНОЙ ЗАДАЧИ АКУСТИКИ

TYULEPBERDINOVA, Gulnur A. ^{1*}; ORALBEKOVA, Zhanar O. ²; GAZIZ, Gulnur G. ³;
MAXUTOVA, Bota A. ⁴; BAITENOVA, Saltanat A. ⁵;

^{1,3,4,5} Al-Farabi Kazakh National University, Department of Informatics, Almaty – Republic of Kazakhstan

² L.N. Gumilyov Eurasian National University, Department of Computer Engineering, Nur-Sultan – Republic of Kazakhstan

* Correspondence author
e-mail: tyulepberdinova@mail.ru

Received 29 August 2019; received in revised form 10 November 2019; accepted 14 March 2020

RESUMO

Atualmente, muitos métodos para resolver problemas inversos decorrentes de eletrodinâmica e acústica têm sido desenvolvidos, mas o desenvolvimento de sistemas práticos é necessário para combinar um grande número de equações que contribuem para a fundamentação de métodos numéricos para resolver vários problemas multidimensionais. Portanto, o principal objetivo do trabalho é uma análise comparativa de métodos numéricos para solucionar o problema acústico inverso unidimensional bem como na busca por resistência acústica. Para atingir esse objetivo, os métodos de descrição e comparação, que contribuíram para a identificação das características da impedância acústica, foram empregados. Além disso, o método da solução de diferença finita, o método de circulação do circuito diferencial e o método de iteração Landweber foram usados. Foi estabelecido que o método de inversão do esquema de diferenças é conveniente para aplicação no caso em que informações adicionais são conhecidas com precisão suficiente e a solução reconstruída é bastante suave. Foi determinado que, se uma dessas condições for violada, o método de reverter o esquema de diferenças se tornará instável. Foram investigados os problemas de correção dos problemas da equação de onda com velocidade complexa nos casos unidimensionais e espaciais. Foram obtidas fórmulas para resolver esses problemas - análogos de fórmulas clássicas. Cálculos numéricos mostraram o tipo de resultados que podem ser esperados do método considerado. O material do trabalho implica o significado prático para os professores universitários das especializações em tecnologia da informação.

Palavras-chave: *função teta de Heaviside, método de inversão de circuito de diferença, método de iteração de Landweber, analógico discreto.*

ABSTRACT

Nowadays, a large number of methods for solving inverse problems arising in electrodynamics and acoustics have been developed, but the development of practical systems is necessary to combine a large number of equations that contribute to the substantiation of numerical methods for solving various multidimensional problems. Therefore, the main goal of the work is a comparative analysis of statistical methods for solving the one-dimensional inverse acoustic problem, as well as in the search for acoustic resistance. To achieve this goal, the means of description and comparison, which contributed to the identification of the characteristics of acoustic impedance, were used. Also, the finite-difference solution method, the differential circuit circulation method, and the Landweber iteration method were used. It was established that the inversion method of the difference scheme is expedient to apply in the case when additional information is known accurately enough, and the reconstructed solution is quite smooth. It was determined that if one of these conditions is violated, the method of reversing the difference scheme becomes unstable. The problems of the correctness of the issues for the wave equation with complex velocity in the one-dimensional and spatial cases were investigated. Formulas for solving these problems were obtained – analogs of classical formulas. Numerical computations show the kind of results that may be expected from the method under consideration. The materials of the paper imply the practical significance for the

Keywords: *Hevisayd's theta-function, final and differential look, method of the circulation of the differential scheme, method of iterations of Landveber, discrete analog.*

АННОТАЦИЯ

К настоящему времени существуют различные методы решения обратных задач, возникающих в электродинамике, акустике, но разработка практических систем необходима для объединения большого числа уравнений, которые способствуют обоснованию численных методов решения многомерных различных задач. Поэтому основная цель работы заключается в сравнительном анализе численных методов решения одномерной обратной задачи акустики, а также в поиске акустического сопротивления. Для достижения поставленной цели авторами были использованы методы описания, сравнения, которые способствовали выявлению особенностей акустического импеданса. Также в работе применены конечно-разностный метод, метод циркуляции дифференциальной схемы и метод итераций Ландвебера. Установлено, что метод обращения разностной схемы целесообразно применять в случае, когда дополнительная информация известна достаточно точно и решение не требует дополнительных подходов. Определено, что при нарушении одного из этих условий метод обращения разностной схемы становится неустойчивым. Исследованы вопросы корректности задач для волнового уравнения с комплексной скоростью в одномерном и пространственном случаях. Получены формулы решения этих задач – аналоги классических формул. Численные расчеты показывают результаты, которые возможно ожидать от использованного метода. Материалы статьи предполагают практическую значимость для преподавателей вузов, которые специализируются на информационных технологиях.

Ключевые слова: *тэта-функция Хевисайда, метод обращения разностной схемы, метод итераций Ландвебера, дискретный аналог.*

1. INTRODUCTION

As is known, most of the inverse problems of geophysics is devoted to determining the speed of sound in the framework of the wave equation or its various approximations. It is assumed that other parameters of the medium, such as the density and absorption of the medium, are constant and known (Evstigneev *et al.*, 2016; Chkadua, 2017; Aliev and Isayeva, 2018; You *et al.*, 2018). Knowledge of this single parameter of the medium – the speed of sound is sufficient in many practical cases. At the same time, it is evident that in many essential inverse problems it is impossible to confine oneself to this approximation and it is necessary to use more accurate models of the structure of the medium and introduce other additional parameters that allow a more adequate description of reality (Gibson, 2018; Safarov, 2018; Pejić *et al.*, 2018). These multi-parameter models provide more complete information about the structure of the medium and are therefore of great interest. Naturally, the processes occurring in such media are described by more complex equations than the wave equation.

The creation and justification of numerical methods for solving inverse and incorrect problems is an urgent problem, firstly, due to the practical importance of reverse and incorrect problems, and secondly, due to the need to create

effective algorithms for solving multidimensional inverse and incorrect acoustics issues and electrodynamics.

It is known that the optimization method is an effective method for solving inverse problems. This method consists in minimizing a specific function concerning the required parameters. The required parameters are the values of the determined quantities at given points in space. Various iterative procedures are used as minimization methods. The quality of one or another numerical minimization method is characterized by efficiency, i.e., the number of operations necessary to obtain a given accuracy of the solution, and the ultimate accuracy with which you can approach the minimum point. The latter determines the ultimate accuracy of solving the inverse problem. Not always, but as a rule, a drop in the efficiency of the algorithm is accompanied by a decline in the accuracy of the solution to the problem.

The one-dimensional return problem of acoustics is considered in "Iterative methods of the solution of the return and incorrect tasks with data on the part of border" (Kabanikhin *et al.*, 2006).

To increase the efficiency of acoustic resistance, a multilevel adaptive algorithm is used. The algorithm is based on dividing the entire algorithm for solving the inverse problem into a series of consecutive levels. When moving from

one level to another, the number of parameters changes adaptively depending on the size of the functional and the rate of convergence – a multi-level adaptive method (Pleshchinskii *et al.*, 2018; Gamzaev, 2019; Leinartas and Shishkina, 2019). This method can only be used to obtain an approximate (trend) solution of the inverse problem since when moving from level to level; the answer is interpolated over several points, i.e., essentially averaging over these points is performed (Equations 1–4), where it is necessary $\sigma(x) > 0, x > 0, \sigma \in C^1[0, \infty)$. It is required to find the solution of a direct task (Equations 1–3) $u(x, t)$ and acoustic rigidity of the environment $\sigma(x)$ according to additional information (Equation 4). It is known (Romanov, 1973), that the solution of the direct problem (Equations 1–3) has the form (Equation 5), Where $\tilde{u}(x, t)$ – continuity $x \geq 0$ and is sufficiently smooth for $t > x > 0$ function, Equation 6 – Heaviside theta function.

This equation is a kind of competitor concerning the equation with the equivalent inverse problem when describing waves in a rectangular channel. Substituting (Equation 5) in (Equations 1–4), the equivalent inverse problem relatively $u(x, t)$ and $s(x)$ is obtained.

The class of nonlinear evolution equations has several additional properties whose origin is related to the main property of this class of nonlinear evolution equations, that is, although temporal evolution is nonlinear in the configuration space, it is connected (by spectral transformation) with simple linear development in spectral space (Equations 7–10).

Thus, this paper aimed to study and substantiate numerical methods for solving a one-dimensional inverse problem of acoustics, since they are important both from a theoretical and a practical point of view.

2. MATERIALS AND METHODS

A difference scheme is a finite system of algebraic equations containing a differential equation and additional conditions (for example, boundary conditions and / or initial distribution). Thus, difference schemes are used to reduce a differential problem of a continuous nature to a finite system of equations, the numerical solution of which is fundamentally possible on computers. Algebraic equations associated with the differential equation are obtained using the difference method, which distinguishes the theory of difference schemes from other numerical

methods for solving differential problems.

The solution of the difference scheme is called the approximate solution of the differential problem. The authors introduce the net $x = ih, t = kh$. represented by the equation (6) in finite difference form (3) (Equation 11) from where having expressed u_{i+1}^k (Equation 12) will be obtained. The authors approximate a boundary condition (7) (Alontseva and Gilev, 2011; Samarskiy, 1971) (Equation 13).

Analytical methods are mainly used to study single-phase or two-phase linear models of various physical processes. It is almost impossible to obtain an exact solution to a nonlinear model using existing analytical methods. In connection with this, numerical methods for solving such problems are increasingly used in modeling, but with their help, it is not always possible to accurately track the law of motion of the phase boundary.

Thus, assuming that all considered functions rather smooth, the authors will write down the return task (Equations 7–10) in a final and differential look (Equations 14–17).

Conclusion of discrete analog of a formula of D'Alembert. The d'Alembert formula can find a solution to the initial – boundary value problem with a homogeneous first-order boundary condition if the primary functions continue along the entire axis odd relative to the origin. A representation of the d'Alembert type here not only provides information on the structure of the general solution but can also be used as the basis for creating a computational scheme for solving the initial-boundary-value problem. Using a known technique (Denisov, 1994; Kabanikhin, 1984; Kabanikhin *et al.*, 2004), discrete analog of a formula of D'Alembert will be received. Shifting indexes in (Equation 14) a chain of equalities (Equations 18-23) will be received. From where (Equation 24) will be obtained. From where D'Alembert's formula in a discrete look (Equations 25–30) will be received or, having made replacement $s = i - m$, (Equation 31) will be obtained.

3. RESULTS AND DISCUSSION:

3.1. Method of the circulation of the differential scheme

The method of circulating the differential scheme is quite natural from the physical point of view, since it uses the theory of characteristics along which, as a rule, the basic information about

the features of solving the direct problem and the medium under investigation is distributed. In the computational aspect (by the number of operations), this method is equivalent to a single solution to the corresponding direct problem and allows parallelization of the calculation procedure (Xu *et al.*, 2016; Guliyev and Nasibzadeh, 2018). Substituting (Equation 31) expression in (Equation 13) and considering (Equation 15), a formula of calculation of unknown function will be received (Kornilov, 2005; Kraht, 2005; Nurseitova and Tyulepberdinova, 2008) (Equations 32–33). The authors will carry out calculations from the border $i = 0$, along with characteristics, as shown in the scheme of Figure 1–15. At first, we will be counted s_0 , then, knowing the value u_0^2, s_1 will be calculated. Further from u_0^4 , calculating along the characteristic, we define s_2 and so on (Appendix 1).

For check of the work of algorithm on the solution of the returned task, the authors will set exact function $s(x)$; then, a direct problem will be solved; a decision trail $x = 0$ will be picked up, thereby function $g(t)$ additional information will be defined. The authors will describe the scheme of the solution of a direct task (Equations 34–38). Here on the known s_i , calculating along with characteristics, we define g_i (Figure 2).

3.2. Method of iterations of Landveber

For check of work of algorithm on the solution of the returned task the authors will set exact function $s(x)$, then a direct problem will be solved by method of the circulation of the differential scheme, a decision trail at $x = 0$, will be picked up, thereby function $g(t)$ – additional information will be defined. Now we will describe computing experiments for various types of functions $s(x)$ (Nurseitova *et al.*, 2010; Samarskiy and Vabishevich, 2004). *Linear function $s(x)$, noise parameter $\varepsilon \approx 0.01$*

For the following parameters $N = 200, l = 1, h = l/N = 0.005$ with function of a look $s(x) = -0.5x - 1$ the direct task was solved and function is received $g(t)$. After the addition of a random error function $g(t)$, I assumed an air results of computing experiment are presented in Figure 3. The authors will carry out the comparative analysis of methods of the solution of the return problem of acoustics (Table 1). Results of numerical calculations for function are shown (Equation 39) with parameters $N = 200, l = 1, h = l/N = 0.005$ and indignation of entrance data $\|\bar{q}_3 - q_3\| = 0.0142$.

The technology for solving the inverse problem for objects with dispersion of sound speed allows us to formulate a more advanced approach to the creation of ultrasonic non-destructive testing techniques. Here you select a frequency range that captures the region with the dispersion of the speed of sound.

4. CONCLUSIONS:

The approximate decision received a method of the circulation of the differential scheme meets to exact better than an approximation of a way of iteration of Landveber, if data exact. Apparently, from Figure 4.4 at inexact data, the method of the circulation of the differential scheme disperses as it is unstable. In Figures 4–13 it is visible that the approximate decision received approximation of a method of iteration of Landveber well meets to exact and at noisy data, though convergence speed the low. Receiving algorithm for discrete analog of a method of iteration of Landveber is followed by more bulky calculations, than approximation of a method of iteration of Landveber, but apparently from the table, discrete analog of a method of iteration of Landveber gives the best approach for twice smaller number of iterations, than approximation of a method of iteration of Landveber. Thus labor input of realization of one iteration approximation of a way of repetition of Landveber and discrete analog of a method of iteration of Landveber have one order, that is this machine time spent for the performance of one iteration has one order.

6. REFERENCES:

1. Aliev, A.B., Isayeva, S.E. *Mathematical Methods in the Applied Sciences*, **2018**, 41(16), 7055-7073.
2. Alontseva, E.A., Gilev, A.A. *Bulletin of Samara State Technical University*, **2011**, 1, 9-13.
3. Chkadua, G. *Mathematical Methods in the Applied Sciences*, **2017**, 40(15), 5539-5562.
4. Denisov, A.M. *Introduction to the theory of inverse problems*. Moscow: Publishing House of Moscow State University named after Lomonosov, **1994**.
5. Evstigneev, R.O., Medvedik, M.Y., Smirnov, Y.G. *Computational Mathematics and Mathematical Physics*, **2016**, 56(3), 483-490.
6. Gamzaev, K. M. *Journal of Engineering*

- Physics and Thermophysics*, **2019**, 92(1), 162-168.
7. Gibson, P.C. *Inverse Problems*, **2018**, 34(7), article number 075013.
 8. Guliyev, H.F., Nasibzadeh, V.N. *Vestnik Tomskogo Gosudarstvennogo Universiteta, Matematika i Mekhanika*, **2018**, 2018(54), 5-16.
 9. Kabanikhin, S.I. *Projection-difference methods of determination of coefficients of the hyperbolic equations*. Novosibirsk: Nauka, **1984**.
 10. Kabanikhin, S.I., Bektemesov, M.A., Nurseitova, A.T. *Iterative methods of the solution of the return and incorrect tasks with data on part of border*. Almaty: International fund of the return tasks, **2006**.
 11. Kabanikhin, S.I., Satybaev, A.D., Shishlenin, M.A. *Direct methods of solving multidimensional inverse hyperbolic problems*. Utrecht: VSP, **2004**.
 12. Kornilov, V.S. *Some inverse problems of identifying the parameters of mathematical models*. Moscow: MGPU, **2005**.
 13. Kraht, L.N. On the issue of problem-based learning and the implementation of interdisciplinary connections at a technical college. *Fundamental Research*, **2005**, 9, 62-63.
 14. Leinartas, E.K., Shishkina, O.A. *Journal of Siberian Federal University - Mathematics and Physics*, **2019**, 12(4), 503-508.
 15. Ieshchinskii, N.B., Pleshchinskaya, I.E., Tumakov, D.N. *Lobachevskii Journal of Mathematics*, **2018**, 39(8), 1099-1107.
 16. Nurseitova, A.T., Nurseitov, D.B., Tyulepberdinova, G.A. *The Messenger TREASURY*, **2010**, 64(1), 139-144.
 17. Nurseitova, A.T., Tyulepberdinova, G.A. *The Messenger of KAZNPU*, **2008**, 21(1), 215-217.
 18. Pejić, D., Gazivoda, N., Ličina, B., Urekar, M., Sovilj, P., Vujičić, B. *Advances in Electrical and Computer Engineering*, **2018**, 18(3), 61-66.
 19. Romanov, V.G. *The return tasks for the differential equations*. Novosibirsk: NGU, **1973**.
 20. Safarov, J.S. *Journal of Siberian Federal University – Mathematics and Physics*, **2018**, 11(6), 753-763.
 21. Samarskiy, A.A. *Introduction to the theory of differential schemes*. Moscow: Nauka, **1971**.
 22. Samarskiy, A.A., Vabishevich, P.N. *Numerical methods for solving inverse problems of mathematical physics*. Moscow: Editorial URSS, **2004**.
 23. Xu, L., Xiao, N., Xie, L. *Automatica*, **2016**, 71, 292-299.
 24. You, X., Li, W., Chai, Y. *Engineering Analysis with Boundary Elements*, **2018**, 94, 79-93.

$$u_{tt} = u_{xx} - 2 \frac{\sigma'(x)}{\sigma(x)} u_x, \quad x > 0, t > 0, \quad (\text{Eq. 1})$$

$$u|_{t=0} \equiv 0, \quad x > 0, \quad (\text{Eq. 2})$$

$$u_x|_{x=+0} = \gamma \delta(t), \quad t > 0, \quad (\text{Eq. 3})$$

$$u|_{x=+0} = g(t), \quad t > 0. \quad (\text{Eq. 4})$$

$$u(x, t) = s(x)\theta(t - x) + \tilde{u}(x, t), \quad (\text{Eq. 5})$$

$$s(x) = -\gamma \sqrt{\sigma(x)/\sigma(+0)}, \quad \theta. \quad (\text{Eq. 6})$$

$$u_{tt} = u_{xx} - 2 \frac{s'(x)}{s(x)} u_x, \quad t > x > 0 \quad (\text{Eq. 7})$$

$$u_x|_{x=0} = 0, \quad t > 0, \quad (\text{Eq. 8})$$

$$u(x, x + 0) = s(x), \quad x > 0, \quad (\text{Eq. 9})$$

$$u|_{x=+0} = g(t), \quad t > 0. \quad (\text{Eq. 10})$$

$$\frac{(u_i^{k+1} - 2u_i^k + u_i^{k-1}))}{h^2} = \frac{(u_{i+1}^k - 2u_i^k + u_{i-1}^k)}{h^2} - 2 \frac{(s_{i+1} - s_{i-1}))}{h(s_{i+1} - s_{i-1}))} \cdot \frac{s_{i+1}^k - s_{i-1}^k}{2h}, \quad (\text{Eq. 11})$$

$$u_{i+1}^k = \frac{(u_i^{k+1} + u_i^{k-1})(s_{i+1} + s_{i-1}) - 2u_{i-1}^k s_{i+1}}{2s_{i-1}}. \quad (\text{Eq. 12})$$

$$\begin{aligned} u_1^k &= u_0^k + h \left. \frac{\partial u}{\partial x} \right|_{x=0} + \frac{h^2}{2} \left. \frac{\partial^2 u}{\partial x^2} \right|_{x=0} + O(h^2) = u_0^k + \frac{h^2}{2} \left(\frac{u_0^{k+1} - 2u_0^k + u_0^{k-1}}{h^2} + 2 \frac{s'(0)}{s(0)} \left. \frac{\partial u}{\partial x} \right|_{x=0} \right) + O(h^2) \\ &= \frac{u_0^{k+1} + u_0^{k-1}}{2} + O(h^2). \end{aligned} \quad (\text{Eq. 13})$$

$$u_{i+1}^k = \frac{(u_i^{k+1} + u_i^{k-1})(s_{i+1} + s_{i-1}) - 2u_{i-1}^k s_{i+1}}{2s_{i-1}}, \quad (\text{Eq. 14})$$

$$u_1^k = \frac{u_0^{k+1} + u_0^{k-1}}{2}, \quad (\text{Eq. 15})$$

$$u_i^i = s_i, \quad (\text{Eq. 16})$$

$$u_0^k = g_k. \quad (\text{Eq. 17})$$

$$u_i^{k+1} = u_{i-1}^{k+2} + u_{i-1}^k - u_{i-2}^{k+1} + h^2 Q_{i-1}^{k+1},$$

$$u_i^{k+1} = u_{i-1}^{k+2} + u_{i-1}^k - u_{i-2}^{k+1} + h^2 Q_{i-1}^{k+1}, \quad (\text{Eq. 18})$$

$$u_{i-1}^{k+2} = u_{i-2}^{k+3} + u_{i-2}^{k+1} - u_{i-3}^{k+1} + h^2 Q_{i-2}^{k+2}, \quad (\text{Eq. 19})$$

$$u_{i-j+1}^{k+j} = u_{i-j}^{k+j+1} + u_{i-j}^{k+j-1} - u_{i-j-1}^{k+j} + h^2 Q_{i-j}^{k+j}, \quad (\text{Eq. 20})$$

$$\vdots \quad j = i - 2 \quad (\text{Eq. 21})$$

$$u_3^{k+i-2} = u_2^{k+i-1} + u_2^{k+i-3} - u_1^{k+i-2} + h^2 Q_2^{k+i-2}, \quad (\text{Eq. 22})$$

$$u_2^{k+i-1} = u_1^{k+i} + u_1^{k+i-2} - u_0^{k+i-1} + h^2 Q_1^{k+i-1}, \quad (\text{Eq. 23})$$

$$u_{i+1}^k = u_i^{k-1} + u_1^{k+i} - u_0^{k+i-1} + h^2 \sum_{j=1}^i Q_j^{k+i-j}. \quad (\text{Eq. 24})$$

$$u_i^{k-1} = u_{i-1}^{k-2} + \frac{g^{k+i-1} - g^{k+i-3}}{2} + h^2 \sum_{j=1}^{i-1} Q_j^{k+i-j-2}, \quad (\text{Eq. 25})$$

$$u_i^{k-1} = u_{i-1}^{k-2} + \frac{g^{k+i-1} - g^{k+i-3}}{2} + h^2 \sum_{j=1}^{i-1} Q_j^{k+i-j-2}, \quad (\text{Eq. 26})$$

$$u_{i-m+1}^{k-m} = u_{i-m}^{k-m-1} + \frac{g^{k+i-2m+1} - g^{k+i-2m-1}}{2} + h^2 \sum_{j=1}^{i-m} Q_j^{k+i-j-2m}, \quad (\text{Eq. 27})$$

$$\vdots \quad m = i - 1 \quad (\text{Eq. 28})$$

$$u_2^{k-i+1} = u_1^{k-i} + \frac{g^{k-i+3} - g^{k-i+1}}{2} + h^2 \sum_{j=1}^1 Q_j^{k-i-j+2}, \quad (\text{Eq. 29})$$

$$u_1^{k-i} = u_0^{k-i-1} + \frac{g^{k-i+1} - g^{k-i-1}}{2}. \quad (\text{Eq. 30})$$

$$k = i + 1. \quad (\text{Eq. 31})$$

$$u_{i+1}^k = \frac{g^{k+i+1} - g^{k-i-1}}{2} + h^2 \sum_{m=0}^{i-1} \sum_{j=1}^{i-m} Q_j^{k+i-j-2m}, \quad (\text{Eq. 32})$$

$$u_{i+1}^k = \frac{g^{k+i+1} - g^{k-i-1}}{2} + h^2 \sum_{s=1}^i \sum_{j=1}^s \mathcal{Q}_j^{k-i-j+2s}. \quad (\text{Eq. 33})$$

$$s_{i+1} = s_{i-1} \frac{u_i^{i+2} + s_i}{2s_{i-1} - s_i - u_i^{i+2} + 2u_{i-1}^{i+1}} \quad (\text{Eq. 34})$$

$$u_{i+1}^k = \frac{2u_{i+1}^k s_{i-1} + 2u_{i-1}^k s_{i+1}}{s_{i+1} + s_{i-1}} - u_i^{k-1}, \quad (\text{Eq. 35})$$

$$u_0^{k+1} = 2u_1^k - u_0^{k-1}, \quad (\text{Eq. 36})$$

$$u_i^i = s_i, \quad (\text{Eq. 37})$$

$$u_0^k = g_k. \quad (\text{Eq. 38})$$

$$s(x) = -1/2x - 1, \quad (\text{Eq. 39})$$

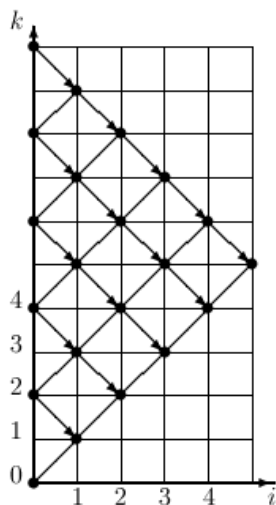


Figure 1. Return task

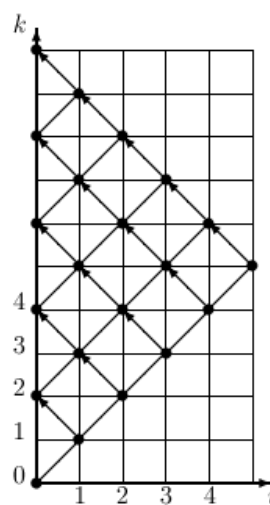


Figure 2. Direct task

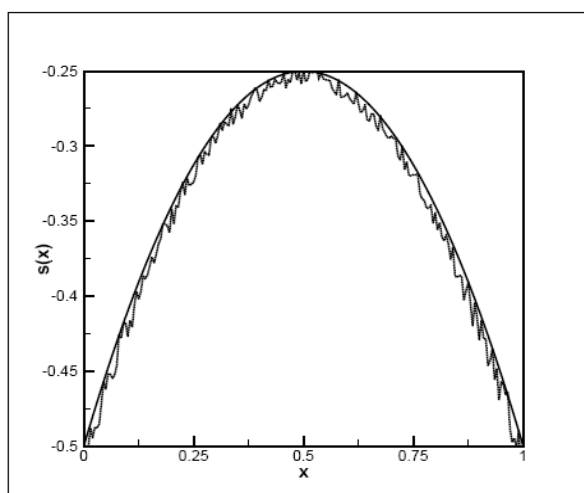


Figure 3. Schedules of restoration parabolic functions $s(x)$ at indignation $\|\tilde{s} - s\| \cong 0.0019$. *The continuous line – the exact decision $s(x)$; the dot line – the approximate decision

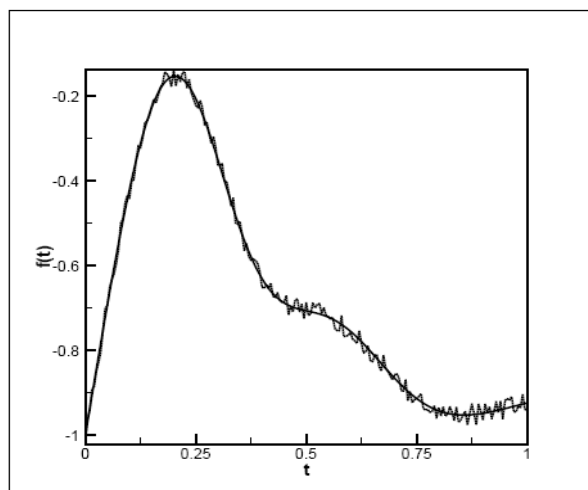


Figure 4. Function graph of additional information $g(t)$ for periodic type of the decision at $\|\tilde{g} - g\| \cong 0.014$. *The continuous line – the exact decision $s(x)$; the dot line – the approximate decision

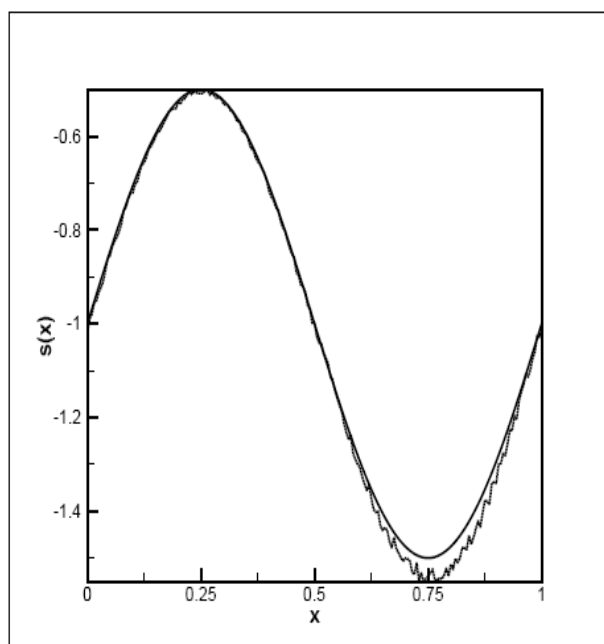


Figure 5. Restoration of periodic function $s(x)$ at $\|\tilde{s} - s\| \cong 0.023$. *The continuous line – the exact decision $s(x)$; the continuous line – the exact decision

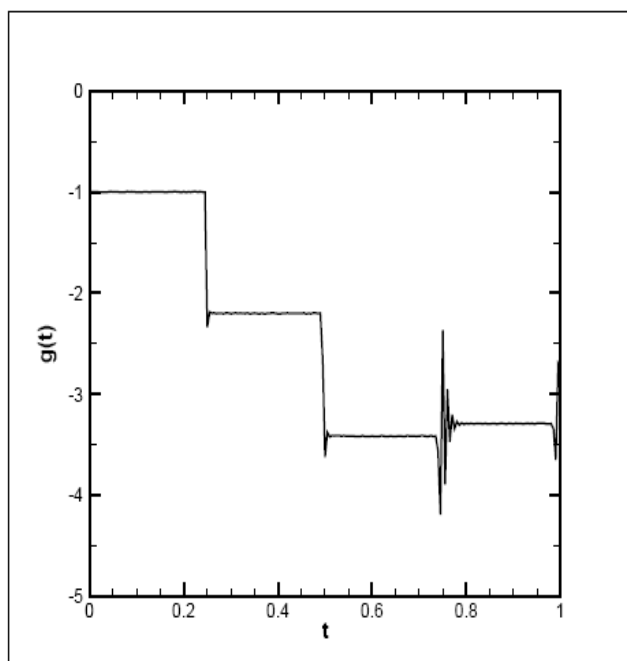


Figure 6. Function graph of additional information $g(t)$ for step type of the decision at $\|\tilde{g} - g\| \cong 0.003$. *The continuous line – exact function $g(t)$; the dot line – the indignant function of additional information

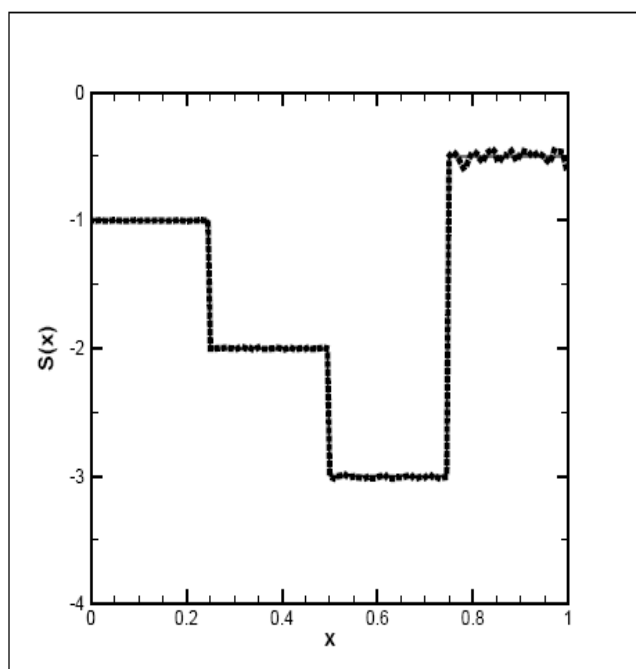


Figure 7. Function restoration $s(x)$ by method a method of the circulation of the differential scheme at $\|\tilde{s} - s\| \cong 0.02$. *The continuous line – exact function $s(x)$; dot line approximate decision

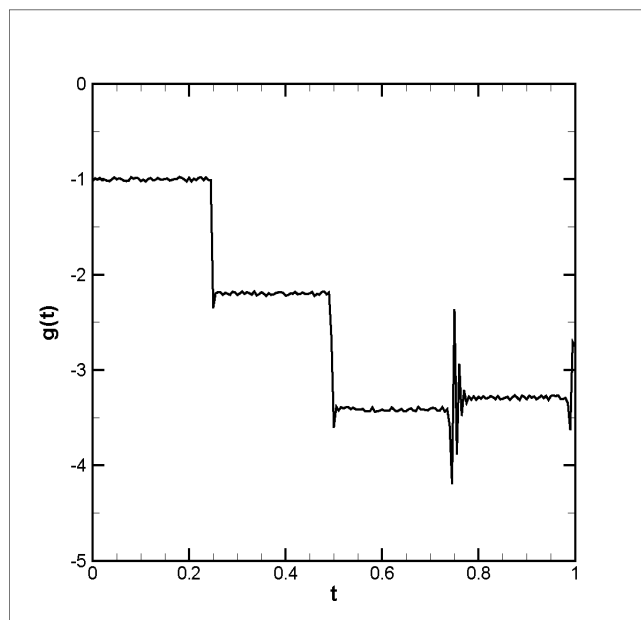


Figure 8. Function graph of additional information $g(t)$ for step type of the decision at $\|\tilde{g} - g\| \cong 0.01$.

*The continuous line – exact function $g(t)$; dot line indignant function of additional information

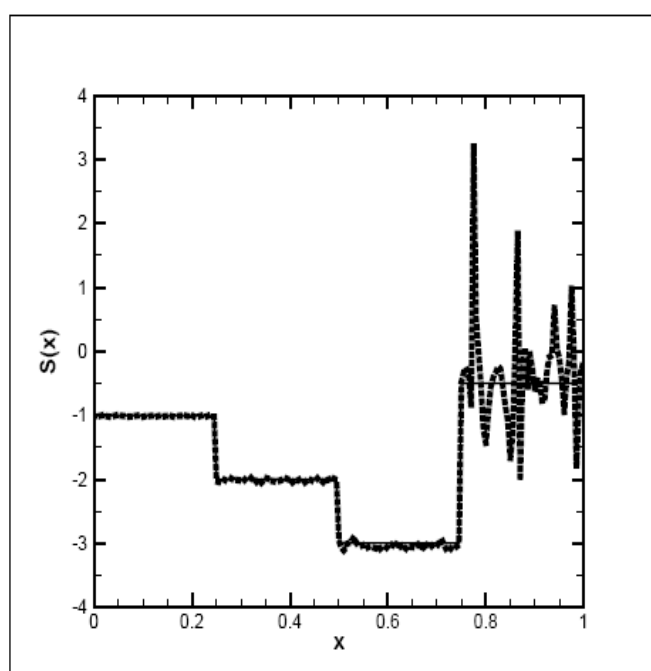


Figure 9. Function restoration $s(x)$ by method a method of the circulation of the differential scheme at $\|\tilde{s} - s\| \cong 0.02$.

*The continuous line – exact function $s(x)$; dot line approximate decision, the circulation of the differential scheme restored by method a method

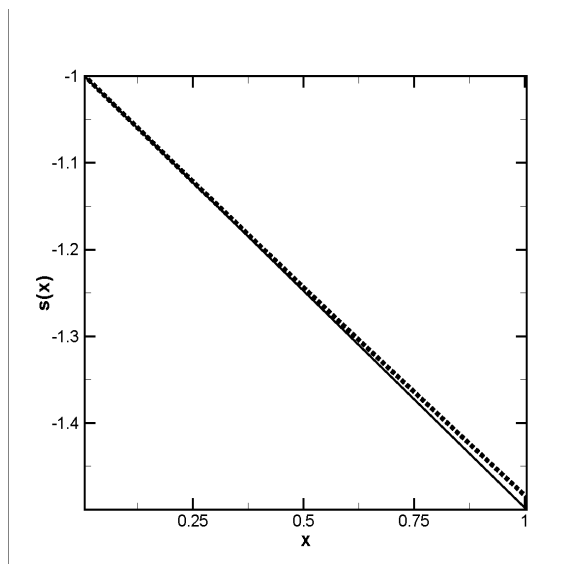


Figure 10. Schedule of restoration of periodic function $s(x)$ by method approximation of a method of iteration of Landveber. *The continuous line – exact function $s(x)$; dashed line – the approximate decision, restored by method approximation of a method of iteration of Landveber

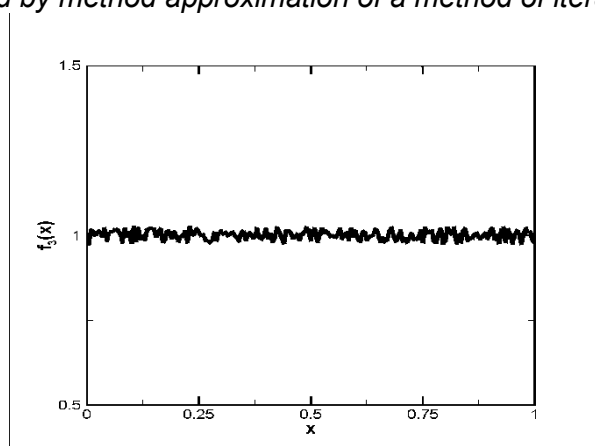


Figure 11. Schedule of noisy function $f_3(x)$

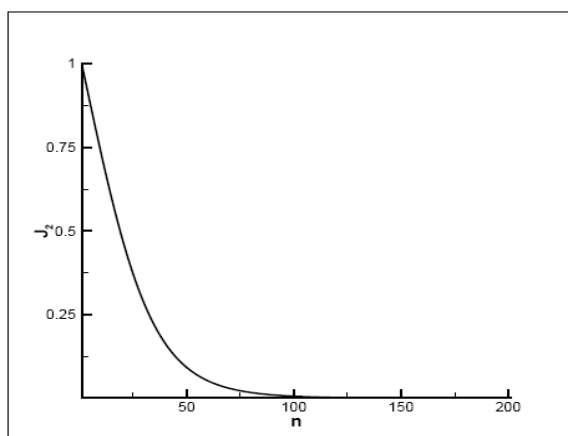


Figure 12. Schedule of functionality $J_2(q^n)$

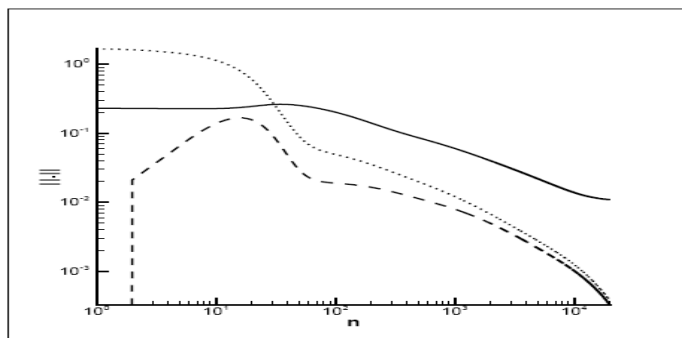


Figure 13. Schedule of functionality of a method approximation of a method of iteration of a method.
 *The continuous line – values of functionality $J_1(q^n)$; dashed line – values of functionality $J_2(q^n)$; the dot line – values of functionality $J_3(q^n)$;

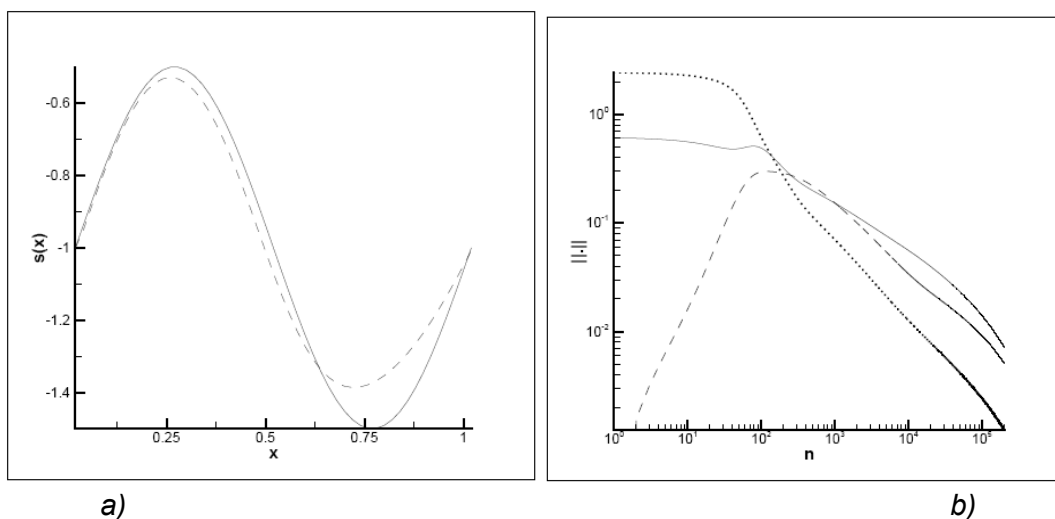


Figure 14. Schedule of restoration of periodic function $s(x)$. *The continuous line – exact function $s(x)$; dashed line – the approximate decision restored by method approximation of a method of iteration of Landveber

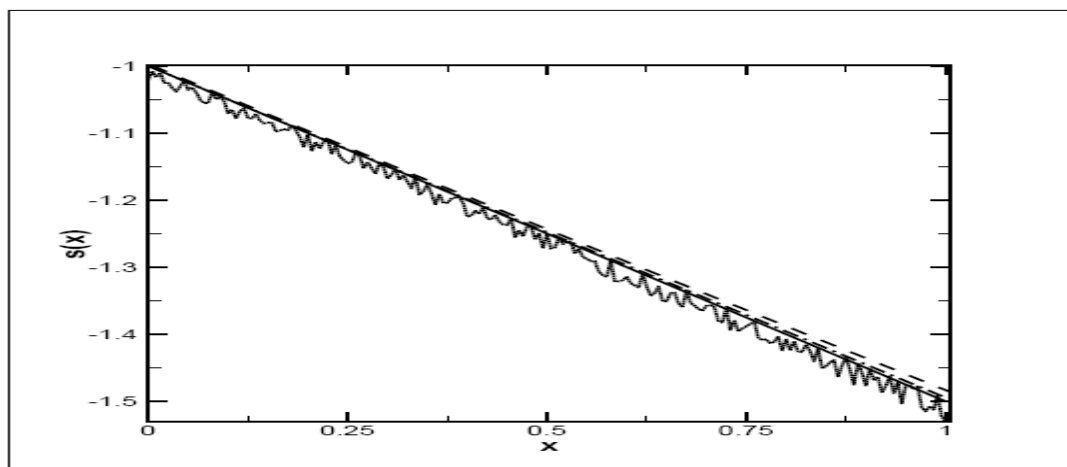


Figure 15. Comparison of various methods. *The continuous line – exact function $s(x)$; the dot line – the approximate decision restored by method method circulation of the differential scheme; dashed line – the approximate decision restored by method approximation of a method of iteration of Landveber; the dash-dotted line – the approximate decision restored by method discrete analog of a method of iteration of Landveber

Table 1. Comparative table of methods

Method	Method circulation of the differential scheme	Approximation of a method of iteration of Landveber	Discrete analog of a method of iteration of Landveber
Criterion			
$\ s - s_{ex}\ $	$1.56 \cdot 10^{-2}$	$9.88 \cdot 10^{-3}$	$2.90 \cdot 10^{-3}$
Scheme	the obvious	the iterative	the iterative
Iterations	-	198	93

Appendix 1

Algorithm of the solution of a Direct task:

1. Value on a Equation 17 is calculated

$$s_0 = u_0^0 = g_0.$$

2. s_1 is calculated:

(a) on a Equation 17 value $u_0^2 = g_2$;

(b) calculating on a Equation 15 value $s_1 = u_1^1 = \frac{u_0^2 + u_0^0}{2}$.

3. s_2 is calculated:

(a) on a Equation 17 value $u_0^4 = g_4$;

(b) calculating on a Equation 15 value $u_1^3 = \frac{u_0^4 + u_0^2}{2}$;

(c) calculating on a Equation 21 value s_2 .

4. s_3 is calculated:

(a) on a Equation 17 value $u_0^6 = g_6$;

(b) calculating on a Equation 15 value $u_1^5 = \frac{u_0^6 + u_0^4}{2}$;

(c) calculating on a Equation 14 value u_2^4 ;

(d) calculating on a Equation 21 value s_3 .

5. And so on, $s_i, i = \overline{4, N}$ is calculated:

(a) on a Equation 17 value $u_0^{2i} = g_{2i}$;

(b) calculating on a Equation 15 value $u_1^{2i-1} = \frac{u_0^{2i} + u_0^{2i-2}}{2}$;

(c) calculating on a Equation 14 along characteristics and value of functions $u_2^{2i-2}, \dots, u_{i-1}^{i+1}$;

(d) calculating on a Equation 21 value s_i .

PROCESSOS DE DEGRADAÇÃO NO SISTEMA Al-Ti-Si SOB CHOQUE TÉRMICO

DEGRADATION PROCESSES IN THE Al-Ti-Si SYSTEM UNDER THERMAL SHOCK

ДЕГРАДАЦИОННЫЕ ПРОЦЕССЫ В СИСТЕМЕ Al-Ti-Si В УСЛОВИЯХ ТЕРМОУДАРА

SKVORTSOV, Arkadiy A.^{1*}; KORYACHKO, Marina V.²; ZUEV, Sergei M.³; RYBAKOVA, Margarita R.⁴;

^{1,4}Moscow Polytechnic University, Department of Mechanics of Materials, Moscow – Russian Federation

²Moscow Polytechnic University, Department of Physics, Moscow – Russian Federation

³Moscow Polytechnic University, Department of Industrial Electronics, Moscow – Russian Federation

* Correspondence author

e-mail: skvortsovaa2009@yandex.ru

Received 28 October 2019; received in revised form 22 January 2020; accepted 12 March 2020

RESUMO

Nos últimos anos, muita atenção dos desenvolvedores de microcircuitos integrados tem sido dada ao desenho de novos tipos de microprocessadores, desenvolvimento e masterização de circuitos tridimensionais multicamadas e criação de dispositivos baseados em semicondutores complexos. O objetivo do presente trabalho é estudar processos térmicos no sistema Al-Ti-Si multicamada até o desenvolvimento de processos de degradação. São considerados os problemas de degradação durante a metalização do alumínio com a deposição de uma subcamada de titânio na superfície de silício. É analisada a evolução dos processos de destruição irreversível do condutor de filme durante a passagem dos pulsos de corrente retangulares com energia de até 300 mJ e duração de 50 ... 1000 μ s. Verificou-se que, sob a influência de um único pulso de corrente retangular com duração não superior a 80 μ s e energia de 85 mJ, o derretimento de um filme de metal é um processo prioritário de destruição da estrutura. O aumento na duração do pulso ($\tau > 80 \mu$ s) altera a prioridade da degradação térmica, e o derretimento de contato se torna o principal mecanismo de destruição estrutural. Também foi descoberto que o recozimento isotérmico leva à melhoria nas propriedades condutoras de calor do sistema e ao aumento nas densidades críticas de corrente. Isso está associado a uma melhoria nas propriedades adesivas da estrutura, bem como a transformações de fase no sistema Al-Ti-Si durante o recozimento. Os resultados do artigo podem ser utilizados em estudos adicionais das propriedades do sistema Al-Ti-Si, bem como na criação de estruturas semicondutoras, levando em consideração propriedades como alta condutividade elétrica, boa processabilidade, ausência de componentes químicos no sistema Al-Si, estabilidade química e tendência à eletromigração, a possibilidade de curto-circuito, alta mobilidade de difusão, baixo ponto de fusão, a incapacidade de conectar o fio por soldagem.

Palavras-chave: *microprocessadores, circuitos integrados tridimensionais, estruturas semicondutoras.*

ABSTRACT

In recent years, much attention of developers of integrated microcircuits is given to designing novel types of microprocessors, development, and mastery of technologies of both multilayer 3D integrated circuits and making devices based on complex semiconductors. The aim of the present work is to study thermal processes in the Al-Ti-Si multilayer system up to the development of degradation processes. The degradation issues in aluminum metallization with titanium sublayer deposited onto silicon surface are considered. The evolution of processes of irreversible destruction of film conductor under passage through it of single square-wave current pulses with energy up to 300 mJ and duration of 50...1000 μ s was analyzed. It was found that, under the action of a single square-wave current pulse with a duration of no more than 80 μ s and energy of 85 mJ, the priority process of structural damage is the melting of the metal film. Increasing pulse duration ($\tau > 80 \mu$ s) changes the priority of thermal degradation, and contact melting becomes the main mechanism of structure damage. It was also found that isothermal annealing leads to improving system heat-conducting properties and increasing critical current densities. This is related to the improvement of adhesion properties of the structure as well as with phase transformations in the Al-Ti-Si system in the course of annealing. The results of the article can be used in further studies of the properties of the Al-Ti-Si system, as well as in the creation of semiconductor structures taking into

account properties such as high electrical conductivity, good processability, the absence of chemical components in the Al-Si system, chemical stability, and a tendency to electromigration, the possibility of short circuit, high diffusion mobility, low melting point, the inability to attach the wire by soldering.

Keywords: *microprocessors, 3D integrated circuits, semiconductor structures.*

АННОТАЦИЯ

В последние годы большое внимание разработчиков интегральных микросхем уделяется проектированию новых типов микропроцессоров, разработке и освоению многослойных трехмерных интегральных схем, созданию устройств на основе сложных полупроводников. Целью данной работы является изучение тепловых процессов в многослойной системе Al-Ti-Si вплоть до развития процессов деградации. Рассмотрены вопросы деградации при металлизации алюминия с нанесением на поверхность кремния подслоя титана. Проанализирована эволюция процессов необратимого разрушения пленочного проводника при прохождении через него одиночных прямоугольных импульсов тока с энергией до 300 мДж и длительностью 50... 1000 мкс. Было установлено, что при воздействии одиночного прямоугольного импульса тока длительностью не более 80 мкс и энергией 85 мДж приоритетным процессом разрушения структуры является плавление металлической пленки. Увеличение длительности импульса ($t > 80$ мкс) меняет приоритет термической деградации, и контактное плавление становится основным механизмом разрушения конструкции. Также было обнаружено, что изотермический отжиг приводит к улучшению теплопроводящих свойств системы и увеличению критических плотностей тока. Это связано с улучшением адгезионных свойств структуры, а также с фазовыми превращениями в системе Al-Ti-Si в процессе отжига. Результаты статьи могут быть использованы при дальнейших исследованиях свойств системы Al-Ti-Si, а также при создании полупроводниковых структур с учетом таких свойств, как высокая электропроводность, хорошая технологичность, отсутствие химических компонентов в системе Al-Si, химическая стабильность и склонность к электромиграции, возможность короткого замыкания, высокая диффузионная подвижность, низкая температура плавления, невозможность прикрепить проволоку пайкой.

Ключевые слова: *микропроцессоры, трехмерные интегральные схемы, полупроводниковые структуры.*

1. INTRODUCTION

In recent years, much attention of developers of integrated microcircuits is given to designing novel types of microprocessors, development, and mastery of technologies of both multilayer 3D integrated circuits and making devices based on complex semiconductors (Topol *et al.*, 2006). Mastery of new semiconductor devices and structures cannot be made without solving the problems of metallization and contact systems (Pedersen *et al.*, 2015). The point is that the role of metallization in modern structures of micro- and nanoelectronics is becoming a key (Chang and Chang, 2010; Okabe *et al.*, 2014; Brincker *et al.*, 2018a; Brincker *et al.*, 2018b; Zhao *et al.*, 2019).

It is known that the performance of logic elements increases with downsizing, while those of interconnections and contacts decrease because of the reduction of the cross-section of film conductors and the growth of their linear resistance and electric capacity. As a result, starting from a certain integration level of semiconductor devices, signal delays in the interconnections may exceed those in the

structures themselves. In addition, as the semiconductor cross-sections decrease, the problems appear that are related to electromigration in thin metal films and contact ohmicity (Kang *et al.*, 2008; Martineau *et al.*, 2014; Macherzyński *et al.*, 2016; De Rose *et al.*, 2018; Homa and Sobczak, 2019; Eslami *et al.*, 2019; Fischer *et al.*, 2019; Chawla *et al.*, 2019; Cruz *et al.*, 2019; Yi *et al.*, 2019). And technological complexities when making modern metallization systems (including the structures involving p-n junctions with small occurrence depth) should also be noted (Garosshen *et al.*, 1985; Macherzyński *et al.*, 2016).

Aluminum films are widely used as material for interconnections and ohmic contacts to silicon when making semiconductor structures (Garosshen *et al.*, 1985). This material has a number of advantages: high electrical conduction, good manufacturability, absence of chemical components in the Al-Si system, chemical stability of aluminum in oxidizing medium, etc. (Ahmad *et al.*, 2019; Kumar *et al.*, 2019; Kumar and Singh, 2019; Sattar *et al.*, 2019; Shuai *et al.*, 2019; Wang *et al.*, 2019b).

However, along with the above

advantages, aluminum metallization has a number of substantial disadvantages. The most important of them are as follows: tendency to electromigration, possibility of short circuit through dielectric in layered metallization systems (because of formation of spurs on a film due to electromigration and Al recrystallization), high diffusion mobility of Al over the grain boundaries, low melting point (577°C) of the eutectic of Al-Si system, low mechanical strength of Al films, impossibility of wire attachment using soldering, etc. (Gupta, 1979; Ahmad *et al.*, 2019). Because of the listed disadvantages, multilayer systems with metal sublayers (including Al) are applied in ICs and transistors with shallow p-n junctions to get the basic current-carrying layer. In this case, usually, the first metal layer (sublayer) has high adhesion to both silicon and silicon dioxide and simultaneously has small solubility and diffusion coefficients in these materials. Titanium meets these requirements. For example, the use of ohmic contacts with titanium sublayer in fast-operating ICs made it possible to increase mean time between failures by a factor of 20 as compared to the Al-Si binary system (Brincker *et al.*, 2015). So the aim of the present work is an investigation of thermal processes in an Al-Ti-Si multilayer system up to the development of degradation processes.

2. MATERIALS AND METHODS

To perform experiments, the structures of the metal-sublayer-semiconductor plate type were formed. Aluminum was the main current-carrying layer because it is the most extended material used for metallization layers in semiconductor structures (Diligenti *et al.*, 1989). Molybdenum, titanium, and nickel were used for metal sublayers that improve the contact, adhesion and barrier properties of current-carrying systems (Macherzyński *et al.*, 2016; Ahmadvand *et al.*, 2019; Alam *et al.*, 2019; Galetz *et al.*, 2019; Liu *et al.*, 2019; Neudeck *et al.*, 2019; Sun *et al.*, 2019; Wang *et al.*, 2019a). Silicon plates doped with phosphorus and oriented along (Mwema *et al.*, 2018) direction, with resistivity $\rho = 0.01 \text{ } \Omega \cdot \text{cm}$ and 60 μm n-epitaxial layer (15 $\Omega \cdot \text{cm}$), served as substrates. Such substrates prevent shunting of metallization layers. Dielectric layers of silicon oxide or silicon nitride were grown preliminary on some substrates.

The deposition of films onto the pre-prepared surface of silicon plates was made by electron-beam evaporation in a single technological cycle (Macherzyński *et al.*, 2016;

Mwema *et al.*, 2018). The substrate temperature ($T = 373 \text{ K}$) and working pressure ($p = 7 \cdot 10^{-4} \text{ Pa}$) were maintained constant in the course of film deposition. They were controlled with a preliminary calibrated platinum-platinum-rhodium (Pt-PtRh) thermocouple (near the sprayed plates) and a vacuum gage. The aluminum (titanium) evaporation rates were $V_1 = 2 \text{ nm/s}$ ($V_2 = 1.5 \text{ nm/s}$). (Hereinafter subscript "1" relates to Al, "2" relates to Ti interlayer and "3" relates to the semiconductor substrate.) Thickness h_1 of Al film was no less than 2 μm ; thickness h_2 of metal sublayer varied in the 80...2000 nm range. Then the test structures described in (Skvortsov *et al.*, 2014; Skvortsov *et al.*, 2016) were made on the prepared multilayer structures using optical photolithography. Investigation of Al-Ti-Si multilayer systems before and after isothermal annealing was made for the obtained test structures (Skvortsov *et al.*, 2014; Skvortsov *et al.*, 2016) from electrical response taken from different their areas at the passage of single square-wave current pulses.

The temperature $T_1(t)$ of the metallization track was calculated from switching oscillograms $U(t)$ taken from an area of the test structure in the course of current pulse passage using Equation (1). Here $R_0 = 0.88 \text{ } \Omega$ is the resistance of metallization track at $T_0 = 290 \text{ K}$ measured by the voltmeter-ammeter method; the area length $\ell = 2.9 \text{ mm}$; Al film thickness $h_1 = 2.1 \text{ } \mu\text{m}$; track width $b = 75 \text{ } \mu\text{m}$; $\alpha = 0.0043 \text{ K}^{-1}$ is the Al temperature coefficient of resistance. The typical experimental curves at passing a sequence of sinusoidal pulses are given in Figure 1. The obtained curves are also described by Equation (2) (Skvortsov *et al.*, 2014). They touch a range of temperatures preceding the beginning of degradation processes related to a thermal overload of the metallization system. Here λ is thermal conductivity; c , d and a are thermal capacity, density and thermal conductivity, respectively. It is evident that parameters related to the thermophysical properties of a thin-film system and silicon matrix depend on temperature. As before (Skvortsov *et al.*, 2016), their mean integral values were used to calculate T_1 . The mean integral value of b is (Equation 3).

It is easy to verify from Equation (2) that dynamics of structure heating depend on current strength, parameters of semiconductor matrix and size-thermal ratio (h_2/λ_2) of a titanium film and intermediate dielectric film. So that the bigger is sublayer thickness, the quicker is heating of metallization tracks.

3. RESULTS AND DISCUSSION:

The results of experiments (Figure 1) fully confirm that as thickness h_2 of titanium sublayer changes from 80 nm to 170 nm, the temperature T_1 of Al film increases from 360 K to 430 K to the moment of pulse shutdown ($t = 500 \mu\text{s}$). This indicates a higher thermal load of multilayer structures as compared with the Al-Si binary system. Moreover, the estimation of values of titanium film thermal conductivity from Equation (2) and experiments (Figure 1) are overvalued. This indicates the necessity of stabilization annealing to improve adhesion and phase transformations in the Al-Ti-Si system. Indeed, preliminary stabilizing annealing at 500 °C in protective nitrogen atmosphere improved parameters of heat transfer of multilayer structures. This reflected in switching oscillograms (Figure 2). The observed improvement of heat sink processes also reflected on the development of thermal degradation of the structure (Dunn *et al.*, 1986; Skvortsov *et al.*, 2016; He *et al.*, 2019).

Earlier it was found out (Skvortsov *et al.*, 2014) that beginning of degradation processes in the studied range of current densities $j = (2-9) \cdot 10^{10} \text{ A/m}^2$ and pulse durations $\tau = (100-1000) \mu\text{s}$ is related to formation of molten zones in a thin-film system and subsequent melting of the total current-carrying layer (at the appropriate power of current pulses). The beginning of thermal damage is attributed to the moment of the abrupt departure of potential $U(t)$ from a monotonic increase in the switching oscillogram (Figure 3). The current density and starting point of irreversible changes in the structure will be called critical j_{cr} and t_{cr} , respectively. As already noted, isothermal annealing of thin-film structures (contributing to the improvement of thermal contact between the layers) has to lead to increasing critical current density j_{cr} at a fixed pulse duration τ . Indeed, the data obtained for the Al-Ti-Si structures confirm this (Figure 4). For single square-wave pulses with a duration of 200 μs and 550 μs , j_{cr} value may increase to 20%.

The observed changes are related to both improvement of adhesion in multilayer structure and active mass transfer (Chen, 2005), with the formation of triple chemical compounds based on titanium disilicide (TiSi_2) and replacement of titanium atoms with silicon atoms and (or) aluminum atoms ($\text{Ti}_x\text{Si}_y\text{Al}_z$). Such atomic rearrangement occurs with the participation of processes of grain boundary diffusion and bulk diffusion and is accompanied by the formation of new phases. All this significantly affects the

electrical and thermal characteristics of the formed multilayer structure and reflects on switching oscillograms and j_{cr} value. As to the character of structure melting after the passage of the current pulse, the melting of aluminum tracks on the Al-Ti-Si system was characterized by regular directivity (Figure 5). Such behavior is related to good adhesion of titanium film to both contacting phases (Al and Si), even without stabilizing annealing. Annealing of the Al-Ti-Si structures did not change melting character; only structure electrical and thermal characteristics varied.

4. CONCLUSIONS:

The article examined the contribution of scientists to the study of the role of metallization in the structures of micro- and nanoelectronics, the operating characteristics of logic elements in various conditions. A characteristic of the use of aluminum in electronics, its positive properties and disadvantages was given. Degradation processes in the Al-Ti-Si system were considered under thermal shock. Heating of a multilayer system at passing through it single square-wave current pulses with a duration of 50...1000 μs and amplitude j to $9 \cdot 10^{10} \text{ A/m}^2$ was analyzed.

For the obtained test structures, a study was performed of Al-Ti-Si multilayer systems before and after isothermal annealing according to the electric response taken from different regions during the passage of one square. It was found that the dynamics of heating the structure depends on the current strength, the parameters of the semiconductor matrix and the size-thermal ratio of the titanium film and the intermediate dielectric film. Accordingly, the bigger the sublayer thickness is, the quicker the heating of metal tracks occurs: when the thickness h_2 of the titanium sublayer changes from 80 nm to 170 nm, the temperature T_1 of the Al film increases from 360 K to 430 K to the moment of pulse shutdown.

It was revealed that isothermal annealing leads to the improvement of heat-conducting properties of the system and, consequently, to increase critical current densities by 20%. This was related to the improvement of adhesive properties of the structure as well as to phase transformations in the Al-Ti-Si system in the course of annealing (atomic rearrangement took place with the participation of grain boundary diffusion and bulk diffusion processes), which affected the electrical and thermal characteristics of the formed multilayer structure and was reflected in the switching of the oscillograms. The melting of aluminum tracks in the Al-Ti-Si system

was characterized by a regular directivity, which was associated with good adhesion of the titanium film to both contacting phases. It was observed that only the structure of electrical and thermal characteristics changed, but the nature of melting did not change.

5. ACKNOWLEDGMENTS:

The reported study was funded by RFBR, according to the research project No. 18-29-27005.

6. REFERENCES:

- Ahmad, S.M., Leong, Ch.S., Winder, R.W., Sopian, K., Zaidi, S.H. *Journal of Electronic Materials*, **2019**, 48(10), 6382–6396.
- Ahmadvand, M.S., Azarniya, A., Madaah Hosseini, H.R. *Journal of Alloys and Compounds*, **2019**, 789, 493–505.
- Alam, M.Z., Durgarao, K.Y., Kumawat, M., Banumathy, S. *Surface and Coatings Technology*, **2019**, 380, 125071.
- Brincker, M., Pedersen, K.B., Kristensen, P.K., Popok, V.N. *IEEE Transactions on Components, Packaging and Manufacturing Technology*, **2018a**, 8(12), 2073–2080.
- Brincker, M., Pedersen, K.B., Kristensen, P.K., Popok, V.N. *Microelectronics Reliability*, **2015**, 55(9–10), 1988–1991.
- Brincker, M., Walter, T., Kristensen, P.K., Popok, V.N. *Journal of Materials Science: Materials in Electronics*, **2018b**, 29(5), 3898–3904.
- Chang, Y.-Y., Chang, C.-P. *Journal of Nanoscience and Nanotechnology*, **2010**, 10(7), 4762–4766.
- Chawla, V., Sidhu, B.S., Rani, A., Handa, A. *Materials and Corrosion*, **2019**, 70(12), 2157–2178.
- Chen, L.J. *Journal of Metals*, **2005**, 57(9), 24–30.
- Cruz, D., Garrido, M.A., Múñez, C.J., Rico, A., Poza, P. *Surface Engineering*, **2019**, 35(9), 792–800.
- De Rose, A., Kraft, A., Eitner, U., Nowotnick, M. *Solder Proceedings of the International Spring Seminar on Electronics Technology*, **2018**, 2018, Article number 8443630.
- Diligenti, A., Bagnoli, P.E., Neri, B., Bea, S., Mantellassi, L. *Solid-State Electronics*, **1989**, 32(1), 11–16.
- Dunn, C.F., Brotzen, F.R., Mcpherson, J.W. *Journal of Electronic Materials*, **1986**, 15(5), 273–277.
- Eslami, M., Deflorian, F., Zanella, C. *Progress in Organic Coatings*, **2019**, 137, 105307.
- Fischer, M., Trant, M., Thorwarth, K., Crockett, R., Patscheider, J., Hug, H.J. *Science and Technology of Advanced Materials*, **2019**, 20(1), 1031–1042.
- Galetz, M.C., Oskay, C., Madloch, S. *Surface and Coatings Technology*, **2019**, 364, 211–217.
- Garosshen, T.J., Stephenson, T.A., Slavin, T.P. *Journal of Metals*, **1985**, 37(5), 55–59.
- Gupta, T.K. *Microelectronics Reliability*, **1979**, 19(4), 337–343.
- He, Y., Yang, X., Yang, X., Xiao, T., Bao, Y., Ma, W., Lv, G. *Materials Science in Semiconductor Processing*, **2019**, 104, Article number 104596.
- Homa, M., Sobczak, N. *Journal of Thermal Analysis and Calorimetry*, **2019**, 138(6), 4215–4221.
- Kang, M.C., Kim, M.W., Kim, K.R., Kim, K.H., Jung, S.Y., Kim, C., Ahn, D.G. *Journal of Computational and Theoretical Nanoscience*, **2008**, 5(8), 1772–1776.
- Kumar, P., Das, B., Singh, A. *Journal of Mechanical Engineering Science*, **2019**, 233(14), 5033–5047.
- Kumar, P., Singh, A. *Fatigue and Fracture of Engineering Materials and Structures*, **2019**, 42(12), 2625–2643.
- Liu, H., Li, S., Jiang, C.-Y., Yu, C.-T., Bao, Z.-B., Zhu, S.-L., Wang, F.-H. *Acta Metallurgica Sinica (English Letters)*, **2019**, 32(12), 1490–1500.
- Macherzyński, W., Stafiniak, A., Paszkiewicz, B., Gryglewicz, J., Paszkiewicz, R. *Physica Status Solidi*, **2016**, 213(5), 1145–1149.

26. Martineau, D., Levade, C., Legros, M., Dupuy, P., Mazeaud, T. *Microelectronics Reliability*, **2014**, 54(11), 2432–2439.
27. Mwema, F.M., Oladijo, O.P., Akinlabi, S.A., Akinlabi, E.T. *Journal of Alloys and Compounds*, **2018**, 747, 306–323.
28. Neudeck, S., Mazilkin, A., Reitz, C., Hartmann, P., Janek, J., Brezesinski, T. *Scientific Reports*, **2019**, 9(1), 5328.
29. Okabe, H., Yoshida, M., Tominaga, T., Fujita, J., Endo, K., Yokoyama, Y., Nishikawa, K., Toyoda, Y., Yamakawa, S. *Materials Science Forum*, **2014**, 778–780, 955–958.
30. Pedersen, K.B., Ostergaard, L.H., Ghimire, P., Popok, V., Pedersen, K. *Microelectronics Reliability*, **2015**, 55(8), 1196–1204.
31. Sattar, M., Batool, M., Khan, Z.S. *Materials Research Express*, **2019**, 6(10), 105545.
32. Shuai, C., Xue, L., Gao, C., Wang, G., Peng, S., Min, A. *Advanced Engineering Materials*, **2019**, 21(7), 1801322.
33. Skvortsov, A.A., Kalenkov, S.G., Koryachko, M.V. *Technical Physics Letters*, **2014**, 40(9), 787–790.
34. Skvortsov, A.A., Zuev, S.M., Koryachko, M.V., Glinskiy, V.V. *Microelectronics International*, **2016**, 33(2), 102–106.
35. Sun, W., Sun, Y., Shah, K.J., Zheng, H., Ma, B. *Journal of Environmental Management*, **2019**, 241, 22–31.
36. Topol, A.W., La Tulipe, D.C., Shi, Jr.L., Frank, D.J., Bernstein, K., Steen, S.E., Kumar, A., Singco, G.U., Young, A.M., Guarini, K.W., Jeong, M. *IBM Journal of Research and Development*, **2006**, 50(4/5), 491–506.
37. Wang, C.J., Koech, P.K., Lin, X.Z. *Journal of the Chinese Institute of Engineers, Transactions of the Chinese Institute of Engineers*, **2019a**, 42(3), 244–253.
38. Wang, M., Tan, Q., Liu, L., Li, J. *Journal of Hazardous Materials*, **2019b**, 380, 120846.
39. Yi, H., Xie, X., Tang, X., Zhao, S., Yang, K., Huang, Y., Yang, Z. *Chemical Engineering Journal*, **2019**, 374, 370–380.
40. Zhao, J., An, T., Fang, C., Bie, X., Qin, F., Chen, P., Dai, Y. *IEEE Transactions on Power Electronics*, **2019**, 34(11), 11036–11045.

$$U(t) = I(t)R_0 \{1 + \alpha [T(t) - T_0]\}. \quad (\text{Eq. 1})$$

$$\Delta T = T_1 - T_0 = \frac{I^2 \bar{R}_l}{S} \left(\frac{h_2}{\bar{\lambda}_2} + \frac{1}{\bar{c}_3 \bar{d}_3} \sqrt{\frac{\tau}{a}} \right) \quad (\text{Eq. 2})$$

$$\bar{b} = \frac{1}{\Delta T} \int_{T_0}^{T_1} b(T) dT \quad (\text{Eq. 3})$$

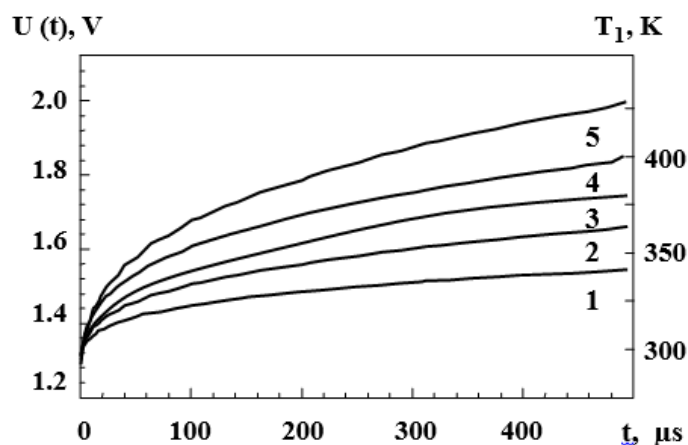


Figure 1. Switching oscillograms of Si-Ti-Al system at different Ti sublayer thicknesses: 1 – $h_2=0$; 2 – $h_2=80$; 3 – $h_2=100$; 4 – $h_2=130$; 5 – $h_2=170$ nm; $j=6.0 \cdot 10^{10}$ A/m²; $h_1=2$ μm; pulse duration of 500 μs

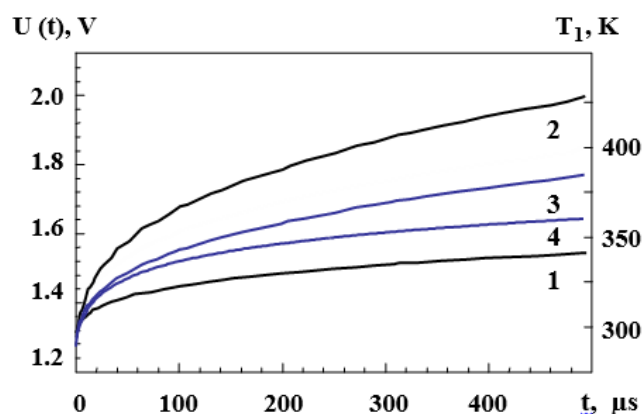


Figure 2. Switching oscillograms of Al-Si (1) and Al-Ti-Si systems with Ti sublayer thickness $h_2=170$ nm (2) after isothermal annealing of the structure at 500 °C for 3 – 60 min.; 4 – 90 min

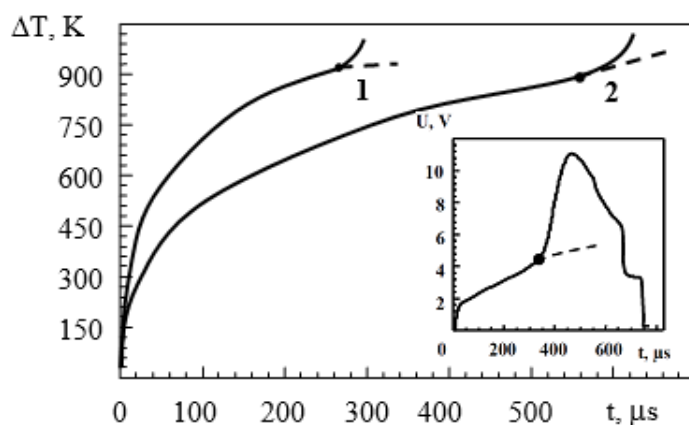


Figure 3. Dynamics of the temperature of aluminum metallization $\Delta T_1(t)=T_1(t)-T_0$ at the passage of a single current pulse with amplitude: 1 – $j=8.7 \cdot 10^{10}$ A/m²; 2 – $7.0 \cdot 10^{10}$ A/m². Insert: switching oscillogram of Si-Ti-Al systems taken at the passage of a single current pulse (duration of 800 μs, the amplitude of $6.4 \cdot 10^{10}$ A/m²)

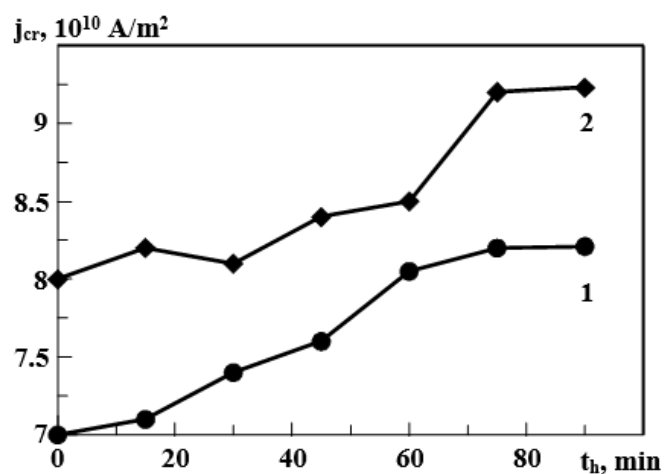


Figure 4. Dependence of critical current density j_{cr} on annealing time t_h of Al-Ti-Si structure in an inert atmosphere at a temperature of 500 °C; duration of square-wave current pulse: 1 – 550 μ s; 2 – 200 μ s

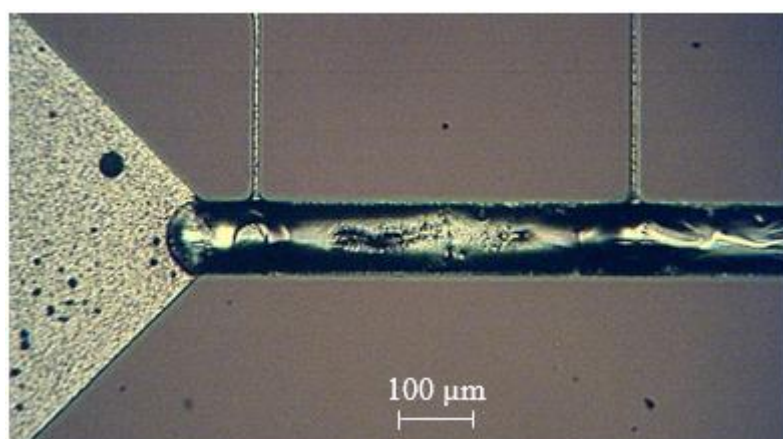


Figure 5. Photograph of thermal degradation of Al-Ti-Si structure after current pulse passage ($j > j_{cr}$)

DIAGNÓSTICO E TRATAMENTO DE DOENÇAS PERIODONTAIS INFLAMATÓRIAS

DIAGNOSIS AND TREATMENT OF INFLAMMATORY PERIODONTAL DISEASES

ДИАГНОСТИКА И ЛЕЧЕНИЕ ВОСПАЛИТЕЛЬНЫХ ЗАБОЛЕВАНИЙ ПАРОДОНТА

UTYUZH, Anatoly S.^{1*}; YUMASHEV, Alexey V.²; ISAKOV, Esenalı I.³; MAKAROV, Alexey L.⁴; MATVEEVA, Elena A.⁵

^{1,2,3,4,5} I. M. Sechenov First Moscow State Medical University (Sechenov University), Department of Prosthetic Dentistry, Moscow – Russian Federation

* Correspondence author
e-mail: uasst@mail.ru

Received 13 September 2019; received in revised form 22 January 2020; accepted 11 March 2020

RESUMO

O diagnóstico prematuro da cavidade oral leva a uma inflamação periodontal subjacente. Portanto, foi levantada uma questão de correção psicológica em pacientes com doenças periodontais inflamatórias, onde foi observado o papel do estado mental e a importância da adição desse componente terapêutico a um programa abrangente para o tratamento de pacientes em clínicas odontológicas. O estudo consistiu em duas etapas: diagnóstica e terapêutica. O primeiro estágio incluiu 76 pacientes que precisavam de um exame para detectar inflamação periodontal; esses pacientes foram examinados usando o dispositivo terapêutico e diagnóstico Fluorit-4S (TDD). A segunda etapa do estudo incluiu 28 pacientes com doenças periodontais inflamatórias. Os pacientes do grupo de estudo (14 pessoas) receberam tratamento usando um método de modulação mesodiencefalo (terapia MDM). Foi comprovada a possibilidade de detecção precoce de inflamação periodontal (mesmo no nível de um processo "latente") usando o dispositivo Fluorit-4S. Maior eficácia terapêutica do tratamento odontológico abrangente em pacientes com inflamação periodontal usando a terapia com Fluorit-4S TDD e MDM foi comprovada em comparação com a estratégia terapêutica padrão em termos de redução mais evidente no desconforto local (em 0,5 pontos em comparação ao grupo controle), diminuição significativa no índice de PMA (um índice que mede a presença ou ausência de inflamação gengival como ocorre nas papilas ou nas gengivas marginais ou anexadas) (em 0,9% em relação ao grupo controle), eliminação mais completa do foco patológico, bem como como uma completa normalização do estado emocional. O uso do Fluorit-4S TDD na prática odontológica permite ao dentista estudar mais de perto os tecidos afetados, resultando em conclusões objetivas sobre os processos patológicos na mucosa oral e, conseqüentemente, na seleção de estratégias terapêuticas adequadas para casos clínicos individuais.

Palavras-chave: *fluorite-4C, modulação de mesodiencefala, espectro infravermelho, método de fisioterapia, área de suprimento sanguíneo.*

ABSTRACT

Untimely diagnosis of the oral cavity leads to an underlying periodontal inflammation. Therefore, it was raised an issue of psychological correction in patients with inflammatory periodontal diseases where it was observed the role of mental state and the importance of the addition of this therapeutic component to a comprehensive program for the treatment of patients in dental clinics is emphasized. The study consisted of two stages: diagnostic and therapeutic. The first stage included 76 patients who needed an examination to detect periodontal inflammation; these patients were examined using the Fluorit-4S therapeutic and diagnostic device (TDD). The second stage of the study included 28 patients with inflammatory periodontal diseases. Patients of the study group (14 people) received treatment using a mesodiencephalic modulation method (MDM-therapy). It was proved the possibility of earlier detection of periodontal inflammation (even at the level of a "latent" process) using the Fluorit-4S device. Higher therapeutic efficacy of comprehensive dental treatment in patients with periodontal inflammation using the Fluorit-4S TDD and MDM-therapy was proved compared to standard therapeutic strategy in terms of more evident reduction in local discomfort (by 0.5 points compared to the control group), more significant decrease in the PMA index (an index that measures the presence or absence of gingival inflammation as occurring on the papillae or the marginal or attached gingivae) (by 0.9% compared to the control group), fuller elimination of the pathological focus, as well as a complete normalization of the emotional state. The use of the Fluorit-4S TDD in dental practice allows dentists to study the affected tissues more closely, resulting in objective conclusions on the pathological processes in the oral mucosa and, accordingly, the selection of adequate therapeutic strategies for individual clinical cases.

Keywords: *fluorit-4S, Mesodiencephalic modulation, Infrared spectrum, Physiotherapeutic method, Area of blood filling.*

АННОТАЦИЯ

Несвоевременная диагностика ротовой полости у пациентов приводит к скрытому воспалению пародонта. Поэтому авторами поднимается вопрос о необходимости психокоррекции пациентов с воспалительными заболеваниями пародонта; отмечена роль психологического состояния у таких пациентов; подчеркивается важность добавления данного компонента лечения в комплексную программу терапии пациентов стоматологических клиник. Проведенное исследование состояло из двух этапов: диагностического и терапевтического. Первый этап включал 76 пациентов, нуждающихся в обследовании для выявления воспаления пародонта, эти пациенты были обследованы с применением лечебно-диагностического комплекса «Флюорит-4С». Второй этап исследования включал 28 пациентов с воспалительными заболеваниями пародонта. Пациенты основной группы (14 человек) получали лечение с помощью метода мезодиэнцефальной модуляции (МДМ-терапии). Авторами доказана возможность более раннего выявления воспаления пародонта (еще на уровне «скрытого» процесса) с помощью комплекса «Флюорит-4С». Доказана более выраженная терапевтическая эффективность комплексного стоматологического лечения у пациентов с воспалением пародонта с помощью комплекса ЛДК «Флюорит-4С» и МДМ-терапии по сравнению со стандартными терапевтическими тактиками в виде более выраженного нивелирования местного дискомфорта (на 0,5 баллов по сравнению с группой сравнения), более выраженного снижения индекса РМА (на 0,9% по сравнению с группой сравнения), более полного устранения патологического очага, а также полной нормализации эмоционального состояния.

Ключевые слова: *флюорит-4С, мезодиэнцефальная модуляция, инфракрасный спектр, физиотерапевтический метод, область кровенаполнения.*

1. INTRODUCTION

In dental practice, periodontal inflammation is one of the most common pathologies. Inflammatory diseases of the tissues which surround the tooth can occur as independent pathologies or as a consequence of reconstructive interventions, for example, dental implantation. The presence of an inflammatory process in the periodontal tissues can lead to local and general discomfort in the form of local pain syndrome and associated impairment of masticatory function, general hyperthermia, impaired psychological state and quality of life, etc. Therefore, timely diagnosis and early therapy of this category of diseases is an integral part of comprehensive dental care (Danilevsky and Borisenko, 2000; Utyuzh *et al.*, 2016a; Utyuzh *et al.*, 2016b; Hajishengallis and Lamont, 2012; Holt and Ebersole, 2005; Grant, 2012; Garaicoa-Pazmino *et al.*, 2019; Marinho *et al.*, 2015; Campbell *et al.*, 2016; Hamilton *et al.*, 2016;). The quality of life of patients who have lost their teeth is significantly reduced. Loss of teeth causes psychological trauma, leads to pronounced aesthetic changes, diseases and exacerbations of the temporomandibular joint and gastrointestinal tract occur.

At present, the detection of patients with inflammatory processes in periodontal tissues at

the early stages of this pathology remains relatively low. This is due to many factors including:

- Psychological unpreparedness of patients to seek dental care at the early stages of the disease. Most often, patients find dental care in cases of severe clinical manifestations of the disease, when they feel a pronounced discomfort, leading to a decrease in the quality of life and psychological well-being. This is often associated with a widespread dentophobia among people which results in a delay in seeking medical advice after the first, still minor, symptoms of the disease (Brogardh-Roth *et al.*, 2017; Kinane *et al.*, 2017; Li *et al.*, 2019; Divaris, 2019; Hiyari *et al.*, 2018; Nibali *et al.*, 2019; Bergan *et al.*, 2014; Bebeko *et al.*, 2015; Moura *et al.*, 2015; Baek *et al.*, 2017; Subramaniam *et al.*, 2016; Wang *et al.*, 2016; Sankaranarayanan *et al.*, 2019; Jeong and Chang, 2015; Chang *et al.*, 2019):

- the absence of clinical manifestations or non-invasive methods for the detection of latent inflammation do not always allow diagnosis of this inflammation during preventive examinations (Tsepov *et al.*, 2008; Gupta *et al.*, 2018; Jepsen and Jepsen, 2016; Iviglia *et al.*, 2019; Echeverría *et al.*, 2019; Trombelli *et al.*, 2015; Page *et al.*, 2014).

The above shows the need to involve new diagnostic methods in the diagnosis of latent inflammations. One of the main principles of the

treatment of inflammatory periodontal diseases is an individual approach to the selection and planning of medical procedures.

The problem of treating patients with periodontal inflammations is complex. A dentist should pay attention both to the condition of the tissues in the mouth and to the psychological state of the patient, which, in patients with periodontal inflammations, often requires correction. Impaired psychological state may be a consequence of dental pathology or, on the contrary, one of the indirect etiopathological components of the inflammation in the mouth (Danilevsky and Borisenko, 2000; Brogardh-Roth *et al.*, 2017; Graziani *et al.*, 2010; D'Aiuto *et al.*, 2004;). Comprehensive treatment involves not only planning but also the mandatory provision of all necessary types of assistance. In this case, it is essential to correctly determine the sequence of measures needed to eliminate the disease and correctly make a forecast for each tooth. However, the involvement of psychologists or psychiatrists in the treatment of patients with dental diseases is not a routine practice in the dental clinic.

Inflammation of periodontal tissues can be observed in the infrared (IR) spectrum. Therefore, according to the authors, the Fluorit-4S therapeutic and diagnostic device (Fluorit-4S TDD) developed in the Scientific and Research Center of Biometric Devices of the Bauman Moscow State Technical University (SRCBD of the BMSTU) can be used to diagnose latent inflammation. Fluorit-4S TDD is intended for infrared diaphanoscopy of biological tissues. It can be used to visualize soft and hard tissues of the oral cavity in the near-infrared spectrum. The principle of action of the device is based on filtration of transmitted or reflected radiation from the examined tissues. Infrared rays can penetrate tissues 3–4 mm deep. Absorbed by the tissues, the energy quantum of infrared radiation is transformed into thermal energy, causing hyperemia. In this case, the main radiation-receiving environment is water contained in the tissues. Due to the increased content of infiltrate in the inflamed tissues, the affected tissues absorb infrared radiation to a greater extent (Zimnyakov, 2007; Kolpakov *et al.*, 2013).

During the development of the inflammatory process in the soft tissues, a region of hyperemia is formed, which is an area of high blood filling due to the expansion of blood vessels, and is characterized by an increased concentration of oxyhemoglobin, hemoglobin, and water, which in turn causes an increase in the absorption coefficient of the inflamed area

(Zimnyakov, 2007; Kolpakov *et al.*, 2013; Ben Amara *et al.*, 2018; Kolenbrander and London, 2013; Boutin *et al.*, 2017; Liu *et al.*, 2018;).

Infrared radiation has demonstrated its efficacy in the treatment of chronic and subacute inflammatory processes in various tissues, resolution of infiltrates after operations and trauma, chronic arthritis, arthrosarthritis of the temporomandibular joint, chronic neuritis, neuralgia, myositis, Setton's stomatitis, trophic, hypogranulating decubitus mouth ulcers, etc. (Kolpakov *et al.*, 2013; Danilevsky *et al.*, 2001). This is due both to the ability of infrared radiation to improve local blood flow, indirectly affecting the regeneration processes in the periodontal tissues and to the photobiostimulation effects of the infrared radiation on the irradiated tissue (Prokhorova *et al.*, 2007; Al-Hebshi *et al.*, 2015; Belstrøm *et al.*, 2016; Caton *et al.*, 2018; Tonetti *et al.*, 2018).

In the diagnostic mode, the radiated wavelength is 0.83–0.9 μm , at a power of 3 mW. The therapeutic effect is achieved with pulse modulation at a frequency of 1–3 kHz; the wavelength is 0.89 μm , and the power is 6 mW (Zimnyakov, 2007; Kolpakov *et al.*, 2013). Therefore, we believe that the Fluorit-4S TDD, the action of which is based on infrared radiation, can be used both for diagnosis and treatment of latent periodontal inflammation.

The issue of correction of the patient's psychological state as part of comprehensive dental care in a dental clinic, in our opinion, can be resolved using physiotherapy methods. We propose to use mesodiencephalic modulation (MDM therapy), a method of physiotherapy based on the targeted action of various pulse currents with a frequency of 10,000 Hz, modulated in the low-frequency range from 20 to 100 Hz, on the subcortical-stem structures of the brain, which leads to the activation and normalization of a number of anti-stress systems of the body and results in normalization of the patient's psycho-emotional state (Karev *et al.*, 2002; Lacigova *et al.*, 2013).

Therefore, this study aimed to seek different ways of psychological correction in patients with dental diseases using the methods available to the dentist as part of comprehensive dental care.

2. MATERIALS AND METHODS

The study was carried out at the Department of Orthopedic Dentistry of the I.M.

Sechenov First Moscow State Medical University, in compliance with the principles of bioethics and deontology, after obtaining informed consent, and consisted of two stages: diagnostic and therapeutic.

At the first stage, 76 patients were examined using the Fluorit-4S TDD (Figure 1). This stage was carried out to establish the diagnostic effectiveness of the Fluorit-4S TDD (Table 1). At this stage, a repeated dental examination of patients was carried out using two methods: clinical and instrumental, using the Fluorit-4S TDD, with two weeks between. The second stage of the study was devoted to the establishment of the therapeutic efficacy of the Fluorit-4S TDD and MDM-therapy as part of comprehensive dental care in patients with periodontal inflammation. For this stage of the study, 28 patients with inflammatory periodontal diseases of various severity, pathological changes in which were detected using the Fluorit-4S TDD at the first stage of the research, were selected.

For a comparative analysis of the efficacy of the Fluorit-4S TDD and MDM-therapy in the treatment of periodontal diseases, the patients selected for the second stage of the study were divided into two groups of 14 people each. The study group (SG) included 14 patients who received therapy using the Fluorit-4S TDD and MDM-therapy. The mean age in the group was 31.4 ± 2.0 years. The course of treatment included 15 sessions of MDM-therapy and infrared radiation therapy using the Fluorit-4S TDD. The sessions using the Fluorit-4S TDD were carried out in the form of a 3-minute irradiation of the affected segment. The meetings of MDM-therapy lasted 30 minutes and were carried out immediately after the sessions using the Fluorit-4S TDD. The course duration was six weeks. The control group (CG) included 14 patients who received standard conservative treatment without the Fluorit-4S TDD and MDM-therapy. The mean age in the group was 32.1 ± 1.8 years. Patients of both groups underwent standard professional oral hygiene procedures before the significant treatment.

The evaluation of the effectiveness of treatment was based on the four following studies:

- subjective assessment (using a five-point scale, where 1 point - no discomfort, 5 points - significant discomfort);
- determination of the papillary-marginal-alveolar index (PMA index);
- infrared diaphanoscopy;

- psychodiagnostic examination using the following psychodiagnostic techniques: Beck Depression Inventory (BDI, A.T. Beck, 1961) – to identify depressive episodes in patients with periodontal inflammation; Beck Anxiety Inventory (BAI, A.T. Beck, 1961) – to identify the presence and severity of anxiety in patients with periodontal inflammation.

Statistical processing of data was carried out using methods of clinical and mathematical statistics (including determination of standard deviation and standard error of the mean, the Fisher exact test, the Student's t-test, and the universal value of the statistical probability – p). Parameters at $p < 0.05$ were considered statistically significant differences.

All procedures performed in studies involving human participants were following the ethical standards of the institutional and national research committee and with the 1964 Helsinki declaration and its later amendments or comparable ethical standards. A study was conducted under the requirements of the ethics committee (Protocol of the meeting of the ethics committee of the Moscow State Medical University No. 110-2019). Informed consent was obtained from all individual participants included in the study (Consent for the publication of clinical data).

3. RESULTS AND DISCUSSION:

During a routine clinical dental examination, periodontal inflammation was diagnosed in 38 patients of all subjects (76 patients). Diagnostic analysis of the mucous membranes of the oral cavity of all patients (76 patients) using the Fluorit-4S TDD showed pathological inflammatory processes, clearly visualized in the infrared spectrum, in the same 38 patients whose inflammation was detected during a routine examination (Table 2).

In 4 other patients (in whom clinical, including visual, manifestations of the inflammatory process were not diagnosed during routine examination), the presence of latent inflammations was found in the infrared spectrum using Fluorit-4S TDD (Figure 2).

Two weeks after the initial examination, the patients were re-examined. A repeated analysis showed the presence of active inflammation in the previously identified four patients who had no clinical manifestations of inflammation in the infrared spectrum during the first examination but latent inflammations were diagnosed using the Fluorit-4S TDD. The remaining 34 patients, who had no signs of inflammation in the infrared

spectrum during the first examination, according to the Fluorit-4S TDD data, were also considered healthy during the second examination. Therefore, our study demonstrated high efficacy of the Fluorit-4S TDD in the detection of "latent" inflammatory processes in the absence of false positive and false negative results (Table 2).

3.1. Study of the therapeutic efficacy of the Fluorit-4S TDD

The study showed a significant improvement in the periodontal condition in the SG compared to the initial; these results were significantly superior compared to the results in the CG. Subjective assessment of the local state of the oral mucosa. In the SG, after the treatment using the Fluorit-4S TDD, a significant subjective improvement in the periodontal condition in the form of reduced discomfort in the oral cavity was diagnosed (from 3.9 ± 0.2 points of discomfort severity to 1.0 ± 0.1 points), which was significantly higher than these parameters in the CG (where discomfort severity changed from 3.9 ± 0.2 points to 1.5 ± 0.2 points) ($p < 0.05$). The difference in the decrease in the severity of local discomfort between the SG and the CG was 0.5 points ($t_{\text{Emp}} = 2.7$) (Table 3).

Objective evaluation using the PMA index In the SG, the mean PMA index before treatment was $59.2 \pm 1.1\%$; after the end of treatment using the Fluorit-4S TDD, this parameter was $7.3 \pm 1.5\%$ (the difference between the measurements was -51.9%), which was positively different from the CG ($p < 0.01$). In the SG, the initial mean PMA index was $60.5 \pm 1.2\%$ and at the end of the study, it was $9.1 \pm 1.4\%$ (the difference between the measurements was -51.0%). Therefore, the decrease in the PMA index in the SG by 0.9% was superior to the CG parameters.

Objective evaluation using infrared diaphanoscopy IR-diaphanoscopy confirmed complete recovery (complete elimination of inflammation) in the SG in 93% of cases (13 people); in the CG, in 43% of cases (6 patients) signs of inflammation persisted, in 57% of cases (8 patients) there was complete recovery, which showed significant differences between the groups ($\phi^*_{\text{emp}} = 2.352$, $p < 0.01$). Therefore, our study demonstrated the high therapeutic efficacy of the Fluorit-4S TDD compared to standard conservative treatment only; subjective and objective examinations confirmed this.

3.2 Study of the therapeutic efficacy of MDM-therapy

The study of the emotional state of patients showed a significantly superior therapeutic effect in the sg compared to the cg. Examination of the level of depression in patients of both groups the depression level, according to the bdi test, did not significantly differ and corresponded to subdepression (14.75 ± 0.45 points in the sg, 14.74 ± 0.68 points in the cg) before the MDM-therapy. Upon completion of MDM-therapy, in all patients in the sg, depressive manifestations resolved (the mean score in the group was 3.22 ± 0.25 points), which significantly differed from the cg, wherein 86% of cases (12 patients) a subdepressive condition persisted (mean score 11.63 ± 0.78).

Study of the level of anxiety according to the bai test, a high level of anxiety was observed in patients of both groups (50.21 ± 0.62 points in the sg, 49.85 ± 0.54 points in the cg) before the beginning of therapy. After the completion of treatment, anxiety resolved in all patients in the sg (mean score in the group was 8.52 ± 0.35 points), whereas in the cg anxiety persisted at the moderate level (24.12 ± 0.42 points), which significantly differed from the cg ($p < 0.01$). Therefore, our study confirms the high therapeutic efficacy of MDM-therapy in the normalization of the emotional state in patients with inflammatory periodontal diseases.

4. CONCLUSIONS:

The study demonstrated the high diagnostic efficacy of the Fluorit-4S TDD in the detection of both active and latent inflammations of periodontal tissues. In 100% of cases, the Fluorit-4S TDD confirmed clinically detected pathologies, as well as diagnosed a pathological process that did not have clinical manifestations. There were no false positive and false negative results of examinations using the Fluorit-4S TDD.

The use of the Fluorit-4S TDD in dental practice allows dentists to study the affected tissues more closely, resulting in objective conclusions on the pathological processes in the oral mucosa and, accordingly, the selection of adequate therapeutic strategies for individual clinical cases. The Fluorit-4S TDD can be recommended for non-invasive diagnosis of inflammatory periodontal diseases, including early stages of the disease without its clinical manifestations, which will ensure timely treatment and minimize complications of the disease.

The high therapeutic efficacy of the Fluorit-4S TDD was established, which supported the use of this system by dentists both as a diagnostic tool

and as a method of physiotherapeutic therapy. In patients treated using the Fluorit-4S TDD, compared to patients who received conservative treatment only, local discomfort was significantly reduced (by 0.5 points), the PMA index was significantly decreased (by 0.9%), and the pathological focus was eliminated, which was confirmed by the infrared diaphanoscopy data.

Significantly higher positive results in patients whose therapeutic strategies included the Fluorit-4S TDD show that the Fluorit-4S TDD can be used as an alternative to a conservative pharmacotherapeutic method in cases when patients have contraindications or allergy history, as well as an additional therapy to guarantee improved treatment outcomes.

The evident therapeutic influence of MDM-therapy on the stabilization of the emotional state of patients with inflammatory periodontal diseases was proved. In patients who received MDM-therapy, a complete recovery of anxiety and depressive symptoms was observed, compared to the control group, which allows the recommendation of this physiotherapeutic method for use in dentistry as part of the comprehensive therapy of patients with inflammatory periodontal diseases.

5. REFERENCES:

- Al-Hebshi, N.N., Nasher, A.T., Idris, A.M., Chen, T. *Journal of Oral Microbiology*, **2015**, 7(1), 28934.
- Baek, J.-S., Yeo, E.W., Lee, Y.H., Tan, N.S., Loo, S.C.J. *Drug Design, Development and Therapy*, **2017**, 11, 1707-1717.
- Bebko, S.P., Green, D.M., Awad, S.S. *JAMA Surgery*, **2015**, 150(5), 390-395.
- Belstrøm, D., Holmstrup, P., Bardow, A., Kokaras, A., Fiehn, N.-E., Paster, B.J. *PLoS ONE*, **2016**, 11(1), e0147472.
- Ben Amara, H., Song, H.Y., Ryu, E., Park, J.S., Schwarz, F., Kim, B.M., Choi, B.-K., Koo, K.-T. *European Journal of Oral Sciences*, **2018**, 126(6), 449-457.
- Bergan, E.H., Tura, B.R., Lamas, C.C. *Intensive Care Medicine*, **2014**, 40(1), 23-31.
- Boutin, S., Hagenfeld, D., Zimmermann, H., El Sayed, N., Höpker, T., Greiser, H.K., Becher, H., Dalpke, A.H. *Frontiers in Microbiology*, **2017**, 8, 340.
- Brogardh-Roth, S., Mansson, J., Ridell, K. *BMC Oral Health*, **2017**, 17(1), 145.
- Campbell, I.K., Leong, D., Edwards, K.M., Razman, V., Ng, M., Goldberg, G.L., Wilson, N.J., Andrews, A.E. *Journal of Immunology*, **2016**, 197(11), 4392-4402.
- Chang, P.-C., Chen, Y.-W., Tu, C.-C., Yen-Ping Kuo, M., Liu, C.-M., Wang, C.-Y. *Journal of the Formosan Medical Association*, **2019**, 118(5), 932-938.
- Consent for the publication of clinical data. https://minzdrav.govmurman.ru/documents/poryadki-okazaniya-meditsinskoy-pomoshchi/5_gingivit.pdf
- D'Aiuto, F., Parkar, M., Andreou, G., Suvan, J., Brett, P.M., Ready, D., Tonetti, M. *Journal of Dental Research*, **2004**, 83(2), 156-160.
- Danilevsky, N.F., Borisenko, A.V. *Periodontal diseases*. Kiev: Zdorov'e, **2000**.
- Danilevsky, N.F., Leontiev, V.K., Nesan, A.F., Rakhniy, Zh.I. *Diseases of the oral mucosa*, Moscow: OAO "Stomatologiya", **2001**.
- Divaris, K. *Advances in dental research*, **2019**, 30(2), 40-44.
- Echeverría, J.J., Echeverría, A., Caffesse, R.G. *Periodontology 2000*, **2019**, 79(1), 200-209.
- Caton, G.J., Armitage, G., Berglundh, T., Chapple, I.L.C., Jepsen, S., Kornman, K., Mealey, B., S. Tonetti, M. *Journal of Clinical Periodontology*, **2018**, 45, 1-8.
- Garaicoa-Pazmino, C., Fretwurst, T., Squarize, C.H., Berglundh, T., Giannobile, W.V., Larsson, L., Castilho, R.M. *Journal of Clinical Periodontology*, **2019**, 46 (8), 830-839.
- Grant, M.M. *Journal of Periodontal Research*, **2012**, 47(1), 2-14.
- Graziani, F., Cej, S., Tonetti, M., Paolantonio, M., Serio, R., Sammartino, G., Gabriele, M., D'Aiuto, F. *Journal of Clinical Periodontology*, **2010**, 37(9), 848-854.
- Gupta, S., Chhina, S., Arora, S.A. *Journal of Oral Biology and Craniofacial Research*, **2018**, 8(2), 98-104.
- Hajishengallis, G., Lamont, R.J. *Molecular Oral Microbiology*, **2012**, 27(6), 409-421.
- Hamilton, J.A., Cook, A.D., Tak, P.P. *Nature Reviews Drug Discovery*, **2016**, 16(1), 53-70.
- Hiyari, S., Green, E., Pan, C., Lari, S., Davar, M., Davis, R., Camargo, P.M., Pirih, F.Q.

- Journal of Bone and Mineral Research*, **2018**, 33(8), 1450-1463.
25. Holt, S.C., Ebersole, J.L. *Periodontology* **2000**, **2005**, 38, 72-122.
 26. Iviglia, G., Kargozar, S., Baino, F. *Journal of Functional Biomaterials*, **2019**, 10(1), 3.
 27. Jeong, J.-S., Chang, M. *Journal of Periodontology*, **2015**, 86(12), 1314-1320.
 28. Jepsen, K., Jepsen, S. *Periodontology* **2000**, **2016**, 71(1), 82-112.
 29. Karev, V.A., Dotsenko, V.I., Voloshin, V.M., Tavtin, I. K. *Med Tekh*, **2002**, 6, 16-20.
 30. Kinane, D.F., Stathopoulou, P.G., Papapanou, P.N. *Nature Reviews Disease Primers*, **2017**, 3, 17-25.
 31. Kolenbrander, P.E., London, J. *Journal of Bacteriology*, **2013**, 175(11), 3247-3252.
 32. Kolpakov, A.V., Makarov, A.L., Spiridonov, I.N. *Science and Education: NE Bauman MSTU Scientific Edition*, **2013**, 12, 297-306.
 33. Lacigova, S., Tomesová, J., Gruberova, J., Rusavý, Z., Rokyta, R. *Neuro Endocrinol Lett*, **2013**, 34(2), 135-142.
 34. Li, J., Xiao, X., Wei, W., Ding, H., Yue, Y., Tian, Y., Nabar, N.R., Wang, M. *Journal of Periodontology*, **2019**, 90(2), 208-216.
 35. Liu, F., Ma, R., Wang, Y., Zhang, L. *Frontiers in Cellular and Infection Microbiology*, **2018**, 8, 243.
 36. Marinho, A.C.S., Martinho, F.C., Leite, F.R.M., Nascimento, G.G., Gomes, B.P.F.A. *Journal of Endodontics*, **2015**, 41(6), 817-823.
 37. Moura, L.A., Ribeiro, F.V., Aiello, T.B., Duek, E.A.D.R., Sallum, E.A., Nociti, F.H., Casati, M.Z., Sallum, A.W. *Journal of Biomaterials Science, Polymer Edition*, **2015**, 26(10), 573-584.
 38. Nibali, L., Bayliss-Chapman, J., Almofareh, S.A., Zhou, Y., Divaris, K., Vieira, A.R. *Journal of Dental Research*, **2019**, 98(6), 632-641.
 39. Page, R.C., Offenbacher, S., Schroeder, H.E., Seymour, G.J., Kornman, K.S., *Periodontology* **2000**, **2014**, 14(1), 216-248.
 40. Prokhorova, E.V., Gemonov, V.V., Druzhinina, R.A. *Russian Journal of Dentistry*, **2007**, 4, 10-12.
 41. Protocol of the meeting of the ethics committee of the Moscow State Medical University No. 110-2019. http://transpl.ru/about_center/science_activity/etika_sovet/polozhenie_o_lokal_nom_eticheskom_komitete/
 42. Sankaranarayanan, R., Saxlin, T., Ylöstalo, P., Khan, S., Knuuttila, M., Suominen, A.L. *European Journal of Oral Sciences*, **2019**, 127(3), 232-240.
 43. Subramaniam, S., Fang, Y.-H., Sivasubramanian, S., Lin, F.-H., Lin, C.-P., *Biomaterials*, **2016**, 74, 99-108.
 44. Tonetti, M.S., Greenwell, H., Kornman, K.S. *Journal of Periodontology*, **2018**, 89, 159-172.
 45. Trombelli, L., Franceschetti, G., Farina, R. *Journal of Clinical Periodontology*, **2015**, 42(S16), 221-236.
 46. Tsepov, L.M., Nikolaev, A.I., Mikheeva, E.A. *Diagnosis, treatment and prevention of periodontal diseases*, Moscow: MEDPress-Infarm, **2008**.
 47. Utyuzh, A.S., Yumashev, A.V., Mikhailova, M.V. *Journal of Global Pharma Technology*, **2016b**, 8(12), 7-11.
 48. Utyuzh, A.S., Yumashev, A. V., Lushkov, R. M. *Clinical Dentistry*, **2016a**, 4, 56-58.
 49. Wang, J., Lv, J., Wang, W., Jiang, X. *Journal of Clinical Periodontology*, **2016**, 43(7), 572-583.
 50. Zimnyakov, D.A. *Optical biomedical diagnostics*, Moscow: FIZMATLIT, **2007**.

Table 1. Fluorit-4S TDD specification

Characteristic	Index
Range of vision	16*12 mm
Wavelength	890 nm
Power consumption	60 W
Control and power unit	
Size	320*120*245 mm
Weight	2 kg

Table 2. Diagnostic ability of a routine method of examination and the Fluorit-4S TDD

Examination / Result	Study population (n=76)			
	Clinically diagnosed periodontal inflammatory diseases		Periodontal inflammatory diseases diagnosed using the Fluorit-4S TDD	
	patients	%	patients	%
Primary examination	38	50.0	42	55.26
False positive results	–	–	–	–
False negative results	4	5.26	–	–

Table 3. Parameters of subjective assessment of local discomfort

Stage of the study	Study groups		t	p
	SG (n=15)	CG (n=15)		
	M±m	M±m		
Before treatment	3.9±0.2	3.9±0.2	0.3	>0.05
After treatment	1.0±0.1	1.5±0.2	2.7	<0.05
t	15.7	9.6		
p	<0.01	<0.01		

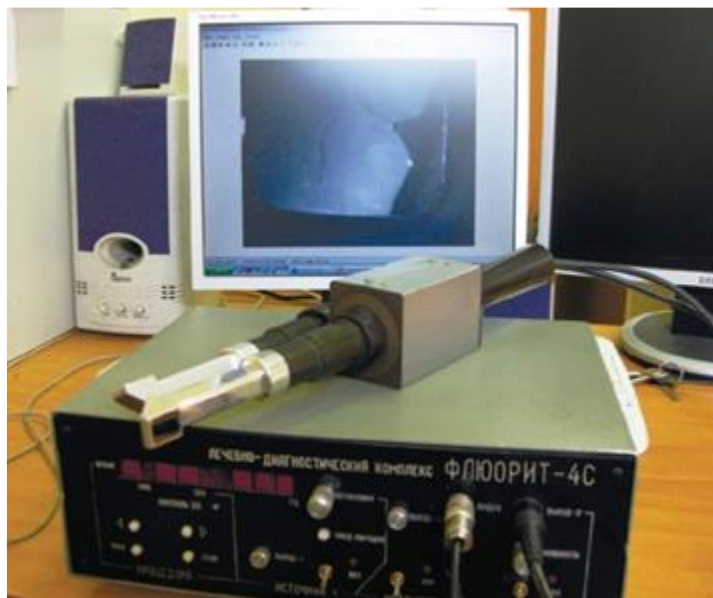


Figure 1. Fluorit-4S therapeutic and diagnostic device (TDD)

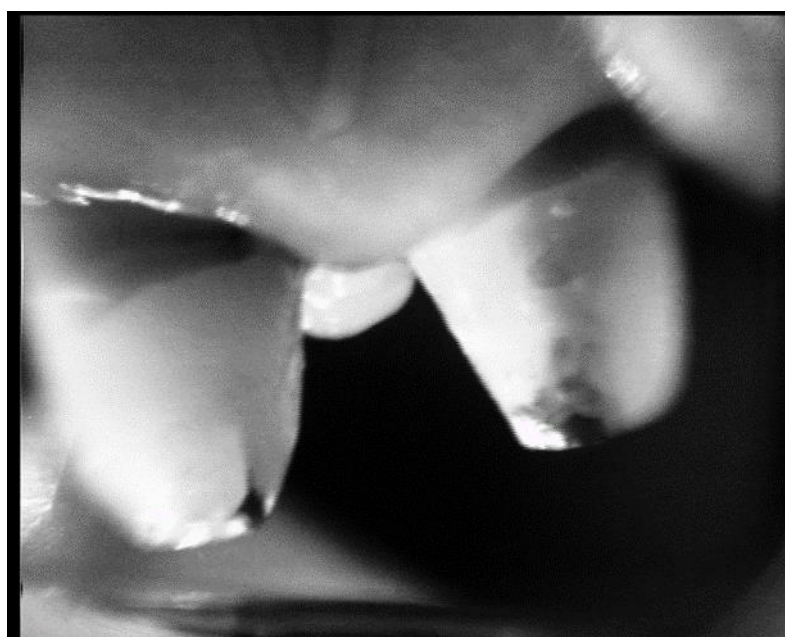


Figure 2. Image obtained using the Fluorit-4S TDD, showing the inflammation of the gum near the tooth 1.1 (left) in the infrared spectrum

AVALIAÇÃO CIENTÍFICA DO RISCO DE SEGURANÇA DOS PRODUTOS BRUTOS DE AÇÚCAR**SCIENTIFIC SECURITY ASSESSMENT OF SAFETY RISK OF RAW SUGAR PRODUCTS****НАУЧНОЕ ОБЕСПЕЧЕНИЕ ОЦЕНКА РИСКА БЕЗОПАСНОСТИ СЫРЬЯ САХАРНОЙ ПРОДУКЦИИ**

ZHAKATAYEVA, Altynay¹; IZTAYEV, Auyelbek ²; MULDABEKOVA, Bayan³; YAKIYAYEVA, Madina⁴ *; HRIVNA Ludek⁵

^{1,2,3,4} Almaty Technological University, Department "Technology of bread and processing industries", 100 Tole Bi st., zip code 050012, Almaty – Kazakhstan

⁵Mendel University in Brno, Department of Food Technology, 1 Zemedelska st., zip code 61300, Brno - Czech Republic

* *Correspondence authors*
e-mail: yamadina88@mail.ru

Received 22 January 2020; received in revised form 10 February 2020; accepted 11 February 2020

RESUMO

A organização adequada do armazenamento de produtos de açúcar bruto permite manter a qualidade do produto e minimizar a perda de massa por muito tempo. As dificuldades estão associadas ao alto conteúdo de água livre nos produtos. Foi estudado o efeito do tratamento com ozônio no armazenamento de longo prazo dos produtos do açúcar bruto, incluindo beterraba sacarina. Amostras de beterraba sacarina foram colhidas na usina de açúcar Koksú, na vila de Balpyk bi, região de Almaty, na República do Cazaquistão. O planejamento dos experimentos fatorial tipo 2^3 , oito protótipos foram elaborados e cada um deles foi processado com diferentes combinações (máx e mín) dos seguintes fatores: x_1 - concentração de ozônio (g/m^3), x_2 - tempo de processamento (min), x_3 - sobrepressão (ati) (o valor da pressão pode ser contado a partir de 0 (pressão absoluta) ou atmosférica (pressão excessiva). Se a pressão é medida em atmosferas técnicas, a pressão absoluta é indicada como ata e a pressão excessiva é indicada como ati). Propriedades físico-bioquímicas, microbiológicas e indicadores de segurança foram determinados para cada amostra de beterraba sacarina: fração mássica de umidade, matéria seca, acidez, pectina, fibra, sacarose, nitrito, metais pesados, pesticidas, micotoxinas, presença de mofo e levedura. Como resultado do estudo, verificou-se que o tratamento com ozônio reduziu significativamente o crescimento de fungos e leveduras, contribui para um aumento no conteúdo de pectina, fibra e sacarose, e uma avaliação de segurança da segurança de produtos de açúcar em bruto foi fornecida cientificamente.

Palavras-chave: *ozônio, tratamento, infecção, microbiologia, doença.*

ABSTRACT

Proper organization of storage of raw sugar products allows for a long time to maintain product quality and minimize loss of its mass. Difficulties are associated with the high content of free water in them. We have studied the effect of ozone treatment on long-term storage of raw sugar products, including sugar beets. Sugar beet samples were taken from the Koksú sugar factory in the village of Balpyk bi, Almaty region of the Republic of Kazakhstan. The plans for full-factor experiments of the type — 2^3 out of eight prototypes — were drawn up and each of them was processed with different combinations (max and min) of the following factors: x_1 - ozone concentration (g/m^3), x_2 - processing time (min), x_3 - overpressure (ati) (the pressure value can be counted from 0 (absolute pressure) or from atmospheric (overpressure). If the pressure is measured in technical atmospheres, then absolute pressure is denoted as ata, and excess pressure is denoted as ati). Physico-biochemical, microbiological properties, and safety indicators were determined for each sample of sugar beet: mass fraction of moisture, dry matter, acidity, pectin, fiber, sucrose, nitrite, heavy metals, pesticides, mycotoxins, the presence of mold and yeast. As a result of the study, it was found that ozone treatment significantly reduces the growth of mold and yeast, contributes to an increase in the content of pectin, fiber and sucrose, and a safety risk assessment of raw sugar products was scientifically provided.

Keywords: ozone, treatment, infection, microbiology, disease.

АННОТАЦИЯ

Правильная организация хранения сырья сахарной продукции позволяет длительное время сохранить качество продукции и свести к минимуму потери ее массы. Трудности связаны с большим содержанием в них воды в свободном состоянии. Нами исследовано влияние озонной обработки на длительные хранения сырья сахарной продукции, в том числе сахарной свеклы. Был проведен отбор проб сахарной свеклы из Коксуского сахарного завода, села Балпык би Алматинской области Республики Казахстан. Составлены планы полнофакторных экспериментов типа 2^3 из восьми опытных образцов и каждые из них обрабатывались с разными сочетаниями (max и min) следующих факторов: x_1 – концентрация озона (г/м^3), x_2 – время обработки (мин), x_3 – избыточное давление (ати) (значение давления может отсчитываться от 0 (абсолютное давление) или от атмосферного (избыточное давление). Если давление измеряется в технических атмосферах, то абсолютное давление обозначается как ата, а избыточное - как ати). По обработанному каждому образцу сахарной свеклы были определены физико-биохимические, микробиологические свойства и показатели безопасности: массовые доли влаги, сухого вещества, кислотности, пектиновых веществ, клетчатки, сахарозы, нитрита, тяжелых металлов, пестицидов, микотоксинов, наличие плесени и дрожжей. В результате исследования были установлены, что озонная обработка заметно снижает рост плесени и дрожжей, способствует к увеличению содержания пектиновых веществ, клетчатки и сахарозы, научно была обеспечена оценка риска безопасности сырья сахарной продукции.

Ключевые слова: озон, обработка, зараженность, микробиология, болезнь.

1. INTRODUCTION

Sugar production is a complex technological process consisting of various stages, which requires the use of special equipment aimed at obtaining high-quality sugar from the corresponding raw materials. It foresees the presence of 3 branches at a sugar factory:

- beet processing (peeling, grinding of beets, diffuse removal of juice from chips);
- juice purification (creating syrup from pure juice + its purification and evaporation);
- food compartment (transformation of syrup into massecuite with further crystallization, jointing, and whitening, drying, and packaging of finished sugar).

In our country, the basis of the raw material base for sugar-producing enterprises is sugar beet. It must be closely monitored for the presence / absence of microorganisms. If the microbiological activity of beets is systematically controlled in the manufacture of sugar, it is possible to establish infectious sources and foci in a timely manner, then take measures to eliminate them, and also correct deviations that occurred in the technological process during the life of organisms (Sapronov *et al.*, 2011; Apasov *et al.*, 2011; Podporinova *et al.*, 2010; Weststrat, 2002).

If there is a microbial defeat of sugar beets, the biological masses of all kinds of microorganisms accumulate in it during storage

and processing. As a result, sugar production has many problems. Saprophyte molds have a destructive effect on the root structure, thereby creating a good environment for the development of bacteria, which, in turn, completes the spoilage process, beets lose their suitability for processing. Bacteria of different groups and species has a decisive influence on the composition of the final metabolic products. Heterofermentative lactic acid bacteria produce dextran polysaccharide. Putrefactive destroy the protein components of the root and therefore contribute to the appearance of hydrogen nitride, dimethyl ketone, and methyl formaldehyde. In the spectrum of the functional activity of butyric acid bacteria - the effect on starch, pectins and sugars with the formation of dimethylketone, alcohol, gas and acidic environments (in particular, butanoic and ethanoic acids). By the way, significant accumulation of gases is a dangerous explosion of a diffusion plant (Stognienko *et al.*, 2012; Sapronov, 2007; Loel *et al.*, 2014; Martindale, 2013).

Determination of the microbiological activity of sugar beet: importance for sugar enterprises. In order to ensure the sanitary and hygienic state of production in such a way that all aspects comply with the regulatory documentation SanERandR 2.3.2.1078-01, it is important to monitor the active microflora and suppress it even at the beginning of processing activities. If this is not done, not only the beets will be unsuitable for work, but also the development of microorganisms in the beet

processing department of the plant, as well as their subsequent accumulation on equipment, will be implemented (Islamgulov *et al.*, 2013; Sapronov *et al.*, 2014; Luterbacher *et al.*, 2005).

When stored at elevated temperatures, this causes intensive respiration of cells and tissues, activates the maturation and aging processes, enhances the evaporation and development of phytopathogenic microflora, which leads to significant losses in mass and product quality. Therefore, during storage, they strive to create conditions that slow down the vital processes of stored products and microorganisms (Manzhesov *et al.*, 2009; Vertush, 2002; Karpov, 2007). The initial control of raw materials in the kagat (or burt - simplified storage of vegetables, root crops in the form of a shaft or foundation pit, covered with straw or tarpaulin) and entering the enterprise looks like a visual inspection. If spoilage is present, determining the nature of microflora becomes relevant (Krylov, 2006; Erkmén, 2001; Lichko *et al.*, 2000).

Most attention should be paid to active fungi that destroy roots. Their standard location is the inside of beets. It is clear that to establish whether there is a problem visually or not will fail. In this case, it is necessary to sow from the inner part of the affected root crop into a nutrient medium with agar and immediately after that, if possible, establish the type of fungus. If a lot of roots with active semi-parasitic fungi are found in the kagat, all beets should be processed out of turn. Plus, measures should be taken to strengthen the fight against infectious damage in the production process, since a number of related microorganisms are a companion of such beets (Shpaar *et al.*, 2000; Ober *et al.*, 2010; Bugaenko, 2002).

Microbiological analysis - the most important segment of sugar production. It allows the timely detection of bacterial microflora, which is dangerous not only for the sugar-producing enterprise but also for various areas of the food industry that use sugar. Sugar contaminated with microorganisms is dangerous for soft drinks, confectionery industry, canning production, and others. Therefore, it is very important to know and use methods for determining microbiological activity and effective control of it (Trisvyatsky *et al.*, 1991; Gagkaeva *et al.*, 2005).

Microorganisms are introduced into it during the bleaching, drying, packaging, and storage of sugar beets. When sugar is washed by centrifugation, the microbes in it are minimized.

Shakes and silos are areas where microflora increases. Microbes come from air masses along with sugar dust. Their control is to take about 300 g of crystalline sugar from every fifth bag. To determine how many microorganisms are present in one gram of sugar, a certain list of dilutions on selective media from the samples is sown (one warmed up for five minutes, the second unheated). Studies of granulated sugar are aimed at determining the following microflora:

- thermophiles (acid-forming aerobes, forming and non-forming hydrogen sulfide anaerobes);
- mesophiles (mucus-forming bacteria, osmotolerant yeast, mycelial fungi).

To protect sugar from negative influences as much as possible, it is important to observe the correct storage conditions. It must be kept in dry rooms with a relative humidity of 50-65% and a temperature of 15-20 °C. The surfaces of silos and premises should be treated with a disinfection agent using a 0.8% solution of the chemical combination cresol + sulfuric acid. To disinfect air and equipment by means of UV radiation (Shkalikov, 2010; Stevanato *et al.*, 2019; Kim *et al.*, 2003; Richardson, 2002).

2. MATERIALS AND METHODS

The following methods were used to determine the physicochemical parameters: the mass fraction of moisture and dry was determined according to GOST 28561-90, acidity according to GOST ISO 750-2013, mass fraction of pectin substances according to GOST 29059-91, mass fraction of sucrose according to GOST 28562-90, mass fraction of nitrite according to GOST 29270-95 and mass fraction fiber according to the Wende method (Timoshenko N.V. *et al.*, 2006). The content of toxic elements in sugar beets was determined: lead and cadmium, according to GOST 30178-96. The content of mycotoxins, including aflatoxin M, was determined according to GOST 30711-2001. The following interstate standards were used to determine microbiological indicators, that is, the content of mold and yeast: GOST 26669-85 Food and taste products. Sample preparation for microbiological analysis; GOST 26670-91 Food Products. Methods for the cultivation of microorganisms; GOST 10444.12-2013 Microbiology of food and animal feeding stuffs. Methods for the detection and colony count of yeasts and molds

A universal ion-ozonation plant has been developed that produces ozone, molecular ions, or an ion-ozone mixture in metered concentrations of certain components of the IOM (ion-ozone mixture). The efficiency of the ion-ozonator installation was obtained by improving and combining the electrical circuits of the ozonator and ionizer installations, the selection of materials, the estimated geometric dimensions and proportions. According to calculations and experimental research, the optimal modes of IOM synthesis were established, the necessary parameters for the impact on the processed product. All this universality is united not only by the similarity and stages of the synthesis of IOM, ionization of water and their interconnected quantum-physical processes that occur in the biological environment during their processing but also in design. Moreover, the synthesis of ozone is accompanied by the formation of ions of different signs of electrical polarity. The factor of the presence of atomic ions, nitrogen oxides, and carbon during the synthesis of ozone has a great influence on the process of negative influence during the processing of products of biological origin (Iztaev, Kulazhanov *et al.*, 2018; Yakiyayeva *et al.*, 2016).

Therefore, there was a need to combine ozone and ion technology to neutralize side effects, harmful impurities of atomic ions, nitrogen and carbon oxides in the synthesis of ozone and in the synthesis of molecular ions with the exception of a high-frequency electromagnetic field or a constant pulsating field with a wavelength that has a harmful effect on the body; radioactive radiation, alpha, beta and especially gamma rays, at least even in the most necessary quantities; emanations of radium - radon, exceeding in content its usual concentration in the external atmosphere; ultraviolet radiation, atomic ozone and nitrogen compounds that accompany the passage of ultraviolet light through the air; metal dust of any dispersion or carbon particles. An important component of the ionosphere is the dielectric pad of the IOM generator, which smoothes the plasma in the discharge gap and is a filter for metal combustion gases (electrodes). The technical effect of increasing ozone concentration, reducing electricity and cost, reducing the size and weight of the structure, as well as obtaining environmentally friendly ozone, molecular, atomic ions, as well as their mixtures is achieved through design solutions that have no analogs in the world (Iztayev, Urazaliev *et al.*, 2018; Iztayev, Yakiyayeva *et al.*, 2018).

Ion-ozonator installation (Figure 1) is necessary for the food and processing industry, microbiological industry, agribusiness, healthcare, medicine, pharmacy, environmental ecology, human ecology, as well as in other areas of national and industrial management since electrically charged particles are synthesized without cumulative harmful substances.

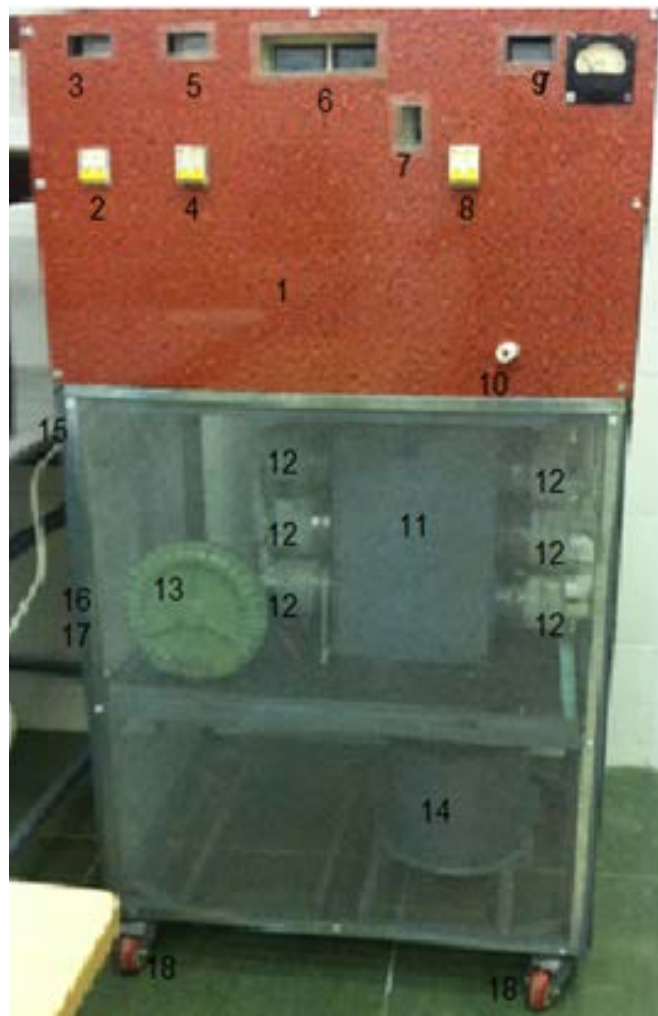


Figure 1. Ion-ozonator installation

The process control panel of the ionosphere 1 consists of:

- control panel for air compression processes (fuse switch 2, voltmeter 3, laboratory autotransformer (latr) not shown);
- ionizer synthesis control panel (fuse switch 4, voltmeter 5, laboratory autotransformer (latr) not shown);
- ozone synthesis control panel (fuse switch 8, voltmeter 9, laboratory autotransformer (latr) not shown);

- pipe for the extraction of ozone, atomic or molecular oxygen ions 10;
- water jacket cooling ozone generators 11;
- ozone generators 12;
- fan 13;
- transformer 14;
- pipe 15 for pouring water into the cooling jacket of ozone generators 12;
- a pipe 16 for taking water from the cooling jacket of ozone generators 12;
- air duct 17 with fan tap 13.

The main node, i.e., the heart of the ion-ozonator installation, is a block of generators of the ion-ozone mixture, and these are ozone generators and a generator of ions of positive or negative polarity, which are performed depending on the quantity, quality and oxidative ability of the processed product. Therefore, in the creation of an ion-ozonized installation, it is necessary to provide - what concentration, what amount of ozone and ions is necessary for the successful processing of products. It is very important to determine the technological process of product processing, to know the structure, humidity, oxidizing ability, temperature, and a very important thing. Also, for the processing of a particular product, it is necessary to control these processes, in connection with this it is necessary to provide a control panel, adjust the concentration of ozone, its amount, how many ions of positive or negative polarity of the electric current, and at what speed electrically charged particles are supplied. This requires a fan, and when processing products under excessive pressure, a compressor of the corresponding capacity.

3. RESULTS AND DISCUSSION

We have studied the effects of ozone treatment on long-term storage of sugar beets. A 2018 sugar beet crop was sampled from the Koksú Sugar Factory. Samples of sugar beets from the 1st degree of infection with bacteria and pests were selected. Sugar beet samples were treated with ozone stream. Plans were made for full-factor experiments of the type - 2^3 out of eight prototypes and each of them was processed with different combinations (max and min) of the following factors: x_1 - ozone concentration (g/m^3), x_2 - processing time (min), x_3 - overpressure (at). Physico-biochemical, microbiological properties,

and safety indicators were determined for each sample of sugar beet: mass fraction of moisture, dry matter, acidity, pectin, fiber, sucrose, nitrite, heavy metals, pesticides, mycotoxins, the presence of mold and yeast. Studies have been conducted to establish technological processing regimes for the destruction of pathogens.

To obtain a mathematical model of the technological process, which is a regression equation, we used a second-order rotatable plan (Box plan), when the number of factors is $K = 3$, the number of experiments of plan 8.

Based on the experimental studies of the process, the following factors are established: x_1 , x_2 , x_3 influencing optimization criteria - acidity, sucrose content, mold content. Next, we performed the coding of the intervals and levels of variation of the input parameters, which are presented in table 1. According to the compiled plan of full-factor experiments, samples of sugar beet from the Koksú sugar factory of the first degree of infection were investigated. The results of the study are shown in table 2.

The planning matrix is presented in table 3.

The coefficient of the regression equation is significant if its absolute value is greater than the confidence interval. Otherwise, it is considered insignificant and can be excluded from further consideration of the mathematical model.

The adequacy of the obtained mathematical regression models was evaluated by the Fisher criterion F_p . The calculated values of F_p are shown in Table 4.

Here:

b - coefficients of regression equations at coded values;

B - coefficients of regression equations at natural factors;

F_p - Fisher's criterion

Comparing the values of confidence intervals from table 3 with the corresponding regression coefficients in table 4, it can be concluded that the effects of the interaction of input factors minor, and they can be neglected.

Next, a search was made for the optimum response functions with the greatest possible accuracy (solution of a compromise problem), while insignificant coefficients were taken into account for constructing a mathematical model, which would be a regression, Equation 1:

$$y = b_0 + b_1x_1 + b_2x_2 + b_3x_3 + b_{12}x_1x_2 + b_{13}x_1x_3 + b_{23}x_2x_3 + b_{11}x_1^2 + b_{22}x_2^2 + b_{33}x_3^2 \quad (\text{Eq. 1})$$

Thus, the regression equations for coded values will accept the following equations (Eq. 2-13):

1. Equations for moisture sugar beet first degree of infection:

$$y_1 = 78,145 - 0,4825x_1 - 1,3425x_2 + 0,29x_3 - 1,535x_1x_2 - 0,0375x_1x_3 + 0,0625x_2x_3 - 0,03x_1x_2x_3 \quad (\text{Eq. 2})$$

2. Equations for dry matter of sugar beet of the first degree of infection:

$$y_2 = 21,8175 + 0,445x_1 + 1,305x_2 - 0,2525x_3 + 1,4975x_1x_2 + 0,075x_1x_3 - 0,025x_2x_3 + 0,0675x_1x_2x_3 \quad (\text{Eq. 3})$$

3. Equations for the acidity of sugar beets of the first degree of infection:

$$y_3 = 3,625 + 1,275x_1 - 1,375x_2 - 0,025x_3 - 0,175x_1x_2 + 0,025x_1x_3 + 0,025x_2x_3 + 0,025x_1x_2x_3 \quad (\text{Eq. 4})$$

4. Equations for the content of pectin substances of sugar beet of the first degree of infection:

$$y_4 = 5,89375 + 1,29625x_1 - 1,21375x_2 - 0,02875x_3 - 1,41625x_1x_2 - 0,00625x_1x_3 - 0,00125x_2x_3 - 0,00375x_1x_2x_3 \quad (\text{Eq. 5})$$

5. Equations for the content of sugar beet fiber of the first degree of infection:

$$y_5 = 6,11375 + 0,69375x_1 - 1,41875x_2 - 0,03375x_3 - 1,65375x_1x_2 + 0,00625x_1x_3 + 0,00875x_2x_3 + 0,00375x_1x_2x_3 \quad (\text{Eq. 6})$$

6. Equations for sucrose content of sugar beet of the first degree of infection:

$$y_6 = 2,36 + 0,0025x_1 - 0,35x_2 + 0,015x_3 + 0,5225x_1x_2 - 0,0025x_1x_3 + 0,0025x_1x_2x_3 \quad (\text{Eq. 7})$$

7. Equations for the content of nitrite sugar beet first degree of infection:

$$y_7 = 550,4125 + 11,7125x_1 - 8,8375x_2 + 0,1375x_3 + 9,0625x_1x_2 + 0,0375x_1x_3 + 0,1875x_2x_3 - 0,2125x_1x_2x_3 \quad (\text{Eq. 8})$$

8. Equations for lead content of sugar beet of the first degree of infection:

$$y_8 = 0,060387 + 0,0062875x_1 - 0,0036375x_2 + 0,0001375x_3 + 0,0014125x_1x_2 + 0,0000625x_1x_3 + 0,0000125x_2x_3 + 0,0000625x_1x_2x_3 \quad (\text{Eq. 9})$$

9. Equations for cadmium content of sugar beet of the first degree of infection:

$$y_9 = 0,0026875 - 0,0006625x_1 - 0,0002125x_2 + 0,0000875x_3 - 0,0003625x_1x_2 - 0,0000125x_1x_3 + 0,0000125x_2x_3 + 0,00000125x_1x_2x_3 \quad (\text{Eq. 10})$$

10. Equations for the content of aflatoxin sugar beet first degree of infection:

$$y_{10} = 0,012625 - 0,000625x_1 - 0,0001125x_2 - 0,000875x_3 + 0,000125x_1x_2 - 0,000125x_1x_3 - 0,000125x_2x_3 + 0,000125x_1x_2x_3 \quad (\text{Eq. 11})$$

11. Equations for the content of sugar beet mold of the first degree of infection:

$$y_{11} = 16,625 - 0,875x_1 - 3,375x_2 + 1,625x_3 - 4,375x_1x_2 - 1,875x_1x_3 + 3,125x_2x_3 - 1,875x_1x_2x_3 \quad (\text{Eq. 12})$$

12. The equations for the content of sugar beet yeast of the first degree of infection:

$$y_{12} = 14,875 - 2,875x_1 - 0,625x_2 + 1,125x_3 + 0,625x_1x_2 - 0,125x_1x_3 + 0,125x_2x_3 + 2,875x_1x_2x_3 \quad (\text{Eq. 13})$$

here:

b – regression equation coefficient

x_1 – ozone concentration, g/m³
 x_2 – ozone treatment time, min
 x_3 – overpressure (cavitation), ati
 y_1 - moisture, %
 y_2 - dry matter, %
 y_3 - acidity, %
 y_4 - pectin substance, %
 y_5 - cellulose, %
 y_6 - sucrose, %
 y_7 - nitrates, mg/kg
 y_8 - Pb – mg/kg
 y_9 - Cd – mg/kg
 y_{10} - aflatoxin, mg/kg
 y_{11} - mold, CFU/g
 y_{12} - yeast, CFU/g

After decoding the independent variables in the equations, regression equations are obtained for natural factors (Eq. 14-16):

1. To determine the acidity of sugar beets of the Koksú sugar factory of the first degree of infection:

$$y_3 = 3,39742947 + 0,2471232x_1 + 0,671098x_2 - 0,05036x_3 + 0,025x_1x_2 - 0,225x_1x_3 + 0,075x_2x_3 - 0,09673x_1^2 + 0,150235x_2^2 - 0,09673x_3^2 \quad (\text{Eq. 14})$$

2. To determine the sucrose content of sugar beets of the Koksú sugar factory of the first degree of infection:

$$y_6 = 2,42959795 + 0,2878224x_1 + 0,247416x_2 + 0,264398x_3 - 0,2125x_1x_2 + 0,1875x_1x_3 - 0,1125x_2x_3 - 0,0213x_1^2 + 0,031623x_2^2 + 0,119823x_3^2 \quad (\text{Eq. 15})$$

3. To determine the mold content of sugar beet of the Koksú sugar factory of the first degree of infection:

$$y_{11} = 18,9442368 + 0,02928x_1 - 0,22253x_2 - 0,46848x_3 + 0,25x_1x_2 - 0,25x_1x_3 - 1,5x_2x_3 + 1,057466x_1^2 - 0,35373x_2^2 + 1,410266x_3^2 \quad (\text{Eq. 16})$$

here:

x_1 – ozone concentration, g/m³
 x_2 – ozone treatment time, min
 x_3 – overpressure (cavitation), ati
 y_3 - acidity, %
 y_6 - sucrose, %
 y_{11} - mold, CFU/g

Thus, given that $F_p < F_{table}$ The model of technological process efficiency can be considered adequate with a 95% confidence probability.

4. CONCLUSIONS

After the canonical transformation of second-order models, canonical regression equations were obtained, values of optimization parameters were calculated on a Microsoft Excel word processor computer, on the basis of which a model was constructed in three-dimensional space, which is a plane that characterizes the dependence of ozone concentration (g/m³), overpressure (ati), processing time, which affect optimization criteria - acidity (degrees), sucrose content (%) and mold content (CFU/g) at 20 °C.

Rotatable planning of the second-order sugar beets of the Koksú sugar factory of the first degree of infection are shown in Table 5.

Based on second-order rotatable planning, a regression equation is obtained for coded, natural factors. The regimes of ozone processing of sugar beet have been optimized in terms of acidity, sugar content, and mold of the first degree of sugar beet infection in the Koksú sugar factory. The results of the study are shown in Figures 2-10.

The analysis of three-dimensional spatial models shows, which are presented in Figures 2-10, that the necessary values of the optimization criterion "y" are achieved in the search area under consideration. This means that the levels of variation of input factors in the design of experiments are accepted quite correctly.

An analysis of the behavior of the obtained three-dimensional surface showed that the following parameters are optimal zones for processing sugar beets:

- when processing with an ozone concentration of 6-8 g/m³, an overpressure of 6-8 ati for 15-20 minutes, the acid content ranges from 0 to 3 degrees;
- when processing with an ozone

concentration of 6-8 g/m³ and an excess pressure of 4-6 at for 10-15 minutes, the sucrose content is 3-10%;

- when processed with an ozone concentration of 6-8 g/m³ for 15-20 minutes, the mold content ranges from 0 to 5 CFU/g.

The analysis of the presented graphs showed that in the three-dimensional model in space there are optimal regions of variable values of ozone concentration (g/m³), overpressure (at), processing time — the values at which sugar beet is processed with optimal acidity (degrees), content sucrose (%) and mold content (CFU/g).

Based on the analysis and comparison of the values, it is possible to recommend generalizing operating parameters of ozone treatment time 15 min, pressure 4 at, ozone concentration of 6 g/m³, which leads to the death of sugar beet microorganisms of the first degree of infection.

The above dependences on the variable parameters of sugar beet processing by ozone flow in the cavitation zone (overpressure) make it possible to predict with sufficient accuracy the change in the values of the optimization criteria in the studied range of factors – acidity (deg), sucrose content (%) and mold content (CFU/g). At the same time, it is possible to establish the dominant influence of each studied factor on the optimization criterion of the process, which allows us to describe with sufficient approximation the optimal processing conditions for sugar beet of the first degree of infection. The results obtained will allow us to optimize the process under study by applying the developed mathematical model.

As a result of the study, it was found that for the storage of raw sugar production, it is necessary to use ozone treatment in the cavitation zone (overpressure). It has been scientifically proven that ozone treatment significantly reduces the growth of mold and yeast, contributes to an increase in the content of pectin, fiber and sucrose while ensuring the safe storage of raw sugar products.

5. REFERENCES

1. Alimkulov, Z., Zhiyenbayeva, S., Muldabekova, B., Batyrbayeva, N. Rational use of wastes from plant products processing. *Bulgarian Journal of Agricultural Science*, **2014**, 20 (3), 532-535.
2. Apasov, I.V., Fomenko, G.K., Putilina, L.N. Efficacy of drugs to increase the safety of sugar beets during storage. *J. Sugar*, **2011**, 4, 37-39.
3. Bugaenko, I.F. The basics of sugar production. M.: International Sugar Company, **2002**, 332.
4. Erkmen, O. Uses of Ozone to Improve the Safety and Quality of Foods. *J. Gıda Teknolojisi*, **2001**, 5 (3), 58–64.
5. Gagkaeva, T. Yu., Levitin, M.M. Current state of mushroom taxonomy of the Gibbe-rella-fujikuroi complex. *J. Mycology and phytopathology*, **2005**, 39(6), 1-14.
6. GOST 26669-85. Food-stuffs and food additives. Preparation of samples for microbiological analyses. M.: Standartinform, **2010**, 66-74.
7. GOST 26670-91. Food products. Methods for cultivation of microorganisms. M.: Standartinform, **2018**, 1-7.
8. GOST 28561-90. Fruit and vegetable products. Methods for determination of total solids or moisture. M.: Standartinform, **2011**, 1-9.
9. GOST 28562-90. Fruit and vegetable products. Refractometric method for determination of soluble dry substances content. M.: Standartinform, **2011**, 166-176.
10. GOST 29059-91. Products of fruit and vegetables processing. Titration method for pectic substances determination. M.: Standartinform, **2011**, 198-202.
11. GOST 30178-96. Raw material and food-stuffs. Atomic absorption method for determination of toxic elements. M.: Standartinform, **2010**, 24-32.
12. GOST 10444.12-2013. Microbiology of food and animal feeding stuffs. Methods for the detection and colony count of yeasts and moulds. M.: Standartinform, **2014**, 1-9.
13. GOST ISO 750-2013. Fruit and vegetable products. Determination of titratable acidity. M.: Standartinform, **2014**, 1-7.
14. Islamgulov, D.R., Ismagilov, R.R., Bikmetov, I.R. Doses of nitrogen fertilizers and technological qualities of root crops. *J. Sugar beet*, **2013**, 3, 17-19.
15. Iztayev, A., Urazaliev, R., Yakiyayeva, M., Maemerov, M., Shaimerdenova, D., Iztayev, B., Toxanbayeva, B., Dauletkeidi, Ye. The investigation of the impact of dynamic deterioration of ozone on grass

- growth and the consequence of ion-ozone cavitation treatment. *Journal of Advanced Research in Dynamical and Control Systems*, **2018**, 10(13), 663-671.
16. Iztayev A., Yakiyayeva M., Kulazhanov T., Kizatova M., Maemerov M., Stankevych, G., Toxanbayeva B., Chakanova Zh. Controlling the implemented mathematical models of ion-ozone cavitation treatment for long-term storage of grain legume crops. *Journal of Advanced Research in Dynamical and Control Systems*, **2018**, 10(13), 672-680.
 17. Iztayev, A., Kulazhanov, T., Yakiyayeva, M., Maemerov, M., Iztayev, B., Mamayeva, L. The Efficiency of Ionocavitation Processing and Storage in the Nitrogen Medium of Oilseeds. *Journal of Advanced Research in Dynamical and Control Systems*, **2018**, 10 (7), 2032–2040.
 18. Karpov, B.A. Technology for post-harvest processing and storage of sugar beets. M.: Agropromizdat, **2007**, 177.
 19. Kim, J. G., Yousef, A. E., Khadre, M. A. Ozone and its Current and Future Application in the Food Industry. *J. Advances in Food and Nutrition Research*, **2003**, 45, 167–218.
 20. Krylov, M.I. Storage of sugar beets. M.: Agropromizdat, **2006**, 77.
 21. Lichko, N.M., Kudrin, V.N., Eliseeva, L.G. Technology of crop production processing. M.: Kolos, **2000**, 552.
 22. Loel, J., Kenter, K., Märlander, B., Hoffmann, C.M. Assessment of breeding progresses in sugar beet by testing old and new varieties in greenhouse and field conditions. *European Journal of Agronomy*, **2014**, 52, 146–156.
 23. Luterbacher, M.C., Asher, M.J.C., Beyer, W., Mandolino, G., Scholten, O.E., Frese, L., Biancardi, E., Stevanato, P., Mechelke, W., Slyvchenko, O. Sources of resistance to diseases of sugar beet in related Beta germplasm: II. Soil-borne diseases. *Euphytica*, **2005**, 141, 49–63.
 24. Manzhesov, V.I., Popov, I.A., Shchedrin, D.S. Storage technology for crop production: a training manual. Voronezh: FGOU VPO VGU, **2009**, 249.
 25. Martindale, W. The sustainability of the sugar beet crop — the potential of add value. *British Sugar Beet Review*, **2013**, 81, 49–52.
 26. Ober, E. S., Rajabi, A. Abiotic stress in sugar beet. *J. Sugar Tech*, **2010**, 12, 294–298.
 27. Podporinova, G.K., Smirnov, M.A., Putilina, L.N. On the question of the safety of root crops in piles. *J. Sugar beet*, **2010**, 7, 35-37.
 28. Richardson, D. P. Functional Food and Health Claims. *J. The world of Functional ingredients*, **2002**, 9, 12–20.
 29. Sanitary and epidemiological rules and regulations SanERandR 2.3.2.1078-01. Hygienic requirements for food safety and nutritional value. approved by the Chief State Sanitary Doctor of the Russian Federation 06.11.2001.
 30. Saprionov N.M. Harvesting and storage of sugar beets: organizational, technological innovation. *J. Sugar*, **2007**, 8, 24-30.
 31. Saprionov, N. M., Berdnikov, A.S., Kosulin, G.S. Storage of sugar beets of modern hybrids using multifunctional preservatives. *J. Sugar production*, **2011**, 8, 26-28.
 32. Saprionov, N. M., Berdnikov, A.S., Kosulin, G.S. Storage of sugar beets in field blades under a polymer cover of multifunctional action. *J. Herald of the Russian Academy of Agricultural Sciences*, **2014**, 6, 73-74.
 33. Shkalikov, V. A. Plant protection against diseases. M.: Kolos, **2010**, 404.
 34. Shpaar, D., Dreger, D., Zakharenko, A. Sugar beet. Minsk.: FUAinform, **2000**, 258.
 35. Stevanato, P., Chiodi, C., Broccanello, Ch., Concheri, G., Biancardi, E., Pavli, O. Sustainability of the Sugar Beet Crop. *J. Sugar Tech*, **2019**, 21(5), 703–716.
 36. Stognienko, O. I., Shamin, A. A. Biotic and abiotic factors in the development of rotten sugar beetroot crops. *J. Sugar beet*, **2012**, 5, 29-32.
 37. Timoshenko N.V. and others. Determination of crude fiber in food products using the FIWE extraction apparatus. Krasnodar: KubSAU, **2006**, 9.
 38. Tolemissova, Z. E., Alimkulov, Z. S. Research of product management quality of feed milling plants of the Republic of Kazakhstan. *International Journal of Mechanical Engineering and Technology*, **2017**, 8(11), 1126-1132.
 39. Trisvyatsky, L.A., Lesik, G.V., Kudrina, V.N. Storage, and technology of agricultural products. M.: Agropromizdat, **1991**, 415.
 40. Vertush, A.N. Ways of intensification of sugar beet production. Minsk.: Unipak, **2002**, 109.

41. Weststrat, J. A., van Poppel, G., Verschuren, P. M. Functional foods, trends, and future. *British Journal of Nutrition*, **2002**, 88(S2), S233–S235.
42. Yakiyayeva, M., Iztaev, A., Kizatova, M., Maemerov, M., Iztaeva, A., Feydengold, V., Tarabaev, B., Chakanova, Zh. Influence of ionic, ozone ion-ozone cavitation treatment on safety of the leguminous plants and oil-bearing crops at the storage. *Journal of Engineering and Applied Sciences*, **2016**, 11(6), 1229-1234.

Table 1. Coding of intervals and levels of variation of input factors

Indicators	Coded value	Factors and their dimension		
		x ₁ – ozone concentration, g/m ³	x ₂ – ozone processing time (min)	x ₃ – overpressure, ati
Upper level	+	6	20	4
Zero level	0	4,5	15	3
Lower level	-	3	10	2
Range of variation		1,5	5,0	1

Table 2. The results of full-factor experiments of type 2³ – sugar beet Koksú sugar factory of the first degree of infection

Experience number	Planning				Indicators											
	x ₀	x ₁ – ozone concentration, g/m ³	x ₂ – ozone treatment time (min)	x ₃ – Overpressure, ati	y ₁ – Moisture, %	y ₂ – dry matter, %	y ₃ – Acidity, %	y ₄ – Pectin substance, %	y ₅ – cellulose, %	y ₆ – Sucrose, %	y ₇ – Nitrates, mg/kg	y ₈ – Pb – mg/kg	y ₉ – Cd – mg/kg	y ₁₀ – Aflatoxin, mg/kg	y ₁₁ – Mold, CFU g	y ₁₂ – Yeast, CFU/g
1	+	6	15	4	75,07	24,93	3,4	4,52	3,72	2,55	562,5	0,0646	0,0015	0,010	9	16
2	+	3	15	4	79,24	20,76	1,1	4,78	5,62	1,5	521,3	0,0492	0,0036	0,011	27	15
3	+	6	5	4	80,76	19,24	6,4	9,79	9,84	2,2	562,1	0,0689	0,0027	0,012	22	10
4	+	3	5	4	78,67	21,33	3,5	4,37	5,14	3,25	556,3	0,0594	0,0033	0,014	15	23
5	+	6	15	2	74,5	25,2	3,3	4,6	3,75	2,52	562,2	0,0643	0,0014	0,012	7	8
6	+	3	15	2	78,4	21,6	1,2	4,82	5,69	1,47	520,3	0,0489	0,0034	0,013	10	18
7	+	6	5	2	80,32	19,68	6,5	9,85	9,92	2,18	561,7	0,0689	0,0025	0,014	25	14
8	+	3	5	2	78,2	21,8	3,6	4,42	5,23	3,21	556,9	0,0589	0,0031	0,015	18	15

$$y_1 = f_1(x_1, x_2, x_3), \quad y_2 = f_2(x_1, x_2, x_3), \quad y_3 = f_3(x_1, x_2, x_3), \dots, \quad y_{12} = f_{12}(x_1, x_2, x_3)$$

Table 3. The matrix of rotatable planning experimental studies of processed sugar beets

Coefficients	y ₁	y ₂	y ₃	y ₄	y ₅	y ₆	y ₇	y ₈	y ₉	y ₁₀	y ₁₁	y ₁₂
b₀	78,145	21,8175	3,625	5,89375	6,11375	2,36	550,4125	0,0603875	0,0026875	0,012625	16,625	14,875
b₁	-0,4825	0,445	1,275	1,29625	0,69375	0,0025	11,7125	0,0062875	-0,0006625	0,000625	0,875	2,875
b₂	-1,3425	1,305	-1,375	1,21375	1,41875	-0,35	8,8375	0,0036375	0,0002125	0,001125	3,375	0,625
b₃	0,29	-0,2525	-0,025	-0,02875	-0,03375	0,015	0,1375	0,0001375	0,0000875	-0,000875	1,625	1,125
b₁₂	-1,535	1,4975	-0,175	1,41625	1,65375	0,5225	9,0625	0,0014125	-0,0003625	0,000125	-4,375	0,625
b₁₃	-0,0375	0,075	0,025	-0,00625	0,00625	-0,0025	0,0375	-6,25E-05	-0,0000125	-0,000125	1,875	-0,125
b₂₃	0,0625	-0,025	0,025	-0,00125	0,00875	0	0,1875	1,25E-05	-0,0000125	-0,000125	3,125	0,125
b₁₂₃	-0,03	0,0675	0,025	-0,00375	0,00375	0,0025	-0,2125	6,25E-05	-1,25E-05	0,000125	-1,875	2,875

Table 4. The coefficients of the regression equations of the output parameters

Optimization criterion	Coefficients	Process
Acidity	With coded factor values	
	b_0	3,397429472
	b_1	0,2471232
	b_2	0,6710976
	b_3	-0,0503616
	b_{12}	0,025
	b_{13}	-0,225
	b_{23}	0,075
	b_{11}	-0,09672538
	b_{22}	0,150234624
	b_{33}	-0,09672538
	With natural factors	
	B_0	-1,7968
	B_1	0,826237728
	B_2	-0,12106203
	B_3	1,173441408
	B_{12}	0,0025
	B_{13}	-0,1125
	B_{23}	0,01500
	B_{11}	-0,02418134
	B_{22}	0,006009385
	B_{33}	-0,09672538
	F_p	4,739616678
Sucrose content	With coded factor values	
	b_0	2,429597952
	b_1	0,2878224

	b_2	0,247416
	b_3	0,2643984
	b_{12}	-0,2125
	b_{13}	0,1875
	b_{23}	-0,1125
	b_{11}	-0,02129722
	b_{22}	0,031622784
	b_{33}	0,119822784
	With natural factors	
	B_0	0,7639
	B_1	0,151552848
	B_2	0,229035859
	B_3	-0,91918387
	B_{12}	-0,02125
	B_{13}	0,09375
	B_{23}	-0,02250
	B_{11}	-0,0053243
	B_{22}	0,001264911
	B_{33}	0,119822784
	F_p	1,927073998
Mold content	With coded factor values	
	b_0	18,9442368
	b_1	0,02928
	b_2	-0,222528
	b_3	-0,46848
	b_{12}	0,25
	b_{13}	-0,25
	b_{23}	-1,5
	b_{11}	1,0574656
	b_{22}	-0,3537344
	b_{33}	1,4102656
	With natural factors	
	B_0	31,5457
	B_1	-3,0327568
	B_2	1,42997568
	B_3	-6,5006048
	B_{12}	0,025
	B_{13}	-0,125
	B_{23}	-0,30000
	B_{11}	0,2643664
	B_{22}	-0,01414938
	B_{33}	1,4102656
	F_p	0,962853903

Table 5. Rotatable planning of the second order acidity of sugar beets of the Koksú sugar factory of the first degree of infection

Name of indicators		x_1	x_2	x_3
Lower levels of factors	(-1)	4	10	3
Upper Factor Levels	(+1)	8	20	5
Main factor levels	(0)	6	15	4
Factor Variation Levels		2	5	1
Relationship		3	3	4

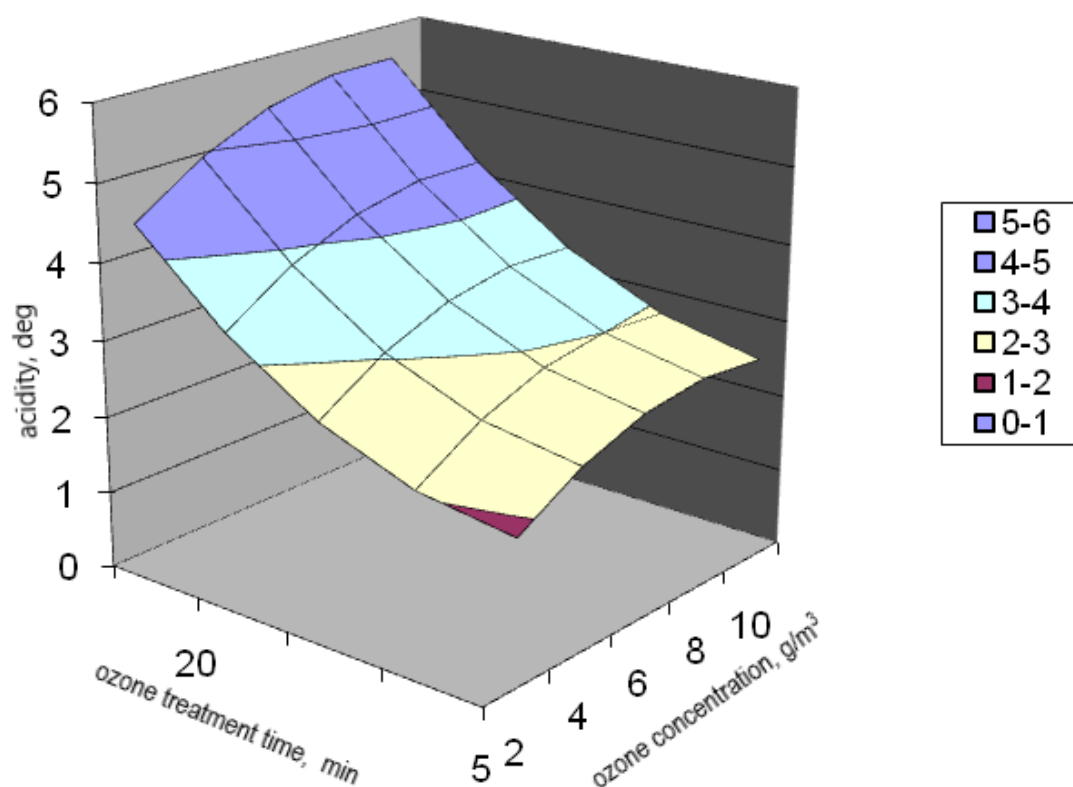


Figure 2. Changes in the acidity content of sugar beets of the Koksú sugar factory of the first degree of infection, depending on the ozone concentration and processing time

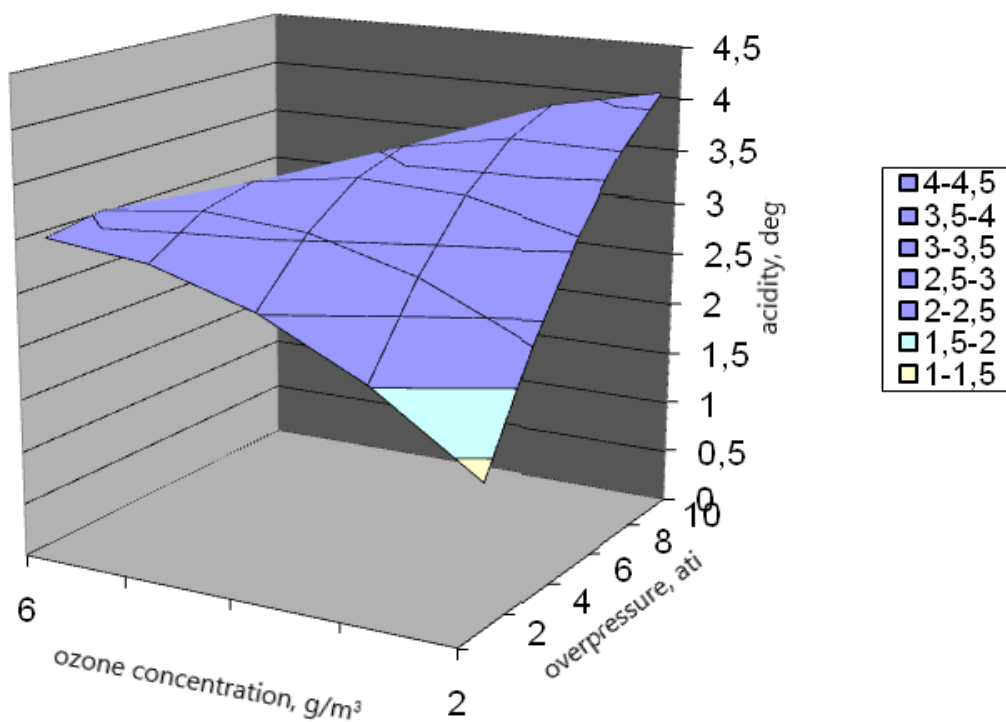


Figure 3. Changes in the acidity content of sugar beets of the Koksú sugar factory of the first degree of infection, depending on the concentration of ozone and pressure concentration

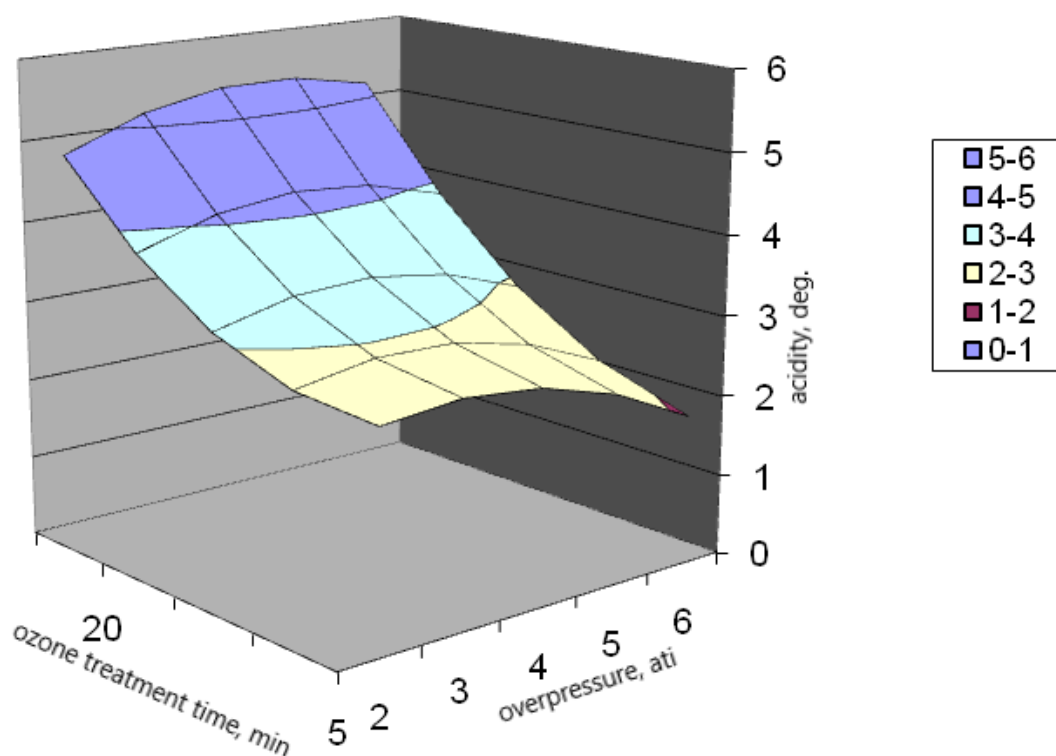


Figure 4. Changes in the acidity content of sugar beets of the Koksú sugar factory of the first degree of infection, depending on the concentration of pressure and processing time

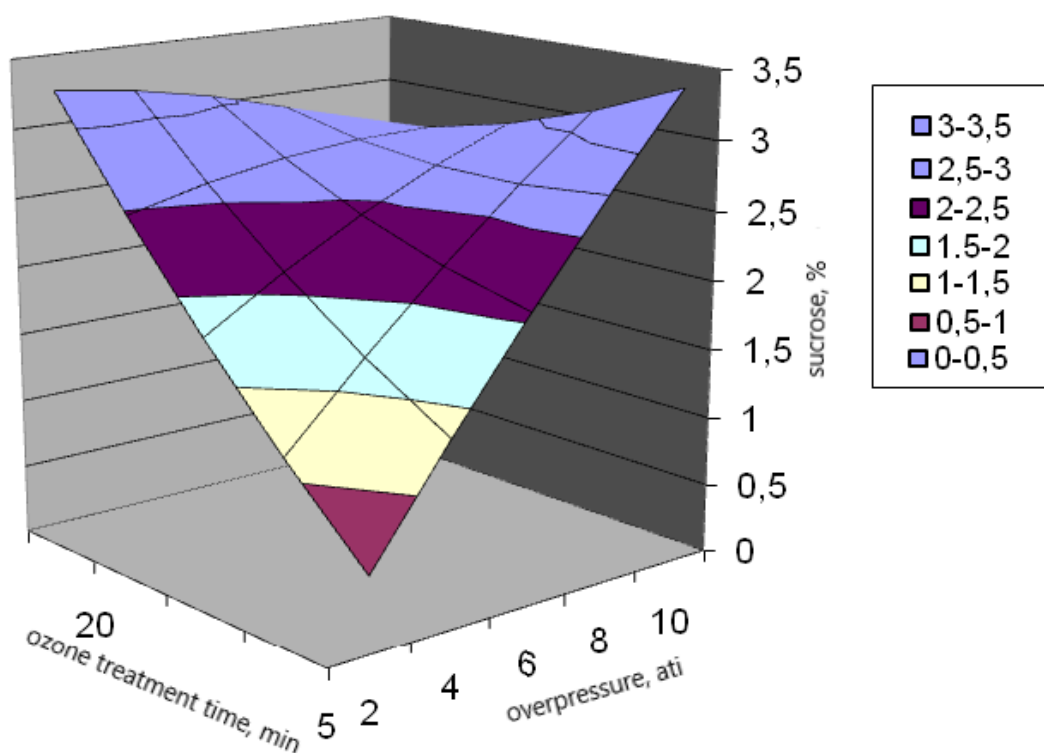


Figure 5. Changes in the sucrose content of sugar beets of the Koksú sugar factory of the first degree of infection, depending on the concentration of pressure and processing time

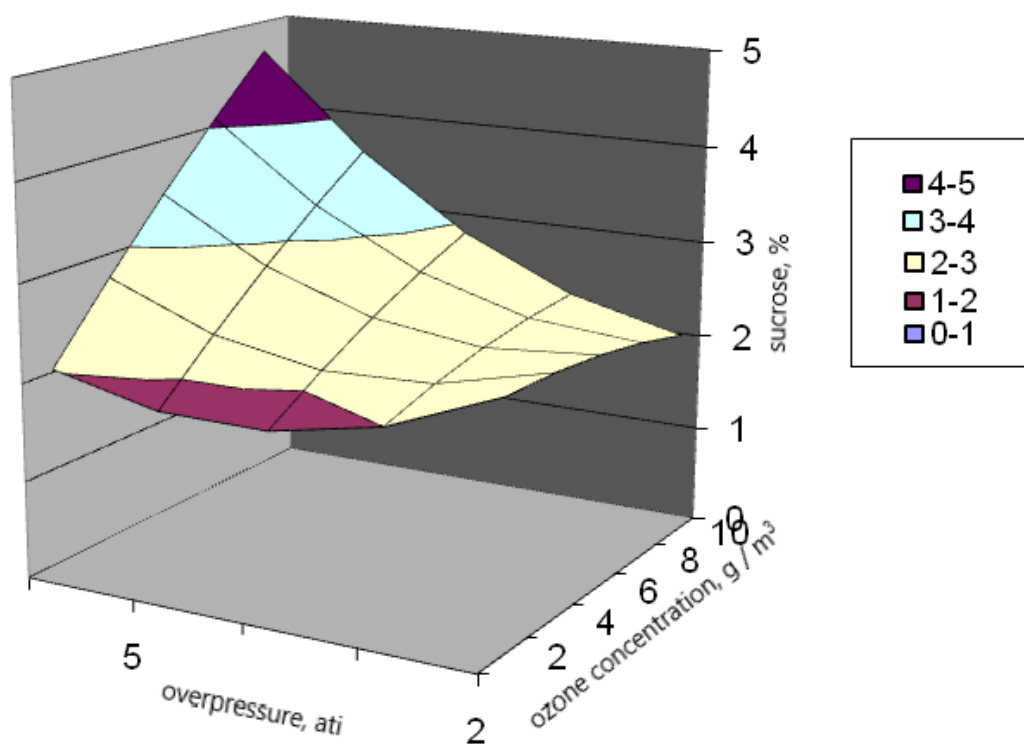


Figure 6. Changes in the sucrose content of sugar beets of the Koksú sugar factory of the first degree of infection, depending on ozone concentration and pressure

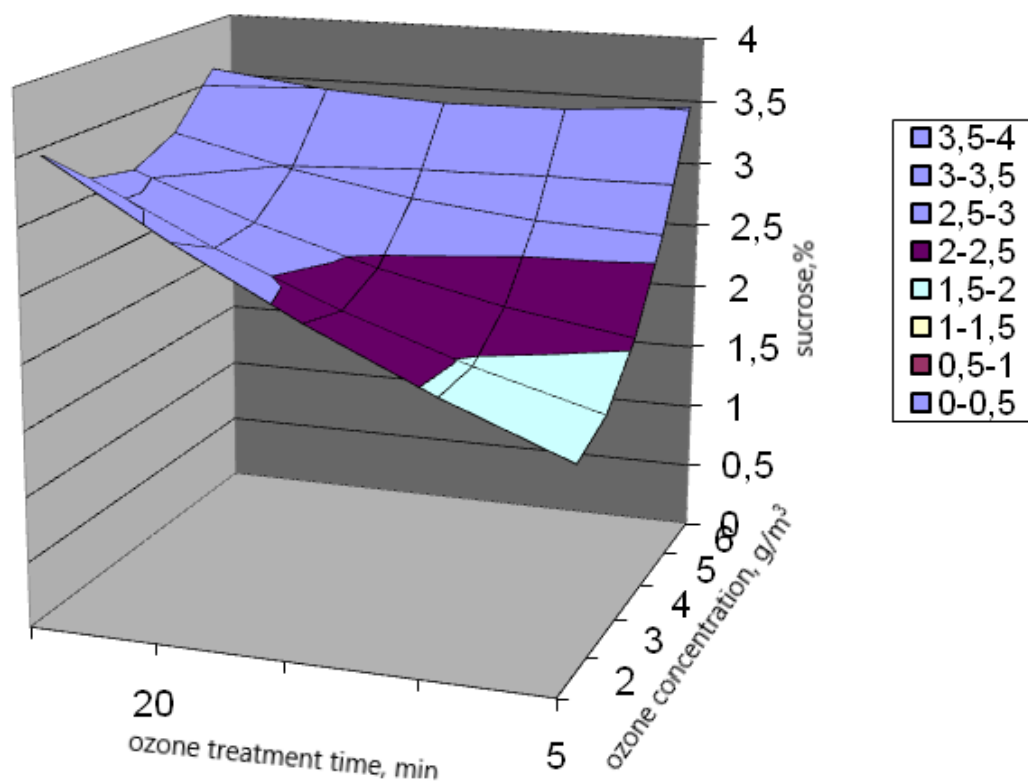


Figure 7. Changes in the sucrose content of sugar beets of the Koksú sugar factory of the first degree of infection, depending on the ozone concentration and processing time

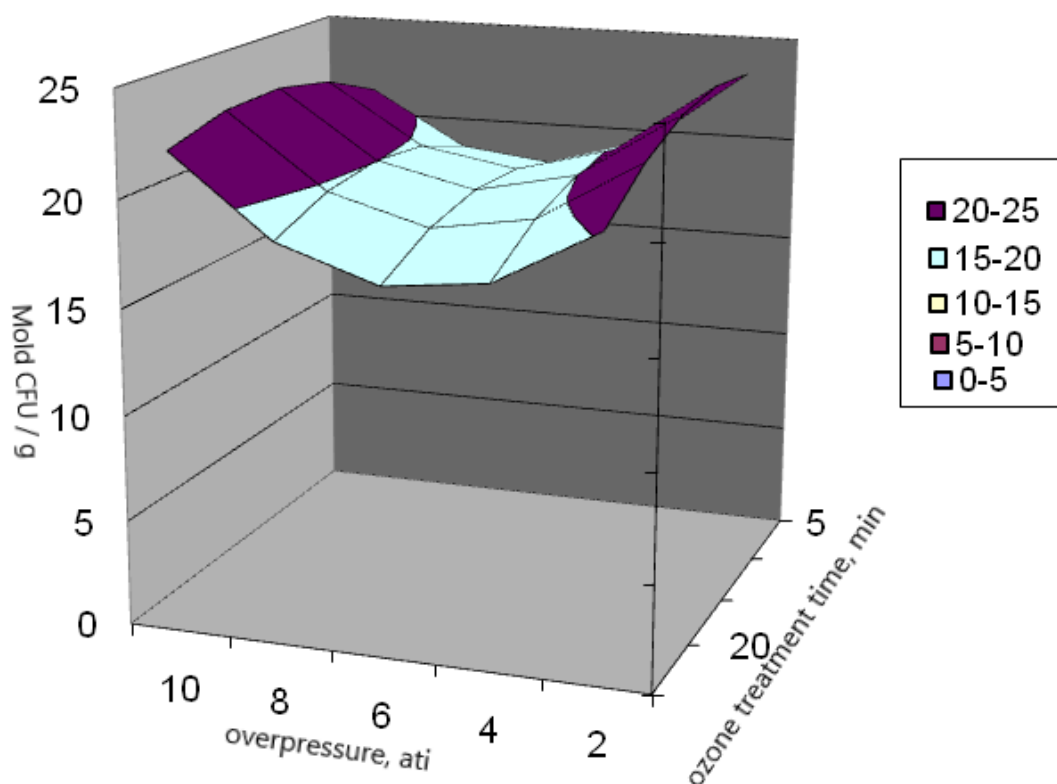


Figure 8. Changes in mold content of sugar beet of the Koksú sugar factory of the first degree of infection, depending on the concentration of overpressure and processing time

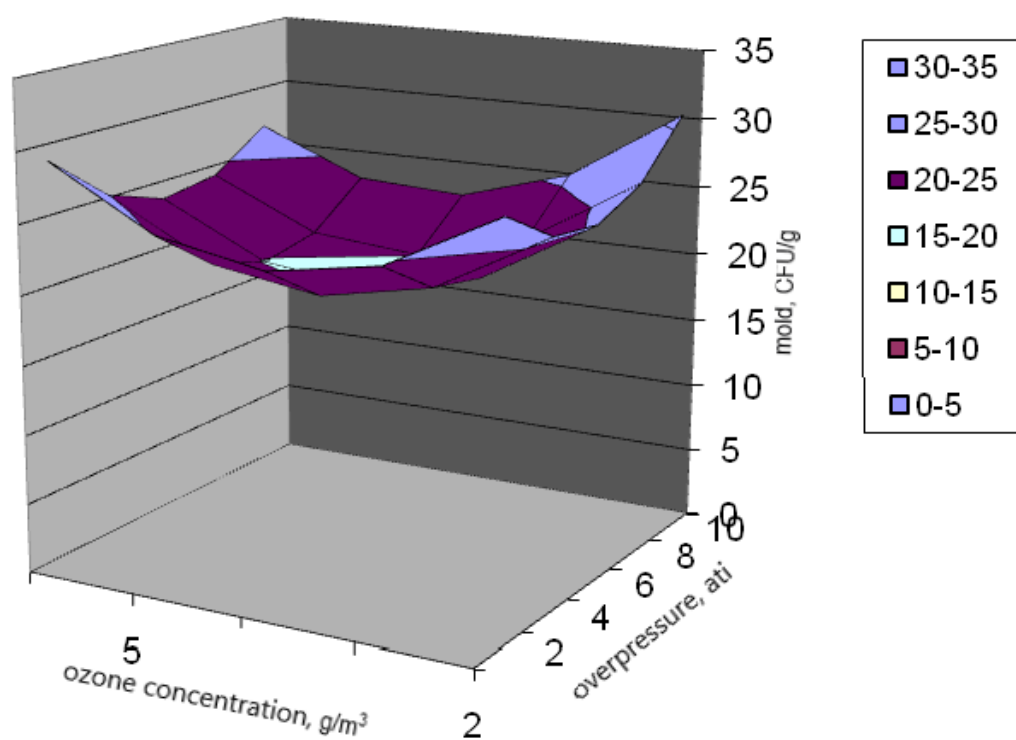


Figure 9. Changes in mold content of sugar beet of the Koksú sugar factory of the first degree of infection, depending on the concentration of ozone and overpressure

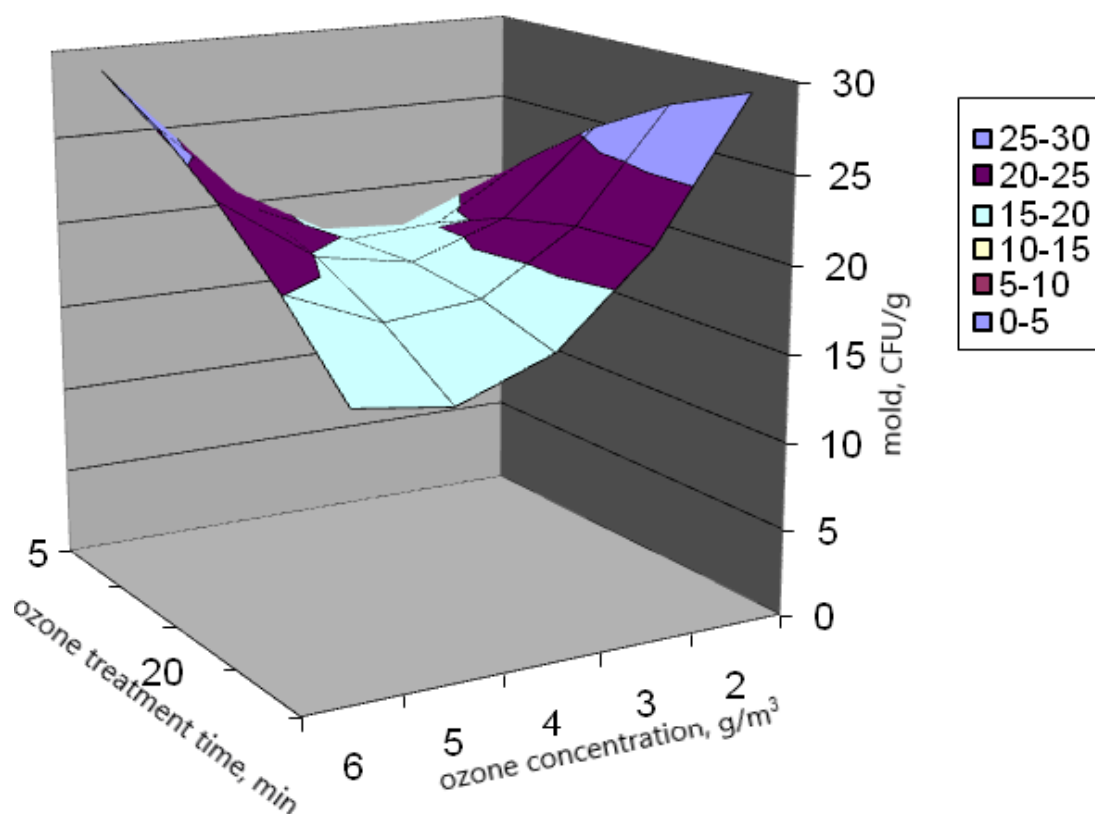


Figure 10. Changes in mold content of sugar beet of the Koksú sugar factory of the first degree of infection, depending on the concentration of ozone and the processing time

MÉTODO DE VALIDAÇÃO PARA DETERMINAÇÃO DE INSETICIDAS ORGANOCLORADOS EM GINSENG USANDO A CROMATOGRAFIA GASOSA ACOPLADA À ESPECTROMETRIA DE MASSA DE DILUIÇÃO ISOTÓPICA (ID-GC-MS)

METHOD VALIDATION FOR ORGANOCHLORINE INSECTICIDES DETERMINATION IN GINSENG BY USING ISOTOPE-DILUTION GAS CHROMATOGRAPHY-MASS SPECTROMETRY (ID-GC-MS)

ARISTIAWAN, Yosi^{1*}; PUTRI RAMADHANINGTYAS, Dillani²; KOMALASARI, Isna³; STYARINI, Dyah⁴; HAMIM, Nuryatini⁵

^{1,5} Badan Standardisasi Nasional, Pusat Riset dan Pengembangan Sumber Daya Manusia

² Lembaga Ilmu Pengetahuan Indonesia, Pusat Penelitian Kimia

^{3,4} Badan Standardisasi Nasional, Direktorat Standar Nasional Satuan Ukuran Termoelektrik dan Kimia

* Corresponding author
e-mail: yosi@bsn.go.id

Received 20 December 2019; received in revised form 21 February 2020; accepted 18 March 2020

RESUMO

Os inseticidas organoclorados ainda são explorados entre os pesticidas mais importantes para fins de proteção de plantas. Conhecidos por serem perigosos para o ser humano e persistentes no meio ambiente, é necessário criar um método preciso para detectar inseticidas organoclorados em alimentos e substâncias ambientais. A espectrometria de massa por cromatografia em fase gasosa de diluição isotópica (ID-GC-MS) é um sistema de medição de acoplamento versátil e método de alta ordem que combina seletividade, sensibilidade e alta precisão. O presente trabalho tem como objetivo mostrar a metodologia da determinação de inseticidas organoclorados (alfa-HCH e gama-HCH) no ginseng usando ID-GC-MS. O método descrito abrangeu a preparação de amostras usando extração com solvente orgânico (hexano), seguido de limpeza com florisil. Após a reconstituição da base de solvente, a medição foi realizada usando ID-GC-MS no parâmetro ideal do instrumento. Usando as condições ideais determinadas, os parâmetros como sensibilidade, linearidade, precisão e exatidão foram estudados para validação do método ID-GC-MS. O limite de detecção e o limite de quantificação do instrumento foram de 0,5 ng/g e 2,0 ng/g para os dois analitos. O método mostrou linearidade com o coeficiente de correlação de 0,999 para alfa-HCH e gama-HCH na faixa de concentração de 1 - 300 ng/g. A precisão variou de 3,0 a 3,7% e 2,4 a 3,3% para alfa-HCH e gama-HCH, respectivamente. As recuperações médias para alfa-HCH e gama-HCH foram encontradas em 98,0 e 95,6%, respectivamente. Após a validação do método, a incerteza de medição da determinação de alfa-HCH e gama-HCH foi avaliada de acordo com o guia EURACHEM GUM com nível de confiança de 95% ($k = 2$). A incerteza expandida na medição de alfa-HCH e gama-HCH foi de 5,4% e 8,2%, respectivamente. Todos esses parâmetros demonstram alta sensibilidade do método oferecido e o sucesso do método descrito na determinação de alfa-HCH e gama-HCH na amostra de ginseng.

Palavras-chave: química analítica, análise orgânica, pesticidas, padrão interno, cromatografia em fase gasosa

ABSTRACT

Organochlorine insecticides are still exploited among the most prominent pesticides for plant protection purposes. Known for having hazardous to humans and persistent in the environment properties, it is necessary to build an accurate method for detecting organochlorine insecticides in food and environmental substances. Isotope-dilution gas chromatography-mass spectrometry (ID-GC-MS) is a versatile coupling measurement system and high order method that combines both selectivity, sensitivity and high accuracy. The present paper aims at showing the methodology of the organochlorine insecticides (alpha-HCH and gamma-HCH) determination in ginseng by using ID-GC-MS. The described method covered sample preparation using an organic solvent (hexane) extraction, followed by florisil cleaning-up. After the reconstitution of the solvent base, the measurement was conducted by using ID-GC-MS in the optimal instrument parameter. Using the determined optimal conditions, the parameters such as sensitivity, linearity, precision, and accuracy were studied for validation of the ID-GC-MS method. The limit of detection and the limit of quantitation of the instrument were 0.5 ng/g and 2.0 ng/g for both

analytes. The method showed linearity with the correlation coefficient of 0.999 for both alpha-HCH and gamma-HCH over the concentration range of 1–300 ng/g. The precision ranged from 3.0 to 3.7% and 2.4 to 3.3% for alpha-HCH and gamma-HCH, respectively. The mean recoveries for alpha-HCH and gamma-HCH were found at 98.0 and 95.6%, respectively. Following method validation, the measurement uncertainty of the alpha-HCH and gamma-HCH determination was evaluated according to EURACHEM GUM guide at a 95 % confidence level ($k = 2$). The expanded uncertainty in the measurement of alpha-HCH and gamma-HCH was 5.4% and 8.2%, respectively. All these parameters demonstrate the high sensitivity of the offered method and the success of the described method in the determination of alpha-HCH and gamma-HCH in ginseng sample.

Keywords: *analytical chemistry, organic analysis, pesticides, internal standard, gas chromatography*

1. INTRODUCTION:

A pesticide is any substance (or in the form of mixtures) from chemical or biological ingredients which are used to control, repel or destroy any pest, or to regulate the growth of the plant (FAO, 2013). The pests are avoided because they can harm during, or otherwise interfering with, the production, processing, storage, or marketing of food, agricultural commodities, wood and wood products, or animal feedstuffs, or which may be administered to animals for the control of insects, arachnids or other pests in or on their bodies (FAO, 2003).

The word pesticide is a parent term to cover all herbicides, fungicides, insecticides, wood preservatives, rodenticides, garden chemicals, and household disinfectants that may be used to destroy some pests (Zacharia & Tano, 2011; EPA, 2009). Insecticides are chemical compounds used in agriculture and are addressed to control and kill insects and related invertebrate pest species (Matsumura, 2009).

The organochlorine group is one class of insecticides that have been used around the world for centuries. Organochlorine pesticides include cyclodienes, DDT-type compounds, and hexachlorocyclohexane (HCH) isomers. Some organochlorine pesticides are members of persistent organic pollutants (POPs) and are classified as the chemicals targeted by the Stockholm Convention (UNEP, 2013). Initially, the use of the chlorinated hydrocarbons or organochlorines was as fire retardants and for dielectrics. As insecticides, the first use of these compounds occurred with the finding that the mixture of benzene and liquid chlorine killed insects in the field (Gupta and Milatovic, 2014).

HCH isomers, also called benzene hexachloride (BHC), are the most common halogenated organic insecticides that have been used for crop protection (Li, 1999; Vijgen, 2006; Simonich and Hites, 1995). The danger of HCHs is contributed by its lipophilic properties and persistence in the environment, causing possibly

bioaccumulated and biomagnified up in the food chain (Berntssen *et al.*, 2012). The residue of HCHs was found at quite significant concentration in soil, air, fish, and mammals because of the usage of HCHs for agricultural purpose (Liu and Meng, 2011; Gong *et al.*, 2004; Concha-Grana *et al.*, 2006; Lammel *et al.*, 2007; Fang *et al.*, 2017). In terms of toxicity for mammals, gamma-HCH is the most toxic, followed by the alpha-, delta-, and beta-isomers when it is acute exposure. Beta-HCH shows the most significant toxicity at the chronic exposure, followed by the alpha-, gamma-, and delta-HCH isomers (Jackovitz and Hebert, 2015). All HCH isomers can cause liver hyperplasia and liver tumors. The International Agency for Research on Cancer (IARC) classifies HCHs as carcinogenic to humans in the Group 2B category (Berntssen *et al.*, 2012). Related to this property, HCH is legally prohibited in many countries (historically since 1981 in the European countries). The use of HCHs has decreased in recent years. However, others, particularly developing countries, still advantage this compound for economic reasons.

With the use of insecticides in the agriculture field and or the existence of pesticides in water and soil, the plant or food is wide open to be contaminated to the compounds. The overall assessment in 12 vegetables and eight fruits is that 73 % contain pesticide residues (Baker *et al.*, 2002). Ginseng, as one of the agriculture commodities, has the same potential to contaminated. This is because ginseng, or its root as the central part in utilization, generally needs 4-6 years (depending on the type of ginseng) to grow and ready for harvest, adequate time for chemical contaminants such as insecticides accumulated in ginseng plant (Yun, 2001). Several papers reported the presence of HCHs and or other organochlorine pesticides in ginseng (Khan *et al.*, 2001; Durgnat *et al.*, 2005; Leung *et al.*, 2005; Lee and Jo, 2012).

Ginseng has a full-range application which is available in many forms and preparations such as fresh root, extracts, capsules, teas, cigarettes,

both alone and in combination with other ingredients. It also appears in Japan, China, Germany, France, Austria, and the UK Pharmacopoeias (Thompson Coon and Ernst, 2002). Ginseng roots as one of the most popular and expensive raw drugs have been advantaged to boost the quality of life (Ellis and Reddy, 2002; Coleman *et al.*, 2003).

Historically, ginseng was first cultivated around 11 BC and had a medical history (as a wild herb) stretching back more than 5000 years (Kennedy and Scholey, 2003). Immune system modulation, anti-stress activity, anti-cancer, anti-aging, a medicine for cardiovascular diseases, improvement of cognitive and physical performance, and sexual function and anti-diabetic activities are the most notable features of ginseng in laboratory and clinical practices (Vogler *et al.*, 1999; Shibata, 2001; Kiefer and Pantuso, 2003; O'Hara *et al.*, 1998). Therefore, rapid, effective, and validated methods for the determination of organochlorine insecticides residues in ginseng that can decrease the product value of ginseng are crucial needed. Moreover, accurate and precise measurements to detect hazard organic contaminants are requisite for ensuring appropriate diagnosis and essential decisions in trade consideration.

Gas Chromatography-Mass Spectrometry instrument is most commonly used to confirm and quantitate the residues of organochlorines in dried fruits, fat-rich cereals, herbal medicine, celery, rape, scallion and spinach (Surma *et al.*, 2014; Rasche *et al.*, 2015; Mao *et al.*, 2012; Zhang *et al.*, 2012;). Mass spectrometry (MS) detector is a powerful analytical tool that has been used successfully for detecting and identifying various volatile organic compounds. One trend in recent years related to the analysis based on MS is the development of isotope dilution mass spectrometry (ID-MS) technique. ID-MS is the optimum analytical method to obtain the accuracy of analytical results through the advantage of spiked target analyte isotope in the sample. By the addition of a known amount of a spike, the amount of analyte in the ID-MS technique is computed based on the change of the isotope ratio, the abundance ratio of two isotopes (Henrion, 1994).

In the analysis of organic and biomolecule compounds, labeled analytes are available commercially in the form of ^{13}C or ^2H (Rodríguez-González and Alonso, 2018). The equilibrium condition of natural and isotopic analyte provides a stable ratio between them in every sub-sample of the mixture along with the sample preparation. The loss during extraction, clean-up, evaporation

will not much affect the accuracy (Sargent *et al.*, 2002). Some successful works employing ID-MS in the determination of organic substances have been published in recent years both GC-based or LC-based (Goldschmidt and Wolf, 2010; Bi *et al.*, 2012; Huertas-Pérez *et al.*, 2019; Huertas-Pérez *et al.*, 2015; Bercaru *et al.*, 2006). However, the challenge in the analysis still presents due to the complex matrix and the shallow maximum residue limits (MRLs) in some regulations.

The goal of this study was to obtain a high order method by using ID-GC-MS for the determination of alpha-HCH and gamma-HCH residue in ginseng roots. The approach to evaluating the measurement uncertainty of the method is also described.

2. MATERIALS AND METHODS:

The organochlorine standard mixture (2000 mg/L), which was used in the validation study, was purchased from SUPELCO. Pure Certified Reference Material (CRM) of lindane was from NMIA, Australia (P1332) and the CRM for α -HCH was from NIST, USA (SRM 2275). The high purity isotope for both Lindane (CLM-1282-S) and α -HCH (CLM-2482-S) was obtained from Cambridge Isotopes Laboratory. The preparations of standard analytical solutions were done by using the gravimetric method.

MERCK supplied analytical grade acetonitrile (ACN), hexane, diethyl ether, florisil, and sodium chloride (NaCl). Sigma Aldrich provided magnesium sulphate (MgSO_4). Ultrapure water (18 MOhm) was produced by a Milli-Q Plus 185 (France).

2.1. Sample Preparation

All the sample preparation was conducted using gravimetric dilution. About 2 grams of ginseng sample was wetted by 10 mL of water for two hours. After two hours, 8 mL of acetonitrile was added to the mixture and the extraction using vortex was applied for 1 minute at room temperature. After the extraction, 4 grams of MgSO_4 and 1 gram of NaCl were added to the mixture and shake vigorously for 30 seconds before centrifuge for 5 minutes at 4000 rpm. A 1 mL of supernatant then filtered by using a 0.2 μm PTFE syringe filter before evaporation using nitrogen gas into dryness. The solid residue was reconstituted with 1 mL of n-hexane. The cleaning up process followed by using 1 gram of activated florisil with 10 mL of n-hexane/diethyl ether (85/15) mixture as eluent. The activated florisil was first

conditioned with n-hexane. The 10 mL of extract was then evaporated again by using nitrogen into dryness, followed by reconstitution with 1 mL of n-hexane. The sample was then ready to be injected into the GC/MS.

In the isotope-dilution experiment, the same treatment was applied, except the labeled standard (isotope solution) was spiked to the sample before the sample extraction step as in the conventional internal standard technique.

2.2. Conditions of GC-MS

A Gas Chromatography-Mass Spectrometry method was developed for their separation and detection. GC-MS was performed using GC Agilent 7890 tandem with MSD 5977A (United States). The chromatographic separation was carried out using an HP-5 MS UI (30 m x 0.250 mm x 0.25 µm). The temperature program was as follows: 70°C as initial temperature and held for 2 min; increased to 150°C at rate of 25°C/min without holding; ramped to 200°C at rate of 3°C/min without holding; and ramped to 280°C at rate of 8°C/min, hold for 10 min. The front inlet pressure was set at a constant flow of 1 mL/min, and 2 µL of sample solution was injected into the GC system. The total run time was 41.9 min. The MS transfer line temperature was held at 280°C.

Mass spectrometric parameters were configured as follows: electron impact ionization with 70 eV energy; ion source temperature, 230°C; MS quadrupole temperature, 150°C, and solvent delay 4 min. The MS system was continuously set in selective ion monitoring (SIM) mode, and each compound was quantified based on peak area using one target and two qualifier ion(s). Retention times of the analytes and complete SIM profile are shown in Table 1. Agilent Masshunter software was used for data processing.

2.3. Validation Method

Initially, the analytical method was validated by using external calibration technique. Linearity for all of the compounds in pure solvent was obtained by plotting the peak area from MS response against the concentration of the corresponding calibration standards between 1 and over 300 ng/g.

Limit of detection (LoD) and limit of quantification (LoQ) were estimated by performing serial dilution method of standard mix solution from the lowest calibration standard with signal to noise (S/N) of 3 and 10, respectively, and observed in 7 times experiment.

Precision was evaluated at two-level concentrations, 20 and 100 ng/g. The relative standard deviation (RSD), and also from the precision of the method, was calculated and compared to the Horwitz equation as the acceptance criteria.

The recovery study was conducted to assess the performance of an analytical procedure or sample preparation. The study was evaluated by spiking analysis, adding the known value to the sample, and measure the substantial value with the usual calibration curve. The authors reviewed the recovery in three different levels of spiking at 50, 300, and 800 ng/g.

After validation of the external calibration, the authors tested the performance of the ID-GC-MS method by checking the linearity firstly. In the ID-MS technique, the calibration curve will cover the plot between the ratio of the concentration of the analyte to concentration of internal standard and the ratio of the area of analyte to internal standard, where the isotope form of HCHs is the internal standard in this case. The HCHs concentration varied in the same range in the external calibration linearity while the isotope was guarded at a level of around 150 ng/g.

The recovery for the ID-GC-MS technique was also evaluated by analyzing CRM from KRISS (ginseng powder), compared the laboratory result with the CRM certificate value and expressed as the percent value.

The authors applied the ID-GC-MS technique to determine the HCHs concentration in the ginseng roots sample, below equation 1. The definition of each parameter in the equation is described in Table 2.

$$C_x = C_z * \frac{m_y * m_{zc}}{m_x * m_{yc}} * \frac{R_B}{R_{Bc}} * \frac{1}{f_d} \quad (\text{Eq. 1})$$

The technique is familiarly known as exact-matching ID-MS. This time-consuming method is capable of reaching a high accuracy result (Sargent *et al.*, 2002).

The evaluation of the measurement uncertainty was studied based on the Guide to the Expression of Uncertainty in Measurement (JCGM, 2008) to consider all parameters in equation 1 that significantly contribute to the account. Other possible sources of uncertainty such as precision (F_p) and different calibration blend (F_{CB}), are accounted for in the final uncertainty budget. The measurement uncertainty (U), which is the expanded uncertainty, was obtained by multiplying the combined standard

possibility of all parameters by a coverage factor, $k = 2$, which gives a confidence level of approximately 95%.

3. RESULTS AND DISCUSSION:

The GC part in this method previously was the developed method for pesticides in black tea analysis (Aryana *et al.*, 2016). Comparing the black tea method, there are minor modifications in this ginseng method due to the different compounds of pesticides and retention time area observation. The change includes the detector the authors employed in the study, which is a mass spectrometry detector, while in the prior research, the authors used μ ECD sensor. The method described in Section 2 gave a satisfying result as the standard mixture of organochlorine has good separation, as shown in Figure 1. The identity of the alpha-HCH and gamma-HCH was confirmed through selective ion monitoring (SIM) mode by the presence of two dominant ion fragments from their particular MS fragmentation within specific time windows. The relative ion intensities of the ions targeted in samples and calibration standards were matched as a confirmation.

The authors obtained LoD and LoQ by injecting HCHs standard solutions (in hexane) at low-level concentration. LoD and LoQ were defined based on the signal-to-noise ratio, higher than 3:1 and 10:1, respectively (Uhrovčík, 2014; NATA, 2006; EMEA, 2006). LoD was determined to be 0.5 ng/g, while LoQ was 2 ng/g for both analytes.

Linearity study was established by the least-squares linear regression analysis of the standard solution set from 1 to 300 ng/g and evaluated by assessing the coefficient of determination (r^2) using ANOVA data analysis ($P < 0.05$). For alpha-HCH and gamma-HCH, the r^2 -values were 0.9999 and 0.9997 respectively and the deviations of all data points in the calibration lines were lower than 10%, described in Figure 2.

Accuracy and precision of the present method were evaluated by recovery and repeatability experiments. Precision was checked by calculating the relative standard deviation (RSD) of the analytical results using standard mixture of 20 and 100 ng/g for each analyte. The experiments were carried out on intra-day observation. The standard mixture solutions at each concentration level was analyzed for five times. The results are listed in Table 3. The peak area of each compound was measured to determine the average values and the RSD (%).

As one of the parameters in the analytical method, recovery is an essential consideration in choosing the appropriate techniques for the calibration laboratory. The term recovery in this article means the amount of substance obtained in the last quantification step (after extraction) to the amount of substance added to the material before extraction and is expressed as a percentage. The authors tested the recoveries of the analytes by using the spiking technique (adding the known amount of the analytes) to the blank matrix. The recovery of the analytes was in the range of 85.5-107.1% with an average value at 98.0 and 95.6% for alpha-HCH and gamma-HCH, respectively. The RSDs of the set of measurements was found at less than 7% for both analytes (Table 3). This recovery criteria meet the satisfactory acceptance as the requirement of the AOAC Guidelines for Single Laboratory Validation of Chemical Methods were set as 80-110% at 100 ng/g. RSDs is also meet the satisfactory criteria which shows value below 22.6%, based on the Horwitz equation in 100 ng/g concentration as the acceptance (Hanley, 2016; Thompson and Lowthian, 1997).

In the application of the ID-GC-MS technique, the authors also checked the linearity profile to show the excellent relationship between the concentration ratio of natural and labeled analyte and the response ratio of natural and labeled analyte. This ratio concept is general in the analytical process by using internal standard calibration (Kościelniak and Wieczorek, 2016). The excellent linearity was described in Figure 3 where r^2 -values for alpha-HCH and gamma-HCH was 0.9995 and 0.9990, respectively. For the other criteria, such as limit of detection, limit of quantitation, and intra-day precision would be in the same range in the previous study (external calibration) since the ID-MS only differs in the calibration technique. To cover the repeatability performance, the deviation of different days observation was taken into account in the uncertainty budget as a method precision parameter.

CRM matrix Ginseng Powder KRISS CRM 108-10-013 was used as quality control material for evaluating the performance of the analytical method for gamma-HCH only, as present in the CRM material. The CRM was analyzed by using the exact matching IDMS technique. The result, as shown in Table 3, shows good performance where the recovery value and the repeatability are in the level of acceptance.

The optimized ID-GC-MS technique was applied to measure alpha-HCH and gamma-HCH in the ginseng roots sample. Figure 4 showed the

chromatogram of the analysis result. The material was found to contain 448.9 ± 24.3 ng/g alpha-HCH and 98.4 ± 8.0 ng/g gamma-HCH. The uncertainties associated with these numbers are expanded (coverage factor $k=2$) to give a 95% confidence interval. The measurement uncertainty for HCHs determination in ginseng roots was evaluated entirely according to the guide to the expression of uncertainty in measurement (GUM) and the ID-MS equation used. Contributors of the overall uncertainty, including the weighing process, both standards and sample, the concentration of HCH standards, repeatability of measurements, dry mass factor and different calibration blend, were taken into consideration.

The uncertainty associated with the method precision, the calibration blend, and the repeatability of the measurement were the three main factors of the uncertainty budget for alpha-HCH and gamma-HCH. In the gamma-HCH's budget, the recovery of the method was also another significant source. This is caused by the parameter from CRM analysis (recovery study), which the authors take into account. Results of ginseng analysis for alpha-HCH and gamma-HCH and its uncertainty in measurement were summarized in Tables 4 and 5. The relative uncertainty was observed at 5.4% and 8.2% for alpha-HCH and gamma-HCH, respectively, representing the unknown true value is located in these interval around the measured result with a confidence level of 95% for each analyte.

4. CONCLUSIONS:

The organic laboratory of sub-directorate of chemical metrology in Indonesia has developed the analytical method for alpha-HCH and gamma-HCH measurement in the range of 1-300 ng/g by using isotope-dilution gas chromatography-mass spectrometry (ID-GC-MS). From the validation study, the proposed method is selective, specific, sensitive, precise, and accurate under the observed level of concentration. The limit of detection and the limit of quantitation values are 0.5 and 2 ng/g, respectively. It can be said the method is entirely reasonable to be advantaged in the trace analysis. The measurement uncertainty was evaluated in this study to obtain the full profile of the analytical process where the relative uncertainty value is 5.4% and 8.2% for alpha-HCH and gamma-HCH, respectively. Future work could focus on participation in the inter-laboratory study to assess and demonstrate the performance of the described method. As a high order method, it would be valuable if the technique can be implied in the accurate and precise determinations such

as assigning a value to a certified reference material.

5. ACKNOWLEDGMENTS:

The authors would like to thank the Ministry of Research, Technology, and Higher Education of the Republic of Indonesia (RISTEKDIKTI) for the financial support through the scheme of the Incentive Research Program for the National Innovation System (05/INS-1/PPK/E4/2019). The authors are also highly indebted to the Research Center for Chemistry - LIPI for excellent cooperation to support a laboratory facility.

6. REFERENCES:

1. FAO; *International code of conduct on the distribution and use of pesticides*; 2013.
2. FAO; *International code of conduct on the distribution and use of pesticides*; 2008.
3. Zacharia; Tano, J.; *Identity, physical and chemical properties of pesticides*; Stoytcheva, M., eds.; IntechOpen: London, 2011.
4. EPA; Pesticides. 2009.
5. Matsumura, F.; *Insecticides*; Resh, V. H.; Cardé, R. T., eds.; Academic Press: London, 2009.
6. Gupta, R. C.; Milatovic, D.; *Insecticides*; Gupta, R. C., eds.; Academic Press; London, 2014.
7. UNEP; *Listing of POPs in the Stockholm Convention*. 2013.
8. Li, Y. F.; *The Science of the Total Environment*. 1999, 232, 121.
9. Vijgen, J.; *The legacy of lindane HCH isomer production*. 2006.
10. Simonich, S. L.; Hites, R. A.; *Science*. 1995, 269, 1851.
11. Berntssen, M. H. G.; Maage, A.; Lundebye, A.-K.; *Contamination of finfish with persistent organic pollutants and metals*; Schrenk, D.; Cartus, A., eds; Woodhead Publishing: London, 2012.
12. Liu, Y.; Meng, F.; *Procedia Environmental Sciences*. 2011, 11, 1296.
13. Gong, Z. M.; Xu, F. L.; Dawson, R.; Cao, J.; Liu, W. X.; Li, B. G.; Shen, W. R.; Zhang, W. J.; Qin, B. P.; Sun, R.; Tao, S.; *Arch. Environ. Contam. Toxicol*. 2004, 46, 432.

14. Concha-Grana, E.; Turnes-Carou, M. I.; Muniategui-Lorenzo, S.; Lopez-Mahia, P.; Prada-Rodriguez, D.; Fernandez-Fernandez, E.; *Chemosphere*. 2006, 64, 588.
15. Lammel, G.; Ghim, Y.-S.; Grados, A.; Gao, H.; Huhnerfuss, H.; Lohmann, R.; *Atmospheric Environment*. 2007, 41, 452.
16. Fang, Y.; Nie, Z.; Die, Q.; Tian, Y.; Liu, F.; He, J.; Huang, Q.; *Chemosphere*. 2017, 178, 340.
17. Jackovitz, A. M.; Hebert, R. M.; *Wildlife Toxicity Assessment for Hexachlorocyclohexane (HCH)*; Williams, M. A.; Reddy, G.; Quinn Jr., M. J.; Johnson, M. S., eds.; Elsevier: Amsterdam, 2015.
18. Baker, B. P.; Benbrook, C. M.; Groth III, E.; Benbrook, K. L.; *Food Additives and Contaminants*. 2002, 19, 427.
19. Yun, T.-K.; *J Korean Med Sci*. 2001, 16, S3.
20. Khan, I. A.; Allgood, J.; Walker, L. A.; Abourashed, E. A.; Schlenk, D.; Benson, W. H.; *J. AOAC Int*. 2001, 84, 936.
21. Durnat, J.-M.; Heuser, J.; Andrey, D.; Perrin, C.; *Food Addit. Contam.* 2005, 22, 1224.
22. Leung, K. S.-Y.; Chan, K.; Chan, C.-L.; Lu, G.-H.; *Phytother. Res*. 2005, 19, 514.
23. Lee, K.-G.; Jo, E.-K.; *Food Chemistry*. 2012, 134, 2497.
24. Coon, J. T.; Ernst, E.; *Drug Safety*. 2002, 23, 323.
25. Ellis, J. M.; Reddy, P.; *The Annals of Pharmacotherapy*. 2002, 36, 375.
26. Coleman, C. I.; Hebert, J. H.; Reddy, P.; *Journal of Clinical Pharmacy and Therapeutics*. 2003, 28, 5.
27. Vogler, B. K.; Pittler, M. H.; Ernst, E.; *Eur J Clin Pharmacol*. 1999, 5, 567.
28. Shibata, S.; *J Korean Med Sci*. 2001, 16, S28.
29. Kiefer, D.; Pantuso, T.; *American Family Physician*. 2003, 68, 1539.
30. O'Hara, M. A.; Kiefer, D.; Farrell, K.; Kemper, K.; *Arch Fam Med*. 1998, 7, 523.
31. Surma, M. K.; Sadowska-Rociek, A. B.; Cieřlik, E. J.; *Food Anal. Methods*. 2014, 7, 366.
32. Rasche, C.; Fournes, B.; Dirks, U.; Speer, K.; *J. Chromatogr. A*. 2015, 1403, 21.
33. Mao, X.; Wan, Y.; Yan, A.; Shen, M.; Wei, Y.; *Talanta*. 2012, 97, 131.
34. Zhang, F.; Yu, C.; Wang, W.; Fan, R.; Zhang, Z.; Guo, Y.; *Analytica Chimica Acta*. 2012, 757, 39.
35. Henrion, A.; *Fresenius J Anal Chem*. 1994, 350, 657.
36. Rodríguez-González, P.; Alonso, J. I. G.; *Isotope Dilution Mass Spectrometry*; Worsfold, P.; Townshend, A.; Poole, C.; Miró, M., eds.; Elsevier: Oxford, 2019.
37. Sargent, M.; Harte, R.; Harrington, C.; *Guidelines for Achieving High Accuracy in Isotope Dilution Mass Spectrometry*; Sargent, M.; Harte, R.; Harrington, C., eds.; Royal Society of Chemistry: Cambridge, 2002.
38. Goldschmidt, R. J.; Wolf, W. R.; *Anal Bioanal Chem*. 2010, 397, 471.
39. Bi, J.; Wu, L.; Yang, B.; Wang, J.; *Anal Bioanal Chem*. 2012, 403, 549.
40. Huertas-Pérez, J. F.; Sejerøe-Olsen, B.; Gokcen, T.; Sandor, F.; Schimmel, H.; Dabrio, M.; *Food Additives & Contaminants: Part A*. 2019, 36, 96.
41. Huertas Pérez, J. F.; Sejerøe-Olsen, B.; Alba, A. R. F.; Schimmel, H.; Dabrio, M.; *Talanta*. 2015, 137, 120.
42. Bercaru, O.; Ulberth, F.; Emons, H.; Vandecasteele, C.; *Anal Bioanal Chem*. 2006, 384, 1207.
43. JCGM; *JCGM 100*. 2008.
44. Aryana, N.; Aristiawan, Y.; Putri, D.; Styarini, D.; *Indones. J. Chem*. 2016, 16, 72.
45. Uhrovčík, J.; *Talanta*. 2014, 119, 178.
46. NATA; *Guidelines for the validation and verification of chemical test methods*. 2006.
47. EMEA; *Validation of Analytical Procedures: Text and Methodology*. 2006.
48. Hanley, Q. S.; *Anal. Chem*. 2016, 88, 12036.
49. Thompson, M.; Lowthian, P. J.; *J. AOAC Int*. 1997, 80, 676.
50. Kościelniak, P.; Wiczorek, M.; *Analytica Chimica Acta*. 2016, 944, 14.

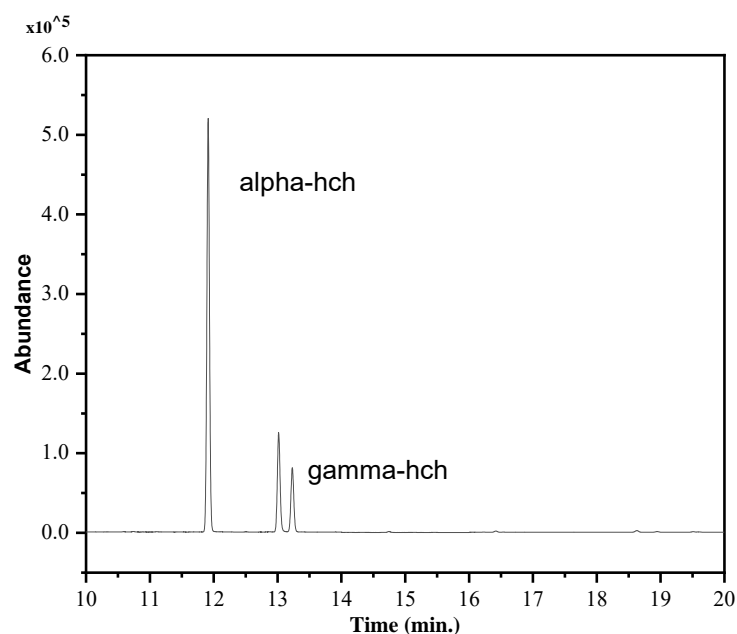


Figure 1. Total ion chromatogram (TIC) of standard mixture of alpha-HCH and gamma-HCH

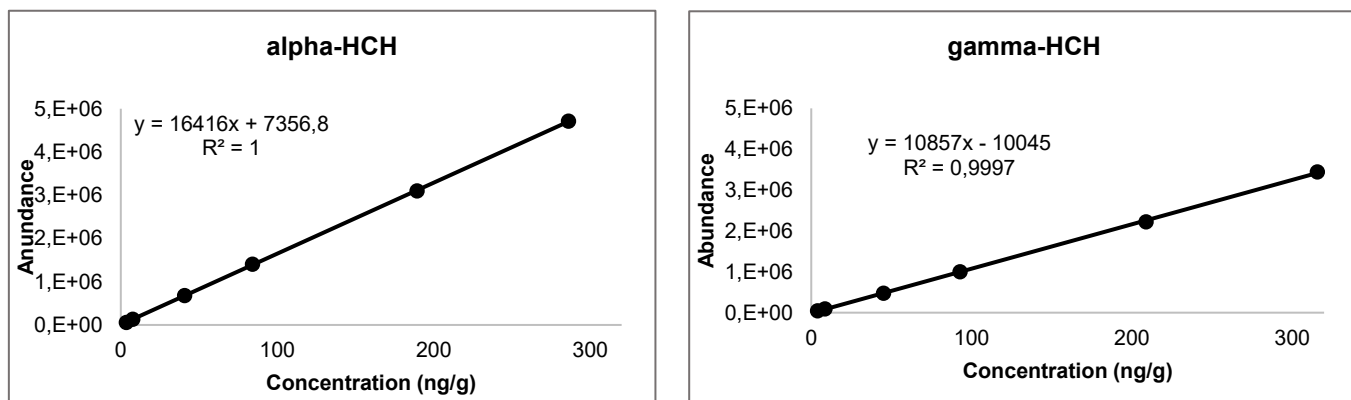


Figure 2. Linearity study for external calibration

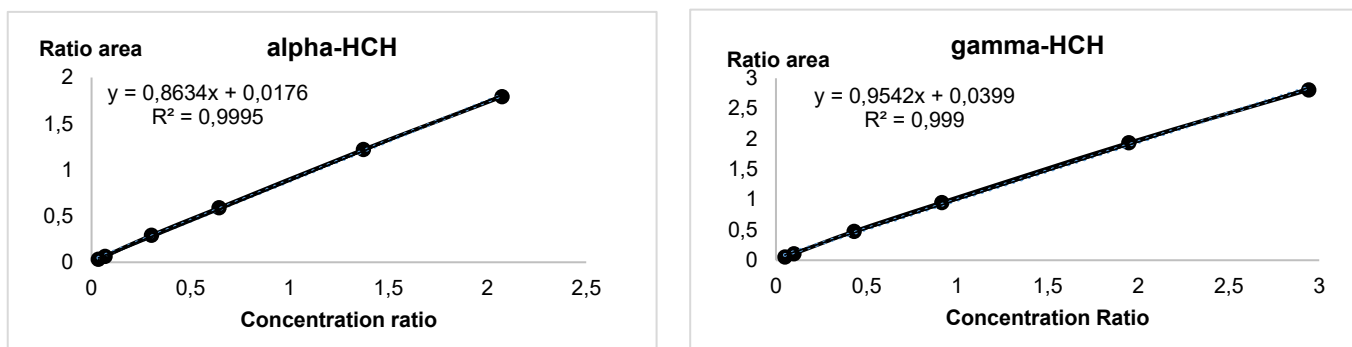


Figure 3. Linearity study for isotope dilution calibration

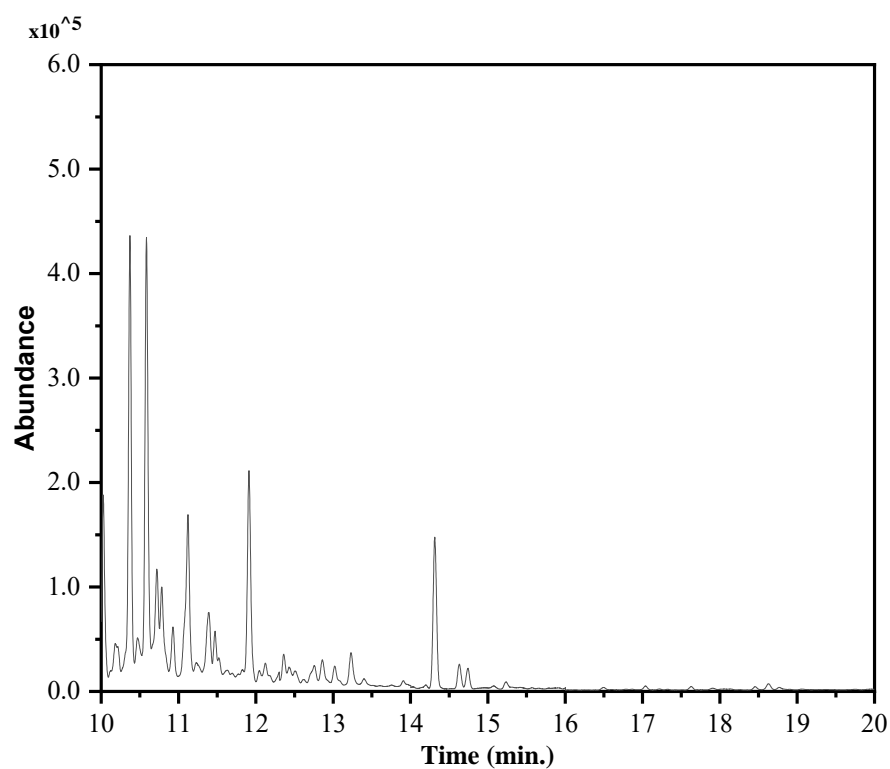


Figure 4. Total ion chromatogram (TIC) of ginseng roots sample in exact-matching ID-GC-MS analysis

Table 1. Ions profile and retention time of analyte

Analyte	Ion (m/z)	Retention time (min)
alpha-HCH	181	11.9
	183	11.9
	219	11.9
¹³ C ₆ alpha-HCH	187	11.9
	189	11.9
	225	11.9
gamma-HCH	181	13.2
	183	13.2
	254	13.2
¹³ C ₆ gamma-HCH	187	13.2
	189	13.2
	260	13.2

Table 2. Parameters definition on ID-MS equation

Parameter	Definition
C_x	mass fraction of HCH analyte in the ginseng sample (dry basis)
C_z	mass fraction of the HCH analyte in the standard solution used for preparing calibration blend
m_y	mass of internal standard solution added to the sample blend
m_{zc}	mass of native HCH calibration standard solution added to calibration blend
m_x	mass of study sample in the sample blend
m_{yc}	mass of internal standard solution added to the calibration blend
R_B	observed native and isotope ion abundance ratio in the sample blend
R_{Bc}	observed native and isotope ion abundance ratio in the calibration blend
f_d	dry mass factor

Table 3. Analytical parameter for the determination of alpha-HCH and gamma-HCH by using ID-GC-MS

Parameter	Analytes	
	alpha-HCH	gamma-HCH
Limit of detection (ppb)	0.5	0.5
Limit of quantitation (ppb)	2.0	2.0
Intraday precision		
%RSD (20 ppb)	3.7	3.3
%RSD (100 ppb)	3.0	2.4
Mean recovery CRM ^a (%)	-	97.8
%RSD recovery CRM	-	2.8
Mean recovery spiked ^b (%)	98.0	95.6
%RSD recovery spiked	7.0	6.0

a) Recovery study obtained using ID-GC-MS technique from CRM analysis

b) Recovery study obtained using external calibration technique from spiking analysis

Table 4. Uncertainty budget for alpha-HCH determination in ginseng roots by exact matching ID-GC-MS

Factor (Unit)	Values	Uncertainty		Sensitivity Coefficients		
	x	u(x)	u(x)/x	dCx/dx	c ² .u(x) ²	#CTV
Method precision	1.00000	0.00966	0.00966	448.94401	18.80711	12.75870%
m_{zc}	0.24985	0.00002	0.00008	1796.83619	0.00145	0.00099%
m_y	0.16508	0.00002	0.00013	2719.59542	0.00333	0.00226%
m_{yc}	0.16934	0.00002	0.00013	-2651.21808	0.00316	0.00215%
m_x	1.73616	0.00002	0.00001	-258.58459	0.00003	0.00002%
C_z	3.00	0.07500	0.02500	149.64800	125.96920	85.45719%
R_B	0.84358	Uncertainties captured in method precision				
R_{BC}	0.87126	Uncertainties captured in method precision				
F_d	0.90770	0.00010	0.00011	-494.59515	0.00255	0.00173%
Calibration blend	1.00000	0.00361	0.00361	448.94401	2.61938	1.77698%
C_x	448.9					
Combined Uncertainty	12.1					
Expanded Uncertainty (k=2)	24.3					
Total				2159.56982	147.40622	100%

Table 5. Uncertainty budget for gamma-HCH determination in ginseng roots by exact matching ID-GC-MS

Factor (Unit)	Values	Uncertainty		Sensitivity Coefficients		
	x	u(x)	u(x)/x	dCx/dx	c ² .u(x) ²	#CTV
Method precision	1.00000	0.01267	0.01267	98.39557	1.55391	9.84514%
m_{zc}	0.13944	0.00002	0.00015	705.64806	0.00022	0.00142%
m_y	0.14478	0.00002	0.00015	679.62908	0.00021	0.00132%
m_{yc}	0.15024	0.00002	0.00014	-654.94436	0.00019	0.00122%
m_x	1.73616	0.00002	0.00001	-56.67428	0.00000	0.00001%
C_z	1.41	0.01084	0.00769	69.82956	0.57262	3.62795%
R_B	0.787	Uncertainties captured in method precision				
R_{BC}	0.961	Uncertainties captured in method precision				
F_d	0.90770	0.000102	0.00011	-108.40098	0.00012	0.00077%
Calibration blend	1.00000	0.03337	0.03337	98.39557	10.78010	68.29970%
Method Recovery	0.9831215		0.017235			
C_x	97	0.016944838	75	100.0848382	2.87615	18.22247%
Combined Uncertainty	98.4					
Expanded Uncertainty (k=2)	4.0					
Total				931.96306	15.78353	100%

COMPOSTOS FENÓLICOS TOTAIS E CAPACIDADE ANTIOXIDANTE *IN VITRO* DA CASCA E POLPA DE ABACAXI PÉROLA E ABACAXI HAVAIANO

TOTAL PHENOLIC COMPOUNDS AND *IN VITRO* ANTIOXIDATING CAPABILITY OF PEARL PINEAPPLE AND HAWAIIAN PINEAPPLE

OLIVEIRA JÚNIOR, Charles Ivo de^{1*}; OIVEIRA, Gustavo Félix²; REZENDE, Gláucia Aparecida Andrade³; ALVES, Blyeny Hatalita Pereira⁴

^{1,2,3,4} Instituto Federal de Educação, Ciência e Tecnologia de Goiás – Campus Itumbiara, Departamento de Química Orgânica.

* Charles Ivo de Oliveira Júnior
e-mail: charlesivo@outlook.com

Received 08 November 2019; received in revised form 10 February 2020; accepted 14 March 2020

RESUMO

O abacaxi tem aceitação pelo seu aroma, sabor e por suas qualidades nutricionais. As pesquisas relacionadas à composição dos alimentos e as substâncias bioativas vem ganhando maior espaço no meio acadêmico devido à preocupação em se manter um estilo de vida mais saudável. O objetivo desse trabalho foi quantificar a presença de compostos fenólicos totais e avaliar a atividade antioxidante *in vitro* na casca e na polpa de abacaxi pérola e havaiano (*Ananas comosus*), cultivados e comercializados na região do triângulo mineiro e sul de Goiás. Esta região foi escolhida devido à proximidade geográfica com a cidade de Itumbiara e por ser uma região com uma destacada produção das duas variedades em estudo. O teor de compostos fenólicos totais foi avaliado através do método de Folin-Ciocalteu e a atividade antioxidante foi avaliada pelo método de sequestros de radicais livres (DPPH• - 2,2-difenil-1-picrilhidrazila). Os testes apontaram valores de 72,53 a 143,90 mg GAE/100g de amostra, para o extrato aquoso e de 62,04 a 165,47 mg GAE/100g de amostra, sendo os maiores valores encontrados para os extratos da casca. Para o teste realizado com o DPPH, para verificação da atividade antioxidante dos extratos aquoso e hidroetanólico, não foi observado um consumo significativo do reagente DPPH. A leitura foi realizada durante 1 hora, sem que o valor medido sofresse alterações substanciais. Portanto maiores estudos necessitam ser realizados para a elucidação da atividade antioxidante em abacaxis.

Palavras-chave: *Substâncias Bioativas; Radicais Livres; DPPH.*

ABSTRACT

The pineapple is praised for its aroma, flavor, and nutritional value. Researches of food composition and bioactive substances gained more space in the academic environment due to a more current severe concern of maintaining a healthier lifestyle. The objective of this paper was to quantify the presence of total phenolic compounds and to evaluate the antioxidant activity *in vitro* in the peel and pulp of two pineapples varieties: the *Abacaxi Pérola* and *Abacaxi Havaiano* (*Ananas comosus*), cultivated and commercialized at the region of the *Triângulo Mineiro* and Southern of Goiás. This region was chosen due to its geographic proximity to the city of Itumbiara, and for being a region with an outstanding production of the subject two varieties. The content of total phenolic compounds was evaluated using the Folin-Ciocalteu method and the antioxidant activity was assessed using the free radical scavenging method (DPPH • - 2,2-diphenyl-1-picrilhidrazil). The tests showed values of 72.53 to 143.90 mg GAE / 100g for each sample, for the aqueous extract and from 62.04 to 165.47 mg GAE / 100g of sample, the highest values being found for the bark extracts. For the test carried out with DPPH, to check the antioxidant activity of aqueous and hydroethanolic extracts, significant consumption of the DPPH reagent was not observed. The reading was performed for 1 hour without the measured value undergoing substantial changes. Therefore further studies need to be carried out to elucidate the antioxidant activity in pineapples.

Keywords: *Bioactive Substances; Free radicals; DPPH.*

1. INTRODUÇÃO

O Brasil é o segundo maior produtor de abacaxi no mundo. Em 2016, a produção da fruta atingiu 2.930.661 de toneladas (EMBRAPA, 2016b). De acordo com dados para produção brasileira de abacaxi em 2016, as cidades de Monte Alegre de Minas, Canápolis e Centralina, no estado de Minas Gerais, ocuparam, respectivamente a 6^a, 9^a e 19^a posição na produção nacional desse fruto, com um total de 136.250 mil frutos produzidos (EMBRAPA, 2016a). A proximidade geográfica da cidade de Itumbiara com a região do triângulo mineiro, torna seus cidadãos potenciais clientes para a comercialização da produção dessas três cidades, principalmente em se tratando do fruto in natura.

As variedades produzidas na região são o abacaxi pérola e o abacaxi havaiano, também conhecido como Smooth Cayenne. Eles apresentam características sensoriais diferentes. O abacaxi havaiano apresenta mais acidez e a polpa é mais amarelada. O abacaxi pérola é pouco ácido, mais adocicado e apresenta a polpa branca. Essas características tornam o abacaxi pérola mais agradável ao paladar do consumidor brasileiro, para o consumo in natura. Já as características do abacaxi havaiano o tornam adequado para industrialização e exportação (Cabral e Junghans, 2003).

Atualmente, a sociedade vem se preocupando em manter uma vida saudável, consequentemente, as pesquisas relacionadas à composição nutricional dos alimentos vêm ganhando espaço. Além dos nutrientes, existem outros componentes que desempenham efeitos positivos nos organismos humanos, como por exemplo, os compostos fenólicos, que desempenham um papel de antioxidante natural (Ota et al., 2016).

De acordo a Tabela Brasileira de Composição de Alimentos – TACO (2011), a composição nutricional do abacaxi cru é: umidade (86,3%), proteínas (0,9g), lipídeos (0,1g), carboidratos (12,3 g), fibras (1,0g), cinzas (0,4g), cálcio (22 mg), magnésio (1 mg) e vitamina C (34,6 g).

Dentre os nutrientes presentes no abacaxi, se destaca a vitamina C (ácido ascórbico). A vitamina C desempenha um papel fundamental na saúde dos seres humanos, pois combate os radicais livres, ou seja, é um antioxidante, auxilia o sistema imunológico, ajuda

na absorção de ferro e na produção de colágeno (Pereira, 2008).

Sousa, Vieira e Lima (2011) realizaram um estudo sobre a capacidade antioxidante e o teor de fenóis totais in vitro de resíduos de polpas de frutas tropicais, entre elas o abacaxi. Nesses ensaios, foram encontradas baixas quantidades de fenóis totais e baixa capacidade antioxidante para esses resíduos. Ota e colaboradores (2016) analisaram as propriedades físico-químicas e o potencial antioxidante da polpa fresca do abacaxi-do-cerrado, afirmando terem encontrado valores superiores de compostos fenólicos e da atividade antioxidante, quando comparado com o abacaxi comum.

O fruto, a parte comercializável da planta, é composto pela polpa, maior parte aproveitada, casca, talo e coroa considerado resíduo orgânico e não tem tido suas utilizações apropriadas, de forma que possam ser aproveitados economicamente. A polpa do abacaxi, em geral, tem aproveitamento máximo tanto na indústria quanto no consumo direto da fruta. A casca do abacaxi normalmente é a parte mais desperdiçada do fruto pela população, no entanto ela pode ser inserida na nutrição humana de diversas formas. A pesquisa de Lima, Souza, Santine e Oliveira (2017), apresenta uma variedade de receitas, dentre elas tem chás, sucos, doces e geleias, receitas saudáveis e com baixo custo financeiro, que podem ser produzidas com a casca do abacaxi.

A progressiva preocupação com o meio ambiente tem estimulado o desenvolvimento de pesquisas que viabilizam a sustentabilidade de impactos causados pelos processos industriais. A indústria de alimentos produz uma vasta quantidade de resíduos orgânicos que podem ser aproveitados. Com isso, identificar a presença de substâncias bioativas e a ação antioxidante da polpa e casca do abacaxi poderá agregar valor de mercado na região e automaticamente reduzir o impacto ambiental (Leite e Pawlowsky, 2015; Ferreira et al., 2016).

Nesse sentido, o objetivo do trabalho foi quantificar os compostos fenólicos totais e determinar a atividade antioxidante da casca e polpa, por meio do sequestro de radicais livres DPPH nos extratos da casca e polpa das duas variedades de abacaxi (pérola e havaiano).

2. MATERIAL E MÉTODOS

2.1. Preparação dos Extratos da Casca e Polpa

Os frutos maduros de abacaxi pérola e abacaxi havaiano foram obtidos diretamente de produtores na cidade de Canápolis (MG). Eles foram transportados até o Laboratório de Química do Instituto Federal de Goiás - Câmpus Itumbiara, lavados em água corrente e processados. O processamento consistiu no descascamento e retirada do cilindro central, obtendo-se as seguintes partes: casca e polpa. A casca e a polpa foram processadas com o auxílio de um aparelho “mixer” doméstico, armazenadas em embalagens plásticas com fechamento hermético e congeladas até o momento das análises. Na Figura 1 são mostradas as etapas do processamento do abacaxi.

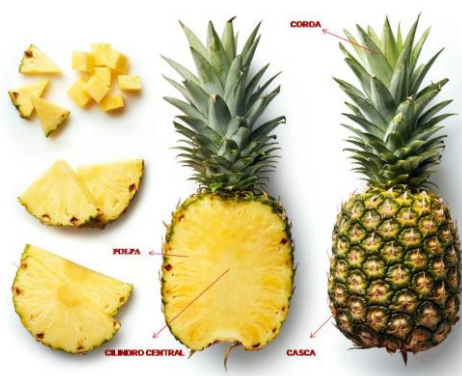


Figura 1. Etapas do processamento do abacaxi

Foram preparados extratos aquosos e hidroetanólico da casca e polpa das duas variedades de abacaxi. Para a preparação dos extratos aquosos foram utilizados 100 mL de água destilada e 20 g de amostra; em seguida, eles foram homogeneizados em frasco Erlenmeyer, usando o agitador magnético durante 1 h à temperatura ambiente ($\pm 25^\circ\text{C}$). A mistura foi centrifugada por 5 min à temperatura ambiente; o sobrenadante filtrado e armazenado em vidro âmbar sob refrigeração a aproximadamente 5°C , para posterior análise. A preparação do extrato hidroetanólico (8:2 água:etanol) seguiu a mesma metodologia (adaptado de Lima, 2008). Todas as análises foram realizadas em até sete dias após a obtenção dos extratos.

2.2. Espectrofotometria no UV-Visível

A espectrofotometria no UV-Visível permite identificar e quantificar cromóforos que exibem a característica de absorver luz na faixa compreendida entre 200 a 850 nm. A espectroscopia na faixa do visível (400 a 850 nm) para compostos fenólicos só é possível através de uma reação específica de modo a se obter um produto colorido em proporção linear ou direta à

quantidade de material fenólico presente nas amostras (Chang, 2000). Estes ensaios colorimétricos têm pontos de absorção máximos pré-definidos. Os ensaios propostos neste trabalho foram realizados em um espectrofotômetro UV/VIS, Modelo UV-380G da marca GEHAKA.

2.3. Determinação de Fenóis Totais pelo Método de Folin-Ciocalteu

Um dos métodos mais utilizados para esta determinação está baseado nos estudos de Singleton e Rossi, que estudaram as características do reagente de Folin-Ciocalteu (Singleton e Rossi, 1965).

O ensaio para a determinação de fenóis totais emprega o reagente de Folin-Ciocalteu, que consiste na mistura dos ácidos fosfomolibdídico e fosfotungstístico, na qual o molibdênio e o tungstênio encontram-se no estado de oxidação 6^+ , porém, em presença de certos agentes redutores, como os compostos fenólicos, formam-se os chamados molibdênio azul e tungstênio azul, nos quais a média do estado de oxidação dos metais está entre 5 e 6 e cuja coloração permite a determinação da concentração das substâncias redutoras, que não necessariamente precisam ter natureza fenólica (Naczek e Shahidi, 2004; Ikawa et al., 2003). Este reagente de cor amarela oxida os fenolatos e reduz os ácidos deste reativo para dar lugar a um complexo azul de molibdênio-tungstênio, registrado a 760 nm.

Para determinação dos fenóis totais foi retirado 0,1 mL dos extratos e diluiu-se com água até o volume de 50,0 mL. Desta solução foi retirada uma alíquota de 0,5 mL que foi transferida para um tubo de ensaio. Adicionou-se 2,5 mL de uma solução aquosa do reagente de Folin-Ciocalteu a 10 % e 2,0 mL de uma solução recém-preparada de carbonato de sódio a 7,5 %. A mistura foi mantida por 5 minutos em banho aquecido a 50°C ; em seguida, foi feita a leitura da absorbância a 760 nm. Fez-se, também, uma curva de calibração com soluções aquosas de ácido gálico em diversas concentrações contra um branco sob as mesmas condições. A concentração das amostras foi determinada a partir da equação da reta obtida. Os resultados estão expressos em equivalentes de ácido gálico.

2.4. Determinação da Atividade Antioxidante

Para determinar a atividade antioxidante exercida em extratos de amostras e substâncias isoladas, um dos métodos mais usados se define por avaliar a atividade seqüestradora ou antioxidante do radical livre DPPH• (Sousa et al., 2007).

A atividade antioxidante foi determinada, através do radical livre estável 2,2-difenil-1-picrilhidrazila (DPPH•) seguindo o método descrito por Brand-Williams et al. (1995) e modificado por Yildirim et al. (2001). Os extratos hidroetanólico e aquoso foram submetidos a 5 diluições sucessivas. Para cada solução, foi tomada uma amostra de 0,10 mL e adicionado 3,90 mL de solução de DPPH• de concentração aproximada de 80 µg mL⁻¹ em metanol. Também, foi feito um branco nas mesmas condições, mas sem o DPPH•. Após a adição do radical DPPH•, as soluções foram deixadas em repouso e suas absorvâncias registradas no comprimento de onda de 517 nm durante uma hora, em intervalos de cinco minutos entre cada leitura. A porcentagem de DPPH-H que reagiu (atividade antioxidante) foi calculada pela expressão:

$$\text{DPPH}_{\text{reagido}}(\%) = \frac{\text{AbvC} - (\text{AbvA} - \text{AbvB}) \times 100}{\text{AbvC}}$$

Onde: AbvC, AbvB e AbvA correspondem às absorvâncias do controle, branco e amostra, respectivamente.

Cálculo do CE₅₀ (quantidade de antioxidante necessário para decrescer a concentração inicial de DPPH. para 50%). Primeiramente será construída uma curva analítica de calibração para o radical DPPH. em diferentes concentrações. Em seguida, serão calculadas as porcentagens de DPPH remanescentes (CE₅₀), ou seja, a quantidade de DPPH• que não reagiu com os antioxidantes através da Equação 1:

$$CE_{50} = \frac{[DPPH]_t}{[DPPH]_{t_0}} \times 100 \quad \text{Eq. 1}$$

Onde: t = tempo onde absorvância do DPPH estável; t₀ = é o tempo zero.

A concentração efetiva média (CE₅₀), que representa a concentração de amostra necessária para sequestrar 50% dos radicais de DPPH., será calculada plotando-se a porcentagem de DPPH-H versus as concentrações dos extratos de cada amostra (Argolo et al., 2004). Para quantificação dos extrativos 1,00 mL dos extratos foi recolhido e seco num frasco tarado a 105 °C, durante 6

horas, resfriado à temperatura ambiente e pesado.

3. RESULTADOS E DISCUSSÃO:

A partir das absorvâncias obtidas para as amostras de ácido gálico em diferentes concentrações conhecidas, foi traçado uma curva de calibração, apresentada na Figura 2. Os valores de fenóis totais encontrados nas amostras são apresentados na Tabela 1.

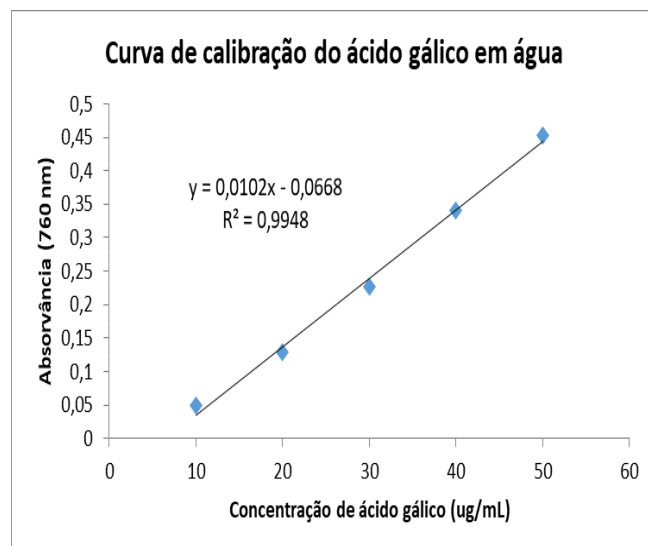


Figura 2. Curva analítica de calibração para o ácido gálico

Tabela 1. Teor de fenóis totais (mg em equivalente de ácido gálico. 100 g⁻¹ de abacaxi) para a polpa e casca das variedades de abacaxi (pérola e havaiano).

Extrato	Pérola	Havaiano
Aquoso – polpa	99,88	72,53
Aquoso – casca	143,90	140,08
Hidroetanólico – polpa	104,00	62,04
Hidroetanólico – casca	165,47	151,55

Fonte: Autoria Própria

Os valores obtidos indicam a presença de maiores teores de fenóis totais nos extratos da casca do abacaxi em ambas às variedades estudadas. Em trabalho realizado por Ota e colaboradores (2016) foram obtidos valores de 186,93±5,22 mg GAE/100g para o abacaxi-do-cerrado (*Ananas comosus*).

Embora os compostos fenólicos estejam associados com a maioria dos antioxidantes naturais (Razavi et al., 2008), muitos outros

compostos estão sendo descobertos. Espécies do gênero Aniba, por exemplo, são conhecidas pelo alto valor econômico e pela composição química do seu óleo, principalmente a espécie a rosaeodora, conhecida como pau-rosa, uma espécie bem explorada e com inúmeras atividades biológicas já descritas (Maia et al., 2007).

Os antioxidantes são um conjunto heterogêneo de substâncias capazes de controlar a produção de radicais livres ($R\cdot$). O termo antioxidante significa “que impede a oxidação de outras substâncias químicas” decorrente das reações metabólicas e fatores exógenos, como raios ultravioletas (Tovani Benzaquen Ingredientes, 2009).

O metabolismo celular normal do corpo é responsável pela produção de radicais livres e outras espécies reativas de oxigênio, que podem causar danos severos a biomoléculas celulares, entre estas a molécula de DNA (Loureiro et al., 2002). Antioxidantes, por sua vez, são substâncias que retardam a velocidade dos processos oxidativos, responsáveis pela formação dos radicais livres, conferindo importantes benefícios à saúde (Pietta, 2000). Estas substâncias podem ser sintéticas ou naturais. No entanto, o uso de antioxidantes sintéticos tem sido evitado devido a suspeita de que estes possam produzir efeitos carcinogênicos (Botterweck et al., 2000). As plantas por sua vez, por possuírem inúmeros compostos, resultantes do seu metabolismo secundário, podem ser fontes de substâncias antioxidantes.

O processo de extração de antioxidantes naturais constitui mecanismo complexo e envolve diversas técnicas, dentre as quais a extração convencional e a supercrítica. Exige controle rigoroso de fatores como a polaridade do solvente utilizado, o tempo e a temperatura de extração, pois pode ocorrer perda ou destruição dos compostos antioxidantes (Andreo e Jorge, 2006).

Vários métodos e técnicas têm sido empregados para determinar a atividade antioxidante in vitro, de modo a aferir uma caracterização e seleção de substâncias e/ou misturas de potencial importância na prevenção de doenças crônico-degenerativas. Dentre estes métodos destacam-se o sistema de co-oxidação do β -caroteno/ácido linoléico e o método de seqüestro de radicais livres, tais como DPPH• - 2,2-difenil-1-picrilhidrazila (Duarte Almeida et al., 2006).

Para o teste realizado com o DPPH, para verificação da atividade antioxidante dos extratos aquoso e hidroetanólico, não foi observado um consumo significativo do reagente DPPH. A leitura foi realizada durante 1 hora, sem que o valor medido sofresse alterações substanciais.

Em estudo realizado por Melo e colaboradores (2008), a capacidade antioxidante do extrato aquoso e acetônico das frutas, foi avaliada no sistema modelo β -caroteno/ácido linoleico, onde, para o abacaxi a porcentagem de inibição foi menor que 20%.

4. CONCLUSÕES:

Com base nos resultados obtidos, pode-se concluir que não foi observada atividade antioxidante nas amostras analisadas, utilizando-se o método de seqüestro de radicais livres DPPH, porém não se pode afirmar que as variedades analisadas não possuem atividade antioxidante, pois não foram testados outros métodos. Maiores estudos necessitam ser realizados para a elucidação da atividade antioxidante em abacaxis.

Os teores de compostos fenólicos totais avaliados nos extratos da casca das duas variedades de abacaxis foram relativamente maiores do que os extratos da polpa. Com base nesses resultados é importante introduzir a casca de abacaxi na alimentação dos seres humanos já que os compostos fenólicos mesmo em pequenas quantidades apresentam ações benéficas para a saúde humana.

5. REFERÊNCIAS:

1. Andreo, D.; Jorge, N. Boletim CEPPA, **2006**, 24, 319.
2. Argolo, A.X.; Santanna A. E.; Pletsch, M.; Coelho, L.C. Bioresource Technology, **2004**, 95, 229.
3. Botterwerck, A. A.; Verhagen, H.; Goldbohm, R. A.; Kleinjans, J.; Brandt, P. A. Food Chemistry Toxicology, **2000**, 38, 599.
4. Brand-Williams, W.; Cuvelier, M. E.; Berset, C. Food Science and Technology, **1995**, 28, 25.
5. Cabral, J. R. S.; Junghans, D. T. EMPRAPA, **2003**.
6. Chang, R. Dissertação de Mestrado, Universidade Federal de Uberlândia, Brasil, **2000**.

7. Duarte-Almeida, J. M.; Santos, R. J.; Genovese, M. I.; Lajolo, F. M. *Ciência e Tecnologia de Alimentos*, **2006**, 26, 446.
8. http://www.cnpmf.embrapa.br/Base_de_Dados/index_pdf/dados/brasil/abacaxi/b32_abacaxi.pdf, acessada em abril **2019**.
9. http://www.cnpmf.embrapa.br/Base_de_Dados/index_pdf/dados/mundo/abacaxi/w1_abacaxi.pdf, acessada em abril **2019**.
10. Ferreira, E. A.; Siqueira, H. E.; Boas, E. V.; Hermes, V. S.; Rios, A. O. *Rev. Bras. Fruticultura*, **2016**, 38, 01.
11. Lima, A. Tese de Doutorado, Universidade de São Paulo, Brasil, **2008**.
12. Loureiro, A. P. M.; Di-Mascio, P.; Medeiros, M. H. G. *Quím. Nova*, **2002**, 25, 777.
13. Lima, P. C. C.; Souza, B. S.; Santine, A. T.; Oliveira D. C. *Holos*, **2017**, 02, 122.
14. Lima, V. L. A. G.; Melo, E. A.; Lima, D. E. S. *Scientia Agricola*, São Paulo, **2002**, 59, 447.
15. Leite, B.; Pawlowsky, U. *Nova Técnica*, **2005**, 10, 96.
16. Lima, V. L. A. G. de; Melo, E. A.; Maciel, M. I. S.; Silva, G. S. B.; Lima, D. E. S. *Revista de Nutrição*, **2004**, 17, 53.
17. Maia, J.G.; Andrade, E.H.; Couto H.A.; Silva, A.C.; Henke C. *Quím. Nova*, **2007**, 30, 1906.
18. Naczek, M.; Shahidi, F. *Journal Chromatography*, **2004**, 1054, 95.
19. Ota, K. C. G. G. Santos, N. C. D.; Durigan, G.; Haminiuk, C. W. I.; Branco, I. G. *Resumos do Congresso Brasileiro de Ciência e Tecnologia de Alimentos*, Gramado, Brasil, **2016**.
20. Pietta, P.G. *Journal of Natural Products*, 2000, 63, 1035.
21. Pereira, V. R. Dissertação de Graduação, Universidade Federal de Pelotas, Brasil, **2008**.
22. Razavi, S. M.; Nazemiyeh, H.; Hajiboland, R.; Kumarasamy, Y.; Delazar, A.; Nahar, L.; Sarker, S. D. *Revista Brasileira de Farmacognosia*, **2008**, 18, 01.
23. Rocha, W. S.; Lopes, R.M.; Silva, D. B.; Vieira, R. F.; Silva, J. P.; Agostine-Costa, T. S. *Revista Brasileira de Fruticultura*, **2011**, 33, 1215.
24. Singleton, V. L.; Rossi, J. A. *Journal for Enology and Viticulture*, **1965**, 16, 144.
25. Sousa, C. M. M.; Silva, H. R. A.; Vieira Jr., G. M.; Ayres, M. C. C.; Costa, C. S.; ARAÚJO, D.S.; CAVALCANTE, L. C. D.; Barros, E. D. S.; Araújo, P. B. de M.; Brandão, M. S.; Chaves, M. H. *Quím. Nova*, **2007**, 30, 351.
26. Sousa, M. S. B.; Vieira, L. M.; Lima, A. *Journal Food Technology*, **2011**, 14, 202.
27. https://www.cfn.org.br/wp-content/uploads/2017/03/taco_4_edicao_ampliada_e_revisada.pdf, acessada em maio **2019**.
28. <http://www.revista-fi.com/materias/83.pdf>, acessada em abril **2019**.
29. Yildirim, A., Kara, A.A. *Food Chemistry*, **2001**, 49, 4083.

PROPRIEDADES DE TRANSPORTE DA PERCOLAÇÃO DE FASE LÍQUIDA EM RAMOS DE POLÍMEROS VÍTREOS ALTAMENTE PERMEÁVEIS

TRANSPORT PROPERTIES OF LIQUID PHASE PERCOLATION CLUSTER IN HIGHLY PERMEABLE GLASSY POLYMERS

ТРАНСПОРТНЫЕ СВОЙСТВА ПЕРКОЛЯЦИОННОГО КЛАСТЕРА ЖИДКОЙ ФАЗЫ В ВЫСОКОПРОНИЦАЕМЫХ СТЕКЛОБРАЗНЫХ ПОЛИМЕРАХ

SOBOLEV Vladimir D.^{1*}; YUSHKIN Alexey A.²; SABBATOVSKIY Konstantin G.³; SERGEEVA Inessa P.⁴;

^{1,3,4} Frumkin Institute of Physical Chemistry and Electrochemistry, Russian Academy of Sciences. Russia.

² Topchiev Institute of Petrochemical Synthesis, Russian Academy of Sciences. Russia.

* Correspondence author

e-mail: vladimir.sobolev@mail.ru

Received 01 December 2019; received in revised form 15 February 2020; accepted 17 February 2020

RESUMO

A porosidade, permeabilidade e condutividade das membranas de poli[1-(trimetilsilil)-1-propino] (PTMSP) em misturas de etanol-água foram determinadas através da análise das características de impedância. Foi calculada a fração crítica de volume da porosidade na qual os canais de condutividade são formados. Quando o teor de álcool na solução aumenta foi de 0,29; quando diminui foi de 0,17. As dependências obtidas indicam que a transferência de matéria na membrana ocorre com os elementos da fase líquida, formando um ramo de percolação à medida que a quantidade de líquido absorvido aumenta. O efeito da histerese foi observado nos valores medidos de porosidade, permeabilidade, condutividade e capacidade. A estrutura porosa de uma membrana seca de PTMSP consiste em elementos de volume livre que não estão conectados entre si. Com aproximadamente 30% de concentração de álcool, através dos canais, começam a se formar, conectando os dois lados da membrana. Nesse caso, a permeabilidade e a condutividade elétrica aumentam como uma função exponencial, em contraste com a porosidade que aumenta linearmente. A fórmula de Lichtenecker e Rother ajudou a calcular as frações de volume das fases condutora e não condutora do sistema. Os valores obtidos da quantidade de líquido na membrana em vários arranjos espaciais dos canais permitiram estabelecer a estrutura dos canais cheios de líquido. A melhor concordância com os valores experimentais foi obtida para a estrutura caótica. Isso é consistente com as idéias existentes sobre a estrutura das membranas estudadas e confirma a suposição de que o ramo de percolação é formado a partir de elementos de volume livre preenchidos com a fase líquida. Os baixos valores observados do potencial zeta e, consequentemente, os baixos valores do componente eletrostático da pressão de cunha indicam que o aumento no tamanho ou no número de canais de transporte está associado a forças não eletrostáticas.

Palavras-chave: membrana, porosidade, impedância, permeabilidade, ramo de percolação.

ABSTRACT

Porosity, permeability, and conductivity of PTMSP membranes in ethanol-water mixtures were determined by analyzing the impedance characteristics. The critical volume fraction of porosity at which through conductivity channels are formed was calculated. When the alcohol content in the solution increases, it was 0.29; when it decreases, it was 0.17. The obtained dependencies indicate that the transfer of matter in the membrane occurs the liquid phase elements, forming a percolation cluster as the amount of sorbed liquid increases. The hysteresis effect was observed in the measured values of porosity, permeability, conductivity, and capacity. The porous structure of a dry PTMSP membrane consists of free volume elements that are unconnected to each other. At ~30% alcohol concentration, through channels, begin to form, connecting both sides of the membrane. In this case, both permeability and electrical conductivity increase as a power function, in contrast to the porosity that increases linearly. Lichtenecker and Rother's formula helped to calculate the volume fractions of the conducting and non-conducting phases in the system. The obtained values of the amount of liquid in the membrane at various spatial arrangements of the channels made it possible to establish the structure of the liquid-filled channels. The best agreement with the experimental values was obtained for the

chaotic structure. This is consistent with the existing ideas about the structure of the studied membranes and confirms the assumption that the percolation cluster is formed from free volume elements filled with the liquid phase. The observed low values of the zeta potential and, consequently, the low values of the electrostatic component of the wedging pressure indicate that the increase in the size or the number of transport channels is associated with non-electrostatic forces.

Keywords: *membrane, porosity, impedance, permeability, percolation cluster.*

АННОТАЦИЯ

Путем анализа импедансных характеристик были определены пористость, проницаемость и проводимость ПТМСР мембран в смесях этанола и воды различной концентрации. Рассчитана критическая объемная доля пористости, при которой происходит образование сквозных каналов проводимости. Для случая, когда содержание спирта в растворе увеличивается, она равна 0,29, а когда уменьшается 0,17. Полученные зависимости свидетельствуют о том, что перенос вещества в мембране осуществляется через элементы жидкой фазы, образующие перколяционный кластер, который формируется по мере увеличения количества сорбированной жидкости, и, в последствие, сохраняется при уменьшении сорбции. Наблюдался эффект гистерезиса в измеренных значениях пористости, проницаемости, проводимости и ёмкости. Пористая структура сухой мембраны из ПТМСР состоит элементов свободного объема практически не связанных друг с другом. При концентрации спирта около 30% начинают образовываться сквозные каналы, соединяющие обе стороны мембраны. При этом и проницаемость и электрическая проводимость возрастают по степенному закону в отличие от пористости, которая увеличивается линейно. Используя формулу Лихтенеккера, были рассчитаны объёмные доли проводящей и непроводящей фазы в системе. Полученные значения количества жидкости в мембране при различных значениях параметра пространственного расположения каналов позволили установить структуру каналов заполненных жидкостью. Наилучшее совпадение с экспериментальными значениями было получено для хаотической структуры каналов. Это согласуется с представлениями о структуре исследованных мембран и подтверждает предположение о том, что перколяционный кластер формируется из элементов свободного объёма, заполненных жидкой фазой. Наблюдаемые низкие значения дзета-потенциала и, следовательно, низкие значения электростатической составляющей расклинивающего давления, свидетельствуют о том, что увеличение размеров или количества транспортных каналов связаны с силами не электростатического характера.

Keywords: *мембрана, пористость, импеданс, проницаемость, перколяционный кластер.*

1. INTRODUCTION

The separation and the purification of liquids have the largest share in the market of membrane processes (Baker, 2012; Nunes and Peinemann, 2006). In filtration or electrodialysis, the membrane wettability is the essential prerequisite of good transport performance. On the other hand, gas-liquid membrane contactors operate efficiently only if the membrane pores are filled with the gas phase, although one or two sides of the membrane stay in contact with the liquid (Drioli *et al.*, 2006).

Depending on the conditions, the same membranes can be used both in membrane contactors and in filtration processes. For example, polytetrafluoroethylene (PTFE) or polyvinylidene fluoride (PVDF) membranes are suitable for both carbon dioxide removals in membrane contactors and for liquid filtration (Curcio and Drioli, 2005; Kang and Cao, 2014; Zaidiza *et al.*, 2016; Mansourizadeh and Ismail,

2009), just as polypropylene, polyethylene, polysulfone, polyetherimide, etc. membranes (Zhang *et al.*, 2006; Faiz *et al.*, 2013; Atchariyawut *et al.*, 2007). In the processes associated with high transmembrane pressure, the upper layer of the membrane is usually made of non-porous (elastomers) or micro-heterogeneous (glassy polymers) materials (Volkov *et al.*, 2008; Marchetti *et al.*, 2014).

In such dense layers, the transfer of matter occurs through the free volume. In flexible chain polymers such as rubbers, free volume elements are dynamically formed due to the statistical fluctuation of polymer segments. If the size of the free volume elements is sufficient, the molecules of the filtered liquid fill them, and the matter flows through the membrane. In glassy polymers, free volume elements are formed during polymer deposition. In the presence of bulky pendant groups and a rigid polymer chain, the dense packing of macromolecules becomes difficult. The most studied polymers of this class

are PIM-1, poly[4-methyl-2-pentyne], and poly[1-(trimethylsilyl)-1-propyne] (Srinivasan *et al.*, 1994; Harms *et al.*, 2012; Budd *et al.*, 2005; Fritsch *et al.*, 2012; Shantarovich *et al.*, 2000; Volkov *et al.*, 2009; Morisato and Pinnau, 1996; Khotimsky *et al.*, 2003). These polymers exhibit large free volume fractions, up to 30%, and more. As a result, free volume elements form coherent pore-like structures that facilitate the transfer of matter in the membrane, thus increasing gas and liquid permeability (Srinivasan *et al.*, 1994; Starannikova *et al.*, 2008; Volkov *et al.*, 2013; Yushkin *et al.*, 2015).

It was previously shown that the transfer of solvents through microporous membranes is nonlinearly related to the content of these solvents in the membrane under equilibrium conditions, i.e., to the solvent sorption (Volkov *et al.*, 2013; Yushkin *et al.*, 2015). It was noted that the sorption of liquid from aqueous ethanol solutions to PTMSP increased in the areas where the concentration of ethanol reached 10–20%, while the flow through the membrane was observed only at alcohol concentrations of greater than 50%. Hydrodynamic flow through the membrane occurs when there are fluid-filled channels connecting the opposite sides of the membrane. In this case, the fluid-filled pores act as conductors that form the system of transport channels. In polymers of internal microporosity, such transport channel systems are the free volume elements.

The situation when the fluid flows through the membrane arises only when sorption reaches critical values, is similar to the percolation theory, which is applied to analyze a wide range of systems (Stanley *et al.*, 1999; Essam, 1980; Parlar and Yortsos, 1988; Berezina and Karpenko, 2000). What also points to this is the finding (Yushkin *et al.*, 2008) that the electrical resistance of membranes decreased for liquids whose permeability increased. In membrane technology, the percolation theory has been widely used in mixtures of electrically conductive and non-conductive materials. The observation of the conductivity threshold in carbon nanotube composites showed that the addition of a certain amount of conductive carbon nanotubes, dispersed in a non-conducting polymer, abruptly increases the conductivity of the system (Bauhofer and Kovacs, 2009; Fangming *et al.*, 2005; Grekhov and Eremin, 2015).

To determine the impedance of a membrane, researchers usually examine the characteristics of an electric circuit in the alternating current mode with and without a

membrane installed (Canas *et al.*, 2001; Coster *et al.*, 1992; Gaedt *et al.*, 2002; Park *et al.*, 2005, 2006; Bannwarth *et al.*, 2015; Sistat *et al.*, 2008; Sedkaoui *et al.*, 2016; Hosseini *et al.*, 2017; Meier *et al.*, 2011). Since solvents have a rather low intrinsic conductivity, electrolytes containing monovalent Na^+ , K^+ , and Cl^- ions are used to improve the measurement sensitivity (Han *et al.*, 2016; Oliot *et al.*, 2016). In the general case, the impedance of the system should be calculated by solving a set of simultaneous equations that describe an equivalent electrical circuit consisting of many elements. However, in most cases, the task is greatly simplified. At low frequencies, the impedance of the system is equal to the summed impedances of the liquid and the membrane (Park *et al.*, 2006).

Previously, the impedance measurements under various conditions were used to assess the thickness of the selective layer in reverse-osmosis and nanofiltration membranes (Canas *et al.*, 2001; Malmgren-Hansen *et al.*, 1989; Asaka, 1990), the porosity of individual membrane layers (Coster *et al.*, 1992; Gaedt *et al.*, 2002), the wetting of membranes (Bannwarth *et al.*, 2015), and also to control the surface contamination (Gaedt *et al.*, 2002; Park *et al.*, 2005; Marbelia *et al.*, 2016). Such data can be obtained by measuring the spectra of electrochemical impedance in a wide frequency range (Canas *et al.*, 2001; Coster *et al.*, 1992; Gaedt *et al.*, 2002; Park *et al.*, 2005, 2006; Bannwarth *et al.*, 2015; Sistat *et al.*, 2008; Malmgren-Hansen *et al.*, 1989; Asaka, 1990).

The aim of this work is to study the patterns of filtration characteristics and conductive behavior of PTMSP associated with the change in the porous structure of the polymer when it swells depending on the properties of the solution in contact with the membrane.

2. MATERIALS AND METHODS

A glassy polymer of internal microporosity poly[1-(trimethylsilyl)-1-propyne] (PTMSP) (Gelest Inc., USA) was used in the experiments. Continuous membranes (films) were made of PTMSP by pouring the polymer solutions (0.5 wt %) in chloroform on to cellophane and drying at room temperature. To remove the tangential stresses after drying, the film samples were kept in butyl alcohol, then placed in ethanol and washed successively in ethanol-water solution, shaving a gradually decreasing concentration of

ethyl alcohol, according to the procedure used in (Volkov *et al.*, 2013). It was previously shown that when filtering ethanol-water solutions through PTMSP, the ratio of components does not change (Volkov *et al.*, 2013). In that research, the experiment with solutions containing NaCl gave a similar result. Therefore, in the calculations, it is assumed that the properties of the liquid in the membrane are the same as in the bulk solution where the membrane was placed.

To study the impedance characteristics of the membrane, it was placed in a cell (Figure 1), having a Teflon body (1), between two platinum electrodes (2, 4). The cell was previously described in detail by Berezkin *et al.*, 2012. The volume on both sides of the membrane (3) was filled with the studied fluid. The membrane was preliminarily kept in the solution for 24 hours, and after that, it was placed in the chamber pre-filled with the solution above the electrode (2). The active membrane area in the cell was 1 cm². It was shown in (Yushkin *et al.*, 2018) that after the membrane is placed in the solution, it takes less than three hours to reach the stationary values of the membrane electrical conductivity. The membrane was placed in the solution 24 hours before measuring the impedance characteristics, and this ensured that the measured values were stationary.

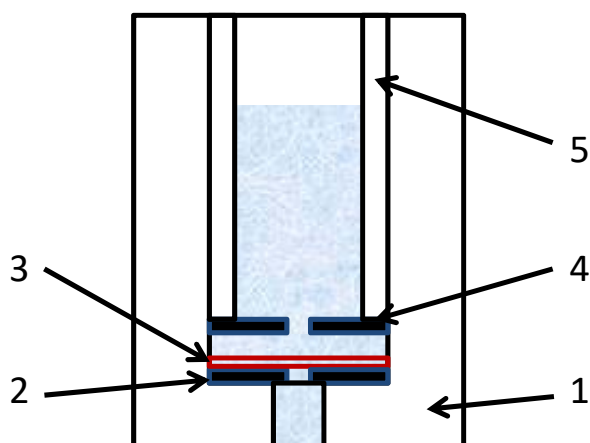


Figure 1. Cell for studying the impedance characteristics of membranes: 1 – cell body, 2 – lower electrode, 3 – membrane, 4 – upper electrode, 5 – sliding cylinder

A Teflon cylinder (5) with an electrode (4) slid into the chamber with the membrane from above. The distance between the electrodes was set remotely with an accuracy of 1 μm. The voltage in the cell and the phase difference between current and voltage were measured with

an accuracy of ~1% in the frequency range from 1 Hz to 2.6 MHz. The impedance characteristics were recorded automatically using the RLC-2010 impedance analyzer.

To measure the PTMSP surface flow potential, a polymethylmethacrylate slit device consisting of two symmetric parts was used (Figure 2).

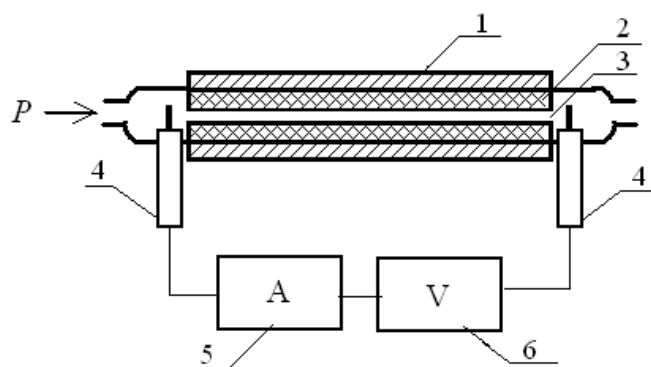


Figure 2. Slit device for measuring the ζ -potential of the membrane surface: 1 – cell body, 2 – membrane, 3 – channel, 4 – silver-chloride electrodes, 5 – multimeter, 6 – voltage source

Two identical PTMSP films (2) were stuck onto the cell body (1). During measurements, the channel width (3) in the device was $b = 2.5$ mm, the channel length was $l = 20$ mm, and the channel height h was altered using gaskets. The height was 70 μm while the membrane was dry, and decreased to 8 μm as the membrane swelled, depending on the percentage content of ethanol. The exact height of the slit was calculated by the flow rate of the solution passing through the channel:

$$h = \frac{\sqrt{12Q\mu l}}{\sqrt{b\Delta p\Delta t}} \quad (\text{Eq. 1})$$

when Q is the volume of fluid passing through the slit at pressure Δp for time Δt , and μ is the solution viscosity.

Silver-chloride electrodes (4) and a multimeter (5), consisting of the U5-12 amplifier (Russia) and the GDM-8246 voltmeter (GW Instek, Taiwan), was used to record the flow potential values. The input impedance of the amplifier in the potential measurement mode was 100 TΩ. The electrical conductivity of the slit was determined by the dependence of the current

on the voltage supplied from the DC power source (6). The method for measuring the ζ -potential is described in (Nebavskaya *et al.*, 2016, 2017).

The mixtures of water and ethanol in various mass concentrations C_0 were used as the liquid phase. To increase the electrical conductivity, 0.5 g/L NaCl was added to the solutions. The conductivity of the mixtures decreases as the ethanol concentration increases, which is associated with the transition from a strong electrolyte (NaCl in water) to a solution with ion associates (NaCl in alcohol). The formation of associates reduces the number of ions, which are the main charge carriers in the system (Harned and Owen, 1950) (Figure 3).

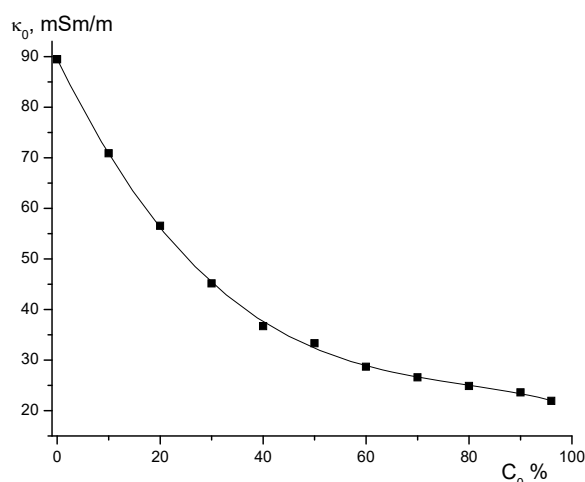


Figure 3. Conductivity κ_0 of ethanol-water solutions with 0.5 g/L NaCl

Before being placed in the cell, the films were kept in the NaCl-water solution for 24 hours. After that, they were placed in the device, filled with the studied mixture, for measuring electrical conductivity. Next, the program for automatic registration of impedance characteristics was launched. Successively increasing the frequency from 1 Hz to 2.66 MHz, the program recorded capacitance (C), conductivity (σ), resistance (R), imaginary ($\text{Im}Z$), and real ($\text{Re}Z$) parts of the complex impedance, and phase shift (ϕ).

After the recording cycle, the sample was placed in the NaCl solution in a mixture of 10% ethanol and 90% water for 24 hours. After that, the entire measurement procedure was repeated. For each sample, the impedance characteristics were measured in ethanol-water solutions, the ethanol concentration changing in the following

order: 0-10-20-30-40-50-60-70-80-90-96-90-80-70-60-50-40-30-20-10-0%.

The electrical conductivity of the membrane κ_m was determined by Equation 2:

$$\kappa_m = \frac{l}{R_m S} \quad (\text{Eq. 2})$$

where R_m is the electrical resistance of the membrane. The through porosity α_r , i.e., the ratio of the electrical conductivity of the membrane to the electrical conductivity of the same layer of volume electrolyte, is equal to $\alpha_r = \kappa_m / \kappa_0$

where κ_0 is the electrolyte conductivity.

The filtration experiments were carried out in dead-end cells previously described in (Volkov *et al.*, 2009), at transmembrane pressure 30 bar and room temperature. The active membrane area in the cells was $33.3 \cdot 10^{-3} \text{ m}^2$. To minimize the concentration polarization effect, the cells were equipped with suspended magnetic anchors and magnetic stirrers that mixed the liquid near the membrane surface. The volume of the primary solution was 800 ml. The membrane permeability was found by the gravimetric method. To do this, a receiving vessel was installed at the cell outlet. The vessel was designed in such a way as to minimize the evaporation of the liquid. The permeability coefficient P was used to characterize the membranes. It was calculated according to Equation 3:

$$P = \frac{m \cdot l}{S \cdot \Delta t \cdot \Delta p} \quad (\text{Eq. 3})$$

where m is the mass of permeate (kg) that passed through a membrane having the area S (m^2) over the period of time Δt (h) under the action of applied transmembrane pressure (Δp). The normalization of the membrane thickness (l) makes this parameter independent of the membrane thickness in the case of symmetrical membranes.

To determine the open porosity of the membrane α_o , i.e., the ratio of the pore volume occupied by the liquid to the membrane volume, 100 μm thick PTMSP films were cast. The mass of dry membranes was measured first, and then

they stayed in the studied solution for one week. The films were soaked in a sealed container in order to exclude the impact of solvent evaporation on the obtained sorption values. Next, the membrane was removed from the studied solution, the excess liquid was removed from its surface with filter paper, and the sample was weighed. The open porosity α_o was calculated by the gravimetric method by the formula:

$$\alpha_o = \frac{m_1 - m_0}{\rho_s V_m} \quad (\text{Eq. 4})$$

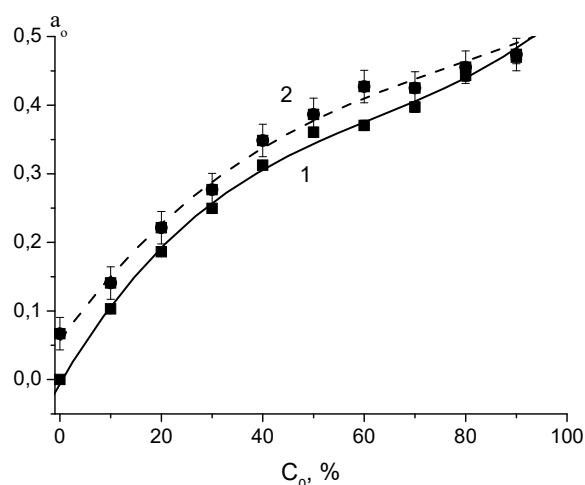
where m_1 is the mass after soaking in the solution, m_0 is the initial mass of the sample, ρ_s is the density of the solution, and V_m is the volume of the membrane.

3. RESULTS AND DISCUSSION

The threshold nature of the water-alcohol mixture flow through PTMSP and other highly permeable glassy polymers has already been shown (Yushkin *et al.*, 2015). This phenomenon is associated with the formation of a percolation cluster through which the liquid is transferred at high concentrations of alcohol.

Figures 4 and 5 demonstrate the dependence of the change in porosity and permeability of the solution on the concentration of ethanol in the solution. The nature of the concentration dependences apparently varies. While the change in porosity occurs at small alcohol concentrations, the permeability is not observed until the alcohol concentration reaches 50%, and only then the permeability manifests itself clearly. From this, it follows that first, the solution fills the existing free volume elements, which are unconnected to each other; and only after the porosity increases to $0.45 \text{ cm}^3/\text{cm}^3$, permeable channels appear and filtration begins. If the alcohol concentration in the solution decreased, the permeability coefficient was higher than with an increased alcohol concentration, i.e., hysteresis was observed. Hysteresis can also be observed when measuring the membrane porosity. In the case of porosity, hysteresis was less pronounced. Moreover, the presence of salt in the solution did not affect the permeability coefficient of the

studied liquids.



Figures 4. Open porosity α_o depending on the ethanol concentration in the solution: 1 – ethanol concentration increasing, 2 – ethanol concentration decreasing.

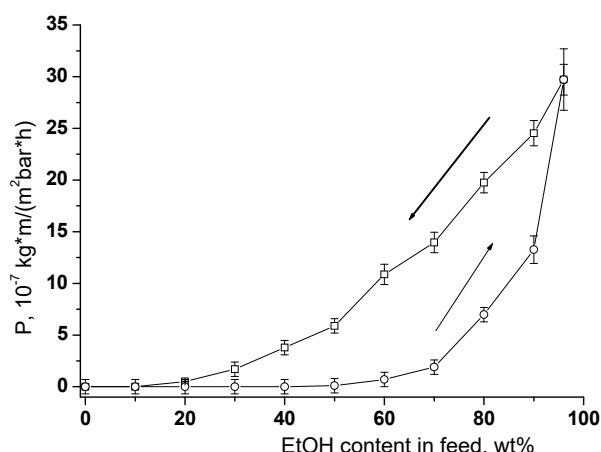


Figure 5. PTMSP permeability in ethanol-water solutions (adapted from (Yushkin *et al.*, 2018))

The wedging pressure in the membrane channels facilitates membrane swelling and formation of through infiltration channels. The main component of the wedging pressure at low electrolyte concentrations is the electrostatic one.

To assess the impact of the electrostatic component of the wedging pressure in the membrane channels on the formation of transport channels, the ζ -potential of the membrane surface was measured depending on the alcohol concentration in the ethanol-water solutions. The measurement showed that the ζ -potential was negative in an aqueous solution (Figure 6), but it

was much less than the potential of a conventional glassy polymer with a relatively small fraction of free volume (Kirby and Hasselbrink, 2004). For polystyrene in a 10^{-3} M KCl solution, the ζ -potential of the surface was -40 mV (Churaev *et al.*, 1988).

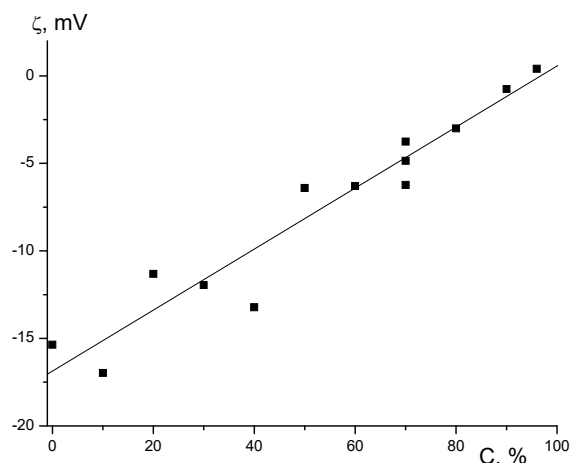
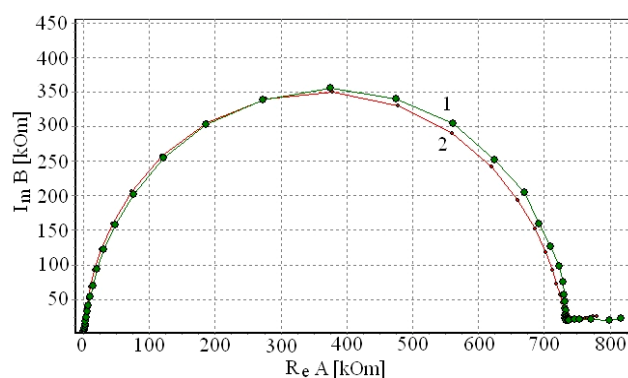


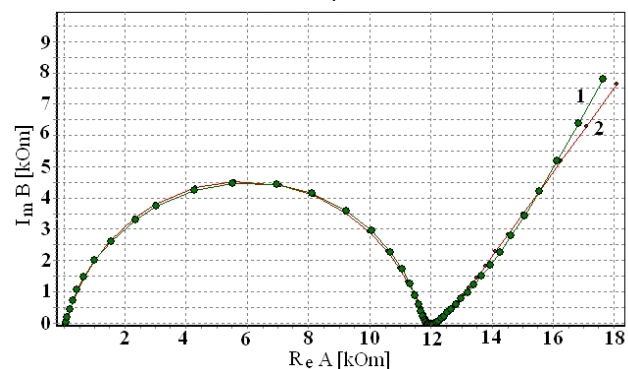
Figure 6. ζ -potential of the membrane surface at the 0.5 g/L NaCl concentration and various alcohol concentrations in the ethanol-water solutions

As the alcohol concentration increases, the ζ -potential of the PTMSP surface decreases in absolute value nearly to zero. Low potential values and, therefore, low electrostatic component values cannot increase the size or the number of transport channels. This means that an increase in the size or the number of transport channels is associated with non-electrostatic forces.

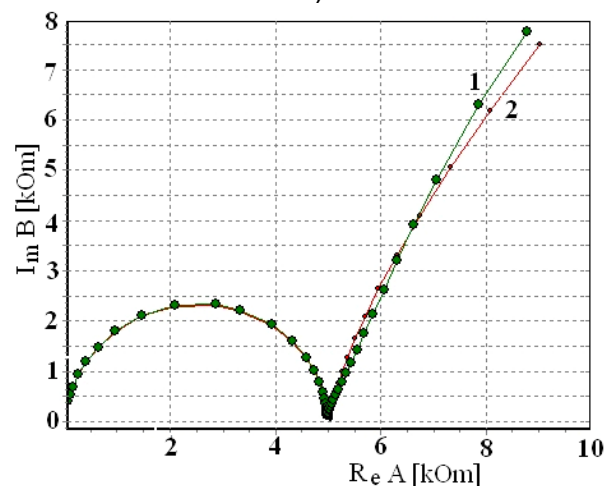
Another method for determining the porous structure of membranes is the impedance spectroscopy. The experiments were carried out with ethanol-water solutions having various alcohol concentrations and the 0.5 g/L NaCl concentration. The presence of salt made it possible to increase the conductivity of the solutions in order to cancel the contribution of the liquid layer between the membrane and the electrodes to the total resistance of the system. First, the capacitance and the resistance of the membrane and the liquid layer above it were measured at different distances between the electrodes and at several frequencies. It was found that the capacitance value or the resistance value, in the extrapolation of the dependences of the capacitance or the resistance to the zero thickness, did not differ from the same values when the electrodes were in direct contact with the membrane. Hence all further measurements were carried out with the electrodes pressed against the membrane.



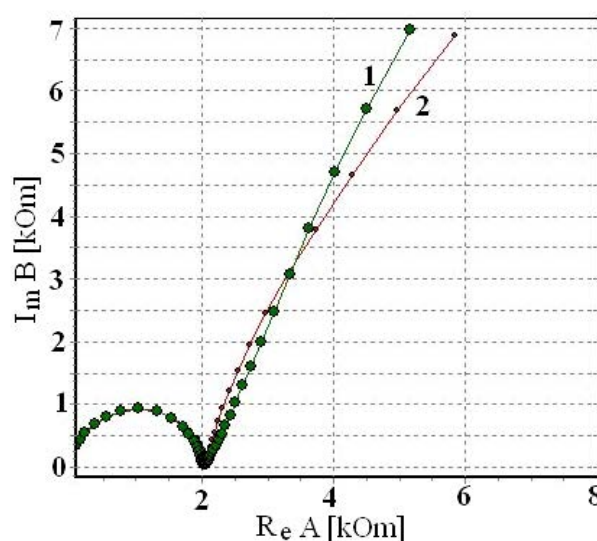
a)



b)



c)



d)

Figure 7. Hodograph curves in Nyquist coordinates for a membrane soaked in solutions with various alcohol concentrations: (a) 10%, (b) 40%, (c) 80 %, (d) 96 %.

Figure 7 shows the impedances of the membrane aged in solutions with various alcohol concentrations. Apparently, there is only one high-frequency arc on the spectrum. According to (Moya, 2016; Rubinstein *et al.*, 2009; Nikonenko and Kozmay, 2011), the high-frequency arc is determined by the geometric capacity of the membrane and its resistance. The characteristic frequency f_g , corresponding to the Nyquist section maximum, including capacitance and parallel resistance, can be determined by Equation 5 (Vorotyntsev, 2002; Barsoukov and Macdonald, 2005):

$$f_g = \frac{1}{2\pi C R_g} \quad (\text{Eq. 5})$$

where R_g is the diameter of the high-frequency arc.

The linear dependences on the right low-frequency part of the graph, which go upward with increasing the alcohol concentration in the solution, are associated with alcohol adsorption on the electrodes. The impedances of such processes can be soundly described by the Frumkin and Melik-Gaykazyan model that considers the impedance of the adsorption process in which diffusion limits the transport of matter to the electrode surface (Grafov and Ukshe, 1973; Stoyanov *et al.*, 1991; Frumkin and Melik-Gaykazyan, 1951). Figure 8 shows the model that presents our experiments very well, where R_m is the membrane resistance, C_m is the membrane capacity, C_{ad} is the adsorption capacity, R_{ct} simulates the resistance of the particles transfer from the solution to the adsorbed state, W is the diffusion limitation, and R_0 is the resistance of the solution between the membrane and the electrodes.

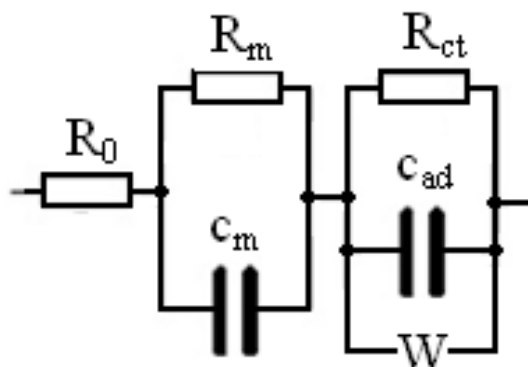
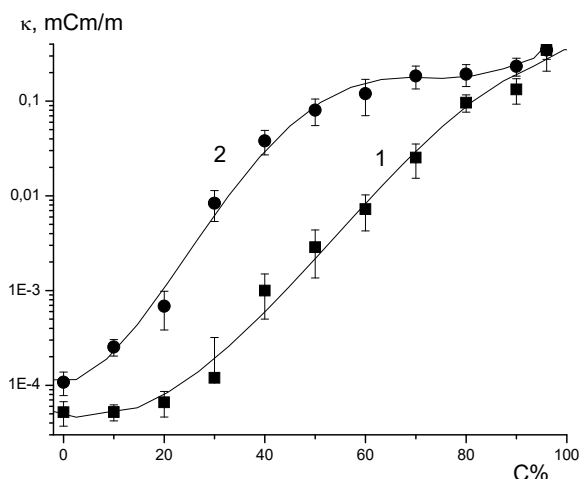


Figure 8. Model for calculating hodograph curves

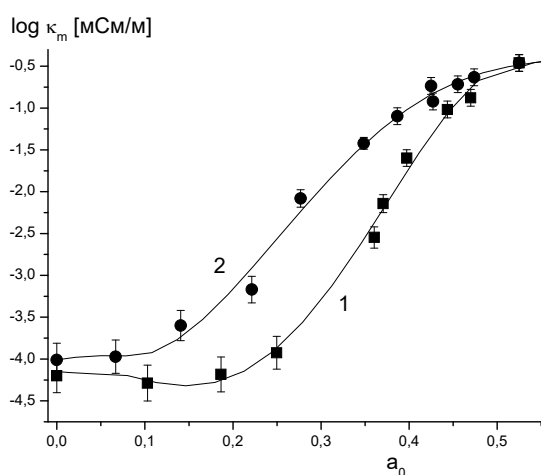
Figure 7 reports the curves 1, which were drawn from the experimental results and which we shall refer to as Curves 1. Curves 2 were calculated using the model shown in Figure 8. The calculations were performed using an equivalent circuit analyzer DCS. The error in determining the parameters does not exceed 1.5–2%.

As illustrated in Figure 7, the resistance R_g , which is determined by extrapolating the hodograph curve to the abscissa axis, practically coincides with the doubled value of R_m , which was calculated according to the model used. As calculations pinpointed, R_0 does not exceed 0.1% of the membrane resistance and, therefore, this value can be neglected. This also proves that it is possible to obtain the impedance characteristics of the membrane when the electrodes in the device are pressed against the membrane.

Figure 9 shows the dependences of the electrical conductivity of the membrane σ_m , calculated from the measured R_m values, depending on (a) the alcohol concentration and (b) the membrane porosity.



a)



b)

Figure 9. Dependence of the electrical conductivity of the membrane on (a) the alcohol concentration and (b) the membrane porosity: Curve 1 – increasing alcohol concentration, Curve 2 – decreasing alcohol concentration.

As can be seen from Figure 9, the conductivity varies nonlinearly at increasing ethanol concentration and increasing membrane porosity. The nature of the dependence changes dramatically at a porosity of about 0.25, the ethanol concentration increasing, and about 0.15, the ethanol concentration decreasing. These values are critical because above them, and percolation clusters are formed from the conductive elements, which provide a sharp increase in electrical conductivity. Similar

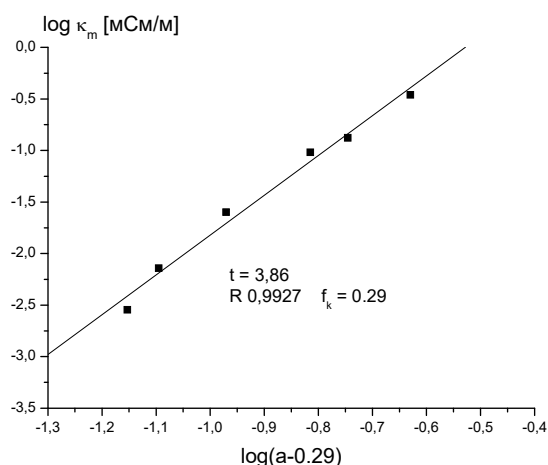
dependencies were obtained in (Vysotskii *et al.*, 1995; Kirkpatrick, 1973). In some cases, the change in properties after the critical point was more abrupt, as in (Berezina and Karpenko, 2000), for ion-exchange membranes, in which additional electrostatic forces occurred due to the presence of charges.

Percolation theory approaches can be used to analyze the obtained data. As shown by theoretical and experimental studies, the electrical conductivity of composites with different ratios of conducting and non-conducting phases near the percolation threshold is described by Equation 6 (Kirkpatrick, 1973):

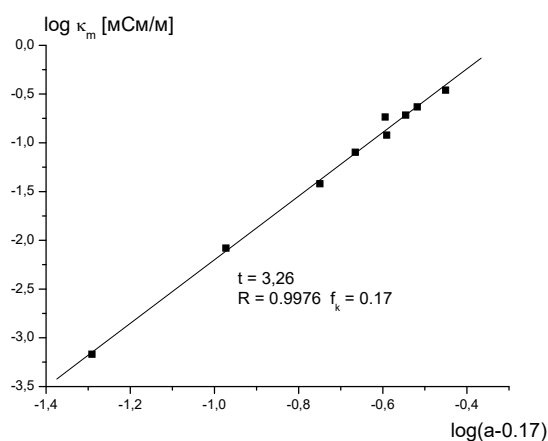
$$\sigma_m = \sigma_0 (f - f_k)^t \quad (\text{Eq. 6})$$

where σ_0 is the factor equal to the specific conductivity of the conductive material, f is the volume fraction of the conductive phase in the composition, f_k is the critical volume fraction of the conductor, and t is the critical conductivity index.

The critical porosity was estimated using the semi-logarithmic dependences shown in Figure 10, which made it possible to calculate the critical volume fraction of porosity a_k at which through conductivity channels are formed. When the alcohol content in the solution increases, $a_k = 0.29$, and when it decreases, $a_k = 0.17$. The critical conductivity index t is $t = 3.86 \pm 0.23$ in the first case and $t = 3.26 \pm 0.085$ in the second case. The critical conductor fraction was determined by the Monte Carlo methods (Kirkpatrick, 1973; Vysotskii *et al.*, 1995; McLachlan *et al.*, 1993; Hsu *et al.*, 1980), and it was found that this value is related to the size and the orientation of particles of both phases, and $f_k = 0.15$ for three-dimensional systems. However, in experiments with a strong asymmetry of the conducting and non-conducting forms, the values can be even larger (Kirkpatrick, 1973; Hsu and Berzins, 1985; Yushkin *et al.*, 2018). Thus, the values obtained agree with the literature data.



a)



b)

Figure 10. Change in the electrical conductivity of the membrane during swelling in the solution in the coordinates $\log \kappa_m - \log(a - a_k)$ with (a) increasing and (b) decreasing alcohol concentration in the solution.

However, the critical conductivity index is much larger than the theoretically calculated one. This may be due to a change in the electrical conductivity of the liquid inside the membrane during its swelling.

If compared, the membrane permeability and the membrane conductivity demonstrate identical relationships. For clarity, Figure 11 shows the values of permeability and conductivity, normalized to the corresponding values for ethanol. The dependence of permeability is bounded from below by a value of 0.01 on the value of ethanol permeability, which is due to the inability to pinpoint such small

transmembrane flows. When measuring the conductivity, there is no such bound, and it was possible to pinpoint a change in the transport characteristics of the membrane at lower ethanol concentrations.

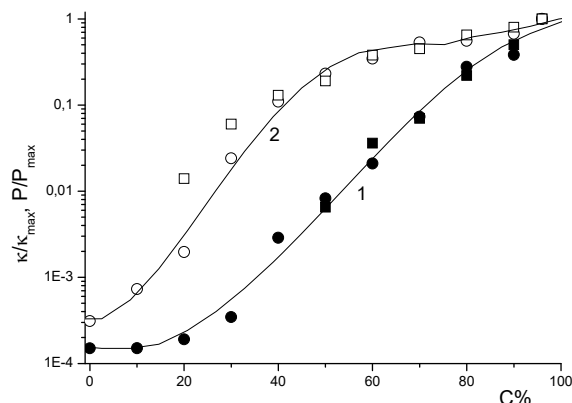


Figure 11. Permeability (squares) and conductivity (circles) of the PTMSP membranes in the ethanol-water solutions

As can be seen, when the ethanol concentration increases, the respective increase in conductivity begins at the ~30% ethanol concentration in the solution, and then the conductivity grows sharply with increasing the alcohol content. When the ethanol concentration decreases, the conductivity decreases slightly until the ethanol concentration reaches 40%, then decreases sharply with decreasing alcohol content, and becomes low at the 20% ethanol concentration. The membrane permeability, in the area where it was possible to measure it, behaves similarly to the conductivity. These data confirm that the conductivity and the permeability of the membrane are provided by the same transport channels formed by the percolation cluster from the liquid phase. The liquid permeability coefficient and the electrical conductivity are provided by the liquid phase inside the membrane and, therefore, the electrical resistance is a good criterion for predicting the transport properties of the membrane. As in (Yushkin *et al.*, 2018), a hysteresis of the membrane properties was observed when the ethanol concentration in the surrounding solution changed upward and downward. One of the mechanisms of the observed hysteresis is related to the fact that during the initial filling of the free volume elements, the largest free volume

elements are filled first, while the percolation cluster is formed at the ~30% ethanol concentration when the isolated elements begin to merge into a network after the smaller elements fill up. On the contrary, in desorption, the liquid first leaves the free volume elements that do not participate in the transfer of matter through the membrane, and the percolation cluster is destroyed at the ~10% ethanol concentration. In the absence of the percolation cluster, the transfer of matter is possible only by the diffusion mechanism, which provides for a significantly lower flow through the membrane.

The deformation of polymer molecules can be another mechanism supporting the hysteresis of hydraulic permeability and electrical conductivity at decreasing alcohol concentrations. Polymer swelling occurs with increasing the pressure in the free volume elements, and the deformation of the supramolecular structures of the polymer can occur, which is similar to the mechanical drawing of the polymer. The molecular orientation, which manifests itself at that, can remain intact for a long time after unloading at a temperature lower than the glass transition temperature. This created the observed hysteresis. It should also be noted that previously hysteresis phenomena were observed in various polymers with internal microporosity (Yushkin *et al.*, 2018), and in hydrophilic cellophane (Yushkin *et al.*, 2015).

Of special interest is the nature of the distribution of liquid-filled channels. A change in the volume fraction of liquid in the membrane entails a change in the dielectric constant of the membrane (ϵ), which can be determined if the capacity and the thickness of the membrane are known.

The ratio of components, including salt, did not change when passing through the membrane under the pressure drop. Based on this, it can be assumed that the concentration of components in the membrane also does not change. Then, it is possible to calculate the volume fractions of the system components (Q_m and Q_s) by Lichtenecker and Rother's mixture formula (Lichtenecker and Rother, 1931):

$$\epsilon^x = \epsilon_m^x \cdot Q_m + \epsilon_s^x \cdot Q_s \quad (\text{Eq. 7})$$

where Q_m and ϵ_m are the volume fraction and the dielectric permittivity of the polymer (membrane material), and Q_s and ϵ_s are the

volume fraction and the dielectric permittivity of the solution in the membrane.

The authors of (Yushkin *et al.*, 2015; Stanley *et al.*, 1999) relied on the assumption that the macroscopic properties of a liquid (by the example of viscosity and density) inside a membrane are close to the properties in a solution. By analogy, we can assume that the dielectric permittivity of the solution in the membrane is equal to the dielectric permittivity of the solution in which the membrane was soaked. The parameter x characterizes the spatial arrangement of the components. The calculations were made for the chaotic arrangement of channels ($x = 0$), for the two extreme cases of layered structures, when the liquid forms channels in the direction of the electric field (perpendicular to the membrane surface) ($x = 1$), and for the case when the liquid is arranged in layers, perpendicular to the field ($x = 1$). The average dielectric permittivity of the membrane ϵ was calculated by the standard formula for a flat capacitor:

$$\epsilon = \frac{C \cdot d}{\epsilon_0 \cdot S} \quad (\text{Eq. 8})$$

where C is the electric capacitance, d is the membrane thickness, ϵ_0 is the dielectric permittivity, and S is the area of the measuring electrodes.

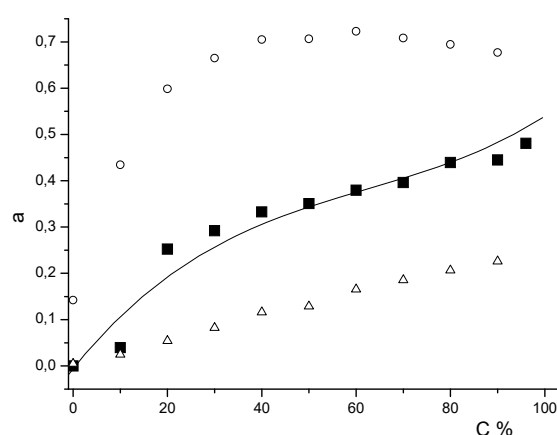


Figure 12. Comparison of the membrane porosity values calculated from the measured membrane capacity at various values of the parameter x , with the values obtained by the weight method:

$x = 1$, circles; $x = 0$, squares; $x = -1$, triangles. The results of porosity measurements by the weight method are taken from Figure 4 and shown in this figure by a solid line.

The obtained amounts of liquid in the membrane, calculated in this way, were compared with the sorption values determined experimentally, and it was found that the calculations at $x \approx 0$ are in the best agreement with the experiment. This means that the channels are randomly distributed inside the membrane.

To assess the influence of transport channels located mainly along the electric field, it is necessary to evaluate through the porosity of the membrane.

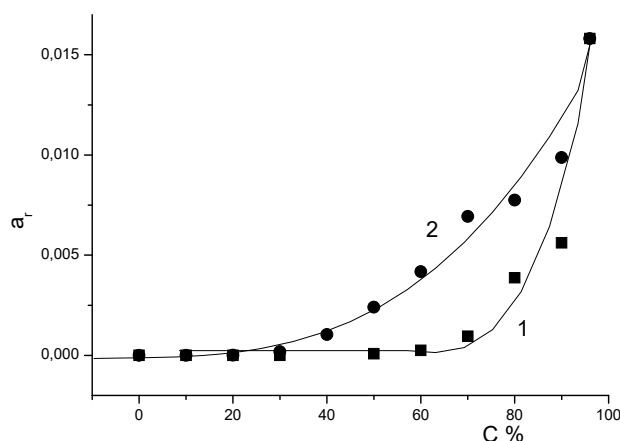


Figure 13. Dependence of the through the porosity of the membrane α_L on the ethanol concentration at the (1) increasing and (2) decreasing alcohol concentrations in the solution.

Through the porosity of the membrane can be estimated by the ratio of the membrane conductivity to the conductivity of the solution layer having the same thickness and area as the membrane. Figure 13 presents such a relationship: the through porosity does not exceed 2% of the total open porosity of the membrane. Hence the through channels do not affect the calculation of the structure by Lichtenecker and Rother's formula (Lichtenecker and Rother, 1931). Therefore, the channels are mostly randomly distributed inside the membrane, and the infiltration channels make up a small part of the total number of filled-liquid

channels. This conclusion is consistent with the ideas about the structure of the studied membranes and the transfer mechanisms in them.

4. CONCLUSION

This study addressed the impedance characteristics of PTMSP membranes in NaCl solutions in ethanol-water mixtures with various alcohol content. The critical porosity was estimated, and the critical volume fraction of porosity α_k at which the through conductivity channels are formed, was calculated. When the alcohol content in the solution increases, $\alpha_k = 0.29$, and when it decreases, $\alpha_k = 0.17$. The critical conductivity index t is $t = 3.86 \pm 0.23$ in the first case and $t = 3.26 \pm 0.085$ in the second case.

The obtained dependencies indicate that the matter is transferred through the liquid phase elements. As the amount of sorbed liquid increases, these elements form a percolation cluster which remains intact at decreased sorption. The porous structure of a dry PTMSP membrane consists of free volume elements that are hardly connected to each other. At low alcohol concentrations, the transfer of liquid between them is possible only due to diffusion. However, even at low alcohol concentrations, the free volume elements are able to expand due to swell, which causes deformation of macromolecules and supramolecular structures of the polymer and a decrease in the length of diffusion gaps. The through channels, connecting both sides of the membrane, begin to form at ~30% alcohol concentration. At the same time, both the permeability and the electrical conductivity grow as a power function, in contrast to the porosity that increases linearly. The hysteresis effect was observed in the measured values of porosity, permeability, conductivity and capacity. With an increase in the alcohol content in the solution, these values are lower than with a decrease. This difference can be attributed to the relaxation of the supramolecular structures of the polymer to the initial state after its swelling. As known, the relaxation of structures in glassy polymers far from the glass transition temperature is very difficult.

Lichtenecker and Rother's formula (Lichtenecker and Rother, 1931) helped to calculate the volume fractions of the conducting and non-conducting phases in the system. The

obtained values of the amount of liquid in the membrane at various spatial arrangements of the channels made it possible to establish the structure of the liquid-filled channels. The best agreement with the experimental values was obtained for the chaotic structure. This is consistent with the existing ideas about the structure of the studied membranes and confirms the assumption that the percolation cluster is formed from free volume elements filled with the liquid phase. Through the porosity of even highly swollen membranes does not exceed 2% of the total open porosity of the membrane. Therefore, the channels are mostly randomly distributed inside the membrane, and the infiltration channels make up a small part of the total number of liquid-filled channels. The observed low values of the zeta potential and, consequently, the low values of the electrostatic component of the wedging pressure indicate that the increase in the size or the number of transport channels is associated with non-electrostatic forces.

5. ACKNOWLEDGMENTS

This research was funded by the Russian Foundation for Basic Research (RFBR project No. 16-08-00839a).

6. REFERENCES

- Asaka, K. Dielectric-properties of cellulose-acetate reverse-osmosis membranes in aqueous-salt-solutions. *J. Membr. Sci.*, **1990**, 50, 71.
- Atchariyawut, S., Jiratananon, R., Wang, R. Separation of CO₂ from CH₄ by using gas-liquid membrane contacting process. *J. Membr. Sci.*, **2007**, 304, 163–172.
- Baker, R. W. Membrane technology and applications, Third Edition. NY, USA: John Wiley & Sons, Inc., **2012**.
- Bannwarth, S., Darestani, M., Coster, H., Wessling, M. Characterization of hollow fiber membranes by impedance spectroscopy. *J. Membr. Sci.*, **2015**, 473, 318.
- Barsoukov, E., Macdonald, J. R. Impedance Spectroscopy Theory, Experiment, and Applications Second Edition Preface. *Impedance Spectroscopy*, **2005**.
- Bauhofer, W., Kovacs, J. Z. A review and analysis of electrical percolation in carbon nanotube polymer composites. *Composites Science and Technology*, **2009**, 69, 1486.
- Berezina, N. P., Karpenko, L. V. Percolation effects in ion-exchange materials. *Colloid J.*, **2000**, 62(6), 749–757.
- Berezkin, V. V., Kiseleva, O. A., Mchedlishvili, B. V., Sobolev, V. D. Electrical conductivity of KCl solutions in pores of track-etched polymer membranes. *Petroleum Chemistry*, **2012**, 52, 636.
- Budd, P. M., Msayib, K. J., Tattershall, C. E., Ghanem, B. S., Reynolds, K. J., McKeown, N. B., Fritsch, D. Gas separation membranes from polymers of intrinsic microporosity. *J. Membr. Sci.*, **2005**, 251, 263.
- Canas, A., Ariza, M. J., Benavente, J. Characterization of active and porous sublayers of a composite reverse osmosis membrane by impedance spectroscopy, streaming and membrane potentials, salt diffusion, and X-ray photoelectron spectroscopy measurements. *J. Membr. Sci.*, **2001**, 183, 135.
- Churaev, N. V., Sergeeva, I. P., Sobolev, V. D., Ulberg, D. E. Investigation of the electrosurface properties of polymers by a capillary electrokinetic method. *Electrokinetic Phenomena'88. Part 1. Drezden: AW DDR Institut für Technologie der Polymere*, **1988**, 277–289.
- Coster, H. G. L., Kim, K. J., Dahlan, K., Smith, J. R., Fell, C. J. D. Characterization of ultrafiltration membranes by impedance spectroscopy.1. Determination of the separate electrical parameters and porosity of the skin and sublayers. *J. Membr. Sci.*, **1992**, 66, 19.
- Curcio, E., Drioli, E. Membrane distillation and related operations. *Separation and Purification Reviews*, **2005**, 34, 35.
- Drioli, E., Criscuoli, A., Curcio, E. Membrane contactors: fundamentals, applications and potentialities. In: E. Drioli, A. Criscuoli, E. Curcio (Eds.). *Membrane Science and Technology, Series 11*. Amsterdam: Elsevier, **2006**.
- Essam, J. W. Percolation theory. *Reports on Progress in Physics*, **1980**, 43, 833.
- Faiz, R. Fallanza, M., Boributh, S., Jiratananon, R., Ortiz, I., Li, K. Long

- term stability of PTFE and PVDF membrane contactors in the application of propylene/propane separation using AgNO₃ solution. *Chem. Eng. Sci.*, **2013**, *94*, 108–119.
17. Fangming, D., Fischer, J. E., Winey, K. I. Effect of nanotube alignment on percolation conductivity in carbon nanotube/polymer composites. *Phys. Rev. B.*, **2005**, *72*, 121404.
 18. Fritsch, D., Merten, P., Heinrich, K., Lazar, M., Priske, M. High-performance organic solvent nanofiltration membranes: Development and thorough testing of thin-film composite membranes made of polymers of intrinsic microporosity (PIMs). *J. Membr. Sci.*, **2012**, *401*, 222.
 19. Frumkin, A. N., Melik-Gaykazyan, V. I. Definition of kinetics of adsorption organic substances on measurements of capacitance and conductivity of border an electrode-solution of alternating current. *Doklady AN USSR*, **1951**, *77*, 855.
 20. Gaedt, L., Chilcott, T. C., Chan, M., Nantawisarakul, T., Fane, A.G., Coster, H. G. L. Electrical impedance spectroscopy characterization of conducting membranes II. *Experimental. J. Membr. Sci.*, **2002**, *195*, 169.
 21. Grafov, B. M., Ukshe, E. A. Electrochemical chains of alternating current. Moscow: Nauka Publ., **1973**.
 22. Grekhov, A. M., Eremin, Y. S. On the threshold concentration of sticks providing formation of a percolating cluster in mixed matrix membranes. *J. Membr. Sci.*, **2015**, *485*, 42.
 23. Han, L., Galier, S., Roux-de Balman, H. Structural properties of cation exchange membranes: Characterization, electrolyte effect and solute transfer. *J. Membr. Sci.*, **2016**, *511*, 207.
 24. Harms, S., Rätzke, K., Faupel, F., Chaukura, N., Budd, P. M., Egger, W., Ravelli, L. Aging and Free Volume in a Polymer of Intrinsic Microporosity (PIM-1). *The Journal of Adhesion*, **2012**, *88*, 608.
 25. Harned, H. S., Owen, B. B. The physical chemistry of electrolytic solutions. NYC: Reinhold, **1950**.
 26. Hosseini, S. M., Jashni, E., Amani, S., Van der Bruggen, B. Tailoring the electrochemical properties of ED ion exchange membranes based on the synergism of TiO₂ nanoparticles-co-GO nanoplates. *J. Colloid Interface Sci.*, **2017**, *505*, 763.
 27. Hsu, W. Y., Barkley, J. R., Meakin, P. Ionpercolation and insulator-to-conductor transition in Nafion perfluorosulfonic acid membranes. *Macromolecules*, **1980**, *13*, 198.
 28. Hsu, W. Y., Berzins, T. Percolation and effective-medium theories for perfluorinated ionomers and polymer composites. *Polym. Phys. Ed.*, **1985**, *23(10)*, 933.
 29. Kang, G., Cao, Y. *J. Membr. Sci.*, **2014**, *463*, 145.
 30. Khotimsky, V. S., Matson S. M., Litvinova E. G., Bondarenko G. N., Rebrov A. I. Synthesis of poly(4-methyl-2-pentyne) with various configurations of macromolecular chains. *Polym. Sci., Ser. A.*, **2003**, *45*, 740.
 31. Kirby, B. J., Hasselbrink, E. F. Zeta potential of microfluidic substrates: 2. Data for polymers. *Electrophoresis*, **2004**, *25(2)*, 203–213.
 32. Kirkpatrick, S. *Rev. Mod. Phys.*, **1973**, *45*, 574.
 33. Lichtenecker, K., Rother, K. Die Herleitung des logarithmischen Mischungsgesetzes des allgemeinen prinzipien der stationären Strömung. *Physikalische Zeitschrift*, **1931**, *32(6)*, 255–260.
 34. Malmgren-Hansen, B., Sørensen, T. S., Jensen, J. B., Hennenberg, M. Electric impedance of cellulose-acetate membranes and a composite membrane at different salt concentrations. *J. Colloid Interface Sci.*, **1989**, *130*, 359.
 35. Mansourizadeh, A., Ismail, A.F.. Hollow fiber gas-liquid membrane contactors for acid gas capture. *Journal of Hazardous Materials*, **2009**, *171*, 38.
 36. Marbelia, L., Mulier, M., Vandamme, D., Muylaert, K., Szymczyk, A., Vankelecom, I. F. J. Polyacrylonitrile membranes for microalgae filtration: Influence of porosity, surface charge, and microalgae species on membrane fouling. *Algal Research*, **2016**, *19*, 128.
 37. Marchetti, P., Jimenez Solomon, M. F., Szekeley, G., Livingston, A. G. Molecular Separation with Organic Solvent Nanofiltration: A Critical Review. *Chemical reviews*, **2014**, *114*, 10735.
 38. McLachlan, D. S., Blaszkiewicz, M., Newnham, R. E. Electrical-resistivity of composites. *J. Am. Ceram. Soc.*, **1990**, *73(M8)*, 2187.
 39. Meier, J. G., Crespo, C., Pelegay, J. L.,

- Castell, P., Sainz, R., Maser, W. K., Benito, A. M. *Polymer*, **2011**, 52, 1788.
40. Morisato, A., Pinnau, I. Synthesis and gas permeation properties of poly(4-methyl-2-pentyne). *J. Membr. Sci.*, **1996**, 121, 243.
 41. Moya, A. A. Electrochemical Impedance of Ion-Exchange Membranes with Interfacial Charge Transfer Resistances. *J. Phys. Chem. C.*, **2016**, 120, 6543–6552.
 42. Nebavskaya, K. A., Sarapulova, V. V., Sabbatovskiy, K. G., Sobolev, V. D., Pismenskaya, N. D., Nikonenko, V. V., Sistat, P. Influence of dzeta-potential of a surface of ionoobmennyy membranes on development of equilibrium and nonequilibrium electroconvection. *Condensed matter and interphases*, **2016**, 18, 374.
 43. Nebavskaya, K. A., Sarapulova, V. V., Sabbatovskiy, K. G., Sobolev, V. D., Pismenskaya, N. D., Sistat, P., Cretin, M., Nikonenko, V. V. Impact of exchange membrane surface charge and hydrophobicity on electroconvection underlimiting and overlimiting currents. *J. Membr. Sci.*, **2017**, 523, 36.
 44. Nikonenko, V. V., Kozmay, A. E. Electrical equivalent circuit of an ion-exchange membrane system. *Electrochim. Acta.*, **2011**, 56, 1262–1269.
 45. Nunes, S. P., Peinemann, K. V., Membrane technology: in the chemical industry. NY, USA: John Wiley & Sons, **2006**.
 46. Oliot, M., Galier, S., Roux-de Balman, H., Bergel, A. Ion transport in microbial fuel cells: Key roles, theory and critical review. *Applied energy*, **2016**, 183, 1682.
 47. Park, J. S., Chilcott, T. C., Coster, H. G. L., Moon, S. H. Characterization of BSA-fouling of ion-exchange membrane systems using a subtraction technique for lumped data. *J. Membr. Sci.*, **2005**, 246, 137.
 48. Park, J. S., Choi, J. H., Woo, J. J., Moon, S. H. An electrical impedance spectroscopic (EIS) study on transport characteristics of ion-exchange membrane systems. *J. Colloid Interface Sci.*, **2006**, 300, 655.
 49. Parlar, M., Yortsos, Y. C. Percolation theory of vapor adsorption desorption processes in porous materials. *J. Colloid Interface Sci.*, **1988**, 124, 162.
 50. Rubinstein, I., Zaltzman, B., Futerman, A., Gitis, V., Nikonenko, V. Reexamination of electrodiffusion time scale. *Phys. Rev. E - Stat. Nonlinear, Soft Matter Phys.*, **2009**, 79, 021506.
 51. Sedkaoui, Y., Szymczyk, A., Lounici, H., Arous, O. A new lateral method for characterizing the electrical conductivity of ion-exchange membranes. *J. Membr. Sci.*, **2016**, 507, 34.
 52. Shantarovich, V. P., Kevdina, I. B., Yampolskii, Y. P., Alentiev, A. Y. Positron annihilation lifetime study of high and low free volume glassy polymers: Effects of free volume sizes on the permeability and permselectivity. *Macromolecules*, **2000**, 33, 7453.
 53. Sistat, P., Kozmay, A., Pismenskaya, N., Larchet, C., Pourcelly, G., Nikonenko, V. Low-frequency impedance of an ion-exchange membrane system. *Electrochimica Acta*, **2008**, 53, 6380.
 54. Srinivasan, R., Auvil, S. R., Burban, P. M. Elucidating the mechanism(s) of Gas-transport in polu[1-(trimethylsilyl)-1-propyne] (PTMSP) membranes. *J. Membr. Sci.*, **1994**, 86, 67.
 55. Stanley, H. E., Andrade, J. S., Havlin, S., Makse, H. A., Suki, B. Percolation phenomena: a broad-brush introduction with some recent applications to porous media, liquid water, and city growth. *Physica A: Statistical Mechanics and its Applications*, **1999**, 266, 5.
 56. Starannikova, L., Pilipenko, M., Belov, N., Yampolskii, Y., Gringolts, M., Finkelshtein, E. Addition-type polynorbornene with Si(CH₃)₃ side groups: Detailed study of gas permeation and thermodynamic properties. *J. Membr. Sci.*, **2008**, 323, 134.
 57. Stoyinov, Z. B., Grafov, B. M., Savova-Stoyinov, B. S., Elkin, V. V. Electrochemical impedance. Moscow: Nauka Publ., **1991**.
 58. Volkov, A., Yushkin, A., Grekhov, A., Shutova, A., Bazhenov, S., Tsarkov, S., Khotimsky, V., Vlugt, T. J. H., Volkov, V. Liquid permeation through PTMSP: One polymer for two different membrane applications. *J. Membr. Sci.*, **2013**, 440, 98.
 59. Volkov, A. V., Korneeva, G. A., Tereshchenko, G. F. Organic solvent nanofiltration: Prospects and applications. *Uspekhi khimii*, **2008**, 77(11), 1053–1064.
 60. Volkov, A. V., Parashchuk, V. V., Stamatialis, D. F., Khotimsky, V. S., Volkov, V. V., Wessling, M. High

- permeable PTMSP/PAN composite membranes for solvent nanofiltration. *J. Membr. Sci.*, **2009**, 333, 88.
61. Vorotyntsev, M. A. Impedance of thin films with two mobile charge carriers. Interfacial exchange of both species with adjacent media. Effect of the double layer charges. *Electrochim. Acta.*, **2002**, 47, 2071.
 62. Vysotskii, V. V., Pryamova, T. D., Roldugin, V. I., Shamurina, M. V. Percolation transitions and conductivity mechanisms in metal-filled polymer-films. *Colloid J. V.*, **1995**, 57, 610.
 63. Yushkin, A., Grekhov, A., Matson, S., Bermeshev, M., Khotimsky, V., Finkelstein, E., Budd, P. M., Volkov, V., Vlugt, T. J. H., Volkov, A. Study of glassy polymers fractional accessible volume (FAV) by extended method of hydrostatic weighing: Effect of porous structure on liquid transport. *React. Funct. Polym.*, **2015**, 86, 269.
 64. Yushkin, A., Grekhov, A., Matson, S., Bermeshev, M., Khotimsky, V., Finkelstein, E., Budd, P. M., Volkov, V., Vlugt, T. J. H., Volkov, A. *React. Funct. Polym.*, **2015**, 86, 269.
 65. Yushkin, A., Vasilevsky, V., Khotimskiy, V., Szymczyk, A., Volkov, A. Evaluation of liquid transport properties of hydrophobic polymers of intrinsic microporosity by electrical resistance measurement. *J. Membr. Sci.*, **2018**, 554, 346.
 66. Zaidiza, D. A., Wilson, S. G., Belaissaoui, B., Rode, S., Castel, C., Roizard, D., Favre, E. Rigorous modeling of adiabatic multicomponent CO₂ post-combustion capture using hollow fiber membrane contactors. *Chemical Engineering Science.*, **2016**, 145, 45.
 67. Zhang, H.-Y., Wang, R., Liang, D. T., Tay, J. H., Modeling and experimental study of CO₂ absorption in a hollow fiber membrane contactor. *J. Membr. Sci.*, **2006**, 279, 301–310.

EFEITO DE PESTICIDAS NO NÍVEL DE DANOS AO MTDNA EM CABEÇAS DE ABELHAS (*BOMBUS TERRESTRIS* L.)

PESTICIDES EFFECT ON THE LEVEL OF MTDNA DAMAGE IN BUMBLEBEES HEADS (*BOMBUS TERRESTRIS* L.)

ВЛИЯНИЕ ПЕСТИЦИДОВ НА УРОВЕНЬ ПОВРЕЖДЕНИЯ мтДНК В ГОЛОВЕ ШМЕЛЕЙ (*BOMBUS TERRESTRIS* L.)

SYROMYATNIKOV, Mikhail Yurievich^{1, 2, 3*}, GUREEV, Artem Petrovich¹, MIKHAYLOV, Evgeny Vladimirovich³, PARSHIN, Pavel Andreevich³, POPOV, Vasily Nikolaevich^{1, 2}

¹ Federal State Budgetary Educational Institution of Higher Education Voronezh State University, Voronezh, Russian Federation

² Federal State Budgetary Educational Institution of Higher Education Voronezh State University of Engineering Technologies, Voronezh, Russian Federation

³ Federal State Funded Research Institution All-Russian Research Veterinary Institute of Pathology, Pharmacology and Therapy, Voronezh, Russian Federation

* Correspondence author

e-mail: mikhailsyromyatnikov@yandex.ru

Received 06 December 2019; received in revised form 12 February 2020; accepted 18 February 2020

RESUMO

O zangão é um dos polinizadores mais importantes para plantas consumidas por seres humanos. Atualmente, existe um risco significativo de extinção para vários polinizadores, incluindo abelhas. Uma das causas mais prováveis é o efeito tóxico dos pesticidas. O efeito mutagênico de pesticidas no DNA de abelhas não foi estudado. O objetivo deste trabalho foi estudar a genotoxicidade de pesticidas para DNA em cabeças de abelhas *Bombus terrestris*. Os autores descobriram que, se adicionados às mitocôndrias isoladas das abelhas, os pesticidas direcionados às mitocôndrias causavam menos danos que os pesticidas de amplo espectro. A maior quantidade de dano ao mtDNA foi causada pela adição de Malathion e Difenconazole às mitocôndrias isoladas. Além disso, os insetos que consumiram xarope com pesticidas apresentaram mais danos à cabeça do que quando o pesticida foi adicionado às mitocôndrias isoladas. Malathion e Cypermethrin demonstraram efeitos genotóxicos significativos *in vivo*. O difenconazol causou danos graves ao mtDNA, enquanto a deltametrina não teve nenhum efeito genotóxico. Entre os pesticidas direcionados às mitocôndrias, Fenazaquin e Pyridaben demonstraram a maior genotoxicidade. O clorfenapir, o hidrametilnona e o tolfenpiradado não apresentaram genotoxicidade do mtDNA. Foi observado um aumento no número de cópias do mtDNA em insetos que consumiram xarope de açúcar com Deltametrina e Tolfenpirita. Esse aumento é provavelmente um efeito compensatório em resposta à inibição da respiração mitocondrial. Este estudo constatou que, em geral, pesticidas de amplo espectro (Difenconazol, Deltametrina, Esfenvalerato, Malathion e Cipermetrina) demonstram maior genotoxicidade do mtDNA em cabeças de abelhas em comparação com pesticidas direcionados às mitocôndrias (Fenazaquina, Clorfenapir, Hydramethylnon, Pyridaben e Pyridaben).

Palavras-chave: pesticidas, abelhas, cabeça, mtDNA, danos, genotoxicidade..

ABSTRACT

Bumblebees are one of the most important pollinators for plants consumed by humans. Currently, there is a significant risk of extinction for several pollinators, including bumblebees. One of the most likely causes is the toxic effect of pesticides. The mutagenic effect of pesticides on the DNA of bumblebees has not been studied. The aim of this work was to study the genotoxicity of pesticides for DNA in *Bombus terrestris* heads. The authors found that if added to bumblebees' isolated mitochondria, mitochondrial-directed pesticides caused less damage than broad-spectrum pesticides. The greatest amount of mtDNA damage was caused by adding Malathion and Difenconazole to isolated mitochondria. Moreover, insects that consumed syrup with pesticides displayed more damage to the head than when the pesticide was added to isolated mitochondria. Malathion and

Cypermethrin demonstrated significant genotoxic effects *in vivo*. Difenoconazole caused severe damage to mtDNA, while Deltamethrin did not have any genotoxic effect. Among mitochondria-targeted pesticides, Fenazaquin and Pyridaben demonstrated the highest genotoxicity. Chlorfenapyr, Hydramethylnone, and Tolfenpyrad did not show mtDNA genotoxicity. An increase in the number of copies of mtDNA was observed in insects that consumed sugar syrup with Deltamethrin and Tolfenpyrad. This increase is probably a compensatory effect in response to inhibition of mitochondrial respiration. This study found that, in general, broad-spectrum pesticides (Difenoconazole, Deltamethrin, Esfenvalerate, Malathion, and Cypermethrin) demonstrate greater mtDNA genotoxicity in bumblebees' heads compared with mitochondria-targeted pesticides (Fenazaquin, Chlorfenapyr, Hydramethylnon, Pyridaben, and Tolfenpyrad).

Keywords: pesticides, bumblebees, head, mtDNA, damage, genotoxicity.

АННОТАЦИЯ

Шмели являются одним из важнейших опылителей растений, потребляемых в пищу человеком. В настоящее время в мире наблюдается тенденция вымирания опылителей, в том числе шмелей. Одной из наиболее вероятных причин такого явления – токсическое действие пестицидов. Мутагенное действие пестицидов на ДНК шмелей практически не изучено. Целью данной работы явилось изучение генотоксичности пестицидов для ДНК в головах шмелей *Bombus terrestris*. Выявлено, что при добавлении к изолированным митохондриям шмелей митохондриально-направленные пестициды вызывали меньшее количество повреждений, чем пестициды широкого спектра действия. Наибольшее количество повреждений мтДНК вызывало добавление к изолированным митохондриям малатиона и дифеноконозола. При этом потребление насекомыми сиропа с пестицидами индуцирует большее количество повреждений в голове, чем добавление пестицида к изолированным митохондриям. Значительный генотоксический эффект *in vivo* демонстрировали малатион и циперметрин. Сильные повреждения мтДНК вызывал дифеноконозол, в то время как дельтаметрин не оказывал никакого генотоксического эффекта. Среди митохондриально-направленных пестицидов наибольшую генотоксичность проявляли феназахин и пиридабен. Хлорфенапир, гидраметилнон и толфенпирад не проявляли генотоксичность в отношении мтДНК. Увеличение количества копий мтДНК наблюдалось у насекомых, которые потребляли сахарный сироп с дельтаметрином и толфенпирадом. Увеличение количества копий мтДНК, возможно, является компенсаторным эффектом в ответ на ингибирование митохондриального дыхания. Установлено, что в целом пестициды широкого спектра действия (дифеноконозол, дельтаметрин, эсфенвалерат, малатион, циперметрин) демонстрируют большую генотоксичность в отношении мтДНК в головах шмелей по сравнению с митохондриально-направленными пестицидами (феназахин, хлорфенапир, гидраметилнон, пиридабен, толфенпирад).

Ключевые слова: пестициды, шмели, голова, мтДНК, повреждения, генотоксичность.

1. INTRODUCTION

Bumblebees are the most important pollinators of entomophilous crops, both in the open and closed ground, capable of pollinating plants even in cool and windy weather (Berger *et al.*, 1998; Goodell & Thomson, 2007; Thomson & Goodell, 2002). Bumblebees for commercial use have been produced since the mid-1980 (Velthuis & van Doorn, 2006). Commercial bumblebee farming is currently undergoing intensive development (Lye *et al.*, 2011). Bumblebees and bees are becoming a popular research subject in light of the threatening crisis of declining pollinator populations in the world (Biesmeijer *et al.*, 2006; Potts *et al.*, 2010; Thomann *et al.*, 2013; Connelly *et al.*, 2015; Rhodes, 2018), which is already a matter of food security for humans (Klein *et al.*, 2007). One of the main reasons for this decline is the widespread use of pesticides (Rortaisa *et al.*, 2005). At the same time, the simultaneous effect of pathogens on pollinators

leads to a synergistic increase in the harmful effect of pesticides on insects (Grassl *et al.*, 2018).

Pesticides may affect the nervous systems of organisms. A number of pesticides, such as carbamates, organophosphates, etc., influence the nervous system (Keifer & Firestone, 2007). There is a study that has shown the association between exposure to pesticides and neurological dysfunction (Kamel & Hoppin, 2004). The neurotoxicity of pesticides has also been proved for bees, so it was found that exposure to pesticides can impair a bee's spatial working memory (Samuelson *et al.*, 2016). Exposure to cholinergic pesticides impairs olfactory learning and memory in bees (Williamson & Wright, 2013). Moreover, the toxic effect of pesticides can be mediated by mitochondria (Singh *et al.*, 2018; Salama *et al.*, 2014).

There are a number of pesticides whose

mechanism of action is associated with the inhibition of the electron transport chain (ETC) of mitochondria. Chlorfenapyr is an insecticide that disrupts oxidative phosphorylation in mitochondria. Chlorfenapyr inhibits the production of adenosine triphosphate (ATP), causing the death of the target organism (Raghavendra *et al.*, 2011). Tolfenpyrad inhibits ETC complex I (NADH dehydrogenase) in mitochondria (Simon, 2015). Hydramethylnone also acts as a mitochondrial respiration inhibitor (Hollingshaus, 1987). It is believed that it inhibits the flow of electrons in mitochondria to the levels of ETC complex III (Simon, 2008). Pyridaben is also a mitochondria-directed pesticide, and its target is mitochondrial ETC complex I (Navarro *et al.*, 2010; Sherer *et al.*, 2007). Fenazaquin, like Pyridaben, inhibits mitochondrial ETC complex I (Lümmen, 1998). The authors have previously shown that fungicides can affect isolated bumblebee mitochondria (Syromyatnikov *et al.*, 2017).

The mutagenic effect of pesticides on the DNA of bees and bumblebees has been poorly studied. The genotoxicity of pesticides on bumblebees has not been studied. Meanwhile, it is known that exposure to pesticides may lead to various forms of DNA damage (Marcelino *et al.*, 2019; Bolognesi, 2003). Of particular interest is the study of the genotoxicity of pesticides of various classes, including mitochondria-targeted, on the level of DNA damage in bumblebee heads. The centers of the bumblebee's nervous system and sense organs are located in its head. Therefore, the aim of this work was to study the genotoxicity of pesticides on the DNA in bumblebees' heads using long-range PCR, which is based on the amplification of long fragments of mitochondrial DNA.

2. MATERIALS AND METHODS

2.1. The object of the study

Tekhnologii Shmelevodstva LLC (Voronezh, Russia) provided male bumblebees (*Bombus terrestris* L.). The bumblebees were kept in cylindrical cages (diameter: 14 cm, height: 7 cm) with a mesh bottom and a lid, at a temperature of 27 °C, and at a relative humidity of 55%, and there were no more than ten bumblebees in each cage.

All experimental procedures with insects were performed in accordance with the rules set by Voronezh State University Ethical Committee on Biomedical Research (Section of Animal Care

and Use, protocol 42-04 dated September 16, 2019).

2.2. In vitro pesticide toxicity study

The toxicity of the following commonly used, commercially available broad-spectrum pesticides were studied: Difenoconazole, Deltamethrin, Esfenvalerate, Malathion, Cypermethrin, and some mitochondria-targeted pesticides (Fenazaquin, Chlorfenapyr, Hydramethylnon, Pyridaben, and Tolfenpyrad). All by Sigma-Aldrich, USA.

Mitochondria from bumblebees were isolated according to the protocol described previously (Syromyatnikov *et al.*, 2013). Intact mitochondria used a mixture of five mmol/L of malate and five mmol/L of pyruvate as a substrate for respiration. Each pesticide, at a concentration of 50 µM, was added to tubes with intact mitochondria. Mitochondria with respiratory substrates and pesticides were incubated for an hour at a temperature of 37 °C. Afterward, the total DNA was isolated from mitochondria by DiaGene DNA isolation kit (Dia-M, Russia).

2.3. The study of the pesticides' toxicity on bumblebees

The concentration of pesticide added to the syrup fed to the bumblebees was preliminarily selected empirically (data not published) so that the mortality of the bumblebees did not exceed 10%. As a result, 1 mg of the investigated substances was dissolved in 0.5 ml of 99% DMSO; after which the resulting solution was added to 10 ml of 60% sugar syrup. The pesticide concentration of 1 mg / 10 ml is the concentration that the bumblebee can potentially come into contact with on plants (Girolami *et al.*, 2009). The control solution contained 10 ml of 60% sugar syrup with 0.5 ml of DMSO. The bumblebees were placed in cylindrical cages (diameter: 14 cm, height: 7 cm) with a mesh bottom (so that the bumblebees would meet the feeder filled with syrup) and a lid; there were 10 bumblebees in each cage. The bumblebees were kept at a temperature of 27–28.5 °C with an air humidity of 55%–68%. DNA was extracted from the bumblebees' heads 24 hours after the experiment.

2.4. DNA isolation and long-range PCR

Afterward, the total DNA was isolated from mitochondria by DiaGene DNA isolation kit (Dia-M, Russia). The amount of oxidative damage was assessed using long-chain PCR on a CFX96 Touch™ Real-Time PCR Detection System thermocycler (made by Bio-Rad, USA) using the Encyclo polymerase kit (Evrogen,

Russia). The reaction conditions were as follows: initial denaturation at 95 °C for five minutes, 35 cycles with denaturation at 95 °C for 10 seconds, annealing the primers at 59 °C for 30 seconds, and elongation at 66 °C for five minutes. The number of lesions was evaluated in fragments corresponding to mitochondrial genes *Cox1* and *Cox2* F: 5'-CCCCAGATATAGCTTTTCCTC-3'; R: 5'-CCAGGAATTGCATCAACTTT-3' (product length is 2,083 bps) and *Nad6*, *Nad1*, *CybB* F: 5'-CGCTATTGCTGGCACTAATTT-3'; R: 5'-AAATTATTCAGAAACAAAATGGAAA-3' (fragment length is 2,013 bps). A short fragment (99 bps) was used as a reference, which was amplified using primers: F: 5'-TCCATGGGATTCATGTTCTT-3'; R: 5'-CAAAATTAATATGATGAATTGAAGAG-3'.

The amount of DNA damage per 10,000 bps was calculated by Equation 1:

$$X = (1 - 2^{-(\Delta\Delta Cq)}) * 10,000 \text{ bp/fragment length, bp.}$$

Where, X - the amount of damage/10 kbp; $\Delta\Delta Cq$ - ΔCq between the control and the experimental long fragments divided by ΔCq between the control and the experimental short fragments.

2.5. Estimated number of mtDNA copies

The number of mtDNA copies was estimated using real-time quantitative PCR using a CFX96 Touch™ Real-Time PCR Detection System (Bio-Rad, USA) using the qPCRMix-HS SYBR + LowROX kit (Evrogen, Russia). The following mtDNA fragments were amplified using the following pair of primers: F: 5'-TCCATGGGATTCATGTTCTT-3'; R: 5'-CAAAATTAATATGATGAATTGAAGAG-3' and genomic DNA using the following pair of primers: F: 5'-AGAACCTCCGTATCCCCTTCG-3'; R: 5'-AGCCTACCAFTGCTGAAC-3'.

The reaction conditions were as follows: initial denaturation at 95 °C for 5 minutes, then 35 cycles with denaturation at 95 °C for 10 seconds, annealing the primers at 59 °C for 30 seconds, and elongation at 66 °C for 30 seconds. Normalized mtDNA level relative to nuclear DNA was calculated using standard formula $2^{-(\Delta\Delta Cq)}$ (Yuan *et al.*, 2006).

2.6. Statistical processing

Statistical processing of the results was carried out using the software package Statistica 10 (StatSoft.Inc, USA). The normality of data distribution was determined using the Shapiro-

Wilk test. The distribution quantity value is presented as the median (Q1 and Q3 quartiles). A comparison of the number of injuries was carried out using the nonparametric Mann-Whitney U-test. The value of the number of mtDNA copies is presented as the mean \pm standard error of the mean. The number of mtDNA copies was compared using the parametric Student's T-test. The work discusses statistically significant differences ($p < 0.05$).

3. RESULTS:

3.1. In vitro pesticide toxicity

The greatest amount of mtDNA damage was caused by the addition of Malathion (median 1.63 (0.71; 2.60), $p < 0.05$) and Difenconazole (median 1.52 (0.52; 2.30), $p < 0.05$) compared with the control (median -0.07 (-0.10; 0.06)) (Figure 1).

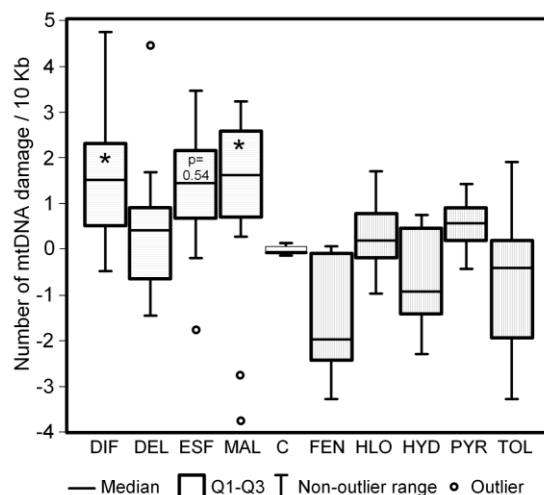


Figure 1. The amount of damage to mtDNA/10 kbp when pesticides are added to isolated mitochondria in vitro. * $p < 0.05$ differences compared with the control are statistically significant according to the Mann-Whitney test. Dif – Difenconazole; Del – Deltamethrin; Esf – Esfenvalerate; Mal – Malathion; C – Control; Fen – Fenazaquin; Hlo – Chlorfenapyr; Hyd – Hydramethylnon; Pyr – Pyridaben; Tol – Tolfenpyrad.

The addition of Esfenvalerate caused damage in intact mitochondria (median (1.45 (0.70; 2.17))), but the data are statistically insignificant ($p = 0.58$). Deltamethrin, as well as Fenazaquin, Chlorfenapyr, Hydramethylnone, Pyridaben, and Tolfenpyrad, did not cause damage to mtDNA when added to intact mitochondria.

3.2. In vivo pesticide toxicity

When bumblebees consumed pesticides, Esfenvalerate caused the largest amount of mtDNA damage (median 4.80 (4.47; 4.92), $p < 0.05$). Significant genotoxic effect was demonstrated by Malathion (median 4.78 (4.20; 4.84), $p < 0.05$) and Cypermethrin (median 4.78 (3.31; 4.84), $p < 0.05$). Difenconazole caused severe mtDNA damage (median 3.98 (3.49; 4.97), $p < 0.01$), while Deltamethrin also had no genotoxic effect. Among mitochondria-targeted pesticides, Fenazaquin (median 2.92 (1.37; 4.54), $p < 0.05$) and Pyridaben (median 2.18 (0.97; 2.69), $p < 0.05$) showed the highest genotoxicity. Chlorfenapyr, Hydramethylnon, and Tolfenpyrad did not show genotoxicity with respect to mtDNA (Figure 2).

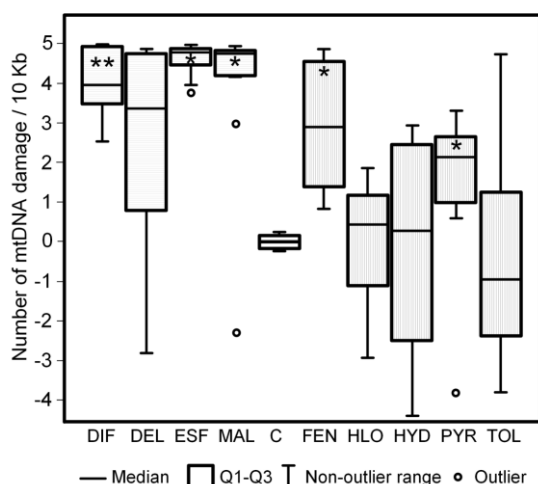


Figure 2. The amount of damage to mtDNA/10 kbp when bumblebees consumed pesticides. * $p < 0.05$; ** $p < 0.01$ differences compared with the control are statistically significant according to the Mann-Whitney test. Dif – Difenconazole; Del – Deltamethrin; Esf – Esfenvalerate; Mal – Malathion; C – Control; Fen – Fenazaquin; Hlo – Chlorfenapyr; Hyd – Hydramethylnon; Pyr – Pyridaben; Tol – Tolfenpyrad.

3.3. Change in the number of copies of mtDNA in bumblebees heads when consuming pesticides

The effect of pesticides on the number of mtDNA copies was not the same. Deltamethrin increased the number of copies of mtDNA by 37%, and Tolfenpyrad by 74% (both $p < 0.05$). Esfenvalerate caused a decrease in the number of mtDNA copies by 34%, and Pyridaben by 38% (both $p < 0.05$) (Fig. 3).

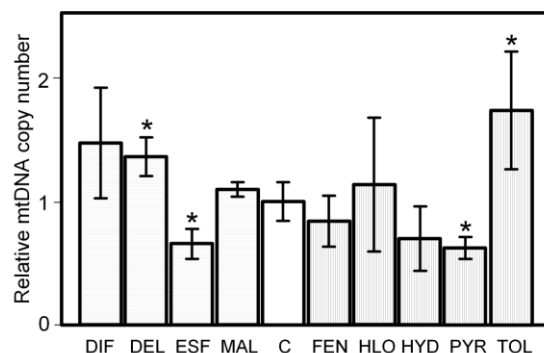


Figure 3. The number of mtDNA copies when bumblebees consumed pesticides. * $p < 0.05$ differences compared with the control are statistically significant according to Student's T-Test. Dif – Difenconazole; Del – Deltamethrin; Esf – Esfenvalerate; Mal – Malathion; C – Control; Fen – Fenazaquin; Hlo – Chlorfenapyr; Hyd – Hydramethylnon; Pyr – Pyridaben; Tol – Tolfenpyrad.

Difenconazole, Malathion, Fenazaquin, Chlorfenapyr, and Hydramethylnon did not show a statistically significant effect on the number of mtDNA copies.

4. DISCUSSION:

The results showed that mitochondrial-directed pesticides cause less damage than pesticides with a wide exposure profile if added to bumblebees' isolated mitochondria (Fig. 1). Mitochondria-directed pesticides, mainly blocking the respiration of mitochondria, can explain this. In turn, a decrease in the respiration rate caused, for example, by dissociation of the inner mitochondrial membrane, may be associated with a decrease in the rate of production of reactive oxygen species (ROS), which are the main damaging factors (Cadenas *et al.*, 2018).

Insect consumption of pesticide syrup induces more damage to the head than adding pesticide to isolated mitochondria (Figures 1 and 2). This may be due to the characteristics of the nervous tissue, which is one of the most metabolically active tissues in the body (Herculano-Houzel, 2011). Among mitochondria-targeted pesticides, Pyridaben, and Fenazaquin (Figure 2) cause mtDNA damage. Pyridaben is known to increase oxidative stress due to the selective inhibition of ETC complex I (Navarro *et al.*, 2010), which causes serious damage to the DNA in mammals (Ebadi Manas *et al.*, 2013). Therefore, its toxicity to insect mtDNA is obvious. Fenazaquin is also an inhibitor of mitochondria

ETC complex I (Lümmen, 1998), and its mechanism of genotoxicity is probably similar to Pyridaben.

A change in the number of mtDNA copies can be a compensatory effect of mitochondria in response to stressful conditions induced by the consumption of pesticides. It is noteworthy that an increase in the number of copies of mtDNA was observed in insects that consumed sugar syrup with Deltamethrin and Tolfenpyrad (Figure 3). Deltamethrin is the only broad-spectrum pesticide that did not cause a statistically significant increase in mtDNA damage, and Tolfenpyrad is the only pesticide whose damage value (median -0.96 (-2.43; 1.24)) was lower than that of the control, though the differences are not statistically significant (Figure 3). An increase in the number of mtDNA copies is probably a compensatory effect in response to inhibition of mitochondrial respiration. It has been shown previously that many cytotoxic agents, such as Hexavalent Chromium (VI) (Zhong *et al.*, 2017), Methamphetamine (Valian *et al.*, 2016), Tert-Butyl Hydroperoxide (Rasbach & Schnellmann, 2007), Buthionine Sulfoximine (Lee *et al.*, 2000), Doxorubicin, Mitoxantrone (Kluza *et al.*, 2004) and ROS (Gutsaeva *et al.*, 2006) are able to activate mitochondrial biogenesis as a compensatory reaction in mammalian cells. It is likely that some pesticides have a similar effect on insects, but this issue needs further study.

In contrast, Esfenvalerate and Pyridaben caused a decrease in the number of mtDNA copies (Figure 3). Esfenvalerate is the most genotoxic of the studied pesticides *in vivo* and one of the most toxic when added *in vitro*. Pyridaben and Fenazaquin, mitochondria-targeted pesticides that showed genotoxicity when bumblebees consumed the syrup, also led to a decrease in the number of mtDNA copies, though the data were not statistically significant for Fenazaquin.

5. CONCLUSIONS:

Broad-spectrum pesticides demonstrate greater mtDNA genotoxicity in bumblebee heads compared to mitochondria-targeted pesticides. We have shown that broad-spectrum pesticides on the whole cause 4.9 times more mtDNA damage than mitochondria-targeted pesticides. In this case, the most toxic pesticides caused a decrease in the number of copies of mtDNA, while when exposed to less toxic pesticides, it was observed an increase in the number of mtDNA, which is probably a compensatory response of the cell in response to inhibition of

mitochondrial respiration.

6. ACKNOWLEDGMENTS:

This work was supported by a grant from the Russian Science Foundation (project 18-76-00027).

7. REFERENCES:

1. Berger, L. A., Vaissiere, B. E., Moffett, J. O., Merritt, S. J.; *Environmental Entomology*. **1988**, 17(5), 789-794. <https://doi.org/10.1093/ee/17.5.789>.
2. Biesmeijer, J. C., Roberts, S. P., Reemer, M., Ohlemüller, R., Edwards, M., Peeters, T., Schaffers, A. P., Potts, S. G., Kleukers, R., Thomas, C. D., Settele, J., Kunin, W. E.; *Science*. **2006**, 313(5785), 351-354. <https://doi.org/10.1126/science.1127863>.
3. Bolognesi, C.; *Mutation Research*. **2003**, 543(3), 251-272. [https://doi.org/10.1016/S1383-5742\(03\)00015-2](https://doi.org/10.1016/S1383-5742(03)00015-2).
4. Cadenas, *et al.*; *Biochimica et Biophysica Acta (BBA) - Bioenergetics*. **2018**, 1856(9), 940-950. <https://doi.org/10.1016/j.bbabi.2018.05.019>.
5. Connelly, H., Poveda, K., Loeb, G., *Agriculture Ecosystems & Environment*. **2015**, 211, 51-56. <https://doi.org/10.1016/j.agee.2015.05.004>.
6. Ebadi Manas, G., Hasanzadeh, S., Najafi, G., Parivar, K., Yaghmaei, P.; *Iranian Journal of Reproductive Medicine*. **2013**, 11(8), 605-610. PMID: 24639796.
7. Goodell, K., Thomson, J. D.; *Entomologia Generalis*. **2007**, 29(2-4), 237-252. <https://doi.org/10.1127/entom.gen/29/2007/237>.
8. Girolami, V., Mazzon, L., Squartini, A., Mori, N., Marzaro, M., Di Bernardo, A., Greatti, M., Giorio, C., Tapparo, A.; *Journal of Economic Entomology*. **2009**, 102(5), 1808-1815. <https://doi.org/10.1603/029.102.0511>.
9. Grassl, J., Holt, S., Cremen, N., Peso, M., Hahne, D., Baer, B.; *J Invertebr Pathology*. **2018**, 159, 78-86. <https://doi.org/10.1016/j.jip.2018.10.005>.
10. Gutsaeva, D. R., Suliman, H. B., Carraway, M. S., Demchenko, I. T., Piantadosi, C. A.; *Neuroscience*. **2006**, 1437(2), 493-504.

- <https://doi.org/10.1016/j.neuroscience.2005.07.061>.
11. Herculano-Houzel, S.; *PLoS One*. **2011**, 6(3), e17514. <https://doi.org/10.1371/journal.pone.0017514>.
 12. Hollingshaus, J. G.; *Pesticide Biochemistry and Physiology*. **1987**, 27(1), 61-70. [https://doi.org/10.1016/0048-3575\(87\)90096-4](https://doi.org/10.1016/0048-3575(87)90096-4).
 13. Kamel, F., Hoppin, J. A.; *Environmental Health Perspectives*. **2004**, 112(9), 950–958. <https://doi.org/10.1289/ehp.7135>.
 14. Keifer, M. C., Firestone, J.; *J. Agromedicine*. **2007**, 12(1), 17-25. https://doi.org/10.1300/J096v12n01_03.
 15. Klein, A. M., Vaissière, B. E., Cane, J. H., Steffan-Dewenter, I., Cunningham, S. A., Kremen, C., Tscharntke, T.; *Biological sciences*. **2007**, 274(1608), 303–313. <https://doi.org/10.1098/rspb.2006.3721>.
 16. Kluza, J., Marchetti, P., Lancel, S., Gallego, M., Fournier, C., Loyens, A., Beauvillain, J., Bailly, C.; *Oncogene*. **2004**, 23(42), 7018-30. <https://doi.org/10.1038/sj.onc.1207936>.
 17. Lee, H. C., Yin, P. H., Lu, C. Y., Chi, C. W., Wei, Y. H.; *The Biochemical Journal*. **2000**, 348(2), 425-432. <https://doi.org/10.1042/0264-6021:3480425>.
 18. Lümnen, P.; *Bioenergetics*. **1998**, 1364(2), 287-296. [https://doi.org/10.1016/S0005-2728\(98\)00034-6](https://doi.org/10.1016/S0005-2728(98)00034-6).
 19. Lye, G. C., Jennings, S. N., Osborne, J. L., Goulson, D.; *Journal of Economic Entomology*. **2011**, 104, 107-114. <https://doi.org/10.1603/EC10092>.
 20. Marcelino, A. F., Wachtel, C. C., Ghisi, N. C.; *International journal of environmental research and public health*. **2019**, 16(3), 358. <https://doi.org/10.3390/ijerph16030358>.
 21. Navarro, A., Bandez, M. J., Gomez, C., Repetto, M. G., Boveris, A.; *J Bioenerg Biomembr*. **2010**, 42(5), 405-412. <https://doi.org/10.1007/s10863-010-9309-4>.
 22. Potts, S. G., Biesmeijer, J. C., Kremen, C., Neumann, P., Schweiger, O., Kunin, W. E.; *Trends in Ecology & Evolution*. **2010**, 25(6), 345-53. <https://doi.org/10.1016/j.tree.2010.01.007>.
 23. Raghavendra, K., Barik, T. K., Sharma, P., Bhatt, R. M., Srivastava, H. C., Sreehari, U.; *Malar J*. **2011**, 10(16). <https://doi.org/10.1186/1475-2875-10-16>.
 24. Rasbach, K. A., Schnellmann, R. G.; *The Journal of Biological Chemistry*. **2007**, 282, 2355-2362. <https://doi.org/10.1074/jbc.M608009200>.
 25. Rhodes, C. J.; *Science Progress*. **2018**, 101(2), 121-160. <https://doi.org/10.3184/003685018X15202512854527>.
 26. Rortaisa, A., Arnolda, G., Halmb, M., Touffet-Briensb, F.; *Apidologie, Springer Verlag*. **2005**, 36(1), 71-83. <https://hal.archives-ouvertes.fr/hal-00892118>.
 27. Salama, M., El-Morsy, D., El-Gamal, M., Shabka, O., Mohamed, W. M.; *Annals of neurosciences*. **2014**, 21(3), 85–89. <https://doi.org/10.5214/ans.0972.7531.210303>.
 28. Samuelson, E. E. W., Chen-Wishart, Z. P., Gill, R. J., Leadbeater, E.; *Scientific reports*. **2016**, 6, 38957. <https://doi.org/10.1038/srep38957>.
 29. Sherer, T. B., Richardson, J. R., Testa, C. M., Seo, B. B., Panov, A. V., Yagi, T., Matsuno-Yagi, A., Miller, G. W., Greenamyre, J. T.; *J Neurochem*. **2007**, 100(6), 1469-1479. <https://doi.org/10.1111/j.1471-4159.2006.04333.x>.
 30. Simon, J. Yu.; *The Toxicology and Biochemistry of Insecticides*, 1st ed., CRC Press, 2008.
 31. Simon, J. Yu.; *The Toxicology and Biochemistry of Insecticides*, 2nd ed., CRC Press, 2015.
 32. Singh, N., Lawana, V., Luo, J., Phong, P., Abdalla, A., Palanisamy, B., Rokad, D., Sarkar, S., Jin, H., Anantharam, V., Kanthasamy, A. G., Kanthasamy, A.; *Neurobiology of Disease*. **2018**, 117, 82-113. <https://doi.org/10.1016/j.nbd.2018.05.019>.
 33. Syromyatnikov, M. Y., Kokina, A. V., Lopatin, A. V., Starkov, A. A., Popov, V. N.; *Pestic Biochem Physiology*. **2017**, 135, 41-46. <https://doi.org/10.1016/j.pestbp.2016.06.007>.
 34. Syromyatnikov, M. Y., Lopatin, A. V., Starkov, A. A., Popov, V. N.; *Biochemistry (Mosc)*. **2013**, 78, 909-914. <https://doi.org/10.1134/S0006297913080075>.
 35. Thomann, M., Lambert, E., Devaux, C., Cheptou, P. O.; *Trends in plant science*. **2013**, 18(7), 353-359. <https://doi.org/10.1016/j.tplants.2013.04.002>.
 36. Thomson, J. D., Goodell, K.; *Journal of Applied Ecology*. **2002**, 38(5), 1032-1044. <https://doi.org/10.1046/j.1365-2664.2001.00657.x>.
 37. Valian, N., Ahmadiani, A., Dargahi, L.; *Journal of Cellular Biochemistry*. **2016**,

- 118(6), 1369-1378.
<https://doi.org/10.1002/jcb.25795>.
38. Velthuis, H. H. W., van Doorn, A.; *Apidologie, Springer Verlag*. **2006**, 37(4), 421-451.
<http://dx.doi.org/10.1051/apido:2006019>.
39. Williamson, S. M., Wright, G. A.; *Journal of Experimental Biology*. **2013**, 216(10), 1799–1807. [https://doi:10.1242/jeb.083931](https://doi.org/10.1242/jeb.083931).
40. Yuan, J.S., Reed, A., Chen, F., Stewart, C.N. Jr.; *BMC Bioinformatics*. **2006**, 7, 85.
41. Zhong, X., de Cassia da Silveira, E Sa R., Zhong, C.; *International journal of molecular sciences*. **2017**, 18(9), 1877. [https://doi:10.3390/ijms18091877](https://doi.org/10.3390/ijms18091877).

AVALIAÇÃO DAS PERSPECTIVAS DE ESTUDAR E USAR COGUMELOS DO AZERBAIJÃO COMO PRODUTORES EFICAZES DE SUBSTÂNCIAS BIOLÓGICAMENTE ATIVAS

ASSESSMENT OF THE PROSPECTS OF STUDYING AND USING MUSHROOMS OF AZERBAIJAN AS EFFECTIVE PRODUCERS OF BIOLOGICALLY ACTIVE SUBSTANCES

ОЦЕНКА ПЕРСПЕКТИВЫ ИЗУЧЕНИЯ И ИСПОЛЬЗОВАНИЯ ГРИБОВ АЗЕРБАЙДЖАНА КАК ЭФФЕКТИВНЫХ ПРОДУЦЕНТОВ БИОЛОГИЧЕСКИ АКТИВНЫХ ВЕЩЕСТВ

BAKHSHALIYEVA, Konul Farrukh¹; NAMAZOV, Nizami Rza²; HASANOVA, Arzu Rasul²; MAMMADOVA, Fidan Rasim³; MURADOV, Panah Zulfigar^{1*}

¹ Institute of Microbiology of Azerbaijan National Academy of Sciences. Azerbaijan.

² Sumgait State University. Azerbaijan

³ Baku State University. Azerbaijan

* Correspondence author

e-mail: muradov.imanas@bk.ru

Received 06 December 2019; received in revised form 30 January 2020; accepted 20 February 2020

RESUMO

Na pesquisa realizada, os macromicetes xilotróficos foram pesquisados como produtores potenciais de substâncias ativas biológicas usadas hoje em dia para diversos fins nas práticas mundiais que se espalham no Azerbaijão e algumas de suas características (atividade biológica de metabólitos sintetizados, toxicidade, atividade antimicrobiana) dinâmica da formação de biomassa.). Ficou claro que fungos como *Ganoderma lucidum* (Curtis) P. Karst., *Laetiporus sulphureus* (Bull.) Murrill, *Pleurotus ostreatus* (Jacq.) P. Kumm, *Schizophyllum commune* Fr e *Trametes versicolor* (L.) Lloyd consideravam uma perspectiva O produtor de substâncias ativas biológicas está amplamente espalhado nas florestas do Azerbaijão, e algumas delas são até espécies dominantes de xilomicobióticos inerentes à natureza do Azerbaijão. Como resultado de estudos com cepas isoladas desses fungos, foi demonstrado que, tanto na solução de cultura (CS) quanto nos micélios vegetativos (VB), existem metabólitos com atividade biológica. O resultado da pesquisa também ficou claro que a atividade antimicrobiana da SC em todos os casos é maior do que nos extratos de água ou álcool da biomassa seca (1,1-1,2 vezes), embora defina a atividade biológica geral dos extratos de VB para a relação de *Paramecium caudatum* dá um efeito de aumento mais alto. Além disso, as cepas ativas selecionadas não ficam atrás das cepas conhecidas em termos da quantidade de biomassa formada (até 8,7 g/l em 7 dias) e manifestações de formas de atividade biológica. Isso fornece uma base séria para realizar a produção de substâncias biologicamente ativas para finalidades diferentes (alimentos, rações, medicamentos e outras) em sua base.

Palavras-chave: substâncias biologicamente ativas, macromicetes xilotróficos, biomassa, efeitos tóxicos, atividade antimicrobiana.

ABSTRACT

In the carried out of the research, Xylotroph macromycetes have been researched as a perspective producer of biological active substances used for various purposes today in world practice which spread in Azerbaijan and some of their features (the biological activity of synthesized metabolites, toxicity, antimicrobial activity and dynamics of biomass formation). It became clear that fungi such as *Ganoderma lucidum* (Curtis) P. Karst., *Laetiporus sulphureus* (Bull.) Murrill, *Pleurotus ostreatus* (Jacq.) P. Kumm, *Schizophyllum commune* Fr and *Trametes versicolor* (L.) Lloyd considered as a perspective producer of biological active substances is widely spread in the forests of Azerbaijan, and some of them are even dominant species of xylomicobiot inherent in the nature of Azerbaijan. As a result of studies with isolated strains of these fungi, it was shown that

both in the culture solution (CS) and in the vegetative mycelia (VB), there are metabolites with biological activity. The result of research also became clear that antimicrobial activity of CS in all cases is higher than in water or alcohol extracts of dry biomass (1,1-1,2 times), although it defines the overall biological activity of VB extracts to the relationship of *Paramecium caudatum* gives a higher increase effect. In addition, the selected active strains do not lag behind the known strains in terms of the amount of biomass formed (up to 8.7 g/l in 7 days) and manifestations of forms of biological activity. This gives a serious basis to realize the production of biologically active substances for different (food, feed, medical and other) purposes on their basis.

Keywords: *biologically active substances, Xylotroph macromycetes, biomass, toxic effects, antimicrobial activity.*

Резюме

В ходе работы ксилотрофные макромицеты были исследованы как перспективный продуцент биологически активных веществ, используемых сегодня для различных целей в мировой практике, которые распространены в Азербайджане, и некоторые особенности (биологическая активность синтезируемых метаболитов, токсичность, антимикробная активность и динамика образования биомассы) их. Стало ясно, что такие грибы, как *Ganoderma lucidum* (Curtis) P. Karst., *Laetiporus sulphureus* (Bull.) Murrill, *Pleurotus ostreatus* (Jacq.) P. Kumm, *Schizophyllum commune* Fr и *Trametes versicolor* (L.) Lloyd является перспективные продуценты биологически активных веществ и широко распространен в лесах Азербайджана, а некоторые из них являются даже доминирующими видами ксиломиобиот, присущими природе Азербайджана. В результате исследований с выделенными штаммами данных грибов было показано, что как в культуральной жидкости (КЖ), так и в вегетативном мицелии (ВМ) присутствуют метаболиты с биологической активностью. В результате исследований также выяснилось, что антимикробная активность КЖ во всех случаях выше, чем в водных или спиртовых экстрактах сухой биомассы (в 1,1-1,2 раза), хотя она определяет общую биологическую активность экстрактов ВМ по отношению *Paramecium caudatum* дает более высокий эффект увеличения. Кроме того, отобранные активные штаммы не отстают от известных штаммов по количеству образующейся биомассы (до 8,7 г/л за 7 дней) и проявлениям форм биологической активности. Это дает серьезную основу для реализации производства биологически активных веществ различного (пищевого, кормового, медицинского и др.) назначения на их основе.

Ключевые слова: биологические активные вещества, ксилотрофные макромицеты, биомассы, токсигенность, антимикробные активности

1. INTRODUCTION

Fungi one of the valuable sources of biologically active substances and these substances synthesized by them have serious perspectives to obtained the healing nutrients products and pharmacologically active preparations (Cao *et al.*, 2018, Muszyńska *et al.*, 2018, Sum Winnie *et al.*, 2019, Sharif *et al.*, 2018) . Mentioned above encountered in the vegetative mycelium of fungi, as well as in the fruits bodies formed in natural conditions (Millar *et al.*, 2019, Stadler and Hoffmeister, 2015, Sułkowska-Ziaja K. *et al.*, 2018). Although the number of fungi species that can form macroscopic fruits is about 14,000 (Chang, 2006), according to literature, their 2,000 are edible and 700 important as medicine (Jilinskaya, 2015).

In natural conditions, the fruity body (FB) formed by the fungi is either one-year or perennial (Bondartseva, 1998), and their reserves

are limited and cannot be reached all year round. On the other side, the deterioration of the ecological situation causes fungi to contain substances that are dangerous to human health (Kokkoris *et al.*, 2019), which limits the use of FB formed in the natural environment. The above-mentioned shortcomings are possible to overcome using strains taken to pure culture from FB of fungi.

Xylotropic macromistates that combining a group of fungi known to science and form macroscopic FB is one of the most widely studied objects in recent years (Aliyeva, 2019, Cör, Knez, and Knez Hrničič, 2018, Rahi and Malik, 2016) , which is due to the fact that they are attract attention as a prospective producers (Baeva *et al.*, 2019, Gargano *et al.*, 2017, Taofiq *et al.*, 2017) of substances used for food, feed, medical, as well as technical purposes (leather, detergent and cleaning powders, insulating materials and so on. products). A number of researches (Osinska-Jaroszuk *et al.*, 2015, Ugbogu *et al.*, 2019, Kryczyk-Poprawa *et al.*, 2019, Wu *et al.*,

2019) have shown that their use for these purposes are ecologically safe (Ritota and Manzi, 2019, Wan and Li, 2012), economically affordable (Grimm and Wösten 2018), technically easy and even some results have already reached the production level (Sekan *et al.*, 2019). Interestingly, results reached to the production level covers almost all of the above-mentioned areas (Gehlot and Singh, 2018).

The number of fungi considered to be promising in the industry or in scientific researches is too small compared with the species known to science, and the usefulness or significance of some fungi for medicinal or for some purpose is to determine in results of general use in folk medicine or in episodic research.

The Xylotrophic macromycetes have been widely spread in the territory of the Republic of Azerbaijan, and the number of species registered in researches up to date is more than 200 (Akhundova, N.A. *et al.*, 2019, Aliyeva, 2019, Garayeva, 2017). Among them also are encountered species like as *Ganoderma lucidum*, *Laetiporus sulphureus*, *Lentinus edodes*, *Pleurotus ostreatus*, *Schizophyllum commune*, *Trametes versicolor* that are used on an industrial scale for different purposes in world practice (Hapuarachchi *et al.*, 2018, Hyde *et al.*, 2019, Özdal *et al.*, 2019, Saltarelli *et al.*, 2015), as well as in the stage of study as promising producers. In Azerbaijan is also encountered researches fungi registered as producers of BAS, and the main focus of research in this direction is focused on the perspective of their produces of hydrolase and oxidases (Musayeva, 2019). In recent times also is encountered research materials directed to the study of some fungi as a producer of polysaccharides (Muradov *et al.*, 2018). The vast majority of Xylotrophic fungi known in Azerbaijan as well as in the world were not only poorly studied as BAS producers, many of them have not been involved in this study.

On the other side, researches have shown that quantitative indicator of ability to synthesize these or other BAS of separate strains belonging to the same species of fungi changes even at the level of strain (Bandara *et al.*, 2019, Rahi and Malik, 2016, Zhou *et al.*, 2016). This allows noting the ability to find more efficient strains of known species spreading in a particular region, which allows noting that new research in this direction in Azerbaijan is actual.

The purpose of this study is to study the possibility of effective biotechnological use of

Xylotrophic macromycetes living in the natural forests of Azerbaijan as potential producers of biologically active substances, by preliminary assessment of their antimicrobial activity, their lack of metabolites with toxic action, as well as studying the dynamics of grow their biomass in culture.

2. MATERIALS AND METHODS

As an objects of the research were used strains belongs to the selected FB of fungi such as *Ganoderma lucidum*, *Laetiporus sulphureus*, *Pleurotus ostreatus* and *Schizophyllum commune* collected from the different areas of Azerbaijan (Azerbaijan part of the Greater Caucasus - GC, Small Caucasus - SC, Hirkan National Park - HNP, Kura-Araz lowland - KA).

Collection of FB, primary description of the body fetus in the field, identification, taken to the pure cultures from MC, as well as the cultivation of fungi were carried out according to known methods (Bondartseva, 1998, Handbook of Mycological, 2006, Ko Y-F. *et al.*, 2017, Netrusov *et al.*, 2005) and those used in our previous work (Akhundova *et al.*, 2019, Muradov *et al.*, 2018).

To evaluate the germination process has been used a nutrient environment, which composition was as follows: (g/l): Carbon source (depending on the purpose, mono-, di-, polysaccharides, wheat bran, wood crumbs, and others) – 10, peptone – 3, NH_4NO_3 – 1,5, $\text{MgSO}_4 \cdot 7\text{H}_2\text{O}$ – 0,5, NaCl – 0,5, KH_2PO_4 – 0,4. Sterilization condition is 0,5 atm, 0,5 hr. Environment after sterilization pH = 5,6.

The amount of formed biomass has been identified, bringing it to the permanent weight at the 105°C and was expressed with g/l.

As a source of BAS has been used both culture solution (CS), as well as from the formed vegetative biomass (VB) of fungi. During the use of VB, biomass has been researched extracted separately with water (WE_1) and alcohol (AE_2). The extraction of mushroom materials was carried out according to the method specified in the work of Alvarez *et al.* (2014).

The toxicity of the biologically active metabolites obtained from solutions (CS, WE_1 , and AE_2) has been clarified in relation to *Tetrahymena pyriformis* (a ciliate protozoan) and at the same time, was used from apparatus of BioLaT-3 and a computer with software AutoCiliataXP (Jilinskaya, 2015). For this, into

the outside circle of the device's tablet are added 10 µl infusor culture and 0,5 ml of the tested solution as control was used as the primary nutrient medium. After 24 hours, the activated BioLaT-3 device was carried out counting of cells.

The assessment was carried out (Table 1) in accordance with the following main criteria (K_1 and K_k), which, for its calculation, was used from such as:

$$K_1 = N_2 / N_1 K_k \quad (\text{Eq. 1})$$

$$K_k = N_{1k} / N_{2k} \quad (\text{Eq. 2})$$

In equations 1 and 2, the N_1 and N_{1k} are the number of infusors in the samples and in the control, respectively, before exposure, N_2 and N_{2k} are the number of infusors in the samples and in the control, respectively, after exposure.

Bactericidal and fungicidal properties have been identified based on the ability growth of test cultures (Bhalodia and Shukla, 2011; De Lira Mota *et al.*, 2012). Thus, the fungicidal activity was determined based on the amount of biomass taken from the test cultures (*Candida albicans*, *Aspergillus fumigatus*, *A.niger*, *Fusarium oxysporium* and *Penicillium cuclopium*), the bactericidal activity was determined based on the optical density of the cultured solution obtained from test cultures (*Bacillus subtilis*, *Staphylococcus aureus*, *Escherichia coli*, *Pseudomonas aeruginosa*) during cultivation, compared to control.

All experiments were performed in 4 replicates and all the data were statistically analyzed (Kobzar, 2006). For processing, the following equation 3 was used:

$$m / M = P \leq 0.05 \quad (\text{Eq. 3})$$

In Equation 3, M is the average repetition rate, m is the standard deviation, and P is the Student criterion.

3. RESULTS AND DISCUSSION:

The Republic of Azerbaijan belongs to the less forested countries, and only 10,4% of its territory is covered with forests, 85 % of which is

mountain and 15 % plain forests (Mamedov and Khalilov, 2002). The main trees in these forests are oak, beech, and hornbeam. This and other trees (for example, ash-tree, iron tree, lime, different fruit trees) spread in our forest at the same time is characterized as settlements and feeding places of fungi, primarily Xylotropic macromyxes. Therefore, firstly xylomyobiota of trees participating in the formation of natural forests located in ecologically different areas of Azerbaijan were evaluated according to the use of fungi in the world practice as a producer of BAS or for use in production. It has become clear that most of the xylotroph macromycetes used today as BAS producers for different purposes are found in the forests of Azerbaijan, and some of them are even dominant species of xylomicobiot inherent in the nature of Azerbaijan (Table 2).

As seen, today, among the most promising mushrooms in the world, only *Inonotus obliquus* (Fan *et al.*, 2012; Géry *et al.*, 2018) are not found more accurately not before us, not in our research this mushroom was not registered. Analog thought can be said about *L. eddodos* (Bisen *et al.*, 2010). It is true that preparations (those with pharmacological activity) taken from *I.obliquus* fungi are obtaining from its sterile FB (reproductive part, which the hemanophore layer does not develop), although has been noted that the drug "Befungin" taken from it has a severe effect on tumor diseases its use today for this purpose is not so useful (Jilinskaya, 2015). Other fungi are currently studied as a promising producer of both intensive cultivation and producer of BAS.

Fungi as a producer of biologically active substances used for the production of various preparation on an industrial scale, as well as promising serious prospects in this direction (Gargano *et al.*, 2017, Muszyńska *et al.* 2018) are widely spread. Although all of the registered fungi by the distribution on the substrate are eutroph, different from each other by remaining features, this diversity gives itself both in their growth, as well as in the quantitative indication of biological activity of the metabolites they synthesize, which is confirmed with data presented below.

It should be noted that the mycelium of Xylotrophic macromycetes in the vegetative growth phase also has biological activity (Nikitina *et al.*, 2017), for this reason, their strains which have fast growth rate, more precisely forms more biomass is considered most promising. For this reason, first of all, it has been evaluated fungi strains taken to the pure culture by these

aspects. From the results became clear that the biomass of fungi formed during cultivation in the liquid nutrient medium different in quantity, and this distinction is also observed between strains belonging to the same species (Table 3). As seen, by formation biomass, the highest indicator belongs to the strains of *Sch.comune* and the minimal to the *L.sulphureus*. Taking into consideration the likelihood of biosynthetic activity and formed metabolites of each fungus that has different activity and characteristics for further research, it was considered appropriate to select one active strain of each species, namely those forms more biomass.

In studies have also been conducted optimization of medium for selected strains such as *G.lucidum* AS-4, *L.sulphureus* AS -7, *P.ostreatus* AH-12, *Sch.comune* AH -17 and *T.versicolor* AN -23 and were defined component compositions of medium which is generally favorable for all of them: Carbon source - wheat bran - 8, source of additional nitrogen - peptone – 1,2 and NH_4NO_3 – 0,7, $\text{MgSO}_4 \cdot 7\text{H}_2\text{O}$ – 0,3 and KH_2PO_4 – 0,1.

It should be noted that others as a source of carbon, especially glucose is a suitable substrate for growth, which is one of the facts that have been confirmed in studies, but there is another reason why we preferred to wheat bran. Thus, bran is a material produced from the wheat in the process of obtaining flour and is useful for human health (Babu *et al.*, 2018; Stevenson *et al.*, 2012). These components contained in biomass during its general use are causing to increase in the probability of evaluating this from the positive side. The real evaluation of this in the future should be carried out research in other aspects.

Cultural solution CS and biomass VB of active strains obtained during cultivation in optimum environments were studied both by general biology and antimicrobial activities in subsequent studies. From the results became clear that both in the CS and VB (general and antimicrobial) have metabolites that have biological activity, and the quantitative indicator of their effectiveness is characterized by different indicators depending on both selected and tested cultures. So that, solutions obtained from all active producer shows relatively low activity to bacteria used as test cultures (30-35 % reduction compared to the control), and in all of the cases, it can be assessed as a weak and moderate bactericidal activity. But related to test fungi is observed as an average (37-50 %) and strong (50-62 %) fungicidal effects.

From the result of research became clear that antimicrobial activity of CS in all cases is higher than in water or alcohol extracts of dry biomass (1,1-1,2 times), although it defines the overall biological activity of VB extracts to the relationship of *Paramecium caudatum* gives a higher increase effect (Table 4). As seen, the growth effect of the materials obtained from the separate strains differs from each other by quantitative indications, but this difference is not too significant.

The discovery of a relatively high growth effect when using CS allows us to note that metabolites with antimicrobial activity are extracellular and are characterized by low molecular weight. So that, a sufficient amount of first metabolites in biomass and to use this by other living things as foodstuffs become easier. Those that synthesized as a manifestation form of adaptive properties and characterized as mainly second metabolites (Keller, 2019, Macheleidt *et al.*, 2016) are secreted out of fungi cells.

Apparently, the characterization of the growth effect of strains with similar indicators is due to the fact that the metabolites that caused the growth effect or contain compounds are similar to the extent that these facts are true, future studies will clarify.

Finally, in relation to the data presented in Table 4, an issue it can be said that none of the strains selected as an active producer is observed metabolites with toxic effects and the presence of biological activity components in all received materials is no doubt.

4. CONCLUSIONS:

Thus, from the carried out of research became clear that today the majority of Xylotropic macrometers as a promising producer of BAS used for various purposes in the world practice is also widely spread in Azerbaijan. Thus, the absence of metabolites with toxic effects as in CS as well as in the VB and possession their both general and antimicrobial activity in the future a serious basis for the organization of various BAS production based on them.

5. REFERENCES:

1. Akhundova, N.A., Orucova, S. B., Bahshaliyeva, K. F., Muradov, P.Z.,

- Rahimov, E.A. *Advances in Bioscience and Biotechnology*, **2019**, 10, 179-17.
2. Aliyeva, B.N. *Advances in Life Sciences*, **2019**, 9(2): 15-19
 3. Álvarez, S.P.O., Cadavid, D.A.R., Sierra, D.M.E., Orozco, C.P.O., Vahos, D.F.R., Ocampo, P.Z., Atehortúa, L. *BioMed Research International*, **2014**, ID 169071, 7 pages.
 4. Babu, Ch.R., Ketanapalli, H., Beebi, Sh.Kh., Kolluru, V.Ch. *Adv Biotech & Micro*, **2018**, 9(1).
 5. Baeva, E., Bleha, R., Lavrova, E., Sushytskiy, L., Copíková, J., Jablonsky, I., Klouček, P., Synytsya, A. *Molecules*, **2019**, 24, 2740.
 6. Bhalodia, N.R., Shukla, V. J. *J Adv Pharm Technol Res*, **2011**, 2(2), 104–109.
 7. Bandara, A.R., Rapior, S., Mortimer, P.E., Kakumyan, P., Hyde, K.D., Xu, J. *Mycosphere*, **2019**, 10(1), 579–607.
 8. Bisen, P.S., Baghel, R.K., Sanodiya, B.S., Thakur, G.S., Prasad, G.B. *Curr Med Chem.*, **2010**, 17(22), 2419-30.
 9. Bondartseva, M. A. *The determinant of mushrooms of Russia. The order is aphylophoric*. Saint Petersburg, Nauka, 1998, p. 391.
 10. Chang, Sh.–T. *International Journal of Medicinal Mushrooms*, **2006**, 8(4), 297–314.
 11. Cao, Y., Xu, X., Liu, S., Huang, L., Gu, J. *Frontiers in Pharmacology*, **2018**, 9(1217).
 12. Cör, D., Knez, Ž., Knez Hrnič, M. *Molecules*, **2018**, 23(3), 649.
 13. De Lira Mota, K.S., Pereira, F.D.O., De Oliveira, W.A., Lima, I.O., Lima, E.D.O. *Molecules*, **2012**, 17, 14418–14433.
 14. Fan, L., Ding, S., Ai, L., Deng, K. *Carbohydr Polym.*, **2012**, 90, 870-874.
 15. Garayeva, S. C., Naghiyeva, S. E., Huseynova, N. H., Mamedaliyeva, M. K. *Transaction of the Institute of Microbiology of Azerbaijan National Academy of Sciences*, **2017**, 15(2), 53–56.
 16. Gargano, M.L., van Griensven, L.J.L.D., Isikhuemhen, O.S., Venturella, G., Lindequist, U., Wasser, S.P., Zervakis, G.I. *Plant Biosystem*, **2017**, 151(3), 548–565.
 17. Gehlot, P., Singh, J. *Fungi, and their Role in Sustainable Development: Current Perspectives*. Springer Nature Singapore Pte.Ltd., 2018, 779.
 18. Géry, A., Dubreule, C., André, V., Rioult, J.P., Bouchart V., Heutte N., Eldin de Pécoulas, P., Krivomaz, T., Garon, D. *Integr Cancer Ther*, **2018**, 17(3), 832–843
 19. Grimm, D., Wösten, H.A.B. *Appl Microbiol Biotechnol.*, **2018**, 102(18), 7795–7803.
 20. *Handbook of Mycological Methods*, 2006.
 21. Hapuarachchi, K.K., Elkhateeb, W.A., Karunarathna, S.C., Cheng, C.R., Bandara, A.R., Kakumyan, P., Hyde, K.D., Daba, G.M., Wen T.C. *Mycosphere*, **2018**, 9(5), 1025–1052.
 22. Hyde, K.D., Xu, J. *Fungal Diversity*, **2019**, 97, 1–136.
 23. Jilinskaya, N.V., *Antimicrobial properties of basidiomycetes Fomitopsis officinalis (Vill.: Fr.) Bond. et Sing., Fomitopsis pinicola (Sw.: Fr.) P. Karst. and Trametes versicolor (L.: Fr.) Lloyd: assessment of the prospects for use in food technology*. Abstract of dissertations Ph.D. Moscow, 2015, 22.
 24. Keller N.P. *Nat Rev Microbiol.*, **2019**, 17(3), 167–180.
 25. Kobzar, A. I. *Applied Mathematical Statistics. For engineers and scientists*. Moscow, Fizmatlit, 2006, 816.
 26. Kokkoris, V., Ioannis, M., Polemisb, E., Koutrotsiosb, G., Zervakisb, G.I. *Science of The Total Environment*, **2019**, 685(1), 280-296.
 27. Ko, Y-F., Liao, J.C., Lee, C.S., Chiu, C.Y., Martel, J., Lin, C.S., Tseng, S.F., Ojcius, D.M., Lu, C.C., Lai, H.C., Young, J.D. *PLoS ONE*, **2017**, 12(1), e0168734.
 28. Kryczyk-Poprawa, A., Żmudzki, P., Maślanka, A., Piotrowska, J., Opoka, W., Muszyńska, B. *Biotech*, **2019**, 9(6), 207.

29. Macheleidt, J., Mattern, D.J., Fischer, J., Netzker, T., Weber, J., Schroeckh, V., Valiante, V., Brakhage, A.A. *Annu. Rev. Genet.* **2016**, 50, 371–392
30. Mamedov, G. S., Khalilov, M. E. *Forest of Azerbaijan*. Baku, Science, 2002, 472.
31. Millar, B. C., Nelson, D., Moore, R. E., Rao, J. R., Moore, J. E. *Int J Mycobacterial*, **2019**, 8(1), 93-97.
32. Muszyńska, B., Katarzyna, K., Radović, J., Sułkowska-Ziaja, Krakowska K., Gdula A., Argasińska, J.W., Kundaković, T. *Eur Food Res Technol.*, **2018**, 244, 2255–2264.
33. Muradov, P. Z., Garayeva, S.C., Naghiyeva, S.E., Abasova, T.S., Bakshaliyeva, K.F., Alibeyli, N.S. *Journal of Advanced Research in Biological Sciences*, **2018**, 5(8), 1–4.
34. Musayeva, V.H. *Int. J. Adv. Res. Biol. Sci.*, **2019**, 6(8), 35-39.
35. Netrusov, A. I., Egorova, M.A., Zagharuk, L.M. *Practice on Microbiology: Textbook for students of higher educational institutions*. Moscow, Academy, 2005, 608.
36. Nikitina, V.E., Loshchinina, E.V. and Vetchinkina, E.P. *Int J Mol Sci.*, **2017**, 18(7), 1334.
37. Osińska-Jaroszuk, M., Jarosz-Wilkolazka, A., Jaroszuk-Ścisel, J., Szaląpata, K., Nowak, A., Jaszek, M., Ozimek, E., Majewska, M. *World J Microbiol Biotechnol*, **2015**, 31(12), 1823-44.
38. Özdal, M., Gülmez, Ö., Özdal, Ö.G., Algur O.F. *Food and Health*, **2019**, 5(1), 12-18.
39. Rahi, D., Malik, D. *Journal of Mycology*, **2016**, 1-18.
40. Ritota, M., and Manzi P. *Sustainability*, **2019**, 11, 5049.
41. Saltarelli, R., Ceccaroli, P., Buffalini, M., Vallorani, L., Casadei, L., Zambonelli, A., Iotti, M., Badalyan, S., Stocchi, V. *Journal of Molecular Microbiology and Biotechnology*, **2015**, 25(1), 16-25.
42. Sekan, A.S., Myronycheva, O.S., Karlsson, O., Gryganskyi, A.G., Blume, Y. *PeerJ*, **2019**, 7, e6664.
43. Sharif, S., Huma, T., Shah, A.A., Afzal, G., Rashid, S., Shahid, M., Mustafa, G. *Food Science & Nutrition*, **2018**, 6(8), 2170-2176.
44. Stadler, M., Hoffmeister, D. *Front. Microbiol.*, **2015**, 6, 127.
45. Stevenson, L., Phillips, F., O'sullivan, K., Walton, J. *Int J Food Sci Nutr.*, **2012**, 63(8), 1001–1013.
46. Sum, Winnie, C., Abwao, S., Matasyoh Josphat, C. *African Journal of Biotechnology*, **2019**, 18, 112-123.
47. Taofiq, O., Heleno, S.A., Calhella, R.C., Alves, M.J., Barros, L., González-Paramás, A.M., Barreiro, M.F., Ferreira, I.C.F.R. *Food and Chemical Toxicology*, **2017**, 108, 139-147.
48. Ugbogu, E. A., Akubugwo, I.E., Ude, V.C., Gilbert, J., Ekeanyanwu, B. *Toxicol Res*, **2019**, 35(2), 181-190.
49. Wan, C., Li, Y. *Biotechnol Adv.*, **2012**, 30, 1447–1457.
50. Wu, Y.-L., Han, F., Luan, Sh.-Sh., Ai, R., Zhang, P., Li, H., Chen, L.-X. *J Agric Food Chem*, **2019**, 67(18), 5147-5158.
51. Zhou, S., Wang, M., Feng, O., Lin, Y., Zhao, H. *SpringerPlus*, **2016**, 5, 1966.

Table 1. Assessment of toxicity of obtained solution with respect to the *Tetrahymena pyriformis* infusion

Growth coefficient of <i>Tetrahymena pyriformis</i> infusion within 24 hours of exposure (K_1)	Assessment of toxicity
$K_1 \leq 0,5$	Solution is toxic
$K_1 \geq 0,9$	The solution is not toxic

Table 2. The general characteristic of Xylotrophic macromycetes located in the natural forests of Azerbaijan and considered promising as a perspective BAS in the world

No	Recorded species	Registered area	Characterization according to highlight substrate	Ecological relationship, the color of the decay	Characterization according to the distribution degree	Hyphal system
1	<i>Ganoderma lucidum</i>	BC, HNP	Evrytroph	Saprotroph, white	Casual and rare species	Trimitik
2	<i>Laetiporus sulphureus</i>	BC, HNP, SC		Polytroph, brown	Frequently encountered	Dimitik
3	<i>Pleurotus ostreatus</i>	BC, HNP, SC, KA		Polytroph, white	Frequently encountered	Dimitik
4	<i>Schizophyllum commune</i>	BC, HNP, SC, SC		Polytroph, white	Dominant	Dimitik
5	<i>Trametes versicolor</i>	BC, HNP, SC, KA		Saprotroph, white	Dominant	Trimitik

Table 3. Evaluation of Xylotroph macromycetes by the amount of biomass formed in the liquid nutrient medium

No	The name of the registered species	Number of checked strains	The total amount of formed biomass (7 day, g/l)
1	<i>G.lucidum</i>	5	5.2-7.8
2	<i>L.sulphureus</i>	5	4.5-6.5
3	<i>P.ostreatus</i>	5	6.6-8.4
4	<i>Sch.commune</i>	5	6.5-8.7
5	<i>T.versicolor</i>	5	5.8-8.1

Table 4. Toxic activity of strains of *Xylotrophic macromysacies* selected as an active producer in relation to *Tetrahymena pyriformis*

Nº	Recorded species	The number of primary cells (cell/300 µl)	The number of cells after 16 hours (cell/µl)	Increase coefficient
<i>VB (Extraction with water)</i>				
1	<i>G.lucidum</i> AS-4	160	319	2.00
2	<i>L.sulphureus</i> AS -7	145	290	2.00
3	<i>P.ostreatus</i> AH-12	150	314	2.09
4	<i>Sch.commune</i> AH -17	148	320	2.16
5	<i>T.versicolor</i> AN -23	156	315	2.02
6	Water	147	185	1.26
<i>VB (Extraction with 1 % alcohol)</i>				
1	<i>G.lucidum</i> AS-4	151	405	2.68
2	<i>L.sulphureus</i> AS -7	157	408	2.60
3	<i>P.ostreatus</i> AH-12	152	398	2.62
4	<i>Sch.commune</i> AH -17	149	410	2.75
5	<i>T.versicolor</i> AN -23	143	356	2.49
6	Alcohol	137	167	1.22
<i>CS</i>				
1	<i>G.lucidum</i> AS-4	159	290	1.82
2	<i>L.sulphureus</i> AS -7	162	298	1.84
3	<i>P.ostreatus</i> AH-12	142	250	1.76
4	<i>Sch.commune</i> AH -17	155	287	1.85
5	<i>T.versicolor</i> AN -23	158	275	1.74
6	The liquid nutrient medium	140	201	1.43

INTEGRANDO O COMPONENTE LINGUO-CULTURAL E O MÉTODO DO MAPA DA MENTE PARA DESENVOLVER UM E-DICIONÁRIO TRILÍNGUE DE TERMOS BIOLÓGICOS

INTEGRATING THE LINGUOCULTURAL COMPONENT AND MIND-MAP METHOD TO DEVELOP A TRILINGUAL E-DICTIONARY OF BIOLOGICAL TERMS

KALIZHANOVA, Anna^{1*}; MARYSHKINA, Taissiya²; ISHMURATOVA, Margarita³; IBRAYEVA, Bayan⁴; SEMBIYEV, Kurmangazy⁵;

^{1,2}Department of Foreign Languages and Intercultural Communication of the Private Institution, Bolashaq Academy

³Department of Botany of Karaganda State University named after E.A. Buketov

⁴Department of Foreign Languages and Intercultural Communication of Bolashaq Academy

⁵Department of Kazakh Language and Literature of Bolashaq Academy

* Corresponding author
e-mail: kalizhanova.bsu@bk.ru

Received 02 December 2019; received in revised form 06 February 2020; accepted 14 March 2020

RESUMO

O projeto nacional *Trinity of Languages* anunciado no Cazaquistão promoveu a educação multilíngue em todo o país. O projeto requer a implementação de ferramentas rigorosas de aprendizado para dominar os idiomas cazaque, russo e inglês no trilinguismo. Um dicionário eletrônico para ser usado no aprendizado integrado de conteúdo e idioma está entre as modernas ferramentas eletrônicas promovidas em um ambiente escolar trilingue. Um dicionário eletrônico biológico fácil de usar ajudará os alunos do ensino médio a compreender conceitos básicos nas ciências naturais. O artigo tem como objetivo descrever como analisar e sistematizar o material lexicográfico selecionado para o desenvolvimento de um dicionário eletrônico trilingue de termos biológicos para os alunos das escolas do Cazaquistão. A determinação das fontes do vocabulário selecionado foi baseada em uma abordagem línguo-cultural, que destaca o aspecto cultural incorporado na língua, e o mapeamento mental, que permite desconstruir graficamente tópicos complexos. Vinte e oito itens foram selecionados para cobrir o curso da escola de biologia, que foram posteriormente analisados e sistematizados para apresentar consistentemente características genéricas e de espécies através do mapeamento mental. Em seguida, a unificação orgânica dos itens e os parâmetros de composição do e-dicionário foram determinados. As descobertas obtidas mostraram que um componente linguístico é incorporado em um dicionário eletrônico trilingue de termos biológicos, retirados dos livros didáticos relevantes das escolas cazaque e russa (notas 6 a 11). Os itens selecionados são classificados e sujeitos à análise línguo-cultural em grupos conceituais que podem mostrar *phytonyms* e *zoonima*. Os itens são fornecidos com um comentário linguístico-cultural adequado, retirado de livros e sites de referência em inglês. Os grupos conceituais e comentários linguísticos são exibidos no mapa mental *Coggle* usado para a formação de quadros do dicionário eletrônico. O componente línguo-cultural proposto incorporado no dicionário eletrônico é raro em outros dicionários eletrônicos trilingues existentes, pois se concentra principalmente no material lexicográfico e em sua representação visual. No geral, o dicionário eletrônico trilingue criado no software de mapeamento mental é uma ferramenta eletrônica eficaz para os alunos do ensino médio estudarem termos biológicos com seus comentários linguísticos.

Palavras-chave: trilingüismo; e-dicionário; unidades lexicográficas; componente línguo-cultural; mapa mental.

ABSTRACT

The national project *Trinity of Languages* announced in Kazakhstan has brought forward multilingual education throughout the country. The project requires the implementation of rigorous learning tools to master the Kazakh, Russian and English languages within trilingualism. An e-dictionary to be used in content and language integrated learning is among modern e-tools promoted in a trilingual school environment. A user-friendly biological e-dictionary will help high school learners grasp fundamental concepts in natural sciences. The article aims to describe how to analyze and systemize the lexicographic material selected for developing a trilingual e-dictionary

of biological terms for Kazakhstani school learners. Determining sources of vocabulary chosen was based upon a linguocultural approach, which highlights the cultural aspect embodied in the language, and mind-mapping, which allows deconstructing complex topics graphically. Twenty-eight items were selected to cover the biology school course, which was later analyzed and systemized to consistently present generic and species features via mind-mapping. Then organic unification of the items and compositional parameters of the e-dictionary were determined. The obtained findings show that a linguocultural component is embedded in a trilingual e-dictionary of biological terms that are taken from relevant Kazakh and Russian school textbooks (grades 6–11). The selected items are classified and subject to linguocultural analysis in conceptual groups which may show phytonyms and zoonima. The items are supplied with an adequate linguocultural commentary taken from English-language reference books and websites. The conceptual groups and linguistic analysis are displayed via the mind map *Coggle* used for the e-dictionary frame formation. The proposed linguocultural component embedded in the e-dictionary is rare in other existing trilingual e-dictionaries since they focus primarily on lexicographic material and their visual representation. Overall, the trilingual e-dictionary created in mind-mapping software is an effective e-tool for high school learners to study biological terms with their linguocultural commentaries.

Keywords: *trilingualism; e-dictionary; lexicographic units; linguocultural component; mind map*

1. INTRODUCTION:

The Republic of Kazakhstan announced the national project called the Trinity of Languages in 2006 (Chukenayeva *et al.*, 2016). This project introduced a new tier of secondary and higher educational institutions, including the Nazarbayev Intellectual Schools and Nazarbayev University. Since then, the project has become the basis of multilingual education in Kazakhstan (Kosybaeva *et al.*, 2017), which means a large-scale introduction of trilingualism throughout the country. In particular, Kazakh is designated as the official language, Russian functions as the language of intercultural communication, and English is selected as the language of business.

This idea supports the government's activities to ensure industrialization and sustainable economic growth revealed in the 100 Concrete Steps to Implement Five Institutional Reforms document published in 2015 ("President Nazarbayev unveils ...", 2015). Since then implementation of this Plan of Nation has been demonstrating a steady increase in industrial production, mining and quarrying, manufacturing, and agriculture. The volume of transportation and communication services, retail and wholesale trade has also risen (State programs, 2018). In the era of globalization, foreign investment brings about technology development and subsequent industrial restructuring, which enable to improve economic output (Dave, 2007; Vanderhill *et al.*, 2019). Hence, people must have a good command of the Kazakh, Russian and English languages to be fully involved in activities boosting industrialization and sustainable economic growth of Kazakhstan (Kulgildinova *et al.*, 2018; Thomas, 2015).

The reforms embodied in the Plan of Nation substantiate the need to create effective, efficient, and fast methods to learn and master the languages. In this regard, the development of rigorous learning tools is required. Among them is a dictionary that helps teach any language and assess the level of language competence. In a dictionary, it is essential to "maintain consistency and predictability when the nature of language requires each concept to be treated individually" (Niininen *et al.*, 2017, p. 451). Any dictionary should reflect the cultural aspect of society since students have to struggle against cultural and social discrepancies in a trilingual environment (Haim, 2019; Rohmatillah, 2016). Following the trilingual policy in Kazakhstan, enculturation of the young generation is also a top priority (Kassymova, 2017) and the method of integrated teaching of subject and language should be the primary method of language teaching in the country (Syrymbetova *et al.*, 2017; Ongarbaeva *et al.*, 2015).

The transition from general to higher education in Kazakhstan involves using trilingual dictionaries when teaching general and specialized subjects. Trilingual educational dictionaries have proved to be useful to learn foreign languages so terminological trilingual ones are actively being developed for use in various spheres of human activity (Mazhitayeva *et al.*, 2016). Accurately, in 2013 the Ministry of Foreign Affairs of Kazakhstan presented Kazakh-English-Russian and Russian-Kazakh-English dictionaries containing word-combinations and terms related to diplomacy, modern politics to diplomats, translators, teachers, and students (Nur-Sultan, 2013).

A search for relevant teaching techniques and the development of information technology

should go hand in hand to produce a user-friendly dictionary for learners (Rohmatillah, 2016). Therefore, it is vital to create a trilingual electronic dictionary (e-dictionary) that encompasses a broad range of videos, photos, and audio data from both linguistic and cultural contexts (Granger, 2012). Detailed information on each term, visualization of term relations, and real-life usage examples (Horák *et al.*, 2019) contribute to the success of an e-dictionary. The mind-map concept explains the visual representation of the data as well as ideas associated with them (Wang & Dostál, 2018). In this way, the dictionary will assist in sampling lexicographic material relevant to multilingual education. This dictionary will be especially convenient to use within the school curriculum since such mind maps will draw learners' attention to the studied material in a beneficial way (Akçadağ, 2010).

Trilingual e-dictionaries are indispensable when there is a shortage of relevant school subject textbooks (Suleimenova *et al.*, 2018) and Kazakh-Russian-English dictionaries in Kazakhstani state schools due to a recent introduction of the national language policy. High school students have to grasp basic concepts in natural sciences in English when immersed in content and language integrated learning (Syrymbetova, 2017; Ydyrys *et al.*, 2019). In particular, chemistry, physics, computer science, and biology will be taught in English since 2019 ("Textbooks in English," 2017). So such students' knowledge of Kazakh and Russian used in secondary schools will help them better understand life and physical science in high school.

There is an urgent need to design a biological e-dictionary to bridge the gap of insufficient subject textbooks where the main concepts of biology as a life science should be displayed. Therefore, it is of vital importance to implement a project to create an e-dictionary of biological terms with the embedded linguocultural component. This component is supposed to offer students not only all the necessary lexicographic information about a particular biological name as mind maps but also peculiarities of its representation in Kazakh, Russian, and English linguacultures.

The article aims to describe how to analyze and systemize the lexicographic material selected for developing a trilingual e-dictionary of biological terms for Kazakhstani school learners. The authors intend to produce the dictionary (Russian-Kazakh-English, English-Russian-Kazakh, and Kazakh-Russian-English) that encompasses the entire Kazakh school biology curriculum in an

electronic form. Within the research aim, it is proposed to analyze the current situation with trilingualism in the Kazakh education system. Next, it is planned to describe the initial stage of creating a biological trilingual e-dictionary, with the linguocultural aspect and mind-mapping technique considered. Finally, it is intended to present the findings relevant to the main steps of the stage. In particular, the focus is on the selection and analysis of lexicographic units from the school biology curriculum in Kazakhstan. Then organic unification of the lexicographic material is determined and compositional parameters of the e-dictionary are established.

Driving forces of developing a trilingual e-dictionary are transition from bilingualism to trilingualism within the Kazakh national education system (Amalbekova, 2013). Trilingualism in Kazakhstan is a unique project intended to help students and teachers switch immediately between Kazakh, Russian, and English (Yeskeldiyeva & Tazhibayeva, 2015). Implementation of the trilingualism project in the Nazarbayev Intellectual Schools throughout Kazakhstan enabled to introduce and execute the plan in general schools all over the country.

Large-scale changes in the education system require the recruitment of trained personnel capable of teaching humanitarian and natural subjects in different languages. The staff should also be able to update teaching methods to meet global best practices. As noted by Jantassova (2015), a working knowledge of English alongside the Kazakh and Russian languages now forms the basis for ensuring a high level of educational quality nationally and consequently the development of international cooperation. Indeed, upgrading teaching skills within Kazakhstan is a top priority nowadays although educators face a 'switching codes' issue because of the transition to trilingualism (Ishmuratova, 2016).

On the other hand, teaching aids, including a library fund for schools, have not adapted adequately to the new realities so far. Of course, changes in teaching methods require designing new teaching aids, renewal of school library funds, and providing access to scientific literature and reference books that conform to multilingualism principles (Kosybaeva *et al.*, 2017). A lack of specialized literature on subjects in English as well as printed and online terminological dictionaries explain the need to supply the educational process with working materials on the topics. Akhmetova (2018) states that glossaries of terms and thesauruses present terminology that can only be

systematized and unified, but not standardized.

Baynieva and Umurzakova (2015) highlight the apparent shortage of relevant trilingual dictionaries in both regular schools and universities within Kazakhstan. The researchers also state that students' acquisition of communicative and linguistic competencies directly depends upon their mastery of the initial vocabulary of all the three languages. In their opinion, the use of trilingual dictionaries at schools and universities will help increase the level of Kazakh, Russian, and English spoken among students and teachers. Moreover, the Bologna Process necessitates the creation and use of e-learning tools to contribute to the development of general cultural and professional language competencies among students (Sysoeva, 2011). A published trilingual dictionary, as well as its electronic version, will, therefore, contribute to the Kazakh education system.

Zhakupova (2012) presents a review of state-of-the-art lexicographic products that include expanded capabilities. She notes that new dictionaries can capture a lot of information including a lexicographic description of words, even borrowed, inadequate, and old ones. These words should correspond to reality, history, and culture of native people. In the researcher's view, a multilingual dictionary organically continues the tradition of anthropocentric lexicography and is characterized by an extensive range of educational possibilities. A large number of users demand an ordered sequence of information that can be expanded by including texts in other languages from an empirical base. However, Yataeva (2016) claims that the structure and organization of an e-dictionary is entirely different from traditional paper counterparts. Indeed, the 'hypertext' of an e-dictionary allows a user to populate 'information zones' according to specific needs (p. 136).

Over the past decade, e-dictionaries have gone far ahead and have become increasingly popular with users as a tool of language learning in the digital era (Liu, 2017). It is also claimed that Macmillan Education announced the publication of only online dictionaries in 2012 (Frommer & Finegan, 2013). Online dictionaries are user-friendly (Müller-Spitzer *et al.*, 2012) since they mean an easy search, a vast database, constant upgrade, and accessibility. A dictionary in one's computer, tablet, laptop, or mobile phone allows accessing information about the language without carrying massive volumes of printed versions.

Despite the evident advantages of e-

dictionaries for learning, they do not seem to be a universal tool for each learner. Disregarding students' psychological and age peculiarities can lead to their unproductive work in class. Lew and Mickiewicz (2013) assert that the use of dictionaries is a two-way game, in which the players are the dictionary itself and the dictionary user. They add that the game proceeds smoothly only if they both perform well. Such performance is nevertheless not typical of schoolchildren so the focus should be on the visual representation, which is lacking in most dictionaries.

The contemporary schoolchildren are referred to the generation Z, who heavily uses gadgets in everyday life. Therefore, such learners develop a genuine visual culture and are immersed in online communication (Stanciu *et al.*, 2016). The learners are early adaptors of technology in the digitalized world so they tend to interact virtually, as Mladkova (2017) acknowledges. She also informs about the fact that such students often experience difficulty in comprehending long and complex texts. Nevertheless, they prefer to deal with short well-structured texts and animated pictures (Lew & Doroszevska, 2009).

The reviewed sources about e-dictionaries demonstrate current deficiencies in presenting lexicographic material in a way similar to that in a printed version. Neglecting some essential skills to work with dictionaries will result in the effective use of the e-learning tool to master foreign languages in content and language integrated learning. For schoolchildren, it is essential to lookup complete, short, and precise information supported with visual data as the standard vocabulary data will not appeal to school-age learners (Commodari, 2016). In turn, a brand-new innovative approach is required when designing an e-dictionary for the Generation-Z learners. In particular, developers must use bright, efficient, and picturesque materials such as infographics, presentations, mind maps, and ready-to-use structures. So the optical interface and graphics execution are advocated for.

As regards a trilingual e-dictionary of biological terms presented as thesaurus, convenient methods of displaying information are important as well. Besides, various criteria for searching for and grouping material should be taken into consideration. Of course, a trilingual e-dictionary of biological terms should encompass a linguocultural component, per the new educational policy of Kazakhstan.

2. MATERIALS AND METHODS:

It is planned to implement three main stages. They include determining sources of vocabulary selected to be included in the e-dictionary, designing and creating a printed version of a trilingual dictionary, and developing an electronic version and a web version of the dictionary.

This article reveals the first stage of the investigation, which involves creating high-quality, innovative products. This activity demands a specific approach, which should help them distinguish from other similar ones. In the context of the research, a linguocultural plan and mind-mapping are prioritized. As regards the linguocultural approach, it highlights the cultural aspect embodied in language. Culturally marked words have an impact on people who use them in their language (Bolt *et al.*, 2017) so their inclusion in an e-dictionary will demonstrate cultural specificity reflected in the language. The creation of the proposed trilingual dictionary will require the use of linguistic research methods including typological approaches, functional, parametric, and structural analyses, as well as language construction for an integrated dictionary model.

The dictionary model should reflect the peculiarities of different types of dictionaries. For instance, linguoculturological dictionaries include specific elements of the language, which are known as realities. There are also dictionaries of phraseological units, thematic dictionaries, dictionaries of nicknames, those of proper names. However, such dictionaries seem to be in demand only among people aimed at mastering the language at an advanced level. Or those who have once come across fragments of the language, which they do not understand, can address such dictionaries.

Next, mind-mapping allows deconstructing complex topics with the help of graphical representation of constituent issues and related themes (Kernan *et al.*, 2017). This approach enables learners to identify the item and select its specific aspect of their work. Application of the mind-map method is advantageous since it allows comprehending the chosen idea alongside with the visual representation of all sub-topics and interconnections. In recent years, the potential of mind-mapping has been considerably enlarged through the development of the relevant software. It enables the creation of digital mind maps, which are also attractive outside the classic scope of supporting learning (Dirnberger, 2016).

To achieve the research aim, it is necessary to specify the initial stage of the investigation: determining sources of vocabulary selected to be included in the e-dictionary. The methods of collecting linguistic data and their interpretation are employed here. Specifically, the primary task of this stage is to select and analyze lexicographic units related to biological terms from the Kazakh school curriculum. It is expected to select 28 items to cover the biology school course (from 1998 till 2017), including textbooks, tutorials, guides, school terminological dictionaries, etc. After selecting the vocabulary, it is necessary to conduct a preliminary analysis of biological concepts and terms. Then it is crucial to systematize them to consistently present generic and species features via mind-mapping.

Concerning the stage, organic unification of the lexicographic units should be determined, with linguocultural commentaries to accompany them taken into consideration. It is also necessary to specify compositional parameters of the e-dictionary for schoolchildren, schoolteachers, students, and university professors, which are based on mind-mapping.

3. RESULTS AND DISCUSSION:

During the initial stage of the research, it is intended to analyze and systemize the lexicographic material selected for developing a trilingual e-dictionary of biological terms for Kazakhstani school learners. Selection of the lexicographic material within the stage is based upon the cultural aspect of learning foreign languages. Usually, members of one culture easily perceive all information. Alternatively, those who study the language often find themselves in a predicament since they do not know the mentality and cultural characteristics of native speakers. As a result, communication fails. According to Shrestha (2014), "since culture comprises language as its part and it finds its survival in the expression of language, it can be said that culture and language are intricately interwoven" (p. 55).

The project participants acknowledge that each language is given a specific role in the case of trilingualism. English, for instance, is highly required in the professional field. The younger generation will be forced to learn the language along with the study of a discipline. About all the necessary materials for a school biology course, students will study it in English. Unlike in regular English classes, they will encounter neither English mentality nor cultural peculiarities to help them grasp both new concepts and a variety of

associated values. For example, the word monkey is translated as обезьяна (obezyana) into Russian. However, few schoolchildren know that the Russian verb обезьяничать (obezyannichat), which means frivolous childish behavior, has the same analog in English to monkey.

Another example is the biological term cloaca, which has a similar equivalent in Russian. However, the following linguocultural explanation helps memorize this term: cloaca defines sewage or surface water. There are numerous examples of similarities of cultures so they contribute to the assimilation of a separate nomination. Also, they give an idea of another cultural mentality and standard parallels in the worldview.

Creating a trilingual dictionary of biological terms incorporates a linguocultural component, which is consistent with the State Program of Education Development in the Republic of Kazakhstan for 2011–2020. This component determines the selection of lexicographic units presenting biological terms for school learners. All sections of the e-dictionary should contain lexicographic material from the school biology curriculum. It will be necessary to cover material from botany, ecology, zoology, physiology, anatomy, genetics, evolution, and molecular biology. The lexicographic content should be taken from the relevant Kazakh and Russian textbooks used in 6–11 grades at schools. The textbooks should be granted official approval to be used in the educational process (Appendix 1). Besides, it will be essential to examine English-language reference books within this discipline (Appendix 2). Another source of the lexicographic material is English-language websites that address this topic (Appendix 3).

Additional preparatory work will comprise the classification of the obtained data as well as linguocultural analysis of the selected terms. These processes demonstrate how the lexicographic units of biological terms can be analysed. Conceptual groups should distribute the subject keywords. The possible subject groups can be presented as origin of terms (compost – from Latin composites, which means compound), phraseological units (перекрыть кислород – close the oxygen, which means to block any action of people), the cultural meaning (in the United Kingdom, the bear and staff feature on the heraldic arms of the county of Warwickshire; bears appear in the canting arms of two cities, Bern and Berlin). The conceptual groups may show phytonyms and zoonima (Bunny Rabbit, Grey Wolf, Nanny Goat, Hafoc-wyrt, Hara-Wyrt, Gold-Wyrt, etc.).

The next step is to create an adequate linguocultural commentary to maintain organic unification of the selected lexicographic units. With this in mind, it is necessary to choose the texts that correspond to the logical and semantic structure of both the biology school course and academic requirements. Sources of the documents are English-language reference books and websites used for selecting the relevant lexicographic units. It is essential to consider such criteria for choosing the texts as language, time, mode, medium, domain (“Dictionaries,” 2013). An example of such a text is as follows: Commonly, animals, which means all animals, except humans. People differ in what they consider an animal: some would say that humans are distinct from animals (creationists, for example), while others would say that humans are animals (evolutionists, for instance). Some do not include lizards as animals; others do not include insects. The selected biological terms and linguocultural commentaries should be supported with illustrations.

The obtained linguistic data should be systemized under the compositional parameters of the e-dictionary. In this vein, it is necessary to prepare the relevant glossary articles, group the lexicographic material by sections and edit it, create a design directory, collate and correct illustrations, as well as edit the list of words (including adjustments, layout, and printing), and distribute the catalog.

However, an attempt to fill an article of a standard form with all elements selected for the funding project may be unreasonable. This attempt may result in obtaining an excessively heavy layer of information, which will cause students to feel anxiety and fatigue. In turn, the mind-map structure allows breaking up the elements into easily perceivable parts and enables them to add a linguocultural component.

Web software is chosen for organic unification of the selected lexicographic units. The software allows ordering and structuring information similarly to the standard mind map called Coggle for the e-dictionary frame formation. There are offered e-dictionary entries and ways to present them, delete and add parts as well as change their position simply and understandably. In other words, this collaborative application encourages producing a specific composition. It meets average schoolchildren’s demands to study biology in English, which is to perceive and comprehend information about a biological term in one clear concept (Figure 1).

Since the mind map is a remarkable way to

introduce the vocabulary information, it is a good idea to separate all aspects of a biological term and turn them into a much more comfortable way to spot. Above all, visual areas prove to be beneficial for e-dictionary users since the visual representation allows splitting the data into short, understandable fragments. In other words, the proposed page layout presents an expedient meaning segmentation. Specifically, the ready-made logical model of a biological term is advantageous for learners since it makes its analysis and comprehension more accessible and simplifies the extraction of the word meaning. Within the trilingual e-dictionary, such a page layout keeps all the fragments of information in the same basic blocks. These blocks contribute to supporting communication among all the languages.

The advantages of creating a mind map substantiate the need to use it as a design entry of the trilingual e-dictionary of biological terms (Figure 2). In the attempt to present only the primary information in the e-dictionary, there are chosen such elements as pronunciation, meaning, cultural models, a picture or a video, an association, and synonyms and antonyms if there are any. Once entering a request, a student is expected to obtain a vivid picture showing the required information.

Students' interaction with the biological e-dictionary demands specific skills. Nesi's research findings (2015) allow outlining four main ones. The first skill involves interpreting morphological and syntactic information. Next, students should understand the definition or translation. As regards the third skill, it is vital to interpret information about collocations. Deriving knowledge from examples is another essential skill.

The findings suggest that the dictionary is an effective e-tool used in content and language integrated learning. It is especially so when there is a lack of relevant specialized literature on the school subject of biology in English as well as printed and online terminological dictionaries. Now the priority is on students' and teachers' needs to switch immediately between Kazakh, Russian, and English within trilingualism. In this context, schools have to recruit trained personnel able to update teaching methods to meet global best practices. Using tools of language learning in the digital era means promoting trilingual e-dictionaries in both regular schools and universities within Kazakhstan.

The page layout of the trilingual e-dictionary of biological terms reflects linguocultural

aspects of the selected and analyzed lexicographic units. This lexicographic material is systemized via the mind-mapping method. In this way, the findings show successful completion of the main tasks connected with creating a new way of dictionary entry organization, which is suitable for students of the current generation Z. This way corresponds to the students' demands to utilize products with such characteristics of information metabolism as fast, short, precise and visual. Employing such products in the educational process enables to develop learners' critical thinking and analytical skills, which undoubtedly affect the quality of learning and students' future academic achievements.

The search for articles devoted to trilingual dictionaries in journals indexed in Scopus and Web of Science since 2014 shows that researchers focus on both lexicographic material and the visual representation. However, rare articles highlight the linguocultural component embedded in the e-dictionary. Only Salipande (2018) emphasizes the cultural aspect of language preservation when investigating the lexical level of the Lopez Agta language. This idea is reflected in a trilingual thematic visual dictionary, which embraces such languages as Agta, Filipino, and English, although the researcher's aim differs from the authors' it is achieved through the linguocultural component of lexicographic units and their visual representation in the printed thematic dictionary.

As regards the visual representation of an e-dictionary, AlQallaf (2018) designs a sign language bilingual dictionary explicitly for hearing impaired and deaf individuals. The Arabic and American sign languages require a web-based platform where such individuals can communicate with others. High accessibility of visual interface enables its developers to integrate the dictionary with a new sign language. Therefore, the potential of the web-based dictionary to become trilingual is rather high. Despite the evident benefit of the visual representation of the e-dictionary, the researcher does not specify the linguocultural component of lexicographic units.

Another platform makes a trilingual online technical dictionary advantageous for Georgian learners. As Margalitadze (2018) claims, a Multilingual Dictionary Management System is specially developed to create Georgian online terminological dictionaries. The researcher uses English, Russian, and Georgian to present specialized vocabulary of different domains. The focus is on terminological synonymy and polysemous words as well as new terminology,

which requires the introduction of collocations and examples of the usage of the term. Still, the researcher does not identify the linguocultural component and seems to restrict the visual representation of technical terms.

Torrent *et al.* (2014), who cover such domains as soccer, tourism, and the World Cup within the Copa 2014 Frame Net Brazil project, develop the sports e-dictionary. The researchers implement the trilingual annotation to populate the Copa 2014 database. They also create the Translation relation, a computational solution to deploy frames as interlingual representations concerning Portuguese, Spanish, and English. Although the researchers promote multilingual lexicographic annotation for their e-dictionary, they do not establish the cultural aspect relative to the thematic lexicographic material.

Dollah *et al.* (2017) center on a mobile application on iOS and Android to develop the trilingual glossary of such terms as Islamic banking and finance. The rapid prototype instructional design model is the basis of developing the mobile terminology glossary app. Here the stress is on the visual representation rather than the linguocultural component of lexicographic units from the Malay, Arabic, and English languages.

So the current publications revealing trilingual e-dictionaries posit some deficiencies mostly relative to the linguocultural component of the lexicographic material embedded in the web software. On the other hand, data about specific web platforms can help further address the visual representation of the selected content.

4. CONCLUSIONS:

The introduction of trilingualism throughout Kazakhstan has caused to tackle a difficult task. It involves integrating the teaching of the biology school course, three languages (Kazakh, Russian, and English), and the cultural aspect. These ideas are considered when developing a trilingual e-dictionary of biological terms primarily for high school learners. Enculturation of the young generation known as the generation Z makes the authors of the article include the linguocultural component in the selected lexicographic material. This component is lacking in most trilingual thematic e-dictionaries, which makes the current research outstanding. Additionally, the visual representation, which is insufficient in most printed dictionaries, should be prioritized in the biological e-dictionary for school learners. Optical interface and graphics execution are presented via mind-mapping to display the biological terms to

advantage.

Overall, this article reveals the first stage of the investigation, which means determining sources of vocabulary selected to be included in the e-dictionary. Selection of the lexicographic material within the scene is based upon the cultural aspect of learning foreign languages. Primarily the article describes how to select and analyze lexicographic units relative to biological terms from the Kazakh school curriculum. The linguocultural component reveals the cultural aspect of learning foreign languages, which allows perceiving another cultural mentality and standard parallels in the worldview. Also, there is a classification of the obtained data and linguocultural analysis of the selected terms.

Next, there was determined organic unification of the lexicographic units by creating an adequate linguocultural commentary. There were also identified compositional parameters of the e-dictionary based on mind-mapping, which is a design entry of the trilingual e-dictionary of biological terms. Systemization of the obtained linguistic data was done via the web software Coggle for the e-dictionary frame formation.

As regards the second stage, it is planned to design and create a printed version of the trilingual dictionary during the second year of work on the funding project. With this in mind, a philological method will help prepare the glossary articles, systemize materials by sections and edit them, create a design directory, collate and correct illustrations, as well as edit the list of words (including adjustments, layout, and printing) and distribute the catalog.

During the third stage, it is proposed to design an electronic version of the dictionary and its web version. In this vein, it is meant to differentially group the materials and search for several variants of each criterion. The first step of the stage will involve creating a software platform that includes both a creative and intuitive interface. Secondly, it is planned to develop a specialized search system that emphasizes the needs of the research process. Thirdly, it is necessary to identify the critical features of all the information contained in the e-dictionary. This will enable description of mechanisms for analyzing entries as search engine parameters are developed. Lastly, it is proposed to form a structural resource database.

The stage of direct application of the mind-map dictionary structure is scheduled for the third year of the funding project. Additional verifications of representing the ideas, consultation with

students and teachers will be required. There may be some technical problems associated with programming this kind of dictionary page. There might be additional elements for a dictionary entry that should be included in the trilingual dictionary. These and other questions can be solved only during practical work with the funding project.

The trilingual e-dictionary of biological terms is planned to be only web-based. The project participants are in search of web-programmers who will manage to create the relevant e-dictionary and will further assist in developing a mobile application. The web-based dictionary and mobile app will bring the funding project closer to students by satisfying the needs of the generation Z to have information readily available.

5. REFERENCES:

1. Akçadağ, T. *Bilig*, **2010**, 53, 29-50.
2. Akhmetova, M. *The Journal of Language Research and Teaching Practice*, **2018**, 2(2), 1-12. doi:10.32788/jlrtp.02.6-15.
3. AlQallaf, A.H. *Journal of Engineering Research*, **2018**, 6(2), 84-102.
4. Amalbekova, M. *Middle East Journal of Scientific Research*, **2013**, 14(9), 1152-1155. doi:10.5829/idosi.mejsr.2013.14.9.2228.
5. Baynieva, K.T., Umurzakova, A. Z. *International Journal of Applied and Fundamental Research*, **2015**, 8(4), 776-779. (in Russian).
6. Bolt, I.V., Szerszunowicz, J. *Neofilologia dla przyszłości*, **2017**, 2, 229-242.
7. Chukenayeva, G., Smagulova, G., Sarbasova, K., Rakhimova, A., Saduakasova, S., Turysbekova, A. *Journal of Language and Literature*, **2016**, 7(3), 5-13. doi:0.7813/jll.2016/7-3/1.
8. Commodari, E. *Perceptual and Motor Skills*, **2016**, 122(3), 855-870. doi: 0.1177/0031512516652034.
9. Dave, B. *Kazakhstan – Ethnicity, Language and Power*. London: Routledge, 2007. doi:10.4324/9780203014899.
10. *Dictionaries: An International Encyclopedia of Lexicography*. (Gouws, R. H., Heid, U., Schweikard, W., Wiegand, H. E. Eds.). Berlin/Boston: Walter de Gruyter, 2013.
11. Dirnberger, D. *World Patent Information*, **2016**, 47, 12-20. doi:10.1016/j.wpi.2016.08.004.
12. Dollah, N.H., Ghalib, M.F.M., Sahrir, M.S., Hassan, R., Zakaria, A.W., Omar, Z. *International Journal of Interactive Mobile Technologies*, **2017**, 11(3), 145-161. doi:10.3991/ijim.v11i3.6620.
13. Frommer, P.R., Finegan, E. *Looking at Languages: A Workbook in Elementary Linguistics*. Stamford, USA: Cengage Learning, 2014.
14. Granger, S. Electronic lexicography – from challenge to opportunity. In S. Granger., M. Paquot (Eds), *Electronic Lexicography*. Oxford: Oxford University Press, 2012. doi:10.1093/acprof:oso/9780199654864.001.0001.
15. Haim, O. *Intercultural Education*, **2019**, 30(5), 510-530. doi: 10.1080/14675986.2019.1598095.
16. Horák, A., Baisa, V., Rambousek, A., Suchomel, V. *International Journal on Artificial Intelligence Tools*, **2019**, 28(2), 1950008. doi:10.1142/S0218213019500088.
17. Ishmuratova, M.Yu. *Proceedings of Youth and Current Global Issues*, **2016**, 341-346. (in Russian).
18. Jantassova, D. *Procedia – Social and Behavioral Sciences*, **2015**, 177, 136-141. doi:10.1016/j.sbspro.2015.02.364.
19. Kassymova, G. *Turkish Online Journal of Educational Technology*, **2017**, 17, 591-595.
20. Kernan, W. D., Basch, C. H., Cadoret, V. *Pedagogy in Health Promotion*, **2017**, 4(2), 101-107. doi:10.1177/2373379917719729.
21. Kosybaeva, U., Shayakhmetova, M., Utebayev, I., Syzdykova, N., Abishev, Z., Orazbekova, R. *Espacios*, **2017**, 38(35). Retrieved from <http://www.revistaespacios.com/a17v38n35/a17v38n35p28.pdf>.
22. Kulgildinova, T., Zhumabekova, A., Shabdenova, K., Kuleimenova, L., Yelubayeva, P. *XLinguae*, **2018**, 11(1), 332-341. doi:10.18355/XL.2018.11.01.28.
23. Lew, R., Doroszewska, J. *International Journal of Lexicography*, **2009**, 22(3), 239-257. doi:10.1093/ijl/ecp022.
24. Lew, R., Mickiewicz, A. From paper to electronic dictionaries: Evolving dictionary

- skills. In Kwary, D. A., N. Wulan, L. Musyahda (Eds), *Lexicography and Dictionaries in the Information Age. Selected Papers from the 8th ASIALEX International Conference*, 2013, (79-84). Surabaya: Airlangga University Press. Retrieved from: https://www.researchgate.net/publication/265252133_From_paper_to_electronic_dictionaries_Evolving_dictionary_skills.
25. Liu, X. *Lexikos*, **2017**, 27, 287-309. doi:10.5788/27-1-1404.
 26. Margalitadze, T. *EURALEX Proceedings*, **2018**, 339-350. <http://euralex.org/wp-content/themes/euralex/proceedings/Euralex%202018/118-4-2995-1-10-20180820.pdf>.
 27. Mazhitayeva Sh., Akhmetova A., Zhunusova A., Azhigenova S. *Bulletin of the Peoples' Friendship University of Russia. Education Issues Series: Languages and Specialty*, **2016**, 4, 50-56. Retrieved from <http://journals.rudn.ru/polylinguality/article/view/14659/13730>.
 28. Mladkova, L. *Proceedings of the 18th European conference on knowledge management (ECKM 2017)*, **2017**, 1-2, 698-703.
 29. Müller-Spitzer, C., Koplenig, A., Töpel, A. Online dictionary use: Key findings from an empirical research project. In S. Granger, M. Paquot (Eds.), *Electronic Lexicography*. Oxford: Oxford University Press, 2012. doi:10.1093/acprof:oso/9780199654864.003.0020.
 30. Nesi, H. The specification of dictionary reference skills in Higher Education. In *Dictionaries in Language Learning: Recommendations, National Reports and Thematic Reports from the TNP Sub-Project 9: Dictionaries*, 2015, (53-67). Berlin: Freie Universität. Retrieved from <https://pureportal.coventry.ac.uk/files/3940949/Nesi1999.pdf>.
 31. Niininen, S., Nykyri, S., Suominen, O. *Journal of Documentation*, **2017**, 73(3), 451-465. doi:10.1108/JD-06-2016-0084.
 32. Nur-Sultan *Kazakh Foreign Ministry presented trilingual diplomatic dictionaries. Kazakhstan 2050*. Retrieved from <https://strategy2050.kz/en/news/4250>.
 33. Ongarbaeva, A.T., Kondybaeva, M.R., Sebeopova, R.M., Smanov, B.U., Karimova, G.S. *Journal of Language and Literature*, **2015**, 6(4), 337-342. doi:10.7813/jll.2015/6-4/62.
 34. *President Nazarbayev unveils 100 concrete steps to implement five institutional reforms* (June 2, 2015). Retrieved from https://www.inform.kz/en/president-nazarbayev-unveils-100-concrete-steps-to-implement-five-institutional-reforms_a2782614.
 35. Salipande, A. L. *2nd Advanced Research on Business, Management and Humanities (ARBUHUM)*, **2018**, 24(4), 2392-2394. doi:10.1166/asl.2018.10961.
 36. Shrestha, K. *Journal of NELTA*, **2016**, 21(12), 54-60. Retrieved from <https://www.nepjol.info/index.php/NELTA/article/view/20201/16601>.
 37. Stanciu, D., Stefan, L. *Pour une Europe forte, renover les structures économiques, entrepreneuriales, politiques, territoriales et éducatives*, **2016**, 289-298.
 38. State programs: Government of Kazakhstan on results of activities for 2017 (June 20, 2018). Retrieved from <https://primeminister.kz/en/news/all/16716>.
 39. Suleimenova, E. D., Kozhamkulova, G.E., Urazaevac K.B. *Journal of Siberian Federal University. Humanities & Social Sciences*, **2018**, 6, 987-1001. doi:10.17516/1997-1370-0288.
 40. Syrymbetova, L.S., Zhumashev, R.M., Nugmetuly, D., Shunkeyeva, S.A., Zhetpisbayeva, B.A. *Novosibirsk State Pedagogical University Bulletin*, **2017**, 7(4), 72-92. doi:10.15293/2226-3365.1704.05 (in Russian).
 41. Sysoeva, L.A. *Journal of International Scientific Publications: Educational Alternatives*, **2011**, 9(2), 127-134. Retrieved from <https://www.scientific-publications.net/download/educational-alternatives-2011-2.pdf>.
 42. Textbooks in English to be introduced in Kazakh schools (February 6, 2017). *Kazinform*. Retrieved from https://www.inform.kz/en/textbooks-in-english-to-be-introduced-in-kazakh-schools_a2996346.
 43. Thomas, M. *Central Asian Survey*, **2015**, 34(4), 456-483. doi:10.1080/02634937.2015.1119552.

44. Torrent, T.T., Salomão, M.M.M., Da Silva Matos, E.E., Gamonal, M.A., Gonçalves, J., De Souza, B.P., Gomes, D.S., Peron-Corrêa, S.R. *Constructions and Frames*, **2014**, 6(1), 73-91. doi:10.1075/cf.6.1.05tor.
45. Vanderhill, R., Joireman, S.F., Tulepbayeva, R. *Europe – Asia Studies*, **2019**, 71(4), 648-670. doi:10.1080/09668136.2019.1597019.
46. Wang, X., Dostál, J. *ACM Conference Proceedings series*, **2018**, 150-153. doi:10.1145/3291078.3291121
47. Yataeva, E.V. *Bulletin of the Chelyabinsk State Pedagogical University*, **2016**, 10, 135-140.
48. Yeskeldiyeva, B.Y., Tazhibayeva, S.Z. *Asian Social Science*, **2015**, 11(6), 56-64. doi:10.5539/ass.v11n6p56
49. Ydyrys, A., Srail, S., Ydyrys, S., Basygarayev, Z., Mautenbaev, A., Baidaulet, T. *Universal Journal of Educational Research*, **2019**, 7(8), 1698-1706.
50. Zhakupova, A.D. *Russian Journal of Lexicography*, **2012**, 2, 66-75. (in Russian).

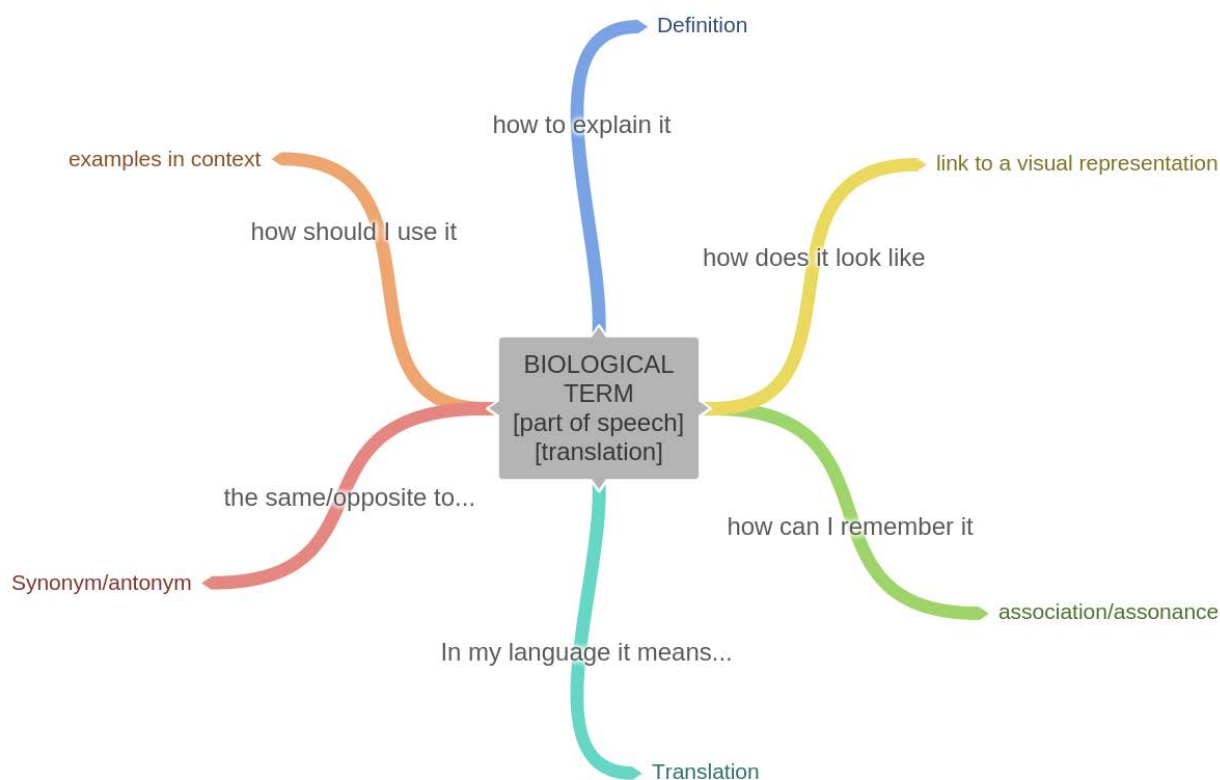


Figure 1. The Coggle mind map of a biological term

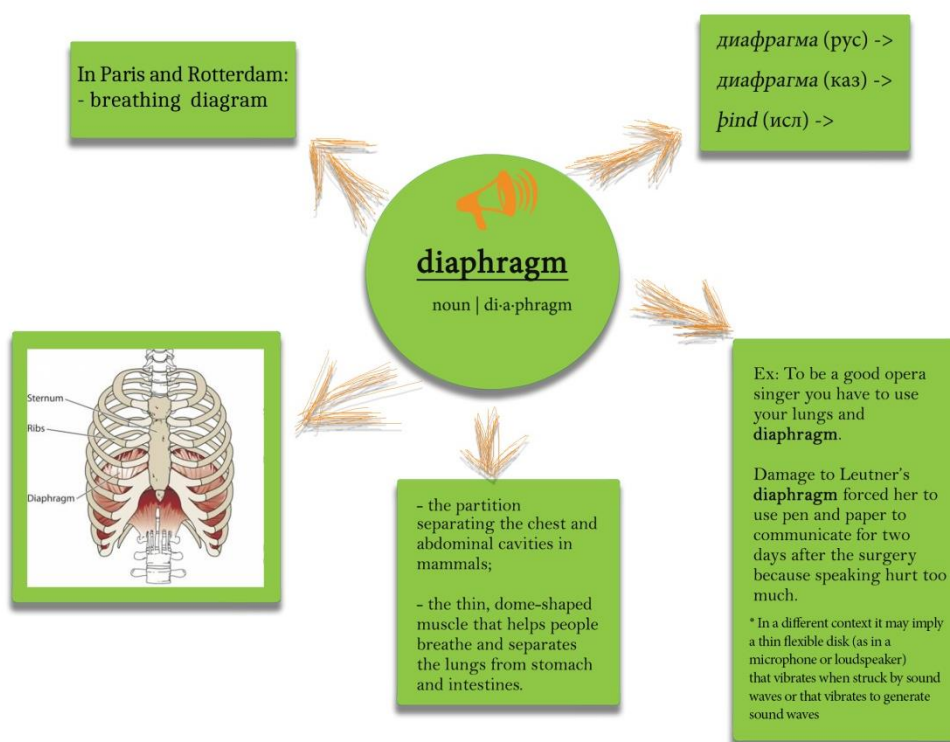


Figure 2. A design entry of the trilingual e-dictionary of biological terms

Appendix 1. List of textbooks of Biology 6-11 grades

- Ochur, E., Kurmanalieva, Zh. (2017). Biology. Textbook. 6th grade. Almaty: Mektep. p. 147.
- Shildebaev, Zh., Kozhantaeva, Zh., Amanzholova, L. (2013). Biology. Almaty: Mektep. p. 116.
- Solovieva, A., Alina, A., Ibraimova, B. (2017). Biology. Textbook. 7th grade. Almaty: Atamyra. p. 230.
- Soloviev, A.R., Ibraimova, B.T. (2018). Biology. Textbook. 8th grade. Almaty: Atamyra. p. 220.
- Alimkulova, R., Satimbekov, R., Solovieva, A. (2016). Biology. Textbook. 8-9th grade. Almaty: Atamyra. p. 250.
- Ermetov, B., Sagintaev, A., Kendzhi, B., Akhmetova, A., Nuralieva, L., Dzhiilkaidarova, A., Karimova, N. (2017). Biological bilingual textbook. 8th grade. Astana: Mektep. p. 200.
- Sartaev, A., Gilmanov, M. (2014). General biology. Textbook. 10th grade. Almaty: Mektep. p. 245.
- Satimbekov, R., Shildebaev, Zh. (2015). Biology. Textbook. 11th grade. Almaty: Mektep. p. 215.
- Kovshar, A., Solovieva, A. (2015). Biology. Textbook. 11th grade. Almaty: Atamyra. p. 270.

Appendix 2. List of English-language reference books

- Renu, E., Sekar, T., Sankar, T.P., Munusamy, T.S. (2006). Botany. Textbook. Tamil Nadup. p. 159.
- Robertson, K.R., Downie, S.R. Mason, S.L. (2014). Botany. Master Naturalists. p. 50.
- Shipunov, A. (2017). Introduction to Botany. Lecture notes. North Dakota, USA: Minot State University. p. 173.
- Sologub, L.I. (2003). Zoology in English. Textbook. Samaata: Samara University Publishing House. p. 73.
- Naumov, D.V. (2015). Zoology. Textbook for schools. Moscow: Mir. p. 216.
- Ishmuratova, M.Yu., Tusupova, G.S. (2016). Russian-English-Kazakh dictionary of biological botany terms (6th grade).Karaganda: . p. 24..
- Alzhanova, R.K., Tusupova, G.S. (2018). English-Russian-Kazakh glossary (biology 8th grade). Karaganda: ShOD Daryn. p. 12.
- Interactive style training manual Biology – Animal. – Astana, 2018. – 2.3 Gb.
- Sadykova, A.R. (2012). English for biotechnologists and biologists. Textbook. Izhevsk: . p. 238.
- Afanasieva, I . et al. (1979). English-Russian biology dictionary. Moscow: Russkoe slovo. p. 732.
- Damblton, K.U. (2000). Russian-English dictionary. Minsk-Kiev: Tekhnicheskii slovari. p. 525.
- Zarikov, M.D., Elemesov, K., Kaimov, K. (1991). Russian-Kazakh dictionary of biological terms. Almata-Ata: Rauan. p. 125.

Appendix 3. English-language websites

- sbio.info
- cellbiol.ru
- bioword.narod.ru
- ebio.ru
- virtulab.net
- biology-online.ru
- biology-online-org
- biodata.ru
- faunaflora.ru
- cengage.com
- khanacademy.org
- ibiology.org
- biology.ru
- biologydictionary.net

RACIONAMENTO ECOLÓGICO DE DOSES DE UMA PREPARAÇÃO CONTENDO CARBONO DE MÚLTIPLOS COMPONENTES ATRAVÉS DE CONTEÚDO DE METAIS PESADOS E ATIVIDADE MICROBIOLÓGICA DO SOLO**ECOLOGICAL RATIONING OF DOSES OF A MULTICOMPONENT CARBON-CONTAINING PREPARATION THROUGH HEAVY METAL CONTENT AND SOIL MICROBIOLOGICAL ACTIVITY**

KHUSAINOV, Abilzhan¹; SARSENOVA, Anara²; SINDIREVA, Anna³; YESSENZHOLOV, Baurzhan^{1*}; ZHARKINBEKOV, Temirkhan¹;

¹ Sh. Ualikhanov Kokshetau State University. Kazakhstan.

² LLC Scientific-Production Association "AgroBioTechnovatsii." Russia.

³ Tyumen State University. Russia.

* *Corresponding author*

e-mail: yessenzholov.ksu@bk.ru

Received 27 January 2020; received in revised form 20 February 2020; accepted 12 March 2020

RESUMO

O artigo trata dos resultados da regulação ecológica de doses introduzidas em uma preparação multicomponente contendo carbono para a queima de metais pesados e a atividade microbológica do solo. A relevância da pesquisa está baseada, por um lado, na degradação global, degaseificação e redução da fertilidade do solo. Por outro lado, é o acúmulo global de resíduos de produção e consumo. O objetivo deste estudo foi avaliar o efeito de doses do produto das cinzas, escórias e negro de carbono sobre o pH, teor de metais pesados e a atividade microbológica do chernossolo no cultivo de trigo de primavera. Os experimentos foram conduzidos em uma zona murada do norte do Cazaquistão. O pH do solo foi determinado por um método potenciométrico; a atividade microbológica do solo pela aplicação de floe; a microflora foi explicada pela semeadura da suspensão do solo em meio nutriente sólido e os metais pesados foram determinados por voltametria por decapagem. Bactérias utilizando compostos orgânicos de nitrogênio; microrganismos que consomem nitrogênio mineral; oligonitrófilos; bactérias que mobilizam fosfatos minerais; microrganismos destruidores de celulose; nitrificação; e cogumelos foram estudados. Observou-se que a preparação estudada contribui para a neutralização do solo e a ativação de processos microbiológicos. De acordo com as evidências, pode-se verificar que a preparação de cinzas e negro de carbono afeta ambigualmente o número de microrganismos. Observou-se um aumento no número de bactérias amonizantes, agentes nitrificantes e no coeficiente de transformação da matéria orgânica, bem como um aumento na disponibilidade de solo com nitrogênio facilmente hidrolisado. O teor de metais pesados não excedeu a concentração máxima admissível. Assim, o uso de um produto à base de cinzas, escórias e negro de fumo para fertilizar solos negros da terra nas culturas de trigo da primavera é ambientalmente seguro.

Palavras-chave: *chernossolo comum, metais pesados, trigo de primavera, extrato aquoso de pH, microorganismos.*

ABSTRACT

The article deals with the results of environmental regulation of doses introduced into a multicomponent carbon-containing preparation for the burning of heavy metals and the microbiological activity of the soil. The relevance of the research is based on, on the one hand, in global degradation, degasification and reduction of soil fertility. On the other hand, it is the worldwide accumulation of production and consumption waste. This study aimed to assess the effect of doses of the product from ash, slag, and carbon black on pH, heavy metal content, and microbiological activity of ordinary chernozem soil for cultivating spring wheat. The experiments were conducted in a walled-zone of Northern Kazakhstan. Soil pH was determined by a potentiometric method, the application of floe discovered the microbiological activity of the soil, the microflora was accounted for by sowing the soil suspension on solid nutrient media, and heavy metals were determined by stripping voltammetry. Bacteria utilizing organic nitrogen compounds; microorganisms consuming mineral nitrogen; oligonitrophils; bacteria mobilizing mineral phosphates; cellulose-destroying microorganisms; nitrification and mushrooms were studied. The studied preparation was observed to contribute to the neutralization of the soil, and the activation of

microbiological processes. According to the evidence, it can be verified that the preparation of ash and carbon black ambiguously affects the number of microorganisms. An increase in the number of ammonifying bacteria, nitrifying agents and the coefficient of transformation of organic matter, as well as an increase in the availability of soil with easily hydrolyzed nitrogen, were noted. The content of heavy metals did not exceed the maximum permissible concentration. Thus, the use of a product based on ash, slag, and carbon black to fertilize black earth soils on spring wheat crops are environmentally safe.

Keywords: *Ordinary chernozem soil, heavy metals, spring wheat, aqueous extract pH, microorganisms.*

1. INTRODUCTION:

Currently, coal is one of the primary sources of energy for most countries worldwide. Long-term use of coal leads to the accumulation of its residues in the form of ash and slag in significant quantities. The combustion of coal, peat and their mixtures for energy purposes (VNITSSMV and NITSPURO, 2011) generate ash and slag waste (ASW).

Vast quantities of ASW accumulate in the dumps that occupy large areas of land and their maintenance requires significant expenses. For example, the stock of accumulated ASW in the Akmola region is about 599.2 thousand tons, of which 423.4 thousand tons of ASW was generated by industrial, and suburban and residential sectors contributed the remaining. These wastes are stored around the city on unique ash dumps, occupy vast territories and exert a negative impact on the soil and water bodies (Khusainov, 2001).

Nevertheless, ash and slag are valuable and can be effectively used as secondary raw materials. According to Maiti and Prasad (2016) (2016), different countries have extensive experience in using them in various sectors of the economy. In 2012, in India it was used 63% of the total accumulated ash and slag, in China was 67% (2010), in the USA was 38.4% (2011), in EU countries was 32% (2010) and in Germany was 91.4% (2010). 2.5% ash and slag is used in agriculture as a fertilizer.

In the Republic of Kazakhstan, the utilization of ash and slag requires an operational solution because currently, only about 10-15% of the ASW of enterprises is recycled to produce cement, cinder blocks, and other building materials. An integrated approach to the processing of ASW can give a significant boost to the economy of Kazakhstan. Therefore, it is necessary to develop industrial technologies for the use of ASW, as well as to develop a set of marketing measures to promote ASW-based products.

Ash and slag are waste of the fifth hazard class, i.e., almost safe and quite useful in the

production of building materials, in construction of roads, and recultivation of disturbed lands (Dik and Soboleva, 2006). Among other things, ash and slag can be sources of valuable rare-earth elements, as well as oxides of silicon, aluminum, and iron. One of the possible ways to solve the issue of ASW from heat power stations is to use it as a fertilizer for agriculture (Berezin *et al.*, 2012).

The use of ASW to preserve soil fertility holds promise in agriculture because besides enhancing soil fertility, it solves the problems of utilization of local waste produced (Satybaldin, 2001). However, many scientists believe that this type of trash can be toxic to the environment and their use as a fertilizer is associated with the danger of soil contamination with heavy metals, changes in the pH of the environment, as well as a decline in soil microbiological activity (Cruz-Paredes *et al.*, 2017; Korcak, 2001; and others).

Therefore, the development of measures for the use of ASW as fertilizer should be accompanied by an assessment and prediction of the soil chemical composition and plants growing on it, as well as associated microbiological activity as a valuable bioindicator of the soil condition. Also, there is a need for scientific substantiation of the used ASW doses as fertilizer on specific soils for certain crops.

This article assessed the environmental impact of the application of ash, slag, and carbon black preparation as a fertilizer for soft spring wheat on chernozem soil in Northern Kazakhstan. The Objectives of this study were:

- to evaluate the effect of ash, slag, and carbon black preparation in different doses on the acidity of black earth soils;
- to establish the impact of the preparation in varying doses on the microbiological activity of black earth soils;
- to carry out environmental rationing of preparation doses on the heavy metals content in the soil.

This study is the first to assess the chernozem soil of Northern Kazakhstan in terms of ash, slag and carbon black preparations in

different doses on the response of the soil environment and the microbiological activity of the soil, as well as the ecological rationing on the heavy metals content in the soil. The use of ash, slag, and carbon black preparations to fertilize chernozem soils will improve soil fertility by enriching it with carbon and microelements for better spring wheat productivity, neutralize the soil environment and activate microbiological processes in the soil.

2. MATERIALS AND METHODS:

Chernozem soil, the preparation of ashes and carbon black, and spring soft wheat variety (*Shortandinskaya 95*, improved). *AgroBionov* preparation was used in powder form, which includes low-calcium ash of Ekibastuz coal, and carbon black. Chemical composition of fly ash from Ekibastuz coal deposits consisted of SiO₂, 62.9%; Fe₂O₃, 6.35%; Al₂O₃, 26.35%; CaO, 1.9%; MgO, 0.9%; SO₃, 1.2%; Na₂O, 0.23%. Macro- and microelement composition of ash consisted of elements in descending order as K > Fe > Al > Mg > Ca > Mn > Sr > Pb > Co > Zn > Cu > Sn > As > Ni > Cd > Hg. Technical carbon consists of more than 99% carbon (Sarsenova, 2013).

The experiment was conducted as per the guidelines of the educational research and production center, "Elite" of Kokshetau State University named after S. Ualikhanov.

The field under investigation is located 32 km north of Kokshetau. The soil cover of the experimental plot is ordinary chernozem soil, with medium carbonate and heavy loamy composition. The arable layer of soil contains 3.96% humus, and the soil solution is slightly alkaline (pH - 7.9).

The easily hydrolyzed nitrogen and mobile phosphorus contents were estimated to be 46 mg·kg⁻¹ and 17 mg·kg⁻¹, respectively. The degree of availability of easily hydrolyzed nitrogen, according to Tyurin and Kononova, was estimated to be medium, and mobile phosphorus according to Machigin was estimated to be low. The heavy metal content before sowing did not exceed the permissible concentration.

The experiment was carried out four sets as follows:

- control without fertilizer applications;
- P16 (1/10 of the estimated dose), as the background;
- on the mineral background, agrobiont preparation was applied in doses of 100, 200, 300, 400, 500 kg·hectare⁻¹ as the primary

treatment before sowing. The plot area was 125 m² (5 x 25 m), and the reference area was 100 m² (4 x 25 m).

The experiment used soft spring wheat of Shortandinskaya 95 variety with an improved medium-late type of ripening and a vegetation period of 95-100 days. This variety has a complex of economically valuable traits, such as high-yield, drought-resistance, resistance to diseases and pests.

The agroclimatic zoning experimental field belongs to a slightly moist, moderately warm zone. According to long-term average data, the hydrothermal coefficient is 0.8-1.0; the sum of active temperatures above 10 °C - 2200-2500 °C; the length of the growing season is 135-140 days. Under the conditions of 2018, the average daily temperature during the growing season (May-October) was 15.1 °C, compared with the long-term average daily temperature (16.22 °C) lower than by 1.12 °C. During the growing season, 242 mm of atmospheric precipitation fell, which is 31 mm more than the average long-term data (211 mm).

In the experiments, observations, counts, and analyses were carried out after collecting the soil samples from the 0-20 cm layer according to GOST 28168-89 before sowing during the tillering stages and full ripeness of soft spring wheat.

The pH of the aqueous extract of the soil samples (GOST 26423-85, GOST 26483-85, GOST 26490-85) (Gosstandart of the USSR, 2011, 1985a, 1985b) was determined by a potentiometric method. The content of heavy metals was determined by stripping voltammetry at the National Center of Examination of the Regional Public Health Department, Ministry of Health, Republic of Kazakhstan, Akmola region (GOST 50686-94, GOST 50683-94) (Gosstandart of the USSR, 1994a, 1994b).

The number of soil microorganisms was accounted for by sowing soil suspension on solid nutrient media, meat-peptone agar (MPA) for bacteria utilizing organic nitrogen compounds, starch ammonia agar (SAA) for microorganisms consuming mineral nitrogen, Mishustina's medium for oligonitrophilia, Muromtsev-Gerretsen medium for bacteria mobilizing mineral phosphates, Getchinson medium for cellulose-degrading microorganisms, water agar with the addition of double ammonium-magnesium salt of phosphoric acid for nitrifying agents, Czapek's medium, acidified with magnesium phosphoric acid for nitrifying agents (Aristovskaya *et al.*, 1962).

Statistical analyses of the results were carried out using Microsoft Excel.

3. RESULTS AND DISCUSSION:

The results of our study show that the preparation (drug) in different doses significantly changed the response of 0-40 cm of the soil layer. Furthermore, an increase in the preparation dose from 100 to 500 kg·hectare⁻¹, led to a decrease in the pH from 7.5 to 7.1, while the control pH remained at 7.9.

A correlation was found between the pH of the aqueous extract and the doses of the applied preparation (correlation coefficient $r = -0.76$). That is, the studied development reduced the pH from slightly alkaline to neutral, which can be explained by the chemical composition of the preparation (Figure 1).

The evaluation of microbiological diversity showed that the number of microorganisms ranged from 515.3 to 580.1 million CFU·g⁻¹ of soil. In terms of ecological-trophic groups, the proportion of bacteria per MPA of the total number in the control was 9.69%, the background of + 100 kg·hectare⁻¹ was 14.29%, the microorganisms on SAA were 10.99% and 12.27%, oligonitrophils were respectively 39%, 71%, and 35.03%, phosphate-mobilizing 39.59% and 38.39%, cellulose-destroying 0.02%, respectively.

The above data indicates that with the use of the preparation, a tendency towards slight redistribution of the primary groups of agronomically essential microorganisms in the chernozem soil was observed.

Besides the analyses of relative microbial ratios, the absolute value of the number of bacteria is of particular interest. Figures 2 and 3 show the effect of the preparation at a dose of 100 kg·hectare⁻¹ on the number of microorganisms.

The obtained data indicate that the preparation of ash, slag, and carbon black ambiguously affects the number of microorganisms in the soil. A comparative analysis shows that the total number of microorganisms in the fertilized variant is less than in control by an average of 11.8%. Also, a decrease in oligonitrophils, phosphate-mobilizing, and cellulose-degrading microbes were observed by 21.6%, 13.8%, and 38%, respectively. At the same time, compared to the control, the number of ammonifying bacteria and nitrifying agents increased by 23.6% and 77.2%, respectively, which contributed to the improved nitrogen dietary

regime of spring wheat.

The studied preparation did not contribute to increase in the number of phosphorus-mobilizing microorganisms and, consequently, improve the dietary phosphorus regime of spring wheat. Therefore, phosphorus fertilizers were applied in the background at the rate of P₁₆. The drug mineralization coefficient of the variant P₁₆+100 kg·hectare⁻¹ was estimated to be lower than that of the control by 23.9% (Table 1).

The transformation ratio of organic matter (PM) was calculated as the product of the ratio MPA/SAA * (MPA + SAA).

In our studies, we evaluated heavy metals that are the primary group of environmental pollutants (Table 2).

The results of laboratory studies show that the introduction of the product from ash, slag, and carbon black does not contribute to excess of heavy metals in the soil maximum permissible concentration (MPC) for the studied elements, although it was accompanied by an increase in Pb and Zn content by the harvest period with increasing dose of the preparation (Figure 4 and Figure 5). The most significant accumulation of Pb was noted after the introduction of the preparation in doses of 400 and 500 kg·hectare⁻¹, which exceeded the levels estimated in control by 321.4% and 357.1%, respectively.

In a comparative assessment of heavy metal content in soil samples taken in summer and autumn periods, the lead content in all variants increased by the harvest period. For other elements, an absolute dependence could not be established. Thus, the zinc content in the fall compared with summer samples of the control and the background decreased by 45.6% and 52.7%, respectively. Contrarily, an increase from 166.7% to 363.6% in the Zn content, was observed in the variants after the use of the preparation. The highest values were noted for the options "background + 100 kg·hectare⁻¹" and "background + 400 kg·hectare⁻¹", while the Zn content exceeded that of the control by 378.4%.

When using the drug at a dose of 100 kg/ha against the background of phosphorus fertilizer at a dose of 16 kg/ha of the active substance, due to the activation of microbiological processes in the soil and increasing the availability of its easily hydrolyzed nitrogen, the yield of spring wheat increased by 21.8% and amounted to 1.43 t/ha (control 1.19 t/ha).

The influence of ash and slag on the physical, chemical and biological properties of the

soil has been comprehensively studied by scientists from India, China, and Poland (Ciecko *et al.*, 2009; Ferreira *et al.*, 2003; Fulekar, 1993; Gracia *et al.*, 1995; Kalra *et al.*, 1997; Lai *et al.*, 1999; Menon *et al.*, 1993; Pandey and Singh, 2010; Phung *et al.*, 1979; Ram and Masto, 2010; Singh *et al.*, 2010; Vincini *et al.*, 1994; Właśniewski, 2009).

While conducting the current study, we paid particular attention to changing the soil environment under the influence of the preparation of ash, slag, and carbon black, since there is no consensus on this issue in the scientific literature. Several scientists (Etiégni and Campbell, 1991; Ohno and Susan Erich, 1990) note that ASW significantly affects soil acidity. For example, the studies of Adriano *et al.* (1980) and El-Mogazi *et al.* (1988) show that modeling the interacting processes of ash and slag with the soil changed its acidity to a value close to neutral. The authors indicated that in the variants with a more massive amount of ash and slag, the pH of the salt changed towards alkalinity. Scientists believe that the introduction of ash and residue into the soil changes the acidity of the soil rather quickly, in the very first year of application. Such a change in acidity can be explained by the easily accessible, high calcium content in ash and slag. Moreover, ash can loosen the soil and change its structure; therefore, the determination of soil pH is a crucial stage of field research.

The product of ash, slag, and carbon black in this study had a positive effect on soil acidity. Ash is highly alkaline and thus neutralizes excess soil acidity (Asmare and Markku, 2016; Sheoran *et al.*, 2014). Moreover, the use of fly ash improves the soil pH and also increases the content of organic carbon and organic matter (Sarangi *et al.*, 2001). Similar results were obtained in studies by Buddhe *et al.* (2014), where a close correlation (-0.83) was established between the doses of ash and slag and the pH value, which enabled the authors to conclude about the positive effect of ash on the pH of the soil environment. The economic role of ash in neutralizing the soil environment has also been emphasized, which makes it possible to use unproductive, empty acidic lands in rural and forest areas after ash and slag reclamation (Saraswat and Chaudhary, 2014).

Changes in the combination of factors that reflect the agrochemical characteristics of the soil under the influence of the preparation can affect the biological activity of the soil. Therefore, the use of the preparation of ash, slag, and carbon black as fertilizer must be assessed for its effect on the microbiota of ordinary chernozem soil, more so,

because there are very few similar, available studies.

When assessing the impact of fertilizers on the soil microbiota, determining the number of microorganisms of various ecological-trophic groups and the nature of changes (increase or decrease), it is not always possible to consider these changes as a uniquely positive or negative phenomenon.

Studies on microorganisms through environmental parameters make it possible to reproduce the biological reactions of organisms under different geochemical conditions and to get answers to unclear questions that arise when studying organisms in their natural environment (Koval'skiy, 1974).

Adriano *et al.* (1978), J. W. C. Wong, and M. H. Wong (1990), and Saffigna *et al.* (1989) report that ash reduces soil microbiological activity. On the contrary, Schutter and Fuhrmann (2001) state that ash increases microbial activity.

The extent of microbiological processes in the soil is determined not only by the number of microorganisms but primarily by their activity. In this regard, it is vital to study the effect of the applied mineral fertilizers on the rate of the essential microbiological processes in the soil. Studies (Kalra *et al.*, 1997) showed that a 5% concentration of fly ash in soil increased microbial activity, while the addition of more significant amounts of fly ash inhibited biological processes. However, research conducted by Vincini *et al.* (1994) showed that the concentration of FA in soil higher than 10% still enhanced microbial activity in the soil.

To assess the activity of microbiological processes, we calculated coefficients reflecting the dominant activity of a particular group of microflora. Microorganisms using mineral forms of nitrogen (growing on SAA) indicate the coefficient of mineralization (ratio SAA/MPA).

A higher coefficient of mineralization (>1), indicates better immobilization processes, which may be due to either a very high supply of ammonia nitrogen in the soil (this may be due to robust ammonifiers) or with organic matter deficient in nitrogen (straw, bark, etc.).

In agrocenosis, too high the Mishustin coefficient (>3-5) may indirectly indicate an increase in the rate of decomposition of humus, a specific soil organic matter (Kazeev *et al.*, 2016).

According to Mukha (1980), the PM value indicates the directionality of the microbiological

transformation process of plant residues either towards the synthesis of humic substances or towards mineralization of organic matter. Therefore, it reflects the potential intensity of accumulation of humic substances in the soil (Korobova, 2013). This may be because the studied preparation contributes, at least, to the preservation of humus in the soil.

Pollution due to heavy metals is one of the possible aspects of the impact of ASW on the environment. According to many studies, in ASW, heat from power plants, several times higher than the original coal, can increase the content of toxic (Be, Hg, As, F), and potentially toxic (Mn, Pb, V, Ni, Co, Cr, Cd, Se) elements (Mjajina, 2004).

The presence of calcium, magnesium, zinc, iron, and other elements makes fly ash a source of trace elements when used as a fertilizer. Its use helps to increase crop yields from 15 to 200% or higher (Kumar, 2009).

Along with the study of soil fertility, there is interest in the effects of heavy metals on soil and plants, since elements such as Fe, Mn, Cu, Zn, and Mo are vital for plants, animals, and humans. Being trace elements, they also have a dual effect on the soil-plant system, and their insufficient content in the soil leads to a slowdown in the growth and development of plants, while, their excess may cause inhibition of plant growth and chemical pollution of the soil. However, heavy metals do not harm plants if the concentration of their available forms in the soil does not exceed the MPC. The application of fly ash for soil fertilization is associated with plant growth and yield increase (Ajaz and Tiyaqi, 2003; Iyer and Scott, 2001; Khan and Khan, 1996; Singh and Agrawal, 2010; Singh *et al.*, 2010).

Jacek Antonkiewicz and Robert Pelka (2014) assessed the ash and slag deposits and observed that the content of heavy metals did not exceed the MAC. Likewise, Mukhanbet *et al.* (2016) indicated that when ash and slag were introduced at a dose of 400 kg·hectare⁻¹, the heavy metal content in the chernozem soil of northern Kazakhstan did not exceed the MPC.

As trace elements, Zn and Cu are crucial for average growth and development of plants (Zacccone *et al.*, 2007). Thus, both their abundance and scarcity in the soil are dangerous. Therefore, the excess of these heavy metals compared to that in control, in this case, cannot be definitively considered as pollution.

4. CONCLUSIONS:

In modern times, intensive development of industrial activity, energy, housing, and communal complex, lead to the generation of large volumes of waste, including ash and slag waste. They can be used efficiently, in particular, to improve soil fertility and the productivity of the plants cultivated on them. Studies have shown the possibility of effective use of the preparation based on ash and black carbon as a fertilizer on ordinary chernozem soil in Northern Kazakhstan. In particular, the increase in soil fertility was associated with a change in pH to neutral and an increase in the number of ammonifying bacteria and nitrifiers, which facilitate the improvement of the nitrogen regime of spring wheat. Lastly, the heavy metal content did not exceed the MPC.

5. ACKNOWLEDGMENTS:

This research work was funded by the Committee of Science and Science of the Republic of Kazakhstan (Contract No. 213 dated March 19, 2018). The authors are grateful to Khamova O. F., Head of the Microbiology Laboratory of the Federal State Budgetary Institution, Siberian Research Institute of Agriculture (Omsk, the Russian Federation), who provided advice on the microflora of the chernozem soil of Western Siberia and Northern Kazakhstan.

6. REFERENCES:

1. Adriano, D.C.; Page, A.L.; Elseewi, A.A.; Chang, A.C.; Straughan, I.; *J. Environ. Qual.* **1980**, *9*, 333–344, doi:10.2134/jeq1980.00472425000900030001x.
2. Adriano, D.C.; Woodford, T.A.; Ciravolo, T.G.; *J. Environ. Qual.* **1978**, *7*, 416–421.
3. Ajaz, S.; Tiyaqi, S.; *Arch. Agron. Soil Sci.* **2003**, *49*, 457–461, doi:10.2134/jeq1978.00472425000700030025x.
4. Antonkiewicz, J., Pelka, R.; *Soil Sci. Annu.* **2014**, *65*, 118–125, doi:10.1515/ssa-2015-0003.
5. Aristovskaya, T.V.; Vladimirskaia, M.E.; Gollerbax, M.M.; Katanskaya, G.A.; Kashkin, P.N.; Klupt, S.E.; Lozina-Lozinskij, L.K.; *Bol'shoj praktikum po mikrobiologii [Large workshop on Microbiology]*, Vysshaya shkola [High

Scool]: Moscow, **1962**.

6. Asmare, M.; Markku, Y.H.; *Afr. J. Agric. Res.* **2016**, *11*, 87–99, doi:10.5897/ajar2015.9632.
7. Buddhe, S.T.; Thakre, M.G.; Chaudhari, P.R.; *Am. J. Eng. Res.* **2014**, *3* (6), 298–304.
8. Berezin, L.V.; Li, M.A.; Shevcov, V.R. in: *Materialy IV nauchno-prakticheskogo seminara "Zoloshlaki TJeS: udalenie, transport, pererabotka, skladirovanie" [Proceedings of the IV scientific-practical seminar "Ash and slag TPP: removal, transport, processing, warehousing"]*, Moscow, April 19 – 20, Izdatel'skij dom MJel: Moscow, **2012**, 103–105.
9. Chechina, O.N.; *Izvestiya Samarskogo nauchnogo tsentra Rossiyskoy akademii nauk: Sotsianye, gumanitarnye, mediko-biologicheskie nauki* **2018**, *4* (61), 75–80.
10. Ciecko, Z.; Zolnowski, A.C.; Kulmaczewska, J.; Chelstowski, A.; *Zeszyty Problemowe Postępow Nauk Rolniczych* **2009**, *535*, 73–83.
11. Cruz-Paredes, C.; López-García, Á.; Rubæk, G.H.; Hovmand, M.F.; Sørensen, P.; Kjølner, R.; *Sci. Total Environ.* **2017**, *575*, 1168–1176, doi:10.1016/j.scitotenv.2016.09.194.
12. Dik, E.P.; Soboleva, A.N.; *Elektricheskie stancii [Electrical stations]* **2006**, *1*, 9–13.
13. El-Mogazi, D.; Lisk, D.J.; Weinstein, L.H.; *Sci. Total Environ.* **1988**, *74*, 1–37, doi: 10.1016/0048-9697(88)90127-1.
14. Etiégni, L.; Campbell, A.G.; *Bioresour. Technol.* **1991**, *37*, 173–178, doi:10.1016/0960-8524(91)90207-z.
15. Ferreira, C.; Ribeiro, A.; Ottosen, L.; *J. Hazard. Mater.* **2003**, *96*, 201–216.
16. Fulekar, M.H.; *Indian J. Environ. Prot.* **1993**, *13*, 85–192.
17. Gosstandart of the USSR; GOST 26483-85 *Soil. Preparation of salt extract and determination of its pH according to the method of Ts/NAO*, GOST dated March 26, 1985 No. 268383-85, Standards Publ.: Moscow, **1985a**.
18. Gosstandart of the USSR; GOST 26490-85 *Soil. Determination of mobile sulfur according to the Ts/NAO method*, GOST dated March 26, 1985 No. 26490-85, Standards Publ.: Moscow, **1985b**.
19. Gosstandart of the USSR; GOST R 50686-94 *Soil. Determination of mobile zinc compounds by the method of Krupsky and Alexandrova in the modification of Ts/NAO*, GOST R dated June 23, 1994 No. 50686-94, Standards Publ.: Moscow, **1994a**.
20. Gosstandart of the USSR; GOST R 50683-94 *Soil. Determination of mobile compounds of copper and cobalt according to the method of Krupsky and Alexandrova in the modification of Ts/NAO*, GOST R dated June 23, 1994 No. 50683-94, Standards Publ.: Moscow, **1994b**.
21. Gosstandart of the USSR; GOST 26423-85. *Soil. Methods for determining the specific electrical conductivity, pH and the solid residue of the aqueous extract*, GOST dated February 08, 1985 No. 26423-85, Standardinform: Moscow, **2011**.
22. Gracia, G.; Zabaleta, I.; Canibano, J.G.; Gyeyo, M.A.; *Coal Abstr.* **1995**, *95*, 32–46.
23. Iyer, R.S.; Scott, J.A.; *Resour. Conserv. Recycl.* **2001**, *31*, 217–228.
24. Kalra, N.; Joshi, H.C.; Chaudhary, A.; Choudhary, R.; Sharma, S.K.; *Bioresour. Technol.* **1997**, *61*, 39–41.
25. Kazeev, K.Sh.; Kolesnikov, S.I.; Akimenko, Ju.V.; Dadenko, E.V.; *Metody biodiagnostiki nazemnyh ekosistem: monografiya [Methods of bio-diagnostics of ground-based ecosystems: monograph]*, Southern Federer University: Rostov-na-Donu, **2016**.
26. Khan, M.R.; Khan, M.W.; *Environ. Pollut.* **1996**, *92*, 105–111.
27. Khusainov, A.T.; *Agrojekologicheskoe sostojanie chernozemnyh pochv Severnogo Kazakhstana [Agroecological condition of the chernozem soil of northern Kazakhstan]*, Kokshetau, **2001**.
28. Korcak, R.F. in: Wright, R.W.; Kemper, W.D.; Millner, P.D.; Power, J.F.; Korcak, R.F. eds., *Agricultural Uses of Municipal, Animal, and Industrial Byproducts*, U.S. Department of Agriculture, Agriculture Research Service: Washington, DC, **2001**, 103–119.
29. Korobova, L.N. in: Korobova, L.N.; Tanatova, A.V.; Ferapontova, S.A.;

- Shindelov, A.V., eds., *Scientific Guidelines on the Use of Microbiological Indicators for Assessing the Condition of Arable Soil of Siberia*, NGAU: Novosibirsk, **2013**.
30. Koval'skiy, V.V.; *Geokhimicheskaya ehkologiya: Ocherki [Geochemical Ecology: Essays]*, Nauka: Moscow, **1974**.
 31. Kumar, V. in: *Materialy II Nauchnoprakticheskogo Seminara "Zoloshlaki TJeS: Uдалenie, Transport, Pererabotka, Skladirovanie" [Proceedings of the II Scientific-Practical Seminar "Ash and Slag TPP: Removal, Transport, Processing, Warehousing"]*, Izdatel'skiy dom Mjel: Moscow, **2009**.
 32. Lai, K.M.; Ye, D.Y.; Wong, J.W.C.; *Water Air Soil Pollut.* **1999**, *113*, 261–272.
 33. Maiti, D.; Prasad, B.; *Appl. Ecol. Env. Res.* **2016**, *14*, 185–212.
 34. Menon, M.P.; Sajwan, K.S.; Ghuman, G.S.; James, J.; Chandra, K.; *J. Environ. Sci. Health., Part A: Environmental Science and Engineering and Toxicology* **1993**, *28*, 2167–2182.
 35. Mjajina, V.I.; *PhD thesis*, Chita, **2004**.
 36. Mukha, V.D. in: *Scientific Works of Kharkiv Agricultural Institute*, Vol. 273, Kharkiv Agricultural Institute: Kharkiv, **1980**.
 37. Mukhanbet, A.K.; Khusainov, A.T.; Elubayev, S.Z.; Balgabayev, A.M.; Khusainova, R.K.; *Biosci., Biotech. Res. Asia* **2016**, *13*, 1007–1015, doi:10.13005/bbra/2127.
 38. Ohno, T.; Susan Erich, M.; *Agric. Ecosyst. Environ.* **1990**, *32*, 223–239.
 39. Pandey, V.C.; Singh, N.; *Agric. Ecosyst. Environ.* **2010**, *136*, 16–27.
 40. Phung, H.T.; Lam, H.V.; Page, A.L.; Lund, L.J.; *Water Air Soil Pollut.* **1979**, *12*, 247–254.
 41. Ram, L.C.; Masto, R.E.; *J. Environ. Manage.* **2010**, *91*, 603–617.
 42. Saffigna, P.; Powlson, D.; Brookes, P.I Thomas, G.; *Soil Biol. Biochem.* **1989**, *21*, 759–765, doi:10.1016/0038-0717(89)90167-3.
 43. Sarangi, P.K.; Mahakur, D.; Mishra, P.C.; *Bioresour. Technol.* **2001**, *76*, 199–205, , doi:10.1016/S0960-8524(00)00127-9.
 44. Saraswat, P.K.; Chaudhary, K.; *Eur. J. Biotechnol. Bioscience* **2014**, *2*, 72–78.
 45. Sarsenova, A.A.; *Pat. RU 2494137 C2*, **2013**.
 46. Satybaldin, A.A.; *Vestnik sel'skokhozyaystvennoy nauki Kazakhstana [Bulletin of Agricultural Science of Kazakhstan]* **2001**, *5*, 3-7.
 47. Schutter, M.E.; Fuhrmann, J.J.; *Soil Biol. Biochem.* **2001**, *33*, 1947–1958.
 48. Sheoran, H.S.; Duhan, B.S.; Kumar, A.; *J. Agroecol. Nat. Resour. Manag.* **2014**, *1*, 98–103.
 49. Singh, A.; Agrawal, S.B.; *Ecotoxicol. Environ. Saf.* **2010**, *73*, 1950–1958.
 50. Singh, R.P.; Gupta, A.K.; Ibrahim, M.H.; Mittal, A.K.; *Rev. Environ. Sci. Biotechnol.* **2010**, *9*, 345–358.
 51. Vincini, M.; Carini, F.; Silva, S.; *Bioresour. Technol.* **1994**, *49*, 213–222.
 52. VNITSSMV, NITSPURO. GOST R 54098-2010. *Resursosberezhenie. Vtorichnye material'nye resursy. Terminy i opredeleniya [State Standard R 54098-2010. Resource-saving. Secondary material resources. Terms and definitions]* Standartinform Publ.: Moscow, **2011**.
 53. Właśniewski, S.; *Ochrona Środowiska i Zasobów Naturalnych [Environmental Protection and Natural Resources]* **2009**, *41*, 479–488.
 54. Wong, J.W.C.; Wong, M.H.; *Agric. Ecosyst. Environ.* **1990**, *30*, 251–264, doi:10.1016/0167-8809(90)90109-q.
 55. Zacccone, C.; Cocozza, C.; Dorazio, V.; Plaza, C.; Cheburkin, A.; Miano, T.; *Talanta* **2007**, *73*, 820–830.

Table 1. The Effect of the Drug on the Orientation of Soil-Microbiological Processes

Variant	Number of microorganisms		SAA/MPA	MPA+SAA	MPA/SAA	PM
	in MPA million CFU.g ⁻¹	on SAA million CFU.g ⁻¹				
Control	56.2	63.7	1.13	119.9	0.88	105.5
Field + 100	73.6	63.2	0.86	136.8	1.16	158.7

Table 2. Effect of ash, slag and carbon black preparation on heavy metal content in the soil (mg.kg⁻¹)

Variants	Pb		Cd		Zn		Cu		As	
	summer	autumn	summer	autumn	summer	autumn	summer	autumn	summer	autumn
MPC	32		0.5		23		33		2.0	
Control	0.49	0.56	0	0	0.68	0.37	0	0	0	0.016
P ₁₆ - field	0.44	1.2	0	0.01	0.72	0.34	0	0	0	0
Field + 100, kg.ha ⁻¹	0.69	1.1	0	0.03	0.87	1.4	0.07	0.04	0	0
Field + 200, kg.ha ⁻¹	-	1.1	-	0	-	0.57	-	0	-	0
Field + 300, kg.ha ⁻¹	0.52	1.3	0	0.02	0.33	1.2	0.09	0.14	0.01	0.003
Field + 400, kg.ha ⁻¹	-	1.8	-	0	-	1.4	-	0	-	0
Field + 500, kg.ha ⁻¹	0.72	2.0	0	0	0.6	1.0	0.07	0	0	0

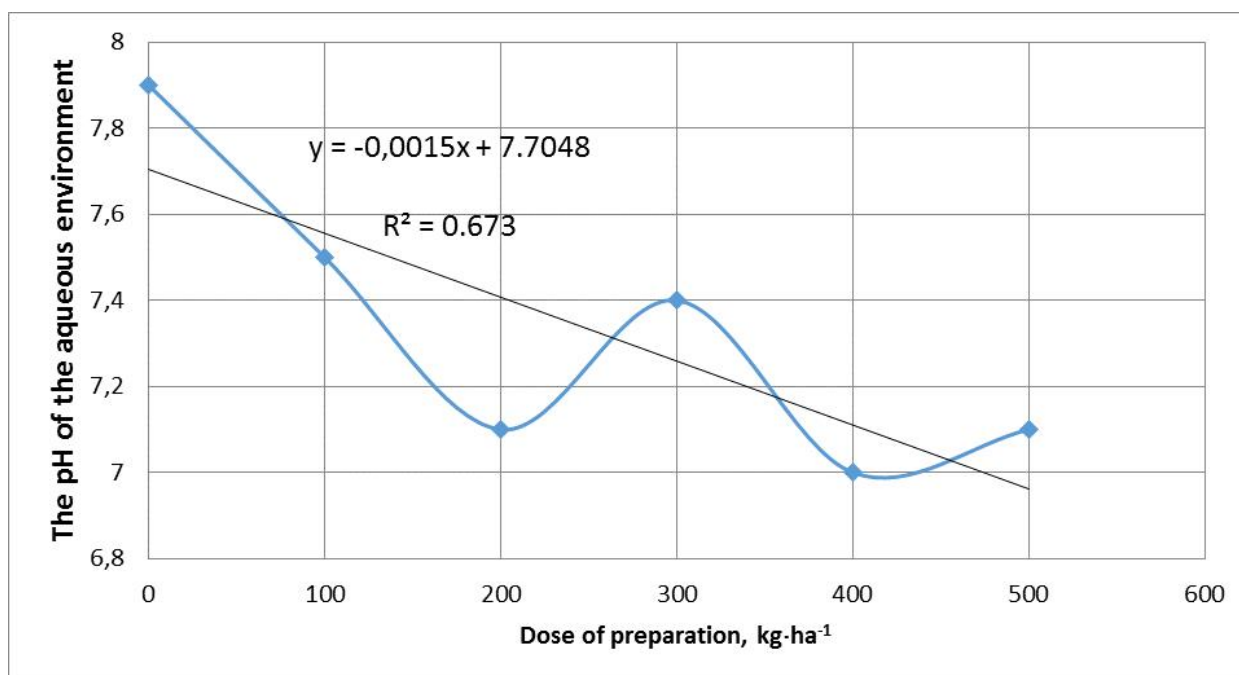


Figure 1. Effect of the Ash, Slag, and Carbon Black Preparation on the PH of the Aqueous Extract of Ordinary Chernozem Soil and on Spring Wheat Crops

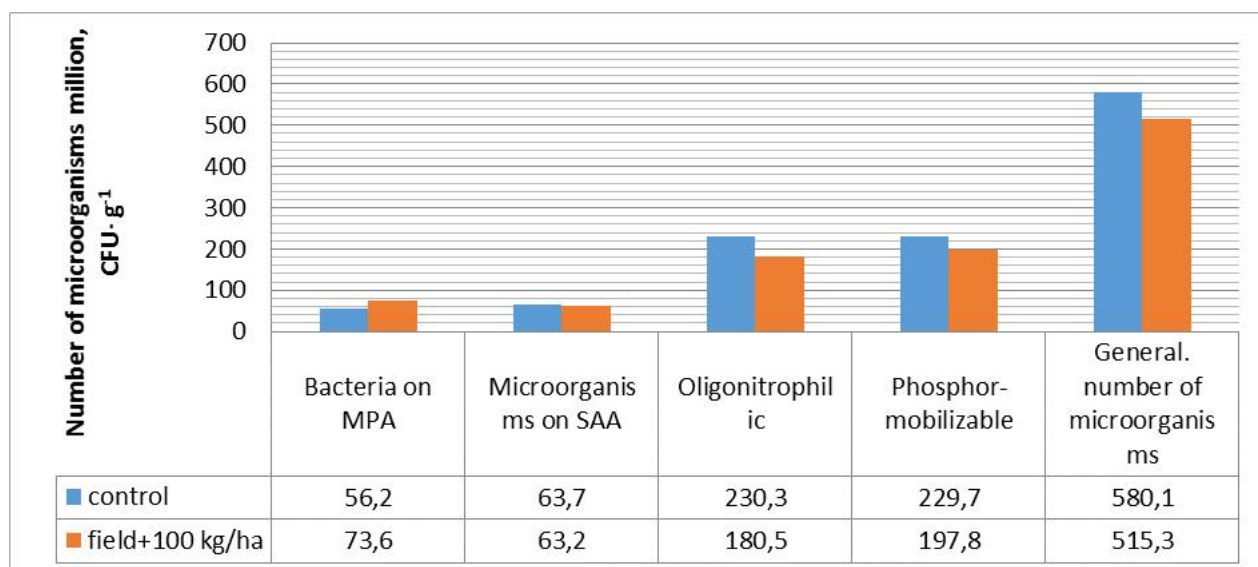


Figure 2. Effect of the Preparation of Ash, Slag, and Carbon Black on the Number of Microorganisms in Ordinary Chernozem Soil

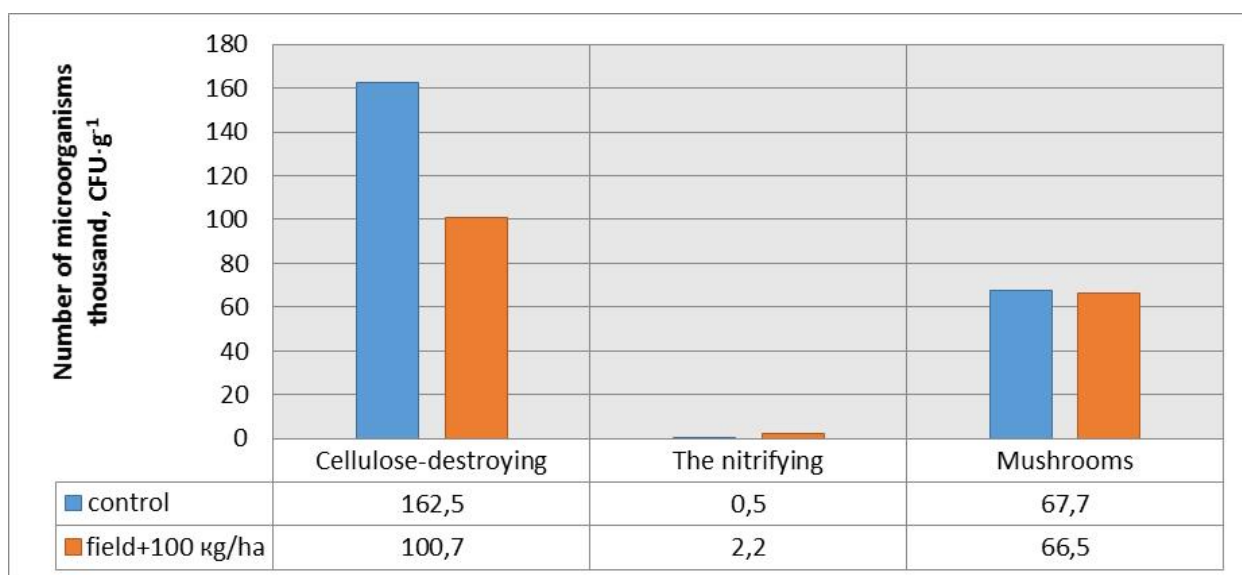


Figure 3. Effect of the Preparation of Ash, Slag, and Carbon Black on the Number of Cellulose-Degrading, Nitrifying Bacteria, and Fungi in Ordinary Chernozem Soil

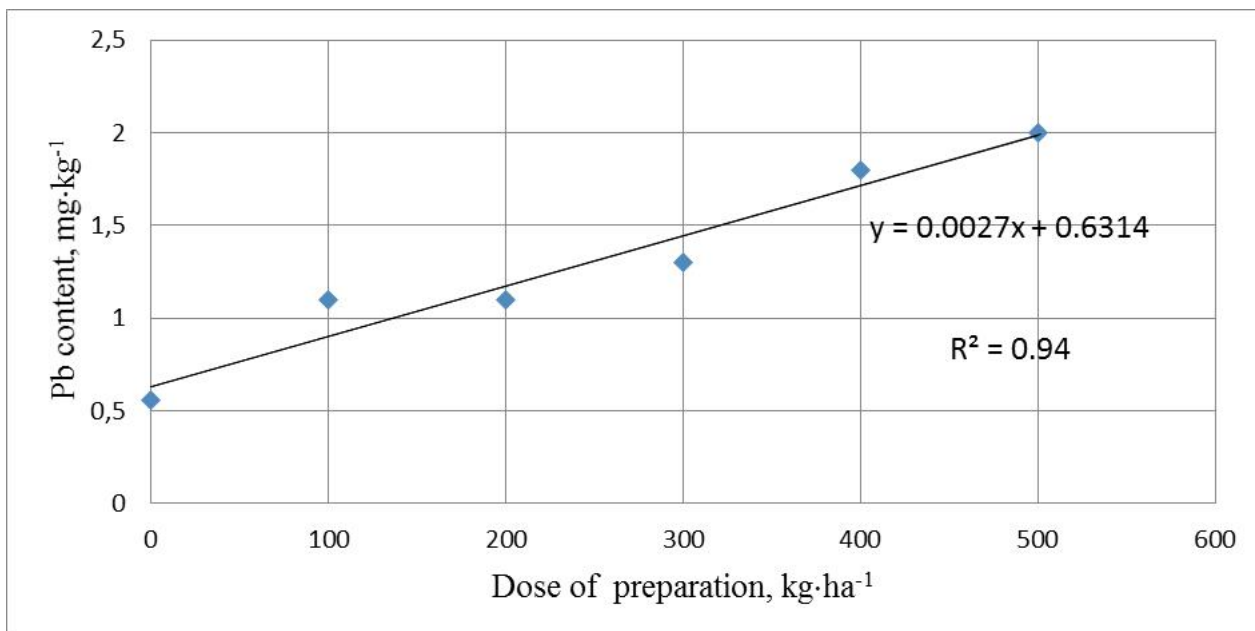


Figure 4. The Content of Pb in the Soil

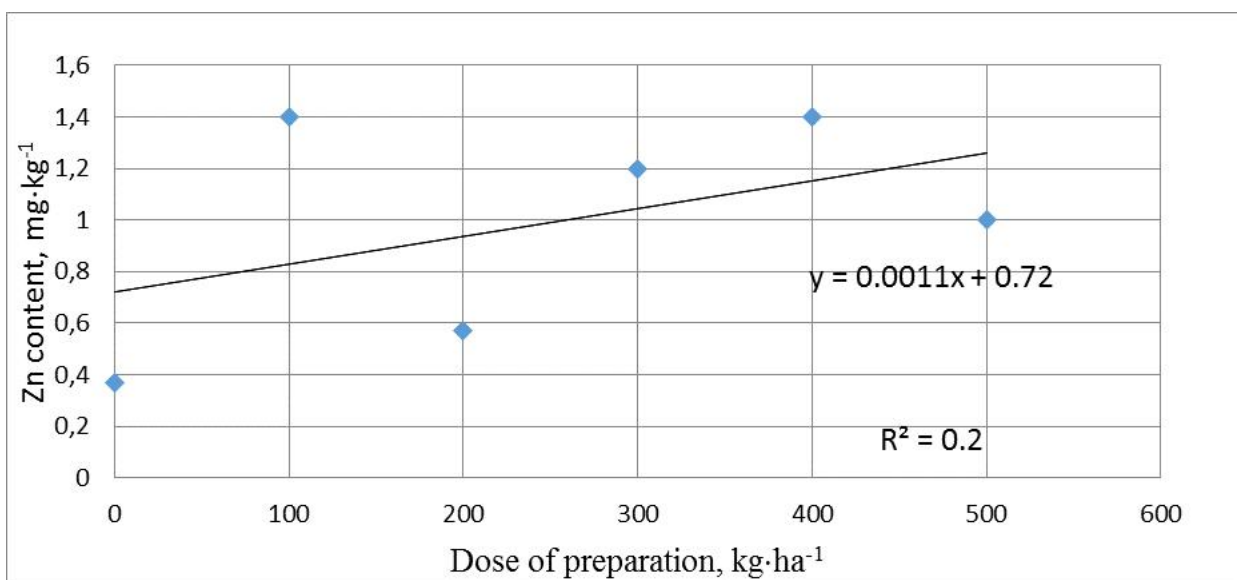


Figure 5. The Content of Zn in the Soil

APLICAÇÃO DE NANOMATERIAIS À BASE DE TITANATO DE SÓDIO PARA ADSORÇÃO DE CORANTES

APPLICATION OF SODIUM TITANATE BASED NANOMATERIALS FOR DYE ADSORPTION

OLIVEIRA, Adriene Kelly Gois ^{1*}, SANTOS, Adriana Paula Batista², CALDEIRA, Vinícius Patrício da Silva³

^{1,3} Programa de Pós-Graduação em Ciências Naturais - Universidade Estadual do Rio Grande do Norte

² Departamento de Química - Universidade do Estado do Rio Grande do Norte

* Autor correspondente

e-mail: adrieneoliveira21@gmail.com.br

Received 04 November 2019; received in revised form 05 February 2020; accepted 08 March 2020

RESUMO

A aplicação de nanomateriais à base de titanato de sódio para adsorção de corantes merece ser investigada por ser uma técnica inovadora e de baixo custo. Além disso, a contaminação de efluentes por corantes orgânicos pode causar danos ambientais e de saúde pública devido sua toxicidade e recalcitrância. Então, a fim de conter o impacto ambiental causado por estes efluentes, é preciso o desenvolvimento de novas tecnologias de remoção. Uma alternativa para a remediação desse problema encontra-se na aplicação da técnica de adsorção por meio da utilização de nanomateriais de titanato de sódio. Estes nanomateriais possuem elevada área superficial, espaços entre as camadas e taxas de transferência de carga interfaciais eficientes, o que os torna excelentes adsorventes. Desse modo, o presente trabalho teve por objetivo sintetizar nanomateriais de titanato de sódio e investigar seu uso para a remoção de corantes orgânicos do meio aquoso. Os materiais foram sintetizados através do método hidrotérmico, sem o uso de direcionador de estrutura, utilizando o dióxido de titânio como material de partida em meio alcalino (NaOH 10M). Tais materiais foram estudados, mediante seu uso na remoção de poluentes orgânicos em meio aquoso onde se constatou a formação de morfologia fibrilar para todos os materiais obtidos. Através da técnica de difração de Raios-X foi verificada a formação de quatro fases cristalográficas de titanatos lamelares, predominantemente, de titanato dissódico, com simetria monoclinica. Em suma, os resultados comprovaram que houve a formação de nanomateriais de titanato. Com efeito, os testes para a remoção do azul de metileno apresentaram promissora atividade adsorptiva dos materiais obtidos em relação ao óxido de partida, removendo até 81% do corante em 30 min. Os nanomateriais de titanato mostraram-se eficientes para remediação de ecossistemas aquáticos contaminados por este poluente orgânico, além disso, os dados coletados tornam-se referência para trabalhos futuros.

Palavras-chave: corantes; adsorção; nanomateriais; titanato de sódio.

ABSTRACT

The application of sodium titanium-based nanomaterials for the adsorption of dyes deserves to be invested by an innovative and low-cost technique. Also, contamination of effluents by used dyes can cause damage and public health due to their toxicity and recalcitrance. So, an end of environmental impact impacted by these effluents, it is necessary or the development of new technologies of removal. An alternative to remedy this problem is found in the application of the adsorption technique through the use of sodium titanium nanomaterials. These factors do not have surface areas, spaces between and charge transfer rates of efficient interfaces, or what significantly increases the adsorbents. Thus, the present work aimed to synthesize sodium titanium nanomaterials and to investigate their use for the removal of dyes or gum from the aqueous medium. The materials were synthesized using the hydrothermal method, without the use of a structured guide, using titanium dioxide as the starting material in the alkaline medium (10M NaOH). These materials were studied, using their use in the removal of organic pollutants in aqueous medium, where it verified the formation of fibrillar morphology for all the materials used. Through the X-ray diffraction technique, it was confirmed the establishment of four crystallographic phases of lamellar titanates, predominantly, of disodium titanate, with monoclinic symmetry. In short, the results proved that there was a formation of titanate nanomaterials. Tests to remove methylene blue are promising for the adsorptive activity of the captured materials concerning the

starting oxide, removing up to 81% of the dye in 30 min. Titanium nanomaterials are efficient to remedy aquatic ecosystems contaminated by this organic pollutant; in addition, the collected data become a reference for future studies.

Keywords: dyes; adsorption; titanate nanomaterials.

1. INTRODUÇÃO:

A baixa disponibilidade de água doce no planeta e sua utilização para diversas atividades básicas do cotidiano e produção industrial, tem acarretado na escassez e poluição dos recursos hídricos e, tal situação, segundo dados coletados pela *World Water Assessment Programme* (WWAP), em 2014, tem se tornado cada vez mais grave, tendendo a piorar nas próximas décadas (Castelo, 2018).

E, para Fagnani *et al.*, (2013) e Lopez (2006), uma das indústrias que utiliza maior volume de água é a têxtil, além disso, a mesma possui alta taxa de poluição. Isso ocorre, devido os vários processos de produção têxtil, que utilizam água doce e, vão desde a lavagem, tingimento, branqueamento e colagem até o acabamento final do tecido, consumindo elevados volumes de água, o que leva ao descarte de grandes volumes de efluentes, geralmente de cor intensa, alta concentração de compostos orgânicos e grandes variações na composição (Ganodermaieri, *et al.*, 2005; Revankar e Lele, 2007; Chen, 2016). Com efeito, 700 mil toneladas de efluentes, contendo 10 mil tipos de corantes, são despejados sem tratamentos físicos e químicos adequados (Vinu e Madras, 2009).

As indústrias têxteis são responsáveis pela geração de diversos compostos recalcitrantes, entre eles, o corante sintético, azul de metileno. Estes corantes são utilizados para tingimento, mas não se aderem totalmente à fibra natural ou sintética durante o processo e, conseqüentemente, ocorre seu desprendimento durante a etapa de lavagem. Gerando assim, efluentes coloridos, os quais, quando descartados inadequadamente em recursos hídricos prejudica a vida aquática, pois absorvem a luz solar reduzindo sua disponibilidade para os processos fotossintéticos, o que diminui o oxigênio e provoca a interrupção da cadeia alimentar aquática (Orzechowski *et al.*, 2018).

Com efeito, técnicas adequadas para o tratamento dos efluentes gerados pelas indústrias têxteis, antes do descarte, são necessárias. As tecnologias físicas e químicas mais utilizadas para a remoção de corantes em

efluentes são a adsorção por carbono ativado, aluminas e zeólitas, o uso de membranas, coagulação-floculação e troca iônica; no entanto, estes tratamentos, apenas transferem compostos orgânicos da fase líquida para a fase sólida ou gasosa, necessitando de um tratamento adicional envolvendo a regeneração do adsorvente ou a substituição da membrana, aumentando assim os custos do tratamento (Tang; An, 1995; Konstantinou; Albanis, 2004; Pires, 2009).

Segundo Ribas (2016), Entre as técnicas citadas, “a adsorção apresenta várias vantagens, como alta eficiência de remoção da cor, facilidade de operação, tratamento contínuo de grandes volumes de efluentes e possibilidade de recuperação do corante e do adsorvente”.

Para Schwarz *et al.*, (2015), a utilização de nanomateriais de titanato revelam-se promissores para o tratamento de efluentes contaminados por corantes orgânicos sintéticos, envolvendo etapas de adsorção (Affam e Chaudhuri, 2013). Em vista disso, Lai (2014), relata que os nanomateriais sintetizados a partir do óxido de titânio, como, nanotubos e nanofitas de titanato de sódio, têm sido vastamente estudados em tratamentos ambientais, atuando na purificação de ar e água, degradação de metais pesados e remediação de resíduos perigosos. Os nanomateriais de titânio, em razão de sua elevada área superficial específica, espaços entre as camadas, taxas de transferência de carga interfaciais eficientes, tornam-se excelentes materiais adsorventes, além disso, possuem método de síntese economicamente viável (Dong *et al.*, 2013).

Entre os nanomateriais de titânio, as nanofitas e nanotubos de titanato de sódio atraem a atenção de estudiosos; as nanofitas devido sua elevada proporção de espessura nanométrica e largura, compostas por algumas camadas de titanato (compostas por Ti, O, H e Na) empilhadas (Ma *et al.*, 2005; Zhang e Liu, 2010; Zhang *et al.*, 2010 e Wang, 2015). Por sua vez, os nanotubos de titanato apresentam forma tubular e são atraentes para a comunidade científica por fornecerem acesso a três diferentes regiões de contato, que são as superfícies internas e externas e as

extremidades do tubo; tais propriedades conferem tanto aos nanotubos quanto as nanofitas uma maior capacidade de adsorção. (Xiong (2010); Schwarz *et al.*, 2015).

Diante do exposto, o objetivo deste trabalho foi sintetizar, caracterizar e aplicar nanomateriais de titanato de sódio na adsorção do corante orgânico azul de metileno, a fim de avaliar o comportamento da remoção do corante em relação ao tipo de nanomaterial utilizado.

2. MATERIAIS E MÉTODOS:

2.1 Sínteses das nanoestruturas de titanato de sódio

Os nanotubos e nanofitas de titanato de sódio foram sintetizados através do método hidrotérmico, livre de templates, utilizando o procedimento empregado por Silva (2012), para a síntese dos nanotubos e, o procedimento utilizado por Wang *et al.* (2015), com adaptações, para a síntese das nanofitas. Inicialmente 1,0g de dióxido de titânio (TiO_2) foi disperso em solução de NaOH 10 M, essa mistura foi então, homogeneizada e mantida em estufa, para tratamento hidrotérmico. Após a reação hidrotérmica, os precipitados brancos formados foram, então, lavados com água destilada, até atingir pH neutro e, posteriormente, secos em estufa. Apesar de as etapas de síntese serem semelhantes houve variações de tempo e temperatura do tratamento hidrotérmico, com a finalidade de obter diferentes nanoestruturas de titanato de sódio. Sendo assim, o tratamento hidrotérmico dos nanotubos foi realizado a 150°C por 36 h e a amostra foi designada como TTNT, já as nanofitas, foram obtidas a 160°C por 120 h e a amostra foi designada como TTNF (Figura 1).

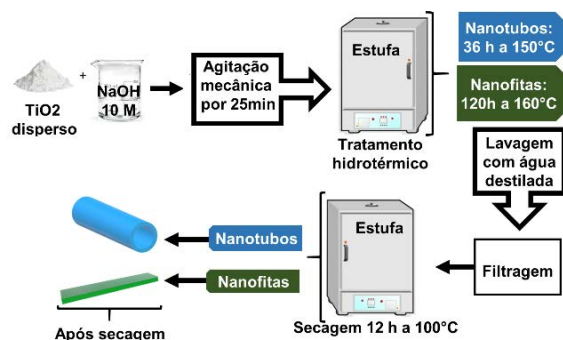


Figura 1. Esquema que ilustra todas as etapas e parâmetros de sínteses hidrotérmica alcalina utilizadas no trabalho. Fonte: Autoria própria.

2.2 Caracterizações

Os materiais obtidos foram caracterizados por Microscopia Eletrônica de Varredura (MEV), Espectroscopia de Energia Dispersiva de Raios-X (EDS), Difração de Raios-X (DRX) e Análise Termogravimétrica (TG/DTG). As imagens de MEV do óxido de titânio foram capturadas em um microscópio da TESCAN, modelo MIRA 3, já o MEV e EDS dos materiais sintetizados, foram obtidos em microscópio de varredura FEG Quanta 450 ambiental, dispersando previamente as amostras, com um processador ultrassônico e posteriormente, colocando-as em porta amostras por intermédio de uma fita de carbono, e em seguida submetendo-as à metalização com uma fina camada de ouro. As medidas de DRX foram realizadas pelo método de varredura, de 2θ de 1 a 90° , em equipamento da Rigaku modelo Mini Flex II, radiação $\text{Cu K}\alpha$, passo de 0.02 graus/s e tempo de 1s. Os dados de DRX do TiO_2 foram submetidos a refinamento automático, através do método de Rietveld, utilizando o software Maud e a carta cristalográfica nº 7206075. Os dados das nanoestruturas foram comparados à cartas cristalográficas (nº 2110464 - 4336945 - 2310730 - 2310331) para identificação das fases cristalinas presentes nos materiais, na qual as cartas cristalográficas foram fornecidas pelo banco de dados *Inorganic Crystal Structure Database* (ICSD). As curvas TG/DTG foram realizadas em equipamento da Shimadzu, modelo TGA-50, com aproximadamente 5,0 mg de amostra, aquecimento de $10^\circ\text{C}/\text{min}$ até 900°C , em fluxo de $100\text{ mL}/\text{min}$ de atmosfera inerte de N_2 . O equipamento de espectroscopia de reflectância UV-Vis utilizado para medir as energias dos materiais foi o espectrofotômetro de UV-Vis da Shimadzu, modelo 46 UV-2600 com feixe duplo. A eficiência adsorptiva foi calculada conforme a equação 1.

$$(\%) = \frac{C_i - C_t}{C_i} * 100 \quad (\text{eq.1})$$

em que: C_i = concentração inicial do corante (mg/L); C_t = concentração do corante ao final do teste adsorptivo (mg/L).

2.3 Testes de adsorção

Os testes de adsorção foram realizados em um reator simples, fechado e em seu interior havia um béquer contendo o material disperso na solução de corante. Na abertura do béquer havia uma tampa de Polipropileno expandido

(isopor), com aberturas para a retirada de alíquotas e também para a introdução do sensor de temperatura. O processo de realização dos testes, ocorreu pela dispersão do catalisador no béquer contendo a solução de corante, sendo a mistura, submetida à agitação mecânica com um agitador magnético que mantinha o sistema em constante e contínua agitação.

Testes experimentais, variando a quantidade de adsorventes (100 mg, 50 mg e 20 mg), a concentração das soluções (10 ppm e 20 ppm) e tempo (120 min, 30 min e 15 min), foram realizados com a finalidade de verificar quais as melhores condições de adsorção para o corante em relação aos adsorventes empregados. Com base nos resultados destes testes, observou-se que ocorreu um decaimento da concentração do corante de forma mais linear usando 20 mg de catalisador, o que proporciona uma melhor verificação do comportamento adsorptivo do material. Em relação a concentração da solução, uma vez que, a absorvância no espectrofotômetro UV-Vis para este corante só é possível de ser analisada até 10 ppm, para utilizar uma solução de 20 ppm seria necessário diluir a amostra e utilizar o fator de correção em seguida, o que aumentaria a margem de erro. No que diz respeito ao tempo, com base nos testes realizados constatou-se que aos 30 min é atingido equilíbrio reacional. Durante todos os testes houve o monitoramento da temperatura.

Para a realização dos testes adsorptivos, inicialmente, 20 mg de adsorvente (TiO_2 , TTNT e TTNF3), foi disperso em 50 mL da solução de corante azul de metileno a 10 ppm. Então, a mistura, cujo pH resultante era 10, foi submetida à agitação mecânica constante e contínua. A Figura 2 mostra o esquema do processo de adsorção.



Figura 2. Esquema representativo dos testes adsorptivos com o corante azul de metileno. Fonte: Autoria própria.

A agitação ocorria em velocidade de 350 rpm (velocidade satisfatória para atingir o

equilíbrio adsorção/dessorção), em ausência de radiação por 30 min. Alíquotas eram retiradas e levadas à centrifuga, sendo que, o precipitado formado, bem como, o sobrenadante, retornavam para o sistema reacional, logo após ser realizada a leitura do sobrenadante em um espectrofotômetro Uv-Vis, modelo Mini 1240 da Shimadzu, com absorvância de 664 nm. Durante todo o teste houve monitoramento contínuo da temperatura do sistema, que variou de 21 a 42 °C.

3. RESULTADOS E DISCUSSÃO:

3.1 Caracterizações dos materiais

3.1.1. Microscopia Eletrônica de Varredura (MEV) e Espectroscopia de energia Dispersiva de Raios-X (EDS)

Por meio das micrografias eletrônicas de varredura para o dióxido de titânio, (Figura 3), identificou-se a presença de partículas aglomeradas, com diâmetro micrométrico.

Cuja a ampliação da imagem (Figura 3a), exibe monocristais de anatásio (TiO_2), na forma de partículas esféricas com diâmetro de 23,1 μm , em conformidade com o encontrado na literatura (Ma *et al.*, 2005). Já as micrografias dos nanotubos (TTNT) sintetizados a partir do TiO_2 , bem como, o EDS, são apresentados na Figura 4.

As micrografias para este material podem ser descritas morfológicamente como filamentos fibrosos, entrelaçados e aglomerados em direções aleatórias, característicos de estruturas unidimensionais de titanato, tais como, as nanotubulares encontradas na literatura (Gao *et al.*, 2008; Natarajan *et al.*, 2013). Estes resultados demonstram que, a síntese utilizada foi eficiente, uma vez que, as micrografias revelam alto rendimento da morfologia fibrilar, totalmente distinta da morfologia esférica do óxido de partida mostrada na Figura 3. As micrografias das nonofitas (TTNF) são exibidas na Figura 5. A morfologia observada exibe uma rede de filamentos fibrosos, entrelaçados em direções aleatórias, com a formação de aglomerados, semelhante aos TTNT's.

As imagens revelam, sobretudo, uma maior distribuição morfológica qualitativa, bem como um pequeno aumento no tamanho desse

material (331,1 nm) quando comparado aos nanotubos (310,5 nm), exibidos na Figura 4. A morfologia exata dos materiais obtidos só poderá ser confirmada através de análise de Microscopia Eletrônica de Transmissão (MET). No entanto, é possível observar a diferença morfológica entre ambos os materiais sintetizados e o óxido de partida, o que confirma a formação de materiais nanoestruturados de titanato, cujas características são semelhantes às descritas na literatura para as morfologias desejadas.

A técnica de EDS, por sua vez, mostrou a presença de sódio na composição dos materiais nanoestruturados, o que é um forte indício de que a síntese foi bem-sucedida, uma vez que, a presença desse elemento corresponde a substituição dos átomos de hidrogênio pelos átomos de sódio durante o tratamento hidrotérmico em meio fortemente alcalino, sendo essa a reação necessária para a obtenção das nanoestruturas desejadas. (Bavykin *et al.*, 2009)

3.1.2 Difração de Raios-X (DRX)

O difratograma do óxido de partida (TiO_2), utilizado como fonte de titânio nas sínteses, é apresentado na Figura 6.

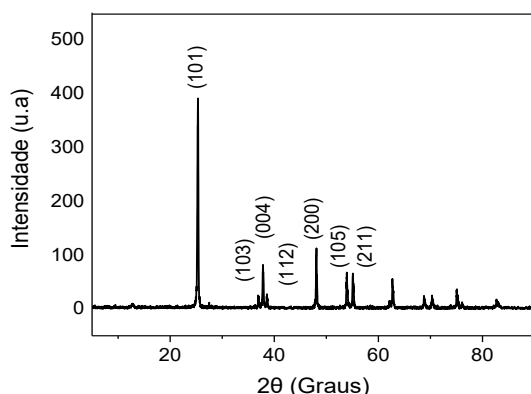


Figura 6. Difratograma da titânia anatase.

É possível observar picos de reflexão bem definidos, dado que, uma das reflexões apresenta alta intensidade ($2\theta=25,3^\circ$) e é característica de óxidos de titânio. Apenas uma fase cristalográfica foi encontrada, a anatase, sendo esta identificada, ao relacionar os picos de reflexão (Tabela 1) com os dados da carta cristalográfica nº 7206075.

Através dos dados da carta cristalográfica realizou-se o refinamento dos

dados de DRX da estrutura do TiO_2 com função automática, por intermédio do método de Rietveld. Os resultados são apresentados na Figura 7, com sua estrutura química identificada e os parâmetros de rede exibidos na Tabela 2, confirmando assim, a estrutura cristalina de fase anatase do TiO_2 utilizado como fonte de titânio.

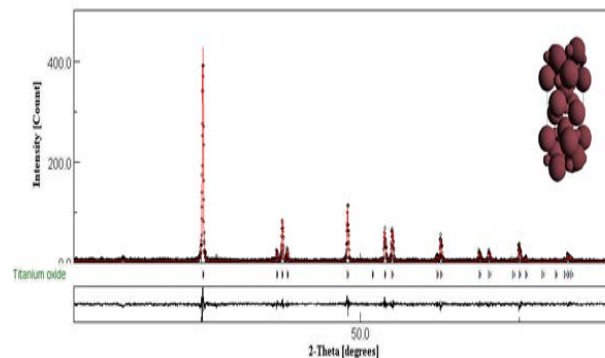


Figura 7. Refinamento estrutural de TiO_2 , apresentando uma única fase anatase.

Diante dos difratogramas das amostras de nanotubos e nanofitas de titanato de sódio apresentados na Figura 8, é possível observar que, há quatro reflexões largas e bem características, sendo esse um padrão difração semelhante ao de titanatos lamelares do tipo $\text{A}_2\text{Ti}_n\text{O}_{2n+1}$, podendo A corresponder à átomos de hidrogênio ou sódio (Junior, 2007).

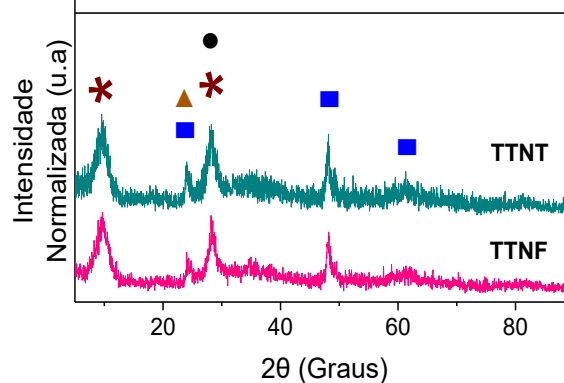


Figura 8. Difratogramas de Raios-X das amostras do TTNT e TTNF nas fases cristalinas $\text{Na}_2\text{O}_3\text{Ti}_{1.25}$ ■; $\text{H}_2\text{O}_7\text{Ti}_3$ ▲; $\text{Na}_2\text{O}_{19}\text{Ti}_9$ ●; e $\text{Na}_2\text{O}_7\text{Ti}_3$ *.

Esse padrão de difração é diferente do observado para o TiO_2 , o qual apresenta apenas uma fase cristalográfica e picos bem mais intensos e definidos (Silva, 2012). É possível verificar, também o desaparecimento do pico de reflexão de elevada intensidade, característico do óxido de partida, sendo esse um forte indício de que ocorreu transformação estrutural no material. O que corrobora com as micrografias,

onde observou-se a distinção morfológica, partindo de uma estrutura esférica do óxido (Figura 3) para estruturas fibrilares (Figuras 4 e 5). Visto que, com base nas duas técnicas de caracterização, verifica-se que mudanças estruturais são acompanhadas por mudanças morfológicas após a síntese hidrotérmica realizada.

Comparando os dados dos difratogramas com cartas cristalográficas disponíveis no banco de dados ICSD, é possível presumir a existência de uma mistura de fases cristalinas, todas com estrutura monoclinica, porém, as fases de titanatos de sódio são predominantes (ver Tabela 3), principalmente, o titanatodissódico ($\text{Na}_2\text{O}_3\text{Ti}_{1.25}$).

Contudo, existem fatores que prejudicam o entendimento da estrutura cristalina de nanoestruturas de titanato. Tal como, os diferentes arranjos cristalinos das formas protonadas de ácidos polititânicos ($\text{A}_2\text{Ti}_n\text{O}_{2n+1}$). Uma outra questão, é o tamanho reduzido dos cristais que remete em um baixo valor da área de coerência, provocando o alargamento das reflexões e instabilidade dos materiais, os quais podem sofrer alterações durante o tratamento (Bavykin *et al.*, 2006; Bagnara, 2011).

3.1.3 Análises Termogravimétricas (TG/DTG)

As curvas de TG/DTG do óxido de titânio e dos materiais obtidos são exibidos na Figura 9. A princípio, pode ser observada a distinção entre as curvas termogravimétricas dos materiais sintetizados e do óxido de partida (TiO_2), uma vez que, neste não há nenhum evento térmico significativo. Os materiais sintetizados apresentaram três eventos de perda de massa em função da temperatura. As perdas de massa inferiores a 100°C , correspondem a saída de água fisissorvida presente na superfície dos materiais.

Por sua vez, as perdas entre 100 - 250°C são decorrentes da liberação da água quimissorvida entre as lamelas dos materiais. E, por fim, acima de 250°C até 600°C as perdas de massa são provocadas, tanto presença de água quimissorvida entre as lamelas quanto pela desidroxilação que ocorre na superfície dos materiais (Junior, 2007). A Tabela 4, mostra o percentual das perdas de massa em função da temperatura para todas as amostras.

Em suma, não ocorreram grandes diferenças nos eventos de perda de massa nas nanoestruturas de titanato de sódio, o que corresponde com os difratogramas de Raio-X, onde constatou-se que as fases predominantes correspondem a titanatos de sódio de composições distintas. Diante das baixas perdas de massa verificadas nos materiais sintetizados e pelas mesmas serem constituídas apenas da saída de água, conjectura-se que os mesmos apresentam excelente estabilidade térmica.

3.1.4 Aplicação na remoção de corantes via adsorção

Nas Figuras 10 e 11 são apresentados os valores correspondentes aos testes de adsorção de AzM na em solução com concentração de 10 ppm, em 20 mg de TiO_2 , TTNT e TTNF, durante 60 min.

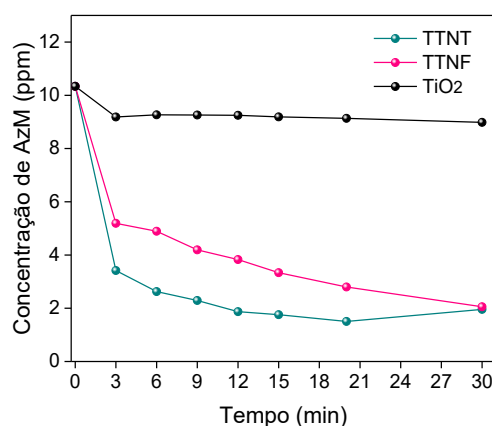


Figura 10. Concentração de AzM, em função do tempo, para os adsorventes TiO_2 , TTNT e TTNF.

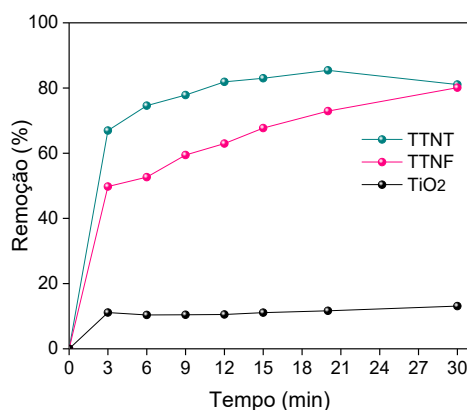


Figura 11. Percentual de remoção (%) de AzM, em função do tempo, para os adsorventes dióxido de titânio (TiO_2), nanotubos de titanato (TTNT) e (C) nanofitas de titanato (TTNF).

Inicialmente, é observada uma rápida, entretanto, gradual adsorção do corante pelos nanomateriais sintetizados, o que ocorre, devido a forte interação eletrostática entre o sítio catiônico presente no corante azul de metileno e as áreas de contato na superfície dos nanomateriais (Figura 12).

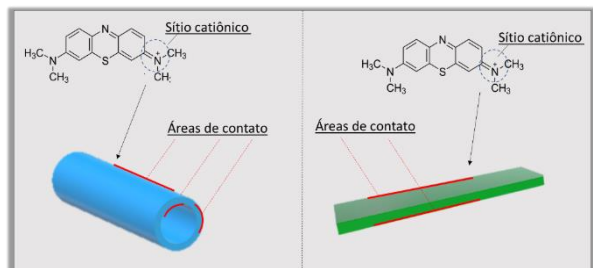


Figura 12. Esquema representativo da molécula de corante interagindo com a superfície dos adsorventes.

Além disso, a capacidade adsorviva dos mesmos se mostra superior ao óxido de partida durante todo o teste de adsorção, dada a concentração e o percentual de remoção do corante pelo óxido ao final do teste, que removeu apenas 13% do corante, o que corresponde a 8,98 ppm. Já a adsorção dos nanotubos e nanofitas no decorrer dos testes foi satisfatória, pois o TTNT removeu 81% do corante, chegando à concentração de 1,97ppm, e a TTNF removeu 80,1% do corante, atingindo a concentração final de 2,05 ppm. Esse melhor resultado de adsorção para os nanotubos em comparação com as nanofitas, possivelmente, é devido a porosidade dos nanotubos, já que a estrutura nanotubular oferece regiões de contato externas e internas, o que aumenta a área superficial e contribui muito para a adsorção. Esse melhor desempenho de remoção do AzM pelos TTNT's pode ser mais um indicativo de que a morfologia nanotubular de interesse foi obtida para esse material.

4. CONCLUSÕES:

Através das caracterizações morfológicas, estruturais e térmicas as sínteses dos nanomateriais foram eficazes. Os resultados de MEV indicaram que as morfologias desejadas podem ter sido obtidas, através do método hidrotérmico utilizado, contudo, a confirmação morfológica dos nanomateriais só poderá ser feita através da análise de MET. Através dos difratogramas de Raios-X, foram vistos picos de reflexão distintos das reflexões do óxido de

partida, com presença de mais de uma fase cristalográfica de titanatos lamelares de sódio. As perdas de massa observadas nas análises de TG/DTG comprovaram que os materiais obtidos possuem em sua constituição moléculas de água física e quimicamente sorvidas. Os materiais sintetizados apresentaram elevado potencial adsorvivo para o corante azul de metileno, removendo até 81% (TTNT) e 80,1% (TTNF), sendo o desempenho destes muito superior ao óxido de partida que removeu apenas 13% do corante. Isso demonstra que os mesmos podem se mostrar excelentes adsorventes de corantes catiônicos, uma vez que ocorre interação eletrostática entre eles.

5. AGRADECIMENTOS:

Ao Laboratório de Catálise, ambiente e materiais, ao Laboratório Análises Magnética e Óptica, a Universidade Federal Rural do Semi-Árido e a Universidade Federal do Ceará.

6. REFERÊNCIAS:

1. Affam, A. C; Chaudhuri, M. J. *Environ manage.*, **2013**, 130-160.
2. Bagnara, M. Dissertação de Mestrado, Universidade Federal do Rio Grande do Sul, Brasil., **2011**.
3. Bavykin, D. V; Friedrich, J. M; Walsh, F. C. J *Adv Mater.*, **2006**, 18, 2807-2824.
4. Bavykin, D. V; Friedrich. J. M; Walsh F. C. J. *Adv. Mater.*, **2006**, 18, 2807-2824.
5. Castelo, Jeremiah. *World Water Reserve*, **2018**. <https://worldwaterreserve.com/water-crisis/percentage-of-drinkable-water-on-earth/>.
6. Chen, L; Wang, L; Wu, X; Ding, X. A. *J. Clean. Prod.*, **2016**, 12, 006.
7. Costa, T. M. S; Lima, M. S; Filho, J. F. C; Silva, L. J; Santos, R. S; Junior, G. E.L. J. *Photochem Photobiol A.*, **2018**, 364, 461-71.
8. Dong, P; Wang, Y; Liu, B; L. Guo; Huang, Y; Yin, S. *Am. Ceram. Soc. Bull.*, **2012**, 2011-2013.
9. Fagnani, E; Gudagnini, R. A; Silva, G.A; Guimarães, R. *Holos.*, **2013**, 13, 85-97.

10. Ganodermaieri, G., Cennamo, G., Sannia, G. *Enzyme Microb. Technol.*, **2005**, 36, 17-24.
11. Gao, T. *J. Phys. Chem. A.*, **2008**, 112, 9272–9277.
12. Júnior, E. M. Tese de Doutorado, Universidade Federal do Rio Grande do Norte, Brasil, **2007**.
13. Konstantinou, I.K., Albanis, T. A. *Appl. Catal. B.*, **2004**, 49, 1-14.
14. Lai, C. W; Juan, J. C; Ko, W. B; Bee, S; Hamid, A. *Int j. photoenergy.*, **2014**, doi.org/10.1155/2014/524135.
15. LOPEZ, M.J.; GUIADO, M.C.; VARGAS-GARCIA; ESTRELLA, F.S.; MORENO, J. *Enzyme Microb. Technol.*, **2006**, 40, 42-45.
16. Ma, R., Fukuda, Sasaki, T., Osada, Y. *J. Phys. Chem. B.*, **2005**, 109, p. 6210– 6214.
17. Ma, R; Fukuda, S. T; Osada, Y. *J. Phys. Chem. B.*, **2005**, doi: 10.1021/jp044282r, 6210– 6214.
18. Natarajan, T; Bajaj. K; Tayade, R. *Elec. Suplit. Mater* supplementary., **2013**, doi.org/10.1007/s11051-013-1669-3, 11051-1669.
19. Orzechowski, T. *MATEC Web Conf.*, **2018**, 1029, 25-314.
20. Pires, A. I. V. F. Dissertação de Mestrado, Universidad Complutense de Madrid, **2009**.
21. Revankar, M.S., Lele, S.S. *Bioresour. Technol.*, **2007**, 98, 775-780.
22. Schwarz, S.C; Sanches, A.C; Fagan, S. B; RAFFIN, R.P; BULHÕES, L.O.S. *Disci. Sci.*, **2015**, 16, 277-283.
23. Silva, E. F. Tese de Doutorado, Universidade Federal do Rio Grande do Norte, Brasil, **2012**.
24. Tang, W.Z., An, H. *Chemosphere.*, **1995**, 31, 4157-4170.
25. Vinu, R; Madras, G. *Environ. Sci. Technol.*, **2009**, 43, 473–479.
26. Wang, J; Liu, W; Yin, G; Li, H. *Colloid. Surf. a physicochem eng. asp. Colloid surface a. Coll surf A.*, **2012**, 414, 9–16.
27. WWAP (United Nations World Water Assessment Programme)/UN-Water. *Nature-Based Solutions for Water.*, **2018**.
28. Xiong, L. Yan, Y.; Mai, J.; Sun, W.; Zhang, C.; Wei, D.; Chen, Q.; Ni, J. *Chem. Eng.*, **2010**, 156, 313-320.
29. Zhang, D., Kim, C., Kang, Y. *J. J. Phys. Chem. A.*, **2010**, 114, 8294–8301.
30. Zhang, X., Liu, W. *Bioresour. Technol.*, **2010**, 5, 1895–1907.

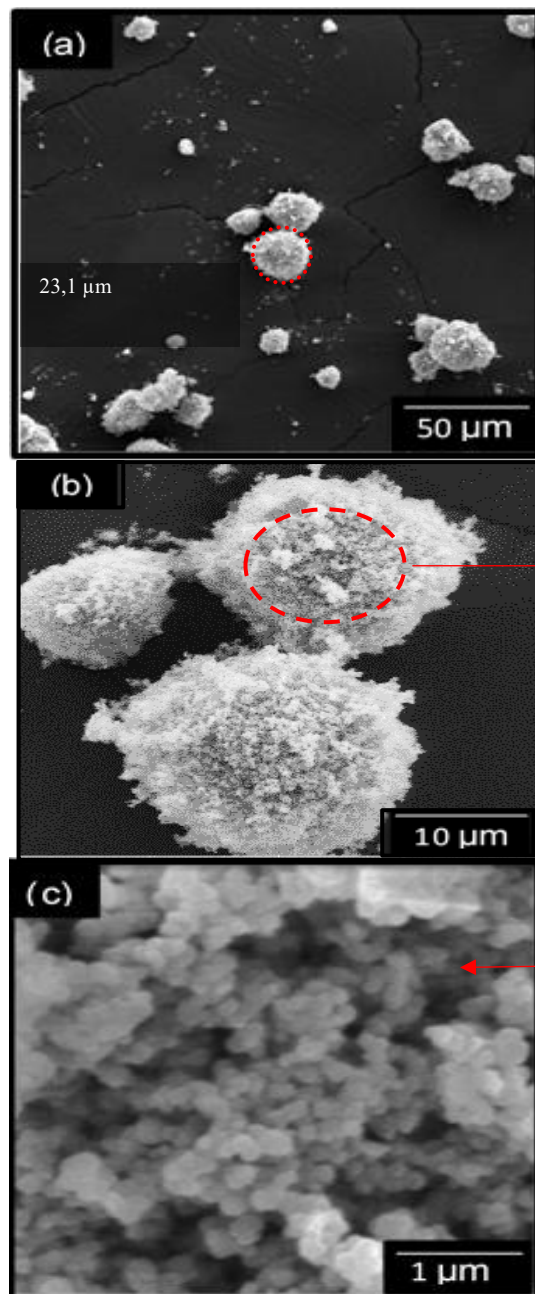


Figura 3. Imagens de MEV do TiO_2 ampliado 1.000 vezes (a) 5.000 vezes (b) e 50.000 vezes (c).

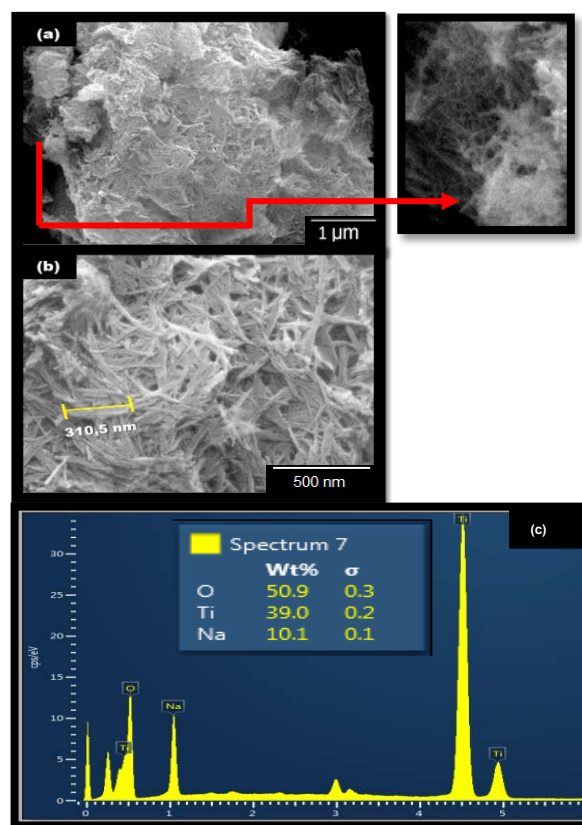


Figura 4. Imagens de MEV dos TTNT, ampliado 65.000 vezes (a) e 200.00 vezes (b).

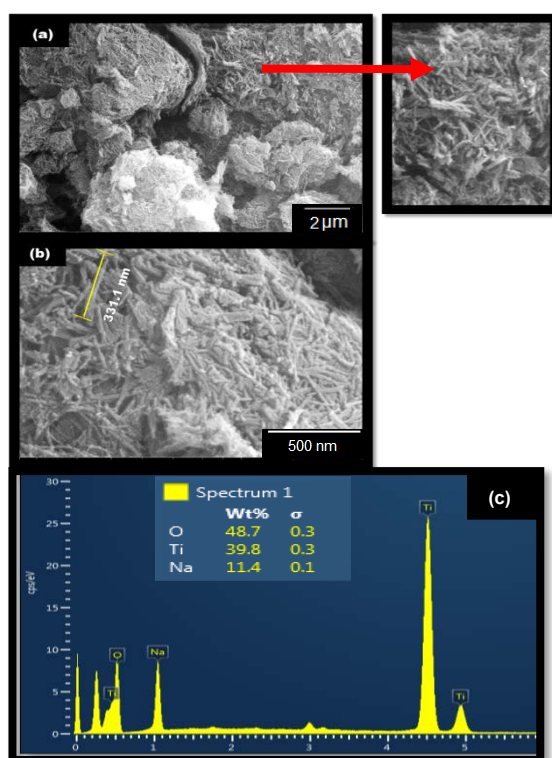


Figura 5. Imagens de MEV das TTNF, ampliado 65.000 vezes (a) e 200.000 vezes (b) e o Resultado médio da análise química quantitativa por EDS (c).

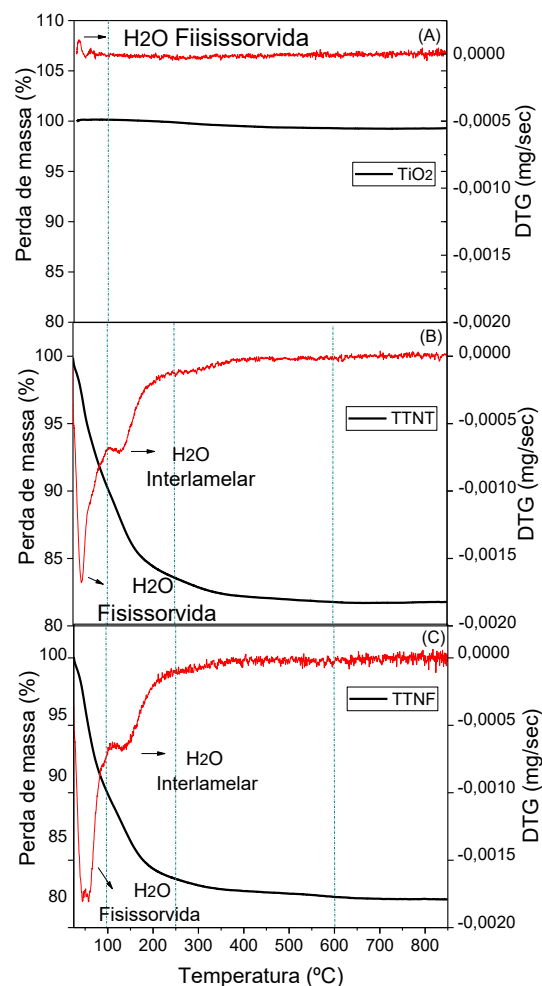


Figura 9. Curvas de TG e DTG das amostras (A) dióxido de titânio (TiO_2), (B) nanotubos de titanato (TTNT) e (C) nanofitas de titanato (TTNF).

Tabela 1. Picos de reflexão do dióxido de titânio (TiO_2).

2 theta	d(A°)	2 theta	d (A°)
25.3	3.517	62.1	1.666
36.9	2.430	62.6	1.493
37.7	.378	68.7	1.480
38.5	2.332	70.2	1.364
48.0	1.892	75.0	1.338
53.8	1.758	76.0	1.279
55.0	1.700	82.6	1.250

Tabela 2. Parâmetros estruturais para o TiO_2 , obtidos pelo refinamento estrutural automático utilizando o método Rietveld.

Fase Cristalográfica	TiO_2 Anatase
Simetria	Tetragonal
Volume de célula	136.38 Å ³
Parâmetros de rede / nm	$a = b = 3,78$; $c = 9,52$; $\beta = 90^\circ$

Tabela 3. Estruturas químicas para o TTNT (obtidas através de refinamento estrutural pelo método de Rietveld) e seus respectivos parâmetros de rede.

ICSD (n°)	Fases Cristalográficas	Percentual de fases (%)	Tamanho do Cristalito	Parâmetros de rede / nm			
				a	b	c	β
210464	Titanatodissódico $\text{Na}_2\text{O}_3\text{Ti}_{1,25}$	62,5	53.8 nm	2.24	3.77	13.3	137.1°
4336945	Trititanato protônico $\text{H}_2\text{O}_7\text{Ti}_3$	4,91	41.0 nm	15.7	3.49	9.04	101.3°
2310730	Trititanato de sódio $\text{Na}_2\text{O}_7\text{Ti}_3$	27,4	29.1 nm	8.94	3.69	9.66	113.0°
2310331	Nonatitanato de sódio $\text{Na}_2\text{O}_{19}\text{Ti}_9$	5,03	36.2 nm	11.5	3.65	15.7	105.1°

Tabela 4. Quantificação das etapas de perda de massa obtidas da curva TG.

Amostras	% de perda de massa		
	(25-100°C)	(100-250°C)	(250°C-600°C)
TiO_2	0,1	-----	-----
TTNT	9,8	6,5	1,8
TTNF	12,7	6,7	1,8

ANÁLISE EXPERIMENTAL DE UM SISTEMA SOLAR TÉRMICO UTILIZANDO NANOFLUIDO HÍBRIDO DE PRATA E DIÓXIDO DE TITÂNIO.

EXPERIMENTAL ANALYSIS OF A SOLAR HEAT SYSTEM USING HYBRID SILVER NANOFLUID AND TITANIUM DIOXIDE.

AMORIM NETO, Juarez Pompeu de^{1*}; LIMA, Ricardo José Pontes²; ROCHA, Paulo Alexandre Costa³; MARINHO, Felipe Pinto⁴; SILVA, Maria Eugênia Vieira da⁵

^{1,2,3,4,5} Universidade Federal do Ceará, Departamento de Engenharia Mecânica, Laboratório de Energia Solar e Gás Natural, Fortaleza – CE, Brasil.

* Autor correspondente

e-mail: juarezneto33@hotmail.com

Received 09 January 2020; received in revised form 20 February 2020; accepted 16 March 2020

RESUMO

A população mundial está cada vez mais atenta com as questões ambientais que envolvem nosso planeta. Em busca de soluções que venham contribuir para conservação do meio ambiente está o uso das energias renováveis que estão em grande expansão sendo o uso da energia solar uma solução para esse propósito. O trabalho teve como objetivo avaliar a capacidade de absorção energética de um nanofluido híbrido de prata e dióxido de titânio utilizados para absorção solar direta em uma "Parede Solar". Os experimentos realizados foram expostos por um período de 16 horas por vários dias. Várias concentrações foram analisadas, onde fixou-se uma concentração de 23,2 ppm de dióxido de titânio e variou a prata em 0,40625 ppm, 0,8125 ppm, 1,625 ppm e 3,25 ppm correspondendo a uma fração molar de 3%, 6%, 12% e 25% respectivamente. Uma análise no perfil de temperatura foi feito, onde observou-se uma melhor aproveitamento da amostra com fração molar de 12% que obteve um ganho de temperatura de 8,3°C correspondendo a 14,9% de ganho. Uma análise na razão de energia armazenada foi analisada, observando um boa resposta dos nanofluidos no início da incidência solar e um máximo de energia armazenada para a amostra de 6%. Outra métrica analisada foi a taxa de absorção específica que alcançou valor máximo de 0,009293 KW/g. O trabalho mostrou que para o preparo do nanofluido híbrido, nem sempre aumentar a concentração da prata implicou em melhores resultados e através das análises de perfil de temperatura e métricas de análise, concluiu-se que uma concentração de prata de 0,8125 ppm juntamente com uma concentração de 23,2 ppm (fração molar de 6%) consegue-se melhores ganhos para uso do nanofluido na parede solar.

Palavras-chave: *Energias Renováveis, Energia Solar, Parede Solar, Nanopartículas*

ABSTRACT

The world population is increasingly aware of environmental issues involving our planet. In search of solutions that will contribute to the conservation of the environment, you can use the renewable energies that are in great expansion, being the use of solar energy a solution for this purpose. This study aimed to evaluate the energy absorption capacity of a hybrid silver nanofluid and titanium dioxide used for direct solar absorption in a "Solar Wall." The experiments performed were exposed for 16 hours for several days. Various concentrations were analyzed, where a concentration of 23.2 ppm titanium dioxide was set, and silver varied to 0.40625 ppm, 0.8125 ppm, 1.625 ppm, and 3.25 ppm corresponding to a 3% molar fraction. 6%, 12% and 25% respectively. An analysis of the temperature profile was made, which showed a better utilization of the sample with a 12% molar fraction that obtained a temperature gain of 8.3 ° C corresponding to a 14.9% gain. An analysis of the stored energy ratio was analyzed, observing a good response of nanofluids at the early solar incidence and a maximum stored energy for the sample of 6%. The other metric analyzed was the specific absorption rate that reached a maximum value of 0.009293 KW / g. The work showed that for the preparation of hybrid nanofluid, not always increasing the silver concentration implied better results and through temperature profile analysis and energy analysis metrics, it was concluded that a silver concentration of 0.8125 ppm together With a concentration of 23.2 ppm (6% molar fraction) better gains are obtained for the use of nanofluid in the solar wall.

Keywords: Renewable Energy, Solar Energy, Solar Wall, Nanoparticles.

1. INTRODUÇÃO

Atualmente há uma grande preocupação com as questões ambientais que envolvem a população mundial, já que existe uma alta degradação em virtude do uso de combustíveis fósseis, a geração de energia proveniente de fontes convencionais causou uma degradação ambiental que pode ser vista através de poluição, chuva ácida, aquecimento global, etc (Suman *et al.*, 2015). Em virtude desse problema, a busca por energias renováveis vem aumentando significativamente nos últimos anos, onde tem sido um objeto de estudo por cientistas e profissionais (Bazdidi-Tehrani *et al.*, 2018). A energia solar é umas das principais fontes de energia renovável e ela pode contribuir para conservação do meio ambiente de duas maneiras, tanto para conversão de energia térmica em eletricidade como para aquecimento de água através de várias tecnologias, Além disso é uma das fontes de energia renovável mais abundante do mundo e disponível de forma gratuita (Gorji e Ranjbar, 2017; Choudhary *et al.*, 2020).

O aproveitamento de energia térmica para aquecimento de águas se dá por meio do uso de coletores solares, onde a eficiência de um coletor é um parâmetro de estudo muitas vezes limitado (Bandarra Filho *et al.*, 2014). O processo de aquecimento em coletores solares tradicionais não é tão eficiente devido a existência de resistências térmicas no processo, onde o conceito de absorção direta da radiação solar promete aumentar a capacidade de absorção e assim reduzir as perdas térmicas para o ambiente (Beicker *et al.*, 2018). Diversos coletores solares estão sendo testados para melhorias em seu funcionamento, dentre as pesquisas recentes pode-se encontrar resultados para o desempenho térmico de um coletor solar de placa plana em Choudhary *et al.* (2020). Qin *et al.* (2019) analisou o desempenho de um coletor solar parabólico. Natividade *et al.* (2019) avaliou a eficiência de um coletor solar de tubo evacuado. Wang *et al.* (2018) e Hatami e Jing (2017) fizeram um estudo para coletores solares de absorção direta. Sahota e Tiwari (2017) analisaram um coletor solar híbrido fotovoltaico/térmico.

Outro fator limitante para a eficiência de trabalho de um coletor solar, além do tipo de geometria, é o tipo de fluido utilizado, onde a utilização de nanofluidos é uma solução viável para substituição dos fluidos convencionais, buscando assim a alta performance desses coletores (Ebrahimi-Moghadam *et al.*, 2018; Raj e Subudhi, 2018; Vakili *et al.*, 2017; Zayed *et al.*,

2019). Os nanofluidos são fluidos com nanopartículas dispersas, onde essas partículas variam de tamanho (1 – 100 nm). Essas nanopartículas podem ser de diversos materiais, tais como o metal, não metal, óxido, carboneto, mistura de nanopartículas (fluido híbrido), etc. Devido ao seu pequeno tamanho em uma superfície considerável, o nanofluido apresenta uma vantagem na capacidade de absorção de calor e assim as perdas em coletores podem ser minimizadas (Mehrali *et al.*, 2015)

Atualmente, diversas pesquisas vêm sendo realizadas para mostrar as melhorias do uso de nanofluidos em coletores solares. O nanotubo de carbono foi usado em Mahbubul *et al.* (2018) e mostrou uma melhoria de 66% na eficiência de um coletor solar de tubo evacuado, o óxido de zinco foi utilizado em Kaya *et al.* (2018) mostrando uma melhoria de 62,87% na eficiência de um coletor solar evacuado de tubo em U, o CeO_2 que aumentou a temperatura do nanofluido em 37,3% em relação à água em Sharafeldin e Gróf (2018), o óxido cuproso que aumentou em 24% a condutividade térmica em Wei *et al.* (2009) e a prata que obteve um aumento máximo de 99,7% na eficiência de conversão fototérmica em comparação com o fluido base (Amjad *et al.*, 2018). Também foram realizados estudos com nanofluidos híbridos, que são novos tipos de nanofluidos que podem ser preparados utilizando duas ou mais nanopartículas, tais como o óxido de grafeno que foi misturado com o ouro e melhorou em 10,8% a eficiência de geração de vapor em Fu *et al.* (2017). Outro trabalho que apresentou resultados positivos foi sobre o nanofluido híbrido alumina-cobre que melhorou em 12,11% a condutividade térmica (Suresh *et al.*, 2011). Karami (2018) mostrou que a utilização do nanofluido híbrido Fe_3O_4/SiO_2 aprimorou a eficiência de um coletor solar para 21,7%.

Além do tipo de nanofluido estudado, muitas melhorias nas eficiências de coletores solares são encontradas quando se modificam a concentração das nanopartículas no fluido base, resultando em uma conversão fototérmica diferente (Javadi *et al.* 2013), onde a eficiência de um coletor solar está diretamente relacionada com a concentração de nanofluidos (Ozsoy e Corumlu, 2018). Mas algumas pesquisas realizadas por Yu *et al.* (2017) mostraram que esse aumento de concentração dos nanofluidos podem ter algumas limitações. Os inconvenientes mais comuns citados por Sreekumar *et al.* (2019) são os custos elevados, processo demorado para síntese do nanofluido, menor estabilidade e maior viscosidade, onde a estabilidade tem um impacto

direto na absorção óptica.

Esse trabalho busca analisar o estudo do nanofluido híbrido de dióxido de titânio (TiO_2) juntamente com a prata, buscando assim a melhor concentração de trabalho na absorção solar direta em um aparato denominado “Parede Solar”.

2. MATERIAIS E MÉTODOS:

2.1. Preparação dos nanofluidos

Existem diversas técnicas de preparação dos nanofluidos como exposto em Rocha *et al.* (2019). Entre elas podem ser citadas a sonificação (Sen *et al.*, 2019), redução química (Mohammadpoor *et al.*, 2019), síntese por líquidos iônicos (Thaokar *et al.*, 2013), pirólise a laser (Huminic *et al.*, 2015), método poliol (Becerra *et al.*, 2015), microemulsão reversa (Foroughi *et al.*, 2015), síntese hidrotérmica assistida por micro-ondas (Hu *et al.*, 2011) e rota sonoquímica para síntese de nanofluidos (Jeong *et al.*, 2004). O preparo do dióxido de titânio foi por dispersão de nanopartículas por meio de sonificação e o de prata foi por redução química de nitrato de prata para formar as nanopartículas dentro do próprio nanofluido.

2.2. Configuração Experimental

Um aparato denominado “Parede Solar” como em Amorim Neto *et al.* (2019) foi construído para captação dos dados, onde o mesmo apresenta uma estrutura de alumínio com quatro placas de vidro na célula inferior (duas internas e duas externas) e mais quatro na célula superior de forma análoga. Os vidros externos possuem 4 mm de espessura, 8 mm de espessura para os vidros internos, comprimento de 1000 mm e altura de 1000 mm, a Figura 1 detalha a Parede Solar.

Na célula inferior do experimento foi inserida água destilada na quantidade de 3,5 L e na célula superior foi inserido o nanofluido de estudo também no mesmo volume. Para aferição das temperaturas dos fluidos foram utilizados 6 termopares do tipo K com precisão de $0,1^\circ\text{C}$, onde três foram colocados na célula inferior e mais três na superior, conforme coloração amarela na Figura 1. Além da temperatura dos fluidos, foram coletadas as temperaturas ambiente e de sensação térmica, sendo representada pela coloração vermelha e preta respectivamente, onde também foram usados sensores do tipo K com mesma precisão. Os experimentos foram realizados no Laboratório de Energia e Gás

Natural (LESGN) da Universidade Federal do Ceará na cidade de Fortaleza (Latitude: $03^\circ 43' 02''$ Sul, Longitude: $38^\circ 32' 35''$ Oeste) entre os dias 20/06/2019 e 16/10/2019 no período de 5:30 até 21:30, já que nesse intervalo de tempo ainda se conseguia verificar um diferencial de temperatura do nanofluido em comparação com a água destilada. O experimento tinha uma de suas faces voltadas para leste e outra para oeste de tal forma que o aproveitamento da radiação solar fosse aproveitado antes e depois de 12:00.

Os nanofluidos foram utilizados em diversas concentrações. A prata foi testada com 0,40625 ppm ($3,86 \times 10^{-5}$ mol/l), 0,8125 ppm ($7,71 \times 10^{-5}$ mol/l), 1,625 ppm ($1,54 \times 10^{-4}$ mol/l), 3,25 ppm ($3,09 \times 10^{-4}$ mol/l) e 6,5 ppm ($6,17 \times 10^{-4}$ mol/l), e de TiO_2 nas concentrações de 1,45 ppm ($7,71 \times 10^{-5}$ mol/l), 2,9 ppm ($1,54 \times 10^{-4}$ mol/l), 5,8 ppm ($3,07 \times 10^{-4}$ mol/l), 11,6 ppm ($6,17 \times 10^{-4}$ mol/l) e 23,2 ppm ($1,23 \times 10^{-4}$ mol/l). Como as partículas de prata e dióxido de titânio apresentam densidades diferentes foi preferível comparar a performance dos mesmos em função da sua concentração molar, já que os valores são iguais quando se compara os nanofluidos da menor para maior concentração.

Buscando ainda a melhor performance dos nanofluidos, foi feito uma análise híbrida da prata e do titânio, fixando a concentração de TiO_2 em 23,2 ppm e dopando com diversas concentrações de prata (0,40625 ppm – 0,8125 ppm – 1,625 ppm e 3,25 ppm), correspondendo a fração molar de aproximadamente 3%, 6%, 12% e 25% respectivamente, similar a pesquisa de Yu e Xuan (2018) que usou o nanofluido de prata disperso na superfície do óxido de cobre. A concentração do dióxido de titânio se manteve constante pois experimentos anteriores foram feitos de forma isolada para a prata e para TiO_2 mostrando a superioridade da prata, e assim buscou-se melhorar gradativamente o TiO_2 fazendo a dopagem com prata. Alguns trabalhos fizeram esse estudo de nanofluidos híbridos e mostrou a melhoria deles (Lenert; Wang, 2012; Duan *et al.*, 2018; Farajzadeh *et al.*, 2018).

2.3 Taxa de Absorção Específica (SAR) e Energia Armazenada (SER)

Identificando a concentração ideal de nanopartículas, é possível identificar a capacidade da nanopartícula de gerar energia térmica por unidade de massa e assim evitar o uso de concentrações elevadas de forma desnecessária. A taxa de absorção específica (SAR) vai descrever esse comportamento (Zeiny *et al.*, 2018; Zhang *et al.*, 2014). A Equação 1

descreve o cálculo de SAR.

$$SAR = \frac{m_{fb}c_{fb}}{1000m_{np}} \left(\frac{\Delta T_{nf}}{\Delta t} - \frac{\Delta T_{fb}}{\Delta t} \right) \quad (1)$$

onde m representa a massa, c o calor específico, T a temperatura e t o tempo. Os subscritos fb , np e nf representam o fluido base, nanopartícula e nanofluido respectivamente. A Equação 1 descreve o cálculo de SAR.

Outra métrica de avaliação da nanopartícula foi avaliada nesse trabalho, a taxa de energia armazenada (SER) mostrado em Peng., *et al.* (2011), que avalia a energia absorvida devido à presença de nanopartícula, por meio da Equação 2.

$$SER = \frac{T_{nf}(t) - T_{nf}(0)}{T_{fb}(t) - T_{fb}(0)} \quad (2)$$

3. RESULTADOS E DISCUSSÕES:

3.1 Análise do perfil de temperatura

A melhoria analisada no início desse trabalho foi o quanto o nanofluido conseguiu superar a água destilada em temperatura de aquecimento durante toda exposição à radiação solar. A figura 2 mostra o resultado da diferença de temperatura entre o nanofluido híbrido e a água, onde percebe-se que quanto maior a fração molar de prata inserida no dióxido de titânio, maior é ganho de temperatura, resultados similares mostraram que uma maior fração em volume implicava em uma maior condutividade térmica dos nanofluidos (Ranga Babu *et al.*, 2017). A fração molar de 3% (0,40625 ppm de prata – 23,2 ppm de TiO_2) conseguiu um ganho de 6,4°C em comparação com a água, onde esse ganho representa uma melhoria de 11,6%, já uma fração molar de 25% (3,25 ppm de prata – 23,2 ppm de TiO_2) conseguiu um ganho de 9,9°C, sendo representado por uma melhoria de 18,3%. Além de mostrar o ganho de temperatura do nanofluido, a Figura 2 mostra o perfil de temperatura que o experimento apresenta ao longo do dia, onde percebe-se uma alta queda de temperatura por volta de meio dia, isso se deve a inclinação dos raios solares em relação às células que contém o nanofluido.

A Tabela 1 mostra todos os comparativos entre as concentrações dos nanofluidos isolados e do híbrido. Quando se aumenta a fração molar de prata no dióxido de titânio, o ganho de

temperatura sempre melhora, partindo de 11,6% até 18,3%, o mesmo acontece com os nanofluidos isolados. Outro fator relevante que se pode destacar da Tabela 1 é que o nanofluido híbrido sempre se torna melhor que a prata, com exceção da fração molar de 25%, onde a prata supera o nanofluido híbrido, tornando desnecessário o preparo do mesmo quando se deseja um ganho de temperatura e assim a fração molar de 12% se torna ideal para essa situação, onde pode-se destacar que a fração molar de 12% obteve um ganho de 8,3°C e a fração molar de 6% obteve um ganho de 7,8°C podendo-se considerar ganhos bem similares. Algumas pesquisas também foram realizadas com os nanofluidos de dióxido de titânio e prata. Said *et al.*, (2015) utilizou o nanofluido TiO_2 para melhorar a eficiência de um coletor solar variando a concentração do nanofluido e fluxo de massa. Kiliç *et al.* (2018) Utilizou o mesmo nanofluido (TiO_2) para avaliar o desempenho de um coletor solar de placa plana, onde chegou-se em uma eficiência de 48,67% contra uma de 36,20% para a água pura. Gan *et al.* (2018) utilizou o nanofluido TiO_2 para melhorar o desempenho de um coletor solar de tubo evacuado aumentando sua eficiência em 16,5%. Chaji *et al.* (2013) utilizou TiO_2 para avaliar o desempenho de um coletor solar de placa plana, onde obteve uma melhoria na eficiência de 15,8%. O nanofluido de prata também foi estudado por Lazarus *et al.* (2015) visando melhorias em um coletor solar de placa plana, onde conseguiu um aumento no coeficiente de transferência de calor por convecção de 18,4%. Comparando com os resultados desse trabalho, pode-se verificar que os nanofluidos de prata e TiO_2 obtêm resultados superiores que o da água para diversas aplicações, sendo elas para absorção direta ou em uso de coletores solares diversos. Em função disso combinou-se as duas melhorias alcançando resultados mais eficientes com a mistura dos nanofluidos.

3.2 Análise de SER

Resultados foram analisados para verificar a quantidade de energia que foi absorvida devido à presença das nanopartículas, que é a taxa de energia armazenada (SER). A Figura 3 mostra como varia SER em função do tempo, onde o resultado deixa claro a grande capacidade do nanofluido em absorver energia nas primeiras horas do dia, mas logo em seguida essa capacidade cai para todas as amostras. Os pontos mais altos de SER são observados no início do dia, pois é nesse momento que há uma maior variação de temperatura do nanofluido em relação

à água. Outro resultado observado é que a fração molar de 6% obteve os melhores índices de energia absorvida, e para o SER mostrou-se superior aos demais experimentos.

A Figura 4 mostra como variou essa razão de energia armazenada em função da fração molar do nanofluido. Esse resultado mostra que nem sempre acrescentar uma quantidade a mais de prata implica em uma maior energia armazenada, sendo desnecessário uma fração de molar de 12% e 25% para o nanofluido híbrido quando se deseja um maior SER.

3.3 Análise de SAR

Outra métrica relevante para analisar a capacidade fototérmica do nanofluido híbrido foi o SAR (Taxa de absorção específica), que calcula a capacidade de absorção energética que cada partícula tem além de mostrar a eficiência de conversão fototérmica em função da concentração de nanopartículas imersa no fluido base. A Figura 5 mostra como varia SAR em função da fração molar do nanofluido híbrido, onde percebe-se que a quantidade SAR aumenta para a amostra de 6% e logo em seguida reduz tendendo a uma estabilidade por volta de 0,009 KW/g. Os resultados de Beicker *et al.* (2018) e Bandarra Filho *et al.* (2014) mostraram que SAR diminui com a concentração até o momento de se estabilizar, mas esses resultados foram encontrados em amostras de nanofluidos isolados. O nanofluido híbrido de prata com dióxido de titânio obteve um aumento em SAR e logo em seguida uma redução, isso pode ser devido ao fato das interações de partículas diferentes. A fração molar de 6% mais uma vez apresentou melhores resultados.

4. CONCLUSÕES:

O trabalho mostrou o a capacidade fototérmica do nanofluido híbrido de dióxido de titânio e prata, onde foram analisados o ganho de temperatura do nanofluido em relação à água, razão de energia armazenada (SER) e taxa de absorção específica (SAR).

Com relação ao ganho de temperatura, foram analisadas 4 frações molares (3%, 6%, 12% e 25%), onde a fração molar de 25% apresentou um maior ganho de temperatura sendo representado por 18,3% esse ganho, mas a prata isoladamente nas mesmas concentrações apresentou um ganho de 19,3%, mostrando assim a inviabilidade do nanofluido híbrido para essa concentração molar, em contrapartida as frações

molares de 6% e 12% conseguiram resultados superiores ao da prata, obtendo ganhos de 14,3% e 14,9%. Nessas condições de perfil de temperatura, o nanofluido híbrido apresentou os melhores resultados com uma fração molar de 6% (0,8125 ppm de prata e 23,2 ppm de dióxido de titânio) e de 12% (1,625 ppm de prata e 23,2 ppm de dióxido de titânio).

Na análise de SER observou-se uma maior razão de energia absorvida para a fração molar de 6%, onde o nanofluido apresentou boa resposta nas primeiras horas de experimento.

A análise da taxa de absorção específica comprovou mais uma vez o bom comportamento do nanofluido híbrido com fração molar de 6%, onde essa amostra mostrou uma melhor resposta para o SAR, apresentando uma máxima de 0,009293 KW/g.

A escolha da melhor concentração de prata no nanofluido híbrido foi de 0,8125 ppm em uma concentração de 23,2 ppm de TiO₂, onde outras concentrações não apresentaram ganhos superiores.

Esse estudo mostrou como buscar melhorias em nanofluidos, onde uma junção entre duas nanopartículas ainda sim pode alcançar resultados mais expressivos. Algo que pode ser analisado em trabalhos futuros seria uma análise de viabilidade econômica dos nanofluidos em função do ganho que os mesmos podem obter.

5. AGRADECIMENTOS:

Este estudo foi financiado em parte pela Coordenação de Aperfeiçoamento de Pessoal de Nível Superior – Brasil (CAPES) – código financeiro 001, e pelo Conselho Nacional de Desenvolvimento Científico e Tecnológico (CNPq), órgãos governamentais brasileiros. O suporte recebido é reconhecido com gratidão.

6. REFERÊNCIAS:

1. Amjad, M. et al. Experimental photothermal performance of nanofluids under concentrated solar flux. *Solar Energy Materials And Solar Cells*, v. 182, p.255-262, ago. **2018**.
2. Amorim Neto, J. P. et al. Analysis and comparison between regression models for temperature estimation of solar collectors operating with nanofluids. *XL cilmace ibero-latin american congress on computational methods in engineering*. **2019**, Natal.

3. Bandarra Filho, E. P. et al. Experimental investigation of a silver nanoparticle-based direct absorption solar thermal system. *Energy Conversion and Management*, v. 84, p.261-267, ago. **2014**.
4. Bazdidi-Tehrani, F., Khabazipur, A., Vasefi, S. I. Flow and heat transfer analysis of TiO₂/water nanofluid in a ribbed flat-plate solar collector. *Renewable Energy*, v. 122, p.406-418, jul. **2018**.
5. Becerra, A. et al. Preparation of poly (vinyl chloride)/copper nanocomposite films with reduced bacterial adhesion. *Procedia Materials Science*. **2015**.
6. Beicker, C. L. I. et al. Experimental study of photothermal conversion using gold/water and MWCNT/water nanofluids. *Solar Energy Materials and Solar Cells*, v. 188, p.51-65, dez. **2018**.
7. Chaji, H. et al. Experimental Study on Thermal Efficiency of Flat Plate Solar Collector Using TiO₂/Water Nanofluid. *Modern Applied Science*, v. 7, n. 10, 24 set. **2013**.
8. Choudhary, S; Sachdeva, A; Kumar, P. Investigation of the stability of MgO nanofluid and its effect on the thermal performance of flat plate solar collector. *Renewable Energy*, v. 147, p.1801-1814, mar. **2020**.
9. Duan, H. et al. Effect of plasmonic nanoshell-based nanofluid on efficiency of direct solar thermal collector. *Applied Thermal Engineering*, v. 133, p.188-193, mar. **2018**.
10. Ebrahimi-Moghadam, A., Mohseni-Gharyehsafa, B., Farzaneh-gord, M. Using artificial neural network and quadratic algorithm for minimizing entropy generation of Al₂O₃-EG/W nanofluid flow inside parabolic trough solar collector. *Renewable Energy*, v. 129, p.473-485, dez. **2018**.
11. Farajzadeh, E; Movahed, S; Hosseini, R. Experimental and numerical investigations on the effect of Al₂O₃/TiO₂H₂O nanofluids on thermal efficiency of the flat plate solar collector. *Renewable Energy*, v. 118, p.122-130, abr. **2018**.
12. Foroughi, F. et al. A designed magnetic CoFe₂O₄-hydroxyapatite core-shell nanocomposite for Zn (II) removal with high efficiency. *Ceramics International*, v. 41, n. 5, p.6844-6850, jun. **2015**.
13. Fu, Y. et al. Investigation on enhancing effects of Au nanoparticles on solar steam generation in graphene oxide nanofluids. *Applied Thermal Engineering*, v. 114, p.961-968, mar. **2017**.
14. Gan, Y. Y. et al. Thermal conductivity optimization and entropy generation analysis of titanium dioxide nanofluid in evacuated tube solar collector. *Applied Thermal Engineering*, v. 145, p.155-164, dez. **2018**.
15. Gorji, T. B; Ranjbar, A. A. Thermal and exergy optimization of a nanofluid-based direct absorption solar collector. *Renewable Energy*, v. 106, p.274-287, jun. **2017**.
16. Hatami, M; Jing, D. Evaluation of wavy direct absorption solar collector (DASC) performance using different nanofluids. *Journal Of Molecular Liquids*, v. 229, p.203-211, mar. **2017**.
17. Hu, L. et al. Microwave-assisted one-step hydrothermal synthesis of pure iron oxide nanoparticles: magnetite, maghemite and hematite. *Journal Of Sol-gel Science And Technology*, v. 60, n. 2, p.198-205, 24 set. **2011**.
18. Huminic, A. et al. Thermal conductivity, viscosity and surface tension of nanofluids based on FeC nanoparticles. *Powder Technology, Bucharest*, v. 284, p.78-84, nov. **2015**.
19. Javadi, F. S; Saidur, R; Kamalisarvestani, M. Investigating performance improvement of solar collectors by using nanofluids. *Renewable And Sustainable Energy Reviews*, v. 28, p.232-245, dez. **2013**.
20. Jeong, S. H. et al. A Sonochemical Route to Single-Walled Carbon Nanotubes under Ambient Conditions. *American Chemical Society*. v. 126, n. 49, ago. **2004**.
21. Karami, M. Experimental investigation of first and second laws in a direct absorption solar collector using hybrid Fe₃O₄/SiO₂ nanofluid. *Journal Of Thermal Analysis And Calorimetry*, v. 136, n. 2, p.661-671, 16 ago. **2018**.
22. Kaya, H., Arslan, K., Eltugral, N. Experimental investigation of thermal performance of an evacuated U-Tube solar collector with ZnO/Ethylene glycol-pure water nanofluids. *Renewable Energy*, v.

- 122, p.329-338, jul. **2018**.
23. Kiliç, F. et al. Effect of titanium dioxide/water nanofluid use on thermal performance of the flat plate solar collector. *Solar Energy*, v. 164, p.101-108, abr. **2018**.
 24. Lazarus, G. et al. Heat transfer performance of silver/water nanofluid in a solar flat-plate collector. *Journal Of Thermal Engineering*, v. 1, n. 2, p.104-123, 1 fev. **2015**.
 25. Lenert, A., Wang, E. N. Optimization of nanofluid volumetric receivers for solar thermal energy conversion. *Solar Energy*, v. 86, n. 1, p.253-265, jan. **2012**.
 26. Mahbubul, I. M. et al. Carbon nanotube nanofluid in enhancing the efficiency of evacuated tube solar collector. *Renewable Energy*, v. 121, p.36-44, jun. **2018**.
 27. Mehrli, M. et al. Effect of specific surface area on convective heat transfer of graphene nanoplatelet aqueous nanofluids. *Experimental Thermal And Fluid Science*, v. 68, p.100-108, nov. **2015**.
 28. Mohammadpoor, M. et al. Investigating heat transfer properties of copper nanofluid in ethylene glycol synthesized through single and two-step routes. *International Journal Of Refrigeration*, v. 99, p.243-250, mar. **2019**.
 29. Ozsoy, A., Corumlu, V. Thermal performance of a thermosyphon heat pipe evacuated tube solar collector using silver-water nanofluid for commercial applications. *Renewable Energy*, v. 122, p.26-34, jul. **2018**.
 30. Peng, H; Ding, G; Hu, H. Effect of surfactant additives on nucleate pool boiling heat transfer of refrigerant-based nanofluid. *Experimental Thermal And Fluid Science*, v. 35, n. 6, p.960-970, set. **2011**.
 31. Qin, C; Kim, J. B; Lee, B. J. Performance analysis of a direct-absorption parabolic-trough solar collector using plasmonic nanofluids. *Renewable Energy*, v. 143, p.24-33, dez. **2019**.
 32. Raj, P., Subudhi, S. A review of studies using nanofluids in flat-plate and direct absorption solar collectors. *Renewable And Sustainable Energy Reviews*, v. 84, p.54-74, mar. **2018**.
 33. Ranga Babu J. A. et al. Thermodynamic analysis of hybrid nanofluid based solar flat plate collector. *World Journal Of Engineering*, p.00-00, 28 dez. **2017**.
 34. Rocha, P. A. C. et al. A review on nanofluids: preparation methods and applications. *Tchê Química*, Porto Alegre, v. 16, n. 31, p.365-380, jan. **2019**.
 35. Sahota, L; Tiwari, G. N. Review on series connected photovoltaic thermal (PVT) systems: Analytical and experimental studies. *Solar Energy*, v. 150, p.96-127, jul. **2017**.
 36. Said, Z. et al. Performance enhancement of a Flat Plate Solar collector using Titanium dioxide nanofluid and Polyethylene Glycol dispersant. *Journal Of Cleaner Production*, v. 92, p.343-353, abr. **2015**.
 37. Sen, B. et al. Influence of Al₂O₃ and palm oil-mixed nano-fluid on machining performances of Inconel-690: IF-THEN rules-based FIS model in eco-benign milling. *The International Journal Of Advanced Manufacturing Technology*, v. 103, n. 9-12, p.3389-3403, 3 maio **2019**.
 38. Sharafeldin, M. A; Gróf, G. Evacuated tube solar collector performance using CeO₂/water nanofluid. *Journal of Cleaner Production*, v. 185, p.347-356, jun. **2018**.
 39. Sreekumar, S. et al. Investigation on influence of antimony tin oxide/silver nanofluid on direct absorption parabolic solar collector. *Journal Of Cleaner Production*, v. 249, nov. **2019**.
 40. Suman, S; Khan, M. K; Pathak, M. Performance enhancement of solar collectors—A review. *Renewable And Sustainable Energy Reviews*, v. 49, p.192-210, set. **2015**.
 41. Suresh, S. et al. Synthesis of Al₂O₃-Cu/water hybrid nanofluids using two step method and its thermo physical properties. *Colloids And Surfaces A: Physicochemical and Engineering Aspects*, v. 388, n. 1-3, p.41-48, set. **2011**.
 42. Thaokar, R., Deshmukh, R., Mehra, A. Ionic Liquid Assisted Synthesis and Crystal Habit Control of Cobalt Accicular Nanoparticles. *Advanced Materials Manufacturing & Characterization*, Mumbai, v. 2, n. 1, p.105-109, mar. **2013**.
 43. Vakili, M. et al. Experimental investigation

- and modeling of thermal conductivity of CuO–water/EG nanofluid by FFBP-ANN and multiple regressions. *Journal Of Thermal Analysis And Calorimetry*, v. 129, n. 2, p.629-637, 27 fev. **2017**.
44. Wang, D. et al. Magnetic Photothermal Nanofluids with Excellent Reusability for Direct Absorption Solar Collectors. *Acs Applied Energy Materials*, v. 1, n. 8, p.3860-3868, 6 jul. **2018**.
45. Wei, X. et al. Synthesis and thermal conductivity of Cu₂O nanofluids. *International Journal Of Heat And Mass Transfer*, v. 52, n. 19-20, p.4371-4374, set. **2009**.
46. Yu, F. et al. Dispersion stability of thermal nanofluids. *Progress In Natural Science: Materials International*, v. 27, n. 5, p.531-542, out. **2017**.
47. Yu, X; Xuan, Y. Investigation on thermo-optical properties of CuO/Ag plasmonic nanofluids. *Solar Energy*, v. 160, p.200-207, jan. **2018**.
48. Zayed, M. E. et al. Factors affecting the thermal performance of the flat plate solar collector using nanofluids: A review. *Solar Energy*, v. 182, p.382-396, abr. **2019**.
49. Zhang, H. et al. Photothermal conversion characteristics of gold nanoparticle dispersions. *Solar Energy*, v. 100, p.141-147, fev. **2014**.
50. Zeiny, A. et al. A comparative study of direct absorption nanofluids for solar thermal applications. *Solar Energy*, v. 161, p.74-82, fev. **2018**.

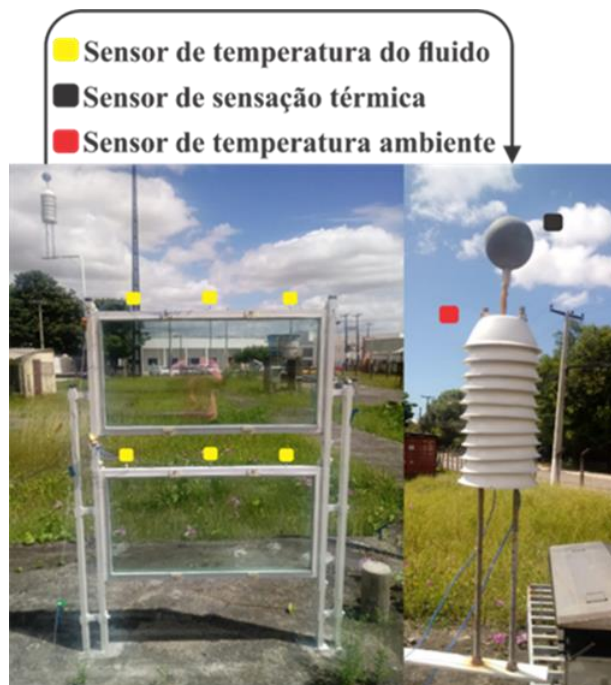


Figura 1. Parede Solar para aquisição dos dados de temperatura

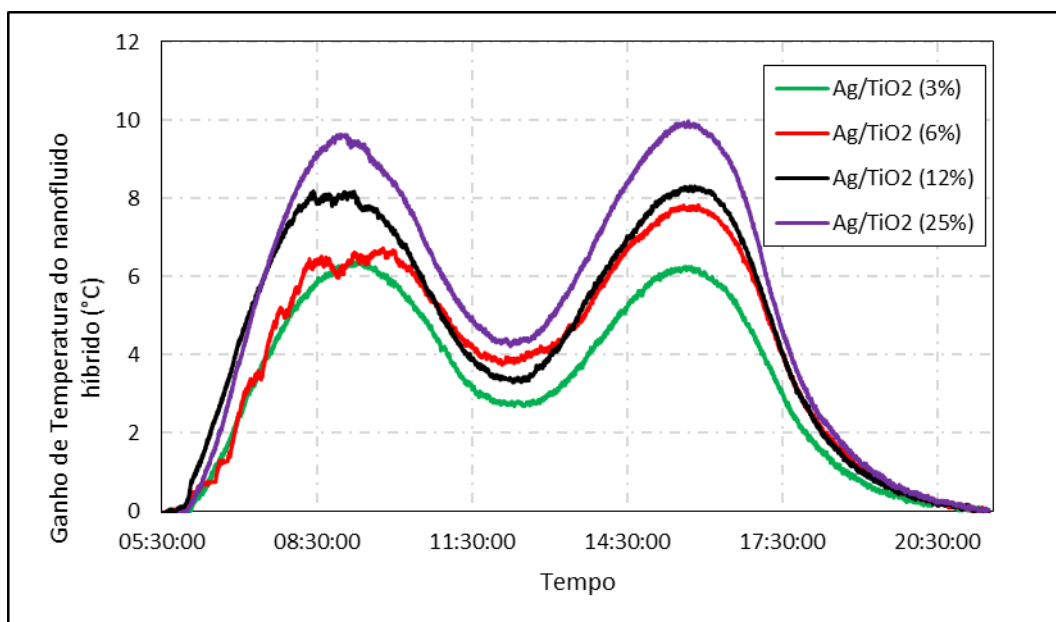


Figura 2. Ganho de temperatura do nanofluido híbrido em relação à água.

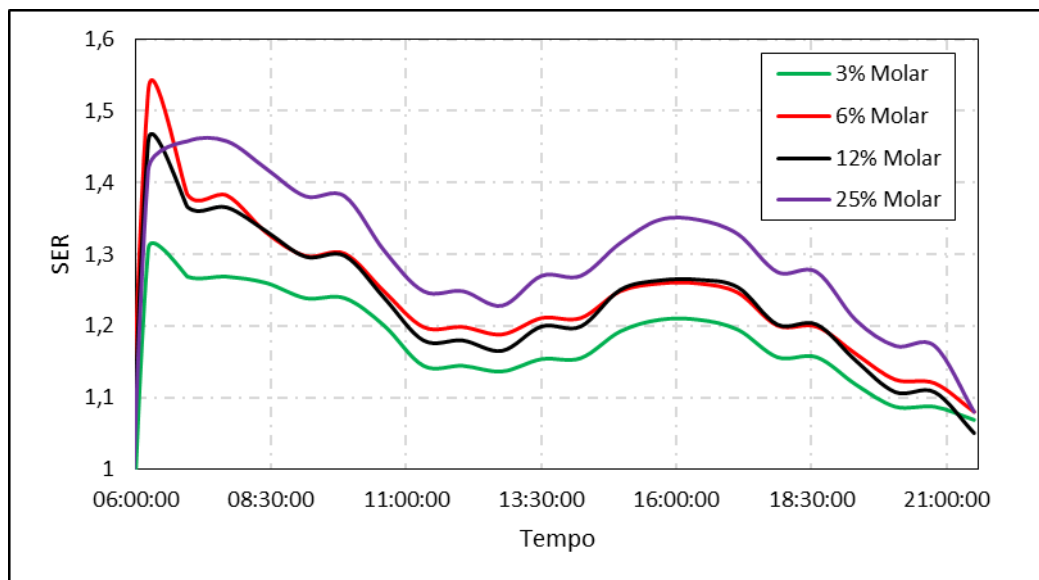


Figura 3. Razão de energia armazenada devido à presença de nanopartículas

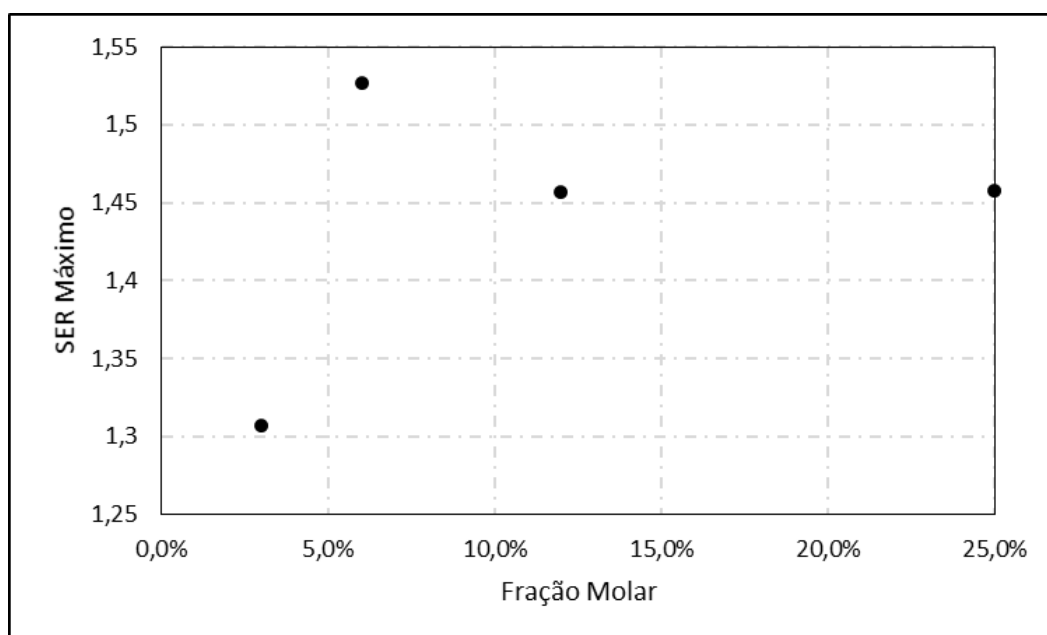


Figura 4. Razão de energia absorvida em função da concentração de prata no dióxido de titânio (23,2 ppm)

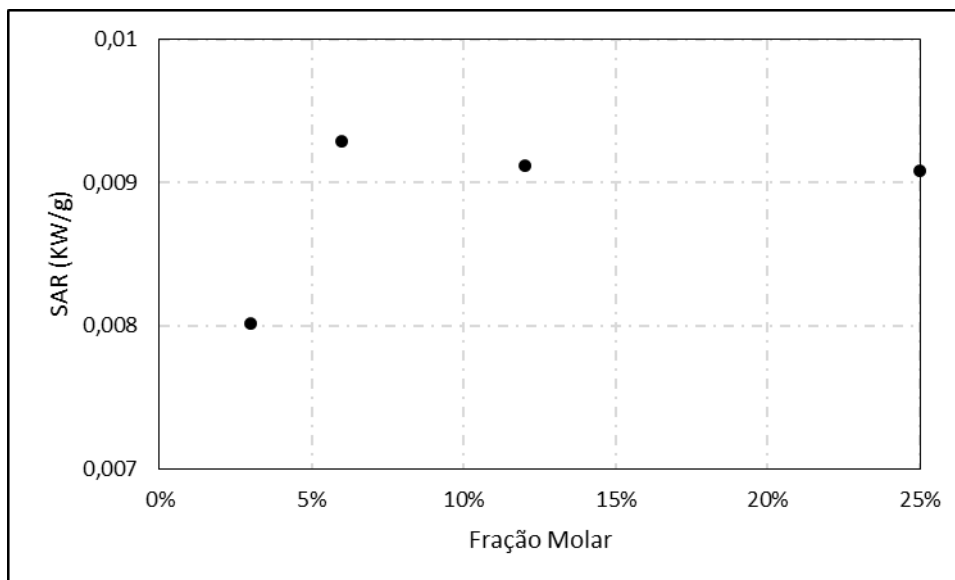


Figura 5. Taxa de absorção específica por unidade de massa em função da fração molar do nanofluido híbrido

Tabela 1. Comparativo entre nanofluidos híbridos e isolados

Nanofluidos (Comparativos)	Ganho de Temperatura (°C) e ganho percentual
Prata (0,40625 ppm)	2,8 - (5,2%)
TiO ₂ (23,2 ppm)	2,7 - (5%)
Híbrido (Fração Molar 3%)	6,4 - (11,6%)
Prata (0,8125 ppm)	5,7 - (10,6%)
TiO ₂ (23,2 ppm)	2,7 - (5%)
Híbrido (Fração Molar 6%)	7,8 - (14,3%)
Prata (1,625 ppm)	6,5 - (11,7%)
TiO ₂ (23,2 ppm)	2,7 - (5%)
Híbrido (Fração Molar 12%)	8,3 - (14,9%)
Prata (3,25 ppm)	10,2 - (19,3%)
TiO ₂ (23,2 ppm)	2,7 - (5%)
Híbrido (Fração Molar 25%)	9,9 - (18,3%)

ALTERAÇÕES ESTRUTURAIS E DE FASE NAS CAMADAS DE SUPERFÍCIE DA COBERTURA MULTICOMPONENTE RESISTENTE AO CALOR DO REVESTIMENTO DE ÍONS DE PLASMA NI-CR-AL-Y APÓS MODIFICAÇÃO POR FEIXES DE ELÉTRONS DE CORRENTE FORTE COM DURAÇÃO DE MICROSSEGUNDOS**STRUCTURAL AND PHASE CHANGES OF THE SURFACE LAYERS OF HEAT-RESISTANT MULTICOMPONENT COATING OF ION-PLASMA COATING Ni-Cr-Al-Y AFTER MODIFICATION BY HIGH-CURRENT ELECTRON BEAMS MICROSECOND DURATION****СТРУКТУРНО-ФАЗОВЫЕ ИЗМЕНЕНИЯ ПОВЕРХНОСТНЫХ СЛОЕВ ЖАРОСТОЙКОГО МНОГОКОМПОНЕНТНОГО ПОКРЫТИЯ ИОННО-ПЛАЗМЕННОГО ПОКРЫТИЯ NI-CR-AL-Y ПОСЛЕ МОДИФИЦИРОВАНИЯ СИЛЬНОТОЧНЫМИ ЭЛЕКТРОННЫМИ ПУЧКАМИ МИКРОСЕКУНДНОЙ ДЛИТЕЛЬНОСТИ**

BYTSENKO, Oksana A.^{1,2*}; STESHENKO, Igor G.³; PANOV, Vladimir A.⁴; TISHKOV, Victor V.⁵; MARKOV, Alexey B.⁶;

¹Chernyshev Moscow Machine-Building Enterprise, Design Department of Research and Reliability, Moscow – Russian Federation

^{2,5}Moscow Aviation Institute (National Research University), Department of Aircraft Robotic Systems, Moscow – Russian Federation

^{3,4}Chernyshev Moscow Machine-Building Enterprise, Moscow – Russian Federation

⁶Tomsk Scientific Center SB RAS, Tomsk – Russian Federation

* Correspondence author
e-mail: oksiwear@yandex.ru

Received 06 November 2019; received in revised form 18 February 2020; accepted 11 March 2020

RESUMO

O desenvolvimento da engenharia aeroespacial e da engenharia mecânica depende diretamente do desenvolvimento de novos materiais metálicos e tecnologias avançadas. O problema de criação dos materiais e seus tipos de processamento para aumentar o nível de propriedades operacionais é relevante em relação à complicação e à rigidez das condições de trabalho das tecnologias modernas. Uma das tarefas mais importantes da construção de aeronaves modernas é aumentar as propriedades operacionais da camada superficial. O objetivo do artigo é elucidar a influência de feixes de elétrons de corrente forte com duração de microssegundos nas alterações estruturais e de fase nas camadas de superfície da cobertura multicomponente resistente ao calor do revestimento de íons de plasma Ni-Cr-Al-Y sob várias condições. Utilizando um complexo de métodos de pesquisa metalofísica, os estados físico-químico e de fase estrutural da camada superficial foram estudados antes e após a modificação das amostras. Essas amostras foram revestidas com revestimentos de plasma de íons condensados resistentes ao calor de três composições diferentes usando nove feixes de elétrons de alta corrente em nove modos com diferentes valores de energia eletrônica e número de pulsos no intervalo selecionado de energia eletrônica. Uma análise das mudanças na fase estrutural que ocorrem durante a modificação foi realizada. Amostras cilíndricas de alvos feitos de liga de níquel resistente ao calor ZhS36 revestida com revestimento multicomponente condensado por íon-plasma SDP-2 + VSDP-16. Essas amostras foram usadas de acordo com a tecnologia serial, ambas com subsequente modificação usando feixes de elétrons de alta corrente e sem modificação. Verificou-se que o cromo no estado inicial está desigualmente distribuído: o cromo está presente nas partículas, a matriz é empobrecida no cromo. Os resultados do estudo podem ser úteis para os cientistas que estudam as propriedades do revestimento de íons de plasma multicomponente resistente ao calor Ni-Cr-Al-Y e o efeito de feixes de elétrons de corrente forte nele, bem como para a fabricação de materiais mais resistentes ao calor em engenharia aeroespacial e engenharia mecânica.

Palavras-chave: irradiação de feixe de elétrons de corrente forte, revestimentos de íões de plasma condensado, estado estruturais e de fase, estudo de microestrutura.

ABSTRACT

The development of aerospace engineering and mechanical engineering directly depends on the development of new metal materials and advanced technologies. The problem of creating materials and their types of processing to increase the level of operational properties is relevant in connection with the complication and tightening of working conditions of modern technologies. One of the most important tasks of contemporary aircraft construction is to increase the operational properties of the surface layer. The purpose of the article is to elucidate the effect of high-current electron beams of microsecond duration on changes in the surface layers of the heat-resistant multicomponent ion-plasma coating Ni-Cr-Al-Y under various conditions. Using a complex of metallophysical research methods, the physicochemical and structural-phase states of the surface layer were studied before and after modification of the samples. These samples were coated with heat-resistant condensed ion-plasma coatings of three different compositions using nine high-current electron beams in 9 modes with different values of electron energy and number of pulses in the selected interval of electron energy. An analysis of the structural phase changes occurring during modification was carried out. Cylindrical samples of targets made of heat-resistant nickel alloy ZhS36 coated with ion-plasma condensed multicomponent coating SDP-2 + VSDP-16. These samples were used according to serial technology, both with subsequent modification using high-current electron beams and without modification. It was found that chromium in the initial state is unevenly distributed: chromium is present in the particles; the matrix is depleted in chromium. The research results can be useful for scientists to study the properties of heat-resistant multicomponent ion-plasma coatings Ni-Cr-Al-Y and the effect of high-current electron beams on it, as well as for the manufacture of more heat-resistant materials in aerospace engineering and mechanical engineering.

Keywords: *high-current electron beam irradiation, condensed ion-plasma coatings, structural-phase state, microstructure study.*

АННОТАЦИЯ

Развитие аэрокосмической техники и машиностроения напрямую зависит от разработки новых металлических материалов и передовых технологий. Проблема создания материалов и их видов обработки для повышения уровня эксплуатационных свойств, является актуальной в связи с усложнением и ужесточением условий труда современных технологий. Одной из важнейших задач современной авиации является повышение эксплуатационных свойств поверхностного слоя. Цель статьи является исследование влияние высокопоточных электронных пучков микросекундной длительности на изменения поверхностных слоев термостойкого многокомпонентного ионно-плазменного покрытия Ni-Cr-Al-Y в различных условиях. Были проведены исследования структурно-фазового состояния цилиндрических образцов из жаропрочного никелевого сплава ZhS36 с нанесенным ионно-плазменным конденсированным многокомпонентным покрытием SDP-2 + VSDP-16 как с последующей модификацией с использованием высокопоточных электронных пучков по различным режимам облучения, так и без модификации. Было обнаружено, что хром в исходном состоянии распределен неравномерно: хром присутствует в частицах, матрица обеднена хромом. Результаты исследования могут быть полезными для ученых, исследующих свойства термостойкого многокомпонентного ионно-плазменного покрытия Ni-Cr-Al-Y и влияние высокопоточных электронных пучков на него, а также для изготовления более термостойких материалов в аэрокосмической технике и машиностроении.

Keywords: *высокопоточное электронно-лучевое облучение, конденсированные ионно-плазменные покрытия, структурно-фазовое состояние, исследование микроструктуры.*

1. INTRODUCTION:

The development of aerospace engineering, including aviation weapons, as well as other branches of engineering, is mostly provided by the development of new metal materials and advanced technologies (Kablova, 2006; Terentyev *et al.*, 2012; Galoyan *et al.*, 2014; Muboyajyan and Budinovsky, 2017; Nesterov, 2018). With ever-increasing complication and toughening of working conditions of modern technology, the problem of creating materials and their processing types, which along with high

strength, increase the level of performance properties has become extremely urgent (Tishkov and Firsanov, 2011; Baranov *et al.*, 2007; Kimura *et al.*, 2016; Abraimov, 2017; Korsmik *et al.*, 2018; Bogdan *et al.*, 2019). It is known that the most loaded and expensive parts and assemblies are parts and assemblies of gas turbine flow path (first of all, the blades and disks of the compressor and turbine), thus, increasing the operational properties of the surface layer has become the most important task of modern aircraft manufacturing (Voyevodin *et al.*, 2017; Yurishcheva *et al.*, 2018; Sapozhkov and

Burakova, 2018; Rechenko *et al.*, 2019; Imashuku and Wagatsuma, 2019; Tarellyk *et al.*, 2019).

The solution to this problem is attempted using several approaches: development of promising, highly alloyed, polycrystalline and single crystal alloys; modernization of methods for manufacture, molding, and processing of products and blanks; development of new ways of surface treatment of parts and applying various protective coatings to their surface, including coatings from nanomaterials (Muboyajyan *et al.*, 2012; Matveev *et al.*, 2013; Ovchinnikov and Yakimov, 2016; Gadlov *et al.*, 2017; Shaidurova *et al.*, 2017; Buckhurst and Kaspersen, 2017; Batsikadze *et al.*, 2017). Besides, intensive research is being performed on the creation of all-metal discs with blades, and these technologies have already found widespread application at leading enterprises in the aviation industry, both in several European countries and in the USA.

At present, special attention is paid to the development of high-intensity methods of surface engineering of engineering parts of a fairly wide range, as well as their extremely rapid implementation of technological processes created on their basis in the industry. One of the demanded tools for surface engineering can be using high-current pulsed electron beams (HCPEB) of microsecond duration to modify the surface and near-surface layers of parts (Novikov *et al.*, 2010; Uglov *et al.*, 2011; Shulov *et al.*, 2012; Gromov *et al.*, 2013; Shulov *et al.*, 2014; Shulov *et al.*, 2015). The study of the effect of HCPEB irradiation on the surface of the layers of the heat-resistant multicomponent ion-plasma coating Ni-Cr-Al-Y under various conditions, as well as the analysis of structural-phase changes occurring upon modification, were the objectives of this work. Also, cylindrical target samples of heat-resistant nickel alloy ZhS36 coated with ion-plasma condensed multicomponent coating SDP-2 + VSDP-16 were the objects of research.

2. MATERIALS AND METHODS:

Cylindrical target samples of heat-resistant nickel alloy ZhS36 coated with ion-plasma condensed multicomponent coating SDP-2 + VSDP-16 were used with serial technology as with subsequent modification using high-current electron beams (samples under conv. No. 3 and No. 4), and without modification (about samples per conv. No. 1) (Paykin *et al.*, 2008; Bytsenko *et al.*, 2015; Bytsenko *et al.*, 2017a). Then, irradiation was carried out on a unique complex automated electron-beam installation "RITM-SP" in 9 modes

with electron energies in the range from 20 to 25 keV, namely 20, 22 and 25 keV with the number of pulses 5, 10 and 20, respectively each value of the electron energy, followed by stabilizing heat treatment (Hsu *et al.*, 2016; Kudryashov *et al.*, 2016; Shmorgun *et al.*, 2016; Tarasenko *et al.*, 2016; Shmorgun *et al.*, 2017a; Min *et al.*, 2017; Shmorgun *et al.*, 2017b; Sinitsyn *et al.*, 2017; Fähsing *et al.*, 2017; Zakirov *et al.*, 2017; Kozyr *et al.*, 2018; Blinkov *et al.*, 2018; Rechenko *et al.*, 2018; Kashapova *et al.*, 2018; Guchenko *et al.*, 2019).

Complex research of the physicochemical and structural phase states was carried out using the following methods (Bytsenko *et al.*, 2016; Bytsenko *et al.*, 2017b): X-ray diffraction analysis to determine the level of residual stresses and phase composition of surface layers on Rigaku D / MAX-2500 diffractometer. The diffraction patterns were registered in monochromatized Cu K alpha radiation in the Bragg-Brentano geometry. The scanning range in the range of angles 2θ 10 degrees - was 100 degrees. The diffraction patterns were decoded using the specialized Jade 5 program and the PDF-2 database. The work was carried out following MM 1.595-17-222-2004. The calculation of residual stress values was performed according to the $\sin^2\psi$ method. Stresses were determined automatically according to 10 values of the angle ψ in the range of angles from 0 degrees to 40 degrees from angular position by approximating the function of Gauss; study of the surface condition using laser confocal microscope LEXT OLS 3100 with subsequent processing of the obtained images using software; raster electron microscopy. This research method was performed using VERIOS 460 scanning electron microscope with an X-MAX 80 energy dispersive X-ray microanalyzer, quantitative X-ray micro spectral analysis (MRSA) to determine the local quantitative and qualitative composition of the material of the surface and subsurface layers before and after modification using HCPEB.

3. RESULTS AND DISCUSSION:

After modifying the target surface according to the selected modes during visual inspection, it was established that, depending on the irradiation mode, the samples have different surface: with high electron energy and a large number of pulses, the surface is shiny, when irradiated with lower-energy electrons and with fewer vibrations, the surface of the samples matte.

An analysis of the microstructure of the

coating after surface modification (by optical microscopy) revealed the presence of a large number of chips of the modified layer when the surface was irradiated with electrons with an energy of 25 keV, regardless of the number of pulses. The thickness of the modified layer increases with an increasing number of pulses: at 5 pulses, the thickness of the modified layer is $\sim 5 \mu\text{m}$; at 20 pulses, it is $\sim 10 \mu\text{m}$. When the surface is irradiated with electrons with energies of 22 and 20 keV, shearing of the modified layer occurs at number of pulses of 20. The thickness of the modified layer at 22 keV was $\sim 10 \mu\text{m}$, at 20 keV - $\sim 5 \mu\text{m}$. When the electron energy was 22 keV and 20 keV and the number of pulses was 10, the modified layer had a thickness of about $5 \mu\text{m}$. At the number of pulses 5, the modified layer has thickness of less than $5 \mu\text{m}$, and at an electron energy of 20 keV, the surface was altered by fragments (there were areas, especially in depressions on the surface of samples where there was no layer). Based on performed studies, the mode was chosen: electron energy - 20 keV, and several pulses was 10.

The study of the surface of samples after irradiation using a laser confocal microscope showed a significant decrease in surface roughness of the samples compared to the original samples (without modification). It should be mentioned that for the selected irradiation mode and final heat treatment, only single cracks were observed, i.e., this mode is optimal and allows to level technological defects during coating that was present on the original samples (the presence of droplet phase, pores, etc.) Figure 1). To assess microstructure on samples of ZhS32 single-crystal alloy with multicomponent coating SDP2 + VSDP16 before and after obtaining high-current beams (HCPEV), the level of residual stresses was estimated. To establish a phase composition of both the initial coating and the modified coating, a qualitative phase analysis was performed using x-ray diffraction analysis.

In the diffractogram of the sample (conv. No. 1) with the initial coating, the main phase is the β phase (NiAl) of cubic modification with a lattice period $a = 0.286 \text{ nm}$. The second phase of gamma-prim (Ni_3Al) with a lattice period $a = 0.357 \text{ nm}$ and chromium carbide Cr_{23}C_6 . Also, the diffraction pattern contains chromium carbide (Cr_3C_2), the intensity of diffraction lines of this phase is weak and traces of tungsten oxide (WO) (Figure 2). From the diffractogram of the irradiated sample (conv. No. 3), it can be seen that the main phase is the β phase (NiAl) with a lattice period $a = 0.286 \text{ nm}$. There are also weak diffraction lines in

insufficient numbers for unambiguous identification (Figure 3a). The diffraction pattern of another irradiated sample (conv. No. 4) contains the β phase (NiAl) with a lattice period $a = 0.286 \text{ nm}$ and weak diffraction lines of γ 'phase (Ni_3Al) with a lattice period $a = 0.357 \text{ nm}$ and a Ni_3 phase Y (Figure 3b).

As can be seen from the data presented after irradiation, the structure of the surface layer is represented mainly by the β phase, which determines the heat resistance of the coating. Extra straining (OH) in all samples is tensile: for the specimen Conv. No. 1 - $+384 \pm 89 \text{ MPa}$, for the sample Conv. No. 3 - $+853 \pm 112 \text{ MPa}$, for the sample Conv. No. 4 - $+424 \pm 62.5 \text{ MPa}$. The level of OH in the original sample Conv. No. 1 and the irradiated sample is quite close (taking into account possible deviations), and the OH value in sample No. 3 is much higher than in the other two samples (conv. No. 1 and conv. No. 4). The presence of high level of residual tensile straining is associated with presence of defects before irradiation (the presence of a droplet phase, pores, and low cohesion of individual particles and adhesion of the coating to the substrate — in this case, the first coating layer — SDP2) acts as a substrate, as well as defects formed during irradiation of the crater and peeling of the coating due to poor adhesion of dusty coating with the substrate. The data obtained are presented in Table 1. Single cracks are observed in all coatings, which is associated with the presence of tensile stresses after treatment with high-current electron beams. The increase in electron energy and some pulses leads to an increase in the number of cracks in the coating.

The fact of the peeling of the coating after irradiation of the sample Conv. No. 3 was discovered after ultrasonic washing (petroleum ether, 10 min) immediately after irradiation. Then, a study was made of the microstructure of the coating material and X-ray spectral analysis (MRSA) of the surface-modified layer of irradiated samples, as well as samples without irradiation, using optical and scanning electron microscopy (SEM). Studies have shown that after YCPEB irradiation there was a modified layer, and it represented a slightly etched surface layer with depth of 3 to $5 \mu\text{m}$, the microstructure of which was mainly represented by beta phase, the layer was homogeneous, had no defects in the form of pores, and there were no laminations with discontinuities. When studying the microstructure of the surface layer using SEM, it was found that modified layer consists of three zones: the first is external (from 2 to $3 \mu\text{m}$), the second is

intermediate (from 0.4 to 0.6 μm) and 3rd (from 0.6-0.8 μm) - the zone of thermal influence, transitional to the bulk of the substrate (Figure 4).

The distribution of alloying elements in the coating was studied by X-ray mapping, which made it possible to determine the spatial distribution of alloying elements. Analysis of distribution maps of chemical elements demonstrates that nickel and aluminum are evenly distributed in the coating. Chromium in the initial state is unevenly distributed: chromium is present in particles; the matrix is depleted in chromium. After irradiation, the surface layer (irradiated layer) has a uniform distribution of all the above elements (Figure 5).

4. CONCLUSIONS:

The comprehensive approach to the analysis of physicochemical and structural-phase states of the material of the samples before and after irradiation with high-current pulsed electron beams using methods of analytical microscopy and x-ray diffraction analysis was implemented. X-ray diffraction analysis helped to determine the level of residual stresses and phase composition of surface layers on the Rigaku D / MAX-2500 diffractometer. Analytical microscopy was used in obtaining images to assess the local quantitative and qualitative structure of the materials. Based on the research, the optimal mode for modifying heat-resistant multicomponent condensed ion-plasma coating SDP2 + VSDP16 (the electron energy was 20 keV, the number of pulses was 10) was chosen. It was established that, when irradiated with high-current electron beams, a modified layer with a depth of up to 5 μm was obtained, consisting of three zones: external, intermediate, and heat-affected zone, which transitions into the bulk of substrate.

The dependence of the irradiation regime on the surface of the samples was found. With high electron energy and a large number of pulses, the surface is shiny; when irradiated with lower-energy electrons and fewer pulses, the surface of the samples is dull. It was concluded that the number of microcircuits of the modified layer upon irradiation of the surface by electrons and its independence on the number of pulses. The pattern was observed in the following: the thickness of the modified layer increases with increasing number of pulses. During X-ray diffraction analysis, the structure of the modified layer was found to be represented mainly by the β phase (NiAl), and there were also weak diffraction lines of γ 'phase (Ni₃Al).

Studies have shown that the presence of a high level of residual tensile stress is associated with the presence of defects before irradiation acting as a substrate, and defects formed during irradiation of the crater and peeling of the coating. It was found that the modified layer consists of three zones: external, intermediate, and heat-affected zone, which passes into the bulk of the substrate. When conducting spatial mapping on samples in the initial state (without irradiation), it was established that nickel and aluminum were evenly distributed in the coating. Chromium was unevenly distributed, it was present in the particles, and the matrix was depleted in chromium. After irradiation, the surface layer had a uniform distribution of all of the above elements.

5. ACKNOWLEDGMENTS:

The authors would like to thank the staff of the Laboratory of Metallophysical Research of the All-Russian Institute of Aviation Materials (FSUE "VIAM") E.V. Filonova, A.N. Raevskikh, N.A. Belova for conducting microstructural research. The scientific work was performed with the financial support of the Russian Federal Property Fund (grant No. 14-08-97046 - р_поволжье_a).

6. REFERENCES:

1. Abraimov, N.V. *Protection of Metals and Physical Chemistry of Surfaces*, **2017**, 53(7), 1222–1226.
2. Baranov, N.A., Nesterov, V.A., Polyansky, V.V. *Bulletin of the Moscow Aviation Institute*, **2007**, 14(1), 13–19.
3. Batsikadze, T., Garibashvili, V., Kandelaki, A., Mikadze, G., Mikadze, O., Mirijanashvili, Z. *Bulletin of the Georgian National Academy of Sciences*, **2017**, 11(4), 48–53.
4. Blinkov, I.V., Volkhonskii, A.O., Chernogor, A.V., Sergevnin, V.S., Belov, D.S., Polyanskii, A.M. *Inorganic Materials*, **2018**, 54(5), 437–445.
5. Bogdan, M., Błachnio, J., Spychała, J., Zasada, D. *Engineering Failure Analysis*, **2019**, 105, 337–346.
6. Buckhurst, M., Kaspersen, S.J. *Corrosion and Prevention*, **2017**, Sydney, Australia, Code 134213.
7. Bytsenko, O.A., Filonova, E.V., Markov, A.B. *News of Materials Science. Science*

and Technology, **2017a**, 2(26), 9.

8. Bytsenko, O.A., Filonova, E.V., Markov, A.B., Belova, N.A. *11th International Conference "Interaction of Radiation with Solids", Minsk, Belarus, 2015*, 194–195. <http://elib.bsu.by/handle/123456789/120259>.
9. Bytsenko, O.A., Filonova, E.V., Markov, A.B., Belova, N.A. *Electronic Journal*, **2016**, 6(42), Article 10. <http://viam-works.ru>.
10. Bytsenko, O.A., Grigorenko, V.B., Lukina, E.A., Morozova, L.V. *Aviation Materials and Technologies*, **2017b**, S5, 498–515.
11. Fähsing, D., Rudolphi, M., Konrad, L., Galetz, M.C. *Oxidation of Metals*, **2017**, 88(1–2), 155–164.
12. Gadalog, V.N., Emel'yanov, S.G., Safonov, S.V., Vornacheva, I.V., Filonovich, A.V. *Russian Engineering Research*, **2017**, 37(9), 751–753.
13. Galoyan, A.G., Muboyadzhyan, S.A., Kashin, D.S. *Aviation Materials and Technologies*, **2014**, S5, 45–55.
14. Gromov, A.N., Shulov, V.A., Bytsenko, O.A., Teryaev, D.A., Teryaev, A.D., Engelco, V.I. *Strengthening Technologies and Coatings*, **2013**, 10(106), 23–25.
15. Guchenko, S.A., Eremin, E.N., Zavatskaya, O.N., Ch Laurinas, V., Yurov, V.M. *Journal of Physics: Conference Series*, **2019**, 1260(6), 062009.
16. Hsu, W.-L., Murakami, H., Yeh, J.-W., Yeh, A.-C., Shimoda, K.A. *Journal of the Electrochemical Society*, **2016**, 163(13), C752–C758.
17. Imashuku, S., Wagatsuma, K. *Corrosion Science*, **2019**, 154, 226–230.
18. Kablova, E.N. (Ed.). *Cast blades of gas turbine engines (alloys, technology, coatings)*. Moscow: Nauka, **2006**.
19. Kashapova, R.S., Lyadov, N.M., Kashapov, R.N., Kashapov, L.N., Kashapov, N.F., Faizrahmanov, I.A. *IOP Conference Series: Materials Science and Engineering*, **2018**, 412(1), 012008.
20. Kimura, T., Sawa, T., Kamijyo, T. *Materials Science Forum*, **2016**, 874, 439–444.
21. Korsmik, R.S., Turichin, G.A., Klimova-Korsmik, O.G., Alekseeva, E.V., Novikov, R.S. *Journal of Physics: Conference Series*, **2018**, 1109(1), 012023.
22. Kozyr, A.V., Konevtsov, L.A., Kononov, S.V., Kovalenko, S.V., Ivashenko, V.I. *Letters on Materials*, **2018**, 8(2), 140–145.
23. Kudryashov, A.E., Potanin, A.Y., Lebedev, D.N., Sukhorukova, I.V., Shtansky, D.V., Levashov, E.A. *Surface and Coatings Technology*, **2016**, 285, 278–288.
24. Matveev, P.V., Budinovskiy, S.A., Muboyadzhyan, S.A., Kosmin, A.A. *Aviation Materials and Technologies*, **2013**, 2, 12–15.
25. Min, P.G., Sidorov, V.V., Budinovskiy, S.A., Vadeyev, V.E. *Inorganic Materials: Applied Research*, **2017**, 8(1), 90–93.
26. Muboyajyan, S.A., Aleksandrov, D.A., Gorlov, D.S., Egorova, L.P., Bulavintseva, E.E. *Aviation Materials and Technologies*, **2012**, S1, 71–81.
27. Muboyajyan, S.A., Budinovskiy, S.A. *Aviation Materials and Technologies*, **2017**, 7, 39–54.
28. Nesterov, V.A. "XLIV Gagarin Science Conference": materials of the conference. Moscow Aviation Institute, Moscow, **2018**.
29. Novikov, A.S., Paykin, A.G., Shulov, V.A., Bytsenko, O.A., Teryaev, D.A., Teryaev, A.D., Engelco, V.I., Tkachenko, K.I. *Strengthening Technologies and Coatings*, **2010**, 3, 34–38.
30. Ovchinnikov, V.A., Yakimov, A.S. *High Temperature*, **2016**, 54(6), 851–857.
31. Paykin, A.G., Krainikov, A.V., Shulov, V.A. *Physics and Chemistry of Materials Processing*, **2008**, 3, 56–60.
32. Rechenko, D.S., Gritsenko, B.P., Popov, A.Y., Balova, D.G. *Journal of Physics: Conference Series*, **2018**, 1050(1), 012067.
33. Rechenko, D.S., Popov, A.Y., Titov, Y.V., Balova, D.G., Gritsenko, B.P. *Journal of Physics: Conference Series*, **2019**, 1260(6), 062020.
34. Sapozhkov, S.B., Burakova, E.M. *IOP Conference Series: Materials Science and Engineering*, **2018**, 441(1), 012042.
35. Shaidurova, G.I., Vasilyev, I.L., Shevyakov, Y.S. *Key Engineering Materials*, **2017**, 743, 135–137.
36. Shmorgun, V.G., Bogdanov, A.I., Taube,

- A.O., Novikov, R.E. *Solid State Phenomena*, **2017a**, 265, 211–214.
37. Shmorgun, V.G., Iskhakova, L.D., Bogdanov, A.I., Taube, A.O. *Metallurgist*, **2017b**, 60(9–10), 1113–1119.
 38. Shmorgun, V.G., Trykov, Y.P., Bogdanov, A.I., Taube, A.O. *IOP Conference Series: Materials Science and Engineering*, **2016**, 116(1), 012018.
 39. Shulov, V.A., Engelko, V.I., Gromov, A.N., Teryaev, D.A., Bytsenko, O.A., Shirvanyants, G.G. *News of Higher Educational Institutions. Powder Metallurgy and Functional Coatings*, **2014**, 1, 43–49.
 40. Shulov, V.A., Engelko, V.I., Gromov, A.N., Teryaev, D.A., Bytsenko, O.A., Shirvanyants, G.G. *Russian Journal of Non-Ferrous Metals*, **2015**, 56(3), 333–338.
 41. Shulov, V.A., Roditelev, V.I., Bytsenko, O.A. *News of Higher Educational Institutions. Physics*, **2012**, 12(3), 245–247.
 42. Sinitsyn, D.Y., Anikin, V.N., Eremin, S.A., Yudin, A.G. *Refractories and Industrial Ceramics*, **2017**, 58(2), 194–201.
 43. Tarasenko, Y.P., Tsareva, I.N., Berdnik, O.B., Fel', Y.A., Krivina, L.A. *Journal of Machinery Manufacture and Reliability*, **2016**, 45(3), 252–257.
 44. Tarel'nyk, V., Konoplianchenko, I., Martsynkovskyy, V., Zhukov, A., Kurp, P. Comparative tribological tests for face impulse seals sliding surfaces formed by various methods. In: V. Ivanov, Y. Rong, J. Trojanowska, J. Venus, O. Liaposhchenko, J. Zajac, I. Pavlenko, M. Edl, D. Perakovic (Eds.), *Advances in design, simulation and manufacturing. DSMIE 2018* (pp. 382–391). Springer: Cham, **2019**.
 45. Terentyev, V.V., Ionov, A.V., Bolkhovitin, M.S. *Russian Engineer*, **2012**, 5, 44–47.
 46. Tishkov, V.V., Firsanov, V.V. *Bulletin of Tula State University: Engineering*, **2011**, 5–1, 261–266.
 47. Uglov, V.V., Koval, N.N., Kuleshov, A.K., Ivanov, Yu.F., Teresov, A.D., Soldatenko, E.A. *X-ray, Synchrotron and Neutron Studies*, **2011**, 4, 50–58.
 48. Voyevodin, V.M., Zmii, V.I., Rudenkyi, S.G. *Powder Metallurgy and Metal Ceramics*, **2017**, 56(3–4), 198–209.
 49. Yurishcheva, A., Astapov, A., Lifanov, I., Rabinskiy, L. *Key Engineering Materials*, **2018**, 771, 103–117.
 50. Zakirov, I.F., Zhirenkina, N.V., Mustaeva, I.A., Obabkov, N.V., Pashkov, L.S., Yurin, D.V. *AIP Conference Proceedings*, **2017**, 1886, 020046.

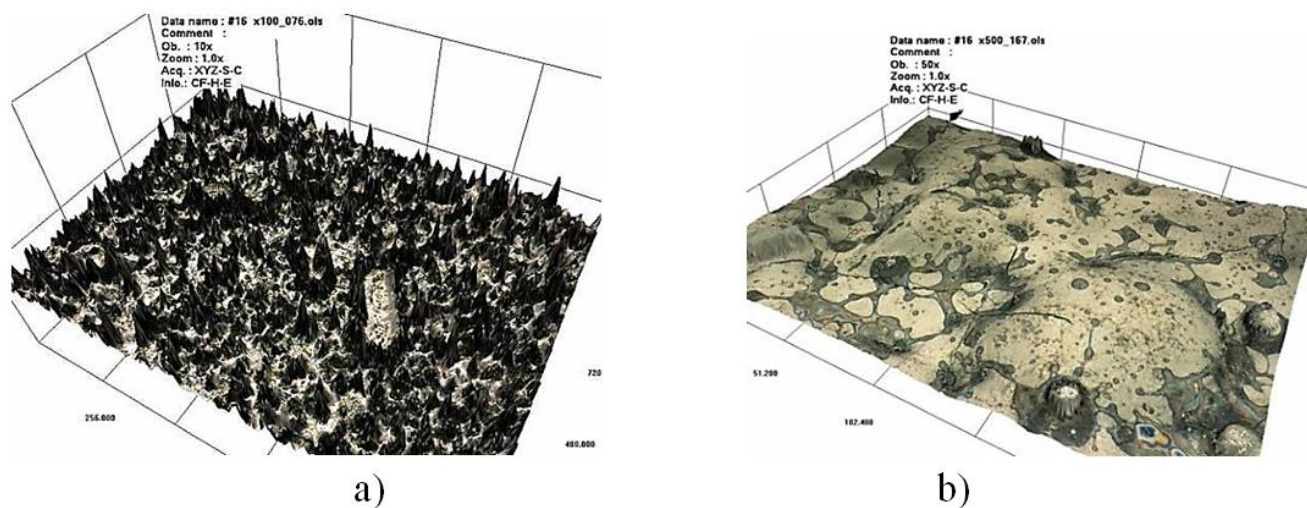


Figure 1. The surface of the samples coated with SDP 2 + VSDP 16: a) - the original sample conv. No. 1; b) the sample after irradiation conv. No. 3

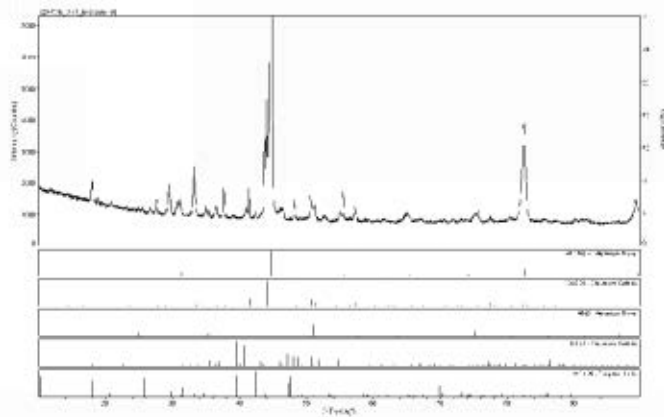


Figure 2. Diffraction spectrum and stroke - diagram of initial sample No. 1

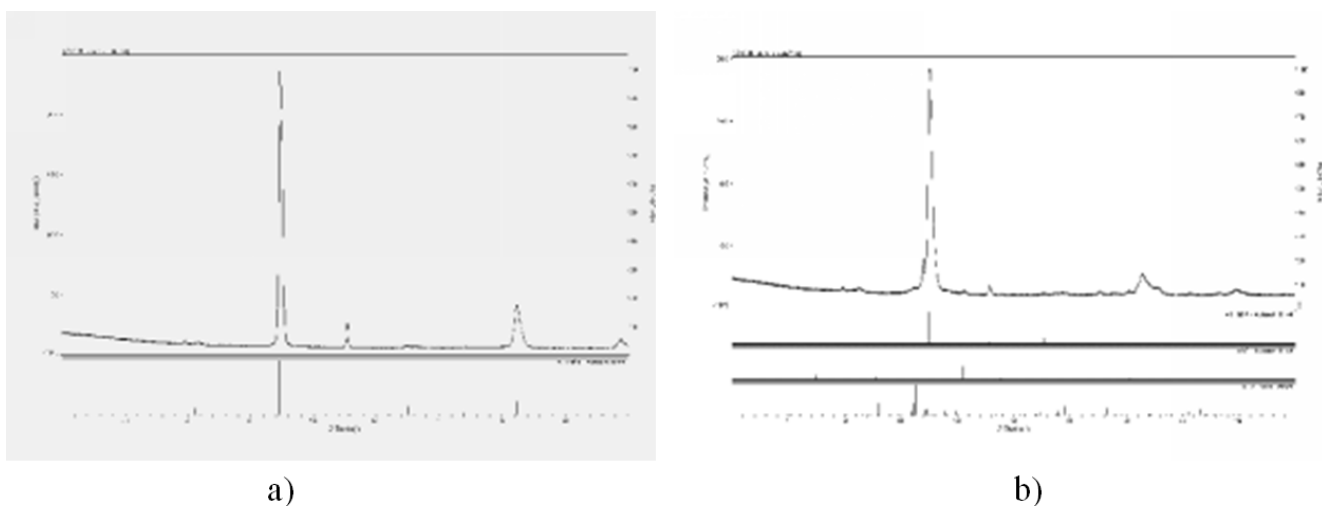


Figure 3. Diffraction spectra and bar charts of irradiated samples with SDP2 + VSDP16 coating, irradiation mode $E = 20$ keV, number of pulses 10: a) sample conv. No. 3 and b) sample conv. No. 4

Table 1. Results of measuring residual stresses in the samples before and after irradiation

No.	Conventional sample number	condition	The value of residual stresses level, MPa
1	1	Initial state	+384 ± 89
2	3	After irradiation according to E = 20 keV mode, number of pulses 10	+853 ± 112
3	4	After irradiation according to E = 20 keV mode, number of pulses 10	+424 ± 62.5

AVALIAÇÃO EXPRESSA DO MECANISMO DE SORÇÃO EM MATERIAIS QUE CONTÊM TURFA

EXPRESS EVALUATION OF SORPTION MECHANISM ON PEAT CONTAINING MATERIALS

GEVORGYAN, Silva A.^{1*}; HAYRAPETYAN, Sergey S.²; HAYRAPETYAN, Martin S.³; KHACHATRYAN, Hambardzum G.⁴^{1,2,3,4} Yerevan State University, Armenia

* Correspondence author

e-mail: gevorgyan.ysu@mail.ru

Received 10 February 2020; received in revised form 26 February 2020; accepted 13 March 2020

RESUMO

A turfa é um sorvente eficaz de metais pesados devido à sua alta capacidade de troca catiônica. O uso de sorventes de turfa tem muitas vantagens. É um adsorvente barato, acessível e eficaz para uma ampla gama de poluentes ambientais. Além disso, pode ser usado separadamente ou como um absorvente combinado e constituintes complexos; no entanto, também possui várias desvantagens, como resistência mecânica insuficiente e baixa estabilidade química das partículas de turfa. Para superar essas deficiências, vários métodos de modificação de turfa foram desenvolvidos (por exemplo, turfa modificada com quitosana, que é usada como um absorvente para remoção de metais pesados, como turfa). As propriedades de sorção por troca iônica de sorventes a base de turfa e turfa modificada com quitosana foram avaliadas pelo método do medidor de pH. Uma amostra de turfa ativada por ácido também foi investigada. Os experimentos foram realizados em modo estático, utilizando amostras de turfa natural colhidas no lago Sevan (próximo à cidade de Vardenis, na região de Gegharkunik, na República da Armênia). Também foi realizado um estudo semelhante sobre a resina de troca catiônica KU-2-8. O objetivo deste artigo foi a avaliação expressa do mecanismo de sorção de sorventes de turfa. O trocador de cátions foi transferido para a forma H^+ por tratamento com HCl (1N). Alterações no perfil de pH em função do tempo de exposição indicam sua identidade com o padrão da alteração de pH do trocador de cátions. Verificou-se que a ativação ácida da turfa (exposição de uma amostra de turfa em HCl 1N por 10-16 horas) aumenta sua capacidade de adsorção. Nesse caso, a diminuição máxima no pH é pH = 2,33, 1,44 pontos mais baixo que na turfa (pH = 3,77) e 0,95 pontos mais que no cationita KU-2-8. Isso indica que os sorventes à base de turfa podem ser regenerados. A turfa modificada com quitosana apresentou deterioração na capacidade de sorção. Nesse caso, pH min = 3,9, o que mostra que a sorção na quitosana não é de troca iônica por natureza.

Palavras-chave: turfa, trocador de cátions, sorvente, sorção, mecanismo de sorção.

ABSTRACT

Peat is an effective sorbent of heavy metals, which is due to its high cation-exchange ability. The use of peat sorbents has many advantages. It is an inexpensive, affordable, and effective sorbent for a wide range of environmental pollutants. Also, it can be used either separately or as a combined sorbent and complex constituents; however, it also has several disadvantages, such as insufficient mechanical strength and low chemical stability of peat particles. To overcome these shortcomings, various methods of peat modification have been developed (e.g., peat modified with chitosan, which is used as a sorbent for heavy metals removal like peat). The ion-exchange sorption properties of sorbents on the base of peat and chitosan - modified peat were evaluated by the method of pH meter. An acid-activated peat sample was also investigated. The experiments were carried out in a static mode using natural peat samples taken from the Lake Sevan (near the city of Vardenis of the Gegharkunik region of the Republic of Armenia). Also, a similar study was conducted on KU-2-8 cation exchange resin. The purpose of this article was the express evaluation of the sorption mechanism of peat sorbents. Cation exchanger was transferred to the H^+ form by treatment with HCl (1N). Changes in the pH profile as a function of the exposure time indicate their identity with the pattern of the pH change of the cation exchanger. It was found that acid activation of peat (exposure of a peat sample in HCl 1N for 10-16 hours) increases its adsorption capacity. In this case, the maximum decrease in pH is pH = 2.33, which is 1.44 points lower than for peat (pH = 3.77) and 0.95 points more than for KU-2-8 cationite. This indicates that sorbents based on peat can be regenerated. Chitosan-modified peat exhibits deterioration in sorption capacity. In this case, pHmin = 3.9, which shows that sorption on chitosan is not ion-exchange in nature.

1. INTRODUCTION:

The use of sorbents based on waste and natural materials is a very urgent problem and is of great interest since resource-saving and environmental protection are priority directions in modern science and technology, and the use of waste on an industrial scale is economically valuable (Imaga, Abia, 2015a; Imaga, Abia, 2015b; Ezuma, 2014; Cheng, Yu, Wang, Chen, Guo, 2014).

The effectiveness of the sorbent depends on the presence of a well-developed surface and the presence of active sites on this surface. The efficiency of the adsorption process depends not only on the amount of sorbent but also on the chemical nature of its surface, the presence of one or another type of active centers on the surface (Klimov, Buzaeva, 2011, p. 22-25; Novoselova, Sirotkina, 2008a, p. 251; Lishtvan, Dudarchik, Kovrik, Smychnik, 2007, p. 38-42).

Among the disadvantages of natural materials and wastes used as a source material for the sorption materials, is their heterogeneity not only from a structural point of view but also their surface. As a rule, such materials have different functional surface groups, which ultimately determine the sorption properties of sorbents derived from them. Characterize these groups becomes relevant to understand the sorption mechanism of such systems better. Therefore, the purpose of this article is to develop express and cheap methods for determining the sorption mechanism of sorption materials obtained based on peat (Cochrane, Lu, Gibb, Villaescusa, 2006, p. 198; Novoselova, Sirotkina 2008b, p. 64-77; Kalmykova, Stromvall, Steenari 2008, p. 885).

The presence of peat in the composition of a large number of biologically active compounds and many reactive functional groups causes a growing interest in the development of peat sorbents (Lyngsie, Borggaard, Hansen, 2014; Sen Gupta, Curran, Hasan, Ghosh, 2009, p. 954).

Adsorption is an effective method for removing metal ions from contaminated water. Organic components of peat, in particular humic substances, are primarily responsible for providing active adsorption sites on which various mechanisms bound metals. It is believed that the adsorption of metal on peat occurs through a combination of physical adsorption, ion exchange and complexation (Dada, Adekola, Odebunmi,

2017; Fernandes, Almeida, Menezes, Debacher, Sierra 2007, p. 412–419; Sieczka, Koda, 2016; Poznyak, Shimanskaya, 2012).

Among organo-mineral compounds, the most complex is the complex compounds called chelates. Chelation is considered as an equilibrium reaction between metal ions and functional groups of an organic molecule, in which more than one bond forms between the components (Semendyaeva, Marmulev, Dobrotvorskaya, 2011; Hayrapetyan, Gevorgyan, Hayrapetyan, Bareghamyan, Pirumyan, 2016; Batista *et al.*, 2009; Lishtvan, Dudarchik, Kovrik, Smychnik, 2007).

The adsorption complexes of organic substances with the mineral part of peat can be divided into two types: organic films on minerals, resulting from the adsorption of humic substances, insoluble complexes of humic substances with non-silicate forms of sesquicrate oxides (Fe_2O_3 , Al_2O_3). In the formation of insoluble products, the primary mechanism is the adsorption of humic substances. The creation of complexes from mineral colloids and humic substances is possible due to the interaction through cations, primarily through iron ions (Hayrapetyan *et al.*, 2016; McLaughlin, Bartholomew, 2007).

It is believed that the primary mechanism of peat sorption is ion-exchange; however, because on the surface of peat, there are many other functional groups (alcohol, aldehyde, carboxyl, ketone, and phenolic) peat also has pronounced complexing properties. Therefore, along with ion exchange, their complexation is added, as a result of which a high degree of sorption is observed (Gondar, Lopez, Fiol, Antelo, Arce, 2005; McLaughlin, Bartholomew, 2007; Lee, Park, Ahn, Chung, 2015; Sen Gupta, Curran, Hasan, Ghosh, 2009).

This hypothesis is based on the functional groups that exist on the humic acid molecule. However, there are no experimental methods that support this hypothesis. The goal of this article was to confirm this statement empirically.

2. MATERIALS AND METHODS:

The choice of pH-meter as a way to study the processes of ion exchange during the contact of the electrolyte with the test materials is dictated, firstly, because the procedure for measuring pH is effortless and very inexpensive, and secondly, ion

exchange is always accompanied by a change in the pH of the medium. The recording of such changes lies at the heart of the methodology of the experiment.

As a criterion, we selected the study of changes in the pH of the model solution in the presence of a robust cation-exchange resin (KU-2-8). The use of cation exchanger serves as a standard for comparing the results obtained.

As a model solution using a 0.1N solution of NaCl. 1 g of peat is placed in different flasks, and 20, 50, 100, 200, 500 ml of the model solution are added, respectively. The pH of the first solution was measured at the initial time, and then after 10, 20, 30, 60, and 1440 minutes. Similar procedures are carried out with peat treated with 1N HCl solution, and with peat modified with chitosan.

The pH value of 0.1 N NaCl and the initial peat is, respectively; pH (0.1 N NaCl) = 5.85, pH (peat) = 4.17.

Samples of peat are dried in a dryer at a temperature of 1050°C to constant weight, then, after grinding, fractionated, passed through sieves.

Activation with hydrochloric acid: a solution of 1N HCl was prepared, added to the sample, and kept for 24 hours. They were then washed with distilled water until neutral pH and air-dried in a dryer at 1050°C.

Peat modification was carried out according to the procedure given in the work by Gevorgyan and Hayrapetyan (2017).

Initially, peat was dried at room temperature. 90 ml of chitosan solution in citric acid (3 g / l) was added to the mass of peat (about 100 g) and dried at room temperature; the pH of the sorbent was 6-7.

To prevent the humates from leaching, an NH_4OH solution with pH = 8–9 was prepared, and 100 ml of the solution was added to a peat-chitosan sorbent (pH = 8–9): the sorbent was dried at room temperature. A solution consisting of 50 ml of water and 15 ml of formaldehyde was added to the peat-chitosan sorbent and left for 2 hours, and then washed with 1000 ml of distilled water, dried in air, then in a dryer at a temperature of 1050°C.

3. RESULTS AND DISCUSSION:

Based on the results, in Figure 1, a curve of pH change depending on the volume of 0.1 N NaCl and the duration of exposure of a suspension

of natural peat in the amount of one gram are plotted.

From Figure 1, it follows that with the addition of 20 ml of the model solution, a relatively sharp decrease in pH is observed (from 5.85 to 3.77-4.17). And with an increase in the exposure time, the first minimum pH value changes from (from 4.17 to 3.77), which is natural; since it takes some time to reach an equilibrium state. In Figure 1, curve of zero exposure in the range from 10 ml to 30 ml gives a loop. The remaining curves with different exposure times do not differ significantly. For greater clarity, Table 1 shows the data based on which the above curves were constructed.

Figure 2 shows the profile of pH change depending on the volume of 0.1 n NaCl suspensions of natural peat, as well as cation exchanger KU-2-8. In contrast to the above experiments, pH values were measured immediately after each addition of a 0.1N NaCl solution at zero exposure. From Figure 2 that after the addition of 10 ml of solution, a decrease in pH is observed (from 5.85 to 3.8) in the case of peat and with an increase in the volume of 0.1 n NaCl of the solution, a gradual increase in pH is observed. For cation, the pH reaches 1.38. It is essential to note the fact that both curves are very similar to each other, which indicates the identity of the sorption processes of Na^+ ions on both materials. The location of the second curve is almost three pH points lower, which is natural since the ion-exchange capacity of pure cation exchanger is much higher than the ion-exchange capacity of any other materials that do not have special attached functional groups (in the case of cation-exchanger-sulfo-groups).

Table 2 presents the data based on which the above curves were constructed. Besides, pH data is shown depending on the time of exposure of the suspension.

It was a similar picture in the case of using natural peat; however, a decrease in pH to 2.5-2.75 is observed. In the case of natural peat, these values were 3.77-4.17. The difference is: $(3.77-2.5) \div (4.17-2.75) = 1.27-1.42$. This difference indicates that as a result of acid treatment, the active centers (including ion exchange) are released from the adsorbed ions of different metals, which leads to an increase in the adsorption capacity, i.e., more Na^+ ions undergo ion exchange at such centers, as a result of which the model solution becomes more acidic because the number of H^+ ions in the solution increases as a result of ion exchange. The next important difference in the pH profile of activated peat is that the zero curve is identical in appearance to the

others, it is only located on top of all the curves, which is natural since it is shown above that the curves with longer exposures are located lower than the curves responsible for short exposures.

The observed loop in the figures can be explained by the fact that at zero exposure, several adsorption centers do not have time to "release," which leads to the formation of such a loop.

With an increase in the exposure time (after 10 minutes), it seems that as a result of Na^+ competition, these centers are already free, and the ion exchange process proceeds smoothly.

Figure 3 shows the profile of the pH change depending on the volume of the suspension of acid-activated peat in 0.1 N NaCl solutions. The pH was measured directly after adding each portion of 0.1 N NaCl solutions (no exposure time). There is a decrease to pH 2, 64. A similar picture is observed in the case of the use of natural sorbent, however, while decreasing the pH to 3.8. It can be assumed that the acid treatment of peat increases the sorption capacity of the sorbent.

Compared with Figure 2, it can be stated that the curve of pH dependence on the number of the model solution as compared to the curve for acid-activated peat is intermediate between the curves for activated peat and cationite. By the way, here, the "behavior" of the curves is identical.

When comparing the ion-exchange properties of four types of samples (natural peat, acid-activated peat, peat modified by chitosan and cation exchanger KU-2-8 (Figure 4)), it follows that the pH-change profile for the cation exchanger lies below the peat sample curves, which is understandable.

What is important here is the fact that all curves are visually identical, that is. pH curve for the cation exchanger can act as a standard. This identical behavior of peat and peat-containing materials with a cation exchanger indicates that sorption on these systems has a cation exchange character.

Sorption on chitosan does not carry an ion-exchange mechanism, as compared with samples of untreated and activated peat, the pH decrease is the lowest.

There are no similar studies in the literature, although understanding the sorption mechanism is an important issue for understanding the processes in terms of the selectivity of the interaction of the adsorbate with the adsorbent. Therefore, the creation of a simple, inexpensive way to assess the mechanism of

sorption of sorbents is an important task.

The method of the experiment is reduced to comparing the profile of the change in the pH of the solution in the presence of a cation exchanger (as a standard) and the pattern of the difference in the pH of the solution in the presence of samples.

The fact that the electrolyte pH changes (0.1 N NaCl) in the presence of a cation exchanger indicates ionic exchange of Na^+ for H^+ , as a result of which H^+ accumulates in the solution, which causes a decrease in pH. There is no other explanation for the reduction of the pH of the electrolyte solution, i.e., a decrease in pH indicates ion exchange. On the other hand, when building a profile of change in the pH of the electrolyte, a clear picture of the pH depending on the amount of electrolyte is traced, i.e., the classic cation exchanger has a clearly defined pH change.

It is assumed that if the test samples also have such a pH change profile as the standard (cationite), then it can be assumed that ion exchange takes place, i.e., such systems have an ion-exchange mechanism of sorption.

Figure 5 presents the formula of humic acid. It follows from the formula that humic acid, in addition to other functional groups, also has carboxyl groups, it is assumed that these groups are responsible for ion exchange and these groups provide the cation-exchange mechanism for the sorption of peat and peat-containing materials.

It was noted above that acid activation leads to the curing of the sorption capacity of peat materials, this suggests that after removing sorbed cations from the surface of peat-containing materials as a result of acid treatment, the carboxyl groups become H^+ forms, which increases their ion-exchange capacity.

This, in turn, means that peat sorbents can be regenerated with the help of acids, which is typical of classical cation exchangers.

There is practically no research of this kind in the literature; therefore, there are no interpretations of the results in the scientific literature on this subject.

We have developed a simple method for assessing the cation-exchange mechanism of sorbents that can be used for other types of sorbents (not only peat). This method is simple, inexpensive, and express.

4. CONCLUSIONS:

A simple, inexpensive method for

evaluating the sorption mechanism of sorbents was proposed, the essence of which is reduced to the identity of the pH change profiles of these materials with the pH change profile of the cation exchanger, and since they are identical in shape, it is assumed that ion exchange takes place.

Peat materials were used as sorption systems. It was established that the treatment of peat with hydrochloric acid increases its sorption capacity, i.e., active sorption centers as a result of acid treatment are released, which leads to an increase in sorption capacity. On the other hand, after modifying the peat surface with chitosan, its sorption capacity decreases, that is, part of the active ion-exchange centers on the peat surface is screened as a result of chitosan binding on the surface. The decrease in the sorption capacity of such systems indicates that sorption on chitosan is not ion exchange in nature.

A simple, express method has been developed for assessing the ion-exchange mechanism of sorption of sorbents, which can be used to characterize not only peat materials. This method allows you to quickly evaluate the mechanism of sorption without the use of expensive instruments and reagents. Therefore, such studies can be useful and can contribute to the knowledge of the properties of sorbents.

5. REFERENCES:

1. Batista, A.P.S., Romão, L.P.C., Arguelho, M.L.P.M., Garcia, C.A.B., Alves, J.P.H., Passos, E.A., Rosa, A.H. *Journal of Hazardous Materials*, **2009**, 163(2-3), 517–523.
2. Benavente, M. *Adsorption of Metallic Ions onto Chitosan: Equilibrium and Kinetic Studies*, Stockholm, Sweden, 2008.
3. Boddu, V. M., Abburi, K., Talbott, J. L., Smith, E. D., Haasch, R. *Water Research*, **2007**, 42(3), 633-642.
4. Cao, W., Easley, C.J., Ferrance, J.P., Landers, J.P. *Anal. Chem.*, **2006**, 78, 7222-7228.
5. Cheng, D., Yu, J., Wang, T., Chen, W., Guo, P. *Polish Journal of Environmental Studies*, **2014**, 23(5), 1527-1535.
6. Cochrane, E.L., Lu, S., Gibb, S.W., Villaescusa, I. *J. Haz. Mat.*, **2006**, 137, 198-206.
7. Dada, A.O., Adekola, F.A., Odebunmi, E.O. *Cogent Chemistry*, **2017**, 3(1).
8. Dhawade, P., Jagtap, R. *Der Chemica Sinica*, **2012**, 3(3), 589-601.
9. Elmorsi, T.M., Mohamed, Z.H., Shopak, W., Ismaiel, A.M. *Journal of Environmental Protection*, **2014**, 5(17), 1667-1681.
10. El-Sayed, G. O., Mohammed T. Y., El-Sayed, O. E. *Advances in Applied Science Research*, **2011**, 2(4), 283-290.
11. Ezuma, I. *Journal of Applied Sciences and Environmental Management*, **2014**, 18(3), 443-448.
12. Fernandes, A.N., Almeida, C.A.P., Menezes, C.T.B., Debacher, N.A., Sierra, M.M.D. *J. Haz. Mat.*, **2007**, 144, 412–419.
13. Gevorgyan, S.A., Hayrapetyan, S.S. *Proceedings of the Yerevan State University: Chemical and Biological Sciences*, **2017**, 51(1), 17-20.
14. Goh, S.C., Chia, C.H., Zakaria, S., Yusoff, M., Haw, C.Y., Ahmadi, Sh., Huang, N.M., Lim, H.N. *Materials Chemistry and Physics*, **2010**, 31-35.
15. Gondar, D., Lopez, R., Fiol, S., Antelo, J. M., Arce, F. *Geoderma*, **2005**, 126(3-4), 367-374.
16. Hayrapetyan, S.S., Gevorgyan, S.A., Hayrapetyan, L.S., Bareghamyan, S.F., Pirumyan, G.P. *Chemical Journal of Armenia*, **2016**, 69(3), 257-265.
17. Imaga, C.C., Abia, A.A. *Journal of Multidisciplinary Engineering Science and Technology*, **2015a**, 2(1), 316-323.
18. Imaga, C.C., Abia, A.A. *Global Journal of Science Frontier Research: B Chemistry*, **2015b**, 15(1), 24-37.
19. Kalmykova, Y., Stromvall, A.M., Steenari, B.M. *J. Haz. Mat.*, **2008**, 152, 885-891.
20. Kalyan, S., Sharma, P. K., Garg, V. K., Kumar, N., Varshney, J. *Der Pharmacia Sinica.*, **2010**, 1(3), 195-210.
21. Klimov, Ye.S, Buzaeva, M.V. Prirodnyye sorbenty i kompleksy v ochildke stochnykh vod [Natural sorbents and complexones in wastewater treatment]. Ulyanovsk: UIGTU [Ulyanovsk State Technical University], 2011.
22. Lee, S.-J., Park, J.H., Ahn, Y.-T., Chung, J.W. *Water, Air, Soil Pollution*, **2015**, 226(2).
23. Li, F., Du, P., Chen, W., Zhang, S. S. *Anal. Chim. Acta.*, **2007**, 585, 211-218.
24. Lishtvan, I.I., Dudarchik, V.M., Kovrik, S.I., Smychnik, T.P., *Journal of Water Chemistry*

- Technology, **2007**, 29, 38-42.
25. Lyngsie, G., Borggaard, O.K., Hansen, H.C.B. *Water Research*, **2014**, 51, 256-265.
 26. McLaughlin, R.A., Bartholomew, N. *Soil Science Society of America Journal*, **2007**, 71(2), 537-544.
 27. Molvinger, K., Quignard, F., Brunel, D., Boissiere, M., Devoisselle, J.M. *Chem. Mater.*, **2004**, 16, 3367-3372.
 28. Novoselova, L. Yu., Sirotkina, E.E. *Solid Fuel Chemistry*, **2008a**, 42, 251-262.
 29. Novoselova, L., Sirotkina, E., *Chemistry of Solid Fuel*, **2008b**, 4, 64-77.
 30. Obike, A.I., Igwe, J.C., Emeruwa, C.N., Uwakwe, K.J. *Journal of Applied Sciences and Environmental Management*, **2018**, 22(2), 182 – 190.
 31. Poznyak, S.S., Shimanskaya, A.A. *Mazyrskaga dzyarzhaŭnaga pedagagichnaga ŭniversiteta [Bulletin of the Mozyr State Pedagogical University]*, **2012**, 2, 37-44.
 32. Raafat, D., Bargaen, K. V., Haas, A., Sahl, H. G. *Appl. Environ. Microb.*, **2008**, 74(12), 3764-3773.
 33. Semendyaeva, N.V., Marmulev, A.N., Dobrotvorskaya, N.I. *Methods for studying soil and soil cover: studies: Allowance*. Novosibirsk: NGAU Publishing House, 2011.
 34. Sen Gupta, B., Curran, M., Hasan, S., Ghosh, T.K. *Journal of Environmental Management*, **2009**, 90(2), 954-960.
 35. Serag, H., Edrees, G. *European Journal of Experimental Biology*, **2011**, 1(4), 87-92.
 36. Sieczka, A., Koda, E. *Applied Sciences*, **2016**, 6(10), 269.
 37. Silva, S.S., Ferreira, R.A.S., Fu, L., Carlos, L.D., Mano, J.F., Reis, R.L., Rocha, J. *J. Mater. Chem.*, **2005**, 15, 3952-3961.
 38. Stevenson, F.J. *Extraction, fractionation, and general chemical composition of soil organic matter*. In F.J. Stevenson (Ed.), *Humus Chemistry. Genesis, Composition, Reactions*. New York: John Wiley and Sons, 26-54, 1982.
 39. USA, patent 7,547,473 B32 B5/66, 2009
 40. Yeh, J.T., Chen, C.L., Huang, K.S. *Mater. Lett.*, **2007**, 61, 1292-1295.

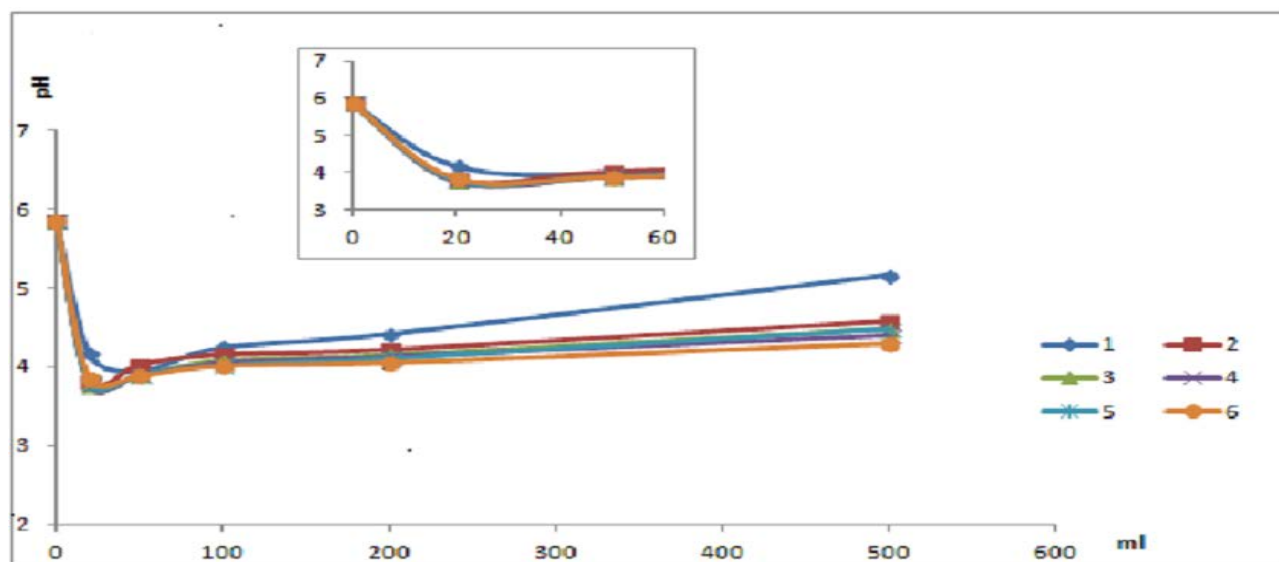


Figure 1. Profile of change in the pH of a suspension of natural peat depending on the amount of a solution of 0.1N NaCl and the time of exposure: 1 - 0 min, 2 - 10 min, 3 - 20 min, 4 - 30 min, 5 – 60 min, 6 - 24 h, amount of peat 1g

Table 1. The change in pH of the suspension of natural peat depending on the volume of the solution of 0.1 N NaCl and the exposure time.

ml	pH ₀	pH _{10minutes}	pH _{20minutes}	pH _{30minutes}	pH _{60minutes}	pH _{1440minutes}
20 ml	4.17	3.81	3.77	3.77	3.79	3.85
50 ml	3.95	4.02	3.89	3.89	3.90	3.89
100 ml	4.25	4.15	4.08	4.05	4.02	4.02
200 ml	4.42	4.21	4.15	4.13	4.11	4.06
500 ml	5.16	4.57	4.48	4.40	4.48	4.30

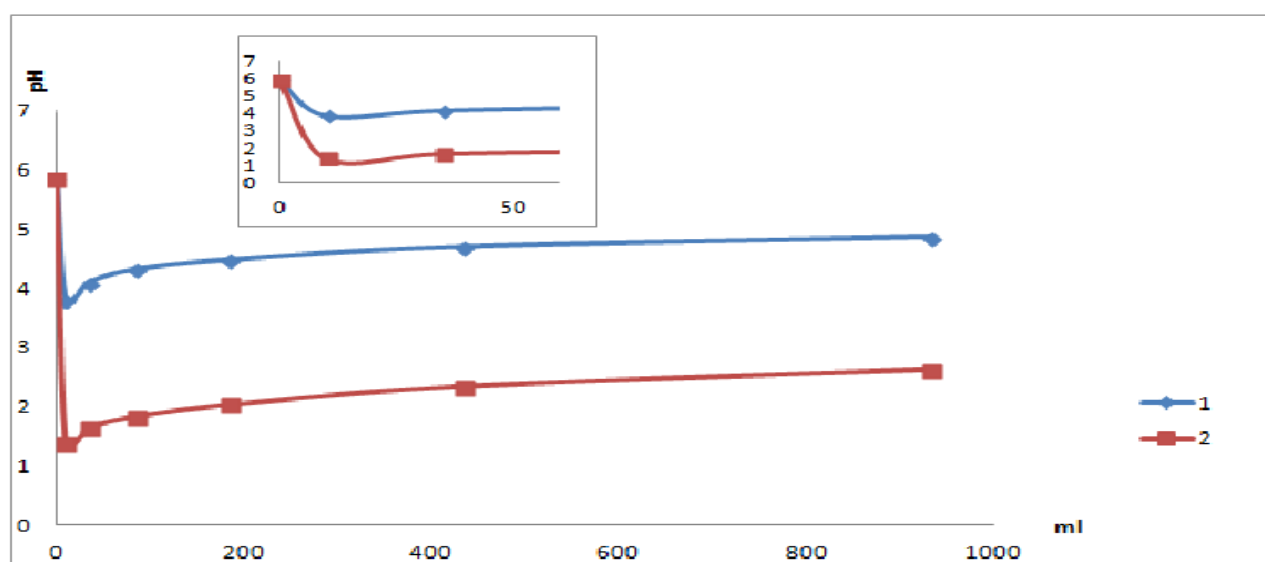


Figure 2. Profile of change in the pH of a suspension of natural peat depending on the amount of a solution of 0,1N NaCl compared to cation exchanger: 1 - Natural peat; 2 - KU-2-8 cation exchanger.

Table 2. The change in pH of the suspension of peat activated with acid depending on the volume of the solution of 0.1 N NaCl and the exposure time.

ml	pH ₀	pH _{10minutes}	pH _{20minutes}	pH _{30minutes}	pH _{60minutes}	pH _{1440minutes}
20 ml	2,75	2,50	2,33	2,48	2,47	2,51
50 ml	3,06	2,83	2,78	2,75	2,74	2,76
100 ml	3,32	3,08	2,95	2,92	2,90	2,92
200 ml	3,60	3,27	3,18	3,15	3,12	3,10
500 ml	3,82	3,57	3,49	3,45	3,43	3,41
1000 ml	4,21	3,80	3,72	3,68	3,66	3,60

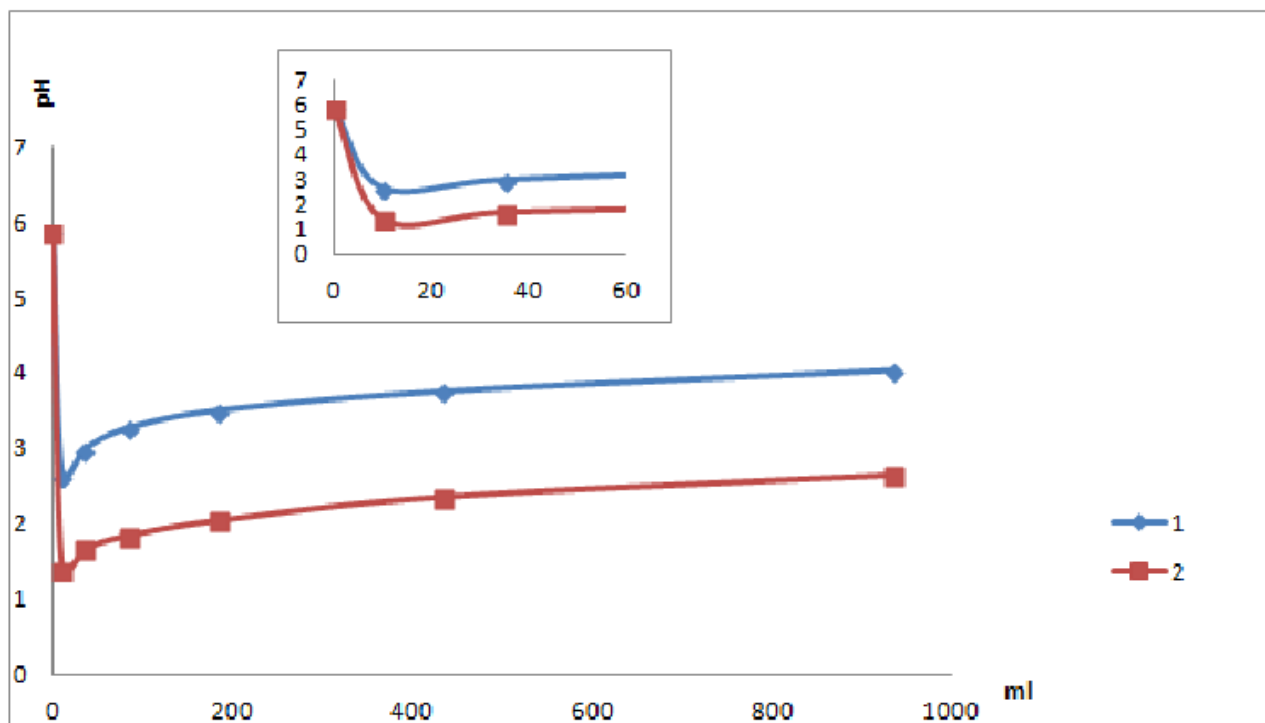


Figure 3. Profile of change in the pH of a suspension of peat activated with acid depending on the amount of a solution of 0.1N NaCl compared to cation exchanger: 1 - Natural peat; 2 - KU-2-8 cation exchanger

Table 3. The change in pH of the suspension of peat modified with chitosan depending on the volume of the solution of 0,1 N NaCl and the exposure time

ml	pH ₀	pH _{10мин}	pH _{20мин}	pH _{30мин}	pH _{60мин}	pH _{1440мин}
20 ml	4,00	3,83	3,80	3,80	3,77	3,77
50 ml	4,15	3,90	3,84	3,82	3,79	3,79
100 ml	4,33	4,14	4,11	4,08	4,06	4,06
200 ml	4,60	4,29	4,17	4,16	4,11	4,10
500 ml	4,91	4,53	4,43	4,39	4,33	4,31
1000 ml	5,13	4,73	4,64	4,59	4,54	4,54

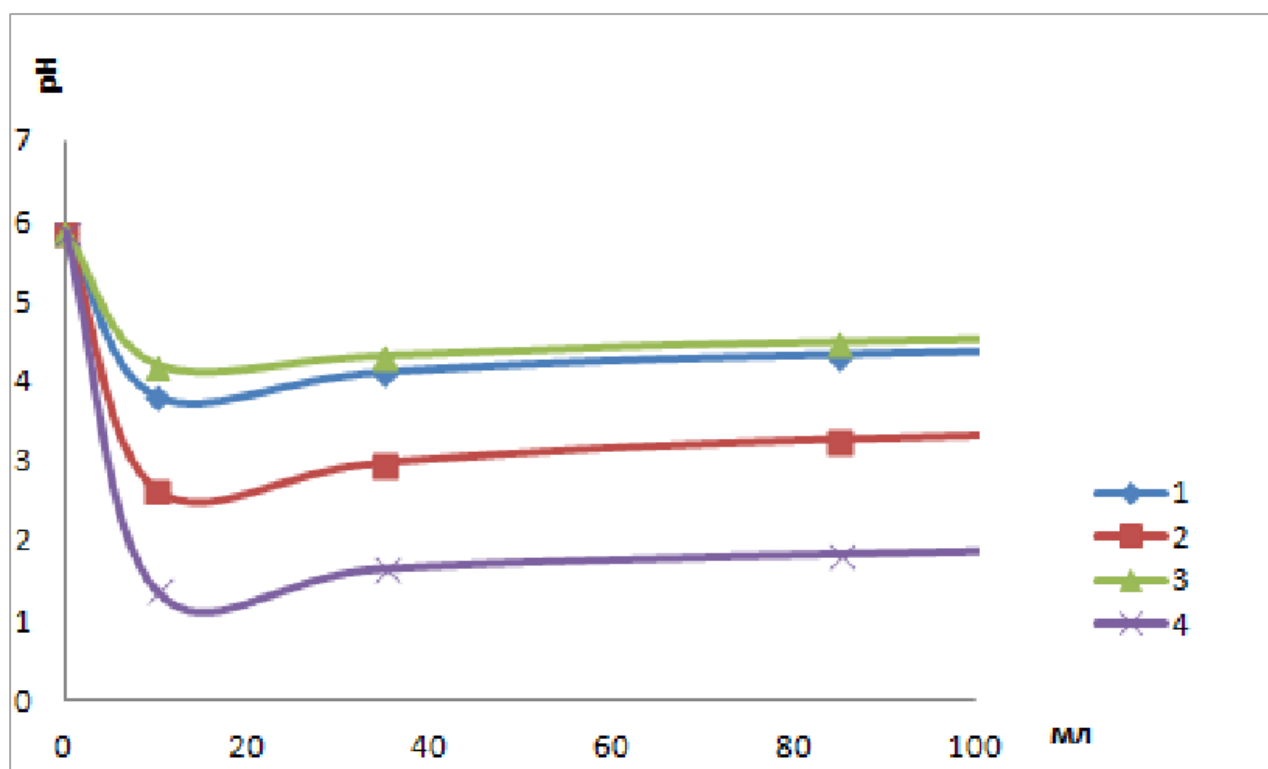


Figure 4. The profile of changes in the pH of a suspension: 1 - Natural peat; 2 - Peat activated with acid; 3 - Modified by chitosan; 4 - Cation exchanger KU-2-8

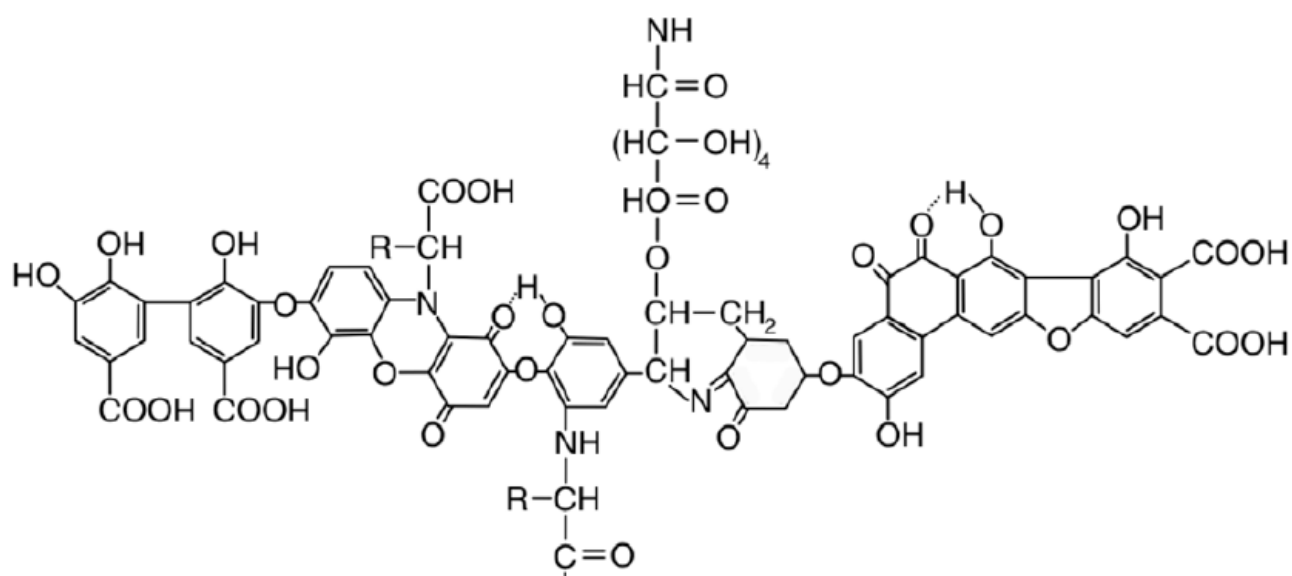


Figure 5. The formula of humic acid (Stevenson, 1982)

APOCYNIN, AN INHIBITOR OF THE NADPH OXIDASE COMPLEX

APOCININA, UM INIBIDOR DO COMPLEXO DE NADPH OXIDASE

GIONGO, Camila Nascimento ^{1*}; LOPES, Vanessa Falchetti ²; GRIGOLETTO, Diana Fortkamp ³; MIRANDA, Eduardo Hösel ⁴.

¹Midwestern Parana State University, Laboratory of Pharmaceutical Nanotechnology, Guarapuava, PR, Brazil

* Autor correspondente
e-mail: camilangiongo@gmail.com

Received 14 January 2020; received in revised form 24 February 2020; accepted 18 March 2020

RESUMO

A apocinina é um composto fenólico isolado originalmente da planta *Picrorhiza kurroa* Royle (PK). Tal composto tem sido amplamente investigado pelo seu potencial terapêutico para doenças que envolvem processos inflamatórios ou estresse oxidativo devido à sua capacidade em inibir o complexo multienzimático NADPH oxidase. Este complexo consiste em duas proteínas transmembrana (Nox2 e p22phox) e quatro proteínas citosólicas reguladoras (p67phox, p47phox, p40phox e GTPase-Rac) e sua ativação ocorre após o estímulo de células fagocíticas pela mediação da enzima mieloperoxidase (MPO). O NADPH oxidase é um complexo enzimático que produz ânion superóxido a partir de oxigênio molecular. Em vias paralelas catalisadas por enzimas, o ânion superóxido é precursor de espécies reativas de oxigênio (EROs). Essas espécies oxidantes, quando em excesso, podem atuar modificando o estado redox de moléculas de DNA, proteínas ou lipídeos desempenhando um papel central no desenvolvimento de patologias crônicas e complicações diversas de saúde como por exemplo, problemas vasculares, hiperglicemia, diabetes, hipertensão, mal de Alzheimer e câncer. Apocinina, previamente ativada por MPO, bloqueia o complexo enzimático e impede a formação dessas espécies oxidativas. Nesse sentido, a função biológica central do composto consiste em modular a ação do NADPH oxidase promovendo um efeito positivo na prevenção/remediação de doenças de caráter inflamatório.

Palavras-chave: *antioxidante; neutrófilos, mieloperoxidase, anti-inflamatório, acetovanilona.*

ABSTRACT

Apocynin (C₉H₁₀O₃) is a phenolic compound isolated from the plant *Picrorhiza kurroa* Royle ex Benth. Such a compound has been extensively investigated for its therapeutic potential in diseases involving inflammatory processes or oxidative stress due to its ability to inhibit the NADPH oxidase multienzyme complex. This complex consists of two transmembrane proteins (Nox2 and p22phox) and four cytosolic regulatory proteins (p67phox, p47phox, p40phox, and GTPase-Rac) and their activation occurs after the stimulation of phagocytic cells by the mediation of the enzyme myeloperoxidase (MPO). NADPH oxidase is the only enzyme complex that is intended for the production of superoxide anion that is precursor of highly oxidizing substances classified as reactive oxygen species (ROS). NADPH oxidase is an enzyme complex that produces superoxide anion from molecular oxygen. At the same time, the superoxide anion is a precursor to reactive oxygen species (ROS) catalyzed by enzymes. These oxidative species, when in excess, can induce burst, causing irreparable tissue damage. They can act by modifying the redox state of DNA, protein or lipid molecules, playing a central role in the development of chronic pathologies and various health complications. One can cite vascular problems, hyperglycemia, diabetes, hypertension, Alzheimer's disease, and cancer, among others. Apocynin, previously activated by MPO, blocks the enzyme complex and prevents the formation of these oxidative species. Therefore, the central biological function of compound is to modulate the action of NADPH oxidase, promoting a positive effect in the prevention/remediation of inflammatory diseases.

Keywords: *antioxidant, neutrophils, myeloperoxidase, anti-inflammatory, acetovanillone*

1. INTRODUCTION:

The plant *Picrorhiza kurroa* royle ex Benth. is traditionally used by Ayurvedic medicine (Kapahi *et al.*, 1993; Katoshi *et al.*, 2011). It is a small perennial herb that belongs to the Scrophulariaceae family (Katoshi *et al.*, 2011) and grows in the Indian trans-Himalayas and at high altitude, being a rare and endangered medicinal plant (Kala, 2000; Gangola *et al.*, 2013). Because it is a species that lives at high altitudes, oxidative stress can be one of the main limiting factors in its growth and productivity (Polle and Rennenberg, 1992). Oxidative stress occurs when there is an imbalance between the generation of oxidizing compounds and the performance of antioxidant defense systems (Birben *et al.*, 2012). Thus, the production of a highly antioxidant system by the plant provides resistance against the biotic and abiotic stresses (Gangola *et al.*, 2013), eliminating the excess of reactive oxygen species (ROS) (Poljsak *et al.*, 2013). Among the compounds with recognized antioxidant activity is apocynin (Sun *et al.*, 2017; Tanriverdi *et al.*, 2017). Apocynin is a natural substance that was isolated from a root extract of *P. kurroa* in 1971 (Basu *et al.*, 1971) and gained extensive attention from researchers due to the medicinal properties attributed to its species of origin (Stefanska and Pawliczak, 2008). The same compound had previously been described by Schmiedeberg (1883) when it was isolated from the roots of the plant *Apocynum cannabinum* L.

Years later, Simons *et al.* (1990) found that *P. kurroa* root extracts decreased *in vitro* the inflammatory response of lymphocytes stimulated by *Phytolacca americana* L, and found that the incubation of non-activated neutrophils with apocynin did not significantly influence their ability to produce O²⁻. This fact suggests that cells that do not release ROS after activation are relatively insensitive to this compound so that apocynin would have selective action. The main conclusion of Simons *et al.* (1990) was that the methoxy-substituted catechols, which include apocynin, present action only when previously activated by myeloperoxidase (MPO).

These findings have led to several similar studies of interest (Kim *et al.*, 2011; Maiocchi *et al.*, 2017; Qin *et al.*, 2017) for the application of apocynin as an anti-inflammatory drug metabolically activated by neutrophils that would have action only at the site of inflammation. Given the importance of these studies, this review aims to provide an overview of the mechanism of action

and biological applications of apocynin.

2. MATERIALS AND METHODS:

2.1 Inflammatory process mediated by neutrophils

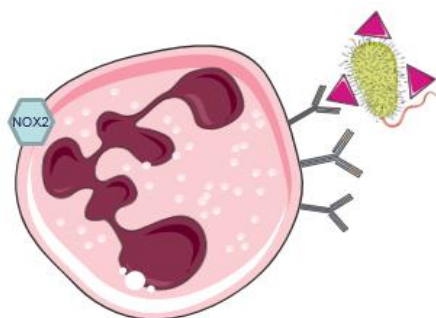
Neutrophils are abundant circulating leukocyte cells that make up the innate immune system (Kolaczowska and Kubes, 2013). They represent the mainline of defense of the body and constitute 40 to 60% of the population of white blood cells (Wright *et al.*, 2010). Neutrophils belong to a family whose hallmark is the presence of granules in their cytosol. The granules are lysosomal organelles with antimicrobial enzymes (Amulic *et al.*, 2012), with azurophilic granules due to the presence of the enzyme myeloperoxidase (MPO), which has the characteristic dark green color (Schultz and Kaminker, 1962).

Neutrophils are produced by the myeloid stem cells of the red bone marrow and remain circulating in the bloodstream until its activation (Nathan, 2006). The action of neutrophils begins with the pathogen-associated molecular patterns (PAMPs), released by invading microorganisms, and damage-associated molecular patterns (DAMPs), derived from damaged cells (Nourshargh and Alon, 2014).

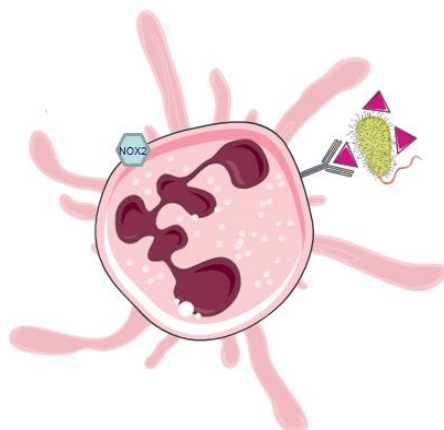
These factors stimulate the expression of selectins and the activation of integrins (Sun *et al.*, 2017), which are transmembrane proteins mediating cell adhesion and binding in the extracellular matrix, as well as cell-cell interaction (Amulic *et al.*, 2012). In this way, the integrins allow the transmigration of the neutrophils by the endothelial cells near the site of inflammation, a mechanism called diapedesis or homing (Filippi *et al.*, 2016; Gong *et al.*, 2017; Leach, Morton, and Sansom, 2017). Both sterile lesions (DAMPs) and infectious lesions (PAMPs) activate similar receptors, which result in phagocytosis, destruction, and subsequent elimination of the pathogen through clearance of debris by the phenomenon of exocytosis or clasmocytosis (Nourshargh and Alon, 2014; Marki *et al.*, 2015). Phagocytic recognition of microbial pathogens is mediated by pathogen recognition receptors (PRRs) (Kumar and Sharma, 2010). PRRs are genetically encoded proteins found mainly in the plasma membrane and in the cytoplasm of phagocytes that recognize conserved ligands in microorganisms, the PAMP's, and DAMP's (Panday, 2014).

At the site of infection, these membrane receptors recognize immunoglobulins and bind to opsonized microorganisms, leading to pseudopodia formation and onset of phagocytosis (Wright *et al.*, 2010) (Figure. 1).

(a)



(b)



(c)

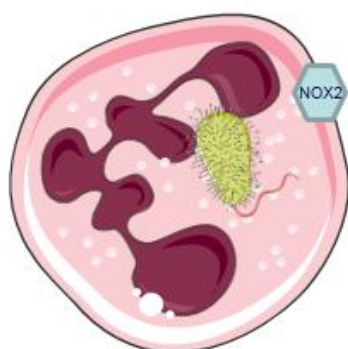


Figure 1. (a) Neutrophil membrane receptors in recognition of opsonized pathogens (b). Formation of pseudopodia and onset of phagocytosis of the pathogen by the neutrophil (c). Establishment of the phagosome for later release of lysosomal enzymes and destruction of the pathogen. Source: (Lim, Grinstein and Roth, 2017). Images edited with the content of images made available in LES LABORATOIRES SERVIER.

Although PRRs are critical for immunological surveillance and to contribute to the increase of neutrophil functions, phagocytosis is more efficient in the presence of opsonins (Kobayashi, Malachowa and Deleo, 2017).

Opsonins are proteins that make up the complement system, in which IgM and IgG are prominent. They adsorb to the pathogen (Gordon, 2016) and function as an immunostimulant to promote bacterial phagocytosis, generate an oxidative burst and stimulate neutrophils to produce interleukin-8 (Katzenmeyer, Szott and Bryers, 2017). Interleukin-8 is a pro-inflammatory chemical mediator that exerts a significant regulatory effect on the development of inflammation (Baggiolini, Clark-Lewis, 1992), in which, at low concentrations, it stimulates the release of L-selectin and increases the expression of integrins and in higher levels results in the onset of oxidative burst (Amulic *et al.*, 2012; Qin, 2017).

However, interleukin-8 represents only one of the regulatory mechanisms of the complex cascade chemical signaling of mediators, fundamental in the recruitment and activation of neutrophils (Nauseef and Borregaard, 2014). PRRs include various receptor proteins such as Toll-like (TLRs), nucleotide-binding, and oligomerization domain (NOD)-like receptors (NLRs), RIG-I-type and C-type lectin (Panday, 2014). Receptors responsible for this regulatory activity mainly involve recruitment and activation of neutrophils and consequent assembly of the enzymatic complex NADPH oxidase and activation of the oxidative explosion in Nox2 during phagocytosis (Hogan and Wheeler, 2014).

2.2. NADPH oxidase system

NADPH (nicotinamide adenine dinucleotide phosphate) oxidase is a large multienzyme complex translocated in the neutrophil cell membrane (Jiang, 2014). These complexes are formed by a heterodimeric flavocytochrome immersed in a cytosolic membrane, known as cytochrome b 558 (consisting of Nox2 and p22phox) and four cytosolic regulatory proteins: p47phox, p67phox, p40phox and GTPase-Rac (Pick, 2014a). This protein, when disposed of as a monomer, is inactive (Figure 2), and requires activators to develop its physiological activity (Pick, 2014b). For the assembly of the massive complex, Nox2 interacts with the small transmembrane protein p22phox which has a shielding function for protein

folding (Brandes, Weissmann and Schröder, 2014).

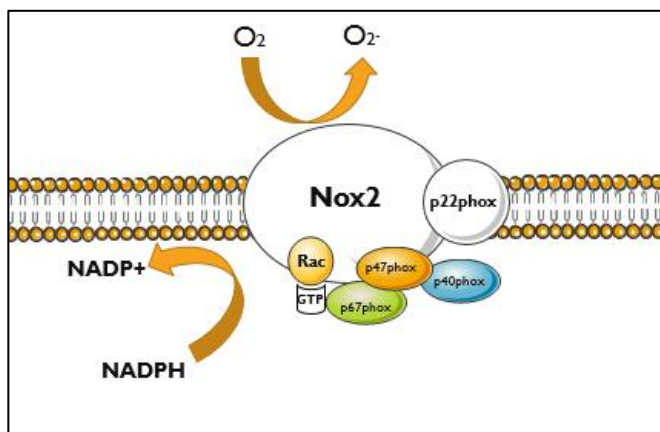


Figure 2. Activated NADPH oxidase enzyme complex. Adapted from Brandes; Weissmann; Schröder, (2014). Source: Images edited with content of images made available in LES LABORATOIRES SERVIE.

In the early stages, p47phox translocates the ternary complex of cytosolic proteins to the newly formed phagosome, which translocates p67phox to the membrane (Pick, 2014b) (Figure 2). The p67phox subunit should interact with Nox2. For this, the regulatory protein RAC must be active (Brandes, Weissmann and SCHRÖDER, 2014). Rac involvement is expressed in the RacGDP-RhoGDI Complex Translocation to the membrane, subsequent RacGDP dissociation from RhoGDI, followed by RacGTP binding to p67phox, promoting interaction with Nox2 (Pick, 2014b). Once assembled, the electron transport in Nox2 (Chan *et al.*, 2009) and the electron flow along a redox gradient, from NADPH to oxygen, leads to the reduction of a molecular oxygen electron (O_2) in superoxide anion (O_2^-) (Pick, 2014a).

2.3 Reactive oxygen species (ROS)

Oxidative stress is the imbalance between oxidant species and antioxidants, in favor of oxidants, leading to a rupture of redox signaling and molecular damage (Sies, 2017). The oxidant species can act by modifying the redox state of DNA, protein, or lipid molecules (Schieber and Chandel, 2014) and play a central role in the development of chronic pathologies and various health complications. As an example, one can cite vascular problems (Munzel *et al.*, 2014; Montezano *et al.*, 2015); hyperglycemia, *diabetes mellitus* (Hur *et al.*, 2010; Rains and Jain, 2011;

Zhang *et al.*, 2016), hypertension (Chan and Chan, 2014; Wu and Harrison, 2014; Togliatto, 2017), Alzheimer's disease (Dumont and Beal, 2011); cancer (Glasauer and Chandel, 2014) among other inflammatory diseases (Schieber and Chandel, 2014; Marín, 2017; Rhaman, 2017).

Among the species responsible for causing this damage are the superoxide anion produced from molecular oxygen and the NADPH multienzyme system (Chan *et al.*, 2009). There are also other species, which originate from the superoxide anion through enzymatic reactions classified as reactive oxygen species (ROS) (Lugrin *et al.*, 2014; Sies, 2017). The formation of ROS by NADPH oxidase complex occurs in the sizeable transmembrane protein Nox2 (Brandes, Weissmann and Schröder, 2014) and is associated with phagocyte formation, pathogen death and activated inflammatory processes (Dupré- Crochet and Nüße, 2013).

These processes initiate the oxidative explosion that generates an amplification of the conversion of O_2 to O_2^- and the subsequent formation of other ROS catalyzed by enzymes also derived from neutrophils (Nauseef, 2017). The superoxide anion is a weak oxidant, but it is the precursor of an uncontrollable series of reactions with free radicals (Lushchak, 2014). As an example, the recombination reaction of superoxide anion radicals catalyzed by the enzyme superoxide dismutase (SOD), which has as a product the reactive oxygen species hydrogen peroxide (H_2O_2) (Sies, 2017). H_2O_2 , in turn, is a precursor to other ROS. The MPO enzyme catalyzes the oxidation of Cl^- and H_2O_2 to generate the oxidant hypochlorous acid (HOCl) (Winterbourn *et al.*, 2006). H_2O_2 is also responsible for damaging ferritin, releasing the ion Fe^{2+}/Fe^{3+} , which can induce Fenton reactions and the generation of hydroxyl radicals (OH^\bullet) and the peroxide radical (OH_2^\bullet), which are species with high oxidant potential (Yoon *et al.*, 2011). Besides, these species lead to inflammatory responses in H_2O_2 concentrations in the range of 0.1 to 1 μM , leading to growth arrest and cell death by several mechanisms, leading to an amplification of the inflammation (Sies, 2017).

Another route of ROS formation, parallel to those previously described, is the reaction of the O_2^- anion with nitric oxide (NO^\bullet), activated neutrophil pro-inflammatory cytotoxin, forming the peroxide nitrite radical ($ONOO^\bullet$) (Guzik, Korbout and Adamek-Guzik, 2003), a reactive nitrogen species (RNS). The nitrite peroxide is cytotoxic,

affects mitochondrial function, and triggers cell death through oxidation and nitration reactions (Radi, 2013). In addition to the above mentioned oxidative species, other reactive intermediates are formed through hydrogen peroxide, in which some use MPO catalysis (Figure 3). In the presence of hydrogen peroxide and bromide, thiocyanate, tyrosine or nitrite, it occurs the formation of hypobromous acid (HOBr) and hypothiocyanite (HOSCN) of the tyrosyl radicals and reactive nitrogen intermediates (ONOO•) (Odobasic, Kitching and Holdsworth, 2016).

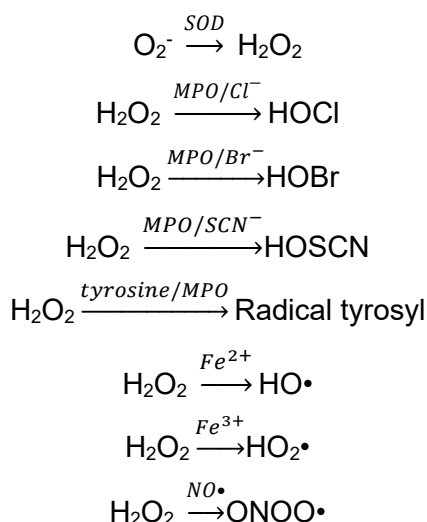


Figure 3. Reactive species generated through the enzymatic complex NADPH oxidase during an oxidative explosion. Source: Adapted from (Sareila *et al.*, 2011; Odobasic, Kitching and Holdsworth, 2016).

This whole process of neutrophil activation and the production of ROS is a highly regulated process by peptides and regulatory proteins to trigger the antimicrobial action of neutrophils. Therefore, this process is vital to maintain immune homeostasis and host health (Kobayashi, Malachowa and Deleo, 2017). In inflammatory processes, in which many neutrophils are stimulated by activating Nox2, an excess of reactive species (ROS and RNS) is generated during the burst (Lugrin *et al.*, 2014). Thus, it is necessary to reestablish the redox equilibrium, because all the substances reported, have a high oxidizing capacity and are responsible for causing irreparable damage to the tissues of hosts (Sareila *et al.*, 2011; Odobasic, Kitching and Holdsworth, 2016; Sies, 2017). Damage ranges from molecular and cellular modifications to cell death through apoptosis and necrosis (Kobayashi, 2017).

Castor, Locatelli, and Ximenes (2010) reported apocynin metabolically activated by MPO during neutrophil activation, avoiding the exacerbated production of these oxidants during the burst.

2.4 Apocynin

After being isolated from the *P. kurroa* plant the same compound was isolated from several plant sources, such as, for example, *Corallodiscus flabellata* Craib) B. L. Burt (Feng *et al.*, 2004), *Sargentodoxa cuneata* (Oliv.) Rehder & E. H. Wilson (Tian *et al.*, 2005), *Allium cepa* L. (Xiao and Parkin, 2007), *Polygonum orientale* L. (Li, 2011), *Ziziphora clinopodioides* Lam. (Senejoux *et al.*, 2012), *Scutellaria ramosissima* Popov (Mamadalieva *et al.*, 2013), *Solanum erianthum* D. Don (Chen *et al.*, 2013), *Pelargonium endlicherianum* Fenz (Karatoprak *et al.*, 2017) and *Iris tectorum* Maxim. (Zhang *et al.*, 2017). The apocynin (C₉H₁₀O₃), CAS 498-02-2, is a phenolic compound belonging to the class of methoxy catechols, it is the 4-hydroxy-3-methoxyacetophenone compound (Figure 4a), commonly known as acetovanilone (RAM, 2013). It is indicated as a pro-compound, due to the need for a pre-activation mediated by the enzyme myeloperoxidase and has as a product the apocynin radical (Almeida *et al.*, 2012). In the work developed by Maiocchi *et al.* (2017) suprapharmacological concentrations of apocynin did not significantly affect the initial rate or extent of NO consumption catalyzed by MPO in diluted human plasma. They did not affect the NO• intake rate in protein-free buffer systems containing urate and tyrosine, which are peroxidase substrates and attenuated the initial rate of NO uptake in the presence of urate, tyrosine, and ascorbate. In contrast, apocynin significantly accelerated the consumption of NO• in the absence of physiological substrates of myeloperoxidase.

According to the author, this is due to the fact of its ability to increase the NO• consumption in the absence of competing peroxidase substrates, since it does not stimulate the competition for the consumption of the enzyme and, therefore, the MPO becomes available to the activation of apocynin (Maiocchi *et al.*, 2017). Consequently, it is evident the dependence relationship between the presence of the MPO enzyme and the inhibitory action of apocynin, establishing a direct correlation between the cellular MPO level and the inhibition of ROS generation through the apocynin radical

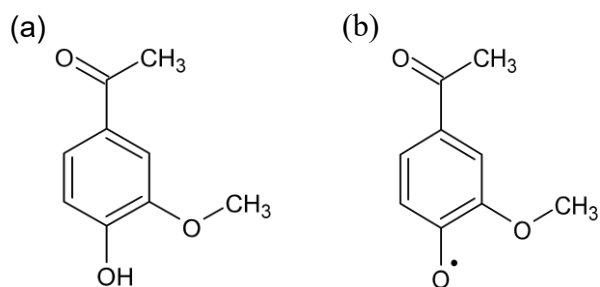
(Odobasic, Kitching and Holdsworth, 2016).

The mechanism proposed for this relationship justifies that the apocynin radical formed via enzymatic conversion (Figure 4b) is highly useful to oxidize thiolic groups (SH) (Castor, Locatelli and Ximenes, 2010).

Ximenes *et al.* (2007) suggest that the reactivity of the apocynin radical with thiol compounds may be involved in the inhibitory effect on the NADPH oxidase complex. The ability of apocynin to inhibit the aggregation of the NADPH oxidase complex in Nox2 is linked to the oxidation of these SH groups since such thiol groups are essential for the migration of the p47phox cytosolic fraction to the membrane (Kanegae *et al.*, 2007).

The apocynin radical further establishes a bond with a second radical, forming a dimeric product, the diapocynin (Figure 4c). Several authors indicate the apocynin dimer as the real inhibitor of NADPH oxidase (Castor, Locatelli and Ximenes, 2010; Dranka *et al.*, 2013; Potje, 2017; Pérez *et al.*, 2017).

According to Pérez *et al.* (2017), the inactivation of p47phox occurs more strongly with the apocynin dimers since the bonds between the aromatic rings of diapocynin allow the interactions with the aromatic residues W193, W263, F209, W204 and Y274 in p47phox, which are the terminals where p22phox turns on. The same author further justifies the increased inhibition of NADPH oxidase due to the increased hydrophobicity of the apocynin dimer over the parent compound. These studies corroborate with that reported by Potje (2017), in which the levels of nitric oxide, ROS, and calcium in aortic endothelial cells stimulated by diapocynin by apocynin were evaluated. The results presented by the author indicated that diapocynin showed a higher antioxidant capacity than apocynin, concerning the promotion of hypotensive effects without alteration of heart rate. Also, both compounds were effective in increasing NO• and also decreased RO levels in endothelial cells.



(c)

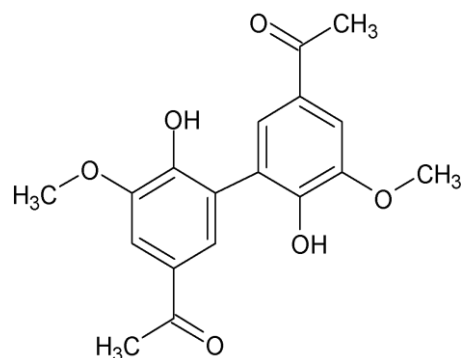


Figure 4. (a) Apocynin Structure, (b) Structure of the Apocynin radical, (c) Structure of the dimeric compound formed as the product of the interaction of two apocynin radicals. Source: (Castor, Locatelli and Ximenes, 2010; Pérez *et al.*, 2017).

In the study reported by Marín *et al.* (2017), diapocynin was chemically synthesized and tested in macrophages stimulated by lipopolysaccharide in an ulcerative colitis model. In this case, diapocynin showed inhibitory activity similar to apocynin, but more expressive. Dimer reduced levels of ROS production and inflammation mediation, such as tumor necrosis factor alpha (TNF-α), interleukin-6 (IL-6) and interleukin-8 (IL-1β), as well as inhibited the enzymatic expression of nitric oxide synthase (iNOS) and cyclooxygenase (COX-2), which act in the synthesis of nitric oxide and prostaglandins, intensifying inflammation. The results reported suggest that oxidation products, or transient species generated during the oxidation of apocynin, prevent migration of the p47phox component to the membrane, avoiding the assembly of NADPH. In this way, the operation of this complex is prevented (Dranka *et al.*, 2013; Potje, 2017; Pérez *et al.*, 2017; Marín, 2017).

Since the pre-activation of apocynin occurs through neutrophil myeloperoxidases that are recruited and activated during the occurrence of inflammation, the anti-inflammatory activity of apocynin makes this compound active in the locus of action of inflammation (Castor, Locatelli and Ximenes, 2010; Aratani, 2018). In according Stefanska *et al.* (2010), anti-inflammatory activity was demonstrated in a variety of cellular and animal models with a significant reduction of all inflammation parameters. Besides, the importance of advances in studies that refer to the development of apocynin-based drugs is due to the central role of Nox2 activity in inflammation. This, therefore, is closely linked in the modulation

of redox signaling pathways (Kim *et al.*, 2012), acting in the prevention and treatment of the most diverse diseases, such as neuronal dysfunction and degeneration and neuroinflammation. Diseases range from strokes, Alzheimer's disease, and Parkinson's disease, to psychiatric disorders (Simonyi, 2012). Due to the characteristics listed, many health problems can be improved by the action of apocynin. Some of the results of studies that have been conducted in recent years with the compound apocynin/ radical/ dimer in disease models encompassing oxidative disorders and/or inflammation are set out in Table 1.

3. RESULTS AND DISCUSSION:

3.1 Apocynin against the effects of ischemia injuries

Oxidative stress is one of the first biochemical changes after ischemia injury; such a factor contributes to the deterioration of the injury leading to other secondary damage (Sun *et al.*, 2017). In this sense, apocynin supplementation has shown essential benefits regarding the mitigation of oxidative stress and its consequent effects on post-injury in ischemic accidents. In vivo, apocynin application studies show the significant reduction in NADPH oxidase activity and the resulting reduced generation of ROS in pulmonary ischemia (Chiang, Chuang and Liu, 2011), ischemic myocardial injury (LUO *et al.*, 2012) for ischemia/reperfusion (I / R) and torsion / destruction (T / D) in testis (Şener *et al.*, 2015; Ozbek *et al.*, 2015), ischemic kidney injury (Choi *et al.*, 2015; Hu *et al.*, 2017), spinal cord injury (Sun *et al.*, 2017) and cerebral ischemia (Kapoor *et al.*, 2018).

Other significant effects of apocynin on ischemia is that the compound has been shown to significantly reduce the activity of the enzyme myeloperoxidase (MPO) which has catalytic activity in the production of reactive oxygen species (Şener *et al.*, 2015; Ozbek *et al.*, 2015; Sun *et al.*, 2017), and also present significant decrease in malonaldehyde (MDA) levels, the end product of lipid peroxidation (Choi *et al.*, 2015; Şener *et al.*, 2015; Ozbek *et al.*, 2015; Hu *et al.*, 2017; Sun *et al.*, 2017). Besides, several studies point to a significant increase in glutathione peroxidase (GSH) and superoxide dismutase (SOD), enzymes responsible for free radical scavenging (Şener *et al.*, 2015; Ozbek *et al.*, 2015; Hu *et al.*, 2017 ; Sun *et al.*, 2017; Kapoor *et al.*,

2018).

Corroborating these reported biochemical indices and proving the effectiveness of in vivo application of apocynin in attenuating biochemical alterations after apocynin injury proved to be efficient in hemodynamics, lung injury indices, and activation of attenuated apoptotic pathways (Chiang, Chuang and Liu, 2011), myocardial infarction size and significantly smaller apoptosis ratio of cardiomyocytes (Luo *et al.*, 2012), reversal of histopathological changes (Ozbek *et al.*, 2015), serum and renal zinc levels, urea nitrogen in the reduced blood (BUN) and serum creatinine (Scr) (Hu *et al.*, 2017) and restoration of mitochondrial membrane potential and reduction of behavioral deficits in ischemic animals for post cerebral ischemia (Kapoor *et al.*, 2018).

Furthermore, a recent study has shown that the up-regulation of NADPH / NOX2 expression and activity is likely a molecular mechanism responsible for the developmental origins of cardiovascular disease in the offspring of diabetic mothers. In this research, the compound apocynin acted in the prevention and reduction of apoptosis rates, ROS generation and infarction providing a new hypothesis that could be tested in future clinical studies (Zhang *et al.*, 2018).

3.2 Apocynin in cancer treatment

Anticancer agents derived from natural products activate or inhibit various pathways leading to suppression of tumor growth, apoptosis induction, and antimetastatic and antiangiogenic activity. These include prevention of DNA damage, inhibition of microtubule assembly, antimigration, anti-invasion, inhibition of cell growth, tumor tissue proapoptosis as well as enzymatic inhibition of topoisomerase for cell replication.

As shown in table 1, apocynin has been reported as an agent with antioncongenic properties with measurement of biological markers directly attributed to the proposed mechanism of action for compound, as the decrease in generation of ROS (Suzuki, 2013) and inflammatory signaling such as nuclear-κB factor (Komyia *et al.*, 2015; Byun *et al.*, 2016). As activities attributed to tumor growth suppression and metastatic activity factors (Suzuki *et al.*, 2013; Komyia *et al.*, 2015; Jantaree *et al.*, 2017).

In researching suppression of prostate cancer in rats, Suzuki *et al.*, (2013) focus on

clusterin precursor, belonging to deregulated genes, which is known to be related to tumorigenesis in many locations. The decreased clusterin expression in the ventral prostate occurred in the apocynin-treated rats' group. In this research, apocynin reduced Ki-67 labeling index and cyclin D1 expression, indicating that ROS generation is related to cell proliferation in rat prostate lobes. Also, NADPH oxidase regulates plasma adiponectin, the concentration of which may be negatively correlated with prostate cancer progression.

According to Suzuki *et al.* (2013), in rats with induced prostate cancer (TRAP), the activation of p38 MAPK (P38 mitogen-activated protein kinases) and ERK1/2 (extracellular signal-regulated kinase) in prostate tissue and their inactivation by prostate cancer were previously detected. Apocynin reduced cell proliferation and induced apoptosis in the prostate tissue, being active in suppressing prostate cancer.

Horemans *et al.* (2017) investigated the action of apocynin on the suppression of oncogenic activity induced by the presence of *H. pylori*. As a result, the histopathological analysis showed high infectious burden and severe gastritis after infection in control animals and immunohistochemistry confirmed the presence of *H. pylori* in all infected stomachs. The untreated and uninfected group had normal gastric histology, indicating that apocynin has no direct effect on stomach tissue. For infected animals, the administration of apocynin in stearic acid showed a significant decrease in abscess formation in the stomach cavity compared to the control group, thus suggesting that apocynin can positively modulate the process by reducing tissue damage induced by *H. Pylori*.

According to the results reported by Byun (2016), administration of apocynin has been investigated as a prevention of non-melanoma skin cancer, to provide new ways to prevent skin damage caused by UVB rays. The NADPH oxidase inhibitor suppressed UVB-induced skin cancer training. While UVB irradiation-induced the expression of critical carcinogenic factors in skin cells, or apocynin treatment reduced serious effects, thus inhibition of NADPH oxidase activity by apocynin was considered responsible for attenuation of signaling pathways during infection of the skin and carcinogenesis, such as signaling Akt, which regulates survival and tumor growth, and the expression factor NF-kB of inflammation.

In work reported by Jantaree *et al.* (2017)

with HepG2 cells from human hepatocellular carcinoma, apocynin and diapocynin were effective in inhibition of migration and invasion, thus effective in antimetastatic effect. During attack and movement, the cell surface binds to the extracellular matrices of cancer cells (ECM) by a family of cell surface receptors, integrins. Integrin-ECM interactions activate downstream signaling including the FAK, PI3K / Akt, ERK and NF-kB signaling pathways. The results showed that the invasion assay induced the phosphorylation of FAK, Akt and ERK proteins in HepG2 cells, while both the apocynin monomeric compound and its dimer specifically suppressed FAK and Akt phosphorylation. These results indicate that diapocynin and its monomeric form act on the same targets with differential power, inhibiting FAK and cell-ECM activated PI3K / Akt signaling, and these compounds are active in preventing metastasis (Jantaree *et al.*, 2017).

Paul *et al.* (2020) investigated the action of apocynin in suppressing the progression of pulmonary carcinoma in vitro and in vivo. Along with the identification of targets and the underlying mechanisms, the property of the compound to bind to tubulin protein and stabilization of cellular microtubules was investigated avoiding mitosis and, consequently, angiogenic activity. As a result, apocynin showed selective cytotoxicity relative to lung cancer cells rather than normal fibroblast cells.

Apocynin also inhibited oncogenic properties, including growth, proliferation, polyp formation, invasion, and spheroid formation in lung cancer cells. In addition, in other established features, apocynin is a novel and potent component for binding to tubulin and depolymerizing that of cellular microtubules. Depolymerization was the mechanism that triggered autophagy-mediated apoptotic cell death, which in turn slowed the progression of lung cancer. Moreover apocynin has shown tumoricidal characteristics inhibit pulmonary tumorigenesis in mice as well. Tubulin-microtubule balance with apocynin may be the primary regulator of catastrophic cellular catabolic processes to mitigate lung carcinoma (Raul *et al.*, 2020).

Considering all the apocynin-listed anticancer activity pathways in the articles cited, it is evident that reactive generation of oxygen species is found to be associated with tissue damage and DNA damage, with neoplastic transformation, aberrant growth and tumor proliferation. In this sense, apocynin deserves

more attention as a chemopreventive drug and also promising for cancer treatment.

3.3 Apocynin in the treatment of dysfunctions from *Diabetes mellitus* (DM)

Increasing reactive oxygen species by activating NADPH oxidase contributes to the development of diabetic complications (Olukam *et al.*, 2018). Diabetes-induced hyperglycemia causes damage to various organs and is associated with vascular and heart disease, responsible for increased morbidity and mortality (Gimenes *et al.*, 2018). Several mechanisms are involved in these effects, including increased or increased production of reactive oxygen species (ROS) produced by NADPH oxidase. In this context, the action of apocynin as an inhibitor of this enzyme complex is a compound with the potential to detect the adverse effects caused by this metabolic syndrome.

According to the results proposed by Gimenes *et al.*, 2018, apocynin showed a modulation activity of systemic antioxidant enzymes by decreasing SOD and GSH activity in control rats and restoring SOD activity in diabetic rats. Therefore, the compound had an influence on streptozotocin-induced cardiac remodeling in diabetic rats, attenuating systolic and diastolic dysfunction in diabetic rats. Also, Apocynin did not alter cardiac structures or myocardial and ventricular functions in normoglycemic rats.

The study reported by Qiu *et al.*, (2016) was developed to focus on unraveling the role of NADPH oxidase in the *diabetes mellitus* setting in addition to the potential benefits of apocynin in diabetic atrial remodeling. The inducibility of atrial fibrillation was increased in the DM group and significantly reduced by apocynin. In addition, the apocynin caused atrial structural remodeling in diabetic rabbits. Western blot analysis indicated that apocynin reduced the increased protein expression of TGF- β , NF- κ B, P-p38, P-JNK, ERK, and P-ERK, which are expressions induced by metabolic syndrome.

Another finding of apocynin action for the treatment of cardiac dysfunction caused by DM, the study proposed by Liang *et al.* (2018), sought to explore the mediated mechanism of ROS production and events in atrial fibrillation induced by diabetes. Western blotting was performed to detect the expression of NADPH oxidase subunits, including Rac1 (regulatory subunit), p22phox and gp91phox (structural subunits). As a result,

apocynin markedly suppressed expression of Rac1 activator but did not affect the expression of the p22phox and gp91phox structural subunits in NADPH stimulated by high glucose levels and H₂O₂ deferment.

In addition, Liang *et al.* (2018) report on the expression and activity of key factors involved in mitogen-activated protein kinase (MAPK) signaling, in which high glucose and H₂O₂ stimulation induced an increase in MMP9 expression. The addition of apocynin markedly reduced the expression of this marker of cellular reproduction. Also, apocynin addition did not induce low MMP2 expression while combined treatment of glucose and H₂O₂ induced increased MMP2 expression. Corroborating these results, glucose and H₂O₂ stimulation promoted cell proliferation and apocynin addition inhibited this increase in atrial fibroblast proliferation induced by high glucose and H₂O₂ stimulation. Therefore, the promoter effects of high glucose and H₂O₂ stimulation were attenuated by apocynin. These results led the author to the conclusion that hyperglycemia and oxidative stress-induced increased proliferation of atrial fibroblasts, leading to cardiac tissue fibrosis and cardiac function dysfunction, including atrial fibrillation. All these effects are alleviated by apo administration, further stating that such results provide the basis for the antioxidative therapy of atrial fibrillation caused by DM.

In addition to the factors mentioned referring to cardiac dysfunctions caused by diabetes mellitus, other consequences generated by this syndrome also presented improvements in apocynin administration. The work reported by Olukam *et al.* (2018) investigated the potential of the protective effect of apocynin on diabetic neuropathy in rats and its precise mechanism of action at the molecular level. Treatment with apocynin increased the dose-dependent pain threshold, showed increased expression of catalase and NOX-p47phox protein in the spinal cord, and was able to increase sciatic nerve conductance and blood flow in diabetic rats.

Another health complication that is a consequence of diabetes Mellitus is retinopathy. Retinopathy is a common complication of diabetes that affects the retina due to the high blood sugar content. Recent studies have shown that the presence of advanced oxidative species is the cause of retinal damage leading to the leakage of tiny blood vessels or act as signaling molecules to trigger neovascularization and apocynin is

presented as an NADPH oxidase inhibitor in various Nox isoforms corresponding to a potential compost for the treatment of this complication (Peng *et al.*, 2019).

In the development of diabetic retinopathy, expression of the inflammatory markers NF- κ B and toll-like receptor 4 occurs. Treatment of rat models with streptozotocin-induced diabetes retinopathy has improved the rates of biochemical markers as well as histological markers. After twelve weeks of apocynin treatment, cell apoptosis, oxidative stress and retinal inflammation were alleviated. Apocynin treatment improved the adverse effects of retinopathy in rats, decreased TLR4 / NF- κ B marker expression by apocynin are involved in this process (Wang *et al.*, 2019).

After proving apocynin as an adjunct in the treatment of many effects caused by metabolic syndrome, the results presented by Chan *et al.*, (2017) show apocynin as an active compound in preventing the generation of type 2 diabetes mellitus. As presented by the author, elevations in C-reactive protein (CRP) levels are positively correlated with the progress of type 2 diabetes mellitus. Purified human CRP impairs insulin secretion in isolated mouse islets and insulin-secreting NIT-1 cells from dose and time dependent ways. CRP increased the production of NADPH oxidase-mediated ROS, which simultaneously promoted the production of nitrotyrosine (indicator of reactive nitrogen species) which decreases cellular viability and insulin secretion in islets and secretory insulin cells. In this research, the apocynin compound considerably reversed the PCR-stimulated RNS ageration, indicating the action of apo on redox signaling and inactivation of RNS and NF- κ B and the reversal in the production of proinflammatory cytokines that cause cell damage.

4. CONCLUSIONS:

The *in vivo* results of apocynin has a broad spectrum of beneficial effects against various biological markers or pathophysiological processes. These include the markers used to monitor the inhibition of NADPH complex activity, such as increased activity of antioxidant enzymes GSH and SOD, decreased MDA content, decreased cell death by necrosis and apoptosis, as well as decreased expression of inflammatory biomarkers TNF- α , IL-6 e IL-1 β , beyond other markers specific to each disease.

The present results are of evaluation in various diseases, such as degenerative diseases, cancer, ischemia, hypertension, diabetes, among many other health problems. Thus, apocynin has been describing as active in the prevention and stabilization of diseases and in the reduction of secondary damage rates in cases of chronic diseases. These notes highlight the potential of apocynin as an excellent compost of its pharmacological properties. However, despite all these promising results that highlight the future potential of this substance, there are controversies about the real mechanism of action *in vivo* that occurs with this compound to obtain these beneficial biomarker indices. Some studies indicate the pro-oxidant activity of apocynin (Castor, Locatelli and Ximenes 2010; Wong *et al.*, 2015). That, once oxidized by MPO enzymes, they are activated and become capable of inducing oxidation of the NADPH enzyme complex, but also of various classes of biomolecules. Concomitantly inhibiting the NADPH complex, apocynin can act as an oxidant by initiating a deleterious intracellular oxidative process.

The same authors also reported that the apocynin radical is capable of oxidizing the endogenous substrate of the NADPH oxidase enzyme complex, and this culminates in necessary implications for the apocynin mechanism as an NADPH oxidase inhibitor. The depletion of its substrate would block NADPH oxidase from superoxide anion production. However, it is known that chemical interaction may also contribute to redox cell imbalance and that NADPH oxidation involves the NADP \cdot intermediate (NADP radical), which is also capable of initiating a prooxidant process, reducing molecular oxygen to the superoxide anion (Castor, Locatelli and Ximenes, 2010).

Apocynin has therapeutic potential against diseases involving inflammation or oxidative stress. Its antioxidant activities, however, are not well characterized and vary according to the experimental context, cell type, and NADPH oxidase system. In cells treated with a pro-oxidative and cytotoxic protein aggregate, the first evidence that apocynin has a more significant inhibitory effect on reactive nitrogen species levels compared to hydrogen peroxide levels (Wong, Fong, and Vieira, 2015). In addition, apocynin does not have a high free radical scavenging capability. However, it has a high scavenging capacity for non-radical oxidizing species, such as HOCl and H₂O₂. Thus, if a peroxidase is expressed or added to cells, depletion of H₂O₂ by

apocynin may represent an additional pathway for its biological effects (Petrônio *et al.*, 2013).

The results obtained for research on the action of apocynin in humans are scarce. It reinforces the need for further studies for this natural compound because, although there are controversies about its mechanism of action, the anti-inflammatory and antioxidant activities in the models presented are significant. However, the tremendous potential of apocynin to inhibit NADPH oxidase has been described in the literature based on results from *in vivo* applications. Apocynin can decrease superoxide anion production of activated neutrophils, while phagocytosis capacity is not affected. Also, it is vital to highlight the regulatory role of neutrophil myeloperoxidase enzyme in the activation of apocynin and, consequently, in the inhibition of the generation of reactive oxygen species that mediated inflammatory processes and cause intense and irreversible cell damage. Thus, apocynin has the potential for the prevention and treatment of several health complications presented in this review. Therefore, the importance of further studies with these compounds is emphasized.

5. ACKNOWLEDGEMENTS:

The authors are grateful to CNPq for the scholarship granted to D. F. Grigoletto (159815/2018-5) and CAPES for the scholarship given to E. H. Miranda.

6. REFERENCES:

1. ABDELMAGEED, Marwa E.; EL-AWADY, Mohammed S.; SUDDEK, Ghada M.. Apocynin ameliorates endotoxin-induced acute lung injury in rats. **International Immunopharmacology**, [s.l.], v. 30, p.163-170, jan. 2016. Elsevier BV. <http://dx.doi.org/10.1016/j.intimp.2015.12.006>.
2. ABDELRAHMAN, Rs. Protective effect of apocynin against gentamicin-induced nephrotoxicity in rats. **Human & Experimental Toxicology**, [s.l.], v. 37, n. 1, p.27-37, 24 jan. 2017. SAGE Publications. <http://dx.doi.org/10.1177/0960327116689716>.
3. ALMEIDA, A.C.; VILELA, M.M.S.; CONDINO-NETO, A.; XIMENES, V.F.. The Importance of Myeloperoxidase in Apocynin-Mediated NADPH Oxidase Inhibition. **Isrn Inflammation**, [s.l.], v. 2012, p.1-7, 2012. Hindawi Limited. <http://dx.doi.org/10.5402/2012/260453>.
4. AMULIC, B.; CAZALET, C.; HAYES, G.L.; METZLER, K.D.; ZYCHLINSKY, A. Neutrophil Function: From Mechanisms to Disease. **Annual Review Of Immunology**, [s.l.], v. 30, n. 1, p.459-489, 23 abr. 2012.
5. ARATANI, Yasuaki. Myeloperoxidase: Its role for host defense, inflammation, and neutrophil function. **Archives Of Biochemistry And Biophysics**, [s.l.], v. 640, p.47-52, fev. 2018.
6. BAGGIOLINI, Marco; CLARK-LEWIS, Ian. Interleukin-8, a chemotactic and inflammatory cytokine. **Febs Letters**, [s.l.], v. 307, n. 1, p.97-101, 27 jul. 1992.
7. BASU, K., DASGUPTA, B., BHATTACHARYA, S.K. AND DEBNATH, P.K. Chemistry and pharmacology of apocynin, isolated from *Picrorhiza kurroa* Royle ex Benth. **Current Science**. V. 40, n. 22, p. 603-604, 1971.
8. BIRBEN, E.; SAHINER, U.M.; SACKESSEN, C.; ERZURUM, S.; KALAYCI, O. Oxidative Stress and Antioxidant Defense. **World Allergy Organization Journal**, [s.l.], v. 5, n. 1, p.9-19, jan. 2012. Elsevier BV. <http://dx.doi.org/10.1097/wox.0b013e3182439613>.
9. POLJSKAK, Borut; IUPUT, Dušan; MILISAV, Irina. Achieving the Balance between ROS and Antioxidants: When to Use the Synthetic Antioxidants. **Oxidative Medicine And Cellular Longevity**, [s.l.], v. 2013, p.1-11, 2013.
10. BRANDES, Ralf P.; WEISSMANN, Norbert; SCHRÖDER, Katrin. Nox family NADPH oxidases: Molecular mechanisms of activation. **Free Radical Biology And Medicine**, [s.l.], v. 76, p.208-226, nov. 2014.
11. BYUN, S.; LEE, E.; JANG, Y.J.; KIM, Y.; LEE, K.W. The NADPH oxidase inhibitor apocynin inhibits UVB-induced skin carcinogenesis. **Experimental**

- Dermatology**, [s.l.], v. 25, n. 6, p.489-491, 18 abr. 2016.
12. CASTOR, Lidyane Regina Gomes; LOCATELLI, Kátia Andreza; XIMENES, Valdecir Farias. Pro-oxidant activity of apocynin radical. **Free Radical Biology And Medicine**, [s.l.], v. 48, n. 12, p.1636-1643, 15 jun. 2010.
 13. CHAN, E.C.; JIANG, F.; PESHAVARIYA, H.M.; DUSTING, G.J. Regulation of cell proliferation by NADPH oxidase-mediated signaling: Potential roles in tissue repair, regenerative medicine, and tissue engineering. **Pharmacology & Therapeutics**, [s.l.], v. 122, n. 2, p.97-108, maio 2009. Elsevier BV. <http://dx.doi.org/10.1016/j.pharmthera.2009.02.005>.
 14. CHAN, P., WANG, Y., CHEN, Y., HSU, W., TIAN, Y., HSIEH, P. Importance of NADPH oxidase-mediated redox signaling in the detrimental effect of CRP on pancreatic insulin secretion. **Free Radical Biology And Medicine**, [s.l.], v. 112, p.200-211, nov. 2017. Elsevier BV. <http://dx.doi.org/10.1016/j.freeradbiomed.2017.07.032>.
 15. CHAN, Samuel Hh.; CHAN, Julie Y.h.. Brain Stem NOS and ROS in Neural Mechanisms of Hypertension. **Antioxidants & Redox Signaling**, [s.l.], v. 20, n. 1, p.146-163, jan. 2014. Mary Ann Liebert Inc. <http://dx.doi.org/10.1089/ars.2013.5230>.
 16. CHEN, Y.C.; LEE, H.Z.; CHEN, H.C.; WEN, C.L.; KUO, Y.H.; WANG, G.J. anti-inflammatory Components from the Root of Solanum erianthum. **International Journal Of Molecular Sciences**, [s.l.], v. 14, n. 6, p.12581-12592, 14 jun. 2013. MDPI AG. <http://dx.doi.org/10.3390/ijms140612581>.
 17. CHIANG, Chi-huei; CHUANG, Chiao-hui; LIU, Shiou-ling. Apocynin attenuates ischemia-reperfusion lung injury in an isolated and perfused rat lung model. **Translational Research**, [s.l.], v. 158, n. 1, p.17-29, jul. 2011.
 18. CHOI, E.K.; JUNG, H.; KWAK, K.H.; YEO, J.; YI S.J.; PARK, C.Y. Effects of Allopurinol and Apocynin on Renal Ischemia-Reperfusion Injury in Rats. **Transplantation Proceedings**, [s.l.], v. 47, n. 6, p.1633-1638, jul. 2015.
 19. DRANKA, B.P.; GIFFORD, A.; GHOSH, A.; ZIELONKA, J.; JOSEPH, J.; KANTHASAMY, J. Diapocynin prevents early Parkinson's disease symptoms in the leucine-rich repeat kinase 2 (LRRK2R1441G) transgenic mouse. **Neuroscience Letters**, [s.l.], v. 549, p.57-62, ago. 2013.
 20. DUMONT, M.; STACK, C.; ELIPENHALI, C.; CALINGASAN, N.Y.; WILLE, E.; BEAL, M.F. Apocynin administration does not improve behavioral and neuropathological deficits in a transgenic mouse model of Alzheimer's disease. **Neuroscience Letters**, [s.l.], v. 492, n. 3, p.150-154, abr. 2011.
 21. DUPRÉ-CROCHET, Sophie; ERARD, Marie; NÜBE, Oliver. ROS production in phagocytes: why, when, and where?. **Journal Of Leukocyte Biology**, [s.l.], v. 94, n. 4, p.657-670, out. 2013.
 22. FENG Wei-sheng *, ZHENG Xiao-ke, LIU Yun-bao, LI Jun. Isolation and structural identification of C-glycosylflavones from Corallodiscus flabellata. **Acta Pharmaceutica Sinica**, 39(2), 110–115, 2004.
 23. FILIPPI, Marie-dominique. Mechanism of Diapedesis. **Advances In Immunology**, [s.l.], p.25-53, 2016.
 24. GANGOLA, Manu Pratap. Components of antioxidant system of Picrorhiza kurrooa exhibit different spatio-temporal behavior. **Molecular Biology Reports**, [s.l.], v. 40, n. 12, p.6593-6603, 22 set. 2013. Springer Nature.
 25. GIMENES, R.; GIMENES, C.; ROSA, C.M.; XAVIER, N.P.; CAMPOS, D.H.S.; FERNANDES, A.A.H. Influence of apocynin on cardiac remodeling in rats with streptozotocin-induced diabetes mellitus. **Cardiovascular Diabetology**, [s.l.], v. 17, n. 1, p.1-12, 17 jan. 2018. Springer Nature. <http://dx.doi.org/10.1186/s12933-017-0657-9>.
 26. GLASAUER, Andrea; CHANDEL, Navdeep S.. Targeting antioxidants for

- cancer therapy. **Biochemical Pharmacology**, [s.l.], v. 92, n. 1, p.90-101, nov. 2014. Elsevier BV. <http://dx.doi.org/10.1016/j.bcp.2014.07.017>.
27. GONG, Y.; ZHANG, Y.; FENG, S.; LIU, X.; LÜ, S.; LONG, M. Dynamic contributions of P- and E-selectins to β 2-integrin-induced neutrophil transmigration. **The FASEB Journal**, [s.l.], v. 31, n. 1, p.212-223, jan. 2017. FASEB. <http://dx.doi.org/10.1096/fj.201600398rrr>.
 28. GORDON, Siamon. Phagocytosis: An Immunobiologic Process. **Immunity**, [s.l.], v. 44, n. 3, p.463-475, mar. 2016. Elsevier BV. <http://dx.doi.org/10.1016/j.immuni.2016.02.026>.
 29. GRATON, M.E.; POTJE, S.R.; TROIANO, J.A.; VALE, G.T.; PERASSA, L.A.; NAKAMUNE, A.C.M.S. Apocynin alters redox signaling in conductance and resistance vessels of spontaneously hypertensive rats. **Free Radical Biology And Medicine**, [s.l.], v. 134, p.53-63, abr. 2019. Elsevier BV. <http://dx.doi.org/10.1016/j.freeradbiomed.2018.12.026>.
 30. GUZIK, T. J.; KORBUT, R.; ADAMEK-GUZIK, T. Nitric oxide and superoxide in inflammation and immune regulation. **Journal of Physiology and Pharmacology: An Official Journal of the Polish Physiological Society**, v. 54, n.4, p. 469-487, dec, 2003. <https://doi.org/10.1385/1-59259-374-7>.
 31. ISMAIL, H.; SCAPOZZA, L.; RUEG, U. T.; DORCHIES, O. Diapocynin, a putative NADPH oxidase inhibitor, ameliorates the phenotype of a mouse model of Duchenne muscular dystrophy. **Neuromuscular Disorders**, [s.l.], v. 24, n. 9-10, p.822-822, out. 2014.
 32. HOGAN, Deborah; WHEELER, Robert T.. The complex roles of NADPH oxidases in fungal infection. **Cellular Microbiology**, [s.l.], v. 16, n. 8, p.1156-1167, 7 jul. 2014. Wiley. <http://dx.doi.org/10.1111/cmi.12320>.
 33. HOREMANS, T.; BOULET, G.; KERCKHOVEN, M.; BOGERS, J.; THYS, S.; VERVAET, C. In-vivo evaluation of apocynin for prevention of Helicobacter pylori-induced gastric carcinogenesis. **European Journal Of Cancer Prevention**, [s.l.], v. 26, n. 1, p.10-16, jan. 2017.
 34. HOU, L.; SUN, F.; HUANG, R.; SUN, W.; ZHANG, D.; WANG, Q. Inhibition of NADPH oxidase by apocynin prevents learning and memory deficits in a mouse Parkinson's disease model. **Redox Biology**, [s.l.], v. 22, p.101134-101146, abr. 2019.
 35. HU, B.; WU, Y.; TONG, F.; LIU, J.; SHEN, X.; SHEN, R.; XU, G. Apocynin Alleviates Renal Ischemia/Reperfusion Injury Through Regulating the Level of Zinc and Metallothionein. **Biological Trace Element Research**, [s.l.], v. 178, n. 1, p.71-78, 1 dez. 2016.
 36. HUR, J.; SULLIVAN, K. A.; SCHUYLER, A.D.; HONG, Y.; PANDE, M.; STATES, D.J.; JAGADISH, H.V.; FELDMAN, E.L. Literature-based discovery of diabetes- and ROS-related targets. **Bmc Medical Genomics**, [s.l.], v. 3, n. 1, p.49-49, 27 out. 2010.
 37. IMPELLIZZERI, D.; ESPOSITO, E.; MAZZON, E.; PATERNITTI, I.; DI PAOLA, R.; BRAMANTI, P. Effect of apocynin, a NADPH oxidase inhibitor, on acute lung inflammation. **Biochemical Pharmacology**, [s.l.], v. 81, n. 5, p.636-648, mar. 2011.
 38. JANTAREE, P.; LIRDPRAPAMONGKOL, K.; KAEWSRI, W.; THONGSORNKLEEB, C.; CHOOWONGKOMON, K.; ATJANASUPPAT, K. Homodimers of Vanillin and Apocynin Decrease the Metastatic Potential of Human Cancer Cells by Inhibiting the FAK/PI3K/Akt Signaling Pathway. **Journal Of Agricultural And Food Chemistry**, [s.l.], v. 65, n. 11, p.2299-2306, 8 mar. 2017.
 39. JIANG, Joy X.. NADPH Oxidases in Chronic Liver Diseases. **Advances In Hepatology**, [s.l.], v. 2014, p.1-8, 2014. Hindawi Limited. <http://dx.doi.org/10.1155/2014/742931>.
 40. KALA, Chandra Prakash. Status and conservation of rare and endangered medicinal plants in the Indian trans-Himalaya. **Biological Conservation**, [s.l.],

- v. 93, n. 3, p.371-379, maio 2000. Elsevier BV. [http://dx.doi.org/10.1016/s0006-3207\(99\)00128-7](http://dx.doi.org/10.1016/s0006-3207(99)00128-7).
41. KANEGAE, M.P.P.; FONSECA, L.M.; BRUNETTI, I.; SILVA, S.O.; XIMENES, V.F. The reactivity of ortho-methoxy-substituted catechol radicals with sulfhydryl groups: Contribution for the comprehension of the mechanism of inhibition of NADPH oxidase by apocynin. **Biochemical Pharmacology**, [s.l.], v. 74, n. 3, p.457-464, ago. 2007. Elsevier BV. <http://dx.doi.org/10.1016/j.bcp.2007.05.004>.
 42. KAPAH, B. K.; SRIVASTAVA, T. N.; SARIN, Y. K.. Description of Picrorhiza Kurroa, A Source of the Ayurvedic Drug Kutaki. **International Journal Of Pharmacognosy**, [s.l.], v. 31, n. 3, p.217-222, jan. 1993. Informa UK Limited. <http://dx.doi.org/10.3109/13880209309082945>.
 43. KAPOOR, M.; SHARMA, N.; SANDHIR, R.; NEHRU, B. Effect of the NADPH oxidase inhibitor apocynin on ischemia-reperfusion hippocampus injury in rat brain. **Biomedicine & Pharmacotherapy**, [s.l.], v. 97, p.458-472, jan. 2018. Elsevier BV. <http://dx.doi.org/10.1016/j.biopha.2017.10.12>.
 44. KARATOPRAK, G. Ş.; GÖGER, F.; YERER, M.B.; KOŞAR, M. Chemical composition and biological investigation of Pelargonium endlicherianum root extracts. **Pharmaceutical Biology**, v. 55, n. 1, p. 1608–1618, dec. 2017.
 45. KATOCH, Meenu. Effect of altitude on picroside content in core collections of Picrorhiza kurroa from the north western Himalayas. **Journal Of Natural Medicines**, [s.l.], v. 65, n. 3-4, p.578-582, 24 fev. 2011.
 46. KATZENMEYER, Kristy N.; SZOTT, Luisa M.; BRYERS, James D.. Artificial opsonin enhances bacterial phagocytosis, oxidative burst and chemokine production by human neutrophils. **Pathogens And Disease**, [s.l.], v. 75, n. 6, p.771-775, 7 jul. 2017. Oxford University Press (OUP). <http://dx.doi.org/10.1093/femspd/ftx075>.
 47. KIM, S.Y.; MOON, K.A.; JO, H.Y.; JEONG, S.; SEON, S.H.; JUNG, E. Anti-inflammatory effects of apocynin, an inhibitor of NADPH oxidase, in airway inflammation. **Immunology And Cell Biology**, [s.l.], v. 90, n. 4, p.441-448, 28 jun. 2011. Wiley. <http://dx.doi.org/10.1038/icb.2011.60>.
 48. KOBAYASHI, Scott D.; MALACHOWA, Natalia; DELEO, Frank R.. Influence of Microbes on Neutrophil Life and Death. **Frontiers In Cellular And Infection Microbiology**, [s.l.], v. 7, p.159-9, 1 maio 2017. Frontiers Media SA. <http://dx.doi.org/10.3389/fcimb.2017.00159>.
 49. KOLACZKOWSKA, Elzbieta; KUBES, Paul. Neutrophil recruitment and function in health and inflammation. **Nature Reviews Immunology**, [s.l.], v. 13, n. 3, p.159-175, mar. 2013. Springer Nature.
 50. KOMIYA, M.; FUJI, G.; MIYAMOTO, S.; TAKAHASHI, M.; ISHIGAMORI, R.; ONUMA, W. Suppressive effects of the NADPH oxidase inhibitor apocynin on intestinal tumorigenesis in obese KK-Ay and Apc mutant Min mice. **Cancer Science**, [s.l.], v. 106, n. 11, p.1499-1505, 16 out. 2015.
 51. KUMAR, V.; SHARMA, A. Neutrophils: Cinderella of innate immune system. **International Immunopharmacology**, [s.l.], v. 10, n. 11, p.1325-1334, nov. 2010.
 52. LEACH, Joshua; MORTON, Jennifer P.; SANSOM, Owen J.. Neutrophils: Homing in on the myeloid mechanisms of metastasis. **Molecular Immunology**, [s.l.], p.30615-30616, dez. 2017.
 53. LEE, S.H.; CHOI, B.Y.; KHO, A.R.; JEONG, J.H.; HONG, D.K.; KANG, D.H. Inhibition of NADPH Oxidase Activation by Apocynin Rescues Seizure-Induced Reduction of Adult Hippocampal Neurogenesis. **International Journal Of Molecular Sciences**, [s.l.], v. 19, n. 10, p.3087-3087, 9 out. 2018.
 54. LI, Yongjun. Chemical constituents in herb of *Polygonum orientale* II. **China Journal Of Chinese Materia Medica**, [s.l.], p.458-461, 15 fev. 2011.
 55. LIU, J.J.; LU, Y.; PING, N.N.; LI, X.; LIN, X.; LI, C. Apocynin ameliorates pressure

- overload-induced cardiac remodeling by inhibiting oxidative stress and apoptosis. **Physiol Res.** v 24; n. 66, p.741-752., 26 oct, 2017. Elsevier.
56. LIM, Justin J.; GRINSTEIN, Sergio; ROTH, Ziv. Diversity and Versatility of Phagocytosis: Roles in Innate Immunity, Tissue Remodeling, and Homeostasis. **Frontiers In Cellular And Infection Microbiology**, [s.l.], v. 7, p.1-12, 23 maio 2017.
 57. LUGRIN, J.; ROSENBLATT-VELIN, N.; PARAPANOV, R.; LIAUDET, L. The role of oxidative stress during inflammatory processes. **Biological Chemistry**, [s.l.], v. 395, n. 2, p.203-230, 1 jan. 2014. Walter de Gruyter GmbH. <http://dx.doi.org/10.1515/hsz-2013-0241>.
 58. LUO, X.; JI, S. K.; LIU, B.; ZHANG, H. F. YANG, Z.B. NADPH oxidase inhibitor apocynin attenuates ischemia/reperfusion induced myocardial injury in rats. **Zhonghua Xin Xue Guan Bing Za Zhi**, v. 40, n.12, p. 991-996, dec, 2012.
 59. LUSHCHAK, Volodymyr I.. Free radicals, reactive oxygen species, oxidative stress and its classification. **Chemaraico-biological Interactions**, [s.l.], v. 224, p.164-175, dez. 2014.
 60. MAIOCCHI, S.,L.; MORRIS, J.C.; REES, M.D.; THOMA, S.T. Regulation of the nitric oxide oxidase activity of myeloperoxidase by pharmacological agents. **Biochemical Pharmacology**, [s.l.], v. 135, p.90-115, jul. 2017.
 61. MAMADALIEVA, N.; VINCIGUERRA, V.; OVIDI, E.; TIEZZI, A. Identification and isolation of non-polar compounds from the chloroform extract of *Scutellaria ramosissima*. **Natural Product Research**, [s.l.], v. 27, n. 21, p.2059-2062, nov. 2013. Informa UK Limited.
 62. MARÍN, M.; Gimeno, C.; Giner, R.M.; Ríos, J.L.; Máñez, S.; Recio, M.A.C. Influence of Dimerization of Apocynin on Its Effects in Experimental Colitis. **Journal Of Agricultural And Food Chemistry**, [s.l.], v. 65, n. 20, p.4083-4091, 16 maio 2017. American Chemical Society (ACS).
 63. MARKI, A.; ESKO, J. D.; PRIES, A. R. ley, k. Role of the endothelial surface layer in neutrophil recruitment. **Journal Of Leukocyte Biology**, [s.l.], v. 98, n. 4, p.503-515, 15 maio 2015.
 64. MONTEZANO, A.C.; LIS, M.D.; TSIROPOULOU, S.; HARVEY, A.; BRIONES, A.M.; TOUYZ, R.M. Oxidative Stress and Human Hypertension: Vascular Mechanisms, Biomarkers, and Novel Therapies. **Canadian Journal Of Cardiology**, [s.l.], v. 31, n. 5, p.631-641, maio 2015. Elsevier BV.
 65. MUNZEL, T.; GORI, T.; BABISCH, W.; BASNER, M. Cardiovascular effects of environmental noise exposure. **European Heart Journal**, [s.l.], v. 35, n. 13, p.829-836, 9 mar. 2014.
 66. NATHAN, Carl. Neutrophils and immunity: challenges and opportunities. **Nature Reviews Immunology**, [s.l.], v. 6, n. 3, p.173-182, 17 fev. 2006. Springer Nature.
 67. NAUSEEF, W. M. (2017). The neutrophil NADPH oxidase. **Hydrogen Peroxide Metabolism in Health and Disease**, p. 237 – 277, oct. 2017.
 68. NAUSEEF, William M; BORREGAARD, Niels. Neutrophils at work. **Nature Immunology**, [s.l.], v. 15, n. 7, p.602-611, jul. 2014. Springer Nature. <http://dx.doi.org/10.1038/ni.2921>.
 69. NOURSHARGH, Sussan; ALON, Ronen. Leukocyte Migration into Inflamed Tissues. **Immunity**, [s.l.], v. 41, n. 5, p.694-707, nov. 2014. Elsevier BV. <http://dx.doi.org/10.1016/j.immuni.2014.10.008>.
 70. ODOBASIC, Dragana; KITCHING, A. Richard; HOLDSWORTH, Stephen R.. Neutrophil-Mediated Regulation of Innate and Adaptive Immunity: The Role of Myeloperoxidase. **Journal Of Immunology Research**, [s.l.], v. 2016, p.1-11, 2016. Hindawi Limited. <http://dx.doi.org/10.1155/2016/2349817>.
 71. OLUKMAN, M.; ONAL, A.; CELENK, F.G.; UYANIKGIL, Y.; CAVUSOGLU, T.; ULKER, S. Treatment with NADPH oxidase inhibitor apocynin alleviates diabetic neuropathic pain in rats. **Neural Regeneration Research**, [s.l.], v. 13, n. 9, p.1657-1664, 2018. Medknow. <http://dx.doi.org/10.4103/1673-5374.232530>.

72. OZBEK, O.; ALTINTAS, R.; POLAT, A.; VARDI, N.; PARLAKPINAR, H.; SAGIRD, M. The Protective Effect of Apocynin on Testicular Ischemia-Reperfusion Injury. **Journal Of Urology**, [s.l.], v. 193, n. 4, p.1417-1422, abr. 2015. Ovid Technologies (Wolters Kluwer Health). <http://dx.doi.org/10.1016/j.juro.2014.11.086>.
73. OZER, M.A.; POLAT, N.; OZEN, S.; OGUREL, T.; PARLAKPINAR, H.; VARDI, N. Histopathological and ophthalmoscopic evaluation of apocynin on experimental proliferative vitreoretinopathy in rabbit eyes. **International Ophthalmology**, [s.l.], v. 37, n. 3, p.599-605, 5 ago. 2016.
74. PANDAY, A.; SAHOO, M.K.; OSORIO, D.; BATRA, S. NADPH oxidases: an overview from structure to innate immunity-associated pathologies. **Cellular & Molecular Immunology**, [s.l.], v. 12, n. 1, p.5-23, 29 set. 2014. Springer Nature. <http://dx.doi.org/10.1038/cmi.2014.89>
75. PENG, J., XIONG, S., DING, L., PENG, J., XIA, X. Diabetic retinopathy: Focus on NADPH oxidase and its potential as therapeutic target. **European Journal Of Pharmacology**, [s.l.], v. 853, p.381-387, jun. 2019. Elsevier BV. <http://dx.doi.org/10.1016/j.ejphar.2019.04.038>.
76. PERASSA, L.A.; GRATON, M.E.; POTJE, S.R.; TROIANO, J.A.; LIMA, M.S.; VALE, G.T. Apocynin reduces blood pressure and restores the proper function of vascular endothelium in SHR. **Vascular Pharmacology**, [s.l.], v. 87, p.38-48, dez. 2016. Elsevier BV. <http://dx.doi.org/10.1016/j.vph.2016.06.005>.
77. PÉREZ, M.E.M.; RODRÍGUEZ, M.H.; PÉREZ, L.C.C.; FRAGOSO-VÁZQUEZ, M.J.; CORREA-BASURTO, J. PADILLA-MARTÍNEZ I.I.; LUNA, D.M.; JIMÉNEZ, E.M. Aromatic Regions Govern the Recognition of NADPH Oxidase Inhibitors as Diapocynin and its Analogues. **Archiv Der Pharmazie**, [s.l.], v. 350, n. 10, p.1700041-1700041, 21 ago. 2017. Wiley. <http://dx.doi.org/10.1002/ardp.201700041>.
78. PETRÔNIO, Maicon. Apocynin: Chemical and Biophysical Properties of a NADPH Oxidase Inhibitor. **Molecules**, [s.l.], v. 18, n. 3, p.2821-2839, 1 mar. 2013. MDPI AG. <http://dx.doi.org/10.3390/molecules18032821>.
79. PICK, Edgar. Cell-Free NADPH Oxidase Activation Assays: "In Vitro Veritas". **Neutrophil Methods And Protocols**, [s.l.], p.339-403, 2014a. Humana Press. http://dx.doi.org/10.1007/978-1-62703-845-4_22.
80. PICK, Edgar. Role of the Rho GTPase Rac in the activation of the phagocyte NADPH oxidase. **Small Gtpases**, [s.l.], v. 5, n. 1, p.27952-27952, jan. 2014b. Informa UK Limited. <http://dx.doi.org/10.4161/sgtp.27952>.
81. POTJE, S.R.; TROIANO, J.A.; GRATON, M.E.; XIMENES, V.F.; NAKAMUNE, A.C.M.S.; ANTONIALI, C. Hypotensive and vasorelaxant effect of Diapocynin in normotensive rats. **Free Radical Biology And Medicine**, [s.l.], v. 106, p.148-157, maio 2017. Elsevier BV. <http://dx.doi.org/10.1016/j.freeradbiomed.2017.02.026>.
82. QIN, Y.; LI, M.; FENG, X.; WANG, J. CAO, L. SHEN, X. K. Combined NADPH and the NOX inhibitor apocynin provides greater anti-inflammatory and neuroprotective effects in a mouse model of stroke. **Free Radical Biology And Medicine**, [s.l.], v. 104, p.333-345, mar. 2017. Elsevier BV. <http://dx.doi.org/10.1016/j.freeradbiomed.2017.01.034>.
83. QIU, J.; ZHAO, J.; LI, J.; LIANG, X.; YANG, Y.; ZHANG, Z. Apocynin attenuates left ventricular remodeling in diabetic rabbits. **Oncotarget**, [s.l.], v. 8, n. 24, p.38482-38490, 27 mar. 2017. Impact Journals, LLC. <http://dx.doi.org/10.18632/oncotarget.16599>.
84. QIU, J.; ZHAO, J.; LI, J.; LIANG, X.; YANG, Y.; ZHANG, Z. NADPH oxidase inhibitor apocynin prevents atrial remodeling in alloxan-induced diabetic rabbits. **International Journal Of Cardiology**, [s.l.], v. 221, p.812-819, out. 2016. Elsevier BV. <http://dx.doi.org/10.1016/j.ijcard.2016.07.132>.
85. RADÍ, Rafael. Peroxynitrite, a Stealthy Biological Oxidant. **Journal Of Biological**

- Chemistry**, [s.l.], v. 288, n. 37, p.26464-26472, 16 jul. 2013. American Society for Biochemistry & Molecular Biology (ASBMB).
http://dx.doi.org/10.1074/jbc.r113.472936.
86. RAINS, Justin L.; JAIN, Sushil K.. Oxidative stress, insulin signaling, and diabetes. **Free Radical Biology And Medicine**, [s.l.], v. 50, n. 5, p.567-575, mar. 2011. Elsevier BV.
http://dx.doi.org/10.1016/j.freeradbiomed.2010.12.006.
 87. RAHMAN, M.M.; MUSE, A.Y.; KHAN, I.O.; AHMED, I.H.; SUBHAN, N.; REZA, H.M. Apocynin prevented inflammation and oxidative stress in carbon tetra chloride induced hepatic dysfunction in rats. **Biomedicine & Pharmacotherapy**, [s.l.], v. 92, p.421-428, ago. 2017. Elsevier BV.
http://dx.doi.org/10.1016/j.biopha.2017.05.101.
 88. RAM, Shri. (2013). A bibliometric assessment of apocynin (*Apocynum cannabinum*) research **Annals of Library and Information Studies**, v. 60, p. 149-158, sept. 2013.
 89. RIBEIRO, M.S.P.; SILVA, D.P.; UEHARA, I.A.; RAMOS-JUNIOR, E.S. The use of apocynin inhibits osteoclastogenesis. **Cell Biology International**, [s.l.], p.1-12, 13 fev. 2019. Wiley.
http://dx.doi.org/10.1002/cbin.11110.
 90. SALEEM, Nikhat; PRASAD, Anamika; GOSWAMI, Shyamal K.. Apocynin prevents isoproterenol-induced cardiac hypertrophy in rat. **Molecular And Cellular Biochemistry**, [s.l.], v. 445, n. 1-2, p.79-88, 18 dez. 2017. Springer Nature.
http://dx.doi.org/10.1007/s11010-017-3253-0.
 91. SAREILA, O.; KELKKA, T.; PIZZOLLA, A.; HULTQVIST, M.; HOLMDAHL, R. NOX2 Complex-Derived ROS as Immune Regulators. **Antioxidants & Redox Signaling**, [s.l.], v. 15, n. 8, p.2197-2208, 15 out. 2011. Mary Ann Liebert Inc.
http://dx.doi.org/10.1089/ars.2010.3635.
 92. SCHIEBER, Michael; CHANDEL, Navdeep.. ROS Function in Redox Signaling and Oxidative Stress. **Current Biology**, [s.l.], v. 24, n. 10, p.453-462, maio 2014. Elsevier BV.
http://dx.doi.org/10.1016/j.cub.2014.03.034.
 93. SCHMIEDEBERG, O. Über die wirksamen bestandtheile der wurzel von *Apocynum cannabinum* L. **Arch. Exp. Path. Pharm**, v. 16, p.161-164; 1883.
 94. SCHULTZ, Julius; KAMINKER, Kenneth. Myeloperoxidase of the leucocyte of normal human blood. I. Content and localization. **Archives Of Biochemistry And Biophysics**, [s.l.], v. 96, n. 3, p.465-467, mar. 1962. Elsevier BV.
http://dx.doi.org/10.1016/0003-9861(62)90321-1.
 95. ŞENER, T.E.; YÜKSEL, M.; ÖZYILMAZ-YAY, N; ERCAN, F. Apocynin attenuates testicular ischemia-reperfusion injury in rats. **Journal Of Pediatric Surgery**, [s.l.], v. 50, n. 8, p.1382-1387, ago. 2015. Elsevier BV.
http://dx.doi.org/10.1016/j.jpedsurg.2014.11.033.
 96. SENEJOUX, F.; DEMOUGEOT, C.; KERRAM P.; AISA, H.A.; BERTHELOT, A.; BÉVALOT, F.; GIRARD-THERNIER, C. Bioassay-guided isolation of vasorelaxant compounds from *Ziziphora clinopodioides* Lam. (Lamiaceae). **Fitoterapia**, [s.l.], v. 83, n. 2, p.377-382, mar. 2012. Elsevier BV.
http://dx.doi.org/10.1016/j.fitote.2011.11.023.
 97. SIES, Helmut. Hydrogen peroxide as a central redox signaling molecule in physiological oxidative stress: Oxidative eustress. **Redox Biology**, [s.l.], v. 11, p.613-619, abr. 2017. Elsevier BV.
http://dx.doi.org/10.1016/j.redox.2016.12.035.
 98. SIMONS, J.M.; HART, B.A.; CHING, T.R.I.; DIJK, H.V.; LABADIE, R.P. METABOLIC activation of natural phenols into selective oxidative burst agonists by activated human neutrophils. **Free Radical Biology And Medicine**, [s.l.], v. 8, n. 3, p.251-258, jan. 1990. Elsevier BV.
http://dx.doi.org/10.1016/0891-5849(90)90070-y.
 99. SIMONYI, Agnes. The neuroprotective effects of apocynin. **Frontiers In Bioscience**, [s.l.], v. 4, n. 6, p.2183-2193, 2012. Frontiers in Bioscience.
http://dx.doi.org/10.2741/e535.

100. STEFANSKA, J.; SOKOLOWSKA, M.; SARNIAK, A.; WLODARCZYK, A.; DONIEC, Z.; NOWAK, D. Apocynin decreases hydrogen peroxide and nirtate concentrations in exhaled breath in healthy subjects. **Pulmonary Pharmacology & Therapeutics**, [s.l.], v. 23, n. 1, p.48-54, fev. 2010. Elsevier BV. <http://dx.doi.org/10.1016/j.pupt.2009.09.003>.
101. SCHMIEDEBERG, O. Über die wirksamen bestandtheile der wurzel von Apocynum cannabinum L. **Arch. Exp. Path. Pharm.** v.16, p.161-164; 1883.
102. STEFANSKA, J.; PAWLICZAK, R.. Apocynin: Molecular Aptitudes. **Mediators Of Inflammation**, [s.l.], v. 2008, p.1-10, 2008. Hindawi Limited. <http://dx.doi.org/10.1155/2008/106507>.
103. SUN, Yijun. Therapeutic effect of apocynin through antioxidant activity and suppression of apoptosis and inflammation after spinal cord injury. **Experimental And Therapeutic Medicine**, [s.l.], v. 13, n. 3, p.952-960, 25 jan. 2017. Spandidos Publications. <http://dx.doi.org/10.3892/etm.2017.4090>.
104. SUN, J.; MING, L.; SHANG, F.; SHEN, L.; CHEN, J.; JIN, Y. Apocynin suppression of NADPH oxidase reverses the aging process in mesenchymal stem cells to promote osteogenesis and increase bone mass. **Scientific Reports**, [s.l.], v. 5, n. 1, p.18572-18572, 21 dez. 2015. Springer Nature. <http://dx.doi.org/10.1038/srep18572>.
105. SUZUKI, S.; SHIRAGA, K.; SATO, S.; PUNFA, W.; NAIKI-ITO, A.; YAMASHITA, Y. Apocynin, an NADPH oxidase inhibitor, suppresses rat prostate carcinogenesis. **Cancer Science**, [s.l.], v. 104, n. 12, p.1711-1717, 28 out. 2013. Wiley. <http://dx.doi.org/10.1111/cas.12292>.
106. TIAN, R.; DING, Y. PENG, Y. Y. LUN, N. Myeloperoxidase amplified high glucose-induced endothelial dysfunction in vasculature: Role of NADPH oxidase and hypochlorous acid. **Biochemical And Biophysical Research Communications**, [s.l.], v. 484, n. 3, p.572-578, mar. 2017. Elsevier BV. <http://dx.doi.org/10.1016/j.bbrc.2017.01.132>.
107. TANRIVERDI, L.H.; PARLAKPINAR, H.; OZHAN, O.; ERMIS, N.; POLAT, A.; VARDI, N. Inhibition of NADPH oxidase by apocynin promotes myocardial antioxidant response and prevents isoproterenol-induced myocardial oxidative stress in rats. **Free Radical Research**, [s.l.], v. 51, n. 9-10, p.772-786, 3 out. 2017. Informa UK Limited. <http://dx.doi.org/10.1080/10715762.2017.1375486>.
108. TIAN, Y.; ZHANG, H. J.; TU, A.P.; DONG, J. X. Phenolics from traditional Chinese medicine *Sargentodoxa cuneata*. **Yaoxue Xuebao**, v.40, n. 7, p. 628-631, jul. 2005.
109. TOGLIATTO, Gabriele; LOMBARDO, Giusy; BRIZZI, Maria Felice. The Future Challenge of Reactive Oxygen Species (ROS) in Hypertension: From Bench to Bed Side. **International Journal Of Molecular Sciences**, [s.l.], v. 18, n. 9, p.1988-2005, 15 set. 2017. MDPI AG. <http://dx.doi.org/10.3390/ijms18091988>.
110. TORRES, Miguel Angel. ROS in biotic interactions. **Physiologia Plantarum**, [s.l.], v. 138, n. 4, p.414-429, abr. 2010. Wiley. <http://dx.doi.org/10.1111/j.1399-3054.2009.01326.x>.
111. WIECZFINSKA, Joanna; PAWLICZAK, Rafal. Thymic stromal lymphopoietin and apocynin alter the expression of airway remodeling factors in human rhinovirus-infected cells. **Immunobiology**, [s.l.], v. 222, n. 8-9, p.892-899, ago. 2017. Elsevier BV. <http://dx.doi.org/10.1016/j.imbio.2017.05.010>.
112. WINTERBOURN, C.C.; HAMPTON, M.B.; LIVESEY, J.H.; KETTLE, A.J. Modeling the Reactions of Superoxide and Myeloperoxidase in the Neutrophil Phagosome. **Journal Of Biological Chemistry**, [s.l.], v. 281, n. 52, p.39860-39869, 30 out. 2006. American Society for Biochemistry & Molecular Biology (ASBMB). <http://dx.doi.org/10.1074/jbc.m605898200>.

113. WONG, Shaun P.; FONG, Vai Hong; VIEIRA, Amandio. Activities of apocynin in cytotoxicity assays of potential pathological relevance. **Biomedicine & Pharmacotherapy**, [s.l.], v. 76, p.6-10, dez. 2015. Elsevier BV. <http://dx.doi.org/10.1016/j.biopha.2015.10.007>.
114. WRIGHT, H.L.; MOOTS, R.J.; BUCKNALL, R.C.; EDWARDS, S.W. Neutrophil function in inflammation and inflammatory diseases. **Rheumatology**, [s.l.], v. 49, n. 9, p.1618-1631, 24 mar. 2010. Oxford University Press (OUP). <http://dx.doi.org/10.1093/rheumatology/keq045>.
115. WU, Jing; HARRISON, David G.. Oxidative Stress and Hypertension. **Blood Pressure And Arterial Wall Mechanics In Cardiovascular Diseases**, [s.l.], p.175-191, 2014. Springer London. http://dx.doi.org/10.1007/978-1-4471-5198-2_15.
116. XIAO, HANG; PARKIN, KIRK L.. Isolation and identification of potential cancer chemopreventive agents from methanolic extracts of green onion (*Allium cepa*). **Phytochemistry**, [s.l.], v. 68, n. 7, p.1059-1067, abr. 2007. Elsevier BV. <http://dx.doi.org/10.1016/j.phytochem.2007.01.021>.
117. XIN, R.; SUN, X.; WANG, Z.; YUAN, W.; JIANG, W.; XIANG, Y. Apocynin inhibited NLRP3/XIAP signalling to alleviate renal fibrotic injury in rat diabetic nephropathy. **Biomedicine & Pharmacotherapy**, [s.l.], v. 106, p.1325-1331, out. 2018. Elsevier BV. <http://dx.doi.org/10.1016/j.biopha.2018.07.036>.
118. XIMENES, V.F.; KANEGAE, M.P.P.; RISSATO, R.S.; GALHIANE, M.S. The oxidation of apocynin catalyzed by myeloperoxidase: Proposal for NADPH oxidase inhibition. **Archives Of Biochemistry And Biophysics**, [s.l.], v. 457, n. 2, p.134-141, jan. 2007. Elsevier BV. <http://dx.doi.org/10.1016/j.abb.2006.11.010>.
119. YOON, J.H.; AN, S.H.; KYEONG, I.G.; LEE, M.S.; KWON, S.C. KANG, J.H. Oxidative modification of ferritin induced by hydrogen peroxide. **Bmb Reports**, [s.l.], v. 44, n. 3, p.165-169, 31 mar. 2011. Korean Society for Biochemistry and Molecular Biology - BMB Reports. <http://dx.doi.org/10.5483/bmbrep.2011.44.3.165>.
120. ZAHIRUDDIN, Sultan. Pharmacokinetics and comparative metabolic profiling of iridoid enriched fraction of *Picrorhiza kurroa* – An Ayurvedic Herb. **Journal Of Ethnopharmacology**, [s.l.], v. 197, p.157-164, fev. 2017. Elsevier BV. <http://dx.doi.org/10.1016/j.jep.2016.07.072>.
121. ZHANG, Chun-lei. Apocynin derivatives from *Iris tectorum*. **Journal Of Asian Natural Products Research**, [s.l.], v. 19, n. 2, p.128-133, 12 jan. 2017. Informa UK Limited. <http://dx.doi.org/10.1080/10286020.2016.1268128>.
122. ZHANG, J.; WANG, X.; VIKASH, V.; YE, Q.; WU, D.; LIU, Y. ROS and ROS-Mediated Cellular Signaling. **Oxidative Medicine And Cellular Longevity**, [s.l.], v. 2016, p.1-18, 2016. Hindawi Limited. <http://dx.doi.org/10.1155/2016/4350965>.

Table 1. Beneficial effects of apocynin and its radical and dimeric on disease models.

Medical complication	Biological markers and decreased effects of the disease	References
Models of ischemia		
Pulmonary ischemia	Reduction of NADPH oxidase activity; Suppress the generation of ROS; Hemodynamic monitoring indices of attenuated lung lesions; Attenuated apoptotic indices.	(Chiang and Chuang, 2011)
Myocardial ischemia	Reduction of NADPH oxidase activity; Significantly smaller myocardial infarction size; The proportion of cardiomyocyte apoptosis reduced; Reduction of myocardial mRNA, expression of VOP1 and NOX2 proteins, serum CK, myocardial NOX, and caspase-3 activity.	(Luo <i>et al.</i> , 2012)
Injury by ischemia / reperfusion (I/ R) and torsion / distortion (T/ D) in testicles	Inhibits the generation of free radicals and increases antioxidant defense; Reduction of NADPH oxidase activity; Reduction of MPO activity and malonaldehyde levels (MDA); Significant increase in glutathione (GSH) and SOD activity.	(Şener <i>et al.</i> , 2015; Ozbek <i>et al.</i> , 2015)
Renal Ischemia	Decrease in MDA levels; Significant increase of GSH and SOD; Lower levels of zinc in serum and renal tissues; Reduction of blood urea nitrogen (BUN) and serum creatinine (Scr).	(Choi <i>et al.</i> , 2015; Hu <i>et al.</i> , 2016)
Ischemic injury in the spinal cord	Reduction of NADPH oxidase activity; Reduction of MPO activity and MDA levels; Significant increase in GSH and SOD.	(Sun <i>et al.</i> , 2017)
Stroke induced by ischemia/ reperfusion (I/ R)	Significant attenuation in Nox2 and ROS levels; It avoids increases in cyclooxygenase (COX2) and inducible nitric oxide synthase (iNOS) in the cortex induced by I / R; Suppression of expression of inflammatory expression proteins, including NLRP3 ASC, caspase-1, IL-1 β and IL-18 in the ischemic cortex; Inhibits the activation of NF-kB; Significant blockade of increases in NOx2 and NOX4 protein levels induced by I / R; Reduction of infarct volume, Improvement in post-stroke survival; Recovery of neurological functions.	(Qin <i>et al.</i> , 2017)
Cerebral ischemia	Reduction of NADPH oxidase activity; Increased GSH and SOD; Restoration of mitochondrial membrane potential; Reduction of behavioral deficits in post cerebral ischemia; Mitochondrial injury attenuation; Restoration of MMP and mitochondrial enzymes.	(Kapoor <i>et al.</i> , 2018)

Cancer		
Prostate cancer	<p>Reduction of ROS;</p> <p>The number of carcinomas in the ventral and lateral prostates were significantly reduced;</p> <p>Inhibition of the production of reactive oxygen species in the human prostate cancer cell line (LNCaP);</p> <p>Blockage of cell growth by inducing G0 / G1 stop with negative regulation of clusterin and cyclin D1.</p>	(Suzuki <i>et al.</i> , 2013)
Intestinal cancer	<p>Reduction of loci of colorectal aberrant crypts in KK-A (and) obese mice;</p> <p>Reduction in the number of intestinal polyps in Min mice;</p> <p>Decreased induced levels of nitric oxide synthase mRNA in polyp tissues;</p> <p>Suppression of nuclear-κB factor transcriptional activity <i>in vitro</i>.</p>	(Komiya <i>et al.</i> , 2015)
Skin cancer	<p>Apocynin significantly reduced expression of major carcinogenic factors in skin cells;</p> <p>Suppression of UVB-induced COX-2 promoter activity;</p> <p>Inhibition of UVB-induced phosphorylation of p38, ERK, JNK and Akt in a dose-dependent manner;</p> <p>Attenuation of signaling pathways involved in skin inflammation and carcinogenesis.</p>	(Byun <i>et al.</i> , 2016)
<i>Helicobacter pylori</i> stomach-Induced cancer	<p>Reduction of <i>H. pylori</i>-activated gastritis;</p> <p>Reduced neutrophil infiltration in the colon mucosal region;</p> <p>Decreased <i>H. pylori</i>-induced well abscess formation;</p> <p>No indication of drug toxicity.</p>	(Horemans <i>et al.</i> , 2017)
Metastasis	<p>Regulation of the invasion process by inhibiting phosphorylation of FAK and Akt and consequent suppression of metastasis in a model of hepatocellular carcinoma by apocynin dimer.</p>	(Jantaree <i>et al.</i> , 2017)
Consequential effects of <i>Diabetes mellitus</i>		
Atrial fibrillation in <i>Diabetes mellitus</i>	<p>A marked reduction in the inducibility of atrial fibrillation (AF);</p> <p>Atrial structural remodeling attenuation in diabetic rabbits;</p> <p>Reduction of DM-induced protein expression of TGF-β, NF-κB, P-p38, P-JNK, ERK, and P-ERK.</p>	(Qiu <i>et al.</i> , 2016)
Vascular and myocardial dysfunction in the <i>Diabetes mellitus</i>	<p>Reduction of serum NO, MPO and MDA levels;</p> <p>Reduced protein expression levels of rac1 and nuclear factor-κB;</p> <p>Transforming growth factor-β, p38, P-p38, and metalloproteinase-9;</p> <p>Increased levels of SOD.</p>	(Qiu <i>et al.</i> , 2017)
Cardiac remodeling in <i>Diabetes mellitus</i>	<p>The increased diastolic function of the left ventricle;</p> <p>Restoration of serum antioxidant enzyme activity: glutathione, peroxidase, SOD, and catalase;</p> <p>Improvement of ventricular diastolic function and myocardial contractile function.</p>	(Gimenes <i>et al.</i> , 2018)

Neuropathy in <i>Diabetes mellitus</i>	<p>Relief of diabetic neuropathic pain;</p> <p>Increased conductance of sciatic nerve and blood flow in diabetic rats;</p> <p>Decreased expression of Nox-p47phox;</p> <p>Reduction of nNOS and iNOS immunoreactivity;</p> <p>Increased immunoreactivity S-100 (Schwann cell marker);</p> <p>Increased expression of Nox and catalase in the spinal cord.</p>	(Olukman <i>et al.</i> , 2018)
Nephropathy in <i>Diabetes mellitus</i>	<p>Reduction of renal damage and improvement of renal function;</p> <p>Negative regulation of NLRP3 expression in the renal cortex;</p> <p>Negative regulation of XIAP expression in the renal cortex;</p> <p>Attenuation of renal fibrosis.</p>	(Xin <i>et al.</i> , 2018)
Vascular diseases		
Hypertension	<p>Significant reduction of mean arterial pressure in spontaneously hypertensive rats (SHR);</p> <p>Improvement of the hypotensive effect of impaired acetylcholine (ACh) in SHR;</p> <p>Decreased levels of oxidative stress;</p> <p>Normalization of the overexpression of Nox2 and its p47phox subunit in SHR aortas.</p>	(Perassa <i>et al.</i> , 2016)
Hypotensive effect	<p>Promoting hypotensive effects without altering heart rate;</p> <p>Induction of independent and endothelium-dependent relaxation;</p> <p>Decreased levels of ROS in endothelial cells.</p>	(Potje <i>et al.</i> , 2017)
Hypertension	<p>Reduction of blood pressure;</p> <p>Prevention of the development of endothelial dysfunction;</p> <p>Reduction of Ang II pressure effects;</p> <p>Increased plasma antioxidant capacity;</p> <p>Decreased production of Nox-dependent aortic and mesenteric oxidants;</p> <p>Overexpression of Nox2 and p47phox;</p> <p>Increased levels of plasma and aortic nitrate / nitrate;</p> <p>Increased endothelial modulation of Ang II vasoconstriction in arteries of resistance to SHR.</p>	(Graton <i>et al.</i> , 2019)
Neurological diseases		
Alzheimer's disease	<p>Improvement in cerebrovascular behavior and function;</p> <p>Reduction of oxidative stress;</p> <p>Reduction of carbonyl levels in the cerebral cortex.</p>	(Dumont <i>et al.</i> , 2011)
Rescue of reduced neurogenesis after seizures	<p>Reduction of oxidative injury induced by seizures;</p> <p>Reduction of neuronal death;</p> <p>Increased hippocampal neuronal survival newly generated by reduced superoxide production following seizures;</p> <p>Increased neuroblast production following seizures.</p>	(Lee <i>et al.</i> , 2018)
Parkinson's disease	<p>Significant improvement of learning and memory deficits;</p>	(Hou <i>et al.</i> , 2019)

	Improvement in hippocampal neurodegeneration and alpha-synuclein pathology in the hippocampus; Reduction of microglial activation; Inhibition of activation of signal transducers and activators of transcription pathways 1 (STAT1) and nuclear factor kappa B (NF-κB), two key regulatory factors for microglial M1 inflammatory response.	
Cardiac diseases		
Cardiac remodeling induced by pressure overload	Inhibition of collagen deposition; Level reduction of metalloproteinase (MMP-2); Reduction of NADPH oxidase activity; Reduction of the apoptotic index of cardiomyocytes; Reduction of ROS production.	(Liu <i>et al.</i> , 2017)
Cardiac hypertrophy	Blockade of the hypertrophic responses evidenced by the HW / BW ratio, HW / TL ratio, echocardiogram, and histopathology; Reduction of transcription levels of p22-phox; Restoration of glutathione level; Prevention of increased mRNA levels of various markers of hypertrophy, including ANP, BNP, β-MHC, and ACTA-1; Reduction of oxidative stress in the heart.	(Saleem <i>et al.</i> , 2018)
Other diseases of inflammatory character		
Bronchial asthma	Inhibition of the expression of transforming growth factor beta (TGF-β) and arginase I induced by rhinovirus; Significant increase in mRNA expression of tissue inhibitors of TIMP-1 metalloproteinases.	(Wieczfinska and Pawliczak, 2017)
Potential for osteogenesis	Reversal of the aging process in mesenchymal stem cells; Increased bone mineral density and total bone volume; Reduced expression of p53; Partial inversion of the aging process and the increase of the osteogenic potential.	(Sun <i>et al.</i> , 2015)
Proliferative vitreoretinopathy (PVR)	Significant decrease in the formation of PVR in histopathological and ophthalmoscopic examinations.	(Ozer <i>et al.</i> , 2016)
Colitis	Protection against inflammatory bowel disease; Reduction of ROS production levels and TNF-α, IL-6 and IL-1β flags; Inhibition of expression of nitric oxide synthase (iNOS) and cyclooxygenase (COX-2); Decreased NO production and prostaglandins (PGE2).	(Marín <i>et al.</i> , 2017)
Nephrotoxicity	Improvement in tissue morphology; A significant decrease in 24-h urine volume, renal somatic index (RSI), urine protein, lactate dehydrogenase (LDH), creatinine (Cr), blood urea nitrogen (BUN), nitric oxide (NO) and malondialdehyde (MDA). Significant elevation in SOD and renal CCr activity;	(Abdelrahman, 2017)
Liver dysfunction	Decreased activities of alanine aminotransferase, aspartate aminotransferase, and alkaline phosphatase;	(Rahman <i>et al.</i> , 2017)

	<p>Considerable reduction of oxidative stress markers MDA, MPO, NO, and apoptotic levels;</p> <p>Restoration of antioxidant enzymes catalase and SOD;</p> <p>Prevention of infiltration of inflammatory cells and fibrosis;</p>	
Osteoclastogenesis	<p>Decrease in the number of cells positive for tartrate resistant acid phosphatase (TRAP) and the area of osteoclasts;</p> <p>Inhibition of osteoclastogenesis by RANK-RANKL-related signaling pathways;</p> <p>Decrease in osteoclast markers;</p> <p>Reduces intracellular calcium concentration.</p>	(Ribeiro <i>et al.</i> , 2019)

DESENVOLVIMENTO DA COMPOSIÇÃO E TECNOLOGIA PARA A PRODUÇÃO DE DROGAS ENCAPSULADAS COM BASE EM 3,7-DIAZABICICLO[3.3.1]NONANO

DEVELOPMENT OF THE COMPOSITION AND TECHNOLOGY FOR THE PRODUCTION OF ENCAPSULATED DRUGS BASED ON 3,7-DIAZABICYCLO[3.3.1]NONANE

РАЗРАБОТКА СОСТАВА И ТЕХНОЛОГИИ ПОЛУЧЕНИЯ КАПСУЛИРОВАННОГО ЛЕКАРСТВЕННОГО СРЕДСТВА НА ОСНОВЕ 3,7-ДИАЗАБИЦИКЛО[3.3.1]НОНАНА

BRKICH, Galina Eduardovna¹; PYATIGORSKAYA, Natalia Valeryevna²; DEMINA, Natalya Borisovna³; BAKHRUSHINA, Elena Olegovna⁴; LAVROV, Mstislav Igorevich⁵;

^{1,2,3,4} Sechenov First Moscow State Medical University, Moscow - Russia.

⁵ Lomonosov Moscow State University, Moscow – Russia.

* Correspondence author

e-mail: brkich@yandex.ru

Received 18 December 2019; received in revised form 15 February 2020; accepted 26 February 2020

RESUMO

Os seguintes fatores biológicos e farmacêuticos influenciam a eficácia terapêutica e a bioequivalência de medicamentos: propriedades físico-químicas de uma substância farmacêutica, biodisponibilidade, meio de dosagem, via de administração, natureza dos excipientes, sua compatibilidade, bem como condições tecnológicas de produção, incluindo a preparação de formulários de medicamentos. Antes da produção em massa de um medicamento, os parâmetros e características tecnológicas da substância farmacêutica devem ser cuidadosamente estudados e comprovados cientificamente. Este trabalho é dedicado ao estudo das propriedades tecnológicas de uma substância farmacêutica original baseada no derivado de 3,7-diazabíciclo [3.3.1]nonano com o nome químico IUPAC 6-[4metoxi-3-(1H-pirazol-1-ilmetil)benzil]-1,11dimetil-3,6,9-triazatriciclo[7.3.1.1]tetradecano-4,8,12-trion, usado como substância ativa para o desenvolvimento da composição e tecnologia para a preparação de formas de dosagem orais em forma de cápsula. O artigo apresenta os resultados do desenvolvimento e teste de um medicamento sob a forma de cápsulas da substância farmacêutica original da ação nootrópica do 3,7-diazabíciclo[3.3.1]nonano, que é praticamente insolúvel em água. O estudo identificou e avaliou as propriedades tecnológicas e biológicas de uma substância farmacêutica que podem afetar a atividade farmacológica na produção de uma forma de dosagem. O estudo examinou os principais indicadores: solubilidade, tamanho de partícula, fluidez, densidade aparente. As características tecnológicas da substância farmacêutica são estudadas não apenas por certos valores das características indicadas, mas também pelos valores dos índices de Hausner e Carr. Os dados obtidos sugerem o conteúdo e o progresso de outras etapas do desenvolvimento farmacêutico. A presença da fase de atraso na dissolução de cápsulas de hipromelose em meio com pH de 1,2 e taxas de desintegração relativamente baixas em meios com pH de 1,2, pH 4,5 e pH 6,8 serviu de base para a escolha de cápsulas de gelatina. A forma farmacêutica desenvolvida atende aos modernos requisitos farmacopéicos, incluindo a cinética de dissolução: de acordo com os resultados obtidos, em 45 minutos (77,6 ± 2,5)% da substância passa para o meio de dissolução com um pH de 4,5. Os resultados do estudo são utilizados para desenvolver um esquema tecnológico para a obtenção da forma de dosagem de 3,7-diazabíciclo[3.3.1]nonano, seus indicadores e padrões de qualidade.

Palavras-chave: *ampaquinas, drogas nootrópicas, derivados do 3,7-diazabíciclo[3.3.1]nonano, desenvolvimento farmacêutico de formas farmacêuticas, cápsulas.*

ABSTRACT

The following biological and pharmaceutical factors influence the therapeutic efficacy and bioequivalence of drugs: physicochemical properties of a pharmaceutical substance, bioavailability, type of dosage form, route of administration, nature of excipients, their compatibility, as well as technological conditions of production, including the preparation of drug forms. Before mass production of a drug, the technological parameters and characteristics of the pharmaceutical substance must be carefully studied and scientifically substantiated. This work is devoted to the study of the technological properties of an original pharmaceutical substance based on the derivative of 3,7-diazabicyclo[3.3.1]nonane with the chemical name IUPAC 6-[4methoxy-3-(1H-pyrazol-1-

ylmethyl) benzyl] -1,11dimethyl-3,6,9-triazatricyclo[7.3.1.1]tetradecane-4,8,12-trion, used as an active substance for the development of the composition and technology for the preparation of oral dosage forms in capsule form. The article presents the results of the development and testing of a drug in the form of capsules of the original pharmaceutical substance of the nootropic action of 3,7-diazabicyclo[3.3.1]nonane, which is practically insoluble in water. The study identified and evaluated the technological and biological properties of a pharmaceutical substance that can affect the pharmacological activity in the production of a dosage form. The study examined the key indicators: solubility, particle size, flowability, bulk density. The technological characteristics of the pharmaceutical substance are studied not only by certain values of the indicated characteristics but also by the values of the Hausner and Carr indices. The data obtained suggest the content and progress of further stages of pharmaceutical development. The presence of the lag phase when dissolving hypromellose capsules in a medium with a pH of 1,2 and relatively low disintegration rates in media with a pH of 1,2, pH 4,5, and pH 6,8 served as the basis for the choice of gelatin capsules. The developed dosage form meets modern pharmacopoeial requirements, including the dissolution kinetics: according to the results obtained, in 45 minutes ($77,6 \pm 2,5$)% of the substance passes into the dissolution medium with a pH of 4,5. The results of the study are used to develop a technological scheme for obtaining the dosage form of 3,7-diazabicyclo[3.3.1]nonane, its indicators, and quality standards.

Keywords: *ampakines, nootropic drugs, derivatives of 3,7-diazabicyclo[3.3.1]nonane, pharmaceutical development of dosage forms, capsules.*

АННОТАЦИЯ

На терапевтическую эффективность и биоэквивалентность лекарственных средств влияют следующие биологические и фармацевтические факторы: физико-химические свойства фармацевтической субстанции, ее биодоступность, вид лекарственной формы, путь введения, природа вспомогательных веществ, их совместимость, а также технологические условия производства, в том числе при получении лекарственных форм. Перед серийным производством лекарственного средства должны быть тщательно изучены и научно обоснованы технологические параметры и характеристики фармацевтической субстанции. Настоящая работа посвящена изучению технологических свойств оригинальной фармацевтической субстанции на основе производного 3,7-диазабицикло[3.3.1]нонана с химическим названием IUPAC 6-[4метокси-3-(1Н-пиразол-1-илметил)бензил]-1,11диметил-3,6,9-триазатрицикло[7.3.1.1]тетрадекан-4,8,12-триона, используемую в качестве действующего вещества для разработки состава и технологии получения лекарственной формы для перорального применения в форме капсул. В статье приведены результаты разработки и испытаний лекарственного средства в форме капсул оригинальной фармацевтической субстанции ноотропного действия 3,7-диазабицикло[3.3.1]нонана, обладающей низкими технологическими характеристиками, практически нерастворимой в воде. В исследовании были определены и оценены технологические и биологические свойства фармацевтической субстанции, способные оказать влияние на фармакологическую активность при производстве лекарственной формы. В исследовании были изучены ключевые показатели: растворимость, размер частиц, сыпучесть, насыпную плотность. Технологические характеристики фармацевтической субстанции исследованы не только по определенным значениям указанных характеристик, но и по величинам индексов Хауснера и Карра. Полученные данные позволили предположить содержание и ход дальнейших этапов фармацевтической разработки. Наличие лаг-фазы при растворении гипромелозных капсул в среде с pH 1,2 и относительно низкими показателями распадаемости в средах с pH 1,2 pH 4,5 и pH 6,8 послужило основанием выбора желатиновых капсул. Разработанная лекарственная форма отвечает современным фармакопейным требованиям, в том числе по кинетике растворения: согласно полученным результатам за 45 минут в среду растворения с pH 4,5 переходит ($77,6 \pm 2,5$) % субстанции. Результаты исследования используются для разработки технологической схемы получения лекарственной формы 3,7-диазабицикло[3.3.1]нонана, ее показателей и норм качества.

Ключевые слова: *ампакины, ноотропные лекарственные средства, производные 3,7-диазабицикло[3.3.1]нонана, фармацевтическая разработка лекарственных форм, капсулы.*

1. INTRODUCTION

In the last 15 years, stroke remains one of the leading causes of death in the world. According to WHO statistics, in 2015, the death rate in the world from stroke amounted to 6,24 million people, which is exceeded the same

indicator in 2000 (5,41 million) by 15,3% (World Health Organization, 2019; Powers, *et al.*, 2018; Hui *et al.*, 2020).

Expanding the possibilities of treating patients who suffered acute brain hypoxia or other cerebrovascular diseases is a crucial task of

pharmaceutical development (Clarkson *et al.*, 2011; Schitine *et al.*, 2012; Su *et al.*, 2016; Gudasheva *et al.*, 2016; Pyatigorskaya *et al.*, 2018). In recent years, tricyclic derivatives of 3,7-diazabicyclo[3.3.1]nonane- ampakines - which are positive allosteric modulators of glutamate AMPA receptors (PAM-AMPA), have attracted the attention of researchers. Drugs of a similar structure provide the production of neurophilic factors and have a nootropic effect (Rumyantseva *et al.*, 2014; Selyavko, Tsvetkova, 2016; Sernov, Gatsura, 2000).

As a result of the studies carried out by the project developers, computer modeling and optimization of over 200 new structures of the PAM-AMPA receptor - derivatives of 3,7-diazabicyclo[3.3.1]nonane, potentially possessing positive modulatory activity to AMP receptors, was carried out, and the synthesis of the most promising of them was performed (selected by simulation results). Approaches to the synthesis of 3,7-diazabicyclo[3.3.1]nonane derivatives have been developed, which, according to docking data, bind well to the AMPA receptor modulator sites. Based on the analysis of the spatial structure of the AMPA receptor, its complexes with the known PAM AMPA receptor, and the results of their molecular docking, it was shown that compounds of derivatives of 3,7-diazabicyclo[3.3.1]nonane can be highly effective AMPA receptor modulators with pronounced physiological effect (Lavrov, 2011; Zapolski *et al.*, 2018).

Physiological researches of the synthesized derivatives of 3,7-diazabicyclo[3.3.1]nonane (bispidine) showed high positive modulation activity against AMPA receptors in vitro tests performed by electrophysiological method, and in vivo tests showed pronounced neuroprotective properties, a significant improvement in memory and cognitive functions in animals (Zefirov *et al.*, 2013).

It is assumed that indications for the use of the obtained compounds, positive AMPA receptor modulators, will include acceleration and improvement of the quality of convalescence after cerebral catastrophes since the acute phase and the phase of convalescence are provided by various pathogenetic mechanisms (Hebert *et al.*, 2016; Zakharov, 2014; Skrebitsky *et al.*, 2008; Denisov *et al.*, 2013).

The section "Pharmaceutical development" in the application for registration of the drug makes possible to present information obtained by applying scientific approaches and managing

quality risks in the development of a product and production process. Pharmaceutical development includes comprehensive experimental studies aimed at the scientific justification of the composition of the drug in a particular dosage form, the technological process and its control, the choice of packaging materials, and also contains a study of the physicochemical, biological and microbiological properties of the product. The methodological approach of the pharmaceutical development, currently adopted in the world, is standardized in ICH Q8 Guidelines "Pharmaceutical Development" (Pharmaceutical Development Q8(R2), 2009).

The aim of this work was to develop the drug "3,7-diazabicyclo[3.3.1]nonane" of appropriate quality and justification of the production process with specified functional characteristics.

2. MATERIALS AND METHODS

Pharmaceutical substance based on the derivative 3,7-diazabicyclo[3.3.1]nonane with the chemical name IUPAC 6-[4methoxy-3- (1H-pyrazol-1-yl-methyl) benzyl] -1,11 dimethyl-3,6, 9-triazatricyclo[7.3.1.1]tetradecane-4,8,12-trione, synthesized in the Department of Chemistry, Lomonosov Moscow State University.

Excipients.

Protanal CR 8133® sodium alginate, manufactured by FMC BioPolymer, USA, having a viscosity of 100-300 centipoise (2% solution), with a particle size (0,104-0,125 mm) and an M / G block ratio of 30-40 / 60-70.

Partially pregelatinized Lycatab PGS® corn starch from Roquette, France. The particle size is 100 microns. Sodium Starch Glycolate Colloidal silicon dioxide (Aerosil) with a surface area of 200 m²/g. Calcium chloride is used as a granulating substance.

Gelatin capsules / HPMC № 3 CAPSUGEL. Capsules filling were performed using a Profiller 2007 manual capsule filling machine (Capsuleconnection, LLC, USA). The solvents and reagents used in the work corresponded in quality to the requirements of Russian Pharmacopeia.

Determination of the particle size of the powder of the substance and the granulate was carried out on the installation for the sieve test of ERWEKA PSS, Germany. Determination of tap density was carried out on a tester "SVM 121" company Erweka GmbH, Germany. Determination of low-ability and angle of repose was carried out on a low-ability tester ERWEKA GTB, Germany,

the size of the outlet of the funnel - 10 and 25 mm; Determination of moisture load was determined using a laboratory instrument AND MS-70 Moisture Analyzer. Drying temperature - 105 °C. Accuracy of determination – 0,01% / min. Granulation was carried out on a laboratory mixer-granulator with a high shear force. The determination of the decay rate was carried out on a "swing basket" type ZT 220 from Erweka GmbH, Germany.

Three media were used: 0,1 M hydrochloric acid solution with pH = 1,2; acetate buffer with pH = 4,5; and phosphate buffer with pH = 6,8. Additionally, 1% of Tween 80 was added to each medium. The medium temperature was (37 ± 0,5) ° C. The volume was 800 ml, and the experiment was carried out without using caps.

The study of the comparative dissolution kinetics was carried out using instrument "arm mixer" at a rotation speed of the stirrer of 50 rpm.

The kinetics of dissolution was studied in three buffer media: with pH = 1,2 (0,1 M hydrochloric acid solution); with pH = 4,5 (acetate buffer) and with pH = 6,8 (phosphate buffer), according to the design of Product specification file the dissolution medium is 0,1 M hydrochloric acid. Since the substance is insoluble in water, 1% Tween-80 was added to the medium. Samples were taken after 5, 10, 15, 30, and 45 minutes in 10 ml portions. The same volume of the corresponding buffer solution was added to the dissolution medium to maintain the volume. The obtained samples were cooled at room temperature, filtered through a blue ribbon paper filter, discarding the first 5 ml of filtrate. The content of the substance in each sample was determined by HPLC.

To obtain statistically reliable results, the study was performed on 6 capsules. The dissolution medium was prepared in accordance with general monograph 1.3.0003.15 "Buffer solutions" (State Pharmacopoeia XIV of Russian Federation). Method of quantitative determination of the released substance. The conditions of the analysis are shown in Tables 1 and 2.

3. RESULTS AND DISCUSSION

The great significance of the dosage form in ensuring the therapeutic performance of drugs has been seriously proven, and today there is no doubt (Zefirov *et al.*, 2013; Demina, 2017; Menshikov, 1986). The rationale of the composition and technology of the dosage form of the original pharmaceutical substance was carried out by

taking into account technological and physic and chemical characteristics.

The substance of 3,7-diazabicyclo[3.3.1]nonane is a white, odorless, amorphous powder. It is well soluble in chloroform, acetonitrile, methylene chloride, acetone, dimethylsulfoxide, dimethylformamide, ethyl alcohol, and methyl alcohol. Slightly soluble in diethyl ether, dioxane. Almost insoluble in purified water. Solubility data allow the substance to be classified in the II / IV class of the Biopharmaceutical classification system. The low solubility of the substance will serve as a factor limiting the absorption. To improve the therapeutic performance of such substances, various technologies have been developed to increase both solubility and dissolution rates (Demina, 2015). The results characteristics of the substance of 3,7-diazabicyclo[3.3.1]nonane are shown in Table 3.

Table 3. Averaged results of determining the technological characteristics of the substance of 3,7-diazabicyclo[3.3.1]nonane, obtained from measurements of 6 samples

Indicator, unit of measure	Magnitude
Particle size	Less than 100 microns
Flowability, g / s	1, 7±0,2*
Tap density before compaction, g / ml	0,15±0,03
Tap density after compaction, g / ml	0,24±0,02
Angle of repose, degrees	45±3
Humidity, %	0,22±0,3
Carr Index	37,4±0,2
Haussner index	1,59±0,2

*The obtained value is the hole diameter of the funnel - 10 mm.

The results indicate low technological properties of the substance (low-ability, angle of repose single, tap density). Moreover, the powder is dusty and electrified. Based on the calculated values of the Carr and Haussner indices, the low-ability of the substance was rated as "very bad."The obtained information on the characteristics of the substance of 3,7-diazabicyclo[3.3.1]nonane served to choice dosage form - capsules. In the production of capsules, compared to tablets, the active substance is not subjected to stressful technological effects (moistening, drying, pressing), which can adversely affect on release from the dosage form and, possibly, later on,

bioavailability (Demina, 2015).

The experimentally established dosage of 3,7-diazabicyclo[3.3.1]nonane was 15 mg, which is fully consistent with the selected dosage form but justifies the inclusion of excipients. Excipients substances were selected based on their compliance with modern standards of quality, safety and manufacturing. The main filler was sodium alginate. Alginates are high-molecular polysaccharides obtained by extraction and subsequent precipitation with sodium chloride or potassium chloride from Phaeophyceae brown algae, capable of gelation, which is widely used in various dosage forms: pastes, gels, and creams, as well as a release regulator from solid dosage forms. Alginates have mucoadhesive properties that have a positive impact on the efficiency of the insoluble medicinal substance (Kirzhanova *et al.*, 2016). Pregelatinized corn starch is included in the powder mixture as a universal filler and disintegrant, as well as to increase flowability. Sodium starch glycolate was used as a disintegrant to ensure the disintegration of the compacted contents of capsules. As a result, to ensure the release of the active substance in normalized values when conducting an analysis on the "Dissolution" indicator. Aerosil was used as a glidant. The small size of the particles and a large specific surface area prevent the caking of powdered materials and contribute to the redistribution of moisture in the material during granulation. Calcium chloride served as a granulating agent. The composition of 3,7-diazabicyclo[3.3.1]nonane capsules is shown in Table 4.

The powder mixture was granulated before filling into capsules. Perforce to granulating was justified by obtaining a homogeneous composition of the bulk product for the preparation of the contents of the capsules. Due to the low solubility of the substance, not traditional viscous solutions of bonding agents were used as the granulating liquid, but purified water and 95% ethyl alcohol, in which the substance is soluble. Excipients: sodium alginate, pregelatinized starch, and sodium starch glycolate were mixed. The substance was added and again thoroughly mixed, granulated, powdered with aerosil and calcium chloride, previously sifted through a sieve with 0,315 mm holes. The mixture left to distribute moisture in a closed bin for 10-12 hours. It was found during the experiment that the formation of granules when the powder mixture is moistened with purified water, in which the substance is insoluble, proceeds only through pregelatinized corn starch and partially sodium alginate. The resulting

product is represented by particles of irregular shape, among which both granules and free particles of substance were present (Swarbrick, 2016; Qualicaps, 2011; Technical Reference File Hard Gelatin Capsules, 2010; Hojava *et al.*, 2013, Gad *et al.*, 2013; Bykovsky *et al.*, 2015; Knitter *et al.*, 2014; Harmonized tripartite guidance ICH Q6A, 2000). Using 95% ethanol as a granulating liquid, in which the substance is well soluble, the granules have a more rounded shape and a smooth surface, there are no particles of the substance in the product. In this case, not only fillers but also pharmaceutical substances take part in the formation of granules due to their dissolution in 95% ethanol. The technique used made it possible to ensure uniformity of dosing, which is extremely important in the manufacture of dosage forms with a low dosage of the substance. The amount of moisturizing liquid used in the granulation process was exactly determined during the experiment for each composition and did not exceed 5% of the total mass of the powder mixture. Averaged results of the determination of the characteristics of the technological granules, obtained as a result of measurements of 6 samples, are given in Table 5.

Table 5. Averaged results of determining the technological characteristics of the granulate, obtained as a result of measurements of 6 samples

Indicator, unit of measure	Magnitude
Particle size	100 to 315 microns
Flowability, g / s	5,91±0,04
Tap density before compaction, g / ml	0,44±0,03
Tap density after compaction, g / ml	0,51±0,03
Angle of repose, degrees	35±2
Humidity, %	0,22±0,04
Carr Index	13,72±0,02
Haussner index	1,16±0,02

The results indicate good technological properties of the granulate: the flowability compared with the substance increased from 1,7 to 5,9 g / s, the tap density before compaction increased from 0,15 to 0,44 g / ml, the tap density after compaction - from 0,24 to 0,51 g / ml. Based on the calculated values of the Carr and Haussner indices, the flowability of the substance was rated as "good". The averaged results of the release of the substance from the hypromellose capsules into the medium with pH = 1,2 (0,1 M hydrochloric acid

solution, 1% Tween 80), obtained on the basis of the study of 6 samples, are shown in Table 6 and in Figure 1.

The lack of release at the first 5 minutes is caused by the dissolution of the HPMC capsule shell, which is confirmed visually. In general, the results of the determination of the kinetics of dissolution show a significant improvement in the solubility of the insoluble substance as a result of the granulation technology used: in 45 minutes, $64,75 \pm 3,0$ substances pass into the dissolution medium pH 1,2. However, the result obtained is below the pharmacopeial standards. The lag phase in the kinetics of dissolution in the first 5 minutes may be the reasons for that, due to the solubility of HPMC capsules and the limited solubility of the substance in the medium, as evidenced by the plateau phase of the dissolution curve at 20-45 minutes. As such the presence of the lag phase during releasing of the substance from the hypromellose capsules, a comparative study of their disintegration with disintegration from gelatin capsules in dissolution media was carried out, the results are presented in Table 7.

Table 7. Averaged results of determining the disintegration of gelatin and hypromellose capsules obtained on 6 samples

Capsules material	Disintegration time, min		
	pH 1,2	pH 4,5	pH 6,8
HPMC	5 min	13 min 30 seconds	5 min 7 seconds
Gelatin	1 min 45 seconds	2 min 25 seconds	4 min

It can be seen from the data in the table that the gelatin capsules disintegrate faster than the hypromellose capsules, and therefore in the further experiment, gelatin capsules were used. Based on the results of studying the dissolution kinetics in a medium with a pH of 1,2, the volume of the medium was increased to 800 ml, which is recommended for poorly soluble substances. The kinetics of the dissolution of 3,7-diazabicyclo[3.3.1]nonane from gelatin capsules into the medium with pH = 4,5 is shown in Table 8 and in Figure 2.

The release of a substance in the medium with a pH of 4,5 is more intense than in the medium with a pH of 1,2. $37,8 \pm 2,1$ of the substance was already found at the 5 minutes in the medium with pH 4,5, at the 15 minutes - $(72,6 \pm 2,2)\%$. In an acidic medium, during this time, 1% and $(50,15 \pm 2,20)$ of the substance are released from the dosage form, respectively. In just 45 minutes,

$(77,6 \pm 2,5)\%$ of the substance passes into the dissolution medium, and this corresponds to the pharmacopeial standards. The slowing down of dissolution after 15 minutes is obviously related to the achievement of the limit of solubility of the substance. It is shown that the developed technology provides the necessary indicators for the release of a substance from the dosage form, which will have a positive impact on the bioavailability of the drug. Table 9 and Figure 3 show the results of studying the kinetics of the dissolution of 3,7-diazabicyclo[3.3.1]nonane from gelatin capsules to a medium with a pH of 6,8.

In the medium with a pH 6,8, as well as in the medium with a pH 4,5, there is an intensive release of the substance in the first 5 minutes, which is ensured by the rapid solubility of gelatin capsules. In general, the dissolution of the substance is somewhat slow, by the 45th minute $(63,32 \pm 2,3)\%$ was found in the medium.

4. CONCLUSIONS

The results of the determination technological characteristics of the pharmaceutical substance 3,7-diazabicyclo[3.3.1]nonane served as a justification for the development of the composition of the dosage form - a capsule. The developed dosage form corresponds to modern requirements for pharmacopoeial quality levels, including release kinetics: according to obtained results, in 45 minutes $(77,6 \pm 2,5)\%$ of the substance passes into the dissolution medium with a pH of 4,5, which corresponds to the pharmacopeial standards. It should be noted that the substance is very little soluble in water, increasing its solubility is achieved as a result of the proposed technology for obtaining the dosage form. The results of the study served as the basis for the development process map of obtaining the dosage form of 3,7-diazabicyclo[3.3.1]nonane, indicators, and quality standards. Thus, as a result of the granulation technology used, selection of excipients and the dosage form, it was possible to obtain the standard dosage form "3,7-diazabicyclo[3.3.1]nonane capsules 15 mg", which corresponds to the pharmacopoeial requirements.

6. REFERENCES:

1. World Health Organization. *Global Health Observatory (GHO) data. Top 10 causes of death: Situation and trends.* http://www.who.int/gho/mortality_burden_di

- sease/causes_death/top_10/en/, accessed September 3, **2019**.
2. Powers, W.J. et al.; *Stroke*. **(2018)**, DOI: 10.1161/STR.0000000000000158
3. Hui, C., Tadi, P., Patti, L.; *Ischemic Stroke*. In: StatPearls [Internet]. Treasure Island (FL): StatPearls Publishing; **2020** Jan-. Available from: <https://www.ncbi.nlm.nih.gov/books/NBK499997/>
4. Clarkson, A. et al.; *J Neurosci*. **2011**, 31(10). 3766-3775.
5. Schitine, C. et al.; *Eur J Neurosci*. **2012**. 35(11).1672-1683.
6. Su, C. et al. *Anesthesiology*. **2016**. 125. 1030-1043.
7. Gudasheva, T.A. et al.; *Doklady Akademii Nauk*. **2016**. 471(1). 106-108.
8. Pyatigorskaya, N.V.; Brkich, G.E.; Lavrov, M.I.; Palyulin, V.A.; *J. Pharm. Sci. & Res.*, **2018**, 10(5), 1103-1106.
9. Rumyantseva, S.A., Silina, E.V., Orlova, A.S., Bolevich, S.B.; *Bulletin of regenerative medicine*. 2014. 3: 91-92.
10. Selyavko, L.E., Tsvetkova, L.S.; A device for working with paired cards during classes on the restoration and preventive training of memory in patients with a neurological clinic. In: *Selected Issues of Neurorehabilitation: Proceedings of the VIII International Congress "Neurorehabilitation 2016" (Moscow, June 8-10, 2016)*. Moscow: Union of Rehabilitologists of Russia, **2016**: 328-330.
11. Sernov, L.N., Gatsura, V.V.; *Elements of Experimental Pharmacology*, Moscow. 2000, 145-151.
12. Lavrov, M.I.; *Ph.D. thesis*, Lomonosov Moscow State University, Moscow, Russia, **2011**.
13. Zapolski, M.E., Karlov, D.S., Palyulin, V.A., Grigoriev, V.V., Brkich, G.E., Pyatigorskaya, N.V., Lavrov, M.I.; *Mendeleeev Communication*. **2018**; 28(3):311-313.
14. Zefirov, N.S.; Palyulin, V.A.; Lavrov, M.I.; Zapolsky, M.E.; *Tricyclic derivatives of 3,7-diazabicyclo[3.3.1]nonanes potentially possessing pharmacological activity, pharmaceutical compositions based on them and method of their application* 2013. (RF patent No. RU 2480470 C2).
15. Hebert D. et al; *Int J Stroke*. **2016**; 11(4). 459-484.
16. Zakharov, V.V.; *Effective pharmacotherapy*. **2014**. 42. 6-14.
17. Skrebitsky, V.G. et al.; *Experimental neurology*. **2008**. 2(2). 23-27.
18. Denisov, I.N. et al.; Diagnosis and tactics for stroke in general medical practice, including primary and secondary prevention: clinical recommendations] Approved. at the IV All-Russian Congress of General Practitioners (Family Doctors) of the Russian Federation. Kazan. **2013**. 33 p.
19. *Pharmaceutical Development Q8(R2)*. International Conference on Harmonisation of Technical Requirements for Registration of Pharmaceuticals for Human Use. ICH Harmonised Tripartite Guideline. **2009**. https://database.ich.org/sites/default/files/Q8_R2_Guideline.pdf, accessed September 3, 2019.
20. State Pharmacopoeia XIV of Russian Federation. 1.3.0003.15 "Buffer solutions". <https://pharmacopoeia.ru/ofs-1-3-0003-15-bufernye-rastvory/>, accessed September 3, 2019.
21. Demina, N.B.; *Drug Development & Registration*, **2017**, 2, 56-62.
22. Menshikov, V.V. ed.; *Directory of laboratory research methods*. Moscow. **1986**.
23. Demina, N.B.; Development of technology for the production of tablets. In: *Pharmaceutical development. Concept and practical recommendations* (pp. 83-134). Perot Publishing: Moscow, **2015**.
24. Kirzhanova, E.A.; Pechenkin, M.A.; Demina, N.B.; Balabushevich, N.G.; *Vestnik Moscow Universities: Khimiya*, **2016**, 57(2), P.37-45.
25. Swarbrick, J. ed.; *Encyclopedia of Pharmactutical Technology*. Third Edition. New York-London: Informa healthcare. **2016**. 406-418
26. Qualicaps. *The two-piece gelatin capsule Handbook*. Qualicaps. **2011**. 43.
27. Technical Reference File Hard Gelatin Capsules, 3rd edition. CAPSUGEL. **2010**. 55.
28. Hojava, M.V. ; Demina, N.B.; Skatkov, S.A.; Kemenova, V.A.; Technological aspects of moisture-activated granulation. *Pharmacy*. **2013**. 4. 34-36.
29. Gad, S.K.; Aladysheva, Z.I.; Belyaev, V.V.; Pyatigorskaya, N.V.; Production of medicines. Quality control and regulation. Saint Petersburg: Profession, **2013**. 960.
30. Bykovsky, S.N., Vasilenko, I.A., Demina, N.B., Shokhina, I.E., Novozhilova, O.V., Meshkovsky, A.P., Spitsky, O.R. Pharmaceutical development: concept and practical recommendations. Scientific and practical guidance for the pharmaceutical industry. Moscow: Publishing House of Perot. **2015**. 472.

31. Knitter, H.-J., Birch, N.S., Yarushok, T.A., Shokhin, I. E. *Development and registration of medicines*. **2014**. 1 (6) 36-46.
32. Harmonized tripartite guidance ICH Q6A "Specifications: analysis procedures and acceptance criteria for new drugs and new dosage forms. Chemical substances". **2000**.

Table 1. *Chromatographic conditions of analysis*

Chromatographical column:	POROSHELL 120 EC-C18, 2.1*50mmID, 2.7µm
Eluent A:	0,1 % TFAinMeCN (0.1 % trifluoroacetic acid in acetonitrile)
Eluent B:	0,1 % TFAinH ₂ O (0.1 % trifluoroacetic acid in water)
Sample quantity:	20 µL/ Needle wash with MeCN
Flow rate:	1,0 mL/min
Chromatography time:	12 мин
Column Temperature:	25°C
Autosampler temperature:	4 °C
Detectors wavelength:	233nm/Bw4nm; Ref:400nm/Bw100nm.

Table 2. *Elution mode*

Gradient elution		
Time, min	Eluent A, %	Eluent B, %
0	0.0	100.0
1.0	0.0	100.0
7.0	100.0	0.0
9.0	100.0	0.0
9.1	0.0	100.0
12.0	0.0	100.0

Table 4. *Excipients in the composition of the drug "3,7-diazabicyclo[3.3.1]nonane, 15 mg capsules", their qualifications and purpose*

No	Component Name	Method of control	Purpose
1.	Sodium alginate	Eur. Ph.	Filler
2.	Pregelatinized corn starch	Eur. Ph	Filler, granulometry substance
3.	Sodium starch glycolate	Eur. Ph.	Disintegrant
4.	Colloidal silicon dioxide	Eur. Ph.	Sliding, moisture distributor
	Calcium chloride	Pharmacopoeial monograph 42-2567-00	Granulating substance
<i>Gelatin capsules</i>		CAPSUGEL, USA	
5.	Gelatin		Capsule material
6.	Titanium Dioxide (E171)		Dye
7.	Triacetin		Plasticizer
8.	Polysorbate 80		Plasticizer
	<i>Hypromelous Capsules (HPMC)</i>	CAPSUGEL, USA	
	Hydroxypropylmethylcellulose		
	Plasticizer (internal standard of the manufacturer)		

Table 6. Dissolution of 3,7-diazabicyclo[3.3.1]nonane from hypromellose capsules into the medium with a pH 1,2

Test sample	Release substance, %					
	5 min	10 min	15 min	20 min	30 min	45 min
3,7-diazabicyclo[3.3.1]nonane 15 mg, capsules	1±1	35,9±1,8	50,15±2,20	61,87±2,15	63,36±1,98	64,75±3,0

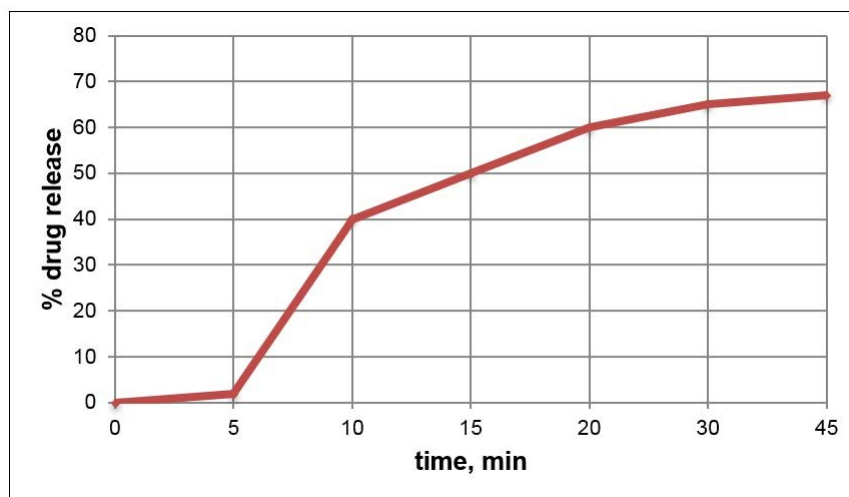


Figure 1. The average dissolution profile of the drug “3,7-diazabicyclo[3.3.1]nonane 15 mg capsules”. Dissolution medium - hydrochloric acid buffer solution with a pH 1,2

Table 8. Dissolution of 3,7-diazabicyclo[3.3.1]nonane from gelatin capsules into the medium with pH = 4,5

Test sample	Release substance, %					
	5 min	10 min	15 min	20 min	30 min	45 min
3,7-diazabicyclo[3.3.1]nonane 15 mg, capsules	37,8±2,1	64,5±1,5	72,6±2,2	73,7±2,5	75,6±1,9	77,6±2,5

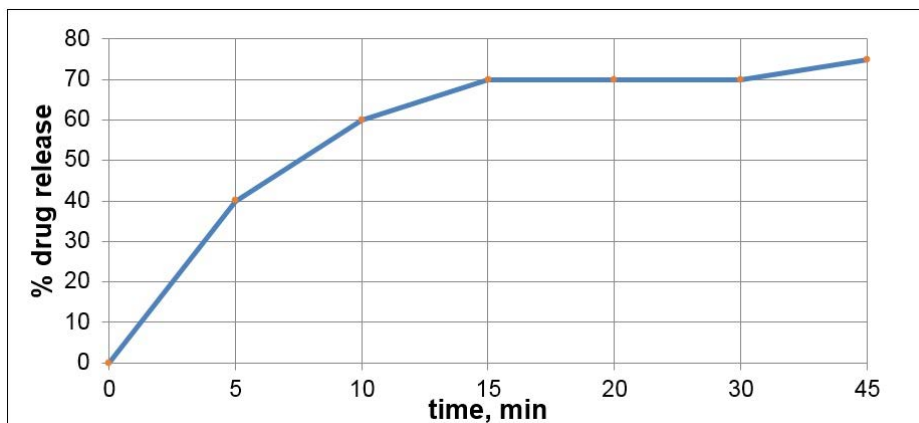


Figure 2. Averaged dissolution profile of the drug “3,7-diazabicyclo[3.3.1]nonane 15 mg capsules”. Dissolution medium - acetate buffer solution with pH 4,5

Table 9. Dissolution of 3,7-diazabicyclo[3.3.1]nonane from gelatin capsules into the medium with pH 6,8

Test sample	Release substance, %					
	5 min	10 min	15 min	20 min	30 min	45 min
3,7-diazabicyclo[3.3.1]nonane 15 mg, capsules	35,54±2,2	44,23±3,0	54,40±2,87	58,71±2,0	60,10±3,1	63,32±2,3

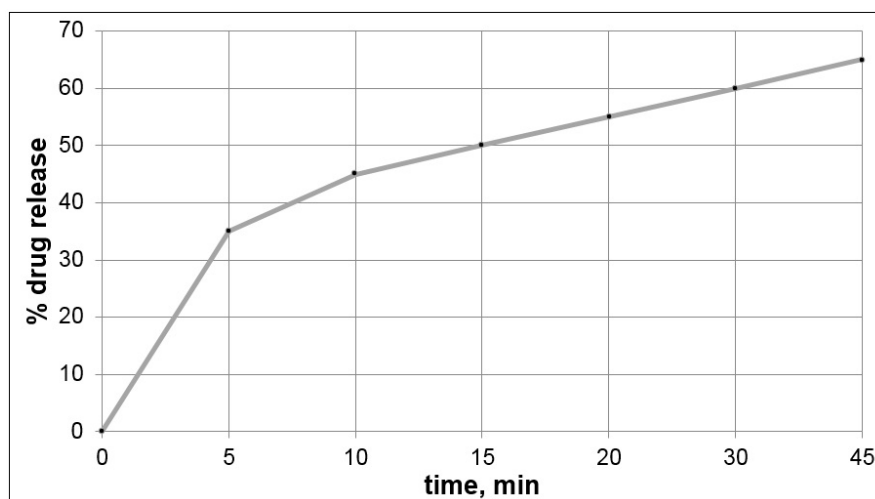


Figure 3. The average dissolution profile of the drug “3,7-diazabicyclo[3.3.1]nonane 15 mg capsules”. The dissolution medium is a phosphate buffer solution with pH 6,8

GANHO E MELHORIA DA LARGURA DE BANDA DE FRAGMENTO RETANGULAR DA ANTENA MICROSTRIP

GAIN AND BANDWIDTH ENHANCEMENT OF RECTANGULAR PATCH MICROSTRIP ANTENNA

تحسين التحصيل وعرض الحزمة للهوائي الشريطي المستطيل

AL-SHAHEEN, Ahmad Hashim^{1*}¹Department of Physics, College of Science, University of Misan, Maysan, Iraq.

* Correspondence author

e-mail: prof.dr.ahmad@uomisan.edu.iq

Received 21 January 2020; received in revised form 28 February 2020; accepted 11 March 2020

RESUMO

As antenas de *microstrip* são muito populares para enviar e transmitir ondas eletromagnéticas em muitos sistemas de comunicação. A antena *microstrip* tem vantagens e desvantagens, como qualquer outro tipo de antena. Dentre as vantagens estão o baixo peso, configuração plana de baixo perfil, baixos custos de fabricação e fácil conexão com circuitos de microondas. A antena remota é adequada para aplicações que são sistemas de comunicação sem fio, telefones celulares, *paggers*, sistemas de radar e sistemas de comunicação via satélite. A antena proposta foi projetada e simulada via HFSS. O substrato da antena, que está entre o remendo dos dois condutores e o plano do solo, é Duroide da constante dielétrica de $\epsilon_r = 2,2$ e perda tangente de $\tan \delta = 0,0009$. As dimensões são 20 mm para comprimento e largura; a altura é de 1,5 mm. O patch das dimensões são 16 mm e 15 mm para comprimento e largura, respectivamente. Neste artigo, a nova técnica foi introduzida para aumentar o ganho e a largura de banda da antena de microponto retangular. Uma nova técnica baseia-se no tratamento de um adesivo como monopolo; o estudo paramétrico feito pela variação do parâmetro é a altura do adesivo em relação ao substrato. O ganho e a largura de banda aumentam quando o ângulo entre a borda do patch e o substrato é aumentado. Embora o ganho tenha aumentado para o ângulo de inclinação de até 20° e depois tenha diminuído suavemente com o aumento do ângulo, os resultados simulados mostram uma mudança significativa na comparação de ganho e largura de banda com a antena de reticulação retangular tradicional. Os resultados mostram um aumento do ângulo de inclinação, aumento da largura de banda e ganho. Esta antena pode ser usada na banda K para aplicativos de comunicação sem fio.

Palavras-chave: *Microstrip, ganho, largura de banda, antena monopolar, banda K*

ABSTRACT

Microstrip antennas are very popular for sending and transmitting electromagnetic waves in many communication systems. The microstrip antenna has advantages and disadvantages, like any other antennas. There many benefits like low weight, low profile planar configuration, low costs of fabrication, and easy to connect with microwave circuits. The patch antenna is suited for applications, which are wireless communications systems, cellular phones, *paggers*, radar systems, and satellite communications systems. The proposed antenna is designed and simulated via HFSS. The antenna substrate, which is between the two conductors' patch and ground plane, is Duroid of the dielectric constant of $\epsilon_r = 2.2$ and tangent loss of $\tan \delta = 0.0009$, the dimensions are 20 mm for both length and width; the height is 1.5 mm. The patch of sizes is 16 mm and 15 mm for length and width, respectively. In this article the new technique has been introduced to enhance the gain and bandwidth of the rectangular patch microstrip antenna, a new technique is based on creating a patch as a monopole, the parametric study done by varying the parameter δ is the height of the patch concerning the substrate. The gain and bandwidth are increased when the angle between the patch edge and the substrate is increased. While the benefit increased for tilt angle up to 20° and then decreased smoothly with angle increased, the simulated results show a significant change in the gain and bandwidth comparison with traditional rectangular patch microstrip antenna. The results show an increasing tilt angle increased bandwidth and gain. This antenna can be used in the K band for wireless communication applications.

Keywords: *Microstrip, Gain, Bandwidth, Monopole antenna, K-band*

للوهائي الشريطي العديد من الخواص الجيدة و أخرى غير الجيدة، مثل أي نوع من الهوائيات الأخرى. هناك العديد من المزايا مثل خفة الوزن و شكله مستو بسيط و قلة كلفة التصنيع وسهولة الربط مع الدوائر المايكرووية. الهوائي المشع مناسب للتطبيقات مثل أنظمة الاتصالات اللاسلكية و الهوائيات النقالية و الاستشعار و أنظمة الرادار و أنظمة الاتصالات الفضائية. الهوائي المقترح صمم وتمت محاكاته بواسطة برنامج " High Frequency Structure " Simulator HFSS. المادة العازلة بين المادتين الموصلة (المشع والقاعدة) للهوائي هي نوع تجاري Douriod تمتلك ثابت عزل $\epsilon_r = 2.2$ وظل فقد كهربائي $\tan \delta = 0.0009$ ، أبعادها 20 mm لكل من الطول والعرض، ارتفاع المادة العازلة هو 1.5 mm. أبعاد الجزء المشع من الهوائي 16 mm و 15 mm للطول والعرض على التوالي. قدمت في هذا البحث تقنية جديدة لتحسين التحصيل وعرض الحزمة للهوائي الشريطي المستطيل، تعتمد التقنية الجديدة على معالجة الهوائي كقطب أحادي، تمت دراسة تأثير العامل δ ، وهو ارتفاع المشع عن الطبقة العازلة. ازداد كل من التحصيل وعرض الحزمة عند زيادة الزاوية إلى ما فوق 20° وتزداد بزيادة الزاوية فوق ذلك، نتائج المحاكاة بينت تغيير معنوي في التحصيل وعرض الحزمة مقارنةً بالهوائي الشريط المستطيل الاعتيادي. يستخدم هذا الهوائي في الحزمة الترددية K لتطبيقات الاتصالات اللاسلكية.

الكلمات المفتاحية: هوائي شريطي، التحصيل، عرض الحزمة، هوائي أحادي القطب، حزمة K

1. INTRODUCTION:

Microstrip antenna is the tool for sending and transmitting electromagnetic waves as a part of the communication systems. Each antenna has advantages and disadvantages, like any other antennas. There many gains such as low weight and profile planar configuration, low fabrication costs, the capability to integrate with microwave circuits. The microstrip patch antenna is very well suited for applications such as wireless communications systems, cellular phones, pagers, Radar systems, and satellite communications systems (Patil, 2012). On the other hand, the disadvantage of narrow bandwidth is, however, the main drawback of the microstrip patch antenna (Xiong *et al.*, 2012).

Many techniques have been introduced and developed to enhance bandwidth and gain for the microstrip antenna due to its disadvantages which listed previously from many researchers (Kharade and Patil, 2012; Islam *et al.*, 2013; Ms. Priyanka and Srivastava, 2013; Urgunde *et al.*, 2014; Saurabh *et al.*, 2013; Bhardwaj *et al.*, 2014; Rabbani and Ghafouri-Shiraz, 2014; Kumar *et al.*, 2014). The primary technique to the enhanced bandwidth of the microstrip antenna which is using slots in patch or ground plane or both, other methods are based on utilized from the metamaterial concept to broadening the bandwidth impedance of the antenna, while, many researchers are using the configurable patch or ground plane (Arora *et al.*, 2017; Pothugunti and Viswanadham, 2017; Al-Ahmadi and Khraisat, 2019; Bhanumathi and Swathi, 2019; Al-Shaheen, 2019), different methods are presented rather than the previous are mentioned (Bakr *et al.*, 2019; Satyanarayana and Shankaraiah, 2018; Bhukya and Pabbu, 2019).

The concept of the modified monopole antenna to enhance both the gain and bandwidth of the rectangular patch microstrip antenna in comparison with the traditional one was used.

The idea of this proposed antenna was to allow several modes to be excited on the antenna's patch at the same time. This was achieved by making the two edges of the patch to be movable by varying the angle between the edges and the antenna's substrate. This bring about

to get an optimum angle, which is provided the best antenna performance such as bandwidth and gain.

2. MATERIALS AND METHODS:

To design the patch antenna, the formulas of the rectangular patch antenna were used (Figure 1), as follows from Equations 1 to 7 (Balanis, 2016). The length of a rectangular patch antenna is in the range,

$$0.333\lambda < L < 0.5\lambda \quad (\text{Eq.1})$$

where λ being the free-space wavelength. While the thickness of the patch is usually in between,

$$0.003\lambda_0 \leq h \leq 0.05\lambda_0 \quad (\text{Eq.2})$$

The dielectric constant of the substrate (ϵ_r) is typically as; $2.2 \leq \epsilon_r \leq 12$. The parameters of a Rectangular Microstrip Patch Antenna for practical design are described in Equations 3-6 as:

1. The width (W_p)

$$W_p = \frac{c}{2f_0 \sqrt{\frac{(\epsilon_r + 1)}{2}}} \quad (\text{Eq.3})$$

2. The effective Dielectric constant (ϵ_{reff})

$$\epsilon_{\text{eff}} = \frac{\epsilon_r + 1}{2} + \frac{\epsilon_r - 1}{2} \left[1 + 12 \frac{h}{W} \right]^{-1} \quad (\text{Eq.4})$$

3. The correction length due to the fringing fields of Microstrip antenna is

$$\Delta L = 0.412 \frac{\left(\frac{W}{h} + 0.264 \right) (\epsilon_{\text{eff}} + 0.3)}{(\epsilon_{\text{eff}} - 0.258) \left(\frac{W}{h} + 0.8 \right)} \quad (\text{Eq.5})$$

4. The length of the patch is

$$L_p = L_{\text{eff}} - 2\Delta L \quad (\text{Eq.6})$$

where

$$L_{\text{eff}} = \frac{c}{2f_0 \sqrt{\epsilon_{\text{eff}}}} \quad (\text{Eq.7})$$

In the case of microstrip antenna, the bandwidth BW of the antenna is proportional to its quality factor Q and given by (Kumar and Ray, 2003) (Equation 8),

$$BW = \frac{VSWR - 1}{Q \sqrt{VSWR}} \quad (\text{Eq.8})$$

where VSWR is voltage standing wave ratio. The percentage bandwidth of the patch antenna in terms of its dimensions and substrates parameters is given as Hamad, 2012 (Equation 9).

$$BW\% = \frac{Ah}{\lambda_0} \sqrt{\frac{W}{L}} \quad (\text{Eq.9})$$

where A is between 180 to 220 according to the ratio of the substrate height and dielectric constant and the operating frequency as Equation 10

$$A = \begin{cases} 180; & \frac{h}{\lambda_0 \sqrt{\epsilon_r}} \leq 0.045 \\ 200; & 0.045 \leq \frac{h}{\lambda_0 \sqrt{\epsilon_r}} \leq 0.075 \\ 220; & \frac{h}{\lambda_0 \sqrt{\epsilon_r}} \geq 0.075 \end{cases} \quad (\text{Eq.10})$$

The proposed antenna was designed and simulated via the High-Frequency Structure Simulator (HFSS). This software resolves the Maxwell's equations in the near field based on the two different numerical methods one of them is finite element method and the other is method of moment MoM to solve the integrodifferential equations to find the current distribution and the near and far-field component of the electric and magnetic fields. Add to that the circuit parameters such as the scattering matrix, Voltage Standing Wave Ratio (VSWR) and input impedance, etc. The software has a graphical tool to demonstrate the results in graph mode in two and three dimensions. Also, one can animate the current and field distribution on the structure under the test. The antenna substrate Duroid of the dielectric constant of $\epsilon_r = 2.2$ and tangent loss of $\tan \delta = 0.0009$, the dimensions are 20 mm for both length and width; the height is 1.5 mm. The patch is selected to be perfect electric conductor PEC, which is suitable for simulating the antenna; the dimensions of patch are 16 mm and 15 mm for length and width, respectively, as shown in Figure 2. The ground plane dimension is the same as the substrate dimensions; the material used to simulate the ground plane to study the variation of the electric field is also the PEC.

The antenna is a probe center feed coaxial cable connector to achieved 50Ω input impedance to get a proper impedance matching between the antenna and other microwave circuits. The HFSS provides a parametric study to get the optimum parameters to get excellent performance for the antenna, by varying the angle between the patch edge and the substrate to change the angle between 0° to 70° (Figure 3).

3. RESULTS AND DISCUSSION:

Using the HFSS software to simulate the effect of the proposed antenna in the K band applications, the result of the traditional patch antenna is shown in Figure 4 which is illustrate the return loss, it can be seen from the Figure the proper impedance matching was achieved the reflection coefficient, return loss, is about -50 dB, which is reflected that the maximum power transfer to the load (antenna). It can also be seen that the bandwidth is about 0.82 GHz at 12.26 GHz resonance frequency. Now the parametric study was done by varying the parameter δ , which is done by it to get the sufficient angle between the edge and the substrate, as shown in Figure 5. The range δ is from 0.5 to 7.5 to vary the angle θ from 3.5° to 70° , the effect of this parameter on the proposed antenna performances, such as the return loss, and the realized gain of depicted of the some selected cases, in Figure 6.

It can be seen from Figure 6 that the bandwidth increased with an increased tilt angle, while the gain increased for tilt angle up to 20° , the increase in both gain and bandwidth is due to allow the surface currents and the fringing field to many exciting modes and then contribute to enhancing them. And then decreased with angle increased, as depicted in Figure 7. After the proposed antenna simulated via HFSS with parametric study by varying the angle as observed previously, the results showed the importance of both gain and bandwidth. It can be seen that the bandwidth is increased up to 9 GHz when the angle increased. Also, the gain increased up to 5 dB. The complete results are listed in table 1.

4. CONCLUSIONS:

Microstrip antenna has many disadvantages, such as the narrow bandwidth. In this paper, the concept of the modified monopole antenna to enhance both the gain and bandwidth of the rectangular patch microstrip antenna in comparison with the traditional one was used. The idea of this proposed method is to varying the angle between two sides of the patch to get the optimum angle to get the best bandwidth and gain. The results show that increase tilt angle increased bandwidth and gain is about 8 dB in the range of movable patch sides of 10 to 30° , the bandwidth is about 0.82 GHz at 12.26 GHz resonance frequency. This antenna can be used in the K band frequency applications.

6. REFERENCES:

1. Al-Shaheen, AHA. *ARPN Journal of Engineering and Applied Sciences*. **2019**, **14**(6):1249-1254.
2. Arora C, Pattnaik SS, Baral RN. *Progress in Electromagnetics Research*. **2017**;76:73-85.
3. Balanis CA. *Antenna theory: analysis and design*. John Wiley & sons; **2016** Feb 1.
4. Bakr MS, Großwindhager B, Rath M, Kulmer J, Hunter IC, Abd-Alhameed RA, Witrissal K, Boano CA, Römer K, Bösch W. *IET microwaves, antennas & propagation*. **2019**,13(8):1142-50.
5. Bhardwaj D, Sharma K, Gulati G, Dixit M. *IJERT*. **2014**, 3(11):1072-1076.
6. Islam MT, Ullah MH, Singh MJ, Faruque MR. *Materials*. 2013,6(8):3226-40.
7. Hamad KA. *ARPN Journal of Engineering and Applied Sciences*. **2012**,7(3):292-7.
8. Al-Ahmadi A, Khraisat YS. *Applied Physics Research*. **2019**,11(1):35.
9. Kharade AR, Patil VP. *IOSR Journal of Electronics and Communication Engineering*. **2012**, 2(6).
10. Kumar G, Ray KP. Artech house; **2003**.
11. Priyanka NS, Srivastava MN. *International Journal of Advancements in Research & Technology*. **2013**, 2(5).
12. Rabbani MS, Ghafouri-Shiraz H. *In2nd IET Annual Active and Passive RF Devices Seminar* **2014** Oct 29 (pp. 1-4). IET.
13. Bhukya DR, Pabpu U. *International Journal of Management, Technology And Engineering*. **2019**, IX(II):235-242.
14. Urgunde KR, Jadhav HL, Pawar AJ. *IJESRT*. **2014**,13(2):684-687.
15. Patil VP. *International journal of engineering sciences & emerging technologies*. **2012**, 3(2):1-2.
16. Xiong H, Hong JS, Peng YH. *Radioengineering*. **2012**,21(4):993-998.
17. Saurabh AK, Kumar S, Srivastava DK. *International Journal of Advanced Research in Computer and Communication Engineering*. **2013**,2(12):4570-4.
18. Kumar S, Beniwal NS, Srivastava DK. *International Journal of Advanced Research in Computer and Communication Engineering*. **2014**,3(1).
19. Bhanumathi V, Swathi S. *ICTACT Journal on Microelectronics*. 2019;4(4):669-75.
20. Pothugunti S, Viswanadham C. *Int. J. Elec&Elec.Eng&Telcomm*. **2017**,6(2):24-29.
21. Satyanarayana R, Shankaraiah N. *International Journal of Applied Engineering Research*. **2018**,13(6):3867-3880.

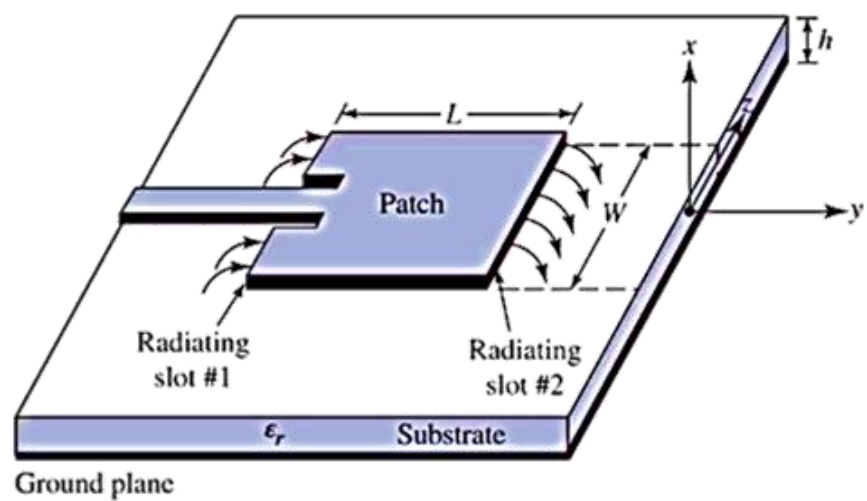


Figure 1. Rectangular patch microstrip antenna.

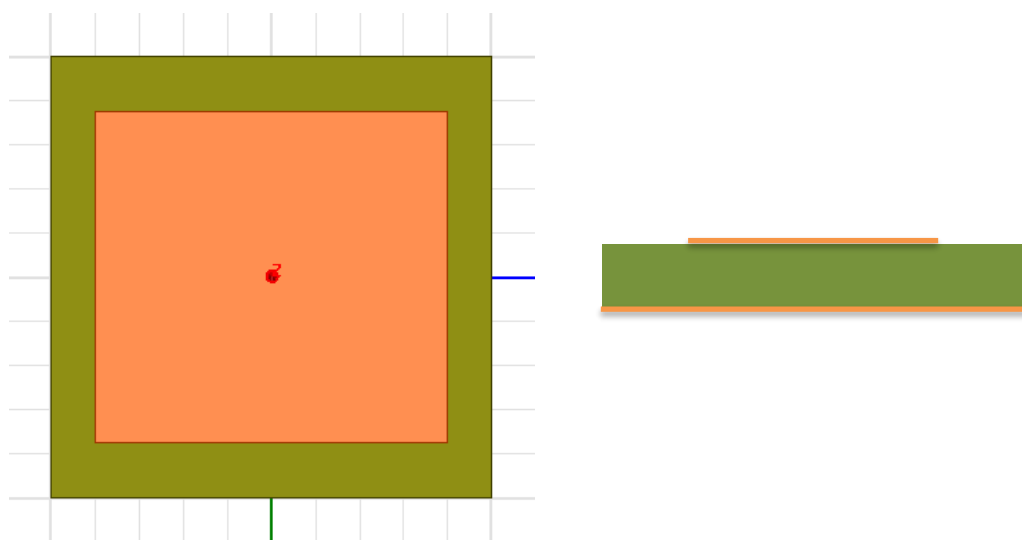


Figure 2. Proposed antenna with angle $\theta = 0^\circ$.

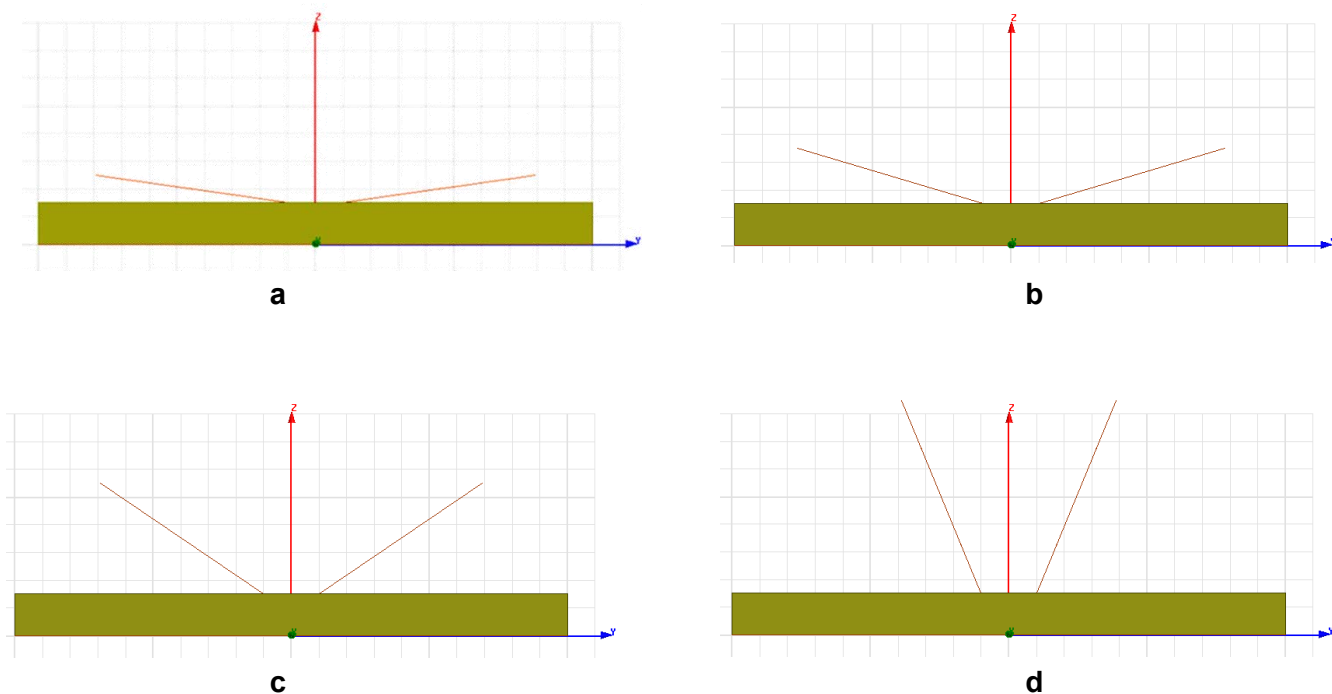


Figure 3. Patch tilts concerning the substrate (a) $\theta = 7^\circ$, (b) $\theta = 14.5^\circ$, (c) $\theta = 30^\circ$ and (d) $\theta = 61^\circ$.

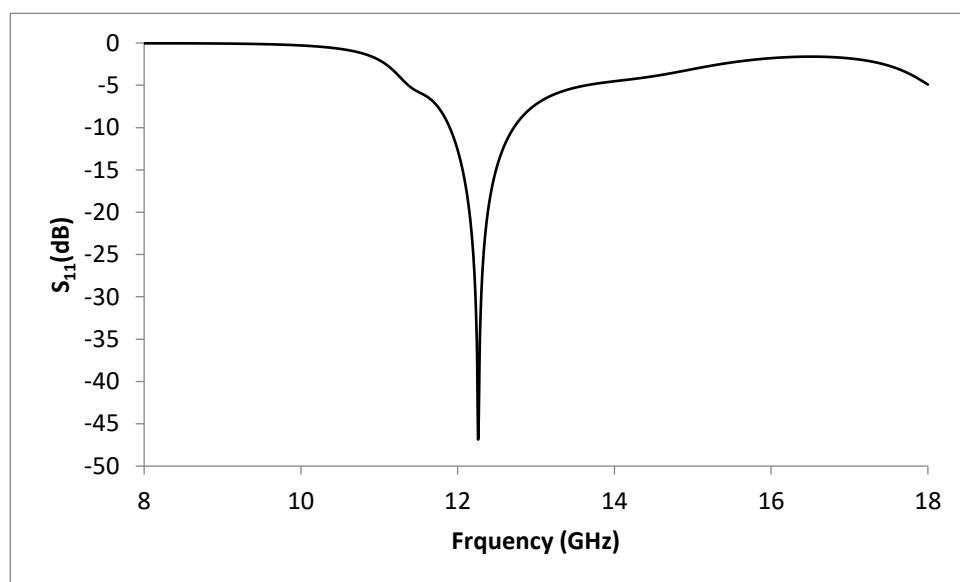


Figure 4. The return loss of the proposed antenna.

$$y = L \cos \theta$$

$$\theta = \sin^{-1}(\delta/L)$$

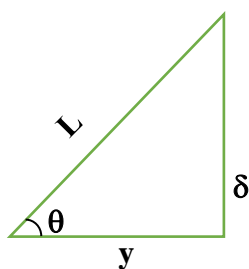
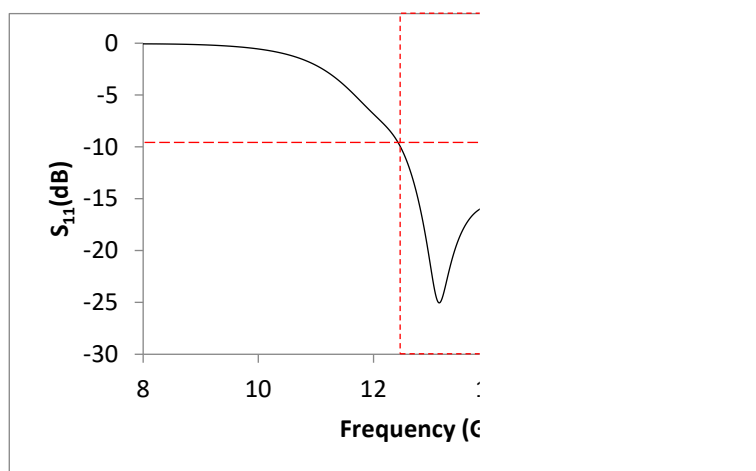
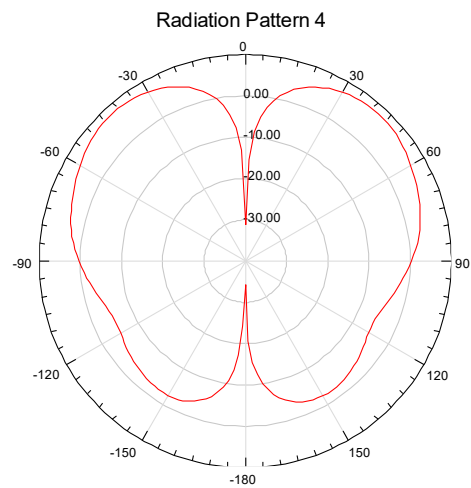


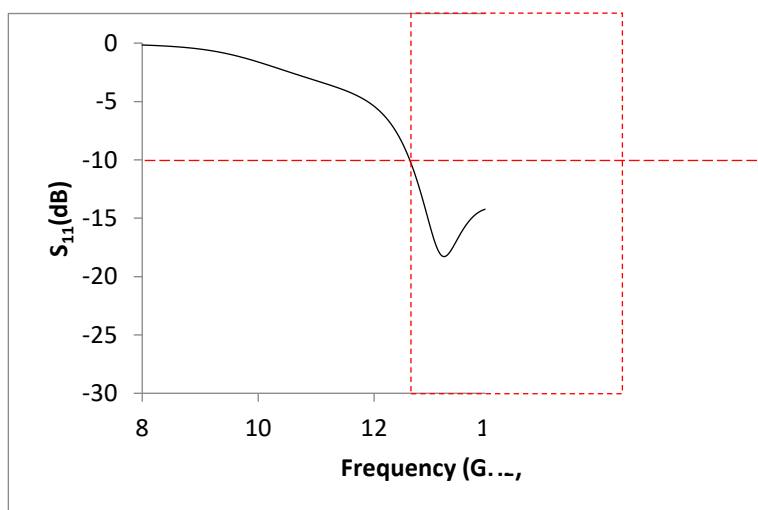
Figure 5. Patch geometry.



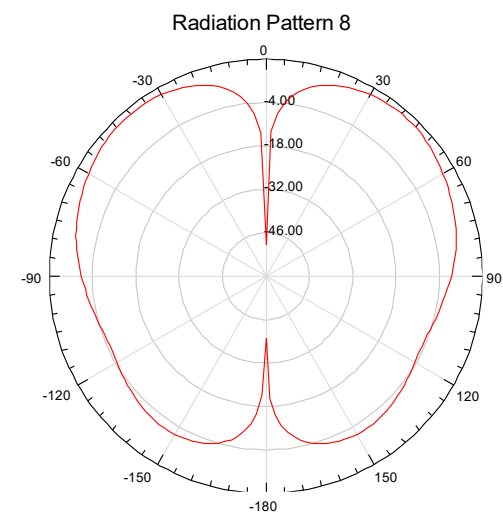
a



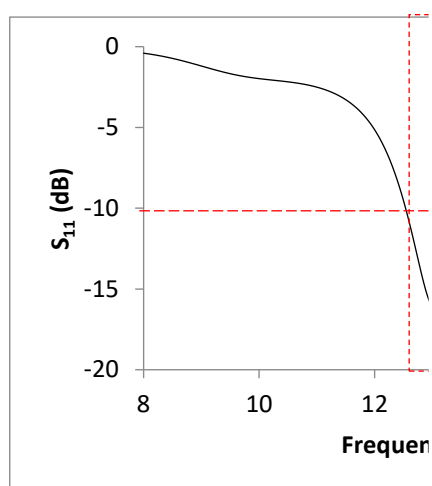
Cur
dB/Realized
Setup1: Sweep
delta=1mm Freq=



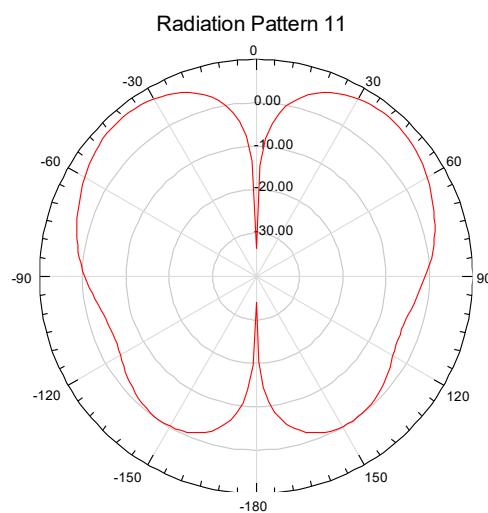
b



dB/
Setup1: S
delta=3mm



c



Cur
dB/Realized
Setup1: Sweep
delta=5mm Freq=

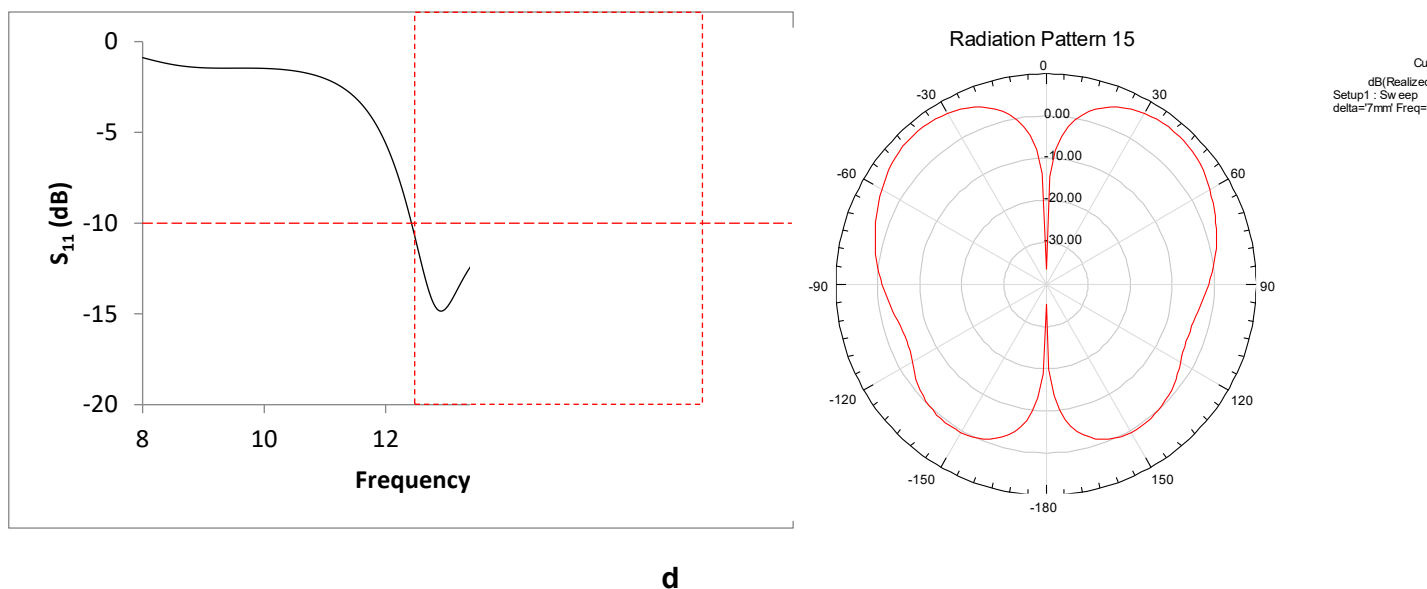


Figure 6. Return loss and realized gain vis. tilt angle; (a) $\theta = 70^\circ$, (b) $\theta = 14.5^\circ$, (c) $\theta = 30^\circ$ and (d) $\theta = 61^\circ$

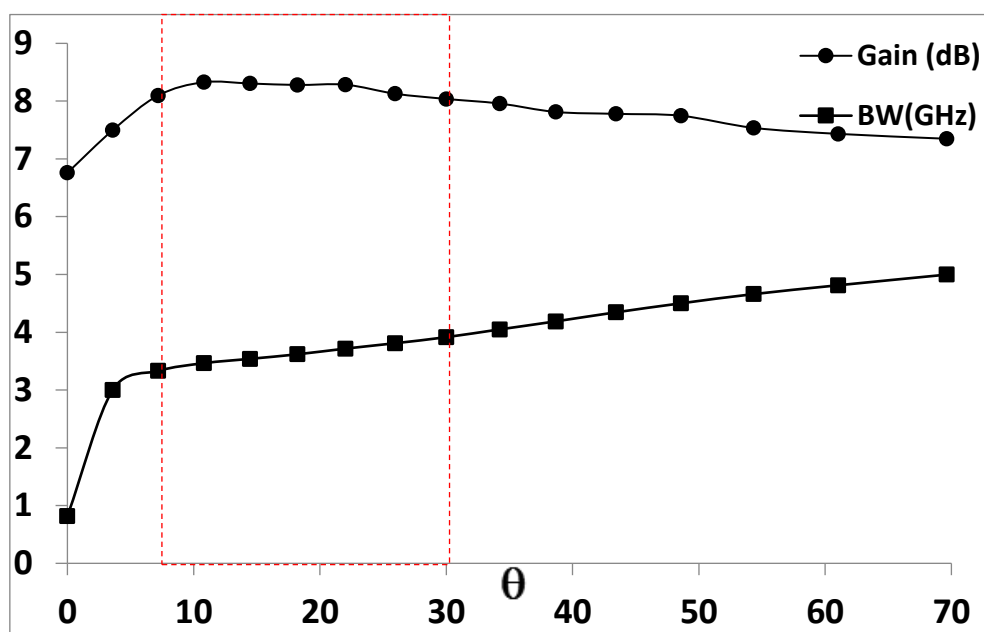


Figure 7. Bandwidth and realized gain vis. angle θ .

Table 1. Bandwidth and realized gain vis. angle θ

δ	θ (deg.)	BW (GHz)	Gain (dB)	δ	θ (deg.)	BW (GHz)	Gain (dB)
0	0	0.8182	6.7599	4	30	3.9147	8.0379
0.5	4	3.0008	7.4961	4.5	34	4.0489	7.9583
1	7	3.3300	8.0968	5	39	4.1884	7.8125
1.5	11	3.4645	8.3279	5.5	43	4.3447	7.7799
2	14	3.5400	8.3051	6	49	4.5006	7.7464
2.5	18	3.6180	8.2797	6.5	54	4.6597	7.5373
3	22	3.7169	8.2847	7.0	61	4.8132	7.4334
3.5	26	3.8097	8.1282	7.5	70	4.9973	7.3485

INFLUÊNCIA DA MINERALIZAÇÃO DA ÁGUA NA PRODUTIVIDADE DE ZOOPLÂNCTON NOS RESERVATÓRIOS DA REGIÃO DE AKMOLA

INFLUENCE OF WATER MINERALIZATION ON ZOOPLANKTON PRODUCTIVITY IN RESERVOIRS OF AKMOLA REGION

AUBAKIROVA, Gulzhan^{1*}; ADILBEKOV, Zhanat²; NARBAYEV, Serik³;

^{1,3}Department of Hunting and Fisheries, Faculty of Veterinary Sciences and Animal Husbandry, S.Seifullin Kazakh Agro-Technical University, Nur-Sultan, Kazakhstan

²Department of Veterinary Sanitation, Faculty of Veterinary Sciences and Animal Husbandry, S.Seifullin Kazakh Agro-Technical University, Nur-Sultan, Kazakhstan

* Corresponding author
e-mail: kadr_90.taz@mail.ru

Received 10 February 2020; received in revised form 03 March 2020; accepted 24 March 2020

RESUMO

O efeito da mineralização da água na produtividade do zooplâncton nos reservatórios da região de akmola é um estudo muito relevante. A composição química das águas naturais está indissociavelmente ligada à composição e estrutura do solo que, por sua vez, se formou durante a longa evolução da crosta terrestre sob a influência do clima. As águas naturais têm uma variedade excepcionalmente ampla de composição química qualitativa e quantitativa. A base para a sistematização nas classificações existentes é a quantidade de mineralização, o componente ou grupo predominante, a relação entre diferentes valores de concentrações de íons diferentes, a presença de quantidades aumentadas de quaisquer componentes específicos dos regimes de gás e sal. A relevância do trabalho se deve ao estudo insuficiente do potencial de pesca de reservatórios de tamanho médio no norte do Cazaquistão. O objetivo do trabalho foi estudar a mineralização da água como fator determinante da vida dos organismos aquáticos. Como resultado desta pesquisa, os dados confirmaram a posição de que os fatores que determinam a vida dos organismos aquáticos são a mineralização da água. Para caracterizar o zooplâncton em toda a área do lago, foram coletadas amostras levando em consideração diferentes estações. O número de organismos individuais na amostra foi determinado. O grau de mineralização dos lagos na região de Akmola foi indicado. O coeficiente de correlação para características no par "mineralização - abundância de zooplâncton" foi calculado como $r = -0,96$ e no par "mineralização - biomassa de zooplâncton" $r = -0,85$. Ao analisar os dados obtidos, observou-se uma relação inversa entre mineralização da água e abundância de zooplâncton. Quando a mineralização da água aumenta 4,03% em julho, o número de organismos zooplanctônicos diminui de 170,03 para 152,6 mil cópias/m³. Quando a salinidade da água do lago Uyali - Shalkar aumenta de 362 (maio) para 508 mg/l (julho), a biomassa do zooplâncton diminui de 6,02 para 5,73 mg/m³.

Palavras-chave: zooplâncton, lago, mineralização, biomassa, produtividade.

ABSTRACT

The effect of water mineralization on zooplankton productivity in the reservoirs of the Akmola region is a very relevant study. The chemical composition of natural waters is inextricably linked to the composition and structure of the soil, which, in turn, was formed during the long evolution of the earth's crust under the influence of climate. Natural waters have a wide variety of qualitative and quantitative chemical composition. The basis for systematization in existing classifications are the amount of mineralization, the predominant component or group, the relationship between different values of concentrations of various ions, the presence of increased amounts of any specific elements of the gas and salt regimes. The relevance of the work is due to insufficient study of the fishing potential of medium-sized reservoirs in Northern Kazakhstan. The work aimed to study the mineralization of water as a factor determining the life of aquatic organisms. As a result of this research, data confirmed the position that the factors that determine the viability of marine organisms are the mineralization of water. To characterize zooplankton across the entire lake area, samples were taken, taking into account different stations. The number of individual organisms in the sample was determined. The degree of mineralization of lakes in the Akmola region was indicated. The correlation coefficient for features in the "mineralization – zooplankton abundance" pair was calculated as $r = -0.96$, and in the "mineralization – zooplankton biomass" pair $r = -0.85$. When analyzing the data obtained, it was observed an inverse relationship

between water mineralization and zooplankton abundance. When water mineralization increases by 4.03% in July, the number of zooplankton organisms decreases from 170.03 to 152.6 thousand copies/m³. When the salinity of the Uyali - Shalkar lake water increases from 362 (May) to 508 mg/l (July), the zooplankton biomass decreases from 6.02 to 5.73 mg/m³.

Keywords: zooplankton, lake, mineralization, biomass, productivity.

1. INTRODUCTION:

The intensity of life processes in lake ecosystems is due to a variety of abiotic factors and processes, ultimately, their biological productivity.

The most important conditions that determine the life of aquatic organisms are temperature, light, the content of nutrients, etc. Marine organisms are interconnected with elements of the abiotic environment; a change in one system of connections inevitably causes a change in another (Brzoska, 2012).

Kazakhstan has excellent opportunities to use internal reservoirs for fish farming. On the territory of the Republic, there are a large number of reservoirs, with the full development of which a significant increase in the catches of valuable fish species is possible (Aubakirova *et al.*, 2019).

However, in many regions of Kazakhstan, until now, the fishery use of natural reservoirs is almost undeveloped or poorly developed. This is due to insufficient study of their biological resources. The need to build lake fish farming in Kazakhstan is obvious. It is dictated by the fact that this will allow you to get high-quality fish products at a relatively low cost.

The development of zooplankton is determined by interrelated and dependent on many factors conditions, the main of which are: the presence of a food substrate, growth, and reproduction conditions. In different reservoirs, these conditions are formed under the influence of the type of reservoir, as well as climatic and weather factors (Popov, 2002).

The main factors that determine the development of populations of different organisms of plankton communities are various. It is considered that for phytoplankton-light, biogenic substances, temperature, for bacteria-organic substrate and temperature, for zooplankters-filters-food substrate-Phyto-, bacterioplankton, and temperature; for predatory forms-the presence of a sufficient number of prey organisms. In some lakes, in specific periods for the development of zooplankton, the main limiting factor is the oxygen regime. Also, in each

community, there are species (even among closely related forms) that respond almost oppositely to the environmental factors that determine their life activity. Thus, among the blue-green (cyanobacteria), mainly thermophilic summer forms, there is *R. Oscillatoria*, represented by many species that can develop at low temperatures. The same group of ways with different responses to environmental conditions are among the protozoans, rotifers, cladocerans, and copepods. The more diverse in space and time the conditions of the reservoir environment, the more ecologically heterogeneous its plankton community (Rice *et al.*, 2012).

The southern location of the lakes contributes to the effect of more intense insolation, especially in low-snow winters. Reservoirs in the Middle zone of the European part are mainly lakes in the Upper Volga basin, located at latitude 58-60°. The difference in the latitudinal location of the upper Volga and TRANS-Baikal lakes is about 8°. This creates a significant advantage in the supply of insolation for TRANS-Baikal lakes. Besides, according to available data, the thickness of the snow cover in the Upper Volga lakes can exceed 70 cm, while in the TRANS-Baikal lakes, its width does not exceed 30 cm (Tikhomirov, Egorov, 1977; Bondarenko, 2009). Thus, for the development of phytoplankton under the ice in the lakes of Transbaikalia, compared with the lakes of the Upper Volga, there are definite advantages in the intensity and duration of solar insolation.

It is accepted that the year-round cycle of the lake is divided into two periods: "vegetation" (ice-free) and subglacial. It is known that usually in the lakes of the Middle zone of the European part, the open water period is more extended than the subglacial one. Environmental conditions in reservoirs during these periods differ fundamentally. The temperature under the ice varies from 0 to +5°C, while in the open water period from 0 to +32°C. The subglacial period is characterized by maximum transparency, weak insolation, minimal dynamics of the water environment, reverse temperature stratification, and specific production processes (Riviere, 2012).

First of all, this applies to lakes located near large industrial cities, the supply of the population with high-quality fish products should be a particular concern of the state. These reservoirs include lakes in the Akmola region of Northern Kazakhstan. Therefore, at this stage, there is a question of mass study of medium and small reservoirs of Kazakhstan for the needs of the fishing industry.

2. MATERIALS AND METHODS:

The content for this work was collected zooplankton samples in the lakes of the Akmola region (lakes Uyaly-Shalkar, Shnet, Shelkar, Maidan dam). During the expedition trips to the lakes, 320 hydrobiological and 120 hydrochemical samples were collected and processed.

Hydrochemical observations were carried out simultaneously with the central hydrobiological studies. Sampling was carried out from the surface and bottom layers of water according to generally accepted methods, that is, water was taken from depths of 30-40 cm and collected in a plastic container with a volume of 1 liter. All dishes were pre-prepared according to the rules for preparing containers before sampling to prevent contamination.

The determination of dissolved oxygen and biochemical oxygen demand was carried out by the iodometric method, according to the Winkler and thermooxidation (Figure 1). The study of the oxygen regime was carried out both from the surface of the reservoir and from the depth of the lake, to calculate the value of the oxygen balance.

Permanganate oxidation was performed using the Kubel method. This method is based on the oxidation of organic substances present in the sample with a known amount of potassium permanganate solution with a concentration of 0.01 mol/l EQ. When boiling in a sulphuric acid medium for 10 minutes, potassium permanganate that has not reacted is reduced with oxalic acid. The excess oxalic acid was titrated with a solution of potassium permanganate. This method, used in the analysis of drinking and slightly polluted natural water, is widely used because of its relative simplicity.

The study of turbidity and transparency was carried out using the "font" method. The definition of turbidity is based on determining clarity by measuring the maximum height of the water column, at which it is already possible to visually

distinguish a black font or an alignment mark (for example, a black cross) on a white background. Based on the value of water transparency determined in the analysis, the value of water turbidity for phormazine (EMF) and kaolin (mg/l) was determined using the calibration schedule. This method is used for clean and low-polluted waters and allows you to assess the transparency of water in almost any conditions and on any body of water, regardless of its depth, the presence of bridges, weather conditions, etc.

Determination of the total hardness as the total molar concentration of the equivalents of calcium and magnesium cations was determined by the titrimetric method. The decision is based on the reaction of calcium and magnesium salts with the reagent-Trilon B. The analysis was performed at pH 10-10.5 in the presence of a dark blue chromic acid indicator (acid chromic-blue T). The role of the indicator in determining the overall hardness is that when it is added to the analyzed water, a reaction initially occurs as a result of which all the calcium and magnesium is bound by the indicator to form a compound colored red. Further, during titration, as Trilon B is added, a more substantial colorless complex with calcium (magnesium) is established, the complex with the indicator is destroyed, and the indicator is released, coloring the solution blue.

The determination of carbonates, hydrocarbonates, and alkalinity was carried out by the titrimetric method. The resolution is based on the reaction of carbonate and bicarbonate ions with hydrogen ions in the presence, as indicators of phenolphthalein and a mixture of bromocresol green and methyl red (mixed indicator). The corresponding amount of acid consumed for the phenolphthalein titration (VF) is equivalent to free alkalinity (Schsv); the amount of acid consumed for the mixed indicator titration (VSM) is total alkalinity (Scho). Based on the results of titration, the values of free and total alkalinity of water were determined, which made it possible to calculate the concentrations of carbonate and bicarbonate ions. Concentrations of carbonate and bicarbonate ions allow us to calculate the carbonate hardness of water, which is the total content of soluble salts of carbonates and hydrocarbonates. The pH of the water was measured by the pH meter testo 206 (Testo AG Germany) (Alekin, 1970; Shishkina, 1974; Balushkina, 1979).

Zooplankton was collected by filtering 50-600 liters of water through the small Apstein network (using mill gas No. 70). Once every ten days. Filtered 50 liters of water. The samples

were fixed with four percent formalin with addition. Each zooplankton sample was marked with the sample number, date, place of collection, and volume of filtered water (Kiselev, 1980; Life of freshwater, 1956).

In each reservoir, zooplankton samples were collected at three points. To identify the taxonomic composition and count the number of zooplankton, samples were analyzed in the Bogorov chamber (freshwater Life., 1956) according to the Bogorov-Gensen method (CIT. by Moruzi *et al.*, 2008). If necessary, the sample was diluted with water. Then, to account for large and small species, the sample was viewed in full. Zooplankton organisms were determined using the following determinants: E. F. Manuilova (1964), L. A. Kutikova (1970), E. V. Borutsky, and others. (1991), "Determinant of freshwater invertebrates of the European part of the USSR" (1977), "Determinant of freshwater invertebrates of Russia..." (1995, 1994), N. M. Korovchinsky (2004). Determination of the naupliar and Junior copepodite stages of oarfoots was carried out up to the suborder (Kiselev, 1980; Moruzi *et al.*, 2008; Manuilova, 1964; Kutikova, 1970; Borutsky, 1991; Korovchinsky, 2004).

To account for rare large forms, as well as ovulatory individuals, the sediment was viewed. To determine the production of zooplankton, 50 specimens of each species were measured, taking into account the stage of development and gender. It is noted (Galkovskaya, 2005) that filtration of bathometric samples through the network (compared to sedimentary samples) leads to a noticeable understatement of the number and biomass, since large mobile crustaceans can avoid fishing gear, and small rotifers and Copepoda naupliars are not held by gas with a mesh greater than 45 microns. Therefore, when calculating the biomass for rotifers, a conversion factor of 2.0 was used; for crustaceans-1.5 with a population of less than 1 thousand copies/m³. Additionally, to reduce the error, when sampling water was filtered through a network located in the water (only its upper edge was above the water) so that rotifers under pressure were not forced through the cells of the net.

Since samples were taken by filtering the volume of water through the Apstein network, the population of each species was calculated as follows:

$$N_i = n_{np} * 1000 / V_{np},$$

where N_i – the number of species in the sample,

ex./m³; n_{np} – the number of organisms of the species in the sample, ex.; V_{np} – the volume of filtered water, l.

Data on the biomass of each zooplankton species was obtained by multiplying the individual mass of each organism (w_i) by its number (N_i):

$$B = \sum N_i * w_i$$

Measurements of the organisms were measured under a binocular microscope according to age stages: adult forms, young (Guide., 1983, 1992). The calculation of the individual mass of organisms in the sample was performed using the formula (balushkina, Vinberg, 1979a, 1979b)

$$w = q * l^b,$$

Where w - the body mass of the organism, mg; l - the body length of the organism, mm; q - the body mass at the body length. Equal to 1 mm; b - exponent (for isometric growth (Rotifera) is 3, for allometric growth (Copepoda, Cladocera) - more or less than 3). For rotifers, the q values proposed by A. Ruttner-Kolisko (1977) were used. The weight of Copepoda nauplii was calculated with the formula of a rotational ellipsoid: $V = 4/3 a * b * c$ where a , b , c – 1/2 of length, width, and height of body, mm, assuming a specific gravity of animals equal to 1.

A Petersen dredger took samples of zoobenthos with a ground capture area of 1/40 m². Sample processing with determination of species composition and number of organisms was performed using conventional methods (Sharapova, Falomeeva, 2006).

To assess species diversity, the Shannon index was used (Shannon, 1963), since it is considered the most informative and convenient. It is assumed that the index values higher than 3 - corresponds to clean waters, from 1 to 3 – moderately polluted; less than 1 – dirty (Ruttner-Kolisko, 1977; Sharapova *et al.*, 2006; Shannon *et al.*, 1961).

The Shannon index quantifies the structure of the community and is calculated using the formula:

$$H = - \sum n_o * \log_2 n_o,$$

n_o – relative number of species in the sample.

Statistical processing of the material was performed using the Microsoft Excel application package. The average value (\bar{x}), the error of the

average value (\bar{S}), the standard deviation (σ), and the coefficient of variation (Cv) were calculated. The difference in average values was estimated using the student's criterion and the probability P, which was recognized as statistically significant at $P \geq 0.95$, using the algorithms of A. N. Plokhinsky (1961), G. F. Lakin (1973), and L. A. Vasilyeva (2004).

3. RESULTS AND DISCUSSION:

To assess the biological resources of small freshwater reservoirs in Northern Kazakhstan, we conducted monitoring studies of many reservoirs in the Akmola region. Their hydrochemical regime, mineralization, and classification of reservoirs by trophic levels were studied. The species composition, number, and biomass of zooplankton communities were identified. Dependencies between individual parameters of the hydrochemical regime and indicators characterizing the well-being of hydrobiont communities were established.

Since the development of zooplankton is significantly affected by water mineralization, we evaluated this relationship.

When analyzing the data obtained, we tried to identify the relationships between various parameters that characterize the chemical quality of water (mineralization) and parameters that describe the state of zooplankton communities (number, biomass).

It is known that environmental conditions influence many properties of living organisms. The high-confidence effect of the amount of mineral substances in water on the biomass of zooplankton communities was found to be 94 %.

Table 1 shows the results of a study of the mineralization of lakes in the Akmola region. According to the classification of I. V. Baranov (Alekin, 1970, 1973), the studied water of the lake. Shnet, Shelkar, Uyaly-Shalkar, Maidan square is medium-mineralized (table.1). As a result of observations, it was found that the level of mineralization in the lake. Uyaly-Shalkar is significantly higher (from 362-532 mg/l). The lowest rates were observed in the lake Chelkar of Arshaly district (186-305 mg/l).

The results of these studies suggest that the degree of mineralization of water, the studied lakes, can be attributed to fresh since the amount of ions contained in the water does not exceed 1g/kg.

The influence of water mineralization on zooplankton productivity was studied on the example of lake Uyaly-Shalkar.

The dependence of the level of zooplankton development on the total water mineralization in lake Uyaly-Shalkar is shown in Figure 2. The higher the mineralization, the lower the number. A similar trend is observed for the "mineralization – biomass" pair.

When analyzing the data obtained, we observed an inverse relationship between water mineralization and zooplankton abundance. When water mineralization increases by 4.03% in July, the number of zooplankton organisms decreases from 170.03 to 152.6 thousand copies/m³.

When the salinity of the Uyaly - Shalkar lake water increases from 362 (May) to 508 mg/l (July), the zooplankton biomass decreases from 6.02 to 5.73 mg/m³.

To confirm this, the correlation coefficient was calculated in these pairs of features; in the pair "mineralization – zooplankton number," it was $r = -0.96$, and in the pair "mineralization – zooplankton biomass" $r = -0.85$.

4. CONCLUSIONS:

Thus, when studying the features of the hydrochemical regime for organoleptic limiting parameters in three reservoirs, the hydrochemical scheme of water was within the normal range. When considering the influence of the hydrochemical regime on the example of water mineralization on productivity, we noted that with an increase in water mineralization in July by 4.03%, the number of zooplankton organisms decreases from 170.03 to 152.6 thousand copies/m³. A similar trend is observed for the "mineralization – biomass" pair.

According to the classifier of O. A. Alekin oz. Uyaly-Shalkar belongs to the hydrocarbonate class, a group of calcium, of the first type; oz. Snet – sulphate class, group of calcium of the first type; oz. Shelkar - to the chloride class, sodium group, of the second type; Maidan dam-of the hydrocarbonate class, calcium group, of the second type.

6. REFERENCES:

1. Aubakirova., Pishenko, B.S. Maikanov. *Mediterranean journal of Social Sciences*, **2014**, 5, 2607-2611.

2. Adilbekov, Aubakirova, Inirbayev and Dzhamanbayev. Fish Fauna and Assessment of Fish Safety in the Reservoirs of Akmola Region of Northern Kazakhstan. *Pakistan J. Zool.*, **2019**, vol. 51(5), pp 1919-1925.
3. Alekin, O. A. Fundamentals of hydrochemistry.- Leningrad: Gidrometizdat, **1970**.- 444 p.
4. Borutsky, E. V. Determinant of Calanoida of fresh waters of the USSR. - L.: Nauka, **1991**. – 504 p.
5. Bondarenko N.A. (2009) Ekologiya i taksonomicheskoe raznoobrazie planktonnykh vodoroslei v ozerakh gornykh oblastei Vostochnoi Sibiri. Avtoref. dokt. diss. Ecology and taxonomic diversity of planktic algae in the lakes of the East Siberian mountainous regions Borok. 2009. –p.45.
6. Brzoska, M.M., Moniuszko-Jakoniuk. *Fd. Chem. Toxicol.*, **2001**, 39: 967–980.
7. Balushkina, E. V., the Relationship between body mass and length in planktonic animals. General principles of studying aquatic ecosystems. - L., **1979**. - Pp. 169-172.
8. Culotta, V.C., Gitlin, J.D. *McGraw-Hill, Wash.*, **1999**, 210-221.
9. Corbel, M.J.. *J. Fish Biol.*, **1975**, 7: 539-563.
10. Determinant of freshwater invertebrates of the European part of the USSR. - L.: Gidrometeoizdat, **1977**. – 486 p.
11. Galkovskaya, G. A. Community of rotifers of pelagic zooplankton of stratified lakes: structural indicators and ways of inclusion in trophic networks. Rotifers (taxonomy, biology and ecology): TEZ. and materials of the IV Intern. Conf. by rotifers (Borok, 6-8 Dec. 2005) - Borok, **2005**. - Pp. 37-38.
12. Kiselev, I. A. Plankton of seas and continental reservoirs. L.: Nauka, **1980**. – 440 p.
13. Kutikova, L. A. Rotifers of the USSR fauna (Rotatoria). - L.: Nauka, **1970**. – 744 p.
14. Korovchinsky, N. M. Branched crustaceans of the order Ctenopoda of the world fauna (morphology, systematics, ecology, zoogeography). - M.: T-vo nauch. ed. KMC, **2004**. – 410 p.
15. Lakin, G. F., Biometrics. -M.: Higher. SHK., **1973**. – 342 p.
16. Lisitsyn A., Makangali K., Uzakov Y., Taeva A., Konysbaeva D., Gorbulya, V (2018) Study of the National Cooked Smoked Meat Products While Tests with Laboratory Animals at the Pathology Models with the Purpose to Confirm the set of Biocorrective Features. Current Research in Nutrition and Food Science journal 6(2): 536-551.
17. Makangali, K. Konysbaeva, D.; Zhakupova, G.; Gorbulya, V.; Suyundikova, Zh. Study of sea buckthorn seed powder effect on the production of cooked-smoked meat products from camel meat and beef. *Periodico Tchê Química*, **2019**, 16: 130-139.
18. Moruzi, I. V. Practicum on Hydrobiology. Novosibirsk. state agrarian. UN-T.- Novosibirsk, **2008**.- Pp. 17-43.
19. Manuilova, E. F. Branched crustaceans (Cladocera) of the fauna of the USSR. - M.; L: Nauka, **1964**. – 328 p.
20. Popov, P.A., **2002**. *Assessment of the ecological status of water bodies methods of actioncialis*. Novosibirsk, NSU.
21. Plokhinsky, A. N. Biometrics. SB as USSR, Novosibirsk, **1961**. – 364 p.
22. Restek Corporation. Example dSPE Cleanup: PAHs in Infant Formula QuEChERS Products Fast, Simple Sample Prep for Multiresidue Pesticide. **2012**
23. Rice, E.W., Baird, R.B., Eaton, A.D. and Clesceri, L.S. Standard Methods For The Examination Of Water And Wastewater. **2012**. Method 6440b y Method 6410B.
24. Ruttner-Kolisko, A. Suggestions for biomass calculations of plankton rotifers. *Archive Hydrobiologia*. - **1977**. - No. 8. - P. 71-76.
25. Riv'er I.K. (2012) Holodnovodnyi zooplankton ozer basseina Verhnei Volgi. The coldwater zooplankton of the Upper Volga basin lakes. Izhevsk, -p. 390.
26. Shishkina, L. A. Hydrochemistry. M.; L.: Hydrometeoizdat, **1974**.- 326 p.
27. Sharapova L. I. Methodological guide for hydrobiological fisheries research of reservoirs in Kazakhstan (plankton, zoobenthos). Almaty, **2006**. - 300 s.
28. Shannon, K. Works on information theory and Cybernetics. - Moscow: Foreign

- literature, **1963**. – 860 p.
29. Tornero, V., Hanke, G. Chemical Contaminants Entering the Marine Environment from Sea-Based Sources: A Review With a Focus on European Seas. *Marine Pollution Bulletin*. **2016**, 06.091
 30. Tihomirov A.I., Egorov A.N. Termicheskie rezhim i teplozapasy (1977) The thermal regime and thermal resources. *Ozero Kubenskoe*. L., -p. 257–285.
 31. Vasilyeva, L. A. Statistical methods in biology. Textbook for the course of lectures "Biometrics". - Novosibirsk, **2004**. - 128 p.
 32. Virbickas, Y.B., Vosyliene, M.Z. and Kazlauskienė, N.P. *Fish Biochem.*, **2000**, 48-
 - 50.
 33. World Health Organization. Guidelines for drinking-water quality. **2011**.

Table 1. Water mineralization in the lakes of Akmola region, mg/dm³

Reservoirs	Mineralization, mg / l		
	May	July	September
Oz.Shnet	256 \pm 3,32	445 \pm 4,01	413 \pm 5,26
Oz.Shelkar	186 \pm 2,13	261 \pm 3,22	305 \pm 4,0
Oz.Uyaly-Shalkar	362 \pm 4,02	508 \pm 6,24	462 \pm 5,44
Maidan Square	302 \pm 4,0	387 \pm 4,04	463 \pm 5,62



Figure 1. The study of the hydrochemical regime of water was carried out using the NKV-12 Express laboratory

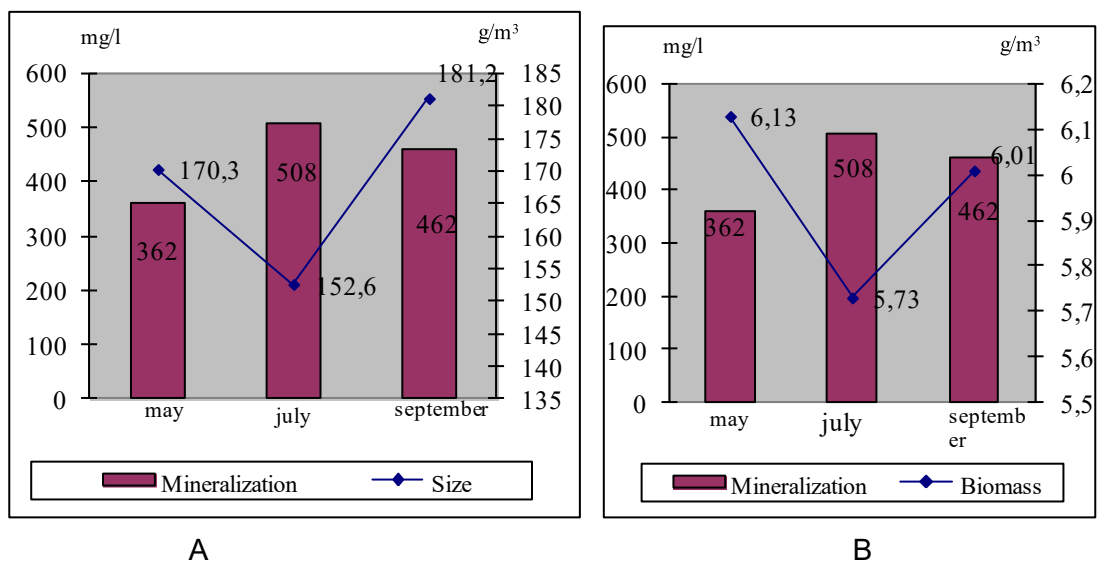


Figure 2. Influence of water mineralization (A - on the number of zooplankton, B - for zooplankton biomass)

SÍNTESE, CARACTERIZAÇÃO, ATIVIDADE ANTIFÚNGICA E RELACIONAMENTO ESTRUTURA-ATIVIDADE: ESTUDO DE ALGUMAS BASES MONO E DI-SCHIFF

SYNTHESIS, CHARACTERIZATION, ANTIFUNGAL ACTIVITY AND STRUCTURE - ACTIVITY RELATIONSHIPS: STUDY OF SOME MONO- AND DI-SCHIFF BASES

JASIM, Ekhlas Q.¹; DHAIF, Hawraa K.²; MUHAMMAD-ALI, Munther A.^{3*}

^{1,3}Basrah University, College of Pharmacy, Pharmaceutical Chemistry Department. Iraq

²Basrah University, College of Education for Pure Science, Department of Chemistry. Iraq

*Corresponding author
e-mail: muntheralamery@yahoo.com

Received 03 January 2020; received in revised form 17 February 2020; accepted 10 March 2020

RESUMO

As bases de Schiff (SB) são tipos importantes de compostos orgânicos e possuem ampla gama de atividades biológicas devido ao uso comercial e farmacêutico. As diferentes atividades desses compostos chamaram a atenção de pesquisadores e os induziram a sintetizar e estudar novos tipos desses compostos. Duas séries de derivados da base Schiff foram sintetizadas pelas reações de condensação de aldeídos salicilaldeído substituído, 4- (N, N-dimetilamino) benzaldeído ou 2,4-dimetoxibenzaldeído com ácido 2-amino-5-iodobenzoico (1:1) ou com 3,5 Ácido 5-diaminobenzoico (1:2) em etanol absoluto como solvente. Diferentes técnicas analíticas caracterizaram a estrutura das bases de Schiff sintetizadas como, por exemplo, Transformada de Fourier por Infravermelho (FT-IR), e Ressonância Magnética Nuclear de Próton ¹H-NMR. A pureza dos compostos sintetizados foi testada por microanálise elementar (CHN) e cromatografia em camada delgada (TLC). As propriedades estruturais das moléculas estudadas foram investigadas teoricamente através da realização da teoria funcional da densidade (DFT) usando o software HyperChem. A lipofilicidade dos compostos testados mostrou que os compostos 2c, 2b, 2a e 1c apresentam valores de logP inferiores a (5), 2,90, 3,78, 3,82 e 4,57, respectivamente, enquanto 1b e 1a possuem valores de logP superiores a (5), 5,01 e 5,03, respectivamente. A distribuição de carga de Mulliken mostrou que o átomo de oxigênio carbonílico do grupo carboxílico é mais negativo (~ -0,4) em comparação com outros átomos de oxigênio (~ -0,3) em todos os compostos selecionados. O diagrama de energia dos orbitais moleculares de fronteira e seu intervalo de banda forneceram indicações sobre a reatividade química e a estabilidade cinética das moléculas. Os compostos sintetizados foram testados quanto a efeitos antifúngicos contra *Aspergillus niger* e *Candida albicans*, o que indicou que os compostos apresentavam boa atividade antifúngica.

Palavras-chave: Atividade microbiana, HOMO-LUMO, HyperChem, SAR, Schiff-Base.

ABSTRACT

Schiff bases (SB) are an important type of organic compounds and have a wide range of biological activities due to commercial and pharmaceutical trading uses. The different activities of these compounds induced the researchers to synthesized and studied new types of these compounds. Two series of Schiff base derivatives were synthesized by the condensation reactions of substituted aldehydes salicylaldehyde, 4-(N,N-dimethylamino)benzaldehyde or 2,4-dimethoxybenzaldehyde with 2-amino-5-iodobenzoic acid (1:1) or with 3,5-diaminobenzoic acid (1:2) in ethanol absolute as a solvent. Different analytical techniques characterized the structure of the synthesized Schiff bases; for instance, Fourier transform infrared FT-IR and proton nuclear magnetic resonance ¹H-NMR. The purity of the synthesized compounds was tested by elemental microanalysis CHN and thin layer chromatography TLC. The structural properties of the studied molecules were investigated theoretically by performing density functional theory (DFT) using the HyperChem software. The lipophilicity of the tested compounds showed that the compounds 2c, 2b, 2a, and 1c have logP values less than (5), 2.90, 3.78, 3.82 and 4.57, respectively, whereas, 1b and 1a have logP values higher than (5), 5.01 and 5.03, respectively. The Mulliken charge distribution showed that the carbonyl oxygen atom of the carboxylic group is more negative (~ -0.4) as compared to other oxygen atoms (~ -0.3) in all selected compounds. Frontier molecular orbitals energy

diagram and their bandgap provided indications about chemical reactivity and kinetic stability of the molecules. The synthesized compounds were tested for antifungal effects against *Aspergillus niger* and *Candida albicans*, which indicated that the compounds had good antifungal activity.

Keywords: Microbial activity, HOMO-LUMO, HyperChem, SAR, Schiff-Base.

1. INTRODUCTION:

The problem of microbial resistance is still the aim of the development of market antibiotics and enhance the drug companies to release a new type of medical agents to reduce the microbial infections (Al-Amiery *et al.*, 2009). It is, therefore, necessary to explore further, novel antifungal formulations to control fungal infections (Kathiravan *et al.*, 2012). The compounds called Schiff-base, imine, or azomethine function present in diverse natural compounds and non-natural derivatives are critical for their biological activities. These types of compounds were synthesized by direct condensation of primary amines with an aldehyde or ketone compounds (da Silva *et al.*, 2011).

SBs are, in reality, known to have a wide range of biological properties such as antibacterial (Kangah *et al.*, 2.17; Al Momani *et al.*, 2013), anticancer (Abd-Elzaher *et al.*, 2016), antiviral (Kumar *et al.*, 2010), antifungal (Chohan and Hanif, 2013; Bharti *et al.*, 2010), antiparasitic (Al-Kahraman *et al.*, 2010) in addition to other biological performances (Abu-Dief and Mohamed, 2015). On the other hand, their structures offer a high probability of structural change, implying a high degree of molecular diversity, which remains very useful for the development of new, less toxic and potent therapeutic agents (Kangah *et al.*, 2.17).

Recently, the studies, including quantitative structure-activity relationship (QSAR), are great importance in the field of modern chemistry and biochemistry. To obtain a significant correlation, it is essential to use the appropriate descriptors, whether they are empirical, theoretical, or derived from easily obtainable experimental characteristics of structures. These descriptors refer to the molecular properties and can thus provide exact information about the physicochemical nature of the chemical systems under investigation (Thakur *et al.*, 2004).

In this paper, two series of Schiff bases were synthesized and characterized. Their antifungal activities were evaluated against *Aspergillus niger* and *Candida albicans* by the disc diffusion method. The study of structure-activity relationships (SAR) between the antifungal activity and the structural properties were also evaluated.

2. MATERIALS AND METHODS:

2.1. Materials and Reagents

All chemicals used in this study were of reagent grade (supplied either by Sigma-Aldrich or Fluka) and used without further purification.

2.2. Characterization

Uncorrected melting points were performed by one side sealed capillary tubes. Bruker model ultra-shield (Switzerland) was used to scan ¹H-NMR spectra using 500MHz, at Tehran University, Islamic Republic of Iran. The solvent used was deuterated DMSO, and TMS was an internal standard. Shimadzu FT-IR model 8400 Spectrophotometer was used to record the FT-IR spectra using KBr disc at the Department of Pharmaceutical Chemistry, Pharmacy College, Basrah University. The CHN analysis measurements for the synthesized compounds were performed at the analytical Laboratory of Tehran University, Iran, using the EuroVector model EA3000A (Italy).

2.3. Synthesis

2.3.1. Synthesis of Schiff-bases Series 1 (S1)

2.3.1.1. Synthesis of (E)-2-((2-hydroxybenzylidene)amino)-5-iodobenzoic acid 1a

To the mixture of 0.01mole (1.31g) 2-amino-5-iodobenzoic acid dissolved in 15ml ethanol, 0.01mole (0.53ml) salicylaldehyde in 15ml ethanol was added. The mixture was stirring at room temperature for one hour. The resulting yellow precipitate was filtered off and washed with cold methanol to remove the not reacted materials. The product was crystallized from ethanol and dried at room temperature (Scheme 1). The characterizations of the prepared compound 1a were listed in Table 1.

2.3.1.2. Synthesis of (E)-2-((4-(dimethylamino)benzylidene)amino)-5-iodobenzoic acid 1b

To the mixture of 0.01mole (1.31g) 2-amino-5-iodobenzoic acid dissolved in 15ml ethanol, 0.01mole (0.745g) 4-(N, N-dimethylamino)benzaldehyde in 15ml ethanol was added. The mixture was stirring at room temperature for one hour. The resulting red precipitate was formed after 30 min, which filtered off and washed with cold methanol to remove the not reacted materials.

The product was crystallized from ethanol and dried at room temperature (Scheme 1). The characterizations of the prepared compound 1b were listed in Table 1.

2.3.1.3. Synthesis of (E)-2-((2,4-dimethoxybenzylidene)amino)-5-iodobenzoic acid 1c

To the mixture of 0.01mole (1.31g) 2-amino-5-iodobenzoic acid dissolved in 15ml ethanol and 0.2ml of glacial acetic acid, 0.01mole (0.83g) 2,4-dimethoxybenzaldehyde in 15ml ethanol was added. The mixture was refluxed for 30min then stirred for 3h. The volume of the resulting solution was reduced, the yellow precipitate was filtered off and washed with cold methanol to remove the not reacted materials. The product was crystallized from ethanol and dried at room temperature (Scheme 1). The characterizations of the prepared compound 1c were listed in Table 1.

2.3.2. Synthesis of Schiff-bases Series 2 (S2)

2.3.2.1. Synthesis of 3-(((E)-2-hydroxybenzylidene)amino)-5-(((Z)-2-hydroxybenzylidene)amino) benzoic acid 2a

A solution of 3,5-diaminobenzoic acid 0.01mole (0.75g) in 40ml warm ethanol and 10 ml ethanol solution of salicylaldehyde 0.01mole (1.05ml) was refluxed for 1 h. A green precipitate was formed. The reaction was stirred at room temperature for farther 2 h to complete reaction. The product was filtered and recrystallized from ethanol and then dried at room temperature (Scheme 2). The characterizations of the prepared compound 2a were listed in Table 1.

2.3.2.2. Synthesis of 3,5-bis(((E)-4-(dimethylamino)benzylidene)amino)benzoic acid 2b

A solution of 3,5-diaminobenzoic acid 0.01mole (0.75g) in 40ml warm ethanol and 20 ml ethanol solution of 4-(N,N-dimethylamino)benzaldehyde 0.01mole (1.49g) with 0.5ml of glacial acetic acid was refluxed for 3 h. On cooling on ice bath the reaction mixture, the brown product was filtered and recrystallized from ethanol and then dried (Scheme 2). The characterizations of the prepared compound 2b were listed in Table 1.

2.3.2.2. Synthesis of 3,5-bis(((E)-2,4-dimethoxybenzylidene)amino)benzoic acid 2c

A solution of 3,5-diaminobenzoic acid 0.01mole (0.75g) in 40ml warm ethanol and 20 ml ethanol solution of 2,4-dimethoxybenzaldehyde 0.01mole (1.66g) with 1ml of glacial acetic acid was refluxed for 3 h. On cooling the reaction mixture to room temperature, the yellowish-green product was filtered and recrystallized from ethanol and then dried (Scheme 2).

The characterizations of the prepared compound 2c were listed in Table 1.

2.4. Preliminary antifungal assay

The antifungal activity of the prepared Schiff-bases compounds was tested against the pathogenic fungus *Aspergillus niger* and *Candida albicans* at a concentration of 1000 µg/ml in dimethyl sulfoxide solvent by using the agar diffusion method. The medium used in this respect was Sabouraud dextrose agar. Fluconazole used as a standard drug.

Wells (6 mm in diameter) were cut using a stainless sterile cutting device (cork borer), and 100 µl of each compound was added to each well. Plates were incubated at 25°C for 72 h, inhibition zone diameters in mm were measured (M-Ali, 2008).

3. RESULTS AND DISCUSSION:

3.1. Synthesis of compounds

The Schiff base compounds S1 were prepared from condensation of 2-amino-5-iodobenzoic acid three aldehydes, salicylaldehyde, 4-(N,N-dimethylamino)benzaldehyde or 2,4-dimethoxybenzaldehyde in ethanol, (Scheme 1). The yield of the reactions was (74-86%). The prepared compounds were soluble in ethanol, methanol, and CHCl₃. The second series of Schiff base compounds S2 were prepared with good yield (68-88%) by condensation two moles of the three aldehydes above with 3,5-diaminobenzoic acid using ethanol as solvent, (Scheme 2). The products were colored compounds that were soluble in ethanol.

3.2. ¹H-NMR spectra

¹H-NMR spectra of some of the prepared compounds were performed in deuterated dimethyl sulfoxide solutions with tetramethylsilane as an internal standard. Table 2 represents the ¹H-NMR data spectra of the prepared compounds. All these spectra showed a signal at 2.5 ppm, which was due to the DMSO solvent and another signal at 3.33 ppm due to dissolved water in DMSO (Gottlieb *et al.*, 1997).

All compounds showed characteristic singlet signals in the range 8.156-9.657 ppm attributed to the proton of the azomethine group, which matched with the works of literature (Issa *et al.*, 2009).

For the compounds 1a and 2a, there are characteristic downfield signals referred to the intramolecular hydrogen-bonded proton of phenolic fragment -OH at 10.259 and 12.786 ppm, respectively (Jadeja *et al.*, 2016).

Two types of aliphatic signals appeared in high field range, which attributed to methyl groups attached to two types of atoms nitrogen and oxygen. Compounds 1b and 2b gave singlet signals at 3.040 and 2.955 ppm, respectively, which referred to protons of CH₃N-fragment with an integrated value of six protons. Whereas, compounds 1c and 2c showed singlet signals at 3.857 and 3.774 ppm, respectively, which referred to protons of CH₃O- groups with an integrated value of twelve protons.

All compounds didn't give signals at greater than 13 ppm attributed to protons of carboxylic acid because of DMSO solvent interactions (Abraham *et al.*, 2006).

All compounds showed multiplet signals in the range 6.420-8.526 ppm, which attributed to protons of aromatic systems.

3.3. IR spectra

FT-IR spectral data (in KBr pellets) of the compounds are given in Table 3. The IR spectra of the Schiff bases show medium or strong intensity absorption bands at 1600–1620 cm⁻¹ assigned to C=N stretching mode. The presence of aromatic rings ν (C=C) has been identified by their characteristic ring vibrations at 1581–1500 cm⁻¹ region. The presence of medium-strong bands particular of ν (C=O) for carboxylic acid at the range of 1728-1681 cm⁻¹ confirms the proposed Schiff base framework in compounds 1b, 1c, 2b, and 2c and these bands absence in the compounds 1a and 2a.

The broad bands in the range of about 3400 cm⁻¹ in the spectra of the compounds 1a and 2a demonstrates the formation of the OH...N intramolecular hydrogen bond between the salicyl part OH proton and the nitrogen atoms of azomethine groups (Bilge *et al.*, 2009).

The characteristic ν (C-H) modes of ring residues are observed at near 3050 cm⁻¹. The range about 1300 cm⁻¹ in the spectra of the compounds 1b, 1c, 2b and 2c show bending vibrations bands attributed to ν (C-H) of methyl groups in the –OCH₃ and –NCH₃ fragments, whereas, weak bands referred to stretching vibration of an aliphatic C-H bond in the range about 2900 cm⁻¹.

3.4. Optimization of molecular geometries

The molecules that formed from the reaction between substituted benzaldehydes (1) and monoaminocarboxylic acid (2) or diaminocarboxylic acid (3). As shown in Scheme 1, these molecules can be classified into two series: mono- Schiff bases (4) and di- Schiff bases (5), as shown in Scheme 3. The synthesized Schiff bases compounds have been optimized to study their theoretical properties using the Hyperchem program by the PM3 method.

Three-dimensional structures and IUPAC names of mono- Schiff bases (4) and for di- Schiff bases (5) are shown in Figure 1. The calculated molecular properties of compounds are shown in Table 4.

3.5. Lipophilicity

Lipophilicity is a physicochemical property of principal importance in drug discovery and development. It affects three phases of drug activity - its pharmaceutical, pharmacokinetic, and pharmacodynamic action (Rutkowska *et al.*, 2013). log P is related to the lipophilicity of compounds and is useful to predict the absorption of drugs across the intestinal epithelium. Log P must be smaller than 5 for a good drug candidate, are based on the observation that the most orally absorbed compounds have log P < 5 (Hughes *et al.*, 2008).

The compounds 1c, 2a, 2b, and 2c have logP values less than 5, whereas 1a and 1b have logP values greater than 5 (Table 4).

3.6. Mulliken atomic charges

The Mulliken atomic charges for the compounds calculated by the PM3 method are presented in Figure 2 and Table 4. The Mulliken charge distribution shows that the carbonyl oxygen atom of the carboxylic group is more negative (~ -0.4) as compared to other oxygen atoms (~ -0.3) in all selected compounds. Whereas, nitrogen atoms in the azomethine group have charge distribution lower than of oxygen in carboxyl, hydroxyl or methoxy groups. It has also been observed that some C atoms are positive, and some are negative.

3.7. Electric dipole moments

The polar molecule has a feature of dipole moment, which refers to electric charge distribution, which relates to the electric field. The polarity is the individual property of the particular molecule that independent of the surrounding area. A dipole moment is largely depending on the difference in electronegativity and distance between the charge separation.

According to Tab. 4, the dipole moments values show that mono- Schiff bases (S1) (2.851-5.525 D) generally have bigger electrical moments than di-Schiff bases (S2) (2.609-3.201 D). Whereas dipole moment is a vector, in symmetrical molecules such as di- Schiff bases (S2) bond dipole moments with the same value cancel each other's. For example, dipole moments of 1a and 2a can be compared. The rank of dipole moment for S1, 1a (5.525 D) > 1c (3.678 D) > 1b (2.851D), whereas, for S2 2a (3.201D) > 2c (2.803D) > 2b (2.609D).

3.8. Global reactivity descriptors

The HOMOs and LUMOs are known as Frontier molecular orbitals (FMOs), which played an essential role in evaluating molecular chemical stability, chemical reactivity, and hardness-softness of the molecule (Tanga *et al.*, 2011).

The determination of energies of the HOMO (π donor) and LUMO (π acceptor) are essential parameters in quantum chemical calculations. The HOMO is the orbital that primarily acts as an electron donor, and the LUMO is the orbital that mainly acts as the electron acceptor.

These molecular orbitals are also called the frontier molecular orbitals (FMOs). ϵ_{HOMO} and ϵ_{LUMO} are computed by the HyperChem software using the MP3 method, as shown in Figure 3.

Other quantum chemical parameters of organic compounds are obtained from calculations such as separation energies ΔE , absolute electronegativities χ , chemical potentials Π , absolute hardness η , global electrophilicity ω , absolute softness σ , global softness S and additional electronic charge (ΔN_{max}) according to the following equations (Yousef *et al.*, 2012; Porchelvi and Muthu, 2015). All quantum chemical parameters of the prepared compounds are listed in Table 5.

$$\Delta E = \epsilon_{\text{LUMO}} - \epsilon_{\text{HOMO}}$$

$$\chi = -1/2 (\epsilon_{\text{LUMO}} + \epsilon_{\text{HOMO}})$$

$$\Pi = -\chi$$

$$\eta = (\epsilon_{\text{LUMO}} - \epsilon_{\text{HOMO}}) / 2$$

$$\omega = \chi^2 / 2\eta$$

$$\Delta N_{\text{max}} = -\Pi / \eta$$

$$\sigma = 1/\eta$$

$$S = 1/2\eta$$

The ϵ_{HOMO} and ϵ_{LUMO} and their neighboring orbitals are all negative (as listed in Table 5), which indicates that the prepared molecules are stable (Yousef *et al.*, 2012; Yousef *et al.*, 2013).

The energy gap (ΔE) represents the chemical reactivity of compounds. For a system, the lower value of ΔE makes it more reactive or less stable. As depicted in Table-4, for compounds in group S1, 1c (7.888) > 1a (7.792) > 1b (7.428). For compounds in group S2, 2a (7.9984) > 2c (7.9959) > 2b (7.6542). Therefore, compound 1c is more stable compared with 1a and 1b in the series S1. Whereas, compound 2a is more stable compared with 2b and 2c.

Electrophilicity index ω is one of the most important quantum chemical descriptors in describing the activity. The electrophilicity adequately quantifies the biological activity of drug-receptor interaction. This new reactivity index measures the stabilization in energy when the system acquires an additional electronic charge from the environment. High values of electrophilicity index increase the electron-accepting

abilities of the molecules (Prabhakaran and Palanivel, 2016).

Thus, the electron-accepting abilities of compounds in the series S1 are arranged in the following order: 1a (3.207) > 1c (3.118) > 1b (2.995). The same arrange for series S2 2a (2.967) > 2c (2.823) > 2b (2.777).

The importance of η and σ is to measure the molecular stability and reactivity (N'dri *et al.*, 2018). The chemical hardness (softness) value of compound 1b ($\eta = 3.714$ eV) is the lowest among studied molecules. Thus, it appears that compound 1b is more reactive than all the studied compounds in two series. Whereas, the compound 2a ($\eta = 3.9992$ eV) is more stable than all compounds in two series.

The concepts of the parameters χ and Π are related to each other. The inverse of the global hardness is designated as the softness σ . Also, we note that compound 1a has its value of electronegativity ($\chi = 4.999$ eV), which is higher than other compounds' value, so it is the best electron acceptor that corresponded with the value of electrophilicity index ω .

3.9. Antifungal activity

In vitro antifungal effects of the investigated compounds were tested against two fungal species (*Aspergillus niger* and *Candida albicans*). The screening results indicate that all compounds exhibited antifungal activities. As shown in Table 5 and Figure 4 These good inhibitory may be attributed to the hydrogen bond formation of the azomethine fragment with the active sites of various constituents of cell which lead to interference with normal cellular processes (Prasad *et al.*, 2011; Thangadurai and Natarajan, 2001; Dharmaraj *et al.*, 2001).

It can be noted that compounds with -OH groups in the ortho position (1a and 2a) showed the most significant inhibitory effect against two types of fungi compared to other compounds (Ragenovic *et al.*, 2001). The activity of all compounds were more significant value against *C. albicans* than *A. niger*, which may be referred to as the high resistance of *A. niger* than *C. albicans*.

The results showed (Table 6) that the activity of all compounds was less than the activity of standard drug fluconazole.

4. CONCLUSIONS:

The two series of Schiff bases compounds (S1 and S2) were synthesized with good yields and high purity. The synthesized compounds gave promising antifungal activity against the tested fungal. There is a clear relationship between the structure of compounds

and the activity depending on the values of charges of groups and moieties, lipophilicity, and electronic dipole moments.

5. ACKNOWLEDGEMENTS:

The authors thank the help of the biologists group in Central Laboratory, College of Pharmacy, Basrah, Iraq, for antifungal study.

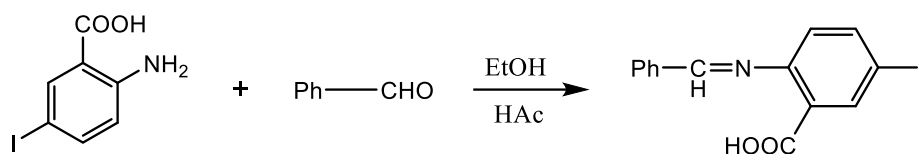
6. CONFLICTS OF INTEREST:

Three authors had declared no conflicts of interest.

7. REFERENCES:

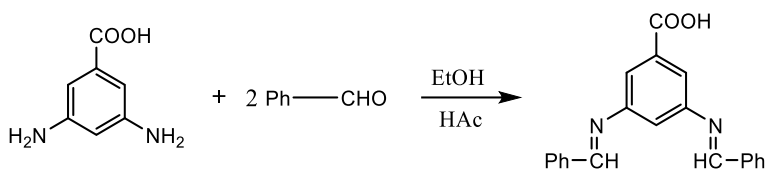
1. Abd-Elzaher, M.M., Labib, A.A., Mousa, H.A., Moustafa, S.A., Ali, M.M., El-Rashedy, A.A. Synthesis, anticancer activity and molecular docking study of Schiff base complexes containing thiazole moiety. *Beni-suef university journal of basic and applied sciences*, **2016**, 5, 85-93.
2. Abraham, R.J., Byrne, J.J., Griffiths, L., Perez, M. ¹H chemical shifts in NMR: Part 23, the effect of dimethyl sulphoxide versus chloroform solvent on ¹H chemical shifts. *Magnetic Resonance in Chemistry*, **2006**, 44, 491-509.
3. Abu-Dief, A.M., Mohamed, I.M. A review on versatile applications of transition metal complexes incorporating Schiff bases, *Beni-suef university journal of basic and applied sciences*, **2015**, 4, 119-133.
4. Al Momani, W.M., Taha, Z.A., Ajlouni, A.M., Abu Shaqra, Q.M., Al Zoubi, M. A study of *in vitro* antibacterial activity of lanthanides complexes with a tetradentate Schiff base ligand. *Asian Pacific Journal of Tropical Biomedicine*, **2013**, 3(5), 367-370.
5. Al-Amiery, A.A., Mohammed, A., Ibrahim, H., Abbas, A. Study the biological activities of tribulus terrestris extracts. *World Academy Science, Engineering and Technology*, **2009**, 57, 433-435.
6. Al-Kahraman, Y.M., Madkour, H.M., Ali, D., Yasinza, M. Antileishmanial, Antimicrobial and Antifungal Activities of Some New Aryl Azomethines, *Molecules*, **2010**, 15, 660-671.
7. Bharti, S.K., Nath, G., Tilak, R., Singh, S.K. Synthesis, anti-bacterial and anti-fungal activities of some novel Schiff bases containing 2,4-disubstituted thiazole ring. *European Journal of Medicinal Chemistry*, **2010**, 45, 651-660.
8. Bilge, S., Kilic, Z., Hayvali Z., Hokelek, T., Safran, S. Intramolecular hydrogen bonding and tautomerism in Schiff bases: Part VI. Syntheses and structural investigation of salicylaldehyde and naphthaldehyde derivatives. *Journal of Chemical Sciences*, **2009**, 121, 989-1001.
9. Chohan, Z.H., Hanif, M. Antibacterial and antifungal metal-based triazole Schiff bases. *Journal of Enzyme Inhibition and Medicinal Chemistry*, **2013**, 28, 944-953.
10. da Silva, C.M., da Silva, D.L., Modolo, L.V., Alves, R.B., de Resende, M.A., Martins, C.V., de Fatima, A. Schiff bases: A short review of their antimicrobial activities. *Bioorganic and Medicinal Chemistry*, **2011**, 2, 1-8.
11. Dharmaraj, N., Viswanathamurthi, P., Natarajan, K. Ruthenium(II) complexes containing bidentate Schiff bases and their antifungal activity. *Transition Metal Chemistry*, **2001**, 26, 105-109.
12. Gottlieb, H.E., Kotlyar, V., Nudelman, A. NMR Chemical Shifts of Common Laboratory Solvents as Trace Impurities. *Journal of Organic Chemistry*, **1997**, 62, 7512-7515.
13. Hughes, J.D., Blagg, J., Price, D.A., Bailey, S., Decrescenzo, G.A., Devraj, R.V., Ellsworth, E., Fobian, Y.M., Gibbs, M.E., Gilles, R.W., Greene, N., Huang, E., Krieger-Burke, T., Loesel, J., Wager, T., Whiteley, L., Zhang, Y. Physicochemical drug properties associated with *in vivo* toxicological outcomes. *Bioorganic & Medicinal Chemistry Letters*, **2008**, 18, 4872-4875.
14. Issa, Y.M., Hassib, H.B., Abdelaal, H.E. ¹H NMR, ¹³C NMR and mass spectral studies of some Schiff bases derived from 3-amino-1,2,4-triazole. *Spectrochimica Acta Part A*, **2009**, 74, 902-910.
15. Jadeja, J.J., Gondaliya, M.B., Mokariya, D.M., Shah, M. Spectral characterization and biological activity studies of Schiff's base of 1,5-dimethyl-2-phenyl-2,3-dihydro-1H-pyrazol-4-amine and its metal complexes. *World Scientific News*, **2016**, 47(2), 123-150.
16. Kangah, N.J., Koné, M.G., Kodjo, C.G., N'guessan, B.R., Kablan, A.L., Yéo, S.A., Ziao, N. Antibacterial Activity of Schiff Bases Derived from Ortho-Diaminocyclohexane, Meta-Phenylenediamine, and 1,6-Diaminohexane: Qsar Study with Quantum Descriptors. *International Journal of Pharmaceutical Science Invention*, **2017**, 6(3), 38-43.
17. Kathiravan, M.K., Salake, A.B., Chothe, A.S., Dudhe, P.B., Watode, R.P., Mukta, M.S., Gadhwe, S. The biology and chemistry of antifungal agents: a review. *Bioorganic and Medicinal Chemistry*, **2012**, 20, 5678-5698.
18. Kumar, K.S., Ganguly, S., Veerasamy, R., De Clercq, E. Synthesis, antiviral activity and

- cytotoxicity evaluation of Schiff bases of some 2-phenyl quinazoline-4(3H)-ones. *European Journal of Medicinal Chemistry*, **2010**, 45, 5474-5479.
19. M-Ali, M.A. *Ph.D. Thesis*, Basrah University, Iraq, **2008**.
 20. N'dri, J.S., Koné, M.G., Kodjo, C.G., kablan, A.L., Affi, S.T., Ouattara, L., Ziao, N. Theoretical Study of the Chemical Reactivity of Five Schiff Bases Derived From Dapsone by the DFT Method, *Chemical Science International Journal*, **2018**, 22(4), 1-11.
 21. Porchelvi, E.E., Muthu, S. Vibrational spectra, molecular structure, natural bond orbital, first-order hyperpolarizability, thermodynamic analysis, and normal coordinate analysis of Salicylaldehyde p-methylphenylthiosemicarbazone by density functional method, *Spectrochimica Acta Part A: Molecular and Biomolecular Spectroscopy*, **2015**, 134, 453-464.
 22. Prabhakaran, N.R., Palanivel, C. Synthesis, spectral characterization (FT-IR and NMR) and DFT (Molecular structure, HOMO-LUMO, NLO) computational studies on some novel (E)-N-phenyl-3,5-dichloropyridin-4-amine and its derivatives, *World Scientific News*, **2016**, 46, 244-259.
 23. Prasad, K., Kumar, L., Shekar, S., Prasad, M., Revanasiddappa, H. Oxovanadium complexes with bidentate N, O ligands: Synthesis, characterization, DNA binding, nuclease activity and antimicrobial studies. *Chemical Sciences Journal*, **2011**, 12, 1-10.
 24. Ragenovic, K.C., Dimova, V., Kakurinov, V., Molnar, D.G., Buzarovska, A. Synthesis, Antibacterial and Antifungal Activity of 4-Substituted-5-Aryl-1,2,4-Triazoles. *Molecules*, **2001**, 6, 815-824.
 25. Rutkowska, E., Pajak, K., Jozwiak, K. Lipophilicity- Methods of Determination and its Role in Medicinal Chemistry, *Acta Poloniae Pharmaceutica - Drug Research*, **2013**, 70 (1), 3-18.
 26. Tanga, G., Zhaoa, J., Li, R., Zhanga, Z., Synthesis, characteristic and theoretical investigation of the structure, electronic properties, and second-order nonlinearity of salicylaldehyde Schiff base and their derivatives. *Spectrochimica Acta Part A*, **2011**, 78, 449-457.
 27. Thakur, A., Thankur, M., Kakani, N., Joshi, A., Thakur, S., Gupta, G. Application of topological and physicochemical descriptors: QSAR study of phenylamino-acridine derivatives. *ARKIVOC xiv*, **2004**, 36-43.
 28. Thangadurai, T., Natarajan, K. Mixed ligand complexes of ruthenium(II) containing α,β -unsaturated- β -ketoamines, and their antibacterial activity. *Transition Metal Chemistry*, **2001**, 26, 500-504.
 29. Yousef, T.A., Abu El-Reash, G.M., El Morshedy, R.M. Quantum chemical calculations, experimental investigations and DNA studies on (E)-2-((3-hydroxynaphthalen-2-yl)methylene)-N-(pyridin-2-yl) hydrazinecarbothioamide and its Mn(II), Ni(II), Cu(II), Zn(II) and Cd(II) complexes, *Polyhedron*, **2012**, 45, 71-85.
 30. Yousef, T.A., Abu El-Reash, G.M., El Morshedy, R.M. Structural, spectral analysis and DNA studies of heterocyclic thiosemicarbazone ligand and its Cr(III), Fe(III), Co(II) Hg(II), and U(VI) complexes, *Journal of Molecular Structure*, **2013**, 1045, 145-159.



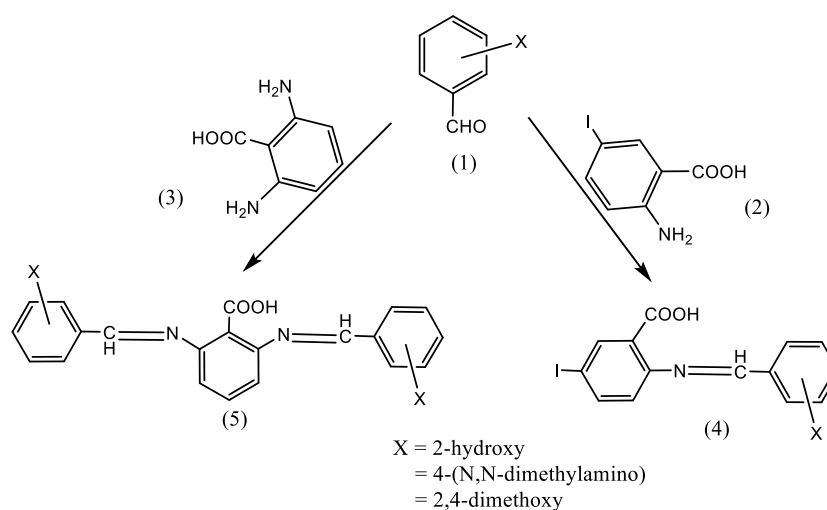
	1a	1b	1c
Ph =			
Name	2-[(E)-(2-hydroxybenzylidene)amino]-5-iodobenzoic acid	2-[(E)-[4-(dimethylamino)benzylidene]amino]-5-iodobenzoic acid	2-[(E)-(2,4-dimethoxybenzylidene)amino]-5-iodobenzoic acid

Scheme 1. Synthesis of Schiff-bases S1



	2a	2b	2c
Ph =			
Name	3-[(E)-(2-hydroxybenzylidene)amino]-5-[(Z)-(2-hydroxybenzylidene)amino]benzoic acid	3,5-bis(((E)-4-(dimethylamino)benzylidene)amino)benzoic acid	3,5-bis(((E)-2,4-dimethoxybenzylidene)amino)benzoic acid

Scheme 2. Synthesis of Schiff-bases S2



Scheme 3. Synthesis of Schiff base S1 and S2

Table 1. The characterization of the prepared Schiff-base compounds

Compd.	Molecular formula	M.Wt (g/mol)	Crystal Color	m. p. (°C)	Yield (%)	Elemental analysis Found (Calcd.)		
						C%	H%	N%
1a	C ₁₄ H ₁₀ INO ₃	367.14	Yellow	236-238	82	45.80 (45.75)	2.75 (2.69)	3.82 (3.85)
1b	C ₁₆ H ₁₅ IN ₂ O ₂	394.21	Red	210-212	86	48.75 (49.54)	3.84 (3.68)	7.11 (7.61)
1c	C ₁₆ H ₁₄ INO ₄	411.20	Yellow	220-223	74	46.74 (47.35)	3.43 (3.34)	3.41 (3.58)
2a	C ₂₁ H ₁₆ N ₂ O ₄	360.37	Pale yellow	>260	78	69.99 (70.25)	4.48 (4.31)	7.77 (7.85)
2b	C ₂₅ H ₂₆ N ₄ O ₂	414.51	Red	187-190	88	72.44 (71.76)	6.32 (6.51)	13.52 (13.66)
2c	C ₂₅ H ₂₄ N ₂ O ₆	448.48	Yellowish gray	113-114	68	66.95 (66.25)	5.39 (5.41)	6.25 (6.47)

Table 2. ¹H-NMR data of the prepared compounds

Compd.	δ ppm				
	-OH	CH=N	-OCH ₃	-NCH ₃	Aromatic
1a	10.259 (s)	8.867 (s)			8.120-6.600 (m)
1b		9.664 (s)		3.040 (s)	8.245-6.597 (m)
1c		8.156 (s)	3.857 (s)		8.156-6.590 (m)
2a	12.786 (s)	9.115 (s)			7.851-6.957 (m)
2b		9.657 (s)		2.955 (s)	8.526-6.420 (m)
2c		8.785 (s)	3.774 (s)		7.997-6.579 (m)

ppm: part per million, s: singlet signal, m: multiplet signal

Table 3. Characteristic IR spectral bands of the prepared compounds

Compd.	ν (C-H) ar. str.	ν (C-H) alip. str.	ν(C=O)	ν (C=N)	ν (C=C)	ν(C-N)	ν(C-O)	ν (C-H) ar. bend.
1a	3055 w		1705 m	1616 s	1554 m	1184 m	1153 m	763 m
1b	3021 w	2850 w	1681 m	1604 s	1581 s 1535 s	1188 m	1165 m	817 m
1c	3018 w	2947 w 2839 w	1708 m	1600 s	1570 m 1500 m	1284 m	1207 m	825 m
2a	3074 w		1728 s	1612 s	1581 s 1504 m	1273 s	1207 m	844 m
2b	3035 w	2924 w	1685 m	1603 s	1550 s	1199 m	1168 m	821 m
2c	3055 w	2989 w	1689 s	1620 s	1589 m 1570 s	1280 m	1253 m	756 s

w: weak, m: medium, s:strong

Table 4. Calculated molecular properties of compounds

Comp.	MW	Volume (Å ³) /Area (Å ²)	Charge O atom	μ (Debye)	logP
1a	367.14	783.31/476.45	[O(18) -0.428] [O(19) -0.263] [O(16) -0.223]	5.525	5.03
1b	394.21	904.07/539.77	[O(17) -0.412] [O(18) -0.311]	2.851	5.01
1c	411.20	904.55/539.30	[O(17) -0.407] [O(18) -0.315] [O(19) -0.193] [O(21) -0.187]	3.678	4.57
2a	360.37	1029.42/618.25	[O(9) -0.409] [O(8) -0.301] [O(26) -0.233] [O(27) -0.232]	3.201	3.82
2b	414.51	1256.44/737.13	[O(9) -0.406] [O(8) -0.307]	2.609	3.78
2c	448.48	1283.59/754.12	[O(24) -0.402] [O(25) -0.312] [O(26) -0.188] [O(28) -0.189]	2.803	2.90

Table 5. The calculated quantum chemical parameters of the prepared compounds

Comp.	ϵ_{HOMO}	ϵ_{LUMO}	ΔE	χ	P_i	η	ω	σ	s	ΔN_{max}
1a	-8.895	-1.103	7.792	4.999	-4.994	3.896	3.207	0.256	0.128	1.281
1b	-8.431	-1.003	7.428	4.717	-4.717	3.714	2.995	0.269	0.134	1.270
1c	-8.904	-1.016	7.888	4.960	-4.960	3.9442	3.118	0.253	0.126	1.257
2a	-8.872	-0.873	7.9984	4.872	-4.872	3.9992	2.967	0.250	0.125	1.218
2b	-8.438	-0.783	7.6542	4.611	-4.611	3.8271	2.777	0.261	0.130	1.204
2c	-8.749	-0.753	7.9959	4.751	-4.751	3.9979	2.823	0.250	0.125	1.194

Table 6. Inhibition zone of the prepared compounds and standard drug at 1000 µg/ml against *Aspergillus niger* and *Candida albicans*

Compound	Inhibition zone (mm)	
	<i>A. niger</i>	<i>C. albicans</i>
1a	27	28
1b	18	22
1c	19	23
2a	23	25
2b	14	16
2c	20	23
FLC	35	38

FLC: fluconazole

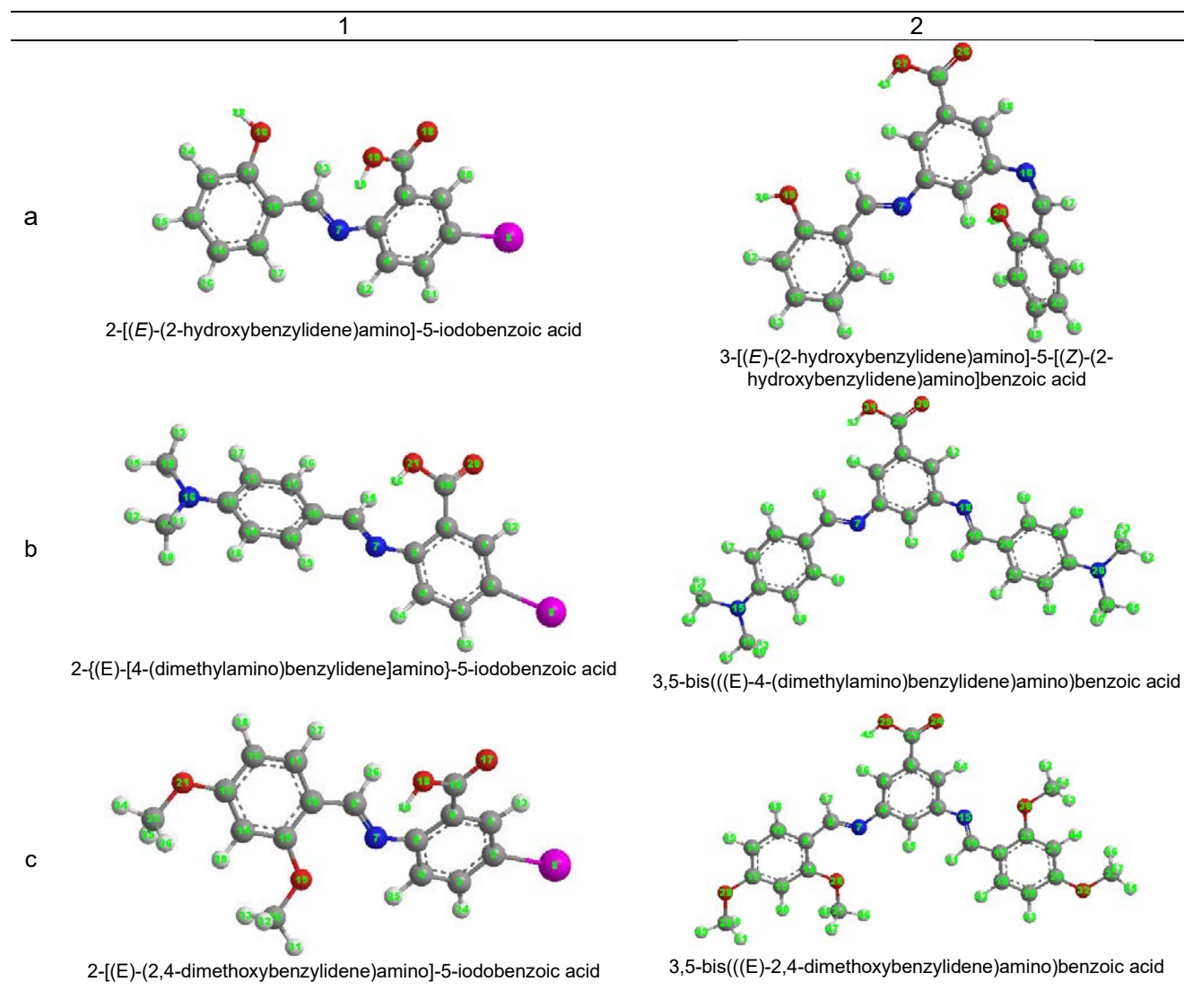


Figure 1. Three-dimensional structures and IUPAC names for mono- Schiff bases S1 and di- Schiff bases S2

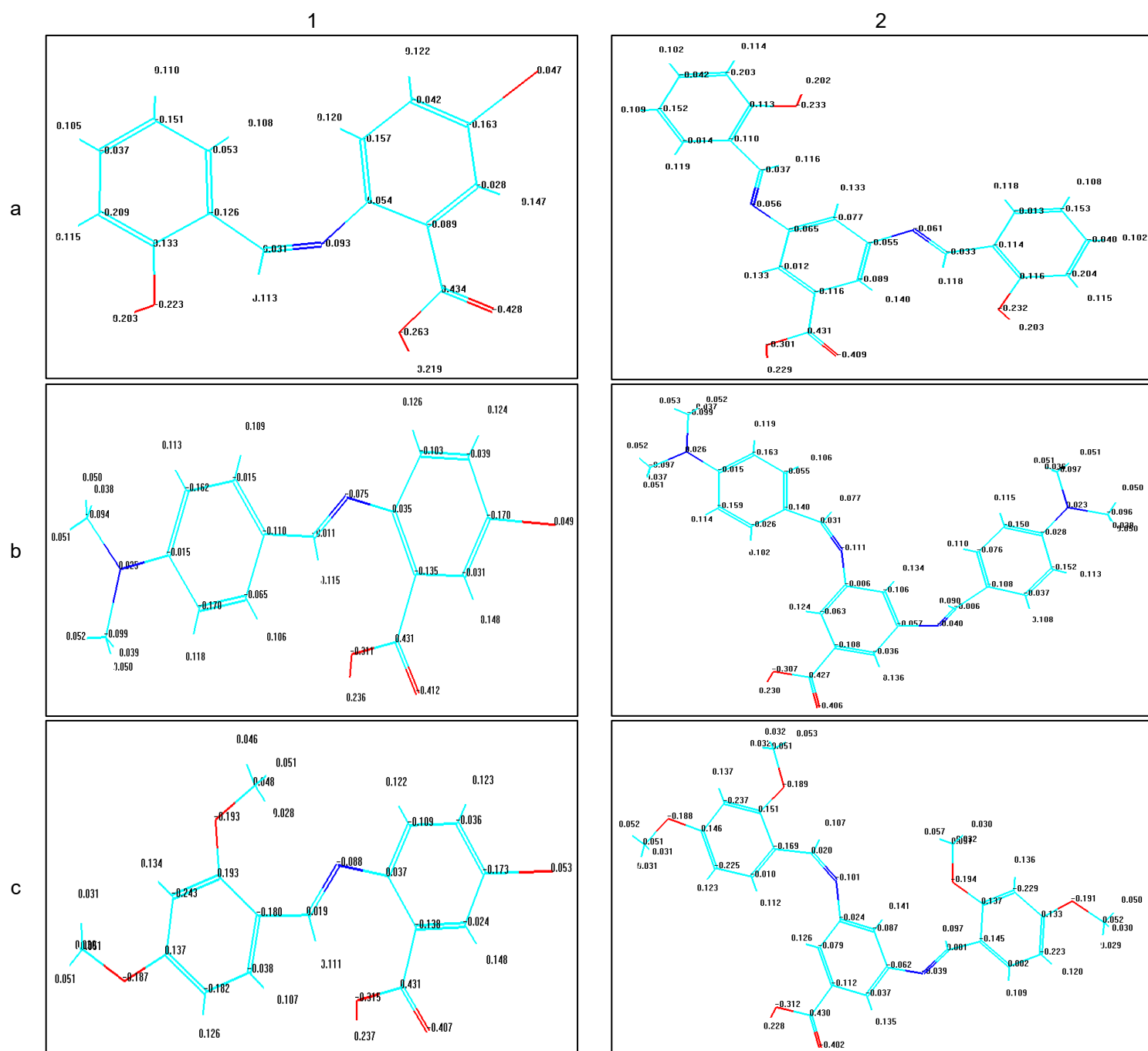


Figure 2. Atomic charges distribution of the compounds

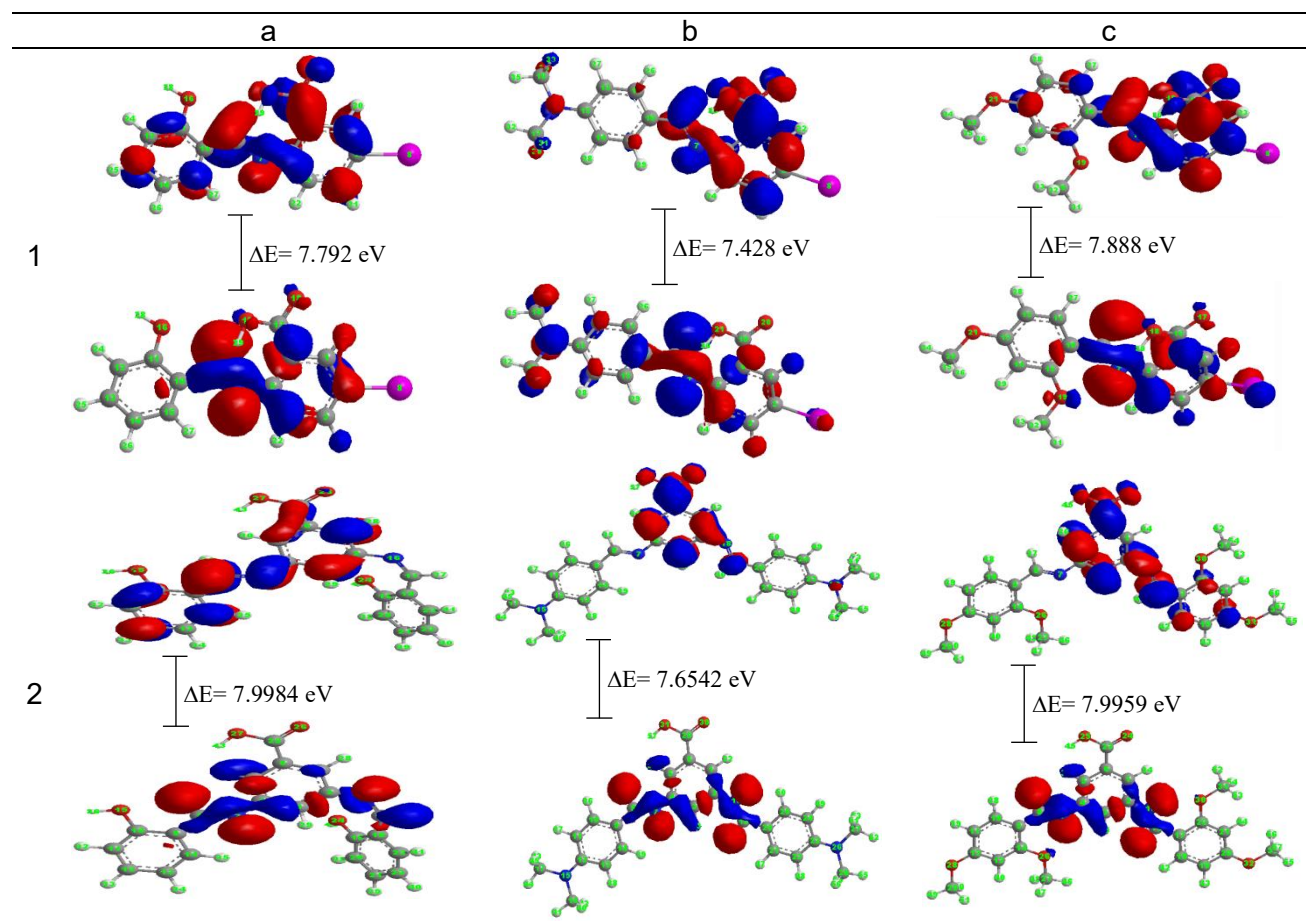


Figure 3. The highest occupied and lowest unoccupied molecular orbitals of the compounds

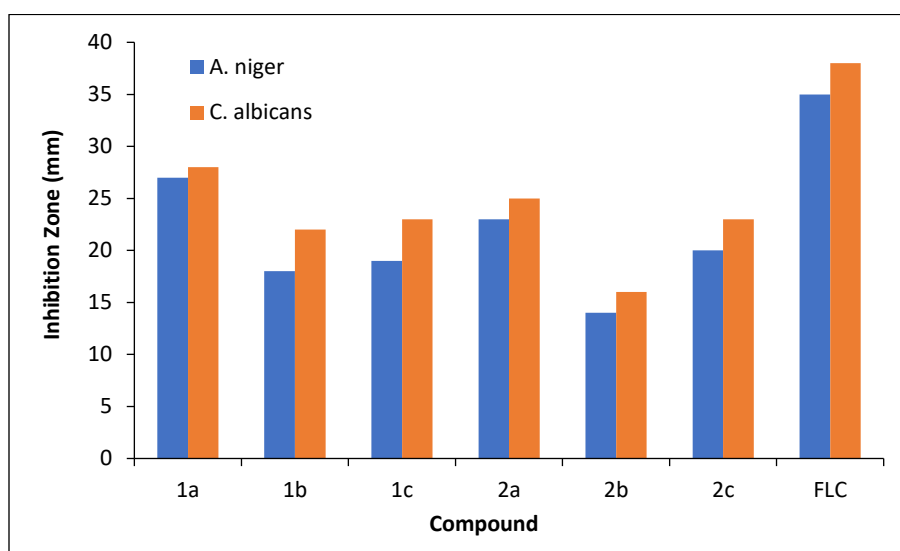


Figure 4. The effect of the compounds toward the tested organism *A. niger* and *C. albicans*

SUBSTANCIAÇÃO E SELEÇÃO DE UM INIBIDOR PARA EVITAR A FORMAÇÃO DE DEPÓSITOS DE ASFALTO-RESINA-PARAFINA

SUBSTANTIATION AND SELECTION OF AN INHIBITOR FOR PREVENTING THE FORMATION OF ASPHALT-RESIN-PARAFFIN DEPOSITS

ОБОСНОВАНИЕ И ВЫБОР ИНГИБИТОРА ДЛЯ ПРЕДУПРЕЖДЕНИЯ ОБРАЗОВАНИЯ АСФАЛЬТОСМОЛОПАРАФИНОВЫХ ОТЛОЖЕНИЙ

KHAIBULLINA, Karina Shamilevna^{1*}; SAGIROVA, Lyaisan Rustamovna²; SANDYGA, Mikhail Sergeevich³;

^{1,2,3} St. Petersburg Mining University, St. Petersburg. Russian Federation.

* Correspondence author
e-mail: khaibullina_k@mail.ru

Received 12 January 2020; received in revised form 16 February 2020; accepted 12 March 2020

RESUMO

Atualmente, a maioria dos campos de petróleo está em estágio avançado de desenvolvimento, o que está associado a vários desafios durante a produção de produtos de reservatório, incluindo a formação de depósitos de asfalto-resina-parafina (ARPD) em sistema de “zona de formação de fundo de poço”. Apesar de o problema da formação de depósitos orgânicos existir há mais de 60 anos, ele ainda é relevante hoje. Atualmente, para impedir a formação de ARPD, inibidores divididos em métodos baseados no uso de agentes umectantes, modificadores, depressores e dispersantes são amplamente utilizados na prática de campo. A composição de inibidores geralmente inclui surfactantes e, de acordo com a experiência de campo, surfactantes não iônicos, a saber, poliésteres, são amplamente utilizados para impedir a formação de ARPD. No entanto, pouco se sabe sobre inibidores com um efeito combinado, por exemplo, possuindo propriedades dispersoras de depressores em relação à ARPD. A partir do exposto, o trabalho visa desenvolver um inibidor combinado com propriedades dispersoras de depressores para impedir a formação de ARPD. A propriedade de dispersão do reagente desenvolvido em relação às partículas de asfalto foi determinada usando métodos capilares e foto colorimétricos. Os estudos foram conduzidos para determinar o impacto do reagente no ponto de congelamento. Foi realizada uma avaliação quantitativa do processo de sedimentação usando a instalação “haste fria”, e foram apresentados os resultados de estudos da resistência à corrosão desenvolvida por inibidor de reagente de ARPD. A temperatura da saturação do óleo com parafina foi determinada por 2 métodos. O método direto - observação visual (microscópio Axio Lab A1) e o método indireto - reogoniometria para determinar a viscosidade cinemática do óleo (analisador de viscosidade HVM-472 (Walter Herzog GmbH, Alemanha)). Assim, foi desenvolvido um inibidor de ARPD (IN-1) compreendendo um copolímero de etileno com α -olefinas ou polímeros de ésteres de ácidos acrílico, metacrílico ou cianoacrílico, um emulsificante de emulsões de óleo em água invertidas e um solvente. O inibidor desenvolvido, com propriedades de dispersão do depressor, é capaz de reduzir o ponto de congelamento de óleo no inverno e desacelerar a precipitação de cristais de parafina em equipamentos de poços e na zona de formação de fundo de poço (BHFZ).

Palavras-chave: depósitos de asfalto-resina-parafina, reagentes tensoativos, inibidor, zona do fundo do poço, razão de floculação

ABSTRACT

Currently, most oil fields are under the late stage of development, which is associated with some challenges during the production of reservoir products, including the formation of asphalt-resin-paraffin deposits (ARPD) in the “well – bottom-hole formation zone” system. Even though the problem of organic deposits creation has existed for more than 60 years, it is still relevant today. Currently, to prevent the formation of ARPD, inhibitors divided into methods based on the use of wetting agents, modifiers, depressors, and dispersants are widely used infield practice. The composition of inhibitors often includes surfactants, and according to field experience, non-ionic surfactants, namely, polyesters, are widely used to prevent the formation of ARPD. However, little is known about inhibitors with a combined effect, for example, possessing depressor-dispersing properties concerning ARPD. Proceeding from the above, the work is aimed to develop a combined inhibitor with depressor-dispersing properties to prevent the formation of ARPD. The dispersing property of the prepared reagent for asphaltene

particles was determined using capillary and photocolorimetric methods. The studies were conducted to assess the impact of the reagent on the freezing point. A quantitative assessment of the sedimentation process using the "Cold rod" installation was performed, and the results of studies of the developed ARPD reagent-inhibitor corrosion resistance were presented. Two methods determined the temperature of oil saturation with paraffin: the direct approach – visual observation (Axio Lab A1 microscope) and the indirect approach – rheogoniometry to determine the kinematic viscosity of oil (HVM-472 viscosity analyzer (Walter Herzog GmbH, Germany)). Thus, an ARPD inhibitor (IN-1), comprising a copolymer of ethylene with α -olefins or polymers of acrylic, methacrylic, or cyanoacrylic acid esters, an emulsifier of inverted oil-in-water emulsions and a solvent, was developed. The developed inhibitor, having depressor-dispersing properties, is capable of reducing oil-freezing point in winter and of slowing down the precipitation of paraffin crystals in well equipped and in the bottom-hole formation zone (BHFZ).

Keywords: *asphalt-resin-paraffin deposits, surface-active reagents, inhibitor, bottom-hole zone, flocculation ratio.*

АННОТАЦИЯ

На сегодняшний день большинство нефтяных месторождений находятся на поздней стадии разработки, которая сопровождается рядом осложнений при добыче пластовой продукции, в том числе образованием асфальтосмолопарафиновых отложений (АСПО) в системе «скважина-призабойная зона пласта». Несмотря на то, что проблема формирования органических отложений существует уже более 60 лет, на сегодняшний день она является актуальной. Сегодня широко используются в промышленной практике ингибиторы для предотвращения образования АСПО, которые подразделяются на методы, основанные на применении смачивающих добавок, модификаторов, депрессаторов и диспергаторов. В состав ингибиторов зачастую входят поверхностно-активные вещества, и как показывает промышленный опыт, неионогенные ПАВ имеют широкое применение для предупреждения образования АСПО, а именно полимеры сложных эфиров. Однако, на сегодня мало известно ингибиторов, обладающими комплексным действием, например, депрессорно-диспергирующими свойствами по отношению к АСПО.. Диспергирующая способность разработанного реагента по отношению к асфальтовым частицам определялась с помощью двух методов: «капиллярный» и фотоколориметрический. Проводились исследования по определению влияния реагента на температуру застывания. Была проведена количественная оценка процесса осадкообразования на установке «Холодный стержень», а также представлены результаты исследований антикоррозионных свойств разработанного реагента-ингибитора АСПО. Температура насыщения нефти парафином определялась 2 метода: прямой метод – визуальная оценка (микроскопа Axio Lab A1) и косвенный метод – реологические исследования по определению кинематической вязкости нефти (Анализатор вязкости HVM-472 (Walter Herzog GmbH, Германия)). Таким образом, был разработан ингибитор АСПО (ИН-1), содержащий сополимер этилена с α -олефинами или полимеры сложных эфиров акриловой, метакриловой или цианакриловой кислот, эмульгатор обратных водонефтяных эмульсий и растворитель. Разработанный ингибитор обладает диспергирующими и депрессорными свойствами, способный уменьшить температуру застывания нефти в зимнее время и выпадение кристаллов парафина в скважинного оборудования и ПЗП.

Ключевые слова: *асфальтосмолопарафиновые отложения, поверхностно-активные вещества, ингибитор, призабойная зона пласта, коэффициент флоккуляции.*

1. INTRODUCTION:

To date, the development of the oil industry in the Russian Federation is characterized by a significant decrease in oil production. This is since most of Russia's oil fields are under the late stage of development. Oil production is often associated with unwanted formation of organic deposits, such as asphalt-resin-paraffin deposits, in the BHFZ, on the walls of underground well equipment, and in the above-ground lines of the oil and gas gathering and processing system. Although the problem of organic deposits formation has existed for more than 60 years, it is still relevant today (Struchkov, 2018).

The formation of ARPD occurs in two ways. It can be either with the formation and growth of paraffin crystals on a solid surface or the formation and growth of paraffin crystals in the flow of reservoir fluid, with their subsequent adhesion to a solid surface. Paraffin crystals cannot form solid deposits. The binding elements during the formation of solid deposits are asphaltenes, resins, and mechanical impurities, included in ARPD composition. The composition and strength of deposits depend on the composition and properties of reservoir fluid, geological, physical, and technological conditions of an oil field development. In oil production, the composition of ARPD mainly consists of 40 - 60% solid paraffin

and less than 10% microcrystalline paraffin, 10 - 56% resins and asphaltenes, water, sand, and inorganic salts (Dubey *et al.*, 2017).

ARPD, in well equipped and the BHFZ, are formed at the change in thermobaric conditions when the reservoir is cooled, resulting from the injection of cold water. A decrease in pressure below the pressure of oil saturation with gas results in the vigorous evolution of gas directly in the BHFZ, an increase in oil density, a decrease in phase permeability, and the formation of ARPD. Besides, the creation of ARPD is affected by the reservoir fluid flow rate, change in the composition of oil during its degassing, state of tubing, and many other factors (Sychugov *et al.*, 2019).

Preventing the formation of ARPD during oil production is carried out in two ways: 1) removal of already formed deposits; 2) preventing scaling. Methods for removing ARPD include thermal methods (steam injection, flushing with hot oil or water as a heat carrier, the use of electric furnaces, induction heaters, etc.), mechanical methods (the use of scraping tools, scratchalizers mounted on rods), chemical methods (the use of organic solvents or detergents to remove ARPD) (Zhang *et al.*, 2019).

The most widely used methods for removing ARPD are chemical methods of removal, namely, the use of organic ARPD solvents. When choosing the most efficient way for removing ARPD, the composition, structure, and properties of these deposits must be accounted for. Nonetheless, the existence of extensive diversity of techniques for removing ARPD fails to completely solve the problem of the formation of ARPD in well equipment (Turbakov *et al.*, 2014).

The standard classification renders possible to specify the following methods for preventing the formation of ARPD: the use of protective coatings (coating of pipes with epoxy resins, finely crushed glass, bakelite varnish, resins, the use of glass-reinforced plastic rods); physical methods (vibrational, ultrasonic methods, exposure to magnetic, electric and electromagnetic fields); chemical methods (wetting agents, modifiers, depressors, and dispersants) (Cuesta *et al.*, 2013; Mali *et al.*, 2014).

The principle of operation of wetting agents is based on the formation of a hydrophilic film on the solid surface of well equipment, which in turn prevents the adhesion of paraffin crystals to the pipes and creates conditions sufficient for their removal by fluid flow. Modifiers, when interacting with paraffin crystals, changing their wettability,

keep them in a suspended, dispersed state, make them more round, compared to their initial needle-like or diamond shape. The principle of operation of depressors resides in the adsorption of their molecules on paraffin crystals, thereby complicating the process of combining thereof into a single system. Dispersants increase the thermal conductivity of oil and slow down the process of paraffin crystallization (Babalyan *et al.*, 1983).

To prevent the formation of ARPD in oil fields, a chemical method for protecting down-hole equipment, based on the use of specially selected chemical reagents – ARPD inhibitors, which are surfactants of ionic or non-ionic classes, is used. Ionic surface-active reagents (surfactants) are divided into cationic and anionic. Anionic surfactants dissociate in water into ions (positively charged cation and negatively charged anion). Negatively charged anion has surface activity. The most typical anionic surfactants, used in the oil industry, are alkyl aryl sulfonates (sulfonyl), alkyl sulfonates, alkyl sulfates, etc. Cationic surfactants also dissociate in water into ions, but in contrast to anionic surfactants, cations, positively charged ions, have surface activity. Examples of cationic surfactants include as follows: aliphatic amines – salts of hydrochloric acid, imidazoline derivatives, etc. Non-ionic surfactants do not dissociate in water into cations and anions. Nonylphenol ethoxylates, ethoxylated fatty alcohols, and acids block copolymers of ethylene and propylene oxides (disolvans, separols), amines are used as non-ionic surfactants (Babalyan *et al.*, 1983; Bikkulov *et al.*, 1997; Rogachev *et al.*, 2000).

Reservoir water often has a high content of alkaline-earth metal chlorides (calcium, magnesium). Therefore, in contrast to anionic surfactants, non-ionic surfactants, which do not chemically react with alkaline-earth metal salts, are often used in oil fields (Dubey *et al.*, 2017; Fang *et al.*, 2014).

Currently, surfactants are widely used in field practice, with various dosing techniques being applied, and according to field experience and patent research data, nonionic surfactants, namely, polyesters are widely used to prevent the formation of ARPD. Proceeding from the above, we have analyzed known and practically applied ARPD inhibitors, and as a result a reagent was developed and tested for its inhibiting property with respect to ARPD. The results of these tests, inter alia, confirmed its inhibiting property. The test results made it possible to optimize the composition of the new reagent and proved its high performance in preventing the formation of ARPD compared to other known inhibitors (RF

patent No. 2388785, RF patent No. 2027730, RF patent No. 2104391, etc.). The new ARPD reagent-inhibitor was assigned a reference designation of IN-1.

A copolymer of ethylene with α -olefins or polymers of acrylic, methacrylic or cyanoacrylic acids esters represented by general formula $(-CH_2-CR'(COOR)-)_n$ ($R' = H$ — acrylates, $R' = CH_3$ — methacrylates, $R' = CN$ — cyanoacrylates); an emulsifier of inverted oil-in-water emulsions and a solvent were chosen as components included in the composition of IN-1. These components were chosen due to their wide applicability and high efficiency in terms of preventing the formation of ARPD.

A copolymer of ethylene with α -olefins (polyvinyl acetate) with a molecular weight of 500-100000 has depressor properties. The dispersant used is an emulsifier of inverted oil-in-water emulsions Yalan E-2 brand A (conc.), manufactured according to TU 2458-00122650721-2009 with rev.1. The solvent serves as a binding element to better dissolve the two components.

This work aimed to develop a combined inhibitor with depressor-dispersing properties to prevent the formation of ARPD. Thus, an ARPD inhibitor (IN-1), comprising a copolymer of ethylene with α -olefins or polymers of acrylic, methacrylic, or cyanoacrylic acid esters, an emulsifier of inverted oil-in-water emulsions and a solvent, was developed. The developed inhibitor, having depressor-dispersing properties, is capable of reducing oil-freezing point in winter and of slowing down the precipitation of paraffin crystals in well equipped and the BHFZ.

2. MATERIALS AND METHODS:

The "capillary" method, which qualitative characteristic is the flocculation ratio, was used to assess the effect by the developed IN-1 inhibitor reagent on asphaltene in oil. The technique involves applying a drop of solution through a narrow capillary on filter paper, capable of trapping large dispersed particles in the center of a spreading drop. By visual inspection of the spot on the paper, after absorbing a drop of oil, it is possible to conclude whether or not there are aggregates of asphaltene particles. Uniform coloring of the spot confirms the absence of such aggregates and heterogeneous coloring witnesses in favor of their presence. By variation in the spot type, when the IN-1 is added in oil, its effect on asphaltene can be assessed (Khabibullin *et al.*, 1992).

Degassed oil with a density of 916 kg/m^3 , oil viscosity of $97.2 \text{ MPa}\cdot\text{s}$, with the following content of resins (12.5%), paraffins (3.7%), and asphaltene (1.69%) was chosen as the object of the research.

The dispersing ability of the IN-1 reagent relative to asphaltene particles can also be assessed via the photocolorimetric method. The studies were performed using the UNICO 2100 spectrophotometer (United Products and Instruments, USA). From the entire wavelength spectrum (300-1000 nm), an average length (500 nm) was chosen to build a graph for the dependence of light absorption coefficient and optical oil density on the IN-1 reagent concentration in oil.

The studies performed were aimed to determine the IN-1 reagent effect on such a key technological parameter of paraffin oil as the congealing point. The studies were carried out according to the state standard GOST 20287 (method B), without dehydration and pre-heating the product to a temperature of $(50 \pm 1)^\circ\text{C}$. An oil model, with paraffin content of 5 wt.%, was used as paraffin oil. The reagent was added in oil in the amount of 0.1 to 1.5 wt.%.

The sedimentation process quantitative assessment was carried out using the "Cold finger" installation. To assess the IN-1 reagent performance, paraffin oil with a density of 916 kg/m^3 was used. Before the experiment, "cold fingers," before being lowered in oil, were treated with petroleum ether and then with acetone. Oil with the IN-1 reagent was poured into metal cups. The studies were implemented by adding the IN-1 reagent in oil in the amount of 0.1 to 1.5 wt.%. For comparison purposes, reagent-free oil was used. The volume of oil in the cups was chosen in such a manner that the "cold fingers" were immersed in oil by at least one-half. The bath temperature was set at 37°C , the "cold finger" temperature was 12°C , and the duration of a single experiment made 60 minutes.

To study the developed ARPD reagent-inhibitor corrosion resistance, an oil model with varied IN-1 content (from 0.1 to 2 wt.%) was used. The model of oil, typical for oil fields of the Republic of Tatarstan, was used. The study of the ARPD inhibitor corrosion resistance was carried out under the state standards GOST 9.908-85, GOST R 9.905-2007, and GOST R 9.907-2007. The permissible corrosive activity for St-20 steel, according to a static test at 20°C , should not exceed $0.2 \text{ g/m}^2\cdot\text{h}$. The experiments were carried out at room temperature (20°C) and reservoir

temperature (37°C).

There is no uniform standard for measuring the temperature of oil saturation with paraffin. Therefore, two methods for determining this parameter were used during the study, including a direct method – a visual estimation, and an indirect method – rheogoniometry for determining the kinematic viscosity of oil.

The IN-1 reagent was dissolved in oil at different concentrations (from 0.1 to 1.5 wt.%). For its complete dissolving, oil was heated to 60°C. Then oil samples with the IN-1 were gradually cooled from 60°C to 18°C. The microstructure of oil with the reagent was studied using an Axio Lab A1 microscope at a magnification of 400 times. The IN-1 reagent-free oil sample was used as a check specimen for comparison purposes. The experiments were carried out for paraffin oils with a paraffin content of 5 wt.% and 7 wt.%.

The indirect method for determining the temperature of oil saturation with paraffin via rheogoniometry involved determining the kinematic viscosity of oil with and without adding the IN-1 at a gradual decrease in temperature. The experiment was carried out using the viscosity analyzer HVM-472 (Walter Herzog GmbH, Germany) according to the state standard GOST 33-2000 (ISO 3104-94), ASTM D445. The determination of the kinematic viscosity of oil with the reagent was implemented within the temperature range from 60°C to 20°C. The IN-1 reagent-free oil sample was used as a check specimen for comparison purposes. A paraffin oil model was used (5 wt.% of paraffin). The reagent concentration in oil made 0.2 wt.%.

3. RESULTS AND DISCUSSION:

The dispersing ability of the studied ARPD inhibitor relative to asphaltene particles was determined by two independent methods, i.e. “capillary” and photocolorimetric methods (Tica *et al.*, 2019, Rahman *et al.*, 2017; Ma *et al.*, 2019; Shatalova *et al.*, 2014;). The results of studying the IN-1 reagent effect on asphaltenes in oil using the “capillary” method are presented in Figure 1.

As is seen from Figure 1, when the IN-1 reagent is added to oil, with the increase in its concentration (from 0 to 4 wt.%), the flocculation ratio of asphaltenes in oil decreases, which witnesses in favor of a decrease in the size of their particles resulting from the dispersing effect of this reagent.

The results of studying the dispersing

ability of the IN-1 reagent relative to asphaltene particles using the photocolorimetric method are presented in Figure 2.

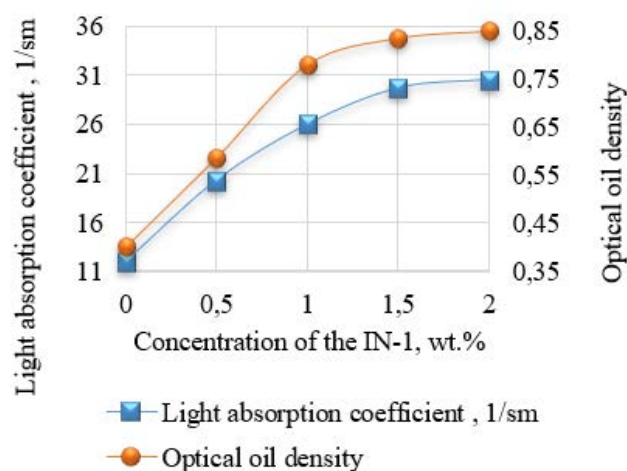


Figure 2. Dependence of light absorption coefficient and optical oil density on the IN-1 reagent concentration in oil

As is seen from Figure 2, oil optical density increases upon adding the ARPD inhibitor, which is due to an increasing degree of dispersion of the main light-absorbing particles in oil – asphaltenes. The results of studying the IN-1 reagent effect on the congealing point of oil are presented in Table 1.

Based on the research findings, it can be concluded that the IN-1 reagent has high depression ability, it's adding in paraffin oil under consideration in the amount of 0.1 wt.% to 1.5 wt.% results to a significant decrease in oil congealing point (by an average of 10°C), approximating it to the average ambient temperature during winter, typical for the main oil-producing regions of the Russian Federation.

The results of studying the sedimentation process using the “Cold finger” installation are presented in Table 2. As is seen from Table 2, the developed ARPD IN-1 inhibitor in oil composition can prevent the sedimentation process by 8.3-45.8%, depending on its weight content in oil. One of the requirements applicable to ARPD inhibitors is their low corrosive activity relative to the metal surface. The results of determining the corrosion rate are presented in Table 3.

As is seen from Table 3, the values of corrosion rate at temperatures of 20°C and 37°C do not exceed the specified standard. When adding the IN-1 in oil, its ability to inhibit the corrosion rate was revealed (at 20°C, by 2.3 times; at 37°C, by 3.3 times). The ARPD inhibitor in combination with oil can be recommended for fields with a reservoir temperature of 37°C (for example, Romashkinskoye field).

Wax crystals occurrence on the walls of down-hole equipment is possible only after oil cooling to a temperature, below the temperature of oil saturation with paraffin. Reaching the saturation temperature is followed by the precipitation, as a solid phase, of the most high-melting paraffins (ceresins), which intensively begin to form deposits (Bikkulov *et al.*, 1997; Struchkov *et al.*, 2019; Struchkov *et al.*, 2018; Joshi *et al.*, 2005; Campbell *et al.*, 2003; Shagiakhmetov *et al.*, 2018). Therefore, when selecting a reagent for removing and preventing the formation of ARPD, the temperature of oil saturation with paraffin is deemed to be an important parameter.

The dependence of the temperature of oil saturation with paraffin on the IN-1 concentration in oil is presented in Figure 3.

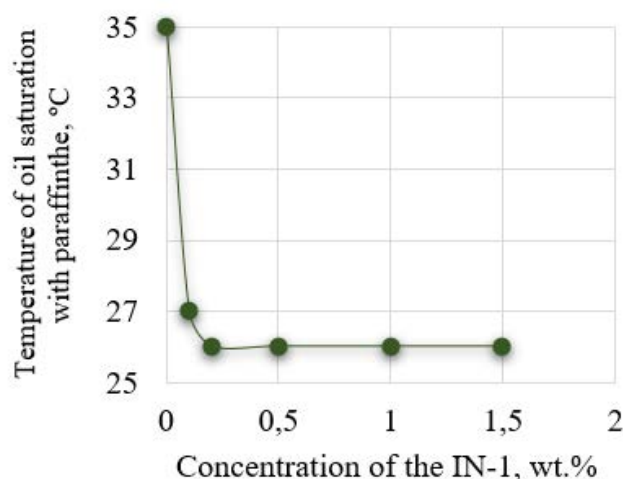


Figure 3. Dependence of the temperature of oil saturation with paraffin on the IN-1 concentration in oil

As is seen from Figure 3, the temperature of oil saturation with paraffin for the IN-1 reagent-free oil made 35°C. The optimal concentration of the inhibitor (0.2 wt.%), at which the temperature of oil saturation with paraffin virtually remains unchanged, was determined. Upon adding the IN-1, the temperature of oil saturation with paraffin decreased by 8°C.

With the increase in paraffin content in oil up to 7 wt.%, the temperature of oil saturation with paraffin increased by 4°C (from 35 to 39°C), i.e. proportionally increasing with the increase in paraffin content. Figure 4 illustrates the micrographs of paraffin oil (7 wt.%) with the IN-1, added in the amount of 0.2 wt.%, and without the IN-1. Micrographs were taken at a temperature of 37°C (average reservoir temperature of Tatarstan fields). As is seen from the micrographs in Figure 4, the introduction of the IN-1 reagent (0.2 wt.%)

into paraffin oil inhibits the formation of wax crystals. The results of studying the temperature of oil saturation with paraffin using rheogoniometry are presented in Figure 5.

As is seen from Figure 5, the temperature of oil saturation with paraffin without adding the IN-1 is 35°C, with a further decrease in temperature, a sharp increase in the kinematic viscosity of oil is observed. Upon adding the IN-1 reagent in oil, the temperature of oil saturation with paraffin decreases from 35 to 26°C. When the temperature drops below 26°C, there is a sharp increase in oil viscosity due to the structure formation process. To confirm the rheogoniometry results, micrographs of paraffin oil were taken using a microscope with and without adding the IN-1 reagent at temperatures of 25 and 30°C (Figure 6).

As is seen from Figure 6b, at the temperature of 30°C in oil with adding the IN-1 reagent, virtually no solid particles are observed, and when the temperature decreases to 25°C, their occurring is observed (Figure 6a). From Figure 6, it can be assumed that occurring the first solid particles of paraffin in oil with adding the IN-1 reagent takes place at a temperature of 26°C.

As is confirmed by the results of rheogoniometry and microscopical analysis, adding the IN-1 reagent in paraffin oil causes a significant decrease in the temperature of oil saturation with paraffin, therefore the IN-1 reagent can be recommended for practical application as the ARPD inhibitor. Thus, while implementing the laboratory research, the ARPD inhibitor (IN-1), containing a copolymer of ethylene with α -olefins or polymers of acrylic, methacrylic or cyanoacrylic acid esters, an emulsifier of inverted oil-in-water emulsions and a solvent, has been developed. The developed inhibitor has dispersing and depressor properties, capable to reduce the congealing point of oil in winter and precipitation of wax crystals in the well equipment and the bottom-hole zone.

4. CONCLUSIONS:

1. An ARPD inhibitor (IN-1), comprising a copolymer of ethylene with α -olefins or polymers of acrylic, methacrylic or cyanoacrylic acid esters, an emulsifier of inverted oil-in-water emulsions and a solvent, was developed.

2. The dispersing property of the studied ARPD inhibitor with respect to asphaltene particles was determined using two independent methods, i.e. "capillary" and photocolorimetric. During the study of the impact of IN-1 reagent on

asphaltenes in oil by the “capillary” method, it was revealed that when IN-1 reagent is added to oil with an increase in its content (from 0 to 4 wt.%), the flocculation ratio of asphaltenes in oil decreases, which witnesses in favor of a decrease in the size of their particles resulting from the dispersing ability of this reagent. During the study of the impact of IN-1 reagent on asphaltenes in oil by the photocolorimetric method, it was revealed that when IN-1 reagent was added in an amount of 0 to 2 wt.%, the values of optical density gradually increased. The optical density of oil increases upon adding ARPD inhibitor, which is due to a rise in the dispersion degree of the main light-absorbing particles in oil - asphaltenes.

3. According to the results of studies of the impact of IN-1 reagent on oil-freezing point, it can be concluded that IN-1 possesses high depressor properties, it's adding to the studied paraffin oil in an amount of 0.1 to 1.5 wt.% results to a significant decrease in oil-freezing point (by an average of 10°C), approximating it to an average ambient temperature in winter, typical for the main oil-producing regions of the Russian Federation.

4. When adding IN-1 in oil, it was revealed that IN-1 is capable of slowing down the corrosion rate (at 20°C by 2.3 times, at 37°C by 3.3 times). The ARPD inhibitor, in combination with oil, can be recommended for the fields with a reservoir temperature of 37°C.

5. When IN-1 reagent is added in oil, the temperature of oil saturation with paraffin decreases from 35 to 26°C. When the temperature drops below 26°C, there is a sharp rise in oil viscosity, due to the process of structuring occurring therein. The results of the performed rheogoniometry and microscopic studies witness in favor of the fact that adding IN-1 reagent to paraffin oil results to a noticeable decrease in the temperature of its saturation with paraffin, thereby the IN-1 reagent can be recommended for practical use as an ARPD inhibitor.

5. REFERENCES:

1. Al-jasmi A. (2014). Evaluation of Artificial Lift Modes for Heavy Oil Reservoirs, (June) 10-12.
2. Babalyan, G.A., Levi B.I., Tumasyan A.B., Halimov E.M. (1983). Oil field development via the use of surfactants. M.: Nedra, p. 216.
3. Bikkulov, A.Z., Nigmatullin R.G., Kamalov A.K., Sholom V.Yu. (1997). Organic oil deposits and their utilization, Ufa, p. 180.
4. Campbell G.J., Griffin J.M. and Chemex S.P.E. (2003). Hydrocarbon. Solvent Treatment for Inhibiting Paraffin and Suspending Asphaltenes in Oil Wells (SPE) 1-7 81004.
5. Cuesta J.J., Ortega J.D., Supply T.D.A., Service S.A. (2013). SPE 165008 Selection Criteria and New Technologies on The Artificial Lift Systems For Heavy Oil And Extra Heavy Oil Wells In Colombia.
6. Dubey A., Chi Y., Daraboina N. and Sarica C. (2017). SPE-187252-MS Investigating the Performance of Paraffin Inhibitors under Different Operating Conditions.
7. Fang F., & Babadagli T. (2014). Three Dimensional Visualisation of Solvent Chamber Growth in Solvent Injection Processes: An Experimental Approach 1-20.
8. Khabibullin, Z.A., Khusainov Z.M., Lanchakov G.A. (1992). Protection against paraffin deposits in oil production, – Ufa: USPTU, p. 105.
9. Ma, S. Z., Mahfud, M., & Altway, A. (2019). Parameter for scale-up of extraction Cymbopogon nardus dry leaf using microwave assisted hydro-distillation. *Journal of Applied Engineering Science*, 17(2), 126-133.
10. Novikova, N. V., Barmuta, K. A., Kaderova, V. A., Il'Yaschenko, D. P., Abdulov, R. E., & Aleksakhin, A. V. (2016). Planning of new products technological mastering and its influence on economic indicators of companies. *International Journal of Economics and Financial Issues*, 6(8Special Issue), 65-70.
11. Rahman, P. A. (2017). Using a specialized Markov chain in the reliability model of disk arrays RAID-10 with data mirroring and striping. *IOP Conference Series: Materials Science and Engineering*, 177(1), <https://doi.org/10.1088/1757-899X/177/1/012087>
12. Rogachev, M.K., & Kondrasheva N.K. (2000). Rheology of oil and oil products: Study guide. – Ufa: Publishing house USPTU, p. 89.
13. Sychugov, A. A., Akhmetshin, E. M., Grishin, V. M., Shpakova, R. N., & Plotnikov, A. V. (2019). Algorithm

- determine trust value to the distributed information systems elements. *Journal of Mechanical Engineering Research and Developments*, 42(2), 6-9. doi:10.26480/jmerd.02.2019.06.09
14. Struchkov I.A., Rogachev M.K., Kalinin E.S., & Roschin P.V. (2019). Laboratory investigation of asphaltene-induced formation damage. *Journal of Petroleum Exploration and Production Technology*, 9(2), 1443-1455.
 15. Struchkov I.A., & Rogachev M. K. (2018). The challenges of waxy oil production in a russian oil field and laboratory investigations. *Journal of Petroleum Science and Engineering*, 163, 91-99.
 16. Sanjay M., Simanta B. and Kulwant S. (1995). Paraffin Problems in Crude Oil Production and Transportation: A Review SPE Production & Facilities 10 50-54.
 17. Shagiakhmetov A., Tananykhin D., & Terleev A. (2018). Development of water-shutoff composition on the basis of carboxymethyl cellulose for fractured and fractured-porous oil and gas reservoirs. *Acta Technica CSAV (Ceskoslovensk Akademie Ved)* (ISSN: 00017043), 63 (3), pp. 475-480.
 18. Shatalova, T. N., Chebykina, M. V., Zhirnova, T. V., & Bobkova, E. U. (2014). Base of instruments for managing energy resources in monitoring activity of industrial enterprises. *Advances in Environmental Biology*, 8(7), 2372–2376.
 19. Turbakov M.S. and Riabokon E.P. (2014). SPE-171295-MS Improving of Cleaning Efficiency of Oil Pipeline from Paraffin.
 20. Tica, S., Živanović, P., Bajčetić, S., Milovanović, B., & Nađ, A. (2019). Study of the fuel efficiency and ecological aspects of CNG buses in urban public transport in Belgrade. *Journal of Applied Engineering Science*, 17(1), 65-73.
 21. Vranješ, B., & Todić, M. (2019). A model of analysis of the occupational safety and health system in the production system. *Journal of Applied Engineering Science*, 17(3), 264-272.
 22. Zhang, Z., Gao, W., Yun, B., Lu, X., Chen, S., Gu, X. (2019). Wax inhibitor screening by differential scanning calorimeter for high wax content crude oil. *IOP Conference Series: Earth and Environmental Science*, 2019.

Table 1. Variation in the congealing point of paraffin oil, containing the ARPD inhibitor

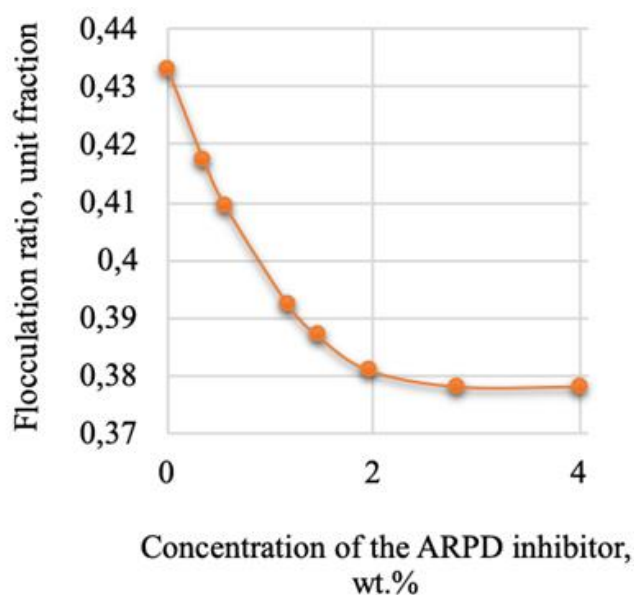
No.	Concentration of the inhibitor in oil, wt.%	Congeeing point, °C	Depressor effect ΔT , °C
1	0	-23	0
2	0.1	-28	5
3	0.5	-32	9
4	1	-39	16
5	1.5	-45	22

Table 2. Inhibitory ability of the IN-1 reagent relative to ARPD

No.	Concentration of the inhibitor in oil, wt.%	Inhibitory ability, %
1	0	—
2	0.1	8.3
3	0.5	25.0
4	1	37.5
5	1.5	45.8

Table 3. The results of determining the ARPD inhibitor corrosion rate in oil

Temperature, °C		Concentration of the IN-1, wt.%				
		0	0.1	0.5	1	1.5
V_c , g/m ² ·h	20	0.0756	0.0325	0.0342	0.0311	0.0318
	37	0.1134	0.0362	0.0369	0.0336	0.0324

**Figure 1.** Dependence of the flocculation ratio of asphaltenes in oil on the content of the IN-1 reagent therein in different concentrations

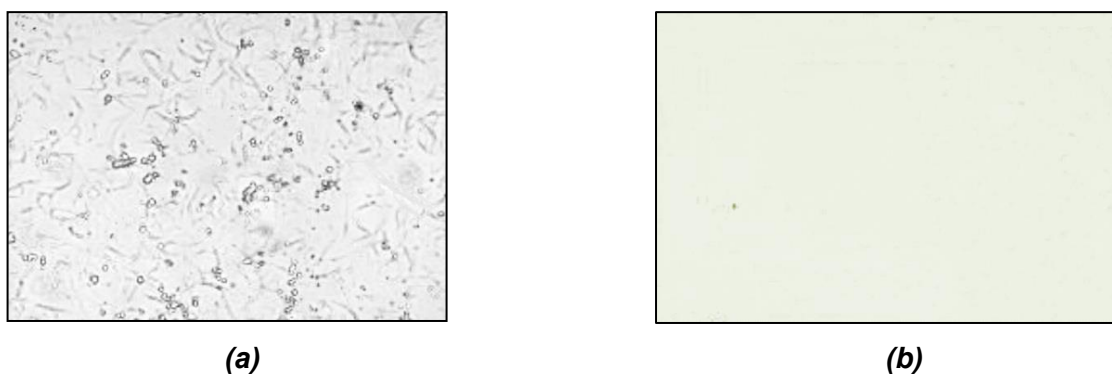


Figure 4. Micrographs at a temperature of 37°C (a) of oil (7 wt.% of paraffin), without the IN-1; (b) of oil with the IN-1, added in the amount of 0.2 wt. %

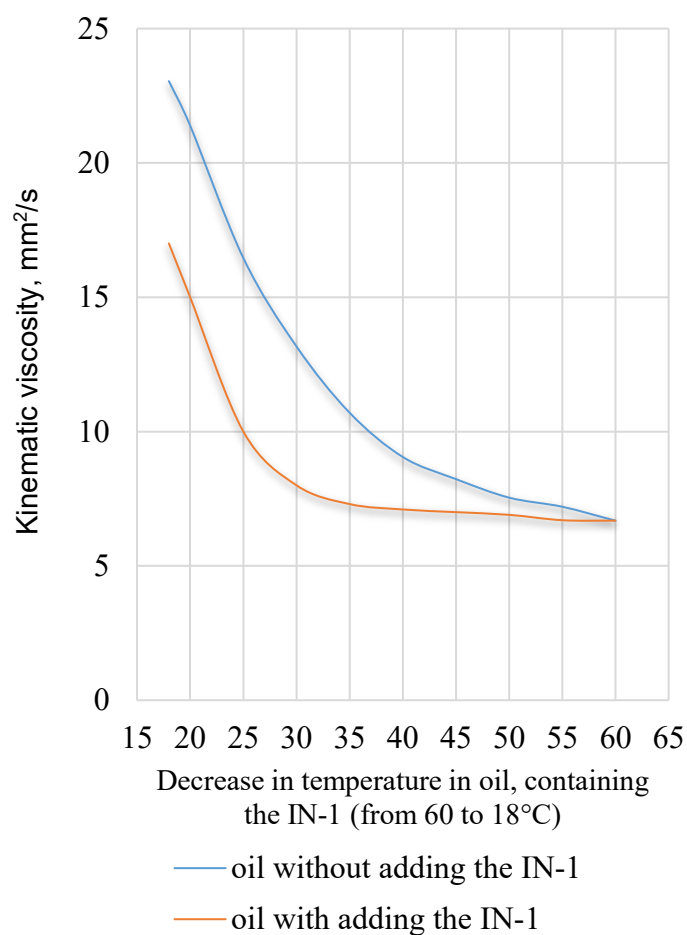


Figure 5. Dependence of kinematic viscosity of oil with and without adding the IN-1 on temperature



(a)



(b)

Figure 6. Micrographs of paraffin oil with adding the IN-1 at a temperature of: **(a)** 25°C; **(b)** 30°C

EFEITO DE COMPOSTOS ORGÂNICOS E INORGÂNICOS DE IODO NA
PRODUTIVIDADE DE PORCOS E NA QUALIDADE DA CARNE

EFFECT OF ORGANIC AND INORGANIC IODINE COMPOUNDS ON PIG PRODUCTIVITY
AND MEAT QUALITY

ИЗУЧЕНИЕ МЯСНОЙ ПРОДУКТИВНОСТИ И КАЧЕСТВА МЯСА ПРИ
ИСПОЛЬЗОВАНИИ В РАЦИО-НАХ СВИНЕЙ НА ОТКОРМЕ ОРГАНИЧЕСКИХ И
НЕОРГАНИЧЕСКИХ СОЕДИНЕНИЙ ЙОДА

BOLSHAKOVA, LARISA SERGEEVNA^{1*}; LISITSYN, ANDREY BORISOVICH²; CHERNUHA,
IRINA MIHAILOVNA³; SHELEPINA, NATALIA VLADIMIROVNA⁴; PARSHUTINA, INNA
GRIGOREVNA⁵;

^{1,4,5}Orel State University of Economy and Trade, 12 Oktyabrskaya Street, 302028, Orel – Russia.

^{2,3}V.M. Gorbato Federal Research Center for Food Systems, 26 Talalikhina Street, 109316, Moscow - Russia.

* Correspondence author
e-mail: ogietitf@yandex.ru

Received 12 June 2020; received in revised form 22 February 2020; accepted 06 March 2020

RESUMO

O objetivo deste estudo foi desenvolvido para examinar a eficiência de vários compostos de iodo nas dietas alimentares de porcos. O impacto dos compostos inorgânicos e orgânicos de iodo - iodato de potássio e proteína do leite iodado, que faz parte do aditivo alimentar "ProstTM" ("Innbiotech", Rússia) - no crescimento, produtividade e rendimento de carne magra porcos de engorda foram estudados. A composição físico-química e o valor biológico da carne foram estudados. O acúmulo de iodo no tecido muscular dos animais foi avaliado. Verificou-se que a proteína do leite iodado contribuiu para um crescimento mais intensivo do que a fonte inorgânica de iodo. Especificamente, os animais alimentados com a forma orgânica de iodo foram superiores em termos de peso de carcaça e valor de produção de tecido muscular e de gordura. Comparados ao grupo controle, os grupos experimentais de porcos demonstraram um rendimento de tecido muscular de 0,45%. Verificou-se também que fontes orgânicas de iodo têm um impacto positivo na composição química da carne; os animais alimentados com a forma orgânica de iodo superaram os que receberam iodo inorgânico em termos de substância seca da carne, teor de proteínas e teor de gordura. O nível de iodo no tecido muscular de porcos que receberam iodo orgânico foi consideravelmente mais alto, superando aqueles que receberam a fonte de iodo inorgânico em termos da presença de aminoácidos essenciais em seu tecido muscular.

Keywords: iodo, iodato de potássio, proteína do leite iodado, alimentação de suínos, qualidade da carne.

ABSTRACT

The aim of this study was designed to examine the efficiency of various iodine compounds in pigs' diets. The impact of inorganic and organic iodine compounds – potassium iodate and iodated milk protein, which is a part of the "ProstTM" feed additive ("Innbiotech", Russia) – on the growth, meat productivity and lean meat yield of fattening pigs was studied. The physico-chemical composition and biological value of the meat were studied. The accumulation of iodine in animal muscle tissue was assessed. It was found that iodized milk protein contributed to more intensive growth than the inorganic iodine source. Specifically, animals fed the organic form of iodine were superior in terms of carcass weight and yield value of muscle and fat tissue. Compared to the control group, the experimental groups of pigs demonstrated a muscle tissue yield of 0.45%. Organic sources of iodine were also found to have a positive impact on the chemical composition of meat; animals fed the organic form of iodine surpassed those receiving inorganic iodine in terms of their meat's dry substance, protein content and fat content. The level of iodine in the muscle tissue of pigs receiving organic iodine was considerably higher, and these pigs surpassed those receiving the inorganic iodine source in terms of the presence of essential amino acids in their muscle tissue.

Keywords: *iodine, potassium iodate, iodated milk protein, pig feeding, quality of meat.*

АННОТАЦИЯ

В работе проведено исследование эффективности использования в рационе свиней в период откорма различных соединений йода. С этой целью было изучено влияние неорганического соединения йода в форме йодата калия и органического - в виде молочного йодированного белка, входящего в состав кормовой добавки "ПростTM" ("Иннбиотех", Россия), на динамику живой массы и интенсивность роста откармливаемых свиней, выход постного мяса. Исследованы физико-химический состав, биологическая ценность мяса. Оценено накопление йода в мышечной ткани животных. В результате исследования установлено, что использование органической йодсодержащей добавки способствовало более интенсивному росту молодняка свиней по сравнению с животными, в рацион которых входил йод в неорганической форме. Животные, получавшие с кормом молочный йодированный белок, отличались большей массой. Выход мышечной ткани у животных опытных групп был достоверно выше по сравнению с контролем на 0,44%. Опытные животные достоверно превышали контроль по содержанию в мясе сухого вещества, белка и жира. В мышечной ткани свиней, получавших в составе основного рациона йодсодержащую добавку в органической форме, содержание йода было значительно выше по сравнению с животными контрольной группы. Опытные животные превосходили контроль по содержанию незаменимых аминокислот в белках мышечной ткани.

Ключевые слова: *йод, йодат калия, молочный йодированный белок, откорм свиней, качество мяса.*

1. INTRODUCTION

Problems with food quality affect complex aspects related to the economy, the social sphere, environment, and the development of the agro-industrial complex. The search for progressive and efficient technologies for feeding animals based on the latest scientific advancements and providing for the use of new bioavailable and stable fodder supplements with iodine is topical given the present conditions of intensifying meat production.

Providing agricultural animals with all the necessary essential nutrients, including mineral substances, is mandatory for increasing meat productivity and improving meat quality (Gorlov *et al.*, 2005; Savenko *et al.*, 2006). Georgievskii (1981), Underwood (1977), and Annenkov (1981) suggested that iodine is a vital microelement. According to reports from EFSA (2005) and SCF (2002), iodine deficit influences thyroid function, causing a decrease in the quantity of hormones the thyroid produces. As a result of protein, carbohydrate, and lipid exchange, iodine deficiency leads to problems in the reproductive system, decreased resistance to viruses, and a number of diseases, as well as excess mortality among livestock stores (Kondrakhin, 1989; McDowell, 2003). Lisitsyn *et al.* (2007), Flachowsky (2007), Flynn *et al.* (2003) and Mahan (1990) noted that iodine deficiency in feeds contributes to a decrease in the iodine content of agricultural animal products. Given that food products of animal origin are the main dietary

iodine source for humans, iodine supply for agricultural animals is not only important to their production and health but also has social importance.

Studies by Khaziakhmetov (2006), Godfrey (1988), and Rojas-Cano *et al.* (2014) focused on the impact of natural and complex synthetic vitamin and mineral agents on the productivity and metabolism of pigs. Rossi *et al.* (2010) and Schöne *et al.* (1988) noted the importance of improving feed additives and sought new prospective preparations with the potential to enhance the efficiency of pig breeding.

Inorganic forms of iodates and iodides are the most common iodine-containing feed additives (Iodobrom, Russia, Ajay-SQM Chile SA, Chile, Sichuan Jindian Chemical Company Limited, China, Deepwater Chemicals Corporation, USA). However, the propensity of iodide ions to photochemically or catalytically (in the presence of ions of transition metals) oxidize down to molecular iodine leads to a considerable loss of iodine during the storage of animal feed (Kuznetsov *et al.*, 1992). In addition, during the storage of premixes and finished feed, some of the iodide ions are converted into copper iodide, CuI, that is insoluble in water, which reduces the biological availability of iodine (Sedykh & Minko, 1975). The above difficulties are caused by the specifics of iodides' chemical behavior. The use of iodates does not solve the problem since they are known to rapidly convert to iodides in the presence of reducing agents. The most appropriate method uses resistant and easily assimilable organic

iodine compounds as the micro-element feed additive (Banoch *et al.*, 2012).

The objective of this study was to investigate the effects of feeding fattening pigs, either an inorganic iodine compound in the form of potassium iodate or an organic compound in the form of iodate milk protein on meat productivity and quality.

2. MATERIALS AND METHODS

The care and use of animals under experiment were performed in accordance with ethical norms and principles and in strict accordance with the research protocol and current regulatory documents (GOST 33044-2014, 2015; National Research Council, 1996; Directive 2010/63/EU, 2010). The study was approved by the Ethics Committee of Orel State University of Economy and Trade (Orel, Russian Federation).

Yorkshire pigs that were 4 months of age were used in this experiment. Three groups of 20 pigs were formed. Groups were selected according to the counterparts' principle. The length of the experiment was 104 days, including 5 days for the preparatory period and 99 days for the principle period. All groups of pigs were fed the same diet. The combined feed contains wheat, barley, corn, soybeans, peas, wheat meal, fish meal, yeast, and mineral and vitamin additives. The chemical composition of the feed was balanced for all major nutrients and adjusted for periods of fattening.

The pigs in the reference group were fed a diet supplemented with 1.4 mg of iodine per head per day. The pigs in the first experimental group were fed the "Prost™" diet supplemented with 0.7 mg of iodine per head per day. The pigs in the second experimental group were fed the "Prost™" diet supplemented with 1.4 mg of iodine per head per day.

The "Prost™" feed additive, which was made by "Inbiotech", Russia, is intended for enriching combined feed with organic iodine or for direct introduction into the diet of farm animals and poultry. The feed additive contains 7 g/kg of iodine. "Prost™" consists of dextrose (glucose) monohydrate (66%) and iodized milk powder protein. Iodinated protein is obtained using the method patented by Ljublinskij *et al.* (2002), which involves mixing protein raw material with an aqueous solution of inorganic iodine with enzyme treatment. A mixture of skim and fresh milk proteins of various natural origins was used as the raw protein material. Iodinated milk protein

contains iodine in bound form as mono- and diiodotyrosines, which are similar to natural organic iodine compounds.

This feed additive is characterized by resistance to light and heat; thus, it has a high degree of stability in long-term storage.

Sanitary, hygienic, and zootechnical requirements were complied with; the animals were clinically healthy and were kept and cared for in identical conditions.

The intensity of the growth and development of stores was defined according to the results of monthly weighing and calculation of absolute (by the difference between the final and initial weight of the animal in kg), and daily average (by dividing the absolute increase by the number of days of the experiment, g) body weight. Once a month, clinical and physiological indicators (body temperature, pulse rate, and breath rate) were measured before and after weighing.

After 104 days, the pigs were slaughtered, and body weight before slaughter, in kg; carcass weight (the weight of the animals after slaughter and evisceration, including viscera and internal raw fat in kg); slaughter yield (the ratio of the dead weight to the weight of the animal before slaughter, in percent); hot and chilled (after 24 hours of storage at $4 \pm 2^\circ\text{C}$) carcass weight in kg; carcass yield (the ratio of the hot carcass weight to the weight before the slaughter, in percent); weight of muscle tissue, fat, bones, and internal fat in kg; thickness of fat above the 6 & 7th chest vertebrae in mm; meatiness index (ratio of the muscle weight to the bone weight); and lean index (the ratio of the muscle weight to the fat weight) was determined.

To conduct chemical analysis, samples of the longissimus dorsi muscle were collected. The moisture content of the samples was determined by drying the hitch until its weight remained constant at a temperature of $105 \pm 2^\circ\text{C}$. Fat content was determined by extracting it from the dry hitch using ether and a Soxhlet extraction apparatus. The protein content was determined using Kjeldahl's method for determining total nitrogen content (GOST 25011-81). The mineral content was determined by mineralizing the samples in a muffle furnace at $550 \pm 25^\circ\text{C}$ for 5 to 6 hours and determining the percentage of ash in the weight of the initial sample. The content of amino acids was determined using an automatic amino acid analyzer LC 3000 manufactured by Eppendorf – Biotronilc (Germany). The total iodine content was determined by preliminary preparation of the sample by alkaline

mineralization, followed by the analysis of the aqueous solution of the mineralized sample using cathodic inversion voltammetry. In the process of sample mineralization, followed by ultraviolet irradiation of the mineralized sample solution, all forms of iodine are converted into iodide ions. Iodide ions are concentrated on a silver-modified electrode in the form of slightly soluble settlement, followed by cathode sludge recovery with linearly changing potential. The resulting cathodic peak with a negative potential of 0.4 ± 0.05 V is the analytical signal. The content of iodide ions in the solution of the prepared sample is determined by adding to a tested mixture of iodide ions. The iodotyrosine content was determined by drying and degreasing the samples, enzymatic hydrolysis of the sample with *Streptomyces griseus* proteases, extracting, and clearing iodotyrosines from the sample using the method of solid-phase extraction, followed by derivatization of the extract, and analysis by high-performance liquid chromatography coupled with a mass spectrometer. Analytes are identified by the absolute time of retention of chromatograph iodotyrosine peaks recorded in multiple reaction monitoring modes. The content of iodotyrosines is determined by the area of the chromatograph peaks in the analyzed samples.

Water-binding power was determined by pressing a weighed amount of meat on a sheet of filter paper with a 1 kg weight for 10 minutes, followed by determination of the weight of pressed-out moisture against the area of the wet stain. Weight loss during heat treatment was determined by the relative percent difference of the weight of meat (50 g) before and after heat treatment at 100°C for 60 minutes. pH was determined with a potentiometer and the aid of a pH-meter at a depth of 4-5 cm. Sensory meat evaluation was determined by a 5-point scale; for meat, by five criteria (appearance, smell, taste, texture, and juiciness), where 1 is the worst, and body weight is the best; and for both, by four criteria (appearance, smell, taste, and richness), where 1 is the worst, and 4 is the best. The biological value of the protein was determined by amino acid score, calculated as the ratio of the content of certain essential amino acids in the studied protein (g/100 g of protein) to the content of this amino acid in the reference protein (g/100 g of the reference protein) established by the FAO/WHO (Lipatov *et al.*, 2001).

The data were statistically analyzed, and a validity test was applied at three levels of probability (Glantz, 1998). A bilateral paired Student's t-test was used for assessing the

statistical significance of the method of a statistical hypothesis, which was a special case of ANOVA used for assessing the importance of the differences between the two datasets (Banoch *et al.*, 2012). The comparison was made at the 5% level of significance ($P < 0.05$).

The t value was calculated according to Equation 1 (Nürnberg *et al.*, 1998):

$$t_{emp} = \frac{X_{1av} - X_{2av}}{\sqrt{\frac{S^2}{n} + \frac{S^2}{n}}}, \quad (\text{Eq. 1})$$

where

X is the mean,

S^2 is the combined estimate of variance,

and n is the sample size.

$$S^2 = \frac{1}{2}(S_1^2 + S_2^2), \quad (\text{Eq. 2})$$

where $S_{1(2)}$ is the standard deviation.

If $t_{emp} < t_{crit}$, the null hypothesis is accepted; otherwise, the alternative hypothesis is accepted (t_{crit} is the reference value). The critical value of t depends on the significance level and on the number of degrees of freedom. The number of degrees of freedom k was determined by Equation 3.

$$k = 2(n-1) \quad (\text{Eq. 3})$$

A significance level of 5% ($P < 0.05$) was adopted.

3. RESULTS AND DISCUSSION

3.1. Dynamics of Body Weight and Intensity of Pigs' Growth

Bodyweight is the most important indicator of the meat productivity of animals.

The research results indicated that the bodyweight of animals in the experimental groups was higher than that in the control group (Table 1).

The bodyweight of animals in group I was significantly higher (5 kg or 4.42%) ($P < 0.05$) than that of animals in the control group.

The absolute gain and an average daily gain in body weight of pigs in group I was higher (4.4%) than that of pigs in the control group.

No significant difference was observed in the bodyweight of animals in group II compared to that in the control group.

Clinical and physiological indicators of the animals were also measured during the weighing process. It was found that their body temperature

increased slightly, as did pulse and breathing rate. However, the changes in these indicators remained within the normal physiological range in all groups.

3.2. Slaughter Characteristics and Meat Characteristics of the Experimental Pigs

Three pigs from each group were slaughtered to assess meat productivity. The results showed that the introduction of iodated milk protein to the diet of pigs did not have a significant impact on their slaughter characteristics (Table 2).

The slaughter yield (72%) and carcass yield (70%) of pigs in the control group and experimental groups I and II were similar.

To a large extent, morphological composition defines the market and food value of pig carcasses. In the process of this study, it was determined that the meat and fat content of pig carcasses varied according to the iodine compounds they consumed (Table 3).

Thus, compared to pigs in the control group, the pigs in experimental groups had improved muscle tissue yield of 0.45% ($P < 0.05$). The fat yield of pigs was significantly higher, by 0.39%, in experimental group I and lower, by 0.1%, in experimental group II compared to that in the control group.

The meatiness index of pigs in the control group was lower than those of experimental groups I and II by 7% and 3.1%, respectively ($P < 0.05$). The lean index was significantly lower in experimental group I, by 13%, and significantly higher in experimental group II, by 4.6%, compared to that in the control group.

The obtained data indicate higher meat productivity in pigs treated with the organic form of iodine.

3.3. Processing Characteristics, Chemical Composition and Biological Value of the Meat

This study explored the technological characteristics of the meat that determine, to a certain degree, its culinary and gastronomic characteristics (Table 4).

No significant differences in processing characteristics were found between the experimental groups. Thus, the influence of iodine on the functional and technological characteristics of pork is not confirmed.

In the course of sensory analysis, the appearance, odor, taste, texture, and juiciness of cooked meat and the appearance, smell, taste,

and richness of broth were evaluated on a 5-point scale. No difference between the groups was established by these indicators. The overall score of cooked meat was between 4.0 and 4.25 points, and that of broth was between 4.36 and 4.56 points.

Among the objective methods for characterizing the quality of meat, the analysis of its chemical composition is one of the most useful (Table 5).

The pork from groups I and II contained significantly greater quantities of dry substance than that from the control group, by 5.82% ($P < 0.05$) and 4.73% ($P < 0.05$), respectively; similarly, the protein content was 1.4% ($P < 0.05$) and 1.1% ($P < 0.05$), respectively, greater than the control group, as was the fat content: 4.47% ($P < 0.05$) and 3.7% ($P < 0.05$), respectively. Higher fat content in the meat of animals receiving an organic source of iodine can be taken as evidence of its more active participation in lipid exchange compared to iodine from inorganic sources. These results confirm the findings of Nürnberg *et al.* (1998).

The total iodine content and mono- and diiodotyrosine content of pigs in groups I and II were considerably higher than those of pigs in the control group. The total iodine content in the muscle tissue of animals from experimental groups I and II was higher than that of animals from the control group by 26.8% ($P < 0.05$) and 72.1% ($P < 0.05$), respectively. Monoiodotyrosines were 200% and 419% higher, and diiodotyrosines were 386% and 724% higher in groups I and II, respectively, than those in the control group. In the calculation of balance in the supply and utilization of iodine in the body of the animals, we relied on the results of Franke *et al.* (2008), who reported that the bulk of ingested iodine is accumulated in the thyroid gland and the muscle tissue of pigs. The accumulation of iodine in bone tissue is not significant (Lipatov *et al.*, 2001). Calculations showed the benefits in the first experimental group. A total of 12.4% of the total iodine supplied in the feed remained in the muscle tissue of the animal, which is more than that of the second experimental group (7.3%) and 3.3 times more than that of the reference group. Flachowsky (2007) stated that iodine accumulation in animal tissues does not exceed 1% of the total amount introduced with food. The content of all forms of iodine in the muscle tissue of experimental group II animals was significantly higher than that of animals in group I and the reference group. These results confirm the conclusions of various researchers regarding the better absorption and

more intensive accumulation of iodine from organic sources in the bodies of animals. For example, Banoch *et al.* (2012) observed a similar effect when alga *Chlorella* spp., which is rich in iodine, was added to pig feed rather than potassium iodide, without noticing any significant influence of iodine introduced with the feed on the quality of pork.

Not only the quantity of protein in the meat but also its quality is of substantial importance. This factor is characterized by the amount of essential amino acids in the protein and the degree to which this approaches the optimal levels recommended by the FAO/WHO (Lipatov *et al.*, 2001). Figure 1 shows the amino acid content of the proteins.

The results of the present study show that the amount of essential amino acids contained in the muscle tissue of animals in the control group was significantly lower than that of the animals in experimental groups I and II (16.7% and 7.1%, respectively, $P < 0.05$). It was also determined that animals in groups I and II surpassed the animals in the control group in terms of the content of almost all essential amino acids, except phenylalanine and threonine in experimental group I and leucine, isoleucine, and phenylalanine in experimental group II. The most considerable benefit that experimental group I animals had over control pigs were in levels of the amino acids lysine (45.9%), isoleucine (14%), methionine (140%), and valine (27.4%). Experimental group II pigs surpassed control group animals mostly in terms of lysine (38.8%) and methionine (139.5%) content.

Table 6 shows the biological values of the studied samples. Essential amino acids were higher in the experimental group I and II animals than those in control group animals. In the experimental group I, the score of only one amino acid (valine) was lower than 100%. Limited amino acids in the proteins of control group animals include methionine + cysteine and valine and isoleucine in the proteins of experimental group II animals. Overall, indices of essential amino acids/nonessential amino acids and essential amino acids/total amino acids were higher in the proteins of animals from experimental groups I and II.

Thus, the results clearly demonstrate that the meat of animals fed iodine in the form of iodated milk protein was of higher biological value than that of animals given iodine in an inorganic form.

This study has clearly demonstrated the

practical advantages of using an organic form of iodine, namely, iodated milk protein (an ingredient of the "ProstTM" feed additive produced by "InnbioTech", Russia), over inorganic sources in the diet of fattening pigs.

The use of the organic iodine-containing additive at an estimated level of 0.7 mg of iodine per day contributed significantly to the more intensive growth of pigs in comparison with animals whose diet contained iodine in an inorganic form.

The introduction of an additive containing iodized milk protein into the diet of pigs had a positive effect on their meat productivity, which can be observed in the greater yield of muscle and adipose tissues in pigs in the experimental groups compared to the yield in pigs in the control group.

The positive impact of the organic iodine source on the chemical composition of the pork was also demonstrated. Animals in experimental groups I and II surpassed those in the control group in terms of the dry substance, protein content, and fat content of their meat.

Animals in the experimental groups also surpassed those in the control group in terms of the content of essential amino acids in the proteins of their muscle tissue, demonstrating the higher biological value of the meat.

The level of iodine in the muscle tissue of pigs in both groups receiving an organic iodine feed additive was significantly higher than that of the animals in the control group. It should be noted that doubling the dosage of organic iodine introduced with the feed in the form of the feed additive "ProstTM" does not increase the share of iodine in the muscle tissue or cause any significant improvement in the quality of the carcass or meat. Therefore, a dosage of 0.7 mg of iodine per head per day is recommended for pork producers.

A number of questions related to using organic forms of iodine require further investigation. Research aiming at clarifying the basic physiological and biological mechanisms of fixing and metabolizing inorganic and organic iodine in the bodies of animals is of great scientific interest.

4. CONCLUSIONS

This study thus demonstrates the advantages of using an organic form of iodine – namely, iodated milk protein – in the process of raising pigs.

According to the ICCIDD (International

Council for the Control of Iodine Deficiency Disorders) report completed in 2011, the population in Russia is experiencing iodine deficiency; the median iodine urinary excretion (IUE) is observed to be in the range of 50 and 99 µg/l vs. the normative lower limit of 100 µg/l [Bost *et al.*, 2014]. Pork with an iodine content of 112-153 µg/kg can be a reliable source of iodine in the diet of Russian people.

5. ACKNOWLEDGMENTS

Proofreading and language editing services provided by Ginevra House.

6. REFERENCES

1. Annenkov, B.; Mineral Feeding of Pigs. In *Mineral Nutrition of Animals* (pp. 355-389). **1981**. <http://dx.doi.org/10.1016/B978-0-408-10770-9.50017-3>.
2. Banoch, T.; Svoboda, M.; Kuta, J.; Salakova, A.; Fajt, Z.; *Acta Vet. Brno*. **2012**, 81, 339-346. <http://dx.doi.org/10.2754/avb201281040339>.
3. Bost, M.; Martin, A.; Orgiazzi, J.; *Trace Elem. Med.* **2014**, 15(4), 3-7.
4. Directive 2010/63/EU of the European Parliament and of the Council of 22 September 2010 on the protection of animals used for scientific purposes. Official Journal of the European Union. **2010**. <https://eur-lex.europa.eu/legal-content/en/TXT/?uri=CELEX:32010L0063>
5. FEEDAP Panel, EFSA. Opinion of the Scientific Panel on Additives and Product or Substances Used in Animal Feed on the Request from the Commission on the Use of Iodine in Feeding Stuffs. *EFSA Journal*. **2005**, 3(2), 168.
6. Flachowsky, G.; *Lohmann Information*. **2007**, 42(2), 47-59.
7. Flynn, A.; Moreiras, O.; Stehle, P. Fletcher RJ, Müller DJ, Rolland V.; *Eur. J. Nutr.* **2003**, 42, 118.
8. Franke, K.; Schöne, F.; Berk, A.; Leiterer, M.; Flachowsky, G.; *Eur. J. Nutr.* **2008**, 47, 40.
9. Georgievskii, V.; The Physiological Role of Microelements. In *Mineral Nutrition of Animals* (pp. 171-224). **1981**. <http://dx.doi.org/10.1016/B978-0-408-10770-9.50010-0>.
10. Glants, S.; *Medical and Biological Statistics*. Practice: Moscow, **1998**.
11. Godfrey, N.; Choosing Pig Feeds. South Perth. Farmnote, Western Austral, dep. of agriculture, **1988**, 129/88.
12. Gorlov, I.F.; Vodiannikov, I.F.; Struk, V.N.; Zlepkin, A.F.; Vodyannikova, V.V.; Shnaider, A.V.; *Methods to Increase Efficiency of Pork Production and Improve Its Quality: Recommendations*. Bulletin of the Russian Academy of Agricultural Sciences: Moscow, **2005**.
13. GOST 33044-2014. Principy nadležashhej laboratornoj praktiki [State Standard 33044-2014. Principles of good laboratory practice]. Moscow: Standartinform; **2015**. 12 p.
14. Khaziakhmetov, F.S.; *Agricultural Biology. Series: Biology of Animals*. **2006**, 6, 123-124.
15. Kondrakhin, I.P.; *Foodborne and Endocrine Diseases of Animals*. VO Agropromizdat: Moscow, **1989**
16. Kuznetsov, S.G.; Bataeva, A.P.; Ovcharenko, G.A.; Aukhatova, S.N.; *Selskokhozyaistvennaia biologiya*. **1992**, 2, 31-39.
17. Lipatov, N.N.; Saginaw, G.Y.; Bashkirov, O.N.; *Storage and Processing of Agricultural Products*. **2001**, 8, 11-14.
18. Lisitsyn, A.B.; Sizenko, E.I.; Chernukha, I.M.; Aleksakhina, V.A.; Semenova, A.A.; Durnev, A.D.; *Meat and Healthy Nutrition*. VNIIMP: Moscow, **2007**.
19. Ljublinskij, S.; Savchik, S.; Smirnov, S.; *The Method of Obtaining Biologically Active Food Supplements. Patent No. 2212155 of the Russian Federation*. 2002.
20. Mahan, D.C.; *J. Ani. Sci.* **1990**, 68, 573-582.
21. McDowell, L.; Chapter 1 - General Introduction. In *Minerals in Animal and Human Nutrition* (pp. 1-32). <http://dx.doi.org/10.1016/B978-0-444-51367-0.50004-0>. **2003**.
22. National Research Council. *Guide for the Care and Use of Laboratory Animals -- Russian Version*. **1996**. Washington, DC: The National Academies Press. <https://doi.org/10.17226/10498>.
23. Nürnberg, K.; Wegner, J.; Ender, K.; *Livest. Prod. Sci.* **1998**, 56(2), 145-156. [http://dx.doi.org/10.1016/S0301-6226\(98\)00188-2](http://dx.doi.org/10.1016/S0301-6226(98)00188-2).
24. Rojas-Cano, M.; Ruiz-Guerrero, V.; Lara, L.; Nieto, R.; Aguilera, J.; *Anim. Feed Sci. Technol.* **2014**, 191, 83-90. <http://dx.doi.org/10.1016/j.anifeedsci.2014.01.018>.

25. Rossi, R.; Pastorelli, G.; Cannata, S.; Corino, C.; *Anim. Feed Sci. Technol.* **2010**, 162(1-2), 1-11. <http://dx.doi.org/10.1016/j.anifeedsci.2010.08.013>.
26. Savenko, N. A.; Lisitsyn, A.B.; Tatulov, Yu.V.; Voskresenskiy, S.B.; *Meat Industry.* **2006**, 6, 22-24.
27. SCF. *Opinion of the Scientific Committee of Food on Tolerable Upper Intake Level of Iodine*. European Commission, Directorate C. 2002. https://ec.europa.eu/food/sites/food/files/safety/docs/sci-com_scf_out146_en.pdf, accessed August 2020.
28. Schöne, F.; Lüdke, H.; Hennig, A.; Jahreis, G.; *Anim. Feed Sci. Technol.* **1988**, 22(1-2), 45-59. [http://dx.doi.org/10.1016/0377-8401\(88\)90073-9](http://dx.doi.org/10.1016/0377-8401(88)90073-9).
29. Sedykh, L.; Minko L.; *Mukomolno-elevatornaya i kombikormovaya promyshlennost.* **1975**, 3, 30-31.
30. Underwood, E.; Iodine. In *Trace Elements in Human and Animal Nutrition* (pp. 271-301). <http://dx.doi.org/10.1016/B978-0-12-709065-8.50015-8>. **1977**.

Table 1. Body Weight and Weight Gain (n=20)

Indicator	Group		
	Control	Group I	Group II
Body weight, kg:			
at the beginning	47.55±7.52	49.65±7.77	48.95±8.98
at the end	113.25±6.63	118.25±7.41*	115.59±8.07
Body weight gain, kg:			
Absolute	65.7±2.08	68.6±1.9*	66.64±3.68
Average daily, g	631.69±19.96	659.6±18.27*	640.81±35.37

* The difference in indicators is statistically significant (P<0.05) compared to the control group

Table 2. Slaughter Characteristics of Experimental Pigs (n=3)

Indicator	Group		
	Control	Group I	Group II
Body weight before slaughter, kg	110.09±3.1	111.68±2.79	110.21±3.52
Hot carcass weight, kg	77.09±2.07	78.18±2.0	77.12±2.5
Internal fat weight, kg	2.23±0.21	2.53±0.2	2.48±0.13
Slaughter weight, kg	79.32±1.89	80.71±2.16	79.6±2.61
Thickness of fat on the level of the 6-7 th scapula vertebrae, mm	22.27±1.86	24.42±3.35	23.1±2.65

Table 3. Morphological Composition of Experimental Pigs' Carcasses (n=3)

Indicator	Group		
	Control	Group I	Group II
Chilled carcass weight, kg	75.76±2.07	76.87±2.0	75.79±2.49
Muscle tissue weight, kg	63.49±1.82	64.76±1.62	63.85±1.95
Muscle tissue yield, %	83.8±0.11	84.25±0.12*	84.25±0.21*
Fat weight, kg	1.92±0.08	2.25±0.07*	1.85±0.10
Fat yield, %	2.54±0.03	2.93±0.01*	2.44±0.05*
Bones' weight, kg	10.35±0.18	9.85±0.32	10.09±0.44
Bone yield, %	13.66±0.14	12.82±0.12*	13.31±0.15*
Fleshing index	6.14±0.07	6.57±0.07*	6.33±0.09*
Leanness index	33.02±0.37	28.74±0.14*	34.54±0.85*

* The difference in indicators is statistically significant (P<0.05) compared to the control group

Table 4. Processing Characteristics of Experimental Pigs' Meat

Indicator	Group		
	Control	Group I	Group II
Water binding capacity, %	62.62±4.5	63.88±4.68	64.9±3.63
Loss of weight during thermal conditioning, %	35.57±0.92	35.35±0.68	35.12±0.49
pH (24 hours after slaughter)	6.13±0.11	6.05±0.48	6.19±0.14

Table 5. Chemical Composition of Experimental Pigs' Meat

Indicator	Group		
	Control	Group I	Group II
Moisture, %	74.51±0.52	68.69±0.62	69.78±0.54
Dry substance, %	25.49±0.39	31.31±0.41*	30.22±0.35*
Protein, %	22.15±0.56	23.55±0.26*	23.25±0.37*
Fat, %	2.23±0.49	6.7±0.35*	5.93±2.02*
Ashes, %	1.11±0.05	1.06±0.02	1.04±0.08
Total iodine, mkg/100 g	8.83±0.72	11.2±0.98*	15.2±0.62*
Monoiodotyrosine, ng/ 100 g	9.53±1.66	28.57±3.04*	49.5±4.91*
Diiodothyrosine, ng/ 100 g	2.2±0.95	10.71±1.23*	18.13±4.37*

* The difference in indicators is statistically significant ($P < 0.05$) compared to the control group

Table 6. Indicators of Biological Value of Muscle Tissue Proteins

Indicator	Group		
	Control	Group I	Group II
Amino acid score, %			
Lysine	98.33±6.17	137.66±4.24*	136.01±5.95*
Leucine	127.12±3.38	127.88±2.41	117.29±3.82*
Isoleucine	99.06±3.83	108.37±3.19*	79.72±3.78*
Phenylalanine + Tyrosine	151.52±7.78	133.87±3.48*	137.87±2.43*
Methionine + Cysteine	66.68±6.26	108.99±11.01*	116.42±8.62*
Valine	80.36±4.93	98.24±8.42*	87.49±4.39
Threonine	154.86±7.55	143.33±12.8	157.89±8.44
Amino acid index of essential amino acids /nonessential amino acids	0.516±0.005	0.616±0.017*	0.571±0.007*
Amino acid index of essential amino acids /total amino acids	0.340±0.002	0.381±0.006*	0.363±0.003*

* The difference in indicators is statistically significant ($P < 0.05$) compared to the control group

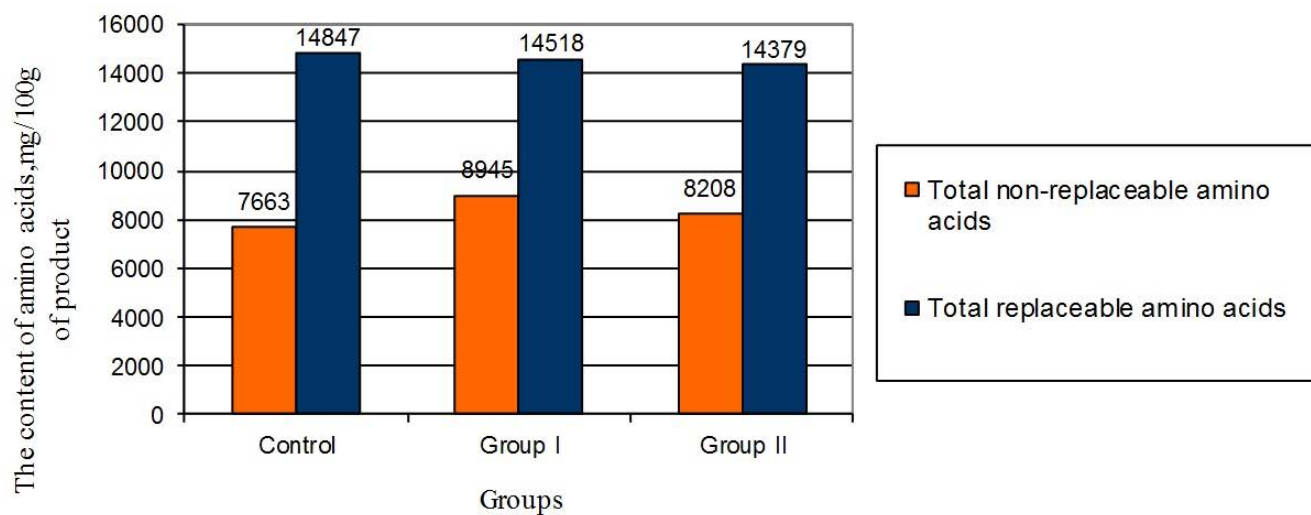


Figure 1. The ratio of basic amino acids (mg/100 g of product) in pork

CONDIÇÕES CONFORMACIONAIS DE MACROMOLECULAS QUITOSANAS E SUA INFLUÊNCIA NA EFICIÊNCIA DO PROCESSO DE POLIMERIZAÇÃO DA QUITOSANA COM 2-HIDROXIETIL METACRILATO E N-VINILPIRROLIDONA

CONFORMATIONAL CONDITIONS OF CHITOSAN MACROMOLECULES AND THEIR INFLUENCE ON THE EFFICIENCY OF CHITOSAN POLYMERIZATION PROCESS WITH 2-HYDROXYETHYL METHACRYLATE AND N-VINYLPYRROLIDONE

КОНФОРМАЦИОННЫЕ СОСТОЯНИЯ МАКРОМОЛЕКУЛ ХИТОЗАНА И ИХ ВЛИЯНИЕ НА ЭФФЕКТИВНОСТЬ ПРОЦЕССА ПОЛИМЕРИЗАЦИИ ХИТОЗАНА С 2-ГИДРОКСИЭТИЛМЕТАКРИЛАТОМ И N-ВИНИЛПИРРОЛИДОНОМ

APRYATINA Kristina V.^{1*}; TKACHUK Ekaterina K.²; SMIRNOVA Larisa A.³

^{1,2,3} Lobachevsky State University of Nizhni Novgorod, Department of Macromolecular Compounds and Colloid Chemistry at the Faculty of Chemistry

* Correspondence author
e-mail: apryatina_kv@mail.ru

Received 19 December 2019; received in revised form 22 February 2020; accepted 06 March 2020

RESUMO

A modificação da quitosana com polímeros sintéticos biocompatíveis é importante para o desenvolvimento de materiais médicos biodegradáveis com um conjunto de propriedades sob medida. A questão da influência da conformação de macromoléculas de polissacarídeos na síntese e nas propriedades dos produtos híbridos permanece aguda. As transições conformacionais de quitosana e sua influência no processo de polimerização enxertada de 2-hidroxietyl metacrilato e N-vinilpirrolidona sobre o polímero e as propriedades de seus copolímeros foram estudadas. Para interpretar as peculiaridades das propriedades das soluções de quitosana, sua viscosidade foi determinada pelo método de viscometria rotacional; as transições conformacionais dos polissacarídeos poliméricos foram investigadas pelo método da espectrofotometria; as características dimensionais das partículas de polímero foram avaliadas pelo método de espalhamento dinâmico da luz. Os copolímeros foram caracterizados pelos métodos de espectroscopia de IV e cromatografia de penetração em gel. A transição conformacional da hélice-espiral da macromolécula de quitosana foi sensível ao pH e à temperatura. O tamanho efetivo das macromoléculas de quitosana para a conformação da hélice foi 14-35% maior do que para a conformação espiral. O rendimento de copolímero enxertado (98%) foi significativamente maior nas soluções de quitosana, onde suas macromoléculas estavam na conformação da espiral. Os resultados obtidos permitem que os pesquisadores criem condições ideais durante o desenvolvimento de materiais biomédicos à base de copolímero, com características aprimoradas.

Palavras-chave: quitosana, conformação, modificação, a eficiência da polimerização.

ABSTRACT

Modification of chitosan with biocompatible synthetic polymers is important for the development of biodegradable medical materials with a tailor-made complex of properties. The issue of the influence of a polysaccharide macromolecule conformation on the synthesis and properties of the hybrid products remains acute. Conformational transitions of chitosan and their influence on the process of grafted polymerization of 2-hydroxyethyl methacrylate and N-vinylpyrrolidone onto the polymer and the properties of their copolymers were studied. To interpret the peculiarities of chitosan solutions properties, their viscosity was identified by the method of rotational viscometry; conformational transitions of the polymer polysaccharides were investigated by the method of spectrophotometry; dimensional characteristics of the polymer particles were assessed by the method of dynamic light scattering. Copolymers were characterized by the methods of IR-spectroscopy and gel-penetrating chromatography. Helix-coil conformational transition of the chitosan macromolecule was pH and temperature-sensitive. The effective size of the chitosan macromolecules for helix conformation was 14-35% larger than for the coil conformation. The grafted copolymer yield (98%) was significantly higher in the solutions of chitosan, where its macromolecules were in the coil conformation. The obtained results allow the researchers

to create optimal conditions during the development of the copolymer-based biomedical materials with improved characteristics.

Keywords: *chitosan, conformation, modification, the efficiency of polymerization.*

АННОТАЦИЯ

Модификация хитозана биосовместимыми синтетическими полимерами актуальна для разработки биоразлагаемых медицинских материалов с индивидуальным комплексом свойств. Остается открытым вопрос о влиянии конформации макромолекулы полисахарида на синтез и свойства гибридных продуктов. Исследованы конформационные переходы макромолекул хитозана и их влияние на процесс привитой полимеризации 2-гидроксиэтилметакрилата и N-винилпирролидона на полимер, а также свойства их сополимеров. Для интерпретации особенностей свойств растворов хитозана изучили их вязкость методом ротационной вискозиметрии; конформационные переходы макромолекул полимера исследовали методом спектрофотометрии; размерные характеристики макромолекул полимера оценивали методом динамического рассеяния света. Соплимеры были охарактеризованы методами ИК-спектроскопии и гель-проникающей хроматографии. Конформационный переход клубок-спираль макромолекул хитозана чувствителен к pH среды и температуре. Эффективный размер макромолекул хитозана для спиральной конформации был на 14-35% больше, чем для конформации клубка. Выход привитого сополимера (98%) был значительно выше в растворах хитозана, где его макромолекулы находились в конформации рыхлого клубка. Полученные результаты позволяют исследователям подбирать оптимальные условия при разработке биомедицинских материалов с улучшенными характеристиками на основе сополимеров хитозана.

Ключевые слова: *хитозан, конформация, модификация, эффективность полимеризации.*

1. INTRODUCTION

Presently, chitosan, a natural-based polymer obtained by deacetylation of chitin, is widely used in different areas of bioengineering, medicine, pharmacology, and industry, primarily, due to unique properties of this polysaccharide, availability, and renewability of its crude material.

Due to hydrogen bonding between the functional groups of chitosan macromolecules, chitosan is poorly soluble in water, because this bonding is stronger than between the molecules of chitosan and water. Never the less, the high content of polar groups provides high hygroscopic properties of chitosan (Smotrina *et al.*, 2015).

Amino groups in macromolecules provide good solubility of the polysaccharide in water solutions of organic and some inorganic acids (HCl). It can strongly hold a solvent in its structure, as well as diluted and suspended particles (Skryabin, 2013). The diversity of functional groups and the specifics of the chitosan structure determine the number of properties of this polymer, like absorptive, chelate, and complex formatting.

Such properties as high biological activity, biocompatibility, biodegradability, and muco-adhesiveness make chitosan an attractive object for the application in different areas.

Chitosan-based hydrogels with different structures are synthesized due to the formation of ions complexes with negatively charged molecules (sulfates, citrates, phosphates) and metal ions Pt^{2+} , Pd^{2+} , and Mo^{6+} , polyelectrolyte complexes (with proteins, heparin, chondroitin sulfate, carboxymethylcellulose, etc.) or due to the formation of polymer bonds between chitosan and other water-soluble nonionic polymers (polyvinyl alcohol) (Skryabin, 2013; Wu *et al.*, 2017; Liu *et al.*, 2018). The obtained hydrogels can be used as the basis for the development of wound healing bandages due to its compatibility with living tissues, viscoelastic nature, and capacity for the controlled release of the diluted substances. There are a number of studies going on the possible application of chitosan as a polymer matrix for drug delivery systems because the majority of substances are characterized by low permeability through biological membranes (Quiñones *et al.*, 2018; Wang *et al.*, 2017; Cánepa *et al.*, 2017; Huang *et al.*, 2017). Chitosan-based biological systems can be used for transport of proteins/peptides, growth factors, anti-inflammatory drugs, antibiotics, antitumor, and other drugs to the diseased cells. Chitosan is used as a filler for pills and capsules that provide the controlled release of the active substance due to the combination of diffusion and slow decomposition of the macromolecule polymer matrix (Skryabin, 2013; Chavana *et al.*, 2017; Lin

and Yeh, 2010). Chitosan is believed to be a highly potential component in tissue engineering (skin, bone, cartilage, nerve, liver tissues) due to its biocompatibility. It provides mechanical strength, steadily degrades facilitating the growth of new tissue, and acts as a cellular and molecular scaffold for the migration and cultivation of the required cells (Lian *et al.*, 2009; Ilbasmi-Tamer *et al.*, 2017; Ribeiro *et al.*, 2017). There are studies on the application of polysaccharides for the production of new biodegradable suture material (Cruz *et al.*, 2016; Li and Tang, 2016). Chitosan is used as a substance that contributes to weight loss and improves cholesterol metabolism and intestinal motility (Tuma *et al.*, 2011). Polymer and its derivatives are widely used in cosmetics as a moisturizer, gelling, film-forming, and anti-inflammatory agents (Aranaz *et al.*, 2018). During the past decade, the interest in the use of chitosan in the composition of hemostatic agents, like "Celox™" and "HemCon ChitoGauze PRO", increased.

Despite numerous studies on the properties of chitosan and chitosan derivatives and the success of the implementation of the obtained results, there are still some tasks that require improvement and further development. Among them, there are chitosan-based hemostatic and wound healing biodegradable materials with the tailor-made complex of properties and good physicochemical parameters. One of the solutions is seen as graft copolymerization of chitosan with biocompatible synthetic polymers. In this aspect, the issue remains relevant to the influence of the conformational condition of chitosan macromolecules on the synthesis of hybrid products and copolymer-based hemostatic and wound healing agents.

Protonation of chitosan amino groups of different degrees is observed at chitosan dilution in media with different pH. This property is determined by different conformational models of its macromolecules in the solution (from the coil to helix), which was confirmed by many studies (Fedoseeva *et al.*, 2008; Franca *et al.*, 2008; Morris *et al.*, 2009; Slivkin *et al.*, 2014; Costa *et al.*, 2015; Desbrieres *et al.*, 2001). It is known that the conformational model of the molecules in different pH media determines the size of macromolecules in the solution. It should be considered that chitosan macromolecule conformation can significantly influence the process of polysaccharide modification by monomers, as well as on the properties of final

products.

The aim of the present study was to establish the conformational transitions of chitosan macromolecules and their influence on the process of chitosan modification by graft polymerization with 2-hydroxyethyl methacrylate (HEMA) and N-vinylpyrrolidone (VP) and on the properties of their final products.

2. MATERIALS AND METHODS

The following substances were used in the study. Chitosan – poly ((1,4)-2-amino-2-deoxy)- β -D-glucose, as such, obtained from crab shells (OJSC "Bioprogress", Moscow, Russia) with different MW - 1.10×10^5 , DD = 0.82 and 2.20×10^5 , DD = 0.82.

Mass fraction of minerals in chitosan did not exceed 0.1%, moisture content - 6%, insoluble compounds - 0.1%.

Chitosan solution was prepared with acetic acid of "chemical purity" GOST 61-75 (99.5%, density 1.049 g/cm^3), hydrochloric acid (HCl) of "chemical purity" (36.8 wt% at 20°C , density – 1.19 g/cm^3).

Modification of chitosan was performed by graft polymerization with HEMA (content of the main component 99.9%, produced by «Sigma-Aldrich»; before the synthesis, the monomer underwent vacuum distillation with full condensation in the headspace at lower pressure) and VP (content of the main component 99.9%, produced by «Sigma-Aldrich»).

Tetrahydrate cerium sulfate (IV) was used as an initiating system for graft copolymerization. The initiator was soluble in water.

Homopolymer extraction was performed in a Soxhlet apparatus by isopropyl alcohol. Isopropyl alcohol had the purity of GOST 9805-84 (CJSC Khimreaktiv).

Dynamic viscosity of chitosan solutions was measured by rotational viscosimeter Brookfield DV-II+ Pro with spindle shafts № 18 and № 31. The precision of viscosity measurement was $\pm 1.0\%$ of the upper range limit.

The authors studied the dependence of chitosan solution dynamic viscosity on the MW of polymer, concentration, temperature, and medium pH. Aqueous acetic acid solutions of chitosan with different concentrations of the polymer (from 1 to 4 wt%) were prepared in the

media with pH ranging from 3.3 to 5.0. Before the measurement, the solutions were kept for 48 hours.

The apparent activation energy of the solution viscous flow (ΔE_a , kJ/mol) was calculated by the equation of Arrhenius-Frencel-Eyring:

$$\eta = A \cdot \exp \cdot \left(\frac{\Delta E_a}{RT} \right) \quad (\text{Eq. 1})$$

Where A – constant, R – universal gas constant (J/mol×K), T – temperature (K), $\eta = \eta_{\max}$.

Conformational transitions of chitosan were established by the spectrophotometric method. For the analysis, 0.03 wt% aqueous solutions of chitosan in hydrochloric acid with MW of the polymer 2.2×10^5 and 1.0×10^5 were prepared. The readings of pH-meter Mettler Toledo LE902 ranging from 3.3 to 6.0 were recorded, and the transmittance spectra of the solutions were registered by the IR and visible spectrophotometer UV-1650 (Shimadzu) during the introduction of some amount of 2.5% NaOH solution.

Dimensional features and polydispersity of chitosan particles in over-diluted chloride solutions were established by the method of DLS with the particle size and zeta potential analyzer Nano Brook Omni (Brookhaven Instruments Corporation, USA). The particle diffusion coefficient of the dispersed phase in the liquid was identified by the analysis of the correlation function of the diffused light intensity fluctuations. The most important parameter, established during the investigation of quasielastic light scattering, was the diffusion coefficient (D). The size of the spherical noninteracting particles was calculated by the Stokes-Einstein Equation 2.

$$D = \frac{k_B T}{6\pi\eta R} \quad (\text{Eq. 2})$$

Where k_B – Boltzmann's constant; T – absolute temperature; η – shear viscosity of the medium with the suspended particles of R radius.

Graft copolymerization of HEMA (VP) onto chitosan was performed at constant stirring in a three-neck round-bottomed flask equipped with a backflow condenser and placed in a temperature-controlled thermostat. The concentration of

chitosan in acetic acid solutions in all the tests was equal to 3 wt%, medium pH ~4.8 and 3.3, reaction temperature 60°C. HEMA (VP) was introduced into the system after the temperature establishment in the reactor. The ratio [monomer]/[glucosamine] was equal to 1.2, 2.4, 4.8 mol/(molar ratio), respectively. The initiator was introduced into the medium. The system was kept for 15 minutes for the establishment of the required temperature of the solution. Further, the weighted sample of the initiator was added. In all the cases, the concentration of the initiator was equal to 5×10^{-3} mol/L. The synthesis was going on for 2 hours. After that, the temperature in the thermostat was raised to 80°C, and the system was kept for 30 minutes until the completion of the HEMA (VP) polymerization process. During the synthesis, the probes were taken at certain time intervals, precipitated with isopropyl alcohol, and centrifuged for the separation of the precipitation. The level of HEMA (VP) conversion was established by the analysis of the residual monomer by the method of gas chromatography. The concentration of the residual monomer was performed by the gas chromatograph GCMS-QP2010, Shimadzu equipped with a thermal conductivity detector and the system of computer readings registration. The column: Equity-1 (length - 30 m, diameter – 0.25 mm, sorbent particles size – 0.25 μm), gas vehicle: helium (He). The rate of the gas vehicle in the column was 1 ml/min; the temperature of the column for HEMA (VP) identification was 230°C.

The synthesis of grafted copolymers HEMA (VP) with chitosan was established by IR-spectroscopy (spectrophotometer "Perkin-Elmer"). The samples of the reaction products were used for the analysis. The authors got a homopolymer poly-HEMA (PVP) extracted in the Soxhlet apparatus. The extraction was performed by isopropyl alcohol for 36 hours. The time was established by the blank test of poly-HEMA (PVP) extraction from the precipitated physical mixture of the respective homopolymers. Further, the samples were dried out by vacuuming to the fixed mass.

After the extraction, the efficiency (relation of the mass of the grafted copolymer to the mass of the total polymerized monomer) and the degree of grafting (the relation of the mass of the grafted polymer to the mass of chitosan) of HEMA (VP) onto chitosan were established.

The degree of grafting (DG) was calculated by the Equation 3. The effectiveness of the grafting (EG) can be calculated by the Equation 4.

MW of the copolymers was established by the method of gel permeation chromatography (GPC) with high-performance liquid chromatograph CTO20A/20AC (Shimadzu, Japan), software module LC-Solutions-GPC, column Tosoh Bioscience TSKgelG3000SWxl with the pore diameter 5 μm , and evaporative light-scattering detector ELSD-LT II. 0.5 M acetic acid solution was used as an eluent. The flow rate was 0.8 ml/min. MW was calculated based on narrow disperse samples of dextran in the range of MW from 1×10^3 to 4.1×10^5 Da (Fluca).

Chitosan-based and chitosan copolymer-based films were obtained by casting their solution on a lavsan substrate in the conditions of even evaporation of the solvent to the fixed-mass at room temperature (lavsan substrate is another name for a smooth polyethylene terephthalate (PET) surface. In our work, the polymer films were obtained by casting a chitosan and copolymer solutions onto smooth lavsan substrates). Further, the films were exposed to vacuum for 4-6 hours at $t=30^\circ\text{C}$ in the vacuum chamber.

Mechanical properties of the film (break strength σ and tension strain ϵ) were established with a tensile testing machine ZWIC Z005 (Germany) at the rate of extension 50 mm/min.

3. RESULTS AND DISCUSSION

The universal technological step in the synthesis of chitosan-based and chitosan derivatives-based materials is the dilution of polysaccharides in aqueous acid solutions. The most available and widespread component in the preparation of chitosan solutions is acetic acid.

The authors (Morris *et al.*, 2009) reviewed the experimental data obtained by different researchers, and theoretical calculations showed that conformational conditions of chitosan macromolecules were different depending on the medium pH: coil – to the pH values up to ~ 3.6 and helix – up to pH values ~ 4.8 -5.5. The analyses of the reactions of chitosan copolymerization with HEMA and VP in the solution were performed in different conformational conditions of polysaccharide macromolecules – helix and coil. Since grafted copolymerization involved different MW of chitosan, it was relevant to develop the method of efficient identification of certain conditions (MW, pH) of conformational conditions of chitosan macromolecules.

A complex of studies was performed for the interpretation of the peculiarities of chitosan solutions:

- Evaluation of the dependence of dynamic viscosity of the chitosan solutions on the pH of the medium;
- Identification of chitosan macromolecules effective sizes by the method of DLS;
- Investigation of temperature-related dependences between dynamic viscosity of chitosan solutions and macromolecules in different conformations and identification of energy of activation of polymer solution viscous flow;
- Evaluation of optical properties of the chitosan solutions.

Chitosan sample with $\text{MW}=1.1 \times 10^5$ and DD 0.82 was used for the evaluation of medium pH influence on the viscosity property of moderately concentrated solutions of the polysaccharide (Figure 1).

The observed dependence of the chitosan solution viscosity on the medium pH was not linear, and the curve was divided into three areas: $\text{pH} < 3.4$ – the curve was steadily going upwards, $\text{pH} = 3.8$ – the curve plateaued, and then went on going steadily upwards. It can be suggested that such a curve structure is associated with the conformational condition of chitosan macromolecules: helix – at $\text{pH} > 4$, coil – at $\text{pH} = 3.3 - 3.5$. Cooperative destruction of hydrogen bonds inside a molecule at some “critical” degree of protonation results in conformational transition helix-coil and provides the polymer macromolecule size change, which is confirmed by the method of DLS. Thus, the conformational condition of a macromolecule significantly influences the viscosity of polymer solutions.

The effective diameter of chitosan macromolecules in different pH media was established by the DLS method (Table 1).

It is shown in Table 1 that chitosan macromolecule in helix conformation, regardless of MW, is characterized larger effective diameter than in coil conformation. Thus, macromolecules of chitosan with $\text{MW} = 1.1 \times 10^5$ in 4.8 medium pH (helix conformation) have the size ~ 624 nm, and in 3.3 medium pH (coil conformation) they have the size ~ 537 nm. It should be noticed that the increase in WM of a polymer leads to a significant increase in the difference in size (Table 1). It must be mentioned that the MW of chitosan

diversely influence on the size of its macromolecules: the molecules in coil conformation with twofold different MW are similar in size, while the molecules in helix conformation, the molecule sizes are different by ~ 30%. In the last case, the authors cannot exclude the association of macromolecules that also provides increased values. However, the experiment was performed in over diluted solutions of chitosan with the polysaccharide concentration, not more than 0.03 wt%. In this case, the influence of the association can be ignored, and the conformation of the molecule remains unchanged. In this particular case, the authors believe that is correct to fix the sizes that are determined by the diffusion rotation of the extended polysaccharide chains, whereas, in the coil conformation, the diffuse rotation of a macromolecule reflects its actual size that is determined by the radius of its radius of gyration. The respective calculations on the radius of gyration by the equation of Flory-Fox based on the values of inherent viscosity confirmed the last statement.

Different conformational conditions of the polysaccharide macromolecules in various pH media are also observed in the studies of the temperature-dependent viscosity of moderately concentrated chitosan solutions (Figure 2).

Within the range of temperatures from 0 to 30°C, the viscosity of solutions of chitosan in the helix conformation exceeds the viscosity of solutions of the polysaccharide in the coil conformation at the same concentration of the polysaccharide (3 wt%) and MW=1.1×10⁵ (Figure 2). At T = 10°C, the viscosity of the solutions is two times different. This can be explained by strong inter-chain interaction between the extended macromolecules in helix conformation, and as a result, by the increased resistance of the flow. As the temperature rises, the viscosity of chitosan solutions in both systems decreases.

Based on the temperature dependence data, the apparent activation energy of the chitosan solutions viscous flow for different conformational models of the macromolecules (ΔE_1 – helix, ΔE_2 – coil) was calculated by the Arrhenius-Frenkel-Eyring equation and the semilog coordinates of the dependence of the viscosity on the temperature (Figure 3).

The apparent activation energy (ΔE_a) of the viscous flow of the liquid is equal to the height of some potential of the energetic barrier that has to be exceeded by one mol of particles for a successive transition from one position of

equilibrium to the other. ΔE_a parameter measures the intensity of intermolecular interaction in solutions, i.e., it is an indirect characteristic of polymer systems structure stability in solutions. The observed difference in the activation energy of the viscous flow of the chitosan solutions was the Equations 5 and 6.

$$\Delta E_1 = (36.5 \pm 0.4) \text{ kJ/mol} - \text{pH} = 4.8 \quad (\text{Eq. 5})$$

$$\Delta E_2 = (31.1 \pm 0.3) \text{ kJ/mol} - \text{pH} = 3.3. \quad (\text{Eq. 6})$$

The higher value of ΔE_a shows that inter-chain interaction between chitosan molecules that involve hydrogen bonds is stronger in the helix conformation.

This tendency agrees with the published data on other natural polysaccharides and their derivatives, in particular, on cellulose and its ethers. In the range of temperature ~50°C, the disruption of macromolecule associates in the helix conformation begins, and the viscosity values in both systems are getting closer. This fact can be explained not only by the disruption of the associates but also by the disruption of hydrogen bonds between the links of polymer chains, which leads to the conformational helix-coil transition. It should be mentioned that this effect can also be determined by the disruption of hydrogen bonds. To prove this suggestion, the authors performed a spectrophotometric analysis of chitosan solutions.

Spectrophotometric analysis is known to be used for the evaluation of the dynamics of protein molecules in a solution. In the present study, for the first time, this method was used for the identification of chitosan macromolecules conformation. During the investigation of the solution viscosity (Figure 2), the authors suggested that its values were getting closer due to cooperative disruption of hydrogen bonds inside a macromolecule and, thus, by the conformational helix-coil transition. For this reason, the change in optical transmission of the solutions in a wide range of temperatures was studied (Figure 4). Precise, systematic decrease of optical transmission in the range from 60 to 75 °C was observed. Thus, the obtained data indicates the fact that conformational helix-coil transition is temperature-sensitive.

$$DD = 0.82; MW = 1.1 \times 10^5 \quad (\text{Eq. 7})$$

The changes in optical density of the diluted chitosan solutions in a wide range of MW dependence from the medium pH were evaluated at $T = \text{const.}$

In all the cases, the authors observed a sudden change in the optical transmission ratio at medium pH 3.4. The character of the curves was similar for all the chitosan samples with the same DD. Figure 5 illustrates the typical picture of optical density change in all the samples with MW 2.2×10^5 and 1.1×10^5 (DD = 0.82) depending on the pH of the medium.

There are two sharp transitions observed within the curves (Figure 5) at pH values ~ 3.4 and $4.8 - 6$. The results are reproduced in multiple replications. The first minimum at pH = 3.4 completely coincides with both MW of chitosan and lies within the same area of pH values that were registered by the authors (Fedoseeva *et al.*, 2008) based on the viscometric data. Unlike the mentioned study, the results of the present spectrophotometric analysis showed that chitosan macromolecule conformational transition helix-coil was fixed very precisely. For the first time, it was shown that at similar DD, that transition did not depend on the MW. After the minimum, the curve did not reach the baseline optical transmission ratio, which is probably, associated with a more intensive light scattering by the macromolecules in a helix conformation. The second minimums on the curves were different for the samples with various MW: the bigger the MW of chitosan was, the earlier the change in optical transmission was observed. The second minimum was characterized by the chitosan macromolecule conformational helix-globule transition. This is explained by the fact that at a slight increase in the medium pH above the minimum point of the curve, precipitation is observed, the solution clears, and the ratio of optical transmission becomes close to one of the solvent. Conformational helix-globule transition at the pH value of polymer precipitation was different for chitosan with various MW, as well as the threshold value of the medium pH that corresponds to the precipitation of the polymer. For chitosan with MW = 1.0×10^5 , this transition was observed at pH = 5.7, while the macromolecules with twofold higher MW collapsed already at pH = 5.0. These test results explain the anomaly revealed during the study of chitosan solution viscosity. In the range of pH $\sim 5.0 - 5.2$, the lower the viscosity of chitosan solutions is, the heavier their MW is at similar DD.

The obtained results indicate the

prospects of application of spectrophotometric analysis for the precise identification of conformational transition of chitosan macromolecules when the medium pH is changed. It was shown that the interaction of chitosan macromolecules by means of hydrogen bonds in the helix conformation was stronger than in the coil conformation. The fact that macromolecules of chitosan at the medium pH = 4.8 (helix conformation) are bigger in size than at the medium pH = 3.3 (coil conformation) allows the preparation of solutions with reproducible viscous properties in different conditions.

The development of hemostatic and wound healing chitosan-based compositions is limited by the fact that chitosan is soluble only in aqueous acid solutions and is characterized by low physicomechanical properties. These issues can be solved by the modification of chitosan.

The modification of chitosan was performed by graft polymerization with HEMA and VP. Due to hydrophilic properties and low toxicity, the polymers HEMA and VP have good biocompatibility and are used in medicine (Ma and Lee, 2009; Dong, 2008; Teodorescu and Bercea, 2015). The modification of chitosan via copolymerization can result in the synthesis of water-soluble (expanding) hybrid products or gels.

The influence of components ratio and chitosan conformation (pH of the medium) on the process of graft polymerization was studied. Cerium sulfate (IV) was used as an initiating agent during graft polymerization. The concentration of the initiator in all the reaction mixtures was 5×10^{-3} mol/L.

This initiator was chosen because, in the mentioned concentration, it did not disrupt the chains of the polysaccharide. Ce^{4+} containing initiator compounds, used in grafted polymerization of monomers onto chitosan, are known (Pourjavadi *et al.*, 2003; Yilmaz *et al.*, 2007; Metzler *et al.*, 2015). However, it should be mentioned that the researchers describe the initiation process differently. The authors (Yilmaz *et al.*, 2007) proposed the mechanism of grafting via oxidation and chitosan chain breakdown (Scheme 1).

The authors (Metzler *et al.*, 2015) do not exclude the involvement of chitosan amino groups, as well as hydroxyl groups, in the process of vinyl monomers polymerization onto chitosan (Scheme 2). In this case, the degree of grafting at copolymerization does not exceed 71%.

The degree of monomer HEMA transformation during its graft polymerization onto chitosan, when the macromolecules of the polysaccharide have helix conformation (pH 4.8), is evaluated below. The complete reaction (Figure 6, a) was observed at the ratio of $[HEMA]/[chitosan] = 4.8 \text{ mol}/(\text{molar ratio})$: the degree of monomer transformation was ~81%, while at other ratios, the degree of transformation was less than 5%.

The significant influence of chitosan macromolecules conformation on the characteristics of the process was observed. The degree of HEMA transformation in helix conformation was 81% (Figure 6, a). It significantly increased to 96% during the process that involved chitosan in coil conformation (Figure 6, b) in analog conditions of synthesis. Besides, in this case, the change in the phase state of the reaction media was observed. During all the process when chitosan macromolecules were in helix confirmation, the system had the properties of a homogenous solution. On the contrary, when chitosan macromolecules were used in coil conformation, at the initial stages of the process, the system had the properties of a colloid solution. Probably, intra and intermolecular interactions within a helix conformation limit the availability of the reactive centers of chitosan, which leads to the synthesis of a significant amount of the homopolymer. MW of the grafted copolymers was also different: in the synthesis with chitosan macromolecule helix confirmation, it was equal to $(2.0-2.5) \times 10^5$, for coil conformation - $(4.0-600) \times 10^5$. It can be suggested that the difference in the phase state of the synthesized products is explained by their limited solubility due to higher MW of the grafted copolymer chains and, as a result, higher concentration and strong interaction.

Grafted polymerization is characterized by the degree and efficiency of polymerization (DP and EP). The highest polymer outcome was observed when chitosan macromolecules were used in coil conformation. In this synthesis, the EP was equal to 98% and DP – to 390% (Table 2).

Grafted copolymer synthesis was confirmed by the results of IR spectroscopy. The spectrum of the original chitosan molecule (Figure 7, 1) contained the stripes that corresponded to the valence vibration of amid functional groups at 1652 cm^{-1} , 1563 cm^{-1} . Besides, the stripes typical for polysaccharides were observed at 1153 cm^{-1} , 1077 , and 1034 cm^{-1} (functional group C-O-C). The stripes observed

at 1379 cm^{-1} belong to the vibrations of the acetamide group. The synthesized product, cleaned from the homopolymer, leaves the stripes typical for HEMA and chitosan. A stripe appears in the spectrum (Figure 7, 2) at 1736 cm^{-1} , which corresponds to the vibrations of HEMA carbonyl ($-C=O$) groups.

Chitosan modification was also performed by the method of graft polymerization with VP. As a result, it was established that to provide water-soluble properties of the copolymer (pH = 7), it was sufficient to have the concentration of the components that did not exceed the value of $[monomer]/[glucosamine] - 1.0 \text{ mol}/(\text{molar ratio})$. This ratio provided minimum content of the synthetic fragment in the structure of the copolymer and the required characteristics, like biocompatibility, water solubility, and capacity for further modification of the copolymer for the creation of chitosan derivatives based wound healing and hemostatic materials.

The study of the kinetics of VP graft polymerization onto chitosan was performed in two temperature modes (60°C and 70°C) and two medium pHs (4.8 and 3.3), at a different molar ratio of the monomer to the links of glucosamine. Cerium sulfate (IV) was used as an initiating system. The degree of VP conversion in the process of polymerization is presented in Figure 8.

The difference in the kinetics of grafted polymerization at 60°C , when the macromolecules of chitosan were in different conformational conditions, was more evident in the case of VP polymerization than HEMA polymerization. The degree of monomer conversion (VP) in different transitions of the polysaccharide conformations differed by more than 40%. The grafted polymerization of VP onto chitosan, performed at 70°C , was characterized by close values of the ultimate depth in monomer transition of both chitosan helix and coil conformation. It cannot be excluded that, in this case, the process is cooperative due to the simultaneous helix-coil conformational transition of chitosan macromolecules. The process, when macromolecules of chitosan were in coil conformation, was characterized by a higher rate. The depth of VP transition at 70°C reaches 80% 25 minutes after the beginning of the process and 98% after the completion of the process.

It similar to the process of polymerization with HEMA and is explained by the fact that chitosan macromolecules in the coil conformation form more available reactive sites as compared

to chitosan macromolecules in helix conformation (pH = 4.8) that form stronger intermolecular interaction due to hydrogen bonds.

Thus, the association of the molecules could be observed during the process of polymerization. The best VP grafted polymerization parameters onto chitosan were obtained when macromolecules of chitosan were in the coil conformation (as in the case with HEMA polymerization): the depth of VP conversion was 98% and EP was 94% (Table 3).

3.1 Investigation of physical-mechanical properties of copolymers.

Chitosan copolymers, modified by grafted copolymerization, can be used as the components of new wound-healing materials in different forms: film and fiber products, gels, sponges, membranes, etc. Hence, it is necessary to investigate their physicochemical (mechanical strength and deformation) properties.

Chitosan (tensile strength 27 MPa) barely expresses any deformation properties (Table 4). HEMA film, obtained with the $\text{Ce}(\text{SO}_4)_2$ in reactive media with different pH (i.e., helix or coil conformation of chitosan macromolecule), is characterized by the improved physicochemical properties in comparison with the original polysaccharide: they are more resistant to deformation (up to 33-35 MPa) 0.35 – 4%. The film, cast from the solutions of chitosan in the coil conformation, has better physicochemical properties due to a higher degree of polymerization.

Chitosan-VP graft copolymers film is two times more tensile as compared to the original chitosan (Table 5): burst stress values reach 60 MPa at 4% deformation.

To increase the elasticity of the film, glycerin was used as a flexibilizer. In practice, it is enough to introduce 0.5 wt% of glycerin into the polymer structure, which allows for the application of the obtained material in the composition of bandaging materials in medicine and veterinary.

In general, it can be concluded that copolymer film, cast from the solutions with chitosan coil conformation, is slightly more tensile and elastic as compared to the one obtained from the solutions with chitosan helix conformation.

4. CONCLUSION

The obtained results showed that spectral analysis was feasible for the identification of the coil-helix and helix-globule conformational transition of chitosan macromolecules in aqueous acidic solutions. Conformational transition is pH-dependent, temperature-sensitive, and does not depend on the chitosan MW at the same degree of deacetylation. Dependence of the depth, degree, and efficiency of the HEMA and VP graft polymerization onto chitosan on the conformational model of its macromolecules allows the researchers to develop new chitosan-based and chitosan derivatives-based biomedical materials with a tailor-made complex of properties.

5. ACKNOWLEDGMENTS

The present study was financed by the Ministry of Education and Science of the Russian Federation (№ 4.3760.2017).

6. REFERENCES

1. Aranaz, I., Acosta, N., Civera, C., Elorza, B., Mingo, J., Castro, C., Gandía, M. L., Caballero, A. H. Cosmetics and Cosmeceutical Applications of Chitin, Chitosan and Their Derivatives. *Polymers*, **2018**, 10(2), 213.
2. Cánepa, C., Imperiale, J. C., Berini, C. A., Lewicki, M., Sosnik, A., Biglione, M. M. Development of a Drug Delivery System Based on Chitosan Nanoparticles for Oral Administration of Interferon- α . *Biomacromolecules*, **2017**, 18(10), 3302–3309.
3. Chavana, C., Bala, P., Pal, K., Kale, S. N. Cross-linked chitosan-dextran sulphate vehicle system for controlled release of ciprofloxacin drug: An ophthalmic application. *OpenNano*, **2017**, 2, 28–36.
4. Costa, C. N., Teixeira, V. G., Delpech, M. C., Souza, J. V. S., Costa, M. A. S. Viscometric study of chitosan solutions in acetic acid/sodium acetate and acetic acid/sodium chloride. *Carbohydrate Polymers*, **2015**, 133, 245–250.
5. Cruz, R. C., Diniz, L. G., Lisboa, H. M., Fook, M. V. Effect of different carboxylic acids as solvent on chitosan fibers production by wet spinning. *Materia*, **2016**, 21(2), 525–531.

6. Desbrieres, J., Brugnerotto, J., Heux, L., Rinaudo, M. Overview on structural characterization of chitosan molecules in relation with their behavior in solution. *Macromolecular Symposia*, **2001**, 168(1), 1–20.
7. Dong, W. Development of a new type of biodressing for burns, human hair keratin-collagen sponge-complex. *The Faseb Journal*, **2008**, 22, 1432–1437.
8. Fedoseeva, E. N., Smirnova, L. A., Fedoseev, V. B. The viscosity of chitosan solutions and its reaction capacity. *Journal of Lobachevskiy Nizhniy Novgorod University*, **2008**, 4, 59–64.
9. Franca, E. F., Lins, R. D., Freitas, L. C. G., Straatsma, T. P. Characterization of Chitin and Chitosan Molecular Structure in Aqueous Solution. *J. Chem. Theory Comput.*, **2008**, 4(12), 2141–2149.
10. Huang, G., Liu, Y., Chen, L. Chitosan and its derivatives as vehicles for drug delivery. *Journal Drug Delivery*, **2017**, 24(2), 108–113.
11. Ilbasimis-Tamer, S., Çiftçi, H., Tu, M. R., Degim, T., Tamer, U. Multiwalled Carbon nanotube-Chitosan Scaffold: Cytotoxic, apoptotic, and necrotic effects on chondrocyte cell lines. *Curr Pharm Biotechnol*, **2017**, 18(4), 327–335.
12. Li, X.-Q., Tang, R.-C. Crosslinked and Dyed Chitosan Fiber Presenting Enhanced Acid Resistance and Bioactivities. *Polymers*, **2016**, 8, 119.
13. Lian, Q., Li, D., Jin, Z., Wang, J., Li, A., Wang, Z., Jin, Z. Fabrication and in vitro evaluation of calcium phosphate combined with chitosan fibers for scaffold structures. *J. Bioact. Compat. Polym.*, **2009**, 24, 113–124.
14. Lin, H.-Y., Yeh, C.-T. Controlled release of pentoxifylline from porous chitosan-pectin scaffolds. *Drug Delivery*, **2010**, 17, 313–321.
15. Liu, H., Wangab, C., Li C., Qina, Y., Wanga, Z., Wang, J. A functional chitosan-based hydrogel as a wound dressing and drug delivery system in the treatment of wound healing. *RSC Adv.*, **2018**, 8, 7533–7549.
16. Ma, Y., Lee, P. Investigation of suspension polymerization of hydrogel beads for drug delivery. *Iran Polym. J.*, **2009**, 18(4), 307 – 313.
17. Metzler, M., Chylińska, M., Kaczmarek, H. Preparation and characteristics of nanosilver composite based on chitosan-graft-acrylic acid copolymer. *Journal of Polymer Research*, **2015**, 22, 146.
18. Morris, G. A., Castile, J., Smith, A., Adams, G. G., Harding, S. E. Macromolecular conformation of chitosan in dilute solution: A new global hydrodynamic approach. *Carbohydrate Polymers*, **2009**, 76, 616–621.
19. Pourjavadi, A., Mahdavinia, G. R., Zohuriaan-Mehr, M. J., Omidian, H. Modified chitosan. I. Optimized cerium ammonium nitrate-induced synthesis of chitosan-g-polyacrylonitrile. *J. Appl. Polym. Sci.*, **2003**, 88, 2048–2054.
20. Quiñones, J. P., Peniche, H., Peniche, C. Chitosan Based Self-Assembled Nanoparticles in Drug Delivery. *Polymers*, **2018**, 10(3), 235–268.
21. Ribeiro, J. C. V., Vieira, R. S., Melo, I. M., Araújo, V. M. A., Lima, V. Versatility of Chitosan-Based Biomaterials and Their Use as Scaffolds for Tissue Regeneration. *The Scientific World Journal*, **2017**, 2017, 1–25.
22. Skryabin, K. G. *Chitosan*. Moscow: Center Publ. “Bioengineering”, **2013**.
23. Slivkin, A. I., Belenova, A. S., Shatalov, G. V., Kuznetsov, V. A., Slivkin, D. A., Firsova, L. I. The study of chitosan solution properties. *Journal of VSU Chemistry Biology Pharmacy*, **2014**, 1, 134–137.
24. Smotrina, T. V., Smotrin, V. A., Stoyanov, O. V. Fine structure and hydrophilic properties of thermally modified polysaccharides 1. Water sorption by thermally modified polysaccharides. *Journal of technical university*, **2015**, 18(16), 18–21.
25. Teodorescu, M., Bercea, M. Poly(vinylpyrrolidone) – A Versatile Polymer for Biomedical and Beyond Medical Applications. *Polymer-Plastics Technology and Engineering*, **2015**, 54(9), 923–943.
26. Tuma, J., Marounek, M., Dušková, D., Copíková, J., Synytsya, A. Chitosan Derivatives as Bile Acid and Cholesterol Sorbents. *J. Chitin Chitosan*, **2011**, 16(4), 262–270.
27. Wang, J., Kong, M., Zhou, Z., Yan, D., Yu, X., Chen X., Feng, C., Liu, Y., Chen, X. Mechanism of Surface Charge Triggered Intestinal Epithelial Tight Junction Opening Upon Chitosan Nanoparticles for Insulin Oral Delivery. *Carbohydr. Polym.*, **2017**, 157, 596–602.
28. Wu, T., Li, Y., Lee, D. S. Chitosan-based composite hydrogels for biomedical applications. *Macromolecular Research*, **2017**, 25(6), 480–488.

29. Yilmaz, E., Adali, T., Yilmaz, O. Grafting of poly(triethylene glycol dimethacrylate) onto chitosan by ceric ion initiation. *Reactive and*

Functional Polymers, **2007**, 67(1), 10.

EQUATIONS

$$DG = \frac{m(\text{grafted polymer}) - m(\text{chitosan})}{m(\text{chitosan})} \times 100 \% \quad (\text{Eq. 3})$$

$$EG = \frac{m(\text{grafted polymer}) - m(\text{chitosan})}{m(\text{grafted polymer}) - m(\text{chitosan}) + m(\text{homopolymer})} \times 100\% \quad (\text{Eq. 4})$$

where $m(\text{grafted polymer})$ – the mass of the copolymer in the sample, $m(\text{chitosan})$ – the mass of chitosan in the probe, $m(\text{homopolymer})$ – the mass of homopolymer extracted from the sample

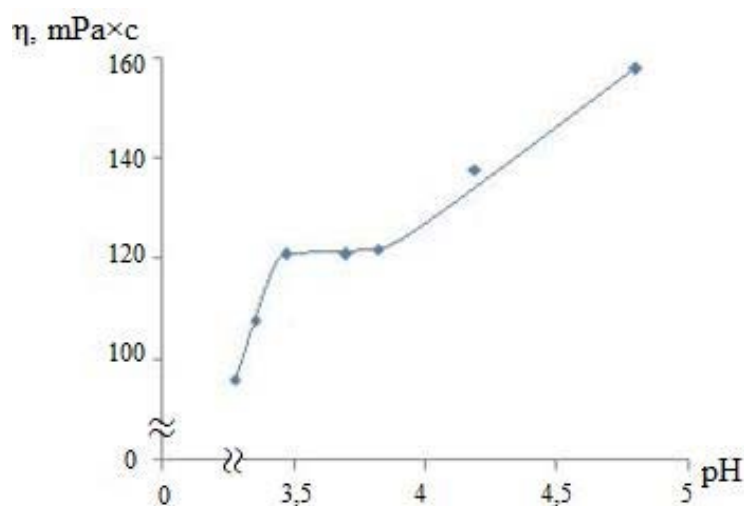


Figure 1. Dependence of the dynamic viscosity of 3 wt% chitosan solution on the medium pH, $MW = 1.1 \times 10^5$, $DD = 0.82$. $T = 25^\circ\text{C}$

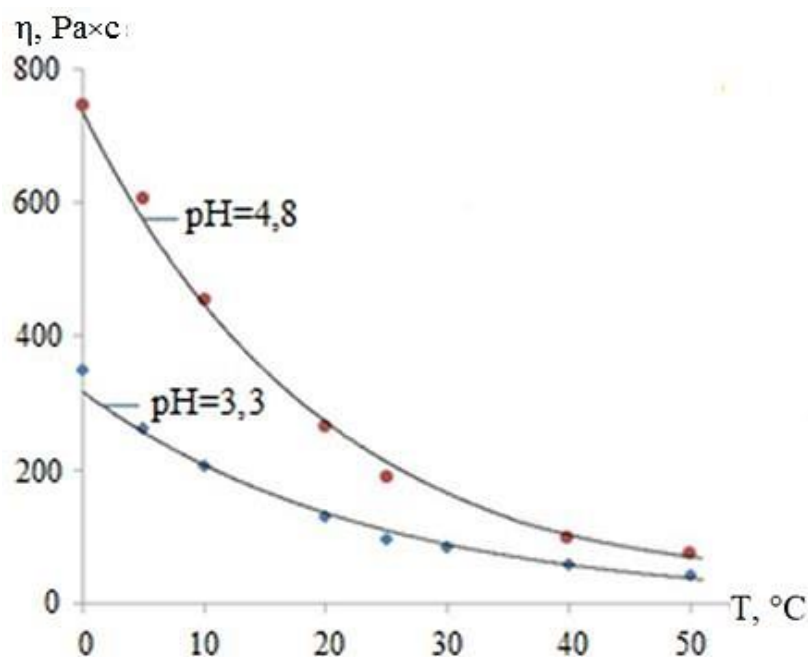


Figure 2. Dependence of solution dynamic viscosity on the temperature in the chitosan samples with $MW = 1.1 \times 10^5$: curve 1 – molecular helix conformation; curve 2 – molecular coil conformation.

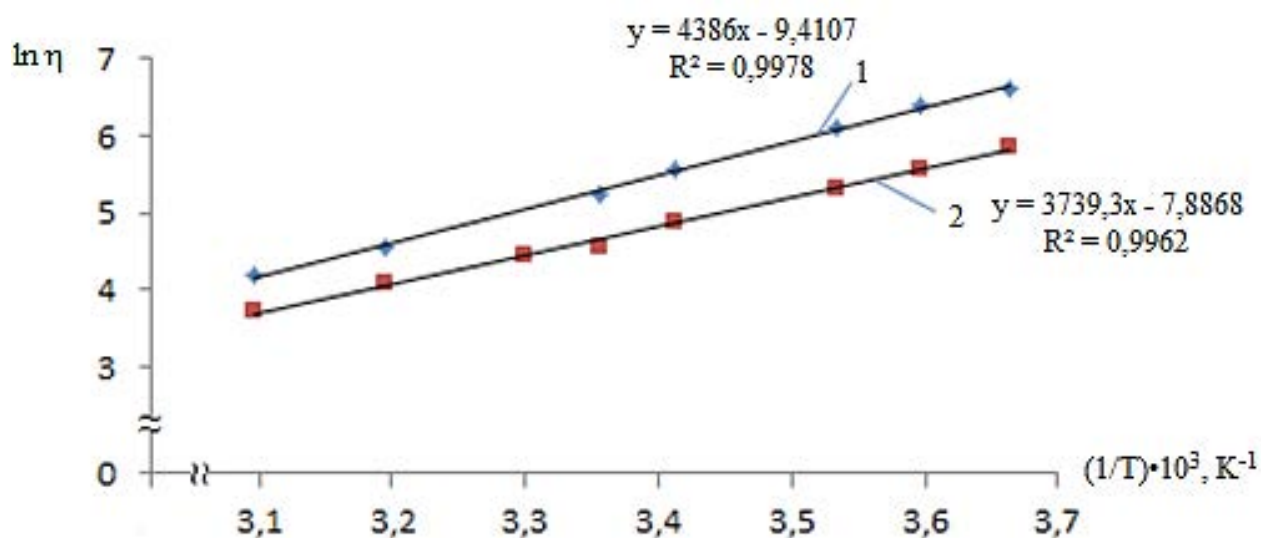


Figure 3. Dependence of $\ln \eta$ on $1/T$ in the samples of chitosan with $MW = 1.1 \times 10^5$. 1 - pH = 4.8; 2 - pH = 3.3

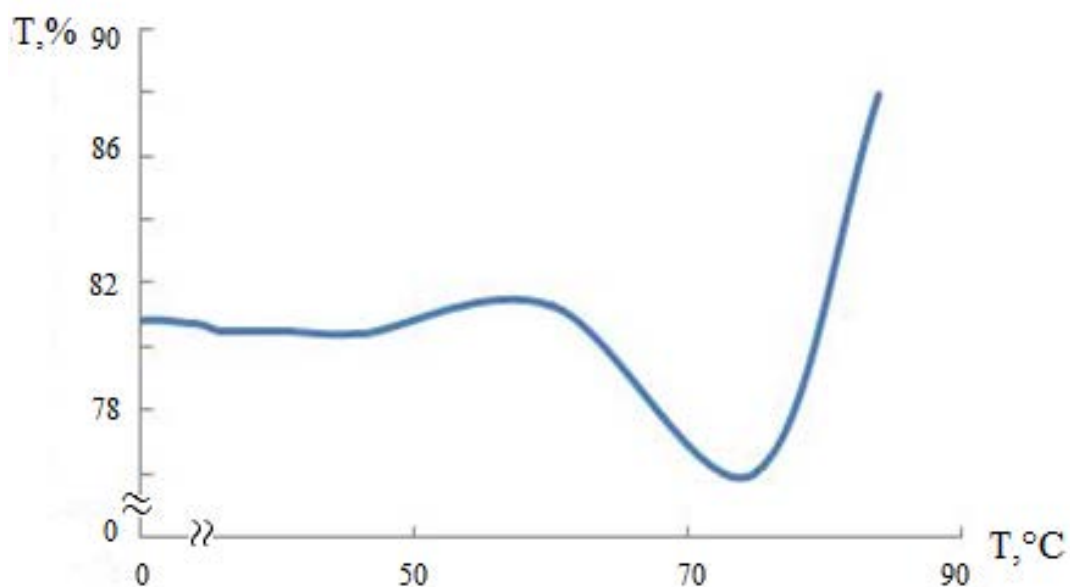


Figure 4. Dependence of optical transmission of 0.03 wt% chitosan solution on the temperature.

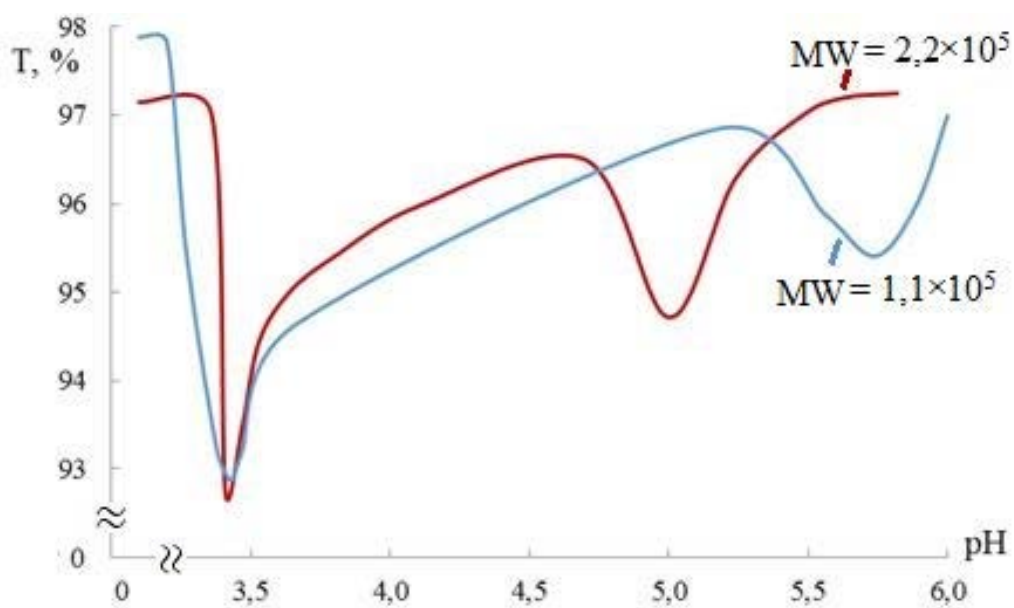


Figure 5. Changes in optical transmission of 0.03 wt% chitosan solution depending on the pH of the medium. DD = 0.82. T = 25°C

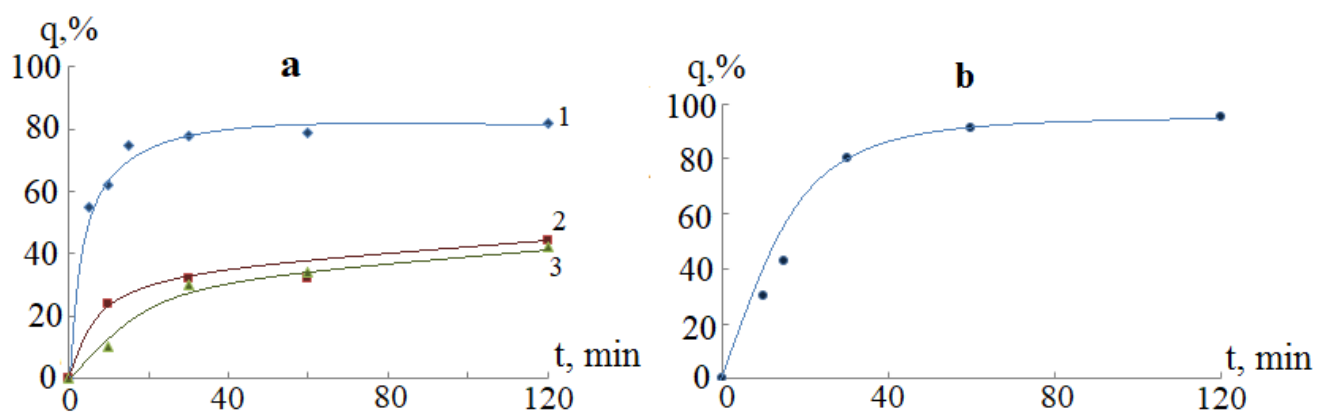


Figure 6. Time-dependent changes in HEMA transformation during graft polymerization onto chitosan with $Ce(SO_4)_2$ as an initiator. $T = 60^\circ C$. a – $pH = 4.8$; $[HEMA]/[chitosan] = 4.8$ (1); 2.4 (2); 1.2 (3) (mol/(molar ratio)). b – $pH = 3.3$; $[HEMA]/[chitosan] = 4.8$ mol/(molar ratio)

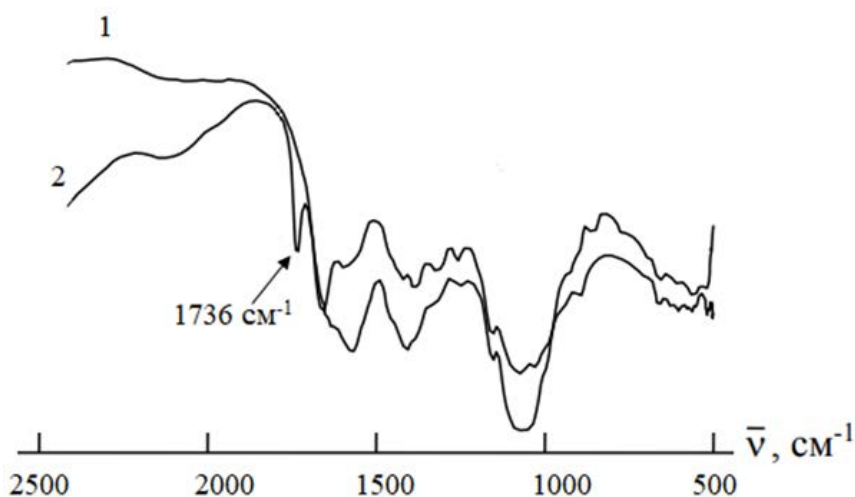


Figure 7. IR spectra of chitosan (1) and chitosan-HEMA copolymer (2).

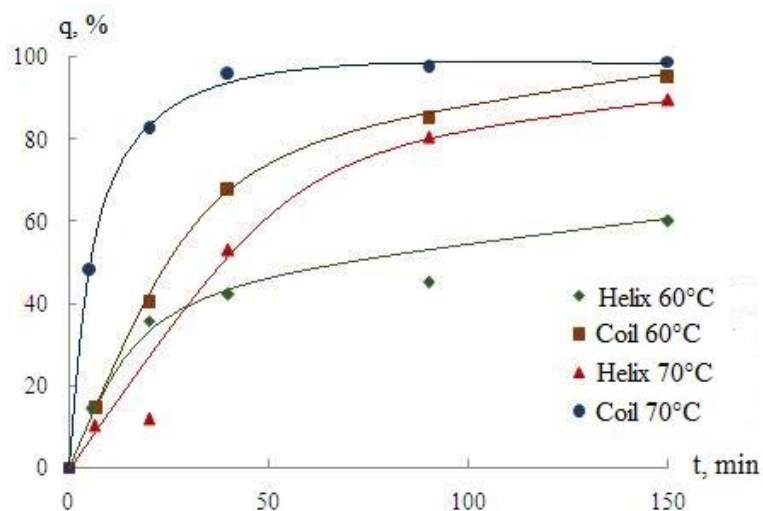
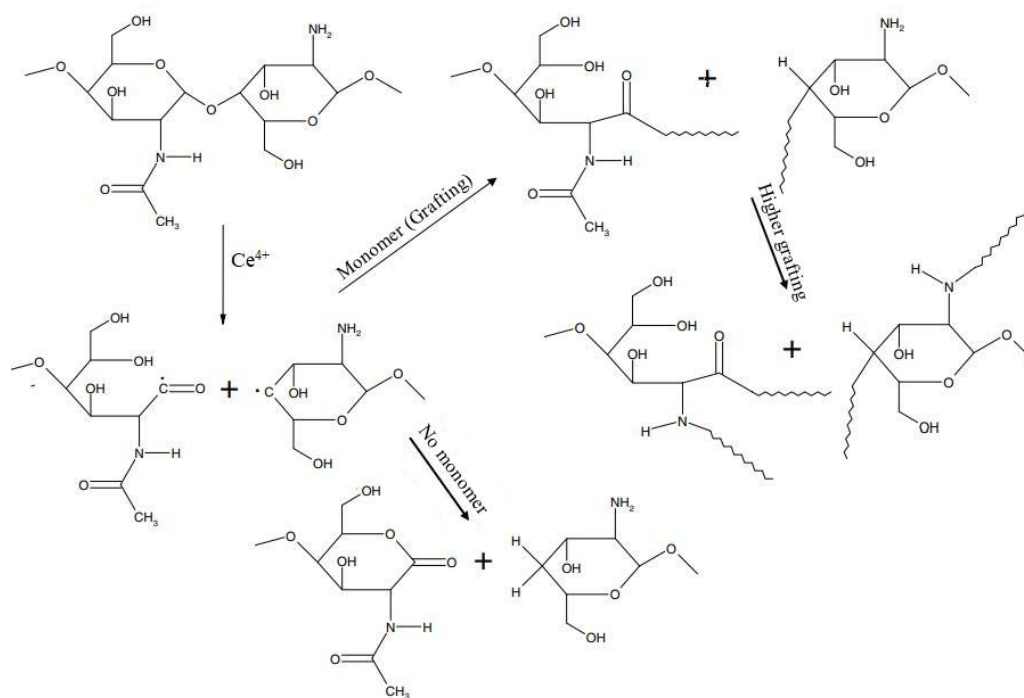
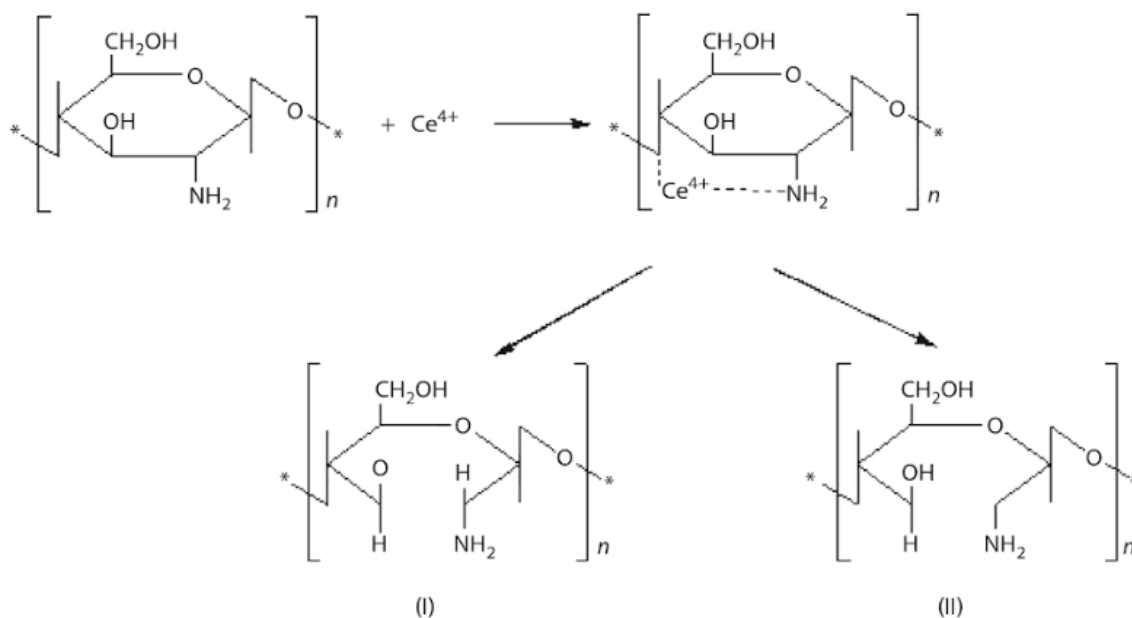


Figure 8. Degree of VP conversion in the process of polymerization onto chitosan with $Ce(SO_4)_2$ as an initiator. $[VP]/[chitosan] = 1.0$ mol/(molar ratio)



Scheme 1. The scheme of the mechanism of graft polymerization onto chitosan with cerium ions as an initiator



Scheme 2. The mechanism of chitosan initiation with cerium ions

Table 1. Effective diameter of chitosan macromolecules in different pH media. $\omega(\text{chitosan}) = 0.03\%$. Polydispersity ~ 1.25

MW of chitosan	Effective diameter, nm pH=4.8 (conformation – helix)	Effective diameter, nm pH=3.3 (conformation – coil)
1.1×10^5	623.9	536.9
2.2×10^5	868.9	546.5

Table 2. DP and EP in grafted polymerization of HEMA onto chitosan, $[\text{chitosan}] = 3 \text{ wt}\%$, $[\text{HEMA}]/[\text{chitosan}] = 4.8 \text{ mol}/(\text{molar ratio})$. Initiator – Ce^{4+}

Conformation of macromolecules	q, %	DP, wt%	EP, wt%
Helix (pH 4.8)	81	300	91
Coil (pH 3.3)	96	390	98

Table 3. The degree and efficiency of VP grafted polymerization onto chitosan, $\omega(\text{chitosan}) = 3 \text{ wt}\%$

Initiating system, temperature	Conformation of macromolecules	$[\text{VP}]/[\text{chitosan}]$, mol/(molar ratio)	q, %	DP, wt%	EP, wt%
$\text{Ce}(\text{SO}_4)_2$ 60°C	Helix (pH=4.8)	1.0	53	20,5	58
$\text{Ce}(\text{SO}_4)_2$ 60°C	Coil (pH=3.3)	1.0	95	44	70
$\text{Ce}(\text{SO}_4)_2$ 70°C	Helix (pH=4.8)	1.0	85	45	80
$\text{Ce}(\text{SO}_4)_2$ 70°C	Coil (pH=3.3)	1.0	98	61	94

Table 4. Physicomechanical properties of chitosan and chitosan-HEMA grafted copolymers

Initiator	pH of the reaction medium	DP	σ , MPa	ϵ , %
-	4.8	0	25.0 -27.0	1.9
$\text{Ce}(\text{SO}_4)_2$	4.8	300	32.5	3.5
$\text{Ce}(\text{SO}_4)_2$	3.3	390	35.0	4.2

Table 5. Physicomechanical properties of grafted chitosan-VP copolymers

$[\text{VP}]/[\text{chitosan}]$, mol/(molar ratio)	pH of the solution	σ , MPa	ϵ , %
1.00	4.8	53.4	2.6
1.00	3.3	60.0	4.0

OPORTUNIDADES MODERNAS DE FARMACOTERAPIA ATEROSCLEROSE: NOVAS DIREÇÕES**MODERN OPPORTUNITIES OF ATHEROSCLEROSIS PHARMACOTHERAPY: NEW DIRECTIONS****СОВРЕМЕННЫЕ ВОЗМОЖНОСТИ ФАРМАКОТЕРАПИИ АТЕРОСКЛЕРОЗА: НОВЫЕ НАПРАВЛЕНИЯ**

DUTOVA, Svetlana Vyacheslavovna^{1*}; SARANCHINA, Julia Vladimirovna²;
KILINA, Oksana Yuryevna³; KHANARIN, Nikolai Vladimirovich⁴;
KULAKOVA, Tatiana Sergeevna⁵;

^{1,2,3,4,5} Katanov Khakass State University Russian Federation

* Correspondence author

e-mail: coluria@mail.ru.

Received 15 December 2019; received in revised form 27 February 2020; accepted 06 March 2020

RESUMO

Apesar das realizações bem-sucedidas da medicina aplicada moderna e da aplicação de medicamentos hipolipidêmicos na prática clínica nos últimos 50 anos, a questão da prevenção e tratamento da doença vascular aterosclerótica (DVA) permanece sem solução. A implementação da teoria da imunopatogênese da aterosclerose, comprovada experimentalmente por estudos modernos, permite que os especialistas ampliem as possibilidades de farmacoterapia e farmacoprevenção para DVA. Assim, o objetivo do presente estudo foi analisar novas direções no desenvolvimento de medicamentos antiateroscleróticos (DAA) com atividade patogênica que suprimia a inflamação autoimune crônica nas áreas de lesão aterosclerótica dos vasos. No decorrer do estudo, foram realizadas a busca e análise das publicações nas bases de dados Web of Science, PubMed e RSCI (Russian Science Citation Index) para o período de 2016-2018. De acordo com a análise realizada, os alvos moleculares mais importantes para a DAA são citocinas pró-inflamatórias e anti-inflamatórias que desenvolvem um desequilíbrio em pacientes com DVA. Assim, os fármacos baseados em anticorpos monoclonais ao fator de necrose tumoral α (TNF α) e interleucinas pró-inflamatórias (1 β , 17A), utilizados no tratamento da artrite reumatóide e psoríase, podem ser utilizados para o tratamento da DVA. As interleucinas recombinantes 6, 13, 19 e substâncias que suprimem a expressão de fatores reguladores de interferon também exercerão um efeito antiaterogênico. Os estudos sobre a modelagem da patogênese da DVA em animais consanguíneos mostraram que outros alvos moleculares para DAA poderiam ser enzimas envolvidas no metabolismo lipídico e de células imunes. Eles incluem a enzima 1 requerente de inositol, a proprotéina convertase subtilisina / Kexin tipo 9 e as enzimas da família paraoxonase. Além disso, a revisão inclui a discussão sobre a aplicação bem-sucedida de medicamentos baseados em anticorpos monoclonais ao TNF α (infliximabe), IL-17A (secukinumabe) e IL-1 β (canacinumabe), bem como os medicamentos com atividade anti-enzimática (evolocumabe e darapladib), na prática clínica para o tratamento da DVA. O conhecimento moderno sobre os mecanismos moleculares da imunopatogênese pode fundamentar o desenvolvimento de fármacos para farmacoterapia patogênica e a farmacoprevenção para as complicações da DVA. A solução mais eficaz seria a indicação de medicamentos que afetam o desequilíbrio de citocinas e processos metabólicos nas células imunológicas.

Palavras-chave: aterosclerose, farmacoterapia, medicamentos antiateroscleróticos, interleucinas, enzimas, placas ateroscleróticas.

ABSTRACT

Despite the successful achievements in modern applied medicine and the application of hypolipidemic drugs into clinical practice for the past 50 years, the issue of prevention and treatment of atherosclerotic vascular disease (AVD) remains unsolved. Implementation of the theory of immunopathogenesis of atherosclerosis that was experimentally proved by modern studies allows the specialists to expand the possibilities of pharmacotherapy and pharmacoprevention for AVD. Thus, the aim of the present study was to analyze new directions in the development of anti-atherosclerotic drugs (AAD) with a pathogenetic activity that suppressed chronic autoimmune inflammation in the areas of atherosclerotic damage of vessels. In the course

of the study, the search and analysis of the publications in the databases Web of Science, PubMed, and RSCI (Russian Science Citation Index) for the period of 2016-2018 were performed. According to the performed analysis, the most perspective molecular targets for AAD are pro-inflammatory and anti-inflammatory cytokines that develop a disbalance in patients with AVD. Thus, the drugs that are based on monoclonal antibodies to the tumor necrosis factor α (TNF α), and pro-inflammatory interleukins (1 β , 17A), used for the treatment of rheumatoid arthritis and psoriasis, can be used for the treatment of AVD. Recombinant interleukins 6, 13, 19, and substances that suppress the expression of interferon regulatory factors will also exert an antiatherogenic effect. The studies on the modeling of the pathogenesis of AVD in inbred animals showed that other molecular targets for AAD could be enzymes involved in the lipid and immune cells metabolism. They include inositol-requiring enzyme 1, proprotein convertase subtilisin/Kexin type 9, and the enzymes of paraoxonase family. Besides, the review includes the discussion of the successful application of drugs based on monoclonal antibodies to TNF α (infliximab), IL-17A (secukinumab) and IL-1 β (canakinumab), as well as the drugs with anti-enzymatic activity (evolocumab and darapladib), in clinical practice for the treatment of AVD. The modern knowledge on molecular mechanisms of immunopathogenesis can give grounds for the development of drugs for pathogenetic pharmacotherapy and pharmacoprevention for the complications of AVD. The most effective solution would be the indication of drugs that affect the disbalance of cytokines and metabolic processes in the immune cells.

Keywords: *atherosclerosis, pharmacotherapy, anti-atherosclerotic drugs, interleukins, enzymes, atherosclerotic plaques.*

АННОТАЦИЯ

Несмотря на успехи современной практической медицины и использование в клинической практике гипOLIпидемических лекарственных средств в течение почти 50 лет, проблема профилактики и лечения atherosclerotic vascular disease (AVD) остается нерешенной. Использование постулатов теории иммунопатогенеза атеросклероза, экспериментально подтвержденной современными исследованиями, позволяет расширить возможности фармакотерапии и фармакопрофилактики AVD. В связи с этим целью данного исследования явился анализ новых направлений в создании анти-атеросклеротических лекарственных средств (AAD) с патогенетическим действием, которые бы угнетали развитие хронического аутоиммунного воспаления в области атеросклеротического поражения сосудов. Для реализации цели был проведен поиск и анализ статей по базам данных Web of Science, PubMed и РИНЦ за период 2016-5-2018гг. Согласно проведенному анализу наиболее перспективными молекулярными мишенями для AAD являются провоспалительные и противовоспалительные цитокины, между которыми при AVD развивается дисбаланс. Поэтому лекарственные средства на основе моноклональных антител к фактору некроза опухолей альфа и провоспалительным интерлейкинам (1 β , 17A), используемые для лечения ревматоидного артрита и псориаза, могут быть использованы и при AVD. Противоатерогенным эффектом будут обладать и рекомбинантные интерлейкины 6, 13, 19 и вещества, угнетающие экспрессию interferon regulatory factor. По результатам изучения патогенеза AVD при моделировании этого патологического процесса у инбредных животных установлено, что другими молекулярными мишенями для AAD могут послужить ферменты, участвующие в обмене липидов и метаболизме иммунных клеток. Это inositol-requiring enzyme 1, proprotein convertase subtilisin/kexin type 9 и ферменты семейства paraoxonase. Кроме того, в обзоре обсуждаются результаты успешного применения в клинической практике для лечения AVD лекарственных средств на основе моноклональных антител к TNF α (инфликсимаба), IL-17A (секукинумаба) и IL-1 β (канакинумаба); а также препаратов с антиферментативной активностью (эволюкумаба и дарапладиба). Таким образом, на основе современных данных о молекулярных механизмах иммунопатогенеза вполне реальна разработка лекарственных средств для патогенетической фармакотерапии и фармакопрофилактики осложнений AVD. Для этой цели наиболее эффективно будет применение лекарственных средств, влияющих на дисбаланс цитокинов и обменные процессы в иммунных клетках

Keywords: *атеросклероз, фармакотерапия, анти-атеросклеротические лекарственные средства, интерлейкины, ферменты, атеросклеротическая бляшка.*

1. INTRODUCTION

Despite the successful achievements in modern applied medicine and the application of hypolipidemic drugs into clinical practice for the past 50 years, the issue of prevention and

treatment of atherosclerotic vascular disease (AVD) remains unsolved.

The analysis of the results of clinical observations after the patients with AVD and the studies on the modeled atherosclerosis (AS) in

animals revealed significant inconsistency with the lipid theory of AS pathogenesis (stereotype, focality, and localization of the process independent of the character of dyslipidemia; possibility of the development of AS in patients with normal lipid metabolism; simultaneous presence of atherosclerotic plaques (AP) of different maturity and they are under endothelial location; AVD relapse after the coronary artery bypass graft surgery) and brought proves in favor of the theory of immunopathogenesis (Kilessa, 2012).

The main role in the pathogenesis of AVD plays the process of autoimmune inflammation, which is confirmed by numerous facts on the protective properties of low-density lipoproteins (LDL) and cholesterol (Ch) in patients with bacterial and viral infections (Kovalenko, 2010). According to the concept of the immunopathogenesis of AS, the degree and reversibility of the vascular walls damage, and the stability of the formed AP are determined by the balance interleukins, interferons, TNFs, and colony-stimulating factors that regulate the interaction of the immune cells (Karagodin, 2014). As a rule, lipid disorders associated with AVD can be considered as one of the most important manifestations of the non-specific congenital immune response to the infectious agents (Kovalenko, 2010).

The abovementioned information can give grounds to the development of new approaches to the pharmacotherapy and pharmacoprevention of AVD. The aim of the present review was to describe modern tendencies in the pharmacotherapy of AS.

2. MATERIALS AND METHODS

In the course of the study, the search and analysis of the publications in the databases Web of Science and PubMed. The search query consisted of different combinations of keywords: «atherosclerosis + interleukins», «atherosclerotic plaques + interleukins», «atherosclerosis + pharmacotherapy», «anti-atherosclerotic drugs», «atherosclerosis + enzymes». Totally, 29 original articles were selected that contained the primary results of the studies and 9 review articles.

The search was also performed in the database RSCI (elibrary.ru – scientific electronic library) for the period of 2010-2018. The authors retrieved 10 review articles and 12 original articles that satisfied the search query

3. RESULTS AND DISCUSSION

3.1. Drugs that affect the synthesis and effects of cytokines

It is known that the disorders in the balance between the pro-inflammatory and anti-inflammatory cytokines lead to the induction of self-maintaining mechanisms of chronic inflammation in patients with AS. Hence, one of the main possible directions in the immunotherapy of AS can be the modification of the cytokine effects (Tedgui and Mallat, 2001; Beshpalova et al., 2013; Alexopoulos and Kaggi, 2014).

There is evidence of the prevalence of cytokines in the serum of patients with AS. These cytokines determine the polarization of the immune response to the activation of T-helper 1 (Th1) lymphocytes. These are anti-inflammatory cytokines (interleukin-1 (IL-1), interleukin-8 (IL-8), tumor necrosis factor-alpha (TNF α)) that enhance the migration of leukocytes to the focus of the immune inflammation, stimulate the migration and proliferation of smooth muscle cells as well as contribute to the apoptosis of immune-competent cells in the AP and enhance their destabilization (von Vietinghoff and Ley, 2010; Ershova et al., 2011; Ait-Oufella et al., 2011; Arabidze, 2013; Sineglazova, 2012; Shalenkova et al., 2013; Fatkhullina et al., 2016).

Besides, the hyperproduction of pro-inflammatory cytokines in patients with progressing AS is one of the main causes of acute disturbance of the regulation of the immune reactions and further progressing of a systemic inflammatory process in the arteries, which explains the relapse of AP in patients after endarterectomy (Curtiss and Tobias, 2009; Zaporozhec et al., 2012; Ramji and Davies, 2015).

The described facts are also confirmed by the results of the tests on the cytokines content in the samples of the arteries affected by AP. Thus, the results, obtained by the method of flow cytometry, revealed the increase in the expression of interleukin-2 (IL-2), interleukin-17 (IL-17) and interferon-gamma (INF γ) CD8 and CD4-T-lymphocytes found in the samples of AP in comparison with the blood cells (Grivel et al., 2012). In the samples of cultivated AP taken from the patients with AVD of carotid arteries, the content of TNF α positive cells was significantly higher than in the samples of the circulating lymphocytes. It should be mentioned that

unstable AP contained more CD4 T-lymphocytes, that express TNF α and IFN γ , than stable ones (Profumo *et al.*, 2013).

It was also established that the samples with unstable AP, taken from the areas of coronary arteries in men with coronary AS with a stable effort angina II-IV FC, had a significantly higher concentration of pro-inflammatory cytokines: interleukin-1 β (IL-1 β), interleukin-18 (IL-18), interleukin-6 (IL-6) and IL-8. It should be mentioned that the unstable AP of the dystrophic-necrotic type also had a significantly higher level of TNF α (Ragino *et al.*, 2011; Ragino *et al.*, 2012). Similar results were obtained during the study of the atherosclerotic areas of carotid arteries in humans (Shishkina *et al.*, 2014). Besides, the experiments on the modeled AS in animals with inhibited pro-inflammatory cytokines indicated the slowdown of the process of the development and progression of the disease (Tedgui and Mallat, 2001; Ershova *et al.*, 2011; Miossec, 2009).

Thus, one of the targets for anti-atherosclerotic drugs (AAD) can be pro-inflammatory cytokines.

It is known that one of the key roles in the pathogenesis of AS and ischemic heart disease plays a pro-inflammatory cytokine TNF α , which inhibits the synthesis of apolipoprotein A-1 (ApoA1) in hepatocytes leading to the decrease in the high-density lipoprotein (HDL) in blood, and induces the apoptosis of vascular smooth muscle cells (VSMC) by inhibiting the expression of connexins resulting in the destabilization of AP (Kovalenko *et al.*, 2010; Tang and Fang, 2017). Hence, the inhibition of this cytokine should have a favorable pathogenetic effect in patients with AS. As a result of a short-term indication of infliximab (drug based on monoclonal antibodies to TNF α) to 33 patients with rheumatoid arthritis, there was an increase in the HDL in plasma by 0.12 mmol/L in two weeks and a significant decrease in the index of atherogenicity (Popa *et al.*, 2007). Apart from infliximab, there are other drugs that reduce the effects of TNF α like etanercept, adalimumab, golimumab, and certolizumab (Geiler *et al.*, 2011; Tousoulis *et al.*, 2016). Presently, it is proved that the treatment of patients with autoimmune diseases (psoriasis, rheumatoid arthritis) with anti-TNF α agents improves the function of endothelium in arteries (Tousoulis *et al.*, 2016; Avgerinou *et al.*, 2011; Spinelli *et al.*, 2014).

IFN γ also plays an important role in the immunopathogenesis of AS stimulating the uptake of modified lipoproteins by the

macrophages and the development of foam cells. The experiment on the cross-breeding of IFN γ -deficient and LDLR-deficient mice (LDL receptor-deficient) on the cholesterol diet showed that there was a significant decrease in the level of IFN γ , which led to the reduction of AP size in several areas of the aorta and relative decrease in the macrophage and VSMC count in the AP that were formed earlier. The authors suggested that the inhibition of the effects of IFN γ -producing T-lymphocytes in the vascular walls was a potentially beneficial strategy for the control of AS (Buono *et al.*, 2003).

Further, in the experiment with inbred mice of IRF3-/-ApoE-/- line (apolipoprotein E knockout with impossibility to synthesize interferon regulatory factor 3, IRF3), the influence of IRF3 was established on the secretion of the molecules of adhesion by the endothelial cells and further infiltration of the vascular walls by macrophages in subjects with AS. IRF3 deficit led to the inhibition of the secretion of the molecules of adhesion in the vascular cells and expression of the molecules of intercellular adhesion, which resulted in the reduction of infiltration of the damaged arterial wall by macrophages. The authors of the study believed that IRF3 could be also used as a potential target for the development of AAD (Liu *et al.*, 2017).

It was also proved that interleukin-17 (IL-17) exerted pro-atherogenic effect due to its capacity to enhance the production of IL-1 β , IL-6, IL-12, and INF γ by macrophages (Ouyang *et al.*, 2008; Chen *et al.*, 2010; Kozlov, 2016). Inhibition of the effects of IL-17 reduces the manifestations of AVD in animal models, but there were no clinical trials performed (Erbel, *et al.*, 2016). Presently, a drug based on monoclonal antibody (MA) to IL-17A (secukinumab) was developed that can expand the therapeutic possibilities for patients with AS. The results of the performed clinical studies on subjects with ankylosing spondylitis showed that secukinumab had low immunogenicity, and its safety profile nearly similar to the one placebo (Jerdes, 2016). Brodalumab (antagonist of IL-17 receptors) and Ixekizumab (MA to IL-17A), used for the treatment of psoriasis, can be also potential AAD considering the pro-inflammatory character of IL-17 (Tousoulis *et al.*, 2016; Coimbra *et al.*, 2014).

In 2018, the results of the randomized controlled clinical study of canakinumab (human anti-IL-1 β MA) were published. The study included more than 10,000 patients with preceding myocardial infarction, an elevated level of C-reactive protein (CRP), and Ch LDL (despite

the therapy with statins). The results revealed the reduction of the primary endpoint of the death caused by the myocardial infarction or stroke by 15% (in the dose of 150 mg or 300 mg every 3rd month). There were no statistically significant changes in the cholesterol of low-density lipoproteins (Ch LDL) registered. Still, the level of CRP and IL-6 significantly decreased. The analysis of the secondary endpoint (a necessity in urgent revascularization) showed even more significant results with a relative reduction of the risk by 17% in comparison with the median. Besides, canakinumab demonstrated the importance of inflammation in patients with multiple systemic disorders. The inhibition of IL-1 β by canakinumab also reduced the mortality rate from lung cancer by more than a half, depending on the indicated dose (Lorenzatti and Servato, 2018).

There is less data on the application of drugs with anti-IL-6 effect. Tocilizumab (MA to the membrane and circulating IL-6), indicated to patients with rheumatoid arthritis in the course of a randomized study, increased total HDL, Ch LDL and triglycerides (Tousoulis *et al.*, 2016; Kawashiri *et al.*, 2011). But the application of tocilizumab also led to the improvement of endothelial function and reduction of aorta stiffness (Tousoulis *et al.*, 2016; Protogerou, 2011). There is an ongoing study on the possibility of an indication of tocilizumab to patients with rheumatoid arthritis and cardiovascular risk factors (Tousoulis *et al.*, 2016).

Another approach to the reduction of disbalance of cytokines in patients with AS can be based on the stimulation of the expression of anti-atherogenic (anti-inflammatory) cytokines. There are some published data that proves an anti-atherogenic role in the expression of interleukin-4 (IL-4), interleukin-13 (IL-13), and interleukin-1 (IL-19) in subjects with AS.

The positive effect of IL-4 and IL-13 lies in the enhancement of polarization of macrophages to a phenotype M2 (involved in the immune reactions of T-helper 2 (Th2), which stimulates the processes of proliferation and angiogenesis) that stimulates the tissue regeneration after the inhibition of inflammatory reaction (Bobryshev *et al.*, 2016; Zhao *et al.*, 2016; Chen *et al.*, 2017). The anti-atherogenic effect of IL-13 was proved by the results of the study on AS-prone mice that could not secrete IL-13, and that developed significantly bigger and more mature AP. A deficit of IL-13 also led to the accelerated development of AVD in LDLR-deficit mice without the influence on Ch in plasma. An indication of IL-

13 to animals limited the chemotaxis of macrophages to AVD foci and favorably modulated the morphology of the existing AP by increasing the content of collagen and decreasing the macrophage count. Besides, the experiments in vitro showed that the activated IL-13 macrophages (phenotype M2) had higher clearance to the oxidized LDL in comparison with M1 macrophages activated by IFN γ (Cardilo-Reis *et al.*, 2012).

The study on the IL-19 knockout mice showed that the deficit of this interleukin activated the proliferation of VSMC and synthesis of pro-inflammatory cytokines (including IL-1 β and TNF α). This fact allowed the authors to suggest the application of IL-19 as a potent suppressor of AS development (Fatkhullina, 2016). In 2016, a group of scientists from Medical Universities of Philadelphia and New-York conducted a study on the capability of exogenous IL-19 to reduce the progression of AVD. LDLR-knockout mice were given feed with increased content of Ch for 12 weeks and, further, given recombinant IL-19 for eight more weeks. The analyses of AVD in mice from the test group (receiving IL-19) revealed the key parameters of the AS regression: reduction of total macrophage count and increase in the M2 macrophage count. Additional studies showed that IL-19 played an important role in the regulation of lipid metabolism of macrophages by means of gamma-receptor regulation of Ch absorption that depended on peroxisome proliferates and increase in the outflow of Ch mediated by ATP-binding cassette transporter (ABCA1) (Gabunia *et al.*, 2016).

Besides, IL-19 plays an important role in the proliferation and transformation of VSMC, in particular, induces the expression of muscle-specific miRNA (miR133a) in these cells that can reduce the expression of low-density lipoprotein receptor adapter protein 1 (LDLRAP1) – an adaptor protein that is necessary for the internalization of LDLR. Thus, IL-19 reduced the accumulation of lipids in VSMC and the uptake of oxidized LDL in the miR133a-dependent mechanism (Gabunia *et al.*, 2016).

Herman *et al.* (2016) in their study, showed that the anti-inflammatory IL-19 reduces the function of mRNA-stability protein HuR in human VSMC, which could also reduce their capacity to proliferation (Herman *et al.*, 2016; Herman *et al.*, 2018). Thus, currently, the following mechanisms of anti-atherogenic activity of IL-19 were established:

- Th2-polarization of the immune response,

- regulation of the role of macrophages in the development of inflammation,
- regulation of macrophages lipid metabolism,
- the decrease in leukocyte adhesion,
- suppression of the expression of the genes of pro-inflammatory cytokines,
- reduction of neointimal hyperplasia by means of the reduction of activation of VSMC (Gabunia *et al.*, 2016; Gabunia *et al.*, 2017).

The interest of the researchers is also attracted by the possibility of target delivery of recombinant IL-19 to the foci of ADV by means of adenoviruses during the modeling of AS in animals. Presently, despite a positive effect of anti-inflammatory cytokines during the modeling of AS in animals, the anti-inflammatory cytokines drugs are not obtained yet (Tousoulis *et al.*, 2016; Tian *et al.*, 2008).

3.2. Drugs that affect enzymatic activity

The second important direction in the development of AAD can become the regulation of the activity of the enzymes that play an important role in the metabolism of immune cells involved in chronic autoimmune inflammation. In this aspect, kinase/endoribonuclease inositol-requiring enzyme 1 (IRE1) can be considered as a perspective target for the drugs. This enzyme is the most conservative regulator of the activity of the protein of a homeostatic regulatory net that reacts to a metabolic overload of endoplasmic reticulum in the conditions of the metabolically induced chronic inflammatory process (AS, diabetes mellitus, metabolic syndrome). IRE1 is also one of the most important regulators of the expression of pro-atherogenic genes that has cytoprotective and pro-apoptotic functions and is activated after the accumulation of lipids and proteins with a damaged quaternary structure in the endoplasmic reticulum. The method of the sequencing of ribonucleic acid (RNA) of macrophages was used to establish that IRE1 regulated the expression of numerous pro-atherogenic genes. Hence, AAD inhibitors of IRE1 could be used for the prevention of activation of the inflammatory process by macrophages in the vascular endothelium under the effect of lipid-induced stress (Pavlova *et al.*, 2014; Tufanli *et al.*, 2017). During the modeling of AS in inbred ApoE-knockout mice, it was established that the introduction of IRE1 inhibitors significantly reduced the production of IL-1 β and IL-18, the activity of Th1 immune response, and

size of AP without the changes in lipid profile of plasma. The authors believed that the pharmacologic modulation of the activity of IRE1 could contribute to the slowdown of the progression of AS (Tufanli *et al.*, 2017). Presently, several substances with the activity of IRE1 inhibitors based on the aromatic or heteroaromatic hydroxy aldehydes are obtained (Pavlova *et al.*, 2014).

Another target for AAD can be the enzymes of the paraoxonase (PON) family. These enzymes prevent the oxidation of lipids to LDL by means of their hydrolysis, inhibit the differentiation of monocytes in macrophages, and uptake of the oxidized LDL by the macrophages and their conversion to foam cells. Besides, the enzymes of the PON family regulate some functions of macrophages: stabilize their mitochondria, contribute to their differentiation to M2 phenotype, and prevent the induction of their apoptosis. The increase in the expression and/or activity of PON can contribute to the metabolism of Ch in macrophages and weaken the inflammatory process in the vascular endothelium (Watson *et al.*, 1995; Whit and Anantharamaiah, 2017).

When the new facts were obtained on the regulation of the expression of LDLR on the hepatocytes surface, that provide the clearance of LDL from the bloodstream, a new target for ADD was identified that took part in the destruction of the receptors to LDLR – proprotein convertase subtilisin/Kexin type 9 (PCSK9) (Kuharchuk and Bazhan, 2013). A recent clinical study on the application of evolocumab (PCSK9 inhibitor) showed a decrease in the Ch LDL level in patients by 70% and more.

In comparison with the apheresis of LDL, two-week injection therapy with this drug proved to be more effective, less expensive, and less invasive without serious side effects (Kawashiri *et al.*, 2017). The analysis of the results obtained in other clinical studies on the evaluation of the effects of PCSK9 inhibitors in patients with a high risk of cardio-vascular disorders showed that there was a positive effect of this pharmacological group on the levels of Ch, LDL in blood, AP volume, decrease in CD rate, and total mortality rate (Kawashiri *et al.*, 2017; Karpov and Talickij, 2015; Schmidt *et al.*, 2017; Karpov, 2017).

Another enzyme was described that could be used as a target for AAD - lipoprotein-associated phospholipase A2 (Lp-PLA2) – that was secreted primarily by macrophages. This

enzyme hydrolyzes phosphatidylcholine on the surface of LDL in plasma. The increase in the activity of Lp-PLA2 leads to the intensive expression of the products of peroxidation and, as a result, to the enhancement of the inflammatory process in the altered vascular walls (Kuharchuk and Tararak, 2010). An inhibitor of Lp-PLA2 (darapladib (GlaxoSmithKline, UK)) was developed. According to the results of the study, published by the manufacturer, the indication of darapladib led to a relative decrease (6%) in the development of myocardial infarction or stroke in patients. The study on drug effectiveness is ongoing (White *et al.*, 2014).

Presently, the results of some clinical studies on potential AAD drugs are published (Table 1).

It was established that anti-cytokine drugs used for the treatment of systemic autoimmune diseases (rheumatoid arthritis, ankylosing spondylitis, psoriasis, acute gouty arthritis, ulcerative colitis) significantly influenced on the mortality rate from CD and the parameters that characterized the presence of AVD.

Thus, the application of AAD – MA to pro-inflammatory cytokines (infliximab, etanercept, adalimumab, golimumab, canakinumab) and their receptors (anakinra, tocilizumab) led to the increase in the HDL level, decrease in the CRP and IL-6 levels, decrease in the atherogenic index, and improvement of the endothelial function (Popa *et al.*, 2007; Geiler *et al.*, 2011; Tousoulis *et al.*, 2016; Avgerinou *et al.*, 2011; Spinelli *et al.*, 2014; Jerdes, 2016; Lorenzatti and Servato, 2018; Kawashiri *et al.*, 2011; Protogerou *et al.*, 2011). Indication of tocilizumab to patients with rheumatoid arthritis in the course of pharmacotherapy resulted in a decrease in LDL, CH LDL levels, and reduction of aortic stiffness (Geiler *et al.*, 2011; Kawashiri *et al.*, 2011; Protogerou *et al.*, 2011). The authors did not reveal any data on the drugs that decreased the expression of IFN γ .

Despite the proven anti-atherogenic activity on AS models, the drugs based on anti-inflammatory cytokines are still not developed and clinically not tested.

When it comes to AAD (enzymes inhibitors), presently, there are only three drugs (evolocumab, alirocumab, darapladib) that are clinically tested in patients with lipid metabolic disorders and CD. The application of evolocumab and alirocumab led to a statistically significant decrease in the level of Ch LDL and the risk of CD development (Kawashiri *et al.*, 2017; Karpov

and Talickij, 2015; Schmidt *et al.*, 2017; Karpov, 2017). The introduction of darapladib to the treatment plan did not show any significant progress in patients with CD (White *et al.*, 2014).

There are some data on the substances with anti-enzymatic activity towards IRE1 (Pavlova *et al.*, 2014), but there are no drugs developed.

Thus, there are some potential targets for the development of innovative AAD drugs that would exert the pathogenetic effect on the process of the development of AVD, and they, certainly, need further investigation.

4. CONCLUSION

Further development of pharmacotherapy for AS can be directed to the influence on the realization of adaptive (shift of cytokine profile to Th2 immune response) and congenital (enhancement of macrophages differentiation to M2 phenotype, regulation of lipid metabolism of macrophages) immune reactions, as well as on the activity of enzymes that play an important role in the metabolism of the immune cells and regulation of the lipid metabolism.

The analysis of the retrieved publications showed that new approaches to the pharmacotherapy of AS were based on different aspects of the theory of immunopathogenesis. According to the performed analysis, the most perspective new directions in the development of AS pharmacotherapy were the following:

- influence on the synthesis and effects of cytokines,
- inhibition, and induction of the activity of the enzymes that take part in the lipid metabolism of immune cells.

The results of the ongoing upscale studies give hope that the application of new AAD drugs in pathogenetic therapy for AS could reduce the risk of complications in patients with AVD.

5. ACKNOWLEDGMENTS

The results were obtained in the framework of the state tasks of the Ministry of Education and Science of the Russian Federation (task number 17.9545.2017 / CU).

6. REFERENCES

1. Kilessa, V.V. Atherosclerosis in the aspect of recapitulation. *Crimea Journal of Experimental and Clinical Medicine*, **2012**, 2(3-4), 17-22.
2. Kovalenko, V.N.; Talaeva, T.V.; Bratus' V.V. Cholesterol and atherosclerosis: traditional views and modern ideas. *Ukrainian Journal of Cardiology*, **2010**, 3, 7-35 (in Russian).
3. Karagodin, V.P.; Bobryshev, Ju.V.; Orehov, A.N. Inflammation, immunocompetent cells, cytokines – a role in atherogenesis. *Patogenez*, **2014**, 12 (1), 21-35.
4. Tedgui, A.; Mallat, Z. Anti-inflammatory mechanisms in the vascular wall. *Circ. Res.*, **2001**, 88(9), 877-887. doi: 10.1161/hh0901.090440.
5. Bespalova, I.D.; Rjazanceva, N.V.; Kaljuzhin, V.V.; Afanas'eva, D.S.; Murashev, B.Ju.; Osihov, I.A. Systemic inflammation in the pathogenesis of metabolic syndrome and associated diseases. *Siberian Medical Journal*, **2013**, 2, 5-9.
6. Alexopoulos, N.; Kaggi, D. Visceral adipose tissue AS a source of inflammation and promoter of atherosclerosis. *Atherosclerosis*, **2014**, 233(1), 104-112. doi: 10.1016/j.atherosclerosis.2013.12.023.
7. von Vietinghoff, S.; Ley, K. Interleukin 17 in vascular inflammation. *cytokine. Growth factor Rev.*, **2010**, 21(6), 463-469. doi: 10.1016/j.cytogfr.2010.10.003.
8. Ershova, O.B.; Belova, K.Ju.; Novikova I.V.; Baranov, A.A.; Nazarova, A.V.; Romanova, M.A. The role of cytokines in the development of cardiovascular osteoporosis and osteoporosis: review of the literature. *Osteoporosis and bone diseases*, **2011**, 3, 33-35 doi: 10.14341/osteo2011333-35.
9. Ait-Oufella, H., Taleb, S., Mallat, Z., Tedgui, A. Recent advances on the role of cytokines in atherosclerosis. *Arterioscler. Thromb. Vasc. Biol.*, **2011**, 3: 969-979. doi: 10.1161/ATVBAHA.110.207415.
10. Arabidze, G.G. Clinical immunology of atherosclerosis - from theory to practice. *Journal of Atherosclerosis and dyslipidaemias*, **2013**, 1, 4-19.
11. Sineglazova, A.V. Interleukin 1 β and coronary atherosclerosis in women with rheumatoid arthritis. *Sovremennye problemy nauki i obrazovaniya*, ISSN - 2070-7428, **2012**, 3, 64.
12. Shalenkova, M.A.; Muhametova Je.T.; Mihajlova, Z.D. Role of markers of necrosis and inflammation in predicting acute forms of coronary heart disease *Klinicheskaja medicina*, ISSN: 0023-2149, **2013**, 11, 14-19 (in Russian).
13. Fatkhullina, A.R.; Peshkova, I.O.; Koltsova, E.K. The role of cytokines in the development of atherosclerosis. *Biochemistry (Moscow)*, **2016**, 81(11), 1358-1370, doi: 10.1134/S0006297916110134.
14. Curtiss, L.K., Tobias, P.S.J. Emerging role of Toll-like receptors in atherosclerosis. *J. Lipid Res.*, **2009**, 50, 340-345, doi: 10.1194/jlr.R800056-jlr200.
15. Zaporozhec, T.S.; Majstrovskij, K.V.; Rapovka, V.G.; Ivanushko, L.A.; Smolina, T.P.; Gazha, A.K. Assessment of the systemic inflammatory response in patients with obliterating atherosclerosis of the vessels of the lower limbs. *Tihookeanskij medicinskij zhurnal*, **2012**, (1), 72-77.
16. Ramji, D.P.; Davies, Th.S. Cytokines in atherosclerosis: Key players in all stages of disease and promising therapeutic targets. *Cytokine & Growth Factor Reviews*, **2015**, 26, 673-685, doi:10.1016/j.cytogfr.2015.04.003.
17. Grivel, Zh.Sh.; Ivanova, O.I.; Pinegina, N.V.; Blank, P.S.; Shpektor, V.; Margolis, L.B.; Vasileva, E.Yu. A new method for analyzing the cellular composition of atherosclerotic plaques. *Creative Cardiology*, **2012**, 1, 26-40.
18. Profumo, E.; Buttari, B.; Tosti, M.E.; Tagliani, A.; Capiano, R.; D'Amati, G.; Businaro, R.; Salvati, B.; Riganò R.I.; Plaque-infiltrating T lymphocytes in patients with carotid atherosclerosis: an insight into the cellular mechanisms associated to plaque destabilization. *J Cardiovasc Surg (Torino)*, **2013**, 54 (3), 349-357.
19. Ragino, Jul.; Chernjavskij, A.M.; Polonskaja, Ja.V.; Volkov, A.M.; Kashtanova, E.V. The content of proinflammatory cytokines, chemoattractants and destructive metalloproteinases in different types of unstable atherosclerotic plaques. *Journal of Atherosclerosis and dyslipidaemias*, **2011**, 1, 23-27.

20. Ragino, Jul.; Chernjavskij, A.M.; Polonskaja, Ja.V.; Volkov, A.M.; Kashtanova, E.V. Activity of the inflammatory process in different types of unstable atherosclerotic plaques. *Bulletin of experimental biology and medicine*, **2012**, 153(2), 150-153, doi: 10.1007/s10517-012-1672-1
21. Shishkina, V.S.; Chelombit'ko, M.A.; Efremova, Ju.E.; Fedorov, A.V.; Il'inskaja, O.P.; Tararak, Je.M. Cytokines of the pro and anti-inflammatory subpopulations of macrophages and their significance in the formation and stabilization of atherosclerotic plaques in the carotid arteries of a person. *Russian cardiology bulletin*, **2014**, 9(4), 62–72.
22. Miossec, P. IL-17 and Th17 cells in human inflammatory disease. *Microbes Infect.*, **2009**, 11(5), 625-630, doi: 10.1016/j.micinf.2009.04.003.
23. Tang, M.; Fang, J. TNF- α regulates apoptosis of human vascular smooth muscle cells through gap junctions. *Molecular medicine reports*, **2017**, 15(3), 1407-1411, doi: 10.3892/mmr.2017.6106.
24. Popa, C.; van den Hoogen, F.H.J.; Radstake, T.R.; Netea, M.G.; Eijlbouts, A.E.; den Heijer, M.; van der Meer, J.W.; van Riel, P.L.; Stalenhoef, A.F.; Barrera, P. Modulation of lipoprotein plasma concentrations during long-term anti-TNF therapy in patients with active rheumatoid arthritis. *Ann. Rheum. Dis.*, **2007**, 66, 1503-1507, doi:10.1136/ard.2006.066191.
25. Geiler, J.; Buch, M.; McDermott, M.F. Anti-TNF treatment in rheumatoid arthritis. *Curr Pharm Des.*, **2011**, 17, 3141–3154, doi:10.2174/138161211798157658.
26. Tousoulis, D.; Oikonomou, E.; Economou, E.K.; Crea, F.; Kaski J.C. Inflammatory cytokines in atherosclerosis: current therapeutic approaches. *European Heart Journal*, **2016**, 37, 1723–1735, doi:10.1093/eurheartj/ehv759.
27. Avgerinou, G.; Tousoulis, D.; Siasos, G.; Oikonomou, E.; Maniatis, K.; Papageorgiou, N.; Paraskevopoulos, T.; Miliou, A.; Koumaki, D.; Latsios, G.; Therianiou, A.; Trikas, A.; Kampoli, A.M.; Stefanadis, C. Anti-tumor necrosis factor α treatment with adalimumab improves significantly endothelial function and decreases inflammatory process in patients with chronic psoriasis. *Int J Cardiol.*, **2011**, 151, 382–383, doi:10.1016/j.ijcard.2011.06.112.
28. Spinelli, F.R.; Di Franco, M.; Metere, A.; Conti, F.; Iannuccelli C.; Agati, L., Valesini G. Decrease of asymmetric dimethyl arginine after anti-TNF therapy in patients with rheumatoid arthritis. *Drug Dev Res.*, **2014**, 75(1), 67–69, doi:10.1002/ddr.21200.
29. Buono, C.; Come, C.E.; Stavrakis, G.; Maguire, G.F.; Connelly, Ph.W.; Lichtman, A.H. Influence of interferon γ on the extent and phenotype of diet-induced atherosclerosis in the LDLR-deficient mouse. *Arterioscler. thromb. Vasc. Biol.*, **2003**, 23, 454-460, doi:10.1161/01.atv.0000059419.11002.6e.
30. Liu, H.; Cheng, W.L.; Jiang, X.; Wang, P.X.; Fang, C.; Zhu, X.Y.; Huang, Z.; She, Z.G.; Li, H. Ablation of interferon regulatory factor 3 protects against atherosclerosis in apolipoprotein E-deficient mice. *Hypertension*, **2017**, 69(3), 510-517, doi:10.1161/hypertensionaha.116.08395.
31. Ouyang, W.; Kolls, J.K.; Zheng, Y. The biological functions of T helper 17 cell effector cytokines in inflammation. *Immunity*, **2008**, 28, 454-467, doi: https://doi.org/10.1016/j.immuni.2008.03.004.
32. Chen, S.; Shimada, K.; Zhang, W.; Huang, G.; Crother, T.R.; Arditi, M. IL-17A is proatherogenic in high-fat diet-induced and Chlamidia pneumonia infection-accelerated atherosclerosis in mice. *J. Immunol.*, **2010**, 185(9), 5619-5627, doi:10.4049/jimmunol.1001879.
33. Kozlov, V.A. Suppressor cells – the basis of immunopathogenesis autoimmune diseases. *Medical immunology*, **2016**, 18(1), 7-15, doi:10.15789/1563-0625-2016-1-7-14.
34. Erbel, C.; Chen, L.; Bea, F.; Wangler, S.; Celik, S.; Lasitschka, F.; Wang, Y.; Böckler, D.; Katus, H.A.; Dengler, T.J. *J Immunol.*, **2009**, 183, 8167–8175, doi: 10.4049/jimmunol.0901126.
35. Jerdes, Sh.F. Interleukin 17A is a new target of anti-cytokine therapy for ankylosing spondylitis. *Scientific and practical rheumatology*, **2016**, 54 (S1), 60-66.
36. Coimbra, S.; Santos-Silva, A.; Figueiredo, A. Brodalumab: an evidence-based review of its potential in the treatment of moderate-to-severe psoriasis. *Core Evidence*, **2014**, 9, 89–97, doi:10.2147/ce.s33940.

37. Lorenzatti, A.; Servato, M.L. Role of Anti-inflammatory interventions in coronary artery disease: understanding the canakinumab anti-inflammatory thrombosis outcomes study (CANTOS). *European Cardiology Review*, **2018**, 13(1), 38-41, doi:10.15420/ecr.2018.11.1.
38. Kawashiri, S.Y.; Kawakami, A.; Yamasaki S.; Imazato, T.; Iwamoto, N.; Fujikawa, K.; Aramaki, T.; Tamai, M.; Nakamura, H.; Ida, H.; Origuchi, T.; Ueki, Y.; Eguchi, K. Effects of the anti-interleukin-6 receptor antibody, tocilizumab, on serum lipid levels in patients with rheumatoid arthritis. *Rheumatol Int.*, **2011**, 31, 451-456, doi:10.1007/s00296-009-1303-y.
39. Protogerou, A.D.; Zampeli, E.; Fragiadaki, K.; Stamatelopoulos, K.; Papamichael, C.; Sfikakis, P.P. A pilot study of endothelial dysfunction and aortic stiffness after interleukin-6 receptor inhibition in rheumatoid arthritis. *Atherosclerosis*, **2011**, 219, 734-736, doi:10.1016/j.atherosclerosis.2011.09.015.
40. Bobryshev, Y.V.; Ivanova, E.A.; Chistiakov, D.A.; Nikiforov, N.G.; Orekhov, A.N. Macrophages and Their Role in Atherosclerosis: Pathophysiology and transcriptome analysis. *BioMed Research International*, **2016**, 2016, 1-13, doi:10.1155/2016/9582430.
41. Zhao, X.N.; Li, Y.N.; Wang, Y.T. Interleukin-4 regulates macrophage polarization via the MAPK signaling pathway to protect against atherosclerosis. *Genetics and molecular research*, **2016**, 15 (1), 2-9, doi:10.4238/gmr.15017348.
42. Chen, Y.; Liu, W.; Wang, Y.; Zhang, L.; Wei, J.; Zhang, X.; He, F.; Zhang, L. Casein kinase 2 interacting protein-1 regulates M1 and M2 inflammatory macrophage polarization. *Cellular signalling*, **2017**, 33, 107-120, doi: 10.1016/j.cellsig.2017.02.015.
43. Cardilo-Reis, L.; Gruber, S.; Schreier, S.M.; Drechsler, M.; Papac-Milicevic, N.; Weber, C.; Wagner, O.; Stangl, H.; Soehnlein, O.; Binder, C.J. Interleukin-13 protects from atherosclerosis and modulates plaque composition by skewing the macrophage phenotype. *Molecular Medicine*, **2012**, 4, 1072-1086, doi:10.1002/emmm.201201374.
44. Gabunia, K.; Ellison, S.; Kelemen, S.; Kako, F.; Cornwell, W.D.; Rogers, T.J.; Datta, P.K.; Ouimet, M.; Moore, K.J.; Autieri, M.V. IL-19 Halts progression of atherosclerotic plaque, polarizes, and increases cholesterol uptake and efflux in macrophages. *American Journal of Pathology*, **2016**, 186 (5), 1361-1374, doi:10.1016/j.ajpath.2015.12.023.
45. Herman, A.; Haines, D.; Autieril, M.V. The Anti-Inflammatory Cytokine IL-19 Reduces mRNA-stability protein HuR function in human vascular smooth muscle cells. *Conference materials «Experimental Biology Meeting»*, 2016, April 02-06, San Diego, CA.
46. Herman, A.B.; Vrakas, C.N.; Ray, M.; Kelemen, S.E.; Sweredoski, M.J.; Moradian, A.; Haines, D.; Autieri, M.V. FXR1 Is an IL-19-Responsive RNA-Binding Protein that Destabilizes Pro-inflammatory Transcripts in Vascular Smooth Muscle Cells. *Cell Rep*, **2018**, 24(5), 1176-1189, doi:10.1016/j.celrep.2018.07.002.
47. Gabunia, K.; Herman, A.B.; Ray, M.; Kelemen, S.E.; England, R.N.; DeLa Cadena, R.; Foster, W.J.; Elliott, K.J.; Eguchi, S.; Autieri, M.V. Induction of MiR133a expression by IL-19 targets LDLRAP1 and reduces oxLDL uptake in VSMC. *Journal of Molecular and Cellular Cardiology*, **2017**, 105, 38-48, doi:10.1016/j.yjmcc.2017.02.005.
48. Tian, Y.; Sommerville, L.J.; Cuneo, A.; Kelemen, S.E.; Autieri, M.V. Expression and suppressive effects of interleukin-19 on vascular smooth muscle cell pathophysiology and development of intimal hyperplasia. *Am J Pathol.*, **2008**, 173, 901-909, doi: 10.2353/ajpath.2008.080163.
49. Pavlova, O.V.; Moskovcev, A.A.; Klement'eva, T.S.; Myl'nikova, A.N.; Solov'eva, I.N. Suppression of ribonuclease IRE1 activity - a new approach in the treatment of certain types of cancer. *Uspekhi v himii i himicheskoy tekhnologii*, **2014**, XXVIII(9), 76-79 (in Russian).
50. Tufanli, O.; Akillilar, P.T.; Acosta-Alvear, D.; Kocaturk, B.; Onat, U.; Hamid, S.M.; Çimen, I.; Walter, P.; Weber, C.; Erbay, E. Targeting IRE1 with small molecules counteracts progression of atherosclerosis. *Proceedings of the national academy of sciences of the united states of America*, **2017**, 114(8), 1395-1404,

- doi:10.1073/pnas.1621188114.
51. Watson, A.D.; Berliner, J.A.; Hama, S.Y.; La Du B.N.; Faull, K.F.; Fogelman, A.M.; Navab, M. Protective effect of high density lipoprotein associated paraoxonase. Inhibition of the biological activity of minimally oxidized low density lipoprotein. *J Clin Invest.*, **1995**, 96(6), 2882-2891, doi:10.1172/jci118359.
 52. Whit, C.R.; Anantharamaiah, G.M. Cholesterol reduction and macrophage function: role of paraoxonases. *Current opinion in lipidology*, **2017**, 28(5), 397-402, doi:10.1172/jci118359.
 53. Kuharchuk, V.V.; Bazhan, S.S. Proprotein convertase subtilisin/kexin type 9 (PCSK9) – a regulator of low-density lipoprotein receptor expression]. *Journal of Atherosclerosis and dyslipidaemias*, **2013**, 2(11), 19-26.
 54. Kawashiri, M.A.; Nohara, A.; Higashikata, T.; Tada, H. Impact of evolocumab treatment on low-density lipoprotein cholesterol levels in heterozygous familial hypercholesterolemic patients withdrawing from regular apheresis. *Atherosclerosis*, 2017, 265, 225-230, doi: 10.1016/j.atherosclerosis.2017.09.011. Epub 2017 Sep 9.
 55. Karpov, Yu.A.; Talickij, K.A. Evolokumab - a representative of a new class of lipid-lowering drugs]. *Novosti kardiologii*, 2015, 4, 21-26.
 56. Schmidt, A.F.; Pearce, L.S.; Wilkins, J.T.; Overington, J.P.; Hingorani, A.D.; Casas, J.P. PCSK9 monoclonal antibodies for the primary and secondary prevention of cardiovascular disease. *Cochrane Database of Systematic Reviews*, 2017, 4, doi:10.1002/14651858.CD011748.pub2.
 57. Karpov, Yu.A. Evolocumab and regression of atherosclerotic lesion according to intravascular ultrasound of the coronary arteries. *Novosti kardiologii*, **2017**, 2, 2-9.
 58. Kuharchuk, V.V.; Tararak, E.H. Atherosclerosis: from A. L. Myasnikov to the present day. *Russian Cardiology Bulletin*, 2010, 5(17), 12-20.
 59. White, H.D.; Held, C.; Stewart, R.; Tarka, E.; Brown, R.; Davies, R.Y.; Budaj, A.; Harrington, R.A. (The stability investigators). Darapladib for preventing ischemic events in stable coronary heart disease. *N Engl J Med.*, **2014**, 370, 1702-1711, doi:10.1056/nejmoa1315878.

Table 1. Characteristics of new targets for the treatment of as and aad

Nº	Target	Drug	Used for therapy	The results of clinical studies in patients with AVD
1	TNF α	Infliximab Etanercept Adalimumab Golimumab	Rheumatoid arthritis, ulcerative colitis, ankylosing spondylitis, psoriasis	increased HDL level decreased atherogenic index, decreased endothelial dysfunction
2	IFN γ	—*	—	—
3	IRF3	—	—	—
4	IL-17A	Secukinumab Ixekizumab	Psoriasis, active ankylosing spondylitis	—
5	IL-17R	Brodalumab	Psoriasis	—
6	IL-1 β	Canakinumab	Acute podagric arthritis, juvenile idiopathic arthritis	decreased CRP and IL-6 levels decreased mortality rate from CD
7	IL-1Ra	Anakinra	Rheumatoid arthritis	decreased CRP and IL-6 levels decreased CD recurrence and mortality rate
8	IL-6	Tocilizumab	Rheumatoid arthritis	decreased LDL, and Ch LDL levels decreased improved endothelial function and decreased aortic stiffness
9	IL-13	—	—	—
10	IL-19	—	—	—
11	IRE1	—	—	—
12	PON	—	—	—
13	PCSK9	Evolocumab Alirocumab	Primary hyperlipidemia, hypercholesterinemia, mixed dyslipidemia	decreased Ch LDL level decreased risk of developing CD
14	Lp-PLA2	Darapladib	CD	decreased LDL level, decreased AP volume, decreased risk of developing CD, the general mortality rate

* – No information.

List of abbreviations:

AAD – anti-atherosclerotic drugs
ApoA-I – apolipoprotein A-I
ApoE – apolipoprotein E
AP – atherosclerotic plaques
AS – atherosclerosis
AVD – atherosclerotic vascular disease
CD – cardiovascular diseases
CRP – C-reactive protein
Ch – cholesterol
IL – interleukin
INF γ – interferon-gamma
IRE 1 – inositol-requiring enzyme 1
IRF3 – interferon regulatory factor
HDL – high-density lipoprotein
LDL – low-density lipoprotein
LDLR – low-density lipoprotein receptor
Lp-PLA2 – lipoprotein-associated phospholipase A2
MA – monoclonal antibody
PCSK9 – proprotein convertase subtilisin/Kexin type 9
PON – paraoxonase
Th – T-helper cells
TNF α – Tumor necrosis factor
VSMC – Vascular smooth muscle cell

EFEITO DO SELÊNIO NA ESTRUTURA SUPRAMOLECULAR E CARACTERÍSTICAS TÉRMICAS DA FIBROÍNA BOMBYX MORI L

THE EFFECT OF SELENIUM ON THE SUPRAMOLECULAR STRUCTURE AND THERMAL CHARACTERISTICS OF FIBROIN BOMBYX MORI L

ЭФФЕКТ СЕЛЕНА НА НАДМОЛЕКУЛЯРНОЙ СТРУКТУРЕ И ТЕПЛОВЫЕ ХАРАКТЕРИСТИКИ ФИБРОИН BOMBYX MORI L

SHUKURLU, Yusif H.*;

¹ Sheki Regional Scientific Center of the National Academy of Sciences of the Republic of Azerbaijan,
24 L. Abdullayev Str., zip code AZ 5500, Sheki – Azerbaijan Republic

* Correspondence author
e-mail: yusifsh@hotmail.com

Received 12 December 2019; received in revised form 20 February 2020; accepted 08 March 2020

RESUMO

O enriquecimento da estrutura molecular da fibroína da seda pelo átomo de selênio levou a um aumento na ramificação da macromolécula da fibroína. Como resultado, a fração amorfa da microfibrila da fibroína aumenta, o que leva a um aumento nas características de resistência do fio da seda. Ao mesmo tempo, essa mudança na estrutura supramolecular da fibroína envolvendo o átomo do selênio nos permitiu estudar o mecanismo de duas modificações para cristalização de microfibrilas da fibroína. Com base em estudos sobre o uso da análise gravimétrica térmica e análise de estrutura de raios X e as alterações relativas na proporção de regiões amorfas e cristalinas, chegamos à conclusão de que as microfibrilas da fibroína consistem principalmente em cristalitos com cadeias crescentes. Alternam-se ao longo do eixo da microfibrila com camadas amorfas, cujos tamanhos são menores que os tamanhos de cristalitos dobrados. Portanto, os cristalito dobrado não pode ser localizado em camadas amorfas entre os cristalitos com cadeias crescentes ao longo do eixo da microfibrila. Como resultado, a capacidade de dobrar seções ramificadas da macromolécula diminui, isto é, o CFC diminui. Isso aumenta a proporção de microfibrilas amorfas na fibroína. No modelo proposto pelos autores, segmentos da macromolécula não cristalizada na forma de cristalito com cadeias crescentes, localizada nas laterais do núcleo central e anexada a ele, restauram sua estrutura dobrada – na forma de dobras de uma placa de cristalitos.

Palavras-chave: *biodegradabilidade, domínios cristalinos, folha beta de Pauling-Corey, polímero, fios adjacentes.*

ABSTRACT

The enrichment of the molecular structure of silk fibroin by selenium atom led to an increase in the branching of fibroin macromolecule. As a result, the amorphous fraction of fibroin microfiber increases which leads to an increase in the strength characteristic of the silk thread. At the same time, this change in the supramolecular structure of fibroin involving a selenium atom has enabled us to study the two-modification mechanism for crystallizing fibroin microfibers. Based on studies on the use of temperature-gravimetric and X-ray diffraction (XRD) analysis and relative changes in the proportion of amorphous and crystalline regions, we came to the conclusion that fibroin microfibrils consist mainly of extended crystallites CSC – crystallites with the stretched chains. They alternate along the axis of microfiber with amorphous layers, the sizes of which are smaller than the sizes of the folded crystallites (CFC). Therefore, CFC cannot be located in amorphous layers between the CSC along the microfiber's axis. As a result, the ability to fold branched sections of the macromolecule decreases, that is, CFC decreases. This increases the proportion of amorphous areas of microfibers of the fibroin. In the model, which is proposed by author non-crystallized in the form of CSC, segments of a macromolecule, on the sides of the central core and attached to it, restored their crystal structure (CFC) – with folded conformation of chains.

Keywords: *silk fibroin microfibers, selenium enrichment, Pauling-Corey beta-sheet, biopolymer, crystallization with "shish-kebab" morphology, adjacent filaments.*

АННОТАЦИЯ

Обогащение молекулярной структуры фиброина шелка атомом селена привело к увеличению разветвленности макромолекулы фиброина. В результате аморфная фракция микроволокон фиброина увеличивается, что приводит к увеличению прочностных характеристик шелковой нити. В то же время это изменение надмолекулярной структуры фиброина с участием атома селена позволило нам изучить механизм двух модификаций для кристаллизации фиброиновых микроволокон. Основываясь на исследованиях по использованию температурно-гравиметрического и рентгеноструктурного анализа (РСА) и относительных изменений в пропорции аморфных и кристаллических областей, мы пришли к выводу, что фиброиновые микрофибриллы состоят в основном из протяженных кристаллитов КРЦ – кристаллитов с растянутыми цепями. Они чередуются вдоль оси микрофибры с аморфными слоями, размеры которых меньше размеров складчатых кристаллитов (КСЦ). Следовательно, КСЦ не может быть расположен в аморфных слоях между КРЦ вдоль оси микрофибры. В результате уменьшается способность складывать разветвленные участки макромолекулы, то есть снижается количество КРЦ. Это увеличивает долю аморфных участков микроволокон в фиброине. В модели, которая предложена авторам, некристаллизованные в виде КРЦ, сегменты макромолекулы, расположенные по бокам центрального ядра и прикрепленные к нему, восстанавливают их кристаллическую структуру (КСЦ) – при сложной конфигурации цепей.

Ключевые слова: микрофибриллы фиброина шелка, разветвление селеном, бета-лист Полинга-Кори, полимер, кристаллизация с морфологией «шашлык», смежные нити.

1. INTRODUCTION

At present, it has become possible to use silk fiber waste (SW) for the development of silk fibroin (SF) films that exhibit differentiated behavior in terms of biodegradability, mechanical strength, and other specific properties (Jaramillo-Quiceno *et al.*, 2017). The authors of (He *et al.*, 1999), are using new technology – foaming. Bombyx mori SF single crystals are obtained in metastable polymorph of silk I. They found that weak acidic conditions in the solution from which the foam was obtained contribute to the formation of silk II, while neutral to weak basic solutions contribute to the formation of silk I. During foaming, more dilute solutions contribute to the formation of silk II while more concentrated solutions (about 7 wt.% or more) contribute to the formation of silk I.

The author of (Fossey *et al.*, 1991) proposed a new model structure for the form of silk I, the crystalline domains of fibroin of silk Bombyx mori and also for the corresponding crystalline form of poly (L-Ala-Gly), which make up the structure of silk II. The main difference between the two structures is the orientation of the side chains of adjacent filaments in each sheet. In the Pauling-Corey beta-sheet and in the structure of silk II called the “register” structure, the Ala side chains of each strand point to the same side of the sheet. In the silk structure I, called the “off-register”, the side chains of Ala residues in adjacent strands point to opposite sides of the

sheet. Thus, according to the authors, some of the secondary structures obtained in the regenerated SF materials include crystalline and amorphous structures. Since crystalline structures include the dominant conformation of β -turns (silk I) and the insoluble structure formed by folded β -sheets (silk II).

The authors of (Jaramillo-Quiceno *et al.*, 2017) estimated the presence of crystalline (silk I and silk II) and amorphous structures by using XRD and Attenuated Total Reflection and Fourier Transform Infra-Red (ATR-FTIR) spectroscopy. The thermal properties of SF films were studied by DSC. According to the FTIR and XRD results, the presence of silk structure I in SF wastes is greater than in SF cocoons. Differences in the enthalpy of crystallization peaks on DSC curves show that SF cocoons have a higher content of amorphous structures than SF wastes, etc. It is known that SF is widely used to create three-dimensional matrices that contribute to the restoration of damaged organs and tissues, biodegradable cell carriers, drugs, etc. (Agapova, 2017). In this regard, our researchers continue to thoroughly study the structural features of this biopolymer.

Thus, we present our results obtained in the study of the effect of selenium on the molecular and supramolecular structures of silk fibroin. Note that in the mid-seventies of the last century, June Magoshi and Shigeo Nakamura investigated the thermal decomposition of SF (Jun Magoshi and Nakamura, 1975). It was shown that decomposition occurs with the formation of

endothermic and exothermic peaks. They explained that the endothermic shift observed at 448K on the DSC curve (curves on the differential scanning calorimetry) was due to the glass transition. The exothermic peak at 485K was recognized by them as crystallization, which was subsequently confirmed by XRD analysis. It was shown that the endothermic peak at 553K is a decomposition of the polymer.

Comparative changes in the supramolecular structure of fibroin microfibrils, ordinary and enriched selenium atoms were studied. At the same time, we used various research methods: we studied the accumulation of free radicals during deformation and irradiation of a silk thread with a full spectrum of an ultraviolet lamp with electron- paramagnetic absorption; we used the spin probe method to determine the degree of change in the proportion of amorphous and crystalline parts of microfibrils, the combined effects and impacts of ultraviolet radiation and selenium on fibroin structure. Also, we carried out tests for deformation strength, thermomechanical and electrical strength. We used differential scanning calorimetry, X-ray diffractometry and infrared spectroscopy to study the crystalline modifications of fibroin (Abdullaev *et al.*, 1978; Abdullaev *et al.*, 1980; Bakirov *et al.*, 1981a; Bakirov *et al.*, 1981b; Shukurov (Shukurlu) *et al.*, 1981). We found that when silk fibrin is enriched with selenium, selenium atoms actively enter to the primary structure of fibroin and change the supramolecular structure, that is, it leads to a change in the relative amounts of crystalline and amorphous sections of fibroin microfibrils.

In this paper, the effect of selenium on the supramolecular structure and the quantitative change in the modification of crystallites of fibroin *Bombyx mori* L. are summarized.

2. MATERIALS AND METHODS

The thermophysical properties of fibroin were studied on an OD-102 system derivatograph (VNR, MOM – Paulik-Paulik-Erdey derivatograph in platinum crucibles), which uses the derivative thermogravimetry (DTG) curve and thus, makes it possible to separate the superimposing thermal effects that are inseparable neither on the differential thermal analysis (DTA) nor on the thermogravimetric (TG) curves (Kadri *et al.*, 2017). A slight change in mass which is almost not observed on the thermogravimetric curves, can easily be detected by the peaks on the DTG curve. The DTG curve allows one to quantitatively determine the fraction of individual effects since

the minima – the horizontal sections of this curve – correspond to the lowest rate of change in mass, i.e., the boundary between the two effects. The thermogravimetric curve informs more accurately about the processes accompanied by a change in the mass of the test substance (Zhang *et al.*, 2017; Kostrobij *et al.*, 2018). Alumina calcined at 1270K was used as a reference. The atmosphere in the furnace is air, the initial temperature is room temperature, the heating rate is 10 deg/min, the sensitivity of the device: T (temperature) – 773K; thermogravimetric analysis (TGA) – 200; differential thermogravimetric analysis (DTGA) – 1/5; differential thermal analysis (DTA, which shares much in common with differential scanning calorimetry (DSC)) – 1/3. Weighed portions of fibroin amounted to 170mg, its crystalline part – 250mg (Shi *et al.*, 2018; Steffi *et al.*, 2018).

To assess the quantitative ratio of the two crystalline modifications and their sizes, we used DRON-2 stationary X-ray diffractometer (was released in 1978) with CuK α radiation with rectified voltage 37kV (λ = 0.154nm) which allowed us to measure the intensities of the XRD beam in a given direction and diffraction angle 2θ . The Debye-Scherrer method ("powder" method) was used for the XRD analysis of fibroin. As a sample, the powder of the crystalline part of fibroin was used.

3. RESULTS AND DISCUSSION:

The end effect on the DTA curve with a minimum of about 360K is observed for all samples and characterizes fibroin dehydration (Jun Magoshi and Nakamura, 1975; Xudayberdiyeva, 2009). The plateau with a fracture at 490K in the temperature range of 450-490K is caused by amorphous regions present in the structure, and its length for fibroin enriched with selenium (Figure 1b) is much larger than for the control (not enriched with selenium) sample (Figure 1a). This confirms the conclusion made above about the increase in the proportion of amorphous parts in experimental samples of fibroin. The exothermic peak of DTA which is about 550K (in the temperature range of 490-560K), characterizes the crystallization of molten amorphous parts of the polymer. In the initial stage of the melting of a polycrystalline substance, a two-phase state forms and the heat capacity sharply changes.

Therefore, an exothermic peak is revealed before the endo-melting effect (upon disordering). Such a peak is not clearly visible for fibroin (Figure 2), unlike its crystalline part (Figure 1). This is

probably due to the specificity of the ratio of the volume fraction of amorphous and crystalline sections of the polymer. From the very beginning of the creation of this method, specialists aimed to use DTA curves to determine quantitative ratios. Quantitative evaluations of the DTA curves were scientifically substantiated by the researchers Speil, Berkelgammer, Pask and Davis, and attempts to improve the method were reflected in the works of Kerr and Coop, Barshed, Berg, Feldvarine, Klibursky. Moreover, many researchers looked for reliable relationships between the height of the peak of the DTA curve and the content of the desired component in the sample.

Currently, the basis of the quantitative evaluation is the area bounded by the curves and the mainline. This method of quantification is correct, but it is very inaccurate and difficult. In practice, it turns out that a quantitative evaluation of DTA curves by this method can only be carried out with an accuracy not more than 5-10%. In addition, it is known that due to the DTA method, it is easy to establish the direction and magnitude of the change in enthalpy associated with chemical reactions and other processes occurring in the test substance under the influence of heat. On the other hand, by using the TGA method, it is possible to determine with high accuracy the nature and magnitude of the change in the mass of the polycrystalline sample material with an increase in temperature.

Due to the TGA curve, it is also possible to perform stoichiometric calculations or percentage calculations. Based on the listed possibilities of the mentioned methods, an idea emerged about their simultaneous use for studying the transformations in the matter that occur under the influence of elevated temperatures.

According to the TGA and DTGA curves, in the crystalline part of the fibroin enriched with selenium mass loss occurs more slowly (Figures 1b and 2b) than in the control one (not enriched with selenium) (Figures 1a and 2a). This is due to the stabilizing effect of selenium. A sharp kink is observed on the TGA curves of the crystalline part of fibroin for control samples at 570K, and on the DTA curves this is characterized by two minima at 560 and 580K. The observation of two minima for polymers in the melting region, in most cases, testifies to the presence of two types of crystallites in them – with the stretched chains (CSC) and with the folded chains (CFC) (Keller, 1967; Keller, 1968; Davidson and Wunderlich, 1969; Keller, 1975).

Based on this, it can be assumed that when a silkworm cocoon is produced, due to the influence of a filament stretch, pressure of the caterpillar spinneret, a peculiar structure of the silk-secreting part and a velocity gradient, the crystallization of fibroin occurs (an orientation process) which is accompanied by the formation of two modifications (bicomponent crystallization) – CSC and CFC.

With an increase in temperature in the chamber of a derivative gravimeter, the crystallites with elongated fibroin chains begin to break down first and after that the crystallites with folded chains. Thereby, the depth and width of the minimum DTGA of the low-temperature region corresponding to the destruction (disordering) of the CSC is much larger than the minimum of the CFC in the high-temperature region. In the case of fibroin enriched with selenium, the minimum corresponding to CFC almost disappears (Figure 2b). Therefore, when selenium is introduced into the structure of fibroin, the amount of CFC decreases, and due to this a predominant increase in the proportion of the amorphous part of the polymer occurs.

To obtain information on polymorphic crystallization, on the relative arrangement of various phases in microfibrils and their relative sizes in fibroin, we performed X-ray diffraction studies of fibroin (Shukurov (Shukurlu) *et al.*, 1981; Shukurlu, 1997). The object of the study was the crystalline part of the fibroin of the control and experimental samples. As a sample, the powder of the crystalline part of fibroin was used. In Figure 3, X-ray diffraction patterns are shown. It is seen that the intensity of the reflexes at 2θ which equal to 21.8; 24.4 and 37.2 degrees for fibroin enriched with selenium (curve 3b in Figure 3), is much less (Note that the reflex at 28.6 degrees matches with the reflection reflex of the glass cuvette of the X-ray diffractometer). In the remaining reflexes, noticeable differences are not observed. By comparing the results with thermal analysis and literature data (Lazarides, 1980; Monshi *et al.*, 2012), it can be stated that wide reflections correspond to crystallites with the stretched chains (CSC) while narrow reflections correspond to crystallites with folded chains (CFC).

Using the Scherrer formula that relates the size of small particles (crystallites) to the width of diffraction peaks, we determined only the size of crystalline particles of fibroin with an amorphous coating, such as this method is used to measure the size of polymer-coated nanoparticles (Shukurlu, 2006). As can be seen from Figure 3 the half-width of narrow reflexes is several times

smaller than that of wide reflexes ($\beta\text{CSC} = 0.103$; $\beta\text{CFC} = 0.016$). Consequently, the size of the CFC is almost ~ 6.5 times larger than that of the CSC ($\text{LCSC} = 1.366\text{nm}$; $\text{LCFC} = 8.821\text{nm}$). It is usually believed that the integrated intensity of reflexes is directly proportional to the number of corresponding regions. According to Figure 3, the area under wide reflexes is 15 times larger than the area under narrow reflexes. Consequently, the amount of CSC is significantly (approximately 15 times) greater than that of CFC.

4. CONCLUSIONS:

Based on X-ray diffraction analysis, it was found that the size of the CFC in the microfibril is 4.2 times larger than the size of the CSC, but their number is 15 times less. When selenium is introduced into the structure of fibroin, the number and size of CSC remain constant while the number of CFC decreases by 2.5 times (according to the area of the intensity of narrow reflexes) and as a result, the proportion of amorphous sites increases by 10%.

Thus, based on the above studies, it can be concluded that fibroin microfibrils are composed mainly of CSC. They alternate along the axis of microfibrils with amorphous layers which are smaller in size than the CSC. Therefore, the CFC cannot be located in amorphous layers i.e. between the CSC along the microfibril axis. This suggests that the formation of the fibroin fiber first forms a central core of crystallites with stretched chains (CSC). With the introduction of selenium into the structure of fibroin, new lateral branches are formed in the macromolecules, which cannot enter the crystal lattice at all. As a result, the ability to fold decreases, and (due to a decrease in the number of CFCs) the proportion of amorphous sites increases. Such a model of fibroin microfibrils is presented in Figure 4. At the lateral sides of this model, the non-crystallized segments of molecules included in the central core restore their folded structure (cross- β -shape). The crystallization of such segments of fibroin macromolecules occurs in the form of CFCs with the formation of microfibrils in the form of a structure called "micro shish-kebab".

5. REFERENCES:

1. Abdullaev, G. B., Bakirov, M. Ya., Mamedov, Sh. V., Shukurov (Shukurlu), Yu. G. *News of Azerbaijan SSR AS. Series of Physical and Technical and Mathematical Sciences*, **1980**, 2, 86-90.
2. Abdullaev, G. B., Bakirov, M. Ya., Mamedov, Sh. V., Shukurov, (Shukurlu), Yu. G. *Scientific reports of AN Azerbaijan SSR*, **1978**, 34(11), 20-24.
3. Agapova, O.I. *Modern technologies in medicine*, **2017**, 9(2), 192-204.
4. Bakirov, M.Ya., Mamedov, Sh.V., Shukurov, (Shukurlu) Yu.G. *Shelk*, **1981a**, 3, 16-17.
5. Bakirov, M.Ya., Shukurov (Shukurlu), Yu.G., Ismailova, R.S., Mamedov, Sh.V. *Shelk*, **1981b**, 4, 27-28.
6. Davidson, T., Wunderlich, B. *Journal of Polymer Science. Part A-2: Polymer Physics*, **1969**, 7, 2051-2059.
7. Fossey, S.A., Némethy, G., Gibson, K.D., Scheraga, H.A. *Biopolymers and Cell*, **1991**, 31(13), 1529-1541.
8. He, S.J., Valluzzi, R., Gido, S.P. *International Journal of Biological Macromolecules*, **1999**, 24(2-3), 187-195.
9. Jaramillo-Quiceno, N., Catalina Álvarez-López, C., Restrepo-Osorio, A. *Procedia Engineering*, **2017**, 200, 384-388. <https://doi.org/10.1016/j.proeng.2017.07.054>
10. Jun Magoshi, J., Nakamura, S. *Journal of Applied Polymer Science*, **1975**, 19(4), 1013-1015. <https://doi.org/10.1002/app.1975.070190410>.
11. Kadri, I., Derbel, M.A., Naïli, H., Roisnel, T., Rekik, W. *Chemical Papers*, **2017**, 71(11), 2063-2073.
12. Keller, A. *Journal of Polymer Science: Polymer Symposia*, **1975**, 51, 7-44.
13. Keller, A. *Reports on Progress in Physics*, **1968**, 31, 623-705.
14. Keller, A., Machin, M. J. *Journal of Macromolecular Science*, **1967**, B1, 41-91.
15. Kostrobij, P., Grygorchak, I., Ivashchyshyn, F., Markovych, B., Viznovych, O., Tokarchuk, M. *Journal of Physical Chemistry A*, **2018**, 122(16), 4099-4110.
16. Lazarides, E. *Nature*, **1980**, 283, 249-256.
17. Monshi, A., Foroughi, M. R., Monshi, M.R. *World Journal of Nano Science and Engineering*, **2012**, 2, 154-160. <http://dx.doi.org/10.4236/wjnse.2012.23020>
18. Shi, Y., Li, Z., Shi, J., Zhang, F., Zhou, X., Li, Y., Holmes, M., Zhang, W., Zou, X. *Sensors and Actuators, B: Chemical*, **2018**, 260, 465-474.

19. Shukurlu, Yu. G. *Some features of the supramolecular structure of silk fibroin*. Sheki: Sheki Regional Scientific Center of the National Academy of Sciences of Azerbaijan. Republic, **1997**.
20. Shukurlu, Yu.G. *Structural Proteins*. Baku: Elm, **2006**.
21. Shukurov (Shukurlu), Yu.G., Kerimov, T.M., Bakirov, M.Ya., Mamedov, Sh.V. *News of Azerbaijan SSR AS. Series of Physical and Technical and Mathematical Sciences*, **1981**, 1, 110-113.
22. Steffi, C., Wang, D., Kong, C.H., Wang, Z., Lim, P.N., Shi, Z., San Thian, E., Wang, W. *ACS Applied Materials and Interfaces*, **2018**, 10(12), 9988-9998.
23. Xudayberdiyeva, D. B. *Textile Industry Technology*, **2009**, 2(314), 56-61.
24. Zhang, X., Jia, C., Qiao, X., Liu, T., Sun, K. *Polymer Testing*, **2017**, 62, 88-95.

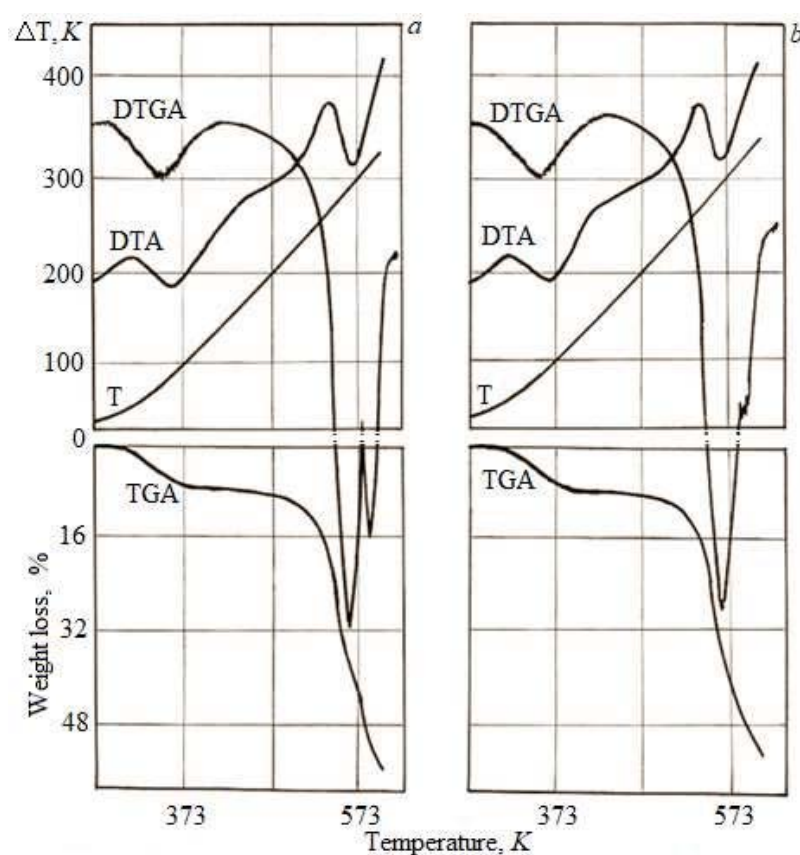


Figure 1. Derivative gravimetric crystalline curves parts of silk fibroin: a – for control (not enriched with selenium); b – for experimental samples

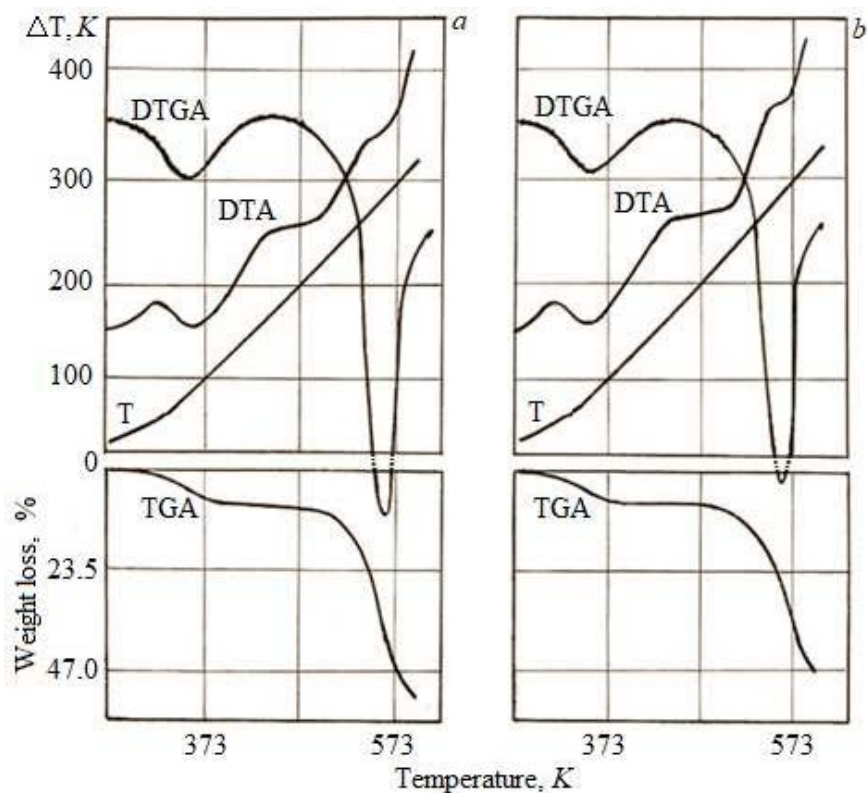


Figure 2. Derivative gravimetric curves of silk fibroin: *a* – for control (not enriched with selenium); *b* – for experimental samples

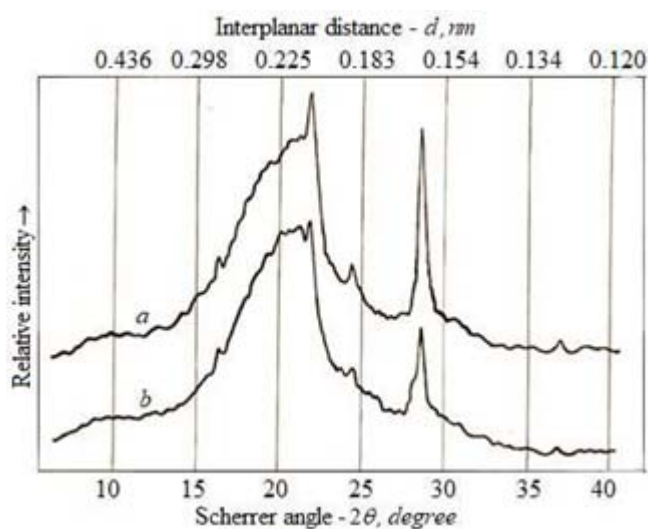


Figure 3. X-ray diffraction patterns of silk fibroin: *a* – for control (not enriched with selenium); *b* – for experimental samples

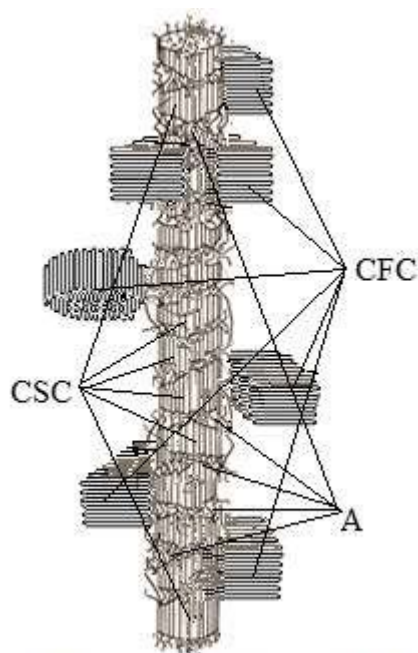


Figure 4. Packing model of silk fibroin macromolecules forming microfibrils: CSC – crystallites with the elongated chains; CFC – crystallites with the folded chains; A – amorphous sites

PATRIMÔNIO MATEMÁTICO DE AL-FARABI E UMA ABORDAGEM ALGORITMICA À SOLUÇÃO DE PROBLEMAS EM CONSTRUÇÕES GEOMÉTRICAS NO AMBIENTE GEOGEBRA**AL-FARABI'S MATHEMATICAL LEGACY AND ALGORITHMIC APPROACH TO RESOLVING PROBLEMS REGARDING GEOMETRICAL CONSTRUCTIONS IN GEOGEBRA ENVIRONMENT****МАТЕМАТИЧЕСКОЕ НАСЛЕДИЕ АЛЬ-ФАРАБИ И АЛГОРИТМИЧЕСКИЙ ПОДХОД К РЕШЕНИЮ ЗАДАЧ НА ГЕОМЕТРИЧЕСКИЕ ПОСТРОЕНИЯ В СРЕДЕ GEOGEBRA**

BIDAIBEKOV, Yessen^{1*}; GRINSHKUN, Vadim²; BOSTANOV, Bektas³; UMBETBAYEV, Kairat⁴; MYRSYDYKOV, Yerles⁵;

^{1,3,4} Abai Kazakh National Pedagogical University, Department of Informatics and Informatization of Education, 13 Dostyk Ave., zip code 050010, Almaty – Republic of Kazakhstan

² Moscow City University, Department of Informatization of Education, 4 Vtoroy Selskohoziastvenny Proezd, zip code 129226, Moscow – Russian Federation

⁵ Nazarbayev Intellectual School, 21/1 Hussein ben Talal Str., zip code 010000, Astana – Republic of Kazakhstan

* Correspondence author
e-mail: esen_bidaibekov@mail.ru

Received 22 December 2019; received in revised form 05 March 2020; accepted 09 March 2020

RESUMO

Al-Farabi deixou uma herança científica rica para as gerações futuras, incluindo pesquisas em vários campos da ciência. Atualmente seus trabalhos ainda são úteis, pois são de grande interesse para a comunidade científica. A relevância deste estudo, que se liga aos desenhos geométricos feitos por Al-Farabi para o ensino moderno de matemática e engenharia, reside no uso exclusivo da abordagem algorítmica para resolver problemas matemáticos e pesquisas aplicadas. Essas abordagens algorítmicas permitem criar as ferramentas de aprendizagem didáticos com base no uso da tecnologia de processamento de informações. Um dos princípios básicos de Al-Farabi é o estudo e a consideração da matemática em termos de fenômenos e processos naturais, bem como todos os tipos de sua implementação prática. Este artigo é dedicado ao estudo da herança matemática de Al-Farabi em relação a problemas geométricos de construção, bem como ao desenvolvimento de métodos para resolvê-los usando modernas tecnologias da informação, em particular, usando o sistema de geometria dinâmica GeoGebra, que é um ambiente para resolver problemas matemáticos projetado para estudar, transformar e visualizar os modelos geométricos de objetos. O artigo científico fornece os exemplos de solução de problemas de construção geométrica usando uma bússola matemática e uma régua, baseadas no algoritmo de construção geométrica de Al-Farabi. Os autores gostariam de familiarizar o público-alvo com os algoritmos desenvolvidos por Al-Farabi e sua implementação de software. Para isso, foi criado um portal científico e educacional para pesquisadores interessados, e os educadores podem encontrar muitas informações úteis e interessantes.

Palavras-chave: *herança matemática de Al-Farabi, GeoGebra, problemas de construção geométrica, trigonometria, portal educacional.*

ABSTRACT

Al-Farabi had left a rich scientific heritage for the succeeding generations including studies in various scientific areas. So far, his proceedings are still valuable being of great interest in the scientific society. The actuality of analyzing the problems with regard to geometric constructions accomplished by Al-Farabi for modern mathematical and engineering education lies in the unique character of Al-Farabi's efforts involving the use of the algorithmic approach for resolving mathematical problems and application-oriented researches. These algorithmic approaches enable the creation of didactic teaching techniques based on the use of information processing

technology. One of the main Al-Farabi's principles is to study and consider the mathematics in terms of natural phenomena and processes as well as all types of its practical implementation. This article pursues studying Al-Farabi's mathematical heritage concerning geometrical construction problems as well as the development of their solution methods using modern information technology, in particular, using the GeoGebra dynamic geometry system which is a problem-solving environment designed for studying, conversion and visualization of geometric object models. This scientific article shows examples of resolving geometric construction problems using only a mathematical compass and a ruler by the Al-Farabi's procedures as well as problems for dividing squares and spheres and giving Al-Farabi's visual evidence of proving Ptolemy's theory from trigonometry area. The authors are interested in a targeted audience to familiarize themselves with algorithms developed by Al-Farabi and this software implementation; for this purpose, a scientific-education portal has been designed for the concerned researches and pedagogues may find out a lot of useful and interesting information.

Keywords: Al-Farabi's mathematical heritage, GeoGebra, geometric construction problems, trigonometry, educational portal

АННОТАЦИЯ

Аль-Фараби оставил богатое научное наследие для будущих поколений, включая исследования в различных научных областях. И сегодня его труды по-прежнему ценны тем, что представляют большой интерес для научного общества. Актуальность данного исследования, которое связано с геометрическими конструкциями, выполненными Аль-Фараби для современного математического и инженерного образования, заключается в уникальном использовании алгоритмического подхода для решения математических задач и прикладных исследований. Эти алгоритмические подходы позволяют создавать дидактические средства обучения, основанные на использовании технологии обработки информации. Одним из основных принципов Аль-Фараби является изучение и рассмотрение математики с точки зрения природных явлений и процессов, а также всех видов ее практической реализации. Эта статья посвящена изучению математического наследия Аль-Фараби в отношении задач геометрического построения, а также разработке методов их решения с использованием современных информационных технологий, в частности, с использованием системы динамической геометрии GeoGebra, которая является средой решения математических задач, предназначенной для изучения, преобразования и визуализации геометрических моделей объектов. В научной статье приведены примеры решения задач геометрического построения с использованием циркуля и линейки, которые основаны на алгоритме геометрического построения Аль-Фараби. Авторы заинтересованы в том, чтобы целевая аудитория ознакомилась с алгоритмами, разработанными Аль-Фараби, и их программной реализацией. С этой целью был создан научно-образовательный портал для заинтересованных исследователей, и педагоги могут найти много полезной и интересной информации.

Ключевые слова: математическое наследие аль-Фараби, GeoGebra, проблемы геометрического построения, тригонометрия, образовательный портал.

1. INTRODUCTION

Al-Farabi was one of the founders of the social and philosophic Thoughts of the East, including Central Asia and the Republic of Kazakhstan. Following in Aristotle footsteps, Al-Farabi had studied many scientific areas and written a lot of valuable academic papers in which physics and mathematical studies are given due attention. Al-Farabi was one of the first commentators of Ptolemy's thesis, "Almagest" playing a big role in developing trigonometrical concepts and methods in the Mideast countries during the medieval period. The attractiveness of Al-Farabi's analysis of geometric construction problems in contemporary education (including mathematics and engineering) lies in the unique character of Al-Farabi's studies involving the use

of the algorithmic approach for resolving mathematical problems and their application-oriented specificity. These algorithmic approaches enable the creation of didactic teaching techniques based on the use of information processing technology. As for application-oriented specificity, one of the main features of Al-Farabi's studies is to study and consider the mathematics in terms of natural phenomena and processes as well as all types of its practical implementation (Bidaibekov *et al.*, 2017; Grinshkun *et al.*, 2019).

Many scientists from different countries have been studying Al-Farabi's heritage during this millennium representing a large scale and responsible job (Baya'a and Daher, 2013; Kamalova and Kiseleva, 2015). One of the followers is Audanbek Kubesov being a famous

scientist in the science and pedagogics area of the Islamic East. His monograph "Al-Farabi's mathematical heritage" (Kubesov, 1975a) is well known to scientific society, highly appraised by foreign researches of Al-Farabi's heritage (Kubesov *et al.*, 2015) being a great value as a scientific effort in which Al-Farabi's mathematical proceedings have been deeply, comprehensively and systematically studied. Kubesov was occupied in Al-Farabi's trigonometry and showed how to calculate values of trigonometric functions by a certain algorithm in a sexagesimal numerical system. He noted, "from the academic perspective the Al-Farabi's geometrical treatise is still actual for today. If processed and added in accordance with the requirements of contemporary pedagogical science, there is no doubt that this thesis becomes a particularly valuable tool to resolve construction problems for students studying in higher education institutes. It is certain that explanation of Al-Farabi's theory of geometric constructions using results of reduced problems will enable to improve the quality of student math training inasmuch as all Al-Farabi's geometric constructions problems are algorithmically represented".

Though Al-Farabi's scientific heritage has been studied for several centuries until the middle of the last century philosophical efforts of the great thinker were studied for the most part of study cases. Al-Farabi's heritage was accumulated and issued in 1972 under the name "Mathematical treatises of Al-Farabi". These mathematical treatises include five parts (Kubesov, 1975a; Salgozha, 2017), of which the second and the third parts are considered in this scientific article: "Book of attachments to "Almagest" including studies in trigonometry area; "Book of spiritual sophisticated techniques and natural secrets regarding peculiarities of geometric figures" (Kirichenko, 2005; Ziatdinov and Kabaca, 2010).

This scientific article is devoted to showing the ways of effective application of geometrical constructions and fundamental trigonometry described in the Al-Farabi's mathematical heritage via comparing them with the Kubesov's studies (Adler, 1940; Kubesov, 1975a; Pinaevskaya, 2012), taking into account achievements of contemporary theoretical mathematics applying advanced teaching methods and new information technologies. In this regard, the "GeoGebra" system is used with "Divider Compass", "Ruler" and "Pencil" are designed as tools with the function of their computer animation to show geometrical constructions reflecting acts "as in real life".

2. MATERIALS AND METHODS

2.1. E-learning modalities of teaching Al-Farabi's mathematical heritage

The results of studies of Al-Farabi's mathematical heritage are published on the scientific and educational portal "Al-Farabi's mathematical heritage" available through the link <http://al-farabi.kaznpu.kz>. In the future, it's planned to update the portal and translate it into different languages (Geiler, 1999; Ziatdinov, 2010; Rakhimzhanov *et al.*, 2015). E-Training Device (ETD) is described on the portal enabling to demonstrate the realistic performance of Al-Farabi's geometrical constructions in "GeoGebra" environment, i.e., there is an opportunity to show a step-by-step procedure of building constructions using a divider compass and a ruler: <http://al-farabi.kaznpu.kz/kz/page/93/#page>.

As a rule, geometrical problems regarding construction are resolved using the usual divider compass and a ruler, that is not provided in the "GeoGebra" environment (Meduov and Janaberdieva, 2016). Construction problems in the second part of this Article are resolved using "Divider Compass", "Ruler" and "Pencil" tools. "GeoGebra" is a universal environment designed for resolving academic and research problems, analysis, conversion and visualization of models of geometrical objects. Process of learning trigonometry using GeoGebra dynamical geometry is based on strengthening of theoretical knowledge through training with studying elements, modeling of geometrical forms and holding various experiments (Bidaibekov *et al.*, 2016d). Scientific and educational portal "Al-Farabi's mathematical heritage" covering fourteen trigonometric problems of Al-Farabi, provides for E-Training Device specifically designed to learn the Al-Farabi's trigonometry (Figure 1).

Now considering a process of animation of geometric constructions using "Divider Compass", "Ruler" and "Pencil" tools in the "GeoGebra" environment.

2.2. Animation of geometric constructions using "Divider Compass", "Ruler" and "Pencil" tools in "GeoGebra" environment

Functions of animating implementation of geometric constructions using a divider compass and a ruler are not realized in the "GeoGebra" environment. If there is a need for resolving problems related to construction, there is no opportunity to show a process of geometric

construction in the animation form, only the final results of geometric constructions may be demonstrated. It is worth noting that "GeoGebra" has options for creating macro objects in Javascript language which enables for expanding opportunities to create animation. Using algorithms to build regular polygons shown in Al-Farabi's mathematical treatises, it was analyzed the animation of a process of performing construction steps using (?) a divider compass and a ruler. Let's turn our attention to the stages of this process implementation. *Development of "Ruler", "Divider Compass" and "Pencil" tools:*

1. Development of "Ruler" tool. *Step 1.* Mark arbitrary points A and B and draw a straight line f through them. *Step 2.* Draw two circles c and d with centers of the circle in the points A and B and with equal radiuses (to be specific, let them be equal 2). Let's designate the points where these circles are crossing the straight line f , being on either sides of A and B, as C and D. *Step 3.* Draw line tangents c and d in the points C and D to the circles and mark points F and E on these line tangents at the same distance from the points C and D accordingly (to be specific let this be equal 1). *Step 4.* Draw a polygon (rectangle) CDEFC shaded in random colors (Figure 2). *Step 5.* Open menu "Tools → Create New Tool ...". *Step 6.* In the tab "Output Objects" choose "Quadrilateral g1: Polygon C, D, E, F" (Figure 3). *Step 7.* In tab "Input Objects" choose "Point A" and "Point B" (Figure 4). *Step 8.* Specify the tool name (tab "Name & Icon"), and it's calling command and finish the tool creation process.

2. Development of "Divider Compass" tool. To develop "Divider Compass" tool, the following procedure in "GeoGebra" environment shall be followed (Figure 5): *Step 1.* Points shall be chosen in such a way so that I and J ($I = (4, 8)$, $J = (14, 8)$), whereas coordinates of these points to be equal ordinates. The role of these two points is to determine two central points of the circles during the construction process. *Step 2.* Draw a line segment h connecting the points I and J. *Step 3.* Draw two circles k and p with centers in the points I and J with equal radiuses. Radiuses of these circles specify the divider compass width. *Step 4.* Draw lines i and j , perpendicular to the line segment h running through the points I and J. *Step 5.* Let's mark the points of contact of the circle k with the line i and the line segment h as K and L, accordingly. *Step 6.* Let's mark the junction points of the circle at P with the line j and the line segment h as N and M, accordingly. *Step 7.* Determine the middle points of the line segments KL and NM and mark them as points O and P, accordingly. *Step 8.*

Draw the lines l and m by the points I and O and points J and P, accordingly. *Step 9.* Identify the middle points of the line segments KO and NP and mark them as points Q and R, accordingly. *Step 10.* Draw lines n and q by the points Q and R parallel to the lines l and m . *Step 11.* Mark the crossing points of the lines n and m , q and l as S and T, accordingly and draw lines r and s through these points perpendicular to the line segment h . *Step 12.* Mark the crossing points of the lines r and s , n and m and q and l as points U, W, B_1 , and V, accordingly. *Step 13.* Draw a polygon through the points I, Q, S, and W. *Step 14.* Draw a polygon through the points J, B_1 , T, and P. *Step 15.* Draw a polygon through the points W, B_1 , U, and V.

As a result, a picture of divider compass shows up as follows: To convert the completed constructions in the tool, the same commands from the menu shall be performed as for the construction of "Ruler" tool (Tools/Create New Tool...). But here the points I and J shall be placed in the icon "Input Objects". The names of the polygons drawn in the last steps shall be indicated in the icon "Output Objects" (Courant and Robbins, 2001). Then enter its name "Asha" in the icon "Name and sign". Thereby a divider compass is converted into a tool to be used in macros.

3. Development of "Pencil" tool. To develop "Pencil" tool, first of all, the following procedure shall be carried out in "GeoGebra" environment (Figure 6):

Step 1. Mark the points K_1 and L_1 , with the same ordinates and connecting them with the line segment j_2 . *Step 2.* Mark the point M_1 on the line segment j_2 . *Step 3.* Draw circles p_2 and q_2 with the center in the point M_1 with different radiuses. The radius of circle q_2 specifies the pencil length, whereas the radius of circle p_2 specifies the pencil's tip height. *Step 4.* Draw the circle r_2 with the central point M_1 and the line l_2 , perpendicular to the line segment j_2 . *Step 5.* A polygon constructed through the points of crossing of the circle and the lines is the "Pencil" tool. The next step: by executing commands of converting into tools as in the previously described tool making procedures, the drawn picture (Figure 6) is converted in the "Pero" tool to be used in macros. As a result of executing the foregoing steps, the "Pero" tool is obtained.

Process of programming codes in macros animating the divider compass and the ruler is described below:

1. Process of programming. To use prepared in advance divider compass and ruler and pencil as animation in constructing actions, a

scenario shall be written in Javascript syntax. In this regard, any object may be outlined via executing the command "Object Properties" using the right mouse button, open the following icon (Figure 7). Whenever necessary, these functions (subprogram) written in the section "Global JavaScript" are animated through the programs written in the section "On Click".

2. *Animated execution of construction steps.* To begin with, let's place the buttons, as shown in the picture below, using standard options of the "GeoGebra" environment (Figure 8). Then, after pressing the button, the program code will be generated, which may open the function of the required constructing action.

3. RESULTS AND DISCUSSION:

Intensive math development in the East during IX-XV centuries preconditioned development of mathematical sciences in Europe in changing times. Academic papers of Eastern scientists hold a specific place in the Renaissance era in Europe. Abu Nasr Al-Farabi holds a special place among the scientists around this time. The majority of his precious academic papers is not preserved to the present day. In school books and encyclopedia of history released until now, they describe that elementary geometry and trigonometry were developing only in ancient Greece. In addition, Indian, Arabic, Uzbek mathematicians have made their contribution to the development of these math sciences. It is disappointing that the name of a great mathematician who made so many discoveries in mathematics studied and is one of the first scientists introducing such concepts as functions of sines and cosines, tangent and cotangent in the mathematics, the greatest scientist and thinker, the second Aristotle of the East, Abu Nasr Al-Farabi was not mentioned as a mathematician at all.

Mathematical papers of Al-Farabi were discovered during the 1950-1960 period in the archives of European countries and were mentioned in the academic papers of Mashanov, Kubesov (Kubesov, 1975a) as well as other scientists and became available in public for scientific society. However, in math school books, there are no references to the mathematical innovations discovered by him, particularly his "Mathematical treatises" (Kubesov, 1947). Al-Farabi has a large and systematized trigonometry developed out of the need for resolving various problems of mathematical astronomy and geography. These data are set forth in the

treatises of a great Greek astronomer Ptolemy "Book of attachments to Almagest" ("Almagest" is a treatise of a great Greek astronomer Ptolemy living in the 2nd-century a.d.) (Kubesov, 1975b). The importance of studies by mathematical treatises of Al-Farabi in foreign countries is proven by creating a digital copy (Kubesov, 1967) in the library of Michigan University in the USA. It's undeniable that this copy (digitalized on 11th of July 2007, contains 246 pages) owned by the University is one of the indications of its importance (Bidaibekov *et al.*, 2016c). Meanwhile, by no means unimportant, the fact of possessing a digitalized copy of the Al-Farabi's book "Mathematical Treatises" by Michigan University (digitalized on 1st of February 2010, contains 523 pages), published under the scientific supervision of A. Kubesov and also possessing of a digitalized copy of the Al-Farabi's book "Comments to Ptolemy's Almagest" by the University of California (digitalized on 27th of August 2008, contains 324 pages).

On the whole, the mathematical heritage of Al-Farabi and its realization in the "GeoGebra" environment are hard to cover within one scientific article limits. For this reason, it is consider expedient to focus on methods of geometrical constructions and trigonometry deemed to be the most interesting in Al-Farabi's scientific heritage (Bostanov and Umbetbaev, 2017).

3.1 Geometrical construction problems of Al-Farabi in GeoGebra environment

The teaching content of the geometric Figure construction algorithm is realized on the basis of the "Book of sophisticated spiritual techniques and natural secrets regarding peculiarities of geometric figures" in Al-Farabi's mathematical treatises. The book manuscript was borrowed from the library of Uppsala University, Sweden. Data regarding this Al-Farabi's manuscript were found out in the monographs of A. Kubesov being one of the first scientists who discovered this manuscript (Bidaibekov *et al.*, 2016a; Bidaibekov *et al.*, 2016c). The manuscript is written in the Arabic language. (Figure 9). The manuscript was translated into the Kazakh language within the framework of the research and development project devoted to studying the Al-Farabi's academic papers (Kubesov *et al.*, 2015).

All problems exemplified in the Book (Bidaibekov *et al.*, 2016c) are based on algorithms for constructing geometric figures using a divider compass and a ruler, the Book itself (Bidaibekov *et al.*, 2016c) comprises of the following sections

(Kubesov, 1975a): on locating the center. On defining the circle center; on drawing equal-sided figures; on the drawing, figures fit in a circle; on drawing a circle fit in Figure circle; on drawing a circle fit in figures; on the drawing, particular figures fit in other figures; on dividing triangles; on dividing quadrangles; on dividing and making squares; on dividing spheres.

In all these sections, geometrical construction problems were sorted out by from “simple to complicated” principle, showing readymade algorithms for geometrical construction to resolve more than a hundred problems. All these problems are presented with no proof. The presentation of problems in the algorithmic form simplifies the geometrical construction process in the “GeoGebra” environment. Let’s look into some of these problems below (Umbetbaev, 2015).

8th problem from the Third section “Methods of drawing figures fit in a circle”. Drawing an equilateral pentagon fit in a circle. Let’s define the point D as the circle center and draw its diameter line AC , further let’s draw the line DB perpendicular to the line segment AC . Divide AD into two halves at the point E . Let’s define the point E as the center and mark the point G at distance EB , mark the point F at distance BG , whereupon arc BF is obtained making one-fifth of the circle. Drawing arcs JF , JK , KH , and HB by arc length equal to BF , building line segments FB , BH , HK , KJ , JF , and an equilateral pentagon $BFJKH$ is obtained (Figure 10).

Analysis. Let’s assume that an equilateral pentagon is fit into a circle with the center located in the point D and radius BD , herewith $BD \perp AC$. In the problem of determining the sides of a regular pentagon, two additional circles are required to build.

Al-Farabi’s construction algorithm:

- 1) Draw a circle ($D; \forall R = BD$) $|D \in BD$;
- 2) $AC \perp BD$;
- 3) $E, E \in AC$, and $EA = ED$;
- 4) Circle $_1$ (E ; Equation 1);
- 5) Circle $_1 \cap AC = G$;
- 6) Circle $_2$ (B ; Equation 2);
- 7) Circle $_2 \cap$ Circle $_1 = F$ and K ;
- 8) BF – sought-for side of the pentagon and Equation 3 (these line segments shown in the picture are not equal);
- 9) let’s draw the rest sides without changing radius equaling to BF .
- 10) $BFNMK$ is the sought-for regular pentagon.

Proof. As follows from the formula for determining the radius of a regular pentagon with fit in a circle, Equation 4. So. Equation 5 Let’s designate the radius of the given circle as R , then Equation 6, where: Equation 7, \Rightarrow Equation 8, or Equation 9 (1). According to the drawing pattern, Equation 10 and Equation 11. The hypotenuse of a right-angled triangle Equation 12. As a radius by construction pattern: Equation 13. By the line segment measuring property: Equation 14; Equation 15.

The hypotenuse of right-angled triangle $\triangle BDG$: Equation 16 As a radius by construction pattern: Equation 17. Now it’s required to prove Equation 18. Let’s consider the right-angled triangle $\triangle BDF$, where the circumscribed circle has Equation 19. According to the Cosine Theorem, it is presented: Equation 20 or Equation 21 $\Rightarrow \dots$ Equation 22 \Rightarrow Equation 23 \Rightarrow Equation 24 \Rightarrow Equation 25 \Rightarrow Equation 26 \Rightarrow Equation 27. It means that (1) and (21-27) have equal left sides; therefore, their right sides are also equal: Equations 25–29. This is, which was to be proved (Kubesov, 1975a).

Note. The radius of the circle may be chosen randomly. In such a case, an unlimited number of pentagons may be constructed using the methods described above. These pentagons are equal to each other (according to the property of turning – conversion of motion). Therefore it is common to say that there is only one solution to this problem.

3rd problem from the sixth subsection “Methods for constructing other figures fit in certain other figures”. The third method for fitting a triangle into an equilateral rectangle. If you like, divide each of the lines AD and BC into halves at the points E and G , connect EG , and assume the point A as the center and draw an arc BH at distance AB . Draw the lines CF and AI equal to the doubled line GH . Draw the lines BI , BF , and FI ; it will be obtained an equilateral triangle BFI fit in the square $ABCD$ (Figure 11).

Construction algorithm:

1. Construct a square $ABCD$.
2. Divide the lines AD and BC into halves at the points E and G .
3. Connect point E with point G .
4. Assume the point A as the center; draw a circle with radius equaling AB .
5. Mark the point where the circle is crossing the line EG as H .
6. Beginning from the point A along the arc AD , mark the point I at a distance equaling $2GH$.
7. Beginning from the point C along the arc

CD mark the point F at a distance equaling $2GH$.

8. Connect the points B and I , B and F , F , and I with line segments.

The built triangle $\triangle BFI$ is an equilateral triangle fit in square $ABCD$.

Mathematical rationale: By construction design $\triangle ABI$ and $\triangle FCB$ are equal, therefore $\angle ABI = \angle FBC = 15^\circ$, it means that $\angle FBI = 60^\circ$ and inasmuch as the triangles are equal, Equation 30. It turns out that the built triangle $\triangle BFI$ is equilateral.

Analysis: line segment GH is the mean line of $\triangle BCF$, since by construction design Equation 31. For that reason, to fit the equilateral triangle in the given square, location of the point of crossing lines F with line BH and line segment CD , as well as the construction of an equilateral triangle by the line segment BF is an optional solution for this problem.

9th problem in the seventh subsection, "Triangle dividing methods." As for how to construct a triangle in the middle of triangle ABC similar to the latter and equaling its half by size or one third or otherwise, let's take the point D in its middle and connect points A and D , B and D and continue to draw the line AD in its direction towards the point E so that the line segment AE to be equal to a half of the line AD , or one third, or one fourth. Draw a semicircle on the line ED , restore a perpendicular line AG , and make the line DH equal to the line segment AG . The same procedure shall be done with other lines; as a result, was obtain the points H , F , and J . After connecting these points, it will be obtained a triangle HFJ constructed inside the triangle ABC , which is required to obtain (Figure 12).

Construction algorithm: As for how to construct a triangle in the middle of triangle ABC similar to the latter and equaling its half by size or one third or otherwise, the following procedure is provided:

1. Mark the point D in the middle of this triangle
2. Connect point A and point D
3. Connect point B and point D
4. Connect point D and point C
5. Continue the line AD towards point E , so that the line AE to be equal to a half or one third and one-fourth of the line AD .
6. Draw a semicircle along the line ED
7. Draw the perpendicular AG
8. Draw the line segment DH equal to the line segment AG .

After accomplishing this procedure with other lines, the points H , F and J are obtained.

Connect these points, and we will obtain the triangle HFJ which was required to fit into the triangle ABC .

Mathematical rationale: The right-angled triangle EDG is under study. Here the altitude drawn to the hypotenuse of the right-angled triangle will divide this triangle into similar triangles. Let's mark the line segment $AC = a$, $AB = b$, $\angle CAB = \alpha$. According to the given value, Equation 32. Equation 33 \rightarrow Equation 34, i.e., Equation 35; it follows by the Thales theory that Equation 36. As for the areas of the figures ABC and HFJ , Equations 37, 38. Equation 39 \rightarrow Equation 40 \rightarrow Equation 41. From here, it follows logically that the area of the triangle HFJ equals half of the triangle ABC . The same as proof of the triangle equaling to one third or other parts of it. This is which was to be proved.

15th problem in the eighth subsection "Rectangular dividing methods." As for how to divide in equal parts (parts equal by area) the parallelogram $ABCD$ by the line running through the point located outside, for example, the point E , then first of all A and C are connected, the line AC is divided into halves at the point G and the line EGF is drawn. Now the line EGF will divide the Figure $ABCD$ into equal halves see (Figure 13).

Construction algorithm: As for how to divide the parallelogram $ABCD$ into equal parts by the line running through the point located outside, for example, the point E , it's required to follow the procedure described below:

1. Draw the line segment AC .
2. Divide the line segment AC at point G in halves.
3. Draw the line EGF . Then the line EGF will divide the Figure $ABCD$ into halves.

Mathematical rationale: Let's mark the point of crossing the lines EF and AD as K : $EF \cap AD = K$. Subject to the second triangle equality feature, $\triangle AKG = \triangle GDH$: "If one side of the first triangle and two adjacent angles equal to the respective side and two adjacent angles of the second triangle, then these two triangles are equal in size; under the conditions of problem Equation 42; $\angle AGK = \angle CGF$ — vertical angles; $\angle GAK = \angle GCF$ — crossing angles. Then, $S_{AKG} = S_{CFG}$."

Subject to the second triangle equality feature, $\triangle ACD = \triangle CBA$: "If three sides of one triangle are equal to the respective three sides of the other triangle, then these triangles are equal in size; by parallelogram definition, its opposite sides are equal to each other whereas its diagonal is the

common side of both triangles". Then, $S_{ACD} = S_{CBA}$. So Equation 43, Equation 44. Then, $S_{KDCF} = S_{AKFB}$. This is which was to be proved. Now let's demonstrate algorithms for resolving particular problems regarding the construction of geometric figures in the "GeoGebra" environment.

7th problem in the ninth subsection "On dividing and arranging squares." If it is necessary to arrange a square out of ten equal squares, then ten will be composed of two squares, one of them – nine, its root – three and the other one – a unit with its side – unit. Let's divide them into halves along the diagonal. Four squares will be left out of the ten squares. Let's arrange a square using the four squares, locate it in the middle, and apply triangles to its sides. As a result, a square is obtained with each side is the hypotenuse of the triangle, i.e., the root often sees (Figure 14). By analogy, let's arrange one square out of seventeen equal squares (Figure 15).

6th problem in the tenth subsection "Sphere dividing methods". Procedure for dividing a sphere into four equal equilateral and equiangular triangles. How to divide a sphere into four equal triangles with equal sides and angles if the sphere diameter is already known? If the sphere diameter is the line segment AB , let's draw a semicircle on the line AB , draw the line AC equaling to a third of the line segment AB , draw the line CD perpendicular to the line AB ; this line crosses the semicircle ADB at the point D . Let's take a randomly chosen point E on the circle, assume it as the pole and draw the circle FGH at distance BD , divide it into three equal sectors at the points G, H, F and draw arcs of a bigger size running through the pole and each of the points G, H and F altogether crossing at the point I and draw arcs of a bigger size running through each two of the points G, H and F . Then it is obtained a sphere divided into four equal equilateral and equiangular triangles. These triangles are IHF, IHG, FIG , and GHF (Figure 16). *What's required to construct:* dividing a sphere into four equal regular spherical triangles. *Construction algorithm:* construction using Al-Farabi's method (Figure 17):

- 1) the sphere diameter equals to the line segment AB ,
- 2) draw a semicircle on the line segment AB ,
- 3) measure and draw the line segment A , equating to one-third of A , Equation 45;
- 4) draw the line segment CD in such a way so that $CD \perp AB$,
- 5) $(O; r = OD = OE) \cap CD \cap ADB = D$, here ADB – semicircle;

- 6) $\forall E \in$ belongs to the semicircle.
- 7) Circle $(E, \text{Equation 46}) \cap \text{Circle}_1 = FGH$,
- 8) Divide the Circle $_1$ at the points G, H, F into three equal parts;
- 9) draw circles of a bigger size through the center of this sphere J and also through each pair of the points G, H , and F ;
- 10) four equal regular spherical triangles JHF, JHG, FJG , and GHF – these are the sought-for figures.

Process dividing a sphere into four parts in 3D space in the "GeoGebra" environment is depicted in Figures 18, 19.

9th problem in the tenth section "Sphere dividing methods". With regard to dividing a sphere into twenty equal parts to obtain an equilateral and equiangular triangle. As for how to divide a sphere into twenty equal parts to obtain an equilateral and equiangular triangle, first of all, draw a big circle $ABCD$ with poles at the points H and G . Divide this circle into ten equal parts; these parts are $AB, BC, CD, DE, EF, FI, IK, KL, LM$, and MA . Let's determine the points A and B as the poles and draw two circles at a distance up until the arc BC from the side of H pole crossing each other at the point Z . Draw intercrossing circles from the side of H pole at the point Z . and from the side of G pole at the point Q in each of the ten parts of a big circle divided into ten equal parts. There will be five points from the side of H pole marked Z and five points from the side of G pole marked Q . Connect both these points, i.e., Z and Q to the arcs of the big circle. Ten triangles will appear with vertexes Z and Q and bases QQ and ZZ . Further, draw arcs of the big circle through each point Z and pole H , and through each point, Q and pole G . Five spherical triangles appear with vertex at the point H , and five spherical triangles appear with vertex at the point G . In such a manner, a sphere is divided into twenty equilateral and equiangular triangles (Figure 20).

What's required to construct: divide a sphere into twenty equal parts being regular spherical triangles. *Construction algorithm:* construction using Al-Farabi's method (Figure 21):

1. First, draw a big circle of $ABCD$ sphere with poles at the points H and G (extreme points of diameter):
2. Divide this circle into ten equal parts; these parts are: $AB, BC, CD, DE, EF, FI, IK, KL, LM$, and MA ;
3. Points A and B are assumed to be the poles and draw two circles at a distance up until the arc BC from the side of H pole crossing each other at the point Z ;

4. Points *B* and *C* are assumed to be the poles and draw two circles at a distance up until the arc *BC* from the side of *G* pole crossing each other at the point *Q*;

5. Draw intercrossing circles from the side of *H* pole at the point *Z*. and from the side of *G* pole at the point *Q* in each of the ten parts of a big circle divided into ten equal parts.

6. There will be five points from the side of *H* pole marked *Z* and five points from the side of *G* pole marked *Q*;

7. Connect *Z* and *Q* to arcs of the big circle;

8. Ten triangles will appear with vertexes *Z* and *Q* and bases being *QQ* and *ZZ* lines;

9. Draw arcs of the big circle through each point *Z* and pole *H* and through each point *Q* and pole *G*;

10. Five spherical triangles appear with vertex at the point *H*, and five spherical triangles appear with vertex at the point *G*.

11. These twenty regular spherical triangles lying on the sphere surface are the sought-for figures.

3.2 Al-Farabi's trigonometry in "GeoGebra" environment

Al-Farabi was one of the first commentators of "Almagest" in the Eastern countries during the medieval period. His "Book of attachments" enclosed to the treatise "Comments to Ptolemy's Almagest" preserved as a unique manuscript. So far, both these treatises have not been republished in other languages or studied. The teaching content of Al-Farabi's trigonometry is identified by "Mathematical treatises of Al-Farabi" based on Chapters of the treatise "Comments to Almagest" or Al-Farabi's "Book of attachments" where, in particular, basic trigonometric notions and calculations are considered, i.e., in its first Chapter containing trigonometric data of "Almagest" cited from thirteen books (Bidaibekov *et al.*, 2016c).

Ptolemy's "Almagest" and the hand-written variant of Al-Farabi's Comments to Ptolemy's Almagest" are kept in the British Museum of London (No. 7474, No. 7368). Accuracy of the discovered data (Kubesov, 1947) enabled us to find and acquire access to the original of this manuscript written in the Arabic language. Figure 22 shows the "Almagest" book cover and start page (Bidaibekov *et al.*, 2017).

Al-Farabi has rather developed trigonometry created by him due to the need for developing mathematical methods required for resolving problems in mathematical astronomy and geography. Al-Farabi was one of the first

commentators of the "Almagest" book. His "Book of attachments" (كتاب اللواحق – Book of attachments), enclosed to the treatise "Comments to Almagest" (شرح المجستي – Explain the Tentacle) preserved as the only one hand-written manuscript in the British Museum of London (Bidaibekov *et al.*, 2016d).

Trigonometry issues are considered by Al-Farabi in his first book "Comments to Almagest" Al-Farabi slightly upgraded Ptolemy's trigonometry system to facilitate understanding of complicated mathematical manipulations encountered everywhere (in the comments to Almagest), replacing chords by sines and designating a sine as half of the doubled chord. For example, if *BD* – arc chord, $BD = 2a$ (Figure 23), then *BC* – line value of arcsine $AB = \alpha$, that is Equation 47. Therefore Al-Farabi, while citing "Almagest" has been continuously replacing arc chord 2α by arcsine α throughout the text. Though such a replacement as it is doesn't look so significant, however, the transition from chord to semi-chord facilitated a large scale implementation of various trigonometric functions in astronomy such as cosine, tangent, cotangent related to sides and angles of a right-angled triangle fit in the circle.

It is worth noting that a special training course for Al-Farabi's trigonometry organized on the basis of "Nazarbayev Intellectual School of Chemistry and Biology" as an optional course to "Math" subject includes teaching how to resolve Al-Farabi's geometrical construction problems using universal interactive mathematical package "GeoGebra". Students learned how to use the acquired knowledge in academic research activity and held top places in a scientific competition among Almaty city school students. This fact evidences the obvious need for using information and communication technology while learning how to resolve geometrical construction problems and trigonometric problems.

It is understood that school students in their prevailing majority are reluctant to study math curriculum subjects. One of the reasons leading to such reluctance is the conservative approach used for teaching math subjects. During recent years, noticeable changes have been observed in the process of teaching many other subjects, including the newest information technologies and instructional design theory motivating students to study into school themes and making them more interesting. However abstractive nature of trigonometric notions makes information technologies quite difficult to use since before applying such technologies, the students lack

basic knowledge about mathematical concepts (Kubesov, 1975b).

In this regard, during recent years, interactive mathematics environments, which are computer software applications providing an animation of changing certain mathematical objects, are being actively used. "GeoGebra" dynamic geometry system provides for not only geometrical illustrations as visual aids for effective understanding of problem solutions but also most important, ensures wide range and purposeful application of such visual aids in cognitive activity being a cognitive-visual method in forming knowledge, skills, and know-how available for the students (Bidaibekov *et al.*, 2016b). For example, while proving the well known Ptolemy's theory, Al-Farabi argues as follows: "in each quadrangle with circumscribed circle multiplication of each of opposite sides by another if summed will be equal to multiplication of the quadrangle's diagonals", i.e., if quadrangle $ABCD$ is fit into a circle, then: Equation 48 (Figure 24).

The liveliness of the object created in the "GeoGebra" environment, the opportunity to visualize all acquired findings while proving facilitates its study. This shows the effectiveness of using the "GeoGebra" environment for teaching Al-Farabi's trigonometry. At changing positions of the points B and C along the circle as shown in Figure 24, one can notice that the line segments EF and GH change to the same extent. This is visual proof of the correctness of Al-Farabi's formulation. Apart from the mentioned options, interactive mathematical packages also have other opportunities, such as alteration of line type and color, demonstration of the movement pattern of geometrical objects (Kamalova *et al.*, 2016).

4. CONCLUSIONS

As for the uniqueness of Al-Farabi's efforts, one can notice his researches carried out in applied areas using an *algorithmic approach*, which, in the author's opinion, enables to create didactic e-learning aids for studying fundamental geometry. It should also be stated that research and methodological studies with regard to opportunities, methods, and techniques for implementation of Al-Farabi's mathematical heritage collected and systematized by Kubesov in today's mathematical education system just began and inadequate so far.

The authors believe that systematized trigonometry set forth in emerging from the need for resolving various problems of mathematical astronomy and geography; first comments to

Ptolemy's "Almagest" book written by of Al-Farabi; methods for dividing figures into several components without using a divider compass and a ruler; calculation of $\sin 1^\circ$ value and resolving other problems will be interesting for students studying mathematics. As for Al-Farabi's algorithms, the authors can only hope that they will be useful at studying the construction of geometrical figures using a divider compass and a ruler and also promote expanding the limits of knowledge on geometrical constructions in the scholar geometry curriculum.

6. REFERENCES:

1. Adler, A. *Theory of geometric constructions*. Leningrad: Uchpedgiz, **1940**.
2. Baya'a, N.F., Daher, W.M. *International Journal of Emerging Technologies in Learning (IJET)*, **2013**, 8(1), 46-51.
3. Bidaibekov, Ye., Kamalova, G., Bostanov, B., Umbetbaev, K. Information technology in teaching mathematical heritage of Al-Farabi. In: *CEUR Workshop Proceedings (CEUR-WS.org): Selected Papers of the XI International Scientific-Practical Conference Modern Information Technologies and IT Education (SITITO 2016)*. Moscow: Lomonosov Moscow State University, **2016a**, 426-439.
4. Bidaibekov, Ye., Kamalova, G., Bostanov, B.G., Umbetbaev, K.U. 2016. Geometric heritage of Al-Farabi in education. In: A. Ashyralyev (Ed.). *Third International Conference on Analysis and Applied Mathematics (ICAAM 2016)*. Almaty: Institute of mathematics and mathematical modeling, **2016b**, 426-439.
5. Bidaibekov, Ye.Y., Kamalova, G.B., Bostanov, B.G., Salgozha, I.T. 2017. On teaching techniques available for students to learn Al-Farabi's mathematical heritage during after class time. In: *Proceedings of IX International Scientific and Methodical Conference "Info – Strategy 2017: Community. State. Education"*. Samara: OOO "Knizhnoye Izdatel'stvo", **2017**, 270-275.
6. Bidaibekov, Ye.Y., Kamalova, G.B., Bostanov, B.G., Umbetbaev, K.U. *Al-Farabi's trigonometric heritage*. Almaty: Kazakh National Pedagogical University after Abai, **2016c**.
7. Bidaibekov, Ye.Y., Oshanova, N.T., Torebekova, R.K. *Annals of Kazakh National*

- Pedagogical University after Abai. Series "Physico-mathematical sciences", 2016d, 4(56): 44-50.*
8. Bostanov, B.G., Umbetbaev, K.U. Using Al-Farabi's mathematical heritage in teaching "GEOGEBRA" environment program. In: *Proceedings of International Scientific and Methodical Conference "Actual problems and tendencies of innovations in today's science and education dedicated to the 60th anniversary of professor T.A. Turmambekov"*. Turkistan: Akhmet Yassawi International Kazakh-Turkish University, **2017**, 39-43.
 9. Courant, R. Robbins, G. *What is mathematics?* Moscow: MTSNMO, **2001**.
 10. Geiler, V.A. *SJE*, **1999**, 12, 115-118.
 11. Grinshkun, V., Bidaibekov, E., Koneva, S., Baidrakhmanova, G. *European Journal of Contemporary Education*, **2019**, 8(1), 25-42.
 12. Kamalova, G.B., Bostanov, B.G., Umbetbaev, K.U. On using computer program "GeoGebra" for teaching Al-Farabi's mathematical heritage. In: *Proceedings of I-st International Scientific and Methodical Conference "Informational support for education and e-learning methods – 2016"*. Krasnoyarsk: SFU, **2016**, 199-204.
 13. Kamalova, G.B., Kiseleva, Ye.A. *Al-Farabi's geometrical heritage for applying in today's education: Teaching aid*. Almaty: Kazakh National Pedagogical University after Abai, **2015**.
 14. Kirichenko V. *Compasses and ruler Construction and Galois theory*. Dubna: Summer school "Modern mathematics", **2005**.
 15. Kubesov, A. (Ed.). *Al-Farabi's Comments to Ptolemy's "Almagest" book*. Alma-Ata: Dj Al Dabbagh, **1975b**.
 16. Kubesov, A. *Education and Labor*, **1967**, 1, 10-12.
 17. Kubesov, A. *Math in School?* **1975a**, 5, 46-48.
 18. Kubesov, A., Bidaibekov, Ye.Y., Bostanov, B.G., Bilal, Sh., Umbetbaev, K.U. *Geometrical construction problems*. Almaty: Kazakh National Pedagogical University after Abai, **2015**.
 19. Kubesov, A.K. *Al-Farabi's mathematical heritage*. Alma-Ata: Science, **1947**.
 20. Meduov, E.U., Janaberdieva, S.A. *Materials of the I International scientific and practical conference "Science of the XXI century-a look into the future"*, Stavropol: Logos, **2016**, 110-114.
 21. Pinaevskaya, T.A. The use of ICT technologies in mathematics lessons. In: *Pedagogical skills: materials of the II international conference*. Moscow: Buki-Vedi, **2012**.
 22. Rakhimzhanov, Ye.Ye., Zhaksylykov, A.Ye., Umbetbaev, K.U. On designing e-teaching aids by Al-Farabi's geometrical heritage and educational portal. In: *Proceedings of VII International Scientific and Methodical Conference "Mathematical modeling and information technologies in education and science" (MM ITES) dedicated to the 70th anniversary of professor Bidaibekov Ye.Y and 30th anniversary of school arithmetic*. Almaty: KazNPU named after Abai, Publishing House "Ulagat", **2015**, 519-522.
 23. Salgozha, I.T. *Materials of international scientific-practical conference "Actual problems and trends of innovation in modern science and education"*. Turkistan, **2017**, 478-481.
 24. Umbetbaev, K.U. Review of Al-Farabi's geometrical heritage. In: N.I Pak (Ed.). *Youth and science of XXI century: XVI Russian-wide (with international participation) academic and research forum for students, Ph.D. candidates and young scientists: Proceedings of Russian-wide youth Conference (with international participation) "Innovative aids and teaching methods in the area of information and communication technology"*. Krasnoyarsk: Krasnoyarsk State Pedagogical University after V.P. Astafyev, **2015**, 254-258.
 25. Ziatdinov, R. *Geometric modelling and projective geometry problems with Geogebra*. 2010.
https://www.researchgate.net/publication/270447932_Geometric_modelling_and_projective_geometry_problems_with_Geogebra, accessed January 2020.
 26. Ziatdinov, R., Kabaca, T., *3rd International Conference on "Innovations in Learning for the Future 2010: e-Learning" (First Eurasia Meeting of GeoGebra (EMG))*, Istanbul, **2010**, 128-143.

$$r_1 = EB \quad (\text{Eq. 1})$$

$$r_2 = BG \quad (\text{Eq. 2})$$

$$F = BK \quad (\text{Eq. 3})$$

$$R = \frac{a_n}{2 \sin \frac{180^\circ}{n}}, \quad (\text{Eq. 4})$$

$$R = \frac{a_5}{2 \sin \frac{180^\circ}{5}} = \frac{a_5}{2 \sin 36^\circ} \quad (\text{Eq. 5})$$

$$R = \frac{a_5}{2 \sin 36^\circ} \quad (\text{Eq. 6})$$

$$a_5 = 2R \sin 36^\circ \quad (\text{Eq. 7})$$

$$\sin 36^\circ = \frac{a_5}{2R} \quad (\text{Eq. 8})$$

$$\sin \frac{\angle BDF}{2} = \frac{a_5}{2R} \quad (\text{Eq. 9})$$

$$DB = R \quad (\text{Eq. 10})$$

$$ED = \frac{R}{2} \quad (\text{Eq. 11})$$

$$\triangle BDE \quad BE = \sqrt{R^2 + \left(\frac{R}{2}\right)^2} = \frac{R\sqrt{5}}{2}; \quad BE = \frac{R\sqrt{5}}{2}. \quad (\text{Eq. 12})$$

$$EG = BE; \Rightarrow EG = \frac{R\sqrt{5}}{2} \quad (\text{Eq. 13})$$

$$DG = EG - ED = \frac{R\sqrt{5}}{2} - \frac{R}{2}; \quad (\text{Eq. 14})$$

$$DG = R \cdot \frac{\sqrt{5}-1}{2} \quad (\text{Eq. 15})$$

$$BG = \sqrt{R^2 + \left(R \frac{\sqrt{5}-1}{2}\right)^2} = \sqrt{\frac{4R^2 + R^2(5-2\sqrt{5}+1)}{4}} = \frac{\sqrt{10R^2 - 2R^2\sqrt{5}}}{2} = \frac{R}{2} \sqrt{10 - 2\sqrt{5}} \quad (\text{Eq. 16})$$

$$BF = BG = \frac{R}{2} \sqrt{10 - 2\sqrt{5}} \quad (\text{Eq. 17})$$

$$a_5 = \frac{R}{2} \sqrt{10 - 2\sqrt{5}} \quad (\text{Eq. 18})$$

$$BD = DF = R \quad (\text{Eq. 19})$$

$$BF^2 = DB^2 + DF^2 - 2DB \cdot DF \cdot \cos \angle BDF \quad (\text{Eq. 20})$$

$$\frac{R}{2} \sqrt{10 - 2\sqrt{5}}^2 = R^2 + R^2 - 2 \cdot R \cdot R \cdot \cos \angle BDF \quad (\text{Eq. 21})$$

$$\left(\frac{R}{2} \sqrt{10 - 2\sqrt{5}}\right)^2 = 2R^2(1 - \cos \angle BDF) \quad (\text{Eq. 22})$$

$$\left(\frac{R}{2} \sqrt{10 - 2\sqrt{5}}\right)^2 = 2R^2 \cdot 2 \cdot \frac{1 - \cos \angle BDF}{2} \quad (\text{Eq. 23})$$

$$\left(\frac{R}{2}\sqrt{10-2\sqrt{5}}\right)^2 = 4R^2 \cdot \sin^2 \frac{\angle BDF}{2} \quad (\text{Eq. 24})$$

$$\frac{R}{2}\sqrt{10-2\sqrt{5}} = 2R \cdot \sin \frac{\angle BDF}{2} \quad (\text{Eq. 25})$$

$$\sin \frac{\angle BDF}{2} = \frac{\frac{R}{2}\sqrt{10-2\sqrt{5}}}{2R}; \quad (\text{Eq. 26})$$

$$\sin \frac{\angle BDF}{2} = \frac{\sqrt{10-2\sqrt{5}}}{4} \quad (\text{Eq. 27})$$

$$\frac{a_5}{4} = \frac{\sqrt{10-2\sqrt{5}}}{4} \quad (\text{Eq. 28})$$

$$a_5 = \sqrt{10-2\sqrt{5}}. \quad (\text{Eq. 29})$$

$$BF=BI \quad (\text{Eq. 30})$$

$$CF=2GH. \quad (\text{Eq. 31})$$

$$AE = \frac{1}{2}AD. \quad (\text{Eq. 32})$$

$$\frac{EA}{AG} = \frac{AG}{AD} \quad (\text{Eq. 33})$$

$$AG = \frac{AD}{\sqrt{2}}, \quad (\text{Eq. 34})$$

$$DH = \frac{AD}{\sqrt{2}} \quad (\text{Eq. 35})$$

$$HJ = \frac{AB}{\sqrt{2}} \quad (\text{Eq. 36})$$

$$S_{ABC} = \frac{1}{2}AC \cdot AB \cdot \sin \angle CAB \quad (\text{Eq. 37})$$

$$S_{ABC} = \frac{1}{2}a \cdot b \cdot \sin \alpha; \quad (\text{Eq. 38})$$

$$S_{HFJ} = \frac{1}{2}AG \cdot AH \cdot \sin \angle CAB \quad (\text{Eq. 39})$$

$$S_{HFJ} = \frac{1}{2} \frac{a}{\sqrt{2}} \cdot \frac{b}{\sqrt{2}} \cdot \sin \alpha \quad (\text{Eq. 40})$$

$$S_{HFJ} = \frac{1}{4}a \cdot b \cdot \sin \alpha \quad (\text{Eq. 41})$$

$$G = GC \quad (\text{Eq. 42})$$

$$S_{KDCF} = S_{ACD} - S_{AKG} + S_{CFG} = S_{ACD} \quad (\text{Eq. 43})$$

$$S_{AKFB} = S_{CBA} + S_{AKG} - S_{DFG} = S_{CBA} \quad (\text{Eq. 44})$$

$$AC = \frac{1}{3}AB \quad (\text{Eq. 45})$$

$$r=BD \quad (\text{Eq. 46})$$

$$\sin \alpha = \frac{1}{2} \cdot chd 2\alpha. \quad (\text{Eq. 47})$$

$$AD \cdot BC = AC \cdot BD - AB \cdot CD \quad (\text{Eq. 48})$$

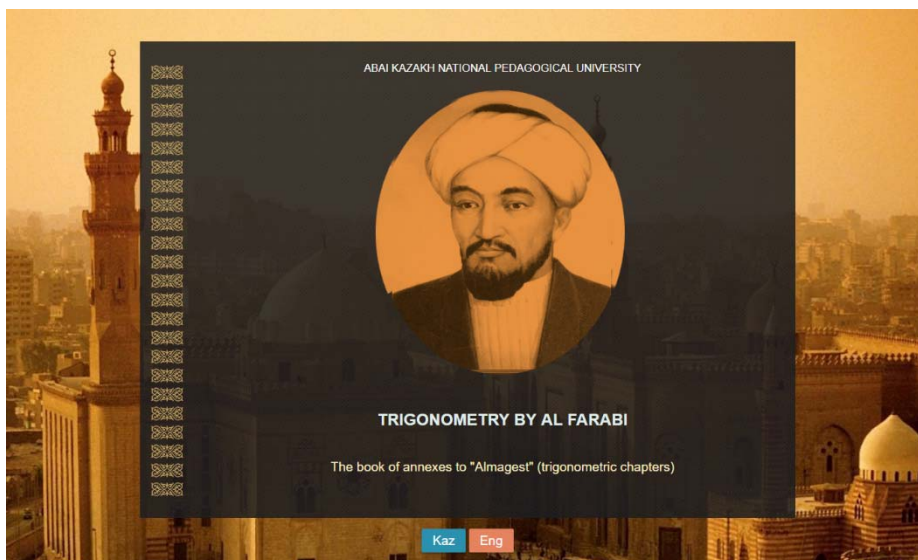


Figure 1. The interface of the E-Training Device

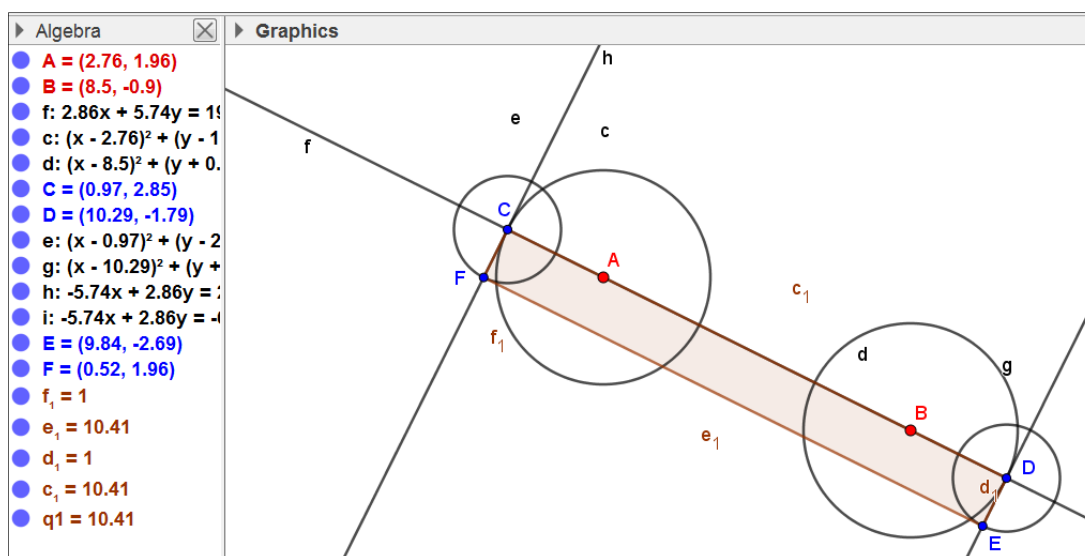


Figure 2. Preparing "Ruler" tool

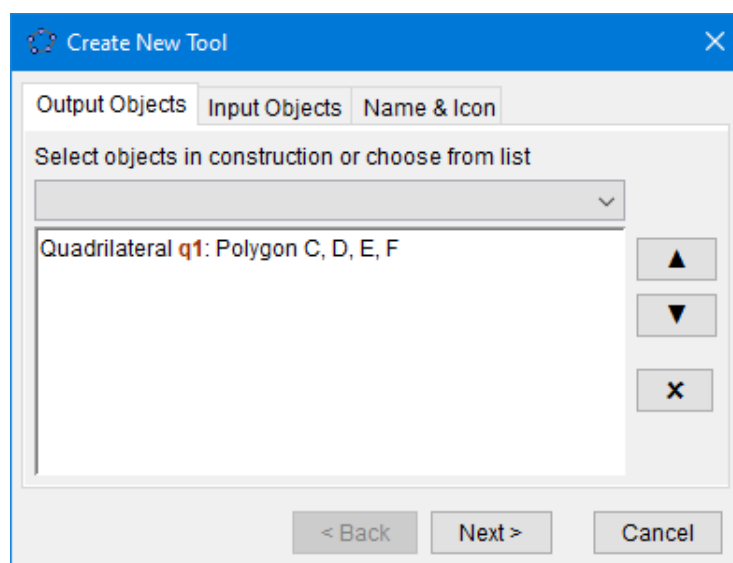


Figure 3. Setting up Output Objects of "Ruler" tool

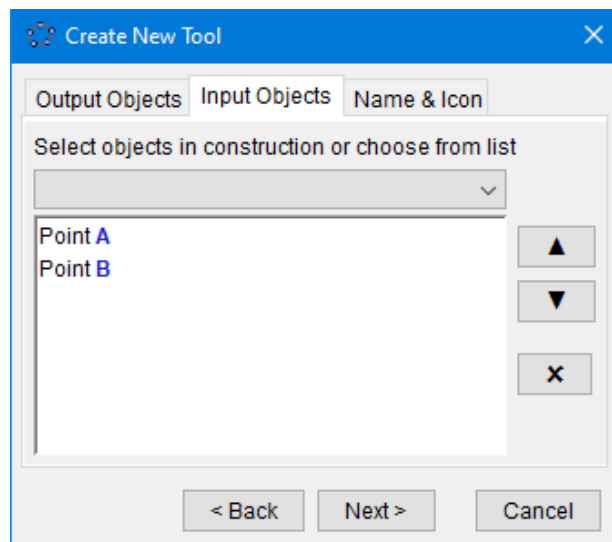


Figure 4. Setting up Input Objects of “Ruler” tool

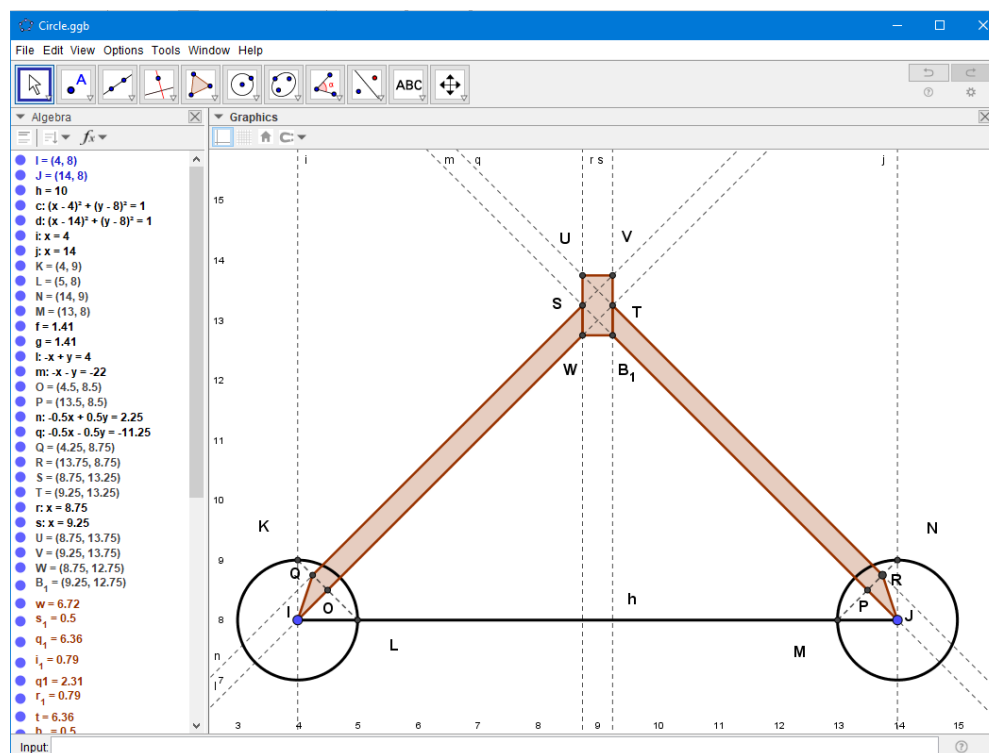


Figure 5. “Divider Compass” tool

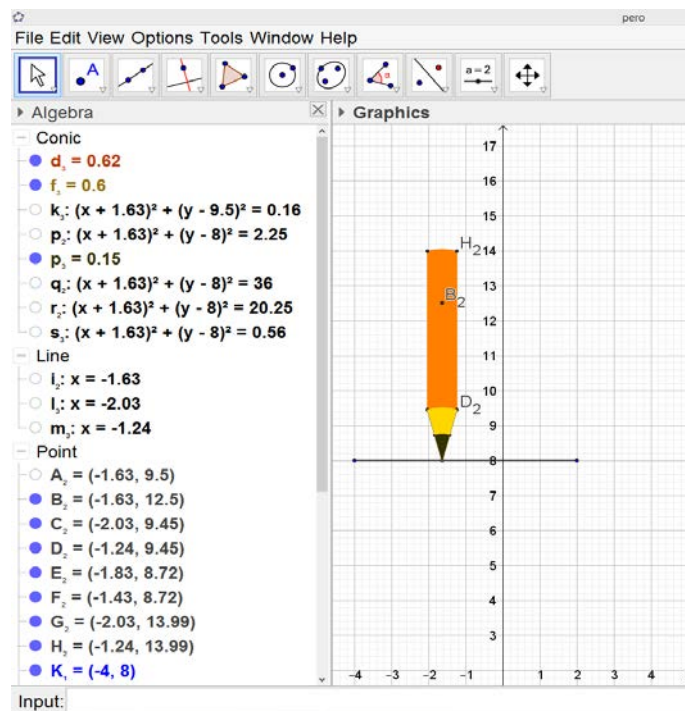


Figure 6. "Pencil" tool

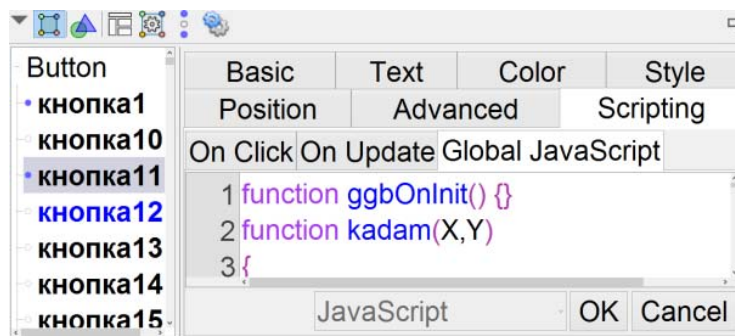


Figure 7. Programming icon

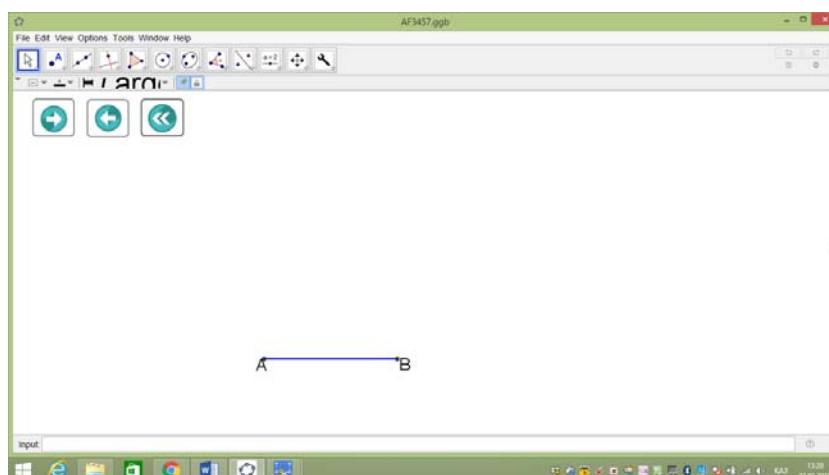


Figure 8. Buttons to make constructions



Figure 9. The first page of Al-Farabi's "Book of spiritual sophisticated techniques and natural secrets regarding peculiarities of geometric figures"

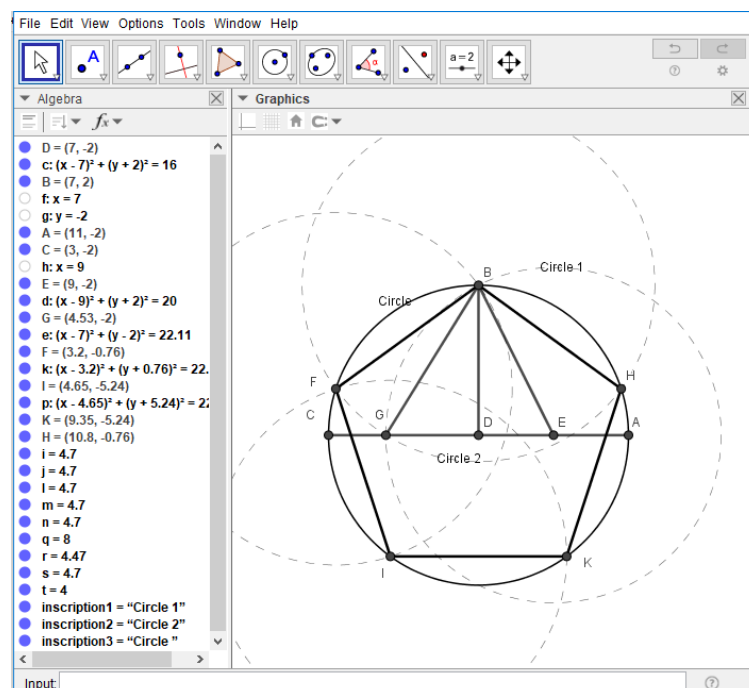


Figure10. Drawing an equilateral pentagon fit in a circle

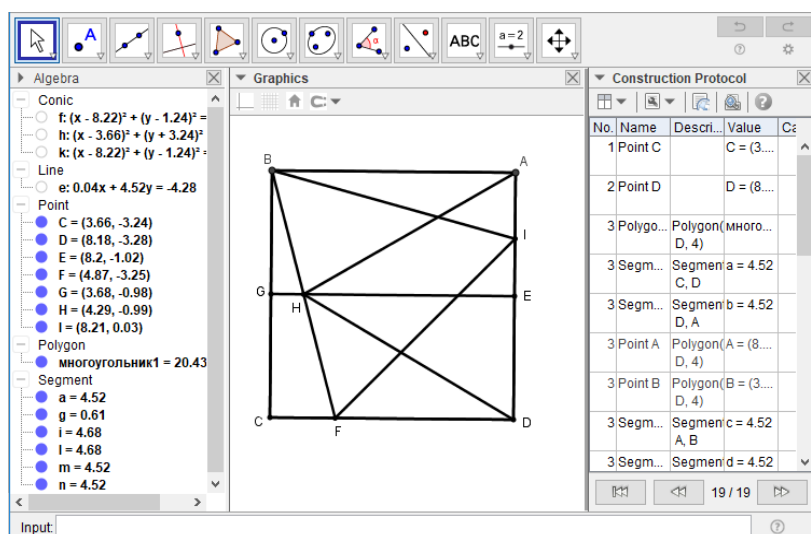


Figure 11. The third method for fitting a triangle into an equilateral rectangle

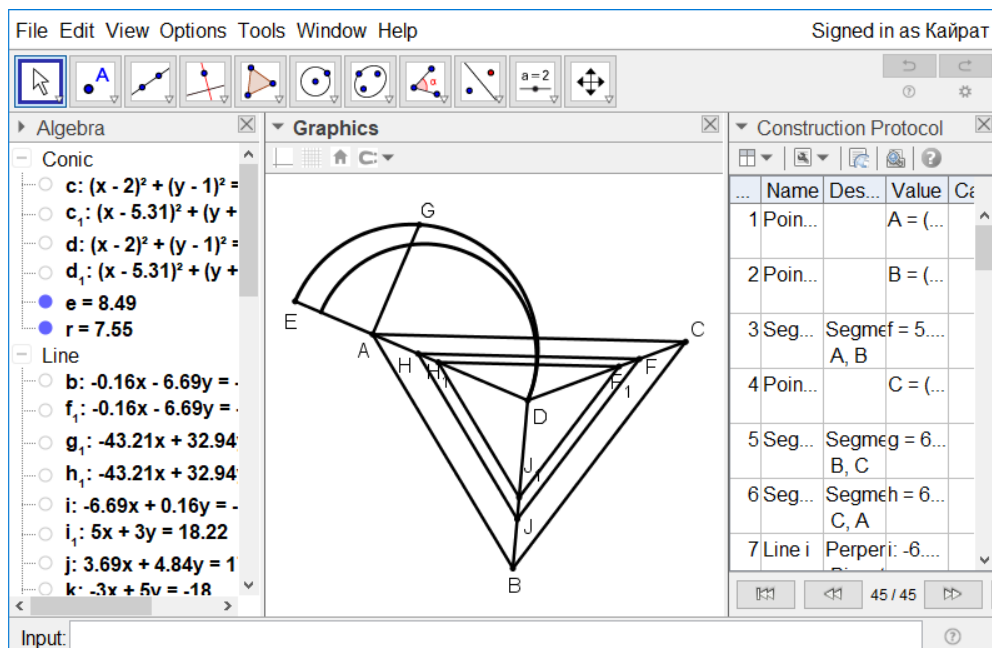


Figure 12. Procedure for constructing triangles inside the triangle ABC similar and equaling its half, one third, or otherwise

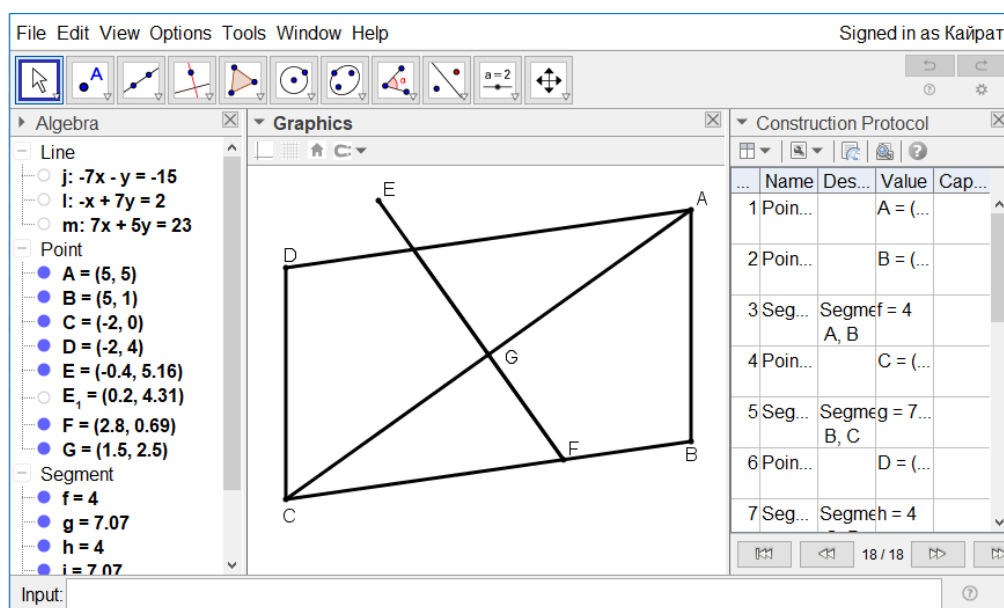


Figure 13. Dividing the parallelogram by a line

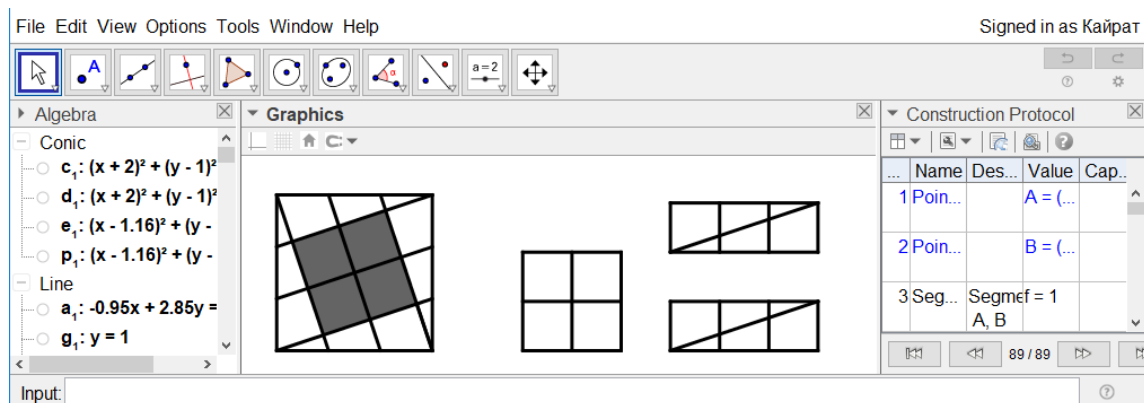


Figure 14. Arranging a square out of ten equal squares

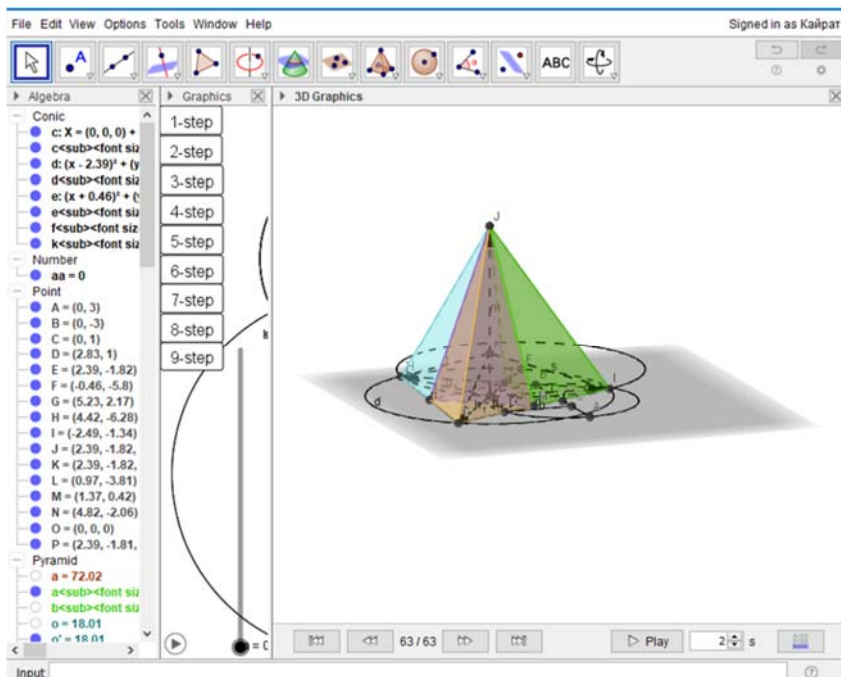


Figure 18. Procedure for dividing a sphere into four parts to obtain an equilateral and equiangular triangle

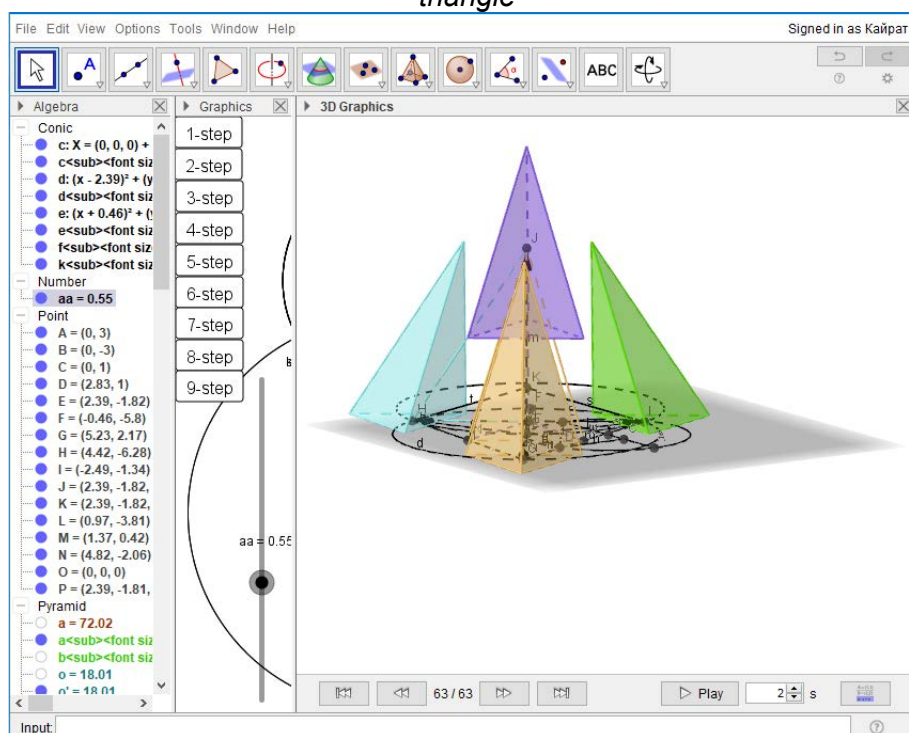


Figure 19. Procedure for dividing a sphere into four parts to obtain an equilateral and equiangular triangle

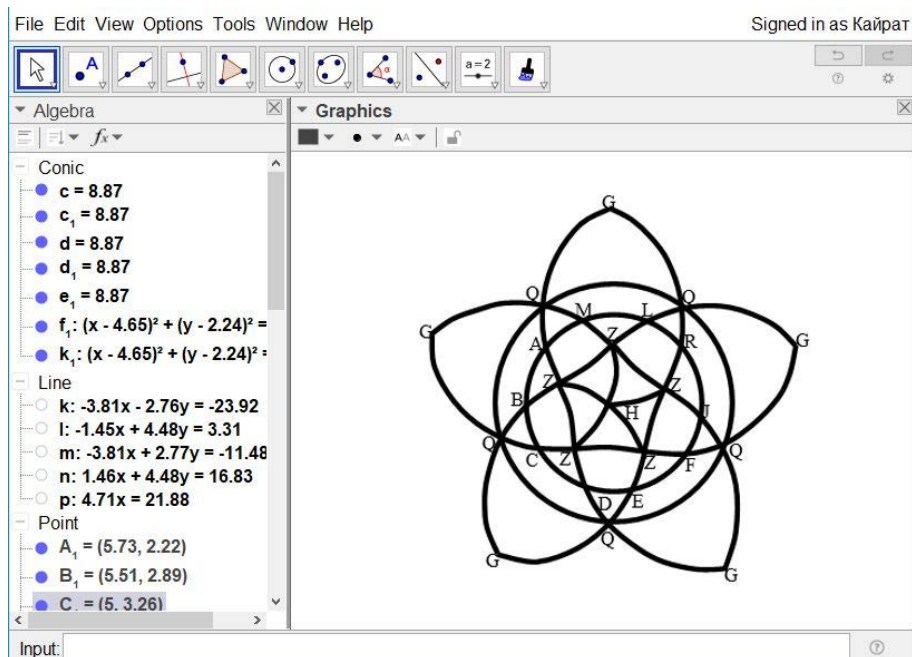


Figure 20. Procedure for dividing a sphere into twenty equal parts to obtain an equilateral and equiangular triangle

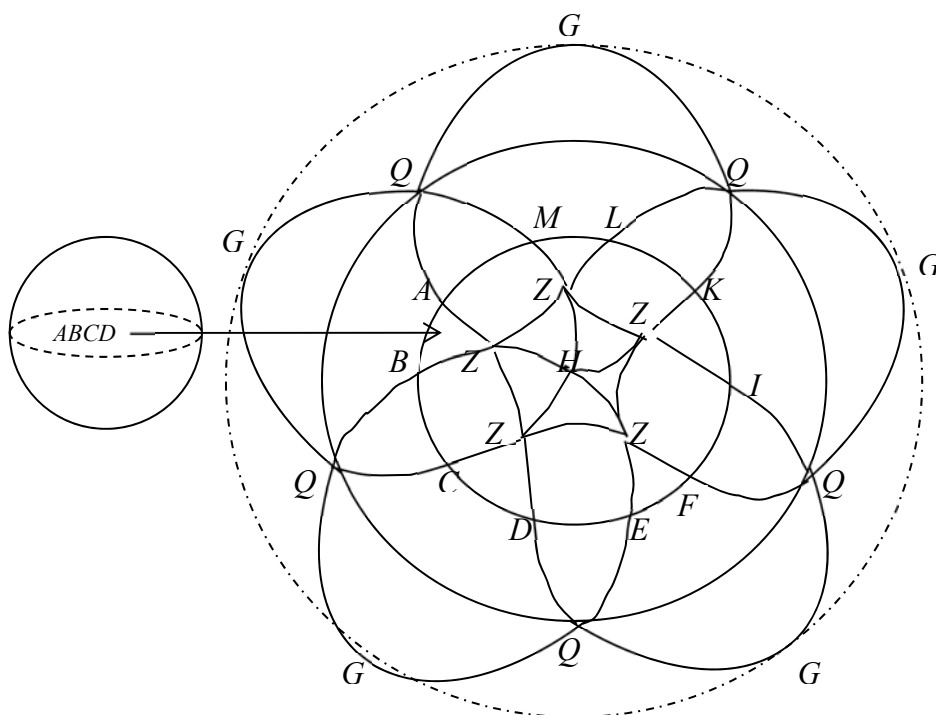


Figure 21. Dividing a sphere into twenty equal parts



Figure 22. Start page of "Almagest" book with a seal indicating ownership of the British Museum

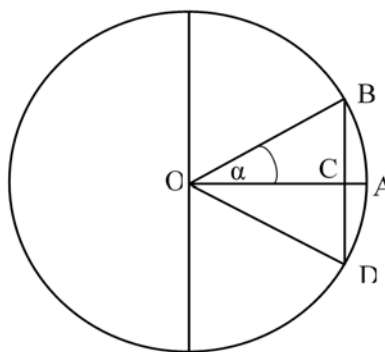


Figure 23. Replacing a chord by a sine

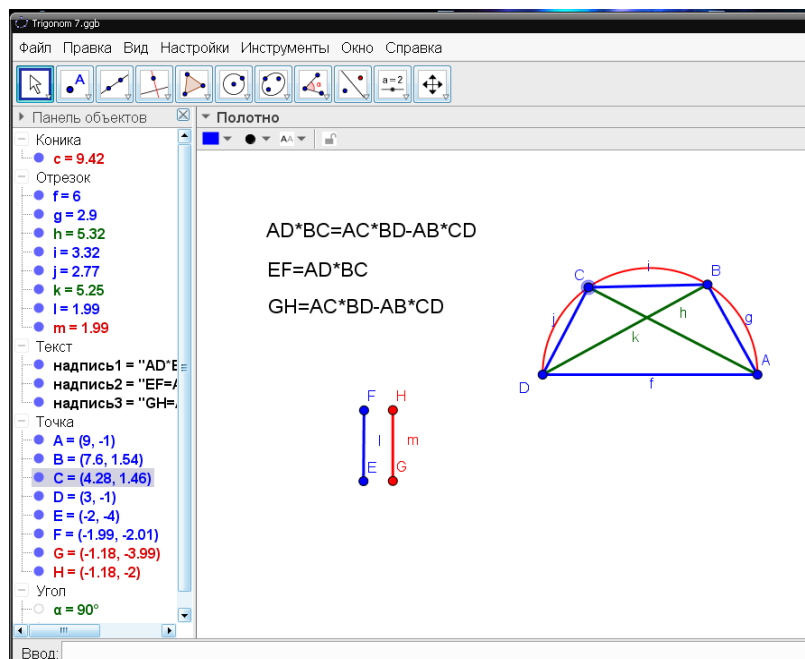


Figure 24. Determining of chord value with the known difference between chords of the other two arcs

SÍNTESE ULTRASSÔNICA DIRETA DE NANOCOMPOSITOS WO₃/TiO₂ E APLICANDO-OS NA FOTODECOLORIZAÇÃO DO CORANTE AMARELO DE EOSINA

DIRECT ULTRASONIC SYNTHESIS OF WO₃/TiO₂ NANOCOMPOSITES AND APPLYING THEM IN THE PHOTODECOLORIZATION OF EOSIN YELLOW DYE

تحضير المتراكبات النانوية لـ (TiO₂WO₃) مباشرةً بواسطة موجات فوق الصوتية وتطبيقها للزالة اللونية بالضوء لصبغة الايوسين الصفراء

Thaqeef Murtada Jawad¹ and Luma Majeed Ahmed^{1*}

¹ Chemistry Department, College of Science, University of Kerbala, Karbala, Iraq.

* Correspondence author

e-mail: luma.ahmed@uokerbala.edu.iq

Received 12 January 2020; received in revised form 22 February 2020; accepted 08 March 2020

RESUMO

Esta pesquisa relatou um método direto, ecológico, econômico e simples de usar um instrumento ultrassônico como uma técnica verde para combinar WO₃ com TiO₂ nas proporções 0,5:1, 0,25:1 e 0,16:1 como compósitos 1, 2 e 3, respectivamente. Os dados de difração de raios-X em pó, identificaram os tamanhos médios dos retículos cristalinos dos WO₃ comerciais, TiO₂ comerciais e dos nanocompósitos de WO₃/TiO₂ preparados nas diferentes proporções, entre 17,897 nm e 48,672 nm. A análise de Microscopia de Força Atômica (MFA) observou que a morfologia da superfície de todas as amostras estudadas é esférica. Os tamanhos médios de cristal e os tamanhos dos compósitos preparados estão na faixa dos nanômetros, e esses valores aumentam com o aumento da quantidade de TiO₂ nos nano-compósitos preparados. A incorporação de W com Ti na matriz ocorreu com sucesso; porque o raio iônico do W⁶⁺ é menor que o do Ti⁴⁺. Foram investigados os valores de intervalo de banda para todas as amostras. Os intervalos de banda dos nanocompósitos preparados 1, 2, 3 e TiO₂ ocorrem como um tipo indireto, enquanto o intervalo de banda do WO₃ é encontrado como tipo direto. As amostras estudadas foram testadas utilizando-as como fotocatalisadores na descoloração de uma solução aquosa do corante amarelo eosina E_{descol.}%. A sequência de descoloração cresce da esquerda para a direita, conforme: E_{descol.}% (compósito 3) < E_{descol.}% (WO₃) < E_{descol.}% (TiO₂) < E_{descol.}% (compósito 2) < E_{descol.}% (compósito 1). A atividade do WO₃ é inibida com a adição de H₂O₂ à solução aquosa do corante amarelo de eosina devido à formação de ácido peroxotungstico (WO₃H₂O₂.H₂O ou WO₂(O₂)H₂O.nH₂O), mas a superfície modificada por incorporação de TiO₂, melhora a atividade, portanto, o nano-composto 1 na proporção de 0,5: 1 recebe uma eficiência máxima de fotodecoloração desse corante e passa de 25,11% para 73,88%.

Palavras-chave: Trióxido de tungstênio; Dióxido de titânio; Nanocompósito; Síntese verde; Eosina Corante amarelo.

ABSTRACT

This research reported a direct, environmentally friendly, economical, and simple method of using an ultrasonic instrument as a green technique to combine WO₃ with TiO₂ in ratios 0.5:1, 0.25:1, and 0.16:1 as composites 1, 2 and 3 respectively. Powder X-Ray Diffraction data identified the mean crystalline sizes of the commercial WO₃, commercial TiO₂, and of the prepared WO₃/TiO₂ nanocomposites in the different ratios in ranged from 17.897 nm to 48.672 nm. AFM analysis noted the surface morphology for all studied samples is spherical. The mean crystal sizes and practical sizes for prepared composites are found to be in the nanometer range, and these values rise with the raising in the TiO₂ quantity in prepared nano-composites. The incorporated of W with Ti in the matrix is successful happened; because the ionic radius of W⁶⁺ is fewer values than it for Ti⁴⁺. The band gaps values for all samples have been investigated. The band gaps of prepared nanocomposites 1, 2, 3, and TiO₂ are occurred as an indirect type, while the band gap of WO₃ is found as direct type. The studied samples were tested by using them as photocatalysts in the decolorization of an aqueous solution, the eosin yellow dye E_{decol.}%. The sequence of decoloration grows from the left to the right as: E_{decol.}% (composite 3) < E_{decol.}% (WO₃) < E_{decol.}% (TiO₂) < E_{decol.}% (composite 2) < E_{decol.}% (composite 1). The activity

of WO₃ is inhibited with addition of H₂O₂ to the aqueous solution of eosin yellow dye because of the formation of peroxotungstic acid (WO₃H₂O₂.H₂O or WO₂(O₂)H₂O.nH₂O), but the modified surface by incorporation of TiO₂, improves the activity hence, nano-composite 1 in the ratio of 0.5:1 is given a maximum photodecolorization efficiency of this dye and changed from 25.11% to 73.88%.

Keywords: Tungsten Trioxide; Titanium dioxide; Nanocomposite; Green synthesis; Eosin Yellow dye.

المخلص:

نشر في هذا البحث بان استخدام جهاز الموجات فوق الصوتية كطريقة سهلة الاستخدام، صديقة للبيئة، اقتصادية وبسيطة، لذا يعتبر كتقنية خضراء، لدمج WO₃ مع TiO₂ ونسب 1:0.25 و 1:0.5 و 1:0.16 كمتراكبات 1، 2، و 3 على التوالي. شخّصت نتائج حيود الأشعة السينية للباودر بان معدل الحجوم البلورية للـ WO₃ التجاري، و TiO₂ التجاري، والنسب المختلفة المحضرة من المتراكبات النانوية (TiO₂WO₃) كان بمدى من 17.897 نانومتر الى 48.672 نانومتر. لوحظ من خلال نتائج تحليل الـ AFM مورفولوجية السطح لجميع العينات المدروسة بكونها دائرية الشكل. وجد ان جميع العينات المدروسة لها معدل حجوم بلورية وحجوم جسيمات ضمن المدى النانوي، اذ تزداد قيمها بزيادة كمية الـ TiO₂ في عينات المتراكبات النانوية المحضرة. تمت عملية تراكب W مع Ti في الشبكية بنجاح، لكون نصف القطر الايوني لـ W⁶⁺ يكون لها اقل قيمة نسبة الى نصف القطر الايوني لـ Ti⁴⁺. خمنت قيم فجوات الطاقة للعينات المدروسة. ظهر بان فجوات الطاقة غير مباشرة للمتراكبات النانوية 1، 2، و 3 المحضرة ولـ TiO₂ ايضا، بينما كانت فجوة الطاقة من نوع المباشر لـ WO₃. اختبرت العينات المدروسة باعتبارها عوامل مساعدة ضوئية لدراسة الازالة اللونية لصبغة الايوسين الصفراء من محلولها المائي، اذ كان تسلسل النسبة المئوية للازالة اللونية E_{decol.}% كالآتي:

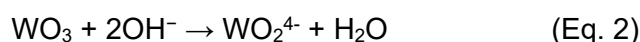
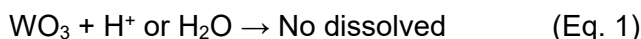
$$E_{decol.}\% (\text{composite } 3) < E_{decol.}\% (\text{WO}_3) < E_{decol.}\% (\text{TiO}_2) < E_{decol.}\% (\text{composite } 2) < E_{decol.}\% (\text{composite } 1)$$

ثبطت كفاءة الـ WO₃ عند اضافة H₂O₂ الى المحلول المائي لصبغة الايوسين الصفراء بسبب تكون حامض فوق اوكسيد التنكستن بهيئة H₂O₂.WO₃.H₂O.nH₂O(O₂)H₂O، ولكن بتحويل سطحه بالتداخل مع TiO₂ ادى الى تحسين الفعالية، لذلك اعطى المتراكب النانوي 1 ذي النسبة (1:0.5) اعلى كفاءة للازالة اللونية لهذه الصبغة، وقد تغيرت القيمة من 25.11% الى 73.88%.

الكلمات المفتاحية: ثلاثي اوكسيد التنكستن، ثنائي اوكسيد التيتانيوم، المتراكب النانوي، التخليق الاخضر، صبغة الايوسين الصفراء.

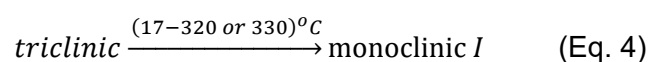
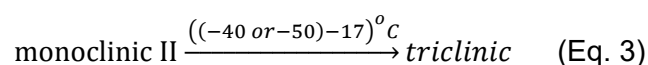
1. INTRODUCTION

The tungsten trioxide (WO₃) also known as tungsten (VI) oxide is one of the transition metal oxides, which is classified as an n-type semiconductor with a wide range of band gap between 2.5 eV to 2.8 eV at room temperature (Yan *et al.*, 2015; Huang *et al.*, 2014; Walle *et al.*, 2012). In addition, it is chemically stable, non-toxic, insoluble in water, and acidic medium, but it can be dissolved in strong alkali solutions or HF, as represented in Equations 1 and 2 (Cotton *et al.*, 1980; Rollinson *et al.*, 1975; Lassner *et al.*, 1999)



The tungsten trioxide is also called as tungstic acid, and is a highly condensed and amorphous substance with a reduced water content, that depends on the ratios of WO₃: H₂O such (1:2), (1:1) and (2:1) for WO₃.2H₂O (white color), WO₃.H₂O (yellow color) and 2WO₃.H₂O (orange-yellow color) respectively. The second ratio (1:1) is the most common, and it is an amorphous yellow powder. Therefore, it can be

used as a pigment for bright yellow glasses, in ceramics and paints (Lassner *et al.*, 1999; Rao, 2013). The crystal structure of WO₃ depends on the temperature; the triclinic (δ-WO₃) appears in the range of temperatures from -50 to 17 °C. The monoclinic form consists of two types: monoclinic II (ε-WO₃) and monoclinic I (γ-WO₃), the first is synthesized at temperatures ranging from -143 °C to -50 °C, while the second type appears in the range of temperatures from 17 °C to 330 °C, the last type (i.e., γ-WO₃) is recognized as the most common, as the commercial form of WO₃ structure, and it is highly thermally stable up to 150 °C. The orthorhombic form (β-WO₃) is prepared in temperatures ranging from 320 °C to 740 °C, and the tetragonal form (α-WO₃) appears in temperatures above 740 °C (Rollinson and *et al.*, 1975; Lassner and *et al.*, 1999; Rao, 2013; Cazzanelli and *et al.*, 1999). As represented in Equations 3 to 6.



monoclinic $I \xrightarrow{(330-740)^\circ C} orthorhombic$ (Eq. 5)

$orthorhombic \xrightarrow{Above (740)^\circ C} tetragonal$ (Eq. 6)

The WO_3 pure or modified - bulk or nanoparticle - have been extensively utilized in fields such as gas-sensors (Staerz *et al.*, 2018; Leidinger *et al.*, 2015), self-cleaning surfaces (Garlisi *et al.*, 2015; Bianchi *et al.*, 2013), photocatalyst for water splitting (Kalanur, 2019; Stoll *et al.*, 2017), dye-sensitized solar cells (Zheng *et al.*, 2010; Yong *et al.*, 2013), antibacterial agents (Syed *et al.*, 2010; Stankic *et al.*, 2016), photoelectron-catalysis (Goulart *et al.*, 2019), used as a new anode material for lithium-ion batteries (Li and Fu, 2010).

In order to improve the photocatalytic activity of the WO_3 , the WO_3 has been incorporated with the TiO_2 by using the Microwave-assisted hydrothermal process (Ren *et al.*, 2011), Sol-gel method (Cabrera *et al.*, 2012; Dominguez *et al.*, 2017), co-precipitation (Luévanó Hipolito *et al.*, 2014). In this work, the purpose is to improve the properties of WO_3 by incorporating it with TiO_2 as a composite in different ratios (0.5:1), (0.25:1), and (0.16:1) by using a direct ultrasonic synthesis. The morphology and optical properties for the commercial WO_3 , the commercial TiO_2 , and their composites of (WO_3/TiO_2) as photocatalysts are ongoing.

2. MATERIALS AND METHODS

In this research, all chemicals were employed as received without any additional purification. The tungsten trioxide (WO_3), as $WO_3 \cdot H_2O$ (yellow color), and the titanium dioxide (TiO_2) as rutile were purchased from Riedel-De-Haen AG, Seelze, Hannover, Germany. Suitable compounds to determine the light intensity in photoreaction experimental was used without any purification. Eosin yellow dye (Acid red 87 dye) was supplied by CDH from India, with the molecular composition $C_{20}H_6Br_4Na_2O_5$, and molecular weight 691.86. The Eosin yellow dye has some unique physical and chemical characteristics, which are listed in Table 1.

In this research, the essential instruments, which were employed to prepare and investigate the characterizations consisted of a sensitive balance model (BL 210 S, Sartorius, Germany), X-Ray Diffraction spectrophotometer model Lab

X- XRD 6000 (Shimadzu, Japan), hot plate stirrer model Heido (Mr. Hei-Standard, Germany), UV-Visible spectrophotometer model AA-1800 (Shimadzu Japan), centrifuge (Hettich- Universal II, Germany), AFM model AA 3000 (Advanced Angstrom Inc., USA), and ultrasound model DAIHAN (Scientific, Korea).

2.1. Synthesis of the (WO_3/TiO_2) composites

Based on the ultrasonic technique with using (ultrasonic, 60 kHz, type DAIHAN Scientific, Korea), a series of steps, as in Figure 1, were performed to synthesize the WO_3/TiO_2 composites in the ratios of 0.5:1, 0.25:1 and 0.16:1. The ultrasonic method is an active method, used to generate sufficient energy for a bond formed. The WO_3 suspension solution and the TiO_2 suspension solution that dissolved in distilled water (type IV reagent water) were mixed in the ultrasound reactor for 5 hours.

2.2 Application of prepared (WO_3/TiO_2) composites on decolorization of eosin yellow dye solution.

After analyzed the morphology using AFM and the optical properties using the Tuce equation of prepared (WO_3/TiO_2) composites, it's found that the composites were successfully prepared as nano-photocatalysts. The active path to test the influence of the TiO_2 chosen to be combined with WO_3 is implemented, which raised the photocatalytic activity with the application of them as a composite on the decolorization of an aqueous solution of eosin yellow dye.

Exactly 0.1000 g of TiO_2 , or WO_3 , or (WO_3/TiO_2) composites (0.5:1, or 0.25:1 or 0.16:1) were added to 100 mL of 5 ppm of eosin yellow dye solutions with the natural dye solution pH (6.09) and then mixed the dye solution with photocatalyst together to produce a homogeneous suspension solution with using a Teflon bar and a magnetic stirrer. The formed mixture was allowed to stay in the dark for 30 min to get ready for the photocatalytic step (Ahmed *et al.*, 2018a; Marhoon *et al.*, 2019; Kzar *et al.*, 2019). In a wooden box, a 250 watts UV-A lamp (Radium-Germany) was applied over the mention suspensions solutions at regular intervals time with a light intensity equal to $2.66 \cdot 10^{-7}$ Einstein s^{-1} . Approximately 2.5 ml of the mixture was collected in a plastic test tube. And then, the photocatalyst was separated by centrifuge from the dye solution twice at 4000 rpm for 15 minutes. The dye solution was analyzed using the UV-Vis spectrophotometer (AA-1800, Shimadzu) to determine the residual

concentration of eosin yellow dye at a maximum wavelength (516 nm (Ahmed, 2018). The kinetic study of this photodecolorization was implemented by calculating the apparent rate constant (k_{app}) (Hussein *et al.*, 2018; Ahmed *et al.*, 2018b) and photodecolorization efficiency ($E_{decol.}\%$) (Jasim, and Ahmed, 2019; Rangel *et al.*, 2018) used from C_o and C_t , referring to the initial concentration of eosin yellow dye without illumination (dark reaction for 30 min) and the concentration of the same dye in according with Equations 7 and 8 at t time of illumination.

$$\ln\left(\frac{C_o}{C_t}\right) = k_{app}.t \quad (\text{Eq.7})$$

$$E_{decol.}\% = \left(\frac{C_o - C_t}{C_o}\right) \times 100 \quad (\text{Eq.8})$$

3. RESULTS AND DISCUSSION:

In order to prove that the nanocomposites 1, 2, and 3 were successfully prepared, the characteristics of prepared nanocomposites were studied and compared with the commercial WO_3 and the commercial TiO_2 .

3.1. Structural characterization

The X-ray diffraction (XRD) analysis was carried out on Lab X- XRD 6000, Shimadzu X-ray diffraction spectrophotometer with a Cu K α radiation source at λ equal to 1.540 Å. On the basis of the resulted peaks in Figure 2, that found the peaks of the commercial WO_3 and the commercial TiO_2 are sharp, but the peaks of the all prepared composites are broad and have low intensities that indicated the gain on nanocomposites from WO_3/TiO_2 . The mean crystal sizes (L) in nm for all the samples was calculated from the Debye-Scherrer, Equation 9 (Ahmed *et al.*, 2014; Ahmed *et al.*, 2012; Mahammed *et al.*, 2017).

$$L = \frac{k \lambda}{\beta \cos \theta} \quad (\text{Eq. 9})$$

In Equation 9, λ is the wavelength of Cu as the source of the instrument in (nm), β is the full width at half maximum intensity in (radian), k is shaped constant, and θ is the Bragg diffraction angle.

The mean crystalline sizes of the WO_3 , TiO_2 , and the prepared WO_3/TiO_2 composites 1, 2, and 3 were found equal to 17.897 nm, 48.672

nm, 40.084 nm, 43.456 nm, and 42.703 nm respectively. The addition of TiO_2 in different ratios for WO_3 leads to raising the mean crystal size and improvement of the optical properties. The peaks positions at 2θ equal to 27.46° , 36.10° , 41.26° , 54.34° , 56.32° , and 69.02° were beyond the diffractions of the TiO_2 at (110), (101), (111), (211), (220) and (301). The highest peak at crystal planer (110) with 2θ was equal to 27.46° corresponds to the rutile phase, which is in agreement with the standard diffraction data (JCDs card No. 00-021-1276) (Filippo *et al.*, 2015). On the other hand, XRD peaks at 2θ equal to 16.60° , 25.72° , 34.24° , 34.99° , 49.68° , 52.74° , 56.29° , 57.24° , and 62.78° which assigned to (020), (111), (200), (131), (202), (222), (311), (113) and (133) plane as orthorhombic $\text{WO}_3 \cdot \text{H}_2\text{O}$ phase (JCDs card No. 00-043-679) (Elnouby *et al.*, 2013). The incorporation between WO_3 and TiO_2 was proved by the redshift occurred toward the essential position peaks with 2θ from 27.46° , 54.34° and 36.10° to $(27.56^\circ - 27.60^\circ)$, $(54.42^\circ - 54.46^\circ)$ and $(36.19^\circ - 36.23^\circ)$, this change ensured that the metal bond was generated between W and Ti in the crystal lattice (Ahmed *et al.*, 2014; Mohammed and Ahmed, 2018; Fakhri and Ahmed, 2019).

3.2. Surface Morphology of photo-catalysts

The atomic force microscopy images are presented in Figure 3. It was noted that the particle sizes of the WO_3 and the TiO_2 are 65.310 nm and 56.220 nm, respectively. Besides, the particle sizes of the prepared WO_3/TiO_2 composites are increased when compared to those of the WO_3 and TiO_2 . This change is due to the agglomeration of WO_3 and TiO_2 particles in the matrix, and the particle sizes of the composites 1, 2, and 3 are equal to 71.270 nm, 93.160 nm, and 94.290 nm for the ratios 0.5:1, 0.25:1 and 0.16:1 respectively. The elevation in the particle sizes for the prepared composites increases when it is increased the ratio of TiO_2 that is attributed to the high ionic radius of the Ti^{4+} (0.61 Å) (Ahmed *et al.*, 2014; Ghosh and Biswas, 2003), making it suitable to be incorporated with W^{6+} with low ionic radius (0.51 Å) (Ghosh and Biswas, 2003).

In Figures 3 and 4, the TiO_2 has more roughness average than the roughness average of the prepared composites 1, 2, and 3. This is due to the inverse relation between average roughness value and particle size. Hence, TiO_2 has a smaller practical size (56.220 nm), so it has the highest roughness value (27.9 nm).

3.3. Optical properties of photocatalysts

The optical band gaps of all the samples in this research were obtained from the absorption coefficient (α) data in Equation 10, which was calculated by analyzing the variation on the absorbance of suspension solution (A) Tauc relation in Equation 11 depends on the Plank's constant (h), the frequency (ν) of the incident photon, the optical constant (k), m is a constant value which is equal to $\frac{1}{2}$ and 2 for a direct transition and indirect transition respectively (Fakhri and Ahmed, 2019; Tauc *et al.*, 1996).

$$\alpha = 2.3026 A/t \quad (\text{Eq. 10})$$

$$\alpha h\nu = k(h\nu - E_g)^m \quad (\text{Eq. 11})$$

The optical band gap deduced from the Tauc plot was displayed in Figure 11. Hence, the linear variation of $(\alpha h\nu)^2$ vs. $h\nu$ indicated that the transition in TiO_2 is indirect allowed and all composites 1, 2 and 3 are indirect allowed also, but, the linear variation of $(\alpha h\nu)^{1/2}$ vs. $h\nu$ indicated that the transition in WO_3 is direct allowed with band gap equal to 2.719 eV. Moreover, the optical band gaps for the prepared composites 1, 2, and 3 were found to be an indirect band gap, and the band gap values decrease compared to the band gap of TiO_2 alone (3.063 eV), they are equal to 2.765 eV, 2.837 eV, and 2.988 eV respectively.

3.4. Effect of using the different photocatalysts on the Photo- decolorization of eosin yellow dye

A series of photo-experiments have been conducted in order to detect the best photocatalytic activity behavior of studied samples primarily, there are a series of photo-experiments were performed. The activities of commercial TiO_2 , WO_3 , and prepared composite 1 are roughly identical in the constant rate values shown in figure 7, but the composite 1 is more effective than that for other samples. This is due to many reasons: first, the WO_3 surface defect raises with forming a composite, which results in the depressed in the recombination process by increasing a surface ability to move the charge from the high conductive band of TiO_2 to the low conductive band of WO_3 . While, the positive charge in WO_3 valance band leaps during combined to the valance band of TiO_2 (Asim *et al.*, 2013; Sajjad *et al.*, 2003). In Figure 6, this

case is displayed schematically. The second cause illustrated that the addition of TiO_2 during combined would elevate the acidity of the WO_3 surface, leading to the formation of high amounts of hydroxyl radicals in present light (Asim *et al.*, 2013; Sajjad *et al.*, 2003). The basic start for the photoreaction is Hydroxyl radical. The third cause is based on the reduced band gap since the two semiconductors were combined. Consequently, the lower conductive band in a vacuum owns the new band gap for a new case, and its operation is elevated toward the use of visible light. Therefore, W^{+5} may be generated during the electron transfer to the reducible species surface. That will assist and improve the optical properties of the photocatalyst (Sajjad *et al.*, 2003). The efficiency of WO_3 increases from 18.951 % to 25.1119 % at 90 min, with combined it with TiO_2 and generated a composite 1.

3.5. Effect of H_2O_2 addition on photocatalysts in eosin yellow dye Photo- decolorization

Now the effect of hydrogen peroxide addition will be studied after the best composite was chosen, which was prepared in using an ultrasonic technique. Figure 8 demonstrates the efficiency of photocatalytic for eosin yellow dye decolorization, which declines with the use of TiO_2 and WO_3 , but the efficiency of this reaction increases with the use of composite 1. This action due to the WO_3 can be reacted with hydrogen peroxide and produced Peroxotungstic acid such as $(\text{WO}_3 \cdot \text{H}_2\text{O}_2 \cdot \text{H}_2\text{O}$ or $\text{WO}_2 (\text{O}_2) \cdot \text{H}_2\text{O} \cdot n\text{H}_2\text{O})$ (Pecquenard *et al.*, 1998), which will inhibit its photoactivity of it because Peroxotungstic acid is used as inorganic photoresists (Pecquenard *et al.*, 1998; Kudo *et al.*, 1991).

Alternatively, peroxotungstic acid assumes that the produced peroxo polytungstate anions are linked together by a hydrogen bond (Pecquenard *et al.*, 1998). This anionic species can reduce the acidity of the WO_3 surface and decline the adsorption of hydroxyl ion, which necessary to form hydroxyl radical under UV-light. On the other hand, the H_2O_2 addition to the TiO_2 suspension solution did not improve the decolorization rate constant and efficiency of the decolorization of eosin yellow dye. That attitude to self-decomposition of H_2O_2 or acting as a scavenger for hydroxyl radicals has finally formed water and liberated oxygen free molecules (Hussein *et al.*, 2018; Ahmed *et al.*, 2018b; Kumar *et al.*, 2011; Mashkour *et al.*, 2011). Inversely, the addition of H_2O_2 to suspension solution of composite 1 leads to improve the

photodecolorization from 25.11% to 73.887. This due to raising the WO_3 acidity following the combination with TiO_2 and induced a high hydroxyl radical species (Asim *et al.*, 2013; Sajjad *et al.*, 2003). This species will increase the probability of the chromophoric group electrophilic attack in studied dye (Arslan *et al.*, 2000).

3.6. Mechanism of photodecolorization of eosin yellow dye

Initially, when UV-A light focuses on surface of dye suspension solution containing photocatalysts such as WO_3 , or TiO_2 or WO_3/TiO_2 nanocomposite, this leads to the formation of hydroxyl radical and other species such as superoxide anion and peroxide radical, which will starts the attachment with the chromophore groups in the dye and induces the decolorization of dye with continuous irradiation from its solution for 90 min. But with irradiation, the dye generated CO_2 and H_2O at the solution pH of reaches to 7 for several hours. The suggested mechanism for decolorization of eosin yellow dye was indicated in Figure 9 (Ahmed, 2018).

4. CONCLUSIONS

The results indicated that the composites prepared using the direct ultrasonic method in distilled water were actually prepared using different ratios of 0.5:1, 0.25:1, and 0.16:1 from WO_3 with the TiO_2 as composites 1, 2 and 3 respectively. It is dependent on the energy provided by the ultrasonic instrument. The phase composition and morphologies of all commercial and prepared samples were estimated by XRD and AFM. The agglomeration between the WO_3 and the TiO_2 was obtained. Hence, the AFM analysis deduced to the particle sizes of prepared composites 1, 2, and 3 were much larger than those of their components alone with smaller surface roughness.

The roughness of the TiO_2 with a small particle size value was considered to have a maximum value. In the primary experiments, the raised of the efficiency of photocatalytic decolorization (E%) of the eosin yellow dye from aqueous solution using the studied photocatalysts was sequenced to:

E% composite 3 < E% WO_3 < E% TiO_2 < E% composite 2 < E% composite 1, and when H_2O_2 is added the sequences will be WO_3 < TiO_2 < composite 1.

5. ACKNOWLEDGMENTS:

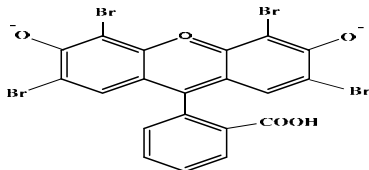
The researchers gratefully acknowledge to the university of Kerbala, college of science, for implementing the assistance during performed this project in graduate labs. Also, the distinction acknowledgment goes to Dr. Abed Al-Kareem Al-Samaraee (the University of Baghdad, College of Science, department of chemistry) and Dr. Ayad Fadi Al-Kaim (the University of Babylon, College of Science for women, department of chemistry) to perform some essential analyses such as AFM analysis and UV-Visible spectrophotometer with Labsphere diffuse reflectance accessory.

6. REFERENCES:

1. Yan, A. H; Huang, F.; Zhao, H.; Li, Q. C.; Wang, C. Y.; Zhang, J.; Chen, F.; Ma, J. Materials Research Innovations, 2015,19, 1183.
2. Huang, C. C.; Su, Y. H; Tu, S. L.; Yung, T. W.; Ke Y. F.; Chen, T. H. Materials Research Innovations, 2014, 18 S, S3-72.
3. Waller, M. R.; Townsend, T.K.; Zhao, J.; Sabio, E. M.; Chamousis, R. L.; Browning, N. D.; Osterloh, F. E. Chem. Mater. 2012, 24, 698.
4. Cotton, F. A.; Wilkinson, G.; Murillo, C. A.; Bochmann, M.; Advanced Inorganic Chemistry, 4th edition, John Wiley & Sons, New York,1980.
5. Rollinson, C. L.; The Chemistry of Chromium, Molybdenum, and Tungsten, volume 21 of Pergamon Texts in Inorganic Chemistry, 1st Edition, Pergamon Press, UK, p. 763, 1975.
6. Lassner, E.; Schubert, W. Tungsten Properties, Chemistry, Technology of the Element, Alloys, and Chemical Compounds, 1st ed., Kluwer Academic / Plenum Publishers, New York, pp: 147-159, 1999.
7. Rao, M. C. Journal of Non-Oxide Glasses. 2013, 5(1), 1.
8. Cazzanelli, E.; Vinegoni, C.; Mariotto, G.; Kuzmin, A.; Purans, J. Journal of Solid State Chemistry. 1999, 143, 24.
9. Staerz, A.; Somacescu, S.; Epifani, M.; Russ, T. Weimar, U.; Barsan, N. Proceedings. 2018, 2 (826), 1.
10. Leidinger, M.; Huotari, J.; Sauerwald, T.; Lappalainen, J.; SchMütze, A. AMA Conferences 2015, Sensor 2015 and IRS² 2015, 2015, 723.
11. Garlisi, C.; Scandura, G.; Alabi, A.;

- Aderemi, O.; Palmisano, G. J. *Adv. Chem. Eng.* 2015, 5(1), 1.
12. Bianchi, C. L.; Gatto, S.; Nucci, S.; Cerrato G.; Capucci, V. *Advances in Materials Research.* 2013, 2(1), 1.
13. Kalanur, S. S. *Catalysts.* 2019, 9(456), 1.
14. Stoll, T.; Zafeiropoulos, G.; Dogan, I.; Genuit, H.; Lavrijsen, R.; Koopmans, B.; Tsampas, M. N. *Electrochemistry Communications*, 2017, 82, 47.
15. Zheng, H.; Tachibana, Y.; Kalantar-zadeh, K. *Langmuir.* 2010, 26(24), 19148.
16. Yong, S.; Nikolay, T.; Ahn, B. T.; Kim, D. K. *Journal of Alloys and Compounds*, 2013, 547, 113.
17. Syed, M. A.; Manzoor, U.; Shah, I.; Bukhar, S. H. A. *New Microbiologica*, 2010, 33, 329.
18. Stankic, S.; Suman, S.; Haque, F.; Vidic, J. *J. Nanobiotechnol.* 2016, 14(73), 1.
19. Goulart, L. A.; Alves, S. A.; Mascaro, L. H. *Journal of Electroanalytical Chemistry*, 2019, 839, 123.
20. Li, W.; Fu, Z. *Applied Surface Science*, 2010, 256, 2447.
21. Ren, G.; Gao, Y.; Yin, J.; Xing A.; Liu, H. *J. Chem. Soc. Pak.* 2011, 33(5), 666.
22. Cabrera, R. Q.; Latimer, E. R.; Kafizas, A.; Blackman, C. S.; Carmalt, C. J. Parkin, I. P. *Journal of Photochemistry and Photobiology A: Chemistry.* 2012, 239, 60.
23. Dominguez, S. Huebra, M.; Han, C.; Campo, P.; Nadagouda, M.N.; Rivero, M.J.; Ortiz, I.; Dionysiou, D. D. *Environ Sci Pollut Res.* 2017, 24, 12589.
24. Luévánó Hipolito, E.; Martínez-de la Cruz, A.; López-Cuellar, E.; Yu, Q.L.; Brouwers, H.J.H. *Materials Chemistry and Physics.* 2014, 148, 208.
25. Ahmed, L. M. *Asian J. Chem.* 2018, 30(9), 2134.
26. Ahmed, L. M.; Jassim, M. A.; Mohammed, M. Q.; Hamza, D. T., *Journal of Global Pharma Technology.* 2018, 10, 248.
27. Marhoon, A. A.; Saeed S. I.; Ahmed, L. M. *Journal of Global Pharma Technology.* 2019, 11, 9, 76.
28. Kzar, K. O.; Mohammed, Z. F.; Saeed, S. I.; Ahmed, L. M.; Kareem, D. I.; Hadyi, H.; Kadhim, A. J. *AIP Conf. Proc.* 2019, 2144, 020004-1.
29. Hussein, Z. A.; Abbas, S. K.; Ahmed, L. M. *IOP Conference Series: Materials Science and Engineering*, 2018, 454, 1.
30. Ahmed, L. M.; Saeed, S. I.; Marhoon, A. A., *Indones. J. Chem.* 2018, 18(2), 272.
31. Jasim, K. M.; Ahmed, L.M. *IOP Conf. Ser.: Mater. Sci. Eng.* 2019, 571, 012064.
32. Rangel, E. M.; Carvalho, C. De O.; Arsand, D. R. *PERIÓDICO TCHÊ QUÍMICA*, 2018, 15 (29), 7.
33. Ahmed, L. M.; Ivanova, I.; Hussein, F. H.; Bahnemann, D. W. *International Journal of Photoenergy*, 2014, 1.
34. Ahmed, L. M.; Hussien, F. H.; Mahdi, A. A. *Asian Journal of Chemistry.* 2012, 24(12), 5564.
35. Mahammed, B. A.; Ahmed, L. M. *Journal of Geoscience and Environment Protection.* 2017, 5, 101.
36. Filippo, E.; Carlucci, C.; Capodilupo, A. L.; Perulli, P.; Conciauro, F.; Corrente, G. A.; Gigli, G.; Ciccacrell, G. *Materials Research.*, 2015, 18(3), 473.
37. Elnouby, M.; Kuruma, K.; Nakamura, E.; Abe, H.; Suzuki, Y.; Naito, M. *Journal of the Ceramic Society of Japan*, 2013, 1(10), 907.
38. Mohammed, B. A.; Ahmed, L. M. *Journal of Global Pharma Technology*, 2018, 10(7), 129.
39. Fakhri, F. H.; Ahmed, L. M. *Indones. J. Chem.* 2019, 19(4) 936.
40. Ghosh, D. C.; Biswas, R. *Int. J. Mol. Sci.*, 2003, 4, 379.
41. Tauc, J.; Grigorovici, R.; Vancu, A. *Phys. Stat. Sol.*, 1996, 15, 627.
42. Asim, N.; Badeiei, M.; Ghoreishi, K. B.; Ludin, N. A.; Zonooz M. R. F.; Sopian, K. *Advances in Fluid Mechanics and Heat & Mass Transfer.* 2013, 110.
43. Sajjad, A. K.; Shamaila, L. S.; Tian, B.; Chen, F. Zhang, J. *Applied Catalysis B: Environmental.* 2009, 91, 397.
44. Pecquenard, B.; Castro-Garcia, Livage, S. J.; Zavalij, P. Y.; Whittingham, M. S.; Thouvenot, R. *Chem. Mater.* 1998, 10, 1882.
45. Kudo, T.; Oi, J.; Kishimoto, A.; Hiratani, M. *Materials Research Bulletin*, 1991, 26(8) 779.
46. Kumar, B. N.; Anjaneyulu, Y.; Himabindu, V. *J. Chem. Pharm. Res.*, 2011, 3(2), 718.
47. Mashkour, M. S.; Al-Kaim, A. F.; Ahmed L. M.; Hussein, F. H. *Int. J. Chem. Sci.*, 2011, 9(3), 969.
48. Arslan, I.; Balcioglu, I. A.; Bahnemann, D. W., *Applied Catalysis B: Environmental*, 2000, 26(3) 193.

Table 1. The Distinctive Physical And Chemical Characteristics of The Eosin Yellow Dye (Ahmed, 2018).

Values	Parameters
	Structure
2-(2,4,5,7-tetrabromo-6-oxido-3-oxo-3H-xanthen-9-yl)benzoate xanthene	IUPAC name
brilliant red-brown powder dye slightly yellowish in aqueous solution	Class
Acidic	Natural
(515-518) nm	λ_{max}

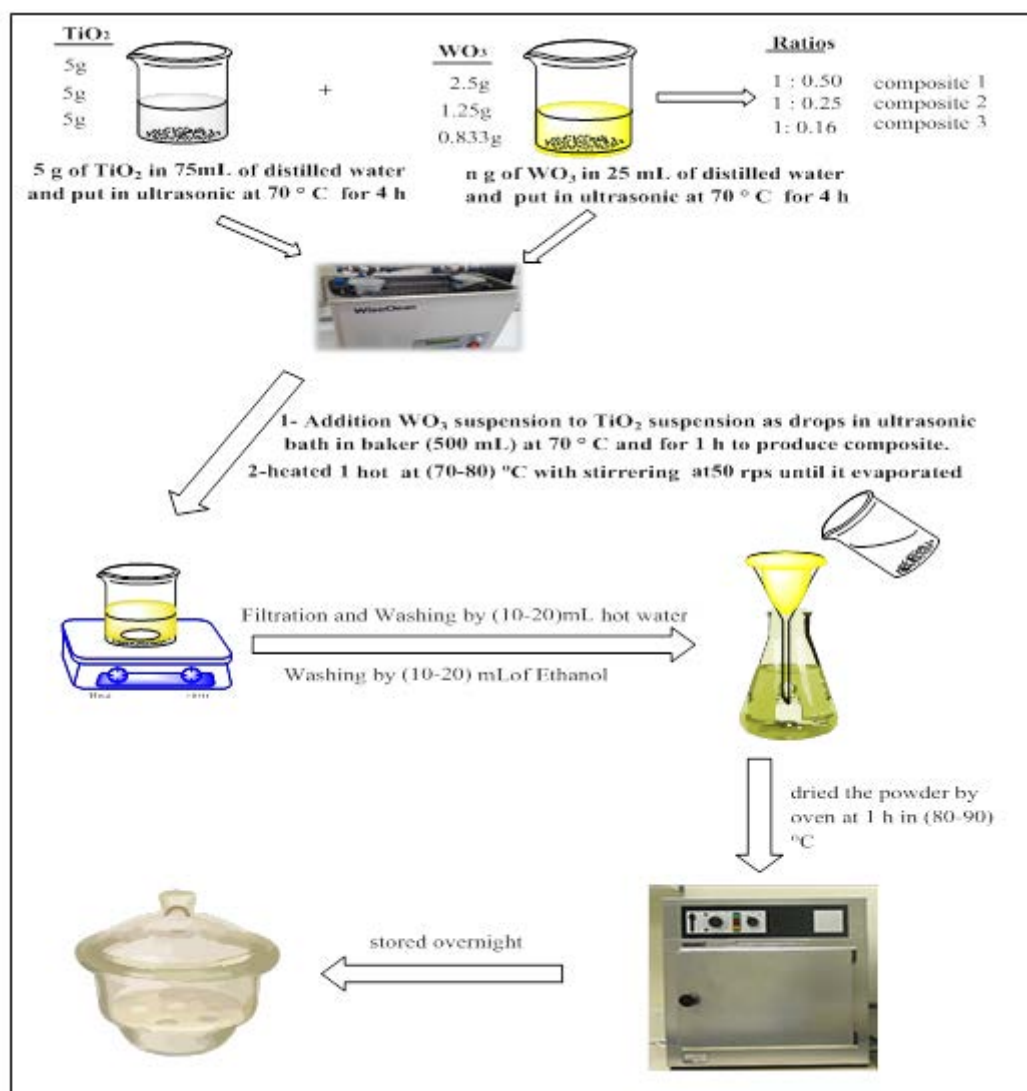


Figure 1. The schematic for full steps of prepared WO₃/TiO₂ composites

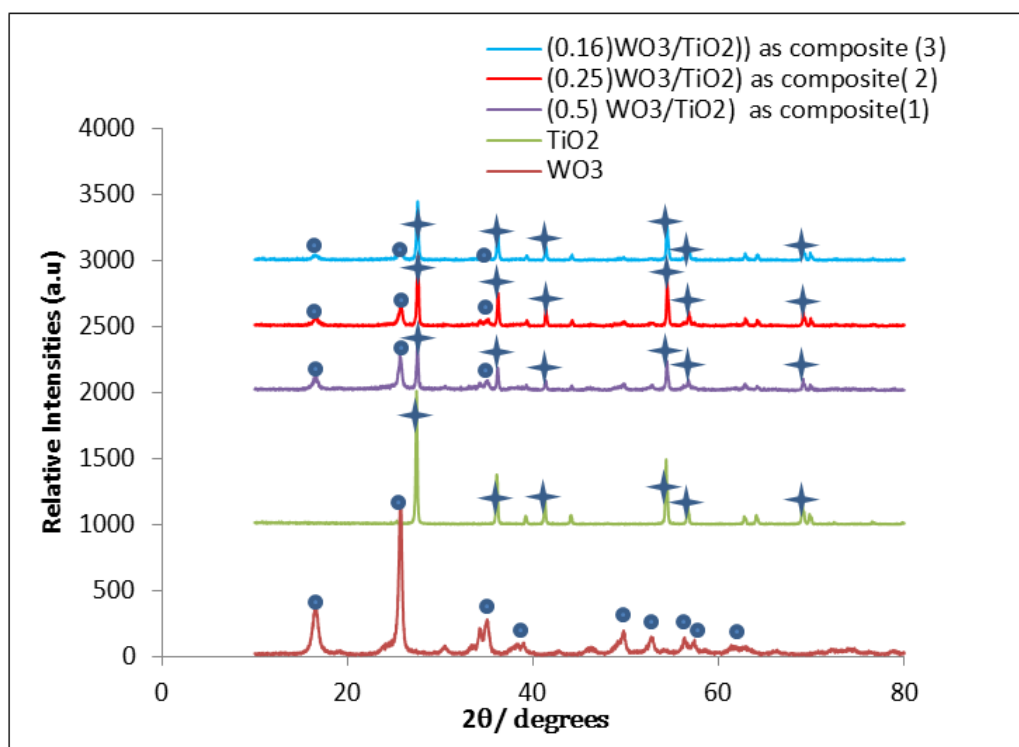


Figure 2. XRD pattern of commercial WO_3 and commercial TiO_2 and its prepared nanocomposites.

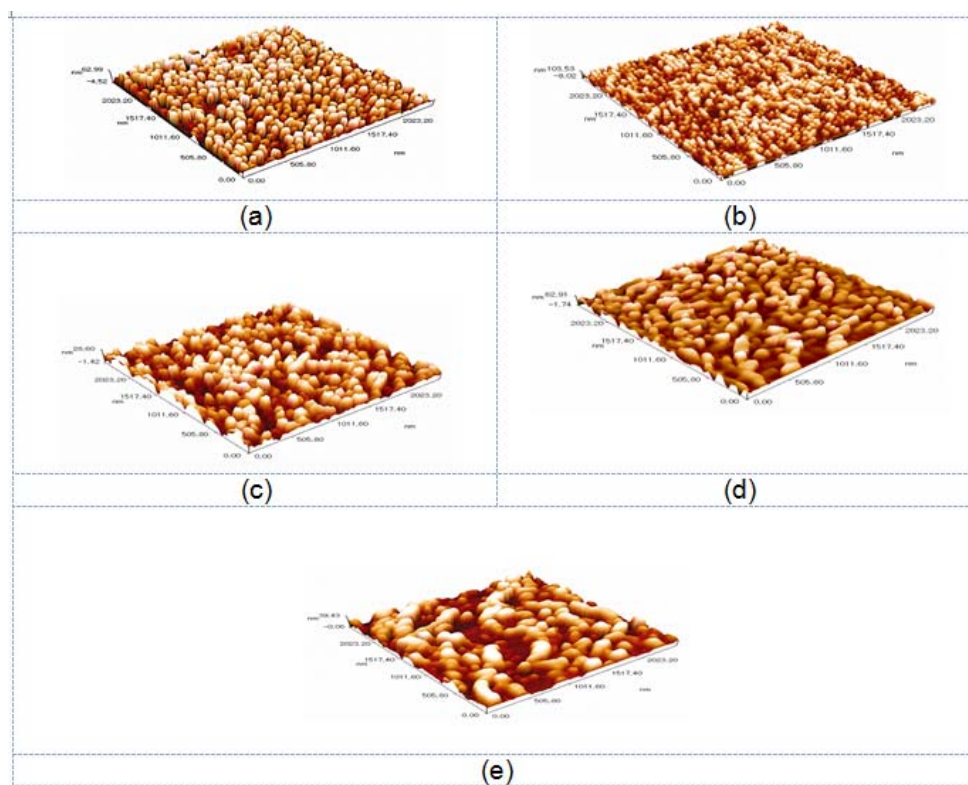


Figure 3. Three-dimensional AFM image of (a) commercial WO_3 , (b) commercial TiO_2 , (c) $(\text{WO}_3/\text{TiO}_2)$ composite 1 (0.5:1), (d) $(\text{WO}_3/\text{TiO}_2)$ composite 2 (0.25:1), and (e) $(\text{WO}_3/\text{TiO}_2)$ composite 3 (0.16:1).

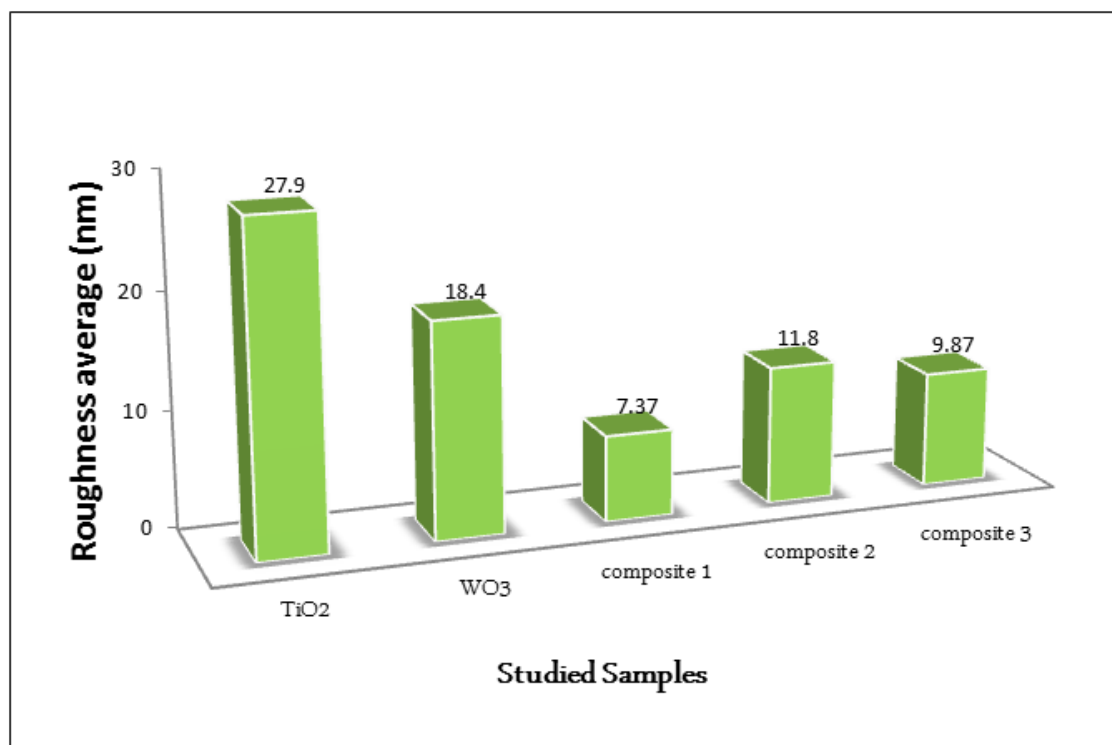


Figure 4. The roughness averages with the studied samples (depended on particle sizes).

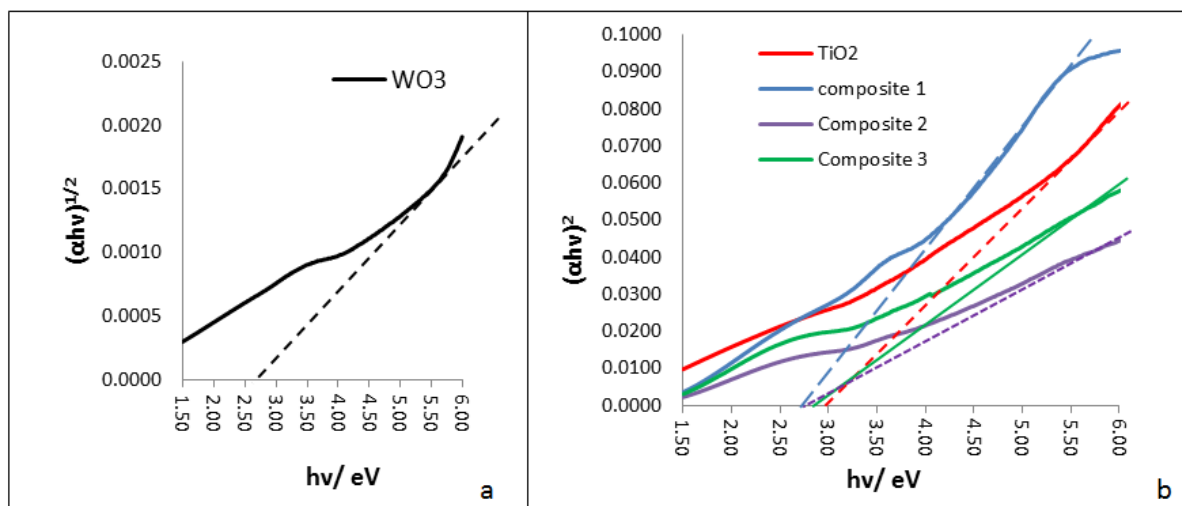


Figure 5. Tauc plot a) for WO₃ as a direct band gap. b) for TiO₂ and prepared (WO₃/ TiO₂) composites 1,2, and 3 as indirect band gaps.

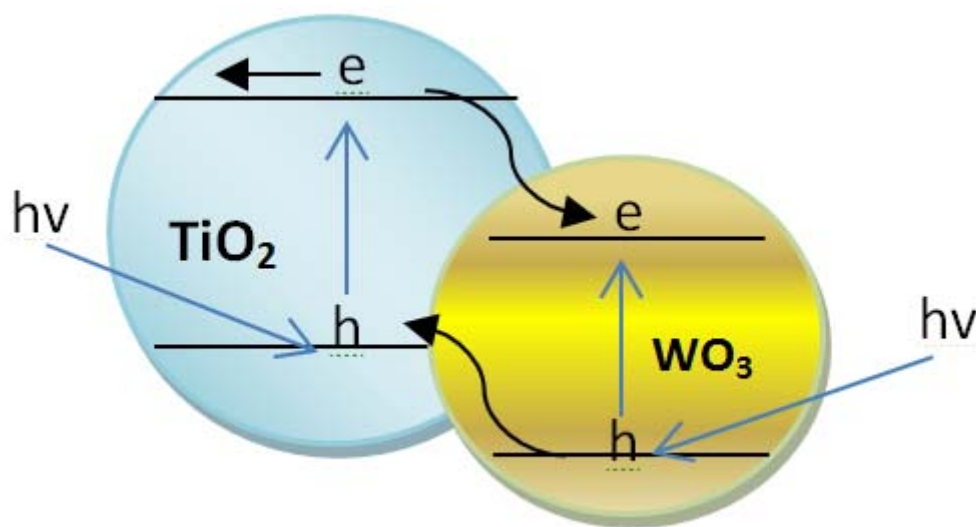


Figure 6. Charge transfer between WO_3 and TiO_2 .

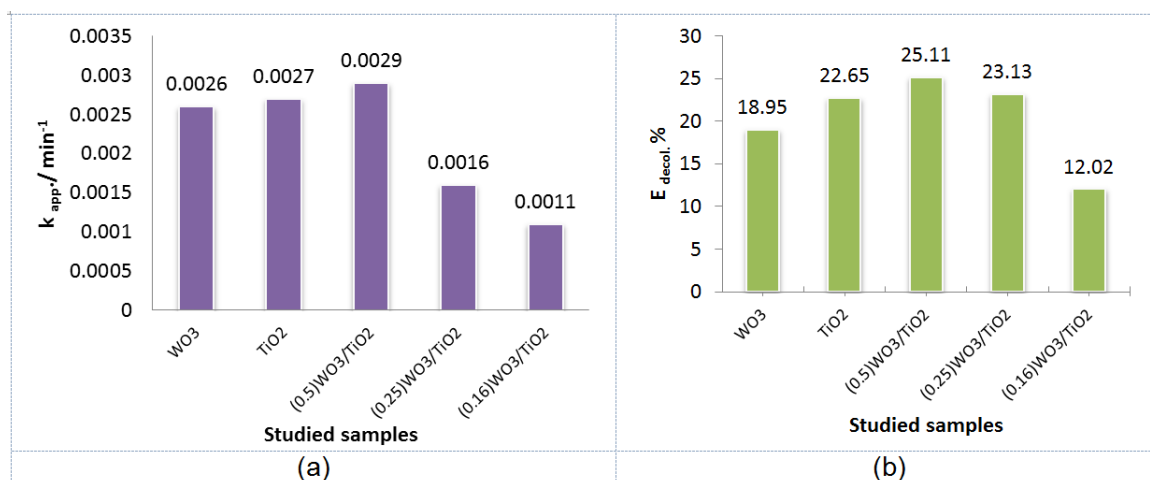


Figure 7. Photocatalytic decolorization of eosin yellow dye with employing WO_3 , TiO_2 and prepared $(\text{WO}_3/\text{TiO}_2)$ composites 1,2 and 3 nanoparticle. at 25°C , 200 mg of catalyst's dose, initial pH 6.09 and 5ppm of eosin yellow dye (a) Relation between appearance rate constant and studied samples and (b) $E_{decol. \%}$ for 90 min verse studied samples.

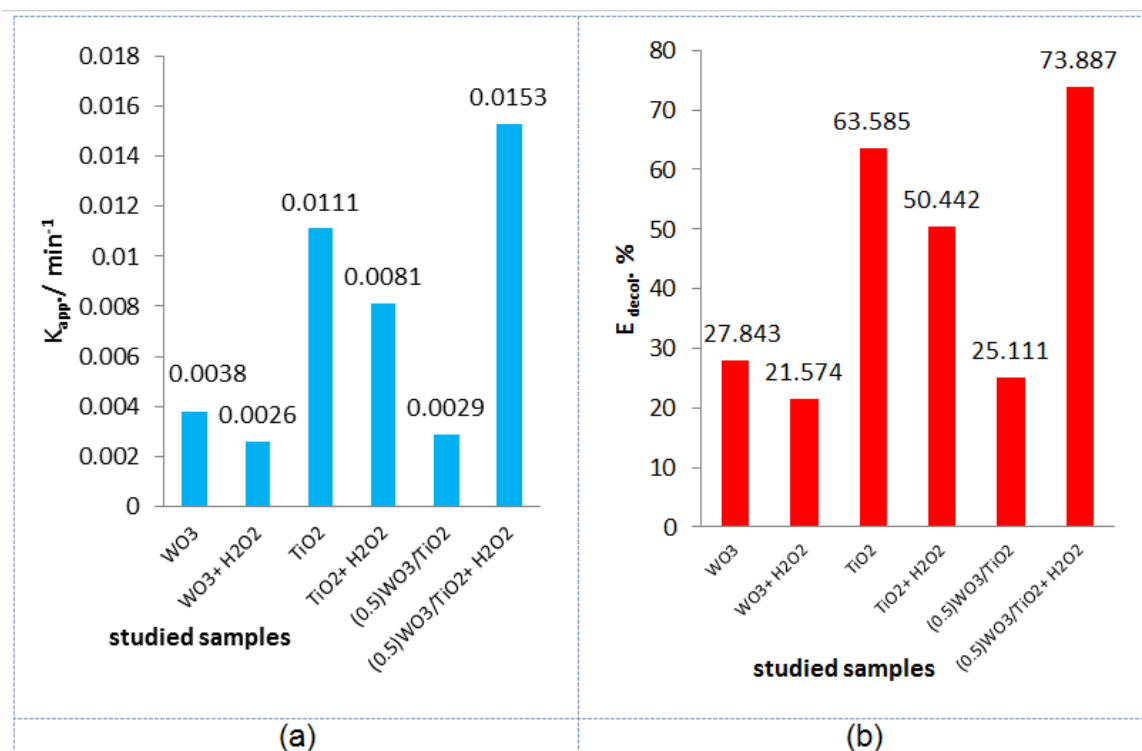


Figure 8. Effect of using H₂O₂ on Photocatalytic decolorization of eosin yellow dye with employing optimum dose 500 mg WO₃, 500 mg TiO₂, and 200 mg prepared (WO₃/TiO₂) composite 1nanoparticle as best doses. At 10⁻² mmol of H₂O₂, 25 °C, 5ppm of eosin yellow dye, and initial pH 6.09 (a) Relation between appearance rate constant and studied samples and (b) $E_{decol} \%$ for 90 min verse studied samples.

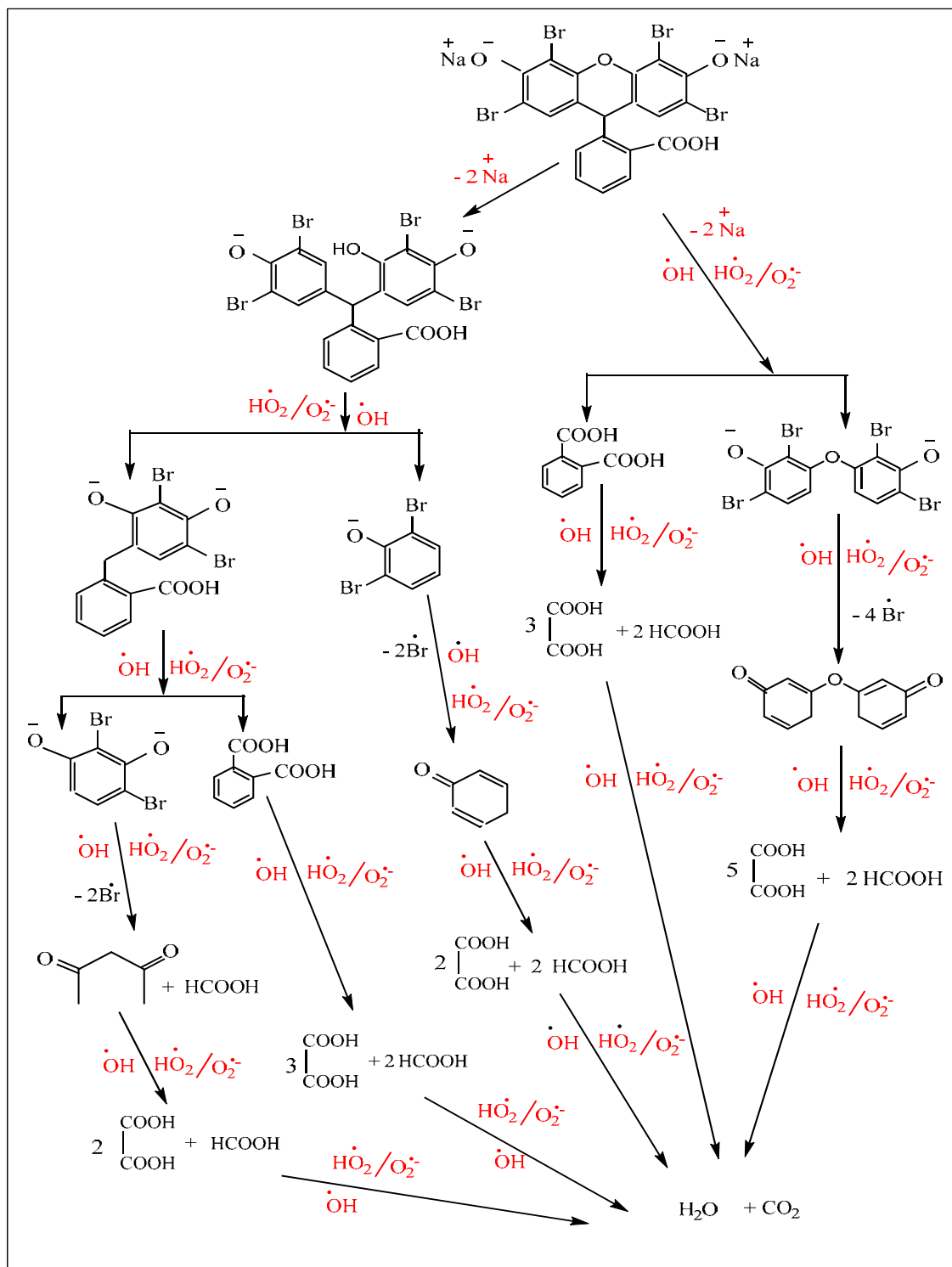


Figure 9. The schematic diagram for the most probable decolorization mechanism of eosin yellow dye in the presence of UV/ WO_3 , or TiO_2 or WO_3/TiO_2 nanocomposite.

JUSTIFICATIVA PARA A SELEÇÃO DE UM SISTEMA ÓTIMO DE DESENVOLVIMENTO DE CAMPO DE ÓLEO NA PARTE ORIENTAL DO MAR DE PECHORA E SEU CÁLCULO**RATIONALE FOR SELECTION OF AN OIL FIELD OPTIMAL DEVELOPMENT SYSTEM IN THE EASTERN PART OF THE PECHORA SEA AND ITS CALCULATION****ОБОСНОВАНИЕ ВЫБОРА И РАСЧЕТ ОПТИМАЛЬНОЙ СИСТЕМЫ РАЗРАБОТКИ НЕФТЯНОГО МЕСТОРОЖДЕНИЯ ВОСТОЧНОЙ ЧАСТИ ПЕЧОРСКОГО МОРЯ**

SABUKEVICH, Violetta Sergeevna^{1*}; PODOPRIGORA, Dmitry Georgievich²;
SHAGIAKHMETOV, Artem Maratovich³

^{1,2,3}Saint-Petersburg Mining University, Department of Development and operation of oil and gas fields. Russian Federation.

** Corresponding author*

e-mail: violettasabukevich@mail.ru

Received 14 January 2020; received in revised form 03 March 2020; accepted 12 March 2020

RESUMO

A justificativa para a seleção e o cálculo do sistema ideal para o desenvolvimento do campo de petróleo do Mar de Pechora é uma tarefa técnico-científica extremamente difícil. Condições climáticas severas da região do Ártico, cobertura de gelo, limites de formação de poços, taxas lentas de perfuração para campos de petróleo *offshore* e afastamento das bases de suprimentos multiplicam o custo dos projetos e criam dificuldades significativas no projeto de engenharia do sistema de desenvolvimento de campo. Para resolver esses problemas, é preciso usar tecnologias altamente eficientes para o desenvolvimento de campos de petróleo *offshore*, o que garantirá a produção intensiva de petróleo, obtendo assim receitas significativas para pagar as despesas. O objetivo deste trabalho é fornecer a base para a seleção e calcular o sistema ótimo de desenvolvimento para um campo de petróleo na parte oriental do mar de Pechora. A solução das tarefas foi realizada com base nas características identificadas no desenvolvimento de campos de petróleo *offshore* do Ártico, na análise de dados geológicos e físicos no campo de petróleo, em um conjunto de trabalhos teóricos, analíticos e em modelagem matemática. A modelagem matemática foi realizada usando métodos padrão e adaptados para o cálculo de sistemas de desenvolvimento de campos de petróleo. Com base nos dados recebidos, concluiu-se que o sistema linear de poços horizontais é ideal para o desenvolvimento do campo. A vazão crítica e inicial dos poços horizontais e os indicadores tecnológicos básicos foram calculados em função do tempo. A estimativa do fluxo de caixa descontado e do índice de lucro descontado demonstrou que o projeto de investimento pode ser iniciado. Como o campo de petróleo está agora sob exploração suplementar, os dados obtidos na pesquisa podem ser aplicados para projetar o sistema de desenvolvimento de campos de petróleo assim que sua exploração industrial for aprovada.

Palavras-chave: *Zona de prateleira do Ártico, o mar de Pechora, sistema de desenvolvimento.*

ABSTRACT

Rationale for selection and calculation of the optimal system for the development of the Pechora Sea oil field is an extremely difficult scientific-technical task. Severe climate conditions of the Arctic region, ice cover, well stock formation limits, slow rates of drilling for offshore oil fields, and remoteness from supply bases multiply the cost of projects and create significant difficulties in engineering design the field development system. To solve these problems, one needs to use highly efficient technologies for offshore oil fields development, which will ensure intensive oil production, thus obtaining significant revenues to pay off the expenses. The purpose of this work is to provide the basis for selection as well as calculate the optimum development system for an oil field in the eastern part of the Pechora Sea. The solution of the tasks was carried out on the basis of the features identified in the development of Arctic offshore oil fields, the analysis of geological and physical data on the oil field, a set of theoretical, analytical works, and mathematical modeling. Mathematical modeling was performed using standard and adapted methods for calculating oil field development systems. Based on the data received, it was concluded that it is the linear system of horizontal wells, which is optimal for the field development. Horizontal wells critical and initial flow rate and basic technical indicators have been calculated versus time. The estimation of the discounted cash flow and the discounted profit index has demonstrated that the investment project can be

initiated. Since the oil field is now under supplementary exploration, the data obtained in the research can be applied for designing the oil field development system as soon as its industrial exploitation is approved.

Keywords: *Arctic shelf zone, the Pechora Sea, development system.*

АННОТАЦИЯ

Обоснование выбора и расчет оптимальной системы разработки нефтяного месторождения Печорского моря является исключительно сложной научно-технической задачей. Суровый арктический климат, тяжелые ледовые условия, ограничения по формированию фонда скважин, невысокие темпы разбуривания месторождений и значительная удаленность от баз обеспечения многократно увеличивают стоимость проектов и создают значительные трудности при проектировании системы разработки месторождения. Для решения этих проблем необходимо применение высокоэффективных технологий разработки нефтяных месторождений, которые обеспечат интенсивную добычу нефти для достижения больших объемов выручки с целью окупаемости понесенных затрат. Цель данной работы – обосновать выбор и рассчитать оптимальную систему разработки нефтяного месторождения восточной части Печорского моря. Решение поставленных задач осуществлялось на основе выявленных в работе особенностей освоения арктических шельфовых нефтяных месторождений, анализа геолого-физических данных о нефтяном месторождении, комплекса теоретических, аналитических работ и математического моделирования, выполненного с использованием стандартных и адаптированных методов расчета систем разработки нефтяных месторождений. На основе полученных данных был сделан вывод, что оптимальной для разработки месторождения является линейная система горизонтальных скважин. Проведены расчеты начального дебита горизонтальных скважин, критического дебита, дан прогноз изменения давления на контуре питания и основных технологических показателей разработки. Оценка накопленного дисконтированного денежного потока и дисконтированного индекса доходности показала, что инвестиционный проект может быть принят к реализации. В связи с тем, что месторождение в настоящее время находится в доразведке, полученные в статье сведения могут быть использованы при проектировании системы разработки нефтяного месторождения после принятия решения о начале его промышленного освоения.

Ключевые слова: *Арктический шельф, Печорское море, система разработки.*

1. INTRODUCTION:

In recent years, the Arctic region is entering a new stage of its development connected with the exploitation of its offshore natural resources. The development of the Arctic shelf zone oil fields is the strategic target for Russia. In the long term they are to replenish the depleting onshore resources (Vasil'cov and Vasil'cova, 2018).

The Pechora Sea is one of the richest in hydrocarbons areas of the Arctic shelf zone. Three average-sized and large oil fields have been discovered in its eastern part apart from the Prirazlomnoye field which is being developed at present. However, the development of the Arctic shelf zone oil fields requires the solution of a number of particular problems (Prokhorova *et al.*, 2016; Shatalova *et al.*, 2014). The latter include severe climate conditions of the Arctic region, hard ice conditions, well stock formation limits, slow rates of drilling for oil fields and remoteness from providing stations. All of these multiply the cost of projects and create obstacles for their implementation. To solve these problems one needs to use highly efficient technologies for the field development which are to ensure intensive oil

recovery thus obtaining significant revenues to pay off the expenses (Carayannis *et al.*, 2019; Vasil'cov and Vasil'cova, 2018; Yemelyanov *et al.*, 2018, 2019).

The main target of this work was to provide the basis for selection as well as calculate the optimum development system capable of intensive oil production with minimal expenses on its construction for an oil field in the eastern part of the Pechora Sea.

2. LITERATURE REVIEW:

2.1 Geological and physical characteristics of the field

The oil field under examination is located in the eastern part of the Pechora Sea, to the south of the Novaya Zemlya archipelago, 80 km north of the mainland (Figure 1). The seabed in the area of the oil field is a low-lying coastal plain sloping gently to the north-west. The sea floor sediments are represented by fine dust sand underlied by loam and clays. Sea depths in the area vary between 25 and 45 metres. The region is seismically stable (Dzyublo, 2009; Yefremkin *et*

al., 2009; Zhuravlyov *et al.* 2014). The coldest month of the year is January with average temperature of -8 degrees C°, the warmest is July with +7 degrees C°. Average annual temperature is -2 degrees C°. The strongest winds in the area are observed in November to February with the average monthly velocity being 8 metres per second. Maximum wind speed is up to 28 m/s gusting up to 40 m/s. Ice cover season lasts from November to June. Ice thickness averages between 0,5 and 0,7 metres, reaching the thickest point of up to 1,2 metres. Prevailing height of hummocks is 1,0 – 1,5 metres (4 metres maximum) (Myuller *et al.*, 2003; Terziyev *et al.* 1991).

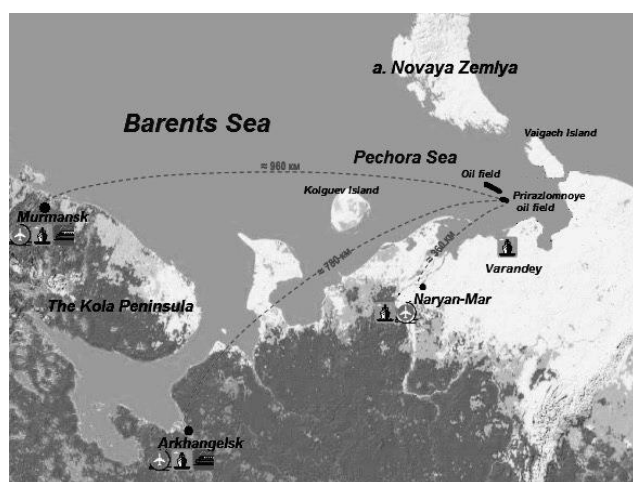


Figure 1. Overview map of the area

The oil field is associated with a massive oil reservoir located in Carboniferous sediments (Figure 2). Its structure is a long and narrow anticlinal fold. The size of the reservoir is estimated 45 km long, 2, 0 – 2,5 km wide and 160 m high. Water-oil contact (hereinafter – WOC) is established on the floor of the marginal oil-saturated layer at the point of minus 3285 metres (Dzyublo, 2009; Zhukov *et al.*, 2009).

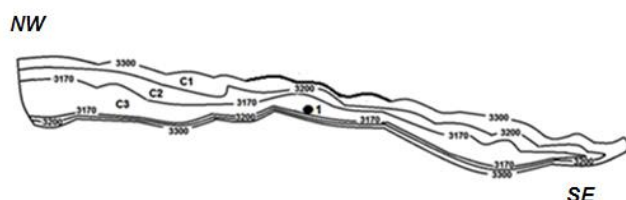


Figure 2. Oil field diagram (Zhukov *et al.*, 2009).

Legend ● 1 Prospective borehole; —3200— roof isolines of productive horizons; C1, C2, C3 are target oil-bearing layers represented by carbonate rocks in C1 –C3 horizons.

Productive reservoir bed is associated with the sediments of Serpukhov and Bashkir floors of the Lower Carboniferous period. The reservoir is

mainly made up of grained, silt-grained limestones and stretches throughout the field (Abstract on the feasibility study (draft), 2020). The reservoir is of fractured and porous type. Additional characteristics of the reservoir are given in table 1. The overlying seals are represented by the Kungurian sediments of the Lower Perm period (Zhukov *et al.*, 2009). An exploration well was drilled within the oil field. During the exploratory drilling while layers was testing the oil flow rate was received 168 m³ a day, gas -29264m³ a day, gas factor 174m³/m³. The recovered oil is light, sulfurous, paraffinic and low in tar. Its density is 0,842 gr/cm³. The geophysical research of the Middle and Upper Carboniferous sediments suggests that they contain industrial oil reserves which have not been confirmed so far by drilling and testing of the layers (Dzyublo, 2009; Tanygin *et al.* 2014; Zhuravlyov *et al.* 2014).

Since the field under examination is located in the area with hard ice conditions, the only possible method of its development is to install gravity-based structure (hereinafter – GBS) (Wang *et al.*, 1994).

2.2 The basis for the field development system selection

Developing the Arctic offshore fields has a number of features. To begin with, the projects are highly capital – intensive. Launching such projects is preceded by costly and time-consuming engineering, research and construction activities in the severe climate and hard ice conditions (Matskevitch, 2007). For instance, the engineering of the Prirazlomnoye oil and gas field, also located in the Pechora Sea, was estimated to be 3 billion dollars by its developers PAO “Gazpromneft” (public joint stock company) (Forbes, 2013). Of which 1,5 are the costs of GBS and 1,5 are drilling expenditures. Therefore, it is essential to apply highly efficient technologies for the field development which are to ensure intensive oil recovery thus obtaining significant revenues to pay off the expenses (Gazprom neft, 2020). Alongside this, development systems are traditionally required to provide high degree of oil extraction (Alkhimov *et al.* 2008; Hermawan *et al.*, 2019; Seyyedattar *et al.* 2019; Lin *et al.*, 2019; Rahman, 2017).

The development systems engineering is complicated by the limits of well stock formation, which depends on the GBS capabilities. High cost of drilling also influences the number of wells (Shandrygin and Dubrovsky, 2015). The price of a single Arctic shelf well construction is more than 50 million dollars. Companies involved in the

extraction of hydrocarbons in the Arctic shelf zone, have to develop and implement new technologies constantly in order to reduce the number of wells and hence diminish the drilling expenses and improve the economics of the projects (Osisanya, 1997).

Field development systems are constructed on the basis of inclined directional wells with long horizontal section (hereinafter – horizontal wells) (Ozkan and Raghavan, 1990). As practice shows, such systems only are capable of providing profitable oil extraction on the Arctic shelf zone due to the fast rates of development (Lacy *et al.*, 1992; Joshi and Ding, 1996; Thakur, 1999).

The Pirazlomnoye field, where all the production and injection wells have long horizontal section, may serve as an example to this. A 6474 metre long well with horizontal deflection from the vertical axis of 4989 metres was drilled on the field in 2018. Maximum horizontal deflection length wells is planned 6300 metres. Also, highly technological multi-hole “fishbone” well is being drilled on the field. Figure 3 shows the distribution of horizontal wells on the Pirazlomnoye field, 6m variant (Figure 3).

From the analysis of the pattern of wells distribution it can be concluded that it was developed taking into account the size of the oil field, besides, the position of production and injection wells is influenced by the profitability of drilling. The tasks are solved, such as: maximum resource involvement, obtaining high coverage rate and oil recovery factor and introducing water into the reservoir using injection wells for compensation of extracted oil (Alkhimov *et al.* 2008; Lin *et al.*, 2019; Alekseev *et al.* 2017).

Finding wellheads of all wells within the limited area of GBS influences the direction of well drilling. That is, if an oil-bearing structure is represented by a long narrow anticlinal fold such fields on land are generally developed by systems of cross-sectional horizontal wells. For instance, the Mikhailovskoye oil field which is located in Bashkiria (Figure 4) (Berdin, 2001). However, offshore fields are commonly developed by systems of wells with long horizontal sections, drilled lengthwise the oil-bearing structure (Figure 3). Drilling transverse wells from GBS is also possible but has some disadvantages. Wells like that will be 10-15% longer which will increase the cost of drilling and thus harm the economics of the project. The trajectory of wells will be very complicated; hence the management and control of wells will be hard to perform which can result in

accidents and even loss (Giannesini, 1988).

The selection of the development system is complicated by low projected rates of drilling on the field. The experience of the Pirazlomnoye field exploitation demonstrates that no more than 4 wells on average can be drilled annually on one GBS in the Arctic shelf zone. This could be explained by difficulties in organising logistics operations aimed at delivery of equipment and stuff for drilling to GBS, especially in winter months (Alkhimov *et al.* 2008; Oganov, 2005).

Assuming that the field is associated with a long narrow anticlinal fold and specific features of the Arctic shelf oil fields exploitation it is evident that the development of the oil field under examination must be conducted using linear system of horizontal wells comprising one row of production wells, placed centrally and lengthwise the oil-bearing structure and two rows of injection wells placed along the oil-bearing boundary from its southern and northern sides. The proportion of production and injection wells is 1:1 (Kuznetsova *et al.*, 2017).

Since the deflection of wells from the vertical axis reaches 6300 m on the Pirazlomnoye field, the length of the field section for development could be up to 12 km (Figure 5).

3. MATERIALS AND METHODS:

Calculating optimum length of horizontal sections. Since the main criterion of the Arctic shelf zone drilling is its economic profitability, the length of horizontal sections of wells should be calculated on the basis of accumulated discounted cash flow estimation (hereinafter – *NPV*). Thus the optimum length of the horizontal sections will be the one at which *NPV* is the largest (Osisaniya, 1997; Mukhametshina *et al.*, 2005).

3.1 Calculus of cash flow

Oil production (in million tonnes per year) is determined at the flow rate of the well corresponding to the length of the horizontal section of the well; cash flow is calculated by multiplying the amount of recovered oil by oil cost per one ton in dollars.

$$NPV = \sum CF_i \alpha - CE \quad (1)$$

where CF_i – cash flow in i – year (in dollars); α – discount factor; CE – capital expenditures in dollars.

$$\alpha = \frac{1}{(1+E)^{t-1}} \quad (2)$$

where E – discount rate, %; t – sequence number of the year of project implementation.

The total cost of a well construction was attributed to capital expenditures, taking into account the complication factor when drilling a horizontal section.

After obtaining data, a graph is drawn, showing the correlation between NPV and the length of a horizontal section. The length value of the horizontal section of a well at the inflection point will be optimal (Dosunmu *et al.* 2015; Tadeu *et al.*, 2019; iannesini 1988; Rahman and Bobkova, 2016).

3.2 Calculating horizontal wells initial flow rate

Horizontal wells initial flow rate (hereinafter – initial rate) has been calculated using Joshi's method (Joshi, 1991; Ahmed 2010).

Initial rate is computed by

$$Q_{oh} = \frac{0,00708 h k_h \Delta P}{\mu_0 B_0 \left[\ln(Z) + \left(\frac{B^2 h}{L} \right) \ln \left(\frac{h}{2r_w} \right) \right]} \quad (3)$$

where B – the factor characterizing the bed anisotropy; L – the length of a horizontal section, ft; μ_0 – oil viscosity, cP; B_0 – oil formation volume factor, bbl/STB; h – effective stratum thickness, ft; r_w – wellbore radius, ft; ΔP – pressure drop from the drainage boundary to wellbore, psi; k_h – horizontal permeability, md; k_v – vertical permeability, md.

Bed anisotropy factor is determined by

$$B = \sqrt{\frac{k_h}{k_v}}, \quad (4)$$

Z – parameter is found by the formula:

$$Z = \frac{a + \sqrt{a^2 - (L/2)^2}}{(L/2)} \quad (5)$$

where a – half the major axis of the drainage ellipse.

$$a = (L/2) \sqrt{0,5 + \sqrt{0,25 + \left(2r_{eh}/L \right)^4}} \quad (6)$$

where r_{eh} – horizontal well drainage radius, ft.

3.3 Calculating horizontal wells critical flow rate

The value of the production rate at which water cone is stationery and water breakthrough are not available is called critical. To calculate the horizontal wells critical flow rate (hereinafter – critical rate) Chaperon's method has been used (Chaperon 1986; Ahmed 2010).

The critical rate is determined by the formula:

$$Q_{oc} = 0,0783 \cdot 10^{-4} \left(\frac{L q_c^*}{r_{eh}} \right) (\rho_w - \rho_0) \frac{k_h [h - (h - D_b)]^2}{\mu_0 B_0}, \quad (7)$$

$$Q_{oc} = 0,0783 \cdot 10^{-4} \left(\frac{L q_c^*}{r_{eh}} \right) (\rho_w - \rho_0) \frac{k_h [h - (h - D_b)]^2}{\mu_0 B_0}, \quad (8)$$

where L – the length of a horizontal section, ft; q_c^* – dimensionless function; r_{eh} – horizontal well drainage radius, m; ρ_0 – oil density, lb/ft³; ρ_w – water density, lb/ft³; μ_0 – oil viscosity, cP; B_0 – oil formation volume factor, bbl/STB; k_h – horizontal permeability, md; h – effective stratum thickness, ft; D_b – distance between the WOC and the horizontal well, ft.

Dimensionless function is found by Joshi's formula (Joshi, 1991; Ahmed 2010):

$$q_c^* = 3,9624955 + 0,0616438 \cdot \alpha'' - 0,000504 \cdot (\alpha'')^2 \quad (8)$$

α'' parameter is found by the formula:

$$\alpha'' = \left(\frac{r_{eh}}{h} \right) \sqrt{\frac{k_v}{k_h}} \quad (9)$$

α'' values lie within the framework: $1 \leq \alpha'' < 70$ and $2r_{eh} < 4L$.

3.4 Calculating horizontal well breakthrough time

To estimate the horizontal well breakthrough time Papatzacos' method has been applied (Papatzacos *et al.*, 1991; Høyland *et al.*, 1989; Ozkan 1990). The time to water breakthrough as expressed in days is calculated by the formula:

$$t_{BT} = \frac{22758,528 h m \mu_0 t_{DBT}}{k_v (\rho_w - \rho_0)} \quad (10)$$

where ρ_0 – oil density, lb/ft³; ρ_w – water density, lb/ft³; h – effective stratum thickness, ft; μ_0 – oil viscosity, cP; m – porosity, fraction, %; t_{DBT} – dimensionless breakthrough time; k_v – vertical permeability, md.

The dimensionless breakthrough time t_{DBT} is determined by the formula:

$$t_{DBT} = 1 - (3q_D - 1) \ln \left(\frac{3q_D}{3q_D - 1} \right) \quad (11)$$

The dimensionless rate (q_D) is determined by the formula:

$$q_D = \frac{20333,66\mu_0 B_0 Q_0}{Lh(\rho_w - \rho_0)\sqrt{k_v k_h}} \quad (12)$$

where μ_0 – oil viscosity, cP; B_0 – oil formation volume factor, bbl/STB; Q_0 – oil flow rate, STB/day; L – the length of a horizontal section, ft; h – effective stratum thickness, ft; ρ_0 – oil density, lb/ft³; ρ_w – water density, lb/ft³; k_h – horizontal permeability, md; k_v – vertical permeability, md.

3.5 Forecast of pressure variations at the well drainage boundary

In order to estimate pressure variations at the well drainage boundary during the oil field development Y. Zheltov's method has been used, taking into account the fact that in the time of drilling t^* which is 3 years, the volumes of water coming from the edge water zone and liquid withdrawal from the formation are variables in time (Zheltov 1998; Laperdin, 2013).

The calculations have been done for:

- the period of increasing liquid yield – $0 \leq t \leq t^*$;
- the period of constant liquid yield – $t^* \leq t \leq t^{**}$;
- the period of first water injections into the edge water zone; while the current liquid withdrawal is partially compensated by water injections into the bed and its inflow from the edge water zone – $t^{**} \leq t \leq t^{***}$;
- the period in which oil is forced out only by water injection into the edge water zone – $t \geq t^{***}$.

It has been assumed that the area of the field under consideration has an ellipsoidal shape. In order to define the external boundary radius, we have represented the field as a circle whose radius has been calculated basing on the ellipse perimeter. A circle area is larger than that of an ellipse; consequently, the former was diminished to be equal to the latter. Thus we got the external

boundary radius equal to the circle radius reduced to the area of the original ellipse (R , m) (Gimatudinov *et al.*, 1983).

Boundary pressure with $0 \leq t \leq t^*$ is determined by the formula:

$$p_{con}(\tau) = p_0 - \frac{\mu_w \alpha_0 R^2}{2\pi k h X} J(\tau) \quad (13)$$

where R – external boundary radius, m; p_0 – formation pressure, psi; μ_w – water viscosity, cP; α_0 – annual extraction from newly introduced wells, m³/year²; X – piezoconductivity quotient, ft²/sec; k – fracture formation permeability, md; h – effective stratum thickness, m.

Thus, the reduced time τ is determined by the formula:

$$\tau = \frac{Xt}{R^2} \quad (14)$$

where t – years.

The value of the integral $J(\tau)$ is calculated by the formula:

$$J(\tau) = 0,5\tau - 0,178[1 - (1 - \tau)^{-2,81}] + 0,487[(1 + \tau) \lg(1 + \tau) - \tau] \quad (15)$$

The boundary pressure with $t^* \leq t \leq t^{**}$ is determined by the formula:

$$p_{con}(\tau) = p_0 - \frac{\mu_w \alpha_0 R^2}{2\pi k h X} [J(\tau) - J(\tau - \tau^*)] \quad (16)$$

The boundary pressure with $t^{**} \leq t \leq t^{***}$ is determined by the formula:

$$p_{con}(\tau) = p_0 - \frac{\mu_w \alpha_0 R^2}{2\pi k h X} [J(\tau) - J(\tau - \tau^*)] - \frac{\mu_w \alpha'_0 R^2}{2\pi k h X} J(\tau - \tau^{**}) \quad (17)$$

where α'_0 – conversion factor.

The boundary pressure with $t \geq t^{***}$ is determined by the formula:

$$p_{con}(\tau) = p_0 - \frac{\mu_w \alpha_0 R^2}{2\pi k h X} [J(\tau) - J(\tau - \tau^*)] - \frac{\mu_w \alpha'_0 R^2}{2\pi k h X} [J(\tau - \tau^{**}) - J(\tau - \tau^{***})] \quad (18)$$

3.6 The main indicators of the field development

The calculation of technological indicators of the field development was made using TatNIPIneft (Tatar Scientific Research and Design Institution) methodology (hereinafter – method) for the model of a layer-by-layer and zonally heterogeneous in its reservoir properties bed

(Laperdin, 2013). Apart from layer-by-layer heterogeneity the oil field development indicators are influenced by the difference between oil and water viscosity, as well as incomplete water-oil displacement. The effect of these factors is determined by a complex value – calculated layer-by-layer heterogeneity. While calculating horizontal wells are replaced by vertical ones considering the production rate of horizontal and vertical wells (Borisov *et al.*, 1964).

3.7 Calculation of development indicators

The density of well pattern is determined by the formula:

$$S_c = \frac{S}{n_0} \quad (19)$$

where S – oil-bearing area, m²; n_0 – total number of wells in the field.

The ratio of production and injection wells at which the maximum amplitude production rate is achieved can be calculated by the formula:

$$\bar{m} = \frac{\alpha + 1}{\alpha} \sqrt{\mu_*} \quad (20)$$

where α – the indicator taking into account differences between average recovery factor of extraction and injection wells (depends on zonal heterogeneity); μ_* – the quotient accounting mobility of the displacing agent (water) and oil in bed conditions.

$$\alpha = \frac{1}{U_3^2} \left[0,3 - \frac{0,02}{U_3^2} \right] \quad (21)$$

where U_3^2 – zonal heterogeneity.

$$\mu_* = \frac{\mu_0}{\mu_w} [1 - 1,5(1 - K_2)] \quad (22)$$

where μ_0 – oil viscosity, cP; μ_w – water viscosity, cP; K_2 – water-oil displacement factor.

The maximum rate of recoverable oil reserves withdrawal is reached when the initial ratio of production and injection wells is $m = 1,2 \cdot \bar{m}$.

The relative well injectivity factor (v) of the wells selected for injection purposes is determined by the formula:

$$v = \frac{\alpha + 1}{\alpha + 1 - \frac{m}{m+1}} \quad (23)$$

The relative wells productivity function (φ) is determined by the formula:

$$\varphi = \frac{1}{\frac{1}{v\mu_*} + \frac{1}{1+m-v}} \cdot \frac{1}{m+1} \quad (24)$$

The amplitude production rate of the whole oil reservoir under examination is determined by the formula:

$$q_0 = 365 K_{av} n_0 \Delta p \varphi \quad (25)$$

where K_{av} – average productivity quotient, tonnes/day·Pa; Δp – pressure differential between production and injection bottom-holes, Pa.

3.8 Calculation of oil reserves exploitation characteristics

Mobile oil reserves (Q_m) are determined by the formula:

$$Q_m = Q_b K_1 K_2 \quad (26)$$

where Q_b – balance oil reserves (in million tonnes); K_1 – well pattern factor showing the share of oil bed volume under this well distribution; K_2 – water-oil displacement factor.

$$K_1 = 1 - a \cdot S \quad (27)$$

where a – constant quotient ($a=0,2$); S – one well area, km².

The estimated layer-by-layer heterogeneity of the bed is determined by the factor (U_p^2), which is calculated by the formula:

$$U_p^2 = U_1^2 + (U_1^2 + 1) \frac{(U_3^2 + 1)}{\left(\frac{U_3^2}{4} + 1\right)} \cdot \frac{2,2}{m+1} \quad (28)$$

where U_1^2 – layer-by-layer heterogeneity.

The marginal share of water in liquid rate of production well is calculated by the formula:

$$A = \frac{A_2}{(1 - A_2)\mu_{0z} + A_2} \quad (29)$$

where A_2 – marginal mass share of water, %, μ_{0z} – a factor which takes into account distinctions between a displacing agent and reservoir oil in mobility in μ_* times and density in ρ_* times.

$$\rho_* = \frac{\rho_w}{\rho_0} \quad (30)$$

where ρ_0 – oil density, lb/ft³; ρ_w – water density, lb/ft³.

$$\mu_{0z} = 0,5(1 + \mu_*)\rho_* \quad (31)$$

Mobile oil exploitation factor (K_3) under the given layer-by-layer bed heterogeneity (U_p^2) and marginal share of the agent (A) is:

$$K_3 = K_{n3} + (K_{k3} - K_{n3})A \quad (32)$$

$$K_{n3} = \frac{1}{1,2 + 4,2U_p^2} \quad (33)$$

$$K_{k3} = \frac{1}{0,95 + 0,25U_p^2} \quad (34)$$

Estimated total liquid withdrawal in fractions of mobile oil reserves (F) is determined from the ratio:

$$F = K_{n3} + (K_{k3} - K_{n3}) \ln \frac{1}{1 - A} \quad (35)$$

Initial recovered liquid (Q_{F0}) and oil (Q_0) reserves are determined by the formulas:

$$Q_{F0} = Q_m F \quad (36)$$

$$Q_0 = Q_m K_3 \quad (37)$$

Mass recovered liquid reserves (Q_{F02}) under surface conditions will be:

$$Q_{F02} = Q_0 + (Q_{F0} - Q_0) \cdot \mu_{0z} \quad (38)$$

Average mass fraction of water in total liquid recovery is determined by the formula:

$$A_{av} = 1 - \frac{Q_0}{Q_{F02}} \quad (39)$$

Oil recovery factor is determined by the formula:

$$K_{ro} = \frac{Q_0}{Q_b} = K_1 K_2 K_3 \quad (40)$$

3.9 Estimating oil and water production rates dynamics

In order to estimate oil production within the task under consideration the process of the field development has been divided into the following stages:

- Stage 1 – the stage of field commissioning (lasts 3 years). New production wells are started (3 wells a year). The development is conducted in the depletion mode and reservoir pressure does not go below the saturation pressure, with elastic regime prevailing;
- Stage 2 – the stage of extraction with constant production rate (lasts 3 years). A system of reservoir pressure support, which consists of 9 injection wells, is formed;
- Stage 3 – the stage lasts until the maximum water cut. Under the Arctic shelf

condition it averages 95%;

The current oil production rate is determined by the formula:

$$q_t = \frac{\frac{q_0}{Q_0}}{1 + 0,5 \frac{q_0}{Q_0}} \left[Q_0 \frac{n_{t0}}{n_0} - (q_1 + q_2 + \dots + q_{t-1}) \right] \quad (41)$$

The estimated current liquid rate under reservoir conditions is determined by the formula:

$$q_{tF} = \frac{\frac{q_0}{Q_{F0}}}{1 + 0,5 \frac{q_0}{Q_{F0}}} \left[Q_{F0} \frac{n_{t0}}{n_0} - (q_{F1} + q_{F2} + \dots + q_{F(t-1)}) \right] \quad (42)$$

The mass current liquid rate under surface conditions is determined by the formula:

$$q_{tF2} = q_t + (q_{tF} - q_t) \mu_{0z} \quad (43)$$

On the third stage the calculations are made with $\frac{n_{t0}}{n_0} = 1$ (n_{t0} – the number of operating wells in t – year) (Laperdin, 2013).

The fourth stage of the field development could also be distinguished. The rate of oil withdrawal amounts 1-2% from the initially extracted reserves, while the water cut exceeds 95%. Oil production rate at this stage is determined by the formula:

$$T_d = \frac{q_t}{Q} \quad (44)$$

where Q – accumulated oil production in million tone; t – year.

3.10 Simplified calculating economic efficiency of the project implementation

Economic efficiency of the project is estimated by calculating the accumulated discounted cash flow and discounted profitability index.

Discounted cash flow PV is calculated by the formula:

$$PV = P \cdot \alpha \quad (45)$$

where P – profit in million dollars; α – discount factor.

The profit is determined by the formula:

$$P = B - \gamma - CE \quad (46)$$

where CE – capital expenditures in dollars; B – product sales revenue in dollars; γ – conditionally-variable cost of oil production in million dollars.

Revenue on product sales is determined by the formula:

$$B = Q \cdot C \quad (47)$$

where Q – annual oil production in million tonnes; C – the price of oil sale in dollars per 1 tonne.

Conditionally-variable cost of oil production is determined by the formula:

$$\gamma = Q \cdot C' \quad (48)$$

where C' – the cost of oil production in dollars per 1 tonne.

The accumulated discounted cash flow is determined by the formula:

$$NPV = \sum PV \quad (49)$$

Discounted profitability index is determined by the formula:

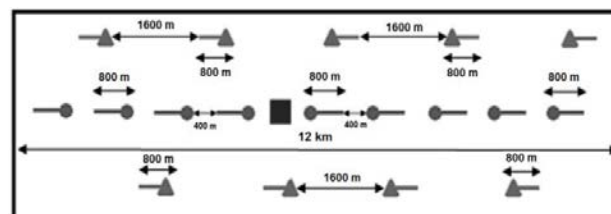
$$DPI = 1 + \frac{NPV}{(\sum CE) \cdot \alpha} \quad (50)$$

4. RESULTS AND DISCUSSION:

Source data for calculations are provided in table 2.

1. Calculation of optimal length of horizontal sections is based on the discounted cash flow rate estimation using the formulas 1 and 2. In order to make calculations, the cost of 1 meter well drilling has been agreed as 6178 dollars without taking into account the complication factor when drilling a horizontal section. The total cost of a well construction, 50,4 million dollars, has been included in capital expenditures taking into account the complication factor, when drilling a horizontal section. Basing on the obtained data, a graph has been drawn (Figure 6) according to which the optimal horizontal section of wells on the oil field is 800 meters long.

Basing on the calculated length of horizontal section, we can represent the schematically linear system of the field development (Figure 7).



Legend:

- Horizontal injection well
- Horizontal production well
- GBS

Figure 7. The system of the field development diagram

2. The initial rate was determined according to the Joshi's method by the formulas 3-6.

$$Q_o = 486,5 \text{ m}^3 \text{ per day.}$$

3. The critical rate was determined according to the Chaperon's method by the formulas 7-9.

$$Q_{oc} = 3,42 \text{ m}^3 \text{ per day}$$

The low value of the critical rate is caused by the relatively fast water breakthrough to horizontal wells. The obtained value was not used in further calculations being much smaller than initial rate. The initial rate was used instead.

4. The horizontal well breakthrough time as expressed in days was calculated according to the Papatzacos' method by the formulas 10-12.

$$t_{BT} = 122 \text{ days}$$

5. The pressure at the well drainage boundary in the course of the field development was determined using Y. Zheltov's method taking into account the fact that in the period of oil field development ($t^* = 3$ years) the volumes of water coming from the edge water zone and liquid withdrawal from the formation are variables in time.

Well drainage boundary radius $R = 2547,5$ m. Evaluation of pressure variations at the well drainage boundary has been made by the formulas 13-18 and are shown in table 3. While calculating horizontal wells were replaced by vertical ones with 1 horizontal well being equal to 3 vertical wells. This replacement was made due

to the correlation between the calculated horizontal well initial flow rate (486,5 m³ per day) and prospective vertical well flow rate (168 m³ per day).

Field development indicators were calculated by the formulas 19-25 and are represented in table 4.

Oil reserves exploitation parameters were determined by the formulas 26-40 and are represented in table 5.

The dynamics of basic technological indicators was determined by the formulas 41-44 and is represented in table 6.

The oil recovery factor value for the whole period of the field development is represented in figure 8.

The field development schedule is presented in figure 9.

Oil recovery rate after 25 years of development $T_d=0,0087 \rightarrow 0,87\%$. Consequently, after 25 years of exploitation the field passed to the fourth stage with the rate of oil withdrawal being lower than 1% and product water cut of 84,63%.

Economic efficiency of the field development has been determined according to the formulas 45-50. Capital expenditures are presented in table 7.

In the first year of exploitation the capital expenditures will be 2111,2 million dollars. These costs comprise the price of GBS, ice-class tankers, supply vessels and 3 wells (50,4 million dollars each).

Three wells are planned to be drilled annually between the second and the sixth years, with capital expenditures being 151,4 million dollars. Subsequently capital expenditures are 0.

1. The cost of oil production is accepted to be 219,9 dollars per 1 tonne.
2. The cost of oil sale is accepted to be 806,3 dollars per 1 tonne.
3. Annual operational expenditures on the project implementation have been accepted to be 100 million dollars.
4. The project funding is provided by the company's own resources.
5. The project is expected to be launched in 2031.

Estimated economic outcome of the field development is provided in table 8. The given calculations incorporate the whole period of the

field development (39 years). The accumulated discounted cash flow graph on the annual basis is given in figure 10.

It should also be mentioned that no project involving hydrocarbon recovery on the Arctic shelf can be implemented in the Russian Federation under the current tax system. Tax incentives are required for all such projects. Consequently, the current assessment was carried out without considering tax contribution.

At present there are no generally accepted principles and approaches to design and implement systems of Arctic shelf oil field development with specified features (Khaibullina, 2016). This has become the issue of concern while writing the given research paper.

5. CONCLUSIONS:

The present research paper studied the oil field situated in the eastern part of the Pechora Sea on the Russian Arctic shelf zone. Basing on the obtained geological and physical data about the oil reservoir structure and revealed specific features of the Arctic offshore oil field development, the optimum system of the field exploitation has been selected and analysed. The following conclusions have been drawn:

1. The oil field is associated with a massive oil reservoir located in Carboniferous sediments. Its structure is a long and narrow anticlinal fold. The size of the reservoir is estimated 45 km long, 2,0 – 2,5 km wide and 160 m high. The oil of the oil field is light with the density of 0,842 gr/sm³, sulfurous, paraffinic and low in tar. One prospective borehole has been drilled on the locality. The field is undergoing additional exploration.
2. The field is located in the area under hard ice conditions with ice thickness reaching 1,2 m in its upmost period. As a result, the only feasible way of the field development is to install the gravity-based structure.
3. Production and injection wells stock formation is limited by the potential of the gravity-based structure, which is the only possible one for oil recovery on the given field, and the high cost of drilling (50,4 million dollars a well).
4. The field development system needs to be engineered using inclined directional wells, since such a system solely is capable of providing profitable oil production on the

- Arctic shelf zone due to the fast rate of the field exploitation. By doing so we involve the maximum of resources in the process of development, acquire high coverage rate, oil recovery factor and necessary withdrawal compensation by introducing water into the reservoir through injection wells.
5. The rate of drilling is not expected to be fast. No more than four wells can be drilled on the field per 1 year. This can be explained by difficulties in organising logistics operations to deliver equipment and other stuff necessary for drilling to GBS, especially in winter.
 6. Since oil-bearing structure is represented by long and narrow anticlinal fold, the field development is made feasible by using the linear system of horizontal wells, drilled lengthwise the oil-bearing structure.
 7. Due to the identified geological and physical features of the oil-bearing structure as well as the specificity of the field development and engineering, the linear system of horizontal wells will be the most favorable one for its exploitation. This system consists of one row of production wells, placed centrally and lengthwise the oil-bearing structure and two rows of injection wells placed along the oil-bearing boundary from its southern and northern sides; production and injection wells ratio is 1:1.
 8. The optimal length of the horizontal section of wells is 800 m, calculated on the accumulated discounted cash flow assessment. With this taken into account, the designed linear development system consists of 9 production and 9 injection horizontal wells. The approximate length of the field section under development could be up to 12 km.
 9. The horizontal wells initial flow rate, calculated using Joshi's method is 486,5 m³ per day.
 10. The horizontal wells critical flow rate, calculated using Chaperon's method is 3,42 m³ per day. The low value of the critical rate is caused by the relatively fast water breakthrough to horizontal wells.
 11. The horizontal wells breakthrough time as expressed in days and calculated by using Papatzacos' method is 122 days.
 12. The boundary pressure for the whole period of the field development (39 years) goes down from 36 MPa to 13,26 MPa.
 13. By the 39th year of the field development, the following output will have been achieved: the ultimate mass share of water - 95%, oil recovery factor - 0,549 (54,9%), accumulated oil recovery - 11,875 million tonnes, accumulated liquid recovery - 31,219 million tonnes.
 14. By the end of the extraction from the field, the accumulated discounted cash flow will have become 257,56 million dollars, profitability index - 1,09. Consequently, the investment project can be accepted for implementation. The project payback period will be slightly over 10 years.
 15. The field development is feasible with oil price being a minimum of 110 dollars per barrel.
 16. The field development is unfeasible without tax benefits to the project being provided.

6. REFERENCES:

1. *Abstract on the feasibility study (draft) of the Pirazlomnaya GBS*. Retrieved from <https://docplayer.ru/29631772-Referat-1-po-tehniko-ekonomicheskomu-obosnovaniyu-teo-proektu-mlsp-pirazlomnaya.html> 12.01.2020.
2. Alekseev, A.D., Zhukov, V.V., Strizhnev, K.V., Cherevko, S.A. (2017). Research of hard-to-recovery and unconventional oil-bearing formations according to the principle «In-situ reservoir fabric». *Journal of Mining Institute*, 228, 695-704. doi: 10.25515/PMI.2017.6.695
3. Alkhimov, R.G., Semyonov, A.M., Chernov, Y.Y. (2008). The means of the Pechora sea offshore oil field development. Proc. Conf. «Oil and gas field development: state, problems and prospects» (pp. 94-102). Moscow: VNIIGAZ.
4. Ahmed, T.H. (2010). *Reservoir engineering handbook* (4th ed). Burlington, USA: Elsevier Inc.
5. Berdin, T.G. (2001). *Oil and gas field development by means of horizontal wells*. Moscow: Nedra-Business Centre (limited liability company).
6. Borisov, Y.P., Pilatovsky, V.P., Tabakov,

- V.P. (1964). *Oil field development by means of horizontal and branched wells*. Moscow: Subsoil.
7. Carayannis, E., Ilinova, A., Chanysheva, A. (2019). Russian Arctic offshore oil and gas projects: methodological framework for evaluating their prospects. *Journal of the Knowledge Economy*. doi: <https://doi.org/10.1007/s13132-019-00602-7>
 8. Chaperon, I. (1986). Theoretical study of coning toward horizontal and vertical wells in anisotropic formations: subcritical and critical rates. Paper presented at the SPE Annual technical conference and exhibition, 5-8 October, New Orleans, Louisiana, USA. doi: <https://doi.org/10.2118/15377-MS>
 9. Dosunmu, I.T., & Osisanya, S.O. (2015). An economic approach to horizontal well length optimization. Paper presented at the Abu Dhabi international petroleum exhibition and conference, 9-12 November, Abu Dhabi, UAE. doi: <https://doi.org/10.2118/177866-MS>
 10. Dzyublo, A.D. (2009). Geological and geophysical research and natural reservoir models of the Barents – Karsk region aiming at accumulating hydrocarbon resource base. Dissertation abstract for the doctor degree in geological and mineralogical sciences. Moscow, Russia.
 11. Forbes. (2013). *Gazprom began to produce oil at the Prirazlomnoye field*. Retrieved from <https://www.forbes.ru/news/249023-gazprom-zapustil-dobychu-nefti-na-prirazlomnom-mestorozhdenii> 12.01.2020.
 12. Gimatudinov Sh.K. et al. (1983). *A guide to oil field development and exploitation design. Oil recovery*. Moscow: Subsoil.
 13. Giannesini, J.F. (1988). Horizontal wells cut offshore production costs. Paper presented at the Offshore South East Asia show, 2-5 February, Singapore. doi: <https://doi.org/10.2118/17656-MS>
 14. Høyland, L.A., Papatzacos, P., Skjaeveland, S.M. (1989). Critical rate for water coning: correlation and analytical solution. *SPE Reservoir Engineering*, 4(04). doi: <https://doi.org/10.2118/15855-PA>
 15. Hermawan, H., Hadiyanto, H., Sunaryo, S., Kholil, A. (2019). Analysis of thermal performance of wood and exposed stone-walled buildings in mountainous areas with building envelop variations. *Journal of Applied Engineering Science*, 17(3), 321-332.
 16. Joshi, S.D. (1991). *Horizontal well technology*. Tulsa, Oklahoma, USA: PennWell publishing company.
 17. Joshi, S.D., Ding, W. (1996). Horizontal well application: reservoir management. Paper presented at the International conference on horizontal well technology, 18-20 November, Calgary, Alberta, Canada.
doi: <https://doi.org/10.2118/37036-MS>
 18. Khaibullina, K. (2016). Technology to Remove Asphaltene, Resin and Paraffin Deposits in Wells Using Organic Solvents. *Society of Petroleum Engineers*. doi:10.2118/184502-STU
 19. Kuznetsova, A.N., Gunkin, A.S., Rogachev, M.K. (2017). Dynamic modeling of surfactant flooding in low permeable argillaceous reservoirs. *IOP Conference Series: Earth and Environmental Science*, 87, 052014. doi:10.1088/1755-1315/87/5/052014
 20. Laperdin, A.N. (2013). *Design methods and regulation of development processes. Guidelines for practical training in the discipline «Met hods of design and regulation of development processes for masters studying in the field of training «Oil and gas business»*. Almet'yevsk: Almet'yevsk state oil institute, Russia.
 21. Lacy, S., Ding, W., Joshi, S.D. (1992). Horizontal well applications and parameters for economic success. Paper presented at the SPE Latin America petroleum engineering conference, 8-11 March, Caracas, Venezuela. doi: <https://doi.org/10.2118/23676-MS>
 22. Lin, H., Chen, Y., Chiu, V., Peter, C.Y. (2019). A decision model for a quality-assured EPQ-based intra-supply chain system considering overtime option. *Journal of Applied Engineering Science*, 17(3), 362-372.
 23. Matskevitch, D. (2007). Technologies for Arctic offshore exploration and development. *SPE Projects, facilities and construction*, 2(02). doi:

- <https://doi.org/10.2118/102441-PA>
24. Mukhametshina, R.Y., et al. (2005). The explanation of prospective horizontal borehole length taking into account the existing wells exploitation, the case study of Entelskaya area, Mamontovskoye field. *Oil and gas engineering*, 3, 179-184, Russia.
 25. Myuller, E.B., et al. (2003). *Reference data on wind and storm modes in Barents, Okhotsk and Caspian seas*. Saint-Petersburg: Russian maritime shipping register.
 26. Oganov, G. (2005). The first national experience in engineering and construction of wells with a significant bore deflection from the vertical on the Russian Arctic offshore. Retrieved from <https://oilcapital.ru/news/markets/26-08-2005/pervyy-otechestvennyy-opyt-proektirovaniya-stroitelstva-skvazhin-s-bolshim-otkloneniem-stvola-ot-vertikalina-arkticheskoy-shelfe-rossii> 12.01.2020.
 27. Osisanya, S.O. (1997). Economic analysis of horizontal wells. Paper presented at the SPE Production operations symposium, 9-11 March, Oklahoma City, Oklahoma, USA. doi: <https://doi.org/10.2118/37495-MS>
 28. Ozkan, E., Raghavan, R. (1990). Performance of horizontal wells subject to bottomwater drive. *SPE Reservoir Engineering*, 5(03).
doi: <https://doi.org/10.2118/18559-PA>
 29. Papatzacos, P., Herring, T.R., Martinsen, R., Skjaeveland, S.M. (1991). Cone breakthrough time for horizontal wells. *SPE Reservoir Engineering*, 6(03).
doi: <https://doi.org/10.2118/19822-PA>
 30. Gazprom neft. (2020). *Proekt Prirazlomnoe*. Retrieved from <https://www.gazprom-neft.ru/company/major-projects/prirazlomnoe/> 12.01.2020.
 31. Rahman, P.A. (2017). Analysis of the mean time to data loss of nested disk arrays RAID-01 on basis of a specialized mathematical model. *IOP Conference Series: Materials Science and Engineering*, 177(1). doi: <https://doi.org/10.1088/1757-899X/177/1/012088>
 32. Rahman, P.A., Bobkova, E.Y. (2016). Reliability model of fault-tolerant data processing system with primary and backup nodes. *IOP Conference Series: Materials Science and Engineering*, 124(1). doi: <https://doi.org/10.1088/1757-899X/124/1/012023>
 33. Seyyedattar, M., Zendehboudi, S., Butt, S. (2019). Technical and non-technical challenges of development of offshore petroleum reservoirs: characterization and production. *Natural Resources Research*. doi: <https://doi.org/10.1007/s11053-019-09549-7>
 34. Shandrygin, A.N., Dubrovsky, D.A. (2015). Strategy for fast tracking development of Arctic oil-gas offshore field. Paper presented at the OTC Arctic technology conference, 23-25 March, Copenhagen, Denmark.
doi: <https://doi.org/10.4043/25544-MS>
 35. Shatalova, T.N., Chebykina, M.V., Zhirnova, T.V., Bobkova, E.U. (2014). Base of instruments for managing energy resources in monitoring activity of industrial enterprises. *Advances in Environmental Biology*, 8(7), 2372–2376.
 36. Tadeu, P., Fernandez Batanero, J., Tarman, B. (2019). ICT in a Global World. *Research in Social Sciences and Technology*, 4(2). Retrieved from <https://ressat.org/index.php/ressat/article/view/431> 12.01.2020.
 37. Tanygin I.A, et al. (2014). Dolginskoye field geological structure detailing. *Oil Industry*, 4, 36-40, Russia.
 38. Terziyev, F.S., et al. (1991). *Hydrometeorology and hydrochemistry of the USSR Seas. Vol. 1. Barents Sea*. Leningrad, USSR: *Hydrometeorology*.
 39. Thakur, G. (1999). Horizontal well technology - a key to improving reserves. *Journal of Canadian Petroleum Technology*, 38(10). doi: <https://doi.org/10.2118/99-10-05>
 40. Vasil'cov, V.S., Vasil'cova, V.M. (2018). Strategic planning of Arctic shelf development using fractal theory tools. *Journal of Mining Institute*, 234, 663-672. doi: 10.31897/PMI.2018.6.663
 41. Wang, A.T., Poplin, J.P., Heuer, C.E. (1994). Hydrocarbon production concepts for dynamic annual sea ice regions.

Hydrotechnical construction, 28(8), 472.

doi: <https://doi.org/10.1007/BF01487456>

42. Yefremkin, I.M., Holmianskij, M.A., Zelenovskij, P.S. (2009). Geoecological characteristic of the south Barents Sea section (Dolginskaya area). *St.Petersburg University Bulletin*, 7(3), 49-57.
43. Yemelyanov, V., Yemelyanova, N., Nedelkin, A. (2018). Diagnostic system to determine lining condition. Paper presented at the MATEC Web of Conferences, 172.
doi:10.1051/matecconf/201817204001
44. Yemelyanov, V., Fatkulin, A., Titov, V., Nedelkin, A., Degtyarev, A. (2019). Software for weight estimation of the transported liquid iron. Paper presented at the Proceedings of the 2019 IEEE Conference of Russian Young Researchers in Electrical and Electronic Engineering (ElConRus), 28-31 January, St. Petersburg, Russia, 381-384.
doi:10.1109/ElConRus.2019.8657011
45. Zheltov, Y. (1998). *Oil field development. A textbook for universities* (2nd ed.). Moscow: Subsoil Publishing house.
46. Zhukov, A.P., Zhemchugova, V.A., Epov, K.A., Berbenev, M.O., Kholodilov, V.A. (2009). Features of the geological structure and hydrocarbon productivity of the Dolginsky field. Proc. The 14th Geological coordinating meeting reports at OAO "Gazprom" (open joined-stock company) (pp 48-74). Moscow, Russia.
47. Zhuravlyov, V.A., et al. (2014). *State geological map of the Russian Federation. 1:1 000 000 (the third generation). North*

Karsk Barents Sea sector. Page R – 39, 40 – Kolguyev island, strait Karskiye Vorota. St. Petersburg: Map-making factory VSEGEI (All-Russia scientific research institute).

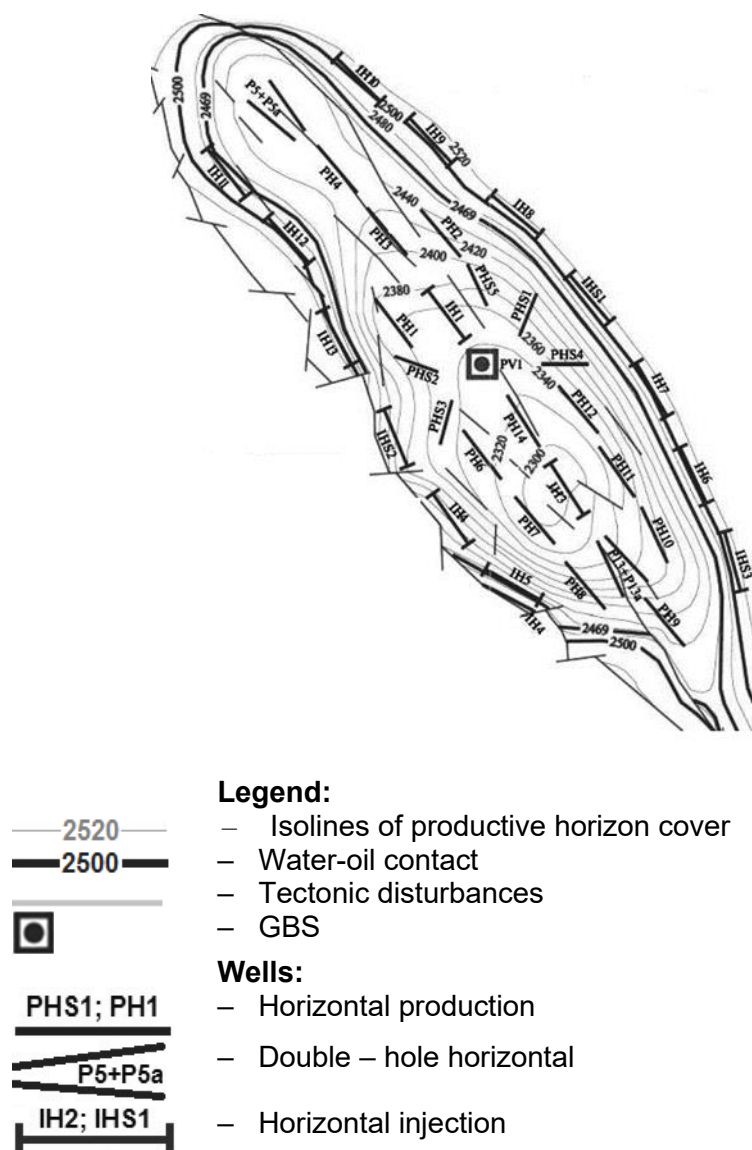


Figure 3. Distribution pattern of horizontal sections of wells on the Prirazlomnoye field. Variant 6 m (Alkhimov et al. 2008)

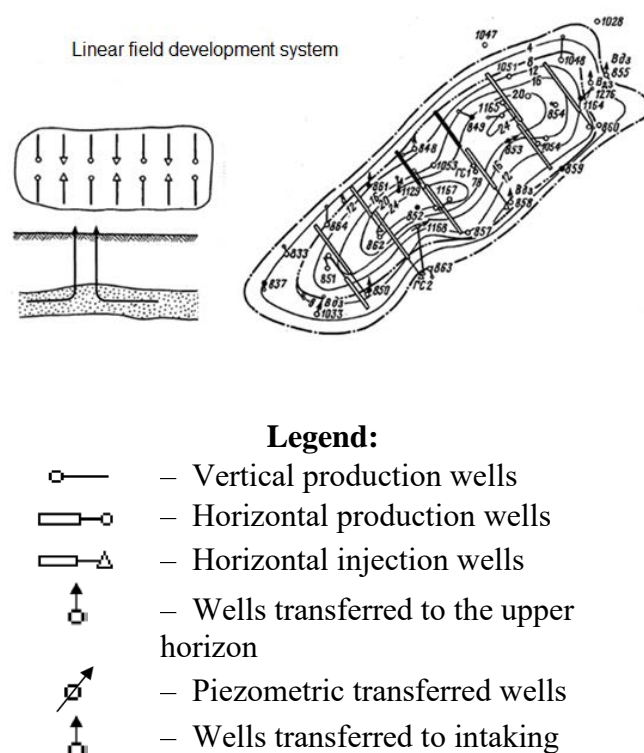


Figure 4. The system of the Mikhailovskoye oil field development (Berdin, 2001)

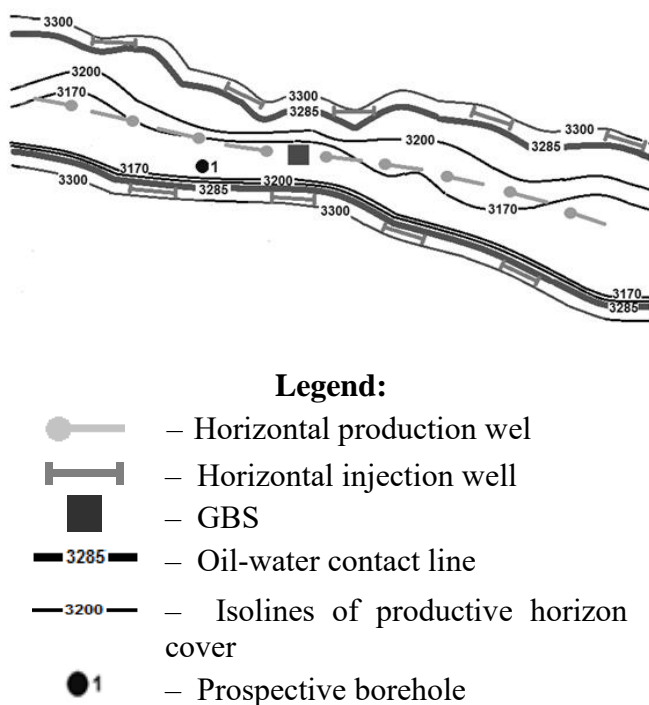


Figure 5. Linear field development system

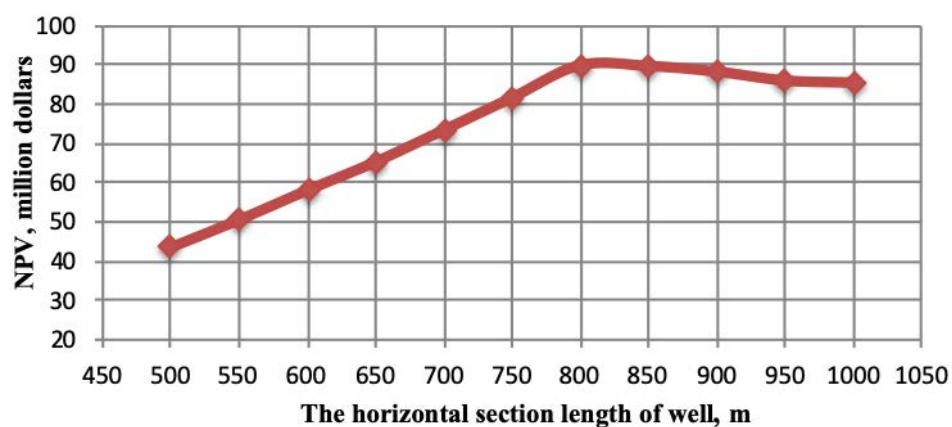


Figure 6. The graph shows the NPV dependency on the horizontal section length of well

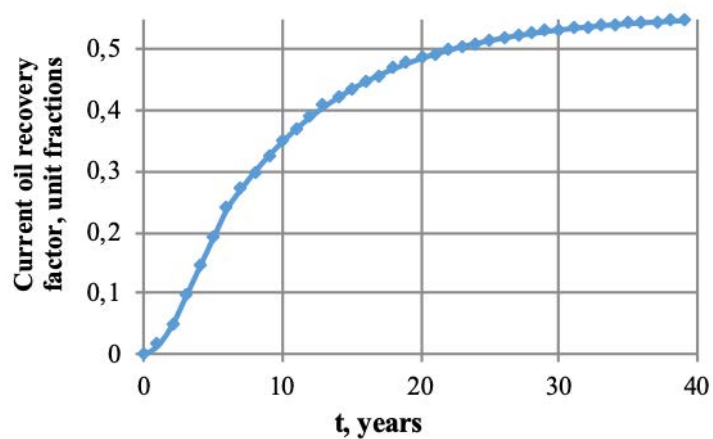


Figure 8. Oil recovery factor for the whole period of the field development

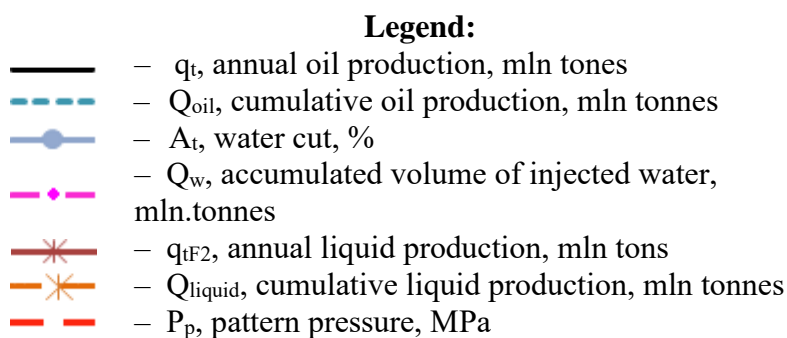
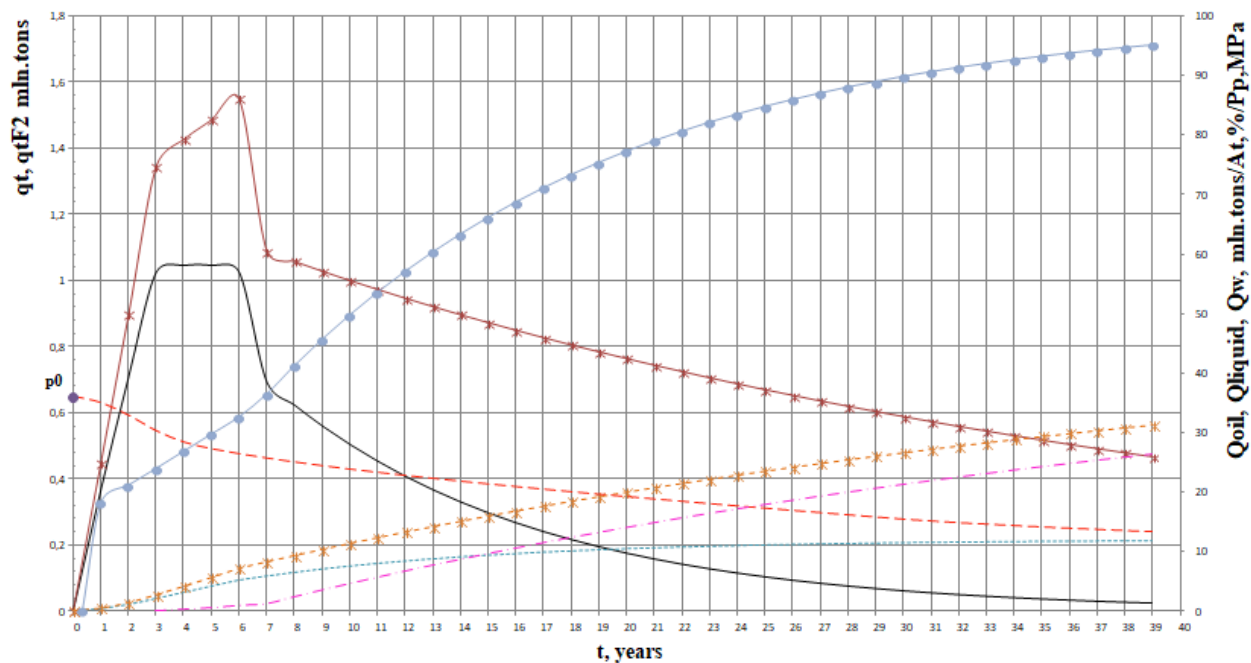


Figure 9. Field development schedule

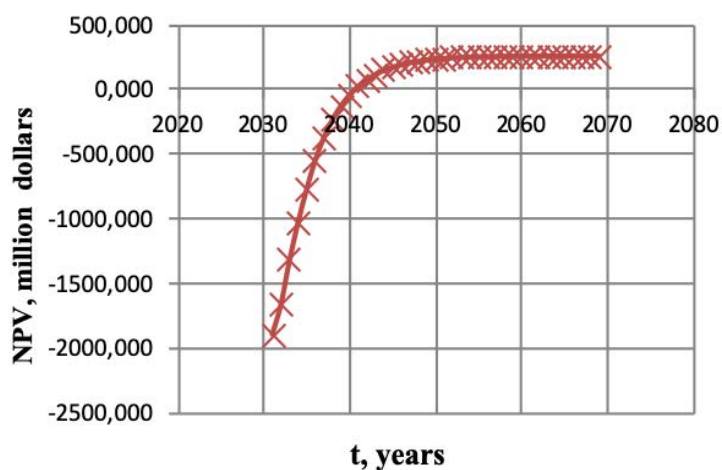


Figure 10. Annual breakdown of accumulated discounted cash flow

Table 1. Geologic characteristics of the reservoir bed in the field

Formation age	Effective oil-saturated thickness of permeable alternations, m	Reservoir temperature, C°	Saturation pressure, MPa	Formation pressure, MPa	Base oil volume factor	Gas content, m ³ / tonne	Oil density on surface gr/cm ³	Dynamic oil viscosity, MPa·c	Porosity, fraction, %	Permeability factor, sq.mic.	Oil saturation factor, unit fractions (OSF)
C ₁	18,8	84	14,9	36	1,32	125	0,842	0,62	8%	5·10 ⁻³	0,8

Table 2. Source data for calculations

Parameter	Value in Russian units of measure	Value in British units of measure
Water viscosity, μ_w	1 mPa·s	1 cP
Oil viscosity, μ_o	0,62 mPa·s	0,62 cP
Production well radius, r_w	0,09685 m	0,318 ft
Effective stratum thickness, h	18,8 m	61,68 ft
Porosity, fraction, m	8%	8%
Formation water density, ρ_w	1100 kg/m ³	68,67 lb/ft ³
Oil density, ρ_o	842 kg/m ³	52,56 lb/ft ³
Pressure drawdown, ΔP	5,86 MPa	849,92 psi
Oil formation volume factor, B_o	1,32	1,32 bbl/STB
Horizontal permeability, k_h	$1,21 \cdot 10^{-15} \text{ m}^2$	1,21 md
Vertical permeability, k_v	$4,62 \cdot 10^{-15} \text{ m}^2$	4,62 md
Fracture formation permeability, k	$5 \cdot 10^{-15} \text{ m}^2$	5 md
Distance to water-oil contact (WOC), D_b	15,24 m	50 ft
Horizontal well drainage radius, r_{eh}	408,4 m	1339,8 ft
Initial water saturation, S_{ws}	0,2	0,2
Residual oil saturation, S_{os}	0,3	0,3
Annual extraction from newly introduced wells, α_o	$0,533 \cdot 10^6 \text{ m}^3/\text{year}^2$	$0,533 \cdot 10^6 \text{ m}^3/\text{year}^2$
Piezoconductivity quotient, X	0,09 m ² /s	0,0084 ft ² /sec
Oil-bearing area, S	20388936 m ²	219464680,6 ft ²
Reservoir volume, V	488049000 m ³	17235252464 ft ³
Total number of wells, n_o	18 horizontal	18 horizontal
Water-oil displacement factor, K_2	0,81	0,81
Zonal heterogeneity, U_3^2	0,39	0,39
Layer-by-layer heterogeneity, U_1^2	0,1	0,1
Average productivity quotient, K_{av}	$4,1 \cdot 10^{-5} \text{ t/day} \cdot \text{Pa}$	$4,1 \cdot 10^{-5} \text{ t/day} \cdot \text{Pa}$
Marginal mass share of water, A_2	95%	95%
Saturation pressure, P_s	14,9 MPa	2161,06 psi
Formation pressure, p_o	36 MPa	5221,35 psi
Geological oil reserves of the developed field sector, Q_g	23,61 million tonnes	23,61 million tonnes

Table 3. Forecast of pressure variations at the well drainage boundary (boundary pressure)

t, sec, ·10 ⁶	τ	J(τ)	$\tau - \tau^*$	J($\tau - \tau^*$)	$\tau - \tau^{**}$	J ($\tau - \tau^{**}$)	$\tau - \tau^{***}$	J ($\tau - \tau^{***}$)	P _p , MPa
31,54	0,437	0,146	-	-	-	-	-	-	34,946
63,08	0,875	0,438	-	-	-	-	-	-	32,837
94,62	1,312	0,800	-	-	-	-	-	-	30,220
126,16	1,750	1,210	0,437	0,146	-	-	-	-	28,314
157,7	2,187	1,656	0,875	0,438	-	-	-	-	27,194
189,24	2,624	2,134	1,312	0,800	-	-	-	-	26,360
220,78	3,062	2,638	1,750	1,210	0,437	0,146	-	-	25,637
252,32	3,499	3,165	2,187	1,656	0,875	0,438	-	-	24,970
283,86	3,937	3,714	2,624	2,134	1,312	0,800	-	-	24,354
315,4	4,374	4,281	3,062	2,638	1,750	1,210	-	-	23,778
346,94	4,811	4,866	3,499	3,165	2,187	1,656	-	-	23,235
378,48	5,249	5,467	3,937	3,714	2,624	2,134	-	-	22,719
410,02	5,686	6,084	4,374	4,281	3,062	2,638	-	-	22,224
441,56	6,124	6,714	4,811	4,866	3,499	3,165	-	-	21,748
473,1	6,561	7,357	5,249	5,467	3,937	3,714	-	-	21,288
504,64	6,998	8,013	5,686	6,084	4,374	4,281	-	-	20,841
536,18	7,436	8,680	6,124	6,714	4,811	4,866	-	-	20,406
567,72	7,873	9,358	6,561	7,357	5,249	5,467	-	-	19,981
599,26	8,311	10,047	6,998	8,013	5,686	6,084	-	-	19,565
630,8	8,748	10,746	7,436	8,680	6,124	6,714	-	-	19,157
662,34	9,185	11,454	7,873	9,358	6,561	7,357	-	-	18,757
693,88	9,623	12,172	8,311	10,047	6,998	8,013	-	-	18,362
725,42	10,060	12,898	8,748	10,746	7,436	8,680	-	-	17,973
756,96	10,498	13,633	9,185	11,454	7,873	9,358	-	-	17,590
788,5	10,935	14,376	9,623	12,172	8,311	10,047	-	-	17,210
820,04	11,372	15,126	10,060	12,898	8,748	10,746	-	-	16,835
851,58	11,810	15,885	10,498	13,633	9,185	11,454	-	-	16,464
883,12	12,247	16,650	10,935	14,376	9,623	12,172	-	-	16,096
914,66	12,685	17,423	11,372	15,126	10,060	12,898	-	-	15,731
946,2	13,122	18,202	11,810	15,885	10,498	13,633	-	-	15,369
977,74	13,559	18,988	12,247	16,650	10,935	14,376	0,437	0,146	15,052
1009,28	13,997	19,780	12,685	17,423	11,372	15,126	0,875	0,438	14,778
1040,82	14,434	20,579	13,122	18,202	11,810	15,885	1,312	0,800	14,526
1072,36	14,871	21,384	13,559	18,988	12,247	16,650	1,750	1,210	14,290
1103,9	15,309	22,194	13,997	19,780	12,685	17,423	2,187	1,656	14,066
1135,44	15,746	23,010	14,434	20,579	13,122	18,202	2,624	2,134	13,853
1166,98	16,184	23,832	14,871	21,384	13,559	18,988	3,062	2,638	13,648
1198,52	16,621	24,659	15,309	22,194	13,997	19,780	3,499	3,165	13,452
1230,06	17,058	25,492	15,746	23,010	14,434	20,579	3,937	3,714	13,263

Table 4. Basic field development indicators

S _c , km ² per 1 well	\bar{m}	m	α	μ_*	v	φ	q ₀ , million tonnes per year
0,48	3,68	4,42	0,22	0,44	3,014	0,16	1,28

Table 5. Oil reserves exploitation parameters

K ₁	Q _m , million t.	K _{ro}	U _p ²	μ_{oz}	A	K _{n3}	K _{k3}	K ₃	F	Q ₀ , million t.	Q _{F0} , million t.	Q _{F02} , million t.	ρ_*	A _{av}
0,904	18,53	0,604	0,87	0,94	0,95	0,205	0,856	0,82	3,44	15,29	63,84	61,06	1,306	0,75

Table 6. The dynamics of basic technological indicators

Years, t	Production, million tonnes		Accumulated production, million tonnes		Water injection, million tonnes		Encroachment, A_t , %	Current oil recovery factor, unit fractions
	Oil, q_t	Liquid, q_{tF_2}	Oil $\sum Q_{oil}$	Liquid $\sum Q_{liquid}$	Annual q_w	Accumulated $\sum Q_w$		
1	0,367	0,449	0,367	0,449	-	-	18,15	0,017
2	0,708	0,897	1,075	1,346	-	-	21,12	0,050
3	1,024	1,346	2,099	2,691	-	-	23,92	0,097
4	1,024	1,399	3,122	4,090	0,251	0,251	26,82	0,145
5	1,024	1,457	4,146	5,547	0,255	0,506	29,71	0,194
6	1,024	1,519	5,170	7,066	0,410	0,916	32,59	0,241
7	0,696	1,090	5,866	8,156	1,199	1,199	36,17	0,273
8	0,626	1,060	6,491	9,215	1,166	2,365	40,95	0,302
9	0,563	1,030	7,054	10,246	1,133	3,498	45,39	0,327
10	0,506	1,002	7,560	11,248	1,102	4,601	49,50	0,351
11	0,455	0,975	8,015	12,223	1,072	5,673	53,31	0,372
12	0,409	0,948	8,425	13,171	1,043	6,716	56,84	0,390
13	0,368	0,923	8,793	14,094	1,015	7,731	60,11	0,407
14	0,331	0,898	9,124	14,992	0,988	8,720	63,13	0,422
15	0,298	0,874	9,422	15,867	0,962	9,681	65,93	0,436
16	0,268	0,851	9,690	16,718	0,936	10,617	68,53	0,448
17	0,241	0,829	9,931	17,546	0,911	11,529	70,93	0,460
18	0,217	0,807	10,147	18,353	0,887	12,416	73,15	0,469
19	0,195	0,786	10,342	19,139	0,864	13,280	75,20	0,478
20	0,175	0,765	10,517	19,904	0,842	14,122	77,09	0,486
21	0,158	0,745	10,675	20,649	0,820	14,942	78,85	0,494
22	0,142	0,726	10,817	21,375	0,798	15,740	80,47	0,500
23	0,127	0,707	10,944	22,082	0,778	16,518	81,97	0,506
24	0,115	0,689	11,059	22,770	0,758	17,275	83,35	0,511
25	0,103	0,671	11,162	23,441	0,738	18,013	84,63	0,516
26	0,093	0,654	11,255	24,095	0,719	18,732	85,81	0,520
27	0,083	0,637	11,338	24,732	0,701	19,433	86,90	0,524
28	0,075	0,621	11,413	25,352	0,683	20,115	87,91	0,528
29	0,067	0,605	11,481	25,957	0,665	20,781	88,84	0,531
30	0,061	0,589	11,541	26,546	0,648	21,429	89,70	0,533
31	0,055	0,574	11,596	27,120	0,632	22,060	90,50	0,536
32	0,049	0,560	11,645	27,680	0,616	22,676	91,23	0,538
33	0,044	0,545	11,689	28,225	0,600	23,276	91,91	0,540
34	0,040	0,531	11,729	28,757	0,585	23,860	92,53	0,542
35	0,036	0,518	11,765	29,275	0,570	24,430	93,11	0,544
36	0,032	0,505	11,797	29,780	0,555	24,985	93,64	0,545
37	0,029	0,492	11,826	30,272	0,541	25,527	94,13	0,547
38	0,026	0,480	11,852	30,751	0,528	26,054	94,58	0,548
39	0,023	0,467	11,875	31,219	0,514	26,568	95	0,549

Table 7. Capital expenditures on the field development

The basic means name	Cost in millions dollars
Gravity based structure (GBS)	1500
Drilling of 18 wells	907,2
Ice-class tankers for oil transportation (2 units)	210
Ice-class supply vessels (2 units)	100
Transit station (tanker)	150
Total capital expenditures	2867,2

Table 8. Estimated economic outcome of the field development

Year	Q, million tonnes	B, million dollars	γ , million dollars	P, million dollars	α	PV, million dollars	NPV, million dollars
2031	0,367	296,011	80,730	-1895,919	1,000	-1895,919	-1895,919
2032	0,708	570,575	155,611	263,763	0,870	229,360	-1666,560
2033	1,024	825,483	225,132	449,151	0,756	339,623	-1326,937
2034	1,024	825,483	225,132	449,151	0,658	295,324	-1031,613
2035	1,024	825,483	225,132	449,151	0,572	256,804	-774,809
2036	1,024	825,483	225,132	449,151	0,497	223,307	-551,502
2037	0,696	560,968	152,991	407,977	0,432	176,380	-375,122
2038	0,626	504,517	137,596	366,922	0,376	137,939	-237,183
2039	0,563	453,748	123,749	329,998	0,327	107,877	-129,306
2040	0,506	408,087	111,296	296,790	0,284	84,366	-44,939
2041	0,455	367,021	100,097	266,924	0,247	65,980	21,040
2042	0,409	330,087	90,024	240,063	0,215	51,600	72,640
2043	0,368	296,870	80,965	215,906	0,187	40,354	112,995
2044	0,331	266,996	72,817	194,179	0,163	31,560	144,554
2045	0,298	240,128	65,490	174,639	0,141	24,681	169,235
2046	0,268	215,964	58,899	157,065	0,123	19,302	188,538
2047	0,241	194,231	52,972	141,259	0,107	15,096	203,634
2048	0,217	174,686	47,642	127,044	0,093	11,806	215,439
2049	0,195	157,107	42,847	114,260	0,081	9,233	224,672
2050	0,175	141,297	38,536	102,762	0,070	7,221	231,893
2051	0,158	127,078	34,658	92,421	0,061	5,647	237,539
2052	0,142	114,291	31,170	83,120	0,053	4,416	241,956
2053	0,127	102,789	28,033	74,756	0,046	3,454	245,409
2054	0,115	92,446	25,212	67,233	0,040	2,701	248,111
2055	0,103	83,143	22,675	60,467	0,035	2,112	250,223
2056	0,093	74,776	20,393	54,383	0,030	1,652	251,875
2057	0,083	67,251	18,341	48,910	0,026	1,292	253,167
2058	0,075	60,484	16,496	43,988	0,023	1,010	254,177
2059	0,067	54,397	14,836	39,562	0,020	0,790	254,968
2060	0,061	48,923	13,343	35,581	0,017	0,618	255,585
2061	0,055	44,000	12,000	32,000	0,015	0,483	256,069
2062	0,049	39,572	10,792	28,780	0,013	0,378	256,447
2063	0,044	35,590	9,706	25,884	0,011	0,296	256,742
2064	0,040	32,009	8,730	23,279	0,010	0,231	256,974
2065	0,036	28,788	7,851	20,936	0,009	0,181	257,154
2066	0,032	25,891	7,061	18,830	0,008	0,141	257,296
2067	0,029	23,285	6,351	16,935	0,007	0,111	257,406
2068	0,026	20,942	5,711	15,231	0,006	0,086	257,493
2069	0,023	18,835	5,137	13,698	0,005	0,068	257,560

Basing on the obtained data:

$NPV = 257,56$ million dollars.

$DPI = 1,09$.

Cost recovery period is expected to be slightly over 10 years.

The accumulated discounted cash flow graph on the annual basis is given in figure 10.

ASPECTOS CLÍNICOS E IMUNOLÓGICOS DA ADAPTAÇÃO DO RECÉM-NASCIDO DE MÃE COM INFECÇÃO INTRAUTERINA**CLINICAL AND IMMUNOLOGICAL ASPECTS OF NEWBORN ADAPTATION BORN FROM MOTHERS WITH INTRAUTERINE INFECTION****КЛИНИКО-ИММУНОЛОГИЧЕСКИЕ АСПЕКТЫ АДАПТАЦИИ НОВОРОЖДЕННОГО ОТ МАТЕРЕЙ С ВНУТРИУТРОБНОЙ ИНФЕКЦИЕЙ**

ZHUMALINA, Akmaral K.^{1*}; TUSUPKALIEV, Balash T.²; ZAME, Yuliya A.³; VOLOSHINA, Lyudmila V.⁴; DARZHANOVA, Klara B.⁵

^{1,2,4} West Kazakhstan Marat Ospanov Medical University, Department of Children's Diseases, Aktobe – Republic of Kazakhstan

³ West Kazakhstan Marat Ospanov Medical University, Center for Continuing Professional Development, Aktobe – Republic of Kazakhstan

⁵ West Kazakhstan Marat Ospanov Medical University, Department of Normal and Topographic Anatomy with Operative Surgery, Aktobe – Republic of Kazakhstan

** Correspondence author*

e-mail: Zumalina@mail.ru

Received 22 January 2020; received in revised form 10 March 2020; accepted 27 March 2020

RESUMO

Hoje, cerca de 40% das crianças estão infectadas com infecções congênitas. As condições imunológicas das crianças no período neonatal estão amplamente associadas à natureza da gravidez em suas mães. O objetivo deste trabalho foi estudar as características clínicas e imunológicas em recém-nascidos de mães com infecção congênita. 48 bebês foram observados. Os recém-nascidos foram divididos em dois grupos: grupo 1 – 33 recém-nascidos de mães infectadas com infecção por citomegalovírus, grupo 2 – 15 recém-nascidos de mães saudáveis. O diagnóstico de infecção congênita é verificado com base em um questionário para mulheres grávidas, dados ambulatoriais de mulheres grávidas e recém-nascidos, testes sorológicos, reação em cadeia da polimerase (PCR), imunoensaio enzimático (IEE), bem como imunidade celular e imunidade humoral. A história somática e obstétrica-ginecológica das mães foi cuidadosamente coletada e avaliados os fatores de risco para o desenvolvimento de complicações no período inicial de adaptação. Como resultado do estudo, verificou-se que na estrutura dos fatores de risco em gestantes com infecções congênitas, são de grande importância a idade de 30 anos, patologia dos órgãos genitais e período extragenital durante a gravidez, abortos espontâneos e gravidez não desenvolvida, os abortos. As infecções virais associadas (CMV, citomegalovirus) predominam na estrutura da infecção congênita. A análise indica uma carga significativa da história perinatal em crianças com fatores infecciosos e fatores de hipóxia perinatal. Os principais sintomas clínicos de infecções congênitas entre as crianças examinadas são o período neonatal precoce, asfixia prematura, sintomas urinários, período neonatal tardio, que diferem no polimorfismo dos sintomas. Durante esse período, um órgão específico do sistema nervoso central é detectado. Em recém-nascidos com infecções congênitas, os parâmetros imunológicos são inibidos (CD4+, Cd8+, Cd19+).

Palavras-chave: imunidade, parâmetros imunológicos, história perinatal, infecção, sintomas clínicos.

ABSTRACT

Today about 40 % of babies are infected with intrauterine infections. The immune statuses of children during the neonatal period are largely associated with the patterns of pregnancies in their mothers. This work aimed to study clinical and immunological features in newborns of mothers with intrauterine infection. 48 infants were observed. Neonates were divided into two groups: group 1 – 33 newborns from mothers infected with cytomegalovirus infection, group 2 – 15 children from healthy mothers. The diagnosis of intrauterine infection was verified on the basis of survey questionnaire for pregnant women, outpatient data of pregnant women and neonates, serologic study, PCR, ELISA, and the cellular immunity and humoral immunity. Somatic and obstetric and gynecological history of mothers was thoroughly collected and the risk factors for the development of complications

in the early period of adaptation were assessed. The result of the study revealed that the structure of risk factors in pregnant women with intrauterine infections is of great importance the age of 30 years, genital and extragenital pathology during pregnancy, spontaneous abortions and non-developing pregnancy, abortion. Associated viral infections (CMV, Cytomegalovirus) predominate in the structure of congenital infection. The analysis indicates significantly burdened perinatal anamnesis in children infectious factors and factors of perinatal hypoxia. The leading clinical symptoms for intrauterine infections among the examined children are in the early neonatal period prematurity asphyxia, urinary symptoms, late neonatal period differ polymorphism symptomatic. In this period reveals a specific organ of the Central nervous system. In newborns with intrauterine infections observed inhibition of immunological indicators (CD4+, Cd8+, Cd 19+).

Keywords: *immunity, immunological indicators, perinatal history, infection, clinical symptoms.*

АННОТАЦИЯ

Актуальность данного исследования заключается в том, что сегодня около 40 % детей заражены внутриутробными инфекциями. Иммунные состояния детей в неонатальном периоде в значительной степени связаны с характером беременности у их матерей. Целью данного исследования является изучение клинических и иммунологических особенностей у новорожденных матерей с внутриутробной инфекцией. Под нашим наблюдением было 48 младенцев. Новорожденные были разделены на две группы: группа 1 – 33 новорожденных от матерей, инфицированных цитомегаловирусной инфекцией, группа 2 – 15 детей от здоровых матерей. Диагноз внутриутробной инфекции верифицируется на основе опросного листа для беременных, амбулаторных данных беременных и новорожденных, серологического исследования, ПЦР, ИФА, а также клеточного иммунитета и гуморального иммунитета. Соматический и акушерско-гинекологический анамнез матерей был тщательно собран и оценены факторы риска развития осложнений в раннем периоде адаптации. В результате проведенного исследования выяснилось, что в структуре факторов риска у беременных с внутриутробными инфекциями большое значение имеет возраст 30 лет, патология половых органов и экстрагенитальный период при беременности, самопроизвольные аборт и неразвивающаяся беременность, аборт. В структуре ВУИ преобладают связанные вирусные инфекции (ЦМВ, вирус простого вируса). Анализ свидетельствует о значительном отягощении перинатального анамнеза у детей инфекционными факторами и факторами перинатальной гипоксии. Ведущими клиническими симптомами внутриутробных инфекций раннего неонатального периода являются недоношенность, асфиксия, мочевого синдромы; поздний неонатальный период отличается полиморфизмом симптоматики: гипертензионно-гидроцефальный, судорожный и желтушный синдромы. У новорожденных при внутриутробных инфекциях наблюдается угнетение иммунологических показателей (CD4+, Cd8+, Cd19+).

Ключевые слова: *иммунитет, иммунологические показатели, перинатальный анамнез, инфекция, клинические симптомы*

1. INTRODUCTION:

According to many authors, the prevalence of intrauterine infections in the human population can reach 10 to 22 % (Shabalov, 2006; Hwang *et al.*, 2019; Stagno *et al.*, 1981; Helmo *et al.*, 2018; Schleiss and Marsh, 2018; Redko, 2015; Ashorn *et al.*, 2018; Britt, 2018; Mamyrbayeva *et al.*, 2017; Bocharova *et al.*, 2019; Wang *et al.*, 2011). Unfortunately, now only 60 % of children are born healthy. Subsequently the number of healthy children aged up to one year is reduced to 29 % (Makarov *et al.*, 2004). It is intrauterine infection (IUI) that largely determines the rates of stillbirth, early neonatal mortality, and morbidity in newborns and infants (Dolgushina *et al.*, 2017). According to various authors, the early neonatal morbidity associated with IUI is 5.3–27.4 %, stillbirth 14.9–16.8 % (Zile *et al.*, 2019), and IUI-related perinatal mortality reaches 65.6 %

(Stetsyuk and Andreeva, 2006; Isakov *et al.*, 2006; Perepelitsa, 2018). Specific antibodies to CMV in pregnant women are detected in 40 % in developed countries and in 100 % of cases in developing countries (Kitsak, 2005; Sial and Patel, 2000; Zhukova *et al.*, 2018; Damato and Winnen, 2002).

It has been proven that the intrauterine infectious agents include more than 27 types of bacteria, many viruses, parasites, 6 species of fungi, 4 species of protozoa, etc. Mycoplasmas (17-50 %) and viruses (herpes simplex virus 7-47 %, enteroviruses 8-17 %, cytomegalovirus 28-91.6 %) are considered to be the predominant antenatal pathogens, and intranatal infections are caused by chlamydia (2-25 %), group B streptococcus (3-12 %), listeria (1-9 %), conditionally pathogenic microorganisms (9- 14.7 %) (Polucci *et al.*, 2009). An intrauterine infection contamination shall mean the supposed

fact of intrauterine microbial fetal penetration without signs of infectious fetal disease, and IUI is the established fact of intrauterine microbial fetal penetration, in which the pathophysiological changes which are specific for the infectious disease occurred in the fetus and newborn prenatally or shortly after birth (Bonaros *et al.*, 2008; Kemp, 2014).

Despite the improvement of the basic parameters which characterize the specific weight of infections (Sukhanova and Sklyar, 2007) in the structure of perinatal and gynecological morbidity (Orekhov, 2002; Volodin, 2001), herpes infection remains the main cause of neonatal morbidity and mortality (Lutoshin, 2005; Subramaniam and Britt, 2018). Herpes virus infections are opportunistic infections, when a virus can exist for a long time in the human body, it may not reveal itself and cause any pathological phenomena, but when the body protective functions decrease, the virus begins to multiply intensely and impair various organs and systems (Ovchinnikova *et al.*, 2018).

The immune systems of newborns are physiologically depressed. According to the WHO, herpes infection is considered one of the most common congenital viral diseases (Volodin, 2002). Herpes infection is an infection that causes spontaneous miscarriage, premature birth, missed abortion, congenital malformations of newborns, fetopathy. The study of the timely early detection of herpes virus infection in women of reproductive age and pregnant women can help to prevent intrauterine fetal viral infections and reduce the number of overt forms of infection in newborns and reduce deaths (Zhumalina *et al.*, 2014; Orekhov, 2002; Borovkova, 2005). In addition, the prognosis of intrauterine transmission depends on the gestational age at which the infection occurred, the characteristics of the pathogen (its pathogenic and immunogenic properties), the type of maternal infection (primary or secondary), the functional state of the mother's immune system (Coppola *et al.*, 2019; Tyutyunnik *et al.*, 2014), the integrity of the uteroplacental barrier, etc.

Due to the incompetent immune system of infants, the basic protective functions are performed by passively acquired serum and secretory antibodies (Kadieva, 2007; Fowler *et al.*, 1992). Functional immaturity of lymphocytes, incompetent cell cooperation in the formation of the immune response, and physiological immunosuppression highly predispose newborns to infection (Carbone, 2016). This is the reason of fundamental study of pathology and development of treatment management and prognosis. Therefore, the purpose of this study was to

analyse the clinical and immunological characteristics of children born from mothers with intrauterine infection.

2. MATERIALS AND METHODS:

Retrospective and prospective studies of women observed in antenatal care, maternal care departments, and clinics and their newborns were conducted. 48 newborns were followed.

All procedures performed in studies involving human participants were in accordance with the ethical standards of the institutional and national research committee (Local Ethics Committee No. WHC-72(23)) of the West Kazakhstan Marat Ospanov Medical University and with the 1964 Helsinki declaration and its later amendments or comparable ethical standards.

According to the research policy of this university, the committee does not require any official supporting document, therefore, informed consent, in which the research and its outcomes are clearly and well explained, was obtained from all individual participants included in the study. The obtained research data will be used for study clinical and immunological features in newborns of mothers with intrauterine infection.

Newborns were divided into two groups: Group 1 included 33 children born from mothers infected with cytomegalovirus infection, Group 2 had 15 children born from healthy mothers (conditionally healthy children). Inclusion criteria: children aged up to 1 month; with positive markers for CMV; hepatitis B vaccination in the first 24 hours of age. Exclusion criteria: children with established causes of jaundice (current overt infection process, breast milk jaundice, etc.); children with congenital malformations; children with physiological jaundice.

Somatic and obstetric and gynecological history of mothers was thoroughly collected, clinical observation was performed. The laboratory test material was venous and capillary blood. Blood was sampled upon the informed consent of parents (mother and father) with the study explained. Blood of newborns was taken in the morning before feeding: 1 ml of venous blood for polymerase chain reaction (PCR), 2 ml of venous blood in the first 7-8 days of age for the cellular and humoral immunity state (determination of T, B-lymphocytes and their subpopulations).

The diagnosis of intrauterine infection was verified on the basis of a questionnaire for pregnant women, outpatient data for pregnant

women and newborns, serological studies, PCR, ELISA and the state of cellular and humoral immunity (determination of T, B-lymphocytes and their subpopulations). Statistical data were processed using:

1. nonparametric Mann-Whitney U-test. The Mann-Whitney test assumes that the studied variables are measured, at least in an ordinal scale (ranked). U-test is calculated as the sum of indicators of pairwise comparison of the first sample elements with the second sample elements. U-test is the most powerful (sensitive) nonparametric method for independent samples. Together with the U-test, z-value (for the normal distribution) and the corresponding p-value are shown
2. descriptive statistics of quantitative data in groups,
3. comparison of groups on PC using MS Excel, EpiData database,
4. licensed statistical program SAS 9.2.

The differences between the groups were significant if the error probability was less than 5 % ($p < 0.05$).

3. RESULTS AND DISCUSSION:

One of the effective ways to predict and diagnose IUI in newborns is to identify intrauterine infection risk factors in pregnant women (Boppana *et al.*, 2011; Zavattoni *et al.*, 2016; Tabata *et al.*, 2016; Wagner *et al.*, 2014; Revello *et al.*, 2008; Stehel *et al.*, 2008). Therefore, we performed a retrospective analysis of 160 outpatient medical records of pregnant women. 34 patients who were considered to be at risk of fetal infection and who had perinatal risk factors for the delivery of newborns with intrauterine infections were selected. Outpatient medical records of pregnant women were reviewed, and the perinatal risk factors that could cause fetal infection and the course of pregnancy were studied. The following data were studied: primipara, abortion, spontaneous miscarriage, missed abortion (non-developed pregnancy), maternal age (30-34 years and above), uterine scarring, aggravation of existing chronic maternal diseases, acute infectious genital diseases, CMV carrier status, acute viral diseases during pregnancy, threatened abortion, polyhydramnios, anemia, colpitis.

According to the analysis, the following premorbid factors were identified. As can be seen from Figure 1, in the group of risk factors that characterize the reproductive health of pregnant

women, the share of missed abortion (30 %) was the largest followed by spontaneous miscarriage and primipara (8 %). Medical abortions and threatened miscarriage were observed in 5 % and 3 %, respectively.

In the group of risk factors that occur during pregnancy, the most intense risk is anemia (22 %). The same risk group included 18 % for acute infectious genital diseases, 9 % for colpitis, 6 % for polyhydramnios, and only 3 % for acute viral infections during pregnancy among women infected with herpes virus (Figure 2).

As for the pregnant women's somatic health, when the risk factors were graded, a larger percentage is represented by chronic inflammatory diseases (chronic gastritis, chronic cholecystitis, COPD) (6 %). CMV carrier status and uterine scarring are 5 % and 4 %, respectively (Figure 3).

The maternal age (30-34 and above) was the most interesting social factors, its specific gravity was 45 %. Other social factors, such as marital status (single, divorced), bad habits (mother's smoking), mother's age under 18, and unintended pregnancy were not considered, since there were isolated cases in outpatient cards of pregnant women. A comparative analysis of the frequency of risk factors showed that 22 mothers (62.9 %) whose children were observed had a latent persistent CMV infection. We noticed that in the late neonatal period icteric syndrome persisted in 33 (48.5 %) children, 16 (23.5 %) had hepatomegaly, and 7 (10.3 %) had splenomegaly. It can be seen that maternal infection and latent persistence of CMV with hypoxic disorders cause protracted hyperbilirubinemia.

The leading neurological syndromes in infected children in the early neonatal period were muscle hypotension, depression and hypertensive hydrocephalus syndrome. The findings in the peripheral blood test of infected children included: left deviation in WBC differential in 12 (17.6 %) children, anemia in 2 (2.9 %) children, thrombocytosis in 2 (2.9 %) children, thrombocytopenia in 1 (1.5 %) child. Urinary syndrome manifested as proteinuria and leukocyturia in 7 (10.3 %) children, microhematuria in 1 (1.5 %) (Chen *et al.*, 2019). According to literature data (De la Calle *et al.*, 2018; Pereira *et al.*, 2014; Seidel *et al.*, 2017), children with CMVI in the late neonatal period develop specific inflammatory changes in the form of meningoencephalitis, pneumonia, hepatitis, nephritis. Our analysis has confirmed these data.

The greatest specific weight among all

syndromes was caused by the nervous system disorders. They were observed in 20 (29.4 %) children and manifested as encephalopathies, various congenital malformations (hydrocephalus, microcephaly) (De Bie and Boucoiran, 2019; Ximenes *et al.*, 2019). In the late neonatal period, hypertensive hydrocephalus and convulsive syndromes were significantly more common in children. We examined the immunological status, evaluated the cellular component of the immune system of newborns infected from mothers of CMVI. We determined the lymphocyte phenotype (main subpopulations) – CD3, CD4, CD8, CD19. The table shows that a significant ($p=0.038044$) increase in the general population of T-lymphocytes (CD3+) was found in the study and control groups: 73.8 ± 6.9 in the study group and 67 ± 8.1 in the control group (Tables 1 and 2).

An increase in the level of T-lymphocytes is seen in the figure of range (Figure 4).

The count of T-helpers (CD4+) in Group 1 (study group) is slightly lower compared to Group 2 (control group), however, the differences are not significant ($p=0.910538$), we can suggest immunological deficiency (Figure 5).

The depression of CD4+ subpopulation of T-lymphocytes may be the result of the direct selective action of intrauterine infections on these cells or serve as the background on which infection occurs. The relationship of the level of lymphocyte subpopulations with infection contamination of the newborns can be established. A more pronounced decrease in Group 1 (study) compared with Group 2 (control) of newborns ($p=0.000004$) when the data of T-cytotoxic lymphocyte count (CD8 +) is interpreted (Figure 6).

In Group 1 (study) group and Group 2 (control), a decrease in B-lymphocyte count (CD19+) was observed, but lower in the study group (8.37 ± 2.5) than in the control group (9.81 ± 3.5) (Figure 7).

Thus, in our study, specific immune system disorders were identified in Group 1 (study), which are characterized by an increase in CD3+, a decrease in CD4+, CD8+, and a decrease in CD19+ proving the impact of intrauterine infections on the immune system of infected newborns; a decrease in T-lymphocytes (CD4+, CD8+) indicates that the fetus was infected antenatally and as a result of exposure to the infection in utero.

4. CONCLUSIONS:

1. In the structure of risk factors, the age above 30 years, extragenital and genital pathologies during pregnancy, spontaneous miscarriages and missed abortion, pregnancy termination are of great importance in pregnant women with intrauterine infections (herpes viruses and CMV). Associated viral infections (CMV, herpes simplex virus) are prevailed in the IUI structure.

2. The analysis indicates a significantly aggravated perinatal history in children by infectious and perinatal hypoxia factors. The leading clinical manifestations of intrauterine infections in the children examined were as follows:

- prematurity, asphyxia, urinary syndromes in the early neonatal period.
- the late neonatal period is characterized by the symptom polymorphism: hypertensive hydrocephalus syndrome, convulsive and icteric syndromes. In the same period, specific central nervous system disorders, urinary and respiratory system disorders, and gastrointestinal disorders are detected.

3. Intrauterine exposure to factors may result in impaired formation of immunocompetent structures and be accompanied by activation of the fetal immune system and early synthesis of antibodies, which can be regarded as a complex of protective reactions or premature overstrain.

The obtained data on the clinical and immunological characteristics of newborns which were born from mothers with intrauterine infection will give deeper understanding of the intrauterine process pathogenesis. They can also be used when antiviral drugs are prescribed and can be used in the prevention of congenital cytomegalovirus and herpes infections in newborns.

5. REFERENCES:

1. Ashorn, P., Hallamaa, L., Allen, L.H., Ashorn, U., Chandrasiri, U., Deitchler, M., Zeilani, M., Dewey, K. G. *Maternal and Child Nutrition*, **2018**, 14(3), 125-85.
2. Bocharova, I.I., Zarochentseva, N.V., Belaya, Y.M., Malinovskaya, V.V., Vodovatova, V.A., Budykina, T.S., Milovanov, A.P., Keshyan, L.V. *Voprosy Ginekologii, Akusherstva i Perinatologii*, **2019**, 18(4), 66- 73.

3. Bonaros, N., Mayer, B., Schachner, N., Laufer, G., Kocher, A. *Clinical Transplantation*, **2008**, 22(1), 89–87.
4. Boppana, S.B., Ross, S.A., Shimamura, M., Palmer, A.L., Ahmed, A., Michaels, M.G., Britt, W.J., Fowler, K.B. *New England Journal of Medicine*, **2011**, 364(22), 2111-2118.
5. Borovkova, E.I. *Russian Bulletin of the Obstetrician and Gynecologist*, **2005**, 4(566), 9–10.
6. Britt, W.J. *Seminars in Perinatology*, **2018**, 42(3), 155-167.
7. Carbone, J. *Transplantation*, **2016**, 100, 11-18.
8. Chen, C., Essien, M.D., Johnson, A.J., Lee, G.T., Chou, F. *Journal of Maternal-Fetal and Neonatal Medicine*, **2019**.
9. Coppola, T., Mangold, J.F., Cantrell, S., Permar, S.R. *Vaccines*, **2019**, 7(4), 129.
10. Damato, E.G., Winnen, C.W. *Journal of Obstetric, Gynecologic, and Neonatal Nursing*, **2002**, 31(1), 86-92.
11. De Bie, I., Boucoiran, I. *Journal of Obstetrics and Gynaecology Canada*, **2019**, 41(6), 855-861.
12. De la Calle, M., Baquero, F., Rodriguez, R., González, M., Fernández, A., Omeñaca, F., Barth, J. L. *Journal of Maternal-Fetal and Neonatal Medicine*, **2018**, 31(16), 2226-2229.
13. Dolgushina, V.F., Dolgushin, I.I., Kurnosenko, I.V., Lebedeva, Y.V. *Akusherstvo i Ginekologiya*, **2017**, (1), 40-45.
14. Fowler, K.B., Stagno, S., Pass, R.F., Britt, W.J., Alford, C.A., Boll, T.J. *New England Journal of Medicine*, **1992**, 326(10), 663-667.
15. Helmo, F.R., Alves, E.A.R., Moreira, R.A.D.A., Severino, V.O., Rocha, L.P., Monteiro, M.L.G.D.R., Machado, J.R Corrêa, R.R.M. *Journal of Maternal-Fetal and Neonatal Medicine*, **2018**, 31(9), 1227-1233.
16. Hwang, J.S., Friedlander, S., Rehan, V.K., Zangwill, K.M. *Journal of Perinatology*, **2019**, 39(5), 690-696.
17. Isakov, V.A., Arkhipova, E.I., Isakov, D. V. *Human herpesvirus infections: a guide for physicians*. St. Petersburg: SpetsLit, **2006**.
18. Kadieva, F.G. *Clinical and immunological features of newborns with intrauterine growth retardation, from mothers infected with herpes viruses*. Astrakhan: Dagestan State Medical Academy of Roszdrav, **2007**.
19. Kemp, M.W. *Frontiers in Immunology*, **2014**, 5, 574.
20. Kitsak, V.Ya. *Pregnant viral infections: fetal and newborn pathology*. Novosibirsk: Koltsovo, **2005**.
21. Lutoshin, I.S. *Russian Bulletin of Perinatology and Pediatrics*, **2005**, 4, 32–36.
22. Makarov, O.V., Bakhareva, I.V., Taranets, A.N. *Obstetrics and Gynecology*, **2004**, 1, 10–13.
23. Mamyrbayeva, M.A., Zhumagaliyeva, G.D., Altyinnik, N.A., Dmitrashchenko, A.A. *Asian Journal of Pharmaceutics*, **2017**, 11(1), 136-145.
24. Orekhov, K.V. *Intrauterine infections and pathology of the newborn*. Moscow: Medpraktika, **2002**.
25. Ovchinnikova, M.A., Lipatov, I.S., Santalova, G.V., Tezиков, Y.V. *Jurnal Infektologii*, **2018**, 10(1), 70-79.
26. Pereira, L., Pettitt, M., Fong, A., Tsuge, M., Tabata, T., Fang-Hoonver, J., Kauvar, L.M., Ogunyemi, D. *Journal of Infectious Diseases*, **2014**, 209(10), 1573-1584.
27. Perepelitsa, S.A. *Obshchaya Reanimatologiya*, **2018**, 14(3), 54-67.
28. Polucci, A.K., Nartov, P.V., Shvaichenko, A.A., Volobueva, O.V., Lyadova, T.I. *Herpesvirus infection*. Moscow: Eksmo, **2009**.
29. Redko, I. *Georgian Medical News*, **2015**, 248, 12-15.
30. Revello, M.G., Campanini, G., Piralla, A., Furione, M., Percivalle, E., Zavattoni, M., Gerna, G. *Journal of Medical Virology*, **2008**, 80(8), 1415-1425.
31. Schleiss, M.R., Marsh, K.J. *Avery's diseases of the newborn: Tenth edition*, **2018**, 482-526.
32. Seidel, V., Feiterna-Sperling, C., Siedentopf, J., Hofmann, J., Henrich, W.,

- Bührer, C., Weizsäcker, K. *Medical Microbiology and Immunology*, **2017**, 206(5), 347-354.
33. Shabalov, N.P. *Neonatology. Volume 2*. Moscow: ME Dress-Inform, **2006**.
 34. Sial, I.G., Patel, R. *Clinical Microbiology Reviews*, **2000**, 13(1), 83–121.
 35. Stagno, S., Pass, R.F., Alford, C.A. *Birth Defects Original Article Series*, **1981**, 17(1), 31-50.
 36. Stehel, E.K., Shoup, A.G., Owen, K. E., Jackson, G.L., Sendelbach, D.M., Boney, L.F., Sánchez, P.J. *Pediatrics*, **2008**, 121(5), 970-975.
 37. Stetsyuk, O.U., Andreeva, I.V. *Farmateka*, **2006**, 14(129), 3–18.
 38. Subramaniam, A., Britt, W.J. *Clinical Obstetrics and Gynecology*, **2018**, 61(1), 157-176.
 39. Sukhanova, L.P., Sklyar, M.S. *Social Aspects of Population Health*, **2007**, 4, 1–60.
 40. Tabata, T., Petitt, M., Fang-Hoover, J., Zydek, M., Pereira, L. *American Journal of Pathology*, **2016**, 186(11), 2970-2986.
 41. Tyutyunnik, V.L., Kan, N.E., Lomova, N.A., Karapetyan, T.E., Kogan, E.A., Shchyogolev, A.I. *Bulletin of Experimental Biology and Medicine*, **2014**, 158(1), 74–76.
 42. Volodin, N.N. *Diagnostic, treatment, and prevention protocols for intrauterine infections in newborn infants*. Moscow: VUNMTS MZ RF, **2001**.
 43. Volodin, N.N. *Protocol for the diagnosis, treatment and prevention of intrauterine infections in newborns*. Moscow: GOU VUNMTS MZ RF, **2002**.
 44. Wagner, N., Kagan, K.O., Haen, S., Schmidt, S., Yerlikaya, G., Maden, Z., Jahn, G., Hamprecht, K. *Journal of Maternal-Fetal and Neonatal Medicine*, **2014**, 27(2), 209-214.
 45. Wang, C., Zhang, X., Bialek, S., Cannon, M.J. *Clinical Infectious Diseases*, **2011**, 52(2), 11-13.
 46. Ximenes, A.S.F.C., Pires, P., Werner, H., Jungmann, P.M., Rolim Filho, E.L., Andrade, E.P., Tonni, G., Araujo Júnior, E. *Journal of Maternal-Fetal and Neonatal Medicine*, **2019**, 32(3), 493-501.
 47. Zavattoni, M., Rustico, M., Tassis, B., Lombardi, G., Furione, M., Piralla, A., Baldanti, F. *Journal of Medical Virology*, **2016**, 88(1), 120-126.
 48. Zhukova, L.I., Kovalevskaya, O.I., Gorodin, V.N., Shakhverdyan, Y.G. *Klinicheskaya Laboratornaya Diagnostika*, **2018**, 63(1), 51-54.
 49. Zhumalina, A.K., Tusupkaliev, B.T., Zame, Yu.A., Iliysova, A.B. *Clinical aspects of the manifestations of CMV infection in children of the neonatal period*. Opole: Publishing House WSZiA, **2014**.
 50. Zile, I., Ebela, I., Rumba-Rozenfelde, I. *Medicina*, **2019**, 55(7), 326.

Table 1. Parameters of Cellular Immunity in Newborns

	Group 1 (study group)	Group 2 (control group)
CD3+	73.8 ±6.9	67±8.1
CD4+	37.1 ±4.2	38.6±4.4
CD8+	17.5±4.2	25.7±1.6
CD19+	8.37 ±2.5	16.4±0.3

Table 2. Values of the General Population of T-lymphocytes in Newborns

Variable	Mann-Whitney U-test (complete blood test and CD) Group by variables Specified criteria are significant at p <0.05000								
	Total ranks Group 1	Total ranks Group 2	U	Z	p-level	Z adjusted	p- level	N Group 1	N Group 2
CD3+	902.0000	274.0000	154.0000	2.06858	0.038586	2.07439	0.038044	33	15
CD4+	814.0000	362.0000	242.0000	0.11121	0.911447	0.11236	0.910538	33	15
CD8+	601.5000	574.5000	40.5000	- 4.59314	0.000004	- 4.62756	0.000004	33	15
CD19+	767.5000	408.5000	206.5000	- 0.90083	0.367677	- 0.92111	0.356996	33	15

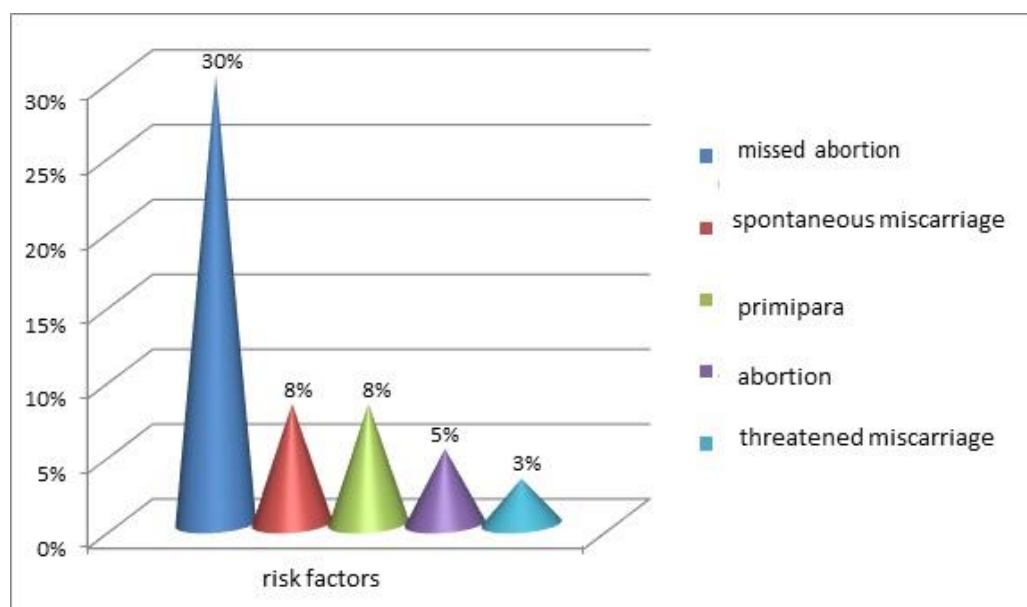


Figure 1. Pregnant Reproductive Health

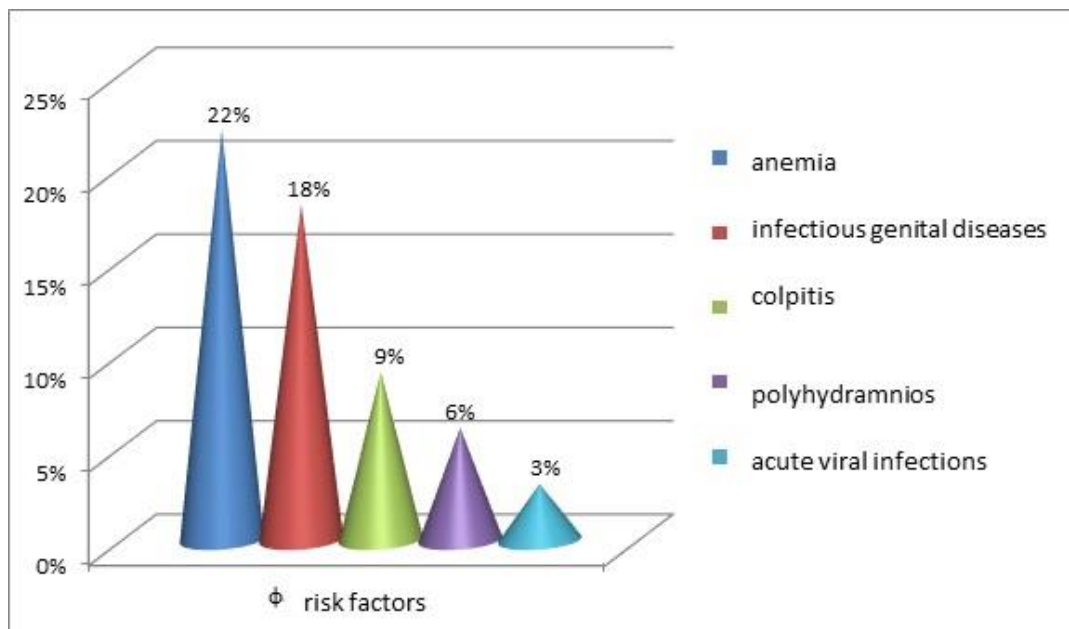


Figure 2. Risk Factors during Pregnancy

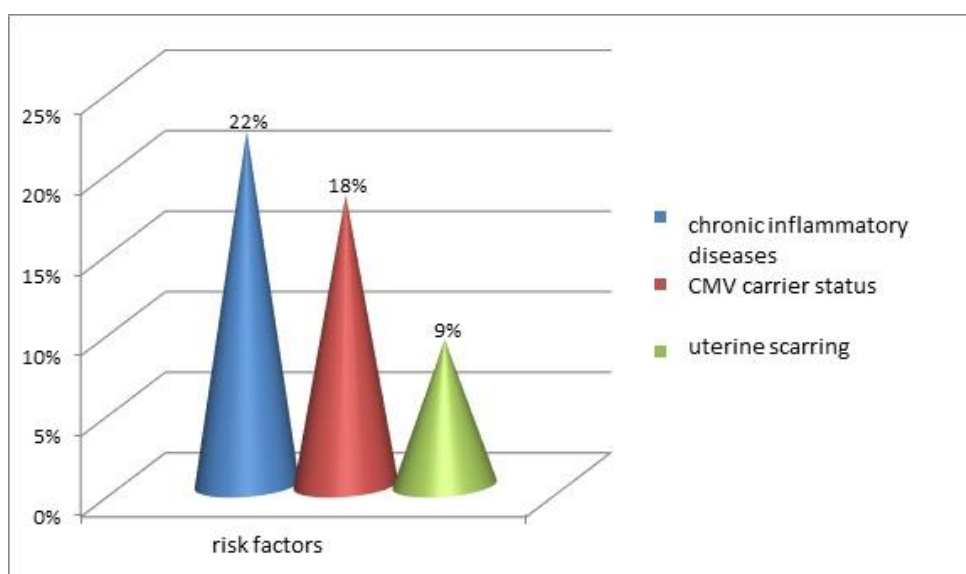


Figure 3. Women's Somatic Health Risk Factors

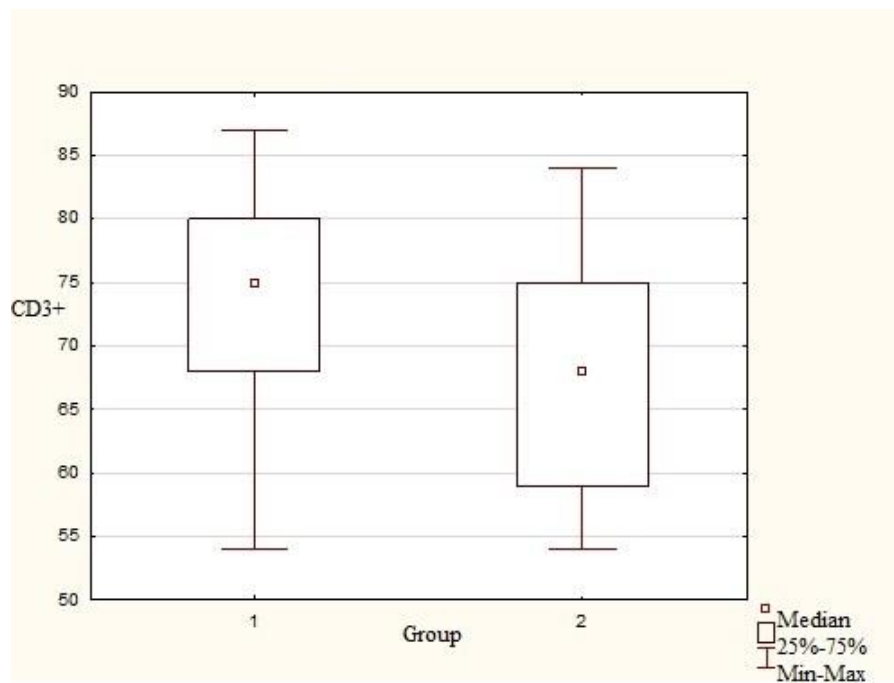


Figure 4. Range by Groups of Variables: CD3+

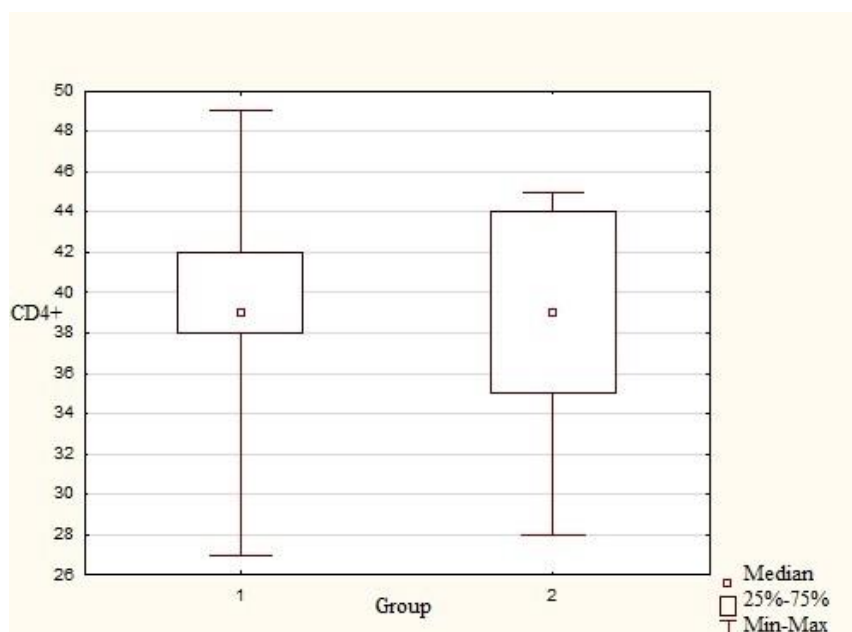


Figure 5. Range by Groups of Variables: CD4+

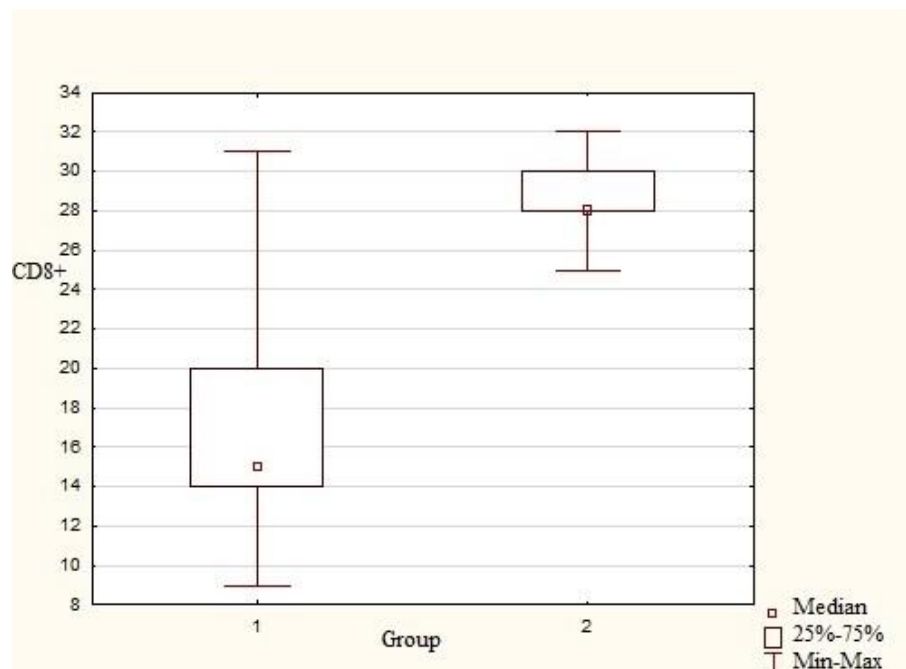


Figure 6. Range by Groups of Variables: CD8+

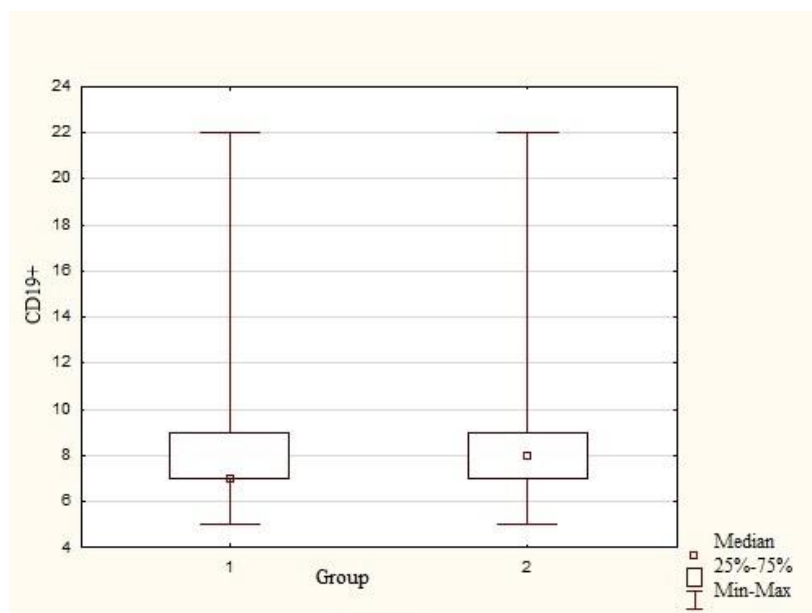


Figure 7. Range by Groups of Variables: CD19+

AVALIAÇÃO DA HABILIDADE DE CRESCIMENTO DE *ARTHROSPIRA* SP. EM SAIS DE METÁIS PESADOS E SEU EFEITO EM ALGUNS COMPONENTES CELULARES

EVALUATION OF *ARTHROSPIRA* SP. GROWTH ABILITY ON HEAVY METAL SALTS AND THEIR EFFECT ON SOME CELLULAR COMPONENTS

تقييم قدرة نمو جنس *Arthrospira* على املاح المعادن الثقيلة وتأثيرها على بعض المكونات الخلوية

Hiba Khaleel Saeed Al-Shakarchi^{1*} and Yousef Jabbar Al-Shahery²

¹Department of Biophysics, College of Science, University of Mosul, Mosul, Iraq.

²Department of Biology, College of Education for Pure Science, University of Mosul, Mosul, Iraq.

* Correspondence author

e-mail: hiba.khaleel@uomosul.edu.iq

Received 06 January 2020; received in revised form 25 February 2020; accepted 09 March 2020

RESUMO

Arthrospira sp. é um microorganismo aquático e fotossintético amplamente empregado como complemento alimentar, devido ao seu rico conteúdo de nutrientes, proteínas e carboidratos. Neste estudo, uma cepa local de cianobactéria do gênero *Arthrospira* foi isolada do solo iraquiano, na região da cidade de Mosul, usando o Meio No. 10 de Chu. A taxa de crescimento, bem como os efeitos sobre a biomassa e o conteúdo de componentes celulares das proteínas, carboidratos e clorofila dessa cepa, foram avaliadas apenas no meio de melaço ou suplementadas com sais de ferro, cobre, níquel, cádmio e cobalto após quinze dias de incubação. Os resultados mostraram que a melhor taxa de crescimento (1,09 OD), o maior valor de biomassa (120,0 mg / l), teor de proteínas (297,2 mg / l), teor de clorofila (14,9 mg / l) e teor de carboidratos (400,0 mg / l) de *Arthrospira* sp. foi alcançado após quinze dias de incubação. Foi observado que a adição de sais de ferro, cobre, níquel, cádmio e cobalto ao melaço aumentou o conteúdo de biomassa, proteínas e carboidratos de *Arthrospira* sp. Observou-se que a maior concentração de biomassa (1960 mg/l) foi obtida quando *Arthrospira* sp. cultivadas em melaço suplementado com níquel. Além disso, nenhum dos sais metálicos adicionados ao meio de melaço aumentou o teor de proteína de *Arthrospira* sp. Por outro lado, a adição de cobre, níquel e cobalto ao meio mostrou um efeito adverso no teor de proteína. Foi demonstrado que a adição de sais de ferro no meio do melaço aumentou os carboidratos e o teor de clorofila de *Arthrospira* sp. Esses resultados sugerem que *Arthrospira* sp. pode ser utilizado para a biorremediação da poluição por metais pesados no ambiente e nas instalações industriais.

Palavras-chave: *Arthrospira*, cianobactéria, melaço, sais de metais pesados, poluentes.

ABSTRACT

Arthrospira sp. is an aquatic and photosynthetic microorganism that is extensively employed as a food supplement due to its rich contents of nutrients, proteins, and carbohydrates. In this study, a local strain of cyanobacterium of the genus *Arthrospira* was isolated from the Iraqi soil, in the region of Mosul city, using the Chu's Medium No. 10. The growth rate, as well as the effects on biomass and cellular component contents of proteins, carbohydrates, and chlorophyll of this strain, were evaluated on the molasses medium alone or supplemented with iron, copper, nickel, cadmium and cobalt salts after fifteen days of incubation. The results showed that the best growth rate (1.09 OD), the highest value of biomass (120.0 mg/l), proteins content (297.2 mg/l), chlorophyll content (14.9 mg/l) and carbohydrates content (400.0 mg/l) of *Arthrospira* sp. was achieved after fifteen days of incubation. Generally, it was observed that adding iron, copper, nickel, cadmium, and cobalt salts into the molasses medium increased the contents of biomass, proteins, and carbohydrates of *Arthrospira* sp.. It was noticed that the highest biomass concentration (1960 mg/l) was obtained when *Arthrospira* sp. grown on molasses medium supplemented with nickel. Also, none of the metal salts added to the molasses medium increased the protein content of *Arthrospira* sp.. Conversely, adding copper, nickel, and cobalt to the medium showed an adverse effect on the protein content. It was shown that adding iron metal salts into the molasses medium increased the carbohydrates and the chlorophyll contents of *Arthrospira* sp.. These results suggest that

Arthrospira sp. can be utilized for the bioremediation of heavy metals pollution in the environment and industrial sites.

Keywords: *Arthrospira*, cyanobacterium, molasses medium, Heavy Metal Salts, Pollutants.

الملخص

يعتبر جنس *Arthrospira* من الكائنات الحية الدقيقة المائية والقادرة على التمثيل الضوئي والتي تستخدم على نطاق واسع كمكملات غذائية بسبب محتوياتها الغنية من المواد الغذائية والبروتينات والكربوهيدرات. في هذه الدراسة، تم عزل سلالة محلية من البكتيريا الخضراء المزرقة للجنس *Arthrospira* من تربة عراقية في مدينة الموصل باستخدام الوسط Chu رقم 10. تم تقييم معدل النمو، وكذلك التأثير على محتويات الكتلة الحيوية والمكونات الخلوية من البروتينات والكربوهيدرات والكلوروفيل على هذه السلالة، على وسط دبس السكر وحده أو بعد إضافة أملاح المعادن التالية الحديد، النحاس، النيكل، الكاديوم، والكوبالت بعد خمسة عشر يوماً من الحضانة. أظهرت النتائج أن أفضل معدل نمو (1.09 كثافة ضوئية)، أعلى قيمة للكتلة الحيوية (120.0 ملغم / لتر)، محتوى البروتينات (297.2 ملغم / لتر)، محتوى الكلوروفيل (14.9 ملغم / لتر) ومحتوى الكربوهيدرات (400.0 ملغم / لتر) للجنس *Arthrospira* تم تحقيقه بعد خمسة عشر يوماً من الحضانة. عموماً، لوحظ أن إضافة أملاح معادن الحديد، النحاس، النيكل، الكاديوم، والكوبالت في وسط دبس تزيد من محتويات الكتلة الحيوية والبروتينات والكربوهيدرات للجنس *Arthrospira*. لوحظ أنه تم الحصول على أعلى تركيز للكتلة الحيوية (1960 مجم / لتر) عند تنمية جنس *Arthrospira* على دبس السكر المضاف إليه النيكل. بالإضافة إلى أن أي من الأملاح المعدنية المضافة إلى وسط دبس لم تزيد من محتوى البروتين للجنس *Arthrospira*. وعلى العكس، فإن إضافة النحاس والنيكل والكوبالت إلى الوسط أظهرت تأثيراً سلبياً على محتوى البروتين. وقد تبين أن إضافة أملاح معدن الحديد في وسط دبس السكر زاد من محتوى الكربوهيدرات والكلوروفيل للجنس *Arthrospira*. تشير النتائج إلى أن بالإمكان استخدام جنس *Arthrospira* في المعالجة البيولوجية للتلوث بالمعادن الثقيلة في البيئة والمواقع الصناعية.

الكلمات المفتاحية: *Arthrospira*، البكتيريا الخضراء المزرقة، وسط دبس السكر، أملاح المعادن الثقيلة، الملوثات.

1. INTRODUCTION

Cyanobacteria are a broad group of organisms that were previously included with algae in the classification of the plant kingdom. Currently, they fall within the group of negative eubacteria to Gram stain (Kozhevnikov and Kozhevnikova 2011). Cyanobacteria are the cause of damage to the aquatic environment or to the lives of aquatic life, or even to human life. They are one of the dangerous, polluting sources to the water, especially the liquefaction water, through releasing of many toxins, and this leads to harm to the lives of millions of people on the globe (Cabral, 2010). In addition, they threaten the aquatic organisms in their environments such as fish and invertebrates, and thus they affect the lives of humans and even animals that feed on these aquatic organisms (Schirmer et al., 2011).

On the other hand, cyanobacteria have countless benefits. Many of them are sources for the production of economically essential materials, which encourage their cultivation and the production of biomass. Cyanobacteria are tremendous sources of many organic acids, cosmetics, enzymes, monosaccharides, and polysaccharides, and are also sources of many pharmaceutical and industrial materials (Markou et al., 2012). Cyanobacteria are able to convert their mod of nutrition from autotrophic to saprophytic. This unique characteristic enables these organisms to take advantage of utilizing the carbon sources available in the nutritional

medium to produce biomass. Therefore, the production of this biomass can then be exploited economically for different purposes and at the same time to remove different pollutants resulting from various industrial activities such as sugar production factories, tanning plants and meat productions (Habib et al., 2008).

In recent years, cyanobacteria have been utilized to get rid of the toxic effects of industrial waste residues containing toxic materials such as heavy metals. Cyanobacteria have various mechanisms in response to the toxic effects of these substances, and their resistance mechanisms are different according to the type of cyanobacterial strain and the type of pollutant (Rathinam et al., 2010). Some cyanobacteria showed their ability to secrete extracellular compounds that have the potential to bind to heavy metals. Heavy metals and ions have the ability to combine with functional groups that are found in bioactive molecules such as OH, NH₄, COOH, PO₄, and SH, and convert them into forms that cannot enter the living cells, or reduce the effectiveness of the ions by controlling the permeability of the cell membranes (Pereira et al., 2011).

These mechanisms, which cyanobacteria use to resist the toxic effect of minerals or prevent them from entering the cell, are known as exclusion. Moreover, many cyanobacterial strains have the ability to remove the toxic effect inside their cells by forming peptide compounds that are rich in SH. In the case of exposure to high concentrations of minerals or when exposed to

sub-lethal concentrations, they lead to the production of peptide compounds that are rich in GSH (Rastogi *et al.*, 2015). In both cases, these compounds are called Phyto-chelating compounds, which are rich in cysteine amino acid.

Cyanobacteria possess a large number of genera and species that can be exploited to be used as ion metals bioremediation agents due to their ability to accumulation ion metals in their bodies (Godlewska *et al.*, 2019). However, since there were limited studies about bacteria from the local environments of Mosul city (Al-Qatan *et al.*, 2019), so, this study aimed to isolate a pure local strain of the genus *Arthrospira* and to study its ability to utilize the molasses as a medium of growth and to evaluate adding some heavy metals on some cellular components of *Arthrospira* sp.

2. MATERIALS AND METHODS

The Materials and Methods for this study as shown below in paragraphs:

1. Isolation and cultivation of *Arthrospira* sp.

Soil samples were collected from the local environment of Mosul city (Iraq); soil sample was mixed, and a suspension of 1 g (dry weight equivalent) in 10 ml of sterile water was prepared (Prasanna, 2017). One ml of the soil suspension was then diluted serially (three-fold) and used in the isolation of the bacteria by standard spread-plate dilution method described by (Seeley *et al.*, 1970; Banoon and Ali, 2018). Each diluted cultured was poured on Chu's Medium No. 10 agar and incubated at 28 ± 1 °C, light 2500 Lux for 15 days, or till appear the growth. The Chu's Medium No. 10 was used for the initial isolation of the Cyanobacteria and for the purification and the cultivation of *Arthrospira* sp. The medium was prepared according to (Chu, 1942) by weighting (40 g calcium nitrate, 25 g magnesium sulfate, 5 g dipotassium phosphate, 20 g sodium carbonate, 25 g sodium silicate, and 8 g iron chloride) (BDH, UK) and 10% Agar-Agar (Himedia, India). The components were dissolved in one L (final volume) of distilled water (reagent water type IV, ASTM D1193), and the pH adjusted to 7.6-7.8, then sterilize by autoclaving at 15 lbs pressure (121 °C) for 15 minutes (Aryal, 2015). After fifteen days (appearance of the growth); One colony was picked from agar plates then cultured on Chu10 agar and incubated at 28 ± 1 °C, light 2500 Lux for 15 days for purification, the subcultured on the Chu10 solid agar was

repeated several times to obtain a pure representative colony according to shape of colony, appearance and microscopic examination using compound Microscope (Olympus Cx21, Germany). Then a pure colony of the *Arthrospira* sp. was picked up and cultured in 10 ml of Chu broth media at 28 ± 1 °C, light (250 lux) at 100 rpm for 15 days for obtaining the *Arthrospira* sp. inoculum, which is used in subsequent experiments.

2. Preparation the Molasses medium

The culture media was distilled water (reagent water type IV), plus 20% (v/v) Zarrouk's medium (Zarrouk, 1966). Each component of the Zarrouk medium was sterilized separately by autoclaving at 121 °C for 15 min. After cooling, the solutions were mixed, and the medium was supplemented with $0.75 \text{ g}\cdot\text{L}^{-1}$ of concentrated molasses (Table 1) that obtained from the Iraqi sugar industry at Mosul city, this medium was divided into 95 ml for each flask and inoculated with 5 ml of Chu 10 broth medium containing the *Arthrospira* sp. To study the growth ability of *Arthrospira* sp. in the molasses medium with heavy metals salts and to study their effects on some cellular components, different gradual concentrations (mg/l) of the following heavy metal salts; iron chloride ($\text{FeCl}_2\cdot 6\text{H}_2\text{O}$), copper chloride ($\text{CuCl}_2\cdot 6\text{H}_2\text{O}$), nickel chloride ($\text{NiCl}_2\cdot \text{H}_2\text{O}$), cadmium chloride (CdCl_2) and cobalt (CoCl_2) were prepared and added to the medium and incubated at 28 ± 1 °C, light 2500 Lux for fifteen days.

3. Analysis Methods

The *Arthrospira* sp. biomass concentration was daily determined by measuring the optical density using spectrophotometry (Labomed Inc, USA), where 1 ml of the culture medium was taken for measuring at ($\lambda_{\text{max}} = 670 \text{ nm}$) (Costa *et al.*, 2002). The pH of the cultures was measured every two days using a digital pH meter (Sartorius, Germany) (Schmidell *et al.*, 2001). The carbohydrates content (mg/L) was estimated by the "phenol-sulfuric acid" method (Dubois *et al.*, 1951) By taking (10) ml of the culture and then mixing by an ultrasonic homogenizer (Sonic Ruptor 400, USA). Then the mixed culture was centrifuged at 3000 rpm for ten minutes after centrifuging 1 ml of the supernatant, one ml of phenol solution (5%), and 5 ml of concentrated sulfuric acid were added. The mixture was then vortexed and incubated in a water bath for 30

minutes, measured by spectrophotometry at 477 nm, and then carbohydrate concentrations were calculated in the samples based on the standard curve using glucose. The Mackinney (1941) method was used to estimate the total chlorophyll content by taking five ml of the culture and pelleted by centrifuging at 3500 rpm for two minutes. The pellet was homogenized with 5 ml of 80% of acetone and incubated in a water bath at 70 °C for 2 minutes. Next, it was centrifuged at 3500 rpm for 5 minutes, and the clear supernatant was taken and read at 665 nm in a spectrophotometer (Labomed Inc, USA) against acetone as blank. The chlorophyll content was calculated using Equation 1.

Chlorophyll content = optical density at 665 nm × 13.9 (Eq. 1)

(13.9 is a constant derived from the absorption coefficient). The protein content of *Arthrospira sp.* was estimated according to the Lowry method, most widely used to estimate the amount of proteins (Lowry *et al.* 1951).

3. RESULTS AND DISCUSSION:

From the results, it was found that *Arthrospira sp.* contains multicellular cylindrical trichomes with a blue-green color (Figure 1). However, these characterizations are typical morphology for the genus *Arthrospira* that were described by Tomaselli *et al.*, 1996.

3.1. Effect of different incubation periods

This experiment was designed to see the ability of *Arthrospira sp.* to exploit the byproduct of molasses to grow *Arthrospira sp.* as a liquid nutritional medium during different incubation times. The results showed that the best growth (1.09 OD) of *Arthrospira sp.* was achieved after fifteen days of incubation (Table 2). Additionally, the highest value of biomass (120.0 mg/l), the highest proteins content (297.2 mg/l), the highest chlorophyll content (14.9 mg/l) and the highest carbohydrates content (400.0 mg/l) were recorded at the same incubation period at the final pH (8.92). These results confirmed that the best growth of the studied species achieves the best protein, chlorophyll, and carbohydrate content as well as possessing the best biomass and higher pH value.

3.2. Effect of heavy metal salts

The growth rate, biomass, protein content, chlorophyll content, and carbohydrates content were evaluated after fifteen days of incubation in molasses medium without and with supplements of different metals salts. From the results, it was observed that adding metal salts into molasses has a variable effect on the growth rate (Figure 2), biomass, and cell components of *Arthrospira sp.* (Figure 3). In general, concentrations of biomass, protein content, and carbohydrates content were increased by adding the metal salts into the molasses medium.

The highest biomass concentration (1960 mg/l) was obtained when *Arthrospira sp.* grown on molasses medium supplemented with nickel chloride (Figure 4). Similarly, adding cadmium, copper, cobalt, and iron chloride into molasses medium were also increased the biomass concentrations of *Arthrospira sp.* To 1801 mg/l, 1734 mg/l, 1640 mg/l and 1626 mg/l accordingly. Although metals induce biosynthesis of some compounds by cyanobacterial strains, they may also have detrimental effects in high concentrations. Nickel plays an important role in many metabolic activities of cyanobacteria. Nickel is directly coordinated by proteins (Ragsdale, 2009) or through the tetrapyrrole ring of coenzyme F₄₃₀, which coordinates a nickel atom in methyl-coenzyme M reductase (MCR); MCR is a nickel tetrahydrocorphinoid (coenzyme F₄₃₀) containing enzyme concerned in the biological synthesis and anaerobic oxidation of methane. MCR catalyzes the conversion of methyl-2-mercaptoethanesulfonate (methyl-SCoM) and N-7-mercaptoheptanoylthreonine phosphate (CoB₇SH) to CH₄ and the corresponding heterodisulfide (CoBS-SCoM) (Wongnate and Ragsdale, 2015; Scheller *et al.*, 2013; Kobayashi and Shimizu 1999). Nickel serves as a cofactor in an enzyme urease, which is needed to use urea as a nitrogen source (Oliveira and Antia, 1984; Collier *et al.*, 1999; Miazek *et al.*, 2015). Studies have shown that metals, such as cadmium, copper and cobalt, at low concentrations had a stimulatory effect on growth of cyanobacteria (Mann *et al.*, 2002; Shanab *et al.*, 2012; Dupont *et al.*, 2012; Twining and Baines, 2013) and these are consistent with the results obtained in the present study.

On the other hand, the addition of iron and cadmium metals had no effect on increasing the protein content of *Arthrospira sp.* as the concentrations were almost similar (Figure 5). It was also noticed that copper and cadmium had the most negative effect on proteins and carbohydrates contents compared with molasses

medium alone as the concentrations were 85 mg/l and 243 mg/l accordingly (Figure 5 and 6). Copper is a metal necessary for the proper growth and development of plants (Sunda, 1989). It is an essential microelement for cyanobacteria because it is an integral component of plastocyanin in the photosynthetic electron-transport chain. However, high concentrations of copper are effective as a cyanocide and are usually used for removing undesired cyanobacterial growth in water reservoirs and drainage systems (Surosz and Palinska, 2004). On the other hand, cadmium is known to be one of the most hazardous rare metals in the environment because of its high toxicity to all components of aquatic communities (Vymazal, 1987) and has received widespread of attention because of its accelerated release into the environment as the result of industrial pollution (Surosz and Palinska 2004; Wieczorek *et al.*, 2018).

It was shown that adding iron and nickel metals into molasses medium increased the carbohydrates content of *Arthrospira* sp. from 400 mg/l in molasses medium to 557 and 463 mg/l (Figure 6) accordingly. However, it is well known that iron is an essential metal for most organisms, including cyanobacteria (Zhang *et al.*, 2018). Iron is involved in the biosynthesis of chlorophyll and phycobilin pigments, electron transport reactions, and inorganic nitrate assimilation (Greene *et al.* 1992; Li *et al.*, 2016). This is very obvious in the present results as the chlorophyll content was higher in the molasses medium supplemented with iron chloride (Figure 3). Our findings were agreed with other studies about the effect the industrial pollutants on the efficacy of cyanobacteria (Abdel-Raouf *et al.*, 2012). However, the heavy metals resistance genes for this exotic strain need to be sequenced or RAPD-typing or detect the resistance genes for further studies as recommended by Salih and Shafeek, 2019; Banoon *et al.*, 2019; Aziz *et al.*, 2019).

4. CONCLUSIONS:

This work has demonstrated that the *Arthrospira* sp. isolated from the Iraqi environment, in the region of Mosul city was able to grow on the byproducts of industrial sugar waste (molasses) alone or supplemented with heavy metals. In this study, it was observed that the addition of iron, copper, nickel, cadmium, and cobalt metals into the molasses medium increased the biomass content. Moreover, while adding iron and nickel metals into the molasses

medium increased the carbohydrates content of *Arthrospira* sp., adding copper, nickel, and cobalt decreased the protein content of *Arthrospira* sp. compared to the molasses medium. This study suggested that this local strain of cyanobacteria can be used as a reliable biological system for bioremediation of heavy metals pollution in the environment.

5. ACKNOWLEDGMENTS:

The authors are very grateful to the University of Mosul, and the College of Science for their provided facilities, which helped to improve the quality of this work.

6. REFERENCES:

1. Abdel-Raouf N., Al-Homaidan A.A., Ibraheem I.B. *Saudi journal of biological sciences*. **2012**,19(3):257-75.
2. Al-Qatan M.A., Al-Khayyat M.Z., Saeed H.K. *Biochem. Cell. Arch.* **2019**,19(1):1415-1418.
3. Aryal, S. "MacConkey Agar-Composition, Principle, Uses, Preparation and Colony Morphology. Microbiologyinfo. 30 de Septiembre." **2015**.
4. Aziz Z.S., Banoon S.R., Hassain A.S. *Arctic*. **2019**, 72(12):58-76.
5. Banoon, S. R., and Ali, Z.M. *Al-Kufa University Journal for Biology*. **2018**, 10(2):157-167.
6. Banoon S. R., Kadhim Z. K., Aziz Z. S., Jameel Z. I., EWadh R. M. *Indian Journal of Public Health Research & Development*. 2019,10(9): 1300-1305.
7. Cabral J.P. *International journal of environmental research and public health*. 2010, 7(10):3657-703.
8. Chu S. P. *J. Ecol.*, **1942**,30: 284-325.
9. Clarke M.A. Syrups. In: Caballero B., Trugo L.C., Finglas P.M. (eds.) *Encyclopedia of food sciences and nutrition* (2ed). *Academic Press*; **2003**. p. 5711-5717.
10. Collier J.L., Brahamsha B., Palenik B. *Microbiology*. **1999**,145(2):447-59.
11. Costa J.A., Colla L.M., Duarte Filho P., Kabke K., Weber A. *World Journal of Microbiology and Biotechnology*. **2002**,18(7):603-7.
12. Dubois M., Gilles K.A., Hamilton J.K., Rebers P.A., Smith F. *Nature*. **1951**, 168(4265):167.

13. Dupont C.L., Johnson D.A., Phillippy K., Paulsen I.T., Brahmsha B., Palenik B. *Appl. Environ. Microbiol.* **2012**, 78(22):7822-32.
14. Godlewska K., Michalak I., Pacyga P., Baśladyńska S., Chojnacka K. *World Journal of Microbiology and Biotechnology*. **2019**, 35(6):80.
15. Greene R.M., Geider R.J., Kolber Z., Falkowski P.G. *Plant Physiology*. **1992**, 100(2):565-575.
16. Habib M.A., Parvin M., Huntington T.C., Hasan M.R. *Aquac. Circ.* **2008**(1034).
17. Kobayashi M., Shimizu S. *European Journal of Biochemistry*. **1999**, 261(1):1-9.
18. Kozhevnikov I.V., Kozhevnikova N.A. *Inland Water Biology*. **2011**, 4(2):143-52.
19. Li P., Wu J., Qian H. *Environmental Earth Sciences*. **2016**, 75(8):698.
20. Lowry O.H., Rosebrough N.J., Farr A.L., Randall R.J. *Journal of biological chemistry*. **1951**, 193:265-75.
21. Mann E.L., Ahlgren N., Moffett J.W., Chisholm S.W. *Limnology and Oceanography*. **2002**, 47(4):976-88.
22. Markou G., Chatzipavlidis I., Georgakakis D. *World Journal of Microbiology and Biotechnology*. **2012**, 28(8):2661-70.
23. Mackinney G. *J. biol. Chem.* **1941**, 140(2):315-22.
24. Miazek K., Iwanek W., Remacle C., Richel A., Goffin D. *International journal of molecular sciences*. **2015**, 16(10):23929-23969.
25. Oliveira L., Antia N.J. *British phycolological journal*. **1984**, 19(2):125-134.
26. Prasanna R. *IJARIT*. **2017**, 3 (1):175-178.
27. Pereira S., Micheletti E., Zille A., Santos A., Moradas-Ferreira P., Tamagnini P., De Philippis R. *Microbiology*. **2011**, 157(2):451-458.
28. Ragsdale SW. *Journal of Biological Chemistry*. **2009**, 284(28):18571-18575.
29. Rastogi R.P., Madamwar D., Incharoensakdi A. *Frontiers in microbiology*. **2015**, 6:1254.
30. Rathinam A., Maharshi B., Janardhanan S.K., Jonnalagadda R.R., Nair B.U. *Bioresource technology*. **2010**, 101(5):1466-1470.
31. Salih T.S., Shafeek R.R. *Jordan Journal of Biological Sciences*. **2019**, 12(5).
32. Scheller S., Goenrich M., Thauer R.K., Jaun B. *Journal of the American Chemical Society*. **2013**, 135(40):14975-14984.
33. Schirrmeister B.E., Antonelli A., Bagheri H.C. *BMC evolutionary biology*. **2011**, 11(1):45.
34. Schmidell W., Lima A.U., Aquarone E., Borzani W. *Biocnologia industrial*. São Paulo. **2001**;3.
35. Seeley H.W., Vandemark P.J., Van Demark P.J. *Microbes in action: A laboratory manual of microbiology*. **1970**.
36. Shanab S., Essa A., Shalaby E. *Plant signaling & behavior*. **2012**, 7(3):392-399.
37. Sunda W.G. *Biological Oceanography*. **1989**, 6(5-6):411-442.
38. Surosz W, Palinska KA. *Archives of environmental contamination and toxicology*. **2004**, 48(1):40-48.
39. Tomaselli L., Palandri R.M., Tredici M.R. *Algological Studies/Archiv für Hydrobiologie*. **1996**, Supplement Volumes:539-548.
40. Twining B.S., Baines S.B. *Annual review of marine science*. **2013**, 5:191-215.
41. Vymazal J. *Toxicity assessment*. **1987**, 2(4):387-415.
42. Wieczorek J., Baran A., Urbański K., Mazurek R., Klimowicz-Pawlas A. *Environmental geochemistry and health*. **2018**, 40(6):2325-2342.
43. Wongnate T., Ragsdale S.W. *Journal of Biological Chemistry*. **2015**, 290(15):9322-9334.
44. Zarrouk C. Contribution à l'étude d'une cyanophycée. Influence de divers facteurs physiques et chimiques sur la croissance et la photosynthèse de *Spirulina maxima*. (Setchell et Gardner) Geitler. Thèse de doctorat, **1966**, Univ Paris, 83 p.
45. Zhang S., Zheng X., Zhang W., Song Q., Zheng Z., Luo X. *Water, Air, & Soil Pollution*. **2018**, 229(10):336.

Table 1: Approximate Component of chemical analysis of molasses medium according to Clarke (2003)

Main constituents	Components	Normal range
water		17-25%
Sugars	Sucrose	30-40%
	Glucose (dextrose)	4-9%
	Fructose (levulose)	5-12%
	Other reducing substances (as invert)	1-4%
	Total reducing substances (as invert)	10-25%
Other carbohydrates	Gums, starch, pentosans, also traces of hexitols; myoinositol, d-mannitol, and uronic acids.	2-5%
Ash	As carbonates	7-15%
	Bases: Potassium oxide (30–50%), Calcium oxide (7–15%), Magnesium oxide (2–14%), Sodium oxide (0.3–9%), Metal oxides (as ferric) (0.4–2.7%) Acids: Sulfur trioxide (7–27%), Chloride (12–20%), Phosphorus pentoxide (0.5–2.5%), Silicates and insolubles (1–7%)	
Nitrogenous compounds	Crude protein (as N \times 6.25)	2.5-4.5%
	True protein	0.5-1.5%
	Amino acids, principally aspartic and glutamic acids, including some pyrrolidine carboxylic acids	0.3-0.5%
	Unidentified nitrogenous compounds	1.5-3.0%
Nonnitrogenous	Aconitic acid (1–5%), citric, malic, oxalic, glycolic	1.5-6.0%
	Mesaconic, succinic, fumaric, tartaric	0.5-1.5%
Wax, sterols, and phosphatides		0.1-1.0%
Vitamins	Thiamin (B ₁)	2-10 ppm
	Riboflavin (B ₂)	1-6 ppm
	Pyridoxine (B ₆)	1-10 ppm
	Nicotinamide	1-25 ppm
	Pantothenic acid	2.25 ppm
	Folic acid	10-50 ppm
	Biotin	0.1-2 ppm

Table 2: Effect of incubation periods on the growth rate, biomass, proteins, chlorophyll, and carbohydrates contents of *Arthrospira* sp.

Incubation period (days)	Final pH	Growth rate (OD)	Biomass mg/l	Proteins content mg/l	Chlorophyll content mg/l	Carbohydrates content mg/l
3	7.71	0.21	211.0	80.0	7.3	103.0
5	7.72	0.32	332.0	82.3	9.6	183.0
7	7.90	0.49	389.0	89.0	11.3	199.0
9	8.01	0.65	401.0	122.0	11.9	256.0
11	8.09	0.77	539.0	189.2	12.7	301.0
13	8.33	0.99	805.0	238.3	12.9	360.0
15	8.92	1.09	120.0	297.2	14.9	400.0
17	8.80	0.89	109.0	223.0	13.6	323.0

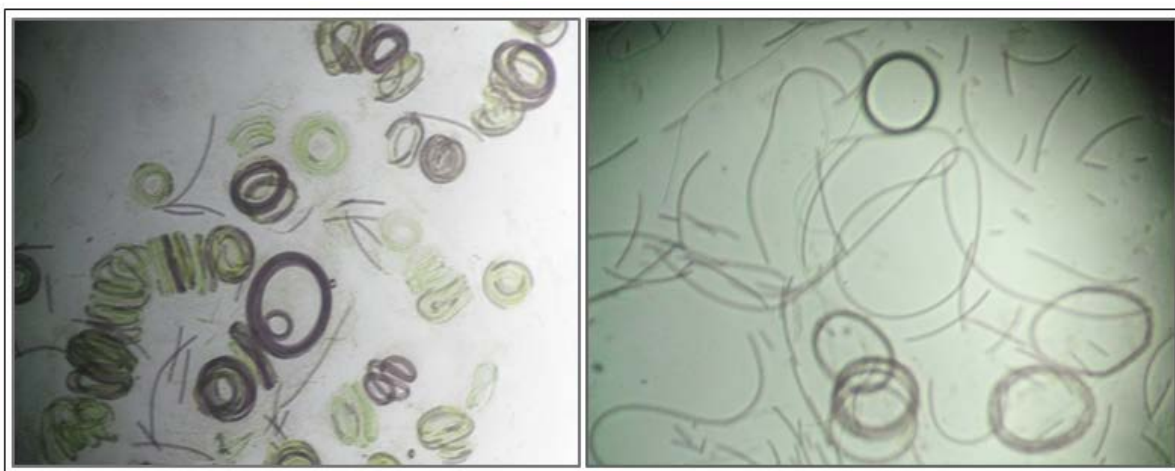


Figure 1: Light microscopy (magnification 10X) of *Arthrospira* sp. from the Chu's No. 10 agar medium (left) and from the Chu's No. 10 broth medium (right).

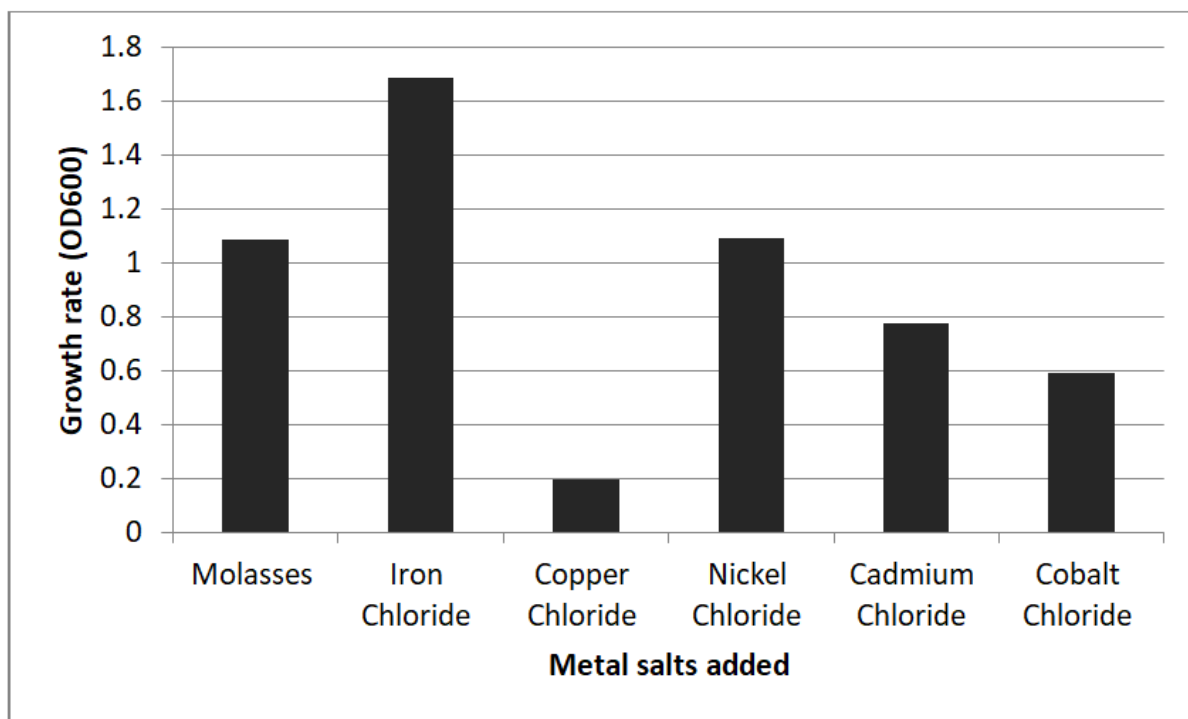


Figure 2: Growth rate of *Arthrospira* sp. grown on molasses medium alone or supplemented with different metals after fifteen days of incubation.

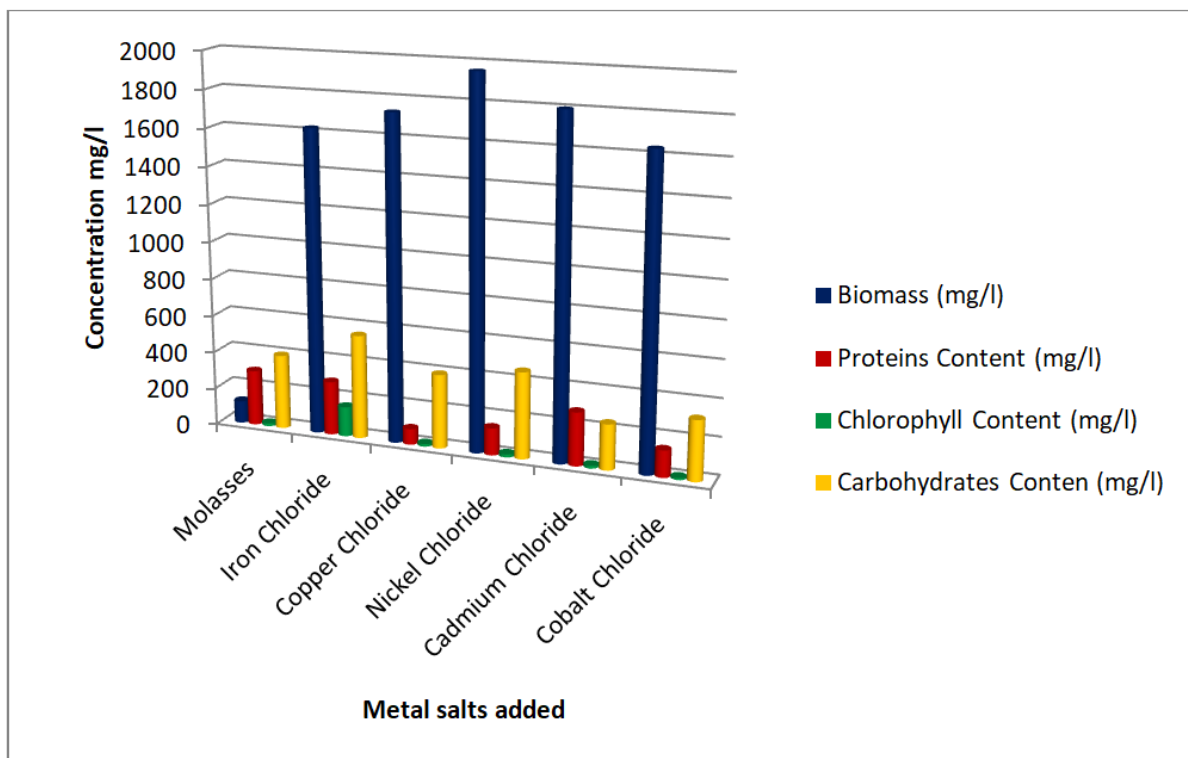


Figure 3: Biomass, protein content, chlorophyll content, and carbohydrates content of *Arthrospira* sp. grown on molasses medium alone or supplemented with different metals after fifteen days of incubation.

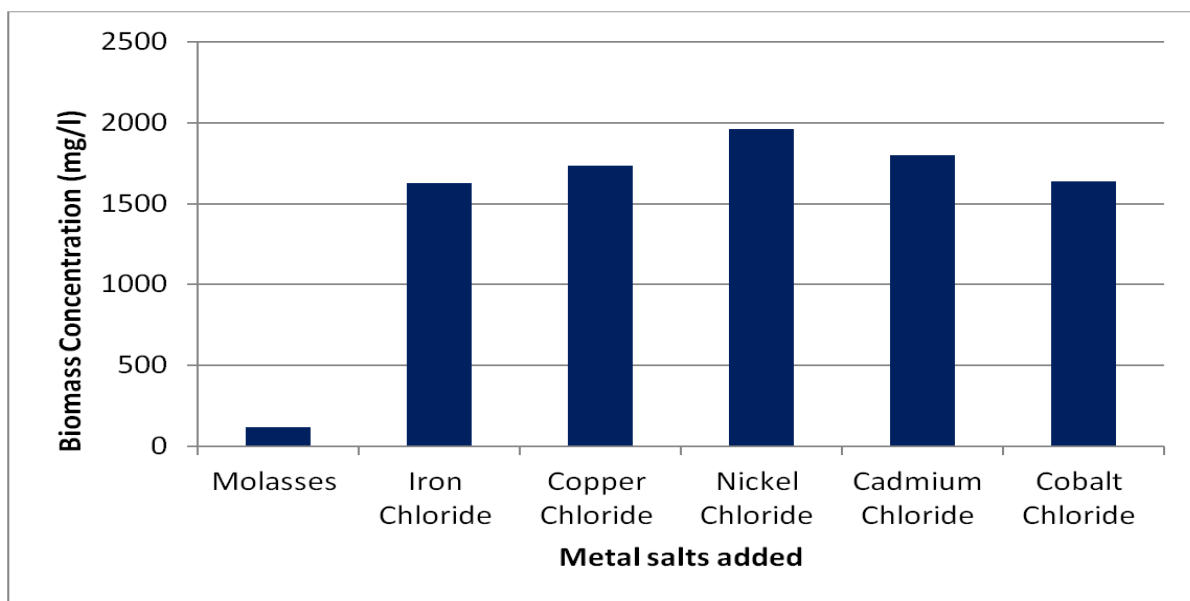


Figure 4: Biomass concentration of *Arthrospira* sp. grown on molasses medium alone or supplemented with iron, copper, nickel, cadmium, and cobalt chloride, respectively, after fifteen days of incubation.

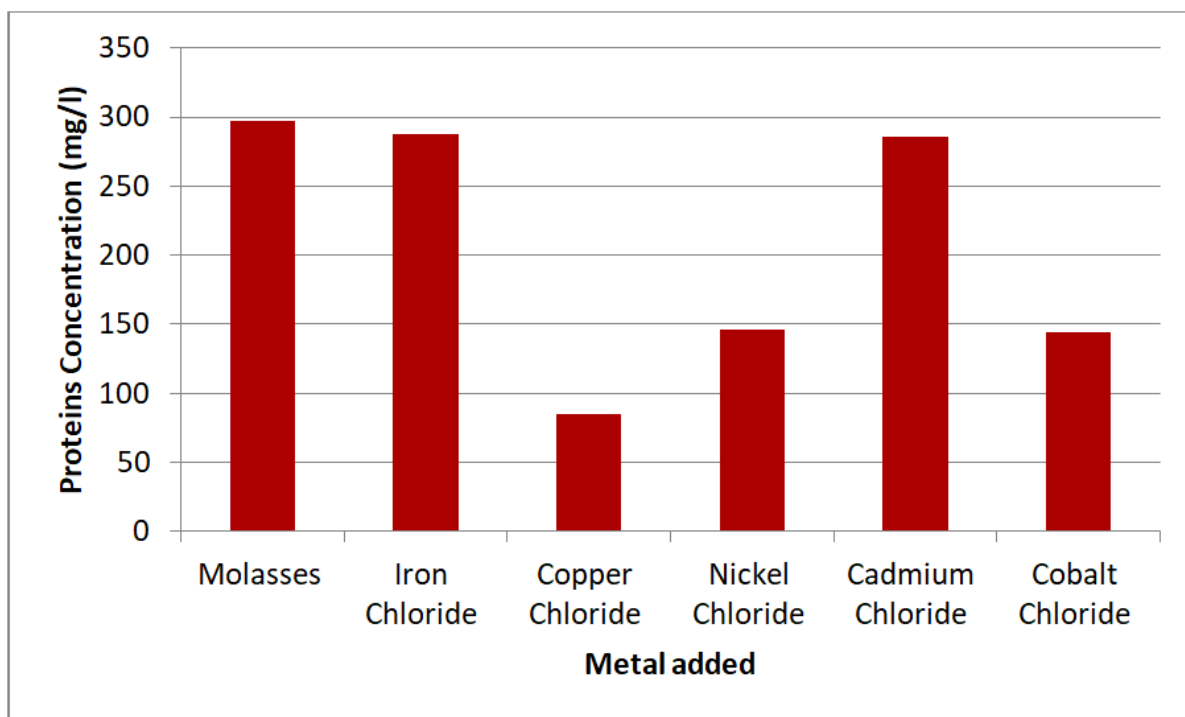


Figure 5: Proteins content of *Arthrospira* sp. grown on molasses medium alone or supplemented with iron, copper, nickel, cadmium, and cobalt chloride, respectively, after fifteen days of incubation.

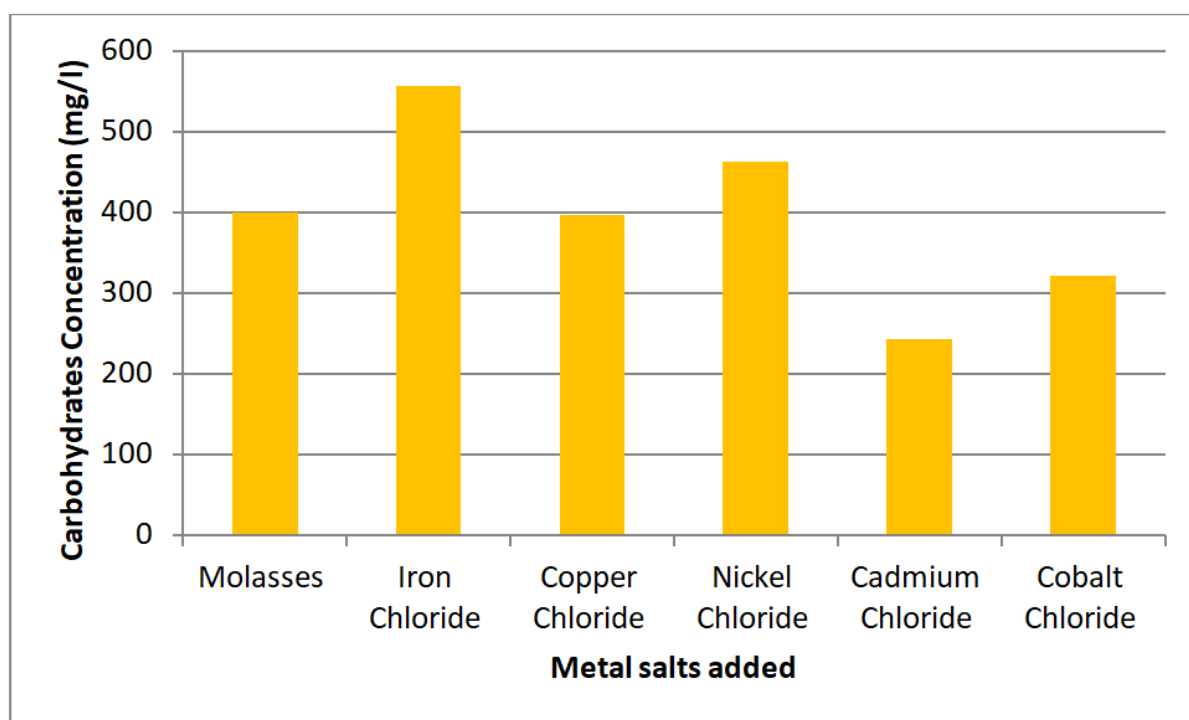


Figure 6: Carbohydrates content of *Arthrospira* sp. grown on molasses medium alone or supplemented with iron, copper, nickel, cadmium, and cobalt chloride, respectively, after fifteen days of incubation.

AGREGADO LEVE E CONCRETO A BASE DE ESCÓRIAS, COM ALTO CONTEÚDO RESIDUAL DE COMBUSTÍVEL

LIGHTWEIGHT AGGREGATE AND ASHES SLAG BASED CONCRETE WITH HIGH RESIDUAL FUEL CONTENT

ЛЕГКИЙ ЗАПОЛНИТЕЛЬ И БЕТОН НА ОСНОВЕ ЗОЛОШЛАКА С ВЫСОКИМ СОДЕРЖАНИЕМ ОСТАТОЧНОГО ТОПЛИВА

ZHUGINISSOV, Maratbek T.¹; ZHUMADILOVA, Zhanar O.²

^{1,2} Satbayev University, Institute of Architecture and Civil Engineering, Department of Civil Engineering and Building Materials, 22 Satpayev Str., zip code 050013, Almaty – Republic of Kazakhstan (phone: +77771388677)

** Corresponding author
e-mail: zhanar_85@mail.ru*

Received 14 November 2019; received in revised form 30 December 2019; accepted 10 March 2020

RESUMO

Os materiais de escória de cinzas na composição química e mineralógica são em grande parte idênticos às matérias-primas minerais naturais. Eles são uma fonte de poluição ambiental, representam uma ameaça à saúde pública e uma ameaça à flora e fauna das áreas circundantes. O desperdício de cinzas de escória contém uma grande quantidade de combustível não queimado. Em algumas cinzas, o teor de combustível não queimado pode representar de 20 a 40%. Nesse caso, é aconselhável usá-lo como matéria-prima para a produção de agregados porosos artificiais. O artigo apresenta os resultados de estudos sobre o desenvolvimento de tecnologia de agregados leves baseados em escória de cinzas com alto teor de combustível residual. Para desenvolver a tecnologia do agregado leve, a escória de cinzas foi usada pela Nova Zinc LLP (região de Karaganda, Cazaquistão), na qual o teor de carvão não queimado é de até 75%. Com base na escória de cinzas, foram obtidos agregados leves usando tecnologias de queima e não queima. Pela tecnologia de torrefação (queima), os agregados foram obtidos queimando a uma temperatura de 1000 e 1100 °C. Os agregados obtidos têm uma densidade aparente de 395-687 kg/m³ e uma resistência à compressão no cilindro de 0,5-2,4 MPa. Por tecnologia não queima, o cimento Portland M400 foi usado como adstringente. Após o endurecimento, os agregados têm uma densidade aparente de 400-600 kg/m³ e uma resistência à compressão de 0,65-1,5 MPa no cilindro. Amostras de concreto leve com densidade de 1200 e 1700 kg/m³, resistência à compressão de 80 (B5) e 120 kg/cm² (B7,5) e coeficientes de condutividade térmica de 0,43 e 0,67 W/m·°C com base no agregado leve não queimado, respectivamente. O agregado leve e o concreto leve em suas propriedades funcionais atendem aos requisitos dos documentos regulamentares.

Palavras-chave: *tecnologia de queima, temperatura, tecnologia de clínquer, fichário, endurecimento, densidade aparente, resistência.*

ABSTRACT

Ashes slag materials in the chemical and mineralogical composition are largely identical to natural mineral raw materials. They are a source of environmental pollution, pose a threat to public health, and a threat to the flora and fauna of the surrounding areas. Ashes slag waste contains a large amount of unburned fuel. In some ashes, the content of unburned fuel can reach 20-40%. In this case, it is advisable to use it as a raw material for the production of artificial porous aggregates. The paper presents the results of studies on the development of lightweight aggregate technology based on ashes slag with a high residual fuel content. To develop the technology of lightweight aggregate, ashes slag was used by Nova Zinc LLP (Karaganda region, Kazakhstan), in which the content of unburned coal is up to 75%. Based on ashes slag, lightweight aggregates were obtained using burning and non-burning technologies. By roasting (burning) technology, aggregates were obtained by burning at a temperature of 1000 and 1100 °C. The aggregates obtained have a bulk density of 395-687 kg/m³ and a compressive strength in the cylinder of 0.5-2.4 MPa. By non-burning technology Portland cement M400 was used as an astringent. After hardening, the aggregates have a bulk density of 400-600 kg/m³ and a

compressive strength of 0.65-1.5 MPa in the cylinder. Samples of light concrete with a density of 1200 and 1700 kg/m³, a compressive strength of 80 (B5) and 120 kg/cm² (B7.5), and thermal conductivity coefficients of 0.43 and 0.67 W/m·°C were obtained on the basis of the non-fired light aggregate, respectively. Lightweight aggregate and lightweight concrete in their functional properties meet the requirements of regulatory documents.

Keywords: *burning technology, temperature, clinker technology, binder, hardening, bulk density, strength.*

АБСТРАКТ

Золошлаковые материалы по химическому и минералогическому составу во многом идентичны природному минеральному сырью. Они являются источником загрязнения окружающей среды, представляют опасность для здоровья населения и угрозу растительному и животному миру близлежащих районов. Золошлаковые отходы содержат в своем составе большое количество несгоревшего топлива. В некоторых золах содержание несгоревшего топлива может достигать 20-40%. В этом случае ее целесообразно применять как сырье для производства искусственных пористых заполнителей. В статье приведены результаты исследований по разработке технологии легкого заполнителя на основе золошлака с высоким содержанием остаточного топлива. Для разработки технологии легкого заполнителя применялся золошлак ТОО «Nova Цинк» (Карагандинская обл., Казахстан), в котором содержание несгоревшего угля составляет до 75%. На основе золошлака получены легкие заполнители по обжиговой и безобжиговой технологиям. По обжиговой технологии заполнители получали обжигом при температуре 1000 и 1100 °С. Полученные заполнители имеют насыпную плотность 395-687 кг/м³ и прочность при сдавливании в цилиндре 0,5-2,4 МПа. По безобжиговой технологии в качестве вяжущего компонента применялся портландцемент М 400. После твердения заполнители имеют насыпную плотность 400-600 кг/м³ и прочность при сдавливании в цилиндре 0,65-1,5 МПа. На основе безобжигового легкого заполнителя получены образцы легких бетонов с плотностью 1200 и 1700 кг/м³, прочностью на сжатие 80 (B5) и 120 кг/см² (B7.5) и коэффициентами теплопроводности 0,43 и 0,67 Вт/м·°С, соответственно. Легкий заполнитель и легкие бетоны по своим функциональным свойствам отвечают требованиям нормативных документов.

Ключевые слова: *обжиговая технология, температура, клинкерная технология, вяжущее, твердение, насыпная плотность, прочность.*

INTRODUCTION

Ashes slag materials in the chemical and mineralogical composition are largely identical to natural mineral raw materials. The level of disposal of this waste in Russia is about 4-5%; in a number of developed countries - about 50%, in France and Germany - 70%, and in Finland - about 90% of their current output. Dry ash is mainly used in these countries, and government policies are being pursued to encourage their use. So, in Poland, the price of land for ash dumps is sharply increased. Therefore, thermal power plants pay extra to consumers in order to reduce their own costs for their storage. In China, ash is delivered to consumers free of charge, while in Bulgaria ash itself is free. In the UK, there are five regional centers for the sale of ashes (Putilin, 2003).

The content of ashes slag material dumps requires high operating costs, which affect the increase in the cost of energy production. They are a source of environmental pollution, pose a threat to public health, and a threat to flora and

fauna of the surrounding areas. Of particular danger are ash dumps located near water basins (rivers and lakes), due to the possible breakthrough of dams. The essential argument against the construction of new fuel power stations (FPS) is often the need to create ash dumps near them. Their use in industry, the construction industry, and agriculture is one of the strategic ways to solve the environmental problem in the zone of FPS operation. Therefore, the development of building materials technology using ash and slag is an urgent task.

The purpose of this study is to develop lightweight aggregate technology and concrete based on ashes slag (AS) with a high content of residual fuel.

One of the first in world practice, American researchers began to use ash for the production of bricks (Antipin, 1969; Reidelbachl, 1970). The American company "TekoledyCorp" developed brick compositions from various industrial wastes such as ash, foundry sands, asbestos wastes, furnace slags (Suleimenov, 2004).

The author of (Malykhin, 2019) conducted experiments to strengthen clay soils using an ash-slag mixture of Novokemerovskaya fuel power center (FPC) and cement M400 CEMII/A-Sh 32.5B of the Topkinsk plant. The greatest water resistance and durability in a water-saturated state are possessed by samples reinforced with 25% AS and 15% cement.

Every year, 3.1 million tons of cement are replaced annually in Germany by A&S dumps. Thanks to this, the resources and energy necessary for the production of cement are saved, and the costs of silos, transportation, and wages are paid back (Malykhin, 2019).

South Africa, with financial state support, is carrying out experimental construction of routes from fly ash (Brooks, 2009). It is proved that mixtures of fly ash with inert materials (sand, rice husk, etc.) reach from 50 to 70% of the strength of materials reinforced with cement.

The American Coal Ash Association and the Municipal Solid Waste Management Group co-sponsor the Coal Firing Partnership. The project is intended to help construction organizations and energy companies understand the environmental benefits and potential consequences of using coal combustion products for various purposes, as well as stimulate their useful use (Lindon, 2015).

Currently, domestic and near-abroad scientists conduct research on the development of compositions and technology of lightweight aggregates, concrete, mortars, and ceramic bricks using ash and slag waste (Maximov, 2004; Denisov, 2008; Turkina, 2009; Gilyazidinova, 2010; Montaeva, 2012; Maksakov, 2012; Lokhova, 2012; Mestnikov, 2013; Abramov, 2013; Netesa, 2013; Malchik, 2015; Kadyrbekov, 2016; Malchik, 2016; Dmitriev, 2017). So, at the Jurgen Institute of Technology (Malchik, 2016), research was conducted on the use of AS in brick production. The optimal percentage ratio for adding ash and slag waste is 15%, at a burning temperature of 1000 °C. In this case, the compressive strength of the samples is 125 kg/cm² without ash and 110 kg/cm² with ash. The thermal conductivity of samples without ash is 0.85 W/m·°C, with ash - 0.76 W/m·°C.

In (Dmitriev, 2017), the introduction of AS waste and rice husk ash into a gas concrete mixture was proposed, which allows to increase the strength, crack resistance of aerated concrete by hardening and compaction of concrete due to the higher particle density. This increases the resistance of aerated concrete to high

temperatures, that is, increase its fire resistance.

MATERIALS AND METHODS

As the main raw material used AS of the enterprise LLP "Nova Zinc" (Karaganda region, Kazakhstan).

For the manufacture of lightweight aggregate by roasting (burning) technology, local loam and highly plastic bentonite clay were used.

For the manufacture of lightweight aggregate by non-firing technology, Portland cement CEM I 32.5 H (Government standard - GOST 31108-2003), gypsum, and liquid glass corresponding to GOST 13078-81 were used as a binder. To accelerate the setting time of cement concrete, calcium chloride (CaCl₂) was used.

To make mixtures, the ashes slags was dried in an oven at a temperature of 100-110 °C to a residual moisture content of 3-4% and then subjected to grinding in a laboratory ball mill until it passes through a 1.25 sieve.

When compiling clay-ash-slag mixtures, the dried clay was crushed and sieved through a sieve of 0.63. To obtain aggregate granules, ash and clay were mixed in certain proportions, and then the mixture was moistened with water until a formable mass was obtained, from which granules with a diameter of 10-20 mm were made using a laboratory granulator. After drying at a temperature from 100 to 105 °C for 1 to 2 hours in an oven, the pellets were fired in a SNOL 1.6 / 1300 muffle furnace at temperatures of 900, 1000, and 1100 °C for 1 hour. After that, their density and strength were determined. In the preparation of clinker-based mixtures, AS were mixed with Portland cement in certain proportions, then the mixture was moistened with water to obtain a workable mixture, from which granules with a diameter of 10-20 mm were also made. Hardening accelerators were added to the mixture along with mixing water. After molding, the granules were kept in a humid environment for 7 and 14 days. After that, their density and strength were determined.

X-ray phase analysis (X-ray PA) was carried out on a DRON-3M diffractometer using C system-K α radiation. The sensitivity of the methods is from 1% to 2%. X-ray PA powder diffraction samples were subjected to passing through a sieve of 100 holes/mm. Radiographs were identified using reference data (Mikheev, 1957).

Differential thermal analysis (DTA) was carried

out on a "Deridalograf" Q-1500 D instrument of the Paulik and Erden system (Hungary) at a temperature change of 7.5 and 10 deg/min.

The physical-mechanical properties of the lightweight aggregate were determined by the method (GOST 9758-2012). The physical-mechanical properties of lightweight concrete were determined by the method (GOST 25820-2014). The thermal conductivity of lightweight concrete was determined using an ITP MG4 100 device.

3. RESULTS AND DISCUSSION

In the technical conditions for the use of ash from FPS as a fine aggregate for structural heat-insulating lightweight concrete (Technical conditions TC-21-33-1-73), the requirements for the grain composition and content of harmful impurities are given. In particular, fuel residues in ash obtained from burning brown coal are allowed no more than 5%, and from burning coal and anthracite up to 12% (by weight). Often in ashes, there is more unburned fuel - up to 20-40%. At the same time, the possibilities of using ash as a filler are limited, especially for reinforced structures. In this case, it is advisable to use it as a raw material for the production of artificial porous aggregates. The maximum permissible content of fuel residues in the ash, suitable for the production of alumina expanded clay, should not exceed 17%. At the excess amount of carbon, the granules melt, and the quality of the aggregate deteriorates (Dvorkin, 2007).

This paper presents the results of studies on the development of compositions and technological parameters of light aggregate and light concrete based on the ashes slag of a FPC enterprise of Nova Zinc LLP (Karaganda region, Kazakhstan). Ashes slag is a loose wet mass of black color, which is removed after burning into the ashes slag dump by the method of hydraulic removal. The black color and the specific gloss of the ashes slag grains indicate the presence of a significant amount of unburned coal. The specific activity of natural radionuclides of AS is 33.0 Bq/kg, which is below the limit, in this regard, they can be used in housing construction without restrictions. The bulk density of ashes slag in its natural state is 632 kg/m³. The bulk density of ground and sieved through a sieve of 1.25 ashes slag is 440 kg/m³. The chemical compounds of ashes slag were determined by X-ray local spectral analysis (X-ray LA) using a JCTXA-733 electron probe microanalyzer. In (Table 1) shows the results of a chemical analysis of the initial AS.

The carbon content (C) is from 73.8 to 75.1%. According to the X-ray PA, the initial ashes slag in small amounts contains β - quartz (SiO_2) with lines d, Å: 4.26-3.35-2.45-2.28-2.12-1.672-1.542-1.454; mullite ($3\text{Al}_2\text{O}_3 \cdot 2\text{SiO}_2$) with lines d, Å: 5.41-3.83-3.35-2.70-2.52-2.28-2.20-2.12-1.840-1.523; anorthite ($\text{CaO} \cdot \text{Al}_2\text{O}_3 \cdot 2\text{SiO}_2$) with lines d, Å: 4.06-3.83-3.21-3.13-2.52; hematite ($\alpha\text{-Fe}_2\text{O}_3$) with lines d, Å: 2.70-2.20 (Figure-1).

In (Table 2) shows the results of the chemical analysis of ash after burning at a temperature of 1000 °C.

After burning at 1000 °C in ashes slag, the residual fuel content is up to 43%. The peak intensities of quartz, mullite, anorthite, and hematite increased significantly. In addition, additional peaks of quartz d, Å: 1.814-1.607-1.378; of mullite d, Å: 2.84-2.01-1.607; of anorthite d, Å: 3.65-1.835-1.480-1.350 and hematite d, Å: 1.679 (Figure-1).

In (Figure-2) shows the result of differential thermal analysis (DTA) of the initial ashes slag. The thermal-analytical curve has endo- and exothermic effects. The endothermal effect at 120 °C is associated with the loss of physically bound water. The endothermal at 460 °C is associated with the softening of the glass phase.

Neoplasms in the thermogram are not observed. DTA showed that ashes slag weight loss is 70%. In (Table 3) shows the composition of the charges and the properties of the aggregate based on ash and loam after firing.

As can be seen from the table, lightweight aggregates obtained from mixtures No.4, 5, 6, and 7 in terms of bulk density and strength correspond to the requirements for lightweight aggregates. Figure 3 shows photographs of lightweight aggregates. As can be seen in the photographs, the aggregate samples from compound No.1 completely crumble. Granules of lightweight aggregates obtained from formulations No. 2 and 3 have a presentation. However, their surface crumbles, and they have low strength (easily crushed by fingers). This is due to the fact that in these compounds, the content of unburned coal is in the range of 42-56%, which burns intensively at a temperature of 900-1000 °C and significantly reduces the sintering ability of clay particles. Lightweight aggregate based on compound No.4 has satisfactory strength and can be used for the manufacture of lightweight concrete of low grades. The most optimal properties are lightweight aggregates obtained on the basis of compounds No. 5, 6, and 7.

Highly flexible bentonite clay has a high binding ability, but this alone did not give positive results. Aggregates containing 60-80% ashes slag also do not have the strength and easily crumble when squeezed by hand. Here the same effect of burning residual coal appears, which prevents clay sintering. However, samples with a content of 40-50% ash after firing at 1000 °C have a bulk density of 370-410 kg/m³ and a compressive strength in the cylinder of 1.2-1.7 MPa, which is two times higher than the strength of aggregates using loam.

For the manufacture of aggregate using clinker technology, almost all ashes and ashes slag mixtures obtained from the combustion of various types of coal can be used. For the preparation of mixtures, ashes slag were used 1-1.25 mm thick fractions. Using Portland cement as a binder, mixtures of 4 series were prepared. One series of compositions contained Portland cement and ashes slag; 2 series of compositions contained ashes slag, Portland cement and gypsum (mixed binder); 3 series of compositions contained ashes slag, Portland cement, and water glass; 4 series of compositions contained ashes slag, Portland cement and calcium chloride (CaCl₂). In the preparation of mixtures with Portland cement W/C, the ratio was 0.4-0.45. Water glass and CaCl₂ were introduced into the mixture with mixing water.

The addition of gypsum instead of part of the cement does not give positive results. With a mixed binder content of 25%, the aggregate has a bulk density of 514 kg/m³ and strength of 0.5 MPa, and after 14 days of hardening, its strength decreases to strength when the granules are easily crushed by fingers.

The addition of liquid glass (20-30%) together with water promotes rapid solidification; after 3 days of hardening under natural conditions, light aggregate granules acquired strength sufficient for its transportation and storage. The compressive strength in the cylinder after 14 days of hardening is 0.47-0.72 MPa. The addition of calcium chloride gives positive results. After hardening for 14 days in the air, the compressive strength in the filler cylinder is 1.2-1.3 MPa (Table 4).

Figure 4 shows samples of lightweight aggregates obtained by clinker technology based on Portland cement. The aggregate obtained on the basis of compound No.3 was used to calculate the composition of lightweight concrete according to the method described in the literature (Skramtaev, 1970).

The calculation showed that for the manufacture of 1m³ of light concrete, it is required: Portland cement - 385 kg; ashes slag aggregate - 265 kg; the rest: calcium chloride, quartz sand, and water. In order to replace quartz sand with ashes slag, the calculation of the flow rate of ashes slag by volumetric mass was performed. According to the calculation, the ashes slag flow rate was 290 kg instead of quartz sand.

Concrete samples were molded in the form of cubes measuring 100x100x100 mm on a laboratory vibrating table for 10-15 seconds. After molding, the samples were kept in metal form for 10-12 hours, then released from the molds. Further hardening of the products was carried out at room temperature for seven days, then the average density and strength of concrete were determined. Figure 5 shows the sample cubes of lightweight concrete obtained with quartz sand and with ashes slag sand.

After 21 days of hardening, the average density and strength of concrete were determined. The average density of concrete with quartz sand is 1700 kg/m³, and the average density of concrete with ashes slag sand is 1200 kg/m³. The compressive strength of concrete with quartz sand is 120 kg/cm², the strength of concrete with ashes slag sand is 80 kg/m². According to the values of compressive strength, they correspond to the brands M100 (B7.5) and M75 (B5), respectively. Determination of thermal conductivity showed that concrete on quartz sand has a thermal conductivity coefficient of 0.67 W/m·°C, concrete on ashes slag sand - 0.43 W/m·°C.

4. CONCLUSIONS

1. According to the requirements for ashes slag materials for the production of light aggregates and concrete, the residual fuel content should not exceed 10-17%. The ashes slag "Nova Zinc" LLP accepted for the study is characterized by a high content of residual fuel, which is up to 75%, i.e., 3-4 times higher than regulatory requirements.

2. For the first time, lightweight aggregates based on ashes slag with a high content of residual fuel were obtained. The optimal compounds of fired and non-fired lightweight aggregates are determined, as well as the technical parameters of their manufacture.

3. It has been found that for the manufacture of lightweight aggregate by firing, moderately

ductile loams, and highly ductile bentonite clay can be used. When using loam, the optimal content of ashes slag in the ceramic mass is 25-50%. When using bentonite clay, the content of ashes slag in the ceramic mass is 40-50%.

4. Using burning technology using loam, aggregates with a bulk density of 395-700 kg/m³, and compressive strength in the cylinder of 0.5-2.7 MPa were obtained. The light aggregates on bentonite clay after burning at 1000 °C have a bulk density of 370-410 kg/m³ and compressive strength in the cylinder of 1.2-1.7 MPa, which is two times higher than the strength of the aggregates using loam after burning at the same temperature.

5. With an increase in the content of ashes slag in the ceramic mass of more than 50%, as a result of intense burning of residual fuel in the temperature range 900-1100 °C, the sintering ability of clay particles decreases, which leads to a significant decrease in the strength of lightweight aggregate.

6. By clinker technology, using Portland cement as a binder, a aggregate with a bulk density of 595-600 kg/m³, and a compressive strength of 0.65-0.8 MPa in the cylinder was obtained. The addition of CaCl₂ as a cement hardening accelerator gives positive results. After three days of hardening in air, the strength of the light aggregate is 0.5-0.6 MPa, after 14 days - 1.2-1.3 MPa.

7. Using clinker aggregate and quartz sand, lightweight concrete samples were produced with a compressive strength of 120 kg/cm², an average density of 1700 kg/m³, and thermal conductivity of 0.67 W/m·°C. When replacing quartz sand with ashes slag sand, lightweight concrete was obtained with a compressive strength of 80 kg/cm², an average density of 1250 kg/m³, and thermal conductivity of 0.43 W/m·°C.

8. Indicators of the properties of light concrete samples in medium density and strength meet the requirements of GOST 25820-2014 "Light concrete". Technical conditions (TC) and their average density can be attributed to structural and structural-thermal insulation. Concrete strength class B7.5 and B5, respectively.

5. ACKNOWLEDGMENTS:

The authors are grateful to the leadership of

the Satbayev University for creating the conditions for carrying out this work.

6. REFERENCES:

1. Putilin E.I., Tsvetkov V.S. Overview of domestic and foreign experience in the application of waste from solid fuel combustion at TPP. Alliances. M. - 2003. - 60 p.
2. Antipin A.N. The use of fly ash from fuel power plants in the USA // Building Materials. - 1969. - No. 3. - P. 39.
3. Reidelbachl A. An industrial evaluation of fluash brics // Inform. Cite / Mines. U.S. Dep / Inter. - 1970. - №8488. - P. 198-200.
4. Suleimenov Zh.T., Zhuginisov M.T. Technology of silicate facing and structural materials based on technogenic raw materials. Tutorial. Taraz: TarSU named after M.Kh. Dulati. - 2004. - 216 p.
5. Malykhin R.N. Application of ash and slag waste in the road construction of Kuzbass // Young scientist. - 2019. - No. 15. - P. 41-44.
6. Brooks R. M. Soil stabilization with fly ash and rice husk ash. // International Journal of Research and Reviews in Applied Sciences. - 2009. - Vol. 1(3). - P. 209-217.
7. Lindon K. A. Properties and use of coal fly ash: Use of fly ash for road construction, runways and similar projects. - London, 2015. - 132 p.
8. Patent No.2232141. A method of obtaining a lightweight aggregate / Maximov B.A. (RU), Petrov V.P. (RU), Korenkova S.F. (RU). Published 06/10/2004.
9. Denisov D.Yu., Kovkov I.V., Abdrakhimov V.Z. The use of coal flotation waste in the production of expanded clay. Bashkir chemical journal. - 2008. Volume 15. - No. 2. - P. 107-109.
10. Turkina I.A. Technogenic waste in the production of building materials / Concrete technology. - 2009. - No.1. - P. 16-17.
11. Gilyazidinova N.V., Santalova T.N., Rudkovskaya N.Yu. Obtaining lightweight

aggregates for concrete based on fly ash TPP / Izv. universities. North Caucasus. region. Tech. Sciences. - 2010. - No. 2. P.123-127.

12. Montaeva A.S., Schuchkin S.V., Montaev S.A. et al. Study of a ceramic composition to obtain a lightweight aggregate. Materials of the conference "Successes in modern science." - 2012. - No. 6. - P. 40-41.

13. Maksakov A.V. Granular nanostructured aggregate based on raw materials of various compositions for lightweight concrete / Author Abstract. Belgorod: BSTU them. V.G. Shukhov. - 2012. - 26 p.

14. Lokhova N.A., Boeva N.V. Lightweight aggregate based on modified liquid glass and dispersed wastes of metallurgy and heat power engineering. Systems. Methods Technologies. - 2012. - No. 1 (13). - P. 139-143.

15. Mestnikov A.E., Fedorov V.I. Lightweight waste paper and liquid glass filler. International Journal of Applied and Basic Research. - 2013. - No. 8. - P. 136-137.

16. Abramov A.K., Efimov V.I. Production of aggregates for lightweight concrete from coal preparation waste. Izvestiya TulGU. Earth sciences. - 2013. - Issue. 2. - P. 95-102.

17. Netesa N.I., Palanchuk D.V., Netesa A.N. Lightweight concrete with fly ash of Dnieper Dnieper TPP. Science and transport progress. Bulletin of the Dnepropetrovsk National University of Railway Transport. - 2013. - No. 5 (47). - P. 137-142.

18. Malchik A. G., Litovkin S. V. [Electronic resource] = Investigation ash and slag waste for use as a of recyclable waste / International Journal of Applied and Basic Research. 2015. - No. 9. - Part 1. - P. 23-27.

19. Kadyrbekov A.M. Use of ash and slag waste from the CHPP of Pavlodar region. Bulletin of the Innovative Eurasian University. - 2016. - No. 1 ISSN 1729-536X. - P. 129-132.

20. Malchik A.G., Litovkin S.V., Rodionov P.V. Study of the technology for processing ash and slag waste from thermal power plants in

the production of building materials // Modern high technology. - 2016. - No. 3 (1). - P. 60-64.
21. Dmitriev I.I., Kirillov A.M. Ash and slag waste in the composition of concrete // StroyMnogo. - 2017. - No. 3 (8).

22. Mikheev I.A. Radiographic determinant of minerals. - Moscow, 1957. - 860 p.

23. GOST 9758-2012. Inorganic porous aggregates for construction work. Test Methods. - Moscow: Interstate Standard. - 2013.

24. GOST 25820-2014 Light concrete. Technical conditions - Moscow: Standartinform. - 2015.

25. Dvorkin L.I., Dvorkin O.L. Building materials from industrial waste. Training manual. - Rostov-on-Don: Phoenix. - 2007. - 368 p.

26. Skramtaev B.G., Burov V.D., Panfilova L.I., Shubenkin P.F. Examples and tasks of building materials. - M.: Higher school. - 1970. - 232 p.

Table 1. The chemical compound of the initial of ashes slag

SiO ₂	Al ₂ O ₃	TiO ₂	CaO	MgO	Fe ₂ O ₃	Na ₂ O	K ₂ O	SO ₃	Cl-ion
6.48	2.99	0.18	1.08	0.26	1.21	0.24	0.18	0.57	0.05

Table 2. The chemical compound of ashes slag, burned at 1000 °C

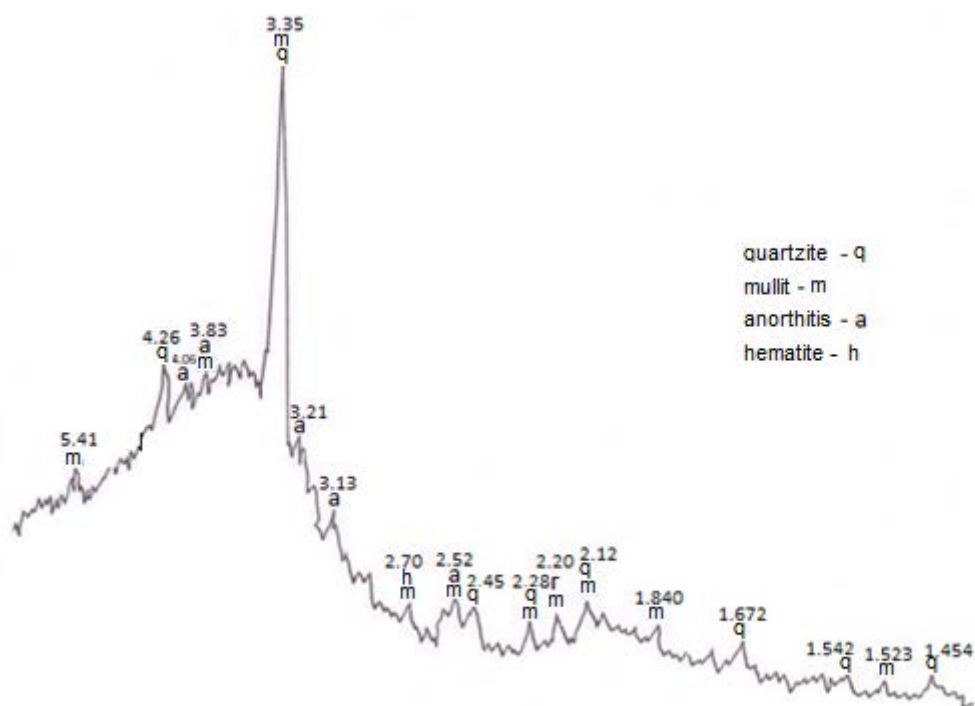
SiO ₂	Al ₂ O ₃	TiO ₂	CaO	MgO	Fe ₂ O ₃	Na ₂ O	K ₂ O	SO ₃	Cl-ion
24.27	11.34	0.53	3.77	1.01	3.97	0.71	0.66	1.3	-

Table 3. The compounds and properties of aggregates with loam

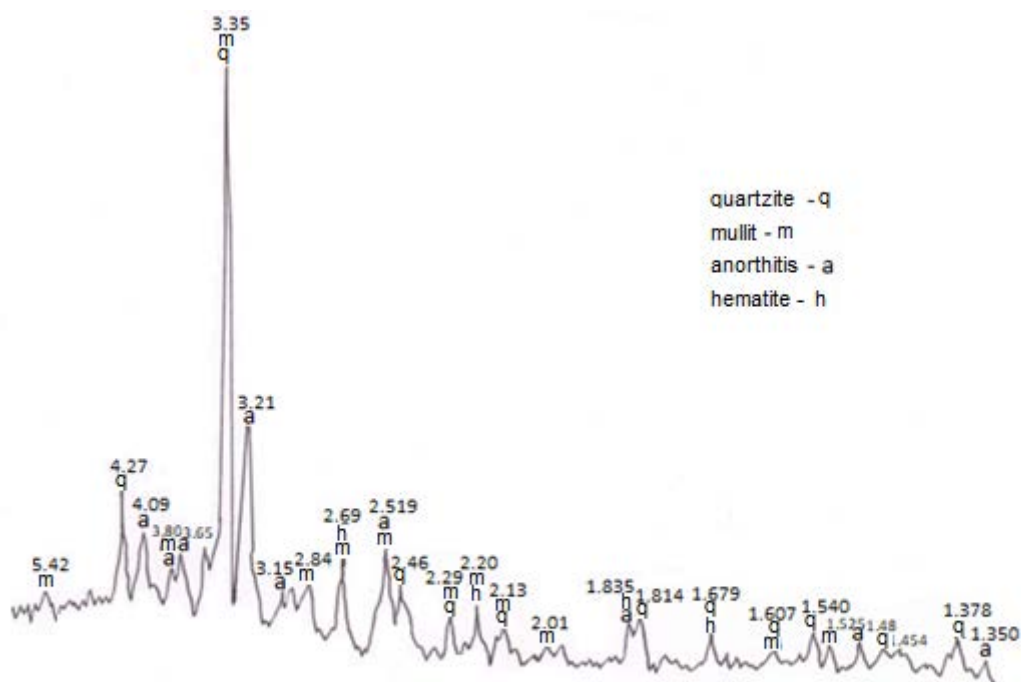
No.	Compound	1000 °C		1100 °C	
		Bulk density, kg/m ³	The compressive strength in the cylinder, MPa	Bulk density, kg/m ³	The compressive strength in the cylinder, MPa
1	Ashes slag (AS) – 80 % Loam – 20 %	impossible to determine	Granules crumble	impossible to determine	Granules crumble
2	AS – 70 % Loam – 30 %	325	Granules are easily crushed by fingers	314	Granules are easily crushed by fingers
3	AS – 60 % Loam – 40 %	415	Granules are crushed by fingers	400	Granules are crushed by fingers
4	AS – 50 % Loam – 50 %	441	0.55	395	0.5
5	AS – 40 % Loam – 60 %	511	0.9	495	0.8
6	AS – 30 % Loam – 70 %	658	1.6	670	1.5
7	AS – 25 % Loam – 75 %	700	2.7	687	2.4

Table 4. The optimal compounds and properties of aggregates with Portland cement

No.	Compound	ρ, bulk density	R, compressive strength in the cylinder, MPa	Hardening conditions
1	AS – 75 % Cement – 25 %	595	0.65	In a humid environment T= 22...25 °C. 14 days
2	AS – 70 % Cement – 30 %	600	0.80	In a humid environment T= 22...25 °C. 14 days
3	AS – 75 % Cement – 25 % CaCl ₂ – 3%	585	1.2	At room temperature, 14 days
4	AS – 70 % Cement – 30 % CaCl ₂ – 3%	590	1.5	At room temperature, 14 days



a



b

Figure 1. Diffraction patterns of the initial (a) and burned (b) ashes slag

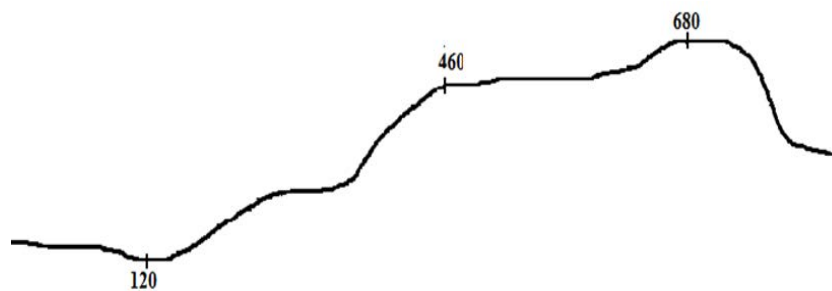


Figure 2. The thermogram of the original ashes slag



a



b



c



d



e



f

Figure 3. Samples of aggregates after burning at a temperature of 1000 °C: a - compound No. 1, b - compound No.3, c - compound No. 4, d - No. 5, e – No.6, f – No.7. (see table 3)



a

b

a - compound No. 2, b - compound No. 3. (see table 3)



SÍNTESE DOS NANOCOMPOSITOS ESPINÉLIO Mn_3O_4 E ESPINÉLIO Mn_3O_4/ZrO_2 E USANDO-OS NA DECOLORIZAÇÃO FOTO-CATÁLICA DO COMPLEXO $Fe(II)$ -(4,5-DIAZAFLUOREN-9-ONA 11)

SYNTHESIS OF SPINEL Mn_3O_4 AND SPINEL Mn_3O_4/ZrO_2 NANOCOMPOSITES AND USING THEM IN PHOTO-CATALYTIC DECOLORIZATION OF $Fe(II)$ -(4,5-DIAZAFLUOREN-9-ONE 11) COMPLEX

تحضير السبيل Mn_3O_4 والمترابكات النانوية للسبيل ZrO_2/Mn_3O_4 واستخدامهم في الازالة اللونية المحفزة ضوئياً لمعقد $Fe(II)$ -(4,5-DIAZAFLUOREN-9-ONE 11)

HAYAWI, Mohammed Kareem¹; KAREEM, Mohanad Mousa², and AHMED, Luma Majeed ^{3*}

^{1,3}Department of Chemistry, College of Science, University of Kerbala, Karbala, Iraq.

²Department of Chemistry, College of Science, University of Babylon, Babylon, Iraq.

* Correspondence author

e-mail: lumamajeed2013@gmail.com

Received 05 January 2020; received in revised form 03 March 2020; accepted 10 March 2020

RESUMO

A estrutura de espinélio Mn_3O_4 e as partículas de nano-compósitos de espinélio Mn_3O_4/ZrO_2 foram sintetizadas com sucesso como fotocatalisadores, empregando o processo de co-precipitação e a técnica ultrassônica, respectivamente. A morfologia dos fotocatalisadores preparados foi distinguida usando a tecnologia de difração de raios-X (DRX) e microscopia de força atômica (AFM) e indicou que os tamanhos médios de cristal e tamanho de partícula para todas as amostras estudadas eram nanométricas. Além disso, as propriedades ópticas dos fotocatalisadores obtidos foram investigadas usando um espectrofotômetro UV-Vis com acessório de refletância difusa Labsphere para medir as distâncias de banda deles. Com base na equação de Tauc, foram determinados os intervalos de banda (Bg) para os fotocatalisadores estudados. Os intervalos de banda são indiretos para todas as amostras e aumentam os valores para os nanocompósitos com o aumento da quantidade de ZrO_2 . Portanto, a sequência dos valores de lacunas de banda é: Bg espinélio Mn_3O_4 < Bg Comp.1 < Bg Comp.2 < Bg Comp.3 < Bg ZrO_2 , e igual a 2,21 eV < 3,15 eV < 4,51 eV < 4,26 eV < 5,29 eV. A pesquisa revelou que as partículas de nanocompósitos de espinélio Mn_3O_4 e espinélio Mn_3O_4/ZrO_2 eram partículas quase esféricas e esféricas, respectivamente. Além disso, foi realizada com sucesso a incorporação da partícula espinélio Mn_3O_4 com a partícula ZrO_2 , comprovada por análises de DRX e AFM. Este trabalho descobriu que a resposta da reação fotocatalítica pelo emprego do complexo $Fe(II)$ -(4,5-Diazafluoren-9-ona 11) como material modelo sob lâmpada UV-A com o uso dos fotocatalisadores estudados. Os experimentos fotográficos primários para esses fotocatalisadores descobriram que a descoloração do complexo $Fe(II)$ -(4,5-Diazafluoren-9-ona 11) não é ativa sem a adição de H_2O_2 , essa atitude se deve à estabilidade muito alta desses complexos por ter uma estrutura octaédrica, que foi comprovada com o uso do método da razão molar. Considerando que, após a adição de H_2O_2 à solução aquosa desse complexo, verificou-se que a atividade com o nanocompósito de espinélio Mn_3O_4/ZrO_2 3 era o ativo duplo do que com o espinélio Mn_3O_4 sozinho e a sequência da eficiência da descoloração por fotoelétricos (E%) está sendo: E% composto 3 < E% composto 2 < E% composto 1 < E% espinélio Mn_3O_4 .

Palavras-chave: *Espinélio Mn_3O_4 ; Nano-composto espinélio Mn_3O_4/ZrO_2 ; ZrO_2 ; Síntese verde e complexo $Fe(II)$ -(4,5-Diazafluoren-9-ona 11).*

ABSTRACT

The spinel structure Mn_3O_4 and the spinel Mn_3O_4/ZrO_2 nano-composites particles were synthesized successfully as photocatalysts by employing the co-precipitation process and ultrasonic technique, respectively. The morphology of the top mention prepared photocatalysts was distinguished using X-ray diffraction (XRD) technology and atomic force microscopy (AFM) and indicated that the mean crystal sizes and particle sizes for all studied samples were nanometric. In addition, the optical properties of the obtained photocatalysts were

investigated using a UV-Visible spectrophotometer with Labsphere diffuse reflectance accessory to measure the bandgaps of them. Based on the Tauc equation, the bandgaps (Bg) for the studied photocatalysts were determined. The bandgaps are indirect for all samples, and it is increased in values for the nanocomposites with the increasing the ratio of ZrO_2 . So, the sequence of bandgaps values is: Bg spinel Mn_3O_4 < Bg Comp.1 < Bg Comp.2 < Bg Comp.3 < Bg ZrO_2 , and equal to $2.21\text{ eV} < 3.15\text{ eV} < 4.51\text{ eV} < 4.26\text{ eV} < 5.29\text{ eV}$. The research revealed that the spinel Mn_3O_4 and the spinel Mn_3O_4/ZrO_2 nano-composites particles were quasi-spherical and spherical particles respectively. Moreover, the incorporation of spinel Mn_3O_4 particle with ZrO_2 particle was successfully carried out that was proved by XRD and AFM analyses. This work discovered that the photocatalytic reaction response via employing Fe(II)-(4,5-Diazafluoren-9-one 11) complex as model material under UV-A lamp with the use of the studied photocatalysts. The primary photo experiments for these photocatalysts found that the decolorization of Fe(II)-(4,5-Diazafluoren-9-one 11) complex is not active without addition of H_2O_2 , that attitude is due to the very high stability of these complex with having an octahedral structure, which was proved with using mole ratio method. Whereas, after the addition of H_2O_2 to the aqueous solution of these complex, the activity with using the spinel Mn_3O_4/ZrO_2 nanocomposite 3 was found to be the double active than that using the spinel Mn_3O_4 alone, and the sequence of photo-decolorization efficiency (E%) is being: E% composite 3 < E% composite 2 < E% composite 1 < E% spinel Mn_3O_4

Keywords: Spinel Mn_3O_4 ; Spinel Mn_3O_4/ZrO_2 nano-composite; ZrO_2 ; Green synthesis and Fe(II)-(4,5-Diazafluoren-9-one 11) complex.

المخلص

حضر تركيب السبيل Mn_3O_4 وجسيمات المتراكبات النانوية للسبيل $ZrO_2 \setminus Mn_3O_4$ بنجاح كعوامل مساعدة ضوئية باستخدام طريقة الترسيب المصاحب وتقنية الموجات فوق الصوتية على التوالي. ميزت الخواص المورفولوجية للعوامل الضوئية المحضرة والمشار إليها اعلاه بوساطة تقنية حيود الاشعة السينية (XRD) ومجهر القوة الذرية (AFM) وأشارت الى كون معدل الحجوم البلورية وحجوم الجسيمات لجميع العينات المدروسة هي مواد نانوية. بالإضافة الى ايجاد الخواص الضوئية للعوامل المساعدة الضوئية من خلال استخدام تقنية مطيافية الاشعة المرئية وفوق البنفسجية مع الانعكاس الانتشاري لغرض قياس فجوات الحزم لها. بالاعتماد على معادلة تاوس، حددت فجوات الطاقة (Bg) للعوامل المساعدة الضوئية المدروسة. وجد بان فجوات الطاقة من النوع غير المباشر لجميع العينات، اذا تزداد قيمتها للمتراكبات بزيادة نسبة ZrO_2 لذلك يكون تسلسل قيمها كالآتي: Bg spinel Mn_3O_4 < Bg Comp.1 < Bg Comp.2 < Bg Comp.3 < Bg ZrO_2 ، و تساوي الى $2.21\text{ eV} < 3.15\text{ eV} < 4.51\text{ eV} < 4.26\text{ eV} < 5.29\text{ eV}$. كشف هذا البحث كون السبيل Mn_3O_4 والمتراكبات النانوية للسبيل $ZrO_2 \setminus Mn_3O_4$ هي شبه كروية وكروية الشكل على التوالي. بالإضافة الى ذلك، وجد بان عملية التداخل بين جسيمات السبيل Mn_3O_4 وجسيمات ZrO_2 تمت بنجاح وقد اثبتت بوساطة تحاليل XRD و AFM. في هذا العمل اكتشف بان هنالك استجابة خلال التفاعل المحفز ضوئيا باستخدام معقد Fe(II)-(4,5-Diazafluoren-9-one 11) كموديل للدراسة بوجود مصباح UV-A باستخدام العوامل المساعدة الضوئية المدروسة. وجد من خلال التجارب الضوئية الاولى بان الازالة اللونية لمعقدات Fe(II)-(4,5-Diazafluoren-9-one 11) تكون غير فعالة بدون استخدام H_2O_2 مع هذه العوامل المساعدة الضوئية، ويعزا ذلك للاستقرارية العالية للمعقد وتركيبه الثماني والذي اثبت باستخدام طريقة النسب المولية. ولكن بعد اضافة الـ H_2O_2 الى المحلول المائي لهذه المعقدات، وجد بان الفعالية باستخدام المتراكب رقم 3 من السبيل $ZrO_2 \setminus Mn_3O_4$ كانت ضعف مقارنة بالفعالية لدى استخدام السبيل Mn_3O_4 لوحدة، حيث كان تسلسل النسبة المئوية للازالة اللونية (E%) كالآتي: composite 3 < composite 2 < composite 1 < spinel Mn_3O_4

الكلمات المفتاحية: السبيل Mn_3O_4 ، والمتراكبات النانوية للسبيل $ZrO_2 \setminus Mn_3O_4$ ، والتخليق الأخضر، ومعقدات Fe(II)-(4,5-Diazafluoren-9-one 11)

1. INTRODUCTION

The Mn_3O_4 (Hausmannite) is a standard spinel compound, indicating the distribution of Mn(II) in tetrahedral and Mn(III) in octahedral locations, this coupling compound can also be written as $Mn^{2+}O.Mn_2^{3+}O_3$ ($MnO.Mn_2O_3$) formula (Goodenough and Loeb, 1955; Fritsch *et al.*, 1998). Despite the Mn(II) and Mn(III), there are large magnetic moments, but Mn_3O_4 is considered a paramagnetic as low as 72 K, but it is ferromagnetic at below 43 K and connected by covalent forces to create a spinel structure with semi-covalent exchange (Goodenough and Loeb, 1955; Boucher *et al.*, 1971a; Boucher *et al.*, 1971b). The structure of spinel Mn_3O_4 is arranged in the unit cell as 24 cations with 32 oxygen

atoms (Fritsch *et al.*, 1998; Pike *et al.*, 2007). The common crystal structure of the spinel Mn_3O_4 is tetragonal with lattice parameters (a equal to b) = 5.762 Å but c = 9.4696 Å (Pike *et al.*, 2007). At 1170 °C , Mc Murdie (McMurdie *et al.*, 1950). found that the tetragonal crystal structure can be translated into a cubic crystal structure.

There are varies routes to prepare the spinel Mn_3O_4 as bulk and nanoparticles catalysts such as soft template self-assembly (Zhang *et al.*, 2010), a hydrothermal method (Yao *et al.*, 2018; Shah *et al.*, 2016), gas-liquid reaction method (Cui *et al.*, 2014), precipitation method (Vijayalakshmi *et al.*, 2014), chemical bath deposition method (Zhao *et al.*, 2015) and using the microwave irradiation technique (Bousquet-

Berthelin *et al.*, 2015). The spinel Mn_3O_4 is considered to be one of the most stable oxides of manganese, thus raising the interest in its use as electrode materials (Themsirimongko *et al.*, 2016; Bikkarolla *et al.*, 2014), as poisonous metal adsorption (Silva *et al.*, 2012) and as a catalyst in multiple oxidation and reduction reactions (Li *et al.*, 2013). The spinel Mn_3O_4 surface is modified by integrating it with other metal oxides as a composite to enhance the effectiveness of the reactions such as NiO (Rahaman *et al.*, 2000), CdO (Deepa *et al.*, 2013), Fe_2O_3 (Mohammad *et al.*, 2014), Al_2O_3 (Asif *et al.*, 2015) and ZnO (Senthilkumar *et al.*, 2015).

The purposes of this work are; to prepare the spinel Mn_3O_4 by the precipitation method, to prepare its composite with ZrO_2 by the ultrasonic method as a green technique, to measure the morphology and optical properties of both, and to exam them on photodecolorization of a colored solution prepared from Fe(II)-(4,5-Diazafluoren-9-one 11) complex, which is high stable.

2. MATERIALS AND METHODS

All the chemicals were used as received without further purification, Manganese (II) acetate tetrahydrate $\text{Mn}(\text{CH}_3\text{COO})_2 \cdot 4\text{H}_2\text{O}$, Sodium carbonate (Na_2CO_3) were purchased from BDH Company, England. 1,10-Phenanthroline, Potassium oxalate ($\text{K}_2\text{C}_2\text{O}_4 \cdot \text{H}_2\text{O}$), and Zirconium(IV) oxide were supplied from Riedel-De-Haen AG, Seelze, Hannover, Germany. Iron (II)sulfate heptahydrate ($\text{FeSO}_4 \cdot 7\text{H}_2\text{O}$), Iron (III)sulfate hydrate ($\text{Fe}_2(\text{SO}_4)_3 \cdot \text{H}_2\text{O}$), Hydrogen peroxide (H_2O_2), Absolute ethanol ($\text{C}_2\text{H}_5\text{OH}$), Hydrochloric acid (HCl) and Sodium hydroxide (NaOH) were of analytical grade and obtained from various sources. Fe(II)-(4,5-Diazafluoren-9-one 11) complex were prepared in the physical-chemistry laboratory at the University of Kerbala, college of science, department of chemistry, as shown in Equation 1.

The metal: ligand ratio is 1:3, and it has high stability constant equal to 7.575×10^4 , this value was calculated from data of mole ratio (Hadjioannoy *et al.*, 1988; Ingle *et al.*, 1988) at wavelength 510 nm or FeL_3 , as represented in Figure 1 and Equations 2 to 4.

2.1. Instrumentation

The main instruments that were applied in the study of the characterization of the prepared nanomaterials were an X-Ray Diffraction Spectroscopy, model Lab X- XRD 6000, Shimadzu, Japan. A UV-Visible

spectrophotometer, model AA-1800, Shimadzu Japan. An AFM, model AA 3000, Advanced Angstrom Inc., USA. A UV-Visible spectrophotometer with Labsphere diffuse reflectance accessory (Varian Cary 100 Scan, Laposphere- 99-010, Maryland United States). Furthermore, a furnace (type Muffle furnace Size-Tow Gallenkamp, England), a pH meter (type OAICTON-2100, Singapore), a ultrasonic bath (DAIHAN Scientific, Korea), a centrifuge (Hettich-Universal II- Germany), a magnetic stirrer (Heido-MrHei-Standard, Germany), and a sensitive balance (BL 210 S, Sartorius, Germany) were employed as essential and simple instruments in this procedure.

2.2. Synthesis of the Spinel (Mn_3O_4) as photocatalyst

A 1 M solution of sodium carbonate (precipitating agent) was added as drop by drop in the solution of $\text{Mn}(\text{CH}_3\text{COO})_2 \cdot 4\text{H}_2\text{O}$ under vigorous mixing, and constant heating from 70°C to 75°C . From this mixture, the Manganese was precipitated as MnCO_3 under controlled pH (9.0). The produced suspension was stirred for 2 hours at the constant temperature to complete the digestion process. After that, a pale pink precipitate of MnCO_3 was filtered using Wattman filter paper no. 1, washed with hot reagent water type IV, and then it was dried at 120°C for 24 hours. After that, the obtained powder of MnCO_3 was well crushed by using a mortar and later oxidized under burn at 600°C with a suitable quantity of oxygen, which leads to producing a dark brown powder from the spinel Mn_3O_4 . The growth of the spinel Mn_3O_4 was elucidated on the happening of the hydrolysis stage of $\text{Mn}(\text{CH}_3\text{COO})_2 \cdot 4\text{H}_2\text{O}$ and then the oxidation stage of the produced MnCO_3 by the chemical reactions described by Equations 5 and 6 (Palache *et al.*, 1944).

2.3. Synthesis of the (Spinel $\text{Mn}_3\text{O}_4/\text{ZrO}_2$) nanocomposites as photocatalysts

After the preparation of the spinel Mn_3O_4 , the spinel $\text{Mn}_3\text{O}_4/\text{ZrO}_2$ nanocomposites were directly prepared by using an ultrasonic technique, which provides the reaction with the necessary energy to combine them. The prepared spinel Mn_3O_4 and commercial ZrO_2 were employed as starting precursors for preparing these nano-composites in ratios of $\text{Mn}_3\text{O}_4:\text{ZrO}_2$ equal to (1:2), (1:3) and (1:4) respectively. The mention ratios of the nanocomposites were prepared directly by using ultrasonic as a green technique that has appropriate energy to generate the bond between Mn and Zr in a crystal lattice.

Exactly 2.5 g, or 1.66 g, or 1.25 g of Mn_3O_4 was dispersed in distilled water using an ultrasonic bath at a frequency equal to 60 kHz for 4 h. On the other hand, (5.0) g of ZrO_2 was also dispersed in distilled water at the same conditions, which deemed as enough energy for bonding Mn with Zr in a crystal lattice. These solutions were combined, and then ultrasonically irradiated for 1 h. The produced suspension was stirred at 70 °C for 30 min, and it produced a dark gray precipitate. The final precipitate was washed with hot distilled water (reagent water type IV) several times, filtered and dried at 100 °C.

The structural characteristics of all studied samples were examined at an X-ray diffractometer with Cu $\text{K}\alpha$ radiation ($\lambda = 0.15406$ nm). The morphology of photocatalyst and photocomposite was performed by atomic force microscopy. The bandgaps for all samples were calculated from the data of using UV-Visible spectrophotometer with Labsphere diffuse reflectance accessory.

2.4. Application of the spinel Mn_3O_4 and the spinel $\text{Mn}_3\text{O}_4/\text{ZrO}_2$ nanocomposites on the decolorization of colored solution.

This application was implemented using a homemade photoreactor, which consisted of a Philips UV-A lamp (400 watts) with a light intensity equal to 3.189×10^{-7} Einstein. s^{-1} , wooden box, magnetic stirrer, Teflon bar, 500 mL Pyrex glass beaker, and fan. As represented in scheme 1. The 0.1 g of the spinel Mn_3O_4 and Spinel $\text{Mn}_3\text{O}_4/\text{ZrO}_2$ nanocomposites were added to 50 mL from a solution of Fe(II)-(4,5-Diazafluoren-9-one 11) complex with 0.5% to 30% of H_2O_2 . This photoreaction was first performed in the dark as a physical adsorption process, for 15 min at 15 °C, to contact the active sites of the prepared photocatalyst with the complex and the H_2O_2 .

Samples of approximately 2.5 mL of the mixture were collected every 5 min of irradiation and separated two times by centrifuge. The clear solution was analyzed using a UV-visible spectrophotometer at 510 nm. The rate constant of this photoreaction (Hussein *et al.*, 2018; Ahmed *et al.*, 2018 a) and the efficiency of decolorization (Ahmed *et al.*, 2018 b; Kzar *et al.*, 2019; Rangel *et al.*, 2018) were calculated using Equations 7 and 8.

$$\ln\left(\frac{A_0}{A_t}\right) = k_{app}.t \quad (\text{Eq. 7})$$

$$E_{decol.}\% = \left(\frac{A_0 - A_t}{A_0}\right) \times 100 \quad (\text{Eq. 8})$$

In Equations 7 and 8, A_0 is the initial concentration of complex without illumination (dark reaction for 15 min), and A_t is the concentration of the complex at time t (in min) of illumination.

3. RESULTS AND DISCUSSION:

In order to investigate the crystalline phases of the synthesized catalyst samples, the X-Ray powder diffraction analysis was performed, results in Figure 2. All the strong and sharp diffraction peaks were successfully refined with the tetragonal phase of Mn_3O_4 (Vijayalakshmi *et al.*, 2014; Zhao *et al.*, 2015) that is compatible with the reference JCPDS 24-0734, which is referred no new peaks of impurities were observed (Zhao *et al.*, 2015; Li *et al.*, 2013). The mean crystallite size (L) of the prepared spinel Mn_3O_4 nanoparticle was detected from the significant (211), (103) and (224) diffraction peaks with the employing the Debye-Scherrer Equation (9) (Rangel *et al.*, 2018; Mohammed and Ahmed., 2018; Fakhri and Ahmed, 2019).

$$L = \frac{k \lambda}{\beta \cos \theta} \quad (\text{Eq. 9})$$

Where, λ is the wavelength of Cu as the source of the instrument in (nm), k is shaped constant, β is the full width at half maximum intensity in (radian), and θ is the Bragg diffraction angle.

The mean crystallite size of the prepared spinel Mn_3O_4 nanoparticle was calculated to be equal to 32.775 nm.

The XRD peaks in Figure 3 proved that the nanocomposites of the prepared spinel Mn_3O_4 nanoparticle with commercial ZrO_2 in ratios (1:2), (1:3) and (1:4) respectively, were actually created between Mn bond and Zr bond in crystal lattices. The mean crystallite sizes for all mention prepared photocatalysts are estimated as 25.411 nm, 25.7504 nm, and 12.994 nm, respectively. Moreover, new peaks at 2θ equal to 23.80° -23.90°, 28.12° -28.18°, 31.34°-31.40°, 39.96°- 40.26°, 49.50°-50.04° are noted at miller indexes (110), (011), (111), (020), (012), (022) corresponding to the m- ZrO_2 phases (Vaizogullar *et al.*, 2016) (JCPDS 37-1484). For the Mn_3O_4 , the peak for 44.3° at (220) is shifted to a high 2θ value when nanocomposites are created, that attitude to incorporate two metals (Mn with Zr)

into the new bond. This behavior is consistent with the study in references (Mahammed and Ahmed, 2017; Ahmed *et al.*, 2014).

3.1. Surface Morphology of photocatalyst

The Atomic force microscopy (AFM) images were displayed in Figure 4, it is noted that the particle size of Mn_3O_4 is 58.33 nm. It is smaller than that values for $\text{Mn}_2\text{O}_3/\text{ZrO}_2$ nanocomposites 1, 2, and 3, which equals 93.71 nm, 88.24 nm, and 73.14 nm, respectively. This is attributed to the low ionic radius of the Mn^{2+} (0.66 Å) and Mn^{3+} (0.64 Å) compared with the ionic radius of Zr^{4+} (0.747 Å) (Ghosh and Biswas, 2003). Moreover, $\text{Mn}_3\text{O}_4/\text{ZrO}_2$ nanocomposites have more agglomeration than the Mn_3O_4 sample.

3.2. Optical Absorption Study

Based on the extrapolation of the peaks of samples employing the Tauc equation plots (Fakhri and Ahmed, 2019; Brijnandan *et al.*, 2017; Augustine and Nnabuchi, 2017) in Figure 5, the indirect bandgaps for spinel Mn_3O_4 , and its nanocomposites 1, 2 and 3 with ZrO_2 were detected and discovered to rise from approximately 2.1 eV for Mn_3O_4 to 3.75 eV, 4.51 eV and 4.65 eV for nanocomposites 1, 2 and 3 respectively. The increase of bandgaps is indicated to decreased the mean crystal size of nanoparticles, so composite 3 is having the maximum bandgap 4.65 eV with less mean crystal size (12.994 nm) and particle size (73.14 nm).

3.4. Photocatalytic decolorization of Fe(II)- (4,5-Diazafluoren-9-one 11) complex

In order to evaluate the photocatalytic activity of the prepared spinel Mn_3O_4 nanoparticles and its nanocomposites 1, 2, and 3, the decolorization of Fe(II)-(4,5-Diazafluoren-9-one 11) complex was performed without and with presence H_2O_2 (strong oxidant agent), according to Equations 10-12.

The addition of H_2O_2 will produce further hydroxide radical (Ahmed *et al.*, 2018 c) under UV-A light.



Figure 6 illustrates that the rate of reaction and the decolorization efficiency of Fe(II)-(4,5-Diazafluoren-9-one 11) complex increase with addition H_2O_2 and using the incorporated of Mn_3O_4 with ZrO_2 as nano-composite 1, nano-composite 2 and nano-composite 3. That due to raising the acidity of the Mn_3O_4 surface via

incorporated it with ZrO_2 crystal lattice. That increases the amount of produced hydroxyl radical at pH 4 (natural pH of Fe(II) solution) in the presence of hydrogen peroxide, as shown in Equations 10 and 11 (Abbas *et al.*, 2019; Ahmed *et al.* 2012). The efficiency of the photodecolorization of this complex with the use of nano-composite 3 is twice the amount than the use of prepared Mn_3O_4 and reached 40% in 1 h that due to have it a low mean crystal size and particle size compared with other synthesis nano-composite (Fakhri and Ahmed, 2019).

4. CONCLUSIONS:

On the depended of the occurred results, the following conclusions may be written:

- 1- The prepared spinel Mn_3O_4 and the spinel $\text{Mn}_3\text{O}_4/\text{ZrO}_2$ nanocomposites have been synthesized by the precipitation method and the direct ultrasonic method, respectively.
- 2- The XRD data conclude that the spinel Mn_3O_4 is actually prepared by precipitation method and should be tetragonal with an indirect bandgap equal to 2.1 eV.
- 3- All the prepared samples are polycrystalline and contain from 3 to 6 crystals.
- 4- The mean crystal size and particle size for spinel Mn_3O_4 are lower than for prepared nanocomposites 1, 2, and 3 readies with significant indirect band gaps of 3.15 eV, 4.51 eV, and 4.62 eV respectively.
- 5- The nanocomposite 3 is more active in the photodecolorization of Fe(II)-(4,5-diazafluoren-9-one 11) complex in the presence of H_2O_2 compared with other samples, and the photoreaction for this obeys to first-order kinetics.

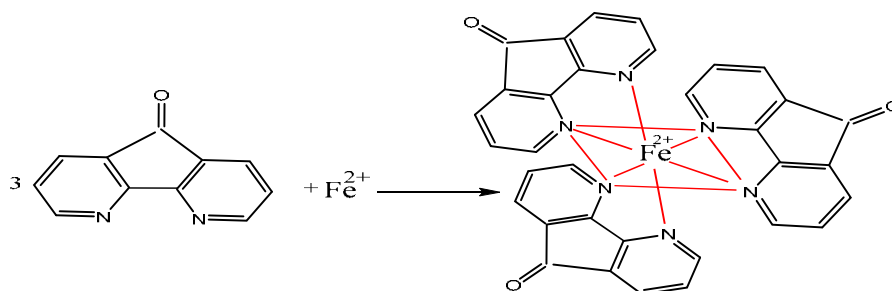
5. ACKNOWLEDGMENTS:

The authors are grateful to all the persons who assisted in this project during performed it at the University of Kerbala, college of science, department of chemistry, the University of Babylon, college of science and College of science for women, department of chemistry.

6. REFERENCES:

1. Goodenough, J. B.; and Loeb, A. L. Physical Review. 1955, 98(2), 391.

2. Fritsch, S.; Sarrias, J.; Rousset, A.; Kulkarni, G. U. *Materials Research Bulletin*. 1998, 33(8), 1185.
3. Boucher, B.; Buh, R.; Perrin, M. *Journal of Physics and Chemistry of Solids*. 1971, 32(10), 2429.
4. Boucher, B.; Burl, R.; Perrin, M. *Journal of Applied Physics*. 1971, 42, 1615.
5. Bricker, O. *Am. Mineral*. 1965, 50, 1296.
6. Pike, J.; Hanson, J.; Zhang, L.; and Chan, S. *Chem. Mater.*, 2007, 19, 5609.
7. McMurdie, H.; Barbara, F.; Sullivan, M.; Mauer, F., A., *Part of the Journal of Research of the National Bureau of Standards*, 1950, 45, 35.
8. Zhang, P.; Zhan, Y.; Cai, B.; Hao, C.; Wang, J.; Liu, C.; Meng, Z.; Yin, Z.; and Chen, Q. *Nano Res.* 2010, 3, 235.
9. Yao, J.; Cheng, Y.; Zhou, M.; Zhao, S.; Lin, S.; Wang, X.; Wu, J.; Lia, S.; and Wei, H. *Chem. Sci.*, 2018, 9, 2927.
10. Shah, H. U.; Wang, F.; Toufiq, A. M.; Khattak, A. M.; Iqbal, A.; Ghazi, Z. A.; Ali, S.; Li, X.; Wang, Z. *Int. J. Electrochem. Sci.* 2016, 11, 8155.
11. Cui, X.; Li, Y.; Li, S.; Sun, G.; Ma, J.; Zhang, L.; Li, T.; Ma, R. J. *Chem. Sci.* 2014, 126(3), 561.
12. Vijayalakshmi, S.; Pauline, S. *International Journal of ChemTech Research*. 2014, 6(7), 3813.
13. Zhao, J.; Xu, L.; Xie, T.; Xie, C. *Chin. J. Geochem.* 2015, 34(1), 55.
14. Bousquet-Berthelin, C.; Stuerger, D., J. *Mater. Sci.*, 2005, 40, 253.
15. Themsirimongko, S.; Promsawan, N.; Saipanya, S. *Int. J. Electrochem. Sci.*, 2016, 11, 967.
16. Bikkarolla, S. K.; Yu, F.; Zhou, W.; Joseph, P.; Cumpson, P.; Papakonstantinou, P. J. *Mater. Chem. A*. 2014, 1.
17. Silvaa, G. C.; Almeida, F. S.; Ferreira, A. M.; Ciminella, V. S. T. *Materials Research*. 2012, 1.
18. Li, X.; Yang, L. *Advanced Materials Research*, 2013, 750-752, 1822.
19. Rahaman, H.; Barman, K.; Jasimuddin, S.; Ghosh, S. K. *J. Appl. Phys.*, 2000, 87, 1318.
20. Deepa, G.; Mahadevan, C. K. *IOSR Journal of Applied Physics*, 2013, 5, 15.
21. Mohammad, S.H.; Haris, K.; Hassan, M.F.; Hayati Idris, N. *European International Journal of Science and Technology*, 2014, 3(9), 61.
22. Asif, S. A.; Khan, S. B.; Asir, A. M. *Nanoscale Research Letters*. 2015, 10, 355.
23. Senthilkumar, P.; Rajeswari, P.; and Dhanuskodi, S. *Materials, Devices, and Applications XIV*, 2015, 9347, 9347IV-1.
24. Hadjiioannoy, T. P.; Christian, G. D.; Efstathion, C. E.; and Nikolelis, D. P. *Problem and Solvent in Analytical Chemistry*, Pergamon Press, New York, 1988, 341.
25. Ingle, J. D.; Stanley, R. C., *Spectrochemical Analysis*, Prentice Hall, New York, 1988, 386.
26. Palache, C.; Berman, H.; and Frondel, C.; *Dana's system of mineralogy*, 7th edition, I, 1944, 712.
27. Hussein, Z. A.; Abbas, S. K.; and Ahmed, L. M. *IOP Conference Series: Materials Science and Engineering*. 2018, 454, 1.
28. Ahmed, L. M.; Jassim, M. A.; Mohammed, M. Q. and Hamza, D.T. *Journal of Global Pharma Technology*, 2018, 10, 248.
29. Ahmed, L. M. *Asian J. Chem.*, 2018, 30(9), 2134.
30. Kzar, K. O.; Mohammed, Z. F.; Saeed, S. I.; Ahmed, L. M.; Kareem, D. I.; Hadyi, H. and Kadhim, A. J. *AIP Conf. Proc.*, 2019, 2144, 020004-1.
31. Rangel, E. M.; Carvalho, C. De O.; Arsand, D. R. *PERIÓDICO TCHÊ QUÍMICA*. 2018, 15 (29), 7-81.
32. Mohammed, B. A., and Ahmed, L. M. *Journal of Global Pharma Technology*. 2018, 10(7), 129.
33. Fakhri, F. H., and Ahmed, L. M., *Indones. J. Chem.*, 2019, 19(4), 936.
34. Vaizoğullar, A.I.; Balci, A.; Uğurlu, M. and Karaoğlu, M. H. *AKU J. Sci. Eng.* 2016, 16, 54.
35. Mahammed, B. A.; and Ahmed, L. M. *Journal of Geoscience and Environment Protection*. 2017, 5, 101.
36. Ahmed, L. M.; Ivanova, I.; Hussein, F. H.; and Bahnemann, D. W. *International Journal of Photoenergy*. 2014, 1.
37. Ghosh, D. C., and Biswas, R. *Int. J. Mol. Sci.* 2003, 4, 379.
38. Brijnandan, M., Dehiya, S., and Yadav, A. *International Journal of Engineering Technology Science and Research*. 2017, 4(7), 370.
39. Augustine, C.; and Nnabuchi, M., N. *Journal of Non - Oxide Glasses*. 2017, 9(3), 85.
40. Ahmed, L. M., Saeed, S. I., and Marhoon, A. A. *Indones. J. Chem.* 2018, 18(2), 272.
41. Abbas, S. K., Hassan, Z. M., and Ahmed,

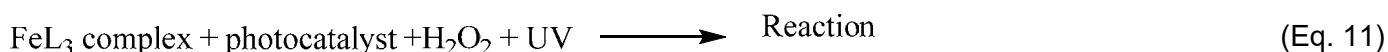
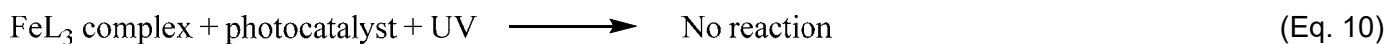
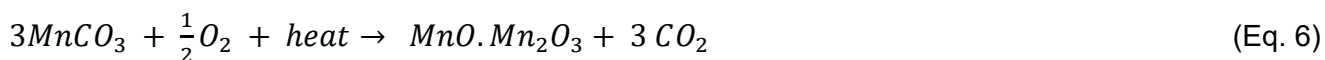
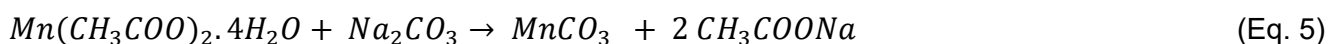


$$k_{\text{instability}} = \frac{[\text{Fe}^{2+}][\text{L}]^3}{[\text{FeL}_3]} = \frac{\left[1 - \frac{A}{A_{\text{max}}}\right]^4}{\left[\frac{A}{A_{\text{max}}}\right]} \times C_{\text{Fe}^{2+}} \quad (\text{Eq. 3})$$

$$= \frac{\left[1 - \frac{0.10}{0.172}\right]^4}{\left[\frac{0.10}{0.172}\right]} \times 2.5 \times 10^{-3} = 1.320 \times 10^{-5} \text{ M}$$

$$k_{\text{stability}} = \frac{1}{k_{\text{instability}}} \quad (\text{Eq. 4})$$

$$= \frac{1}{1.320 \times 10^{-5}} = 7.575 \times 10^4 \text{ M}^{-1}$$



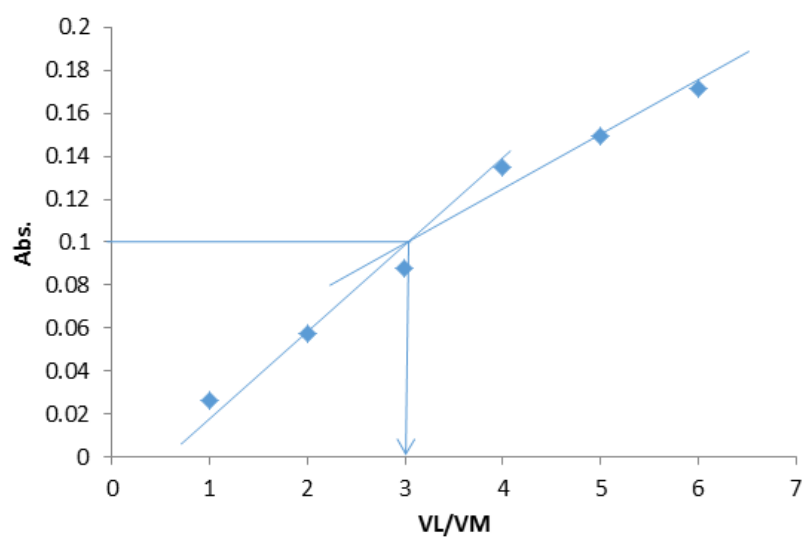
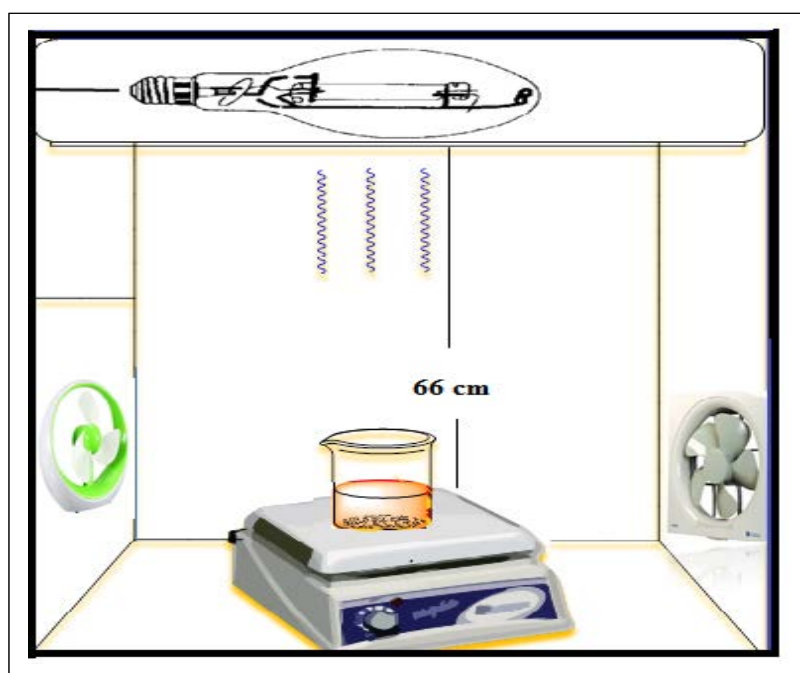


Figure 1. Mole ratio method for ligand: Fe(II).



Scheme 1. Schematic diagram of Homemade Photocatalytic Reactor Unit

Figure 3. XRD pattern of prepared spinel Mn_3O_4 nanoparticle and his nanocomposites with ZrO_2 .

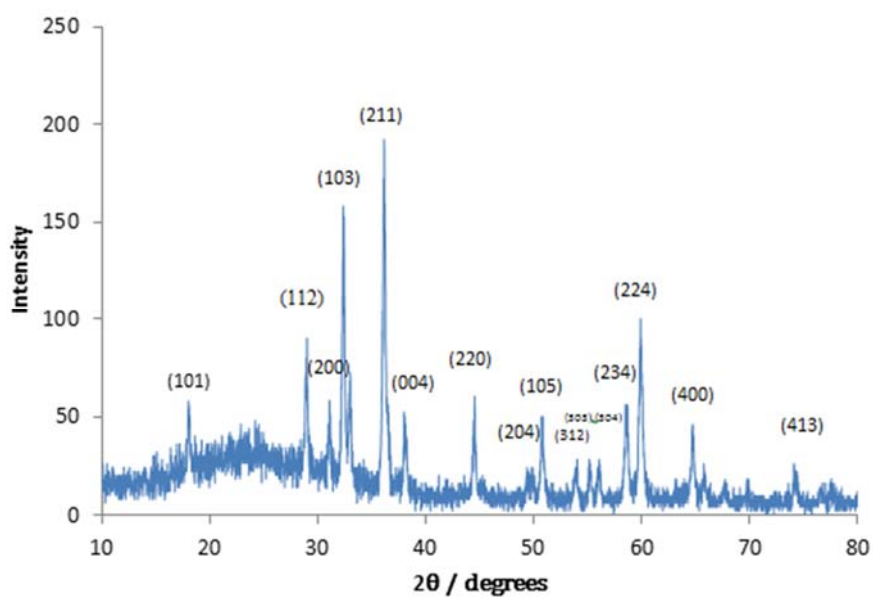


Figure 2. XRD pattern of prepared spinel Mn_3O_4 nanoparticle.

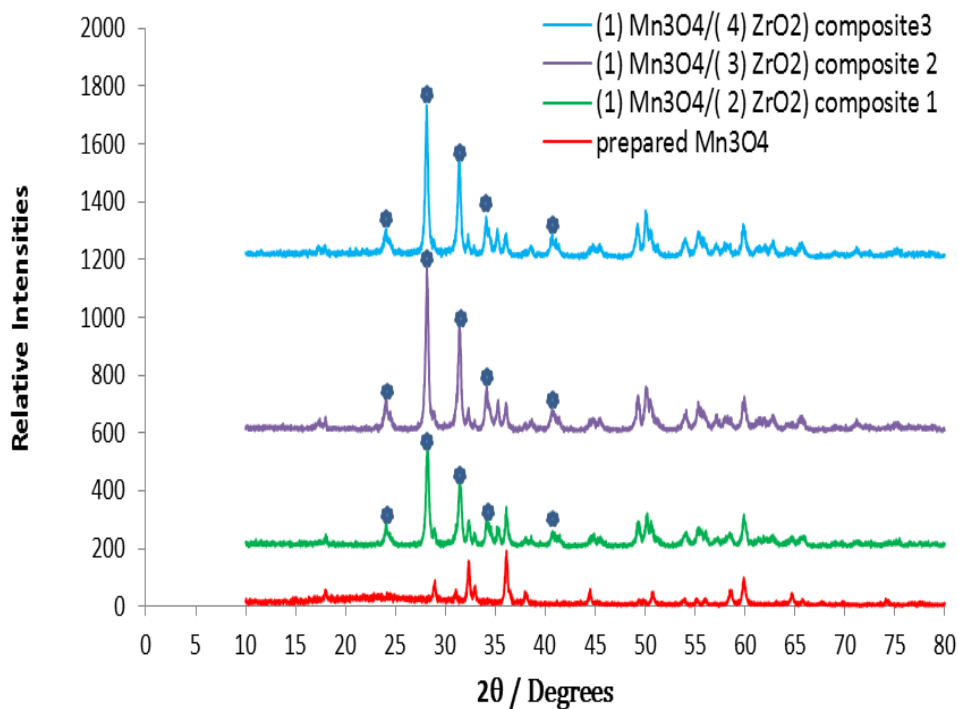


Figure 3. XRD pattern of prepared spinel Mn_3O_4 nanoparticle and his nanocomposites with ZrO_2 .

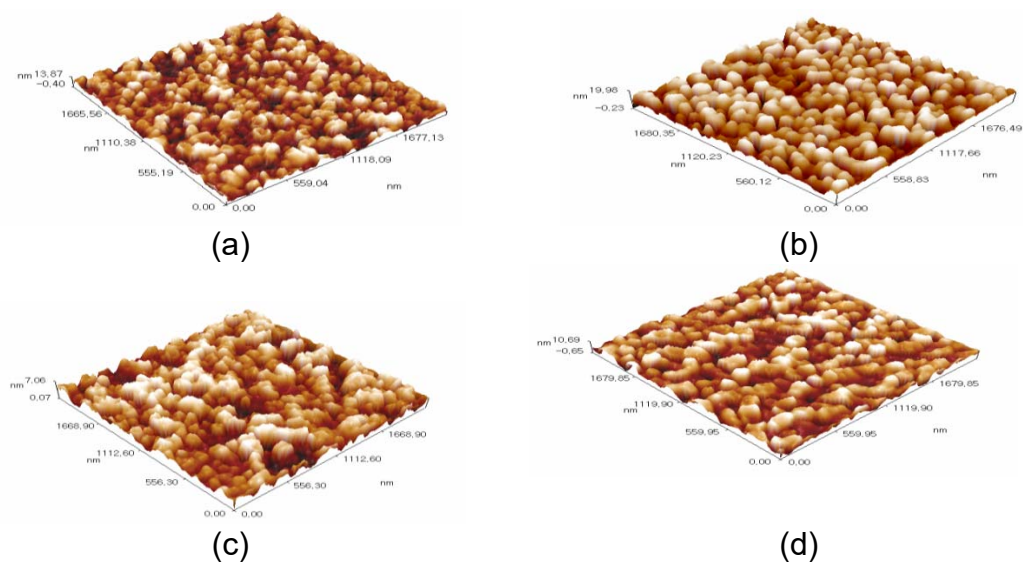


Figure 4. AFM Analysis of prepared spinel Mn_3O_4 nanoparticle (a) and his nanocomposites 1, 2 and 3 with ZrO_2 in (b),(c), and (d), respectively.

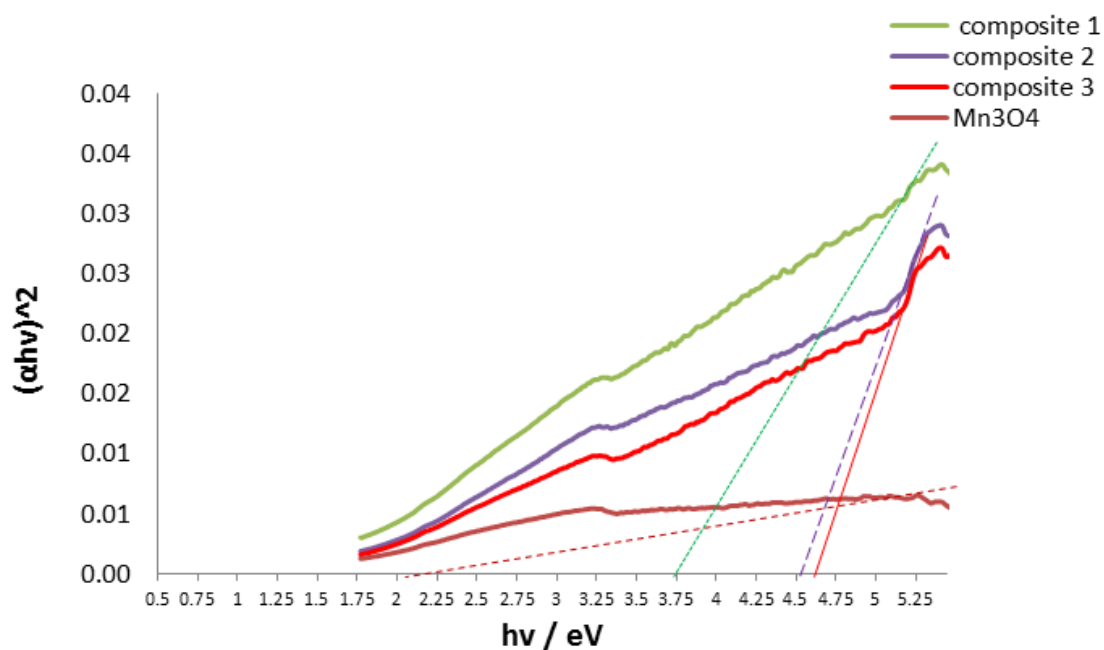


Figure 5. The bandgap of prepared spinel Mn_3O_4 nanoparticle and his nanocomposites 1, 2, and 3.

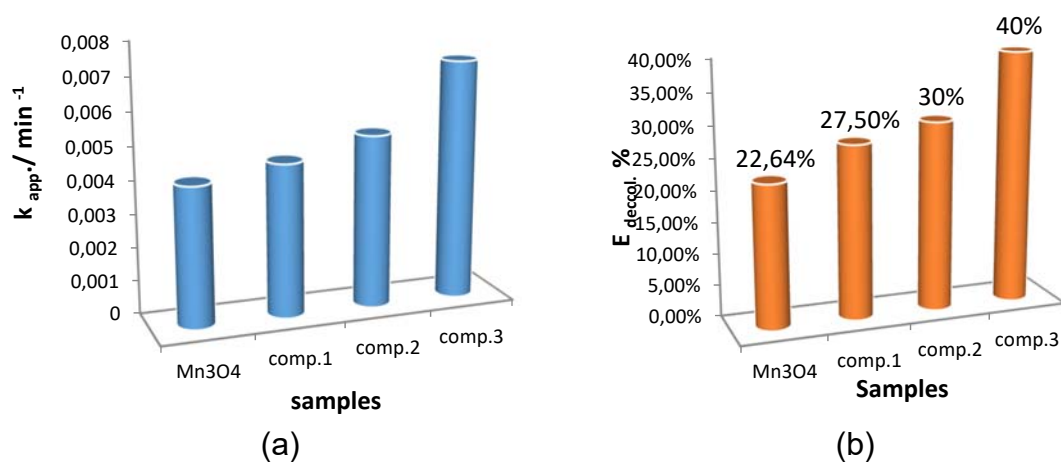


Figure 6. Photocatalytic decolorization of Fe(II)-(4,5-Diazafluoren-9-one 11) complex by using prepared spine Mn₃O₄ nanoparticle and his nanocomposites 1,2 and 3. (a) Relation between rate constant and samples and (b) $E_{decol.} \%$ verse samples.

SEPARAÇÃO MAGNÉTICA SECA DE MINÉRIO DE MAGNETITA

DRY MAGNETIC SEPARATION OF MAGNETITE ORES

СУХАЯ МАГНИТНАЯ СЕПАРАЦИЯ МАГНЕТИТОВЫХ РУД

CHOKIN, Kanat Sh.^{1*}; YEDILBAYEV, Abdraman I.²; YEDILBAYEV, Baimurat A.³;
YUGAY, Vladimir D.⁴

¹ Satbayev University, Institute of Physics and Technology, Almaty – Republic of Kazakhstan

²⁻⁴ Gornoe Buro LLP, Almaty – Republic of Kazakhstan

**Correspondence author
e-mail: kanatch@mail.ru*

Received 22 December 2019; received in revised form 20 February 2020; accepted 14 March 2020

RESUMO

A relevância do artigo reside no fato de que a separação magnética seca (SMS) é o principal método de enriquecimento de minérios de magnetita. A falta de máquinas e dispositivos industriais eficientes para separar os minérios de magnetita de granulação fina significa que a SMS é usada principalmente como uma operação de pré-concentração para as classes razoavelmente grandes. O objetivo do estudo é investigar a possibilidade de utilizar um novo modelo de separador magnético no processo de concentração a seco de minério de magnetita do depósito de Bapy. Este artigo apresenta os estudos teóricos e experimentais de um novo modelo de separador magnético. Foi realizada uma modelagem matemática do processo de separação magnética do dispositivo para avaliar os parâmetros de acordo com os quais o separador de laboratório foi posteriormente fabricado. Para o estudo experimental das propriedades desse sistema magnético, foi construído o separador magnético de laboratório. A possibilidade de usar o novo separador magnético no processo de beneficiamento a seco de minério de magnetita do depósito de Bapy foi investigada. O esquema industrial implementado consiste na esmagamento de minério e beneficiamento em dois estágios nos separadores magnéticos de tambor seco. O estudo dos indicadores de enriquecimento do separador magnético foi realizado utilizando o minério de ferro do depósito de Bapy, que é magnetita monomineral. Para o estudo, foram selecionadas as misturas da classe menos 0,1 mm com um teor de ferro de $\alpha = 50\%$ e $\alpha = 40\%$. Como resultado do estudo, foram obtidos os indicadores de enriquecimento em escala laboratorial. Assim, a melhoria do esquema de enriquecimento é reduzida ao isolamento de um produto pequeno e seu enriquecimento subsequente usando um novo modelo de separador magnético. Assim, o separador magnético apresentado é adequado para processamento a seco de minério de magnetita esmagado.

Palavras-chave: separador magnético, classificador pneumático, campo magnético do separador, suscetibilidade magnética de partículas, velocidade da correia.

ABSTRACT

The relevance of the paper is that dry magnetic separation (DMS) is the main beneficiation method of magnetite ores. The lack of efficient industrial-grade machines and apparatus for separating fine-grained magnetite ores means that DMS is used mainly as a pre-concentration operation for fairly large classes. The aim of the research is to study the possibility of using a new magnetic separator model in the process of dry beneficiation of magnetite ore from the Bapy deposit. This paper presents theoretical and experimental studies of a new model of a magnetic separator. The mathematical modeling of the magnetic separation process of the device was carried out to evaluate the parameters in accordance with which a laboratory separator was subsequently manufactured. For the experimental study of the properties of this magnetic system, a laboratory magnetic separator was built. The possibility of using a new magnetic separator in the process of dry beneficiation of magnetite ore from the Bapy deposit was investigated. The industrial scheme being implemented consists in ore crushing and two stage dressing on dry drum magnetic separators. The study of beneficiation indicators of the magnetic separator was carried out using iron ore of the Bapy deposit, which is mono-mineral magnetite. For the study, mixtures of the minus 0.1 mm class were selected with the iron content $\alpha = 50\%$ and $\alpha = 40\%$. As a result of the research, beneficiation indicators were obtained on a laboratory scale. Therefore, the improvement

of the beneficiation scheme is reduced to the isolation of a small product and its subsequent beneficiation using a new model of magnetic separator. Thus, the presented magnetic separator is suitable for dry processing of crushed magnetite ore.

Keywords: *magnetic separator, pneumatic louver classifier, magnetic field of the separator, magnetic susceptibility of particles, belt speed.*

АННОТАЦИЯ

Актуальность статьи заключается в том, что сухое магнитное разделение (СМС) является основным методом обогащения магнетитовых руд. Отсутствие эффективных промышленных машин и устройств для отделения мелкозернистых магнетитовых руд означает, что СМС используется в основном в качестве операции предварительного концентрирования для довольно больших классов. Целью исследования является изучение возможности использования новой модели магнитного сепаратора в процессе сухого обогащения магнетитовой руды месторождения Бапы. В данной статье представлены теоретические и экспериментальные исследования новой модели магнитного сепаратора. Математическое моделирование процесса магнитной сепарации устройства проводилось для оценки параметров, в соответствии с которыми впоследствии был изготовлен лабораторный сепаратор. Для экспериментального исследования свойств этой магнитной системы был построен лабораторный магнитный сепаратор. Исследована возможность использования нового магнитного сепаратора в процессе сухого обогащения магнетитовой руды с месторождения Бапы. Реализуемая промышленная схема состоит в дроблении руды и двухступенчатой обогащении на сухих барабанных магнитных сепараторах. Исследование показателей обогащения магнитного сепаратора проводилось с использованием железной руды месторождения Бапы, которая представляет собой мономинеральный магнетит. Для исследования были выбраны смеси класса минус 0,1 мм с содержанием железа $\alpha = 50\%$ и $\alpha = 40\%$. В результате исследования были получены показатели обогащения в лабораторном масштабе. Таким образом, усовершенствование схемы обогащения сводится к изоляции небольшого продукта и его последующему обогащению с использованием новой модели магнитного сепаратора. Таким образом, представленный магнитный сепаратор подходит для сухой переработки измельченной магнетитовой руды.

Ключевые слова: *магнитный сепаратор, пневматический классификатор, магнитное поле сепаратора, магнитная восприимчивость частиц, скорость ленты.*

1. INTRODUCTION

Dry magnetic separation (DMS) is the primary beneficiation method of magnetite ores, especially in places where water resources are scarce. Such is the situation at the Bapy ore deposit in Kazakhstan. The lack of efficient industrial-grade machines and apparatus for separating fine-grained magnetite ores means that DMS is used mainly as a pre-concentration operation for fairly large classes (Duman *et al.*, 2019; Chang and Cheng, 2019; Fan *et al.*, 2019; Eliopoulos and Economou-Eliopoulos, 2019). Thus, at the Bapy deposit, the -10mm grade ore is brought to an iron concentration of 52-54% by means of DMS, using traditional drum separators. This industrial product is the final commercial product. However, the iron content of the class of -0.3 mm drops to 42-46%. These results can be further improved by beneficiating individual finer classes. However, the use of traditional separators lowers the recovery of mineral particles (Karthaus *et al.*, 2019; D'Souza *et al.*, 2018; Zhang *et al.*, 2018).

A negative effect on the process of magnetic separation of small classes is exerted by the influence of a magnetic field on the behavior of particles, i.e., magnetic flocculation. The rotation of the magnetic field in the separators improves the situation and contributes to the destruction of magnetic agglomerations (Li *et al.*, 2015; Vorob'ev *et al.*, 2018; Zhao *et al.*, 2017a). It is possible to improve the current situation in DMS by improving the technology of dry magnetic beneficiation of crushed magnetite ores. Studies are underway in this direction (Urick, 2018; Edathil *et al.*, 2018; Tang *et al.*, 2020). It should be noted the development of work on the separation of magnetite ores in suspension (Sedinkina *et al.*, 2014; Yu *et al.*, 2017; Shahrokhi *et al.*, 2019).

In (Chokin *et al.*, 2012), a method was proposed where the finely ground material is loosened and crumbled into separate particles in a device for creating a dusty air mixture, and magnetic separation of particles is made from a dusty air mixture, which is blown at a constant speed into an inhomogeneous magnetic field and moves there along a path defined by a special

reflector, which ensures the movement of the dusty air mixture in the separation zone with the opposite action of centrifugal and magnetic forces (Kovalenker *et al.*, 2019; Kenzhaliev *et al.*, 2019). Particles having a magnetic susceptibility value above a certain value, depending on the ratio of these forces, are extracted from the overall flow into the magnetic product, and the residual dust-air mixture is removed from the separation zone. Traditionally, a magnetic separator is a magnetic system around which a non-magnetic drum rotates. Ore is fed from the top to a rotating non-magnetic drum and, due to centrifugal force, gangue particles bounce off the drum, and magnetic particles remain on it (Liu *et al.*, 2019; Liang *et al.*, 2019).

In (Chokin *et al.*, 2017), a new separator was proposed, the fundamental difference of which is that ore is fed into the magnetic field from the bottom along the inner surface of the carrier tape, which envelopes the drum and is separated from it by a certain distance. This gap is a separation area. Shredded ore is pressed to the belt centrifugally. Due to the magnetic force, magnetite particles detach from the surface of the carrier tape and are attracted to a rotating non-magnetic drum, and the waste remains on the tape. Thus, in the first case, beneficiation occurs due to the fact that non-magnetic particles leave the drum, and in the second, vice versa – the magnetic particles in the opposite direction leave the surface of the tape and are attracted to the rotating drum.

2. MATERIALS AND METHODS

In the present work, theoretical and experimental studies of this magnetic separator (Chokin *et al.*, 2017; Zhao *et al.*, 2017b) for dry beneficiation of magnetites are carried out. The beneficiation indices obtained on a model laboratory separator are obtained. The discussed method of magnetic separation of finely divided magnetic separation is shown schematically in Figure 1. The magnetic separator consists of: a movable drum of non-magnetic material “1”, a stationary magnetic system “2” installed inside it and consisting, for example, of permanent magnets with alternating polarity, a conveyor with a bearing surface “3”, which is a convex cylindrical surface with a generatrix parallel to the axis of the drum, a divider “4”, which separates the magnetic “5” and non-magnetic “6” fractions and the feeder tray “7”.

The device operates as follows. Bulk material is fed by the feeder “7” to the moving belt

of the conveyor “3” and moves it into the magnetic field. Centrifugal force presses the particles against the inner surface of the conveyor belt. In the separation zone, a magnetic force acts on the magnetic particle to counteract the centrifugal force. Magnetic particles are attracted by the magnetic field to the surface of the rotating drum “1”, moved by the drum to the zone of absence or significant weakening of the magnetic field, where they are separated from the surface of the drum, and non-magnetic particles remain on the moving conveyor belt and are transferred by it to the receiver for the non-magnetic fraction.

The proposed device for magnetic separation allows adjusting the selectivity of separation according to the magnetic properties of the particles. This is achieved by changing the centrifugal force acting on the particles, which counteracts the magnetic force of attraction. By changing the speed of movement of the reflector tape, it is possible to efficiently isolate the magnetic fraction of particles with a wide range of values of the magnetic susceptibility of the particles.

The study of beneficiation indicators of the magnetic separator was carried out using iron ore of the Bapy deposit, which is mono-mineral magnetite. The matrix components of the ores are diopside and serpentine. The mineralogical and petrographic analysis allows us to evaluate the effectiveness of magnetic separation (Parian *et al.*, 2016; Lund *et al.*, 2015; Li *et al.*, 2016a; Yu *et al.*, 2015). Such observations determined in diopside and serpentine the frequent presence of thin dispersed (pulverized) disseminated magnetite with sizes in the range of 1-5 microns. As a result, fine dusty particles of silicates, 10-50 microns in size, can stick together with the same but larger particles of magnetite, which to some extent, complicates magnetic separation, especially in the air. Magnetite grains, in this case, have a shell of weakly magnetic dust, in which the content of magnetite iron is much lower than in standard ores. Ore is difficult to process. With the wet magnetic separation of class minus 0.1 mm, the maximum iron content in the concentrate does not exceed 62%. The physical reason for the difficult beneficiation, apparently, is due to the fact that the proportion of grains in intergrowths in the class of -0.1 +0.071 mm is 27%, and in the class of -0.071 mm – 17%.

In (Sedinkina *et al.*, 2014), a mixture of magnetite and quartz was used to determine the beneficiation parameters of the magnetic separator in suspension. In the present work, due to the absence of magnetite, it was replaced with

concentrate with an average iron content of 60.6%. It was received as follows. At first, the initial ore was taken with a particle size of minus 10 mm with an average iron content of 54%. Then crushing and grinding were carried out to a class of -0.1 mm. The required amount of 60.6% Fe concentrate was obtained by preliminary magnetic separation of the crushed ore in the laboratory magnetic separator under study. After that, the mixture was prepared from the obtained concentrate and construction chamotte fines of the same class by thorough mixing (Li *et al.*, 2016b; Schlüter and Saboktakin, 2016). Unfortunately, in contrast to magnetic properties and density, such a mixture is inferior to a mixture using magnetite, which ultimately reduces the measured beneficiation indices. For the study, mixtures of the minus 0.1 mm class were selected with the iron content $\alpha = 50\%$ and $\alpha = 40\%$. The first option was used to assess the ability of the separator for dry beneficiation of the industrial fields of the Bapy deposit. The second mixture with $\alpha = 40\%$ expanded the measurement range. Table 1 shows the beneficiation at various speeds of the tape.

In line 1, beneficiation indicators correspond to a magnetic system with a full set of magnets. It can be seen that with an increase in the speed of the tape, the iron content β in the final product increases with some decrease in ε extraction. Note that β does not change at speeds greater than 7.6 m/s. Apparently, this is due to the fact that in the test mixture prepared from 60.6% Fe concentrate, magnetite splices have a rather high lower limit of the concentration of iron in the splices. Real ore has a set of splices with a wider difference in iron concentrations. Then, with an increase in velocity over 7.6 m/s, intergrowths with a low concentration of Fe will be cut off, and β will increase.

Rows 2 and 3 present the result of measuring the beneficiation indices for the magnetic system from which one magnet is removed. This option was theoretically considered earlier and is shown in fig. 2 and 3. A comparison of the indicators in lines 1 and 2 indicates that shaking the particles on the drum when passing through a region with a low magnetic field strength leads to some purification of the magnetic product. In this case, the extraction drops. The data obtained in the study of separation of the mixture with a particle size of -0.1 mm with increased content of gangue rock $\alpha=40\%$ (row 3) indicate a good extraction of the magnetic product. It, of course, falls in comparison with $\alpha=50\%$, but, nevertheless, remains quite high.

3. RESULTS AND DISCUSSION:

Mathematical modeling of particle motion in a magnetic field and experimental verification allows us to evaluate the effectiveness of the magnetic separator (Charikinya *et al.*, 2017; Thiagu and Dhanasekaran, 2014; Zhang *et al.*, 2020). For this purpose, authors consider the movement of particles in a space bounded by two cylindrical surfaces, namely, internal and external (Figure 1). If a particle has a certain specific magnetic susceptibility χ , and in a moving space, there is a magnetic field of intensity H , which weakens in the direction from the inner surface to the outer, then the motion of the particles will be quite complicated. The magnetic field will attract a particle of mass m with a magnetic force F_{mag} , as described in Equation 1.

$$F_{mag} = m\mu_0\chi H \text{ grad}H \quad (\text{Eq. 1})$$

where μ_0 is the magnetic constant, equal to $1.256 \cdot 10^{-6}$ H/m, χ is the specific magnetic susceptibility, m^3/kg . The direction of action of the force is determined by the gradient and, in this case, is directed from the surface of the tape towards the drum. Another force acting on the particle is the force of gravity, as in Equation 2.

$$F_g = mg \quad (\text{Eq. 2})$$

Where g is the acceleration of gravity, in this separator, the tape and non-magnetic drum rotate in the same direction with the same angular velocity. The small gap between them allows us to assume that the air layer in this gap also moves with the same angular velocity. In this case, authors can neglect the air resistance acting on the moving particle in this gap, because particle velocity relative to airflow will be negligible. The magnetic field of the separator is considered to be two-dimensional/cylindrical since the length of the magnetic system in the axial direction has a significant extension. Then, in the cylindrical coordinate system, the particle trajectory is a function of two coordinates: radius R and polar angle ϕ .

$$\begin{cases} \frac{d^2r}{dt^2} = F_r(r, \phi) + r\left(\frac{d\phi}{dt}\right)^2 - g\cos\phi \\ r\frac{d^2\phi}{dt^2} = F_\phi(r, \phi) + g\sin\phi - 2\frac{dr}{dt}\frac{d\phi}{dt} \end{cases} \quad (\text{Eq. 3})$$

Where $F_r(r, \phi)$ and $F_\phi(r, \phi)$ are the radial and angular projections of the specific magnetic force, respectively. Border conditions:

$$\frac{d\varphi}{dt} = -\omega_1, \text{ for } r = R_1; \quad (\text{Eq. 4})$$

$$\frac{d\varphi}{dt} = -\omega_2, \text{ for } r = R_2; \quad (\text{Eq. 5})$$

where R_1 is the radius of the rotating non-magnetic drum, R_2 is the radius of curvature of the tape:

$$R_1 \leq r \leq R_2 \quad (\text{Eq. 6})$$

Initial condition

$$t=0, \varphi=\pi;$$

$$r = R_2;$$

$$\frac{d\varphi}{dt} = -\omega_2 = -V/R_2. \quad (\text{Eq. 7})$$

The calculation is carried out to the condition $\varphi = 0$. The authors decided to elaborate on the calculation of the magnetic field. As previously noted, the field is considered cylindrical. It is convenient to calculate such a system under the assumption that, due to the high anisotropy constant, the rotation of the magnetization vector is impeded. Authors can assume that there are no space charges and that the source of the field is constituted only by surface charges located on the arcs of the circles of the pole ends. In (Tolmachev, 1974), a method for calculating such magnetic systems was described, which was applied in this paper.

The mathematical modeling of the magnetic separation process of the device, the scheme of which is shown in Figure 1, was carried out to evaluate the parameters in accordance with which a laboratory separator (Figure 4) was subsequently manufactured. It was initially assumed that the outer radius of the non-magnetic drum constitutes 100 mm, the radius of the arc of the circumference of the outer pole ends is 94.5 mm.

Used components from leading manufacturers (Nord, SKF), which have high-performance characteristics. It is made using both ferrite and modern high-energy Nd-Fe-B neodymium magnets, which ensures the value of magnetic induction on the drum surface in the range of 50-500 mT. In the manufacture of used stainless shell 6 mm thick of steel 12X18H10T, which can significantly increase its service life and operation. Three standard drum diameters are manufactured: 900, 1200, 1500 mm with a working zone length from 1000 mm to 3000 m. The cost of operation depends on the frequency of use, load, and type of magnetic separator.

The available Nd-Fe-B magnets were 15x20x80 mm with a residual magnetic induction of ~ 300 mT. The magnetic susceptibility of the mixture χ_{cp} depends on the concentration of magnetite in the intergrowths and the magnetic field strength. In accordance with (Karmazin *et al.*, 1999), the magnetic susceptibility at each point of the separated space was calculated using the formula:

$$\chi_{cp} = k_2 H^2 + k_1 H + k_0, \quad (\text{Eq. 8})$$

where k_2 , k_1 , k_0 are the coefficients, depend on the concentration of magnetite in the intergrowths α_m , and N is the local magnetic field strength. These calculations do not take into account the dependence of the magnetic susceptibility on the particle size, which is characteristic of small particles as a manifestation of the transition of a multi-domain structure to a single domain (Yurov, 2009; Bonyadi and Sadeghi, 2020; Cournède *et al.*, 2020). The mathematical modeling of the magnetic separation process is reduced to a system (3) of particle motion equations, which was solved numerically by the fourth-order Runge-Kutta method. Initial data: initial position (values of R and φ) of the particle at the inlet of the separator, iron concentration in intergrowths α , magnetite density 5 g/cm³ and empty rock 2.8 g/cm³. The initial particle velocity is equal to the speed of the tape. Next, the trajectory of the particle during the separation time is traced. Of interest is the case when several Nd-Fe-B magnets are replaced by a weaker magnet, for example, ferrite or one magnet, in general, is removed and a "dip" of the magnetic field is formed in its place. Figure 2 shows the radial component of the magnetic force acting on the particle when one Nd-Fe-B magnet is removed from the system. Figure 3 shows the calculated trajectories of the intergrowths of magnetite particles with $\alpha = 57\%$ Fe in the separation field (Figure 2) with different belt speeds.

Of particular interest in this calculation is the fact that the particles located on the magnetic drum and passing over the area with the missing magnet are detached from the drum, and then, upon falling into the region where the magnetic force increases, again gravitate to the drum. All particles in this area are shaken. If a non-magnetic particle enters the drum during the separation process and is held on top of the drum by a magnetic particle from above, then shaking releases particles of waste rock. They subsequently return to the tape. Thus, the

magnetic fraction is cleaned of waste rock particles that accidentally hit the drum.

For the experimental study of the properties of this magnetic system, a laboratory magnetic separator (Figure 4) was built with the parameters defined above. The operating mode of the magnetic separator is determined by the frequency of rotation of the non-magnetic drum in a magnetic field or, equivalently, the speed of the tape. This parameter affects the magnitude of the centrifugal force acting on the ore particles. In this geometry of the separator, the angular velocity of rotation of the non-magnetic drum was 3.5 times slower than the speed of the engine. The maximum engine speed was 2800 rpm, which corresponds to 780 rpm of rotation of a non-magnetic drum or 9.5 m/s belt speed.

The possibility of using a new magnetic separator in the process of dry beneficiation of magnetite ore from the Bapy deposit was investigated. The industrial scheme being implemented consists of ore crushing and two-stage dressing on dry drum magnetic separators. An industrial product with a grain size of -10 mm with an average iron content of 52-54% is shipped at the outlet. The lowest concentration of Fe has a small class. Therefore, the improvement of the enrichment scheme is reduced to the isolation of a small product and its subsequent enrichment using a new magnetic separator.

For the industrial selection of a small class, the application of the air classification method is technically and economically promising. For this purpose, a pneumatic louver classifier with reverse air suction was manufactured (Ponomarev, 2015; Sun *et al.*, 2020; Gahrouei *et al.*, 2020). The fractional separation of the intermediate product of the initial size -10 mm in the air classifier is shown in Figure 5.

The yield of a finer product with a size of approximately minus 300 μm was $\sim 14\%$. The total iron content $\beta = 54\%$. Moreover, in the large class – $\beta = 55.6\%$ Fe, and in the isolated small product, the iron concentration is much lower, only $\beta = 44\%$ Fe. The aim of the experiment was to raise the iron content in the fine product to 56%. In this case, the total iron content in the intermediate product will increase by about 2% without additional grinding operations and high financial costs. In a magnetic separation experiment, a 1 kg sample was used. Table 2 shows the data of the magnetic separation of the selected small product at different speeds of the tape.

It is notable that increasing the speed of the tape from 4 m/s to 9.5 m/s increases the average

concentration of iron in the magnetic product from 53.4% at 58%. Unfortunately, the speed of 9.5 m/s was the maximum speed of the tape in this geometry and the configuration of the magnetic separator. The purification of product No. 1, carried out at the same speeds, slightly increased the iron content in the concentrate from 53.4% to 55%. A similar conclusion can be made about the product obtained at 9.5 m/s when there is a change from 58% to 59.3%. Thus, the speed of the tape determines a certain upper limit of beneficiation. It should be noted that the cleaning of product No. 2 at a higher speed of the tape leads to content of $\beta = 59\%$ Fe in the final product, and the same operation performed at a higher speed of the tape of the first separation gives a slight increase in the final product $\beta = 59.3\%$ Fe. But in the first instance, the recovery ϵ was 92%, and in the second, it decreased slightly to 90.9% with comparable iron content.

4. CONCLUSIONS:

Thus, according to the optimal beneficiation scheme, in order to achieve higher beneficiation rates, it is desirable to carry out the process in two stages. At the first stage, beneficiation is carried out at a belt speed of 4-5 m/s, and the subsequent cleaning of the magnetic product of the first stage is carried out at an increased speed of 9-10 m/s. But to achieve the goal of 56% Fe, it is enough to carry out beneficiation in one stage at a belt speed of 8.4 m/s.

The possibility of using a new magnetic separator model in the process of dry beneficiation of magnetite ore from the Bapy deposit was studied. The industrial scheme being implemented consists of ore crushing and two-stage dressing on dry drum magnetic separators. An industrial product with a grain size of -10 mm with an average iron content of 52-54% is shipped at the outlet. Finer classes have the lowest Fe content. Therefore, the improvement of the beneficiation scheme is reduced to the isolation of a small product and its subsequent beneficiation using a new model of magnetic separator. Thus, the presented magnetic separator is suitable for dry processing of crushed magnetite ore. Note that the higher speed of the tape increases the performance of the device.

5. ACKNOWLEDGMENTS:

The results of the article were procured in the course of implementation of the project

AR05134706 "Development of innovative technology for direct reduction of iron ore using solid fuels and construction of a laboratory-scale technological system for its complete redistribution from beneficiation to the production of metalized iron", performed within the framework of grant financing for 2018-2020 from the state budget of the Republic of Kazakhstan.

6. REFERENCES:

1. Bonyadi, Z., Sadeghi, R. *Journal of Asian Earth Sciences*, **2020**, 189, Article number 104152.
2. Chang, Q., Cheng, X. *Chinese Journal of Environmental Engineering*, **2019**, 13(9), 2152-2163.
3. Charikinya, E., Robertson, J., Platts, A., Becker, M., Lamberg, P., Bradshaw, D. *Minerals Engineering*, **2017**, 107, 53-62.
4. Chokin, K.Sh., Edilbaev, A.I., Edilbaev, B.A., Yugay, V.D. Eurasian patent No. 025638. *Device and method for magnetic separation*, **2017**.
<https://www.eapo.org/ru/publications/bulletin/ea201701/HTML/025638.html>, accessed December 2019.
5. Chokin, K.Sh., Edilbaev, A.I., Yugay, V.D. Eurasian patent No. 016328. *The method of magnetic separation and device for its implementation*, **2012**.
<https://www.eapo.org/rus/bulletin/ea201204/HTML/016328.html>, accessed December 2019.
6. Cournède, C., Gattacceca, J., Rochette, P., Shuster, D.L. *Earth and Planetary Science Letters*, **2020**, 533, Article number 116042.
7. D'Souza, R., Vats, T., Chattree, A., Siril, P.F. *Renewable Energy*, **2018**, 126, 1064-1073.
8. Duman, F., Sahin, U., Atabani, A.E. *Fuel*, **2019**, 256, Article number 115935. DOI: 10.1016/j.fuel.2019.115935
9. Edathil, A.A., Shittu, I., Hisham Zain, J., Banat, F., Haija, M.A. *Journal of Environmental Chemical Engineering*, **2018**, 6(2), 2390-2400.
10. Eliopoulos, D.G., Economou-Eliopoulos, M. *Minerals*, **2019**, 9(12), Article number 759.
11. Fan, R., Min, H., Hong, X., Yi, Q., Liu, W., Zhang, Q., Luo, Z. *Journal of Hazardous Materials*, **2019**, 364, 780-790.
12. Gahrouei, Z.E., Labbaf, S., Kermanpur, A. *Physica E: Low-Dimensional Systems and Nanostructures*, **2020**, 116, Article number 113759.
13. Karmazin, V.V., Bikbov, M.A., Bikbov, A.A. *Mountain News and Analysis Bulletin*, **1999**, 4, 9-12.
14. Karthaus, J., Elfgen, S., Leuning, N., & Hameyer, K. *International Journal of Applied Electromagnetics and Mechanics*, **2019**, 59(1), 255-261.
15. Kenzhaliev, B.K., Kvyatkovskii, S.A., Kozhakhmetov, S.M., Sokolovskaya, L.V., Kenzhaliev, É.B., Semenova, A.S. *Metallurgist*, **2019**, 63(7-8), 759-765.
16. Kovalenker, V.A., Plotinskaya, O.Y., Kiseleva, G.D., Minervina, E.A., Borisovskii, S.E., Zhilicheva, O.M., Yazykova, Y.I. *Geology of Ore Deposits*, **2019**, 61(6), 559-579.
17. Li, L., Liu, T., Liu, X. 2015. *Mining Engineering*, **2015**, 13(6), 23-26.
18. Li, Q.-L., Han, L.-N., Chang, L.-P., Bao, W.-R., & Wang, J.-C. *Modern Chemical Industry*, **2016a**, 36(9), 28-31.
19. Li, Z., Lun, Q., Wang, Q., Zhang, L. *Journal of Harbin Institute of Technology*, **2016b**, 48(3), 33-38.
20. Liang, Z., Yi, L., Huang, Z., Lu, B., Jiang, X., Cai, W., Tian, B., Jin, Y. *Powder Technology*, **2019**, 356, 691-701.
21. Liu, D.-F., Shi, X.-J., Tang, C.-J., Cao, H.-P., Li, J. *Journal of Iron and Steel Research International*, **2019**, 26(11), 1154-1161.
22. Lund, C., Lamberg, P., Lindberg, T. *Minerals Engineering*, **2015**, 82, 61-77.
23. Parian, M., Lamberg, P., Rosenkranz, J., *International Journal of Mineral Processing*, **2016**, 154, 53-65.
24. Ponomarev, V.B. *Calculation and design of equipment for air separation of bulk materials*, Yekaterinburg: Ural Federal University, **2015**.
25. Schlüter, H., Saboktakin, M. *Journal of Pharmacy and Nutrition Sciences*, **2016**, 6(4), 126-143.
26. Sedinkina, N.A., Pavelin, A.V., Khisametdinova, D.N., Mubaryakov, R.S. *Actual Problems of Modern Science, Technology and Education*, **2014**, 1, 39-42.
27. Shahrokhi, B., Pirdashti, M., Managhebi, M. *Iranian Journal of Science and Technology, Transaction A: Science*, **2019**, 43(6), 2807-

2813.

28. Sun, Y., Zhang, X., Han, Y., Li, Y. *Powder Technology*, **2020**, 361, 571-580.
29. Tang, Z., Gao, P., Li, Y., Han, Y., Li, W., Butt, S., Zhang, Y. *Powder Technology*, **2020**, 361, 591-599.
30. Thiagu, G., Dhanasekaran, R. *Journal of Theoretical and Applied Information Technology*, **2014**, 64(2), 386-392.
31. Tolmachev, S.T. *University News. Electromechanics*, **1974**, 10, 1071-1076.
32. Urick, D. United States Patent Application No. 20180093279. *Magnetic separator apparatus*, **2018**. <http://appft1.uspto.gov/netacgi/nph-Parser?Sect1=PTO2&Sect2=HITOFF&p=1&u=%2Fnetacgi%2FPTO%2Fsearch-bool.html&r=2&f=G&l=50&co1=AND&d=PG01&s1=%22dry+magnetic+separator%22&s2=air&OS=%22dry+magnetic+separator%22+AND+air&RS=%22dry+magnetic+separator%22+AND+air>, accessed December 2019.
33. Vorob'ev, V.A., Ivanov, E.N., Larionov, A.N., Ryazanov, M.A. Dry technologies of ore preparation as a tool for increasing extraction of valuable components. In *XXIX International Mineral Processing Congress (IMPC 2018)* (pp. 708-715), Moscow: IMPC, **2018**.
34. Yu, L., Zhang, S., Zhang, M., Chen, J. *Applied Surface Science*, **2017**, 425, 46-55.
35. Yu, X., Zhang, Z.-L., Zheng, S.-Y. *Biosensors and Bioelectronics*, **2015**, 66, 520-526.
36. Yurov, V.M. *Modern Problems of Science and Education*, **2009**, 4, 152-155.
37. Zhang, T., Yuan, Y., Cui, X., Yin, H., Gu, J., Huang, H., Shu, J. *Journal of Polymer Science, Part B: Polymer Physics*, **2018**, 56(9), 751-761.
38. Zhang, X., Han, Y., Sun, Y., Lv, Y., Li, Y., Tang, Z. *Mineral Processing and Extractive Metallurgy Review*, **2020**, 41(2), 117-129.
39. Zhao, H.L., Wang, X.M., Wei, H.G. *Nonferrous Metals (Mineral Processing Section)*, **2017a**, 10(9), 87-89.
40. Zhao, Y., Wang, X., Liu, L., Liang, W. *Acta Materiae Compositae Sinica*, **2017b**, 34(1), 121-128.

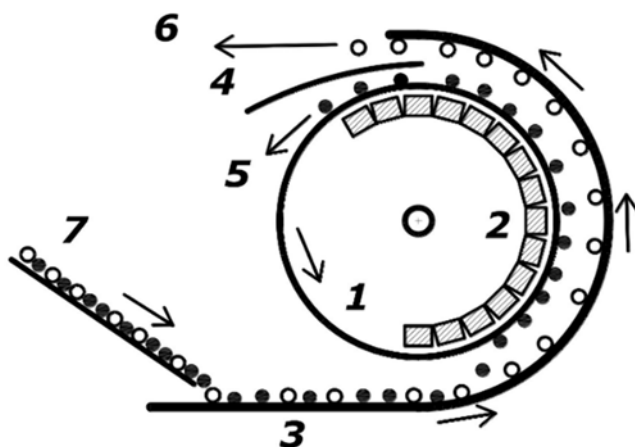


Figure 1. Magnetic separator circuit

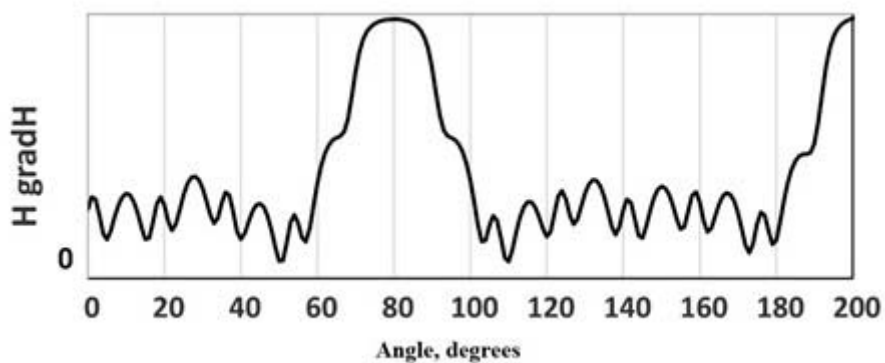


Figure 2. Radial component of magnetic force

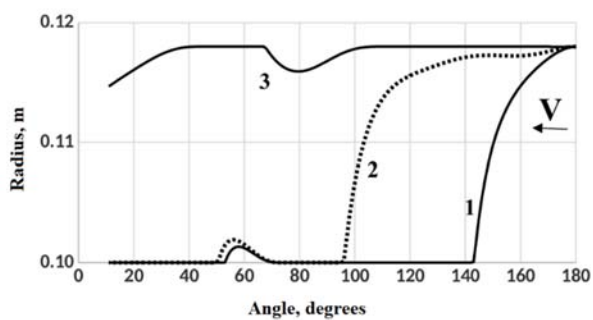


Figure 3. The trajectories of the growths of magnetite particle aggregates with $\alpha_M = 57\%$ Fe in the separator field with different belt speeds V : 1 – 8.5 m/s; 2 – 9.5 m/s; 3 – 10.5 m/s

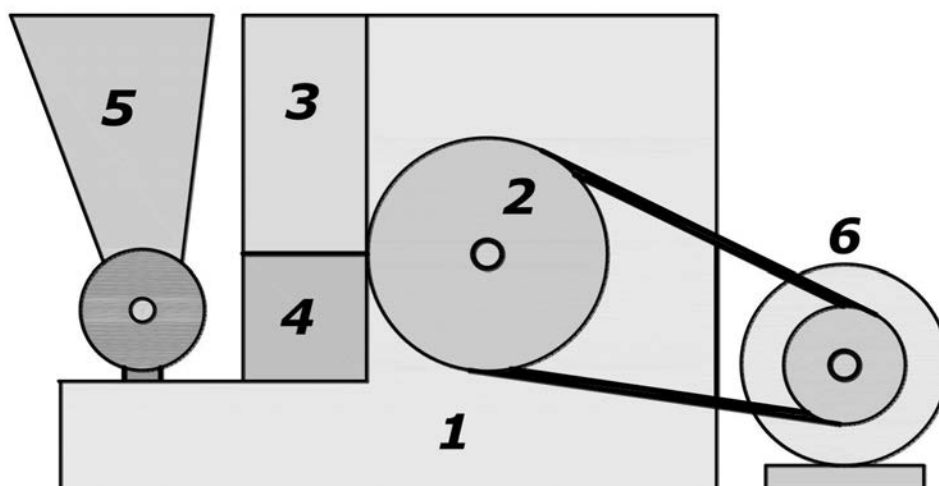


Figure 4. Laboratory magnetic separator: 1 - trunk, 2 - pulley, 3 - waste rock receiver, 4 - concentrate receiver, 5 - feeder, 6 - electric motor

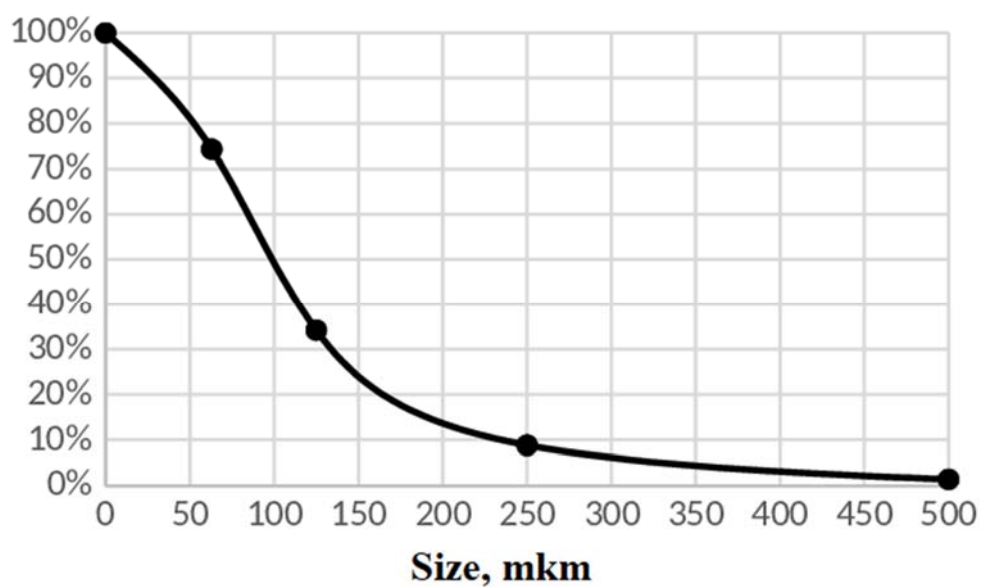


Figure 5. The degree of fractional extraction into a fine product during air classification

Table 1. Beneficiation figures

No.	$\alpha, \%$	The speed of the tape, m/s											
		3,8			5,7			7,6			9.5		
		$\gamma, \%$	$\beta, \%$	$\epsilon, \%$	$\gamma, \%$	$\beta, \%$	$\epsilon, \%$	$\gamma, \%$	$\beta, \%$	$\epsilon, \%$	$\gamma, \%$	$\beta, \%$	$\epsilon, \%$
1	50	86.1	57.1	98.3	81.0	59.3	96.1	74.6	61.2	91.3	70.5	61.3	86.4
2	50	83.0	57.8	95.9	78.9	59.4	93.8	72.4	61.3	88.8	70.4	61.3	86.3
3	40	69.9	55.5	96.9	62.4	58.6	91.4	59.6	60.8	90.7	-	-	-

Table 2. Magnetic separation results at various belt speeds

No.	Belt speed, m/s	β	ϵ
1	4	53.4%	94.5%
Recycling No. 1	4	55.0%	93.6%
2	4.8	54.0%	94.2%
Recycling No. 2	9.5	59.0%	92.0%
3	7.6	55.7%	93.4%
4	9.5	58.0%	92.2%
Recycling No. 4	9.5	59.3%	90.9%

**DESENVOLVIMENTO DE MATERIAIS DE ENSINO-APRENDIZAGEM DE FÍSICA
BASEADOS EM TECNOLOGIA CIENTÍFICA DE ENGENHARIA E MATEMÁTICA PARA
DESENVOLVER HABILIDADES DE APRENDIZAGEM DO SÉCULO XXI****DEVELOPMENT OF PHYSICS LEARNING TEACHING MATERIALS BASED ON SCIENCE
TECHNOLOGY ENGINEERING AND MATHEMATICS TO DEVELOP 21ST CENTURY
LEARNING SKILLS**YULIANTI, Dwi^{1*}; WIYANTO²; RUSILOWATI, Ani³; NUGROHO, Sunyoto Eko⁴;^{1,2,3,4} Universitas Negeri Semarang, Postgraduate Studies, Department of Natural Science Education. Indonesia.** Corresponding author
e-mail: yulifis04@yahoo.com*

Received 28 January 2020; received in revised form 10 March 2020; accepted 23 March 2020

RESUMO

O aprendizado baseado na tecnologia científica de engenharia e matemática (STEM) foi amplamente implementado no aprendizado para ajudar os alunos a entenderem o aprendizado no século XXI. O desenvolvimento de materiais de ensino é uma maneira de implementá-los, mas esses materiais de ensino devem estar de acordo com as competências do currículo de 2013 e aplicar os valores e conceitos contidos na aprendizagem no século XXI. Este estudo teve como objetivo descrever as características do material didático de aprendizagem de física baseado em STEM para desenvolver habilidades de aprendizado do século XXI e testar a legibilidade e a viabilidade. Esse estudo foi dividido em quatro etapas (estudos preliminares, planejamento, desenvolvimento e testes). O design do teste usa o *One Group* Pré-Teste e Pós-Teste. Os sujeitos dos ensaios em pequenos e grandes grupos foram estudantes do quinto semestre do Programa de Estudos em Educação Física *Universitas Negeri Semarang*. Os materiais de ensino apresentam dados sobre os antecedentes da importância das habilidades de aprendizagem STEM e do século XXI, material STEM e habilidades de aprendizado do século XXI, STEM e exemplos baseados no ensino de aprendizagem de física. Os resultados do teste de viabilidade, utilizando um questionário, mostraram que o material didático estava na categoria viável. Os resultados dos testes de legibilidade, usando um teste de *cloze* e um gráfico de *Raygor*, mostraram que o material didático estava incluído na categoria de fácil compreensão.

Palavras-chave: *STEM, materiais didáticos, legibilidade, viabilidade, materiais didáticos de aprendizagem.***ABSTRACT**

Learning based on Science Technology Engineering and Mathematics (STEM) has been widely implemented in learning to assist students in understanding learning in the 21st century. Developing teaching materials is one way to implement them, but these teaching materials must be in accordance with competencies in the 2013 curriculum and apply the values and concepts contained in learning in the 21st century. This study aimed to describe the characteristics of physics learning teaching material based on STEM to develop 21st Century Learning Skills and testing readability and feasibility. This study was divided into four stages (preliminary studies, planning, development, and testing). The trial design uses One Group Pretest-Posttest. The subjects of the small and large group trials were students of the fifth-semester Physics Education Study Program Universitas Negeri Semarang. The teaching materials showed data about the importance of STEM and 21st-century learning skills, STEM material, and 21st Century Learning Skills, and Physics Learning Teaching based STEM and examples. The results of the feasibility test using a questionnaire showed that the teaching material was in the category of feasible. Readability test results using a cloze test and Raygor graphic showed that the teaching material included in the easy to understand category.

Keywords: *STEM, teaching materials, readability, feasibility, learning teaching materials.*

1. INTRODUCTION:

The 21st-century learning and innovation skills, known as 4C skills, are soft skills that need to be developed in every individual. Kivunja (2015) states that 4C is a super skill which is the core skill because it can help students to develop and demonstrate a good understanding of career skills, information, media, and technology. The Ministry of Education and Culture of the Republic Indonesia has adopted the concept of 21st-century education, in developing the 2013 curriculum for Senior High Schools (SMA) and Madrasah Aliyah (MA), namely 21st Century Skills (Trilling and Fadel, 2009). The US-Based Partnership for 21st Century Skills (P21) and (Beers, 2011) identify the competencies required in the 21st century, namely Communication, Collaboration, Critical Thinking, and Creativity, which is abbreviated as "the 4C".

Lundeberg & Jacobson (2016) mentioned that communication as a gate of 21st-century skills. Communication skills become one of the important considerations in the world of education and work. Metusalem *et al.* (2017) states that the importance of communication skills for personal, academic, and professional success is recognized in the elements of current standards and educational practices. According to Hoon, Fadzlin, & Singh (2017), communication skills and class management can influence the success of class activities and student learning. Collaboration is expressed as a coordinated and synchronous activity that is the result of ongoing efforts to build and maintain a shared conception of an issue (Rosen, Ferrara, & Mosharraf, 2016). Collaboration is carried out to achieve common goals. Lai *et al.* (2017) revealed that collaboration and teamwork focus on the process of interacting and requiring individuals to work together towards shared goals. The role of collaboration in learning is stated by Ronfeldt, Farmer, McQueen, & Grissom (2015) that can provide benefits for students. Students will get better achievement if they study in a strong collaborative environment. Woodland & Hutton (2012) states that collaboration can produce greater innovation while conserving resources to achieve common goals.

Critical thinking has a role in the world of education, especially for students. The benefits in students according to Bassham, Irwin, Nardone, & Wallace (2010) that it can help them do better learning in class by increasing their ability to understand, build, and criticize an argument. Critical thinking skills in students influence their

learning outcomes. Siburian, Corebima, Ibrohim, & Saptasari (2019) stated that students' critical thinking skills need to be empowered in learning, so students get more optimal learning outcomes. Creative thinking skills are very necessary in life. Creative thinking is a high-level thinking ability (Kotzer & Elran, 2012). Creative thinking skills are needed for someone to be able to innovate. The benefits of creative thinking skills are also mentioned by Siburian *et al.* (2019) that it has tangible benefits for improving students' understanding of concepts, which can ultimately contribute to cognitive learning outcomes.

The development of 21st-century learning skills can be implemented through the Science Technology Engineering and Mathematics (STEM) approach (Bybee, 2010; Elliot *et al.*, 2001; Gülhan and Şahin, 2016; Kennedy and Odell, 2014; Morrison, 2006; Olivarez, 2012; Roberts, 2012; Sahin *et al.*, 2014; Yamak *et al.*, 2014). STEM is an acronym for Science, Technology, Engineering, and Mathematics, which was introduced by the National Science Foundation (NSF) in the 1990s (Bybee, 2013). STEM is an approach to education that aims to integrate the four disciplines of science (S), technology (T), engineering (E), and mathematics (M) (Ercan, Altan, Taştan, & Dağ, 2016). The STEM approach not only focuses on the interdisciplinary integration of S, T, E, and M, but also focuses on systematic thinking, openness to communication, ethical values, research, production, creativity, problems, intersection of knowledge and skills in science, technology, engineering, and mathematics (Çengel, Alkan, & Yildiz, 2019). The advantage of integrating STEM into all class-level curricula was mentioned by Meyrick (2011) that STEM provides students with the experience and knowledge to determine their future careers, understand the principles of engineering design for completing problem-based projects and deepen students' understanding of 21st-century skills.

This means that in the 2013 curriculum, the STEM approach can be applied specifically to physics learning in schools. The achievement of the learning and competency objectives expected by the 2013 curriculum requires model innovation, approaches, and learning strategies, this means that physics teachers are required to be able to design learning that can deliver students to achieve the expected competencies. In order for teacher candidates to teach physics using the STEM approach to develop 21st-century learning skills, teaching materials needed for learning STEM-based Physics are integrated into

21st-century learning skills. This study aimed to describe the characteristics of Physics Learning Teaching Material Based on Science Technology Engineering and Mathematics (STEM) to develop 21st Century Learning Skills, and testing readability and feasibility.

2. MATERIALS AND METHODS:

The research was conducted at the Department of Physics Education FMIPA Universitas Negeri Semarang. The research subjects were 150 of fifth-semester students who were taking Basic Courses and Learning Processes in Physics I. The subjects of this research were divided into four classes consisted of 35-40 students. The subjects were all classes or population studies and chosen because they will get material about Learning Teaching Methods. When taking research data, classes are held in parallel so that the time and conditions are the same. The research method used was research and development (R & D). The research procedure used is four stages, namely the preliminary study planning, development, and trial phases. The preliminary study phase analyses the Semester Learning Plan and observes the material on the teaching materials used in the lecture process. The planning stage compiles a draft of teaching materials to be developed. The development phase includes the process of preparing STEM-based physics learning teaching materials to develop 21st-century learning skills. The trial phase consisted of small and large scale trials, including readability, feasibility. The validation sheet is used to determine the feasibility of teaching materials using a Likert scale. The Cloze test is used to determine the readability of teaching materials, Raygor graphic, to determine the level of readability.

3. RESULTS AND DISCUSSION:

Learning materials Science Technology Engineering and Mathematics (STEM) integrated learning skills of the 21st century. STEM-based learning materials developed, consisting of five chapters, numbered 63 pages and is divided into three parts: introduction, content, and closing. The introduction consists of the title page, preface, table of contents, Graduates Learning Subjects, and Learning Objectives. The body consists of five chapters, cover consisting of a Bibliography, Glossary, and Index. Printed materials use A4 paper (29.7 cm × 21 cm) because it has a size that fits the needs of

learning. According to (Prastowo, 2015), paper size to print learning materials should be able to accommodate the needs of the learning that has been set. Typography writing materials using Times New Roman font size 12 pt. According to (Mudzakir, 2009), one of the components of the consummation of learning materials print is 12-14 pt font size for this type of Times New Roman or comparable to the type of the other. Learning materials, special titles, and subchapters, type, and size of letter customized to your needs.

Readability level measurement results using Raygor graphic indicates that the materials are appropriate for the level of the fifteen and above, which means according to the university level. As Gyasi (2013) states, readable text produces greater comprehension, retention, reading speed, and motivates readers. (Muslich, 2010) preparation of the textbook should pay attention to the linguistic elements related to the readability. In this formula the readability, sentence length and word difficulties identified as the main determinant of the readability of the text (Zamanian and Heydari, 2012). The readability of a text depends on how easy the text it is understood by the reader (Fry, 2002). There are a variety of methods and different approaches that can be used to assess the level of readability of reading materials. The most common approach in assessing the readability is the use of the formula. These formulas give educators the estimated difficulty of books and other texts. Most readability formulas are combining two components of semantic difficulty and the difficulty of the syntax (Freahat, 2014).

The appropriateness of materials from seven aspects, i.e. the content, the presentation of the material, component 4C, STEM skills, physics-based STEM learning components, completeness of presentation and language. The results of the analysis of the feasibility of the learning materials are presented in Table 1.

Based on the results of the analysis of the test of feasibility, materials-based STEM meets the eligibility standard print materials that are set by the Badan Standarasi Nasional Pendidikan (BSNP). Standard assessment defined (BSNP, 2014); the feasibility of the print materials can be assessed based on aspects of content, presentation, and linguistic. The achievement eligibility categories can also be caused by the process of the preparation of learning materials that have been adapted to the guidelines set forth by the Department of national education.

Aspects of the feasibility of the content

consist of elements of completeness, depth of content, the accuracy of the facts, and the concept of developmental science, fitness, and contextual. Materials physics-based STEM learning consistently presents material associated with the approach of the STEM and 21st-century learning skills. STEM-based learning, able to develop the ability to think creatively and improve the creativity of students (Lestari, 2018; Pertiwi, 2017).

Aspects of the presentation of the material consists of concept, systematics, user-centered, and coherence as well as motivation. The content in the materials presented in order from the general concept headed to more specialized concepts regarding the application of the approach STEM. In addition, the materials are presented with examples of illustration that comes in the form of images that support the learning material. According to (Cook 2008), illustration in the learning materials can help students absorb knowledge and understand concepts.

Aspects of component skills 4C consists of the urgency of skills and 4C aspect. This needs to be supplied to the candidates because of the role of teachers in the 21st century should be shifted from the patterned "planter of knowledge," leading to a role as mentors, directors discussion and measuring student learning progress (Hampson, 2011). (Luthvitasari, 2012) research shows that project-based learning can improve aspects of critical thinking skills, creative thinking, and generic skills of students. Research results (Duran and Sendag, 2012), learning associated with aspects of the STEM can develop critical thinking ability significantly. Critical thinking ability evolves because supported by the existence of the problem presented in the materials, including the questions and discussions. The problems are presented with customized aspects of STEM students and facilitate discussions to find a solution to any problem. Research results (DeJarnette, 2012), collaborating learning problems and aspects of the STEM can attract and train the ability of critical thinking.

Aspects of STEM components consist of the urgency approach STEM and elements in the STEM learning materials. This is important because its existence in learning materials suitably (Reeve, 2013), as an interdisciplinary approach on STEM learning, direct students to use science, technology, engineering, and mathematics in the context of a real-time to connect between school, work, world, and globalized world, so develop a STEM literacy

delivering learners able to compete in the knowledge-based era. STEM materialized in certain situations when learning science (including physics) involves activity the authentic problem-solving in the context of social, cultural, and functional (Roberts, 2012).

Aspects of physics-based STEM learning component, consisting of the physics-based STEM learning and examples of learning physics-based STEM. In the example presented episodes of learning materials to high school students who have tested the feasibility and readability. On the learning materials, students are invited to discuss, create projects, problem-solving. According to research (Yuliaty, 2011), several activities such as discussing and making projects can improve student learning outcomes. The result is also supported by the results of research (Roberts, 2012), which reveals a STEM-based learning can add to the learning experience through practice and apply the General principles of the material being studied, so growing creativity, curiosity and encourage cooperation among students. Moreover, Yildirim's research results (2016) approach to STEM has a positive impact on learning outcomes in school, students 'interests and motivation, critical thinking skills, problem-solving skills, students' attitudes toward learning, and also scientific process skills. In addition, learning using the STEM approach based on Sari, Alici, & Şen's (2017) research has proven to be effective in the learning process carried out and helps students to develop 21st-century skills, create a more pleasant classroom atmosphere, increase student interest in the engineering profession, and help students choose their future careers.

Aspect of completeness in presentation consists of the cover, table of contents, evaluation questions, bibliography, glossary, and index. The linguistic aspect consists of the appropriateness of the sentence structure, the term of the word, the meaning of wholeness, connecting between the chapter and the section later, correctness of grammar, spelling, and its terms. Materials are organized using a straightforward Indonesian Language, communicative, and pay close attention to the spelling rules of the Ejaan Bahasa Indonesia (EBI). It is in accordance with the terms of the advanced materials (Depdiknas, 2008); materials components include readability, clarity of information, as well as conformity with the Indonesian language rule, which is good and correct.

Based on the results of the analysis of the

test data readability, obtained an average score of 82.17% readability. According to the criteria of readability Rankin & Culhane, materials physics-based STEM learning included in easy to understand categories. According to (Lucy, 2014) readability resulting from the interaction between the various factors that make the text can be understood, while according to (Jatnika, 2007), the level of readability is influenced by two factors, namely: the language regarding word choice, waking up sentence, the order of the paragraphs and other grammatical elements, as well as factors relating to the form of the grammar of the letters or typography. In General, the structure of the sentences used in the learning materials in accordance with the rules of Indonesian Language and the ability of students.

According to (Suryadi, 2007) that in general, causal factors in the level of readability in learning materials consists of word choice, sentence, the order of the paragraphs, and other grammatical elements, as well as the form of the letter such as grammar is concerned the size of letters, the density of the lines, the width of the pias, and other visual layout elements. According to (Graves and Graves, 2003), factors that affect the readability of the text including the complexities of vocabulary; sentence structures and texts; text length and elaboration; coherence and unity; knowledge of the content and a required background; the suitability of the audience; the quality and passion of writing; and interest.

4. CONCLUSIONS:

The characteristics of teaching materials, containing material about the background of the importance of STEM and 21st-century learning skills, STEM material and 21st Century Learning Skills, STEM-based Physics learning teaching and examples. The results of the feasibility test using a questionnaire show that the teaching material is in the category of proper use. Readability test results using a ride test and Raygor graph show the teaching material included in the easy to understand category. Physics learning materials based STEM to develop 21st-century learning skills can be used by students (university level). Besides, learning materials developed viable to use and easy to understand.

5. REFERENCES:

1. Basham, J.D., Israel, M., and Maynard, K.

- Journal of Special Education Technology*, **2010**, 25(3): 9 – 19.
2. Beers, S. *21st Century Skills: Preparing Students for Their Future*. **2011**.
3. BSNP. *Instrumen Penilaian Buku Teks Pelajaran Tahun 2014*, Badan Standar Nasional Pendidikan: Jakarta, **2014**.
4. Bybee, R.W. *Tech. Eng. Teacher*. **2010**, 70, 30-5.
5. Çengel, M., Alkan, A., and Yildiz, E.P. *International Journal of Higher Education*, **2019**, 8(3): 257-267.
6. Cook, M. *Electronic J. Sci. Educ.* **2008**, 12(1), 39-54.
7. DeJarnette, N. *Educ.* **2012**, 133(1), 77-84.
8. Depdiknas. *Panduan Pengembangan Bahan Ajar*, Depdiknas: Jakarta, **2014**.
9. Duran, M. and S, Sendag. *Creative Educ.* **2012**, 3(2), 241-50.
10. Elliott, B., Oty, K., McArthur, J., and Clark, B., *Int. J. Math. Edu. Sci. Tech.*, **2001**, 32(6), 811-816.
11. Ercan, S., Altan, E.B., Taştan, B., and Dağ, I. *Journal of Turkish Science Education*, **2016**, 13: 30-43.
12. Freahat, N.M. *Theory Prac. Lang. Studies*, **2014**, 4(10), 2042-2050.
13. Fry, E. *Reading Teacher*, **2002**, 56(3), 286-291.
14. Graves, M.F. and Graves, B.B. *Scaffolding Reading Experiences: Designs for Student Success*. Norwood, MA: Christopher-Gordon, **2003**.
15. Gülhan, F. and Şahin, F. *Int. J. Hum. Sci.*, **2016**, 13(1), 602-620.
16. Gyasi, W.K., *J. Research and Method in Edu*, **2013**, 2(1): 09-19.
17. Hampson, M., Patton, A., and Shanks, L. *Ten Ideas for 21st Century Education*, Innovation Unit: London, **2011**.
18. Hoon, T.S., Fadzlin, N., Singh, P. *Asian Journal of University Education*, **2017**, 13 (1): 67-78.
19. Jatnika, A.W. *J. Sosioteknologi*, **2007**, 10(6), 192-200.
20. Kennedy, T.J. and M.R.L. Odell. *Sci. Edu. Int.*, **2014**, 25(3), 246-258.
21. Kivunja, C. *Exploring the Pedagogical*

- Meaning and Implications of the 4Cs "Super Skills" for the 21st Century through Bruner's 5E Lenses of Knowledge Construction to Improve Pedagogies of the New Learning Paradigm, 2015.*
22. Kotzer, S., and Elran, Y. Learning and teaching with Moodle-based E-learning environments, combining learning skills and content in the fields of Math and Science & Technology. 1st Moodle Research Conference, **2012**.
 23. Lai, E., DiCerbo, K., and Foltz, P. Skill for Today: What We Know About Teaching and Assessing Collaboration. Pearson: London, **2017**.
 24. Lestari, T.P., Sarwi and Sumarti, S.S. *J. Primary Educ.*, **2018**, 7(1), 18-24.
 25. Lucy, S. *South African J. Childhood Educ.* **2014**, 4(2), 154-175.
 26. Lundeborg, and Jacobson, V. *Educational Leadership and Administration: Teaching and Program Development*, **2016**, 27, 82-100.
 27. Luthvitasari, N., N, Made D.P., and Linuwih, S. *J. Innov. Sci. Educ.*, **2012**, 1(2), 92-97.
 28. Metusalem, R., Belenky, D.M., and DiCerbo, K. *What We Know About Teaching and Assessing Communication*. Pearson: London, **2017**.
 29. Meyrick, K.M. *Meridian K-12 School Computer Technologies Journal*, **2011**, 14 (11).
 30. Morrison, J. *TIES STEM Education Monograph Series: Attributes of STEM Education*, MD TIES: Baltimore, **2006**.
 31. Mudzakir, A.S. *J. Bahasa dan Sastra*, **2009**, 9(1), 34-46.
 32. Muslich, M. *Text Book Writing: Dasar-Dasar Pemahaman, Penulisan, dan Pemakaian Buku Teks*, Ar-Ruzz Media: Yogyakarta, **2010**.
 33. Olivarez, N., *Doctoral Dissertation*, Texas A & M University, Texas, **2012**.
 34. Pertiwi, R.S., Abdurrahman and Rosidin, U. *J. Pemb. Fisika*, **2017**, 5(2), 11-19.
 35. Prastowo, A. *Panduan Kreatif Membuat Bahan Ajar Inovatif*, Diva Press: Yogyakarta, **2015**.
 36. Reeve, E.M. *Implementing Science, Technology, Mathematic and Engineering (STEM) Education in Thailand and in ASEAN*, Institute for the Promotion of Teaching Science and Technology: Bangkok, **2013**.
 37. Roberts, A. *Tech. Eng. Teacher*, **2012**, 71(8), 1-5.
 38. Ronfeldt, M., Farmer, S.O., McQueen, K., and Grissom, J.A. *American Educational Research Journal*, **2015**, 52 (3): 47 – 514.
 39. Rosen, Y., Ferrara, S., and Mosharraf, M. *Handbook of Research on Technology Tools for Real World Skill Development*. IGI Global: Hershey PA (USA), **2016**.
 40. Sahin, A., Ayar, M.C. and Adiguzel, T. *Educ. Sci. Theory Prac.*, **2014**, 14(1), 309-322.
 41. Sari, U., Alici, M., and Şen, Ö.F. *Electronic Journal of Science Education*, **2017**, 22(1): 1-20.
 42. Sen, C., Ay, Z.S., Kiray, S.A. *Research Highlights in STEM Education*, **2018**, 81-100.
 43. Siburian, J., Corebima, A.D., Ibrohim, and Saptasari, M. *Eurasian J. Educ. Res.*, **2019**, 81: 99-114.
 44. Suryadi, A. *J. Sosiologi*, **2007**, 6(10), 196-200.
 45. Trilling, B., and Fadel, C. *21st Century Skills: Learning for Life in Our Times*, Jossey-Bass: San Fransisco, **2009**.
 46. Woodland, R.H., and Hutton, M.S. *American J. Evaluation*, **2012**, 33(3): 366-383.
 47. Yamak, H., Bulut, N., and Dundar, S.J. *Gazi Educ. Fac.*, **2014**, 34(2), 249-265.
 48. Yildirim, B. *J. Edu. and Practice*, **2016**, 7(34): 23-33
 49. Yulianti, D.I., Yulianti, D., and Khanafiyah, S. *J. Pend. Fisika Indonesia*, **2011**, 7, 23-27.
 50. Zamanian, M., and Heydari, P. *Theory Prac. Lang. Studies*, **2012**, 2(1), 43-53.

Table 1. *The analysis result of the feasibility of learning materials*

No	Aspect	Results	Criteria
1	Contents	84.80%	Feasible
2	Presentation of material	85.12%	Very feasible
3	4C component skill	83.30%	Feasible
4	STEM component	84.30%	Feasible
5	Physics-based STEM Learning	85.62%	Very feasible
6	Completeness of Presentation	85.67%	Very feasible
7	Language	82.43%	Feasible
	Average	84.40%	Feasible

VARIABILIDADE ESPACIAL DE PROPRIEDADES FÍSICAS E MECÂNICAS DE MASSA ROCHOSA NO CAZAQUISTÃO CENTRAL**SPATIAL VARIABILITY OF PHYSICAL AND MECHANICAL PROPERTIES OF ROCK MASS IN CENTRAL KAZAKHSTAN****ПРОСТРАНСТВЕННАЯ ИЗМЕНЧИВОСТЬ ФИЗИКО-МЕХАНИЧЕСКИХ СВОЙСТВ МАССИВА ГОРНЫХ ПОРОД В ЦЕНТРАЛЬНОМ КАЗАХСТАНЕ**

ABETOV, Auez E.^{1*}; UZBEKOV, Abylay N.²; GRIB, Nicolay N.³; MELNIKOV, Andrey E.⁴; MALININ, Yury A.⁵;

^{1,2} Satbayev University, Department of Geophysics, 22-a Satpaev Str., zip code 050013, Almaty – Republic of Kazakhstan

^{3,4,5} Nerungri Technical Institute (branch) of North-Eastern Federal University, Department of Geophysics, 16 Kravchenko Str., zip code 678960, Neryungri – Russian Federation

* Correspondence author

e-mail: a.uzbekov@stud.satbayev.university

Received 20 December 2019; received in revised form 01 March 2020; accepted 22 March 2020

RESUMO

A eficiência e a qualidade das operações de perfuração e detonação no desenvolvimento de depósitos minerais dependem amplamente da variabilidade das propriedades da massa rochosa. Graças a um estudo detalhado de vários objetos geológicos – depósitos minerais ou elementos estruturais da crosta terrestre de qualquer ordem, até uma camada ou bloco, é possível criar os modelos digitais tridimensionais. O artigo considera a possibilidade de variabilidade espacial das propriedades da massa rochosa no Cazaquistão Central utilizando a modelagem matemática com uso de dados do arquivo de controle de processo de perfuração do sistema Aquila da unidade de perfuração DH-M. Para avaliar a estrutura e condição do maciço, foi construído um modelo digital de uma seção bidimensional, que mostra a variabilidade espacial das propriedades físicas e mecânicas. A aproximação pseudo-linear entre os vetores dos arquivos foi selecionada como um método para construir seções bidimensionais. O artigo mostra a aplicação do método matemático de interpolação pseudo-linear, que permite avaliar com um grau suficiente de confiabilidade as propriedades físicas e mecânicas (PFM) das rochas no espaço entre poços e entre linhas da massa rochosa. Com base nos resultados do estudo, foi desenvolvido um software que fornece uma avaliação rápida e eficaz das propriedades físicas e mecânicas da massa rochosa, com visualização do resultado. A abordagem e o software desenvolvidos podem ser usados para aumentar a eficiência das operações de perfuração e detonação pelas empresas de mineração existentes, bem como na implementação de estudos científicos e industriais sobre modelagem matemática do estado da massa rochosa.

Palavras-chave: *previsão de variabilidade espacial, propriedades físicas e mecânicas de rochas, modelo geológico tridimensional digital, processo de perfuração, software.*

ABSTRACT

The efficiency and quality of drilling and blasting operations in the development of mineral deposits largely depend on the variability of the properties of the rock mass. With a detailed study of various geological objects—mineral deposits or structural elements of the earth's crust of any order, up to a single layer or block, it is possible to create three-dimensional digital models. The article considers the possibility of spatial variability of rock mass properties in Central Kazakhstan by means of mathematical modeling using data from the drilling process control file of the Aquila system of a DH-M drilling rig. To assess the structure and condition of the rock mass, it was constructed two-dimensional sections digital model, which shows the spatial variability of physical and mechanical properties. A pseudolinear approximation between the file vectors is chosen as a method for constructing two-dimensional sections. The application of the mathematical method of pseudo-linear interpolation is shown, which allows with a sufficient degree of reliability to evaluate the physical and mechanical properties (PMP) of the rocks in the inter-well and inter-interval space of the rock mass. Based on the results of the study, the software was

developed that provides an operational and effective assessment of the physical and mechanical properties of the rock mass with the visualization of the result. The developed approach and software can be used to improve the efficiency of drilling and blasting operations of existing mining enterprises, as well as in the implementation of scientific and industrial research on mathematical modeling of state of the rock mass.

Keywords: *prediction of spatial variability, physical and mechanical properties of rocks, digital three-dimensional geological model, drilling process, software.*

АННОТАЦИЯ

Эффективность и качество буровзрывных работ при разработке месторождений полезных ископаемых во многом зависят от изменчивости свойств горного массива. Благодаря детальному изучению различных геологических объектов – месторождений полезных ископаемых или структурных элементов земной коры любого порядка, вплоть до одного слоя или блока, можно создавать трехмерные цифровые модели. В статье рассматривается возможность пространственной изменчивости свойств горного массива в Центральном Казахстане с помощью математического моделирования с использованием данных из файла управления процессом бурения системы Aquila буровой установки ДН-М. Чтобы оценить структуру и состояние горного массива, была построена цифровая модель двумерной секция, которая показывает пространственную изменчивость физико-механических свойств. Псевдолинейное приближение между векторами файлов выбрано в качестве метода построения двумерных сечений. Показано применение математического метода псевдолинейной интерполяции, который позволяет с достаточной степенью достоверности оценивать физико-механические свойства (ФМП) горных пород в межскважинном и междурядном пространстве массива горных пород. На основе результатов исследования было разработано программное обеспечение, которое обеспечивает оперативную и эффективную оценку физико-механических свойств горного массива с визуализацией результата. Разработанный подход и программное обеспечение могут быть использованы для повышения эффективности буровзрывных работ действующих горных предприятий, а также при осуществлении научных и промышленных исследований по математическому моделированию состояния массива горных пород.

Ключевые слова: *прогноз пространственной изменчивости, физико-механические свойства горных пород, цифровая трехмерная геологическая модель, процесс бурения, программное обеспечение.*

1. INTRODUCTION

The efficiency and quality of drilling and blasting operations in the development of mineral deposits largely depend on the variability of the properties of the rock mass (Liu *et al.*, 2017; Chicco *et al.*, 2019). Since the study of natural and technogenic variability of the rock mass is carried out mainly by a selective method, using a network of natural and artificial outcrops, the set of initial data is limited and has a random nature (Chen *et al.*, 2017; Jiang *et al.*, 2017; Uyanik *et al.*, 2019). The limited experimental data and discreteness of observation networks lead to the need to create generalized models (Zhang *et al.*, 2018; Menegoni *et al.*, 2019; Xu *et al.*, 2019). The peculiarity of modeling of mining and geological structures that are modeled, but representations about them or variability of properties observed at the studied level of the object structure. The complexity of the spatial variability of physical and mechanical properties and limitations of empirical data prevent the direct application of deterministic models (Qiu *et al.*, 2019; He *et al.*, 2019). The manifestation of

random variability of the studied properties testifies not to the absence of geological regularities, but only the lack of knowledge at this stage of the study of the subsoil (Grib, 1999; Mordensky *et al.*, 2018; Baldík *et al.*, 2018).

With a detailed study of various geological objects-mineral deposits or structural elements of the earth's crust of any order, up to a single layer or block, it is possible to create three-dimensional digital models (Zhang *et al.*, 2019; Zhang and Shen, 2019; Wu *et al.*, 2019). Their development significantly facilitates the research process by visualizing the structure of the contact surfaces of individual layers and sections in any planes, and adjusting the model as new mining and geological information is obtained (Alekseev *et al.*, 2003; Grib, 2013; Grib and Kuznetsov, 2018; Kovaleva *et al.*, 2018).

In the general case, the creation of the model is carried out in the following sequence: models of the relief of the earth's surface of the blasting block and the network of wells are formed, then the places of their intersection of geological

boundaries and heterogeneities are attached to the wellbores. Interpolation predicts the configuration of boundaries in the inter-well space within the block, which is a connected area. At the final stage of development, it becomes possible to create two-dimensional cross-sections of the variability of physical and mechanical properties with depth and strike, in this case, on the basis of the vectors of the “drilling process control files” F of the “Aquila” system of the DM-H drilling rig obtained by drilling blast holes, further files (Martynov, 2011).

2. MATERIALS AND METHODS

Modern computer technologies allow visualizing the values of physical and mechanical properties corresponding to each point of a two-dimensional section of a geological body. For this reason, to assess the structure and condition of the rock mass, it was sufficient to construct not a complete three-dimensional digital model, but its approximation by two-dimensional sections, which show the spatial variability of physical and mechanical properties: the velocity of elastic waves (V_p), the pressure strength (σ_p), the tension strength (σ_t), the volume density (ρ).

A pseudolinear approximation between the file vectors is chosen as a method for constructing two-dimensional sections: let Y_1 and Y_2 be the observed values at points X_1 and X_2 , and the authors want to estimate the values of Y' at point X' . Considering the dependence in the intermediate points linear, the calculations are carried out according to Equation 1 (Korobeynikov, 2009; Martynov, 2011; Kuznetsov *et al.*, 2018).

It is assumed that the difference of values in two adjacent points is a linear function of the distance between them. The method gives satisfactory results when the number of evenly spaced points and observation points is approximately equal. If the source data is irregular and intermediate values have to estimate for each pair of observations, then linear interpolation is justified. In previous studies (Alekseev *et al.*, 2003), linear interpolation was used to construct models of homogeneous blocks.

Analyzing the experimental results (Alekseev *et al.*, 2003) establishing links and dependencies between the physical and mechanical properties of the drilled rocks and the values of the “drilling process control file” F, which were performed for overburden rocks of the Centralny Kazakhstansky, Slavgorodsky, Kenterlausky sections at the experimental site,

where 15 wells were drilled at a distance of 1 m from each other, and wells 1, 3, 5, 7, 9, 11, 13 and 15 were drilled by the DM-H drilling rig using the Aquila system, and wells 2, 4, 6, 8, 10, 12, 14 were drilled by the exploration drilling machine with full core selection throughout the trunk wells. The study of physical and mechanical properties of core samples from wells 12-14 was carried out in the petrophysical laboratory. According to the test results, the following parameters of physical and mechanical properties were obtained:

- the velocity of propagation of elastic longitudinal waves in rock V_p , km/sec;
- compressive strength of rocks on compression σ_p and tension σ_t MPa;
- volume density of rocks, δ_o g/cm³;
- porosity coefficient, %;
- humidity, %.

Next, a regression analysis was performed between the data of the “drilling process control file” F, and the experimentally obtained values of physical and mechanical properties (Alekseev *et al.*, 2003).

The established correlations are described by the regression equation of the form (Equation 2).

The correlation coefficient between the parameters of the file vectors varies within $0.5 < R < 0.95$, the coefficient of variation $S/X \leq 0.2$ – with confidence not lower than 95%. Where: S is the mean square deviation, X is the mean. This was the basis to consider the exploding block as a connected geological body, and to build its model in the form of a smooth manifold of dimension ≥ 3 . The spread of the parameters of the file vectors is explained by the natural heterogeneity and technogenic fracturing of rocks. The regression of the species is constructed (Equation 3).

Where: X-the average values of the studied parameters calculated for all analyzed wells, and Y-the variance estimate of the average values of the studied parameters; parameters: $A = -0.1941769$, $B = 3.225438 \cdot 10^{-2}$. The correlation coefficient for this regression is $R = 0.9014131$, which according to the theory of A.B. Vistelius (1980), means that the entire exploding block was formed as a result of one process and that the block is of one petrographic composition.

Processing, interpretation, modeling of the structure, composition, and state of the rock mass are based on the assumption that the three-dimensional geological space can be successfully

approximated by a system of two-dimensional layers (Matheron, 2009; Demyanov, 2010). In work (Alekseev *et al.*, 2003), the method of approximation of three-dimensional distributions of parameters of physical and mechanical properties by means of two-dimensional sections is offered. Not random variability allows estimating the character of anisotropy of properties of a massif of rocks and consistency of its structure in various directions. Its characteristic serves as the basis for the choice of distances between wells and the design of the charge mass. Random variability has a direct impact only on the statistical evaluation of the average characteristics of physical and mechanical properties, the anisotropy of which is manifested in the difference of non-random variability of the studied parameter in different directions. A measure of the anisotropy I is the ratio of the average number n of heterogeneity elements intersected by lines drawn in a given direction to the lengths of these lines l within the studied block (Equation 4).

Thus, the ideas about the anisotropy of the properties and structure of the rock mass depend on their natural properties and on the location of the wells of the drilled network. As a tool for constructing two-dimensional sections, it was used the Delphi programming environment and the package of functions of the OpenGL open graphic library (Flenov, 2011; Ginsburg and Purnomo, 2015), the capabilities of which allow us to obtain reliable and visual pictures of sections. The developed application program allows to quickly build two-dimensional sections and maps of arbitrary orientation to determine the most informative types of sections and maps. In addition, the current version of the program allows to visualize cracks in blocks (provided that the angle of incidence of the crack is not very large (Equation 5), where h is the distance between the horizontal lines, l is the distance between the wells).

3. RESULTS AND DISCUSSION:

The program of an automated geological modeling system divided into three blocks: input-output, matrix transformation, and forecasting geological boundaries. The input-output unit writes to the matrix information file about one section on the same network: a series of wells, output of this information, and construction of sections of iso-areas. At the same time, control is carried out on the minimum and maximum permissible values to eliminate typical errors. In the construction of contours, interpolation is applied using the method of rectangles and trapeziums. Variation in scale,

additional smoothing of the boundaries of iso-areas, their display in different colors are provided. In the absence of information in certain parts of the numerical model on the map of iso-areas, these areas are marked in white.

When visualizing strength sections, the interpolation points are evenly spaced at a specified interval. At these points, the values of physical and mechanical properties are determined by interpolation and used as initial points within a square with a side equal to the step of the network model. The data conversion unit is developed on the basis of the established correlations of physical and mechanical properties of rocks with the data of the file F. Regression equations are obtained for four parameters: σ_P , σ_T , V_p , δ_0 (Equations 6-9).

Where F_n -values was taken from the drilling control file of the machine "Aquila" (Vistelius, 1980; Korobeynikov, 2009). The program provides data input from a file and from the keyboard. The data is presented in the form of Table 1, in which the first column is the parameter F_n (entered by the user), the columns (σ_P , σ_T , V_p , δ_0) are calculated according to the above formulas.

In practice, three methods are used to describe maps of isolines: coordinates of vertices of polygons approximating the isolines; coordinates of characteristic points of the surface; numerical matrices, the elements of which are the depths or altitudes of the described surface in the nodes of a rectangular network. Based on the data obtained from the "drilling process control file" of the Aquila system, we adopted the third method-the description of the contour maps in the nodes of the rectangular network. At the same time, the maximum angle of bodies described by contact surfaces cannot exceed (Equation 10), where ΔH is the depth difference at neighboring points, ΔL is the horizontal step of the network.

It should be emphasized that the contact surfaces can be described large relative to the applied network of the body, as with a small number of points that fall into the contour, the approximation may be unacceptably rough. The density of the network should ensure satisfactory accuracy of determining the contact surface at any point of the site by linear interpolation of the matrix elements corresponding to the nodes of the cell within which the defined point is located (Matheron, 2009; Demyanov, 2010; Martynov, 2011; Moiseev, 2011). When interpolating, the following technique will be applied. It is natural to assume that in the center of the cell, the value is equal to the average of the values specified in the

nodes (Matheron, 2009; Demyanov, 2010; Martynov, 2011; Moiseev, 2011). Based on this in the center of the cell (Figure 1), set a point with a value equal to the average value. Now it is possible to form four triangles in a cell, and within each of them, it is possible to determine the values by drawing planes through the known values at the vertices of the triangle.

Let's introduce notation (Equation 11). Then it is easy to get expressions to calculate the values within the first – fourth triangle, respectively (Equations 12-15).

Similar results can be obtained by linear interpolation in two mutually perpendicular directions. The resulting surface will not be a plane, so the interpolation is called pseudolinear (Matheron, 2009; Demyanov, 2010; Martynov, 2011; Moiseev, 2011). Experience shows that depending on the complexity of the relief of contact surfaces, the density of the network should be sufficiently detailed (Alekseev *et al.*, 2003; Kutuzov, 2011; Fokin, 2015). Therefore, to display two-dimensional vertical sections along the rows of wells, a uniform network with a step of $Y = 8\text{ m}$ and a step of $X = 0.5\text{ m}$ is used, condensed to a uniform network with steps of 0.05 m and 0.1 m along the x and Y axes, respectively. This thickening of the network avoids complex and time-consuming calculations of the passage of isolines and proceed to the direct display of the values of the resulting matrix pixel by pixel, using the capabilities of OpenGL (Figure 2).

4. CONCLUSIONS:

To represent a three-dimensional image of the results of calculations of the interpolation of physical and mechanical properties of rocks, a cube is used, the faces of which are two-dimensional sections along the rows of the block under study. Each pair of opposite faces contains the same number of displayed wells. A separate image is constructed for each pair of wells. After building images of all pairs of wells displayed in the volumetric figure, the resulting textures are superimposed on the faces of the cube in accordance with the spatial position. After displaying the image on the screen, the user can rotate the cube with the cursor keys, studying in detail the images of each pair or three faces, which allows to more clearly represent the spatial variability of physical and mechanical properties in the block under study.

Thus, using the data file management system drilling Aquila drilling machine DH-M, their correlation with the strength and elastic

characteristics of rocks, pseudobinary mathematical method of interpolation and the proposed software may reliably predict physical and mechanical properties of rocks in the interwell space that is prepared for the explosion of the unit, to determine the optimal conditions for blasting.

5. REFERENCES:

1. Alekseev, G.F., Grib, N.N., Samokhin, D.A. *Management of a Complex of Drilling and Blasting Operations in Difficult Mining and Geological Conditions of the South Yakutsk Basin*. Yakutsk: YF GU Publishing House of the SB RAS, **2003**.
2. Baldík, V., Krumlová, H., Buriánek, D., Kryštofová, E., Janderková, J., Sedláček, J., Novotný, R., Dostalík, M. *Geological Research in Moravia and Silesia*, **2018**, 25(2), 108-112.
3. Chen, J., Li, X., Zhu, H., Rubin, Y. *Engineering Geology*, **2017**, 228, 214-223.
4. Chicco, J.M., Vacha, D., Mandrone, G. *Remote Sensing*, **2019**, 11(2), article number 179.
5. Demyanov, V.V. *Geostatistics: Theory and Practice*. Moscow: Nauka, **2010**.
6. Flenov, M.E. *Bible Delphi*. Saint Petersburg: BHV-Petersburg, **2011**.
7. Fokin, V.A. *Methodological Aspects of the Analysis of Technological Information in the Production of Drilling and Blasting Operations in Quarries*. Apatity: Kola scientific center of RAS, **2015**.
8. Ginsburg, D., Purnomo, B. *OpenGL ES 3.0. Developer's Guide*. Moscow: DMK Press, **2015**.
9. Grib, N.N. *Development of Methods for Predicting Technological Characteristics of Coal, Lithological Composition and Physical and Mechanical Properties of Carbon-Containing Rocks of the South Yakut Basin According to Geophysical Data*. Neryungri: Yakut State University, **1999**.
10. Grib, N.N. *Fundamental Research*, **2013**, 6-2, 397-401.
11. Grib, N.N., Kuznetsov, P.Yu. *Coal*, **2018**, 1-2018, 68-74. DOI: 10.18796/0041-5790-2018-1-68-73
12. He, M., Li, N., Zhang, Z., Yao, X., Chen, Y., Zhu, C. *International Journal of Rock Mechanics and Mining Sciences*, **2019**, 116,

64-74.

13. Jiang, H., Mo, Z., Hou, X., Wang, H. *Sains Malaysiana*, **2017**, 46(11), 2215-2221.
14. Korobeynikov, A.F. *Theoretical Bases of Modeling of Mineral Deposits*. Tomsk: TPU Publishing house, **2009**.
15. Kovaleva, T., Drobinina, E., Koriakina, A. *International Multidisciplinary Scientific GeoConference Surveying Geology and Mining Ecology Management, SGEM*, **2018**, 18(1.2), 27-34.
16. Kutuzov, B.N. *Methods of Blasting. Part 2. Blasting in Mining and Industry*. Moscow: Gornaya kniga: MSU Publishing House, **2011**.
17. Kuznetsov, N., Fedotova, I., Pak, A. *Geomechanics and Geodynamics of Rock Masses*, **2018**, 1, 653-658.
18. Liu, Q., Lei, G., Lu, C., Peng, X., Zhang, J., Wang, J. *Yanshilixue Yu Gongcheng Xuebao/Chinese Journal of Rock Mechanics and Engineering*, **2017**, 36, 3140-3147.
19. Martynov, E.V. *Mathematical Methods of Modeling Parameters of Geological Processes and Phenomena*. Murmansk: MGTU Publishing house, **2011**.
20. Matheron, J. *Fundamentals of Applied Geostatistics*. Izhevsk: Institute of computer technologies, **2009**.
21. Menegoni, N., Giordan, D., Perotti, C., Tannant, D.D. *Engineering Geology*, **2019**, 252, 145-163.
22. Moiseev, N.N. *Mathematical Problems of System Analysis*. Moscow: URSS, **2011**.
23. Mordensky, S.P., Villeneuve, M.C., Farquharson, J.I., Kennedy, B.M., Heap, M.J., Gravley, D.M. *Journal of Volcanology and Geothermal Research*, **2018**, 367, 46-62.
24. Qiu, P., Li, X., Ning, J., Wang, J., Yang, S. *Energies*, **2019**, 12(22), article number 4282.
25. Uyanık, O., Sabbağ, N., Uyanık, N.A., Öncü, Z. *Bulletin of Engineering Geology and the Environment*, **2019**, 78(8), 6003-6016.
26. Vistelius, A.B. *Fundamentals of Mathematical Geology*. Moscow: Nauka, **1980**.
27. Wu, Z., Guo, F., Li, J. *Arabian Journal of Geosciences*, **2019**, 12(15), article number 467.
28. Xu, W., Zhang, Y., Li, X., Wang, X., Zhang, P. *Environmental Earth Sciences*, **2019**, 78(16), article number 516.
29. Zhang, P., Du, K., Tannant, D.D., Zhu, H., Zheng, W. *Engineering Geology*, **2018**, 239, 109-118.
30. Zhang, R., Yu, Z., Khayone, L. *Journal of the Mine Ventilation Society of South Africa*, **2019**, 72(1), 6-10.
31. Zhang, X., Shen, Z. *Journal of Visual Communication and Image Representation*, **2019**, 59, 334-346.

$$Y' = \frac{(Y_2 - Y_1)(X' - X_1)}{X_2 - X_1} + Y_1 \quad (\text{Eq. 1})$$

$$y = \frac{x}{a + b \cdot x} \quad (\text{Eq. 2})$$

$$Y = f(X) = \frac{X}{A + BX} \quad (\text{Eq. 3})$$

$$l = n// \quad (\text{Eq. 4})$$

$$\text{tg}\varphi \leq h// \quad (\text{Eq. 5})$$

$$\sigma_P = 165,313 \cdot \text{EXP} \left(\frac{27,11714}{F_n} \right) + 2,018, \text{ (MPa)}, \quad (\text{Eq. 6})$$

$$Vp = 5,112606 \cdot \frac{F_n}{(13,34124 + F_n)} + 0,08, \text{ (km/c)}, \quad (\text{Eq. 7})$$

$$\delta_0 = \frac{F_n}{(1,204589 + 0,3686797 \cdot F_n)} - 0,0576, \text{ (g/cm}^3\text{)}, \quad (\text{Eq. 8})$$

$$\sigma_T = \left(\frac{F_n}{(3,255616 + 0,688612 \cdot F_n)} \right)^6 + 1,299, \text{ (MPa)}, \quad (\text{Eq. 9})$$

$$\alpha = \text{arctg} (\Delta H / \Delta L), \quad (\text{Eq. 10})$$

$$\beta = (y - y_1) / \Delta y \quad (\text{Eq. 11})$$

$$F_1(x, y) = (1 - \alpha - 0,5\beta)F_1 - (\alpha - 0,5\beta)F_4 + 0,5\beta F_3 + 0,5\beta F_2 \quad (\text{Eq. 12})$$

$$F_2(x, y) = (1 - \beta - 0,5\alpha)F_1 - (\beta - 0,5\alpha)F_2 - 0,5\alpha F_3 + 0,5\alpha F_4, \quad (\text{Eq. 13})$$

$$F_3(x, y) = (\alpha + \frac{1+\beta}{2})F_3 + (\alpha - \frac{1-\beta}{2})F_2 + \frac{1-\beta}{2}F_1 + \frac{1-\beta}{2}F_4, \quad (\text{Eq. 14})$$

$$F_4(x, y) = (\beta - \frac{1+\alpha}{2})F_3 - (\beta - \frac{1-\alpha}{2})F_4 + \frac{1-\alpha}{2}F_1 + \frac{1-\alpha}{2}F_2, \quad (\text{Eq. 15})$$

Table 1. Example of calculation of physical and mechanical properties

F_n	V_p, km/sec	δ₀g/cm³	σ_P, MPa	σ_T, MPa
7.84	1.968	1.914	7.220	0.653
18.96	3.077	2.313	41.570	2.566
48.64	4.088	2.541	96.682	5.476
29.71	3.604	2.443	68.379	3.967
44.08	4.000	2.525	91.377	5.189
33.338	3.727	2.470	75.309	4.332

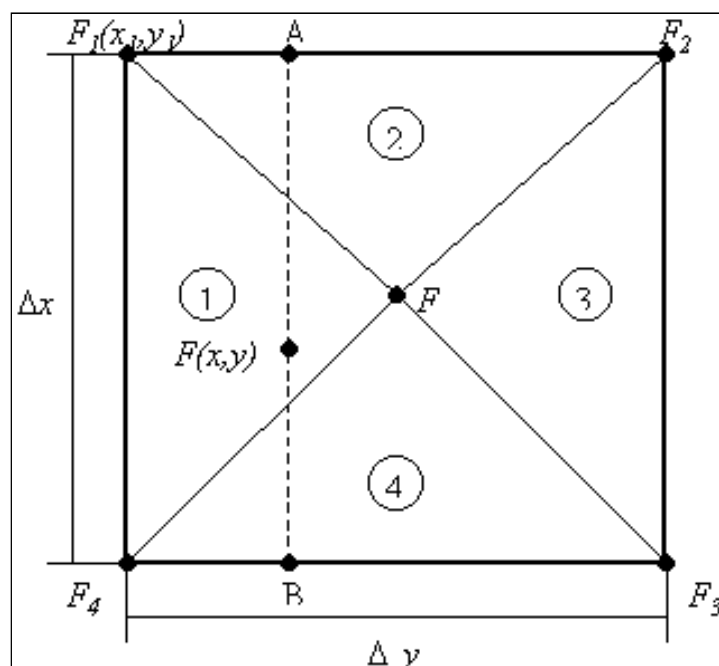


Figure 1. The interpolation cell; 1-4 the numbers of triangles

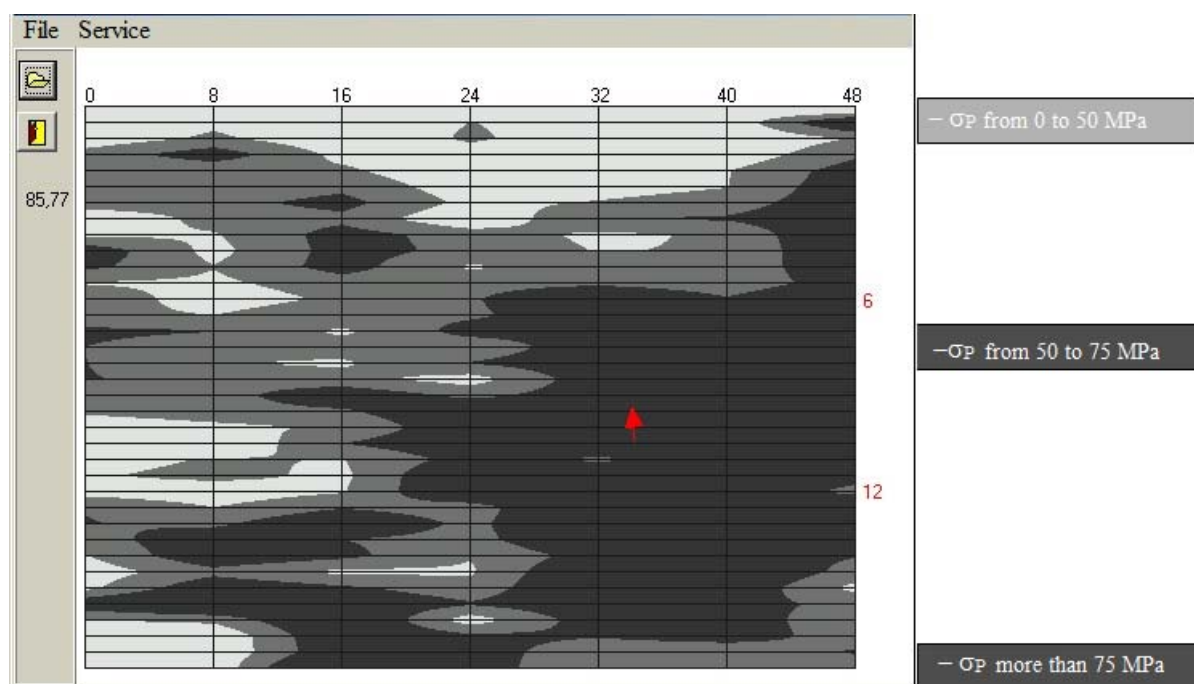


Figure 2. General view of the running program window

INVESTIGAÇÃO DE COMPLEXIDADE SOCIAL (ISC): PROJETO INSTRUCIONAL PARA REFORÇAR AS COMPETÊNCIAS CRÍTICAS E CRIATIVAS (CCT) NA QUÍMICA

INQUIRY SOCIAL COMPLEXITY (ISC): DESIGN INSTRUCTIONAL TO EMPOWERMENT CRITICAL AND CREATIVE THINKING (CCT) SKILLS IN CHEMISTRY

PERDANA, Ryzal^{1*}; Budiyo²; Sajidan³; Sukarmin⁴, RUDIBYANI, Ratu Betta⁵

¹, Doctoral Program of Educational Science, Sebelas Maret University, Ir. Sutami St. 36A, Surakarta, Central Java, Indonesia

^{2,3,4} Teacher Training and Education Faculty of Sebelas Maret University, Ir. Sutami St. 36A, Surakarta, Central Java, Indonesia

⁵ Teacher Training and Education Faculty of Universitas Lampung, Prof. Dr. Sumantri Brojonegoro St. 1, Bandar Lampung, Lampung, Indonesia

* Correspondence author
e-mail: ryzalperdana2009@gmail.com

Received 29 January 2020; received in revised form 11 March 2020; accepted 22 March 2020

RESUMO

Para preparar as pessoas para viverem no século 21 com sucesso, é necessário mais do que o conteúdo da matéria. É muito importante que as pessoas saibam como aplicar suas habilidades e conhecimentos através do pensamento crítico, usando o conhecimento em novas situações, compreendendo novas ideias, colaborando, comunicando, resolvendo problemas, tomando decisões e assim por diante. Esta pesquisa é uma inovação da educação disruptiva que visa projetar modelos de aprendizagem que possam capacitar as habilidades de pensamento crítico dos alunos por meio de análise descritiva com base em dados e revisão da literatura. Este estudo utilizou uma amostra de 180 estudantes do ensino médio na cidade de Surakarta, Indonésia. Os resultados da medição das habilidades de pensamento crítico dos alunos na categoria são muito escassos em todos os aspectos, como, por exemplo, 52,80% dos aspectos de análise, 37,28% dos aspectos de inferência, 45,16% dos aspectos de explicação, 35,01% dos aspectos de autorregulação estão em critérios muito baixos e 41,14% dos aspectos de interpretação em critérios muito ruins. Os resultados da medição das habilidades de pensamento criativo dos alunos também mostram categorias muito preocupantes em todos os aspectos que os envolvem a saber: 45,83% no aspecto da fluência, 42,50% no aspecto da flexibilidade, 44,86% no aspecto da originalidade e 47,50% no aspecto da elaboração, todos em muito baixo critério. Os resultados da revisão de literatura também descobriram que o modelo de *design* dos professores de química não maximizou a capacidade de pensar criticamente, de modo que ele precisa de um design de aprendizado que possa capacitar habilidades de pensamento crítico. Através de um estudo bibliográfico baseado em dados, foi formulado um modelo de complexidade social (ISC) para capacitar habilidades de pensamento crítico.

Palavras-chave: *Investigação de Complexidade Social (ISC), Pensamento Crítico, Pensamento Criativo, Química.*

ABSTRACT

To prepare people to live in the 21st century successfully, it is needed more than subject contents. It is very crucial for the people to know in how to apply their skills and knowledge by critical thinking, using knowledge in new situations, comprehending new ideas, collaborating, communicating, problems solving, decision making and so on. This research is an innovation of disruptive education that aims to design learning models that can empower students' critical thinking skills through descriptive analysis based on data and literature review. This study used a sample of 180 high school students in the city of Surakarta, Indonesia. The results of the measurement of students' critical thinking skills in the category are very lacking in all aspects, for instance, 52.80% of analysis aspect, 37.28% of inference aspects, 45.16% of explanation aspect, 35.01% of self-regulation aspect are in very low criteria as well as 41.14% of interpretation aspects in very poor criteria. The results of measurement of students' creative thinking skills also shows very concerning category in all aspects involving: fluency of 45.83% of fluency aspect, 42.50% of flexibility aspect, 44.86% originality aspect, and 47.50% of elaboration aspect are all in very low criteria. Literature review results also found that chemistry teachers' design model has not maximized

the ability to think critically so that it needs a learning design that can empower critical thinking skills. Through a data-based literature study a form of inquiry social complexity (ISC) model was formulated to empower critical thinking skills.

Keywords: *Inquiry Social Complexity (ISC), Critical Thinking, Creative Thinking, Chemistry.*

1. INTRODUCTION:

21st Century learning requires schools to change teacher-centered learning methods into student-centered learning; this is intended to get students who can think critically, deductively, and inductively in learning science in the era of disruption (Affandi and Sajidan, 2017; Trilling and Fadel, 2009). The learning methods carried out conventionally, namely through memorization at this time are not following the paradigm of 21st-century learning (Zivkovil, 2016). 21st Century learning must be able to empower higher-order thinking skills, which consist of critical and creative thinking skills (Trilling and Fadel, 2009; Rubdiyani and Perdana, 2019).

Critical thinking skills are self-regulation in producing something by interpreting, analyzing, evaluating and inferring, as well as using explanations, concepts, methodologies, criteria or considerations that form the basis of conclusions (Facione, 2011). Critical thinking skills are very important to be empowered in the world of education because it allows students to get a more complex understanding of information. Besides, students can also communicate the results of their thoughts through sharing with others as well as describing socially critical thinking (Dwyer, Hogam, and Stewart, 2014; Forawi, 2016). It becomes very essential among practical competences and formative one in the new educational context (Zuriguel *et al.*, 2015). As a complex activity, it requires to build coherent arguments by involving the educators in the organisation of assessments and learning activities (Daly, 2001). It includes the information for analysis, making decision, and reflection (Von Colln-Applying and Guilano, 2017). It is crucial to make provision of quality care with professional responsibility (Paul, 2014). It is also underscore the flexibility as the different in conceptualising the term of critical thinking skills (Kahlke and Eva, 2018). It should be a skill that is possessed inherently that should be designed its strategies to perform this ability (Carvalho *et al.*, 2017). It will have positive effects on their care behaviours and self- reflection (Chen *et al.*, 2018). The development of critical thinking skills becomes challenge both for educator and student for knowledge transmission (Johanns *et al.*, 2017).

The educators play the role as the contextual and social factors affecting students' critical thinking skills (Raymond *et al.*, 2018). It will enhance their ability to solve problems that needs to think deductively, provide interpretations, and draw inferences (Cui *et al.*, 2018).

Critical thinking skills have six aspects, including Analysis, Inference, Interpretation, Explanation, Self-regulated, and evaluation (Facione, 2011). Based on the understanding and aspects of critical thinking skills shows that critical thinking skills are defined as thinking skills to understand concepts, apply, synthesize, and evaluate new knowledge or information obtained. This can be understood that not all new information that is used as knowledge that is believed to be the truth is used as a benchmark in thinking and acting. In addition to critical thinking skills, creative thinking skills must also be empowered by each student to be successful in the 21st century (Ataizi and Donmez, 2014; Ledward and Hirata, 2011).

Creative thinking skills are a result of thinking that leads to new insights, new approaches, new perspectives, or new ways to understand, think and produce new ideas or ideas (Facione, 2011, Hartono and Sauber, 2015, Anwar *et al.*, 2012). Creative thinking will make students see the world differently and will be happy to experiment to get something new (Anna, Bob, and Mike, 2001). Creative thinking skills are one aspect that must be possessed by every human being to be able to solve problems (Aldig & Arseven, 2017). This shows a person's ability to solve problems correlates with creative thinking skills and achievement towards success (Miller, 2003).

Based on the explanation, it shows that it is important to empower critical and creative thinking skills, which can be implemented in learning. In developed countries, critical and creative thinking skills become one of the competencies of educational goals, even as one of the main goals to be achieved (Zubaidah, 2010). Whereas in Indonesia, the empowerment of critical and creative thinking skills is applied through the implementation of the 2013 curriculum, as an effort to improve higher-order thinking skills (Rudibyani and Perdana, 2019). The

implementation of the 2013 curriculum is a reference for learning centered on students, so it is expected to be able to empower not only cognitive abilities but also aspects of attitudes and skills (Nastiti, Rahardjo, Susanti, and Perdana, 2018).

The results of the study (Subagia, 2013) showed problems that could occur in the implementation of the 2013 curriculum, including 1) the habits of teaching teachers, 2) facilities learning support, 3) preparation of learning, 4) implementation of learning and 5) assessment of learning outcomes. The most frequent weakness is that the implementation of learning is not directed at critical and creative thinking skills (Clorawati, Rohiat, and Amir, 2017), this is due to the habits of teachers who teach conventionally. Whereas critical thinking and creative skills can be empowered through science learning (Zubaidah, 2010), one of them is in chemistry subjects. Therefore, the aim of this study was to design learning models that can empower students' critical thinking skills to prepare people to live in the 21st century successfully.

2. MATERIALS AND METHODS:

2.1. Study Design and Ethical Approval

The qualitative study was designed through a cross-sectional concept where the qualitative description of an experience or event that remain close to participants' accounts (Sandelowski, 2000), and establishes pragmatic approach to have policy making, inform practice and refine or develop interventions (Neergaard, Olesen, Andersen, & Sondergaard, 2009).

This research was carried out by the recommendations of the Department of Secondary and Special Education Management (BP2MK) of Central Java province which permits the letter of acceptance to conduct and gather the data for research. It is done by the agreement of all samples from 180 high school students in the city of Surakarta, Indonesia. The study protocol accepted its ethical approval from the Research Ethics Committee of the Ministry of Education and Culture.

Data collection was carried out using instruments in the form of tests of critical and creative thinking skills, totaling ten items on acid-base chemical materials and salt hydrolysis. The instrument test was first performed an analysis of the instrument quality aided by the Quebec User Evaluation of Satisfaction with Assistive Technology (Quest) program (Demers, Lambrou,

Ska, and Demers, 2000). Reliability estimation using the QUEST program is calculated based on items called item separation indexes and based on testees called person separations (Aminah, 2017). The reliability estimation results obtained the value of person reliability of 0.78 and item reliability of 0.75, so it can be concluded that the consistency of the answers from both the testee or from the items has high reliability.

The next criterion is that an item is said to be fit if the value of the MNSQ INFIT is in the range of 0.70 to 1.30 (Aminah, 2017). The output results of the MNSQ INFIT value are presented in Figure 1. Based on Figure 1 shows that the results of the analysis of the test instruments used, overall the items have large support for the total score. This data illustrates that as a whole the items used are accepted, and can be used as a tool for data retrieval.

3. RESULTS AND DISCUSSION:

3.1. Critical Thinking Skills

Critical thinking is reflective of decision making wisdom in solving problems about what to believe and carrying out intellectual processes (Facione, 2011). Based on this definition it can be understood that critical thinking processes require a higher level of cognitive skills in information processing (Choy and Cheah, 2009). Facione (2011) divides critical thinking skills into 6 types that must be mastered to be possessed by someone, so that a person will have good critical thinking skills, skills that must be possessed of six aspects of critical thinking skills, namely Analysis, Inference, Interpretation, Explanation, Self-regulated, and evaluation (Facione, 2011).

The analysis aspect is the skill of identifying the intentions of the conclusions in the relationship between questions and concepts, the description or form of questions expected to express beliefs and decision experiences and reasons, and information and opinions (Facione, 2011). The aspect of Inference that is the ability to identify and select elements needed to form reasonable conclusions or form hypotheses to pay attention to relevant information and reduce the consequences arising from data, questions, principles, evidence, judgment, beliefs, opinions, concepts, descriptions, questions or other forms of representation (Facione, 2011).

Interpretation aspects, namely the ability to understand, express meaning, statement from various experiences, situations, and data, events as well as decisions, conversion of beliefs and

rules, procedures or criteria (Facione, 2011). Explanation aspects, namely the ability to state the results of a person's judgment process to justify the reasons based on evidence, concepts, methodologies, certain criteria in reasonable consideration, and the ability to present reasons in the form of convincing arguments (Facione, 2011).

The aspect of self-regulation is that one's awareness monitors one's cognition, the elements used in the thought process and the results that are developed, specifically applying the skills of analyzing and evaluating one's ability to conclude with questions, confirmations, validations and corrections (Facione, 2011). Evaluation aspect is the skill to assess the credibility of a question or other presentation with a value or to describe one's perception, experience, situation, decision, belief and to assess the logic power of an expected inferential relationship or actual inferential relationship including statements, descriptions, questions, or other forms of representation (Facione, 2011).

3.2. Creative Thinking Skills

Creative thinking skills make students see the world differently and will be happy to experiment to get something new (Anna, Bob, and Mike, 2001), and is one of the domains in the concept of higher-level thinking (HOTS). So the creative thinking skills of most experts argue is one important factor in achieving success (Glaveanu, 2018). It can be understood that the creative thinking skills acquired by a person are achieved in personal and professional life. For example the success of innovative institutions that can develop in a complex and dynamic work environment; the success of developed countries that can foster creative industry sectors that can compete healthily and invest in research and development (Glaveanu, 2018).

Indicators of creative thinking skills from four aspects namely Fluency, Flexibility, Originality, and Elaboration (Torrance, Ball, and Safter, 1992). Fluency is the ability to generate a number or many ideas (Torrance, 1980). Flexibility is the ability to produce diverse ideas (Torrance, 1980). Originality is the ability to generate responses to ideas that are not common among most or rare/unique (Torrance, 1980). Elaboration is the ability to develop and issue ideas (Torrance, 1980).

3.2.1 Field Study

Aspects of critical thinking skills used in conducting field studies, using aspects of Facione (2011) which consists of six aspects of critical thinking skills, namely Analysis, Inference, Interpretation, Explanation, Self-regulated, and evaluation (Facione, 2011). Test results on 180 students in the MA city of Surakarta also showed that critical thinking skills were still relatively low, in the analysis aspect of 60.83% the criterion was very lacking, the inference aspect was 43.19% the criterion was very lacking, the interpretation aspect was 46.25% with very poor criteria, the explanation aspect of 52.08% criteria is very less, the self-regulation aspect of 39.44% criteria is very less and the evaluation aspect of 46.39% the criterion is very less.

Aspects of critical thinking skills used in conducting field studies, using aspects of Torrance consisting of four aspects namely Fluency, Flexibility, Originality, and Elaboration (Torrance, 1980, 1992). Test results on 180 students also showed that the creative thinking ability of students in the MA city of Surakarta was still low, the fluency aspect was 46.81% the criterion was very lacking, the flexibility aspect was 48.81%, the original aspect was 46.39% the criterion was very less, the elaboration aspect of 46.94% criteria is very lacking. Therefore, an appropriate teaching model to train students' creative thinking skills is needed in learning activities.

The results of the measurement of high-level skills of high school students (Istiyono, Mardapi, and Suparno, 2014) that are still in the sufficient category. The solution that should be done to overcome the problem will be less fulfilled indicators of critical thinking abilities and creative thinking abilities of students is to choose an innovative learning model (Rudibyani and Perdana, 2019; Perdana, Budiyo, Sajidan, and Sukarmin, 2019). One of them is inquiry learning model (Perdana, Budiyo, Sajidan, and Sukarmin, 2019; Perdana, Budiyo, Sajidan, Sukarmin, and Atmojo, 2019).

3.2.2 Empowerment of Critical and Creative Thinking Skills

The development of science and technology today has led to higher-order thinking skills. As a result of the development of a global mindset that seeks to produce human beings who are professional and able to solve problems as well as possible. High-level thinking skills are basically divided into critical and creative thinking skills. The inquiry learning model provides

opportunities for students to develop ways of active learning by discovering and investigating their own knowledge (Perdana, Budiyo, Sajidan, and Sukarmin, 2019; Perdana, Budiyo, Sajidan, Sukarmin and Atmojo, 2019). The inquiry model helps practitioners understand important factors and the relationship between activities that are interrelated with learning (Wenning, 2005). The inquiry learning model facilitates students to make them interested in learning. This learning model spurs students to get their own discoveries (Perdana, Budiyo, Sajidan, Sukarmin, and Atmojo, 2019).

Activities in inquiry learning include several activities, including: (1) exploration, in this case, the teacher has the role of asking questions and problems that will be solved by students; (2) introduction to the concept, in this activity students collect information relating to experiences in daily life; (3) application of concepts, in this activity the teacher exposes students to new situations based on exploration activities and application of concepts (Perdana, Budiyo, Sajidan, and Sukarmin, 2019; Perdana, Budiyo, Sajidan, Sukarmin, and Atmojo, 2019).

The inquiry learning model has stepped in observation, manipulation, generalization, verification, application (Wenning, 2005). In this step there is no situation where students can interact and communicate effectively with other individuals to construct the knowledge they will get (Perdana, Budiyo, Sajidan, and Sukarmin, 2019).

Children develop their thinking ability through external factors rather than passive form internal (Vygotsky, 1978), so we need a learning model that can accommodate students to interact with each other based on effective communication indicators to gain wider knowledge. The Inquiry Social Inquiry model (ISC) learning model is obtained from the results of the literature review thinking (Perdana, Budiyo, Sajidan, Sukarmin, and Atmojo, 2019). Here are pictures of thoughts obtained from the study:

Figure 2 shows that the elements of social complexity are weak at all levels of inquiry, students who have high levels of cognitive are weak, so it is necessary to add an element of social complexity from the study of some literature, because social elements are very important to do in learning to empower the abilities of students from the low level to the high level in cognitive and skills (Trif, 2015; Russo, Verna, and Wolbert, 2015). The ability of a child is influenced by the ability to solve problems and exchange

information with others who know more about it will be clearer (Wooand Reeves, 2007). In this case, the teacher can be used as a source to guide and give students the opportunity to find out how far students understand in studying the lesson. The Design Inquiry Social Complexity (ISC) is presented in Figure 3.

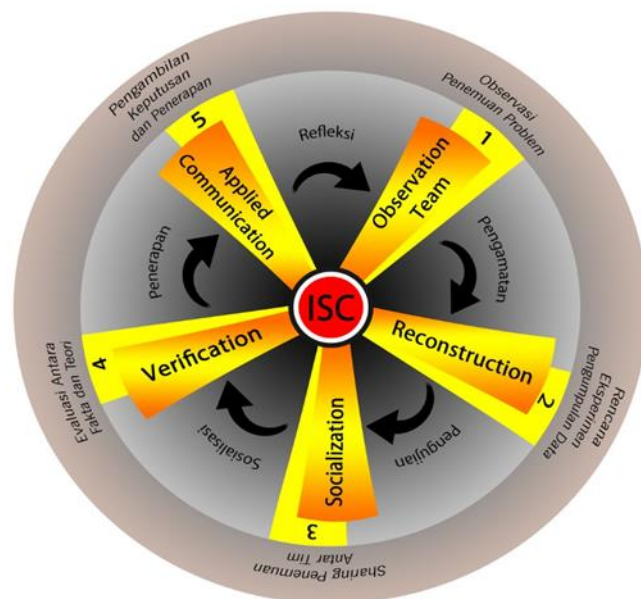


Figure 3. Design Model Inquiry Social Inquiry (ISC)

ISC Model display according to Figure 2 in a circle, each syntax clearly visible, equipped with the main learning activities in each syntax with a colorful, adding to the attractiveness of the model design. Arrows clockwise, describing the syntax sequence marked with a number at each step. According to experts who validate the model, the design of the model is considered attractive, and in the picture, there are also elements that are also new. According to the syntax revision, the learning activities were improved in the syntax of team observation, reconstruction, and applied communication. Activities in learning using the inquiry social complexity model:

- 1) Observation Team: students work together in teams to observe phenomena that have been provided by the teacher in the form of video/demonstration of events to bring up problems that will be researched and studied in learning. At this stage the students detect and produce a unique idea from a question or situation they face.
- 2) Reconstruction: students in each team create ideas and collect data both qualitatively and quantitatively. Data collection is done through the preparation of practicum tools and materials

made by students in groups. At this stage, students are able to identify the truth between questions and concepts and can state decisions with the right information.

- 3) Socialization: students in small groups express ideas between groups on the data collected, 1 participant in the group stays in the group then other members play a role in finding the results of other groups through sharing which is presented by other groups which will then be explained again by him to his group friends about what participants get from sharing other groups, each student has an important role to participate effectively in the group. At this stage, students are able to explain the truth between the data with the applicable theories and can defend their opinions to be accepted by others.
- 4) Verification: Students in the team conduct tests and analyze the truth of the facts they find by linking them with the theoretical basis they already know from the previous stage. At this stage, students are able to assess the credibility of the question or presentation by describing a person's perceptions, experiences, situations, decisions, beliefs and assessing the logic power of actual inferential relationships or other forms of representation. In addition students are able to describe something in more detail to be understood by others.
- 5) Applied Communication: students in groups express their opinions using oral or written through the media presentations from the results of group discussions in turn to then be agreed on the truth with the teacher's direction which is true in learning and can be applied in everyday life. At this stage, students are able to make or accomplish things in a different way but are of truth or usefulness.

4. CONCLUSIONS:

The results showed that critical and creative thinking skills were in a low category, which is below 50%. The solution that should be done to empower students' critical thinking skills and creative thinking skills is to choose an innovative learning model. One innovative learning model is the inquiry model, but there are weaknesses in that model. In this model there is no situation where students can interact and communicate effectively with other individuals, so we need a learning model that can accommodate students to interact with each other. The learning model that can be used is the Inquiry Social Complexity (ISC), learning model.

5. ACKNOWLEDGMENTS:

I want to thank my research colleague at Sebelas Maret University, who were willing to cooperate in completing this research. I also want to thank all those who have helped both material and moral so that this research can be carried out well.

6. REFERENCES:

1. Afandi. and Sajidan, Stimulasi Keterampilan Berpikir Tingkat Tinggi, 1st ed. Surakarta: UNS Press, **2017**.
2. B. Trilling and C. Fadel, "21st Century Skills: Learning for life in our times. Sanfransisco," Jossey-Bass, **2009**, 256.
3. S. Zivkovil, "A Model of Critical Thinking as an Important Attribute for Success in the 21st Century," *Procedia - Soc. Behav. Sci.*, **2016**, 232,102–108.
4. R. Betta Rudibyani and R. Perdana, "The Effect of Problem Solving Models to Improve High Levels of Skills Ability Students," *J. Phys. Conf. Ser.*, **2019**, 1175,1.
5. P. Facione, "Critical thinking: What it is and why it counts. 1998," Insight Assessment, Pearson Educ., **2011**, 9,1–28.
6. C. P. Dwyer, M. J. & Hogam, and I. Stewart, "An integrated critical thinking framework for the 21st century," *Think. Ski. Creat.*, **2014**, 12, 43–52,.
7. S. A. Forawi, "Standard-based science education and critical thinking," *Think. Ski. Creat.*, **2016**, 20, 52–56.
8. M. Ataizi and M. Donmez, "Book Review: 21st Century Skills -Learning for Life in Our Times," *Contemp. Educ. Technol.*, **2014**, 5, 3, 271–274,.
9. B. C. Ledward and D. Hirata, "An overview of 21 st century skills," *Pacific Policy Res. Cent.*, **2011**, 2–5.
10. B. Hartono and Subaer, "Profil Kreativitas Mahasiswa Berdasarkan Gaya Berpikirnya dalam Memecahkan Masalah Fisika di Universitas Negeri Makasar," *Indones. J. Appl. Phys.*, **2015**.
11. G. M. Anwar, M. Nadeem., Muhammad Aness., Asma Khizar., Muhammad Naseer., "Relationship of Creative Thinking with the Academic Archivments of

- Secondary School Students," *Int. Interdiscip. J. Education*, **2012**, 1, 3.
12. C. Anna, J. Bob, and L. Mike, *Creativity in Education*. New York: Continuum, **2001**.
 13. E. Aldig and A. Arseven, "The Contribution of Learning Outcomes for Listening to Creative Thinking Skills," *J. Educ. Learn.*, **2017**, 6, 3, 41,.
 14. G. E. Miller, *Handbook of Psychology: Educational Psychology*. New York: John Wiley & Sons, Inc, 2003.
 15. S. Zubaidah, "Berpikir kritis: Kemampuan berpikir tingkat tinggi yang dapat dikembangkan melalui pembelajaran sains," *Semin. Nas. Sains 2010 dengan Tema "Optimalisasi Sains untuk Memberdayakan Manusia,"* no. June, **2010**, 1–14.
 16. D. Nastiti, S. B. Rahardjo, V. H. Elfi Susanti, and R. Perdana, "The need analysis of module development based on search, solve, create, and share to increase generic science skills in chemistry," *J. Pendidik. IPA Indones.*, **2018**, 7, 4, 428–434.
 17. I. W. Subagia, "Implementasi Pendekatan Ilmiah Dalam Kurikulum 2013 Untuk Mewujudnyatakan Tujuan Pendidikan Nasional," in *Seminar Nasional FMIPA UNDIKSHA III*, **2013**, 16–29.
 18. A. R. Clorawati, S. Rohiat, and H. Amir, "Implementasi Kurikulum 2013 Bagi Guru Kimia," **2017**, 1, 2, 132–135.
 19. L. Demers, R. Weiss-Lambrou, B. Ska, and L. Demers, "Item Analysis of the Quebec User Evaluation of Satisfaction with Assistive Technology (QUEST)," *Assist. Technol.*, **2000**, 12, 2, 96–105.
 20. N. S. Aminah, *Assesmen Pembelajaran Fisika*, 1st ed. Surakarta: UNS Press, **2017**.
 21. N. C. Facione and P. A. Facione, "Analyzing Explanations for Seemingly Irrational Choices: Linking Argument Analysis and Cognitive Science," *Int. J. Appl. Philos.*, **2001**, 15, 2, 267–287.
 22. N. Facione and P. A. Facione, "Critical Thinking and Clinical Reasoning in the Health Sciences: A Teaching Anthology," *Crit. Think. Clin. Judgm.*, pp. 1–9.
 23. S. C. Choy and P. K. Cheah, "Teacher perceptions of critical thinking among students and its influence on higher education," *Int. J. Teach. Learn. High. Educ.*, **2009**, 20, 2, 198–206.
 24. V. P. Glăveanu, "Educating which creativity?," *Think. Ski. Creat.*, **2018**, 27, 25–32.
 25. E. P. Torrance, "Growing up creatively gifted: A 22-year longitudinal study," *Creat. Child Adult Q.*, **1980**, 5, 170, 148–158.
 26. E. P. Torrance, O. Ball, and H. T. Safter, *Torrance test of creative thinking streamlined scoring guide figural a and B*. Bensenville. Illinois: Scholastic Testing Service, Inc., **1992**.
 27. E. Istiyono, D. Mardapi, and Suparno, "Pengembangan Tes Kemampuan Berpikir Tingkat Tinggi (PysTHOTS) Peserta Didik SMA," *J. Penelit. Dan Eval. Pendidik.*, **2014**, 18, 1, 1–12.
 28. R. Perdana, Budiyono, Sajidan, and Sukarmin, "Measuring level of inquiry (LoI) in senior high school surakarta city," *IOP Conf. Ser. Earth Environ. Sci.*, **2019**, 243, 1.
 29. Z. Z. Flor, R. K., Bitu, A., Monir, K. C., & Zohreh, "The Effect of Teaching Critical and Creative Thinking Skills on the Locus of Control and Psychological Well-being in Adolescents," *Procedia - Soc. Behav. Sci.*, **2013**, 82, 52–56.
 30. P. G. Rivas, "Strategies for Teaching and Dissemination of Artistic Heritage by Promoting Critical and Creative Thinking Among Future Primary Education Teachers," *Procedia - Soc. Behav. Sci.*, , **2017**, 237, 717–722.
 31. R. Perdana, Budiyono, Sajidan, Sukarmin, and I. R. W. Atmojo, "A conceptual of teaching models inquiry-based social constructivism (IbSC)," *IOP Conf. Ser. Earth Environ. Sci.*, **2019**, 243, 1.
 32. C. J. Wenning, "Implementing Inquiry-Based Instruction in the Science Classroom: A New Model for Solving the Improvement-of-practice Problem," *J. Phys. Teach. Educ. Online*, **2005**, 2, 4, 9–15.
 33. C. J. Wenning, "Levels of inquiry: Hierarchies of pedagogical practices and inquiry processes," *J. Phys. Teach. Educ. Online*, **2005**, 2, 3, 3–11.

34. C. J. Wenning, "Levels of Inquiry Model of Science Teaching : Learning sequences to lesson plans," *J. Phys. Teach. Educ. Online*, **2011**, 6, 2, 17–20.
35. L. S. Vygotsky, *Mind in Society: The Development of Higher Psychological Processes*. London: Harvard University Press, **1978**.
36. L. Trif, "Training Models of Social Constructivism. Teaching Based on Developing A Scaffold," *Procedia - Soc. Behav. Sci.*, **2015**, 180, 978–983.
37. M. F. Russo, J. Vernam, and A. Wolbert, "Sandplay and storytelling: Social constructivism and cognitive development in child counseling," *Arts Psychother.*, **2006**, 33, 3, 229–237.
38. Neergard, M.A., Olesen, F., Andersen, R.S., & Sondergaard. J. "Qualitative description: The poor cousin of health research". *BMC Medical Research methodology*, **2009**, 9, 52.
39. Sandelowski, M, "Whatever happened to qualitative description?" *Research in Nursing and Health*, **2000**, 23,334-340.
40. Y. Woo and T. C. Reeves, "Meaningful interaction in web-based learning: A social constructivist interpretation," *Internet High. Educ.*, **2007**,10, 1, 15–25.
41. E. Zuriguel, M.T. Lluch, A. Falco, M. Puig, C. Moreno, J. Roldan, "Critical thinking in nursing: scoping review of the literature", *Int. J. Nurs. Pract.*, **2015**, 21, 6, 820-830.
42. W. M. Daly, "The development of an alternative method in the assessment of critical thinking as an outcome of nursing education", *J. Adv. Nurs.*, **2001**, 36,1,120-130.
43. Von Colln- Appling, D. Giuliano,"A concept analysis of critical thinking: a guide for nurse educators", **2017**, 49, 106-109.
44. S. A. Paul, "Assessment of critical thinking: a delphi study". *Nurse educ*, **2014**, 34,1357-1360.
45. R. Kahlke, K. Eva, "Constructing critical thinking in health profession education". *Perspect. Med. Educ*, **2018**, 7,3,156-165.
46. D. P. S. R. P. Carvalho, L. C. Cruz, G. K. P. Mafra, A. I. C. Rego, A. F. Vitor, V. E. P. Santos, A. I. P. Cogo, M. A. Junior Ferreira, "Strategies used for the promotion of critical thinking in nursing undergraduate education: a systematic review". *Nurse Educ. Today*, **2017**, 57, 103-107.
47. S. Y. Chen, H. C. Chang, H. C. Pal, "Caring behaviours directly and indirectly affect nurisng students' critical thinking". *Scand. J. Caring Sci*, **2018**, 32, 1, 197-203.
48. B. Johans, A. Dinkens, J. Moore, "A systematic review comparing open-book and closed-book examinations: evaluating effects on development of critical thinking skills". *Nurse Educ. Prac*, **2017**, 27, 89-94.
49. C. Raymond, Profetto- McGrath, J. Myrick, W. B. Stream, "Balancing the seen and unseen: nurse educator as role model for critical thinking". *Nurse Educ. Pract*, **2018**, 31, 41-47.
50. C. Cui, Y. Li, D. Geng, H. Zhang, C. Jin, "The effectiveness of evidence-based nursing on development of nursing students' critical thinking: a meta analysis". *Nurse Educ. Today*, **2018**, 65, 46-53.

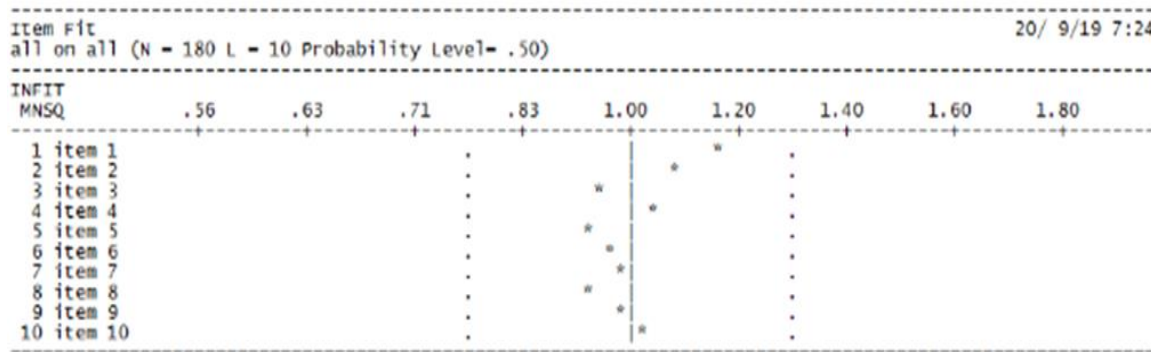


Figure 1. Output of Quest analysis results on MNSQ INFIT values

Model of Inquiry	Discovery Learning	Interactive Demonstration	Inquiry Lesson	Inquiry Laboratory	Real-Word Application	Hypothetical Inquiry
Student Skills	Rudimentary Skills	Basic Skills	Intermediate Skills	Integrated Skills	Culminating Skills	Advanced Skills
S I N T A C	Observation Manipulation Generalization Verification Application					
cognitive	Low	Intellectual Sophistication				High
Teaching Activity	Teacher	Locus of Control				Student
Social Complexity	Deep	Intermediate				Shadow

Figure 2. Literature review of the level of inquiry, level of cognitive, teaching activity and level of social complexity (Perdana, Budiyo, Sajidan, Sukarmin, and Atmojo, 2019).

CARACTERÍSTICAS COMPARATIVAS DA SEGURANÇA DOS MÉTODOS DE
IMUNOTERAPIA SUBLINGUAL E PARENTERALCOMPARATIVE CHARACTERISTICS OF SAFETY OF SUBLINGUAL AND PARENTERAL
IMMUNOTHERAPY METHODSСРАВНИТЕЛЬНАЯ ХАРАКТЕРИСТИКА БЕЗОПАСНОСТИ СУБЛИНГВАЛЬНОГО И
ПАРЕНТЕРАЛЬНОГО МЕТОДОВ ИММУНОТЕРАПИИSALTABAYEVA, Ulbossyn^{1*}; YUMASHEV, Alexei²¹ Astana Medical University, Department of Children Diseases, Nur-Sultan – Republic of Kazakhstan² I.M. Sechenov First Moscow State Medical University (Sechenov University), Department of Prosthetic Dentistry, Moscow – Russian Federation

* Correspondence author

e-mail: s.ulbosyn@mail.ru

Received 06 February 2020; received in revised form 07 March 2020; accepted 28 March 2020

RESUMO

Entre um número significativo de alergias, a alergia ao pólen é a mais comum entre crianças e adultos. A alergia ao pólen leva principalmente à irritação do nariz e dos olhos, mas também pode causar dores de cabeça, fraqueza, fadiga e diminuição do tempo de atenção. Uma reação alérgica aguda pode causar o choque anafilático, ou seja, uma queda acentuada da pressão arterial com risco de vida. Essas e muitas outras consequências das reações alérgicas sugerem a necessidade de criar os medicamentos que possam curar uma pessoa alérgica ou interromper a manifestação de reações alérgicas. O objetivo do artigo foi estudar a segurança da imunoterapia específica para alérgenos. Os métodos de pesquisa incluem análise da comparação da eficácia de dois métodos de imunoterapia, comparação da segurança dos métodos sublingual e parenteral de administração de vacinas alérgicas e uma avaliação comparativa da segurança dos tipos de imunoterapia específica para alérgenos. O estudo envolveu 228 pacientes com severidade variável da febre do feno, entre os quais as crianças de 5 a 18 anos e os adultos (113 pacientes eram homens, 115 eram mulheres). O estudo mostrou que a imunoterapia sublingual aumenta a segurança do tratamento e é um bom substituto para a imunoterapia parenteral, especialmente em crianças. Estudos também confirmaram as evidências científicas bem conhecidas sobre a segurança da imunoterapia sublingual em pacientes com febre do feno. Concluiu-se que a imunoterapia sublingual aumenta a segurança do tratamento e é um bom substituto para o método de imunoterapia parenteral específica para alérgenos, principalmente em pacientes pediátricos, enquanto apresenta várias vantagens, como redução significativa de reações adversas, alta eficiência e conveniência de administração, grande compromisso do paciente e confiança no tratamento, e eliminação da transmissão da infecção.

Palavras-chave: febre do feno, segurança, imunoterapia sublingual específica para alérgenos, imunoterapia parenteral específica para alérgenos.

ABSTRACT

Among a significant number of allergies, the most common among children and adults is pollen allergy. Pollen allergies primarily lead to irritation of the nose and eyes, but can also cause headaches, weakness, fatigue, and decreased attention span. In an acute allergic reaction, anaphylactic shock can occur, that is, a life-threatening sharp drop in blood pressure. These and many other consequences of allergic reactions imply the need to create drugs that could cure a person of allergies or stop the manifestation of allergen reactions. The aim of the article was to study the safety of allergen-specific immunotherapy. The research methods included an analysis of the comparison of the effectiveness of two immunotherapy methods, a comparison of the safety of sublingual and parenteral methods of administering allergic vaccines, a comparative assessment of the safety of types of allergen-specific immunotherapy. The study involved 228 patients with varying severity of hay fever, among whom were children from 5 to 18 years old and an adult population (113 patients were men, 115 were women). The study revealed that sublingual immunotherapy increases the safety of treatment and is a good substitute for parenteral immunotherapy, especially in children. The studies have also confirmed well-known

scientific evidence on the safety of sublingual immunotherapy in patients with hay fever. It was concluded that sublingual immunotherapy increases the safety of treatment and is a good substitute for the parenteral allergen-specific immunotherapy method, especially in pediatric patients, while having several advantages, such as a significant reduction in adverse reactions, high potency, and a convenient mode of administration, greater patient commitment and trust in treatment, and the elimination of infection transmission.

Keywords: *pollinosis, safety, sublingual allergen-specific immunotherapy, parenteral allergen-specific immunotherapy.*

АННОТАЦИЯ

Среди разнообразного числа аллергий наиболее распространенной среди детей и взрослых является аллергия на пыльцу. Аллергия на пыльцу в первую очередь приводит к раздражению носа и глаз, но также может вызывать головные боли, слабость, усталость и снижение концентрации внимания. При острой аллергической реакции может возникнуть анафилактический шок, то есть опасное для жизни резкое падение артериального давления. Эти и многие другие последствия аллергических реакций предполагают необходимость создания лекарств, которые могли бы вылечить человека от аллергии или остановить проявление аллергических реакций. Целью статьи является изучение безопасности аллерген-специфической иммунотерапии. Методы исследования включают анализ сравнения эффективности двух методов иммунотерапии, сравнение безопасности сублингвальных и парентеральных методов введения аллергических вакцин, сравнительную оценку безопасности типов аллерген-специфической иммунотерапии. В исследовании приняли участие 228 пациентов с различной степенью тяжести сенной лихорадки, среди которых были дети от 5 до 18 лет и взрослое население (113 пациентов были мужчины, 115 – были женщины). Исследование показало, что сублингвальная иммунотерапия повышает безопасность лечения и является хорошей заменой парентеральной иммунотерапии, особенно у детей. Исследования также подтвердили хорошо известные научные данные о безопасности сублингвальной иммунотерапии у пациентов с поллинозом. Были сделан вывод о том, что сублингвальная иммунотерапия повышает безопасность лечения и является хорошей заменой метода парентеральной аллерген-специфической иммунотерапии, особенно у педиатрических пациентов, при этом она обладает рядом преимуществ, таких как значительное снижение побочных реакций, высокая эффективность и удобство способ введения, большая приверженность пациента и доверие к лечению, а также устранение передачи инфекции.

Ключевые слова: *поллиноз, безопасность, сублингвальная аллерген-специфическая иммунотерапия, парентеральная аллерген-специфическая иммунотерапия.*

1. INTRODUCTION:

In the etiological structure of allergic diseases, pollen allergy is one of the leading places. Due to its high prevalence, pollen allergy in children and adults remains one of the significant problems of pediatrics and clinical allergology. Pollinosis significantly reduces the quality of life of patients in the spring-summer period of the year, disrupting its medical and social adaptation. A sharp surge in the incidence over the past two decades is associated with an increase in the allergenic load on humans, which is associated largely with environmental pollution, including atmospheric air, drinking water, food and soil, chemicals that act as allergens, and the current century will be the age of allergies, taking the scale of the medical and social problem (Shvetsova and Korotkova, 2017; Waldron and Kim, 2020).

The incidence of allergies has risen sharply over the past 30 years, especially in developed countries. According to WHO, from 2001 to 2010,

the number of allergic people in the world increased by 20%. By 2025, according to WHO, 50% of the world's population will already suffer from this ailment. Now, according to the European Academy of Allergology and Clinical Immunology (EAACI), there are 150 million chronic allergy sufferers in Europe (20% of the population). Growth rates depend on the specific country and the diet of its inhabitants. The spread of allergies is especially noticeable in Western countries. In Britain, between 1995 and 2016, the incidence of allergies increased five-fold. In Kazakhstan, pollinosis is mainly caused by weeds. An allergic reaction to wormwood, quinoa and ragweed is almost 23% of all residents who are allergic to flowering. In the second place – cereals (10.46%), in third – the pollen of trees (11.06%) (Carlson and Coop, 2019).

Allergens can cause very diverse reactions that can seriously affect a person's life. Some people have a runny nose and sneezing. Others have itchy, unsightly rashes or swelling and trouble breathing (Tosca *et al.*, 2020; Dick *et al.*,

2020; Penagos and Durham, 2019). Sometimes an allergic reaction can be life threatening. Anaphylaxis can occur, which, in the absence of immediate treatment, can be fatal. Today, allergen-specific immunotherapy is the only one alternative method for the treatment of hay fever, recognized by many domestic and foreign allergists. It is known that one of the most important requirements of pharmacotherapy for patients is safety. Sublingual immunotherapy is especially indicated for children, due to its greater safety compared to other approaches of ASIT (Saltabayeva and Morenko, 2015).

2. MATERIALS AND METHODS:

Surveys were carried out on the basis of the National Scientific Center for Motherhood and Childhood, in the medical and health center "Umit" and the Astana City Children's Hospital N1. The study involved 228 patients with varying degrees of severity of hay fever, among whom were children from 5 to 18 years old and an adult population (113 patients were males, 115 were females). The average age was 23.5 ± 0.9 years, the minimum age was 5 years, the maximum was 60 years. The studied respondents were randomized into two groups: group 1 included 126 (55.3%) patients who took sublingual immunotherapy, group 2 included 102 (44.7%) patients who received parenteral immunotherapy.

All procedures performed in studies involving human participants were in accordance with the ethical standards of the institutional and national research committee and with the 1964 Helsinki declaration and its later amendments or comparable ethical standards. Informed consent was obtained from all individual participants included in the study.

The safety of sublingual and parenteral allergen-specific immunotherapy was assessed by the frequency and severity of undesirable local and systemic reactions. In the manufacturer's instructions for use of the drug, the effects are described only in the form of general malaise, drowsiness, fatigue and fever.

3. RESULTS AND DISCUSSION:

Over 3 years of observations, were noted both local and systemic adverse events. Local adverse events (AEs) were presented with PIT in the form of hyperemia, itching and infiltration at the injection site, with SLIT – in the form of edema of the oral mucosa at the site of the allergen, lip swelling, itching in the mouth, sore throat and

numbness of the tongue. Hives, bronchial obstruction, rhinoconjunctivitis, nausea, fatigue were attributed to systemic adverse reactions (Saltabayeva *et al.*, 2016b).

When SLIT local adverse events developed, as a rule, within 5-10 minutes after application of the allergen without disrupting the general well-being of the patient. With duration of local AE up to 15-30 minutes, was recommended the continuation of the course without changing the treatment regimen, with repeated relapsed AE repeated the previous dose of the drug of the same concentration. With persistent conservation of local AEs, it was recommended to return to the dose at which there was no development of exacerbations, and to continue the course of treatment starting from this dose. In the absence of the effect of this technique, we prescribed a course of treatment on the background of antihistamines, after passing the "critical concentration" symptomatic drugs were canceled.

Systemic adverse events were stopped by standard methods, then they recommended continuation of the course with a mandatory change in the treatment regimen: the immunotherapy was repeated starting from the administration of the minimum dose of the previous allergen concentration. With the re-development of common AEs, the threshold dose of allergic vaccine, which was later regarded as an individual threshold dose, took an allergen concentration that did not cause the development of common AEs. This dose was "maximal" for the patient, and was administered during the maintenance phase. During the use of sublingual ASIT, most undesirable reactions were resolved mostly on their own, without requiring discontinuation of treatment or correction of the dose regimen.

When conducting 1 course SLIT in 1 group of patients on the background of sublingual ASIT, local adverse events (swelling of the oral mucosa at the site of the allergen, lip swelling, itching in the mouth, sore throat, numbness of the tongue) developed in 35 (27.75%) treated patients with pollinosis (Table 1). All AEs lasted for 5-15 minutes after the application of the allergen and passed on their own within 30 minutes. 18 (14.29%) patients developed general AEs (hives, bronchial obstruction, rhinoconjunctivitis, nausea, fatigue), which were of a mild nature and were stopped within 24 hours without requiring a change in treatment regimen or discontinuation of therapy.

These reactions were described in the instructions for use of the drug and were expected

during the study. In studies of some scholars, when conducting SLIT, local undesirable phenomena, such as swelling of the vocal fold, swelling and burning of the lips, burning of the tongue, swelling of the tongue and the mucous membranes of the mouth, were noted in 15.1% of respondents, general AE cough, nausea, vomiting, heartburn) – in 30% of patients (Haiduk, 2013; Baranov *et al.*, 2002). As a rule, general AEs were light in nature, and did not require the cancellation of therapy. In studies by other authors, local adverse reactions such as burning, itching, tingling, and swelling in the oral cavity were observed in 20% of patients where the reactions were mild, occurred immediately after taking the allergen, and passed on their own within 30 minutes (Goryachkina and Nenasheva, 2008). Systemic reactions in the form of acute urticaria, lung respiratory discomfort were detected in 12.5% of patients. According to other scientists, systemic reactions in the form of coughing, shortness of breath, nasal congestion and local – in the form of itching in the eye area occurred in 14.2 and 5.7% of treated patients, respectively (Revyakina, 2007).

During the 2nd course of SLIT, local reactions in the form of edema of the oral mucosa at the site of allergen, lip swelling, itching in the mouth, sore throat, numbness of the tongue and general, such as rhinoconjunctivitis, fatigue, occurred in 16 (12.7%) and 3 (2.38%) patients, respectively. Total complications during the 2nd course of immunotherapy were recorded in 19 (15.08%) patients. All AEs were lightweight, and did not require the termination of immunotherapy. During the last 3rd course of SLIT, mainly local AEs (itching in the mouth, sore throat) occurred in 9 (7.14%) patients, and in general 2 (1.59%), in the form of rhinoconjunctivitis. Total AEs were observed in 11 (8.73%) patients. During the study, not a single serious adverse event was recorded (Figure 1) (Saltabayeva and Morenko, 2017).

Analysis of adverse events in the group of patients who received parenteral ASIT showed that during the 1st course of immunotherapy, AE was observed in 62 patients (60.78%), systemic reactions – in 26 (25.49%) patients. Of these, 19 patients developed systemic reactions 15–30 minutes after the administration of allergic vaccines and were presented as localized hives, rhinoconjunctivitis, bronchial obstruction with a decrease in EFM to 60%. The development of generalized hives occurred in 3 patients (2.94%), bronchial obstruction in 4 patients (3.92%), rhinoconjunctivitis in 11 (10.78%) people. According to the classification of systemic

reactions that occur during injection therapy, these AHs were attributed to the lungs (1 point) and moderate (2 points) systemic reactions (Table 2).

Local adverse reactions were noted in 36 (35.29%), of them in 3 (2.94%) patients in the form of infiltrate more than 30 mm with the introduction of PIT at a dilution of 1:10. These patients required discontinuation of immunotherapy for the period of treatment with a further change in treatment regimen.

Undesirable reactions during the 2nd course were detected in 38 (37.25%) patients. Systemic reactions occurred in 10 (9.80%) patients: generalized urticaria in 1 (0.98%) patient and an attack of bronchial asthma with a decrease in peak expiratory flow rate to 40% in 2 (1.96%) patients, rhinoconjunctivitis in 6 (5.88%), fatigue in 1 (0.98%), which were regarded as severe, but not life-threatening (Saltabayeva, 2017).

Local adverse events occurred in 27.45% (28 patients) of cases in the form of itching, swelling, hyperemia at the injection site and infiltration of more than 30 mm at the injection site. The analysis of AE has shown that they developed, as a rule, in violation of the diet (the use of causally significant allergens – honey, halva, nuts). Therapy of systemic reactions was carried out according to recommended standards, after normalization of the patients' condition; the course was continued according to an individual scheme. During the last 3rd course of PIT, local AEs manifested in 10 (9.80%) patients, common – in 3 (2.94%). Total AEs were noted in 13 (12.74%) patients (Figure 2) (Saltabayeva *et al.*, 2016a).

The frequency of local reactions during the 1st and 2nd course PIT was not significantly different. With the development of local reactions, a course of antihistamines was recommended, with continued immunotherapy, the dose of the allergen was repeated, at which the local reaction developed. With the recurrence of a local reaction, they took a break for 2-3 days, followed by a repeat dose of allergic vaccine (Figure 3).

Analysis of the comparison of the effectiveness of the two methods of immunotherapy showed that with sublingual immunotherapy, the dose of the collected allergen is much higher than that of parenteral immunotherapy. Undesirable local and systemic reactions during PIT (60.78%) were manifested 1.5 times more often compared to sublingual (42.07%) type of therapy.

Important for us was the comparison of the safety of sublingual and parenteral methods of

allergic vaccine administration. Local suburbs with sublingual immunotherapy were presented mainly as a local reaction in the oral cavity with duration of no more than 30 minutes and as requiring medical correction. Systemic adverse events in sublingual immunotherapy were attributed to the lungs and did not require discontinuation of immunotherapy and changes in the treatment regimen. During the parenteral type of ASIT, local AEs required correction of the immunotherapy regimen. With the development of systemic reactions with the parenteral administration of an allergen, both light systemic AEs and moderate and severe but not life-threatening reactions took place. This complication of the parenteral ASIT method required the discontinuation of treatment and the development of an individualized treatment regimen, but none of the patients had treatment discontinued (Saltabayeva, 2016a).

In a comparative assessment of studying adverse events in patients with pollinosis of different ages, the following values were obtained, as shown in Figures 4 and 5.

In the study of the safety of ASIT species for a three-year period in the age subgroup from 5 to 18 years showed that against the background of SLIT 41.27%, against the background of PIT 76.60% ($p < 0.001$), in the subgroup from 18 to 45 years on the background of SLIT in 52.17%, on the background of PIT in 67.50% ($p < 0.05$), in the subgroup from 45 to 60 years on the background of SLIT in 58.82%, on the background of PIT in 73.33% of patients local adverse events were reported with pollinosis ($p < 0.001$).

According to the results of observation of patients with pollinosis, systemic adverse reactions in the age period from 5 to 18 years were detected on the background of SLIT in 17.46%, on the background of PIT in 42.55% ($p < 0.01$), in the age subgroup from 18 up to 45 years on the background of SLIT in 19.67%, on the background of PIT at 35.00% ($p < 0.01$), in the age subgroup from 45 to 60 years on the background of SLIT on 17.65%, on the background of PIT on 33.33% of the surveyed respondents ($p < 0.001$).

According to the above data, during the three-year period, it became known that, against the background of parenteral ASIT, local AEs were observed 1.9 times more often in patients aged 5 to 18, systemic AEs 2.4 times 45 years old local AEs 1.3 times, systemic ones 1.8 times; at the age of 45 to 60 years old local AEs are 1.2 times more often and systemic ones 1.9 times more than sublingual allergen-specific immunotherapy ($p < 0.001$; $p < 0.01$; $p < 0.001$).

In the analysis of adverse events, it was found that in patients with pollinosis of all the studied groups, they manifested themselves at high doses of the administered allergens and when the diet was disturbed during the course of immunotherapy, i.e. use of cross food allergens that have common antigens with pollen from pollen.

Our research also confirmed the well-known scientific data on the safety of sublingual immunotherapy in patients with pollinosis. In this multicenter, randomized, placebo-controlled study, this high safety was indicated by Durham S.R. and his co-authors, who established in 2012 that sublingual immunotherapy is well tolerated by patients, reducing the symptoms of pollinosis and improving the quality of life (Durham *et al.*, 2012). Similar results were previously obtained in the work of other foreign scientists, where the vaccine was well tolerated by patients with minor local side effects, and the clinical manifestations of SLIT were a safe alternative for the parenteral type of immunotherapy and, moreover, were used fairly easily at home (Calderon *et al.*, 2011; Saltabayeva, 2016b; Saltabayeva *et al.*, 2017).

4. CONCLUSIONS:

Summarize the data discussed in the Results and Discussion showing the relevance of the work and how different it is from others researches. Also, point out the benefits and improvements that can be observed in order to develop new scientific standards that can change something in the related field.

Thus, a more frequent occurrence of both local and systemic adverse reactions during the parenteral type of immunotherapy compared with sublingual was reliably established. The favorable effect of ASIT on the course of concomitant allergic pathology manifested itself in a decrease in the frequency and severity of exacerbations of allergic diseases, which, of course, made it possible to reduce the volume of basic therapy. It should be noted that comparatively undesirable effects were more often noted when using parenteral ASIT in the form of systemic reactions, and with sublingual administration – more of a local character. However, local adverse events in most cases were resolved on their own, without the use of drug therapy and changes in treatment tactics. However, systemic adverse events, registered with parenteral form of ASIT, required the appointment of short courses of antihistamines and the use of local glucocorticosteroids.

Therefore, analyzing the above studies, were concluded that sublingual immunotherapy increases the safety of treatment and is a good substitute for the parenteral ASIT method, especially in pediatric patients, while having several advantages, such as a significant reduction in adverse reactions, high potency, and a convenient mode of administration, greater patient commitment and trust in treatment, and the elimination of infection transmission.

5. REFERENCES:

1. Baranov, A. A., Bogomilsky, M. R., Revyakina, V. A. *Allergic Rhinitis in Children: A Guide for Doctors*. Moscow: Nauka, **2002**.
2. Calderon, M. A., Casale, T. B., Togias, A., Bousquet, J., Durham, S. R., Demoly, P. *Journal of Allergy and Clinical Immunology*, **2011**, 127(1), 30-38.
3. Carlson, G., Coop, C. *Annals of Allergy, Asthma and Immunology*, **2019**, 123(4), 359-365.
4. Dick, K., Briggs, A., Ohsfeldt, R., Sydendal Grand, T., Buchs, S. *Journal of Medical Economics*, **2020**, 23(1), 64-69.
5. Durham, S. R., Emminger, W., Kapp, A., de Monchy, J. G., Rak, S., Scadding, G. K., Wurtzen, P. A., Andersen, J. S., Tholstrup, B., Riis, B., Dahl, R. *The Journal of Allergy and Clinical Immunology*, **2012**, 7, 717-725.
6. Goryachkina, L. A., Nenasheva, N. M. *Local Allergen-Specific Immunotherapy*. Moscow: Miklos, **2008**.
7. Haiduk, I. M. *Respiratory Allergies in Children: Epidemiology, Approach to Treatment and Prevention*. Saint Petersburg: Saint Petersburg Academician I.P. Pavlov State Medical University, **2013**.
8. Penagos, M., Durham, S. R. *Current Opinion in Allergy and Clinical Immunology*, **2019**, 19(6), 594-605.
9. Revyakina, V. A. *Russian Allergic Journals (Attachment)*, **2007**, 4, 31-38.
10. Saltabayeva, U. *Materials of the 2nd International Conference of Medical Students and the 18th International Scientific and Practical Conference*, **2016a**, 2, 143-157.
11. Saltabayeva, U. Sh. *Comparative Evaluation of the Effectiveness of the Types of Allergen-Specific Immunotherapy for Pollinosis*. Astana: Astana Medical University, **2017**.
12. Saltabayeva, U. Sh. *Materials of the 58th International scientific-practical conference young scientists and students*, **2016b**, 1, 276-277.
13. Saltabayeva, U. Sh., Morenko, M. A. *Materials of IX International scientific conference Eurasian Scientific Association "Prospects for the modernization of modern science"*, **2015**, 1, 17-18.
14. Saltabayeva, U. Sh., Morenko, M. A. *Materials of the XVIIth Intern. National Scientific Congress "Asthma and Allergies"*, **2017**, 1, 12-16.
15. Saltabayeva, U., Garib, V., Morenko, M., Rosenson, R., Ispayeva, Zh., Gatauova, M., Zulus, L., Karaulov, A., Gastager, F., Valenta, R. *International Archives of Allergy and Immunology*, **2017**, 173(2), 93-98.
16. Saltabayeva, U., Morenko, M., Garib, V., Rozenson, R. *Materials of the European Academy of Allergy and Clinical Immunology Annual Congress*, **2016a**. <https://www.eaaci.org/>, accessed December 2019.
17. Saltabayeva, U., Morenko, M., Garib, V., Rozenson, R. *Materials of the Annual Meeting of the OEGAI*, **2016b**, 4, 51-56.
18. Shvetsova, E. S., Korotkova, T. S. *Modern Problems of Science and Education*, **2017**, 4, 26-33.
19. Tosca, M. A., Olcese, R., Licari, A., Ciprandi, G. *Pediatric Allergy and Immunology*, **2020**, 31(S24), 46-48.
20. Waldron, J., Kim, E. H. *Immunology and Allergy Clinics of North America*, **2020**, 40(1), 135-148.

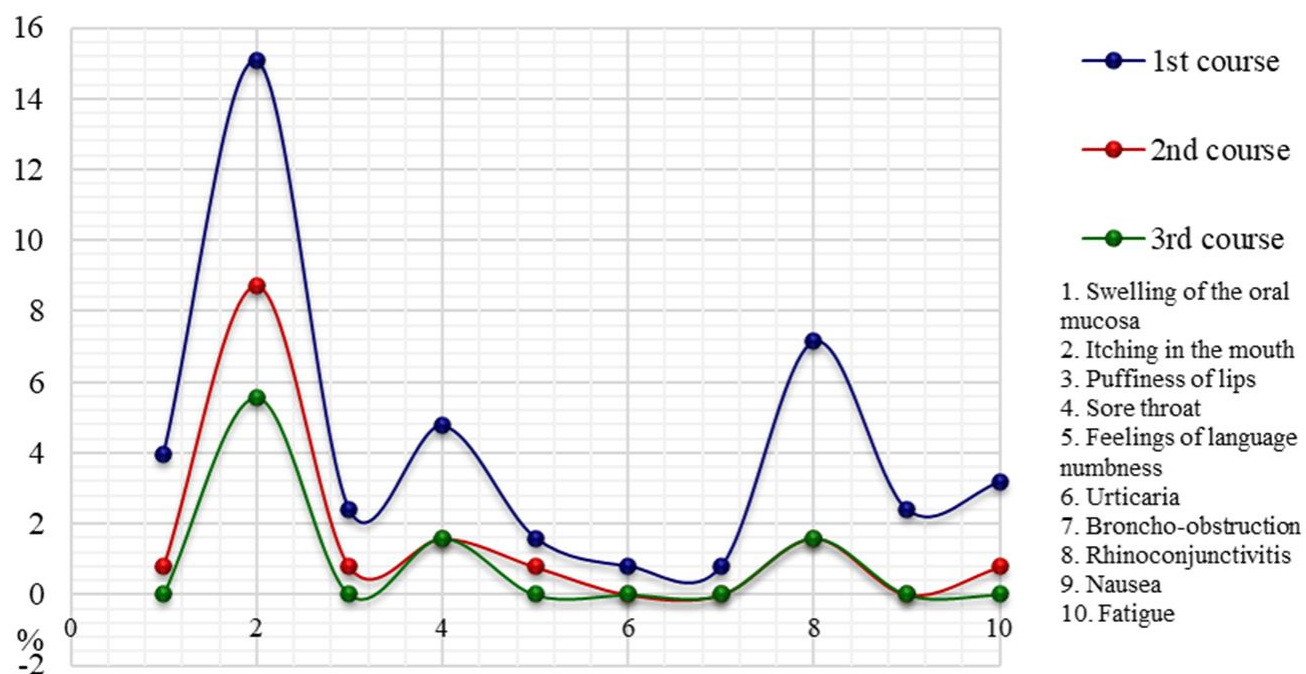


Figure 1. Undesirable effects on the background of SLIT

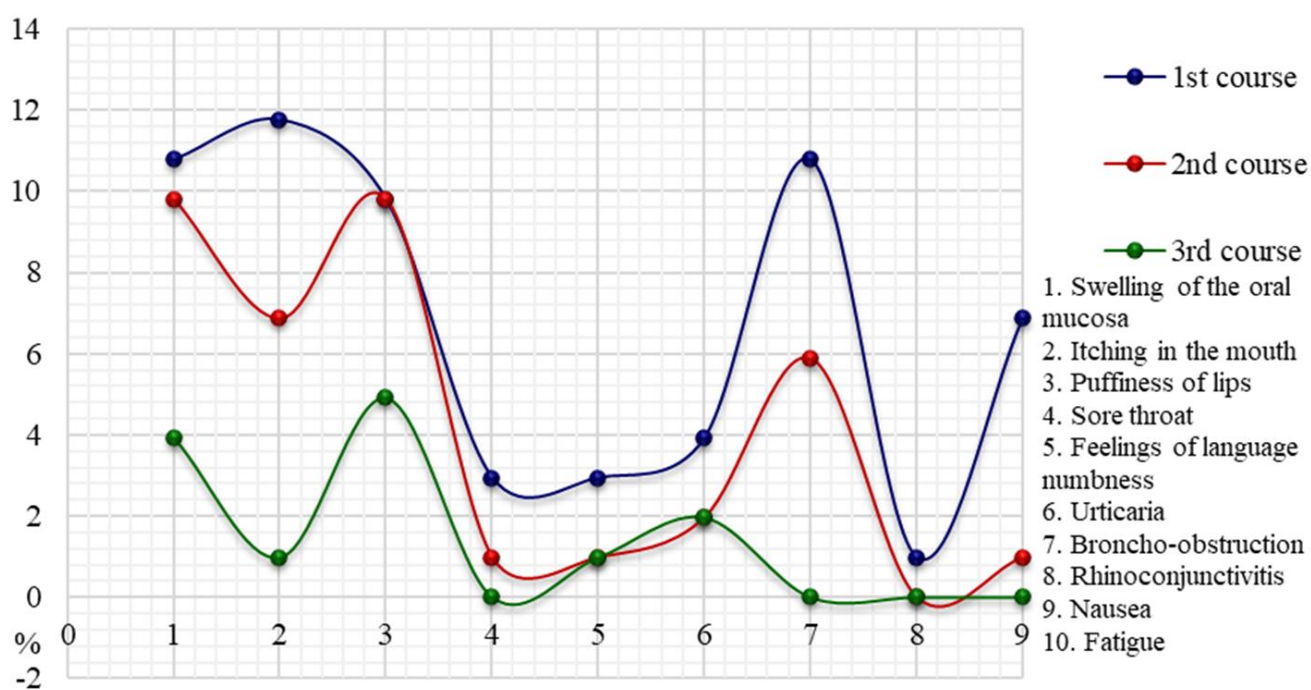


Figure 2. Undesirable effects on the background of PIT

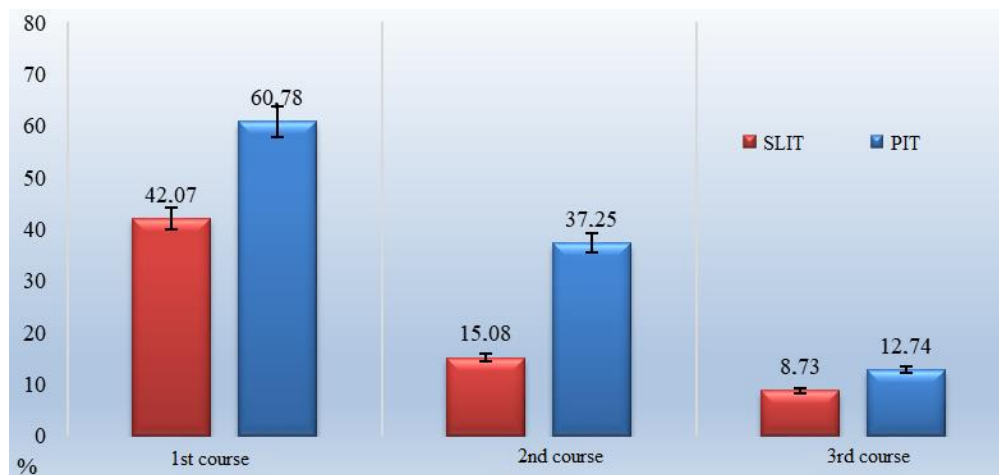


Figure 3. Comparative dynamics of undesirable reactions on the background of SLIT and PIT

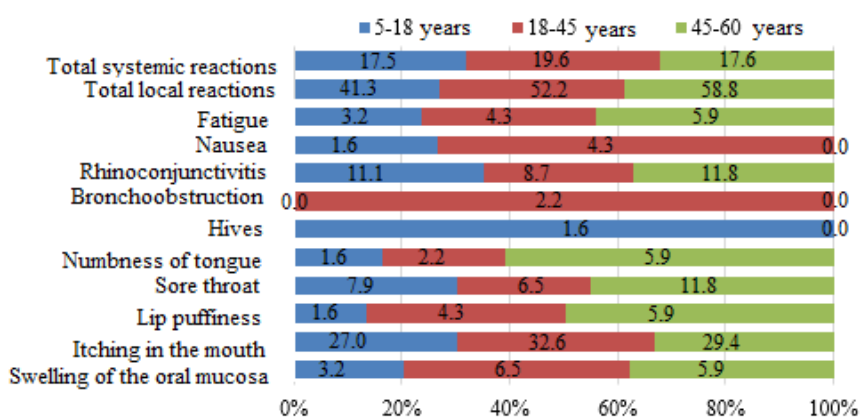


Figure 4. Evaluation of local and systemic adverse events in patients of different age groups against the background of SLIT

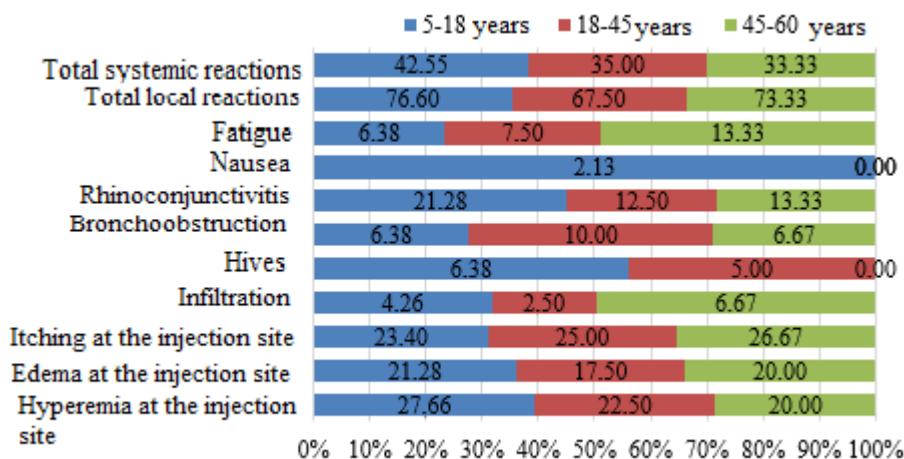


Figure 5. Evaluation of local and systemic adverse events in patients of different age groups on the background of SLIT

Table 1. The frequency of local and systemic adverse reactions during sublingual immunotherapy in patients with pollinosis

Adverse events	1 st course SLIT N=126, (%)	2 nd course SLIT N=126 (%)	3 rd course SLIT N=126 (%)	P value
<i>Local</i>				
Swelling of the oral mucosa	5(3.97)	1(0.79)	0(0.00)	<0.001*
Itching in the mouth	19(15.08)	11(8.73)	7(5.55)	<0.001*
Lip puffiness	3(2.38)	1(0.79)	0(0.00)	<0.05
Sore throat	6(4.76)	2(1.59)	2(1.59)	<0.01
Feelings of numbness of the tongue	2(1.59)	1(0.79)	0(0.00)	<0.05
Total	35(27.78)	16(12.70)	9(7.14)	<0.001*
<i>Systemic</i>				
Hives	1(0.79)	0(0.00)	0(0.00)	<0.05
Bronchoobstruction	1(0.79)	0(0.00)	0(0.00)	>0.05
Rhinoconjunctivitis	9(7.14)	2(1.59)	2(1.59)	<0.001*
Nausea	3(2.38)	0(0.00)	0(0.00)	<0.05
Fatigue	4(3.17)	1 (0.79)	0(0.00)	<0.01
Total	18(14.29)	3 (2.38)	2(1.59)	<0.001*
Total	53(42.07)	19(15.08)	11(8.73)	<0.001*

*High statistically significant

Table 2. The frequency of local and systemic adverse reactions during parenteral immunotherapy in patients of the control group

Undesirable effects	1 st course SLIT N=102 (%)	2 nd course SLIT N=102 (%)	3 rd course SLIT N=102 (%)	P value
<i>Local</i>				
Hyperemia at the injection site	11(10.78)	10(9.80)	4(3.92)	<0.01
Edema at the injection site	12(11.76)	7(6.86)	1(0.98)	<0.001*
Itching at the injection site	10(9.80)	10(9.80)	5(4.90)	<0.05
Infiltration	3(2.94)	1(0.98)	0(0.00)	<0.05
Total	36(35.29)	28(27.45)	10(9.80)	<0.001*
<i>Systemic</i>				
Hives	3(2.94)	1(0.98)	1(0.98)	<0.05
Bronchus obstruction	4(3.92)	2(1.96)	2(1.96)	<0.05
Rhinoconjunctivitis	11(10.78)	6(5.88)	0(0.00)	<0.001*
Nausea	1(0.98)	0(0.00)	0(0.00)	<0.05
Fatigue	7(6.86)	1 (0.98)	0(0.00)	<0.01
Total	26(25.49)	10(9.80)	3(2.94)	<0.001*
Total	62(60.78)	38(37.25)	13(12.74)	<0.001*

* High statistically significant

ALTERAÇÕES SAZONAIS E A LONGO PRAZO DO ÍNDICE DE VEGETAÇÃO DE TERRAS ARÁVEIS DA REGIÃO DE BRYANSK (RÚSSIA CENTRAL): REGULARIDADES E FATORES DINÂMICOS**SEASONAL AND LONG-TERM CHANGES OF VEGETATION INDEX OF ARABLE LANDS OF BRYANSK REGION (CENTRAL RUSSIA): REGULARITIES AND DYNAMICS FACTORS****СЕЗОННЫЕ И МНОГОЛЕТНИЕ ИЗМЕНЕНИЯ ВЕГЕТАЦИОННОГО ИНДЕКСА ПАХОТНЫХ ЗЕМЕЛЬ БРЯНСКОЙ ОБЛАСТИ (ЦЕНТРАЛЬНАЯ РОССИЯ): ЗАКОНОМЕРНОСТИ И ФАКТОРЫ ДИНАМИКИ**

LOBANOV, Grigory V.^{1*}; AVRAMENKO, Marina V.²; PROTASOVA, Alina P.³; DROZDOV, Nikolai N.⁴

^{1,2,3,4} Bryansk State University named after academician I.G. Petrovsky; Department of Geography, Ecology and Land Management, 14 Bezhitskaya Str., zip code 241036, Bryansk – Russian Federation

* Correspondence author
e-mail: lobanov_grigorii@mail.ru

Received 16 January 2020; received in revised form 16 March 2020; accepted 26 March 2020

RESUMO

Existem vários fatores diferentes que afetam o desenvolvimento sustentável da agricultura. Uso eficiente dos recursos terrestres e hídricos, levando em consideração as ameaças que podem surgir como resultado das mudanças climáticas, bem como a dinâmica do crescimento e desenvolvimento das plantas. Os índices de vegetação desempenham um papel importante no monitoramento das variações da vegetação. Este artigo fornece informações sobre as mudanças sazonais e de longo prazo no EVI (índice de vegetação expandida) de terras aráveis em Bryanskaya Óblast. O objetivo do artigo é identificar a dinâmica sazonal do indicador, os intervalos de sua variabilidade, as prováveis causas das diferenças entre anos 2000-2018. Neste artigo, os métodos de pesquisa físicos e químicos foram usados para calcular o conteúdo de húmus, as características da topografia da superfície e as características do uso agrícola com base nos materiais cartográficos e de origem; a composição e densidade do solo foram determinadas usando trabalho de campo. Apresenta-se o material resumido sobre as alterações nos valores de EVI para o período sem neve como um todo e para os intervalos individuais da pesquisa (18 por ano) em 2000-2018. É descrito o mecanismo da influência de várias condições da vegetação edáfica sobre as diferenças de suavização no EVI ao longo de vários anos com diferentes condições meteorológicas. São apresentados os resultados da análise de fatores da dinâmica de longo prazo, o papel das flutuações climáticas de curto prazo, a diminuição progressiva das chuvas e mudanças na composição de espécies de culturas na dinâmica de longo prazo. EVI é demonstrado.

Palavras-chave: *índice vegetativo expandido, terras aráveis, dinâmica sazonal das condições da vegetação, dinâmica de longo prazo dos fatores da vegetação, agrocenose.*

ABSTRACT

There are a number of different factors that affect the sustainable development of agriculture. Efficient use of land and water resources, taking into account the threats that may arise due to climate change, as well as the dynamics of plant growth and development. Vegetation indices play an important role in monitoring vegetation variations. This article provides information on seasonal and long-term changes in the EVI (Enhanced Vegetation Index) of arable land in the Bryansk region. The purpose of the article is to discern the course of the seasonal dynamics of the index, the ranges of its variability, probable causes of differences between 2000-2018. In this article, physicochemical research methods were used to calculate the humus content, surface topography characteristics, and agricultural use features based on cartographic and stock materials, and the soil composition and density were determined through fieldwork. Summarized material on changes in EVI values for a snowless period as a whole and for individual filming intervals (18 per year) in 2000-2018 is presented. The mechanism of the influence of a variety of edaphic vegetation conditions on smoothing the differences in EVI over a series of

years with different meteorological conditions has been described. The results of the analysis of the factors of the long-term dynamics are presented, the role of short-term climatic fluctuations, a progressive decrease in the amount of precipitation, and changes in the species composition of grain crops in the long-term dynamics of EVI are demonstrated.

Keywords: *enhanced vegetation index, seasonal dynamics, conditions, factors, agroecosystem.*

АННОТАЦИЯ

Существует ряд различных факторов, которые влияют на устойчивое развитие сельского хозяйства. Эффективное использование земельных и водных ресурсов с учетом угроз, которые могут возникнуть в результате изменения климата, а также динамики роста и развития растений. Индексы растительности играют важную роль в мониторинге вариаций растительности. В данной статье представлена информация о сезонных и долгосрочных изменениях EVI (расширенного индекса растительности) пахотных земель в Брянской области. Целью статьи является выявление динамики сезонной динамики показателя, диапазонов его изменчивости, вероятных причин различий между 2000-2018 гг. В этой статье физико-химические методы исследования использовались для расчета содержания гумуса, характеристик топографии поверхности и особенностей сельскохозяйственного использования на основе картографических и исходных материалов, а состав и плотность почвы определялись с помощью полевых работ. Представлен обобщенный материал об изменениях значений EVI для бесснежного периода в целом и для отдельных интервалов съемок (18 в год) в 2000-2018 гг. Описан механизм влияния различных условий эдафической растительности на сглаживание различий в EVI в течение ряда лет с различными метеорологическими условиями. Представлены результаты анализа факторов многолетней динамики, роли кратковременных климатических колебаний, прогрессивного уменьшения количества осадков и изменения видового состава зерновых культур в многолетней динамике. EVI демонстрируется.

Ключевые слова: *расширенный вегетативный индекс, пахотные угодья, сезонная динамика условий вегетации, многолетняя динамика факторов вегетации, агроценоз.*

1. INTRODUCTION

Sustainable agricultural development is recognized as one of the main conditions for the practical implementation of the goals outlined in the Millennium Declaration (Resolution adopted by the General Assembly..., 2015). The principles of such development, in particular, are the efficient use of land and water resources of agriculture; climate change-related threats are based on up-to-date information on the dynamics of farmland productivity (Bobylev and Grigoryev, 2016; Liu *et al.*, 2014; Trushkov *et al.*, 2019). On their basis, ideas about the significance of individual factors of vegetation are formed; the conformity of management decisions to changes in environmental conditions is assessed; the dynamics of the state of agro-landscapes is forecasted. An important source of information on farmland productivity comes from multi-zone satellite filming (Ambika and Mishra, 2019; Jaafar and Ahmad, 2015; Reyes-Díez *et al.*, 2015; Rokni and Musa, 2019). The "specialization" of satellite images as a source of information is associated with wide possibilities for analyzing the state and dynamics of agroecosystems of large regions with an area of tens of thousands of square kilometers,

with a distraction from local variability of vegetation factors. The experience of satellite filming for sustainable agriculture in Central Russia is relatively small, but at the same time, it is interesting for the wide variety of edaphic conditions and the instability of weather conditions both within the growing season and in a number of years (Biewer *et al.*, 2009; Grzegozewski *et al.*, 2017; Sarmah *et al.*, 2018; Sobhani *et al.*, 2018).

The primary material for the analysis of long-term changes in the productivity of arable land by remote methods is data on the geographical distribution of vegetation indices (VI). Vegetation indices are a family of indicators that express the ratio of the spectral brightness of the surface in the red and near-infrared range. The indicative properties of the indices are theoretically justified by the dependence of the surface absorption intensity in the red spectrum on the concentration of chlorophyll molecules. The content of chlorophyll characterizes the physiological state of plants, and through it – the primary productivity of the vegetation cover. The value of productivity, in turn, characterizes the intensity and direction of the processes occurring in the landscape. The distribution of vegetation indices in space reflects differences in factors

affecting the growth and development of plants (edaphic, climatic). Based on theoretical ideas about the nature of vegetation indices, their dynamics over time follow seasonal and long-term changes in the state of landscapes. The integrated nature of vegetation indices determines interest to apply them in remote monitoring of natural landscapes and agricultural land (Wardlow *et al.*, 2007; Cherepanov, 2011; Terekhin and Posternak, 2019; Panigrahi *et al.*, 2019).

Over the decades of operation of remote monitoring programs, a lot of factual material has been collected on the distribution of vegetation indices. Based on the interpretation of their differences in time and space, models are constructed that explain the differences in the VI in space and time within the boundaries of one region or type of landscape. The spatial resolution of surveys in satellite monitoring programs allows tracking the dynamics of VI at the level of a large region, agricultural land, or individual arable land. Studies of indicator properties, patterns of VI distribution in space and time are at an empirical level. For some types of natural and cultural communities, relationships between the distribution of VI in space with the species composition, age structure, and direction of changes in productivity have been established and justified (Tsalyuk *et al.*, 2017; Zewdie *et al.*, 2017; Cho *et al.*, 2014). At a qualitative and quantitative level, relationships have been established between individual spectral and other topographic, physical, physicochemical surface characteristics that affect the distribution of vegetation indices (Cabello *et al.*, 2012a). Methods are being developed for applying information on vegetation indices to agricultural management (Sakharova *et al.*, 2015; Kern *et al.*, 2018; Nagy *et al.*, 2018).

At the same time, modern models of the distribution of index values are distinguished by a low level of generalization, "tied" to the features of the structure and dynamics of the landscapes of the model territory. The possibilities of transferring methods and approaches from other objects of study are limited, first of all, in explaining the reasons for the differences in vegetation indices of surface areas in space and time. A low level of theoretical generalizations retains the relevance of studying the factors of the distribution of VI of objects at the regional and local levels or their types. Information on the geographical distribution and dynamics of indexes of individual territories form the basis for evaluating higher-level processes. In particular, the study of the dynamics of VI contributes to the creation of a general picture of changes in the productivity of

landscapes of large regions under conditions of modern climate warming (Dubovyk *et al.*, 2015; Gopp *et al.*, 2018; Phompila *et al.*, 2015; Zhao *et al.*, 2020).

Changes in the productivity of arable land agroecosystems are revealed in the differences in the distribution of VI in a series of satellite images of the territory taken at the same time intervals. Distributions are compared according to the average values of the index, the variation range, and the statistical characteristics of the deviation. Seasonal changes in the distribution can be seen in the pictures, repeated after a few days or one or two weeks (depending on the phase of vegetation). Long-term changes in vegetation indexes are manifested in two aspects: features of seasonal dynamics in years with different vegetation conditions and differences in distribution characteristics in images repeated after a year. The seasonal dynamics of vegetation indexes reflect a regular change in the state of agroecosystems, which is interpreted unambiguously – as a change in the physiological state of plants in development phases. The interpretation of long-term dynamics is a much more difficult task for territories with a wide variety of vegetation conditions and different specialization of agricultural enterprises (Cabello *et al.*, 2012b).

A comparison of the dynamics of the VI of the surface of the plots with different types of plants, natural conditions of vegetation, and land use features allows highlighting the changes determined by local causes and processes of regional and (or) global rank. The influence of the latter is manifested in similar changes in the productivity of sites with unequal vegetation conditions and species composition of plants (Piedallu *et al.*, 2018; Chen *et al.*, 2015; Mengue *et al.*, 2019). The causes of differences in dynamics are rarely detected by statistical methods due to the wide variety of vegetation conditions and the weak connection between the productivity dynamics and the factors determining it. To explain the local features of seasonal and long-term dynamics of vegetation, one has to resort to a detailed study of the conditions of heat and moisture supply. Along with natural factors, the state of cultivated vegetation is determined by the features of the farming system, which is understood as technical, technological, and organizational decisions in the use of arable land affecting their productivity. Natural factors act on the dynamics of productivity through short-period fluctuations in meteorological conditions of vegetation and long-term steady changes in the climate system. The fluctuations in heat and

moisture supply are consistent with alternating periods of high and low VI values in a number of years (Lobanov *et al.*, 2018; Lobanov *et al.*, 2019). The directed long-term changes are manifested in productivity shifts, which are explained by steady shifts in the heat and moisture supply of cultivated plants. Changes in the agricultural system affect the distribution of VI through the development of agricultural machinery, crop cultivation technologies, and especially the demand for agricultural products. At the level of individual farms, changes are manifested in a change in land structure, crop rotation, intensity, and direction of land reclamation. Changes determine rapid changes in the value of the state of agrocenoses; therefore, vegetation indexes of arable land plots can vary greatly from year to year. The separation of the contribution of natural and technical and economic factors to the dynamics of productivity is revealed by involving materials on the state of agricultural production of the model territory. Therefore, the aim of this study was to identify the dynamics of the seasonal dynamics of the indicator, the ranges of its variability, and the probable causes of differences between 2000-2018.

2. MATERIALS AND METHODS

The patterns of changes in vegetation indexes over time are considered for arable land in the Bryansk region – a region with an area of 34.5 thousand square km located in the southwestern part of Russia, in the northern part of the river Dnieper basin. The territory of the Bryansk region is stretched for 250 km from west to east, 150 km from north to south. The relief is flat, with heights of watershed surfaces from 240-260 m in the north and east, to 140-160 m in the southwest (Rybalsky *et al.*, 2007) (Figure 1). The average temperature at the beginning of the 21st century is 7.1°C, and the minimum temperature is – 28.4°C, the maximum +38.3°C, 630 mm of precipitation falls annually, mainly in the form of rain. Snow cover is usually set in September, destroyed in March. The nature of the relief determines small differences in the main climatic within the region, but long-term climate variability is very high. Quasi-rhythmic fluctuations of the main climatic characteristics are characteristic with a frequency of several years (Climatic Data, 2019). A slight growth trend is expressed in temperature changes from the beginning of the century, on the contrary, the amount of precipitation decreased by 25%. A significant part of the watersheds is occupied by arable land. Many lands are ploughed up from the Middle Ages

(10-13 centuries) so that the natural low-fertile soils of the southern part of the forest zone are significantly transformed.

The primary research material was the data of the MOD13 product – data of multi-stage automatic processing of medium resolution satellite images obtained by the MODIS spectroradiometer (Earth Explorer, 2019). The product provides information on the distribution of the maximum values of Enhanced vegetation index (EVI) for intervals of 16 days with a spatial resolution of 250 m, after geometric and atmospheric correction and linkage of the satellite image to the coordinate system. The index value (EVI) is determined through the ratio of the spectral brightness of the surface in the near-infrared, red, and blue range with correction factors (Equation 1):

$$EVI = G \times \frac{NIR - Red}{NIR + C_1 \times Red - C_2 \times Blue + L} \quad (\text{Eq. 1})$$

Where NIR, Red, Blue – the spectral brightness coefficients in the near-infrared region, the red, blue region of the spectrum; G, C₁, C₂, L empirical coefficients equal respectively to 2.5; 6.0; 7.5 and 1.0, respectively (Huete *et al.*, 1999; Huete *et al.*, 2002; Justice *et al.*, 2002).

The use of MOD13 as a source of primary research material corresponds to the level of diversity of natural and economic conditions for the growth and development of plants. The average resolution of the images allows for tracking the main patterns of changes in the index values in time and space for arable land; Moreover, local differences in the spectral characteristics of the surface, which greatly complicate the distribution pattern, are not specifically considered. The study uses satellite images of the surface in the time interval from the second decade of February to early December. From mid-December to early March, the surface is usually covered with snow, although the timing of snow cover may vary from year to year by several weeks.

A correct interpretation of the differences in the index in time and space on the terrain is provided by information on vegetation conditions on 255 key plots of arable land with an area of 150 hectares each. For the plots, the mechanical composition and density of soil compaction (fieldwork), the content of humus (by physicochemical methods), the characteristics of the surface topography, and the features of agricultural use (from cartographic and stock materials) are determined. The selection of key objects reflects the diversity of combinations of

natural and economic factors of vegetation.

The relief of the territory occupied by arable land is mostly homogeneous. Arable lands occupy flat or slightly inclined (up to 2°) watershed surfaces in the southern part of the forest zone. The lithological composition of parent rocks and the mechanical composition of soils are much more diverse. Fine-grained sands, sandy loams, and light loams are typical, soils on heavy mechanical composition and large sands are rarely ploughed. The prevalence of loamy and sandy loamy arable soils is explained by the history of the development of the territory. For arable land, first of all, elevated, well-drained areas with a flushing water regime were used, such a direction of the use of the territory has been preserved to this day. The average humus content varies from 0.8 to 4.5%, depending on a combination of natural and anthropogenic factors.

The natural fertility of soils on the watersheds generally decreases from convex, elevated areas, composed of loessoid loams and sandy loams, to flat, relatively low, folded water-ice sands. The characteristics of arable soils in the region are strongly altered by long-term agricultural development. The most significant effect on the soil occurs in the second half of the 20th century in connection with the targeted improvement of agrochemical characteristics by the introduction of fertilizers and a decrease in acidity. Despite the decrease in the activity of regulating the properties of soils in the 90s of the 20th century, the humus content on many arable lands exceeds the average value for natural soils. At the same time, there are plots of arable land with a low humus content and a dense surface horizon that have lost fertility due to surface erosion and the removal of nutrients from the crop (Mameev *et al.*, 2016).

The sown area is occupied by crops – winter and spring wheat, spring barley, oats, corn for grain; buckwheat, oilseed crops are less common. The ratio of grain areas has changed from the beginning of the century – the proportion of crops of spring crops and corn has increased. At the beginning of the first decade of the 21st century, the areas under crops of winter rye and wheat were correlated as 5 to 3; in the second one, as 1 to 2. The rational selection of crops partially compensates for the adverse changes in vegetation conditions due to climate fluctuations. Differences in vegetation conditions are manifested in fluctuations in the yield of grain crops, which varies significantly over the years and seasons.

3. RESULTS AND DISCUSSION:

The EVI values of key areas vary in the shooting interval by a value from a few to the first hundred percent. The differences are explained by the unequal species composition of crops, the geographical features of the thermal and water regimes of soils, and the technology of agricultural work. The composition of crops affects the distribution of EVI through physiological differences in the growth and development of varieties and species of agricultural plants – the rate of biomass accumulation, changes in the projective cover over time, and photosynthesis rate. Differences in the thermal and water regimes determine the favorable conditions for the growth and development of plants, and through them, the timing of the onset of vegetation stages in crops of different species composition. The composition of technological methods (selection of crops, terms of tillage, use of fertilizers, plant protection products) sets the timing of vegetation and the state of vegetation, as well as natural factors – over a wide range. A wide variety of options for combining natural and economic conditions is consistent with the “colorful” picture of the distribution of EVI values in space, the explanation of which is not limited to one- or two-factor models. At the same time, the absolute value of the index and its position in the ranked series of values are in good agreement with information on the differences in arable land.

The distribution of the average long-term values of the VI by the intervals is presented in Figure 2. The direction and magnitude of changes in the index are in good agreement with ideas about physical processes in agro-landscapes.

In late winter and early spring, the average EVI value is explained by the ratio of the areas of plots still covered with snow and freed from it. The surface of the latter can be open (under “steam”) or occupied by winter crops. The values of EVIs of surfaces of different types are usually significantly different: with a snow cover close to zero with open soil under the steam of less than 0.2, under winter crops about 0.2. At this time, the projective cover under crops is small. Therefore, the average spectral characteristics are close to those for open soil. EVI growth is driven by the gradual, uneven destruction of snow cover. The difference between the dates of snow cover melting in the southwest (the warmest part of the region) and the north (the coldest part) is two weeks. First, elevated, well-heated sections of the southern exposure are freed from snow, then – flat surfaces, the last –

lowering and flat watershed surfaces with weak drainage.

The snow melting provides an increase in the index values usually until mid-April; depending on weather conditions – until early April – early May. With the growth of winter crops and the beginning of vegetation of spring crops, EVI values grow rapidly over 3–4 weeks and reach 0.40–0.45 in mid-May. The index growth is provided by an increase in the area of cereal leaves and projective cover. In late May - early June, index growth slows. The EVI values reach a maximum (0.5–0.6), change little overtime for some time, and gradually decrease at the end of summer and autumn with a decrease in vegetation activity. The decline in EVI values begins in the second half of summer, due to a decrease in the leaf (photosynthetic) surface as the grains ripen, and decreases to values characteristic of the open soil surface by early November due to a decrease in the photosynthetic activity of winter crops. A critical factor in the rate of decline of EVI values is moisture availability.

The values of VI in years with a drought in the second half of summer (2010) decrease after the maximum faster than the average for a long period and then reach a plateau. In late summer and early fall, the rate of decrease in EVI is affected by grain harvesting and soil preparation for sowing winter crops. Treated open soil areas with a low EVI value reduce the average index values. At the end of the calendar autumn – the beginning of the calendar winter, the average EVI values decrease to 0.2–0.1. The spectral properties of the surface are determined by the ratio of the areas with the open surface of the soil, crop residues, and crops of winter cereals. With the establishment of snow cover, EVI values tend to zero 0, and sometimes they become negative – with high water content in the snow. The seasonal dynamics of EVI differ in a number of years in the amplitude of values, the duration of periods of growth, decline and relative stability, and the rate of change of vegetation.

The average EVI values for the entire shooting period (from February to December) slightly increase in a number of years – from 0.30 to 0.32 (Figure 3).

A small increase is formed by the small amplitude of fluctuations in the index values in the intervals near the maximum vegetation (the first half of the calendar summer). The EVI values in the intervals near the borders of the vegetation period (beginning of spring and late autumn) vary quite noticeably in a number of years – by several tens of percent, but their contribution to the

general trend is small due to small absolute values. The distribution of EVI values relative to the long-term average is unstable in a series of years in two aspects. The first is the inconstancy of periods of high and low index values in a certain interval, the duration of which is from one to four years. The second is the unequal position of the index values relative to the annual average for the year as a whole and for individual intervals of the growing season. In years with high (or low) average EVI values, intervals of the growing season with the opposite position of the index values are distinguished (Table 1).

The amplitude of average EVI values in 2000–2018 varies widely – from 0.39 to 0.58, depending on the time of destruction (less often – formation) of the snow cover and favorable weather conditions for vegetation in spring. The lower limit of EVI values determines the duration of snow cover. The index value for the open soil surface is significantly higher than for areas covered with snow; therefore, their ratio of areas determines the EVI value in early spring or late autumn.

The upper limit of EVI is determined by the meteorological conditions of spring. The maximum values of the index correspond to the winter ripening phase, which usually occurs in mid-June (12 years out of 19). Less often, the maximum occurs in early June or early July, and the values change in a series of years no more than 10%. Minor differences are probably due to two reasons. The first is uneven, and in some cases, multidirectional, the influence of weather on vegetation conditions over time intervals of different durations (from several days to the phenological season). In wet years, the best conditions for plant growth and development are characteristic of well-drained areas; in dry, on the contrary, for arable land covered with poorly permeable soils and muds; soils that retain moisture. The second reason is the great variability of the weather at the beginning of the growing season. Seasonal spring warming occurs unevenly, gives way to severe cold, which dramatically slows down the vegetation. Typically, the maximum values of vegetation are less in years with long and strong cooling in April and May.

EVI values are steadily increasing until the time of the beginning of active vegetation (mid-April), with the maximum growth rate occurring in late February – early March. The direction of the dynamics of the index at the end of winter is in good agreement with the increase in average temperature and, accordingly, the early periods of

snow cover destruction. The large variability of the snow cover melting dates determines the largest (in the period from February to December) amplitude of the EVI values. The percentage deviation of the VI from the mean annual values exceeds 150%.

In the middle of spring (April), the dynamics of EVI values and temperatures are multidirectional: an increase in the index occurs against a background of lower air temperatures. The increase in EVI in this period is due to the long "protracted" spring, which is typical for Central Russia in the second decade of the 21st century. The middle of spring at the end of the 2nd decade is colder than at the beginning of the century, but as a rule, active vegetation is already going on in arable lands in April. The values of the index in late spring (late April – mid-May) as a whole increase in agreement with the trend of temperature growth, which provides more favorable vegetation conditions. However, the growth rate of EVI values directly depends on the amount of precipitation. A significant increase is noted in April (temperature and precipitation increase) and insignificant in May (temperature rises, but precipitation decreases). The dynamics of the index is in good agreement with the well-known regularity of functioning of the agro-landscapes of Central Russia – the amount of water in the soil in spring acts as a critical factor at the beginning of the growing season in the south of the forest and north of the forest-steppe zone. In recent decades, the amount of moisture in the soil has been decreasing due to frequent thaws and small reserves of water in the snow by the beginning of melting.

Near the vegetation maximum (June-July), the EVI values change little in a number of years. The difference between maximums and long-term average values does not exceed 5.5% – the smallest deviation in comparison with other shooting periods. In general, the index values slightly decrease from the beginning of the century to the present. Quasi-rhythmic oscillations with a frequency of 2-3 years overlap the trend. Fluctuations are caused by a rhythmic change in humidification conditions (a combination of temperature and precipitation). According to the dynamics of weather conditions, rhythm is better expressed in the first half of June and mid-July, worse at the border of the months. In June, the dynamics of EVI values are associated mainly with meteorological conditions of previous weeks. Low index values in June are preceded by periods of dry and (or) cold weather. In July, low index values are typical for shooting intervals with low rainfall and high temperatures. The lack of moisture in

combination with high temperatures creates the least favorable conditions for vegetation, and therefore, in dry and hot years, the index values tend to a minimum. Rare years with exceptionally high rainfall in early summer (more than 200 mm in late June – early July 2011) also have low index values.

The vegetation recession period (late July – late August) is also characterized by the constancy of EVI values. The average deviation from perennial values does not exceed 6%. The rhythm of fluctuations is less pronounced than during the maximum of vegetation. Several isolated minima and maxima of EVI values alternate with periods of weak index changes lasting several years. The change in the index, as well as in the previous phase of the growing season, is determined by humidification conditions and agrotechnical measures. The periods of dry and hot weather coincide in time with the lows of vegetation or precede them.

In late August – mid-September, the pattern of the distribution of the vegetation index is affected by soil preparation for winter crops. The timing of the start of soil cultivation and sowing strongly depends on the moisture content of the last months of summer and weather forecasts for the beginning of autumn. Therefore, they differ in time by one to two weeks. Differences are reflected in the quasi-rhythmic distribution of index values over a series of years. The low values of the index most often correspond to the worst wetting conditions, sometimes in combination with low temperatures. In October, the long-term dynamics of the index is due to differences in winter vegetation conditions; the average deviation in a number of years is 12%. The general direction of changes is poorly expressed, however, the meteorological conditions of mid-autumn have noticeably changed since the beginning of the century – a steady decrease in temperature of 1-2°C is combined with a small amount of precipitation of 10-20 mm. Apparently, the conditions of autumn differences in heat and moisture do not fundamentally affect the speed of vegetation, therefore, the average value of the index varies slightly. Low values in a number of years are due to a sharp deterioration in the supply of crops with heat and vegetation conditions in September. The long-term dynamics of EVI in November is mainly due to the difference in the timing of snow cover. The spectral properties of the early albeit unstable snow cover reduce the average EVI to 0.1-0.0 (depending on the fraction of the area occupied by snow).

4. CONCLUSIONS:

The nature of the long-term dynamics of the index allows considering short-term fluctuations in meteorological conditions as an important factor in changing the primary productivity of arable lands agroecosystems. Changes in the heat and moisture supply of cultivated plants significantly affect the average value of the index, despite the wide variety of natural conditions of vegetation and local characteristics of the farming system. Differences in EVI values in the spring in a series of years are determined mainly by temperature fluctuations; in the middle and at the end of the growing season – humidification conditions. At the same time, the distribution of the average values of the index in a series of years – average for the year as a whole or part of the growing season – as a rule is not explained solely from the meteorological conditions of the growing season during the survey. The value of the index, and presumably, the primary productivity of the land is affected by the state of vegetation factors in the weeks preceding the filming interval. The influence can be traced mainly at a qualitative level, and it is difficult to formalize, but it is often a necessary component of a consistent model of EVI dynamics.

There is no pronounced trend in the change in average annual EVI values from the beginning of the 21st century. The index values fluctuate with a small amplitude relative to the long-term average with insignificant changes in heat supply and a steady decrease in rainfall. A steady decrease in moisture supply has a weak effect on the average values of EVI, probably due to changes in the composition of grain crops from the beginning of the century – the use of spring wheat and maize less demanding on moisture, as well as the growth of agricultural technology in general. The findings are consistent with statistics on increasing agricultural land productivity.

The idea of the scale, direction, and reasons for the long-term dynamics of the EVI of a large region (in this case, the Bryansk region) is a prerequisite for the development of a consistent model of the influence of natural and technological-economic factors of vegetation on the productivity of agroecosystems.

5. ACKNOWLEDGMENTS:

The study was performed as part of the work on the state task 5.8588.2017/БЧ – "Use of multi-zone satellite filming as a source of information about the structure, seasonal and

long-term dynamics of landscapes in the upper Dnieper region".

6. REFERENCES:

1. Ambika, A. K., Mishra, V. *Geophysical Research Letters*, **2019**, 46(22), 13441-13451.
2. Biewer, S., Erasmi, S., Fricke, T., Wachendorf, M. *Precision Agriculture*, **2009**, 10(2), 128-144.
3. Bobylev, S. N., Grigoriev, L. M. *Sustainable Development Goals of UN and Russia*. Moscow: Analytical Center under the Government of the Russian Federation, **2016**.
4. Cabello, J., Alcaraz-Segura, D., Ferrero, R., Castro, A. J., Liras, E. *Journal of Arid Environments*, **2012a**, 79, 76-83.
5. Cabello, J., Segura, D. A., Ferrero, R., Castro, A. J., Liras, E. *Journal of Arid Environments*, **2012b**, 79, 76-83.
6. Chen, Y., Mo, W., Luo, Y., Mo, J., Huang, Y., Ding, M. *Nongye Gongcheng Xuebao/Transactions of the Chinese Society of Agricultural Engineering*, **2015**, 31(9), 187-194.
7. Cherepanov, A. S. *Geomatics*, **2011**, 3, 98-102.
8. Cho, J., Lee, Y.-W., Han, K.-S. *Remote Sensing Letters*, **2014**, 5(1), 37-45.
9. *Climatic Data*, **2019**. <https://rp5.ru>, accessed December 2019.
10. Dubovyk, O., Landmann, T., Erasmus B. F. N., Tewes, A., Schellberg, J. *International Journal of Applied Earth Observation and Geoinformation*, **2015**, 38, 175-183.
11. *Earth Explorer*, **2019**. <https://earthexplorer.usgs.gov>, accessed December 2019.
12. Gopp, N. V., Savenkov, O. A., Nechaeva, T. V., Smirnova, N. V. *Izvestiya – Atmospheric and Ocean Physics*, **2018**, 54(9), 1152-1157.
13. Grzegozewski, D. M., Uribe-Opazo, M. A., Johann, J. A., Guedes, L. P. C. *Engenharia Agricola*, **2017**, 37(3), 541-555.
14. Huete, A. R., Justice, C., van Leeuwen, W. *MODIS Vegetation Index (MOD 13) Algorithm Theoretical Basis Document*

- (ATBD) Version 3.0. Greenbelt: NASA Goddard Space Flight Center, **1999**.
15. Huete, A., Didan, K., Miura, T., Rodriguez, E. P., Gao, X., Ferreira, L. G. *Remote Sensing of Environment*, **2002**, 83(1/2), 195-213.
 16. Jaafar, H. H., Ahmad, F. A. *International Journal of Remote Sensing*, **2015**, 36(18), 4570-4589.
 17. Justice, O., Townshend, J. R. G., Vermote, E. F., Masuoka, E., Wolfe, R. E., Saleous, N., Roy, D. P., Morisette, J. T. *Remote Sensing of Environment*, **2002**, 83, 3-15.
 18. Kern, A., Barcza, Z., Marjanović, H., Árendás, T., Fodor, N., Bónis, P., Bognár, P., Lichtenberger, J. *Agricultural and Forest Meteorology*, **2018**, 260/261, 300-320. doi: 10.1016/j.agrformet.2018.06.009.
 19. Liu, S.-L., Dong, Y.-H., An, N.-N., Wang, J., Zhao, H.-D. *Chinese Journal of Applied Ecology*, **2014**, 25(11), 3263-3269.
 20. Lobanov, G. V., Avramenko, M. V., Charochkina, A. Y., Drozdov, N. N. *Journal of Environmental Management and Tourism*, **2019**, 10(3), 669-679.
 21. Lobanov, G. V., Trishkin, B. V., Avramenko, M. V., Charochkina, A. Yu., Protasova, A. P. *Journal of Environmental Management and Tourism*, **2018**, 9(1), 34-39.
 22. Mameev, V. V., Torikov, V. E., Sycheva, I. V. *Scientific Journal of Federal State Budgetary Educational Institution of Higher Education "Bryansk State Agrarian University"*, **2016**, 1(53), 3-13.
 23. Mengue, V. P., Fontana, D. C., da Silva, T. S., Zanotta, D., Scottá, F. C. *Revista Brasileira de Engenharia Agrícola e Ambiental*, **2019**, 23(11), 812-818.
 24. Nagy, A., Fehér, J., Tamás, J. *Computers and Electronics in Agriculture*, **2018**, 151, 41-49.
 25. Panigrahi, S., Verma, K., Tripathi, P. *Soft Computing*, **2019**, 23(17), 7699-7713.
 26. Phompila, C., Lewis, M., Ostendorf, B., Clarke, K. *Remote Sensing*, **2015**, 7(5), 6026-6040.
 27. Piedallu, C., Chéret, V., Denux, J. P., Perez, V., Azcona, J. S., Seynave, I., Gégout, J. C. *Science of the Total Environment*, **2018**, 651, 2874-2885. doi: 10.1016/j.scitotenv.2018.10.052.
 28. *Resolution adopted by the General Assembly on 25 September 2015*, **2015**. <https://undocs.org/en/A/RES/70/1>, accessed December 2019.
 29. Reyes-Díez, A., Alcaraz-Segura, D., Cabello-Piñar, J. *Revista de Teledetección*, **2015**, 2015(43), 11-29.
 30. Rokni, K., Musa, T. A. *Catena*, **2019**, 178, 59-63.
 31. Rybalsky, N. G., Samotesov, E. D., Mityukov, A. G. *Natural resources and the environment of the constituent entities of the Russian Federation*. Moscow: Research Institute-Nature. **2007**.
 32. Sakharova, E. Yu., Sladkhih, L. A., Kulik, E. N. *Interexpo Geo-Siberia, 2015*, 1, 47-52.
 33. Sarmah, S., Jia, G., Zhang, A., Singha, M. *Remote Sensing Letters*, **2018**, 9(12), 1195-1204.
 34. Sobhani, B., Abad, B., Kefayat Motlagh, O. M. *Applied Ecology and Environmental Research*, **2018**, 16(4), 3861-3872.
 35. Terekhin, E. A., Posternak, T. S. *Sovremennye Problemy Distantionnogo Zondirovaniya Zemli iz Kosmosa*, **2019**, 16(4), 161-172.
 36. Trushkov, A. V., Odabashyan, M. Y., Kazeev, K. S., Kolesnikov, S. I. *Agronomy Research*, **2019**, 17(6), 2438-2444.
 37. Tsalyuk, M., Kelly, M., Getz, W. M. *ISPRS Journal of Photogrammetry and Remote Sensing*, **2017**, 131, 77-91.
 38. Wardlow, B., Egbert, St. L., Kastens, J. H. *Central Great. Remote Sensing of Environment*, **2007**, 108, 290-310.
 39. Zewdie, W., Csaplovics, E., Inostroza, L. *Applied Geography*, **2017**, 79, 167-178.
 40. Zhao, J., De Notaris, C., Olesen, J. E. *Agriculture, Ecosystems and Environment*, **2020**, 290, 106786.

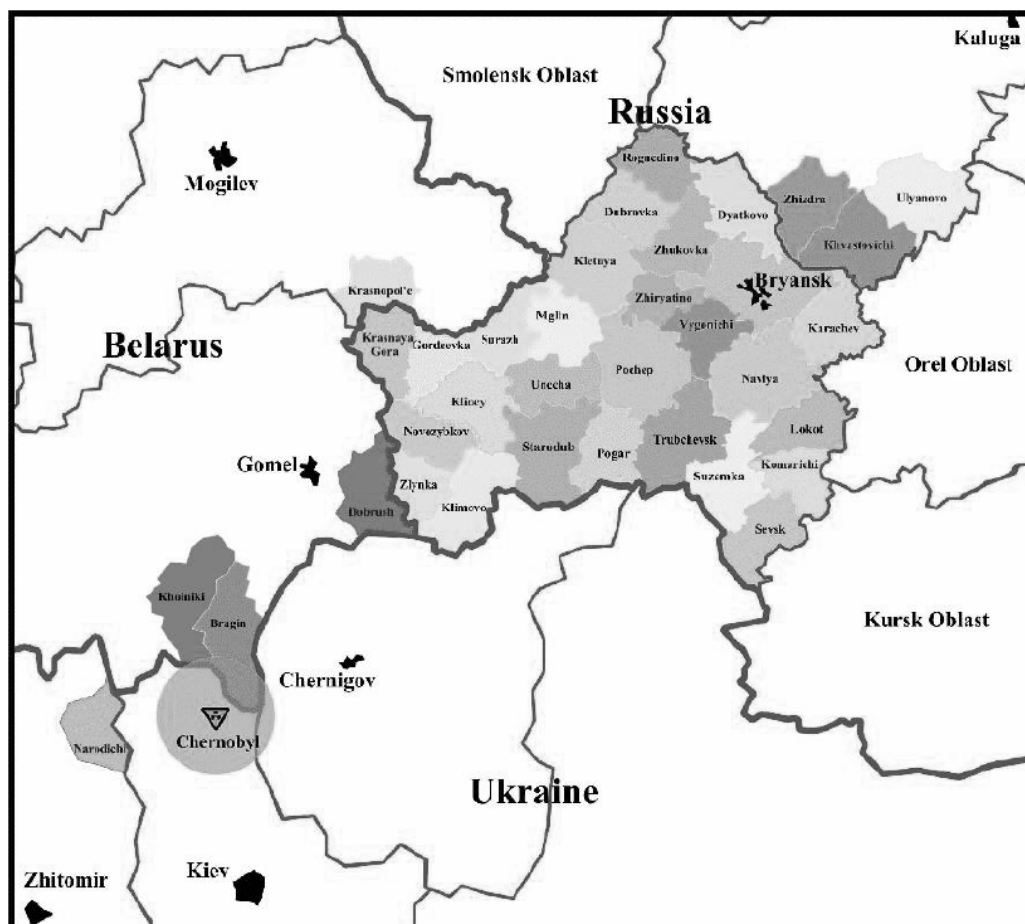


Figure 1. Map of the districts of the Bryansk region of the Russian Federation

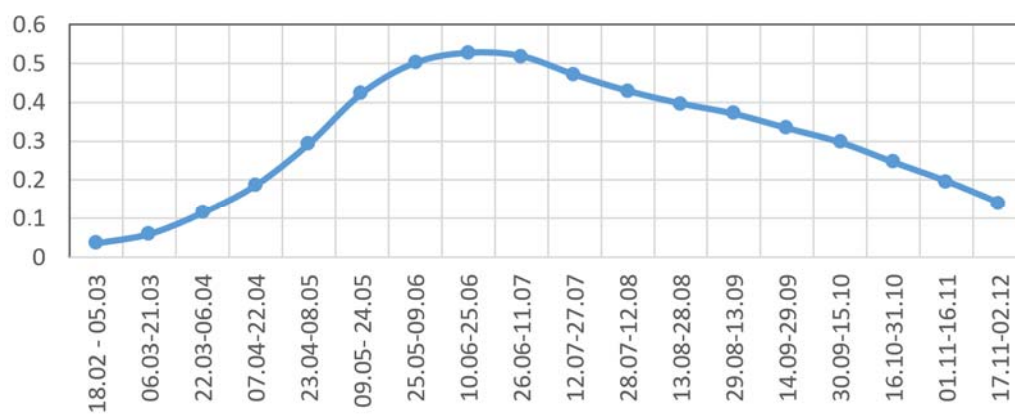


Figure 2. Seasonal dynamics of EVI values

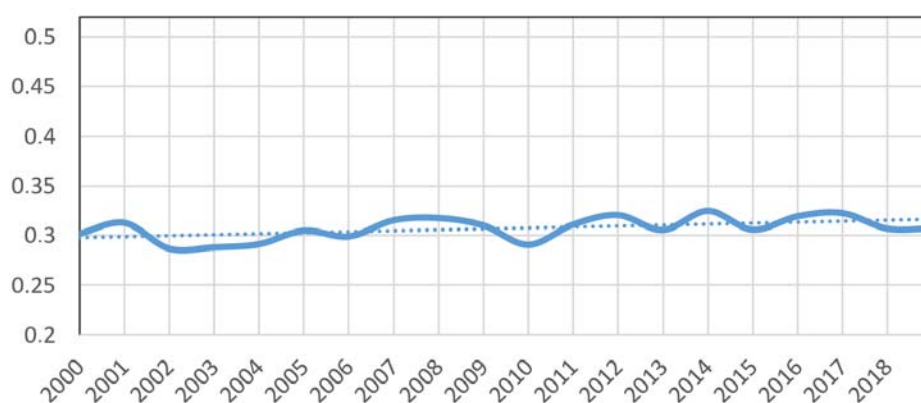


Figure 3. Long-term changes in the average EVI. Dotted line – linear trend.

Table 1. The ratio of EVI values for filming intervals to long-term trends

Years	Filming intervals																	
	I	II	II	IV	V	VI	VII	VIII	IX	X	XI	XII	XIII	XIV	XV	XVI	XVII	XVIII
2000	l	l	l	h	h	l	l	l	l	h	h	h	h	h	h	h	l	h
2001	l	l	h	h	h	h	h	l	h	h	h	h	h	h	h	h	h	l
2002	h	h	h	h	h	h	h	l	l	l	l	l	l	l	l	l	l	h
2003	l	l	l	l	l	l	l	h	l	h	h	h	h	h	h	h	h	l
2004	l	l	l	l	l	l	s	h	h	h	h	l	l	l	l	l	h	l
2005	l	l	h	l	l	h	l	h	h	h	h	h	h	l	l	l	h	l
2006	l	l	h	l	l	l	l	h	h	h	h	h	h	h	h	h	l	h
2007	l	h	h	h	h	h	h	h	h	l	s	h	h	h	h	h	l	l
2008	h	h	h	h	h	h	h	s	h	l	l	l	l	l	l	h	h	l
2009	l	l	h	s	l	l	l	h	h	h	h	h	h	h	h	h	h	l
2010	l	l	l	l	l	h	h	l	l	l	l	l	l	s	h	h	l	h
2011	l	l	l	l	l	l	s	l	l	h	h	h	h	h	h	h	h	h
2012	l	l	h	l	h	h	h	l	h	l	l	h	h	h	h	l	h	h
2013	l	l	l	l	l	h	h	h	h	l	h	s	l	l	l	s	h	h
2014	h	h	h	h	h	h	h	h	h	l	l	l	l	l	l	l	h	h
2015	h	h	h	l	l	l	l	l	l	h	l	l	s	l	h	h	l	h
2016	h	h	h	h	h	l	l	l	h	h	l	l	h	h	h	l	l	l
2017	h	h	h	h	h	l	l	l	l	h	h	h	h	h	l	h	l	l
2018	l	l	l	l	h	h	h	l	s	h	h	h	s	l	h	l	h	L

*Filming intervals: I – 18.02 – 05.03; II- 06.03-21.03; III- 22.03-06.04; IV- 07.04-22.04; V- 23.04-08.05; VI – 09.05- 24.05; VII – 25.05-09.06; VIII – 10.06-25.06; IX – 26.06-11.07; X- 12.07-27.07; XI – 28.07-12.08; XII- 13.08-28.08; XIII – 29.08 – 13.09; XIV – 14.09-29.09; XV – 30.09-15.10; XVI – 16.10-31.10; XVII – 01.11-16.11 XVIII – 17.11-02.12

** Deviation of EVI values from a long-term trend: h – upward; l – downwards; s – corresponds to a long-term trend.

ESTUDO ESTRUTURAL DE COMPLEXOS DE HEXAFLUOROACETILACETONA, PIRAZOL E DERIVADOS DE PIRAZOL COM ALGUNS METAIS POR FT-IR E ¹H-RMN

STRUCTURAL STUDY OF COMPLEXES FROM HEXAFLUOROACETYLACETONE, PYRAZOLE, AND ITS PYRAZOLE DERIVATIVE WITH SOME METALS BY FT-IR, AND ¹H-NMR

دراسة تركيبية من معقدات الهكسوفلورواسيتايل اسيتون، البيروزول، و مشتق البيروزول مع بعض الفلزات بواسطة FT-IR و ¹H-NMR

Jassim Abas Al-Hilfi^{1*}, Zaidoon Jawad Kahdim¹, Tahseen Saddam Fandi¹, and Luma M. Ahmed²

¹Department of Chemistry, College of Science, University of Misan, Maysan, Iraq

²Department of Chemistry, College of Science, University of Kerbala, Kerbala, Iraq

* Correspondence author

e-mail: jassimal-hilfi@uomisan.edu.iq

Received 12 January 2020; received in revised form 28 February 2020; accepted 11 March 2020

RESUMO

As formações complexas em série de níquel (II) ou cobalto (III) com hexafluoroacetilacetona, pirazol, 3,5-dimetilpirazol e 3,5-bis(trifluorometil)-1H-pirazol foram preparadas. O primeiro passo da reação incluiu a síntese do complexo a partir da utilização de hexafluoroacetilacetona como um ligante com Co(III) ou Ni(II) um metal, de spin alto com doação de π e forma enol do ligante. O complexo formado foi identificado por FT-IR, espectroscopia de ¹H-RMN e cálculo de suscetibilidade magnética. Considerando que o segundo passo para a produção do complexo dependia da mistura de água com pirazol e usando-os como ligantes com Co(III) ou Ni(II) um metal, de spin alto com doação e um átomo de nitrogênio aromático é doador do ligante. Na terceira etapa, o complexo foi produzido misturando água com 3,5-bis(trifluorometil)-1H-pirazol como ligante com Co(III) ou Ni(II) um metal, de spin baixo. A investigação dos complexos preparados e dos ligantes utilizados foi realizada comparando os resultados de espectroscopia de ¹H-RMN de FT-IR. Além disso, o cálculo da suscetibilidade magnética também foi empregado. Os resultados da espectroscopia de ¹H-RMN e suscetibilidade magnética provaram que os complexos produzidos são diamagnéticos, quando o ligante inclui o grupo CF₃. Ao mesmo tempo, os complexos produzidos são paramagnéticos, quando o ligante não contém o grupo CF₃, que é formado com a mistura de água e 3,5-dimetilpirazol como ligante, ou água e pirazol como ligante, com Co(III) ou Ni(II) como metal. Todos os ligantes nos complexos paramagnéticos possuíam um átomo doador e outro o átomo receptor no pirazol que é um átomo de nitrogênio aromático. Portanto, todos os complexos de alta rotação preparados não eram evidentes no espectro de ¹H-RMN, porque os picos parecem ninhados que, devido ao alto tempo de relaxamento de ¹H-RMN de T₁, e a investigação resultou em dois picos de atribuição. Esse comportamento é uma atitude para ocorrer o fenômeno da forma cetona e da forma enol usando os espectros de ¹H-RMN, e é um acoplamento evidente entre o átomo de hidrogênio ou carbono com um átomo de flúor.

Palavras-chave: hexafluoroacetilacetona, complexos de Co(III) e Ni(II), espectros de FT-IR e ¹H-RMN.

ABSTRACT

The series complex formation nickel(II) or cobalt(III) with hexafluoroacetylacetone, pyrazole, 3,5-dimethylpyrazole, and 3,5-bis(trifluoromethyl)-1H-pyrazole were prepared. The first reaction step included the synthesis of the complex using hexafluoroacetylacetone as a ligand with Co(III) or Ni(II), metals with high spin with π donate and enol-form of the ligand. This formed complex was identified by FT-IR, ¹H-NMR spectroscopy, and magnetic susceptibility calculation. Whereas, the second reaction step to produce the complex depended upon mixing water and pyrazole and using it as ligands with Co(III) or Ni(II) a metal, which is a high spin with one donate and the another is aromatic nitrogen atom in a ligand. In the third reaction step, the complexes were produced by mixing water with 3,5-bis(trifluoromethyl)-1H-pyrazole as a ligand with Co(III) or Ni(II) as low spin

metal. The analysis of these prepared complexes and their used ligands were done by comparing the results using $^1\text{H-NMR}$ and FT-IR spectroscopies. Besides, the magnetic susceptibility calculation was also employed. The results of $^1\text{H-NMR}$ spectroscopy and magnetic susceptibility proved that the produced complexes are diamagnetic when the ligand includes the CF_3 group. At the same time, the produced complexes are paramagnetic, when the ligand without the CF_3 group, which is formed the mixture of water and 3,5-dimethylpyrazole as ligand or water and pyrazole as a ligand with Co(III) or Ni(II) as metal. All the ligands in the paramagnetic complexes were one donate, and another the donated atom in pyrazole is an aromatic nitrogen atom. Therefore all prepared high spin complexes were not evident in the $^1\text{H-NMR}$ spectrum because the peaks appear broad that due to high T_1 relaxation $^1\text{H-NMR}$ time, and the investigation turned out two assignment peaks. This behavior is an attitude to happen the ketone form and enol form phenomenon by using $^1\text{H-NMR}$ spectra, and its an evident assignment coupling between hydrogen or carbon atom with a fluorine atom.

Keywords: hexafluoroacetylacetone, complexes Co(III) Ni(II) , FT-IR, and $^1\text{H-NMR}$ spectra.

المخلص:

حضرت سلسلة من معقدات النيكل (II) أو الكوبلت (III) مع هكسوفلورواستيتايل اسيتون، والبيرازول، و 3،5-ثنائي مثيل بيرازول، و 3،5-بس(تراي فلورومثيل)-1-هيدروجين-البيرازول. تضمنت خطوة التفاعل الاولى تحضير المعقد باستخدام الليكاند هكسوفلورواستيتايل اسيتون مع فلز الكوبلت (III) أو النيكل (II)، حيث يكون سلوك الليكاند عالي البرم ومانح لمزدوجين الكترونيين (ثنائي المنح) وعلى شكل اينول فورم. شُخصت المعقدات المتكونة بواسطة مطيافية FT-IR و مطيافية $^1\text{H-NMR}$ وحسابات الحساسية المغناطيسية. بينما تضمنت الخطوة الثانية، تحضير معقد بالأعتماد على استخدام مزيج من الماء و البيرازول كلكاندات مع فلز الكوبلت (III) أو النيكل (II)، إذ تكون الفلزات عالية البرم وتحوي ليكاند مانح لزوج إلكتروني وليكاند اخر تكون فيه الذرة المانحة ذرة النيتروجين الاروماتية. في الخطوة الثالثة، حضرت المعقدات من مزيج متكون من تفاعل الماء و 3،5-بس(تراي فلورومثيل)-1-هيدروجين-بيرازول كاليكاندات مع فلز الكوبلت (III) أو النيكل (II) واطئة البرم. تم تشخيص هذه المعقدات المحضرة من الليكاندات المستخدمة عن طريق مقارنة النتائج بواسطة مطيافية $^1\text{H-NMR}$ ومطيافية FT-IR. بالإضافة الى ذلك فقد استخدمت حسابات الحساسية المغناطيسية لهم. برهنت نتائج مطيافية $^1\text{H-NMR}$ والحساسية المغناطيسية بأن المعقدات المتكونة هي دايا مغناطيسية (الفلز واطيء البرم)، عندما يحوي الليكاند على مجموعة CF_3 ، بينما تكون المعقدات الناتجة بارا مغناطيسية (الفلز عالي البرم)، عندما لا يحوي الليكاند على مجموعة CF_3 ، والتي تتكون من مزيج من الماء و 3،5-بس(تراي فلورومثيل)-1-هيدروجين-البيرازول كلكاند او ليكاند من الماء والبايروزول مع فلز الكوبلت (III) أو النيكل (II). تكون جميع الليكاندات في المعقدات البارامغناطيسية مانحة لمزدوج إلكتروني واحد، والآخر في البيرازول فان ذرة النيتروجين الاروماتية هي الذرة المانحة. لذلك تكون جميع المعقدات عالية البرم المحضرة غير واضحة في طيف $^1\text{H-NMR}$ ، لظهور حزم عريضة والتي تُعزى لزمان الاسترخاء السريع للبروتونات في الرنين النووي المغناطيسي، وشُخصت اشارتين مهمة. غُزي هذا السلوك الى حدوث ظاهرة الكيتون فورم والاينول فورم باستخدام اطياف $^1\text{H-NMR}$ ، والتي اعطت ازدواج مميز لذرة الهيدروجين او ذرة الكربون مع ذرة الفلور.

الكلمات المفتاحية: هكسوفلورواستيتايل اسيتون، معقدات الكوبلت (III) النيكل (II)، مطيافية FT-IR و مطيافية $^1\text{H-NMR}$.

1. INTRODUCTION

Hexafluoroacetylacetone was used as a chelating agent in this work. It has been widely used as a chelating agent for the determination of neptunium and plutonium and the extraction of lanthanides and actinides. The IUPAC name of hexafluoroacetylacetone is 1,1,1,5,5,5-hexafluoro-2,4-pentanedione. It was one of the β -diketone derivatives in which two CF_3 groups substituted R_1 and R_2 β -diketone ligands have been extensively studied in coordination as well as organometallic chemistry for several decades and are the precursors for various heterocyclic compounds such as pyrazole and imidazole. The presence of electron-withdrawing groups, such as CF_3 groups, favors the enol form (Burdett and Rogers, 1964). When four or more fluorine atoms are present in the molecule, the enolization is complete (Pashkevich *et al.*, 1981). For instance, 100% of the molecules of hexafluoroacetylacetone are in the enol form. Also, phenyl groups favor the enol form (Reid J.C, Calvin, 1950). It was already about 100% of

the molecules of dibenzoylmethane are in the enol form. For their compounds, the lower the polarity of the solvent, the higher is the percentage of the enol form. In CCl_4 , 94% of the acetylacetone molecules are present in the enol form, whereas, in acetonitrile, this value is reduced to 36%. The amount of enol form decreases with increasing temperatures. As the degree of enolization increases, the acidity of the enol proton decreases (Hammond *et al.*, 1959). In the case of unsymmetrically-substituted β -diketones, two different enol forms are possible (Lowe Jr. and Ferguson, 1965). It has been shown that benzoylacetylacetones (with different substituents in the *para*-position of the phenyl group) are enolized towards the phenyl group. The acidity of the β -diketone depends on the substituents. Because of the presence of the two carbonyl groups, the proton on the α -carbon is quite acidic, and relatively weak bases can remove it. However, by compulsion of acetylacetone and benzoylacetylacetone, the enolization is accessed towards the phenyl group, but in the flour acetylacetone, it accesses the CF_3 group. In general, the techniques that

can be used in studying the enolization and tautomerism in β -dicarbonyl compounds are ^1H -NMR, FT-IR, and U.V. spectrophotometry. Nevertheless, the most powerful method is ^1H -NMR. β -diketone and their metal complexes have several applications in different fields. The rare-earth β -diketones are used as ^1H -NMR shift reagents (Morrill, 1986; Hinckley, 1969). Ketoamines and their metal(II) complexes continue to attract attention because of their unique catalytic and coordination properties (Schrock *et al.*, 1999; Graf *et al.*, 1999; Guérin *et al.*, 1998; Stabnikov *et al.*, 2003; Baidina *et al.*, 2004a; Baidina *et al.*, 2003). β -diketones can be used, e.g., for the preparation of ketoimines (by condensation with amines), thioketones, and various heterocyclic compounds (e.g., pyrimidine derivatives) (Baidina, 2004b).

2. MATERIALS AND METHODS

2.1 preparation of tris(hexafluoroacetylaceton)cobalt(III) and the bis (hexafluoroacetylaceton)nickel(II) as first reaction step

The tris(hexafluoroacetylaceton)cobalt(III) or bis(hexafluoroacetylaceton)nickel(II) were prepared as in the Equation 1 according to the literature with changed in precursor materials (Sharma *et al.*, 2003; Woods *et al.*, 2004). It was altered the amount of reactants and reflux times. Exactly (29.317 mg, 0.1177 mmol) from $\text{Co}(\text{CH}_3\text{COOH})_2 \cdot 4\text{H}_2\text{O}$ or (43.92 mg, 0.1765 mmol) from $\text{Ni}(\text{CH}_3\text{COOH})_2 \cdot 4\text{H}_2\text{O}$ were dissolved in 5 mL ethanol and 1 mL acetic acid, and then added to the hexafluoroacetylaceton (73.5 mg, 0.353 mmol). The suggested structure of the product is shown in Figure 3. It was confirmed by FT-IR, ^1H -NMR spectroscopy, and magnetic susceptibility calculated.

2.2 preparation of triaquatripyrazole cobalt(III) or diaqua dipyrazole nickel(II) as second reaction step

The triaquatripyrazolecobalt(III) or diaquadi-pyrazolenickel(II) were prepared as in the Equation 2 according to the literature with changed in precursor materials (Sharma *et al.*, 2003; Woods *et al.*, 2004), amount of reactants, and reflux times. $\text{Co}(\text{CH}_3\text{COOH})_2 \cdot 4\text{H}_2\text{O}$ or $\text{Ni}(\text{CH}_3\text{COOH})_2 \cdot 4\text{H}_2\text{O}$ (165.74 mg, 0.66 mmol or 248.86 mg, 1 mmol respectively) in 14 mL ethanol was added to the pyrazole (136 mg, 2 mmol). The suggested structure of the product is presented in Figures 5 and 6. The structure was confirmed by FT-IR spectroscopy, and the

magnetic susceptibility was calculated.

2.3 Preparation of 3,5-bis(trifluoromethyl)-1H-pyrazole

The compound was prepared as in Equation 3, according to the literature with changes in the precursor materials (Clark, 2010; Al-Mathkuri *et al.*, 2018), amount of reactants, rate of solvents, and reflux times. Hexafluoroacetylaceton (780.22 mg, 3.75 mmol) in 14 mL ethanol, toluene, and THF were added to the hydrazine (120.19 mg, 3.75 mmol). The suggested structure of the product is shown in Figure 8. It was confirmed by FT-IR. spectroscopy and the magnetic susceptibility was calculated.

2.4 Preparation of the diaquabis(hexafluoroacetylaceton)nickel(II) as the third reaction step

The diaquabis(hexafluoroacetylaceton)nickel(II) was prepared in Equation 4 according to the literature with a change in the precursor materials (Sharma *et al.*, 2003; Woods *et al.*, 2004), amount of reactions, and reflux times. $\text{Co}(\text{CH}_3\text{COOH})_2 \cdot 4\text{H}_2\text{O}$ or $\text{Ni}(\text{CH}_3\text{COOH})_2 \cdot 4\text{H}_2\text{O}$ (83.43 mg, 0.335 mmol or 483.86 mg, 1.944 mmol respectively) in 15 mL ethanol was added to the 3,5-bis(trifluoromethyl)-1H-pyrazole or 3,5-methylpyrazole (338.0 mg, 1.6598 mmol or 560 mg, 5.833 mmol respectively). One suggests that the structure of the product is shown in Figure 8. It was confirmed by FT-IR, ^1H -NMR spectroscopy, and the magnetic susceptibility was calculated.

3. RESULTS AND DISCUSSION:

The ^1H -NMR spectrum of a hexafluoroacetylaceton sample is shown in Figure 1. The spectrum in DMSO as a solvent at 0 °C using TMS as an internal reference. The appearance of the single peak (significant peak) at 6.480 ppm was assigned to a vinylic proton, the peak at 2.055 ppm attribute to a CH_2 keto-form, the peak at 10.868 ppm attributed to a OH enol-form (Al-Hilfi *et al.*, 2019).

All prepared complexes were magnetic susceptibility to figure out the physics of the magnetic behavior, and the results were paramagnetic of all prepared complexes from pyrazole and 3,5-dimethylpyrazole as ligands while it was diamagnetic of all prepared complexes from 3,5-bis(trifluoromethyl)-1H-pyrazole, therefore the hybridization of the prepared complexes from pyrazole and 3,5-

dimethylpyrazole as ligands with Co or Ni as a metal was sp^3d^2 and sp^3 respectively, while it is of prepared complexes from 3,5-bis(trifluoromethyl)-1H-pyrazole as a ligand with Co or Ni as a metal was d^2sp^3 and dsp^2 respectively. The ^{13}C -NMR spectrum of a hexafluoroacetylacetone sample is shown in Figure 2. The spectrum of hexafluoroacetylacetone in DMSO as a solvent at 0 °C with the using TMS as the internal reference. The spectrum shown three peaks (because coupling with fluoride) at range 26.288-35.144 ppm assigned to CH_2 ketone-form, multi peaks (because coupling with fluoride) at range 91.704-95.238 attributed to CH enol-form, carbon of CH enol-form splitting more than carbon of CH_2 keto-form with fluoride are because enol-form is resonance system more than is resonance system keto-form, and enol-form is two forms a structure of hexafluoroacetylacetone, while one form is keto-form. Multi peak around at 124 ppm attributed to CF_3 groups, multi peaks around at 159 ppm assigned to carbonyl groups. Figures 1 and 2, respectively, confirm the ligand of the starting material. At Tables 1 and 2, some spectral data of the starting material ligand and its complex (Walmsley and Walmsley, 2005; Pavia *et al.*, 2009).

At Figure 4, the 1H -NMR spectrum of the pyrazole sample, the spectrum appeared triplet peak at 6.369 ppm due to proton number 8, doublet peak at 7.657 ppm assigned to protons number 7 and 9, whereas proton of NH group disappeared because tautomerism between two nitrogen atoms while its appeared in spectra 6 and 7 of two complexes prepared from pyrazole as a ligand with nickel or cobalt as a metal respectively, and appeared shifting in complexes spectra in Table 3. Table 3 appears different between ligand with complexes more than Table 1 may be attributed to the lone pair donor of the nitrogen atom in aromatic while in Table 1 was aliphatic. Therefore it may be assigned to the aromatic system defect, and the 1H -NMR spectra of complexes were high resolution of protons coupling may because of shift reagent of metals (Pavia *et al.*, 2009). At Table 4, appears triplet peak at 6.867, 7.038, 7.208 ppm because of the coupling between the proton with fluoride attributed to the aromatic proton of pyrazole while its peak appears broad peak at 7.473 ppm in the complex.

The results in Figures (11-13) and Table 5 revealed that the complex of 3,5-bis(trifluoromethyl)-1H-pyrazole with Ni(II) was successfully prepared by the analysis of the positions of the peaks (Silverstein and Bassler,

1962; Nakamoto, 1970; CHACÓN *et al.*, 2018; Santorum *et al.*, 2018). The shift in the peaks in Table 5 is proven that the complex with Ni(II) was prepared from 3,5-bis(trifluoromethyl)-1H-pyrazole as a ligand with nickel(II) (Silverstein and Bassler, 1962; Nakamoto, 1970).

4. CONCLUSIONS:

In the first reaction step, the prepared complexes were paramagnetic. Hence the complex formed from nickel as a metal whose hybridization was sp^3 , and whereas the complex formed from cobalt as a metal whose hybridization was sp^3d^2 . The prepared complexes were π donating, their two bonds between the ligand and the transition metal are one bond covalent a charge, and two bonds donate.

In the second reaction step, the prepared complexes were paramagnetic. Hence the complex formed from nickel as a metal whose hybridization was sp^3 , and whereas the complex formed from cobalt as a metal whose hybridization was sp^3d^2 . The prepared complexes contained from one donate ligand and another donated ligand (one bond donated for neutralizing the metal) between the ligand and the transition metal.

In the third reaction step, the prepared complexes were diamagnetic. Hence the complex formed from nickel as a metal whose hybridization was dsp^2 , and whereas the complex formed from cobalt as a metal whose hybridization was d^2sp^3 .

The prepared complexes consisted of one donate ligand and another donated ligand (one bond donate as neutral of metal) between the ligand and the transition metal.

The FT-IR spectra indicated that the complex between 3,5-bis(trifluoromethyl)-1H-pyrazole and Ni(II), were successfully synthesized.

5. ACKNOWLEDGMENTS:

The authors wish to acknowledge the College of Science staff at University of Misan in supporting this work in their laboratories.

6. REFERENCES:

1. Burdett J. L., Rogers M. T. *Journal of the American Chemical Society*. **1964**, 86(11):2105-9.

2. Pashkevich K. I., Saloutin V. I., Postovskii I. Y. *Russian Chemical Reviews*. **1981**, 50(2):180.
3. Reid J. C., Calvin M. *Journal of the American Chemical Society*. **1950**, 72(7):2948-52.
4. Hammond G. S., Borduin W. G., Guter G.A. *Journal of the American Chemical Society*. **1959**, 81(17):4682-6.
5. Lowe Jr J. U., Ferguson L. N. *The Journal of Organic Chemistry*. **1965**, 30(9):3000-3.
6. Morrill T.C. Lanthanide shift reagents in stereochemical analysis. New York: VCH; **1986**.
7. Hinckley C. C. *Journal of the American Chemical Society*. **1969**, 91(18):5160-2.
8. Schrock R. R., Seidel S. W., Schrodi Y., Davis W. M. *Organometallics*. **1999**, 18(3):428-37.
9. Graf D. D., Schrock R. R., Davis W. M., Stumpf R. *Organometallics*. **1999**, 18(5):843-52.
10. Guérin F., McConville D. H., Vittal J. J., Yap G. A. *Organometallics*. **1998**, 17(23):5172-7.
11. Stabnikov P. A., Baidina I. A., Sysoev S. V., Vanina N. S., Morozova N. B., Igumenov I.K. *Journal of Structural Chemistry*. **2003**, 44(6):1054-61.
12. Baidina I. A., Zharkova G. I., Pervukhina N. V., Gromilov S.A., Igumenov I. K. *Journal of Structural Chemistry*. **2004a**, 45(4):678-687.
13. Baidina I. A., Gromilov S. A., Zharkova G. I., Stabnikov P. A. *Journal of Structural Chemistry*. **2003**, 44(3):448-56.
14. Baidina I. A., Stabnikov P. A., Vasiliev A. D., Gromilov S. A., Igumenov I. K. *Journal of Structural Chemistry*. **2004b**, 45(4):671-677.
15. Sharma S., Rai A. K., Singh Y. *Phosphorus, Sulfur, and Silicon*. **2003**, 178(11):2457-63.
16. Woods J. A., Osowole A. A., Odunola O. A. *Synthesis and Reactivity in Inorganic and Metal-Organic Chemistry*. **2004**, 34(8):1471-85.
17. Clark, J. Stephen. "Heterocyclic Chemistry." **2010**.
18. Walmsley J. A., Walmsley F. *Journal of the Korean Chemical Society* **2005**, 49(1).
19. Pavia D. L., Lampman G. M., Kriz G. S., Vyvyan J. A. Introduction to spectroscopy. 4th edition, Cengage Learning. **2009**, USA.
20. Silverstein R. M., Bassler G. C. *Journal of Chemical Education*. **1962**, 39(11):546.
21. Nakamoto, Kazuo. "Infrared spectra of inorganic and coordination compounds." **1970**.
22. CHACÓN C., HENAO J.A., JAMALIS J., RIVAS P., VELÁSQUEZ W., DELGADO G.E. *Periódico Tchê Químico*. **2018**, 15 (29) :292-299.
23. Santorum N., Fabara A., Pilaquinga F., Ampudia S., Jara E., Meneses L. *Periódico Tchê Química*. **2018**, 15(29):309-18.
24. Al-Hilfi J. A., AL-Furiji H. S., Saleh A. T. *ARCTIC Journal*. **2019**, 72(9):149-163.
25. Al-Mathkuri T. S., Al-Jubori H. M., Saleh A. T. *Oriental Journal of Chemistry*. **2018**, 34(4):2031-42.

Table 1. ¹H-NMR chemical shifts in ppm of hexafluoroacetylacetone and complex from hexafluoroacetylacetone as a ligand with cobalt as a metal (Pavia *et al.*, 2009)

Assigned protons	Chemical Shifts of ligand	Chemical Shifts of complex
Vinyl proton	6.48	7.176
Proton CH ₂ moiety	2.055	2.397

Table 2. ¹³C NMR chemical shifts in ppm of hexafluoroacetylacetone and complex from hexafluoroacetylacetone as a ligand with cobalt as a metal (Walmsley and Walmsley, 2005)

Assigned carbons	Chemical Shifts of ligand	Chemical Shifts of complex
The carbon of the CH group	Multi peak around at 94.00	Two peaks at 94.337-94.770
carbon CH ₂ group	Three peaks at 26.288-30.435-35.144	33.065
Carbon C=O group	Two peaks at 159.147-159.656	Two peaks at 148.255-207-418

Table 3. ¹H-NMR chemical shifts, in ppm, of pyrazole and complex from pyrazole as a ligand with nickel as a metal (number 1) or cobalt as a metal (number 2).

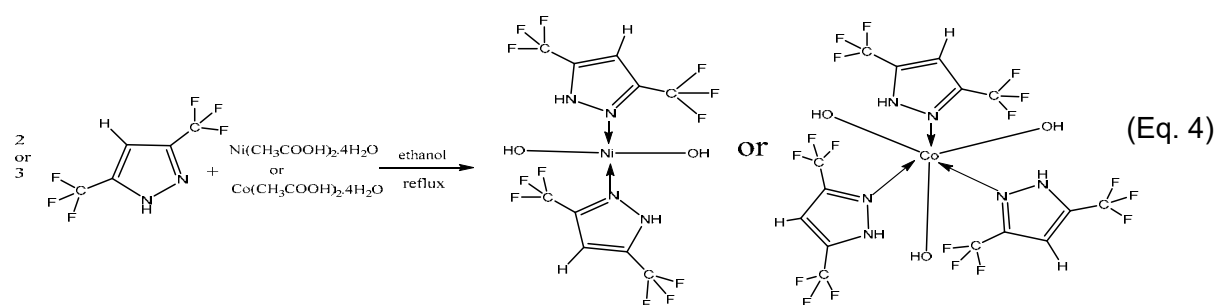
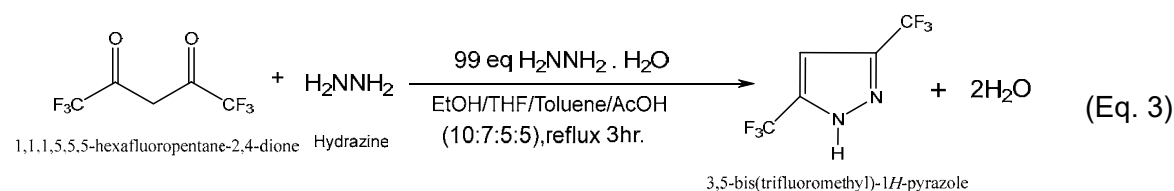
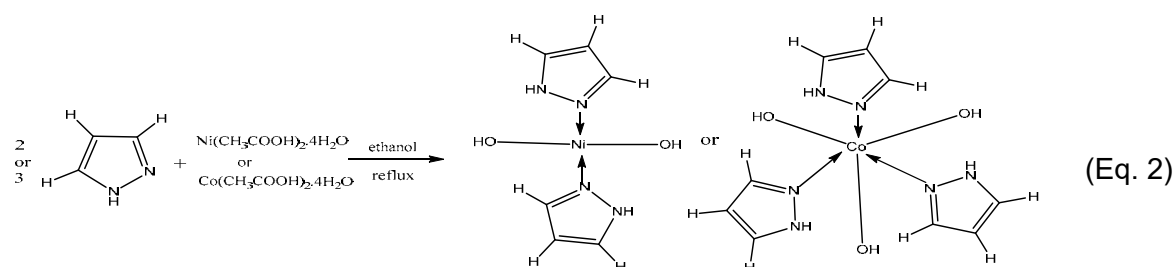
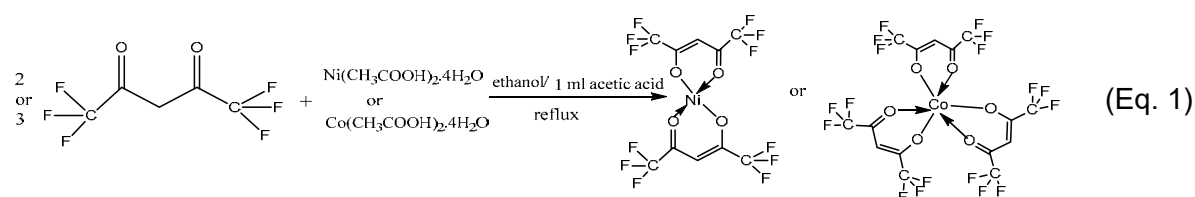
Assigned protons	Chemical Shifts of pyrazole	Chemical Shifts of complex number 1	Chemical Shifts of complex number 2
Proton number 8	6.369	4.007	3.992
Protons number 7 and 9	7.657	4.722	4.676
Proton number 6	12.3	Brood; disappeared	7.335

Table 4. ¹H-NMR chemical shifts, in ppm, of 3,5-bis(trifluoromethyl)-1*H*-pyrazole and complex from 3,5-bis(trifluoromethyl)-1*H*-pyrazole as a ligand with nickel as a metal.

Assigned protons	Chemical Shifts of pyrazole	Chemical Shifts of complex
Aromatic proton(triplet peak)	6.867,7.038,7.208	7.473
The proton of the NH group	8.389	10.34

Table 5. FT-IR bands in cm^{-1} of hexafluoroacetylacetone, 3,5-trimethylpyrazole, and complex from 3,5-bis(trifluoromethyl)-1*H*-pyrazole as a ligand with nickel as a metal.

functional group names assigned	FT-IR bands of hexafluoroacetylacetone	FT-IR bands of pyrazole	FT-IR bands of complex
$\nu(\text{C-F})$ stretching (strong peak)	1138.11-1178.55	-	1136.11
$\nu(\text{C-N})$ stretching (strong peak)	-	1305.85	1242.20
$\nu(\text{C=O})$ stretching	Brood band at 1650	-	-
$\nu(\text{N-H})$ stretching (strong peak)	-	3200.01	Brood band at 3400.62



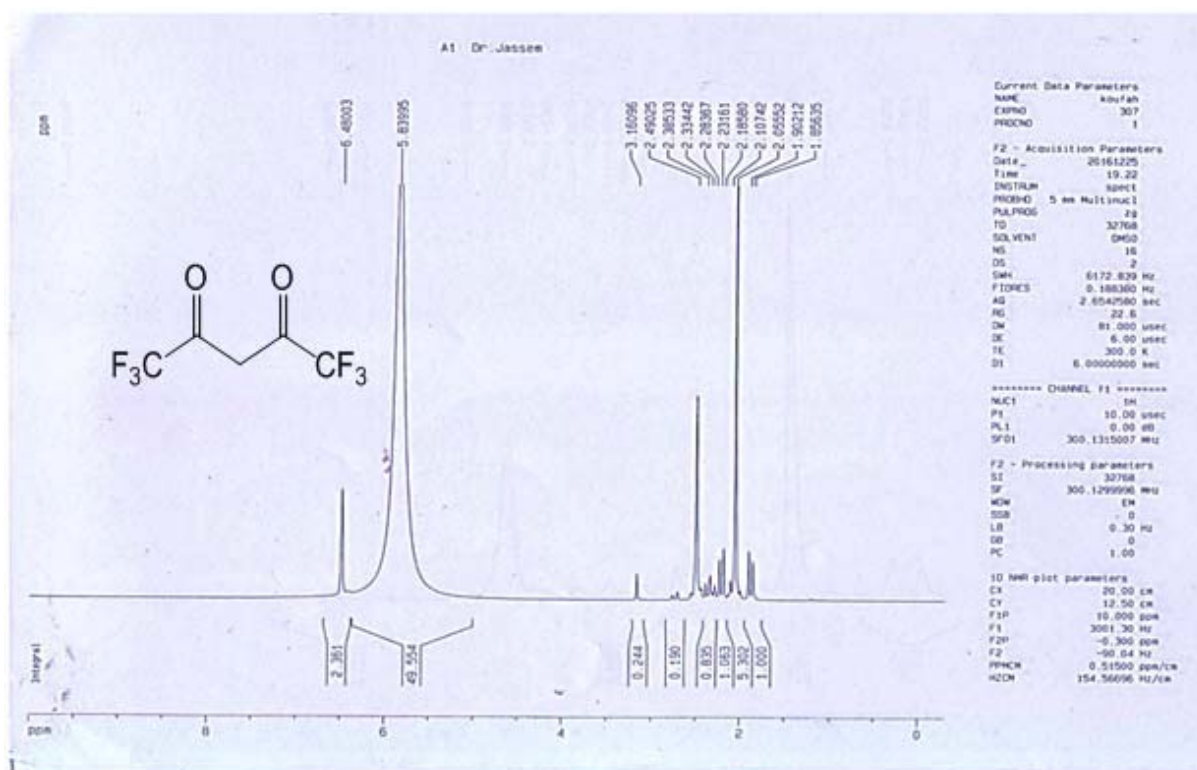


Figure 1. ^1H -NMR spectrum of a hexafluoroacetylacetone.

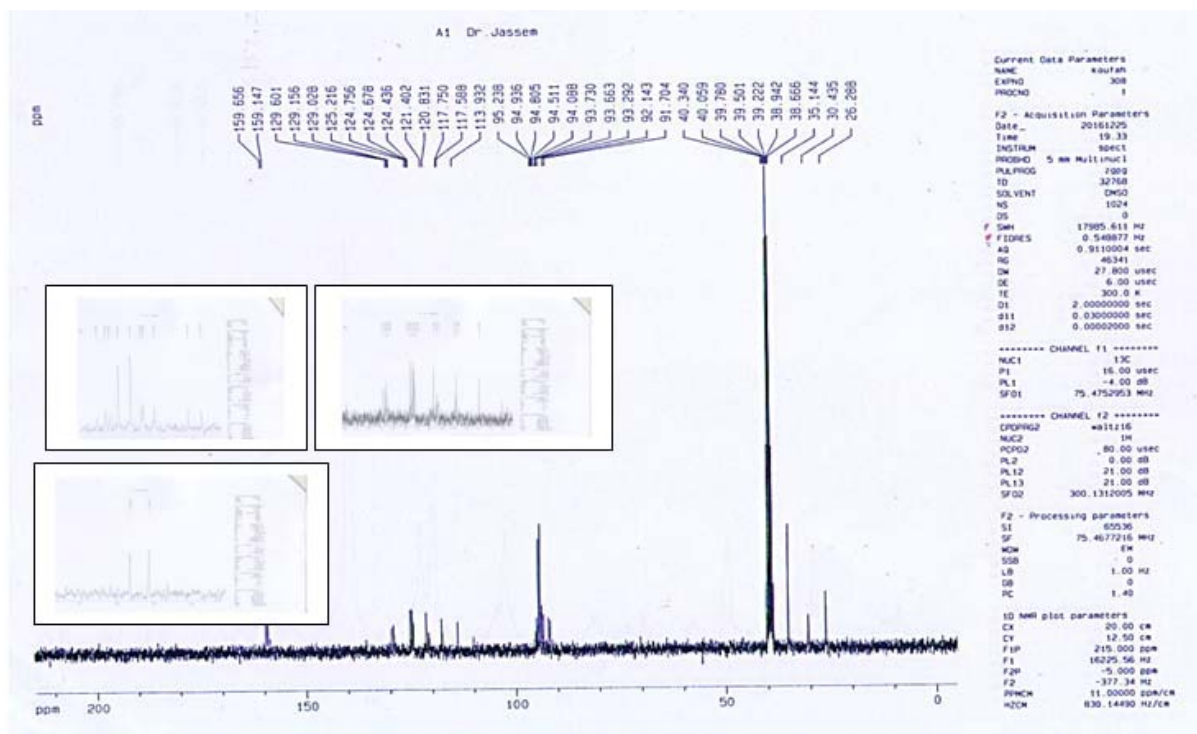


Figure 2. ^{13}C -NMR spectrum of a hexafluoroacetylacetone with three spectra expands it.

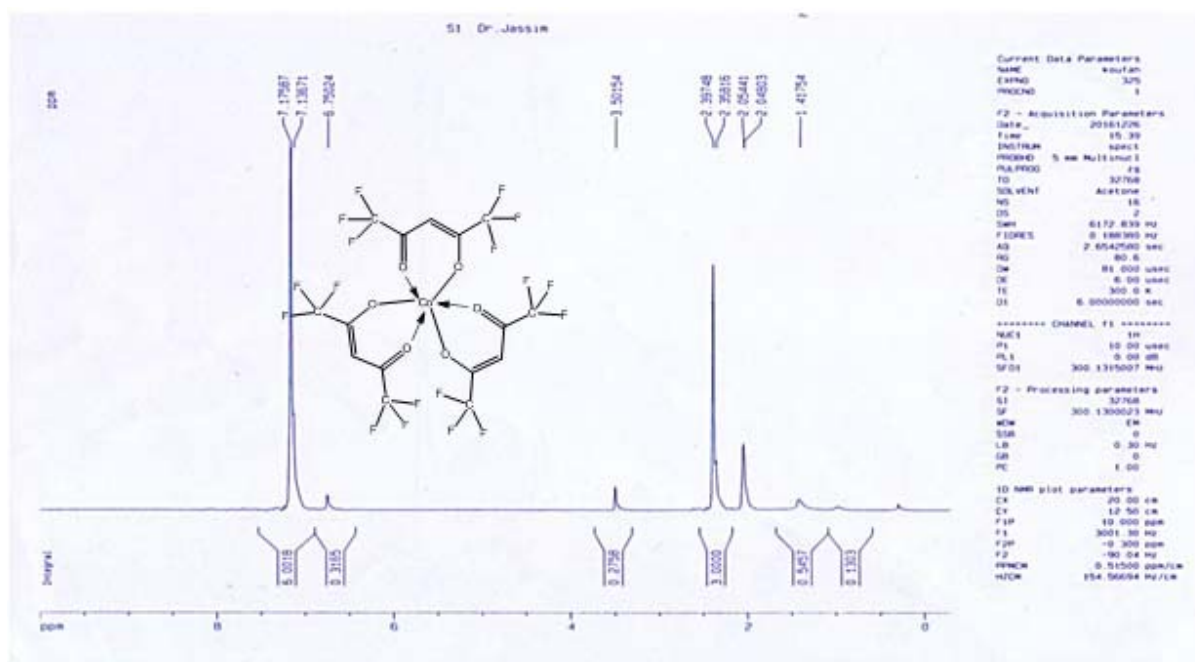


Figure 3. ^1H -NMR spectrum of complex prepared from hexafluoroacetylacetone as a ligand and nickel as a metal.

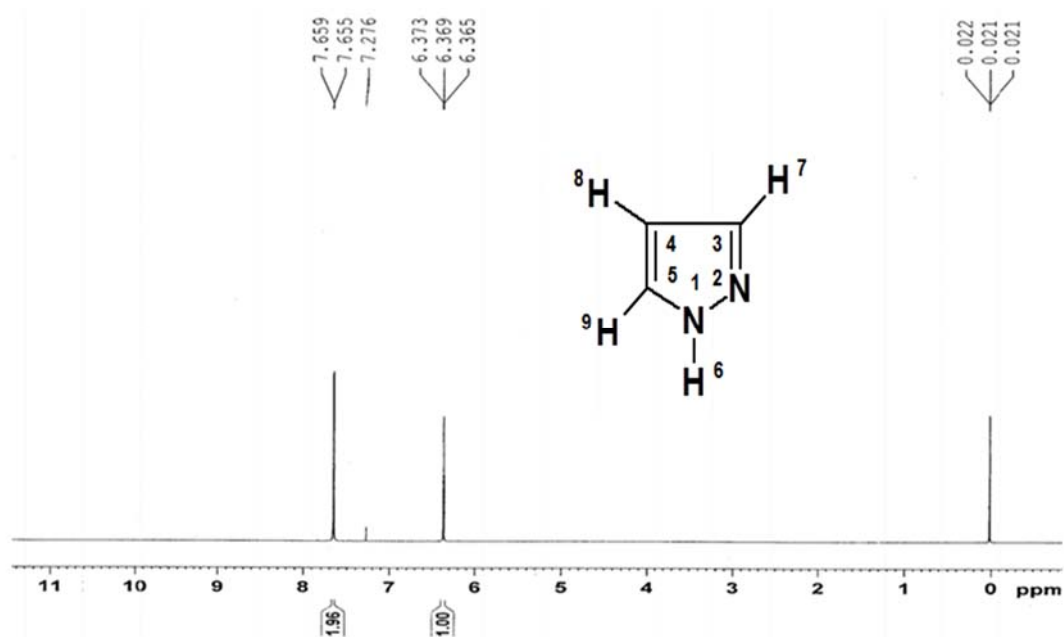


Figure 4. ^1H -NMR spectrum of pyrazole (Clark, 2010)

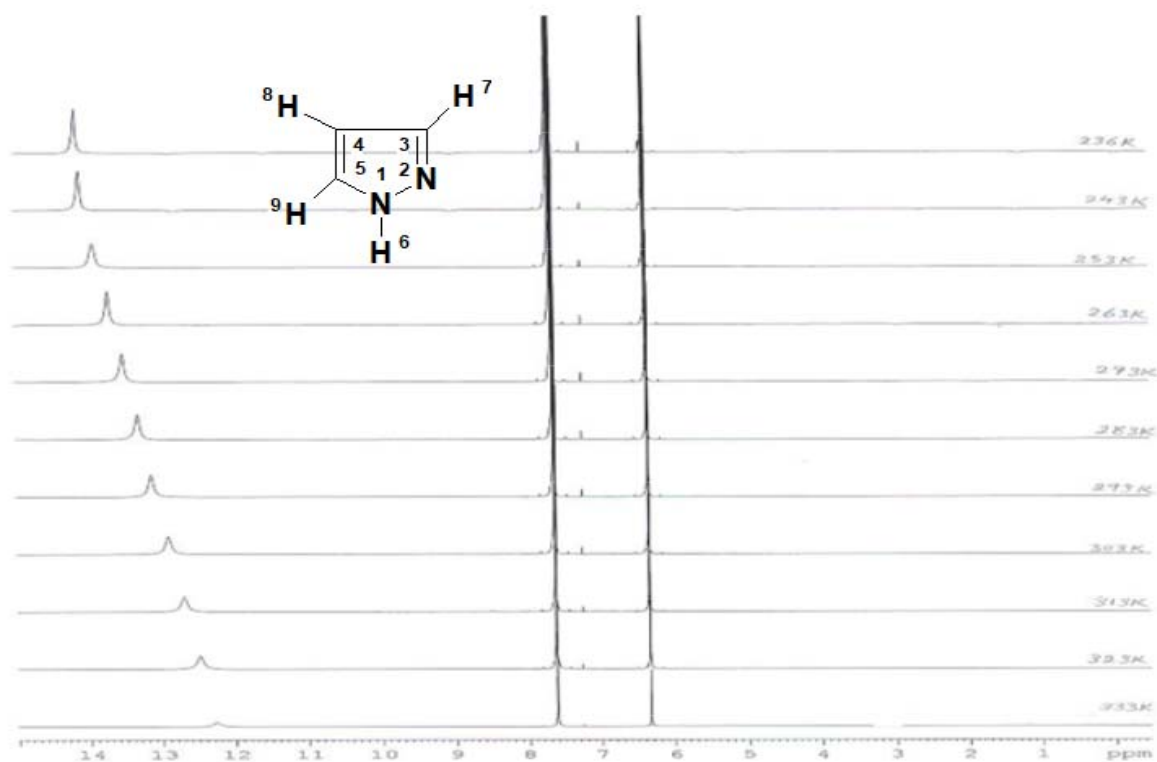


Figure 5. DNMR spectrum of pyrazole (Clark, 2010)

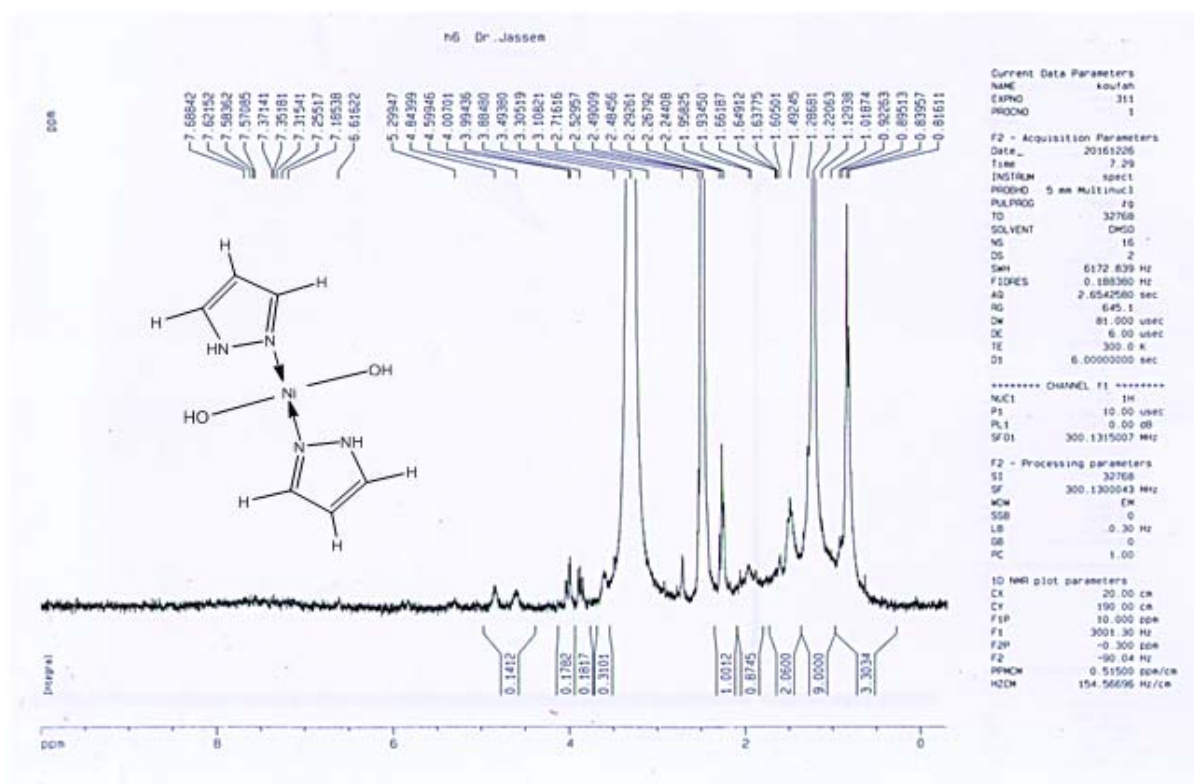


Figure 6. ^1H -NMR spectrum of complex prepared from pyrazole as a ligand and nickel as a metal.

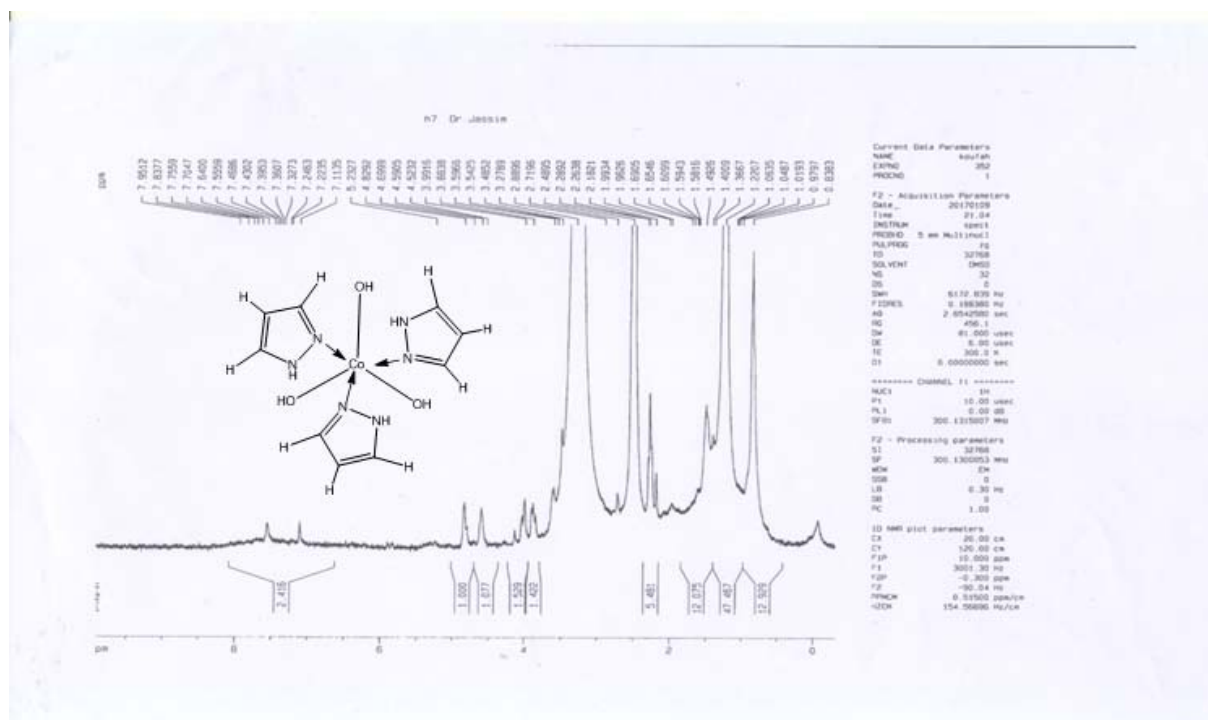


Figure 7. ^1H -NMR spectrum of complex prepared from pyrazole as a ligand and cobalt as a metal.

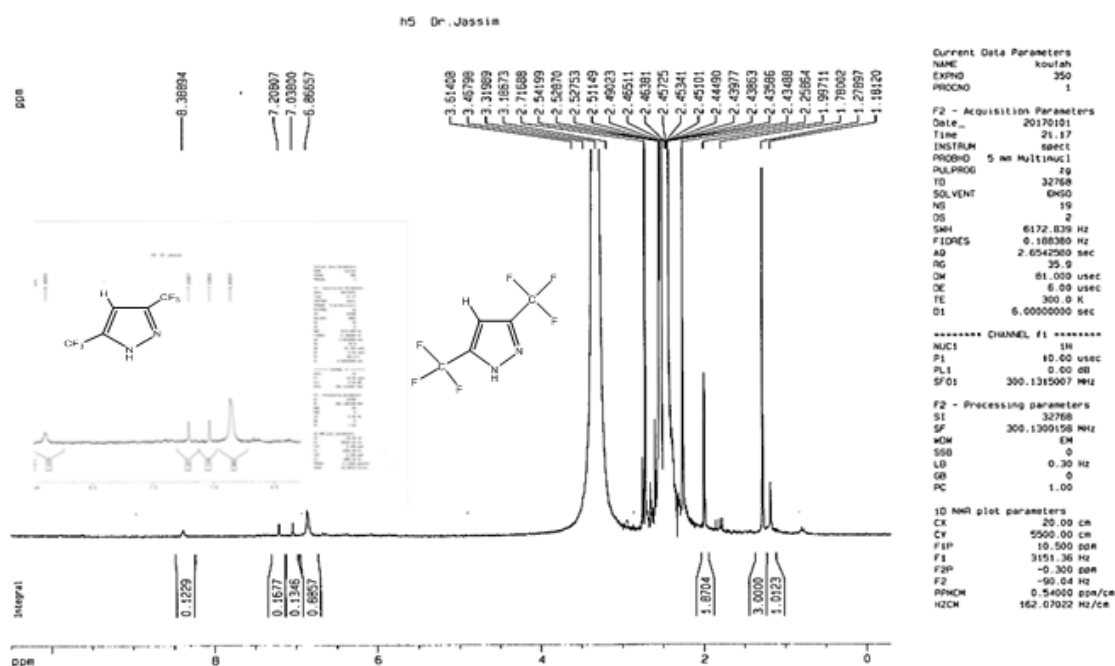


Figure 8. ^1H - NMR spectrum of 3,5-bis(trifluoromethyl)-1H-pyrazole with expansion region at 6.5-8.5 ppm.

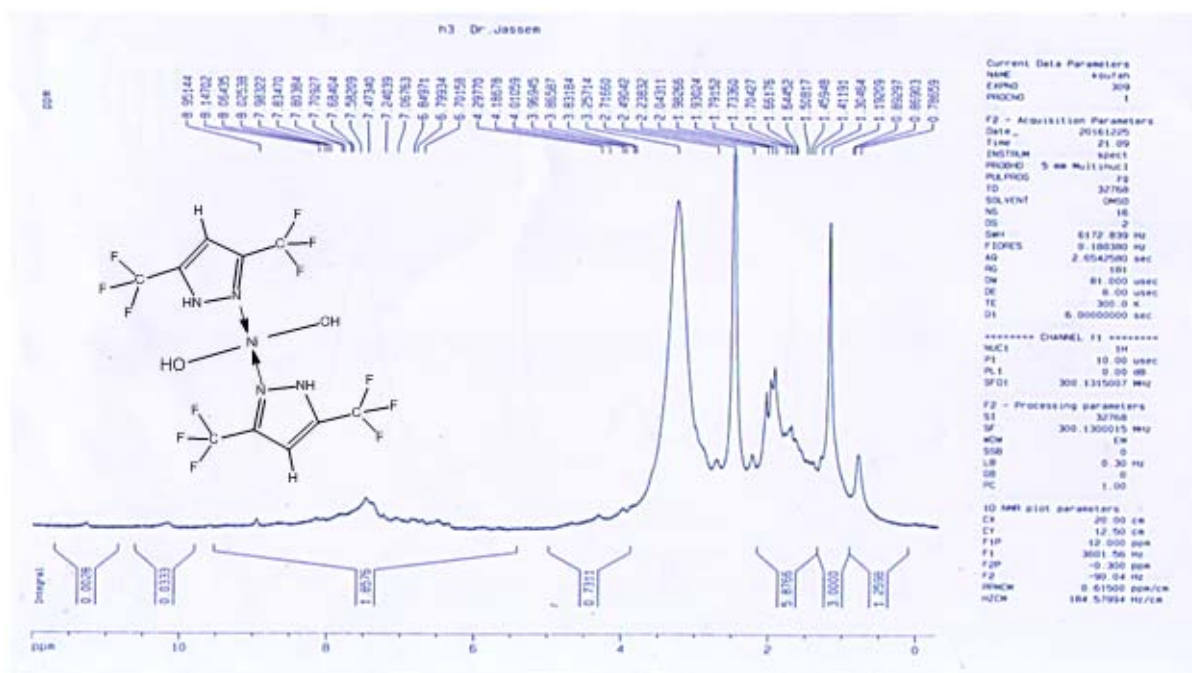


Figure 9. ^1H -NMR spectrum of complex prepared from 3,5 bis(trifluoromethyl)-1H-pyrazole as a ligand and nickel as a metal.

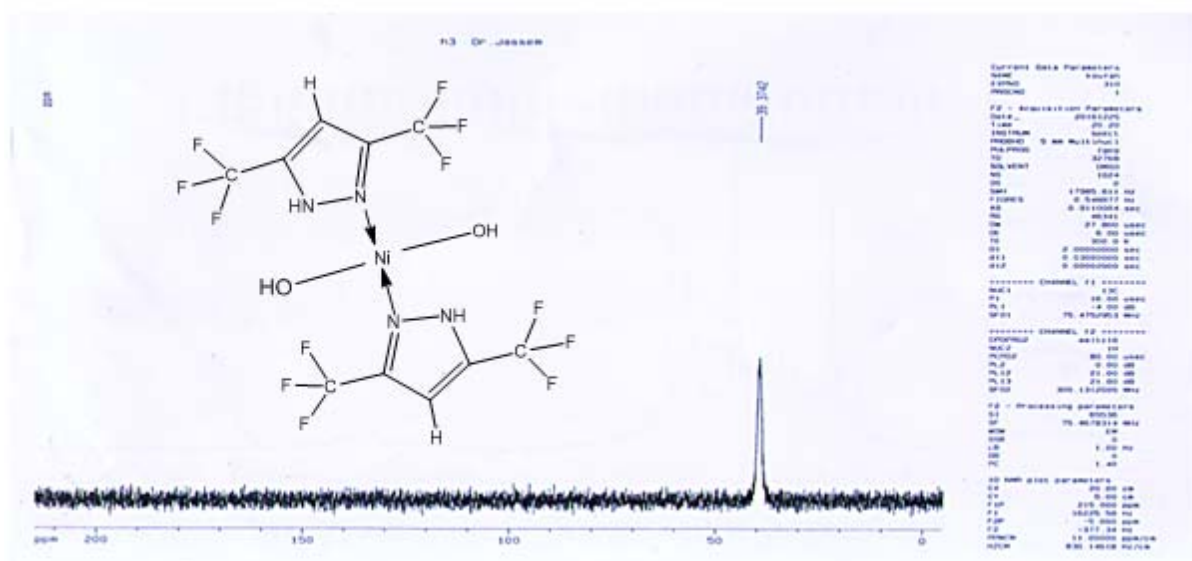


Figure 10. ^{13}C -NMR spectrum of complex prepared from 3,5-bis(trifluoromethyl)-1H-pyrazole as a ligand and nickel as a metal.

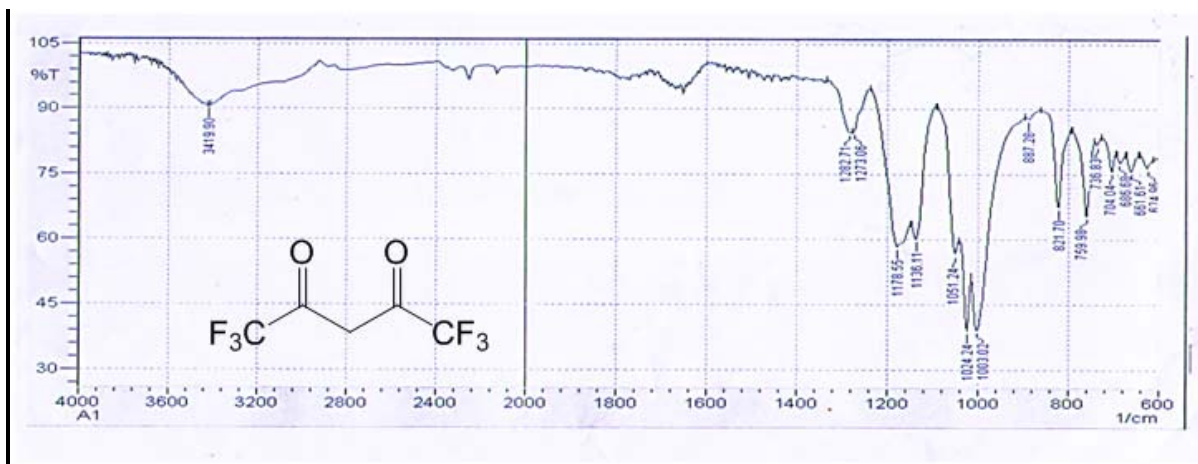


Figure 11. The FT-IR spectrum of hexafluoroacetylacetone.

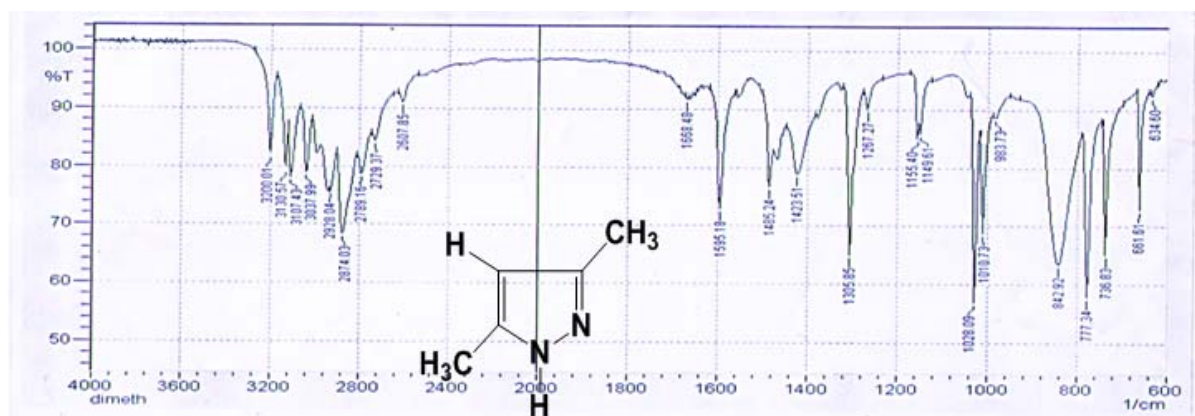


Figure 12. The FT-IR spectrum of 3,5-dimethylpyrazole.

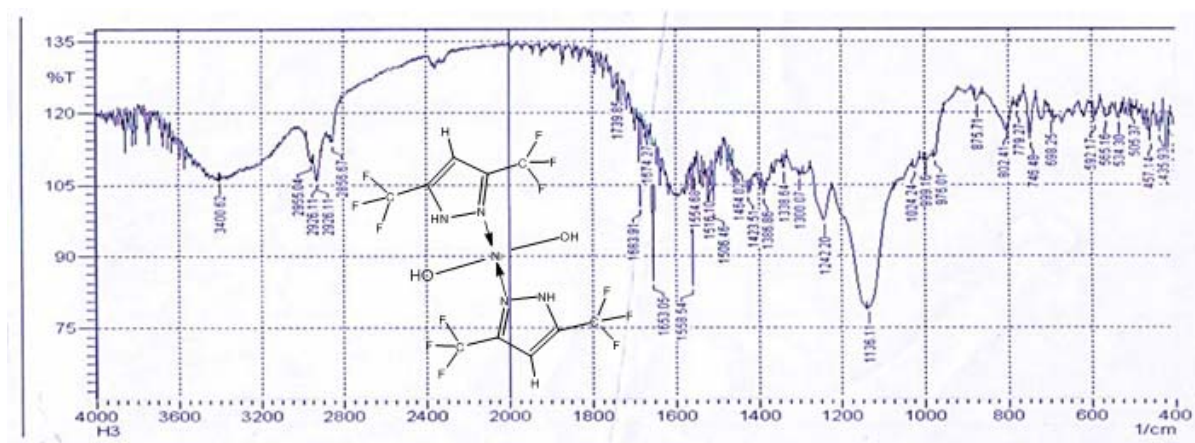


Figure 13. FT-IR spectrum of complex prepared from 3,5-bis(trifluoromethyl)-1H-pyrazole as a ligand and nickel as a metal.

DESENVOLVIMENTO DE UM INIBIDOR DE DEPÓSITO DE ASFALTO-RESINA-PARAFINA E SUBSCANTIAÇÃO DOS PARÂMETROS TECNOLÓGICOS DE SUA INJEÇÃO NA ZONA DE FORMAÇÃO DE FURO INFERIOR**DEVELOPMENT OF AN ASPHALT-RESIN-PARAFFIN DEPOSITS INHIBITOR AND SUBSTANTIATION OF THE TECHNOLOGICAL PARAMETERS OF ITS INJECTION INTO THE BOTTOM-HOLE FORMATION ZONE****РАЗРАБОТКА ИНГИБИТОРА АСФАЛЬТОСМОЛОПАРАФИНОВЫХ ОТЛОЖЕНИЙ И ОБОСНОВАНИЕ ТЕХНОЛОГИЧЕСКИХ ПАРАМЕТРОВ ЕГО ЗАКАЧКИ В ПРИЗАБОЙНУЮ ЗОНУ ПЛАСТА**

KHAIBULLINA, Karina Shamilevna^{1*}; KOROBOV, Grigory Yurievich²; LEKOMTSEV Aleksandr Viktorovich³;

^{1,2} St. Petersburg Mining University, St. Petersburg. Russian Federation

³ Perm National Research Polytechnic University, Perm, Russian Federation.

* Correspondence author
e-mail: khaibullina_k@mail.ru

Received 10 February 2020; received in revised form 11 March 2020; accepted 23 March 2020

RESUMO

O problema da formação de depósitos de asfalto-resina-parafina (ARPD) em campos de petróleo dentro do sistema “poço - zona de formação de fundo de poço” ainda é relevante. Para impedir a formação de ARPD no sistema “zona de formação de fundo de poço - poço”, os inibidores de ARPD devem ter propriedades de alta adsorção e baixa dessorção em relação à rocha. A composição de inibidores geralmente inclui surfactantes. Os surfactantes não iônicos, ou seja, os poliésteres são amplamente utilizados para evitar a formação de ARPD. No entanto, atualmente, pouco se sabe sobre inibidores com um efeito combinado, por exemplo, possuindo propriedades dispersoras de depressoress em relação à ARPD. O trabalho objetivou desenvolver um inibidor combinado possuindo não apenas propriedades dispersoras de depressoress, mas também boas propriedades de adsorção e dessorção em relação à rocha para impedir a formação de ARPD. O artigo apresenta os resultados da pesquisa sobre o desenvolvimento de um inibidor da ARPD, bem como da determinação de suas propriedades dispersoras, inibidoras e corrosivas do depressor; a temperatura da saturação de óleo com parafina também foi determinada. Os estudos da adsorção do inibidor da ARPD foram realizados pelos métodos estático e dinâmico. Já o processo de dessorção do inibidor foi estudado por filtragem de óleo através de uma amostra saturada da rocha usando um modelo a granel e um material do núcleo. O impacto da taxa de fluxo de fluido na taxa de dessorção do inibidor foi estudado. Foram calculados os parâmetros tecnológicos da injeção da solução inibidora da ARPD na zona de formação do fundo dos poços de produção. A composição desenvolvida possui altas propriedades inibidoras em relação à ARPD, propriedades dispersoras de depressoress, baixa atividade corrosiva em relação a uma superfície metálica e é capaz de reduzir a temperatura de saturação de óleo com parafina.

Palavras-chave: *depósitos de asfalto-resina-parafina, inibidor, zona de formação de fundo de poço, temperatura de saturação de óleo com parafina, adsorção, dessorção.*

ABSTRACT

The problem of the formation of asphalt-resin-paraffin deposits (ARPD) in oil fields within the “well – bottom-hole formation zone” system is still relevant. To prevent the formation of ARPD in the “bottom-hole formation zone – well” system, the ARPD inhibitors must have high adsorption and low desorption properties concerning the rock. The composition of inhibitors often includes surfactants. Nonionic surfactants, namely, polyesters, are widely used to prevent the formation of ARPD. However, currently, little is known about inhibitors with a combined effect, for example, possessing depressor-dispersing properties for ARPD. This work aimed to develop a combined inhibitor possessing not only depressor-dispersing properties but also having good adsorption and desorption properties to the rock to prevent the formation of ARPD. The paper presents the research results on the development of an ARPD inhibitor, as well as the effects of determination of its depressor-

dispersing, inhibiting, and corrosive properties; the temperature of oil saturation with paraffin is determined as well. The studies of the ARPD inhibitor adsorption were carried out by the static and dynamic methods. In contrast, the process of the inhibitor desorption was studied by oil filtering through a saturated sample of the rock using a bulk model and core material. The impact of the fluid flow rate on the inhibitor desorption rate was studied. The technological parameters of the ARPD inhibitor solution injection into the bottom-hole formation zone of production wells were calculated. The developed composition has high inhibiting properties concerning the ARPD, depressor-dispersing properties, low corrosive activity for a metal surface, and is capable of lowering the temperature of oil saturation with paraffin.

Keywords: *asphalt-resin-paraffin deposits, inhibitor, bottom-hole formation zone, temperature of oil saturation with paraffin, adsorption, desorption.*

АННОТАЦИЯ

На сегодняшний день проблема образования асфальтосмолопарафиновых отложений (АСПО) на нефтяных месторождениях в системе «скважина-призабойная зона пласта» является актуальной. Чтобы предотвратить образование АСПО в системе «призабойная зона - скважина», ингибиторы АСПО должны обладать высокими адсорбционными и низкими десорбционными свойствами по отношению к породе. В состав ингибиторов часто входят поверхностно-активные вещества. Неионогенные поверхностно-активные вещества, а именно полимеры сложных эфиров, широко используются для предотвращения образования АСПО. Однако, в настоящее время мало известно об ингибиторах с комбинированным эффектом, например, обладающих депрессорно-диспергирующими свойствами по отношению к АСПО. Работа направлена на разработку ингибитора комбинированного действия, обладающего не только депрессорно-диспергирующими свойствами, но также обладающего хорошими адсорбционными и десорбционными свойствами по отношению к породе для того, что предотвратить образование АСПО. В статье представлены результаты исследований по разработке ингибитора АСПО, а также определены его депрессорно-диспергирующие, ингибирующие и коррозионные свойства; температура насыщения нефти парафином. Исследования адсорбции ингибитора АСПО проводились статическим и динамическим методами. Процесс десорбции ингибитора был изучен путем фильтрации нефти через насыщенный образец породы с использованием насыпной модели и кернового материала. Было изучено влияние скорости течения жидкости на скорость десорбции ингибитора. Рассчитаны технологические параметры закачки раствора ингибитора АСПО в призабойную зону пласта добывающих скважин. Разработанный состав обладает высокими ингибирующими свойствами по отношению к АСПО, депрессорно-диспергирующими свойствами, низкой коррозионной активностью по отношению к металлической поверхности и способен снизить температуру насыщения нефти парафином.

Ключевые слова: *асфальтосмолопарафиновые отложения, ингибитор, призабойная зона пласта, температура насыщения нефти парафином, адсорбция, десорбция.*

1. INTRODUCTION:

Oil production at the fields of the Russian Federation is often associated with unwanted formation of asphalt-resin-paraffin deposits in the bottom-hole formation zone, on the walls of underground well equipment, and in the above-ground lines of the oil and gas gathering and processing system (Yemelyanov *et al.*, 2018, 2019; 2020; Plaskova *et al.*, 2019;).

Currently, chemical methods are the most widely used to prevent the formation of ARPD. Their principle of operation is based on adsorption processes, occurring at a boundary of a liquid and solid surface. Thus, chemical methods are divided by this feature into methods based on the use of wetting agents, modifiers, depressors, and dispersants.

The principle of operation of wetting agents is based on the formation of a hydrophilic film on the solid surface of well equipment, which in turn prevents the adhesion of paraffin crystals to the pipes and creates conditions sufficient for their removal by fluid flow. Modifiers, when interacting with paraffin crystals, changing their wettability, keep them in a suspended, dispersed state, make them rounder, compared to their initial needle-like or diamond shape. The principle of operation of depressors resides in the adsorption of their molecules on paraffin crystals, thereby complicating the process of combining thereof into a single system. Dispersants reduce oil-freezing point. Dispersants increase the thermal conductivity of oil and slow down the process of paraffin crystallization. Due to the increase in duration for paraffin crystals being in a dispersed suspended state, the possibility of removal thereof

from the well equipment at the wellhead increases (Windyandari *et al.*, 2018;).

To date, the use of ARPD inhibitors to protect well equipment and the BHFZ is a matter of urgency. However, it is often the case that their cost is high, most of the components, included in their composition, are toxic, and an individual selection of reagents for oils with different properties is required. According to field experience, when dosing the ARPD inhibitor for the well bottom-hole, it often enters the reservoir fluid after the formation of paraffin solid phases has begun. This is because the creation of ARPD can occur earlier than the reservoir fluid enters the well, namely in the BHFZ and in the pore space of the oil reservoir.

Despite the diversity of scientific papers devoted to the study of methods for removing organic deposits in oilfield equipment, as of today, the technique for preventing the formation of ARPD by dosing inhibitors in the BHFZ remains poorly studied and unsubstantiated. To solve this problem, it is expedient to use the known technique for preventing scaling, wherein the inhibitor is dosed in the BHFZ (Antipin *et al.*, 1987; Kashchavtsev *et al.*, 2004; Mishchenko 2007; Faskhutdinov *et al.*, 1996).

According to the technique for preventing the formation of ARPD by the injection of reagents into the BHFZ, the duration of the inhibitor removal is determined by the processes of its adsorption and subsequent desorption. In this case, the inhibitor removal by the reservoir fluid up to a minimum effective concentration determines the period of protection of the oilfield equipment from ARPD and the time between injections, when injecting it into the BHFZ. The efficiency of the inhibitor use and the frequency of its injection are determined by the duration of its adsorption-desorption processes occurring in the BHFZ; therefore, to select and substantiate the technique, these processes need to be studied (Solazzi and Zrnić, 2017; Kopish and Marques, 2020).

The study aimed at determining the efficiency of the use of the ARPD inhibitor, as well as its adsorption and dispersing properties with respect to the rock, have been conducted.

2. MATERIALS AND METHODS:

A chemical composition, with a reference designation of IN-1, was developed by us as an ARPD inhibitor, wherein the IN-1 is a composition based on a mixture of olefins and the product of

the interaction between unsaturated fatty acids and complex ethylene amines, amino alcohols and mixtures thereof. The ARPD inhibitor (IN-1) acts as a blocking agent to prevent the formation of heavy paraffins, which have a tendency towards sedimentation in fluids under the action of a gravitational field or centrifugal forces and does not require harsh conditions. For better dissolving in oil, it is sufficient to heat the IN-1 reagent to a temperature of 30-40°C.

Besides, an indirect method for determining the temperature of oil saturation with paraffin, via rheogoniometry, was used to determine the kinematic viscosity of oil with and without adding the IN-1 at a gradual decrease in temperature. To determine the adsorption properties of the IN-1 reagent, a bulk formation model, which is quartz sand, was chosen as the adsorbent. Its grain-size composition with a particle diameter of 0.25-0.1 mm – 85 wt.%; 0.1-0.05 mm – 15 wt.%. The IN-1 reagent was preliminary dissolved in a paraffin oil model, at different concentrations (0.05–2%). Since the ARPD formation begins with the separation of the solid phase of paraffin, only the paraffin oil model was used during the studies. Using the EASYDROP system for measuring the contact angle of wetting and interfacial (surface) tension, the surface tension was measured at the boundary with distilled water, followed by the construction of a calibration curve, that allows one to determine the studied reagent concentration in the fluid by the changes in the surface tension (Neizvestnaya *et al.*, 2018; Szafarczyk, 2019; Prodanova *et al.*, 2019;).

The studies of the ARPD inhibitor (IN-1 reagent) adsorption were carried out by two methods: static – using a bulk model and dynamic – using core material, which renders possible to specify the amount of the inhibitor adsorption on pore walls, referred to the pore surface area. A well-known technique for determining the reagent adsorption under static conditions was used during the studies (Babalyan *et al.*, 1983). The inhibitor equilibrium concentration in the solution after adsorption is determined by the change in the surface tension of the fluid with increasing concentration of this substance in the solution using the calibration curve (Figure 3). The study of the ARPD inhibitor adsorption on the core pore walls under dynamic conditions was conducted as follows. An oil-saturated core was placed in the core holder, through which oil, with the ARPD inhibitor (5 wt.%) dissolved therein, was subsequently pumped until the inhibitor concentration at the core holder inlet and outlet

became equivalent. Samples were periodically taken to determine the surface tension at the boundary with distilled water, and the values obtained were used to determine the ARPD inhibitor concentration in oil.

The process of the IN-1 inhibitor desorption was studied by oil filtering through a saturated sample of the rock via two methods: using a bulk model and core material. To determine the desorption process, samples of the bulk model (50 g) were placed in separation test flasks, with subsequent injection of the inhibiting solution – oil with the IN-1 inhibitor dissolved therein (20 wt.%). The concentration of the inhibitor was selected empirically. When its concentration in oil exceeds 20%, the reagent is quickly removed at the initial stages of filtration, which is economically unprofitable. When the inhibitor concentration in oil is less than 20%, the amount of pore volumes of oil, needed for the reagent removal, is halved. Therefore the time of the reagent presence in the rock as well as the reagent efficiency is reduced.

To achieve adsorption equilibrium, the inhibited bulk model was left for a day. The inhibiting solution desorption was implemented by passing through the inhibited bulk model of oil without reagent. The volumetric flow rate of the fluid through the rock was 3 ml/min. At the outlet of the separation test flask, 3 ml of working solution was taken to be analyzed for the ARPD inhibitor content. Oil was injected until its percentage content in the bulk model pores became constant. The impact of the fluid flow rate on the inhibitor desorption rate was studied. The studies were carried out at various volumetric flow rates of the fluid (from 0.5 to 3 ml/min). The research results are presented in Figure 5.

Proceeding from the obtained results of laboratory studies of the ARPD inhibitor adsorption-desorption processes, it is possible to calculate the technological parameters of squeezing the solution, inhibiting the ARPD, into the BHFZ of production wells.

To calculate the amount of the ARPD inhibitor for injection into the BHFZ, the formula, proposed in scientific papers by Antipin Yu.V., Ibragimov G.Z., and Khisamutdinov N.I., was accepted for determining the amount of the scaling inhibitor with injection into the BHFZ (Antipin *et al.*, 1987; Ibragimov and Khisamutdinov, 1983; Rahim, 2018; Jasińska, 2019).

$$m_{\text{инг}} = Q_{\text{сж}} \cdot (1 - \beta) \cdot C_{\text{эф}} \cdot t \cdot \rho_{\text{ж}} \cdot A \quad (1)$$

where: $m_{\text{инг}}$ is the calculated amount of the ARPD inhibitor for injection into the BHFZ, kg; $Q_{\text{сж}}$

is a well productivity by the fluid, m³/day; $C_{\text{эф}}$ is the ARPD inhibitor concentration in the produced fluid, ensuring the required protective effect in the system, kg/m³; t is the planned time for the inhibitor removal from the formation (120-180 days); $\rho_{\text{ж}}$ is the produced fluid density, kg/m³; β is a volumetric fraction of water in the produced well products.

Formula 1 contains a coefficient A , considering the unevenness of the scaling inhibitor removal from the BHFZ. According to the scientific papers by Antipin Yu.V., Ibragimov G.Z., and Khisamutdinov N.I., it is recommended to take it from 1.5 to 2 (Kashchavtsev and Mishchenko, 2004; Lateef *et al.*, 2019; Zakki *et al.*, 2019;), without the choice of a specific value being substantiated.

Proposed is a graphical method for determining the coefficient A depending on the fluid volumetric flow rate (well production rate), according to experimental diagrams for the dependence of the ARPD inhibitor concentration in oil at the core holder outlet on the number of pore volumes of pumped oil. The coefficient A is determined as the ratio of the volume of the ARPD inhibitor removed from the formation during its uneven removal to the hypothetical volume of the ARPD inhibitor during uniform removal.

In the diagram, this will be determined as the area ratio of the Figures, bounded by the functions $f_1(n)$ and $f_2(n)$:

$f_1(n)$ is the curve of the ARPD inhibitor desorption at uneven removal;

$f_2(n)$ is the hypothetical curve of the ARPD inhibitor desorption at uniform removal.

3. RESULTS AND DISCUSSION:

It was revealed that the developed chemical composition IN-1 has high inhibiting properties with respect to the ARPD, possesses depressor-dispersing properties, has low corrosive activity with respect to a metal surface, and reduces the temperature of oil saturation with paraffin.

To determine the temperature of oil saturation with paraffin via rheogoniometry, a paraffin oil model was used (5 wt.% of paraffin). The reagent concentration in oil made 0.2 wt.%. The diagram for the dependence of oil viscosity on temperature, according to which, by the subsequent use of the indirect method, the temperature of oil saturation with paraffin was

determined, was built.

The research results are presented in Table 1 and Figures 1 and 2. The temperature of oil saturation with paraffin for paraffin oil (5 wt.% of paraffin) was determined via rheogoniometry and the method of visual observation. The temperature of oil saturation with paraffin for the IN-1 reagent-free oil made 35°C. The optimal concentration of the inhibitor (0.2%), wherein the temperature of oil saturation with paraffin virtually remains unchanged, was determined. Upon adding the IN-1, the temperature of oil saturation with paraffin decreased by 8°C. With the increase in paraffin content in oil up to 7 wt.%, the temperature of oil saturation with paraffin increased by 4°C (from 35 to 39°C), i.e., proportionally increasing with the increase in paraffin content. Micrographs of paraffin oil (7 wt.%) with the IN-1, added in the amount of 0.2 wt.%, and without the IN-1, were made. The micrographs were taken at a temperature of 37°C (average formation temperature of Tatarstan fields). As is seen from the micrographs in Figure 1, upon injection of the developed ARPD inhibitor (0.2 wt.%) into paraffin oil, the process of paraffin crystals formation slows down.

As is seen from Figure 2, the temperature of oil saturation with paraffin without adding the IN-1 is 35°C; with a further decrease in temperature, a sharp increase in the kinematic viscosity of oil is observed. Upon adding the ARPD inhibitor in oil, the temperature of oil saturation with paraffin decreases from 35 to 26°C. Thus, it can be concluded that the developed IN-1 reagent can act as the ARPD inhibitor to prevent the formation of deposits in well equipment and the BHFZ.

As is seen from Figure 3, the highest rate of increase in the IN-1 inhibitor adsorption is observed in the range of low values of its initial concentration in oil. This is since the IN-1 inhibitor has a high surface tension to the bulk model. When adding the inhibitor in the amount from 0.5 to 1%, the adsorption isotherm approaches the "plateau" region, i.e., the adsorption equilibrium. The adsorption equilibrium occurs at the reagent concentration of more than 0.5%. It means that when IN-1 is added in the amount of more than 0.5%, the inhibitor rate of advance will be equal to the rate of injection. The value of the limiting adsorption, wherein the entire surface of the adsorbent is filled with adsorbate, made 0.0147 ml/g (0.219 ml/m²).

Figure 4 presents the dynamics of changes in the ARPD inhibitor concentration in oil at the core holder outlet. The value of the limiting

adsorption on core material under dynamic conditions made 0.520 ml/m². The results of the study of the ARPD inhibitor adsorption on a core sample used under a dynamic mode, as well as under a static one, prove that the developed reagent has adsorption properties with respect to the rock.

The results of studying the impact of the fluid flow rate on the inhibitor desorption rate confirm that with an increase in the fluid volumetric flow rate, the rate of the inhibitor desorption from the formation increases as well. For example, when the fluid flow rate increases from 0.5 ml/min to 3 ml/min, the reagent removal time reduces by 19 times. When calculating the technological parameters of the inhibiting solution injection into the BHFZ, it is necessary to take into account the fluid filtration rate (volumetric flow rate) in the BHFZ.

Studies of the inhibitor desorption from the pore walls, depending on the different length of the bulk model, were carried out. Two samples of the bulk model, with a length of 3.5 and 7 cm, were studied. The fluid volumetric flow rate made 0.5 ml/min. The research results are presented in Figure 6.

As is seen from Figure 6, at the bulk model length of 3.5 cm, the time of the ARPD inhibitor removal until the minimum effective concentration is achieved makes approximately 600 minutes, and at the bulk model length of 7 cm – 1300 minutes. Thus, it can be concluded that an increase in the volume of the formation, being treated with the solution, inhibiting the ARPD, results to a proportional increase in the time of the inhibitor removal.

The ARPD inhibitor (20%) was injected into a core with a different volume of pumped oil after the inhibitor was squeezed. The oil filtration rate made 0.5 ml/min. The impact of the volume of pumped oil on the subsequent inhibitor desorption from the core pore walls was studied. The dependence of the ARPD inhibitor relative concentration in oil at the core holder outlet on the volume of pumped oil is presented in Figure 7.

The results obtained make it possible to conclude that when injecting the inhibitor into the BHFZ, it is necessary to squeeze it into the formation using at least 5 ... 10 times the volume of displacement fluid, to reduce the loss of the inhibitor at the initial stage of well operation after treatment. It is recommended to use oil as a displacement fluid.

Furthermore, the ARPD inhibitor was

injected into the core, with its subsequent squeezing with oil in the amount of 10 pore volumes at different volumetric flow rates. The research results are presented in Table 2.

Table 2. Impact of the fluid volumetric flow rate on the duration of the ARPD inhibitor protective effect

$Q_{\text{көрн}}$, ml/min	0.5	1	2	3
n, units	200	127	61	35

where $Q_{\text{көрн}}$ is the fluid volumetric flow rate by the core; n is the number of pore volumes of the pumped oil until a minimum effective concentration of the ARPD inhibitor is achieved.

The determination of the coefficient A at oil volumetric flow rate of 0.5 ml/min (0.00072 m³/day) is graphically presented in Figure 8, and analytically shown in formula (2).

$$A = \frac{S_1}{S_2} = \frac{\int_{n_{i-1}}^{n_i} f_1(n) dn}{\int_{n_{i-1}}^{n_i} f_2(n) dn} = \frac{\sum C_i \cdot (n_i - n_{i-1})}{C_{\min \text{ эф}} \cdot (n_i - n_{i-1})} \quad (1)$$

where S_1 is the area of the Figure, bounded by the function $f_1(n)$; S_2 is the area of the Figure, bounded by the function $f_2(n)$; n_i is the number of pore volumes of oil pumped through the core, fr.unit; C_i is the inhibitor concentration at the time of selection from the core holder, %; $C_{\min \text{ эф}}$ is the minimum effective concentration of the ARPD inhibitor, %.

The range of the fluid volumetric flow rates by the core was taken, corresponding to the average range of well production rates. The calculation results are presented in Table 3.

In Table 3, the coefficient A correlates with the fluid volumetric flow rate by the core. It is necessary to recalculate the fluid volumetric flow rate by the core during plane-parallel filtration flow to the well production rate during plane-radial filtration. The complexity resides in the fact that the fluid filtration rate in the BHFZ differs at different distances from the well. Therefore, it is proposed to compare the fluid filtration rate in the core with the average logarithmic rate of the fluid filtration in the BHFZ.

The average logarithmic rate of the fluid filtration ($V_{\text{cp.log}}$) is derived from formula (3):

$$V_{\text{cp.log}} = \frac{v_1 - v_2}{\ln \frac{v_2}{v_1}} = \frac{\frac{Q}{F_1} - \frac{Q}{F_2}}{\ln \frac{R}{r}} = \frac{Q \cdot (R - r)}{2 \cdot \pi \cdot h \cdot R \cdot r \cdot \ln \frac{R}{r}} = \frac{Q_{\text{скв}}}{2 \cdot \pi \cdot h \cdot r \cdot \ln \frac{R}{r}} \quad (2)$$

where U_1 is the fluid filtration rate near the well wall with a radius r , m/s; v_2 is the fluid filtration rate in the BHFZ at a distance R from the well, m/s; R is the radius of squeezing (based on the experience of preventing scaling via the technique of injecting the inhibitor in the BHFZ, to achieve good results, it is sufficient to squeeze the inhibitor solution 1-2 m deep into the formation) (Antipin *et al.*, 1987; Lyushin *et al.*, 1983; Radoičić and Jovanović, 2018); h is an opened effective formation thickness, m; since $R \gg r$, then $R - r \approx R$.

The fluid filtration rate by the core is derived from formula (4):

$$v_{\text{көрн}} = \frac{4 \cdot Q_{\text{көрн}}}{\pi \cdot d_{\text{көрн}}^2} \quad (3)$$

The core with a diameter of $d_{\text{көрн}} = 0.03$ m was used.

By equating formulae (3) and (4), we get the equation, relating the fluid flow rate in the core to the well production rate (formula 5):

$$Q_{\text{скв}} = \frac{8 \cdot Q_{\text{көрн}} \cdot h \cdot r \cdot \ln \frac{R}{r}}{d_{\text{көрн}}^2} = 8888,88 \cdot Q_{\text{көрн}} \cdot h \cdot r \cdot \ln \frac{R}{r} \quad (4)$$

Proceeding from the obtained results of laboratory studies, it is recommended to use in calculations $Q_{\text{көрн}} = 0.5$ ml/min, since, under these conditions, the ARPD inhibitor gradual desorption from the rock pores takes place, the inhibitor is released and enters the well with the formation fluid, providing the requirements for the prevention of the ARPD formation in the BHFZ and, accordingly, in the well.

Therefore, considering the results and recommendations of laboratory studies, taking into account the values of the fluid volumetric flow rate by the core, the well production rate will be calculated according to the following formula:

$$Q_{\text{CKG}} = 6,4 \cdot h \cdot r \cdot \ln \frac{R}{r} \quad (5)$$

Thus, the results of experimental studies of adsorption-desorption processes make it possible to determine the amount of the developed ARPD inhibitor (IN-1), required for injection into the BHFZ, taking into account the well productivity, unevenness of the inhibitor removal from the BHFZ, and the volume of displacement fluid.

4. CONCLUSIONS:

1. The developed chemical composition IN-1 has high inhibiting properties with respect to the ARPD, possesses depressor-dispersing properties, and has low corrosive activity with respect to a metal surface.
2. The temperature of oil saturation with paraffin for paraffin oil was determined via rheogoniometry and the method of visual observation. Upon adding the ARPD inhibitor in oil, the temperature of oil saturation with paraffin decreases from 35 to 26°C. The developed IN-1 reagent can act as the ARPD inhibitor to prevent the formation of deposits in well equipment and in the BHFZ.
3. During the study of the ARPD inhibitor adsorption properties with respect to the rock, under static conditions, the value of the limiting adsorption, when the entire surface of the adsorbent is filled with adsorbate, made 0.0147 ml/g (0.219 ml/m²). The value of the limiting adsorption on core material under dynamic conditions made 0.520 ml/m². The results of the study of the ARPD inhibitor adsorption, on a core sample, under a dynamic mode, as well as under a static one, prove that the developed reagent has adsorption properties with respect to the rock.
4. The results of studying the impact of the fluid flow rate on the inhibitor desorption rate prove that with an increase in the fluid volumetric flow rate, the rate of the inhibitor desorption from the formation increases as well. An increase in the volume of the formation, being treated with the solution, inhibiting the ARPD, results to a proportional increase in the time of the inhibitor removal. When injecting the inhibitor into the BHFZ, it is necessary to squeeze it into the formation using at least 5 ... 10 times the volume of displacement fluid, to reduce the loss of the inhibitor at the initial stage of well operation after treatment. It is recommended to use oil as a displacement

fluid.

5. Based on the obtained results of laboratory studies of the ARPD inhibitor adsorption-desorption processes, the paper presents calculations for the technological parameters of squeezing the solution, inhibiting the ARPD, into the BHFZ, and substantiates the choice of coefficient A, which accounts the inhibitor uneven removal from the BHFZ, depending on the fluid volumetric flow rate (well production rate). Coefficient A is determined graphically, according to diagrams for the dependence of the ARPD inhibitor concentration in oil at the core holder outlet on the number of pore volumes of pumped oil.

5. REFERENCES:

1. Antipin Yu.V., Valeev M.D., Syrtlanov A.Sh. (1987). Prevention of complications in water-cut oil production. Ufa: Bashk. Book publishing house, 168 p.
2. Babalyan, G.A., Levi B.I. *et al.* (1983). Oil field development via the use of surfactants. M.: Nedra.
3. Faskhutdinov R.A., Antipin Yu.V., Islanova G.Sh. (1996). Patent 2070910 (RF) Composition for preventing deposition of inorganic salts in oil and gas production from wells, No. 36.
4. Ibragimov G.Z., & Khisamutdinov N.I. (1983). Reference book on the use of chemical agents in oil production. M.: Nauka, 1983, p. 226.
5. Jasińska, M. (2019). Recognition and description of synergy conditions in team work in view of the grounded theory. *Entrepreneurship and Sustainability Issues*, 7(1), 375-397. doi:10.9770/jesi.2019.7.1(27)
6. Kashchavtsev V.E., & Mishchenko I.T. (2004). Salt formation in oil production. M., 432 p.
7. Kopish, M., & Marques, W. (2020). Leveraging Technology to Promote Global Citizenship in Teacher Education in the United States and Brazil. *Research in Social Sciences and Technology*, 5(1), 45-69. Retrieved from <https://ressat.org/index.php/ressat/article/view/440>

8. Lateef, A. O., Bin, M. S. H., & Ademola, F. J. (2019). Performance assessment based on Intelligent power management for standalone PV system in remote area of Ibadan, Nigeria. *Journal of Applied Engineering Science*, 17(1), 52-60.
9. Lyushin S.F., Glazkov A.A., Galeeva G.V., Antipin Yu.V., Syrtlanov A.Sh. (1983). M.: VNIIOENG,. 100 p. (Oilfield engineering. Overview, issue 11 (29))
10. Mishchenko I.T. (2007). Borehole oil production. M.: Oil and gas. 826 p.
11. Neizvestnaya D.V., Kozlova N.N., Prodanova N.A. (2018). Application of CVP-Analysis at the Water Transport Organizations. *Helix*. 2018. Vol. 8(1). Pages 2811-2815. DOI 10.29042/2018-2811-2815
12. Plaskova, N. S., Prodanova, N. A., Samusenko, A. S., Erzinkyan, E. A., Barmuta, K. A., & Shichiyakh, R. A. (2019). Investment decisions formation: Innovative assets. *International Journal of Engineering and Advanced Technology*, 9(1), 2913-2916. doi:10.35940/ijeat.A1213.109119
13. Prodanova, N., Savina, N., Kevorkova, Z., Korshunova, L., & Bochkareva, N. (2019). Organizational and methodological support of corporate self-assessment procedure as a basis for sustainable business development. *Entrepreneurship and Sustainability Issues*, 7(2), 1136-1148. doi:10.9770/jesi.2019.7.2(24)
14. Radoičić, G., & Jovanović, M. (2018). Determination of heavy machines performances by using a measuring system with telemetric synchronization and transmission of signals. *Journal of Applied Engineering Science*, 16(4), 454-463.
15. Rahim, R. (2018). Applied Pohlig-Hellman algorithm in three-pass protocol communication. *Journal of Applied Engineering Science*, 16(3), 424-429.
16. Szafarczyk, A. (2019). Kinematics of mass phenomena on the example of an active landslide monitored using GPS and GBInSAR technology. *Journal of Applied Engineering Science*, 17(2), 107-115.
17. Solazzi, L., & Zrnić, N. (2017). Design of a high capacity derrick crane considering the effects induced by load application and release. *Journal of Applied Engineering Science*, 15(1), 15-24.
18. Yemelyanov, V. A., Yemelyanova, N. Y., Morozova, O. A., & Nedelkin, A. A. (2018). Specialized computer system to diagnose critical lined equipment. Paper presented at the *Journal of Physics: Conference Series*, 1015(5) doi:10.1088/1742-6596/1015/5/052032
19. Yemelyanov, V. A., Nedelkin, A. A., & Olenov, L. A. (2019). An object-oriented design of expert system software for evaluating the maintenance of lined equipment. Paper presented at the 2019 International Multi-Conference on Industrial Engineering and Modern Technologies, FarEastCon 2019, doi:10.1109/FarEastCon.2019.8934414
20. Yemelyanov, V., A. Nedelkin, and N. Yemelyanova. (2020). Expert System Software for Assessing the Technical Condition of Critical Lined Equipment. *Advances in Intelligent Systems and Computing*. Vol. 1115 AISC. doi:10.1007/978-3-030-37916-2_92.
21. Windyandari, A., Dwi, H. G., & Suharto, S. (2018). Design and performance analysis of B-series propeller for traditional purse seine boat in the north coastal region of Central Java Indonesia. *Journal of Applied Engineering Science*, 16(4), 494-502.
22. Zakki, F. A., Suharto, S., Myung, B. D., & Windyandari, A. (2019). Performance on the drop impact test of the cone capsule shaped portable tsunami lifeboat using penalty method contact analysis. *Journal of Applied Engineering Science*, 17(2), 233-244.

Table 1. The results of the determination of depressant-dispersing, inhibiting and corrosive properties of the ARPD inhibitor (the IN-1 reagent)

No.	The inhibitor concentration in oil, %	Oil-freezing point, °C	Depressor effect ΔT , °C	Inhibiting property, %	The inhibitor corrosion rate (mm/year) at temperature:	
					20°C	37°C
1	0	-23	0	0	0.0756	0.1134
2	0.1	-28	5	8.3	0.0325	0.0362
3	0.5	-32	9	25	0.0342	0.0369
4	1	-39	16	37.5	0.0311	0.0336
5	1.5	-45	22	45.8	0.0318	0.0324

Table 3. The results of determining the coefficient A at different volumetric flow rates of the fluid

The fluid volumetric flow rate ($Q_{\text{көрп}}$), ml/min	The coefficient of the inhibitor removal unevenness (A), units
0.5	1.4
1	2.2
2	4.6
3	8

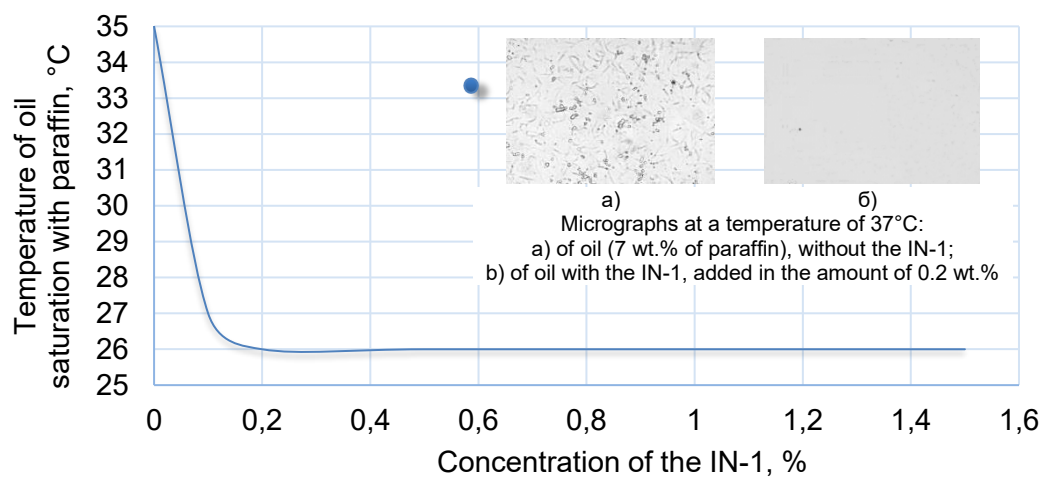


Figure 1. Dependence of the temperature of oil saturation with paraffin on the IN-1 concentration in oil

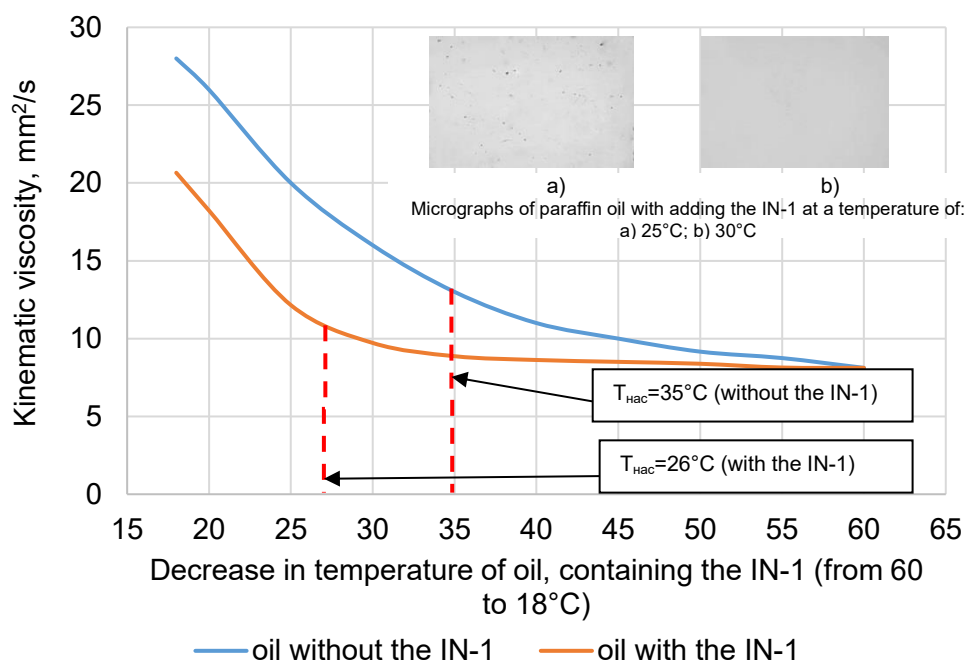


Figure 2. Dependence of kinematic viscosity of oil, with and without adding the IN-1, on temperature

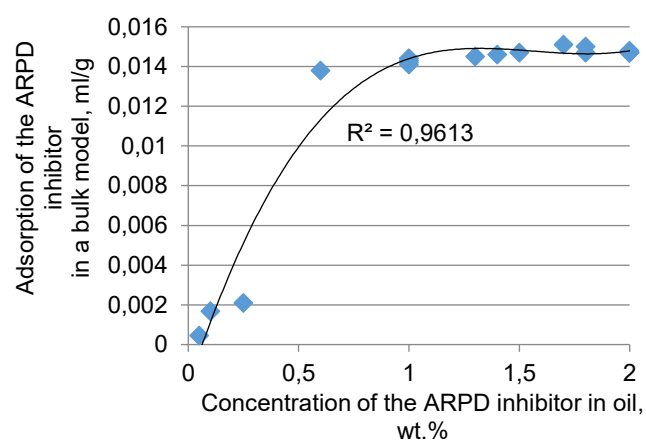


Figure 3. Adsorption of the ARPD inhibitor (IN-1 reagent) on the surface of the bulk model depending on its concentration in oil

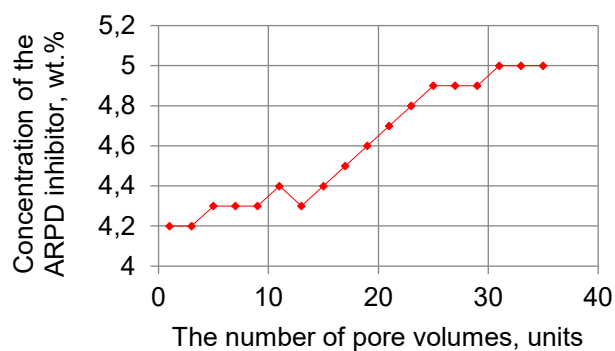


Figure 4. Dynamics of changes in the ARPD inhibitor concentration in oil at the core holder outlet

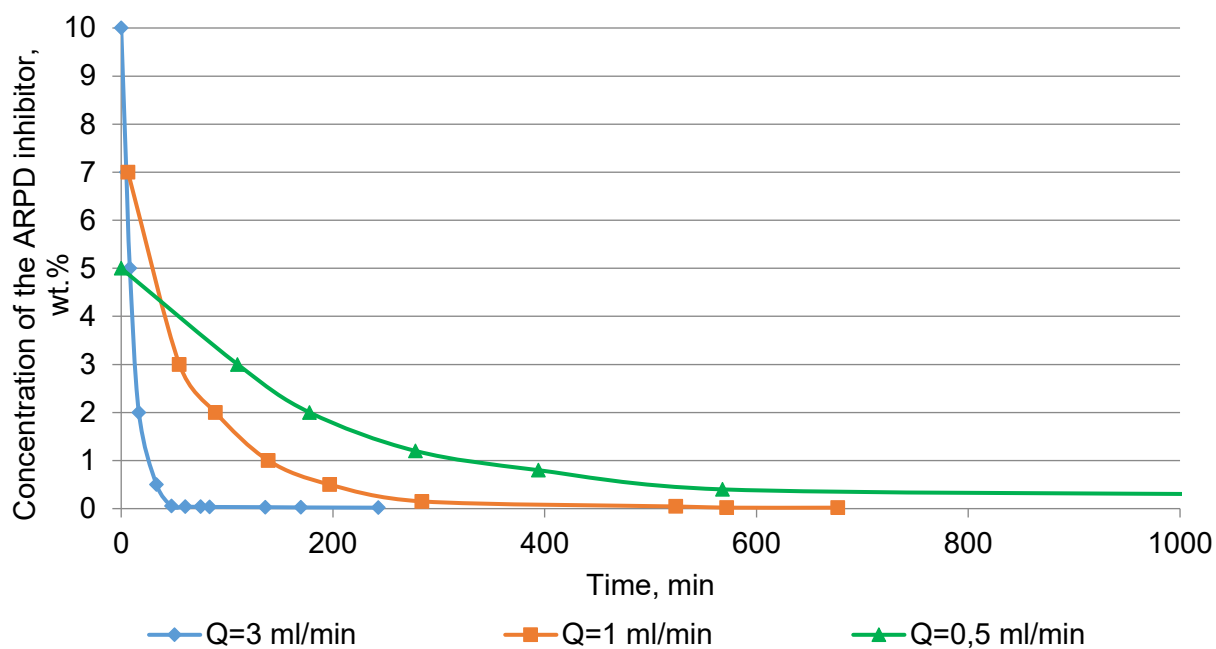


Figure 5. Profile of the ARPD inhibitor removal when changing the fluid volumetric flow rate by the core

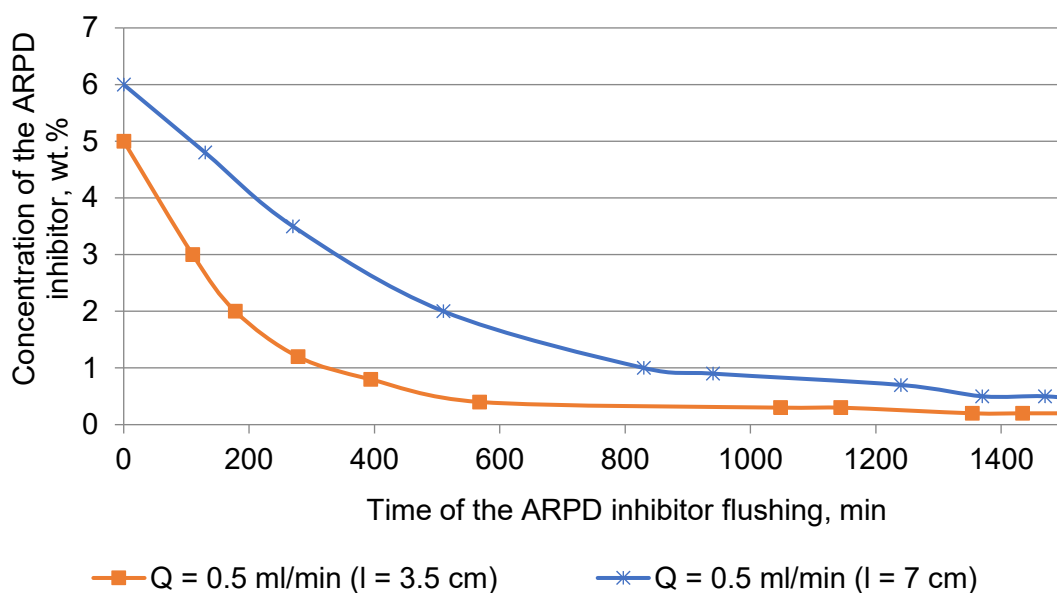


Figure 6. Profile of the ARPD inhibitor removal at a change in the bulk model length depending on the time of the ARPD inhibitor flushing with oil

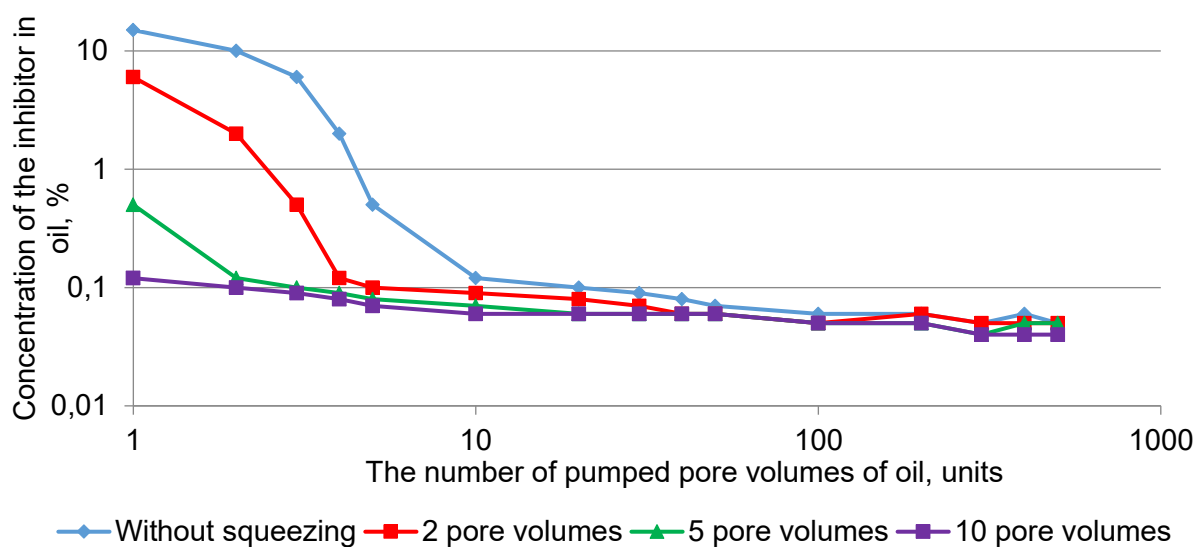


Figure 7. Dependence of the ARPD inhibitor concentration in oil at the core holder outlet on the number of pumped pore volumes of oil

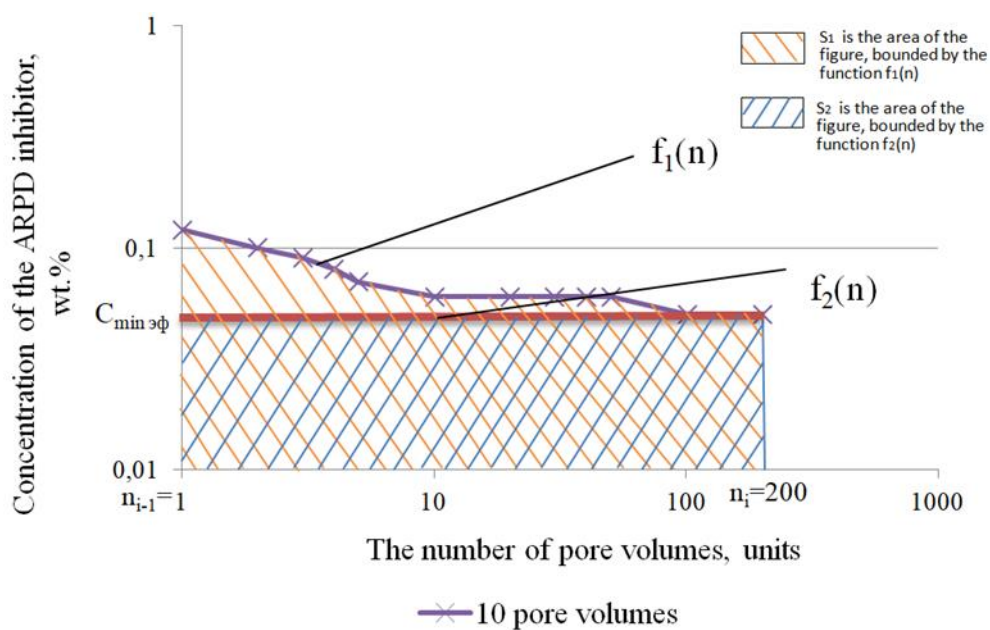


Figure 8. Determination of the coefficient A in a graphical manner at the fluid volumetric flow rate by the core of 0.5 ml/min

DETALHES DA TECNOLOGIA DE CONTROLE DE POÇO DURANTE A OPERAÇÃO EM CONDIÇÕES COMPLICADAS

SPECIFICS OF WELL KILLING TECHNOLOGY DURING WELL SERVICE OPERATION IN COMPLICATED CONDITIONS

ОСОБЕННОСТИ ТЕХНОЛОГИИ ГЛУШЕНИЯ СКВАЖИН ПРИ ПОДЗЕМНОМ РЕМОНТЕ В ОСЛОЖНЕННЫХ УСЛОВИЯХ

MARDASHOV, Dmitry^{1*}; ISLAMOV, Shamil²; NEFEDOV, Yury³^{1,2,3} Saint Petersburg Mining University, Development and Operation of Oil and Gas Fields, St. Petersburg, Russia

* Corresponding author

e-mail: Mardashov_DV@pers.spmi.ru

Received 29 January 2020; received in revised form 11 March 2020; accepted 26 March 2020

RESUMO

O processo das operações de controle de poços no campo de condensado de petróleo e gás na província de Volga-Ural é complicado devido a diversas condições como reservatório de carbonato fraturado, pressão do reservatório anormalmente baixa, alta relação gasóleo, alto teor de sulfeto de hidrogênio, fraturamento com ácido e tratamentos com ácido clorídrico. Durante o processo de controle de poço, observam-se avanços significativos de gás e perda de fluido neste campo, o que requer uso significativo de composições de bloqueio (até 50-100 m³ por poço único) e aumenta os custos de serviço do poço. O objetivo deste trabalho foi aumentar a eficiência da extração de poços durante o serviço, estudando os mecanismos que ocorrem perto da zona do poço durante este processo. A aplicação da análise estatística e multifatorial dos processos de abate de poços foi realizada de 2018 a 2019, o que permitiu destacar as principais razões para o baixo sucesso desses trabalhos. Os resultados do cálculo mostraram que o estado de tensão próximo ao poço difere significativamente do campo de tensão regional e varia de acordo com a pressão gerada no poço, que por sua vez afeta a atividade de fraturas próximas ao poço. Os mecanismos revelados que ocorrem perto da zona do poço, juntamente com os testes laboratoriais e piloto das composições de bloqueio, podem ser usados para melhorar as operações de serviço do poço no campo de condensado de petróleo e gás na província de Volga-Ural. Neste trabalho, concluiu-se que é importante usar a abordagem geomecânica para aumentar a eficiência de abate de poços em combinação com um complexo de testes reológicos e de filtragem de laboratório de composições bloqueadoras.

Palavras-chave: *operação de serviço de poço, modelagem geomecânica, análise multifatorial, fluido de emulsão invertida, gel de polímero reticulado.*

ABSTRACT

The process of the well killing operations in the oil and gas condensate field in Volga-Ural province is complicated due to several conditions like fractured carbonate reservoir, abnormally low reservoir pressure, high gas-oil ratio, high hydrogen sulfide content, acid fracturing, and hydrochloric acid treatments requirement. During the well killing process, significant gas breakthroughs and fluid loss are observed in this field, which requires significant usage of blocking compositions (up to 50-100 m³ per single well) and increases the well service costs. The aim of this work was to increase the well killing efficiency during well service by studying the mechanisms that take place near the wellbore zone during this process. The application of statistical and multifactor analysis of well-killing processes were conducted from 2018 to 2019, which allowed highlighting the main reasons for the low success of these works. The calculation results showed that the stress state near the well significantly differs from the regional stress field and varies depending on the generated pressure in the well, which in turn affects the activity of fractures near the wellbore. The revealed mechanisms that take place near the wellbore zone coupled with the laboratory and pilot tests of the blocking compositions can be used to improve the well service operations at the oil and gas condensate field in the Volga-Ural province. In this work, it was concluded that it is important to use the geomechanical approach to increase the well killing efficiency in combination with a complex of laboratory rheological and filtration tests of blocking compositions.

Keywords: *well service operation, geomechanical modeling, multifactor analysis, invert emulsion fluid, cross-*

АННОТАЦИЯ

Процесс глушения скважин на нефтегазоконденсатном месторождении Волго-Уральской провинции сопровождается осложненными условиями: трещинно-поровый карбонатный коллектор; аномально-низкое пластовое давление; высокий газовый фактор; высокое содержание сероводорода; проведение кислотных гидроразрывов пласта и солянокислотных обработок. На данном месторождении в процессе глушения наблюдаются значительные прорывы газа и поглощения жидкостей пластом, что подразумевает большие объемы закачки блокирующих составов (до 50-100 м³ на 1 скважину) и, соответственно, приводит к удорожанию данной операции при подземном ремонте скважин. Целью данной работы является повышение эффективности глушения нефтяных скважин в осложненных условиях путем изучения механизмов, происходящих в прискважинной зоне при подземном ремонте. Использование статистического и многофакторного анализа процессов глушения скважин за период 2018-2019 гг. позволило выделить основные причины низкой успешности данных работ. Результаты расчетов показали, что напряженное состояние вблизи скважины существенно отличается от регионального поля напряжений и меняется в зависимости от создаваемого давления в скважине, что в свою очередь влияет на активность трещин вблизи ствола скважины. Выявленные механизмы, происходящие в прискважинной зоне, в сочетании с лабораторными исследованиями и опытно-промышленными испытаниями блокирующих составов, могут быть использованы для совершенствования процесса организации работ по глушению скважин в условиях нефтегазоконденсатного месторождения Волго-Уральской нефтегазоносной провинции. В данной работе сделан вывод о важности использования геомеханического подхода для повышения эффективности глушения нефтяных скважин в сочетании с комплексом лабораторных реологических и фильтрационных исследований блокирующих составов.

Ключевые слова: *глушение скважин, геомеханическое моделирование, многофакторный анализ, жидкости глушения, инвертно-эмульсионный раствор, сшитый полимерный состав.*

1. INTRODUCTION:

Development complexity of the oil and gas condensate field in Volga-Ural province is primarily due to geological characteristics since carbonate fractured reservoirs with a high gas-oil ratio and high hydrogen sulfide content dominate in productive formations. The presence of fractures in the creation requires a unique, differentiated approach to planning operations for killing wells associated with the choice of the type of blocking composition. Currently, manufacturers of chemical reagents offer many brands of various blocking compositions for well killing operation, but not all of them satisfy the requirements for such technological fluids. Therefore, the correct selection of blocking compositions for killing wells requires careful laboratory research for specific objects of the planned application. Failure to comply with the above conditions when planning activities at the well may lead to the loss of significant volumes of process fluids, increase the repair and response time, which, ultimately, will lead to an increase in the cost of well service operations (Ling and Yumashev, 2018; Yemelyanov et al., 2019 a,b). Thus, the justification of using blocking compositions for well killing in the conditions of oil and gas condensate field in the Volga-Ural province is especially important in connection with the difficult

geological, technological and technical conditions for the operation of production wells: fractured carbonate reservoir, abnormally low formation pressure, high gas-oil ratio, high hydrogen sulfide content, acid fracturing and hydrochloric acid treatments requirement (Zambrano *et al.*, 2018; Lushpeev and Margarit, 2018; Gil-Martín *et al.*, 2017).

In such complicated conditions, the main task is to control the fluid loss during well killing operations. In world practice, two basic physical principles are used to reduce fluid loss during well service: increasing the blocking fluids viscosity and Blocking of pores (fractures) and channels of filtration by solid particles (Dandekar, 2013; Rogachev and Kondrashev, 2016; Petrov *et al.*, 2008; Ryabokon, 2009; Galimkhanov, 2019; Volkov, 2019). These principles are implemented in blocking compositions, which are aqueous solutions, emulsions, crosslinked polymer gels, and dispersed systems with solid or gas phases (Figure 1) (Islamov *et al.*, 2019).

Calculation of the stress state of the rock in the near-wellbore zone based on geomechanical modeling can make a significant contribution to the optimization of well killing processes. Among the works on the assessment of the stress state in the near-wellbore zone can be distinguished (Elchin *et al.*, 2019; Lakatos *et al.*, 2013; Fischer *et al.*, 1973;

Dorman and Udvary, 1996; Bouts *et al.*, 1997; Orlov *et al.*, 1991; Musabirov *et al.*, 2019).

2. MATERIALS AND METHODS:

2.1 Multifactor analysis of the well killing efficiency

Modern methods of data analysis were used to assess different factors that influence the killing of wells efficiency. They allowed finding factors that have a significant effect on the result of geological and technological procedures. Algorithm for analysis can be divided into several steps. The first step is selecting factors that can theoretically influence the success of operation and which are available for analysis. It is important to choose geological and physical factors describing properties of the bed near the well's area and technological factors relating terms of root properties of well-killing success.

The criterion of "well-killing success" can take two values: "successfully" - if the well was successfully well killed in 1 cycle, and "unsuccessfully" - if the well was not well killed in 1 cycle.

The next step is forming of dataset with experimental observations. The first steps of evaluation in construction the mathematic model are creating correlation matrix and factors selection with its construction results; the elements are definitely having a linear relationship with an experimental value (coefficient of correlation over 0.5 at the scale of Chaddock (Tague, 2000; Gmurman, 2003; Cameron and Trivedi, 2013; Chaddock, 1925)). The next step is a search of the mathematic model by stepwise regression (Cameron and Trivedi, 2013), which will describe a change of observable value objectively (selected on a coefficient of determination (Saunders *et al.* 2012) with its scaled analog considering the complexity of the model). The following step is the comparison of the model's predictions with real values. A principal diagram of the selected analysis is shown in Figure 2 (Legkokonets *et al.*, 2018).

The analysis of the well killing efficiency at the oil and gas condensate field in the Volga-Ural province was carried out in two main directions that have different criteria for the effectiveness of well-killing operation (Figure 3) (Legkokonets *et al.*, 2018):

1. Multifactor analysis of the well killing efficiency (with the criterion of effectiveness "Ramp-up time of the operation mode").

2. Analysis of the reasons for repeated well killing (with the effectiveness criterion "Number of well-killing cycles").

Moreover, multifactor analysis was carried out only according to data for 2018-2019.

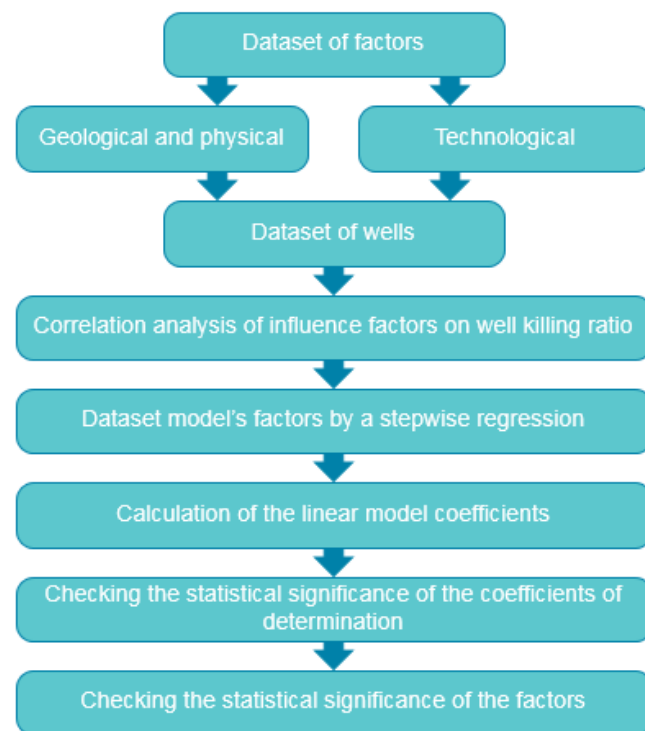


Figure 2. Analysis workflow (Legkokonets *et al.*, 2018)

Multifactor analysis was carried out on a sample of wells No.1, compiled according to the following criteria:

1. The number of well-killing cycles – 1.
2. Excluded wells that have taken measures to oil production intensification, which could affect the criterion for the effectiveness of response time (acid treatment, hydraulic fracturing, sidetracking, drifting gas, regime change, optimization of underground equipment, etc.).
3. Excluded wells with a fluid flow rate of less than 1 m³/day.
4. Wells are excluded that lack data for at least one of the selected factors.
5. Wells are excluded where the method of operation is a flowing (small sample of wells).
6. Wells entered from drilling excluded.

Analysis of the reasons for repeated well killing was carried out on a sample of wells No.2, which include:

1. The number of well-killing cycles – 1.
2. Wells entered from drilling excluded.

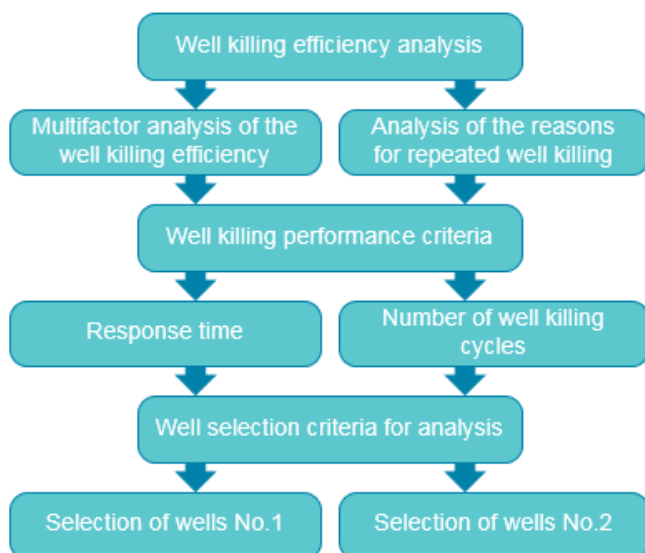


Figure 3. Flow chart analysis of the well killing efficiency (Legkokonets *et al.*, 2018)

2.2 Geomechanical analysis of the well killing efficiency

Productive horizons P_{IV} - P_V of the oil and gas condensate field in Volga-Ural province are presented by fractured carbonate reservoir. Therefore, the correct quantitative assessment of the conductive activity of fracturing is a criterion for the success of well killing. A geomechanical approach was used to evaluate the activity of fractures.

The rock, in a natural occurrence, is in severe stress conditions due to vertical and horizontal stresses associated with the weight of the overlying rocks, as well as tectonic and chemical processes. A well, like a rock excavation, is a local stress concentrator. The stress state in the neighborhood of the well will differ significantly from the regional stress field far from it. The conductive activity of the fracture near the well depends on the values and orientation of the near well bore stress field, as well as on the spatial orientations of the fracture relative to the path of the well (Alzayer *et al.*, 2019).

According to the data of microimages, zones with two characteristic fracture distributions are present in the reservoir (Figure 4) (Ovcharenko *et al.*, 2017). Ordered fracturing prevails in the south-western and north-eastern region of the oil and gas condensate field in the Volga-Ural province. In contrast, multidirectional fracturing is characteristic in the central zone of the reservoir.

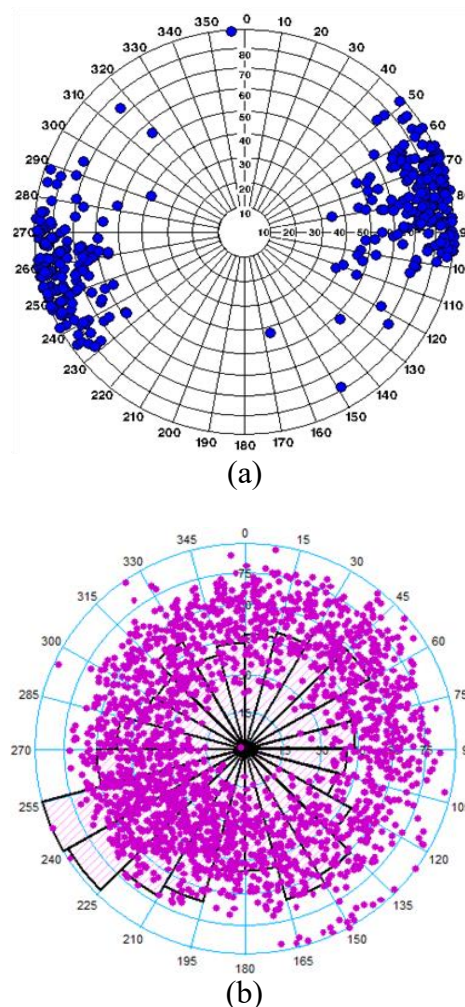


Figure 4. Typical fracture orientation distribution types for oil and gas condensate field in the Volga-Ural province: (a) ordered fracturing; (b) multidirectional fracturing (Ovcharenko *et al.*, 2017)

These features of the observed natural fracture are associated with tectonic regimes that existed in the field at the time of fracture formation and are a separate topic for research that is beyond the scope of this article (Maxwell *et al.*, 2016).

3. RESULTS AND DISCUSSION:

Analysis of the well-killing efficiency in production wells at the oil and gas condensate field in the Volga-Ural province for 2018-2019 showed an increase in the efficiency of well killing in 2019 relative to 2018 (Figure 5) (Islamov *et al.*, 2019). It should also be noted that the decrease in the share of unsuccessful well killing operations for geological reasons, which indicates the success of the planned activities.

Analysis of the influence well-killing fluids on the ramp-up time depending on the method of their

operation was carried out only for wells that did not have a change in the method of operation, and there was no effect on the bottom-hole formation zone in the after well service period. Also, only wells that were well killed with an invert emulsion fluid (IEF) or a crosslinked polymer gel (CPG) from the first cycle were analyzed. The analysis showed that IEF have the least negative effect on production wells during well killing process (Figure 6).

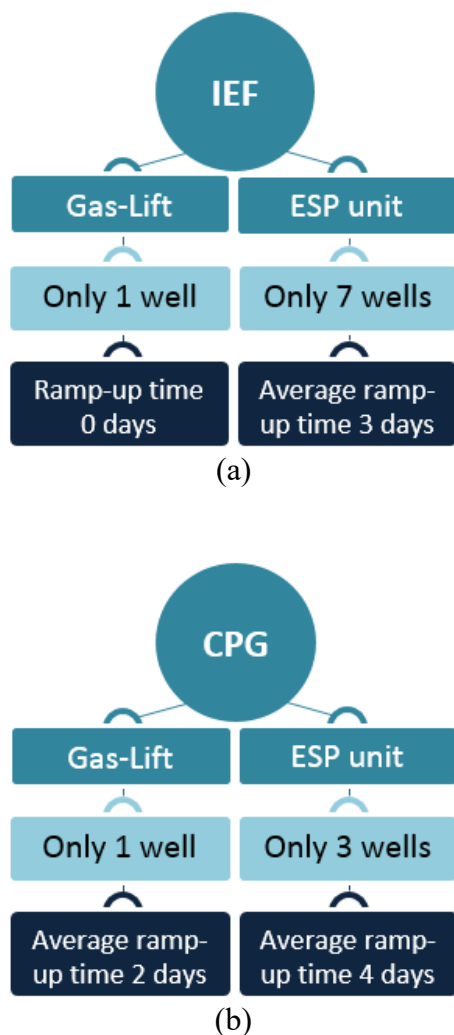


Figure 6. Analysis of the influence of well-killing fluids on the ramp-up time depending on the method of their operation: (a) invert emulsion fluid; (b) crosslinked polymer gel

Based on multifactor analysis, it was possible to determine the parameters that have the most significant impact on the success of well killing. Among the analyzed factors were data obtained by the results of geophysical and hydrodynamic studies of wells and direct measurements, as well as data collected by the results of geological, hydrodynamic, and geomechanical modeling. Figure 7 shows the most important of them (Legkokonets *et al.*, 2018):

- fracture intensity for fractures of various types (different geometry);
- azimuth of well;
- fracture opening;
- volume of invert emulsion fluid – injected volume of blocking composition;
- volume of crosslinked polymer gel – injected volume of blocking composition.

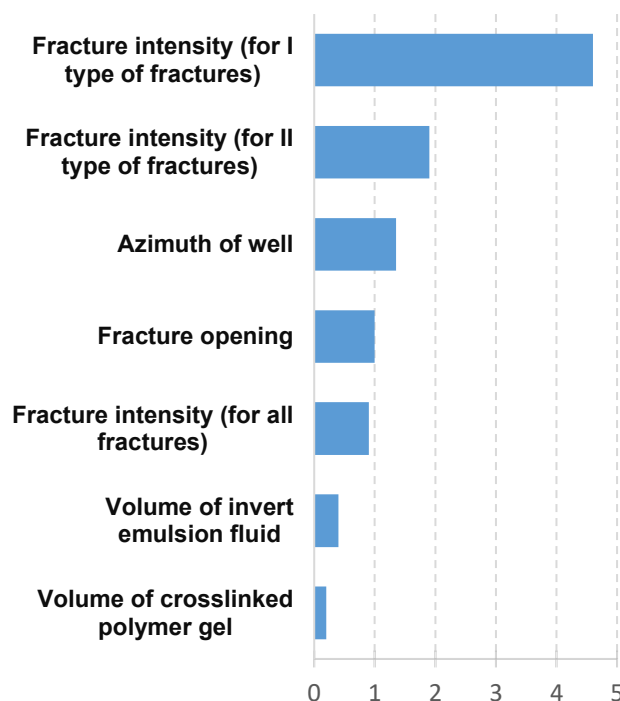


Figure 7. Diagram of the influence of factors on the success of well killing

In that framework, an example of well No.1007-1 of the oil and gas condensate field in the Volga-Ural province using geomechanical tools was used to analyze the conductive activity of fractures crossing its horizontal wellbore. The calculation was carried out with a reservoir pressure anomaly coefficient of 0.8. The well is located in a region with a low fracture density, and the distribution of the fracture propagation is an ordered type (Figure 4a). In the analysis, two wells with the type of fractures (I and II) were considered (Table 1).

Table 1. Characteristics of fractures for well No.1007-1

Type	Azimuth of the falling fractures	Fracture strike azimuth	Angle of incidence
I	260°	170°	80°
II	230°	140°	60°

Type I fracture (Figure 8) presents the fracture extension, which is most prevalent for well No.1007-1 (Ovcharenko *et al.*, 2017).

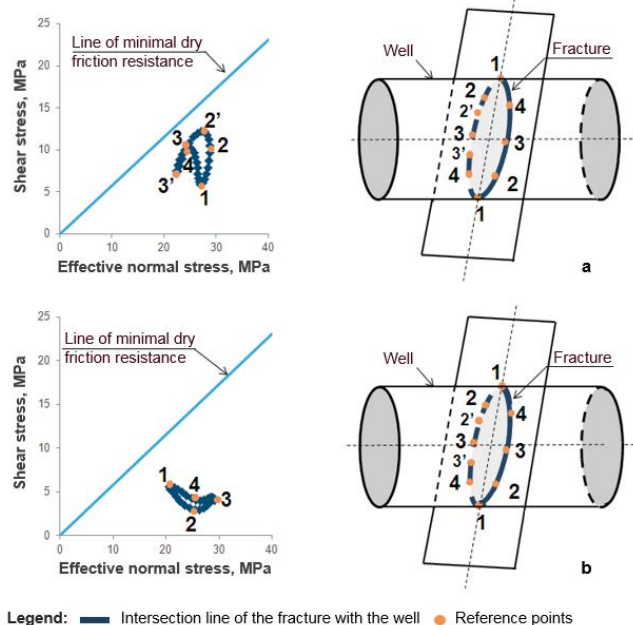


Figure 8. I type fracture stress diagram: (a) during the operation of the well (depressed); (b) during well-killing process (at a pressure of injection well-killing fluid)

Type I fracture activity analysis results in the conditions of dynamic (when the well is working on a depression) and static (after well-killing process) are presented in Figures 8a and 8b. The dependence shown in the figures describes the value of normal and shear stresses at the line of intersection of the surface of the fracture with the cylindrical wellbore wall. The straight line represents the so-called line of minimum dry friction resistance for rocks in the interval of the target reservoir (Rahman and Bobkova, 2016; Shatalova *et al.*, 2015; Yemelyanov *et al.*, 2019; Maulana *et al.*, 2019). If at the fracture point the combination of standard and shear stress exceeds the line of minimum dry friction resistance, then this region of the fracture experiences displacement along the surface, and in this region the fracture becomes conductive due to the tensile strain arising. As can be seen from Figures 8a and 8b, the "reference points" 1, 2, 3, and 4 are located below the straight line in both cases: both in depression and well-killing process. Thus, the fracture of the I type of well No.1007-1 does not fall into the active conducting state in the considered range of bottom hole pressures.

Type II fracture (Figure 9) represent the least prevailing direction of fractures for well No.1007-1 (Ovcharenko *et al.*, 2017). The results of the analysis of the conductive activity of a Type II

fracture under dynamic and static conditions (when the well is working on depression, hydrostatic pressure, and repression) are presented in Figures 9a-9c. According to the results obtained, the combination of normal and shear stress exceeds the line of minimum dry friction resistance of a given rock (red dots) on depression and at a pressure of injection of the well-killing fluid, i.e., in dynamics, this fracture is in an open (active conducting) state. The active zones of the fracture crossing the wellbore are indicated by red dots (Figures 9a and 9c). As can be seen from Figure 7a, when the depression is active, there is a part of the crack, to which points 2', 3, 4, 4' belong. In static conditions (after well-killing process), the fracture is entirely in a closed (non-active) state (Figure 9b).

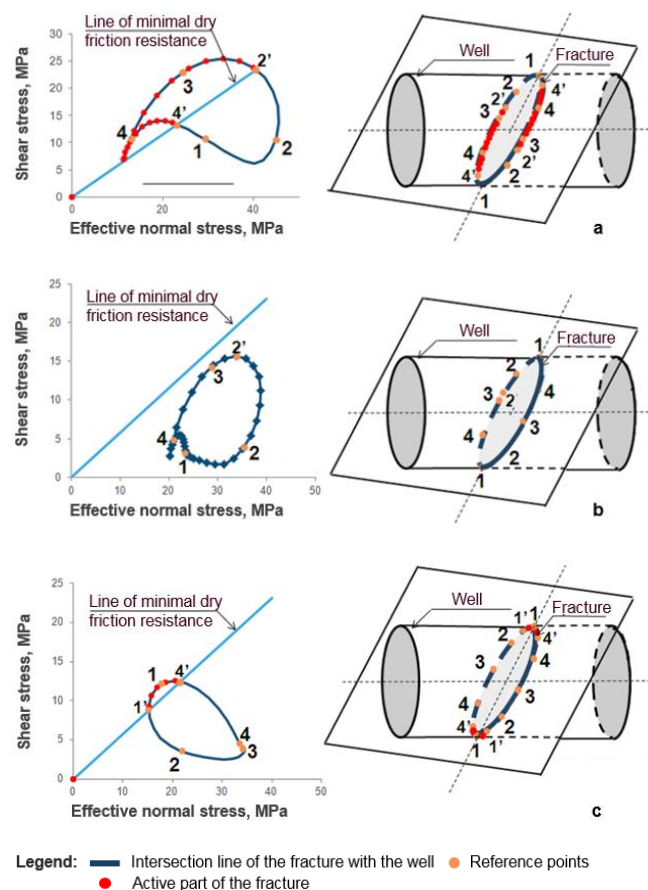


Figure 9. Type II fracture stress diagram: (a) during the operation of the well (depressed); (b) during well shutdown process (at hydrostatic pressure); (c) during well-killing process (at a pressure of injection well-killing fluid)

When squeezing the well killing fluid into the well, the bottom hole pressure rises, and the fracture again goes into the active (open) state. However, according to the results presented in Figure 9c, the location of the core relative to the wellbore walls (points 4'-1-1') has changed at the fracture. It is logical to assume that the blocking

composition during well-killing operation (when creating repression) penetrates into the zone of the fracture that is not active during well operation (points 4'-1-1'). When a well is discharged after well killing, a breakthrough of gas from a fracture region that is not fixed by a blocking composition (points 2'-3-4-4') is possible. It can be assumed that for this well, all well killing processes were successful due to the low intensity of fractures of this type (Kumar *et al.*, 2019).

In the analysis, we used the distribution of fractures obtained using the interpretation of the microimager. For wells that did not have this well logging complex, it is proposed to use the statistical distribution of fracture orientations obtained from the geomechanical fracture model.

Knowing the active zones in the fracture, it is possible to qualitatively determine the places and nature of the penetration of blocking compounds in the bottom hole formation zone by conducting a set of laboratory rheological and filtration studies.

4. CONCLUSIONS:

1. To increase the efficiency of well killing at the oil and gas condensate field in the Volga-Ural province, to make an informed choice of the most effective blocking compositions and technologies for their application is necessary, which is recommended taking into account the analysis of field data, the results of geomechanical modeling, laboratory studies, and also based on the results of pilot field tests.

2. Geomechanical modeling confirmed the results of the multifactor analysis, which indicated a close relationship between the success of well-killing operation, the well path, and the type of fracturing.

3. The stress state near the well differs significantly from the regional stress field and varies depending on the generated pressure in the well, which in turn affects the activity of fractures near the wellbore.

4. The presence of the image of resistances or a calibrated geomechanical model of fracturing allows us to predict actively conducting sections of fractures near the wellbore at various values of downhole pressure.

5. An integrated approach to solving the problems of well killing in complicated geological, physical, and technological conditions for the development of oil and gas condensate field is needed, consisting in a combination of geomechanical modeling methods with laboratory

and field tests.

5. REFERENCES:

1. Alzayer, Y., Alnazghah, M. & Zahm, C. (2019). 3D Reservoir-Scale Forward Geomechanical Modeling of Differential Compaction Fractures. *SPE Middle East Oil and Gas Show and Conference*, doi: 10.2118/195079-MS, 18-21 March. Bahrain: Manama.
2. Bouts, M.N., Ruud, A.T. & Samuel, A.J. (1997). Time Delayed and Low-Impairment Fluid-loss Control Using a Succinoglycan Biopolymer with an Internal Acid Breaker. *SPE Journal*, doi: 10.2118/31085-PA, 21-23 December. Texas: Houston.
3. Cameron, C.A. & Trivedi, P.K. (2013). *Regression Analysis of Count Data*. 2nd ed. Cambridge: Cambridge University Press.
4. Chaddock, R.E. (1925). *Principles and Methods of Statistics*. Cambridge: Houghton Mifflin Company.
5. Dandekar, A.Y. (2013). *Petroleum Reservoir Rock and Fluid Properties*. Boca Raton: CRC press.
6. Dorman, J. & Udvary, F. (1996). Comparative Evaluation of Temporary Blocking Fluid Systems for Controlling Fluid Loss Through Perforations. *SPE Formation Damage Control Symposium*, doi: 10.2118/31081-MS, 14-15 February. Louisiana: Lafayette.
7. Elchin, F.V., Azizagha, A.A., Vugar, V.G. & Nurana, V.N. (2019). Water Shutoff Using Crosslinked Polymer Gels. *SPE Annual Caspian Technical Conference*, doi: 10.2118/198351-MS, 16-18 October. Baku: Azerbaijan.
8. Fischer, P.W., Gallus, J.P., Krueger, R.F., Pye, D.S., Simmons, F.J. & Talley, B.E. (1973). An Organic "Clay Substitute" for Nondamaging Water Base Drilling and Completion Fluids. *Fall Meeting of the Society of Petroleum Engineers of AIME*, doi: 10.2118/4651-MS, 1-3 October. Las Vegas: Nevada.
9. Galimkhanov, A., Okhotnikov, D., Ginzburg, L., Bakhtin, A., Sidorov, Y., Kuzmin, P., Kulikov, S., Veliyev, G. & Badrawi, M. (2019). Successful Implementation of Managed Pressure Drilling Technology Under the Conditions

- of Catastrophic Mud Losses in the Kuyumbinskoe Field. *SPE Russian Petroleum Technology Conference*, doi: 10.2118/196791-MS, 22-24 October. Russia: Moscow.
10. Gmurman, V.E. (2003). *Theory of Probability and Mathematical Statistics*. 9th ed. Moscow: Higher School of Economics.
 11. Gil-Martín, L. M., Fernandez-Ruiz, M. A., & Hernandez-Montes, E. (2017). A discussion on the stiffness matrices used in tensegrity structures. *Journal of Applied Engineering Science*, 15(3), 383-388.
 12. Islamov, S.R., Bondarenko, A.V. & Mardashov, D.V. (2019). Substantiation of a Well Killing Technology for Fractured Carbonate Reservoirs. *Youth Technical Sessions Proceedings: VI Youth Forum of the World Petroleum Council - Future Leaders Forum*. CRC Press/Balkema, Taylor & Francis Group, pp. 256-264. United Kingdom: London
 13. Kumar, A., Shrivastava, K., Manchanda, R. & Sharma, M. (2019). An Efficient Method for Modeling Discrete Fracture Networks in Geomechanical Reservoir Simulation. *SPE/AAPG/SEG Unconventional Resources Technology*, doi: 10.15530/urtec-2019-1083, 22-24 July. Colorado: Denver.
 14. Lakatos, I.J., Lakatos-Szabo, J., Szentes, G., Vadaszi, M., Vago, A. (2013). Novel Water Shutoff Treatments in Gas Wells Using Petroleum External Solutions and Microemulsions. *SPE European Formation Damage Conference & Exhibition*, doi: 10.2118/165175-MS, 5-7 June. The Netherlands: Noordwijk.
 15. Legkokonets, V.A., Islamov, S.R. & Mardashov, D.V. (2018). Multifactor Analysis of Well Killing Operations on Oil and Gas Condensate Field with a Fractured Reservoir. *Topical Issues of Rational Use of Mineral Resources*. CRC Press/Balkema, Taylor & Francis Group, pp. 111-118. United Kingdom: London.
 16. Ling, V. V., & Yumashev, A. V. (2018). Estimation of worker encouragement system at industrial enterprise. *Espacios*, 39(28)
 17. Lushpeev, V., & Margarit, A. (2018). Optimization of oil field development process based on existing forecast model. *Journal of Applied Engineering Science*, 16(3), 391-397.
 18. Maxwell, S.C., Lee, B.T. & Mack, M. (2016). Calibrated Microseismic Geomechanical Modeling of a Horn River Basin Hydraulic Fracture. *50th U.S. Rock Mechanics/Geomechanics Symposium*, ARMA-2016-626, 26-29 June. Texas: Houston.
 19. Maulana, M., Hanova, Y., Waruwu, A., & Ratama, P. E. (2019). Simplified method for prediction of settlement in bamboo piles-reinforced peat under embankment. *Journal of Applied Engineering Science*, 17(1), 35-42.
 20. Musabirov M.Kh., Kuryashov D.A., Garifov K.M., Dmitriyeva A.Y. & Abusalimov E.M. (2019). *Developing Structure-Forming Colloidal Systems for Matrix Acidizing of Porous-Fractured Carbonate Reservoirs*. *Oil Industry Journal*, 6, 71-73.
 21. Orlov, G.A., Kendis, M.Sh. & Glushchenko, V.N. (1991). *Application of Invert Emulsions in Oil Production*. Moscow: Nedra.
 22. Ovcharenko, Yu.V., Gumerov, R.R., Bazyrov, I.Sh., Kunakova, A.M., Mardashov, D.V., Gunkin, A.S. & Legkokonets, V.A. (2017). *Well Killing Specifics in Conditions of Fractured and Porous Carbonate Reservoirs of the Eastern Part of the Orenburgskoye Oil-Gas-Condensate Field*. *Oil Industry Journal*, 12, 59-62.
 23. Petrov, N.A., Soloviev, A.Ya., Sultanov, V.G., Krotov, S.A. & Davydova, I.N. (2008). *Emulsion Solutions in Oil and Gas Processes*. Moscow: Chemistry.
 24. Rahman, P. A., & Bobkova, E. Y. (2016). Reliability model of fault-tolerant data processing system with primary and backup nodes. *IOP Conference Series: Materials Science and Engineering*, 124(1). <https://doi.org/10.1088/1757-899x/124/1/012023>
 25. Rogachev, M.K. & Kondrashev, A.O. (2016). *Substantiation of the Technology of In-Situ Waterproofing in Low-Permeability Reservoirs*. *Journal of Mining Institute*, 217, 55-60.
 26. Ryabokon, S.A. (2009). *Technological Fluids for Completion and Well Service*

Operations. Krasnodar: Prosveshcheniye-Yug.

27. Shatalova, T. N., Chebykina, M. V., Zhirnova, T. V., & Bobkova, E. Y. (2015). Methodological problems in determining the basic features of the sample set controlling the activities of the enterprise. *Mediterranean Journal of Social Sciences*, 6(3S4), 261–268. <https://doi.org/10.5901/mjss.2015.v6n3s4.p261>
28. Tague, J.R. (2000). Multivariate Statistical Analysis Improves Formation Damage Remediation. *SPE Annual Technical Conference and Exhibition*, doi: 10.15530/urtec-2019-1083, 1-4 October. Texas: Dallas.
29. Volkov, V., Turapin, A., Ermilov, A., Vasyutkin, S., Fomin, D. & Sorokina, A. (2019). Experience of Gas Wells Development in Complex Carbonate Reservoirs in Different Stages of Development. *SPE Russian Petroleum Technology Conference*, doi:10.2118/196915-MS, 22-24 October. Russia: Moscow.
30. Yemelyanov, V. A., Yemelyanova, N. Y., Nedelkin, A. A., Glebov, N. B., & Tyapkin, D. A. (2019a). Information system to determine the transported liquid iron weight. Paper presented at the Proceedings of the 2019 IEEE Conference of Russian Young Researchers in Electrical and Electronic Engineering, ElConRus 2019, 377-380. doi:10.1109/ElConRus.2019.8656693
31. Yemelyanov, V. A., Nedelkin, A. A., & Olenov, L. A. (2019b). An object-oriented design of expert system software for evaluating the maintenance of lined equipment. Paper presented at the 2019 International Multi-Conference on Industrial Engineering and Modern Technologies, FarEastCon 2019, doi:10.1109/FarEastCon.2019.8934414
32. Zambrano, C. J. R., Kovshov, S., & Lyubin, E. (2018). Assessment of anthropogenic factor of accident risk on the main oil pipeline Pascuales - Cuenca in Ecuador. *Journal of Applied Engineering Science*, 16(3), 307-312.

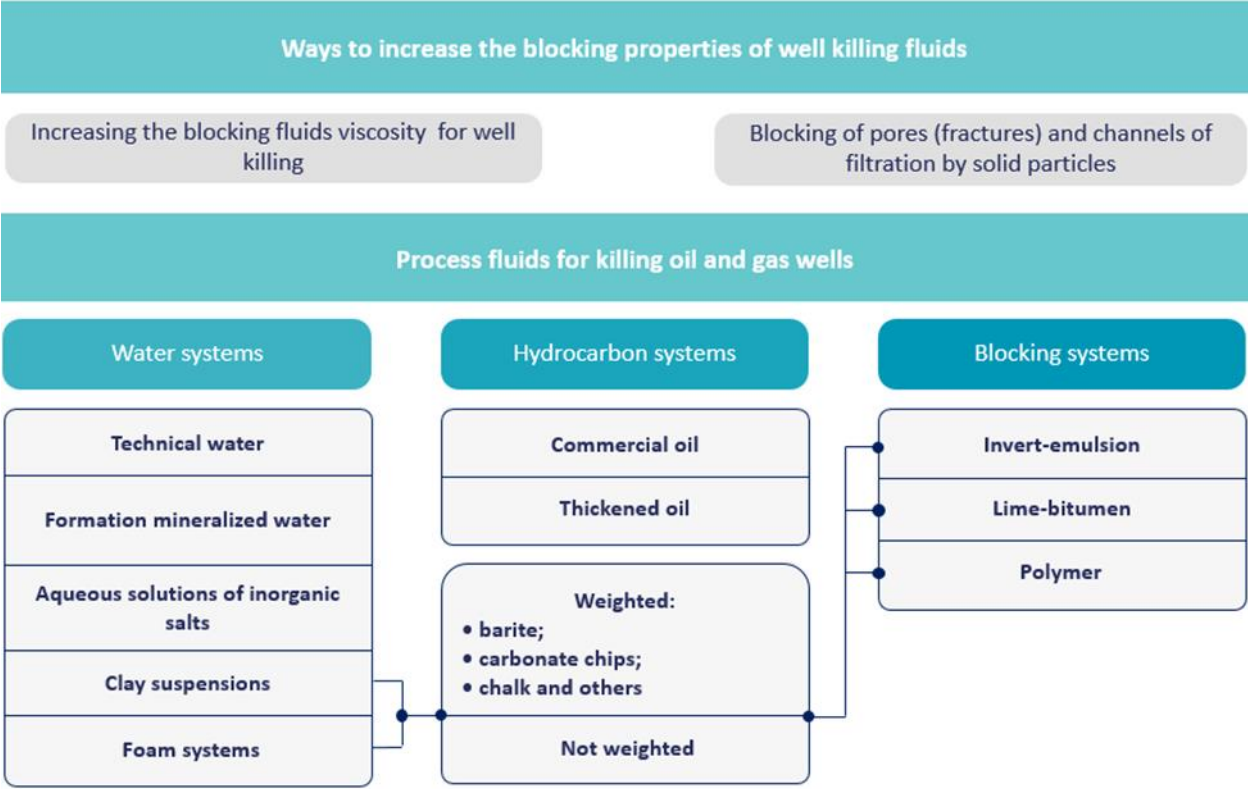


Figure 1. Main types of well killing fluids (Islamov et al., 2019)

Ratio of successful (in 1 cycle) and unsuccessful (more than 1 cycle) well killing operations

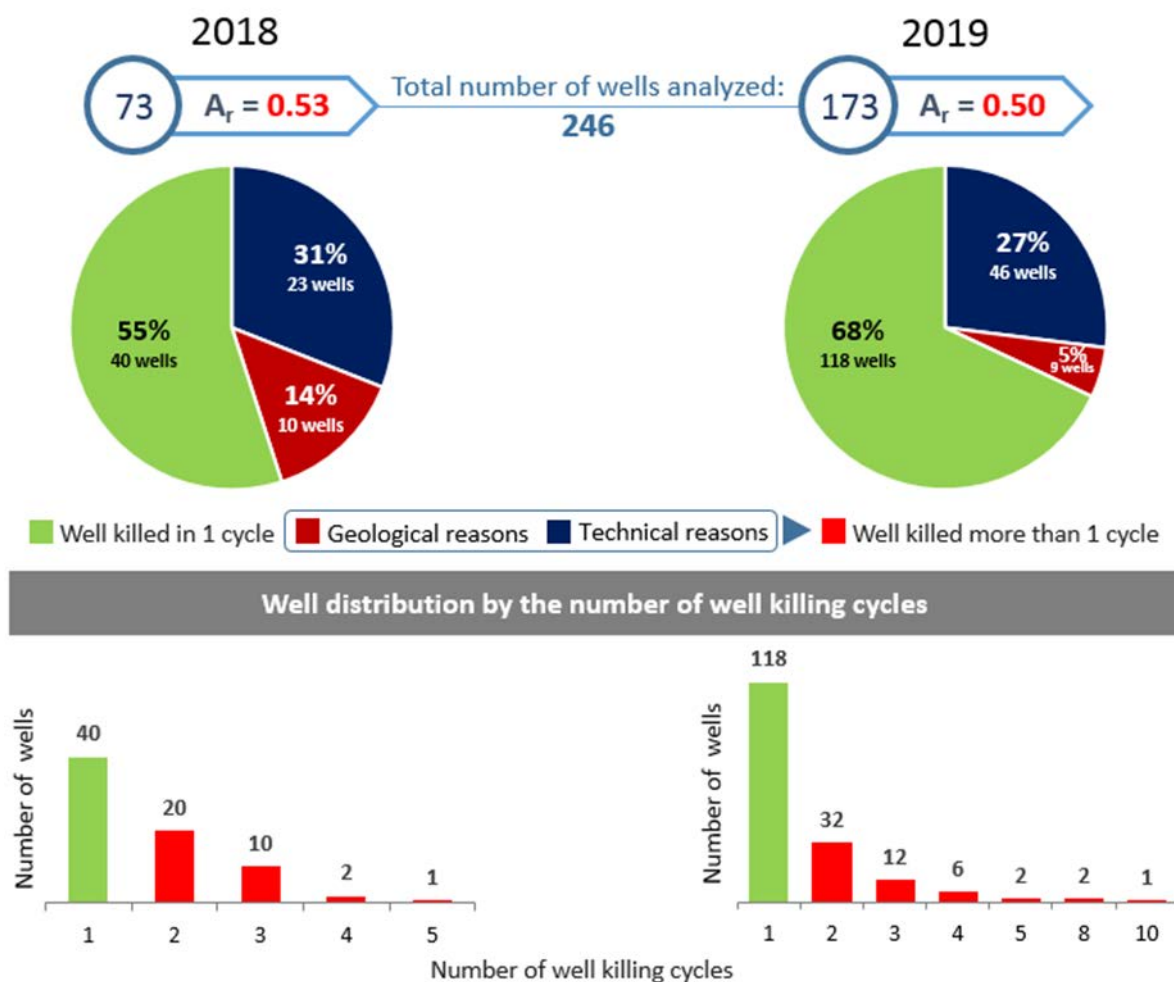


Figure 5. Well killing results at the oil and gas condensate field in the Volga-Ural province for 2018-2019 (Islamov et al., 2019)

ESTIMATIVA DE SUPERFÍCIE ESPECÍFICA DE MCCC NO PROCESSO DE OXIDAÇÃO A BAIXA TEMPERATURA

CCCM SPECIFIC SURFACE ESTIMATION IN PROCESS OF LOW-TEMPERATURE OXIDATION

ОЦЕНКА УДЕЛЬНОЙ ПОВЕРХНОСТИ УУКМ В ПРОЦЕССЕ НИЗКОТЕМПЕРАТУРНОГО ОКИСЛЕНИЯ

POGODIN, Veniamin A.^{1*}; ASTAPOV, Alexey N.²; RABINSKIY, Lev N.³

¹⁻³ Moscow Aviation Institute (National Research University), Department of Advanced Materials and Technologies for Aerospace Application, Moscow – Russian Federation

* Correspondence author
e-mail: pogodin@yandex.ru

Received 22 December 2019; received in revised form 26 February 2020; accepted 19 March 2020

RESUMO

O processo de oxidação a baixa temperatura de materiais compósitos carbono-carbono (MCCC) com uma matriz de pirocarbono foi examinado. A oxidação em temperaturas de 450 a 700 °C é caracterizada por queima interna da fase de carbono, sem uma mudança perceptível no volume externo das amostras experimentais. Foi realizada análise de resistência à oxidação dos componentes estruturais do MCCC. O MCCC e a área superficial específica das fibras de carbono foram estimados pela adsorção a baixa temperatura de nitrogênio e criptônio usando o modelo Brunauer-Emmett-Teller e a teoria do modelo funcional da densidade. A distribuição do tamanho dos poros foi calculada pelo método semi-empírico de Horvath-Kawazoe. Um aumento significativo (cerca de 10 a 15 vezes) na área superficial específica do material compósito, juntamente com um aumento no volume livre ~ 5%, foi acompanhado por uma perda de peso total de cerca de 5%. Alterações específicas da área superficial ocorrem como resultado do ataque anisotrópico da superfície das fibras de carbono com a formação de microporos com uma faixa de diâmetro de 0,5–2,0 nm. Embora os macroporos sejam formados principalmente devido à oxidação do resíduo de pirólise do ligante termoendurecível, eles não contribuem para o aumento específico da superfície, mas apenas fornecem acesso aos microporos. A evolução da microporosidade leva a um aumento do grau de descontinuidade estrutural e, finalmente, à perda do limite de contato matriz-carga. Como resultado, um enfraquecimento geral das características mecânicas do material deve ser observado. Assim, a degradação oxidativa está intimamente relacionada ao aumento do espaço vazio. Um estudo de acompanhamento está em andamento. De fato, permanece uma questão em aberto: saber se o processo oxidativo ocorre diferentemente nos microporos de diâmetro inferior a 2 nm e como ele pode contribuir para o comportamento da resistência ao estresse oxidativo do CCCM.

Palavras-chave: *oxidação, microporos, BET, DFT, MCCC, área superficial específica.*

ABSTRACT

The low-temperature oxidation process of carbon-carbon composite materials (CCCM) with a pyrocarbon matrix has been examined. Oxidation at temperatures of 450 to 700 °C is characterized by internal burnout of the carbon phase without a noticeable change in the experimental samples external volume. Oxidation resistance analysis of CCCM structural components was performed. CCCM and carbon fibers specific surface area were estimated by the low-temperature adsorption of nitrogen and krypton using the Brunauer–Emmett–Teller model and the theory of density functional model. Pore size distribution was calculated by the semi-empirical Horvath–Kawazoe method. A significant increase (about 10-15 times) in specific surface area of the composite material, together with a rise in free volume ~5%, was accompanied by total weight loss of about 5%. Specific surface area changes occur as a result of anisotropic etching of carbon fibers surface with the formation of micropores with 0.5–2.0 nm diameter range. Although macropores are formed mainly due to the oxidation of thermosetting binder pyrolysis residue, they do not contribute to the specific surface increase but solely provide access to micropores. Microporosity evolution leads to an increase of structural discontinuity degree and, ultimately, to the loss of matrix-filler contact boundary. As a result, an

overall weakening of material mechanical characteristics is to be noted. Thus, oxidative degradation is closely related to the increase in void space. A follow-up study is on-going. In fact, an open question remains, namely whether the oxidative process occurs differently in the micropores of diameter less than 2 nm and how it may contribute to the oxidative stress resistance behavior of CCCM.

Keywords: oxidation, micropores, BET, DFT, CCCM, specific surface area.

АННОТАЦИЯ

Исследован процесс низкотемпературного окисления углерод-углеродных композиционных материалов (УУКМ) с пироуглеродной матрицей. Окисление при температурах от 450 до 700 °C характеризуется внутренним выгоранием углеродной фазы без заметного изменения внешнего объема экспериментальных образцов. Проведен анализ стойкости к окислению структурных компонентов УУКМ. Удельная поверхность УУКМ и углеродных волокон оценивалась методом низкотемпературной адсорбции азота и криптона с использованием модели Брунауэра–Эммета–Теллера и теории функционала плотности. Распределение пор по размерам было рассчитано полуэмпирическим методом Хорвата–Кавазое. Значительное увеличение (примерно в 10-15 раз) удельной поверхности композиционного материала вместе с увеличением свободного объема ~5% сопровождалось общей потерей массы около 5%. Изменение удельной площади поверхности происходит в результате анизотропного травления поверхности углеродных волокон с образованием микропор диаметром 0,5 – 2,0 нм. При этом макропоры, образующиеся главным образом за счет окисления пиролизного остатка термореактивного связующего, не способствуют увеличению удельной поверхности, а лишь обеспечивают доступ к микропорам. Эволюция микропористости приводит к увеличению степени структурной неоднородности и в конечном итоге к потере контакта на границе матрица-наполнитель. В результате следует отметить общее ослабление механических характеристик материала. Таким образом, окислительная деградация приводит к увеличению пористости. В настоящее время исследование продолжается. На самом деле остается открытым вопрос, а именно, происходит ли окислительный процесс в микропорах диаметром менее 2 нм другим образом, и как этот процесс влияет на устойчивость УУКМ к окислению.

Ключевые слова: окисление, микропоры, БЭТ, DFT, УУКМ, удельная поверхность.

1. INTRODUCTION

Carbon-carbon composite materials (CCCM) are the basis for the creation of aerospace products that are operated under supercritical thermal, mechanical, and aerogasodynamic loads (Jin *et al.*, 2018; Terentieva *et al.*, 2011; Astapov and Terentieva, 2016; Yurishcheva *et al.*, 2018). The main task in the technology of super-temperature carbon materials is to provide effective protection against oxidation under conditions of high-velocity flow around high-enthalpy flows of oxygen-containing gases (Astapov and Rabinskiy, 2017; Terentieva and Astapov, 2018; Astapov *et al.*, 2019a; Astapov *et al.*, 2019b). Along with thermal spraying processes, chemical vapor deposition, and chemical vapor infiltration (Jin *et al.*, 2018; Yurishcheva *et al.*, 2018; Kiryukhantsev-Korneev *et al.*, 2017; Kiryukhantsev-Korneev *et al.*, 2018), slip protection coatings are widely used to protect CCCM (Astapov and Terentieva, 2016; Terentieva and Astapov, 2018; Astapov *et al.*, 2019a; Kablov *et al.*, 2017; Bankovskaya *et al.*, 2018).

The known technical solutions based on silicide, boride, carbide systems, and their compositions, as a rule, provide CCCM protection from oxidation above 1200-1300 °C and are ineffective below 700 °C. The boron oxide coatings (McKee, 1986) and phosphorus oxide coatings (Luthra, 1988) inhibit the diffusion of oxygen at low temperatures but evaporate or interact with carbon phase above 1000 °C. The lack of a unified approach to protecting CCCM consists in a complex oxidation mechanism, which depends on a number of parameters: (i) ambient temperature, (ii) oxygen partial pressure, (iii) nature of the oxidizing agent, (iv) structure and chemical composition of the carbon phase, and (v) mechanical stresses at the phase boundary. CCCM is an architecturally complex material represented by the following phases: (i) graphitized carbon fibers (CF), (ii) amorphous pyrolysis residue (PR) of a thermoset or pitch binder, and pyrocarbon (PC) matrix, whose structure depends on the regimes and hardware design of the deposition process. The CF properties substantially influenced by the

precursor, the carbonization conditions, and the degree of graphitization.

The impact of the listed factors for oxidation resistance of CCCM estimated through analysis of porosity, specific surface area, and macrokinetics parameters of rate-controlling step at chemical and physical processes. Indicative in this regards are the works (Swaminathan-Gopalan *et al.*, 2019; Swaminathan-Gopalan *et al.*, 2018) devoted to mathematical modeling of the adsorption mechanism FiberForm® CF bulk oxidation, taking into account the evolution of their porous surface. The physical meaning for the dimension of the carbon oxidation rate constant by adsorbed oxygen atoms corresponds to the dimension of the specific surface per unit time reduced to the molar concentration [$\text{m}^2/\text{mol}\times\text{sec}$].

The specific surface of carbon materials depends on the structure and production technology. For nanoscale forms of carbon (nanotubes, graphene), the specific surface area exceeds $2000 \text{ m}^2/\text{g}$; for catalysts, activated carbons, and soots, it is $500\text{--}1500 \text{ m}^2/\text{g}$. Pyrographite and glassy carbon are characterized by a minimal specific surface area and the lack of open porosity, its the reason for their resistance to oxidation up to 700°C (Appen, 1976). The porosity nature of the phase carbon graphitized has a distinctive feature. According to the IUPAC classification (Dubinina, 1953; Dubinina, 1958), the pores forming the specific surface are mainly represented by slit micropores with a size of $0.5\text{--}2 \text{ nm}$. Amorphous forms of carbon show a wide variety of pores in size (micro-, meso-, macropores) and morphology: cylindrical, bottle-shaped, and spherical.

The study of the formal kinetics of CCCM oxidation is complicated by its heterophasic nature. CCCM structural components are characterized by different oxidative stability. Hence, the calculated values of the rate constant, activation energy, the oxidation reaction order are additive indicators and can not correspond to real values. Therefore, set up true mechanism CCCM heterogeneous oxidation, the staging, nature of the ongoing processes, and their mutual influence is really a difficulty. For example, the kinetics of the carbon materials oxidation at various conditions has been studied in detail for CF of varying degrees of graphitization (Govorov *et al.*, 2015), graphite (Rosner and Allendorf, 1965), C/SiC composites, and PC (Halbig, 2004). The rate constants, activation energy values, and the order of reactions are established. In the research of Ismail (1991), the nature of the

change in the specific surface area of CF of various manufacturers during the oxidation process was examined in detail, the volume and size of micropores of various morphologies were estimated, and the effect of alkali metals on the oxidation kinetics at temperatures of $500\text{--}950^\circ\text{C}$ was studied. At the present time, the region of reaction flowing for carbon materials heterogeneous oxidation have been determined depending on the temperature and oxygen pressure.

Despite the complete quantitative description for the oxidation kinetics and the extensive results in mathematical modeling ongoing processes, a number of questions remain that cause active discussions. The S-shaped kinetic profile at $450\text{--}700^\circ\text{C}$ indicates a complex mechanism with an induction effect or the autocatalysis phenom in the oxidation of CF and carbon composites with PC or ceramic matrix (Naslain *et al.*, 2004; Kumar and Kandasubramanian, 2019). A disadvantage in a complete understanding of the reaction mechanism and key factors affecting the oxidation rate limits the use of carbon materials in oxidizing media.

Due to the heterogeneous nature of the CCCM oxidation process, one of the main parameters determining its rate is the value boundary of the phase interface through which mass transfer proceeds (Kamyar *et al.*, 2019; Lee *et al.*, 2019). The complex influence of phase boundary consists of the fact that its only active part, the proportion of which varies with time, is involved in the process of low-temperature oxidation. Moreover, these changes are non-linear and difficult to predict. Therefore, conducting studies of structural changes in the surface and obtaining quantitative estimates is an urgent task for understanding and refining the mechanism of carbon materials oxidation.

The purpose of this work was to study structural changes in the CCCM carbon phase at the initial stages of low-temperature oxidation by estimating the specific surface area and analyzing the microstructure.

2. MATERIALS AND METHODS

A CCCM with a PC matrix INCARBO® (Russia) was used as the object of study. The CCCM was obtained on the basis of a carbon fabric CF UKN-M-3K (LLC Argon, Russia) based on polyacrylonitrile (PAN) precursor. The main characteristics of CF are presented in Table 1.

The prepregs were obtained by layering, and the phenol-formaldehyde resin was used as a binder. After the resin carbonization (binder mass loss was 40 wt.% at 1100 °C), PC bulk impregnation was carried out in methane medium at a residual pressure of 10–40 mm Hg in four cycles for 8 hours at 1300–1600 °C. The check was carried out by changing the mass of the workpiece at each stage of the technological redistribution.

The PC phase was obtained by the deposition of films with a thickness of 3–4 mm on an isostatic graphite substrate at a temperature of 1600 °C and a methane pressure of 30–40 mm Hg. The films were separated from the substrate by thermal shock. The determination of the porosity and the apparent CCCM density was carried out by hydrostatic weighing according to GOST R ISO 12985-2-2014 (ISO 12985-2: 2000). The weighing of the samples was carried out on an analytical balance GR-202 (AND, Japan) with an accuracy of 10^{-4} g. The CCCM samples were oxidized in an LHT04/17 SW chamber furnace (Nabertherm, Germany) with a working volume of 4 under isothermal conditions. The thermocouple TPR (type B) acted as a temperature sensor. Weighed samples in corundum boats were loaded into a furnace heated to operating temperature, kept at the isotherm for a predetermined time, cooled together with the furnace to 20 °C, removed from the furnace, and re-weighed. The oxidation was carried out in an air duct and in a mixture of air with helium at a flow rate of 70–220 ml/min.

The oxidation kinetics of CCCM, CF, and PC were studied by synchronous thermal analysis using an STA 449 F3 Jupiter instrument (Netzsch, Germany) in the thermogravimetric mode together with the differential scanning calorimetry mode on the isotherm. The samples were heated in open crucibles from Al_2O_3 with a volume of 0.085 ml at a linearly increasing furnace temperature at a rate of 20 °C/min. The oxidation was carried out in the air and in a mixture of air and helium at a gas flow rate of 70–220 ml/min. An empty crucible was used as a reference. The temperatures of the sample and the reference were measured using built-in S-type thermocouples made of Pt-Rh alloys. The change in mass of the samples was recorded with an accuracy of 1 µg. The balance drift over the entire temperature range did not exceed 10 mg/h.

For oxidation in a furnace, samples with sizes of 26.4×26.4×2.8 mm and 4.0×60×2.8 mm were used, and for thermal analysis, samples with sizes of 4.0×3.6×2.8 mm were used. Dried

air supplied from a high-pressure cylinder through a desiccant was used as an oxygen source. Due to the low carbon dioxide content (0.03 vol.%), the effect of CO_2 on the oxidation reaction rate and chemical interaction with the carbon phase was neglected. Helium gas was used with a purity of 99.99999 vol.% (grade 7.0). To quantify the rate of mass loss, it was used the change in the mass of the sample as a result of the oxidation per unit of time with respect to the initial mass, [g/g×sec]. When analyzing volumetric bodies, it is customary to use the concept of the volumetric surface [m^{-1}], but since the quantitative assessment of the oxidation reaction was a change in mass, it was used the concept of a specific surface, reduced to the mass of the sample, [m^2/g]. The value of the total surface S_{tot} was expressed according to the measurement data through the product of the specific surface S_{sp} determined by the Brunauer-Emmett-Teller (BET) method and the mass of the sample.

The specific surface area of CCCM and CF were determined by the adsorption of nitrogen and krypton using the single point BET method on three independent devices: NOVA 1000e (Quantachrome Instruments, USA), Sorbi®-MS (META LLC, Russia), ASAP 2020 Plus Physisorption (Micromeritics, USA), and according to the density functional theory (DFT) by the quantum-chemical method of modeling adsorption on heterogeneous surfaces on an ASAP 2020 Plus Physisorption device (Micromeritics, USA). In this case, a graphite surface model with slit-like pores was used for calculations. Various ways for determining the specific surface, which were described above, were used due to the fact that, according to the BET theory, it is very difficult to obtain objective results in the presence of micropores (Rouquerol *et al.*, 1999). According to the results of calculations using DFT, the pore size distribution was obtained by the semi-empirical Horvath-Kawazoe method. The optical microscopy of the samples was performed in bright field mode using an inverted Olympus GX51 microscope (Olympus Life Science GmbH, Germany). The microstructural studies were performed on a Zeiss Supra 40VP scanning electron microscope (Carl Zeiss Group, Germany) in the secondary electron mode at an accelerating voltage of 10 kV and a beam current of 445 pA.

3. RESULTS AND DISCUSSION:

Figure 1 shows the mass loss data for low-temperature oxidation of CF of the UKN-M-3K grade, CCCM with PC matrix (CC), and PC phase. The obtained results for CF of the UKN-M-3K grade are in good agreement with the data on the oxidation of CF of the T-300 grade given in (Halbig, 2004). Despite the low oxidative stability of CF, the mass loss for CCCM based on them is much lower. According to the calculation of the activation energy of the CCCM oxidation reaction (Fig. 1), CF and, a carbonized PR of phenol-formaldehyde resin is predominantly oxidized. According to the optical microscopy, the cross-sectional structure of the initial CCCM samples with a PC matrix is relatively solid - without shells and voids (Fig. 2, b, c). However, numerous cracks were revealed on the surface of the samples (Fig. 2, a). They result from the relaxation of thermal stresses arising at the pyro-densification stage due to the difference in the linear thermal expansion coefficients of the CF and PC matrices in combination with a high modulus of elasticity and low CF elongation.

With a total CCCM mass loss due to oxidation of about 5% (Table 2), there were no visual changes in the structure of the surface layer (Fig. 2, d). No traces of oxidation were detected on the PC matrix surface. In volume, burnup occurs along the "CF-PR-PC" phase boundary and is accompanied by the formation of air channels oriented along CF (Fig. 2, f). The reason for this is the low oxidative stability of the amorphous PR low-temperature binder - phenol-formaldehyde resin. The oxidation of the PC matrix is less pronounced, since the oxidative stability of PC is higher, as can be seen from the data presented in Fig. 1. The analysis of the optical microscopy data allowed to say that, during low-temperature oxidation, the linear dimensions and volume of the samples remain almost unchanged. The change in density and porosity during the oxidation process occurs due to the loss of CF mass, binder residues, and the opening of closed pores. Table 2 summarizes that the values of apparent density and open porosity after the oxidation are proportional to mass loss. With a total mass loss of about 5%, the proportion of the free volume of the samples increased by almost 5%. Based on this, one can understand that the fraction of closed macropores in the CCCM structure is insignificant. This is consistent with the microscopy data.

The established increase in the specific surface area of CCCM during the low-

temperature oxidation (Table 2) is an unobvious and important circumstance. Under the assumption that the geometrical dimensions of the samples remain unchanged during oxidation, the area of their external surface S_{ext} remains constant. However, the value of the total surface S_{tot} , taking into account both the external and internal (concentrated in the material pores) surface, undergoes significant changes. The calculated data on the total surface of CCCM samples before and after oxidation, obtained through the product of the specific surface S_{sp} (Table 2) by the corresponding mass of the sample, are presented in Table 3. It is possible to note that, as a result of oxidation, the total surface of CCCM increases by order of magnitude relative to its value for the initial samples and differs by four orders of magnitude from the surface area. Thus, as a result of the increase in the inner surface of the CCCM, its outer surface becomes a negligible value in comparison with the surface concentrated in micropores.

The works of K.L. Luthra (1988) and P.L. Walker *et al.* (1959) contain the results of attempts to make estimates of the specific surface area of carbon materials through their porosity. The most objective estimates of the change in the specific surface during CF oxidation are given by M.K.I. Ismail (1991). It was shown (Ismail, 1991) that in some cases, the specific surface area of CF can increase up to 60 m²/g, while for CCCM, according to our data (Table 2), its increase is less pronounced. The oxidation of CCCM is a heterogeneous process. Therefore, it is supposed to bring the calculated reaction rate to the interface through which chemical interaction and mass transfer are carried out. With a significant difference in the external and volume surfaces (10^3 – 10^4 times), the influence of macrokinetic parameters on the oxidation rate at temperatures below 700 °C must be estimated, taking into account the nature of the change in specific surface.

The reason for the increase in the specific surface during oxidation and the total weight loss of the samples is the formation of micro- and mesopores with sizes of 0.5–2 nm and 2–50 nm (according to the IUPAC classification (Dubinina, 1953; Dubinina, 1958)), respectively. Macropores do not contribute to the specific surface; they provide access to meso- and micropores. Analyzing the oxidation resistance of the structural components of CCCM, one can conclude that macropores are formed as a result of oxidation of PR phenol-formaldehyde resin,

and micro- and mesopores are formed as a result of oxidation of the CF surface. Such selective oxidation of CCCM breaks the contact at the "matrix–filler" interface. Therefore, control of the specific surface will allow an assessment of the kinetic stability of composite materials during oxidation.

Since the BET theory does not take into account the phenomenon of condensation of adsorbed gas in micropores (Rouquerol *et al.*, 1999; Carrot *et al.*, 1987), when they are present in the structure of the samples, the measurement results are distorted relative to reality. Therefore, the obtained data on the specific surface of CCCM (Table 2) were refined by the DFT calculation data and on the equipment of various manufacturers. The study was conducted on CCCM samples and individual CF. The measurement data averaged over four samples in each series are presented in Table 4. One can see that the specific surface values, according to BET and DFT, differ significantly. This is probably due to the presence of micropores on the CF surface. The BET data measured on NOVA 1000e and Sorbi®-MS showed good convergence. Additionally, according to DFT, the pore size distribution was calculated using the semi-empirical Horvath–Kawazoe method. The resulting estimates for CCCM after oxidation are shown in Table 5.

The microstructural heterogeneity of the studied objects and the significant measurement errors associated with it make it difficult to obtain reliable quantitative estimates of the specific surface area and pore distribution. However, qualitative changes in the structure of carbon materials during low-temperature oxidation are clearly visible. So, the BET specific surface area changes that we established (Tables 2, 4) are not consistent with the oxidation scheme proposed by M.C. Halbig (2004). According to Halbig's scheme, CF degradation in the composite matrix proceeds uniformly - with a decrease in the fiber cross-section and correlates with mass loss. As a result, the specific surface area of the reinforcing CF is reduced during the oxidation process. That is, the model proposed by Halbig (2004) takes into account only the macroporosity of the C/SiC composite and does not consider possible changes in the specific surface. At the same time, the nature of structural changes during micro- and macroporosity differs fundamentally.

In view of the noted difficulties in assessing the specific surface area and pore size distribution, additional studies of CCCM samples were carried out before and after oxidation using

scanning electron microscopy. The results are selectively presented in Figure 3. It can be seen that CF after CCCM oxidation has a more relief microstructure with a developed surface in comparison with a smoother surface of the initial fibers. This indirectly indicates the effect of etching the CF surface with oxygen, accompanied by the appearance of microcavities and ledges. The formation of mesopores 2–50 nm in size is not observed; the presence/absence of micropores has not been visually established due to insufficient resolution of the microscope. This result is not consistent with the obtained pore size distribution data (Table 5). Apparently, the heterophase structure of the composite material affects the results of measurements of the specific surface and data on the distribution and volume of micropores.

The formation of micropores in the process of low-temperature oxidation is possible by several mechanisms. According to Ismail (1991), a CF structure is characterized by closed microporosity; as the surface oxidizes, the pores open, and the specific surface increases. The most likely explanation for the appearance of micropores is proposed by K.L. Luthra (1988), as an anisotropic etching of the CF surface. The reasons for the manifestation of anisotropy and the mechanism of the appearance of micropores with boundary sizes of 0.8–1.2 nm (Ismail, 1991) are poorly studied and constitute a subject for future scientific discussion. The most plausible hypothesis seems to be expressed by Naslain *et al.* (2004) and Walker *et al.* (1959). Anisotropic oxidation of the carbon surface is due to defects in the structure of the fiber and the presence of impurities. It becomes apparent to a lesser extent as the degree of graphitization of the carbon phase of the fibers increases.

Thus, the low-temperature degradation of CCCM is due to an increase in the number of micropores on the CF surface. As a result, with a slight loss of mass, a substantial increase in the volume surface is observed. Its value is 10^3 – 10^4 times greater than the external surface area. At the macro level, the contact between the PC matrix and CF is broken in the structure of the composite material. This, together with an increase in the degree of structural discontinuity as a result of the formation and development of microporosity, leads to a decrease in the work aimed at breaking the binding forces in the "fiber–matrix" system and the work of pulling out the fibers from the matrix. The consequence is a decrease in the mechanical properties of CCCM both at room temperature (tensile strength, yield

strength) and at elevated temperatures (creep strength, tensile strength).

4. CONCLUSIONS:

The oxidation of CCCM based on PAN fibers with a PC matrix at temperatures of 450 to 700 °C is voluminous and is accompanied by a significant change in porosity and specific surface with no visible signs of oxidation from the outside. The process of low-temperature oxidation of CCCM is anisotropic in nature at the macro- and microstructural levels. At the macro level, this is manifested in various oxidative stability of the structural components of the composite material - CF, PC matrix, and PR thermosetting binder. At the micro-level, this is manifested by anisotropic etching of the CF surface, accompanied by an increase in microporosity. Macropores do not contribute to the value of the specific surface, but only provide access to meso- and micropores.

The oxidation of CCCM proceeds predominantly along the CF-PR-PC phase boundary and results in the rupture of the contact between the matrix and the filler. This, together with an increase in the degree of structural discontinuity due to the formation and development of microporosity, leads to a decrease in the kinetic stability of the composite material and the loss of its mechanical properties.

5. ACKNOWLEDGMENTS:

This work was carried out as part of the RSF grant for the event "Research by scientific groups led by young scientists" of the Presidential Program for Research Projects (Agreement No. 19-79-10258 of 08.08.2019).

6. REFERENCES:

1. Appen, A.A. *Temperature-resistant inorganic coatings*, Leningrad: Khimiya, **1976**.
2. Astapov A.N., Rabinskiy, L.N. *Solid State Phenomena*, **2017**, 269, 14-30. DOI: 10.4028/www.scientific.net/SSP.269.14.
3. Astapov, A.N., Lifanov, I.P., Rabinskiy, L.N. *High Temperature*, **2019a**, 57(5), 744-752. DOI: 10.1134/S0018151X19050018.
4. Astapov, A.N., Terentieva, V.S. *Russian Journal of Non-Ferrous Metals*, **2016**, 57(2), 1-173. DOI: 10.3103/S1067821216020048.
5. Astapov, A.N., Zhestkov, B.E., Lifanov, I.P., Rabinskiy, L.N., Terentieva, V.S. *Arabian Journal for Science and Engineering*, **2019b**, 44(6), 5323-5334. DOI: 10.1007/s13369-018-3585-4.
6. Bankovskaya, I.B., Nikolaev, A.N., Kolovertnov, D.V., Polyakova, I.G. *Physics and Chemistry of Glass*, **2018**, 44(5), 509-515. DOI: 10.7868/S0132665118050086.
7. Carrot, P.J.M., Roberts, R.A., Sing, K.S.W. *Carbon*, **1987**, 25(1), 59-68. DOI: 10.1016/0008-6223(87)90040-6.
8. Dubinina, M.M. Methods for studying the structure of finely dispersed and porous bodies. *Proceedings of the Meeting*, July 25-29; Moscow, Russia, **1953**, 164-166.
9. Dubinina, M.M. Methods for studying the structure of finely dispersed and porous bodies. *Proceedings of the Second Meeting*, June 13-18; Moscow, Russia, **1958**, 296-298.
10. Govorov, A.V., Galiguzov, A.A., Tikhonov, N.A., Malakho, A.P., Rogozin, A.D. *New Refractories*, **2015**, 11, 34-39.
11. Halbig, M.C. Oxidation kinetics and strength degradation of carbon fibers in a cracked ceramic matrix composite. *28th International Conference on Advanced Ceramics and Composites B: Ceramic Engineering and Science Proceedings*, January 25-30; Florida, USA, **2004**, 137-146.
12. Ismail, M.K.I. *Carbon*, **1991**, 29(6), 777-792. DOI: 10.1016/0008-6223(91)90017-D.
13. Jin, X., Fan, X., Lu, C., Wang, T. *Journal of the European Ceramic Society*, **2018**, 38(1), 1-28.
14. Kablov, E.N., Zhestkov, B.E., Grashchenkov, D.V., Sorokin, O.Yu., Lebedeva, Yu.E., Vaganova, M.L. *Thermophysics of High Temperatures*, **2017**, 55(6), 704-711. DOI: 10.7868/S0040364417060059.
15. Kamyar, N., Rezaee, S., Shahrokhian, S., Amini, M.M. *Journal of Colloid and Interface Science*, **2019**, 555, 655-666.
16. Kiryukhantsev-Korneev, Ph.V., Iatsyuk, I.V., Shvindina, N.V., Levashov, E.A., Shtansky, D.V. *Corrosion Science*, **2017**, 123, 319-327. DOI: 10.1016/j.corsci.2017.04.023.
17. Kiryukhantsev-Korneev, Ph.V., Potanin, A.Yu. *Russian Journal of Non-Ferrous Metals*, **2018**, 59(6), 698-708. DOI: 10.3103/S106782121806010X.

18. Kumar, C.V., Kandasubramanian, B. *Industrial and Engineering Chemistry Research*, **2019**, 58(51), 22663-22701.
19. Lee, S., Park, G., Kim, J.G., Paik, J.G. *International Journal of Aeronautical and Space Sciences*, **2019**, 20(3), 620-635.
20. Luthra, K.L. *Carbon*, **1988**, 26(2), 217-224. DOI: 10.1016/0008-6223(88)90040-1.
21. McKee, D.W. *Carbon*, **1986**, 24(6), 737-741. DOI: 10.1016/0008-6223(86)90183-1.
22. Naslain, R., Guede, A., Rebillat, F., Le Gallet, S., Lamouroux, F., Filipuzzi, L., Louchet, C. *Journal of Materials Science*, **2004**, 39(24), 7303-7316. DOI: 10.1023/B:JMSC.0000048745.18938.d5.
23. Rosner, D.E., Allendorf, H.D. *Carbon*, **1965**, 3(2), 153-156. DOI: 10.1016/0008-6223(65)90042-4.
24. Rouquerol, F., Rouquerol, J., Sing, K. *Adsorption by powders and porous solids*, Cambridge: Academic Press, **1999**. DOI: 10.1016/B978-0-12-598920-6.X5000-3.
25. Swaminathan-Gopalan, K., Borner, A., Murray, V.J., Poovathingal, S., Minton, T.K., Mansour, N.N., Stephani, K.A. *Carbon*, **2018**, 137, 313-332. DOI: 10.1016/j.carbon.2018.04.088.
26. Swaminathan-Gopalan, K., Stephani, K.A., Ferguson, J., Borner, A., Panerai, F., Mansour, N.N. Effective oxidation model for light-weight carbon preform ablators. *AIAA SciTech Forum*, January 7-11; San Diego, USA, **2019**, 63-67.
27. Terentieva, V.S., Astapov, A.N. *Russian Journal of Non-Ferrous Metals*, **2018**, 59(6), 709-718.
28. Terentieva, V.S., Eremina, A.I., Astapov, A.N., Leipunskii, I.O., Pshechenkov, P.A. *Composites: Mechanics, Computations, Applications*, **2011**, 2(3), 247-270.
29. Walker, P.L. Jr., Rusinko, F. Jr., Austin, L.G. Gas reactions of carbon. In Eley, D.D., Selwood, P.W., Weisz, P.B. (Eds.): *Advances in Catalysis. Vol. 11* (pp. 133-221), New York: Academic Press, **1959**.
30. Yurishcheva, A.A., Astapov, A.N., Lifanov, I.P., Rabinskiy, L.N. *Key Engineering Materials*, **2018**, 771, 103-117. DOI: 10.4028/www.scientific.net/KEM.771.103.

Table 1. Properties of the CF UKN-M-3K based on the PAN precursor

Linear density, tack	190
The diameter of the filament, μm	7
Modulus of elasticity, GPa	225
Specific breaking load at the break of a loop, cN/tack	10
Tensile stress, GPa	3.5
Density, g/cm^3	1.75
Processing temperature, $^{\circ}\text{C}$	1500
A specific surface according to BET, m^2/g	1.35

Table 2. The apparent density ρ_{app} , open porosity P_o and specific surface area S_{sp} by BET (NOVA 1000e) of CCCM samples in the initial state and after oxidation at $T = 570^{\circ}\text{C}$, $PO_2 = 0.6 \text{ atm}$ for 190 min

No.	Mass loss, %	ρ_{app} , g/cm^3		P_o , %		S_{sp} , m^2/g	
		Before oxidation	After oxidation	Before oxidation	After oxidation	Before oxidation	After oxidation
1	-4.985	1.52	1.46	2.6	7.8	1.18	14.26
2	-4.801	1.50	1.46	2.7	7.4	1.07	14.39
3	-3.922	1.51	1.47	2.7	7.4	1.15	13.62
4	-4.839	1.52	1.46	2.7	7.7	1.01	13.87

Table 3. The calculated data on the total surface area of CCCM samples by BET in the initial state and after oxidation at $T = 570^{\circ}\text{C}$, $\text{PO}_2 = 0.6 \text{ atm}$ for 190 min

No.	Sample mass, g		External surface S_{ext} , cm^2	Total surface S_{tot} , cm^2	
	Before oxidation	After oxidation		Before oxidation	After oxidation
1	0.983	0.934	8.077	11599.4	133188.4
2	1.083	1.031	8.991	11588.1	148360.9
3	0.969	0.931	8.016	11143.5	126802.2
4	1.054	1.003	8.644	10645.4	139116.1

Table 4. Data on the specific surface area of samples by nitrogen adsorption (CCCM) and krypton adsorption (CF)

Sample	Specific surface S_{sp} , m^2/g	BET		DFT	
		NOVA 1000e	Sorbi®-MS	ASAP 2020 Plus Physisorption	
CCCM	Before oxidation	1.3	1.2	<1	-
	After oxidation				
	At $T = 570^{\circ}\text{C}$ (mass loss 5%)	14.0	13.0	10.5	7.5
CF	Before oxidation	0.8	<1	<1	-
	After oxidation				
	At $T = 570^{\circ}\text{C}$ (mass loss 5%)	29.4	32.1	24.6	19.6

Table 5. Pore size distribution for CCCM after oxidation at $T = 570^{\circ}\text{C}$ (mass loss 5%) obtained by the semi-empirical Horvath–Kawazoe method

Volume available for gas adsorption – $0.01 \text{ cm}^3/\text{g}$	0.5–2 nm micropores	2–50 nm mesopores
Share, %	25–35	65–75

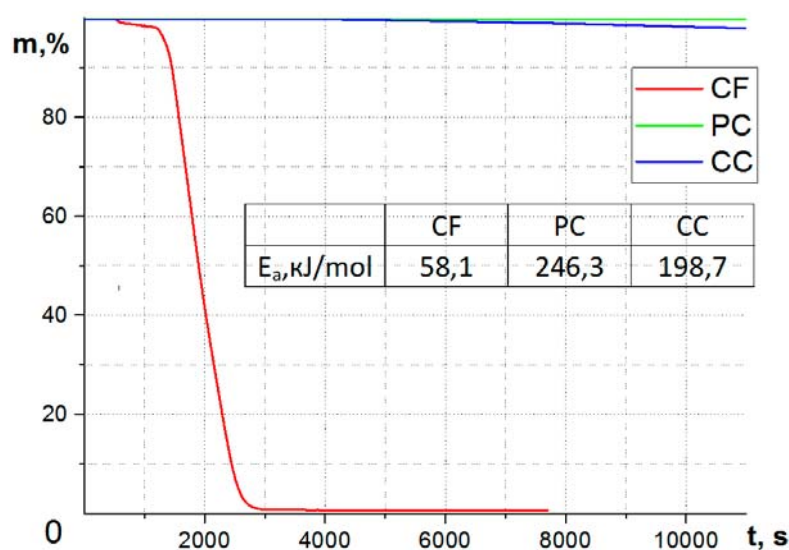


Figure 1. Data on mass loss during oxidation at $T = 570^{\circ}\text{C}$, $\text{PO}_2 = 0.6 \text{ atm}$ for CF of the UKN-M-3K grade, CCCM with PC matrix (CC), and PC phase (PC)

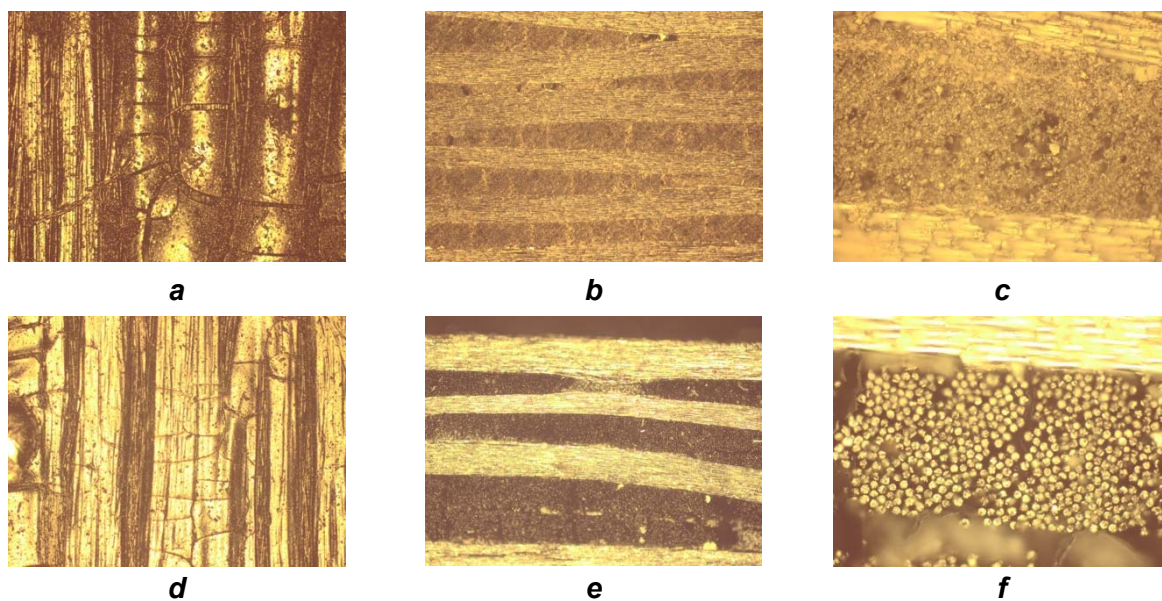


Figure 2. The structure of CCCM according to optical microscopy in the initial state (a, b, c) and after oxidation at $T = 570^{\circ}\text{C}$, $\text{PO}_2 = 0.6 \text{ atm}$ for 190 min. (d, e, f): a, d - x50; b, e - x100; c, f - x500

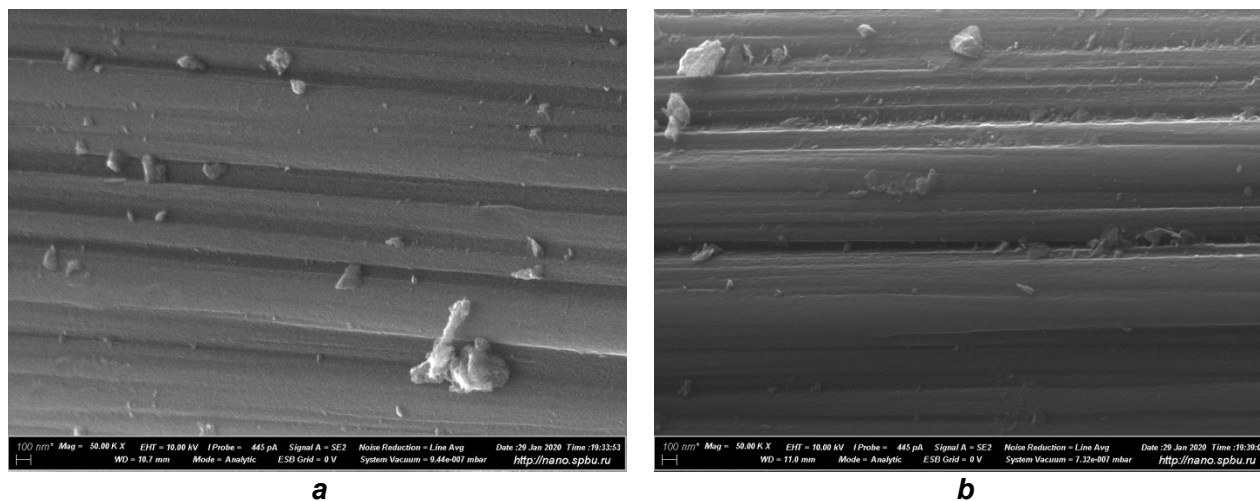


Figure 3. Microstructure of CF in secondary electrons before (a) and after (b) oxidation of CCCM at $T = 570^{\circ}\text{C}$ (mass loss 5%)

SOCIEDADE DIGITAL: NOVOS DESAFIOS PARA A EDUCAÇÃO

DIGITAL SOCIETY: NEW CHALLENGES FOR EDUCATION

ЦИФРОВОЕ ОБЩЕСТВО: НОВЫЕ ВЫЗОВЫ ДЛЯ ОБРАЗОВАНИЯ

GAPSALAMOV, Almaz Rafisovich¹; BOCHKAREVA, Tatyana Nikolaevna²; AKHMETSHIN, Elvir Munirovich^{3*}; VASILEV, Vladimir Lvovich⁴; ANISIMOVA, Tatyana Ivanovna⁵;

^{1,3,4} Kazan Federal University, Elabuga Institute of KFU, Economics and Management Faculty, Economics and Management Department. Russia.

² Kazan Federal University, Elabuga Institute of KFU, Psychology and Pedagogy Faculty, Pedagogy Department. Russia.

⁵ Kazan Federal University, Elabuga Institute of KFU, Mathematics and Natural Sciences Faculty, Mathematics and Applied Computer Science Department. Russia.

* Corresponding author
e-mail: elvir@mail.ru

Received 28 January 2020; received in revised form 16 February 2020; accepted 15 March 2020

RESUMO

O mundo entrou em uma nova fase de desenvolvimento - a era da sociedade digital. Sob a influência de uma nova rodada de progresso tecnológico, os mecanismos e práticas da ordem mundial assim como equipamentos e tecnologias estão mudando. Atualmente, a gama de inovações não se limita a uma ou duas indústrias; as mudanças abrangem quase tudo - setores de telecomunicações, informação e comunicação, nanotecnologia, espaço, bioengenharia, robótica, etc. O objetivo da pesquisa é estudar os processos de mudança do paradigma do desenvolvimento social sob a influência da formação de uma sociedade digital. O artigo analisa o conceito de "sociedade digital", mostra como as ferramentas da economia digital são usadas para justificar uma mudança de paradigma no desenvolvimento social da geração moderna. A metodologia de pesquisa é baseada em uma abordagem funcional sistemática e estrutural. A pesquisa é composta por métodos gerais de pesquisa científica que incluem análise, síntese, abstração, métodos de análise sistêmica, complexa, lógica, estrutural, comparativa e estatística. Como resultado da análise, são formuladas abordagens para a definição de economia digital, apresentadas as etapas do desenvolvimento da sociedade digital, identificadas as trajetórias de mudanças tecnológicas na era digital e formulados problemas que inibem o processo de digitalização.

Palavras-chave: *sociedade digital, economia digital, digitalização, tecnologias digitais, prioridades nacionais, educação.*

ABSTRACT

The world has entered a new phase of development – the era of digital society. Under the influence of a new round of technological progress, the mechanisms and practices of the world order, as well as equipment and technologies, are changing. The range of innovations today is not limited to one or two industries; changes cover almost everything – telecommunications, information and communication sectors, nanotechnology, space, bioengineering, robotics, etc. The research aims to study the processes of changing the paradigm of social development under the influence of the formation of a digital society. The article analyzes the concept of "digital society," shows how the tools of the digital economy are used to justify a paradigm shift in social development for the modern generation. The research methodology is based on a systematic and structural-functional approach. Also, methods of sociological survey and statistical processing of information were used. As a result of the analysis, plans to the definition of the digital economy are formulated, the stages of development of digital society are presented, the trajectories of technological changes in the digital era are identified, and problems that inhibit the digitalization process are formulated.

Keywords: *digital society, digital economy, digitalization, national priorities, education.*

АННОТАЦИЯ

Мир вступил в новую фазу своего развития – эпоху цифрового общества. Под воздействием нового витка технологического прогресса меняются механизмы и порядки мироустройства, техника и технологии. Спектр нововведений сегодня не ограничивается одной или двумя отраслями, изменения охватывают практически всё что нас окружает – это отрасли телекоммуникации, информатизации и связи, нанотехнологии, космос, биоинженерия, робототехника и многое-многое другое. Целью работы является исследование процессов изменения парадигмы общественного развития под воздействием становления цифрового общества. В статье анализируется понятие "цифровое общество", показано, как используются инструменты цифровой экономики для обоснования смены парадигмы общественного развития для современного поколения. Методология исследования построена на системном и структурно-функциональном подходе. Кроме того, были использованы методы социологического опроса и статистической обработки информации. В результате анализа сформулированы подходы к определению цифровой экономики, представлены этапы развития цифрового общества, определены траектории технологических изменений в цифровую эпоху и сформулированы проблемы, препятствующие процессу цифровизации.

Ключевые слова: цифровое общество, цифровая экономика, цифровизация, национальные приоритеты, образование.

1. INTRODUCTION:

The world is witnessing not just quantitative changes in the sectoral nature of economic management. In essence, there is an exponential increase in the technological, engineering, and product range, and all this is occurring in the context of ongoing globalization and an open policy of national institutions. At the same time, the subsequent gigantomania of large corporations takes place – the volume of their capital increases at a rapid pace; as a result, state institutions are leveled more and more (Abdrakhmanova *et al.*, 2019; Maximov *et al.*, 2019).

An essential feature of modern transformation is the period of its passing (Biserova and Shagivaleeva, 2019). If the previous ups of social and technological development spanned an extended period, for the whole of humanity (not for individual countries), continuing for centuries, then the modern technological breakthrough is a momentous change that has already occurred over a decade. The planet has not yet known in its history such an increase in scientific knowledge and its applied use (Magsumov, 2014, 2019).

For Russia, this situation is a new challenge. An economically, socially, technologically weakened state that has not recovered from the crisis events of the 1990s – early 2000s, today must accomplish the impossible – to become one of the leading countries in the race for the "digit." The new qualitative growth of the state or its further decline depends on this. In this regard, the presented

research will aim to study the processes of changing the paradigm of social development under the influence of the formation of a digital society.

2. LITERATURE REVIEW:

The widespread dissemination of research in the sphere of the digital economy has begun relatively recently. This is explained by many reasons, among which the timing of the beginning of the digital era and the unpreparedness of researchers for the processes that occur today are essential. Despite this, in the literature, there is a relatively large layer of research devoted to the problems of changing the paradigm of social development.

The modern world has come to a new stage in its development – the period of digitalization. The content of the world economy is changing; the living conditions of every person on the planet are changing (Saenko *et al.*, 2019). New technologies will absorb old ones; new professions will sweep away the old and unclaimed. Gandini's book "The reputation economy: Understanding knowledge work in a digital society" (Gandini, 2016) shows that digital technologies are not only mediators of production and organizational processes, opening up new paths to satisfy supply and demand, but they actually contribute to the spread of cultural concepts of labor and values that promise to become the new industry standard.

According to Ilie (2019), computer society is a new stage in human civilization, a new way of life of the highest quality, which involves the

intensive use of information in all spheres of human activity and existence, which has a severe economic and social impact. Information society provides its members with broad access to information, a new way of working, and knowledge, which increases the likelihood of economic globalization and increases social cohesion (Jarrah, 2019; Sycheva *et al.*, 2019; Tarman, 2016). Technological support for the new society consists of the convergence of three sectors: information technology, communication technology, digital content production. Technological advances have allowed the emergence of new multimedia services and applications that combine sound, image, and text and use all means of communication (telephone, fax, television, and computers). The development of these new means of communication and information technology is an important factor in increasing the competitiveness of economic agents, opening up new prospects for better organization of work and creating new jobs (Yamova *et al.*, 2019; Fedulova *et al.*, 2019; Nikolaichuk *et al.*, 2017). At the same time, new prospects are emerging for the modernization of public services, healthcare, environmental management, and new ways of communication between public administration institutions and citizens. Broad access to education and culture – for all social categories, regardless of age or geographical location – can also be achieved with the help of new technologies. Some scholars (Low *et al.*, 2019) generally understand the digital economy as a living creature. They propose a multi-level analysis to study efforts aimed at creating a rational living society by examining the structure of the technology of environmental organizations.

At the same time, it should be noted that not all scholars accept the concept of the new digital era, and some of them criticize the conceptual apparatus that is used in science. In “Digital economy: Beautiful, but imaginary, concept” Astafyev and Sokolov (Astafyev & Sokolov, 2020; Ipatov *et al.*, 2019) give their vision of digital economy and digitalization processes, and offer applied tools for researching these processes.

The problems of providing resources for the new economy are of particular interest in the academic community. Digilina and Lebedeva (2020) suggest that the role of economic resources is changing significantly. In industrial societies, the driver of economic development is predominantly human (labor) resources and financial resources, but knowledge and people are

the drivers of economic progress in the digital economy. The transition to new conditions is a labor-intensive, complex, and significant process that ensures sustainable development and stimulates the competitiveness of economic entities. Technological resources are critical to the digital economy; besides, the identification and formulation of requirements that are necessary for the transition from an industrial society are of particular importance.

Many researchers (Malakhova *et al.*, 2018; Popkova & Gulzat, 2020) reflect on the implications of the digital era; others argue over its legal nature (Krönke, 2019; Tarakanov *et al.*, 2019; Solovykh *et al.*, 2019).

A significant number of researchers attempt to conduct a comparative analysis of the process of digitalization by countries. Benčič *et al.*, using developed and developing countries as leaders in their categories and occupying middle and peripheral positions, consider integrated indicators of digital competitiveness, which are highlighted and calculated by IMD as of 2018 (Benčič *et al.*, 2020). The research methodology includes an analysis of variations (calculation of the direct average, standard deviation, and the coefficient of variation), forecasting, and scenario analysis. The authors concluded that in developed countries, the basis of digital competitiveness of the economy is a high level of integration of information and communication technologies and devices, and a low interest of the business in digital modernization is an obstacle to its growth. The opposite situation has occurred in developing countries – a low level of integration of information and communication technologies and devices with a high interest in digital modernization on the part of the business.

In continuation of this study, Chazhaeva *et al.* (2020) attempted to rank countries moving along the path of digitalization and highlighted the threats that impede this process (Chazhaeva *et al.*, 2020). The study attempts to identify the prospects for bringing the digital economy model in line with current requirements for its sustainability and work out some recommendations for managing its threats (Zlivko *et al.*, 2018; Shikhnaieva *et al.*, 2019; Yemelyanov *et al.*, 2018). In conclusion, the idea is formulated that the practical implementation of the digital economy model does not guarantee its sustainable development – its growth can occur according to one of three scenarios: stable (no fluctuations in GDP growth rates in stable prices, for example, in Indonesia and China); unstable development and crisis (bright fluctuations in GDP

growth rates in real terms – for example, in Venezuela and Russia); sustainable growth (the most preferred scenario, which provides for an increase in GDP growth rates in real terms – for example, in Singapore and the USA). Social and technological factors largely determine the scenario for the development of the digital economy.

A special place in the studies is devoted to the consideration of the role of states in the process of digitalization of the economy. Studies on the theoretical features of building a digital economy in Russia are particularly interesting in this regard. In “The algorithm of modern Russia’s transition to a digital economy” (Shulus *et al.*, 2020), an algorithm is proposed for the transition of modern Russia to a digital economy, which will overcome barriers through the joint efforts of the state, business, and society. The main attention is paid to the formation of effective demand for breakthrough digital technologies. It includes three consecutive stages: the development of information society, the formation of technological reserves, and the introduction of advance digital technologies. Kuznetsova *et al.* (2020) consider modern time a period of transformation in Russia, which is significant in the context of the development of a market efficient, innovative economy (Kuznetsova *et al.*, 2020). To lead Russia out of the polysystem crisis along the path of sustainable economic growth, according to the authors, it is necessary to apply a systematic and integrated approach: entering the path of sustainable growth of the level and quality of national human capital (Aleshko *et al.*, 2019); diversification of the economy and creation of an effective national innovation system and an innovative economy or a knowledge economy; decriminalization of the country (Goryushkina *et al.*, 2019; Lafer and Tarman, 2019). The modernization of the traditional industries and the service sector as a result of the penetration of information technology and digitization of economic processes will create the basis for the formation of new markets and new conditions for the functioning of the Russian market, as well as new approaches to analytics, forecasting, and management decisions. An important sector in the transition to digitalization will remain the industry.

A similar study that characterizes the potential of the Russian economy during the transition to a digital economy is presented in Bezdudnaya *et al.* (2020). The study provides a quantitative assessment of the level of use of production potential in the regions of the Russian Federation over a long period of time. The authors’

criteria for diagnosing the degree of development of advanced technologies are presented; general conclusions on the real level of introduction of advanced technologies at the enterprises of the Russian Federation in dynamic and spatial aspects are formulated; some prerequisites for the development of further research in the field of monitoring regional imbalances, developing additional combined indicators and studying the effectiveness of the realization of production potential in the territories during the transition of the national economic system to modernization are identified (Kolmakov, 2019; Voronkova *et al.*, 2019).

In conclusion of the historiographic analysis, the authors would like to move on to studies that consider not the global processes of the impact of digitalization on the world economy or the economy of individual countries, but the worldview problems that the new era brings and the reflection of these processes on the quality of public life. In Guryanova *et al.* (2020), the problem of the individual’s change in the conditions of modern society and economy is considered (Guryanova *et al.*, 2020). The influence of digitalization on a person and the resulting problems of the ideological, psychological, and social nature are shown. That study also analyzes the dialectical interactions of the real and virtual worlds, the human mind and artificial intelligence, the on-line and off-line communication. Their relationships are the most complex humanitarian problem of digital society. Homo digital is characterized as a product of digitization and the owner of fundamentally new qualities and value orientations. The authors are convinced that the right human values are vital to the digital world (Dobrovolskienė *et al.*, 2017). Their misinterpretation leads to the victory of consumer ideology and social degradation. Equality and humanism, by contrast, are considered the core values of modern society (Frolova *et al.*, 2019; Ishchenko and Magsumov, 2019; Mullins, 2019). However, it cannot yet be called “humanistic.” For this, fundamental human values must be applied in digitalization conditions. The real progress of humanity is possible based on self-improvement, development of human consciousness, intelligence, and moral qualities.

In “The impact of the digital economy on the quality of life” (Razumovsky *et al.*, 2020), the issues related to the development of digital economy in current conditions, as well as the degree of impact of digitalization on the quality of public life, are examined. The main vectors and directions of the development of information and

communication technologies, as well as the prospects for using the digitalization of the economy, are presented. The main problems that impede the implementation of the digital economy in resolving the issues of public socio-economic life are identified.

3. MATERIALS AND METHODS:

In work, general scientific research methods were used: analysis and synthesis, deduction and induction, the relationship of historical and logical processes, the search for cause-effect relationships, the systemic and structural-functional approach, the laws of dialectics.

Also, a questionnaire was developed for conducting a sociological survey (table 1). The data obtained were processed using statistical research methods. The factors that have the highest impact on the digitalization process in education and the economy have been identified as objects of study, secondary general and professional educational institutions, universities, and enterprises of the real sector of the economy were considered. The questionnaire was sent to 50 schools, 10 colleges, 20 universities, 100 enterprises of the Russian Federation. 90% of the profiles were returned with answers. A total of 300 people were interviewed. The questionnaire was anonymous and did not require obtaining consent to the processing of personal data. The purpose of the study was to identify the most relevant trends in the development of digital technologies in the opinion of all members of the public: pupils, teachers, students, teachers, workers, specialists, and leaders. It was important to evaluate the general understanding of the country's population about the course of the formation of a new digital society and the necessary educational digital competencies.

As a result of statistical processing of the obtained information, the current trends in the development of the digital economy and education were identified, as well as the most important factors determining the essence and design of the new digital society were identified. The results and conclusions are presented in this article

4. RESULTS AND DISCUSSION:

4.1. The concepts of "digital economy" and "digital society"

The term "digital economy" has entered the terminology very tightly. At the same time, in the

scientific literature, one can find such words with the same meaning as "diginomica," "Internet economy," and "web economy" (Teryokhin, 2018; Ziyadin *et al.*, 2020).

To date, there has not been a single, well-established definition of the concept of a "digital economy". Most researchers are inclined to the idea of qualitative and quantitative growth of technologies related primarily to the spread of the Internet. For example, the digital economy is understood as "a global network of economic and social activities that are supported through platforms such as the Internet, as well as mobile and sensor networks" (Australia's Digital Economy: Future Directions, 2019), or "an economy capable of providing high-quality ICT infrastructure and mobilizing ICT capabilities for the benefit of consumers, business and the state" (Technology Isn't Working, 2019), or "activities for the creation, dissemination, and use of digital technologies and related products and services; technologies for the collection, storage, processing, search, transmission and presentation of data in electronic form" (Abdrakhmanova *et al.*, 2019, 13-14).

However, the presented definitions seem to the authors not entirely accurate. Under the influence of technological changes, the structure of society, its institutions, and, ultimately, the entire state and public system are changing. The previous economic, social, and political mechanisms will be updated with new ones. This suggests that evaluating the digital economy only from a technology innovation perspective is not entirely true.

In this regard, it will be more accurate for the authors to accept a definition where the digital economy is understood as "a new way of economy based on knowledge and digital technologies, within the framework of which new digital skills and opportunities are being developed in society, business and state" (Development of digital economy in Russia, 2016).

The authors agree with the part of this definition, which speaks of a new economic structure based on knowledge and digital technologies. Transformational changes taking place in the world are modifying the entire ecosystem and leave an imprint on all spheres of human life (Nelyubina *et al.*, 2018; Ziyadin *et al.*, 2018; Prause and Atari, 2017). However, the second part of the definition, where the formation of digital skills is prescribed, dramatically narrows the subject field of the ongoing processes. Today, the changes in which digital competencies are

formed are only a small element of the current global events (Korableva *et al.*, 2019). In the authors' opinion, it is crucial to see the digitalization of the economy from the perspective of global processes in the context of the exponential growth of technology and knowledge in the world, but not in individual countries.

This implies the broader concept of "digital society," by which the authors mean a new type of social and economic relations based on the creation and use of knowledge and digital technologies, the main form of ownership of which being the intellectual property of large corporations. It is the format of relations that is being built in the modern world.

4.2. Stages of development of the new society

A distinctive feature of the new time will be its transience and unpredictability. The growth of global knowledge and its massive introduction in the form of a high-tech product will contribute to cardinal changes in the lifestyle of the entire population of the planet.

Today the world is witnessing the first stage of the formation of a new order (Figure 1). It is associated primarily with technological changes taking place in the world. New technologies and high-tech products are being introduced into people's lives at high speed, and people get the opportunity to use them now, and not over a time lag. Just to imagine, in the old days, innovations would reach end users (by no means all) after a long period; now, the situation is different. Everyone touches the products of the new era at every moment, at one's discretion. An example is Pokemon Go game, which got 50 million players within 19 days. Against the background of cars (62 years), phones (50 years), or bank cards (28 years), 19 days is an instance (Delyukin, 2018).

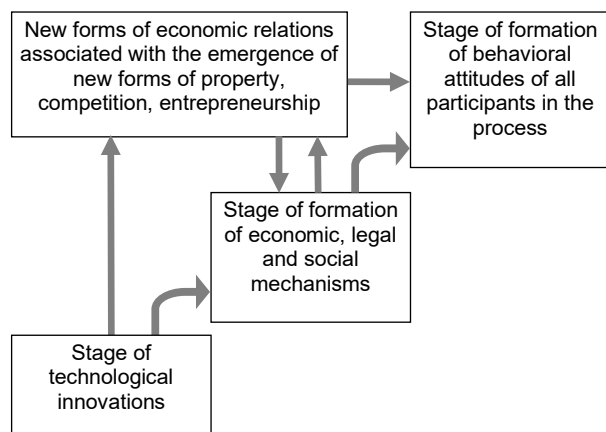


Figure 1. The staged model of digital society formation. Source: Compiled by the authors.

The appeared superstructure in the movement scheme along the stages of the formation of "digital society" explains all the inconsistency, difficulty, and unevenness of this process. New technologies are in such a way changing the traditional economic relations, regular market transactions, traditional forms of appropriation that the formation of financial and legal regulatory mechanisms is impossible without the formation of new structures of economic relations. It is impossible to convert such economical relations into the existing legal form as adequate legal forms have not yet been developed. This explains the lagging of the second stage, and especially the third stage, behind the rapid development of the first stage. Therefore, in existing academic studies of the digital economy phenomenon in relation to the prospects of the existing economic model, there is a certain impasse. It is impossible to build a model of "digital society" within the existing economic paradigm. New approaches to the organization of economic relations, a change in thinking, a transition to a new social system adequate to the nature and challenges of the digital economy are required.

Despite this progress, the world community itself and public institutions have not yet been able to rebuild. People still live in the realities and conditions of the 20th century; in the mass consciousness, there is no adequate understanding of the processes occurring. The vast majority of modern society does not understand or underestimates the events that take place in the modern world. However, this is temporary; very soon, society will plunge into the maelstrom of new epochal upheavals.

Automation of production processes, computerization, and, finally, digitalization, level human labor. Only modern, highly qualified specialists and managers are becoming in demand in modern society. As a result, the masses of people today have either lost their jobs already or will lose them in the near future. The volume of information received and transmitted increases manifold, so an average person no longer always has the opportunity to trace it and use it for its intended purpose. Many other things are also occurring that are going to change the established view of the world.

Despite this, one can already speak about the beginning of the second stage of a new way of the digital economy. In essence, this is the formulation of economic, legal, and social mechanisms for the functioning of new relations. In particular, legal institutions aimed at protecting intellectual property are being formed; in the

globalizing world, cross-border cooperation is being built between states and businesses; countries agree on common ways to combat cybercrime, etc. Why this stage is highlighted separately and, in the authors' opinion, is late, is explained very simply. Recent scientific discoveries and innovations have multiplied, in many areas, as a result of which society simply does not have the time to turn them into an appropriate legal form, to control (or even restrain) them.

Finally, the third stage, to which modern society has not yet come, in the authors' opinion, is seen in building a "frame" of the behavioral attitudes of all participants in the process. Understanding by all participants of the importance of the changes that are taking place and their involvement in this process will undoubtedly be an essential criterion for integrating national economies into the canvas of digital society.

Today it is becoming increasingly apparent that the role of national economies is gradually losing importance. This is especially evident when it comes to the economic movement of information. On this occasion, Vedin puts "...The nature of the relationship between globalization and the information economy is similar to the formation of national economic complexes in the era of the industrial revolution and the formation of the capitalist order of production. In other words, the global economy in the information era is the national economy in the era of industrial capitalism. Of course, industrial capitalism initiated the internationalization of production. But globalization and internationalization have a fundamental difference. If the internationalization of production was accompanied by an increase in the role of nation-states, then globalization means a decline in the role of the nation-state as the central subject of international economic relations" (Vedin, 2002).

With a general decline in the importance of national institutions, property institutions began to change. A new system of appropriation is emerging in society that coexists and interacts with traditional forms of ownership. The authors agree with the researchers that the institutions of ownership will change in two main directions: 1) the transformation of traditional forms of ownership as a result of the emergence of new objects and methods of appropriation (especially intellectual property); 2) the appearance of a qualitatively new property relationship between society and an individual regarding the appropriation and development of a universal

(general human) productive force (Vedin, 2002). However, in the second point, the authors make some adjustment. In essence, the appearance of qualitatively new changes will occur mainly not between society and an individual, but between an organization and a corporation.

The importance of public and private property institutions in the form that operated during the 20th and beginning of the 21st century and coped with their role began to decline markedly. The strong, often uncontrolled growth of transnational corporations, a change in their role in the global economy, as well as in the political sphere, is undoubtedly changing the institutions of property. Megacorporations today are fighting for the possession of a highly intellectual product, new technologies, protecting their secrets with all their might. In many ways, this is also useful for the state – the burden of developing new products and technologies is laid on the shoulders of private companies. As a result, society is gradually approaching such a stage of its development when the importance of not already personal private property becomes the prerogative of social development, but the protection of the property of large corporations. Accordingly, state institutions themselves follow the support and protection of these forms of property.

Personal private property of individual citizens or even companies is becoming a thing of the past; obtaining and using knowledge, and subsequently, directly the product of this knowledge, is gradually becoming the prerogative of several large companies. Employees of these enterprises, as carriers of this knowledge, will have the ability to create, store (in some cases, even sell it), but these will only be "crumbs from a big pie". Talking about information at the company, Bill Gates wrote: "...so that the top management of the company realizes the importance of free dissemination of knowledge, otherwise no efforts in this direction will bring success" (Gates, 2000), but the authors emphasize – within the company, as outside the company knowledge of one employee can be immediately reset. In the context of high-tech products and technologies, it is impossible for individual scientists and engineers to have a complete understanding and knowledge of products today. It is corporations that collect this knowledge bit by bit, concentrate it and create a finished product, and, as a result, become its copyright holder.

4.3. The trajectories of technological change in the new era

Consider the critical trajectories of the

development in the new era, which reflect its modern character. These include preservation of digital national sovereignty; advantage in using national digital technologies; the presence of a single digital space; development of digital competencies of players, the formation of a unified knowledge system; free, equal and non-discriminatory access of each player to digital assets; formation and development of new digital values and culture while preserving traditional, social, national values and culture (Ageev *et al.*, 2017).

All trends are somehow tied to the implementation and use of digital technology. Researchers classify as common (or through) areas the following (the authors use the report of scholars from the Institute for Statistical Studies and Economics of Knowledge of the National Research University Higher School of Economics, published in 2019):

- use of technologies for the collection, processing, and storage of structured and unstructured arrays of information based on big data;

- development and implementation of artificial intelligence, that is, a software system capable of perceiving information with a certain degree of autonomy, learning and making decisions based on the analysis of large data arrays, including imitating human behavior (Polyakova *et al.*, 2019a,b);

- implementation of distributed registry technologies (blockchain) based on algorithms and protocols for decentralized storage and processing of transactions, structured as a sequence of linked blocks without any possibility of their subsequent change;

- development and application of quantum technologies based on quantum effects, which allow radically changing the methods of transmission and processing of large data arrays;

- use of new production technologies that increase the efficiency of resource use, design and manufacture of individualized items, the cost of which is comparable to the cost of mass-produced goods;

- introduction of the mass industrial Internet capable of uniting devices in the manufacturing sector, equipped with sensors and capable of interacting with each other and/or the external environment without human intervention;

- development, improvement, and implementation of components of robotics (industrial robots) with three or more degrees of

mobility (freedom), built on the basis of sensors and artificial intelligence, able to perceive the environment, control their actions and adapt to its changes;

- development and implementation of wireless communication technologies based on data transmission through a standardized radio interface without using a wired network connection;

- development and use of virtual reality technologies based on computer modeling of a three-dimensional image or space, through which a person interacts with a synthetic ("virtual") environment with subsequent sensory feedback (Abdrakhmanova *et al.*, 2019, 13-14).

Meantime, it should be understood that these areas are practically not tied to any industries or sectors of the economy, which means that the scope of application of new technologies will become widespread.

4.4. Findings

The result of the study was an understanding of the inevitability of fundamental changes in both global and national ecosystems. Under the influence of digitalization, the economic, social, cultural, and even political order of states is changing.

Digitalization has embraced almost all sectors of the economy and is very quickly transforming the life of every person and society as a whole. Changes affect the technology of collection, processing, and storage of information, automation, and robotization of production processes, wireless technology, and much, much more.

At the same time, along with the processes of digitalization, the nature of public institutions is changing. The institution of property is gradually transforming, and the role and importance of states are decreasing due to the increasing role of transnational corporations.

This process is happening in three stages: the stage of technological innovations; the stage of formation of economic, legal and social mechanisms; and the stage of formation of behavioral attitudes of all participants in the process.

5. CONCLUSIONS:

The formation of a new order will require cardinal changes in the education system.

Previous tools and mechanisms in the new realities may turn out to be not only useless but also harmful. Already today, in many countries of the world, some problems are inhibiting the digitalization process. These include a lack of specialists with new digital skills and competencies; lack of educational programs that can meet the needs of the modern society. Even problems such as boredom or burnout from learning are a brake on new relationships. The national education system faces the question: how to educate children further? All this taken together defines the national educational strategies, the main requirements of which include definition of a common goal, which means understanding by all participants of the importance of ongoing processes; competitive education; compulsory continuing education; development of new units for assessing the quality of education; preservation of intellectual information; creation of existing tools for monitoring incoming and outgoing information; formation of a basic level of competence of the able-bodied population of the country in the field of foreign languages, programming, etc.

Undoubtedly, all these events should go hand in hand with the widespread digital potential that has been accumulated in the country.

Against the background of the large-scale effects of digitalization in the public space, the concept of a "digital economy" has appeared. The authors carried out a historiographic analysis of the works on the disclosure of the essence of the concepts of "digital society" and "digital economy." It has been shown that various scientists have different approaches to the definition of these concepts, sometimes even rejecting the existing conceptual apparatus that is used in science. The role of the state in the process of digitalization has also been analyzed. Not only global digitalization processes but also worldview problems of the new era have been considered.

From the definition of the term, the authors proceeded to formulate the stages of development of digital society. A statement has been put that modern society goes through the first stage associated with technological changes and goes into the second stage – the scene of formation of economic, legal, and social mechanisms.

The key trajectories of the development in the new era have been considered: preservation of digital national sovereignty; advantage in using national digital technologies; the presence of a single digital space; development of digital competencies of players, formation of a unified

knowledge system; free, equal and non-discriminatory access of each player to digital assets; formation and development of new digital values and culture while preserving traditional, social, national values and culture. The new era gives rise to new problems, the mechanisms for solving which have not yet been developed. First of all, this concerns the sphere of education, which should prepare personnel for the future digital economy, but at the given moment, it is still in the old realities. Thus, the validity of the paradigm shift in the social development of digital society has been examined.

6. ACKNOWLEDGMENTS:

The reported study was funded by RFBR, project number 19-29-07037.

7. REFERENCES:

1. Alajmi, M. A. **2019**. The impact of E-portfolio use on the development of professional standards and life skills of students in the Faculty of Education at Princess NouraBint Abdul Rahman University, Entrepreneurship and Sustainability Issues 6(4) 1714-1735. [http://doi.org/10.9770/jesi.2019.6.4\(12\)](http://doi.org/10.9770/jesi.2019.6.4(12))
2. Abdrakhmanova, G.I., Vishnevsky, K.O., Gokhberg, L.M. et al. What is a digital economy? Trends, competencies, measurement. HSE Report to XX Apr Int. scientific conf. on the problems of economic and social development (Moscow, April 9-12, 2019). In L. M. Gokhberg (Ed.). Moscow: Publishing House of the Higher School of Economics. **2019**. Retrieved from https://www.hse.ru/data/2019/04/12/1178004671/2_Цифровая_экономика.pdf
3. Ageev, A. I., Aver'yanov, M. A., Evtushenko, S. N., & Kochetova, E. Yu. Digital Society: Architecture, Principles, Vision. Economic strategies, 1, 114-125. **2017**. Retrieved from http://www.inesnet.ru/wp-content/mag_archive/2017_01/es2017-01-114-126_Ageev_Averyanov_Yevtushenko_Kochetova.pdf
4. Aleshko, R., Petrova, L., Ivanova, E., Plotnikova, A., Melnikov, M., & Antonov, V. Human capital in the digital economy format. *International Journal of Engineering and Advanced Technology*,

- 2019, 9(1), 7517-7523. doi:10.35940/ijeat.A2201.109119
5. Astafyev, I. V., & Sokolov, D. P. Digital economy: Beautiful, but imaginary, concept. *Lecture Notes in Networks and Systems*, 2020, 87, 230-237. doi:10.1007/978-3-030-29586-8_27
6. Australia's Digital Economy: Future Directions. Australian Government. Office of the Australian Information Commission. 2019. Retrieved from https://www.oaic.gov.au/images/document/s/migrated/migrated/sub_broadband_digital_economy.pdf
7. Benčič, S., Kitsay, Y. A., Karbekova, A. B., & Giyazov, A. Specifics of Building the Digital Economy in Developed and Developing Countries. *Lecture Notes in Networks and Systems*, 2020, 87, c. 39-48. doi:10.1007/978-3-030-29586-8_5
8. Bezdudnaya, A. G., Gundorova, M. A., Gerashchenkova, T. M., Gerasimov, K. B., & Fraimovich, D. Y. Analyzing the use of the production potential in the Russian Federation's territories during the transition to the digital economy. *Lecture Notes in Networks and Systems*, 2020, 87, 185-192. doi:10.1007/978-3-030-29586-8_22
9. Chazhaeva, M. M., Serebryakova, A. A., Tashkulova, G. K., & Atabekova, N. K. Sustainable Development of the Digital Economy on the Basis of Managing Social and Technological Threats. *Lecture Notes in Networks and Systems*, 2020, 87, 49-56. doi:10.1007/978-3-030-29586-8_6
10. Delyukin, E. Infographics: eight major trends shaping the future of the global economy. (2018, December 29). Vc.ru. 2018. Retrieved from <https://vc.ru/finance/54677-infografika-vosem-glavnyh-trendov-formiruyushchih-budushchee-mirovoy-ekonomiki>
11. Dobrovolskienė, N.; Tvaronavičienė, M.; Tamošiūnienė, R. 2017. Tackling projects on sustainability: a Lithuanian case study, Entrepreneurship and Sustainability Issues 4(4): 477-488. [http://doi.org/10.9770/jesi.2017.4.4\(6\)](http://doi.org/10.9770/jesi.2017.4.4(6))
12. Digilina, O. B., & Lebedeva, D. V. Resource provision of the digital economy. *Lecture Notes in Networks and Systems*, 2020, 87, 352-358. doi:10.1007/978-3-030-29586-8_41
13. Fedulova, I., Ivanova, V., Atyukova, O., & Nosov, V. Inclusive education as a basis for sustainable development of society. *Journal of Social Studies Education Research*, 2019, 10(3), 118-135.
14. Gandini, A. *The Reputation Economy: Understanding Knowledge Work in Digital Society. The reputation economy: Understanding knowledge work in digital society* (Book). London: Palgrave Macmillan. 2016. doi:10.1057/978-1-137-56107-7
15. Gates, B. Business with the speed of thought. Moscow: Publishing House EKSMO-Press, 2000.
16. Goryushkina, N., Petrova, L., Khudyakova, T., Tchuykova, N., Klimovskikh, N., Voinova, N. Diversification and its Role in Improving Hotel Industry Businesses Competitiveness. *International Journal of Recent Technology and Engineering*, 2019, 8(4), 605-609.
17. Guryanova, A., Khafiyatullina, E., Petinova, M., Astafeva, N., & Guryanov, N. Social, psychological and worldview problems of human being in digital society and economy. *Lecture Notes in Networks and Systems*, 2020, 87, 244-250. doi:10.1007/978-3-030-29586-8_29
18. Ilie, M. Digital economy and its impact on the society. *Paper presented at the Proceedings of the 33rd International Business Information Management Association Conference, IBIMA 2019: Education Excellence and Innovation Management through Vision 2020*, 2019, 6642-6650.
19. Ipatov, Y., Krevetsky, A., Andrianov, Y., & Sokolov, B.. Creation of image models for evolving objects on dynamically changing scenes. *Journal of Applied Engineering Science*, 2017, 15(4), 540-545.
20. Jarrah, H. Y. Six thinking hats: An analysis of the skill level of Jordanian vocational education teachers and the extent of skill application. *Space and Culture*, India, 7(1), 2019, 170-185. doi:10.20896/saci.v7i1.470
21. Korableva, O., Durand, T., Kalimullina, O., & Stepanova, I. Studying user satisfaction with the MOOC platform interfaces using the example of coursera and open education platforms. *Paper presented at the ACM International Conference*

- Proceeding Series*, **2019**, 26-30. doi:10.1145/3322134.3322139
22. Krönke, C. Public procurement law as digitalization consequential law: Likewise, a contribution to the theory of public procurement law. [Vergaberecht als digitalisierungsfolgenrecht: zugleich ein beitrage zur theorie des vergaberechts] *Verwaltung*, **2019**, 52(1), 65-98. doi:10.3790/verw.52.1.65
 23. Kuznetsova, S. N., Kuznetsov, V. P., Kozlova, E. P., Potashnik, Y. S., & Tsymbalov, S. D. Transformational Period of Russian Development in the Digital Economy. *Lecture Notes in Networks and Systems*, **2020**, 91, 663-669. doi:10.1007/978-3-030-32015-7_74
 24. Lafer, S., & Tarman, B. Editorial 2019: (2)1, Special Issue. *Journal of Culture and Values in Education*, 2(1), **2019**, i-v. Retrieved from <http://cultureandvalues.org/index.php/JCV/article/view/34>
 25. Low, M. P., Chung, C. Y., Ung, L. Y., Tee, P. L., & Kuek, T. Y. Smart living society begins with a holistic digital economy: A multi-level insight. *Paper presented at the 2019 7th International Conference on Information and Communication Technology, ICoICT 2019*, **2019**. doi:10.1109/ICoICT.2019.8835199
 26. Malakhova, E. V., Garnov, A. P., & Kornilova, I. M. Digital economy, information society and social challenges in the near future. *European Research Studies Journal*, **2018**, 21, 576-586.
 27. Mullins, R. Using Dewey's Conception of Democracy to Problematize the Notion of Disability in Public Education. *Journal of Culture and Values in Education*, **2019**, 2(1), 1-17. Retrieved from <http://cultureandvalues.org/index.php/JCV/article/view/24>
 28. Nikolaichuk, L. A., Malyshkov, G. B., & Sergeev, I. B. **2017**. Integration of economic aspects into the teaching system for disciplines in the field of natural resource management and environmental protection. *International Journal of Applied Engineering Research*, 12(6), 928-931.
 29. Nelyubina, E. G., Safina, L. G., Bobkova, E. Y., Korobejnikova, E. V., & Melysheva, E. P. Integrative-project model of environmental education in the training system of the students. *International Journal of Economics and Financial Issues*, 6(1S), **2016**, 249-255.
 30. Popkova, E. G., & Gulzat, K. Contradiction of the digital economy: Public well-being vs. cyber threats. *Lecture Notes in Networks and Systems*, 87, **2020**, 112-124. doi:10.1007/978-3-030-29586-8_13
 31. Prause, G.; Atari, S. On sustainable production networks for Industry 4, Entrepreneurship and Sustainability Issues, **2017**, 4(4): 421-431. [http://doi.org/10.9770/jesi.2017.4.4\(2\)](http://doi.org/10.9770/jesi.2017.4.4(2))
 32. Razumovsky, V. M., Sultanova, A. V., Chechina, O. S., & Nikonorova, S. A. The impact of the digital economy on the quality of life. *Lecture Notes in Networks and Systems*, **2020**, 87, 417-423. doi:10.1007/978-3-030-29586-8_48
 33. Shikhnaieva, T., Brezhnev, A., Saidakhmedova, M., Brezhneva, A., & Khachaturova, S. **2019**. Intellectualization of educational information systems based on adaptive semantic models doi:10.1007/978-3-319-92363-5_8
 34. Saenko, N., Voronkova, O., Volk, M., & Voroshilova, O. The social responsibility of a scientist: Philosophical aspect of contemporary discussions. *Journal of Social Studies Education Research*, **2019**, 10(3), 332-345.
 35. Shulus, A. A., Zarudneva, A., Yatsechko, S., Fetisova, O. The Algorithm of Modern Russia's Transition to the Digital Economy. *Lecture Notes in Networks and Systems*, **2020**, 87, 57-63. doi:10.1007/978-3-030-29586-8_7
 36. Solovykh, N. N., Koroleva, I. V., Stompeleva, E. S., Terskaya, G. A., & Aliev, V. M. Digital economy and socio-economic contradictions of information society. *Studies in Computational Intelligence*, **2019**, 826, 655-662. doi:10.1007/978-3-030-13397-9_70
 37. Tarakanov, V. V., Inshakova, A. O., & Dolinskaya, V. V. Information society, digital economy and law. *Studies in Computational Intelligence*, **2019**, 826, 3-15. doi:10.1007/978-3-030-13397-9_1
 38. Tarman, B. Innovation and Education. *Research in Social Sciences and Technology*, **2016**, 1(1). Retrieved from <http://ressat.org/index.php/ressat/article/vi>

39. Technology Isn't Working. The Economist Newspaper Limited. **2019**. Retrieved from <https://www.economist.com/news/special-report/21621237-digital-revolution-has-yet-fulfil-its-promise-higher-productivity-and-better>
40. Teryokhin, K. Digital Economy in Russia. (2018, November 19). RusCoins.info. **2018**. Retrieved from <https://ruscoins.info/faq/cifrovaya-ekonomika-v-rossii/>
41. The development of the digital economy in Russia. World Bank Office in Russia (2016, December 20). World Bank Group. **2016**. Retrieved from <https://www.vsemirnyjbank.org/ru/events/2016/12/20/developing-the-digital-economy-in-russia-international-seminar-1>
42. Vedin, N. V. Post-industrial society: the establishment of a new system of appropriation. *Problems of the Modern Economy*, **2002**, 1(1), 63-65.
43. Volchik, V.; Maslyukova, E. **2019**. Trust and development of education and science, Entrepreneurship and Sustainability Issues 6(3): 1244-1255. [http://doi.org/10.9770/jesi.2019.6.3\(27\)](http://doi.org/10.9770/jesi.2019.6.3(27))
44. Yamova, O. V., Maramygin, M. S., Sharova, I. V., Nesterenko, J. N., & Sobina, N. V. Integral valuation of an enterprise's competitiveness in the industrial economy. *European Research Studies Journal*, **2018**, 21, 777-787.
45. Ziyadin, S., Ermekbaeva, B., Supugaliyeva, G., & Doszhan, R. Transformation of basic indicators of socio-economic processes in the digital economy. Paper presented at the Proceedings of the 31st International Business Information Management Association Conference, IBIMA 2018: Innovation Management and Education Excellence through Vision 2020, **2018**, 2009-2017.
46. Ziyadin, S., Suieubayeva, S., & Utegenova, A. Digital transformation in business. Lecture Notes in Networks and Systems, **2020**, 84, 408-415. doi:10.1007/978-3-030-27015-5_49
47. Zlivko, S.D., Magsumov, T.A., & Maksimov Ya.A. Kodifikatsiya uzual'nykh i rechevykh osobennostey upotrebleniya inoyazychnykh neologizmov [Codification of usual (lexicographical) and speech features of the use of foreign-language neologisms]. *Sovremennye issledovaniya sotsialnykh problem* [Modern Studies of Social Issues], **2018**, 10(3-3): 151-159.

Table 1. Questions for analysis of current trends in the development of the digital society, digital economy and education

Question	Answer options
1. Personal data (age, gender)	Age: _____ Gender: _____
2. The organization in which you work / study	_____ _____
3. What do you mean by "digital economy"	1. Business based on the use of digital technologies; 2. Government and business services provided in the digital environment; 3. Promotion of digital products and services on the market Other _____
4. What do you mean by "digital education"	1. Distance learning using digital technologies 2. The use of digital technology in the educational process 3. The process of continuous learning under the influence of the development of digital technologies 4. Other _____
5. What do you mean by "digital society"	1. A society based on knowledge and new digital technologies 2. A society dominated by relationships in virtual reality and on the Internet 3. A society in which human and artificial intelligence exist 4. Other _____
6. Point out the most important characteristic of modern society	1. The speed of change 2. Innovation 3. Continuing education 4. Digitalization of all processes 5. Other _____
7. What factor, in your opinion, has a negative impact on the development of the "digital society"	1. Limited economic and financial resources 2. Low digital literacy of the population and business 3. Lack of sufficient information and technological infrastructure 4. Misunderstanding by government authorities of current development trends 5. Other _____
8. Mark the most important state task in the context of the formation of a single, global digital society	1. Preservation of national sovereignty 2. Creating conditions for free information exchange 3. Information security 4. Improving the quality of education using digital technology 5. Support for a digital business 6. Creating a new digital culture and digital values Other _____
9. Mark the most important threat to the development of digital education	1. Excessive enthusiasm for virtual reality, loss of physical activity

10. Mark the most important global trend in the development of a digital society

2. Reducing the role of personal communication, increasing the psychological dependence on digital services
3. The decline in the quality of education due to loss of control over the educational process
4. The loss of highly qualified personnel due to the dominance of foreign educational systems in the digital environment
5. Other _____

1. Erasing national borders through a single digital space
2. Reducing the role of private property by increasing the total resource of knowledge
3. Transformation of traditional institutions into digital analogues (digital money, digital government, digital business, digital universities, digital banks)
4. The emergence of new types of fraud in the digital environment
5. Other _____

ANÁLISE DAS RAZÕES DA PRESSÃO ENTRE COLUNAS COM O EXEMPLO DE CAMPO DE ZHANAZHOL

INTERCASING PRESSURE CAUSES ANALYSIS ON THE EXAMPLE OF ZHANAZHOL FIELD

АНАЛИЗ ПРИЧИН МЕЖКОЛОННЫХ ДАВЛЕНИЙ НА ПРИМЕРЕ МЕСТОРОЖДЕНИЯ ЖАНАЖОЛ

MAKHMETOVA, Ardak S.^{1*}; AGZAMOV, Farit A.²; KOMLEVA, Svetlana F.³; ISMAILOV, Abdulakhat A.⁴; ISMAILOVA, Jamilyam A.⁵;

^{1,5} Satbayev University, Department of Petroleum Engineering, Almaty – Republic of Kazakhstan

^{2,3} Ufa State Petroleum Technological University, Department of Oil and Gas Well Drilling, Ufa – Russian Federation

⁴ LLP “SIC Petroleum Engineering Consulting”, 12 Tagzym Str., zip code 050063, Almaty – Republic of Kazakhstan

* Correspondence author
e-mail: ada.makhmetova@gmail.com

Received 06 February 2020; received in revised form 10 March 2020; accepted 26 March 2020

RESUMO

As pressões entre colunas nos poços de gás e petróleo operacionais são um dos problemas mais significativos, pois perturbam o equilíbrio ecológico dos territórios do campo, levam à perda de fluido de formação e representam um perigo para o pessoal. Apesar da melhoria contínua da tecnologia de construção de poços em muitos campos de petróleo e gás, os fluxos entre colunas e manifestações de fluidos na boca ainda são um tipo comum de complicação. Infelizmente, a maioria dos métodos para a eliminação das pressões entre colunas envolve a injeção de compostos selantes no espaço entre colunas a partir da boca, que é um método extremamente ineficaz, pois fecha os sinais visíveis, mas não exclui suas causas. Portanto, o estudo das causas da pressão terá um significado acadêmico e prático, uma vez que a maneira mais eficaz não é eliminar, mas impedir as pressões entre colunas durante a construção e completação do poço. Neste artigo, a ocorrência de pressão no reservatório é considerada no exemplo dos poços do campo de Zhanazhol. Foi realizado um estudo de 40 poços na região. Para determinar o grau de influência de fatores geológicos, técnicos, tecnológicos, físico-químicos e mecânicos na ocorrência das pressões entre colunas, foram utilizados os procedimentos de análise estatística e de correlação, análise da composição do fluido intermediário e análise de material de campo. Com base nos resultados disponíveis, foram apresentados os métodos e técnicas possíveis da ocorrência das pressões entre colunas, bem como os princípios que poderiam ser usados para evitar a pressão durante a construção e operação do poço.

Palavras-chave: *espaço anular, pressão anular, equilíbrio ecológico, fluidos de reservatório, curvas de recuperação de pressão.*

ABSTRACT

In the operational reserve of gas and oil wells, formation pressure (ICP) is one of the most significant problems, since it violates the ecological balance of the field areas, leads to the loss of formation fluid and is dangerous for personnel. Despite the continuous improvement of well construction technology at many oil and gas fields, adjacent flows and fluid effects at the wellhead are still a common type of complication. Unfortunately, the majority of methods for the ICP elimination involves the injection of sealing compounds into the inter casing from the wellhead, which is an extremely inefficient technique, since it covers visible signs, but does not exclude their causes. Therefore, the study of the causes of pressure will have both academic and practical significance, since the most effective way is not to eliminate, but to prevent PMS during the construction and completion of the well. In this paper, the occurrence of pressure in the reservoir by the example of wells of the Zhanazholsky field was considered. The research of 40 wells in a given region was conducted. To determine the degree of influence of geological, technical, technological, physicochemical and mechanical factors on the occurrence of ICP,

statistical and correlation analysis procedures, an analysis of the composition of the intermediate fluid, and analysis of field material were used. Based on the available results, possible methods and ways for the ICP occurrence were shown, and also principles were formulated that could be used to prevent pressure during construction of wells and further exploitation.

Keywords: *annular pressure, annular space, ecological equilibrium, formation fluids, pressure recovery curves.*

АННОТАЦИЯ

Межколонные давления (МКД) в эксплуатационном фонде газовых и нефтяных скважин являются одной из наиболее значимых проблем, поскольку нарушают экологическое равновесие территорий месторождений, приводят к потере пластового флюида и представляют опасность для персонала. Несмотря на постоянное совершенствование технологии строительства скважин на многих нефтяных и газовых месторождениях, межколонные перетоки и флюидопроявления на устье все ещё остаются распространённым видом осложнений. К сожалению, большинство методов ликвидации МКД предполагает закачку герметизирующих составов в межколонное пространство с устья, что является крайне неэффективным приёмом, поскольку закрывает видимые признаки, но не исключает их причины. Поэтому изучение причин давления будет иметь как академическое, так и практическое значение, поскольку наиболее эффективным способом является не устранение, а предотвращение МКД во время строительства и заканчивания скважины. В данной работе рассмотрено возникновение МКД на примере скважин месторождения Жанажол. Было проведено исследование 40 скважин в данном регионе. Для определения степени влияния геологических, технических, технологических, физико-химических и механических факторов на возникновение МКД использовались процедуры статистического и корреляционного анализа, анализ состава межколонного флюида и анализ полевого материала. На основе имеющихся результатов были показаны возможные источники и пути возникновения МКД, а также сформулированы принципы, которые можно было бы использовать для ликвидации и предотвращения МКД во время строительства скважин и их дальнейшей эксплуатации.

Ключевые слова: *межколонное давление (МКД), межколонное пространство, экологическое равновесие, флюидопроявления, кривые восстановления давления.*

1. INTRODUCTION:

The complication of inter casing pressure treatment is due to the variety of their causes and the multitude of migration routes of formation fluids from the reservoir to the wellhead. Among the causes of annular pressure are the productive formation operation mode, temperature fluctuations in the well during operation, external pressures of plastic clay rocks, or salts (Gao *et al.*, 2013). In this case, the leakage of the casing head packer, the leakage of the cement ring, or casing string should be distinguished as the paths of fluids movement that create the ICP.

Unfortunately, the majority of methods for the ICP elimination involves the injection of sealing compounds into the inter casing from the wellhead, which is an extremely inefficient technique, since it covers visible signs, but does not exclude their causes. In this regard, the most effective way is not the elimination, but the ICP prevention during the construction and completion of the well.

The analysis of field data for the main gas producing regions shows that the number of wells, especially gas wells, in which inter casing pressure occurs, is vast (Govier and Fogarasi, 1975; Curtis, 2002). As the duration of field development

increases, the number of such wells, generally, increases. The most significant percentage of wells with inter casing pressure is typical for underground gas storage facilities. Moreover, the time of occurrence (detection) of ICP can be from several hours to several months.

Despite the continuous improvement of well construction technology in many oil and gas fields, inter casing flows, and fluid exposure at the wellhead still remain a common type of complication (Peffer *et al.*, 1988). Since the causes of inter casing pressure (ICP) may be common, let us consider them for further details.

The authors of (Mavlyutov *et al.*, 1984; Bulatov *et al.*, 1969; Bulatov, 2017; Mamadzhano and Halfin, 1963; Malevanskiy, 1963; Davies *et al.*, 2014; Glover, 2009; Adams and MacEachran, 1994; Dong and Chen, 2017; Mwang'Ande *et al.*, 2019; Baynham *et al.*, 2003) works subdivide the ICP into two groups. The first group includes inter casing shows caused by the direct flow of fluid (gas, oil) from the production horizons through the cement ring (Brown *et al.*, 2016), the gaps between the cement ring and wellbore, between the cement stone and casing strings. The second one is fluid shows arising due to the leakage or depressurization of casing strings in the process

of well operation. The authors of (Bulatov *et al.*, 1969; Bulatov, 2017; Mamadzhanov and Halfin, 1963; Malevanskiy, 1963; Liu *et al.*, 2014; Brownlow *et al.*, 2017; Lackey and Rajaram, 2019; Pattillo *et al.*, 2004; Narozhnyy and Ilyenko, 2017) consider the channels in the contact zone as the main paths of gas shows through the annular space, which arise when the quality of cementing of the column is low and the presence of thick mudcake, as well as channels in the cement stone, formed as a result of water separation.

According to the researchers (Bulatov, 1990; Chernenko and Kuksov, 1972; Rakhimbayev, 1976; Bulatov, 1971; Levain *et al.*, 1980), immediately after punching the cement slurry into the annular space, suspended solid cement particles begin to sediment, and the free mixing fluid displaced from the cementing system forms filtration streams in the pore space. The system forms a series of areas with increased porosity connected by channels of different diameters, lengths, and configurations. At the same time, cement stone is in the process of hydration due to contraction (Raikhel and Konrad, 1979) sweeps away water from the mudcake to form a network of canals in a dried crust.

According to (Bulatov, 2008; Vidovskiy and Bulatov, 1977; Halal and Mitchell, 1993), the appearance of pressure at the wellhead may be associated with a decrease in the "active" pressure column of the cement slurry on the wellbore walls during its hardening, as well as filtration of excess mixing water into the formation. Researchers (Agzamov *et al.*, 2011) associate one of the main reasons for the failure of lining wells with contraction. When hardening in a closed volume, such as the inter casing of wells or the space close to dense and impermeable rocks, contraction can lead to a vacuum inside the hardening stone, shrinking deformations in it, leakage of the contact zones or an increase in the permeability of the cement stone.

The reasons for the inter casing showings, according to (Krylov *et al.*, 1981; Mamedov, 1990; Fattakhov, 1991), can be various technological operations carried out in the well: pressure integrity testing and perforation of casing strings, drilling out a cement column, deepening the wellbore, etc.

Thus, the analysis of scientific and technical literature (Țicleanu *et al.*, 2014; Bamberger and Oswald, 2012; Howarth *et al.*, 2011; Lu *et al.*, 2016; Cocuzza *et al.*, 2012; Tariq *et al.*, 2019; Bellarby *et al.*, 2013) allows to identify the main factors that are considered the most

reasonable in explaining the reasons for the inter casing showings:

1) Technological factors due to the penetration of fluid into the cement slurry as a result of a decrease in operating pressure on the formation, formation of channels between the cement ring and the string while reducing the pressure in it wait-on-cement time (WOC time), a low degree of drilling fluid displacement from the inter casing.

2) Physical and chemical factors caused by changes in the micro- and macrostructure of the cement slurry during its hardening, especially in contact with the "pinched" drilling mud or mudcake under conditions of high temperatures and pressures.

3) Technical factors associated with the formation of a channel between the cement ring and casing strings due to their deformation during pressure integrity testing of the casing and other technological operations.

Therefore, the study aimed to consider in detail the causes of inter casing pressure and develop recommendations for preventive measures to eliminate them.

2. MATERIALS AND METHODS:

To identify the degree of influence of geological, technical, technological, physicochemical and mechanical factors on the occurrence of ICP, the research was conducted in which statistical analysis procedures were applied using the STATGRAPHICS application software package (Leach and Adams, 1993).

The analysis was subjected to 40 wells, in which the inter casing pressure was recorded and were divided into groups depending on the degree of pressure of the P-shaped casing. Among them: 19 wells with Pinter casing ≤ 10.0 MPa, 11 wells with Pinter casing ≤ 20.0 MPa.

At the first stage from the whole well fund the more detailed actual material was collected on wells, in which the ICP value exceeds 2.0 MPa. The primary analysis was carried out on the array, which includes all the wells of the production fund with the value of ICP higher than 2.0 MPa.

To assess the degree of influence of various factors on the value of the inter casing pressure, elasticity coefficients were calculated, which showed that for the analyzed data set, the following factors had the most significant influence on the value of the inter casing pressure:

- power of the strong brine exposure

complex;

- the depth of the descent of the intermediate string;
- the depth of descent of the production string;
- density of the washing liquid;
- the volume of cement slurry.

Particular attention in the analysis was paid to the types of casing heads (CG) installed in the wells. In this case, it was taken into account that in fields with ICP, due to the leakage of CG, the value of ICP should be equal to the intercasing pressure (Ma, 2006).

When processing an array of data, a correlation analysis procedure was applied, which made it possible to conclude the degree of statistical relationship between factors using a sample. Since to assess the statistical significance of many factors, a larger amount of initial data is necessary to evaluate the effect on the ICP values by various groups of factors (geological, technological, properties of drilling fluids, properties of cement slurry and cementing technology).

Initial data and a list of analyzed factors are given in Table 1. The analyzed data included:

- dependent factors (performance indicators), namely – the value of the ICP (numerical variable, MPa);
- independent factors affecting performance indicators, including geological, technical and technological, physical and chemical, mechanical, etc. (42 factors in total), the degree of influence of which on the occurrence of ICP could be assessed by statistical methods.

3. RESULTS AND DISCUSSION:

According to the geological information (Passey *et al.*, 2010), there are no other reservoirs in the crosssection that contain oil or gas (except for the productive formation) and that are capable of becoming a source of ICP (Guseynov *et al.*, 2005). Therefore, the number one source is the productive formation. Another source of ICP can also be a strong brine exposure horizon occurring in the interval of salts.

The source of the ICP can also be a liquid located outside the production string and pushed out during the flow of the salt mass and plastic clays that are in the Kunguri interval. Fluid outside the production string can create ICP also due to thermal expansion as a result of warm formation fluid lifting into the cooled upper part of the well. Analysis of the composition of the intercasing fluid

will help to clarify these assumptions (Oudeman and Kerem, 2004; Bloys *et al.*, 2007; Azzola *et al.*, 2004).

Wellhead equipment leakage is one of the most likely causes. This is testified by the large amount of bibliographic and field data obtained at other fields, as well as some experience of the Zhanazhol field, when, after repairing the well and replacing the sealing elements of the casing head ICP decreased or disappeared. At the same time, the experience of other fields shows that for a given reason for the occurrence of ICP, its value is usually equal to the annular pressure. Analysis of field material showed that these values are not equal, i.e. this factor can be excluded as the cause of ICP.

Leakage of the production string is not excluded, although it seems unlikely, since pipes that are used for casing are of increased tightness of threaded connections, recommended for gas wells. Leakage of the cement ring, considered as the main cause of ICP. It is also necessary to take into account the impact of variable loads on the lining of the well in the form of pressure integrity test, perforation, development, flow stimulation, installation of underground equipment. As a rule, these technological operations are accompanied by loads correlated even with the strength of the column and the matrix of cement stone, although the zone of adhesion of the cement ring with casing metal is the most vulnerable point in the intercasing isolation.

The composition of the intercasing fluid. These can be gas, oil, hydrocarbon liquid, strong brine, liquid used for mixing cement slurry, pore liquid of cement stone, circulation liquid or its filtrate, brine water from the overlying horizons, etc. The probe (in except of the gas) should be collected during the periodical ICP discharge and be transmitted for analysis. The composition of the annular fluid will help to determine the most likely source of ICP and the path of fluid inflow. The volume of fluid leaked from the intercasing space is necessary for evaluating the reservoir characteristics of the ICP source. The recovery rate of ICP will determine the source of the ICP and the path of fluid flow.

The presence or absence of ICP for the intermediate string. This information is very important for assessing the tightness of the lining of the well (the cement ring and its contact zones), since there is a high probability of destruction of the cement ring behind the intermediate string and the conductor when drilling with the rotor under the following columns.

Simultaneous control of the annular pressure when measuring the pressure in the inter casing. Date of the first detection of ICP in wells will allow you to specify the source of the ICP. To detect the causes of ICP it is proposed to use the following Table 1. Identification of the ICP source and the fluid-conducting channel with the greatest probability is more possible only with a comprehensive assessment of all the information characterizing this type of complication.

1. In case of leakage of wellhead equipment, it should be oil or gas entering the inter casing from the annular space. If the pressure in the inter casing is higher than the saturation pressure, then the more likely fluid will be oil. ICP discharge time should be short for a few minutes only. The pressure recovery time makes up several hours due to the small length of the channel, so that the ICP is comparable to the annular pressure.

2. In case of leakage of the production string, the outgoing fluid may be oil or gas if the cement slurry height raises up to the wellhead. The fluid may be mud, located above the cement stone if the height of the cement slurry does not reach the wellhead. Depending on the location of the leak, there will be different rates of pressure build-up. If the leakage occurs in the non-cemented zone, the pressure build-up rate is fast enough. If the leakage occurs in the cemented zone, the rate of pressure build-up will slow due to fluid filtration in the cemented zone. Moreover, the higher the quality of cementing and the height of the cement rise, the longer the pressure is restored. With the passage of oil through the leakage of the cement ring there may change the composition of oil and gas in the direction of reducing the content of hydrogen sulfide, which is partially neutralized by the hardening products of cement.

3. In the case of a cement ring leakage, the composition of the formation fluid depends on the assignment of the well. In the case of injection wells, water is more likely, the one that is similar in composition to the injected water, as well as a mixture of oil and water, a mixture of water and mud that remains above the cement grout. The value of the ICP should be correlated with the injection pressure. Depending on the flushing of the channel, the pressure build-up rate can reach from several hours to several days. In these wells it is necessary to pay attention to the sealing of the annular space, because the efficiency of reservoir pressure maintenance is sharply reduced, since there is a high probability that water to be pumped into other layers.

In production wells, the most likely fluid from the inter casing will be oil, gas and mud. Oil and gas may not contain hydrogen sulfide. The pressure value maintained lower than the annular may correlate with the reservoir pressure in the productive horizon.

If, due to the leakage of the cement ring, the strong brine exposure horizon shows, the composition of the fluid from the inter casing should coincide with the composition of the strong brine, and the pressure should correlate with the pressure of the strong brine exposure horizon. In case of the cement ring leakage, the pressure growth rate in all cases is slowed down due to the filtration of fluids in the cement stone. To carry out preventive maintenance of the ICP sources and fluid penetration paths, samples were taken and analyzed from the annular space of the wells.

Based on the available results, possible methods and ways for the ICP occurrence were shown, in particular:

- leakage of the casing head may occur in 3 wells;
- leakage of the cement ring may occur in 13 wells;
- casing string leakage may occur in 2 wells.

Since the main cause of the inter casing pressure is the leakage of the cement ring, then it is worth paying particular attention to it. First, it is necessary to establish the height of the cement ring behind the production string. Next, it is necessary to evaluate the injectivity of the inter casing by the injection of fluid (water or oil) and evaluate the possibility of pumping the sealing compound into the inter casing.

With a small height of the cement ring, the recommended method for the elimination of ICP consists in that the fluid located there is pumped out from the inter casing of the well. After that, the gelling sealant is pumped into inter casing. In this case, the injected suspension should be of low structural strength. With a small volume of annular space and a certain injectivity, it is possible to pump the sealing compound into the inter casing from the wellhead. The last way to eliminate the ICP may be the injection of a sealant into the inter casing above the productive formation through unique holes in the casing string.

Since the elimination of the leakage of the cement ring is a very complicated and expensive procedure, it is necessary to find out the possibility of the operation of wells with ICP under tight control of the fluid composition, pressure values, dynamics of their changes. It is necessary to

determine the maximum possible pressure value to prevent the intermediate tubing burst. Taking into account the method of drilling and work carried out inside the casing string, it is necessary to predict the growth of the number of wells with ICP for this reason.

Therefore, it is necessary to improve the technology of cementing of wells under construction. This may be the application of cementing technology with a movable packer (Agzamov *et al.*, 1989), the use of self-healing cements (Ismagilova *et al.*, 2017), the use of carbon swellable packers placed on the casing string above the dangerous horizon.

In general, the fact of the ICP presence in the well does not in pose itself a danger or a threat if there is no uncontrolled showing of hydrogen sulfide-containing fluid at the wellhead or around it.

For certain specific measures for each well with ICP, it is important to assess the causes of the occurrence of ICP and its value as a percentage to the ultimate pressure (UP) relative to the previous column. The following system can be used:

- Category 1: wells in which the measured inter casing pressure is 100% or higher of UP.
- Category 2: wells in which the measured inter casing pressure ranges from 50 to 100% of the UP.
- Category 3: wells in which the measured inter casing pressure is from 25 to 50% of the UP.
- Category 4: all other wells with ICP.

The following principles can be used to make decisions in this regard:

- Category 1: perform a control release and/or well killing, perform workover the well or well abandonment, and carry out a control release of the ICP, if it is necessary to ensure the safe conduct of work. Perform daily monitoring.
- Category 2: if the annular pressure communicates with the productive formation and it exceeds 50% of the UP, then to include the well in the well killing schedule. To release ICP if it necessary to ensure the safe conduct of work. Perform daily monitoring.
- Category 3: in case of ICP occurs due to the formation, and it raises up to 50% of the UP, it is necessary to continue to conduct weekly monitoring and to release the ICP, if it is necessary to ensure the safe conduct of work.
- Category 4: Perform weekly monitoring.

4. CONCLUSIONS:

1. The occurrence of ICP in gas and oil wells is one of the most common and significant complications in the development of fields that require correct solutions for the reason of affecting the environment, production and safety of personnel.

2. Technological, physical, chemical and technical factors influence the appearance of the ICP in the wellbore.

3. To solve the ICP problem, firstly it is necessary to carry out diagnostics, which makes it possible to identify the causes of the occurrence of the ICP, its source, paths of the fluids and to take appropriate decisions.

4. The main causes of ICP are leaks in the cement ring, leaks in the production string, leaks in the wellhead equipment, and each of these causes corresponds to a certain type of fluid.

5. Four categories of wells can be distinguished depending on the value of the ICP, and each category corresponds to recommendations for making decisions on the further operation of the wells.

6. Most technologies for the elimination of ICP involve the injection of sealants from the wellhead, which only eliminates the visible signs of the ICP occurrence, but does not eliminate its source. Therefore, the most effective is not the elimination of the ICP but the prevention of its occurrence during the construction of wells and their further operation.

5. REFERENCES:

1. Adams, A.J., MacEachran, A. *SPE Drilling and Completion*, **1994**, 9(3), 210-216.
2. Agzamov, F.A., Izumkhambetov, B.S., Tokunova, E.F. *Chemistry of Cement and Drilling Fluids*. Saint-Petersburg: Nedra, **2011**.
3. Agzamov, F.A., Mavlyutov, M.R., Shmelyev, P.S. *The method of cementing casing. Author's license No. 1454959 SSSR, MKI3 E21 B33/13*, **1989**.
4. Azzola, J.H., Tselepidakis, D.P., Pattillo, P.D., Richey, J.F., Tinker, S.J., Miller, R.A., Segreto, S.J. *Proceedings - SPE Annual Technical Conference and Exhibition*, **2004**, 1899-1905.
5. Bamberger, M., Oswald, R.E. *New Solutions*, **2012**, 22(1), 51-77.

6. Baynham, R., Levie, D., Calderoni, A., Molaschi, C., Zausa, F. A novel concept for casing centralization in lean profile™ applications, *Offshore Mediterranean Conference and Exhibition, OMC*, **2003**.
7. Bellarby, J., Kofoed, S., Marketz, F. *SPE/IADC Drilling Conference Proceedings*, **2013**, 2, 1562-1573.
8. Bloys, B., Gonzalez, M., Hermes, R., Bland, R., Foley, R., Tijerha, R., Davis, J., Cassel, T., Daniel, J., Robinson, I., Billings, F., Eley, R. *SPE/IADC Drilling Conference, Proceedings*, **2007**, 1, 113-122.
9. Brown, J., Kenny, N., Slagmulder, Y. Unique cement design to mitigate trapped annular pressure TAP between two casing strings in steam injection wells, *Society of Petroleum Engineers - SPE Heavy Oil Conference and Exhibition*, **2016**.
10. Brownlow, J.W., Yelderman, J.C., Jr., James, S.C. *Groundwater*, **2017**, 55(2), 268-280.
11. Bulatov, A.I. *Detective biography of oil and gas wells casing tightness*. Krasnodar: Prosveshhenie-Yug, **2008**.
12. Bulatov, A.I. *Formation and Operation of Cement Stone in the Well*. Moscow: Nedra. **1990**.
13. Bulatov, A.I. *Gas Industry*, **2017**, 12, 24-27.
14. Bulatov, A.I., Kuksov, A.K., Obozin, O.N., Novohatskiy, D.F., Golovenko, N.G. *Drilling*, **1971**, 2, 7.
15. Bulatov, A.I., Ryabchenko, V.I., Sibirko, I.A., Sidorov, N.A. *Gas Shows in Wells and Control and Their Treatment*. Moscow: Nedra, **1969**.
16. Chernenko, A.V., Kuksov, A.K. *Oil and Gas Economy*, **1972**, 10, 4.
17. Cocuzza, M., Pirri, C., Rocca, V., Verga, F. *American Journal of Applied Sciences*, **2012**, 9(6), 784-793.
18. Curtis, J.B. *AAPG Bulletin*, **2002**, 86(11), 1921-1938.
19. Davies, R.J., Almond, S., Ward, R.S., Jackson, R.B., Adams, C., Worrall, F., Herringshaw, L.G., Gluyas, J.G., Whitehead, M.A. *Marine and Petroleum Geology*, **2014**, 56, 239-254.
20. Dong, G., Chen, P. *Journal of Natural Gas Science and Engineering*, **2017**, 37, 85-105.
21. Fattakhov, Z.M. *Abstracts of the reports of the Scientific and Technical Conference TECHNOGEN*, **1991**, 1, 36-37.
22. Gao, D., Qian, F., Zheng, H. *Computer Modeling in Engineering and Sciences*, **2013**, 89(1), 1-15.
23. Glover, P. *Leading Edge*, **2009**, 28(1), 82-85.
24. Govier, G.W., Fogarasi, M. *Journal of Canadian Petroleum Technology*, **1975**, 14(44), 28-41.
25. Guseynov, F.A., Ivakin, R.A., Gadzhibekov, G.M., Griguletsky, V.G. *Neftyanoe Khozyaystvo - Oil Industry*, **2005**, 6, 120-121.
26. Halal, A.S., Mitchell, R.F. *Drilling Conference - Proceedings*, **1993**, 179-190.
27. Howarth, R.W., Santoro, R., Ingraffea, A. *Climatic Change*, **2011**, 106(4), 679-690.
28. Ismagilova, E.R., Agzamov, F.A., Abbas, A.D. *Georesources*, **2017**, 19(2), 129-134.
29. Krylov, D.A., Marabayev, N.A., Talamanov, Ye.N., Burkhailo, V.A., Serenko, I.A. *Drilling*, **1981**, 7, 18-21.
30. Lackey, G., Rajaram, H. *Water Resources Research*, **2019**, 55(1), 298-323.
31. Leach, C.P., Adams, A.J. New method for the relief of annular heat-up pressures, *Production Operations Symposium*, **1993**, 819-826.
32. Levain, D.K., Thomas, E.U., Bezner, H.P., Tolpe, D.K. *Oil, Gas and Petrochemistry Abroad*, **1980**, 10, 8-17.
33. Liu, Y., Ren, G., Xue, C., Guan, Z., Hu, L. *Natural Gas Industry*, **2014**, 34(9), 64-69.
34. Lu, S., Zhang, Y., Li, J., Ju, Y. *Bulletin of Mineralogy Petrology and Geochemistry*, **2016**, 35(1), 28-36.
35. Ma, H. *Well Testing*, **2006**, 15(2), 21-24+76.
36. Malevanskiy, V.D. *Open gas Fountains and Their Treatment*. Moscow: Gostoptehizdat, **1963**.
37. Mamadzhanov, U.D., Halfin, V.E. *Oil Economy*, **1963**, 1, 22-24.
38. Mamedov, A.A. *Preventing Casing*

- Faulting*. Moscow: Nedra, **1990**.
39. Mavlyutov, M.R., Kravtsov, V.M., Ovchinnikov, V.P., Agzamov, F.A. *The Analysis of the Annulus Gas Shows Causes and Ways to Improve the Quality of Tubing Cementation in the Conditions of Hydrogen Sulfide Aggression*. Moscow: All-Russian Scientific Research Institute for Organization, Management and Economics of the Oil and Gas Industry Open Institute, **1984**.
 40. Mwang'Ande, A.W., Liao, H., Zeng, L. *Journal of Energy Resources Technology, Transactions of the ASME*, **2019**, 141(10).
 41. Narozhnyy, I.M., Ilyenko, E.P. *20th IEEE International Conference on Soft Computing and Measurements*, **2017**, 310-311.
 42. Oudeman, P., Kerem, M. *11th ADIPEC: Abu Dhabi International Petroleum Exhibition and Conference - Conference Proceedings*, **2004**, 665-674.
 43. Passey, Q.R., Bohacs, K.M., Esch, W.L., Klimentidis, R., Sinha, S. From oil-prone source rock to gas-producing shale reservoir - geologic and petrophysical characterization of unconventional shale-gas reservoirs, *Society of Petroleum Engineers - International Oil and Gas Conference and Exhibition*, China, **2010**.
 44. Pattillo, P.D., Coteles, B.W., Morey, S.C. *Proceedings - SPE Annual Technical Conference and Exhibition*, **2004**, 189-195.
 45. Peffer, J.W., Miller, M.A., Hill, A.D. *SPE Production Engineering*, **1988**, 3(4), 643-655.
 46. Raikhel, V., Konrad, D. *Concrete. Part 1. Properties. Engineering. Testing*. Moscow: Stoyizdat, **1979**.
 47. Rakhimbayev, Sh.M. *Technical Properties of Cement Slurries Adjustment*. Tashkent: Fan, **1976**.
 48. Tariq, Z., Mahmoud, M., Abdurraheem, A. *Journal of Petroleum Exploration and Production Technology*, **2019**.
 49. Ţicleanu, M., Nicolescu, R., Ion, A. *International Multidisciplinary Scientific Geo Conference Surveying Geology and Mining Ecology Management*, **2014**, 1(5), 299-306.
 50. Vidovskiy, A.L., Bulatov, A.I. *Pressure in the Cement Stone of Deep Wells*. Moscow: Nedra, **1977**.

Table 1. Diagnostic table of inter casing pressure

No.	ICP source	ICP cause	ICP characteristics			
			Fluid type for ICP	$P_{\text{annular}}/P_{\text{intercasing}}$ rate	Release time	The recovery rate of the P_{IC} to the original value
1	Production well. Productive formation	Cement ring leakage	Oil Gas, circulation fluid when cement slurry does not reach the wellhead	$P_{\text{annular}} \geq P_{\text{intercasing}}$	1–20 min	Slowly up to several days or weeks
2	Injection well. Productive formation	Cement ring leakage	Pumped water Water + oil Water + mud	$P_{\text{annular}} \geq P_{\text{intercasing}}$	1–20 min	Slowly up to several days or weeks
3	Strong brine exposure interval	Cement ring leakage	Brine water, Brine water + mud	$P_{\text{annular}} \neq P_{\text{intercasing}}$ $P_{\text{intercasing}} = P_{\text{formation}} - \rho g h$	1–10 min	Slowly up to several days
4	Casing head	Casing head packer leakage	Oil, gas	$P_{\text{annular}} \approx P_{\text{intercasing}}$	5–10 min	Fast for a few hours
5	Production interval	Casing string leakage	Oil, Gas, Mud	$P_{\text{annular}} \geq P_{\text{intercasing}}$	1–10 min	Slowly up to several days if the leak is below the cement level
6	Clay solution in intercasing	Temperature fluctuations	Mud	$P_{\text{annular}} \neq P_{\text{intercasing}}$	1–10 min, decreases when the well is stopped	Increases at bringing well into production

NÍVEIS SÉRICOS DE IL-8 EM PACIENTES COM GASTRITE CRÔNICA ATIVA E DOENÇA ÚLCERA PÉPTICA

SERUM LEVELS OF IL-8 IN PATIENTS WITH CHRONIC ACTIVE GASTRITIS AND PEPTIC ULCER DISEASE

ПОКАЗАТЕЛИ СЫВОРОТОЧНОГО ИЛ-8 У БОЛЬНЫХ ХРОНИЧЕСКИМИ АКТИВНЫМИ ГАСТРИТАМИ И ЯЗВЕННОЙ БОЛЕЗНЬЮ

BELAIA, Olga Fedorovna^{1*}; GUTKIN, Denis Sergeevich²; KAREVA, Elena Nikolaevna^{1,3}; VOLCHKOVA, Elena Vasilyevna¹; VAKHRAMEEVA, Maria Sergeevna⁴

¹ Sechenov First Moscow State Medical University, Russian Federation.

² Burdenko Penza Regional Clinical Hospital, Penza, Russian Federation.

³ Pirogov Medical Research University, Moscow, Russian Federation.

⁴ Gamaleya National Research Center for Epidemiology and Microbiology, Moscow, Russian Federation.

* Correspondence author
e-mail: ofbelaya@mail.ru

Received 20 December 2019; received in revised form 01 March 2020; accepted 13 March 2020

RESUMO

A maioria dos pesquisadores descobre associações entre *H. pylori* (Hp) e a produção sérica de IL-8 com o estágio da inflamação crônica. Os dados sobre os níveis de IL-8 na gastrite crônica (GC) e na úlcera gastroduodenal (GDU) são insuficientes, e frequentemente controversos. Todos os pacientes com gastrite crônica ativa (GCA) e GDU foram divididos em 4 subgrupos: pacientes com GDU e infecção por Hp de acordo com métodos comuns (GDU+Hp), pacientes com GDU e sem infecção por Hp documentada (GDU), pacientes com CAG e encontraram infecção por Hp de acordo com métodos comuns (GCA+Hp) e pacientes com CAG sem infecção por Hp documentada (GCA). Os níveis séricos mais altos de IL-8 foram observados em pacientes com GDU+Hp, enquanto os mais baixos foram observados em pacientes com CAG. Os homens têm os níveis mais baixos de IL-8 no subgrupo GCA+Hp em comparação com outros subgrupos. Os valores de IL-8 foram significativamente diferentes dos valores mais altos nas mulheres. A taxa de antígeno O fecal do *H. pylori* LPS encontrada no teste de coaglutinação é de 86%. Os níveis mais altos de antígeno O do *H. pylori* LPS foram detectados no subgrupo GCA. Em pacientes com GDU + Hp, os níveis de antígeno O do *H. pylori* LPS foram significativamente maiores em comparação com o subgrupo GDU. Portanto, pacientes com GDU, especialmente aqueles com GDU+Hp e com GCA, têm produção ativa de IL-8. A coaglutinação para detectar o antígeno O do *H. pylori* LPS nas fezes usadas junto com métodos comuns aumenta a probabilidade de confirmar que os pacientes (especialmente aqueles com gastrite crônica) estão infectados com esse micróbio.

Palavras-chaves: Infecção por *H. pylori*, gastrite crônica, úlcera péptica, interleucina 8, antígeno O de *H. pylori*, diagnóstico

ABSTRACT

The majority of researchers discover associations between *H. pylori* (Hp) and serum IL-8 production with the stage of chronic inflammation. Data on IL-8 levels in chronic gastritis (CG) and a gastroduodenal ulcer (GDU) are insufficient, and often controversial. All patients with chronic active gastritis (CAG) and GDU were divided into 4 subgroups: patients with GDU and found Hp infection according to common methods (GDU+Hp), patients with GDU and no documented Hp infection (GDU), patients with CAG and found Hp infection according to common methods (CAG+Hp), and patients with CAG with no documented Hp infection (CAG). The highest serum IL-8 levels were seen in patients with GDU+Hp, whereas the lowest ones were observed in patients with CAG. Men have the lowest IL-8 levels in the CAG+Hp subgroup as compared with other

subgroups. The IL-8 values were significantly different from higher values in women. The rate of fecal O-antigen of *H. pylori* LPS found using the coagglutination test is 86%. The highest levels of O-antigen of *H. pylori* LPS were detected in the CAG subgroup. In patients with GDU+Hp, the levels of O-antigen of *H. pylori* LPS were significantly higher as compared with the GDU subgroup. So patients with GDU, especially those with GDU+Hp, and with CAG, have active IL-8 production. Coagglutination to detect O-antigen of *H. pylori* LPS in feces used along with common methods increases the probability to confirm that the patients (especially those with chronic gastritis) are infected with this microbe.

Keywords: *H. pylori* infection, chronic gastritis, peptic ulcer disease, interleukin 8, O-antigen of *H. pylori*, diagnostics

АННОТАЦИЯ

Большинство исследователей отмечают связь присутствия *H. pylori* (Hp) и уровней IL-8 в сыворотке крови со степенью хронического воспаления. Несмотря на то, что IL-8 интенсивно изучается при различных заболеваниях, имеется недостаточно сведений о его уровнях при хронических гастритах (ХГ) и язвенной болезни желудка и двенадцатиперстной кишки (ЯБ), кроме того, полученные результаты порой носят противоречивый характер. У больных хроническими активными гастритами (ХАГ, включая эрозивные гастродуодениты) и ЯБ повышение сывороточных уровней IL-8 (выше 62 пг/мл) наблюдается у большинства больных (90%). Присутствие Hp общепринятыми методами установлено у 33,3% пациентов с хроническими гастритами и у 61,7% пациентов с ЯБ. Все больные ХАГ и ЯБ были разделены на 4 подгруппы: больные ЯБ с выявленной инфекцией Hp по данным общепринятых методов (ЯБ+Hp), больные ЯБ без подтвержденной Hp-инфекции (ЯБ), больные ХАГ с выявленной инфекцией Hp по данным общепринятых методов (ХАГ+Hp) и больные ХАГ без подтвержденной Hp-инфекции (ХАГ). Наиболее высокие уровни сывороточного ИЛ8 выявлены у больных ЯБ+Hp, наиболее низкие - у больных ХАГ. У мужчин, в целом, отмечены наиболее низкие уровни IL-8 в подгруппе больных ХАГ+Hp, в сравнении с другими подгруппами, и эти показатели IL-8 достоверно отличались от более высоких показателей у женщин. Частота выявления в кале ЛПС/О-антигена Hp методом коагглютинации - 86%. Наиболее высокие уровни ЛПС/О-антигена Hp выявлены у больных в подгруппе ХАГ. У больных ЯБ+Hp уровни ЛПС/О-антигена Hp были достоверно выше, чем в подгруппе ЯБ. Полученные данные свидетельствуют, что у больных ЯБ, особенно при ЯБ+Hp и больных ХАГ наблюдается активная продукция IL-8. Применение метода коагглютинации для выявления ЛПС/О-антигена *H. pylori* в кале, в дополнение к общепринятым методам, увеличивает вероятность подтверждения инфицирования этим микробом, особенно у больных хроническими гастритами.

Ключевые слова: инфекция *H.pylori*, хронический гастрит, язвенная болезнь, интерлейкин 8, О-антиген *H.pylori*, диагностика.

1. INTRODUCTION

Helicobacter pylori (Hp) is the most widespread infection in humans. This microaerophilic gram-negative bacterial infection causes chronic gastritis, gastroduodenal ulcer, stomach cancer, and MALT-lymphoma (McColl, 2010; Rehman, 2020). Gastric mucus is the basic primary colonization site of *H. pylori*. However, the microbe can penetrate even deeper tissues, submucous membranes of the stomach, where it is found next to endothelial cells (Kusters *et al.*, 2006).

Almost all people infected with *H. pylori* develop chronic gastric inflammation. In this case, the gastric mucus is infiltrated with neutrophils and macrophages (Sipponen, 1993; Vinagre *et al.*, 2018; Israel and Peek, 2001). In patients with chronic nonatrophic gastritis, the activity of inflammation depends on gastric mucus Hp

colonization; the inflammation intensity is decreased against the background of reduced bacterial content (Ageeva *et al.*, 2011).

This inflammation is caused by cytokines and chemokines, including interleukin-1 β , tumor necrosis factor- α (TNF- α), IL-8, and IL-6. IL-8 (Kononov, 2006; Sun *et al.*, 2014; de Brito *et al.*, 2018; Serrano *et al.*, 2007), which is a powerful angiogenic and chemoattractive agent, a key mediator of Th1-type immune response overexpressed in gastric epithelial cells during infection with *H. pylori*, is necessary to differentiate and recruit effector cells into the focus of Hp-associated inflammation (Crabtree, 1996; Naumann and Crabtree, 2004).

The mechanism used by *H. pylori* to stimulate IL-8 induction in gastric epithelial cells and chronic inflammation is examined intensively [3]. The stomach has a greater mucus surface;

thus, it is believed that chronic inflammation caused by *H. pylori* cannot be limited but have systemic effects due to the action of serum inflammatory cytokines (Bayraktaroglu *et al.*, 2004).

H. pylori of primary endothelial cells stimulate the secretion of key inflammatory cytokines in humans, IL-6, and IL-8. Endothelial cells play a decisive role in the innate immune response, wound healing, and oncogenesis. IL-8 is secreted by *H. pylori*-infected endothelial cells 10-20 times more actively as compared to gastric epithelial cells infected with *H. pylori* (Tafreshi *et al.*, 2018).

It must be noted that the level of interleukin depends not just on gene polymorphism (Saes *et al.*, 2017; Kang *et al.*, 2009) but also on a microorganism genotype. In particular, it is known that the highest IL-8 content is found when the organism is infected with Hp CagA-strains (Siregar *et al.*, 2015; Lee *et al.*, 2013; Higashi *et al.*, 2004).

IL-8 is significantly activated in tumors and their microenvironment. It also acts as a key regulator of proliferation, angiogenesis, and metastasis. IL-8 regulates the cellular transmission of signals in cancer development and progression irrespective of chemotaxis during an inflammatory process. The expression of IL-8 makes stomach cancer resistant to chemotherapy. There is a close association between gastric cancer and *H. pylori*, with IL-8 levels indicating the unfavorable prognosis (Pece *et al.*, 1997).

Although the majority of authors note an association between Hp, IL-8 levels and stage of chronic inflammation along with the stage of neutrophil infiltration (Kononov, 2006; Siregar *et al.*, 2015; Nagashima *et al.*, 2015), some data and opinions oppose these provisions (Bayraktaroglu *et al.*, 2004; Zimmerman, 2018).

Data on IL8 levels in various diseases are limited and sometimes controversial. Thus, we examined serum levels of IL-8 in patients with chronic gastritis and gastroduodenal ulcer depending on confirmation of Hp infection with common methods and based on the presence of O-antigen of *H. pylori* LPS in stools according to coagglutination tests on immunological plates.

Purpose: To determine the levels of serum IL-8 in in-patients with chronic gastritis and gastroduodenal ulcer when Hp-infection is confirmed with common methods and based on the presence of O-antigen of *H. pylori* LPS in stools.

2. MATERIALS AND METHODS

Ninety-five patients of the gastroenterological department were examined (37 men and 58 women with a mean age of 59). Fifty-three of them were diagnosed with chronic active gastritis (CAG, including erosive gastroduodenitis; 17 men and 36 women), whereas 42 had a gastroduodenal ulcer (GDU, 20 men and 22 women).

To confirm the diagnosis, the following laboratory and instrumental methods of examination were used: clinical blood analysis, blood chemistry, Helpful test (AMA, Russia), urea breath test, test for fecal occult blood, blood group and Rh factor, fibro gastro duodenoscopy (Olympus xq40, Japan) with a cytological examination of the biopsy specimen, and abdominal ultrasound imaging (Sonoscape s8, China, GE Vivid 7, USA). Special blood tests for detecting and determining the level of IL-8 using the enzyme-linked immunosorbent assay and analysis of feces for O-antigen of *H. pylori* LPS during the agglutination test were carried out.

To find the dependence between the found levels of serum IL-8 and fecal LPS/O-antigen levels all the patients with CAG and GDU were subdivided into 4 subgroups: patients with GDU and found Hp infection using common methods (GDU+Hp) (16 blood samples), patients with GDU but without confirmed Hp (GDU) (52 blood samples), patients with CAG and Hp found using common methods (GDU+Hp) (25 blood samples), and patients with CAG but without confirmed Hp (CAG) (58 blood samples).

Surface epithelium with signs of dystrophia, chronic inflammation, edematous mucous layer, and leucocytic infiltration was found during a microscopic examination of 5 biopsy samples taken from the affected site of the antral section and duodenal bulb in CAG.

Cellular detritus, degenerative changes, inflammatory infiltrate elements, focal necrosis limited with granulation tissue, stromal edema, layers of the surface-foveolar epithelium in GDU with proliferative and dystrophic changes, leucocytic infiltration, atrophic fragments, and mucus dysplasia were discovered during a microscopic examination of biopsy samples in GDU.

The patients obtained proton pump inhibitors (PPI), antacids, H-2 receptor blocking agents. When Hp infection was confirmed, eradication therapy was given according to the National recommendations on diagnostics and

treatment of acid-dependent and *Helicobacter pylori*-associated diseases (VI Moscow agreements, dated 24-25 November 2016).

One hundred fifty-one blood serum samples were examined to detect the level of IL-8 using the EIA and test systems produced by the «Cytokine» company. Paired blood samples were obtained from patients with CAG and GDU upon their hospitalization, and also in 3-4 days after the first blood test.

Detection of O-antigen of *H. pylori* LPS in coprofiltrates of patients (149 samples) was done during a coagglutination test (CAT) using diagnostic agents prepared in accordance with the patent (Belaia *et al.*, 2001).

The test was done using immunological plates with a round (U-shaped) bottom. Every coprofiltrate sample was titrated twice (in phosphate buffer saline, 0.15M, pH=7.4) with 2 rows of plates. Coagglutination diagnostic was added in one row, and 1% unsensitized staphylococcus suspension was added to the other row. The plate was covered and put on air-bath at 37°C for 12 hours. A positive reaction is indicated by the formation of visible agglutinate clumps at 2+. Four-fold or greater dilution with a diagnostic showed the presence of O-antigen of *H. pylori* LPS in the sample as compared to the control reagent.

All patients included in the study gave informed consent to the inpatient examination. Confidentiality was preserved.

The digital data underwent statistical processing using common methods of variation statistics, Student's t criterion, and programs of Microsoft Word and Microsoft Excel.

3. RESULTS AND DISCUSSION

Confirmation of Hp infection by conventional methods did not exceed 30%.

Increased levels of serum IL-8 (above 0.062 ng/ml) were found in the majority of patients (90%). As mentioned above, all patients with CAG and GDU were subdivided into 4 subgroups: patients with GDU and found Hp using common methods (GDU+Hp), patients with GDU and no confirmed Hp (GDU), patients with CAG and found Hp using common methods (CAG+Hp) and patients with CAG with no confirmed Hp (CAG).

During the study it was found out that the highest levels of serum IL-8 were detected in patients with GDU+Hp ($p \leq 0.05$) (the same

tendency was seen for the first stool sample), the lowest levels were found in patients with CAG (without detection of Hp using common methods). No significant differences were found between the mean IL-8 levels in the first and second stool samples due to a small time interval (3-4 days). Only a weak, insignificant tendency to lower IL-8 levels was detected during the second analysis (Table 1).

When results obtained during analyses 1 and 2 are combined, levels of IL-8 in patients with GDU+Hp were significantly higher than those in patients with GDU but without Hp detected using common methods (0.50 ± 0.09 and 0.32 ± 0.04 , respectively; $p \leq 0.05$), and higher than those in patients with CAG+Hp (0.50 ± 0.09 and 0.30 ± 0.05 , respectively; $p \leq 0.05$). In patients with GDU and CAG, the mean levels of IL-8 were similar (0.32 ± 0.04 and 0.30 ± 0.04 , respectively) and significantly lower than in patients with GDU +Hp ($p \leq 0.05$).

The levels of serum IL-8 were examined in patients of both sexes during two blood serum analyses (Table 2). In men with Hp detected using common methods, the levels of IL-8 in GDU+Hp were significantly higher than in CAG+Hp (0.46 ± 0.07 and 0.20 ± 0.04 , respectively, $p \leq 0.05$). This influenced the aggregate level of IL-8 (both in men and in women) where the levels of IL-8 in GDU+Hp were significantly higher than those in patients with GDU (0.50 ± 0.09 and 0.32 ± 0.04 , respectively, $p \leq 0.05$), CAG+Hp (0.50 ± 0.09 and 0.30 ± 0.05 , respectively, $p \leq 0.05$) and CAG (0.50 ± 0.09 and 0.30 ± 0.04 , respectively, $p \leq 0.05$).

According to the aggregate value obtained in two analyses, the levels of IL-8 in women were significantly higher than in men (CAG+Hp) (0.40 ± 0.07 and 0.20 ± 0.04 , respectively, $p \leq 0.05$). No significant differences were found between men and women with GDU, CAG, and GDU+Hp.

Thus, men with CAG+Hp have lower levels of IL-8 as compared with other subgroups. These IL-8 values were significantly different from those in women.

To establish the dependence between the detected levels of serum IL-8 and fecal LPS/O-antigen, the levels of the antigen were examined in 4 subgroups of patients mentioned above (Table 3).

The total rate of fecal LPS/O-antigen detection was 86%. The highest levels of fecal O-antigen of *H. pylori* LPS were found in CAG patients (lg10 reverse antigen titre – 1.473 ± 0.111) and in the general group of patients with CAG and

CAG+Hp (1.452±0.092). Patients with GDU+Hp and CAG+Hp had identical or lower levels of O-antigen of *H. pylori* LPS (1.400±0.180 and 1.400±0.167, respectively). Patients with GDU+Hp had significantly higher

Helicobacter pylori cause chronic gastritis, gastroduodenal ulcer, stomach cancer, and MALT-lymphoma (McColl, 2010). Chronic gastric inflammation, characterized by gastric mucous infiltration with neutrophils and macrophages (Kusters *et al.*, 2006), is due to cytokines and chemokines including interleukin-1 β , IL-8, and IL-6, tumor necrosis factor- α (TNF- α), which are produced under the influence of *H. pylori* pathogenicity factors (Siregar *et al.*, 2015; Naito *et al.*, 2005; Sharma *et al.*, 1995).

The majority of researchers notice a relationship between the presence of *H. pylori* alongside with serum IL-8 levels and the rate of chronic inflammation with the rate of neutrophil infiltration (Siregar *et al.*, 2015). IL-8 is a powerful angiogenic and chemoattractive agent, a key mediator of Th1-type immune response overexpressed in gastric epithelial cells influenced by *H. pylori* and epithelial cells (Sharma *et al.*, 1995). Although widely studied in any disease, data on IL-8 levels in chronic gastritis (CG) and a gastroduodenal ulcer (GDU) are insufficient and often controversial.

According to the current study of serum IL-8 levels in patients with chronic active gastritis (CAG, including erosive gastroduodenitis) and a gastroduodenal ulcer (GDU), its increased levels were found in the majority of patients (90%), while Hp-infection using conventional methods was detected in no more than 30% of patients. Thus, the increased concentration of serum IL-8 was seen even in those patients for whom the presence of Hp wasn't confirmed using common methods.

The highest levels of serum IL-8 were found in those with GDU+Hp ($p \leq 0.05$), the lowest ones in those with CAG. Men generally had the lowest levels of IL-8 in CAG+Hp as compared to other subgroups. These IL-8 values were significantly different from higher values in women.

The total detection rate of fecal LPS/O-antigen of *H. pylori* was 86%, and this level was higher than the confirmation of Hp infection by conventional methods. The highest levels of fecal O-antigen of *H. pylori* LPS were found in CAG patients, and this level of O-antigen was higher than that in patients with GDU.

Patients with GDU+Hp had significantly

higher levels of O-antigen of *H. pylori* LPS as compared to patients with GDU. Patients with GDU+Hp and CAG+Hp had similarly low levels of O-antigen of *H. pylori* LPS. In the aggregate, the levels of O-antigen of *H. pylori* LPS in GDU were significantly inferior to those in CAG. This could be due to more intense destruction of gastric Hp, making it impossible to detect whole microbial cells when using common methods of Hp diagnostics, while when they are destroyed, there is a greater amount of free O-antigen in the feces. This is probably the reason for significantly higher levels of O-antigen of *H. pylori* LPS in CAG as compared to GDU.

Thus, among patients with a peptic ulcer disease who had their *H. pylori* infection confirmed with the common methods, the mean levels of fecal O-antigen of *H. pylori* were higher in GDU+Hp than in GDU, whereas the levels of IL-8 were the highest in GDU as compared with other subgroups. Patients with CAG had the highest levels of O-antigen/LPS and relatively low levels of IL-8. We believe that the level of O-antigen in feces is not a determining factor in stimulating the production of IL-8 in patients with chronic active gastritis and peptic ulcer disease.

At the same time, it was found that an intermediate metabolite of LPS *Helicobacter pylori* inner core heptose biosynthesis (HBP) modulates host cell responses by CagT4SS-dependent translocation. The authors suggest that HBP is a major factor leading to the activation of cellular responses. This response is connected to the human cellular adaptor protein TIFA (Stein *et al.*, 2017).

As known from experiments in CagA and/or CagL knockout bacterial lines, extracellular CagA might induce IL-8 production by AGS cells (Fazelli *et al.*, 2016; Zeng *et al.*, 2020).

The C-terminal coiled-coil region of the *H. pylori* CagL protein, a protein described to be located on the tip of the T4SS-pilus, is responsible for *H. pylori*-induced IL-8 secretion via the transforming growth factor (TGF)- α activated epidermal growth factor-receptor (EGF-R) signaling pathway and the bridging of the T4SS to its human target cells. This novel bacterial-host recognition sequence allows a new insight into how *H. pylori* induce the inflammatory response in gastric epithelial cells and facilitate the development of precancerous conditions (Tafreshi *et al.*, 2018; Wiedemann *et al.*, 2016; Lee *et al.*, 2016). Outer inflammatory protein A (OipA) of *Helicobacter pylori* is regulated by host cell contact and mediates CagA translocation and interleukin-

8 response only in the presence of a functional cag pathogenicity island type IV secretion system (Horridge *et al.*, 2017).

There is insufficient data on the effect of LPS Hp on IL-8 levels (Stein *et al.*, 2017; Pece *et al.*, 1997). Despite the low immunological potential, an array of proinflammatory cytokines (IL-8, IL-1, and TNF- α) are produced both in vitro and in vivo following the stimulation of mucosal cells with *H. pylori* organisms (Pece *et al.*, 1997). The highest levels of fecal O-antigen of *H. pylori* LPS were found in CAG patients, while the level of IL-8 was the highest in the group of ulcers, indicating a mismatch between the levels of O-antigen in feces and IL-8 in serum. Nonetheless, the detection of *H. pylori* O antigen in feces has diagnostic value, especially in patients with CAG in the lack of detection of Hp by conventional methods.

4. CONCLUSION

The vast majority of patients (90%) have elevated levels of IL-8. According to the data obtained, more active IL-8 production was found in peptic ulcer disease, especially when *H. pylori* was detected using common methods.

The rate of fecal *H. pylori* O-antigen in the coagglutination test was 86%. The highest levels of O-antigen of *H. pylori* LPS were detected in the CAG subgroup, and in total in patients with CAG compared with DGU. In patients with GDU+Hp, the levels of O-antigen of *H. pylori* were significantly higher as compared with the GDU subgroup.

Simultaneous use of the coagglutination test to detect fecal O-antigen of *H. pylori* and common methods make the infection confirmation highly probable, especially in chronic gastritis (almost until the level of infection confirmation in peptic ulcer disease).

5. ACKNOWLEDGMENTS

Supported by the Russian Academic Excellence Project 5-100

Conflict of interest: The authors declare there is no conflict of interest.

6. REFERENCES

- Ageeva, E. S.; Shtygasheva, O. V.; Pulikov, A. S.; Butorin, N. N. The role of IL-1 and IL-8 in pathomorphosis of the mucous coat of stomach at the *Helicobacter pylori*-associated gastritis. *Acta Biomedica Scientifica*, 2011, 77(1), part 1, 16-17
- Bayraktaroglu, T.; Aras, A. S.; Aydemir, S.; Davutoglu, C.; Ustundag, Y.; Atmaca, H.; Borazan, A. Serum levels of tumor necrosis factor- α , interleukin-6, and interleukin-8 are not increased in dyspeptic patients with *Helicobacter pylori*-associated gastritis. *Mediators Inflamm.*, 2004, 13, 25-28. DOI: 10.1080/09629350410001664789
- Belaia, Y.A.; Belaia, O.F.; Petrukhin, V.G. Method of obtaining diagnostic agents to detect *Helicobacter pylori* antigens during a coagglutination test. Patent RU No. 2186394, 31 January 2001.
- Crabtree, J. E. Gastric mucosal inflammatory responses to *Helicobacter pylori*. *Aliment Pharmacol. Ther.*, 1996, Suppl. 10, 29–37. DOI: 10.1046/j.1365-2036.1996.22164003.x.
- de Brito, B. B.; da Silva, F.A. ; de Melo, F. F. Role of polymorphisms in genes that encode cytokines and *Helicobacter pylori* virulence factors in gastric carcinogenesis. *World J Clin Oncol*, 2018, 9(5) 83-89.
- Fazelli, Z.; Alebouyeh, M.; Tavirani M.R.; Azimirad, M.; Yadegar, A. *Helicobacter pylori* CagA induced interleukin-8 secretion in gastric epithelial cells. *Gastroenterol Hepatol Bed Bench*, 2016, 9(Suppl. 1), 42-46, PMID: 28224027.
- Higashi, H; Nakaya, A.; Tsutsumi, R.; Yokoyama, K.; Fujii, Y.; Ishikawa, S.; Higuchi, M.; Takahashi, A.; Kurashima, Y.; Teishikata, Y.; Tanaka, S.; Azuma, T.; Hatakeyama, M. *Helicobacter pylori* CagA induces Ras-independent morphogenetic response through SHP-2 recruitment and activation. *J Biol Chem.*, 2004, 279(17), DOI: 10.1074/jbc.m309964200.
- Horridge, D.N.; Begley, A.A.; Kim, J.; Aravindan, N.; Fan, K.; Forsyth, M.H. Outer inflammatory protein an (OipA) of *Helicobacter pylori* is regulated by host cell contact and mediates CagA translocation and interleukin-8 response only in the presence of a functional cag pathogenicity island type. *Pathog Dis.*, 2017, 75(8), DOI: 10.1093/femspd/ftx113.
- Israel, D.A.; Peek, R.M.; Review article: pathogenesis of *Helicobacter pylori*-induced gastric inflammation. *Aliment Pharmacol Ther.*, 2001, 15, 1271-1290.
- Kang, J. M.; Kim, N.; Lee, D. H.; Park, J. H.; Lee, M. K.; Kim, J.S.; Jung, H. C.; Song, I.S.

- The effects of genetic polymorphisms of IL-6, IL-8, and IL-10 on *Helicobacter pylori*-induced gastroduodenal diseases in Korea. *J Clin Gastroenterol.*, 2009, 43(5), 420-428, DOI: 10.1097/MCG.0b013e318178d1d3.
11. Kononov, A.V. Inflammation as the basis of *Helicobacter pylori*-associated diseases. *Arkhiv patologii*, 2006, 68 (5), 3–10.
 12. Kusters, J.G.; van Vliet, A.H.; Kuipers, E.J. Pathogenesis of *Helicobacter pylori* infection. *Clin. Microbiol. Rev.*, 2006, 19, 449–490. doi: 10.1128/CMR.00054-05.
 13. Lee, H.; Su Y.L.; Huang B.S.; Hsieh F. T.; Chang Y.H.; Tzeng S.R.; Hsu C.H.; Huang P.T.; Lou K.L.; Wang Y.T.; Chow L.P. Importance of the C-terminal histidine residues of *Helicobacter pylori* GroES for Toll-like receptor 4 binding and interleukin-8 cytokine production. *Scientific reports*, 2016, 6, 37367; DOI: 10.1038/srep37367.
 14. Lee, K. E.; Khoi, P. N.; Xia, Y.; Park, J. S.; Joo, Y. E.; Kim, K. K.; Choi, S. Y.; Jung, Y. D. *Helicobacter pylori* and interleukin-8 in gastric cancer. *World J Gastroenterol*, 2013, 19(45), 8192-8202. DOI: 10.3748/wjg.v19.i45.8192.
 15. McColl, K.E. Clinical practice. *Helicobacter pylori* infection. *N Engl J Med.*, 2010, 362, 1597-604, DOI: 10.1056/NEJMcp1001110.
 16. Nagashima, N.; Iwatani, S.; Cruz, M.; Abreu, J.A.J.; Tronilo, L.; Rodríguez, E. Differences in interleukin-8 expression in *Helicobacter pylori*-infected gastric mucosa tissues from patients in Bhutan and the Dominican Republic *Hum Pathol.*, 2015, 46(1), 129–136, PMID:25454482, DOI:10.1016/j.humpath.2014.10.006.
 17. Naito, Y.; Ito, M.; Watanabe, T.; Suzuki, H. Biomarkers in patients with gastric inflammation: a systematic review. *Digestion*, 2005, 72(2-3), 164–180, DOI: 10.1159/000088396
 18. Naumann, M.; Crabtree, J. E. *Helicobacter pylori*-induced epithelial cell signalling in gastric carcinogenesis. *Trends Microbiol*, 2004, 12, 29-36, DOI: 10.1016/j.tim.2003.11.005.
 19. Pece, S.; Giuliani, G.; Di Leo, A.; Fumarola, D.; Antonaci, S.; Jirillo, E. Role of lipopolysaccharide and related cytokines in *Helicobacter pylori* infection. *Recenti Prog Med.*, 1997, 88(5), 237-241.
 20. Rehman, S. “*Helicobacter pylori*: A Short Literature Review”. *EC Gastroenterology and Digestive System*, 2020, 7.2, 1-9.
 21. Saes, M.; de Labio, R.W.; Rasmussen, L.T., Payão, S.L.M. Interleukin 8 (-251 T>A) polymorphism in children and teenagers infected with *Helicobacter pylori*. *Journal of Venomous Animals and Toxins including Tropical Diseases*, 2017, 23, 1-3, DOI: 10.1186/s40409-017-0113-z.
 22. Serrano, C.; Diaz M.I.; Valdivia, A.; Godoy, A.; Pena, A.; Rollan, A. Relationship between *Helicobacter pylori* virulence factors and regulatory cytokines as predictors of clinical outcome. *Microbes Infect.*, 2007, 9, 428-3.
 23. Sharma, S. A.; Tummuru, M.K.; Miller, G.G.; Blaser, M.J. Interleukin-8 response of gastric epithelial cell lines to *Helicobacter pylori* stimulation in vitro. *Infect Immun.*, 1995, 63, 1681-1687.
 24. Sipponen, P. Long-term evaluation of *Helicobacter pylori*-associated chronic gastritis. *Eur. J. Gastroenterol. Hepatol.*, 1993, 5(Suppl 1), 93–97.
 25. Siregar, G. A.; Halim, S.; Sitepu, R. R. Serum TNF- α , IL-8, VEGF Levels in *Helicobacter pylori* Infection and Their Association with Degree of Gastritis. *Acta Medica Indonesiana*, 2015, 47 (2), 120-126.
 26. Stein, S.C.; Bats, E.F.S.H.; Murillo, T.; Speidel, Y.; Coombs, N.; Josenhans, C. *Helicobacter pylori* modulates host cell responses by CagT4SS-dependent translocation of an intermediate metabolite of LPS inner core heptose biosynthesis. *PLoS Pathog*, 2017, 13(7), e1006514. DOI: /10.1371/journal.ppat.1006514.
 27. Sun, Q.; Sun, F.; Wang, B.; Liu, S.; Niu, W.; Liu, E.; Peng, C.; Wang, J.; Gao, H.; Liang, B.; Niu, Z.; Zou, X.; Niu, J. Interleukin-8 promotes cell migration through integrin $\alpha\beta 6$ upregulation in colorectal cancer. *Cancer Lett.*, 2014, 354(2), 245-53. DOI: 10.1016/j.canlet.2014.08.021.
 28. Tafreshi, M.; Guan, J.; Gorrell, R.J.; Chew, N.; Xin, Y.; Deswaerte, V.; Rohde, M.; Daly, R.J.; Peek, R.M.Jr.; Jenkins, B.J.; Davies, E.M.; Kwok, T. *Helicobacter pylori* Type IV Secretion System and Its Adhesin Subunit, Cag L, Mediate Potent Inflammatory Responses in Primary Human Endothelial Cells. *Front. Cell. Infect. Microbiol*, 2018, 8, 22, DOI: 10.3389/fcimb.2018.00022.
 29. VI National guidelines for the diagnosis and treatment of acid-related and *Helicobacter pylori*-associated diseases (VI Moscow agreement). *Experimental and Clinical Gastroenterology Journal*, 2017, 2(138), 3-21.
 30. Vinagre, R.M.D.F.; Vinagre, I.D.F.; Vilar-e-Silva, A.; Fecury, A.A.; Martins, L.C. *Helicobacter pylori* infection and immune profile of patients with different gastroduodenal

diseases. *Arq Gastroenterol*, 2018, 55(2), 122-127, [dx.doi.org/10.1590/S0004-2803.201800000-21](https://doi.org/10.1590/S0004-2803.201800000-21).

31. Wiedemann, T.; Hofbaur, S.; Loell, E.; Rieder, G. A C-terminal coiled-coil region of CagL is responsible for *Helicobacter pylori*-induced IL-8 expression. *European Journal of Microbiology and Immunology*, 2016, 3, 186–196, DOI: 10.1556/1886.2016.00020.
32. Zeng, B.; Chen, C.; Yi, Q.; Zhang, X.; Wu, X.; Zheng, S.; Li, N.; She, F. N-terminal region of *Helicobacter pylori* CagA induces IL-8 production in gastric epithelial cells via the β 1 integrin receptor. *Med Microbiol*, 2020, Feb 25, DOI: 10.1099/jmm.0.001088. [Epub ahead of print]
33. Zimmerman, Ya.S. Peptic ulcer: a critical analysis of modern state of the problem. *Experimental and Clinical Gastroenterology Journal*, 2018, 149(1), 80-89.

Table 1. Mean serum levels of IL-8 in the course of chronic gastritis and a gastroduodenal ulcer (ng/ml)

IL-8 ng/ml	GDU+Hp	CAG+Hp	GDU	CAG
Analysis 1	0.46±0.11 n=10	0.32± 0.07 n=13	0.32±0.05 n=29	0.34±0.05 n=33
Analysis 2	0.4±0.15 n=6	0.30±0.07 n=12	0.31±0.04 n=23	0.25±0.05 n=25
Total	0.50±0.09 n=16	0.30±0.05 * n=25	0.32±0.04 * n=52	0.30±0.04 * n=58
Overall	0.36±0.05 n=41		0,31±0,03 n=110	

Note: *) statistical significance in comparison with patients suffering from GDU+Hp ($p \leq 0.05$)

Table 2. Mean levels of serum IL-8 in patients with chronic active gastritis and gastroduodenal ulcer depending on the gender and in the aggregate

Patients:	Mean IL-8 levels in blood serum (ng/ml)				
	GDU	GDU + Hp	CAG	AG + Hp	Total
Men Analysis 1	0,32±0,09 n=13	0,43± 0,14 n=7	0,36±0,10 n=8	0,19±0,06 n=7	0,33±0,05 n=35
Men Analysis 2	0,35±0,06 n=11	0,45 ±0,23 n=4	0,30±0,06 n=6	0,22±0,18 n=4	0,33±0,05 n=25
Men Analysis 1+2	0,34±0,05 n=24	0,46±0,07 n=11	0,33±0,06 n=14	0,20±0,04 * n=11	0,33±0,03 n=60
Women Analysis 1	0,32±0,07 n=16	0,43±0,22 n=3	0,33±0,05 n=25	0,47±0,1 n=6	0,35±0,04 n=50
Women Analysis 2	0,26±0,06 n=12	0,42±0,01 n=2	0,24±0,07 n=19	0,40±0,10 n=8	0,28±0,04 n=41
Women Analysis 1+2	0,30±0,05 n=28	0,43±0,12 n=5	0,30±0,04 n=44	0,40±0,07 ** n=14	0,32±0,03 n=91
Total (M+F, 2 analyses)	0,32±0,04 & n=52	0,50±0,09 n=16	0,30±0,04 & n=58	0,30±0,05 & n=25	0,32±0,02 n=151
Total	0,32 ± 0,03 n = 68		0,31 ± 0,03 n = 83		0,32±0,02 n=151

Note. The significance of differences in comparison with: *) a subgroup of men with Hp GDU ($p = 0.004$); **) the respective subgroup of men ($p = 0.04$); &) the 'total' subgroup with Hp GDU ($p \leq 0.05$)

Table 3. Mean levels of fecal O-antigen of *H. pylori* LPS during the coagglutination test (Ig10 reverse antigen titer) in patients with CAG and GDU depending on the association of the disease with *H. pylori* (according to common methods)

Mean levels of LPS/O-antigen	GDU+Hp	GDU	CAG+Hp	CAG
	1,400 ± 0,180 n = 16	1,000 ± 0,080 * n = 52	1,400 ± 0,167 n = 23	1,473 ± 0,111 ** n = 58
Total	1,195 ± 0,076 n = 68		1,452 ± 0,092 # n = 81	

Note. The significance of differences in comparison with: *) patients with GDU+Hp ($p = 0.026$); **) patients with GDU ($p = 0.00$); &) all patients with GDU ($p = 0.00$)

INTELIGÊNCIA INTERPESSOAL DE ESTUDANTES DA ESCOLA PROFISSIONAL EM APRENDIZAGEM QUÍMICA: UM ESTUDO DE CASO**INTERPERSONAL INTELLIGENCE OF VOCATIONAL HIGH SCHOOL STUDENTS ON CHEMISTRY LEARNING: A CASE STUDY**ASTUTI, Elsa Ari¹; WORO, Sumarni^{2*}; WIYANTO³^{1,2}Universitas Negeri Semarang, Mathematics and Science Faculty, Chemistry Department. Indonesia.³Universitas Negeri Semarang, Mathematics and Science Faculty, Physic Department. Indonesia.

* Corresponding author

e-mail: worosumarni@mail.unnes.ac.id

Received 10 February 2020; received in revised form 04 March 2020; accepted 24 March 2020

RESUMO

A inteligência interpessoal é a inteligência social que mostra a capacidade de criar bons relacionamentos com amigos ou com o meio ambiente. De fato, essa inteligência não foi treinada ao máximo na aprendizagem na escola, especialmente na química, embora a inteligência seja importante o suficiente para aprimorar a capacidade da criança de socializar com seu ambiente. O objetivo deste estudo foi identificar as reais condições da inteligência interpessoal dos estudantes na Escola Profissional de Farmácia da cidade de Semarang. Uma pesquisa foi realizada no ano acadêmico 2018/2019 com uma amostra de 57 alunos da Escola Profissional de Farmácia Classe XII da cidade de Semarang, na Indonésia, que haviam aprovado como participantes. A amostragem foi realizada aleatoriamente. As técnicas de coleta de dados foram realizadas por observação, avaliação por pares e autoavaliação ao aplicar o aprendizado de química. Os resultados mostraram que 56% dos estudantes possuíam baixa inteligência interpessoal com base nas observações feitas e, de acordo com os resultados da análise da pesquisa com instrumentos de avaliação por pares, havia 59% dos estudantes também categorizados como baixos para essa capacidade. Os resultados da pesquisa com instrumentos de autoavaliação também mostraram que 56% dos estudantes possuíam baixa inteligência interpessoal. A baixa inteligência está principalmente nos indicadores da capacidade de fazer, responder perguntas e fornecer respostas. Esse fato é relativamente semelhante à literatura que revela que 50% dos estudantes têm inteligência interpessoal com uma categoria média-baixa. Portanto, a conclusão é que, na realidade, essa inteligência ainda é baixa.

Palavras-chave: *Inteligência interpessoal, inteligência social, aprendizado de química.***ABSTRACT**

Interpersonal intelligence is social intelligence that shows one's ability to create good relationships with friends or the environment. In fact, this intelligence has not been maximally trained in learning at school, especially in chemistry learning, even though the intelligence is important enough to hone the child's ability to be able to socialize with their environment. The purpose of this study was to identify the real conditions of students' interpersonal intelligence in Pharmacy Vocational High School in the city of Semarang. A survey was performed in the academic year 2018/2019 with a sample of 57 students of class XII Pharmacy Vocational High School in the city of Semarang, Indonesia, who had given their approval as participants. Sampling was done randomly. Data collection techniques were carried out by observation, peer assessment, and self-assessment when applying chemistry learning. The results showed that 56% of students had low interpersonal intelligence based on observations and, according to the results of survey analysis with peer assessment instruments, there were 59% of students also categorized low for this capability. The survey results with self-assessment instruments also showed 56% of students had low interpersonal intelligence. Low intelligence is mainly in the indicators of the ability to ask, answer questions, and provide answers. This fact is relatively similar to the literature, which reveals that 50% of students have interpersonal intelligence with a medium-low category. So the conclusion is that in reality, this intelligence is still low.

Keywords: *Interpersonal intelligence, social intelligence, chemistry learning.*

1. INTRODUCTION:

Interpersonal intelligence is an intelligence that is important and useful for education and learning in the 21st century. Interpersonal intelligence is a person's ability to interact with others. This intelligence is suitable to be applied in learning as one of the skills that can help students to socialize. Learning that integrates intelligence is unique because it pays attention to the potential and characteristics of each student (Utami, 2019).

Considering the beneficial effects obtained by students by having interpersonal intelligence both now and in the future, it is deemed to be essential to identify students' interpersonal intelligence (Astuti *et al.*, 2019).

Learning about interpersonal intelligence has been applied to curricula in many countries around the world (Utami, 2019). Interpersonal intelligence is social intelligence (Handayani, 2019; Mahmud *et al.*, 2018) that is someone's skill in creating a good relationship with their environment (Suthatorn & Charoensukmongkol, 2018; Safitri & Sriyanto, 2019).

Interpersonal intelligence is intelligence that is shown by the child's ability to socialize with other people well, such as being easy to get along with, understanding other people, and cooperating with others (Utami, 2019; Agustika *et al.*, 2019). The components of interpersonal intelligence, in general, are the purpose of learning affective aspects in education (Lorenzo *et al.*, 2019) in school, including chemistry learning.

Components of interpersonal intelligence include organizing groups, negotiating problem-solving, establishing personal relationships, and conducting social analysis (Shearer, 2019). Characteristics and indicators of interpersonal intelligence that are implemented during the learning process, namely: students pay attention to the teacher's explanation attentively, students determine problem-solving by the problem, students take the initiative to express opinions, students become members of an orderly group, students help their friends difficulty in doing the task, students respond to solving the proposed problem and its reasons (Pertiwi, 2018; Sari, 2019).

Each individual owns interpersonal intelligence. This intelligence is vital to be developed in everyday life because every human being lives together in groups and needs others (Kusumaningrum, 2019). Interpersonal intelligence is also an influential element in education in schools because students will interact

or interact with other friends (Hsu & Beasley, 2019). Interpersonal intelligence is shown by the ability of students to socialize (Rusmayadi, 2019). With interpersonal intelligence, a person must be able to establish good relations with the surrounding environment so that it can be said that interpersonal intelligence is the key to dealing with other people (Wulansuci, 2019).

The beneficial effect on the achievement of children's interpersonal intelligence is the success of interacting with others (Suryana, 2019), understand other people well (Yerizon, 2018), can handle problems, understand and recognize prejudices, like group work, give feedback, and empathize, easy to get along with others and love to make friends (Astuti *et al.*, 2019). Not only that, students can get excellent academic achievements in the future because students already know the potential they have (Nurtika, 2019) even to college and at work (Wulansuci, 2019).

If interpersonal intelligence is not well developed, children tend to be less sensitive, less caring, selfish, and often offend others. Children who fail to develop interpersonal experiences many obstacles in the social world such as behavior difficulties at school, delinquency, ignorance, peer rejection, emotional challenges, bullying, difficulties in friends, aggressiveness, problems in interpersonal relationships, poor self-concept, failure academic, concentration difficulties, isolation from peers, and depression (Prakoso, 2019).

Interpersonal intelligence is essential for students both at this time and when they have graduated later, especially for Vocational High School (SMK) students. Vocational level students are individuals who are in adolescence. One of the roles of adolescent developmental tasks plays a role in social life, such as developing interpersonal intelligence, both individuals and groups, and mastering the ability to carry out social purposes. With interpersonal intelligence, vocational students can easily interact with friends at school and in the future when continuing their careers, especially for students of SMK Pharmacy. Interpersonal intelligence possessed by SMK Pharmacy graduates will describe a positive or good self-image, then the individual will feel safe and respect oneself and will undoubtedly be able to respect others, the image of the others, the physical environment, the environment social, condition or condition of a person when communicating and body language (Kemala & Sukmawati, 2019).

Based on research conducted by Sari (2019), (Johar *et al.*, 2019) (Syasmita *et al.*, 2019) shows that the interpersonal intelligence of students is still in the low category. Research (Johar *et al.*, 2019) revealed that more than 50% of students with a major in health have interpersonal intelligence with a medium-low category.

Given the importance of interpersonal intelligence for vocational students, therefore it is necessary to know how the interpersonal intelligence profile of students. The purpose of the research to be achieved is to determine the ability to socialize with other people that students have had so far in the field of education, which later on, if found to be still low, can be improved in further learning.

2. MATERIALS AND METHODS:

A survey was carried out in the academic year 2019 with a sample of class XII Vocational Pharmacology in the city of Semarang, Central of Java, Indonesia. Sampling was done randomly. Samples obtained as many as 57 students (after agreeing to participate in this survey) of whom 9% male and 91% female; 22% of students have parents as farmers, 35% as civil servants, and 43% as entrepreneurs. Data collection techniques were carried out by observation, peer assessment, and self-assessment. Each of these refers to Shearer (2019), which is adapted to the learning activities carried out in research schools, namely cooperation, responsibility, listening to others, asking questions, answering questions, and providing assistance in answering questions during the discussion.

Data collection instruments (Appendix 4) with all of these indicators were given a score based on the rating scale (score 1-4) so that the maximum score is 24. The scores obtained on the observation sheet are totaled then divided by the total score and determine the students' interpersonal intelligence criteria at class intervals in table 1.

Table 1. Criteria for interpersonal intelligence

Interval skor	Criteria
18 > score ≥ 24	Very high
12 > score ≥ 18	High
6 > score ≥ 12	Low
0 > score ≥ 6	Very low

The same data analysis was performed on

the data obtained on the self-assessment and peer-assessment sheets.

Besides, the data obtained were analyzed per indicator, each indicator on the three instruments added up and divided by the total score, then made in the form of a percentage (%) and determine the criteria at certain class intervals (Sugiyono, 2017).

Table 2. Criteria for Student Interpersonal Intelligence Assessment

Indicator score (%)	Criteria
75 ≤ score < 100	Very high
50 ≤ score < 75	High
25 ≤ score < 50	Low
0 ≤ score < 25	Very low

3. RESULTS AND DISCUSSION:

The results showed that 25% of students live in suburban areas, and 75% of students live in downtown areas. Also, the students studied have identified that 43% of students have low achievement, 40% of students have moderate performance, and 17% of students have high achievement. The results of the interpersonal intelligence of students in this study, there are six aspects of assessment that are tailored to the implementation of learning to uncover students' interpersonal knowledge. The six points are working together, taking responsibility, listening to others, asking questions, answering questions, and providing assistance in answering questions during the discussion. The results of observations of the interpersonal intelligence of students are shown in Table 3.

Table 3. Recapitulation of observations of students' interpersonal intelligence

Criteria	Number of learners (children)	Percentage of learners (%)
Very high	5	9
High	19	33
Low	32	56
Very low	1	2

Based on data from Table 3, it can be seen that as many as 56% of students have interpersonal intelligence with a low category. Thus it can be said that the majority of students

have low interpersonal intelligence. The same result was found by Purwanto (2019) that as many as more than 50% of students have interpersonal intelligence with low categories. This is indicated because students have not dared to create active conversations in the classroom, are less involved in delivering arguments, even slow to absorb information. Learners are more silent during the learning process, waiting to be appointed by the teacher to express their opinions in class and ashamed (Syarifatunnisa, 2019).

The low data of students' interpersonal intelligence is also found in peer assessments that have been distributed to students. The results of students' interpersonal intelligence on the peer assessment instrument are shown in table 4.

Table 4. Recapitulation of students' interpersonal intelligence by peer assessment

Criteria	Number of learners (children)	Percentage of learners (%)
Very high	5	9
High	17	31
Low	34	59
Very low	1	2

In table 4, it can be seen that as many as 59% of students have a low level of interpersonal intelligence. The low interpersonal intelligence was also revealed by Saputra, *et al.* (2018) and Wulandari, *et al.* (2018), there is a close relationship between students' low interpersonal intelligence and learning outcomes. Students with low interpersonal intelligence, low learning outcomes, including learning outcomes in learning chemistry. Learning chemistry as part of natural science requires students to use scientific methods in the implementation of learning, which is often done practicum or experiment that is usually conducted by groups or groups. If students cannot work well together, their work will not be maximal. Sometimes these learners experience misunderstandings or misinterpretations of what their classmates are conveying (Syarifatunnisa, 2019).

The same data was also found in the self-assessment instrument given to students to assess themselves against interpersonal intelligence indicators. The results are shown in Table 5.

Table 5. Recapitulation of students' interpersonal intelligence by self-assessment

Criteria	Number of learners (children)	Percentage of learners (%)
Very high	5	9
High	19	33
Low	32	56
Very low	1	2

There are more than 50% of students who have low interpersonal intelligence. Furthermore, the same results were also shown by Nisa, *et al.* (2019) the low interpersonal intelligence is mostly caused by three main factors, namely lack of interaction and communication within the family, not being accepted in peer groups so that they tend to experience difficulties in socializing and communicating, and trouble working in groups/discussions. In general, students who have low interpersonal intelligence show signs such as; can not get along, like being alone/lacking, lacking sensitivity to friends and the environment, tend to be selfish, challenging to trust others, and sometimes even act in ways that offend others (Ulfah, 2018).

Data recapitulation of observations of students' interpersonal intelligence of each indicator is shown in Figure 1.

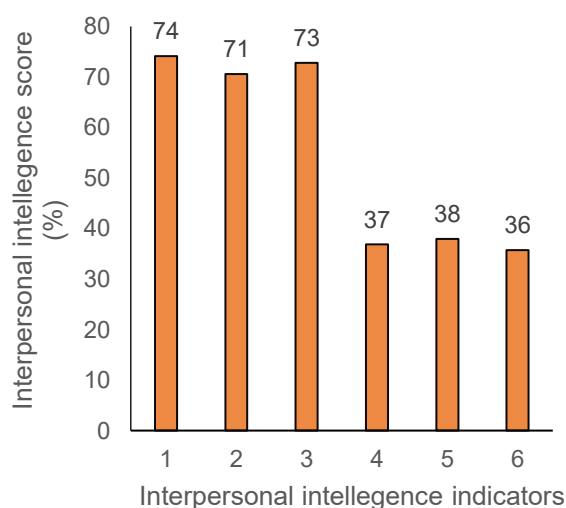


Figure 1. Observation Results of Students' Interpersonal Intelligence Legend: (1) Collaborate during discussions; (2) Responsible for conducting discussions from the beginning to the end of the discussion; (3) Listen to others when there is a group presenting and when discussing

(question and answer); (4) Asking when the discussion; (5) Answering questions during the discussion; (6) Provide assistance in answering questions during the discussion.

Based on Figure 1, it can be seen that the students' interpersonal intelligence on indicators work together, listen to other people, and are responsible when the discussion is high. In the implementation of the group discussion stage, there is a functional interaction between students and students and students and teachers. Collaboration with group members gives them a sense of responsibility for their learning and the learning of group members (Syarifatunnisa, 2019).

Based on data in figure 1, the next indicator is the aspect of asking questions, answering questions, and providing assistance in answering questions during the discussion. These three aspects are in the low category. The same findings were revealed in the study (Pratiwi *et al.*, 2019) and Palupi *et al.* (2020). Students tend to be still reluctant to ask questions even though they do not understand the material presented by the teacher. This can occur due to (1) lack of space for students to pour the questions that will be asked (the media / LKPD does not provide students the opportunity to develop questioning skills); (2) the learning that is carried out still tends to be teacher-oriented with the teacher still more dominant in mastering learning; (3) learning material tends to be based only on students' books and lacks additional resources from various sources; (4) lack of use of innovative and contextual learning media that is suitable with the subject matter (Susilowati, 2019). Also, the habit or culture that formed by itself in the class that is only a few students who actively asked and answered during the discussion.

4. CONCLUSIONS:

The interpersonal intelligence of high school students in chemistry learning is still low with aspects that are low in their ability to question during discussions, ask questions during conversations, and provide assistance in answering questions during discussions, so in the next chemistry, learning needs to be improved.

5. ACKNOWLEDGMENTS:

Author declare many thanks to all lecturer at Departement of Chemical Education, Semarang State University, Indonesia for the fruitful discussion to the content of the manuscript.

6. REFERENCES:

1. Agustika, G. N. S., Aryati, N. M. A. & Wiarta, I. W. *Journal of Education Research and Evaluation*, **2019**, 3(3), 147-156.
2. Astuti, E., Sri, W., Sri, K. & Kasmui. *Journal of Education and Learning*, **2019**, 13(4), 502-209.
3. Handayani, S. S. A. D. *Jurnal Ilmu-ilmu Sejarah, Sosial Budaya dan Kependidikan*, **2019**, 6(1), pp. 63-73.
4. Hsu, S. Y. & Beasley, R. E. *Australasian Journal of Educational Technology*, **2019**, 35(1), 149-162.
5. Johar, N., Ehsan, N. & Khan, M. A. *Emotional Intelligence and Academic Performance*, **2019**, 69(3), pp. 455-59.
6. Kemala, R. P. & Sukmawati, I. *Jurnal Neo Konseling*, **2019**, 1(3), 1-6.
7. Kusumaningrum, F. A. *Management Science Letters*, **2019**, 9(9), 1645-1654.
8. Lorenzo, R. D., Venturelli, G., Spiga, G. & Ferri, P. *Acta Biomed for Health Professions*, **2019**, 90(4), 32-43.
9. Mahmud, N. *et al. Journal of Physics: Conference Series*, **2018**, 1321(2), 1-7.
10. Nisa, E., Rusilowati, S. & Wardani, S. *Journal of Primary Education*, **2019**, 8(1), pp. 161-168.
11. Nurtika, E. *Jurnal Pendidikan Raudhatul Athfal*, **2019**, 2(1), 1-10.
12. Palupi, B. S., Slamet, S., Triyanto, Rukayah, *International Journal of Emerging Technologies in Learning*, **2020**, 15(1): 200-212.
13. Pertiwi, N. A. S. *Science Education Journal*, **2018**, 2(1), 37-53.
14. Pratiwi, I. K., Nur, W. K., Dama, N. & Supeno. *Jurnal Pembelajaran Fisika*, **2019**, 8(4), 269-274.
15. Prakoso, A. A. & T. *Jurnal Pendidikan untuk Semua*, **2019**, 8(2), 1-7.
16. Purwanto, T. *Jurnal Kajian Pendidikan dan Pengajaran*, **2019**, 5(2), 174-182.
17. Rusmayadi. *Early Childhood Education Journal of Indonesia*, **2019**, 2(1), 23-30.
18. Safitri, N. & Sriyanto. *Journal of*

- Humanities and Social Studies*, **2019**,3(1), pp. 1-4.
19. Sari, S. *The 1st Multi-Disciplinary International conference University Of Asahan*, **2019**, 596(508), 1004-1012.
 20. Shearer, C. *International Journal of Psychological Studies*, **2019**,11(3), 1-26.
 21. Sugiyono, 2017. *Metode Penelitian Pendidikan Pendekatan Kuantitatif, Kualitatif, dan R & D*. Bandung: Alfabeta.
 22. Suryana. *Jurnal Inspirasi*, **2019**,10(1), 78-97.
 23. Susilowati, E. & S. *Jurnal Riset Teknologi dan Inovasi Pendidikan*, **2019**, 2(1), 243-255.
 24. Suthatorn, P. & Charoensukmongkol, P., 2018. *Journal of Human Resources in Hospitality and Tourism*, **2019**,10(24), 1-22.
 25. Syarifatunnisa, S. A. *Issues in Mathematics Education*, **2019**, 3(1), 29-48.
 26. Syasmita, I., Setiawan, D. & Saragi, D. *Budapest International Research and Critics in Linguistic and Education*,**2019**,2(4), 603-615.
 27. Ulfah, M. *Jurnal Pendidikan Anak Usia Dini*, **2018**,7(7), 554-562.
 28. Utami, S. W. *Prosiding Seminar Nasional & Call Paper*, **2019**,1(1), 251-257.
 29. Wulansuci, G. L. R. H. R. *Jurnal Pengabdian Masyarakat Ilmu Keguruan dan Pendidikan*, **2019**, 2(2), 60-66.
 30. Yerizon, P. A. A. S. M. *International Electronic Journal of Mathematics Education*,**2018**,13(3), pp. 97-101.
 31. Yue, X. Y. *International Journal of Innovation Education and Research*, **2018**,7(5), 248-257.

APPENDIX 1

SHEET OF OBSERVATION OF INTERPERSONAL INTELLIGENCE OF STUDENTS

Theory:

Time:

IDENTITY

Observer Name:

Position / institution:

Instructions:

1. The researcher is requested to fill in the practicum time and observer's identity.
2. Following are some statement items to assess students' interpersonal intelligence observed when conducting discussions
3. The researcher is requested to provide an assessment by putting a checkmark (v) in the column provided following the assessment rubric.

[illegible]

APPENDIX 2

STUDENTS SELF-ASSESSMENT SHEET

Name:

Class / No:

Semester:

Hint: Put a checkmark in the score column according to the actual situation.

No.	Statement	Score			
		4	3	2	1
1	I collaborate during discussions				
2	I am responsible during discussions				
3	I listen to other people during discussions				
4	I ask questions during discussions in a class				
5	I answer questions during discussions				
6	I assist in answering questions during discussions				
Score total					

APPENDIX 3

STUDENTS PEER-ASSESSMENT SHEET

Name of friend rated:

Appraiser's name:

Class:

Semester:

Hint: Put a checkmark (✓) in the score column according to its actual whereabouts.

No.	Statement	Score			
		4	3	2	1
1	My friend works together during a discussion				
2	My friend is responsible during discussions				
3	My friend listens to other people when discussing				
4	My friend asks questions when discussing in a class				
5	My friend answers questions during the discussion				
6	My friend assists in answering questions during the discussion				
Score total					

APPENDIX 4

ASSESSMENT RUBRIC SHEET OF OBSERVATION, SELF-ASSESSMENT, AND PEER-ASSESSMENT OF INTERPERSONAL INTELLIGENCE OF STUDENTS

No.	The observed aspect	Criteria	Score
1.	Cooperation (during discussion)	Learners want to work together in solving problems in worksheet (all questions are answered)	4
		Learners want to work together in solving problems in worksheets (all questions are solved) but by managing others.	3
		Learners want to work together in solving problems in worksheet (80% of questions solved)	2
		Students do not wish to cooperate in solving problems in worksheet (50% of questions solved)	1
2.	Empathy processing during discussion (Responsible for discussion)	Learners conduct discussions per the instructions of the teacher with focus (without doing anything else).	4
		Learners conduct discussions under the instructions of the teacher while looking at the work of other groups	3
		Learners conduct analyses by the guidance of the teacher while doing other things (such as talking to different groups of friends, asking other groups about answers)	2
		Students do not conduct discussions following instructions from the teacher but do other things such as playing mobile.	1
3.	Listen to other people (during discussions in 1 class)	Students sit quietly listening and paying attention to other groups who are presenting in front of the class with focus	4
		Students sit quietly listening and paying attention to other groups who are giving in front of the class while doing other things (such as busy themselves with their work / completing assignments at worksheet)	3
		Students sit quietly listening but do not pay attention to other groups who are presenting in front of the class (such as playing cellphones, reading comics, reading novels)	2
		Students do not listen and do not pay attention to other groups who are presenting in front of the class (such as talking to friends, busy alone).	1
4.	Requests and questions (when discussing in 1 class)	Students provide questions and input/suggestions to the group presenting in front of the class	4
		Students give queries but do not offer input/advice to the group offering in front of the class	3
		Students only give input/suggestions to the group presenting in front of the class	2
		Learners do not provide questions and do not provide input/advice to the group offering in front of the class.	1
5.	Give feedback (provide answers to	Students can answer and explain answers to questions raised by other groups appropriately.	4
		Learners can answer and explain answers to questions raised by other groups but are not quite right.	3

	questions) during the discussion	Learners can answer from questions raised by other groups but cannot explain it.	2
		Learners cannot answer and explain answers to questions raised by other groups correctly.	1
6.	Empathy processing (providing help to answer questions) during discussions	Students assist with answers (additional answers as reinforcement) politely (ask permission in advance) and answers given correctly.	4
		Students provide answers to help (additional answers as reinforcement) but are less polite (do not ask permission first), and the answers are given precisely.	3
		Students provide answers (additional answers as reinforcement) but are not polite (do not ask permission first), and the answers given are not appropriate.	2
		Students do not provide help answers (additional answers as reinforcement).	1

EFICÁCIA DA APLICAÇÃO DE SAPROPEL EM DIETAS DE GANSOS

EFFECTIVENESS OF SAPROPEL APPLICATION IN DIETS OF GEESE

ЭФФЕКТИВНОСТЬ ИСПОЛЬЗОВАНИЯ САПРОПЕЛЯ В РАЦИОНАХ ГУСЕЙ

KHAZIEV, Danis^{1*}; GADIEV Rinat¹; GALINA, Chulpan²; VALITOV, Farit¹; KAZANINA, Marina¹; KOPYLOVA, Svetlana¹; IVANOV, Efim¹

¹ Federal State Budgetary Education Institution of Higher Education “Bashkir State Agrarian University”. Russia

² Bashkir Scientific Research Institute of Agriculture of the Ufa Federal Research Centre of the Russian Academy of Sciences. Russia

* Correspondence author
khazievdan11@rambler.ru

Received 10 February 2020; received in revised form 04 March 2020; accepted 22 March 2020

RESUMO

Tornou-se uma prática para as indústrias avícolas usarem diferentes substâncias biologicamente ativas, reduzindo os custos gerais para aumentar a qualidade dos produtos avícolas. Infelizmente, nem todas as substâncias biologicamente ativas são seguras e têm preços razoáveis. O uso de sapropel para compensar a falta de substâncias minerais e vitamínicas nas dietas de gansos de diferentes faixas etárias ainda não foi estudado. Neste estudo, o efeito do suplemento mineral e vitamínico sapropel nas qualidades produtivas e reprodutivas dos gansos do rebanho parental foi estudado para encontrar sua taxa ideal na dieta dos ganso. O alvo da pesquisa foram os gansos brancos húngaros no segundo ano. Os pássaros foram divididos em quatro grupos com 50 cabeças cada. A dieta de cada grupo incluiu de 3,0% a 9,0% de sapropel. Os seguintes métodos de pesquisa foram utilizados no trabalho: zootécnico, fisiológico, biológico, hematológico, morfológico, estatístico e econômico. A melhor taxa de sapropel na dieta dos gansos do rebanho parental foi de 6,0% do peso das forragens. Proporcionou uma maior taxa de sobrevivência do rebanho em 2,0%, aumento da produção de ovos em 7,5%, taxa de eclosão em 5,4%, melhor composição morfológica do sangue, digestibilidade e utilização de nutrientes da dieta. A produção de gosling de um dia aumentou 17,5%, enquanto os custos de forragem por unidade de produção diminuíram. Como resultado, os indicadores econômicos da produção de carne de ganso aumentaram 9,8%.

Palavras-chave: *rebanho criador; aditivo alimentar; substâncias minerais; produtividade; sapropel.*

ABSTRACT

It has become a practice for poultry industries to use different biologically active substances while reducing overall costs to increase poultry product quality. Unfortunately, not all the biologically active substances are safe and have reasonable prices. The use of sapropel to compensate for the lack of mineral and vitamin substances in the diets of geese of different age groups hasn't been studied yet. In this study, the effect of the mineral and vitamin supplement sapropel on the productive and reproductive qualities of geese of the parent flock was studied to find its optimal rate in the goose diet. The research target was Hungarian white geese in their second year. Birds were divided into four groups with 50 heads each. The diet of each group included from 3.0% to 9.0% sapropel. The following research methods were used in work: zootechnical, physiological, biological, hematological, morphological, statistical, and economical. The best sapropel rate in the diet of geese of the parental flock was found to be 6.0% of the fodder weight. It provided a higher survival rate of the crowd by 2.0%, increased egg production by 7.5%, hatching rate by 5.4%, improved morphological blood composition, digestibility, and diet nutrient utilization. Day-old gosling production climbed by 17.5% while fodder costs per unit of production declined. As a result, the economic indicators of goose meat production increased by 9.8%.

Keywords: *breeder flock; feed additive; mineral substances; productivity; sapropel.*

АННОТАЦИЯ

В настоящее время перед лицом растущей конкуренции на мировом рынке наиболее остро стоит

вопрос обеспечения продовольственной безопасности, где ключевую роль играет развитие аграрного сектора, в частности, птицеводства. Для повышения продуктивности и качества продукции птицы на фоне снижения общих затрат в практику промышленного птицеводства вошло использование различных по содержанию и действию биологически активных веществ, однако не все они обладают должной безопасностью и доступной стоимостью, поэтому в последнее время все больше внимания начали обращать кормовым добавкам природного происхождения, таким как бентониты и гуминовые соединения, среди них особый интерес представляет сапропель. В настоящее время не изученным является использование сапропеля для компенсации недостатка минерально-витаминных веществ в рационах гусей различных возрастных групп. Целью исследований, результаты которой представлены в этой статье, явилось изучение влияния минерально-витаминной добавки сапропель на продуктивные и воспроизводительные качества гусей родительского стада и установление оптимального уровня его включения в состав их рациона. Объектом исследования продолжительностью 130 дней выступили гуси белой венгерской породы второго года использования – четыре группы птиц по 50 голов в каждой с уровнем включения сапропеля от 3,0% до 9,0%. Методологической основой исследований послужили ранее проведенные работы зарубежных и отечественных ученых по изучаемой теме. При выполнении работы использовались общепринятые методы: эксперимент, сравнение, анализ, обобщение; специальные методы: зоотехнические, физиологические, биологические, гематологические, морфологические, статистические и экономические. По результатам исследований установлена оптимальная доза включения сапропеля в состав рациона гусей родительского стада в объеме 6,0% от массы комбикорма, что способствовало повышению сохранности поголовья на 2,0%, яйценоскости – на 7,5%, вывода гусят – на 5,4%, улучшению морфологического состава крови, переваримости и использования питательных веществ рациона, увеличению объема производства суточного молодняка на 17,5% при уменьшении удельных затрат кормов на единицу продукции, что в конечном счете, повысило экономические показатели производства мяса гусей на 9,8%.

Ключевые слова: *родительское стадо, кормовая добавка, минеральные вещества, продуктивность, сапропель*

1. INTRODUCTION:

Unlike other sectors of agriculture, poultry farming generates more and more annual output due to the growth of poultry population and a steadily improving productivity in addition to the intensification of the entire production process all around the globe (Burova *et al.*, 2019; Fisinin *et al.*, 2017; Gabitov *et al.*, 2018a, 2018b).

Fisinin *et al.* (2017) argue that higher production of eggs and poultry meat would ensure food independence and address the social issue of the availability of animal source proteins for all social strata.

Goose production is a branch of poultry farming that is prominent in terms of precociality, feed conversion, viability, and fattening capacity. The primary challenge it faces today, as well as the entire poultry industry, is to reduce production costs and increase productivity by providing a more comprehensive and useful use of essential nutrients in feed material (Gadiev *et al.*, 2019).

With a shift to high technologies in goose breeding, geese are deprived of replenishing natural biologically active substances, macronutrients, and micronutrients. It makes it necessary to balance poultry diets by adding vitamin and mineral supplements or manufactured premixes, which affects the cost of feed and,

consequently, the finished product (Prasai *et al.*, 2016). There is a clear need for inexpensive and easy-to-use alternative sources of biologically active substances.

Sapropels are a good source of diet replenishment with the necessary nutrients for growing geese (Rumyantsev *et al.*, 2017; Shtin, 2005). Sapropels and their products are environmentally friendly, non-toxic, and contain essential nutrients (Stankevica *et al.*, 2016).

Sapropels (gyttja or dy) are centuries-old freshwater sediments, which contain up to 15% of organic substances (Kurzo *et al.*, 2004; Obuka *et al.*, 2015) and are formed of benthos, i.e., remnant phytoplankton and zooplankton, and fractions of soil humus (Kurzo, 2005; Rutina *et al.*, 2013; Vincevica-Gaile and Stankevica, 2018). Sapropels can only develop in stagnant fresh waters, at bottoms of stagnant lakes with reduced oxygen availability (Lacis, 2003; Obuka *et al.*, 2015).

According to Obuka *et al.* (2015) and Rumyantsev *et al.* (2017), sapropels or lake muck consists of detritus material, different kinds of plankton, insect chitin, and higher plant spores found in lake environments. The sapropel color vary from light pink to dark brown depending on the maximum content of certain substances. A high natural content of phosphorus makes it dark blue that turns light blue after drying. Sapropels

can be found in shallow overgrown post-glacial lakes and vast river valleys while they are quite rare in permafrost meltwater reservoirs, mountainous areas, and drylands.

Sapropels are widely used throughout the world that makes them an essential natural resource. Lake muck is applied in agriculture, horticulture, forestry, animal husbandry, chemical and construction industries, spa services sector, production of beauty products, and coagulants (Stankevica and Klavins, 2013).

The widespread use of sapropels allows them to be used as a national strategic natural resource. In contrast, processed products of sapropels may be exported worldwide as fertilizers, feed additives, raw materials for chemistry and construction, medicinal clay, etc.

Sapropels are considered to be a kind of geological formations that occur at the bottom of a reservoir during the entire period of its existence. However, according to Leinerte (1988), the development of sapropels strongly depends on the lake type; their deposition can occur with substances in high energy environments, which is widely observed in autotrophic lakes.

Stankevica and Klavins (2013) and Stankevica *et al.* (2016) distinguish between autochthonous sapropels accumulated due to the lake biomass deposits and allochthonous ones, where sediments include a large amount of humic substances, which enter the lake from the surrounding areas and marshes. Autochthonous sapropels with maximum organic matter content are thought to be more valuable because the initial biomass, its biochemical degradation and conversion into organic substances do not create polycyclic aromatic hydrocarbons, such as benzo(a)pyrene, which is characteristic of soil, peat and, particularly, coal humic substances.

The global scientific community proposes multiple classifications of sapropels, depending on their composition. For example, Potenje (1920) identified two groups of sapropels, such as "sapropels" being thick fine-grained sediments containing 25% to 90% of organic matter and mineral deposits, and "sapropelites" consisting of diatomaceous earth, lime, iron, and sands.

Pidoplizko and Grisuk (1962) classify lacustrine sediments into the seven types as listed below:

- pastelike, heavy, gray, or bluish-gray, clayey gyttja with high mineral levels, usually deposited in lakes naturally;
- calcareous sapropels with an ash content

of more than 35% (including 50% to 65% of CaO), found in groundwater discharge areas with high calcium concentrations; they are greenish-gray and usually form grayish-white incoherent mixture after drying;

- grained green or greenish-gray silicate sapropels with a higher ash content of more than 30%;

– mixed sapropels with the most top ash content (about 70% – 80%), which can contain large amounts of calcium and silicates, clay fractions and calcium; these mixed lacustrine sediments are formed of planktonic organisms and may be grayish, dark-green, blue-green, or grayish-brown;

– organic sapropels (fine detritus gyttja) with a low ash content no more than 30%. They are green, or greenish-brown, if they contain some hummus, and occur in water bodies lacking ample mineral matter supplies;

– coarse detritus gyttja with a low ash content, accumulated in lakes with plenty of aquatic plants in addition to plankton organisms; it is usually dark green with potential traces of higher aquatic plants;

– peat sapropels occurring when peat deposits come into contact with the lake, or as a result of overgrowing of autotrophic coastal water bodies; peat sapropels are brown transitional formations between sapropels and peats with residual material from bulrush, sedge grasses, horsetail and other plants, characterized by a very low ash content (8–10%) and a high level of decomposition (about 25–30%).

For years, sapropels have been deposited at bottoms of freshwater ponds and accumulated great amounts of different organic, mineral and biologically active substances. In terms of their composition, sapropels are a unique product containing proteins (up to 23%), minerals (calcium and phosphorous), trace elements (iron, manganese, magnesium, copper, sulfur, cobalt, etc.), vitamins, and humic compounds.

Quisenberry (1968) and Rumyantsev *et al.* (2017) find sapropels to be a functional feed additive for agricultural animals and poultry because of the high content of different macro- and trace elements.

As a substrate rich in minerals and vitamins, sapropels can be considered a good vitamin and mineral feed for poultry. Indeed, experiments conducted to add sapropels to poultry diets showed a significant increase in body weight, egg size, and life expectancy (Stankevica *et al.*,

2019).

Lake muck has been found to be an active feed additive in animal husbandry. However, there is still not enough knowledge of what effect sapropels can have on productive and reproductive characteristics of geese in different age and sex groups.

Based on the above, the aim of the given paper was to study the effect of the mineral and vitamin supplement sapropel on the productive and reproductive qualities of geese of the parent flock and to find its optimal rate in the goose diet.

2. MATERIALS AND METHODS:

2.1. Object and materials of study

Studies have been carried out on Hungarian white geese grown for two years at Bashkirska ptitsa, Limited Liability Company of Blagovarsky District, Republic of Bashkortostan. The study was conducted in accordance with the ethical principles approved by the Animal Experiments Ethics Committee of Federal State Budget Educational Institution of Higher Education «Bashkir State Agrarian University» (Protocol №5 of 14th December 2018).

Healthy poultry were collected for studies, based on their age, sex, fertility, body weight, and condition. Geese of parent flock were divided by analogy into one control and three experimental groups. Each group included 50 birds with one gander per 3 hens, this is the minimum number of birds to obtain reliable data. Geese of the control group were given complete feed without sapropel. The feed of experimental groups 1, 2, and 3 was supplemented with sapropel in the dose of 3.0, 6.0, and 9.0% of feed mass, respectively. The study lasted 130 days.

2.2. Conditions of the study

Geese of the control and experimental groups had identical feeding conditions and were raised according to the recommendations of the All-Russian Research and Technological Poultry Institute (Sergiyev Posad) except for the study factor. Poultry were kept in solar houses with deep-litter unchangeable nests. Nest cushions were filled with chaff.

2.3. Methods of study

The study was performed under standard methods, such as experiment, comparison, analysis, synthesis, and special ones:

zootechnical, physiological, biological, hematological, morphological, statistical, and economical.

The survival rate (%) was analyzed by day-to-day control of dead and cull birds with the determination of mortality reasons; body weight (g) by monthly weighing during the laying period; egg-laying capacity of average bird by dividing the amount of laid eggs in a group for a specific time by an average goose stock for the same period of time; morphological and physical-chemical indicators of eggs were assessed under methodological recommendations of the All-Russian Research and Technological Poultry Institute (ARRTPI); results of hatching were studied according to manual for biological control of poultry eggs hatching (ARRTPI, 2014); egg embryonation (%) – ratio of embryonated eggs to hatching eggs; hatched birds (%) – ratio of hatched certified birds to hatching eggs; content of carotenoid and vitamins in the yolk – by using standard methods of Skurikhin and Shabaev (1996). The morphological composition of blood was analyzed by conventional methods of Sukhanova and Azaubayeva (2017), digestibility and feed nutrient utilization (%) by conducting digestible trials following ARRTPI methodology. Laboratory tests were performed in analytic laboratories of Bashkir State Agrarian University and Bashkir Research Institute of Agriculture.

A cost-effectiveness analysis of sapropel application in goose farming was based on the results of research and production studies, actual prices for the period of studies.

2.4. Data analysis

The data under research, received during the studies, have been processed using a variation statistics method on a PC using Microsoft Excel software. Statistical significance of differences was calculated using Student's t-test with three confidence levels: $p < 0.05$; $p < 0.01$; $p < 0.001$.

3. RESULTS AND DISCUSSION:

One of the factors determining the poultry's genetically determined productivity is the usefulness of feeding. Numerous studies have proved that including various feed additives and biologically active substances in diets favorably affects the poultry productivity and poultry product quality, helps to enhance the body's resistance to adverse environmental factors.

According to many authors, sapropel is a good source of diet enrichment with the necessary

components for breeding and keeping poultry (Rumyantsev *et al.*, 2017; Shtin, 2005). As a substrate rich in minerals and vitamins, sapropel is an environmentally friendly mineral-and-vitamin feed for poultry (Stankevica *et al.*, 2016).

The data received in this paper shows the results of a comprehensive scientific analysis of the effects of sapropel in a dose of 3.0, 6.0, and 9.0% of the feed weight on reproductive and productive qualities of the parent flock geese. The methodological basis for the study was previous works by foreign and domestic researchers on this topic.

Sapropel in mixed feed of the goose parent flock in the amount of 6.0% per the combined feed weight has been found to raise the survival rate of poultry by 2.0% ($p < 0.05$), which is equal to 96%. Bailey *et al.* (2006) also found in their studies that the use of montmorillonite clay as NovaSil PLUS additive allowed protecting broiler chickens from aflatoxicosis and increasing the livestock preservation.

When keeping geese of experimental groups, no adverse effect of sapropel on the goose live weight parameters has been recorded. However, at the end of the productive period, a slight decrease in live weight was observed in all groups, both in males and females. A relatively higher reduction of live weight was observed in females of the 2nd experimental group in June (by 1.3%) at the confidence level of $p < 0.05$, due to high rates of their egg production. This phenomenon indicates a correlation between the live weight and egg productivity.

The results of the research by Mikulioniene and Balezientiene (2012) also show that the use of sapropel as a feed additive had a positive effect on the live weight, the digestive tract development, the digestibility of nutrients, and the quality of gosling and duckling meat. Thus, the ducklings' diet added with 6% of sapropel and the goslings' food without the same (the control group, CG) provided for the most effective feed conversion (3.62 and 3.83, respectively). The diet based on feed added with 9% of sapropel ensured the most significant body weight: 1.931 g and 2.704 g for ducklings aged 40 and 50 days; 1.766 g and 3.772 g for goslings aged 20 and 60 days, respectively. Adding sapropel increased the body weight by 9% in 50-day ducklings and 60-day goslings by 5% and 9%, respectively. The ducklings' diet added with 9% of sapropel improved the feed digestibility along with the highest meat output (66.7%), increasing the CG weight by 1.6%. Also, there was an increased content of fat and duck meat fat by

1.7% and 1.1%, respectively. However, the gosling meat quality parameters were better in the CG than in the 4th experimental group added with 9% of sapropel; it was probably due to their higher body weight and nutritional needs, as compared to ducklings. Besides, the presence of essential amino acids in sapropel is confirmed in the amount of 47% to 60% of their total number. The availability of a large number of nutrients allows for the use of sapropel as a natural, environmentally friendly mineral-and-vitamin feed supplement of natural origin.

Bayurov (2018), in his research, established the beneficial effects of liquid sapropel extract (ES-2) on broiler chickens. According to this author, adding sapropel in the poultry diet increased the chicken growth rate, enhanced the body resistance, and livestock preservation.

Researchers Ezhkova *et al.* (2018) also found the positive effect of sapropel on broiler chicken's body. Thus, for their study, they formed seven groups of 10-day chickens, 120 birds in each. The birds in the control group I received complete mixed feed (OP). The birds in the experimental group II received OP + feed sapropel at the dose of 3.0% to the dry matter of the diet. The birds in the experimental groups III, IV, V, VI, and VII, received 3.0; 2.4; 1.8; 1.2, and 0.6% of nanostructured sapropel added to their diet, respectively. The additive was given for 30 days – until the technological slaughter of chickens for meat. According to the research results, it was found that the relative increase in the poultry weight was more considerable in the experimental groups than in the control group (2,190.0 g) by 1.1...8.2%; the weight of the whole bird without giblets, by 14.5...175.1 g. The slaughter yield of experimental broilers was 1.7...2.1% higher than in the control group (70.5%), except for the group III, where it was 0.5% lower. The meat of experimental broilers had an increased content of essential amino acids by 1.7...8.7%, nonessential amino acids, by 2.4...12.5%, with the same values in the control group equal to 27.68 and 31.67 g/kg, respectively. The ratio of essential and non-essential amino acids in the poultry meat of the experimental groups was 1.15...1.18; in the control group, 1.14; the protein quality indicator was 4.56...4.64; in the control group, 4.51, respectively. The economic efficiency per 1 ruble of costs amounted to when using sapropel in the dose of 3.0% – 2.1 rubles, nanostructured sapropel in the treatments of 3.0; 2.8; 1.8; 1.2 and 0.6% – 1.1; 2.4; 3.5; 3.8, and 4.2 rubles, respectively (Ezhkova *et al.*, 2018).

The impact of sapropel on body weight was

also studied in pigs on feed. Thus, according to Mikulionienė and Baležentienė (2009) addition of 200-400 g of sapropel in the diet (treatment group) allowed increasing the total body weight of pigs by 12% and decreasing their food consumption by 12% compared to pigs of the control group.

There is a positive effect of sapropel on the egg productivity and the goose hatching eggs quality. The data on the egg-laying capacity by months are shown in Figure 1. As follows from Figure 1, adding sapropel in the feed for parent flock poultry had a positive effect on poultry egg productivity in all experimental groups in the first month of use compared to their peers in the control group. In the first month of egg-laying (February) noted an increase in egg-laying by 15.2–24.2% ($p < 0.001$) among poultry in the experimental groups, where the birds received mixed feed added with sapropel within the range of 3% to 9%, as compared to the control group.

The total goose egg productivity in the experimental groups met the breed standard, and, based on the productivity records, it was within the range of 49.2 to 51.6 pcs. It should be noted that increasing the content of sapropel added up to 9% (the 3rd experimental group) did not contribute to further increase in poultry production and, to some extent, it resulted in its decrease. Goose egg production in the 3rd experimental group decreased during the last two months of productivity, as compared to peers in the control group, by 4.2 ($p < 0.05$) and 9.5% ($p < 0.01$), respectively. When adding sapropel in the amount of 6% of the combined feed weight (the 2nd experimental group), goose egg productivity per average layer was, in general, 51.6 pcs., which is higher by 3.6 pcs. Or 7.5% ($p < 0.01$), as compared to the control group.

The hatching process effectiveness is greatly affected by the morphological composition of eggs and their biological value; therefore, the assessment was made according to these criteria. As it was expected, adding sapropel to the poultry's diet had no significant effect on the main morphological parameters of eggs. However, there was a slight increase of the egg weight in the experimental groups by 0.96–1.12%, due to higher specific weight of the yolk by 1.83 – 2.48% and that of the shell by 4.45–5.38%.

When assessing the biological value of hatching eggs, adding sapropel into the goose mixed feed in the amount of 6.0% of its weight confidently increased the content in vitamin A in eggs by 8.5% ($p < 0.01$); vitamin B2, by 6.3% ($p < 0.01$), and carotenoids, by 11.9% ($p < 0.01$),

which indicates the advisability of using sapropel in this dose.

Producing sound and high-quality hatching eggs is an essential factor in goose breeding. Accounting of the hatching egg production showed that its highest level was recorded in the 2nd experimental group; the difference with the control group was 2.0% ($p < 0.05$). For the first and third experimental groups, it was 0.2% and 0.7%, in favor of the experimental groups.

The use of sapropel positively affected the egg fertilization, which increased to 4.8% ($p < 0.01$) in the second experimental group, and by 1.1% and 1.9% ($p < 0.05$) in the first and third experimental groups, respectively. This fact confirms the favorable effect of sapropel on the egg-laying capacity. In turn, better egg-laying capacity favorably affected the hatching results. Thus, goslings output increased in the experimental groups by 0.38–5.43% ($p < 0.05$), and hatchability, by 1.49–1.91%. The best hatching results were recorded in the 2nd experimental group, where the content of the sapropel added was 6% of the mixed feed weight. Along with sapropel, the researchers' attention has long been attracted by such natural clay minerals as bentonite and kaolinite due to their environmental friendliness and low cost (Adamis *et al.*, 2005; Almquist *et al.*, 1967; Erwin *et al.*, 1957).

Experiments held on hens, when adding bentonite and kaolinite into their diet, showed that poultry significantly increased their body weight, egg size, and lifetime. However, they consumed fewer calories than in the control group (Quisenberry, 1968). At the same time, the use of kaolin increased the feed caloric value even slightly better than bentonite; however, without a visible effect on the growth and the carcass quality. Effective kaolins are estimated at two calories of metabolizable energy per gram. However, according to the above author, the main positive effect is probably due to a decreased rate of feed passage through the bird's intestinal tract.

Researchers Pasha *et al.* (2008) also determined the effect of diets containing various doses of sodium bentonite on broiler chickens' productivity. Their study involved 280 one-day chickens, which were randomly divided into 7 experimental groups: A (control); B, and C (0.5% and 1.0% of sodium bentonite, respectively); D and E (0.5% and 1.0% of sodium bentonite + 0.5% and 1.0% of gentian (respectively); F and G (0.5% and 1.0% of sodium bentonite + 0.5% and 1.0% of acetic acid, respectively). According to the research results, it was found that birds who

received the diet with sodium bentonite treated with 0.5% or 1.0% acetic acid significantly increased their live weight gain ($P < 0.05$), reduced feed consumption per unit of product, and increased the protein digestibility ratio, as compared to the control and other experimental groups.

As known, feed is a significant part of the total cost of growing and keeping poultry, which accounts on average for more than 70% of all costs and, accordingly, the feed utilization by the poultry body affects the entire production performance. Accounting of the feed costs per unit of products showed that the poultry in the 1st and 2nd experimental groups consumed 0.4–1.6 kg or 2.5–10.1% less feed ($p < 0.05$) to produce ten eggs. The use of feed components was determined based on the digestibility and utilization of feed nutrients by carrying out balance experiments. Based on the data obtained, it should be noted that the use of sapropel as a feed additive in the goose diet increased the digestibility and utilization of the primary feed nutrients (Table 1).

The use of sapropel as a feed additive in the goose diet has been found to increase the digestibility and utilization of the main feed nutrients. Thus, the digestibility of protein increased by 0.4–4.9% ($p < 0.001$), fat, by 0.2–1.6% ($p < 0.01$), and fiber, by 0.4–2.6% ($p < 0.01$). In terms of nitrogen, calcium, and phosphorus utilization, we noted the same tendency in the experimental groups. Thus, adding sapropel in the goose diet increased the use of nitrogen to 6.2% ($p < 0.001$), calcium, to 8.7% ($p < 0.001$), and phosphorus, to 1.6% ($p < 0.05$).

Among the experimental groups, the best results in terms of digestibility and utilization of feed components were that of geese in the 2nd experimental group, where the level of sapropel added was 6.0% of the mixed feed weight. It should be noted that increasing the level of sapropel added to 9.0% of the mixed feed weight did not provide any further improvement in the utilization of feed components.

Gous (2010) also stated the opportunities to improve the use of feed nutrients. Thus, according to this researcher, over the past 50 years, genetics has shown success in improving potential bird growth indicators, and, probably, further genetic progress is possible in the future. However, to maximize the potential growth of fast-growing crosses, nutritionists will need to change their feeding method. It is assumed that, with some manipulation of the nutrient content in the feed, nutritionists will be able to support these genetic

changes. In the future, feed restrictions may occur immediately after hatching, when the intestinal volume does not allow consuming a sufficient amount of the usual starting feed, but so that a chicken could fully grow, revealing its full potential.

Blood, ensuring the constancy of the body's internal environment and the connection between its parts, plays an essential role in metabolism. The general health status of a bird can be assessed through blood counts. Therefore, we studied the morphological composition of the goose blood when consuming mixed feeds with different levels of sapropel, the results of which are presented in Table 2.

It was demonstrated that goose hematological parameters in all groups were within the physiological standards and corresponded to clinically healthy poultry. At the same time, these parameters were slightly higher in the experimental groups than in the control group, which indicates a positive effect of sapropel on hematopoiesis in their body. Thus, the level of hemoglobin in the goose blood in the experimental groups increased by 2.9–9.1% ($p < 0.05$); the number of red blood cells increased by 0.7–1.7%; white blood cells, by 1.9–6.3%, as compared to the control group, whereas the best indicators were recorded in the experimental group -2, making 132.2 g/L, $3.01 \times 10^{12}/L$, and $25.84 \times 10^9/L$, respectively. Therefore, the use of sapropel-enriched diets increased the level of hemoglobin and blood cells, which, in turn, has a favorable effect on the redox processes in the goose body.

The positive effect of sapropel on the poultry body was revealed in the research by other authors. Thus, Losyakova *et al.* (2018) studied slaughter indicators of Ross 308 cross broiler chickens, whose diet included sapropel-based feed additives. The control broiler chickens received mixed feed without additives; the 2nd group, mixed feed with the addition of 1% (by weight) sapropel extract into drinking water; the 3rd and 4th groups, mixed feed partially replaced (by weight) with the studied additives: poultry in the 3rd group received 2.5% of frozen sapropel; the 4th group, 10% of additional green feed with sapropel mass. The study lasted 56 days. The most regular results were obtained in young hens, where broiler chickens in the experimental groups exceeded the control group by all studied slaughter indicators. Among the chickens of the experimental groups, the advantage was observed in the 3rd group. With no differentiation by gender, poultry in the experimental groups exceeded the control group by such valuable indicators as the weight of the pectoral and

femoral muscles, the weight of the heart, and gizzard stomach.

Along with using sapropel as a feed additive for farm animals and poultry, it is added to finished products to increase their nutritional value. Thus, Gorelik *et al.* (2017) studied the chemical and mineral composition of a new fermented-milk biological product with sapropel powder. They added sapropel in the form of powder to the fermented milk formulation in the amount of 1.5% of the total weight. According to the results of their investigation, the researchers found that the protein content in the new fermented-milk biological product was significantly higher (20.95%) than in the control sample (18.40%) with a decrease in moisture content to 76.0–76.3% against 79.50% in the control group. At the same time, the nutritional value of the final product increased to 15.3 kcal or 16.4% due to the high protein and fat content (Gorelik *et al.*, 2017, Chernitskiy *et al.*, 2019).

A high ability of sapropel to biogenic stimulation and its protective properties was indicated. Thus, Kurzo (2005) and Makarov *et al.* (2017) argue that the use of sapropel promotes tissue repair processes; it has an anti-inflammatory effect in case of burns and corneal diseases, stimulates respiration, and inhibits free radical activity. Therefore, sapropel preparations as biological stimulants are becoming perspective in different branches of the economy, including healthcare, agriculture, and veterinary medicine (Stankevica *et al.*, 2019, Vorobyev *et al.*, 2019).

Along with assessing the sapropel effects on the manifestation of economically useful traits and biological parameters in the parent flock of geese, it is also important to evaluate its economic efficiency in this age and gender group. For this purpose, an industrial validation of the sapropel effectiveness in the parent flock diets of Hungarian white geese was conducted on the premises of the Bashkirskaya Ptitsa, LLC, located in the Blagovar District, the Republic of Bashkortostan. The results are presented in Table 3.

The study was conducted on two groups of geese with different types of feeding. There were 1,000 birds in each group with 3 hens per 1 male. Geese of the first group received mixed feed without sapropel; birds in the second group got feed with sapropel in the amount of 6.0% of the feed weight. The poultry of both studied groups had the same keeping and feeding conditions consistent with the recommendations of the All-Russian Research and Technological Institute of Poultry Breeding (Sergiev Posad), except for the

studied factor.

The results of the industrial validation confirmed the positive effect of sapropel on the reproductive qualities of the goose parent flock. Thus, geese fed with sapropel showed a higher egg productivity per average layer, i.e., 49.1 eggs, which is higher by 7.2% ($p < 0.01$) compared to the group that did not receive sapropel. This has resulted in higher gross egg production and the total yield of hatching eggs by 9.8% ($p < 0.01$) and 2.3% ($p < 0.05$), respectively. Better productive parameters, that increased the number of standard-quality goslings by 3,850 birds or 17.46% ($p < 0.01$), had a positive impact on the economic indicators of geese raising. Thus, the cost of one-day goslings reduced by 7.1%; the revenue and profit from their selling increased by 17.5% and 153,439.3 rubles, respectively, whereas the sector's profitability grew by 9.8%.

4. CONCLUSIONS:

The results of the conducted research prove that adding sapropel in the diet of the parent flock of geese promoted a complete satisfaction of the body's needs for nutrients and improved metabolic processes, as evidenced by the poultry's highly productive and reproductive qualities. The optimal rate of sapropel in the goose diet was found to be 6.0% of the mixed feed weight. It enhances a survival rate of poultry by 2.0%, egg production by 7.5%, the number of goslings hatched by 5.4%, improved the morphological composition of blood and the diet nutrients utilization. The production rate of one-day goslings was found to be higher by 17.5% while reducing the cost of feed per unit of products. This ultimately increased the sector's profitability by 9.8%.

5. REFERENCES:

1. Adamis, Z., Fodor, J., Williams, R. B. *Bentonite, Kaolin, and Selected Clay Minerals*, World Health Organization: Geneva, **2005**.
2. Almquist, H. J., Christensen, H. L., Maurer, S. **1967**, 39(20), 54.
3. Bailey, C. A., Latimer, G. W., Barr, A. C., Wigle, W. L., Haq, A. U., Balthrop, J. E., Kubena, L. F. *JAPR Research Report*, **2006**, 15(2), 198.
4. Bayurov, L. I. *Poultry*, **2018**, 11–12, 29.
5. Burova, D., Akopyan, A., Roiter, L. *IOP Conference Series: Earth and Environmental Science*, **2019**, 274, 1.

6. Erwin, E. S., Elam, C. J., Dyer, A. *Journal of Animal Science*, **1957**, 16(4), 858.
7. Ezhkova, A. M., Yapparov, I. A., Ezhkov, V. O., Yapparov, A. Kh., Fayzrakhmanov, R. N. *Achievements of science and technology of the agro-industrial complex*, **2018**, 7(32), 59.
8. Fisinin, V. I., Roiter, Ya. S., Roiter, L. M., Akopyan, A. G. *Poultry and Poultry Products*, **2017**, 2, 67.
9. Gabitov, I., Mudarisov, S., Gafurov, I., Ableeva, A., Negovora, A., Davletshin, M., Rakhimov, Z., Khamaletdinov, R., Martynov, V., Yukhin, G. *Journal of Engineering and Applied Sciences*, **2018a**, 13, 8338.
10. Gabitov, I. I., Saifullin, R. N., Farhshatov, M. N., Negovora, A. V., Mudarisov, S. G., Khasanov, E. R., Galiullin, R. R., Gabdrafiqov, F. Z., Yunusbaev, N. M., Valiev, A. R. *Journal of Engineering and Applied Sciences*, **2018b**, 13, 6478.
11. Gadiev, R. R., Khaziev, D. D., Galina, Ch. R., Farrakhov, A. R., Farhutdinov, K. D., Dolmatova, I. Y., Kazanina, M. A., Latypova, G. F. *AIMS Agriculture and Food*, **2019**, 4(2), 349.
12. Gorelik, O. V., Shatskikh, E. V., Rebezov, M. B., Kanareikina, S. G., Kanareikin, V. I., Likhodeevskaya, O. E., Andrushechkina, N., Kharlap, S. Yu., Temerbayeva, M., Dolmatova, I. A., Okuskhanova, E. K. *Annual Research & Review in Biology*, **2017**, 4, 1.
13. Gous, R. M. *Livestock Science*, **2010**, 130(1), 25.
14. Kurzo, B., Hajdukiewicz, K., Krasnoborskaya, O. *Limnological Review*, **2004**, 4, 125.
15. Kurzo, B. V. *Regularity of Development and Problems in Using Sapropel*, Belarusian Science: Minsk, 2005.
16. Lacis, A. *Thesis of the 61st Conference of University of Latvia*, LU, Riga, 2003.
17. Leinerte, M. *The lakes are burning!* Zinatne: Riga, 1988.
18. Losyakova, E. V., Arzhankova, Yu. V., Nikolaeva, S. Yu. *Bulletin of the Ulyanovsk State Agricultural Academy*, **2018**, 3(43), 151.
19. Makarov, S. V., Nikolaev, I. A., Maksimyuk, N. N. *Young Scientist*, **2017**, 20, 170.
20. Mikulioniene, S., Balezentiene, L. *Veterinary and Zootechnics*, **2009**, 48(70), 37.
21. Mikulioniene, S., Balezentiene, L. *Veterinary and Zootechnics*, **2012**, 60(82), 45.
22. Obuka, V., Sinka, M., Klavins, M., Stankevica, K., Korjamins, A. *IOP Conference Series: Materials Science and Engineering*, **2015**, 96, 1.
23. Pasha, T. N., Mahmood, A., Khattak, F. M., Jabbar, T. M. A., Khan, A. D. *The Turkish Journal of Veterinary and Animal Sciences*, **2008**, 32(4), 245.
24. Pidoplizko, A. P., Grisuk, R. I. *Chemistry and Genesis of Peat and Sapropel*, **1962**, 1, 258.
25. Potenje, G. *Sapropelites*, Oil and Shale Farm: Petrograd, 1920.
26. Prasai, T. P., Walsh, K. B., Bhattarai, S. P., Midmore, D. J., Van, T. T., Moore, R. J., Stanley, D. *PLoS One*, **2016**, 11(4), e0154061.
27. Quisenberry, J. H. *Clays and Clay Minerals*, **1968**, 16, 267.
28. Rumyantsev, V. A., Mityukov, A. S., Kryukov, L. N., Yaroshevich, G. S. *Doklady Earth Sciences*, **2017**, 473(2), 482.
29. Rutina, L., Stankevica, K., Klavins, M. *71th Scientific Conference of University of Latvia*, Riga, University of Latvia, 2013.
30. Shtin, S. M. *Lake Sapropelites and their Complete Exploitation*, Moscow State Mining University: Moscow, 2005.
31. Skurikhin, V. N., Shabaev, S. V. *Methods for analysis of vitamins A, E, D and carotene in the feed, biological objects and animal products*, Right ed., Chemistry: Moscow, 1996.
32. Stankevica, K., Klavins, M. *Material Science and Applied Chemistry*, **2013**, 29, 109.
33. Stankevica, K., Vincevica-Gaile, Z., Klavins, M. *Agronomy Research*, **2016**, 14(3), 929.
34. Stankevica, K., Vincevica-Gaile, Z., Klavins, M. *Agronomy Research*, **2019**, 17(3), 850.
35. Sukhanova, S. F., Azaubayeva, G. S. *Bulletin of Poltava State Agrarian Academy*, **2017**, 1–2, 63.
36. Vincevica-Gaile, Z., Stankevica, K. *Environmental Geochemistry and Health*, **2018**, 40, 1725.
37. Chernitskiy, A., Shabunin, S., Kuchmenko, T., Safonov, V. *Turkish Journal of Veterinary and Animal Sciences*, **2019** 43(6), 707.
38. Vorobyev, V. I., Vorobyev, D. V., Zakharkina, N. I., Polkovnichenko, A. P., Safonov, V. A. *Asia Life Sciences*, **2019**, 28(1), 99.

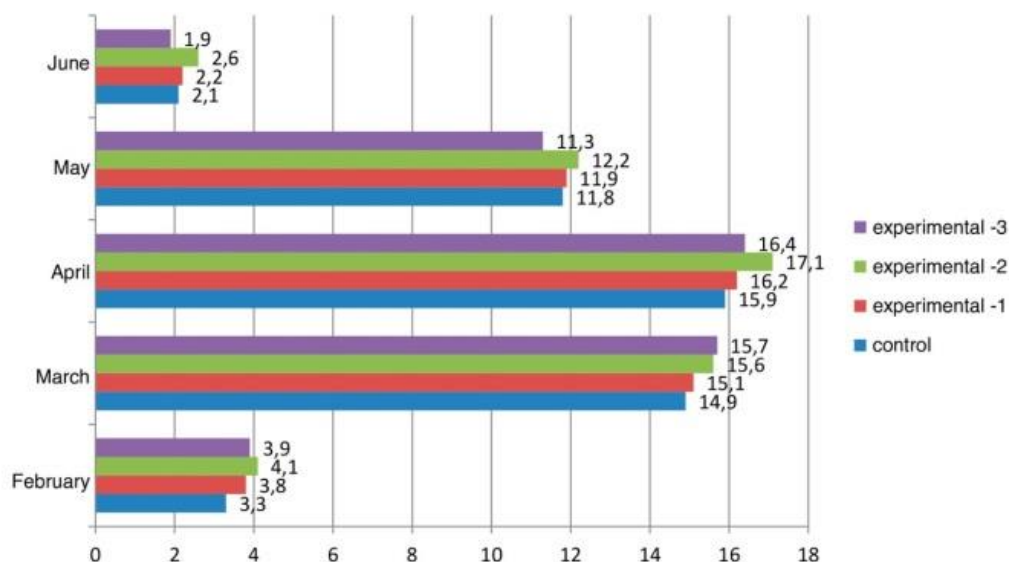


Figure 1. Goose egg productivity per average layer, pcs.

Table 1. Generalized utilization indicators of the mixed feed nutrients

Group	Digestibility, %				Utilization, %	
	protein	fat	fiber	nitrogen	calcium	phosphorus
control	78.3±0.38	55.8±0.18	53.1±0.16	46.9±0.41	41.6±0.52	38.3±0.18
experimental -1	78.6±0.42	55.9±0.19	53.3±0.23	47.2±0.35	42.3±0.19	38.4±0.15
experimental -2	82.1±0.46***	56.7±0.21**	54.5±0.26**	49.8±0.39***	45.2±0.47***	38.9±0.13*
experimental -3	79.7±0.48*	56.1±0.08	53.7±0.24	48.3±0.46*	42.8±0.38	38.6±0.12

Confident differences with control: * – $p < 0.05$; ** – $p < 0.01$; *** – $p < 0.001$

Table 2. Morphological composition of goose blood at the peak of productivity (in April)

Group	Hemoglobin, g/L	Red blood cells, $\times 10^{12}/L$	White blood cells, $\times 10^9/L$
Control	121.2±1.39	2.96±0.19	24.31±1.98
Experimental -1	124.8±1.31	2.98±0.21	24.79±2.06
Experimental -2	132.2±1.44*	3.01±0.26	25.84±2.11
Experimental -3	128.6±1.34*	2.98±0.24	25.81±2.04

* – $p < 0.05$

Table 3. Results of the industrial use of sapropel in the husbandry of the parent flock geese

Indicator	Diet type	
	Basic diet without sapropel	Basic diet added with sapropel in the amount of 6.0% by weight of feed
Total goose stock, birds.	1,000	1,000
including females, birds	750	750
males, birds	250	250
Egg production by average layer, pieces	45.8±0.56	49.1±0.53***
Gross egg production – total, pieces	32,564	35,757
Hatching egg output, %	94.8	97.1
Goslings hatched, %	67.71	72.43
Number of one-day goslings, birds	22,049	25,899
Feed consumption – total, kg	81,121	83,903
Feed cost – total, rubles	42,1829.2	43,6295.6
Sapropel cost, rubles	0	5,191.68
Cost of a one-day gosling, rubles	51.7	48.0
Egg production cost – total, rubles	1,138,938.8	1,243,442.5
Revenue – total, rubles	1,477,280.0	1,735,223.0
Profit, rubles	338,341.2	491,780.5
Profitability, %	29.7	39.5

*** – $p < 0.001$

MODELO ESTRUTURAL E FUNCIONAL DA METODOLOGIA DE PREPARAÇÃO DE PROFESSORES DE QUÍMICA PARA A APLICAÇÃO DE TECNOLOGIAS DE NUVEM NA ATIVIDADE PROFISSIONAL**STRUCTURAL AND FUNCTIONAL MODEL OF THE METHODOLOGY FOR PREPARING FUTURE CHEMISTRY TEACHERS FOR THE USE OF CLOUD TECHNOLOGIES IN PROFESSIONAL ACTIVITIES****СТРУКТУРНО-ФУНКЦИОНАЛЬНАЯ МОДЕЛЬ МЕТОДИКИ ПОДГОТОВКИ БУДУЩИХ УЧИТЕЛЕЙ ХИМИИ К ПРИМЕНЕНИЮ ОБЛАЧНЫХ ТЕХНОЛОГИЙ В ПРОФЕССИОНАЛЬНОЙ ДЕЯТЕЛЬНОСТИ**

SHYIAN, Nadiia I.^{1*}; KRYVORUCHKO, Alina V.²; STRYZHAK, Svitlana V.³; KRYKUNOVA, Valentyna Ye.⁴; ANTONETS, Oleksandr A.⁵

^{1, 2, 3} Poltava V.G. Korolenko National Pedagogical University, Department of Chemistry and Methods of Teaching Chemistry, 2 Ostrogradski Str., zip code 36000, Poltava – Ukraine

⁴ Poltava State Agrarian Academy, Department of Biotechnology and Chemistry, 1/3 Skovorody Str., zip code 36000, Poltava – Ukraine

⁵ Poltava State Agrarian Academy, Department of Plant Production, 1/3 Skovorody Str., zip code 36000, Poltava – Ukraine

* Correspondence author
e-mail: chemisnada@gmail.com

Received 21 December 2019; received in revised form 16 March 2020; accepted 29 March 2020

RESUMO

A relevância do estudo deve-se às especificidades de percepção e assimilação de informações pelas crianças em idade escolar (a propensão da geração jovem ao pensamento de clipe) e a um número insuficiente de estudos que revelam as características teóricas e processuais da formação da preparação dos professores de química para usar tecnologias de nuvem em atividades profissionais. O objetivo do artigo é desenvolver um modelo estrutural e funcional da metodologia para preparar futuros professores de química para o uso de tecnologias de nuvem nas atividades profissionais e em seus testes. O método principal para estudar este problema é o método de modelagem, que nos permite considerar o problema em estudo como um processo organizado e focado de desenvolvimento profissional de futuros professores de química e formação da competência no campo das tecnologias de informação e comunicação (TIC), refletindo a capacidade e a vontade do professor. Professor de química usa tecnologia de nuvem em atividades profissionais. O modelo desenvolvido permite não apenas formar o conhecimento dos estudantes sobre as funções das tecnologias em nuvem, mas também visa preparar futuros professores de química para novas condições de atividade profissional. A análise dos resultados da pesquisa mostrou a efetividade do modelo proposto da metodologia para a preparação de futuros professores de química para o uso de tecnologias de nuvem nas atividades profissionais, o que foi confirmado pela dinâmica positiva dos níveis de preparação entre os estudantes do grupo experimental. Os materiais do artigo podem ser úteis para professores e estudantes de instituições de ensino superior, professores de instituições de ensino e especialistas no campo da educação.

Palavras-chave: *modelo estrutural e funcional, tecnologias de nuvem, treinamento profissional, futuros professores de química.*

ABSTRACT

The relevance of the study is due to the specifics of perception and assimilation of information by schoolchildren (the young generation's penchant for clip thinking) and the insufficient number of studies that reveal the theoretical and substantive-procedural features of the formation of preparedness of future chemistry teachers for the use of cloud technologies in professional activities. The purpose of the article is to develop a structural-

functional model of the methodology for preparing future chemistry teachers for the use of cloud technologies in professional activities and its testing. The leading method for studying this problem is the modeling method, which allows to consider the problem under study as a focused, organized process of improving the professional competence of future chemistry teachers and the formation of ICT competency, reflecting the ability and willingness of a future chemistry teacher to use cloud technologies in professional activities. The developed model allows not only to form students' knowledge about the functions of cloud technologies but also aims to prepare future chemistry teachers for new conditions of professional activity. Analysis of the results of the study showed the effectiveness of the proposed model of the methodology for preparing future chemistry teachers for the use of cloud technologies in professional activities, which were confirmed by the positive dynamics of the levels of readiness formation among students of the experimental group. Article materials may be useful for teachers and students of higher educational institutions, teachers of institutions of general secondary education, specialists in the field of education.

Keywords: *structural-functional model, cloud technology, training, future chemistry teachers.*

АННОТАЦИЯ

Актуальность исследования обусловлена спецификой восприятия и усвоения информации школьниками (склонность молодого поколения к клиповому мышлению) и недостаточным количеством исследований, раскрывающих теоретические и предметно-процедурные особенности формирования подготовленности будущей химии. учителя по использованию облачных технологий в профессиональной деятельности. Целью статьи является разработка структурно-функциональной модели методики подготовки будущих учителей химии к использованию облачных технологий в профессиональной деятельности и ее тестирование. Ведущим методом изучения этой проблемы является метод моделирования, который позволяет рассматривать исследуемую проблему как сфокусированный, организованный процесс повышения профессиональной компетентности будущих учителей химии и формирования компетентности в области ИКТ, отражающий способность и готовность будущего. Учитель химии использует облачные технологии в профессиональной деятельности. Разработанная модель позволяет не только формировать у студентов знания о функциях облачных технологий, но и направлена на подготовку будущих учителей химии к новым условиям профессиональной деятельности. Анализ результатов исследования показал эффективность предложенной модели методики подготовки будущих учителей химии к использованию облачных технологий в профессиональной деятельности, что было подтверждено положительной динамикой уровней формирования готовности у студентов экспериментальной группы. Материалы статьи могут быть полезны преподавателям и студентам высших учебных заведений, преподавателям общеобразовательных учреждений, специалистам в области образования.

Ключевые слова: *структурно-функциональная модель, облачные технологии, профессиональная подготовка, будущие учителя химии.*

1. INTRODUCTION

Modern information and communication technologies in educational institutions of Ukraine used in the development of electronic educational resources for educational, scientific and managerial purposes have determined the pedagogical community to highlight the issue of updating approaches to the formation of the educational environment of institutions of general environmental education and implementation of a cloud-based learning environment (Litvinova, 2014; Mkrttchian *et al.*, 2019; Sinex *et al.*, 2016; Blue and Tirota, 2011; Cvetkovic *et al.*, 2017; Li *et al.*, 2019; Ovchinnikova *et al.*, 2019; Parmigiani *et al.*, 2019; Zeng, 2016).

This requires a teacher to solve a set of pedagogical tasks aimed at facilitating the assimilation by students of educational material and consideration of the specifics of perception and assimilation of information by the modern generation (Zhitenova, 2019; Collins, 2017; Barak, 2017; Orehovački *et al.*, 2019; Vikhrova, 2017; Wang, 2017). Consequently, new directions appear in the teacher's work: preparing materials of various subjects, modeling processes, creating drawings, mind maps. (Bulvinskaya *et al.*, 2016; Golubeva, 2016; Estapa *et al.*, 2016; Robertson, 2013; Schwenz and Miller, 2014; Zheng *et al.*, 2015).

Modern realities in the education system require a teacher to theoretically comprehend and

justify the use of cloud services in chemistry education (Babenko, 2018b; Astafieva *et al.*, 2019; Chamrat, 2019; Kholoshyn *et al.*, 2019; Oddone, 2016; Park and Han, 2016). However, an analysis of practice showed that only a small part of teachers has knowledge of the methodology for creating electronic teaching materials and use them in the educational process. This is mainly due to the inability to use online services and the lack of guidelines for chemistry teachers to create them (Olakanmi, 2017; Qi and Zhao, 2017; Rusmansyah *et al.*, 2019; Sadvakassova and Serik, 2017; Spirin *et al.*, 2018; Tsai *et al.*, 2014).

The aim of the study was to present a structural-functional model of the methodology for preparing a future chemistry teacher for the use of cloud technologies in professional activities in the unity of motivational-target, organizational, content-procedural, and productive-corrective blocks, based on the use of cloud technologies, which allow creating one's own electronic educational materials (visual teaching aids, interactive tasks, and posters, web-quests, didactic and methodological materials, e-portfolio) and include motivational-organizational, cognitive-activity and reflexive stages.

2. MATERIALS AND METHODS

In the research process, the following methods were used: theoretical (analysis, synthesis, generalization and systematization, modeling); diagnostic (observation, testing, survey, conversation, interviewing, questioning); empirical (the study of educational and normative documents, generalization and systematization of the pedagogical experience of teachers and teachers of secondary schools) experimental (ascertaining, formative, generalizing stages) statistical (methods of mathematical statistics).

All procedures performed in studies involving human participants were in accordance with the ethical standards of the institutional and national research committee and with the 1964 Helsinki declaration and its later amendments or comparable ethical standards. Informed consent was obtained from all individual participants included in the study.

The experimental base of the research was the V. G. Korolenko National Pedagogical University. In addition, individual elements of the methodology were tested on the basis of the Poltava State Agrarian Academy.

The leading research method is the modeling method, which allows us to consider the

problem under study as a focused, organized process of improving the professional competence of future chemistry teachers, which consists in the ability and willingness of a future chemistry teacher to use cloud technologies in professional activities. This method involves working in such three stages:

–At the first stage of the study, a theoretical analysis of the existing methodological approaches in the philosophical, psychological and pedagogical scientific literature was conducted, the pedagogical experience of the professional training of future chemistry teachers was studied, and the design plan was formulated.

–At the second stage, a model of the methodology for preparing future chemistry teachers for the use of cloud technologies in professional activities was developed, pedagogical conditions for the implementation of a model of the methodology for preparing future chemistry teachers for the use of cloud technologies in professional activities were identified and substantiated, the pedagogical experiment was conducted and analyzed, conclusions were clarified.

–At the third stage, quantitative and qualitative processing of the obtained data was conducted, the main points and conclusions of the experimental study were generalized and systematized.

3. RESULTS AND DISCUSSION:

3.1. The structure and content of the model

The methodology of preparing future chemistry teachers for the use of cloud technologies in professional activities is presented in the form of a model in the unity of motivational-targeted, organizational, content-procedural and effective-correcting blocks (Figure 1). The motivation-target block includes the goal (the formation of the preparedness of future chemistry teachers for the use of cloud technologies in professional activities).

Achieving the goal of the developed model of the methodology is based on consideration of the leading conceptual provisions, in accordance with which the authors construct training aimed at enhancing the study and application of cloud technologies in professional activities by future chemistry teachers: competency, activity, personality-oriented, systemic, practice-oriented approaches. The goal and methodological approaches determine the tasks, the selection of the content of the disciplines of the vocational

training cycle, forms, methods, and training tools. The organizational block discloses pedagogical conditions and stages of preparation of future chemistry teachers for the use of cloud technologies in professional activities.

The content-procedural block includes the content filling of the disciplines of the vocational training cycle with relevant topics; workshop "Using Google Classroom", the training course "Cloud Technologies in Education"; master classes: "Modern tools for creating didactic visual aids", "Application of Google cloud services for the development of research competence", which systematizes knowledge about various cloud technologies in education, reflects the forms, methods, and means of forming the preparedness of future chemistry teachers to use cloud technologies in professional activity.

The resulting-correcting block of the model provides for both the assessment by experts and the students' mutual and self-assessment of the results achieved in the learning process, the establishment of compliance with their tasks in accordance with the developed criteria and indicators of the preparedness of the future chemistry teacher to use cloud technologies in professional activities. The research results were analyzed on the basis of the developed criteria and indicators of the preparedness of a future chemistry teacher to use cloud technologies in professional activities:

- motivational criterion (formedness of students' motivation and the necessity for the use of cloud technologies in professional activities, interest in the problem of using cloud technologies in professional activities),
- content criterion (completeness and depth of knowledge, the efficiency of knowledge),
- activity criterion (operational skills, the ability to use tools to create one's own electronic training materials),
- reflexive criterion (formedness of skills to analyze their own educational activities and their results, evaluate their own preparation for the use of cloud technologies in professional activities and the creation of electronic educational materials)

These criteria are the basis for identifying high, sufficient, and low levels of preparedness.

Thus, the developed model of the methodology sets the goal to form the preparedness of future chemistry teachers for the use of cloud technologies in professional activities. The result is the preparedness of future chemistry

teachers to use cloud technology in professional activities, which is presented by the criteria and preparedness formation levels. The content of the training is the knowledge that forms the basis of the individual components of preparedness: motivational, cognitive, active, reflexive, formed during lectures, practical, laboratory classes, work with mentors, the work of creative groups of teachers and students, in the process of consultation, independent and individual work, research activities, pedagogical practice, during masterclasses with the use of practice-oriented teaching methods on motivational-organizational cognitive-activity and reflexive stages. The pedagogical conditions for the implementation of the model of the methodology for preparing future chemistry teachers for the use of cloud technologies in professional activities are determined.

3.2. Stages of model implementation

The introduction of the presented model provided the following stages of experimental work:

- determination of the initial level of preparedness of future chemistry teachers for the use of cloud technologies in professional activities using methods of testing, questionnaires, pedagogical observation, statistical processing of research results;
- development and implementation of methodological support for the formation of preparedness of future chemistry teachers for the use of cloud technologies in professional activities in the process of studying the disciplines of the vocational training cycle: the content of disciplines, methodological recommendations and selection of online sources on practical issues of using cloud services, a system of professionally oriented tasks for the development of visual didactic tools and individual and group research projects using cloud technology; research tasks for laboratory studies, e-portfolio. The introduction of methodological support ensured the students' practical mastery of the necessary theoretical knowledge and skills for the effective application of cloud technologies in the professional activities of future chemistry teachers;
- determining the level and dynamics of the formation of the preparedness of the future chemistry teacher for the use of cloud technologies.

The preparatory stage of the study was to develop and adjust the experimental model, to prepare teachers of the disciplines of the

vocational training cycle to form the preparedness of future chemistry teachers to use cloud technologies in their professional activities.

The level of the studied preparedness of future chemistry teachers was determined in accordance with the selected criteria and indicators. To check the formation of the motivational criterion, the authors used observation methods, conversations, questionnaires, a test to determine the focus on the acquisition of knowledge (Ilyin, 2002), a scale for assessing the need for achievement (Shiyan, 2018b). To diagnose the formation of the cognitive criterion, students were monitored on the functions and main components of cloud technologies, an analysis of the implementation of complex research tasks (the method of element-wise and operational analysis by A. Usova (2006)), analysis of the results of the current, modular and final control. The formation of the activity criterion was checked by analyzing the practical actions of students in carrying out individual research tasks, using methods of expert assessments, observation, interviews, the method of "Incomplete decisions" (Friedman *et al.*, 1988). Formedness of the reflexive criterion was diagnosed according to the method of A. Karpov (2004) and by questioning students.

At the ascertaining stage of the pedagogical experiment (the 2016-2017 academic year), it was established that only 10.88% of students have a high level of motivation and need to develop knowledge, skills, and abilities to apply cloud technologies in professional activities; 2.72% of students have a high level of knowledge about cloud technologies and tools; 2.04% of students are able to use cloud technology and create their own electronic educational resources; 23.81% of students recognize the importance of using cloud technology in their professional activities (Derkach and Starova, 2017). The formative stage of the pedagogical experiment (the 2017-2018 academic year) was conducted in accordance with the developed model of the methodology for preparing future chemistry teachers for the use of cloud technologies in professional activities. The effectiveness of the model was tested in two ways: a sequential and parallel experiment. The number of students who took part in the pedagogical experiment at its formative stage was 147 people, of which the experimental (75 people) and control (72 people) groups were formed.

The motivational-organizational stage of the methodology was aimed at students recognizing the importance of using cloud technologies in future professional activities, developing their interest in creating their own electronic

educational resources (Babenko and Komar, 2018). For this purpose, electronic educational resources were used in laboratory studies. To maintain interest in acquiring new knowledge and practical skills as a permanent incentive mechanism for cognition, electronic educational resources were chosen in such a way that their content corresponded to the cognitive needs of future chemistry teachers, was interesting, accessible and at the same time complex, thereby encouraging students to work with cloud computing technology.

Students were also offered interactive exercises, crosswords, web quests, puzzles, and the like. The motivation trainings for creating an electronic portfolio also turned out to be effective at this stage, where they considered the possibilities of using e-portfolios to develop creativity, present their own achievements and increase competitiveness in the labor market, focused on the detailed disclosure of the principles of maintaining an electronic portfolio by students during their training, on tools, creating an electronic portfolio based on cloud services.

Before students created an electronic portfolio, the structure of which was determined by the topics provided by the work programs of the disciplines, it was proposed to use such cloud services as Blogger.com. and Sites.google.com. Students also did hands-on learning of the Google Classroom Learning Management System in the "Using Google Classroom" workshop. The indicated forms, methods, and teaching aids contributed to the formation of interest in obtaining new knowledge and practical skills for their further productive use, formed the desire for self-improvement, as well as establishing communication, optimizing teamwork, which subsequently had a positive impact on the organization of effective student activities the team.

At the cognitive-activity stage of the model, the methods formed the knowledge system of future chemistry teachers about the basic components of a cloud-based learning environment, studied the characteristics, functionality and tools of cloud services (Derkach, 2011; Derkach, 2013). For this purpose, lectures-visualisations, interactive lectures were used. Lectures were held using technical teaching aids, namely, demonstration of the elements of lecture material using various types of cloud technologies: a multimedia system (screen, laptop, projector) or a multimedia board.

The laboratory works were conducted using

the appropriate software: a multimedia board, Google Chrome, online services, the Google Classroom learning management system. Methodological recommendations for the laboratory work included the following components: topic, purpose, equipment description, list of training results, instructions for conducting practical works, resources and files for the use of video materials and a virtual (simulation) experiment (if necessary), visual material of theoretical information topics for show students visualization examples, characteristics of their usage in the learning process, comparison and evaluation of visual identical chemical content created by different instruments. Control over the implementation of tasks and consultations took place, except for the audience, in the online mode of the Google Classroom learning management system. The means of controlling knowledge and skills in chemical disciplines were diversified using cloud services (tests, computational and graphic tasks, interactive tasks, logical exercises, research tasks, quests) with commenting and self-control.

Particular attention was paid to mastering by future teachers the skills of planning and organizing independent work in order to achieve maximum productivity, which is an important factor in successfully preparing for classes, completing additional tasks, studying external resources (LearningApps.org, Flippity). Group working methods were implemented by a combination of research and design activities using the popular Google Forms and Kahoot services to search for topics and posed a research problem, Padlet service for organizing a discussion of the problem, Google Docs services, and Google Sheets for joint creation, editing, formatting of documents and adding comments, Mindmeister.com, Mindomo.com, Bubbl.us services for visualizing materials, Prezi, Canva, Padlet services for presenting the results.

Additional tasks related to future professional activities were proposed for laboratory studies, which took into account the real professional functions of a chemistry teacher, the solution of which required the use of observation skills, analysis, synthesis and generalization of the necessary information, brainstorming methods, mind mapping, inverted training, research method, project method, portfolio, computer modeling. The development of the content and tools of cloud services was facilitated by the training course "Cloud Technology in Education". The workshops were also effective: "Modern tools for creating didactic visual aids", "Use of Google cloud

services for the development of research competence," and others.

At the reflexive stage, self-analysis and adequate self-esteem of students were facilitated by the creation of an e-portfolio, student forums and chats, and pedagogical mentoring. For the presentation by students of personal achievements in educational activities, the authors used such cloud services as Resume and Kartatalanta.ru. Student forums with participation of stakeholders helped future chemistry teachers establish their own level of preparedness for professional activity with the requirements of employers. Participation in student scientific conferences and seminars, working with mentors, provided students with practical experience in presenting research results, and testing the created electronic educational resources in real conditions of a comprehensive school.

The conducted experimental work made it possible to prove the effectiveness of the identified pedagogical conditions for the implementation of the developed model of the methodology for preparing future chemistry teachers for the use of cloud technologies in professional activities.

It was proved that by implementing the first condition – using Google Classroom to create virtual interaction between the participants of the educational process – there was an expansion of communication tools and ensuring feedback efficiency, planning of the educational process, storage of files and links to information sources, distribution of educational materials, creation of educational content, organization of students' joint work, effective communication between students and a teacher, creation of virtual educational communities in the organization and questionnaires, surveys, monitoring and evaluation of learning outcomes.

Users in the virtual classroom also interacted through gaming activities, namely the organization of web quests. For students, they offered, for example, the methodical quest "Interactive exercises in chemistry", which included working with computer programs and using the Internet, including cloud technology. Each participant received a task that included creating a mind map using Mindmeister.com, creating exercises, crosswords using Learning Apps, creating tests using Google Forms on the relevant topics, then switched to an e-class and sent the completed task to the teacher. A teacher immediately checked the assignment and set the score (encoded letter of the alphabet). Students composed words from encrypted letters and

published them in the classroom. The team jointly summed up the results of each assignment, the participants exchanged materials to achieve a common goal – to create a collection of interactive exercises in chemistry.

The implementation of the second pedagogical condition – the use of cloud services for the organization of educational and research activities of future chemistry teachers – contributed to the practical preparation of students for future professional activities, due to which there were a better understanding and perception of educational material by students, the acquisition of professional experience in the classroom by involving them in creative oriented activities. The directions of using cloud services for organizing the educational activities of future chemistry teachers are proposed, namely: learning management, systematization, and presentation of educational material, communication of participants in the educational process, monitoring, and evaluation. In order to attract future chemistry teachers to organize research, the authors used Google's cloud services to select research information resources (Google Academy, Google Books), create electronic notebooks (One Note), save a lot of information and work with documents (Google Drive), conducting online surveys (Google Form), electronic document management (Gmail, Google Docs), planning support and organization of work (Google Calendar).

Implementation of the third pedagogical condition – providing pedagogical support for students to create their own electronic learning resources (visual teaching aids, interactive tasks, and posters, web-quests, didactic and methodological materials, e-portfolio.) during classes and in extracurricular activities – contributed to the disclosure of the personal potential of a future teacher by providing specific assistance to him in overcoming difficulties in learning, in self-determination and self-realization of a personality of a future specialist, attracting them to active, creative work (the implementation of individual and group research projects with the subsequent presentation of the results at a meeting of the regional round table "Cloud Services in Education", conducting master classes on creating didactic visual teaching aids, interactive electronic exercises and posters in chemistry for students, teachers, schoolchildren, work with mentors.).

The main ways of providing pedagogical support to future chemistry teachers during classes and in extracurricular activities were

pedagogical counseling and pedagogical mentoring. The main forms and methods of work of teachers-mentors with students were masterclasses, training, conversations, and discussions on various methodological topics; discussion of the possibilities of using various electronic educational resources in the lessons, joint design of lessons, their detailed analysis; counseling on the organization of educational and cognitive activities and the like. A great role was played by a mentor for future chemistry teachers to test their own developments, research activities, pass pedagogical practice. Based on this, the main attention was paid to supporting the initiative, creative search, independent improvement of the professional competence of future specialists.

According to the results of psychological and pedagogical diagnostics of the phenomenon under study at the formative stage of the experiment in the EG, a significant increase in the level of formation of preparedness of future chemistry teachers to use cloud technologies in professional activities was revealed (Table 1). The reliability of the obtained experimental work data was checked using the χ^2 Pearson criterion. With a confidence probability of $p = 0.01$, comparing the levels of formation of preparedness of future chemistry teachers for the use of cloud technologies of the experimental and control groups showed that $\chi^2_{\text{emp.}} > \chi^2_{\text{cr.}}$ by all criteria.

An analysis of the results of the experimental work showed the effectiveness of the proposed model of the methodology for preparing future chemistry teachers for the use of cloud technologies in professional activities, which is confirmed by the positive dynamics of the levels of preparedness formation among students of the experimental group. In particular, indicators of a high level of the motivational criterion for students of experimental groups increased from 12% to 64%, cognitive – from 2.7% to 24%, activity – from 2.7% to 20%, reflexive – from 24% to 49.3 %. At the same time, the number of students with a low level of preparedness of future chemistry teachers for the use of cloud technologies in professional activities according to all criteria decreased in the experimental group. No significant changes were found in the indicators of the research competence of students in the control group. The reliability of the data obtained is confirmed by the method of mathematical statistics (χ^2 Pearson criterion), which in the experimental groups showed a significant advantage of empirical values of the indicators over critical ones at a probability level of 99%.

A theoretical analysis of the problem under

study in pedagogical theory and practice showed the absence of special studies on the preparation of future chemistry teachers for the use of cloud technologies in professional activities. However, the studies of N. Burinskaya (1987), L. Velichko (2013), V. Starosta (2006), N. Shiyan (2018a), O. Yaroshenko (Yaroshenko et al., 2016) are devoted to the formation of general pedagogical skills of a future chemistry teacher. ICT, as a means of teaching chemistry, was considered in their works by T. Derkach (2016), E. Babenko (2018a), E. Ratkevich (1998), N. Titarenko (2004).

Pedagogical conditions contribute to the preparation of future chemistry teachers for the use of cloud technologies in their professional activities: the use of Google Classroom to create virtual interaction between participants in the educational process; use in the process of preparing future chemistry teachers to cloud services for educational and research activities; providing pedagogical support for students to create their own electronic learning resources (visual teaching aids, interactive tasks and posters, web quests, didactic and teaching materials, e-portfolios) during classes and in extracurricular activities.

Using Google Classroom virtual classroom to support the educational process and learning management promotes open access to the educational information environment; filling the content of the virtual classroom with the necessary methodological, educational, methodological and scientific developments; the establishment of the value priorities of future chemistry teachers, in particular, the steady desire to be competent in the chosen profession, internal motivation to use cloud technologies in professional activities, the ability to carry out effective learning activities, and the willingness to take responsibility for its results; the creation of auxiliary ELR (visual materials, practice-oriented tasks, tests, presentations, guidelines, electronic collections, dictionaries.). Building trust with students is facilitated by the fact that the teacher in the virtual classroom acts as a facilitator, as a result of which students can freely express their opinions and defend their own position reasonably. On this basis, the independence and initiative of the participants in the educational process are formed, their personal growth, creative development are stimulated, and skills to navigate in non-standard situations are developed.

4. CONCLUSIONS:

As a result of the study, it can be concluded

that the effectiveness of using cloud services in the process of preparing future chemistry teachers for educational and research activities depends on the correct selection of hardware and software, the integration of methods and forms of activity, and the system of pedagogical tasks. The integration of cloud, research, and design technologies ensures the formation of both subject competence of future specialists and readiness for the introduction of cloud technologies, as it simplifies their understanding and assimilation of the essence of cloud technologies and the mastery of their tools. The creation by students of their own electronic learning resources stimulates the assimilation of new knowledge and new ways of working, improving practical skills, ensures the intensification of cooperation among participants in the educational process, promotes the professional development of future chemistry teachers, and immerses them directly in the field of professional activity.

Meetings with mentors contribute to the realization of the importance of obtaining the necessary theoretical knowledge and practical skills to apply cloud technology in professional activities, providing the opportunity to feel in the role of a teacher, forming personal practical experience, motivation to use cloud technology in solving professionally-oriented tasks, and comparing the level of formation of one's professional competence to requirements of employers and adjusting their own educational trajectory. Students check their own developed electronic educational resources in the real conditions of a general educational institution, find out the feasibility of choosing a tool, and make adjustments to the creation of educational products.

The rapid development of cloud technologies and their inclusion in the practice of modern education indicate the need for special training of future chemistry teachers for the use of cloud technologies in their professional activities. The proposed model of the methodology for preparing future chemistry teachers for the use of cloud technologies in professional activities is focused on the gradual mastery of the basic principles and modern tools of cloud services by students.

Article materials may be useful for teachers and students of higher educational institutions, teachers of institutions of general secondary education, specialists in the field of education. The study does not exhaust all aspects of the formation of the readiness of future chemistry teachers to use cloud technologies in their professional

activities. Prospects for further research include the use of virtual and augmented reality technologies in preparing future chemistry teachers for the use of cloud technologies in professional activities.

5. REFERENCES:

1. Astafieva, M., Bodnenko, D., Proshkin, V. *CEUR Workshop Proceedings*, **2019**, 2387, 507-512.
2. Babenko, O. M. *Actual Nutrition of Natural-Mathematical Education*, **2018a**, 1(11), 175-182.
3. Babenko, O. M. *Topical Issues in Natural and Mathematical Education: Collection of Scientific Papers*, **2018b**, 1(11), 175-182.
4. Babenko, O. M., Komar, O. V. *Natural Sciences*, **2018**, 15, 67-70.
5. Barak, M. *Journal of Science Education and Technology*, **2017**, 26(5), 459-469.
6. Blue, E., Tirotta, R. *TechTrends*, **2011**, 55(3), 31-39.
7. Bulvinskaya, O. I., Divinskaya, N. O., Dyachenko, N. O., Zhabenko, O. V., Linova, I. O., Skiba, Y. A., Chornoivan, G. P., Yaroshenko, O. G. *The Concept and Methodology of Implementation of Research Activities of the Subjects of the Educational Process of Universities*. Kyiv: Higher Education Institute of NAPS of Ukraine, **2016**.
8. Burinskaya, N. M. *Methods of Teaching Chemistry (Theoretical Foundations)*. Kyiv: High School, **1987**.
9. Chamrat, S. *AIP Conference Proceedings*, **2019**, 2081, 030018.
10. Collins, T. J. *Journal of Cleaner Production*, **2017**, 140, 93-110.
11. Cvetkovic, D., Mijatovic, M., Mijatovic, M., Medic, B. *2017 40th International Convention on Information and Communication Technology, Electronics and Microelectronics, MIPRO 2017 – Proceedings*, **2017**, 7973543, 865-869.
12. Derkach, T. M. *European Researcher*, **2013**, 44(3-2), 649-653.
13. Derkach, T. M. *Pedagogika i Psykhologia Professiinoi Osvity*, **2011**, 5, 33-41.
14. Derkach, T. M. *Science, and Education*, **2016**, 12, 99-109. DOI: 10.24195/2414-4665-2016-12-19.
15. Derkach, T., Starova, T. *Science and Education*, **2017**, 6, 51-56. Doi:10.24195/2414-4665-2017-6-8.
16. Estapa, A., Pinnow, R. J., Chval, K. B. *New Educator*, **2016**, 12(1), 85-104.
17. Friedman, L. M., Pushkina, T. A., Kaplunovich, I. Ya. *Studying the Personality of the Student and the Student Teams: A Book for the Teacher*. Moscow: Prosveschenie, **1988**.
18. Golubeva, E. A. *Use of Cloud Services in School Teacher Work*, **2016**. <http://novainfo.ru/article/4449>, accessed December 2019.
19. Ilyin, E. P. *Motivation and Motives*. St. Petersburg: Peter, **2002**.
20. Karpov, A. V. *Psychology of Reflexive Mechanisms of Activity*. Moscow: Institute of Psychology, Russian Academy of Sciences, **2004**.
21. Kholoshyn, I. V., Bondarenko, O. V., Hanchuk, O. V., Shmeltser, E. O. *CEUR Workshop Proceedings*, **2019**, 2433, 403-412.
22. Li, X., Zhang, Y., Xue, Y. *ACM International Conference Proceeding Series*, **2019**, 1, 6-9.
23. Litvinova, S. G. *Information Technology and Teaching Aids*, **2014**, 2, 26-41.
24. Mkrttchian, V., Krevsky, I., Bershadsky, A., Glotova, T., Gamidullaeva, L., Vasin, S. *International Journal of Web-Based Learning and Teaching Technologies*, **2019**, 14(1), 32-52.
25. Oddone, F. *Journal of E-Learning and Knowledge Society*, **2016**, 12(2), 85-99.
26. Olakanmi, E.E. *Journal of Science Education and Technology*, **2017**, 26(1), 127-137.
27. Orehovački, T., Etinger, D., Babić, S. *Advances in Intelligent Systems and Computing*, **2019**, 876, 82-87.
28. Ovchinnikova, M. V., Shilova, L. I., Linnik, E. P. *CEUR Workshop Proceedings*, **2019**, 2522, 145-157.
29. Park, I.-W., Han, J. *Cluster Computing*, **2016**, 19(2), 987-999.
30. Parmigiani, D., Benigno, V., Hidi, A. *TechTrends*, **2019**, 63(6), 669-681.

31. Qi, M., Zhao, Y. *Boletim Tecnico/Technical Bulletin*, **2017**, 55(7), 509-515.
32. Ratkevich, E. Yu. *Ph.D. thesis*, Moscow Pedagogical University, Moscow, **1998**.
33. Robertson, C. *TechTrends*, **2013**, 57(6), 57-60.
34. Rusmansyah, Yu.L., Ibrahim, M., Isnawati, P.B.K. *Journal of Technology and Science Education*, **2019**, 9(1), 59-76.
35. Sadvakassova, A., Serik, M. *Journal of Theoretical and Applied Information Technology*, **2017**, 95(11), 2434-2441.
36. Schwenz, R. W., Miller, S. *Journal of Chemical Education*, **2014**, 91(9), 1362-1367.
37. Shiyan, N. I. *School Chemistry Course and Method of Its Teaching*. Poltava: V.G. Korolenko Poltava National Pedagogical University, **2018a**.
38. Shiyan, N. *Pedagogical Stimulation of Future Teacher to Self-Evaluation of Educational Activity in the Process of Vocational Training*. Poltava: V.G. Korolenko Poltava National Pedagogical University, **2018b**.
39. Sinex, S. A., Chambers, T. L., Halpern, J. B. *MRS Advances*, **2016**, 1(56), 3727-3733.
40. Spirin, O., Oleksiuk, V., Oleksiuk, O., Sydorenko, S. *CEUR Workshop Proceedings*, **2018**, 2104, 294-304.
41. Starosta, V. I. *Teaching Students to Write and Solve Chemistry Problems: Theory and Practice*. Uzhgorod: UzhNU-Grazhda, **2006**.
42. Titarenko, N. V. *Biology and Chemistry at School*, **2004**, 1, 9-11.
43. Tsai, C.-W., Shen, P.-D. *International Journal of Information and Communication Technology Education*, **2014**, 10(1), 89-96.
44. Usova, A. V. *Science and School*, **2006**, 4, 57-59.
45. Velichko, L. P. *XX Carishine Readings: Materials of the International Scientific Conference*, **2013**, 1, 54-57.
46. Vikhrova, O. *Information (Japan)*, **2017**, 20(9), 6313-6324.
47. Wang, J. *Turkish Online Journal of Distance Education*, **2017**, 18(3), 197-213.
48. Zeng, X. *Proceedings – 2016 8th International Conference on Measuring Technology and Mechatronics Automation, ICMTMA 2016*, **2016**, 7488514, 122-125.
49. Zheng, B., Lawrence, J., Warschauer, M., Lin, C.-H. *Technology, Knowledge and Learning*, **2015**, 20(2), 201-229.
50. Zhitenova, N. V. *Physico-Mathematical Education*, **2019**, 1, 55-61.

Table 1. Diagnostic results of the preparedness of future chemistry teachers to the use of cloud technology in professional activities at the ascertaining and formative stages of the experiment

No	Criteria	Experimental group 75 persons, %						Control group 72 persons, %					
		ascertaining stage			formative stage			ascertaining stage			formative stage		
		l	m	h	l	m	h	l	m	h	l	m	h
1	Motivational	41.3	46.7	12	2.7	33.3	64	38.9	51.4	9.7	16.7	62.5	20.8
2	Cognitive	76	21.3	2.7	9.3	66.7	24	76.4	20.8	2.8	52.8	30.5	16.7
3	Activity	78.7	18.6	2.7	17.3	62.7	20	79.2	19.4	1.4	47.2	37.5	15.3
4	Reflexive	45.3	30.7	24	5.4	45.3	49.3	44.4	32	23.6	16.7	45.8	37.5



Figure 1. The model of the methodology for preparing future chemistry teachers for the use of cloud technologies in professional activities

O IMPACTO DA ADESÃO À MEDICAÇÃO NA QUALIDADE DE VIDA RELACIONADA À SAÚDE DE PACIENTES DIABÉTICOS NO REINO DA ARÁBIA SAUDITA: CONCLUSÕES DE UM ESTUDO TRANSVERSAL

THE IMPACT OF MEDICATION ADHERENCE ON HEALTH-RELATED QUALITY OF LIFE OF DIABETIC PATIENTS IN THE KINGDOM OF SAUDI ARABIA: FINDINGS FROM A CROSS-SECTIONAL STUDY

أثر التقيد بالأدوية على الجودة الصحية ذات الصلة بحياة مرضى السكري في المملكة العربية السعودية: نتائج من دراسة متقاطعة

ALSHAYBAN, Dhfer¹; JOSEPH, Royes^{1*}

¹ Department of Pharmacy Practice, College of Clinical Pharmacy, Imam Abdulrahman Bin Faisal University, Dammam, Saudi Arabia.

* Correspondence author
e-mail: rjchacko@iau.edu.sa

Received 20 January 2020; received in revised form 22 February 2020; accepted 14 March 2020

RESUMO

O diabetes é uma doença crônica comum que é considerada um dos problemas de saúde que mais crescem no mundo. A adesão aos medicamentos pode ser um fator importante na redução dessas complicações e na melhoria da qualidade de vida. O objetivo desta pesquisa foi avaliar o impacto da adesão ao tratamento na qualidade de vida relacionada à saúde em pacientes com diabetes tipo 2. Um estudo transversal multicêntrico foi realizado com 368 pacientes com diabetes. A Escala Geral de Adesão à Medicação foi utilizada para avaliar o nível de adesão e o EuroQol-5D para avaliar a qualidade de vida. Os resultados mostram que 19%, 21% e 23% dos pacientes mantiveram baixa adesão à medicação devido ao comportamento intencional ou não intencional do paciente devido a doenças adicionais ou sobrecarga de pílulas e devido a restrições financeiras, respectivamente. No geral, 43% (n = 162) participantes mantiveram alta adesão à medicação e 37% (n = 138) mantiveram baixa adesão à medicação para medicamentos antidiabéticos. Quase um terço (31%) dos pacientes com alta adesão geral apresentou um estado de saúde perfeito em comparação com 4% entre os pacientes com baixa adesão. Além disso, a menor proporção (21%) de pacientes com alta adesão geral apresentou um estado de saúde perfeito em comparação com a dos pacientes com baixa adesão (34%). Além da adesão geral, a associação foi estatisticamente significativa para os domínios relacionados à não adesão devido ao comportamento intencional ou não intencional do paciente (valor de $p < 0,001$) e não adesão devido a doenças adicionais ou sobrecarga de comprimidos (valor de $p < 0,001$) após levar em consideração as características sociodemográficas e clínicas. Em conclusão, os resultados sugerem que os formuladores de políticas devem estabelecer uma intervenção para melhorar a adesão ao tratamento diabético e, assim, melhorar a qualidade de vida dos pacientes diabéticos tipo 2.

Palavras-chave: *Diabete, Adesão, qualidade de vida relacionada à saúde*

ABSTRACT

Diabetes is a common chronic disease that is considered as one of the fastest-growing health problems in the world. Adherence to medications could be an important factor in reducing these complications and improving the quality of life. The purpose of this research was to assess the impact of treatment adherence on health-related quality of life in patients with type 2 diabetes. A multicenter cross-sectional study was carried out among 368 diabetes patients. General Medication Adherence Scale was used to assess the adherence level and EuroQol-5D to assess the quality of life. The results show that 19%, 21%, and 23% of patients had maintained low medication adherence due to patient's intentional or unintentional behavior due to additional diseases or pills burden and due to financial constraints, respectively. Overall, 43% (n=162) participants had maintained high medication adherence, and 37% (n=138) had maintained low medication adherence to antidiabetic drugs. Nearly one-third (31%) of patients with high overall adherence had perfect health state in comparison with 4% among patients with low adherence. Further, the lower proportion (21%) of patients with high overall adherence had

perfect health state in comparison with that among patients with low adherence (34%). In addition to the overall adherence, the association was statistically significant for the domains related to non-adherence due to the patient's intentional or unintentional behavior (p -value<0.001) and non-adherence due to additional diseases or pills burden (p -value<0.001) after taking into account of socio-demographic and clinical characteristics. In conclusion, the findings suggest that the policymakers should establish an intervention to improve adherence to diabetic treatment, and thus improve the quality of life for the type 2 diabetic patients.

Keywords: Diabetes, Adherence, Health-related quality of life

الخلاصة

داء السكري هو مرض مزمن شائع يعتبر من أسرع المشاكل الصحية نمواً في العالم. يمكن أن يكون الالتزام بالأدوية عاملاً مهماً في الحد من هذه المضاعفات وتحسين جودة الحياة. كان الغرض من هذا البحث هو تقييم أثر الالتزام بالعلاج على نوعية الحياة المتعلقة بالصحة لدى مرضى السكري من النوع 2. أجريت لتقييم EuroQoL-5D دراسة مستعرضة متعددة المراكز بين 368 من مرضى السكري. تم استخدام مقياس الالتزام بالأدوية العامة لتقييم مستوى الالتزام وجودة الحياة. أظهرت النتائج أن 19% و 21% و 23% من المرضى قد حافظوا على التزام منخفض بالأدوية بسبب سلوك المريض المتعمد أو غير المتعمد بسبب أمراض إضافية أو عبء حبوب وبسبب القيود المالية، على التوالي. بشكل عام، حافظ 43% (ن = 162) مشاركاً على التزام عالٍ بالأدوية، و 37% (ن = 138) حافظوا على انخفاض التزام الأدوية بالأدوية المضادة لمرض السكر. ما يقرب من ثلث (31%) من المرضى الذين لديهم التزام عام مرتفع لديهم حالة صحية مثالية بالمقارنة مع 4% بين المرضى الذين يعانون من انخفاض الالتزام. علاوة على ذلك، كانت النسبة الأقل (21%) من المرضى الذين لديهم التزام عام عالٍ بحالة صحية مثالية مقارنة بالمرضى من ذوي الالتزام المنخفض (34%). بالإضافة إلى الالتزام العام، كان الارتباط مهماً إحصائياً للنطاقات المتعلقة بعدم الالتزام بسبب سلوك المريض المتعمد أو غير المقصود (القيمة الاحتمالية > 0.001) وعدم الالتزام بسبب أمراض إضافية أو عبء حبوب (قيمة بعد مراعاة الخصائص الاجتماعية والديمقراطية والسريرية. في الختام، تشير النتائج إلى أنه يجب على واضعي السياسات إنشاء تدخل لتحسين ($p < 0.001$) الالتزام بعلاج مرض السكري، وبالتالي تحسين نوعية الحياة لمرضى السكري من النوع

الكلمات المفتاحية: داء السكري، الالتزام، جودة الحياة المتعلقة بالصحة

1. INTRODUCTION

Diabetes mellitus (DM) is a common metabolic disease that is considered as one of the fastest-growing health problems in the world. It results from a complex inheritance-environment interaction together with other risk factors such as lifestyle as lack of exercise, unhealthy diet, obesity, and overweight (Naeem, 2015; Daya, Bayat and Raal, 2016). It has both short and long-term complications such as hypoglycemia and hyperglycemia and cardiovascular diseases. Diabetic patients are prone to suffer from depression. These complications and comorbidities are responsible for significant societal and economic burden, and they have a negative impact on health-related quality of life (HRQoL) (Al-Ghamdi *et al.*, 2018).

Saudi Arabia ranks second-highest in the Middle East and is seventh in the world for the rate of diabetes. It is reported that 7 million of the population have been diagnosed with diabetes, and the number of prediabetes population has reached 3 million (Robert *et al.*, 2016). It has been shown that patients with type 2 DM (T2DM) experienced significantly decreased HRQoL compared with those without diabetes, and their HRQoL further decreases with disease development and complications (Holmes *et al.*, 2000; Koopmanschap and CODE-2 Advisory Board, 2002; Wexler *et al.*, 2006; Grandy and Fox, 2008). Our previous publication on HRQoL of

T2DM patients in the Eastern Province, Saudi Arabia, reported that only one-fifth of the patients were in perfect health state, and more than a quarter were in poor health state (Alshayban and Joseph, 2019).

Improving medication adherence to diabetes medications have the potential to significantly reduce the complications of diabetes and reduce the risk of hospitalization and ER visits, and thus improves HRQoL of the patients (Polonsky and Henry, 2016; Ahmed, Abugalambo and Almethen, 2017; Farhat *et al.*, 2019). Although both adherence to diabetic treatment and HRQoL are important factors for the treatment success of therapeutic interventions (Heng *et al.*, 2015; Daya, Bayat and Raal, 2016), the association between them has rarely been studied in diabetes. A previous study, from the Makkah region of Saudi Arabia, had been reported that a positive association between medication adherence and quality of life among patients with diabetes and hypertension (Khayyat *et al.*, 2019). Since the previous study was focused on patients with multiple chronic conditions and with limited to small sample size, a large-scale study that focuses on T2DM patients is warranted. If a positive relationship is found, more attention can be directed on reinforcing adherence to therapy to improve HRQoL for diabetic patients in Saudi Arabia. Therefore, this study aimed to assess treatment adherence and its association with the quality of life in patients with type 2 diabetes.

2. MATERIALS AND METHODS

2.1. Study setting and subjects

The study setting and methodology were detailed elsewhere (Alshayban and Joseph, 2019). A multicenter cross-sectional study was carried out from November 2017–April 2018. Patients were selected from outpatient clinics of King Fahad Hospital of the University, Khobar, and Family and Community Medicine Centre, Dammam. Hospital records indicate that both hospitals serve patients from several urban and rural areas within the Eastern Province. Patients aged 18 years or older and had T2DM for a minimum of one year were considered. Patients with other chronic/serious illness or pregnancy were excluded. The study was designed to target 385 diabetes patients based on sample size calculation. Ethical approval was obtained from the Institutional Review Board at Imam Abdulrahman Bin Faisal University (IRB-2019-05-391).

2.2. Data Collection

Patients at the waiting lounge of the hospitals were approached and explained the purpose of the study, and informed consent was obtained if they agreed to participate in the study. The questionnaire was administrated in the Arabic language, which is the national language of Saudi Arabia. The questionnaire did not request any information that could identify individual participants during or after data collection.

The study questionnaire had three sections. In the first section, patients' demographic and clinical characteristics were requested. The variables included sex, age in years, education qualification, family income, random blood glucose level, presence of diabetes-related conditions, and type and number of antidiabetic medications used. In the second section, as detailed elsewhere (Alshayban and Joseph, 2019), the HRQoL of participants was assessed using the EQ-5D-5L (Herdman *et al.*, 2011), and the EQ-5D index (Devlin *et al.*, 2018) was derived. Using the EQ-5D-5L, health status was assessed in terms of mobility, self-care, usual activities, pain/discomfort, and anxiety/depression. Patients were classified as with perfect health state if no problem in domains of EQ-5D, slight/moderate health state if problems in one or more domains but not worse than moderate health in any domains, or severe/unable health state if a health status with problems worse than moderate health in some domains (Alshayban and Joseph, 2019).

In the final section, adherence to antidiabetic drugs was measured using the General Medication Adherence Scale (GMAS) (Naqvi *et al.*, 2018). The questionnaire was validated with good reliability and high sensitivity and specificity among Saudi patients with chronic diseases (Naqvi *et al.*, 2019). The questionnaire consists of a total of eleven questions under three-domains. The domains are 1) non-adherence due to patient behavior (unintentional and intentional), 2) non-adherence due to additional disease and pill burden, and 3) non-adherence due to financial constraints. All questions in the GMAS were answered on a 4-point scale (0-3; from always to never) with a higher score indicating a higher medication adherence. The domain-specific score is calculated by summing the scores of relevant individual items. The summative scores may range 0-15, 0-12, and 0-6 for the first, second, and third domains, respectively. A score of greater than or equal to 13, 11, and 6 is regarded as high adherence in first, second, and third domains, respectively. A score of less than or equal to 10, 8, and 4 is regarded as low adherence in first, second, and third domains, respectively. In addition, a score between high and low adherence is referred to as moderate adherence to medications. Overall, medication adherence is calculated by summing scores for all the 11 items in the questionnaire, and it may range from 0 to 33. An overall score of 30–33, 27–29, and less than 27 is regarded as high, good, and low overall medication adherence, respectively.

2.3. Statistical analysis

Data management and analyses were carried out using SPSS Statistics 24.0. Data were summarized as frequency (percentage) and mean (standard deviation) for categorical and continuous variables, respectively. The association of the level of medication adherence on HRQoL was assessed using 1) chi-square test where outcome variable was HRQoL with three levels, 2) multiple logistic regression where outcome variable was a binary variable indicating 'perfect health' or 'not', and 3) multiple linear regression where the dependent variable, EQ-5D index, was transformed using a cubic function to achieve normally distributed residuals. Regression estimates were adjusted for demographic information and clinical characteristics. A p-value of less than 0.05 was considered statistically significant.

3. RESULTS AND DISCUSSIONS

The study was completed by 378 patients;

however, 10 participants were excluded due to incomplete data. The socio-demographic and clinical characteristics of participants were presented in a previous publication (Alshayban and Joseph, 2019). The participants involved an equal proportion of male and female patients; more than two-thirds were older than 50 years. Among the participants, nearly half of them (n=178) had a random glucose level 200 mg/dl or higher; three-fourth (n=286) had complications related to diabetes; more than half (n=224) were on oral antidiabetic medications only; and two-third (n=253) were on multiple antidiabetic medications.

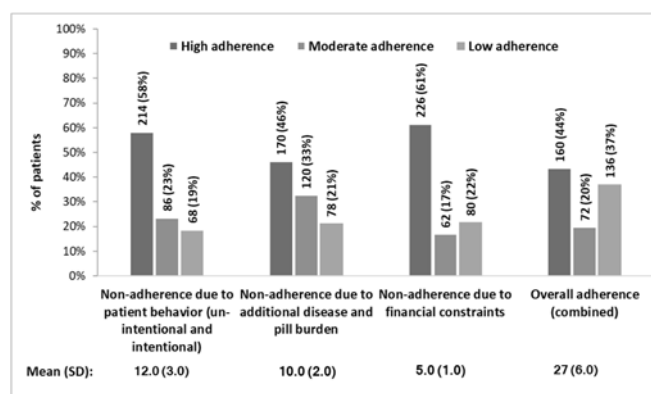


Figure 1. Level of adherence to antidiabetic drugs (measured using GMAS)

The level of medication adherence is summarized in Figure 1. The results show that 19%, 21%, and 22% of patients had maintained low medication adherence due to patient's intentional or unintentional behavior, due to additional diseases or pills burden, and due to financial constraints, respectively. Overall, 44% (n=160) participants had maintained high medication adherence, and 37% (n=136) had maintained low medication adherence to antidiabetic drugs. The mean (standard deviation) overall GMAS score was 27.3 (5.6) on a 0–33 scale.

Table 1 presents the association of level of medication adherence on the level of HRQoL. The results show that the proportion of patients with the perfect health was higher among the high adherence patients, and the proportion of patients with the severe/extreme health was higher among the low adherence patients in comparison with contrary groups. The results were statistically significant for the domains related to non-adherence due to the patient's intentional or unintentional behavior (p-value<0.001) and non-adherence due to additional diseases or pills burden (p-value<0.001). Overall, 31% of patients with high overall medication adherence reported

as having perfect health against the proportion among patients with moderate overall adherence (28%) and with low overall adherence (4%). Further, a lower proportion (21%) of patients with high overall adherence had perfect health state in comparison with that among patients with low adherence (34%).

Table 1. Overall health-related quality of life by the level of medication adherence

Adherence level	Overall health status: n (%)		
	Perfect health	Slight-Moderate	Severe-Extreme
	76 (20.6)	190 (51.6)	102 (27.7)
Non-adherence due to patient behavior (unintentional and intentional)**			
HA (13-15)	66 (30.8)	94 (43.9)	54 (25.2)
MA (11-12)	6 (7)	52 (60.5)	28 (32.6)
LA (<12)	4 (5.9)	44 (64.7)	20 (29.4)
Non-adherence due to additional disease and pill burden**			
HA (11-12)	52 (30.6)	78 (45.9)	40 (23.5)
MA (9-10)	18 (15)	66 (55)	36 (30)
LA (<9)	6 (7.7)	46 (59)	26 (33.3)
Non-adherence due to financial constraints ^{NS}			
HA (6)	54 (23.9)	116 (51.3)	56 (24.8)
MA (5)	10 (16.1)	30 (48.4)	22 (35.5)
LA (<5)	12 (15)	44 (55)	24 (30)
Overall adherence (Cumulative)**			
HA (30-33)	50 (31.3)	76 (47.5)	34 (21.3)
MA (25-29)	20 (27.8)	30 (41.7)	22 (30.6)
LA (<25)	6 (4.4)	84 (61.8)	46 (33.8)

HA – High Adherence; MA-Moderate Adherence; LA-Low Adherence. **p-value<0.001; ^{NS} – not statistically significant

Table 2 presents the adjusted odds ratio and its 95% confidence interval from a multiple logistic regression on an outcome variable indicating 'perfect health' or 'not'. The adjusted odds ratios for the first domain (non-adherence due to patient's intentional or unintentional behavior) indicates that the odds of having perfect health state among patients with moderate medication adherence and among patients with a low adherence were 86% and 91%, respectively, lower than that among patients with high medication adherence (p-value<0.05). Similarly, the adjusted odds ratio for the second domain (non-adherence due to additional disease or pills burden) indicates that the odds of having perfect health state among patients with low medication adherence was 87% lower than that among patients with high medication adherence (p-value<0.05). Overall, the odds of having perfect health state among patients with low medication adherence was 91% lower than those among patients with high medication adherence (p-value<0.05).

Table 2. Adjusted odds ratio for perfect health status and its 95% confidence interval

Adherence level	Odds ratio [#] (95% CI)	p-value
Non-adherence due to patient behavior (unintentional and intentional)		
HA (13-15)	1.0	
MA (11-12)	0.14 (0.05-0.45)	0.001
LA (<12)	0.09 (0.03-0.33)	<0.001
Non-adherence due to additional disease and pill burden		
HA (11-12)	1.0	
MA (9-10)	0.45 (0.21-1.01)	0.051
LA (<9)	0.13 (0.05-0.39)	<0.001
Non-adherence due to financial constraints		
HA (6)	1.0	
MA (5)	0.76 (0.27-2.18)	0.614
LA (<5)	0.52 (0.23-1.21)	0.13
Overall adherence (Cumulative)		
HA (30-33)	1.0	
MA (27-29)	0.91 (0.4-2.07)	0.815
LA (<27)	0.09 (0.03-0.27)	<0.001

HA – High Adherence; MA-Moderate Adherence; LA-Low Adherence. [#]Adjusted for gender, education status, monthly income, no. of comorbidities, type of antidiabetic medication, and random blood glucose level.

Table 3. Results of multiple linear regression model for the cubic function of EQ-5D index

	Regression Coefficient (95% CI)	p-value
Non-adherence due to patient behavior (unintentional and intentional)	0.024 (0.014, 0.033)	<0.001
Non-adherence due to additional disease and pill burden	0.021 (0.010, 0.033)	<0.001
Non-adherence due to financial constraints	0.010 (-0.008, 0.030)	0.268
Overall adherence (Cumulative)	0.011 (0.006, 0.016)	<0.001

[#]Adjusted for age, gender, education status, monthly income, no. of comorbidities, type of antidiabetic medication, and random blood glucose level.

Table 3 presents the results of a multiple linear regression, where the cubic function of the EQ-5D index was the outcome variable. The cubic transformation was carried out to achieve the normality assumption. The adjusted regression coefficients with a 95% confidence interval are reported. The estimates were consistent with the results of the logistic model. It suggests that lower adherence due to patient's intentional or

unintentional behavior, low adherence due to due to additional disease or pills burden, and low overall medication adherence were prone to have a lower EQ-5D index. In specific, for a unit increase in overall adherence score, there was an increase of 0.011 units in the cubic function of the EQ-5D index (p-value<0.001).

4. CONCLUSIONS

To the best of our knowledge, the present study was among the few studies conducted to assess the relationship between both the adherence and the quality of life in Saudi Arabia. The survey gathered responses from a considerable number of patients with almost an equal number of male and female participants. The main finding of this study revealed that there is an association between medication adherence and quality of life among patients with diabetes even after taken into account socio-demographic characteristics. That is, subjects with low medication adherence to treatment may have a lower quality of life compared to those with high medication adherence. These findings are consistent with a previous study that was conducted in primary care clinics in Makkah, Saudi Arabia, that found a strong association between medication adherence and quality of life for participants with chronic diseases (Khayyat *et al.*, 2019).

Not surprisingly, the findings showed a low level of medication adherence among participants due to patient behavior and/or due to additional disease and pill burden. These findings are consistent with the previous studies that documented the same results among Saudi patients with diabetes and/or hypertension (Khayyat *et al.*, 2017, 2019). Furthermore, the results revealed that non-adherence to diabetic medications due to financial constraints was not statistically significant, and this might be because Saudi patients have free access to medications and health care services. These findings conflicted with the findings from previous studies (Adisa and Fakeye, 2014; Polonsky and Henry, 2016; Rezaei *et al.*, 2019), which found that the financial barrier was seen among a significant proportion of patients and might have contributed to low adherence.

Overall, a strong positive correlation between adherence to medication and health-related quality of life was observed. The study considered possible confounding factors age, gender, education status, monthly income, no. of comorbidities, type of antidiabetic medication, and

random blood glucose level (Alshayban and Joseph, 2019) and accounted in the analysis using multiple regression modeling. Importantly, it was found that patients who had a high adherence based on behavior-related non-adherence were mostly in perfect health as compared to those with moderate and low adherence who had a compromised quality of life irrespective of their socio-demographic and clinical characteristics. The findings were supported by a previous cohort study that found side effects and forgetfulness as the most common reasons for non-adherence (Krack *et al.*, 2018).

In a German study involving cardiovascular patients, adherence was significantly associated with HRQoL (Krack *et al.*, 2018). Quality of life tended to drop with decreasing adherence to medications. Further, the adjusted odds ratio for perfect health status indicated that patients with low adherence had less than 20% probability of achieving a perfect health status. Furthermore, with a unit increase in adherence score, there was a significant increase in quality of life score. In a study in Lebanon, it was observed that an increase in QoL would translate into an increase in adherence (Farhat *et al.*, 2019).

Besides, patients who demonstrated high adherence in the face of comorbidities and high pill burden were mostly in perfect health ($p < 0.001$). There was no significant association between financial issues and health status ($p > 0.05$). The finding was likely as Saudi patients do not pay out-of-pocket for the health care service. Hence, economic issues are not a determinant of adherence and may not affect the quality of life (AlQarni *et al.*, 2019).

Despite the fact this present study was among the few studies that explore the association between adherence and quality of life for diabetic patients in Saudi Arabia, it has some limitations. Selection bias is frequently linked to convenient sampling. Therefore, since the hospitals were selected based on our convenient accessibility, the generalization of our findings may be limited. Remarkably, some disease characteristics were not included in our analyses (e.g., HbA1c and duration of illness) due to the fact that most of the patients were not exactly able to remember them.

The study found that adherence was directly associated with HRQoL among diabetes patients in Saudi Arabia. The adherence to antidiabetic medications could be improved if patients are counseled regarding the importance of adherence and its repercussions. This could translate into a better quality of life. Finally, the

study might contribute to the growing body of evidence regarding treatment adherence and its impact on the quality of life, and it might provide important information to Saudi decision-makers to develop an effective intervention that can help in improving both adherence and quality of life for diabetic patients in Saudi Arabia.

5. ACKNOWLEDGMENTS

The authors are greatfull to Dr. Muhammed Aftab for his valuable advice, and Ms. Razan and Ms. Zahra for their help on data collection.

6. REFERENCES

1. Adisa, R. and Fakeye, T. O. (2014) 'Treatment non-adherence among patients with poorly controlled type 2 diabetes in ambulatory care settings in southwestern Nigeria.', *African health sciences. Makerere University Medical School*, 14(1), pp. 1–10. DOI: 10.4314/ahs.v14i1.2.
2. Ahmed, N. O., Abugalambo, S., and Almethen, G. H. (2017) 'Adherence to oral hypoglycemic medication among patients with diabetes in Saudi Arabia.', *International Journal of health sciences. Qassim University*, 11(3), pp. 45–49. Available at: <http://www.ncbi.nlm.nih.gov/pubmed/28936151> (Accessed: 30 April 2018).
3. Al-Ghamdi, S. H., Ahmad, G. A. U., Ali, A. H., Bahakim, N. O., Alomran, S. I., Alhowikan, W. K., Aljuaid, F. F. (2018) 'How do Saudi diabetic patients perceive their illness? A multicenter survey using revised-illness perception questionnaire.', *Journal of family & community medicine. Wolters Kluwer -- Medknow Publications*, 25(2), pp. 75–81. DOI: 10.4103/jfcm.JFCM_63_17.
4. AlQarni, K., AlQarni, E. A., Naqvi, A. A., AlShayban, D. M., Ghorri, S. A., Haseeb, A., ... Jamshed, S. (2019) 'Assessment of Medication Adherence in Saudi Patients With Type II Diabetes Mellitus in Khobar City, Saudi Arabia', *Frontiers in Pharmacology. Frontiers*, 10, p. 1306. DOI: 10.3389/fphar.2019.01306.
5. Alshayban, D. and Joseph, R. (2019) 'Health-related quality of life among patients with type 2 diabetes mellitus in Eastern Province, Saudi Arabia: a cross-sectional study', *PLOS ONE*. DOI: 10.1371/journal.pone.0226169.
6. Daya, R., Bayat, Z. and Raal, F. J. (2016) 'Effects of diabetes mellitus on health-related quality of life at a tertiary hospital in South Africa: A cross-sectional study', *South African Medical Journal. Health & Medical Publishing Group*, 106(9), p. 918. DOI: 10.7196/SAMJ.2016.v106i9.9899.

7. Devlin, N. J., Shah, K. K., Feng, Y., Mulhern, B., & van Hout, B. (2018) 'Valuing health-related quality of life: An EQ-5D-5L value set for England', *Health Economics*, 27(1), pp. 7–22. DOI: 10.1002/hec.3564.
8. Farhat, R., Assaf, J., Jabbour, H., Licha, H., Hajj, A., Hallit, S., & Khabbaz, L. R. (2019) 'Adherence to oral glucose-lowering drugs, quality of life, treatment satisfaction and illness perception: A cross-sectional study in patients with type 2 diabetes', *Saudi Pharmaceutical Journal*, 27(1), pp. 126–132. DOI: 10.1016/j.jsps.2018.09.005.
9. Grandy, S. and Fox, K. M. (2008) 'EQ-5D visual analog scale and utility index values in individuals with diabetes and at risk for diabetes: Findings from the Study to Help Improve Early evaluation and management of risk factors Leading to Diabetes (SHIELD)', *Health and Quality of Life Outcomes*, 6(1), p. 18. DOI: 10.1186/1477-7525-6-18.
10. Heng, J. K., Koh, L. J., Toh, M. P. H. S., & Aw, D. C. W. (2015) 'A study of treatment adherence and quality of life among adults with chronic urticaria in Singapore', *Asia Pacific Allergy*, 5(4), p. 197. DOI: 10.5415/apallergy.2015.5.4.197.
11. Herdman, M., Gudex, C., Lloyd, A., Janssen, M., Kind, P., Parkin, D., & Badia, X. (2011) 'Development and preliminary testing of the new five-level version of EQ-5D (EQ-5D-5L)', *Quality of Life Research*, 20(10), pp. 1727–1736. DOI: 10.1007/s11136-011-9903-x.
12. Holmes, J., McGill, S., Kind, P., Bottomley, J., Gillam, S., & Murphy, M. (2000) 'Health-related Quality of Life in Type 2 Diabetes (T2ARDIS-2)', *Value in Health*, 3, pp. S47–S51. DOI: 10.1046/j.1524-4733.2000.36028.x.
13. Khayyat, S. M., Khayyat, S. M. S., Hyat Alhazmi, R. S., Mohamed, M. M. A., & Abdul Hadi, M. (2017) 'Predictors of Medication Adherence and Blood Pressure Control among Saudi Hypertensive Patients Attending Primary Care Clinics: A Cross-Sectional Study', *PLOS ONE*. Edited by N. C. Barengo, 12(1), p. e0171255. DOI: 10.1371/journal.pone.0171255.
14. Khayyat, S. M., Mohamed, M. M. A., Khayyat, S. M. S., Hyat Alhazmi, R. S., Korani, M. F., Allugmani, E. B., & Abdul Hadi, M. (2019) 'Association between medication adherence and quality of life of patients with diabetes and hypertension attending primary care clinics: a cross-sectional survey', *Quality of Life Research*, 28(4), pp. 1053–1061. DOI: 10.1007/s11136-018-2060-8.
15. Koopmanschap, M., and CODE-2 Advisory Board (2002) 'Coping with Type II diabetes: the patient's perspective', *Diabetologia*, 45(S1), pp. S21–S22. DOI: 10.1007/s00125-002-0861-2.
16. Krack, G., Holle, R., Kirchberger, I., Kuch, B., Amann, U., & Seidl, H. (2018) 'Determinants of adherence and effects on health-related quality of life after myocardial infarction: a prospective cohort study', *BMC Geriatrics*. BioMed Central, 18(1), p. 136. DOI: 10.1186/s12877-018-0827-y.
17. Naeem, Z. (2015) 'Burden of Diabetes Mellitus in Saudi Arabia.', *International Journal of health sciences*. Qassim University, 9(3), pp. V–VI. DOI: 10.12816/0024690.
18. Naqvi, A. A., Hassali, M. A., Rizvi, M., Zehra, A., Iffat, W., Haseeb, A., & Jamshed, S. (2018) 'Development and Validation of a Novel General Medication Adherence Scale (GMAS) for Chronic Illness Patients in Pakistan', *Frontiers in Pharmacology*, 9, p. 1124. DOI: 10.3389/fphar.2018.01124.
19. Naqvi, A. A., AlShayban, D. M., Ghori, S. A., Mahmoud, M. A., Haseeb, A., Faidah, H. S., & Hassali, M. A. (2019) 'Validation of the General Medication Adherence Scale in Saudi Patients With Chronic Diseases', *Frontiers in Pharmacology*, 10. DOI: 10.3389/fphar.2019.00633.
20. Polonsky, W. and Henry, R. (2016) 'Poor medication adherence in type 2 diabetes: recognizing the scope of the problem and its key contributors', *Patient Preference and Adherence*, Volume 10, pp. 1299–1307. DOI: 10.2147/PPA.S106821.
21. Rezaei, M., Valiee, S., Tahan, M., Ebtekar, F., & Ghanei Gheshlagh, R. (2019) 'Barriers of medication adherence in patients with type-2 diabetes: a pilot qualitative study.', *Diabetes, metabolic syndrome, and obesity: targets and therapy*. Dove Press, 12, pp. 589–599. DOI: 10.2147/DMSO.S197159.
22. Robert, A., Al Dawish, M., Braham, R., Musallam, M., Al Hayek, A., & Al Kahtany, N. (2016) 'Type 2 Diabetes Mellitus in Saudi Arabia: Major Challenges and Possible Solutions', *Current Diabetes Reviews*, 13(1), pp. 59–64. DOI: 10.2174/1573399812666160126142605.
23. Wexler, D. J., Grant, R. W., Wittenberg, E., Bosch, J. L., Cagliero, E., Delahanty, L., & Meigs, J. B. (2006) 'Correlates of health-related quality of life in type 2 diabetes', *Diabetologia*, 49(7), pp. 1489–1497. DOI: 10.1007/s00125-006-0249-9.

O SISTEMA EDUCACIONAL NO CONTEXTO DAS TRANSFORMAÇÕES SOCIOECONÔMICAS**THE EDUCATION SYSTEM IN THE CONTEXT OF SOCIO-ECONOMIC TRANSFORMATIONS****СИСТЕМА ОБРАЗОВАНИЯ В УСЛОВИЯХ ОБЩЕСТВЕННО-ЭКОНОМИЧЕСКИХ ТРАНСФОРМАЦИЙ**

GAPSALAMOV, Almaz Rafisovich¹; MERZON, Elena Efimovna²; KUZNETSOV, Maksim Sergeyevich³; VASILEV, Vladimir Lvovich⁴; BOCHKAREVA, Tatyana Nikolaevna^{5*}

^{1,3,4} Kazan Federal University, Elabuga Institute of KFU, Economics and Management Faculty, Russia.

² Kazan Federal University, Elabuga Institute of KFU, Psychology and Pedagogy Faculty, Russia.

⁵ Kazan Federal University, Elabuga Institute of KFU, Psychology and Pedagogy Faculty, Russia.

** Corresponding author
e-mail: tatyana-n-boch@bk.ru*

Received 09 February 2020; received in revised form 26 February 2020; accepted 16 March 2020

RESUMO

O mundo moderno está entrando em um novo estado de desenvolvimento associado ao processo de digitalização. Afeta todos os aspectos da sociedade, muda as fundações tradicionais e impõe novos requisitos para o processo educacional. Os sistemas educacionais nacionais não podem permanecer distantes desse processo. O objetivo deste artigo é estudar o processo de digitalização e seu impacto no sistema educacional do mundo e na Federação Russa. A metodologia do artigo é baseada em uma abordagem sistêmica e estrutural-funcional. A validade dos resultados do estudo é baseada no uso de métodos científicos e especiais populares, incluindo análise, síntese, análise histórica e comparativa. Com base na análise da literatura científica, os autores formaram uma imagem geral do problema em consideração. O trabalho analisa os processos que ocorrem no mundo associados ao início de um novo período histórico. O novo tempo também impõe novos requisitos em vários ramos do conhecimento, atualiza abordagens para o uso de tecnologias da informação modernas e futuras. Um lugar específico é dado à abordagem sinérgica, que é uma alternativa otimista para dominar o conhecimento e as competências da educação digital. No artigo, os autores apontam para o atraso na base teórica do processo de digitalização, o atraso na infraestrutura, deficiências na organização do processo educacional, revelam contradições cognitivas e, ao mesmo tempo, mostram formas possíveis de resolvê-las.

Palavras-chave: *sinérgica, revolução digital, economia do conhecimento, modernização do sistema educacional.*

ABSTRACT

The modern world is entering a new state of its development associated with the digitalization process. It affects all aspects of society, changes the traditional foundations and imposes new requirements for the educational process. National educational systems cannot remain aloof from this process. The purpose of this article is to study the digitalization process and its impact on the education system of the world and the Russian Federation. The methodology of the article is based on a systemic and structural-functional approach. The validity of the results of the study is based on the use of popular scientific and special methods, including analysis, synthesis, historical and comparative analysis. On the basis of the analysis of scientific literature, the authors formed an overall picture of the problem under consideration. The work analyzes the processes occurring in the world associated with the beginning of a new historical period. The new time also imposes new requirements on various branches of knowledge, updates approaches to the use of modern and future information technologies. A particular place is given to the synergistic approach, which is an optimistic alternative to mastering the knowledge and competencies of the digital education. In the article the authors point to the lag in the theoretical base of the digitalization process, the lag in infrastructure, shortcomings in the organization of the educational process, reveal cognitive contradictions and, at the same time, show possible ways to solve them.

Keywords: *synergetics, digital revolution, knowledge economy, modernization of the educational system.*

АННОТАЦИЯ

Современный мир вступает в новое состояние своего развития, связанное с процессом цифровизации. Он затрагивает все стороны жизни общества, меняет традиционные устои и налагает новые требования к образовательному процессу. Не могут остаться в стороне от данного процесса национальные образовательные системы. Целью представленной статьи является исследование процесса цифровизации и его влияние на систему образования мира и Российской Федерации. Методология статьи строится на системном и структурно-функциональном подходе. Достоверность результатов исследования основана на использовании общенаучных и специальных методов, в том числе анализа, синтеза, исторического и сравнительного анализа. На основе анализа научной литературы авторы сформировали общую картину рассматриваемой проблемы. В работе анализируются процессы, происходящие в мире, связанные с началом нового исторического периода. Новое время налагает и новые требования к различным отраслям знания, актуализирует подходы к использованию современных и будущих информационных технологий. Особое место здесь отводится синергетическому подходу, который является оптимистической альтернативой для овладения знаниями и компетенциями в рамках цифрового образования. В статье авторы указывают на отставание теоретической базы процесса цифровизации, отставание инфраструктуры, недостатки в организации образовательного процесса, вскрываются когнитивные противоречия и, одновременно, показаны возможные пути их разрешения.

Ключевые слова: *синергетика, цифровая революция, экономика знаний, модернизация системы образования.*

1. INTRODUCTION:

The beginning of the new century is characterized by reaching important positions in the economic development, based on the innovative knowledge, digital technologies, usage of artificial intelligence, full application of robotic systems with the extended range of adaptation to production. Nevertheless, there are such problems on the way of the scientific and technology progress which have never been faced by the society before - lack of linearity, super-complexity, non-specificity, creation of innovative knowledge bases which meet the requirements of high technologies and large scale of the expanding digital revolution (Alajmi, 2019).

The solutions that can give answers to the whole combination of the interrelated questions are in high demand. At the same time, there are more critical issues related to the appearance of the new digital technologies, knowledge and self-organizing very complex machine systems and large-scale digital infrastructure. It is necessary to create unique and reliable security systems and devices for the defense from cyberattacks (Bulanichev *et al.*, 2007; The program "Digital Economy of the Russian Federation," 2017; Sveiby, 1997).

In the modern world, the efficiency of any organization, including higher education institutions, is defined by mobilization of the staff members' intellect, learning new competencies and acquirement of new knowledge (Korableva *et*

al., 2019 a, b; Ziyadin *et al.*, 2018).

The outstanding foreign and Russian scientists researched the background and conditions of the modern digital revolution development: A. Toynbee, I.R. Prigozhin, (1986), P.F. Drucker, (2003). C. Shannon, R. Ashby, K.E. Swaby, M. Rumisen, G. Haken, and also N.N. Moiseev, V.M. Glushkov, A.A. Samarsky, (1989). S.P. Kurdyumov, (1989), G.G. Malinetskiy, (2002), D.S. Chernovsky, (2004), A.N. Uemova, and others.

The technological features of the new era are "Questions of "unknown complexity" (A. A. Samarsky, 1989); problems of "incredible scale" (S.P. Kurdyumov, 1989); aspects appeared due to the introduction of non-linearity, non-equilibrium, irreversibility, paradox, ambivalence in calculating the effectiveness of the economic processes (I.R. Prigozhin, 1986); problems connected with the transition from cybernetics to synergy, when the chief aim is not the stability in the systems and processes, but their constant change, development, re-engineering (G.G. Malinetsky, 2002).

These technological changes were responded by such organizational answers as research and development; moreover, it was not research of some specific organizations, but studying the trends of development (Johnson and Hinton, 2019). The description of the researched trends in the quantity form becomes so complicated and even impossible that new research methods are needed; it is also necessary

to change traditional ways of solving problems into new ones, which refer to the phase and structural level.

Scientists state that the methods of research which used to be successful are not relevant anymore. The new comprehension of nature is undergoing groundbreaking changes in the direction of diversification, temporality and complexity. The processes linked to contingency and irreversibility, which used to be considered as exceptions, nowadays are beginning to play a significant role (Prigozhin *et al.*, 1986, p. 11). The complexity originates from the non-linearity of the issues under research and the diversity of the possible answers to the questions. The basis of scientific research technology, analysis, and prognosis is compound of mathematical model and simulation experiment on computers (Samarsky *et al.*, 1989, p. 126).

The change of the scientific paradigm in the information sphere due to the progress of computer facilities is inevitable. The development of society and the economy led to the appearance of such a new non-material asset as knowledge. Information technologies speed up the process of integrating knowledge into economic turnover (Rumezen, 2004, p. 18). In the USA, experts in the management, sphere raised a question about managing non-material assets as the central management task in the XXI century. Knowledge is not only a business resource; it is a universal social resource (Drucker, 2003, p. 14).

Thus, society faces a unique resource that changes the material world, yet, it the kind of support that requires specific organization, technology, and management. Information technologies are the product of knowledge evolution on the one hand and an instrument for knowledge management on the other side (Knowledge Management, 2000).

The information revolution brings forth new requirements. In the first place, it is a necessary staff assistance. Besides the users of the end information products, there is a need for specialists that can create computer programs. Computer systems analysts and programmers who will be able to transfer users' tasks into the computer language are required (Pospelov, 1988, p. 14-15).

It is beneficial to study the experience of the countries which are most advanced in the sphere of informatics, robotic systems and system researches, such as Japan, the USA, Singapore, Finland etc (Lysytsia *et al.*, 2019). The Japanese, for example, think that computing techniques

should not be more challenging to use than using a washing machine. The Japanese example shows that people got used to cooperation with a device, considering its compactness, speed of operation, low price, reliability, large memory capacity, optimized architecture and adjusted to the work, not with the numerical but with the symbol information (Pospelov, 1988, p. 22).

Thus, the purpose of the presented article was to analyze the problems, tasks, prospects for the development of the digital revolution and its impact on the economy and education system of the Russian Federation.

2. MATERIALS AND METHODS:

Digital device which allows us to analyze, calculate, experiment, and plan is called a computer of 5-6th generation. This provides the basis for creating the artificial intellect. In the Institute of Applied Automatic Control Engineering named after M.V. Keldysh, applying the methods of computer-oriented experimentation, there were held works on using plasma processing, peaking regimes, non-linear phenomena etc.

This puts the question of acquiring new modes of scientific research and educational process (Gafurov *et al.*, 2020; Safiullin *et al.*, 2019; Suwarni *et al.*, 2020). Notably, the synergy approach to the educational process is more spread nowadays (Bulanichev *et al.*, 2007; Knyazeva *et al.*, 2005; Kuzetsov *et al.*, 1998; Malinetsky *et al.*, 2002; Prigozhin *et al.*, 1986). In this regard, the systematic and structural-functional approaches have become the methodological basis of scientific research. The reliability of the presented research results is ensured by the use of general scientific and special methods, including analysis, synthesis, modeling, content analysis, statistical, historical and others.

The historiographic analysis of works on the impact of digitalization on the modern world is widely used in the work. This method is based on the identification of historical knowledge, its paradigmatic foundations and connections with the historiographic culture of its time. The need for its use is justified by the fact that, based on the observance of the time sequence, the continuity of the change of periods and stages, each fact was analyzed in the process of occurrence, formation and development.

The article also widely used structural-functional analysis. Based on it, conclusions were drawn about cardinal changes in the technological

and information space of our time.

To identify the problems of the impact of the digitalization process on the education system, we used content analysis. This method made it possible to determine the composition and structure of digitalization problems in the world, determine their quantitative significance, and outline priority areas for improving the education system under the influence of emerging trends.

A significant place was given to the synergistic approach to the educational process. The general background of the research was based on a special methodology, the core of which is the guarantor of the continuity of scientific values, on the one hand, and openness to innovation, on the other. Such an open adaptive formation methodology is the methodology of synergetics. It is designed to realize, root the principles of synergetics in the public mind, and adapt them for lay people no longer at the level of metaphors, but constructive principles that help to understand and model reality.

A synergetic approach (synergetic paradigm) was used in relation to the educational process, the mastery and use of knowledge in which takes into account openness, self-organization (search and use in the educational process of those methods that allow you to obtain maximum results in solving specific problems); recognizes non-linearity as a natural stage in the cognitive process, bifurcation of the environment, non-uniformity of decisions, disproportionate responses to small influences.

The system of obtaining knowledge was considered not as the transfer of knowledge from one head to another, but as the production of new knowledge, as a transition to a new quality of understanding of new meanings, mastery of a new categorical apparatus based on logical-structural search and research. The recognition of learning as a cascade of phase and structural ascensions to truth, the recognition of the historical development process as an irreversible convergence of chaos and disordered forms into ordered systems. Synergetics in the educational process has opened up new opportunities for the recognition of an interdisciplinary synthesis of knowledge that dominates processes in a space of interrelated scientific areas. The synergetic approach has opened up the possibility of mastering such "wrong" phenomena as emergence, resonance, ambivalence, chirality, etc. as a normal method of cognition, which expanded the potential of cognition of objects and processes. The synergetic approach proposed by

the authors drew attention to the role of such weak signals in cognition as coordination, synchronization, catalysis (autocatalysis), vibrations (self-oscillations), and modification, which have not yet entered the vocabulary of cognitive and educational programs. Meanwhile, these "weak" signals form strong structures.

It is the synergistic approach that is the most optimistic alternative for acquiring new knowledge and competencies in the digital revolution.

3. RESULTS AND DISCUSSION:

A wide range of knowledge and competencies required to manage the digital revolution requires professional training of students, specialists, and employees of organizations dealing with digital technologies (Figure 1).

It is impossible to compose a classifier and codification of knowledge in one particular article. Moreover, there is a danger of limitation and even loss of information (including digital) resources in Russia. Hacker attacks on the Russian information systems cause a great amount of danger. The security issue is of immediate interest now. For the educational tasks of students training, it is necessary to create bases of knowledge in a specific regime (automated or manual) or to buy them. University education programs should include the necessary training courses. The Ministry of Science and Higher Education should support this process. The selection of information knowledge bases for each particular task should be specific, with the possibility of maximum expansion, with a certain expenditure of funds. Most advanced corporations created programs of knowledge management – Intel, Siemens, IBM, Johnson & Johnson, World Bank Group, British Petroleum, British Telecom, etc. Since the 1980s, in the USSR there existed Reference Information Systems (ZAPSIB, DILOS, POET, GRANIT, MAVR) in which application software packages were developed.

So, the knowledge economy started its existence about forty years ago, but with the transition to digital technologies, the development acquired an intensified character. Digital programming, information distribution, project development got a breakthrough role in the advanced countries and the USSR and the Russian Federation, especially when there was a transition to the computers of 5th and 6th generations.

This transition to the intellectual, self-organizing, self-programming computers raises a question of new types of problems. First of all, there are robotic complexes, remotely piloted vehicles, taking digital issues to space. There has been brought up the question of preparing 2-3 million specialists of the new type. Taking into consideration the difficult demographic situation in Russia, preparing skilled workers for the digital revolution is becoming an issue of vital importance. The solution to this problem should be found by educational institutions, scientific-research institutes, design, and technology institutes.

There is a demand not only for specialists in digital programming but professionals in expert automated systems, control of complex production systems, nanotechnology with automated research and management.

The need for artificial intelligence arose in the 1980s about the attempts to simulate psychophysical, creative, chess-game, research operations, composing literary texts, music, etc. on computers. Modeling of psychophysical processes, in addition to the general theory of systems, system analysis, system synthesis, system dynamics, includes theories of biology, physiology, social economics, the theory of large (TLS), and complex systems (TCS). Models which can simulate way of thinking of specific people or groups of people are in high demand (Polyakova *et al.*, 2019; Neizvestnaya *et al.*, 2018; Abramovich *et al.*, 2019; Shrestha, 2019; Magsumov, 2019; Tarman, 2016; Yemelyanov *et al.*, 2019; Kolawole *et al.*, 2019). Bionic, neurological, neurophysical, neuropsychological attempts to simulate the work of the brain require special devices that started to be used in computers of the 5th and 6th generations.

Artificial intelligence theory is at the stage of being developed. The emergence of automated control systems (ACS), computer-aided design (CAD) systems, network clustering, scaling in 3D, 4D, 5D space require new competencies, knowledge, and strategies. The new paradigm of the cascade of scientific and technological revolutions of the XXI century in the sphere of computer science includes the several trends (Drucker, 2003; Knyazeva *et al.*, 2005; Kuznetsov *et al.*, 1998; Malinetsky *et al.*, 2002; Sturm and Quaynor, (2020):

The information program itself finds the data necessary for its work, converts them into text or voice signals, or transfers it to the relevant executive bodies; the task of searching for the

programs that bring knowledge to the necessary condition is being solved; computer is getting the ability to set aims itself; computer beside the symbolic system of storing and processing data starts to have the "sensor-based" system of data handling, choice of crucial factors of solving problems, ability to recognize images, mental pictures, "see the future";

The person who studies the modern paradigm of information technology should master a systematic approach, including system analysis, system synthesis, system dynamics and, above all, non-linear dynamics (synergetic), as well as cybernetic methods of information security; a logical and mathematical methods of analysis and modeling synthesis; modern languages and procedures of programming; contact and non-contact methods of interaction with a computer; construction of positive (synergetic) and negative (cybernetic) connections in knowledge management systems; master the techniques of overcoming uncertainty, ambiguity, fractal dimension, non-linearity, disequilibrium in the tasks of systematization, structuring, as well as emergence, non-uniqueness of solutions at bifurcation points, building hierarchy of databases, knowledge bases, modeling of objects and processes with a large number of degrees of freedom, ambivalence, chirality; and creating innovative content to expand the digital economy space.

Optic fiber and holographic entered the sphere of digital technologies to store, processing data, and provide its security. That's why these trends should be included in the contents of the educational program for specialist training. The rules of safety suggest storing information in the system that has some branches around the whole net as vibrations of different frequencies (Rumezen, 2004, p. 3).

The interconnection of informatics, optic fiber, and holographic provides new promising opportunities for the digital economy, intelligence systems, and unattended machining. Artificial intelligent robots are getting the ability to change their behavior within a wide range in terms of autonomous management centers. In the future, the conflicts between intelligent systems will constitute more frequent threats and danger than ever (Popper, 1983; Walton, 1997; Sveiby, 1997).

We should expect conflicts of aims, tasks, and interests of the systems functioning in the frame of cybernetics and synergetic. All these facts demand robust programs for providing security and high-speed performance. There will

be a need for the program of coordination of autonomous systems working in the same area and conducting the program ensembles. Complexity, scale, uncertainty, non-linearity, disequilibrium, autocatalysis, self-oscillations of large and complex systems (LTS and CTS), carry threats and challenges, and people who work in the area of intelligent systems and modern informatics should be prepared for it.

Synergetics as science allows us to solve new problems of the information revolution and prepare specialists according to the new requirements with the necessary digital competences. D. Nash, A. Turing, A. Toynbee, S. Hawking, K. Sagan predict the most severe complications that await humanity in the future. This means that a mighty intellectual effort will be required to quench the threats and challenges related to information technologies. To create a security system and neutralize the destructive difficulties and risks of the new information world, it is necessary to remove worldview myths, barriers, gaps, contradictions in the minds of people who generate and consume new ideas and technologies in the information sphere. Information development can be stable, safe and translationally progressive in case people master the methods of self-organization (synergetics). These methods involve the transition of chaos into order, spontaneity in purposefulness. In terms of the digital revolution, the formation of ordered structures can be carried out according to the schemes and principles described by R. Clausius, C. Darwin, E. Schrödinger, A. Einstein, I.R. Prigogine, V.I. Vernadsky, A.A. Bogdanov, A. Bertalanffy, S. Hawking (2004).

In the information sphere, order and chaos are created according to the same schemes and principles that operate in thermal, organic, physical, space, chemical, geological systems. This challenging task must be solved in classrooms, laboratories, at philosophical seminars, and mathematical congresses. The global landscape is such that a particular cannot break out of the whole and dominate it. It is necessary to create a collective mind (Schrodinger, 2019, p. 52). Presumably, to a certain extent, no more than 3% of the part of the Universe surrounding us is available to humanity (Prigozhin *et al.*, 1986, p. 6). Mankind hasn't yet mastered many secrets and laws of nature and does not even try to think about it. Nevertheless, these facts do not relieve us of responsibility for the future (Kuzetsov, 1998, p. 3).

The movement into the future of large complex systems goes through rhythm cascades

imposed on each other. To cause a resonant position of rhythm cascade oscillations and to obtain the maximum synergistic effect, complex management actions on the mega system are required. These are the conditions necessary for minimizing losses and ensuring digital security (Drucker, 2003; Knyazeva *et al.*, 2005; Vu, 2019; Kuzetsov *et al.*, 1998; Malinetsky *et al.*, 2002; Prodanova *et al.*, 2019; Prigozhin *et al.*, 1986). Revolutionary changes in the sphere of computer science, including the digital economy, oblige the generation of the first half of the XXI century to act competently, rationally and consistently in the area of digital technology development.

There are other trends in the information sphere. Scientists encourage us to discover and introduce new methods of cognition without fear (Popper, 1983, p. 27). Hundreds of billions of dollars around the world are spent on the search for adequate methods and developing new ways of describing and modeling. The cognition of the world demands research in all areas (gnoseological, epistemological, ontological, systemological, etc.). A lot of special attention is paid to objects and processes characterized by openness, nonlinearity, irreversibility, nonequilibrium, ambiguity, uncertainty, emergence, synergy, chirality, ambivalence, self-oscillation, auto-catalysis.

There is specific experience in the formation of economic knowledge and the creation of knowledge management systems in Russia - this is the "Strategy for the Development of the information society for 2017-2030." This document was approved by the Decree of the President of the Russian Federation of 9 May 2017 No. 203 (The program "Digital Economy of the Russian Federation," 2017; Decree "On the Strategy for the Development of the Information Society in the Russian Federation for 2017-2030", 2017). In the Russian Federation, centers, technology parks, technopolises in the field of information technology have been arranged. Directive and regulatory documents were created, including "The Digital Economy of the Russian Federation," ratified by order of the Government of the Russian Federation of July 28, 2017 No. 1632-r.

There have been created documentation and structures, scientific centers, technopark structures throughout the country. There were created regional centers with a world level of information technology - Moscow, St. Petersburg, Nizhny Novgorod, Kazan, Yekaterinburg, Novosibirsk, Tomsk, Samara. The Kaspersky Center, dealing with information security systems,

information technology technopolises in Zelenograd, Tomsk; Innopolis in the Republic of Tatarstan won world fame. Some enterprises are making efforts to work on unmanned driving vehicles. In general, Russia makes the top fifty in the ranking of countries' readiness for the digital economy, and make the top forty in the use of innovative results in digital technologies. Russia is lagging in creating a regulatory framework for the digital economy; the level of digital technology usage in business structures is rather low.

4. CONCLUSIONS:

The experience of such countries as the USA, Japan, China, Singapore, and other countries that have achieved the immense success in the field of information revolution proves that the main trends of applying efforts by the advanced countries are formation of the society of knowledge; creation of the digital economy; raising the level of information awareness and digital literacy of the population; creation of new digital technologies, new digital platforms; enhancing the material and technical base of organizations in the field of information technology; increasing attention to environmental safety of the information sphere, a variety of forms, methods of representing the reality; support for creative ways of knowledge presentation; researchers' attention is focused on the breakthrough knowledge in the field of computer science and pattern recognition; growing recognition in the science of the direction known as "creative self-destruction"; the status of paradoxical and intuitive knowledge of our world is reinforced; the interdisciplinarity of knowledge is intensified; and the synergistic approach to cognition becomes dominant.

The main trends of the development of the digital economy in Russia are statutory regulation, the formation of a new regulatory environment that provides a favorable legal regime for the emergence and development of modern technologies; creation of a permanent mechanism for managing changes and competencies (knowledge) in the area of the digital economy regulation; withdrawal of key legal restrictions and the creation of separate institutions aimed at solving the high-priority tasks of creating a digital economy; the formation of a full-scale legislative regulation of relations emerging due to the development of the digital economy; taking actions aimed at stimulating economic activity related to the use of modern technologies, data collection, and use; the formation of a policy of the digital economy development in the territory of the

Eurasian Economic Union, the harmonization of approaches to legal regulation that contribute to the development of the digital economy within the Eurasian Economic Union; and establishment of a methodological basis for the development of competences in the field of digital economy regulation.

Time has propelled knowledge to the top strategic position. Digital technology is one of the contemporary elements of the "knowledge" system. Knowledge management determines the effectiveness of production systems and the quality of life to a large scale. The new scientific paradigm - synergetics - aims at integration, cooperation, blending into mega systems, and their self-organization. This paradigm brings intellectual resources in the activities of staff, harmonization, synchronization, constructive interaction for achieving a common goal. This is entirely applied to knowledge, knowledge management, the knowledge economy, to such an essential part of knowledge as digital technology.

Education proves to be essential in terms of mastering innovative knowledge. For 10 thousand people in Russia, there are 340 university students. On top of that, an extensive army studies at colleges, technical schools, and other educational institutions. The educational process is carried out in technopolises, innopolises, IT- technology parks. While choosing effective forms of education, harmonizing goals, tasks, financing the educational process with the infrastructure, it will not take long to see the results. The experience of India, Singapore, Japan, Finland, and other countries confirms the possibility of optimistic prospects.

5. ACKNOWLEDGMENTS:

The reported study was funded by RFBR, project number 19-29-07037.

6. REFERENCES:

1. Alajmi, M. A. (2019). The impact of E-portfolio use on the development of professional standards and life skills of students in the Faculty of Education at Princess NouraBint Abdul Rahman University, Entrepreneurship and Sustainability Issues 6(4) 1714-1735. [http://doi.org/10.9770/jesi.2019.6.4\(12\)](http://doi.org/10.9770/jesi.2019.6.4(12))
2. Bulanichev, V. A., Serkov, L.A. (2007). Synergetic modeling of educational processes. Yekaterinburg: Institute of Economics, Ural Branch of RAS: AMB

- Publishing House.
3. Chernovsky, D. S. (2004). Synergetics and information. Dynamic information theory. Moscow: URSS.
 4. Chervinskaya, K. R. (2019). Methods of the conceptual analysis of knowledge. Methods and decision-making systems.
 5. Decree of the President of the Russian Federation of May 9, 2017 No. 203 "On the Strategy for the Development of the Information Society in the Russian Federation for 2017-2030"
 6. Dresvyannikov, V. A. (2006). Building a knowledge management system in an enterprise: a training manual. Moscow: KNORUS.
 7. Drucker, P. (2003). Effective Management. Economic Tasks and Optimal Solutions. Translated by. M. Kotelnikova. Moscow: AIR-PRESS.
 8. Gafurov, I. R., Safiullin, M. R., Akhmetshin, E. M., Gapsalamov, A. R., Vasilev, V. L. (2020). Change of the higher education paradigm in the context of digital transformation: from resource management to access control. International Journal of Higher Education, 9(3), 1-16.
 9. Hawking, S. A. (2004). Brief History of Time - St. Petersburg: Amphora.
 10. Johnson, C., & Hinton, H. (2019). Toward a Brilliant Diversity. Journal of Culture and Values in Education, 2(1), 56-70. Retrieved from <http://cultureandvalues.org/index.php/JCV/article/view/27>
 11. Knowledge Management. Research Report (2000).
 12. Knyazeva, E. N., Kurayumov, S. P. (2005). Foundations of synergetics, Synergetic worldview. Moscow: Komkniga.
 13. Korableva, O., Durand, T., Kalimullina, O., & Stepanova, I. (2019a). Usability testing of MOOC: Identifying user interface problems. Paper presented at the ICEIS 2019 - Proceedings of the 21st International Conference on Enterprise Information Systems, 2 468-475.
 14. Korableva, O., Durand, T., Kalimullina, O., & Stepanova, I. (2019b). Studying user satisfaction with the MOOC platform interfaces using the example of coursera and open education platforms. Paper presented at the ACM International Conference Proceeding Series, 26-30. doi:10.1145/3322134.3322139
 15. Lysytsia, N.; Martynenko, M.; Prytychenko, T.; Gron O.; Us M. (2019). Prospects for innovations in marketing of economic educational services in Ukraine, Entrepreneurship and Sustainability Issues 6(4): 1771-1783. [http://doi.org/10.9770/jesi.2019.6.4\(16\)](http://doi.org/10.9770/jesi.2019.6.4(16))
 16. KPMG Consulting (2001). Retrieved from <http://www.kpmg.com>
 17. Kuzetsov, B. L. (1998). Introduction into Economic Synergetics. Naberezhnye Chelny: KamPi Edition.
 18. Malinetsky, G. G. (2002). Order parameters, self-organization and education. Electron. Dan, Moscow: IPM named after M.V. Keldysh, Russian Academy of Sciences.
 19. Parangishvili, I. V., Abramova, N. A., Spiridonov, V. F., Kovriga, S. V., Razbegin, V. L. (1999). Search for approaches to solving problems. Series "Information Russia on the threshold of the XXI century". Moscow: SINTET.
 20. Pikovsky, A., Rosenblum, M., Kurihs, J. (2001). Synchronization, Cambridge University Press.
 21. Popper, K. (1983). Logic and the growth of scientific knowledge. Moscow: Progress.
 22. Pospelov, G. S. (1988). The soul and heart of the latest information technology. Hypotheses. Prognoses (Future Sciences): International Yearbook. Moscow: Knowledge.
 23. Prigozhin, I., Stengers, I. (1986). Order from chaos: A new dialogue between man and nature: Translated from English. Ed. by V.I. Arshinova, Yu.L. Klimontovich and Yu.V. Sachkova. Moscow: Progress.
 24. Rumezen, M. K. (2004). Knowledge Management: Translated from English. Moscow: Publishing House. LLC: Publishing House. LLC; 2004.
 25. Safiullin, M. R., & Akhmetshin, E. M. (2019). Digital transformation of a university as a factor of ensuring its competitiveness. International Journal of Engineering and Advanced Technology, 9(1), 7387-7390.

26. Samarsky, A. A., Kurdyumov, S. P. (1989). Paradoxes of a multivariate nonlinear world - the world around us. Hypotheses. Prognoses (the future of science): International Yearbook. Moscow: Knowledge.
27. Shrestha, M. (2019). Influences of gender and locale on teachers' job satisfaction. *Research in Educational Policy and Management*, 1(1), 17-32. Retrieved from <https://repamjournal.org/index.php/REPAM/article/view/7>
28. Schrodinger, E. (2019). *Quantum Code of the Universe: Translated from English by Migunova E.O.* Moscow: Rodina LLC: 2019.
29. Sturm, E., & Quaynor, L. (2020). A Window, Mirror, and Wall: How Educators Use Twitter for Professional Learning. *Research in Social Sciences and Technology*, 5(1), 22-44. Retrieved from <https://ressat.org/index.php/ressat/article/view/439>
30. Suwarni, Okagbue, H. I., Lydia, E. L., Shankar, K. (2020). Digital Economic Challenges and Economic Growth in Environmental Revolution 4.0. *Journal of Environmental Treatment Techniques*, 8(1), 546-550.
31. Sveiby, K. E. (1997). *The New Organizational Wealth*, San Fransisco.
32. Tarman, B. (2016). Innovation and Education. *Research in Social Sciences and Technology*, 1(1). Retrieved from <http://ressat.org/index.php/ressat/article/view/3>
33. The program "Digital Economy of the Russian Federation" dated July 28, 2017 No. 1632-r.
34. Vaga, T. (2019). *Profiting from Chaos. Using Chaos Theory for Market Timing, Stock Selection and option Valuation.* McGraw-Hill, New York.
35. Vu, T. (2019). Theoretical Constructs and Practical Strategies for Intercultural Communication. *Journal Of Curriculum Studies Research*, 1(1), 43-53. Retrieved from <https://curriculumstudies.org/index.php/Cs/article/view/3>
36. Walton H. (1997). *Measuring Knowledge-Based Assets Publishers?* Sam Francisco.
37. Werbos, P. (1974). *Beyond Regression: New Tools for Prediction and Analysis in the Behavioral Sciences.* PhD Thesis, Dept, of Applied Mathematics. Harvard University: Cambridge: Mass.
38. Wiener, N. (1983). *Cybernetics or Management and communication in the animal and machine.* Translated from English by I.V. Soloviev and G.N. Povarova; Ed. G.N. Povarova. 2nd ed. Moscow: Science; The main edition of publications for foreign countries.
39. Ziyadin, S., Ermekbaeva, B., Supugaliyeva, G., & Doszhan, R. (2018). Transformation of basic indicators of socio-economic processes in the digital economy. Paper presented at the Proceedings of the 31st International Business Information Management Association Conference, IBIMA 2018: Innovation Management and Education Excellence through Vision 2020, 2009-2017.

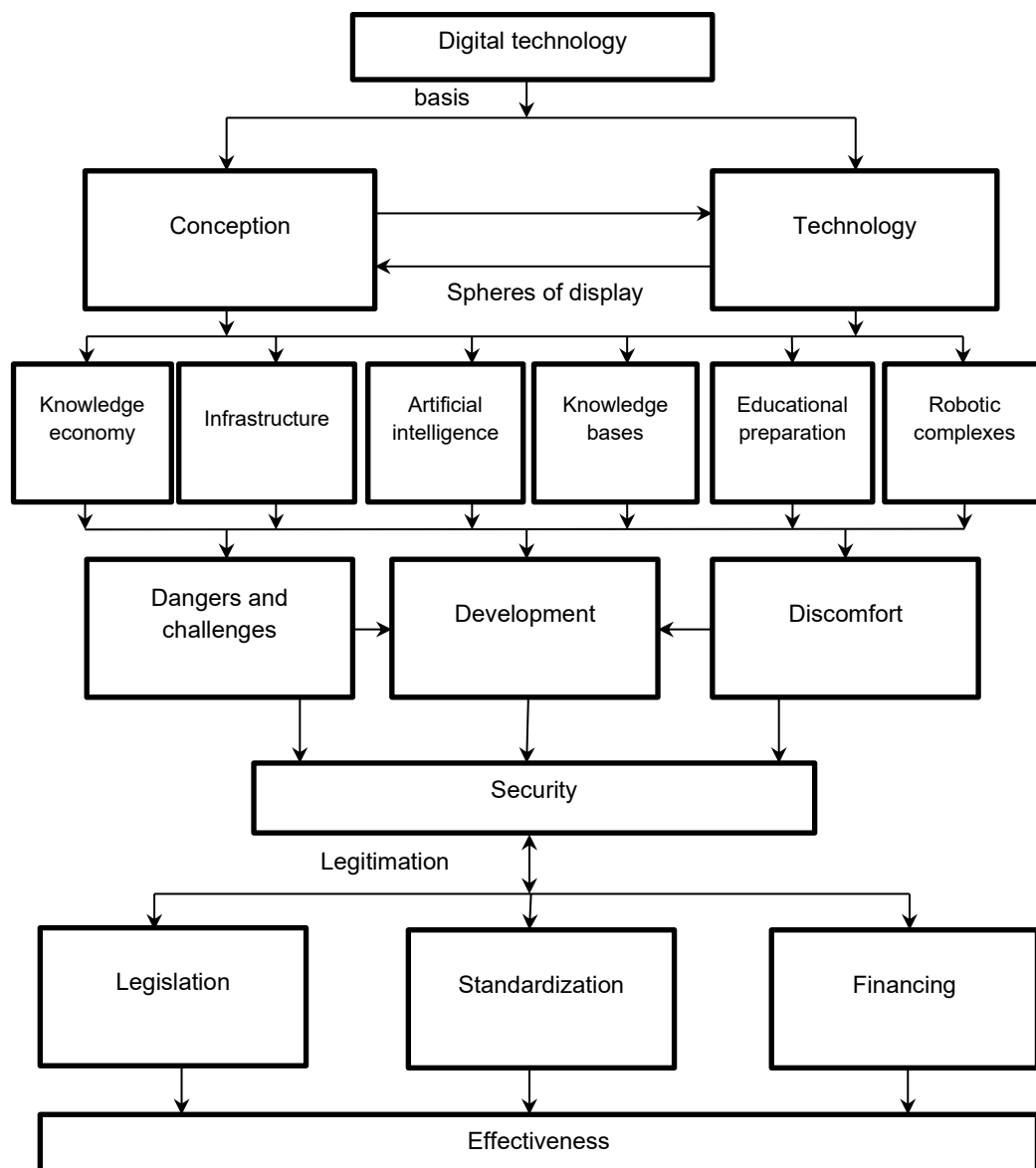


Figure 1. Structure of the digital economy.

Source: developed by the authors.

ESTUDO DO PROBLEMA DE PERDA DE ESTABILIDADE DE ESTRUTURAS CILINDRICAS DE PAREDES FINAS SOB EXPOSIÇÃO TÉRMICA LOCAL INTENSA**RESEARCH OF THE PROBLEM OF LOSS OF STABILITY OF CYLINDRICAL THIN-WALLED STRUCTURES UNDER INTENSE LOCAL TEMPERATURE EXPOSURE****ИССЛЕДОВАНИЕ ЗАДАЧИ ПОТЕРИ УСТОЙЧИВОСТИ ЦИЛИНДРИЧЕСКИХ ТОНКОСТЕННЫХ КОНСТРУКЦИЙ ПРИ ИНТЕНСИВНОМ ЛОКАЛЬНОМ ТЕМПЕРАТУРНОМ ВОЗДЕЙСТВИИ**

KURBATOV, Alexey S.^{1*}; OREKHOV, Alexander A.²; RABINSKIY, Lev N.³; TUSHAVINA, Olga V.⁴; KUZNETSOVA, Ekaterina L.⁵;

^{1,2,3,5} Moscow Aviation Institute (National Research University), Institute of General Engineering Education, Department of Perspective Materials and Technologies of Aerospace Designation, Moscow – Russian Federation

⁴ Moscow Aviation Institute (National Research University), Institute of Aerospace, Department of Managing Exploitation of Space-Rocket Systems, Moscow – Russian Federation

** Correspondence author*

e-mail: defunt@inbox.ru

Received 22 January 2020; received in revised form 20 February 2020; accepted 20 March 2020

RESUMO

Atualmente, a tecnologia de impressão tridimensional está se desenvolvendo rapidamente. Isso se deve à necessidade de criar produtos de formas complexas, cuja produção pelos métodos padrão existentes é muito trabalhosa e desvantajosa e, às vezes, tecnicamente impossível. O objetivo do estudo é estudar o problema da estabilidade de temperatura de uma estrutura cilíndrica de paredes finas sob exposição térmica local não estacionária, simulando o movimento de um ponto de feixe de laser ao longo de uma das extremidades. Para resolver o problema, foi utilizado o método dos elementos finitos. Como as áreas geométricas do cálculo foram parametrizadas, para cada conjunto de parâmetros, sua própria malha de elementos finitos foi usada para todos os tipos de análise. Foi construído um modelo de elemento finito espacial paramétrico de um invólucro cilíndrico preso ao longo da extremidade inferior. O fluxo de calor em movimento local atua no lado oposto, simulando o movimento do feixe de laser durante a formação aditiva do elemento de parede fina. São obtidas as soluções numéricas do problema de condução de calor dinâmico não estacionário, dependências de temperatura espaço-temporais e soluções do problema quase-estático da perda da estabilidade local e completa do estado de equilíbrio do cilindro em vários instantes de tempo devido à ocorrência de tensões compressivas locais durante aquecimento intenso. São obtidas as dependências da potência crítica do fluxo de calor correspondentes à perda de estabilidade na espessura da parede do cilindro e sua altura. Os resultados acima podem ser usados como parâmetros de calibração do processo de criação de estruturas de paredes finas, usando as tecnologias aditivas da classe Laser Melting para produtos que exigem requisitos maiores de precisão de fabricação.

Palavras-chave: *tecnologias aditivas, capacidade de carga, corpos em crescimento, modelagem completa, temperatura de alto gradiente.*

ABSTRACT

Presently, three-dimensional printing technology is developing rapidly. This happens due to the need to create products of complex shape, the production of which by existing standard methods is very difficult and disadvantageous, and sometimes technically impossible. The study aims to investigate the problem of temperature stability of a thin-walled cylindrical structure under unsteady local thermal exposure, simulating the motion of a laser beam spot along one of the ends. To solve the problem, the finite element method was used. Since the geometric areas of calculation were parameterized, then for each set of parameters, its own finite element mesh was used for each type of analysis. A parametric spatial finite element model of cylindrical shell pinched at the bottom end was constructed. The local moving heat flux acts on the opposite side, simulating the movement of a laser beam during the additive formation of a thin-walled element. Numerical solutions of the non-stationary dynamic heat conduction problem were obtained, spatiotemporal temperature dependences were

obtained, and solutions of the quasistatic problem of the loss of both local and complete loss of stability of the equilibrium state of the cylinder at various times due to the occurrence of local compressive stresses during intense heating were obtained. The dependences of critical heat flux power corresponding to the loss of stability on the cylinder wall thickness and its height were obtained. The above results can be used as calibration parameters of the process of creating thin-walled structures using additive technologies of Laser Melting class for products that require increased requirements for manufacturing accuracy.

Keywords: *additive technologies, load-bearing capacity, growing bodies, full-fledged modeling, high-gradient temperature.*

АННОТАЦИЯ

В настоящее время технологии трехмерной печати развивается стремительными темпами. Это связано с необходимостью создавать изделия сложной формы, производство которых существующими стандартными методами весьма трудоемко и невыгодно, а порой и технически неосуществимо. Целью исследования является исследование задачи температурной устойчивости тонкостенной цилиндрической конструкции при нестационарном локальном тепловом воздействии, моделирующим движение пятна лазерного пучка вдоль одного из торцов. Для решения задачи был использован метод конечного элемента. Так как геометрические области расчета были параметризованы, то для каждого набора параметров использовалась своя конечно-элементная сетка для всех типов анализа. Построена параметрическая пространственная конечно-элементная модель цилиндрической оболочки, заземленной по нижнему торцу. На противоположную сторону действует локальный движущийся тепловой поток, моделирующий движение лазерного луча при аддитивном формировании тонкостенного элемента. Получены численные решения нестационарной динамической задачи теплопроводности, получены пространственно-временные зависимости температуры и получены решения квазистатической задачи о потере как местной, так и полной потери устойчивости равновесного состояния цилиндра в различные моменты времени вследствие возникновения локальных сжимающих напряжений при интенсивном нагреве. Получены зависимости критической мощности теплового потока, соответствующие потере устойчивости от толщины стенки цилиндра и его высоты. Приведенные результаты могут применяться в качестве калибровочных параметров процесса создания тонкостенных конструкций методами аддитивных технологий класса Laser Melting для изделий, требующих повышенных требований к точности изготовления.

Ключевые слова: *аддитивные технологии, несущая способность, растущие тела, конечно-элементное моделирование, высокоградиентные температурные поля.*

1. INTRODUCTION:

Presently, three-dimensional printing technology is developing rapidly (You *et al.*, 2017; Jacobs and Lin, 2017; Park *et al.*, 2017; Smith *et al.*, 2018; Tyburec *et al.*, 2019). This happens due to the need to create products of complex shape, the production of which by existing standard methods is very laborious and disadvantageous, and sometimes technically impossible (Kinash *et al.*, 2017; Boitsov *et al.*, 2018; Du *et al.*, 2018). A large number of works have been done on the topic of use of additive technologies, in particular a review (Uriondo *et al.*, 2015; Chen *et al.*, 2017; Etienne and Timiryazev, 2018; Kasatkin *et al.*, 2019; Ostroukh *et al.*, 2019; Teslenko *et al.*, 2019). Additive technologies allow us to create products with mechanical characteristics close to the features of products obtained by traditional methods (Kablov, 2015; Sokolov and Razov, 2018). It is worth noting that, in addition to advantages, additive technologies have a number of disadvantages, residual stresses and

deformations (Buchbinder *et al.*, 2015; Gerasimenko *et al.*, 2017; Leicht *et al.*, 2018; Fedorenko *et al.*, 2019), which reduce load-bearing capacity of products, as well as hardly predicted distortion of the initial shape that occurs during molding (Simagina, 2017; Formalev *et al.*, 2018a; Bahaadini and Saidi, 2018; Kurbatov *et al.*, 2018; Matveenkov *et al.*, 2019; Faizan *et al.*, 2019).

Attempts to develop high-quality mathematical model of growing bodies are associated with problems of adequate comprehensive formulation and large computational resources (Gao *et al.*, 2018; Nahmany *et al.*, 2017; Formalev and Kolesnik, 2019; Kopecki *et al.*, 2019; Cetin and Baykasoğlu, 2019). At the same time, full-fledged modeling based on classical models of mechanics of deformable solids appears impossible or insufficiently accurate (Lomakin *et al.*, 2017; Jin *et al.*, 2017; Rzeszut and Voronoi, 2018; Wen *et al.*, 2018; Xin *et al.*, 2018; Bai *et al.*, 2019). Nonetheless, taking into account high-gradient temperature stresses associated with

heterogeneity of the temperature fields during the synthesis of the product is also possible based on relatively simple models (Khoshdarregi and Altintas, 2018; Li *et al.*, 2018; Li *et al.*, 2019; Gokhale *et al.*, 2019; Sun *et al.*, 2019). In particular, the presence of local areas of compressive stresses can lead to loss of stability of thin-walled products (Ogibalov and Gribanov, 1968; Falta *et al.*, 2018; Iwicki *et al.*, 2019; Basaglia *et al.*, 2019; Ma *et al.*, 2019).

The study aimed to investigate the problem of temperature stability of a thin-walled cylindrical structure under unsteady local thermal exposure, simulating the motion of a laser beam spot along one of the ends.

2. MATERIALS AND METHODS:

The linearized problem of loss of stability of thin-walled cylindrical shell under local edge heating by high-intensity radiation source simulating the action of the laser beam was considered, and the critical power of the source for its different positions on the circuit was calculated (Formalev *et al.*, 2018b). The shell panels in form of circular cylinder in the three-dimensional quasistatic formulation of thermoelasticity problem were considered. External influence follows from solutions of the problem of unsteady heat conduction. Equations of the static equilibrium have the form (Equation 1). Kinematic relationships correspond to geometrically linear theory (Equation 2). The defining equations of linear thermoelastic medium have the form (Equation 3), where the temperature field follows from the solution of the heat conduction problem described below.

Boundary conditions correspond to rigid termination of one of the ends of cylinder; the remaining surfaces are free of bonds (Equation 4). The heat conduction problem can be considered in a non-stationary setting (Equation 5). At boundary conditions corresponding to the absence of heat exchange with the external environment (Equation 6) and in homogeneous initial conditions (Equation 7). At the upper end of the cylinder, the field of heat flux vector with a finite carrier is set, directed along the normal, and decaying according to exponential law. The position of non-zero flux is defined by the point modeling center of the spot of the laser beam (Equation 8) (Rabinskiy and Tushavina, 2019a). The accepted law of distribution of amplitude of heat flux over time is presented in Figure 1. The solution to the heat conduction problem has a general form $T=T(x,y,z,t)$.

The geometric model represents a cylindrical shell with the height and wall thickness specified parametrically (Rabinskiy and Tushavina, 2019b). Tasks can be solved using the finite element method. Since the geometric areas of calculation were parameterized, then for each set of parameters, its own finite element mesh was used for each type of analysis. Volumetric tetrahedral four-node elements formed the grid. The number of nodes for each option was not less than 150.000 (Figure 2).

In the heat conduction problem, initial and boundary conditions (6)-(7) were applied to all surfaces. At the upper limit at point $(R, 0, H)$, heat flow (8) is used. The problem is solved in a dynamic setting. The solution to the problem of heat conduction is a temperature field set table at points corresponding to the nodes of the finite element grid $T=T_{(i,k)}$ (i is the node number, k is the time instant) (Rabinskiy *et al.*, 2019). The linear thermoelasticity problem can be solved numerically in three-dimensional formulation. Lower side surface is rigidly pinched (4). The temperature field is used as a load at a fixed moment of time in accordance with the solution of previous problem.

The obtained solution of thermoelasticity problem corresponds to the subcritical state of the simulated system. The issue of stability of the equilibrium state for the discrete analog of the original problem is considered in bifurcation formulation; that is, it can be reduced to the eigenvalue problem for the operator of homogeneous initial-boundary value problem of bending deformation under strains corresponding to the thermoelasticity problem. Then, the temperature field generated by source (laser) and causing subcritical stress state acts as one-parameter loading of the system. The load parameter will be the coefficient at the amplitude of heat flux, i.e. (Equation 9).

The result of solving the spectral problem can be a set of eigenvalues and eigenvectors of a discrete analogue of the original problem, while the smallest positive value is taken as critical.

3. RESULTS AND DISCUSSION:

The problem was solved for various combinations of wall thickness and cylindrical shell height parameters. The result of integrating the equations of unsteady heat conduction was a solution in the form of isothermal contours similar to concentric circles. At the same time, the density decreased with increasing time (temperature gradients decreased). When calculating linear

thermoelasticity tasks, the obtained stress fields had high gradients at the initial time points, which sharply reduced over time. Since the overall heating of structure increased, the stresses in the embedment zone increased. When solving the task, the effect of the transition of form of loss of stability from local (at short times and high-temperature gradients) to general (at large times and general heating of the structure) was revealed. The various first forms of buckling are demonstrated in Figures 3-4.

The results of solving the spectral problem have demonstrated that over time the value of critical effect decreases, and asymptotically tends to a fixed minimum value. Figure 5 illustrates typical curves for parametric interaction critical values. Based on the results obtained, the following conclusions could be made.

1) when solving the problem, allocation of the model parameter ranges is realized, in which using of given laser heat source with a fixed exposure time at a point is unacceptable ($\lambda < 1$)

2) solving the problem allows us to develop methods for predicting the behavior of thin-walled products during growth, reducing the possibility of appearing of "leashes" and changing the required geometric characteristics at the output.

4. CONCLUSIONS:

Numerical solutions were obtained for the problems of stability loss by thermoelastic thin-walled cylindrical structures during high-intensity edge heating by moving heat source. This problem is an approximation of the model of additive formation of the thin-walled structure by selective laser sintering. The questions were solved by the finite element method in three-dimensional formulation. At the same time, the source was modeled as a field of heat flux vector normal to the side surface of the shell with an amplitude that is isotropically attenuated exponentially.

The quasistatic problem corresponding to heating the structure at various points in time was considered. In the bifurcation formulation of the stability loss problem, the critical values of heat flux power were determined depending on geometric parameters of the model, and the duration of heat source influence. Zones of changes in the form of loss of stability from local to general were identified. It was demonstrated that in the process of laser synthesis, instability zones arise that do not allow using the laser sintering method. The obtained dependencies make it possible to determine the permissible time of

exposure to a laser beam of one zone, taking into account the power of the input stream and geometric dimensions of the product when developing an additive process for thin-walled structural elements based on selective laser sintering.

5. ACKNOWLEDGMENTS:

The reported study was funded by RFBR, according to the research project No 19-08-00938, 20-08-00880.

6. REFERENCES:

1. Bahaadini, R., Saidi, A.R. *European Journal of Mechanics, A/Solids*, **2018**, 72, 298-309.
2. Bai, X., Tang, R.a, Zan, Y., Li, J. *Ocean Engineering*, **2019**, 193, Article number 106584.
3. Basaglia, C., Camotim, D., Silvestre, N. *Structural Stability Research Council Annual Stability Conference 2019*, **2019**, 2, 888-901.
4. Boitsov, B.V., Gavva, L.M., Endogur, A.I., Firsanov, V.V. *Russian Aeronautics*, **2018**, 61(4), 524-532.
5. Buchbinder, D., Meiners, W., Wissenbach, K., Poprawe, R. *Journal of Laser Applications*, **2015**, 27, S29102-1-S29102-7. DOI: 10.2351/1.4906389.
6. Cetin, E., Baykasoğlu, C. *International Journal of Mechanical Sciences*, **2019**, 157-158, 471-484.
7. Chen, L., He, Y., Yang, Y., Niu, S., Ren, H. *International Journal of Advanced Manufacturing Technology*, **2017**, 89(9-12), 3651-3660.
8. Du, X., Liu, W., Yuan, H., Liu, M., Cheng, X. *Jianzhu Jiegou Xuebao/Journal of Building Structures*, **2018**, 39(7), 1-10.
9. Etienne, H., Timiryazev, V.A. *Mining Informational and Analytical Bulletin*, **2018**, 2018(11), 136-144.
10. Faizan, A., Davignon, R., Stamp, R., Murray, S., Raja, L. *Surgical Technology International*, **2019**, 34, 462-468.
11. Falta, J., Janota, M., Sulitka, M. *Procedia CIRP*, **2018**, 77, 175-178.
12. Fedorenko, A.N., Fedulov, B.N., Lomakin,

- E.V. *PNRPU Mechanics Bulletin*, **2019**, 2019(3), 104-111.
13. Formalev, V.F., Kolesnik, S.A. *Journal of Engineering Physics and Thermophysics*, **2019**, 92(1), 52-59.
 14. Formalev, V.F., Kolesnik, S.A., Kuznetsova, E.L. *Composites: Mechanics, Computations, Applications*, **2018a**, 9(3), 223-237.
 15. Formalev, V.F., Kolesnik, S.A., Kuznetsova, E.L. *High Temperature*, **2018b**, 56(3), 393-397.
 16. Gao, B., Yin, Z., Zhao, F., Shang, C. *Journal of Pressure Vessel Technology, Transactions of the ASME*, **2018**, 140(4), Article number 041203.
 17. Gerasimenko, A., Guskov, M., Gouskov, A., Lorong, P., Shokhin, A. *Journal of Vibroengineering*, **2017**, 19(8), 5825-5841.
 18. Gokhale, N.P., Kala, P., Sharma, V. *Journal of the Brazilian Society of Mechanical Sciences and Engineering*, **2019**, 41(12), Article number 569.
 19. Iwicki, P., Rejowski, K., Tejchman, J. *Thin-Walled Structures*, **2019**, 135, 414-436.
 20. Jacobs, C.A., Lin, A.Y. *Plastic and Reconstructive Surgery*, **2017**, 139(5), 1211-1220.
 21. Jin, Y., He, Y., Du, J. *International Journal of Computer Integrated Manufacturing*, **2017**, 30(12), 1301-1315.
 22. Kablov, E.N. *Intelligence & Technology*, **2015**, 2(11), 52-56.
 23. Kasatkin, M.M., Kozhina, T.D., Federov, M.M. *Russian Engineering Research*, **2019**, 39(3), 262-267.
 24. Khoshdarregi, M.R., Altintas, Y. *Journal of Manufacturing Science and Engineering, Transactions of the ASME*, **2018**, 140(4), Article number 041016.
 25. Kinash, O., Abolmaali, A., Park, Y. *Journal of Pipeline Systems Engineering and Practice*, **2017**, 8(2), Article number 04016017.
 26. Kopecki, T., Mazurek, P., Lis, T. *Materials*, **2019**, 12(19), Article number 3230.
 27. Kurbatov, A.S., Orekhov, A.A., Rabinsky, L.N. *Technical Science*, **2018**, 12, 513-519.
 28. Leicht, A., Klement, U., Hryha, E. *Materials Characterization*, **2018**, 143, 137-143.
 29. Li, Z., Tang, Y., Tang, F., Chen, Y., Chen, G. *Thin-Walled Structures*, **2018**, 123, 214-221.
 30. Li, Z.a, Zheng, J., Meng, L., Zou, X., Hu, X. *Engineering Structures*, **2019**, 196, Article number 109318.
 31. Lomakin, E.V., Lurie, S.A., Belov, P.A., Rabinskiy, L.N. *Doklady Physics*, **2017**, 62(1), 46-49.
 32. Ma, G., Zhao, G., Li, Z., Yang, M., Xiao, W. *International Journal of Advanced Manufacturing Technology*, **2019**, 101(5-8), 1275-1292.
 33. Matveenkov, A.M., Ostrik, A.V., Bakulin, V.N. *Journal of Physics: Conference Series*, **2019**, 1392(1), Article number 012045.
 34. Nahmany, M., Stern, A., Aghion, E., Frage, N. *Journal of Materials Engineering and Performance*, **2017**, 26(10), 4813-4821.
 35. Ogibalov, P.M., Gribanov, V.F. *Heat resistance of plates and shells*. Moscow: Moscow State University, **1968**.
 36. Ostroukh, A.V., Subbotin, B.S., Borisevich, V.B., Ryabchinskii, A.I., Kristal'nyi, S.R. *Russian Engineering Research*, **2019**, 39(8), 710-712.
 37. Park, S.-H., Kang, B.-K., Lee, J.E., Chun, S.W., Jang, K., Kim, Y.H., Jeong, M.A., Kim, Y., Kang, K., Lee, N.K., Choi, D., Kim, H.J. *ACS Applied Materials and Interfaces*, **2017**, 9(14), 12290-12298.
 38. Rabinskiy, L.N., Tushavina, O.V. *INCAS Bulletin*, **2019a**, 11(S1), 203-211.
 39. Rabinskiy, L.N., Tushavina, O.V. *STIN*, **2019b**, 4, 22-26.
 40. Rabinskiy, L.N., Tushavina, O.V., Fedotenkov, G.V. *Asia Life Sciences*, **2019**, 19(1), 149-162.
 41. Rzeszut, K., Voronoi, A. *E3S Web of Conferences*, **2018**, 49, Article number 00049.
 42. Simagina, S.G. *Key Engineering Materials*, **2017**, 746, 16-21.
 43. Smith, D.M., Kapoor, Y., Klinzing, G.R., Procopio, A.T. *International Journal of Pharmaceutics*, **2018**, 544(1), 21-30.
 44. Sokolov, V., Razov, I. *Advances in Intelligent Systems and Computing*, **2018**,

692, 666-678.

45. Sun, J., Zhao, Y., Yang, L., Yu, T. *International Journal of Advanced Manufacturing Technology*, **2019**, 105(5-6), 2087-2101.
46. Teslenko, I.B., Digilina, O.B., Abdullaev, N.V. *IOP Conference Series: Materials Science and Engineering*, **2019**, 483(1), Article number 012093.
47. Tyburec, M., Zeman, J. Novák, J., Lepš, M., Plachý, T., Poul, R. *Materials and Design*, **2019**, 183, Article number 108131.
48. Uriondo, A., Esperon-Miguez, M., Perinpanayagam, S. *Aerospace Engineering*, **2015**, 229(11), 2132-2147.
49. Wen, X., Tan, J.-P., Li, X.-H., Liu, S.-Q. *Binggong Xuebao/Acta Armamentarii*, **2018**, 39(10), 2006-2015.
50. Xin, W., Zhengying, W., Jun, D., Chuanqi, R., Shan, Z., Zhitong, Z. *International Journal of Advanced Manufacturing Technology*, **2018**, 96(5-8), 2367-2372.
51. You, X., Ye, C., Guo, P. *Journal of Micro and Nano-Manufacturing*, **2017**, 5(4), Article number 040901.

$$\frac{\partial \sigma_{rr}}{\partial r} + \frac{1}{r} \frac{\partial \tau_{r\theta}}{\partial \theta} + \frac{\partial \tau_{rz}}{\partial z} + \frac{\sigma_{rr} - \sigma_{\theta\theta}}{r} = 0, \frac{\partial \tau_{r\theta}}{\partial r} + \frac{1}{r} \frac{\partial \sigma_{\theta\theta}}{\partial \theta} + \frac{\partial \tau_{\theta z}}{\partial z} + \frac{\tau_{r\theta}}{r} = 0, \frac{\partial \tau_{rz}}{\partial r} + \frac{1}{r} \frac{\partial \tau_{\theta z}}{\partial \theta} + \frac{\partial \sigma_{zz}}{\partial z} + \frac{\tau_{rz}}{r} = 0 \quad (\text{Eq. 1})$$

$$\begin{aligned} \frac{\partial \sigma_{rr}}{\partial r} + \frac{1}{r} \frac{\partial \tau_{r\theta}}{\partial \theta} + \frac{\partial \tau_{rz}}{\partial z} + \frac{\sigma_{rr} - \sigma_{\theta\theta}}{r} &= 0, \\ \frac{\partial \tau_{r\theta}}{\partial r} + \frac{1}{r} \frac{\partial \sigma_{\theta\theta}}{\partial \theta} + \frac{\partial \tau_{\theta z}}{\partial z} + \frac{\tau_{r\theta}}{r} &= 0, \\ \frac{\partial \tau_{rz}}{\partial r} + \frac{1}{r} \frac{\partial \tau_{\theta z}}{\partial \theta} + \frac{\partial \sigma_{zz}}{\partial z} + \frac{\tau_{rz}}{r} &= 0. \end{aligned} \quad (\text{Eq. 2})$$

$$\begin{aligned} \sigma_{rr} &= \lambda(\varepsilon_{rr} + \varepsilon_{\theta\theta} + \varepsilon_{zz}) + 2\mu\varepsilon_{rr} - (3\lambda + 2\mu)\alpha T, \\ \sigma_{\theta\theta} &= \lambda(\varepsilon_{rr} + \varepsilon_{\theta\theta} + \varepsilon_{zz}) + 2\mu\varepsilon_{\theta\theta} - (3\lambda + 2\mu)\alpha T, \\ \sigma_{zz} &= \lambda(\varepsilon_{rr} + \varepsilon_{\theta\theta} + \varepsilon_{zz}) + 2\mu\varepsilon_{zz} - (3\lambda + 2\mu)\alpha T, \\ \sigma_{r\theta} &= 2\mu\varepsilon_{r\theta}, \sigma_{\theta z} = 2\mu\varepsilon_{\theta z}, \sigma_{rz} = 2\mu\varepsilon_{rz}. \end{aligned} \quad (\text{Eq. 3})$$

$$u_r = u_\theta = u_z = 0, z = 0 \quad (\text{Eq. 4})$$

$$\frac{\partial T}{\partial t} = a \left(\frac{1}{r} \frac{\partial}{\partial r} \left(r \frac{\partial T}{\partial r} \right) + \frac{1}{r^2} \frac{\partial^2 T}{\partial \theta^2} + \frac{\partial^2 T}{\partial z^2} \right) + \frac{Q}{\rho c}, \quad (\text{Eq. 5})$$

$$-nq = 0 \quad (\text{Eq. 6})$$

$$T = 0, t = 0 \quad (\text{Eq. 7})$$

$$q_0 = \frac{2\eta P}{\pi r_0^2} e^{-\frac{2r^2}{r_0^2}} \quad (\text{Eq. 8})$$

$$q_0 = \lambda \frac{2\eta P}{\pi r_0^2} e^{-\frac{2r^2}{r_0^2}} \quad (\text{Eq. 9})$$

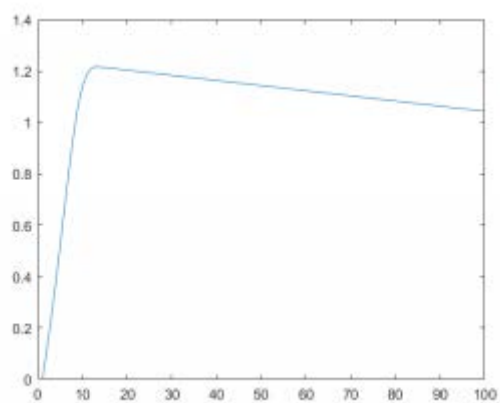


Figure 1. The accepted law of distribution of amplitude of the heat flux in time

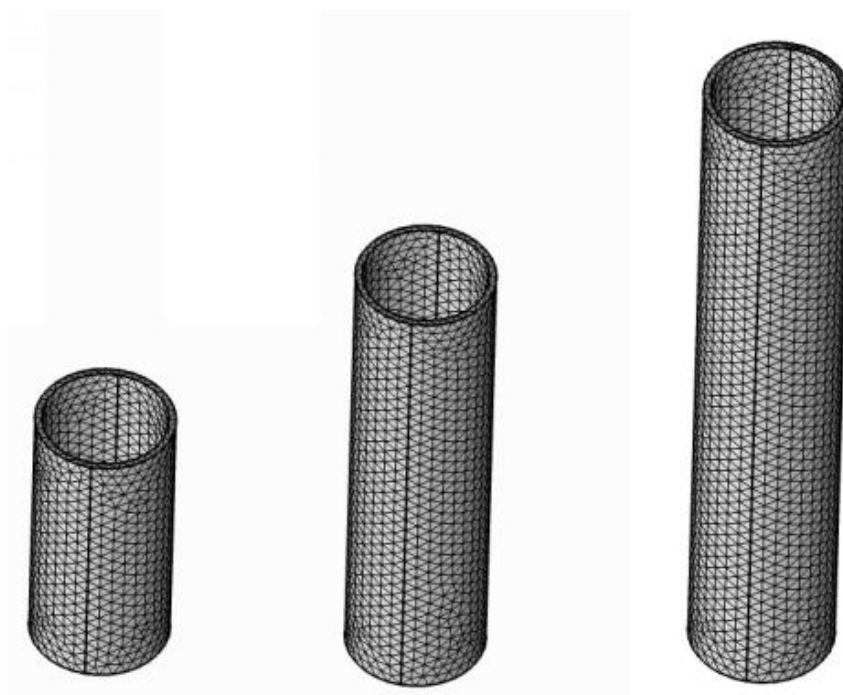


Figure 2. General view of model

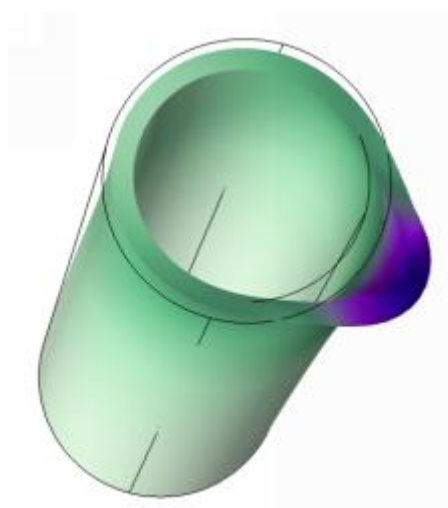


Figure 3. Local form of loss of stability



Figure 4. General form of loss of stability

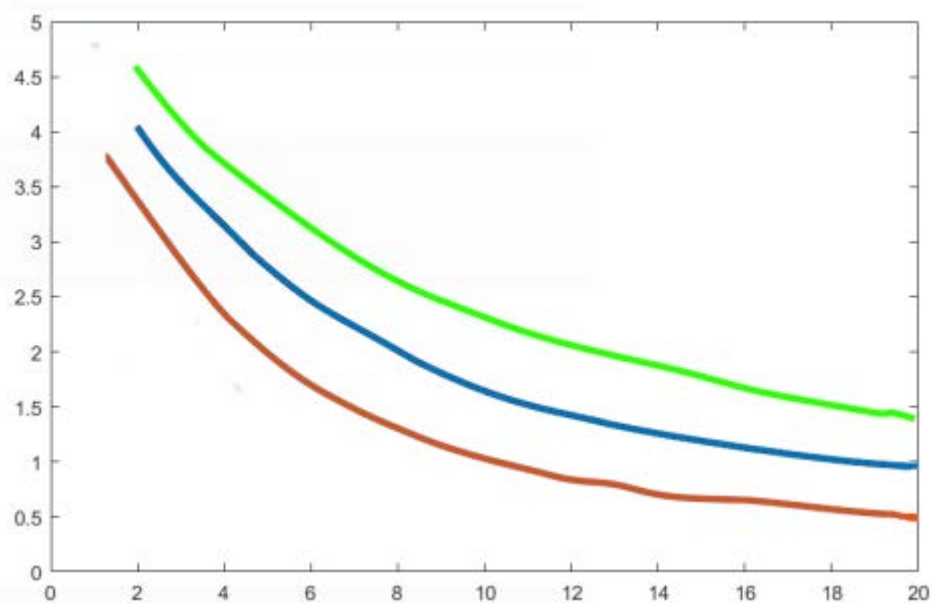


Figure 5. Typical curves of dependence of the critical value of amplitude of heat flux on time

PESQUISA DO MECANISMO DE PRODUÇÃO DE PETRÓLEO A PARTIR DE DEPÓSITOS DE HIDROCARBONETOS COM COLETORES DE BAIXA PERMEABILIDADE**RESEARCH OF THE MECHANISM OF OIL RECOVERY FROM HYDROCARBON DEPOSITS WITH LOW PERMEABILITY RESERVOIRS****ИССЛЕДОВАНИЕ МЕХАНИЗМА НЕФТЕИЗВЛЕЧЕНИЯ ИЗ ЗАЛЕЖЕЙ УГЛЕВОДОРОДОВ С НИЗКОПРОНИЦАЕМЫМИ КОЛЛЕКТОРАМИ**

KUANGALIEV, Zinon A.^{1*}; DOSKASIYEVA, Gulsin S.²; MARDANOV, Altynbek S.³;

^{1,2} Atyrau University of Oil and Gas, Department of Oil and Gas Business, 45A Baimukhanova Str., zip code 060027, Atyrau – Republic of Kazakhstan

³ “KMG Engineering” LLP “Caspimunaigas”, 22A Elorda Ave., ZIP code 060006, Atyrau – Republic of Kazakhstan

* Correspondence author
e-mail: z.kuangaliev@mail.ru

Received 02 February 2020; received in revised form 01 March 2020; accepted 20 March 2020

RESUMO

A maior parte das reservas de difícil recuperação da Rússia está confinada a reservatórios de baixa permeabilidade e carbonatos 73%, óleos altamente viscosos – 12%, vastas zonas localizadas imediatamente abaixo da tampa de gás de depósitos de petróleo e gás cerca de 15% e formações localizadas em grandes profundidades – 7%. O desenvolvimento de tais reservas usando tecnologias tradicionais é economicamente ineficiente. Requer-se o uso de novas tecnologias para seu desenvolvimento e, fundamentalmente, as novas abordagens para o design, levando em consideração as características da extração de reservas de difícil recuperação. O objetivo deste estudo é encontrar as maneiras de aumentar a eficiência do desenvolvimento de reservas de campos com reservatórios de baixa permeabilidade. Para realizar esta tarefa, o campo petrolífero Novobogatinskoye Yugo-Vostochnoye (Sudeste) foi descrito como um exemplo. Foram destacadas as propriedades necessárias das instalações de produção no campo, além de viabilidade econômica e eficiência tecnológica. As reservas envolvidas no desenvolvimento foram determinadas e, graças ao conhecimento das reservas geológicas de petróleo dos depósitos, o potencial fator de recuperação de petróleo foi calculado com a tecnologia de desenvolvimento existente. Como resultado do estudo, foram desenvolvidas as opções de desenvolvimento com os resultados do cálculo de indicadores de projeto para o campo como um todo. Apresenta-se uma comparação dos gráficos de produção e recuperação de petróleo, bem como os padrões de localização. Três opções para os indicadores tecnológicos de desenvolvimento de campo foram calculadas. As figuras mostram os gráficos de produção de petróleo, bem como os padrões de localização. Os autores do estudo concluem qual das opções de desenvolvimento recomendadas pode ajudar a extrair as reservas máximas de petróleo.

Palavras-chave: *coeficiente de recuperação de petróleo, recuperação de petróleo, pressão de saturação, modelo de fluido, fraturamento hidráulico.*

ABSTRACT

The main part of Russia's hard-to-recover reserves is 73% for low-grade and carbonate reservoirs, 12% for high-viscosity oil, about 15% of extensive sub-gas zones of oil and gas deposits and 7% of reservoirs lying at great depths. The development of such stocks with the usage of traditional technologies is economically inefficient. It requires the application of new technologies for their development and fundamentally new approaches to design, taking into account the features of extraction of hard-to-extract reserves (HtER). The purpose of this research is to find ways to improve the performance of low-permeability reservoirs. To accomplish this task, the Novobogatinsk South-Eastern Oil Field has been taken as an example and described. The necessary properties of production facilities in the field are highlighted, along with economic feasibility and technological efficiency. The reserves involved in the development are determined and, thanks to the knowledge of the geological oil reserves

of the deposits, the potential oil recovery factor is calculated with the existing development technology. As a result of the research, development options were worked out with the results of the calculation of design indicators for the field as a whole. The comparison of oil recovery schedules and ORI, as well as the layout of wells, have been presented. As a result of the study, a description of 3 options for the development of design indicators for the field as a whole is given. The figures show oil production graphs, as well as location patterns. The authors of the study conclude which of the recommended development options can help extract maximum oil reserves.

Keywords: *oil recovery index (ORI), oil recovery, saturation pressure, fluid model, fracturing.*

АННОТАЦИЯ

Основная часть трудноизвлекаемых запасов России приурочены к низкопроницаемым и карбонатным коллекторам 73%, высоковязким нефтям – 12%. обширным подгазовым зонам нефтегазовых залежей около 15% и пластам, залегающим на больших глубинах – 7%. Разработка таких запасов с использованием традиционных технологий экономически неэффективна. Она требует применения новых технологий их освоения и принципиально новых подходов к проектированию, учитывающих особенности извлечения трудноизвлекаемых запасов (ТРИЗ). Целью данного исследования является поиск способов повышения эффективности освоения запасов месторождений с низкопроницаемыми коллекторами. Для выполнения поставленной задачи приведено в пример и описано Новобогатинское Юго-Восточное месторождение нефти. Выделены необходимые свойства эксплуатационных объектов на месторождении, наряду с экономической целесообразностью и технологической эффективностью. Определены вовлечённые в разработку запасы и благодаря знаниям о геологических запасах нефти по залежам, рассчитан потенциальный КИН при существующей технологии разработки. В результате исследования разработаны варианты разработки с результатами расчета проектных показателей по месторождению в целом. Представлено сравнение графиков добычи нефти и КИН, а также схемы расположения скважин. Рассчитаны три варианта технологических показателей разработки месторождения. На рисунках представлены графики добычи нефти, а также схемы расположения скважин. А также авторы исследования приходят к заключению, что, третий рекомендуемый вариант разработки способствует максимальному извлечению запасов нефти.

Ключевые слова: *коэффициент извлечения нефти, нефтеотдача, давление насыщения, флюидальная модель, гидроразрыв пласта.*

1. INTRODUCTION

The peculiarity of the deposits located within the Astrakhan-Aktobe uplift zone is the low permeability, high fragmentation, and heterogeneity of the reservoir (Naderi and Babadagli, 2014; Ren and Wang, 2015; Solaimany-Nazar and Zonnouri, 2011). The following developmental difficulties are associated with these factors:

1. The problem of obtaining industrial inflow from the reservoir, there is no period of gushing, production is mechanized at the beginning, and until the end of development.

2. The problem is related to the preparation of well production. Already in the first months of operation, wells produce water products (20-30%), and this entails additional preparation costs.

3. Difficulties with reaching the project level of oil recovery – the need to use thick wells, drilling the side trunks both in the option of sealing the grid and in the version of HS and surface flooding

systems, GTM in significant volumes, the active introduction of flow-deflection technologies, increasing the injection pressure.

4. Low initial oil saturation, in advance – causes low potential oil recovery.

5. Qualitative opening of the productive horizon during drilling is also necessary, due to the fact that the undersaturated collector begins to be intensively saturated with the moisture of the drilling mud, which leads to a sharp decrease in the phase permeability of the reservoir for oil in the BFZ.

6. Ballast water is recovered in large quantities.

The result is a final ORI of about 0.25-0.3. All these factors lead to an increase in the cost of extracted oil. Examples of these phenomena are traced to the following fields: 1. South-Eastern uplift – sub-cornfield of the Novobogatinsk South-East (SEN); 2. Central uplift – the Central Novobogatinsk field; 3. Western uplift – the Novobogatinsk Western field.

The research of the main features of the development of low-permeability reservoirs and the creation of effective technologies for their development are urgent tasks. This circumstance has predetermined the direction of this work research (Alhuraishawy *et al.*, 2018; Li *et al.*, 2018; Zakirov *et al.*, 2016). All the above fields are similar, have low permeability of reservoirs, the porosity of which varies within 16.7-19.5% (Nazari and Honma, 2017; Shelley *et al.*, 2010; Volpin *et al.*, 2014). The gas content varies from 100-150 m³ / t. The saturation pressure is below the current reservoir pressure by 2-10MPa and averages 5-17MPa. The fluid model of the deposit is characterized by light, low-viscosity, low-sulfur, low-paraffin oil (Kuangaliev and Nakpaev, 2019; Kuangaliev and Nakpaev, 2018b; Wang *et al.*, 2017; Wang *et al.*, 2018). Based on the purpose of this study, we identified the main objectives of the work:

1. Research of the mechanism of oil extraction from hydrocarbons with low-permeability reservoirs in the implementation of various schemes for maintaining reservoir pressure.

2. Substantiation of wells grids, zones of their location, rates of hydrocarbon extraction, and sequence of development of reserves when implementing development systems with and without impact on the formation.

3. Research on the impact of layer-by-layer heterogeneity of low-permeability reservoirs on the efficiency of their development with active influence on the process of oil extraction by hydraulic fracturing (fracturing).

The efficiency of the development of an oil field is determined by the accuracy of the choice of method of impact on the productive layer, aimed at increasing or maintaining the mobility of oil. The choice of impact method is based on the available data on the geological and physical conditions of the oil deposit, composition, structure and petrophysical properties of the rocks, and the characteristics of reservoir fluids, taking into account their compliance with the criteria of applicability.

2. MATERIALS AND METHODS

The most common impact method today is water flooding, which provides 95% of oil production in Kazakhstan, due to the restoration of reservoir pressure and the displacement of the whole oil. The main features of the current state of the oil industry in Kazakhstan are an increase in

the share of hard-to-recover reserves in the structure of oil reserves and a lack of experience in the industrial application of enhanced oil recovery methods. In general, four problems are relevant in the fields of the Atyrau region: the high viscosity of oil; high water cut of products; the problem of utilization of oil gas and associated water; The low permeability of reservoirs.

The territory under consideration is located on the south-western slope of the Novobogatinsk dome, complicated by an overhanging cornice of salt, which is monoclinically immersed in the adjacent mold. Let's take a closer look at the Novobogatinsk South-Eastern field. At the Novobogatinsk South-Easternfield, deposits were discovered from the Permian-Triassic to Quaternary age inclusively, including deposits of the Kungurian stage of the Lower Permian (salt), which are embedded in the Permian as deposits in the form of a cornice.

Exploration and, subsequently, production drilling confirmed the industrial oil content of Permotias in the under-eaves conditions. Seven productive horizons were established in the section of the subcarpathian Permotias: RT-IV, RT-V, RT-VI (square A + B), RT-VII, RT-VIII, RT-IX, RT-X. All deposits by the type of natural reservoir are stratified, vaulted, shielded by tectonic disturbances, and the sole of the salt cornice (Figures 1 and 2). The reservoir strata of productive horizons are lithologically represented by sandstones, siltstones, sand, and Alekvrit, varying degrees of cementation. Siltstone of different colors, fine-grained, clay to varying degrees, slightly carbonate, cemented. Sandstones are gray, dark gray, fine-grained, slightly clayey, non-carbonate, micaceous. Sands are light gray, dark gray, slightly carbonated, slightly clay. The type of collector is porous. The sandiness coefficient varies in the range of 0.32-0.55, the dissection coefficient is in the range of 1-10. The pioneer of the Novobogatinsk South-East oilfield is an exploratory well No 1, which in January 1984 produced an inflow of oil with a flow rate of 2.8 tons/day for a 5 mm nozzle.

According to the results of laboratory tests of the core, the values of porosity vary from 0.142 to 0.202 fractions of a unit, the average value across the horizon is 0.167 fractions of a unit, the coefficient of variation is 0.086. The permeability varies from 1.13 to 31.6 × 10⁻³ μm², and the average permeability is 5.81 × 10⁻³ μm², the coefficient of variation is 0.921. According to the GIS results, the average porosity coefficient is 0.198 fractions of units, varying from 0.136 to 0.315 fractions of units, oil saturation on average

is 0.695 fractions of units, varying from 0.461 to 0.862 fractions of units. According to hydrodynamic studies, the horizontal values of permeability vary from 0.023 to $7.363 \times 10^{-3} \mu\text{m}^2$, the average horizontal value is $1.343 \times 10^{-3} \mu\text{m}^2$, and the coefficient of variation is 1.941. The fluid model is characterized by light, low-viscosity, low-sulfur, low-paraffin oil (Table 1).

In total, the oil reserves of the field in categories B + C1 + C2 have reached: geological – 14253 thousand tons, recoverable – 3439 thousand tons. The choice of the most rational development system for both individual deposits and the field as a whole depends on the correct allocation of production facilities. With the selection of production facilities in the field, along with economic feasibility and technological efficiency, the geological structure comes to the fore. A dedicated development object should have sufficient specific oil reserves per unit area of the reservoir and sufficient productivity in order to ensure high well flow rates over a long period of well operation during an anhydrous period and during flooding. In general, two production facilities were allocated at the field:

- I object – horizons RT-IV, RT-V, RT-VI-a, RT-VI-B;
- II object – horizons RT-VII, RT-VIII, RT-IX, RT-X.

A total of 27 wells were drilled at the Novobogatinsk South-East field, of which the production fund is 17 wells, including 11 operating, six wells inactive. The supervisory fund contains three wells, two wells in conservation after drilling. The liquidated fund is five wells; all wells have been abandoned for geological reasons. In the period 2012-2016, the wells of the field were operated with oil production rates of up to 5 tons/day. The maximum average annual production rate was achieved in 2013-2014 (up to 10 tons/day), then a slight decrease in production rate is noted. The main reason for the decrease in oil production rates is the low permeability of the formation.

In general, two wells are currently highly productive in the field, with oil production rates of up to 10 tons/day. According to these wells, hydraulic fracturing was carried out, which gave a positive result. From 1997 to 2005, there was an increase in oil production, which is associated with the commissioning of wells and their active operation (Figure 3). During this period, the stock of producing wells increased from one to six units. Since 2006, there has been a decrease in oil production with subsequent stabilization at the

level of 5.8-6 thousand tons for three years (2006-2008). From 2009 to 2014, oil production is characterized by an increase. The increase in oil production is associated with the commissioning of new production wells from drilling and the implementation of additional geological and technical measures to intensify oil production. From the dynamics of the technical indicators of development, it can be seen that the maximum level of oil production was reached in 2014 and amounted to 18.5 thousand tons. Then, there is a slight decline in annual production due to lack of drilling, reduction in the number of active wells, and low production rate.

The initial reservoir pressure for the I object is 15.6 MPa. Current reservoir pressure averages 12.7 MPa, varying from 10.4 to 16.5 MPa (Table 2). The current bottom-hole pressure, varying in the range of 6.4-10.7 MPa, averages 9.5 MPa. Saturation pressure averages 4.8 MPa. The initial reservoir pressure for the II facility is 19.3 MPa. Current reservoir pressure averages 15.7 MPa, varying from 13.6 to 16.4 MPa. A more noticeable decrease in reservoir pressure, compared with the I object, is associated with more intensive oil production and a three-fold excess of the existing production fund. The current bottom hole pressure averages 9 MPa. The saturation pressure averages 7.3 MPa.

At the beginning of the development in the field, 172.4 thousand tons of oil were produced. The selection rate from the initial recoverable reserves in the field is 0.5%, the selection rate from the currently recoverable reserves is 0.5%, the development of reserves in the field was 5.4% (Table 3). In general, oil-saturated thicknesses in the field vary from 19-146.5 m. The opening of effective oil-saturated thicknesses overall productive horizons is, on average, 30.8% (Table 4) (Kuangaliev and Nakpaev, 2018a).

To determine the values of oil reserves involved in active development with the currently developed development system and applied production technology, according to the method of V.D. Lysenko, the dependences of the specific monthly oil production per well were built on the accumulated oil production based on actual data. This method allows you to determine the amount of oil reserves involved in each facility. Having determined the reserves involved in the development and, knowing the geological oil reserves of the deposits, the potential oil recovery factor was calculated with the existing development technology (Table 5). Under the existing development system, it is impossible to achieve the approved oil recovery index for any of

the development objects, since the involved reserves are lower than the approved recoverable oil reserves (Lysenko, 2000).

3. RESULTS AND DISCUSSION:

Further, on the basis of the "TatNIPIneft" methodology (author V.D. Lysenko), a forecast of technological indicators for the development of production facilities has been made, which is based on a model of a zonal and layer-by-layer heterogeneous formation. The following assumptions have been made in the methodology:

1. the reservoir consists of permeable layers and impermeable layers separating them;
2. in the area of their distribution layers and interlayers consist of square zones, identical in the area;
3. all layers are of the same thickness;
4. layers differ in average permeability, and the distribution of these average values across the layers is completely chaotic, subordinated only to a statistical regularity in the form of a gamma distribution;
5. per layer, within the zones, the permeability values remain constant and change randomly during the transition from one zone to another;
6. in addition to the zonal permeability heterogeneity, the layers can still have a chaotic spread of area zones with zero permeability (discontinuity).

The methodology allows us to evaluate recoverable oil reserves and calculate the dynamics of technological development indicators during the implementation of various formation stimulation systems. In addition, the technique allows you to take into account the difference in the viscosity ratio of oil and water, the effect of a decrease in productivity as a result of a fall in reservoir pressure below the saturation pressure. The calculation of technical indicators in the methodology is carried out according to the following formulas:

the oil flow rate in the t -year (Equation 1):

here q_0^t – current amplitude rate at the middle of the t -th year, t/year ; Q_i – initial recoverable oil reserves put into development by the middle of the t -year, mln tons; $\sum_{i=1}^{t-1} q^i$ – total oil selection for all previous years.

The fluid flow rate in the t -th year (Equation

2): where Q_i^t – initial recoverable liquid reserves introduced into development by the middle of the year; $\sum_{i=1}^{t-1} q_F^i$ – total estimated fluid selection for all previous years.

To calculate the amplitude flow rate use the formula (Equation 3): where τ – working time of the wells; η_{cp} – the average productivity of the wells; n – total number of wells of the operational fund; P_{ch} – bottom hole pressure of injection wells; P_{c3} – bottom-hole pressure of producing wells; φ – the function of the relative productivity of the wells, taking into account the difference in wells in productivity, the relative placement, and the ratio of production and injection wells, the ratio of the mobilities of the displacing agent and oil; ξ_1, ξ_2 – reliability factors taking into account the increase infiltration resistance and, accordingly, the productivity of the layers due to their discontinuity and zonal heterogeneity, as well as the degree of knowledge of the layers.

Recoverable reserves are determined by the formula (Equation 4): where Q_b – balance oil reserves. The oil recovery index (ORI) is calculated by the formula (Equation 5): Index K_1 is called a grip coefficient and depends on the number of production wells and the distance between them (Equation 6): where S^1 – oil square per well of the design grid, km^2 ; w – the share of the non-collector by the square of distribution of the isolated oil layers, unit fractions; d – the size of the square zones' sides that simulate the zonal heterogeneity of the formations (step of random variation of the effective thickness of oil formations), km.

Index K_2 in, the ORI formula indicates the coefficient of oil extraction. The index K_3 is the coefficient of water flooding and is calculated by the formula (Equation 7): where K_{3H} – the proportion of the selection of mobile reserves for the anhydrous period; K_{3K} – the final share of the selection of mobile stocks; A – estimated marginal water cut, unit fraction.

These parameters are determined by the following formulas (Equations 8-10): where V^2 – the square of the variation coefficient of the estimated heterogeneity of reservoir features of the lay; A_2 – the maximum water cut of the production of wells, unit fraction; μ_0 – coefficient taking into account the difference in physical properties of oil and water in reservoir conditions (Equations 11-12): where ρ_w, ρ_H – the density of water and oil, kg/m^3 ; b_H – volumetric coefficient of oil, unit fraction;

To determine the squared coefficient of variation of the calculated heterogeneity of reservoir properties (V^2), it is necessary to establish the actual layer-by-layer and zonal inhomogeneities (Equation 13): where M – the ratio of the lengths of the neutral (the longest) and main (the shortest) streamlines going from the injection well (or from the aquifer) to the producing well; n – the number of sides of the water approach to production wells; V_1^2 – the square coefficient of variation of the actual layer-by-layer inhomogeneity of reservoir properties; V_{sq}^2 – the square of the coefficient of variation of zonal inhomogeneity of reservoir properties (Economides *et al.*, 1994).

This methodology is based on direct field measurements of good operation: productivity coefficients, oil, and fluid production rates, accumulated oil and fluid production, current and accumulated displacement agent injection rates, bottom-hole, and formation pressure. The methodology is a mutually agreed, fairly mobile, and universal equation of the oil and liquid production process, as well as the well stock of the production facility for almost any development system.

The validity of using the methodology is based on many years of effective application and its continuous improvement, thanks to the use of effective mathematical ideas and methods; design scheme of point-focused filtration resistances; distribution functions of a universal type and methods for their transformation and association; substantiation of the mutual independence of existing factors; characteristics of distribution functions with initial moments of various orders of inhomogeneities, etc. (VNII GOST 39-112-80..., 1981; Moufazalov *et al.*, 2000).

The acceptable applicability of the methodology has also been proved by conducting numerous approbations within the framework of technological schemes, development projects, and estimation of hydrocarbon reserves in Kazakhstan's fields, including the Emba region. Based on this technique, three variants of technological forecasting indicators of field development, including the object I (Unified Rules for the Development..., 1996; The Gas Industry Development Program..., 2010), have been calculated. Below is a description of 3 development options with the results of the calculation of design indicators for the field as a whole. Figure 4 shows a graph of oil production and oil recovery index as well as the layout of the wells (Figures 5-7 – the recommended option).

3.1. The first variant (basic)

It provides for the continuation of the development of production objects for the SEU field.

In order to use the potential of the drilled well stock, to increase the oil recovery factor at production facilities, measures are also planned to involve additional oil reserves in the development by:

- developing in the wells the intervals of productive horizons allocated to one production object that has not been previously developed;
- transferring wells from object to object, as a result of the development of reserves.

3.2. The second variant

Additionally, the introduction of new design wells in the amount of 90 units is provided with hydraulic fracturing and taking into account the new understanding of the geological structure of productive horizons and their productive capabilities. The development of the object is also expected to be in natural mode. The location of the project wells was selected, taking into account new ideas about the geological structure of the field. The main purpose of the option is to assess the effectiveness of previously accepted and unrealized design decisions from the point of view of new ideas about the geological structure and the achievement of the approved ORI values. For the projected period, the production fund will be 101 wells.

3.3. The third variant (recommended)

It is envisaged that 80 production wells will be commissioned from drilling with hydraulic fracturing, as well as with the launch of an ESP. Additionally provided is the input from drilling 31 injection wells in order to maintain reservoir pressure. Carbon dioxide was selected as the working agent for injection. For the projected period, the production fund will be 91 wells. Injection well stock – 31 units.

Thus, the largest amount of oil in the field will be produced during the implementation of the third option, which involves the drilling of new wells with hydraulic fracturing and launching of ESP, as well as the use of an injection system with gas injection. According to calculations, the value of the oil recovery factor by the end of development will be 0.483 units, which is significantly higher than the approved value of 0.258 units. The lowest

oil recovery factor is characterized by option one, which involves the development of an object by existing wells (Table 6).

Economic analysis is a special approach that allows you to assess the possible financial and economic consequences of implementing a development option. This analysis allows you to measure the total costs of the investor and the benefits of implementing a development option using the same unit of measure, usually money. The economic analysis allows you to determine the most profitable option for a company-subsoil user and for the state.

When choosing the recommended development option, the following were analyzed: the projected level of oil production, cumulative oil production for a profitable period, the time to reach the economic limit, the payback period of investments, capital investments, operating costs, net profit, accumulated cash flow, and economic indicators. Based on the technical and economic indicators for each option, analysis, and selection of the recommended option for development were carried out. When comparing development options, the best option has turned out to be the option III, according to which the maximum indicators of the accumulated cash flow are obtained – 1,059.6. Million US dollars, net present value – 250.4 million US dollars and total payments to the state for 2061 – 2,480.2 million US dollars.

According to the main provisions of the development system options, the technical indicators were calculated for operational objects and for the field as a whole in three versions. To assess the achieved ORI values, technological indicators for all productive horizons have been additionally calculated for each counting object (horizon). As a recommended option, the III development option is proposed for implementation during the implementation of which the maximum extraction of oil reserves is achieved. When implementing the recommended third development option, the projected level of oil production in the amount of 375.16 thousand tons will be achieved in 2061, the rate of selection will be 10.2%. The cumulative oil production in the field as a whole by the end of the economically viable development period will be 6814.91 thousand tons, the oil recovery index achieved is 0.478 unit fraction.

4. CONCLUSIONS:

According to the main technical and economic indicators for each variant, the analysis and selection of the recommended variant for development have been carried out. While comparing development options, the best option turns out to be the III, from which the maximum accumulated cash flow – 1,059.6. USD has been obtained, net present value – USD 250.4 million, and total payments to the state for 2061 – USD 2 480.2 million.

According to the basic provisions of the variants of the development systems, the calculations of the technical indicators for the operational objects and the field as a whole in three variants have been made. To evaluate the achieved ORI values, calculations of technological indicators for all productive horizons were additionally carried out for each calculated object (horizon).

As a recommended variant, the third variant of development is proposed for implementation, in the course of which the maximum extraction of oil reserves has been achieved. While implementing the recommended third development variant, the projected level of oil production in the amount of 375.16 thousand t will be reached in 2061, the rate of selection will be 10.2%. The accumulated oil production by the field as a whole by the end of the economically profitable development period will make 6814.91 thousand t, achieved by ORI 0.478 unit fraction.

5. REFERENCES:

1. Alhuraishawy, A. K., Bai, B., Wei, M., Geng, J., Pu, J. *Fuel*, **2018**, 220, 898-907.
2. Economides, M. J., Hill, A. D., Ehlig-Economides, C., Zhu, D. *Petroleum Production Systems*. Upper Saddle River: Prentice Hall PTR, **1994**.
3. Kuangaliev, Z. A., Nakpaev, J. S. *Bulletin of Atyrau University of Oil and Gas*, **2019**, 1(49), 68-76.
4. Kuangaliev, Z. A., Nakpaev, J. S. *Conference on the 70th anniversary of T.P. Serikov*, **2018a**, 2, 545.
5. Kuangaliev, Z. A., Nakpaev, J. S. *International Scientific and Practical Conference "Ecology and the Oil and Gas Complex" on the 85th anniversary of MD Diarov*, **2018b**, 1, 514.

6. Li, P., Hao, M., Hu, J., Ru, Z., Li, Z. *Journal of Petroleum Science and Engineering*, **2018**, 171, 340-352.
7. Lysenko, V. D. *Innovative Development of Oil Fields*. Moscow: Nedra, **2000**.
8. Moufazelov, R. Sh., Muslimov, R. Kh., Burtsev, I. B. *Hydromechanics of Joint Work of the Reservoir, Production and Injection Wells*. Kazan: Dom Pechati, **2000**.
9. Naderi, K., Babadagli, T. *Journal of Canadian Petroleum Technology*, **2014**, 53(5), 263-274.
10. Nazari, A. J., Honma, S. *International Journal of GEOMATE*, **2017**, 12(29), 81-88.
11. Ren, T., Wang, F. T. *International Journal of Oil, Gas and Coal Technology*, **2015**, 10(3), 272-292.
12. Shelley, R. F., Lolon, E., Dzubin, B., Vennes, M. *Proceedings – SPE Annual Technical Conference and Exhibition*, **2010**, 2, 1507-1519.
13. Solaimany-Nazar, A. R., Zonnouri, A. *Journal of Petroleum Science and Engineering*, **2011**, 75(3-4), 251-259.
14. *The Gas Industry Development Program of the Republic of Kazakhstan for 2004-2010*. 2004. Decree of the Government of the Republic of Kazakhstan dated June 18, 2004 No. 669. By the Decree of the Government of the Republic of Kazakhstan dated April 14, 2010, No. 302, **2010**.
15. *Unified Rules for the Development of Oil and Gas Fields in the Republic of Kazakhstan*. Decree of the Government of the Republic of Kazakhstan dated June 18, 1996 No. 745, **1996**.
http://base.spininform.ru/show_doc.fwx?rgn=11033, accessed December 2019.
16. VNII GOST 39-112-80 "Oil. Typical Study of Reservoir Oil", Approved by Order of the Ministry of Petroleum Industry of January 23, 1981. No. 603, **1981**.
<http://www.gostrf.com/normadata/1/4293835/4293835390.pdf>, accessed December 2019.
17. Volpin, S. G., Saitgareev, A. R., Kornaeva, D. A., Smirnov, N. N., Kravchenko, M. N., Dieva, N. N. *Neftyanoe Khozyaistvo – Oil Industry*, **2014**, 1, 62-66.
18. Wang, B., Fan, Z., Zhao, J., Lv, X., Pang, W., Li, Q. *Applied Energy*, **2018**, 229, 858-871.
19. Wang, D., Niu, D., Li, H. A. *SPE Journal*, **2017**, 22(5), 1596-1608.
20. Zakirov, S. N., Barenbaum, A. A., Zakirov, E. S., Indrupskiy, I. M., Serebryakov, V. A., Klimov, D. S. *Indian Journal of Science and Technology*, **2016**, 9(42), 104219.

$$q^t = \frac{q_0^t}{Q_i^t + \frac{1}{2}q_0^t} [Q_i^t - \sum_{i=1}^{t-1} q^i] \quad (\text{Eq. 1})$$

$$q_F^t = \frac{q_0^t}{Q_{Fi}^t + \frac{1}{2}q_0^t} [Q_{Fi}^t - \sum_{i=1}^{t-1} q_F^i] \quad (\text{Eq. 2})$$

$$q_0 = \tau \cdot \eta_{cp} \cdot n \cdot (P_{ch} - P_{c3}) \cdot \varphi \cdot \xi_1 \cdot \xi_2 \quad (\text{Eq. 3})$$

$$Q_i = Q_b \cdot ORI, \quad (\text{Eq. 4})$$

$$ORI = K_1 \cdot K_2 \cdot K_3. \quad (\text{Eq. 5})$$

$$K_1 = e^{-\alpha \cdot S^1}, \alpha = \frac{w^2}{d^2} \quad (\text{Eq. 6})$$

$$K_3 = K_{3H} + (K_{3K} - K_{3H}) \cdot A \quad (\text{Eq. 7})$$

$$K_{sq} = \frac{1}{1.2+4.2 \cdot V^2}; \quad (\text{Eq. 8})$$

$$K_{sq} = \frac{1}{0.95 + 0.25 \cdot V^2}; \quad (\text{Eq. 9})$$

$$A = \frac{A_2}{(1 - A_2) \cdot \mu_0 + A_2}, \quad (\text{Eq. 10})$$

$$\mu_0 = \frac{1}{2} \cdot (1 + \mu_*) \cdot \frac{\rho_w}{\rho_H} \cdot b_H \quad (\text{Eq. 11})$$

$$\mu_* = \frac{\mu_H}{\mu_w} \cdot K_2^{1.5} \quad (\text{Eq. 12})$$

$$V^2 = (V_1^2 + 1) \cdot \left(\frac{2}{3} \cdot \frac{(M-1)^2}{M} \cdot \frac{2\mu_*}{1+\mu_*} + 1 \right) \cdot \left(\frac{V_{sq}^2 + 1}{\frac{V_{sq}^2}{n_*} + 1} + 1 \right) - 1 \quad (\text{Eq. 13})$$

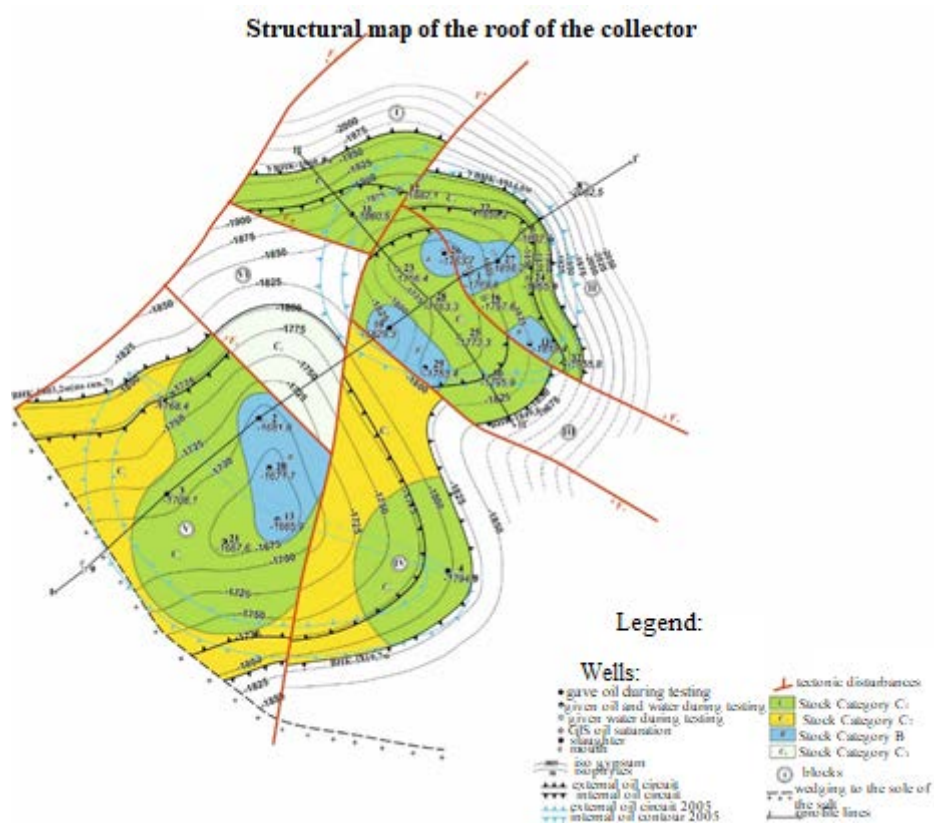


Figure 1. Structural map of the horizon collector roof

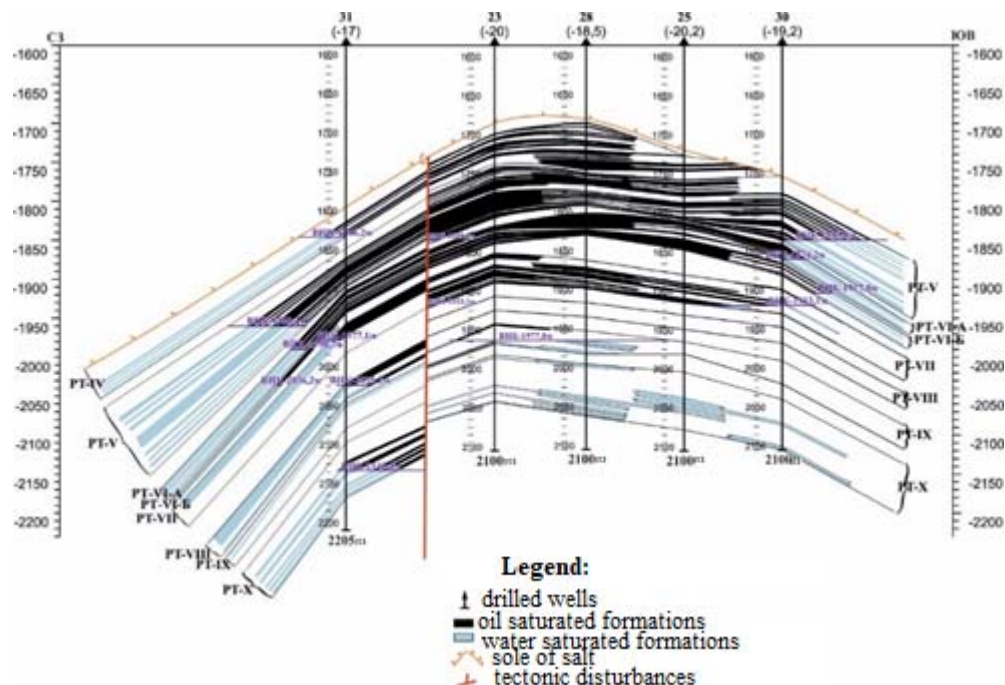


Figure 2. Geological and lithological profile

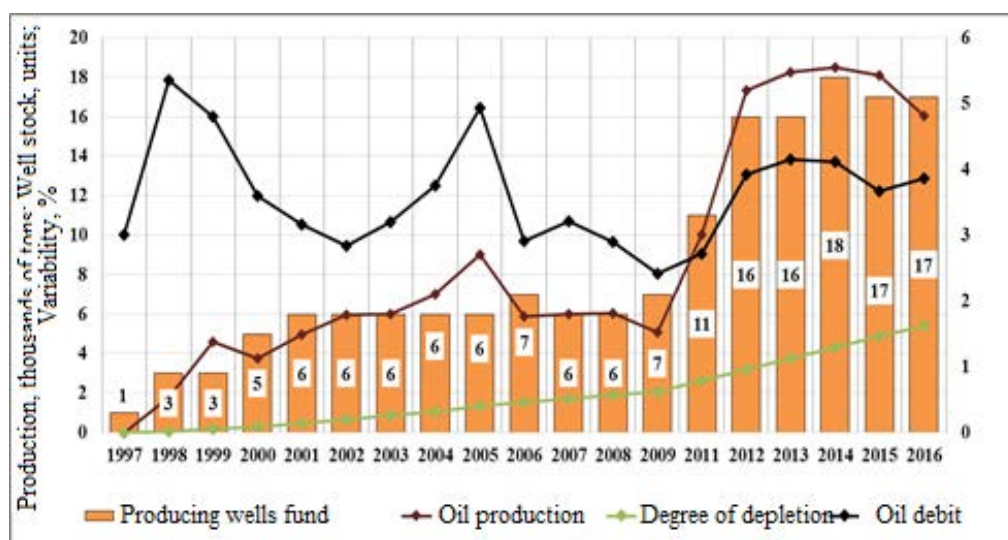


Figure 3. Dynamics of the main technical indicators of field development

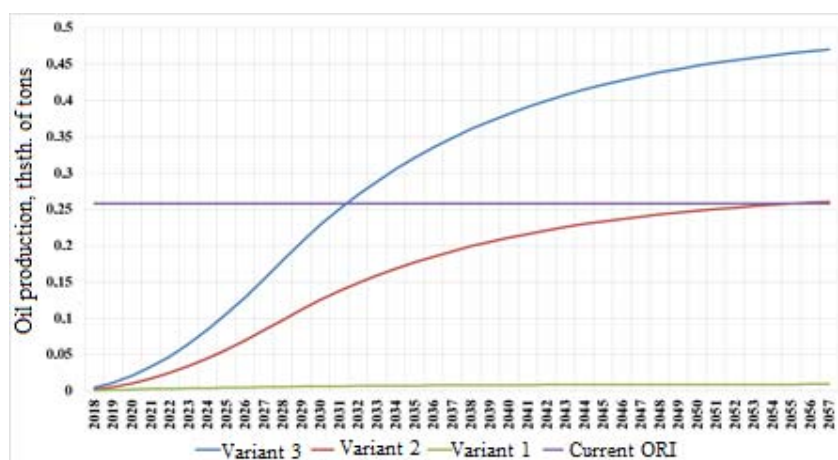


Figure 4. Comparison of the project ORI by development options

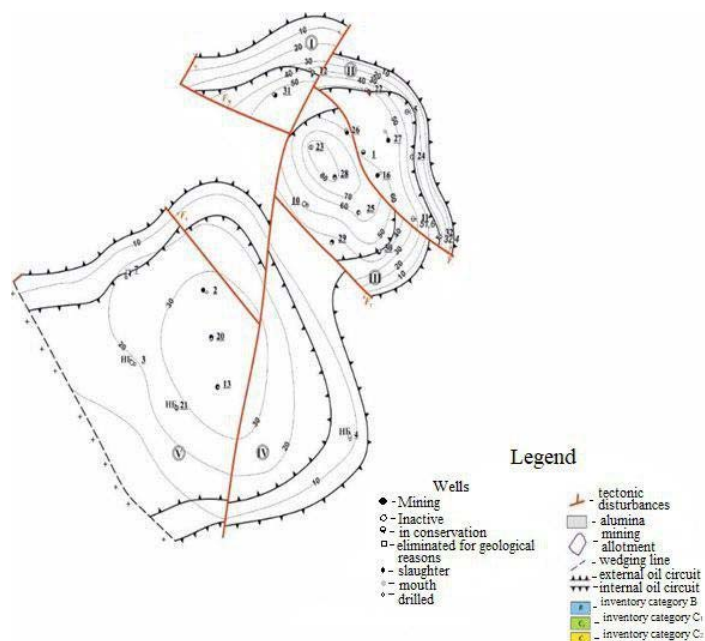


Figure 5. Layout diagram of drilled and project wells according to option 1

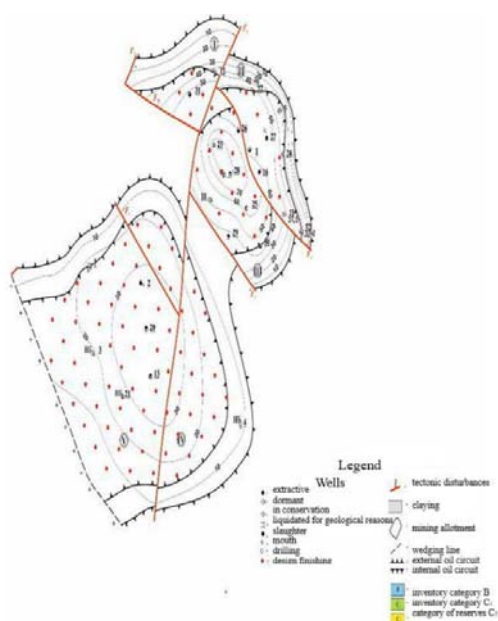


Figure 6. Layout diagram of drilled and project wells according to option 2

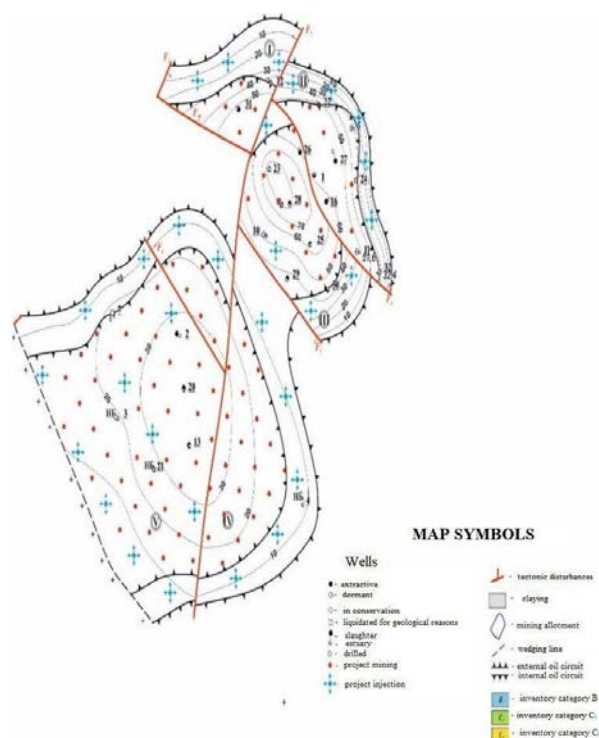


Figure 7. Layout diagram of drilled and project wells according to option 3

Table 1. Physical and chemical features of oil under reservoir conditions

Item	Horizons					
	PT-IV	PT-V	PT-VI-A	PT-VII	PT-IX	PT-X
Bubble point pressure, MPa	7.2	4.9	10.7	11.9	9.0	9
Gas oil ratio, m ³ /t	130.1	135.5	137.6	155.7	170.2	189.3
Volume ratio, u.f.	1.306	1.318	1.326	1.397	1.430	1.337
Density, kg/m ³	656.0	692.0	708.0	686.0	687.0	0.777
Viscosity, Mpa. S	0.64	0.70	0.69	0.68	0.6	0.6
Sample test temperature, °C	43.2	44.8	46.5	47.2	45	47

Table 2. Energy characteristic of the Novobogatinsk South-Eastern deposit

Objects	Figures	Pin, MPa	Years						Deviations, MPa	
			2012	2013	2014	2015	2016	Pin, MPa		
									P _{current} -P _{in}	P _{in} -P _{current}
I	Reservoir pressure, MPa	15.6	14.4	14.2	14.1	13.9	12.7	4.8	7.9	2.9
	Bottom hole pressure, MPa		11.2	8.6	8.5	9.5	9.5			
	Depression ΔP, MPa		3.2	5.6	5.6	4.4	3.2			
II	Reservoir pressure in the selection zone, MPa	19.3	17.6	17.2	16.8	16.4	15.7	7.3	9.0	3.6
	Bottom hole pressure, MPa		11.1	11.6	8.3	9.3	9.0			
	Depression ΔP, MPa		6.5	5.6	8.5	7.1	6.7			

Table 3. Oil production relating to objects and field as a whole

Development object	Initial reserves, thousand tons		Reservoir oil production, thousand tons	Recoverable reserves, thousand tons		ORI, u.f.		Production, %
	geology.	recov.		geolog.	recov.	conf.	cur.	
I object	3492	917	41.3	3450.7	875.7	0.263	0.012	4.5
II object	8867	2275	131.0	8736.0	2144.0	0.257	0.015	5.8
In general, according to the field	12359	3192	172.4	12187	3020	0.258	0.014	5.4

Table 4. The distribution of the opening degree of effective oil-saturated thickness with perforation

Wells' No	Total effective oil-saturated thickness	Total opening of the effective thickness with perforation		Total unopened oil-saturated thickness	
	(m)	(m)	% from general	(m)	% from general
1	146.5	50	34.1	96.5	65.9
2	32.1	29	90.3	3.1	9.7
3	19.9	15.9	79.9	4.0	20.1
4	22.5	8.5	37.8	14.0	62.2
5	34.1	6	17.6	28.1	82.4
7	21.2	0	0.0	21.2	100.0
10	57.7	37.3	64.6	20.4	35.4
11	103.1	16.3	15.8	86.8	84.2
12	78.9	0	0.0	78.9	100.0
13	34.1	13.3	39.0	20.8	61.0
16	144.5	37.6	26.0	106.9	74.0
20	38.3	28.7	74.9	9.6	25.1
21	30.3	5.9	19.5	24.4	80.5
22	89.9	25.5	28.4	64.4	71.6
23	111.4	17.6	15.8	93.8	84.2
24	58	16.6	28.6	41.4	71.4
25	79.1	10.6	13.4	68.5	86.6
26	100.2	22.9	22.9	77.3	77.1
27	78.2	26.1	33.4	52.1	66.6
28	100.2	12	12.0	88.2	88.0
29	40.7	12.9	31.7	27.8	68.3
30	52.2	7.6	14.6	44.6	85.4
31	85.8	57.8	67.4	28.0	32.6
32	74	45.2	61.1	28.8	38.9
Total	1632.9	503	30.8	1129.6	69.2

Table 5. Comparison of the calculation results of the reserves involved

Object	Oil reserves, thousands of tons				ORI, u.f.		
	geol.	produc.	inv.	rest from inv.	appr.	cur.	Potent.
I object	3492	917	100	817	0.263	0.012	0.029
II object	8867	2275	230.5	2044.5	0.257	0.015	0.026

Table 6. ORI per variants

	K1	K2	K3	ORI
Variant 1	0.159	0.56	0.649	0.058
Variant 2	0.854	0.56	0.549	0.263
Variant 3	0.854	0.645	0.874	0.481

INVESTIGAÇÃO DA COMPOSIÇÃO BIOQUÍMICA DO BORDO DA NORUEGA (*ACER PLATANOIDES L.*) NAS CONDIÇÕES DE ESTRESSE TECNOGÊNICO**AN INVESTIGATION OF THE BIOCHEMICAL COMPOSITION OF NORWAY MAPLE (*ACER PLATANOIDES L.*) IN THE CONDITIONS OF TECHNOGENIC STRESS****ИССЛЕДОВАНИЕ БИОХИМИЧЕСКОГО СОСТАВА НОРВЕЖСКОГО КЛЕНА (*ACER PLATANOIDES L.*) В УСЛОВИЯХ ТЕХНОГЕННОГО СТРЕССА**KUZMIN, Petr A.^{1*}; BUKHARINA, Irina L.²; KUZMINA, Ajgul M.³¹Kazan Federal University, Yelabuga Institute, Russia Federation.²Udmurt State University, Russian Federation..³Izhevsk State Agricultural Academy, Russian Federation.

* Correspondence author

e-mail: petrkuzman84@yandex.ru

Received 24 February 2020; received in revised form 13 March 2020; accepted 24 March 2020

RESUMO

Um número bastante grande de publicações dedicadas ao estudo do papel de substâncias antioxidantes em plantas que crescem sob estresse antropogênico apareceu em revistas científicas. No entanto, esses problemas e questões não são estudados suficientemente. Este estudo teve como objetivo revelar as características da composição bioquímica do bordo norueguês (*Acer platanoides L.*) nas condições das plantações urbanas (pelo exemplo do grande centro industrial da cidade de Naberezhnye Chelny). O artigo apresenta os resultados de investigações sobre características de composição bioquímica do bordo norueguês nas condições de um grande centro industrial, a cidade de Naberezhnye Chelny (República do Tartaristão). Nas condições de carga tecnogênica intensiva, o bordo norueguês apresenta maior atividade da oxidase do ácido ascórbico nos estágios iniciais da vegetação ativa e menor atividade no final da vegetação, em comparação com as plantas nas zonas de controle convencionais (CCZ). Ao mesmo tempo, o teor de ácido ascórbico nas folhas também diminui durante a vegetação das plantas nas plantações da zona tampão de empresas industriais e plantações de tronco. Nas plantações da zona tampão de empresas industriais e plantações de tronco, o bordo norueguês foi caracterizado por um aumento na atividade da polifenol oxidase em comparação com as plantações de controle. O aumento da atividade da polifenol oxidase é acompanhado por uma diminuição no teor de taninos. O bordo norueguês em plantações de tronco apresenta menor atividade de peroxidase em suas folhas nas condições de carga mais intensa em julho do que nas plantações de CCZ e, em agosto, essa atividade é maior do que no grupo controle.

Palavras-chave: *Bordo da Noruega (Acer platanoides L.), atividade de polifenol oxidase, atividade de oxidase de ácido ascórbico, atividade de peroxidase, plantações urbanas.*

ABSTRACT

A reasonably large number of publications devoted to the study of the role of antioxidant substances in plants growing under anthropogenic stress have appeared in scientific journals. However, these problems and issues are not studied sufficiently. This study aimed to reveal the biochemical composition features of Norway maple (*Acer platanoides L.*) in the conditions of urban plantations (by the example of the large industrial center in the city of Naberezhnye Chelny). The paper presents the results of investigations of biochemical composition features of Norway maple in the conditions of a large industrial center, the city of Naberezhnye Chelny (the Republic of Tatarstan). In the circumstances of intensive technogenic load, Norway maple shows higher ascorbic acid oxidase activity at the initial stages of active vegetation and lower activity at the end of vegetation, in comparison with plants in the conventional control zones (CCZ). At the same time, the content of ascorbic acid in the leaves also decreases during the vegetation of plants in the buffer zone plantations of industrial enterprises and trunk plantations. In the buffer zone plantations of industrial enterprises and trunk plantations, Norway maple was characterized by an increase in polyphenol oxidase activity, in comparison with the control plantings. The rise in polyphenol oxidase activity is accompanied by a decrease in the content of tannins. Norway maple in trunk

plantations has lower peroxidase activity in its leaves in the conditions of the most intense load in July than in plantations of CCZ, and in August, this activity is higher than in the control group.

Keywords: Norway maple (*Acer platanoides* L.), polyphenol oxidase activity, ascorbic acid oxidase activity, peroxidase activity, urban plantations.

АННОТАЦИЯ

В научных журналах появилось достаточно большое количество публикаций, посвященных изучению роли антиоксидантных веществ в растениях, растущих в условиях антропогенного стресса. Однако эти проблемы и проблемы недостаточно изучены. Целью данного исследования было выявление особенностей биохимического состава клена обыкновенного (*Acer platanoides* L.) в условиях городских насаждений (на примере крупного промышленного центра в городе Набережные Челны). В статье представлены результаты исследований особенностей биохимического состава клена обыкновенного в условиях крупного промышленного центра, г. Набережные Челны (Республика Татарстан). В условиях интенсивной техногенной нагрузки клен норвежский проявляет более высокую активность оксидазы аскорбиновой кислоты на начальных этапах активной вегетации и более низкую активность в конце вегетации по сравнению с растениями в обычных контрольных зонах (ЗКК). В то же время содержание аскорбиновой кислоты в листьях также уменьшается при вегетации растений на плантациях буферной зоны промышленных предприятий и на стволовых плантациях. На плантациях буферной зоны промышленных предприятий и стволовых насаждениях клен обыкновенный характеризовался повышением активности полифенолоксидазы по сравнению с контрольными насаждениями. Увеличение активности полифенолоксидазы сопровождается снижением содержания дубильных веществ. Клен обыкновенный в стволовых насаждениях имеет более низкую активность пероксидазы в своих листьях в условиях наиболее интенсивной нагрузки в июле, чем на плантациях CCZ, а в августе эта активность выше, чем в контрольной группе.

Ключевые слова: Клен обыкновенный (*Acer platanoides* L.), активность полифенолоксидазы, активность аскорбинатоксидазы, активность пероксидазы, городские плантации.

1. INTRODUCTION:

In recent years, a relatively large number of publications devoted to the study of the role of antioxidant substances in plants growing under anthropogenic stress have appeared in scientific journals. However, these problems and issues are not studied sufficiently. The interaction features of enzymes and secondary metabolites involved in the formation of adaptive reactions of the plant organism are among these issues (Chupakhina *et al.*, 2012; Bukharina *et al.*, 2014; Galves-Valdivieso *et al.*, 2010; Maiti *et al.*, 2016).

Many investigations highlight the relationship between the adaptive capacity of the plant organism and the functioning of the non-enzymatic and enzymatic systems, individual elements of which are such substances as tannins and polyphenol oxidase, ascorbic acid, and ascorbic acid oxidases (Bukharina *et al.*, 2014; John *et al.*, 2008; Gill, Tuteja, 2010; Pachzkowska *et al.*, 2007; Podoprigora, and Korobov, 2017; Ivanova *et al.*, 2019; Rogatchev *et al.*, 2019). Polyphenol oxidase and peroxidase in combination with phenolic substrates, participate in the respiration process at the intermediate stages of hydrogen transfer. It was found that polyphenol oxidase activity increases in damaged

tissues of plants (Shagiakhmetov *et al.*, 2019). Ascorbic acid oxidase contributes to the elimination of reactive oxygen intermediates and participates in the protective reactions of plant organisms in the fight against oxidative stress (Sarika *et al.*, 2005; Ahmad *et al.*, 2010; Hattas, Julkunen-Tiitto, 2012; Kerio *et al.*, 2013;).

For example, during the study of antioxidant properties of the deciduous shrub *Cassia alata* L., scientists have found the features of the work of the enzymatic system and photosynthetic apparatus in different conditions of the abiotic environment. When abiotic stress occurs, catalase, ascorbate peroxidase, and glutathione, reductase activity increases (Ahmed, Anis, 2014). Other investigations have noted the role of antioxidant enzymes, proline, abscisic acid, phenols, and ascorbic acid in poplar plants and green tea. The specific reaction of these samples under stress was revealed, which is manifested in the increase in the activity of antioxidant enzymes and the reduction of the proline and abscisic acid levels (Garcia *et al.*, 2016; Kloseiko, 2016; Li *et al.*, 2014; Podoprigora and Korobov, 2017).

This study aimed to reveal the biochemical composition features of Norway maple (*Acer platanoides* L.) in the conditions of urban plantations (by the example of the large industrial

center in the city of Naberezhnye Chelny).

2. MATERIALS AND METHODS:

The object of investigation was Norway maple (*Acer platanoides* L.). The studied species grows in the city as a part of plantations of different ecological categories: trunk plantations (major highways Avto-1 and the Mira avenue) and the buffer zones (BZ) of industrial enterprises in OAO "KamAZ": foundry and blacksmith plants which are the primary pollutants of the city. The territories of Naberezhnye Chelny local forestry were chosen as conventional control zones (CCZ).

On the basis of sample plots description, (3 in each studied area, laid down by the regular method of different configurations, the size of at least 0.25 hectares, depending on the area of the studied category of plantations), it was made the selection and numbering of accounting plants (10 plants, from which the plants of good average generative ontogenetic condition were selected for biochemical studies) (Rodin *et al.*, 1968; Grishina, Samoylova, 1971). The schematic map of the sample plots location is shown in Figure 1.

The degree evaluation of air pollution in the places of woody plant growth was carried out on the basis of the materials of the "Report on the ecological state of the Republic of Tatarstan". The complex atmosphere impurity index (All=11.6) characterizes the state of air pollution in the city as very high (State..., 2016).

Within the boundaries of sample plots, selection and numbering of at least ten samples for the study of biochemical parameters was carried out. The calculation of the relative life state (RLS) of forest crop in plantations was carried out according to the method by V.A. Alekseev (1990)

$$RLS = \frac{100n_1 + 70n_2 + 40n_3 + 5n_4}{N},$$

where n_1, n_2, n_3, n_4 – the number of healthy, weak, very weak, and dying trees in the sample plot, respectively; 100, 70, 40, 5 – coefficients expressing (in percent) the life state of healthy, weak, very weak and dying trees;

N – the total number of trees in the sample plot (including dead trees). At the value of the relative life state from 100 to 80%, the forest crop is estimated as healthy, at 79-50% – weak, at 49-20% – very weak, at 19% and below – wholly destroyed.

In the period of active vegetation (in June, July, and August), the leaves of the middle

formation on the annual vegetative shoot (from the lower third of the south-facing crown) were taken from the accounting samples. The leaves of the intermediate creation are typical for the plant, developing in the middle zone of the shoot and performing the function of photosynthesis (Korovkin, 2007). In trunk plantations, the part of the south-facing crown was turned towards the roadway of the avenue directly. The selection of leaves was carried out in one day in all types of plantations.

In laboratory conditions, the content of condensed tannins in the leaves of woody plants was determined with the help of the permanganate metrical method (the Leventhal method modified by Kirsanov). The quantitative content of ascorbic acid was established following 24556-89 government standard (Chupakhina, 2000).

Ascorbic acid oxidase activity was determined with the method proposed by D.K. Asamov, S.T. Rakhimova (Ermakov *et al.*, 1987), which is based on the property of ascorbic acid to absorb light with a maximum wavelength of 265 nm. The activity of the enzyme was judged by the reduction of the optical density, taking into account that the degree of oxidation of ascorbic acid is proportional to the amount of the enzyme. Peroxidase activity was determined with the use of the calorimetric method (by A.M. Boyarkin) based on the determination of the benzidine oxidation reaction rate).

Polyphenol oxidase activity was determined by a spectrophotometric method based on the measurement of optical density of reaction products, which formed during the oxidation of pyrocatechol for a certain period of time (Ermakov *et al.*, 1987).

The analyses were carried out in triplicate for each accounting plant. The mathematical analysis of the measurement results was carried out with the use of the statistical package "Statistica 6.0". To interpret the obtained data, the method of variance multiple factor analysis was used (in the subsequent assessment of differences with the numerous comparison LSD test). In the process of comparison and analysis of the obtained results, significant differences between the signs were used (at $P < 0.05$).

3. RESULTS AND DISCUSSION:

In the territory of the study, the excess of the maximum permissible concentration of benz(a)pyrene, formaldehyde, phenols, carbon oxides, and nitrogen was determined. In the buffer

zones of industrial enterprises, the average annual MPC excess was observed for the following substances: carbon oxide – by two times; nitrogen oxides – by 3 times; sulfur dioxide – by 1.2 times; formaldehyde – by 5 times; phenol – by 1.7 times; benz(a)pyrene – by 1.9 times. In the trunk plantations zone, the average annual MPC excess was observed for the following substances: carbon oxide – by 3.4 times; formaldehyde – by 3.8 times; phenol – by 1.4 times; benz(a)pyrene – by 1.5 times.

The characteristics of plantations on the sample plots in the investigated areas are given in Table 1. The state assessment of plantations showed that in CCZ, the forest crop was estimated as healthy. But in buffer zones of industrial enterprises and in trunk plantations, the forest crop was weak. One of the substances with antioxidant properties is ascorbic acid, but the information in the literature is contradictory. In some sources, it is reported that under the influence of technogenic stress, the content of ascorbic acid decreases in others – vice versa.

Variance multiple factor analysis of the research results revealed the reliability of the influence of the complex conditions of the place of growth (significance level $p < 10^{-5}$), the vegetation period ($P < 10^{-5}$), as well as the interaction of these factors ($P < 10^{-5}$), on ascorbic acid oxidase activity in the leaves of Norway maple (Table 2).

The indicator of ascorbic acid oxidase activity in the leaves was compared among the plants growing in different types of plantations, i.e., in the conditions of the influence of anthropogenic load with varying intensity. In June, the activity of ascorbic acid oxidase in urban plantations was higher than among control samples in the park area. Further on, in July and August, Norway maple showed less enzyme activity among trees in the buffer areas of industrial zones and trunk plantations. At the same time, significant differences were found in August in the conditions of buffer zones of industrial enterprises and amounted to 3.17 activity units.

The analysis of the dynamics of ascorbic acid oxidase activity showed that in the zone of conditional control in the leaves of Norway maple, this index increased significantly from June to August.

In the leaves of Norway maple, the activity of this enzyme significantly decreased during the entire period of active vegetation, in the conditions of buffer plantations of industrial enterprises and trunk plantations. Thus, it can be concluded that the increase in ascorbic acid oxidase activity

during the growing season in the zone of conditional control and the decrease in the buffer zones of industrial enterprises and trunk plantations is typical for Norway maple.

Variance multiple factor analysis of the research results showed the reliable influence of the complex conditions of the place of growth ($P = 4.34 \cdot 10^{-5}$), vegetation period ($P < 10^{-5}$), as well as the interaction of these factors ($P < 10^{-5}$), on the content of ascorbic acid in the leaves of woody plants. The Norway maple growing in BZ plantations of the industrial enterprises, the content of ascorbic acid in leaves in comparison with control was higher: in June – by 76.1; in July – by 59.1, in August – by 22.3 mg/%.

The other tendency was observed in trunk plantations: the content of this metabolite, compared with CCZ, was significantly higher in June – by 111.7, in July, no significant differences were found, and in August it was slightly lower – by 9.6 mg% ($NSR_{05} = 6.5$ mg%). Thus, in Norway maple in the conditions of BZ of industrial enterprises and in trunk plantations, the content of this metabolite decreased during the growing season, which indicates the decrease in the activity of redox processes occurring in the leaves of plants. However, some samples in trunk plantations have differences in the dynamics of ascorbic acid content in the leaves. Thus, the increase of the degree of technogenic load leads to the increase in ascorbic acid content in the leaves of Norway maple.

The features of the content of condensed tannins in the leaves of Norway maple in connection with the conditions of the place of growth were investigated in this work as well. Variance multiple factor analysis of the research results revealed the reliability of the influence of the complex conditions of the place of growth ($P < 10^{-5}$), the vegetation period ($P < 10^{-5}$), as well as the interaction of these factors ($P < 10^{-5}$), on the content of condensed tannins in the leaves of Norway maple (Table 3).

Norway maple in all dates of observations (June, July, August) in the trunk plantations showed the significantly lower content of tannins in the leaves compared with the plantings of CCZ: in June – by 0.35; in July – by 1.06, in August – by 0.89 mg/g⁻¹gDW. Among the plantations of buffer zones of industrial enterprises, the picture was different: in June, the content of this substance was higher by 0.11 mg g⁻¹gDW, in July and August, on the contrary, lower, respectively – by 0.78 and 0.94 mg g⁻¹gDW, in comparison with plantations in the zone of conditional control.

The obtained results indicate the intensive use of this metabolite and its possible participation in the processes of adaptation of woody plants under technogenic stress. By the end of the period of the active vegetation of plants in the plantations of each category, the significant increase in the content of condensed tannins in the leaves of all the species of woody plants under investigation was observed ($P < 10^{-5}$).

Such results were observed in both years of research, which confirms the position that the condensed tannins are an active participant in the adaptation processes of Norway maple in the technogenic environment. Thus, the content of tannins in the leaves of Norway maple growing in the plantations of different ecological categories increased throughout the whole growing season.

To find out the cause of high or low content of tannins, intensive consumption of metabolite, or reduction of its synthesis under conditions of intense technogenic load, the activity of the enzyme involved in the synthesis of tannins was analyzed. The indicator of polyphenol oxidase activity in the leaves was compared among the plants growing in different types of plantations. Variance multiple factor analysis of the research results revealed the reliability of the influence of the complex conditions of the place of growth ($P < 10^{-5}$), the vegetation period ($P < 10^{-5}$), as well as the interaction of these factors ($P < 10^{-5}$), on polyphenol oxidase activity in the leaves of Norway maple (Table 2).

In Norway maple in plantations of BZ of the industrial enterprises in August, and in trunk plantations in July and August, the activity of this enzyme was authentically higher than among control samples in park plantations. The most significant differences were in August in the conditions of the most intensive technogenic load of the trunk plantations; they reached 3.07 activity units.

The dynamics of polyphenol oxidase activity in the leaves of Norway maple in plantations of different types have been studied as well. In park plantations, the significant increase in enzyme activity in July was observed and then the considerable decrease in August; the enzyme activity rates, despite a substantial reduction compared to July, were significantly higher than in June.

In buffer zones plantations and trunk plantations, enzyme activity increased in July and further expanded in August. Thus, the investigation of polyphenol oxidase activity in the leaves of Norway maple has allowed finding out

that in August, the highest values of this indicator in the buffer zones plantations, as well as in trunk plantations, are observed in comparison with park plantations.

Peroxidase activity in the leaves of Norway maple in plantations of different types has been studied as well. Variance multiple factor analysis of the research results revealed the reliability of the influence of the complex conditions of the place of growth ($P < 10^{-5}$), the vegetation period ($P < 10^{-5}$), as well as the interaction of these factors ($P < 10^{-5}$), on peroxidase activity in the leaves of Norway maple (Table 2).

Norway maple in plantations of BZ of the industrial enterprises and in trunk plantations in June showed peroxidase activity that was authentically higher than among control samples in park plantations (Figure 2). In July, the action of the enzyme of Norway maple was higher by 0.04 activity units in the plantations of BZ of industrial enterprises. In August, it was lower by 0.04 activity units than in CCZ.

Norway maple showed higher, in comparison with the control, indicators of enzyme activity only in June. In the following months, the enzyme activity of Norway maple in July was lower (by 0.09), and in August – higher (by 0.03 of activity units) than in the CCZ. The dynamics of peroxidase activity in the leaves of Norway maple in plantations of different types have been studied as well. In park plantations, the significant increase in enzyme activity in July was observed and then the decrease in August; the enzyme activity rates, despite a substantial reduction compared to July, were significantly higher than in June.

In the plantations of BZ of industrial enterprises and the trunk plantations, the dynamics of enzyme activity were similar, increased in July, and decreased by August.

4. CONCLUSIONS:

In the conditions of intensive technogenic load, Norway maple shows higher ascorbic acid oxidase activity at the initial stages of active vegetation and lower at the end of vegetation, in comparison with plants of CCZ. At the same time, the content of ascorbic acid in the leaves also decreases during vegetation of plants in the buffer zones plantations of industrial enterprises and trunk plantations. Thus, the increase in the degree of technogenic load leads to an increase in the ascorbic acid content in the leaves of Norway maple.

As for polyphenol oxidase activity and

tannins content, in the buffer zones plantations of industrial enterprises and trunk plantations, Norway maple was characterized by the increase in polyphenol oxidase activity, in comparison with the control plantings. The rise in polyphenol oxidase activity is accompanied by the decrease in the content of tannins, which indicates the active participation of tannins in the adaptive reactions of plants associated with the mechanisms of neutralization of pollutants.

In the plantations of BZ of industrial enterprises and in the trunk plantations in June, peroxidase activity in the leaves is higher than the same indicators of the control samples. Norway maple in trunk plantations has lower peroxidase activity in its leaves in the conditions of the most intense load in July than in farms of CCZ, and in August, this activity is higher than in the control group.

5. ACKNOWLEDGEMENTS:

The research was carried out with the financial support of a grant of the President of the Russian Federation for young candidates of sciences No. 1955.2017.11.

6. REFERENCES:

1. Ahmad P., Jaleel C., Salem M. Roles of enzymatic and non-enzymatic antioxidants in plants during abiotic stress: Crit. Rev. Biotechnol **2010**, 30, 161–175.
2. Ahmed M.R., Anis M. Changes in activity of antioxidant enzymes and photosynthetic machinery during acclimatization of micropropagated *Cassia alata* L. plantlets: In Vitro Cellular and Developmental Biology-Plant **2014**, 50, 601–609.
3. Avdeeva E.V. Green areas in monitoring the environment of a large industrial city (using the example of Krasnoyarsk): author. dis. ... Dr. S.-H. sciences. Krasnoyarsk, **2008**.
4. Bukharina I.L., Kuzmin P.A., Sharifullina A.M. The content of low molecular weight organic compounds in the leaves of trees under man-made loads: Forest science **2014**, 2, 20–26.
5. Bukharina I.L., Zhuravleva A.N., Dvoeglazova A.A., Kamasheva A.A., Sharifullina A.M., Kuzmin P.A. Physiological and Biochemical Characteristic Features of Small-Leaved Lime (*Tilia Cordata* Mill.) in Urban Environment: Research Journal of Pharmaceutical, Biological and Chemical Sciences **2014**, 5(5), 1544–1548.
6. Chupakhina G.N. Physiological and biochemical methods of plant analysis. Kaliningrad, **2000**.
7. Chupakhina G.N., Maslennikova P.V., Skrypnik L.N., Besserezhnova M.I. The reaction of the pigment and antioxidant system of plants to the environmental pollution of Kaliningrad by motor vehicle emissions: Tomsk State University Bulletin. Biology **2012**, 2 (19), 171–85.
8. Ermakov A.I., Arasimovich V.V., Yarosh NP, Peruvsky Yu.V., Lukovnikova G.A., Ikonnikova M.I. Methods of biochemical studies of plants. L.: Agropromizdat, **1987**.
9. Galves-Valdivieso, Mullineaux P.M.G. The role of reactive oxygen species in signalling from chloroplasts to the nucleus: Physiologia Plant **2010**, 138, 430–439.
10. Garcia D.E., Glasser W.G., Pizzi A., Paczkowski S.P., Laborie M.P. Modification of condensed tannins: from polyphenol chemistry to materials engineering: New Journal of Chemistry **2016**, 1, 234–242.
11. Gill S.S., Tuteja N. Reactive oxygen species and antioxidant machinery in Abiotic stress tolerance in crop plants: Plant Physiology Biochem **2010**, 48, 909–930.
12. Grishina L.A., Samoilova E.M. Biomass accounting and chemical analysis of plants. M.: Publishing House of Moscow. gov. University, **1971**.
13. Hattas D., Julkunen-Tiitto R. The quantification of condensed tannins in African savanna tree species Phytochemistry Letters **2012**, 5, 329–334.
14. Ivanova, V., Atukov, I., Vinogradova, N., Shatin, A., & Ivanov, S. (2019). Natural risks and economic vulnerability. Journal of Environmental Management and Tourism, 10(7), 1486-1494. doi:10.14505/jemt.v10.7(39).06
15. John R., Ahmad P., Gadgil K., Sharma S. Effect of cadmium and lead on growth, biochemical parameters and uptake in *Lemnapolyrrhiza* L.: Plant Soil Environ **2008**, 54, 262–270.
16. Kerio L.C., Wachira F.N., Wanyoko J.K.,

- Rotich M.K. Total polyphenols, catechin profiles and antioxidant activity of tea products from purple leaf coloured tea cultivars: *Food Chem* **2013**, 136, 1405–1413.
17. Kloseiko J. Cupric ferricyanide reaction in solution for determination of reducing properties of plant antioxidants: *Food analytical methods* **2016**, 9, 164–177.
 18. Korovkin O.A. Anatomy and morphology of higher plants. Glossary of terms. M.: Drofa, **2007**.
 19. Li X., Yang Y.Q., Sun X.D., Lin H.M., Chen J.H., Ren J., Hu X.Y., Yang Y.P. Comparative physiological and proteomic analyses of poplar (*Populus yunnanensis*) plantlets exposed to high temperature and drought: *Plos one* **2014**, 9, 100–108.
 20. Maiti R., Rodriguez H.G., Sarkar N.C., Kumari A. Biodiversity in Leaf Chemistry (Pigments, Epicuticular Wax and Leaf Nutrients) in Woody Plant Species in North-eastern Mexico, a Synthesis: *Forest Res* **2016**, 5, 170–176.
 21. Neverova O.A., Kolmogorova E.Yu. Woody plants and urbanized environment. Novosibirsk: Science, **2003**.
 22. Pachzkowska M., Kozłowska M., Golinski P. Oxidative stress enzyme activity in *Lemnaca minor* L. exposed to cadmium and lead: *Acta Biologica Cracoviensia. Ser. Botanica* **2007**, 49, 33–37.
 23. Podoprigora, D., & Korobov, G. (2017). Selection of the acidizing compositions for use in terrigenous reservoirs with high carbonate content. *International Journal of Applied Engineering Research*, 12(2), 249–255.
 24. Rodin L.E., Releasov N.P., Bazilevich N.I. Guidelines for the study of the dynamics and the biological cycle in phytocenoses. L.: Science, **1968**.
 25. Rogatchev, M. K., Sukhikh, A. S., & Kuznetsova, A. N. (2019). Filtration tests of surfactant solutions effects on displacement efficiency oil from low-permeable polymictic reservoirs. Paper presented at the Topical Issues of Rational use of Natural Resources - Proceedings of the International Forum-Contest of Young Researchers, **2018**, 125–130.
 26. Sarika A., Sairam R.K., Srivastava G.C., Tyagi Aruna, Meena R.C. Role of ABA, salicylic acid, calcium and hydrogen peroxide on antioxidant enzymes induction in wheat seedlings: *Plant Science* **2005**, 169, 559–570.
 27. State report "On the state of natural resources and environmental protection of the Republic of Tatarstan in 2016" [Electronic resource]. Kazan, **2017**. URL: eco.tatarstan.ru/rus/file/pub/pub_1007315.pdf (appeal date: 08/21/2018)
 28. Voskresenskaja O.L. Ecological and physiological adaptations of the western thuja (*Thuja occidentalis* L.) in urban environments: monograph. Yoshkar-Ola: Mari State University, **2006**.

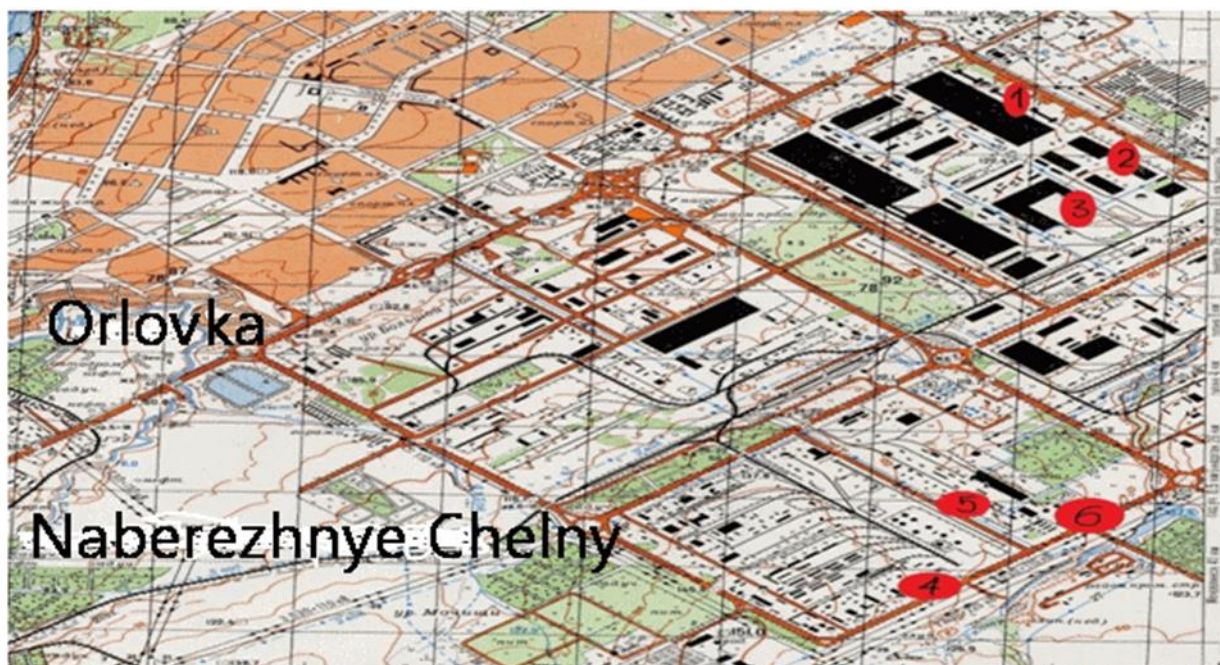


Figure 1. The schematic map of sample plots location (the city of Naberezhnye Chelny): Buffer zones of industrial enterprises: 1, 2, 3 – blacksmith plant; 4, 5, 6 foundry plant; trunk plantations: 7, 8, 9 – Avto-1; 10, 11, 12 – Mira Avenue. The scale is 1:50,000.

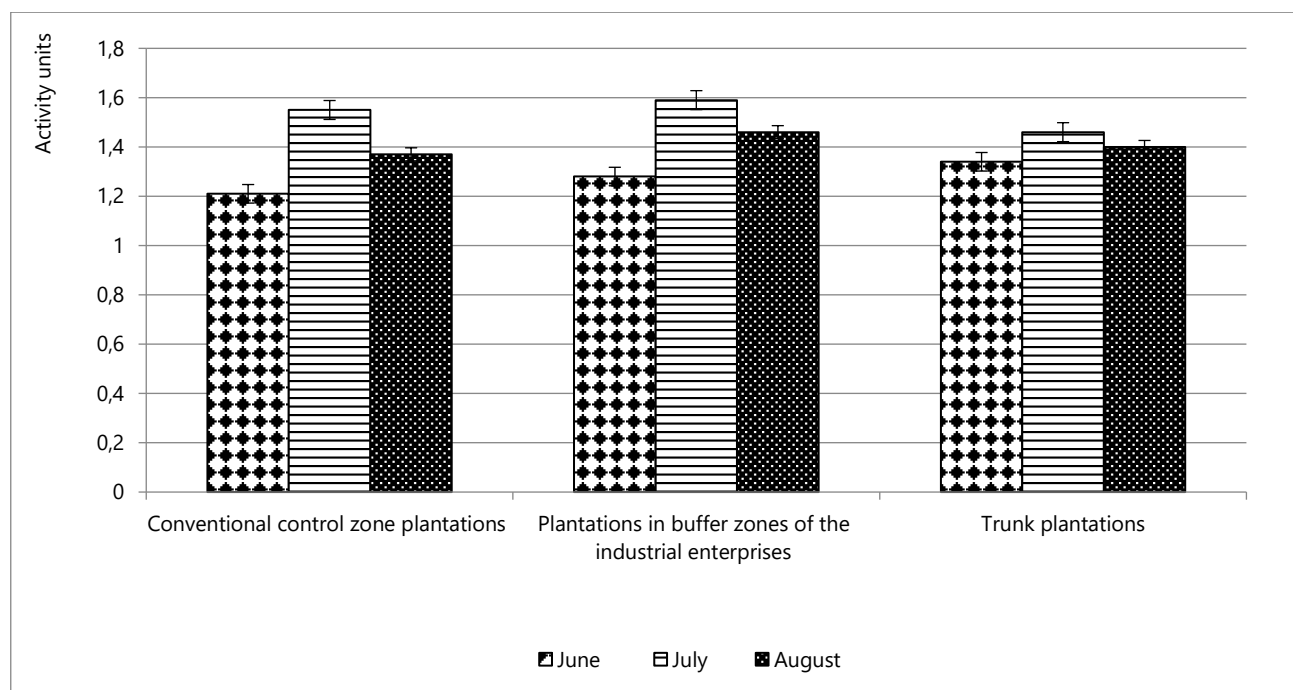


Figure 2. Peroxidase activity in the leaves of Norway maple in plantations of different types, act.un

Table 1. The characteristics of plantations on the sample plots in the investigated areas

Indicators	Sample plot	Investigation area					
		Conventional control zone		Buffer zones		Trunk plantations	
		Naberezhnye Chelny forestry	Grenada park	Blacksmith plant	Foundry plant	Mira Avenue	Avto-1
Trees/shrubs density, pcs./ha	SP No. 1	416/32	336/40	412/20	440/36	464/12	460/12
	SP No. 2	480/28	352/64	440/32	336/52	420/16	420/44
	SP No. 3	388/24	392/56	384/44	392/56	440/28	440/20
Total number of trees/shrubs, pcs.	SP No. 1	104/8	84/10	103/5	110/9	116/3	115/3
	SP No. 2	120/7	88/16	110/8	84/13	105/4	105/11
	SP No. 3	97/6	98/14	96/11	98/14	110/7	110/5
Forest crop normality	SP No. 1	0.7	0.7	0.7	0.8	0.8	0.8
	SP No. 2	0.8	0.7	0.8	0.6	0.7	0.7
	SP No. 3	0.7	0.8	0.7	0.7	0.8	0.8
Relative life state of forest crop, according to the scale by V.A. Alekseev (1990)	SP No. 1	health	health	weak	weak	weak	weak
	SP No. 2	health	health	weak	weak	weak	weak
	SP No. 3	health	health	weak	weak	weak	weak
Plantations age, years	SP No. 1	45	45	35	40	35	40
	SP No. 2	65	40	55	40	45	40
	SP No. 3	60	40	40	35	45	45

Table 2. The content of ascorbic acid and ascorbic acid oxidase activity in the leaves of Norway maple in plantations of different types

Plantations types	Ascorbic acid oxidase activity, act.un.			Ascorbic acid, mg/%		
	June	July	August	June	July	August
Conventional control zone	3.42	4.25	5.62	246.1	199	158.8
Buffer zone	3.66	3.18	2.45	322.2	258.1	181.1
Trunk plantations	3.96	3.58	2.96	357.8	196.7	149.2
NSR ₀₅	0.03			6.5		

Table 3. *The content of condensed tannins and polyphenol oxidase activity in the leaves of Norway maple in different types of plantations*

Plantations types	Polyphenol oxidase activity, act.un.			Condensed tannins, mg/gDW		
	June	July	August	June	July	August
Conventional control zone	0.94	2.92	1.80	4.87	6.90	8.45
Buffer zone	0.96	2.95	3.51	4.98	6.12	7.51
Trunk plantations	0.96	3.41	4.87	4.52	5.84	7.56
NSR ₀₅	0.04			0.04		

MATÉRIA-PRIMA BASE DE RESERVAS DE ÓLEO DE DIFÍCIL EXTRAÇÃO DA RÚSSIA

RAW MATERIAL BASE OF HARD-TO-EXTRACT OIL RESERVES OF RUSSIA

СЫРЬЕВАЯ БАЗА ТРУДНОИЗВЛЕКАЕМЫХ ЗАПАСОВ НЕФТИ РОССИИ

PRISCHEPA, Oleg M.^{1*}; NEFEDOV, Yury V.²; KOCHNEVA, Olga E.³;

^{1,2,3}Saint-Petersburg Mining University, Oil and Gas Geology Department, Saint-Petersburg, Russia

* Correspondence author
e-mail: yurijnefedov@yandex.ru

Received 28 February 2020; received in revised form 15 March 2020; accepted 24 March 2020

RESUMO

A estimativa da parcela das reservas de petróleo difíceis de extrair nos depósitos da Rússia varia de acordo com diferentes fontes em uma faixa bastante ampla (de 30 a 70%). Devido à ausência de uma abordagem comum à sua definição, a variedade de parâmetros utilizados para estimar essa parcela e as condições fundamentalmente diferentes para o desenvolvimento dos grupos de reservas classificadas como difíceis de extrair tornam-se um desafio. Uma parcela significativa das reservas comprovadas de petróleo dos campos de petróleo russos - cerca de 34% (6,3 milhões de toneladas) - pertence a pesados (densidade de óleo superior a 0,871 g/cm³) e superpesados (densidade de óleo superior a 0,895 g/cm³). Em geral, a parcela de óleos de alta viscosidade e super alta viscosidade é de cerca de 13% (2,4 milhões de toneladas). A maior parcela refere-se aos depósitos de três distritos. Em coletores de baixa permeabilidade (permeabilidade inferior a 0,05 μm²), enormes reservas estão concentradas - 8,2 milhões de toneladas ou 44,6% de todo o petróleo. A comparação da extração de petróleo e da estrutura de reservas indica uma boa correlação para a extração de óleo de coletores com baixa permeabilidade em 41,8% com o percentual de reservas em 44,6% assim como correlação relativamente boa em óleo super pesado em 13,4% com porcentagem de reservas em 18% e taxas baixas para óleo de viscosidade super alta em 1,7%, com porcentagem de reservas em 6%. Reservas comprovadas significativas de óleo de alta viscosidade na Rússia indicam a possibilidade de aumentar a produção com a introdução de tecnologias modernas, existentes e comprovadas, sob condições econômicas apropriadas. O envolvimento em larga escala no desenvolvimento apenas dos maiores depósitos de óleo de alta viscosidade permitiria à Federação Russa produzir pelo menos 25 a 30 milhões de toneladas no médio prazo.

Palavras-chave: reservas de difícil extração, HTER, rochas de baixa permeabilidade, base de matérias-primas da Federação Russa.

ABSTRACT

The estimation of the share of hard-to-extract oil reserves in the deposits of Russia varies by different sources, in a fairly wide range (from 30 to 70 %). Due to the absence of a common approach to their definition, the variety of parameters used to estimate this share and fundamentally different conditions for the development of the groups of reserves classified as hard-to-extract become challenging. A significant share of the proven oil reserves of Russian oil fields - about 34 % (6.3 million tons) - belongs to heavy (oil density more than 0.871 g/cm³) and super-heavy (oil density more than 0.895 g/cm³). In general, the share of high-viscosity and super-high-viscosity oils is about 13% (2.4 million tons). The largest share refers to the deposits of three districts. In low-permeable collectors (permeability less than 0.05 μm²), huge reserves are concentrated – 8.2 million tons or 44.6 % of all oil. Comparison of oil extraction and reserves structure indicates a good correlation for oil extraction from low-permeable collectors in 41.8 % with reserves percentage in 44.6 % as well as a relatively good correlation in super-heavy oil in 13.4% with reserves percentage in 18 % and low rates for super-high-viscosity oil in 1.7% with reserves percentage in 6 %. Significant proven reserves of high-viscosity oil in Russia indicate the possibility of increasing production with the introduction of modern, existing and proven, technologies under appropriate economic conditions. Full-scale involvement in the development of only the largest deposits of high-viscosity oil would allow the Russian Federation to produce at least 25-30 million tons in the medium term.

Keywords: hard-to-extract reserves, HTER, low-permeable rocks, raw material base of the Russian Federation.

АННОТАЦИЯ

Оценка доли трудноизвлекаемых запасов нефти в месторождениях России варьирует по разным источникам, в довольно широком диапазоне (от 30 до 70 %). Это обусловлено отсутствием единого подхода к их определению, многообразием параметров, используемых для оценки этой доли и, что более существенно, принципиально разными условиями освоения групп запасов, относимых к трудноизвлекаемым. Существенная доля разведанных запасов нефти месторождений РФ - около 34 % (6,3 млрд т) относится к тяжелым (плотность более 0,871 г/см³) и сверхтяжелым (плотность более 0,895 г/см³). В целом доля высоковязких и сверхвысоковязких нефтей составляет около 13% (2,4 млрд.т.) Наибольшая их часть приурочена к месторождениям трех регионов. В низкопроницаемых коллекторах (с проницаемостью менее 0,05 мкм²) сосредоточены огромные запасы – 8,2 млрд т или 44,6 % всех запасов нефти. Сравнение объемов добычи и структуры запасов свидетельствует о хорошей корреляции по добыче нефти из низкопроницаемых коллекторов 41,8 % при доле запасов в РФ 44,6 %, относительной хорошей корреляции по сверхтяжелой нефти 13,4 % при доле в запасах 18 %, и низких показателях по сверхвысоковязкой нефти - 1,7 % при доле в запасах 6 %. Значительные разведанные запасы высоковязкой нефти в России свидетельствуют о возможности наращивания объемов добычи при внедрении современных, уже имеющихся и апробированных технологий при соответствующих экономических условиях. По оценкам экспертов полномасштабное вовлечение в разработку только наиболее крупных залежей высоковязкой нефти позволило бы России дополнительно добывать не менее 25-30 млн.т. в среднесрочной перспективе.

Ключевые слова: трудноизвлекаемые запасы, ТРИЗ, низкопроницаемые породы, сырьевая база РФ.

1. INTRODUCTION:

The involvement in economic turnover of oil reserves belonging to various groups of hard-to-extract (HTER) has become possible due to advances in technology and changes in market conditions that allow the effective development of such reserves (Shpurov *et al.*, 2006).

Assessment of the possibility of reserves development depends on the use and availability of extraction technologies, which in turn determine the economic characteristics of HTER projects (Prischepa *et al.*, 2011; Shpurov *et al.*, 2014; Zambrano *et al.*, 2018;) makes it necessary to take a more careful approach to their differentiation.

The concept of "hard-to-extract reserves" is subject to significant revision over time (Shpurov *et al.*, 2014). The classification of hard-to-extract reserves, developed by E. M. Halimov and N. N. Lisovsky (Lisovsky *et al.*, 2009) proposed in 1994, established the basic criteria for such reserves require significant refinements with the introduction of tax incentives in 2012, but new technology has allowed cost-effectively develop a certain proportion of reserves that were previously considered ineffective (Shpurov *et al.*, 2014). Accordingly, the criteria that characterize oil reserves as hard-to-extract have been rethought (Muslimov, 2011; Shelepov, 2013; Szydlowski, 2019; Shpurov *et al.*, 2014; Prischepa, 2019; Prischepa, 2016;).

A typical example is given in a retrospective survey of 2014 year by Shpurov I. V. (Shpurov *et al.*, 2014) on the change of the share

of hard-to-extract oil reserves in West Siberia over the past 30 years, indicating that the reserves in the 80-90 years of the twentieth century belonged to hard-to-extract were involved in active production (Kontev *et al.*, 2019). As a result of the use of the latest technologies that became widespread in the late XX - early XXI century, in particular the emergence of hydraulic fracturing technologies, horizontal drilling, and multidimensional digital reservoir models, oil extraction in West Siberia was about 300 million tons, i.e., in 2 times more than expected in accordance with development projects drawn up and approved before 1990.

When discussing the opportunities for the development of projects for the exploration of hard-to-extract oil reserves in recent years, the emphasis is mainly placed on two groups: deposits in low-permeable rocks and deposits of heavy and high-viscosity oil. The solution of the problem of stimulating the production of hard-to-extract reserves in modern conditions is complicated by the lack of a concept (definition) and a classifier for HTER of these two groups (Shpurov *et al.*, 2014).

The most significant role in intensifying of exploration and development of hard-to-extract reserves had to play benefits for the tax on mineral extraction (TME), taking into account the permeability of the collectors (from reduced tax of 20% to completely "reset" for the extremely low permeability of bazhenovskaya, domanic, and hadumskaya formations) and benefits on extraction of heavy and high-viscosity oil. Meanwhile, criteria for hard-to-extract reserves

contained in low-permeability collectors, and reserves of high-viscosity oil with the progress of technology has substantially increased: permeability from 0.03 to 0.002 mm²; by viscosity from 30 to 200 MPa·s. Accordingly, the volume of oil reserves that can be defined as hard-to-extract significantly decreased (from 10.8 billion to 4.7 billion tons, i.e., in 2 - 3 times when using such criteria). The objective of tightening the criteria is shown by the fact that about 60% of the reserves that were previously considered as hard-to-extract are already involved in the development. In 2014, only 4.8 billion of the 10 billion tons that previously belonged to this category remained uninvolved (Neizvestnaya *et al.*, 2018; Yemelyanov *et al.*, 2019a,b, 2020; Voronkova *et al.*, 2019).

At the same time, the share of reserves involved in the development that are classified as hard-to-extract in accordance with the tax code is only 13% (with the exception of depleted reserves) (Shpurov *et al.*, 2014; Lushpeev and Margarit, 2018; Lateef *et al.*, 2019).

A separate category of projects for hard-to-extract reserves that have not yet been developed is projects for unusual HCM accumulations in extremely low-permeable collectors (oil from dense and shale collectors).

A push for development of such projects should have been the allocation of several specialized projects (including big companies - Gazpromneft (the project of The Bazhen technology center), Surgutneftegaz, Tatneft, Rosneft and LUKOIL) that allow testing approaches to technologies for the development of "dense" collectors and so-called "shale" formations, first of all, bazhenovskaya and domanic formations. These measures have played a role in the intensification of study, but in general, especially for the last group of commercially successful projects until now, including due to the uncertainty of the regulatory framework and the development of new methods for assessing reserves (Gutman *et al.*, 2017; Kamenchukov *et al.*, 2019).

Accordingly, in light of that, estimate of the share of hard-to-extract oil deposits in Russia varies in line to different sources, in a fairly wide range (from 30% to 70%) (Prischepa *et al.*, 2011; Yakutseni *et al.*, 2007; Lisovsky *et al.*, 2009; Shpurov *et al.*, 2014; Shelepov, 2013; Muslimov, 2011), due to the lack of a unified approach to their definition, many of the parameters used for the evaluation of this share and, more significantly, the fundamentally different conditions of development of groups of reserves classified as hard-to-extract.

In "The strategy of development of mineral resources of the Russian Federation till 2030", the mention of the 65% share of hard-to-extract reserves in Russia, with none of the classification parameters, indicating that classification of oil reserves with certain properties to be hard-to-extract (density and viscosity of oil, tar, sulfur, and paraffin content, etc.), such share in the structure of reserves is not mentioned.

Due to the fact that reserves can often be classified as hard-to-extract by several classification criteria (heavy and high-viscosity oils, high-tar and sulfur oils, etc.), a simple summation of the volume of reserves of such groups does not allow you to get an idea of the real share of hard-to-extract reserves and their structure (Prodanova *et al.*, 2019).

This study aimed to analyze the share of hard-to-extract oil deposits in Russia, to establish a single approach to their definition, parameters used to estimate this share, and to see the different conditions of development of hard-to-extract reserves.

2. MATERIALS AND METHODS:

The most important parameters used to classify oil reserves as hard-to-extract are the quality characteristics of the fluids. Thus, according to the "Classification of oil and combustible gas reserves", there are oils with deteriorated (in terms of the possibility of development) physical and chemical properties, which include bituminous (density over 0.895 g/cm³) and heavy (0.871-0.895 g/cm³), super-high-viscosity (viscosity over 200 MPa·s) and high-viscosity (from 30.1 to 200 MPa·s), as well as oil with high (more than 500 m³/t) or low (less than 200 m³/t) gas saturation.

The next group of parameters is related to the collector properties of the hydrocarbon-containing strata. Here, the main classification parameters are both the collector capacity itself, which essentially determines the volume of reserves in the strata and such an important characteristic as permeability, which directly affects the development modes and extraction technologies.

In terms of permeability, productive layers are divided into low-permeable (up to 100 mD), medium-permeable (100-500 mD), and high-permeable (more than 500 mD).

There is a large group of parameters that also determines the complexity of development and the need to use special modes or technologies

– this is the occurrence of collectors at low depths and (or) in the permafrost zone, high or extremely low intra-layer temperatures, high water content of the extracted water-oil liquid, etc.

3. RESULTS AND DISCUSSION:

At the beginning of 2019, 3176, fields with deposits containing oil have been identified in the Russian Federation (Prischepa, 2019). Most of the oil reserves are accounted for in 2756 fields of the distributed subsoil fund (96.6% of all drilled developed reserves). Oil extraction in Russia as a whole for the 2018 year amounted to be about 3% of the current drilled developed reserves. In more than half of the multi-deposit oil fields (1720) in Russia, one or more deposits are characterized by properties that make it possible to classify oil reserves as hard-to-extract.

As of 01.01.2019, a significant share of oil reserves is characterized by properties that allow considering them as hard-to-extract. Thus, heavy (more than 0.871 g/cm³) and super-heavy (more than 0.895 g/cm³) oil fields in the Russian Federation amount to be about 34% (6.3 billion tons) of the current drilled industrial extractable reserves, which is significantly different from the estimates of international experts, who estimate 13.4 billion barrels (less than 2 billion m³), probably due to accounting only super-heavy oil, which at the same time is high-viscosity and super-high-viscosity. The largest part of the reserves of heavy and super-heavy oil in absolute terms is concentrated in the deposits of the Urals Federal district (2.9 billion tons, or 45.9 % of all heavy oil reserves in Russia), including the Khanty-Mansi Autonomous region there are 1.7 billion tons (including 0.252 billion tons of super-heavy), the Yamalo-Nenets Autonomous region – 0.995 billion tons (0.958 billion tons of super-heavy); the Volga Federal district – 2.1 billion tons (33.2%); the North-West Federal district – 0.7 billion tons (11.1%) (figure 1). More than 90% of the reserves of heavy and super-heavy oil are concentrated in the fields of 3 specified Federal districts. Since the volumes of total current oil reserves recorded in the respective districts differ significantly, the share of reserves of heavy oil in them varies from 10.5% in the Urals Federal district, 26.8% in the Volga Federal district to 39.9% in the North-Western Federal district. In the Siberian Federal district, with relatively small amounts of recorded reserves, the share of heavy oil is 14.8%.

On a parameter of viscosity (when referring to a group of high-viscosity oil with a viscosity of more than 30 MPa•s and taking into account that

for some fields, data on the quality of raw materials in the State balance are not given for 1092 million tons of extractable reserves or 6% of the oil reserves of the Russian Federation), the current structure of oil reserves in the Russian Federation differs slightly from the structure of distribution of reserves by oil density. So, in the whole of Russia, the share of high-viscosity (30.1-200 MPa•s) and super-high-viscosity (more than 200 MPa•s) oil is respectively 6.0 and 6.9% of extractable commercial reserves, or in the amount of 2378.6 million tons. Most of them are in the deposits of the Volga Federal district (940.9 million tons, or 39.6% of high-viscosity oil reserves of the Russian Federation), the Urals Federal district (902.5 million tons or 37.9%), almost all of them are in the Yamalo-Nenets Autonomous region (818.4 million tons) and the North-Western Federal district (426.3 million tons, 18.1%) (figure 2). In the structure of the reserves of these districts, the lowest share of high – viscosity oil (8.5%) falls on the Urals Federal district, and the largest (25.5 and 31.0%) – on the Volga and the North-Western Federal districts, respectively. It should also be noted that a significant share of Russian oil reserves belongs to the group of high-viscosity (10.1-30.0 MPa•s) – 1115.7 million tons, that most part (892 million tons) is also concentrated in the Volga Federal district.

If we consider the structure of heavy and high-viscosity oil reserves in the section of oil and gas provinces (OGP), most of them are in the Volga-Ural (Republic of Tatarstan, Samara region and Perm region), West Siberian (Yamalo-Nenets and Khanty-Mansi Autonomous regions) and the Timan-Pechora (the Republic of Komi) OGP. Also, a significant share of heavy oil is noted in the reserves of the Okhotsk province (Sakhalin island shelf) (Saitgaleev *et al.*, 2019; Tannady *et al.*, 2019), but since it does not differ in high-viscosity, it is not hard-to-extract.

When comparing the structure of heavy (super-heavy) and high-viscosity (super-high-viscosity) oil, there are significant discrepancies (almost 2 times) in the recorded oil reserves in the Russian Federation as a whole. The volumes of heavy and super-heavy oil reserves of Russia are estimated at 6.3 billion tons, and high-viscosity and super-high-viscosity oil at 3.4 billion tons.

From the point of view of development conditions, super-heavy oils that do not have high-viscosity in layer conditions, in fact, not much differ from heavy and even medium-density oil. The limit of classification for hard-to-extract reserves by the value of oil density used in the previous classification (more than 0.92 g/cm³) met the need

for special extraction technologies to a much greater extent than the recommended limit for super-heavy (bituminous) reserves - more than 0.895 g/cm^3 in the current classification. It is even less correct to classify heavy oil with a density of $0.87 - 0.895 \text{ g/cm}^3$ as hard-to-extract.

When comparing the ratio of super-heavy oil reserves in the Russian Federation (3.3 billion tons) and high-viscosity oil (3.4 billion tons), a good correlation is observed, which is confirmed by an additional comparison of these groups by Federal districts and subjects. Thus, in three Federal districts, the most important largest reserves of heavy and viscous oil, noted the following relationship: in the Urals Federal district - 1210 million tons of super-heavy oil and 939 million tons of high-viscosity and super-high-viscosity oil, in the Volga Federal district, respectively 1255 and 975 million tons, in the North-West Federal district - 541 and 436 million tons. For significant subjects of the Russian Federation, this ratio is as follows: in the Yamalo-Nenets Autonomous region - 958 and 854 million tons, in the Republic of Tatarstan - 689 and 569 million tons, in the Republic of Komi - 329 and 355 million tons, in the Samara region - 135 and 128 million tons.

Thus, when the boundary of the classification of reserves as hard-to-extract changes in density increasing above 0.92 g/cm^3 , the differences between the reserves of super-heavy and high-viscosity oil become even more insignificant. It is important to understand that despite significant reserves of high-density oil (more than 0.87 g/cm^3), for example, in the Khanty-Mansiysk Autonomous Region, the Nenets Autonomous Region, Krasnoyarsk region and Omsk region, such reserves should not be considered as hard-to-extract due to the fact that the oil is not viscous, and its extraction does not require significant additional costs compared to the extraction of lighter oil.

From the point of view of development conditions and, accordingly, the need to use technologies that significantly affect the economic performance of development projects (Prodanova *et al.*, 2019b), 3.3 - 3.4 billion tons of drilled explored reserves of the Russian Federation, which is about 18% of the total drilled reserves, are hard-to-extract in this way.

The largest deposits of heavy oil in Russia are the Russian, the Eastern-Messoyakhskoye and Severo-Komsomolskoye in the Yamalo-Nenets Autonomous region, respectively, 418, 201 and 147 million tons (extractable reserves of

heavy oil); Yarega and Usinsk in the Komi Republic, respectively, 174 and 130 million tons. A separate issue when considering the development of hard-to-extract oil deposits is the issue of sulfur content. Oil extraction with high sulfur content requires the use of specialized equipment; such oil requires high additional costs during processing, and special transportation conditions, which affects the economy of projects and limits its extraction (Gennadyevich *et al.*, 2019).

The share of sulfurous oil (sulfur content 1.0-3.0%) in the explored drilled reserves of the Russian Federation is 27.9%, high-sulfur (more than 3.0%) - 6.0%, i.e., a third of all explored oil reserves of the Russian Federation belong to sulfur and high-sulfur. Almost 80% of the extractable reserves of high-sulfur oil from Russian fields (878.2 million tons) are concentrated in the Volga Federal district (including 511.3 million tons in the Republic of Tatarstan), and another 11.7% is in the Urals Federal district (129.3 million tons in the Khanty-Mansiysk Autonomous region). Taking into account the combination of sulfur and high-sulfur oil, in the Volga Federal district accounts for 3050 million tons (82% of all current registered reserves of the district, including the Republic of Tatarstan - 910.9 million tons and the Perm region - 443.9 million tons); the North-Western Federal district - 681 million tons (almost 50% of the district's reserves).

Consideration of the properties of the oil-containing strata indicates that the low-permeable collectors (less than 0.05 mm^2) contain huge reserves - 8.2 billion tons or 44.6% of all oil reserves of categories A+B1+C1, including the Volga Federal district - 1.1 billion tons (13.4%), the Urals - 6.0 billion tons (75%) and the Siberian - 0.76 billion tons (9.3%). Low-permeability collectors account for more than 56% of the current reserves of West Siberia, almost 30% of the reserves of the Volga-Ural OGP, and 17 % of the oil reserves of the Timan-Pechora province.

One thousand two hundred sixty-five million tons of oil, or 6.8% of the A+B1+C1 reserves, are concentrated in sub - gas deposits, including 650 million tons in the Urals region and 312 million tons in the Siberian Federal district.

Along with heavy and bituminous oil, bitumen is considered as a strategic reserve. The principal difference between super-heavy oil and bitumen is its mobility in the reservoir. Thus, the group of heavy and super-heavy oil includes, as a rule, oil with a viscosity of more than $100 \text{ MPa}\cdot\text{s}$ (Prischepa *et al.*, 2011; Yakutseniet *et al.*, 2007;

Lisovsky *et al.*, 2009), and bitumen has a viscosity exceeding 10000 sP. Many bitumens and super-heavy oil have a higher viscosity in the reservoir. There are many factors that affect the viscosity of hydrocarbons, which include the group composition, the presence of dissolved natural gas, and the temperature and pressure in the layer. In general, the viscosity of heavy oil or bitumen is approximated with the density.

The state balance of mineral reserves of the Russian Federation as of 01.01.2019 includes only three deposits of bitumen and asphaltites, one of which is associated with bituminous dolomites, and one with bituminous sands. Deposits with recorded reserves of bitumen and asphaltites are located only in two districts – Southern and Volga. The recorded reserves are not of industrial value due to their small size.

Huge accumulations of bitumen and heavy oil are known in Eastern Siberia (within three provinces). The main bituminous layers are found in the Vendian-Cambrian, Silurian, Carboniferous, and Permian formations. Clusters (deposits) are poorly studied due to their remoteness and lack of economic interest.

Numerous accumulations of heavy bitumen have been identified within the Volga-Ural province, most of which are shallow deposits of Permian age in the Central and Northern parts of the province. According to R. H. Muslimov and R. R. Ibatullin, the Republic of Tatarstan has the largest natural bitumen resources in Russia; there are 450 deposits in the upper Permian sandstones with reserves of 1.163 billion m³ (7.3 billion barrels) (30-200 MPa·s). Heavy oil and bitumen in this province have high sulfur content (up to 4.5%) and contain metals (V, Ni, Mo).

Since the 80-ies of the last century, two fields of the Volga-Ural OGP - Mordovo-Karmalskoye and Ashalchinskoye fields - have been the testing ground for working out a good method for extracting natural bitumen. The following technologies have been designed and tested on them: core extraction in friable bituminous sandstones specially created by the coredigger; sampling of bituminous wells; initiating intra-layer thermal gas generator, high-frequency electromagnetic field, steam, electric heating installation UESK-100; thermocycler action on the bituminous-saturated layer by air, steam, and steam gas; area injection of air, steam, and steam gas; changes in the direction of filtration flows; extraction of NB by low-temperature oxidation (Muslimov, 2016).

Despite almost 40 years of research on the

geology and extraction of NB from Permian deposits, the problem of starting their development has not been solved. It is concluded that the characteristics of heavy oil and natural bitumen deposits in the Republic of Tatarstan are worse than those in Canada, Venezuela, and the United States: much smaller thickness; lower collector properties; relatively low oil bituminous saturation; high water content; a significant share of hydrocarbons in complex, extremely heterogeneous layers, which does not allow automatic transfer of technologies developed in the West to the bitumen deposits of the Russian Federation. To solve the problem of involvement in economic turnover, of course, the most important is to solve theoretical issues, conduct research and experimental industrial work on the development of bitumen deposits, which is impossible without the participation of the state with direct co-financing on the terms of private-public partnership (Muslimov, 2016).

A significant negative indicator of large developed fields is the high depletion of their reserves, which in general is 56%, and for many large ones reaches 90%. The rest (unprocessed) part of oil reserves can be considered as hard-to-extract.

If we compare the structure of hard-to-extract oil reserves and the extraction of the considered groups, the largest degree of correlation is observed when comparing the volumes of oil in tight collectors – extraction was 214.5 million tons, or 41.8%, the proportion of reserves in such collectors of 44.6%; in sub-gas deposits, respectively 38.3 million tons (7.5%), with the share in reserves of 6.8%; for super-high-viscosity oil (with a viscosity greater than 200 MPa·s) – 8.7 million tons (1.7%) with the share in reserves of 6%, high-viscosity oil (viscosity more than 30 MPa·s) – 30.6 million tons (6%), with the share in the reserves of 12.8%; super-heavy oil with a density of more than 0.895 g/cm³ – 68.8 million tons (13.4%) with a share in reserves of 18%, and taking into account heavy and super-heavy oil with a density of more than 0.87 g/cm³ - 170 million tons (33.2% of extraction) with a share in reserves of 34%.

In the structure of oil extraction in the Russian Federation, due to the introduction of new efficient development technologies (hydraulic fracturing, horizontal drilling, thermal methods, etc.), the share of oil extracted from low-permeable collectors, sub-gas deposits, and heavy and super-heavy oil has increased significantly in recent years (Shelepov, 2013; Shpurov *et al.*, 2014; Prischepa, 2019).

The main methods of development are thermal methods, which include: steam-thermal exposure, intra-layer combustion, hot water injection, steam-cyclic treatment of bottom-hole zones of producing wells, and a combination of these methods with other physical and chemical methods (combined methods).

Heavy oil is extracted in three main oil provinces: the Volga-Ural, the Timan-Pechora, and West Siberia. In all regions, the extraction of heavy and super-heavy oil is growing due to the improvement and application of modern extraction technologies.

In the Volga-Ural province, Ashalchinsky and Mordovo-Karmalsky fields are being developed, which are the oldest developed heavy oil fields. The Yareg and Usinsk super-heavy oil fields are being developed in the Timan-Pechora OGP (the Komi Republic). The Yareg high-viscosity oil field contains about 130 million m³ of heavy oil confined to the Devonian sandstones located at a depth of 180-200 m.

The peculiarity of the development at present is the transition from the long-used mining methods (thermoshaft method, thermocyclic impact) for more than 70 years to purely surface ones. According to LUKOIL, this will lead to a significant increase in the extraction of super-heavy oil at the field – up to 2 million tons per year or more. In conjunction with the second Usinsky field that being developed in the Timan-Pechora OGP, where the proven reserves of high-viscosity oil in the Permian-coal reservoir amount to more than 170 million tons, oil extraction is close to 5 million tons. The total accumulated extraction of high-viscosity oil on the territory of the Komi Republic as of 01.01.2018 exceeded 100 million tons.

4. CONCLUSIONS:

Progress in extraction technologies, combined with benefits for extracting high-viscosity, super-heavy oil, and oil from low-permeable collectors, has led to a significant increase in its extraction (achieving a share in extraction comparable to the structure of current proven reserves) and the possibility of extending this invaluable experience to other projects in Russia, which will significantly support current production in the long term.

Significant proven reserves of heavy and high-viscosity oil in Russia indicate the possibility of increasing extraction volumes with the introduction of modern, existing, and proven technologies under appropriate economic

conditions. This is evidenced by such achievements as a significant increase in the share of heavy oil in the production structure, a sharp increase in the volume of oil extraction from low-permeable collectors in the Russian Federation. At the same time, the rate of extraction of high-viscosity oil, despite the growth, is significantly behind the share of the corresponding structure of oil reserves due to the need to use high-cost technologies (thermal methods, etc.) in the development.

One of the most important measures recommended by the specialists of SRC (Shpurov *et al.*, 2014) and supported by the specialists of the regions with huge volumes of hard-to-extract oil reserves is the creation of a classifier of hard-to-extract reserves, as well as developing a scientifically sound definition of hard-to-extract reserves and its application, including the criteria for the appointment and cancellation of tax incentives for different types of these reserves.

According to experts, full-scale involvement in the development of only the largest deposits of high-viscosity oil would allow Russia to extract at least 25-30 million tons in the medium term (Prishchepa *et al.*, 2011; Muslimov, 2016).

5. REFERENCES:

1. Gutman, I. S., Potemkin, G. N., Postnikov, A.V., Postnikova, O. V., Kozlova, E. V., Alekseev, A.D., Karpov, I. A. *Methodological approaches to reserves calculation and resources evaluation of bazhenovskaya formation*, Oil industry, **2017**, (03), 28-32.
2. Gennadyevich, Y. S., Pakhomova, E. G., & Olegovna, D. K. (2019). Reliability of RC frame-braced systems in dangerous geological conditions. *Journal of Applied Engineering Science*, 17(2), 245-250.
3. Kamenchukov, A., Pugachev, I., Yarmolinsky, A., Vasilyev, A., & Kulikov, Y. (2019). Improving the criteria for determining dates of repair of highways. *Journal of Applied Engineering Science*, 17(1), 8186.
4. Kontev, A., Konteva, O., Kremneva, A., Voronkova, O., Kiseleva, N., & Zhuravlev, P. (2019). Economic and ecological fundamentals for the establishment of the metallurgical complex in siberia in the 18th century. *Journal of Environmental Management and Tourism*, 10(7), 1628-1636. doi:10.14505/jemt.v10.7(39).20

5. Lateef, A. O., Bin, M. S. H., & Ademola, F. J. (2019). Performance assessment based on Intelligent power management for standalone PV system in remote area of Ibadan, Nigeria. *Journal of Applied Engineering Science*, 17(1), 52-60.
6. Lisovsky, N. N., Halimov, E. M. *On the classification of hard-to-extract reserves*, Bulletin of the Central Committee of Rosnedra, **2009**, (6), 33-35.
7. Lushpeev, V., & Margarit, A. (2018). Optimization of oil field development process based on existing forecast model. *Journal of Applied Engineering Science*, 16(3), 391-397.
8. Muslimov, R. H. *Experience of development of resources of super-high-viscosity oils and natural bitumens of the Volga-Ural oil and gas province*, Oil economy, **2011**, (11), 42-47.
9. Muslimov, R.H. *New strategy of oil fields in modern Russia – optimization of production and maximization of EOR*, Oil. Gas. Novations, **2016**, (4), 8-17.
10. Neizvestnaya D.V., Kozlova N.N., Prodanova N.A. (2018). Application of CVP-Analysis at the Water Transport Organizations. *Helix*. 2018. Vol. 8(1). Pages 2811-2815. <https://doi.org/10.29042/2018-2811-2815>
11. Prischepa, O.M., Halimov, E.M. *Hard-to-extract oil: potential, state and opportunities for development*, Oil and gas vertical, **2011**, (5), 24-29.
12. Prodanova, N., Plaskova, N., Popova, L., Maslova, I., Dmitrieva, I., Sitnikova, V., & Kharakoz, J. (2019a). The role of IT tools when introducing integrated reporting in corporate communication. *Journal of Advanced Research in Dynamical and Control Systems*, 11(8 Special Issue), 411-415.
13. Prodanova, N., Savina, N., Kevorkova, Z., Korshunova, L., & Bochkareva, N. (2019b). Organizational and methodological support of corporate self-assessment procedure as a basis for sustainable business development. *Entrepreneurship and Sustainability Issues*, 7(2), 1136-1148. doi:10.9770/jesi.2019.7.2(24)
14. Prischepa, O. M. *State of the raw material base and extraction of hard-to-extract oil reserves in Russia*, Mineral resources of Russia, Economics and management, **2019**, (5,168), 14-20.
15. Prischepa, O. M. *Problems of reproduction of hydrocarbon reserves: the Arctic shelf and (or) hard-to-extract reserves*, Mineral resources of Russia, Economics and management, **2016**, (1, 2), 18-34.
16. Saitgaleev, M., Senchina, N., Sokolova, J. *Application of the method of ion-selective electrodes in exploration work on the sea shelf*, Marine Technologies, Gelendzhik, **2019**, DOI: 10.3997/2214-4609.201901811
17. Shelepov, V. V. *The work of the Central Commission on development at the present stage (to the 50th anniversary of its formation)*, Oil and gas industry, Oil industry, **2013**, (4), 4.
18. Szydlowski A.. (2019). "ORGANON OF DEMOCRACY". *Baltic Humanitarian Journal* Vol. 8 Iss. 4 p. 407 - 411 ISSN: 2311-0066.
19. Shpurov, I. V., Rastrogin, A. E., Bratkova, V. G. *On the problem of developing hard-to-extract oil reserves in West Siberia*, Oil economy, **2014**, (12), 95-97.
20. Tannady, H., Gunawan, E., Nurprihatin, F., & Wilujeng, F. R. (2019). Process improvement to reduce waste in the biggest instant noodle manufacturing company in South East Asia. *Journal of Applied Engineering Science*, 17(2), 203-212.
21. Yakutseni, V. P., Petrova, Yu. E., Sukhanov, A. A. *Dynamics of the share of the relative content of hard-to-extract oil reserves in the general balance*, Oil and gas Geology, Theory and practice, **2007**, (2), <http://www.ngtp.ru/rub/9/023.pdf>
22. Yemelyanov, V., A. Nedelkin, and N. Yemelyanova. (2020). Expert System Software for Assessing the Technical Condition of Critical Lined Equipment. *Advances in Intelligent Systems and Computing*. Vol. 1115 AISC. doi:10.1007/978-3-030-37916-2_92.
23. Yemelyanov, V. A., Nedelkin, A. A., & Olenov, L. A. (2019a). An object-oriented design of expert system software for evaluating the maintenance of lined equipment. Paper presented at the 2019 International Multi-Conference on

24. Yemelyanov, V. A., Yemelyanova, N. Y., Nedelkin, A. A., Glebov, N. B., & Tyapkin, D. A. (2019b). Information system to determine the transported liquid iron weight. Paper presented at the Proceedings of the 2019 IEEE Conference of Russian Young Researchers in Electrical and Electronic Engineering, EIConRus 2019, 377-380. doi:10.1109/EIConRus.2019.8656693
25. U.S. Energy Information Administration, 2016, *Petroleum and other liquids*, http://www.eia.gov/dnav/pet/PET_CRD_CRPDN_ADC_MBBL_A.htm
26. U.S. Energy Information Administration, 2019, *Venezuelan crude oil production falls to lowest level since January 2003*, <https://www.eia.gov/todayinenergy/detail.php?id=39532#>
27. Voronkova, O. Y., Iakimova, L. A., Frolova, I. I., Shafranskaya, C. I., Kamolov, S. G., & Prodanova, N. A. (2019). Sustainable development of territories based on the integrated use of industry, resource and environmental potential. *International Journal of Economics and Business Administration*, 7(2), 151-163.
28. Zambrano, C. J. R., Kovshov, S., & Lyubin, E. (2018). Assessment of anthropogenic factor of accident risk on the main oil pipeline Pascuales - Cuenca in Ecuador. *Journal of Applied Engineering Science*, 16(3), 307-312.

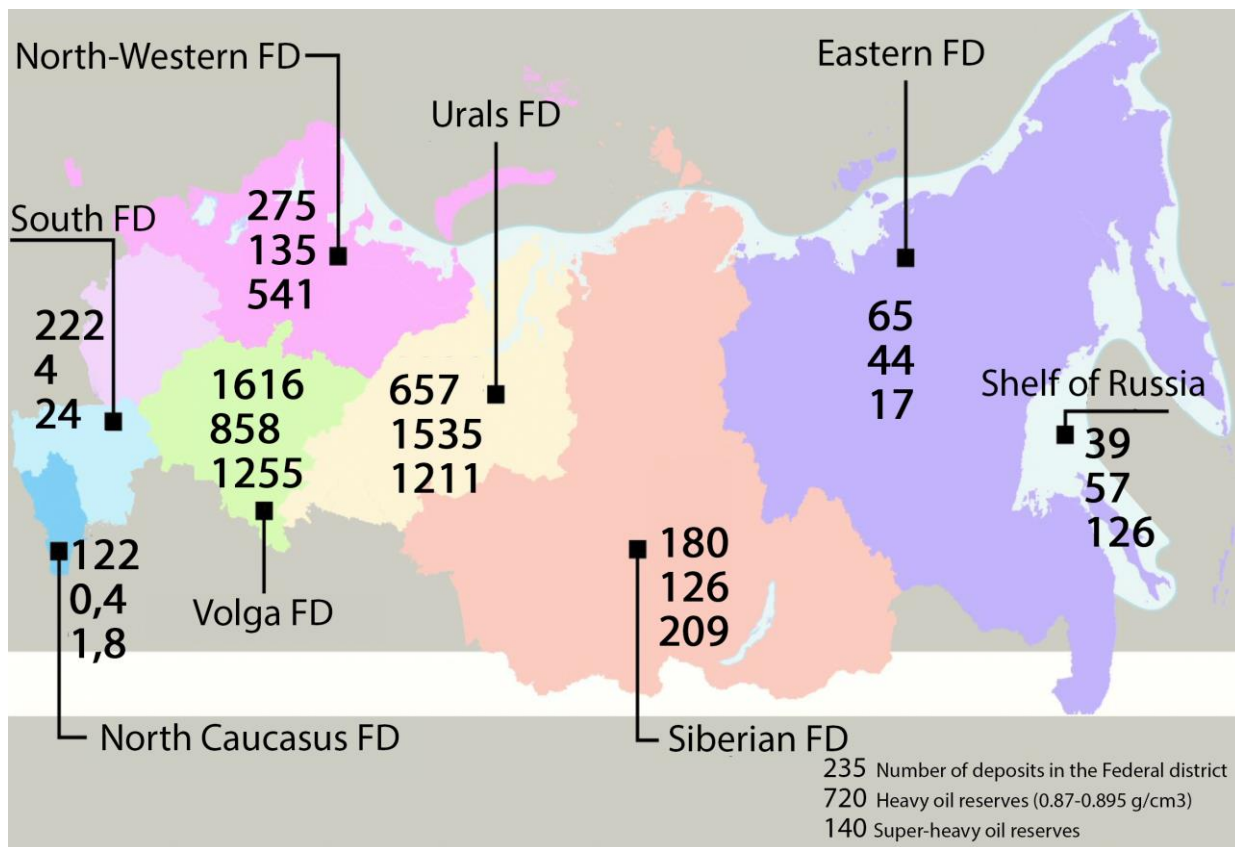


Figure 1. Distribution of heavy and bituminous oil reserves by Federal districts in the Russian Federation

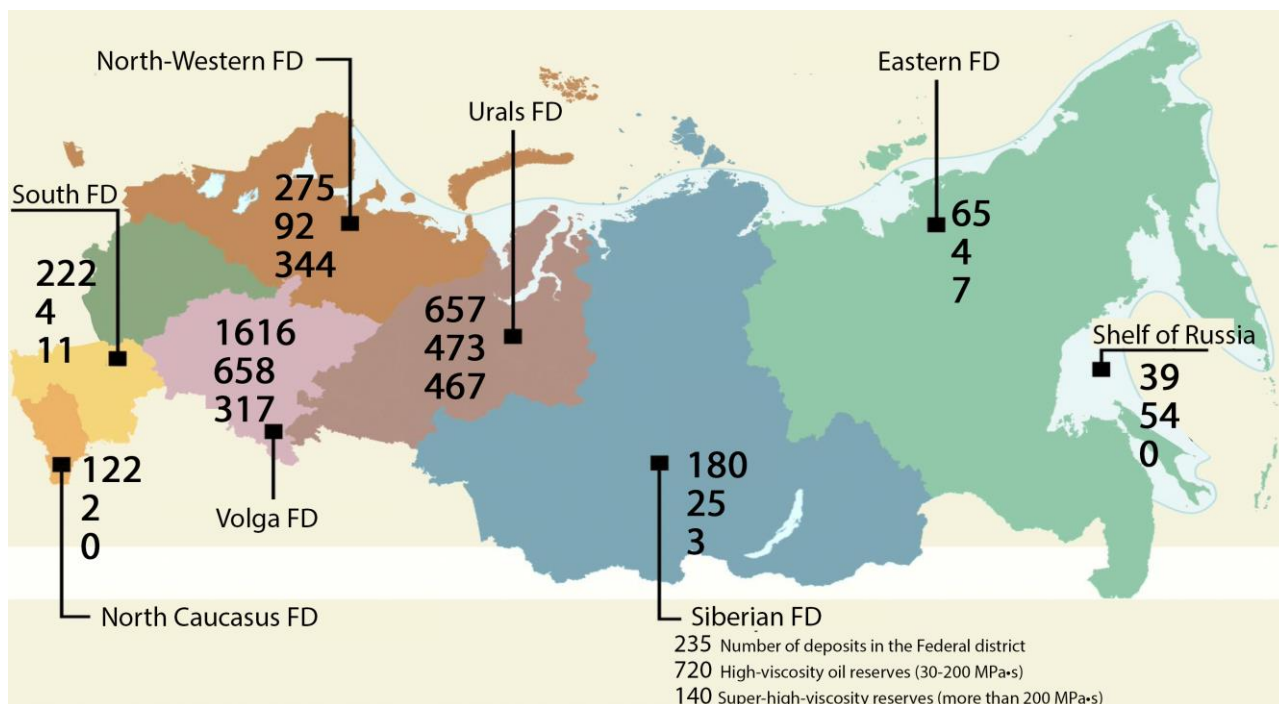


Figure 2. Distribution of high - and super-high-viscosity oil reserves by Federal districts in the Russian Federation

CARACTERÍSTICAS DA DEFORMAÇÃO E DESTRUIÇÃO DE CERÂMICAS POROSAS À BASE DE DIATOMITO

THE FEATURES OF DEFORMATION AND DESTRUCTION OF POROUS DIATOMITE-BASED CERAMICS

ОСОБЕННОСТИ ДЕФОРМАЦИИ И РАЗРУШЕНИЯ ПОРИСТОЙ КЕРАМИКИ НА ОСНОВЕ ДИАТОМИТА

SKVORTSOV, Arkadiy A.^{1*}; LUK'YANOV, Mikhail N.²; SKVORTSOVA, Anna A.³;

^{1,2,3} Moscow Polytechnic University, Department of Mechanics of Materials, 38 Bolshaya Semyonovskaya Str., zip code 107023, Moscow – Russian Federation

* Correspondence author
e-mail: skvortsovaa2009@yandex.ru

Received 15 December 2019; received in revised form 27 February 2020; accepted 28 March 2020

RESUMO

Estudos experimentais e teóricos das propriedades mecânicas de materiais porosos são uma das áreas prioritárias para o desenvolvimento da física da matéria condensada. A cerâmica de diatomito pode servir como matéria-prima para os materiais estruturais de isolamento térmico e os materiais estruturais à prova de som, para os aditivos de certos tipos de cimento e para polimento dos metais e mármore. A cerâmica à base de diatomito também é usada para isolamento térmico na produção de alumínio. A cerâmica de espuma de diatomito é um material poroso promissor. Mas as propriedades da cerâmica de diatomito não são bem conhecidas, o que determina a relevância do estudo. O principal objetivo deste trabalho é estudar a porosidade e os módulos elásticos da cerâmica à base de diatomito, bem como o efeito do tratamento térmico sobre suas propriedades físicas e mecânicas. O trabalho é dedicado ao estudo das propriedades mecânicas de cerâmica porosa à base de diatomito – rocha sedimentar, consistindo principalmente de conchas com micro e nanoporos de 50 nm... 500 µm. Conforme os resultados do estudo da microestrutura de cerâmica porosa à base de diatomito, foi determinada a porosidade média das amostras (~ 50%) e os valores dos módulos elásticos estático (35... 45 GPa) e dinâmico (0,3... 0,8 GPa) foram medidos experimentalmente. Verificou-se que os módulos elásticos diminuem com o aumento da porosidade do material. O experimento mostrou que o módulo elástico do material altamente poroso em consideração era duas ordens de magnitude inferior ao do cristalino. O artigo pode servir como material para um estudo mais aprofundado das propriedades da cerâmica à base de diatomito. Os resultados do estudo também podem ser utilizados para aplicações práticas em isolamento térmico, produção de cimento, polidor de metais e mármore.

Palavras-chave: *material de espuma de diatomito, propriedades mecânicas, microestrutura, lei de Hooke.*

ABSTRACT

The experimental and theoretical investigations of mechanical properties of porous materials are one of the priority areas of development of condensed matter physics. Diatomite ceramics can serve as a raw material for structural heat and sound insulating materials and additives to some types of cement, as a polisher for metals and marble. Diatomite-based ceramics are also used for thermal insulation in aluminum production. The foam-diatomite ceramics is a promising porous material. But the properties of diatomite ceramics are not well studied, which determines the relevance of the study. The main task of the present work is the investigation of porosity and elastic moduli of diatomite ceramics, as well as the effect of thermal treatment on its physical-mechanical properties. The work deals with studying mechanical properties of porous ceramics based on diatomite – a sedimentary rock composed predominantly of shells with micro- and nanopores of 50 to 500 µm. From the results of studying the microstructure of porous diatomite-based ceramics, the average porosity of samples (~50%) was determined, and the values of static (35 to 45 GPa) and dynamic (0.3 to 0.8 GPa) elastic moduli were experimentally measured. It was found that the values of elastic moduli decrease as material porosity increases. The experiment showed that the elastic modulus of the considered high-porous material was two orders of magnitude less than that of the crystalline one.

Keywords: *foam-diatomite material, mechanical properties, microstructure, Hooke's law.*

АННОТАЦИЯ

Экспериментальные и теоретические исследования механических свойств пористых материалов являются одним из приоритетных направлений развития физики конденсированных сред. Диатомитовая керамика может служить сырьем для конструкционных тепло- и звукоизоляционных материалов и добавок к некоторым типам цемента, а также полировкой для металлов и мрамора. Керамика на основе диатомита также используется для теплоизоляции при производстве алюминия. Пенодиатомитовая керамика является перспективным пористым материалом. Но свойства диатомитовой керамики изучены недостаточно, что определяет актуальность исследования. Основной задачей настоящей работы является исследование пористости и модулей упругости диатомитовой керамики, а также влияния термической обработки на ее физико-механические свойства. Работа посвящена изучению механических свойств пористой керамики на основе диатомита – осадочной породы, состоящей преимущественно из оболочек с микро- и нанопорами размером 50 нм... 500 мкм. По результатам изучения микроструктуры пористой керамики на основе диатомита была определена средняя пористость образцов (~ 50%) и экспериментально измерены значения статического (35... 45 ГПа) и динамического (0,3... 0,8 ГПа) модулей упругости. Было обнаружено, что значения модулей упругости уменьшаются с увеличением пористости материала. Эксперимент показал, что модуль упругости рассматриваемого высокопористого материала был на два порядка меньше, чем у кристаллического. Статья может служить материалом для дальнейшего изучения свойств диатомитовой керамики. Результаты исследования также могут быть использованы для практического применения в теплоизоляции, производстве цемента, полировщика для металлов и мрамора.

Ключевые слова: пено-диатомитовый материал, механические свойства, микроструктура, закон Гука.

1. INTRODUCTION

Ceramics is the third most widely used industry material after metals and polymers. It is the most competitive class of materials compared to metals for use at high temperatures (Jones *et al.*, 2016; Rudnev *et al.*, 2016). Ceramics are artificial stone materials and products obtained in the processing of mineral raw materials and subsequent burning at high temperatures. The raw materials for the manufacture of ceramic materials are constituted by a variety of clay rocks (clays).

Most ceramic materials respond to machine processing with difficulty (Nikolaev, 2016; Saprnov *et al.*, 2017; Smelik *et al.*, 2019). Therefore, the main condition for ceramic technology is to obtain practically finished products upon consolidation. To finish the surfaces of ceramic products, abrasive treatment with diamond wheels, electrochemical, ultrasonic and laser processing are used (Yuan *et al.*, 2015; Bilalov *et al.*, 2016; Dashko and Kotiukov, 2018; Soshko and Soshko, 2019). The use of protective coatings is effective as it heals the smallest surface defects – roughness, grooves, etc.

They are classified by a number of attributes:

– according to the purpose, ceramic products are divided into the following types: wall, decoration, roofing, for floors, for cover-ups, road, sanitary, acidproof, heat-insulating, fireproof, and

filling aggregates for concrete;

– according to the structure, ceramic products with a porous and sintered (dense) shard are distinguished. Porous are products with water absorption by weight of more than 5%. These include products of both rough (ceramic wall bricks and stone, products for roofing and ceilings, drainage pipes), and fine (facing tiles, earthenware) ceramics. Products with water absorption by weight less than 5% are referred to as dense. They also include products of both rough (clinker bricks, large-sized cladding plates) and fine (earthenware, semi-porcelain, porcelain) ceramics;

– according to the melting temperature, ceramic materials and products are divided into low-melting (with a melting temperature below 1350°C), high-melting (with a melting point of 1350°C - 1580°C), refractory (1580°C - 2000°C), super-refractory (over 2000°C).

The experimental and theoretical investigations of mechanical properties of porous materials are one of the priority areas of development of condensed matter physics. Now porous ceramics are mostly applied in two areas (Vassileva *et al.*, 2013; Ilina and Shelekhova, 2014; Dong *et al.*, 2016): thermal insulation (Akhtar *et al.*, 2009; Jang *et al.*, 2013) and porosity (as well as related properties) (Van Garderen *et al.*, 2011; Dong *et al.*, 2014). Diatomite ceramics is a typical representative of such materials. Its

basis is diatomite – amorphous material, mostly involving diatom shells (Vassileva *et al.*, 2013; Dong *et al.*, 2016; Wil'deman *et al.*, 2018). The chemical composition of diatomaceous material is presented in Table 1.

It has high porosity, ability to adsorption, low thermal conductivity and sound conductivity, infusibility, and acid resistance (Akhtar *et al.*, 2009). Now diatomite serves as a constructional material with low thermal conductivity (Galzerano *et al.*, 2018; Lyngsie *et al.*, 2019; Hao *et al.*, 2019) used to produce accumulators (Cheng *et al.*, 2019), supercapacitors (Liguori *et al.*, 2017; Li *et al.*, 2019) and antibiotics (Wu and Zhang, 2019). It also serves as raw material for constructional heat-insulating and soundproof materials (Fraine *et al.*, 2019) and additives to some types of cement, as well as a polisher (in the paste composition) for metals and marbles (Ho *et al.*, 2019; Jiang *et al.*, 2019). The diatomite-based ceramics is also used for heat insulation when producing aluminum (Li and Shi, 2019). The foam-diatomite ceramics is a promising porous material. However, its physical-chemical properties (elastic moduli, porosity, etc.) are not sufficiently investigated yet. Therefore, the main task of the present work is the investigation of porosity and elastic moduli of diatomite ceramics, as well as the effect of thermal treatment on its physical-mechanical properties.

2. MATERIALS AND METHODS

Diatomite as a raw material to make foam-diatomite products, is a light porous rock composed of amorphous silica (70-80%) and clay material (30-20%). Amorphous silica is presented by the microscopic leaves of dead ancient water plants – diatoms (Vassileva *et al.*, 2013) whose microphotographs are presented in Figure 1. The apparent density of raw material is usually in the 250-550 kg/m³ range. The materials for investigations were formed products of diatomite ceramics (with porosity over 30% and working temperature range up to 900 °C). It was made from the SiO₂ – and Al₂O₃-based raw material using the standard technology that involved (i) rock drying and crushing, (ii) flask formation with adding a foaming agent, and (iii) burning (Skvortsov *et al.*, 2017; Li and Shi, 2019). The samples (15×15×100 mm parallelepipeds) were made of the material obtained.

Originally, the mass of the samples was measured, and their density was calculated. An analysis of the composition and structure of the sample was performed using a high-resolution

field-emission scanning electron microscope (SEM) JSM 7500F (JEOL) equipped with an EMF detector. Silicon served as an element of optimization. The instrument sensitivity was 0.2-1 at %, depending on the element. The spatial resolution was no less than 1 nm. During shooting, the pressure in the chamber with samples was no more than 9.6×10^{-5} Pa. The compression-test diagrams were registered using a testing machine. The resonance method was used to measure the dynamic elastic moduli (Van Garderen *et al.*, 2011; Dong *et al.*, 2014).

3. RESULTS AND DISCUSSION:

At room temperature, the diatomite ceramics (as most of other ceramics) is a brittle material for which Hooke's law is satisfied. Its elastic modulus E_0 is 71 GPa at zero porosity (Lyngsie *et al.*, 2019; Hao *et al.*, 2019) and may decrease as porosity increases. The typical results of the mechanical tests of the samples are presented in Figure 2. Young's modulus for the given sample is 35 GPa. A microphotograph of its surface is given in Figure 3. It is easy to see a wide range of pore sizes in the material under investigation. Therefore, to estimate ceramics porosity, a morphological analysis of the ceramics studied was performed (Figure 4). The results of the sample studying before and after its deformation are given in Figure 5 and are combined in Table 2.

As expected, deformation promotes the reduction of material porosity. Then dynamic elastic moduli of the samples were measured by applying the resonance method (Dong *et al.*, 2014; Skvortsov *et al.*, 2017). The essence of the method using bending vibrations is as follows. The bending vibrations of variable frequency are excited by an electronic generator and an electro-acoustic transducer in a sample (lying on bearings). These vibrations are taken by another transducer (receiver) and are delivered to an indicator. The generator frequency changes. When the frequency of the natural fundamental oscillations of a sample coincides with the frequency of exciting oscillations, an abrupt increase of oscillation amplitude (resonance) occurs. One can quantify the value of elastic modulus of the given sample by measuring the natural resonant frequency of steady-state vibrations of a solid sample with undisturbed structure: $E = 4 \cdot \pi \cdot 10^{-3} \cdot L^2 \cdot \rho_k \cdot f^2$. Here L is sample length; ρ_k is sample density, and f is the resonant frequency.

The dependence of elastic modulus on

porosity (0-20%) is known (Lou and Stevents, 1999; Akhtar *et al.*, 2010). For high-porous diatomite ceramics, investigations of dynamic elastic modulus dependence on porosity (30-80%) were performed. The obtained results are presented in Figure 5. One can see that elastic modulus of the considered high-porous material is two orders of magnitude less than that of the crystalline one (Lou and Stevents, 1999; Romashin *et al.*, 2004). Similar results were also obtained by measuring the dependence of dynamic elastic modulus on sample density. The results of this set of experiments are shown at the insert of Figure 5. The numerical E values agree with the known literature data on high-porous quartz ceramics (Pivinsky and Romashin, 1974; Lou and Stevents, 1999; Romashin *et al.*, 2004).

4. CONCLUSIONS:

The properties of solids, in contrast to the properties of liquids and gases, are determined not only by the chemical composition but also by the structural features. In this work, the mechanical properties of porous diatomite-based ceramics were experimentally investigated. The values of static (35 to 45 GPa) and dynamic (0.3 to 0.8 GPa) elastic moduli of samples are obtained. Ceramics structure and pore morphology (general, minimum, and maximum area and average pore diameter) were studied, and the values of sample porosity in the 30 to 80% range were determined. The dependences of dynamic elastic modulus of diatomite ceramics on porosity were also studied. It was fixed that (i) the elastic moduli decrease as material porosity increases and (ii) after deformation material porosity decreases. It is found experimentally that the elastic modulus of the considered high-porous material is two orders of magnitude less than that of the crystalline one.

The materials of the paper are of practical importance since industrial ceramics has been used in mechanical engineering, in metallurgy, in the chemical industry, in the woodworking, and in the aviation industry for many decades. The development of this industry has high prospects, which entails an increase in the quality of processing of materials, service life, productivity, wear-resistance, and many other factors. The most important task in the field of production of ceramic products is the establishment of patterns between the structure of the material and its operational properties.

5. REFERENCES:

1. Akhtar, F., Rehman, Y., Bergström, L. *Powder Technology*, **2010**, 201(3), 253–257.
2. Akhtar, F., Vasiliev, P.O., Bergström, L. *Journal of the American Ceramic Society*, **2009**, 92(2), 338–343.
3. Bilalov, D. A., Sokovikov, M. A., Chudinov, V. V., Oborin, V. A., Bayandin, Y. V., Terekhina, A. I., Naimark, O. B. *Journal of Applied Mechanics and Technical Physics*, **2016**, 57(7), 1217–1225.
4. Cheng, H., Cai, N., Wang, M. *Solid State Ionics*, **2019**, 337, 12–18.
5. Dashko, R. E., Kotiukov, P. V. *Paper presented at the Geomechanics and Geodynamics of Rock Masses*, **2018**, 1, 241–248.
6. Dong, G., Su, Zh., Wang, J. *Advanced Materials Research*, **2014**, 850–851, 1355–1359.
7. Dong, L., Zhang, C., Chen, Y., Cao, L., Li, J., Luo, L. *Materials Letters*, **2016**, 171, 108–111.
8. Fraine, Y., Seladji, C., Aït-Mokhtar, A. *Building and Environment*, **2019**, 154, 145–154.
9. Galzerano, B., Verdolotti, L., Capasso, I., Liguori, B. *Materials and Manufacturing Processes*, **2018**, 33(15), 1648–1653.
10. Hao, L., Gao, W., Yan, S., Niu, M., Liu, G., Hao, H. *Materials Chemistry and Physics*, **2019**, 235, 121741.
11. Ho, C.-H., Lo, H.-M., Lin, K.-L., Lan, J.-Y. *Environmental Progress and Sustainable Energy*, **2019**, 38(2), 321–328.
12. Ilina, V.P., Shelekhova, T.S. *Glass, and Ceramics*, **2014**, 66(3–4), 109–112.
13. Jang, D., Meza, L.R., Greer, F., Greer, J.R. *Nature Materials*, **2013**, 12(10), 893–898.
14. Jiang, F., Zhang, L., Jiang, Z., Li, C., Cang, D., Liu, X., Xuan, Y., Ding, Y. *Ceramics International*, **2019**, 45(5), 6085–6092.
15. Jones, B., Thuerey, N., Shinar, T., Bargteil, A. W. *ACM Transactions on Graphics*, **2016**, 35(4), Article number a34.
16. Li, K., Liu, X., Zheng, T., Jiang, D., Zhou, Z., Liu, C., Zhang, X., Zhang, Y., Losic, D. *Chemical Engineering Journal*, **2019**, 370, 136–147.
17. Li, M., Shi, J. *Construction and Building Materials*, **2019**, 194, 287–310.

18. Liguori, B., Capasso, I., Romeo, V., D'Auria, M., Lavorgna, M., Caputo, D., Ilaria Capasso, Verdolotti, L. *Journal of Cellular Plastics*, **2017**, 53(5), 525-536.
19. Lou, J., Stevens, R. *Ceramics International*, **1999**, 25, 281–286.
20. Lyngsie, G., Katika, K., Fabricius, I.L., Hansen, H.C.B., Borggaard, O.K. *Chemosphere*, **2019**, 17, 884–890.
21. Nikolaev, S. *Gornyi Zhurnal*, **2016**, 4, 15-20.
22. Pivinsky, Yu.E., Romashin, A.G. *Quartz ceramics*. Moscow: Metallurgiya, **1974**.
23. Romashin, A.G., Rusin, M.Yu., Borodai, F.Y. *Refractories and Industrial Ceramics*, **2004**, 45(6), 387–391.
24. Rudnev, S. D., Popov, D. M., Kozlov, M. A., Hayatov, R. R. *Theoretical Foundations of Chemical Engineering*, **2016**, 50(1), 106-109.
25. Saprionov, O. O., Buketov, A. V., Zinchenko, D. O., Yatsyuk, V. M. *Composites: Mechanics, Computations, Applications*, **2017**, 8(1), 47-65.
26. Skvortsov, A.A., Luk'yanov, M.N., Novitsan, Y.V. *Solid State Phenomena*, **2017**, 269, 71–77.
27. Smelik, R., van Wermeskerken, F., Krijnen, R., Kuijper, F. *Journal of Defense Modeling and Simulation*, **2019**, 16(3), 255-271.
28. Soshko, O. I., Soshko, V. O. *Progress in Physics of Metals*, **2019**, 20(1), 96-192.
29. Van Garderen, N., Clemens, F.J., Mezzomo, M., Bergmann, C.P., Graule, T. *Applied Clay Science*, **2011**, 52(1–2), 115–121.
30. Vassileva, P.S., Apostolova, M.S., Datcheva, A.K., Ivanova, E.H. *Chemical Papers*, **2013**, 67(3), 342–349.
31. Wil'deman, V. E., Staroverov, O. A., Lobanov, D. S. *Mechanics of Composite Materials*, **2018**, 54(3), 313-320.
32. Wu, Q., Zhang, Z. *Journal of Chemical Technology and Biotechnology*, **2019**, 94(8), 2537–2546.
33. Yuan, W., Yuan, P., Liu, D., Yu, W., Deng, L., Chen, F. *Microporous and Mesoporous Materials*, **2015**, 206(C), 184-193.

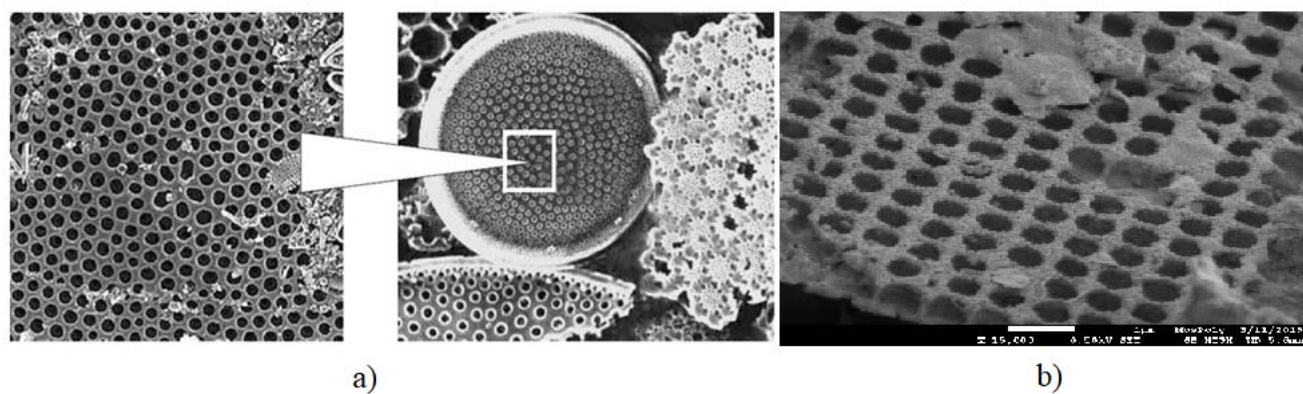


Figure 1. a) Microstructure of a diatoms leaf: right – diatoms leaf (diameter of 0.2 mm); left – leaf porous structure (Vassileva et al., 2013); b) microstructure of a diatoms leaf at the samples.

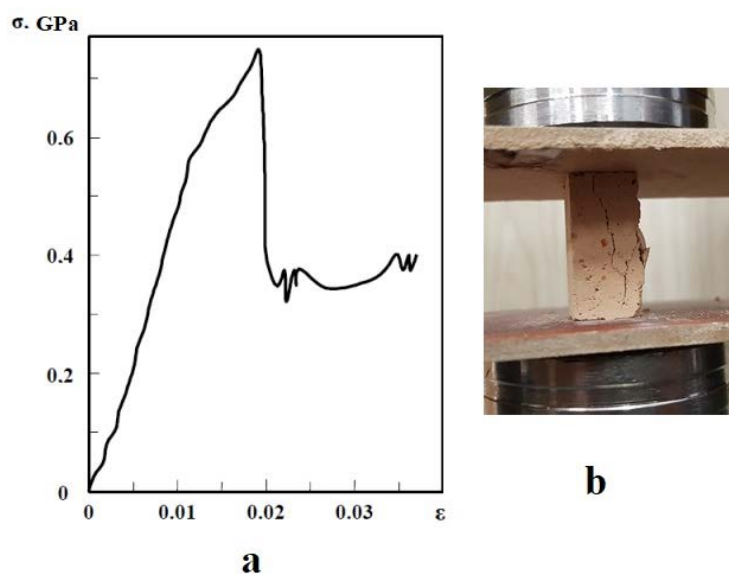


Figure 2. A typical compression-test diagram of diatomite ceramics (a) and a photograph taken at the moment of crack formation at sample compression (b).

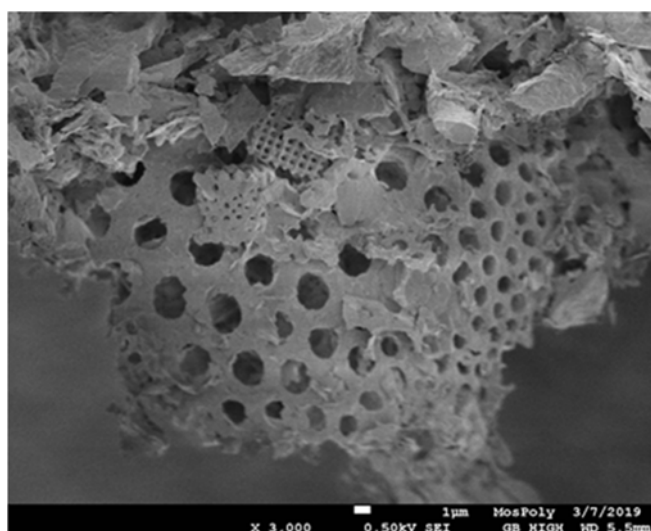


Figure 3. SEM photograph of a sample.

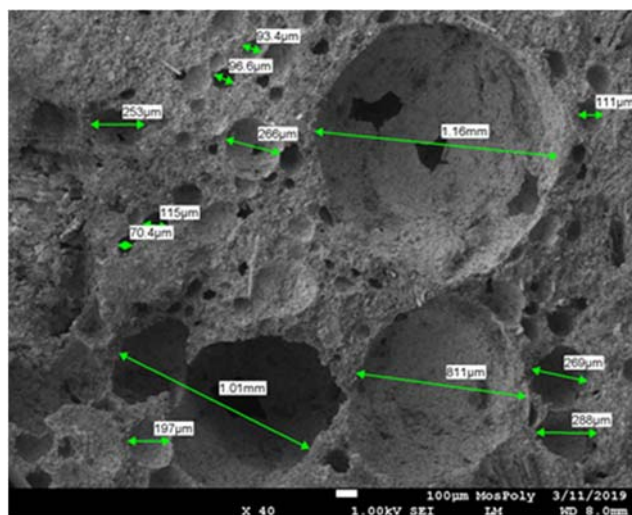


Figure 4. SEM photograph of the sample under consideration with characteristic pore sizes.

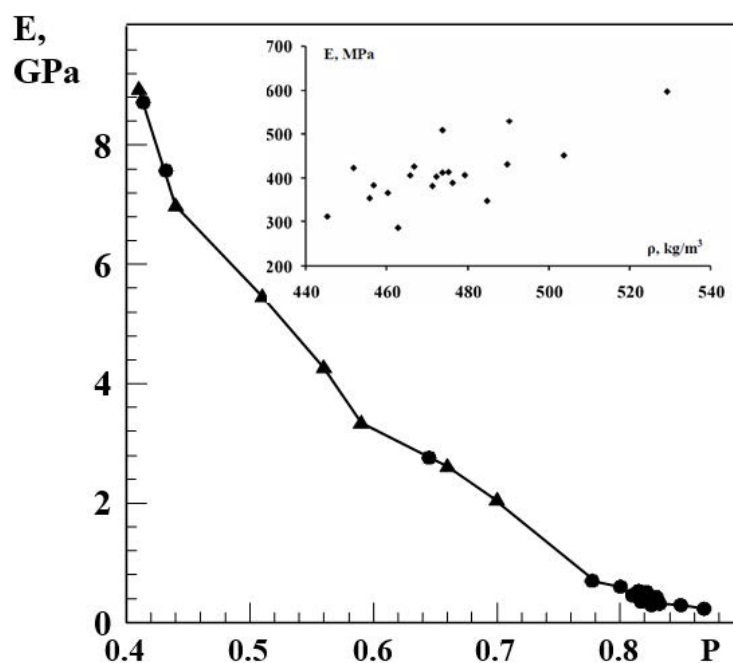


Figure 5. Elastic modulus vs quartz ceramics porosity: ▲ – data from (Cheng et al., 2019), ● – data from this investigation. Insert: (for initial 25×30×120 mm samples of foam-diatomite ceramics) dynamic elastic modulus vs material density.

Table 1. Chemical composition of foam-diatomite ceramics

Compound	Content, %	Compound	Content, %
SiO ₂	86.00	MgO	0.84
Al ₂ O ₃	6.10	CaO	0.32
Fe ₂ O ₃	2.80	TiO ₂	0.29
K ₂ O	1.34	Na ₂ O	0.20

Table 2. General indicators of ceramics pore space.

	Initial	After deformation
Porosity, %	26±5	21±4
Total pore area, μm ²	972 323	1 120 520
Total pore perimeter, μm	7 592 290	3 959 696
Average pore diameter, nm	84	55
Average area, μm ²	0.12	0.10
Average perimeter, μm	0.90	0.34
Minimum pore area, μm ²	0.003	0.001
Maximum pore area, μm ²	88 988	22 784
Permeability coefficient, mm/min	6.3±0.5	7.6±0.5

O ESTUDO DA DEPENDÊNCIA DAS PROPRIEDADES REOLÓGICAS DAS COMPOSIÇÕES DE FORMAÇÃO EM GEL NA ABERTURA DE FENDAS AO MODELAR SEU FLUXO EM UM VISCÔMETRO ROTACIONAL**THE STUDY OF THE DEPENDENCE OF THE RHEOLOGICAL PROPERTIES OF GEL-FORMING COMPOSITIONS ON THE CRACK OPENING WHEN MODELING THEIR FLOW ON A ROTATIONAL VISCOMETER****ИЗУЧЕНИЕ ЗАВИСИМОСТИ РЕОЛОГИЧЕСКИХ СВОЙСТВ ГЕЛООБРАЗУЮЩИХ СОСТАВОВ ОТ РАСКРЫТОСТИ ТРЕЩИНЫ ПРИ МОДЕЛИРОВАНИИ ИХ ТЕЧЕНИЯ НА РОТАЦИОННОМ ВИСКОЗИМЕТРЕ**

SHAGIAKHMETOV, Artem Maratovich^{1*}; PODOPRIGORA, Dmitry Georgievich²; TERLEEV, Andrey Victorovich³;

^{1,2,3}St. Petersburg Mining University, St. Petersburg. Russian Federation.

* Correspondence author
e-mail: artem-shagiakhmetv@mail.ru

Received 12 February 2020; received in revised form 14 March 2020; accepted 24 March 2020

RESUMO

O período atual de produção de petróleo é caracterizado pela deterioração da estrutura das reservas de petróleo devido ao alto corte de água do produto e baixas taxas de produção de petróleo. Para reduzir o aumento do corte de água, são geralmente realizados trabalhos de reparo e isolamento. Isso implica na injeção de sistemas de polímeros reticulados ou o tratamento da zona de formação de fundo de poço com sistemas de polímero-gel. Esse problema é especialmente relevante para reservatórios fraturados, que geralmente são representados por rochas carbonáticas. Este artigo é dedicado ao estudo da dependência das propriedades reológicas das composições formadoras de gel na abertura de fissuras em reservatórios de carbonato. A relevância do trabalho se baseia no rápido envolvimento no desenvolvimento de campos de petróleo com reservatórios de carbonato, o que é complicado por um grande número de trincas de vários tamanhos. Foram descritos os tipos de reservatórios fraturados, as características de desenvolvimento de cada tipo e as complicações na produção de hidrocarbonetos a partir da estrutura de poros fraturados do reservatório. A pesquisa também apontou métodos e tecnologias para limitar o fluxo de água em fendas ou poros de alta permeabilidade. As propriedades reológicas dos fluidos ao se mover dentro de poros e rachaduras foram relatadas. Foi apresentada a dependência de alterações nas propriedades reológicas da composição para limitar o influxo de água à base de carboximetilcelulose no tamanho de poros, cavernas e trincas. A física do movimento e formação de gel dentro dos reservatórios fraturados, que permitirá prever mudanças no tempo de formação do gel e na resistência plástica de cada objeto individualmente, foi reportada. De acordo com este estudo, é possível usar os recursos das propriedades reológicas das composições formadoras de gel para aumentar a eficiência do uso de tecnologias de impermeabilização na produção de poços ou alinhar o perfil de injetividade dos poços de injeção.

Palavras-chave: obras de acabamento e isolamento, composição gelificante, propriedades reológicas, limitação da entrada de água, revisão geral de poços.

ABSTRACT

The current period of oil production is characterized by the deterioration of the structure of oil reserves because of high water cut of the product and low oil production rates. To reduce the increased water cut, repair and insulation works are often performed. This implies in the injection of cross-linked polymer systems or the treatment of the bottom hole formation zone with polymer-gel systems. This problem is especially relevant for fractured reservoirs, which are often represented by carbonate rocks. This article is devoted to the study of the dependence of the rheological properties of gel-forming compositions on the crack opening in carbonate reservoirs. The relevance of the work relies on the rapid involvement in the development of oil fields with carbonate reservoirs which is complicated by a large number of cracks of various sizes. The types of fractured reservoirs, the development features of each type, as well as complications in the hydrocarbon production from the fractured-pore structure of the reservoir were described. The research also pointed methods and technologies for limiting

water flow in cracks or pores of high permeability. The rheological properties of fluids when moving inside pores and cracks were reported. The dependence of changes in the rheological properties of the composition for limiting water inflow based on carboxymethylcellulose on the size of pores, caverns and cracks were presented. The physics of movement and formation of gel inside the fractured reservoirs, which will allow predicting changes in the gel formation time and plastic strength for each object individually was described. According to this study, it is possible to use the features of the rheological properties of gel-forming compositions to increase the efficiency of the use of water-proofing technologies for producing wells, or to align the injectivity profile of injection wells.

Keywords: *workover and insulation works, gelling composition, rheological properties, limitation of water inflow, overhaul of wells.*

АННОТАЦИЯ

Текущий период добычи нефти характеризуется ухудшением структуры запасов нефти из-за высокой обводненности продукта и низких темпов добычи нефти. Для уменьшения повышенной обводненности часто проводятся водоизоляционные работы. Это подразумевает закачку сшитых полимерных систем или обработку призабойной зоны полимерно-гелевыми системами. Эта проблема особенно актуальна для трещиноватых коллекторов, которые часто представлены карбонатными породами. Данная статья посвящена изучению зависимости реологических свойств гелеобразующих композиций от раскрытия трещины в карбонатных коллекторах. Актуальность работы заключается в быстром росте разработки нефтяных месторождений с карбонатными коллекторами, что осложняется большим количеством трещин различного размера. В данной работе описаны типы трещиноватых коллекторов, особенности разработки каждого типа, а также сложности при добыче углеводородов из трещинно-поровой структуры пласта. Исследование также указало методы и технологии для ограничения потока воды в трещинах или порах с высокой проницаемостью. Авторами описаны реологические свойства жидкостей при движении внутри пор и трещин. Представлена зависимость изменения реологических свойств составов для ограничения водопритока на основе карбоксиметилцеллюлозы от размера пор, каверн и трещин. Описана физика движения и образования геля внутри трещиноватых резервуаров, что позволит прогнозировать изменения времени образования геля и пластической прочности для каждого объекта в отдельности. Согласно этому исследованию, можно использовать особенности реологических свойств гелеобразующих композиций для повышения эффективности использования водоизоляционных технологий при добыче нефти из добывающих скважин или для выравнивания профиля приемистости нагнетательных скважин.

Ключевые слова: *ремонтно-изоляционные работы, гелеобразующий состав, реологические свойства, ограничение водопритока, капитальный ремонт скважин.*

1. INTRODUCTION:

The current period of oil production is characterized by the deterioration of the structure of oil reserves, the addition of heterogeneous reservoirs to the development, and the sharp transition of the leading production sites to the final development stage, which is characterized by high water cut of the product and low oil production rates. To reduce the increased water cut, repair and insulation works are often performed. Such an approach implies the injection of cross-linked polymer systems, or the treatment of the bottomhole formation zone with polymer-gel systems (Nikitin and Petuhov 2011; Strizhnev, 2010; Petković *et al.*, 2019).

This problem is especially relevant for fractured reservoirs, which are often represented by carbonate rocks. Owing to their high conductivity, fractures in such oil and gas reservoirs are, as a rule, the main ways of filtering formation fluids, while the majority of hydrocarbon

reserves can be concentrated in a matrix with relatively low permeability (Nazriet *al.*, 2018).

Fracturing of rocks depending on the measurement methods is characterized by: intensity (total width of crack opening per unit length of the well, mm / m); specific water absorption (water absorption by the massif per unit length of the well and unit of hydrostatic head per unit time, l / s • m²); rheometric permeability (drop in air pressure when it spreads in the well per unit length per unit time, Pa / m • s) and other parameters. Depending on the presence of cracks and caverns, the collectors are divided into porous, cavernous porous, cavernous, fissured-porous, fissured-cavernous, fissured-cavernous-porous (Rajss, 2012).

However, most experts (Rajss, 2012, Hanin, 2013; Yemelyanov *et al.*, 2018 a,b;) dwell on the division of reservoirs into fractured-pore and fractured-non-porous. In fractured-porous reservoirs, oil is located inside the blocks of the porous medium, and cracks play the role of

connecting channels through which filtration is carried out. The fractured-non-porous blocks are impermeable and do not contain hydrocarbons; oil is concentrated in a system of connected caverns, through which filtration is carried out.

To generalize and typify the geological and physical characteristics of the reservoir, it is necessary to classify carbonate reservoirs. There are several types of division of carbonate reservoirs:

1. According to the Viktorin V.D. – by collector productivity and its composition (Hanin, 2013);
2. according to Amelin I.D. – by the size of cracks (Gol'f-Raht, 1986);
3. according to Chernitsky A.V. – by the ratio of reserves in the media (Ibatullin, 2011);
4. according to R. Nelson - according to the ratio of reserves in media and the share of their participation in filtration (foreign classification) (Blazhevichet *al.*, 1999).

The main ones are the first and fourth type of classification. The first type is based on the dividing of rocks according to the predominant type of fluid-containing and conductive systems. Viktorin V.D. divided the collectors into high, medium, low and potentially productive, assigned a certain type to each group and assigned them boundary values of porosity and permeability (Hanin, 2013). For example, the low-permeability group is composed of fractured-pore and fractured-cavernous rocks with permeability from 1 to 10 mD, open porosity of 4-8% and oil saturation from 57 to 74%.

According to the Nelson classification, collectors are divided into 4 types depending on the increase or decrease in the effect of cracks. In the first type, the effect of cracks is maximum, therefore, the main reserves are confined to cracks, the matrix of the reservoir has low porosity and permeability. In this type, productivity is associated only with cracks. In the second type, the main reserves are contained in the matrix, cracks provide the main productivity. The matrix of the reservoir has low permeability, but can have both low, medium and, in rare cases, high porosity. In the third type, the matrix of the reservoir contains the main oil reserves, has high permeability and porosity, and cracks complement the matrix permeability. In the latter type, cracks do not contribute to the permeability and porosity of the matrix of the formation but introduce anisotropy into the formation. In this type, productivity is directly dependent on the reservoir

matrix.

Further, depending on what type of reservoir the developed reservoir belongs to, mechanisms of oil displacement from reservoirs are selected. According to Gol'f-Raht (Gol'f-Raht, 1986), the following mechanisms of oil displacement from the matrix are distinguished elastic mode, capillary impregnation, gravity drainage of oil by water, horizontal (displacement due to differential pressure) (Susantiet *al.*, 2018).

When oil is displaced from fractured-porous reservoirs, gravitational drainage of oil by water predominates, and piston displacement occurs in fracture systems. In a pore structure, the process of oil displacement by water or gas is based on the combined action of gravitational and capillary forces. However, the predominance of certain forces largely depends on the nature of the wettability of the rock (Suryonoet *al.*, 2019; Polyakovaet *al.*, 2019):

In hydrophilic reservoirs, water, as a rule, quietly passes into blocks, as a result of which gravitational forces prevail over capillary forces, and as a result, water displaces oil from the pores (Vogrincet and Premrov, 2018).

In hydrophobic reservoirs, due to the action of capillary forces, water cannot penetrate into the blocks, and displacement is possible only if the gravitational force overcomes the resistance of capillary pressure (inlet pressure). The smaller the pore size, the higher the pressure at which water enters the unit. Therefore, it is extremely difficult to displace oil from a hydrophobic, highly fractured reservoir. Experience in the development of deposits with carbonate reservoirs shows that the matrix of the rock due to the hydrophobicity of carbonate rocks is blocked by the displacement agent, and at the same time, production rates in the area with a reservoir pressure maintenance system are sharply worsened (Neizvestnayaet *al.*, 2018).

The main problem with this displacement is the high pressure gradients that lead to an increase in the filtration rate to values higher than critical in the near-wellbore zone, which contributes to the premature breakthrough of the underlying water into the wells and, thereby, the capillary impregnation process is disrupted, which is the most effective method of displacing oil from porous blocks (Hermawanet *al.*, 2019; Zakkiet *al.*, 2019).

For fractured reservoirs when developing oil deposits by water flooding, breakthroughs of injected or formation water through a system of

fractures to producing wells are characteristic. Herewith, oil is displaced from them very efficiently, and the coefficient can reach significant values:

0.8–0.85. Experience shows that oil is also displaced from the matrix of fractured-pore reservoirs, however, the displacement coefficient is relatively low – it does not exceed 0.3 even for hydrophilic reservoirs. Oil displacement from fractured reservoirs occurs under the influence of two most important factors. The first one is transient pressure gradients in the matrix-fracture system. The second one is the process of capillary impregnation. In this case, capillary impregnation itself occurs extremely slowly (Balakin *et al.*, 1988; Strizhnev *et al.*, 2006; Surguchev *et al.*, 1997).

So, this research is aimed at studying the movement and formation of a stable gel depending on the size of the pore space of the carbonate reservoir.

2. MATERIALS AND METHODS:

One of the most important problems in recent decades has been the restriction of water inflow into wells draining a fractured formation, as well as the isolation of a highly conductive single fracture, which connects a production well with an injection well or aquifer. Instant watering of the recovered fluid occurs as a result of the breakthrough of formation and injection waters through highly permeable reservoirs and fractures. Under these conditions, an important task is to restrain water drainage in the highly permeable part and fractures of the reservoir. One of the main methods in the middle of the last century was polymer flooding. This method, due to the property of polymers to increase the viscosity of water, helps to reduce the ratio of the mobility of water and oil, thereby removing the possibility of a breakthrough of water due to heterogeneity of the reservoir. For this operation, it is necessary to pump a significant amount of the composition into the reservoir, therefore this method did not become widespread in water inflow limitation. In view of this factor, technologies with the use of low-volume injections (rims), which lead to the creation of a water-proof screen in the bottom-hole zone of production wells, have gained popularity in reducing the movement of water through cracks and highly permeable layers. For measures to limit water inflow through injection wells, cheaper and more affordable reagents are used (Vlasov *et al.*, 1988; Nikitin 2012; Petrov *et al.*, 1995).

However, the behavior of polymer-gel system under reservoir conditions has been poorly

studied, since until recently it was impossible to conduct experiments under conditions close to reservoir conditions. The advent of modern rotational viscometers allows to simulate the movement of the gel in cracks by adjusting the gap in the measuring system (for example, "plate-plate").

In order to study the behavior of polymer systems in cracks of various openings, a laboratory was conducted to determine the dependence of the rheological properties of polymers on the probable opening of an insulated crack in a laboratory for increasing oil recovery at the Mining University.

Two samples of polymer-gel systems with an assumed different viscosity were taken. To prepare the gelling composition № 1, the following reagents were mixed: a carboxymethyl cellulose polymer, a chromium acetate crosslinker and a copper sulfate catalyst (thickener). All the components are environmentally friendly and harmless. This composition is recommended when limiting water inflow in cracks. To reduce the movement of water in highly permeable interlayers, a gel-forming composition is proposed, consisting of carboxymethyl cellulose polymer, chromium acetate and sodium acetate, which significantly reduces the viscosity of the composition after preparation but during gelation it does not reduce the strength characteristics of the composition.

An Anton Paar MCR 102 rheometer was used, which is highly accurate in studying the properties of various liquids. The device is described in detail in papers (Roshchin, 2014). At this device, it is possible to change the gap in the plate-plate system to simulate the flow of fluid in a crack with an openness of up to 1 mm. In this case, this option was used to study the behavior of the gel-forming composition in the fractures of the formation of different openness.

The experiment was carried out as follows: a sample of a gel-forming composition was placed on the plate with a dispenser, then a certain gap and a formation temperature of 25 °C were established. After that, within 2 minutes, the shear rate linearly increased from 0 to 100 s⁻¹, simulating the movement of the gel along the crack. During the experiment with gel samples № 1 and № 2, the following gaps were established: 1; 0.8; 0.6 and 0.5 mm.

3. RESULTS AND DISCUSSION:

Figure 1 shows graphs of the dependence

of the shear stress of gel №1 on time with an increase in shear rate from 0 to 100 s⁻¹. The graph shows the influence of the established gap on the rheological properties of the gelling composition. This can be explained as follows: firstly, the effect on the gel-forming composition occurs with different masses, changing with a change in the gap. For example, the mass of the gel enclosed in the space between the fixed plate and the rotor plate in the gap of 0.5 mm will be less than the mass of the gel in the gap of 1 mm. Therefore, the transfer of mechanical energy from a viscometer to a gel sample will occur in the same way, however, the ratio of the transferred energy to the mass of the sample will vary significantly.

Reducing the gap from 1 mm to 0.5 mm doubles the energy transferred to the unit mass of the gel used for the experiment. Secondly, at the indicated shear rates, the conversion of mechanical energy into heat is likely, which allows the creation of additional chemical bonds in the gel-forming composition. It is due to such effects that it is possible to substantiate an additional parameter of the selectivity of the composition, which manifests itself in gel strengthening in small cracks and pores, and its further movement along large highly permeable channels, which allows the gel-forming composition to penetrate as deep as possible into the treated area of the reservoir and isolate large highly permeable channels. Due to this, some reagent savings are possible, since it is mainly large cracks that are filtration channels for water that will be insulated.

Also, by the method described above, a less viscous gelling composition № 2 was investigated. Figure 2 shows the dependence of shear stress on the time of gel-forming composition № 2 with a gradual linear increase in shear rate. This graph shows that the addition of sodium acetate to the gel No. 1, consisting of a polymer CMC-500 and a crosslayer of chromium acetate, reduces the viscosity of the composition, without violating the strength characteristics and the dependence of the gel formation time on the opening of cracks.

The smaller difference between the values of the effective viscosity (shear stress) for different crack openings is explained by the fact that the conversion of mechanical energy to thermal energy will first be directed to increase the viscosity in the pore space and then to create additional chemical bonds in the gel-forming composition.

4. CONCLUSIONS:

1. The dependence of the rheological properties of the gel-forming compositions on the crack opening during modeling of their flow on a rotational viscometer was established. Wherein, phenomena have been identified that can play a positive role in the operation of waterproofing work in wells that have uncovered oil or gas formations.
2. It was found that the addition of sodium acetate to the gel-forming composition based on a polymer of carboxymethylcellulose and a crosslinking of chromium acetate reduces the initial viscosity of the initial composition, without violating the dependence of gel formation in pores of various sizes, which allows for selective injection of the gel-forming composition into cracks.
3. The dependence of rheological properties, gel-forming formulations of opening the crack allows us to offer the highest quality gel-forming composition to improve the effective use of waterproofing technology or alignment profile injectivity of injection wells.

5. REFERENCES:

1. Balakin V., Vlasov S., & Fomin A. (1998). Modelirovaniopolimernogozavodneniyasloist o-neodnorodnogoplasta. Neftyanoechozyajstvo. №. 1. – p. 47-48.
2. Blazhevich V. A., & Umetbaev V.G. (1990). Spravochnikma sterapokapital'nomurem ontuskvazhin, M.: Nedra. p.320
3. Gol'f-Raht T.D. (1986). Os novyneftepro myslovo jgeologii, irazrabotkitreshchinov atyhkolle ktorov. Per. s angl. M.: Nedra, p.607
4. Hanin A.A. (2013). Porody-kollektoryne ftiigazaiihizuchenie. M.:RipolKlassik. p.167
5. Hermawan, H., Hadiyanto, H., Sunaryo, S., &Kholil, A. (2019). Analysis of thermal performance of wood and exposed stone-walled buildings in mountainous areas with building envelop variations. Journal of Applied Engineering Science, 17(3), 321-332.
6. Ibatullin R.R. (2011). Tekh nologich eskieprocessyraz rab otk ine ftyanyhm esto roz hdenij. M.: OAO "VNIIIOENG",p.304
7. Nazri, M. F., &Mohd, A. M. Y. (2018).

- Parametric study on transversal slope and short-term deflection of precast segmental box girder conditions by performing static load test. *Journal of Applied Engineering Science*, 16(2), 173-184.
8. Neizvestnaya D.V., Kozlova N.N., & Prodanova, N.A. (2018). Application of CVP-Analysis at the Water Transport Organizations. *Helix*. 2018. Vol. 8(1). Pages 2811-2815. DOI 10.29042/2018-2811-2815
 9. Nikitin M. N. (2012). Obosnovaniye tekhnologii povsheniya nefteotdachizalezhejvys o ko vyazkih neftej v treshchinno-poro vykholl ektorah s primene niemgeleobrazuyushcheg osostavana osnov esilikatanatriya: dis. – SPb.: Nikitin Marat Nikolaevich.
 10. Nikitin M. N., Petuhov A. V. (2011). Geleobraz uyushchijs ostavn osnov esilikatanatriyad lyaogranicheniyav odopritoka v slozhnopo stroenn yhr eshchinnyhko llektorah. *Neftegazo voedelo*. № 5. p. 143-154.
 11. Petrov N.A. Korenyako A.V., YAngirov F.N., Esipenko A.I. (1995). Ogranichenie pritokavody v skvazhinah, M.: VNIIOENG, p.65.
 12. Petković, M., Mihanović, V., & Vujović, I. (2019). Blockchain security of autonomous maritime transport. *Journal of Applied Engineering Science*, 17(3), 333-337.
 13. Polyakova, A. G., Loginov, M. P., Strelnikov, E. V., & Usova, N. V. (2019). Managerial decision support algorithm based on network analysis and big data. *International Journal of Civil Engineering and Technology*, 10(2), 291-300
 14. Rajss L. (2012). Osnovy razrab otkitreshc hinovatyh kollektorov. M.-Izhevsk: Institut ko mp'yut ernyh issledovaniy, p.118
 15. Roshchin P.V. (2014). Obosnovan iekomple ksnoy tekhn ologii obrabotki pr izabojnojz onyplastanazale zhahvyso kovyzakh neftejs treshc hinno-p orovym i kollektorami: dis. kand. tekhn. nauk. -SPb., p.112
 16. Strizhnev K.V. (2010). Remontno-izolyacion nyeraboty v skvazhinah: Teoriya i praktika, SPb.: «Nedra», p. 560
 17. Strizhnev K. V., Strizhnev V. A. (2006). Vybortamponazhnogomaterialadlyaobosnova niyatekhnologii remontno-izolyacionnyh rabot. *Neftyanoe khozyajstvo*. № 9. P. 108-111.
 18. Susanti, D. R., Tambunan, R., Waruwu, A., & Syamsuddin, M. (2018). Studies on concrete by partial replacement of cement with volcanic ash. *Journal of Applied Engineering Science*, 16(2), 161-165.
 19. Suryono, S., Surarso, B., Saputra, R., & Sudalma, S. (2019). Real-time decision support system for carbon monoxide threat warning using online expert system. *Journal of Applied Engineering Science*, 17(1), 18-25.
 20. Surguchev M.L., Kemanov V.I., Gavura N.V. (1987). Izvlecheni enefti iz karbon atnyh koll ektorov. M.: Nedra, p.230
 21. Vlasov S.A., Krasno pevceva N.V., Kagan YA.M. (1998). Novye per spektivy p olimernogoz avodn eniya v Rossii. *Neft yanoeho zyajstvo*. №5. p. 46-49.
 22. Vogrinec, K., & Premrov, M. (2018). Experimental and analytical study of the inter-storey hold-down connections in timber-frame panel buildings. *Journal of Applied Engineering Science*, 16(3), 358-367.
 23. Yemelyanov, V., Yemelyanova, N., & Nedelkin, A. (2018a). Diagnostic system to determine lining condition. Paper presented at the MATEC Web of Conferences, 172 doi:10.1051/mateconf/201817204001
 24. Yemelyanov, V., Tochilkina, T., Vasilieva, E., Nedelkin, A., & Shved, E. (2018b). Computer diagnostics of the torpedo ladle cars. Paper presented at the AIP Conference Proceedings, 2034 doi:10.1063/1.5067351
 25. Zakki, F. A., Suharto, S., Myung, B. D., & Windyandari, A. (2019). Performance on the drop impact test of the cone capsule shaped portable tsunami lifeboat using penalty method contact analysis. *Journal of Applied Engineering Science*, 17(2), 233-244.

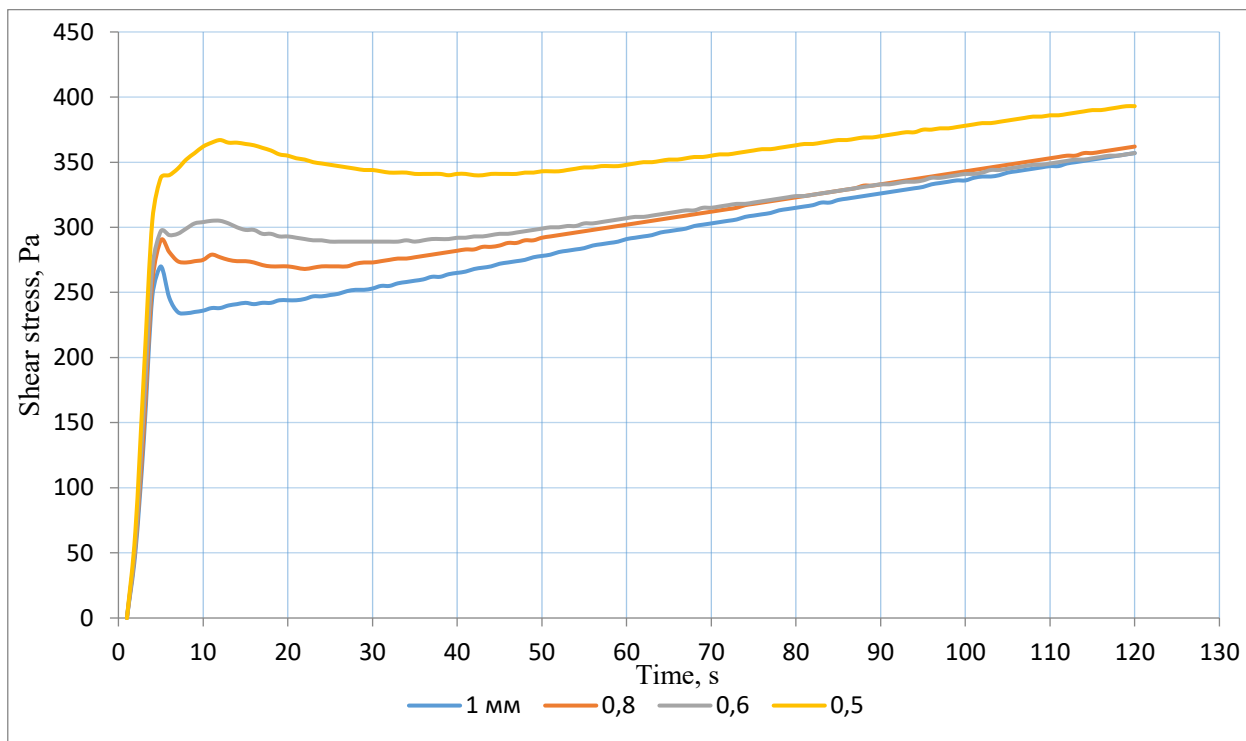


Figure 1. Dependence of the shear stress on time of gelling composition № 1 with a linear increase in shear rate from 0 to 100 s⁻¹

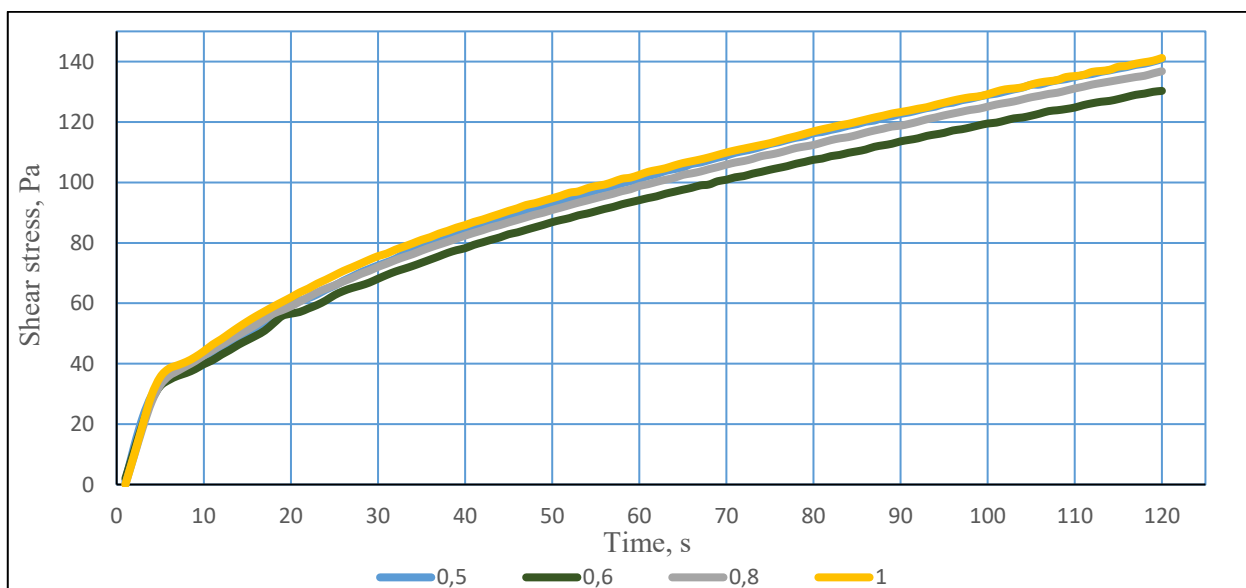


Figure 2. Dependence of the shear stress on time of gelling composition № 2 with a linear increase in shear rate from 0 to 100 s⁻¹

**DISPOSITIVO PARA ESTUDO DAS PROPRIEDADES TERMOFÍSICAS DE MATERIAIS
TÊXTEIS DE VOLUME E SUAS EMBALAGENS PELO MÉTODO DE MODO REGULAR
NO AR****A DEVICE FOR STUDYING THE THERMOPHYSICAL PROPERTIES OF BULK TEXTILE
MATERIALS AND THEIR PACKAGES BY THE REGULAR MODE METHOD IN AIR****УСТРОЙСТВО ДЛЯ ИССЛЕДОВАНИЯ ТЕПЛОФИЗИЧЕСКИХ СВОЙСТВ ОБЪЕМНЫХ
ТЕКСТИЛЬНЫХ МАТЕРИАЛОВ И ИХ ПАКЕТОВ МЕТОДОМ РЕГУЛЯРНОГО РЕЖИМА
В ВОЗДУШНОЙ СРЕДЕ**

TASHPULATOV, Salikh S.^{1*}; SABIROVA, Ziyoda A.²; CHERUNOVA, Irina V.³; NEMIROVA,
Lyubov F.⁴; MUMINOVA, Umida T.⁵

^{1,2,5} Tashkent Institute of Textile and Light Industry, Department of Costume Design, Tashkent – Republic of
Uzbekistan

³ Don State Technical University, Department of Design and Technology, Schakhty – Russian Federation

⁴ MINSP Limited Liability Company, Omsk – Russian Federation

* Correspondence author
e-mail: ssht61@mail.ru

Received 06 February 2020; received in revised form 02 March 2020; accepted 28 March 2020

RESUMO

Os tecidos têxteis têm diferentes propriedades de transferência de calor, que dependem das condições de consumo do produto e de vários tipos de processamento. Tudo isso é de interesse científico para identificar fatores e propriedades de materiais individuais. O objetivo do estudo foi monitorar a transferência de calor através de embalagens de materiais têxteis multicamada em condições térmicas estacionárias e transitórias. Uma propriedade especial dos materiais têxteis reside na capacidade de se deformar sob o seu próprio peso, de modo que uma amostra possa ser colocada entre as células do material com alta resistência ao calor. A transferência de calor é realizada por convecção de calor entre a superfície do material e o ar. Para o estudo, a lei de Fourier foi usada nos cálculos e métodos numéricos para resolver problemas de condução de calor. O programa desenvolvido, criado para pesquisa, permite gravar parâmetros em um computador e usá-los para calcular as propriedades termofísicas da amostra. Como resultado do trabalho, foram apresentados gráficos do estado de embalagem dos materiais e foi proposto um dispositivo que permite determinar os modos que caracterizam as propriedades termofísicas dos materiais utilizados na fabricação de roupas e suas embalagens. O dispositivo permite com alta precisão registrar, gravar e armazenar alterações nos parâmetros em que os estudos foram realizados.

Palavras-chave: *material têxtil, coeficiente de condutividade térmica, condutividade térmica equivalente, propriedades termofísicas, regime térmico regular.*

ABSTRACT

Textile fabrics have different heat transfer properties, which depend on the conditions of consumption of the product and various types of processing. All this is of scientific interest for identifying factors and features of individual materials. The purpose of the study was to track heat transfer through packages of multilayer textile materials in stationary and transient thermal conditions. A particular property of textile materials lies in their ability to deform under their weight so that a sample can be placed between meshes of a material with high heat resistance. Heat transfer is carried out by convective heat transfer between the surface of the material and the air. To conduct this study, the Fourier law was used in the calculations and numerical methods for solving heat conduction problems. The developed program, which was created for the study, permit to write parameters to a computer and uses them to calculate the thermophysical properties of the sample. As a result of the work, graphs of the state of the package of materials were presented, and a device was proposed that allows to determine the modes that characterize the thermophysical properties of the materials used in the manufacture of clothing and

its packages. The device admits with high accuracy to record, record and store changes in the parameters at which studies were conducted.

Keywords: *textile material, thermal conductivity coefficient, equivalent thermal conductivity, thermophysical properties, regular thermal regime.*

АННОТАЦИЯ

Текстильные ткани имеют разные теплообменные свойства, что зависит от условий потребления продукта и различных видов обработки. Все это представляет научный интерес для выявления факторов и свойств отдельных материалов. Целью исследования было отслеживание теплообмена через пакеты многослойных текстильных материалов в стационарных и переходных тепловых условиях. Особое свойство текстильных материалов заключается в их способности деформироваться под действием собственного веса, так что образец может быть помещен между ячейками материала с высокой термостойкостью. Теплопередача осуществляется путем конвективного теплообмена между поверхностью материала и воздухом. Для проведения исследования использовался закон Фурье в расчетах и численные методы решения задач теплопроводности. Разработанная программа, созданная для исследования, позволяет записывать параметры в компьютер и использовать их для расчета теплофизических свойств образца. В результате работы были представлены графики состояния упаковки материалов и предложено устройство, позволяющее определять режимы, характеризующие теплофизические свойства материалов, используемых при изготовлении одежды и ее упаковок. Устройство допускает с высокой точностью регистрировать, записывать и хранить изменения параметров, при которых проводились исследования.

Ключевые слова: *текстильный материал, коэффициент теплопроводности, эквивалентная теплопроводность, теплофизические свойства, регулярный тепловой режим.*

1. INTRODUCTION:

The features of the thermal processes occurring in textile materials under various processing conditions and consumption conditions are of great theoretical and practical interest, both for choosing the optimal processing conditions and for ensuring thermal comfort during operation. This is due to both the variety of textile materials and the conditions of use of clothes, the processes in which can be complex. The thermophysical properties of clothing play an essential role in ensuring the thermal comfort of the user, and in the effectiveness of protection against exposure to low or high temperatures. The design of heat-protective clothing is a multilayer package of materials, the properties of which are determined by the amount of materials, the order of their location and the properties of each layer (Angelova *et al.*, 2017; Cherunova *et al.*, 2018b; Cilveli *et al.*, 2020; Ivashchenko *et al.*, 2017; Labanieh *et al.*, 2019; Liu *et al.*, 2018).

Numerous works have been devoted to studies of the heat-protective properties of materials, the results of which have been successfully used to study the properties of textile materials and theoretical calculations of the relationship between the properties of individual materials and their packages (Kolesnikov, 1964; Bessonova and Zhikharev, 2007; Tsirkina and Nikiforov, 2016), based on the general theory of

heat transfer (Mikheev and Mikheeva, 1977; Carslaw *et al.* 1959; Xu *et al.* 2019), the development of methods research instruments (Carslaw *et al.* 1959; Clulow and Rees, 1968; Tessier, 2017; Ghang, 2001; Sokolovskaya, 2005) by research automation that allowed experimental studies of materials and multilayer packets under various conditions of thermal processes, including with fixing constant parameters in the automatic mode (Cherunova *et al.*, 2018a; Shaid *et al.*, 2019; Cherunova *et al.*, 2015), using a special dummy recreate human thermal comfort (Hunter and Fan, 2015; Osmanov and Sharpar, 2017; Siddiqui and Sun, 2018; Trofimovich *et al.*, 2018; Venkataraman *et al.*, 2016). To examine the relationship between the thermal insulation properties of the individual materials and multilayer package (Matusiak, 2006; Matusiak and Kowalczyk, 2014; Ronald *et al.*, 1987; Liang *et al.*, 2019; Michalak *et al.*, 2009; Sokolovskaya *et al.*, 2012; Sokolovskii and Shablygin, 2015).

However, the methods have the disadvantage that the thermal process in a textile material is examined in contact with a heater, most often a metal one, and it differs from the specific heat exchange of a person with an external (air) environment through a package of textile clothing materials. Therefore, it is advisable to study and evaluate the specificity of thermal processes in textile materials in various conditions, including the air. In the air, drying processes of textile

materials, and textile products, wet-heat treatment; Thus, during the wet-heat treatment, the processing time is determined by the time of heating the package of processed materials and the time of free cooling in the air. During the operation of clothes, an unsteady mode occurs when a person enters a warm room after a cold or vice versa. The work aimed to study the heat transfer through multilayer packets of textile materials in the air under conditions of stationary and non-stationary thermal conditions. For research, a method was proposed, and a device was developed in which the heat packet of air is affected by a package of materials, the power of which can vary (Bartkowiak and Greszta, 2018; Matusiak and Sybilska, 2016; Neves *et al.*, 2017; Seretis *et al.*, 2018; Wazna *et al.*, 2019).

2. MATERIALS AND METHODS:

The method helps to explore the thermal state of the package of materials at various temperature conditions; determine the equivalent coefficient of thermal conductivity, λ_{eq} of multilayer packets. In the device, heat transfer between the surface of the material and the air is carried out by convective heat transfer, and inside the package between the outer layers by heat conduction. The Fourier law and numerical methods for solving heat conduction problems are used in the calculations (Mikheev and Mikheeva, 1977; Carslaw *et al.* 1959; Cremer *et al.*, 2016). Fourier law under stationary thermal conditions (Equation 1).

Where: λ is the thermal conductivity coefficient $W/(m \times K)$; Q is the heat flux power, W ; F is the heat exchange surface area, m^2 ; τ is the time, s ; Δt is the temperature head, temperature difference: $^{\circ}C$; l is the length, m .

The thermal conductivity coefficient λ , $W/(m \times K)$ is a characteristic of the physical properties of the material, is determined by the formula (Equation 2).

Where δ is the thickness of the test sample, m ; q is the heat flux density from the heater, W/m^2 , ΔT is the temperature difference at the sample boundaries, $^{\circ}C$.

It is believed (Kolesnikov, 1964; Deryabina and Lisienkova, 2016; Deryabina and Lisienkova, 2017) that for multilayer packets, the value of the equivalent coefficient of thermal conductivity depends on the values of thermal conductivity and the thickness of individual layers and can be calculated by the formula (Equation 3).

Where: λ_{eq} is the equivalent thermal

conductivity of the multilayer packet $W/(m \times K)$; Δ is the thickness of the package, m ; δ_i is the thickness of an individual layer, m ; λ_i is the thermal conductivity coefficient of an individual layer, $W/(m \times K)$.

The proposed method was based on the method of heating/cooling the material in the air, which is described in (Mikheev and Mikheeva, 1977; Celcar, 2012; Kim *et al.*, 2016; Lizák and Mojumdar, 2013; Lizák and Mojumdar, 2015). The temperature field of the material is determined by the influence of the environment, the physical properties of the materials, the geometrical shape and dimensions of the system in which the process proceeds, as well as its initial thermal state. We accept the studied material package/sample as a single-layer (homogeneous) flat wall with a thickness of Δ , m with unknown thermal conductivity (Kobakov *et al.*, 2017; Peng *et al.*, 2019; Satomi *et al.*, 2016). Characteristics of the materials included in the studied system (device): δ is the thickness, m ; F area m^2 ; λ is the coefficient of thermal conductivity, $W/(m \times K)$; α is the heat transfer coefficient $W/(m \times K)$. Process parameters: temperature of the outer surfaces of the sample, t_{c1} and t_{c2} , $^{\circ}C$; air temperature near the sample surface t_{i1} and t_{i2} , cooling time (heating) τ , with heat transfer: $^{\circ}C$; heat flux power Q , W . The nature of the temperature change is shown in Figure 1.

Before testing, the sample is maintained under normal conditions for 24 hours. Therefore, the initial test conditions are stationary temperature field, temperature head $\Delta t = 0$. Air temperature $t_{i1} = t_{i2}$. On the sample surfaces $t_{c1} = t_{c2}$; time $\tau = 0$. Testing: a heat flow of air of constant power Q_1 is supplied on one side of the package, which ensures a stationary (regular) heat transfer mode. As a result, the air temperature $t_{i1} > t_{i2}$, $(t_{i1} - t_{i2}) > 0$; temperature on sample surfaces $t_{c1} > t_{c2}$, $(t_{c1} - t_{c2}) > 0$. The flow is supplied until the temperature on the surface of the material reaches a predetermined value $t_{c1} = N$, $^{\circ}C$. After which the flow stops. Then the sample cools down, and the parameters are fixed when the temperature difference on the surfaces of the sample is $\sim 1^{\circ}C$; $t_{c1} - t_{c2} = 1^{\circ}C$ the field is stationary. The air temperature is determined t_{i1} , t_{i2} , time is the τ . If the heat fluxes Q_1 and Q_2 are supplied on both sides of the sample, or if $Q_1 > Q_2$, more complex heat transfer processes can be simulated; a stationary or non-stationary temperature field is reached regular and irregular thermal conditions.

The calculation of indicators is carried out according to generally accepted formulas (Mikheev and Mikheeva, 1977; Firšt Rogale *et al.*, 2018). The calculations take into account the heat

flux passing through the walls of the device. A device for implementing the enclosed method is a housing made of heat-permeable material that allows exchange with the environment; sensors are mounted in the housing that transmit data to a computer. The device diagram is shown in Figure 2a, the sensor connection diagram in Figure 2b. The technical solution of the device is protected by the patent for utility model of the Republic of Uzbekistan No. FAP 00950 (Appendix 1), the software is protected by a patent for a computer program No. DGU 02633 (Appendix 2) (Juraev et al., 2012; Rikhsieva et al., 2012).

The housing (1) is made of organic glass with a thickness of 0.08 m with a heat transfer coefficient of 3.6 W/m²K. Case dimensions 0.3 × 0.4 × 0.5 m³. The body is divided into two compartments (8), (9) with a horizontal partition (3), with an opening in which the sample holder (3) is placed (Fig. 1a). The size of the sample is 0.3×0.3 m². A specific property of textile materials (bags) is the ability to deform under their own weight; therefore, the sample (2) can be placed between the grids (13) of a material with high thermal resistance, the distance between the grids can vary from 0.005 m to 0.025 m. The thickness of the material package was determined in a non-contact manner (Nemirova et al., 2008; Cherunova et al., 2019; Gilewicz et al., 2013).

Air is supplied to the compartment by fans (4) and (5) with an adjustable mode, which allows changing the density of the heat flow. When choosing a device, it should be borne in mind that a household hair dryer allows you to set the nominal temperature of the exhaust air in one of three modes: weak 40°C, moderate 55°C, strong 70°C, the nominal capacity is adjustable and leaves from 3×10⁻³ m³/s, up to 16×10⁻³ m³/s, depending on the type of hairdryer. To obtain a higher temperature, building hair dryers should be used. For their fastening in the case above and below there are holes in the form of a truncated cone with a curvilinear generatrix: through the upper hole (6) cold air is supplied from the hairdryer in cooling mode, and a heated air stream (from the hairdryer during heating mode is supplied through the lower hole (7)). The power consumption of hairdryers is measured using electronic power meters (11) and (12). The temperature on the surface of the sample is recorded by contact temperature sensors, thermocouples (10), (15). The air temperature in the compartments is recorded by thermometers. Air supply stops when the temperature, or temperature difference, reaches a certain value — temperature measurement range from 40

to +126°C.

A specially developed program writes parameters to a computer, for which the device is connected via USB to a computer and the USBTermo program opens. By the “measure” command, the measured parameters are shown on the monitor: time, heat flow, air temperature, temperature and temperature difference of the sample surfaces. The results are stored and used to calculate the thermophysical properties of materials. According to the results in Excel, a graph of the thermal state of the test sample can be built (Appendix 1, 2).

3. RESULTS AND DISCUSSION:

Experimental studies on the proposed installation were carried out in the testing laboratory of SentexUz, Republic of Uzbekistan. In this study, hairdryers with a maximum power of 1800 watts were used. with an electronic temperature regulator with an interval of 10°C. Tests were carried out under the following modes of nominal productivity: 3×10⁻³ m³/s, 8×10⁻³ m³/s. Test samples of textile bags included cotton gabardine, cotton wool and cotton lining twill (Table 1).

To reproduce standardized conditions, the flow of heated air into the compartments was stopped when the surface temperature on the “hot” side of the sample was 50°C. Measurements were continued until the temperature difference on the sample surfaces became less than 1.0°C. To assess the accuracy and reproducibility of the results obtained on this device, tested a sample of a package of materials, the results of which are shown in Table 1.

According to the results of statistical data processing, it was found that the relative measurement error is from 4% to 10%. Therefore, the developed device allows the study of the thermophysical properties of materials for clothing and their packages, providing the required accuracy (up to 10%), adopted in studies in the light industry. The error is lower when testing in 2 modes. Table 2 shows the data characterizing the thermal state of the package of materials and the values of the equivalent coefficient of thermal conductivity under various heating conditions under given conditions: heating the surface of the sample in air to 50°C.

A graph of changes in the thermal state of a package of materials during heating and cooling in air is shown in Figure 3.

The obtained experimental data show that

with an increase in the heating power in air, the time for establishing thermal equilibrium in the sample is reduced, which can be taken into account when choosing the parameters of heat treatment of materials and products. The results show that the proposed device allows you to set the modes and measure the parameters characterizing the thermophysical properties of materials and clothing packages, provides high measurement accuracy, reproducibility of the results, as well as the preservation of the results of each experiment.

4. CONCLUSIONS:

As a result of the study, it was found that the developed device facilitates the study of thermophysical properties of materials for clothing and their packaging, providing the necessary accuracy (up to 10%), which was adopted in light industry research. Using the program developed for the study, it is possible to write parameters to a computer and calculate the thermophysical properties of the sample. The method that we used in the research process allowed us to analyze the thermal conditions of the package of materials at different temperatures, as well as to calculate the equivalent thermal conductivity of multilayer packages. The device provides high-precision recording and storage of the results of temperature changes in the sample. The results obtained help to formulate and solve the problems of choosing materials in packages, taking into account thermal conditions.

5. ACKNOWLEDGMENTS:

This study was carried out at the Tashkent Institute of Textile and Light Industry under the State Assignment of the Agency for Science and Technology of the Republic of Uzbekistan under the project OT-A3-63 (2017-2018), Supervisor: Doctor of Technical Sciences, Professor S. Tashpulatov.

6. REFERENCES:

1. Angelova, R. A., Reiners, P., Georgieva, E., Konova, H. P., Pruss, B., Kyosev, Y. *Textile Research Journal*, **2017**, 87(9), 1060-1070.
2. Bartkowiak, G., Greszta, A. *Przegląd Włokienniczy*, **2018**, 72(3), 27-33.
3. Bessonova, N. G., Zhikharev, A. P. *Thermophysical Properties of Materials for Light Industry Products*. Moscow: IITSMGUDT, **2007**.
4. Carslaw, H. S., Jaeger, J. C., Clulow, E. E., Rees, W. H. *Conduction of Heat in Solids*. Oxford: Oxford University Press, **1959**.
5. Celcar, D. *Tekstilec*, **2012**, 55(1), 45-57.
6. Cherunova, I. V., Stenikina, M. P., Cherunov, P. V. *8th International Conference on Textile Composites and Inflatable Structures – STRUCTURAL MEMBRANES 2017*, **2018a**, 1, 210-216.
7. Cherunova, I., Dhone, M., Kornev, N. *COUPLED PROBLEMS 2015 – Proceedings of the 6th International Conference on Coupled Problems in Science and Engineering*, **2015**, 1, 1303-1311.
8. Cherunova, I., Tashpulatov, S., Davydova, Yu. *IOP Conference Series: Materials Science and Engineering*, **2019**, 680, article number 012039.
9. Cherunova, I., Tashpulatov, S., Kolesnik, S. *International Russian Automation Conference*, **2018b**. doi: 10.1109/RUSAUTOCON.2018.8501795.
10. Cilveli, G., Okur, A., Sölar, V. *Fibres and Textiles in Eastern Europe*, **2020**, 28(1), 50-57.
11. Clulow, E. E., Rees, W. H. *Journal of the Textile Institute*, **1968**, 59(6), 285-294.
12. Cremer, L. D., Acosta-Martinez, J., Villarreal, A., Salinas, A., Wei, L., Mao, Y., Lozano, K. *Chemical Fibers International*, **2016**, 66(1), 40-42.
13. Deryabina, A. I., Lisienkova, L. N. *Izvestiya Vysshikh Uchebnykh Zavedenii, Seriya Tekhnologiya Tekstil'noi Promyshlennosti*, **2016**, 2016(1), 94-98.
14. Deryabina, A. L., Lisienkova, L. N. *Izvestiya Vysshikh Uchebnykh Zavedenii, Seriya Tekhnologiya Tekstil'noi Promyshlennosti*, **2017**, 2017(2), 189-192.
15. Firšt Rogale, S., Rogale, D., Nikolić, G. *Textile Research Journal*, **2018**, 88(19), 2214-2233.
16. Ghang, X. Heat-storage and thermo-regulated textiles and clothing. In: *Smart Fibers, Fabrics and Clothing*. Sawston: Woodhead Publishing, **2001**.
17. Gilewicz, P., Dominiak, J., Cichocka, A., Frydrych, I. *Fibres and Textiles in Eastern Europe*, **2013**, 101(5), 80-84.
18. Hunter, L., Fan, J. Improving the comfort of garments textiles and fashion. In: *Materials*,

19. Ivashchenko, I. N., Sevrugina, N. I., Shmalko, S. P. *Gigiena i Sanitariya*, **2017**, 96(4), 324-327.
20. Juraev, A., Tashpulatov, S.Sh., Cherunova, I.V., Rikhsieva, B.A., Bakhriddinova, D.A., Muminova, U.A. Device for determining the thermal conductivity of deformed materials. Patent No. FAR 00950 for FAR 20120134. Published 02.10.2012.
21. Kim, E., Dembsey, N., Godfrey, T. A. *ASTM Special Technical Publication*, **2016**, 1593, 78-101.
22. Kobrakov, K. I., Kuznetsov, D. N., Rodionov, V. I., Sokolovsky, R. R., Fedoseev, A. I. *Izvestiya Vysshikh Uchebnykh Zavedenii, Seriya Tekhnologiya Tekstil'noi Promyshlennosti*, **2017**, 371(5), 52-56.
23. Kolesnikov, P. P. *Thermal Protective Properties of Clothing*. Legkaya industriya, Moscow, **1964**.
24. Labanieh, A. R., Garnier, C., Ouagne, P., Dalverny, O., Soulat, D. *Mechanics and Industry*, **2019**, 20(4), 2019016.
25. Liang, S., Pan, N., Cui, Y., Wu, X., Ding, X. *Textile Research Journal*, **2019**, 89(8), 1455-1471.
26. Liu, S., Gong, J., Xu, B. *Polymers*, **2018**, 10(7), 748.
27. Lizák, P., Mojumdar, S. C. *Journal of Thermal Analysis and Calorimetry*, **2015**, 119(2), 865-869.
28. Lizák, P., Mojumdar, S. C. *Journal of Thermal Analysis and Calorimetry*, **2013**, 112(2), 1095-1100.
29. Matusiak, M. *Fibres & Textiles in Eastern Europe*, **2006**, 14(5), 98-102.
30. Matusiak, M., Kowalczyk, S. *AUTEX Research Journal*, **2014**, 14(4), 299-307.
31. Matusiak, M., Sybilska, W. *Journal of the Textile Institute*, **2016**, 107(7), 842-848.
32. Michalak, M., Felczak, M., Wiecek, B. *Fibres and Textiles in Eastern Europe*, **2009**, 74(3), 84-89.
33. Mikheev, M. A., Mikheeva, I. M. *Fundamentals of Heat Transfer*. Moscow: Energiya, **1977**.
34. Nemirova, L. F., Mironchik, E. V., Kataeva, S. B. *Scientific Bulletin of NSTU*, **2008**, 4(33), 165-175.
35. Neves, S. F., Campos, J. B. L. M., Mayor, T. S. *Applied Thermal Engineering*, **2017**, 117, 109-121.
36. Osmanov, Z. N., Sharpar, N. M. *Fibre Chemistry*, **2017**, 48(5), 379-383.
37. Peng, L., Su, B., Yu, A., Jiang, X. *Cellulose*, **2019**, 26(11), 6415-6448.
38. Rikhsieva, B.A., Musakhanov, A.A. Tashpulatov, S.Sh., Dzhurayev, A., Artikbaeva, N.M., Muminova, U.A. Software for determining the temperature of deformed textile materials and bags. Software Registration Patent No. DGU 02633 according to the application DGU 20120198. Published 11.10.2012
39. Ronald, J., George, M., Lamb, E. R. *Textile Research Journal*, **1987**, 57(12), 721-727.
40. Satomi, K., Kyohei, J., Katsuroku, T. *Journal of Textile Engineering*, **2016**, 62(3), 43-50.
41. Seretis, G. V., Theodorakopoulos, I. D., Manolagos, D. E., Provatidis, C. G. *International Journal of Clothing Science and Technology*, **2018**, 30(2), 195-209.
42. Shaid, A., Wang, L., Padhye, R., Gregory, M. *Hardware X*, **2019**, 5, article number e00060. doi: 10.1016/j.ohx.2019.e00060.
43. Siddiqui, M. O. R., Sun, D. *Clothing and Textiles Research Journal*, **2018**, 36(3), 215-230.
44. Sokolovskaya, T. S. *Fibre Chemistry*, **2005**, 37(1), 59-62.
45. Sokolovskaya, T. S., Shablygin, M. V., Shibarova, E. A. *Fibre Chemistry*, **2012**, 43(5), 381-383.
46. Sokolovskii, R. I., Shablygin, M. V. *Fibre Chemistry*, **2015**, 47(2), 108-116.
47. Tessier, D. Testing thermal properties of textiles. In: *Advanced Characterization and Testing of Textiles*. Sawston: Woodhead Publishing, **2017**.
48. Trofimovich, M. A., Galiguzov, A. A., Yurkov, A. L., Malakho, A. P., Avdeev, V. V., Oktyabr'skaya, L. V., Lepin, V. N., Makarovets, N. A. *Fibre Chemistry*, **2018**, 49(6), 365-371.
49. Tsirkina, O. G., Nikiforov, A. L. *Izvestiya Vysshikh Uchebnykh Zavedenii, Seriya*

50. Venkataraman, M., Mishra, R., Kotresh, T. M., Militky, J., Jamshaid, H. *Textile Progress*, **2016**, 48(2), 55-118.
51. Wazna, M. E. L., Gounni, A., Bouari, A. E. L., Alami, M. E. L., Cherkaoui, O. *Journal of Industrial Textiles*, **2019**, 48(7), 1167-1183.
52. Xu, R., Wang, W., Yu, D. *Composite Structures*, **2019**, 212, 58-65.

$$\lambda = -\frac{[\overline{q}]}{\text{grad } T} = \frac{Q}{F\tau\Delta t/l}, \quad (\text{Eq. 1})$$

$$\lambda = \frac{q \cdot \delta}{\Delta T}, \quad (\text{Eq. 2})$$

$$\lambda_{eq} = \frac{\Delta}{\frac{\delta_1}{\lambda_1} + \frac{\delta_2}{\lambda_2} + \frac{\delta_3}{\lambda_3}} = \frac{\delta_1 + \delta_2 + \delta_3}{\frac{\delta_1}{\lambda_1} + \frac{\delta_2}{\lambda_2} + \frac{\delta_3}{\lambda_3}} \quad (\text{Eq. 3})$$

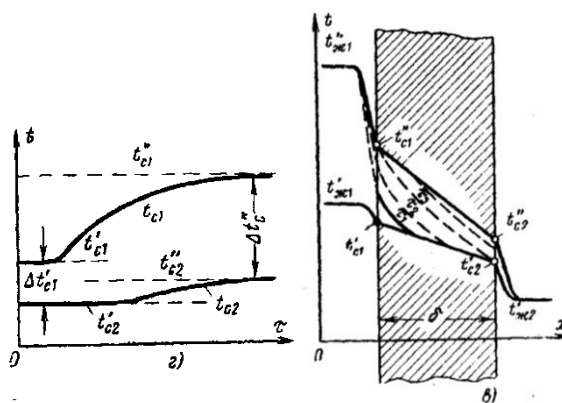


Figure 1. Non-stationary thermal conductivity: nature of temperature change (Mikheev and Mikheeva, 1977)

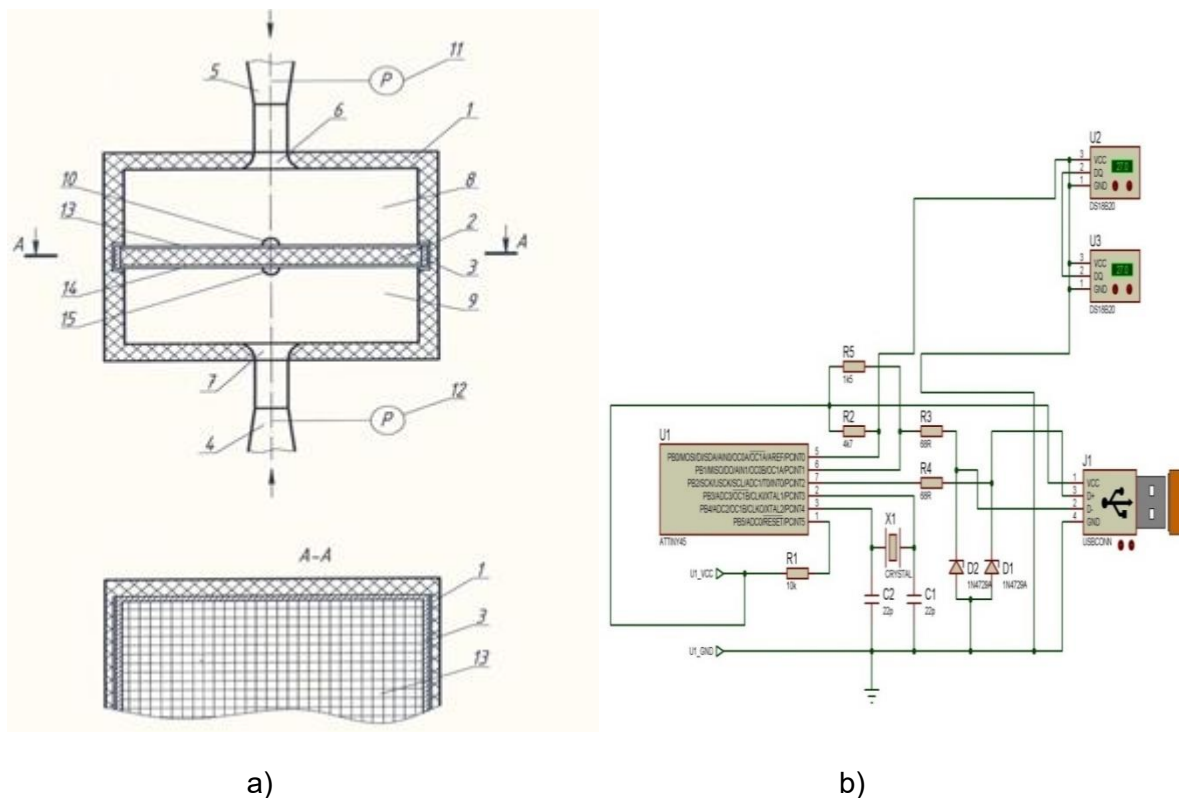


Figure 2. Scheme of the device for studying the thermophysical properties of materials in air: a) technical solution; b) connection of sensors

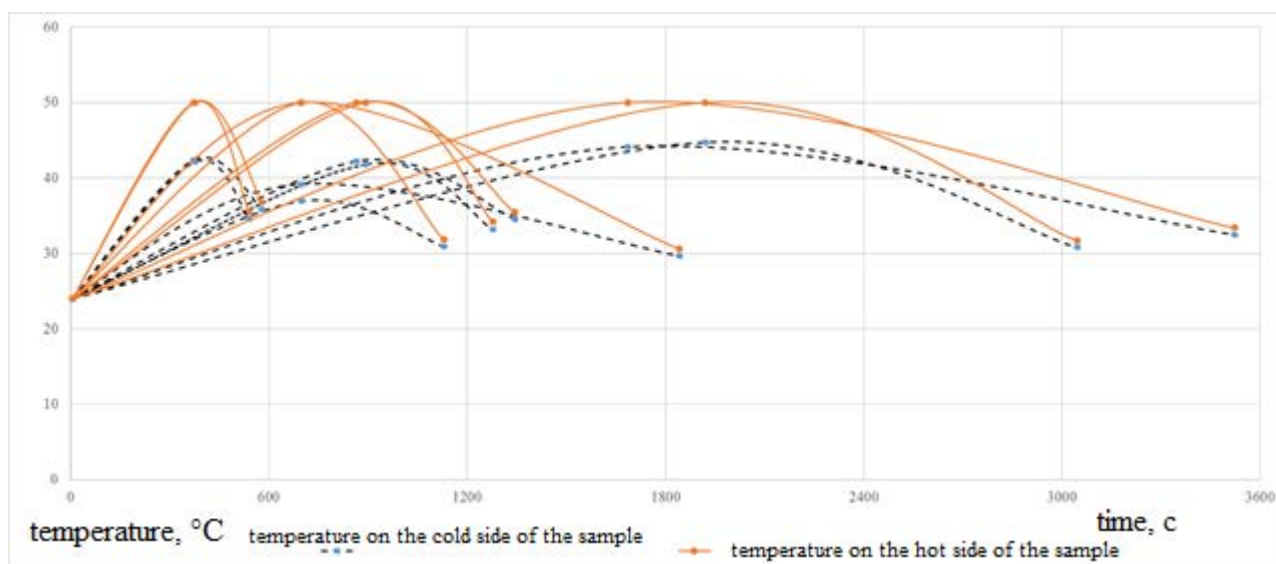


Figure 3. The diagram of the thermal state of packages of textile materials

Table 1. The measurement results of the test parameters of the package of materials

Options	Mode 1. Nominal productivity: $3 \times 10^{-3} \text{ m}^3/\text{s}$														
	Temperature measurement time τ_s , test, No.														
	1			2			3			4			5		
	5	884	1208	5	986	1164	5	832	1432	5	864	1344	5	904	1241
The surface temperature of the upper sample $t_{s1}, ^\circ\text{C}$;	24.3	42.4	31.75	24.43	40.31	32.81	24.3	41.56	35.87	24	42.18	34.56	24	42.48	31.19
lower $t_{s2}, ^\circ\text{C}$	24.4	50	32.68	25.01	50	33.7	24.28	50	36.81	24	50	35.5	24	50	33.16
Temperature drop $\Delta T, ^\circ\text{C}$		7.6	0.93		9.69	0.89		8.44	0.94		7.82	0.94		7.52	0.97
Equivalent thermal conductivity coefficient $\lambda_{eq}, \text{W}/(\text{m} \times \text{K})$	0.05														
Options	Mode 2. Nominal productivity: $8 \times 10^{-3} \text{ m}^3/\text{s}$														
	Temperature measurement time τ_s , test, No.														
	6			7			8			9			10		
	5	369	506	5	404	553	5	327	567	5	380	546	5	399	531
The surface temperature of the upper sample $t_{s1}, ^\circ\text{C}$;	24.2	41.5	36.0	24.43	42.37	34.56	24.13	41.97	33.5	24	42	34.12	24	42.37	34.68
lower $t_{s2}, ^\circ\text{C}$	24.4	50	36.93	25.01	50	35.5	24.9	50.06	34.43	23	50	35.06	24	50.0	35.62
Temperature drop $\Delta T, ^\circ\text{C}$		8.5	0.93		7.63	0.94		8.09	0.93		8	0.94		7.63	0.94
Equivalent thermal conductivity coefficient $\lambda_{eq}, \text{W}/(\text{m} \times \text{K})$	0.045														

Table 2. The measurement results of test parameters of samples of packages of materials

Options	Mode 1. Nominal productivity: 3×10 ⁻³ m ³ /s											
	Temperature measurement time τ, c											
	Sample 1			Sample 2			Sample 3			Sample 4		
	5	89 4	1278	5	1687	3522	5	1921	3046	5	698	1129
The surface temperature of the upper sample t _{s1} ,°C;	24. 2	41. 8	33.2	24. 1	44.1	32.5	24.3	44.7	30.8	2 4	36.9 3	30.9 3
lower t _s ’2, °C	24. 3	50	34.2	23. 9	50	33.4	24.2 8	50	31.7	2 4	50	31.8 7
Temperature drop ΔT,°C		8.2	1.0		5.9	0.9		5.3	0.9		13.0 7	0.94
Equivalent thermal conductivity coefficient λ _{eq} , W/(m×K)	0.036			0.0152			0.143			0.035		

Options	Mode 2. Nominal productivity: 8×10 ⁻³ m ³ /s											
	Temperature measurement time τ, c											
	Sample 1			Sample 2			Sample 3			Sample 4		
	5	37 6	640	5	696	1842	5	864	1344	5	373	579
The surface temperature of the upper sample t _{s1} ,°C;	23. 8	42. 1	34.6	25	39.1 8	29.6 8	24.3	42.3 7	35.8 7	2 4	42.1 8	34.5 6
lower t _s ’2, °C	24. 1	50	35.5 3	25	50	30.6 2	24.2 8	50	36.8 1	2 4	50	35.5
Temperature drop ΔT,°C		7.9	0.93		10.2	0.9		7.62	0.9		7.82	0.94
Equivalent thermal conductivity coefficient λ _{eq} , W/(m×K)	0.05			0.01			0.04			0.02		

APPENDIX

O'ZBEKISTON RESPUBLIKASI INTELLEKTUAL MULK AGENTLIGI
АГЕНТСТВО ПО ИНТЕЛЛЕКТУАЛЬНОЙ СОБСТВЕННОСТИ
РЕСПУБЛИКИ УЗБЕКИСТАН

FOYDALI MODELGA PATENT **№ FAP 00950**
ПАТЕНТ НА ПОЛЕЗНУЮ МОДЕЛЬ

Ushbu patent O'zbekiston Respublikasining Hozirgi vaqtda qabul qilingan qonunlar va qonunlar qabul qilish to'g'risida qabul qilingan qonunlar bilan bog'liq bo'lgan. Настоящий патент выдан на основании Закона Республики Узбекистан «О изобретениях, полезных моделях и промисловых образцах, на полезную модель».

Деформацияланган материалларнинг иссиқлик ўтказувчанлигини аниқлаш учун қўрилма
Устройство для определения теплопроводности деформированных материалов

Telefonoma keldi tushgan sana: **02.10.2012** Telefonoma tashlati: **FAP 2012 0134**
Data postulovchi xabar: Номер заявки:
Ushbu patent: **02.10.2012**
Дата прислуги:
Patent egasi (egalar): **Тошкент тўқимачилик ва енгил саноат институти, UZ**
Патентобладатель(и): **Ташкентский институт текстильной и легкой промышленности, UZ**

Foydali model muallifi(lari): **Джурев Анвар Джуревич, Ташпулатов Салих Шукрович, UZ,**
Автор(ы) полезной модели: **Черунова Ирина Викторовна, RU, Риксиева Барнохон Абдуллоевна, UZ,**
Бакроддинова Дилрабо Аминовна, Мунинова Умида Абдулғаффаровна, UZ

Patent O'zbekiston Respublikasining hozirgi qonunlarida 02.10.2012 yildan boshlab qabul qilinayotgan qonunlar bilan bog'liq bo'lgan. O'zbekiston Respublikasi hukumati tomonidan 12.03.2014 yilda tasdiqlanishiga to'g'ri keladi.

Патент действует на всей территории Республики Узбекистан в течение 5 лет с 02.10.2012 г. при условии ежегодной уплаты пошлины за поддержание в действии. Сохранение и подтверждение срока действия патента Республикой Узбекистан, с.г. Ташкент 12.03.2014 г.

Bosh direktor v.b. **3. Гинсов**
И.о. Генерального директора

Appendix 1. Documents on copyright protection of intellectual activity for a utility model; b) for software

O'ZBEKISTON RESPUBLIKASI INTELLEKTUAL MULK AGENTLIGI
АГЕНТСТВО ПО ИНТЕЛЛЕКТУАЛЬНОЙ СОБСТВЕННОСТИ
РЕСПУБЛИКИ УЗБЕКИСТАН

ELEKTRON HISOBASH MASHINALARI UCHUN YARATILGAN DASTURNING
RASMIY RO'YXATDAN OTKAZILGANLIGI TO'G'RISIDAGI QUVONOMA
СВИДЕТЕЛЬСТВО ОБ ОФИЦИАЛЬНОЙ РЕГИСТРАЦИИ ПРОГРАММЫ ДЛЯ
ЭЛЕКТРОННО-ВЫЧИСЛИТЕЛЬНЫХ МАШИН

№ DGU 02633

Ushbu quvonoma O'zbekiston Respublikasining Hozirgi vaqtda qabul qilingan qonunlar va qonunlar qabul qilish to'g'risida qabul qilingan qonunlar bilan bog'liq bo'lgan. Настоящее свидетельство выдано на основании Закона Республики Узбекистан «О правовой охране программ для электронных вычислительных машин и баз данных» на программу для ЭВМ.

Деформацияланган текст материаллари ва таътирларнинг температурасини аниқлаш учун
Программное обеспечение для определения температуры деформированных текстильных материалов в пакете

Telefonoma keldi tushgan sana: **11.10.2012** Telefonoma tashlati: **DGU 2012 0198**
Data postulovchi xabar: Номер заявки:
Ushbu quvonoma: **11.10.2012**
Дата прислуги:
Patent egasi (egalar): **Тошкент тўқимачилик ва енгил саноат институти, UZ**
Патентобладатель(и): **Ташкентский институт текстильной и легкой промышленности, UZ**

Dastur muallifi(lari): **Риксиева Барнохон Абдуллоевна, Мунинов Азамат Ахмеджанович,**
Автор(ы) программы: **Ташпулатов Салих Шукрович, Джурев Анвар Джуревич, Артемова Мария Муниновна, Мунинова Умида Абдулғаффаровна, UZ**

O'zbekiston Respublikasi elektron hisoblash mashinalari uchun dasturlar ro'yxatidan otkazilganligi to'g'risida qonunlar qabul qilish to'g'risida qabul qilingan qonunlar bilan bog'liq bo'lgan.

Свидетельство о государственной регистрации программы для электронно-вычислительных машин Республики Узбекистан, с.г. Ташкент, 18.11.2012 г.

Bosh direktor v.b. **3. Гинсов**
И.о. Генерального директора

Appendix 2. Documents on copyright protection of intellectual activity for software

CORROSÃO DE MAGNÉSIA DE MATERIAIS DE ENCHIMENTO

MAGNESIA CORROSION OF GROUTING MATERIALS

МАГНЕЗИАЛЬНАЯ КОРРОЗИЯ ТАМПОНАЖНЫХ МАТЕРИАЛОВ

AGZAMOV, Farit A.^{1*}; KABDUSHEV, Arman²; TOKUNOVA, Elvira³; MANAPBAYEV, BAUYRZHAN Zh.⁴; KOZHAGELDI, Bolat Zh.⁵

^{1,3} Ufa State Petroleum Technological University, Department of Oil and Gas Well Drilling, Ufa, Russian–Federation

^{2,4} M.Kh. Dulaty Taraz State University, Department of Oil and Gas Engineering, Taraz – Republic of Kazakhstan

⁵ M.Kh. Dulaty Taraz State University, Department of Electric Power, Taraz – Republic of Kazakhstan

* Correspondence author

e-mail: faritag@yandex.ru

Received 22 January 2020; received in revised form 20 February 2020; accepted 30 March 2020

RESUMO

A questão da corrosão de magnésia de materiais de enchimento em poços de petróleo e gás é muito relevante na construção de poços de petróleo e gás, uma vez que os sais de magnésio podem levar à destruição da pedra de cimento à base de cimento Portland dentro de alguns meses. Ao fixar os intervalos poderosos de depósitos de sal representados por sais de magnésio, o uso de cimentos da magnésia é eficaz. No entanto, as camadas individuais e as camadas contendo os sais de magnésio dissolvidos não são cimentadas individualmente, mas se sobrepõem ao longo de todo o intervalo do orifício aberto com o cimento Portland, que pode ser destruído devido à corrosão de magnésia. A parte principal do trabalho é dedicada ao estudo da corrosão da pedra de cimento Portland em ambientes agressivos de magnésia. Como os indicadores quantitativos que caracterizam o grau de dano à pedra, são tomadas a espessura da camada danificada e o coeficiente de resistência da pedra, caracterizados pela relação da resistência à compressão ou à flexão das amostras de pedra, depois de estar em um ambiente agressivo com a resistência das amostras de controle no mesmo tempo de endurecimento. A resistência à corrosão da pedra de cimento foi avaliada após 8 semanas no ambiente de magnésia agressivo. Além disso, foi estudado o papel da concentração de $MgCl_2$ no mecanismo de danificação da pedra de cimento por corrosão. Propõe-se a redução em relação água/cimento e a adição de argila de paligorskite para reduzir a porosidade da pedra de cimento e a taxa de danos por corrosão. A cinética e os principais fatores que afetam o processo de corrosão foram considerados, uma análise de difração de raios X dos produtos de corrosão e da pedra de cimento não afetada foi realizada.

Palavras-chave: *corrosão de magnésia, pedra de cimento Portland, resistência à corrosão, profundidade de corrosão, paligorskite.*

ABSTRACT

The issue of magnesia corrosion of grouting materials in oil and gas wells is very relevant in the construction of oil and gas wells since magnesia salts can lead to the destruction of Portland cement-based cement stone within few months. When fastening powerful intervals of salt deposits represented by magnesium salts, the use of magnesia cements is effective. However, individual layers and interlayers containing dissolved magnesium salts are not individually cemented, but overlap over the entire interval of the open hole with cement Portland cement, which can be destroyed due to magnesia corrosion. The main aim of the paper is to analyze the corrosion of Portland cement stone in aggressive environments of magnesia. As the quantitative indicators characterizing the degree of stone damage, the thickness of the damaged layer and the stone resistance coefficient are taken, characterized by the ratio of the compressive strength or bending strength of stone samples after being in an aggressive environment to the strength of control samples at the same hardening time. The corrosion resistance of cement stone was assessed after 8 weeks in an aggressive magnesia environment. Also, the role of $MgCl_2$ concentration on the mechanism of corrosion damage to cement stone was studied. The use of reducing the water-cement ratio and adding palygorskite clay to reduce the porosity of cement stone and reduce

the rate of corrosion damage is proposed. The kinetics and the main factors affecting the corrosion process were considered, an X-ray diffraction analysis of corrosion products and unaffected cement stone was carried out.

Keywords: *magnesia corrosion, Portland cement stone, corrosion resistance, corrosion depth, palygorskite.*

АННОТАЦИЯ

Вопрос магниальной коррозии тампонажных материалов в нефтяных и газовых скважинах является весьма актуальным при строительстве нефтяных и газовых скважин, поскольку магниальные соли могут привести к разрушению цементного камня на основе портландцемента в течение нескольких месяцев. При креплении мощных интервалов соляных отложений, представленных солями магния, эффективно применение магниальных цементов. Однако, отдельные пласты и пропластки, содержащие растворенные соли магния, не цементируются индивидуально, а перекрываются по всему интервалу открытого ствола тампонажным портландцементом, который может разрушаться из-за магниальной коррозии. Основная часть работы заключается в изучении коррозии портландцементного камня в агрессивных магниальных средах. В качестве количественных показателей, характеризующих степень поражения камня, приняты толщина поврежденного слоя и коэффициент стойкости камня, характеризующий отношением предела прочности на сжатие или изгиб образцов камня, после пребывания в агрессивной среде, к прочности контрольных образцов в одинаковые сроки твердения. Проведена оценка коррозионной стойкости цементного камня через 8 недель пребывания в магниальной агрессивной среде. Кроме этого, изучена роль концентрации $MgCl_2$ на механизм коррозионного поражения цементного камня. Предложено использование снижение водоцементного отношения и добавки палыгорскитовой глины для уменьшения пористости тампонажного камня и снижения скорости коррозионного поражения. Рассмотрена кинетика и основные факторы, влияющие на процесс коррозии, проведен рентгеноструктурный анализ продуктов коррозии и непораженного цементного камня.

Ключевые слова: *магниальная коррозия, портландцементный камень, коррозионная стойкость, глубина коррозии, палыгорскит.*

1. INTRODUCTION:

To improve the quality of the fastening of wells, it is inevitable to regulate the technological properties of cement slurries using various chemicals (Agzamov *et al.*, 2006; Agzamov *et al.*, 2018). However, the expansion of the drilling zone led to the development of a significant number of fields, in the context of which there are formations represented by solid magnesia salts or solutions of these salts, which reduce the integrity of the well support (Kravets *et al.*, 1979; Agzamov and Izmukhambetov, 2005; Tolkachev *et al.*, 2010). The thickness of magnesia saline deposits varies from several to a thousand meters (Zhuravlev, 1972; Karabalina and Tankibaeva, 1989; Palilu *et al.*, 2019).

The amount and composition of salts in the reservoirs in each individual region vary widely. Typically, saline deposits are represented by bischofite ($MgCl_2 \cdot 6H_2O$), carnallite ($KCl \cdot MgCl_2 \cdot 6H_2O$), kieserite ($MgSO_4 \cdot H_2O$) and epsomite ($MgSO_4 \cdot 7H_2O$). The temperature of salt formations in some regions reaches $160^\circ C$, which enhances the aggressiveness of salts (Mukhin *et al.*, 1976). In salt deposits, brine-forming strata with abnormally high pressures, consisting of saturated saline and containing chlorides, calcium, magnesium, sodium and potassium sulphates and

other salts, are often found. As a rule, the presence of magnesia salts in the section creates serious complications when fastening wells, manifested in: increasing the diameter of the well; the formation of gaps between the cement ring and the wall of the well; plastic flow of salts; thickening of grouting mortar; increasing pressure on the cementing head; destruction of cement stone; inter-reservoir flows and increased water cut of well products; crushing of intermediate or production strings, premature corrosion of casing strings, etc. (Mukhin *et al.*, 1976; Akhmadeev and Danyushevsky, 1981; Danyushevsky *et al.*, 1987).

In wells cemented with Portland cement, casing corrosion is usually observed in places where grouting stone is absent, since Portland cement, having a high pH (more than 12.0), ensures the formation of a protective passivation film on the metal surface (Maksutov *et al.*, 1970; Zagirov, 1982; Tolkachev *et al.*, 2013). It should be noted that the practice of well construction, depending on the thickness of aggressively active sections, uses various types of grouting materials. To fix the intervals represented by magnesium-containing salts, magnesia cements are used, which are shut with aqueous solutions of magnesia salts (Trupak, 1956; Tolkachev *et al.*, 2010; Wang *et al.*, 2019; Calvo *et al.*, 2019), the effectiveness of which is confirmed by practice. At

the same time, aqueous solutions of magnesia salts and magnesia cements have a low pH (less than 7). Therefore casing strings under these conditions require additional protection (Tolkachev *et al.*, 2013).

If there are separate layers and interlayers in the section of the well containing dissolved magnesia salts, there is no practice of using technology for individual cementing of these zones, and cementing is usually carried out along the entire open hole interval with Portland cement, which is the weakest link in the well support and can be destroyed from due to magnesia corrosion (Shahraki *et al.*, 2017; Kujur *et al.*, 2018; Liu *et al.*, 2019a). Therefore, despite the danger of magnesia corrosion in relation to Portland cement, even with a small amount of magnesium, a sufficiently large number of wells under these conditions are cemented by this grouting material. The main aggressive component in the corrosion of cement stone in contact with magnesium salts or their aqueous solutions is magnesium cation (Zaitsev *et al.*, 2016; Xu *et al.*, 2017a; Xu *et al.*, 2017b). As a result of chemical reactions of components of an aggressive environment with cement hydration products, and first of all with calcium hydroxide located in the pore fluid, reaction products are formed that are either removed from the cement stone as a result of diffusion or, precipitating, remain in its pores.

Thus, the main aim of the study is to research the main factors affecting the corrosion process of Portland cement stone in aggressive magnesia media by an experimental method using X-ray crystallography of corrosion products and unaffected cement stone.

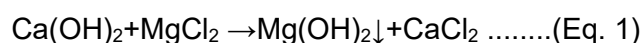
2. MATERIALS AND METHODS:

In studies of the durability of concrete and cement, the corrosion processes of Portland cement are classified into several types (Kind, 1955; Babushkin and Ratnova, 1968; Moskvina *et al.*, 1980; Rakhimbayev *et al.*, 2012; Rakhimbayev, 2012; Rakhimbayev and Tolypina, 2015). Corrosion of the first type is associated with the gradual hydrolysis of cement hydration products, and the leaching of calcium hydroxide. A decrease in calcium hydroxide violates the stability of cement stone hardening products, leading to their subsequent hydrolysis and dissolution. In borehole conditions, this type of corrosion is characteristic of injection wells (Kind, 1955; Agzamov *et al.*, 2011). Corrosion of the second type is characterised in that in the surface layers of cement stone in contact with the aggressive

environment; there is an intensive destruction of the structural elements of hydrated cement stone. In this case, the process of destruction of the surface layers can be complete while maintaining intact stone in the adjacent layers. As a rule, this type is characteristic of the interaction of cement stone with acidic environments. About downhole conditions, this is observed under the action of dissolved hydrogen sulfide or carbon dioxide on the well support (Kind, 1955; Babushkin and Ratnova, 1968; Agzamov *et al.*, 2011).

The third type of corrosion is characterised by the fact that crystalline products accumulate in the pores and capillaries of the cement stone, which are the result of chemical reactions of an aggressive environment with the constituent parts of the cement stone. The growth and accumulation of corrosion products can lead to the development of tensile stresses on the pore walls and destroy the structural elements of the stone. One of the signs of this type of corrosion is the destruction of stone with an increase in volume, which is preceded by an accelerated, in comparison with control samples, increase in strength. In borehole conditions, this type of corrosion can be observed when sulfate media or gaseous hydrogen sulfide acts on a cement stone (Babushkin and Ratnova, 1968; Agzamov *et al.*, 2011).

The damage to the cement stone caused by $\text{Mg}(\text{SO}_4)_2$, according to (Kind, 1955), at low salt concentrations in water is caused by sulfate corrosion, which is dangerous only for Portland cement. At high concentrations of $\text{Mg}(\text{SO}_4)_2$, magnesia-gypsum corrosion is observed, which is also dangerous for other types of cements. This means that with an increase in the Mg^{+2} cation in the solution, it is magnesia corrosion that prevails, the mechanism of which differs from the types of corrosion described above. There are several opinions regarding the corrosion mechanism of Portland cement in magnesia media. When the cement stone comes in contact with an aggressive magnesia medium, chemical reactions occur between the dissolved salt and calcium hydroxide located in the pores of the cement stone and near its surface according to the Equation 1:



Calcium chloride, being a readily soluble product, dissociates into ions, and the Ca^{2+} cation is released into the environment. Chlorine ion remains in the pores of the cement stone and can diffuse further into the cement stone. Depending on the concentration of the aggressive substance, the composition of the cement stone hardening products, its structural characteristics during

magnesia corrosion, the meeting of the flows of aggressive ions with calcium hydroxide, and their subsequent neutralization can occur in different places. It can be outside the cement stone, either inside the stone near its surface or inside the stone at a considerable distance from the surface of the stone. Accordingly, a different mechanism of magnesia corrosion can be observed.

A decrease in calcium hydroxide in the pores of the cement stone upset the equilibrium between solid hardening products and dissolved Ca(OH)_2 , leading to the dissolution and hydrolysis of hardening products and leaching of new portions of calcium hydroxide. In this case, leaching corrosion is observed, leading to the destruction of cement stone due to leaching of calcium hydroxide from it. The corrosion rate will depend on the diffusion rate of calcium cations from the cement stone, i.e., on the porosity of the formed leached layer, which in turn depends on the initial porosity of the cement stone. If cement stone hardening products are easily soluble, for example, highly basic calcium hydro silicates, their hydrolysis occurs quickly, and the zone of penetration of aggressive ions narrows. In this case, the corrosion of cement stone can take place according to the acid mechanism, that is, the destruction of the stone is carried out in layers, and the destruction can achieve full development when stored in closely spaced intact layers of cement stone with almost no change in structure and composition (Moskvin *et al.*, 1980; Kravtsov *et al.*, 1987; Amanbayev *et al.*, 2019; Orynbayev *et al.*, 2019).

The corrosion rate is also determined by the diffusion of aggressive fluids, i.e. the process has diffusion control. The higher the concentration of the solution of magnesia salt, the denser the structure of the membrane formed on the surface of the stone, and the retardation effect depends on its density, strength, and permeability. Another mechanism of damage is associated with the formation of magnesium hydroxide in the pores of cement stone by replacing the calcium cation with magnesium cation. According to (Trupak, 1956), this reaction is accompanied by an increase in the volume of corrosion products, leading to volumetric destruction of the stone. The possibility of volumetric destruction of Portland cement stone upon contact with a magnesia medium was also indicated in the works of V. Danyushevsky (Akhmadeev and Danyushevsky, 1981; Danyushevsky *et al.*, 1987). He noted that osmotic pressure, due to the presence of a semi-permeable shell in the surface layers of cement stone, and leading to the development of high

pressures inside the stone, contributing to its destruction, is a reinforcing factor of magnesia corrosion. In his opinion, magnesium hydroxide (solubility 18.2 mg/l) can accumulate at the border of a cement stone or inside a stone near the surface, forming a semi-permeable septum, leading to osmotic effects.

According to (Kind, 1955), in MgCl_2 solutions, cement stone corrosion proceeds more slowly than in $\text{Mg}(\text{SO}_4)_2$ solutions having a similar concentration of Mg^{2+} ions. This is due to the effect of clogging the pores of the cement stone with magnesium hydroxide deposited on the surface of the cement stone and in pores adjacent to the surface. With a high porosity of the cement stone, the effect of the formation of a mud layer decreases, and the active corrosion of the cement stone under the influence of MgCl_2 begins to appear when the salt content in the solution is about 2%, which corresponds to about 5000 mg/l of MgCl_2 ions (Kind, 1955). If the flow of calcium hydroxide is insufficient due to the low rate of hydrolysis of the hardening products and the low concentration of calcium hydroxide, for example, in slag cement, and the number of aggressive ions is large, then a deeper penetration of magnesium cations into the stone and the formation of poorly soluble precipitate of magnesium hydroxide at a larger thickness inside cement stone.

Thus, when exposed to aggressive environments containing magnesium cations, several types of corrosion can be observed. In particular, it can be corrosion of the first type associated with the leaching of calcium hydroxide from cement stone, corrosion of the second type (acid), as well as corrosion of the third type, accompanied by the accumulation of corrosion products in the pores of the cement stone. During experimental studies, an aqueous solution of MgCl_2 with a concentration of 10% was used as an aggressive medium. The ratio of the volume of aggressive liquid and the volume of cement stone was 10:1, with a weekly update of the aggressive solution. The tested cement samples were prepared from Portland cement solutions with a water-cement ratio (W/C) of 0.4; 0.5; 0.6, which are solid in both water and air. Weekly, three samples were taken from the solution, which was tested for bending and compression. In addition, the depth of corrosion was determined at the fracture of the samples, and the phase composition of hardening products and corrosion products was determined in various layers of cement stone.

3. RESULTS AND DISCUSSION:

The applicability of this method to assess the effect of the aggressiveness of magnesium salts on cement stone is conditioned by the fact that during the reaction of the sample with the medium, hydrolysis and leaching of cement hardening products occur, thereby increasing the pore space and decreasing the strength of the stone (Cano *et al.*, 2015; Thomas *et al.*, 2015; Zhang *et al.*, 2019; Liu *et al.*, 2019b). The depth of corrosion is equal to the penetration depth of magnesium ions and was measured as the boundary of the resulting white products. The effect of H/C on the tensile strength of a cement stone installed in an aggressive environment during compression is shown in Figure 1, which shows that with a decrease in the initial water content of a solution, the strength of a Portland cement stone increases over time (Lee and Lee, 2019; Nikolopoulou *et al.*, 2019).

At the same time, the effect of hardening conditions and the composition of cement stone on the change in the strength of the stone was clearly manifested only due to the change in W/C. This is due to the fact that in the cement stone in the first weeks of hardening, hydration processes actively continue, which competes with destructive corrosion processes (Zhang *et al.*, 2019). Since the structural processes associated with the hydration and hardening of Portland cement during this period proceed faster than corrosion processes, it is not possible to single out the role of the latter during this period. This is quite obvious and does not contradict the basic provisions of hydration and hardening of cements (Danyushevsky *et al.*, 1987; Agzamov *et al.*, 2011; Kravtsov *et al.*, 1987).

The decrease in W/C always reduces the porosity of the cement stone. It increases the corrosion resistance of the cement stone, which confirms the assumption of diffuse control of the process. At the fracture of the samples (Figure 2), zones of different colors are visible. The depth of the corroded zone increases with time. Moreover, with increasing W/C, the depth of the corrosion zone grows (Figures 3 and 4).

At the fracture of the samples shown in Figures 2 and 3, layer-by-layer destruction of the stone, characteristic of the second type of corrosion, is visible. At the same time, a loose white layer about 1 mm thick was formed on the surface of the cement stone, the composition of which, according to the X-ray phase analysis, showed the predominance of brussite $\text{Mg}(\text{OH})_2$, which is a reaction product of MgCl_2 and $\text{Ca}(\text{OH})_2$.

The middle zone of the sample (non-corroded) in its phase composition corresponds to the composition of the control sample of cement stone (Illampas *et al.*, 2019; Liu, 2019; Samsykin *et al.*, 2019). Between these layers inside the stone, a damaged (corroded) layer is distinguished, with a partially changed composition of the phase composition (Table 1). A quantitative analysis of the XRD results, the names of minerals, hardening products, and corrosion products were obtained by processing the diagrams in the TopasDiffrac licensed program. The comparison was carried out by changing the amount of non-hydrated cement minerals, cement hydration products, and corrosion products.

The table shows that in the central non-corroded part of the samples, there are not hydrated cement minerals and their hydration products (Elsayed *et al.*, 2018; Khatami and O'Kelly, 2018; Sögaard *et al.*, 2018; Wu and Zhang, 2018). The presence of corrosion products is not observed. In the middle (corroded) layer, the number of clinker minerals decreased with a simultaneous increase in hydration products. In particular, the number of minerals included in the composition of the initial cement decreased from 76.7% to 27.2%. An increase in the proportion of hardening products may indicate an increase in cement hydration processes with a decrease in pH. Other researchers noted this effect. In particular, some works suggested hardening cement stone when mixing it, for example, with water with dissolved carbon dioxide or dissolved hydrogen sulfide. This is because calcium hydroxide released during hydration of clinker minerals is more quickly neutralized by an acidic medium, and, as a result, causes accelerated hydration of cement minerals to maintain the required concentration of calcium hydroxide solution (Agzamov *et al.*, 2011; Hou *et al.*, 2018; Song *et al.*, 2018; Le and Sun, 2018).

The amount of Portlandite (calcium hydroxide) in these layers does not differ significantly. In the non-corroded layer, this is due to the onset of equilibrium between the solid phase and the pore liquid, and in the corroded layer it is associated with the hydrolysis of the hardening products due to the constant binding of calcium hydroxide from the pore liquid due to the reaction with magnesium chloride (Zou *et al.*, 2018; Liu *et al.*, 2018; Junxiang *et al.*, 2018). In the surface layer of cement stone, calcium hydroxide (oxide) completely went into solution and bound with aggressive ions, due to which only insoluble or poorly soluble compounds remained in this layer, which play a significant role in inhibiting the

corrosion process. These include aluminum and magnesium hydroxide, as well as silicon oxide and a small amount of carbonates. Aluminum hydroxide, which has a larger size than aluminum oxide, reducing pore size, acts as an additional agent that reduces the permeability of the cement stone layer near the border with the aggressive environment. Magnesium hydroxide, in this case, acts as a semipermeable membrane and a binding agent for silicon oxide.

Analysis of the results allows to clarify the idea of the mechanism of corrosion of cement stone in a magnesia medium. A significant value of the content of brussite in the surface sediment (Table 1) indicates the second type of corrosion, during which exchange reactions occur between the components of the cement stone and the mortar, and the resulting reaction products are deposited on the cement surface and in the pores (Moskvin et al., 1980; Rakhimbayev, 2012; Rakhimbayev et al., 2012; Rakhimbayev and Tolypina, 2015;). Corrosion, in this case, can come with braking due to the partial compaction of cement stone with corrosion products. At the same time, no signs of volumetric destruction due to the accumulation of corrosion products inside the cement stone were noted, which may indicate a reaction between calcium hydroxide and magnesium chloride at the surface of the cement stone. This may be evidenced by a small amount of corrosion products in the middle (damaged) layer.

The experiments confirmed that the factors determining the kinetics of the corrosion process are the diffusion rate, the porosity of the stone, and the compaction of the cement stone with reaction products. Since one of the factors determining the kinetics of the corrosion process is the porosity of the stone, an addition of salt-resistant clay – palygorskite in an amount of 3% was used to reduce it. In this case, the W/C of the solution was maintained equal to 0.5. The experiments showed (Figure 5) that corrosion also occurs in layers, but the boundaries of the layers are less noticeable, and the corrosion process slows down. A layer of brussite $Mg(OH)_2$, less than 1 mm thick, also formed on the surface of the cement stone. The results of determining the tensile strength of Portland cement stone and the depth of corrosion of samples containing palygorskite are shown in Figures 6 and 7.

With the same porosity of the stone (due to the same W/C), the corrosion rate of the stone obtained from cement with the addition of palygorskite decreased by 17% compared to the control samples. This is attributed to a slowdown

in the diffusion of aggressive ions into the stone due to the clogging of its pores with swollen, salt-resistant clay. A study of the behavior of cement stone in media with different concentrations of magnesium chloride showed that a concentration of 10% is most interesting for considering the corrosion process, since the corrosion front is at the grouting stone – solution, and second-type corrosion is observed. When the concentration of the aggressive medium is more than 10%, in the experiment with 20%, the corrosion front moves inside the stone, and the corrosion passes to the third type, and, also, $MgCl_2$ begins to crystallize on the surface of the samples (Figure 8).

At concentrations of aggressive medium less than 10%, the corrosion front extends beyond the cement stone, and corrosion occurs only due to the leaching of $Ca(OH)_2$.

4. CONCLUSIONS:

1. The relationship of the kinetics of corrosion damage to Portland cement stone with its structural properties is shown, which makes it possible to control the corrosion rate by reducing the water-cement ratio of the cement slurry.

2. The possibility of reducing the rate of corrosion of cement stone in a magnesia medium using palygorskite additive, which acts as a pore colmatant, has been shown.

3. A change in the mechanism of damage to cement stone in magnesia media depending on the concentration of Mg^{2+} cation has been theoretically substantiated and experimentally shown.

4. Corrosion damage to the cement stone has a layered character, from the intact sample to the corroded layer, which differ in phase composition, and the kinetics of the lesion is characterised by a slowdown in the corrosion rate.

5. It has been shown that on the open stone surface from Portland cement at high concentrations of $MgCl_2$ crystallisation occurs with the formation of a layer that reduces the corrosion rate.

5. REFERENCES:

1. Agzamov, F., Kabdushev, A., Ismailov, A., Betzhanova, A., Karabaeva, A. *Key Engineering Materials*, **2018**, 771, 9-23.
2. Agzamov, F.A., Izmukhambetov, B.S. *Durability of cement stone in corrosive*

- environments*. St. Petersburg: Nedra LLC, **2005**.
3. Agzamov, F.A., Izmukhambetov, B.S., Tokunova, E.F. *Chemistry of grouting and flushing solutions*. St. Petersburg: Nedra, **2011**.
 4. Agzamov, F.A., Kabdushev, A.A., Komleva, S.F., Bayutenov, N.A. *Pollution Research*, **2006**, 35(4), 241-246.
 5. Akhmadeev, R.G., Danyushevsky, V.S. *Chemistry of flushing and grouting liquids*. Moscow: Nedra, **1981**.
 6. Amanbayev, E.N., Alimbayev, B.A., Manapbayev, B.Z., Djanuzakova, R.D. *Manufacturing Technology*, **2019**, 19(3), 359-365. DOI: 10.21062/ujep/296.2019/a/1213-2489/mt/19/3/359.
 7. Babushkin, V.I., Ratinova, V.G. *Physico-chemical processes of corrosion of concrete and reinforced concrete*. Moscow: Stroyizdat, **1968**.
 8. Calvo, W.A., Pena, P., Tomba Martinez, A.G. *Ceramics International*, **2019**, 45(1), 185-196.
 9. Cano, Z. P., Danaie, M., Kish, J. R., McDermid, J. R., Botton, G. A., Williams, G. *Corrosion*, **2015**, 71(2), 146-159.
 10. Danyushevsky, V.S., Aliev, R.M., Tolstykh, I.F. *A reference guide for grouting materials*. Moscow: Nedra, **1987**.
 11. Elsayed, M., Nehdi, M.L., Provost-Smith, D.J., Eissa, O.S. *Construction and Building Materials*, **2018**, 183, 311-324.
 12. Hou, J., Li, H., Liu, L. *Environmental Earth Sciences*, **2018**, 77(18), 636
 13. Illampas, R., Silva, R. A., Charmpis, D. C., Lourenço, P. B., Ioannou, I. *RILEM Bookseries*, **2019**, 18, 1548-1556.
 14. Junxiang, Z., Bo, L., Yuning, S. *International Journal of Mining Science and Technology*, **2018**, 28(3), 505-512.
 15. Karabalina, U.S., Tankibaeva, M.A. (Ed.). *Technology for drilling subsalt wells in the Caspian basin*. Moscow: Nedra, **1989**.
 16. Khatami, H., O'Kelly, B.C. *Construction and Building Materials*, **2018**, 192, 202-209.
 17. Kind, V.V. *Corrosion of cements and concrete in hydraulic structures*. Moscow: Gosenergoizdat, **1955**.
 18. Kravets, S.G., Kritsuk A.A., Matveeva A.M. *Drilling of deep wells in pre-salt and salt deposits*. Moscow: Nedra, **1979**.
 19. Kravtsov, V.M., Kuznetsov, Yu.S., Mavlyutov, M.R., Agzamov, F.A. *Fastening of high temperature wells in corrosive environments*. Moscow: Nedra, **1987**.
 20. Kujur, M. K., Roy, I., Kumar, K., Chintaiah, P., Ghosh, S., Ghosh, N.K. *Materials Today: Proceedings*, **2018**, 5(1), 2359-2366.
 21. Le, H., Sun, S. *Yantu Lixue/Rock and Soil Mechanics*, **2018**, 39, 211-219.
 22. Lee, J., Lee, T. *Materials*, **2019**, 12(22), Article number 3664
 23. Liu, J., Li, Y., Zhang, G., Liu, Y. *Construction and Building Materials*, **2019a**, 227, Article number 116654
 24. Liu, W. *Nature Environment and Pollution Technology*, **2019**, 18(5), 1683-1689.
 25. Liu, Y., Wang, Y., Fang, G., Alrefaei, Y., Dong, B., Xing, F. *Construction and Building Materials*, **2018**, 170, 418-423.
 26. Liu, Z., Yu, J., Yuan, L. *Journal of Materials Science*, **2019b**, 54(1), 265-273.
 27. Maksutov, R.A., Yusupov, I.G., Zagirov, M.M., Akhmetov, Z.M. *Researchers to Production*, **1970**, 7, 40-47.
 28. Moskvina, V.M., Ivanov, F.M., Alekseev, S.N., Guzeev, E.A. *Corrosion of concrete and reinforced concrete. Methods of their protection*. Moscow: Stroyizdat, **1980**.
 29. Mukhin, L.K., Anopin, A.G., Leonidova, A.I. *Drilling*, **1976**, 1, 24-26.
 30. Nikolopoulou, V., Adami, C.-E., Karagiannaki, D., Vintzileou, E., Miltiadou-Fezans, A. *International Journal of Architectural Heritage*, **2019**, 13(5), 663-678.
 31. Orynbayev, S., Amanbayev E., Alimbayev B., Manapbayev B., Beglerova S., Myktybekov B. *News of the National Academy of Sciences of the Republic of Kazakhstan. Series of Geology and Technical Sciences*, **2019**, 4(436), 213-221. DOI: 10.32014/2019.2518-170X.116.
 32. Palilu, J. M., Soegijono, B., Marbun, B. T. H. *Journal of Physics: Conference Series*, **2019**, 1245(1), Article number 012036.
 33. Rakhimbayev, Sh.M. *Concrete and Reinforced Concrete*, **2012**, 6, 16-17.

34. Rakhimbayev, Sh.M., Karpacheva, E.N., Tolypina, N.M. *Concrete and reinforced concrete*, **2012**, 5, 25-26.
35. Rakhimbayev, Sh.M., Tolypina, N.M. *Improving the corrosion resistance of concrete by a rational choice of binder and aggregates*. Belgorod: Izdatelstvo BGTU, **2015**.
36. Samsykin, A.V., Yarmukhametov, I.I., Trofimov, V. E., Agzamov, F. A. *Neftyanoe Khozyaystvo - Oil Industry*, **2019**, 2019(12), 115-117.
37. Shahraki, A., Ghasemi-kahrizsangi, S., Nemati, A. *Materials Chemistry and Physics*, **2017**, 198, 354-359.
38. Sögaard, C., Funehag, J., Abbas, Z. *Nano Convergence*, **2018**, 5(1), Article number 6
39. Song, G., Wang, L., Zhang, Y., Cao, Y., Guo, Y. *Jianzhu Cailiao Xuebao/Journal of Building Materials*, **2018**, 21(4), 529-535.
40. Thomas, S., Medhekar, N. V., Frankel, G. S., Birbilis, N. *Current Opinion in Solid State and Materials Science*, **2015**, 19(2), 85-94
41. Tolkachev, G.M., Galkin, V.I., Kozlov, A.S. *Geology, Geophysics and Oil and Gas Field Development*, **2010**, 12, 34-41.
42. Tolkachev, G.M., Kozlov, A.S., Devyatkin, D.A.. *Bulletin of Perm National Research Polytechnic University. Geology, Oil and Gas and Mining*, **2013**, 9, 49-56.
43. Trupak, N.G. *Cementation of fractured rocks in mining*. Moscow: Metallurgizdat, **1956**.
44. Wang, P., Gong, Z. Y., Hu, J., Pu, J., Cao, W. *J. Surface Engineering*, **2019**, 35(7), 627-634.
45. Wu, X., Zhang, X. *Jianzhu Jiegou Xuebao/Journal of Building Structures*, **2018**, 39(10), 156-163.
46. Xu, Y., Li, Y., Yang, J., Sang, S., Wang, Q. *Metallurgical and Materials Transactions B: Process Metallurgy and Materials Processing Science*, **2017a**, 48(3), 1763-1770.
47. Xu, Y., Li, Y., Yang, J., Sang, S., Wang, Q. *Journal of Alloys and Compounds*, **2017b**, 723, 64-69.
48. Zagirov, M.M. *Works of TatNIPIneft*, **1982**, 50, 10-20.
49. Zaitsev, A. I., Karamysheva, N. A., Nikonov, S. V., Koldaev, A. V., Kazankov, A. Y. *Metallurgist*, **2016**, 59(9-10), 931-940.
50. Zhang, C., Yang, J., Fu, J., Ou, X., Xie, Y., Liang, X. *Journal of Materials in Civil Engineering*, **2019**, 31(7), Article number 06019003
51. Zhang, M., Liu, X., Biswas, K., Warner, J. *Applied Thermal Engineering*, **2019**, 162, Article number 114297
52. Zhuravlev, V.S. *Comparative tectonics of the Pechersk, Caspian, North Sea exagonal depressions of the European Platform*. Moscow: Nauka, **1972**.
53. Zou, L., Håkansson, U., Cvetkovic, V. *International Journal of Rock Mechanics and Mining Sciences*, **2018**, 106, 243-249.

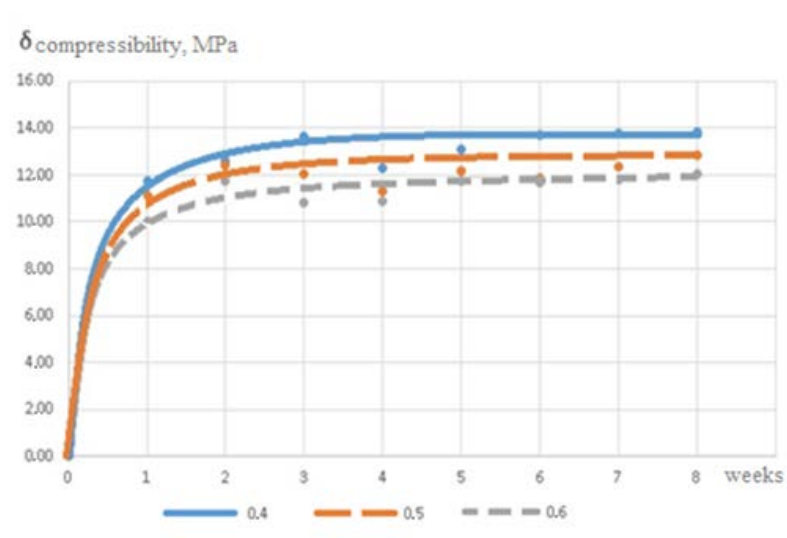


Figure 1. Influences of W/C on cement stone strength in an environment of $MgCl_2$

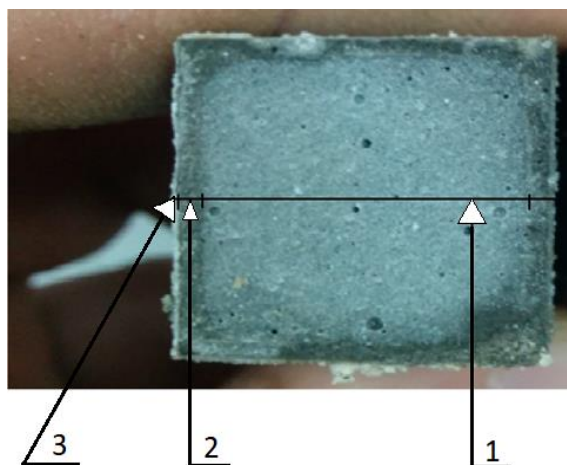


Figure 2. A sample of cement stone after 14 days in a medium of magnesium chloride. 1 – non-corroded part; 2 – corrosion zone; 3 – precipitate of magnesium hydroxide on the surface of the sample

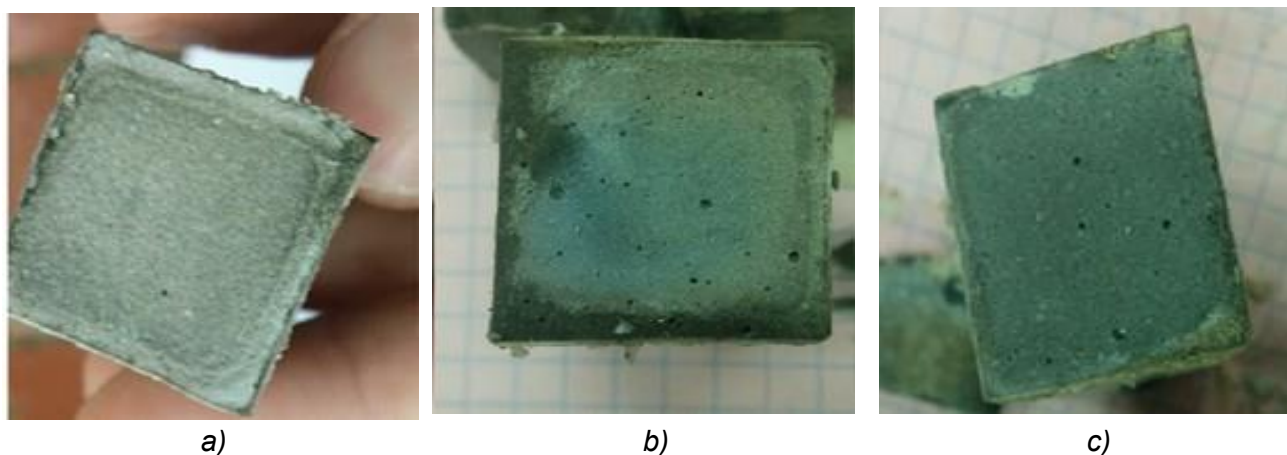


Figure 3. Samples of cement stone after 28 days in an aggressive environment
a – $W/C = 0.6$; b – $W/C = 0.5$; c – $W/C = 0.4$

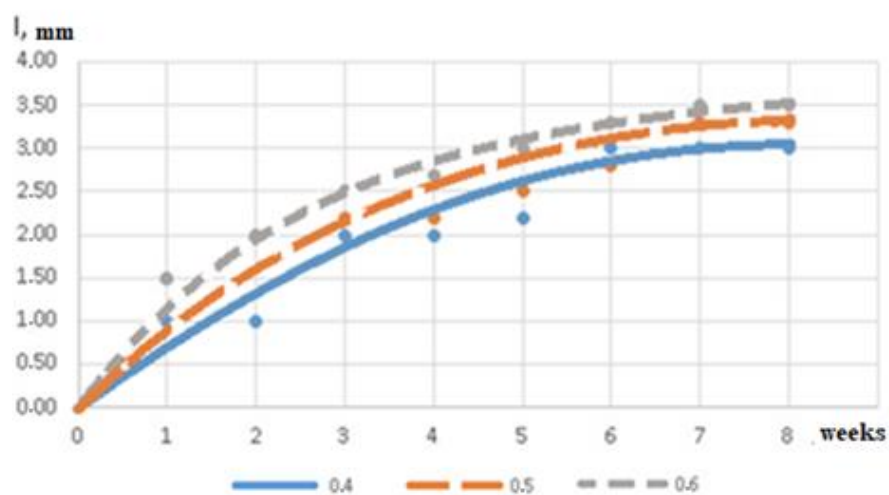


Figure 4. The effects of W/C on the depth of corrosion of cement stone in a medium of $MgCl_2$

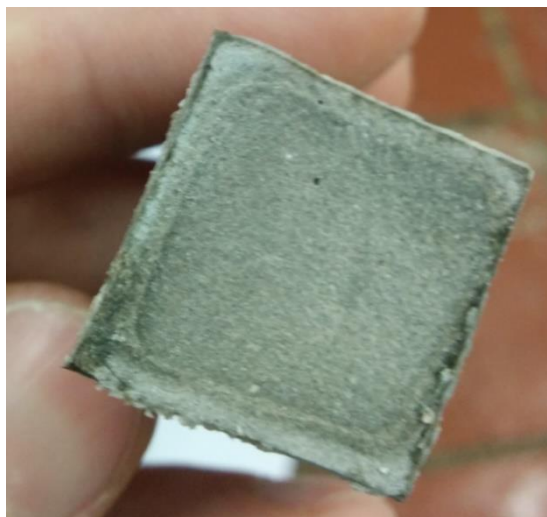


Figure 5. Corrosion of Portland cement with palygorskite

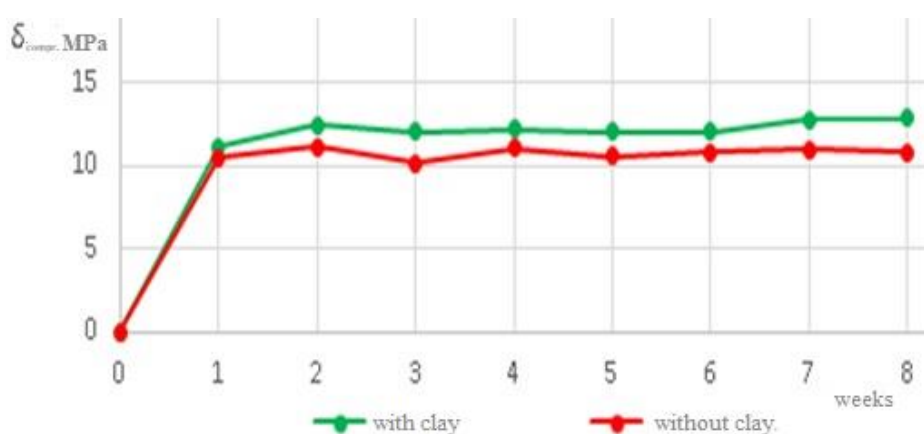


Figure 6. Effect of palygorskite additive on the strength of Portland cement stone in MgCl_2

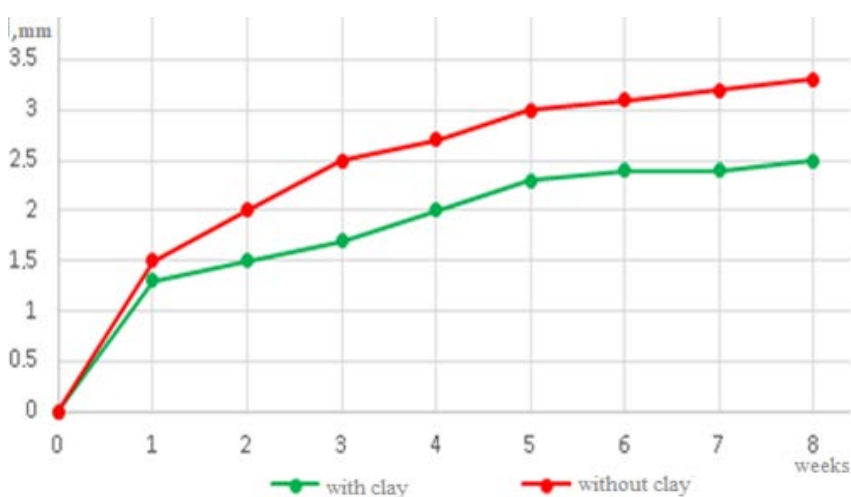


Figure 7. The effect of palygorskite additive on the corrosion depth of Portland cement stone in MgCl_2



Figure 8. Crystal formation of magnesium chloride on a stone surface

Table 1. The results of quantitative X-ray phase analysis

Zone	Formula	Name of compound	%
Non-corroded layer	C ₃ S	monoclinic (NISHI)	47.21
	C ₂ S (sum α , β , γ)	dicalcium silicate	14.59
	C ₄ AF	tetracalcium aluminaferrite	12.67
	C ₃ A _{cubic}	tricalcium aluminate	2.22
	Ca(OH) ₂	portlandite	2.18
	C ₃ S ₃ H	xonolite	7.66
	C ₅ S ₆ H ₅	tobermorite	7.4
	MgCO ₃	magnesite	6.02
Corroded layer	C ₃ S	monoclinic (NISHI)	7.17
	C ₂ S (sum α , β , γ)	dicalcium silicate	11.46
	C ₄ AF	tetracalcium aluminaferrite	7.32
	C ₃ A _{cubic}	tricalcium aluminate	1.2
	C ₁₂ A ₇	mayenite	2.69
	Ca(OH) ₂	portlandite	2.01
	C ₅ S ₆ H ₅	tobermorite	19.54
	C ₃ S ₃ H	rosenhahnite	17.75
	C ₆ S ₃ H	gammaDellaite	12.65
	(Mg,Fe) ₂ Al ₄ Si ₅ O ₁₈	cordierite	9.49
	C ₂ AS	gehlenite	4.57
	SiO ₂	quartz	0.44
	MgCO ₃	magnesite	3.05
	CaCO ₃	vaterite	1.1
	C ₃ S	monoclinic (NISHI)	1.24
	C ₃ A _{cubic}	tricalcium aluminate	0.29
Precipitation	C ₄ AF	tetracalcium aluminaferrite	0.84
	C ₃ ACs ₃ H ₃₁	ettringite	1.71
	Mg(OH) ₂	brucite	54.70
	SiO ₂	silicaLeBail	29.01
	Al(OH) ₃	nordstrandite	8.63
	CaCO ₃	calcite	3.58
	MgO	periclase	0.19

Publication Ethics

Dear readers. We are sorry for the inconvenience, but this manuscript was selected for additional review.

This manuscript may or may not return in a future issue of the journal.

The editorial team is continuously improving the publication practices to ensure fair publication opportunities to all.

The editors are grateful for the understanding of this situation.

Editors.

AVALIAÇÃO DO ESTADO DAS PLANTAS VERDES SOB AS CONDIÇÕES DE URBANIZAÇÃO

EVALUATION OF THE STATE OF GREEN PLANTS UNDER THE CONDITIONS OF URBANIZATION

ОЦЕНКА СОСТОЯНИЯ ЗЕЛЁНЫХ НАСАЖДЕНИЙ В УСЛОВИЯХ УРБАНИЗАЦИИ

AVDEEV, Yuri Mikhailovich^{1*}; GOROVY, Sergey Alekseevich²; KARPENKO, Elena³;
KUDRYAVTSEV, Valery^{4*}; KOZLOVSKY, Lydia⁵;

¹ Vologda State University, Vologda, Russian Federation

² Kuban State Agrarian University named after I.T. Trubilin, Krasnodar, Russian Federation

³ Plekhanov Russian University of Economics, Russian Federation

^{4,5} K.G. Razumovsky Moscow State University of technologies and management, Russian Federation

* Correspondence author
e-mail: avdeevyur@yandex.ru

Received 18 February 2020; received in revised form 29 February 2020; accepted 14 March 2020

RESUMO

A formação de um ambiente urbano ecológico é uma tendência do tempo atual. É necessário solucionar os problemas do paisagismo das cidades, pois, na atual fase, observa-se a deterioração do estado dos espaços verdes e a diminuição da área que eles ocupam. O artigo apresenta dados sobre o estado da vegetação arbórea no maior parque de Vologda (região de Vologda, Rússia). De acordo com os resultados da avaliação dendrométrica no Mira Park, foi revelado o número de tipos de desvantagens em cada espécie de árvore em um determinado diâmetro do tronco. Vale a pena notar que os tipos mais comuns de inconvenientes em tílias no Mira Park são danos mecânicos e fissuras por geada. A investigação foi realizada com base no "Procedimento de levantamento de inventário para plantações urbanas". Na maioria das vezes, os inconvenientes da madeira nessa espécie ocorrem nos diâmetros do tronco na faixa de 40 a 52 cm. Com base na avaliação bioecológica realizada no Mira Park, pode-se afirmar que o maior percentual de bom estado de saúde das árvores foi encontrado no pinheiro - 67,3%, o maior percentual satisfatório de estado de saúde das árvores foi encontrado no olmo - 35,7% e o maior percentual de péssimo estado de saúde das árvores foi encontrado no carvalho - 16,1%. De acordo com os resultados da investigação, pode-se dizer que a maioria das plantas arbóreas está em boas e satisfatórias condições. A maior porcentagem de problemas de saúde foi encontrada em espécies de árvores como carvalho e álamo. Basicamente, existem falhas comuns nas plantações de árvores como danos mecânicos, uma fenda congelada e um tronco curvo. A situação atual no maior parque da cidade de Vologda é estável. No entanto, para melhorar a condição sistemática, é necessário realizar uma série de atividades que devem preservar e diversificar as plantações de árvores e arbustos, além de ajudar a resolver problemas existentes.

Palavras-chave: *ecologia urbana, poluição, plantações urbanas verdes, espécies arbóreas, biodiversidade*

ABSTRACT

The formation of an urban ecological environment is a local trend of the current time. It is necessary to solve the problems of city landscaping since, at the present stage, the deterioration of the state of green spaces and a decrease in the area that they occupy are observed. The article presents data on the state of tree vegetation in the largest park in Vologda (Vologda Region, Russia). According to the dendrometric assessment results in Mira Park, the number of drawback types in each tree species at a specific diameter of the trunk was revealed. It is worth noting that the most common types of drawbacks in linden trees in Mira Park are mechanical damage and frost cleft. The investigation was carried out based on the "Inventory Survey Procedure for Urban Plantations." Most often, wood drawbacks in this species occur on the trunk diameters in the range from 40 to 52 cm. Based on the bioecological assessment performed in Mira Park, it can be stated that the highest percentage of good tree health status was found in pine – 67.3%, the highest percentage of satisfactory tree health status was found in

elm – 35.7% and the highest percentage of poor tree health status was found in oak – 16.1%. According to the results of the investigation, it can be said that most of the tree plants are in good and satisfactory condition. The highest percentage of poor health status was found in tree species such as oak and poplar. There are such common flaws on tree plantations as mechanical damage, a frozen slot, and a curved trunk. The current situation in the biggest park in the city of Vologda is stable. However, to improve the systematic condition, it is necessary to hold some activities that should preserve and diversify the tree and shrub plantations, as well as help to solve existing problems.

Keywords: *urban ecology, pollution, green urban plantations, tree species, biodiversity*

АННОТАЦИЯ

Формирование экологической городской среды является актуальной тенденцией современности. Необходимо решить проблемы городского благоустройства, поскольку на современном этапе наблюдается ухудшение состояния зеленых насаждений и уменьшение площади, которую они занимают. В статье приводятся данные о состоянии древесной растительности крупнейшего парка г. Вологды (Вологодская область, Россия). По итогам проведения дендрометрической оценки в парке Мира выявлено количество видов пороков у каждой древесной породы на определённом диаметре ствола. Стоит отметить, что наиболее встречающиеся виды пороков у липы в парке Мира – это механическое повреждение и морозобоинная трещина. Чаще всего пороки древесины у данной породы встречаются на диаметрах ствола в интервале от 40 до 52 см. Исследование проводилось на основе «Процедуры инвентаризации городских плантаций». На основании проведения биоэкологической оценки, выполненной в парке Мира, можно констатировать, что наибольший балл хорошего санитарного состояния деревьев был выявлен у сосны – 67,3 %, наибольший процент удовлетворительного санитарного состояния деревьев был выявлен у вяза – 35,7 %, наибольший балл плохого санитарного состояния деревьев был выявлен у дуба – 16,1 %. По результатам проведения исследований можно сказать, что большая часть древесных растений находится в хорошем и удовлетворительном состоянии. В основном встречаются такие распространенные недостатки на плантациях деревьев, как механические повреждения, замерзшая щель и изогнутый ствол. Текущая ситуация в самом большом парке города Вологды является устойчивой. Однако, для улучшения общего состояния необходимо выполнять ряд мероприятий, которые должны сохранить и разнообразить древесно-кустарниковые насаждения, а также помочь в решении существующих проблем.

Ключевые слова: *экология города, загрязнение, зелёные городские насаждения, древесные породы, биоразнообразие*

1. INTRODUCTION:

The urban environment is a complex of natural, human-made, and socio-economic factors, which are a radical means of improving the ecology of the city and the human environment. On the lands of settlements, green spaces perform many functions that contribute to the formation of stable conditions for the optimal life of the townspeople (Yu *et al.*, 2019). Green urban plantings are not only the most important element of greening the urban environment, but also a severe urban planning, architectural, planning, and social factor (Voronkova *et al.*, 2019).

A green plantation is a community of trees, shrubs, and grassland vegetation in a particular area (Avdeev *et al.*, 2018; Khamitova *et al.*, 2017a, b; Wang *et al.*, 2018). In urban land, green plantations perform many functions that contribute to the formation of acceptable conditions for various activities of citizens (Pozdnyakov, 2017; Landis and Leopold, 2014).

The urban environment is a system of natural, anthropogenic, and socio-economic factors that can severely affect city residents (Naliukhin *et al.*, 2018a,b; Kozlov *et al.*, 2018). It can be represented as a complex of material and spiritual areas that includes the city itself and has specific features of internal configuration and development (Lomova *et al.*, 2019; Kosenchuk *et al.*, 2019; Hu *et al.*, 2017).

Investigation objective is to assess the state of green plantations by the example of the Vologda city park and make recommendations for improving their territories. To implement the specified objective, the following assignments were set: to analyze the state of tree species in the parks of the city of Vologda; to choose and describe the objects of investigation; to find out the quantitative and percentage distribution of tree species; to identify common tree drawbacks; to offer recommendations for improving the park's territory.

2. MATERIALS AND METHODS:

The investigation area is the city of Vologda, which is located in the North of the European part of Russia. Vologda has an area of 116 square km. The city is situated on both banks of the Vologda River. Urban climate can be called moderately continental, as it is formed in the conditions of a small amount of solar radiation and a strong influence of the Northern seas. Weather in Vologda is unstable: many thaws happen in winter, low temperatures, and temperature differences are observed in spring. Winter in Vologda lasts a long time and is moderately cold (the general period lasts about six months). Autumn and spring in the city are quite cool, and the summer period is warm. The coldest month during the year is January, and the warmest one is July. The air pollution level in the city is quite high. Vehicle exhaust can be called the main source of pollution. Also, large enterprises such as the VologdaGorTeploset, Vologda Optical, and Mechanical Plant, Vologda Bearing Factory, etc. contribute a substantial stake to the deterioration of the urban ecology.

The investigation was carried out at the Vologda city park: Mira Park. Mira Park is the largest park in the city of Vologda. Its area has been increased several times since its creation and currently is 155 hectares (Figure 1).

Mira Park has a vibrant history. It was founded in May 1939 and was named initially as Central Park of Culture and Recreation. About two thousand residents of the city took part in the large-scale event on the construction and arrangement of the park: the citizens planted about five thousand trees and shrubs. After the end of the Great Patriotic War in 1945, Central Park was renamed into Mira Park. In the 1950s-1960s, the park was improved actively. The species composition of plantings was expanded, mass plantings were performed, the park area was planned, and a beach on the bank of the Vologda River was opened.

Today, Mira Park is one of the most visited places. It can be called a favorite recreation place of Vologda residents both in summer and winter. However, the park is of great value not only as a place of leisure and recreation but also as the largest nature reserve of the plant world, with the possibility of penetration of its particular species into the urban environment. Its diversity and originality distinguish the park's flora. In addition to the species that were cultivated by humans, a large number of natural vegetation representatives may be found as well. Mira Park is a complex of

urban phytocenoses and small areas of natural phytocenoses that are presented in the park territory. Rare and exciting specimens of tree, shrub, and grassland vegetation can be found in the park.

The investigation was carried out based on the "Inventory Survey Procedure for Urban Plantations" (The methodology of the inventory of urban green spaces, 1997). This method describes the purposes for which the inventory survey of green plantations is carried out and reveals the procedure for conducting field works. Besides, GOST 2140-81 "Visible Wood Drawbacks. Classification, Terms and Definitions, Methods of Measurement," which describes external defects that can be identified with the naked eye was used during the work (GOST 2140-81, 2006).

During field research (perpetual inventory) at the facility, each tree species was taken into account and identified, on which the taxation diameter of the tree trunk was measured at the height of 1.3 m using a measuring fork. Each tree had a general sanitary condition on a 3-point scale and a variety of defects.

Wood drawbacks are various defects that reduce the quality of the wood structure and reduce the possibility of its use for practical purposes: defects in the wood structure, chemical stains, wood-destroying fungi, biological damage, knots, defects in the shape of the tree trunk, cracks, mechanical damages, foreign deposits, defects obtained in the process of wood machining, casting (Bukharina, 2012).

Landscape and taxation analysis was carried out in the territory of nine parks in Vologda, which included a comprehensive assessment of tree vegetation morphological indicators. In this regard, a continuous inventory survey was conducted. In each park, a dendrometric assessment was carried out, which included fixing such parameters as the specific name of the tree, the diameter of the trunk, the number of trunks on multi-stem specimens. The bioecological assessment assumed identification of the general state of the tree. At the same time, all considered specimens of trees were divided into three groups: (1) Good health status of trees is characterized by high resistance to low temperatures, the normal shape of the trunk and leaves, the correct process of flowering and fruiting, harmonious and bright color of the foliage; (2) Satisfactory health status of trees – these are trees that are characterized by weak growth, the presence of dry shoots in the crown, weak flowering and small leaf size; and (3)

Poor health status of trees – these are trees that have top drying, weak flowering or complete absence of the latter, poor leafing, poor resistance to low temperatures, the presence of various types of damages that appeared due to the activities of insect pests and diseases.

Mira Park is one of the largest and most visited urban parks; its area includes both banks of the Vologda River. During the investigation of this object, landscape and taxation analysis was carried out, which included a comprehensive assessment of tree vegetation morphological indicators. In this regard, a continuous inventory survey was carried out, and a dendrometric evaluation was performed, which included fixing such parameters as the specific name of the tree, the diameter of the trunk, the number of trunks on multi-stem specimens.

3. RESULTS AND DISCUSSION:

In total, 3,017 trees of ten species were found in Mira Park. The predominant species is linden, which makes up 38.8% of the total number of trees growing in the park. The second place is occupied by poplar, which makes up 29.2% of the total number of trees. Birch is in the third-place – 15.1%. The least common species in the park are spruce and rowan. Their percentage of the total number of trees is 1.3 and 0.4%, respectively. The total quantity and percentage distribution of tree species in Mira Park are shown in Table 1.

According to the dendrometric assessment results in Mira Park, the number of drawback types in each tree species at a specific diameter of the trunk was revealed (Marfenin, 2006). The results for each tree species are presented in tables. It is worth noting that the most common types of drawbacks in linden trees in Mira Park are mechanical damage and frost cleft. Most often, wood drawbacks in this species occur on the trunk diameters in the range from 40 to 52 cm.

It can be said that the most common types of drawbacks in poplar trees in Mira Park are a frost cleft and a crooked trunk. Most often, wood drawbacks in this species occur on the trunk diameters in the range from 44 to 52 cm. It should be emphasized that the most common types of disadvantages in birch trees in Mira Park are mechanical damages and frost cleft. Most often, wood drawbacks in this species occur on the trunk diameters in the range from 44 to 48 cm and from 51 and 54 cm.

It is worth noting that the most common types of drawbacks in oak trees in Mira Park are

frost cleft and mechanical damages. Most often, wood drawbacks in this species occur on the trunk diameters in the range from 48 to 51 cm. It can be said that the most common types of cons in larch trees in Mira Park are mechanical damages and a crooked trunk. Most often, wood drawbacks in this species occur on the trunk diameters in the range from 48 to 50 cm. It should be emphasized that the most common types of disadvantages in ash trees in Mira Park are a crooked trunk and mechanical damages. Most often, wood drawbacks in this species occur on the trunk diameters in the range from 45 to 48 cm.

It is worth noting that the most common types of drawbacks in elm trees in Mira Park are mechanical damage and burr. Most often, wood drawbacks in this species occur on the trunk diameters in the range of 46-47 cm. It can be said that the most common types of cons in pine trees in Mira Park are mechanical damages and frost cleft. Most often, wood drawbacks in this species occur on the trunk diameters in the range of 48-49 cm.

It should be emphasized that the most common types of drawbacks in spruce trees in Mira Park are mechanical damages and burr. Most often, wood drawbacks in this species occur on the trunk with a size of 43, 47, and 48 cm. It is worth noting that the most common type of drawbacks in rowan trees in Mira Park is the frost cleft. Most often, wood drawbacks in this species occur on the trunk diameter of 45 cm.

Also, a bioecological assessment was carried out as a part of the investigation, i.e., the general condition was found out for each tree species. All considered specimens of trees were divided into three groups: 1. Good condition – flowering and fruiting of the tree are normal, there is a bright color of the leaves, the tree has high winter hardiness, dry branches are completely absent, the presence of drawbacks was not detected; 2. Satisfactory condition – minor drawbacks in the trees, a small number of dry branches, a lag in the growth of trees are observed; 3. Poor condition – the trees have significant drawbacks, the presence of strong dryness, noticeable damages caused by harmful insects and diseases, weak resistance of the tree to low temperatures. The quantitative and percentage ratio of the health status of all wood species in Mira Park is shown in Table 2.

Based on the bioecological assessment performed in Mira Park, it can be concluded that the highest percentage of good tree health status was found in pine – 67.3%, the highest percentage

of satisfactory tree health status was found in elm – 35.7% and the highest percentage of poor tree health status was found in oak – 16.1%.

In current conditions, green plantations are an integral part of the city's structure and perform many essential functions. Green plantations have the ability to affect the ecology of the urban environment positively, so they should be created in places where people live and work. The fact that the city should be a biocenosis that is not entirely favorable, but at least does not cause harm to people's health has great importance. The organization of parks is one of the solutions to the problem of improving the environmental situation of urban areas (Voronkova *et al.*, 2019). Green plantations are directly involved in creating favorable microclimatic and sanitary and hygiene conditions, and also increase the artistic expressiveness of architectural ensembles (Tetior, 2013).

Parks in urban areas contribute to solving various problems related to environmental sustainability. The primary important function of green urban plantations is to reduce air pollution in the city (Sokolov *et al.*, 2017). Green plantations are an effective means of noise control because tree stands with dense crowns, dense foliage, and a large number of small branches can reduce the noise level significantly. Parks are involved in reducing the dust and gas content of the air, reducing the harmful concentration of gases that are in it (Betancurt *et al.*, 2017; Ferrini *et al.*, 2014). The impact of green plantations located in the park on reducing the concentration of gases in the air is caused by the density of their plantings. The formation of parks with line plantings of woody vegetation, which reach a width of up to 50.0 m, and a height of 15.0 ... 20.0 m, respectively, reduces the pollution of the air basin by 70.0 ... 75.0%.

According to the results of the investigation, it can be said that most of the tree plants are in good and satisfactory condition. The most common species are linden, birch, poplar, and elm. The highest percentage of poor health status was found in tree species such as oak and poplar. The most common types of drawbacks in tree plantations are mechanical damage, frost cleft, and a crooked trunk. Thus, it can be concluded that the current situation in the largest park in the city of Vologda is stable. However, to improve the systematic condition, it is necessary to hold some activities that should preserve and diversify the tree and shrub plantations, as well as help to solve existing problems.

First, plantings need care to improve their quality and create favorable conditions for growth and development. It is necessary to remove shrunk, dry-top, stunted, diseased trees, besides, those species that do not represent decorative value. Second, when treating trees with dry-top shoots, it is necessary to remove the tops and dry branches, and for damaged trees, it is needed to disinfect injuries with a 5.0% solution of copper sulfate. In the place of cuts, the wound should be covered with tree-wound paint (garden putty). In addition, it is necessary to make a complex of organic and mineral fertilizers in the soil under the trees, loosening the soil, sowing perennial grass stands, forming artificial places for nesting birds, feeders, etc. The above-mentioned measures will help to restore and improve the state of the grass cover, as well as its decorative parameters, the appearance of self-seeding of tree species, and increase the growth of woody plants. Third, great attention should be paid to preventive measures, which should consist of regular monitoring of the number of trees of different types and insect pests that should be treated with biological products.

Together with forestry and silvicultural measures, an active agitation campaign should be carried out to protect green plantations from fires, various damages of grass stand, etc. Agitation tools such as periodicals, television and radio broadcasts, and posters should be used. To increase the decorative value of tree plantations, it is necessary to increase biodiversity by introducing new tree species, create flower beds, shrubberies, and lawn coverings that differ in a variety of shapes and colors.

4. CONCLUSIONS:

1. Green plantations are of great importance for preserving and improving the favorable environmental situation in modern cities. They perform many essential functions that help in creating the best microclimatic and hygiene and sanitary conditions for the life of urban citizens. Green plantations directly affect the microclimate of modern cities, actively absorb harmful substances from the air, improve the wind regime in localities, and are important in fighting fires, snow shifts, and soil erosion.
2. Urban parks are the most important components of the general structure of landscaping the city's territories, which perform recreational, architectural, artistic, and other significant functions. Today, urban parks are not only a natural area of urban

space but also a unique territory for communication, a place for outdoor sports, and an area where interesting entertainment events would be held. The main purpose of green urban plantations is to form a recreation for citizens.

3. A large number of trees with poor conditions were found in Mira Park, which has the most significant area among all parks. The most common types of tree drawbacks in this park were frost cleft and mechanical damage, and the highest percentage of poor tree health status in Mira Park was found in oak.

6. REFERENCES:

1. Avdeev Y.M., Hamitova S.M., Kostin A.E., Lukashevich V.M., Lukashevich M.V., Kozlov A.V., Uromova I.P., Trushkova M.A., Davydova Y.Y., Kuzletsov V.A. (2018). Assessing the Properties of Tree Trunks in Forest Phytocenoses Depending on the Soil and the Climatic Conditions on the Territory of the Taiga Zone of the European North of Russia. *Journal of Pharmaceutical Sciences and Research*. Vol. 10. № 5, P. 1288-1291
2. Betancurt, R., Rovere, A. E., & Ladio, A. H. (2017). Incipient domestication processes in multicultural contexts: A case study of urban parks in san carlos de bariloche (argentina). *Frontiers in Ecology and Evolution*, 5(DEC) doi:10.3389/fevo.2017.00166
3. Bukharina, I. L. (2012). Urban plantings: ecological aspect. Udmurt University. 206 p.
4. Ferrini, F., Bussotti, F., Tattini, M., & Fini, A. (2014). Trees in the urban environment: Response mechanisms and benefits for the ecosystem should guide plant selection for future plantings. *Agrochimica*, 58(3), 234-246. doi:10.12871/0021857201432
5. GOST 2140-81 (2006). Visible wood defects. Classification, terms and definitions, measurement methods; enter 01/01/81. - Moscow: Standartinform, 96 p.
6. Hu, Y., Vincent, G., & Chen, X. (2017). How can botanical gardens support sustainable urban development? a case study of shanghai chenshan botanical garden. *Annals of the Missouri Botanical Garden*, 102(2), 303-308. doi:10.3417/D-16-00003A
7. Khamitova S.M., Glinushkin A.P., Avdeev Yu.M., Naliukhin A.N., Beliy A.V., Zavarin D.A., Snetilova V.S., Lebedeva M.A., Danilova E.D., Semykin V.A., Pigorev I.Ya., Lichukov S.D. (2017a). Assessment of microorganisms and heavy metals' content in the soils of arboretum named after Nikolai Klyuev. *International Journal of Pharmaceutical Research and Allied Sciences*. Vol. 6. - № 3. - P. 47-55
8. Khamitova S.M., Glinushkin A.P., Avdeev Yu.M., Naliukhin A.N., Kostin A.E., Kozlov A.V., Uromova I.P., Rudakov V.O., Tesalovskiy A.A., Protopopova E.V., Pigorev I.Y., Polukhin A.A., Sycheva I.I. (2017b). Condition assessment of tree plantations and phytosanitary properties of soils in cedar groves. *International Journal of Pharmaceutical Research and Allied Sciences*. - 2017. Vol. 6. - № 4. - P. 1-7
9. Kosenchuk, O., Shumakova, O., Zinich, A., Shelkovnikov, S., & Poltarykhin, A. (2019). The development of agriculture in agricultural areas of siberia: Multifunctional character, environmental aspects. *Journal of Environmental Management and Tourism*, 10(5), 991-1001. doi:10.14505/jemt.v10.5(37).06
10. Kozlov A.V., Uromova I.P., Koposova N.N., Novik I.R., Vershinina I.V., Avdeev Y.M., Hamitova S.M., Naliukhin A.N., Kostin A.E., Mokretsov Y.V. (2018). Optimization of the Productivity of Agricultural Crops at Application of Natural Minerals as Ameliorants and Mineral Fertilizers on Sod-Podzolic Soils. *Journal of Pharmaceutical Sciences and Research*. Vol. 10. № 3. P.667-680
11. Landis, C. L., & Leopold, D. J. (2014). Natural plant establishment along an urban stream, onondaga creek, new york. *Northeastern Naturalist*, 21(2), 303-322. doi:10.1656/045.021.0211
12. Lomova, L. A., Voronkova, O. Y., Aleshko, R. A., Goneev, I. A., Avdeev, Y., & Sochnikova, I. Y. (2019). Ecological and economic consequences of water pollution. *International Journal of Engineering and Advanced Technology*, 9(1), 7056-7062. doi:10.35940/ijeat.A1925.109119
13. Marfenin, N. N. (2006). Sustainable development of mankind: a textbook. Moscow: Publishing House of Moscow

14. Naliukhin A.N., Glinushkin A.P., Khamitova S.M., Avdeev Yu.M. **(2018a)**. The influence of biomodified fertilizers on the productivity of crops and biological properties of soddy-podzolic soils. *Entomology and Applied Science Letters*. 2018. Vol. 5. № 3. Pp. 1-7
15. Naliukhin A.N., Khamitova S.M., Glinushkin A.P., Avdeev Yu.M., Snetilova V.S., Laktionov Yu.V., Surov V.V., Siluyanov O.V., Belozarov D.A. **(2018b)**. Change in the metagenome of the prokaryotic community as an indicator of the fertility of arable sod-podzolic soils with the use of fertilizers. *Soil Science*. No. 3. P. 331-337.
16. Pozdnyakov, A. **(2017)**. Ecological and economic aspects of planning of urban development. *Journal of Applied Engineering Science*, 15(4), 418-421
17. Sokolov, N., Ezhov, S., & Ezhova, S. **(2017)**. Preserving the natural landscape on the construction site for sustainable ecosystem. *Journal of Applied Engineering Science*, 15(4), 518-523.
18. Tetior, A.N. **(2013)**. Ecology of the urban environment: textbook. Moscow: Publishing Center "Academy", 352 p.
19. The methodology of the inventory of urban green spaces. (1997). Moscow, 1997. 14 p.
20. Voronkova, O. Y., Iakimova, L. A., Frolova, I. I., Shafranskaya, C. I., Kamolov, S. G., & Prodanova, N. A. **(2019)**. Sustainable development of territories based on the integrated use of industry, resource and environmental potential. *International Journal of Economics and Business Administration*, 7(2), 151-163.
21. Wang, W., Zhang, B., Xiao, L., Zhou, W., Wang, H., & He, X. **(2018)**. Decoupling forest characteristics and background conditions to explain urban-rural variations of multiple microclimate regulation from urban trees. *PeerJ*, 2018(8) doi:10.7717/peerj.5450
22. Yu, W., Chen, Y., Wang, X., & Wang, X. **(2019)**. Effects of land pavement on the structure and function of soil microbial community under different tree species.

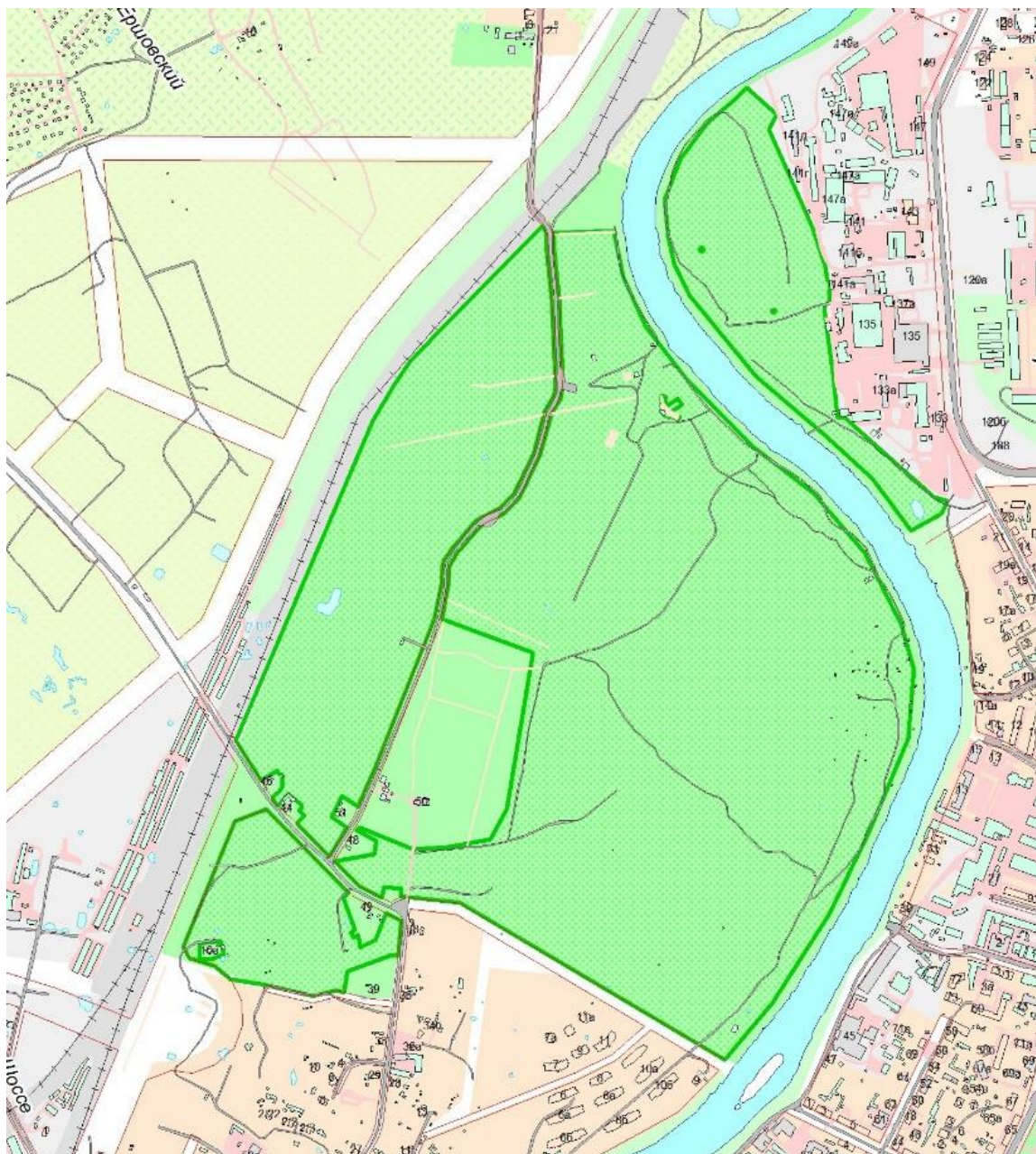


Figure 1. Plan of Mira Park in Vologda. Source <https://vologda.4geo.ru/maps/>

Table 1. Quantitative distribution of tree species in Mira Park

Specific name	The number of trees, pcs.	%
Linden	1,172	38.8
Poplar	880	29.2
Birch	455	15.1
Oak	186	6.2
Larch	92	3

Ash	77	2.6
Elm	56	1.8
Pine	49	1.6
Spruce	39	1.3
Rowan	11	0.4
Total	3,017	100

(Source: Data collected by the authors during the study)

Table 2. Quantitative ratio of health status indicators of wood species in Mira Park

Specific name	Heath status	The number of trees, pcs.	%
<i>Linden</i>	<i>Good</i>	630.0	53.8
	<i>Satisfactory</i>	367.0	31.3
	<i>Bad</i>	175.0	14.9
<i>Poplar</i>	<i>Good</i>	475.0	54
	<i>Satisfactory</i>	278.0	31.6
	<i>Bad</i>	127.0	14.4
<i>Birch</i>	<i>Good</i>	245.0	53.9
	<i>Satisfactory</i>	149.0	32.7
	<i>Bad</i>	61.0	13.4
<i>Oak</i>	<i>Good</i>	101.0	54.3
	<i>Satisfactory</i>	55.0	29.6
	<i>Bad</i>	30.0	16.1
<i>Larch</i>	<i>Good</i>	53.0	57.7
	<i>Satisfactory</i>	27.0	29.3
	<i>Bad</i>	12.0	13
<i>Ash</i>	<i>Good</i>	47.0	61
	<i>Satisfactory</i>	25.0	32.5
	<i>Bad</i>	5.0	6.5
<i>Elm</i>	<i>Good</i>	32.0	57.1
	<i>Satisfactory</i>	20.0	35.7
	<i>Bad</i>	4.0	7.2

<i>Pine</i>	<i>Good</i>	<i>33.0</i>	<i>67.3</i>
	<i>Satisfactory</i>	<i>12.0</i>	<i>24.5</i>
	<i>Bad</i>	<i>4.0</i>	<i>8.2</i>
<i>Spruce</i>	<i>Good</i>	<i>24.0</i>	<i>62.6</i>
	<i>Satisfactory</i>	<i>13.0</i>	<i>33.3</i>
	<i>Bad</i>	<i>2.0</i>	<i>5.1</i>
<i>Rowan</i>	<i>Good</i>	<i>7.0</i>	<i>63.6</i>
	<i>Satisfactory</i>	<i>3.0</i>	<i>27.3</i>
	<i>Bad</i>	<i>1.0</i>	<i>9.1</i>

(Source: Data collected by the authors during the study)

REDUÇÃO DAS CONDIÇÕES DEFEITUOSAS DE OPERAÇÃO DA PLANTA DE ENERGIA EÓLICA AO RESERVAR OS MODOS DE OPERAÇÃO DE ENERGIA ALTERNATIVA**REDUCTION OF DEFECTIVE CONDITIONS OF THE WIND POWER PLANT OPERATION AT RESERVING THE OPERATION MODES OF ALTERNATIVE ENERGY****СНИЖЕНИЕ ДЕФЕКТНЫХ СОСТОЯНИЙ РАБОТЫ ВЕТРОВОЙ УСТАНОВКИ ПРИ РЕЗЕРВИРОВАНИИ РЕЖИМОВ ФУНКЦИОНИРОВАНИЯ АЛЬТЕРНАТИВНОЙ ЭНЕРГЕТИКИ**

SHUYUSHBAYEVA, Nurgul N.^{1*}; SAGIMBAEVA, Shynar Zh.²; MUSSENOVA, Elmira K.³; BIZHANOVA, Karlygash B.⁴; ZHANTURINA, Nurgul N.⁵;

¹ Sh. Ualikhanov Kokshetau State University, Department of Mathematics and Physics – Republic of Kazakhstan

^{2,5} K. Zhubanov Aktobe Regional State University, Department of Physics – Republic of Kazakhstan

³ Buketov Karaganda State University, Department of Physics and Nanotechnologies – Republic of Kazakhstan

⁴ Yessenov University, Department of Natural Sciences – Republic of Kazakhstan

** Correspondence author
e-mail: nn_shuish@mail.ru*

Received 03 February 2020; received in revised form 06 March 2020; accepted 31 March 2020

RESUMO

O ritmo atual da economia global requer um aumento significativo na produção de energia. Ao mesmo tempo, as reservas de combustíveis naturais tradicionais, como gás natural e petróleo, estão sendo gradualmente esgotadas. Portanto, a energia tradicional está sendo substituída por alternativa. O desenvolvimento da tecnologia de operação dos dispositivos que garantem o funcionamento de empresas de energia alternativa baseia-se no fato de que a confiabilidade desses dispositivos deve estar no nível das usinas de energia tradicionais. Cada dispositivo deve não apenas ser tolerante a falhas, mas também fácil de manter. Geralmente, são considerados dispositivos portáteis e independentes, capazes de gerar energia sem manutenção excessiva do equipamento pelo serviço técnico. O artigo objetivou resolver o problema do uso de energia eólica em uma área remota. O principal método de pesquisa foi a análise da teoria dos gráficos. A novidade da pesquisa é determinada pelo fato de oferecer a formação de um modelo que atenda aos padrões de funcionamento no nível dos maiores modelos industriais usados em energia alternativa como um dos objetos da produção pura de energia. Uma usina de geração de energia eólica é usada como uma instalação semelhante. Foi revelado que esse problema deve ser considerado apenas desde que essa instalação produza energia em uma quantidade não inferior a uma amostra semelhante de uma fonte de energia tradicional em consumo por consumidores industriais e padrão. A importância prática do estudo é determinada pelo fato de que cada um dos tipos de instalações projetados possa operar em quase todas as condições e ter alta tolerância a falhas.

Palavras-chave: *energia, consumo, padrão, desenvolvimento, fonte de energia alternativa.*

ABSTRACT

The current pace of the global economy requires a significant increase in energy production. At the same time, the reserves of traditional natural fuels, such as natural gas and oil, are gradually being depleted. Therefore, conventional energy is being replaced by an alternative. Developing the operation technology of the devices that ensure the functioning of alternative energy enterprises is based on the fact that the reliability of such devices should be at the level of traditional power plants. Each device must be not only fault-tolerant but also easy to maintain. It is often considered to be portable and self-contained devices capable of generating energy without excessive maintenance of the equipment by the technical service. The article aimed to solve the problem of using wind energy in a remote area. The leading research method was graph theory analysis. The

novelty of the research is determined by the fact that it offers the formation of a model that will meet the standards of functioning at the level of the most significant industrial models used in alternative energy as one of the objects of pure energy production. A wind power generation plant is used as a similar facility. It was revealed that this issue should be considered only provided that such a facility will produce energy in an amount of not less than a similar sample of a traditional energy source in consumption by both industrial and standard consumers. The practical significance of the study is determined by the fact that each of the designed types of facilities can operate in almost any conditions and have high fault tolerance.

Keywords: *energy, consumption, standard, development, alternative energy source.*

АННОТАЦИЯ

Современные темпы развития мировой экономики требуют значительного увеличения производства энергии. Вместе с тем, запасы традиционных естественных видов топлива, таких как природный газ и нефть, постепенно истощаются. Поэтому на смену традиционной энергетике приходит альтернативная. Формирование технологии работы устройств, которые обеспечивают функционирование предприятий альтернативной энергетикой, основано на том, что надежность подобных устройств должна быть на уровне традиционных энергетических установок. Каждое устройство должно быть не только отказоустойчивым, но также и являться простым для обслуживания. В качестве подобного устройства зачастую рассматриваются портативные и автономные устройства, способные вырабатывать энергию без чрезмерного ухода за оборудованием со стороны технической службы. Целью статьи являлось решение задачи использования энергии ветра в отдаленном районе. Ведущим методом исследования был анализ с помощью теории графов. Новизна исследования определяется тем, что предложено формирование модели, которая будет отвечать стандартам функционирования на уровне крупнейших промышленных моделей, применяемых в альтернативной энергетике в качестве одного из объектов выработки энергии чистого типа. В качестве подобного объекта используется установка ветрового производства энергии. Было выявлено, что следует рассматривать данный вопрос только при условии того, что подобная установка будет производить энергию в количестве не меньшем чем подобный образец традиционного источника энергии в потреблении как промышленными, так и стандартными потребителями. Практическая значимость исследования определяется тем, что каждый из проектируемых видов установки может функционировать практически в любых условиях и обладать высокой отказоустойчивостью.

Ключевые слова: *энергия, потребление, стандарт, развитие, альтернативный источник энергии.*

1. INTRODUCTION:

The most common method of generating electricity for remote loads, both in areas and for special applications, is a diesel engine driving a generator set (Beinke *et al.*, 2017; Heredia *et al.*, 2018; Ballireddy and Modi, 2019). For small loads, a single diesel unit will be sufficient, but a more significant number of diesels will be needed for a larger group of consumers (Zheng *et al.*, 2015; Zhang *et al.*, 2018; Zhang *et al.*, 2019).

It is recommended to use diesel generators with a minimum load of not less than, usually, 40 percent to maintain high efficiency (efficiency), since fuel costs can be significant, which will be expensive, and to minimize machine wear (Kaiser and Snyder, 2012a; Bukar *et al.*, 2019; Rehman *et al.*, 2019). However, given that the load is continually changing and the need to match the load, in many areas, you can find diesels that have the appropriate capacity or are inefficiently used (Chakraborty, 2018). This quite often happens with diesels, for which the

operational demands are not fulfilled. However, diesel units guarantee reliability and long service life (Hau, 2013; Hong *et al.*, 2018; Chen *et al.*, 2017; Can, 2019).

Energy costs tend to be high, often many times higher than for higher-capacity networks (Grigorash *et al.*, 2014; Krasnobaev *et al.*, 2018; Obukhov *et al.*, 2018). Low efficiency is a result of the high cost of diesel fuel, including transportation costs, which are often the dominant factor, and operating and maintenance costs, as diesel systems are usually installed in remote areas. The main advantage of diesel systems is that they are highly reliable (Yang *et al.*, 2013; Sujith and Ramesh, 2017; Dai *et al.*, 2019).

The critical point is that despite the reliability of diesel-electric systems, the energy produced by them has a high cost. This ratio is unlikely to change in the future, with costs likely to rise (Miller and Keith, 2018; Finn and Sandeberg, 2019). The nature of the electrical load in remote areas is of crucial importance and

largely depends on the type of electric machine in the system (Chemekov and Kharchenko, 2013; Grigor'ev *et al.*, 2019; Grigoriev *et al.*, 2019).

Two factors are affecting the system: variability of electrical load; quality of the energy consumed, or "stability" of the network. In the first case, the total load tends to change more or less regularly throughout the day, often peaking during regular working hours and falling to a minimum early in the morning. In addition to the gradual change, there are also fluctuations of much shorter duration caused by the switching on or off powerful electrical equipment. The load can also vary significantly by day of the week or depending on the season of the year. From an economic point of view, it is necessary to know whether the annual change in wind energy potential corresponds to the change in load or there is a significant inconsistency. In the first case, the full potential of wind energy can be used (Tereshkin, 2018; Devederkin *et al.*, 2019). However, the downside of this will be the need to operate the diesel at low load. In case of incomplete compliance, there may be a situation of some advantage for individual systems, so diesel can be better loaded when the need for loads is high, although the downside may be the high cost of diesel fuel.

The second factor – "sustainability" applying – is slightly less obvious, but highly relevant. To properly feed the most potent load, the voltage and frequency of the current must be within the appropriate limits (Perzhabinsky and Karamov, 2017; Semenyutina *et al.*, 2019; Rodina, 2019). Fulfilling this condition is usually not tricky when only diesel generators are used. When other sources of energy, such as wind turbines, are added to the system, the task is more complicated. This is caused primarily by short fluctuations (of the order of seconds or minutes) in the wind speed, which causes corresponding changes in the generation of electricity from the wind energy (Nižetić *et al.*, 2017; Sabir *et al.*, 2019). The ability to account for these fluctuations is a requirement for any wind-diesel system (Essallah *et al.*, 2019; Ochoa and Martinez, 2019).

There are three areas of application of the autonomous power plant: for specialized applications in remote areas, e.g., communications, irrigation, for remote regions of industrialized countries and islands, local power plants in developing countries (Sebastián, 2017; Sivachandran, 2017).

Each has its unique requirements; for

example, the system reliability may be a more valuable property than the cost of energy for systems managed automatically (Deltenre and Runacres, 2019; Fernández-Guillamón *et al.*, 2019; Rabanal *et al.*, 2019). While consumers in industrialized areas expect high levels of energy quality, suitability, and competitiveness, ease of maintenance is a critical factor for the consumers in the countries that are in the process of development (Tsgoev, 2012; Dekkiche *et al.*, 2017; Rudenko *et al.*, 2019).

The article aimed to solve the problem of using wind energy in a remote area.

2. LITERATURE REVIEW:

To solve the problem of using wind energy in a remote area, it is necessary to compensate for the variability of the wind, which can be done with the help of a diesel generator. Such a system would take advantage of the free wind resource, saving a certain amount of fuel consumption, and would supply energy on-demand following the load of the consumer. Ideally, diesel could be used to provide a steady supply of energy in low wind, and WDPP could be used to save diesel when the wind power is sufficient (Wang and Bai, 2010).

The nature of wind energy has a significant impact on the overall efficiency, as well as on the organization of any wind-diesel system. The most significant aspect of this system is wind variability, which occurs over time, ranging from long – term changes (hourly to seasonal) to short-term turbulent fluctuations (seconds to minutes) (Morales Pedraza, 2015). Considering long-term changes, it would be desirable from an economic point of view that the wind speed in the long-term periods corresponds to the load.

While the correspondence between long-term changes in wind power and load can significantly affect the economy of the system, short fluctuations have the most significant impact on the design of the system. Most tasks with a simple combination of wind and diesel are reduced to adapting to this level of wind variability. Wind changes rapidly, leading to significant changes in the energy potential of the system (Tang *et al.*, 2017). This means that the amount of electricity that is affected by changes in a moderate time interval (such as an hour) can be much less than the average of the same range. Through the random nature of wind oscillations, reliable absolute minimum energy values can be guaranteed, although the probability of exceeding and most optimal levels

can be calculated (DeMeo and Steitz, 1990).

Since wind power is continually changing, diesel power also needs to be further modified to provide electricity to a relatively constant load. While the maximum of instantaneous wind energy is less than the load, the required level of energy can be expected from WDPP. WDPP will act as an unwanted load. Thus, in the scope of the diesel, the load will be less than the available wind energy. In addition to wind variability, the load itself can directly change over short time intervals. In much smaller systems, turning on or off any single device significantly affects their operation. When wind power exceeds the load capacity, the management of the system becomes even more complicated (Kaiser and Snyder, 2012b).

However, if the load is not always less than the energy supplied by the WDPP, the diesel should not be in the off state for a long time, because wind energy will sometimes fall to a level below the ability to provide the load. Trying to stop the diesel every time the wind power is above some level will result in having to turn the diesel on and off perhaps hundreds of times per hour. Such a strategy is not acceptable. This would lead to excessive deformation of the engine and starter motor, possibly resulting in their shorter service life (Tanasheva *et al.*, 2018). The pulse ratio could be aligned with some on and off strategy, but this would be at the expense of increased fuel consumption. In practice, the desirability of maintaining a minimum operating time also complicates the problem. It should also be noted that rapid load changes, especially in small networks, can have a similar and, at times, more severe effect than the effect of variable wind energy (Minin, 2012).

Among the autonomous power supply systems based on WDPP with asynchronous generator comprises, in addition to the facility, the control unit of generator start, battery pack with charge controller, inverter equipment, diesel-unit with a synchronous generator as a backup source, and a power matching output parameter of the system with the needs of the consumer. Depending on the production conditions, these component blocks can assemble block diagrams, working separately or in parallel to meet the needs of the consumer.

3. MATERIALS AND METHODS:

A simple method of integrating wind energy into a diesel system is to connect the WDPP to the grid in the same way as to a

massive power grid. Ideally, the operation of such a system is simple. When there is wind, the payload on the diesels is reduced and, if the wind force is strong enough, the diesel can be turned off altogether. When the desired significant fuel economy is achieved, the system should already contain additional components and control systems. It should be borne in mind that, in most cases, one of the key points is to reduce the overall cost of electricity production. Thus, the fuel economy should not be achieved at the expense of a significant increase in the value of the entire system (Conzalez-Rodriguez *et al.*, 2010).

It was analyzing the structural schemes of autonomous power supply systems based on the wind-diesel system and determine the dependence of the load intensity of the power supply channel of the consumer on the degree of its capacity. Let's consider the variants of structural schemes formed with such a set of components (Figure 1).

Such problems can be analyzed using graph theory. The algorithm of functioning of this system, as a set of dependencies, determines the necessary performance of a given process of providing energy to the consumer, we consider with the help of oriented graphs of these structures (Figure 2). The nodes of the graph are the structural components of the system. Ribs – energy flows between nodes, X1 – the flow of wind energy, X2 – the flow of traditional power (fuel), X3 – the flow of energy from batteries, Y1 – the flow of energy needs to the consumer.

The following mathematical methods were also used during the study: linear equations, Erlang equation, probability theory, theory of automatic control, Routh table, etc.

Transformation of energy flows in the system to meet the needs of the passing consumer: according to A (Equation 1), according to B (Equation 2), according to C (Equation 3). Provision of the consumer passes through two interconnected channels. The first is a wind power plant; the second is a diesel generator. In the absence of wind, the provision of the consumer is made at the expense of only the diesel generator. Channel selection, as well as the depth of correction, passes through the synchronization node 6 (Equation 4).

Providing the consumer passes through three interconnected channels: wind turbine, diesel generator, and stored energy in batteries. In the absence of wind, the consumer is only provided due to diesel-generator and

accumulator cells. In the case of discharge of batteries, and the lack of wind, the complete provision of electricity to the consumer is performed by a diesel generator. Channel selection, as well as correction depth, is carried out through the synchronization node 6. The matching coefficients of graph nodes k_1, k_2, k_3, k_4, k_5 , respectively refer to the wind power plant, diesel generator, capacitor bank, controller, storage unit, and inverter is less than 1.

4. RESULTS AND DISCUSSION:

The use of an asynchronous generator in WDPP requires constant correction of energy consumption because it is susceptible to its deficit. Therefore, there is a task of organizing feedback in an autonomous wind power system, which is to ensure the production of a control signal for the restructuring of composite systems to comply with the technological requirements of the consumer. Let's suppose that the processes in this system are linear (Equation 5). Where $z(t)$ – system input value (consumer requirements); $y(t)$ – input value of the system (power supply level); A, B, C – system component parameters.

Then, if at some point in time the state of the system is \bar{x} , and the output value will take the value \bar{y} , the system blocks must have the following parameters $\bar{A}, \bar{B}_1, \bar{B}_2$ and \bar{C} , under which the following conditions would be fulfilled $x(t) - \bar{y}(t) \rightarrow 0$ (Equation 6).

Since this system uses an asynchronous generator with a short-circuited rotor winding and a synchronous generator with permanent magnets of the diesel plant and excitation control is impossible, the feedback parameters are assumed to be single. That is, it is necessary to determine the state of the system under the following condition $x(t) - \bar{x}(t) \rightarrow 0$ (Equation 7).

This requirement is met when $\bar{B}_1 = B$ and in the real part (Equations 8-9). The stability of the system will be ensured when the parameters of the unit \bar{B}_2 (synchronizer, Figure 2) will be controlled and have the property to be observed (at any time to provide the requirements of the consumer on the load power).

Analysis of schemes a and b shows their

limitations in providing energy needs of the consumer and dependence on the presence of a certain level of wind speed. Schemes C and D are almost little dependent on fluctuations in wind energy supply over time because they have an additional source of power supply (diesel generator) and can increase the fill factor of the load graph of the consumer almost to 1.

Relative throughput Q of the system for a single channel system is as follows (Equation 10). Where λ – the intensity of the flow of consumer demand (applications); μ – the power of the flow of wind energy (maintenance). The organization of two-channel and three-channel systems will increase the degree of security of the consumer. According to the Erlang's equation for a two-channel system with failures (Equation 11) and a three-channel system with failures (Equation 12). At $Q = 50\%$, $\rho = 1$, i. e. the intensity of the flow of service and requests is equalized. Compared to a dual channel system, the relative throughput of the system provided $\rho = 1$ is less by 30%.

Figure 3 shows the dependence of (Equation 13) for single- two- and three-channel system. The latter has an advantage over the former since the application execution devices work with less intensity. The probability that the consumer is provided from one unit will be (Equation 14). From two blocks at once (Equation 15), from three blocks (Equation 16). That is, the probability of simultaneous operation of three sources at the same load level has a smaller value than two and one source (Figure 4).

The WDPP used in stand-alone operation consists of two sources of electrical energy: a diesel generator and a wind power plant. The power of the diesel generator can be changed during the process of the plant, depending on the needs of the consumer and on the arrival of wind. The power of the wind power plant is entirely uncontrolled since it depends on the wind speed. As a rule, a wind-diesel system is built according to the following scheme: a wind turbine rotor (with or without a speed controller), an electric generator, a diesel generator (with a fuel supply regulator), an electric energy storage (an electrochemical battery) and a dc-to-dc converter (one-or three-phase industrial frequency). The study of such systems requires considering that they often operate in the mode of commensurate power with the consumer with the pulsating nature of the wind speed change. That is, in the created channel of the energy flow, the above elements of the wind-diesel power plant (WDPP)

are most often in the transition process, which requires determining the boundary of the stability of the consumer's energy supply system. In general, the block diagram of an autonomous WDPP is as follows (Figure 5).

The conversion of wind energy in an autonomous wind-diesel power system follows the standard principle: the mechanical energy of the wind flow is converted by the WDPP rotor into electrical energy by an electric generator in the same way as the mechanical energy in an internal combustion engine when burning fuel. The electrical energy is then used by the consumer either directly or through a dc-to-dc converter. It should be noted that the nature of the load of the consumer can be active (heaters, lighting), capacitive (electrochemical batteries) or active-inductive (an electric drive of technological machines with constant or variable moment of resistance). That is, the functional scheme of an autonomous wind-diesel power plant will consist of five links (Figure 6).

Input f_1 , characterizing the parameters of the wind flow (speed, duration of wind speed gradations, and period of calm) and the boundaries of the zone of useful wind energy. The link output signal W_1 is the input signal of the link W_2 and will be equal to (Equation 17). Where $f(v)$ – wind speed distribution density. If the value f_2 gives the opportunity of entering the zone of production load, f_3 signal is formed, the value of which makes it possible to ensure the implementation of the consumer's production needs (link W_5).

Input f_4 characterizes the parameters and periods of fuel supply. Link output signal W_3 is the input signal of the link W_4 and will characterize the mechanical power that is supplied to the rotor of the generator. If the value f_5 allows entering the zone of production load, f_6 signal is formed, the value of which makes it possible to ensure the implementation of the consumer's production needs (link W_5). Thus, we have a mixed connection of five links, each of which can have internal feedback, but the whole system lacks the main feedback; that is, the system cannot affect the input signal f_1 (the wind flow parameters).

Let's analyze the operation of the above system in the channel of the wind flow and the diesel engine. For this purpose, each component of an autonomous wind-diesel power plant is considered separately, considering the influence of other components. The motion equation for the rotor of a wind power plant or a rotor of a diesel engine, considering the influence of the generator link, is as follows (Equation 18). Where M_p – mechanical torque on the rotor shaft of a wind farm or diesel engine rotor; M_G – electromagnetic torque on generator shaft; J – inertial torque of rotating rotor elements; ω – angular speed of rotation of rotor and generator shafts.

The speed of rotation of the rotor shaft may vary due to changes in wind speed, changes the amount of fuel, and as a result of load change. If the rate of rotation of the rotor shaft, as a result of the action of wind or increased fuel supply increased by $\Delta\omega$, this will change the resulting torque to ΔM , then (Equation 19). As M_p and M_G are nonlinear functional speed ω , applying Taylor series expansion within $t=0$ and limiting ourselves to the first two members, we have as follows (Equation 20). After the substitution of equation (19) to equation (20) and replacement of (Equations 21-22), we have as follows (Equation 23).

From the theory of automatic control, it is known that the system will be stable in the case when (Equation 24) i.e. $\frac{dM_G}{d\omega} > \frac{dM_p}{d\omega}$. This means

that the system will remain stable if the load increases. Moreover, the rate of its rise must exceed the rate of increase in the value of the wind speed or the rate of increase in the fuel supply. If this is not possible, it is necessary to limit the speed of rotation.

As the wind speed or fuel supply decreases, the equation (23) takes the following form (Equation 25) and, after the transformation have as follows (Equation 26). Then, to keep the system stable $\left(\frac{dM_p}{d\omega} > \frac{dM_G}{d\omega}\right)$ it is necessary to provide a condition for reducing the load, and the rate of its decline should be higher than the rate of change in the value of the wind speed or the value of the fuel supply.

The speed of the transient process is affected by the time constant of each system block. The analysis of the processes taking place in the blocks of the functional scheme of an

autonomous wind-diesel power plant (Figure 6) will lead to a differential equation of type (23) describing the first-order aperiodic link (Equation 27). Where T_1, T_2, T_3, T_4, T_5 , – the timing of relevant links and $\xi_1, \xi_2, \xi_3, \xi_4, \xi_5$, – coefficients of self-alignment of the corresponding links.

The total transfer function of the entire system will be as follows (Equation 28). Substituting values of transfer functions of separate links, we have as follows (Equation 29). Opening the brackets and equating the denominator of the transfer function of the system to zero, we obtain the following characteristic equation (30).

The general view of the characteristic equation will be as follows (Equations 31-32). The following coefficients can be derived from the characteristic (Equations 33-38). The stability analysis is carried out using the algebraic Raus criterion. Let's make a Raus table in which the elements are determined from the following equations (39)-(40), where $i \geq 3$ – line number, k – column number (Table 1).

Let's substitute the coefficients and determine the values of the table elements r_3, r_4, r_5, r_6 by the given formulas in algebraic form. The expression to determine the coefficient r_3 is equal to (Equation 41). The expression to determine the coefficient r_4 is presented as follows (Equation 42). The expression to determine the coefficient r_5 is (Equation 43).

Let's find all the c coefficients from the Raus table in algebraic form: coefficient $c_{1,1}$ is equal to α_0 (Equation 44); coefficient $c_{1,2}$ is equal to α_1 (Equation 45); coefficient $c_{1,3}$ is equal to the difference between α_2 and $r_3\alpha_3$ (Equation 46); coefficient $c_{1,4}$ is equal to the difference between α_3 and $r_4c_{2,3}$ (Equation 47); coefficient $c_{1,5}$ is equal to the difference between $c_{2,3}$ and $r_5c_{2,4}$ (Equation 48); coefficient $c_{1,6}$ is equal to α_5 (Equation 49); coefficient $c_{2,1}$ is equal to α_2 (Equation 50); coefficient $c_{2,2}$ is equal to α_3 (Equation 51); coefficient $c_{2,3}$ is equal to the difference between α_4 and $r_3\alpha_5$

(Equation 52); coefficient $c_{2,4}$ is equal to the difference α_5 (Equation 53); coefficient $c_{3,1}$ is equal to α_4 (Equation 54); coefficient $c_{3,2}$ is equal to α_5 (Equation 55). For the stability of a linear stationary system it is necessary and sufficient that all the coefficients of the first column of the Raus table $c_{1,1}, c_{1,2}, c_{1,3}, c_{1,4}, c_{1,5}, c_{1,6}$ were the same sign. If this is not done, the system is unstable.

Analysis of coefficient data in general form ($c_{1,1}, c_{1,2}, c_{1,3}, c_{1,4}, c_{1,5}, c_{1,6}$) is difficult because their algebraic expression is too significant. Therefore, the stability study will be conducted for a specific wind-diesel power system, the parameters of which, as well as the time periods, need to be determined by simulation.

Since all-time steels have a positive sign, coefficient $c_{1,1}$ is the product of all stable times of the system; then respectively the given coefficient will be positive. Sign of coefficients $c_{1,3}, c_{1,4}, c_{1,5}$ is complicated to analyze because algebraic expressions are very cumbersome. Therefore, it is possible to determine the sign of these coefficients only by substituting the corresponding values of time constants and coefficients ξ for a specific system.

Let's analyze the coefficient (Equation 56). If an odd value (one, three, five) is the self-adjustment coefficient ξ will have a negative sign, it is the value $c_{1,6}$ will be negative and therefore the system is not stable. Thus, for the stability of the system, it is necessary that all coefficients ξ had a positive sign, or even value ξ had a negative sign. Let's consider each case in more detail and analyze it (Equation 57).

Coefficient $\xi_1 < 0$ characterizes the first link (WDPP rotor) and indicates a decrease in wind speed, and, accordingly, a reduction in the generated power in the system. Based on this, the system, of course, will lose stability if the load is not reduced. When reducing the load, coefficient ξ_5 will take a negative value, and the system will remain stable. When substituting values, all coefficients c will have a positive sign that indicates the stability of the system (Equation 58).

Coefficient of self-regulation $\xi_2 < 0$ characterizes the second link (WDPP generator)

and indicates a decrease in the generated power in the system. Consequently, the system will lose stability if the load is not reduced. When reducing the load, coefficient ξ_5 will take a negative value, and the system will remain stable. When substituting values, all coefficients c will have a positive sign, which indicates the stability of the system (Equation 59)

$\xi_3 < 0$ characterizes the third link (diesel generator) and shows a decrease in the speed of fuel supply, and, accordingly, a reduction in the generated power in the system. The system will lose stability if the load is not reduced. When reducing the load, coefficient ξ_5 will take a negative value, and the system will remain stable. When substituting values, all the coefficients will have a positive sign, which indicates the stability of the system (Equation 60).

$\xi_4 < 0$ characterizes the fourth link (diesel generator) and indicates a decrease in the generated power in the system. Based on this, the system, of course, will lose stability if the load is not reduced. When reducing the load, coefficient ξ_5 will take a negative value, and the system will remain stable. When substituting values, all the coefficients will have a positive sign, which indicates the stability of the system (Equation 61).

$\xi_5 < 0$ characterizes the fifth link (load) and indicates a decrease in the value of the load. Consequently, the system will lose stability if one does not reduce the value of the generated power. When reducing the energy generation coefficient ξ_2 or ξ_4 will take a negative value, and the system will remain stable. When substituting values, all coefficients c will have a positive sign that indicates the stability of the system.

Let's analyze coefficient $c_{1,2}$ (Equation 45). Since the time intervals T have a positive value, we can say that the coefficient $c_{1,2}$ will be equal to the sum of all self-regulation coefficients multiplied by some value. If all coefficients (Equation 62) are above zero, the system will be stable. Let's consider the case when $\xi_1 < 0$ or $\xi_2 < 0$. So that the system remains sustainable, it is necessary to ensure that the rate of increase of torque on a shaft of a diesel generator (flow of fuel) is greater than the rate of reduction of torque

on a shaft of the wind turbine (wind speed). I. e. it is necessary to compensate for the decrease in wind speed by increasing the fuel supply at a constant load or to reduce the load so that the system does not lose stability.

When $\xi_3 < 0$ or $\xi_4 < 0$ to ensure the stability of the system, it is necessary to compensate the decrease in torque of the diesel generator (fuel) by increasing the torque of wind turbine (wind speed) and the rate of increase must be greater than the rate of changing the torque on diesel generation or by reducing the load in accordance with the change in generation from diesel-generating. When $\xi_5 < 0$ (load link) it is possible to compensate for the replaceable torque on the shaft of the diesel generator (fuel supply) or wind generator (wind speed).

Let's consider coefficient $c_{1,3}$ (formula 46).

All T time intervals are positive values. To simplify the analysis, let's make some assumption: since coefficients ξ_1 and ξ_2 as well as ξ_3 and ξ_4 are part of the same systems, then combine them, i.e. $\xi_1 = \xi_2 = \xi_{1,2}$ and $\xi_3 = \xi_4 = \xi_{3,4}$ respectively. If time intervals and coefficients are not considered, equation 39 takes the following form (Equation 63).

In the case where all the self-regulation coefficients (Equation 64) are above zero, the stability of the system requires meeting the following condition (Equation 65). For other cases and analysis of the coefficients $c_{1,4}$ and $c_{1,5}$ in analytical form is difficult because of the bulkiness of expressions.

5. CONCLUSIONS:

1. As a result, it was analyzed the structural schemes of an autonomous supply system based on a wind-diesel system, which showed that the relative capacity for a three-channel system is 30% less than for a two-channel system, i.e. a three-channel system allows increasing the degree of security of consumer requirements.

2. A mathematical model of the load modes of the wind-diesel system in the conditions of variable rotor speed of the wind turbine and load parameters based on the Raus criterion allows analyzing the nature of the dynamic processes.

3. The autonomous system must have a certain hierarchical subordination, that is, the electrical supply is carried out first from the units that convert wind energy, and only in the case of a decrease in the level of production or a decrease to critical values, a diesel plant is used. If we consider the operation of this system in terms of the queuing theory, it is necessary that the flow of customer requirements was stationary, ordinary, and had no consequences.

4. To study the stability of the system, it is necessary to operate with numerical values. The simulation model will calculate, if necessary, the time constants and coefficients of self-alignment of all the system parts and use them in the study of stability by the Raus criterion.

6. REFERENCES:

- Ballireddy, T.R.R., Modi, P.K. *Lecture Notes in Electrical Engineering*, **2019**, 553, 207-215.
- Beinke, T., Ait Alla, A., Freitag, M. Resource and Information Sharing for the Installation Process of the Offshore Wind Energy. In: H. Lödding, R. Riedel, K.-D. Thoben, G. von Cieminski, D. Kiritsis (Eds.), *Advances in Production Management Systems. The Path to Intelligent, Collaborative and Sustainable Manufacturing*, Cham: Springer International Publishing, **2017**, 268–275.
- Bukar, A.L., Tan, C.W., Lau, K.Y. *Solar Energy*, **2019**, 188, 685-696.
- Can, E. *Environmental Monitoring and Assessment*, **2019**, 191(12), article number 746.
- Chakraborty, T. A MCDM-NBO Approach for Selection of Installation Location for Wave Energy Power Plants. In: M. Majumder (Ed.), *Application of Geographical Information Systems and Soft Computation Techniques in Water and Water Based Renewable Energy Problems*, Singapore: Springer Singapore, **2018**, 121-140. https://doi.org/10.1007/978-981-10-6205-6_6
- Chemekov, V.V., Kharchenko, V.V. *Thermal Engineering*, **2013**, 60(3), 212–216. <https://doi.org/10.1134/S0040601512110031>
- Chen, N., Yu, R., Chen, Y., Xie, H. *IET Renewable Power Generation*, **2017**, 11(4), 403-410.
- Conzalez-Rodriguez, A.G., Serrano-Conzalez, J., Riquelme-Santos, J.M., Burgos-Payán, M., Castro-Mora, J., Persan, S.A. Global Optimization of Wind Farms Using Evolutionary Algorithms. In: L. Wang, C. Singh, A. Kusiak (Eds.), *Wind Power Systems: Applications of Computational Intelligence*, Berlin, Heidelberg: Springer Berlin Heidelberg, **2010**, 53-104. https://doi.org/10.1007/978-3-642-13250-6_3
- Dai, X., Zhang, K., Geng, J., Wang, Y.a, Yuan, K. *Journal of Electrical Engineering and Technology*, **2019**, 14(3), 1063-1074.
- Dekkiche, M., Tahri, T., Bettahar, A., Belmadani, B. *Desalination and Water Treatment*, **2017**, 79, 125-134.
- Deltenre, Q., Runacres, M.C. Installation of a Small Building-Mounted Wind Turbine: A Case Study from Idea to Implementation. In: L. Battisti (Ed.), *Wind Energy Exploitation in Urban Environment*, Cham: Springer International Publishing, **2019**, 71-88.
- DeMeo, E.A., Steitz, P. The U.S. Electric Utility Industry's Activities in Solar and Wind Energy Survey and Perspective. In: K.W. Böer (Ed.), *Advances in Solar Energy: An Annual Review of Research and Development*, Boston, MA: Springer US, **1990**, 1-218. https://doi.org/10.1007/978-1-4613-9948-3_1
- Devederkin, I., Nikitenko, G., Antonov, S., Lysakov, A. *Engineering for Rural Development*, **2019**, 18, 1497-1502.
- Essallah, S., Bouallegue, A., Khedher, A. *Journal of Modern Power Systems and Clean Energy*, **2019**, 7(5), 1115-1128.
- Fernández-Guillamón, A., Gómez-Lázaro, E., Muljadi, E., Molina-García, Á. *Renewable and Sustainable Energy Reviews*, **2019**, 115, 109369.
- Finn, J., Sandeberg, P. AC Offshore Substations Associated with Wind Power Plants. In: T. Krieg, J. Finn (Eds.), *Substations*, Cham: Springer International Publishing, **2019**, 591-728. https://doi.org/10.1007/978-3-319-49574-3_29
- Grigor'ev, A.S., Skorlygin, V.V., Grigor'ev, S.A., Mel'nik, D.A., Losev, O.G., *Journal of Engineering Physics and Thermophysics* **2019**, 92(3), 562-573.
- Grigorash, O.V., Suleimanov, R.A., Kvitko, A.V. *Russian Electrical Engineering*, **2014**, 85(4), 217–221. <https://doi.org/10.3103/S1068371214040063>
- Grigoriev, A.S., Skorlygin, V.V., Grigoriev, S.A., Melnik, D.A., Losev, O.G. *Russian Electrical Engineering*, **2019**, 90(7), 505-508.
- Hau, E. Wind Turbine Installation and Operation. In: *Wind Turbines: Fundamentals, Technologies, Application, Economics*, Berlin,

- Heidelberg: Springer Berlin Heidelberg, **2013**, 719-787. https://doi.org/10.1007/978-3-642-27151-9_18
21. Heredia, F.-J., Cuadrado, M.D., Corchero, C. *Computers and Operations Research*, **2018**, 96, 316-329.
 22. Hong, S., Qvist, S., Brook, B.W. *Energy Policy*, **2018**, 112, 56-66.
 23. Kaiser, M.J., Snyder, B.F. Modeling Offshore Wind Installation Costs. In: *Offshore Wind Energy Cost Modeling: Installation and Decommissioning*, London: Springer London, **2012a**, 159-187. https://doi.org/10.1007/978-1-4471-2488-7_9
 24. Kaiser, M.J., Snyder, B.F. *Maritime Economics & Logistics*, **2012b**, 14(2), 220-248. <https://doi.org/10.1057/mel.2012.5>
 25. Krasnobaev, Y.V., Nepomnyashchii, O.V., Ivanchura, V.I., Pozharkova, I.N., Yablonskiy, A.P. *Bulletin of the Tomsk Polytechnic University, Geo Assets Engineering*, **2018**, 329(11), 61-73.
 26. Miller, L.M., Keith, D.W. *Environmental Research Letters*, **2018**, 13(10), article number 104008.
 27. Minin, V.A. *Thermal Engineering*, **2012**, 59(11), 854-859. <https://doi.org/10.1134/S0040601512110092>
 28. Morales Pedraza, J. The Current Situation and Perspectives on the Use of Wind Energy for Electricity Generation. In: *Electrical Energy Generation in Europe: The Current Situation and Perspectives in the Use of Renewable Energy Sources and Nuclear Power for Regional Electricity Generation*, Cham: Springer International Publishing, **2015**, 221-346. https://doi.org/10.1007/978-3-319-16083-2_5
 29. Nižetić, S., Penga, Ž., Arici, M. *Energy Conversion and Management*, **2017**, 148, 533-553.
 30. Obukhov, S.G., Plotnikov, I.A., Masolov, V.G. *IOP Conference Series: Materials Science and Engineering*, **2018**, 289(1), article number 012026.
 31. Ochoa, D., Martinez, S. *IEEE Latin America Transactions*, **2019**, 17(5), 775-787.
 32. Perzhabinsky, S., Karamov, D. *E3S Web of Conferences*, **2017**, 25, article number 02005.
 33. Rabanal, A., Ulazia, A., Ibarra-Berastegi, G., Sáenz, J., Elosegui, U. *Energies*, **2019**, 12(1), article number 28.
 34. Rehman, A.U., Abidi, M.H., Umer, U., Usmani, Y.S. *Sustainability (Switzerland)*, **2019**, 11(21), article number 6112.
 35. Rodina, L. *E3S Web of Conferences*, **2019**, 124, article number 04024.
 36. Rudenko, N., Ershov, V., Trints, D. *IOP Conference Series: Earth and Environmental Science*, **2019**, 403(1), article number 012123.
 37. Sabir, H., Ouassaid, M., Ngote, N. *2019 8th International Conference on Systems and Control, ICSC 2019*, **2019**, October, 366-371.
 38. Sebastián, R. *IET Renewable Power Generation*, **2017**, 11(2), 296-303.
 39. Semenyutina, A., Lazarev, S., Melnik, K. *World Ecology Journal*, **2019**, 9(1), 1-23. <https://doi.org/https://doi.org/10.25726/NM.2019.66.65.001>
 40. Sivachandran, P. *Journal of Green Engineering*, **2017**, 7(1-2), 1-24.
 41. Sujith, S., Ramesh, V. *International Review of Automatic Control*, **2017**, 10(1), 78-85.
 42. Tanasheva, N.K., Shuyushbayeva, N.N., Mussenova, E.K. *Technical Physics Letters*, **2018**, 44(9), 787-789. DOI: 10.1134/S1063785018090134
 43. Tang, X., Shen, Y., Li, S., Yang, Q., Sun, Y. Mixed Installation to Optimize the Position and Type Selection of Turbines for Wind Farms. In: D. Liu, S. Xie, Y. Li, D. Zhao, E.-S. M. El-Alfy (Eds.), *Neural Information Processing*, Cham: Springer International Publishing, **2017**, 307-315.
 44. Tereshkin, A. *World Ecology Journal*, **2018**, 8(2), 60-70. <https://doi.org/https://doi.org/10.25726/NM.2018.2.2.006>
 45. Tsgoev, R.S. *Russian Electrical Engineering*, **2012**, 83(2), 114-117. <https://doi.org/10.3103/S1068371212020125>
 46. Wang, W., Bai, Y. *Journal of Marine Science and Application*, **2010**, 9(2), 175-180. <https://doi.org/10.1007/s11804-010-9076-y>
 47. Yang, X., Chen, D., Dong, M., Li, T. Design of Control System for Hydraulic Lifting Platform with Jack-Up Wind-Power Installation Vessel. In: Q. Zu, B. Hu, A. Elçi (Eds.), *Pervasive Computing and the Networked World*, Berlin, Heidelberg: Springer Berlin Heidelberg, **2013**, 711-718.
 48. Zhang, G., Wu, B., Maleki, A., Zhang, W. *Solar Energy*, **2018**, 173, 964-975.
 49. Zhang, W., Maleki, A., Rosen, M.A. *Journal of Cleaner Production*, **2019**, 241, article number 117920.

$$\begin{cases} X1 \rightarrow k1X1 \\ X1 > Y1, \\ Y1 \rightarrow 0 \\ X1 \rightarrow 0 \end{cases} \quad (\text{Eq. 1})$$

$$\begin{cases} X1 + X2 \rightarrow k1X1k2X2 \\ X1 + X2 > Y1, \\ Y1 \rightarrow X2 \\ X1 = 0 \end{cases} \quad (\text{Eq. 2})$$

$$\begin{cases} X1 + X3 \rightarrow k1k3k4k5X1 \\ X1 + X3 > Y1, \\ Y1 \rightarrow X3 \\ X1 = 0 \end{cases} \quad (\text{Eq. 3})$$

$$\begin{cases} X1 + X2 \rightarrow k1k3k4k5X1 + k2X2 \\ X1 + X2 > Y1, \\ Y1 \rightarrow X2 + X \\ 1 = 0, \\ Y1 \rightarrow X2 \\ X1 + X3 = 0. \end{cases} \quad (\text{Eq. 4})$$

$$\begin{cases} \frac{dx}{dt} = Ax + Bz, \\ y = Cx \end{cases} \quad (\text{Eq. 5})$$

$$\begin{cases} \frac{dx}{dt} = \overline{Ax} + \overline{B_1z} + \overline{B_2y}, \\ \overline{y} = \overline{Cx} \end{cases} \quad (\text{Eq. 6})$$

$$\frac{d[\bar{x}(t) - x(t)]}{dt} = \bar{Ax} - Ax + (\bar{B}_1 - B)z + B_2y = \bar{Ax} - Ax + \bar{B}_2Cx + (\bar{B}_1 - B)z \rightarrow 0 \quad (\text{Eq. 7})$$

$$\frac{d[\bar{x}(t) - x(t)]}{dt} < 0 \quad (\text{Eq. 8})$$

$$\frac{d[\bar{x}(t) - x(t)]}{dt} = (A - \bar{B}_2C)[\bar{x}(t) - x(t)] \quad (\text{Eq. 9})$$

$$Q = \frac{\mu}{\lambda + \mu} \quad (\text{Eq. 10})$$

$$Q = 1 - \frac{\rho^2}{2!} \frac{1}{\left(1 + \rho + \frac{\rho^2}{2}\right)} \quad (\text{Eq. 11})$$

$$Q = 1 - \frac{\rho^3}{3!} \frac{1}{1 + \rho + \frac{\rho^2}{2!} + \frac{\rho^3}{3!}} \quad (\text{Eq. 12})$$

$$\frac{\lambda}{\mu} = f(Q) \quad (\text{Eq. 13})$$

$$p_1 = \frac{\alpha}{1 + \alpha} \quad (\text{Eq. 14})$$

$$p_2 = \frac{\frac{1}{2!}\alpha^2}{1 + \alpha + \frac{1}{2!}\alpha^2} = \frac{\alpha^2}{1 + (1 + \alpha)^2} \quad (\text{Eq. 15})$$

$$p_3 = \frac{\frac{1}{3!}\alpha^3}{1 + \alpha + \frac{1}{2!}\alpha^2 + \frac{1}{3!}\alpha^3} = \frac{\frac{\alpha^3}{6}}{1 + \alpha + \frac{1}{2}\alpha^2 + \frac{\alpha^3}{6}} \quad (\text{Eq. 16})$$

$$f_2 = \int_0^{\infty} \nu^3 f(\nu) d\nu \quad (\text{Eq. 17})$$

$$j \frac{d\omega}{dt} = M_P - M_G \quad (\text{Eq. 18})$$

$$j \frac{d(\omega_0 + \Delta\omega)}{dt} = M_P - M_G + \Delta M \quad (\text{Eq. 19})$$

$$\begin{cases} M_P(\omega) = M_{P_0} + \left(\frac{dM_P}{d\omega} \right)_0 \Delta\omega + \Delta M \\ M_G(\omega) = M_{G_0} + \left(\frac{dM_G}{d\omega} \right)_0 \Delta\omega \end{cases} \quad (\text{Eq. 20})$$

$$\varphi = \frac{\Delta\omega}{\omega_0} \quad (\text{Eq. 21})$$

$$\mu = \frac{\Delta M}{M_0} \quad (\text{Eq. 22})$$

$$j \frac{\omega_0}{M_0} \frac{d\varphi}{dt} + \varphi \frac{\omega_0}{M_0} \left\{ \left(\frac{dM_G}{d\omega} \right)_0 - \left(\frac{dM_P}{d\omega} \right)_0 \right\} = \mu \quad (\text{Eq. 23})$$

$$\xi = \frac{\omega_0}{M_0} \left\{ \left(\frac{dM_G}{d\omega} \right)_0 - \left(\frac{dM_P}{d\omega} \right)_0 \right\} > 0 \quad (\text{Eq. 24})$$

$$j \frac{d(\omega_0 - \Delta\omega)}{dt} = M_P - M_G - \Delta M \quad (\text{Eq. 25})$$

$$j \frac{\omega_0}{M_0} \frac{d\varphi}{dt} + \varphi \frac{\omega_0}{M_0} \left\{ \left(\frac{dM_P}{d\omega} \right)_0 - \left(\frac{dM_G}{d\omega} \right)_0 \right\} = \mu \quad (\text{Eq. 26})$$

$$\begin{aligned} W_1 &= \frac{k_1}{T_1 p + \xi_1} \\ W_2 &= \frac{k_2}{T_2 p + \xi_2} \\ W_3 &= \frac{k_3}{T_3 p + \xi_3} \\ W_4 &= \frac{k_4}{T_4 p + \xi_4} \\ W_5 &= \frac{k_5}{T_5 p + \xi_5} \end{aligned} \quad (\text{Eq. 27})$$

$$W = (W_1 W_2 W_3 W_4) W_5 \quad (\text{Eq. 28})$$

$$W = \left(\frac{k_1}{T_1 p + \xi_1} \frac{k_2}{T_2 p + \xi_2} + \frac{k_3}{T_3 p + \xi_3} \frac{k_4}{T_4 p + \xi_4} \right) \frac{k_5}{T_5 p + \xi_5} \quad (\text{Eq. 29})$$

$$(T_1 p + \xi_1)(T_2 p + \xi_2)(T_3 p + \xi_3)(T_4 p + \xi_4)(T_5 p + \xi_5) = 0 \quad (\text{Eq. 30})$$

$$\alpha_0 p^5 + \alpha_1 p^4 + \alpha_2 p^3 + \alpha_3 p^2 + \alpha_4 p + \alpha_5 = 0 \quad (\text{Eq. 31})$$

$$\begin{aligned} & (T_1 T_2 T_3 T_4 T_5) p^5 + (\xi_5 T_1 T_2 T_3 T_4 + \xi_4 T_1 T_2 T_3 T_5 + \xi_3 T_1 T_2 T_4 T_5 + \\ & + \xi_2 T_1 T_3 T_4 T_5 + \xi_1 T_2 T_3 T_4 T_5) p^4 + (\xi_4 \xi_5 T_1 T_2 T_3 + \xi_3 \xi_5 T_1 T_2 T_4 + \\ & + \xi_2 \xi_5 T_1 T_3 T_4 + \xi_1 \xi_5 T_2 T_3 T_4 + \xi_3 \xi_4 T_1 T_2 T_5 + \xi_2 \xi_4 T_1 T_3 T_5 + \\ & + \xi_1 \xi_4 T_2 T_3 T_5 + \xi_2 \xi_3 T_1 T_4 T_5 + \xi_1 \xi_3 T_2 T_4 T_5 + \xi_1 \xi_2 T_3 T_4 T_5) p^3 + \\ & + (\xi_3 \xi_4 \xi_5 T_1 T_2 + \xi_2 \xi_4 \xi_5 T_1 T_3 + \xi_1 \xi_4 \xi_5 T_2 T_3 + \xi_2 \xi_3 \xi_5 T_1 T_4 + \\ & + \xi_1 \xi_3 \xi_5 T_2 T_4 + \xi_1 \xi_2 \xi_5 T_3 T_4 + \xi_2 \xi_3 \xi_4 T_1 T_5 + \xi_1 \xi_3 \xi_4 T_2 T_5 + \\ & + \xi_1 \xi_2 \xi_4 T_3 T_5) p^2 + (\xi_2 \xi_3 \xi_4 \xi_5 T_1 + \xi_1 \xi_3 \xi_4 \xi_5 T_2 + \xi_1 \xi_2 \xi_4 \xi_5 T_3 + \\ & + \xi_1 \xi_2 \xi_3 \xi_5 T_4 + \xi_1 \xi_2 \xi_3 \xi_4 T_5) p + \xi_1 \xi_2 \xi_3 \xi_4 + \xi_5 = 0 \end{aligned} \quad (\text{Eq. 32})$$

$$\alpha_0 = T_1 T_2 T_3 T_4 T_5 \quad (\text{Eq. 33})$$

$$\alpha_1 = \xi_5 T_1 T_2 T_3 T_4 + \xi_4 T_1 T_2 T_3 T_5 + \xi_3 T_1 T_2 T_4 T_5 + \xi_2 T_1 T_3 T_4 T_5 + \xi_1 T_2 T_3 T_4 T_5 \quad (\text{Eq. 34})$$

$$\begin{aligned} \alpha_2 = & \xi_4 \xi_5 T_1 T_2 T_3 + \xi_3 \xi_5 T_1 T_2 T_4 + \xi_2 \xi_5 T_1 T_3 T_4 + \xi_1 \xi_5 T_2 T_3 T_4 + \xi_3 \xi_4 T_1 T_2 T_5 + \\ & + \xi_2 \xi_4 T_1 T_3 T_5 + \xi_1 \xi_4 T_2 T_3 T_5 + \xi_2 \xi_3 T_1 T_4 T_5 + \xi_1 \xi_3 T_2 T_4 T_5 + \xi_1 \xi_2 T_3 T_4 T_5 \end{aligned} \quad (\text{Eq. 35})$$

$$\begin{aligned} \alpha_3 = & \xi_3 \xi_4 \xi_5 T_1 T_2 + \xi_2 \xi_4 \xi_5 T_1 T_3 + \xi_1 \xi_4 \xi_5 T_2 T_3 + \xi_2 \xi_3 \xi_5 T_1 T_4 + \xi_1 \xi_3 \xi_5 T_2 T_4 + \\ & + \xi_1 \xi_2 \xi_5 T_3 T_4 + \xi_2 \xi_3 \xi_4 T_1 T_5 + \xi_1 \xi_3 \xi_4 T_2 T_5 + \xi_1 \xi_2 \xi_4 T_3 T_5 \end{aligned} \quad (\text{Eq. 36})$$

$$\alpha_4 = \xi_2 \xi_3 \xi_4 \xi_5 T_1 + \xi_1 \xi_3 \xi_4 \xi_5 T_2 + \xi_1 \xi_2 \xi_4 \xi_5 T_3 + \xi_1 \xi_2 \xi_3 \xi_5 T_4 + \xi_1 \xi_2 \xi_3 4 T_5 \quad (\text{Eq. 37})$$

$$\alpha_5 = \xi_1 \xi_2 \xi_3 \xi_4 \xi_5 \quad (\text{Eq. 38})$$

$$r_i = \frac{c_{1,i-2}}{c_{1,i-1}} \quad (\text{Eq. 39})$$

$$c_{k,1} = c_{k+1,i-2} - r_i c_{k+1,i-1} \quad (\text{Eq. 40})$$

$$r_3 = \frac{(T_1 T_2 T_3 T_4 T_5)}{(T_2 T_3 T_4 T_5 \xi_1 + T_1 T_3 T_4 T_5 \xi_2 + T_1 T_2 T_4 T_5 \xi_3 + T_1 T_2 T_3 T_5 \xi_4 + T_1 T_2 T_3 T_4 \xi_5)} \quad (\text{Eq. 41})$$

$$r_4 = (T_2T_3T_4T_5\xi_1 + T_1T_3T_4T_5\xi_2 + T_1T_2T_4T_5\xi_3 + T_1T_2T_3T_5\xi_4 + T_1T_2T_3T_4\xi_5) /$$

$$/ (T_3T_4T_5\xi_1\xi_2 + T_2T_4T_5\xi_1\xi_3 + T_1T_4T_5\xi_2\xi_3 + T_2T_3T_5\xi_1\xi_4 + T_1T_3T_5\xi_2\xi_4 +$$

$$+ T_1T_2T_5\xi_3\xi_4 + T_2T_3T_4\xi_1\xi_5 + T_1T_3T_4\xi_2\xi_5 + T_1T_2T_4\xi_3\xi_5 + T_1T_2T_3\xi_4\xi_5 -$$

$$- (T_1T_2T_3T_4T_5(T_4T_5\xi_1\xi_2\xi_3 + T_3T_5\xi_1\xi_2\xi_4 + T_2T_5\xi_1\xi_3\xi_4 + T_1T_5\xi_2\xi_3\xi_4 +$$

$$+ T_3T_4\xi_1\xi_2\xi_5 + T_2T_4\xi_1\xi_3\xi_5 + T_1T_4\xi_2\xi_3\xi_5 + T_2T_3\xi_1\xi_4\xi_5 + T_1T_3\xi_2\xi_4\xi_5 +$$

$$+ T_1T_2\xi_3\xi_4\xi_5)) / (T_2T_3T_4T_5\xi_1 + T_1T_3T_4T_5\xi_2 + T_1T_2T_4T_5\xi_3 + T_1T_2T_3T_5\xi_4 +$$

$$+ T_1T_2T_3T_4\xi_5)) \quad (\text{Eq. 42})$$

$$r_5 = (T_3T_4T_5\xi_1\xi_2 + T_2T_4T_5\xi_1\xi_3 + T_1T_4T_5\xi_2\xi_3 + T_2T_3T_5\xi_1\xi_4 + T_1T_3T_5\xi_2\xi_4 +$$

$$+ T_1T_2T_5\xi_3\xi_4 + T_2T_3T_4\xi_1\xi_5 + T_1T_3T_4\xi_2\xi_5 + T_1T_2T_4\xi_3\xi_5 + T_1T_2T_3\xi_4\xi_5 -$$

$$- (T_1T_2T_3T_4T_5(T_4T_5\xi_1\xi_2\xi_3 + T_3T_5\xi_1\xi_2\xi_4 + T_2T_5\xi_1\xi_3\xi_4 + T_1T_5\xi_2\xi_3\xi_4 +$$

$$+ T_3T_4\xi_1\xi_2\xi_5 + T_2T_4\xi_1\xi_3\xi_5 + T_1T_4\xi_2\xi_3\xi_5 + T_2T_3\xi_1\xi_4\xi_5 + T_1T_3\xi_2\xi_4\xi_5 +$$

$$+ T_1T_2\xi_3\xi_4\xi_5)) / (T_2T_3T_4T_5\xi_1 + T_1T_3T_4T_5\xi_2 + T_1T_2T_4T_5\xi_3 + T_1T_2T_3T_5\xi_4 +$$

$$+ T_1T_2T_3T_4\xi_5)) / (T_4T_5\xi_1\xi_2\xi_3 + T_3T_5\xi_1\xi_2\xi_4 + T_2T_5\xi_1\xi_3\xi_4 + T_1T_5\xi_2\xi_3\xi_4 +$$

$$+ T_3T_4\xi_1\xi_2\xi_5 + T_2T_4\xi_1\xi_3\xi_5 + T_1T_4\xi_2\xi_3\xi_5 + T_2T_3\xi_1\xi_4\xi_5 + T_1T_3\xi_2\xi_4\xi_5 +$$

$$+ T_1T_2\xi_3\xi_4\xi_5)) / (T_2T_3T_4T_5\xi_1 + T_1T_3T_4T_5\xi_2 + T_1T_2T_4T_5\xi_3 + T_1T_2T_3T_5\xi_4 +$$

$$+ T_1T_2T_3T_4\xi_5)) / (T_4T_5\xi_1\xi_2\xi_3 + T_3T_5\xi_1\xi_2\xi_4 + T_2T_5\xi_1\xi_3\xi_4 + T_1T_5\xi_2\xi_3\xi_4 +$$

$$+ T_3T_4\xi_1\xi_2\xi_5 + T_2T_4\xi_1\xi_3\xi_5 + T_1T_4\xi_2\xi_3\xi_5 + T_2T_3\xi_1\xi_4\xi_5 + T_1T_3\xi_2\xi_4\xi_5 +$$

$$+ T_1T_2\xi_3\xi_4\xi_5 - ((T_2T_3T_4T_5\xi_1 + T_1T_3T_4T_5\xi_2 + T_1T_2T_4T_5\xi_3 + T_1T_2T_3T_5\xi_4 +$$

$$+ T_1T_2T_3T_4\xi_5) (T_5\xi_1\xi_2\xi_3\xi_4 + T_4\xi_1\xi_2\xi_3\xi_5 + T_3\xi_1\xi_2\xi_4\xi_5 + T_2\xi_1\xi_3\xi_4\xi_5 +$$

$$+ T_1\xi_2\xi_3\xi_4\xi_5 - (T_1T_2T_3T_4T_5\xi_1\xi_2\xi_3\xi_4\xi_5)) / (T_2T_3T_4T_5\xi_1 + T_1T_3T_4T_5\xi_2 +$$

$$+ T_1T_2T_4T_5\xi_3 + T_1T_2T_3T_5\xi_4 + T_1T_2T_3T_4\xi_5))) / (T_3T_4T_5\xi_1\xi_2 + T_2T_4T_5\xi_1\xi_3 +$$

$$+ T_1T_4T_5\xi_2\xi_3 + T_2T_3T_5\xi_1\xi_4 + T_1T_3T_5\xi_2\xi_4 + T_1T_2T_5\xi_3\xi_4 + T_2T_3T_4\xi_1\xi_5 +$$

$$+ T_1T_3T_4\xi_2\xi_5 + T_1T_2T_4\xi_3\xi_5 + T_1T_2T_3\xi_4\xi_5 - (T_1T_2T_3T_4T_5(T_4T_5\xi_1\xi_2\xi_3 +$$

$$+ T_3T_5\xi_1\xi_2\xi_4 + T_2T_5\xi_1\xi_3\xi_4 + T_3T_4\xi_1\xi_2\xi_5 + T_2T_4\xi_1\xi_3\xi_5 +$$

$$+ T_1T_4\xi_2\xi_3\xi_5 + T_2T_3\xi_1\xi_4\xi_5 + T_1T_3\xi_2\xi_4\xi_5 + T_1T_2\xi_3\xi_4\xi_5)) / T_2T_3T_4T_5T_1 +$$

$$+ T_1T_3T_4T_5\xi_2 + T_1T_2T_4T_5\xi_3 + T_1T_2T_3T_5\xi_4 + T_1T_2T_3T_4\xi_5))) \quad (\text{Eq. 43})$$

$$c_{1,1} = T_1T_2T_3T_4T_5 \quad (\text{Eq. 44})$$

$$c_{1,2} = \xi_5T_1T_2T_3T_4 + \xi_4T_1T_2T_3T_5 + \xi_3T_1T_2T_4T_5 + \xi_2T_1T_3T_4T_5 + \xi_1T_2T_3T_4T_5 \quad (\text{Eq. 45})$$

$$\begin{aligned}
c_{1,3} = & T_3T_4T_5\xi_1\xi_2 + T_2T_4T_5\xi_1\xi_3 + T_1T_4T_5\xi_2\xi_3 + T_2T_3T_5\xi_1\xi_4 + T_1T_3T_5\xi_2\xi_4 + \\
& + T_1T_2T_5T_3T_4 + T_2T_3T_4\xi_1\xi_5 + T_1T_3T_4\xi_2\xi_5 + T_1T_2T_4\xi_3\xi_5 + T_1T_2T_3\xi_4\xi_5 - \\
& - (T_1T_2T_3T_4T_5 - (T_4T_5\xi_1\xi_2\xi_3 + T_2T_3T_4\xi_1\xi_5 + T_1T_3T_4\xi_2\xi_5 + T_1T_2T_4\xi_3\xi_5 + \\
& + T_1T_2T_3\xi_4\xi_5 - (T_1T_2T_3T_4T_5 - (T_4T_5\xi_1\xi_2\xi_3 + T_3T_5\xi_1\xi_2\xi_4 + T_2T_5\xi_1\xi_3\xi_4 + \\
& + T_1T_5\xi_2\xi_3\xi_4 + T_3T_4\xi_1\xi_2\xi_5 + T_2T_4\xi_1\xi_3\xi_5 + T_1T_4\xi_2\xi_3\xi_5 + T_2T_3\xi_1\xi_4\xi_5 + \\
& + T_1T_3\xi_2\xi_4\xi_5 + T_1T_2\xi_3\xi_4\xi_5))) / (T_2T_3T_4T_5\xi_1 + T_1T_3T_4T_5\xi_2 + T_1T_2T_4T_5\xi_3 + \\
& + T_1T_2T_3T_5\xi_4 + T_1T_2T_3T_4\xi_5)
\end{aligned}
\tag{Eq. 46}$$

$$\begin{aligned}
c_{1,4} = & T_4T_5\xi_1\xi_2\xi_3 + T_3T_5\xi_1\xi_2\xi_4 + T_2T_5\xi_1\xi_3\xi_4 + T_1T_5\xi_2\xi_3\xi_4 + T_3T_4\xi_1\xi_2\xi_5 + T_2T_4\xi_1\xi_3\xi_5 + \\
& + T_1T_4\xi_2\xi_3\xi_5 + T_2T_3\xi_1\xi_4\xi_5 + T_1T_3\xi_2\xi_4\xi_5 + T_1T_2\xi_3\xi_4\xi_5 - ((T_2T_3T_4T_5\xi_1 + T_1T_3T_4T_5\xi_2 + \\
& + T_1T_2T_4T_5\xi_3 + T_1T_2T_3T_5\xi_4 + T_1T_2T_3T_4\xi_5)(T_5\xi_1\xi_2\xi_3\xi_4 + T_4\xi_1\xi_2\xi_3\xi_5 + T_3\xi_1\xi_2\xi_4\xi_5 + \\
& + T_2\xi_1\xi_2\xi_4\xi_5 + T_1\xi_2\xi_3\xi_4\xi_5 - (T_1T_2T_3T_4T_5\xi_1\xi_2\xi_3\xi_4\xi_5)) / (T_2T_3T_4T_5\xi_1 + T_1T_3T_4T_5\xi_2 + \\
& + T_1T_2T_4T_5\xi_3 + T_1T_2T_3T_5\xi_4 + T_1T_2T_3T_4\xi_5))) / (T_3T_4\xi_5\xi_1\xi_2 + T_2T_4\xi_5\xi_1\xi_3 + T_1T_4\xi_5\xi_2\xi_3 + \\
& + T_2T_3\xi_5\xi_1\xi_4 + T_1T_3\xi_5\xi_2\xi_4 + T_1T_2\xi_5\xi_3\xi_4 + T_2T_3\xi_4\xi_1\xi_5 + T_1T_3\xi_4\xi_2\xi_5 + T_1T_2\xi_4\xi_3\xi_5 + \\
& + T_1T_2\xi_3\xi_4\xi_5 - (T_1T_2T_3T_4T_5(T_4T_5\xi_1\xi_2\xi_3 + T_3T_5\xi_1\xi_2\xi_4 + T_2T_5\xi_1\xi_3\xi_4 + T_1T_5\xi_2\xi_3\xi_4 + \\
& + T_3T_4\xi_1\xi_2\xi_5 + T_2T_4\xi_1\xi_3\xi_5 + T_1T_4\xi_2\xi_3\xi_5 + T_2T_3\xi_1\xi_4\xi_5 + T_1T_3\xi_2\xi_4\xi_5 + T_1T_2\xi_3\xi_4\xi_5))) / \\
& (T_2T_3T_4T_5\xi_1 + T_1T_3T_4T_5\xi_2 + T_1T_2T_4T_5\xi_3 + T_1T_2T_3T_5\xi_4 + T_1T_2T_3T_4\xi_5)
\end{aligned}
\tag{Eq. 47}$$

$$\begin{aligned}
c_{1,5} = & T_5\xi_1\xi_2\xi_3\xi_4 + T_4\xi_1\xi_2\xi_3\xi_5 + T_3\xi_1\xi_2\xi_4\xi_5 + T_2\xi_1\xi_3\xi_4\xi_5 + T_1\xi_2\xi_3\xi_4\xi_5 - \\
& - (T_1T_2T_3T_4T_5\xi_1\xi_2\xi_3\xi_4\xi_5) / (T_2T_3T_4T_5\xi_1 + T_1T_3T_4T_5\xi_2 + T_1T_2T_4T_5\xi_3 + \\
& + T_1T_2T_3T_5\xi_4 + T_1T_2T_3T_4\xi_5) - (\xi_1\xi_2\xi_3\xi_4\xi_5(T_3T_4T_5\xi_1\xi_2 + T_2T_4T_5\xi_1\xi_3 + \\
& + T_1T_4T_5\xi_2\xi_3 + T_2T_3T_5\xi_1\xi_4 + T_1T_3T_5\xi_2\xi_4 + T_1T_2T_5\xi_3\xi_4 + T_2T_3T_4\xi_1\xi_5 + \\
& + T_1T_3T_4\xi_2\xi_5 + T_1T_2T_4\xi_3\xi_5 + T_1T_2T_3\xi_4\xi_5 - (T_1T_2T_3T_4T_5(T_4T_5\xi_1\xi_2\xi_3 + \\
& + T_3T_5\xi_1\xi_2\xi_4 + T_2T_5\xi_1\xi_3\xi_4 + T_1T_5\xi_2\xi_3\xi_4 + T_3T_4\xi_1\xi_2\xi_5 + T_2T_4\xi_1\xi_3\xi_5 + \\
& + T_1T_4\xi_2\xi_3\xi_5 + T_2T_3\xi_1\xi_4\xi_5 + T_1T_3\xi_2\xi_4\xi_5 + T_1T_2\xi_3\xi_4\xi_5)) / (T_2T_3T_4T_5\xi_1 + \\
& + T_1T_3T_4T_5\xi_2 + T_1T_2T_4T_5\xi_3 + T_1T_2T_3T_5\xi_4 + T_1T_2T_3T_4\xi_5))) / (T_4T_5\xi_1\xi_2\xi_3 + \\
& + T_3T_5\xi_1\xi_2\xi_4 + T_2T_5\xi_1\xi_3\xi_4 + T_1T_5\xi_2\xi_3\xi_4 + T_3T_4\xi_1\xi_2\xi_5 + T_2T_4\xi_1\xi_3\xi_5 + \\
& + T_1T_4\xi_2\xi_3\xi_5 + T_2T_3\xi_1\xi_4\xi_5 + T_1T_3\xi_2\xi_4\xi_5 + T_1T_2\xi_3\xi_4\xi_5 - ((T_2T_3T_4T_5\xi_1 + \\
& + T_1T_3T_4T_5\xi_2 + T_1T_2T_4T_5\xi_3 + T_1T_2T_3T_5\xi_4 + T_1T_2T_3T_4\xi_5)(T_5\xi_1\xi_2\xi_3\xi_4 + \\
& + T_4\xi_1\xi_2\xi_3\xi_5 + T_3\xi_1\xi_2\xi_4\xi_5 + T_2\xi_1\xi_2\xi_3\xi_4\xi_5 + T_1\xi_2\xi_3\xi_4\xi_5 - \\
& - (T_1T_2T_3T_4T_5\xi_1\xi_2\xi_3\xi_4\xi_5) / (T_2T_3T_4T_5\xi_1 + T_1T_3T_4T_5\xi_2 + T_1T_2T_4T_5\xi_3 + \\
& + T_1T_2T_3T_5\xi_4 + T_1T_2T_3T_4\xi_5))) / (T_3T_4T_5\xi_1\xi_2 + T_2T_4T_5\xi_1\xi_3 + T_1T_4T_5\xi_2\xi_3 + \\
& + T_2T_3T_5\xi_1\xi_4 + T_1T_3T_5\xi_2\xi_4 + T_1T_2T_5\xi_3\xi_4 + T_2T_3T_4\xi_1\xi_5 + T_1T_3T_4\xi_2\xi_5 + \\
& + T_1T_2T_4\xi_3\xi_5 + T_1T_2T_3\xi_4\xi_5 - (T_1T_2T_3T_4T_5(T_4T_5\xi_1\xi_2\xi_3 + T_3T_5\xi_1\xi_2\xi_4 + \\
& + T_2T_5\xi_1\xi_3\xi_4 + T_1T_5\xi_2\xi_3\xi_4 + T_3T_4\xi_1\xi_2\xi_5 + T_2T_4\xi_1\xi_3\xi_5 + T_1T_4\xi_2\xi_3\xi_5 + \\
& + T_2T_3\xi_1\xi_4\xi_5 + T_1T_3\xi_2\xi_4\xi_5 + T_1T_2\xi_3\xi_4\xi_5)) / (T_2T_3T_4T_5\xi_1 + T_1T_3T_4T_5\xi_2 + \\
& + T_1T_2T_4T_5\xi_3 + T_1T_2T_3T_5\xi_4 + T_1T_2T_3T_4\xi_5)))
\end{aligned}$$

(Eq. 48)

$$c_{1,6} = \xi_1\xi_2\xi_3\xi_4\xi_5 \quad (\text{Eq. 49})$$

$$\begin{aligned}
c_{2,1} = & \xi_4\xi_5T_1T_2T_3 + \xi_3\xi_5T_1T_2T_4 + \xi_2\xi_5T_1T_3T_4 + \xi_1\xi_5T_2T_3T_4 + \xi_3\xi_4T_1T_2T_5 + \\
& + \xi_2\xi_4T_1T_3T_5 + \xi_1\xi_4T_2T_3T_5 + \xi_2\xi_3T_1T_4T_5 + \xi_1\xi_3T_2T_4T_5 + \xi_1\xi_2T_3T_4T_5
\end{aligned}$$

(Eq. 50)

$$\begin{aligned}
c_{2,2} = & \xi_3\xi_4\xi_5T_1T_2 + \xi_2\xi_4\xi_5T_1T_3 + \xi_1\xi_4\xi_5T_2T_3 + \xi_2\xi_3\xi_5T_1T_4 + \xi_1\xi_3\xi_5T_2T_4 + \\
& + \xi_1\xi_2\xi_5T_3T_4 + \xi_2\xi_3\xi_4T_1T_5 + \xi_1\xi_3\xi_4T_2T_5 + \xi_1\xi_2\xi_4T_3T_5
\end{aligned}$$

(Eq. 51)

$$\begin{aligned}
c_{2,3} = & T_5\xi_1\xi_2\xi_3\xi_4 + T_4\xi_1\xi_2\xi_3\xi_5 + T_3\xi_1\xi_2\xi_4\xi_5 + T_2\xi_1\xi_3\xi_4\xi_5 + T_1\xi_2\xi_3\xi_4\xi_5 - \\
& - (T_1T_2T_3T_4T_5\xi_1\xi_2\xi_3\xi_4\xi_5) / (T_2T_3T_4T_5\xi_1 + T_1T_3T_4T_5\xi_2 + T_1T_2T_4T_5\xi_3 + \\
& + T_1T_2T_3T_5\xi_4 + T_1T_2T_3T_4\xi_5)
\end{aligned}$$

(Eq. 52)

$$\begin{aligned}
c_{2,4} &= \xi_1\xi_2\xi_3\xi_4\xi_5 \\
c_{2,5} &= 0 \\
c_{2,6} &= 0
\end{aligned}$$

(Eq. 53)

$$c_{3,1} = \xi_2 \xi_3 \xi_4 \xi_5 T_1 + \xi_1 \xi_3 \xi_4 \xi_5 T_2 + \xi_1 \xi_2 \xi_4 \xi_5 T_3 + \xi_1 \xi_2 \xi_3 \xi_5 T_4 + \xi_1 \xi_2 \xi_3 \xi_4 T_5 \quad (\text{Eq. 54})$$

$$\begin{aligned} c_{3,2} &= \xi_1 \xi_2 \xi_3 \xi_4 \xi_5 \\ c_{3,3} &= 0 \\ c_{3,4} &= 0 \\ c_{3,5} &= 0 \\ c_{3,6} &= 0; \end{aligned} \quad (\text{Eq. 55})$$

$$c_{1,6} = \xi_1 \xi_2 \xi_3 \xi_4 \xi_5 \quad (\text{Eq. 56})$$

$$\begin{aligned} \xi_1 \langle 0; \xi_2 \rangle 0 \\ \xi_3 &> 0 \\ \xi_4 &> 0 \\ \xi_5 &> 0 \end{aligned} \quad (\text{Eq. 57})$$

$$\begin{aligned} \xi_1 &> 0 \\ \xi_2 \langle 0; \xi_3 \rangle 0 \\ \xi_4 &> 0 \\ \xi_5 &> 0 \end{aligned} \quad (\text{Eq. 58})$$

$$\begin{aligned} \xi_1 &> 0 \\ \xi_2 &> 0 \\ \xi_3 \langle 0; \xi_4 \rangle 0 \\ \xi_5 &> 0 \end{aligned} \quad (\text{Eq. 59})$$

$$\begin{aligned} \xi_1 &> 0 \\ \xi_2 &> 0 \\ \xi_3 &> 0 \\ \xi_4 \langle 0; \xi_5 \rangle 0 \end{aligned} \quad (\text{Eq. 60})$$

$$\begin{aligned} \xi_1 &> 0 \\ \xi_2 &> 0 \\ \xi_3 &> 0 \\ \xi_4 &> 0 \\ \xi_5 &< 0 \end{aligned} \quad (\text{Eq. 61})$$

$$\begin{aligned}
\xi_1 &> 0 \\
\xi_2 &> 0 \\
\xi_3 &> 0 \\
\xi_4 &> 0 \\
\xi_5 &> 0
\end{aligned}
\tag{Eq. 62}$$

$$\xi_{1,2} + \xi_{1,2}\xi_{3,4} + \xi_{1,2}\xi_5 + \xi_{3,4}\xi_5 - \frac{(\xi_{1,2}^2(\xi_{3,4} + \xi_5) + \xi_{3,4}^2(\xi_{1,2} + \xi_5) + \xi_{1,2} * \xi_{3,4} * \xi_5)}{\xi_{1,2} + \xi_{3,4} + \xi_5}
\tag{Eq. 63}$$

$$\begin{aligned}
\xi_1 &> 0 \\
\xi_2 &> 0 \\
\xi_3 &> 0 \\
\xi_4 &> 0 \\
\xi_5 &> 0
\end{aligned}
\tag{Eq. 64}$$

$$\xi_{1,2} + \xi_{1,2}\xi_{3,4} + \xi_{1,2}\xi_5 + \xi_{3,4}\xi_5 > \frac{(\xi_{1,2}^2(\xi_{3,4} + \xi_5) + \xi_{3,4}^2(\xi_{1,2} + \xi_5) + \xi_{1,2}\xi_{3,4}\xi_5)}{\xi_{1,2} + \xi_{3,4} + \xi_5}
\tag{Eq. 65}$$

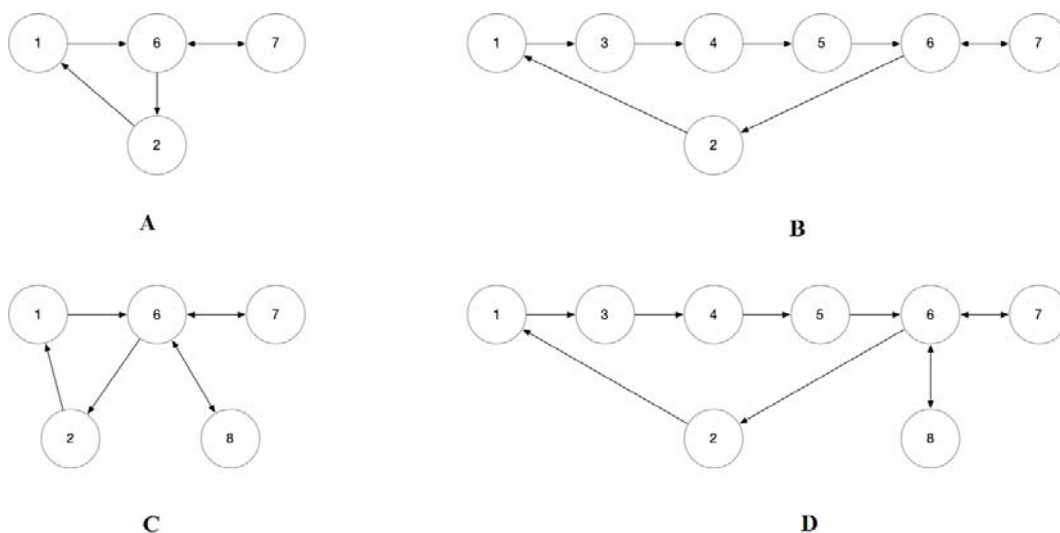


Figure 1. Block Diagrams of Autonomous Power Supply System based on WDPP: 1 – WDPP; 2 – capacitor bank; 3 – controller; 4 – battery pack; 5 – inverter; 6 – synchronizer; 7 – consumer; 8 – diesel generator

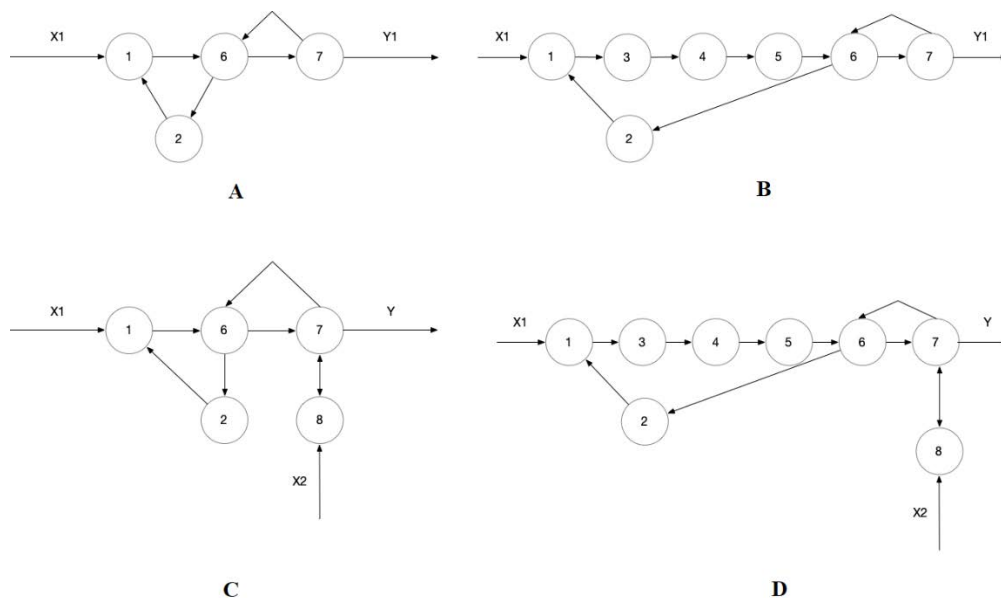


Figure 2. Graphs of Autonomous Power Supply System based on WDPP

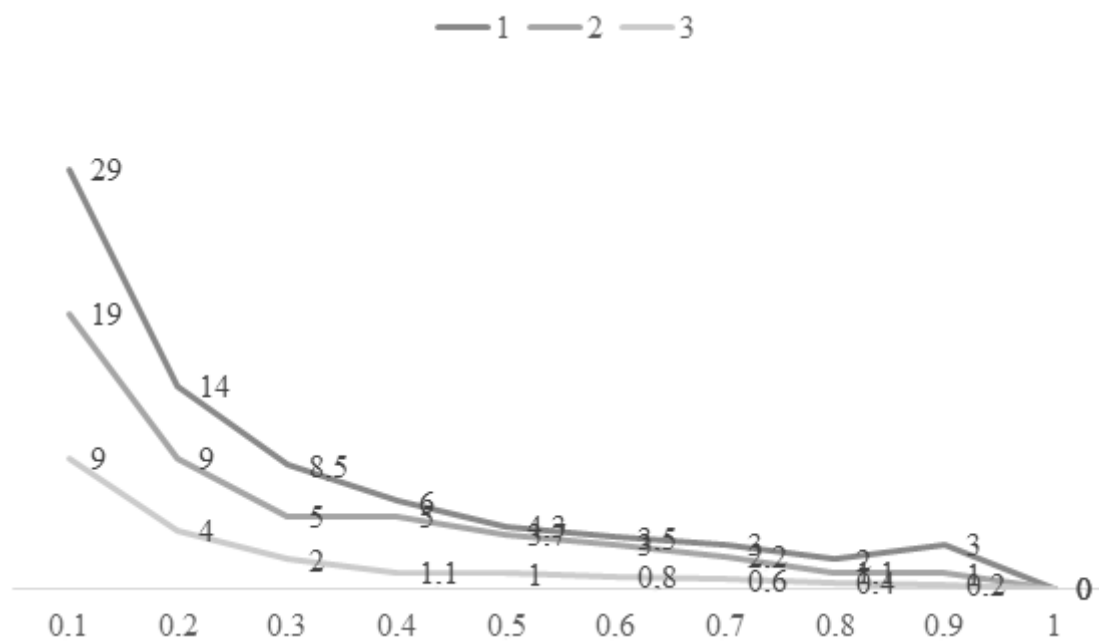


Figure 3. The Dependence of the Load Intensity on the Capacity of a Single-Channel (3), Two-Channel (2), and Three-Channel (1) System

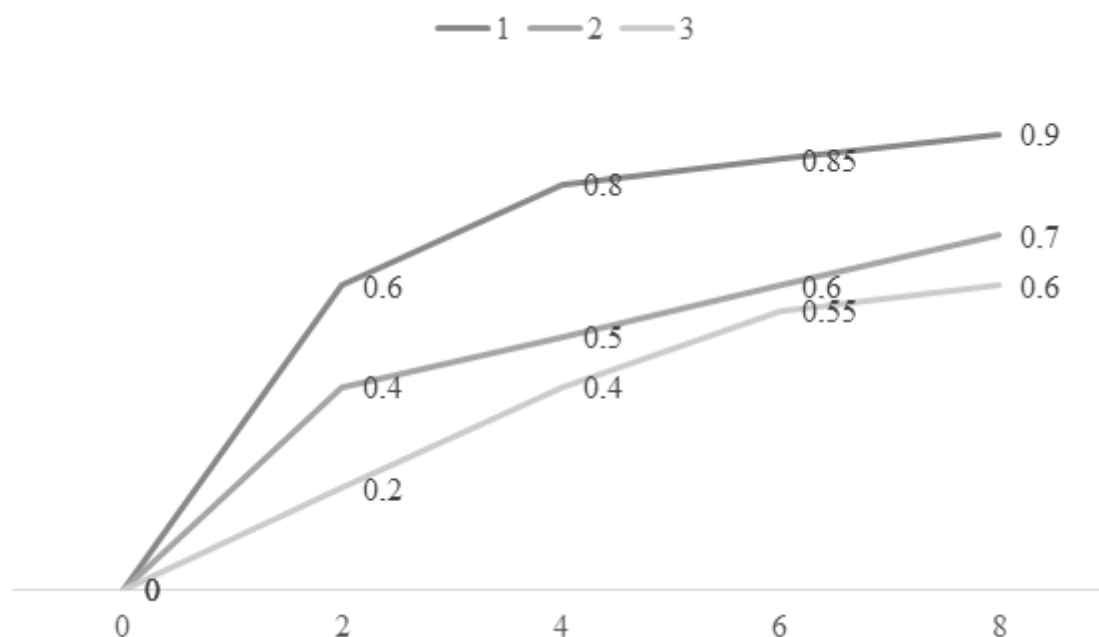


Figure 4. Probability of Power Supply of the Consumer: 1-Probability of Power Supply from One Power Source; 2-Probability of Power Supply of the Consumer from Two Power Sources at the Same Time; 3 – from Three Power Sources

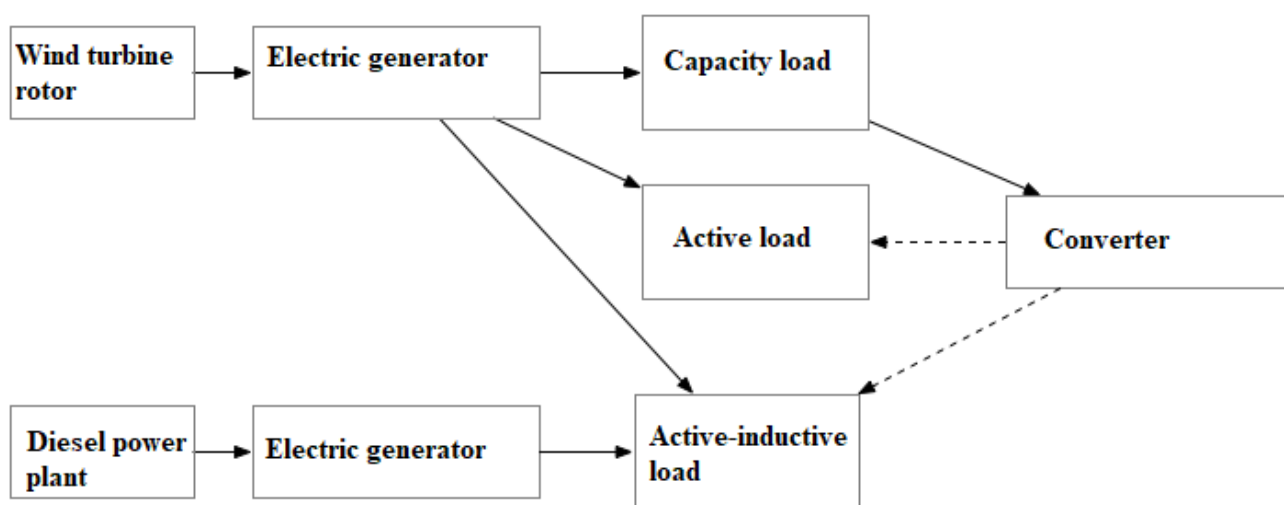


Figure 5. Block Diagram of an Autonomous Wind-Diesel Power System

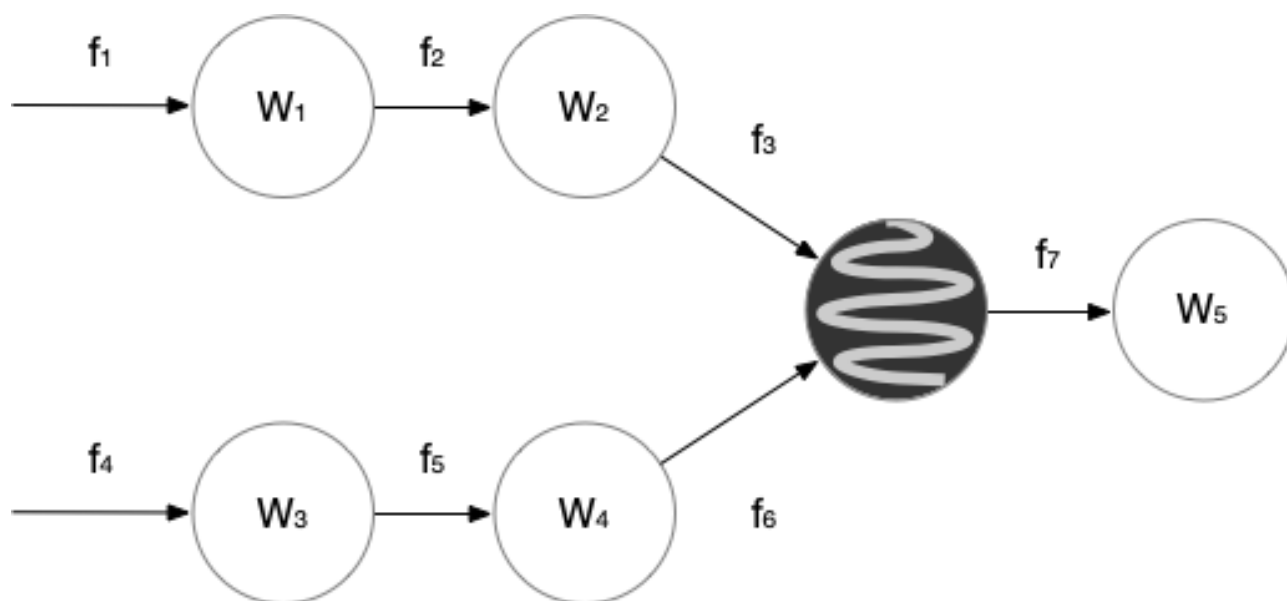


Figure 6. Functional diagram of an autonomous wind-diesel power plant: W_1 – rotor link; W_2 – electric generator link; W_3 – diesel engine link; W_4 – electric generator link; W_5 – load link.

Table 1. Raus Table

r_i	i / k	1	2	3
–	1	$c_{1,1} = \alpha_0$	$c_{2,1} = \alpha_2$	$c_{3,1} = \alpha_4$
–	2	$c_{1,2} = \alpha_1$	$c_{2,2} = \alpha_3$	$c_{3,2} = \alpha_5$
$r_3 = \frac{c_{1,1}}{c_{1,2}}$	3	$c_{1,3} = c_{2,1} - r_3 c_{2,2}$	$c_{2,3} = c_{3,1} - r_3 c_{3,2}$	$c_{3,3} = 0$
$r_3 = \frac{c_{1,2}}{c_{1,3}}$	4	$c_{1,4} = c_{2,2} - r_4 c_{2,3}$	$c_{2,4} = c_{3,2} - r_4 c_{3,3}$	$c_{3,4} = 0$
$r_3 = \frac{c_{1,3}}{c_{1,4}}$	5	$c_{1,5} = c_{2,3} - r_5 c_{2,4}$	$c_{2,5} = 0$	$c_{3,5} = 0$
$r_3 = \frac{c_{1,4}}{c_{1,5}}$	6	$c_{1,6} = c_{2,4} - r_6 c_{2,5}$	$c_{2,6} = 0$	$c_{3,5} = 0$

APLICAÇÃO DO POSTULADO DE NÃO-EQUILÍBRIO PARA CÁLCULAR O NÃO-EQUILÍBRIO DE SISTEMAS DE VÁRIOS GASES E LÍQUIDOS

APPLICATION OF THE POSTULATE OF NONEQUILIBRIUM TO CALCULATE THE NONEQUILIBRIUM OF SYSTEMS OF DISSIMILAR GASES AND LIQUIDS

ПРИМЕНЕНИЕ ПОСТУЛАТА НЕРАВНОВЕШНОСТИ ДЛЯ РАСЧЁТА НЕРАВНОВЕШНОСТИ СИСТЕМ РАЗЛИЧНЫХ ГАЗОВ И ЖИДКОСТЕЙ

RYNDIN, Vladimir V.^{1*};

¹ Toraigyrov Pavlodar State University, Department of Mechanics and Oil and Gas Engineering, Pavlodar – Republic of Kazakhstan

* Correspondence author
e-mail: rvladvit@yandex.kz

Received 06 February 2020; received in revised form 02 March 2020; accepted 29 March 2020

RESUMO

A segunda lei da termodinâmica é baseada no postulado de não-equilíbrio. De acordo com este postulado, existe uma propriedade objetiva da matéria – “não-equilíbrio”, que caracteriza a distribuição desigual da matéria e do movimento no espaço. Todos os processos (reversíveis e irreversíveis) podem ocorrer apenas em sistemas sem equilíbrio. Como uma característica quantitativa de um sistema sem equilíbrio, considera-se o trabalho máximo que pode ser feito quando o sistema sem equilíbrio entra em equilíbrio. A única formulação da segunda lei é dada: quando ocorrem processos reais (irreversíveis), o não-equilíbrio de um sistema isolado diminui e, quando ocorrem processos reversíveis, o não-equilíbrio no sistema de subsistemas de equilíbrio local não muda (o aumento em um tipo de não-equilíbrio é completamente compensado por diminuição em algum outro tipo de não-equilíbrio). Quando o sistema alcança o equilíbrio, o não-equilíbrio desaparece e todos os processos cessam. O artigo fornece uma confirmação calculada das disposições teóricas do conceito de não-equilíbrio e de seu aparato matemático com os exemplos de determinação da perda de não-equilíbrio do sistema durante a mistura isotérmica de gases diferentes e alterações no estado de não-equilíbrio do sistema “solvente puro – solução” quando uma parte do solvente entra em solução. A mistura dos mesmos gases leva ao paradoxo de Gibbs, que também é considerado neste artigo. O conceito de não-equilíbrio foi desenvolvido e as características quantitativas (medidas) do sistema de não-equilíbrio foram introduzidas, permitindo estudar os sistemas de não-equilíbrio que consistem em subsistemas de equilíbrio local nas seções da termodinâmica clássica tão simplesmente como os sistemas de equilíbrio separados.

Palavras-chave: segunda lei da termodinâmica, postulado do não-equilíbrio, valor do não-equilíbrio, paradoxo de Gibbs, cálculo do não-equilíbrio.

ABSTRACT

The postulate of nonequilibrium is at the heart of the second law of thermodynamics. According to this postulate, there is a real property of matter – “nonequilibrium,” which characterizes the uneven distribution of matter and motion in space. All processes (reversible and irreversible) can occur only in nonequilibrium systems. As a quantitative characteristic of the nonequilibrium of the system, the maximum work that can be performed during the transition of the nonequilibrium system to the equilibrium state is considered. The only formulation of the second law is given. When real (irreversible) processes occur, the nonequilibrium of the isolated system decreases, and in reversible processes, the nonequilibrium in the system of locally equilibrium subsystems does not change (the increment of one kind of the nonequilibrium entirely compensated by a decrease in the disequilibrium of some other kind). When the system reaches an equilibrium state, the disequilibrium disappears, and all processes cease. The article provides a calculated confirmation of the theoretical provisions of the concept of nonequilibrium and its mathematical apparatus by examples of determining the loss of the nonequilibrium of system when an isothermal mixing of dissimilar gases, and changes of nonequilibrium of system “pure solvent – solution” in the transition of part of the solvent in the solution. The mixing of the same gases leads to the Gibbs paradox, which is also considered in this paper. The concept of nonequilibrium was developed and the quantitative characteristics (measures) of nonequilibrium of the system were introduced allow to study nonequilibrium systems consisting of locally equilibrium subsystems in the sections of classical thermodynamics as simply as individual

Keywords: *second law of thermodynamics, postulate of nonequilibrium, quantity of nonequilibrium, Gibbs paradox, calculation of nonequilibrium.*

АННОТАЦИЯ

В основе второго закона термодинамики лежит постулат неравновесности. Согласно этому постулату существует объективное свойство вещества – «неравновесность», которое характеризует неравномерное распределение вещества и движения в пространстве. Все процессы (обратимые и необратимые) могут происходить только в неравновесных системах. В качестве количественной характеристики неравновесной системы рассматривается максимальная работа, которую можно выполнить при переходе неравновесной системы в состояние равновесия. Дается единственная формулировка второго закона: когда происходят реальные (необратимые) процессы, неравновесность изолированной системы уменьшается, а в обратимых процессах неравновесность в системе локально равновесных подсистем не изменяется (увеличение одного вида неравновесности полностью компенсируется уменьшением неравновесия какого-либо другого вида). Когда система достигает состояния равновесия, неравновесие исчезает, и все процессы прекращаются. В статье приведено расчётное подтверждение теоретических положений концепции неравновесности и её математического аппарата на примерах определения потери неравновесности системы при изотермическом перемешивании разнородных газов и изменения неравновесности системы «чистый растворитель – раствор» при переходе части растворителя в раствор. Смешивание одних и тех же газов приводит к парадоксу Гиббса, который также рассматривается в данной статье. Была разработана концепция неравновесности и введены количественные характеристики (меры) неравновесности системы, позволяющие изучать неравновесные системы, состоящие из локально равновесных подсистем, в разделах классической термодинамики так же просто, как отдельные равновесные системы.

Ключевые слова: *второй закон термодинамики, постулат неравновесности, количество неравновесности, парадокс Гиббса, расчёт неравновесности.*

1. INTRODUCTION:

All the fundamental laws of physics are based on the philosophical law of conservation of matter and its motion properties. Thus, the first law of thermodynamics (FLT) is an analytical (quantitative) expression of the law of motion conservation when changing its shape. As for the second law of thermodynamics (SLT), it has not been determined so far which property of matter (motion, form of motion or any other property) is quantitatively conserved in the isolated system (IS) when reversible (ideal) processes occur and decreases when irreversible (real) processes occur (Borgnakke and Sonntag, 2009).

Lack of knowledge (misunderstanding) of the SLT essence led to various formulations (about twenty formulations of the SLT were proposed (Putilov, 1971) and an enormous amount of researches on explaining the meaning of these formulations (Reyf, 1972; Bejan, 2016; Ben-Naim, 2010; Chen *et al.*, 2017; Wald, 2001; Martyushev and Seleznev, 2006; Rakopoulos and Giakoumis, 2006; Liu and Liu, 2008; Seifert, 2012; D'Alessio *et al.*, 2016; De Oliveira, 2019; Marboeuf *et al.*, 2019; Ptasiński and Esposito, 2019; Sellitto and Di Domenico, 2019; De Blasio, 2019).

When explaining the SLT formulations,

contradictions arise both within separate textbooks and textbooks of different authors: Andryushchenko (1975); Baehr (1973); Calabrese (2018); Chen and Tsutsumi (2018); Holyst and Poniewierski (2012); Krutov V.I. (Krutov *et al.*, 1991); Vukalovich and Novikov (1968); Novikov (1984); Callen (1985); Fermi (1937); Kirillin V. A. (Kirillin *et al.*, 1983); Kittel (1993); Kondepudi and Prigogine (2015); Krichevsky (1970); Lavenda (2010); Morales-Rodriguez (2016); Moran (Moran *et al.*, 2014); Srivastava (Srivastava *et al.*, 2007).

A single formulation is needed (as in other laws) from which consequently must result (or be deemed redundant) various existing formulations. Such the SLT formulation, based on the postulate “on the existence and change of nonequilibrium”, is given by Ryndin V.V. “The total (complete) nonequilibrium of an isolated system cannot increase – in reversible (ideal) processes it does not change, and in real (irreversible) processes it decreases”. This monograph introduces the concept of nonequilibrium. According to this concept, the cause of all processes is the nonequilibrium, a property of matter caused by the uneven distribution of the concentration of motion in space (Ryndin, 2014).

The following types of nonequilibrium are singled out: thermal and baric, caused by

temperature and pressure difference in space; mechanical (kinetic and potential), electric, chemical, and others. To estimate the nonequilibrium of the whole system consisting of a set of locally equilibrium subsystems, the concept of total nonequilibrium is introduced as a sum of all the types of nonequilibrium of an isolated system (Ryndin, 2014).

Processes in which the total nonequilibrium of IS does not change (the increase in nonequilibrium of one type is fully compensated by the loss of nonequilibrium of other types), and will be those reversible processes that are considered in thermodynamics; in irreversible processes, the nonequilibrium of IS decreases. The analytic expression of the postulate of nonequilibrium (nonequilibrium IS cannot increase) is the following inequality (Ryndin, 2014) (Equation 1), where Λ – nonequilibrium (the amount of nonequilibrium), which means the maximum work obtained by running reversible processes in the adiabatic system (AS) before the full transition of the system to the equilibrium state, or lost work in the IS when the system changes to the equilibrium state.

Whereas the IS can be mentally transformed into an adiabatic system, the loss of the IS nonequilibrium can be defined as the work of the adiabatic system with reversible processes occurring in it, that bring the nonequilibrium system into an equilibrium state. Inequality (Equation 1) is the opposite of Rudolf Clausius inequality (Clausius, 1850) (Equation 2) – total entropy of IS cannot decrease. As a result of this generalization, the dS_{IS} , entropy change used to write the SLT has become one of the characteristics of IS nonequilibrium change.

This article gives the calculated confirmation of the main provisions of the nonequilibrium concept by examples of calculation of the nonequilibrium of systems of dissimilar gases and liquids.

The mixing of homogeneous gases is associated with the Gibbs Paradox. The paradox was formulated by Josiah Willard Gibbs in 1875 at the same time as the version of its explanation (Gibbs, 1982). According to Gibbs, there was nothing paradoxical about the entropy of mixing; the term Gibbs paradox was probably first used by O. Wiedeburg (Wiedeburg, 1894; Gelfer *et al.*, 1975).

Gibbs Paradox is the absence of continuity for entropy when moving from mixing different (dissimilar) gases to mixing identical gases: mixing entropy when moving from ideal gases with an

arbitrarily small degree of difference to identical gases jumps from constant value to zero, which seems unexpected and illogical (Lyuboshits and Podgoretsky, 1971). Sometimes Gibbs paradox is called the apparently nonadditivity of entropy when two volumes of the same ideal gas are combined (Poltorak, 1991; Klimontovich, 1982; Anselm, 1973). To solve the Gibbs paradox means to establish the reasons for the jump in entropy of the ΔS when moving from a mixture of closely similar gases to a mixture of identical gases.

A significant number of various attempts to solve the Gibbs paradox are described in the literature. However, the fact that more and more new paradox solutions are appearing suggests that there is no generally accepted answer to the posed question (Ignatovich, 2010; Haytun, 2010).

2. MATERIALS AND METHODS:

2.1. Nonequilibrium of an isolated system

The concept of nonequilibrium defines an isolated system as a nonequilibrium system consisting of a set of local-equilibrium (quasi-equilibrium) subsystems (heat sources (HS) and heat receivers, work receivers and work sources, work body (WB), ambient medium (AM), finite and small flow elements), that interact with each other but do not interact with other systems that do not belong to the considered isolated system.

Since when real processes take place, the IS tends to the equilibrium state, when the system loses the ability to perform work (to transfer motion in an ordered form), then as a quantitative measure of the nonequilibrium of the system Λ it is accepted the maximum work that could be transferred by the system to the environment when mechanical isolation is removed, i.e. if it is mentally turned into an adiabatic system (Equation 3).

To calculate the maximum (possible) work, values such as thermodynamic potentials, heat exergy and flow exergy are used in thermodynamics. In isolated systems, when real processes take place, there is a transformation of dissipation of ordered motion (OM) into chaotic motion (CHM), i.e. there is dissipation (scattering) of chaotic motion. The equilibrium state in the system occurs when all the OM (work) completely turns into CHM (heat) (Equation 4).

This work is called a possible work, loss of performance, or energy loss. It is estimated through the entropy increase (Equation 5) at the transition of the IS from the nonequilibrium state to

the equilibrium state according to the Gouy-Stodola equation (Equation 6) (Kirillin *et al.*, 1983), where T_{AM} is the temperature of the equilibrium ambient medium (AM) (atmosphere or large waterbody), which does not change at the transition of the nonequilibrium system to the equilibrium state (Equation 7).

In general, when there is no liquid AM, the T_{CBmin} temperature is taken, i.e. the variable body temperature with the lowest temperature (cold body temperature – CB) during the heat exchange or the temperature of the thermodynamic system (WB, HS) during its interaction with the work sources (load, spring, flywheel, capacitor, accumulator, etc.), which alone are not characterized by temperature, and Equation 3 with consideration of Equation 6 becomes as Equation 8.

Change of nonequilibrium (Equation 9) IS (recall: increment (plus sign) (Equation 10), decrease (minus sign) (Equation 11)) at its transition to the equilibrium state it can be represented as the difference between the values of the nonequilibrium in the final state (equilibrium state Λ_2 , where the nonequilibrium is zero (Equation 12) and the initial Λ_1 – nonequilibrium state determined by Equation 8 (Equation 13).

The equation (Equation 13) for changing the IS nonequilibrium in a simple process considering the inequality (Equation 2) for changing the IS entropy (Equation 14) is recorded as follows (Equation 15).

The inequality (Equation 15) confirms the postulate of nonequilibrium (Equation 1) – IS nonequilibrium cannot increase. If we proceed from the primary inequality (Equation 1), then out of (Equation 13) follows the Clausius inequality (Equation 2) (Equation 16). The Equation 13 in differential form for the loss of $(-d\Lambda)$ system nonequilibrium can be recorded as follows (Equation 17) and in integral form (Equation 18).

2.2. The nonequilibrium of the adiabatic system

If in general the thermodynamic potential is indicated by the symbol Π (“pi” Greek), then the amount of the system's nonequilibrium will be determined by the difference between the system's potentials in the nonequilibrium state $\Pi_{noneq.st}$ and the equilibrium state $\Pi_{eq.st}$ (let's call it the “potential difference” $\Delta\Pi^*$), equal to the maximum work of the system during its transition to the equilibrium state (Equation 19).

For the finite loss of nonequilibrium, the

equation (Equation 19) can be recorded as Equation 20. In differential form, this equation will look like Equation 21, where (Equation 22), because all processes stop when the system goes into an equilibrium state and, consequently, changes of all values are equal to zero. The potential difference in the adiabatic system performing the work decreases in any processes (reversible and irreversible). However, only in reversible processes (index “o”) the loss of potential difference equal to the loss of thermodynamic potential will be equal to the maximum external work of the nonequilibrium system (Equation 23).

In the case of irreversible processes, the external (upper index “e”) work of the system results in fewer losses of potential difference (losses of thermodynamic potential) (Equation 24).

Consequently, the general condition of the transition of the system from a more nonequilibrium state to a less nonequilibrium state (more equilibrium) is as follows (Equation 25). According to this formula, the external work is equal to the loss of potential difference, or the loss of thermodynamic potential in reversible processes and less than this loss in irreversible processes.

2.3. Gibbs Paradox

Many specialized works are dedicated to the Gibbs Paradox: Bazarov (1979; 2010), Gelfer (Gelfer *et al.*, 1975); Ignatovich (2010); Lyuboshits and Podgoretsky (1971); Terletsky (1984); Haytun (2010) and others. Let us consider the isothermal mixing of two originally separated ideal gases placed in a box with diathermic (heat-conducting) walls impermeable to the substance and the same partition dividing the box into two parts with different gases; both parts have identical volumes (Equation 26) and contain the same amount of substance (Equation 27) with temperature T and pressure p ; the box is placed in a thermostat with the same temperature T , to achieve equality of gas temperatures during the mixing process, and the partition is equipped with an opening door (flap, crane, valve). Molar heat capacities of gases on both sides of the partition are the same. The assumption of the uniformity of molar heat tanks, volumes of subsystems, and the equality of the substance quantity contained in them is made to simplify the calculations. In the book by Bazarov I.P. a formula for the entropy of mixing is given without using this simplification.

Gibbs has discovered the fact that when identical ideal gases are mixed, there is no change

in entropy, and when dissimilar gases are mixed, there is a jump in entropy (Bazarov, 2010) (Equation 28), where v – substance quantity, mole; R_μ – molar (universal) gas constant, J/(mol.K); k_B – Boltzmann's constant, J/K; N – particle number (atoms, molecules).

This abrupt (discontinuous) behavior of the entropy of mixing ΔS is called the Gibbs Paradox. The paradox here is that when considering the mixing of gases entropy, the mixing of two identical gases cannot be considered as a limiting case of mixing two different gases (the paradox, as we know, is a true statement, which is unusual, contradicts the previously known, and about which it should be said that it cannot be). As noted in the paper (Bazarov, 1979), "the paradox cannot be 'removed' or eliminated, but can be explained or solved". Various solutions to the Gibbs Paradox were proposed.

Solutions that reject the actual existence of the paradox. The reasoning logic of researchers who reject the very existence of the Gibbs paradox is as follows. The paradox comes down to a jump in the behavior of ΔS mixing entropy at a continuous convergence of some parameters characterizing the gases being mixed. If such continuous approximation is contrary to the laws of physics, i.e., if the differences between gases can only change discretely (for example, between the H and He atoms there's no continuous transition), the Gibbs paradox disappears: there's nothing strange about the fact that when gases parameters are changed discretely, their mixtures properties also change discretely (Sommerfeld, 1955; Kedrov, 1969).

Quantum discrete solutions. Today, the discrete quantum solution to the Gibbs Paradox has the most significant number of supporters. It is distinguished from the solutions rejecting the paradox itself by the paradox existence recognition, the discreteness of the mixing entropy is perceived as a natural result of the substance discreteness, the correct dependence of the gas entropy on the number of particles (quantity of substance) follows from the quantum statistics of indistinguishable particles (Haytun, 2010), and the autonomy of the mixing entropy from the properties of gases is considered as an obvious consequence of the assumption of their ideality (Gelfer *et al.*, 1975).

On the experimental discovery of the Gibbs Paradox. Throughout the whole 20th century more and more new approaches have been invented, trying to verify the reality of the Gibbs paradox, and over and over again convincing of the impossibility

of their realization. The Van der Waals hypothesis of the fundamental impossibility of experimentally verifying the existence of the Gibbs Paradox (Waals and Kohnstamm, 1912) remains unproven, but in practice the paradoxical jump of the entropy of mixing still cannot be measured.

3. RESULTS AND DISCUSSION:

3.1. Nonequilibrium of a system of dissimilar gases at the same pressures and temperatures (isothermal mixing – diffusion)

Let's consider two gases divided by partition A into two volumes V' and V'' (Figure 1). Initially (at time t_1) the temperature and pressure of gases are the same (Equation 29). After removing the partition, each gas spreads over the entire volume of (Equation 30) towards each other and at the time t_2 reaches the corresponding pressure (p_2' or p_2''). In the case of ideal gases, the temperature of their T does not change during mixing.

When the gases are mixed, the diffusion (concentration) nonequilibrium is lost, allowing the work to be obtained in the presence of an appropriate device. Such a device can be movable semi-permeable partitions (pistons), each of which is pressurized by only one gas for which the partition is impermeable. Under the appropriate pressures, the pistons-partitions will move from partition A to the end of the cylinder, and the gases will expand while working. So that the temperature of gases when disposing the work from the pistons-partitions to the work receiver (flywheel, spring, load...) does not change, it is necessary to supply heat equal to the work performed, i.e. a heat source (HS) is required.

In such isolated system (HS-WB-WR) when a reversible process is running, the loss of diffusive nonequilibrium in the system "gas–gas" $-\Delta\Lambda_{\text{dif}}$ WB-WB (WB – work body) is compensated for by an increase in the mechanical nonequilibrium of the system working body-work receiver WB-WR $\Delta\Lambda_{\text{mech}}$ (thermal nonequilibrium in all IS does not change (Equation 31), since the process is isothermal and is running at (Equation 32), thus the thermal nonequilibrium of IS does not change (Equation 33).

If the work receivers (WR) are separated from the rest of the system bodies, i.e., consider a non-isolated adiabatic system WB-HS (Figure 1), then in accordance with (Equation 24) the loss of diffusive nonequilibrium AS will be equal to the increase of mechanical nonequilibrium WR, which

in its turn is equal to the external work (Equation 34), performed by AC in a reversible process (index "o") at its transition to an equilibrium state (Equation 35).

The work performed by nonequilibrium AS will consist of the works of isothermal expansion of the 1st W_T and 2nd W''_T gases (Equation 36), where pressures are expressed through volumes using the Clapeyron equation (Equation 37) and (Equation 38), where R (Equation 39) – specific gas constant, J/(kg.K); R_μ – molar gas constant, J/(kg.K); M – molar mass, kg/mole. Since the volume and temperature of the nonequilibrium adiabatic system do not change (isochoric and isothermal process), the maximum operation of such a system at its reversible transition to an equilibrium state will be equal to Helmholtz potential (energy) losses (Equation 20) (Equation 40), where the change in Helmholtz energy of heat source is equal to zero: because it does not perform any external work (Equation 41), then according to the FLT (Equation 42), i. e. (Equation 43).

Specific Helmholtz energy of ideal gas (Equation 44) can be calculated if the expression for entropy is known. In the case of the ideal gas, the expression for specific entropy in the function of temperature T and specific volume is as follows (Kirillin *et al.*, 1983) (Equation 45), where s_o – constant for this gas. By substituting the expression for s in the general formula for Helmholtz specific energy (Equation 44), we'll get Equation 46, where $b(T)$ – the function of only one temperature, since energy expression for the ideal gas depends only on the temperature, i.e. (Equation 47).

By multiplying all the figures (Equation 46) by the mass of the gas and expressing the specific volume of the gas through the complete volume, we obtain the expression for Helmholtz energy in function of temperature, mass, and volume of the ideal gas (Equation 48). By substituting expression (Equation 48) for Helmholtz potential in (Equation 33), given that (Equation 49), we'll get Equation 50.

Comparing expressions (Equation 40) and (Equation 50), we conclude that, indeed, the work of nonequilibrium AS in the case of a reversible isochoric and isothermal process is equal to the Helmholtz energy losses. In the case of a complete transition of nonequilibrium AS to an equilibrium state, it is equal to the diffusive nonequilibrium of such a system (Equation 51).

As there are no such special devices (semi-permeable pistons) in actual practice, all

possible external work at system transition to an equilibrium state is lost, it dissipates inside the system. The entropy increase of an isolated system consisting of two dissimilar gases associated with the loss of concentration nonequilibrium due to diffusion will be determined by the general formula (Equation 8) considering that (Equation 52) and lost work is equal to external work (Equation 50) of adiabatic system (WB-HS) in case of reversible isochoric and isothermal process, i. e. (Equation 53).

For an ideal gas, we can introduce a "body gas constant" (Equation 54), through which specific and molar gas constants are introduced (Equation 55). Considering (Equation 54), the expression (Equation 53) can be recorded as follows (Equation 56).

In the particular case, of equal quantities of gases (Equation 57), remaining before mixing in equal volumes (Equation 58) the ratio (Equation 56) will be as follows (Equation 59), which is similar to the known expression (Equation 28) for entropy jump in the mixing of dissimilar gases. As we can see, calculations of the IS entropy change through lost work (Equation 53) and the entropy values of gases before and after mixing (Equation 28) give the same results, which once again confirms the correctness of formula (Equation 53) for calculating the entropy change of an isolated system.

In the case of a reversible process of equalizing the concentration of gases over the entire cylinder volume in an adiabatic (WB-HS) or isolated system (AS-WR), the change of entropy of these systems is equal to zero, because in the reversible process the heat supplied to WB by HS is equal and opposite in sign to the heat supplied by HS (Equation 60), as well as equal to the temperatures of WB and HS (Equation 61), where the work receiver entropy change ΔS_{WR} is equal to zero, because it does not possess a reserve of chaotic (thermal) motion.

If we take two identical gases at equal pressures and temperatures, separated by a partition, and then remove this partition, the entropy of such a system will not change, although the gas molecules will take up the entire volume. This fact is easily explained by the concept of nonequilibrium. According to the described nonequilibrium concept based on the postulate of nonequilibrium, a change in IS entropy is only possible if the system loses its full (total) nonequilibrium characterized by the lost work. Since there is no nonequilibrium, including concentration (diffusion) nonequilibrium in a

homogeneous gas separated by a partition in two parts at the same pressure and temperature, there can be no lost work (Equation 62) and the entropy increase associated with it: when two portions of the same gas are mixed, the gas-permeable pistons-partitions on both sides will be stationary. Therefore, although technically it is possible to calculate the change of IS entropy, consisting of homogeneous gas, by formula (Equation 28), such calculation does not make sense, because there are no devices working in a full equilibrium system. Since there is no lost work (no change in the nonequilibrium system) when mixing two portions of the same gas, there is no change in entropy (there is no dissipation of ordered motion) of such a system according to (Equation 59).

When two different (dissimilar) ideal gases are mixed with the same molar heat capacity, the system entropy increases by the same value regardless of the degree of difference between the gases. In other words, the mixing entropy during the transition from ideal gases with as little difference as possible to identical gases changes by a jump from a constant value to zero (*paradoxical jump of entropy of mixing*) (Vukalovich and Novikov, 1968). As already mentioned, the autonomy of the entropy of mixing from the nature of gases is considered as an obvious consequence of the assumption of their ideality. Ideal gas is a model of gas, rather than the gas itself, in which there are no interaction forces between the molecules (and in our case with permeable partitions) that could influence the possible mixing work. Therefore, as a special property of an ideal gas (as in the assumption that the internal energy is constant about the gas volume), it should be recognized that the amount of nonequilibrium and entropic difference is constant when mixing dissimilar ideal gases in an isolated system.

3.2. Calculation of change of nonequilibrium of system "pure solvent-solution" at transition of a part of solvent in a solution

Suppose that in a hermetically sealed boiler at a constant temperature T , in two vessels, there is pure solvent and solution of any non-volatile substance (Figure 2).

This system is in an equilibrium state, as the vapor pressure above the solvent p_1 is higher than above the solution p_2 . When a portion of the solvent of a single mass ($m = 1$ kg) evaporates and passes into the solution, the nonequilibrium (specific) of the system decreases by the value of specific external work (Equation 20), which could have been obtained in a reversible process in the

presence of a special device (Equation 63).

Such a device can be a cylinder with a moving piston, which is connected in turn with a special crane to a pure solvent or solution. In the first stage (*a-b*), 1 kg of water evaporates at constant values of pressure (Equation 64) and temperature (Equation 65). To do this, the cylinder is connected by a crane to a vessel containing pure solvent and an isobaric expansion of this steam is performed. As a result of the steam expansion, steam performs a specific work on the piston (Equation 66).

By neglecting the specific volume of water (liquid) compared to the specific volume of steam and considering steam as an ideal gas (Equation 67), we will get Equation 68, where R_{st} – specific gas steam constant, J/(kg.K). In the second stage (*b-c*), there is an isothermal expansion of the steam to the pressure p_2 . In this case, the steam performs a specific work of isothermal expansion over the piston, which is known to be determined by the expression (Equation 69).

In the third stage (*c-d*), there is a condensation of steam, for which the cylinder cavity is connected by a crane to a vessel in which there is a solution at a pressure of p_2 of steam above it, and isobaric compression is performed. As a result, a portion of water weighing 1 kg passes into the solution, with a specific compression work above the steam (the specific volume of condensate – liquid – neglected) (Equation 70).

Since isobaric and isothermal processes are carried out with the supply (removal in compression) of heat, it is necessary to provide for the presence of sources (receivers) of heat exchanging heat with steam (work body) in such a system. Consequently, the nonequilibrium adiabatic system will include the work body (steam in nonequilibrium state in two vessels above both solvent and solution, and in the cylinder – in equilibrium state) and heat sources. To receive the work performed by nonequilibrium AS, it is necessary to provide the work receiver (it can also be used as a source of work during compression). As an AS receiver (source) of work, can be used a special device that provides equality of moments relative to the axis of the cam of constant gravity and variable force of steam pressure on the piston, which ensures the slowness (and thus equilibrium) of the expansion process (Figure 2). The total specific work performed by such nonequilibrium AS, will be equal to the sum of works defined by expressions (Equations 68 – 70), (Equation 71).

Since the volume of nonequilibrium AS in

the process of transition of water solvent in the solution does not change, as well as temperature, such a process will be isochoric and isothermal, and thus the loss of nonequilibrium (specific) system will be equal to the loss of Helmholtz potential (specific), which in its turn is equal to the external specific work of nonequilibrium AS in the reversible process (Equation 72).

As there is no special device for reversible transition of water solvent to solution in actual practice, all possible useful work will be lost (Equation 73). In the case of a natural (irreversible) transition process of solvent into solution, the entropy (specific) of the isolated system consisting only of solvent and solution vessels will increase by the value of (Equation 74).

It is evident from the considered examples that in the presence of special devices reversible processes can take place also in strictly nonequilibrium systems, and not only in the systems close to an equilibrium state as it is generally accepted to count.

4. CONCLUSIONS:

Thus, it was calculated confirmation of the theoretical provisions of the concept of nonequilibrium and its mathematical apparatus by examples of determining the loss of the nonequilibrium of system. The formula for calculating the change in entropy of an isolated system when mixing dissimilar gases, obtained through the lost nonequilibrium (lost work), coincides with the Gibbs formula, which is a practical confirmation of the validity of the postulate of nonequilibrium, which the author used as a basis for the SLT.

When considering the isothermal mixing of two originally separated ideal gases, the following was found: Gibbs Paradox of a jump-like change in the entropy of an isolated system when mixing dissimilar gases is explained by a jump-like loss of nonequilibrium inherent in the ideal gas model, when the interaction forces between gas molecules as well as with the walls are not considered.

Based on the results, the concept of nonequilibrium was developed and introduced quantitative characteristics (measures) of nonequilibrium system allow to investigate nonequilibrium systems consisting of locally equilibrium subsystems in sections of classical thermodynamics as easily as separate equilibrium systems.

This article is a continuation of the author's

concept of nonequilibrium. The above expressions which obtained in the calculations of diffusive nonequilibrium of the dissimilar gases system that is lost as a result of gases isothermal mixing, and also nonequilibrium changes of the "pure solvent – solution" system at transition of a part of solvent to solution can be used in practice.

5. REFERENCES:

1. Andryushchenko, A. I. *Fundamentals of Technical Thermodynamics of Real Processes*, Moscow: Vysshaya shkola, **1975**, 264.
2. Anselm, A. I. *Fundamentals of Statistical Physics and Thermodynamics*, Moscow: Nauka, **1973**, 424.
3. Baehr, H. D. *Thermodynamics: An Introduction to the Basics and Their Technical Applications*, Berlin – Heidelberg – New York: Springer – Verlag, **1973**.
4. Bazarov, I. P. *Methodological Problems of Statistical Physics and Thermodynamics*, Moscow: Publishing House Moscow University, **1979**, 88.
5. Bazarov, I. P. *Thermodynamics*, Saint Petersburg, Moscow, Krasnodar: Doe, **2010**, 384.
6. Bejan, A. *Advanced Engineering Thermodynamics*, Durham: Duke University, **2016**.
7. Ben-Naim, A. *Discover Entropy and the Second Law of Thermodynamics: A Playful Way of Discovering a Law of Nature*, Singapore: World Scientific Publishing Company Incorporated, **2010**.
8. Borgnakke, C., Sonntag, R.E. *Fundamentals of Thermodynamics*, Ann Arbor: University of Michigan, **2009**.
9. Calabrese, P. *Physica A: Statistical Mechanics and its Applications*, **2018**, 504, 31-44.
10. Callen, B. *Thermodynamics and Introduction to Thermostatistics*, New York: John Wiley and Sons, **1985**.
11. Chen, L., Tsutsumi, A. *Chemical Engineering Transactions*, **2018**, 70, 949-954.
12. Chen, Z.-S., Li, C., Wang, G. *Journal of Engineering Thermophysics*, **2017**, 38(8), 1589-1596.
13. Clausius, R. First Memoir. On the Moving

- Force of Heat and the Laws of Heat Which May be Deduced Therefrom. In: *The Mechanical Theory of Heat – with its Applications to the Steam Engine and to Physical Properties of Bodies*, London: John van Voorst, 1 Paternoster Row, **1850**.
14. D'Alessio, L., Kafri, Y., Polkovnikov, A., Rigol, M. *Advances in Physics*, **2016**, 65(3), 239-362.
 15. De Blasio, C. Introduction to entropy and second law. In: *Green Energy and Technology*, Basingstoke: Springer Nature, **2019**.
 16. De Oliveira, M.J. *Revista Brasileira de Ensino de Física*, **2019**, 41(1).
 17. Fermi, E. *Thermodynamics*, New York: Prentice-Hall, Inc, **1937**.
 18. Gelfer, Ya. M., Lyuboshits, V. L., Podgoretsky, M. I. *The Gibbs Paradox and Particle Identity in Quantum Mechanics*, Moscow: Nauka, **1975**, 272.
 19. Gibbs, J. V. *Thermodynamics. Statistical Mechanics*, Moscow: Nauka, **1982**, 584.
 20. Haytun, S. D. *History of the Gibbs Paradox*, Moscow: Komkniga, **2010**, 168.
 21. Hołyst, R., Poniewierski, A. *Thermodynamics for Chemists, Physicists and Engineers*, Dordrecht: Science + Business Media, **2012**.
 22. Ignatovich, V. N. *The Gibbs Paradox from the Point of View of a Mathematician*, Kyiv: Atopol, **2010**, 80.
 23. Kedrov, B. M. *Three aspects of atomistics. I. The Gibbs Paradox, The logical aspect*. Moscow: Nauka, **1969**, 294.
 24. Kirillin, V. A., Sychev, V. V., Sheyndlin, A.E. *Technical Thermodynamics*, Moscow: Energoatomizdat, **1983**, 448.
 25. Kittel, Ch. *Thermal Physics*, New York: John Wiley and Sons, **1993**.
 26. Klimontovich, Yu. L. *Statistical Physics*, Moscow: Nauka, **1982**, 608.
 27. Kondepudi, D., Prigogine, I. *Modern Thermodynamics: From Heat Engines to Dissipative Structures*, New Delhi: John Wiley and Sons, **2015**.
 28. Krichevsky, I. R. *Concepts and Foundations of Thermodynamics*, Moscow: Khimiya, **1970**.
 29. Krutov, V. I., Isayev, S. I., Kozhinov, A. I. *Technical Thermodynamics*, Moscow: Vysshaya Shkola, **1991**.
 30. Lavenda, B. H. *A New Perspective on Thermodynamics*, Berlin: Springer Science + Business Media, **2010**.
 31. Liu, Y., Liu, Y.-J. *Separation and Purification Technology*, **2008**, 61(3), 229-242.
 32. Lyuboshits, V. L., Podgoretsky, M. I. *Advances in Physical Sciences*, **1971**, 105(2), 353-359.
 33. Marbœuf, A., Claisse, A., Le Tallec, P. *Journal of Computational Physics*, **2019**, 390, 66-92.
 34. Martyushev, L. M., Seleznev, V. D. *Physics Reports*, **2006**, 426(1), 1-45.
 35. Morales-Rodriguez, R. *Thermodynamics: Fundamentals and Its Application in Science*, Kongens Lyngby: Technical University of Denmark, **2016**.
 36. Moran, M. J., Shapiro, H. N., Boettner, D. D., Balley, M. B. *Fundamentals of Engineering Thermodynamics*, New York: John Wiley and Sons, **2014**.
 37. Novikov, I. I. *Thermodynamics*, Moscow: Mashinostroenie, **1984**.
 38. Poltorak, O. M. *Thermodynamics in Physical Chemistry*, Moscow: Vysshaya Shkola, **1991**.
 39. Ptaszyński, K., Esposito, M. *Physical Review Letters*, **2019**, 122(15).
 40. Putilov, K. A. *Thermodynamics*, Moscow: Nauka, **1971**.
 41. Rakopoulos, C.D., Giakoumis, E.G. *Progress in Energy and Combustion Science*, **2006** 32(1), 2-47.
 42. Reyf, F. *Statistical Physics: Berkeley Physics Course*, Berkeley: The University in Berkeley, McGraw Hill Book Company, **1972**.
 43. Ryndin, V.V. *The Concept of Nonequilibrium as the Basis of the Second Law of Thermodynamics*, Saarbrücken: LAP Lambert Academic Publishing, **2014**, 454.
 44. Seifert, U. *Reports on Progress in Physics*, **2012**, 75(12).
 45. Sellitto, A., Di Domenico, M. *Continuum Mechanics and Thermodynamics*, **2019**, 31(3), 807-821.
 46. Sommerfeld, A. *Thermodynamics and Statistical Physics*, Moscow: IL, **1955**.
 47. Srivastava, R. C., Subit, K. S., Abhay, K. J. *Thermodynamics: A Core Course*, New Delhi: Prentice-Hall of India Private Limited, **2007**.
 48. Terletsky, Y. P. *Thermophysical Properties of*

Metastable Systems, **1984**, 3-7.

49. Vukalovich, M. P., Novikov, I. I. *Technical Thermodynamics*, Moscow: Energiya, **1968**.

50. Waals, J. D., Kohnstamm, Ph. *Lehrbuch der Thermodynamik*, Zweiter Teil. Leipzig: Verlag von Johann Ambrosius Barth, **1912**, 646.

51. Wald, R. M. *Living Reviews in Relativity*, **2001**, 4, 1-44.

52. Wiedeburg, O. *Annalen der Physik*, **1894**, 289(12), 684-697.

$$d\Lambda_{\text{noneq.IS}} \leq 0 \quad (\text{Eq. 1})$$

$$dS_{\text{IS}} = dS_{\text{noneq.IS}} \geq 0 \quad (\text{Eq. 2})$$

$$\Lambda \equiv \Lambda_{\text{noneq.IS}} \equiv W_{\text{noneq.st} \rightarrow \text{eq.st}}^{\text{max}} \quad (\text{Eq. 3})$$

$$W_{\text{noneq.st} \rightarrow \text{eq.st}}^{\text{max}} = W_{\text{lost}}^{\text{max}} = Q_{\text{diss}} \quad (\text{Eq. 4})$$

$$\Delta S_{\text{noneq.IS} \rightarrow \text{eq.st}} \quad (\text{Eq. 5})$$

$$W_{\text{diss}}^{\text{max}} = W_{\text{noneq.st} \rightarrow \text{eq.st}}^{\text{max}} = T_{\text{AM}} \Delta S_{\text{noneq.st} \rightarrow \text{eq.st}} \quad (\text{Eq. 6})$$

$$T_{\text{AM}} = \text{const} \quad (\text{Eq. 7})$$

$$\Lambda_{\text{noneq.IS}} = W_{\text{diss}}^{\text{max}} = W_{\text{lost}} = W_{\text{noneq.st} \rightarrow \text{eq.st}}^{\text{max}} = T_{\text{CBmin}} \Delta S_{\text{noneq.IS} \rightarrow \text{eq.st}} \quad (\text{Eq. 8})$$

$$\Delta \Lambda = \Lambda_2 - \Lambda_1 \quad (\text{Eq. 9})$$

$$\Delta x = x_2 - x_1 \quad (\text{Eq. 10})$$

$$-\Delta x = x_1 - x_2 \quad (\text{Eq. 11})$$

$$\Lambda_{\text{eq.st}} \equiv 0 \quad (\text{Eq. 12})$$

$$\Delta \Lambda_{\text{noneq.IS}} = \Lambda_{\text{eq.st}} - \Lambda_{\text{noneq.IS}} = -\Lambda_{\text{noneq.IS}} = -W_{\text{noneq.st} \rightarrow \text{eq.st}}^{\text{max}} = -T_{\text{CBmin}} \Delta S_{\text{noneq.IS} \rightarrow \text{eq.st}} \quad (\text{Eq. 13})$$

$$dS_{\text{noneq.IS}} \geq 0 \quad (\text{Eq. 14})$$

$$d\Lambda_{\text{IS}} = -T_{\text{CBmin}} dS_{\text{IS}} \leq 0 \quad (\text{Eq. 15})$$

$$dS_{\text{IS}} \geq 0 \quad (\text{Eq. 16})$$

$$-d\Lambda = \delta W_{\text{lost}} = \delta W_{\text{diss}} = T_{\text{CBmin}} dS_{\text{diss}} \quad (\text{Eq. 17})$$

$$-\Delta \Lambda = W_{\text{lost}} = W_{\text{diss}} = T_{\text{CBmin}} \Delta S_{\text{diss}} \quad (\text{Eq. 18})$$

$$\Lambda_{\text{AS}} = \Delta \Pi^* = \Pi_{\text{noneq.st}} - \Pi_{\text{eq.st}} = W_{\text{noneq.st} \rightarrow \text{eq.st}}^{\text{max}} = W_{\text{max}}^{\text{e}} \quad (\text{Eq. 19})$$

$$\begin{aligned}
-\Delta\Lambda_{AS}^{\max} &= -\Delta(\Delta\Pi^*)_{\max} = \Lambda_1 - \Lambda_2 = \Lambda_{\text{noneq.st}} - \Lambda_{\text{eq.st}} = \Lambda_{\text{noneq.st}} = \\
&= \Pi_{\text{noneq.st}} - \Pi_{\text{eq.st}} = \Pi_1 - \Pi_2 = -\Delta\Pi_{\max} = W_{\text{noneq.st} \rightarrow \text{eq.st}}^{\max} = W_{\max}^e.
\end{aligned}
\tag{Eq. 20}$$

$$-d\Lambda_{AS} = -d(\Delta\Pi^*) = -d\Pi_{\text{noneq.st}} + d\Pi_{\text{eq.st}} = -d\Pi_{\text{noneq.st}} \equiv -d\Pi = \delta W_{\max}^e = \delta W^{e\circ} \tag{Eq. 21}$$

$$d\Pi_{\text{eq.st}} \equiv 0 \tag{Eq. 22}$$

$$\delta W^{e\circ} = \delta W_{\max}^e = -d(\Delta\Pi^*) \tag{Eq. 23}$$

$$\delta W^e < -d(\Delta\Pi^*) = -d\Pi \tag{Eq. 24}$$

$$\delta W^e \leq -d(\Delta\Pi^*) = -d\Pi \tag{Eq. 25}$$

$$V_1 = V_2 = V \tag{Eq. 26}$$

$$v_1 = v_2 = v \tag{Eq. 27}$$

$$\Delta S = 2vR_{\mu} \ln 2 = 2k_B N \ln 2 \tag{Eq. 28}$$

$$p_1' = p_1'' \tag{Eq. 29}$$

$$V = V_2' = V_2'' = V' + V'' \tag{Eq. 30}$$

$$\Delta\Lambda_{\text{therm}} = 0 \tag{Eq. 31}$$

$$T_{WB} = T_{HS} \tag{Eq. 32}$$

$$\Delta\Lambda_{\text{noneq.IS}} = \Delta\Lambda_{\text{noneq.AS}} + \Delta\Lambda_{WR} = \Delta\Lambda_{\text{therm}} + \Delta\Lambda_{\text{dif}} + \Delta\Lambda_{\text{mech}} = 0 \tag{Eq. 33}$$

$$W_{AS \rightarrow \text{eq.st}}^o \tag{Eq. 34}$$

$$-\Delta\Lambda_{\text{noneq.AS}} = -\Delta\Lambda_{\text{dif}} = \Delta\Lambda_{\text{mech}} = W_{AS \rightarrow \text{eq.st}}^o \tag{Eq. 35}$$

$$\begin{aligned}
W_{AS \rightarrow \text{eq.st}}^o &= W_T' + W_T'' = \int_{V'}^V p' dV + \int_{V''}^V p'' dV = m' R' T \int_{V'}^V \frac{dV}{V} + \\
&+ m'' R'' T \int_{V''}^V \frac{dV}{V} = [m' R' \ln(V/V') + m'' R'' \ln(V/V'')] T,
\end{aligned}
\tag{Eq. 36}$$

$$p' = m' R' T / V' \tag{Eq. 37}$$

$$p'' = m'' R'' T / V'' \tag{Eq. 38}$$

$$R = R_{\mu}/M \tag{Eq. 39}$$

$$\begin{aligned}
W_{V,T}^{\max} &= W_{AS \rightarrow \text{eq.st}}^o = -\Delta F_{AS} = -\Delta F_{WB} - \Delta F_{HS} = \\
&= -\Delta F_{WB} = F_{WB1} - F_{WB2} = F_1' + F_1'' - F_2' - F_2''.
\end{aligned}
\tag{Eq. 40}$$

$$W_{\text{HS}} = 0 \quad (\text{Eq. 41})$$

$$Q_{\text{HS}} = \Delta U_{\text{HS}} \quad (\text{Eq. 42})$$

$$-\Delta F_{\text{HS}} = F_{\text{HS}2} - F_{\text{HS}1} = \Delta U_{\text{HS}} - T \Delta S_{\text{HS}} = \Delta U_{\text{HS}} - Q_{\text{HS}} = 0 \quad (\text{Eq. 43})$$

$$f = u - Ts \quad (\text{Eq. 44})$$

$$s(T, v) = c_v \ln T + R \ln v + s_0 \quad (\text{Eq. 45})$$

$$f = u - Ts = u - T(c_v \ln T + R \ln v + s_0) = -RT \ln v + b(T) \quad (\text{Eq. 46})$$

$$b(T) = u - Tc_v \ln T - Ts_0 \quad (\text{Eq. 47})$$

$$F = -mRT \ln v + m b(T) = -mRT \ln(V/m) + B(T) \quad (\text{Eq. 48})$$

$$m'_1 = m'_2 = m', \quad m''_1 = m''_2 = m'', \quad V'_1 = V', \quad V''_1 = V'', \quad V'_2 = V''_2 = V, \quad B'(T) = B''(T) \quad (\text{Eq. 49})$$

$$\begin{aligned} W_{\text{V,T}}^{\text{max}} = W_{\text{AS} \rightarrow \text{eq.st}}^0 = F'_1 + F''_1 - F'_2 - F''_2 = -m' R' T \ln(V'/m') + B'(T) - \\ - m'' R'' T \ln(V''/m'') + B''(T) + m' R' T \ln(V/m') - B'(T) + \\ + m'' R'' T \ln(V/m'') - B''(T) = m' R' T \ln(V/V') + m'' R'' T \ln(V/V''). \end{aligned} \quad (\text{Eq. 50})$$

$$\Lambda_{\text{noneq.AS}} = \Lambda_{\text{dif}} = -\Delta F_{\text{V,T}}^{\text{max}} = W_{\text{AS} \rightarrow \text{eq.st}}^0 \quad (\text{Eq. 51})$$

$$T_{\text{CB}} = T' = T'' = T \quad (\text{Eq. 52})$$

$$\Delta S_{\text{IS}} = W_{\text{lost}}/T = W_{\text{V,T}}^{\text{max}}/T = m' R' \ln(V/V') + m'' R'' \ln(V/V''). \quad (\text{Eq. 53})$$

$$R_{\text{body}} = \frac{pV}{T} = mR = \nu R_{\mu} = \text{const} \quad (\text{Eq. 54})$$

$$R = R_{\text{body}}/m; \quad R_{\mu} = R_{\text{body}}/\nu \quad (\text{Eq. 55})$$

$$\Delta S_{\text{IS}} = W_{\text{lost}}/T = W_{\text{V,T}}^{\text{max}}/T = \nu' R_{\mu} \ln(V/V') + \nu'' R_{\mu} \ln(V/V''). \quad (\text{Eq. 56})$$

$$\nu' = \nu'' = \nu \quad (\text{Eq. 57})$$

$$V' = V'' = V/2 \quad (\text{Eq. 58})$$

$$\Delta S_{\text{IS}} = W_{\text{lost}}/T = W_{\text{V,T}}^{\text{max}}/T = 2\nu R_{\mu} \ln 2 \quad (\text{Eq. 59})$$

$$Q_{\text{WB}} = -Q_{\text{HS}} \quad (\text{Eq. 60})$$

$$\begin{aligned} \Delta S_{\text{IS}} = \Delta S_{\text{WB}} + \Delta S_{\text{HS}} + \Delta S_{\text{WR}} = \Delta S_{\text{AS}} = \Delta S_{\text{WB}} + \Delta S_{\text{HS}} = \\ = Q_{\text{WB}}/T + Q_{\text{HS}}/T = Q_{\text{WB}}/T - Q_{\text{WB}}/T = 0, \end{aligned} \quad (\text{Eq. 61})$$

$$W_{\text{lost}} = 0 \quad (\text{Eq. 62})$$

$$-\Delta\lambda_{\text{noneq.AS}} = w_{\text{noneq.AS}}^{\text{eo}} \quad (\text{Eq. 63})$$

$$p_1 = \text{const} \quad (\text{Eq. 64})$$

$$T = \text{const} \quad (\text{Eq. 65})$$

$$w_{a-b}^p = p_1 (v_{\text{st}} - v_{\text{liq}}) \quad (\text{Eq. 66})$$

$$(p_1 v_{\text{st}} = R_{\text{st}} T) \quad (\text{Eq. 67})$$

$$w_{a-b}^p = p_1 v_{\text{st}} = R_{\text{st}} T \quad (\text{Eq. 68})$$

$$w_{b-c}^T = \int p dv = R_{\text{st}} T \ln(v_c / v_b) = R_{\text{st}} T \ln(p_b / p_c) = R_{\text{st}} T \ln(p_1 / p_2) \quad (\text{Eq. 69})$$

$$w_{c-d}^p = p_2 (v_{\text{liq}} - v_{\text{st}}) = -p_2 v_{\text{st}} = -R_{\text{st}} T \quad (\text{Eq. 70})$$

$$w_{\text{noneq.AS}}^{\text{eo}} = w_{a-b}^p + w_{b-c}^T + w_{c-d}^p = R_{\text{st}} T + R_{\text{st}} T \ln(p_1 / p_2) - R_{\text{st}} T = R_{\text{st}} T \ln(p_1 / p_2) \quad (\text{Eq. 71})$$

$$-\Delta\lambda_{\text{noneq.AS}} = -\Delta f_{V,T} = w_{\text{noneq.AS}}^{\text{eo}} = R_{\text{st}} T \ln(p_1 / p_2) \quad (\text{Eq. 72})$$

$$w_{\text{lost}} = w_{\text{noneq.AS}}^{\text{eo}} = R_{\text{st}} T \ln(p_1 / p_2) \quad (\text{Eq. 73})$$

$$\Delta S = w_{\text{lost}} / T = R_{\text{st}} \ln(p_1 / p_2) \quad (\text{Eq. 74})$$

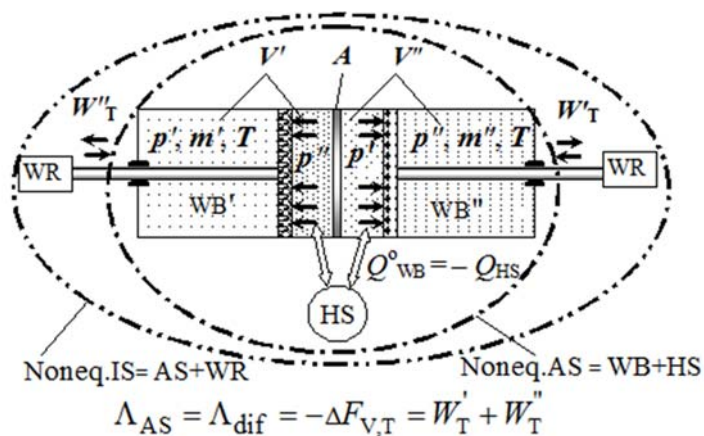


Figure 1. To the calculation of the work of the adiabatic system in transition it to an equilibrium state

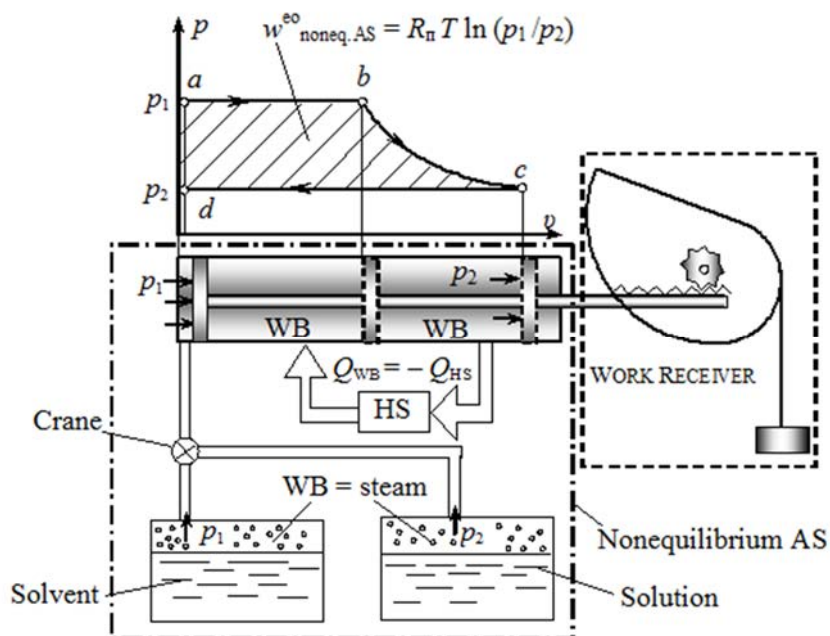


Figure 2. To calculation of change of nonequilibrium of system "pure solvent-solution"

Publication Ethics

Dear readers. We are sorry for the inconvenience, but this manuscript was selected for additional review.

This manuscript may or may not return in a future issue of the journal.

The editorial team is continuously improving the publication practices to ensure fair publication opportunities to all.

The editors are grateful for the understanding of this situation.

Editors.

UMA INVESTIGAÇÃO SOBRE O EFEITO DO VÍRUS INFLUENZA H9N2 NA APOPTOSE DE CÉLULAS TESTICULARES EM EMBRIÃO DE GALINHA USANDO SYBR VERDE PCR EM TEMPO-REAL**AN INVESTIGATION INTO THE EFFECT OF H9N2 INFLUENZA VIRUS ON APOPTOSIS OF TESTICULAR CELLS IN CHICKEN EMBRYO USING SYBR-GREEN REAL-TIME PCR**

بررسی تاثیر ویروس آنفلوآنزای اچ 9 ان 2 به روی آپوپتوز سلولهای بافت بیضه ی جنین جوجه ی مرغ با استفاده از تکنیک مولکولی ریل تایم پی سی آر- سایبرگرین

NAZARABADI, Roshanak Bahrami ^{1,2}; MEHRABANPOUR, Mohammad Javad ^{3*}; EDALATMANESH, Mohammad Amin ⁴; SHARIATI, Mehrdad⁵

¹ Department of Biology, Fars Science and Research Branch, Islamic Azad University, Fars, Iran.

² Department of Biology, Shiraz Branch, Islamic Azad University, Shiraz, Iran.

³ Razi Vaccine and Serum Research Institute Shiraz Branch, Agricultural Research, Education and Extension Organization (AREEO), Shiraz. Iran.

⁴ Department of Biology, College of Sciences, Shiraz Branch, Islamic Azad University, Shiraz, Iran.

⁵ Department of Biology, Kazerun Branch, Islamic Azad University, Kazerun, Iran.

* Correspondence author

e-mail: mehrabanpourj@yahoo.com

Received 03 January 2020; received in revised form 22 March 2020; accepted 29 March 2020

RESUMO

Os vírus da gripe podem induzir a morte celular em seu hospedeiro por apoptose ou necrose. O H9N2 é um subtipo do vírus da gripe aviária (AIV) que pode causar graves danos aos órgãos reprodutivos das galinhas poedeiras. O presente estudo teve como objetivo investigar o efeito do vírus influenza H9N2 na apoptose de células testiculares em embriões de galinha. Para este fim, A/Chicken/Tehran/ZMT-101/99(H9N2) foi inoculado em 210 ovos embrionados com quinze dias de idade postos por galinhas SPF. Em seguida, de acordo com o desenho do experimento, os embriões vivos foram dissecados no 19º e no 21º dia de vida fetal e no 25º dia após o nascimento para estudos patológicos e moleculares e avaliação da expressão gênica no tecido testicular. Os tecidos dissecados foram corados com hematoxilina e eosina (H&E) e estudados sob um microscópio óptico com aumento de 400x. Para estudos moleculares, o RNA viral foi extraído dos tecidos testiculares, replicado por RT-PCR e, finalmente, avaliado o H9N2. Em seguida, a expressão dos genes envolvidos na apoptose das células do tecido testicular foi avaliada por PCR em tempo-real. Estudos patológicos indicaram que o H9N2 causou lesões na orquite do tecido testicular, seminífero e nefrite do hospedeiro. Estudos moleculares também mostraram que a replicação de H9N2 no corpo hospedeiro aumenta a expressão de BAX e Caspase 3 e reduz a expressão de Bcl-2 e Bcl-X_L. Essas mudanças na expressão gênica aumentaram a apoptose e induziram a morte celular no hospedeiro. Em resumo, os resultados do estudo sugeriram que o H9N2 pode aumentar a expressão de genes pró-apoptóticos e reduzir a expressão de genes anti-apoptóticos, resultando em destruição severa do tecido testicular causado pela apoptose celular.

Palavras-chave: Apoptose, H9N2, Vírus da gripe A, PCR verde em tempo real SYBR, Tecido testicular.

ABSTRACT

Influenza viruses can induce cell death in their host through apoptosis or necrosis. The H9N2 is a subtype of the Avian Influenza Virus (AIV) that can cause severe damage to reproductive organs of laying hens. The present study aimed to investigate the effect of the H9N2 influenza virus on apoptosis of testicular cells in chicken embryos. To this end, A/Chicken/Tehran/ZMT-101/99(H9N2) was inoculated to 210 embryonated fifteen-day-old

eggs laid by SPF hens. Then, according to the experiment design, live embryos were dissected on the 19th and 21st days of fetal life and on the 25th day after birth for pathological and molecular studies and evaluation of gene expression in testicular tissue. Dissected tissues were stained with hematoxylin and eosin (H&E) and studied under an optical microscope at 400x magnification. For molecular studies, viral RNA was extracted from testicular tissues, replicated by RT-PCR, and finally evaluated H9N2. Then, the genes expression involved in the testicular tissue cells apoptosis was evaluated through real-time PCR. Pathological studies indicated that H9N2 caused lesions in testicular tissue orchitis, seminiferous, and nephritis of the host. Molecular studies also showed that H9N2 replication in the host body increases BAX and Caspase 3 expression and reduces the expression of Bcl-2 and Bcl-X_L. These changes in gene expression increased apoptosis and induced cell death in the host. In summary, the study findings suggested that H9N2 can increase the expression of pro-apoptotic genes and reduce the expression of anti-apoptotic genes, resulting in severe destruction of testicular tissue caused by cell apoptosis.

Keywords: Apoptosis, H9N2, Influenzavirus A, SYBR Green Real-Time PCR, Testicular tissue

چکیده

ویروس های آنفلوانزا می توانند باعث القا مرگ سلولی در میزبان خود از طریق فرایند آپوپتوزیس یا نکروزیس شوند. تحت تیپ اچ 9 ان 2 ویروس آنفلوانزا پرندگان (AIV) می تواند باعث آسیب شدید در اندام های تولید مثلی مرغ های تخم گذار شود. در این مطالعه کوشش شده است که تاثیر ویروس آنفلوانزا تحت تیپ H9N2 به روی آپوپتوز سلول های بیضه جنین جوجه مورد بررسی قرار گیرد. برای این منظور سویه اچ 9 ان 2 به 210 تخم مرغ جنین دار اس پی اف 15 روزه تلقیح شد سپس طبق الگوی طراحی شده آزمایش ، جنین های زنده در روزهای 19 و 21 جنینی و در روز 25 پس از تولد جهت بررسی اثرات پاتولوژیکی و بررسی مولکولی و بیان ژن بافت بیضه تشریح شدند. بافت های تشریح شده با رنگ هماتوکسیلین و انوزین (H&E) رنگ آمیزی شدند و به وسیله میکروسکوپ نوری با بزرگنمایی X400 مشاهده شدند. جهت بررسی مولکولی ، RNA ویروسی از بافت های بیضه استخراج شد و تکثیر ویروس آنفلوانزا به وسیله تکنیک (ار تی - پی سی آر) با استفاده از پرایمر اختصاصی bp808 مورد بررسی قرار گرفت و در انتها بیان ژن هایی که ممکن است در القای فرایند آپوپتوز نقش داشته باشند و باعث تخریب سلول های بافت بیضه شده اند به وسیله تکنیک مولکولی ریل تایم پی سی آر- سایبرگرین مورد ارزیابی قرار گرفت. بررسی های پاتولوژیکی این آزمایش نشان داد که تحت تیپ اچ 9 ان 2 باعث ایجاد ضایعات بافتی در بافت بیضه میزبان می شود و در بررسی های مولکولی مشخص شد که تکثیر ویروس اچ 9 ان 2 در بدن میزبان باعث افزایش بیان ژن های بکس و کاسپاز 3 و کاهش بیان BCL-2 و BCL-X_L می شود که این تغییرات بیان ژنها ، باعث افزایش فرایند آپوپتوز و القا مرگ سلولی میزبان می شود. به طور خلاصه بررسی های حاصل از این مطالعه نشان داد که تحت تیپ اچ 9 ان 2 می تواند باعث افزایش بیان ژن های پروآپوپتوتیک و کاهش بیان ژن های ضد آپوپتوتیک شود و این امر باعث تخریب شدید بافت های بیضه در اثر القا فرایند آپوپتوز سلولی شود.

کلمات کلیدی : آپوپتوزیس ، اچ 9 ان 2 ، بافت بیضه

1. INTRODUCTION

H9N2 is a subtype of Influenza A virus that causes a contagious infectious disease. The virus belongs to the family of Orthomyxoviridae and the class of Low Pathogenic Avian Influenza Virus (LPAIV) (Abolnik, 2017). This virus has become prevalent among domestic birds in most Asian countries since the mid-1940s, as 5-30% of mortalities among birds have been reported to be caused by H9N2 (Abolnik, 2017; Alexander & Capua, 2008). Many studies have indicated that infection with H9N2 causes mild clinical symptoms in the gastrointestinal tract, respiratory system, and genital organs of infected chickens (Pantin-Jackwood *et al.*, 2015). H9N2 can apply specific effects on the immune system of infected birds that result in the immunity termination followed by a secondary infection (Bano, Naeem, & Malik, 2003). Different studies state that the avian influenza virus can greatly affect the host cell processes, including aging, proliferation, and autophagy, and cell apoptosis (Moon *et al.*, 2017; Qi, Zhang, Wang, & Wang, 2016; Yan *et al.*, 2017). Apoptosis may be induced in different types of

hosts by a wide variety of viruses. Type A (e.g., avian, horse, swine, and human) and also Type B of influenza viruses are capable of inducing apoptosis in different cell lines (Hinshaw, Olsen, Dybdahl-Sissoko, & Evans, 1994; Ito, Kobayashi, Morita, Horimoto, & Kawaoka, 2002; Lowy, 2003). Due to the activation of the apoptotic gene (Fas antigen) in the early stages of infection, type A and B influenza underlie the process of apoptosis induction (Ito *et al.*, 2002). Viruses induce apoptosis in two ways as follows: the intrinsic pathway (mitochondrial/cytochrome C) and the extrinsic pathway (receptor death) (Lowy, 2003). These two mechanisms involve receptors stimulation, kinase/phosphate activation, and release of transcriptional regulatory factors. The main regulators of apoptosis include the Bcl-2 genes, tumor suppressor p53, mitochondria, and caspases (Krajewska *et al.*, 2002). The apoptosis process depends on the release of pro-apoptotic proteins from the intermembrane space of mitochondria and thereby the destruction of the mitochondrial outer membrane, controlled by the Bcl-2 gene (Lalier *et al.*, 2007). Studies show that H9N2 induces apoptosis in chicken's macrophage

cells by non-structural protein NS1 through the receptor's death-inducing pathway (Fas or FasL-mediated) (Xing *et al.*, 2008; Xing *et al.*, 2011). Other studies have also shown that H9N2 causes tissue damage and excessive apoptosis in chicken's oviduct. Influenza virus causes different pathological changes in host tissues, including testicular tissue. However, it is not yet clearly specified how H9N2 triggers apoptosis in testicular tissue of the chicken embryo. Therefore, it is necessary to scrutinize the molecular mechanisms of H9N2-induced apoptosis. Hence, the aim of the present study was to investigate the effects of avian influenza virus (H9N2) on the expression of pro-apoptotic and anti-apoptotic genes in testicular tissue of the chicken embryo.

All experiments of this project have been performed with the approval of the Ethics Committee for the Protection of Laboratory Animals of Shiraz Islamic Azad University. (IR.IAUSHIRAZ.8346.95.942)

2. MATERIALS AND METHODS

2.1. Preparation of virus strain

Virus A/chicken/Tehran/ZMT-101/99 (H9N2) is a strain of influenza isolated from infected birds in Iran. The virus was propagated by inoculating 11 day-olds embryonated Specific Pathogenic Free (SPF) chicken eggs for 48h at 35°C. The virus was screened to exclude the presence of the other infected agent such as bacteria and common virus poultry, as previously described. The allantoic fluid was harvested and subsequently titrated according to the Reed and Muench method (OIE, 2012). In this study, H9N2 was provided by Razi Vaccine and Serum Research Institute Iran- South Branch (Shiraz).

2.2. Preparation of specific-pathogen-free (SPF) embryonated eggs

For this study, 210 SPF embryonated eggs were purchased from a company SPF chicken center of Venky, India. These eggs were free from any pathogenicity and even the maternal antibody titer. The eggs were kept in a hatching machine under optimal temperature (35.6 °C) and humidity (65%) for 15 days, and then they were used for AIV inoculation (OIE, 2012).

2.3. EID50

Before performing any test, the EID50 of AIV (H9N2) was determined. For this purpose, ten consecutive dilutions of the virus from 10^{-1} through 10^{-10} were prepared, and 200 mL of each dilution

was injected into five embryonated eggs aged 9-11 days. After five days, the EID50 level was calculated based on REED & MUENCH table (OIE, 2012).

2.4. Experiment design

H9N2 was administered to 180 embryonated fifteen-day-old eggs laid by SPF hens, 30 of which were regarded as the control. In the test group, 100 μ L of the virus (with a dilution of 10^{-4}) was injected into eggs. In addition, 30 embryonated eggs in the control group received 100 μ L of PBS.

After inoculation, the eggs were examined daily to determine whether the embryo was alive and the dead embryos were discarded. On the 19th day of embryonic life, 140 embryos in the test group remained alive, 70 of which were removed from the egg and dissected. In addition, 12 out of 24 alive embryos in the control group were dissected. The eggs with alive embryo were kept in a hatching machine until the 21st day when the chicks were born. Then testicular tissue of 37 male embryos from the test group and ten male embryos from the control group was sampled for molecular and pathological studies (Table 1). The eggs were hatched on the 21st day, and the chickens were kept under standard temperature and humidity for 25 days. After this period, the chickens of both groups were euthanized, and their testicular tissue was removed. (Ito *et al.*, 2002; xing *et al.*, 2008)

2.5. Pathological examination of embryo and chicken testicle

To study the pathological characteristics of testicular tissue of embryos and chickens after a viral infection, it is necessary to prepare the tissue based on standard methods (Bonfante *et al.*, 2017). To this end, uninfected and infected chicken tissues were cut into 5 μ m blocks and fixed in 10% buffered formalin solution for 48h, routinely processed, and embedded in paraffin wax. In the end, testicular sections were stained with Hematoxylin and Eosin (H&E). Finally, samples were studied under an optical microscope (Bonfante *et al.*, 2017).

2.6. RNA extraction

To perform Real-Time PCR, viral RNA was extracted from testicular tissue (0.19) by using an RNA extraction kit (High pure viral RNA kit, Roche Applied Science Mannheim, Germany) according to the manufacturer's instructions then reverse

transcribed into cDNA. In order to ensure the optimum quality of the extracted RNA and determine its concentration, the absorbance of each sample at 260 and 280 nm was determined using a Picodrop Microliter UV/Vis Spectrophotometer (Sigma-Aldrich Corporation).

2.7. cDNA synthesis

cDNA of the extracted RNA was synthesized using the Ki622 Fermentas kit. To this end, the reaction was incubated at 25°C for 5 minutes and then at 42°C for 60 minutes. Finally, reaction tubes were placed at 70°C for 5 minutes in order to inactivate the RT enzyme

2.8. RT-PCR and H9N2 detect

The definitive presence of H9N2 in tissue samples was confirmed using RT-PCR (Reverse Transcriptase Polymerase Chain Reaction). For this purpose, using a primer that produces 808 bp after the RT-PCR process if there is H9N2.

2.9. Evaluation of apoptotic genes expression using SYBR-Green real-time PCR

The expression of desired genes was measured through SYBR-Green real-time PCR. To this end, all primers were designed by Allele ID-7.8. In this reaction, beta-actin was used as the internal control gene. Real-time PCR was performed using ABI Step One Applied Biosystem (USA).

The components of the real-time PCR reaction were prepared and adjusted according to the instructions of the device kit. The final volume of the reaction mix was considered to be 25 µL that contained 12.5 µL of PCR Master Mix, 1 µL of forwarding primer, 1 µL of reverse primer, 30 ng (6 µL) of cDNA, and 4.5 µL of RNase-free water. The PCR program included initial denaturation at 95°C for 10 min, 40 cycles of denaturation at 95°C for 30 seconds, annealing at 56°C for 60 seconds, and extension at 72°C for 30 seconds. The ABI Step One also delivered us the melting curve at the end.

3. RESULTS AND DISCUSSIONS

3.1. Virus EID50

Considering the protocol provided by OIE and the REED & MUENCH calculation table, the EID50 value for H9N2 was obtained $10^{-6} \log_{10}$. None of the embryo and chicken testicular tissue samples in the control group showed significant

microscopic changes.

3.2. Pathological study of embryo and chicken testicular tissue

H&E staining technique was employed for the pathological study of tissue samples. The results showed that replication of H9N2 leads to tissue lesions such as orchitis and seminiferous with the accumulation and infiltration of inflammatory mononuclear cells (Figure 1).

3.3. RT-PCR for the definitive detection of the virus exists in the host tissue

RT-PCR was used to definitively determine the existence of the virus in the testicular tissue of chicken. The formation of specific bands in the range of 808 bp indicated the presence of the virus in testicular tissues (Figure 2). Then, the best annealing temperature for this reaction was determined through the gradient PCR technique at 60°C.

3.4. Determination of the RT-PCR and standard curve efficiency

After confirmation of primers and definitive report of the presence of H9N2 in the host testicular tissue, the DNA concentration for evaluation of genes expression was determined to be 25 ng for each reaction. In all reactions, equal amounts of DNA and internal control gene (beta-actin) were used depending on the desired gene type. Hence, genomic RNA was used as the sample extracted from the H9N2 isolate to determine the test accuracy. The optimal temperature of annealing was adjusted to 60°C, and the optimal concentration of primers was determined to be 1 µL in 12.5 µL of the reaction mix. After 40 cycles of replication, the melting curve (T_m) was obtained 86.3°C for caspase 3, 87.1°C for Bcl-X_L, 83°C for BAX, 85.4°C for Bcl-2, and 78.5°C for beta-actin. Then, the standard curve was plotted in order to determine the line slope and coefficient of determination (R^2) for each gene. According to the line slope and coefficient of determination (R^2), the efficiency of reactions was greater than 90%.

3.5. Expression of apoptotic genes after virus inoculation

The findings showed that injection of the H9N2 virus could significantly increase the expression of BAX and caspase3 genes in embryos and chickens; so that the BAX gene was expressed greater than the control gene by 1094

times in embryos ($p=0.014$) and 1.92 times in chickens ($p=0.007$) and the caspase three gene was expressed greater than the control gene by 3.34 times in embryos ($p<0.001$) and 1.25 times in chickens ($p<0.001$) (Figure 3). The results also indicated that the injection of the virus caused a reduction in the expression of Bcl-2 and Bcl-X_L, representing the increased apoptosis process. Compared to the control gene, the reduction in gene expression was lower by 0.29 times in embryos ($p<0.001$) and 0.52 times in chickens ($p=0.012$) in Bcl-2 and by 0.53 times in embryos ($p<0.001$) and 0.64 times in chickens ($p=0.045$) in Bcl-X_L (Figure 3). As shown in (Figure 3), the inoculation of H9N2 increases the expression of apoptotic genes and reduces the expression of anti-apoptotic genes in embryos and chickens.

3.6. Discussions

Apoptosis is an important physiological mechanism for homeostasis and mitochondrial pathways. The apoptosis is generally induced by two pathways: the mitochondrial pathway and the death receptor pathway (Hinshaw *et al.*, 1994). An important point about the process of cell apoptosis is that the host cells take advantage of apoptosis to limit the activity of the influenza A virus by removing infected cells. However, viruses use apoptosis to maintain their own survival and proliferation in the host (Wurzer *et al.*, 2003). Shahsavandi *et al.* showed that H9N2 induces apoptosis in human cells through the mitochondrial pathway, and NS1 from the avian influenza virus (H9N2) can induce death receptor-mediated apoptosis in macrophage of chicken (Shahsavandi, Ebrahimi, Sadeghi, Mosavi, & Mohammadi, 2013).

The apoptosis process depends on the release of pro-apoptotic proteins from the intermembrane space of mitochondria and, thereby, the destruction of the mitochondrial outer membrane, controlled by Bcl-2 genes (Lalier *et al.*, 2007). The Bcl-2 protein family includes the genes encoding anti-apoptotic proteins, including Bcl-2, Bcl-X_L, Bcl-W, MCL-1, BFL-1, and Bcl-B and the genes encoding pro-apoptotic proteins such as Bid, Bik, Bok, Bad, Bak, and BAX (Krajewska *et al.*, 2002). Pro-apoptotic proteins like BAX located on the mitochondrial outer membrane cause this layer to be permeable to apoptosis activating factors, including cytochrome C (Gross, 2016; Lalier *et al.*, 2007). Another category of pro-apoptotic proteins is activated by extracellular or intracellular access, which is divided into 2 types of activator and sensor, based on the stress. Activators play a role in apoptosis induction (Gross, 2016). Another factor contributing to the

induction of apoptosis is caspases. By cleaving the activators, active caspases cause further mitochondrial permeability, the release of cytochrome C, and finally, the formation of the apoptosome complex (Elmore, 2007). Primary caspases, such as caspase 8 and caspase 9, activates downstream effector caspases, including caspase 3, caspase 6, and caspase 7, that cut a series of cell proteins, and then apoptosis takes place (Iwai, Shiozaki, & Miyazaki, 2013; Krajewska *et al.*, 2002; Xing *et al.*, 2011). Studies have reported that Poly (ADP-ribose) polymerase (PARP) is one of the main cleavage sites of caspase 3 in vivo (Schultz-Cherry, Dybdahl-Sissoko, Neumann, Kawaoka, & Hinshaw, 2001).

The present study aimed to investigate four categories of genes involved in H9N2-induced apoptosis in embryos and chickens of SPF laying hens. The studied genes were selected from two categories including anti-apoptotic proteins encoding genes (Bcl-2 and Bcl-X_L) and pro-apoptotic proteins encoding genes (BAX and caspase 3). In addition, beta-actin was employed as the internal control gene. In this study, H9N2 was inoculated to embryonated fifteen-day-old eggs laid by SPF hens, and testicular tissue of embryos and chickens were sampled at preset intervals in order to investigate pathologic effects and expression of the genes involved in cell apoptosis. It is noteworthy that the expression of genes was measured through SYBR Green real-time PCR. The findings corroborate the results of previous studies regarding the attack of influenza virus to tissues containing specific receptors, including epithelial cells, decreased expression of anti-apoptotic genes, and increased expression of pro-apoptotic genes, resulting in apoptosis and cell death in the host tissue. In a study conducted by Doustar *et al.* (2004), it was shown that the attack of H9N2 to SPF hens leads to defects in lymphoid tissues caused by apoptosis and necrosis in these areas, especially in the spleen tissue (Doustar, 2004). Wang J. also reported that H9N2-induced infection causes severe tissue damage to the oviduct of laying hens as a result of apoptosis and changes in the expression of inflammatory factors (Wang *et al.*, 2015).

Bonfante *et al.* investigated the pathologic effects of the H9N2 influenza virus on the reproductive organs of laying hens. They found that some regions of the oviduct tissue were necrotized and epithelial cells were damaged due to the influenza virus (Bonfante *et al.*, 2017). She was also reported that HPAI viruses could cause necrosis and inflammation in the trachea and lungs (Moon *et al.*, 2017). On the other hand,

Hadipour *et al.* found that the H9N2 influenza virus causes edema, hyperemia, secretion of heterophile antibodies, destruction of cilia, and hyperplasia of epithelial tissue in the trachea (Hadipour, 2010). According to the observations of Swayne *et al.* (2013), H9N2 can result in necrosis, edema, and hypertension of kidney tubules, especially proximal tubules; this was also confirmed by other authors (Swayne & Spackman, 2013). In this study, the effect of the influenza virus on testicular tissue was investigated for the first time, and the results indicated the infiltration of mononuclear inflammatory cells and hyperemia with necrosis in this area.

The findings suggest that the H9N2 influenza virus can cause pathological lesions in the testicles, although its effects were not as severe as those reported in the trachea and lung tissues. Perhaps the H9N2 influenza virus causes fewer lesions in the testicular tissue than respiratory tissue, due to its tissue tropism or tendency. In terms of the role of apoptosis in cell death, Ito *et al.* (2002) stated that apoptosis or necrosis are the main factors involved in cell death of hens infected with influenza A virus. They reported that apoptosis causes cell death in the liver, kidney, and brain of the host, which is corroborated by the occurrence of viral antigens in apoptosis-degraded organs (Ito *et al.*, 2002). Qi *et al.* reported that the NS1 protein of H9N2 could induce apoptosis through the mitochondrial pathway and finally causes the destruction of epithelial cells in the oviduct of hens (Qi *et al.*, 2016). Different tissues of chicken have been sampled for the examination of apoptosis in previous studies.

4. CONCLUSIONS:

The present study was the first one that investigated the effect of apoptosis on testicular tissue in embryo and chickens. Molecular studies and evaluation of gene expression indicated that the expression of anti-apoptotic genes (Bcl-2 and Bcl-X_L) reduced, but the expression of pro-apoptotic genes (BAX and caspase 3) increased. This intensified the process of cell apoptosis in testicular tissue and caused testicular tissue destruction and tissue lesions such as orchitis and seminiferous with the accumulation and infiltration of inflammatory mononuclear cells. This study suggested that H9N2 induces apoptosis in the host body through BAX and caspase3 proteins. In other words, H9N2 induces apoptosis through the mitochondrial pathway by modulating the Bcl-2 proteins encoding gene family and cause tissue

lesions.

5. ACKNOWLEDGMENTS:

The authors would like to thank the Razi Vaccine and Serum Research Institute Shiraz Branch, Agricultural Research, Education, and Extension Organization (AREEO), Shiraz. Iran.

6. REFERENCES:

1. Abolnik, C. *Onderstepoort. J. Vet. Res.*, **2017**, *84*, 1-7.
2. Alexander, D., Capua, I. *WPSJ*, **2008**, *64*, 513-32.
3. Bano, S., Naeem, K., Malik, S. *Avian. Dis.*, **2003**, *47*, 817-22.
4. Bonfante, F., Cattoli, G., Leardini, S., Salomoni, A., Mazzetto, E., Davidson, I., Haddas, R., Terregino, C. *Avian. Pathol.*, **2017**, *46*, 488-96.
5. Doustar, Y., dissertation, Tehran University, Tehran, **2004**.
6. Elmore, S. *Toxicol. Pathol.*, **2007**, *35*, 495-516.
7. Gross, A. *Biochim. Biophys. Acta*, **2016**, *1857*, 1243-46.
8. Hadipour, M. *Iran. Braz. J. Poult. Sci.*, **2010**, *12*, 160-64.
9. Health, W. O. f. A. Paris, France, **2012**.
10. Hinshaw, V. S., Olsen, C. W., Dybdahl-Sissoko, N., Evans, D. J. *Virology*, **1994**, *68*, 3667-73.
11. Ito, T., Kobayashi, Y., Morita, T., Horimoto, T., Kawaoka, Y. *Virus. Res.*, **2002**, *84*, 27-35.
12. Iwai, A., Shiozaki, T., Miyazaki, T. *Biochem. Biophys. Res. Commun.*, **2013**, *441*, 531-37.
13. Krajewska, M., Mai, J., Zapata, J., Ashwell, K. W., Schendel, S., Reed, J. Krajewski, S. *Cell. Death. Differ.*, **2002**, *9*, 145.
14. Lalier, L., Cartron, P.-F., Juin, P., Nedelkina, S., Manon, S., Bechinger, B., Vallette, F. M. *Apoptosis*, **2007**, *12*, 887-96.
15. Lowy, R. J. *Int. Rev. Immunol.*, **2003**, *22*, 425-49.
16. Moon, H.-J., Nikapitiya, C., Lee, H.-C., Park, M.-E., Kim, J.-H., Kim, T.-H., Yoon, J.-E., Cho, W.-K., Ma, J. Y., Kim, C.-J. *Sci. Rep.*, **2017**, *7*, 4875.
17. Pantin-Jackwood, M. J., Costa-Hurtado, M., Miller, P. J., Afonso, C. L., Spackman, E., Kapczynski, D. R., Shepherd, E; Smith,

- D., Swayne, D. E. *Vet. Microbiol*, **2015**, 177, 7-17.
18. Qi, X., Zhang, H., Wang, Q., Wang, J. J. *Gen. Virol*, **2016**, 97, 3183-92.
19. Schultz-Cherry, S., Dybdahl-Sissoko, N., Neumann, G., Kawaoka, Y., Hinshaw, V. S. *J. Virol*, **2001**, 75, 7875-81.
20. Shahsavandi, S., Ebrahimi, M. M., Sadeghi, K., Mosavi, S. Z., Mohammadi, A. *Biomed. Res. Int*, **2013**.
21. Swayne, D. E., Spackman, E. *Dev. Biol (Basel)*, **2013**, 135, 79-94.
22. Wang, G., Yu, Y., Tu, Y., Tong, J., Liu, Y., Zhang, C., Chang, Y., Wang, S., Jiang, C., Zhou, E.-M. *PLoS. One*, **2015**, 10, e0128292.
23. Wurzer, W. J., Planz, O., Ehrhardt, C., Giner, M., Silberzahn, T., Pleschka, S., and Ludwig, S. *EMBO. J*, **2003**, 22, 2717-28.
24. Xing, Z., Cardona, C. J., Li, J., Dao, N., Tran, T., Andrada, J. J. *Gen. Virol*, **2008**, 89, 1288-99.
25. Xing, Z., Harper, R., Anunciacion, J., Yang, Z., Gao, W., Qu, B., Guan, Y., Cardona, C. J. *Am. J. Respir. Cell. Mol. Biol*, **2011**, 44, 24-33.
26. Yan, Y., Su, C., Hang, M., Huang, H., Zhao, Y., Shao, X., Bu, X. *Virol. J*, **2017**, 14, 190.

Table 1. Experimental design

Group	Egg type	Antigen type	Antigen dilution	Injection dosage	Embryo age (day)	Embryo total number	Dead embryo number	Number of embryos at 19 days old			Number of embryos at 21 days old		Number of chickens at 25 days old	
Control	SPF	PBS	-	100 µL	15	30	6	Number of dissected embryos	Number of males	Number of remaining embryos	Number	Number of live births	Number	Number of males
								12	8	12	12	10	9	5
Test	SPF	H9N2	10 ⁻⁴	100 µL	15	180	40	Number of dissected embryos	Number of males	Number of remaining embryos	Number	Number of live births	Number	Number of males
								70	27	70	70	58	55	22

Table 2. Primer sequence used to detect H9N2 in RT-PCR

Genes	Primer Sequences	Sizes (bp)
H9 Serotype	Forward: 5'-AGCAAAAGCAGGGGAAGTCC-3'	808
	Reverse: 5'-CCATACCATGGGGCAATTAG-3'	

Table 3. Design of primers used in real-time PCR

Genes	Primer Sequences	Sizes (bp)
Bcl-2	Forward: 5'- TTCCGTGATGGGGTCAACTG-3' Reverse: 5'- CCACAAAGGCATCCCATCCT-3'	187
Bcl-xl	Forward: 5'- GATGCGCGAAAGGTCGGAT-3' Reverse: 5'- CCCGGTTACTGCTGGACATT-3'	141
Caspase 3	Forward: 5'- TGGTATTGAAGCAGACAGTGGA-3' Reverse: 5'- GGAGTAGTAGCCTGGAGCAGTAGA-3'	103
BAX	Forward: 5'- GTGATGGCATGGGACATAGCTC-3' Reverse: 5'- TGGCGTAGACCTTGCGGATAA-3'	90
Beta-Actin	Forward: 5'- TATTGCTGCGCTCGTTGTTG-3' Reverse: 5'- ACCAACCATCACACCCTGAT-3'	127

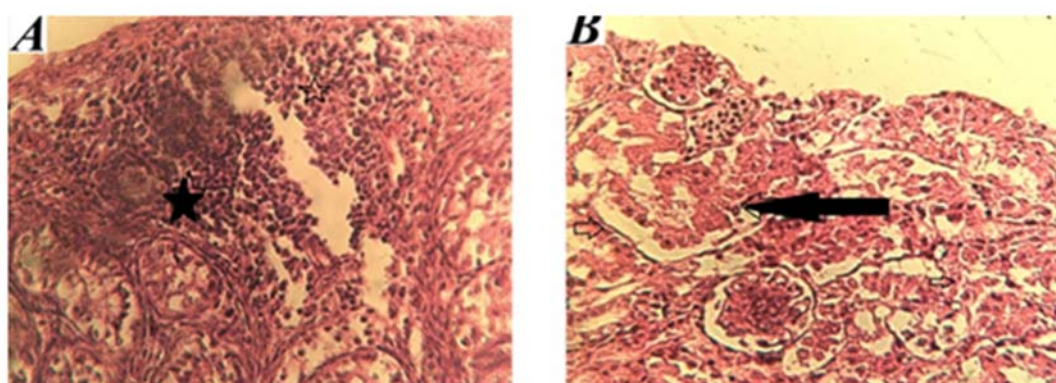


Figure 1. Lesions caused by H9N2 replication in testicular tissue of embryo and chicken (H&E staining, 400x magnification)

A: Orchitis (infiltration of inflammatory mononuclear cells)

B: Orchitis with seminiferous tubules necrosis.

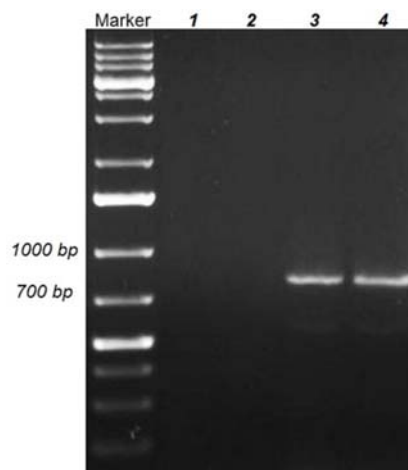


Figure 2. Electrophoresis gel obtained from RT-PCR

Line 1: Non-infectious tissue of embryo and chicken

Lane 2: Non-infectious testicular tissue of embryo and chicken

Lanes 3 and 4: Testicular tissue of embryo and chicken infected with H9N2

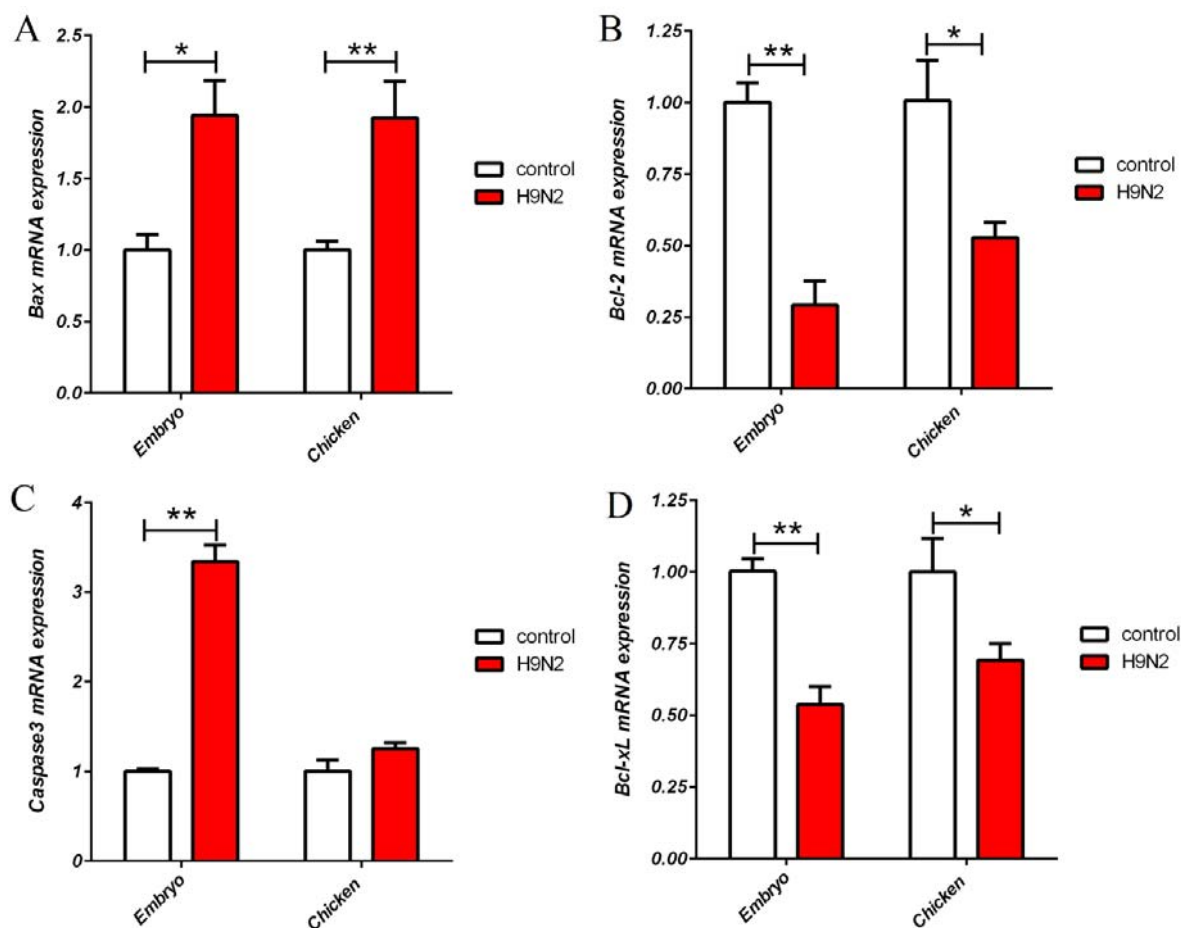


Figure 3. Changes in the expression of genes associated with cell apoptosis in embryos and chickens. White charts belong to the control group, and colored charts represent the increase or decrease in gene expression compared to the control. A, B, C, and D represent the gene expression for the Bax, Bcl-2, Caspase3, and Bcl-xL genes, respectively.

COMPOSIÇÃO DE AMINOÁCIDOS DE FARINHA POLI-CEREAL NÃO CONVENCIONAL PARA MASSA

THE AMINO ACID COMPOSITION OF UNCONVENTIONAL POLY-CEREAL FLOUR FOR PASTA

АМИНОКИСЛОТНЫЙ СОСТАВ НЕТРАДИЦИОННОГО ПОЛИЗЛАКОВОГО СЫРЬЯ ДЛЯ ИЗГОТОВЛЕНИЯ МАКАРОННЫХ ИЗДЕЛИЙ

OSPANOV, Abdymanap^{1*}; MUSLIMOV, Nurzhan²; TIMURBEKOVA, Aigul¹; MAMAYEVA, Laura¹; JUMABEKOVA, Gulnara³

¹Kazakh National Agrarian University, Republic of Kazakhstan

²Kazakh Research Institute of Food and Processing Industry, Republic of Kazakhstan

³M. Kh. Dulaty Taraz State University, Republic of Kazakhstan

* Correspondence author
e-mail: obdymanap@yahoo.com

Received 06 January 2020; received in revised form 22 February 2020; accepted 22 March 2020

RESUMO

Os produtores de massas conhecem três formulações de massa para fabricar produtos de massa com o valor nutricional e biológico aumentado a partir de matérias-primas não convencionais de poli-cereais. Essas formulações para massas compõem misturas de farinha de cereais/legumes com adição de glúten de trigo seco. A mistura de farinha foi formulada através do método de *design* que permite regular o conteúdo de nutrientes no produto para atender aos requisitos de nutrição racional e adequada e proporcionar um efeito terapêutico e preventivo. Este artigo explora a cinética de secagem de massas a partir de matérias-primas não convencionais e relata a qualidade e as propriedades do consumidor para massas. Os resultados mostram que, com o aumento da porcentagem de glúten de trigo seco na mistura de farinha de cereais, a porcentagem de aminoácidos essenciais e não essenciais na mistura também aumenta. A Formulação No. 1 fornece uma mistura com a porcentagem máxima de aminoácidos nela. O referido máximo é significativamente superior à concentração total de aminoácidos (% em peso) em uma mistura feita de acordo com as formulações 2 e 3. O aumento do glúten de trigo seco de 15% para 35% leva a um aumento acentuado na concentração de aminoácidos essenciais (triptofano e lisina). Não foi detectado um aumento significativo em outros aminoácidos essenciais (valina, isoleucina, leucina, metionina, treonina, fenilalanina).

Palavras-chave: *glúten de trigo seco; aminoácidos essenciais; tecnologia de processamento de alimentos; produtos de massa; matérias-primas poli-cereais.*

ABSTRACT

Pasta producers know three pasta formulations for making pasta products with the increased nutritional and biological value from unconventional poly-cereal raw materials. These pasta formulations composite flour mixtures of cereal/legumes with added dry wheat gluten. The flour mix was formulated through the design method that allows regulating the content of nutrients in the product to meet the requirements of rational and adequate nutrition and provide a therapeutic and preventive effect. This article explores the drying kinetics of pasta from unconventional raw materials and reports on the quality and consumer properties of pasta. Results show that with the percentage of dry wheat gluten increasing in the poly-cereal flour mix, the percentage of both essential and non-essential amino acids in the mix also increases. Formulation No. 1 provides a mix with the maximum percentage of amino acids in it. The said maximum is significantly higher than the total concentration of amino acids (% by weight) in a mix made according to formulations No. 2 and No. 3. The increase in dry wheat gluten from 15% to 35% leads to a sharp increase in the concentration of essential amino acids (tryptophan and lysine). A significant increase in other essential amino acids (valine, isoleucine, leucine, methionine, threonine, phenylalanine) was not detected.

Keywords: *dry wheat gluten; essential amino acids; food processing technology; pasta products; poly-cereal raw materials.*

АННОТАЦИЯ

Производителям макаронных изделий известны три рецептуры для производства макаронных изделий с повышенной пищевой и биологической ценностью из нетрадиционного цельносмолотого сырья. Эти пастообразные составы представляют собой смеси цельносмолотого зерна злаковых и крупяных культур с добавлением сухой пшеничной клейковины (СПК). В основу составления состава мучных смесей положена методология конструирования, позволяющая регулировать содержание нутриентов в продукте, удовлетворяющих требованиям рационального и адекватного питания, обеспечивая лечебно-профилактическую направленность. Изучена кинетика процесса сушки макаронных изделий из нетрадиционного сырья; дана качественная характеристика макаронных изделий и определены их потребительские свойства. Установлено, что увеличение процентного содержания СПК в мучной полизлаковой смеси в целом увеличивает процентное содержание как незаменимых, так и заменимых аминокислот. При этом рецептура № 1 отличается максимальными значениями процентного содержания группы аминокислот, что значительно выше значений общей массовой доли содержания аминокислотного состава, чем в рецептурах № 2 и № 3. Показано, что увеличение процентного содержания СПК с 15 до 35 % приводит к резкому увеличению массовой доли содержания таких незаменимых аминокислот как триптофан и лизин. Значительного увеличения содержания других незаменимых аминокислот (валин, изолейцин, лейцин, метионин, треонин, фенилаланин) не обнаружено.

Ключевые слова: *сухая пшеничная клейковина; незаменимые аминокислоты; технология пищевой промышленности; макаронные изделия; ползерновое сырье.*

1. INTRODUCTION

The current state of the art of the pasta industry allows producing a wide range of pasta products. Pasta goes in various shapes and sizes and is made according to various formulations. Classic pasta is made from durum wheat flour, sometimes with various vegetative additives (Bigliardi and Galati, 2013; Capozzi *et al.*, 2012; Iztaev *et al.*, 2018; Ospanov *et al.*, 2014).

On the pasta market, domestic producers run their business next to the representatives from countries outside and inside the former Soviet Union. Pasta products stand out not only with high consumer properties and with high-quality packaging materials but also with the price policy. Prices for pasta are fixed specifically for particular segments of the population (Koryachkina, 2006).

There are various ways to improve pasta production. For example, pasta products can be enriched with dietary fiber, minerals, organic acids, vitamins, and antioxidants by adding vegetative raw materials (legumes, vegetables or berries) (Gull *et al.*, 2018; Padalino *et al.*, 2017; Zheng *et al.*, 2016). For the same enrichment purpose, producers may use other types of additives. To enrich pasta with biologically active substances, they use a lactic acid starter or milk whey. To enrich pasta with minerals, producers use eggshell waste. The yeast is used to increase the protein content. Tomato-based products, if

added, increase the mineral content of a product. There was a pasta-enriching method designed to solve the problem of iodine deficiency in the country. This method implies the fortification of pasta products with seaweed (Ivanišová *et al.*, 2018; Ostrikov *et al.*, 2018; Spinelli *et al.*, 2019).

Additionally, to the nutritional improvement of pasta-like products, studies are focused on the improvement of pasta pressing and cooking techniques. Because various additives significantly change the structural and mechanical properties of the dough, the cooking properties of pasta will be different in different pasta products made from the different dough (Cubadda *et al.*, 2007; Doxastakis *et al.*, 2007; Lucisano *et al.*, 2012). This is why new formulations should embrace the full cycle of pasta production, from the preparation of raw materials and flour mix formulation to the production and assessment of consumer properties of a cooked product (Ospanov *et al.*, 2017; Ospanov *et al.*, 2017).

When the product range increased due to the introduction of unconventional raw materials into production, the wholemeal pasta became of greater interest (Chillo *et al.*, 2008). Now, pasta is produced with the inclusion of wheat bran (Brennan *et al.*, 2008). This direction should be promoted in Kazakhstan without restrictions because of the high grain potential of this country. In 2017–18, for example, the grain harvest in Kazakhstan amounted to 19.3 million tons.

Thus, the pasta industry should be on the way towards the expansion of the product range with products from new types of raw materials, such as the unconventional poly-cereal raw materials. Pasta pressing, dough forming, pasta drying, and pasta cooking technologies should also be improved. The purpose of this research is to study the amino acid composition of a poly-cereal flour mixture for pasta dough, as well as to investigate the drying kinetics of pasta from unconventional raw materials.

2. MATERIALS AND METHODS

Analytical studies were conducted in the research laboratory of the 'Technology of Processing Industries' research center, attached to the Kazakh National Agrarian University, and in the research laboratory of the AgriTech Hub, which cooperates with the University.

The rheological properties of poly-cereal dough were studied using modern devices, such as the AlveoConsistograph (CHOPIN Technologies, France) and the farinograph (Brabender, Russia). Pasta from unconventional poly-cereal raw materials was made using the laboratory press machine (Germany).

Dry wheat gluten (hereinafter referred to as DWG) was added to the pasta formulation to improve the technological properties of the dough (Ospanov *et al.*, 2018a, 2018b). The amino acid composition was measured separately in various single-ingredient flour samples and in the poly-cereal flour mixtures afterward. The first stage of experimental studies was aimed at determining the limiting essential and non-essential amino acids both in the wholemeal flour (ground from cereal/legumes) and in the flour with added DWG. The next step was to determine the proportion of essential amino acids (EAA) in the reference of "ideal" protein (amino acid score). After determining the amount of non-essential amino acids both in the wholemeal flour and in DWG, their composition was compared between the two given raw materials.

A review of protocols for testing cereal crop varieties was made to form a database of nutritional information for pasta from poly-cereal raw materials. For the same purpose, the granted quality assurance certificates were analyzed. The resulting database allowed rationalizing the unconventional pasta formulations. The quality of raw materials and pasta was assessed in accordance with regulatory documents. The nutritional value of poly-cereal flour was

determined using originally designed software (Ospanov *et al.*, 2013).

3. RESULTS AND DISCUSSION:

Figure 1 shows the total concentrations of essential amino acids in cereals/legumes and in DWG by weight. While in cereal flour (corn, barley, oats, buckwheat, millet), the total concentration of essential amino acids are low, in flour ground from legumes, it is almost twofold higher. The total concentration of essential amino acids in DWG reaches a high of 12.653% by weight.

The comparative diagram showcases an amino acid profile of the wholemeal flour against the amino acid profile of flour with added DWG (Figure 2). The comparative analysis includes essential amino acids, such as valine, isoleucine, leucine, lysine, methionine, threonine, tryptophan, and phenylalanine. In flour ground from cereals, the level of essential amino acids is insignificant. In flour ground from legumes, the level of essential amino acids is significantly higher by contrast: valine, isoleucine, leucine, lysine, threonine, and phenylalanine hit the maximum. However, tryptophan and methionine were not significant. The flour with added DWG was high in lysine and valine.

Figure 3 shows that the concentration of non-essential amino acids is almost twofold higher than the concentration of essential amino acids. As in the previous experiment, flour ground from legumes is higher in non-essential amino acids than flour ground from cereals. The flour with added DWG is also high in non-essential amino acids.

The comparative diagram showcases an amino acid profile of the wholemeal flour against the amino acid profile of flour with added DWG (Figure 4). The comparative analysis includes non-essential amino acids.

Figure 4 shows that flour samples ground from corn, barley, and oat contain the highest concentrations of glutamic acid and proline. Other non-essential amino acids turned to be insignificant. The flour samples ground from buckwheat and millet contain the highest concentration of non-essential amino acids. However, these samples of flour are lower in glutamic acid and proline but higher in other non-essential amino acids (alanine, arginine, aspartate, glycine, and serine). Flour ground from legumes contains concentrations that are significantly different from previous values. The analysis suggests that all non-essential amino

acids, except histidine, hit the maximum. In this case, glutamic and aspartic acids stand out against other non-essential amino acids. The flour with added DWG higher concentrations of glycine, glutamic acid, proline, and serine.

The next step was to evaluate the amino acid profile of three different formulations with DWG added in different amounts. These formulations were labeled as Formulation No. 1, Formulation No. 2, and Formulation No. 3 with regard to the percentage of added DWG (15%, 25%, and 35%, respectively).

First, this evaluation touched upon the essential amino acids (Figures 5-7), then upon the non-essential amino acids (Figures 8-10). Figures 5-7 show that with an increase in DWG from 15% to 35%, the total concentration of essential amino acids becomes higher in all three flour mixtures.

In Formulation No. 1, comprising 15% of DWG, the total concentration of essential acids amounts to 6.124% by weight. With an increase to 25% of DWG, the total concentration of essential amino acids becomes higher, up to 7.39% by weight. With a further increase, up to 35%, the total concentration of essential amino acids becomes even higher, reaching 8.653% by weight (Figure 5).

Formulations No. 2 and No. 3 showed a pattern similar to one displayed by Formulation No. 1 (Figures 6 and 7). These figures show that an increase in DWG leads to an increase in the total concentration of essential amino acids. Figures 8-10 show that with an increase in DWG from 15% to 35%, the total concentration of non-essential amino acids becomes higher in all three flour mixtures.

This research shows that with an increasing percentage of DWG in the poly-cereal flour, both essential and non-essential amino acids become higher in concentration. Upon that, Formulation No. 1 stands out with the maximum concentrations of amino acids. At this point, we can state with certainty that Formulation No. 1 has the best amino acid composition.

The amino acid score was calculated for each of these three formulations. To accomplish this objective, the level of each essential amino acid was determined in the reference of "ideal" protein (Figures 11-13).

Figure 11 shows the laboratory concentrations of essential amino acids in the Formulation No. 1 with added DWG (15%, 25%, and 35%). From Figure 11, it follows that with an increase in DWG, Formulation No. 1 contained a

higher total concentration of tryptophan, threonine, and lysine. On the background of a significant increase in these amino acids, the increase in valine concentration was less impressive. The level of other amino acids did not change.

Figure 12 shows the laboratory concentrations of essential amino acids in the Formulation No. 2 with added DWG (15%, 25%, and 35%). The presented values show a slight increase in the concentration of essential amino acids in the Formulation No. 2. However, this increase was driven mainly by two amino acids – tryptophan and lysine. Changes that occurred in the concentration of essential amino acids in the Formulation No. 3 after the introduction of DWG are presented in Figure 13.

Figure 13 shows that with a DWG fraction increasing from 15% to 35%, tryptophan and lysine concentrations in Formulation No. 3 show a sharp increase. Such an impressive change was not observed in the concentrations of other essential amino acids (valine, isoleucine, leucine, methionine, threonine, and phenylalanine).

The concentrations of non-essential amino acids were also analyzed (Figures 14-16).

Figure 14 shows those changes that occurred in the concentrations of non-essential amino acids in the poly-cereal flour made according to Formulation No. 1 with added DWG (15%, 25%, and 35%). The diagram in Figure 14 shows that glutamic acid, proline, and serine tend to hit the maximum of the possible concentration in all formulations. A slight increase was observed in the level of glycine and histidine. The concentration of tyrosine, cysteine, alanine, arginine, and aspartate did not change significantly.

Figure 15 shows those changes that occurred in the concentrations of non-essential amino acids in the poly-cereal flour made according to Formulation No. 2 with added DWG (15%, 25%, and 35%). According to the diagram, significant changes occurred in the concentration of serine, proline, and glutamic acid. The remaining amino acids showed less significant changes in the concentration.

Figure 16 shows the three-dimensional model of changes that occurred in the concentration of non-essential amino acids in the poly-cereal flour made according to Formulation No. 3 with added DWG (15%, 25%, and 35%). The 3D model shows that with an increase in DWG from 15% to 35%, the concentration of glutamic acid, serine, and proline became higher. The

concentrations of the remaining non-essential amino acids remained almost within the same limits. The total concentration of non-essential amino acids did not show any significant change.

This research shows that DWG, added to the Formulations (No. 1, No.2 and No.3) at the level from 15% to 35%, leads to an increase in the concentration of specific amino acids. The most significant concentration increment was displayed by tryptophan, threonine, and lysine (essential amino acids), as well as by glutamic acid, serine, and proline (non-essential amino acids).

In this study, the resulting product, with reduced gluten content, is of acceptable quality. In conventional paste production, which involves durum wheat, gluten network formation is crucial to texture, but reaching quality in the gluten-free paste is a challenge (Mariotti *et al.*, 2011). In poly-cereal, mostly water-soluble, paste, weaker interactions between wheat proteins, mainly glutenins and gliadins, and proteins of other cereals can cause increased loss of weight during cooking (Phongthai *et al.*, 2017; Rizzello *et al.*, 2017). Paste formulations in this study (Figure 13) contain essential amino acids in the amount higher than recommended by WHO/FAO/UNU for adults (WHO/FAO/UNU, 2007). Thus, products prepared in accordance with these formulations demonstrate sufficient consumer qualities, and there is no need to add additional protein-rich components to the flour, which is what other authors do.

Laleg *et al.* (2016) investigated the composition of amino acids in bean flour paste, and this allowed achieving compliance with the requirements of WHO/FAO/UNU (2007). However, the well-known anti-nutritional properties of legumes (Gupta, 1987; Nosworthy *et al.*, 2016) do not make this approach optimal. An alternative attempt to enrich paste with essential amino acids at the expense of animal proteins (Desai *et al.*, 2018) does not seem successful either due to obvious problems – short shelf life. Moreover, adding animal raw materials to the paste will make it unsuitable for vegan diets that are associated with many health benefits, including significantly lower risks of developing heart disease, high blood pressure, stroke, and diabetes.

4. CONCLUSIONS:

To sum up, poly-cereal pasta formulations are a promising innovation that can carve out a niche in the market due to obvious competitive

advantages.

This research studied the amino acid composition of single-ingredient flour samples and a poly-cereal flour mixture for pasta dough. The analysis of diagrams suggests that the amino acid profile includes the following essential amino acids: valine, isoleucine, leucine, lysine, methionine, threonine, tryptophan, and phenylalanine. In flour ground from cereals, the total concentration of essential amino acids is insignificant. In flour ground from legumes, the level of essential amino acids is significantly higher by contrast: valine, isoleucine, leucine, lysine, threonine, and phenylalanine hit the maximum. However, tryptophan and methionine were not significant. The flour with added DWG was high in lysine and valine.

This research shows that with an increasing percentage of DWG in the poly-cereal flour, both essential and non-essential amino acids become higher in concentration. Upon that, the Formulation No. 1 stands out with the maximum concentrations of amino acids, which is significantly higher than in Formulations No.2 and No. 3.

Research results showed that the increase in dry wheat gluten from 15% to 35% leads to a sharp increase in the concentration of tryptophan and lysine. The concentration of other essential amino acids (valine, isoleucine, leucine, methionine, threonine, phenylalanine) did not change significantly.

5. ACKNOWLEDGMENTS:

This article was supported by the RK Ministry of Education and Science grant within the framework of the 2018-2020 R&D project: "The Development of Technology for Producing Pasta with Unconventional Poly-Cereal Raw Material" (state registration number 0118RK00310).

6. REFERENCES:

1. Bigliardi, B., Galati, F. (2013). *Innovation trends in the food industry: the case of functional foods*. Trends Food Sci. Technol., 31(2), 118–129.
2. Brennan, M. A., Merts, I., Monroe, J., Woolnough, J., Brennan, C. S. (2008). *Impact of guar and wheat bran on the physical and nutritional quality of extruded breakfast cereals*. Starch-Stärke, 60(5), 248-256.
3. Capozzi, V., Russo, P., Fragasso, M., De Vita, P., Fiocco, D., Spano, G. (2012). *Biotechnology and pasta-making: lactic acid*

bacteria as a new driver of innovation. Front. Microbiol., 3: 94.

4. Chillo, S., Laverse, J., Falcone, P. M., Del Nobile, M. A. (2008). *Quality of spaghetti in base amaranthus wholemeal flour added with quinoa, broad bean and chick pea*. J. Food Eng., 84(1), 101-107.

5. Cubadda, R. E., Carcea, M., Marconi, E., Trivisonno, M. C. (2007). *Influence of gluten proteins and drying temperature on the cooking quality of durum wheat pasta*. Cereal Chem., 84(1), 48-55.

6. Desai, A. S., Brennan, M. A., Brennan, C. S. (2018). *Amino acid and fatty acid profile and digestible indispensable amino acid score of pasta fortified with salmon (*Oncorhynchus tshawytscha*) powder*. Eur. Food Res. Technol., 244(10), 1729–1739.

7. Doxastakis, G., Papageorgiou, M., Mandalou, D., Irakli, M., Papalamprou, E., D'Agostina, A., Resta, D., Boschini, G., Arnoldi, A. (2007). *Technological properties and non-enzymatic browning of white lupin protein enriched spaghetti*. Food Chem., 101(1), 57-64.

8. Gull, A., Prasad, K., Kumar, P. (2018). *Nutritional, antioxidant, microstructural, and pasting properties of functional pasta*. Journal of the Saudi Society of Agricultural Sciences, 17(2), 147-153.

9. Gupta, Y. P., (1987). *Anti-nutritional and toxic factors in food legumes: a review*. Plant Foods Hum. Nutr., 37(3), 201-228.

10. Ivanišová, E., Košec, M., Brindza, J., Grygorieva, O., Tokár, M. (2018). *Green barley as an ingredient in pasta: Antioxidant activity and sensory characteristics evaluation*. Contemporary Agriculture, 67(1), 81–86.

11. Iztaev, B. A., Iskakova, G. K., Umirzakova, G. A., Magomedov, G. O. (2018). *Expansion of the range of pasta products through the use of vegetable raw materials*. Vestnik Voronežskogo Gosudarstvennogo Universiteta Inženernyh Tehnologij, 80(1), 173-180.

12. Koryachkina, S. Ya. (2006). *Pasta products: ways to improve the quality and nutritional value*. Trud Publishing House, Oryol.

13. Laleg, K., Cassan, D., Barron, C., Prabhasankar, P., Micard, V. (2016). *Structural, culinary, nutritional, and anti-nutritional properties of high protein, gluten-free, 100% legume pasta*. PLoS One, 11(9), e0160721.

14. Lucisano, M., Cappa, C., Fongaro, L., Mariotti, M. (2012). *Characterization of gluten-free pasta through conventional and innovative methods: evaluation of the cooking behavior*. J. Cereal Sci., 56(3), 667-675.

15. Mariotti, M., Iametti, S., Cappa, C., Rasmussen, P., Lucisano, M. (2011). *Characterization of gluten-free pasta through conventional and innovative methods: Evaluation of the uncooked products*. J. Cereal Sci., 53(3), 319-327.

16. Nosworthy, M. G., Tulbek, M. C., House, J. D. (2017). *Does the concentration, isolation, or deflavoring of pea, lentil, and faba bean protein alter protein quality?* Cereal Foods World, 62(4), 139-142.

17. Ospanov, A. A., Muslimov, N. Zh., Timurbekova, A. K., Jumabekova, G. B. (2013). *Formulating poly-cereal flour mixture for high-quality products (computer-aided calculation)*. Research, Results, 3, 121-131.

18. Ospanov, A., Gaceu, L., Timurbekova, A., Muslimov, N., Dzhumabekova, G. (2014). *Innovative technologies of grain crops processing*. Infomarket, Brasov.

19. Ospanov, A., Muslimov, N., Timurbekova, A. (2017). *Technology of manufacturing of whole-milled flour: Textbook*. Almanach Publishing House, Almaty.

20. Ospanov, A., Muslimov, N., Timurbekova, A., Jumabekova, G., Kamzabekov, S. (2017). *Research efficiency extrusion process flour poly-cereal mixture*. Research, Results, 1, 24-30.

21. Ospanov, A., Muslimov, N., Timurbekova, A., Jumabekova, G. (2018a). *Research of rheological behaviour of the dough from poly-cereal flour mix for the manufacture of pasta*. Scientific Journal KazNau of Research and Results, 3(79), 63-69.

22. Ospanov, A., Muslimov, N., Timurbekova, A., Jumabekova, G. (2018b). *Rheological properties of dough from poly-cereal flour mixture for pasta*. Research, Results, 3, 43-46.

23. Ostrikov, A. N., Shakhov, S. V., Ospanov, A. A., Muslimov, N. Z., Timurbekova, A. K., Jumabekova, G. B., Matevey, Y. Z. (2018). *Mathematical modeling of product melt flow in the molding channel of an extruding machine with meat filling feeding*. J. Food Process Eng., 41(8): e12874.

24. Padalino, L., Conte, A., Lecce, L., Likyova, D., Sicari, V., Pellicano, T. M., Poiana, M., Del Nobile, M. A. (2017). *Functional pasta with tomato by-product as a source of antioxidant compounds and dietary fiber*. Czech J. Food Sci., 35(1), 48-56.

25. Phongthai, S., D'Amico, S., Schoenlechner, R., Homthawornchoo, W., Rawdkuen, S. (2017). *Effects of protein enrichment on the properties of rice flour-based*

gluten-free pasta. Food Sci. Technol., 80, 378-385.

26. Rizzello, C. G., Losito, I., Facchini, L., Katina, K., Palmisano, F., Gobbetti, M., Coda, R. (2016). *Degradation of vicine, convicine, and their aglycones during fermentation of faba bean flour*. Sci. Rep., 6, 32452.

27. Rizzello, C. G., Verni, M., Koivula, H., Montemurro, M., Seppa, L., Kemell, M., Katina, K., Coda, R., Gobbetti, M. (2017). *Influence of fermented faba bean flour on the nutritional, technological and sensory quality of fortified pasta*. Food & Function, 8(2), 860-871.

28. Spinelli, S., Padalino, L., Costa, C., Del Nobile, M. A., Conte, A. (2019). *Food by-products to fortified pasta: A new approach for optimization*. J. Clean Prod., 215, 985-991.

29. WHO/FAO/UNU (2007). *Protein and amino acid requirements in human nutrition. WHO technical report series 935*. World Health Organization. Available from: <http://apps.who.int/iris/handle/10665/43411>, Accessed: 15/12/2019.

30. Zheng, Y., Dandin, T., Hernandez, G. (2016). *Effect of dietary fiber on in vitro bioavailability of minerals in fiber-enriched pasta products*. J. Nutr. 133(1), 1-4.

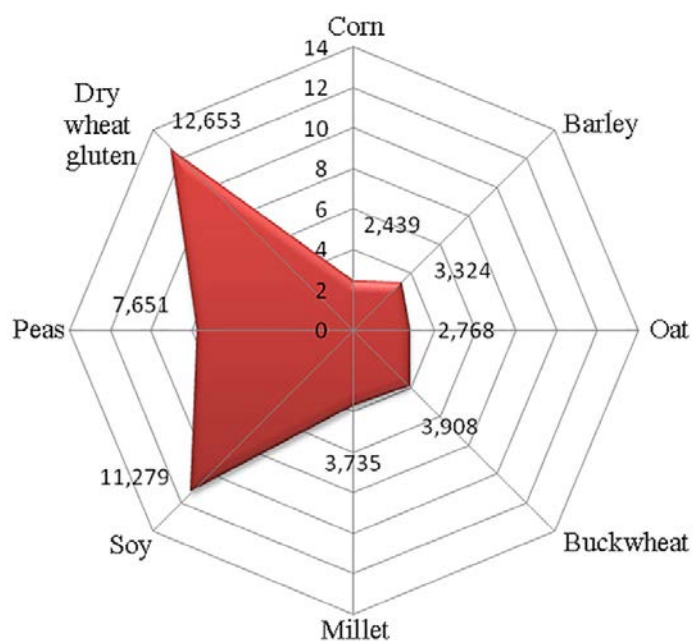


Figure 1. Total Concentration of Essential Amino Acids in Cereals/Legumes and in DWG, % by Weight.

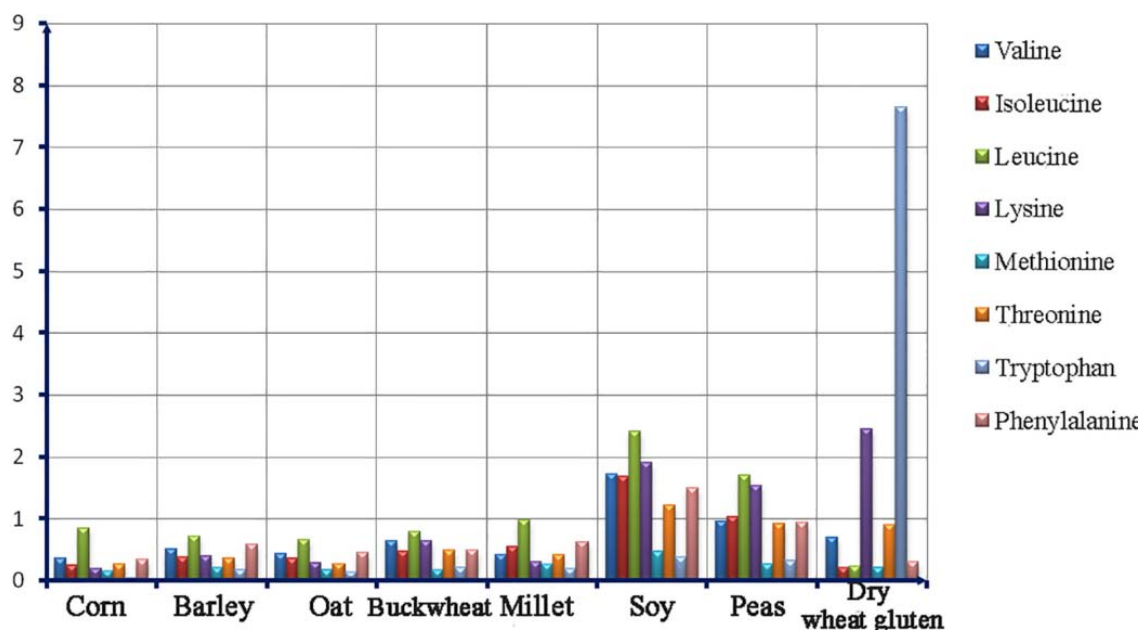


Figure 2. Essential Amino Acid Profile: Wholemeal Flour (Ground from Cereals/Legumes) vs. Flour with added DWG, % by Weight.

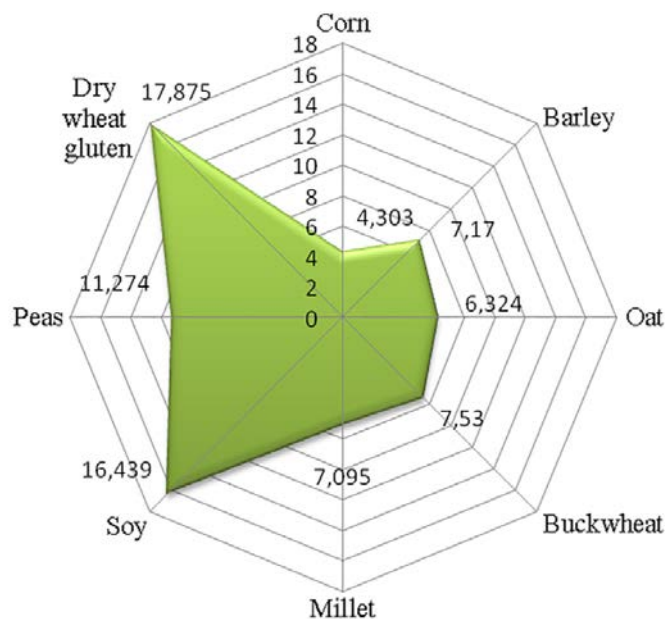


Figure 3. Total Concentration of Non-Essential Amino Acids in Cereals/Legumes and in DWG, % by Weight.

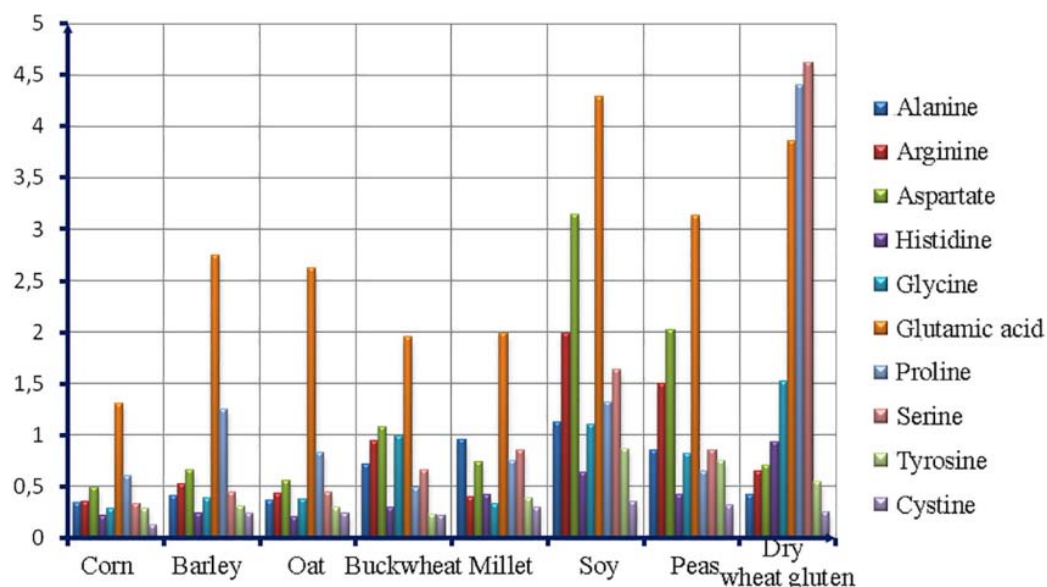


Figure 4. Essential Amino Acid Profile: Wholemeal Flour (Ground from Cereals/Legumes) vs. Flour with added DWG, % by Weight.

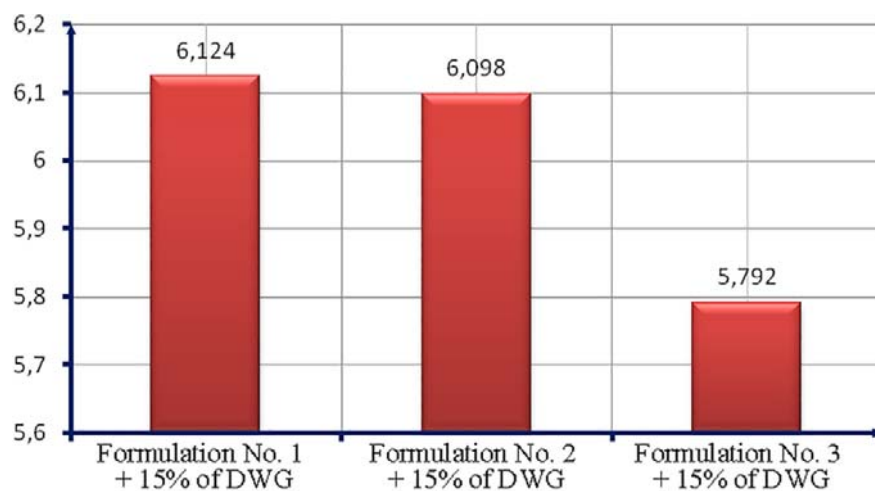


Figure 5. Total Concentration of Essential Amino Acids in Formulations (No. 1, No. 2 and No. 3) with added DWG (15%).

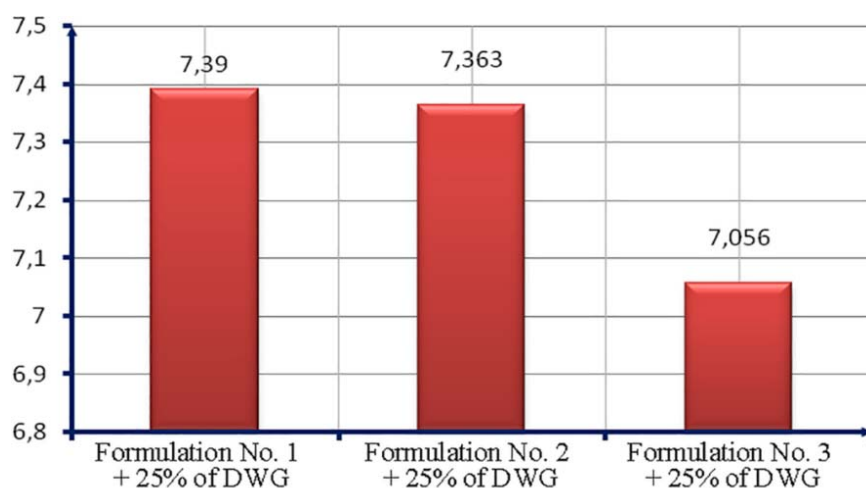


Figure 6. Total Concentration of Essential Amino Acids in Formulations (No. 1, No. 2 and No. 3) with added DWG (25%).

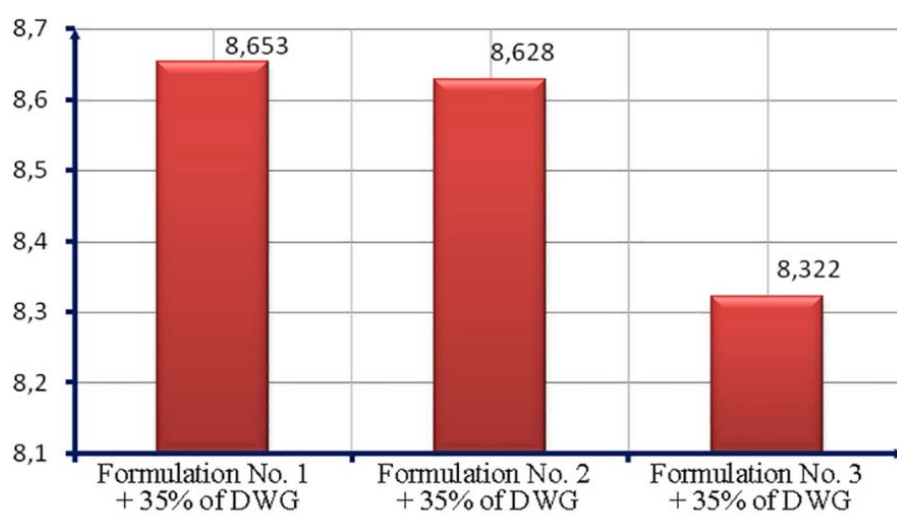


Figure 7. Total Concentration of Essential Amino Acids in Formulations (No. 1, No. 2 and No. 3) with added DWG (35%).

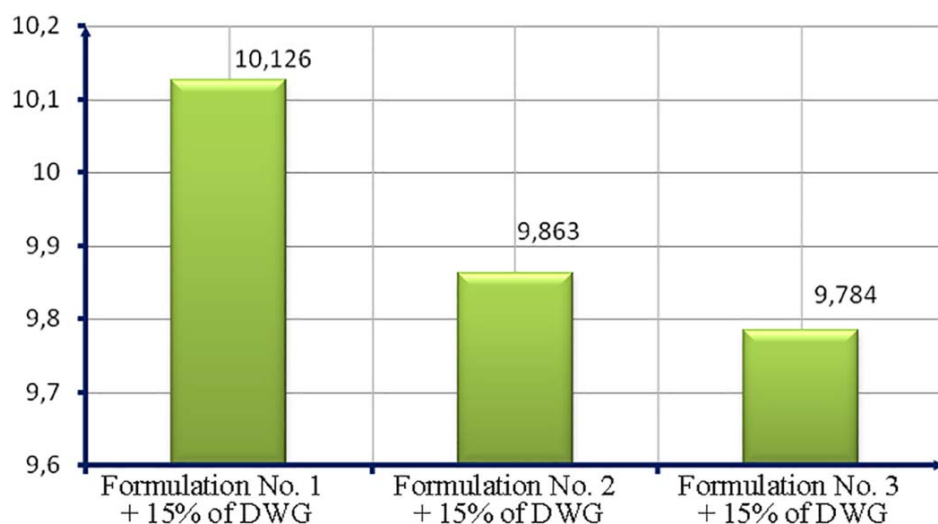


Figure 8. Total Concentration of Non-Essential Amino Acids in Formulations (No. 1, No. 2 and No. 3) with added DWG (15%).

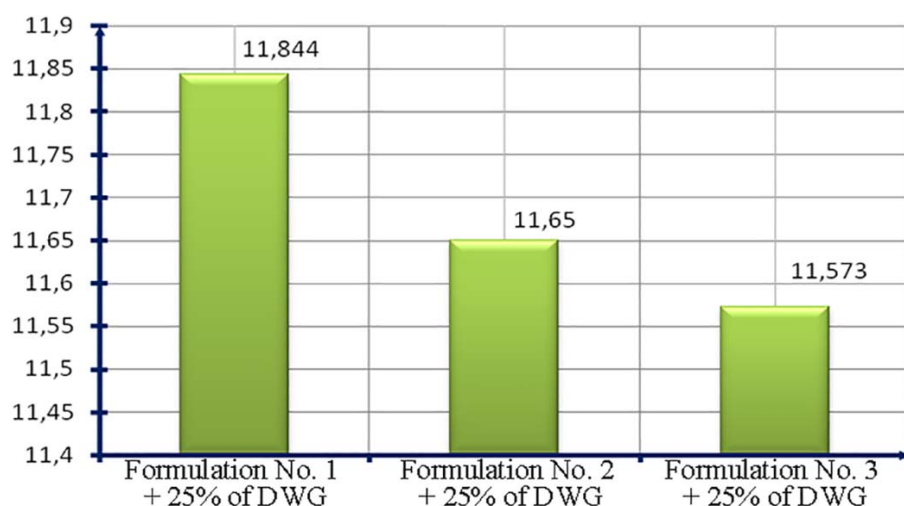


Figure 9. Total Concentration of Non-Essential Amino Acids in Formulations (No. 1, No. 2 and No. 3) with added DWG (25%).

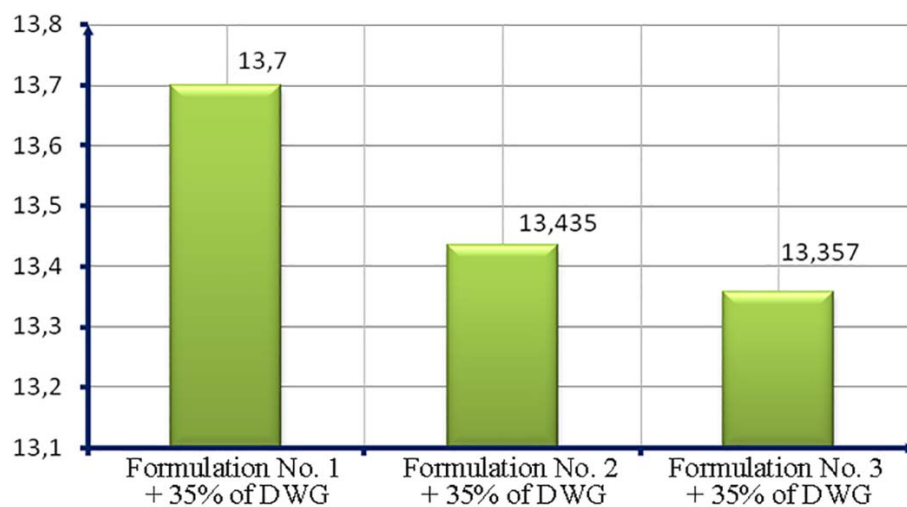


Figure 10. Total Concentration of Non-Essential Amino Acids in Formulations (No. 1, No. 2 and No. 3) with added DWG (35%).

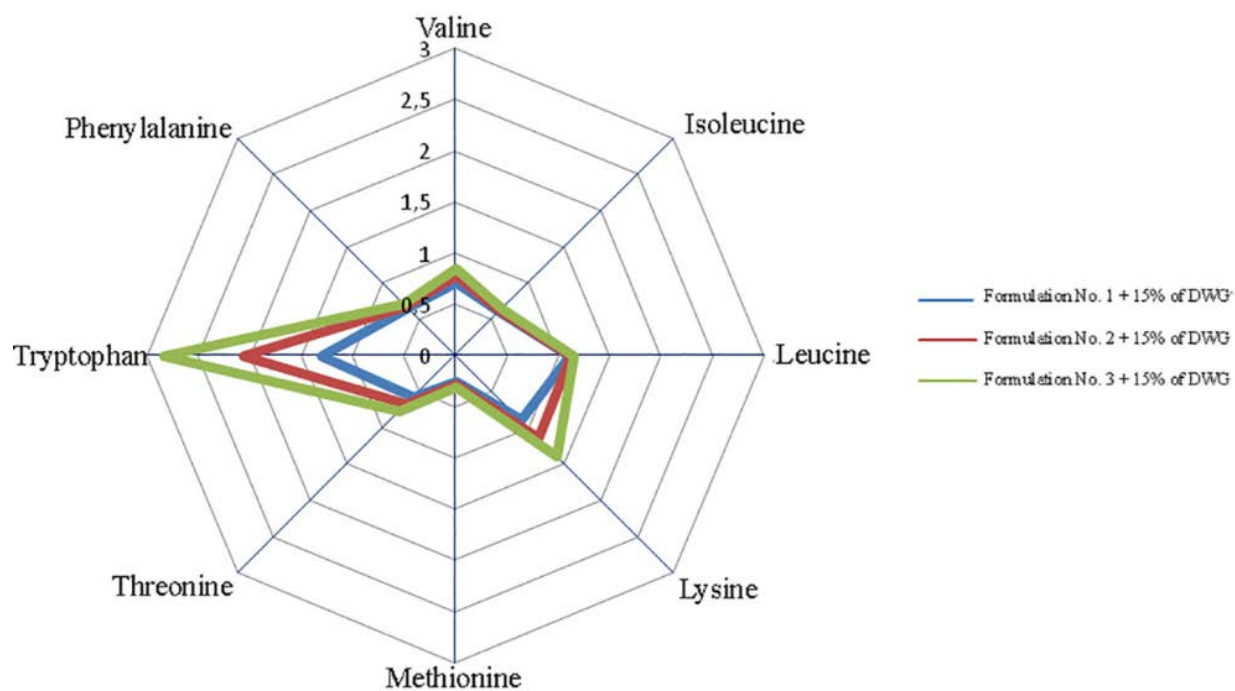


Figure 11. The Concentrations of Essential Amino Acids in Formulation No. 1 with added DWG (15 %, 25 %, and 35 %).

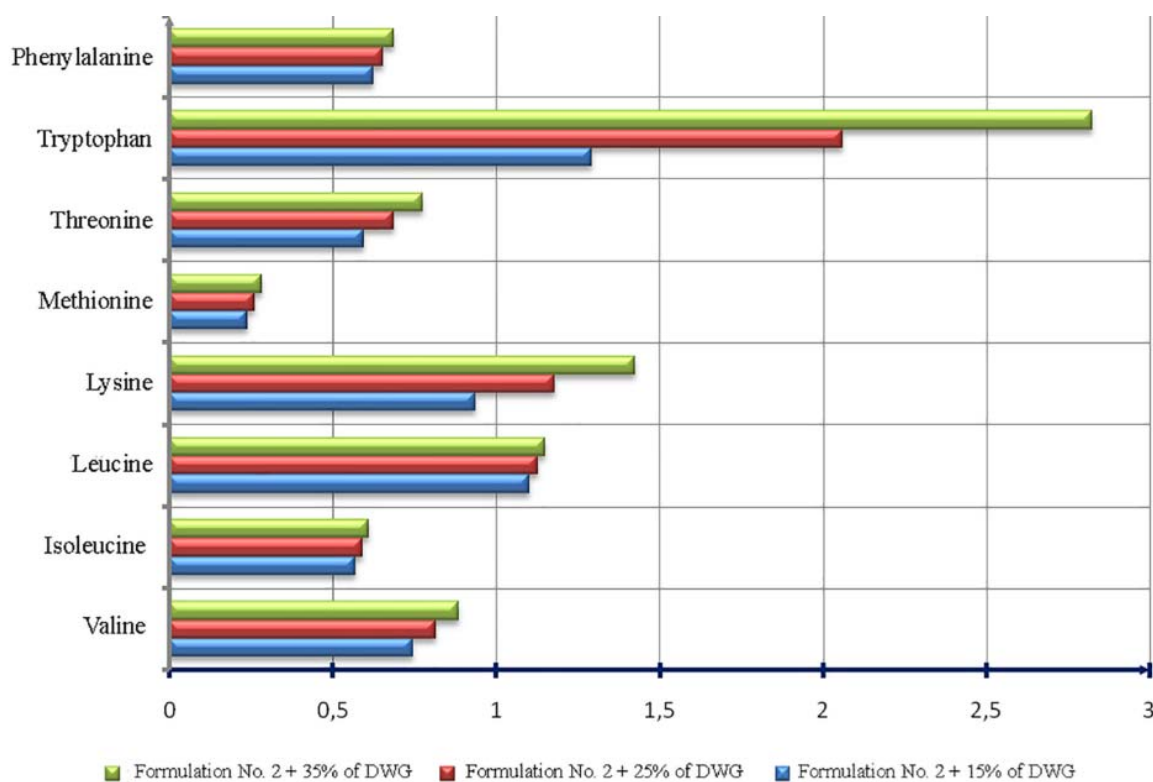


Figure 12. The Concentrations of Essential Amino Acids in Formulation No. 2 with added DWG (15 %, 25 %, and 35 %).

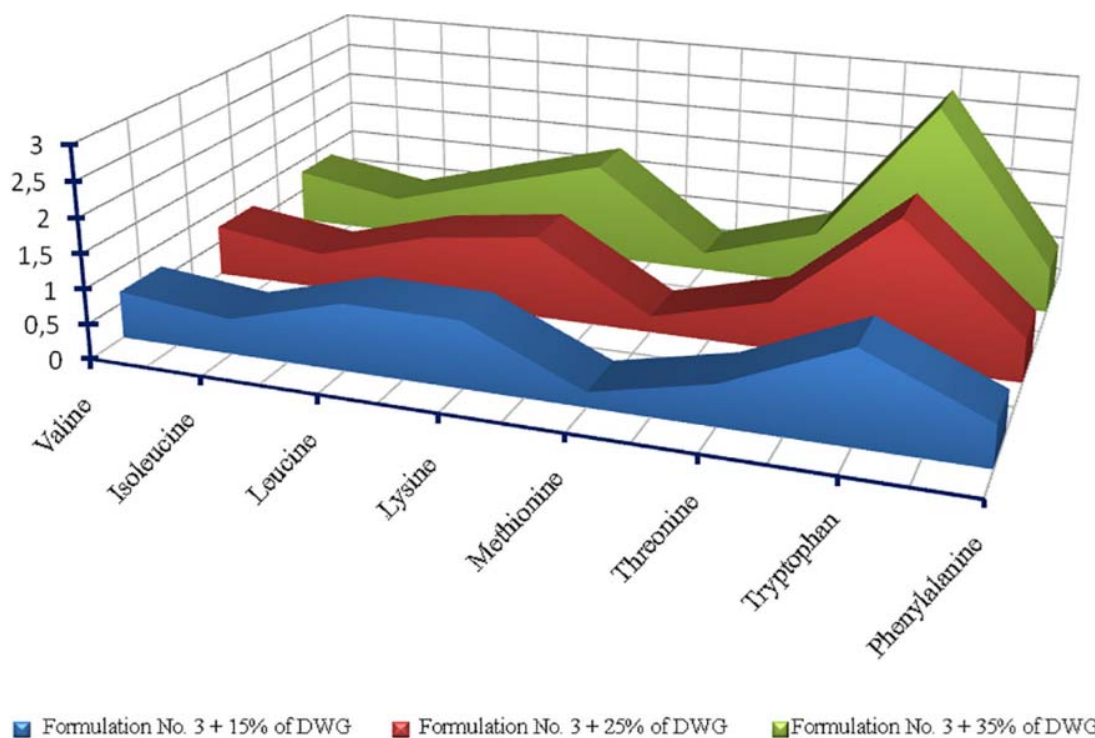


Figure 13. The Concentrations of Essential Amino Acids in Formulation No. 3 with added DWG (15 %, 25 %, and 35 %).

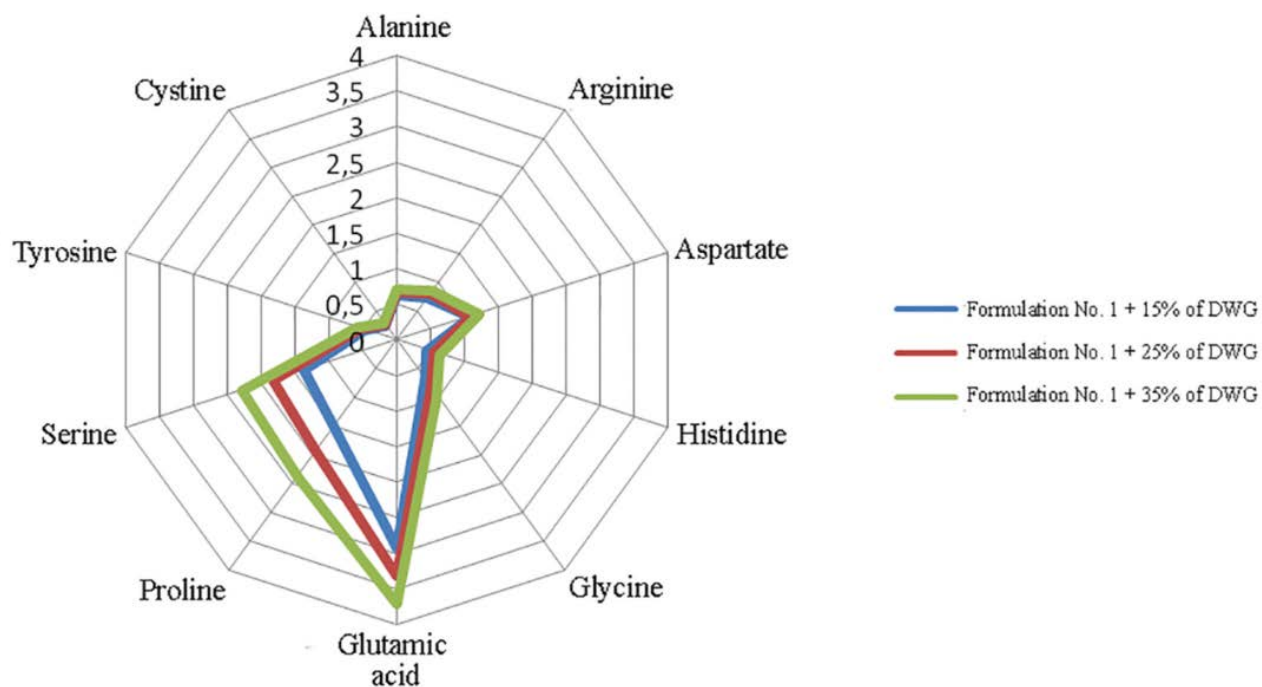


Figure 14. The Concentrations of Non-Essential Amino Acids in the Formulation No. 1 with added DWG (15 %, 25 %, and 35 %).

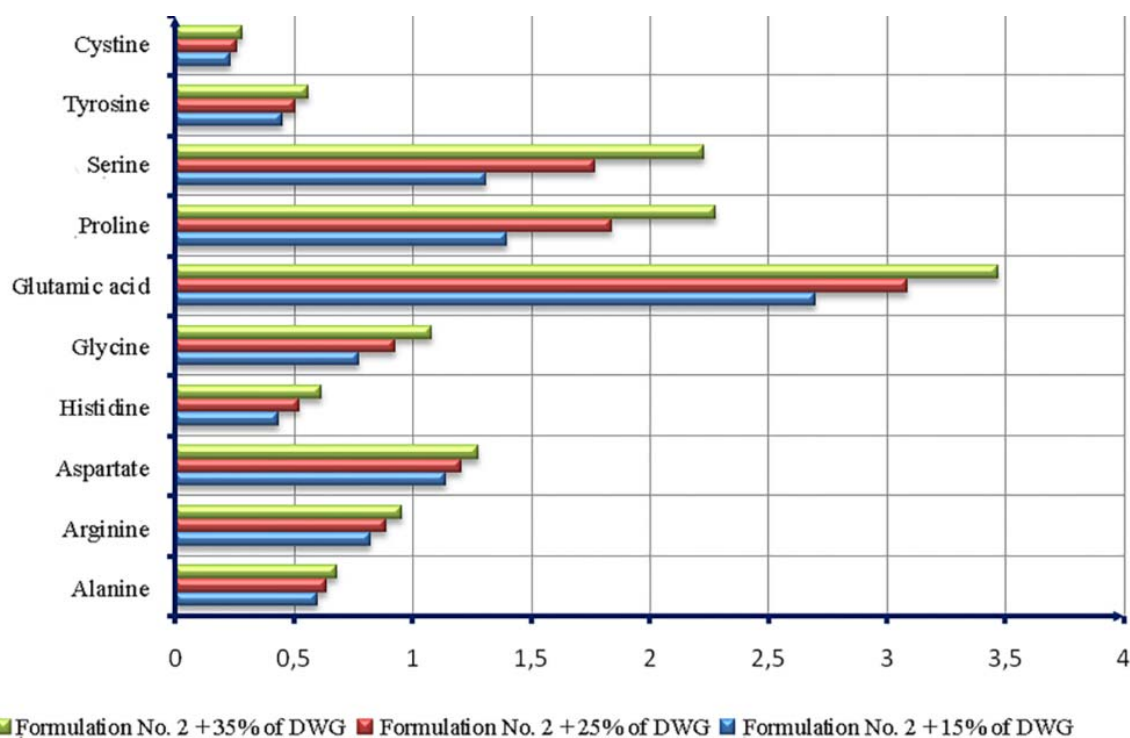


Figure 15. The Concentrations of Non-Essential Amino Acids in the Formulation No. 2 with added DWG (15 %, 25 %, and 35 %).

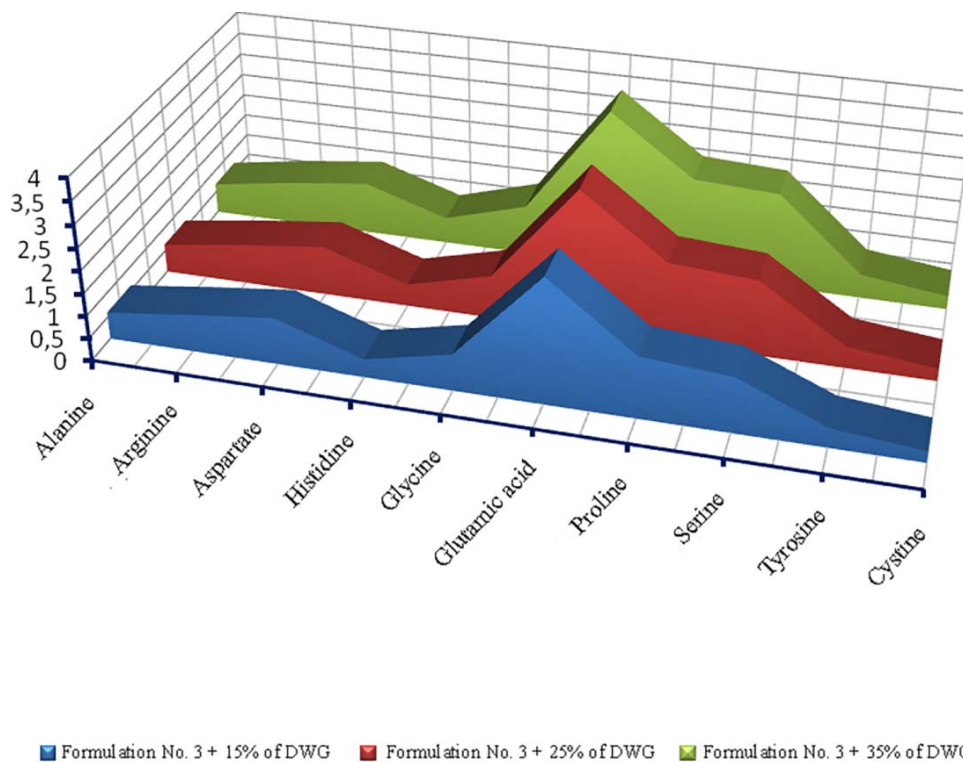


Figure 16. The Concentrations of Non-Essential Amino Acids in the Formulation No. 3 with added DWG (15 %, 25 %, and 35 %).

A TOMOGRAFIA DE EMISSÃO DE POSITRONS NO DIAGNÓSTICO PRECOCE DOS TRANSTORNOS METABÓLICOS DO MIOCÁRDIO EM PACIENTES RESISTENTES À INSULINA COM DOENÇA HEPÁTICA GORDUROSA NÃO ALCOÓLICA**THE POSITRON EMISSION TOMOGRAPHY IN EARLY DIAGNOSTICS OF THE METABOLIC MYOCARDIAL DISORDERS IN INSULIN-RESISTANT PATIENTS WITH NON-ALCOHOLIC FATTY LIVER DISEASE****ПОЗИТРОННО-ЭМИССИОННАЯ ТОМОГРАФИЯ КАК ЭФФЕКТИВНЫЙ МЕТОД РАННЕЙ ДИАГНОСТИКИ МЕТАБОЛИЧЕСКИХ НАРУШЕНИЙ МИОКАРДА У ПАЦИЕНТОВ С НЕАЛКОГОЛЬНОЙ ЖИРОВОЙ БОЛЕЗНЬЮ ПЕЧЕНИ**

ROYTBERG, Grigory Efimovich¹; SHARKHUN, Olga Olegovna^{2*}; PLATONOVA, Oksana Evgenyevna³; STEPANOVA, Anna Alexandrovna⁴;

^{1,2} Pirogov Russian National Research Medical University, Moscow, Russian Federation

^{3,4} Joint Stock Company «Medicina», Moscow, Russian Federation

* Correspondence author
e-mail: olga_sharkhun@mail.ru

Received 19 December 2019; received in revised form 20 February 2020; accepted 19 March 2020

RESUMO

Recent studies demonstrated the Hepato-cardiac relationship in patients with non-alcoholic fatty liver disease as subclinical, structural, and functional alterations in the heart. However, the mechanisms underlying the changes in the cardiovascular system are understudied and not clear. The aim of the study was to assess glucose metabolism, its perfusion in the cardiomyocytes and the detection of the myocardial dysfunction in patients with fatty liver disease and insulin resistance using the positron emission tomography with fludeoxyglucose. During the study, 18 patients (14 men and 4 women, mean age 52 ± 4.2 years) with the non-alcoholic fatty liver disease and the insulin resistance ($\text{HOMA-IR} > 2.6$) were examined. There were 12 patients in the control group. Echocardiography revealed various types of the left ventricular cardiac remodeling in the study group: 44.4% of patients with eccentric hypertrophy, 38.9% with concentric hypertrophy, and 16.7% with the concentric remodeling. In this group, there was a pronounced diffuse uneven distribution of the radiopharmaceutical. In addition, zones of hypometabolism and paradoxical accumulation of glucose were detected. Thus, it was shown that in patients with non-alcoholic fatty liver disease and insulin resistance, the intensity and nature of glucose metabolism in cardiomyocytes changed, indicating the presence of myocardial metabolic dysfunction. We believe that the systemic insulin resistance metabolic processes were disturbed not only in the liver cells but also in the cardiomyocytes. As a result of the metabolic dysfunction, the geometric parameters of the heart are changed, and various types of cardiac remodeling are formed.

Palavras-chave: *fatty liver disease, insulin resistance, metabolic dysfunction.*

ABSTRACT

Recent studies demonstrated the Hepato-cardiac relationship in patients with non-alcoholic fatty liver disease as subclinical, structural, and functional alterations in the heart. However, the mechanisms underlying the changes in the cardiovascular system are understudied and not clear. The aim of the study was to assess glucose metabolism, its perfusion in the cardiomyocytes and the detection of the myocardial dysfunction in patients with fatty liver disease and insulin resistance using the positron emission tomography with fludeoxyglucose. During the study, 18 patients (14 men and 4 women, mean age 52 ± 4.2 years) with the non-alcoholic fatty liver disease and the insulin resistance ($\text{HOMA-IR} > 2.6$) were examined. There were 12 patients in the control group. Echocardiography revealed various types of the left ventricular cardiac remodeling in the study group: 44.4% of patients with eccentric hypertrophy, 38.9% with concentric

hypertrophy, and 16.7% with the concentric remodeling. In this group, there was a pronounced diffuse uneven distribution of the radiopharmaceutical. In addition, zones of hypometabolism and paradoxical accumulation of glucose were detected. Thus, it was shown that in patients with non-alcoholic fatty liver disease and insulin resistance, the intensity and nature of glucose metabolism in cardiomyocytes changed, indicating the presence of myocardial metabolic dysfunction. We believe that the systemic insulin resistance metabolic processes were disturbed not only in the liver cells but also in the cardiomyocytes. As a result of the metabolic dysfunction, the geometric parameters of the heart are changed, and various types of cardiac remodeling are formed.

Keywords: *fatty liver disease, insulin resistance, metabolic dysfunction.*

АННОТАЦИЯ

Недавние исследования продемонстрировали гепатокардиальные отношения у пациентов с неалкогольной жировой болезнью печени как субклинические структурные и функциональные изменения в сердце. Однако механизмы, лежащие в основе данных изменений, недостаточно изучены и не совсем понятны. Целью исследования было оценить метаболизм глюкозы, ее перфузию в кардиомиоцитах и выявление дисфункции миокарда у пациентов с неалкогольной жировой болезнью печени и инсулинорезистентностью с использованием метода позитронно-эмиссионной томографии с использованием фтордезоксиглюкозы. В нашем исследовании было обследовано 18 пациентов (14 мужчин и 4 женщины, средний возраст $52 \pm 4,2$ года) с НАЖБП и инсулинорезистентностью (HOMA-IR > 2,6). В контрольной группе было 12 пациентов. Эхокардиография выявила различные типы ремоделирования левого желудочка в основной группе: 44,4% пациентов с эксцентрической гипертрофией, 38,9% с концентрической гипертрофией и 16,7% с концентрическим ремоделированием. В контрольной группе пациентов с ремоделированием сердца не было. В этой группе при проведении позитронно-эмиссионной томографии установлено равномерное распределение фторглюкозы в сердечной мышце, и структура миокарда была относительно однородной. В основной группе наблюдалось выраженное диффузное неравномерное распределение радиофармпрепарата. Кроме того, были обнаружены зоны гипометаболизма и парадоксального накопления глюкозы. Мы полагаем, что при системной инсулинорезистентности метаболические процессы нарушаются не только в клетках печени, но и в кардиомиоцитах. В результате метаболической дисфункции изменяются геометрические параметры сердца и формируются различные типы ремоделирования сердца.

Ключевые слова: *жировая болезнь печени, инсулинорезистентность, метаболическая дисфункция.*

1. INTRODUCTION

Presently, positron-emission tomography (PET) is widely used in different areas of medicine, for example, in oncology, for the diagnostics of tumors of different localization, in cardiology, for the evaluation of the myocardium damage and myocardial blood supply rate, in neurology, for the diagnostics of Alzheimer disease (Usov *et al.*, 2014; Buziashvili and Buziashvili, 2014; Cohn, 1998). The method allows the specialists to combine computer tomography and the introduction of short half-life isotopes that are necessary for the evaluation of the functional activity of the studied tissue. The main advantage of the method is the possibility of the evaluation of energetic metabolic disturbances of the studied organ (Nikiforov, 2017; Yoshinaga and Tamaki, 2007).

Energetic metabolism of the myocardium is a many-staged process that includes the

formation of a highly allergic compound, adenosine triphosphoric acid (ATP), in mitochondria, intercellular transport of ATP molecules and their utilization during the energy-dependent vital processes (Parmon and Ryzhova, 2014; Sergienko and Babev, 2011). The main metabolic sources of biological synthesis of ATP are long-chained free fatty acids (FFA) and glucose that provide normal functioning of the enzymes of the breathing chain in mitochondria and regulate the process of oxidative phosphorylation with the formation of ATP (Usov *et al.*, 2014; Ryotberg and Sharkhun, 2017b). In normal physiologic conditions, the utilization of fatty acids and carbohydrates is absolutely balanced and depends on the availability of each of these substrates. When the consumption of oxygen is sufficient (60-80%), ATP is synthesized due to the oxidation of long-chained FFA. However, in comparison with glucose, fatty acids are considered to be a less feasible source of

energy because, for the oxidation of the same amount of ATP, it is required to spend 10% more oxygen. The involvement of FFA in energy metabolism is reduced during physical load, in stress situations, in smokers, in the condition of hypoxia, and in patients with hyperglycemia or hyperinsulinemia. Insulin resistance in tissues and disturbance of glucose transport are associated with mitochondrial dysfunction and, as a result, the disturbances of energy metabolism in cells, including cardiomyocytes. In such conditions, the rate of beta-oxidation of FFA significantly decreases, and glycolysis becomes the main source of ATP for the cells (Bokeria, 2010; Yoshinaga and Tamaki, 2007). Hence, the quantitative evaluation of the utilization rate of glucose can be used for the study of the activity of this metabolic pathway for the evaluation of the functional status of the myocardium. Presently, the most informative method is positron emission tomography with fluorodeoxyglucose (^{18}F -FDG). When ^{18}F -FDG gets into a cell, it phosphorylates due to hexokinase to fluorodeoxyglucose-6-phosphate, a compound that does not get involved in further metabolic reactions. Since it cannot penetrate through a cellular membrane, the transport of ^{18}F -FDG to a cell is irreversible. Thus, the accumulation of ^{18}F -FDG in the myocardium correlates with the consumption of glucose and can be used for the estimation of the rate of its utilization and identification of the activity of glycolysis.

It is established that the disturbance of carbohydrate and lipid metabolism is determined pathogenically by the condition of the liver (Björnsson *et al.*, 2013; Musso *et al.*, 2012). According to the opinion of the leading organizations in hepatology, the presence of the signs of hepatic steatosis and the absence of secondary fat accumulation is treated as non-alcoholic fatty liver disease (NAFLD). NAFLD is closely associated with metabolic syndrome and its components: abdominal obesity, dyslipidemia, hyperglycemia, atherosclerosis, and arterial hypertension. In its turn, NAFLD is not only an additional risk factor for the development of cardiovascular diseases but also a factor that determines the outcome of liver disease (Ryotberg and Sharkhun, 2017b). There are data on the presence of Hepato-cardiac associations that are characterized by the change in the geometry of the heart, structural-functional parameters of the heart, and diastolic dysfunction in patients with NAFLD (Björnsson *et al.*, 2013; Musso *et al.*, 2012). However, the mechanisms underlying the alteration in the cardiovascular system remain understudied and unclear, which

defines the aims and tasks of further studies.

The aim of the present study was to evaluate glucose metabolism, condition of its perfusion in the myocardium, and myocardial dysfunction in patients with non-alcoholic fatty liver disease and insulin resistance.

2. MATERIALS AND METHODS

The authors examined two groups of patients at the clinics of JSC "Medicine". Group I included 18 patients with clinical and laboratory-instrumental signs of NAFLD. Group II (control group) included 12 people who did not have signs of NAFLD and met the study exclusion criteria. The study exclusion criteria were diabetes mellitus 1 and 2 types, lipid metabolism disorders (including congenital disorders and hypolipidemic therapy), arterial hypertension that requires therapeutic correction, ischemic heart disease, obesity of II and III degrees, serious somatic diseases at the stage of decompensation, and hormonal replacement therapy.

NAFLD was diagnosed based on the performed examination as a diagnosis of the exclusion of other hepatic pathology in patients with ultrasound signs of fatty hepatosis. Insulin resistance (IR) in patients was evaluated with a laboratory model of the evaluation of homeostasis (HOMA-IR) by Equation 1.

$$\text{HOMA-IR} = (\text{G}_{\text{bf}} \cdot \text{I}_{\text{bm}}) / 22.5 \quad (\text{Eq. 1})$$

Where G_{bf} = (Glucose before meal (mmol/L); I_{bm} = Insulin before the meal (mcU/ml))/22.5

According to the recommendation of the WHO, in the clinical practice, the upper quartile of the HOMA-IR distribution index in the general population is to be used for the evaluation of IR. Thus, threshold resistance to insulin, expressed in HOMA-IR, is defined as 75 percentile of its cumulative populational distribution. In the present study, the threshold value of HOMA was 2.6 points. IR was diagnosed in patients at HOMA-IR higher than 2.6 points.

All the patients had an echocardiographic study performed with an apparatus "Vivid E80" ("GE Healthcare"). The main geometry parameters of the left ventricle (LV) included the

end-diastolic dimension of LV, crosscut dimension, longitudinal dimension of VL in diastole (DLV), left ventricular posterior wall thickness, interventricular septum thickness in diastole (ISTD). Parameters of the geometry of LV were used for the calculations of indexes reflecting the process of its remodeling: sphericity index – the relation of the cross-sectional dimension of LV to its long axis, myocardial mass index (MMI) of LV (was identified by the formula of R. Devereux and N. Reichek), index of the relative thickness of the wall (RTW) – the ratio of a sum of LV PWT and IWST to LV EDD. Depending on the values of these indexes, different types of LV geometry remodeling are identified (by the classification of A. Ganau, 1992): normal geometry of LV ($RWT \leq 0.42$ and $MMI \leq 95 \text{ g/m}^2$ for women and $\leq 115 \text{ g/m}^2$ for men), concentric hypertrophy of LV: $RWT > 0.42$ and $MMI > 95 \text{ g/m}^2$ for women and $> 115 \text{ g/m}^2$ for men; eccentric hypertrophy: $RWT \leq 0.42$ and $MMI > 95 \text{ g/m}^2$ for women and $> 115 \text{ g/m}^2$ for men, concentric remodeling: $RWT > 0.42$ and $MMI \leq 95 \text{ g/m}^2$ for women and $\leq 115 \text{ g/m}^2$ for men.

All PET-CT studies were performed with "Biograph mCT Flow 64-4R PET/CT system" (Siemens Healthcare, Germany). The procedure was performed before a meal at rest for the exclusion of the negative influence of hyperinsulinemia on the accumulation of radiopharmaceutical agent (RPA) in the myocardium. The study was performed in a static mode on a reconstructed image that clearly visualized the left ventricle. For the analysis, the zones of interest were chosen that corresponded to the myocardium of LV. The image processing was performed by the cut sections that were formed by the vertical, horizontal, and short axes of LV with a section cut the thickness of 0.5 cm. Visual analysis of the images was performed with a color scale that allowed the authors to evaluate the intensity of RPA accumulation in focus, its localization, dimensions, contours, and character of the drug distribution.

3. RESULTS AND DISCUSSION

Eighteen patients were selected in the study group (14 men and 4 women, average age 52 ± 4.2 years old). All the patients were preliminary examined and had clinical and laboratory-instrumental signs of NAFLD revealed. There were two forms of this disease revealed: nonalcoholic steatosis (liver fatty degeneration at a normal level of aminotransferases) and nonalcoholic steatohepatitis (with an increase in

the level of hepatic enzymes in the blood) in 12 and 6 patients, respectively. The calculated laboratory index HOMA-IR exceeded the threshold values in all the patients from the study group and was equal to 4.41 ± 3.8 , which indicated insulin resistance in this category of patients. The control group included 12 patients (5 men and 7 women, average age 44 ± 6.5 years old) that did not have signs of NAFLD. The patients did not have signs of disturbances of carbohydrate metabolism and insulin resistance (HOMA-IR 1.29 ± 0.98).

Echocardiogram in patients from the study group revealed the alterations of the heart chambers dimensions in comparison with the control group. Thus, average values of LV EDD were 4.87 ± 0.38 cm vs. 4.73 ± 0.32 ($p < 0.05$), average values of LV longitudinal dimension (DLV) were 7.87 ± 0.86 vs. 8.38 ± 0.50 ($p < 0.05$). The Index of sphericity (IS) of LV, as a relation of a cross-section of LV to its long axis, in normal condition does not exceed 0.6 and characterize an ellipsoid shape of LV. In the present study, the patients with NAFLD and IR had an average IS higher than the norm and significantly different from the patients in the control group: 0.62 ± 0.06 vs. 0.58 ± 0.05 , ($p < 0.05$). In the majority of patients from the study group, this parameter was higher than 6 in 13 out of 18 patients, which was 72.2%. The increase in the IS was higher than 0.6, which indicated the alterations in the geometry of the heart with a tendency to the formation of spherical shape.

The average values of LV PWT and IVST were 0.99 ± 0.12 cm and 1.01 ± 0.13 cm, respectively, in the control group. The calculation of the index of relative wall thickness (RWT) of LV (relation of a sum of LV PWT and IVST to LV EDD) in 7 out of 18 (38.9%) patients from the study group showed higher values of normal values. In the control group, these values did not exceed the normal value in all the patients. LV MMI was calculated automatically. According to the Russian Medical Society on Arterial Hypertension (2013), LV MMI in men did not exceed 115 g/m^2 , in women - 95 g/m^2 . In the present study, the average values of the LV MMI parameter exceeded the norm only in the group of patients with IR and NAFLD and were equal to $116.61 \pm 11.03 \text{ g/m}^2$ and $96.03 \pm 7.46 \text{ g/m}^2$, respectively. Based on the obtained data, the indexes RWT and LV MMI were used for the evaluation of the heart geometry and establishment of the type of LV remodeling. The distribution of patients by different types of remodeling is presented in Table 1.

Table 1. Distribution of the remodeling types of the left ventricle in the studied group.

Geometric model of LV	Echocardiogram parameters	Number of patients
Eccentric hypertrophy	RWT \leq 0.42 MMI $>$ 95g/m ² ♀, >115g/m ² ♂	n=8 44.4%
Concentric hypertrophy	RWT > 0.42 MMI $>$ 95g/m ² ♀, >115g/m ² ♂	n=7 38.9%
Concentric remodeling	RWT > 0.42 MMI \leq 95g/m ² ♀, \leq 115g/m ² ♂	n=3 16.7%

The results of the performed examination showed that in the study group, the hypertrophic variants of the remodeling prevailed. In 44.4% (8/18) of patients, it was eccentric hypertrophy and 38.9% (7/18) of patients – concentric hypertrophy of LV. Concentric remodeling of LV was observed only in 16.7% (3/18) of patients. Prognostically hypertrophic variants of the heart geometry were less favorable in terms of the development of rhythm disturbances and persistent arterial hypertension.

In the control group, PET-CT with 18F-FDG showed even distribution of RPA in the myocardium. The myocardium structure was relatively consistent. This picture was taken as a variant of normal, even glucose uptake by cardiomyocytes. The analysis of the character of the distribution of RPA in the group of patients with NAFLD and IR showed the following alterations. The authors evaluated the density of hepatic tissue that was lower than the normal level and equal to 38.4 \pm 3.2 HU (at normal values of liver density 50 HU). The evaluation of the metabolic activity of myocardium in this group of patients and visual analysis revealed an expressed uneven diffusive distribution of RPA. Such manifestations primarily reflect anatomic (histologic) inconsistency of the myocardium. It is not always associated with the reduction of myocardial blood circulation, and in the present study, the heterozygosity of the distribution of RPA can indicate zones of fibrosis or fat tissue in the myocardium. Such diffusive inconsistency of the image in 12 patients (66.7%) from this group

revealed the zones of hypometabolism (decrease in the accumulation of RPA). The area of these zones did not exceed 12.24 cm² (maximum value). Such a decrease in the glucose uptake by the myocardium was observed in patients with concentric (5 patients) and eccentric (7 patients) hypertrophy of LV. Along with the patients that had a decreased accumulation of RPA, there were patients with minor (5-7 mm) zones of paradoxical accumulation of glucose. In 2 patients (11.1%), zones of hypermetabolism (7.8 and 3.4 cm) with increased accumulation of RPA were revealed. However, they did not form sectors that corresponded to a pool of a certain artery, and, probably, they were the reflections of the zones of fatty infiltration or fibrotic alterations in the myocardium. Echocardiogram showed that these patients had a concentric type of remodeling of LV. Thus, it was established that patients with NAFLD and IR with altered geometry of the heart, the sphericity of LV myocardium, and different type of remodeling in cardiomyocytes had an intensity and character of glucose metabolism changed, which indicates myocardial metabolic dysfunction.

Presently, a close association between NAFLD and metabolic syndrome and its components is established. In patients with NAFLD, lipid and carbohydrate metabolism disturbances aggravate, atherogenic types of dyslipidemias develop, the risk of atherosclerosis and the incidence rate in patients with arterial hypertension increase (Roytberg *et al.*, 2017a; Lazebnik *et al.*, 2017; Drapkina, 2011). Recent studies demonstrated the formation of hepatocardial associations in patients with fatty hepatosis in the form of structural-functional alterations in the heart. It was shown that patients with NAFLD had early left ventricular diastolic dysfunction developed (Bonapace *et al.*, 2012; Mantovani *et al.*, 2015), dimensions of heart chambers, and interventricular septum thickness altered (Drapkina, 2011). Besides, the patients with steatohepatitis had altered hemodynamics in the form of luminal narrowing of the aorta that was associated with atherosclerosis and mitral and aortal valves alterations of atherosclerotic nature in comparison with patients that did not have hepatic disorders. According to the published data, patients with NAFLD have elevated risk of the development of cardiovascular events (myocardial infarction, arrhythmia, stroke, sudden cardiac arrest, congestive heart failure). However, pathways and mechanisms of mutual influence of the structural-functional condition of the liver and heart in patients with metabolic disorders remain unclear.

The authors of the present study analyzed the possible mechanisms underlying the alterations in the myocardium in patients with fatty degeneration of the liver. Since NAFLD is associated with the sensitivity of tissues to insulin, the study group included patients with two main criteria: clinical and laboratory-instrumental signs of NAFLD and signs of IR diagnosed by the index HOMA-IR. It can be suggested that in patients with systemic IR, metabolic processes get disturbed not only in hepatocytes but also in cardiomyocytes, the rate of glucose utilization, and its transmembrane transport to cardiomyocytes changes. The development of metabolic dysfunction leads to alterations in the geometry of the heart and the formation of different types of remodeling of LV (Figure 1).

The study of perfusion and metabolism of glucose in the myocardium is an important mechanism in the understanding of pathophysiological grounds of structural-functional alteration in the heart and its remodeling in patients with NAFLD and IR. PET-CT with ¹⁸F-FDG showed diffusive heterogeneity of the perfusion of the isotope marked glucose in all the patients from this group, a decrease in the uptake of glucose by cardiomyocytes in 66.7% of cases and its paradoxical accumulation in 22.2%. The defects of perfusion were observed in 37.5% of cases. However, they did not form sectors that corresponded to a respective pool of a certain artery. Probably, these defects reflect the zones of fibrosis or fatty inclusions. Probably, they are observed due to the alterations in the microcirculatory bloodstream. The pathology of intramural microvessels like arterioles, capillaries, venules, and arteriole-venular anastomosis, that provide blood filling, intervascular exchange, and tissue homeostasis in the myocardium, play an important role in this processes (Drapkina, 2011; Yoshinaga and Tamaki, 2007). According to the published data, patients with metabolic syndrome had pathologic alterations in 30-50% of cases (biopsy of the myocardium) (Cunningham, 2006; Yamamoto, 2002). It is suggested that the pathogenesis of the coronary circulation disorders is based on the reversible processes (endothelial dysfunction, rheological blood disorders, diastolic dysfunction, disbalance in the vegetative nervous system) and irreversible alterations (vascular walls remodeling, the imbalance between the number of capillaries and the mass of heart, like heart hypertrophy) (Cohn, 1998). Perfusion disorders in the myocardium in patients with insulin resistance can also be associated with endothelial dysfunction of the vessels, in particular, decrease in the production

of endogenous vasodilator nitrogen oxide that is produced by the endothelium (Usov *et al.*, 2014; Buziashvili and Buziashvili, 2014). Thus, a complex of the mechanisms that are pathogenetically associated with insulin resistance, metabolic disorders, and pathological alterations in the liver plays an important role in the development of metabolic dysfunction of the myocardium.

4. CONCLUSION

The results of the present study showed that patients with NAFLD and IR had altered geometry of the heart and prognostically unfavorable hypertrophic types of left ventricle remodeling (eccentric, concentric hypertrophy of LV). Hepato-cardiac associations are based on the disturbed sensitivity of cardiomyocytes to insulin and glucose metabolism disorders that contribute to the development of metabolic myocardial dysfunction. Presently, it is difficult to evaluate the cause-effect relations in the Hepato-cardiac associations. However, it is clear that NAFLD is a predictor of heart dysfunctions due to the decrease in glucose metabolism in cardiomyocytes. Further studies are needed for the understanding of clinical importance of the identification of perfusion-metabolic alterations in the myocardium and their prognostic significance.

5. REFERENCES

1. Altehoefer, C.; Vom Dahl, J.; Bares, R.; Stöcklin, G. L.; Büll, U. Metabolic mismatch of septal beta-oxidation and glucose utilization in left bundle branch block assessed with PET. *J. Nucl. Med*, **1995**, 36, 2056–2059
2. Bokeria, L. A.; Shurupova, I. V.; Asladini, I. P. Evaluation of the perfusion and metabolism in patients with dilated cardiomyopathy. *Creative cardiology*, **2010**, 1, 43-54.
3. Bonapace, S.; Perseghin, G.; Molon, G.; Canali, G.; Bertolini, L.; Zoppini, G.; Barbieri, E.; Targher, G. Nonalcoholic fatty liver disease is associated with left ventricular diastolic dysfunction in patients with type 2 diabetes. *Diabetes Care*, **2012**, 35 (2), 389-95.
4. Björnsson, E.; Treeprasertsuk, S.; Treeprasertsuk, S. NAFLD fibrosis score: a prognostic predictor for mortality and

- liver complications among NAFLD patients. *World J Gastroenterol*, **2013**, 19(8), 1219–1229.
5. Buziashvili, Y. I.; Buziashvili, V. Y. Possibilities of modern methods of visualizations in patients with ischemic heart disease. *Cardiosomatics*. **2014**, 3-4, 20-26.
 6. Cohn, J. N. Arteries, myocardium, blood pressure and cardiovascular risk: towards a revised definition of hypertension. *J. Hypertens*, **1998**, 16, 12, Pt. 2., 2117-2124.
 7. Cunningham, K. S.; Veinot, J. P.; Butany, J. An approach to endomyocardial biopsy interpretation. *J. Clin. Pathology*, **2006**, 59(2), 121-129.
 8. Drapkina, O. M. PAAC and fibrosis. Hepato-cardiac relations. *Russian medical journal*, **2011**, 19(18), 1136-1139.
 9. Lazebnik, L. B.; Radchenko, V. G.; Golovanova, E. V. Zvenigorodskaya, L. A.; Konev, Yu. V.; Seliverstov, P. V.; Sitkin, S. I.; Tkachenko E. I.; Avaluyeva, E. B.; Aylamazyan, E. K.; Vlasov, N. N.; Grinevich, V. B.; Korniyenko, E. A.; Novikova, V. P.; Khoroshinina, L. P.; Zhestkova, N. V.; Oreshko, L. S.; Dudanova, O. P.; Dobritsa, V. P. Nonalcoholic fatty liver disease: clinics, diagnostics, treatment (recommendations for therapists, 2nd edition). *Therapy*, **2017**. 3, p.5-23.
 10. Mantovani, A.; Pernigo, M.; Bergamini, C.; Bonapace, S.; Lipari, P.; Pichiri, I.; Bertolini, L.; Valbusa, F.; Barbieri, E.; Zoppini, G.; Bonora, E.; Targher, G. Nonalcoholic Fatty Liver Disease Is Independently Associated with Early Left Ventricular Diastolic Dysfunction in Patients with Type 2 Diabetes. *PLoS ONE*, **2015**, 10(8), 234-239.
 11. Musso, G.; Cassader, M.; Rosina, F.; Gambino, R. Impact of current treatments on liver disease, glucose metabolism and cardiovascular risk in non-alcoholic fatty liver disease (NAFLD): a systematic review and meta-analysis of randomized trials. *Diabetologia*, **2012**, 55(4), 885–904.
 12. Nikiforov, V.S. Methods of cardiovascular visualization in the diagnostics of ischemic heart disease. *Consilium medicum*, **2017**, (01), 18-24.
 13. Parmon, E. V.; Ryzhova, D.V. Evaluation of the metabolism and perfusion of myocardium in patient with non-coronarogenic ventricular rhythm disturbances. *Arterial hypertension*, **2014**, 20(3), 189-200.
 14. Roytberg, G. E.; Sharkhun, O. O. Evaluation of the risk factors for non-alcoholic fatty liver disease. *Practicing doctor*, **2017a**, 1, 58-62.
 15. Ryotberg, G. E.; Sharkhun, O. O. Peculiarities of the progression of liver damage in patients with insulin resistance. *Medical almanac*, **2017b**, 1 (46), 65-68.
 16. Sergienko, V. B.; Babev, F. Z. Positron-emission tomography in the evaluation of metabolism of the myocardium. *Atherosclerosis and dyslipidemia*, **2011**, 26-31.
 17. Usov, V. U.; Arkhangelskiy, V. A.; Fedorenko, E. V. The evaluation of viability of the damaged myocardium in cardiosurgical patients: comparison of the possibilities of magnet-resonance and emission tomography. *Complex problems of cardiovascular diseases*, **2014**, 3, 124-132.
 18. Yamamoto, S.; James, T. N.; Kawamura, K.; Nobuyoshi, M. Cardiocytic apoptosis and capillary endothelial swelling as morphological evidence of myocardial ischemia in ventricular biopsies from patients with angina and normal arteriograms. *Coron. Artery Dis*, **2002**, 13(1), 25-35.
 19. Yoshinaga, R.; Tamaki, N. Imaging myocardial metabolism. *Gurr. Opin. Biotechnoll*, **2007**, 18i, 52-59.

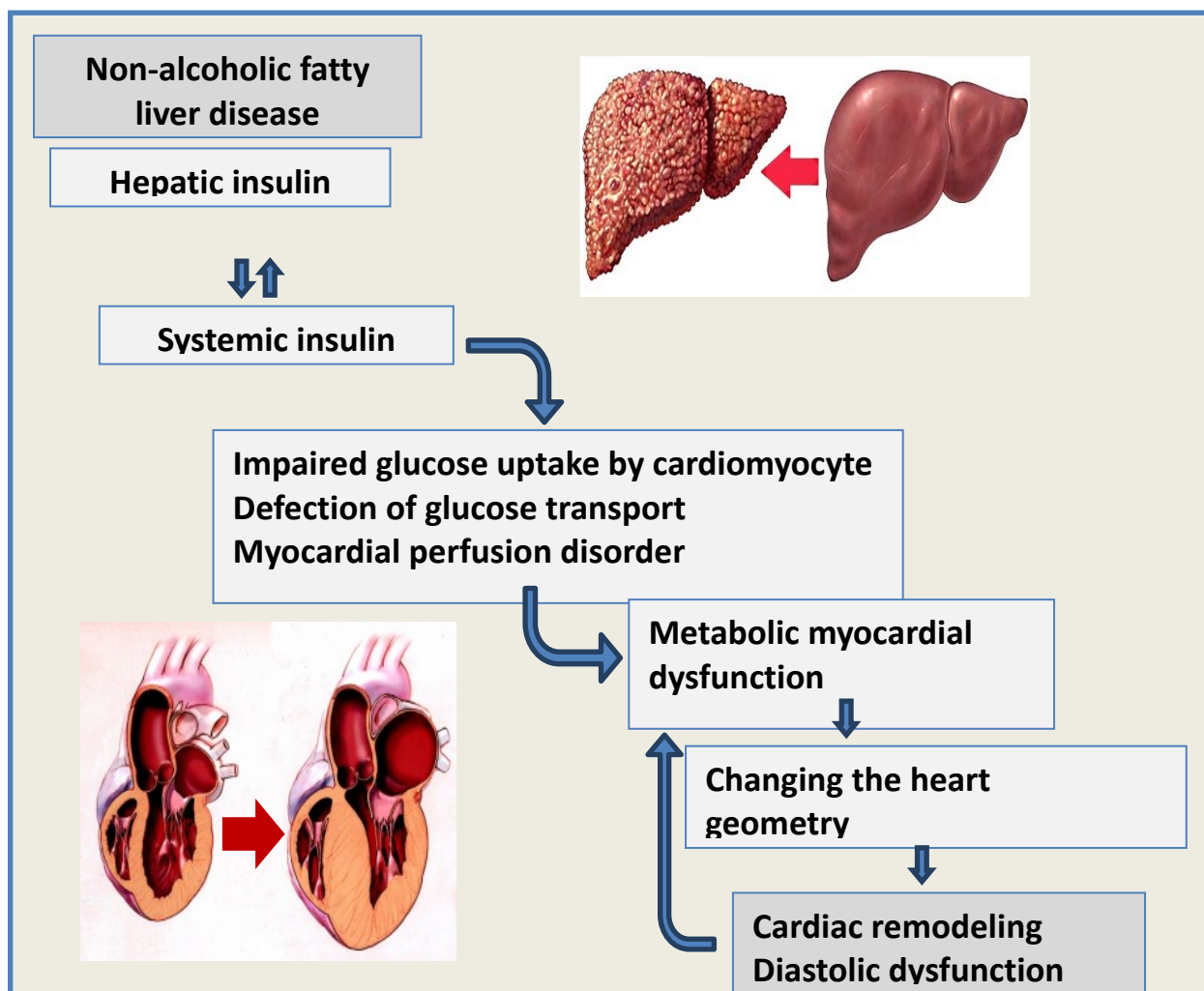


Figure 1. Development of Hepato-cardiac relations in patients with NAFLD and insulin resistance.

AVALIAÇÃO DOS EFEITOS DE MITIGAÇÃO DE *GLOMUS MOSSEAE* EM *TRITICUM AESTIVUM* L., CV. CHAMRAN SOB ESTRESSE SECA**EVALUATION OF MITIGATION EFFECTS OF *GLOMUS MOSSEAE* ON *TRITICUM AESTIVUM* L., CV. CHAMRAN UNDER DROUGHT STRESS****ارزیابی اثرات بهبود دهنده *GLOMUS MOSSEAE* روی *TRITICUM AESTIVUM* L., CV. CHAMRAN تحت تنش خشکی**

BITARAF, Negin¹; SAADATMAND, Sara^{*2}; MEHREGAN, Iraj³; AHMADVAND, Rahim⁴;
EBADI, Mostafa⁵

¹⁻⁴Islamic Azad University, Science and Research Branch, Faculty of Science, Biology Department. Iran.

⁵Seed and Plant Improvement Institute, Agricultural Research, Education and Extension Organization. Iran.

* Correspondence author

e-mail: saadatmand.srbiau@gmail.com

Received 19 January 2020; received in revised form 20 March 2020; accepted 26 March 2020

RESUMO

O objetivo principal deste estudo foi avaliar a resposta fisiológica e de tolerância à seca associadas ao crescimento de *T. aestivum* L., cv. Mudan de Chamran com *G. mosseae* em folhas e raízes. As mudas micorrízicas arbusculares (MA) ou não-MA sob condições normais ou em stress hídrico foram avaliadas quanto aos parâmetros de crescimento, teor relativo de água (TRA), classificação do soluto, peroxidação lipídica e antioxidantes enzimáticos e não enzimáticos. Os resultados refletiram a crescente influência da MA nas mudas sob estresse hídrico: micorrização de zero e 32,25% em mudas não-MA e MA, respectivamente, peso fresco e peso seco das mudas (28,5 e 27,34%, respectivamente) e raízes (28,86 e 31,68%, respectivamente), TRA (55,15%), concentração de fósforo nas brotações e raízes (69,25 e 95,36%), teor total de proteínas solúveis e carboidratos nas brotações (52,63 e 15,80%, respectivamente) e raízes (30,65 e 9,80%, respectivamente), catalase (28,66 e 31,43%), superoxidase dismutase (28,44 e 15,27%), glutathione redutase (44,62 e 18,84%), ascorbato peroxidase (15,58 e 39,49%) e redução no acúmulo de prolina de parte aérea e raiz (45,01 e 44,03%) e peroxidação lipídica (52,27 e 57,26%) em comparação com plântulas estressadas não inoculadas. Pigmentos fotossintéticos, incluindo clorofila a (77,28%), clorofila b (51,70%), clorofila total (66,76%), carotenóides (51,75%) e metabólitos secundários antioxidantes, como compostos fenólicos totais (36,25%), teor total de flavonóides (30%) e o teor total de antocianina (29,52%) aumentou adicionalmente nas folhas bandeira de plantas MA estressadas pela água. Considerando todos os resultados deste estudo, é possível concluir que a inoculação MA de plantas de trigo pode aliviar consideravelmente os efeitos nocivos do estresse por déficit hídrico.

Palavras-chave: mudas de trigo, déficit hídrico, micorriza arbuscular, antioxidantes enzimáticos, estresse oxidativo.

ABSTRACT

The main aim of this study was to evaluate physiological and growth-associated drought tolerance responses of mycorrhiza inoculated *T. aestivum* L., cv. Chamran seedlings with *G. mosseae* in flag leaves and roots. The arbuscular mycorrhizal (AM) or non-AM wheat seedlings under normal or water-stressed conditions were assessed for growth parameters, relative water content(RWC), solute aggradation, lipid peroxidation, and enzymatic and non-enzymatic antioxidants. Outcomes reflected the enhancing influence of AM on seedlings

under drought stress: mycorrhization of zero and 32.25% in non-AM and AM seedlings, respectively, fresh weight and dry weight of shoots (28.5 and 27.34%, respectively) and roots (28.86 and 31.68%, respectively), RWC (55.15%), phosphorus concentration in shoots and roots (69.25 and 95.36%), total soluble protein and carbohydrate content in shoots (52.63 and 15.80%, respectively) and roots (30.65 and 9.80%, respectively), catalase (28.66 and 31.43%), superoxidase dismutase (28.44 and 15.27%), glutathione reductase (44.62 and 18.84%), ascorbate peroxidase (15.58 and 39.49%) and reduction in proline accumulation of shoot and root (45.01 and 44.03%) and lipid peroxidation (52.27 and 57.26%) by comparison to non-inoculated stressed seedlings. Photosynthetic pigments including chlorophyll a (77.28%), chlorophyll b (51.70%), chlorophyll total (66.76%), and carotenoid (51.75%) and antioxidative secondary metabolites such as total phenolic compounds (36.25%), total flavonoid content (30%) and total anthocyanin content (29.52%) additionally increased in flag leaves of water-stressed AM plants. Taking into account all the results of this study, it can be concluded that AM inoculation of wheat plants may considerably alleviate the harmful effects of water deficit stress.

Keywords: wheat seedlings, water deficit, arbuscular mycorrhiza, enzymatic antioxidants, oxidative stress.

چکیده

هدف اصلی این مطالعه ارزیابی واکنش‌های فیزیولوژیکی و رشدی-مرتبط با مقاومت به خشکی در برگ پرچم و ریشه گیاهچه‌های *T. aestivum* L., cv. Chamran تحت شرایط تنش آبی و تنش آب از نظر پارامترهای رشدی، محتوای نسبی آب (RWC)، تجمع مواد محلول، پراکسیداسیون چربی و آنتی‌اکسیدان‌های آنزیمی و غیر آنزیمی مورد ارزیابی قرار گرفتند. نتایج منعکس کننده اثر افزایشی و بهبود دهنده AM روی گیاهچه‌های تحت تنش آبی نسبت به شاهد به قرار زیر بود: مایکوریزایی شدن ریشه‌ها صفر و 32/5% به ترتیب در گیاهچه‌های با-AM و بدون AM، وزن تر و خشک شاخساره (5/28 و 27/34%)، به ترتیب و ریشه‌ها (28/86 و 31/68%)، به ترتیب، RWC (55/15%)، به ترتیب، غلظت فسفر در شاخساره و ریشه (25/69 و 36/95%)، به ترتیب، کل پروتئین‌های محلول و محتوای کربوهیدرات در شاخساره (63/52 و 80/15%)، به ترتیب و ریشه (65/30 و 80/9%)، به ترتیب، کاتالاز (28/66 و 31/43%)، به ترتیب، سوپر اکسید دیسموتاز (44/28 و 27/15%)، به ترتیب، گلوکاتایون ریدوکتاز (62/44 و 84/18%)، به ترتیب، آسکوربات پروکسیداز (58/15 و 49/39%)، به ترتیب، کاهش پرامترها از جمله کاهش تجمع پرولین در شاخساره و ریشه (45/01 و 44/03%)، به ترتیب و مالون آلدنید (27/52 و 26/57%)، به ترتیب، نسبت به گیاهچه‌های تلقیح نشده مشاهده گردید. بعلاوه رنگرزی‌های فتوسنتزی، شامل کلروفیل a (77/28%)، کلروفیل b (51/70%)، کلروفیل کل (76/66%) و کارتنوئید (70/51%) و متابولیت‌های ثانویه آنتی‌اکسیدانی مانند ترکیبات فنولی کل (25/36%)، محتوای فلاونوئید کل (30%) و محتوای آنتوسیانین کل (52/29%) در برگ پرچم گیاهچه‌های مورد تنش آبی واقع شده تلقیح شده با AM افزایش نشان داد. با مد نظر قرار دادن نتایج مطالعه کنونی، می‌توان نتیجه گرفت که تلقیح گیاهچه‌های گندم با AM می‌توان به نحوه موثری اثرات منفی کمبود آب را جبران نماید.

کلیدواژه‌ها: گیاهچه گندم، کمبود آب، آرباسکولار مایکوریزا، آنتی‌اکسیدان‌های آنزیمی، تنش اکسیداتیو

1. INTRODUCTION

Environmental abiotic stresses are of the most important performance-reducing factors for agricultural products (Hameed *et al.*, 2014; Mathur *et al.*, 2019). Among them drought stress as the most ubiquities abiotic stress along with the lack of soil nutrients, in many semi-arid regions of the world imposing serious restriction on yield at a world-scale of wheat (*T. aestivum*) as a critically important staple crop that provides over 20% protein and calories for over half of the world's population (Kumaraswamy and Shetty, 2016; Smith, 2017).

Further, to a large extent, in semi-arid areas where wheat is the main crop, drought stress is a constant threat that could occur at any growth stage (Wang *et al.*, 2015; Saeidi *et al.*, 2017). To this end, strategies to assist crops in coping with oxidative stress-driven by drought and ameliorate its impacts involve the utilization of symbiosis fungi species are essential. Drought stress besides a

considerable reduction in wheat growth and yield negatively affects a wide range of other critical physiological and biochemical mechanisms (Kumaraswamy and Shetty 2016; Antoniou *et al.*, 2017). Water deficit stress evokes osmotic and oxidative stress, in addition to a decrement in growth rate, biosynthesis of protein, and photosynthetic potential (Wang *et al.*, 2018).

Moreover, generating a great deal of reactive oxygen species (ROS) under drought stress is more than common which is majorly responsible for peroxidation of lipids in the membrane that has disruption of cell membrane integrity as aftermath (Hameed *et al.* 2014; Jajic *et al.*, 2015; Wang *et al.*, 2019). The intensity of drought stress tolerance is more depends on the developmental phase and genetics (Ashraf and Foolad, 2007). Numerous metabolical strategies utilized by plants to develop important modifications at the molecular and biochemical levels and properly react drought stress generally by fortifying the enzymatic and non-enzymatic

defensive antioxidant mechanisms. In the case of enzymatic antioxidants, a rich literature exists that shows an enhance in activities of ascorbate peroxidase (APX), catalase (CAT), glutathione reductase (GR) or superoxide dismutase(SOD) to eliminate the harmful ROS generated under drought stress (Götz *et al.*, 1999; Hajiboland *et al.*, 2010; Amiri *et al.*, 2017; Chiappero *et al.*, 2019). Additionally, incrementing in non-enzymatic antioxidants, including accumulation of amino acids particularly proline as a crucial proteinogenic and plant secondary compounds such as phenolics and anthocyanin (Tattini *et al.*, 2004; Khalil *et al.*, 2018; Chiappero *et al.* 2019). Also, biosynthesis of some substances, namely generally known as regular responses, water-stressed plants (Bandurska 2000; Szabados and Savoure 2010).

Improving the drought resistance of wheat plants can indeed have a profound influence on their growth and grain yield under water-deficit stress. The results of current studies have shown that soil inoculation with arbuscular mycorrhizal (AM) fungi can cause a significant improvement in the nutrition absorption of plants (Alvarez *et al.*, 2009; Hajiboland *et al.*, 2010; López-Ráez 2016; Mathur *et al.*, 2019). Which is possible by creating a symbiotic relationship through a vast network of hyphae in the soil and the rhizosphere surrounding which aim to improve the absorption of phosphorus, nitrogen, and transport of those elements to the host plant, enhancing water uptake, reducing the negative impact of environmental pollution, incrementing resistant to pathogens and positively contributing in growth and function of host plants in sustainable agricultural systems (Evelin *et al.*, 2009; Santander *et al.*, 2017; Mathur *et al.*, 2019). Further, AM inoculation, as an applicable economically efficient, might mitigate the destructive impacts of drought through improving the enzymatic antioxidant and aggregation of compatible solutes (Jiang and Zhang 2002; Laxa *et al.*, 2019). AM has been observed to enhance the drought stress tolerance in plants by increasing photosynthetic pigments, RWC, protein accumulation, and myriad other stress tolerance-related modifications (Xu *et al.*, 2009; Mathur *et al.*, 2019).

Considering the growing risk of drought stress in semi-arid wheat farms which has experienced significant reductions in growth and yield as the aftermath, and the essentiality of research in this area to find breakthroughs, in this study we aimed to examine the influence of inoculated AM fungus (*Glomus mosseae*) on

alleviating the negative effects imposed by drought stress on *T. aestivum* cv. Chamran under greenhouse condition.

2. MATERIALS AND METHODS

Wheat (*T. aestivum* cv Chamran) seeds (obtained from Seed and Plant Improvement Institute, Karaj, Iran) using 1% (v/v) sodium hypochlorite for 5 min disinfected then Benomyl 10%(fungicide) was applied on seeds for further sterilization and washed with distilled water three times. Then, the seeds were sown in plastic pots (20 seeds per pot, thinned and uniform ones selected) filled with 1 kg of 3-time autoclaved sterilized soil mixture (perlite/field soli 2:1 (v/v) ratio). At the first irrigation, all pots received 200 cc of water than the 16 pots divided into two groups including eight were non-inoculated which a half received normal irrigation (100 cc of water, two times a week, considered as control) and the rest subjected to water stress (50cc of water, two times a week), the other eight pots were inoculated and had the same treatments as the first group. For mycorrhization of each pot, 12.5 g of *G. mosseae* spores (acquired from Agriculture Department of Islamic Azad University Rafsanjan Branch, Iran) was blended with the soil mixture before sowing seeds. Pots placed at Germinator with a light density of roughly 100 $\text{lmol}\cdot\text{m}^{-2}\cdot\text{s}^{-1}$ day/night temperatures of $25 \pm 1/ 18 \pm 1$ °C under a 16 h photoperiod in a greenhouse. After germination of seeds, pots received Hoagland solution containing: 5 ml/L KNO_3 , 5 ml/L $\text{Ca}(\text{NO}_3)_2$, 2 ml/L MgSO_4 , 1 ml/L KH_2PO_4 , 1 g/L MnCl_2 , 1 g/L ZnSO_4 , 1 g/L CuSO_4 , 1 g/L Na_2MoO_4 , 2 g/L Fe-EDDHA, and 1 g/L H_3BO_3 two times, once one week after sown seeds and another three weeks later. The duration of the experiment completed in 7 weeks, afterward, the samples of flag leaves and roots were taken.

2.1 Growth parameters

The fresh weight (FW) and dry weight of flag leaf and underground parts were determined using a digital scale to weigh the fresh plant tissues individually then oven-dried them at 70 °C throughout 72 h.

2.2 RWC

To evaluate the water status fresh weight (FW) of leaves, four mature leaves were obtained instantly. Afterward, the leaves were soaked in distilled water for four h under 25 °C to measure turgid weight(TW). Then, to obtain dry weight (DW), specimens were dried by the oven for 24 h at 80 °C. Equation 1 was used to calculate RWC (Tofighi *et al.*, 2017).

$$\text{RWC} = (\text{FW} - \text{DW}) / (\text{TW} - \text{DW}) \quad (\text{Eq. 1})$$

2.3 Phosphorus concentration

A mixture of 5 mL of extracted material and 10 mL of Barton reagent with a final volume of 50 mL. After keeping samples at room temperature, phosphorus (P) contents were evaluated using a spectrophotometer (Perkin Elmer, Lambda 25, UV/VIS) at 420 nm using a standard curve. The preparation of Barton reagent was based on the method introduced by He and Dijkstra (2014).

2.4 Estimation of AM colonization

To study the symbiosis and to obtain Arbuscular mycorrhization (AM%) of *G. mossea*, one-centimeter fragments of the wheat root was bleached at 10% KOH solution for seven min, then using a 5% solution of the vinegar and dye the root segments stained (Vierheilig *et al.*, 1998). To evaluate the colonization percentage, 40 fragments of 1 cm stained roots on slides and using a light microscope (Norris and Ribbons 1972). Ultimately, the percentage of mycorrhization was determined using a method described by Beltrano and Ronco (2008).

2.5 Total carbohydrate

The determination of soluble carbohydrates of flag leaves was carried out based on the method previously described by Lee *et al.* (2008). To this end, samples were taken from flag leaf oven-dried at 80 °C for 48h. Five mL distilled water added to 1 gram of derived tissue then placed in a 90 °C warm water bath for one h. Afterward, eliminate the residual, the samples were centrifuged for 15 min at 5000 rpm, then, 5 mL of the solution added to a mixture of 95 mL distilled water and 2 mL of resorcinol acid 0.1% composed of 0.5 g of resorcinol, 300 mL of pure ethanol, and 100 mL of concentrated hydrochloric acid. The solution was incubated in a warm water bath at 80 °C for 5 min then immediately placed at cold water. For standard solution, inulin was used. Using spectrophotometer (Perkin Elmer, Lambda 25, UV/VIS) at wavelength 520 nm, soluble carbohydrate concentration was determined.

2.6 Estimation of photosynthetic pigments

To estimate pigments involved in the photosynthetic process including, chlorophyll (Chl) a, Chl b, total Chl and carotenoids (Car) contents employing spectrophotometric procedure as Parry *et al.*, (2014) described. To extract the photosynthetic pigments, fresh leaf tissues were homogenized with 95% ethyl alcohol in a test tube

at 5000 rpm for 5 min at 60 °C. Then the final volume adjusted into 10 mL with 95% ethyl alcohol and at the absorbance of 663, 644, and 452 nm (Perkin Elmer, Lambda 25, UV/VIS), the concentration of chlorophylls and Car were measured and expressed as mg/g FW.

2.7 Total soluble protein

The total protein concentration of extracts obtained from flag leaves by homogenizing them with liquid nitrogen then centrifuged at 14,000 rpm for 15 min at 4 °C, measured by Coma colorant Brilliant Blue-G reagent 250 in 95% ethanol and 85% orthophosphoric acid. Bovine plasma gamma globulin protein (BSA; Merck, Germany) was used as a standard protein curve. For this purpose, the enzymatic surfactant liquid extracted, added to 2.5 mL of Bradford reagent (Merck, Germany) and the mixture of tube contents and placed at dark for 15 min. The absorbance of samples at wavelength 595 nm employing spectrophotometer (Perkin Elmer, Lambda 25, UV/VIS) was read, and the total protein concentration was calculated by comparing it to the standard curve.

2.7 Free proline

Using Bates *et al.*, (1973) method, the free proline concentration was measurement. 250 mg of plant tissue frozen in liquid nitrogen, then 5 mL of sulfosalicylic acid 3% was added. Using Whatman filter paper, the blend filtered. One mL of the mixture was added to the equal volume of acetic acid Glacial and ninhydrin reagent (Sigma-Aldrich, Germany) and kept in a hot water bath at 100 °C. Reactions have begun by placing test tubes in an ice bath. 2 mL toluene mixed with that solution and Vertex for 15 seconds. After keeping samples at 25 °C, two separate layers were formed. Finally, the absorbance of the upper colored layer (containing free proline) was read at 520 nm with the aim of a spectrophotometer (Perkin Elmer, Lambda 25, UV/VIS). The standard curve for measuring proline concentration was prepared using standard solutions.

2.8 Enzymatic antioxidants

An amount of half a gram of fresh tissue of flag leaf was homogenized in 2 mL of 50 mM potassium phosphate buffer (pH 7) in ice-cold condition, afterward, at 12,000 for 20 min at 4 °C the mixture was centrifuged. The obtained supernatant was utilized to measure different antioxidant enzymes; APX, CAT, SOD, and GR. APX: its activity determined using Nakano and Asada (1981) spectrophotometric method at 290 nm. To extract APX, 25 mM phosphate buffer with seven pH containing 0.1 mM EDTA (Ethylenediaminetetraacetic acid; Merck,

Germany) was used. The results expressed as $\text{mg}^{-1} \text{ protein min}^{-1}$. The determination of CAT activity was based on Aebi (1984) procedure. The reaction mixture prepared using 50 mM potassium phosphate buffer (pH 7.0), 30% (w/v) H_2O_2 , and 100 μL of enzyme extract. Increment in absorbance rate at 420 nm for 1 min in a single unit was considered as enzyme activity, which expressed as $\text{mg}^{-1} \text{ protein min}^{-1}$. SOD: for extraction of SOD at 4 °C, 50 mM phosphate buffer with seven pH, including 0.1 mM EDTA was used. SOD activity was evaluated according to the Kaushal and Wani (2016) method by spectrophotometer at 560 nm and expressed as $\text{mg}^{-1} \text{ protein min}^{-1}$. GR: evaluation of GR was based on the modified method of Foyer and Halliwell (1976). An amount of 75 μL extracts procured from leaf tissue in addition to 1.5 mL KNa-phosphate buffer solution (0.05 M, pH 7.8), 0.75 mL 3 mM 5,5'-dithio-bis-(2-nitrobenzoic acid) (DTNB, Merck, Germany), 0.15 mL NADPH (Nicotinamide adenine dinucleotide phosphate; Merck, Germany) (2 mM), and 0.15 mL oxidized glutathione (GSSG; 20 mM; Sigma-Aldrich Chemie, Steinheim, Germany) prepared. GSSG was mixed with the reaction and the increment in absorbance was monitored at 412 nm for 3 min. The non-GR related NADPH oxidation during the evaluation was considered. The final enzymatic activity mentioned as μmol of oxidized NADPH per 1 gram of FW for 1 min. These indicators were all determined using a spectrophotometer (Perkin Elmer, Lambda 25, UV / VIS).

2.9 Lipid peroxidation

To determine the concentration of malondialdehyde (MDA) in the flag leaves, the method described by Xu *et al.* (2013) was used. First 0.5 g fresh leaves homogenized in 20% thiocloroacetic acid (TCA; Sigma-Aldrich Chemie, Steinheim, Germany) solution contained 0.5% thiobarbituric acid for four then the mixture for 25 min at 95 °C placed in the Ben Marie bath. Afterward, the mixture cooled in an ice bath and using a spectrophotometer (Perkin Elmer, Lambda 25, UV / VIS) the absorbance of the solutions was read at 532 nm. The target matter to absorb in this wavelength is the red complex (TBA-MDA), the absorbance of the other nonspecific pigments was measured at 600 nm and subtracted. To calculate the concentration of MDA the extinction coefficient ($155 \text{ mM}^{-1} \text{ cm}^{-1}$) and determined with Equation 2.

$$\text{MDA } (\mu\text{mol g}^{-1} \text{ Fw}) = [\text{A}_{532} - \text{A}_{600} / 155] \times 1000$$

(Eq. 2)

2.10 Total Phenolic Content

Using the Folin–Ciocalteu method, total phenolic content (TPC) was evaluated (Singleton *et al.*, 1999). 125 μL of methanol extract mixed with 375 μL of water and 2.5 ml of Folin-Ciocalteu reagent 10% (Sigma-Aldrich Chemie, Steinheim, Germany). After 6 min, after 2 ml, 5.7% sodium carbonate was added. The absorbance of the mixture after incubation for 90 min at the dark condition was measured at a wavelength of 765 nm using the Spectrophotometer (Perkin Elmer, Lambda 25, UV / VIS). Finally, TPC is calculated using the standard curve and expressed as Mg of Gallic acid equivalent gram of DW (mg GAE/g DW).

2.11 Total Flavonoid Content

The aluminum chloride colorimetric method was used to determine total flavonoid content (TFC) Lamaison and Carnet (1990). To 0.5 ml of each extract (10 mg/ml), 1.5 ml of methanol, 0.1 ml of aluminum chloride solution in 10% ethanol, 0.1 ml of 1 M potassium acetate and 2.8 ml of distilled water were added. The mixture was read 30 min after incubation at room temperature at 415 nm (Perkin Elmer, Lambda 25, UV/VIS). Quercetin (Sigma-Aldrich Chemie, Steinheim, Germany) was used for the calibration curve, and the final results are expressed as mg of quercetin equivalents (QE) per gram of DW (mg QE/g DW).

2.12 Anthocyanin

For the assay, extracts obtained from methanol solvent: hydrochloric acid (98: 2 v / v) was centrifuged at 1000 rpm for 20 min. 0.5 ml of solution with 49.5 ml of 1mM 2N-morpholino ethane sulfonic acid buffer with a pH of 1 and 4.5 in 50 ml balloons, and after 30 min absorbance measured with a spectrophotometer (Perkin Elmer, Lambda 25, UV / VIS) at 510 nm. Concentrations of anthocyanins were reported in milligrams of cyanidin-3-glucoside per gram fresh weight (mg cyanidin-3-glucoside/g FW) (Farooq *et al.*, 2009).

2.2 Statistical analysis

The experimental design used in this experiment was a completely randomized factorial design with four replicates. All other assays were conducted in triplicate. Variance analysis was carried out utilizing the SAS statistical package (version 9.4; SAS Institute, Cary, NC, USA). Tukey's range test assessed differences among treatments at the level of 1% and 5%.

3. RESULTS AND DISCUSSION:

3.1 Mycorrhization

Mycorrhizal inoculation (AM%) of *G. mosseae* in roots of inoculated wheat seedlings was assessed (Table 1). The seedlings grown under N+M and D+M that were AM-inoculated showed high mycorrhization (73.46 and 38.25%, respectively). The mycorrhization in water-stressed seedlings decreased almost to half of its value in well-irrigated pots. Since the soil mixture overall autoclaved to eliminate the possible effect of other factors, therefore, the non-AM plants under water stress and control showed no mycorrhization in their roots.

3.2 Growth indicators and RWC of leaves

Imposing drought stress considerably changed the intensity of stress-associated physiological responses in *T. aestivum* cv. Chamran plants. The decline in growth parameters observed in plants under drought stress which could be attributed to the inhibitory impact of water shortage on cell enlargement and photosynthesis potential of the plant (Xu *et al.*, 2009; Wang *et al.*, 2018). The results indicated the negative influence of drought stress on growth as it reflected in shoot and root FW as compared to controls (Table 1). Whereas, Mycorrhizal inoculation had positive impacts on improving growth parameters in which FW of shoot and root were 28.5% and 28.68%, respectively, and showed significant difference with those subjected to drought stress with no *G. mosseae* inoculation. Similarly, the DW content of shoots and roots also followed the same paradigm (Table 1; 27.34% and 31.68%). However, plants inoculated with *G. mosseae* either under normal conditions or drought stress had higher values in comparison to the other two treatments. Inoculation of wheat plants with *G. mosseae* significantly contributed to improving the RWC % of plants subjected to the drought stress in comparison with non-inoculated plants. In N+M treatment, the highest RWC observed with a significant difference at $P < 0.05$ Tukey's test. While RWC of leaves of seedlings under drought with no AM decreased to 40.75% and raised significantly in water-stressed AM-plants up to 70.95% (Figure 1). Notable mitigation in negative effects of drought stress on plant growth was observed in inoculation with AM. Through positively influencing the availability of nutrients for the roots (data not shown) and improving water uptake, *G. mosseae* inoculation generates several metabolic improvements which increase in biosynthesis of proteins as critical aftermath prevents from growth reduction

in plants subjected to drought stress (Nadeem *et al.*, 2014; López-Ráez 2016; Zhang *et al.*, 2019).

Of the renowned effect of AM on plants is the improvement of nutrient content in particular P, which is the cornerstone of resistance against stresses, specifically drought (Augé 2001; Giri *et al.*, 2007). Further, the results of this experiment showed a markedly decrease in water content of leaf of water-stressed plants, probably owing to a decline in the osmotic potential of cells. By positively affecting the availability of water, AM fungi found to be contributed in enhancing RWC of leaves of plants subjected to water stress, besides, rectified intergradation of the membrane and influencing the biosynthesis of phytohormones, namely declining ABA which causes improvement of leaf water status, are other potential possibilities. Similar findings previously reported by other scholars (Ortiz *et al.*, 2015; Zhou *et al.*, 2015; Rahimi *et al.*, 2017; Chandrasekaran *et al.*, 2019).

3.3 P concentration

The concentration of P in shoots and roots (69.25% and 95.36%, respectively) of AM-plants under drought stress were significantly higher compared with water-stressed non-inoculated plants at $P < 0.05$ Tukey's test (Table 1). AM inoculation considerably increased P content of shoots and roots of normally irrigated by over 100% in comparison to those under drought stress. In this study also the P content in inoculated and non-inoculated wheat plants notably enhanced, possibly due to the fact that under drought stress the mobility of nutrients and soil moisture decreased which ends up with limiting available P (Danielsen and Polle 2014; He and Dijkstra 2014) and its where that mycorrhiza with extended hyphae can aim to keep the nutrition supply continue (Alvarez *et al.* 2009; Evelin *et al.* 2009; Danielsen and Polle 2014).

3.4 Total soluble proteins, carbohydrates and proline

Concentration changes in compounds involved in osmoregulation of the cell, including total soluble proteins, carbohydrates, and proline content of wheat flag leaf and root under conditions of D, D+M, N, and control (Table 1) were studied. Comparison of the means of the constituents mentioned above indicated that except for proline they all followed a similar pattern of physiological response in which their content enhanced considerably (total soluble proteins: 52.63% and 30.65%; total soluble carbohydrates: 15.80% and 9.45% in leaf and root, respectively) in both leaf and root of wheat plants inoculated

with *G. mosseae* under drought stress when compared to the water-stressed non-AM plant. Whereas, the values of proline observed in AM-plants were significantly lower (45.01% and 44.03%, leaf and root, respectively) than non-AM plants. Additionally, the concentration of total soluble proteins, carbohydrates, and increment in proline was higher in aerial parts than roots.

The water-stressed wheat plants had a dramatically decreased level of total soluble protein possibly owing to the reduction in photosynthetic activity of leaves under stress condition (Sara *et al.*, 2012), whereas, inoculated plants with AM under normal or stressed conditions had a higher but statistically insignificant concentration of total soluble protein, which mirrors the positive effects of AM on preventing the decrease of biosynthesis mechanisms under stress through improving the content of photosynthetic pigments. Reduction in the uptake of mineral elements essential for the biosynthesis process or proteolysis under drought stress leads to a decrease in soluble proteins (El-Komy *et al.*, 2003; Abdelmoneim *et al.*, 2014; Delshadi *et al.*, 2017).

Of the essential osmoprotectants in plants subjected to abiotic stress is proline which its accumulation is a fundamental reaction with the antioxidant capability and effective in tranquilizing homeostasis under stress condition (Bandurska 2000; Szabados and Savoure 2010; Antoniou *et al.* 2017). In the present study, the proline content in non-inoculated water-stressed plants notably increased while otherwise observed in inoculated plants under either normal irrigation or stressed. A similar pattern has been reported in previous studies (Abdelmoneim *et al.* 2014; Chiappero *et al.* 2019), the effect of mycorrhizal inoculation by *G. mosseae* on the accumulation of proline can be a good indication that plants inoculated with AM were experienced less drought stress-associated metabolic modifications, therefore, required a lower quantity of proline for osmotic adjustment in compare to non-treated plants with AM (Asrar *et al.*, 2012). Consequently, it can be concluded that elevation in proline content is not needlessly associated with improving resistance to drought stress (Lutts *et al.*, 1999), at least in the case of cv. Chamran. In accordance to our results, Porcel and Ruiz-Lozano (2004) recorded a decrease in proline concentration in AM-inoculated *Glycine max* L. Additionally, similar results have been reported by Asrar *et al.* (2012) in *Antirrhinum majus* L. and Amiri *et al.* (2017) in *Pelargonium graveolens* L. There is some ambiguity in the actual association of proline with tolerance to

stresses (Ashraf and Foolad 2007; Benitez *et al.*, 2016), while some scholars postulated that increase in proline level is indeed related to a specific level of tolerance, while others have found the proline aggregation as a signal of injury (Hien *et al.*, 2003; Silvente *et al.*, 2012). Carbohydrates are of the critical primary compounds to promote various physiological tolerant processes under abiotic stresses (Amiri *et al.* 2017). Induction the biosynthesis of soluble carbohydrates under water deficit has been commonly reported, particularly in AM-inoculated plants which are possible owing to the positive influences on improving photosynthetic performance that results in higher assimilation and synthesis of free carbohydrates (Lee *et al.* 2008) in addition to enhancing carbon fixation and enzymatic functions (Hameed *et al.* 2014; López-Ráez 2016). Thus, the aggregation of soluble carbohydrates may have contributed in enhancing the physiological capability of cv. Chamran to tolerate drought stress.

3.5 MDA

Lipid peroxidation intensity decreased significantly by 52.27% and 57.26%, respectively, in shoots and roots of AM-inoculated plants under drought stress in comparison with water-stressed non-AM plants (Table 1). Mycorrhizal inoculation resulted in decrementing the MDA level in shoots and roots (significant at $P < 0.05$ Tukey's test). Control of AM on MDA seems to be higher in roots as compared to flag leaves.

3.6 Enzymatic activities

A marked enhancement in enzymatic activity of CAT, SOD, GA, and APX in roots and flag leaves of wheat plants as a result of mycorrhizal inoculation by *G. mosseae* observed (CAT: 28.66% and 31.43%; SOD: 28.44; GR: 44.62% and 18.84%; APX: 39.49% and 15.58%, respectively) in comparison to non-inoculated plants under water stress (Table 1). These increases for enzymatic antioxidants were always equal or higher in shoots than roots, by comparison. Also, the activity of these antioxidant enzymes was much lower in well-irrigated AM-plants when compared to AM and non-AM plants under stress.

The major source of negative effects of drought stress and abiotic stress overall is the generation an excessive level of ROS that leads to lipid peroxidation which has MDA as a byproduct and perfect indication of membrane degradation, dysfunctioning or peroxidation of lipids in the membrane (Xu *et al.* 2013; Laxa *et al.* 2019; Wang *et al.* 2019). The concentration of MDA in shoot and root of water-stressed wheat plants

significantly increased while remarkably lessened in AM inoculated plants under normal or drought stress conditions in consistent to Porcel and Ruiz-Lozano (2004), Chiappero *et al.* (2019). Also, the MDA in roots was lower than shoots, which reflects less oxidative damage to the roots, which was in agreement with Zhu *et al.*, (2011). The abundance of ROS in particular hydrogen peroxide (H_2O_2), and superoxide radicals (O_2^-) under normal condition constantly suppressed by antioxidants while when plant subjected to drought stress the ROS generation radically increases to a level that harms the vital organs such as photosynthesis system, lipids of membranes and cause mutation in DNA (Lushchak 2014; Jajic *et al.* 2015; Chiappero *et al.* 2019). Generally, in response to such an increase, the level of antioxidant enzymes (i.e., SOD, APX, GR, and CAT) rises significantly. The activities of these enzymes have been shown to be elevated even under moderate water stress (Jiang and Zhang 2002). The participation of the aforementioned antioxidants, CAT, APX, and GR, is through the simultaneous act to the production of water and oxygen from H_2O_2 (Gratão *et al.*, 2005) or SOD as a defensive initiative mechanism against ROS, by dismutating O_2^- to H_2O_2 and O_2 . The AM inoculation found to be effective in increasing the antioxidant enzymes in wheat seedlings subjected to drought stress or those grown under normal conditions. Improving antioxidant activity in AM inoculated plants under drought stress also observed by Khalafallah and Abo-Ghalia (2008) in water-stressed wheat seedlings or in *Pistacia vera* L. Abbaspour *et al.*, (2012) inoculated with AM.

3.7 Photosynthetic pigments

The photosynthetic pigments in leaves as a critical measure to understand the effects of drought stress in wheat plants were evaluated (Table 2). The content of Chl a, b, total and Car in flag leaves of wheat inoculated with *G. mosseae* and subjected to drought stress almost all followed a similar paradigm and incremented compared to non-inoculated plants under drought stress (Chl a: 77.28%; Chl b: 51.70%; total: 66.76% and Car: 51.75%), statistically significant at $P < 0.05$ Tukey's test. In non-AM plants subjected to drought stress experienced a considerable reduction in photosynthetic pigments.

A major part of dry weight in wheat produced by flag leaf, therefore, enhancing its photosynthetic potential can have a substantial impact on growth and yield as it has become of the interest of plant breeders in wheat (Yang *et al.*, 2007; Xu *et al.* 2013). In this investigation, the content of pigments: Chl a, b, and total in wheat

plants inoculated with AM was significantly higher in comparison to non-inoculated AM. Given the importance of a high concentration of Chl in photosynthesis, it can be postulated that AM inoculation enhancing the growth rate in inoculated or non-inoculated through increasing or stabilizing the content of Chl in plants under normal or stress condition. The outcomes of the current study are inconsistent with published researches claiming the growth improvement of mycorrhizal plants under drought stress (Garmendia *et al.*, 2017; Hao *et al.*, 2019; Mathur *et al.* 2019). Car is potent photoprotection compounds in which intensification of its biosynthesis can effectively help plants to cope with stress through detoxification of reactive oxygen species (ROS) (Götz *et al.* 1999; Hashimoto *et al.*, 2016; Paliwal *et al.*, 2017). In accordance with that argument, the result of this study strongly indicated the improvement in Car concentration in the flag leaf of wheat plant inoculated with AM under water stress condition. Photosynthetic apparatus heavily relies on Car to protect them from the attack of ROS, which otherwise the photosynthesis rates in drought stress conditions drop dramatically. Our investigation revealed that photosynthetic pigments content in cv. Chamran enhanced considerably with the aim of AM inoculation. In numerous similar assessments, photosynthetic pigments, more often than not, increased with AM inoculation in comparison with non-inoculated plants under water stress (Al-Karaki *et al.*, 2004; Kaya *et al.*, 2009; Hajiboland *et al.* 2010; Hao *et al.* 2019).

Phenolic compounds as a large group of secondary plant metabolites have long known for their significant contribution in plant tolerance under various stresses which often is due to their high antioxidant activity and quenching ROS (Amiri *et al.* 2017; Khalil *et al.* 2018; Chiappero *et al.* 2019). Evaluation the phenolic, flavonoid and anthocyanin compounds in this study revealed the increase of these valuable photo protectors in both inoculated and non-inoculated wheat seedlings under drought stress in which the content of TPC, TFC, and TAC as a notable source of antioxidant activity remarkably enhanced in flag leaves of wheat inoculated with mycorrhizal fungus *G. mosseae* (Table 2). The improvement in those abovementioned bioactive constituents in water-stressed AM-plants was 36.35%, 30%, and 24.52% higher in comparison to non-inoculated plants. The difference of TAC content was not statistically significant between treatments, while TPC and TFC showed the highest increase in all treatment when compared to control with D+M

treatments, which in agreement with the results of previous studies on various species inoculated with AM such as incrementing TFC in *Ligustrum vulgare* L. (Tattini *et al.* 2004), TAC in *Oryza sativa* L. (Farooq *et al.* 2009) or TPC in *Mentha pulegium* L. (Oueslati *et al.*, 2010) and *Thymus vulgaris* L. (Khalil *et al.* 2018). The information on ATC of wheat under drought stress is rare, in this respect, our results can greatly contribute to encouraging scholars to consider this essential secondary chemical in further relevant studies.

4. CONCLUSION

The threat of abiotic stresses, drought, in particular, is ubiquitous and is annually responsible for a large portion of crop losses, therefore, addressing this challenging issue through efficient strategies as exploiting the considerable potential of AM is pivotal especially for main food crops which in this study mycorrhizal inoculation an important widely cultivated versatile cultivar of wheat in Iran, cv. Chamran observed to be significantly positive in improving the capability of seedlings to cope with osmotic stresses imposed by water deficiency and enhanced traits associated with growth, osmoprotectants, and strongly inhibited MDA, notably improved enzymatic antioxidants as well as secondary metabolites that possess antioxidant activity. Considering the capability of cv. Chamran to provide high yield in either well-watered or arid farming, the results of this study. Indeed, for the first time presented an insight into physiological responses of this cultivar to drought and remarkable benefits of AM inoculation, which can be important from an economic perspective. Additionally, further investigations urgent by using various irrigation regimes or inoculation with other mycorrhizal bacteria. It's critical to conduct a complimentary, carefully designed field experiment to assess the quality and quantity of grain yield.

5. ACKNOWLEDGMENT

We wish to thank Azad Islamic University Science and Research Branch for supplying laboratory equipment to this investigation.

6. REFERENCES

1. Abbaspour, H., Saeidi-Sar, S., Afshari, H., Abdel-Wahhab, M. A. *Journal of Plant Physiology*, 2012, 169(7):704-709.
2. Abdelmoneim, T., Moussa, T. A., Almaghrabi, O., Alzahrani, H. S., Abdelbagi, I. *Life Sci J*, 2014, 11:10-17.
3. Aebi, H. *Methods Enzymol*, 1984, 105:121-126.
4. Al-Karaki, G., McMichael, B., Zak, J. *Mycorrhiza*, 2004, 14:263-269.
5. Alvarez, M., Huygens, D., Olivares, E., Saavedra, I., Alberdi, M., Valenzuela, E. *Physiologia plantarum*, 2009, 136(4):426-436.
6. Amiri, R., Nikbakht, A., Rahimmalek, M., Hosseini, H. *Journal of Plant Growth Regulation*, 2017, 36(2):502-515.
7. Antoniou, C., Chatzimichail, G., Xenofontos, R., Pavlou, J. J., Panagiotou, E., Christou, A., Fotopoulos, V. *Journal of Pineal Research*, 2017, 62(4):e12401.
8. Ashraf, M., Foolad, M. R. *Environmental, and Experimental Botany*, 2007, 59(2):206-216.
9. Asrar, A.-W., Abdel-Fattah, G., Elhindi, K. *Photosynthetica*, 2012, 50:305-316.
10. Augé, R. M. *Mycorrhiza*, 2001, 11(1):3-42.
11. Bandurska, H. *Acta Physiologiae Plantarum*, 2000, 22(4):409-415.
12. Bates, L. S., Waldren, R. P., Teare, I. D. *Plant and Soil*, 1973, 39(1):205-207.
13. Beltrano, J., Ronco, M. G. *Brazilian Journal of Plant Physiology*, 2008, 20(1):29-37.
14. Benitez, L. C., Vighi, I. L., Auler, P. A., do Amaral, M. N., Moraes, G. P., dos Santos Rodrigues, G., da Maia, L. C., de Magalhães Júnior, A. M., Braga, E. J. B. *Acta Physiologiae Plantarum*, 2016, 38(11):267.
15. Chandrasekaran, M., Chanratana, M., Kim, K., Seshadri, S., Sa, T. *Front Plant Sci*, 2019, 10:457.
16. Chiappero, J., Cappellari, L. d. R., Sosa Alderete, L. G., Palermo, T. B., Banchio, E. *Industrial Crops and Products*, 2019, 139:111553.
17. Danielsen, L., Polle, A. *Environmental, and Experimental Botany*, 2014, 108:89-98.
18. Delshadi, S., Ebrahimi, M., Shirmohammadi, E. *Journal of Plant Interactions*, 2017, 12(1):200-208.
19. El-Komy, H. M., Hamdia, M. A., Abd El-Baki, G. K. *Biologia Plantarum*, 2003, 46(2):281-287.
20. Evelin, H., Kapoor, R., Giri, B. *Annals of botany*, 2009, 104(7):1263-1280.
21. Farooq, M., Wahid, A., Basra, S. M. A., Islam-ud-Din. *Journal of Agronomy and Crop Science*, 2009, 195(4):262-269.
22. Foyer, C. H., Halliwell, B. *Planta*, 1976, 133(1):21-25.

23. Garmendia, I., Gogorcena, Y., Aranjuelo, I., Goicoechea, N. *Journal of plant growth regulation*, 2017, 36(4):855-867.
24. Giri, B., Kapoor, R., Mukerji, K. G. *Microbial Ecology*, 2007, 54(4):753-760.
25. Götz, T., Windhövel, U., Böger, P., Sandmann, G. *Plant Physiol*, 1999, 120(2):599-604.
26. Gratão, P. L., Polle, A., Lea, P. J., Azevedo, R. A. *Functional plant biology*, 2005, 32(6):481-494.
27. Hajiboland, R., Aliasgharzadeh, N., Laiegh, S. F., Poschenrieder, C. *Plant and Soil*, 2010, 331(1):313-327.
28. Hameed, A., Wu, Q.-S., Abd-Allah, E. F., Hashem, A., Kumar, A., Lone, H. A., Ahmad, P. *Alleviation of Soil Stress by PGPR and Mycorrhizal Fungi*. Miransari, M., eds.; Springer New York, New York, 2014.
29. Hao, Z., Xie, W., Jiang, X., Wu, Z., Zhang, X., Chen, B. *Agronomy*, 2019, 9(10):572.
30. Hashimoto, H., Uragami, C., Cogdell, R. J. *Subcell Biochem*, 2016, 79:111-139.
31. He, M., Dijkstra, F. A. *New Phytologist*, 2014, 204(4):924-931.
32. Hien, D. T., Jacobs, M., Angenon, G., Hermans, C., Thu, T. T., Son, L. V., Roosens, N. H. *Plant Science*, 2003, 165(5):1059-1068.
33. Jajic, I., Sarna, T., Strzalka, K. *Plants (Basel)*, 2015, 4(3):393-411.
34. Jiang, M., Zhang, J. *J Exp Bot*, 2002, 53(379):2401-2410.
35. Kaushal, M., Wani, S. P. *Annals of microbiology*, 2016, 66(1):35-42.
36. Kaya, C., Ashraf, M., Sonmez, O., Aydemir, S., Tuna, A. L., Cullu, M. A. *Scientia Horticulturae*, 2009, 121(1):1-6.
37. Khalafallah, A., Abo-Ghalia, H. H. *J Appl Sci Res*, 2008, 4:559-569.
38. Khalil, N., Fekry, M., Bishr, M., El-Zalabani, S., Salama, O. *Plant Physiology and Biochemistry*, 2018, 123:65-74.
39. Kumaraswamy, S., Shetty, P. *Agricultural Reviews*, 2016, 37(4).
40. Lamaison, J., Carnet, A. *Pharm Acta Helv*, 1990, 65(1):315-320.
41. Laxa, M., Liebthal, M., Telman, W., Chibani, K., Dietz, K.-J. *Antioxidants (Basel)*, 2019, 8(4):94.
42. Lee, B. R., Jin, Y. L., Jung, W. J., Avice, J. C., Morvan-Bertrand, A., Ourry, A., Park, C. W., Kim, T. H. *Physiol Plant*, 2008, 134(3):403-411.
43. López-Ráez, J. A. *Planta*, 2016, 243(6):1375-1385.
44. Lushchak, V. I. *Chemico-Biological Interactions*, 2014, 224:164-175.
45. Lutts, S., Majerus, V., Kinet, J.-M. *Physiologia Plantarum*, 1999, 105(3):450-458.
46. Mathur, S., Tomar, R. S., Jajoo, A. *Photosynthesis Research*, 2019, 139(1):227-238.
47. Nadeem, S. M., Ahmad, M., Zahir, Z. A., Javaid, A., Ashraf, M. *Biotechnology Advances*, 2014, 32(2):429-448.
48. Nakano, Y., Asada, K. *Plant, and Cell Physiology*, 1981, 22(5):867-880.
49. Norris, J. R., Ribbons, D. W. (1972) *Methods in microbiology*. Academic Press.
50. Ortiz, N., Armada, E., Duque, E., Roldán, A., Azcón, R. *Journal of plant physiology*, 2015, 174:87-96.
51. Oueslati, S., Karray-Bouraoui, N., Attia, H., Rabhi, M., Ksouri, R., Lachaal, M. *Acta Physiologiae Plantarum*, 2010, 32(2):289-296.
52. Paliwal, C., Mitra, M., Bhayani, K., Bharadwaj, S. V. V., Ghosh, T., Dubey, S., Mishra, S. *Bioresource Technology*, 2017, 244:1216-1226.
53. Parry, C., Blonquist Jr., J. M., Bugbee, B. *Plant, Cell & Environment*, 2014, 37(11):2508-2520.
54. Porcel, R., Ruiz-Lozano, J. M. *J Exp Bot*, 2004, 55(403):1743-1750.
55. Rahimi, A., Jahanbin, S., Salehi, A., Farajee, H. *Journal of Biological Sciences*, 2017, 17(1):28-34.
56. Saeidi, M., Moradi, F., Abdoli, M. *Arid land research and management*, 2017, 31(2):204-218.
57. Santander, C., Aroca, R., Ruiz-Lozano, J. M., Olave, J., Cartes, P., Borie, F., Cornejo, P. *Mycorrhiza*, 2017, 27(7):639-657.
58. Sara, K., Hossein, A., Masoud, S. J., Hassan, M. *Journal of Stress Physiology & Biochemistry*, 2012, 8(3).
59. Silvente, S., Sobolev, A. P., Lara, M. *PLOS ONE*, 2012, 7(6):e38554.
60. Singleton, V. L.; Orthofer, R.; Lamuela-Raventós, R. M.; *Methods in enzymology*, Elsevier: Amsterdam, 1999.
61. Smith, S. *Agricultural Commodities*, 2017, 7(3):27.
62. Szabados, L., Savoure, A. *Trends Plant Sci*, 2010, 15(2):89-97.
63. Tattini, M., Galardi, C., Pinelli, P., Massai, R., Remorini, D., Agati, G. *New Phytologist*, 2004, 163(3):547-561.
64. Tofighi, C., Khavari-Nejad, R. A., Najafi, F., Razavi, K., Rejali, F. *Physiology and Molecular Biology of Plants*, 2017, 23(3):557-564.
65. Vierheilig, H., Coughlan, A. P., Wyss, U., Piché, Y. *Appl Environ Microbiol*, 1998, 64(12):5004-5007.

66. Wang, X., Liu, H., Yu, F., Hu, B., Jia, Y., Sha, H., Zhao, H. *Scientific Reports*, 2019, 9(1):8543.
67. Wang, X., Zhao, C., Guo, N., Li, Y., Jian, S., Yu, K. *Spectroscopy Letters*, 2015, 48(7):492-498.
68. Wang, Z., Li, G., Sun, H., Ma, L., Guo, Y., Zhao, Z., Gao, H., Mei, L. *Biology Open*, 2018, 7(11):bio035279.
69. Xu, C., Yin, Y., Cai, R., Wang, P., Ni, Y., Guo, J., Chen, E., Cai, T., Cui, Z., Liu, T., Yang, D., Wang, Z. *Photosynthetica*, 2013, 51(1):139-150.
70. Xu, Z., Zhou, G., Shimizu, H. *J Exp Bot*, 2009, 60(13):3737-3749.
71. Yang, X., Chen, X., Ge, Q., Li, B., Tong, Y., Li, Z., Kuang, T., Lu, C. *Journal of Plant Physiology*, 2007, 164(3):318-326.
72. Zhang, Z., Zhang, J., Xu, G., Zhou, L., Li, Y. *New Forests*, 2019, 50(4):593-604.
73. Zhou, Q., Ravnskov, S., Jiang, D., Wollenweber, B. *Plant Growth Regulation*, 2015, 75(3):751-760.
74. Zhu, X., Song, F., Liu, S. *J Food Agric Environ*, 2011, 9(2):583-587.

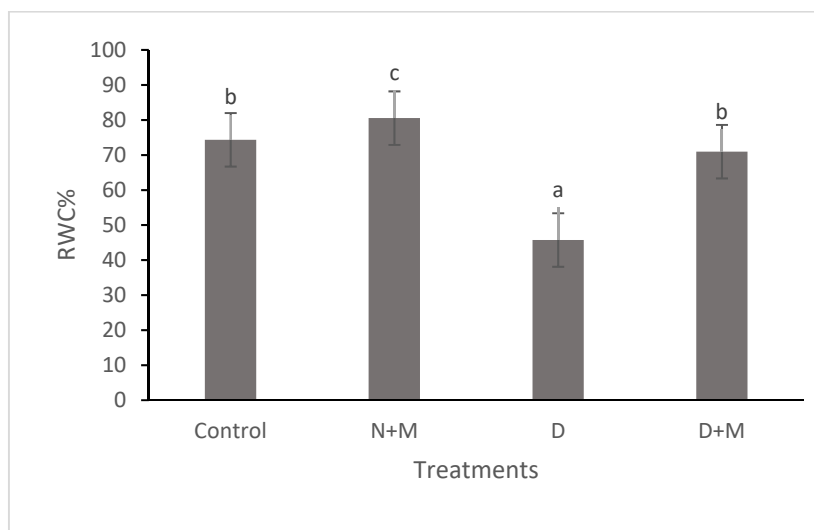


Figure 1: Effect of water deficiency and inoculation with *G. mosseae* on RWC of seedlings of *T. aestivum* cv. Chamran. Different letters indicate significant differences at $P < 0.05$

Table 1. Effect of water deficiency and inoculation with *G. mosseae* on Mycorrhization, FW, DW, P, total soluble protein, carbohydrates and free proline, MDA, CAT, SOD, GR and APX in flag leaves and roots of seedlings of *T. aestivum* cv. Chamran.

Parameters	Treatments			
	Control	N+M	D	D+M
Mycorrhization	0±0.0a	73.46± 2.49c	0±0.0a	38.25±1. 2b
Flag leaf				
Shoot freshweights	0.5732±0.0018b	0.6139±0.0011b	0.4283±0.0027a	0.5491±0.0019b
Shoot dry weights	0.0627±0.0011a	0.0717±0.001a	0.0596±0.0014a	0.0759±0.0015a
P concentration	2.2193±0.1263ab	2.9718±0.1794b	1.4719±0.1329a	2.4913±0.1825b
Total soluble protein	4.7166±0.879b	4.8535±0.715b	3.1874±0.366a	4.8650±0.436b
Proline	1.4250±0.686a	1.5600±0.637a	2.4825±0.896b	1.3650±0.484a
Total soluble carbohydrates	4.4862±0.208a,b	5.0222±0.482a	6.3746±0.465b,c	7.3821±0.539c
MDA	0.1339±0.002b	0.1032±0.049a	0.1828±0.008c	0.0781±0.001a
CAT	121.2050±3.611b	129.2650±5.064a	147.3225±5.813c	189.5525±7.154d
SOD	83.2400±2.014b	95.3475±7.010a	123.4325±3.175c	158.5375±11.013d
GR	0.2900±0.010b	0.3475±0.015a	0.4375±0.013c	0.6325±0.008d
APX	8.1525±1.146a	10.9300±0.914b	13.0085±1.1628c	18.1458±1.277d
Root				
Root fresh weights	0.0938±0.0005a	0.1254±0.001b	0.0739±0.001a	0.0951±0.0013a
Root dry weights	0.0116±0.0007a	0.0186±0.0004b	0.0103±0.0006a	0.0135±0.0009b
P concentration	1.9426±0.1893b	2.3358±0.1127b	1.1832±0.1922a	2.3115±0.1327b
Total soluble protein	3.2447±0.301b	3.5211±0.765b	2.6252±0.500a	3.4301±0.448b
Proline	1.2150±0.025a	1.5350±0.707ab	1.9075±0.021b	1.0675±0.214a
Total soluble carbohydrates	3.2162±0.298a	3.7745±0.148a,b	4.2171±0.261b	4.5485±0.259b
MDA	0.1138±0.002a	0.0936±0.010a	0.1582±0.008a	0.0744±0.001a
CAT	109.3829±3.027a	112.9725±9.056b	130.4075±8.201c	171.4025±5.019 d
SOD	79.0500±5.970a,b	88.0650±5.176a	118.0925±4.062b	136.1350±7.018c
GR	0.0825±0.004a	0.1000±0.013a	0.0950±0.004a	0.1129±0.003a
APX	5.0975±0.127a	6.8732±0.119ab	7.0375±0.185b	7.9233±0.241b

Values represent the mean ± SE of four replicates. Different letters indicate significant differences at P<0.05
 Note: Mycorrhization: %; Shoot fresh weights: g; Shoot dry weights: g; P concentration: mg g⁻¹DW; Total soluble protein: mg g⁻¹DW; Proline: mg g⁻¹DW; Total soluble carbohydrates: mg g⁻¹DW; MDA: μM g⁻¹ FW; CAT: mg⁻¹ protein min⁻¹; SOD: mg⁻¹ protein min⁻¹; APX: mg⁻¹ protein min⁻¹; GR: μmol of oxidized substrate/(g fr wt min).

Table 2. Effect of water deficiency and inoculation with *G. mosseae* on photosynthetic pigments (Chl a, b, and total), phenolic compounds (phenol and flavonoid), and anthocyanin content in flag leaves of seedlings of *T. aestivum* L., cv. Chamran.

Parameters	Treatments			
	CONTROL	N+M	D	D+M
Chl a	1.3786±0.109a	1.4085±0.046a	1.0514±0.068a	1.8648±0.126b
Chl b	0.9484±0.048a	0.9573±0.055a	0.7388±0.019a	1.1203±0.090a
Chl t	2.3270±0.096b	2.3658±0.199b	1.7902±0.216a	2.9851±0.396c
Car	0.6520±0.114a	1.0086±0.142a	0.9336±0.152a	1.4095±0.036b
TPC	16.9639±1.967a	36.5472±4.307c	34.7000±2.993b	47.2833±5.551d
TFC	12.7150±1.853a	19.0519±1.471b	27.5071±1.936c	35.7548±3.250d
TAC	0.7803±0.028a	0.6864±0.077a	0.7424±0.081a	0.9242±0.060a

Values represent mean ± SE of four replicates. Different letters indicate significant differences at $P < 0.05$ Note: Chl a, Chl b, Chl t, Car: mg/g FW; TPC: mg GA/g DW; TFC: mg QE/g DW; TAC: mg cyanidin-3-glucoside/g FW.

EXTRAÇÃO E DETERMINAÇÃO DE TEBUCONAZOL EM AMOSTRAS AMBIENTAIS DA CIDADE DE KARBALA NO IRAQUE E EM SUA FORMULAÇÃO USANDO CROMATOGRAFIA LÍQUIDA DE ALTO DESEMPENHO (HPLC)

EXTRACTION AND DETERMINATION OF TEBUCONAZOLE IN ENVIRONMENTAL SAMPLES FROM THE CITY OF KARBALA, IRAQ AND IN ITS FORMULATION USING HIGH- PERFORMANCE LIQUID CHROMATOGRAPHY (HPLC)

استخلاص وتقدير التبيكونازول في نماذج ومستحضرات بيئية في مدينة كربلاء / العراق باستخدام تقنية الكروماتوغرافيا السائلة عالية الاداء (HPLC)

SHAHEED, Ihsan Mahdi^{1*} and DHAHIR, Saadiyah Ahmed²

¹ University of Baghdad, Faculty of Science, Department of Chemistry, Baghdad. Iraq.

² University of Baghdad, Faculty of Science for women, Department of Chemistry, Baghdad. Iraq.

* Correspondence author

e-mail: ihsan.aldahan@uokerbala.edu.iq

Received 06 January 2020; received in revised form 10 March 2020; accepted 26 March 2020

RESUMO

O triazol, o pesticida tebuconazol, foi determinado em sua formulação e também nas amostras de água do rio coletadas de diferentes áreas agrícolas da cidade de Kerbala, no Iraque, usando o método de cromatografia líquida de alta eficiência (HPLC) desenvolvido com detecção visível por UV, fase móvel de composição era uma mistura de acetonitrila: metanol (50:50 v/v) e a coluna era C18 (250 cmx4.6mm, 5µm). Também foi utilizada a microextração dispersivo líquido-líquido modificada (DLLME), considerada um método ecológico, para a extração de tebuconazol a partir de amostras de água utilizando acetonitrila e clorofórmio como extração de solventes e agente dispersivo, respectivamente. A linearidade para manter a curva de calibração foi alcançada a partir de (0,1-70) µg·mL⁻¹ com um limite de detecção (0,053) µg·mL⁻¹ e limite de quantificação (0,174) µg·mL⁻¹. Três níveis de concentração de pico (1,0, 5,0 e 10) µg·mL⁻¹ foram utilizados para a validação do método. O desvio padrão relativo (RSD%) foi (0.294-0.813)% e a porcentagem de recuperação foi (100.001-100.005). Os estudos de formulação para duas concentrações diferentes (10 e 40) µg·mL⁻¹, preparados a partir da formulação de tebuconazol (Raxil ODS2 a 2%), proporcionam uma recuperação percentual aceitável entre (98.956-99.833). O método desenvolvido pode ser usado com precisão para a determinação de tebuconazol em amostras de água e na formulação eficaz de tebuconazol.

Palavras-chave: *Dispersivo, formulação, HPLC, apiciforme e tebuconazol.*

ABSTRACT

The triazole, tebuconazole pesticide, was determined in its formulation and also in the river water samples collected from different agriculture areas in the Iraqui city of Kerbala using developed high-performance liquid chromatography method(HPLC) with UV-visible detection, The mobile composition phase was a mixture of acetonitrile:methanol (50:50 v/v) and the column was C18 (250 cmx4.6mm,5µm). Also modified dispersive liquid-liquid microextraction (DLLME), which is regarded as an ecological -friendly method, was used for the extraction of tebuconazole from water samples using acetonitrile and chloroform as solvents extraction and dispersive agent, respectively. Linearity to maintain the calibration curve was achieved from (0.1-70) µg·mL⁻¹ with a limit of detection(0.053) µg·mL⁻¹ and limit of quantification (0.174) µg·mL⁻¹. Three spiked levels of concentration (1.0, 5.0, and 10) µg·mL⁻¹ were used for the validation of the method. The relative standard deviation (RSD%) was (0.294-0.813)%, and the percentage recovery was (100.001-100.005). The formulation studies for two different concentrations (10 and 40) µg·mL⁻¹, which prepared from tebuconazole formulation (Raxil ODS2 2%), gave acceptable percentage recovery between (98.956-99.833). The developed method can be used accurately for the

determination of tebuconazole in water samples and in the formulation of tebuconazole effectively.

Keywords: Dispersive, formulation, HPLC, spiked, and tebuconazole.

الملخص

الترابازول , مبيد التبيكونازول, تم تقديره في محاليله وكذلك في نماذج من مياه النهر جمعت من مناطق زراعية مختلفة في مدينة كربلاء / العراق باستخدام تقنية كروماتوغرافيا السائلة عالية الأداء وباستخدام الكاشف في المنطقة المرئية وفوق البنفسجية . تركيب الطور المتحرك هو عبارة عن مزيج من الاسيتونتريل : ميثانول (50:50 حجم/حجم) والكولوم المستعمل من نوع C18 بابعاد (250 سم x 4.6 ملم x 5 مايكرو ملم) . وكذلك تم استخدام طريقة تشتت سائل-سائل المايكروية, التي تعتبر من طرق الاستخلاص الصديقة للبيئة, لاستخلاص التبيكونازول من نماذج الماء باستخدام الاسيتونتريل والكوروفورم كمحاليل للاستخلاص والتشتت . الخطية لمنحني المعايرة تم الوصول إليها عند تراكيز (0.1-70) ملي مايكرو/ مل وكان حد الكشف (0.053) ملي مايكرو/ مل وحد الكشف الكمي (0.174) ملي مايكرو/ مل. ثلاث تراكيز (5.0, 10.0 و 10.0) مايكرو غرام/ مل تم استعمالها لتقييم الطريقة . الانحراف المعياري النسبي كان (0.294-0.813) ونسبة الاسترجاع كانت (100.001-100.005). تمت دراسة المحاليل للتبيكونازول لتركيزين (10 و 40) ملي مايكرو/ مل , والتي حضرت من محاليل التبيكونازول (راكسيل 2% ODS2) وأعطت نسب استرجاع بين (98.956-99.833). الطريقة المحدثة يمكن تطبيقها بدقة لتقدير التبيكونازول في نماذج الماء وكذلك في محاليل التبيكونازول بكفاءة .

الكلمات المفتاحية: تشتت , محاليل , HPLC , spiked , تبيكونازول .

1. INTRODUCTION

Triazole was, synthesized by Fisher in 1878, consist of three nitrogen atoms in positions 1,2, and 4 forming five membranes heterocyclic ring, its weak properties made it soluble in all organic solvent. Triazoles have many applications in agriculture, medicine and industry when fused with pyrimidines, triazine, pyridazine and pyrazine. (Maddila et al., 2013). Hydrocarbon backbone in triazole bounded with nitrogen in position1. The chiral center, due to the presence of nitrogen in the triazole ring, gives this compound its bioactivity when it is used as fungicides against fungal disease in different crops (SHAH et al., 2006; Subova et al., 2006). Generally, all formulations of triazole were found as a racemic mixture, thus gives triazole enantioselectivity phenomena, Although there is an exception in some of the triazole pesticides, which consist of one enantiomer, such as uniconazole and diniconazole (Wang et al., 2010).

Triazole regarded as the most interesting heterocyclic compounds that inter in the constituent of cell and living matter (Palmer et al., 2012).

Tebuconazole (TEB) (figure 1), (R,S)-1-*p*-chlorophenyl-4,4-dimethyl-3-(1*H*-1,2,4-triazol-1-ylmethyl)pentan-3-ol, is a triazole fungicide used to control different plant diseases but has a toxic effect on the organisms in the water environment (Yu et al., 2013).

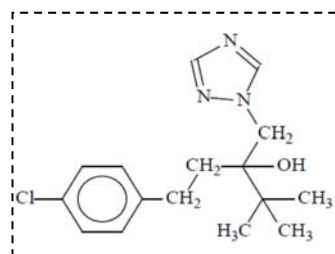


Figure 1: Chemical structure of tebuconazole

Risk assessment for the triazole fungicides became necessary due to the toxicological properties of tebuconazole especially in children and farmers through the ingestion of contaminated food and also due to the inappropriate treatment done without following safety instruction leading to remaining the residue in food after harvest (Liu, 2017, Lutsevich et al., 1995, Oliva et al., 2007).

Various methods were reported for the determination of tebuconazole to monitor its residues in the different environmental samples. These methods includes gas-liquid chromatography (Patil et al., 1992, Vorpsi et al., 2011, Farajzadeh et al., 2014), Liquid chromatography-mass spectrophotometry (Caldas et al., 2011, Khalil and Huat, 2013, Kundu et al., 2011), gas chromatography-mass spectrophotometry (Liu et al., 2011, Dong and Hu, 2014), High-performance liquid chromatography (Rao et al., 2012, Caldas et al., 2009).

2. MATERIALS AND METHODS

2.1. Reagents and chemicals

Tebuconazole standard (purity > 99%) was supplied by Dr. Ehrenstorfer GmbH company. Water, Acetonitrile, and methanol for HPLC analysis with purity (> 99.9%) were purchased from the Sigma-Aldrich company. Tebuconazole Formulation (Raxil ODS₂ 2%) was obtained from Karbala Agriculture Department. Orthophosphoric acid (85%) was provided from Merck (Darmstadt, Germany), hydrochloric acid (36w/v%) from HIAMEDIA, and Sodium hydroxide (99%) from B.H.D company.

2.1.1. Preparation of Formulation Solution

One milliliter from tebuconazole formulation (Raxil ODS₂ 2%), obtained from Karbala Agriculture Department, was diluted with 100 mL methanol, then different volumes were taken for this solution to prepare different concentration of tebuconazole for HPLC analysis. All solutions were kept in 4°C.

2.1.2. Preparation of Standards Solutions

The calculated amount of standard tebuconazole was diluted with methanol to prepare (1000 µg·mL⁻¹). Series solutions from the stock solution ranged from (0.5 - 200) µg·mL⁻¹ were prepared in 5 mL volumetric flask for studying the calibration curve. All solutions were kept in 4°C.

2.1.3. preparation of sodium hydroxide (0.1 M)

Sodium hydroxide (NaOH) was prepared by dissolving 0.4 g of sodium hydroxide in 100 mL distilled water.

2.1.4. preparation of orthophosphoric acid (0.1M)

Orthophosphoric acid (H₃PO₄) was prepared by diluting 0.680 mL of concentrated orthophosphoric acid in 100 mL distilled water.

2.1.6. Modified Dispersive liquid-liquid microextraction method (DLLME)

Five milliliters of water samples, collected from different agriculture areas in Kerbala city/ Iraq, were filtered and the filtrates were transferred to a glass centrifuged test tube (10mL) with a screw and spiked with different concentrations of standard tebuconazole (1.0, 5.0 and 10) µg·mL⁻¹. Sodium chloride (5% v/v, 0.5 mL) was added as

salting-out agent. A mixture of acetonitrile (1 mL) and chloroform (100 µL) was added to the spiked samples as solvent extraction and dispersant agent, respectively. The final solution was vortexed for 2 minutes, followed by shaking by hand for 10 minutes, then centrifuged at 5000 rpm for 15 minutes. Two layers were separated. The aqueous layer removed by microsyringe and the organic layers, which contain tebuconazole as droplets, were diluted with 0.5 mL of acetonitrile for HPLC analysis injection after filtration through Millipore filter paper 0.45 µm. The same procedure was applied for river water samples collected from different agriculture areas from Kerbal city / Iraq without spiking as a controller.

2.2. INSTRUMENTATION

Double beam UV-spectrophotometer-1800, Shimadzu. Digital balance, Denver-TP-214. High-performance liquid chromatography (HPLC) 20 AD Shimadzu equipped with UV-detector. Ultrasonic cleaner, KQ200E. pH-meter, Hanna-pH211. Centrifuge, C2 series.

2.3. METHOD VALIDATION

2.3.1. Chromatographic conditions

High-performance liquid chromatography system (LC-20AD, SHIMADZU Corporation) equipped with an autosampler, hyper sail ODS C18 column (25cmx4.6mm, 5 µm), and UV-Visible detector was used for analysis. The composition of the mobile phase was acetonitrile:methanol (50:50 v/v) at pH 5.0 using H₃PO₄/NaOH (0.1M) for adjusting the pH. The flow rate was 0.8 mL/min, and the volume of injection was 20 µL at λ_{max} 220 nm.

2.3.2. Wavelength selection

Standard tebuconazole solutions (50 and 10) µg·mL⁻¹, prepared in methanol from stock solution, were scanned from 190-800 nm. It was found there are two peaks that appear, low-intensity peak at λ_{max} 268 and high-intensity peak at λ_{max} 220 nm (figure 2). The peak at 220 nm was chosen for optimization due to its high intensity.

2.3.3. Limit of Detection (LOD) and Limit of Quantification (LOQ)

Limit of detection (LOD) is the lowest

concentration of analyte detected by the proposed method but may not be quantified, on the other hand, the limit of quantification(LOQ) is the lowest concentration of analyte that can be detected quantitatively with high precision and accuracy. LOD and LOQ measured due to the ratio of noise(N) to signal(S) of the baseline. LOD calculated if the ratio (N/S=3), while LOQ calculated when the ratio (N/S=10).

2.3.4. Precision and Accuracy

The precision of results in the proposed method represented by the repeatability of injection samples (n=5) and measured by relative standard deviation value (RSD%), while recovery percentage represents accuracy. Different concentrations (0.5,10 and 50) $\mu\text{g}\cdot\text{mL}^{-1}$ from tebuconazole standard were prepared and tested for validation study by injection in HPLC devise under optimum conditions(n=5).

3. RESULTS AND DISCUSSION

3.1. Method development

Some preliminary investigations were performed, which included tested two types of columns (C18 and C8) to perform the best response and acceptable peak shape and capacity. It was found that the best separation was manyained by using C18 column rather than C8 coolumn. Also, different ratios of solvents (methanol, acetonitrile, and water) with different compositions ranged from (90:10 v/v) to (50:50 v/v) were tested for the best separation. Mobile phase with composition of acetonitrile:methanol (50:50 v/v) was chosen for optimization according to the highest response, good peak shape and acceptable capacity factore and resolution (figure 3) . All preliminary investigations were maintained at flow rate $1\text{mL}\cdot\text{min}^{-1}$ and the injection volume of $20\mu\text{L}$ at $\lambda_{\text{max}}220\text{nm}$.

3.2. Method validation

3.2.1. Effect of pH

The mobile phase with different pH ranging from (3.0-8.0) were studied for the best response, tebuconazole ($50\mu\text{g}\cdot\text{mL}^{-1}$) was injected, and the pH justified by using NaOH/phosphoric acid (0.1M).

Table 1. Effect of pH.

pH	Retention time (tR) (min.)	Peak area	Capacity (k)	Tailing factor (TF)
3.0	2.883	1825538	0.765	1.166
4.0	2.773	1802392	0.864	1.079
5.0	2.722	1872780	0.935	1.004
6.0	2.731	1776323	0.903	1.021
7.0	2.763	1755021	0.934	0.951
8.0	2.902	1011624	0.972	1.162

Results illustrated in Table 1 and figure 4 proved that pH 5.0 was the best choice according to the good resolution, acceptable peak shape and capacity, for that pH 5.0 was used for optimization.

3.2.2. Effect of flow rate

At pH 5.0, tebuconazole with concentrarion ($50\mu\text{g}\cdot\text{mL}^{-1}$) was injected (n=3) at various flow rate ranged from (0.3 -1.5) mL/min.

Table 2. Effect of flow rate.

Flow rate mL/min	Retention time(tR) (min.)	Peak area	Capacity (k)	Tailing factor (TF)
0.5	5.372	3511399	0.974	1.211
0.8	3.315	2293504	0.981	1.024
1.0	2.662	1864464	0.894	1.223
1.3	2.221	1473194	0.921	1.332
1.5	1.782	1181085	0.916	1.361

From results in table 2 and figure 5, the highest response obtained was at flow rate $0.5\text{ mL}\cdot\text{min}^{-1}$,but at this flow rate an acceptable vaule of tailing factor obtained. Flow rate at $0.8\text{ mL}/\text{min}$ was adopted for optimization as a result of maintaining good symmetric shape, acceptable capacity, and short retention time (Table 2).

3.2.3. Effect of volumes injection

Different volumes eanged from (5.0-25.0 μL) of tebuconazole standard of concentration ($50\mu\text{g}\cdot\text{mL}^{-1}$) were injected(n=3) to HPLC system at optimum conditions. The results explained in table 3 and figure 6.

Table 3. Effect of volume injection.

Volume (μL)	Retention time(t _R) (min.)	Peak area	Capacity (k)	Tailing factor (TF)
5	3.313	520218	1.028	2.155
10	3.318	881235	0.990	1.394
15	3.328	1656336	0.937	1.280
20	3.331	2282035	0.987	1.086
25	3.335	2850382	0.906	1.277

Result in Table 3 and figure 6 explained that after injection the volume of 20 μL the tailing factor was increased and an acceptable peak shape was obtained due to overloaded of the column which affected the shape of peak and baseline stability, while up to 20 μL the responses were increased systematically with improvement in peak shape, for that the volume 20 μL was chosen for optimization.

3.2.4. Linearity

For linearity study, series solutions ranged from (0.1-100) μg·mL⁻¹ were prepared from the stock solution of standard tebuconazole and injected (n=3) into the HPLC system. The calibration curve was maintained by plotting peaks area against concentrations (figure 7). All solutions were filtered through a 0.45 μm Millipore filter.

Table 4. Analytical parameter for the Tebuconazole calibration curve.

λ max (nm)	220
Linearity range (μg mL ⁻¹)	0.1-70
Limit of detection (μg mL ⁻¹)	0.072
Limit of quantification (μg mL ⁻¹)	0.240
Regression Equation	y = 60592x + 126273
Slope	60592
Correlation coefficient (R ²)	0.9997

Linearity was achieved at concentration ranged from (0.1-70) μg mL⁻¹ after that deviation observed from Lambert's law with correlation coefficient (0.9997). The limit of detection and limit of quantification are 0.072 and 0.240 μg mL⁻¹, respectively (table 4).

3.2.5. Precision and Accuracy

At optimum conditions, three concentration

levels of tebuconazole (0.5, 10 and 50) μg·mL⁻¹ were injected (n=5). The results sorted in Table 5.

Table 5. Precision and Accuracy for the modified method.

Conc. (μg·mL ⁻¹)	Retention time(t _R) (min.)	Recovery %	RSD %
0.5	3.331	100.007	0.929
10.0	3.330	100.000	0.045
50.0	3.331	100.002	0.453

From results in Table 5, good recovery (100.000-100.007) and low RSD% values (0.045-0.929) were obtained, for that this method was accurate to determine the amount of tebuconazole in environmental samples.

3.3. Application

The optimized method was applied for the determination of tebuconazole in spiked river water samples (1.0, 5.0, and 10) μg·mL⁻¹ collected from different agriculture areas in Kerbala City / Iraq and in its formulation (Raxil 2%) (Tables 6-7) and (figures 8-10).

Table 6. Recovery of Tebuconazole in water samples spiked with three different levels.

Spiked level (μg·mL ⁻¹)	Amount found (μg·mL ⁻¹)	Recovery % (n=5)
0	Not detected	-
1.0	0.839	83.184
5.0	4.546	90.904
10.0	9.659	96.594

Table 7. Recovery of Tebuconazole in the formulation.

Formulation (μg·mL ⁻¹)	Amount found (μg·mL ⁻¹)	Recovery % (n=5)
10.0	9.892	98.956
30.0	29.250	97.502

Result in table 6 explained that there is no detection for tebuconazole was obtained for water samples collected from different agriculture area due to the very low concentration of tebuconazole in these samples. For spiked samples the percentage recoveries were ranged from (83.184-96.594) while the percentage recoveries for different prepared concentration of formulation

(table 7) were ranged from (97.503-98.956).

4. CONCLUSION

The sensitive, selective, and accurate method was developed to extract and determine the tebuconazole in the water sample. Tebuconazole residues in six samples collected from different agriculture area in Kerbala City / Iraq was not detected due to the very low concentrations of the residues in water samples. Good recoveries and relative standard deviations values were obtained which made the proposed method can be applied successfully for the determination of tebuconazole in environmental samples and in its formulations.

5. ACKNOWLEDGMENTS

The authors thank the support from the staff of the College of Science for Women/ Chemistry Department for providing requirements and also thank the staff of the department of agriculture for their cooperation and support.

6. REFERENCES:

1. Caldas, S. S., Bolzan, C. M., Cerqueira, M. B., Tomasini, D., Furlong, E. B., Fagundes, C., Primel, E. G. *Journal of agricultural and food chemistry*, **2011**, 59, 11918-11926.
2. Caldas, S. S., Demoliner, A., Primel, E. G. *Journal of the Brazilian Chemical Society*, **2009**, 20, 125-132.
3. Dong, B., Hu, J. *International Journal of Environmental Analytical Chemistry*, **2014**, 94, 493-505.
4. Farajzadeh, M. A., Mogaddam, M. R. A., Ghorbanpour, H. *Journal of Chromatography A*, **2014**, 1347, 8-16.
5. Khalil, N. H. H. B., Huat, T. G. *Agricultural Chemistry. IntechOpen*, **2013**.
6. Kundu, C., Goon, A., Bhattacharyya, A. *Journal of Environmental Protection*, **2011**, 2, 424.
7. Liu, B. *IOP Conference Series: Materials Science and Engineering*, **2017**. IOP Publishing, 012060.
8. Liu, X., Wang, X., XU, J., Dong, F., Song, W., Zheng, Y. *Biomedical Chromatography*, **2011**, 25, 1081-1090.
9. Lutsevich, A., Bender, K., Reshet'ko, O. *Ekspertimental'naia i klinicheskaia farmakologiya*, **1995**, 58, 51-55.
10. Maddila, S., Pagadala, R., B Jonnalagadda, S. *Letters in Organic Chemistry*, **2013**, 10, 693-714.
11. Oliva, J., Payá, P., Cámara, M. Á., Barba, *Journal of Environmental Science and Health*, **2007**, 42, 775-781.
12. Palmer, M. H., Camp, P. J., Hoffmann, S. V., Jones, N. C., Head, A. R., Lichtenberger, D. L. *The Journal of chemical physics*, **2012**, 136, 094310.
13. Patil, V. B., Sevalkar, M. T., Padalikar, S. V., *Analyst*, **1992**, 117, 75-76.
14. Rao, T. N., Reddy, E., Satish, P., NAGACHANDRUDU, S., Parvathamma, T. *International journal of chemical and analytical science*, **2012**, 3, 1565-1568.
15. Shah, J., Jan, M. R., Bashir, N. *Analytical sciences*, **2006**, 22, 145-146.
16. Subova, I., Assandas, A. K., Icardo, M. C., Calatayud, J. M. *Analytical sciences*, **2006**, 22, 21-24.
17. Vorpsi, V., Harizaj, F., Vladi, V. *Research Journal of Agricultural Science*, **2011**, 43.
18. Wang, C., Zhang, N., Li, L., Zhang, Q., Zhao, M., Liu, W. *The Pharmacological, Biological, and Chemical Consequences of Molecular Asymmetry*, **2010**, 22, 612-617.
19. Yu, L., Chen, M., Liu, Y., Gui, W., Zhu, G. *2013. Aquatic toxicology*, **2010**, 138, 35-42.

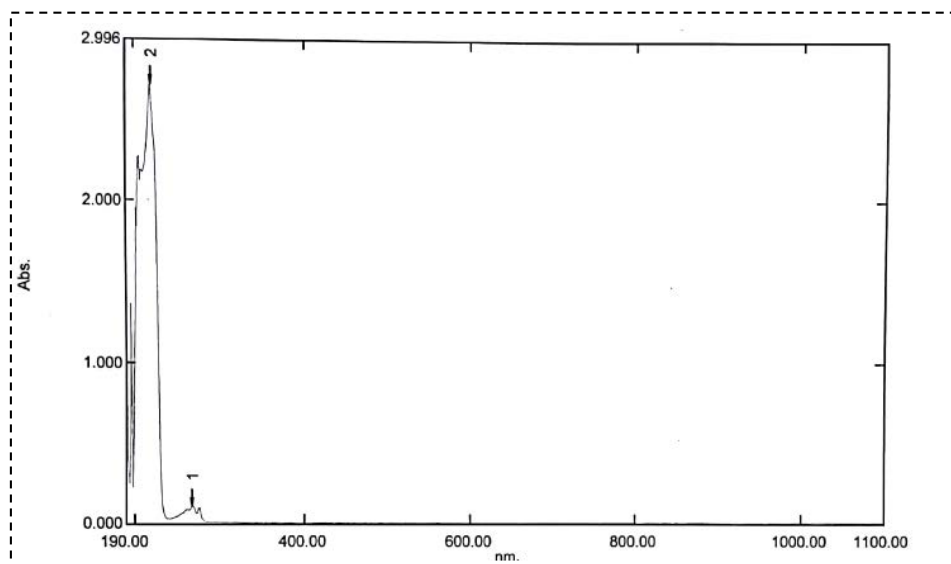


Figure 2: UV-visible spectra of Tebuconazole

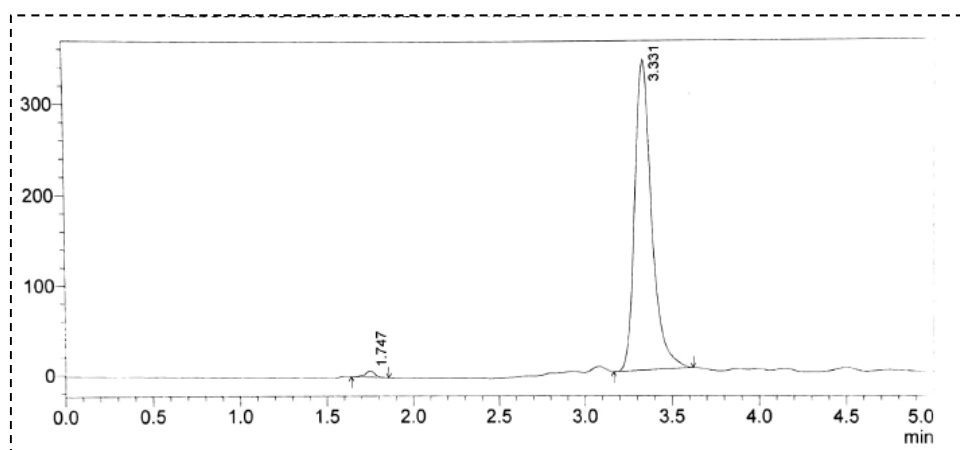


Figure 3. Chromatogram of standard Tebeconazole

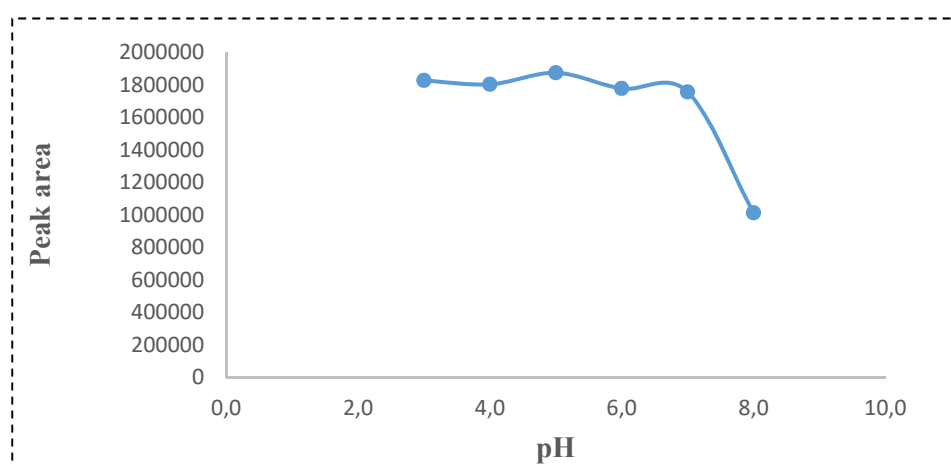


Figure 4. Effect of pH

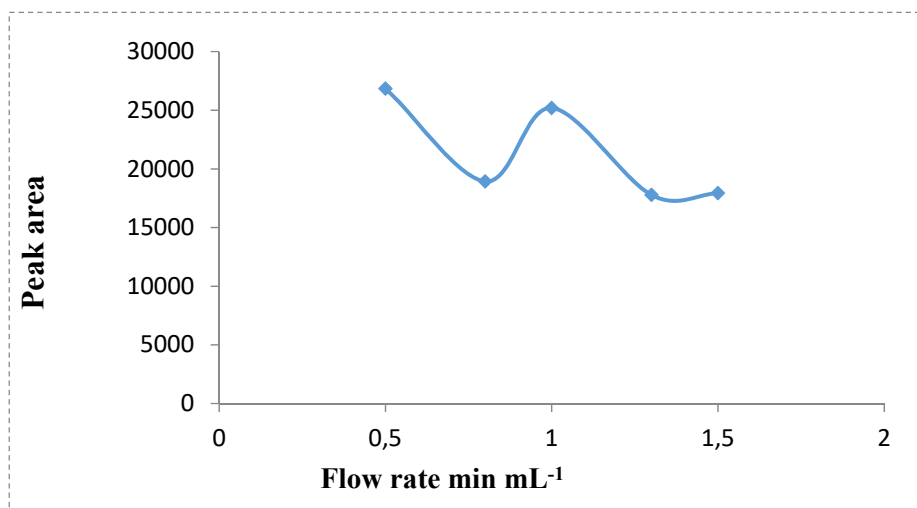


Figure 5. Effect of Flow rate

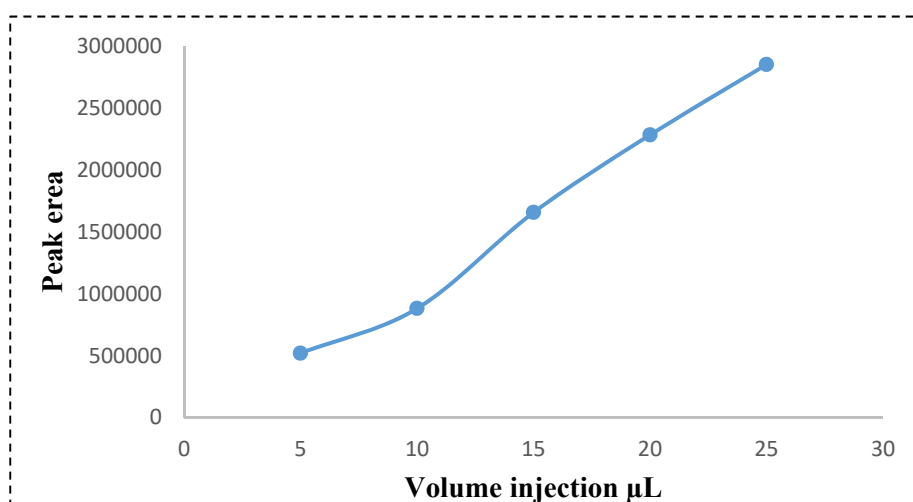


Figure 6. Effect of volume injection

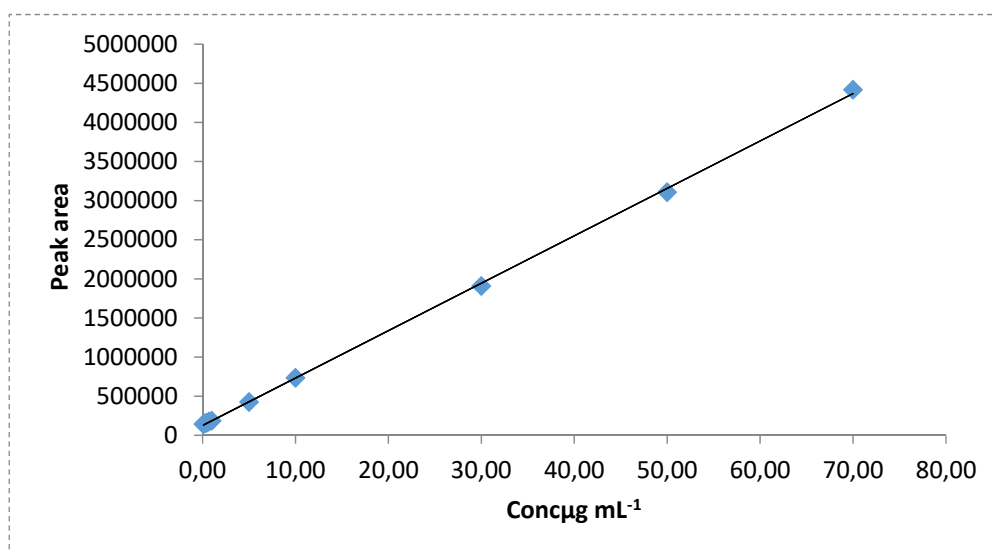


Figure 7. Calibration curve for α-Cypermethrin standards

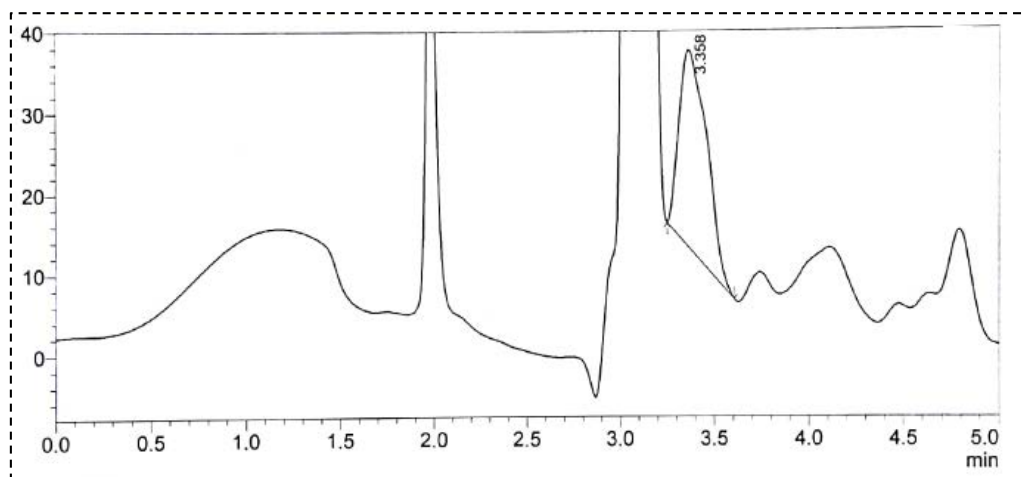


Figure 8. Chromatogram of spiked water sample(1.0) $\mu\text{L mL}^{-1}$

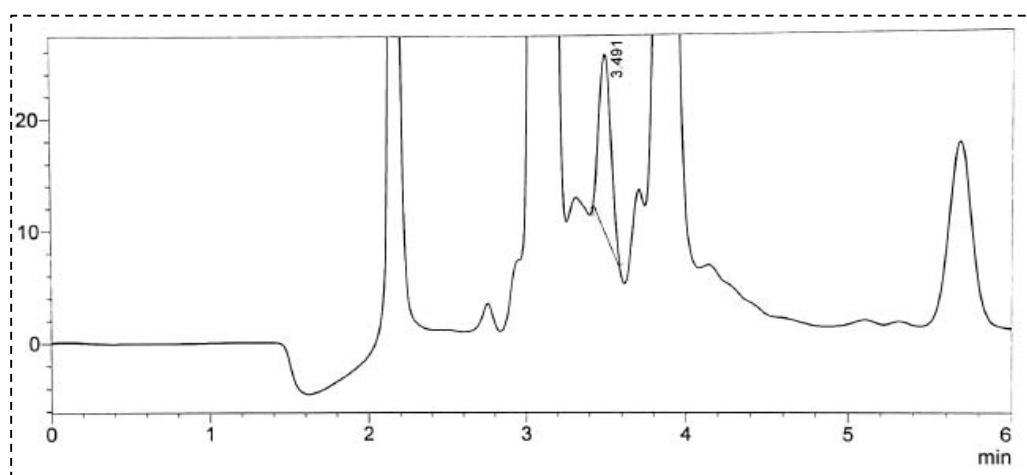


Figure 9. Chromatogram of spiked water sample(5.0) $\mu\text{L mL}^{-1}$

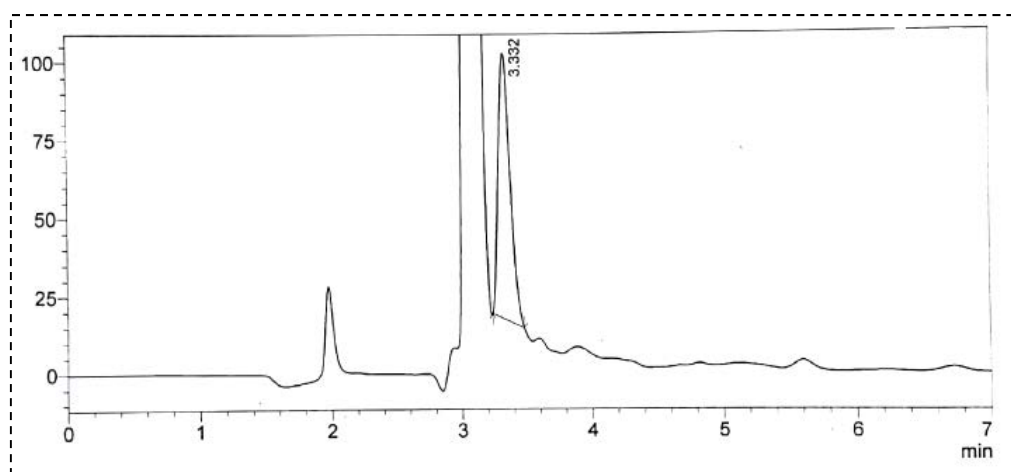


Figure 10. Chromatogram of spiked water sample(10.0) $\mu\text{L mL}^{-1}$

INVESTIGAÇÃO DE DEFORMAÇÕES PERMANENTES EM COMPOSITOS NANOMODIFICADOS APÓS A MOLDAGEM EM TEMPERATURAS ELEVADAS

INVESTIGATION OF PERMANENT STRAINS IN NANOMODIFIED COMPOSITES AFTER MOLDING AT ELEVATED TEMPERATURES

ИССЛЕДОВАНИЕ ОСТАТОЧНЫХ ДЕФОРМАЦИЙ В НАНОМОДИФИЦИРОВАННЫХ КОМПОЗИТАХ ПОСЛЕ ФОРМОВАНИЯ

BABAYTSEV, Arseniy V.^{1*}; KUZNETSOVA, Ekaterina L.²; RABINSKIY, Lev N.³; TUSHAVINA, Olga V.⁴;

^{1,3} Moscow Aviation Institute (National Research University), Department of Engineering Graphics, 4 Volokolamskoe shosse, zip code 125993, Moscow – Russian Federation

² Moscow Aviation Institute (National Research University), Institute of General Engineering Education, Department of Perspective Materials and Technologies of Aerospace Designation, 4 Volokolamskoe shosse, zip code 125993, Moscow – Russian Federation

⁴ Moscow Aviation Institute (National Research University), Institute of Aerospace, Department of Managing Exploitation of Space-Rocket Systems, 4 Volokolamskoe shosse, zip code 125993, Moscow – Russian Federation

* Correspondence author
e-mail: Ar77eny@gmail.com

Received 12 January 2020; received in revised form 14 November 2020; accepted 24 March 2020

RESUMO

Este trabalho investiga o efeito da nanomodificação do carbono no estado de tensão-deformação residual (ETD) após a moldagem. Uma das maneiras de reduzir tensões residuais e deformidades é a nanomodificação. O objetivo principal foi determinar o grau de influência dos parâmetros de nanomodificação no ETD residual. No âmbito deste estudo, foram feitas 4 placas. Duas placas foram feitas com um aglutinante convencional com assentamento [010/9010] e [010/4510] e duas placas com um material de ligação modificado com a mesma estrutura de camada. Para as placas fabricadas, as deformações foram medidas em cada um dos quatro lados, durante o qual foram obtidas deformações residuais nos painéis de fibra de carbono nano modificada para as camadas consideradas com e sem material de ligação modificado. Para analisar o estado de tensão-deformação residual, foi realizado um cálculo numérico e analítico. O cálculo numérico foi realizado pelo método dos elementos finitos para o caso em que a palca é fixada no ponto do centro geométrico, sem carga de energia, e a carga de temperatura é uma diferença de 100 °C. Um cálculo analítico foi realizado para o caso em que a placa está livre de fixação e carga de energia externa, e a carga de temperatura é uma diferença de 100 °C. Durante o estudo, variantes das propriedades físico-mecânicas da monocamada foram obtidas usando o *software* Digimat e o método de média de Mori-Tanaka. Os resultados obtidos pelos métodos analíticos e numéricos têm boa correlação entre si e, no decorrer da comparação com o experimento, foi determinado um método para calcular as características da monocamada mais próxima do resultado experimental. Com base nos resultados obtidos, foram tiradas conclusões sobre a possibilidade de reduzir ETD residual e a deformação em estruturas com esquemas de reforço assimétrico, utilizando uma matriz contendo nanopartículas de carbono.

Palavras-chave: *materiais compósitos, partículas de tamanho nano, nano modificação, deformações, deformidades residuais, tensões residuais, ETD.*

ABSTRACT

This work investigates the effect of carbon nanomodification on the residual stress-strain state (SSS) after molding. One of the ways to reduce residual stresses and deformities is nanomodification. The main objective was to determine the degree of influence of the nanomodification parameters on the residual SSS. Within the framework of this study, 4 slabs were made. Two slabs are made of a conventional binder with laying [0₁₀/90₁₀] and [0₁₀/45₁₀] and two slabs of a modified binding material with the same layer structure. For the fabricated plates,

deflections were measured on each of the four sides, during which residual strains were obtained in the panels of nanomodified carbon fiber for the considered layings with and without modified binding material. To analyze the residual stress-strain state, a numerical and analytical calculation was performed. The numerical calculation was carried out by means of the finite element method for the case when the slab is fixed at the point of the geometric center, with no power load, and the temperature load is a difference of 100 °C. An analytical calculation was carried out for the case when the slab is free from fastening and external power load, and the temperature load is a difference of 100°C. During the study, variants of the physicommechanical properties of the monolayer were obtained using the Digimat software and the Mori-Tanaka averaging method. The results obtained by analytical and numerical methods have a good correlation between each other, and in the course of comparison with the experiment, a method for calculating the characteristics of the monolayer that was closest to the experimental result was determined. On the basis of the obtained results, conclusions were made on the possibility of reducing residual SSS and deformation in structures with asymmetric reinforcement schemes using a matrix containing carbon nanoparticles.

Keywords: *composite materials, nanosized particles, nanomodification, deformations, residual deformations, residual stresses, SSS.*

АННОТАЦИЯ

В работе исследуется влияние наномодификации углепластика на остаточное напряженно-деформированное состояние (НДС) после формования. Одним из способов снижения остаточных напряжений и деформаций является наномодификация. Основной задачей является определение степени влияния параметров наномодификации на остаточное НДС. В рамках данного исследования изготавливались 4 плиты. Две плиты выполнены из обычного связующего с укладкой $[0_{10}/90_{10}]$ и $[0_{10}/45_{10}]$ и две плиты из модифицированного связующего, с такой же структурой слоев. Для изготовленных пластин измерялись прогибы по каждой из четырех сторон, в ходе которого были получены остаточные деформации в панелях из наномодифицированного углепластика для рассматриваемых укладок с модифицированным связующим и без. Для анализа остаточного напряженного деформированного состояния проводился численный и аналитический расчет. Численный расчет проводился методом конечных элементов для случая, когда пластина закреплена в точке геометрического центра, силовая нагрузка отсутствует, температурная нагрузка – перепад 100°C. Аналитический расчет проводился для случая, когда пластина свободна от закрепления и внешней силовой нагрузки, температурная нагрузка – перепад на 100°C. В процессе исследования были получены варианты физико-механических свойств монослоя с использованием программы Digimat и метода осреднения Мори-Танак. Результаты, полученные аналитическим и численным методами, имеют хорошую корреляцию между собой, а в ходе сопоставления с экспериментом был определен метод расчета характеристик монослоя наиболее приближенный к экспериментальному результату. На основе полученных результатов были сделаны выводы о возможности снижения остаточного НДС и поводом в структурах с несимметричными схемами армирования при использовании матрицы содержащей углеродные наночастицы.

Ключевые слова: композитные материалы, наноразмерные частицы, наномодификация, поводки, остаточные деформации, остаточные напряжения, НДС.

1. INTRODUCTION

The paper investigates the effect of carbon-fiber-reinforced plastic nanomodification on the permanent stress-strain state (SSS) after molding. The creation of polymer composites based on nanomodified binders has long been one of the research priorities in the field of CM manufacturing technologies, and significant progress has been achieved in this area (Hsu and Herakovich, 1977; Zweben, 1977; Ditcher *et al.*, 1981; Manders and Bader, 1981; Christensen, 1982; Hucho *et al.*, 1994; Bakis *et al.*, 2002; Yerramalli and Waas, 2003; Gojny *et al.*, 2005; Fatykhov *et al.*, 2006; Stavichenko, 2007; Zhang

et al., 2007; Ma *et al.*, 2008; Zhang *et al.*, 2009; Jean *et al.*, 2011; Dong and Davies, 2012; Gururaja and Hari Rao, 2012; Raghavulu Thirumalai *et al.*, 2013; Afanasiev *et al.*, 2014; Sathishkumar *et al.*, 2014; Harik, 2014; Swolfs *et al.*, 2014; Jagannatha and Harish, 2015; O'Brien and Zaghi, 2018; Üstündağ *et al.*, 2019; Kurchatov *et al.*, 2019; Bulychev, 2019a; Bulychev, 2019b; Solyaev *et al.*, 2019; Babaytsev and Zotov, 2019). The development of CMs that improve their operational limits is based on reinforcing two or more fibers into a single polymer matrix, which leads to an improved material system called hybrid composites with a wide variety of material properties (Christensen, 1982). The study of the

mechanical characteristics of hybrid composites with glass fibers of $\pm 45^\circ$ and stainless steel $0^\circ/90^\circ$ is no less important when using similar structures (Gururaja and Hari Rao, 2012). In this study, hybrid and non-hybrid composites of various obstacles, fiber content, and weave types were fabricated and subjected to hysteretic tensile loads. The current state of hybrid composite materials, their technology, in terms of material properties, has an obvious advantage with an emphasis on various applications (Ditcher *et al.*, 1981).

As a rule, composites are molded at elevated temperatures, after which they are cooled to operating temperature. Due to the high anisotropy of the physicomaterial properties during cooling, the composite layers shrink unevenly in thickness and direction (Stavichenko, 2007). This leads to the appearance of residual deflections and internal stresses in composite parts (Hsu and Herakovitch, 1977; Ditcher *et al.*, 1981; Fatykhov *et al.*, 2006; Stavichenko, 2007; Üstündağ *et al.*, 2019). One of the ways to reduce residual stresses and strains is nanomodification (Raghavalu Thirumalai *et al.*, 2013; Sathishkumar *et al.*, 2014; Kurchatov *et al.*, 2019; Bulychev, 2019a; Bulychev, 2019b; Solyaev *et al.*, 2019; Babaytsev and Zotov, 2019). The introduction of nanosized particles into the composition of the composite or its components (fiber or binder) allows not only to increase its physical and mechanical properties, but also to improve the picture of the residual stress-strain state.

The main task is to determine the degree of influence of the nanomodification parameters on the residual VAT.

2. MATERIALS AND METHODS

To study the effect of carbon nanomodification, 4 plates were made, characterized by layering and a binder. Two plates are made of a conventional binder with laying $[0_{10}/90_{10}]$ and $[0_{10}/45_{10}]$, and two plates are of a modified binder with the same layer structure. For the manufactured plates, deflections were measured on each of the four sides, during which residual strains were obtained in the panels of nanomodified carbon fiber.

To analyze the residual stress-strain state, a numerical and analytical calculation was performed. Based on the simulation result, the result obtained was compared with each other and with the experiment for the corresponding version of the stacking under consideration.

The studies used fullerene black produced by "Nanopolimer" (Russia). This fullerene black without other additives contains 10% of C60 and C70 fullerenes and 100% carbon. The black density is 0.3 g/cm^3 . The carbon-fiber-reinforced plastic sample was made using EDT-10. Epoxy binder (Russia) and carbon fibers NTA-40 (Toho Tenax Co. Ltd.). Typical matrix properties are as follows: Young's modulus is 2–3 hPa, Poisson's constant is 0.35, and the ultimate stress is 20–25 MPa. In order to obtain nanomodified samples, a binder heated to 90°C without hardeners was added to fullerene black (0.2 wt.%). In the manufacture of samples, the matrix was mixed with a paddle mixer for 30 minutes, followed by ultrasonic dispersion for 5 minutes to reduce agglomeration.

For the experimental study, four plates were made: two plates with $[0_{10}/90_{10}]$ and $[0_{10}/45_{10}]$ with a modified binder and two plates with $[0_{10}/90_{10}]$ and $[0_{10}/45_{10}]$ with a conventional binder. Due to the high anisotropy during cooling after molding, internal stresses arose in the plates and, as a result, leashes. The resulting deflections of the plates were measured on each of the four sides, Figure 1. To measure the deflection of the plate, it was fixed on a flat surface at two extreme points, and the deflection was measured in the center of the side with a caliper. Table 1 presents the results of measurements of the deflections of the manufactured plate with the layer structure $[0_{10}/45_{10}]$ and with the layer structure $[0_{10}/90_{10}]$.

For analytical calculation, we considered a plate free from fastening and external power load, and the temperature load is a difference of 100°C .

Numerical calculation is carried out using the finite element method. The plate under consideration was fixed at the point of the geometric center, there was no power load, and the temperature load was a difference of 1000°C .

3. RESULTS AND DISCUSSION:

3.1. Numerical and analytical modeling of residual strains in panels with asymmetric styling

We will carry out numerical and analytical modeling of residual strains in panels with asymmetric styling. A multilayer panel of a polymer composite with anisotropy due to the non-symmetry of the properties of the structure of the package in thickness is considered. For the panel, we introduce the x, y, z coordinate system so that the x, y axes are centered around the reinforcement plane, and the z-axis is directed along with the panel thickness. Generally, six

internal force factors arise in the panel: $N_x, N_y, N_{xy}, M_x, M_y, M_{xy}$. Physical relations, in this case, will be the following (Equation 1).

Where $N_x^T, N_y^T, N_{xy}^T, N_x^H, N_y^H, N_{xy}^H$ – linear forces caused by thermal deformation (index T) and initial layers tension (index H); $M_x^T, M_y^T, M_{xy}^T, M_x^H, M_y^H, M_{xy}^H$ – linear moments caused by thermal deformation (index T) and initial layers tension (index H); B_{mn}, C_{mn}, D_{mn} – panel generalized rigidities ($m, n = 1, 2, 3$); $\varepsilon_x, \varepsilon_y, \varepsilon_{xy}$ – panel linear strains in the reference plane; $\kappa_x, \kappa_y, \kappa_{xy}$ – panel curvature in the reference plane.

The relation between the panel strains in the reference plane with displacements u_0, v_0 (Equation 2). Relationship between panel curvature and standard rotation angles θ_x, θ_y (Equation 3). The relationship between standard rotation angles with deflection w has the following form (Equation 4). Where ψ_x, ψ_y – lateral shears.

Panel generalized rigidities are defined as follows (Equations 5-8). Where e – reference plane coordinate (for an asymmetric panel is chosen arbitrarily); $m, n = 1, 2, 3, r = 0, 1, 2$. Formulae for the force and moment caused by temperature fields (Equations 9-10). Where (Equations 11-12): Z_k – coordinate of k layer, counted from the reference plane; N – number of layers; $b_{ij}^{(k)}$ – linear stiffness of k layer, referenced to the panel axes (x, y); ($i, j = 1, 2, 3$); ΔT – temperature drop due to cooling; $\overline{\alpha}_1^{(k)}, \overline{\alpha}_2^{(k)}, \overline{\alpha}_3^{(k)}$ – coefficients of linear thermal expansion of k layer in the panel axes.

Similarly, we record the force and moment from the initial tension (Equations 13-14). Where (Equations 15-16): $\overline{\varepsilon}_{H1}^{(k)}, \overline{\varepsilon}_{H2}^{(k)}, \overline{\varepsilon}_{H3}^{(k)}$ – initial layers' strains in the panel axes.

The linear stiffness for k layer in the case of an asymmetric panel are as follows (Equations 17-18). The coefficients of linear thermal expansion for k layer, as well as layer strains caused by the initial tension, in the panel axes, are determined by appropriate transformation (Equations 19-20). In the above formulae, $m^{(k)}$ and $n^{(k)}$ are the trigonometric functions of $\varphi^{(k)}$ layers' orientation angle relative to the x panel (Equation 21).

We will consider a flat panel without initial curvature with free of load and fixing edges, subject to the temperature field evenly distributed

over the thickness (Yerramalli and Waas, 2003; Raghavalu Thirumalai *et al.*, 2013; Sathishkumar *et al.*, 2014; Harik, 2014; Swolfs *et al.*, 2014). The reference surface coincides with the median surface. The orthotropic composite structure $B_{13} = B_{31} = 0$ and $C_{13}, C_{31}, C_{23}, C_{32}, D_{13}, D_{31}$ coefficients are small and can be neglected. Taking this into consideration, the physical relations for the orthotropic composite structure in the expanded form will look like (Equations 22-23).

Thus, in the case of the orthotropic composite structure, the determination of the deformed state splits into 2 independent problems of finding the deflections (curvature component κ_x, κ_y) and twist (κ_{xy}).

3.2. Determination of stress in layers using Hooke's law

Stresses in the layers are determined by Hooke's law using the curvature and deformation components obtained from (Equation 1), i.e. (Equations 24) (Harik, 2014; Sathishkumar *et al.*, 2014; Swolfs *et al.*, 2014; Babaytsev and Zotov, 2019; Bulychev, 2019b). In this case, z_k is the coordinate of the layer's median surface, i.e., $z_k = (Z_k - e) - h_k/2$. To move to the $\sigma_1, \sigma_2, \tau_{12}$ stresses in the layer axes, it is necessary to use the transformation formulae when turning the coordinate axes (Equation 25).

As it is evident from the physical relations (1) in multilayer panels with asymmetric lay-up, layers subject to tension-compression will cause the panel bending. Such complex behavior of panels in highly loaded structures can lead to a decrease in their efficiency. In addition, the molding of such panels will be accompanied by the permanent temperature flexural strains (buckling) (Hsu and Herakovich, 1977; Ditcher *et al.*, 1981; Fatykhov *et al.*, 2006; Stavichenko, 2007; Üstündağ *et al.*, 2019).

Panels with a symmetrical layers' arrangement, i.e., when the same layer ($N-k$) corresponds to the layer (k), where N is the total number of layers in the panel. Taking this into account, we write the formulae for generalized stiffness in the following simplified form (Equation 26).

The Z_k coordinate is then counted from the $e=h/2$ medial plane, and the sum is calculated only by half the panel. The physical relations (Equation 1) for an orthotropic panel with load-free edges will then take such a form (Equations 27-28). From (Equation 28), it is easy to see that the molding of flat panels with a symmetrical panel structure will

not lead to their buckling.

As a result of the study, we can distinguish the algorithm in the analytical analysis of the residual stress-strain state, conditionally divided into the main stages:

1. The calculation of the stiffness characteristics of the package according to Equations 5, 17-21;
2. Determination of internal force factors caused by the initial tension and temperature difference according to Equations 23-26;
3. Determination of the components of deformations and curvature from physical relations (Equation 1);
4. Calculation of stresses in composite layers using Hooke's law (Equations 24, 25).

As the calculated characteristics of the monolayer used in the simulation, the values obtained from the assumption that the reinforcing particles of fullerene soot are absolutely solid and not destroyed, and at the same time have the shape of a sphere, are used. Therefore, a spherical inclusion model was used to model the properties of the filled matrix using the Digimat-MF program using the Mori-Tanaka averaging method (Zweben, 1977; Ditcher *et al.*, 1981; Christensen, 1982; Hucho *et al.*, 1994; Gojny *et al.*, 2005; Stavichenko, 2007; Jean *et al.*, 2011; Gururaja and Hari Rao, 2012; Jagannatha and Harish, 2015). The calculation was carried out with the effective volume content (volume content of the filler + volume content of the interfacial layer, under the assumption that their properties are equal). The effective volumetric content was selected, taking into account the results obtained at the test entrance: 1) in terms of tensile strength; 2) in modulus. In the course of this, the value of the average Young's modulus of the packet was obtained, but it differs from the test. It is known that when using test data for unidirectional material in the calculation of the properties of a layered package, errors can occur. Therefore, it is usually necessary to use the stiffness data of several package options with different layer stackings (Bulychev, 2019b). In this work, for the properties of a monolayer, we will use an overestimated value of the transverse modulus equal to 28 GPa, which is more than the experimental data obtained on unidirectional samples (6.5 GPa). In this case, it is possible to reliably describe the obtained experimental data on the Young's modulus of the composite samples with symmetric stacking $[0^\circ, 90^\circ]$ (Manders and Bader, 1981; Ditcher *et al.*, 1981; Christensen, 1982; Bakis *et al.*, 2002; Ma *et*

al., 2008; Gururaja and Hari Rao, 2012; Afanasiev *et al.*, 2014; O'Brien and Zaghi, 2018).

For numerical and analytical calculations, the calculation was carried out for four variants of the physicomaterial characteristics of the monolayer taking into account two stacking options using the properties of a monolayer of pure carbon fiber and nanomodified carbon fiber, Table 2. A total of 8 calculations were performed for the stacking option $[0_{10}/45_{10}]$, the calculation results of deflections are presented in Table 3 and 8 of the calculations for $[0_{10}/90_{10}]$, the calculation results of the deflections are presented in Table 4.

The results of the distribution of normal stresses between the layers for laying $[0_{10}/45_{10}]$ and $[0_{10}/90_{10}]$ are given in Figure 2. The results obtained by analytical and numerical methods are the same. However, the greatest similarity with experimental data is provided by 4 methods for determining the effective properties of a monolayer. The residual deformations and stresses for laying $[0_{10}/90_{10}]$ are 25-46% higher than in laying $[0_{10}/45_{10}]$. At the same time, nanomodified composites, to a greater extent, reduce residual strains and stresses for laying $[0_{10}/45_{10}]$, about 26%.

4. CONCLUSIONS:

Investigation of the residual stress-strain state of structural elements made of carbon fiber reinforced plastic using the values of thermoelastic characteristics of composite monolayers identified on the basis of the developed methods revealed the possibility of reducing the residual SSS and leach in structures with asymmetric reinforcement schemes using a matrix containing carbon nanoparticles.

The results obtained by analytical and numerical methods are identical. The most similar to experimental data is the fourth method for determining the effective properties of a monolayer. This method is a model of spherical inclusions for modeling the properties of a filled matrix using the Digimat-MF program and the Mori-Tanaka averaging method taking into account the results of physical and mechanical tests.

Using the proposed model of thermoelasticity of the layered composite, it was also found that the addition of nanoparticles within the range recommended by the standard range of 10% only leads to a slight increase in the longitudinal elastic modulus and the shear modulus of the monolayer.

The obtained result showed the possibility of improving the mechanical properties of carbon fiber samples with a nanomodified binder, as well as the possibility of taking into account the effect of carbon nanomodification on the residual stress-strain state (SSS) after molding. The process of further reducing residual deformations and stresses by adding nanosized particles to the composition of the composite or its components (fiber or binder) takes place. However, this process is non-linear and requires further investigation, taking into account the models used to calculate the results obtained.

5. ACKNOWLEDGMENTS:

The work was carried out with the financial support of the state project of the Ministry of Education and Science project code 9.9074.2017/BCh.

6. REFERENCES:

1. Afanasiev, A.V., Nguen, D.Q., Solyaev, Y.O., Dudchenko, A.A. *Nanomechanics Science and Technology: An International Journal*, **2014**, 5(3), 229-238.
2. Babaytsev, A.V., Zotov, A.A. *Russian Metallurgy (Metally)*, **2019**, 13(1), 1452-1455, DOI: 10.1134/S0036029519130020
3. Bakis, C.E., Bank, L.C., Brown, V.L., Cosenza, E., Davalos, J.F., Lesko, J.J., Machida, A., Rizkalla, S.H., Triantafillou, T.C., *Journal of Composites Constructions*, **2002**, 6(2), 73-87.
4. Bulychiev, N.A. *Bulletin of the Lebedev Physics Institute*, **2019a**, 46(7), 219-221.
5. Bulychiev, N.A. *International Journal of Hydrogen Energy*, **2019b**, 44(57), 29933-29936.
6. Christensen, R.M. *Mechanics of composite materials*. New York: A. Wiley-Interscience Publication John Wiley&Sons, **1982**.
7. Ditcher, K., Rhodes, F.E., Webber, J.P.H. *Journal of Strain Analysis*, **1981**, 16, 43-51.
8. Dong, Ch., Davies, I.J. *Materials and Design*, **2012**, 37, 450-457.
9. Fatykhov, M.A., Enikeev, T.I., Akimov, I.A. *Bulletin of OSU*, **2006**, 2(2), 87-92.
10. Gojny, F.H., Wichmann, M.H.G., Fiedler, B.K., Schulte, K. *Composites Science and Technology*, **2005**, 65, 2300-2313.
11. Gururaja, M.N., Hari Rao, A.N. *International Journal of Soft Computing and Engineering*, **2012**, 1(6), 352-355.
12. Harik, V. *Trends in Nanoscale Mechanics: Mechanics of Carbon Nanotubes, Graphene, Nanocomposites and Molecular Dynamics*. Berlin: Springer, **2014**.
13. Hsu, P.W., Herakovich, C.T. *Composite Materials*, **1977**, 5, 442-428.
14. Hucho, C., Kraus, M., Maurer, D., Müller, V., Werner, H., Wohlers, M., Schlögl, R. *Molecular Crystals and Liquid Crystals*, **1994**, 245(1), 277-282.
15. Jagannatha, T.D., Harish, G. *International Journal of Mechanical Engineering and Robotics Research*, **2015**, 4(2), 131-137.
16. Jean, A., Willot, F., Cantournet, S., Forest, S., Jeulin, D. *International Journal for Multiscale Computational Engineering*, **2011**, 9(3), 271-303.
17. Kurchatov, I.S., Bulychiev, N.A., Kolesnik, S.A. *International Journal of Recent Technology and Engineering*, **2019**, 8(3), 8328-8330.
18. Ma, C., Ji, L.J., Zhang, R.P., Zhu, Y.F., Zhang, W., Koratkar, N. *Carbon*, **2008**, 46, 706-710.
19. Manders, P.W., Bader, M.G. *Journal of Materials Science*, **1981**, 16, 2233-2245.
20. O'Brien, C., Zaghi, A.E., Mechanical Characteristics of Hybrid Composites with $\pm 45^\circ$ Glass and $0^\circ/90^\circ$ Stainless Steel Fibers. University of Connecticut. Materials (Basel), **2018**, 4;11(8), Article number E1355.
21. Raghavalu Thirumalai, D.P., Andersen, T.L., Markussen, Ch.M., Madsen B., Lilholt H. Tensile and compression properties of hybrid composites – A comparative study. *Proceedings of the 19th International Conference on Composite Materials (ICCM19) (pp. 1029-1035)*. Canadian Association for Composite Structures and Materials, Montréal, Canada, **2013**.
22. Sathishkumar, T.P., Naveen, J., Satheeshkumar, S. *Journal of Reinforced Plastics and Composites*, **2014**, 33(5), 454-471.
23. Solyaev, Y., Lurie, S., Koshurina, A., Dobryanskiy, V., Kachanov, M. *International Journal of Engineering Science*, **2019**, 134, 66-76.
24. Stavichenko, V.G. *Technological Systems*, **2007**, 4, 7-11.

25. Swolfs, Y., Gorbatiikh, L., Verpoest, I. *Composites Part A: Applied Science and Manufacturing*, **2014**, 67, 181-200.
26. Üstündağ, O., Gook, S., Gumenyuk, A., Rethmeier, M. *Procedia Manufacturing*, **2019**, 36, 112-120.
27. Yerramalli, C.S., Waas, A.M. Compressive behavior of hybrid composites. *Proceedings of 44th AIAA/ASME/ASCE/AHS structures, Structural Dynamics and Materials Conference*, Norfolk, Virginia, **2003**.
28. Zhang, W., Picu, R.C, Koratkar, N., *Journal of Applied Physics*, **2007**, 91(19), 193-109.
29. Zhang, W., Srivastava, I., Zhu, Y.F., Picu, R.C., Koratkar, N. *Small*, **2009**, 5(12), 1403–1407.
30. Zweben, C. *Journal of Materials Science*, **1977**, 12, 1325-1337.

$$\begin{pmatrix} N_x \\ N_y \\ N_{xy} \\ M_x \\ M_y \\ M_{xy} \end{pmatrix} = \begin{pmatrix} B_{11} & B_{12} & B_{13} & C_{11} & C_{12} & C_{13} \\ B_{21} & B_{22} & B_{23} & C_{21} & C_{22} & C_{23} \\ B_{31} & B_{32} & B_{33} & C_{31} & C_{32} & C_{33} \\ C_{11} & C_{12} & C_{13} & D_{11} & D_{12} & D_{13} \\ C_{21} & C_{22} & C_{23} & D_{21} & D_{22} & D_{23} \\ C_{31} & C_{32} & C_{33} & D_{31} & D_{32} & D_{33} \end{pmatrix} \times \begin{pmatrix} \varepsilon_x \\ \varepsilon_y \\ \varepsilon_{xy} \\ \kappa_x \\ \kappa_y \\ \kappa_{xy} \end{pmatrix} - \begin{pmatrix} N_x^T \\ N_y^T \\ N_{xy}^T \\ M_x^T \\ M_y^T \\ M_{xy}^T \end{pmatrix} - \begin{pmatrix} N_x^H \\ N_y^H \\ N_{xy}^H \\ M_x^H \\ M_y^H \\ M_{xy}^H \end{pmatrix}. \quad (\text{Eq. 1})$$

$$\varepsilon_x = \frac{\partial u_0}{\partial x}; \varepsilon_y = \frac{\partial v_0}{\partial y}; \varepsilon_{xy} = \frac{\partial u_0}{\partial y} + \frac{\partial v_0}{\partial x}. \quad (\text{Eq. 2})$$

$$\kappa_x = \frac{\partial \theta_x}{\partial x}; \kappa_y = \frac{\partial \theta_y}{\partial y}; \kappa_{xy} = \frac{\partial \theta_x}{\partial y} + \frac{\partial \theta_y}{\partial x}. \quad (\text{Eq. 3})$$

$$\theta_x = \psi_x - \frac{\partial w}{\partial x}; \theta_y = \psi_y - \frac{\partial w}{\partial y}, \quad (\text{Eq. 4})$$

$$B_{mn} = I^{(0)}_{mn}, \quad (\text{Eq. 5})$$

$$C_{mn} = I^{(1)}_{mn} - eI^{(0)}_{mn}, \quad (\text{Eq. 6})$$

$$D_{mn} = I^{(2)}_{mn} - 2eI^{(1)}_{mn} + e^2 I^{(0)}_{mn}, \quad (\text{Eq. 7})$$

$$I^{(r)}_{mn} = \int_0^h b_{mn} Z^r dt = \frac{1}{r+1} \sum_{k=1}^N b_{mn}^{(k)} (Z_k^{r+1} - Z_{k-1}^{r+1}), \quad (\text{Eq. 8})$$

$$N_x^T = \sum_{j=1}^3 N_{1j}^T, N_y^T = \sum_{j=1}^3 N_{2j}^T, N_{xy}^T = \sum_{j=1}^3 N_{3j}^T, \quad (\text{Eq. 9})$$

$$M_x^T = \sum_{j=1}^3 M_{1j}^T, M_y^T = \sum_{j=1}^3 M_{2j}^T, M_{xy}^T = \sum_{j=1}^3 M_{3j}^T, \quad (\text{Eq. 10})$$

$$N_{ij}^T = \Delta T \sum_{k=1}^N [b_{ij}^{(k)} \overline{\alpha_j^{(k)}} (Z_k - Z_{k-1})]; \quad (\text{Eq. 11})$$

$$M_{ij}^T = \Delta T \sum_{k=1}^N b_{ij}^{(k)} \overline{\alpha_j^{(k)}} \left[\frac{1}{2} (Z_k^2 - Z_{k-1}^2) - e(Z_k - Z_{k-1}) \right]; \quad (\text{Eq. 12})$$

$$N_x^H = \sum_{j=1}^3 N_{1j}^H, N_y^H = \sum_{j=1}^3 N_{2j}^H, N_{xy}^H = \sum_{j=1}^3 N_{3j}^H, \quad (\text{Eq. 13})$$

$$M_x^H = \sum_{j=1}^3 M_{1j}^H, M_y^H = \sum_{j=1}^3 M_{2j}^H, M_{xy}^H = \sum_{j=1}^3 M_{3j}^H, \quad (\text{Eq. 14})$$

$$N_{ij}^H = \sum_{k=1}^N [b_{ij}^{(k)} \overline{\varepsilon_{ij}^{(k)}} (Z_k - Z_{k-1})]; \quad (\text{Eq. 15})$$

$$M_{ij}^H = \sum_{k=1}^N b_{ij}^{(k)} \overline{\varepsilon_{ij}^{(k)}} \left[\frac{1}{2} (Z_k^2 - Z_{k-1}^2) - e(Z_k - Z_{k-1}) \right]; \quad (\text{Eq. 16})$$

$$\begin{aligned} b_{11}^{(k)} &= [\overline{E_1} m^4 + \overline{E_2} n^4 + 2(\overline{E_1} \nu_{12} + 2G_{12}) m^2 n^2]^{(k)} \\ b_{22}^{(k)} &= [\overline{E_1} n^4 + \overline{E_2} m^4 + 2(\overline{E_1} \nu_{12} + 2G_{12}) m^2 n^2]^{(k)} \\ b_{12}^{(k)} &= b_{21}^{(k)} = [\overline{E_1} \nu_{12} + [\overline{E_1} + \overline{E_2} - 2(\overline{E_1} \nu_{12} + 2G_{12})] m^2 n^2]^{(k)} \\ b_{13}^{(k)} &= b_{31}^{(k)} = [mn [\overline{E_1} m^2 - \overline{E_2} n^2 - (\overline{E_1} \nu_{12} + 2G_{12}) (m^2 - n^2)]]^{(k)}, \\ b_{23}^{(k)} &= b_{32}^{(k)} = [mn [\overline{E_1} n^2 - \overline{E_2} m^2 + (\overline{E_1} \nu_{12} + 2G_{12}) (m^2 - n^2)]]^{(k)} \\ b_{33}^{(k)} &= [(\overline{E_1} + \overline{E_2} - 2\overline{E_1} \nu_{12}) m^2 n^2 + G_{12} (m^2 - n^2)]^{(k)} \end{aligned} \quad (\text{Eq. 17})$$

$$\begin{aligned} E_1^{(k)} &= \frac{E_1^{(k)}}{1 - \nu_{12}^{(k)} \nu_{21}^{(k)}}, \\ E_2^{(k)} &= \frac{E_2^{(k)}}{1 - \nu_{12}^{(k)} \nu_{21}^{(k)}}, \end{aligned} \quad (\text{Eq. 18})$$

$$\begin{pmatrix} \overline{\alpha_1} \\ \overline{\alpha_2} \\ \overline{\alpha_3} \end{pmatrix}^{(k)} = \begin{pmatrix} m^2 & n^2 \\ n^2 & m^2 \\ 2mn & -2mn \end{pmatrix}^{(k)} \begin{pmatrix} \alpha_1 \\ \alpha_2 \end{pmatrix}^{(k)}, \quad (\text{Eq. 19})$$

$$\begin{pmatrix} \overline{\varepsilon_{H1}} \\ \overline{\varepsilon_{H2}} \\ \overline{\varepsilon_{H3}} \end{pmatrix}^{(k)} = \begin{pmatrix} m^2 \\ n^2 \\ 2mn \end{pmatrix}^{(k)} (\varepsilon_H)^{(k)}. \quad (\text{Eq. 20})$$

$$\begin{aligned} m^{(k)} &= \cos(\varphi^{(k)}), \\ n^{(k)} &= \sin(\varphi^{(k)}). \end{aligned} \quad (\text{Eq. 21})$$

$$\begin{cases} 0 = B_{11}\varepsilon_x + B_{12}\varepsilon_y + C_{11}\kappa_x + C_{12}\kappa_y - N_x^T - N_x^H \\ 0 = B_{12}\varepsilon_x + B_{22}\varepsilon_y + C_{21}\kappa_x + C_{22}\kappa_y - N_y^T - N_y^H \\ 0 = C_{11}\varepsilon_x + C_{12}\varepsilon_y + D_{11}\kappa_x + D_{12}\kappa_y - M_x^T - M_x^H \\ 0 = C_{21}\varepsilon_x + C_{22}\varepsilon_y + D_{21}\kappa_x + D_{22}\kappa_y - M_y^T - M_y^H \end{cases} \quad (\text{Eq. 22})$$

$$\begin{cases} 0 = B_{33}\varepsilon_{xy} + C_{33}\kappa_{xy} - N_{xy}^T - N_{xy}^H \\ 0 = C_{33}\varepsilon_{xy} + D_{33}\kappa_{xy} - M_{xy}^T - M_{xy}^H \end{cases} \quad (\text{Eq. 23})$$

$$\begin{pmatrix} \sigma_x \\ \sigma_y \\ \tau_{xy} \end{pmatrix}^{(k)} = \begin{pmatrix} b_{11} & b_{12} & b_{13} \\ b_{21} & b_{22} & b_{23} \\ b_{31} & b_{32} & b_{33} \end{pmatrix}^{(k)} \begin{pmatrix} \varepsilon_x + \kappa_x \cdot z_k - \overline{\alpha_1}^{(k)} \cdot \Delta T - \overline{\varepsilon_{H1}}^{(k)} \\ \varepsilon_y + \kappa_y \cdot z_k - \overline{\alpha_2}^{(k)} \cdot \Delta T - \overline{\varepsilon_{H2}}^{(k)} \\ \varepsilon_{xy} + \kappa_{xy} \cdot z_k - \overline{\alpha_3}^{(k)} \cdot \Delta T - \overline{\varepsilon_{H3}}^{(k)} \end{pmatrix} \quad (\text{Eq. 24})$$

$$\begin{pmatrix} \sigma_1 \\ \sigma_2 \\ \tau_{12} \end{pmatrix}^{(k)} = \begin{pmatrix} m^2 & n^2 & 2mn \\ n^2 & m^2 & -2mn \\ -mn & mn & (m^2 - n^2) \end{pmatrix}^{(k)} \begin{pmatrix} \sigma_x \\ \sigma_y \\ \tau_{xy} \end{pmatrix}^{(k)} \quad (\text{Eq. 25})$$

$$\begin{aligned} B_{mn} &= 2 \sum_{k=1}^{N/2} b_{mn}^{(k)} (Z_k - Z_{k-1}) \\ D_{mn} &= \frac{2}{3} \sum_{k=1}^{N/2} b_{mn}^{(k)} (Z_k^3 - Z_{k-1}^3) \\ C_{mn} &= 0 \end{aligned} \quad (\text{Eq. 26})$$

$$\begin{cases} 0 = B_{11}\varepsilon_x + B_{12}\varepsilon_y - N_x^t - N_x^H \\ 0 = B_{12}\varepsilon_x + B_{22}\varepsilon_y - N_y^t - N_y^H \\ 0 = D_{11}\kappa_x + D_{12}\kappa_y \\ 0 = D_{21}\kappa_x + D_{22}\kappa_y \end{cases} \quad (\text{Eq. 27})$$

$$\begin{cases} 0 = B_{33}\varepsilon_{xy} - N_{xy}^t - N_{xy}^H \\ 0 = D_{33}\kappa_{xy} \end{cases} \quad (\text{Eq. 28})$$

Table 1. Comparison of deflections for lay-up $[0_{10} / 45_{10}]$ and lay-up $[0_{10} / 90_{10}]$ with and without nano

		Lay-up experiment $[0_{10}/45_{10}]$	Lay-up experiment $[0_{10}/90_{10}]$
Deflection on the long side, mm	With nano	5.85	4.35
	Without nano	5.95	3.2
Deflection on the short side, mm	With nano	4.1	2.1
	Without nano	3.7	2.75

Table 2. Material stress-strain properties

No.		E_{11} [MPa]	E_{22} [MPa]	G_{12} [MPa]	ν_{12}	$\alpha_1 \times 10^{-6}$ K^{-1}	$\alpha_2, \alpha_3 \times 10^{-6}$ K^{-1}	G_{23} [MPa]
1	Carbon fiber-reinforced plastic	129960	7056	2658	0.593	0.7	42	2214
	Nanomodified carbon fiber-reinforced plastic	135130	19078	8225	0.567	3.4	44	6085
2	Carbon fiber-reinforced plastic	129510	5211	1917	0.596	0.46	42	1632
	Nanomodified carbon fiber-reinforced plastic	129760	6266	2337	0.594	0.6	42	1965
3	Carbon fiber-reinforced plastic	129500	4730	2050	0.29	0.19	20	1670
	Nanomodified carbon fiber-reinforced plastic	129750	5700	2500	0.29	0.26	20	2010
4	Carbon fiber-reinforced plastic	129500	4730	2050	0.29	-10.4	20	1670
	Nanomodified carbon fiber-reinforced plastic	129750	5700	2500	0.29	-12	20	2010

Table 3. Comparison of deflections for options 1-4 and lay-up $[0_{10} / 45_{10}]$ with experiment

		1	2	3	4	Experiment
Deflection on the long side, mm	With nano	10.6	6.6	3.2	5.1	4.35
	Without nano	7	5.3	2.8	4.3	3.2
Deflection on the short side, mm	With nano	5.7	3.5	1.7	2.8	2.1
	Without nano	3.8	2.8	1.5	2.3	2.75

Table 4. Comparison of deflections for options 1-4 and lay-up $[0_{10} / 90_{10}]$ with experiment

		1	2	3	4	Experiment
Deflection on the long side, mm	With nano	19.9	12.4	5.6	9.2	5.85
	Without nano	13.3	10	5	7.7	5.95
Deflection on the short side, mm	With nano	10.7	6.7	3	4.9	4.1
	Without nano	7.2	5.4	2.7	4.2	3.7

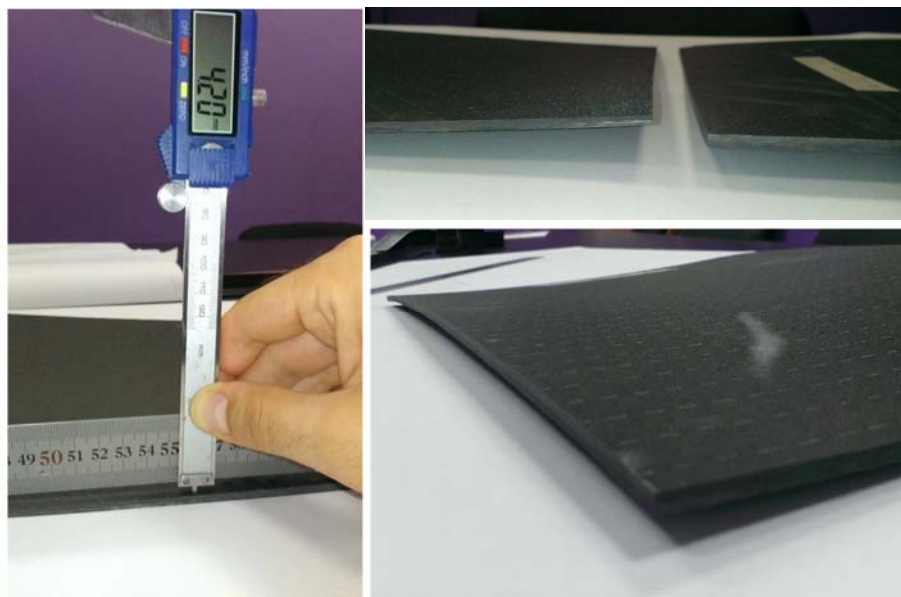


Figure 1. *Measurement of the panel deflection using caliper rule*

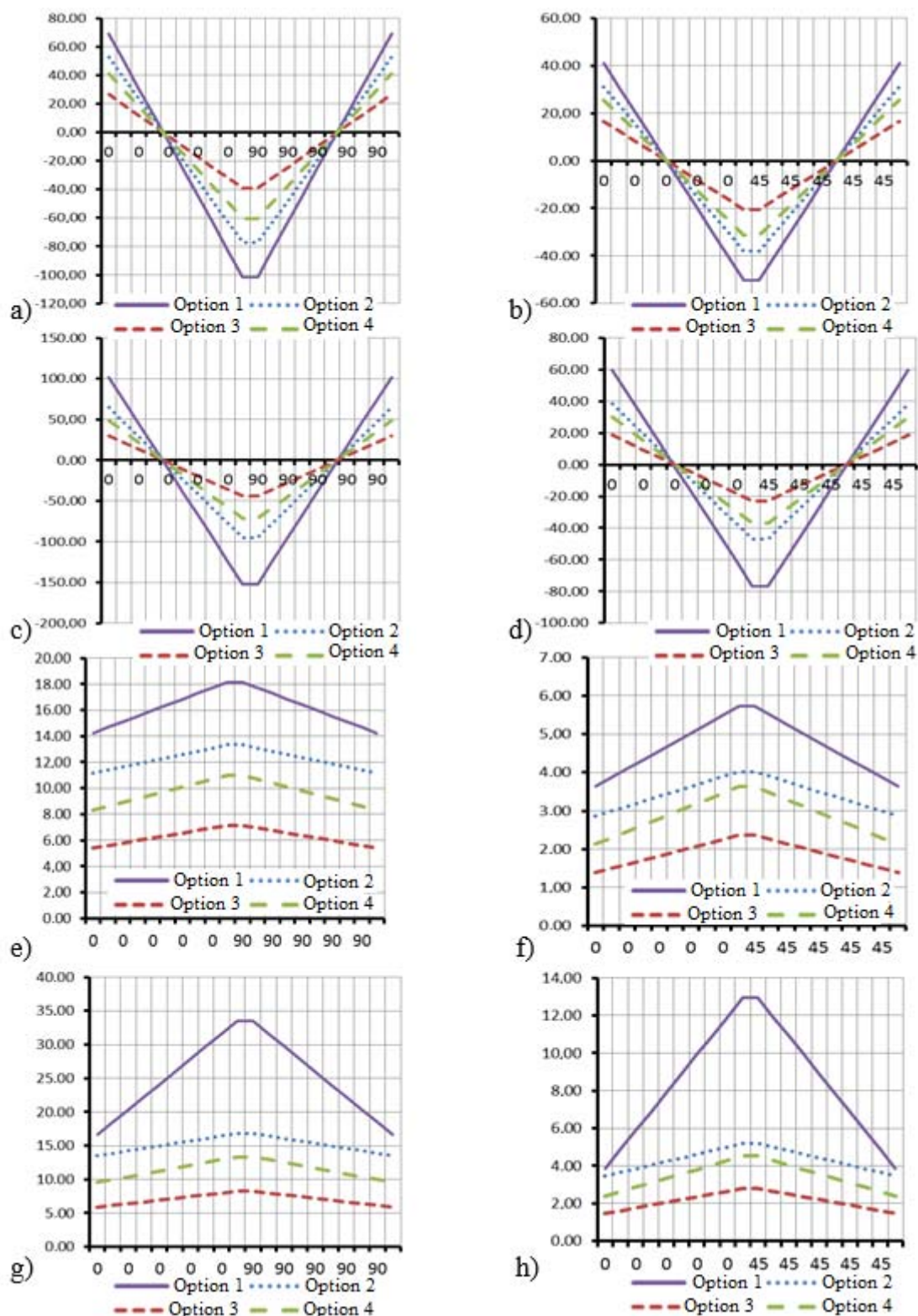


Figure 2. The results of the distribution of normal stresses between the layers for laying $[0_{10}/90_{10}]$: a, e – without nanoparticles; c, g – with nanoparticles and $[0_{10}/45_{10}]$: b, d – without nanoparticles, d, h – with nanoparticles (a, b, c, d – Distribution of normal stresses in the layers σ_1 , MPa; e, f, g, h – Distribution of normal stresses in the layers σ_2 , MPa)

INSTRUCTIONS FOR AUTHORS

We ask authors always to visit the online instructions for the use of the latest instructions available. Manuscripts must be submitted using the template available on the Journal's website.

PREPARATION OF MANUSCRIPTS

1. PREPARATION OF MANUSCRIPTS
2. THE FIRST PAGE OF THE MATERIAL
3. THE CENTRAL TEXT PART OF THE MATERIAL
4. GUIDELINES FOR REFERENCES
5. FIGURES
6. TABLES
7. MATHEMATICAL EXPRESSIONS
8. SUPPLEMENTARY MATERIAL

1. PREPARATION OF MANUSCRIPTS (TEMPLATE):

Please, observe the following points in preparing manuscripts. Papers not conforming strictly to these instructions may be returned to their authors for appropriate revision or may be delayed in the review process.

Readability: Manuscripts should be written in clear, concise, and grammatically correct English (British or American English throughout). The editors can not undertake wholesale revisions of poorly written papers. Every paper must be free of unnecessary jargon and readable by any specialist of the related field. The abstract should be written in an explanatory style that will be comprehensible also to readers who are not experts in the subject matter.

General format: The complete paper has to be written, preferably in Rich Text Format either in an MS-Word (.doc) or a Br.Office (.odt) compatible file. Page size: A4, margins: 2 cm on each side, line spacing: single, font type: Arial. Please leave headers and footers unchanged, since the editors should fill it. Please check guidelines for accurate information based on all different categories (review articles, technical notes, etc.) available. A single file of the whole manuscript should then be submitted through TQJ's email (journal.tq@gmail.com). The Journal no longer accepts submissions in any other form.

The order of the material should be as follows: Title, Author(s), Abstract, Keywords, Main text (Introduction, Review of Literature, Definitions (if any), Materials and Methods, Results, Discussion), Acknowledgements (if any), References, Appendix (if any). This structure of the main text is not obligatory, but the paper must be logically presented. Footnotes should be avoided. The main text must be written with font size 11, Arial, justify. Within each main section, three levels of subheadings are available, and the titles must be bold, bold, and italic, italic, respectively.

The manuscript should contain the whole text, figures, tables, and explanations according to the followings (we suggest using the template file):

2. THE FIRST PAGE OF THE MATERIAL SHOULD BE AS FOLLOWS:

Title: (both in Portuguese and English). The editors can provide the title in Portuguese for those whose Portuguese is not the first language. It should be brief and informative. The title should reflect

the essential aspects of the article, in a preferably concise form of not more than 100 characters and spaces. Font size 12, Arial, capital letters, center alignment.

By-line: Names (size 12, Arial, small capital) of the authors. No inclusion of scientific titles is necessary. In the case of two or more authors, place their names in the same row, separate them with a semicolon (;) and please indicate the corresponding author with * in superscript. The corresponding author should be the one submitting the article online and an e-mail given (only one e-mail) below the addresses of all authors. Authors from different institutions must be labeled with numbers in superscript after the names. Addresses of the authors, phone, and fax number should also be given (size 10). Authors should be grouped by address.

Abstract: (both in Portuguese and English). The editors can provide the translation of the abstract to Portuguese for those whose Portuguese is not the first language. Required for all manuscripts in which the problem, the principal results, and conclusions are summarized. The abstract must be self-explanatory, preferably typed in one paragraph, and limited to max. 200 words. It should not contain formulas, references, or abbreviations. The name ABSTRACT should be written in capital letters, Arial, size 12, bold, left alignment. The abstract should be written font Arial, size 10, justify.

Keywords: (both in Portuguese and English. The editors can provide the keywords in Portuguese for those who Portuguese is not the first language). Keywords should not exceed five, not including items appearing in the title. The keywords should be supplied, indicating the scope of the paper. Size 10, italic, justify, only the word Keywords must be bold, left alignment.

The authors should include Abbreviations and Nomenclature listings when necessary.

3. THE CENTRAL TEXT PART OF THE MATERIAL SHOULD BE AS FOLLOWS:

The words Introduction, Materials, and Methods, Results and Discussion, Conclusion, Acknowledgements, and References must be written in capital letters, Arial, font size 12, left alignment, bold.

Introduction: The introduction must clearly state the problem, the reason for doing the work, the hypotheses or theoretical predictions under consideration, and the essential background. It should not contain equations or mathematical notation. A brief survey of the relevant literature so that a non-specialist reader could understand the significance of the presented results.

Materials and Methods: Provide sufficient details to permit repetition of the experimental work. The technical description of methods should be given when such methods are new.

Results and Discussion: Results should be presented concisely. Also, point out the significance of the results and place the results in the context of other work and theoretical background.

Conclusion: Summarize the data discussed in the Results and Discussion showing the relevance of the work and how different it is from other researches. Also, point out the benefits and improvements that can be observed to develop new scientific standards that can change something in the related field.

Acknowledgments: (if any) These should be placed in a separate paragraph at the end of the text, immediately before the list of references. It may include funding information too.

References: In the text, references should be cited in Harvard style (Author, year). Alternatively, the author's surname may be integrated into the text, followed by the year of publication in parentheses. Cite only essential resources, avoid citing unpublished material. References to papers "in press" must mean that the article has been accepted for publication, at the end of the paper list references alphabetically by the last name of the first author. Please, list only those references that are cited in the text and prepare this list as an automatically numbered list. The word References with size 12, Arial,

bold, capital letters, left alignment.

4. GUIDELINES FOR REFERENCES:

- The Journal uses the APA (American Psychological Association) FORMAT CITATION as follows:

Author's surname, initial(s). (Date Published). **Title of Source.** **Location of publisher:** **publisher.** Retrieved from URL

Author Rules:

1. **Initials are separated and ended by a period.**

Examples: Goldani, E.
De Boni, L.A.B.

2. **Multiple authors are separated by commas and an ampersand.**

Examples: Goldani, E. & De Boni, L.A.B.
Goldani, E., De Boni, L.A.B. & Casanova, K.

3. **Multiple authors with the same surname and initial: add their name in square brackets.**

Example: Goldani, E. [Eduardo]

Date Rules:

1. **Date refers to date of publishing**
2. **If the date is unknown 'n.d' is used in its place.**

Example: De Boni, L.A.B (n.d)

Title Rules:

1. **The format of this changes depending on what is being referenced**

Publisher Rules:

1. **If in the US: the city and two letter state code must be stated.**

Examples: San Diego, CA
Houston, TX
New York, NY

2. **If not in the US: the city and country must be stated.**

Examples: Sydney, Australia
Lisbon, Portugal
Rome, Italy

Retrieved from URL: This is used if the source is an online source

- ✓ The Journal recommend to visit the websites below for a more detailed information.

< <https://www.mendeley.com/guides/apa-citation-guide> >
< <https://libguides.murdoch.edu.au/APA6/all> >
< <https://aut.ac.nz.libguides.com/APA6th/referencelist> >

5. FIGURES:

The number of pictures (including graphs, diagrams, etc.) should not exceed 10 and should be submitted either in JPG or PNG formats. All photographs, charts, and diagrams should be numbered consecutively (e.g., Figure 1) in the order in which they are referred in the text. Caption must appear below the figure (size 11, bold, italic) and should be sufficiently detailed to enable us to understand apart from the text. Explanation of lettering and symbols should be also given in the caption and only exceptionally in the figures. Figures should be of good quality and preferably in black and white. (Color figures will appear in the downloadable files, but all papers will be printed in black and white.) Scanned figures should be at a resolution of 800 dpi/bitmap for line graphs. Diagrams containing chemical structures should be of high graphical quality and always be of the same size so that they can be uniformly reduced. Figures should have a maximum width of one Journal column (8.5 cm) to be inserted on the body of the text so that they can be applied to the standards of the Journal. If the figures exceed 8.5 cm, they will be placed at the end of the article. Also, authors may be requested to submit each figure also as an image file in one of the following formats: jpg or png. For pictures, graphs, diagrams, tables, etc., identical to material already published in the literature, authors should seek permission for publication from the companies or scientific societies holding the copyrights and send it to the editors of TQ along with the final form of the manuscript.

6. TABLES:

Tables should be self-explanatory. They should be mentioned in the text, numbered consecutively (e.g., Table 1) and accompanied by title at the top (size 11, bold, italic). Please insert all the tables in the text, do not enclose huge tables which cannot be fit within the page margins.

7. MATHEMATICAL EXPRESSIONS:

In general, minimize unusual typographical requirements, use solidus, built-up fractions. Avoid lengthy equations that will take several lines (possibly by defining terms of the equation in separate displays). For drawing equations, please use the Equation Editor of Word, if possible. Make subscripts and superscripts clear. Display only those mathematical expressions that must be numbered for later reference or that need to be emphasized. Number displayed equations consecutively throughout the paper. The numbers should be placed in parentheses to the right of the equation, e.g. (Eq. 1).

8. SUPPLEMENTARY MATERIAL:

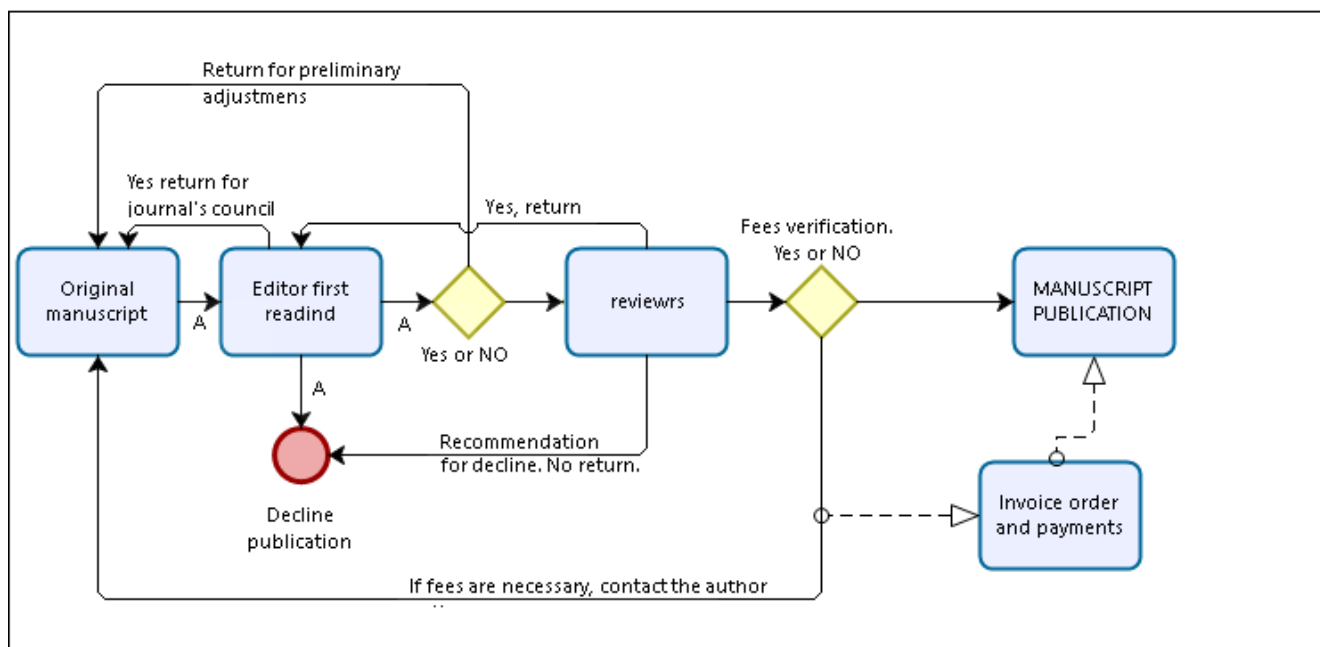
Any Supplementary material (other figures, tables, diagrams, etc.) should be placed at the end of the manuscript and indicated as such. A single.PDF - document, including the supplementary material, should be submitted.

Editors, at any time of the editing process, may ask authors to split off part of the manuscript, presenting it as supplementary material.

PAGE CHARGES (1), DISCOUNTS (2), AND FREE PUBLICATION OPPORTUNITIES (3)

Authors are required to pay a publication fee to share in the costs of production. The fee will be asked if and when the article is accepted for publication. Once full payment has been made (PayPal, Bank Transfer, or Western Union Services), the paper will be published at the Ahead of Print and scheduled for the next available issue. All waivers (as well as the publication fee requests) are applied to the accepted papers after successful peer-review only.

Please observe the flowchart below to understand how we work.



1. PAGE CHARGES PRICES:

*Brazilian authors, USD 110

*Other countries income groups:

High income (or nuclear-capable countries) - USD 300

Upper middle-income USD 250

Lower middle-income USD 120

Lower middle income (Heavily indebted poor countries (HIPC)) USD 100

Low-income USD 100

Low income (Heavily indebted poor countries (HIPC)) USD 80

(*) Classification according to the World Bank list of economies (June 2017)

** Optional page formatting fee + USD 80. If you don't have time or the proper conditions to execute the formatting of your manuscript, we will find someone to do it for you.

2. ADDITIONAL FEES FOR PUBLICATION

a) *Proofreading and / or plagiarism*

If the submitted manuscript has more than 100 grammatical errors or plagiarism greater than 5%, a fee of USD 200 will be charged. This fee does not guarantee publication of the manuscript and is non-refundable.

b) *Alteration of PDF files*

After undergoing the final check of the manuscript file and Pre-Print PDF generation, a USD 100 will be charged with the authors in case they want to change something. For each new change, the fee is charged again.

If there is no need, additional fees are not charged.

3. DISCOUNTS

a) **50% discount** for authors who support other journals from the team (*Southern Brazilian Journal of Chemistry* (this is a 100% free journal)), with 1 manuscript approved for publication;

b) **100% discount** for authors who support other journals from the team (*Southern Brazilian Journal of Chemistry* (this is a 100% free journal)), with 2 manuscripts approved for publication;

c) **Volume discount**, if you are an author/collaborator of the journal, that has published with us 4 manuscripts (paid your full corresponded price), your fifth manuscript will be free of charge. Later the counting cycle restart.

4. FREE PUBLICATION:

a) Young scientists publishing the first manuscript of their career with us. Requirements: Copy of the curriculum with no publications; maximum of 2 authors; join the author alliance program (free).

b) All personal related to the production of the journals, from Brazil and abroad;

c) Long-time collaborators. Authors that have been publishing with us over the last decade, for more than 4 times, will pay no fees. Thank you for working with us for all those years.

d) Paper considered by the Editors of high quality, priority, and relevance for the development of the society shall pay no fees. Note that this condition is a small recognition prize, not something that you may request. Thank you for your comprehension.